

ENCYCLOPEDIA *of AGROPHYSICS*

Edited by

J. Gliński, J. Horabik and J. Lipiec

Glossary
Terms
Included

 Springer

ENCYCLOPEDIA *of*
AGROPHYSICS

Encyclopedia of Earth Sciences Series

ENCYCLOPEDIA OF AGROPHYSICS

About the Editors:

Em. Prof. Jan Gliński, soil scientist, is a full member of the Polish Academy of Sciences. He was Director of the Institute of Agrophysics in Lublin from 1982 to 2003. He was one of the initiators and an active promoter of scientific cooperation between many universities and institutes in Poland and abroad, and organized many international conferences on agrophysics. He has been a member of the ISSS since 1961 and was vice-chairman of the Commission I (Soil Physics) of the ISSS in the period 1986–1990. He is the author or co-author of numerous papers, books, monographs, patents and multilingual dictionaries in the field of agrophysics. He participated actively in eight World ISSS Congresses (1960, 1964, 1974, 1978, 1986, 1990, 1994, and 1998). He serves as the Editor-in-Chief of the journal International Agrophysics (since 1992).

Józef Horabik is Director of the Institute of Agrophysics, Polish Academy of Sciences, in Lublin, Poland. He holds a M.Sc. degree in physics, a Ph.D. in agricultural engineering, and is a professor of Agronomy. He is the Editor-in-Chief of Acta Agrophysica, an Associate Editor of International Agrophysics, and a member of the Editorial Board of the Polish Journal of Soil Science. He works together with over 20 scientific institutions in Poland and abroad. Over 260 scientific publications have been published to which he has contributed. His scientific interests are: applied physics, agrophysics, physical properties of agromaterials, modelling of mechanics of granular solids and food powders.

Jerzy Lipiec is a Professor of Soil Science and Plant Relations at the Institute of Agrophysics of the Polish Academy of Sciences in Lublin, Poland. He received his M.Sc. (1969), Ph.D. (1977) and D.Sc. (1983) in Soil Science from the Agricultural University of Lublin. He contributed widely in research activities in various European countries, Japan, US and international projects. He serves on the advisory boards of several scientific journals and has published over 250 scientific papers. He is author or co-author of several chapters in books, including works as *Soil Physical Conditions and Plant Roots* (CRC Press).

Editorial Board

Winfried E.H. Blum

Institute of Soil Research

University of Natural Resources and Applied Life Sciences (BOKU)

Peter-Jordan-Str. 82

1190 Vienna

Austria

Josse De Baerdemaeker

Division of Mechatronics

Biostatistics and Sensors (MeBioS)

Department of Biosystems, K.U. Leuven

Kasteelpark Arenberg 30

3001 Leuven

Belgium

Charles W. Finkl

Department of Geosciences

Florida Atlantic University

Boca Raton, FL 33431

USA

Stanisław Grundas

Institute of Agrophysics

Polish Academy of Sciences

ul. Doświadczalna 4

20-290 Lublin

Poland

Rainer Horn

Institute for Plant Nutrition and Soil Science

Christian Albrechts University of Kiel

Olshausenstr. 40

24118 Kiel

Germany

Krystyna Konstankiewicz

Institute of Agrophysics

Polish Academy of Sciences

ul. Doświadczalna 4

20-290 Lublin

Poland

Yakov A. Pachepsky

Environmental Microbial and Food Safety Laboratory

Animal and Natural Resource Institute

Beltsville Agricultural Research Center, USDA-ARS

10300 Baltimore Ave, Bldg. 173, BARC-EAST

Beltsville, MD 20705

USA

Evgeny V. Shein

Department of Soil Physics

Moscow State University

Moscow 119992

Russia

Aims of the Series

The *Encyclopedia of Earth Sciences Series* provides comprehensive and authoritative coverage of all the main areas in the Earth Sciences. Each volume comprises a focused and carefully chosen collection of contributions from leading names in the subject, with copious illustrations and reference lists.

These books represent one of the world's leading resources for the Earth Sciences community. Previous volumes are being updated and new works published so that the volumes will continue to be essential reading for all professional earth scientists, geologists, geophysicists, climatologists, and oceanographers as well as for teachers and students. See the dust jacket of this volume for a current list of titles in the *Encyclopedia of Earth Sciences Series*. Go to <http://www.springerlink.com/reference-works/> to visit the "Earth Sciences Series" on-line.

About the Series Editor

Professor Charles W. Finkl has edited and/or contributed to more than eight volumes in the Encyclopedia of Earth Sciences Series. For the past 25 years he has been the Executive Director of the Coastal Education & Research Foundation and Editor-in-Chief of the international *Journal of Coastal Research*. In addition to these duties, he is Research Professor at Florida Atlantic University in Boca Raton, Florida, USA. He is a graduate of the University of Western Australia (Perth) and previously worked for a wholly owned Australian subsidiary of the International Nickel Company of Canada (INCO). During his career, he acquired field experience in Australia; the Caribbean; South America; SW Pacific islands; southern Africa; Western Europe; and the Pacific Northwest, Midwest, and Southeast USA.

Founding Series Editor

Professor Rhodes W. Fairbridge (deceased) has edited more than 24 Encyclopedias in the Earth Sciences Series. During his career he has worked as a petroleum geologist in the Middle East, been a WW II intelligence officer in the SW Pacific and led expeditions to the Sahara, Arctic Canada, Arctic Scandinavia, Brazil and New Guinea. He was Emeritus Professor of Geology at Columbia University and was affiliated with the Goddard Institute for Space Studies.

ENCYCLOPEDIA OF EARTH SCIENCES SERIES

ENCYCLOPEDIA *of* AGROPHYSICS

edited by

**JAN GLIŃSKI
JÓZEF HORABIK
JERZY LIPIEC**

*Institute of Agrophysics
Polish Academy of Sciences
Lublin
Poland*



Springer

Library of Congress Control Number: 2011924206

ISBN: 978-90-481-3584-4

This publication is available also as:

Electronic publication under ISBN 978-90-481-3585-1 and

Print and electronic bundle under ISBN 978-90-481-3586-8

Published by Springer
P.O. Box 17, 3300 AA Dordrecht, The Netherlands

Printed on acid-free paper

Cover illustration: Photo 26814460 from photos.com. © 2011 photos.com

Every effort has been made to contact the copyright holders of the figures and tables which have been reproduced from other sources. Anyone who has not been properly credited is requested to contact the publishers, so that due acknowledgment may be made in subsequent editions.

All Rights Reserved for Contributions on *Hardpan Soils: Management; Soil Penetrometers and Penetrability; Stable Isotopes in Evaluation of Green House Gas Emissions*
© Springer Science + Business Media B.V. 2011

No part of this work may be reproduced, stored in a retrieval system, or transmitted in any form or by any means, electronic, mechanical, photocopying, microfilming, recording, or otherwise, without written permission from the Publisher, with the exception of any material supplied specifically for the purpose of being entered and executed on a computer system, for exclusive use by the purchaser of the work.

Contents

Contributors	xxi	After Harvest Technology	14
Preface	xlv	Aggregate Stability	14
Absorption	1	Aggregation Indices	14
Absorptivity	1	Agricultural Products	14
Acoustic Emission	1	Agricultural Raw Materials	14
Acoustic Tomography	1	Agriculture and Food Machinery, Application of Physics for Improving	14
Adaptable Tillage	1	<i>Leszek Mieszkalski</i>	
Adhesion	1	Agroforestry Systems, Effects on Water Balance in Cropping Zone	26
Adsorption	1	<i>Andrzej Kędziora</i>	
Adsorption Complex	2	Agrogeology <i>Ward Chesworth</i>	29
Adsorption Energy and Surface Heterogeneity in Soils	2	Agrophysical Objects (Soils, Plants, Agricultural Products, and Foods)	34
<i>Zofia Sokołowska and Stefan Sokołowski</i>		<i>Jan Gliński</i>	
Adsorption Energy of Water on Biological Materials	5	Agrophysical Properties and Processes	35
<i>Jiří Bláhovec</i>		<i>Jan Gliński, Józef Horabik and Jerzy Lipiec</i>	
Advection	7	Agrophysics: Physics Applied to Agriculture	35
Aeration of Agricultural Products	7	<i>Jan Gliński, Józef Horabik and Jerzy Lipiec</i>	
<i>Marek Molenda</i>		Air Entry Value	48
Aeration of Soils and Plants	8	Air Flux (Resistance) in Plants and Agricultural Products	48
<i>Witold Stępniewski</i>		<i>Agnieszka Kaleta and Krzysztof Górnicki</i>	
Aerodynamics	13		

vi	CONTENTS		
Air Humidity	49	Biofilms in Soil <i>Mette Burmølle, Annelise Kjøller and Søren J. Sørensen</i>	70
Air Porosity	49		
Algae, the Potential Source of Energy <i>Magdalena Frąc</i>	49	Biofilms in the Food Environment <i>Katarzyna Czaczyk and Kamila Myszka</i>	75
Alkalinity, Physical Effects on Soils <i>Lajos Blaskó</i>	49	Biogas	78
Alternative Sources of Energy from Agriculture Biomass – A European Perspective <i>Piotr Kowalik</i>	52	Biomass	78
Alumino-Silicate Clay Minerals	55	Biomass as an Environmentally Benign Energy Source <i>Keith Openshaw</i>	78
Anaerobiosis	55	Biomechanics	88
Angle of Repose	55	Biomes	88
Anion Exchange Capacity	55	Biospeckle <i>Artur Zdunek</i>	88
Anisotropy of Soil Physical Properties <i>Xinhua Peng</i>	55	Biota	89
Anoxia and Hypoxia	57	Biotechnology, Physical and Chemical Aspects <i>Zdzisław Targoński</i>	89
Anthric Saturation	57	Bound Water	90
Arable Land Use	57	Boussinesq Equation	90
Attenuation	57	Bowen Ratio	91
Atterberg Limits	57	Bragg's Law	91
Available Water (Capacity)	57	Breads: Physical Properties <i>Renata Różyło and Janusz Laskowski</i>	91
Backscattering <i>Bogusław Usowicz</i>	59	Brightness Temperature in Monitoring of Soil Wetness <i>Jerzy Usowicz</i>	93
Bedrock	60	Bruise	94
Bending Properties of Plants <i>Jiří Blahovec</i>	60	Buffer Capacity of Soils <i>Mieczysław Hajnos</i>	94
Bernoulli's Principal	62	Bulk Density of Soils and Impact on Their Hydraulic Properties <i>Shmuel Assouline</i>	95
Binding Force (Plants)	62	Burrow	100
Biochemical Responses to Soil Management Practices <i>Jan Koper and Małgorzata Brzezińska</i>	62	Bypass Flow in Soil <i>Horst H. Gerke</i>	100
Biocolloids: Transport and Retention in Soils <i>Tammo S. Steenhuis, Verónica L. Morales, M. Ekrem Cakmak, Anthony E. Salvucci and Wei Zhang</i>	66		

	CONTENTS	vii	
Caking	107	Coagulation	138
Caliche (Lime-Pan)	107	Cohesion	138
Canopy Structure	107	Colloids	138
Capillarity	107	Color Composite (Multiband Photography)	138
Capillary Fringe	107	Color in Food Evaluation <i>Seong Pal Kang</i>	138
Carbon Losses Under Dryland Conditions, Tillage Effects <i>Félix Moreno, José M. Murillo and Engracia Madejón</i>	108	Color Indices, Relationship with Soil Characteristics <i>Manuel Sánchez-Marañón</i>	141
Carbon Nanotube	110	Compactibility	145
Catchment (Catchment Basin)	110	Compaction of Soil	145
Cation Exchange Capacity	110	Compensatory Uptake	145
Cementation	110	Compressibility	145
Cereals, Evaluation of Utility Values <i>Dariusz Dziki and Janusz Laskowski</i>	110	Compression Index	145
Chemical Imaging in Agriculture <i>Adam Paweł Kuczyński</i>	113	Compression Point	145
Chemical Time Bomb, Relation to Soil Physical Conditions <i>Halina Smal</i>	116	Compression Test, Triaxial Conditioners, Effect on Soil Physical Properties <i>Ryszard Dębicki</i>	145
Chisel	117	Conductivity	148
Clay Minerals and Organo-Mineral Associates <i>Tatiana Victorovna Alekseeva</i>	117	Cone Index	148
Claypan and its Environmental Effects <i>Stephen H. Anderson</i>	122	Confined Compression Test	148
Cleavage Plane	125	Consistency	148
Climate Change: Environmental Effects <i>Miroslav Kutilek</i>	125	Consolidation	148
Climate Risk	135	Contact Area of Agricultural Tyres, Estimation <i>Etienne Diserens and Abdallah Alaoui</i>	148
Climate Stress Mitigation Tillage	135	Continuity Equation	153
Clod	135	Contour-Furrow Irrigation	153
Clusters in Soils <i>David L. Pinskiy</i>	135	Controlled Traffic Farming <i>Thomas Anken and Martin Holpp</i>	153
	135	Conventional Tillage	155
	135	Coulomb's Law	155

viii	CONTENTS	
Coupled Heat and Water Transfer in Soil <i>Joshua L. Heitman and Robert Horton</i>	155	Denitrification 200
Cracking in Soils <i>Pascal Boivin</i>	162	Density 200
Crop Emergence, the Impact of Mechanical Impedance <i>W. R. Whalley and W. E. Finch-Savage</i>	163	Desertification: Indicators and Thresholds 200 <i>Max Kuderna and Adam Zsolnay</i>
Crop Responses to Soil Physical Conditions <i>Jerzy Lipiec, Artur Nosalewicz and Jacek Pietrusiewicz</i>	167	Detachment 207
Crop Rotation	176	Deterministic Model 207
Crop Water Use Efficiency	176	Dew Point 207
Crop Yield Losses Reduction at Harvest, from Research to Adoption <i>Bogusław Szot, Mieczysław Szpryngiel and Jerzy Tys</i>	176	Dielectric Loss Tangent 207
Cropping Systems, Effects on Soil Physical Properties <i>Stephen H. Anderson</i>	180	Dielectric Properties of Agricultural Products 207 <i>Stuart O. Nelson and Samir Trabelsi</i>
Crushing Strength	184	Diffuse Double Layer (DDL) 213 <i>Md. Abdul Mojid</i>
Crust	184	Diffusion in Soils 214 <i>Witold Stępniewski, Henryk Sobczuk and Marcin Widomski</i>
Cultivation Under Screens, Aerodynamics of Boundary Layers <i>Josef Tanny</i>	185	Dilatancy 220
Cumulative Infiltration	187	Discharge 220
Cutan	187	Dispersion 220
Cyclic Compressibility	187	Dispersivity 220
Darcy's Law	189	Diurnal Strains in Plants 220 <i>Pawel Kojas and Tomasz Rusin</i>
Databases on Physical Properties of Plants and Agricultural Products <i>Agnieszka Kaleta and Krzysztof Górnicki</i>	189	DNA in Soils: Mobility by Capillarity 224 <i>Maria Teresa Ceccherini and Giacomo Pietramellara</i>
Databases of Soil Physical and Hydraulic Properties <i>Attila Nemes</i>	194	Double Layer 228
Deflation	200	Drainage 228
Deflocculation	194	Drip Irrigation 228
Degradation of Soil	200	Drought 228
	200	Drought Stress, Effect on Soil Mechanical Impedance and Root (Crop) Growth 228 <i>W. R. Whalley and L. J. Clark</i>
	200	Drying of Agricultural Products 231 <i>Digvir S. Jayas and Chandra B. Singh</i>
	200	Duripan 232

	CONTENTS	ix
Dynamic Load	232	Empirical Model
Earthworms as Ecosystem Engineers <i>Patrick Lavelle</i>	233	Energetically Homogenous (Heterogenous) Surface
Ecohydrology <i>Maciej Zalewski</i>	235	Energy Balance of Ecosystems <i>Andrzej Kędziora</i>
Ecosystem	237	Energy Balance of a Field
Effective Rainfall	237	Enthalpy
Elasticity	237	Entropy
Elastoplasticity	237	Environmental Conserving Tillage
Electrical Conductivity	237	Enzyme
Electrical Double Layer (Diffuse Layer, Double Layer)	237	Enzymes in Soils <i>Małgorzata Brzezińska</i>
Electrical Permeability	237	Erodibility of Soil
Electrical Properties of Agricultural Products <i>Zuzana Hlaváčová</i>	237	Erosion
Electrical Properties of Soils <i>Shmulik P. Friedman</i>	242	Erosivity
Electrical Resistivity	255	Estimation of Quartz Content in Mineral Soils <i>Vlodek R. Tarnawski, Toshihiko Momose, Wey H. Leong and David J. W. Piper</i>
Electrical Resistivity to Assess Soil Properties <i>Guy Richard, Maud Séger, Arlène Besson and Isabelle Cousin</i>	256	Evaporation
Electrical Susceptibility	260	Evapotranspiration
Electrochemical Measurements in Soils <i>Andrzej Bieganowski and Jolanta Cieśla</i>	260	<i>Viliam Novák</i>
Electrokinetic (Zeta) Potential of Soils <i>Mieczysław Hajnos and Jolanta Cieśla</i>	264	Exchange Complex
Electromagnetic Field	267	Exchangeable Ions
Electromagnetic Fields, Impact on Seed Germination and Plant Growth <i>Stanisław Pietruszewski</i>	267	Extrusion, Effect on Physical and Chemical Properties <i>Leszek Mościcki</i>
Elutriation	269	Exudate, Root
Eluviation	270	Fabric
Emissivity	270	Failure
		Fatigue Strength
		Fats: Rheological Characteristics <i>Fernanda Peyronel, Thamara Laredo and Alejandro G. Marangoni</i>

x	CONTENTS	
Fertilizers (Mineral, Organic), Effect on Soil Physical Properties <i>Kuntal Hati and Kalikinkar Bandyopadhyay</i>	296	Funnel Flow 321 Furrow 321
Fick's Law	299	Furrow Erosion 321
Field Water Capacity <i>Karl Vanderlinden and Juan V. Giráldez</i>	299	Furrow Irrigation 321 Gas Exchange In Soils 323
Fingering	300	Gases Sink 323
Firmness	300	Geologic Erosion 323
Fissures	300	Geostatistics 323
Flexural Strength	301	Gibbs Free Energy 323
Flocculation and Dispersion Phenomena in Soils <i>Emil Chibowski</i>	301	Grain Physics 323 <i>Stanisław Gründas, Agnieszka Nawrocka and Josef Pecen</i>
Flooding, Effects on Soil Structure <i>Miguel A. Taboada, Patricia L. Fernández and María F. Varela</i>	304	Grains, Aerodynamic and Geometric Features 327 <i>Bronisława Barbara Kram</i>
Flow	308	Grass Fibers, Physical Properties 333 <i>Majda Sfiligoj Smole and Silvo Hribenik</i>
Flowability	308	Gravimetric Water Content 334
Fluvial Erosion	308	Gravitational Potential 334
Flux	308	Gravity Head (Gravity Potential) 334
Food Freezing	308	Grazing-Induced Changes of Soil Mechanical and Hydraulic Properties 334 <i>Julia Krümmelbein</i>
Food Machinery	308	Greenhouse, Climate Control 338 <i>Istvan Farkas</i>
Fourier's Law	308	Greenhouse Effect 339
Fractal Analysis in Agrophysics <i>Yakov Pachepsky, Fernando San José Martínez and Miguel Angel Martin</i>	309	Greenhouse Gas Fluxes: Effects of Physical Conditions 339 <i>Ryusuke Hatano</i>
Fracture	315	Greenhouse Gases Sink in Soils 351 <i>Teresa Włodarczyk</i>
Fragipan	315	Ground-Penetrating Radar, Soil Exploration 354 <i>Jim Doolittle</i>
Friction	316	Groundwater 355
Friction Phenomena in Soils <i>Rainer Horn</i>	316	Gully (Linear) Erosion 355
Frozen Foods	318	Hardening 357
Fruits, Mechanical Properties and Bruise Susceptibility <i>Margarita Ruiz-Altisent and Guillermo P. Moreira</i>	318	

CONTENTS			xi
Hardpan	357	Hydrophobicity of Soil <i>Paul D. Hallett, Jörg Bachmann, Henryk Czachor, Emilia Urbanek and Bin Zhang</i>	378
Hardpan Soils: Management <i>Warren J. Busscher</i>	357	Hypobaric Storage	384
Hardsetting Soils: Physical Properties <i>Neyde Fabíola Balarezo Giarola, Herdjania Veras de Lima and Alvaro Pires da Silva</i>	360	Hysteresis in Foods <i>Matthew Caurie</i>	384
Harvest Technology	364	Hysteresis in Soil <i>Cezary Ślawiński</i>	385
Heat Advection	364	Ice Erosion (Glacial Erosion, Thermal Erosion)	387
Heat Balance	364	Illuviation	387
Heat Capacity	364	Image Analysis in Agrophysics <i>Magnus Persson</i>	387
Heat Diffusion	364	Imbibition	390
Heat of Condensation	364	Indicator Plants	390
Heat of Sublimation	364	Infiltrability	390
Heat of Vaporization	364	Infiltration Capacity	390
Heat of Wetting	364	Infiltration in Soils <i>Miroslav Kutílek</i>	390
Henry's Law	364	Insolation	393
Hooke's Law	364	Institute of Agrophysics in Lublin: Progress in Agrophysics <i>Józef Horabik and Grzegorz Józefaciuk</i>	393
Horticulture Substrates, Structure and Physical Properties <i>Anna Słowińska-Jurkiewicz and Monika Jaroszuk-Sierocińska</i>	364	Institute of Agrophysics in Saint-Petersburg: Roots of Agrophysics <i>Igor B. Uskov and Victor P. Yakushev</i>	396
Humus	367	Integrated Drainage	399
Hydraulic Diffusivity	367	Interception	399
Hydraulic Gradient	368	Interflow	400
Hydraulic Head	368	Internal Drainage	400
Hydraulic Properties of Unsaturated Soils <i>Martinus Th. van Genuchten and Yakov Pachepsky</i>	368	Interrill Erosion	400
Hydrodynamic Dispersion	376	Intersecting Surfaces Approach (Isa)	400
Hydropedological Processes in Soils <i>Svatopluk Matula</i>	376	Intrinsic Permeability	400
Hydrophobicity	378	Ion Exchange	400

xii	CONTENTS
Ion Hydration	400 Liquid Limit (Upper Plastic Limit, Atterberg Limit) 428
Irrigation and Drainage, Advantages and Disadvantages <i>Lajos Blaskó</i>	400 Loading 428
Irrigation Water Use Efficiency	402 Lodging of Crops 428
Irrigation with Treated Wastewater, Effects on Soil Structure <i>Guy J. Levy</i>	403 Lysimeters: A Tool for Measurements of Soil Fluxes 428 Johann Fank
Isoelectric Point	407 Machine Vision 433
Isotopes	407 Machine Vision in Agriculture 433 John Billingsley
Isotropy and Anisotropy in Agricultural Products and Foods <i>Józef Horabik and Marek Molenda</i>	407 Macropore Flow 436
Kernel	411 Magnetic Properties of Soils 436 Andrey Alekseev
Kinematic Viscosity	411 Magnetic Resonance Imaging in Soil Science 439 Andreas Pohlmeier
Kirchhoff's Laws	411 Magnetic Treatment of Irrigation Water, Effects on Crops 444
Kriging	411 Basant Maheshwari and Harsharn Grewal
Laminar and Turbulent Flow in Soils <i>Henryk Czachor</i>	413 Management Effects on Soil Properties and Functions 447 Rainer Horn
Laminar Flow	413 Mapping of Soil Physical Properties 455 Jan Gliński and Janusz Ostrowski
Land Reclamation	414 Matric Potential 460
Landfill	414 Matrix of the Soil 460
Landslide	414 Measurements Non-Destructive 460
Laplace Equation	414 Mechanical Impacts at Harvest and After Harvest Technologies 460 Zbigniew Ślipek and Jarosław Frączek
Latent Heat	414 Mechanical Resilience of Degraded Soils 464 Heiner Fleige
Layered Soils, Water and Solute Transport <i>H. M. Selim</i>	421 Membranes, Role in Water Transport in the Soil–Root–Xylem System 465 Marian Kargol
Leaching of Chemicals in Relation to Soil Structure <i>Tom M. Addiscott</i>	424 Microbes and Soil Structure 470 Vadakattu Gupta
Least Limiting Water Range (LLWR)	424 Microbes, Habitat Space, and Transport in Soil 472 Karl Ritz
Light Interception by Plant Canopies <i>Pierre Dutilleul</i>	
Liming, Effects on Soil Properties <i>Tadeusz Filipek</i>	

CONTENTS	xiii		
Microcosm	475	Neural Networks in the Modeling of Drying Processes <i>Istvan Farkas</i>	509
Micro-Irrigation	475	Nitrification	511
Microstructure of Plant Tissue <i>Krystyna Konstankiewicz</i>	476	Nondestructive Measurements in Fruits <i>Francisco J. García-Ramos</i>	511
Mineral Fertilizers	481	Nondestructive Measurements in Soil <i>Wojciech M. Skierucha</i>	513
Mineralisation	481	Noninvasive Quantification of 3D Pore Space Structures in Soils <i>Stephan Peth</i>	516
Mineral–Organic–Microbial Interactions <i>Małgorzata Dąbek-Szreniawska and Eugene Balashov</i>	481	Non-Limiting Water Range (NLWR)	520
Mire	483	Non-Thermal Technologies	520
Modeling the Thermal Conductivity of Frozen Foods <i>Vlodek R. Tarnawski, Wey H. Leong and Toshihiko Momose</i>	483	Normal Stress	520
Modulus of Elasticity (Young's Modulus)	489	Numerical Methods (Model)	520
Modulus of Rigidity	489	Ohm's Law	521
Mohre Circle of Stress	489	Online Measurement of Selected Soil Physical Properties <i>Abdul Mounem Mouazen</i>	521
Monitoring Physical Conditions in Agriculture and Environment <i>Wojciech M. Skierucha</i>	489	Organic Carbon in Soil	523
Mualem Equation	492	Organic Dusts, Electrostatic Properties <i>Wiktor Pietrzyk and Marek Horyński</i>	523
Mulching	492	Organic Farming, Effect on the Soil Physical Environment <i>Apostolos Papadopoulos</i>	526
Mulching, Effects on Soil Physical Properties <i>Antonio Jordán, Lorena M. Zavala and Miriam Muñoz-Rojas</i>	492	Organic Fertilizers	528
Munsell Color System	496	Organic Matter	528
Mycorrhizal Symbiosis and Osmotic Stress <i>Juan M. Ruiz-Lozano</i>	496	Organic Matter, Effects on Soil Physical Properties and Processes <i>Rattan Lal</i>	528
Nanomaterials in Soil and Food Analysis <i>Subramanian Viswanathan</i>	499	Ornamental Plants, Physical Properties <i>Paweł Szot</i>	534
Nature Conservation Management <i>Tadeusz J. Chmielewski</i>	503	Ortstein, Physical Properties <i>Jacek Chodorowski</i>	535
Neural Networks in Agrophysics <i>Krzysztof Lamorski</i>	505		

xiv	CONTENTS		
Osmosis	535	Perched Groundwater	561
Osmotic Potential	536	Percolation	561
Overburden Pressure	536	Permafrost	561
Overland Flow <i>Elias Dimitriou</i>	536	Permanent Charge	561
Oxidation-Reduction Reactions in the Environment <i>Zofia Stępniewska</i>	536	Permeability	561
Oxygenology <i>Witold Stępniewski</i>	541	Photosynthesis	561
Packing Density	543	Physical Degradation of Soils, Risks and Threats <i>Winfried E. H. Blum</i>	562
Pan	543	Physical Dimensions and Units Use in Agriculture <i>Wojciech Skierucha, Marcin Widomski, Witold Stępniewski and Bogusław Usowicz</i>	563
Parent Material and Soil Physical Properties <i>Andrzej Mocek and Wojciech Owczarzak</i>	543	Physical Phenomena and Properties Important for Storage of Agricultural Products <i>Marek Molenda and Józef Horabik</i>	567
Partial Pressure	547	Physical Processes	573
Particle Density	547	Physical Properties	573
Particle Film Technology <i>Michael Glenn</i>	547	Physical Properties as Indicators of Food Quality <i>Martin G. Scanlon</i>	573
Particle-Size Distribution	548	Physical Properties of Raw Materials and Agricultural Products <i>Bohdan Dobrzański, Jr. and Rafał Rybczyński</i>	579
Particulate Organic Matter	548	Physical Properties for Soil Classification <i>Johan Bouma</i>	589
pe	548	Physical Protection of Organic Carbon in Soil Aggregates <i>Tiphaine Chevallier</i>	592
Peatlands: Environmental Functions <i>Tadeusz J. Chmielewski and Danuta Urban</i>	548	Physical Quality, Soil	595
Peats and Peatlands, Physical Properties <i>Lech Wojciech Szajdak, Jan Szatyłowicz and Raimo Kõlli</i>	551	Physical (Mechanical) Weathering of Soil Parent Material <i>Stefan Skiba</i>	595
Ped	555	Physico-Chemical Methods for Remediation of Contaminated Soils <i>Toshko Raytchev and Svetla Rousseva</i>	596
Pedon	555	Physics of Near Ground Atmosphere <i>Evgenny V. Shein and Tatiana A. Arkhangelskaya</i>	597
Pedotransfer Functions <i>Yakov Pachepsky and Martinus Th. van Genuchten</i>	556	Physics of Plant Nutrition <i>Evgenny V. Shein</i>	600
Penetrability	561		
Penetration Resistance	561		
Penman Equation	561		
Penman-Monteith Equation	561		

	CONTENTS	xv
Piezometer Head	602	Polish Society of Agrophysics <i>Bogusław Szot</i>
Planck's Law	602	Pore Morphology and Soil Functions
Plant Bending	602	<i>Marcello Pagliai</i>
Plant Biomechanics <i>Tomasz Rusin and Paweł Kojas</i>	602	Pore Size Distribution <i>Miroslav Kutílek</i>
Plant Disease Symptoms, Identification from Colored Images <i>Anyela Valentina Camargo Rodriguez and Jan T. Kim</i>	605	Porosimetry <i>Mieczysław Hajnos</i>
Plant Drought Stress: Detection by Image Analysis <i>Istvan Farkas</i>	608	Porosity
Plant Lodging, Effects, and Control <i>Grażyna Podolska</i>	609	Potential Evapotranspiration
Plant Nutrients	610	Power Spectrum
Plant Physical Characteristics in Breeding and Varietal Evaluation <i>Bogusław Szot and Wojciech Rybiński</i>	610	Precision Agriculture: Proximal Soil Sensing <i>Viacheslav I. Adamchuk and Raphael A. Viscarra Rossel</i>
Plant Root Strength and Slope Stability <i>Sekhar Lukose Kuriakose and L. P. H. van Beek</i>	622	Pre-Compression Stress
Plant Roots and Soil Structure <i>A. Pierret and C. J. Moran</i>	628	Pre-Compression Test
Plant Temperature <i>Piotr Baranowski</i>	632	Preferential Flow
Plant Tropisms, Physics <i>Fernando Migliaccio, Alessio Fortunati and Paola Tassone</i>	633	Pressure Head
Plant Wellness <i>Istvan Farkas</i>	637	Pressure Potential
Plant–Soil Interactions, Modeling <i>Tiina Roose</i>	637	Priming Effects in Relation to Soil Conditions – Mechanisms <i>Evgenia Blagodatskaya and Yakov Kuzyakov</i>
Plastic Limit	639	Proton Nuclear Magnetic Resonance (NMR) Relaxometry in Soil Science <i>Gabriele E. Schaumann</i>
Plasticity	639	Proximal Soil Sensing
Plasticity Number	639	Puddling: Effect on Soil Physical Properties and Crops
Plate Sinkage Test	639	<i>Gunnar Kirchhof, T. P. Tuong and H. B. So</i>
Poiseuille's Law	639	Pugging
		Quality of Agricultural Products in Relation to Physical Conditions <i>Guillermo P. Moreda and Margarita Ruiz-Alcisent</i>
		Radiative Properties

xvi	CONTENTS		
Rainfall Interception by Cultivated Plants <i>Józef Kolodziej</i>	679	Seed	729
Rainfall Water Use Efficiency	681	Seepage	729
Raw Materials	681	Self Similarity	730
Redox Potential (E_h)	681	Sensory Evaluation	730
Reflectivity	681	Shear Strength	730
Remote Sensing of Soils and Plants Imagery <i>Ramsis B. Salama</i>	681	Shear Stress	730
Representative Elementary Volume	693	Sheet Erosion	730
Rheology in Agricultural Products and Foods <i>Jiří Blahovec</i>	693	Sheet Flow	730
Rheology in Soils <i>Wibke Markgraf</i>	700	Shrinkage	730
Rheopexy	705	Shrinkage and Swelling Phenomena in Agricultural Products <i>Bohdan Dobrzański, Jr.</i>	730
Rhizosphere <i>Jerzy Lipiec and Jan Gliński</i>	705	Shrinkage and Swelling Phenomena in Soils <i>Pascal Boivin</i>	733
Rigidity	709	Slaking	735
Rill Erosion	709	Slope Stability	736
Root Length Density	709	Snowmelt Infiltration <i>Yukiyoshi Iwata</i>	736
Root Responses to Soil Physical Limitations <i>A. Glyn Bengough</i>	709	Soil Aeration	736
Root Strength	712	Soil Aggregates	736
Root System Architecture: Analysis from Root Systems to Individual Roots <i>Loïc Pagès</i>	712	Soil Aggregates, Structure, and Stability <i>Apostolos Papadopoulos</i>	736
Root Water Uptake: Toward 3-D Functional Approaches <i>Mathieu Javaux, Xavier Draye, Claude Doussan, Jan Vanderborght and Harry Vereecken</i>	717	Soil Aggregation and Evaporation <i>Barbara Witkowska-Walczak</i>	740
Roughness	722	Soil Biota, Impact on Physical Properties <i>Pascal Boivin and Roxane Kohler-Milleret</i>	740
Runoff	722	Soil Colour Index	742
Salinity, Physical Effects on Soils <i>Lajos Blaskó</i>	723	Soil Compactibility and Compressibility <i>Stephan Peth</i>	742
Scale (Dependency, Invariance)	725	Soil Erodibility	746
Scaling of Soil Physical Properties <i>Asim Biswas and Bing Cheng Si</i>	725	Soil Erosion Modeling <i>John N. Quinton</i>	746
		Soil Functions <i>Winfried E. H. Blum</i>	747

CONTENTS	xvii		
Soil Hydraulic Properties Affecting Root Water Uptake <i>Leilah Krounbi and Naftali Lazarovitch</i>	748	Soil Water Flow <i>Miroslav Kutílek</i>	798
Soil Hydrophobicity and Hydraulic Fluxes <i>Peter Hartmann</i>	754	Soil Water Management <i>Willibald Loiskand and Gerhard Kammerer</i>	802
Soil Parent Material	754	Soil Water Potential (Pressure, Head)	805
Soil Penetrability, Effect on Animal Burrowing <i>Petr Heneberg</i>	754	Soil Welding	805
Soil Penetrometers and Penetrability <i>Francisco J. Arriaga, Birl Lowery and Randy Raper</i>	757	Soil–Plant–Atmosphere Continuum <i>Cezary Ślawiński and Henryk Sobczuk</i>	805
Soil Phases <i>Jan Gliński</i>	760	Soil–Wheel Interactions <i>Hiroshi Nakashima</i>	810
Soil Physical Degradation: Assessment with the Use of Remote Sensing and GIS <i>Stanisław Białousz</i>	761	Soilborne Diseases, Control by Physical Methods <i>Jaacov Katan and Abraham Gamliel</i>	813
Soil Physical Quality <i>Blair M. McKenzie, Judith M. Tisdall and Wendy H. Vance</i>	770	Soils and Plants Aeration	816
Soil Pore	777	Soils and Plants Oxygenation	816
Soil Separates	777	Solar Drying of Biological Materials <i>Istvan Farkas</i>	816
Soil Structure and Mechanical Strength <i>Rainer Horn and Heiner Fleige</i>	777	Solute Transport in Soils <i>Yves Coquet and Valérie Pot</i>	819
Soil Structure, Intersecting Surface Approach, and its Applications <i>Victor Yakov Chertkov</i>	780	Sorption	824
Soil Structure, Visual Assessment <i>Lothar Müller</i>	783	Sorptivity of Soils <i>Budiman Minasny and Freeman Cook</i>	824
Soil Surface Sealing and Crusting <i>Shmuel Assouline</i>	786	Space Soil Physics <i>Robert Heinse</i>	826
Soil Temperature Effect	791	Spatial Variability of Properties and Processes	827
Soil Texture: Measurement Methods <i>Andrzej Bieganowski and Magdalena Ryżak</i>	791	Spatial Variability of Soil Physical Properties <i>Ole Wendoroth, Edwin L. Ritchey, Susmitha Nambuthiri, John H. Grove and Robert C. Pearce</i>	827
Soil Tillage	794	Specific Surface Area of Soils and Plants <i>Zofia Sokołowska</i>	839
Soil Tilth: What Every Farmer Understands but no Researcher Can Define <i>Douglas L. Karlen</i>	794	Stable Isotopes in Evaluation of Greenhouse Gas Emissions <i>Kurt A. Spokas</i>	845
	794	Stable Isotopes, Their Use in Soil Hydrology <i>Peggy Macaigne</i>	849
	794	Standardization in Agrophysics <i>Andrzej Bieganowski and Magdalena Ryżak</i>	854

CONTENTS			
xviii			
Steady Flow	854	Surface-Water Excess	889
Sticky	854	Suspension	889
Stochastic Model	854	Swelling	889
Stokes' Law	854	Temperature Effects in Soil <i>Graeme D. Buchan</i>	891
Stomatal Conductance, Photosynthesis, and Transpiration, Modeling <i>Andrée J. Tuzet</i>	855	Tensile Strength	895
Stratification of Soil Porosity and Organic Matter <i>Alan J. Franzluebbers</i>	858	Tensiometry <i>Krzysztof Lamorski</i>	895
Strength	861	Terrestrial Ecosystem	897
Stress Relaxation	861	Texture	897
Stress–Strain Relations <i>Stephan Peth and Rainer Horn</i>	862	Thermal Capacity	897
Stress–Strain Relationships: A Possibility to Quantify Soil Strength Defined as the Precompression Stress <i>Rainer Horn and Stephan Peth</i>	867	Thermal Conductivity	897
Subdrainage	869	Thermal Diffusivity	898
Subirrigation	870	Thermal Imaging	898
Subsoil	870	Thermal Technologies in Food Processing <i>António A. Vicente and Luís F. Machado</i>	898
Subsoil Compaction <i>Rainer Horn and Heiner Fleige</i>	870	Thermosequence	902
Subsurface Water	873	Thixotropy	903
Surface and Subsurface Waters <i>Todd C. Rasmussen</i>	874	Tillage, Impacts on Soil and Environment <i>Márta Birkás</i>	903
Surface Area	877	Tillage Erosion	906
Surface Charge	877	Jianhui Zhang	906
Surface Properties and Related Phenomena in Soils and Plants <i>Grzegorz Józefaciuk</i>	877	Tillage Pan	909
Surface Roughness, Effect on Water Transfer <i>Frédéric Darboux</i>	887	Tilth	910
Surface Runoff	889	Top Soil	910
Surface Storage Capacity	889	Toposequence	910
Surface Tension	889	Trace Elements in Crops: Effects of Soil Physical and Chemical Properties <i>Holger Kirchmann and Jan Eriksson</i>	910
	889	Traffic Farming	912
	889	Trafficability and Workability of Soils <i>Lothar Müller, Jerzy Lipiec, Ted S. Kornecki and Stephan Gebhardt</i>	912

	CONTENTS	xix	
Transmissivity	924	Visible and Thermal Images for Fruit Detection <i>Duke M. Bulanon, Thomas F. Burks and Victor Alchanatis</i>	944
Transpiration	924		
Transpiration Ratio	924	Visual Assessment	954
Treated Waste Water	924	Vitreosity	954
Triaxial Compression Test <i>Marek Molenda</i>	924	Void Ratio	954
Trickle Irrigation	925	Volumetric Water Content	954
Tropical Fruits and Vegetables: Physical Properties <i>K. P. Baiyeri and F. D. Ugese</i>	925	Vughs	954
Tropical Soils, Physical Properties <i>Charles A. Igwe</i>	934	Water Application Efficiency	955
Tropical Watersheds, Hydrological Processes <i>Juergen Baumann</i>	937	Water Balance in Terrestrial Ecosystems <i>Joanna Sposób</i>	955
Tropisms	938	Water Budget in Soil <i>Alberto Pistocchi</i>	959
Turbidity <i>Ewa A. Czyż and Anthony R. Dexter</i>	938	Water Diffusion	964
Turf	940	Water Effects on Physical Properties of Raw Materials and Foods <i>Piotr P. Lewicki</i>	964
Turgor Pressure	940	Water Erosion: Environmental and Economical Hazard <i>Jerzy Rejman</i>	968
Two-Phase Flow	940	Water in Forming Agricultural Products <i>Jiří Blahovec</i>	971
Underground Runoff	941	Water Management	973
Unsaturated Zone	941	Water Productivity	973
Unsteady Flow	941	Water Release Curve	973
Urban Soils, Functions <i>Thomas Nehls and Gerd Wessolek</i>	941	Water Reservoirs, Effects on Soil and Groundwater <i>Waldemar Mioduszewski</i>	973
Utility Value of Cereals	942	Water Retention Curve	975
Vadose Zone	943	Water Stress	975
Van Der Waals Forces	943	Water Table	975
Van Genuchten Equation	943	Water Uptake and Transports in Plants Over Long Distances <i>Marian Kargol</i>	975
Vapor Pressure	943		
Viscosity	943		

Water Use Efficiency in Agriculture: Opportunities for Improvement <i>Meni Ben-Hur</i>	979	Wetting Front	996
		Wien's Law	996
Water-Repellent	984	Wildfires, Impact on Soil Physical Properties <i>Henryk Czachor</i>	996
Waterlogged Soil	984	Wilting Point	997
Watershed	984	Wind Erosion	997
Weather, Effects on Plants <i>Vlasta Štekauerová</i>	984	<i>Christof Gromke and Katrin Burri</i>	
		Windbreak and Shelterbelt Functions	1000
Wellness	987	<i>Andrzej Kędziora</i>	
Wetlands, Management, Degradation and Restoration <i>Kathrin Kiehl</i>	987	Workability	1004
Wetness	992	X-ray Method to Evaluate Grain Quality <i>Alexander M. Demyanchuk, Leonid P. Velikanov, Michael V. Arhipov and Stanisław Grundas</i>	1005
Wettability	992	Author Index	1011
Wetting and Drying, Effect on Soil Physical Properties <i>Sudhakar M. Rao</i>	992	Subject Index	1013

Contributors

Viacheslav I. Adamchuk
Bioresource Engineering Department
McGill University
21,111 Lakeshore Road
Ste-Anne-de-Bellevue, QC H9X 3V9
Canada
viacheslav.adamchuk@mcgill.ca

Tom M. Addiscott
Soil Science Department
Rothamsted Research
West Common
Harpenden, Herts AL5 2JQ
UK
tom.addiscott@ukf.net

Abdallah Alaoui
Hydrology Group
Department of Geography
University of Bern
Hallerstrasse 12
3012 Bern
Switzerland
alaoui@giub.unibe.ch

Victor Alchanatis
Agricultural Research Organization
Volcani Center
Institute of Agricultural Engineering
Bet Dagan
Israel
victor@volcani.agri.gov.il

Andrey Alekseev
Laboratory Geochemistry and Soil Mineralogy
Institute of Physicochemical and Biological Problems
of Soil Science
Russian Academy of Sciences
Instituskaya street 2
Pushchino, Moscow Region 142290
Russia
alekseev@issp.serpuhov.su

Tatiana Victorovna Alekseeva
Laboratory Geochemistry and Soil Mineralogy
Institute of Physicochemical and Biological Problems
of Soil Science
Russian Academy of Sciences
Institutskaya street 2
Pushchino, Moscow region 142290
Russia
alekseeva@issp.serpuhov.su
tanalekseeva@rambler.ru

Stephen H. Anderson
Department of Soil, Environmental, and Atmospheric
Sciences
University of Missouri
302 ABNR Building
Columbia, MO 65211
USA
AndersonS@missouri.edu

Thomas Anken
Federal Department of Economic Affairs
Agroscope Reckenholz-Tänikon Research Station ART
Tänikon
8356 Ettenhausen
Switzerland
thomas.anken@art.admin.ch

Michael V. Arhipov
 Laboratory of Seed Biophysics
 Agrophysical Research Institute of Russian Academy
 of Agricultural Sciences
 Grazdansky av. 14
 195220 St. Petersburg
 Russia
 sznmc@spb.lanck.net

Tatiana A. Arkhangelskaya
 Department of Soil Physics
 Moscow State University
 Moscow 119991
 Russia
 arhangelskaia@rambler.ru

Francisco J. Arriaga
 U.S. Department of Agriculture-Agricultural
 Research Service
 National Soil Dynamics Laboratory
 411 S.Donahue Drive
 Auburn, AL 36832
 USA
 francisco.arriaga@ars.usda.gov

Shmuel Assouline
 Environmental Physics and Irrigation
 Institute of Soil, Water and Environmental Sciences
 Agricultural Research Organization – Volcani Center
 P.O. Box 6
 Bet Dagan 50250
 Israel
 vwshmuel@agri.gov.il

Jörg Bachmann
 Institute of Soil Science
 Leibniz University of Hannover
 Herrenhaeuser Str. 2
 30419 Hannover
 Germany
 bachmann@ifbk.uni-hannover.de

K. P. Baiyeri
 Department of Crop Science
 University of Nigeria
 Nsukka, Enugu State
 Nigeria
 paul.baiyeri@unn.edu.ng
 paulkayodebaiyeri@yahoo.com

Eugene Balashov
 Agrophysical Research Institute RAAS
 Russian Academy of Agricultural Sciences
 14 Grazhdansky Prospekt, St. Petersburg
 195220 St. Petersburg
 Russia
 Eugene_Balashov@yahoo.co.uk

Kalikinkar Bandyopadhyay
 Central Institute for Cotton Research
 Marutha Malai Main Road
 Coimbatore 641 003, Tamil Nadu
 India
 kk.bandyopadhyay@gmail.com

Piotr Baranowski
 Institute of Agrophysics
 Polish Academy of Sciences
 Doświadczalna 4
 20-290 Lublin
 Poland
 pbaranow@ipan.lublin.pl

Juergen Baumann
 Hydroagricultural Infrastructure (SGIH-GDTT)
 National Water Commission (CONAGUA)
 Av. Insurgentes Sur 2416, Piso 6
 Mexico City, Federal District, D.F 4340
 Mexico
 jh_baumann@web.de

A. Glyn Bengough
 Scottish Crop Research Institute (SCRI)
 Dundee DD2 5DA
 UK
 Glyn.Bengough@scri.ac.uk

Meni Ben-Hur
 Soil Chemistry
 Institute of Soil, Water, and Environmental Sciences
 The Volcani Center, ARO
 P.O. Box 6
 Bet Dagan 50250
 Israel
 meni@agri.gov.il

Arlène Besson
 Institut National de la Recherche Agronomique (INRA)
 Unité de Science du Sol, Centre de Recherche d'Orléans
 BP 20619
 45166 Olivet cedex, Orléans
 France

Stanisław Białousz
 Department of Photogrammetry, Remote Sensing and GIS
 Warsaw University of Technology
 Plac Politechniki 1
 00-661 Warsaw
 Poland
 S.Bialousz@gik.pw.edu.pl

Andrzej Bieganowski
 Institute of Agrophysics
 Polish Academy of Sciences
 Doświadczalna 4
 20-290 Lublin
 Poland
 a.bieganowski@ipan.lublin.pl

John Billingsley
 University of Southern Queensland
 Darling Heights
 Toowoomba, QLD 4350
 Australia
 billings@usq.edu.au

Márta Birkás
 Department of Soil Management
 Institute of Crop Production, Szent István University
 Gödöllő
 2103 Gödöllő
 Hungary
 Birkas.Marta@mkk.szie.hu

Asim Biswas
 Department of Soil Science
 University of Saskatchewan
 Saskatoon, SK S7N 5A8
 Canada
 asim.biswas@usask.ca

Evgenia Blagodatskaya
 Department of Agroecosystem Research
 University of Bayreuth
 95440 Bayreuth
 Germany
 and
 Institute of Physicochemical and Biological Problems
 in Soil Science
 Russian Academy of Sciences
 Pushchino 142290
 Russia
 sblag@mail.ru

Jiří Blahovec
 Department of Physics
 Czech University of Life Sciences
 Kamycka 129
 16521 Prague 6-Suchdol
 Czech Republic
 blahovec@tf.czu.cz

Lajos Blaskó
 Karcag Research Institute of Centre for Agricultural
 and Technical Sciences
 Debrecen University
 Kisujeszállási út 166
 5300 Karcag
 Hungary
 blasko@dateki.hu

Winfried E. H. Blum
 Institute of Soil Research
 University of Natural Resources and Applied Life
 Sciences (BOKU) Vienna
 Peter Jordan Str. 82
 1190 Vienna
 Austria
 winfried.blum@boku.ac.at

Pascal Boivin
 University of Applied Sciences of Western Switzerland
 (HES-SO)
 Rue de la Prairie 4
 1202 Geneva
 Switzerland
 pascal.boivin@hesge.ch

Johan Bouma
 Soil Science Department
 Wageningen University
 Spoorbaanweg 35
 CA 3911 Rhenen
 The Netherlands
 Johan.bouma@planet.nl

Małgorzata Brzezińska
 Institute of Agrophysics
 Polish Academy of Sciences
 ul. Doświadczalna 4
 20-290 Lublin
 Poland
 m.brzezinska@ipan.lublin.pl

Graeme D. Buchan
 Soil and Physical Sciences Department and Centre for Soil
 and Environmental Research
 Lincoln University
 P.O. Box 84, Lincoln University
 Christchurch, 7647 Canterbury
 New Zealand
 Graeme.Buchan@lincoln.ac.nz

Duke M. Bulanon
 Agricultural and Biological Engineering Department
 University of Florida
 Rogers Hall, Museum Road
 Gainesville, FL 32601
 USA
 bulanon@ufl.edu

Thomas F. Burks
 Agricultural and Biological Engineering Department
 University of Florida
 Rogers Hall, Museum Road
 Gainesville, FL 32601
 USA
 tburks@ufl.edu

Mette Burmølle
 Section of Microbiology, Department of Biology
 University of Copenhagen
 Sølvgade 83H
 1307 Copenhagen K
 Denmark
 burmolle@bio.ku.dk

Katrin Burri
 WSL Institute for Snow and Avalanche Research SLF
 Flueelastr. 11
 7260 Davos Dorf
 Switzerland
 burri@slf.ch

Warren J. Busscher
 Agricultural Research Service
 US Department of Agriculture
 Coastal Plain Soil, Water and Plant Research Center
 2611 W Lucas St.
 Florence, SC 29501
 USA
 warren.busscher@ars.usda.gov

M. Ekrem Cakmak
 Soil and Water Laboratory
 Department of Biological and Environmental Engineering
 Cornell University
 164 Riley Robb Hall
 Ithaca, NY 14853
 USA
 mec68@cornell.edu

Anyela Valentina Camargo Rodriguez
 School of Computing
 University of East Anglia
 Norwich NR4 7TJ
 UK
 a.camargo-rodriguez@uea.ac.uk

Matthew Caurie
 Department of Home Economics Education
 University of Education, Winneba
 P.O. Box 25
 Winneba
 Ghana
 caurie1936@yahoo.com

Maria Teresa Ceccherini
 Dipartimento Scienza del Suolo e Nutrizione della Pianta
 Università degli Studi di Firenze
 P.le delle Cascine, 28
 50144 Firenze
 Italy
 mariateresa.ceccherini@unifi.it

Victor Yakov Chertkov
 Division of Environmental, Water, and Agricultural
 Engineering
 Technion – Israel Institute of Technology
 Haifa 32000
 Israel
 agvictor@tx.technion.ac.il

Ward Chesworth
 Department of Land Resource Science
 University of Guelph
 Guelph, ON NIG 2W1
 Canada
 wcheswor@uoguelph.ca

Tiphaine Chevallier
 UMR Eco&Sols, Functional Ecology and
 Biogeochemistry of Soils and Agro-Ecosystems
 Institut de Recherche pour le Développement (IRD)
 BP 64501, 34394 Montpellier
 France
 tiphaine.chevallier@ird.fr

Emil Chibowski
 Maria Curie-Skłodowska University
 Pl. Marii Curie-Skłodowskiej 3/130
 20-031 Lublin
 Poland
 emil.chibowski@umcs.lublin.pl

Tadeusz J. Chmielewski
 Department of Landscape Ecology and Nature
 Conservation
 University of Life Sciences
 Dobrzańskiego 37 St.
 20-262 Lublin
 Poland
 tadeusz.chmielewski@up.lublin.pl

Jacek Chodorowski
Department of Soil Science
Maria Curie-Skłodowska University
Akademicka 19
20-033 Lublin
Poland
jchodor@poczta.umcs.lublin.pl

Jolanta Cieśla
Institute of Agrophysics
Polish Academy of Sciences
Doświadczalna 4 Str
20-290 Lublin
Poland
j.ciesla@ipan.lublin.pl

L. J. Clark
Department of Soil Science
Rothamsted Research
Harpenden, West Common, Hertfordshire AL5 2JQ
UK

Freeman Cook
CSIRO Land and Water
CSIRO Long Pocket Laboratories - Indooroopilly
120 Meiers Road
Indooroopilly, QLD 4068
Australia

Yves Coquet
UMR 1091 INRA/AgroParisTech Environment and
Arable Crops
AgroParisTech
BP 01
78850 Thiverval-Grignon
France
yves.coquet@agroparistech.fr

Isabelle Cousin
Institut National de la Recherche Agronomique (INRA)
Unité de Science du Sol, Centre de Recherche d'Orléans
BP 20619
45166 Olivet cedex, Orléans
France

Henryk Czachor
Institute of Agrophysics
Polish Academy of Sciences
Doświadczalna 4, P.O. Box 201
20-290 Lublin
Poland
hczechor@ipan.lublin.pl

Katarzyna Czaczyk
Department of Biotechnology and Food Microbiology
University of Life Sciences
ul. Wojska Polskiego 28
60-637 Poznań
Poland
kasiacz@up.poznan.pl

Ewa A. Czyż
Department of Soil Science Erosion and Land
Conservation
Institute of Soil Science and Plant
Cultivation (IUNG–PIB)
Czartoryskich 8
24-100 Puławy
Poland
and
Rzeszów University
Aleja Rejtana 16c
35-959 Rzeszów
Poland
ewac@iung.pulawy.pl

Alvaro Pires da Silva
Departamento de Ciência do Solo
Escola Superior de Agricultura “Luiz de Queiroz”
Universidade de São Paulo
Piracicaba – São Paulo
Brazil
apisilva@esalq.usp.br

Małgorzata Dąbek-Szreniawska
Institute of Agrophysics PAN
Polish Academy of Sciences
ul. Doświadczalna 4
20-290 Lublin
Poland
mszreniawska@wp.pl

Frédéric Darboux
UR 0272 Science du sol
INRA, Centre de recherche d'Orléans
CS 40001
45075 Orléans Cedex 2
France
Frederic.Darboux@orleans.inra.fr

Herdjania Veras de Lima
Instituto de Ciências Agrárias
Universidade Federal Rural da Amazônia
Belém – Pará
Brazil
herdjania.lima@ufra.edu.br

Ryszard Dębicki
 Department of Soil Science
 Maria Curie-Skłodowska University
 Pl. Marii Curie-Sklodowskiej 5
 20-032 Lublin
 Poland
 ryszard.debicki@umcs.lublin.pl
 prorekt@poczta.umcs.lublin.pl

Alexander M. Demyanchuk
 Laboratory of Seed Biophysics
 Agrophysical Research Institute of Russian Academy of Agricultural Sciences
 Grazdansky av. 14
 195220 St. Petersburg
 Russia
 alexdem4@ya.ru

Anthony R. Dexter
 Department of Soil Science Erosion and Land Conservation
 Institute of Soil Science and Plant Cultivation (IUNG-PIB)
 Czartoryskich 8
 24-100 Puławy
 Poland
 tdexter2@iung.pulawy.pl

Elias Dimitriou
 Institute of Inland Waters
 Hellenic Centre for Marine Research
 Sounio Ave.
 Anavissos, Attika 19013
 Greece
 elias@ath.hcmr.gr

Etienne Diserens
 Agricultural Engineering Systems Group
 Department of Agricultural Economics and Engineering
 Agroscope Reckenholz-Tänikon ART
 8356 Ettenhausen, Thurgovie
 Switzerland
 etienne.diserens@art.admin.ch

Bohdan Dobrzański, Jr.
 Pomology Department
 University of Life Sciences
 Leszczyńskiego 58
 20-068 Lublin
 Poland
 and
 Institute of Agrophysics
 Polish Academy of Sciences
 Doświadczalna 4
 20-290 Lublin
 Poland
 bdob@ipan.lublin.pl
 b.dobrzanski@ipan.lublin.pl

Jim Doolittle
 USDA-NRCS
 National Soil Survey Center
 11 Campus Blvd., Suite 200
 Newtown Square, PA 19073
 USA
 jim.doolittle@lin.usda.gov

Claude Dousson
 UMR 1114 EMMAH, INRA/UAPV
 Bat. Sol - Domaine St Paul, Site Agroparc
 Avignon cedex 9
 84914 Avignon
 France

Xavier Draye
 Crop Physiology and Plant Breeding
 Earth and Life Institute - Agronomy
 Université catholique de Louvain
 Croix du Sud 2-11
 1348 Louvain-la-Neuve
 Belgium

Pierre Dutilleul
 Department of Plant Science
 McGill University, Macdonald Campus
 21,111 Lakeshore Road
 Ste-Anne-de-Bellevue, QC H9X 3V9
 Canada
 pierre.dutilleul@mcgill.ca

Dariusz Dziki
 Department of Equipment Operation and Maintenance in the Food Industry
 University of Life Sciences
 Doświadczalna 44
 20-288 Lublin
 Poland
 dariusz.dziki@up.lublin.pl

Jan Eriksson
 Department of Soil and Environment
 Swedish University of Agricultural Sciences
 Box 7014
 750 07 Uppsala
 Sweden
 jan.eriksson@mark.slu.se

Johann Fank
 Department of Water Resources Management
 RESOURCES - Institute of Water, Energy, and Sustainability
 Joanneum Research
 Elisabethstraße 16 / II
 8010 Graz, Styria
 Austria
 johann.fank@joanneum.at

Istvan Farkas
 Department of Physics and Process Control
 Szent Istvan University
 Pater K. u. 1
 2103 Gödöllő
 Hungary
 Farkas.Istvan@gek.szie.hu

Patricia L. Fernández
 Facultad de Agronomía
 Universidad de Buenos Aires
 Av. San Martín 4453 (C1417DSE)
 Ciudad Autónoma de Buenos Aires
 Argentina

Tadeusz Filipek
 Department of Agricultural and Environmental Chemistry
 University of Life Sciences
 Akademicka 15
 20-950 Lublin
 Poland
 tadeusz.filipek@up.lublin.pl

W. E. Finch-Savage
 Warwick HRI
 Warwick University
 Wellesbourne, Warwick CV35 9EF
 UK

Heiner Fleige
 Institute for Plant Nutrition and Soil Science
 Christian-Albrechts-University zu Kiel
 Hermann-Rodewaldstr. 2
 24118 Kiel
 Germany
 h.fleige@soils.uni-kiel.de

Alessio Fortunati
 Institute of Agro-Environmental and Forest Biology
 (IBAF)
 National Research Council
 Via Salaria Km 29,300
 Monterotondo, 00016 Rome
 Italy

Magdalena Frąc
 Department of Plant and Soil System
 Institute of Agrophysics Polish Academy of Sciences
 Doswiadczenia 4
 20-290 Lublin
 Poland
 m.frac@ipan.lublin.pl

Jarosław Frączek
 Department of Mechanical Engineering and Agrophysics
 University of Agriculture
 ul. Balicka 120
 30-149 Kraków
 Poland
 Jaroslaw.Fraczek@ur.krakow.pl

Alan J. Franzluebbers
 United States Department of Agriculture
 Agricultural Research Service
 1420 Experiment Station Road
 Watkinsville, GA 30677
 USA
 alan.franzluebbers@ars.usda.gov

Shmulik P. Friedman
 Environmental Physics and Irrigation
 Institute of Soil, Water and Environmental Sciences
 The Volcani Center
 Agricultural Research Organization
 50250 Bet Dagan
 Israel
 vwsfried@agri.gov.il

Abraham Gamliel
 The Laboratory for Pest Management Research
 Institute of Agricultural Engineering
 The Volcani Center
 Agricultural Research Organization
 50250 Bet Dagan
 Israel
 agamliel@agri.gov.il

Francisco J. García-Ramos
 Escuela Politécnica Superior
 University of Zaragoza
 22071 Huesca
 Spain
 fjavier@unizar.es

Stephan Gebhardt
 Institute for Plant Nutrition and Soil Science
 Christian Albrechts University of Kiel
 Hermann-Rodewald-Straße 2
 24118 Kiel
 Germany
 s.gebhardt@soils.uni-kiel.de

Horst H. Gerke
 Institute of Soil Landscape Research
 Leibniz-Centre for Agricultural Landscape Research
 (ZALF) Müncheberg
 Eberswalder Strasse 84
 15374 Müncheberg
 Germany
 hgerke@zalf.de

Neyde Fabíola Balarezo Giarola
Departamento de Ciéncia do Solo e Engenharia Agrícola
Universidade Estadual de Ponta Grossa
Ponta Grossa – Paraná
Brazil
neydef@uepg.br

Juan V. Giráldez
Department of Agronomy
University of Córdoba
Campus de Rabanales
14071 Córdoba
Spain
ag1gicej@uco.es

Michael Glenn
USDA-ARS Appalachian Fruit Research Station
2217
Wiltshire Road Kearneysville
Kearneysville, WV 25430
USA
michael.glen@ars.usda.gov

Jan Gliński
Institute of Agrophysics
Polish Academy of Sciences
ul. Doświadczalna 4
20-290 Lublin
Poland
j.glinski@ipan.lublin.pl

Krzysztof Górnicki
University of Life Sciences (SGGW)
Nowoursynowska 164
02-787 Warszawa
Poland
krzysztof_gornicki@sggw.pl

Harsharn Grewal
School of Natural Sciences, Hawkesbury Campus
Building H3
University of Western Sydney
Locked Bag 1797
Penrith South DC, NSW 1797
Australia
h.grewal@uws.edu.au

Christof Gromke
WSL Institute for Snow and Avalanche Research SLF
Flueelastr. 11
7260 Davos Dorf
Switzerland
gromke@slf.ch

John H. Grove
Department of Plant and Soil Sciences
College of Agriculture
University of Kentucky
Lexington, KY 40546
USA
jgrove@email.uky.edu

Stanisław Grundas
Institute of Agrophysics
Polish Academy of Sciences
ul. Doświadczalna 4
20-290 Lublin
Poland
grundas@ipan.lublin.pl

Vadakattu Gupta
Entomology
CSIRO
PMB No. 2
Glen Osmond, SA 5064
Australia
Gupta.Vadakattu@csiro.au

Mieczysław Hajnos
Institute of Agrophysics
Polish Academy of Sciences
Doświadczalna 4
20-290 Lublin
Poland
m.hajnos@ipan.lublin.pl

Paul D. Hallett
Scottish Crop Research Institute
Invergowrie
Dundee DD2 5DA
UK
paul.hallett@scri.ac.uk

Peter Hartmann
Department of Soils and Environment
Forest Research Institute Baden-Wuerttemberg
Wonnhalde Str. 4
79100 Freiburg, i. Br.
Germany
Peter.Hartmann@forst.bwl.de

Ryusuke Hatano
Laboratory of Soil Science
Graduate School of Agriculture
Hokkaido University Kita-Ku
Kita-ku, Kita 9, Nishi9
Sapporo, 060-8589 Hokkaido
Japan
hatano@chem.agr.hokudai.ac.jp

Kuntal Hati
 Division of Soil Physics
 Indian Institute of Soil Science
 Nabibagh, Berasia Road
 Bhopal 462038, Madhya Pradesh
 India
 kmh@iiss.ernet.in

Robert Heinse
 Department of Plant, Soil and Entomological Sciences
 University of Idaho
 875 Perimeter Dr. Moscow
 Moscow, ID 83844-2339
 USA
 rheinse@uidaho.edu

Joshua L. Heitman
 Soil Science Department
 North Carolina State University
 Raleigh, NC 27695
 USA
 jlheitman@ncsu.edu

Petr Heneberg
 Charles University in Prague
 Ruská 87
 100 00 Prague 10
 Czech Republic
 Petr.Heneberg@lf3.cuni.cz

Zuzana Hlaváčová
 Department of Physics
 Slovak University of Agriculture in Nitra
 Tr. A. Hlinku 2
 Nitra 949 76
 Slovakia
 Zuzana.Hlavacova@uniag.sk

Martin Holpp
 Federal Department of Economic Affairs
 Agroscope Reckenholz-Tänikon Research Station ART
 Tänikon
 8356 Ettenhausen
 Switzerland

Józef Horabik
 Institute of Agrophysics
 Polish Academy of Sciences
 ul. Doświadczalna 4
 20-290 Lublin
 Poland
 j.horabik@ipan.lublin.pl

Rainer Horn
 Institute for Plant Nutrition and Soil Science
 Christian-Albrechts-University zu Kiel
 Olshausenstr. 40
 24118 Kiel
 Germany
 rhorn@soils.uni-kiel.de

Robert Horton
 Agronomy Department
 Iowa State University
 Ames, IA 50011
 USA
 rhorton@ncsu.edu

Marek Horyński
 Department of Computer and Electrical Engineering
 Lublin University of Technology
 Nadbystrzycka Street 38A
 20-618 Lublin
 Poland
 m.horynski@pollub.pl

Silvo Hribernik
 Department of Textile Materials and Design
 University of Maribor
 Smetanova 17
 2000 Maribor
 Slovenia
 silvo.hribernik@uni-mb.si

Charles A. Igwe
 Department of Soil Science
 University of Nigeria
 Nsukka, Enugu State 460001
 Nigeria
 charigwe1@hotmail.com
 charles.igwe@unn.edu.ng

Yukiyo Iwata
 Climate and Land-use Change Research Team
 National Agricultural Research Center for Hokkaido
 Region, NARO
 Sinsei Memuro, Hokkaido 082-0081
 Japan
 iwatayuk@affrc.go.jp

Monika Jaroszuk-Sierocińska
 Institute of Soil Science and Environment Management
 University of Life Sciences
 Akademicka 13
 20-950 Lublin
 Poland
 monika.jaroszuk@up.lublin.pl

Mathieu Javaux
Agrosphere, ICG-4
Institute of Chemistry and Dynamics of the Geosphere
Forschungszentrum Juelich GmbH
52425 Juelich
Germany
and
Earth and Life Institute-Environmental Sciences
Université catholique de Louvain
Croix du Sud, 2, bte 2
1348 Louvain-la-Neuve
Belgium
mathieu.javaux@uclouvain.be

Digvir S. Jayas
Departement of Biosystems Engineering
University of Manitoba
207 Administration Building
Winnipeg, MB R3T 5V6
Canada
digvir_Jayas@Umanitoba.ca

Antonio Jordán
MED_Soil Research Group, Departamento de
Cristalografía, Mineralogía y Química Agrícola
Universidad de Sevilla
c/Profesor García González, 1
41012 Sevilla
Spain
ajordan@us.es

Grzegorz Józefaciuk
Institute of Agrophysics
Polish Academy of Sciences
ul. Doświadczalna 4
20-290 Lublin
Poland
g.jozefaciuk@ipan.lublin.pl

Agnieszka Kaleta
University of Life Sciences (SGGW)
Nowoursynowska 164
02-787 Warszawa
Poland
agnieszka_kaleta@sggw.pl

Gerhard Kammerer
Department of Water, Atmosphere and Environment
Institute of Hydraulics and Rural Water-Management
University of Natural Resources and Life Sciences
Muthgasse 18
1190 Vienna
Austria
gerhard.kammerer@boku.ac.at

Seong Pal Kang
Cognitive Robot Research Center
Korea Institute of Science and Technology
119-801 Samsung Ramian APT Hawalgokdong
Sung-Buk-gu, Seoul-si
Republic of Korea
sp_kang@hotmail.com

Marian Kargol
Independent Department of Environment Protection and
Modelling
The Jan Kochanowski University of Humanities and
Sciences
ul. Świętokrzyska 15
25-406 Kielce
Poland
katamar34@gmail.com

Douglas L. Karlen
National Laboratory for Agriculture and the Environment
(NLA)
2110 University Boulevard
Ames, IA 50011-3120
USA
doug.karlen@ars.usda.gov

Jaacov Katan
Department of Plant Pathology and Microbiology
The Hebrew University of Jerusalem, Food and
Environment
Rehovot, 76100
Israel
Katan@agri.huji.ac.il

Andrzej Kędziora
Institute for Agricultural and Forest Environment
Polish Academy of Sciences
Bukowska 19
60-809 Poznań
Poland
kedan@man.poznan.pl

Kathrin Kiehl
University of Applied Sciences Osnabrück
Postfach 1940
49009 Osnabrück
Germany
k.kiehl@fh-osnabrueck.de

Jan T. Kim
School of Computing
University of East Anglia
Norwich NR4 7TJ
UK
j.kim@uea.ac.uk

Gunnar Kirchhof
School of Land, Crop and Food Sciences
The University of Queensland
Brisbane, QLD 4072
Australia
gunnar@thinksoils.org

Holger Kirchmann
Department of Soil and Environment
Swedish University of Agricultural Sciences
Box 7014
750 07 Uppsala
Sweden
holger.kirchmann@mv.slu.se

Annelise Kjøller
Section of Microbiology
Department of Biology
University of Copenhagen
Sølygade 83H
1307 Copenhagen K
Denmark

Roxane Kohler-Milleret
Institute of Biology, Soil & Vegetation Group
University of Neuchâtel
Rue Emile-Argand 11, Case postale 158
2009 Neuchâtel
Switzerland

Paweł Kojs
Polish Academy of Sciences
Botanical Garden – Center for Biological Diversity
Conservation
Warsaw
Poland
pkojs@op.pl

Raimo Kölli
Department of Soil Science and Agrochemistry
Institute of Agricultural and Environmental Sciences,
Estonian University of Life Sciences
Kreutzwaldi Str. 1a
51014 Tartu
Estonia
raimo.kolli@emu.ee

Józef Kołodziej
Department of Agrometeorology
University of Life Sciences
Akademicka 15
20-950 Lublin
Poland
jozef.kolodziej@up.lublin.pl

Krystyna Konstankiewicz
Institute of Agrophysics
Polish Academy of Sciences
ul. Doświadczalna 4
20-290 Lublin
Poland
konst@ipan.lublin.pl

Jan Koper
Department of Biochemistry
University of Technology and Life Sciences
6 Bernardyńska Str
85-029 Bydgoszcz
Poland
koper@utp.edu.pl

Ted S. Kornecki
USDA-ARS, National Soil Dynamics Lab. Research Unit
411 S. Donahue Drive
Auburn, AL 36832
USA
ted.kornecki@ars.usda.gov

Piotr Kowalik
Department of Sanitary Engineering
Gdansk University of Technology
Narutowicza 11
80-233 Gdańsk, Pommerania
Poland
piotr_kowalik@tlen.pl
pkow@pg.gda.pl

Bronisława Barbara Kram
Institute of Agricultural Engineering
University of Environmental and Life Sciences
ul. Chełmińskiego 37/41
50-630 Wrocław
Poland
Bronislawa.Kram@up.wroc.pl

Leilah Krounbi
Wyler Department of Dryland Agriculture
French Associates Institute for Agriculture and
Biotechnology of Drylands
Jacob Blaustein Institutes for Desert Research
Ben-Gurion University of the Negev
Sede Boqer campus 84990
Israel

Julia Krümmelbein
Soil Protection and Recultivation
Brandenburg University of Technology
Konrad-Wachsmann-Allee 6
03046 Cottbus
Germany
kruemmel@tu-cottbus.de

Adam Paweł Kuczyński
 Institute of Agrophysics
 Polish Academy of Sciences
 ul. Doswiadczałna 4
 20-290 Lublin 27
 Poland
 akucyski@ipan.lublin.pl

Max Kuderna
 wpa Beratende Ingenieure GmbH
 Lackierergasse 1
 1090 Vienna
 Austria
 max.kuderna@wpa.at

Sekhar Lukose Kuriakose
 United Nations University-ITC School for Disaster
 Geo-information Management
 University of Twente
 Hengelosestraat 99, P.O. Box 217
 7500 AE Enschede
 The Netherlands
 sekhar.lk@gmail.com
 lukose11753@itc.nl

Miroslav Kutílek
 Nad Patankou 34
 160 00 Prague 6
 Czech Republic
 miroslav.kutilek@volny.cz

Yakov Kuzyakov
 Department of Agroecosystem Research
 University of Bayreuth
 95440 Bayreuth
 Germany

Rattan Lal
 Carbon Management and Sequestration Center, SENR
 The Ohio State University
 2021 Coffey Road
 Columbus, OH 43210
 USA
 Lal.1@osu.edu

Krzysztof Lamorski
 Institute of Agrophysics
 Polish Academy of Sciences
 ul. Doswiadczałna 4
 20-290 Lublin
 Poland
 k.lamorski@ipan.lublin.pl

Thamara Laredo
 Department of Food Science
 University of Guelph Food and Soft Materials Science
 50 Stone Road East
 Guelph, ON N1G 2W1
 Canada
 tlaredoa@uoguelph.ca

Janusz Laskowski
 Department of Equipment Operation and Maintenance in
 the Food Industry
 University of Life Sciences
 Doświadczalna 44
 20-288 Lublin
 Poland
 janusz.laskowski@up.lublin.pl

Patrick Lavelle
 IRD/UPMC Université Paris 6, CIAT
 Cali
 Colombia
 Patrick.Lavelle@bondy.ird.fr

Naftali Lazarovitch
 Wyler Department of Dryland Agriculture
 French Associates Institute for Agriculture and
 Biotechnology of Drylands
 Jacob Blaustein Institutes for Desert Research
 Ben-Gurion University of the Negev
 Sede Boqer campus 84990
 Israel

Wey H. Leong
 Department of Mechanical and Industrial Engineering
 Ryerson University
 350 Victoria St.
 Toronto, ON M5B 2K3
 Canada

Guy J. Levy
 Institute of Soil, Water and Environmental Sciences
 The Volcani Center
 Agricultural Research Organization
 P.O. Box 6
 50250 Bet Dagan
 Israel
 vwguy@volcani.agri.gov.il

Piotr P. Lewicki
 Department of Food Engineering and Process
 Management
 University of Life Sciences (SGGW)
 Nowoursynowska Str. 159c
 02-776 Warszawa
 Poland
 piotr_lewicki@sggw.pl

Jerzy Lipiec
 Institute of Agrophysics
 Polish Academy of Sciences
 ul. Doświadczalna 4
 20-290 Lublin
 Poland
lipiec@ipan.lublin.pl

Basant Maheshwari
 School of Natural Sciences, Hawkesbury Campus,
 Building H3
 University of Western Sydney
 Locked Bag 1797
 Penrith South DC, NSW 1797
 Australia
b.maheshwari@uws.edu.au

Willibald Loiskandl
 Department of Water, Atmosphere and Environment
 Institute of Hydraulics and Rural Water-Management
 University of Natural Resources and Life Sciences
 Muthgasse 18
 1190 Vienna
 Austria
willibald.loiskandl@boku.ac.at

Alejandro G. Marangoni
 Department of Food Science
 University of Guelph Food and Soft Materials Science
 50 Stone Road East
 Guelph, ON N1G 2W1
 Canada
amarango@uoguelph.ca

Birl Lowery
 Department of Soil Science
 University of Wisconsin-Madison
 1525 Observatory Drive
 Madison, WI 53706
 USA
blowery@wisc.edu

Wibke Markgraf
 Institute for Plant Nutrition and Soil Science
 Christian-Albrechts-University zu Kiel
 Hermann-Rodewald-Str. 2
 24118 Kiel
 Germany
w.markgraf@soils.uni-kiel.de

Peggy Macaigne
 Soil and Water Management and Crop Nutrition Section
 Joint FAO/IAEA Division
 International Atomic Energy Agency (IAEA)
 Wagramer Strasse 5, P.O. Box 100
 1400 Vienna
 Austria
p.macaigne@hotmail.fr
macgyp@hotmail.com

Miguel Angel Martín
 Department of Applied Mathematics in Agricultural
 Engineering
 Technical University of Madrid (UPM)
 Avd. de la Complutense
 28040 Madrid
 Spain
miguelangel.martin@upm.es

Luís F. Machado
 IBB – Institute for Biotechnology and Bioengineering
 Center of Biological Engineering
 Universidade do Minho
 Campus de Gualtar
 4710-057 Braga
 Portugal
flaviomachado@deb.uminho.pt
luis.flaviomachado@gmail.com

Svatopluk Matula
 Department of Water Resources, Food and Natural
 Resources
 Czech University of Life Sciences
 Kamycka 129
 165 21 Prague
 Czech Republic
Matula@af.czu.cz

Engracia Madejón
 Instituto de Recursos Naturales y Agrobiología de Sevilla
 (IRNAS-CSIC)
 P.O. Box 1052
 41080 Sevilla
 Spain

Blair M. McKenzie
 Environment–Plant Interactions
 Scottish Crop Research Institute
 Invergowrie
 Dundee DD2 5DA
 UK
blair.mckenzie@scri.ac.uk

Leszek Mieszkalski
 Department of Agricultural Engineering and Natural Raw Materials
 University of Varmia and Mazury in Olsztyn
 M. Oczapowskiego 11
 10-719 Olsztyn
 Poland
 mieszko@poczta.fm

Fernando Migliaccio
 Institute of Agro-Environmental and Forest Biology (IBAF)
 National Research Council
 Via Salaria Km 29,300
 00016 Monterotondo, Rome
 Italy
 fernando.migliaccio@ibaf.cnr.it

Budiman Minasny
 Food & Natural Resources
 The University of Sydney
 Sydney, NSW 2006
 Australia
 budiman.minasny@sydney.edu.au

Waldemar Mioduszewski
 Department of Water Resources
 Institute of Technology and Life Sciences
 Al. Hrabska 3
 05-090 Raszyn Falenty
 Poland
 w.mioduszewski@itep.edu.pl

Andrzej Mocek
 Department of Soil Sciences and Land Protection
 University of Life Sciences
 Szydłowska 50
 60-656 Poznań
 Poland
 moceka@up.poznan.pl

Md. Abdul Mojid
 Irrigation and Water Management
 Agricultural University
 2202 Mymensingh
 Bangladesh
 ma_mojid@yahoo.com

Marek Molenda
 Institute of Agrophysics
 Polish Academy of Sciences
 ul. Doświadczalna 4
 20-290 Lublin
 Poland
 mmolenda@ipan.lublin.pl

Toshihiko Momose
 Bavarian Environment Agency
 Hans-Högn-Straße 12
 95030 Hof/Saale
 Germany

Verónica L. Morales
 Soil and Water Laboratory
 Department of Biological and Environmental Engineering
 Cornell University
 164 Riley Robb Hall
 Ithaca, NY 14853
 USA
 vlm8@cornell.edu

Chris J. Moran
 Sustainable Minerals Institute
 The University of Queensland
 Cnr Staffhouse and College Roads
 Brisbane, QLD 4075
 Australia
 Chris.moran@uq.edu.au

Guillermo P. Moreda
 Laboratorio de Propiedades Físicas y Tecnologías Avanzadas en Agro-Alimentación (LPF-TAGRALIA)
 Universidad Politécnica de Madrid
 Avda. Complutense, s/n
 28040 Madrid
 Spain
 guillermo.moreda@upm.es

Félix Moreno
 Instituto de Recursos Naturales y Agrobiología de Sevilla (IRNAS-CSIC)
 P.O. Box 1052
 41080 Sevilla
 Spain
 fmoreno@irnase.csic.es

Leszek Mościcki
 Department of Food Process Engineering
 University of Life Sciences
 Doświadczalna str. 44
 20-280 Lublin
 Poland
 leszek.moscicki@up.lublin.pl

Abdul Mounem Mouazen
 Natural Resources Department
 Natural Soil Resources Institute
 Cranfield University
 Cranfield, Bedfordshire MK43 0AL
 UK
 a.mouazen@cranfield.ac.uk

<p>Lothar Müller Leibniz – Centre for Agricultural Landscape Research (ZALF) Institute of Landscape Hydrology Eberswalder Straße 84 15374 Müncheberg Germany lmueller@zalf.de</p>	<p>Thomas Nehls Department Soil Conservation Technische Universität Berlin Salzufer 12, Sekr BK-1 10587 Berlin Germany thomas.nehls@tu-berlin.de</p>
<p>Miriam Muñoz-Rojas Instituto de Recursos Naturales y Agrobiología de Sevilla (CSIC) Avda. Reina Mercedes, 10 41012 Sevilla Spain mirmunroj@alum.us.es</p>	<p>Stuart O. Nelson U.S. Department of Agriculture Agricultural Research Service, Russell Research Center P.O. Box 5677 Athens, GA 30604-5677 USA stuart.nelson@ars.usda.gov</p>
<p>José M. Murillo Instituto de Recursos Naturales y Agrobiología de Sevilla (IRNAS-CSIC) P.O. Box 1052 41080 Sevilla Spain</p>	<p>Attila Nemes Crop Systems and Global Change Laboratory USDA-ARS 10300 Baltimore Avenue, Building 001, BARC-West Beltsville, MD 20705 USA Attila.Nemes@ars.usda.gov</p>
<p>Kamila Myszka Department of Biotechnology and Food Microbiology University of Life Sciences ul. Wojska Polskiego 28 60-637 Poznań Poland kmyszka@up.poznan.pl</p>	<p>Artur Nosalewicz Institute of Agrophysics Polish Academy of Sciences ul. Doświadczalna 4, P.O. Box 201 20-290 Lublin Poland a.nosalewicz@ipan.lublin.pl</p>
<p>Hiroshi Nakashima Agricultural Systems Engineering Laboratory Division of Environmental Science and Technology Graduate School of Agriculture Kyoto University Oiwake-cho, Kitashirakawa, Sakyo-ku Kyoto 606-8502 Japan hiron@kais.kyoto-u.ac.jp</p>	<p>Viliam Novák Institute of Hydrology Slovak Academy of Sciences Racianska 75 Bratislava 85101 Slovakia novak@uh.savba.sk</p>
<p>Susmitha Nambuthiri Department of Plant and Soil Sciences College of Agriculture University of Kentucky Lexington, KY 40546 USA susmitha.agri@gmail.com</p>	<p>Keith Openshaw Formerly Staff Member of the Food and Agricultural Organization (FAO) of the UN Rome Italy and Formerly Staff Member at the World Bank Washington, DC USA kopenshaw@cox.net openshaw.keith@gmail.com</p>
<p>Agnieszka Nawrocka Institute of Agrophysics ul. Doświadczalna 20-290 Lublin Poland a.nawrocka@ipan.lublin.pl</p>	<p>Janusz Ostrowski Institute of Technology and Life Sciences Al. Hrabska 3 05-099 Raszyn Poland j.ostrowski@imuz.edu.pl</p>

Wojciech Owczarzak
 Department of Soil Sciences and Land Protection
 University of Life Sciences
 Szydłowska 50
 60-656 Poznań
 Poland

Yakov A. Pachepsky
 Environmental Microbial and Food Safety Laboratory
 Animal and Natural Resource Institute
 Beltsville Agricultural Research Center, USDA-ARS
 10300 Baltimore Ave, Bldg. 173, BARC-EAST
 Beltsville, MD 20705
 USA
 yakov.pachepsky@ars.usda.gov

Loïc Pagès
 INRA Centre d'Avignon
 UR 1115 PSH Site Agroparc
 84914 Avignon cedex 9
 France
 Loic.Pages@avignon.inra.fr

Marcello Pagliai
 Agricultural Research Council (CRA)
 Research Centre for Agrobiology and
 Pedology (CRA-ABP)
 Piazza M. D'Azzeglio, 30
 50121 Florence
 Italy
 marcello.pagliai@entecra.it

Apostolos Papadopoulos
 Research and Development
 Branston Ltd
 Mere Road
 Branston LN4 1NJ
 UK
 apapadopoulos@branston.co.uk

Robert C. Pearce
 Department of Plant and Soil Sciences
 College of Agriculture
 University of Kentucky
 Lexington, KY 40546
 USA
 rpearce@email.uky.edu

Josef Pecen
 Department of Sustainable Technologies
 Institute of Tropics and Subtropics
 University of Life Sciences Prague
 Kamýcká str. 129
 165 21 Prague 6 - Suchdol
 Czech Republic
 pecen@its.czu.cz

Xinhua Peng
 Institute of Soil Science
 Chinese Academy of Sciences
 P.O. Box 821
 Nanjing 210008
 PR China
 xhpeng@issas.ac.cn

Magnus Persson
 Department of Water Resources Engineering
 Lund University
 Box 22100
 Lund
 Sweden
 magnus.persson@tvrl.lth.se

Stephan Peth
 Institute for Plant Nutrition and Soil Science
 Christian-Albrechts-University zu Kiel
 Olshausenstr. 40
 24118 Kiel
 Germany
 s.peth@soils.uni-kiel.de

Fernanda Peyronel
 Department of Food Science
 University of Guelph Food and Soft Materials Science
 50 Stone Road East
 Guelph, ON N1G 2W1
 Canada
 fsvaikau@uoguelph.ca

A. Pierret
 Institut de Recherche pour le Développement/
 International Water Management Institute
 Ban Nongviengkham
 Vientiane
 Lao PDR

Giacomo Pietramellara
 Dipartimento Scienze del Suolo e Nutrizione della Pianta
 Università degli Studi di Firenze
 P.le delle Cascine, 28
 50144 Firenze
 Italy
 giacomo.pietramellara@unifi.it

Jacek Pietrusiewicz
 Department of Plant Anatomy and Cytology
 Maria Curie-Skłodowska University
 ul. Akademicka 19
 20-033 Lublin
 Poland
 jacekp@poczta.umcs.lublin.pl

Stanisław Pietruszewski
 Department of Physics
 University of Life Sciences
 Akademicka 13
 20-950 Lublin
 Poland
 stanislaw.pietruszewski@up.lublin.pl

Wiktor Pietrzyk
 Department of Computer and Electrical Engineering
 Lublin University of Technology
 Nadbystrzycka Street 38A
 20-618 Lublin
 Poland
 w.pietrzyk@pollub.pl

David L. Pinskiy
 Institute of Physico-Chemical and Biological Problems
 in Soil Science
 Laboratory of Physical-Chemistry of Soils
 Institutskaya 2, Pushchino
 Moscow Region 142290
 Russia
 pinsky@issp.serpukhov.su

David J. W. Piper
 Geological Survey of Canada
 Bedford Institute of Oceanography
 Dartmouth, B2Y 4A2
 Canada

Alberto Pistocchi
 GECOsistema srl
 Viale G.Carducci, 15
 47023 Cesena (FC)
 Italy
 alberto.pistocchi@gecosistema.it

Grażyna Podolska
 Department of Cereal Crop Production
 Institute of Soil Science and Plant Cultivation
 National Research Institute
 Czartoryskich 8 st
 24-100 Puławy
 Poland
 aga@iung.pulawy.pl

Andreas Pohlmeier
 ICG-4, Research Centre
 Wilhelm Johnen Str
 52425 Jülich
 Germany
 a.pohlmeier@fz-juelich.de

Valérie Pot
 UMR 1091 INRA/AgroParisTech Environment and
 Arable Crops
 AgroParisTech
 BP 01
 78850 Thiverval-Grignon
 France
 vpot@grignon.inra.fr

John N. Quinton
 Lancaster Environment Centre
 Lancaster University
 Bailrigg
 Lancaster LA1 4YQUK
 UK
 J.Quinton@Lancaster.ac.uk

Sudhakar M. Rao
 Department of Civil Engineering
 Indian Institute of Science
 Bangalore 560012
 India
 msrao@civil.iisc.ernet.in

Randy Raper
 U.S. Department of Agriculture-Agricultural Research
 Service
 Dale Bumpers Small Farm Research Center
 6883 South State Highway 23
 Booneville, AR 72927
 USA
 randy.raper@ars.usda.gov

Todd C. Rasmussen
 Warnell School of Forestry & Natural Resources
 The University of Georgia
 Athens, GA 30602-2152
 USA
 trasmuss@uga.edu

Toshko Raytchev
 Nikola Poushkarov Institute of Soil Science
 Shosse Bankya 7
 Sofia 1080
 Bulgaria

Jerzy Rejman
 Institute of Agrophysics
 Polish Academy of Sciences
 ul. Doświadczalna 4
 20-290 Lublin
 Poland
 rejman@ipan.lublin.pl

Guy Richard
 Institut National de la Recherche Agronomique (INRA)
 Unité de Science du Sol, Centre de Recherche d'Orléans
 BP 20619
 45166 Olivet cedex, Orléans
 France
 Guy.Richard@orleans.inra.fr

Edwin L. Ritchey
 Department of Plant and Soil Sciences
 College of Agriculture
 University of Kentucky
 Lexington, KY 40546
 USA
 elritc2@uky.edu

Karl Ritz
 Natural Resources Department
 National Soil Resources Institute
 School of Applied Sciences
 Cranfield University
 Cranfield MK43 0AL
 UK
 k.ritz@cranfield.ac.uk

Tiina Roose
 School of Mathematics
 University of Southampton
 University Road
 Southampton SO17 1BJ
 UK
 T.Roose@soton.ac.uk

Svetla Rousseva
 Nikola Poushkarov Institute of Soil Science
 Shosse Bankya 7
 Sofia 1080
 Bulgaria
 svetlarousseva@gmail.com

Renata Rózyło
 Department of equipment operation and maintenance
 in the food industry
 University of Life Sciences
 Doświadczalna 44
 20-280 Lublin
 Poland
 renata.rozylo@up.lublin.pl

Margarita Ruiz-Altisent
 Laboratorio de Propiedades Físicas y Tecnologías
 Avanzadas en Agro-Alimentación (LPF-TAGRALIA)
 Universidad Politécnica de Madrid
 Avda. Complutense, s/n
 28040 Madrid
 Spain
 margarita.ruiz.altisent@upm.es

Juan M. Ruiz-Lozano
 Departamento de Microbiología del Suelo y Sistemas
 Simbióticos
 Estación Experimental del Zaidín (CSIC)
 Prof. Albareda, 1
 18008 Granada, Andalucía
 Spain
 juanmanuel.ruiz@eez.csic.es

Tomasz Rusin
 MTS Systems Corporation
 Elhys sp. z.o.o. ul. Naukowa 45
 02-463 Warsaw
 Poland
 trusin@elhys.com.pl

Rafał Rybczyński
 Institute of Agrophysics
 Polish Academy of Sciences
 20-290 Lublin
 Poland
 rryb@ipan.lublin.pl

Wojciech Rybiński
 Institute of Plant Genetics
 Polish Academy of Sciences
 Strzeszyńska 34
 60-479 Poznań
 Poland

Magdalena Ryżak
 Institute of Agrophysics
 Polish Academy of Sciences
 Doświadczalna 4
 20-290 Lublin
 Poland
 mryzak@ipan.lublin.pl

Ramsis B. Salama
 Managed Water Resources
 7 Fireball Way
 Ocean Reef 6027
 Australia
 ramsis@managedwater.com

Anthony E. Salvucci
 Soil and Water Laboratory
 Department of Biological and Environmental Engineering
 Cornell University
 164 Riley Robb Hall
 Ithaca, NY 14853
 USA
 aes84@cornell.edu

Fernando San José Martínez
 Department of Applied Mathematics in Agricultural Engineering
 Technical University of Madrid (UPM)
 Avd. de la Complutense
 28040 Madrid
 Spain
 fernando.sanjose@upm.es

Manuel Sánchez-Marañón
 Departamento de Edafología y Química Agrícola,
 Facultad de Ciencias
 Universidad de Granada
 Campus Fuentenueva
 18071 Granada
 Spain
 msm@ugr.es

Martin G. Scanlon
 Department of Food Science
 University of Manitoba
 Winnipeg, R3T 2N2
 Canada
 scanlon@cc.umanitoba.ca

Gabriele E. Schaumann
 Department of Environmental and Soil Chemistry
 Institute for Environmental Sciences
 University Koblenz-Landau
 Fortstr. 7
 76829 Landau
 Germany
 schaumann@uni-landau.de

Maud Séger
 Institut National de la Recherche Agronomique (INRA)
 Unité de Science du Sol, Centre de Recherche d'Orléans
 BP 20619
 45166 Olivet cedex, Orléans
 France

H. M. Selim
 School of Plant, Environmental and Soil Sciences
 (SPESS)
 Agricultural Center
 Louisiana State University
 Baton Rouge, LA 70803-2110
 USA
 hselim@lsu.edu

Majda Sfiligoj Smole
 Department of Textile Materials and Design
 University of Maribor
 Smetanova 17
 2000 Maribor
 Slovenia
 majda.sfiligoj@uni-mb.si

Evgeny V. Shein
 Department of Soil Physics
 Moscow State University
 Moscow 119992
 Russia
 e.v.shein@gmail.com

Bing Cheng Si
 Department of Soil Science
 University of Saskatchewan
 Saskatoon, SK S7N 5A8
 Canada
 bing.si@usask.ca

Chandra B. Singh
 Department of Biosystems Engineering
 University of Manitoba
 E2-376 Engineering Building
 Winnipeg, MB R3T 5V6
 Canada

Stefan Skiba
 Department of Pedology and Soil Geography
 Institute of Geography and Spatial Management
 Jagiellonian University
 Gronostajowa 7
 30-387 Cracow
 Poland
 s.skiba@geo.uj.edu.pl

Wojciech M. Skierucha
 Institute of Agrophysics
 Polish Academy of Sciences
 ul. Doświadczalna 4
 20-290 Lublin
 Poland
 w.skierucha@ipan.lublin.pl

Cezary Ślawiński
 Institute of Agrophysics
 Polish Academy of Sciences
 ul. Doświadczalna 4
 20-290 Lublin
 Poland
 cslawin@ipan.lublin.pl

Zbigniew Ślipek
 Department of Mechanical Engineering and Agrophysics
 University of Agriculture
 ul. Balicka 120
 30-149 Kraków
 Poland
 Zbigniew.Slipek@ur.krakow.pl

Anna Słowińska-Jurkiewicz
Institute of Soil Science and Environment Management
University of Life Sciences
Akademicka 13
20-950 Lublin
Poland
anna.jurkiewicz@up.lublin.pl

Halina Smal
Institute of Soil Science and Environment Management
University of Life Sciences
Leszczyńskiego 7
20-069 Lublin
Poland
halina.smal@up.lublin.pl

H. B. So
School of Land, Crop and Food Sciences
The University of Queensland
Brisbane, QLD 4072
Australia

Henryk Sobczuk
Department of Thermal Techniques
Lublin University of Technology
ul. Nadbystrzycka 40b
20-618 Lublin
Poland
h.sobczuk@pollub.pl

Zofia Sokołowska
Institute of Agrophysics
Polish Academy of Sciences
Doświadczalna 4
20-290 Lublin
Poland
zosia@maja.ipan.lublin.pl

Stefan Sokołowski
Department for the Modelling of Physico-Chemical
Processes
MCS University
Lublin
Poland
stefan.sokolowski@gmail.com

Søren J. Sørensen
Section of Microbiology, Department of Biology
University of Copenhagen
Sølvgade 83H
1307 Copenhagen K
Denmark

Kurt A. Spokas
United States Department of Agriculture
Agricultural Research Service
1991 Upper Buford Circle – 439 Borlaug Hall
St. Paul, MN 55108
USA
kurt.spokas@ars.usda.gov

Joanna Sposób
Department of Hydrography
Institute of Earth Sciences
Maria Curie-Skłodowska University
19 Akademicka Str.
20-033 Lublin
Poland
joanna.sposob@poczta.umcs.lublin.pl

Tammo S. Steenhuis
Soil and Water Laboratory
Department of Biological and Environmental Engineering
Cornell University
206 Riley Robb Hall
Ithaca, NY 14853
USA
tss1@cornell.edu

Vlasta Štekauerová
Institute of Hydrology
Slovak Academy of Sciences
Račianska 75
83102 Bratislava 3
Slovakia
stekauer@uh.savba.sk

Zofia Stepniewska
Department of Biochemistry & Environmental Chemistry
The John Paul II Catholic University of Lublin
Kraśnicka 102
20-718 Lublin
Poland
stepz@kul.pl

Witold Stepniewski
Department of Land Surface Protection Engineering
Lublin University of Technology
Nadbystrzycka 40B
20-712 Lublin
Poland
w.stepniewski@pollub.pl

Lech Wojciech Szajdak
Department of Environmental Chemistry
Institute for Agricultural and Forest Environment
Polish Academy of Sciences
ul.Bukowska 19
60-809 Poznań
Poland
szajlech@man.poznan.pl

Jan Szatyłowicz
 Department of Environmental Improvement
 University of Life Sciences (SGGW)
 ul. Nowoursynowska 159
 02-776 Warsaw
 Poland
 jan_szatylowicz@sggw.pl

Bogusław Szot
 Institute of Agrophysics
 Polish Academy of Sciences
 Doświadczalna 4
 20-290 Lublin, Lublin
 Poland
 b.szot@ipan.lublin.pl

Paweł Szot
 Institute of Ornamental Plants and Architecture
 of Landscape
 University of Life Sciences
 Leszczyńskiego 58
 20-068 Lublin
 Poland
 pszot@autograf.pl

Mieczysław Szpryngiel
 University of Life Sciences
 Głęboka 28
 20-612 Lublin
 Poland

Miguel A. Taboada
 INTA, CIRN – CONICET
 Instituto de Suelos
 Los Reseros y Las Cabañas S/N, (1688) Hurlingham
 Villa Udaondo-Castelar, Provincia de Buenos Aires
 Argentina
 and
 CONICET
 Av. Rivadavia 1917 (C1033AAJ)
 Ciudad Autónoma de Buenos Aires
 Argentina
 and
 Universidad de Buenos Aires
 Av. San Martín 4453 (C1417DSE)
 Ciudad Autónoma de Buenos Aires
 Argentina
 mtaboada@cnia.inta.gov.ar

Josef Tanny
 Institute of Soil, Water, and Environmental Sciences
 Agricultural Research Organization
 The Volcani Center
 P.O. Box 6
 Bet Dagan 50250
 Israel
 tanai@volcani.agri.gov.il

Zdzisław Targoński
 Department of Biotechnology
 Human Nutrition and Science of Food Commodities
 University of Life Sciences
 Skromna 8
 20-703 Lublin
 Poland
 zdzislaw.targonski@up.lublin.pl

Vlodek R. Tarnawski
 Division of Engineering
 Saint Mary's University
 923 Robbie St.
 Halifax, NS B3H 3C3
 Canada
 vlodek.tarnawski@smu.ca

Paola Tassone
 Institute of Agro-Environmental and Forest Biology
 (IBAF)
 National Research Council
 Via Salaria Km 29,300
 00016 Monterotondo, Rome
 Italy

Judith M. Tisdall
 Department of Agricultural Sciences
 La Trobe University
 Bundoora, VIC 3086
 Australia
 j.tisdall@latrobe.edu.au

Samir Trabelsi
 U.S. Department of Agriculture
 Agricultural Research Service, Russell Research Center
 P.O. Box 5677
 Athens, GA 30604-5677
 USA
 Samir.trabelsi@ars.usda.gov

T. P. Tuong
 International Rice Research Institute
 DAPO Box 7777
 Metro Manila 1301
 Philippines
 t.tuong@cgiar.org

Andrée J. Tuzet
 Unité Mixte de Recherche, Environnement et Grandes
 Cultures
 Institut National de la Recherche Agronomique (INRA)
 78850 Thiverval Grignon
 France
 tuzet@grignon.inra.fr

Jerzy Tys
 Institute of Agrophysics
 Polish Academy of Sciences
 Doświadczalna 4
 20-290 Lublin, Lublin
 Poland

F. D. Ugese
 Department of Crop Production
 University of Agriculture
 Makurdi, Benue State
 Nigeria
f_ugese@yahoo.com

Danuta Urban
 Institute of Soil Science and Environment Formation
 University of Life Sciences
 Leszczyńskiego 7 St.
 20-069 Lublin
 Poland
danuta.urban@up.lublin.pl

Emilia Urbanek
 Department of Geography
 Swansea University
 Singleton Park
 Swansea SA2 8PP
 UK
e.urbanek@swansea.ac.uk

Igor B. Uskov
 Agophysical Research Institute
 Russian Academy of Agricultural Science
 Grazhdansky pr. 14
 195220 St. Petersburg
 Russia
office@agophys.ru

Bogusław Usowicz
 Institute of Agrophysics
 Polish Academy of Sciences
 ul. Doświadczalna 4
 20-290 Lublin
 Poland
b.usowicz@ipan.lublin.pl

Jerzy Usowicz
 Torun Centre for Astronomy
 Nicolaus Copernicus University
 Gagarina 11
 87-100 Torun
 Poland
ju@astro.uni.torun.pl

L. P. H. van Beek
 Department of Physical Geography
 Utrecht University
 P.O. Box 80. 115
 3508 TC Utrecht
 The Netherlands
r.vanbeek@geo.uu.nl

Martinus Th. van Genuchten
 Department of Mechanical Engineering, COPPE/LTTC
 Federal University of Rio de Janeiro, UFRJ
 Rio de Janeiro RJ CEP 21945-970
 Brazil
rvangenuchten@yahoo.com

Wendy H. Vance
 School of Environmental Science
 Murdoch University
 Murdoch, WA 6150
 Australia
w.vance@murdoch.edu.au

Jan Vanderborght
 Agrosphere, ICG-4, Institute of Chemistry and Dynamics
 of the Geosphere
 Forschungszentrum Juelich GmbH
 52425 Juelich
 Germany

Karl Vanderlinden
 Centro Las Torres-Tomejil
 IFAPA
 Ctra. Sevilla-Cazalla, km 12.2
 41200 Alcalá del Río (Seville)
 Spain
karl.vanderlinden@juntadeandalucia.es

Maria F. Varela
 CONICET
 Av. Rivadavia 1917 (C1033AAJ)
 Ciudad Autónoma de Buenos Aires
 Argentina
 and
 Facultad de Agronomía
 Universidad de Buenos Aires
 Av. San Martín 4453 (C1417DSE)
 Ciudad Autónoma de Buenos Aires
 Argentina

Leonid P. Velikanov
 Laboratory of Seed Biophysics
 Agophysical Research Institute
 Russian Academy of Agricultural Sciences
 Grazdansky av. 14
 195220 St. Petersburg
 Russia
leonidvelikanov@yandex.ru

Harry Vereecken
 Agrosphere, ICG-4, Institute of Chemistry and Dynamics
 of the Geosphere
 Forschungszentrum Juelich GmbH
 52425 Juelich
 Germany

António A. Vicente
 IBB – Institute for Biotechnology and Bioengineering
 Center of Biological Engineering
 Universidade do Minho
 Campus de Gualtar
 4710-057 Braga
 Portugal
 avicente@deb.uminho.pt

Raphael A. Viscarra Rossel
 Division of Land & Water Bruce E. Butler Laboratory
 Commonwealth Scientific and Industrial Research
 Organisation (CSIRO)
 GPO Box 1666
 Canberra, ACT 2601
 Australia
 Raphael.Viscarra-Rossel@csiro.au

Subramanian Viswanathan
 Requimte, Grupo de Reacções e Análises Químicas
 Instituto Superior de Engenharia do Porto
 Rua Dr. António Bernardino de Almeida 431
 4200-072 Porto
 Portugal
 rsviswa@gmail.com

Ole Wendoroth
 Department of Plant and Soil Sciences
 College of Agriculture
 University of Kentucky
 Lexington, KY 40546
 USA
 owendoroth@uky.edu

Gerd Wessolek
 Department Soil Conservation
 Technische Universität Berlin
 Salzufer 12, Sekr BK-1
 10587 Berlin
 Germany
 gerd.wessolek@tu-berlin.de

W. R. Whalley
 Department of Soil Science
 Rothamsted Research
 Harpenden, West Common, Hertfordshire AL5 2JQ
 UK
 richard.whalley@bbsrc.ac.uk

Marcin Widomski
 Department of Land Surface Protection Engineering
 Lublin University of Technology
 Nadbystrzycka 40B
 20-712 Lublin
 Poland
 M.Widomski@wis.pol.lublin.pl

Barbara Witkowska-Walczak
 Institute of Agrophysics
 Polish Academy of Sciences
 Doświadczalna 4
 20-290 Lublin
 Poland
 bwitwal@ipan.lublin.pl

Teresa Włodarczyk
 Institute of Agrophysics
 Polish Academy of Sciences
 ul. Doświadczalna 4
 20-290 Lublin
 Poland
 teresa@ipan.lublin.pl

Victor P. Yakushev
 Agrophysical Institute
 Russian Academy of Agricultural Science
 Grazhdansky pr. 14
 195220 St. Petersburg
 Russia

Maciej Zalewski
 Department of Applied Ecology
 University of Łódź
 Banacha 12/16
 90-237 Łódź
 Poland
 and
 International Institute of Polish Academy of Sciences
 European Regional Centre for Ecohydrology under the
 auspices of UNESCO
 Tylna 390-364
 Łódź
 Poland
 mzal@biol.uni.lodz.pl

Lorena M. Zavala
 MED_Soil Research Group
 Departamento de Cristalografía, Mineralogía y Química
 Agrícola
 Universidad de Sevilla
 Carretera de Utrera, km 1
 41013 Sevilla
 Spain
 lorena@us.es

Artur Zdunek
Institute of Agrophysics
Polish Academy of Sciences
ul. Doświadczalna 4
20-290 Lublin
Poland
a.zdunek@ipan.lublin.pl

Bin Zhang
Institute of Agricultural Resources and Regional Planning
Chinese Academy of Agricultural Sciences
Beijing 100081
PR China
bzhang@caas.ac.cn

Jianhui Zhang
Institute of Mountain Hazards and Environment
Chinese Academy of Sciences and Ministry of Water
Conservancy
P.O. Box 417
Chengdu, 610041 Sichuan
PR China
zjh@imde.ac.cn

Wei Zhang
Soil and Water Laboratory
Department of Biological and Environmental Engineering
Cornell University
164 Riley Robb Hall
Ithaca, NY 14853
USA
wz47@cornell.edu

Adam Zsolnay
German Research Helmholtz Zentrum
Center for Environmental Health
München
Germany
zsolnay-q@web.de

Preface

Agrophysics is the science that studies physical processes and properties affecting plant production. The fundaments of agrophysical investigations are mass (water, air, nutrients) and energy (light, heat) transport in the soil–plant–atmosphere and soil–plant–machine–agricultural products–foods continuums and way of their regulation to acquire biomass of high quantity and quality with sustainability to the environment. Agrophysics has been developing dynamically over the past decades, filling the gap between disciplines like agrochemistry, agrobiology, agroecology, agroclimatology and linking them together. Unlike physics of individual objects like soils, plants, agricultural products and food, agrophysics provides a physical basis to better understand interrelations between the objects.

Understanding physical processes in the agrophysical objects is a pre-requisite for applying new technologies in sustainable land use and environment management, and in the production of healthy agricultural products and food. The recognition of physical phenomena in the agricultural environment allows more efficient use of water and chemicals in agriculture and decreasing biomass losses during harvest, transport, storage and processing. These result in a growing interest in the application of physics for improving the quality of the above mentioned objects. It is therefore considered timely to produce a key resource across the discipline providing a clear explanation of present knowledge in modern agrophysics interfacing with the physical sciences and environmental and food sciences.

The roots of agrophysics are based in Saint Petersburg (Russia) where A.F. Ioffe (1880–1960) founded the principles of a new branch of natural and agricultural sciences and was the founder in 1932 of the Institute of Physics and Agriculture, later called the Institute of Agrophysics. Subsequently, the Institute of Agrophysics of the Polish Academy of Sciences was created in 1968 in Lublin (Poland)

by B. Dobrzański (1908–1987), whose idea was to extend the application of physics not only to soils, but also to agricultural plants and products. Initially the Institute played an important role in the coordination of agrophysical research in Poland and in European countries, and later the cooperation was broadened to numerous scientific institutions worldwide.

The *Encyclopedia of Agrophysics* has been written to portray the agrophysical objects in terms of physical processes and physical properties characterising them. Interactions between the objects are also included. As agrophysical issues become more and more complicated, so will the knowledge and vocabulary required for their clear understanding, discussion and study be extended. Due to the dynamic and rapid growth of agrophysical knowledge, the Encyclopedia considers many new research methods and terms that did not even exist a decade ago.

The Encyclopedia can be helpful in evaluating and improving the quality of soils and agricultural products as well as the technological processes. Moreover, agrophysical terminology can be applied to soil science, agronomy, biophysics, agroecology, agricultural engineering, horticulture, plant science, food science, environmental science, landscape ecology and geography, and thereby it can help collaboration and the flow of information between the disciplines. The Encyclopedia can serve as a reference document for researchers, students of various levels, librarians, policy- and decision-makers, and interested societies working and studying in a range of disciplines related to agrophysics.

The *Encyclopedia of Agrophysics* encloses 261 articles and 400 glossary terms that are arranged in alphabetical order. Each article includes “cross-references” that direct the reader to one or more other articles that may shed more light on the topic.

The *Encyclopedia of Agrophysics* is a result of the efforts of many contributors from throughout the world.

The Editors are very obliged to all Authors who kindly accepted the invitation to contribute and who have inspired the Encyclopedia with their informative contributions.

We appreciate the assistance of the many friends and colleagues who have suggested new issues and terms, helped with definitions as well as provided valuable criticism. Particular thanks go to the Editorial Board of the Encyclopedia and to the anonymous reviewers for many helpful

advice and comments. We are indebted to the Publishing Editors of Springer for many suggestions and kind cooperation.

Jan Gliński
Józef Horabik
Jerzy Lipiec
(Editors-in-Chief)

A

ABSORPTION

The process by which one substance, such as solid or liquid, takes up another substance, such as liquid or gas, through minute pores or spaces between its molecules. Clay minerals can take water and ions by absorption.

ABSORPTIVITY

Absorbed part of incoming radiation/total incoming radiation.

ACOUSTIC EMISSION

The phenomenon of transient elastic-wave generation due to a rapid release of strain energy caused by a structural alteration in a solid material. Also known as stress-wave emission.

Bibliography

McGraw-Hill Dictionary of Scientific & Technical Terms, 6E,
Copyright © 2003 by The McGraw-Hill Companies, Inc.

ACOUSTIC TOMOGRAPHY

A form of tomography in which information is collected from beams of acoustic radiation that have passed through an object (e.g., soil). One can speak of thermo-acoustic tomography when the heating is realized by means of microwaves, and of photo-acoustic tomography when optical heating is used.

Cross-references

[Agrophysics: Physics Applied to Agriculture](#)

ADAPTABLE TILLAGE

See [Tillage, Impacts on Soil and Environment](#)

ADHESION

The attraction between different substances, acting at surfaces of contact between the substances e.g., water and solid, water films and organo-mineral surfaces, soil and the metal cutting surface.

ADSORPTION

A phenomenon occurring at the boundary between phases, where cohesive and adhesive forces cause the concentration or density of a substance to be greater or smaller than in the interior of the separate phases.

Bibliography

Introduction to Environmental Soil Physics (First Edition). 2003.
Elsevier Inc. Daniel Hillel (ed.) <http://www.sciencedirect.com/science/book/9780123486554>

Cross-references

[Adsorption Energy and Surface Heterogeneity in Soils](#)
[Adsorption Energy of Water on Biological Materials](#)
[Solute Transport in Soils](#)
[Surface Properties and Related Phenomena in Soils and Plants](#)

ADSORPTION COMPLEX

Collection of organic and inorganic substances in soil that are capable of adsorbing (absorbing) ions or molecules.

Cross-references

[Adsorption Energy and Surface Heterogeneity in Soils](#)
[Surface Properties and Related Phenomena in Soils and Plants](#)

ADSORPTION ENERGY AND SURFACE HETEROGENEITY IN SOILS

Zofia Sokołowska¹, Stefan Sokołowski²

¹Institute of Agrophysics, Polish Academy of Sciences, Lublin, Poland

²Department for the Modeling of Physico-Chemical Processes, MCS University, Lublin, Poland

Generalities

The potential energy of interaction of a single adsorbate molecule with a solid adsorbent can be described by the function $U(R)$, where $\{R\}$ is a set of coordinates necessary to define the position of the adsorbate molecule. Assuming that the adsorbate molecule is a sphere of diameter σ , its position is given by the Cartesian coordinates of its center, $R = r = (x, y, z)$. For molecules composed of several atoms, one needs to specify a multidimensional vector $\{R\}$ that determines the coordinates of all the atoms (or groups of atoms) building a given molecule. Formally, according to the classical statistical thermodynamics $U(R)$ is the sum of the interactions of N_a interaction centers located within a given adsorbate molecule, with N_s interaction centers located within a solid,

$$U(R) = \sum_{i \in N_s} \sum_{j \in N_a} u(r_{ij}), \quad (1)$$

where r_{ij} is the distance between the interacting centers. Of course, when quantum-mechanical treatment is employed, $U(R)$ is the difference of ground state energies between the molecule at the position $\{R\}$ and the ground state of a separated molecule.

For a selected adsorbate molecule, say a spherical molecule, the potential $U(r)$ can be used to characterize the surface. For a given set of coordinates x, y in the plane parallel (or tangential) to the solid the minimum of the function $U(r)$ with respect to the third coordinate, z , is often called “the adsorption energy,” ε_{ad} . If ε_{ad} is independent of x, y , the corresponding surface is energetically uniform (or homogeneous). For crystalline surfaces ε_{ad} (and, of course, $U(r)$) is a periodic function of x, y . However, there exists a variety of surfaces that are neither uniform nor crystalline. In those cases, $\varepsilon_{ad}(x, y)$ may vary in a quite complicated manner with x, y and we call such surfaces energetically heterogeneous.

Energetically heterogeneous surfaces can be next classified into several groups, among which we can distinguish patchwise and random surfaces. In the case of random surfaces $\varepsilon_{ad}(x, y)$ varies quite randomly with x, y ; for patchwise surfaces $\varepsilon_{ad}(x, y) = \text{constant}$ for x, y within consecutive regions Δ_i . Both random and patchwise surfaces are two limiting cases of surface topography that is defined by spatial correlations between the points x_i, y_i with given values of the energy $\varepsilon_{ad,i}$. We can distinguish correlations between pairs of sites, triples of sites, and so on (Bulnes et al., 2001).

The variation of the energy of adsorption results from several factors: the presence of different atoms or groups of atoms on the surface; geometrical irregularities including the presence of pores of different shape and dimensions, and so on. Of course, geometrical and energetic nonuniformities are correlated and the former is one of principal sources of energetic heterogeneity. Moreover, a given adsorbent may be a quite complex mixture of several interacting chemical species. Both energetic and geometric heterogeneities have a great impact on the adsorption process.

Description of adsorption on energetically heterogeneous surfaces

Accurate modeling adsorption on geometrically nonuniform surfaces is difficult and only in some cases it is possible to construct an adequate model for a solid. When it is possible, then computer simulations can be employed. However, the structure of great majority of environmental adsorbents, and soils in particular (see [Clay Minerals and Organo-Mineral Associates](#); [Organic Matter, Effects on Soil Physical Properties and Processes](#); [Parent Material and Soil Physical Properties](#); [Soil Phases](#)) is extremely complex due to diversified mineral, organic, and ionic composition. Therefore, the application of approximate approaches is necessary. The most widely used methods are based on the so-called integral adsorption isotherm equation.

Suppose we know the function $\theta_l(p, \varepsilon)$ that describes the isotherm (surface coverage) on a uniform surface with the adsorption energy ε . Then, the isotherm on a heterogeneous surface can be approximated as

$$\theta(p) = N_m \int_{\varepsilon_{min}}^{\varepsilon_{max}} \theta_l(p, \varepsilon) \chi(\varepsilon) d\varepsilon, \quad (2)$$

where p is the pressure, $\theta(p, \varepsilon)$ is the global (measured) adsorption isotherm, N_m is the monolayer capacity, and $\chi(\varepsilon)$ is the energy distribution function that yields a fraction of the surface characterized by the adsorption energy ε . The latter function satisfies the normalization condition

$$\int_{\varepsilon_{min}}^{\varepsilon_{max}} d\varepsilon = 1, \quad (3)$$

where $[\varepsilon_{min}, \varepsilon_{max}]$ are the lower and upper integration limits. In many cases, these limits are assumed to be $[\varepsilon_0, \infty)$, where ε_0 is the liquefaction energy of the adsorbate. [Equation 2](#) states that the total adsorption is just a weighted average of the isotherms on model, homogeneous surfaces, characterized by different values of ε . However, it means that the adsorption on each homogeneous surface occurs independently of the adsorption on other surfaces. The last assumption is satisfied only for a patchwise topography, or when the interactions between adsorbed particles are negligibly small. Despite of the above quoted limitations, [Equation 2](#) has been widely used to describe adsorption on heterogeneous surfaces. Note that a quite similar approach is usually used to describe adsorption by porous solids. In the latter case, the weight function is just the pore size distribution function.

If the local adsorption isotherm and the energy distribution function are given by analytical expressions, [Equation 2](#) can be integrated to yield an equation for the total adsorption isotherm. For example, if the local isotherm is just given by the Langmuir equation, $\theta_l(p, \varepsilon) = pK(\varepsilon)/[1 + pK(\varepsilon)]$, where $K(\varepsilon) = K_0 \exp[-\varepsilon/kT]$, k is the Boltzmann constant, T is the temperature, and K_0 is a constant, then one can show that the Temkin isotherm, $\theta(p) = \ln(1 + Kp)^\gamma$, corresponds to a constant energy distribution function; the Freundlich isotherm is associated with an exponential distribution and the Langmuir–Freundlich isotherm, $\theta(p) = Cp^\gamma/[1 + Cp^\gamma]$ – with a quasi-Gaussian distribution (Xia et al., 2006). In the above C , K and γ are constants. Numerous analytical expressions for the total adsorption isotherms obtained from [Equation 2](#) can be found in the monographs of Rudziński and Everett (1992) and Jaroniec and Madey (1988).

The above method of derivation of isotherm equations can be also extended to the case of a multilayer adsorption. The multilayer local adsorption isotherm on a homogeneous surface can be described by the Brunauer, Emmet and Teller (BET) equation (Brunauer et al., 1938)

$$\theta_l(p, \varepsilon) = \frac{1}{1 - x} \frac{c(\varepsilon)x}{1 + [c(\varepsilon) - 1]x}, \quad (4)$$

where $x = p/p_s$ is the relative vapor pressure, p_s is the saturated vapor pressure, and $c(\varepsilon) = \exp[-(\varepsilon - \varepsilon_0)/kT]$. For a quasi-Gaussian energy distribution, we obtain then the multilayer Langmuir–Freundlich isotherm of the form $\theta(x) = [1/(1 - x)\{\tilde{c}x^\gamma/[1 + \tilde{c}x^\gamma]\}]$ with $\tilde{c} = \exp[-(\varepsilon_{min} - \varepsilon_0)/kT]$ (Rudziński and Everett, 1992).

Evaluation of the energy distribution functions from the experimental adsorption isotherms

When the total adsorption $\theta(x)$ is measured experimentally and the local adsorption model is assumed, [Equation 2](#) can be solved (analytically or numerically) with respect to the distribution function $\chi(\varepsilon)$. The main difficulty in evaluating $\chi(\varepsilon)$ is the ill-posed nature of [Equation 2](#) for some of its kernels $\theta_l(p, \varepsilon)$. Therefore, if

meaningful results are to be obtained, special care and the quality of experimental data are required (Jaroniec and Bräuer, 1986). The easiest way to obtain an approximate solution of [Equation 2](#) goes through the so-called condensation approximation, according to which (Rudziński and Everett, 1992)

$$\chi(\varepsilon) = -\partial\theta[p(\varepsilon)]/\partial\varepsilon. \quad (5)$$

The condensation approximation replaces the local adsorption isotherm by a step function, i.e., every pressure is associated with the value of the adsorption energy, $p/p_0 = \exp(\varepsilon/kT)$, that corresponds to one half of the coverage of a given homotactic patch. The basic difficulty in this method is associated with an appropriate numerical differentiation of the total adsorption isotherm, $\theta[p(\varepsilon)]$. One of the methods that has been widely used for that purpose relies on the approximation of the experimental data by the so-called exponential adsorption isotherm (Jaroniec and Bräuer, 1986)

$$\theta(p) = \exp \left[\sum_{n=1}^N B_n (kT \ln(p/p_m))^n \right], \quad (6)$$

where $\{B_n\}$ are the coefficients and the pressure p_m is associated with the minimum adsorption energy via $\varepsilon_{min} = kT \ln(p_m)$. The distribution function resulting from [Equations 5](#) and [6](#) is

$$\chi(\varepsilon) = \left[\sum_{n=1}^N n B_n (\varepsilon - \varepsilon_m)^{n-1} \right] \exp \left[\sum_{n=1}^N B_n (\varepsilon - \varepsilon_m)^n \right]. \quad (7)$$

Approximation of the experimental data using [Equation 6](#) must be carried out under constraint that the function $\chi(\varepsilon)$ is nonnegative for the energies corresponding to the interval of pressures at which the isotherm was measured. Note that the above described method has been next extended to the case of adsorption on fractal surfaces (Sokołowska and Sokołowski, 2008).

The steps that lead to an appropriate solution of [Equation 2](#) must involve a correct choice of the local adsorption isotherm and initial analysis of experimental data with respect to elimination of systematic and random experimental errors. Several numerical procedures for the evaluation of $\chi(\varepsilon)$ from experimental adsorption data have been proposed; numerous of them have been outlined by Jaroniec and Bräuer (1986) and Jaroniec and Madey (1988). One of the most accurate methods is the so-called regularization method (von Szombathely et al., 1992). Note that a quite analogous method was also employed to calculate the pore size distribution from experimental adsorption isotherms (Kowalczyk et al., 2003). Another quite accurate and numerically simple method was developed by Stanley and Guiochon (1993), who employed an expectation–maximization method of parameter estimation to calculate adsorption energy distributions from

experimental adsorption isotherms. The method does not require any prior knowledge of the distribution function, or the analytical expression for the experimental isotherm, requires no smoothing of the isotherm data, and converges with high stability toward the maximum-likelihood estimate. The method is therefore robust and accurate at high iteration numbers. The test calculations carried out by Stanley and Guiochon proved that their method is more accurate than several previous approaches (Jaroniec and Madey, 1988).

One should also mention about an alternative theoretical approach to model adsorption by heterogeneous adsorbents that is based on the concept of quenched-annealed mixtures (Pizio, 2000). In the case of one-component adsorbate, the adsorption system is considered as a two-component mixture, in which one component (adsorbent) is frozen. The application of the so-called replica methodology (Pizio, 2000) allows them to calculate adsorption isotherms. Similarly, a planar heterogeneous surface can be modeled by “quenching” an imaginary “fluid of adsorbing centers” (Rzysko et al., 1999). This approach, although theoretically promising, has been not employed to model experimental data adsorption on environmental materials so far.

Energetic heterogeneity of soils

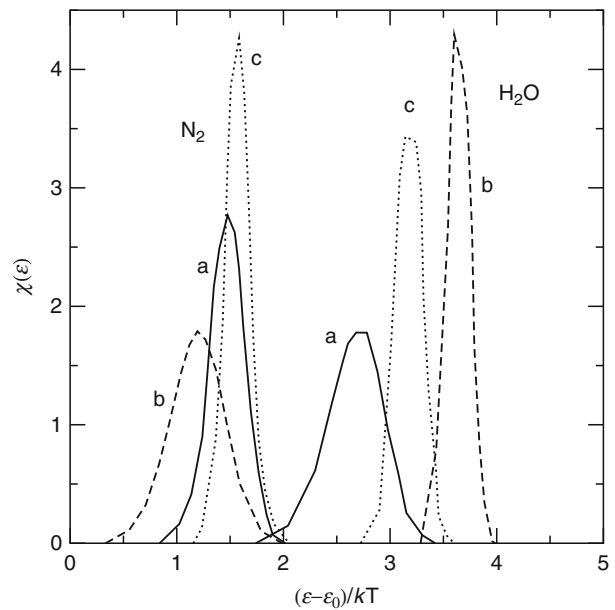
The concepts of adsorbent heterogeneity and the integral adsorption equation in particular have been widely used to study adsorption of vapors by soils (Bottero et al., 1993; Pachepsky et al., 1995; Józefaciuk and Bowanko, 2002; Sokołowska et al., 1999; 2002; Villiéras et al., 2002). The energy distribution functions and the average values of the energy of adsorption, $\langle \varepsilon \rangle$,

$$\langle \varepsilon \rangle = \int d\varepsilon \chi(\varepsilon) \quad (8)$$

obtained from experimental adsorption isotherms have been proved to be useful while discussing the mechanism of adsorption, the role played by selected constituents of soils and soil minerals in the adsorption process, to get insights into the changes in the soils caused by chemical and/or treatment, and so on.

Figure 1 shows exemplary energy distribution functions obtained from the numerical solution of **Equation 2** applied experimental data of nitrogen and water vapor adsorption on alluvial soils (for details see Sokołowska et al., 2002). Of course, the energy of interaction of a single adsorbate particle with adsorbing surface depends on its chemical nature. Consequently, the results for both adsorbates are different. However, the energy distribution functions for nitrogen, as well as for water are described by narrow, Gaussian-like peaks. Such peaks indicate the existence of one major kind of adsorbing centers.

The energy distribution functions and their changes due to the changes or modifications of soils depend on the individual soil properties, but one should remember that function $\chi(\varepsilon)$ provides only a global energetic



Adsorption Energy and Surface Heterogeneity in Soils,
Figure 1 Examples of the energy distribution functions vs. dimensionless energy obtained from adsorption isotherms of nitrogen and water vapor on a sample of alluvial soil by Sokołowska et al. (2002). Labels (a), (b), and (c) denote horizons. (Reprinted from Sokołowska et al. (2002). Copyright (2002), with permission from Elsevier).

characteristic of a given surface. In order to associate its particular peaks to really existing adsorption centers, additional studies, e.g., spectroscopic measurements of adsorbed molecules, are necessary.

Bibliography

- Bottero, J. Y., Arnaud, M., Villiéras, F., Michot, L. J., de Dobato, P., and François, M., 1993. Surface and textural heterogeneity of fresh hydrous ferric oxides in water and in the dry state. *Journal of Colloid and Interface Science*, **159**, 45–52.
- Brunauer, S., Emmett, P. H., and Teller, E., 1938. Adsorption of gases in multimolecular layers. *Journal of the American Chemical Society*, **60**, 309–319.
- Bulnes, F., Ramirez-Pastor, A. J., and Zgrablich, G., 2001. Scaling behavior in adsorption on bivariate surfaces and the determination of energetic topography. *The Journal of Chemical Physics*, **115**, 1513–1521.
- Jaroniec, M., and Bräuer, P., 1986. Recent progress in determination of energetic heterogeneity of solids from adsorption data. *Surface Science Reports*, **8**, 65–117.
- Jaroniec, M., and Madey, R., 1988. *Physical Adsorption on Heterogeneous Solids*. Amsterdam: Elsevier.
- Józefaciuk, G., and Bowanko, G., 2002. Effect of acid and alkali treatment on surface areas and adsorption energies of selected minerals. *Clays and Clay Minerals*, **50**, 771–783.
- Kowalczyk, P., Terzyk, A. P., Gauden, P. A., Leboda, R., Szmechtig-Gauden, E., Rychlicki, G., Ryu, Z., and Rong, H., 2003. Estimation of the pore-size distribution function from the nitrogen adsorption isotherm. Comparison of density functional theory and the method of do and co-workers. *Carbon*, **41**, 1113–1125.

- Pachepsky, Y. A., Polubesova, T. A., Hajnos, M., Sokołowska, Z., and Józefaciuk, G., 1995. Parameters of surface heterogeneity from laboratory experiments on soil degradation. *Soil Science Society American Journal*, **59**, 68–75.
- Pizio, O., 2000. Adsorption in random porous media. In Borówko, M. (ed.), *Computational Methods in Surface and Colloid Science*. New York: M. Dekker, pp. 293–346.
- Rudziński, W., and Everett, D. H., 1992. *Adsorption of Gases on Heterogeneous Surfaces*. London: Academic. Chapters 5–10.
- Rzysko, W., Pizio, O., Sokołowski, S., and Sokołowska, Z., 1999. Application of the Replica Ornstein–Zernike equations to study submonolayer adsorption on energetically heterogeneous surfaces. *Journal of Colloid and Interface Science*, **219**, 184–189.
- Sokołowska, Z., Hajnos, M., Borówko, M., and Sokołowski, S., 1999. Adsorption of nitrogen on thermally treated peat soils: the role of energetic and geometric heterogeneity. *Journal of Colloid and Interface Science*, **219**, 1–10.
- Sokołowska, Z., Borówko, M., Reszko-Zygmont, J., and Sokołowski, S., 2002. Adsorption of nitrogen and water vapor by alluvial soils. *Geoderma*, **107**, 33–54.
- Sokołowska, Z., and Sokołowski, S., 2008. Fractal approach to adsorption/desorption processes on environmental surfaces. In Senesi, N., and Wilkinson, K. J. (eds.), *Biophysical Chemistry of Fractal Structures and Processes in Environmental Systems*. New York: Wiley, pp. 179–220.
- Stanley, B. J., and Guiochon, C., 1993. Numerical estimation of adsorption energy distributions from adsorption isotherm data with the expectation-maximization method. *The Journal of Physical Chemistry*, **97**, 8098–8104.
- von Szombathely, M., Bräuer, P., and Jaroniec, M., 1992. The solution of adsorption integral-equations by means of the regularization method. *Journal of Computational Chemistry*, **13**, 17–32.
- Villiéras, F., Michot, L. J., Bardot, F., Chamerois, M., Eypert-Blaison, C., François, M., Gérard, G., and Cases, L.-M., 2002. Surface heterogeneity of minerals. *Geoscience*, **334**, 597–609.
- Xia, X., Litvinov, S., and Mühlner, M., 2006. Consistent approach to adsorption thermodynamics on heterogeneous surfaces using different empirical energy distribution models. *Langmuir*, **22**, 8063–8070.

Cross-references

- [Adsorption Energy of Water on Biological Materials](#)
[Clay Minerals and Organo-Mineral Associates](#)
[Estimation of Quartz Content in Mineral Soils](#)
[Organic Matter, Effects on Soil Physical Properties and Processes](#)
[Parent Material and Soil Physical Properties](#)
[Soil Phases](#)
[Specific Surface Area of Soils and Plants](#)

ADSORPTION ENERGY OF WATER ON BIOLOGICAL MATERIALS

Jiří Blahovec
 Department of Physics, Czech University of Life Sciences, Prague 6-Suchdol, Czech Republic

Synonyms

Adsorption enthalpy; Adsorption heat; Isosteric heat of sorption

Definition

Adsorption energy (heat) represents the difference between the heat of evaporation the unit quantity of a substance from the product and the heat of evaporation the unit quantity substance from the pure liquid state in the same conditions (temperature, external pressure, product composition, etc.). The SI unit of adsorption energy is $\text{J}\cdot\text{mol}^{-1}$.

The adsorption energy (heat) of water is usually calculated at constant moisture content (isosteric heat of adsorption).

Introduction

The biological materials are not simple substances and/or simple mixtures. Substances in biological materials form aggregates in which they bond one to the other ([Physical Properties of Raw Materials and Agricultural Products](#)). The consequence is that molecules of the individual substances have lower energy in the aggregates than in pure substance. These interactions of the individual substances in the aggregate are described by the chemical potentials ([Daniels and Albery, 1961](#)).

For biological materials, the most important component is water (See also [Water Effects on Physical Properties of Raw Materials and Foods](#); [Water in Forming Agricultural Products](#); [Drying of Agricultural Products](#)) and that is why we deal here only with the adsorption of water. Water vapor in the surrounding air depends on the state of water inside the material. Water from the material can evaporate into the surrounding air or water can condense on the surface of the material. Both processes, evaporation and condensation, lead to equilibrium after some time. In this state, the properties of water inside a material can be described by the properties of water vapor. This equilibrium is related only to the “surface,” most available water being in contact with water vapor; the product usually contains more water that is not in contact with the vapor. This water is usually more bond than the above mentioned more available “surface” water. Different mechanisms of water bonding in biological materials were observed. The most important are participation in solution, adsorption on surfaces (internal and external), adsorption in biological cells, and pore adsorption. Adsorption is not usually very strong when chemical adsorption is excluded.

The state of internal water can be expressed by the relative chemical potential that is termed water potential ([Oertli, 1976](#); [Moore, 1972](#)). This term is in direct relation to the adsorption enthalpy. The state of water vapor in the surrounding air is well described by the relative pressure that is termed water activity ([Daniels and Albery, 1961](#)).

Water potential: adsorption enthalpy

Water potential (Ψ) is directly given by the difference between the chemical potential of water in the material (μ_m) and the chemical potential of pure water (μ_0) in the same conditions:

$$\Psi = \mu_m - \mu_0 \quad (1)$$

The water potential can be expressed either in the usual SI units ($\text{J}\cdot\text{mol}^{-1}$) or it could be recalculated into another SI expression, frequently into pressure (in Pa). The chemical potential is the relative Gibbs potential so that its value represents also the adsorption enthalpy in conditions that the difference between entropy of water in the material and entropy of water in the pure state can be omitted (Daniels and Alberty, 1961). Water potential is frequently used to describe the status of water in living organisms (See *Water Effects on Physical Properties of Raw Materials and Foods*) (Oertli, 1976) and in soil (Blahovec, 2008). Binding of water in the product is expressed by the negative value of water potential.

Water activity

Dimensionless term, water activity (a_w) of water solutions can be simply estimated by the formula (Daniels and Alberty, 1961)

$$a_w = e^{\frac{\Psi}{RT}} \quad (2)$$

where R is the universal gas constant ($8.3145 \text{ J.K}^{-1} \text{ mol}^{-1}$) and T absolute temperature. Water activity then changes from 0 to 1 for water potentials from $-\infty$ to 0. In more complicated materials, water activity can be simply expressed as the ratio of fugacities of the material water (f_m) and pure water (f_0):

$$a_w = \frac{f_m}{f_0} \approx \frac{p_m}{p_0} \quad (3)$$

that could be approximated by the ratio of the partial water vapor pressures (p_m and p_0) above the corresponding water states (Daniels and Alberty, 1961). The definition of water activity by the pressure ratio is fully correct for water vapor described as an ideal gas; the water activity of the material is then given directly by the air humidity being in equilibrium with the material. The difference between water activity based on the fugacity and on the pressure increases with deviations of the water vapor properties from properties of the ideal gas, for example, with increasing moisture content of the material.

Water activity is a crucial parameter for the living activity of agroproducts and the activity of their components (enzymes, microorganisms, etc. – see Karel, 1975b, Fennema, 1976). This is very important for storage of agricultural products (See also *Physical Phenomena and Properties Important for Storage of Agricultural Products; Physical Properties as Indicators of Food Quality*).

Sorption isotherm

The vapor pressure of the solvent in a solution can be expressed by Raoult's Law (Daniels and Alberty, 1961; Karel, 1975a, Moore, 1972) and the relation between moisture content and water activity can be estimated on this base. In real water solutions and/or more complex

materials, this relation is more complicated. It can be obtained experimentally at constant temperature in the form of a sorption isotherm that is the plot of moisture content (usually on dry basis) versus water activity at equilibrium and constant temperature. In most cases, the material is in solid and/or semisolid state (*Rheology in Agricultural Products and Foods*); in this case, the adsorption of water is understood and theoretically analyzed as a surface controlled process, that is, process based on water deposition on the (internal surface) of the material. Van den Berg and Bruin (1981) gave 77 types of different equations that can be used to describe water sorption isotherms in foodstuffs; more than 22 of them are theoretically based on water surface sorption. The most frequent are the Langmuir's isotherm, BET isotherm, and GAB isotherm.

The most frequent way to obtain the sorption isotherm at a sample consists in finding individual points of the sorption isotherm. Each point is obtained by determining the moisture content of a sample (by a gravimetric method) that was kept for long time, up to equilibrium, at constant temperature close to an oversaturated water solution of known water activity (Karel, 1975b).

Isosteric heat of sorption

A set of sorption isotherms obtained at different temperatures is the usual basis for determining the isosteric heat of sorption ΔH , that is, the difference between the heat of evaporation unit quantity of water from the product and the heat of evaporation of a unit quantity of water from the pure water in the same conditions. Isosteric heat of sorption of water is given by formula (Daniels and Alberty, 1961, Blahovec, 2008)

$$\Delta H = \left(R \frac{d(\ln a_w)}{d(\frac{1}{T})} \right)_{MC} \quad (4)$$

where MC denotes that the derivative is calculated at constant moisture content. The experimental values of water activity are usually well given by an exponential function of reciprocal absolute temperature (see Equation 2) so that the isosteric heat of sorption is nearly independent of temperature.

The isosteric heat of sorption in real biological materials increases with decreasing water activity (decreasing moisture content) similarly as the absolute value of the water potential in Equation 2 at least at moisture contents higher than approximately 10% w. b. At lower moisture contents, Equation 2 loses its validity for real biological materials:

$$\Delta H_R \approx -\Psi_R \prec \Delta H_T \approx -\Psi_T \quad (5)$$

where index R denotes water in real biological materials and index T denotes data based on water vapor as an ideal gas.

Direct and indirect methods for determination of the heat of adsorption

Direct methods for the determination of the heat of adsorption meet experimental difficulties when they are applied to biological experimental materials (Heiss, 1968). The biological materials are sensitive to changes of external parameters (temperature, pressure, see also [Stomatal Conductance, Photosynthesis, and Transpiration, Modeling](#)) that usually lead to changes of the physical state of the biological material. Hence, the direct experimental methods have only limited application in the determination of the heat of adsorption of biological materials.

Among indirect methods, the most frequent is the above mentioned method based on the sorption isotherms. From the others, the methods based on the determination of the points of melting and evaporation can be also applied (Daniels and Alberty, 1961; Heiss, 1968). New ways for studying water sorption in biological materials have been developed (e.g., Nelson and Trabelsi, 2005).

The highest values of the isosteric heat of adsorption ($20\text{--}30\text{ kJ}\cdot\text{mol}^{-1}$) are observed in biological materials at low moisture contents (lower than about 5% w.b.). These values are about one half of the heat of vaporization of water ([Water in Forming Agricultural Products](#); Blahovec, 2007; 2008).

Conclusion

The adsorption energy of water (AEW) on biological materials depends on the material moisture content. At higher moisture contents, AEW increases with decreasing moisture content in a similar manner as the absolute value of water potential increases with decreasing water activity. At the lowest moisture contents (less than 5%), the AEW reaches in many cases nearly constant values $20\text{--}30\text{ kJ}\cdot\text{mol}^{-1}$ that represent about half of the heat of evaporation of water.

The AEW is well described by isosteric heat of sorption that could be easily obtained from sorption isotherms measured at different temperatures. Direct methods for measurement of AEW are difficult to apply to AEW of biological materials. Application of physical chemistry to the calculation of AEW usually fails either due to the limited applicability of ideal gas conception or complicated aggregate structure of biological materials.

Bibliography

- Blahovec, J., 2007. Role of water in food and product texture. *International Agrophysics*, **21**, 209–215.
- Blahovec, J., 2008. *Agromaterials. Study Guide*. Prague: Czech University of Life Sciences.
- Daniels, F., and Alberty, R. A., 1961. *Physical Chemistry*. New York: Wiley.
- Fennema, O. R., 1976. Water and ice. In Fennema, O. R. (ed.), *Principles of Food Science, Part II Physical Principles of Food Preservation*, New York: Marcel Dekker, pp. 13–38.
- Heiss, R., 1968. *Halbarkeit und Sorptionsverhalten wasserarmer Lebensmittel*. Berlin: Springer-Verlag.
- Karel, M., 1975a. Equilibrium and rate considerations in processes for food concentration and dehydrations. In Fennema, O. R. (ed.),

Principles of Food Science, Karel, M., Fennema, O.R., and Lund, D. B. (eds.), *Part II Physical Principles of Food Preservation*, New York: Marcel Dekker, pp. 219–236.

Karel, M., 1975b. Water activity and food preservation. In Fennema, O. R. (ed.), *Principles of Food Science*, Karel, M., Fennema, O.R., and Lund, D. B. (eds.), *Part II Physical Principles of Food Preservation*, New York: Marcel Dekker, pp. 237–263.

Moore, W. J., 1972. *Physical Chemistry*. Englewood Cliffs, USA: Prentice Hall.

Nelson, S. O., and Trabelsi, S., 2005. Permittivity measurements and agricultural applications. In Kupfer, K. (ed.), *Electromagnetic Aquametry*. Berlin: Springer Verlag, pp. 419–442.

Oertli, J. J., 1976. The states of water in the plant. Theoretical considerations. In Lange, O. L., Kappen, L., and Schulze, E.-D. (eds.), *Water and Plant Life. Problems and Modern Approaches*. Berlin: Springer-Verlag, pp. 19–31.

Van den Berg, C., and Bruin, S., 1981. Water activity and its estimation in food systems: theoretical aspects. In Rockland, L. B., and Stuards, G. F. (eds.), *Water activity. Influence on Food Quality*. New York: Academic Press, pp. 1–61.

Cross-references

[Drying of Agricultural Products](#)

[Physical Phenomena and Properties Important for Storage of Agricultural Products](#)

[Physical Properties as Indicators of Food Quality](#)

[Physical Properties of Raw Materials and Agricultural Products](#)

[Rheology in Agricultural Products and Foods](#)

[Stomatal Conductance, Photosynthesis, and Transpiration, Modeling](#)

[Water Effects on Physical Properties of Raw Materials and Foods](#)

[Water in Forming Agricultural Products](#)

ADVECTION

See [DNA in Soils: Mobility by Capillarity](#)

Cross-references

[Soil–Plant–Atmosphere Continuum](#)

AERATION OF AGRICULTURAL PRODUCTS

Marek Molenda

Institute of Agrophysics, Polish Academy of Sciences,
Lublin, Poland

Definition

Aeration, that is, forced ventilation of ambient or refrigerated air through stored products is necessary to maintain their quality. The main purpose of aeration is to minimize a risk of storage losses through equalizing temperatures in a bedding in order to minimize moisture movement, to cool product for pest control, and to stop product heating.

Background

Certain biological reactions generate heat and often it is necessary to remove it, that is, to cool the product. Heating

and cooling (see [Heat Diffusion](#)) large amounts of biological material require energy and time so the knowledge about the process is necessary to optimize operations. Heating or cooling is not an uniform inside the volume of layer of material, rather heating or cooling front passes through the material. The velocity and thickness of the front are dependent on the air velocity (see [Air Flux \(Resistance\) in Plants and Agricultural Products](#)), the evaporation rate, the temperature difference, and the sizes of particles (see [Pore Size Distribution](#)). Usually, the air velocity is a crucial factor. In design of processes or equipment mathematical equations describing heating or cooling are used that are derived with necessary simplifying assumptions. Usually, the most important assumptions are as follows: the material is isotropic (see [Isotropy and Anisotropy in Agricultural Products and Foods](#)) in terms of thermal and mass diffusivity; the temperature, moisture content, and porosity of the layer are initially identical in the volume and porosity does not change during the process; the temperature of the moving air does not change observably, walls limiting the considered volume are isolated, and fluctuations of external temperature are negligible. Differential equations are formulated and solved numerically that allow to estimate movement of heat front.

Grain aeration

The process of aeration of grain will be described below as probably the most common at the farm. Grain is good insulator (see [Grain Physics](#)) and heat loss from it is relatively low as compared to other materials. Grain is usually placed in a storage silo in the fall and its portion near the center tends to remain near the temperature at which it came from the dryer or field. The grain near the silo wall tends to cool to near the average outside temperature. With a decrease in the ambient temperature, the difference between the temperature in the center and near the wall produces air currents inside the grain mass. The colder air near the wall is denser and tends to fall, while warmer air flows up through the center of grain mass. Warmer air contains more moisture and when it reaches top center of the silo fill it cools to a point at which it cannot hold all moisture it had absorbed. The excess moisture condenses at the top layer of grain and creates an environment enhancing mold and insect growth. The opposite situation occurs in warmer periods, the moisture condenses near the bottom center of grain mass.

The problem of air currents within the grain mass may be minimized by keeping the temperatures near the center close to the average temperature near the wall of the storage silo (Loewer et al., 1994). To accomplish this aeration fans may be used that pull air down through the grain until the temperature of grain mass is within 5°C of the average monthly temperature. Aeration air can move either up or down through the grain mass. Most fans have the ability to either push or pull, however, airflow volumes and power requirements will often change due to direction. It is not necessary to cool the grain mass below 5°C, because

the activity of typical storage fungi is very low below this temperature. In spring, warming of grain is necessary if extended storage (post June) is required or if the temperature of grain is below 0°C. Typical aeration airflow rates range from 1 to 2 L of air per second per cubic meter of grain (1–2 L/(s m³)). Higher rates should be used (2–6 L/(s m³)) if grain is stored at higher moisture levels or if a large variance in incoming moisture levels exist. An aeration system cannot be considered a drying (see [Drying of Agricultural Products](#)) system since natural air drying rates are at least 10 times longer.

Conclusion

Aeration and controlled atmosphere storage are still under development to elaborate efficient methods for control of temperature and moisture of product, as well as for elaboration of optimum strategies specific for crop, storage structure, and climatic conditions. Currently, investigations are conducted on characterization of bedding anisotropy and including this into strategies of aeration control (Navarro and Noyes, 2001).

Bibliography

- Loewer, O. J., Bridges, T. C., and Bucklin, R. A., 1994. *On-Farm Drying and Storage Systems*. St. Joseph: American Society of Agricultural Engineers.
Navarro, S., and Noyes, R. T., 2001. *The mechanics and Physics of Modern Grain Aeration Management*. Boca Raton: CRC Press.

Cross-references

- [Air Flux \(Resistance\) in Plants and Agricultural Products](#)
[Drying of Agricultural Products](#)
[Grain Physics](#)
[Heat Diffusion](#)
[Isotropy and Anisotropy in Agricultural Products and Foods](#)
[Pore Size Distribution](#)
[Water Effects on Physical Properties of Raw Materials and Foods](#)

AERATION OF SOILS AND PLANTS

Witold Stepniewski

Department of Land Surface Protection Engineering,
Lublin University of Technology, Lublin, Poland

Synonyms

Gas exchange in soils; Oxygenation of soils and plants;
Oxygenology of soils and plants

Definition

Aeration of soils and plants is a term used in wide sense as a name of complex issues related to air transport and distribution in soil and its effect on processes occurring in soil and plants. Sometimes it is used in a narrow sense to denote gas exchange between soil and atmosphere, or only

oxygen content in soil air or even as a name for a process of artificially forcing air into the soil (Gliński and Stepniewski, 1985).

Introduction

In soil medium intensive production, transformations, and consumption of a number of gases, which are transported to and from the atmosphere, take place. These processes are not only important for the production of plant biomass but also play an important environmental role.

The most important soil gasses are oxygen (indispensable for root respiration and important for microbial metabolism and for numerous biochemical and chemical processes) and carbon dioxide (product of oxic respiration of plant roots, microorganisms, and mezo- and macrofauna, as well as anoxic microbial respiration and fermentation). Nitrogen, important for its fixation by some microbes, draws less attention because it is considered as non-limiting due to its abundance.

Soil air contains, moreover, a number of gases occurring in trace amounts such as nitrous oxide (N_2O), nitrogen oxide (NO) and dioxide (NO_2), ethylene, ammonia (NH_3), and hydrogen sulfide (H_2S). An intermediate position occupies methane which under dryland conditions occurs in trace amounts but under wetland conditions and under landfill conditions can occupy a substantial fraction of the soil air. Dependently on the aeration status, the soil can be a source or a sink of greenhouse gasses such as CH_4 and N_2O .

Pathways of gas exchange

There are two essential pathways of the gas transport in the *soil-plant-atmosphere continuum* (see [Soil-Plant-Atmosphere Continuum](#)): the soil pathway and the internal pathway through the plant tissues ([Figure 1](#)). The first one prevails in soils cultivated under dryland conditions, while the plant pathway dominates in natural and constructed wetlands and paddy fields (e.g., Yan et al., 2000). If the soil

is without plants, the downward transport of gases practically ceases while the gases generated in the soil such as CO_2 and CH_4 are released to the atmosphere by ebullition.

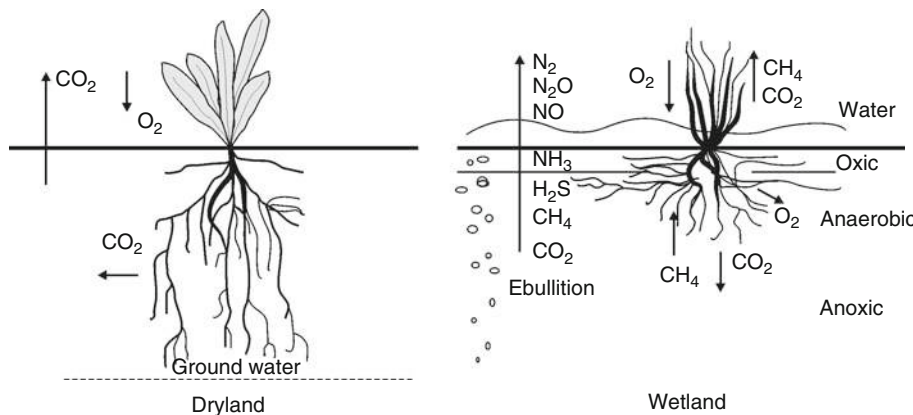
Between these two pathways, there are numerous intermediate situations with different contributions of soil- and plant-mediated transport of gases dependently on the land use and tillage influencing air-filled porosity, gas diffusion coefficient, and air permeability of soil (Stepniewski and Stepniewska, 2009). Agricultural land use is connected mainly with dryland conditions as wetland rice cultivation produces about 20% of food calories (IRRI, 2005). There are also examples of intermediate systems such as midseason drainage of paddy fields to prevent toxicity of sulfides (Kanno et al., 1997), combining cultivation of lowland rice with dry season crops (So and Ringrose-Voase, 2000) as well as so-called system of rice intensification characterized by change from permanent flooding to intermittent irrigation (Dobermann, 2004) to improve the oxygen supply to rice roots (Stoop et al., 2002).

Mechanism of gas exchange

There are two essential mechanisms of gas exchange in soil medium: mass flow or advection (convection) and molecular diffusion. Both these mechanisms can take place in soil pores as well as in plant tissues. The relative contribution of both mechanisms of gas exchange can vary within wide limits dependently on the conditions.

Mass flow

The driving force of mass flow is pressure gradients appearing within soil or plants due to fluctuations of atmospheric pressure, variability of temperature, changes of groundwater depth, infiltration of rainwater, as well as humidity-induced convection in leaves and Venturi convection caused by wind action (Armstrong et al., 1996). Of these drivers only fluctuations of atmospheric pressure may be of importance in the soils with very deep impervious layer.



Aeration of Soils and Plants, Figure 1 Model of the two pathways of gas exchange in the atmosphere-plant-soil continuum. Dryland conditions – oxygen is supplied to the plant roots via the soil. Wetland conditions – oxygen is transported through the tissues of the plant itself.

In case of *laminar flow* (see [Laminar Flow](#)) usually occurring in soil, when the Reynolds's number < 1 (Currie, 1970) the movement of gases is described by Darcy's equation:

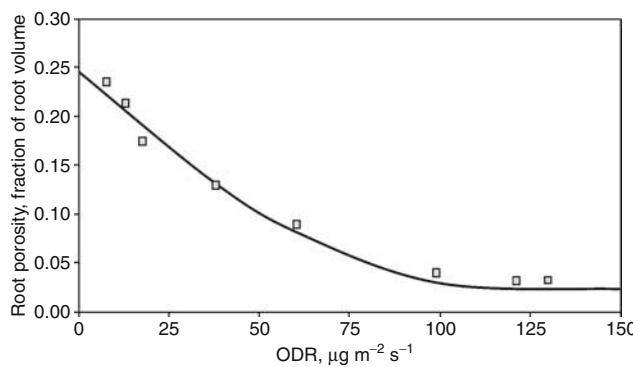
$$\frac{dV}{dt} = -A \frac{k}{\eta} \frac{dp}{dx} \quad (1)$$

where dV/dt is the volumetric rate of gas flow, $\text{m}^3 \text{s}^{-1}$, A is the cross-sectional area of the porous medium, m^2 ; η is the dynamic viscosity of the gas, $\text{kg m}^{-1} \text{s}^{-1}$; dp/dx is the pressure gradient, $\text{Pa m}^{-1} = \text{kg m}^{-2} \text{s}^{-2}$; and k is the air permeability, m^2 .

According to Gliński and Stepniewski (1985), the values of air permeability in soil are within the range of $0.01-500 \times 10^{-12} \text{ m}^2$. Air permeability depends in general terms on the quantity and quality of air-filled pores. The latter term relates to the pore size distribution, continuity, and tortuosity, which, in turn depend on the arrangement of soil particles, on soil bulk density, and water content. Advective gas flow depends on the fourth power of the pore size.

Morphological changes within plants are very important adaptation to flood conditions. They include development of a shallow root system, formation of adventitious roots of high porosity, formation of aerenchyma within roots (Gliński and Stepniewski, 1985), and development of aerial roots or pneumatophores (e.g., Purnobasuki and Suzuki, 2005).

The internal *air flux* ability of the plant tissues can be a permanent feature or it may become apparent or enhanced under oxygen deficiency conditions ([Figure 2](#)). Internal transport of oxygen via plant roots can cover not only oxygen demand of the plant roots, but also can protect the plants against Fe^{2+} and H_2S toxicity (Jayakumar et al., 2005). It should be emphasized that an increase of internal porosity of root tissues increases both air permeability as well as gas diffusion coefficient.



Aeration of Soils and Plants, Figure 2 The relationship between oxygen availability in soil medium as characterized by oxygen diffusion rate (ODR) and the internal porosity of rice roots. (Modified from Ghildyal [1982].)

Diffusion

The basic mechanism of gas exchange in the soil medium and within the plant tissues is the concentration diffusion induced by concentration gradients.

The diffusive flow f_x of a gas within a porous medium is described by the first Fick's law.

$$f_x = -D dC/dx \quad (2)$$

The above equation says that the uniaxial diffusion flow (f_x) of an agent through a unit cross-section, in a unit of time, is proportional to the concentration gradient (dC/dx) and to the diffusion coefficient D characterizing the mobility of the agent in a given medium.

Coefficient of gas diffusion in soil depends on the kind of gas, its temperature, and pressure, and also on the amount of air-filled pores, their continuity, and shape which depend on the spatial arrangement of soil particles and on distribution of water. The diffusive properties of a soil medium are usually characterized by the relative diffusion coefficient D/D_o , being the ratio of gas diffusion coefficient in soil D , to that of the same gas in atmospheric air D_o , under the same pressure and temperature conditions. The D/D_o value does not depend on the temperature, pressure, or the kind of the diffusing gas.

The influence of *soil bulk density* and soil moisture tension on D/D_o is presented in [Figure 3](#). The value of D/D_o in soil is usually below 0.2. It increases with soil moisture tension, and rapidly decreases with soil bulk density. It should be stressed out that gas diffusion coefficient in porous media does not depend on the size of the pores, as long as the pore diameters are greater than the mean free path of the molecules of the gas under consideration. (Gliński and Stepniewski, 1985). This limit is the pore diameter of $0.10 \mu\text{m}$. In the case of soil, pores of that size are emptied of water at soil moisture tension levels over 3 MPa ($\text{pF} > 4.5$), i.e., at moisture contents lower than the permanent wilting point. Thus, gas diffusion within macropores (above $30 \mu\text{m}$) as well in the mezopores ($30-0.2 \mu\text{m}$) containing usually plant available water does not depend on the pore size.

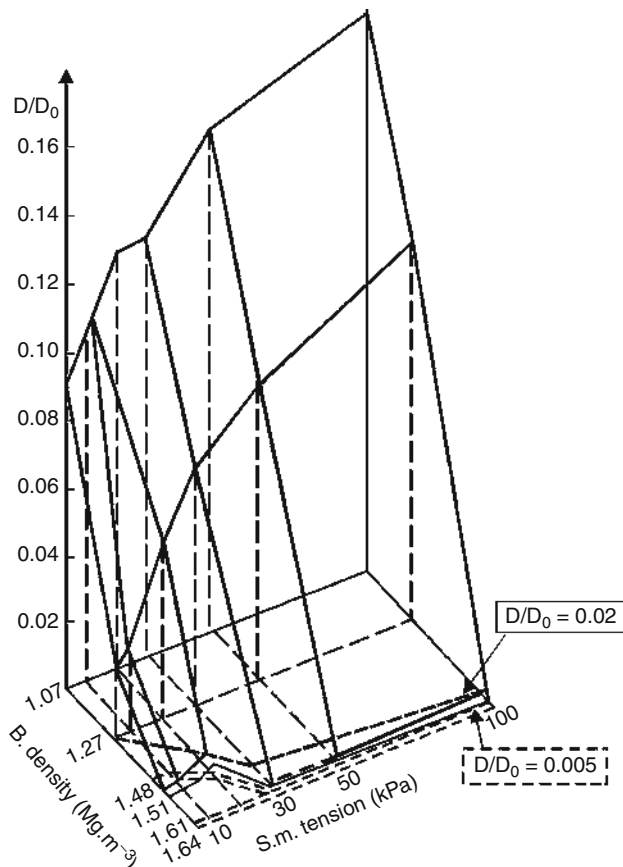
D/D_o usually shows a curvilinear relationship versus E_g , as shown in [Figure 4](#). It can be described by an empirical power model in the following form:

$$\frac{D}{D_o} = \gamma E_g^\mu \quad (3)$$

where γ and μ are empirical coefficients characterizing the porous material.

The author was unable to find literature data related to direct measurements of gas diffusion coefficients within living plant tissues.

It should be underlined that the composition of air within the intra-aggregate pores may differ from that in the inter-aggregate pores due to soil heterogeneity. The former pores contain less oxygen and more

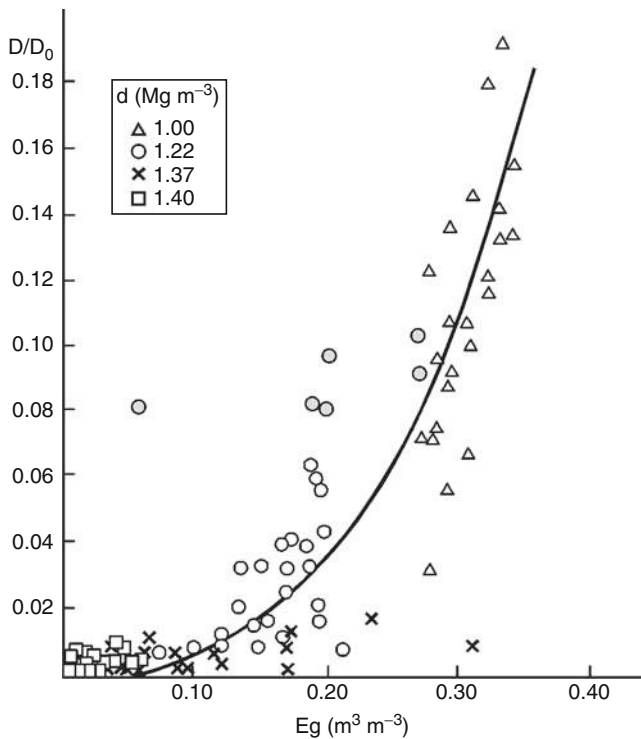


Aeration of Soils and Plants, Figure 3 Dependence of relative gas diffusion coefficient in a loamy textured Phaeozem (Kock, Poland) on soil moisture tension and bulk density. (Modified from Stępniewski [1981].)

carbon dioxide compared to the inter-aggregate pores (e.g., Zausig et al., 1993; Højberg et al., 1994; Horn, 1994; Horn and Smucker, 2005).

Oxygen

Oxygen is taken up by the soil due to respiration of microorganisms and plant roots. Respiration of soil microorganisms depends on the availability of oxygen, organic carbon, and nutrients as well on temperature and water content. The temperature interval for microbial growth ranges from -12°C to 110°C . Microorganisms with respect to their temperature requirements are divided into psychrophilic, mesophilic, and thermophilic (Paul and Clark, 1998). A new term “hyperthermophiles” denotes extreme thermophiles growing in the temperature range from 60°C to 110°C . Soil contains a mixture of different groups of microorganisms and its respiration rate increases two to three times with the increase of temperature by 10°C until the temperatures of break of metabolism (at about 60 – 70°C).

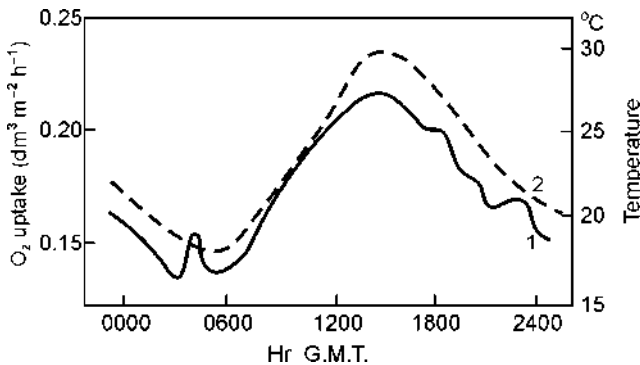


Aeration of Soils and Plants, Figure 4 Relationship of D/D_0 to air-filled porosity E_g of silt Fluvisol at different bulk densities d . (Modified from Stępniewski [1981].)

With respect to oxygen requirements, soil microbes are divided into obligate oxic, facultative anoxic, and obligate anoxic organisms (obligate anaerobes). A special group of microorganisms constitute microaerophiles characterized by oxygen optimum of order 2–10% by volume (Black, 1996). Oxic microorganisms utilize oxygen as a terminal electron acceptor from the cytochrome oxidase.

Soil microbial activity depends both on oxygen and carbon dioxide concentration, independently. Carbon dioxide is a carbon source for autotrophic microflora. Dommergues and Mangenot (1970) reported 2–14% CO_2 as the optimal range for the growth of these bacteria. For other microorganisms, carbon dioxide is an inhibitor of respiration and growth although some microorganisms display metabolic stimulation by low CO_2 concentration and inhibition above a certain CO_2 concentration (Dixon et al., 1998; Sierra and Renault, 1995).

The dependence of microbial respiration on water content shows a maximum corresponding to the range of optimal availability of oxygen and water. With respect to water requirements, the soil microorganisms are divided (Gliński and Stępniewski, 1985) into hydrophilic (disappearance of activity at pore water pressure > -7.1 MPa), mesophilic (disappearance of activity within the pore water pressure interval from -7.1 to -30 MPa), and xerophilic (disappearance of activity at pore water pressures < -30 MPa). Under field conditions, the rate of soil



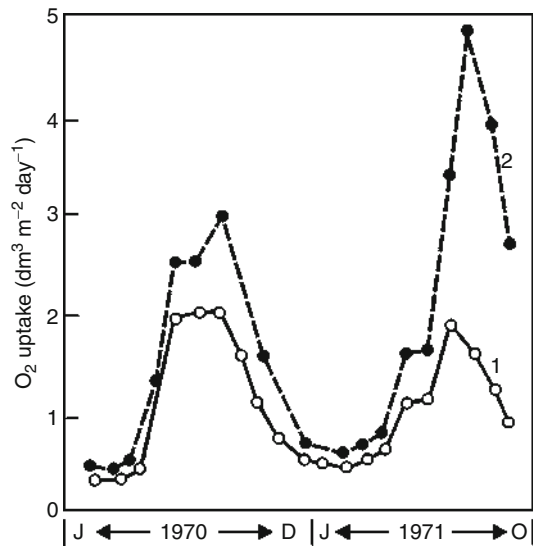
Aeration of Soils and Plants, Figure 5 Diurnal dynamics of soil respiration rate as measured by oxygen uptake and temperature. (Modified from Currie [1975].)

microbial respiration is usually within the range from 0.1 to 10 mg m⁻³s⁻¹ (Gliński and Stępniewski, 1985).

The root respiration rate depends on plant internal factors such as plant type and development stage, root mass distribution, dimensions, and physiological age of the tissue, as well as on external factors such as temperature and the availability of water and nutrients. It should be emphasized that soil microbial activity increases in the presence of plant roots due to production of root exudates being a source of easily available carbon for microorganisms. Respiration rate of the root tissues is about two orders of magnitude of that of the soil itself and ranges from 10 to 50 mg m⁻³s⁻¹ (Gliński and Stępniewski, 1985).

Oxygen uptake by a cropped field is a sum of microbial and root respiration and under field conditions is of order of several tons of oxygen per hectare and year (Gliński and Stępniewski, 1985). Soil respiration under field conditions (Figure 5) shows a maximum in the afternoon and minimum before sunrise. In the moderate climate zone, the annual dynamics of oxygen uptake under field conditions is characterized by a summer maximum (Figure 6). It should be emphasized that the presence of plants may elevate the oxygen uptake more than twice.

The oxygen deficiency in soil affects the plant performance directly by limitation of root respiration, of energy supply, and changing the metabolism in the root tissue itself, as well as indirectly by inducing chemical and biological changes in the surrounding soil (e.g., *oxidation-reduction reactions* (see *Oxidation-Reduction Reactions in the Environment*), accumulation of phytotoxic substances, changes of pH and ion exchange equilibria). Effects of deficient aeration can be manifested in plant roots in the form of ethanol and ethylene generation, reduced water permeability, growth inhibition, and necrosis. The shoot response comprises *stomatal closure*, chlorosis, epinasty, leaf senescence and abscission, partial or complete suppression of *photosynthesis* (see *Photosynthesis*), and growth leading to reduction of biomass and yield (Glinski and Stępniewski, 1985).



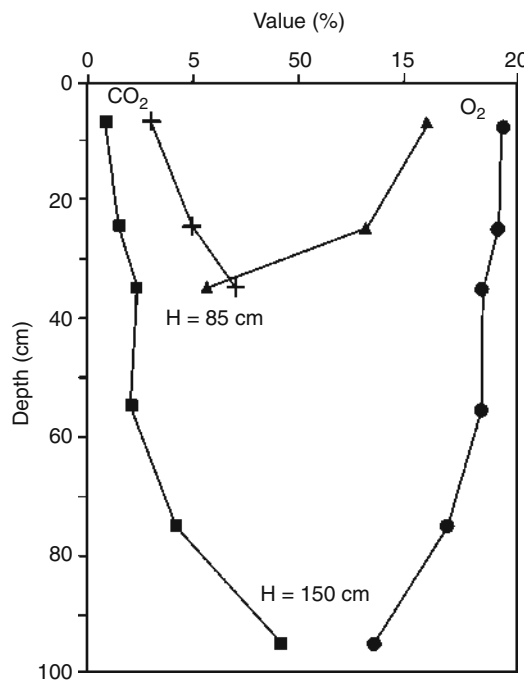
Aeration of Soils and Plants, Figure 6 Annual dynamics of soil respiration as measured by oxygen uptake rate in an uncropped (1) and cropped (2) soil under moderate climate conditions of England. (Modified from Currie [1975].)

Carbon dioxide and other gases

Production of carbon dioxide in soil under oxic conditions is directly related to oxygen uptake and all the factors influencing oxygen uptake affect also the emission of carbon dioxide.

Because of complementary character of oxygen uptake and carbon dioxide production their sum in soil air is usually about 20% by volume (cf. Figure 7). It means that also their fluxes between soil and the atmosphere are approximately equal. Concentration of oxygen in soil air decreases with depth and that of CO₂ increases. The composition of soil air is a decisive factor for microbial and plant metabolism, for many *oxidation-reduction reactions* and oxidation state of numerous soil nutrients, as well as for soil fertility and crop productivity. It should be kept in mind that under anoxia CO₂ can be produced without oxygen consumption (sum of O₂ and CO₂ >20%) and the emission of CO₂ from the soil exceeds the volume of oxygen taken up. However, long-term CO₂ emission under anoxia is reduced, what leads to carbon accumulation in soil.

Soil aeration state effects not only global turnover of oxygen and *fluxes of greenhouse gases* (see *Greenhouse Gas Fluxes: Effects of Physical Conditions*) such as carbon dioxide, methane, and nitrous oxide but also the emission of ammonia, NO_x, and ethylene. Methane emission increases under anoxic conditions. Ethylene is generated within plants under moderate hypoxia. Nitrous oxide is formed and is stable under moderate hypoxia and undergoes decomposition both under oxic conditions and under severe anoxia. Ammonia under oxic conditions undergoes oxidation to nitrates.



Aeration of Soils and Plants, Figure 7 Distribution of oxygen and carbon dioxide concentration in a gley meadow soil (Garbow, near Lublin, Poland) at two levels of ground water on 1971.06.19 (ground water level $H = 85\text{ cm}$) and the same point on 1971.09.04 ($H = 150\text{ cm}$). (From unpublished data of Stepniewski.)

Bibliography

- Armstrong, J., Armstrong, W., Beckett, P. M., Halder, J. E., Lythe, S., Holt, R., and Sinclair, A., 1996. Pathways of aeration and the mechanisms and beneficial effects of humidity – and Venturi-induced convections in *Phragmites australis* (Cav.) Trin. ex Steud. *Aquatic Botany*, **54**, 177–197.
- Black, J. G., 1996. *Microbiology. Principles and Applications*, 3rd edn. Upper Saddle River: Prentice Hall, pp. 144–148.
- Currie, J. A., 1970. Movement of gases in soil respiration. In *Sorption and Transport Processes in Soil*. S.C.I. Monograph No. 37, London: Society of Chemical Industry.
- Currie, J. A., 1975. Soil respiration. *Ministry of Agriculture, Fisheries and Food. Technical Bulletin*, **29**, 461–468.
- Dixon, N. M., Lovitt, R. W., Morris, J. G., and Dell, D. B., 1998. Growth energetic of Clostridium sporogenes NCIB 8053: modulation by CO_2 . *Journal of Applied Bacteriology*, **65**, 119–133.
- Dobermann, A., 2004. A critical assessment of the system of rice intensification (SRI). *Agricultural Systems*, **79**, 261–281.
- Domergues, Y., and Mangenot, F., 1970. *Ecologie Microbienne du Sol*. Paris: Mason.
- Ghildyal, B. P., 1982. Nature, physical properties and management of submerged rice soils, Transections of the 12th International Congress of Soil Science, New Delhi, India. In *Vertisols and Rice Soils of the Tropics, Symposium papers II*, Shri S.N. Mehta, New Delhi, India.
- Gliński, J., and Stepniewski, W., 1985. *Soil Aeration and Its Role for Plants*. Boca Raton: CRC Press.
- Højberg, O., Revsbech, N. P., and Tiedje, J. M., 1994. Denitrification in soil aggregates analyzed with microsensors for nitrous oxide and oxygen. *Soil Science Society of America Journal*, **58**, 1691–1698.
- Horn, R., 1994. Effect of aggregation of soils on water, gas and heat transport. In Schulze, E. E. (ed.), *Flux Control in Biological Systems*. San Diego: Academic, Vol. 10, pp. 335–361.
- Horn, R., and Smucker, A., 2005. Structure formation and its consequences for gas and water transport in unsaturated arable and forest soils. *Soil and Tillage Research*, **82**, 5–14.
- IRRI, 2005. World Rice Statistics. <http://www.rri.org/science/ricestat>.
- Jayakumar, B., Subathra, C., Velu, V., and Ramanathan, S., 2005. Effect of integrated crop management practices on rice (*Oryza sativa* L.) root volume and rhizosphere redox potential. *Agronomy Journal*, **4**, 311–314.
- Kanno, T., Miura, Y., Tsuruta, H., and Minami, K., 1997. Methane emission form rice paddy fields in all of Japanese prefecture. *Nutrient Cycling in Agroecosystems*, **49**, 147–151.
- Paul, E. A., and Clark, F. E., 1998. *Soil Microbiology and Biochemistry*. San Diego: Academic.
- Purnobasuki, H., and Suzuki, M., 2005. Functional anatomy of air conducting network on the pneumatophores of a mangrove plant, *Avicennia marina* (Forst.) Vierh. *Asian Journal of Plant Sciences*, **4**, 334–347.
- Sierra, J., and Renault, P., 1995. Oxygen consumption by soil microorganisms as affected by oxygen and carbon dioxide levels. *Applied Soil Ecology*, **2**, 175–184.
- So, H. B., and Ringrose-Voase, A. J., 2000. Management of clay soils for rain fed lowland rice-based cropping systems: an overview. *Soil and Tillage Research*, **56**, 3–14.
- Stepniewski, W., 1981. Oxygen diffusion and strength as related to soil compaction. II. Oxygen diffusion coefficient. *Polish Journal of Soil Science*, **14**, 3–13.
- Stepniewski, W., and Stepniewska, Z., 2009. Selected oxygen – dependent processes – response to soil management and tillage. *Soil and Tillage Research*, **102**, 193–200.
- Stoop, W. A., Uphoff, N., and Kassam, A., 2002. A review of agricultural research issues raised by the systems for resource-poor farmers. *Agricultural Systems*, **71**, 249–272.
- Yan, X., Shi, S., Du, L., and Xing, G., 2000. Pathways of N_2O emission from rice paddy soil. *Soil Biology and Biochemistry*, **32**, 437–440.
- Zausig, J., Stepniewski, W., and Horn, R., 1993. Oxygen concentration and redox potential gradients in different model soil aggregates at a range of low moisture tensions. *Soil Science Society of America Journal*, **57**, 906–916.

Cross-references

- Air Flux (Resistance) in Plants and Agricultural Products
 Bulk Density of Soils and Impact on Their Hydraulic Properties
 Climate Change: Environmental Effects
 Greenhouse Gas Fluxes: Effects of Physical Conditions
 Greenhouse Gases Sink in Soils
 Laminar and Turbulent Flow in Soils
 Oxidation–Reduction Reactions in the Environment
 Oxygenology
 Soil–Plant–Atmosphere Continuum
 Stomatal Conductance, Photosynthesis, and Transpiration, Modeling

AERODYNAMICS

See *Cultivation Under Screens, Aerodynamics of Boundary Layers; Grains, Aerodynamic and Geometric Features*

AFTER HARVEST TECHNOLOGY

See [Mechanical Impacts at Harvest and After Harvest Technologies](#)

AGGREGATE STABILITY

See [Cropping Systems, Effects on Soil Physical Properties](#)

Cross-references

[Soil Aggregates, Structure, and Stability](#)

AGGREGATION INDICES

Soil aggregation may be determined through the following indices: dispersion ratio, Wischmeier's erodibility index, clay dispersion index, clay flocculation index, geometric mean diameter and mean -weigh diameter.

Bibliography

Igwe, C. A., Akamigbo, F. O. R., and Mbagwu, J. S. C., 1995. The use of some soil aggregate indices to assess potential soil loss in soils of South-Eastern Nigeria. *International Agrophysics*, **9**, 95–100.

AGRICULTURAL PRODUCTS

See [Agophysical Objects \(Soils, Plants, Agricultural Products, and Foods\); Agrophysics: Physics Applied to Agriculture](#)

AGRICULTURAL RAW MATERIALS

See [Physical Properties of Raw Materials and Agricultural Products](#)

AGRICULTURE AND FOOD MACHINERY, APPLICATION OF PHYSICS FOR IMPROVING

Leszek Mieszkalski

Department of Agricultural Engineering and Natural Raw Materials, University of Varmia and Mazury in Olsztyn, Olsztyn, Poland

Definition

Physics is the science concerned with the study of matter and natural forces, such as light, heat, movement.

Design is an intellectual activity; it is the oldest mental process engaged in by man to solve complex problems, develop and improve technical systems, including farming and food processing machines. Design is a process of drawing logical conclusions from empirical observations. It enables man to create artificial objects that support his existence and to introduce technical systems into the natural environment.

A machine is a set of interconnected elements that perform a given set of operations, carry the load and the moment of force to perform useful work as an energetic effect, and transform any type of energy into mechanical energy or mechanical energy into a different type of energy. Motion is transferred by mechanisms.

Introduction

The primary goal of physics is to examine the material world and search for the truth and the fundamental properties of matter on the assumption that the laws of physics are consistent and universal. Physics studies natural objects with the application of universal methods, concepts, and laws. Physical sciences support the design of farming and food processing machines by solving complex problems relating to the physical properties of soil, organic materials, and food products with the use of methods that involve the determination of physical quantities and process descriptions, based on the principles of mechanics, thermodynamics, optics, electrodynamics, electronics, acoustics, and nuclear, molecular, and solid-state physics, as well as the principles of other modern fields of physics.

Rising competition in food production requires product quality growth and production costs reduction. Physical prosperities of raw materials make designing agricultural machinery and food processing machinery difficult. Precise knowledge of raw material prosperities is a condition to create appropriate food processing technologies and machinery. There are many problems to solve in machine designing, e.g., soil degradation, excessive chemicalization, food safety, etc. Sciences as agrophysics, agricultural engineering, food engineering, and other related sciences as mechanics, mechatronics, computer sciences, genetic engineering are used to help with gathering and receiving information for machine designing.

Changing rapidly global economy uses robots on a big scale in food production. Today human work in food production is replaced by machinery with complicated mechanisms, working units, sensors, and board computers. In current mechanical production dynamic development of mechanization, atomization and robotics takes place.

The importance of the physical properties of raw materials and food products in machines designing

Animate and inanimate matter differs as regards the values of state parameters such as temperature, pressure, radiation field intensity, and humidity. Live cells of animate

matter used in the production of food have a highly complex microstructure, and its specific attributes, the observed chemical and biological processes reflect the universal laws of physics. The laws of physics attributed to complex systems imply various characteristic properties that have to be taken into account when designing food processing machines. Raw materials and food products have unique physical characteristics such as stretch, location, velocity, mass, momentum, temperature, color, and chemical and biological attributes. The raw materials used in the production of foodstuffs are examined with the use of physical methods to select the appropriate working parameters of the designed farming and food processing machines. The study of physical phenomena occurring in plant and animal material, i.e., anisotropic objects, in an unstable and an unpredictable environment poses a challenge for contemporary physics which, in addition to investigating the occurring processes, accumulating data and expanding our knowledge base, also aims to expand the intellectual capacity of technical sciences and offers solutions to specific problems. Scientific knowledge should have a practical dimension, and it should satisfy man's nutritional needs. Physical phenomena are described with the involvement of measurable properties, referred to as physical quantities. The process of examining the physical phenomena attributed to raw materials for the food industry can be divided into several stages. The first stage involves the selection of parameters that support the investigation of the studied object's suitability for processing and its description. The method of measuring the selected parameters is determined at the second stage. At the third stage, researchers develop the general concept and the structure of measuring equipment; they select the units of measurement and calibrate tools. At the following stage, measurements are performed at the required level of precision, the results are analyzed, and conclusions are formulated. At successive stages, the obtained results are applied to design and upgrade farming and food processing machines.

The relationship between motion and the force of raw material and food product molecules at the microstructure level is very important during the construction of farming and food processing machines. Motion is described with the use of parameters such as the components of a position vector that changes over time, which are attributed to the discrete morphological elements of a biological object. The measured quantities include distance, angle, and time. The correlation between the above quantities is investigated with the use of mathematical formulas. The human senses do not respond to many physical phenomena, including field and radiation. Such phenomena are often encountered in food processing technology. They are measured with the application of detectors that convert various pulses into observable signals. Detectors are clocks, weighing scales, thermoscopes, baroscopes, electroscopes, spectrometers, microscopes, etc. A measuring device is closely interrelated with the physical quantity that is being measured at a given level of precision.

Measurement precision determines the quality of physical observation. The results of measurements in a discrete system are expressed in the form of a finite set of numbers to which quantitative data are attributed. The studied processes involve recurring phenomena and phenomena that constitute the laws of physics. Those phenomena can be used to formulate theoretical structures and design many practical applications. The laws of physics are expressed in the form of mathematical relations between symbols representing different quantities. The discovery of new, validated laws of physics expressed by equations and inequations supports the examination of the resulting consequences. The application of physics theories in engineering and machine construction, including farming and food processing equipment, is important for the process of designing processing technologies. The physical properties of raw materials are transformed during processing into food products. The principal physical quantities describing a particle of the studied raw material or product are particle mass, vectors of position, and forces applied to those particles. If those quantities are known at a given time, then the velocity and acceleration of particle mass moved by that force is also known. Other quantities include momentum, angular momentum, and torque. Newton's laws of dynamics, described as a system of three quadratic differential equations for unknown time functions, support an infinite number of solutions. A fixed solution can be obtained only by determining the initial conditions.

In the process of building farming and food processing machines with the use of laws of physics that describe the general relationships associated with an infinite number of physically admissible solutions, a specific physical situation at a given point in time should be determined and implemented. Food engineering deals with various objects, including elementary particles, atoms, cells, tissues, ions, molecules, systems of microscopic and macroscopic particles as well as fields. One of the many goals of food engineering is the use of physics theories, namely the laws of physics written down in mathematical form, in a strictly defined environment. The above also applies to farming and food processing equipment, raw materials of plant and animal origin, and end products. For a physics theory to be useful in the process of solving technical problems, the number of predictions has to be consistent with experimental results. Established physics theories are not always fit for use in farming and food engineering. Despite their universal character, the applicability and precision of those theories may be limited in this particular context. If this is the case, a theory has to be adapted to a given situation to ensure a higher level of accuracy and consistency with the experiment. Experiments support the discovery of new physical phenomena and new attributes of technical and biological objects (Shao et al., 2009), and they are of paramount importance in the process of solving technical problems in agriculture, food engineering, and production. The measurements used to determine the physical quantities of the studied

raw materials and food products contribute to the discovery of rules, correlations, structures, and dependencies. These experimental and intellectual methodological operations support the development of new concepts, conceptual structures and theories, the discovery of important phenomena for biological objects and dynamic causal relationships. The acquired knowledge on raw materials and food products, expressed in mathematical form, enables researchers to examine and determine the effect of changes in the physical qualities of the studied objects owing to different factors (conditions), to subject their findings to a critical evaluation and formulate logical conclusions. A physics theory that is free of logical and mathematical contradictions is a venture point for explaining causally connected facts, and it supports the prediction of new, unknown facts.

Many problems in agricultural and food engineering may be solved with the use of data in the existing knowledge database. Scientists developing new farming and food processing machines rely on information describing the physical properties of raw materials and food products as well as established scientific theories and laws of physics. Biological objects have a complex structure. The attributes of complex objects are determined by the laws and properties applicable to their components. Their geometric form follows from the surface structure of the morphological components of a biological object. Physics and its laws are closely related to natural sciences, which is why the laws of science have many applications in agricultural and food engineering, in particular in describing working processes and developing new technologies and machines. A sound theory of elementary particles should support the discovery of new phenomena and laws that may be applied in designing new technologies for processing a given type of raw materials into food products with the anticipated properties. As a rational science supporting the development of formal languages for the precise description of abstract concepts and relations, mathematics plays an important role in the physical description of the actual condition of farming and food processing machines. From among a variety of mathematical equations describing a given phenomenon, scientists have to choose the propositions, concepts, and statements that are fit for use in the process of building models of farming and food processing machines and modeling working processes in food production (Mieszkalski, 1996; Hardin and Searcy, 2009). Many biological objects with technical applications can be described with the use of geometric and mechanical models as discrete structures. A system of spatially distributed mass particles may serve as a model of raw materials and food products. The distance between mass particles is modified under the influence of the applied force. The physical quantities indicating displacement over time are described with the use of mechanics, thermodynamics, and other existing theories.

The design of new farming and food processing machines as well as food processing technologies relies

heavily on mathematical modeling, which will develop as new advances are made in IT and computer systems. A preferred mathematical model for describing physical processes in farming and food engineering should have the widest possible range of applications, it should deliver a high degree of precision and, above all, it should support the prediction of experimentally validated events.

Many discoveries have been made as regards measuring devices for observing the structure of biological objects of plant and animal origin. Small objects in the structure of the studied raw materials are investigated with the use of microscopes. Vast advancements have been made in the field of microscopy, leading to the development of electron and confocal microscopes (Entwistle, 2000; Danilatos and Postle, 1982; Inoue, 1986). New solutions simplifying the observation of the spatial structures of those objects are likely to be introduced in the future. Empirical knowledge on the spatial distribution of particles with a complex shape will contribute to the development of more accurate particle models as well as theories that offer practical implications for farming and food engineering.

Testing raw materials and food products

There is a need to isolate a field of physics dealing exclusively with physical relations in the natural environment, soil, water, air, plants, animals, raw materials of plant and animal origin, and food products. This field – agrophysics – should have its own conceptual system covering a specific field of study.

Agrophysics studies the ecosystem and biological objects that participate in the food production process, which are processed by human activity and whose mathematical, physical, and chemical attributes are described with the use of scientific methods. Agrophysics could further the development of food research by:

- Introducing universal standards applicable to biological objects for food production
- Promoting the development of high-precision research methods investigating the phenomena and properties encountered in the food production process
- Describing physical processes in food production
- Examining the physical properties of farming produce used for food processing
- Investigating mutual relations in the natural environment relating to food production
- Designing new methods that restrict the degradation of the environment where raw materials and food are produced
- Monitoring and storing data on changes in physical quantities characteristic of raw materials and food products during processing
- Developing mathematical models of the processes observed in biological objects that are marked by high variability and anisotropy during food production

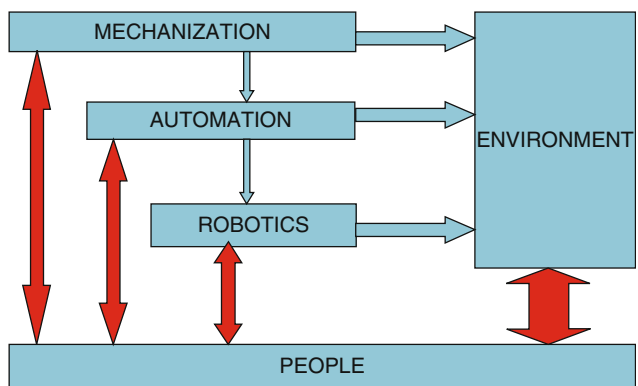
- Developing advanced measuring systems supporting fast and precise measurement of physical properties in automated food production
- Improving physical methods in the area of food production
- Developing new methods for evaluating food quality and safety

Physics supports agricultural engineering that deals mainly with soil – machine – plant systems and breeding animals, as well as food engineering, which investigates the relationships between farming produce and machines, and machines and food products. The relationship between physics, agricultural engineering and food engineering is based on the supply of data from physical experiments for developing new production technologies, preserving and storing food, designing machines, devices, research methods, measuring equipment and apparatuses. Physics will have a growing role in agricultural and food engineering because the progressing drop in employment levels in the farming sector will force farming corporations and local food producers to modernize and expand their resources.

Trends in the development of agricultural machinery and food machinery

There will be a growing demand for new technologies yielding high quality raw materials and food products (Semos, 2004). The interest in new-generation machines will rise. New computer-aided design solutions will shorten design time and cut the relevant costs, while significantly enhancing the quality of the end product. 4D computer-aided design which, in addition to 3D modeling principles, accounts for the time factor, will enable scientists not only to model but also to simulate the kinematics of mechanical motion and the dynamics of changes taking place in machines, raw materials, and food products over time.

According to the National Academy of Engineering, the quality of life in the twentieth century improved dramatically owing to technological progress in areas such as electrification, the invention of mechanical vehicles and airplanes, potable water networks, electronics, radio, television, computers, telephones, paved roads, spaceships, the Internet, medical technology, crude oil processing, lasers and optical fibers, nuclear technology, and state-of-the-art materials. Living standards also improved owing to farming mechanization (ranked 7th), air-conditioning and cooling (ranked 10th) and household equipment (ranked 15th). The twentieth century brought the mechanization era to a close. The current level of technological process supports the construction of machines that may successfully replace human labor. The twenty-first century will witness the development of scientific fields such as information technology, biotechnology, and mechatronics, which will automate and robotize production processes, including farming and the food industry (Figure 1). Physics will play an important role in this



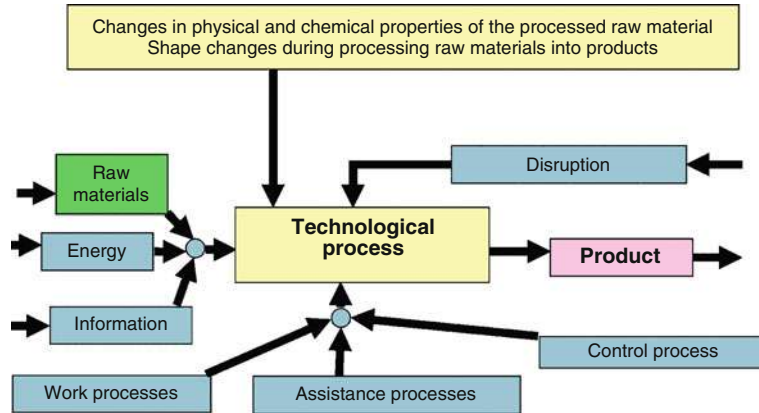
Agriculture and Food Machinery, Application of Physics for Improving, Figure 1 Stages of technical modernization in agriculture and the food processing industry.

process. Highly industrialized countries are entering a new phase of technological advancement marked by automation and robotization of production and services (Liu et al., 2009). Efforts must be made to ensure this progress does not have adverse consequences for the natural environment, which is of fundamental importance for the quality of life on Earth.

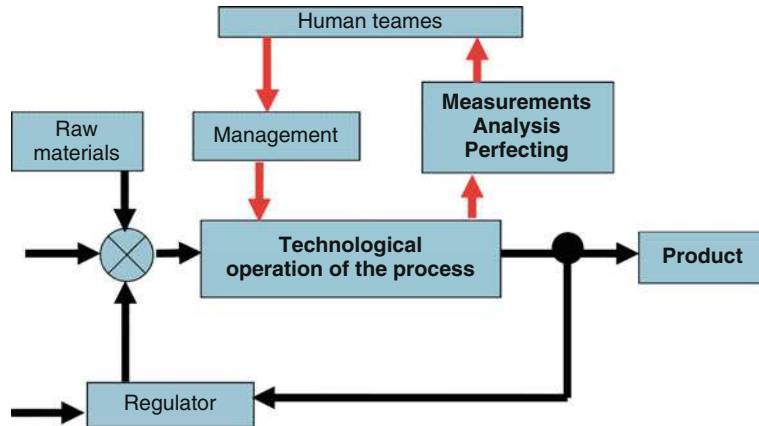
The challenges presently faced by physics, agricultural and food engineering involve rational and pragmatic needs analyses, systematic research, the development of theoretical systems based on the results of scientific experiments and observations, and expanding and building a reliable knowledge base with practical implications leading to the implementation of new concepts. A reliable knowledge base delivers practical results and contributes to an improvement in the quality of life. Scientific progress in new farming and food processing technologies can be used to ensure social demands and can be implemented on a mass scale.

In the process of dynamic civilizational development, science should be independent and free of any political influences in order to deliver unbiased solutions at every stage of development of new technologies and machines. Above all, scientific advancement should support the establishment of a sustained relationship between artificial systems, the natural environment, and man (Arvanitoyiannis et al., 2000; Ravertz, 2002). In designing optimal design, decisions must be taken, having a serial structure which affects the quality of the proposed agricultural machinery and food machinery. This process has very serious consequences as it determines the final quality of farming and food processing machines. Scientific teams designing farming and food processing machines rely on data that deliver information on the physical and chemical properties of soil, plants, animals, and end products (Mieszkalski, 1997). Physics must fill the existing knowledge gaps in a structured way to support technology process design and then the machine design (Figure 2).

A technological process is a dynamic system where the set of input data accounts for raw materials, energy, and



Agriculture and Food Machinery, Application of Physics for Improving, Figure 2 Block diagram of a technological process.



Agriculture and Food Machinery, Application of Physics for Improving, Figure 3 Block diagram of a technological process operation.

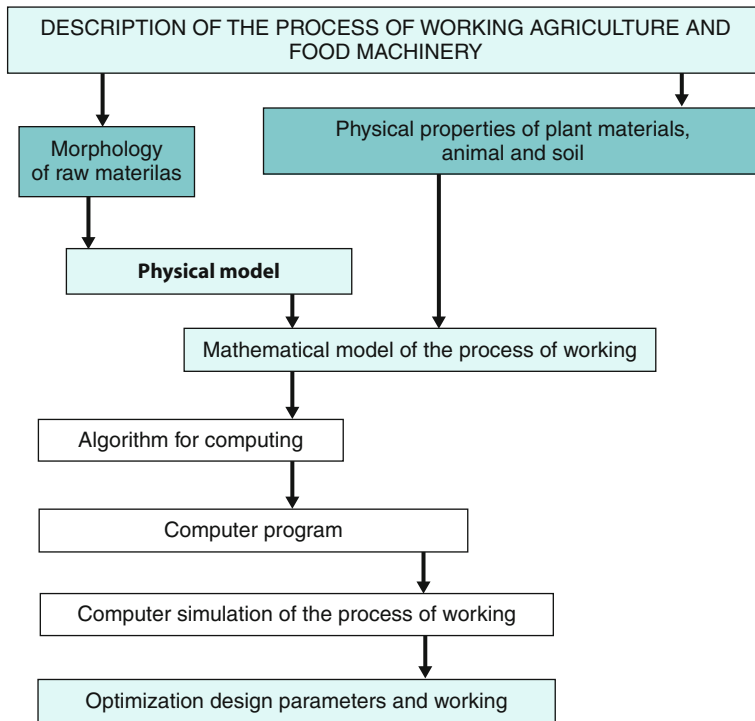
information, and the set of output data comprises end products and waste. In the initial design phase, the technological process and the process line supplying farming and food processing machines have to be thoroughly evaluated to guarantee the highest quality of the end product. Scientists should develop structural solutions to search for appropriate solutions in the design process of machines farming and food processing machines.

A well-designed process that accounts for economic, ergonomic, environmental, and social criteria consists of a series of activities that modify the physical and chemical parameters and the shape of the processed materials, and facilitate the search for new structural solutions. A thorough examination and a detailed description of the technological process should underlie all research efforts in physics, agricultural engineering, and food processing engineering (Figure 3).

Every working process in the food processing industry comprises many complex and interconnected factors. Their impact on the technological process is determined

by the physical condition of the processed plant and animal material as well as the kinematic and dynamic parameters of the processing system. An algorithm describing the technological process of a machine is presented in Figure 4 (Mieszkalski, 1998a). The food production process involves physical events and phenomena. A physical phenomenon is an event during which the form of a biological object is transformed by modifying its physical properties. The occurrence of a physical phenomenon requires electrical, magnetic, gravitational and particle interactions as well as friction. A phenomenon is a unitary event, an existing fact. The physical state of a material object embodies its quality, form, level, quantity, number, and location at a given time. The technological process of a farming and food processing machine encompasses a number of constituent processes, which form a sequence of actions and measures required to achieve the planned goal.

In the technological process of a machine, the processing of raw materials into food products involves



Agriculture and Food Machinery, Application of Physics for Improving, Figure 4 Block diagram of a farming machine's technological process.

the modification of their physical and chemical properties. Those changes and their course have to be taken into account at the stage of designing the working process as the quality of the end product can be modified during that phase. An analysis of the food production process relies on the results of research involving a verified mathematical model that constitutes a formal basis for the computer-aided simulation of that process. A computer simulation is a method of investigating an empirical system which, in view of the objective of modeling, may replace natural experiments in the process of acquiring information on the efficacy of the analyzed technical system. This research method will have a growing role in the design of farming and food processing machines. The precision of computer simulations is determined mainly by the degree of accuracy delivered by the mathematical model, the description of input data, errors, and the applied simplifications. Physical sciences are of utmost importance in this type of research. By selecting the appropriate research methods, physics theories and other cognitive instruments, scientists are able to explain how physical quantities affect vital changes in the physical properties of raw materials and food products. Computer simulations involve the use of software based on algorithms that allow the user to generate a history of raw material stocks and monitor the progress in machine construction. It should be noted that a simulated working process is merely an approximated representation of the real process rather than its faithful replication. By relying on

computer simulations as a research method in designing technological processes and machines, scientists select a sequential system of events and simulate elementary processes in a given order. The majority of simulations rely on the fixed time-step method and the discrete event method. In the fixed time-step method, events take place in steps that increase by a fixed time increment. In the discrete event method, a growing time increment is attributed to the next event. The results of a computer simulation are verified experimentally.

Technical progress will also modify the structural solutions applied to farming equipment. There will be growing demand for new-generation farming machines equipped with satellite navigation, board computers, and feedback control systems. GPS navigation and the development of computer technology will create new prospects for intelligent farming machines. The operating conditions and the requirements imposed on such equipment will be determined by physics and agricultural engineering. We must create a design-effective system for controlling and managing agricultural production while ensuring that the technical advancements in farming directly contribute to the quality of the end product. In the near future, precision farming will become the leading branch of agriculture. Many tractors, fertilizer distributors, seeding machines, and combines for harvesting cereal and root crops are equipped with electronic and data transmission systems. Farming and food processing machines are turning into complex mechatronic systems. We are witnessing the

rapid development of remote control solutions for farming machines supplying raw materials for the food production industry. A machine that is a programmable mechatronic system (Mieszkalski, 1998a) equipped with sensors receives signals from the environment during the working process. Those signals are processed and interpreted in view of the existing situation and possible control errors, after which they are transmitted to the machine's steering unit to maintain adequate working parameters and optimize the movement of working elements. In systems equipped with feedback control, the operator is no longer required to directly control the machine's operating parameters. The operator enters into a relationship with a mechatronic system by inputting system data and controlling processed output data. In a mechatronic system, sensors generate signals on the physical quantities of a working process that involves the machine and raw materials. After processing, the signal is transmitted to the steering unit, which modifies working parameters accordingly. Physics also aims to devise new solutions for sensors analyzing the physical condition of the processed plant and animal raw materials. One of such examples is the electronic nose, which monitors changes in the aroma of farming produce during storage. This solution involves artificial neural networks that have been trained to detect the age of grain (Zhang and Wang, 2008).

The contemporary GIS technology with 3D spatial data and the option of developing numerical terrain and field maps, crop maps, and soil nutrient maps are the stepping stone on the road to developing remotely controlled machines (Karimi et al., 2008). Technological progress in farming production will further the development of sensors for measuring and, when coupled with the possibilities offered by IT systems, monitoring the characteristic properties of the soil, plants, and the atmosphere. Physics and agricultural engineering will propose a variety of new solutions in the area of machine and sensor construction.

Tractors have played and continue to play a vital role in farming. Their horsepower ranges from 30 to around 650. Tractors with the highest output weigh around 20 t. The dynamic growth of physics, farming, biological, technical, and IT sciences has visibly furthered the development of the tractor industry. The leading manufacturers of farming equipment have been conducting intensive research into

the design of driverless tractors. The most important considerations that have to be taken into account in the design of modern tractors are steering systems, control systems as well as ergonomic solutions (Drakopoulos and Mann, 2008). Similar problems have to be tackled as regards other types of farming and food processing equipment.

The requirements imposed on agricultural machines will change owing to the vast variation in the size of farming areas. The main problem is the selection of production technologies and machines that would not lead to the degradation of soil and the natural environment. Heavy-duty, self-propelled farming machinery delivering a high productive yield is developed to cater to the needs of large commercial farms. The problem of excessive pressure exerted on soil by farming equipment, in particular heavy-duty machines, has not been solved to date. Designers are short of ideas for building an innovative drive system. The existing choice is limited to wheel and caterpillar drive systems (Figure 5). Farming machinery is becoming heavier, and it exerts a growing load on the soil. The intensive use of contemporary machines leads to soil rolling, structural damage, and degradation. Machines weighing 20 t, mostly potato harvesters, exert a highly negative effect on loosened soil by compacting it excessively (Figure 6). Vehicles transporting the harvested crops to the place of storage also contribute to soil damage.

Soil fragmentation and structural damage caused by rotary and swirl harrows are also a serious problem (Figure 7). Disk blades of rotary and swirl harrows used in simplified farming systems produce a cycloidal motion and exert an uneven effect on the soil (Figures 8 and 9) (Mieszkalski, 1998b). There are no effective solutions protecting harrows against damage when the disk blade hits a hard obstacle, such as a rock.

Global climate change will have a growing impact on agriculture. In many regions, milder winters marked by fewer days with below-zero temperatures and less snow undermine the purpose of deep fall plowing. A detailed analysis of the effect of plowing on the dynamics of soil changes in view of climate change will contribute to the search for new cultivation technologies, including methods that do not rely on plows.

The challenge for designers is to develop new technologies to minimize the adverse effects of chemicalization of



Agriculture and Food Machinery, Application of Physics for Improving, Figure 5 Wheels and caterpillars in farming machines.



Agriculture and Food Machinery, Application of Physics for Improving, Figure 6 Excessive soil compaction caused by farming machines.



Agriculture and Food Machinery, Application of Physics for Improving, Figure 7 Harrow rotor's effect on the soil.

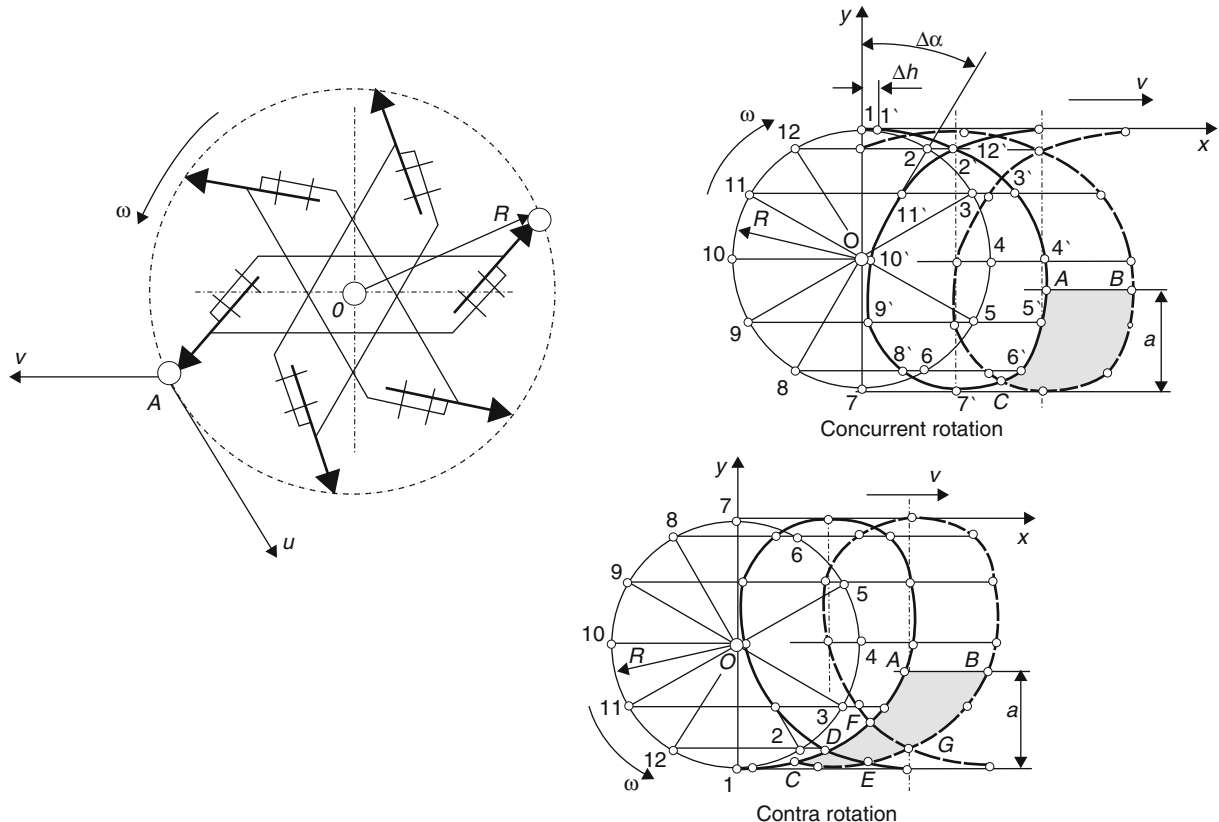
food products and production in general. We must prevent environmental degradation of not reducing the standards of living. Environmental contamination caused by physical, chemical, and biological factors applied in the growing of farm produce and the food processing industry poses a mounting problem. The production of wheat grain, for example, involves around six chemical treatments. Designers are faced with the challenge of inventing machines and equipment that support such technological processes.

The problem of excessive chemicalization is also encountered in the food processing industry. The applied pesticides and mineral fertilizers systematically introduce toxic substances to the soil across large areas. An

interesting alternative is the use of optical sensors in electronic weed control systems, which selectively spray herbicides on crop plantations (Celen et al., 2008). The failure to observe waiting periods makes the soil, plants, seeds, and crops susceptible to the deposition of toxins. As a result, harmful substances enter the food chain of humans and breeding animals. Despite the application of precision farming methods (soil fertility maps, board computers), the disks of fertilizer distributors do not spread the fertilizer evenly across the field. There is a dire need for new methods of protecting plants against weeds and pests that do not rely on chemicals and minimize environmental contamination. Precision agriculture offers such a solution. New methods are also needed for the early detection of disease sources and pest development stages to support the quick implementation of treatment methods that do not involve chemicals. Image analysis coupled with precision pesticide application is an innovative option. For the needs of farming production, chemicals should be regarded as medical treatment, not a method of increasing crop yield that disregards quality considerations. Product chemicalization in the food processing industry adds to the problem. Appropriate solutions should be offered by science, in particular agrophysics, agricultural engineering, and food engineering.

Combines for harvesting grain, potatoes, carrots, and beets are part of a rapidly developing market of farming machines. Advanced solutions are implemented in the group of combine harvesters whose main working elements have not been upgraded in the past 150 years. The introduced modifications include double-rail axial threshing mechanisms, double-cylinder threshing units, straw shaker supports, belt conveyors instead of worm conveyors in combine headers, laser remote control systems for guiding combines, and many other solutions. In designing, it is important to ask and seek answers for questions, for example: Is a combine harvester the ultimate solution? Should threshing take place in the field? How can the seed ripening period be prolonged? Can grain harvesting be mechanized or automated with the use of modern technology that replaces combines and economizes the harvesting process? Modern combine harvesters are equipped with board computers for controlling and monitoring the machine's working parameters and the quality of harvesting operations. Satellite navigation systems support the generation of digital yield maps (Fulton et al., 2009). Combine harvesters are also equipped with vision systems comprising several video cameras outside the machine for surveying the harvested area.

By-products of the farming process, such as straw, are also an important consideration in view of the changes taking place in agricultural practice. Straw is pressed in the field, and its density reaches around 180 kg m^{-3} . Various structural solutions for straw presses are available. Presses are equipped with control units for monitoring the compacting process and its working parameters. Straw used as an energy resource is compacted into pellets with density of up to $1,400 \text{ kg m}^{-3}$ as well as into briquettes



Agriculture and Food Machinery, Application of Physics for Improving, Figure 8 Motion trajectory of rotary harrow disk blades.

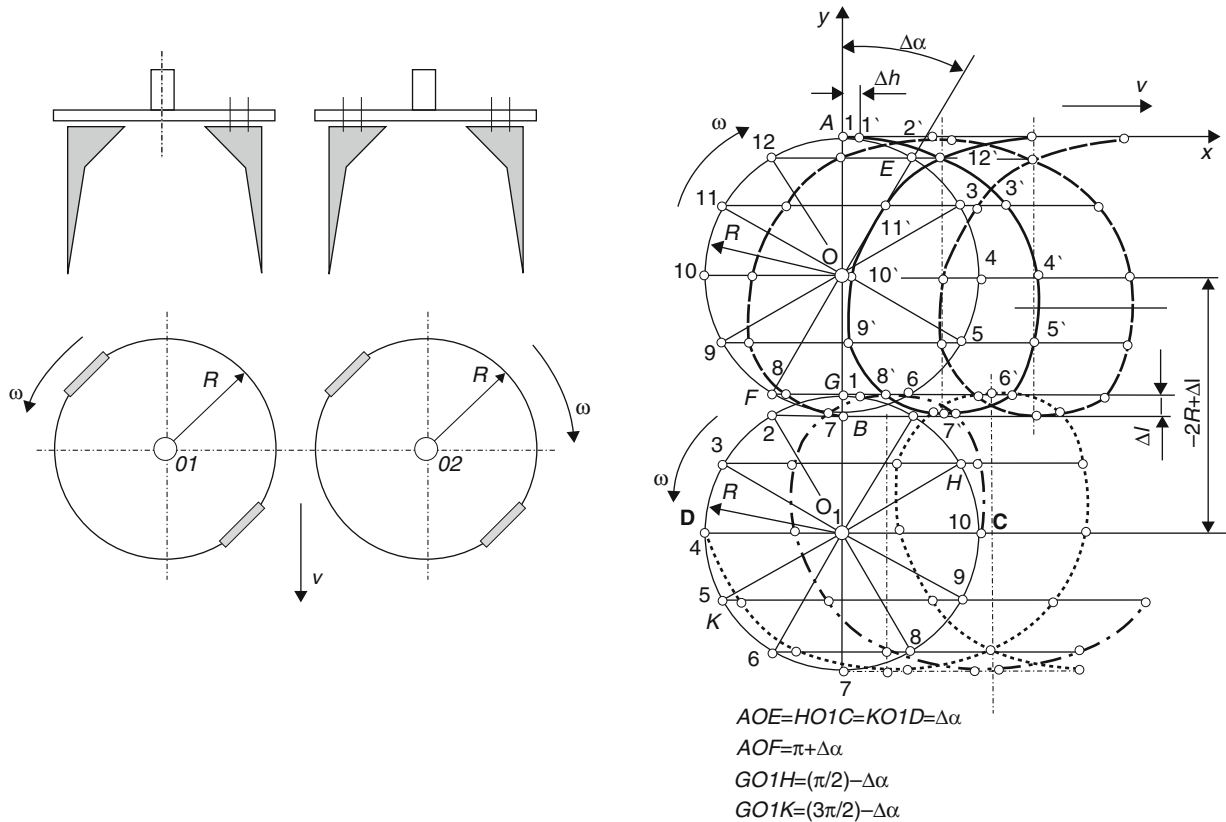
with density of around 700 kg m^{-3} . New briquetting techniques will soon be developed with the involvement of, for example, straw rolling, to produce briquette density of 500 kg m^{-3} or higher.

Significant progress is also noted in numerical methods for data processing and process virtualization in farming and food production. Production lines with a feedback control signal are implemented in food processing plants.

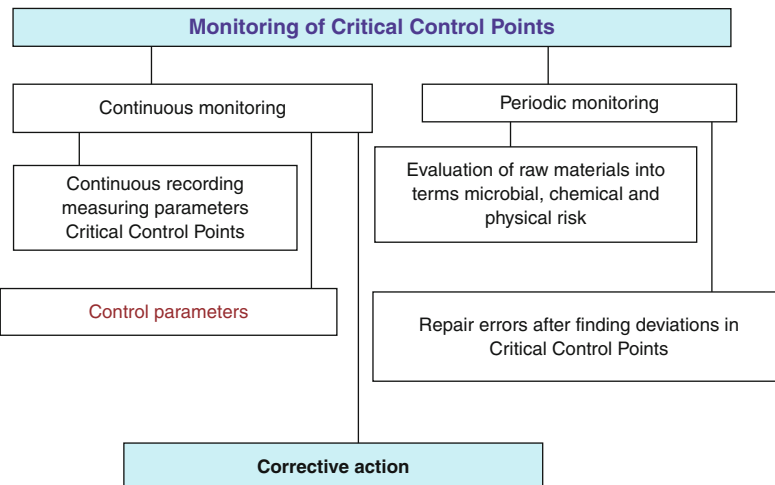
Production of raw materials and food processing technologically must be adapted to quality management requirements. Food processing plants implement HACCP systems for analyzing biological, chemical, and physical threats and for measuring and monitoring critical parameters that significantly affect food safety and quality. Risk evaluation in food production poses another challenge. The task of food engineering, agricultural engineering, physics, and other sciences is to devise methods ensuring the safe application of chemicals, food additives, and bio-engineered foods. The selection of adequate risk evaluation methods in the food industry is a difficult process because food products contain a high number of ingredients, which form a variety of combinations (Brock et al., 2003; Blaha, 2001). Biotechnology plays an increasingly important role in food production, and it involves the modification of the natural ingredients of foodstuffs (Taylor, 2003). Various branches of science, including

food engineering, agricultural engineering, and physics, search for effective and transparent production methods that guarantee the safety of bio-engineered products that have not been mass produced to date. Food safety systems monitor the value of critical parameters at control points of the production line to ensure that qualitative requirements are met. Critical parameters are monitored continuously and periodically with the use of principles of mathematical statistics (Figure 10). Continuous monitoring supports production with a feedback control signal. The production process is observed by experts on computer screens. Many operations are performed on fully automated lines. Automated systems are tested on grafted tomato seedlings for monitoring the external features of plants during growth (Chiu et al., 2008). Camera vision systems are used to classify farming produce by determining its physical properties such as length, diameter, curvature, flower color, flower size, and surface damage (Chong et al., 2008).

Robots are increasingly often used in food production. New robots equipped with complex kinematic systems, sensory devices, vision cameras, and complex control algorithms have a growing number of applications in the food industry. They are used for object grabbing with pressure control, transporting, packaging, palletizing, production line work (e.g., carcass dressing), cooling plant



Agriculture and Food Machinery, Application of Physics for Improving, Figure 9 Motion trajectory of swirl harrow disk blades.



Agriculture and Food Machinery, Application of Physics for Improving, Figure 10 Block diagram of monitoring physical quantities and working parameters during a technological process.

operations, etc. Greenhouses were the first farming sites to introduce mobile robots (González et al., 2009).

In an era marked by dynamic changes in the global culture, which is becoming dominated by politics, free

market principles, consumerism, temporary solutions, and the flood of information that dulls our senses, scientists have to ask precise questions and search for the answers. Modern technology and economy cannot replace

quality. The most urgent task for physics, agricultural and food engineering is the search for effective production methods that guarantee the highest quality of both raw materials and the end product. The above will be determined by their willingness to tackle complex problems. In an era marked by growing production, higher work efficiency, and soaring competition, we need to reflect and develop a rational approach to technological progress in line with the following motto: "to produce, but without doing harm to nature and mankind".

The process of building contemporary machines relies on data from various fields of science. Physics plays an important role in this process by searching for new structural materials, methods for determining their physical properties, and the displacement of elementary particles under the influence of internal and external forces. As regards the design of farming and food processing machines, the role of physics is to find new mechanisms and new methods of kinematic and dynamic analyses. The determination of trajectory, speed and acceleration, and the search for motion that meets a given set of kinematic conditions are very important considerations in the kinematics of mechanisms. Dynamics is also of paramount significance in the construction of farming and food processing machines as it determines changes in force over time during operation and the correlation between motion and the forces acting on different parts of a machine. The variability of load applied to the working elements of a machine results from the non-homogeneity of the processed biological material. Substrate variability and changes in its spatial configuration affect the load applied to the working elements of a farming machine. The elements of farming and food processing machines are subjected to complex, often nonlinear load. The search for methods of anticipating the behavior of machines and their subassemblies under the influence of variable and stochastic load poses a serious challenge for contemporary physics. New scientific theories in the field of nonlinear system dynamics need to be formulated. The working process of farming and food processing machines is the result of many complex relations between the machine, its operator, and the operating environment. Physics should play a fundamental role in the search for relations that are optimal for machines, man, and the environment.

Owing to the vast diversity of farming and food processing machines, the role of physics in the process of designing and modifying all models cannot be described in detail. In this group of machines, a number of work processes have a universal character. The key processes in obtaining plant materials for food production are: soil engaging operations, seedbed preparation, inter-row tillage, spreading of organic and mineral fertilizers, distribution and planting of seeds, seed-potatoes and seedlings, formation of liquid droplet streams for plant protection and stream distribution on plant surface, cutting plant material, reeling, gathering, shaking, raking and transporting stem material, crushing stem material, threshing, separating, and transporting crops. The following general

processes take place in food production: shredding, separation, liquid flow, filtration, pressing, forming, liquid squeezing, movement of solids in liquid, movement of liquids in liquid, agglomeration, hulling, peeling, drilling, cleaning, germination, polishing, removing inedible parts, gravitational and centrifugal separation, straining, settling, classification, transport, mixing and dosing, cleaning, packaging, drying, distilling, extracting, leaching, cooling, freezing, heat processing, and pressure processing. The design of farming and food processing machines relies heavily on data on the physical and chemical properties of soil, raw materials, food products, technological process, and the design methodology. Physics contributes vast amounts of information on the physical properties of soil, raw materials, and food products, and it describes physical phenomena that occur when raw materials are processed into foodstuffs.

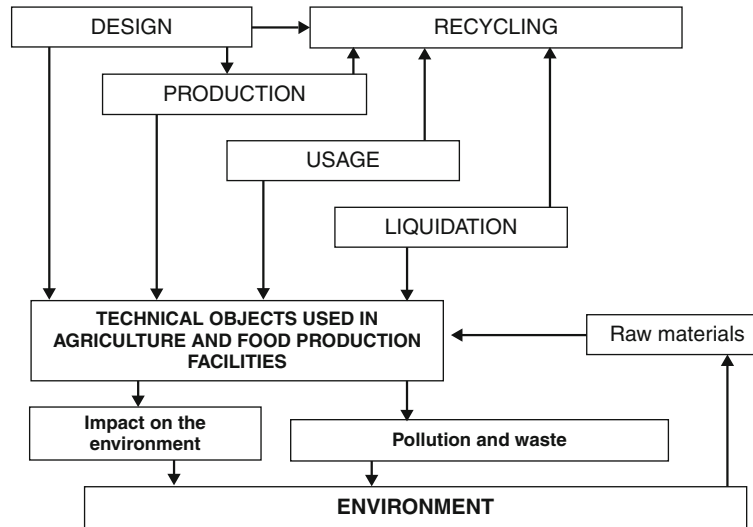
Designers building farming and food processing machines have to account for all stages in the machine's life cycle (Figure 11). The quality of serially structured design decisions determines the usable properties of machines, the safety of operators, and the impact of machines on the natural environment. Farming machines are closely interrelated with the environment throughout their entire working life. The natural environment supplies nonrenewable resources for the production of structural materials. The manufacture, use, and scrapping of farming and food processing machines is a source of waste and pollution that has a highly adverse effect on man and the environment (Park and Kim 2009a, b, c). New solutions are needed for recycling used materials to limit or eliminate the disposal of worn-out machines and lower the demand for new resources. Physical sciences will support the development of new methods for applying recycled materials in the production of brand-new items and protecting the natural environment against the hazards posed by other scientific inventions, such as gamma ray and X-ray radiation.

Above all, the main goal of practical inventions delivered by research in physics should be the well-being of humans and the protection of the natural environment.

Summary

Many problems still await a solution. The greatest challenges involve the standardization of farming sites, determination of the spatial and structural attributes of soil, raw materials and products, protection of food products against negative factors, modeling and computer-aided simulation of food production processes, developing effective methods for evaluating food quality, designing new measuring systems for monitoring, storing and processing data, and effective decision-making at different stages of the food production process.

Use of latest achievements of science is required in studies of physical properties of raw materials and food products. Use of advanced measuring technologies is essential in gaining new information on the raw material and food production. In the production of raw materials



Agriculture and Food Machinery, Application of Physics for Improving, Figure 11 The main stages in the life cycle of a farming and a food processing machine and its impact on the natural environment.

increasing role plays precision farming. Automatization with robots use is developing rapidly. Further interdisciplinary research is needed to achieve safe food product, both produced on an industrial scale and in small manufacturing plants. It is important to search for new food products, and new food technologies in mass and local production. Modern machines should concerned new technologies of food preservation, conservation and food packaging considering positive influence on peoples' health.

Bibliography

- Arvanitoyannis, I. S., Eustratiades, M. M., and Boudouropoulos, I. D., 2000. ISO 9000 and ISO 14000. *Presentation-Analysis of Models of Quality Assurance and Environmental Management, Adaptation to the Food and Drink Industry*. Saloniki: University Studio Press.
- Blaha, T., 2001. Pre-harvest food safety and quality management from agricultural primary production to retail. *Tierarztliche Umschau. Konstancja*: Terra-Verlag GMBH.
- Brock, W. J., Rodricks, J. V., Rulis, A., Dellarco, V. L., Szary, G. M., and Lane, R. W., 2003. Food safety: risk assessment methodology and decision-making criteria. *International Journal of Toxicology*, **22**, 435–451. Philadelphia: Taylor & Francis.
- Celen, I. H., Kilic, E., and Durgut, M. R., 2008. Technical note: development of an automatic weed control system for sunflower. *Applied Engineering in Agriculture*, **24**, 23–27.
- Chiu, Y. C., Chang, M. Y., Wu, G. J., and Chen, C. C., 2008. Development of an automatic outward-feature properties measurement system for grafted tomato seedlings. *Applied Engineering in Agriculture*, **24**, 101–113.
- Chong, V. K., Kondo, N., Ninomiya, K., Nishi, T., Monta, M., Namba, K., and Zhang, Q., 2008. Features extraction for eggplant fruit grading system using machine vision. *Applied Engineering in Agriculture*, **24**, 675–684.
- Danilatos, G. D., and Postle, R., 1982. The environmental scanning electron microscope and its applications. *Scanning Electron Microscopy*, **1982**, 1–16.
- Drakopoulos, D., and Mann, D. D., 2008. A mathematical equation for quantifying control functionality in agricultural tractors. *Journal of Agricultural Safety and Health*, **14**, 377–389.
- Entwistle, A., 2000. Confocal microscopy: an overview with a biological and fluorescence microscopy bias. *Quekett Journal of Microscopy*, **38**, 445–456.
- Fulton, J. P., Sobolik, C. J., Shearer, S. A., Higgins, S. F., and Burks, T. F., 2009. Grain yield monitor flow sensor accuracy for simulated varying field slopes. *Applied Engineering in Agriculture*, **25**, 15–21.
- González, R., Rodríguez, F., Sánchez-Hermosilla, J., and Donaire, J. G., 2009. Navigation techniques for mobile robots in greenhouses. *Applied Engineering in Agriculture*, **25**, 153–165.
- Hardin, R. G., IV, and Searcy, S. W., 2009. Searcy modeling of seed cotton viscoelastic properties. *Transactions of the American Society of Agricultural and Biological Engineers*, **52**, 707–714.
- Inoue, S., 1986. *Video Microscopy*. New York: Plenum.
- Karimi, D., Mann, D. D., and Ehsani, R., 2008. Modeling of straight-line driving with a guidance aid for a tractor-driving simulator. *Applied Engineering in Agriculture*, **24**, 403–408.
- Liu, L., Crowe, T. G., and Roberge, M., 2009. Sensor-based scouting algorithms for automatic sampling tasks in rough and large unstructured agricultural fields. *Transactions of the American Society of Agricultural and Biological Engineers*, **52**, 285–294.
- Mieszkalski, L., 1996. Mathematical models of the faba bean seed hulling process. *Annual Review of Agricultural Engineering*, **1**, 111–117.
- Mieszkalski, L., 1997. The role of the physical properties of seeds in the design of hullers. *International Agrophysics*, **11**, 283–291.
- Mieszkalski, L., 1998a. *Design Methodology of Agricultural Tools and Machines (in Polish)*. Olsztyn: ART.
- Mieszkalski, L., 1998b. *Elements of the Mathematical Description of the Selected Tools Units and Agricultural Machines (in Polish)*. Olsztyn: ART.
- Park, Y. J., and Kim, K. U., 2009a. Reduction of rattle noise of a direct engine-PTO driveline of agricultural tractors: Part I. Measurement and analysis of PTO rattle noise. *Transactions of the American Society of Agricultural and Biological Engineers*, **52**, 15–20.
- Park, Y. J., and Kim, K. U., 2009b. Reduction of rattle noise of a direct engine-PTO driveline of agricultural tractors: Part II.

- Causes of PTO rattle noise. *Transactions of the American Society of Agricultural and Biological Engineers*, **52**, 357–368.
- Park, Y. J., and Kim, K. U., 2009c. Reduction of rattle noise of a direct engine-PTO driveline of agricultural tractors: Part III. Reduction of PTO rattle noise by a torsional damper. *Transactions of the American Society of Agricultural and Biological Engineers*, **52**, 369–374.
- Ravertz, J. R., 2002. Food safety, quality, and ethics. *Journal of Agricultural and Environmental Ethics*, **15**, 255–265.
- Semos, A. B., 2004. *Agricultural Products Manufacturing. Economic-Organization-Production of Foodstuffs*. Saloniki: Zittis Publications.
- Shao, Y., Zhao, C., He, Y., and Bao, Y., 2009. Application of infrared spectroscopy technique and chemometrics for measurement of components in rice after radiation. *Transactions of the American Society of Agricultural and Biological Engineers*, **52**, 187–192.
- Taylor, S. L., 2003. Safety assessment of foods produced through agricultural biotechnology. *Nutrition Reviews*, **61**, 5135–5140.
- Zhang, H., and Wang, J., 2008. Identification of stored-grain age using electronic nose by ANN. *Applied Engineering in Agriculture*, **24**, 227–231.

Cross-references

- [Agophysical Objects \(Soils, Plants, Agricultural Products, and Foods\)](#)
[Agophysical Properties and Processes](#)
[Databases on Physical Properties of Plants and Agricultural Products](#)
[Mechanical Resilience of Degraded Soils](#)
[Monitoring Physical Conditions in Agriculture and Environment](#)
[Organic Farming, Effect on the Soil Physical Environment](#)
[Physical Degradation of Soils, Risks and Threats](#)
[Physical Properties of Raw Materials and Agricultural Products](#)
[Physics of Plant Nutrition](#)
[Precision Agriculture: Proximal Soil Sensing](#)
[Soil–Plant–Atmosphere Continuum](#)
[Soil–Wheel Interactions](#)
[Standardization in Agrophysics](#)
[Tillage Erosion](#)

AGROFORESTRY SYSTEMS, EFFECTS ON WATER BALANCE IN CROPPING ZONE

Andrzej Kędziora
 Institute for Agricultural and Forest Environment, Polish Academy of Sciences, Poznań, Poland

Definition

Many definitions were formulated within last few decades. One of the last definitions was made up by World Agroforestry Centre (ICRAF) in 1993:

Agroforestry is a collective name for land use systems and practices in which woody perennials are deliberately integrated with crops and/or animals on the same land management unit. The integration can be either in a spatial mixture or in a temporal sequence. There are normally both ecological and economic interactions between woody and nonwoody components in agroforestry.

Agroforestry is a land use system that allows for the concurrent production of trees and agricultural crops from the same piece of land (Gordon and Newman, 1997).

Agroforestry should be considered as a dynamic, ecologically based, natural resource management system that, through the integration of trees in farm and rangeland, diversifies and sustains production for increased social, economic, and environmental benefits (Leakey, 1996).

History

It has a rich history of development and has been practiced in some parts of the world for more than 6,000 years. Much recent research into agroforestry has been carried out in the tropics and within the context of developing nations, where land shortages brought about by the rapid growth in population demand that efficient production systems for both wood and food be developed and enhanced.

Agroforestry is an age-old practice throughout the world, but its recognition as a science is nearly 5 decades old. For example, during the Han Dynasty (206 BC to AD 220), administrators recommended that forests be developed to accommodate livestock husbandry and crops, according to varying site conditions. Qi Min Yao Shu reported that during the sixth century, the Chinese scholar tree (*Sophora japonica*) was planted with hemp for the purpose of increasing hemp growth and to improve the form of trees for future roadside plantations (Gordon and Newman, 1997).

In mid-1970s, the International Center for Research in Agroforestry (ICRAF) was created in response to a visionary study in the mid-1970s led by forester John Bene of Canada's International Development Research Centre (IDRC). The study coined the term "agroforestry" and called for global recognition of the key role trees play on farms. This initiation led to the establishment of ICRAF in 1978 to promote agroforestry research in developing countries.

During the 1980s, ICRAF operated as an information council focused on Africa. It joined the Consultative Group on International Agricultural Research (CGIAR) in 1991 to conduct strategic research on agroforestry at a global scale, changing its name from Council to Centre. After joining the CGIAR, the Centre explicitly linked its work to the goals of the CGIAR – reducing poverty, increasing food security, and improving the environment – through two means: overcoming land depletion in smallholder farms of subhumid and semiarid Africa, and searching for alternatives to slash-and-burn agriculture at the margins of the humid tropical forests. In implementing this strategy, the Centre expanded into South America and Southeast Asia while strengthening its activities in Africa.

Within 1990s, ICRAF continued the process of institutional transformation by developing a science culture, building excellent research facilities, and doubling its financial and human resources by 1996. The Centre formally adopted an integrated natural resource management framework for all of its work, and institutionalized its commitment to impact by creating a Development Group dedicated to moving research results onto farmers' fields.

In 2002, the Centre acquired the brand name the “World Agroforestry Centre”; however, the “International Centre for Research in Agroforestry” remains our legal name. The new name reflects the fact that the Centre is now recognized as the international leader in agroforestry research and development. Realistically, however, the Centre cannot possibly provide expertise on all conceivable dimensions of agroforestry – nor do we wish to do so. There are advantages to specialization, which is why the Centre engages in strategic alliances with a range of other institutions. Some of these partners are centers of scientific excellence in specific topics of relevance to agroforestry; others specialize in the effective delivery of research results to farmer’s fields (Technical Advisory, 1993).

Agroforestry

The “art” of agroforestry has evolved over centuries; agroforestry as a formalized approach to land use is more recent. Agroforestry is promoted on the basis that it can provide biological, economic, and social advantages. ICRAF’s Strategic Plan (Technical Advisory, 1993) states “resource-poor rural households benefit from improved soil fertility coming from the introduction of nitrogen-fixing trees in enriched fallows or through interplanting; they gain additional income through sale of tree products such as fruit or timber; and gain improved food security associated with the way the perennial component of agroforestry systems extends the season when green fodder and food supplies are available. The latter benefit has significant implications for the nutritional vulnerability of the poorest groups, especially women and children. At the same time, the quality of the environment is maintained through the maintenance of biological diversity, preservation of water catchments and soil quality, and a halt to the net loss of forested land.”

Agroforestry combines agriculture and forestry technologies to create more integrated, diverse, productive, profitable, healthy, and sustainable land-use systems. It means that trees are intentionally used within agricultural systems. Knowledge, careful selection of species, and good management of trees and crops are needed to maximize the production and positive effects of trees and to minimize negative competitive effects on crops.

Agroforestry must satisfies four requirements: (1) it is a form of multiple cropping, (2) at least one component is a woody perennial, (3) the component interacts biologically, (4) at least one of plant species is managed for forage, annual or perennial crop production (Somarriba, 1992). Agroforestry must be compatible with local socio-cultural practices and serve to improve living conditions in the region.

Agroforestry systems can be advantageous over conventional agricultural and forest production methods through increased productivity, economic benefits, social outcomes, and the ecological goods and services provided.

There are five basic types of agroforestry practices today: alley cropping, silvopasture, windbreaks, riparian

buffers, and forest farming. Within each agroforestry practice, there is a continuum of options available to land-owners depending on their own goals (e.g., whether to maximize the production of interplanted crops, animal forage, or trees).

Alley cropping

Alley cropping, sometimes referred to as “sun systems,” is a form of intercropping, and can be applied by farmers as a strategy to combat soil erosion, to increase the diversity of farmland, as a means for crop diversification and to derive other integrated benefits. In this practice, crops are planted in strips in the alleys formed between rows of trees and/or shrubs. The potential benefits of this design include the provision of shade in hot, dry environments (reducing water loss from evaporation), retention of soil moisture, increase in the structural diversity of the site, and wildlife habitat. The woody perennials in these systems can produce fruit, fuelwood, fodder, or trimmings to be made into mulch.

Alley cropping involves growing crops (grains, forages, vegetables, etc.) between trees planted in rows. The spacing between the rows is designed to accommodate the mature size of the trees while leaving room for the planned alley crops. When sun-loving plants like corn or some herbs will be alley cropped, the alleyways need to be wide enough to let in plenty of light even when the trees have matured.

Like all integrated systems, alley cropping requires skillful management and careful planning. Both the crop and the trees have requirements that sometimes necessitate tradeoffs between them. The design must allow sufficient room for the equipment needed to service each enterprise.

Silvopasture

Silvopastures combine livestock grazing on forage crops or pastures within actively managed tree or shrub crops. Cattle, sheep, and goats are the most common livestock incorporated into silvopasture systems and they may be deployed entirely within a private farm/woodlot silvopasture or through collaborative arrangements between forest licensees and livestock producers on public lands. Tree and pasture combinations are called *silvopastoral agroforestry*. Hardwoods (sometimes nut trees) and/or pines are planted in single or multiple rows, and livestock graze between them. Although both the trees and the livestock must be managed for production, some systems emphasize one over the other. Usually, in the early years of establishment, crops or hay are harvested from the planting. Grazing generally begins after 2 or 3 years, when the trees are large enough that the livestock cannot damage them. In other instances, tree tubes and electric fencing protect the young trees, and grazing begins immediately.

Grazing livestock on silvopasture eliminates some of the costs of tree maintenance. With good grazing management, for example, herbicides and mowing may become unnecessary. Grazing also enhances nutrient cycling and

reduces commercial fertilizer costs; the animals remove few nutrients, and their waste is a valuable input for the trees. Well-managed grazing will increase organic matter and improve soil conditions. However, controlling the number of animals per area, limiting the number of days those animals remain on each site, and avoiding compaction are critical for a successful silvopasture system.

Windbreaks or shelterbelts

Extensive research on windbreaks, also called *shelterbelts*, has been carried out in many countries. Trees are planted in single or multiple rows along the edge of a field to reduce wind effects on crops or livestock. Windbreaks have been shown to reduce wind impact over a horizontal distance equaling at least ten times the height of the trees. Wind and water erosion are reduced, creating a moist, more favorable microclimate for the crop. In the winter the windbreak traps snow, and any winter crops or livestock are protected from chilling winds. Beneficial insects find permanent habitat in windbreaks, enhancing crop protection.

Although the trees compete for available water along the edges between the windbreak and the crop rows, potentially reducing crop yield near the windbreak, the net effect on productivity is positive. In fact, even on land that is well suited for high-value crops, a windbreak can increase the crop yield of the entire downwind field by as much as 20%, even when the windbreak area is included in the acreage total.

Windbreaks can be designed specifically for sheltering livestock. Studies have shown the economic advantages of providing protection from wind chill, a major stress on animals that live outside in the winter. Reduced feed bills, increases in milk production, and improved calving success have resulted from the use of windbreaks. Besides providing protection to crops and livestock, windbreaks offer other advantages. They benefit wildlife, especially by serving as continuous corridors along which animals can safely move.

Any tree species can be used in a windbreak. However, deciduous species, even in multiple rows, will lose effectiveness when they lose their leaves. For year-round use, some of the species selected should be evergreen. Fast-growing trees should be included; it is best to plant deep-rooted, noncompetitive species along the edges. Regular deep chisel plowing along the edges will keep roots from spreading into the crop rows. If some of the trees are harvested periodically, replacements can be planted, establishing a long-term rotation.

Riparian buffers and integrated riparian management

Riparian buffers are managed forest and shrubs belts in areas bordering lakes, streams, rivers, and wetlands. Integrated riparian management systems are used to enhance and protect aquatic and riparian resources as well as generating income from timber and non-timber forest

products. Similar to shelter and timberbelts, integrated riparian management systems can employ a wide variety of tree and shrub species, with specific plantings tailored to suit the specific growing conditions and production opportunities.

Trees, grasses, and/or shrubs planted in areas along streams or rivers are called *riparian buffers* or *filter strips*. These plantings are designed to catch soil, excess nutrients, and chemical pesticides moving over the land's surface before they enter waterways. Such plantings also physically stabilize stream banks. On cropland that is tiled to improve drainage, polluted water can flow directly into streams; constructed wetlands installed in the buffers can capture and clean this drainage water before it enters the stream. Shading the water keeps it cooler, an essential condition for many desirable aquatic species. Buffer strips also provide wildlife habitat and can be managed for special forest products.

Forest farming and special forest products

Forest farming, also known as "shade systems," is the sustainable, integrated cultivation of both timber and non-timber forest products in a forest setting. Forest farming is separate and distinct from the opportunistic exploitation – wild harvest of non-timber forest products. Successful forest farming operations produce mushrooms, maple and birch syrup, native plants used for landscaping and floral greenery (e.g., salal, sword fern, bear grass, cedar boughs, and others), medicinal and pharmaceutical products (e.g., ginseng, goldenseal, cascara, or yew bark), wild berries, and fruit. When a natural forested area is managed for both wood products and an additional enterprise, it becomes an agroforestry system. Besides producing saw timber and pulpwood, woodlands can generate income from many other products. Established forests offer many non-timber "special forest products" that contribute to cash flow without requiring the one-time harvest of old trees. For example, landowners can manage established woods to encourage naturally occurring patches of berries or bittersweet. Or they might plant understory crops adapted to the forest type and climate. Growing mushrooms on logs is another, more labor-intensive, possibility; a canopy of either hardwoods or pine will provide the shade needed to maintain moisture for fruiting.

Benefits

Agroforestry practices may also be employed to realize a number of other associated environmental services, including

- Carbon sequestration
- Odor, dust, and noise reduction
- Wastewater or manure management (e.g., utilizing urban wastewater on intensive, short rotation forests for wood fiber production)
- Green space and visual aesthetics
- Enhancement or maintenance of wildlife habitat

Biodiversity in agroforestry systems is typically higher than in conventional agricultural systems. Agroforestry incorporates at least several plant species into a given land area and creates a more complex habitat that can support a wider variety of birds, insects, and other animals. Agroforestry also has the potential to help reduce climate change since trees take up and store carbon at a faster rate than crop plants.

The resulting biological interactions provide multiple benefits, including diversified income sources, increased biological production, better water quality, and improved habitat for both humans and wildlife. Farmers adopt agroforestry practices for two reasons. They want to increase their economic stability and they want to improve the management of natural resources under their care.

Agroforestry practices can increase farmer's annual incomes. Some increases in revenue come from harvesting different tree crops in different seasons. The result is that income and employment are distributed more evenly throughout the year. There are also many other reasons for growing trees on farms, such as the provision of shade for cooler soil temperatures, reduction of soil moisture loss, and protection of the soil from wind and water erosion. Agroforestry systems can reduce the risk of total crop failure. For example, if the viability of one crop is reduced by pest damage or market failure, the farmer can make up for it by harvesting another crop.

Summary

Land-use options that increase resilience and reduce vulnerability of contemporary societies are fundamental to livelihood improvement and adaptation to environmental change. Agroforestry as a traditional land-use adaptation may potentially support livelihood improvement through simultaneous production of food, fodder, and firewood as well as mitigation of the impact of climate change.

To promote well-being of the society, management of multifunctional agroforestry needs to be strengthened by innovations in domestication of useful species and crafting market regimes for the products derived from agroforestry and ethnforestry systems. Future research is required to eliminate many of the uncertainties that remain, and also carefully test the main functions attributed to agroforestry against alternative land-use options in order to know equivocally as to what extent agroforestry served these purposes.

The ecological integrity of an agroforest is a state of system development in which the habitat structure, natural functions, and species composition of the system are interacting in ways that ensure its sustainability in the face of changing environmental conditions as well as both internal and external stresses (Wyant, 1996).

Bibliography

- Auclair, D., and Dupraz, C. (eds.), 1999. *Agroforestry for Sustainable Land-Use*. Dordrecht: Kluwer Academic, 266 pp.
Gene Garrett, H. E. (ed.), 1992. *Proceedings of the Second Conference on Agroforestry in North America, August 1991*. The

- School of Natural Resources, University of Missouri, MO: Springfield.
Gordon, A. M., and Newman, S. M., 1997. *Temperate Agroforestry Systems*. New York: CAB International, 269 pp.
ICRAF, 1993. *International Centre for Research in Agroforestry: Annual Report 1993*. Kenya: Nairobi, 208 pp.
Leakey, R. R. B., 1996. Definition of agroforestry revisited. *Agroforestry Today*, 8(1), 5–7.
Montagnini, F., and Nair, P. K. R., 2004. Carbon sequestration: an underexploited environmental benefit of agroforestry systems. *Agroforestry Systems*, 61(62), 281–295.
Ramachandran Nair, P. K., 1993. *An Introduction to Agroforestry*. Kluwer Academic (in cooperation with ICRAF). 496 pp.
Rasmussen, P. E., Goulding, K. P. E., Brown, J. R., Grace, P. R., Janzen, H. H., and Körschens, M., 1998. Long-term agroecosystem experiments: assessing agricultural sustainability and global change. *Science*, 282, 893–896.
Somarriba, E., 1992. Revisiting the past: an essay on agroforestry definition. *Agroforestry System*, 19, 233–240.
Technical Advisory Committee, 1993. Report of the first External Programme and Management Review of the International Centre for Research in Agroforestry (ICRAF) (English) Consultative Group on International Agricultural Research, Rome (Italy), vp.
Wiersum, K. F., 1981. Outline of the agroforestry concept. In Wiersum, K. F. (ed.), *Viewpoints in Agroforestry*. Netherlands: Wageningen Agricultural University, pp. 1–23.
Williams, P., 1989. Agroforestry in North America. In *Proceedings of the First Conference on Agroforestry in North America*. Guelph: Department of Environmental Biology, Ontario Agricultural College, University of Guelph.
Wyant, 1996. Agroforestry – an ecological perspective. *Agroforestry Today*, 8, 1.

Cross-references

- [Drought Stress, Effect on Soil Mechanical Impedance and Root \(Crop\) Growth](#)
[Evapotranspiration](#)
[Irrigation and Drainage, Advantages and Disadvantages](#)
[Management Effects on Soil Properties and Functions](#)
[Rainfall Interception by Cultivated Plants](#)
[Tropical Fruits and Vegetables: Physical Properties](#)

AGROGEOLOGY

Ward Chesworth
Department of Land Resource Science, University of Guelph, Guelph, ON, Canada

Synonyms

Agricultural geology; Soil science (obsolete)

Definition

Agrogeology: any and all aspects of earth science that relate to agriculture and are impacted by agriculture.
Anthrobleme: the physical manifestation of human activities on the surface of the earth. From Greek roots meaning "human scar."
Anthropocene: the present geological age, taken to date from the Neolithic Revolution, approximately 10,000 years ago.

Biosphere: the surface and near-surface region of the earth where living organisms exist.

Deposition: the laying down or precipitation of materials at the surface of the earth.

Erosion: the loosening and removal of a rock or soil formation by natural or anthropic agencies.

Malthusian collapse: the state reached when population increases to outrun food resources. Named for the Reverend Thomas Malthus who published An Essay on the Principle of Population in 1798.

Neolithic Revolution: the transformation in human lifestyle that began slightly more than 10,000 years ago, when hunting and gathering began to give way to agriculture as the principal means of food production.

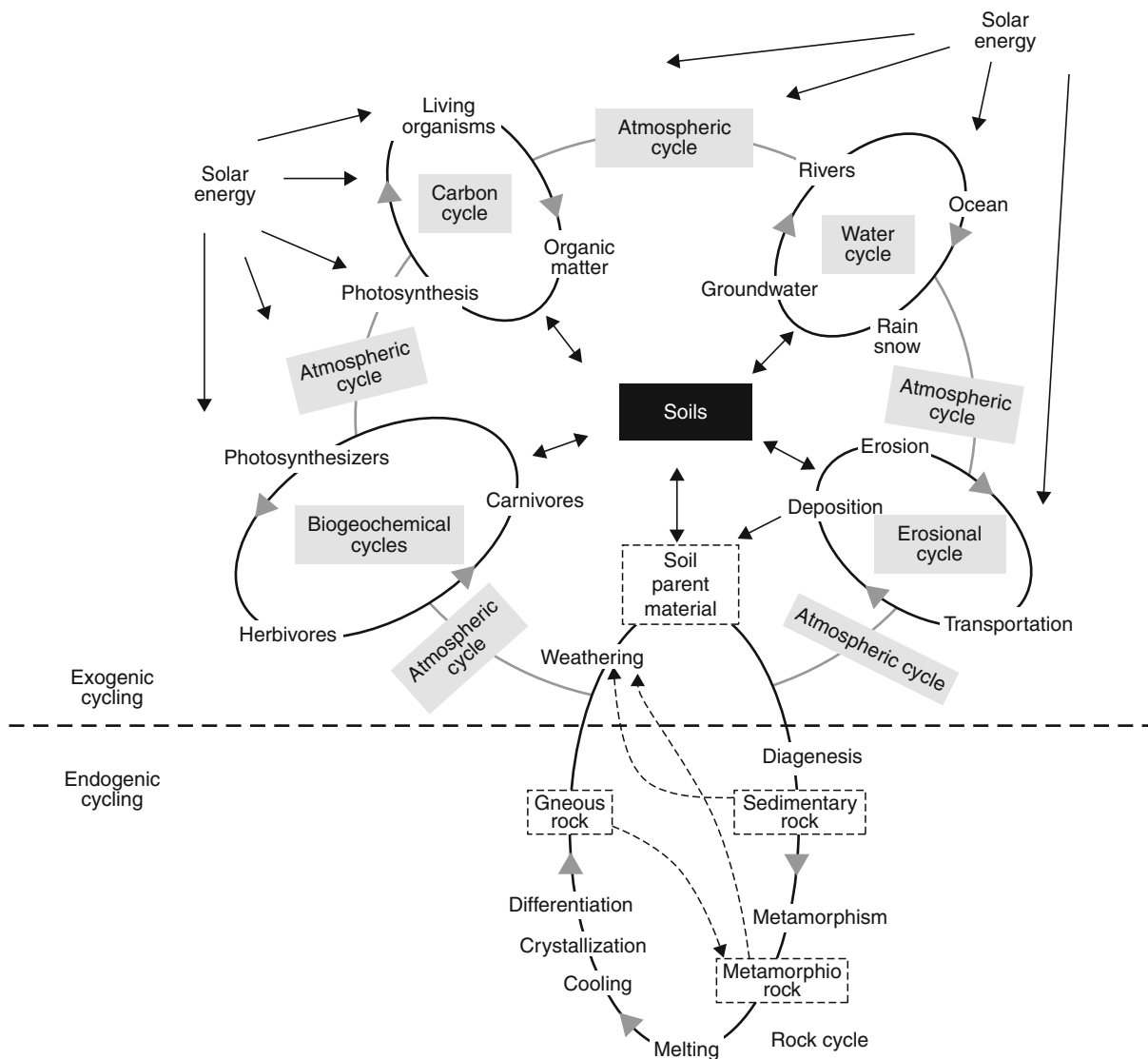
Transport: the movement of the products of weathering and erosion by water, wind, ice or biological (including human) activity.

Weathering: the chemical and physical breakdown of rocks and minerals at the surface of the earth.

Würm: the last ice sheet in Europe, between 24,000 and 10,000 years before the present. Roughly equivalent to the Wisconsinan glaciation in North America. Other local equivalents exist.

Introduction

Agrogeology is concerned with the science of geology in the context of agricultural science. The most obvious



Agrogeology, Figure 1 The centrality of soil in the exogenic, or external geological cycle on the earth, and its relationship with the endogenic, or internal cycle.

connection between the disciplines is soil, the geological substrate for the farmers' crop. But agriculture is massively contingent on geology for other reasons as well. Not only do the common geological processes of the planetary surface – weathering, transport and deposition – form soil in the first place, they are also implicated in the demise of soil, especially by the process of erosion (Chesworth, 2008).

Soil: the primary geological resource of the farmer

The centrality of soil on the earth's land surface is shown in Figure 1. It is an integral component of all major chemical and physical cycles of a geological nature, that take place there. Figure 2 depicts similar relationships, but with an important change of perspective. Seeing soil metaphorically in the neck of an hourglass, emphasizes its strategic position in the biosphere, but, importantly in the present context, emphasizes the vulnerability of the biosphere to any damage to the soil from natural or anthropic activities.

The evolution of soil can be thought of in terms of two geochemical pumps – a proton pump, and an electron pump. Protons are provided by two sources, rainwater (charged with CO₂) and the dissociation of –COOH

groups on the breakdown products of organic matter. The dominant form of electrons in soil is decaying organic matter.

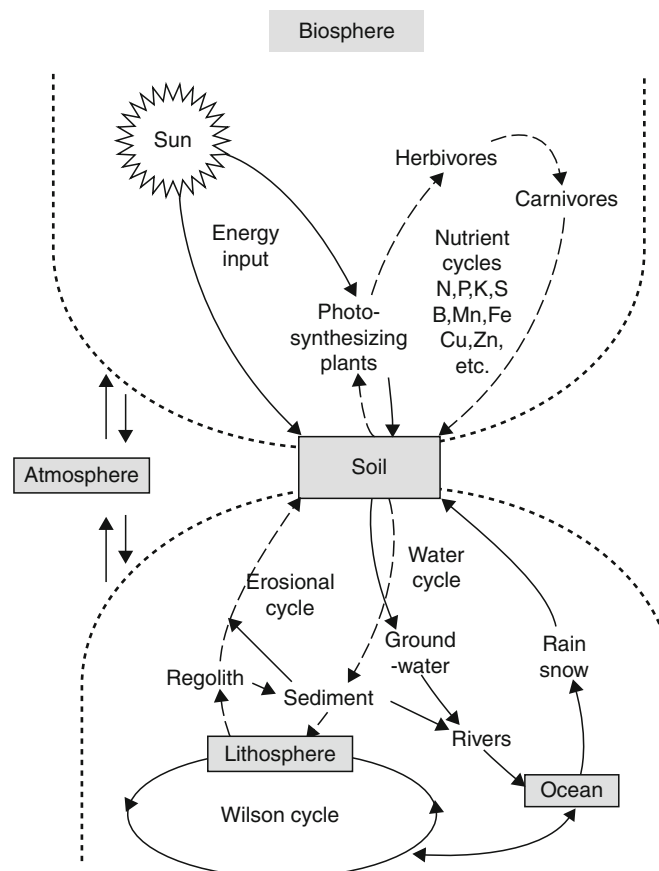
Protons flow from their source to a sink represented by the earth's surface, which acts as a base. A massive titration takes place during weathering, and in humid climates it amounts to an over-titration resulting in a progressive acidification of the soils of the land surface. In arid climates it is an under-titration, and soils progress along a path of alkalinization.

The dominant sink for electrons at the earth's surface, including within the pore space of unsaturated soils, is atmospheric oxygen. When this is unavailable, several ions in high oxidation states, may serve this function, e.g., nitrate, ferric Fe, manganic Mn, and others.

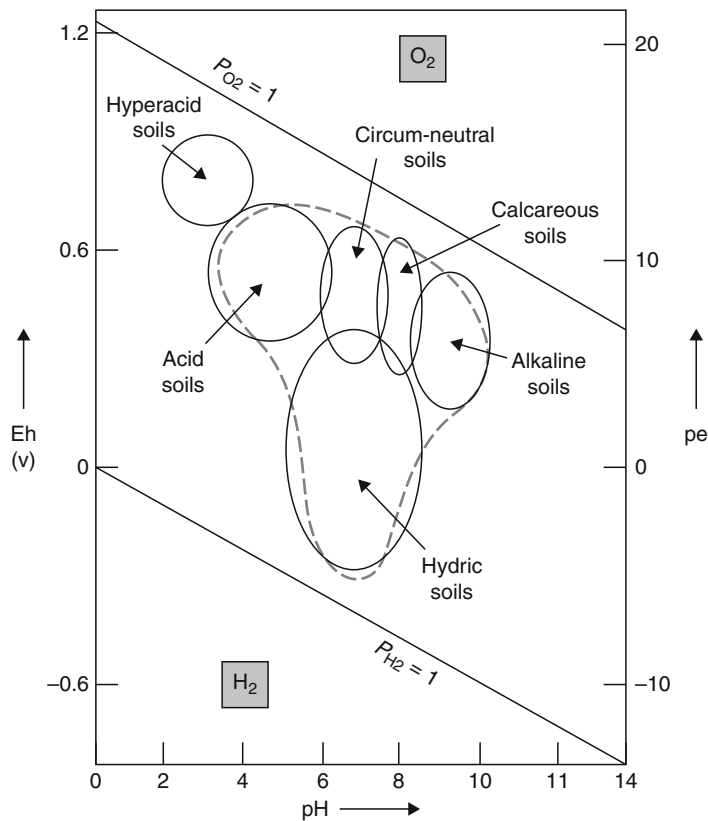
As a result of protons and electrons flowing from source to sink, the geochemical field of soil evolution covers an area of pe–pH space shown in Figure 3.

The geological scar of agriculture

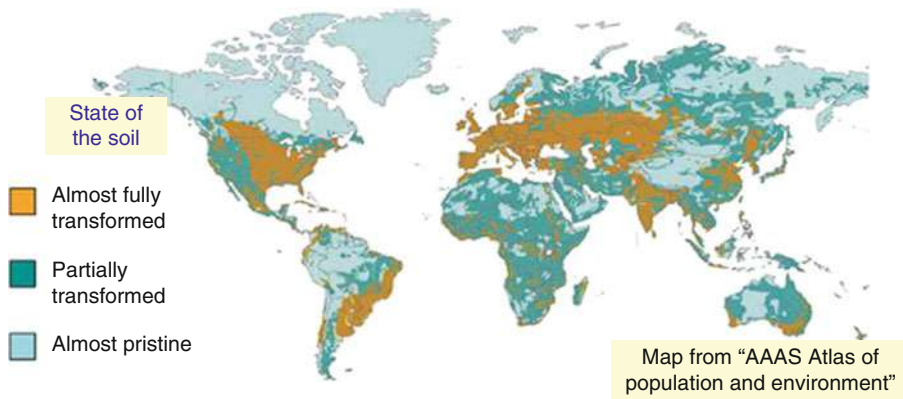
Anthropic effects on soil were relatively minor and local while the genus *Homo* was exclusively hunting and gathering, though when *Homo erectus* learned to control fire



Agrogeology, Figure 2 The hourglass paradigm, showing the critical vulnerability of the biosphere to changes in the soil covering the terrestrial landscape.



Agrogeology, Figure 3 A graphical representation of soils in terms of electron (pe) and proton (pH) variables. Hyperacid soils require a higher concentration of protons than those mentioned in the text, namely by the weathering of sulfides.



Agrogeology, Figure 4 Geological determinism in the pattern of human settlement (the anthroleme, or human scar).

(perhaps as early as 1.8 million years ago), a powerful tool for clearing land became available. It may have been used as such by the hunters and gatherers in order to control the ease with which prey animals were hunted, but with the Neolithic invention of agriculture by *Homo sapiens*, some 10,000–12,000 years ago, it became the principal means by which land was deforested and made ready for cultivation. According to Ruddiman (2010), the agricultural

deforestations that began then, marked the start of a buildup of greenhouse gases in the atmosphere, that received a further boost (as methane) when paddy-rice cultivation became dominant in east Asia about 5,000 years ago. The current threat of global warming may have a long agricultural pedigree.

The earliest agriculturalists for which we have reliable archeological records, practiced their art in the crescent

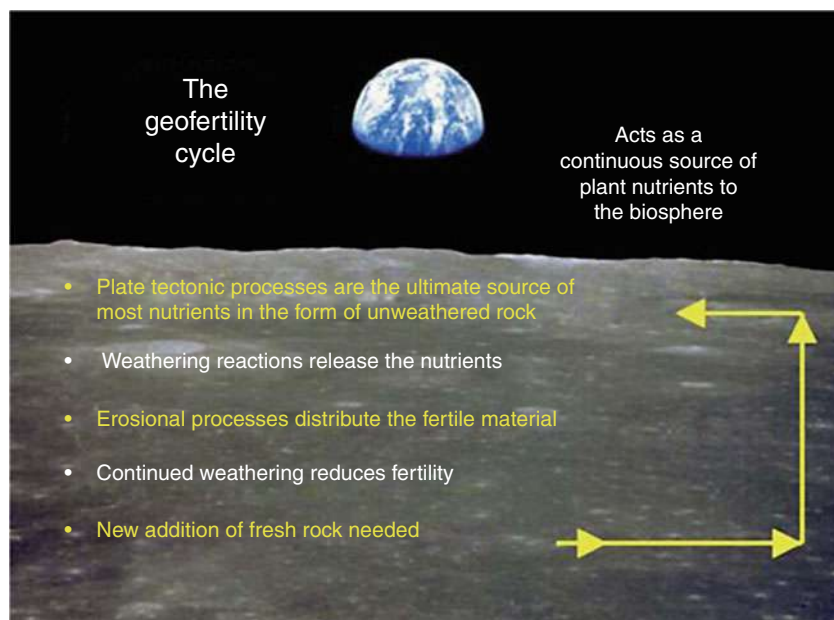
of highland that stretches from the Taurus mountains of southern Turkey to the Zagros mountains of Iran. Çatalhöyük in Turkey is particularly well investigated. Here, farmers depended on the soils developed on geological deposits laid down principally as alluvial fans. They chose light, silty soils that were easy to work, and that were moist for much, if not all of the year. They required no great advancements of technology – no ploughs, no irrigation canals – and they were in a region where the wild progenitors of their crops and farm animals were to be found. Large-scale developments became possible when the farmers, or their technologies migrated into the great river valleys enclosed by the highland rim. The Tigris and Euphrates provided a good source of water and of fertilizing sediments, and the effect was eventually extended onto arid soils when irrigation began to be practiced. It has been surmised that the need to manage water communally was an important impulse in the development of the first civilizations – Sumer, at the head of the Persian Gulf being the earliest on record.

Agriculture spread from its Middle Eastern birthplace to the Nile and the Indus, and because of their dependence on great rivers, the civilizations that developed are commonly referred to as hydraulic civilizations. The advent of agriculture in eastern Asia was probably independent, though it too was based on a large river system, the Huang Ho. In the Americas, farming developed independently of the Old World, and had a geological basis more similar to the agriculture of the Turkish highlands in being based on damp soils on the edges of lakes and wetlands, rather than the soils of large river valleys.

When agriculture expanded into Europe, it took two principal routes and each was facilitated by specific geological circumstances (Chesworth, 2010). The quicker route to the Atlantic was along the Mediterranean, with isolated communities probably developing at the mouths of coastal rivers where wet, light soils could be found. The original sites are probably lost now as a consequence of sea rise as the Würm ice sheet continued to retreat. But isotopic dating confirms that the Mediterranean Coast of Iberia was reached some 7,500 years ago, and the Atlantic coast about a thousand years later. The slower route moved up to the Danube valley and used the light, fertile deposits of loess to cross central Europe to the west. In fact, the footprint stamped on the planet by *H. sapiens*, contains a large component produced by agriculture following the pattern of this important geological sediment, formed by the wind erosion of deposits left by receding ice (Figure 4). Agriculture reached the Atlantic coast of Ireland about 5,000 years ago.

Anthropocene

The early farmers depended in large part on the inherent fertility of the soils they were cultivating. This in turn depends upon the geo-fertility cycle (Figure 5). Following was the simplest technology that allowed a cropped soil to recover fertility (by the weathering of minerals initially provided by the geo-fertility cycle). In essence, this early agriculture depended entirely on renewable resources – sunlight, water, a soil with a good inherent fertility, human muscle. In Egypt, with the Nile as a reliable delivery



Agrogeology, Figure 5 The geo-fertility cycle, the natural means whereby the inherent fertility of the soils of the biosphere is maintained. One major nutrient is not provided by this cycle, nitrogen. That requires the activity of nitrogen-fixing plants in the standing biomass.

system of both water and fertility, agriculture reached as close to a sustainable state as it is likely to get.

Since its Neolithic beginnings, has followed a path from the digging stick, to the ard, the wooden plough, and metal ploughs of increasing power, evolving in tandem with an increasing energy intensiveness, from human to animal muscle, and now to fossil fuel. Over the last 10,000 years or so, we have become the only organism to qualify as a geological force in our own right, a new phenomenon in the geological history of the planet, and one that justifies the recognition of the post Neolithic as a new geological period: the Anthropocene (Crutzen, 2000).

Conclusion

Currently, modern agriculture is utterly dependent on fossil fuels as well as on other nonrenewable geological resources. The rapidly depleting global reserve of natural gas, allows the artificial fixation of nitrogen, a service originally provided in the biosphere by N-fixing organisms. Other nutrient elements are made available by extraction from geological raw materials (phosphorites and potassium-bearing evaporates for example) on an industrial scale. The farming enterprise is now as far from sustainability as it has ever been, and with a world population of almost 7 billion people, a Malthusian collapse of human civilization in its present form, becomes ever more probable.

Bibliography

- Chesworth, W., 2008. Geology and soils. In Chesworth, W. (ed.), *Encyclopedia of Soil Science*. New York: Springer, pp. 209–296.
 Chesworth, W., 2010. Womb, belly and land in the anthropocene. In Martini, P., and Chesworth, W. (eds.), *Landscape and Society*. New York: Springer.
 Crutzen, P. J., 2000. The anthropocene. *Journal de Physique IV*, **12**, 1–5.
 Ruddiman, W. F., 2010. *Plows, Plagues, and Petroleum: How Humans Took Control of Climate*. New edn. Princeton: Princeton University Press.

Cross-references

- [Agophysical Objects \(Soils, Plants, Agricultural Products, and Foods\)](#)
[Alkalinity, Physical Effects on Soils](#)
[Biochemical Responses to Soil Management Practices](#)
[Clay Minerals and Organo-Mineral Associates](#)
[Compaction of Soil](#)
[Cracking in Soils](#)
[Cropping Systems, Effects on Soil Physical Properties](#)
[Desertification: Indicators and Thresholds](#)
[Fertilizers \(Mineral, Organic\), Effect on Soil Physical Properties](#)
[Liming, Effects on Soil Properties](#)
[Management Effects on Soil Properties and Functions](#)
[Mechanical Resilience of Degraded Soils](#)
[Parent Material and Soil Physical Properties](#)
[Physical Degradation of Soils, Risks and Threats](#)
[Rheology in Soils](#)
[Salinity, Physical Effects on Soils](#)
[Soil Aggregates, Structure, and Stability](#)
[Subsoil Compaction](#)
[Soil Structure, Intersecting Surface Approach, and its Applications](#)

[Tillage Erosion](#)

[Tillage, Impacts on Soil and Environment](#)

[Water Erosion: Environmental and Economical Hazard](#)

[Wind Erosion](#)

AGROPHYSICAL OBJECTS (SOILS, PLANTS, AGRICULTURAL PRODUCTS, AND FOODS)

Jan Gliński

Institute of Agrophysics, Polish Academy of Sciences, Lublin, Poland

Definition

Agophysical objects are those materials that play an important role in agricultural production. They are characterized by specific physical properties and undergo various natural and human-induced processes.

Four groups of main agrophysical objects are distinguished: soils, agricultural plants, agricultural products, and foods of plant origin.

Soils represent the greatest group among agrophysical objects. For agricultural crops, they are a medium, which is capable of physically supporting plants and constitutes a magazine for the water and nutrients essential for plant growth (Hillel, 2007; Chesworth, 2008). Soils are formed from the uppermost layer of earth crust (mother rocks) under the influence of five main factors: mother rocks, climate, vegetation, relief, and time. The properties of the soils are, in general, dependent on the above factors and therefore create a mosaic of taxonomic soil units as well over small as large areas, which are combined in very different qualities, quantities, and patterns. Soils are extraordinarily complex media, made up of a heterogeneous mixture of solid, liquid, and gaseous phases, as well as a diverse community of living organisms forming irregularities in their physical structure. They are comprised of different soil horizons (layers), aggregates, cracks, and texture classes. The mass of soil is nonrenewable. Even within the same volume of soil a great heterogeneity and anisotropy can be observed. Most soils are predominantly built of mineral material, but they have upper horizons of organic materials and there is a group of typically organic soils. In the near ground area, *microclimate* of cultivated field is distinguished ([Physics of Near Ground Atmosphere](#)).

From about 300 *agricultural plant* species 14 represent the major crops as a source of foods: wheat (the highest area in the world production), rice, maize, potatoes, barley, cassava, sweet potatoes, soya, beans, tomatoes, sorghum, leguminous grains, oats, millet, and rye (the lowest area in the world production) (Langer and Fill, 1991). Plant structure differs with growing conditions of plants and their individual organs (roots, stems, foliage, and harvestable products). As regards masses of plants, they may be bulk- or stored crops, or chopped or even pressed materials. Some plants, for example, willow, fiber crops,

medicinal plants in the form of dead state, are used as agro-resources for the renewable energy, textile industry, building, and medicine.

Agricultural products are living or dead objects. Within their structure, particles, pores, and cells are distinguished. They have typical macroscopic dimensions and shapes. According to their mechanical properties they are divided into four classes: fluids, semiliquids, semisolids, and solids (Blahovec, 2008). Physical conditions during storage and processing of agricultural products such as temperature, moisture, aeration, and pressure affect their structure and quality.

Plant foods include plant and plant parts eaten as food without or after their processing. There are grain-based foods (cereals, legumes, and nuts), oils from oilseeds, fruits, vegetables, bread, and food extrudate products (Guy, 2001).

Bibliography

- Blahovec, J., 2008. *Agromaterials. STUDY Guide*. Prague: Czech University of Life Sciences.
- Chesworth, W., 2008. *Encyclopedia of Soil Science*. Dordrecht: Springer.
- Guy, R., 2001. *Extrusion cooking*. Boca Raton: CRC Press.
- Hillel, D., 2007. *Soil in the Environment*. Amsterdam: Elsevier.
- Langer, R. H. M., and Fill, G. D., 1991. *Agricultural Plants*. Cambridge: Cambridge University Press.

AGROPHYSICAL PROPERTIES AND PROCESSES

Jan Gliński, Józef Horabik, Jerzy Lipiec
Institute of Agrophysics, Polish Academy of Sciences,
Lublin, Poland

Definitions

Physical process is defined as: "A continuous action or series of changes which alters the material form of matter" and *physical property* as: "Any aspect of an object or substance that can be measured or perceived without changing its identity."

The term *Agrophysical processes and properties* concerns these processes and properties which are used in agrophysics and are relevant to agrophysical objects, i.e., soils, plants, agricultural products, and foods with particular reference to agricultural and environmental applications. Main agrophysical processes and related properties and their technological functions are: aeration, surface phenomena, electricity, mechanics, heat, and hydrology. Some of them are related to all objects or part of them and they have physical quantities expressed in SI units (Scott, 2000; Blahovec, 2008) (see also *Physical Dimensions and Units Use in Agriculture*). Soils which are the most important element of the natural environment undergo changes in their physical properties during natural soil development and also anthropogenic processes such as plowing, compaction, sealing and crusting, erosion, amelioration, loss of humus, salinization, reclamation, and

contamination by inorganic and organic compounds (Blum, 2002; Horn and Baumgartl, 2002). Soil physical processes and properties and resulting soil functions have been specified by Lal and Shukla (2004). Physical processes and related properties of living plants in the field are subjected to environmental pressure, mainly weather conditions (Monteith and Unsworth, 2007) and agricultural products are subjected to technology of food processing (Mohsenin, 1986).

Bibliography

- Blahovec, J., 2008. *Agromaterials. Study Guide*. Prague: Czech University of Life Sciences.
- Blum, W. E. H., 2002. Environmental protection through sustainable soil management – a holistic approach. In Pagliai, M., and Jones, R. (eds.), *Sustainable Land Management – Environmental Protection – A Soil Physical Approach*. Advances in Geocology 35, pp. 1–8, Reiskirchen: Catena Verlag GmbH.
- Horn, R., and Baumgartl, T., 2002. Dynamic properties of soils. In Warrick, A. (ed.), *Soil Physics Companion*. Boca Raton: CRC Press, pp. 17–48.
- Lal, R., and Shukla, M. J., 2004. *Principles of Soil Physics*. Boca Raton: CRC Press.
- Mohsenin, N. N., 1986. *Physical Properties of Plant and Animal Materials*, 2nd edn. New York: Gordon and Breach.
- Monteith, J., and Unsworth, M., 2007. *Principles of Environmental Physics*. San Diego: Academic.
- Scott, H. Don., 2000. *Soil Physics: Agriculture and Environmental Applications*. Ames: Iowa State University Press.

Cross-references

- Agrophysics: Physics Applied to Agriculture
 Air Flux (Resistance) in Plants and Agricultural Products
 Bending Properties of Plants
 Biocolloids: Transport and Retention in Soils
 Bypass Flow in Soil
 Coupled Heat and Water Transfer in Soil
 Flocculation and Dispersion Phenomena in Soils
 Infiltration in Soils
 Organic Matter, Effects on Soil Physical Properties and Processes
 Pedotransfer Functions
 Physical Dimensions and Units Use in Agriculture
 Plant Lodging, Effects, and Control
 Pore Size Distribution
 Shrinkage and Swelling Phenomena in Agricultural Products
 Shrinkage and Swelling Phenomena in Soils
 Solute Transport in Soils
 Water Erosion: Environmental and Economical Hazard

AGROPHYSICS: PHYSICS APPLIED TO AGRICULTURE

Jan Gliński, Józef Horabik, Jerzy Lipiec
Institute of Agrophysics, Polish Academy of Sciences,
Lublin, Poland

Definition

Agrophysics is a science that studies physical processes and properties affecting plant production. The fundaments

of agrophysical investigations are mass (water, air, nutrients) and energy (light, heat) transport in the soil–plant–atmosphere and soil–plant–machine–agricultural products–foods continuums and way of their regulation to reach biomass of high quantity and quality with the sustainability to the environment. The knowledge of physical phenomena in agricultural environment allows increasing efficiency of use of water and chemicals in agriculture and decreasing biomass losses during harvest, transport, storage, and processing.

Short history

The term *agrophysics* was proposed by the Russian physicist A.F. Ioffe (1880–1960) to cover the relations within the soil environment, and especially those of the mass and energy transfer in the soil–plant–atmosphere system (The Agrophysical Institute of the Russian Academy of Agricultural Sciences in Saint-Petersburg: The Roots of Agrophysics). Agrophysics was defined as “a science that studies physical, physicochemical, and biophysical processes in the system ‘the soil – the plants – the active layer of the atmosphere’ as well as main principles of the production process, physical properties of the system components and of various agricultural products.” Over time, it expanded onto other materials, such as agricultural crops, agricultural raw materials and foods, and soil–machine and machine–plant relations. Penman (1948) called attention to the role of physics in agriculture, and later on Przestalski (2001) explicitly argued that “Many phenomena important for agriculture (e.g., soil structure and interactions that determine it, water transport in the soil, transport of water and mineral nutrients in the soil–plant system, effects of the temperature, radiation and other factors on the crop yields, substance permeation through the membranes, and others) which are subjected to physics laws can be investigated with the physical methods only.”

Agrophysics was further developed by Polish scientists B. Dobrzański, J. Gliński, J. Haman, B. Szot, R. Walczak and East European institutions, such as: Institute of Agrophysics of the Polish Academy of Sciences and European Union Centre of Excellence in Lublin “Agrophysics,” Poland ([Institute of Agrophysics in Lublin: Progress in Agrophysics](#)); Agrophysical Institute of the Russian Academy of Agricultural Sciences in Saint-Petersburg (Russia); Czech University of Agriculture in Prague (Czech Republic); Hydrological Institute of the Slovak Academy of Sciences in Bratislava (Slovakia); Agricultural University in Gödöllő (Hungary); Research Institute of Soil Science and Agricultural Chemistry of the Hungarian Academy of Sciences in Budapest (Hungary); N. Pushkarov Institute of Soil Science, Sofia (Bulgaria); Centre of Agricultural Landscape and Land Use Research, Müncheberg (Germany); Institute for Problems of Natural Resources Use and Ecology BAS, Minsk (Belarus); Research Institute for Soil Science and Agrochemistry, Bucharest (Romania); Institute for Soil

Science and Agrochemistry Research, UAN, Kharkiv (Ukraine); and Institute of Physicochemical and Biological Problems of Soil Science and Institute of Basic Biological Problems RAS, Puschino (Russia). This cannot be forgotten about other institutions contributing in the progress of agrophysics, collaborating for many years with the Institute of Agrophysics in Lublin. They are: University of Agricultural Sciences, Institute of Soil Science, Vienna (Austria); Ghent University, Department of Soil Management and Soil Care, Gent (Belgium); University of Guelph, Ontario Agricultural College, Department of Land Resources Sciences (Canada); Institute of Soil Science, Academia Sinica, Nanjing (China); Cranfield University, Silsoe College, Land Resources Division, Silsoe (England); University of Helsinki, Agricultural Chemistry and Physics, and Agrifood Research Centre of Finland, Jokioinen (Finland); Institute of Soil Science, Montfavet (France), Christian Albert University, Institute of Soil Science and Plant Nutrition, Kiel; University Hohenheim, Institute of Soil Science, Stuttgart; Technical University Berlin, Institute Ecology, Department of Soil Science and Soil Protection, Berlin (Germany); Winand Staring Center for Integrated Land, Soil and Water Research SC-DLO, Wageningen (Holland); Institute of Mechanisation of Agriculture CNR, Torino (Italy); Hokkaido University, Laboratory of Soil Science, Sapporo, and Graduate School of Bioagricultural Science, Nagoya (Japan); Institute of Natural Resources and Agrobiology IRNAS-CSIC, Sevilla (Spain); Sweden University of Agricultural Sciences, Department of Soil Science, Uppsala (Sweden); University of Kentucky, Department of Agricultural Engineering, Lexington; and Coastal Plains and Soil Water Conservation Research Center, Florence, South Carolina (USA).

Scientific symposia, conferences, and meetings presented various aspects of agrophysics. The most progressive were the international conferences organized in: Lublin, Poland (1976, 1997) ([Figure 1](#)); Gödöllő, Hungary (1980); Prague, Czechoslovakia (1985); Rostock, East Germany (1989); Bonn, West Germany (1993); Brussels, Belgium (2004); Lublin, Poland (2005). Also many bilateral conferences: Polish–Czechoslovak on “Physics of soil water,” Polish–Hungarian on “Mechanical properties of agricultural materials” and on “Soil degradation,” Polish–French on “Agricultural and hydrological aspects of soil amelioration” were organized since 1973. Most presentations from these conferences were published in various journals, including the International Agrophysics, e.g., Special issue, 1994. Vol. 8, Nos. 1–4.

In Poland, very active is the Polish Society of Agrophysics ([Polish Society of Agrophysics](#)) and an important role in the promotion of agrophysics is played by the journals *International Agrophysics* and *Acta Agophysica*.

Since 2001, every spring international workshops for young scientists, *BioPhys Spring*, are systematically organized, alternately by the Czech University of Agriculture



Agrophysics: Physics Applied to Agriculture, Figure 1 Participants of the 6th International Conference on Agrophysics, (6 ICA), September 15–18, 1997, Lublin, Poland.

in Prague and the Institute of Agrophysics in Lublin. The meetings are oriented on training of young researches and on exchange of professional experience in physics applied to biological, agricultural, and food systems. In 2008, the Slovak University of Agriculture in Nitra and the Szent Istvan University in Gödöllő (Hungary) joined the Organizing Committee of the Workshops, increasing the international level of the event.

Books (Gliński and Stepniewski, 1985; Gliński and Lipiec, 1990; Przestalski, 2009) and a set of monographs on various problems of agrophysics were published within the scope of activity of the Institute of Agrophysics in Lublin and the EU Centre of Excellence “Agrophysics”: Baranowski and Walczak (2004); Bieganowski and Walczak (2004); Bieganowski et al. (2004); Józefaciuk (2004); Józefaciuk et al. (2004); Gliński et al. (2004); Lipiec et al. (2004); Matyka-Sarzyńska and Walczak (2004); Skierucha and Walczak (2004); Skierucha and Malicki (2004); Skierucha et al. (2004); Ślawiński et al. (2004); Stepniewski et al. (2005); Usowicz and Usowicz (2004); Witkowska-Walczak et al. (2004); Baranowski et al. (2005); Horabik and Laskowski (2005a, b); Konstankiewicz and Zdunek (2005); Raytchev et al. (2005a, b); Szot et al. (2005); Włodarczyk and Kotowska (2005); Dobrzanski et al. (2006); and Szymanek et al. (2006). To facilitate access to the worldwide literature on agrophysics, a six-language (English, German, Spanish, French, Polish, and Russian) dictionary on agrophysics, containing 2,800 terms, was elaborated (Dębicki et al., 1991).

Agrophysics is related to the *agrosphere* which is one of the Earth spheres. The Agrosphere Institute ICG-4 of the Forschungszentrum Jülich, Germany, indicates a role of a network of scales and disciplines in the agrosphere. They start with molecule scale to soil column, pedon, field, regional, and superregional scales using NMR, NMR imaging, resistance tomography, and remote sensing methods depending on the scale (<http://www.fz-juelich.de/icg/icg-4/>).

Importance of agophysical research

Agrophysics is developing dynamically, linking knowledge in environmental physics, plant physics, and food physics, filling the gap between such disciplines as agrochemistry, agrobiology, agroecology, and agroclimatology. Agophysical knowledge is useful in agricultural research and practice, especially in agronomy, agricultural engineering, horticulture, food and nutrition technology, and environmental management (Frączek and Ślipek, 2009). Application of agophysical research allows reduction of losses of agricultural products at harvest and post harvest processes and storage.

Progress in agrophysics was possible due to the joined activity of agronomists, physicists, chemists, and biologists, resulting in interdisciplinary approach and solution of theoretical and instrumental problems focused on their practical application in agriculture and natural environment. Agriculture contribution to greenhouse gases production and sink in soils and emission to the

atmosphere is closely connected with soil physical properties (Włodarczyk and Kotowska, 2005).

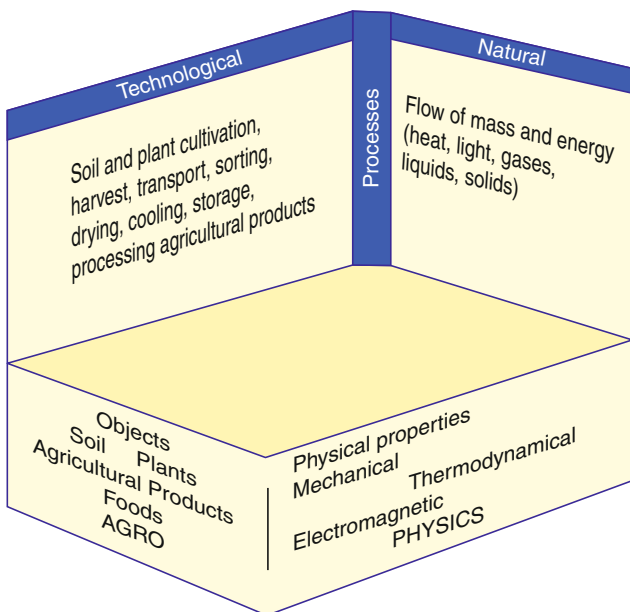
Application of physical methods, laws, and theories for the agricultural problems allowed for more precise description and modeling of the above processes (Haman, 2003).

The area of agrophysical activity may be presented on a three-axial configuration (Figure 2), and the basic scheme of agrophysical research is shown in Figure 3.

Agrophysical knowledge plays an important role in appropriate *processing and storing* of agricultural products and foods which use modern technologies and physical laws that control behavior of biological materials. Agriculture and the food industry belong to largest producers and users of granular materials. Increasing number of processes and operations involving granular materials have resulted in a growing need for new theory and technology. Elaboration of effective design methods of technological processes requires detailed knowledge of physical properties of the processed material as well as proper understanding of interactions with construction materials, e.g., silos (Ravenet, 1981).

Agrophysical objects

The main objects of agrophysical investigations are soils, plants, and agricultural products and foods (see *Agrophysical Objects (Soils, Plants, Agricultural Products, and Foods)*). From the physical point of view, the three states of matter (solid, liquid, gas) can occur in every agrophysical object.

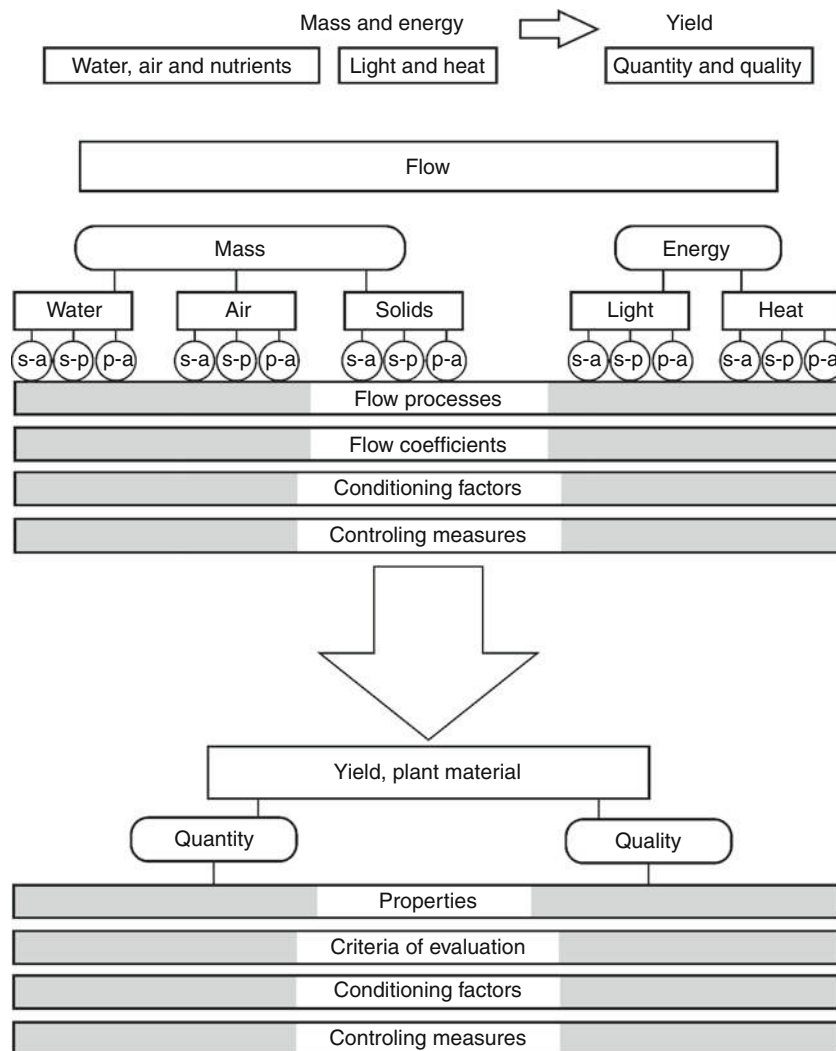


Agrophysics: Physics Applied to Agriculture, Figure 2 Three-dimensional scheme of agrophysical research (Adapted from Gliński, 1992).

Soils

Soils are the central link in the terrestrial environment (Hillel, 2007; Chesworth, 2008) due to their ecological functions (*Soil Functions*). The functions are largely influenced by soil physical characteristic parameters (see *Agrophysical Properties and Processes*) which are well described in many books by e.g., Hillel (1972, 1982, 1998, 2004, 2007); Hanks and Askroft (1980); Gliński and Stepniewski (1985); Gliński and Lipiec (1990); Hartge and Horn (1991); Marshal et al. (1996); Koorevaar et al. (1999); Scott (2000); Shein and Goncharov (2000); Smithson et al. (2002); Warrick (2002); William and Horton (2004); Lal and Shukla (2004). It is enough to mention water, air, and thermal, mechanical, and rheological properties which determine the conditions for crop production, assuming at the same time efficient use of chemicals and agricultural machines. In the evaluation of soil properties and processes, scale (length and time) problems (*Scaling of Soil Physical Properties*) are considered. For water transport in the porous system of soil Kutilek and Nielsen (1994) proposed four length scales, from submicroscopic (10^{-10} to 10^{-8} m) through microscopic (10^{-6} to 10^{-3} m), macroscopic (10^{-1} to 10 m) to watershed (10^2 to 10^4 m and even more). The response time for changes in these parameters is in a broad scale. The changeability of other soil physical characteristics are, e.g., $<10^{-1}$ year for bulk density, total porosity, and composition of soil air, 10^0 – 10^{-1} year for cation exchange capacity, 10^{-1} – 10^2 year for clay mineral associations, $>10^3$ year for texture (Arnold et al., 1990).

Nowadays, worldwide problems closely connected with soil physical properties are soil erosion and compaction. Water and wind erosion are disastrous phenomena in many places. Soil erosion causes tremendous damage, e.g., in America, which loses at the level of 4.8 billion tons of topsoil of agricultural land annually due to erosion (Arnold et al., 1990, p. 78). In Africa, these losses are equal to 700 Mg km^{-2} and in Europe 84 Mg km^{-2} . Closely related with soil erosion are such phenomena as surface soil sealing and crusting, and destruction of soil structure (see *Water Erosion: Environmental and Economical Hazard; Soil Surface Sealing and Crusting*). Soil compaction is a severe problem now due to increasingly using heavier tractors, larger implements, bigger combines, reduced tillage, and no-tillage systems (Horn et al., 2000). Conducting field operations when the soil is too wet, especially in spring and harvesting in the fall increase compaction. Compaction increases soil bulk density and mechanical impedance to root growth and reduces soil macro-porosity, affecting water and air conditions both for plant growth and yield. Nearly all great agroecological programs directed at increasing soil productivity or soil protection against degradation or land conservation include investigations on the physical processes and properties in soils (see *Soil Aggregates, Structure, and Stability; Soil Compactibility and Compressibility; Soil Erosion Modeling; Soil Surface Sealing and Crusting*).



Agrophysics: Physics Applied to Agriculture, Figure 3 Basic scheme of agrophysical research. *a* atmosphere, *p* plants, *s* soil
(Adapted from Gliński, 1992).

Additionally, the variability and large heterogeneity of soil properties gives the view of difficulties to be faced by the physicist dealing with measurements performed in the soil environment (Bieganowski and Walczak, 2004). For this reason, there are still problems concerning standardization of physical methods used in agrophysics (ISO) (see [Standardization in Agrophysics](#)).

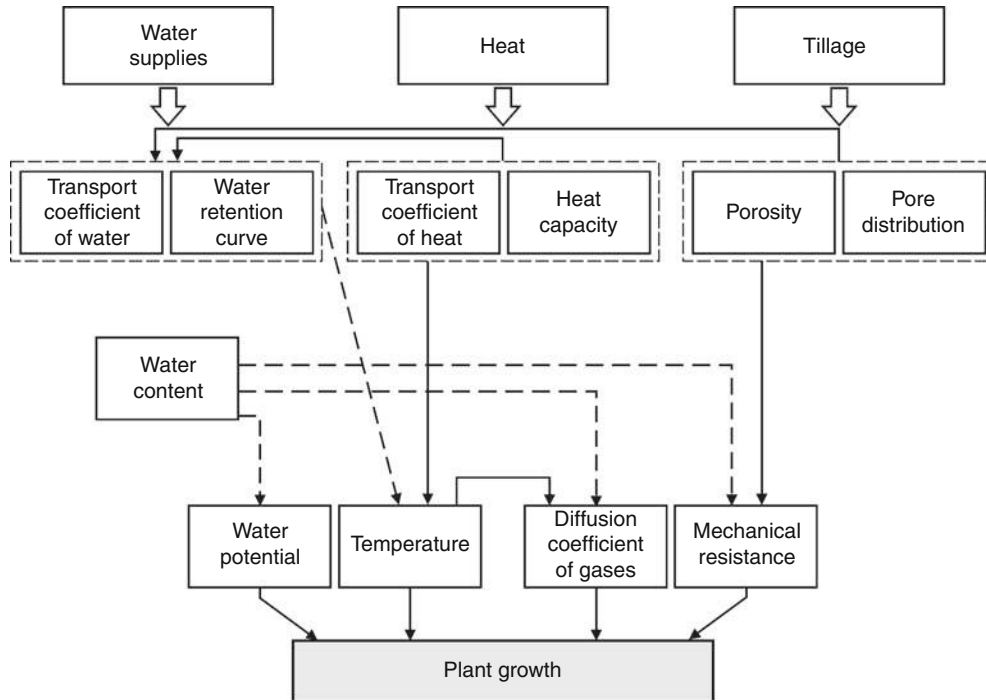
It is worth to mention here the near-ground atmosphere which forms the *microclimate* ([Physics of Near Ground Atmosphere](#)) of a cultivated field with plant canopy, where the processes of evapotranspiration play an important role (Monteith and Unsworth, 2007).

Plants

Productivity of agricultural plants is highly affected by physical factors that are determined by soil tillage, land management, and climate (Szot, 1976; Gliński and

Stepniewski, 1985; Letey, 1989; Gliński and Lipiec, 1990; Lipiec et al., 2004; Gliński et al., 2008) (Figure 4).

Plants differ within themselves and within their organs such as: the root system, stem, foliage, fruit, not to mention the complex structure of each component. Further sharp distinction has to be made as regards the post harvest mass of plants which may be in bulk, stored crops, chopped or even pressed material. The knowledge on the physical properties of plants is useful in plant breeding to improve resistance to lodging and crop productivity and quality (see [Plant Lodging, Effects, and Control](#); [Plant Physical Characteristics in Breeding and Varietal Evaluation](#)). Moreover, plants are important source of biomass for renewable energy production in many countries (see [Alternative Sources of Energy from Agriculture Biomass – a European Perspective](#); [Biomass as an Environmentally Benign Energy Source](#)).



Agrophysics: Physics Applied to Agriculture, Figure 4 Physical factors influencing plant growth (Adapted from Walczak and Zawadzki, 1979).

Agricultural products

Agricultural products are composed of living or harvestable products of plant origin. It is not easy to separate agricultural products from foods. Generally, they are raw materials for foods after their storage and processing, but some of them (vegetables, fruits) can be eaten as fresh foods. Many agricultural products are irregular in shape, with convex and concave parts on different surfaces and a characteristic internal structure consisted of particles, pores, and cells (Blahovec, 2008). The mechanical properties of agricultural products play an important role in the transport, storage, and processing of these materials. Fruit properties, such as porosity, surface area, mass, volume, dimensions, friction, and color are significant in sorting, storing, and packing. Agricultural raw materials, products, and foods must fulfill stringent requirements and standards, including their physical properties, which should be currently and quickly checked during their processing. Agricultural tools and machines used during harvest and transport cause yield losses and mechanical damage (see *Crop Yield Losses Reduction at Harvest, from Research to Adoption*). Physical processes during storage and drying of biological materials may cause their mechanical and biological damage and thus worsening quality. Application of physics provides bases for new technologies on maximal reduction of above-mentioned losses during various operations (Mohsenin, 1986).

Plant foods

Plant foods include plant and plant parts eaten as food without or after their processing (see *Agophysical Objects (Soils, Plants, Agricultural Products, and Foods)*). The knowledge of physical properties affects their quality during post-harvest operations, storing, and processing (Heldman, 2003; Sahin and Sumnu, 2006). Quality of food is the multiparameter attribute related to sensory properties (appearance, texture, taste, and aroma), nutritive values, chemical constituents, mechanical properties, functional properties, and defects. An important physical element of food quality is texture. The texture is a sensory and functional manifestation of the structural, mechanical, and surface properties of foods detected through the senses of vision, hearing, touch, and kinesthesia (Szczesniak, 2002). Texture is affected by the structure of food (Jackman and Stanley, 1995). Texture of plant foods can be attributed mainly to the structural integrity of the cell wall and middle lamella, as well as to the turgor pressure generated within cells by osmosis. It is well known that texture of fruits and vegetables is influenced by cell wall structure (thickness, chemical composition), middle lamella, turgor pressure, parenchyma cells arrangement, quality and volume of intercellular spaces, permeability of cell walls.

Main agrophysical processes, properties, and their technological functions are presented in **Table 1**.

Agrophysics: Physics Applied to Agriculture, Table 1 Main agrophysical processes and properties and their impacts on soil, plants, agricultural products, and food

Physical processes	Physical properties	Impact on soil and plants	Impact on agricultural products and food
Mass transport (water, vapor, air, and chemicals flow; capillary flow, molecular diffusion, osmosis)	Hydraulic conductivity, water diffusivity, vapor diffusivity, air diffusivity, chemicals diffusivity, permeability	Water available to plants, seepage, filtration, drainage, irrigation, flooding, chemical transport, gas emission from soil, aeration, evaporation, respiration, transpiration, weathering, erosion, runoff, soil sealing, and crusting	Chilling, cooling, drying, and fumigation of products in bulk, storage respiration, shelf life
Mass absorption/adsorption (adhesion, cohesion)	Particle size distribution, porosity, surface area, wettability	Waste disposal, gas exchange, coagulation, flocculation, peptization, shrinkage	Drying, hydration, dehydration, storage respiration
Energy transport (heat conduction, convection, radiation)	Thermal conductivity, heat capacity, specific heat, permittivity	Thermal condition	Drying, processing, cooking
Energy absorption/emission (heat conduction, radiation)	Reflectance, absorption, permittivity, dispersion, color indices	Thermal condition, albedo, growing degree-days	Drying, heating, processing
Phase transition (evaporation, condensation, crystallization, melting)	Latent heat, melting heat	Soil freezing/thawing, plant freezing	Freezing, freeze-drying, storage
Mechanical processes (impact, compression, crushing, shearing, tension)	Elasticity, viscosity, plasticity, hardness, density, porosity	Soil tillage, soil aggregation, soil compaction, trafficability, plant lodging, emergence	Harvesting, post-harvest treatment, storage, handling, processing (agglomerating, chopping, mixing, separating)

Agromechanics

Agricultural objects undergo mechanical changes but their cognition is difficult because of the very complicated structure (Koolen and Kuipers, 1983; Husar, 1985; Haman, 1988). Therefore the application of results from engineering mechanics to agromechanics is difficult. The most important areas of agromechanics are related to the strength of agricultural products and to the determination of stresses and strains occurring in the system. Agrophysicists make effort to acquire knowledge on the effects of stresses acting on agricultural objects. In the case of agricultural products, external forces are coming from the effects of a body's own weight, wind force, supporting force, shock, vibration, mechanical interference. Internal forces appear, e.g., between stalk and nodes, stalk and root system in cereals, or tuber and foliage. Examples of stress-strain relations of some agrophysical objects are shown in Figure 5. The tasks connected with the transport and processing of agricultural products, such as baling, milling, grinding, etc., depend fundamentally on the machinery used. In the case of soils, the natural influences and human interventions that cause the stress-strain relations in soils are even more difficult to determine. Advances in applied physics with extended theoretical knowledge are needed to know mutual interactions of machine elements with plants.

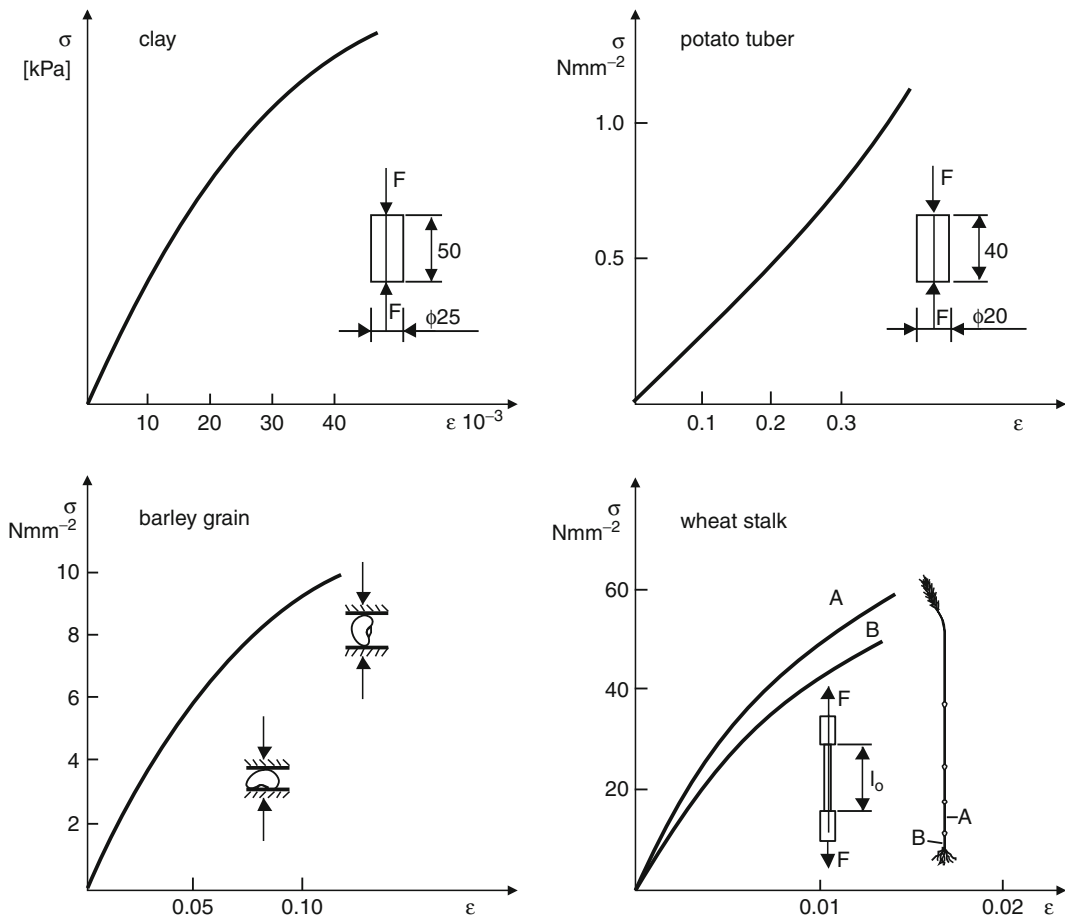
In the conditions of intensive agriculture, problems of the level of *energy use* in various technological processes

are of fundamental significance. Especially soil cultivation and yield harvest consume a lot of energy which can be decreased by applying knowledge of the physical properties of agrophysical objects and machines used.

Main tools in agrophysical research

Measuring methods, instrumentation, and metrology

Study of the multiphase and heterogeneous system of agricultural objects is very complex and therefore needs to adopt many measurement methods and instrumentations used in other scientific disciplines (Gliński and Konstankiewicz, 1991a, b; Walczak, 1993; Blahovec and Kutilek, 2003; Lamorski et al., 2004). The scientists need precise quantitative information concerning the physical behavior and spatial variability of examined objects to create models for practical use after their experimental verification. For this purpose, many advanced methods and measuring tools were recently developed. Some of them are considered in the Encyclopedia of Agrophysics (see *Acoustic Tomography*; *Electrochemical Measurements in Soils*; *Electrical Resistivity to Assess Soil Properties*; *Electromagnetic Fields, Impact on Seed Germination and Plant Growth*; *Fractal Analysis in Agrophysics*; *Ground-Penetrating Radar, Soil Exploration*; *Image Analysis in Agrophysics*; *Nanomaterials in Soil and Food Analysis*; *Neural Networks in Agrophysics*; *Nondestructive Measurements in Fruits*; *Nondestructive*



Agrophysics: Physics Applied to Agriculture, Figure 5 Stress–strain diagrams for clay, potato tuber, barley grain, and wheat stalk (Modified from Husar, 1985).

Measurements in Soil; Nuclear Magnetic Resonance (NMR); Particle Film Technology; Porosimetry; Precision Agriculture: Proximal Soil Sensing; Proximal Soil Sensing; Proton Nuclear Magnetic Resonance (NMR) Relaxometry in Soil Science; Remote Sensing of Soils and Plants Imagery; Tensiometry; Visible and Thermal Images for Fruit Detection; and X-ray Method to Evaluate Grain Quality).

Modeling

In agrophysics, one of the basic methods of investigation is modeling. Modeling, like scientific observation and experimentation, is a method for increasing our understanding of cause-and-effect relationships. It requires classifying the processes involved according to their importance, which results in the creation of a simplified reality (see *Stomatal Conductance, Photosynthesis, and Transpiration, Modeling*).

Generally, the models used in physics and in other life sciences, including agrophysics, can be divided into

physical and mathematical models. The physical models, with regard to the way of description of processes taking place in the environment, can be divided into: real models, analogue models, and phenomenological models (Mazurek et al., 1996).

The *real models* concern field or laboratory experiments (lysimetric and pot studies, greenhouse experiments). The *analogue models* enable the description of a given object, phenomenon, or physical process with the help of another analogous object, phenomenon, or physical process. The analogue models are created to simulate slow real process, e.g., the flow and accumulation of water in a porous medium can have an analogue in the flow and accumulation in a net of resistances and condensers. The *phenomenological models* are constructed when a real process is too complicated for a detailed physical–mathematical description (e.g., evapotranspiration, erosion, biomass production).

Recent development of computer technology and information management (or programming) enhances the importance of mathematical models. A mathematical

model is an equation or set of equations whose solution describes the physical behavior of a related physical system. A mathematical model is always a simplified description, or caricature, of a physical reality expressed in mathematical terms (Weatherley, 2006).

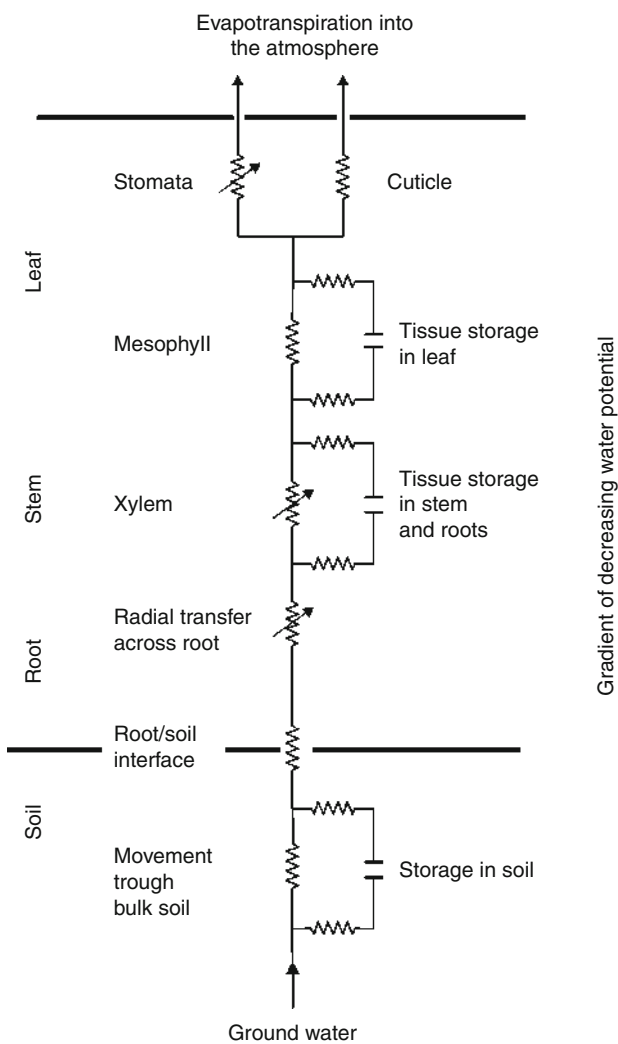
Mathematical models can be divided into mathematical–physical, statistical–physical, and mathematical–statistical models. They may be used for different applications – from pure modeling of transport phenomena in soil to crop growth and yield prediction.

A typical example of mathematical–physical model is the mass and energy transport through the soil–plant–atmosphere system (see *Soil–Plant–Atmosphere Continuum*) as a principal agrophysical phenomenon. It results from a combination of various mechanisms and includes molecular liquid diffusion, molecular vapor diffusion, capillary flow, convective transport, evaporation–condensation, pure hydrodynamic flow, and movement due to gravity. This transport can be described by 3D nonlinear differential equations with coefficients that can be determined experimentally. Water movement through the system was presented as a series of interrelated, independent processes which can be treated as analogous to the flow of electricity through a conducting system (Figure 6).

Complex mathematical–physical models are developed to describe soil, atmosphere, and plant processes responsible for biomass increase, using constitutional mathematical–physical equations (e.g., van Genuchten, 1980). The equations are resulting from the conservation laws, describing a chosen phenomenon in this system, e.g., transport of water, salt, and heat in the soil; soil deformation; and stress as a result of agricultural machines and cultivation tools reaction (Haman and Pukos, 1983; Pukos, 1994; Walczak et al., 1997; Konstankiewicz and Pytka, 2008).

Other examples of mathematical–physical models are models using the discrete element method (DEM) and finite element method (FEM) for modeling physical processes in various media (e.g., grain silos) (Holst et al., 1999a, b).

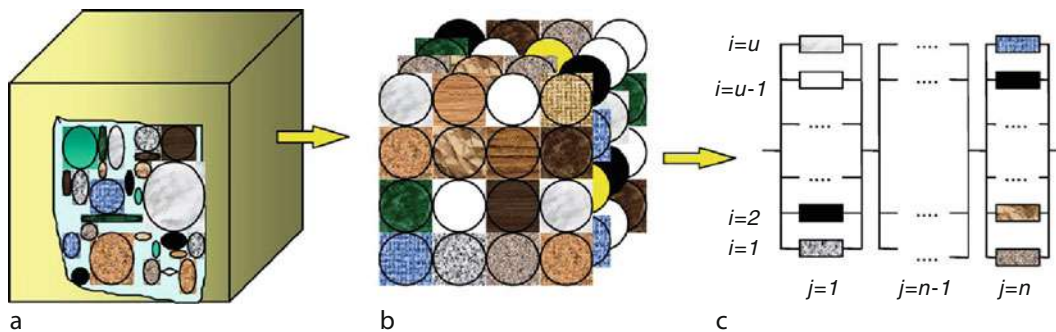
An example of a statistical–physical model is the model of soil thermal conductivity proposed by Usowicz et al. (2006). The model is expressed in terms of heat resistance (see *Ohm's law* and *Fourier's law*), two laws of Kirchhoff, and the polynomial distribution. The volumetric unit of soil in the model (Figure 7a) consists of solid particles, water, and air, and is treated as a system made up of regular geometric figures, spheres, filling the volumetric unit by layers (Figure 7b). It is assumed that connections between the layers of spheres and the layer between neighboring spheres will be represented by serial and parallel connections of thermal resistors, respectively (Figure 7c). Comparison of resultant resistance of the system, with consideration of all possible configurations of particle connections together with a mean thermal resistance of given unit soil volume, allows estimating the thermal conductivity of soil ($\text{Wm}^{-1}\text{K}^{-1}$).



Agrophysics: Physics Applied to Agriculture,
Figure 6 Diagram of water flow from soil to the atmosphere through plants (Adopted from Russel, 1977).

An example of mathematical–statistical models are pedotransfer functions (PTF), being equations or algorithms expressing relationships between soil properties different in the difficulty of their measurement or their availability. PTFs are vital tools to translate data that we have to data that we need in agrophysical research and management applications (*Pedotransfer Functions*). They were extensively used to predict soil hydraulic properties (retention curve, hydraulic conductivity) from basic soil properties such as particle-size distribution, organic matter, and bulk density.

Global warming resulting in climate change and its possible effects on the soil environment and the economy yielded the creation of simulation models concerning also predicted changes of soil parameters. The model of soil water balance, being a combination of mathematical–physical and phenomenological models, was elaborated



Agrophysics: Physics Applied to Agriculture, Figure 7 Schematic diagram of structure of the statistical model where (a) is a unitary volume of soil, (b) is the system of spheres that forms n layers, and (c) is a representation of contacts in layers by u parallel connection of resistors (Usowicz et al., 2006).

for the territory of the European Community within the ACCESS project (Agro-climatic change and European soil suitability – a spatially distributed soil, agro-climatic and soil hydrological model) (Loveland, 1996). One of its submodels on bypass flow in cracking soils was done and experimentally verified (Armstrong et al., 1996; Ślawiński et al., 1996; Walczak et al., 1996; Fernandez et al., 2004).

Mathematical modeling contributes to better understanding of the complex and variable effects of soil and subsoil compaction (Lipiec et al., 2003). Frequently, mechanistic and deterministic models were used. Root growth is often predicted as a function of mechanical resistance and water status of soil and crop yield from interactions of soil water and plant transpiration and assimilation. Modeling of the movement of water and chemicals is based on the Darcy/Richards one-dimensional flow equation. The effect of soil compaction is considered by changing hydraulic conductivity, water retention, aeration, and root growth. The predictability of some models was improved by considering macro-porosity and strength discontinuity (spatial and temporal variability of material parameters) and the relative compaction instead of bulk density. Scarcity of experimental data on the heterogeneity is a constraint in modeling the effects of soil compaction. Further work is needed to develop modeling approaches with consideration of soil structural discontinuities and spatial variation of the input parameters resulting from compaction.

Soil erosion models broadly fit into two groups: empirical and process-based models (see *Soil Erosion Modeling*). The Universal Soil Loss Equation (USLE) (Wischmeir and Smith, 1978) is the most dominant empirical model to predict field-scale erosion rates.

Crop models are mostly based on physiological and climate data without consideration of soil structure (Walczak et al., 1997). To bridge this gap, investigations were carried out in 1992–1995 within the framework of international multilateral projects between Austria, Czech Republic, Hungary, Poland, and Slovak Republic on the role of soil structure functions for sustainable agricultural

biomass production and soil protection (International Agrophysics, Special issue, 1993, Vol. 7, Nos 1–3 and Special issue, 1997, Vol. 11, Nos. 1–2). From the analysis of the models considering soil processes, it resulted that the soil structure parameters appearing most frequently in them are soil water retention, root system parameters, soil compaction and porosity, and unsaturated and saturated water conductivity. Generally, models of plant production include two groups of parameters: soil parameters and plant parameters. At least growth stage and rooting depth are necessary as plant parameters if crop growth should be coupled with soil structure effects. Modeling showed clearly that the effect of the saturated water conductivity and bulk density on crop yield alone was not significant. But, as soon as root distribution was introduced as a plant parameter, a strong effect on the plant growth was detected as an overall consequence of the soil structure status. Physical soil parameters provide the same kind of methodological troubles as all other scientific measurements. But, there is an additional difficulty, which is the fact that structure-dependent parameters cannot be determined from composite, disturbed samples. Each core sample or each in situ measurement has to be treated separately. This creates very specific problems of sampling. However, almost all crop production models assume that soil is a homogeneous substrate. Therefore, it is very important to develop models which also consider soil heterogeneity, time, and spatial variability of soil parameters at various scales.

Food processing technology using innovative strategy needs support from models. Within the EU 7th Framework Program, the multidisciplinary European DREAM project (Design and development of REAListic food Models with well-characterized micro- and macrostructure and composition) is being created at INRA (France) (Ad Litteram, 2009). The physical and mathematical food models developed as a result of the project will serve “as standards that can be applied across all major food categories to facilitate the development of common approaches to risk assessment and nutritional quality for food research and industry.” Also post-harvest and processing

technologies need mathematical models and optimization methods (De Baerdemaeker and Vandewalle, 1995; Agbashlo et al., 2009).

Even models which describe correctly the physical processes in modeled object may not yield accurate results when reliable values of the physical parameters of modeled object are not known. Even if the model has been widely used, uncertainties still arise when it is applied to conditions different than those for which the model was previously tested. Therefore, experimental verification of the model is very important (Fernandez et al., 2004).

Monitoring

Monitoring is the collection of data that allow to determine temporal and spatial variations of physical conditions in agriculture and the environment (see *Monitoring Physical Conditions in Agriculture and Environment*). The increasing pressure on natural resources, sustainability and exhaustion of nonrenewable resources need monitoring which should provide sufficient data for the decision makers. Advances in sensors, computers, and communication devices make it easier to collect useful information about physical conditions in agricultural and natural environment.

Recently, remote sensing technology is rapidly developing for monitoring the world's agricultural production including crop identification, acreage, vigor, density, maturity, growth rates, and yield forecasting, as well as soil physical properties and water availability and quality (see *Remote Sensing of Soils and Plants Imagery; Soil Physical Degradation: Assessment with the Use of Remote Sensing and GIS*).

Research needs and challenges

We present some research needs and challenges to improve agrophysical knowledge and applications.

Soils

Capture the dynamics of soil structure effects and improve quantitative description of surface roughness, crusting, bypass flow, infiltration, deformation resistance (mechanical impedance, crop establishment).

Estimate of the effective soil physical properties of heterogeneous field soil profiles. Integration of directly measured data and indirectly estimated information derived from new noninvasive techniques such as neutron and X-ray radiography, magnetic resonance imaging, electrical resistivity tomography, ground penetrating radar. Microwave remote sensing seems promising for this.

Quantify the size, continuity, orientation, and irregularity of pores by means of image analysis for a broad range of agrophysical applications including water movement and solute transport following human activity.

Visualize and quantify the complex geometry of the pore network and soil structure in 3D on various scales, thus enhancing understanding of the multiple interacting

soil physical, biological, and biogeochemical processes, including flux phenomena.

Quantify coupled soil heat and water transfer (particularly vapor flow components) and associated implications at various scales.

Integrate soil mechanical and conductive (hydraulic) processes affecting the time-dependent strain and the alteration of pore functioning, e.g., aeration and water fluxes. Precompression stress reflects well the stress and strain state for a given predrying intensity and helps the specification of appropriate agricultural machinery to avoid excessive soil and subsoil compaction.

Develop noninvasive soil sensors to alleviate the difficulty in researching below-ground processes (e.g., root development, water movement etc.).

Soil–plant relations

Explain perception of soil physical stress by plants (or plant roots) and the conversion of physical and chemical phenomena into physiological responses.

Determine the combined effects of multiple stresses such as water stress, oxygen stress, and mechanical stress, salinity, and temperature extremes on plant performance.

Develop emerging area of 3D soil–plant functional interactions modeling based on root architecture which allow better understanding of the complex mechanisms controlling water and nutrients fluxes in the soil–plant continuum and increase root uptake efficiency. Advances made in noninvasive measurement techniques can be useful for this.

Evaluate coating effects of increasing temperature and associated changes in soil moisture and rising atmospheric CO₂ on SOM and plant productivity, due to future climatic change.

Manage landscape structure to optimize the use of solar energy, heat and water balance of agricultural areas toward increasing potential for sustainable production of biomass.

Breed plants to develop crop varieties for physically stressed environment, e.g., lodging.

Agricultural products and foods

Determine optimal physical conditions to increase the utility (technological) value during processing and storage.

Improve technology of harvesting, storing and processing to decrease qualitative and quantitative losses using physical methods and modeling approaches.

Deepen knowledge on physical properties through description of macroscopic and microscopic structures and processes.

Technology

Save energy during various technological processes used in agriculture.

Improve construction of machines and devices (equipped with electronics) used in agriculture in terms of effective energy use and environmental protection.

Data use

Develop complete and reliable databases of agrophysical data – a challenging task. They are an invaluable resource for researches, educators, practitioners, and policy makers, and present great opportunities to translate the existing data to the data we need using cost-effective pedotransfer functions (or model approaches).

Develop modeling approaches with consideration of structural discontinuities and spatial variation of the input parameters.

Bibliography

- Ad Litteram DREAM, 2009. *A European project coordinated by the BIA research unit*. Newsletter of the INRA Centre of Angers-Nantes, July 2009, p. 29.
- Aghbashlo, M., Kianmehr, M. H., Khani, S., and Ghasemi, M., 2009. Mathematical modelling of thin-layer drying of carrot. *International Agrophysics*, **23**, 1–5.
- Armstrong, A. C., Legros, J. P., and Voltz, M., 1996. ACCESS-II: detailed model for crop growth and water conditions. *International Agrophysics*, **10**, 171–184.
- Arnold, R. W., Szabolcs, I., and Targulian, V. O., (eds.), 1990. *Global soil change*. Report of an IIASA-ISSS-UNEP Task Force on the Role of Soil in Global Change. IIASA, Laxenburg, Austria.
- Baranowski, P., and Walczak, R. T., 2004. *Method and Methodology for Determination of Basic Physical Characteristics of Porous Media with Application of TDR Technology*. Lublin: Institute of Agrophysics PAS.
- Baranowski, P., Usowicz, B., and Walczak, R. T., 2005. *Evapotranspiration into the Boundary Layer of the Atmosphere*. Lublin: Institute of Agrophysics PAS.
- Bieganowski, A., and Walczak, R. T., 2004. Problems of standardization of soil physics methods. In Józefaciuk, G. (ed.), *Physics, Chemistry and Biogeochemistry in Soil and Plant Studies*. Lublin: Institute of Agrophysics PAS, pp. 31–33.
- Bieganowski, A., Józefaciuk, G., and Walczak, R. T., 2004. *Modern Physical and Physicochemical Methods and Their Applications in Agroecological Research*. Lublin: Institute of Agrophysics PAS.
- Blahovec, J., 2008. *Agromaterials Study Guide*. Prague: Czech University of Life Sciences.
- Blahovec, J., and Kutilek, M. (eds.), 2003. *Physical Methods in Agriculture*. New York: Kluwer Academic.
- Chesworth, W. (ed.), 2008. *Encyclopaedia of Soil Science*. Dordrecht: Springer.
- De Baerdemaeker, J., and Vandewalle, J. (eds.), 1995. *Control Applications in Post-harvest and Processing technology (CAPPT'95)*. A postprint volume from the 1st IFAC/CIGR/EURAGENE/ISHS Workshop, Ostend, Belgium, 1–2 June 1995. International Federation of Automatic Control, Laxenburg (Austria), p. 321.
- Dębicki, R., Fijałkowska, A., Gliński, J., Hajnos, M., Konstankiewicz, K., Kupryś, P., Lipiec, J., and Martin-Aranda, J., 1991. *Dictionary of Agrophysics in Six Languages: English, German, Spanish, French, Polish and Russian*. Lublin: Institute of Agrophysics PAS.
- Dobrzanski, B., jr, Robaczewski, J., and Rybczyński, R., 2006. *Handling of Apple Transport Techniques and Efficiency Vibration, Damage and Bruising, Texture, Firmness and Quality*. Lublin: Institute of Agrophysics PAS.
- Fernandez, J. E., Ślawiński, C., Moreno, F., Lamorski, K., Walczak, R. T., and Vanclooster, M., 2004. Experimental verification of the agrophysical models. In Matyka-Sarzyńska, D., and Walczak, R. T. (eds.), *Basic Problems of Agrophysics*. Lublin: Institute of Agrophysics PAS, pp. 41–49.
- Frączek, Z., and Ślipeć, Z., 2009. Significance of agrophysics in the area of agriculture and technical investigations (in Polish). *Biuletyn Informacyjny PTA*, **29**, 6–16.
- Gliński, J., 1992. Agrophysics in modern agriculture. *International Agrophysics*, **6**, 1–7.
- Gliński, J., and Konstankiewicz, K., 1991. *Methods and Equipment for Agrophysical Investigations. I. Soil*. Problemy Agrofizyki 64, Ossolineum, Wrocław.
- Gliński, J., and Konstankiewicz, K., 1991. *Methods and Equipment for Agrophysical Investigations. II. Plant Material*. Problemy Agrofizyki 65, Ossolineum, Wrocław.
- Gliński, J., and Lipiec, J., 1990. *Soil Physical Conditions and Plant Roots*. Boca Raton: CRC Press.
- Gliński, J., and Stepniewski, W., 1985. *Soil Aeration and Its Role for Plants*. Boca Raton: CRC Press.
- Gliński, J., Józefaciuk, G., and Stahr, K., 2004. *Soil – Plant – Atmosphere Aeration and Environmental Problems*. Lublin: Institute of Agrophysics PAS.
- Gliński, J., Lipiec, J., and Stepniewski, W., 2008. Plant roots and soil physical factors. In Chesworth, W. (ed.), *Encyclopaedia of Soil Science*. Dordrecht: Springer, pp. 571–578.
- Haman, J., 1988. *Soil-Plant-Machine Relations – The Base for Agricultural Machine Design. Physical Properties of Agricultural Materials and Products*. New York: Hemisphere Publishing Corporation, pp. 63–69.
- Haman, J., 2003. Agrophysics (in Polish). *Nauka*, **1**, 53–60.
- Haman, J., and Pukos, A., 1983. Problems of physical equations in agricultural properties of soil. *Zeszyty Problemowe Postępów Nauk Rolniczych*, **220**(II), 337–345.
- Hanks, R. J., and Askroft, G. L., 1980. *Applied Soil Physics*. Berlin: Springer.
- Hartge, K. H., and Horn, R., 1991. *Einführung in die Bodenphysik*. Stuttgart: Ferdinand Enke Verlag.
- Heldman, D. R. (ed.), 2003. *Encyclopedia of Agricultural, Food, and Biological Engineering*. New York: Taylor and Francis.
- Hillel, D., 1972. *Optimizing the Soil Physical Environment towards Greater Crop Yield*. New York: Academic Press.
- Hillel, D., 1982. *Introduction to Soil Physics*. San Diego: Academic Press.
- Hillel, D., 1998. *Environmental Soil Physics*. San Diego: Academic Press.
- Hillel, D., 2004. *Introduction to Environmental Physics*. Amsterdam/Boston: Elsevier/Academic.
- Hillel, D., 2007. *Soil in the Environment*. San Diego: Elsevier.
- Holst, J. M. F. G., Ooi, J. Y., Rotter, J. M., and Rong, G. H., 1999a. Numerical modeling of silo filling I: continuum analyses. *Journal of Engineering Mechanics-ASCE*, **125**, 94–103.
- Holst, J. M. F. G., Ooi, J. Y., Rotter, J. M., and Rong, G. H., 1999b. Numerical modeling of silo filling II: Discrete element analyses. *Journal of Engineering Mechanics-ASCE*, **125**, 104–110.
- Horabik, J., and Laskowski, J., 2005a. *Mechanical Properties of Granular Agro-materials and Food Powders for Industrial Practice. Part I. Characterization of Mechanical Properties of Particulate Solids for Storage and Handling*. Lublin: Institute of Agrophysics PAS.
- Horabik, J., and Laskowski, J., 2005b. *Mechanical Properties of Granular Agro-materials and Food Powders for Industrial Practice. Part II. Material Properties for Grinding and Agglomeration*. Lublin: Institute of Agrophysics PAS.
- Horn, R., van den Akker, J. J. H., and Arvidsson, J. (eds.), 2000. Subsoil compaction – distribution, processes and consequences. *Advances in GeoEcology*, **32**. Catena Verlag, Reiskirchen, Germany 460 p.
- Husar, I., 1985. Agromechanics. *International Agrophysics*, **1**, 23–39.

- Jackman, R. L., and Stanley, D. W., 1995. Perspective in the textural evaluation of plant foods. *Trends in Food Science and Technology*, **6**, 187–194.
- Józefaciuk, G., 2004. *Physics, Chemistry and Biogeochemistry in Soil and Plant Studies*. Lublin: Institute of Agrophysics PAS.
- Józefaciuk, G., Sokołowska, Z., and Hajnos, M., 2004. *Physical Chemistry of Soil: Surface and Pore Properties*. Lublin: Institute of Agrophysics PAS.
- Konstankiewicz, K., and Pytka, J., 2008. Soil engineering. In Chesworth, W. (ed.), *Encyclopedia of Soil Science*. Dordrecht: Springer, pp. 646–656.
- Konstankiewicz, K., and Zdunek, A., 2005. *Micro-structure Analysis of Plant Tissue*. Lublin: Institute of Agrophysics PAS.
- Koolen, A. J., and Kuipers, H., 1983. *Agricultural Soil Mechanics*. Berlin/New York: Springer.
- Koorevaar, P., Menelik, G., and Dirkens, C., 1999. *Elements of Soil Physics*. Amsterdam: Elsevier.
- Kutilek, M., and Nielsen, D. R., 1994. *Soil Hydrology*. Cremblingen-Destedt: Catena Verlag.
- Lal, R., and Shukla, M. J., 2004. *Principles of Soil Physics*. Boca Raton: CRC Press.
- Lamorski, K., Walczak, R., Śląwiński, C., and Witkowska-Walczak, B., 2004. Validation and sensitivity analysis of heat transport model in soil profile. In Bieganowski, A., Józefaciuk, G., and Walczak, R. T. (eds.), *Modern Physical and Physicochemical Methods and their Applications in Agroecological Research*. Lublin: Institute of Agrophysics PAS, pp. 102–109.
- Letey, J., 1989. Relationship between soil physical properties and crop production. *Advances in Soil Science*, **1**, 277–294.
- Lipiec, J., Arvidsson, J., and Murer, E., 2003. Review of modelling crop growth, movement of water and chemicals in relation to topsoil and subsoil compaction. *Soil and Tillage Research*, **73**, 15–29.
- Lipiec, J., Walczak, R., and Józefaciuk, G., 2004. *Plant Growth in Relation to Soil Physical Conditions*. Lublin: Institute of Agrophysics PAS.
- Loveland, P. J., 1996. The ACCESS project: Agro-climatic change and European soil suitability – a spatially distributed soil, agro-climatic and soil hydrological model. *International Agrophysics*, **10**, 145–153.
- Marshall, T. J., Holmes, J. W., and Rose, C. W., 1996. *Soil Physics*. New York: Cambridge University Press.
- Matyka-Sarzyńska, D., and Walczak, R. T., 2004. *Basic Problems of Agrophysics*. Lublin: Institute of Agrophysics PAS.
- Mazurek, W., Walczak, R. T., Sobczuk, H. A., and Baranowski, P., 1996. The model investigation of soil water content and soil water potential impact on radiation temperature of meadow plant cover. *Zeszyty Problemowe Postępów Nauk Rolniczych*, **436**, 93–100.
- Mohsenin, N. N., 1986. *Physical Properties of Plant and Animal Materials*, 2nd edn. New York: Gordon and Breach.
- Monteith, J., and Unsworth, M., 2007. *Principles of Environmental Physics*. San Diego: Academic.
- Penman, H. I., 1948. Physics in agriculture. *Journal of Scientific Instruments*, **25**, 425–432.
- Przestalski, S., 2001. Significance of physics in agricultural science (in Polish). *Postępy Nauk Rolniczych*, **3**, 47–56.
- Przestalski, S., 2009. *Elements of Biophysics and Agrophysics (in Polish)*. Wrocław: Wydawnictwo Uniwersytetu Wrocławskiego.
- Pukos, A., 1994. Quantitative descriptions of structural changes in soil and plant material during deformation. *International Agrophysics*, **8**, 103–112.
- Ravenet, J., 1981. Silo problems. *Bulk Solids Handling*, **1**(4), 667–679.
- Raytchev, T., Józefaciuk, G., Sokołowska, Z., and Hajnos, M., 2005a. *Physicochemical Management of Acid Soils Polluted with Heavy Metals*. Lublin: Institute of Agrophysics PAS.
- Raytchev, T., Józefaciuk, G., Sokołowska, Z., and Hajnos, M., 2005b. *Physicochemical Character of Soil Adsorbents*. Lublin: Institute of Agrophysics PAS.
- Russel, R. S., 1977. *Plant Root Systems: Their Function and Interaction with the Soil*. London: McGraw-Hill.
- Sahin, S., and Sumnu, S. G., 2006. *Physical Properties of Foods, Food Science Text Series*. New York: Springer.
- Scott, H. D., 2000. *Soil Physics: Agriculture and Environmental Applications*. Ames: Iowa State University Press.
- Shein, E. V., and Goncharov, V. M., 2000. *Agrophysics (in Russian)*. Feniks: Rostov-on-Don.
- Skierucha, W., and Malicki, M., 2004. *TDR Method for the Measurement of Water Content and Salinity of Porous Media*. Lublin: Institute of Agrophysics PAS.
- Skierucha, W., and Walczak, R. T., 2004. *Monitoring and Modelling the Properties of Soil as Porous Medium: the Role of Soil Use*. Lublin: Institute of Agrophysics PAS.
- Skierucha, W., Walczak, R. T., and Wilczek, A., 2004. *Monitoring Systems for Verification of Mass and Energy Transport Models in Porous Media*. Lublin: Institute of Agrophysics PAS.
- Śląwiński, C., Sobczuk, H., and Walczak, R. T., 1996. Submodel of bypass flow in cracking soils. Part 1 – theory. *International Agrophysics*, **10**, 189–195.
- Śląwiński, C., Witkowska-Walczak, B., and Walczak, R. T., 2004. *Determination of Water Conductivity Coefficient of Soil Porous Media*. Lublin: Institute of Agrophysics PAS.
- Smithson, P., Addison, K., and Atkinson, K., 2002. *Fundaments of the Physical Environment*, 2nd edn. London/New York: Routledge and Hungry Minds.
- Stepniewski, W., Stepniewska, Z., Bennicelli, R., and Gliński, J., 2005. *Oxygenology in Outline*. Lublin: Institute of Agrophysics PAS.
- Szczesniak, A. S., 2002. Texture is a sensory property. *Food Quality and Preference*, **13**, 215–225.
- Szot, B., 1976. Variability of the mechanical properties of cereal plants. *Zeszyty Problemowe Postępów Nauk Rolniczych*, **203**, 17–26.
- Szot, B., Stepniewski, A., and Rudko, T., 2005. *Agophysical Properties of Lentil (Lens culinaris Medik.)*. Lublin: Institute of Agrophysics PAS.
- Szymańek, M., Dobrzański, B., jr, Niedziółka, I., and Rybczyński, R., 2006. *Sweet Corn Harvest and Technology Physical Properties and Quality*. Lublin: Institute of Agrophysics PAS.
- Usowicz, B., and Usowicz, J. B., 2004. *Spatial and Temporal Variation of Selected Physical and Chemical Properties of Soil*. Lublin: Institute of Agrophysics PAS.
- Usowicz, B., Lipiec, J., Marczewski, W., and Ferraro, A., 2006. Thermal conductivity modelling of terrestrial soil media – a comparative study. *Planetary and Space Science*, **54**, 1086–1095.
- van Genuchten, M. Th., 1980. A closed-form equation for predicting hydraulic conductivity of unsaturated soils. *Soil Science Society of America Journal*, **44**, 892–898.
- Walczak, R. T., 1987. Basic problems of mass and energy transfer in the soil-plant-atmosphere system. *Zeszyty Problemowe Postępów Nauk Rolniczych*, **346**, 11–22.
- Walczak, R., 1993. New aspects of agrophysical metrology (in Polish). *Nauka Polska*, **4**, 74–76.
- Walczak, R. T., and Zawadzki, S., 1979. Soil water as a basic factor of the growth and crop field of plants. *Zeszyty Problemowe Postępów Nauk Rolniczych*, **220**(I), 53–59.
- Walczak, R. T., Sobczuk, H., and Śląwiński, C., 1996. Submodel of bypass flow in cracking soils. Part 2 – experimental validation. *International Agrophysics*, **10**, 197–207.
- Walczak, R. T., Witkowska-Walczak, B., and Baranowski, P., 1997. Soil structure parameters in models of crop growth and field prediction. Physical submodels. *International Agrophysics*, **11**, 111–127.

- Warrick, A. W., 2002. *Soil Physics Companion*. Boca Raton: CRC Press.
- Weatherley, D., 2006. *MATH3203 Lecture 1 Mathematical Modeling and ODEs*. Earth Systems Science Computational Centre, University of Queensland, February 27, 2006.
- William, A. J., and Horton, R., 2004. x. Hoboken: Wiley.
- Wischmeier, W. H., and Smith, D. D., 1978. *Predicting rainfall erosion losses. Agricultural Handbook No. 537*. Washington, DC: USDA Agricultural Research Service.
- Witkowska-Walczak, B., Walczak, R., and Ślawiński, C., 2004. *Determination of Water Potential-Moisture Characteristics of Soil Porous Media*. Lublin: Institute of Agrophysics PAS.
- Włodarczyk, T., and Kotowska, U., 2005. *Nitrogen Transformations and Redox Potential Changes in Irrigated Soil*. Lublin: Institute of Agrophysics PAS.

Cross-references

- [Agophysical Objects \(Soils, Plants, Agricultural Products, and Foods\)](#)
[Agophysical Properties and Processes](#)
[Climate Change: Environmental Effects](#)
[Mineral–Organic–Microbial Interactions](#)
[Monitoring Physical Conditions in Agriculture and Environment](#)
[Plant–Soil Interactions, Modeling](#)
[Soil–Plant–Atmosphere Continuum](#)
[Soil–Wheel Interactions](#)

AIR ENTRY VALUE

The value of water content or potential at which air first enters a porous media.

AIR FLUX (RESISTANCE) IN PLANTS AND AGRICULTURAL PRODUCTS

Agnieszka Kaleta, Krzysztof Górnicki
 University of Life Sciences (SGGW), Warszawa, Poland

Synonyms

Airflow–pressure drop relationship; Resistance to airflow

Definition

The resistance, which has to be overcome by air flying through porous media such as plant tissues and a packed bed of plants and agricultural products (e.g., bulk grain), is defined as a pressure drop per unit depth.

When air is forced through a layer of porous materials, resistance to the flow, the so-called pressure drop, develops as a result of energy lost through friction and turbulence. The prediction to airflow resistance is necessary, for example, to the fan selection for grain drying and aeration systems.

Ergun's model is the most comprehensive model to be used for airflow–pressure drop calculations. Ergun assumed that the pressure loss can be treated as the sum of the viscous and kinetic energy losses. The model is

the sum of equation for laminar flow (this term is a linear function of airflow rate) and equation for turbulent flow (this term is a function of v_0^2) and has the following form:

$$\Delta P = 150 \frac{v_0 \mu}{d_e^2} \frac{(1 - \varepsilon)^2}{\varepsilon^3} + 1.75 \frac{\rho v_0^2}{d_e} \frac{(1 - \varepsilon)}{\varepsilon^3} \quad (1)$$

where ΔP is the pressure drop per unit height, v_0 is the superficial velocity, d_e is an equivalent particle diameter, ε is the bulk porosity, μ is the dynamic viscosity of air, and ρ is the air density. The factors that affect the resistance of porous materials to airflow are among others: material porosity, size distribution of particles and pores, irregularity in particles and pores shape, surface roughness characteristics, orientation of the particles, and tortuosity. Such variables are extremely difficult to measure. For this reason, an empirical approach is often used.

Factors in Ergun's model other than airflow can be lumped into two parameters, so the model becomes an equation with the following form:

$$\Delta P = A_1 v_0 + B_1 v_0^2 \quad (2)$$

where A_1 and B_1 are product-dependent constants obtained from the experiment. When the velocity is small enough ($v_0 < 0.01 \text{ m s}^{-1}$), viscous forces dominate the flow and the equation reduces to Darcy's Law ($\Delta P = A_1 v_0$). The Shedd's equation represents the airflow resistance data over an airflow range of $0.005\text{--}0.3 \text{ m s}^{-1}$ and has the following form:

$$\Delta P = A_2 v_0^{B_2} \quad (3)$$

where A_2 and B_2 are product-dependent constants obtained from the experiment. The constant B_2 lying between 1 and 2 is a compromise between the velocity (v_0) and the (v_0^2) terms in Ergun's model. Hukill and Ives' equation:

$$\Delta P = \frac{A_3 v_0^2}{\ln(1 + B_3 v_0)} \quad (4)$$

where A_3 and B_3 are product-dependent constants obtained from the experiment, is valid for airflow range of $0.01\text{--}2.0 \text{ m s}^{-1}$.

Effects of process parameters on the resistance of, for example, bulk grain and seeds to airflow are generally the following: (1) the resistance to airflow decreases with an increase in product moisture content, (2) dense filling results in an increase in pressure drop, (3) the resistance to airflow through a bed of product in the horizontal direction is, in most cases, smaller than in the vertical direction, (iv) a product mixed with foreign materials offers more resistance to airflow than cleaned one.

Further details are given by Smith (1995) and Pabis et al. (1998).

Bibliography

- Pabis, S., Jayas, D. S., and Cenkowski, S., 1998. *Grain Drying: Theory and Practice*. New York: Wiley.
- Smith, E. A., 1995. Forced air distribution for in-bin drying and aeration. In Jayas, D. S., White, N. D. G., and Muir, W. E. (eds.), *Stored-Grain Ecosystems*. New York: Marcel Dekker, pp. 569–607.

Cross-references

- [Aeration of Agricultural Products](#)
[Aeration of Soils and Plants](#)
[Drying of Agricultural Products](#)
[Grains, Aerodynamic and Geometric Features](#)

AIR HUMIDITY

The amount of water vapor within the atmosphere.

AIR POROSITY

A volume of a material (e.g., soil, plant) that is occupied by pore spaces.

ALGAE, THE POTENTIAL SOURCE OF ENERGY

Magdalena Frac
 Department of Plant and Soil System, Institute of Agrophysics Polish Academy of Sciences, Lublin, Poland

Definition

Algae are a large and diverse group of simple photosynthetic microorganisms. They live in different environments: such as water, soil, but also on snow, and on ice. Algae are very sensitive to different factors, so they can be used as biological and pollution indicators. Algae are useful as fertilizer, important source of food – especially in Asia – and in bioremediation applications. They contain very important chemical compounds, so can be used in industry, especially for cosmetics and pharmaceuticals.

In aspect of the potential energy source, microalgae are sunlight-driven cells that convert carbon dioxide to potential biofuels and high-value bioactivities. Microalgal biomass contains three main compounds: carbohydrates, protein, and natural oils and can provide several different types of renewable biofuels:

- Methane produced by anaerobic digestion of the algal biomass
- Biodiesel derived from microalgal oil
- Ethanol produced by fermentation
- Photobiologically produced biohydrogen

Economics of the fuel production from algae demands that all the biomass is utilized as efficiently as possible. The most simplistic method is methane gas production. Biological and thermal processes are involved in gasification of organic carbon into methane. Ethanol production is most effective for conversion of the carbohydrate fraction. Biodiesel production applies to the natural oil fraction.

The idea of using microalgae as a source of fuel is not new, but it is being taken seriously because of the escalating price of petroleum. The production of microalgal biomass is carried out in closed photobioreactors or in open ponds. Closed photobioreactors have the benefits of better control over environmental conditions (pH, temperature) and biological contaminants and higher cell concentrations.

Bibliography

- Chisti, Y., 2007. Biodiesel from microalgae. *Biotechnology Advances*, **25**, 294–306.
- Miao, X., and Wu, Q., 2006. Biodiesel production from heterotrophic microalgal oil. *Bioresource Technology*, **97**, 841–846.

ALKALINITY, PHYSICAL EFFECTS ON SOILS

Lajos Blaskó
 Karcag Research Institute of Centre for Agricultural and Technical Sciences, Debrecen University, Karcag, Hungary

Synonyms

Basicity; Sodicity

Definition

Alkali or *alkaline soils* have been defined as soils with high pH-value, which is caused by excessive (usually more than 15% of the exchange sites) amount of exchangeable sodium ions or/and soluble salts capable of alkaline hydrolysis. The most injurious alkaline sodium compounds in the soils and irrigation waters are Na_2CO_3 (sodium carbonate) or NaHCO_3 (sodium bicarbonate).

Introduction

Natural and man-induced salt accumulation in the soil profile is a major environmental threat with dramatic negative impacts on agricultural production and sustainability, especially in the arid and semiarid regions of the world.

Alkalinity problems are more common in clay soils than in soils with low colloid content. As a consequence of the relative preponderance of sodium on exchange sites of colloids, the alkaline reaction of the liquid phase and the swelling/shrinking clay minerals, the low fertility of these salt-affected soils, in most cases, are closely related to their unfavorable physical and hydrophysical properties and their extreme moisture regime (Várallyay, 1981).

The sustainable use and management require adequate understanding of the processes causing structural, water regime, and water transport problems of these soils.

Indicators of alkalinity

Exchangeable sodium percentage is for characterizing the relative ratio of sodium in the exchangeable cation complex (ESP). It is defined as

- $\text{ESP} = (\text{exchangeable Na} \times 100 / \text{cation exchange capacity})$
- $\text{ESP} = (\text{exchangeable Na} \times 100 / \Sigma (\text{exchangeable Ca} + \text{Mg} + \text{K} + \text{Na}))$

The exchangeable cations and the exchange capacity are expressed in milliequivalent per 100 g.

The sodium adsorption ratio (SAR) is for characterizing the sodicity of the soil solution or applied irrigation water. It is defined as

$$\text{SAR} = [\text{Na}^+] / ([\text{Ca}^{2+}] + [\text{Mg}^{2+}])^{1/2}$$

The cations in liquid phase of soil or in irrigation water are expressed in milliequivalent per liter.

Besides the widely used alkalinity indicators, the direct determination of soda alkalinity (Soda%) is used for the examination and the qualification of salt-affected soils containing considerable amounts of salts capable of alkaline hydrolysis. The determination is carried out with a suspension of soil in distilled water. The suspension is titrated with 0.1M KHSO_4 till the red color of phenolphthalein disappears. The pH-value can also be an indirect indicator of sodicity. The finely dispersed calcium carbonate may cause slight phenolphthalein alkalinity up to pH 8.5, and above this value, the alkalinity is probably caused by sodium carbonate or bicarbonate (Darab and Ferencz, 1969).

Change of soil physical properties under the influence of alkalinity/sodicity

The influence of sodicity on physical properties varies with clay content and clay mineralogy. In soils with higher content of swelling/shrinking clay minerals, lower exchangeable sodium percentage (ESP) or soda content can cause a more significant physical effect (Shaw and Thorburn, 1985; Várallyay, 1981).

Soil structure properties

There is a general agreement among the soil scientists, that spontaneous clay dispersion and swelling are the major factors that disintegrate the structure of sodic soils.

The increasing dispersion and swelling of bentonite caused by sodium carbonate solution was demonstrated in laboratory experiments (Darab and Ferencz, 1969; Szabolcs et al., 1969). An important conclusion of these experiments is that swelling reached its maximum at a relatively low concentration of sodium carbonate (0.1% m/m), while at a higher concentration it assumed a nearly constant lower value.

The effect of increasing alkalinity (pH) or Sodium Adsorption Ratio (SAR) on clay dispersion was confirmed by several experiments (Chen and Banin, 1975; Frenkel et al., 1978; Bauder and Brock, 2001). While there is an agreement on dispersive effect of sodium on clay minerals, the combined effect of organic material and ESP on the dispersion of clay has been the subject of discussion. Emerson (1954) demonstrated the dispersive effect of organic material in soils with high ESP. Oades (1984) explained the dispersive effect of organic colloids by decreasing the activity of calcium through complexation, and by increasing the negative charge on soil colloids. There are several positive results of experiments where organic materials such as green manure or compost have been used to improve the structure of sodic soils (Chand et al., 1977; Robbins, 1986; Singh and Singh, 1989; Barzegar et al., 1997). Solving this problem needs further researches because of the contradictory results regarding the effect of organic colloids on clay dispersion.

McNeal (1968) revealed that the swelling of soil colloids can be evaluated as an opposite effect of ESP and the salt concentration of the soil solution (EC). The increase of ESP or the decrease of EC causes the increase of the swelling factor. The effect of sodium salt is double. As electrolytes, the neutral sodium salts (NaCl , Na_2SO_4) coagulate the colloids. However as an exchangeable cation, sodium tends to favor dispersion. For the simultaneous evaluation of effect of sodicity and salinity the electrochemical stability index (ESI) was developed. ESI has been suggested as a good measure of dispersive behavior of soils (Hulugalle and Finlay, 2003).

We have only a few data relating to the direct measuring of the change in the pore volume and its distribution under the influence of increasing alkalinity.

Józefaciuk et al. (2002) investigated the effect of alkalization on the pore properties of the soil with sodium hydroxide solution of increasing concentration from 0.001 to 1 mol dm^{-3} . The macropore volume and radius, in general, increased with the increasing alkali concentrations. The mesopore volume in most cases decreased due to the treatments. In general, the average mesopore radius increased under lower concentrations of sodium hydroxide and decreased under higher concentrations.

Lebron et al. (2002) using thin-section-techniques established that the area of the aggregates decreased steeply in the ESP range of 0–5. In the ESP range of 6–55, the area of the aggregates did not change.

Várallyay (1981) investigated the effect of Na_2CO_3 on the water retention of soil. Due to the effect of Na_2CO_3 , the water retention increased with the increasing alkali concentration within the whole suction range. The available moisture range (AMR) – calculated as the difference between the field capacity and the permanent wilting point – increased with the higher ESP values. From the results he concluded that in such cases the main limiting factor of the availability of water is not the low AMR, but the limited water transport.

Transport processes in soils

Surface sealing and crusting are the first impeding factors of water infiltration into the soil. Soil crusting is related to soil texture, organic matter, and sodium content. In arid and semiarid regions, the presence of crusted salt and sodium-affected soils is very common (Bauder and Brock, 1992).

There are several studies in which the decrease of saturated hydraulic conductivity (K) has been related to the increasing Na content (McNeal and Coleman, 1966; Frenkel et al., 1978; Várallyay, 1981; Shainberg and Letey, 1984; Suarez et al., 1984).

Lebron et al. (2002) measured a steep decrease of hydraulic conductivity in the ESP range of 0–5, over this ESP range the hydraulic conductivity did not change. Crescimanno et al. (1995) pointed out that could not be defined a critical ESP threshold relating to the effect of ESP on water transport properties, since there were an almost linear relationships between the soil physical properties and the ESP.

Várallyay (1981) measured the influence of Na_2CO_3 on the unsaturated water conductivity of the soil. The influence of Na_2CO_3 was stronger in the low suction range. The influence of Na_2CO_3 solution decreased with the increasing suction.

Rajkai et al. (1993) measured by means of tension infiltrometer much lower hydraulic conductivity on soil with ESP 15 than on soil with ESP 2 in case of similar clay content. In line with Várallyay's result, the water conductivity difference between sodic and non-sodic soil was higher at low than at high tension.

Consequently it can be established that infiltration and leaching (wet condition, low gradient) are more limited than the upward capillary flow (dry conditions, high gradient) promoting the salt and sodium accumulations in these soils in case of a shallow, saline groundwater.

There are only a few data relating to the effect of alkalinity on gas transport in soils. Stępniewski et al. (1992) measured the oxygen diffusion coefficient and air permeability at different moisture tension of clay soils and at different exchangeable sodium content. These aeration-related soil properties were much worse in the natic B, than in the A horizon. However, an exact quantifying of the relationship between alkalinity and aeration properties needs much more data.

Conclusions

Alkalinity indicates very unfavorable physical properties of soils, especially in soils with high smectite-type clay content. The alkaline pH range and the ESP cause increasing dispersion and swelling of clay minerals. The role of organic colloids in the dispersion processes is not fully clarified. The structural deterioration in sodic soils causes a very limited water transport in the matrix of the wet soil. Salt accumulation can hardly be reversed due to the limited leaching in wet state of the soil. To the contrary, an accelerated bypass water movement can occur in dry state

of the sodic soil due to crack formation. The structural and water movement properties of sodic soils are intensively investigated, but clarifying of some special transport properties (i.e., transport through the cracks and soil aeration properties) needs further researches.

Bibliography

- Barzegar, A. R., Nelson, P. N., Oades, J. M., and Rengasamy, P., 1997. Organic matter, sodicity, and clay type: influence on soil aggregation. *Soil Science Society of America Journal*, **61**, 1131–1137.
- Bauder, J. W., and Brock, T. A., 1992. Crops species, amendment, and water quality effects on selected soil physical properties. *Soil Science Society of America Journal*, **56**, 1292–1298.
- Bauder, J. W., and Brock, T. A., 2001. Irrigation water quality, soil amendment, and crop effects on sodium leaching. *Arid Land Research and Management*, **15**, 101–113.
- Chand, M., Abrol, I. P., and Bhumbra, D. R., 1977. A comparison of the effect of eight amendments on soil properties and crop growth in a highly sodic. *Indian Journal of Agricultural Science*, **47**, 348–354.
- Chen, Y., and Banin, A., 1975. Scanning electron microscope (SEM) observations of soil structure changes induced by sodium calcium exchange in relation to hydraulic conductivity. *Soil Science Society of America Journal*, **120**, 428–436.
- Crescimanno, G., Iovino, M., and Provenzano, G., 1995. Influence of salinity and sodicity on soil structural and hydraulic characteristics. *Soil Science Society of America Journal*, **59**, 1701–1708.
- Darab, K., and Ferencz, K., 1969. *Soil Mapping and Control of Irrigated Areas*. (in Hungarian), Budapest: OMMI.
- Emerson, W. W., 1954. The determination of the stability of soil crumbs. *Journal of Soil Science*, **5**, 235–250.
- Frenkel, H., Goertzen, J. O., and Rhoades, J. D., 1978. Effects of clay type and content, exchangeable sodium percentage, and electrolyte concentration on clay dispersion and soil hydraulic conductivity. *Soil Science Society of America Journal*, **42**, 32–39.
- Hulugalle, N. R., and Finlay, L. A., 2003. EC1:5/exchangeable Na, a sodicity index for cotton farming systems in irrigated and rainfed Vertosols. *Australian Journal of Soil Research*, **41**, 761–769.
- Józefaciuk, G., Hoffmann, C., and Marschner, B., 2002. Effect of extreme acid and alkali treatment on pore properties of soil samples. *Journal of Plant Nutrition and Soil Science*, **165**, 59–66.
- Lebron, I., Suarez, D. L., and Yoshida, T., 2002. Gypsum effect on the aggregate size and geometry of three sodic soils under reclamation. *Soil Science Society of America Journal*, **66**, 92–98.
- McNeal, B. L., 1968. Prediction of the effect of mixed salt solutions on soil hydraulic conductivity. *Soil Science Society of America Journal*, **31**, 190–193.
- McNeal, B. L., and Coleman, N. T., 1966. Effect of solution composition on soil hydraulic conductivity. *Soil Science Society of America Proceedings*, **30**, 308–312.
- Oades, J. M., 1984. Soil organic matter and structural stability: mechanism and implication for management. *Plant and Soil*, **76**, 319–334.
- Rajkai, K., Zsembeli, J., Blaskó, L., and Várallyay, G., 1993. Use of tension infiltrometer and water retention characteristics in the assessment of soil structure. *International Agrophysics*, **7**, 141–154.
- Robbins, C. W., 1986. Sodic calcareous soil reclamation as affected by different amendments and crops. *Agroomy Journal*, **78**, 916–920.
- Shainberg, I., and Letey, J., 1984. Response of soils to sodic and saline conditions. *Hilgardia*, **61**, 21–57.

- Shaw, R. J., and Thorburn, P. J., 1985. Towards a quantitative assessment of water quality for irrigation. In Planning and management of water for agriculture in the tropics. *Fifth Afro-Asian Regional Conference*, Townsville: ICID (International Commission on Irrigation and Drainage), pp. 41–52.
- Singh, M. V., and Singh, K. N., 1989. Reclamation techniques for improvement of sodic soils and crop yield. *Indian Journal of Agricultural Science*, **59**, 495–500.
- Stepniewski, W., Stepniewska, Z., Włodarczyk, T., and Brzezińska, M., 1992. Aeration related properties of six soil profile from Hungary. Final report in the framework of multilateral project of cooperation between Austria–Czecho-Slovakia–Hungary–Poland entitled: *Assessment of Soil Structure in Agricultural Soils*.
- Suarez, D. L., Rhoades, J. D., Lavado, R., and Grieve, C. M., 1984. Effect of pH on saturated hydraulic conductivity and soil dispersion. *Soil Science Society of America Journal*, **48**, 50–55.
- Szabolcs, I., Darab, K., and Várallyay, G., 1969. Methods of predicting salinization and alkalinization processes due to irrigation on the Hungarian Plain. *Agrokémia és Talajtan*, **18**(Suppl.), 351–376.
- Várallyay, G., 1981. Extreme moisture regime as the main limiting factors of the fertility of salt affected soils. *Agrokémia és Talajtan*, **30**, 73–96.

Cross-references

- Aeration of Soils and Plants
 Liming, Effects on Soil Properties
 Shrinkage and Swelling Phenomena in Soils
 Soil Aggregates, Structure, and Stability
 Soil Hydraulic Properties Affecting Root Water Uptake
 Soil Structure and Mechanical Strength
 Soil Structure, Intersecting Surface Approach, and its Applications
 Soil Surface Sealing and Crusting
 Solute Transport in Soils

ALTERNATIVE SOURCES OF ENERGY FROM AGRICULTURE BIOMASS – A EUROPEAN PERSPECTIVE

Piotr Kowalik
 Department of Sanitary Engineering, Gdańsk University of Technology, Gdańsk, Pommerania, Poland

Introduction

Energy is the capacity of a physical system to perform work. Energy appears in many different forms, including chemical energy of fuels, heat, mechanical energy, and electricity, among others. These are related by the fact that conversion can be made from one type of energy to another.

Biomass is a renewable energy resource in the form of solid, liquid, or gas energy carriers. Solid biomass is used mainly for heat, liquid biomass for transport, and gas for electricity production. Biomass is regenerated by energy from the sun and through societal metabolism. In this context, biomass is material originating from vegetation (wood, straw, lignin liquid waste as black liquor, waste paper), from animals (municipal sewage sludge, manure,

dung), and from substances that produce biogas (from anaerobic digestion of manure, sewage sludge, or organic solid waste on the sanitary landfills), bioethanol (from alcoholic fermentation of potatoes or crops), or pyrolytic gas (produced from wood or sewage sludge).

Organic waste material originating from animal metabolism may include biogas from the anaerobic digestion of animal manure or dung, biogas from anaerobic fermentation of sewage sludge in wastewater treatment plants, or biogas from anaerobic digestion of waste on the sanitary landfills. Organic material may be transformed into pyrolytic gas (mainly during the process of gasification of wood), and this pyrolytic gas may drive gas engines for electricity production or may be used in gas boilers for heat production.

Biomass is accumulated mainly in the place of production or processing of the plant material (e.g., surplus straw during the production of grain, waste wood in timber processing, and pulp in the paper industry), or it may be the plant material produced only for purpose of energy, for example, on the fast-growing, short-rotation tree plantations of selected poplar or willow clones.

Biomass is divided into two types of resources:

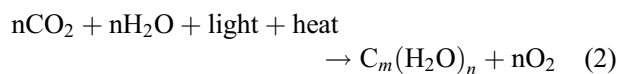
- Primary energy resources, including wood, straw, and sewage sludge (analogous to peat).
- Second-generation biomass that is a processed energy resource, upgraded into the form of biocarbon, biogas, bioethanol, biohydrogen, and pyrolytic gas.

Energy from photosynthesis

Plants have the ability to incorporate atmospheric carbon into biomass through photosynthesis. These molecules can then be used for fuel. This process is roughly exemplified by the following equation:



where PAR is the photosynthetic active radiation (visible light) and 8 quantum of light is needed for transformation of 1 atom of C. The equation takes the form:



The first “block” in building the biomass of plants is glucose, $\text{C}_6\text{H}_{12}\text{O}_6$ ($m = n = 6$), followed by more complex substances like polysaccharides ($m = n = \text{tens/thousands}$), cellulose ($m > n = \text{hundreds/thousands}$), and lignin ($m < n = \text{hundreds/thousands}$).

In the past, black coal $(\text{CH}_2)_n$ was derived from biomass, but today, biogas $(\text{CH}_4)_n$, methanol $(\text{CH}_3\text{OH})_n$, and biohydrogen (H_2) are derived. About 2 Mg of dry wood or straw are equivalent of the energetic value of 1 Mg of black coal. A fossil fuel like black coal has the parameters 25/22/0.8 (25 MJ/kg, 22% ash, 0.8% sulfur), but biomass from plant material (wood or straw) has the parameters 13/3/0.03. Dry sewage sludge has the parameters 14/45/0.8, which is similar to the contents of the coal

waste mud produced during the process of washing of black coal or to the contents of low-quality lignite (brown coal) or dry peat. But in energy production such a material may be utilized, meaning that coal waste mud, low-quality lignite, peat, or dry sewage sludge are considered an energy resource in local solutions.

Energy crops

Energy crops can take many forms and can be converted to a number of different products (Canell, 2003; Sims et al., 2006). Many crop species are multipurpose in that they can be used to produce more than one type of energy product like oil, ethanol, and solid biomass, and they are classified as follows:

1. Oil crops (e.g., rapeseed, linseed, field mustard, hemp) – Vegetable oils can be used directly as heating fuel or refined into transport biofuels such as biodiesel esters.
2. Cereals (e.g., barley, wheat, oats, maize, rye, triticosecale) – Grain can be used to produce ethanol and the straw can be used as a solid fuel (after pelleting, if possible), or for biogas production from feedstock.
3. Starch and sugar crops (e.g., potato, sugar beets, Jerusalem artichoke) – Ethanol can be produced by fermentation, and then is used mainly in blends with gasoline.
4. Cellulose crops (e.g., straw, grass, wood, short-rotation coppice) – The hemicellulose can be reduced to sugar by acid or enzymatic hydrolysis and then fermented to produce ethanol in blends with gasoline or biogas (to produce electricity).
5. Solid energy crops (e.g., whole-crop maize, reed canary grass, silvergrass, willow, poplar) – These crops can be utilized as a whole to produce heat and electricity directly through combustion or indirectly through conversion for use as biofuels like methanol or ethanol.

Such classifications are very useful in the evaluation of the recent biomass market.

In agriculture, solid biomass can be produced from traditional crops like the straw of wheat, rye, or rapeseed, and from grasses. In the timber industry, sawdust and wood chips and shavings are used for biomass (wood used for fuel is usually smaller branches of trees and low-quality timber). From agribusiness, mill cake, brewery grains, pomace of apples, bagasse, beet pulp, fruit stones, husks, molasses, paper, and pulp residues can be obtained.

More than 350 oil-bearing crops have been identified (Demirbas, 2007). Vegetable oils can be used directly or refined to biodiesel. The cereal grains can be used to produce ethanol, and straw can be used as a solid fuel. Sugar and cellulose crops can produce ethanol by fermentation, which is then either used directly or blended with fossil oil. Solid energy crops can be utilized only indirectly through conversion to biofuels. Some of the more common energy crops have been listed by Sims et al. (2006) and Tuck et al. (2006). Discussed here are crops already being grown in Europe or those, although allochthonous,

with potentially high bioenergetic performances. Energy crops are annual and perennial plants, herbaceous or arborescent. Annual crops are mainly cereals or oilseed crucifers of the genus *Brassica*. Less important in terms of cultivated hectares in the EU are sugar beet (*Beta vulgaris* var. *saccharifera*), soybean, hemp, and flax. Perennial crops are herbaceous (e.g., silvergrass, Jerusalem artichoke, giant knotweed), shrubs (e.g., *Rosa multiflora*), or trees (e.g., willow *Salix spp.*, poplar *Populus spp.*, black locust *Robinia pseudoacacia*).

Biomass as a liquid transport biofuel in the form of oil or ethanol is very common. Two technologies exist on the market today. The first is the production of esters from rapeseed oil, creating so-called biodiesel. The second is the production of alcohol in the form of dewatered bioethanol mixed with ordinary gasoline (3.5% bioethanol, 96.5% gasoline) and distributed in the gasoline stations.

Liquid biofuels are produced from crops rich in oil, sugar, or starch. First-generation biofuels were produced as bioethanol from fermentation of maize or potatoes, or as the vegetation oils from rapeseed or soybean. Bioethanol with oil can be used to produce biodiesel, an ester of oils. The second-generation production of bioethanol is based on perennial plants (Reddy et al., 2008) such as switchgrass and silvergrass – these can provide 260% more ethanol per hectare than maize (Heaton et al., 2008) – or microalgae (Schenk et al., 2008) (see *Algae, the Potential Source of Energy*). The global yield for all biomass crops (both herbaceous and woody) ranges from 8 to 22 Mg of dry matter per hectare per year (Ragauskas et al., 2006).

The second generation of biofuels is biogas and biohydrogen. Biogas may be produced by anaerobic digestion in sewage sludge, animal manure, or solid waste dumps.

Biomass for energy in the European Union

According to terminology introduced in the European Union (Grassi et al., 1992; THERMIE, 1995), biomass includes all organic material of biological origin (mainly from vegetation), which may be produced on special energy plantations, or may come from the residues and waste products of forestry, timber production, municipalities, agriculture, and agribusiness (mainly the food-processing industry).

The sources of biomass in the European Union are wood from the fast-growing tree plantations, wood residues from forestry and timber production, manure and dung from animal production, straw produced along with grain, and organic waste in agribusiness during food processing. Organic material in the sewage sludge produced in the municipal wastewater treatment plants is also considered to be biomass. The producers of biomass for energy are agriculture (straw, biogas from animal manure), the forestry and wood processing industry (solid fuel wood), municipalities (waste paper, biogas from the sanitary landfills, or biogas from the wastewater treatment

plants), or industry (residues from the paper and pulp industry, textile industry, food processing industry, etc.).

In the European Union, biomass has been identified as a vast potential reservoir of energy, comprising various organic raw materials of plant origin: forestry production, specific crops, and recycled agricultural, industrial, and household waste. Worldwide, it represents the fourth biggest energy resource (14% of global consumption) (see *Biomass as an Environmentally Benign Energy Source*). However, apart from Austria, Finland, and Sweden, where it plays a significant role, biomass accounts for only 2% of Europe's energy production. Biomass energy can be stored and does not fluctuate, and it has numerous advantages. It is neutral in terms of the greenhouse effect when used for electricity; plants give off the carbon dioxide that they took in while they were growing. A robust biomass industry has considerable potential for job creation and would provide a rationale for developing a common agricultural policy (European Commission, 2006, 2007).

Various European research projects involving conversion technologies (thermochemical, chemical, and biological processes) offer potential for diverse end-users, either as a source of heat and power or in the form of biofuels. Nevertheless, there are logistical problems involved in processing the large volumes of raw materials required to obtain sufficient and economical energy sources. At present, the cost of the energy produced is too high for many applications.

Oilseeds, cereals, starch crops, and solid biofuels will probably increase their growth in northern Europe by 2080, due to increasing temperatures, and will decrease in southern Europe due to increased drought (Tuck et al., 2006). These predictions indicate that the choice of bioenergy crops in southern Europe will be severely reduced in the future unless measures are taken to adapt to climate change.

Conclusion

Barriers to the use of biomass as an energy resource exist, including:

1. Lack of knowledge that the production of heat energy and electricity from cheap residual biomass is very economical and easily competes with conventional fossil fuels.
2. Low prices of conventional fossil fuels that don't account for the negative effects of coal, oil, and natural gas on the environment and human health.
3. Slow progress in the technological development of the most efficient production of heat and power from biomass.
4. Difficulties with the distributing the produced biogas or heat energy and electricity to the state-controlled gas pipe grid or electrical grid or to the district heating distribution pipes.
5. Lack of experience in implementing renewable energy in local energy plans for communities. The dissemination of knowledge about existing pilot programs

and demonstration solutions is important. Until now, there have been a limited number of the success stories and positive solutions, but in the future there will be more examples of installations and commercial applications.

Production of heat and power from biomass is very promising if we take into account the existing positive demonstration plants. Biomass is much more environmentally friendly than any fossil fuel. The technical parameters of the boilers, the positive economical results and relatively short time to payback on investment, and the ecological benefits due to the low level of emission of pollutants into the atmosphere support the increased use of biomass as an energy source.

Bibliography

- Canell, M., 2003. Carbon sequestration and biomass energy offset: theoretical, potential and achievable capacities globally, in Europe and the UK. *Biomass Bioenergy*, **24**, 97–116.
- Demirbas, S. A., 2007. Importance of biodiesel as transportation fuel. *Energy Policy*, **35**, 4661–4670.
- European Commission, 2006. *Renewable Energy Road Map – Renewable Energies in the 21st Century – Building a More Sustainable Future*. EU COM (2006) 848 (final).
- European Commission, 2007. *Biofuels Progress Report – Report on the Progress Made in the Use of Biofuels and Other Renewable Fuels in the Member States of the European Union*. Brussels: Commission of the European Communities.
- Grassi, G., Trebbi, G., and Pike, D. C. (eds.), 1992. *Electricity from biomass*. Newbury, Berkshire: CPL Press.
- Heaton, E. A., Dohleman, F. G., and Long, S. P., 2008. Meeting US biofuel goals with less land: the potential of Miscanthus. *Global Change Biology*, **14**, 2000–2014.
- Ragauskas, A. J., Williams, C. K., Davidson, B. H., Britoske, G., Cairney, J., Eckert, C. A., Frederick, W. J., Hallett, J. P., Leak, D. J., Liotta, C. L., and Tschaplinski, T., 2006. The path forward for biofuels and biomaterials. *Science*, **311**, 484–489.
- Reddy, B. V. S., Kumar, A. A., Wani, S. P., and Sreedevi, T. K., 2008. *Bio-fuel crops research for energy security and rural development in Developing Countries*. Bioenergy Research. doi:10.1007/s12155-008-9022-x.
- Schenk, P. M., Thomas-Hall, S. R., Stephens, E., Marx, U. C., Mussgnug, J. H., Posten, C., Kruse, O., and Hankamer, B., 2008. Second generation biofuels: high-efficiency microalgae for biodiesel production. *Bioenergy Research*, **1**, 20–43.
- Sims, R. E. H., Hastings, A., Schlamadinger, B., Taylor, G., and Smith, P., 2006. Energy crops: current status and future prospects. *Global Change Biology*, **12**, 2054–2076.
- THERMIE, 1995. *Energy from biomass, principles and applications. A THERMIE Programme Action, RES, European Commission, Directorate General for Energy (DGXyII)*. Madrid: IDAE, p. 25.
- Tuck, G., Glendining, M. J., Smith, P., House, J. I., and Wattenbach, M., 2006. The potential distribution of bioenergy crops in Europe under present and future climate. *Biomass Bioenergy*, **30**, 187–197.

Cross-references

- [Agroforestry Systems, Effects on Water Balance in Cropping Zone](#)
[Algae, the Potential Source of Energy](#)
[Biomass as an Environmentally Benign Energy Source](#)

ALUMINO-SILICATE CLAY MINERALS

Clay minerals in which the crystal lattice typically consists of alternating layers of alumina and silica ions in association with oxygen atoms or hydroxide ions. Particles of such minerals typically exhibit negative surface charges, which are usually countered by adsorbed (exchangeable) cations.

Bibliography

Introduction to Environmental Soil Physics (First Edition). 2003. Elsevier Inc. Daniel Hillel (ed.) <http://www.sciencedirect.com/science/book/9780123486554>

Cross-references

[Clay Minerals and Organo-Mineral Associates](#)

ANAEROBIOSIS

Occurring in the absence of molecular oxygen. (I) Growing in the absence of molecular oxygen (such as anaerobic bacteria). (III) in the absence of molecular oxygen (as a biochemical process).

Cross-references

[Aeration of Soils and Plants](#)

[Oxidation-Reduction Reactions in the Environment](#)

ANGLE OF REPOSE

The maximum angle the inclined surface of a cohesionless material can make with the horizontal.

ANION EXCHANGE CAPACITY

The total exchangeable anions that the soil can adsorb.

Cross-references

[Surface Properties and Related Phenomena in Soils and Plants](#)

ANISOTROPY OF SOIL PHYSICAL PROPERTIES

Xinhua Peng
Institute of Soil Science, Chinese Academy of Sciences,
Nanjing, P.R. China

Definition

Anisotropy is the property of being directionally dependent, as opposed to *isotropy*, which means homogeneity

in all directions. It can be defined as a difference in one soil physical property along different directions.

Anisotropic soil does not have the same physical properties when the direction of measurement is changed. Commonly it is used in reference to soil structure, soil strength, and soil permeability changes with direction of measurement.

Causes

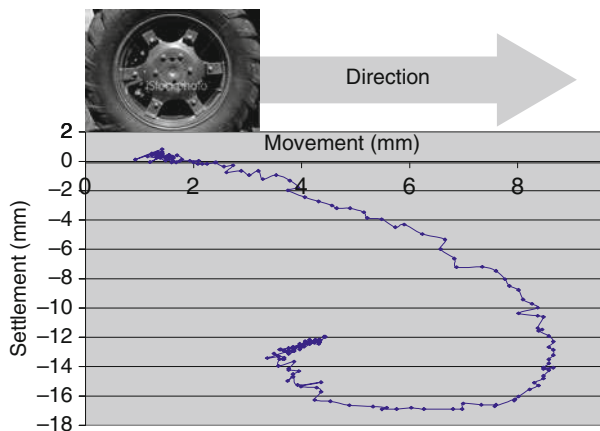
The anisotropy of soil physical properties may be primarily derived from natural pedogenesis. Due to the weathering of rock materials and the input of organic matter into soils, soil profiles can be, in general, defined as a humus-enriched mineral horizon (A), a leached horizon (E), an accumulated horizon (B), and a parent material horizon (C) from the topsoil downward to the less-weathered underlying material. The horizontal layers contain directly dependent soil properties. Human activity may be the secondary factor. Tillage creates a plow layer and a plow pan, which both exaggerate the predominantly horizontal-dependent soil properties. Soil cracks induced by soil shrinkage and swelling and biochannels may be another cause for a vertical-dependent soil structure and the permeability of gas and water. Soil physical properties, which are anisotropic, include soil structure (Pagliai et al., 2004; Dörner and Horn, 2006), soil strength (Peng and Horn, 2008), soil shrinkage and swelling (Bronswijk, 1990; Peng and Horn, 2007), and soil permeability of gas and water (Mualem, 1984; Dabney and Selim, 1987; Dörner and Horn, 2006), and so on. These properties, however, are further interacted each other. For example, the anisotropy of soil structure may result in the directionally dependent soil strength, soil permeability, and soil shrinkage and swelling.

Soil structure

Hydraulic stress by natural wetting and drying cycles and mechanical stress by human tillage management always propagate three-dimensionally through the solid, liquid, and gaseous phases and result in a rearrangement of aggregates, their reformation, or complete destruction. In such case, the stress propagation is linked to an alteration of pore structure and excess soil water is drained off. During the natural wetting and drying cycles, new aggregate formation always starts with a prismatic structure of strongly vertically anisotropic behavior, later followed by a polyhedral and subangular blocky structure with a slight vertical anisotropic to isotropic behavior (Hillel, 1998; Horn et al., 2003). But, after tillage compaction, a platy structure can be formed (Pagliai et al., 2004; Dörner and Horn, 2006).

Soil strength

Mechanical stress from tractor wheeling causes a “kneading effect” of tires, which furthermore enhances an anisotropic soil structure (Figure 1). Aggregates or particles simultaneously move forward and downward. Therefore, the responses of pore structure and soil strength



Anisotropy of Soil Physical Properties, Figure 1 Particles move forward and downward simultaneously during tractor tire running.

to tractor wheeling resulted in anisotropic soil properties. Peng and Horn (2008) reported that agricultural machinery caused soil strength to be more anisotropic in conservation tillage than in conventional tillage.

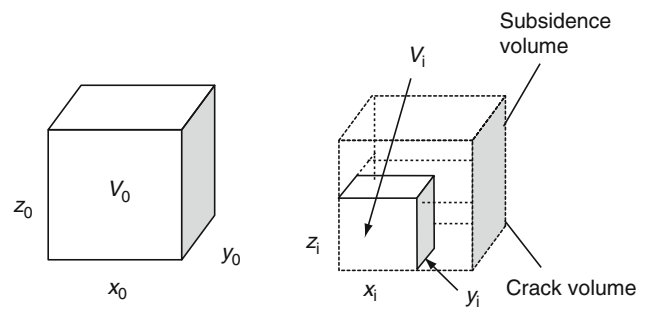
Soil shrinkage/swelling

The anisotropy between the vertical and horizontal deformations during shrinkage and swelling was described by Bronswijk (1990) with the dimensionless geometry factor (Figure 2), r_s , defined by

$$r_s = \ln \frac{V_i}{V_0} / \ln \frac{z_i}{z_0} \quad (1)$$

where V and z are the volume and height of the soil, with the subscript 0 being the initial conditions and subscript i representing the i th step. There are five cases to describe their relationships: (1) $r_s = 1.0$, only vertical deformation; (2) $1.0 < r_s < 3.0$, predominant vertical deformation; (3) $r_s = 3.0$, isotropic deformation; (4) $r_s > 3.0$, predominant horizontal deformation; (5) $r_s \rightarrow \infty$, only horizontal deformation.

Based on the geometry factor, the anisotropy of shrinkage and swelling, increased with water loss and decreased upon wetting (Garnier et al., 1997; Chertkov et al., 2004; Peng and Horn, 2007). A conceptual model about the anisotropy of shrinkage and swelling was proposed by Peng and Horn (2007). At the beginning of drying, water is first drained from macropores by gravity, resulting in a small capillary pressure. The geometry factor shows only vertical shrinkage. As the soil dries further, water is removed from finer pores, causing greater capillary stress and both horizontal and vertical shrinkages. Vertical shrinkage dominates until the soil is dried intensively and only part of the very fine micropores still contains water. At this stage, the heterogeneous distribution of water preferably within soil aggregates and electrostatic attraction produces highly



Anisotropy of Soil Physical Properties, Figure 2 Volume change in vertical and horizontal direction by soil shrinkage.

consolidated platy units. Due to the stress history on the soil the horizontal shrinkage becomes dominant instead of vertical shrinkage, while r_s is a little larger than 3. During swelling, however, the impact of overburden stress on vertical swelling results in the geometry factors exceeding 3.0 during the whole wetting process. At the beginning of wetting, the previously oriented platy soil particles, caused by the shrinkage history, produce the geometry factor greatly exceeding 3.0. If we evaluate the alteration of soil structure during wetting and drying, the shrinkage and swelling processes should be isolated.

Soil permeability

One of the consequences of anisotropic soil structure is a directly dependent permeability of gas and water. Earthworm and roots channels in the plowed layer both cause a preferential flux in a vertical direction (Wiermann et al., 2000; Peng and Horn, 2008). Vertical soil cracks also lead to a vertical predominance of soil permeability, whereas platy soil structure compacted by agricultural machinery induces a mainly horizontal flux (Dörner and Horn, 2006; Horn et al., 2003; Pagliai et al., 2004).

Summary

Anisotropy of soil structure induced either by pedogenesis or by human activity is a basic soil property in nature. However, its consequences have not yet received much attention, particularly when modeling the permeability of gas and water it is often simplified as isotropic. The concept and principle of anisotropic soil physical properties will improve our understanding of dynamic of soil structure and permeability and soil sustainable agricultural management.

Bibliography

- Bronswijk, J. J. B., 1990. Shrinkage geometry of a heavy clay soil at various stresses. *Soil Science Society of America Journal*, **54**, 1500–1502.
- Chertkov, V. Y., Ravina, I., and Zadoenko, V., 2004. An approach for estimating the shrinkage geometry factor at a moisture content. *Soil Science Society of America Journal*, **68**, 1807–1817.

- Dabney, S. M., and Selim, H. M., 1987. Anisotropy of a fragipan soil: vertical vs. horizontal hydraulic conductivity. *Soil Science Society of America Journal*, **51**, 3–6.
- Dörner, J., and Horn, R., 2006. Anisotropy of pore functions in structured Stagnic Luvisols in the Weichselian moraine region in N Germany. *Journal of Plant Nutrition and Soil Science*, **169**, 213–220.
- Garnier, P., Perrier, E., Jaramillo, R. A., and Baveye, P., 1997. Numerical model of 3-dimensional anisotropic deformation and 1-dimensional water flow in swelling soils. *Soil Science*, **162**, 410–420.
- Hillel, D., 1998. *Environmental Soil Physics*. London: Academic.
- Horn, R., Way, T., and Rostek, J., 2003. Effect of repeated tractor wheeling on stress/strain properties and consequences on physical properties in structured arable soils. *Soil and Tillage Research*, **73**, 101–106.
- Mualem, Y., 1984. Anisotropy of unsaturated soils. *Soil Science Society of America Journal*, **48**, 505–509.
- Pagliari, M., Vignozzi, N., and Pellegrini, S., 2004. Soil Structure and the effect of management practices. *Soil and Tillage Research*, **79**, 131–143.
- Peng, X., and Horn, R., 2007. Anisotropic shrinkage and swelling of some organic and inorganic soils. *European Journal of Soil Science*, **58**, 98–107.
- Peng, X., and Horn, R., 2008. Time-dependent, anisotropic pore structure and soil strength in a 10-year period after intensive tractor wheeling under conservation and conventional tillage. *Journal of Plant Nutrition and Soil Science*, **171**, 936–944.
- Wiermann, C., Werner, D., Horn, R., Rostek, J., and Werner, B., 2000. Stress/strain processes in a structured unsaturated silty loam Luvisol under different tillage treatments in Germany. *Soil and Tillage Research*, **53**, 117–128.

Cross-references

- Ecohydrology
 Shrinkage and Swelling Phenomena in Soils
 Soil Aggregates, Structure, and Stability
 Soil Structure and Mechanical Strength
 Tillage, Impacts on Soil and Environment

ANOXIA AND HYPOXIA

Terms anoxia (absence of oxygen) and hypoxia (decrease of oxygen).

Cross-references

- Aeration of Soils and Plants
 Oxygenology

ANTHRIC SATURATION

This special, human-induced aquic condition occurs in soils that are cultivated and irrigated, especially by flood

irrigation. Examples of anthric saturation would be rice paddies, cranberry bogs and treated wetlands.

Bibliography

- Schaetzl, R., and Anderson, S., 2005. Soils: Genesis and geomorphology. Cambridge University Press, p. 492.

ARABLE LAND USE

See [Tillage, Impacts on Soil and Environment](#)

ATTENUATION

The process by which a compound is reduced in concentration over time, through absorption, adsorption, degradation, dilution, and/or transformation.

Bibliography

- Library of Congress Cataloging-in-Publication Data Environmental engineering dictionary and directory/Thomas M. Pankratz <http://www.docstoc.com/docs/2845196/CRC-Press>

ATTERBERG LIMITS

Limits of soil consistency suggested by Albert Atterberg, 1911–1912. See [Consistency](#), [Liquid limit \(upper plastic limit, Atterberg limit\)](#), [Plastic limit](#), and [Plasticity number](#).

Bibliography

- Glossary of Soil Science Terms. *Soil Science Society of America*. 2010. <https://www.soils.org/publications/soils-glossary>

Cross-references

- [Rheology in Soils](#)

AVAILABLE WATER (CAPACITY)

The amount of water released between field capacity (at soil matric potential -33 kPa) and the permanent wilting point (usually estimated by water content at soil matric potential of -1.5 MPa).

Cross-references

- [Field Water Capacity](#)
[Soil Hydraulic Properties Affecting Root Water Uptake](#)

B

BACKSCATTERING

Bogusław Usowicz
Institute of Agrophysics, Polish Academy of Sciences,
Lublin, Poland

Synonyms

Backscatter

Backscattering (or backscatter) is the reflection of waves, particles, or signals back to the direction they came from. Backscattering is defined also as the phenomenon that occurs when radiation or particles are scattered at angles to the original direction of motion of greater than 90°. It is a diffuse reflection due to scattering, as opposed to specular reflection like a mirror. The term is used in several fields of physics, as well as in photography, telecommunication, computer network security, security imaging systems, and e-mail. Backscattering has also important applications in astronomy and medical ultrasonography (Wikipedia).

The incoming waves or particles can be scattered by quite different mechanisms:

- Rayleigh scattering of electromagnetic waves from small particles, diffuse reflection from large particles, or Mie scattering in the intermediate case, causing alpenglow and gegenschein, and showing up in weather radar
- Inelastic collisions between electromagnetic waves and the transmitting medium (Brillouin scattering and Raman scattering), important in fiber optics
- Elastic collisions between accelerated ions and a sample (Rutherford backscattering)

- Bragg diffraction from crystals, used in inelastic scattering experiments (neutron backscattering, X-ray backscattering spectroscopy)
- Compton scattering, used in Backscatter X-ray imaging

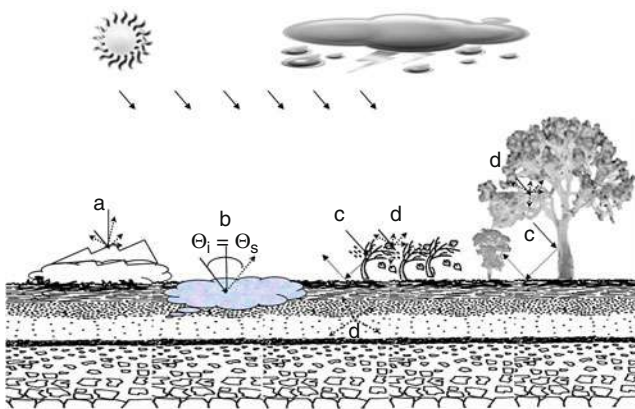
The scattering of rays or particles is more or less isotropic, that is, the incoming rays, particles are scattered randomly in various directions, with no particular preference for backward scattering. In these cases, the term “backscattering” just designates the detector location chosen for some practical reasons (backscatter):

- In X-ray imaging, backscattering means just the opposite of transmission imaging.
- In optical fibers, light can only propagate forward or backward. Forward Brillouin or Raman scattering would violate momentum conservation, so inelastic scattering in optical fibers cannot be anything else but backscattering.
- In inelastic neutron or X-ray spectroscopy, backscattering geometry is chosen because it optimizes the energy resolution.

In other cases, the scattering intensity is enhanced in backward direction. This can have different reasons:

- In alpenglow, red light prevails because the blue part of the spectrum is depleted by Rayleigh scattering.
- In gegenschein, constructive interference might play a role.
- In multiple scattering from suspensions like milk, the enhancement of backscattering is connected with weak localization.

Backscattering occurs in the environment at quite different physical forms and is the result of complex interactions between electromagnetic waves and the land surface, as



Backscattering, Figure 1 Complex interactions between electromagnetic waves and the land surface: (a) diffuse, (b) specular, (c) corner reflection, and (d) volume scattering (Θ_i and Θ_s are incidence angle and reflection angle).

(a) diffuse, (b) specular, (c) corner reflection, and (d) volume scattering (Figure 1).

Bibliography

Backscatter, ©2005–2010 – Backscattering.com, (<http://www.backscattering.com/>).

Wikipedia: <http://en.wikipedia.org/wiki/Backscattering>.

Cross-references

[Brightness Temperature in Monitoring of Soil Wetness](#)

BEDROCK

A solid rock underlying a soil, forming its parent material.

Cross-references

[Parent Material and Soil Physical Properties](#)

[Physical \(Mechanical\) Weathering of Soil Parent Material](#)

BENDING PROPERTIES OF PLANTS

Jiří Blahovec

Department of Physics, Czech University of Life Sciences, Prague 6-Suchdol, Czech Republic

Synonyms

Plant deflection; Plant flexure

Definition

Bending of plants and their parts is understood as a flexure process in which there is a change in the curvature of the plant part. Different views can be used for the

classification of plant bending: Shape and structure of the deflected part

- one-dimensional homogeneous rod (beam) type
- one-dimensional inhomogeneous rod (beam) type
- planar thin (membrane) type
- planar thick homogeneous plate type
- planar thick inhomogeneous plate type

Location of the loading forces

- local forces
- continuous loading

Duration of loading (*Rheology in agricultural products and foods*)

- short-time loading
- long-time loading
- alternating (dynamical) loading

State of plant part (*Drying of agricultural products*)

- natural
- dried
- thermal processed
- chemical processed

Introduction

The bending properties of plants are being studied for a long time, because during plant cultivation and processing, the plants and/or their parts frequently bend. Among the most important properties of this type, are tree windbreak and plant lodging (see [Plant Lodging, Effects, and Control](#)). The physical property connected to both windbreak and lodging resistance is the stem toughness. It plays an important role in harvesting (e.g., hay bailing and fruit shaking harvest) and processing technologies (wood rods and beams, see Kollmann et al., 1968).

Plant bending represents a complicated physical problem, difficult to solve in its complexity. For this reason, plant inhomogeneities are excluded in the actual cases and the problem is solved by methods usually used in material sciences (Boal, 2002).

Theoretical considerations for ideal beam: static elastic case

Theoretical methods describing plant bending follow the methods developed for stress evaluation in beams and plates (Timoshenko and Goodier, 1970; Timoshenko and Woinowsky-Krieger, 1959).

We limit our considerations to a very simple case, where the beam cross section does not change by external loading perpendicular to the beam longitudinal axis. The beam cross section is the same over the whole length of the beam with the same modulus of elasticity E and the second moment of cross-sectional area I to centroidal axis perpendicular to the external forces (the axis lies in the neutral plane). The product EI is then also constant over the whole longitudinal beam axis and is termed bending

toughness T . The Euler Bernoulli's equation for the deformed beam can be written as follows:

$$EI \frac{d^4 u}{dx^4} = w(x) \quad (1)$$

where $u(x)$ is the beam deflection (deformation) in direction perpendicular to the beam longitudinal axis, $w(x)$ distributed load (longitudinal force distribution, in N.m^{-1}), and x is longitudinal beam coordinate. The bending toughness includes information on the beam dimension (second moment of the cross section) and on the beam material (modulus of elasticity see also *Physical Properties of Raw Materials and Agricultural Products*).

In many cases, we can simplify beam loading by external forces taking into account only loading by the bending moment M omitting the shear stresses produced by gradients of the external forces. In this case, the normal stresses σ (in tension and in compression) in a loaded beam can be expressed as follows:

$$\sigma = \frac{My}{I} = E y \frac{d^2 u}{dx^2} \quad (2)$$

where y is the distance of the analyzed point from the neutral plane. Equations 1 and 2 can be integrated depending on the boundary conditions and the relations between external and internal quantities can be obtained as follows for two important cases (see also Mohsenin, 1986):

Type of loading	Beam maximum deflection	Stress
<i>Cantilever</i>		
A beam with one fixed and one free-loaded end F – loading force, l – length of beam	$y = \frac{Fl^3}{3EI}$	$\sigma = \frac{My}{I}$ see Equation 2
<i>Three point beam bending</i>		
A beam supported on the ends and loaded in the center of the beam by a perpendicular force F – loading force, l – length of beam	$y = \frac{Fl^3}{48EI}$	$\sigma = \frac{My}{I}$ see Equation 2

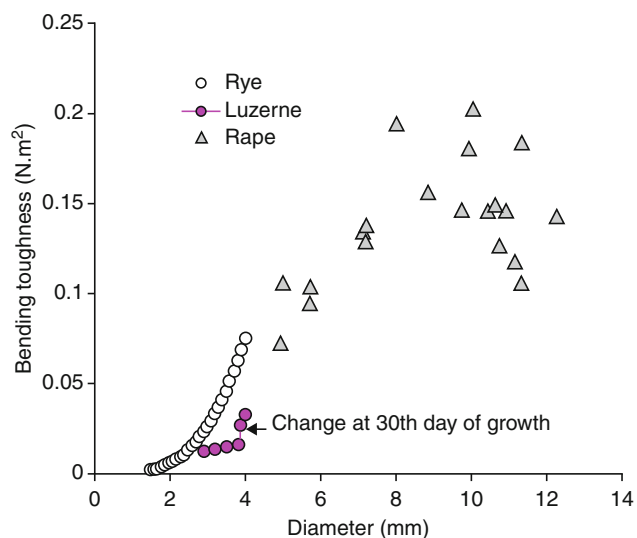
The second moment of the cross section area I depends on the shape of the cross section. For rectangular shape $I = bh^3/12$, where b is the length of the edge perpendicular to the loading force. For circular cross sections, $I = \pi d^4/64$.

The simple formulas in the above table are complicated in more real cases by the direct influence of external "feed" forces that change the stress field in the loaded beam and moreover change the shape of the cross section area (Skubisz, 1982). This type of change is observed at bending of cereal stems similar to thin wall tube. The given formulas can be used only to test very long beams at low levels of loading.

Mechanical properties of plant stalks and trunks

Bending tests of real plant stalks give variable results (see *Plant Biomechanics; Grass Fibers, Physical Properties*). The bending toughness for cereal stalks (rye), rape stem, and the lucerne stalks are given in Figure 1. The figure shows that bending toughness increases with increasing stalk diameter in most cases. For rye, nearly an exact relation was found even if the toughness depends not only on the diameter but also on the thickness of the stem wall and its modulus of elasticity. The results obtained on raw lucerne stalks show that in this state toughness is lower than in the dry state (see *Drying of Agricultural Products*) and illustrate the influence of stalk lignification. The results obtained on the dry rape stems illustrate limitations on the trend of increasing of stem toughness with increasing diameter. The increase in diameter of the rape stem is usually related to the increase of the soft aerenchyma (see *Microstructure of Plant Tissue*) in the stem, which leads to a decreasing mean value of the modulus of elasticity and a decreasing value of the bending toughness. Moreover, the rape stem aerenchyma is frequently destroyed by insects with consequence of toughness decrease, mainly in thick parts of the stems (Skubisz and Blahovec, 1997; Skubisz et al., 1989).

Modulus of elasticity of young soft plants is 1–2 GPa (lucerne) and moves up to values of about 10 GPa for dry cereal stalks and/or stems. This quantity could reach values of 20–30 GPa for special sclerenchymatic parts of the dry stalks (Razdorskij, 1949, *Microstructure of Plant Tissue*). These results are in agreement with the module of elasticity of wood, as obtained in bending test. For moist natural



Bending Properties of Plants, Figure 1 Plot of bending toughness versus diameter for some field plants: dry cereal stem (rye), raw lucerne stalk, dry rape stem (Blahovec, unpublished results). For rye it is quasi-theoretical formula $T = 0.0000995d^4 + 0.00114d^3 - 0.00157d^2 + 0.000504d - 0.0000801$, where d is in mm and T in N.m^2 . At lucerne the effect of its stalk lignification is displayed.

wood, the results are well below 10 GPa (Skubisz et al., 2001; Kollmann et al., 1968) whereas for dry wood ($MC\ d.b. = 12\%$) the values are usually higher than 10 GPa.

Bending tests give data suitable for strength limit estimation. Our unpublished results give 40–50 MPa for dry cereal stalks.

Stationary vibrations of plant stalks

Stationary natural vibration of an elastic beam is given as follows:

$$\omega_i^2 = k_i \frac{EI}{S\rho l^4} = k_i \frac{EI}{ml^3} \quad (3)$$

where ω_i is a natural angular frequency of the mode i with the characteristic constant k_i , S cross section of the beam area, ρ density, l length, and m mass. The characteristic constant is given by fixing of the beam and it is related to different harmonics of the vibration. Equation 3 shows that natural frequencies are proportional to the bending toughness of a beam. Experimentally determined natural frequencies of plant beams can be used to calculate their bending toughness. The natural angular frequencies of wheat stalk internode are about 40 s^{-1} (Dunca, 2008).

Bending of processed plant stalks and their parts

Plants and their parts are frequently bent in basket making, matting, and joinery. In most cases, the plants are processed before bending. The processing is very variable but generally it consists either in separation of the fibrous parts (Microstructure of Plant Tissue; Grass Fibers, Physical Properties) that can be well bent or hydrothermal or chemical modification of the plant parts to increase their inelastic deformability. For hydrothermal processing, hot water or steam is used to increase the temperature of the processed medium up to temperatures between 90°C and 98°C (for details see Kollmann et al., 1968).

Conclusions

The key problem of plant bending is related to rod bending that is modeled by beam bending. A big part of the problems is of elastic character that can be solved in the frame of the theory of elasticity either as a static or as a dynamic problem. Static bending is based on the term “bending toughness” with two subcomponents: the modulus of elasticity and the second moment of the cross-sectional area. The dynamic bending is tightly connected with beam natural frequencies.

Other bending problems have to be solved by numerical methods. Some of the problems are connected with deep changes in plant properties during processing and have to be solved experimentally.

Bibliography

- Blahovec, J., 2008. *Agromaterials. Study Guide*. Prague: Czech University of Life Sciences.
Boal, D., 2002. *Mechanics of the Cell*. Cambridge: Cambridge University Press.

- Dunca, J., 2008. Mechanical properties of cereal stem. *Research in Agricultural Engineering*, **54**, 91–96.
Kollmann, F., Kuenzi, E., and Stamm, A., 1968. *Principles of Wood Technology I. Solid Wood*. New York: Springer -Verlag.
Mohsenin, N. N., 1986. *Physical Properties of Plant and Animal Materials*. Emmaplein: Gordon & Breach Science Publishers Ltd.
Razdorskij, V. F., 1949. *Plant anatomy (in Russian)*. Moskva: Nauka.
Skubisz, G., 1982. *Toughness problems of cereal stems (in Polish)*. Ossoliński, Wroclaw: Zakład Narodowy im. Skubisz, G., and Blahovec, J., 1997. A method for rapid quasi static testing of the mechanical properties of plant stalks. *Zemědělská Technika*, **48**, 93–97.
Skubisz, G., Tys, J., and Blahovec, J., 1989. Mechanical properties of winter rape. *International Agrophysics*, **5**, 205–220.
Skubisz, G., Rudko, T., and Salamon, Z., 2001. Determination of the mechanical properties of blackcurrant shoots. *International Agrophysics*, **15**, 287–291.
Timoshenko, S. P., and Goodier, J. N., 1970. *Theory of elasticity*. New York: McGraw-Hill.
Timoshenko, S., and Woinowsky-Krieger, S., 1959. *Theory of plates and shells*. New York: McGraw-Hill.

Cross-references

- [Drying of Agricultural Products](#)
[Grass Fibers, Physical Properties](#)
[Microstructure of Plant Tissue](#)
[Plant Biomechanics](#)
[Physical Properties of Raw Materials and Agricultural Products](#)
[Plant Lodging, Effects, and Control](#)
[Rheology in Agricultural Products and Foods](#)

BERNOULLI'S PRINCIPAL

The soil water potential decreases in the direction of flow.

BINDING FORCE (PLANTS)

The force to detach the kernel (e.g., rice grain) from the branch.

Bibliography

- Szot, B., Ferrero, A., and Molenda, M., 1998. Binding force and mechanical strength of rice grain. *International Agrophysics*, **12**, 227–230.

BIOCHEMICAL RESPONSES TO SOIL MANAGEMENT PRACTICES

Jan Koper¹, Małgorzata Brzezińska²

¹Department of Biochemistry, University of Technology and Life Sciences, Bydgoszcz, Poland

²Institute of Agrophysics, Polish Academy of Sciences, Lublin, Poland

Definition

Biochemical response: Change in the activity of enzymes induced by external and internal signals.

Soil management: The combination of all tillage operations, cropping practices, fertilizer, lime, and other treatments conducted on or applied to the soil for the production of plants (Glossary of Soil Science Terms, SSSA, <https://www.soils.org/publications/soils-glossary>).

Introduction

Soil provides a habitat for numerous and diverse species of bacteria, fungi, and microfauna and can be viewed as a huge heterogeneous collection of microsites throughout which microorganisms are unevenly distributed (McCarthy et al., 2005). Agricultural management changes soil physical conditions (e.g., aggregate stability and air-water status) and the quantity and quality of plant residues entering the soil, thus strongly modifying the habitat of soil microbes.

Soil biochemical activity

All functions of a cell are based on the fine-tuned action of enzymes that are part of regulatory networks. Owing to the possibility of metabolism regulation, soil microbes persist in changing soil environment. Central to cell regulation is the ability of a cell to adopt the activity of enzymes in response to external and internal signals. In a broad sense, enzyme regulation operates at two main levels, either by changing the enzyme concentration (mechanisms used often for long-term adaptations) or by altering the activity of preexisting enzymes (a quick response to stimuli, allowing short-term changes in the rates of biochemical reactions) (Krauss, 2003).

Enzymes in soil are produced mostly by bacteria, fungi, and plant roots. They are active in soil both intra- and extracellularly (Burns, 1978), and are similar to enzymes in other systems, in that their level and reaction rates are markedly dependent on pH, temperature, redox potential, ionic strength, presence of inhibitor or substrate, etc. (Gliński and Stępniewski, 1985; Dick and Tabatabai, 1993). At low nutrient concentrations, soil microbes may maintain viable populations by growing slowly or by sustaining periods of starvation interspersed by rapid proliferation and increase in metabolism intensity when nutrients become available (McCarthy et al., 2005).

Despite major amounts of introduced enzymes are inhibited by soil constituents or rapidly degraded by soil proteases, the enzymes synthesized by plants, and added to soil with plant residues, may remain active. Thus, it is not surprising that the type of vegetation added to soil can greatly affect soil enzyme activity (Dick and Tabatabai, 1993). Plants also indirectly influence soil biochemical activity. Enzyme activity is considerably greater in the rhizosphere of plants than in bulk soil due to either a specific microflora or the plant root or to both (Nannipieri et al., 2007).

Effect of agricultural management on soil biochemical activity

Biochemical activity of soil organisms is involved in both the stabilization and degradation of soil structure. Agricultural production causes an alteration of natural ecosystems and produces disturbances in abiotic and biotic components (Schjønning et al., 2002; Liu et al., 2006; Melero et al., 2009). There is worldwide interest in assessment of management effects on soil quality. Soil physical, chemical, and biological properties are involved in soil functioning and all have been extensively used to measure soil quality. However, physical and chemical properties usually change very slowly and at a temporal scale are not suitable for short-term management purposes. By contrast, soil biochemical properties respond most rapidly to small changes in soil, and, because are directly related to soil organisms involved in biogeochemical cycles of C, N, P, and S, thereby are considered to be appropriate indicators of soil quality or early indications of soil alteration in both natural and agroecosystems (Pankhurst et al., 1997; Gil-Sotres et al., 2005; García-Ruiz et al., 2008).

Many publications over the last decades have dealt with modification of soil biochemical activity by soil management practices (a few of them are listed in Table 1).

In general, a decline of soil biochemical activity can be observed following soil cultivation with respect to adjacent soils in continuous grass and pasture (Bandick and Dick, 1999; Caravaca et al., 2002). Numerous experiments confirmed that intensive and even reduced tillage resulted in lower enzyme activities than a no-tillage system. Nevertheless, conservation tillage system is still far from reaching the quality levels of the adjacent soils under native vegetation (Roldán et al., 2005). Trasar-Cepeda et al. (2008) observed a much lower biochemical status of 45 cultivated soils than those corresponding to soils under oak forest (*climax* soils), i.e., natural soils of the highest possible quality. However, when the biochemical properties were expressed per unit of organic C, the values for both types of soils were very similar, and for some properties, the values for the cultivated soils were even higher.

The no-tillage system, which allows a great surface accumulation of crop residues, is the most effective for improving soil biochemical status. In cultivated systems, enzyme activity is higher where crops or organic residues were added as compared to treatments without amendments (Bandick and Dick, 1999). Change in the quantity and quality of plant residues in the soil profiles under different practices strongly influences soil microbial processes, and an effect of management practices may vary among different soil depth (Friedel et al., 1996; Kandeler et al., 1999; Geisseler and Horwath, 2009).

The study of Eivazi et al. (2003) was designed to examine the long-term effects of various cropping and management practices (since 1888) on five soil hydrolases. With regard to tillage practice, activities of all tested enzymes were significantly higher for continuous corn

Biochemical Responses to Soil Management Practices, Table 1 Soil enzymes used in studies of the effect of agricultural practices on soil biochemical activity

Management practice	Enzyme	Reference
Tillage	Arylsulphatase; catalase; dehydrogenase; α , β -glucosidase; β -glucosaminidase; o-diphenol oxidase; phosphatase (acid, alkaline); protease; urease; xylanase	Kandeler et al. (1999); Eivazi et al. (2003); Saviozzi et al. (2001) Roldán et al. (2005); Benítez et al. (2006); Bielińska et al. (2008); García-Ruiz et al. (2008); Geisseler and Horwath (2009); Madejón et al. (2009); Melero et al. (2009)
Rotation	Amidase; aminopeptidase; arylsulfatase; catalase; cellulase; chitinase; deaminase; dehydrogenase; α , β -galactosidase; α , β -glucosidase; invertase; peptidase; phosphatases (acid, alkaline); phosphodiesterase; protease; rhodanase; sulfatase; urease; β -xylosidase	Friedel et al. (1996); Koper and Piotrowska (1998); Bandick and Dick (1999); Schjønning et al. (2002); Eivazi et al. (2003); Bending et al. (2004); Gajda and Martyniuk (2005); Trasar-Cepeda et al. (2008)
Fertilization (mineral, organic)	Aminopeptidase; amidase; arylsulphatase; catalase; cellulase; β -cellobiohydrolase; chitinase; deaminase; dehydrogenase; α , β -galactosidase; α , β -glucosidase; N-acetyl- β -glucosaminidase; invertase; phosphatase (acid, alkaline); phosphodiesterase; protease; rhodanase; urease; β -xylosidase	Koper and Piotrowska (1998); Bandick and Dick (1999); Koper and Piotrowska (1999); Vepsäläinen et al. (2001); Eivazi et al. (2003); Koper and Piotrowska (2003); Koper et al. (2004); Jezierska-Tys and Frac (2005); Marx et al. (2005); Nazarkiewicz and Kaniuczak (2008); Skwaryło-Bednarz and Krzepiło (2009)
Liming	Amidase; arylamidase; arylsulfatase; L-asparaginase; L-aspartase; catalase; dehydrogenase; α , β -galactosidase; α , β -glucosidase; L-glutaminase; phosphatase (acid, alkaline); phosphodiesterase; protease; urease	Acosta-Martínez and Tabatabai (2000); Koper et al. (2003); Nazarkiewicz and Kaniuczak (2008)

under no-tillage than for continuous corn under conventional tillage. All enzymes showed significantly higher activity in plots that received manure applications since 1888, regardless of crop type as compared with inorganic fertilization. The highest enzyme activities were found in the 3-year rotation plot which received manure as only source of fertilizer since 1888, and the lowest values in the plot under continuous soybean grown under conventional tillage. The lower activities of soil enzymes in the monoculture than in the rotation system indicates that substantial disturbances occur in the microbial activity under the monoculture (Dick, 1992; Koper and Piotrowska, 1998; Gajda and Martyniuk, 2005).

Animal manure and plant residues usually stimulate soil biochemical activity (Bandick and Dick, 1999; Schjønning et al., 2002; Koper et al., 2004). However, after slurry and FYM application, a specific response was also observed, depending on tested enzyme (Koper and Piotrowska, 1999). Although inorganic fertilizers can increase soil biological activity because of an increased plant biomass production, some evidence suggests that repeated applications of inorganic fertilizer nutrients can suppress production of certain soil enzymes that are involved in the cycling of a given nutrient (Dick, 1992; Nazarkiewicz and Kaniuczak, 2008), or the changes can be negligible (Koper et al., 2004). The intensity of the effect of NPK-fertilization on enzyme activities may differ for rhizosphere and non-rhizosphere soil (Skwaryło-Bednarz and Krzepiło, 2009).

Marx et al. (2005) assessed the effect of long-term nitrogen fertilization on distribution and kinetics of six hydrolases in four particle-size fractions. For non-fractionated soils, N management had a considerable

effect on all enzymes, with the fertilized system having a higher activity than the non-fertilized system. At higher resolution, in the particle size fractions from both fertilizer systems, the same observations were made, except in the coarse sand fraction ($>2,000 \mu\text{m}$), where activities were not significantly different. Soil hydrolases showed a significant fertilization effect in the smaller size fractions, while both clay-size fractions displayed no change in their contents of C_{org} and N_{tot} . This shows that the variation in enzyme activity cannot be solely explained by changes in the organic matter status. What seems clear, at least in the clay-size fraction (2–0.1 μm), is that the enzyme activity is more sensitive as an indicator of treatment effects than are C and N contents. It is unclear, however, whether the higher catalytic potential in the high N system can be attributed to a larger accumulation of enzymes or a more advanced enzyme system with higher activity rates. The same values of Michaelis constant (K_m) were found in the same fractions from the soil under two contrasting fertilizer management regimes, indicating that the K_m was unaffected by soil changes caused by N fertilization (Marx et al., 2005).

The usefulness of soil enzymes as indicators of soil quality has also been criticized because of their seasonal changes and inherent differences in the activity, and sometimes little or inconsistent responses across soil management practices (Wick et al., 1998; Geisseler and Horwath, 2009). However, the enzyme activities show higher sensitivity to soil management practices than do other soil properties. In a long-term study, Kandeler et al. (1999) found that enzyme activities significantly increased in the top 10 cm of the profile after only 2 years of minimum and reduced tillage compared to conventional

tillage. In contrast, significant effects of tillage treatments on microbial biomass, nitrogen (N) mineralization, and potential nitrification were not observed until after 4 years. Besides, soil enzymes are strictly related to nutrient transformations and are easy to measure. Thus, soil biochemical activity is commonly used for assessing the quality or sustainability of agricultural ecosystems (e.g., Roldán et al., 2005). Another option for the evaluation of the impact of soil management on soil ecosystem is to use complex indices calculated by the combinations of different biochemical and physico-chemical soil properties (Koper et al., 2003; Koper and Piotrowska, 2003; Puglisi et al., 2006; Bastida et al., 2008).

Summary

The use of land for agricultural purposes is one of the main causes of soil degradation, and there is therefore worldwide interest in quantifying the loss of soil quality generated by agricultural operations. Soil enzyme activities are increasingly used as indicators of soil quality because of their relationship to decomposition and nutrient cycling, ease of measurement, and rapid response to changes in soil caused by both natural and anthropogenic factors. The enzyme activities show higher sensitivity to the agricultural practices than do physical-chemical properties, and, thus are useful for monitoring of the trends in soil over time and as early indicators of management-induced changes in soil quality. Numerous experiments show that the traditional soil cultivation generates many changes in soil properties and the associated changes in biochemical activity. In quantitative terms, the enzyme activities in soils under intensive cultivation are lower than in soils from undisturbed ecosystems. Soil biochemical activity reflects not only soil properties but also tillage operations, cropping practices, fertilization, liming, and other agricultural treatments.

Bibliography

- Acosta-Martínez, V., and Tabatabai, M. A., 2000. Enzyme activities in a limed agricultural soil. *Biology and Fertility of Soils*, **31**, 85–91.
- Bandick, A. K., and Dick, R. P., 1999. Field management effects on soil enzyme activities. *Soil Biology and Biochemistry*, **31**, 1471–1479.
- Bastida, F., Zsolnay, A., Hernández, T., and García, C., 2008. Past, present and future of soil quality indices: a biological perspective. *Geoderma*, **147**, 159–171.
- Bending, G. D., Turner, M. K., Rayns, F., Marx, M. C., and Wood, M., 2004. Microbial and biochemical soil quality indicators and their potential for differentiating areas under contrasting agricultural management regimes. *Soil Biology and Biochemistry*, **36**, 1785–1792.
- Benítez, E., Nogales, R., Campos, M., and Ruano, F., 2006. Biochemical variability of olive-orchard soils under different management systems. *Applied Soil Ecology*, **32**, 221–231.
- Bielińska, E. J., Mocek, A., and Paul-Lis, M., 2008. Impact of the tillage system on the enzymatic activity of typologically diverse soils. *Journal of Research and Applications in Agricultural Engineering*, **53**, 10–13.
- Burns, R. G., 1978. *Soil Enzymes*. London: Academic.
- Caravaca, F., Masciandaro, G., and Ceccanti, B., 2002. Land use in relation to soil chemical and biochemical properties in a semiarid Mediterranean environment. *Soil and Tillage Research*, **68**, 23–30.
- Dick, R. P., 1992. A review: long-term effects of agricultural systems on soil biochemical and microbial parameters. *Agriculture, Ecosystem and Environment*, **40**, 25–36.
- Dick, W. A., and Tabatabai, M. A., 1993. Significance and potential uses of soil enzymes. In Metting, F. B., Jr. (ed.), *Soil Microbial Ecology*. New York: Marcel Dekker, pp. 93–127.
- Eivazi, F., Bayan, M. R., and Schmidt, K., 2003. Select soil enzyme activities in the historic Sanborn Field as affected by long-term cropping systems. *Communications in Soil Science and Plant Analysis*, **34**, 2259–2275.
- Friedel, J. K., Munch, J. C., and Fischer, W. R., 1996. Soil microbial properties and the assessment of available soil organic matter in a Haplic Luvisol after several years of different cultivation and crop rotation. *Soil Biology and Biochemistry*, **28**, 479–488.
- Gajda, A., and Martyniuk, S., 2005. Microbial biomass C and N and activity of enzymes in soil under winter wheat grown in different crop management systems. *Polish Journal of Environmental Studies*, **14**, 159–163.
- García-Ruiz, R., Ochoa, V., Hinojosa, M. B., and Carreira, J. A., 2008. Suitability of enzyme activities for the monitoring of soil quality improvement in organic agricultural systems. *Soil Biology and Biochemistry*, **40**, 2137–2145.
- Geisseler, D., and Horwath, W. R., 2009. Short-term dynamics of soil carbon, microbial biomass, and soil enzyme activities as compared to longer-term effects of tillage in irrigated row crops. *Biology and Fertility of Soils*, **46**, 65–72.
- Gil-Sotres, F., Trasar-Cepeda, C., Leirós, M. C., and Seoane, S., 2005. Different approaches to evaluating soil quality using biochemical properties. *Soil Biology and Biochemistry*, **37**, 877–887.
- Gliński, J., and Stepniowski, W., 1985. *Soil Aeration and Its Role for Plants*. Boca Raton: CRC Press.
- Jezińska-Tys, S., and Frąc, M., 2005. *Changes in enzymatic activity and the number of proteolytic microorganisms in brown soil under the influence of organic fertilization and cultivation of spring wheat*. 38: Polish Journal of Soil Science, pp. 61–68.
- Kandeler, E., Tscherko, D., and Spiegel, H., 1999. Long-term monitoring of microbial biomass, N mineralisation and enzyme activities of a chernozem under different tillage managements. *Biology and Fertility of Soils*, **28**, 343–351.
- Koper, J., and Piotrowska, A., 1998. *Soil acid phosphatase, catalase and rhodanase activities as affected by different systems of plant cultivation*. 49: Soil Science Annual, pp. 17–21.
- Koper, J., and Piotrowska, A., 1999. Soil organic matter content and enzymatic activity as affected by long-term application of farm-yard manure and slurry. *Humic Substances in Ecosystems*, **3**, 59–65.
- Koper, J., and Piotrowska, A., 2003. Application of biochemical index to define soil fertility depending on varied organic and mineral fertilization. *Electronic Journal of Polish Agricultural Universities, Agronomy*, 6 (Online). Available from World Wide Web: http://www.ejpau.media.pl/volume6/issue1/agronomy/article_06.html.
- Koper, J., Piotrowska, A., and Siwik-Ziomek, A., 2003. Influence of long-term mineral-organic fertilisation on the value of biological indicator of soil fecundity. *Advances of Agricultural Sciences Problem*, **494**, 207–213.
- Koper, J., Lemanowicz, J., and Igras, J., 2004. *The effect of fertilization on the phosphatase activity and the content of some phosphorus forms*. 59/E: Annals UMCS, pp. 679–686.
- Krauss, G., 2003. *Biochemistry of Signal Transduction and Regulation*. Weinheim: Wiley-VCH.
- Liu, X., Herbert, S. J., Hashemi, A. M., Zhang, X., and Ding, G., 2006. Effects of agricultural management on soil organic matter

- and carbon transformation – a review. *Plant, Soil and Environment*, **52**, 531–543.
- Madejón, E., Murillo, J. M., Moreno, F., López, M. V., Arrue, J. L., Alvaro-Fuentes, J., and Cantero, C., 2009. Effect of long-term conservation tillage on soil biochemical properties in Mediterranean Spanish areas. *Soil and Tillage Research*, **105**, 55–62.
- Marx, M. C., Kandeler, E., Wood, M., Wermuth, N., and Jarvis, S. C., 2005. Exploring the enzymatic landscape: distribution and kinetics of hydrolytic enzymes in soil particle-size fractions. *Soil Biology and Biochemistry*, **37**, 35–48.
- McCarthy, A. J., Gray, N. D., Curtis, T. P., and Head, I. M., 2005. Response of the soil bacterial community to perturbation. In Bardgett, R. D., Usher, M. B., and Hopkins, D. W. (eds.), *Biological Diversity and Function in Soils*. Cambridge: Cambridge University Press, pp. 273–294.
- Melero, S., López-Garrido, R., Madejón, E., Murillo, J. M., Vanderlinde, K., Ordóñez, R., and Moreno, F., 2009. Long-term effects of conservation tillage on organic fractions in two soils in southwest of Spain. *Agriculture, Ecosystems and Environment*, **133**, 68–74.
- Nannipieri, P., Ascher, J., and Ceccherini, M. T., 2007. Microbial Diversity and Microbial Activity in the Rhizosphere. *Ciencia del Suelo*, **25**, 89–97.
- Nazarkiewicz, M., and Kaniuczak, J., 2008. *Effect of liming and mineral fertilization on the enzymatic activity of grey-brown podzolic soils formed from loess*. XLI: Polish Journal of Soil Science, pp. 201–207.
- Pankhurst, C. E., Doube, B. M., and Gupta, V. V. S. R., 1997. *Biological Indicators of Soil Health*. New York: CAB International, pp. 419–435.
- Puglisi, E., Del Re, A. A. M., Rao, M. A., and Gianfreda, L., 2006. Development and validation of numerical indexes integrating enzyme activities of soils. *Soil Biology and Biochemistry*, **38**, 1673–1681.
- Roldán, A., Salinas-García, J. R., Alguacil, M. M., Díaz, E., and Caravaca, F., 2005. Soil enzyme activities suggest advantages of conservation tillage practices in sorghum cultivation under subtropical conditions. *Geoderma*, **129**, 178–185.
- Saviozzi, A., Levi-Minzi, R., Cardelli, R., and Riffaldi, R., 2001. A comparison of soil quality in adjacent cultivated, forest and native grassland soils. *Plant and Soil*, **233**, 251–259.
- Schjønning, P., Elmholt, S., Munkholm, L. J., and Debosz, K., 2002. Soil quality aspects of humid sandy loams as influenced by organic and conventional long-term management. *Agriculture, Ecosystems and Environment*, **88**, 195–214.
- Skwarylo-Bednarz, B., and Krzepiło, A., 2009. Effect of different fertilization on enzyme activity in rhizosphere and non-rhizosphere of amaranth. *International Agrophysics*, **23**, 409–412.
- Trasar-Cepeda, C., Leirós, M. C., Seoane, S., and Gil-Sotres, F., 2008. Biochemical properties of soils under crop rotation. *Applied Soil Ecology*, **39**, 133–143.
- Vepsäläinen, M., Kukkonen, S., Vestberg, M., Sirviö, H., and Niem, R. M., 2001. Application of soil enzyme activity test kit in a field experiment. *Soil Biology and Biochemistry*, **33**, 1665–1672.
- Wick, B., Kühne, R. F., and Vlek, P. L. G., 1998. Soil microbiological parameters as indicators of soil quality under improved fallow management systems in South-Western Nigeria. *Plant and Soil*, **202**, 97–107.

Cross-references

- [Biofilms in Soil](#)
[Enzymes in Soils](#)
[Management Effects on Soil Properties and Functions](#)
[Microbes, Habitat Space, and Transport in Soil](#)
[Priming Effects in Relation to Soil Conditions – Mechanisms](#)
[Soil Biota, Impact on Physical Properties](#)

BIOCOLLOIDS: TRANSPORT AND RETENTION IN SOILS

Tammo S. Steenhuis, Verónica L. Morales, M. Ekrem Cakmak, Anthony E. Salvucci, Wei Zhang
Soil and Water Laboratory, Department of Biological and Environmental Engineering, Cornell University, Ithaca, NY, USA

Synonyms

Bacteria; Organic colloids; Protozoa; Viruses

Definitions

Colloids: Particulate matter between the sizes of approximately 10 µm to 1 nm of organic (e.g., viruses, bacteria, microemulsions, nonaqueous phase liquids) or inorganic (e.g., clay particles, mineral precipitates) nature.

Biocolloids: A colloidal entity of organic nature including bacteria, viruses, protozoa, and their respective exudates.

DLVO theory: A balance of van der Waals and electric double layer forces set to describe the stability of colloidal particles in suspension.

Stability: In colloid systems, it is the state in which particles resist flocculation or aggregation for an extended period of time.

Colloid facilitated transport: Typically used to describe the enhanced movement of otherwise immobile contaminants that sorb onto colloid surfaces and therefore travel much further and faster than traditional solute transport models predict.

Why we look at colloid/biocolloid transport in soils

The transport and retention of colloids and biocolloids in soils is of significant interest from the standpoint of groundwater protection, bioremediation of subsurface contamination, and wastewater and drinking water treatments (Ginn et al., 2002; Keller and Auset, 2007). In terms of water treatment, colloidal-sized contaminants need to be removed from wastewater prior to discharge, and biocolloid concentrations must meet drinking water standards for potable water. However, despite the importance of this topic, the transport of pathogens through porous media is still poorly understood.

Colloid systems have special properties that allow them to resist flocculation and aggregation, and will thus remain in a stable suspension for very long periods of time. Due to their particle size, colloids are characterized by a high surface-to-volume ratio, which promotes complexation and sorption of a variety of substances onto their surface. Thus, the hydrological pathways of the soil water in which colloids are suspended/advection, as well as their surface chemistry properties are crucial parameters that determine the fate of colloids in soils.

Most research on biocolloid transport in the subsurface has been focused on the movement of disease-causing

contaminants to drinking water aquifers. The phrase “biocolloid contaminants” is generally used to refer to human pathogens such as viruses (e.g., Hepatitis A, non-A, and non-B) and enterobacteria (e.g., *Escherichia coli*, *Salmonella*, and *Campylobacter*). These pathogens generally enter the soil environment via land-applied wastes and leaking septic systems at or near the soil surface (Steenhuis et al., 2006). The distribution of coliform bacteria in soils often follows the direction of groundwater flow from leaking septic tanks and sewer lines, where a steady supply of nutrients and favorable growth conditions encourage greater bacterial penetration and proliferation (McCarthy and Wobber, 1993). Precipitation facilitates the transport of these pathogens even further, as rainwater infiltrates the soil and carries suspended biocolloids to depths that can reach groundwater aquifers. Although the soil matrix acts as a natural filter for percolating water, the flux of bacteria through soils is governed by a complex set of interrelated physical, chemical, and biological processes, which in turn control cell growth, survival, attachment, and detachment.

Currently, available understanding on the processes that control the transport and retention of colloid particles in soils is being applied toward the advancement of colloid-based strategies for subsurface contaminant mitigation and remediation. Several strategies that rely on effective colloid manipulation include (1) Improved delivery of specific microbes with the ability to scavenge and transform toxic compounds into benign substances, (2) Increased mobility of colloids to change the soil’s permeability to create an *in situ* barrier that will isolate the region of concern, (3) Introduction of surface-active colloids to promote contaminant sorption onto their surface, allowing the colloid sorbed contaminants to move with the flowing groundwater and be more efficiently extracted by pump-and-treat systems (McCarthy and Wobber, 1993).

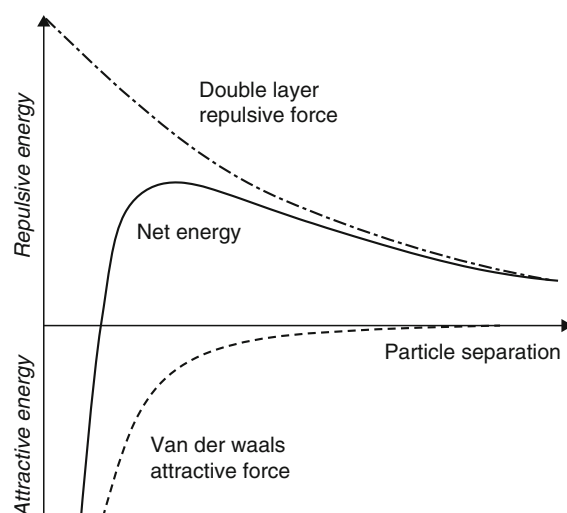
Thus, in cases when biocolloids are either accidentally or purposefully introduced into soils, understanding transport and retention of biocolloids is critical to effectively predict the load and timing of biocolloids arriving to a particular aquifer or contaminated site. To date, accuracy of predicted concentrations is a major challenge in environmental engineering; especially in terms of protecting drinking groundwater resources that become unsafe with minimal biocolloid contamination. In the following sections, a brief review of the primary transport and retention mechanisms of colloids/biocolloids is provided, though it is important to mention that it is an active research area that is constantly advancing our understanding of this complex topic.

Transport and retention processes of biocolloids in soils

Water is the primary carrier of colloids/biocolloids in soils. During transport, colloids can become permanently retained or retarded by a number of physical and chemical mechanisms that affect the behavior of colloids with each

other and the soil media. In addition, colloids tend to be excluded from soil pores in which they physically do not fit, and thus travel mainly through larger pores. For this reason, colloids can reach velocities that are orders of magnitude larger than the average velocity of solutes. Although several theories have been put forward to explain energetically how colloids behave in soils and their likelihood of becoming retained, none of them are found without shortcomings; especially in calculations that aim to predict colloid transport through unsaturated soils where water, air, and soil phases coexist.

Colloid retention in porous media is partially dependent on surface interactions between a colloid and the solid–water interface (SWI), colloids with each other, or a colloid and the air–water interface (AWI). As a colloid or a colloid aggregate collides with an immobile surface in the soil, the probability of attachment is determined by a balance of electrostatic and van der Waals forces between the colloid(s) and the retention site. These surface interactions are calculated by the Derjaguin–Landau–Verwey–Overbeek (DLVO) theory of colloidal stability. The van der Waals and electric double layer energies in DLVO theory are calculated as additive forces that decay with separation distance between charged surfaces/particles (Figure 1). The net energy potential indicates whether the interaction between the two particles will be repulsive (i.e., favorable colloid stability) or attractive (i.e., favorable colloid aggregation and/or surface attachment). Because the classic DLVO theory assumes conditions that are too simple to account for the complexity of natural systems, a significant amount of work has been done to elucidate a more complete set of dominant forces, including hydrogen bonding, hydrophobic effects (i.e., Lewis acid



Biocolloids: Transport and Retention in Soils,
Figure 1 Schematic diagram of the
Derjaguin–Landau–Verwey–Overbeek (DLVO) energy
potential of two approaching colloidal particles.

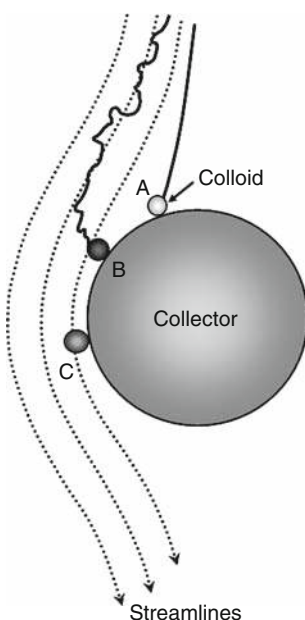
base interactions), and steric interactions (van Oss, 1994; Grasso et al., 2002), often referred to as extended-DLVO forces. However, the applicability of a combination of these additional forces to any colloidal system remains a topic of controversy, and more work on the matter is still needed to specify the dominant mechanisms that control colloidal stability of complex natural systems.

Although DLVO theory has been widely employed to account for the behavior of many colloid systems, the main assumptions of DLVO theory (colloid sphericity, uniform charge density, and impermeable surfaces) are promptly violated when applied to describe biocolloid stability. Biocolloids are inherently nonspherical, soft, deformable, have nonhomogeneous surfaces, and respond to chemical changes in the environment (Ginn et al., 2002; Tufenkji et al., 2006). Thus, biocolloids require an additional set of interaction forces to describe the mechanisms that affect their transport behavior.

The clean bed filtration theory derived by Yao et al. (1971) is the most commonly used approach for predicting particle deposition in a saturated and homogeneous porous media (Rajagopalan and Tien, 1976; Tufenkji and Elimelech, 2004; Tien and Ramarao, 2007; Cakmak et al., 2008). This theory describes the removal of suspended particles onto a single collector surface (i.e., soil grain). According to the theory, a particle moving through a porous medium will collide with a collector by one of three mechanisms (Figure 2): (1) interception, dragging colloids along streamlines; (2) gravitational settling of colloids or aggregates that are denser than the fluid; or (3) Brownian motion of particles. Nonetheless, filtration theory inaccurately predicts the amount of colloids that will become retained in the presence of an energy barrier between the colloid particles and the charged porous medium due to its simplistic pore geometry assumptions (Johnson et al., 2007; Bradford and Torkzaban, 2008). This discrepancy in deposition has more recently been explained with additional retention mechanisms (e.g., colloid wedging between grain-to-grain contacts) in pore structures made up of multiple collectors and the flow dynamics associated with them (Johnson et al., 2007).

A substantial fraction of research to date has focused on colloid transport in saturated porous media; though attention is quickly shifting toward the more complex – and perhaps more important to understand – transport in unsaturated porous media. Interest in unsaturated porous media transport has grown because the vadose zone is the critical connection between surface and shallow contaminant sources and the deeper groundwater (McCarthy and McKay, 2004). In addition to the above-mentioned characteristics that control transport in saturated soils, transport in unsaturated soils is further complicated by the presence of air. This third phase greatly affects colloid partitioning between the water phase, the soil surface, and the interfacial regions in between (e.g., AWI, SWI, and air–water–solid interface), which often act as additional sites for colloid retention (Crist et al., 2005; Zevi et al., 2005; Bradford and Torkzaban, 2008; Gao et al., 2008; Morales et al., 2009; Zevi et al., 2009). Experimental observations indicate that colloid retention in unsaturated soils is generally enhanced, though the mechanisms responsible for retention at the observed sites are still under debate. In addition to the moisture content of the porous medium, wetting history and changes in solution chemistry significantly contribute to the retention mechanisms of colloid transport through soils (DeNovio et al., 2004).

Predictive simulation studies aim to model biocolloid behavior under sets of measurable deterministic field conditions. For simplification purposes, colloids are typically modeled as inert particles suspended in fluid that can be represented with a modified convection–dispersion equation (CDE) containing systematic terms to account for attachment, detachment, and die-off of biocolloids (Elimelech et al., 1995; Tufenkji, 2007). While colloid transport models for saturated porous media are relatively effective and well developed, currently available models for unsaturated porous media are limited and need further improvement (Flury and Qiu, 2008).

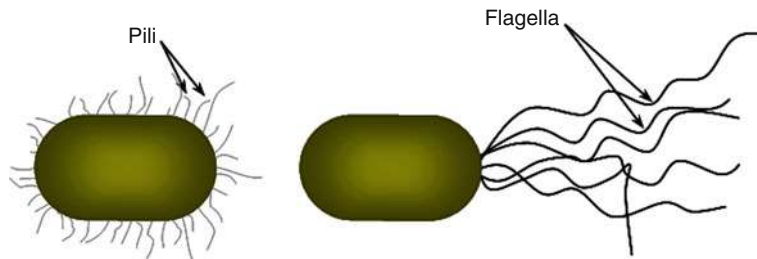


Biocolloids: Transport and Retention in Soils,

Figure 2 Schematic of filtration theory demonstrating colloid sedimentation (A), diffusion (B), and interception (C) onto a single soil-grain collector.

Effect of biofilms and extracellular appendages on biocolloid transport

Biofilms play an important role in the retention of colloids in the subsurface, as they are the prevailing lifestyle of most soil bacteria. Moreover, biofilms promote biocolloid



Biocolloids: Transport and Retention in Soils, Figure 3 Generic bacteria with pili and flagella appendages.

retention by anchoring cells of a colony to soil surfaces (Or et al., 2007), and often act as a nucleation site for suspended biocolloids (Keller and Auset, 2007).

Extracellular appendages or surface structures such as flagella, pili, curli, and polysaccharides are suspected to also play a key role in bacterial transport and retention through soils (Stevik et al., 2004). Short extracellular structures like lipopolysaccharides, curli, and pili (Figure 3) are typically associated with strains that are easily retained in soils, as it is hypothesized that the small appendages are used as sticky arms that help cells hold on to surfaces while biofilm is synthesized to attach the cells more permanently (Rijnarts et al., 1995; Walker et al., 2004, van Houdt and Michiels, 2005). In contrast, structures like flagella and cilia (Figure 3) increase cell motility, and are typically associated with more mobile strains that favor a nomadic lifestyle. As such, biocolloids with these characteristics are carried in suspension by the flowing soil water.

In addition to surface structures, different bacterial strains have diverse physicochemical properties that influence the cell's "stickiness" and ability to form biofilms (Keller and Auset, 2007), and subsequently affect biocolloid transport and retention. Other biological factors that may also affect attachment of microorganisms to immobile surfaces, but which are difficult to monitor in situ include cell growth, death, predation, and biofilm sloughing. Recent research is focused heavily on understanding the factors that support long-term survival of biocolloids in soils and the conditions that induce cell detachment from soil grains, which are related aspects of biocolloid transport that are still not well understood.

Conclusions

This chapter provides an overview of the transport mechanisms that allow biocolloids to move through soils. A vast amount of work has been done to further our understanding of the physical and chemical mechanisms that drive biocolloid transport through porous media. However, one major drawback to currently available knowledge is the accuracy with which models can predict the arrival time and concentration of biocolloids to specific locations in the subsurface, which are critical for protecting groundwater aquifers from contaminants and

for effective bioremediation strategies. In order to address this knowledge gap, basic research is constantly being carried out to discern interrelated effects that are not accounted for with classic DLVO and filtration theory calculations. In addition, technological advances constantly increase our ability for collecting data with improved temporal and spatial resolution, so that the necessary information can be assembled to refine predictive models and effectively monitor biocolloid transport in soils.

Bibliography

- Bradford, S. A., and Torkzaban, S., 2008. Colloid transport and retention in unsaturated porous media: a review of interface-, collector-, and pore-scale processes and models. *Vadose Zone Journal*, **7**, 667–681.
- Cakmak, M. E., Gao, B., Nieber, J. L., and Steenhuis, T. S., 2008. Pore scale simulation of colloid deposition. In Petrone, G., and Cammarata, G. (eds.), *Modeling and Simulation*. Vienna: I-Tech Education and Publishing KG, pp. 55–66.
- Crist, J. T., Zevi, Y., McCarthy, J. F., Troop, J. A., and Steenhuis, T. S., 2005. Transport and retention mechanisms of colloids in partially saturated porous media. *Vadose Zone Journal*, **4**, 184–195.
- deNovio, N. M., Saiers, J. E., and Ryan, J. N., 2004. Colloid movement in unsaturated porous media: recent advances and future directions. *Vadose Zone Journal*, **3**, 338–351.
- Elimelech, M., Gregory, J., Jia, X., and Williams, R. A., 1995. *Particle Deposition and Aggregation – Measurement, Modeling, and Simulation*. Oxford: Butterworth-Heinemann.
- Flury, F., and Qiu, H., 2008. Modeling colloid-facilitated contaminant transport in the vadose zone. *Vadose Zone Journal*, **7**, 682–697.
- Gao, B., Steenhuis, T. S., Zevi, Y., Morales, V. L., Nieber, J. L., Richards, B. K., McCarthy, J. F., and Parlange, J. Y., 2008. Capillary retention of colloids in unsaturated Porous Media. *Water Resources Research*, **44**, W04504.
- Ginn, T. R., Wood, B. D., Nelson, K. E., Scheibe, T. D., Murphy, E. M., and Clement, T. P., 2002. Processes in microbial transport in the natural subsurface. *Advances in Water Resources*, **25**, 1017–1042.
- Grasso, D., Subramaniam, K., Butkus, M., Strevett, K., and Bergendahl, J., 2002. A review of non-DLVO interactions in environmental colloidal systems. *Reviews in Environmental Science and Biotechnology*, **1**, 17–38.
- Johnson, W. P., Tong, M., and Li, X., 2007. On colloid retention in saturated porous media in the presence of energy barriers: The failure of α , and opportunities to predict η . *Water Resources Research*, **43**, W12S13.
- Keller, A. A., and Auset, M., 2007. A review of visualization techniques of biocolloid transport processes at the pore scale under

- saturated and unsaturated conditions. *Advances in Water Resources*, **30**, 1392–1407.
- McCarthy, J. F., and McKay, L. D., 2004. Colloid transport in the subsurface: past, present, and future challenges. *Vadose Zone Journal*, **3**, 326–337.
- McCarthy, J. F., and Wobber, F. J., 1993. *Manipulation of Groundwater Colloids for Environmental Restoration*. Florida: Lewis.
- Morales, V. L., Gao, B., and Steenhuis, T. S., 2009. Grain surface-roughness effects on colloidal retention in the vadose zone. *Vadose Zone Journal*, **8**, 11–20.
- Or, D., Smets, B. F., Wraith, J. M., Dechesne, A., and Friedman, S. P., 2007. Physical constraints affecting bacterial habitats and activity in unsaturated porous media – a review. *Advances in Water Resources*, **30**, 1505–1527.
- Rajagopalan, R., and Tien, C., 1976. Trajectory analysis of deep-bed filtration with sphere-in-cell porous media model. *AIChe Journal*, **22**, 523–533.
- Rijnhaarts, H. H. M., Norde, W., Bouwer, E. J., Lyklema, J., and Zehnder, A. J. B., 1995. Reversibility and mechanism of bacterial adhesion. *Colloid Surface Biointerfaces*, **4**, 5–22.
- Steenhuis, T. S., Dathe, A., Zevi, Y., et al., 2006. Biocolloid retention in partially saturated soils. *Biologia*, **61**, S229–S233.
- Stevik, T. K., Aa, K., Ausland, G., and Hanssen, J. F., 2004. Retention and removal of pathogenic bacteria in wastewater percolating through porous media: a review. *Water Research*, **38**, 1355–1367.
- Tien, C., and Ramarao, B. V., 2007. *Granular Filtration of Aerosols and Hydrosols*. Great Britain: Butterworth-Heinemann.
- Tufenkji, N., 2007. Modeling microbial transport in porous media: Traditional approaches and recent developments. *Advances in Water Resources*, **30**, 1455–1469.
- Tufenkji, N., and Elimelech, M., 2004. Correlation equation for predicting single collector efficiency in physicochemical filtration in saturated porous media. *Environmental Science and Technology*, **38**, 529–536.
- Tufenkji, N., Dixon, D. R., Considine, R., and Drummond, C. J., 2006. Multi-scale Cryptosporidium/sand interactions in water treatment. *Water Research*, **40**, 3315–3331.
- van Houdt, R., and Michiels, C. W., 2005. Role of bacterial cell surface structures in *Escherichia coli* biofilm formation. *Research in Microbiology*, **156**, 626–633.
- van Oss, C. J., 1994. *Interfacial Forces in Aqueous Media*. New York: Marcel Dekker.
- Walker, S. L., Redman, J. A., and Elimelech, M., 2004. Role of cell surface lipopolysaccharides (LPS) in *Escherichia coli* K12 adhesion and transport. *Langmuir*, **20**, 7736–7746.
- Yao, K. M., Habibian, M. T., and O'Melia, C. R., 1971. Water and wastewater filtration: concepts and applications. *Environmental Science and Technology*, **5**, 1105–1112.
- Zevi, Y., Dathe, A., McCarthy, J. F., Richards, B. K., and Steenhuis, T. S., 2005. Distribution of colloid particles onto interfaces in partially saturated sand. *Environmental Science and Technology*, **39**, 7055–7064.
- Zevi, Y., Dathe, A., Gao, B., Zhang, W., Richards, B. K., and Steenhuis, T. S., 2009. Transport and retention of colloidal particles in partially saturated porous media: effect of ionic strength. *Water Resources Research*, **45**, W12403.

Cross-references

[Diffuse Double Layer \(DDL\)](#)

[Electrokinetic \(Zeta\) Potential of Soils](#)

[Hydraulic Properties of Unsaturated Soils](#)

[Layered Soils, Water and Solute Transport](#)

[Microbes, Habitat Space, and Transport in Soil](#)

[Soil Water Flow](#)

[Solute Transport in Soils](#)

[Surface and Subsurface Waters](#)

BIOFILMS IN SOIL

Mette Burmølle, Annelise Kjøller, Søren J. Sørensen
Section of Microbiology, Department of Biology,
University of Copenhagen, Copenhagen K, Denmark

Definition

A biofilm is commonly defined as “a structured community of bacterial cells enclosed in a self-produced polymeric matrix and adherent to an inert or living surface” (Costerton et al., 1999), but this definition has been modified to also include that the cell attachment is irreversible, and that the bacteria living in the biofilm exhibit an altered phenotype with respect to growth rate and gene transcription (Donlan and Costerton, 2002).

Introduction

Biofilms are characterized by being composed of cells that are organized into matrix-enclosed structures that vary in size from smaller microcolonies to large and sometimes “mushroom-shaped” structures, which allow nutrient supply and waste product removal for cells placed in the deeper biofilm layers (Costerton et al., 1987; Donlan and Costerton, 2002; Stoodley et al., 2002; Jefferson, 2004). The biofilm matrix consists of extracellular polymeric substances (EPS), mainly exopolysaccharides, and also of proteins and nucleic acids, and contains up to 97% water (Sutherland, 2001; Stoodley et al., 2002).

It has been estimated that “99% of all microbial activity in open ecosystems is stuck (in biofilms) to surfaces (Potera, 1996)”. Furthermore, bacteria are believed to obtain several advantages by living in biofilms (Jefferson, 2004). Therefore, understanding of biofilm structure, dynamics, and function has become a crucial part not only of microbiology but also of many more or less related research areas. Despite this, little is known about biofilms in soil, which may be due to the difficulties involved in the study of this structurally complex environment at the microscopic scale without disturbing the soil- and biofilm structures.

Bacterial distribution in soil

Bacteria are not evenly distributed in the soil environment. The highest bacterial densities are found near nutrient sources, i.e., on roots or decaying organic material (Foster, 1988; Pearce et al., 1995; Nunan et al., 2003) (see [Microbes, Habitat Space, and Transport in Soil](#)). In the bulk soil, bacteria are found in patches or microcolonies containing low cell numbers, often composed of different bacterial species (Nunan et al., 2003; Grundmann, 2004). However, when exposed to nutrient sources, these microcommunities have the potential of developing into multispecies biofilms with high bacterial density (Nunan et al., 2003). This biofilm-associated fraction may represent the stage of the bacterial life cycle in soil, characterized by metabolic activity, whereas the microcolony

stage is a dormant/survival stage with low activity. If so, cell division and interactions with other bacteria in the active biofilm stage must be of major importance for bacterial adaptation and proliferation in soil.

Why form biofilms in soil?

The physical and chemical conditions faced by bacterial cells in soil may change dramatically over very short time periods, which is why the ability of adaptation and self-protection is crucial for the survival of soil bacteria. Due to the embedment of cells in the biofilm matrix, the biofilm-associated cells are surrounded by a more constant environment than that outside the biofilm (e.g., in the soil water) and may better resist these dramatic changes.

A highly varying parameter in soil is the water content, and soil bacteria are often exposed to drought. However, it has been demonstrated that a soil *Pseudomonas* sp. produced more exopolysaccharides when subjected to desiccation (Roberson and Firestone, 1992) and that biofilm forming (mucoid) strains of different species survived desiccation better than isogenic non-mucoid mutants (Ophir and Gutnick, 1994). These results strongly indicate a protective effect of the biofilm toward desiccation, which is likely to be caused by the moist nature of the biofilm matrix (Sutherland, 2001; Jass et al., 2002).

Another challenge met by soil bacteria is the exposure to antibiotics, which are naturally produced by microorganisms in soil (Hansen et al., 2001), or to heavy metals and other toxic compounds present in plant material (Verbruggen et al., 2009). Generally, bacteria are more resistant to a wide range of antibacterial compounds when present in biofilms, compared to the free-living, planktonic state. This has been attributed to several factors including reduced permeability of the EPS matrix to some compounds and a changed gene and protein expression patterns that up-regulate the stress response (efflux pumps, EPS production, and stress factors) and lead to the formation of the more resistant “persistor cells” (Mah and O’Toole, 2001; Gilbert et al., 2002; Jefferson, 2004). A similar protective effect of biofilms in soil was indicated in a study by Almås et al., where it was demonstrated that the tightly bound bacterial cells (i.e., those present in biofilms or very small soil pores) were more susceptible to trace metals, which indicates a previous protection from the metals in the soil (Almås et al., 2005). The biofilm environment may also serve as protection against protozoan grazing, which is considered to be a very important constraining factor for bacterial growth in many environments, including soil (Ekelund and Rønn, 1994).

Finally, soil bacterial biofilms consist of a mixture of multiple species interacting metabolically and socially, whereby the present bacteria gain several selective advantages (Jefferson, 2004). The fact that different species are present in a high cell density environment increases the possibility of horizontal gene transfer (Sørensen et al., 2005) and this process may be further stabilized by the structural nature of the biofilm. Thus, by organizing in

biofilms, the cells increase their possibility of receiving genes from other bacterial cells – genes that usually encode traits, conferring selective advantages (Sørensen et al., 2005; Burmølle et al., 2008). Hereby the cells adapt even further to the versatile soil environment. The biofilm environment may also offer optimized conditions for quorum sensing, whereby bacteria regulate gene expression according to the cell density. We have demonstrated that intraspecies communication, based on *N*-acyl homoserine lactones, occurs in soil (Burmølle et al., 2005) and inter-species communication, based on universal signal compounds (such as AI-2, Xavier and Bassler, 2003), are likely to play a role in the development and physiology of multispecies biofilms. Additionally, multispecies biofilms are even more resistant to antibacterial compounds than those composed of single species (Burmølle et al., 2006) and the biofilm environment may also serve protection of species that would otherwise be outcompeted (Stewart et al., 1997; Klayman et al., 2009).

Thus, there are many selective advantages gained by soil bacteria by organizing into biofilm communities. From an evolutionary perspective, these may result in an improved fitness for the biofilm-associated bacteria, and it seems likely that the selective pressure in soil has favored bacteria capable of biofilm formation to such extend that the species surviving in the soil are those capable of biofilm formation when exposed to nutrient availability.

How to study soil biofilms

As previously mentioned, *in situ* studies of soil biofilms are complicated because of the complex structure of the soil environment. This, combined with an astonishingly high bacterial number ($\sim 10^9$ cells/g soil) and diversity ($\sim 10^6$ species/g soil) (Torsvik et al., 1990; Gans et al., 2005), imposes challenges and difficulties on such studies. Microscopic analysis of ultrathin soil slices provides information on the distribution of bacteria in the soil (Foster, 1981; Foster, 1988; Nunan et al., 2003), but not on the nature or function of these bacteria. One way to circumvent this is to study aspects of biofilm formation and physiology in the laboratory by use of model systems composed of one or more soil isolates, similar to the studies of the bacterial response to desiccation mentioned above (Roberson and Firestone, 1992; Ophir and Gutnick, 1994). A very commonly used model system is flow cells, where the biofilms are established on glass surfaces and continuously studied by confocal scanning laser microscopy (Møller et al., 1997; Stach and Burns, 2002). This technique has been adapted for studies of soil conditions by addition of sand grains to the medium (Rodriguez and Bishop, 2007). Biofilm establishment in culture tubes allows high-resolution microscopy of structural aspects of biofilm growth (Baum et al., 2009).

Attempts have been made to better mimic the conditions in the soil by establishment of biofilms in different types of bioreactors (Holden et al., 1997; Karamanov et al., 1997; von Canstein et al., 2002; Dunsmore et al., 2004;

Jean et al., 2004). Analysis of the composition and function of the community is then performed with microscopic, molecular methods or by detection of production/removal of various compounds. von Canstein et al. (2002) used a bioreactor to demonstrate that multispecies biofilms were more efficient in reducing mercury than those consisting of only one species. We have, in our group, developed a flow biofilm system, based on isolation and growth of soil bacteria on agar-covered glass slides and supplied with autoclaved soil water as nutrient source, thereby avoiding plate cultivation-dependent isolation and artificial growth medium (Burmølle et al., 2007, Figure 1). The system allowed identification of the dominating species present and studies of biofilm succession. Lünsdorf and co-workers isolated biofilm-forming bacteria on specific slides and showed by microscopy that the cells were organized into small “clay hutches,” possibly serving different functions including protection against protozoan grazing (Lünsdorf et al., 2000, 2001).

These model systems provide important knowledge on biofilm structure, function, diversity, and physiology that are essential in understanding soil biofilms. However, many aspects of how the complexity of soil and diversity of species affect the biofilm are still missing. Regardless of how well the model system is refined, it is impossible to create conditions perfectly reflecting those in soil. Still, we depend on these systems in order to gain more knowledge on soil biofilms.

Succession and diversity of soil biofilms

Biofilms in natural environments are primarily composed of bacteria attaching to surfaces in soil or water, but also fungi, algae, and protozoa are common inhabitants. Most

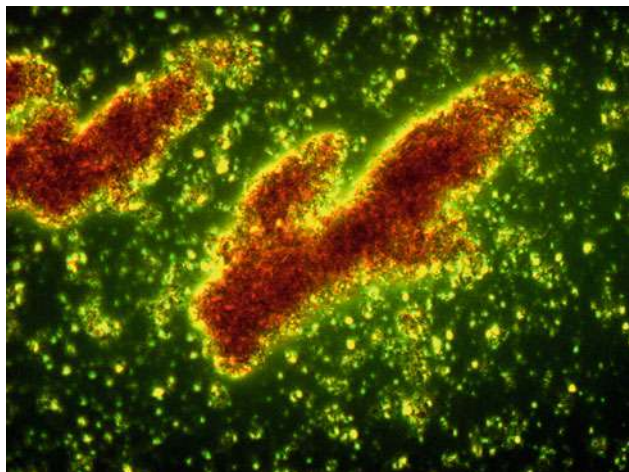
investigations concentrate on bacterial biofilms, but the other taxonomic groups also contribute to the function of the biofilm. Based on experimental work, Jackson (2003) suggested a general model for the development of bacterial biofilms. The species diversity will increase initially but decrease at a later stage when less-competitive species disappear. With time, the resource diversity will increase and competition become less important. At a later stage, interaction between bacteria and predation by protozoa will affect the biofilm diversity (Jackson et al., 2001; Jackson, 2003). By use of the flow biofilm system described above, we followed the succession in an early multispecies biofilm. The observed succession pattern could not be explained by the conceptual model, but we were able to distinguish early, intermediate, and late colonizers in the species present. We also showed that the ability of single species biofilm formation was reflected in the time of appearance in the multispecies biofilm, but that this was not the case for the planktonic growth rate. Thus, it seems that the ability of cell attachment and single species biofilm formation was essential for successful implementation in the multispecies biofilm consortium (Burmølle et al., 2007).

In the few studies of the bacterial species diversity of soil biofilms, a dominance of Gram-negative species was observed (Burmølle et al., 2007), and a similar tendency has been observed in aquatic systems (Hu et al., 2003; Martiny et al., 2003). However, some of these results could be artifacts caused by the fact that the methods used for growth and DNA extraction are optimized for Gram-negative bacteria.

Function of soil biofilms

Biofilms play a dominating role in degradation of decaying organic material in soil. As such degradation usually depends on extracellular enzymes, it makes sense for the degrading organisms to cover the material as much and tight as possible. By nutrient induced establishment of biofilm in soil on or near a degradable source (litter, roots etc.) the bacteria involved have a great advantage compared with the unattached bacteria as they have altered growth rate, physiological capabilities, and metabolic activity (Jass et al., 2002). In the biofilm, bacteria and microfungi act simultaneously in the degradation process; both bacteria and fungi are able to produce a variety of extracellular enzymes to degrade organic matter in soil, e.g., pectinase, amylase, xylanase, cellulase, protease, and lipase (Nannipieri et al., 2002); only fungi are able to attack and degrade recalcitrant ligninolytic compounds (Baldrian, 2006). The resulting soluble nutrients from the different enzymatic processes are later available both for bacteria and other microorganisms.

The bioremediating potential of several soil biofilm consortia has been evaluated. As described above, a multispecies soil biofilm effectively reduced mercury under changing environmental conditions (von Canstein et al., 2002). It has also been demonstrated how a biofilm



Biofilms in Soil, Figure 1 Micrograph showing the morphology of a multispecies biofilm composed of soil bacteria. The biofilm was established by immersion of agar-coated glass slides into soil slurry for 7 days. The attached biofilm was rinsed in a saline solution, stained with crystal violet, and rinsed again, followed by an examination by light microscopy. See Burmølle et al. (2007) for further details.

culture, composed of soil bacteria, were more diverse, both at the species and molecular level, compared to enrichment cultures (Stach and Burns, 2002). In the biofilm, more different polycyclic aromatic hydrocarbon (PAH) degrading species were present, and additionally, a higher diversity of genes involved in PAH degradation was observed. In line with this, bacterial degradation of fenemiphos was demonstrated only to take place within a mixed consortium of six Gram-negative bacteria, and only in the presence of soil particles in the growth medium (Ou and Thomas, 1994). Also, toluene diffusion was facilitated by a *Pseudomonas putida* in an unsaturated biofilm reactor (Holden et al., 1997). In fact, it has been suggested that the biotreatment of soil is improved by immobilization of soil and bacteria in a soil bioreactor, allowing the bacterial cells to form biofilms (Karamanov et al., 1997). Thus, bacterial soil biofilms may be very efficient in bioremediation, which could rely on several factors including the presence of multiple species and the bacteria-surface/soil particle interaction.

Pathogenicity and biofilms in soil

Many opportunistic pathogenic bacteria including *Burkholderia*, *Pseudomonas*, *Salmonella*, *Listeria*, *Campylobacter*, and *Legionella* are naturally occurring in the soil environment (Winfield and Groisman, 2003; Berg et al., 2005; Gray et al., 2006). However, the characterization of these bacteria has focused on their biology and population dynamics in human hosts or in hospital environments, ignoring the impact of the external (non-host) environment. Recent research suggests that the bacterial pathogenicity is greatly affected by the time and conditions faced by the bacteria in these external environments, of which soil is of major importance (Wilson and Salyers, 2003; Walther and Ewald, 2004). As stated above, soil conditions may select for biofilm formation and attachment, which unfortunately also enhance the potential pathogenicity of these bacteria. Additionally, species incapable of surviving in the soil environment on their own may become part of soil biofilms wherein they persist and evolve. This is of particular interest – and concern – with respect to pathogenic bacteria.

Perspectives

There are many reasons for soil bacteria to organize into biofilm communities: They obtain increased protection toward the harsh conditions faced by soil bacteria, they obtain a surrounding environment as stable as possible and, finally, they increase their potential of fast adaptation and maximum nutrient gain. We therefore hypothesize that the biofilm mode of growth is the preferred life style for active bacteria in soil due to evolutionary selective forces.

Studies of soil biofilms are complicated and we depend on ecologically relevant model systems for such studies. These are very fundamental tools for expanding our knowledge of the bacterial life in soil – knowledge useful

for exploiting the potential of bacterial bioremediation and for surveying the development of new aggressive pathogenic bacteria that may become less harmful when we are prepared for their arrival.

Acknowledgments

The authors would like to thank Prof. James I. Prosser (University of Aberdeen) and Dr. Regin Rønn (University of Copenhagen) for providing useful information.

Bibliography

- Almås, A. R., Mulder, J., and Bakken, L. R., 2005. Trace metal exposure of soil bacteria depends on their position in the soil matrix. *Environmental Science and Technology*, **39**, 5927–5932.
- Baldrian, P., 2006. Fungal laccases – occurrence and properties. *FEMS Microbiology Reviews*, **30**, 215–242.
- Baum, M. M., Kainovic, A., O'Keefe, T., Pandita, R., McDonald, K., Wu, S., and Webster, P., 2009. Characterization of structures in biofilms formed by a *Pseudomonas fluorescens* isolated from soil. *BMC Microbiology*, **9**, 103–116.
- Berg, G., Eberl, L., and Hartmann, A., 2005. The rhizosphere as a reservoir for opportunistic human pathogenic bacteria. *Environmental Microbiology*, **7**, 1673–1685.
- Burmølle, M., Hansen, L. H., and Sørensen, S. J., 2005. Use of a whole-cell biosensor and flow cytometry to detect AHL production by an indigenous soil community during decomposition of litter. *Microbial Ecology*, **50**, 221–229.
- Burmølle, M., Webb, J. S., Rao, D., Hansen, L. H., Sørensen, S. J., and Kjelleberg, S., 2006. Enhanced biofilm formation and increased resistance towards antimicrobial agents and bacterial invasion are caused by synergistic interactions in multispecies biofilms. *Applied and Environmental Microbiology*, **72**, 3916–3923.
- Burmølle, M., Hansen, L. H., and Sørensen, S. J., 2007. Establishment and early succession of a multispecies biofilm composed of soil bacteria. *Microbial Ecology*, **54**, 352–362.
- Burmølle, M., Bahl, M. I., Jensen, L. B., Sørensen, S. J., and Hansen, L. H., 2008. Type 3 fimbriae, encoded by the conjugative plasmid pOLA52, enhance biofilm formation and transfer frequencies in *Enterobacteriaceae* strains. *Microbiology*, **154**, 187–195.
- Costerton, J. W., Cheng, K. J., Geesey, G. G., Ladd, T. I., Nickel, J. C., Dasgupta, M., and Marrie, T. J., 1987. Bacterial biofilms in nature and disease. *Annual Reviews of Microbiology*, **41**, 435–464.
- Costerton, J. W., Stewart, P. S., and Greenberg, E. P., 1999. Bacterial biofilms: a common cause of persistent infections. *Science*, **284**, 1318–1322.
- Donlan, R. M., and Costerton, J. W., 2002. Biofilms: survival mechanisms of clinically relevant microorganisms. *Clinical Microbiology Reviews*, **15**, 167–193.
- Dunsmore, B. C., Bass, C. J., and Lappin-Scott, H. M., 2004. A novel approach to investigate biofilm accumulation and bacterial transport in porous matrices. *Environmental Microbiology*, **6**, 183–187.
- Ekelund, F., and Rønn, R., 1994. Notes on protozoa in agricultural soil with emphasis on heterotrophic flagellates and naked amoebae and their ecology. *FEMS Microbiology Reviews*, **15**, 321–353.
- Foster, R. C., 1981. Polysaccharides in soil fabrics. *Science*, **214**, 665–667.
- Foster, R. C., 1988. Microenvironments of soil-microorganisms. *Biology and Fertility of Soils*, **6**, 189–203.

- Gans, J., Wolinsky, M., and Dunbar, J., 2005. Computational improvements reveal great bacterial diversity and high metal toxicity in soil. *Science*, **309**, 1387–1390.
- Gilbert, P., Allison, D. G., and McBain, A. J., 2002. Biofilms in vitro and in vivo: do singular mechanisms imply cross-resistance? *Journal of Applied Microbiology*, **92**(Suppl), 98S–110S.
- Gray, M. J., Freitag, N. E., and Boor, K. J., 2006. How the bacterial pathogen *Listeria monocytogenes* mediates the switch from environmental Dr. Jekyll to pathogenic Mr. Hyde. *Infection and Immunity*, **74**, 2505–2512.
- Grundmann, G. L., 2004. Spatial scales of soil bacterial diversity – the size of a clone. *FEMS Microbiology Ecology*, **48**, 119–127.
- Hansen, L. H., Ferrari, B., Sørensen, A. H., Veal, D., and Sørensen, S. J., 2001. Detection of oxytetracycline production by *Streptomyces rimosus* in soil microcosms by combining whole-cell biosensors and flow cytometry. *Applied and Environmental Microbiology*, **67**, 239–244.
- Holden, P. A., Hunt, J. R., and Firestone, M. K., 1997. Toluene diffusion and reaction in unsaturated *Pseudomonas putida* biofilms. *Biotechnology and Bioengineering*, **56**, 656–670.
- Hu, J. Y., Fan, Y., Lin, Y. H., Zhang, H. B., Ong, S. L., Dong, N., Xu, J. L., Ng, W. J., and Zhang, L. H., 2003. Microbial diversity and prevalence of virulent pathogens in biofilms developed in a water reclamation system. *Research in Microbiology*, **154**, 623–629.
- Jackson, C. R., 2003. Changes in community properties during microbial succession. *Okios*, **101**, 444–448.
- Jackson, C. R., Churchill, P. F., and Roden, E. E., 2001. Successional changes in bacterial assemblage structure during epilithic biofilm development. *Ecology*, **82**, 555–566.
- Jass, J., Roberts, S. K., and Lappin-Scott, H. M., 2002. Microbes and enzymes in biofilms. In Burns, R. G., and Dick, R. D. (eds.), *Enzymes in the Environment. Activity, Ecology, and Applications*. New York: Marcel Dekker, pp. 307–326.
- Jean, J., Tsao, C., and Chung, M., 2004. Comparative endoscopic and SEM analyses and imaging for biofilm growth on porous quartz sand. *Biogeochemistry*, **70**, 427–445.
- Jefferson, K. K., 2004. What drives bacteria to produce a biofilm? *FEMS Microbiology Letters*, **236**, 163–173.
- Karamanov, D. G., Chavarie, C., and Samson, R., 1997. Soil immobilization: New concept for biotreatment of soil contaminants. *Biotechnology and Bioengineering*, **57**, 471–476.
- Klayman, B. J., Volden, P. A., Stewart, P. S., and Camper, A. K., 2009. *Escherichia coli* O157:H7 requires colonizing partner to adhere and persist in a capillary flow cell. *Environmental Science and Technology*, **43**, 2105–2111.
- Lünsdorf, H., Erb, R. W., Abraham, W. R., and Timmis, K. N., 2000. ‘Clay hutches’: a novel interaction between bacteria and clay minerals. *Environmental Microbiology*, **2**, 161–168.
- Lünsdorf, H., Strömpl, C., Osborn, A. M., Bennasar, A., Moore, E. R. B., Abraham, W. R., and Timmis, K. N., 2001. Approach to analyze interactions of microorganisms, hydrophobic substrates, and soil colloids leading to formation of composite biofilms, and to study initial events in microbiogeological processes. *Methods in Enzymology*, **336**, 317–331.
- Mah, T. F., and O’Toole, G. A., 2001. Mechanisms of biofilm resistance to antimicrobial agents. *Trends in Microbiology*, **9**, 34–39.
- Martiny, A. C., Jørgensen, T. M., Albrechtsen, H. J., Arvin, E., and Molin, S., 2003. Long-term succession of structure and diversity of a biofilm formed in a model drinking water distribution system. *Applied and Environmental Microbiology*, **69**, 6899–6907.
- Møller, S., Korber, D. R., Wolfaardt, G. M., Molin, S., and Caldwell, D. E., 1997. Impact of nutrient composition on a degradative biofilm community. *Applied and Environmental Microbiology*, **63**, 2432–2438.
- Nannipieri, P., Kandeler, E., and Ruggiero, P., 2002. Enzyme activities and microbiological and biochemical processes in soil. In Burns, R. G., and Dick, R. P. (eds.), *Enzymes in the Environment: Activity, Ecology, and Applications*. New York: Marcel Dekker, pp. 1–33.
- Nunan, N., Wu, K. J., Young, I. M., Crawford, J. W., and Ritz, K., 2003. Spatial distribution of bacterial communities and their relationships with the micro-architecture of soil. *FEMS Microbiology Ecology*, **44**, 203–215.
- Ophir, T., and Gutnick, D. L., 1994. A role for exopolysaccharides in the protection of microorganisms from desiccation. *Applied and Environmental Microbiology*, **60**, 740–745.
- Ou, L. T., and Thomas, J. E., 1994. Influence of soil organic-matter and soil surfaces on a bacterial consortium that mineralizes fenamiphos. *Soil Science Society of America Journal*, **58**, 1148–1153.
- Pearce, D., Bazin, M. J., and Lynch, J. M., 1995. The rhizosphere as a biofilm. In Lappin-Scott, H. M., and Costerton, J. W. (eds.), *Microbial Biofilms*. New York: Cambridge University Press, pp. 207–220.
- Potera, C., 1996. Biofilms invade microbiology. *Science*, **273**, 1795–1797.
- Roberson, E. B., and Firestone, M. K., 1992. Relationship between desiccation and exopolysaccharide production in a soil *Pseudomonas* sp. *Applied and Environmental Microbiology*, **58**, 1284–1291.
- Rodriguez, S. J., and Bishop, P. L., 2007. Three-dimensional quantification of soil biofilms using image analysis. *Environmental Engineering Science*, **24**, 96–103.
- Sørensen, S. J., Bailey, M., Hansen, L. H., Kroer, N., and Wuertz, S., 2005. Studying plasmid horizontal transfer in situ: a critical review. *Nature Reviews Microbiology*, **3**, 700–710.
- Stach, J. E. M., and Burns, R. G., 2002. Enrichment versus biofilm culture: a functional and phylogenetic comparison of polycyclic aromatic hydrocarbon-degrading microbial communities. *Environmental Microbiology*, **4**, 169–182.
- Stewart, P. S., Camper, A. K., Handran, S. D., Huang, C., and Warnecke, M., 1997. Spatial distribution and coexistence of *Klebsiella pneumoniae* and *Pseudomonas aeruginosa* in biofilms. *Microbial Ecology*, **33**, 2–10.
- Stoodley, P., Sauer, K., Davies, D. G., and Costerton, J. W., 2002. Biofilms as complex differentiated communities. *Annual Reviews of Microbiology*, **56**, 187–209.
- Sutherland, I., 2001. Biofilm exopolysaccharides: a strong and sticky framework. *Microbiology*, **147**, 3–9.
- Torsvik, V., Goksöyr, J., and Daæe, F. L., 1990. High diversity in DNA of soil bacteria. *Applied and Environmental Microbiology*, **56**, 782–787.
- Verbruggen, N., Hermans, C., and Schat, H., 2009. Mechanisms to cope with arsenic or cadmium excess in plants. *Current Opinion in Plant Biology*, **12**, 364–372.
- von Canstein, H., Kelly, S., Li, Y., and Wagner-Dobler, I., 2002. Species diversity improves the efficiency of mercury-reducing biofilms under changing environmental conditions. *Applied and Environmental Microbiology*, **68**, 2829–2837.
- Walther, B. A., and Ewald, P. W., 2004. Pathogen survival in the external environment and the evolution of virulence. *Biological Reviews of the Cambridge Philosophical Society*, **79**, 849–869.
- Wilson, B. A., and Salyers, A. A., 2003. Is the evolution of bacterial pathogens an out-of-body experience? *Trends in Microbiology*, **11**, 347–350.
- Winfield, M. D., and Groisman, E. A., 2003. Role of nonhost environments in the lifestyles of *Salmonella* and *Escherichia coli*. *Applied and Environmental Microbiology*, **69**, 3687–3694.
- Xavier, K. B., and Bassler, B. L., 2003. LuxS quorum sensing: more than just a numbers game. *Current Opinion in Microbiology*, **6**, 191–197.

Cross-references

[Biofilms in the Food Environment](#)
[Microbes, Habitat Space, and Transport in Soil](#)
[Microbes and Soil Structure](#)

BIOFILMS IN THE FOOD ENVIRONMENT

Katarzyna Czaczyk, Kamila Myszka
Department of Biotechnology and Food Microbiology,
University of Life Sciences, Poznań, Poland

Synonyms

Microbial attachment in the food environment

Definition

Biofilms are currently defined as microbial communities (composed from one or many genus of microorganisms), surrounded by self-produced exopolymers and adherent to abiotic and/or biological surfaces (Costerton et al., 1995).

Introduction

In the majority of natural ecosystems, microorganisms have a tendency to adhere to solid surfaces. Following adhesion to a surface, cells may proliferate, form colonies, produce exopolymers (EPS), and finally develop a biofilm. The ability of microorganisms to adhere to solid surfaces has important economic consequences in many fields (contamination of food processing equipment, contamination of biomaterials in medicine, biofouling of marine materials, and wall growth in fermentation processes). Microbial biofilms play a crucial role in a variety of disciplines, including biotechnology, immunology, and biodeterioration. Biofilms are a serious problem in food processing environments. In the food industry, bacteria colonizing the processing equipments are a potential source of food contamination by spoilage or/and pathogenic microorganisms. Biofilms cause serious economical problems such as increase resistance in the liquid flow and heat transfer and increase the corrosion rate on the surface, leading to product and energy losses. In the food industry, bacteria in both biofilms and suspended forms are exposed to stresses such as high or low temperature, dehydration, pressure, and antimicrobial agents. Biofilm formation is a part of the survival strategies of microorganisms in adverse environmental conditions.

Mechanisms of biofilm formation

Biofilm formation is a dynamic process that includes the following steps: initial adhesion (reversible), specific adhesion (irreversible), formation of microcolonies (early stages of biofilm formation), growth of biofilm and finally, detachment of microorganisms from peripheral parts of biofilm. Sometimes, reversible adhesion is

preceded by conditioning of a surface. In the food environment, some organic and inorganic molecules like proteins, carbohydrates, and other constituents may adsorb to the surface, forming conditioning film. There is no clear evidence that microorganisms better attach to the conditioned surface. It depends on the kind of surface and its microtopography. The next step of biofilm formation is the initial attachment of microorganisms to the surface. This process may be active or passive and depends on various factors like microorganism's motility, growth stage, nutrient supply in surrounding environment, and physicochemical properties of the cells. This weakly interaction between surface and microorganisms are referred as reversible adhesion. In irreversible adhesion, hydrophobic/hydrophilic interactions, covalent and ionic bonding, and dipole–dipole interactions play a significant role. The irreversibly attached cells grow, divide, and form microcolonies. During this phase, microorganisms produce extracellular polymers, which help in the anchorage of the cells to the surface. The exopolymer molecules play crucial role in biofilm formation process. They promote specific adhesion, formation of microcolonies, and more advanced stages of biofilm development. The extracellular compounds are responsible for both adhesion and cohesion of microorganisms. Exopolymers strengthen the interactions between the microorganisms themselves (formation of cell aggregates) and between the microorganisms and surface. In the literature, there are clear evidences that the biosynthesis of extracellular proteins and exopolysaccharides are responsible for the morphology and three-dimensional architecture of the biofilms and take part in maintaining structural integrity of biofilms. As the biofilm ages, the attached microorganisms are able to detach and disperse from the biofilm and colonize new niches (Costerton et al., 1995; Lee Wong, 1998; Jefferson, 2004; Branda et al., 2005).

Factors affecting the adhesion of microorganisms to solid surfaces

The process of biofilm formation is dictated by a number of variables including: physico-chemical properties of solid surfaces, hydrophobicity of solid materials and cell surface, extracellular production of polymeric substances (mainly polysaccharides and proteins), environmental factors (temperature, pH, type of media, ionic strength), and other factors (species of microorganisms, microbial growth phase, cultivation conditions, nutrient supply, viability of cells, microbial competition, presence of signaling compounds). A lot of disagreements appeared in the literature relating to factors and its affecting to the adhesion of microorganisms to solid surfaces. These antitheses probably result from species of microorganisms being examined, methods used to detect the attached bacteria to the surfaces, solid surface properties, and differences in experimental conditions (Lindsay et al., 2000; Liu and Tay, 2001; Cabanes et al., 2002; Czaczyk and Myszka, 2007; Fuster-Valls et al., 2008). Recently, scientists have

paid attention to the molecular and genetic basis of biofilm formation. Analysis of expressed genes in response to a specific environment in which microorganisms form a biofilm will help in the production of good quality products.

Problems caused by biofilm in food industry

The biofilm formation on the food products or food contact surfaces leads to serious hygienic problems. A number of reports demonstrate the possibility of biofilm development process by foodborne pathogens like *Salmonella* sp., *Listeria monocytogenes*, *Yersinia enterocolitica*, *Campylobacter jejuni*, *Pseudomonas aeruginosa*, *Legionella pneumophila*, *Escherichia coli* O157:H7, and *Staphylococcus aureus* (Kumar and Anand, 1998; Lee Wong, 1998; Shi and Zhu, 2009). The presence of pathogenic bacteria on the surfaces of food processing equipment is a potential health risk for consumer. The adhesion of nonpathogenic microorganisms to the food products or food contact surfaces may lead to food spoilage. For example, biofilm formation in the dairy industry by nonstarter lactic acid bacteria is a common reason of cheese defects such as gas formation or undesirable flavors.

Studies carried out by different research workers present that biofilm may develop on various food contact surfaces. Microorganisms may be attached to rubber, polypropylene, Teflon, glass, stainless steel, aluminum, and other solid materials. In consequence, biofilm may develop on the floors, walls, water pipes, bends in pipes, conveyor belts, tanks, rubber or Teflon seals, and stainless steel surfaces. If the biofilm is not completely removed from surface, it may be a reason of food contamination by spoilage or/and pathogenic bacteria. Many researchers observed this process in poultry, meat, and dairy products. Biofilm is also responsible for cross-contamination and post-processing contamination (Bower et al., 1996; Kumar and Anand, 1998; Fuster-Valls et al., 2008).

In the food industry, biofilm formed on processing equipment reduces heat exchange, increases friction on movable elements of enginery, and causes limitation in liquid flow, filter blocking, and finally, equipment breakdown. The microbial attachment in drinking water distribution systems decreases water velocity and carrying capacity, causes clogging of pipes, and decreases efficiency of operations. The presence of sulfate-reducing or acid-producing bacteria in biofilms causes corrosion of metal surfaces. All these adverse technological effects have an economic impact on the food industry (Bower et al., 1996; Branda et al., 2005; Shi and Zhu, 2009).

Resistance of biofilms to antimicrobial agents

Resistance of bacterial biofilm to toxic compounds is a very serious problem of modern medicine and industry practice. Microorganisms forming biofilm initiate multilevel resistance mechanisms that protect the cells against antibacterial substances. Biofilms can tolerate antimicrobial agents at concentrations of 10–1,000 times that needed to inactivate genetically equivalent planktonic

bacteria (Jefferson, 2004). Inefficiency of antibacterial compounds on attached cells depends on biofilm structure, environmental factors in which biofilm is formed, the presence of capsule of bacteria, production of degrading enzymes, changes of the molecular targets of the biocides, and the activity of “efflux pumps” proteins. The exopolymers produced by microorganisms in biofilm may bind the disinfectants and prevent its penetration through biofilm (Bower et al., 1996). The process of formation and secretion of signal molecules to the medium by bacteria is also a very relevant aspect. Furthermore, microorganisms deeply embedded in biofilm receive less oxygen and nutrients than cells in suspension. In consequence, they alter physiology (quasi-dormant state) and become less sensitive to sanitizers, antibiotics, and surfactants (Shi and Zhu, 2009).

Removal of biofilms from food contact surfaces

The complete removal of attached microorganisms from food contact surfaces is a very difficult and demanding task. It requires time- and cost-effective cleaning and sanitizing procedures. The effective methods of biofilm removal are combination of mechanical, thermal, chemical, and biological processes. Traditional cleaning of food contact surfaces starts with physical removal of attached bacteria. This is scraping, brushing, or circulating turbulent solutions through the equipment to detach the biofilms. New physical methods are also being developed for the control of biofilms. They include high-pulsed electrical fields, super high magnetic fields, ultrasound treatment, and low electrical fields. The effectiveness of these techniques is high, especially when they are used in combination with organic acids, antibiotics, and other biocides. The chemical methods that are used to remove biofilm from food contact surfaces include the usage of typical groups of disinfectants such as alcohols, aldehydes, oxidizing agents, phenolic, quaternary ammonium compounds, and others. Studies demonstrate that peracetic acid, chlorine, iodine, hydrogen peroxide, and monolaurin are the most efficient in biofilms removal. It has been known that before using chemical sanitizers, mechanical elimination of microorganisms is required. When no mechanical treatment is applied, the effectiveness of disinfectants is not so high. The exopolysaccharides prevent the penetration of these substances through the biofilm by binding them, making it impossible for them to get into the cells. Detergents containing chelating agents like ethylenediaminetetraacetic acid (EDTA) or ethylene glycol tetraacetic acid (EGTA) also improve biofilms removal from food contact surfaces. They bind calcium and magnesium ions and destabilize the microorganisms' outer membranes. New biological strategies for biofilm control have also been devised. They include the usage of biological active compounds like bacteriocins (e.g., nisin) or exopolysaccharide degrading enzymes (Bower et al., 1996; Kumar and Anand, 1998; Burfoot and Middleton, 2009).

Preventing microbial adhesion

Methods of preventing microbial adhesion in food contact surfaces include applying antimicrobial agents, modifying surface hydrophobicity, and designing food contact equipment. Some surfaces impregnated with biocides may prevent microbial colonization for as long as the antimicrobial agents are being released from these materials. Antifoulant paints, which are used to protect the hull of ships from fouling, may be also used to control of biofilm formation on food contact surfaces. For example, antifoulant paints containing silver ions have been successfully applied to control mixed biofilms containing *L. pneumophila*. It has been reported that the applications of lactic acid bacteria cultures, its cell-free supernatants, and bacteriocins prevent the adhesion on the surface of different spoilage and pathogenic microorganisms. In the recent years, food packaging materials containing active compounds have gained practical significance in control of spoilage microorganisms and foodborne pathogens on food surfaces. These active antimicrobial substances incorporated in the packing materials migrate to the food surface and microbial contamination is eliminated (Le Magrex-Debar et al., 2000). Hydrophilic materials such as glass or stainless steel are known to reduce microbial adhesion, and therefore they are often used as food contact surfaces. It is caused by the low interfacial energy characteristic for such materials, and the fact that the cells and surfaces are similarly charged. The low-affinity contact surfaces may be obtained by attaching to them some passivating compounds. It is made by the derivation of the surfaces with polyethylene oxide, noncovalent attachment of some proteins (e.g., milk protein albumin), or treatment materials with surface active or nonionic compounds. The proper design of food contact equipment plays an important role in preventing biofilm formation. Materials which are used as food contact surfaces should be smooth (without any cracks, starches, and topographical defects), resistant for corrosion and damage. Equally important in food equipment design is the cleanability of the surfaces (Bower et al., 1996; Kumar and Anand, 1998; Branda et al., 2005).

Beneficial aspects of biofilms in the food environment

Not all biofilms cause problems in the food industry. They are applied in the production of some food products. Bio-reactors with biofilms (biofilms represent a natural form of cell immobilization) are used to obtain acetic acid, citric acid, ethanol, and polysaccharides. Human gastrointestinal tract is colonized by lactic acid bacteria and *Bifidobacterium* sp., protecting against colonization by pathogenic microorganisms. An appropriate number of these microorganisms creates a healthy equilibrium between the beneficial and potentially harmful microflora in the gut. This probiotic effect is also observed when various fermented foods are consumed. Biofilms are applied in municipal and industrial sewage treatment plants.

Present microorganisms in biofilms biodegrade many compounds (also toxic ones) and minimize the buildup of pollutants. Mixed microbial consortia are used in fluidized beds and trickling filters for wastewater purification. It is important for highly harmful sewage from the food industry (Kumar and Anand, 1998; Morikawa, 2006).

Conclusions

In the last few years, extensive studies have been carried out on various aspects of biofilms in the food environment. Results of these investigations will help fully understand the interactions between microorganisms and biotic or abiotic surfaces. The presence of attached cells or biofilms on food products and food contact surfaces plays a significant role in food safety, especially for minimally processed food and raw food. From this point of view, the increased resistance of microbial biofilms to antimicrobial agents, new strategies should be developed for the control of biofilms. It is found necessary to formulate new cleaning and disinfectant agents for effective biofilm removal.

A better understanding of biofilm formation and the factors affecting this process is needed for the production of microbiologically safe and good quality products in the food industry.

Bibliography

- Bower, C. K., McGuire, J., and Daeschel, M. A., 1996. The adhesion and detachment of bacteria and spores on food-contact surfaces. *Trends in Food Science and Technology*, **7**, 152–157.
- Branda, S. S., Vik, A., Friedman, L., and Kolter, R., 2005. Biofilm: the matrix revisited. *Trends in Microbiology*, **13**, 20–26.
- Burfoot, D., and Middleton, K., 2009. Effects of operating conditions of high pressure washing on the removal of biofilms from the stainless steel surfaces. *Journal of Food Engineering*, **90**, 350–357.
- Cabanes, D., Dehoux, P., Dussurget, O., Frangeul, L., and Cossart, P., 2002. Surface proteins and the pathogenic potential of *Listeria monocytogenes*. *Trends in Microbiology*, **10**, 238–245.
- Costerton, J. W., Lewandowski, Z., Caldwell, D. E., Korber, D. R., and Lappin-Scott, H. M., 1995. Microbial biofilms. *Annual Review of Microbiology*, **49**, 711–745.
- Czaczylk, K., and Myszka, K., 2007. Biosynthesis of extracellular polymeric substances (EPS) and its role in microbial biofilm formation. *Polish Journal of Environmental Studies*, **16**, 799–806.
- Fuster-Valls, N., Hernandez-Herrero, M., Marin-de-Mateo, M., and Rodriguez-Jerez, J. J., 2008. Effect of different environmental conditions on the bacteria survival on stainless steel surfaces. *Food Control*, **19**, 308–314.
- Jefferson, K. K., 2004. What drives bacteria to produce biofilm? *FEMS Microbiology Letters*, **236**, 163–173.
- Kumar, C. G., and Anand, S. K., 1998. Significance of microbial biofilms in food industry: a review. *International Journal of Food Microbiology*, **42**, 9–27.
- Le Magrex-Debar, E., Lemoine, J., Gellé, M. P., Jaqueline, L. F., and Choisy, C., 2000. Evaluation of biohazards in dehydrated biofilms on foodstuff packaging. *International Journal of Food Microbiology*, **5**, 239–243.
- Lee Wong, A. C., 1998. Biofilms in food processing environments. *Journal of Dairy Science*, **81**, 2765–2770.

- Lindsay, D., Brözel, V. S., Mostert, J. F., and von Holy, A., 2000. Physiology of dairy-associated *Bacillus* spp. over a wide pH range. *International Journal of Food Microbiology*, **54**, 46–62.
- Liu, Y., and Tay, J. H., 2001. Detachment forces and their influence on the structure and metabolic behaviour of biofilms. *World Journal of Microbiology and Biotechnology*, **17**, 111–117.
- Morikawa, M., 2006. Beneficial biofilm formation by industrial bacteria *Bacillus subtilis* and related species. A review. *Journal of Bioscience and Bioengineering*, **101**, 1–8.
- Shi, X., and Zhu, X., 2009. Biofilm formation and food safety in food industries. *Trends in Food Science and Technology*, **20**, 407–413.

Cross-references

- [Agriculture and Food Machinery, Application of Physics for Improving Biofilms in Soil](#)
[Microbes and Soil Structure](#)
[Microbes, Habitat Space, and Transport in Soil](#)
[Thermal Technologies in Food Processing](#)

BIOGAS

The gas produced by the anaerobic decomposition of organic matter.

BIOMASS

See *Biomass as an Environmentally Benign Energy Source; Alternative Sources of Energy from Agriculture Biomass – a European Perspective*

BIOMASS AS AN ENVIRONMENTALLY BENIGN ENERGY SOURCE

Keith Openshaw
 Formerly Staff Member of the Food and Agricultural Organization (FAO) of the UN, Rome, Italy
 Formerly Staff Member at the World Bank, Washington, DC, USA

Definitions

Biomass. Any living or dead matter from plants and animals, excluding fossils.

Biomass energy. Energy from living or dead plants and animals in unprocessed or processed forms, excluding fossil fuels.

Introduction

All animals depend on biomass for their direct energy requirements, and since time immemorial biomass has been used to provide energy services to humankind. Biomass energy includes fuelwood, crop residues, leaves, grasses, and dung, plus solid, liquid, and gaseous products

derived from them. About 70% of the population in less developed countries (LDCs) – half the world's population – is dependent on biomass for cooking and water/space heating, the principal uses of household energy. Recently, there has been an upsurge of interest in motor ethanol and biodiesel as a result of concerns about global warming and the increased price of oil.

Biomass is an important fuel in the service and industrial sectors especially in rural areas of LDCs. It is used for: baking, beverage and alcohol preparation, ceramic manufacture, crop drying, food processing, cooking, and in many other formal and informal enterprises. According to the International Energy Agency (IEA, 2009), biomass energy accounts for an estimated 10% of primary energy supply in 2008 for the world as a whole (51.4 ExaJoule (EJ) – 10^{18} J – of which 43.0 EJ are in LDCs). Because of conversion losses, final energy consumption is only about 70% of energy supply. According to the *Renewable 2010 Global Status Report*, and the IEA, final renewable energy consumption accounts for 18% of total energy use in 2008 (63.5 EJ) of which 13% or nearly three quarters (44.8 EJ) is traditional biomass of which 34.9 EJ (78%) is in LDCs (IEA, 2009; Ren21, 2010). Hence, in most developing countries it dominates with over 50% of total energy use. And although much of it is used by the subsistence sector, in many countries it is the most important traded fuel both in terms of employment and value.

Why has so little attention been paid to biomass energy? For energy planners in LDCs, the reliance on unprocessed biomass fuels is a sign of under-development. Biomass is considered a “traditional” fuel that requires relatively more time to use and is more difficult to control than “modern” fuels such as petroleum base energy and electricity. Biomass, especially unprocessed biomass has a relatively low energy value per unit weight unlike fossil fuels (Table 1).

Generally, biomass is unsuited to provide large-scale motive power, heat and illumination – regarded as essential ingredients in the development process. Apart from small energy plantations including palm oil and sugar estates, biomass energy production is very scattered, difficult to monitor and measure, and in many instances it grows despite, rather than because of, “human” intervention. On the other hand, petroleum products and electricity are manufactured in discrete large-scale units that can be controlled and for which special skills and training are required for production and maintenance.

Thus, development agencies, governments, and the private sector often pay scant attention to biomass energy because its production does not lend itself to large, capital-intensive projects. Nor in most instances is its production recorded or its consumption metered and the mechanics of marketing are poorly understood.

Energy terminology

The use of the term “commercial” energy only to describe products of fossil fuels, electricity, and more recently

Biomass as an Environmentally Benign Energy Source, Table 1 Energy value (EV) of biomass, its products, and fossil fuels

Fuel	Unit	Energy value MJ	Unit	EV – MJ
Methane (natural gas) (CH_4)	m^3	35.8	kg	50.1
LPG (propane/butane)	m^3	33.9	kg	47.5
Kerosene, diesel, petrol, etc.	l	32.2 to 37.2	kg	43.5 to 45.0
Coal (brown coal to anthracite)			kg	10.0 to 30.0
Steam coal			kg	26.2
(Electricity)	kWh	3.6		
Crop residues (15% mcwb; 10% ash)			kg	13.0
Dung (15% mcwb; 20% ash)			kg	14.1
Wood (15% mcwb, 1% ash)			kg	15.5
<i>Green biomass</i> (45% mcwb)			kg	8 to 10
Densified wood (7.5% mcwb, 1% ash)			kg	17.0
Wood charcoal (5% mcwb; 4% ash; 85% carbonized)			kg	29.0
Biogas (60% methane) (CH_4 , H_2 , CO_2 , NO_x)	m^3	22.6	kg	30.5
Producer gas (CO , H_2 , CH_4 , CO_2 , NO_x)	m^3	3.6 to 5.5	kg	10.6 to 16.2
Methanol (wood alcohol) (CH_3OH)	l	15.8	kg	20.0
Ethanol ($\text{C}_2\text{H}_5\text{OH}$)	l	21.6	kg	26.9
Gelfuel (ethanol/cellulose mix, + 10% H_2O)	l	18.0	kg	22.3
Plant oil (<i>Jatropha curcas</i> oil)	l	37.4	kg	40.7
Black liquor (pulp mill waste)	l	11.8 to 12.2	kg	12.5 to 13.0

Note: mcwb = moisture content wet basis: wet weight – dry weight/wet weight.

Source: (Openshaw, 1986) revised and updated.

renewable energy from solar, wind, and water is very misleading and ignores the role biomass plays in the monetary economy of developing countries. Charcoal and liquid fuels such as methanol (wood alcohol), ethanol, and now biodiesel have always been commercial products and increasingly, fuelwood, crop residues and dung are being traded. Also, biogas (60% methane) is being produced commercially. Granted, the bulk of rural people in LDCs still collect biomass, principally fuelwood, but many of these same people collect surplus fuel to sell to urban households or rural industries and for these people it is a very important source of income.

While employment figures for fuelwood and charcoal trading are scarce, a survey undertaken in Malawi in 1996/1997 (Openshaw, 1997a, b) estimated that 93,500 full-time people were employed in tree growing/management, production, transport and trade of which 64,530 supplied all urban areas. Household supply accounted for 84,000 for the country and 58,000 for all urban areas. This should be compared to those employed in kerosene, LPG, and electrical production, transport or transmission, and trading for the household sector, an estimated 350–500 people. A repeat survey was undertaken in 2008 (BEST, 2009). This found that full-time employment in growing, production transport and trade was an estimated 133,000 of which 122,000 served the household sector. Thus, woodfuel was and still remains the dominant “commercial” household fuel in Malawi. This is true for many sub-Saharan African (SSA), Latin American, and Asian countries. While there are no definite worldwide estimates, nearly 30 million people may be involved in the commercial production, transport and trade of biomass energy worldwide and it could generate in the region of

US\$ 20 billion annually (This estimate assumes that there are 3 billion biomass users worldwide. It is based on Malawi figures, which estimated that the woodfuel informal sector employs 1 person per 100 users of all biomass energy (purchased and collected). Each employed person generates about US\$ 650 per year. Besides cooking, biomass is used for household heating and by (rural) industries and the service sector. Some wood-rich Developed Countries also use biomass for heating and industrial purposes. So this employment figure and value may be underestimated). And as stated above in many SSA countries, the trade in household biomass energy is much greater than the sale of fossil fuels and electricity. In contrast, according to The Renewable Global Status Report, page 34 (Ren21, 2010), more than three million people are employed in all forms of “modern” renewable energy.

Again, the use of biomass has been widely disregarded by developing agencies. Indeed, the 2002 World Summit on Sustainable Development held in South Africa set a 2015 target for “renewable energy” in LDCs of 15% as part of the Millennium Development Goal (UNDP/WB, 2002). But the definition of renewable energy was mainly confined to solar, wind, and water, and completely ignored “traditional” biomass fuels, which were considered to be “unsustainable”! If biomass fuels are included, then already most LDCs have achieved the 15% renewable energy target.

There is reluctance in development circles to consider biomass as a legitimate energy form that can assist with poverty alleviation and sustainable development. Yet it is universally available, can be grown simply and cheaply close to where it is required, and has a sustainable supply several times that of the annual consumption of fossil fuels. Part of the reluctance to regard it as a viable form

of energy is that it is considered to impose an excessive burden on women and children who collect it and is a health hazard for the user, especially in a confined kitchen. The general consensus is that people who cook with biomass will remain in poverty. Until they use more convenient cooking fuels such as kerosene and LPG and until energy (electricity) access is improved, poor households will not be able to escape the poverty trap. Yet in most, if not all rural areas of the world, kerosene is available, but generally it is used sparingly for illumination purposes. Households are most reluctant to pay for fuel if they can collect it. In urban areas, most fuels are available, but many houses in “shanty towns” do not have grid electricity. It was proposed at the World Bank’s Energy Week in March 2004 (WB, 2004a) and again in March 2006 to subsidize kerosene and liquid petroleum gas (LPG) (WB, 2006) and to spend US\$ 120 billion over the next 10 years on rural electrification (WB, 2004b). (At the 2006 WB Energy Week meeting, it was stated by Prof. Robert Socolow of the Center for Energy and Environmental Studies at Princeton University (USA) that 35 kg of LPG per capita (1.65 GJ/c) should be sufficient to meet the yearly cooking requirements for the average household. Assuming the above figure, the delivered cost of LPG works out at about US\$ 100 for a family of six per year. For the world, about 500 million households containing three billion people cook with biomass (& coal). Thus, the yearly cost of LPG would be about US\$ 50 billion and the cost for a cylinder and 2-burner stove of US\$ 1.5 billion per year on average. This additional use of LPG would add between 82 and 90 million tons of carbon to the atmosphere each year. If past fuel subsidies are used as a pointer, free or subsidized kerosene will be sold as a diesel substitute, etc., and people will still cook with biomass: it will not ease the burden for women, nor reduce kitchen smoke. Also, would some of the US\$ 120 billion be better spent elsewhere on other energy and non-energy initiatives, such as improved stoves? The Global Alliance for Clean Cookstoves – a partnership between the US government and other nations along with charitable foundations – has pledged US\$ 60 million over 5 years to assist national cookstove programs in India, Mexico, and Peru [BBC (News 2010)]. While it is a step in the right direction, it is a paltry sum compared to the proposed investment in rural electrification!

At present a World Bank Group Energy Strategy Approach Paper has as its main thrust, improved energy (electricity) access for developing countries. “Traditional biomass” fuels are considered to be nonrenewable and to be substituted as quickly as possible (WB, 2009). By not treating biomass as a legitimate and renewable carbon-based fuel, an opportunity is being lost to provide employment for low-income rural and urban families.

Hydrogen has been touted as the new and renewable energy of the future, but its impact in LDCs will be negligible, especially in rural areas. Because hydrogen is difficult to handle, it has been suggested that methanol (CH_3OH) be the

“carrier” for hydrogen. Methanol can be produced from the dry distillation of biomass, therefore, why not use methanol directly rather than as a hydrogen carrier?

Each year, plants fix between 57 and 100 billion tons of atmospheric carbon through photosynthesis, of which about half is from land plants and thus potentially available for fuel before it decays and returns to the atmosphere (Hall and Rao, 1994; Sorensen, 1979). Wood is the most convenient form of biomass for energy purposes. For the world as a whole and for developing countries in particular, the annual growth of wood is 3–4 times annual demand (FAO, 1993; FAO, 2007–2009; Hosier, 1993; Openshaw, 1983, 2000a; Soussan, 1991; WB, 1994). It is not the use of wood that is causing “deforestation” but the clearing of land for arable and pastoral agriculture (and urbanization) as a result of population increase and the need to generate cash income. In 2008, about 8.0 billion tons of carbon were burnt in fossil fuels (IEA, 2009), thus even taking energy efficiency and conversion losses into consideration, there is considerable scope to consume much more than the current 1.4 billion tons of “renewable” carbon in biomass used for energy purposes (IEA, 2009). Burning renewable biomass does not add to the accumulation of atmospheric carbon dioxide because if biomass is not used it will decay and CO_2 will be returned to the atmosphere (the Carbon Cycle). If not properly prepared and burnt, biomass (and other fuels) generates products of incomplete combustion that can affect health and contain more damaging greenhouse gases (GHGs) such as methane and oxides of nitrogen. But these are technical problems that can and should be tackled at source rather than proposing alternatives such as fuel switching, most of which are financially and logically unattractive. Thus, biomass energy should be considered environmentally benign as it produces little if any net additional GHGs.

Biomass, rather than being treated as a fuel of the past, should be embraced as a legitimate, renewable, and versatile carbon-based fuel that can be and is used in the unprocessed and processed form or used as a feedstock for electrical generation. After all, all animals, including humans, rely on carbon-based fuel (food) for energy and there is no reason why biomass should not be a significant part of the world’s energy mix in future.

In the last 2–3 years, there has been an upsurge of interest in growing biomass for motor ethanol and biodiesel. The estimated consumption of motor ethanol in 2009 is 76,000 million liters (1,642 PetaJoules [PJ]) and that for biodiesel is 16,600 million liters (657 PJ) (Ren21, 2010), of which 50% is produced in Europe. In Europe, the EU has mandated that renewable energy, especially biofuels be increased significantly by 2020. The European Commission proposes the following targets in a series of documents representing the EU New Energy Policy (EU, 2001):

- Reduce greenhouse gas emissions by 20% in 2020, compared to the 1990 emissions
- Increase the share of renewable energy in the total energy mix from less than 7% in 2006 to 20% by 2020

- Increase the share of biofuels to at least 10% of the total energy content of transport fuels by 2020
- Reduce the global consumption of primary energy by 20% in 2020

Unfortunately, the UN Global Climate Summit in Copenhagen in December 2009 never reached an agreement on GHG reduction. One of the few positive outcomes was a pledge by Developed Nations of US\$ 30 billion over 3 years to help poorer countries mitigate climate change. Some of this money will go to REDD + (reduction of emissions from degradation and deforestation). However, clearing land for agriculture is a principal cause of deforestation. It is hoped that some will also go to help increasing agricultural productivity. With help and improved management, trees can be used to improve agricultural productivity and stabilize the environment, add to the store of organic carbon, and generate additional income; thus, expanded biomass use could be a key ingredient in the initiatives to alleviate poverty.

Carbon sequestration and greenhouse gasses (GHG)

Atmospheric carbon is stored in biomass, particularly woody biomass and in all types of soils. There is a greater accumulation of carbon in forest and woodland soils and to a lesser extent in grassland soils than in arable agricultural soils under similar conditions. Therefore, biomass can be used to sequester atmospheric carbon in the biosphere, while its annual production could be used, for example, as renewable energy or as a carbon store in wood products. There are proposals and actual schemes to sequester carbon dioxide from fossil fuel burning in caves, abandoned mines, porous rocks, and in the ocean to mitigate and eventually stabilize the “global warming effect.” But it may be easier, less costly, and safer to increase the carbon dioxide storage in biomass and soils, while at the same time increasing the supply of wood, etc., for biomass energy!

Unfortunately, because of population pressures, low (subsistence) agricultural productivity and the need to produce cash crops in LDCs, more forest land is being cleared than is being replaced by newly planted or naturally regenerated trees. Therefore, at present, more CO₂ is being released into the atmosphere from forest land clearing, the burning of wood in situ and from former forest soils, than is being sequestered. In order to reduce deforestation, apart from a vigorous policy to slow down and eventually reverse population increase, agricultural productivity, especially in LDCs, has to increase. In part trees and other forms of biomass can play a role. Many plants, including trees and shrubs, fix atmospheric nitrogen; thus nitrogen-fixing trees, judiciously spaced in fields can maintain if not improve agricultural productivity, while at the same time providing stick wood. Also, trees can provide browse and fodder for animals; the manure from these animals can be used directly or indirectly as fertilizer in place of being used as unprocessed fuel as happens in several countries such as India where wood is scarce. Also many countries

have biogas digesters to extract methane from manure. China has an estimated 25 million and India four million digesters (Ren21, 2010). Again, trees can reclaim marginal land and improve the local microclimate through shelterbelts and hedges on rainfed and irrigated arable lands and protect watersheds, thus benefiting lowland agriculture and hydro-dams amongst other things.

This is not to say that chemical fertilizers should not be encouraged. But such agencies as the World Bank are against subsidizing such fertilizers and they are promoting “market driven” solutions. Yet agricultural subsidies in developed countries (DCs) are depressing world market prices and this is leading to “subsidized” food from DCs competing with non-subsidized food from LDCs. The whole theory of comparative advantage is being corrupted by distorted agricultural policies in DCs especially in the EU, Japan, and the USA.

It is not that “traditional” collection and use of biomass energy is unsustainable, rather it is the policies of developed countries and one-sided “market” solutions that are unsustainable: this is accelerating deforestation and keeping many rural communities in poverty. A level playing field with regard to subsidies for agriculture (and energy) will do more for development than the current trade and aid policies. However in 2008/2009, the price of staples such as maize increased considerable because maize was being diverted for motor ethanol production and it had a knock-on effect regarding the price of rice. In the USA, the ethanol producers receive a subsidy and there is an import tax on ethanol produced in Brazil, a much cheaper fuel source. Also tropical forests were being cleared for palm oil production for biodiesel, although this has slowed down due to reduced palm oil prices.

Energy use

According to the International Energy Agency’s official statistics (IEA, 2009), biomass energy supplied 51.4 EJ (10%) of the world’s energy demand in 2008. This is up from the 1997 figure of 44.1 EJ (11%) (IEA, 1999). Many surveys in LDCs have shown that official figures underestimate actual consumption (Openshaw, 1978). Even in developed countries taken as the 29 OECD counties (footnote to Table 2), wood is used as a heating fuel during the winter months and much is not recorded. Therefore, in 2008, the actual primary energy supply of biomass energy may be in the region of 64 EJ or 12% of the energy consumption! Taking this adjustment into consideration, the average primary energy supply for the world in 2008 is 78.5 GigaJoules [GJ, 10⁹ J] per capita. In non-OECD countries, the percentage share of biomass energy rises from 15% to 18%, but the average per capita consumption is only 55 GJ – 29% of the average in OECD countries of 188 GJ/c. In sub-Saharan Africa, biomass fuels account for as much as 80% of energy consumption, but per capita primary energy supply is a low 36 GJ, less than half of the world average and 18% of that of developed countries.

Biomass as an Environmentally Benign Energy Source, Table 2 Estimated world primary energy supply 1997 and 2008
(Units: ExaJoules (10^{18} J) except where stated)

	OECD countries ^a		Non-OECD countries ^b		Total	
	1997	2008	1997	2008	1997	2008
<i>Population (billion)</i>	1.09 (19%)	1.19 (18%)	4.59 (81%)	5.51 (82%)	5.68	6.70
Natural gas	43.3	54.7	36.5	53.7	79.8	108.4
Oil	88.9	84.1	53.2	86.4	142.1	170.5
Coal	43.9	44.5	50.1	94.2	94.0	138.7
<i>Subtotal fossil fuels</i>	176.1	183.3	139.8	234.3	315.9 ^d	417.6 ^e
Per capita fossil (GJ)	161.6	154.0	30.5	42.5	55.6	62.3
Nuclear	22.4	25.2	3.8	4.6	26.2	29.8
Per capita nuclear (GJ)	20.6	21.2	0.8	0.8	4.6	4.4
<i>Renewable energy</i>						
Hydro	4.6	4.7	4.5	6.6	9.1	11.3
Biomass & waste	6.8	8.4	37.3 ^c	43.0 ^c	44.1	51.4
<i>Per-c biomass (GJ)</i>	6.2	7.1	8.1	7.8	7.8	7.7
Geothermal/solar/wind	1.3	2.7	0.3	0.9	1.6	3.6
<i>Subtotal renewables</i>	12.7	15.8	42.1	50.5	54.8	66.3
Per-c. renewables (GJ)	11.7	13.3	9.2	9.2	9.6	9.9
Total	211.2	224.3	185.7	289.4	396.9	513.7
Per capita (GJ- 10^9 J)	193.8	188.5	40.5	52.5	69.9	76.7

^aOECD Countries (29). Australia, Austria, Belgium, Canada, the Czech Republic, Denmark, Finland, France, Germany, Greece, Hungary, Iceland, Ireland, Italy, Japan, Luxembourg, Mexico, the Netherlands, New Zealand, Norway, Poland, Portugal, South Korea, Spain, Sweden, Switzerland, Turkey, the UK, and the USA.

^bThe non-OECD countries include all developing countries except Mexico and Turkey. All the former Soviet Union Countries are non-OECD, although Russia is developed. Likewise, the Gulf States are non-OECD countries, whereas in most, their per capita income is high and are classified as developed. In 1977, Albania, DPR Korea, and Vietnam (populations 103 million) were excluded. In 2008 they were included (populations 109 million).

^cThe biomass total for non-OECD is probably low due to under-recording. A more realistic figure for both time periods is 10 GJ/c or 535 kg in wood equivalent terms. This would increase the overall biomass share by about 3.5% in each time period. In 1997 biomass and waste energy is an estimated 45.9 EJ and 55.1 EJ in 2008 and the total energy consumption 405.5 EJ in 1997 and 525.8 EJ in 2008.

^dThis gives off 22.85 billion tons CO₂, equal to 6.23 billion tons C.

^eThis gives off 29.23 billion tons CO₂, equal to 7.97 billion tons C. There has been a 28% increase in CO₂ emission since 1997 – 2.4% increase per year.

IEAs statistics are in million tons of oil equivalent (TOE). 1 TOE = 41.868 GJ.

Sources: (IEA 1999, 2009).

At present the top 18% of the world's population consume about 44% of the world's annual energy demand and 3.6 times more in per capita consumption of fossil fuels. If the remaining 82% were to approach the energy use of the top 18%, then annual energy consumption would increase by 3.6 times. If this increase is mainly in the form of fossil fuels it could lead to serious if not disastrous environmental consequences. What is more, the world's population may swell to over nine billion by 2050. Therefore, even following the current energy use patterns may mean the world is sitting on an environmental time bomb. This is why trying to stabilize fossil fuel consumption at 1990 levels and having a vigorous policy to expand the use of renewable energy is so important. The Stern Review to the UK Government on the Economics of Climate Change emphasized this (Stern, 2006). But the December 2009 "Global Climate Summit" in Copenhagen did not reach any agreement on fossil fuel stabilization.

Clearly, the developing world must expand its (useful) energy consumption if it is to escape from the present

poverty and under-development traps. And just as important, the developed world must reduce its energy input of fossil fuels. Therefore, it is inappropriate environmentally and may be unwise from an economic standpoint for LDCs to follow the past energy strategies of the "West." Of course there are vested interests in promoting development with a reliance on "modern" fuels. Expanding the use of these fuels requires considerable capital investment. Indeed the World Bank Energy Workshop held in March 2004 proposed that US\$ 120 billion be spent on rural electrification over the next 10 years (WB, 2004a). However, only 3.2% of energy investment was for renewable energy, the bulk of which was for non-biomass energy (WB, 2004b). Developed countries promote capital-intensive energy programs because much of the equipment and technical know-how is supplied from the "West" (and of late from India and China). Also energy planners in LDCs favor such projects for they see them as the way to modernize the country by providing power at the flick of a switch. But in many instances, because of inadequate

tariff structures, poor maintenance, and unauthorized use, electrical supply is usually intermittent with considerable voltage fluctuations.

One justification for low tariffs in LDCs is to assisting the poor. But most poor households do not have electrical connections! Those that do, use electricity very sparingly. In Malawi in 2008, the average household tariff, including tax, was US cents 4.56/kWh. It was estimated that of the 31% of urban households with connections, the rich received a subsidy of about US\$ 638 per year, whereas the poor only got US\$ 44 (BEST, 2009). There is no reason why the rich and middle income households should be subsidized. If poor households need help, then a lifeline tariff is the most equitable way to help.

Similarly, subsidies on fossil fuels generally depress the price of competing (biomass) fuels. This lowers the opportunities for rural people to increase their earnings and increases the chance of the natural resource base being less well managed. In some cases, it leads to trees in watershed areas being felled to expand subsistence agriculture and to obtain cash from the sale of wood. In turn, this affects the water retention capacity and can lead to flash floods during the rainy season and little stream flow in the dry season. For countries with hydro-electricity generation, trash may block the inflow channels during the “flood” period and there may be too little water during the dry season. Thus, hydro-electrical production may be seriously affected.

Energy strategies for LDCs

In LDCs, what options and strategies could energy planners choose in preparing for an expansion of energy use? Can and should they follow the conventional path and mainly plan for the expanded use of fossil fuels and electricity using traditional generating options and switch to non-biomass fuels as quickly as possible? Or should they recognize that biomass is a legitimate, renewable indigenous resource and is one of several options that should be given the importance it deserves in the energy mix of individual countries? After all about 3 billion people cook with biomass and it will be decades, if ever, before a significant switch to non-biomass (cooking) energy is achieved, even if concerted efforts are made by countries and development agencies. And is this the appropriate option to pursue both economically and environmentally?

In most sub-Saharan African countries biomass energy accounts for over 80% of total energy demand. It is the dominant fuel in the household sector and is important in the service and industrial sectors. This same pattern is found in Asian and Latin American countries, although biomass energy use is not as dominant. Even so, biomass accounted for about half of energy consumption in the Philippines in 1989 – 87% in the household sector and one third each in the service and industrial sectors (ESMAP, 1991). There is little chance that this dominance can be replaced rapidly, nor in most cases, is this the best option. Yet governments in general and energy ministries in particular have little detailed knowledge either of the

biomass energy supply situation or the sector demand patterns. This leads to poor planning, misallocation of resources, and erroneous strategies.

Estimates of biomass availability, particularly wood, can vary by a factor of four or more. One estimate in Ethiopia indicated that the country was using considerably more than the annual growth of wood (TFAP, 1996). It was proposed that a massive countrywide plantation program should be undertaken to close the demand/supply gap and that other mitigation measures be undertaken. However, an inventory in 2003 showed that for the country as a whole, the annual growth of wood was more than annual demand (WBISPP, 2003). This inventory pinpointed areas of shortage and surplus. Programs were proposed in these specific areas to meet the shortfall through local community and farmer driven efforts and to increase the off-take of wood in surplus areas. Similar discrepancies were found in Malawi, the Philippines, and Uganda. A carbon sequestration study in 2000 undertaken for the Global Environment Facility (GEF) in Benin, estimated the store of carbon in wood and soils. An inventory of all woody live and dead biomass was undertaken (Openshaw, 2000a). It was determined that stem wood accounted for only 55% of aboveground weight. Therefore, basing the carbon store just on stem weight underestimates the aboveground carbon content in wood by over 80% and considerably underestimates the quantity of wood available for use. Again, in the Philippines, one estimate of sustainable wood supply indicated that there was an annual shortfall of 15 million tons of woodfuel to satisfy demand, whereas a later inventory estimated that there was a surplus of 44 million tons (ESMAP, 1991). This latter information led to a recommendation that biomass consumption should be expanded.

In these countries, the largest cause of deforestation is agricultural clearing. Indeed, an analysis undertaken in all sub-Saharan African countries indicated that 95% or more of deforestation was caused by clearing land for arable agriculture and that the annual growth of wood ranged from 2.6 times more than demand in Southern Africa to nine times more in Western Africa (Openshaw 2004). Therefore, without good supply/demand analyses and proper investigations into the causes of land degradation and energy access, etc., inappropriate and costly solutions are often proposed.

Promote rural electrification and switching from fossil fuels

While it is desirable for people to have energy at the flick of a switch or the turn of a knob, without the (rural) poor having money to pay for these fuels, even if they are subsidized, then it is unlikely that they will use such fuels for household purposes. Therefore, rural electrification should be first targeted for productive and/or health uses. Before village electrification is promoted, people have to be in a position to afford electricity. One way this can occur is to use more fully the natural resources that are available in the surrounding areas.

Electricity, with other forms of energy, can be an engine for growth in the non-household sectors of the economy. The “green revolution” in India was assisted by electrical pump sets that provided irrigation water enabling the growing of two and three crops per year. This provided money for farmers to pay for electricity. This is documented in a 2007 publication on the challenges of rural electrification. It provides pointers for successful rural electrification programs (Barnes, 2007). In future, much more emphasis has to be placed on supplying the increased demand for electricity, especially in rural areas, from renewable forms of energy such as wind, solar, micro-hydro, and biomass. Using biomass in stand-alone projects or as part of grid-based systems will provide jobs to rural people and help with poverty alleviation.

While LPG, natural gas (and biogas) are perhaps the “best” cooking fuels, kerosene is the only fossil fuel that is widely available in rural areas of developing countries. It is a more convenient cooking fuel to use than unprocessed biomass. However, from the many household surveys that were undertaken by the UNDP/WB: Energy Sector Management Assistance Programme (ESMAP), it was found that rural people in general and rural/urban poor in particular were reluctant to purchase fuel for cooking if biomass could be collected. Subsidizing kerosene (and LPG) generally did not lead to it being used for cooking. Rather, it was diverted to other neighboring countries and/or used as a diesel substitute. Where subsidies are proposed, they have to be targeted and the government has to make sure that the target group receives most of the benefit.

One renewable energy source that has been promoted for the last 40 years with little success is solar energy for cooking. A critical analysis was prepared for an *International Conference on World Solar Cooking and Food Processing* held in Italy in 1999. Solar stove initiatives were examined in Africa and India and it was concluded that they are, at best, only marginally successful and have not been cost-effective. Solar cooker initiatives neither solve indoor kitchen pollution nor contribute to the halt of deforestation (Openshaw, 1999).

Treat biomass as a legitimate resource for economic development and poverty alleviation

Biomass, particularly wood, is not only a fuel or a source of industrial wood products, but it has many other uses. Trees can be used to increase agricultural productivity through improved microclimate and/or fertilizer inputs. Many trees have multiple uses: they are used as a source of fodder and animal feed; trees are important for honey, nut, fruit, and medicinal/herbal production and are essential for environmental protection. This versatility is both a strength and weakness.

No single government ministry feels responsible for all the functions of trees and forests and in many instances no one takes responsibility for coordinating these various functions and uses. Forestry departments may undertake the management/inventories of forests under their control, but rarely

will they measure trees on forests and woodlands outside their control. Nor will they ever think about measuring trees (and residues) on non-forest land, particularly agricultural land. Yet these trees are an important source of wood and biomass energy, particularly for rural households; they may account for up to 85% of rural energy and generate income for local people when supplying biomass to industry, the service sector, and urban areas.

However, unless the growing stock and annual yield of trees and other forms of biomass are measured, it is impossible to undertake meaningful planning. Governments, development banks, and private companies would never finance natural gas or oil field development unless they knew the extent of the reserves, but this basic assessment is rarely, if ever, done for the dominant energy resource in many LDCs. This is extremely short-sighted for it can mean either the difference between using a resource that will last indefinitely or mining it over a limited time period with possible adverse environmental and agricultural effects. It may lead to inappropriate investments in tree planting. Therefore, it is important that governments, development agencies, the private sector and individuals co-operate to manage biomass resources sustainably and to target tree planting and other mitigation measures.

Promote sound environmental projects

Countries, development banks, especially the World Bank and the sister regional banks, plus other development agencies such as UNDP, the Global Environmental Fund (GEF), the Food and Agricultural Organisation (FAO) of the UN, the UN Clean Development Mechanism (CDM) and REDD + and the WB Prototype Carbon Fund could and should be strong influences in promoting poverty alleviation linked to sustainable development. Yet in the past and even today some are directly or indirectly supporting initiatives that are environmentally questionable and may be economically dubious. Development banks have long encouraged capital-intensive schemes in the electricity and petroleum sectors. Hydroelectric schemes were promoted without proper watershed protection and refineries were built because of prestige rather than viability. But several initiatives in the agricultural/natural resource sector are questionable. Vietnam was encouraged to grow coffee on a large scale. Many forest areas were cleared to plant the coffee bushes to the detriment of biodiversity and the carbon store and local people were moved from the area. However, the demand for coffee has increased at a much slower pace than the supply and depressed world prices: this adversely affecting all coffee producing nations and especially coffee farmers. In Indonesia, forest areas are being destroyed to make way for palm oil production, and in Brazil forests are cleared for soy beans and pastoral agriculture. Irrigation schemes have been badly planned leading to, for example, sterilization of the soil through surface salt deposits (Pakistan), drastic lowering of water tables (India) and abandonment because of excessive sedimentation in the water, destroying the water pumps (Bangladesh and Kenya).

Therefore, development must be attuned to the environment and its long-term sustainability.

There are many areas of marginal and abandoned agricultural land that can be reclaimed for “biomass crops” rather than clearing forests for oil crops, soy bean and pastoral agriculture. Areas of *Imperata cylindrica* grass an aggressive “weed” species can be reclaimed through the planting of nitrogen-fixing tree species such as *Gliricidia sepium* and *Leucaena leucocephala*. These trees rapidly suppress the weed and it dies, leaving little that can sustain a grass fire (NAS, 1979). The reclaimed land can be used for arable and pastoral agriculture, with some short-rotation trees left to provide mulch, shade and stick wood, etc. Again witchweed (*Striga asiatica*) attacks food crops such as maize and reduces yields considerably. It can be controlled naturally by planting tick-trefoil (*Desmodium sp.*) as a nitrogen-fixing understory. This can then be used as a green manure and/or as an animal feed (NAS, 1979).

Similarly, dry areas including deserts can be reclaimed with *Prosopis sp.* This provides stick wood; the milled pods are protein rich and are sold commercially as animal feed. There are many nitrogen-fixing plants including short-rotation trees that can be grown in all areas of developing countries that can be of environmental benefit and provide tree products (NAS, 1979).

Prospects for motor fuels from biomass in LDCs

An oil-bearing tree species, *Jatropha curcas*, which can be grown on marginal lands, is exciting much interest at present. It is being planted in Africa and Asia. Although it can be grown on dry marginal land, productivity is a function of water availability and soil fertility. *Jatropha* is not a nitrogen-fixing tree; indeed its seed cake is nitrogen-rich and can be used as a fertilizer. This implies that in order to maintain productivity, nitrogen fertilizer has to be added to the soil. *Jatropha* could be inter-cropped with a tree legume and/or NPK fertilizers could be added to the soil (Openshaw, 2000b).

While there are many motor ethanol plants, Brazil is by far the largest producer in LDCs. Out of a 2008 world total production of 67 billion liters, Brazil produces 27 billion liters and the USA 34 billion liters (Ren21, 2010). However, twice as much land is required in the USA to produce the same amount of motor ethanol as in Brazil. Sugar is the main feedstock in Brazil, whereas corn (maize) is the feedstock in the USA. The production cost in Brazil is an estimated US cents 29 per liter and the wholesale price is US 71 cents. About 1.35 L of motor ethanol are required per liter of gasoline. It is estimated that if crude oil prices remain above US\$ 35–40 per barrel (159 L), then ethanol production from Brazil will be competitive with gasoline [(Xavier, 2007); CBS (News, 2006)]. Moreover, bagasse (sugarcane waste) is used to raise heat and power for the factories and to provide surplus electricity to towns.

There are plans to make motor ethanol from wood waste and switch grass, etc., both raw materials being

cheaper than maize (corn). The cellulose in each product will have to be broken down into simple sugars before it is fermented into ethanol. It may be more cost-effective to produce alcohols and hydrocarbons, etc., directly by the dry distillation of cellulose or from the gasification of cellulose. There are pilot projects to produce biomass from algae, cyanobacteria, and artificial photosynthesis in ranaspumin based foam (NPR, 2010; Wendell and Todd, 2010). The biomass can then be turned into liquid fuels and used for motive power, but at present these systems are in the development stages and much more work has to be done to make them economically viable.

Biomass, especially traditional biomass, is the Cinderella of fuels

The production of liquid biomass fuels as substitutes for liquid fossil fuels is receiving considerable attention, but gaseous fuels from fermentation or gasification are also important. However, most energy ministries in LDCs pay particular attention to electricity and petroleum-based fuels. They may even have sections dealing with new and renewable sources of energy such as solar power, wind and water. Few, if any, devote much time to biomass fuels, especially “traditional” biomass use, because in general they assume that they cannot influence the production process and they wrongly think that using such fuels, especially wood, is a principal cause of deforestation. However, through systematic supply and demand surveys, governments can pinpoint areas of surplus and deficit, determine the root causes of deforestation, document current management, conversion and end-use practices, and investigate actual and potential end uses and barriers to promote renewable energy, particularly biomass. Development banks and aid agencies could and should help with such work. This information is essential for compiling meaningful strategies and proposing long-term development initiatives.

Today the main emphasis is on Renewable Energy, which mostly excludes biomass, except using “modern” biomass in discrete initiatives mainly in developed countries. It appears that rather than fostering poverty alleviation, development bodies are promoting rural backwardness and environmental degradation.

Apart from helping governments obtain good biomass supply/demand statistics, development bodies should assist them with rural development plans, especially improving agricultural productivity, promoting greater rural access, providing timely market intelligence, and increasing social services. Expanding biomass use, promoting specific vegetation types and encouraging species selection to improve agricultural and silvicultural production, decreasing the incidence of pests and diseases, and protecting biodiversity and watersheds should be an integral part of rural development. This could be done through training, demonstration and extension at all levels. Farmers, women’s groups, villagers and local entrepreneurs can be shown how better to grow, manage, produce and market their resources on all land use types. Housewives can be shown better kitchen

practices, and encouraged to obtain improved stoves, as part of enhanced village services. Generally, all these initiatives require outside assistance, albeit at a modest level. But usually such assistance will pay off many times over, both environmentally and socially. Also, from a financial standpoint it is mostly very cost-effective.

In some countries, charcoal producers are regarded as destroyers of the forests and woodlands, when in fact they are the producers of an important urban fuel that in many cases use resources that otherwise would ultimately rot or be burnt in situ. In some countries such as Ethiopia and Malawi, charcoal production is illegal. This leads to surreptitious (and generally wasteful) production methods and the fear of confiscation unless bribes are paid: all this adversely affects the price of charcoal and makes producers outlaws, rather than the providers of a demanded product.

Charcoal production can be improved and producers should receive training in woodland management, charcoal production, and in marketing. It should be treated as a legitimate activity that is supplying a renewable and convenient energy form, while generating employment in production, transport, and trading. There are petroleum engineers, electrical engineers, but there are few biomass production engineers (charcoal, methanol/ethanol, biodiesel, biogas/producer gas). Yet these are, or could be, important fuels and their status would be enhanced through systematic university/technical training in the production of these fuels.

The World Bank has stressed the importance of assisting the private sector, and biomass energy production is principally in the hands of the private informal sector and is a fuel consumed by the poor and rural industries. Yet very little help is afforded to such people. Development banks could assist through training, market intelligence, encouraging the removal of inappropriate bans and restrictions, improved infrastructure, and promoting a level playing field regarding fuel subsidies. If world bodies are serious about global warming, they should be promoting carbon taxes on fossil fuels (Stern, 2006).

Similarly, energy conservation is considered to be an important way to reduce fuel costs and decrease pollution. But relatively little effort has been put into improving end-use efficiencies in the household sector. Because biomass stoves are produced mainly by the informal sector, who can ill afford to undertake research and development, governments should assist in this effort, through targeting training in stove manufacture techniques, business management and marketing, providing loans for micro-enterprise development, testing stoves and materials, and undertaking quality control. Governments should also coordinate efforts of health departments and stove manufacturers to reduce indoor air pollution. Some effort is now being made and US 50 million has been proposed to improve stoves in three countries over the next 5 years [BBC (News, 2010)], but this is a meager sum compared to that proposed for rural electrification over the next 10 years – US\$ 120 billion (WB, 2004).

Sustainable development

Various authors have given estimates of the earth's carrying capacity for humans ranging from a low 0.5 billion to a high 14 billion, with the median ranging from 2.1 billion (low) to 5.0 billion (high) (Richards, 2002). The high estimates are based on a much increased use of the net primary production (NPP) from biomass. Already, the world's population may be greater than its carrying capacity and there are wars, fights and disputes over land and water resources.

This year, 2010, is the International Year of Biodiversity. It has been stated that our ecological footprint – what we take out of the planet – is now 1.3 times the biological capacity of earth. Habitats are being destroyed and species are being lost, because of population and economic growth leading to the destruction and degradation of forests, grassland, farmlands, wetlands, rivers, seas, etc. At present, only lip service is given to sustainable development, reclaiming areas that have been degraded, improving agricultural and silvicultural management and productivity, and the sharing of resources within and between countries. If the world is not overtaken by environmental disasters, by 2050, the human population may be 9.2 billion and by then people on average will be nearly three times as wealthy as today! (The World Bank Energy Strategy Approach Paper states that "The world economy is set to grow four-fold by 2050 and — energy-related carbon dioxide emissions will more than double" (WB, 2009). This translates to an overall increase of 2.9 times in per capita wealth assuming the world's population will reach 9.2 billion by 2050.) Their total energy demand, even taking energy efficiency and energy conservation measures into consideration, may be in the region of 1,000 EJ, nearly twice the amount used today (Table 2). By that time, the extraction of liquid fossil fuels may be uneconomic, if they have not been banned, and only coal will be available in quantity. But to foster truly sustainable development, such fossil fuels should not be used. All types of renewable energy and nuclear power will be needed to meet such a demand.

At present, electricity supplies an estimated 16.3% of the energy mix (OECD Countries 20.0%) (IEA, 2009). Of course, by 2050 electricity's share may increase considerably, but solid, liquid and gaseous fuels still will be required to meet the everyday needs of the population. As stated previously, all fossil fuels came from biomass, so biomass can be turned into similar fuels.

Every year plants fix between 57 and 100 billion tons of atmospheric carbon with Richards giving an estimate of about 80 billion tons of atmospheric carbon (Richards, 2002). In theory about half is available for use, before it rots or is burnt in wild fires, etc. The other half is produced in the seas and oceans. Now some of this may be farmed using algae (NPR, 2010). The present consumption of biomass energy is an estimated 55.1 EJ containing 1.5 billion tons carbon (Table 2). (This is the adjusted figure. The IEA figure is 1.4 billion tons of carbon.) Taking into account

the other uses of biomass including food, about 1.8–2.0 billion tons out of a possible 40 billion tons C are presently used. The carbon content in fossil fuels that are burnt annually is about 8.0 billion tons C. (IEA, 2009). Therefore, out of the approximately 38 billion tons C that is theoretical available, at least an additional 10 billion tons C in biomass could be used as fuel (26%); this could sustainably meet a considerable quantity of future energy demand. If the overall conversion efficiency to gaseous, liquid, and solid fuels is 50%, then five billion tons C would be available for motive power, power generation, process heat, and cooking. Thus, biomass energy could be an important and increasing renewable input to sustain development.

Conclusions

In summary, there should be no distinction between energy types. Energy planners and development agencies should attempt to quantify the supply and demand for biomass energy alongside other forms of energy. All fossil fuels came from biomass and thus it can be a feedstock to produce many kinds of renewable substitutes for fossil fuels. By doing this, the importance of the different types and uses of energy will be highlighted. It will bring home to governments not only the problems of quantifying biomass supply and demand, but also the opportunities that biomass presents in encouraging rural people to manage the resource sustainably, thus promoting rural development and poverty alleviation.

Second, because biomass production impinges on forestry, agriculture, energy, environment, industry and development, it is important to have a multidisciplinary approach so that planning and policy can be influenced by biomass energy specialists.

Third, it must be recognized that biomass is a versatile multipurpose commodity that can be turned into gaseous, liquid, and solid products both for energy and non-energy purposes or used directly as a fuel or feedstock for steam generation, process heat, and electrical generation. It can be produced indefinitely and, therefore, is a renewable *carbon-based fuel* that does not increase GHG: this cannot be overemphasized. The potential available carbon in the annual growth of biomass – 40 billion tons C – is many times that given off from the annual burning of fossil fuels (8.0 billion tons C). Thus, there is considerable scope to substitute much more biomass energy for fossil fuels, thereby reducing GHG accumulation.

Fourth, trees, shrubs, bamboo, etc., are a store of atmospheric carbon both in the living biomass and the soil beneath the biomass, as well as in wood products, etc. Such plants can be used to sequester more atmospheric carbon than at present. Wood is a convenient store of solar energy that can be used when required and/or left to perform other functions such as watershed management, habitat conservation, and environmental protection.

Fifth, biomass can be and is grown, managed, and used by rural people with little capital inputs, but with income

generating possibilities and to ensure energy availability nearby. Trees, etc., can assist agricultural productivity, land reclamation, and environmental protection. They can provide energy for industries and the service sectors, thus assisting sustainable rural development.

Sixth, global warming, mainly caused by burning fossil fuels, but exacerbated by deforestation, has to be checked through aggressive action by all nations of the world, especially OECD countries.

Seven, in order to slow down and eventually halt deforestation, agricultural productivity has at least to keep pace with population increase. However, it is important that action be taken to slow down and eventually reverse population increase. Already, with the present living standards, the earth's carrying capacity for the human population may be exceeded.

Eight, while the promotion of "modern" energy is receiving priority, it will do little to help the bulk of poor people living in tropical countries. Modest investments in time, money, good governance, and policy reform could reverse the deforestation trend. Bringing the poor into partnership with government and providing more opportunities to earn money from all aspects of tropical forests, plantations, woodlands, and trees outside the forest could reap great environmental and economic rewards and help alleviate poverty.

Finally and most importantly, biomass is a local resource that is environmentally benign. It is an important fuel in many developing countries, which can be produced indefinitely. Its importance is also increasing in developed countries that see it as a means of greenhouse gas mitigation. Because it is a renewable and versatile carbon-based fuel that can be grown universally, it should be promoted as a form of energy that truly can support sustainable development. This lesson could and should be followed especially by the developed and "emerging" nations of the world.

Bibliography

- Barnes D. F. (ed.), 2007. The challenge of rural electrification: strategies for developing countries. Washington D.C.: Resources for the Future Press, & ESMAP/WB, pp. 345.
- BBC News, 2010. Science and Environment. Global bid to tackle cooking smoke. 21 Sept. 2010. <http://www.bbc.co.uk/news/science-environment-11381760>?
- BEST, 2009. Malawi: Biomass Energy Strategy Study. A Report Prepared for the Government of Malawi (GoM). The EU, Brussels, Belgium.
- CBS News, 2006. Brazil is World's Ethanol Superpower. CBS News USA. 13 March 2006. www.cbsnews.com/stories/2006/03/13/tech/main1394254.shtml
- ESMAP, 1991. *The Philippines: Household Energy Supply and Demand. UNDP/WB Energy Sector Management Assistance Programme*. Washington, DC: The World Bank.
- EU, 2001. European Union Directive 2001/77/EC. Brussels, Belgium.
- FAO, 1993. Forest Resource Assessment 1990: tropical countries. Forest paper 112. FAO, Rome.
- FAO, 2007–2009. *State of the world's forests 2007, 2008, 2009*. Rome: FAO.

- Hall, D. O., and Rao, K. K., 1994. *Photosynthesis*, 5th edn. Cambridge: Cambridge University Press, p. 211.
- Hosier, R. H., 1993. *Forest energy in Pakistan: the evidence for sustainability*. Washington DC: HESS. UNDP/WB.
- IEA, 1999. *International Energy Agency: Key World Energy Statistics 1997*. Paris: IEA.
- IEA, 2009. *International Energy Agency: Key World Energy Statistics 2008*. Paris: IEA.
- NAS, 1979. *US National Academy of Sciences. Tropical Legumes: Resources for the Future*. Washington, DC: NAS, p. 332.
- NPR, 2010. US National Public Radio program: Science Friday, 30 April 2010. Biofuel Roundup. <http://www.sciencefriday.com/program/archives/201004305>
- Openshaw, K., 1978. Woodfuel: a time for reassessment. Natural Resources Forum, Vol. 3, No. 1 (October 1978). UN, New York. Reprinted as Chapter 6 in Smil, V., and Knowland, W. E. (eds.), 1980. *Energy in the Developing World: The Real Energy Crisis*. UK: Oxford University Press, pp. 386.
- Openshaw, K., 1983. *An inventory of biomass in Kenya*. Stockholm, Sweden: Beijer Institute (Swedish Academy of Sciences).
- Openshaw, K., 1986. *Concepts and methods for collecting and compiling statistics on biomass used as energy*. Paper Presented to a Workshop at a UN Statistical Office Workshop at FAO HQ, Rome, Sept/Oct 1986. Published in the Proceedings. UN Statistical Office. New York.
- Openshaw, K., 1997a. *Malawi: Woodfuel Production, Transport and Trade; A Consolidated Report*. A report prepared for the GoM. Alternative Energy Development (now part of International Resources Group [IRG]), 1211 Connecticut Avenue NW, Suite 700, Washington, DC.
- Openshaw, K., 1997b. *Malawi: biomass energy strategy study*. A report prepared for the World Bank. AED/IRG, 1211 Connecticut Avenue NW, Suite 700, Washington, DC.
- Openshaw, K., 1999. Solar stoves: are they a viable technology? AED/IRG, 1211 Connecticut Avenue NW, Suite 700, Washington, DC.
- Openshaw, K., 2000a. *Gov. of Benin/WB & GEF. A baseline survey of organic carbon in woody biomass and soils on different land-use types in the project areas. Benin: PGFTR Project*. Washington, DC: World Bank.
- Openshaw, K., 2000b. A Review of *Jatropha curcas*: an Oil Plant of Unfulfilled Promise. Biomass and Bioenergy 19 (2000) 1–15. Pergamon Press, UK.
- Openshaw, K., 2004. Natural Resources: Population Growth & Sustainable Development in Africa, Ch. 11. In Low Pak, Sum (ed.), *Climate Change and Africa*. Cambridge: Cambridge University Press, p. 369.
- Ren21, 2010. Renewables Global Status Report 2009. REN 21 Secretariat, Paris.
- Richards, G., 2002. Human Carrying Capacity of Earth. Institute for Lifecycle Environmental Assessment. ILEA leaf Winter 2002 issue. USA.
- Sorensen, B., 1979. *Renewable Energy*. London: Academic, p. 683.
- Soussan, J., 1991. *Philippines household energy strategy: fuelwood supply and demand*. Washington, DC: UNDP/WB ESMAP. World Bank.
- Stern, N. [Sir], 2006. *Stern Review on the Economics of Climate Change*. Cambridge, UK: Cambridge University Press, pp. 700.
- TFAP, 1996. *Ethiopia: Tropical Forestry Action Plan*. Rome, Italy: FAO.
- UNDP/WB, 2002. *World Summit on Sustainable Development. Cape Town, South Africa 2002*. New York: UNDP.
- WB, 1994. *Estimating Woody Biomass in Sub-Saharan Africa*. Washington, DC: The World Bank [WB].
- WB, 2004a. Proceedings. The World Bank Energy Week Workshop. WB, Washington, DC.
- WB, 2004b. Renewing our Energy Business. WB Group Energy Program Implementation Progress Report 2001–03. WB, Washington, DC.
- WB, 2006. Proceedings. The World Bank Energy Week Workshop. WB, Washington, DC.
- WB, 2009. Energy Strategy Approach Paper. October 2009. WB, Washington, DC. <http://web.worldbank.org/>
- WBISPP, 2003. *Ethiopia: Woody Biomass Inventory and Strategic Planning Project (WBISPP)*. A report prepared for the Government of Ethiopia. TecSult, International Ltd., Quebec, Canada.
- Wendell, D., and Todd, J., 2010. *Artificial photosynthesis in Ranaspumin*. Cincinnati: University of Cincinnati.
- Xavier, M. R., 2007. *The Brazilian Sugarcane Ethanol Experience No 3*. 1001 Connecticut Avenue N.W. Washington, DC 20036, USA: Competitive Enterprise Institute.

Cross-references

- [Algae, the Potential Source of Energy](#)
[Alternative Sources of Energy from Agriculture Biomass – a European Perspective](#)
[Greenhouse Gas Fluxes: Effects of Physical Conditions](#)
[Greenhouse Gases Sink in Soils](#)

BIOMECHANICS

See [Plant Biomechanics](#)

BIOMES

The world's major communities, classified according to the predominant vegetation and characterized by adaptations of organisms to that particular environment. Land biomes area: forests ($41 \times 10^6 \text{ km}^2$), grasslands ($30 \times 10^6 \text{ km}^2$), savannas/woodlands ($17 \times 10^6 \text{ km}^2$), deserts ($30 \times 10^6 \text{ km}^2$), crop fields ($17 \times 10^6 \text{ km}^2$), wetland ($7 \times 10^6 \text{ km}^2$).

Bibliography

- Campbell, N. A., 1996. *Biology*, 4th Edition. The Benjamin/Cummings Publishing Company, Inc., Menlo Park, California.
- Yiqi Luo and Xuhui Zhou, 2006. *Soil respiration and the environment*. Elsevier, Amsterdam.

BIOSPECKLE

Artur Zdunek
Institute of Agrophysics, Polish Academy of Sciences,
Lublin, Poland

Definition

Biospeckle is phenomenon of interference pattern formation when a biological specimen is irradiated by a coherent light.

When a coherent laser illuminates a rough surface, the scattered light exhibits mutual interference and forms randomly distributed bright and dark spots of variable shapes called speckle pattern. When the laser coherent light impinges on the surface of biological material, it can pass through one or more layers (e.g., air space, skin, and cell walls), each of them will act as a stationary diffuser. If particles within the biological material are in motion, the speckle pattern exhibits spatial and temporal fluctuations and is said to “boil” or “twinkle.” This phenomenon is called biospeckle.

BIOTA

See [Soil Biota, Impact on Physical Properties](#)

BIOTECHNOLOGY, PHYSICAL AND CHEMICAL ASPECTS

Zdzisław Targoński

Department of Biotechnology, Human Nutrition and Science of Food Commodities, University of Life Sciences, Lublin, Poland

Definitions

Biotechnology – any technical application that uses biological systems, living organisms, or derivations thereof to make or modify products or processes for specific use.

Bioprocess – any process that uses complete living cells or their components (e.g., bacteria, enzymes, chloroplasts) to obtain desired products.

Biorefinery – the coproduction of a spectrum of bio-based products (food, feed, materials, chemicals) and energy (fuels, power, heat) from biomass.

Physical aspects

Various definitions of biotechnology are known (Purohit, 2005); however, biotechnology is best defined as a process, which enables its exponents to convert raw materials into final products when the raw material and/or a stage in the production process involves biological entities. Most commercial processes used in the chemical industry are applicable to bioprocesses.

A bioprocess includes an upstream process, biological reaction (fermentation process), and a downstream process. An upstream process consists of various stages of processing and preparing biological materials before the production stage including organisms and enzyme screening, gene screening, cloning, transformation, cell line development, medium design, cleaning, sterilization, filtration, and feed control. The core, a biotechnological process, is a biological reaction in a bioreactor. The organisms require strict chemical and physical factors

in a bioreactor for growth as well as for the production of biomass and metabolites. The physical processes used in bioreactors are as follows: agitation, absorption and desorption of gas, oxygen transfer, and heat exchange. The goal of process control is the optimal utilization of biological systems for biosynthesis, transformation, and biodegradation. A variety of online sensors is used in bioprocesses, which are temperature, bioreactors back pressure, gas flow rate, agitation rate, dissolved oxygen and carbon dioxide, pH, redox potential, and optical density (Alford, 2006).

A downstream process consists of various processing stages that occur after the completion of the production stage and includes cell lysis, solid–liquid clarification, product isolation, product purification, formulation, and packaging of products (Misha and Dubrey, 2009). There are two methods of cell lysis that can be used: chemical (osmotic shock, addition of chemicals, detergents, enzymes) and physical (compression and/or shear, high pressures homogenizer, bead mill, ultrasonication). Biological products are separated and based on one or several physical or physicochemical properties, which are as follows:

- Size, for example, filtration, centrifugation, membrane separation, gel filtration
- Density, for example, flotation, centrifugation, sedimentation
- Diffusivity, for example, membrane separation, extraction
- Shape, for example, flocculation, sedimentation
- Polarity, for example, extraction, precipitation, crystallization
- Electrostatic charge, for example, adsorption
- Mobility, for example, electrophoresis
- Steric hindrance, for example, filtration
- Volatility, for example, distillation, pervaporation

In the formulation of the end product, lyophilization, adding of excipients and package are used as the main processes.

Chemical aspects

Chemistry has had a fundamental role in almost every aspect of modern society. However, the chemical industry has come under increasing pressure to make production more eco-friendly. Green chemistry is a chemical philosophy encouraging the design of products and processes that reduce or eliminate the use and generation of hazardous substances (Anastas and Warner, 1998). As for white biotechnology, it links green chemist and bio-based production. Also known as industrial biotechnology, it is the modern use and the application of biotechnology for the sustainable processing and production of chemicals, materials, and fuels (Hatti-Kaul et al., 2007). Biotechnology can both replace existing chemical processes and allow the production of new products. A concretization of white biotechnology is a concept of a biorefinery. A biorefinery is a facility that systematically obtains products such as

valuable chemicals, fuels, and materials through microbial fermentation of sugar produced by decomposing biomass as renewable resources (Kamm and Kamm, 2004).

Fossil reserves are finite and increasingly expensive as raw materials. A change in the feedstock from hydrocarbons to biological molecules will alter the technological basis of the world industry. Plants offer a sustainable solution; thanks to photosynthesis, complex products are renewable and can be obtained cheaply and in large quantities. Biomass will play a major role in the next generation of chemical industry which, contrary to petroleum refineries, does not use crude oil to obtain similar products. Biomass can be subdivided into several groups of substances, such as cellulose, starch, hemicelluloses, protein, oil, and lignin. The majority of all biomass found in nature is carbohydrates, which remain to be a flexible raw material. Biotechnological transformation, as well as classical chemical transformation, has also been explored. Nowadays, only a small number of chemicals are produced from renewable resources via fermentation (Haveren et al., 2008). The biotechnological production of lactic acid, acetic acid, and ethanol is a process that is currently applied on a technical scale, which can compete with petrochemical routes. Various technological processes used in the production of many chemicals such as butadiene, butandiol, acrylic acid, propane, and succinic acid from renewable resources are technologically feasible, yet, they remain uneconomical.

Biocatalysis is one of the branches of chemical biotechnology. The increasing contribution of biotechnology in industrial chemistry means discovering enzymes and new synthetic routes to fine and bulk chemistry (Arnold and Glieder, 2003). Current applications of enzyme biocatalysis are dominated by enantioselective bioconversion for fine chemical production. However, an enzyme can have other functions, including the production, degradation, and modification of polymers.

Chemical biotechnologists are generating new molecules with the aim of applying them to the production of foods, pharmaceuticals, materials, and consumer products. By cloning genes from different sources in new ways inside the engineered host, pathways to rare or even unknown metabolites have been found.

Summary

Biotechnology, being an interdisciplinary science, is largely based on physical and chemical processes used in the preparation of organisms and substrates for conducting a biological process as well as various individual operations with the aim of obtaining an end product. Bioprocess control is based to a considerable degree on sensors that use physical and chemical properties of specific media. Chemical biotechnology is going to play a more and more significant role in generating bioenergy and chemicals with the use of renewable plant biomass serving as raw material. The progress in metabolic paths is going to enable one to obtain compounds in a natural way – an innovation in the field of biotechnology.

Bibliography

- Alford, J. S., 2006. Bioprocess control: advances and challenges. *Computers and Chemicals Engineering*, **30**, 1464–1475.
- Anastas, P., and Warner, J., 1998. *Green Chemistry. Theory and Practice*. New York: Oxford University Press.
- Arnold, F. H., and Glieder, A., 2003. Chemistry and biotechnology: a productive union meets new challenges. *Currents Opinion in Biotechnology*, **14**, 567–569.
- Hatt-Kaul, R., Tornvall, U., Gustafsson, L., and Borjesson, P., 2007. Industrial biotechnology for the production of biobased chemicals – a cradle-to-grave perspective. *Trends in Biotechnology*, **25**, 119–124.
- Haveren, J., Scott, E. L., and Sanders, J., 2008. Bulk chemicals from biomass. *Biofuels, Bioproducts and Biorefining*, **2**, 41–57.
- Kamm, B., and Kamm, M., 2004. Principles of biorefineries. *Applied Microbiology and Biotechnology*, **64**, 137–145.
- Misha, N., and Dubrey, A., 2009. *Bioseparation Technology*. CRC PR INC.
- Purohit, S. S., 2005. *Biotechnology. Fundaments and Applications*. Agrobios (India).

Cross-references

- [Algae, the Potential Source of Energy](#)
[Alternative Sources of Energy from Agriculture Biomass – a European Perspective](#)
[Biofilms in the Food Environment](#)
[Biofilms in Soil](#)
[Enzymes in Soils](#)
[Microbes and Soil Structure](#)
[Microbes, Habitat Space, and Transport in Soil](#)

BOUND WATER

The thin layer of water tightly adsorbed onto the surface of clay particles, presumed by some investigators to be more rigid than the bulk water that resides in the wider pore spaces between the particles

Bibliography

- Introduction to Environmental Soil Physics. (First Edition). 2003. Elsevier Inc. Daniel Hillel (ed.) <http://www.sciencedirect.com/science/book/9780123486554>

BOUSSINESQ EQUATION

An equation describing pressure distribution in uniform elastic materials. It is used in soil mechanics to estimate the stresses at any point within the soil profile due to a concentrated load applied to the surface.

Bibliography

- Introduction to Environmental Soil Physics. (First Edition). 2003. Elsevier Inc. Daniel Hillel (ed.) <http://www.sciencedirect.com/science/book/9780123486554>

BOWEN RATIO

An index that is proportional to the ratio of temperature gradient to vapor pressure gradient in the atmosphere above a field. It is relatively low when the field is wet and the evaporation rate is high, i.e., when the temperature gradient is small relative to the vapor pressure gradient. When the field is dry, the humidity gradients tend to be low and much of the received solar energy goes to warming the soil, hence the temperature gradients tend to be steep and the Bowen ratio becomes large.

Bibliography

Introduction to Environmental Soil Physics. (First Edition). 2003. Elsevier Inc. Daniel Hillel (ed.) <http://www.sciencedirect.com/science/book/9780123486554>

Cross-references

[Energy Balance of Ecosystems](#)

BRAGG'S LAW

The relationship between x-ray wavelength (λ), the crystal planar spacings (d), and the x-ray beam incident angle(θ) when diffraction occurs: $n\lambda = 2 d \sin\theta$.

BREADS: PHYSICAL PROPERTIES

Renata Różyło, Janusz Laskowski

Department of Equipment Operation and Maintenance in the Food Industry, University of Life Sciences, Lublin, Poland

Definition

Physical properties of bread – bread properties that can be measured or calculated from instrument readouts.

Introduction

Bread is one of the fundamental food products, necessary in human nutrition. It is produced through baking dough made of flour, water, possibly also salt and other additives. The dough is usually subjected to fermentation, either natural or with the help of leavening agents.

Depending on the basic material used, bread is generally classified as wheat bread, rye bread, mixed grain bread, and others – as pertains to the raw materials, the technology applied, etc. Bread quality depends on the properties of the raw materials and on the technological parameters applied in the process of production. The quality assessment of bread makes use of determinations of its physical properties, among which the most frequently tested are the volume, weight, and specific weight (true

density) of bread. Estimations of the quality of bread crumb take into consideration such features as its structure, moisture, and mechanical properties (firmness (hardness), gumminess, chewiness, cohesiveness, resilience, springiness, etc.). Whereas, estimations of the quality of bread crust are based on such parameters as color and mechanical properties of crust as determined in testing by means of a variety of instruments. The results of determinations of the physical properties of bread permit verification of the effect of the raw materials and the process parameters on the quality of bread.

Determination of physical properties of bread

Measurement of volume is used for the determination of the specific volume which is a quotient of volume and weight of bread, as well as for the determination of true density of bread, through division of its weight by its volume (Esteller et al., 2006). Bread volume measurement can be made in accordance with the methods consisting in bread volume measurement by means of granular materials, e.g., millet or rapeseed. Poppy seed is less frequently used for the purpose. The most commonly used devices operating on the principle of displaced seeds include the Fornet apparatus (Tamba – Berehoui et al., 2004), the Sa-Wa apparatus (Sadowska et al., 2003), very popular in Poland, and the Chopin apparatus (Carr et al., 2006).

Currently the latest generation apparatus for bread volume measurement have been introduced, where the object studied is scanned with the ultrasonic method or by means of laser beam.

The volume of bread is affected by the process of dough fermentation, during which carbon dioxide is released, leavening the dough and causing an increase in bread volume. Whereas, poorly risen dough subjected to baking will yield bread of small volume. Extended process of fermentation has a negative effect on the plasticity of gluten, yielding loafs of reduced volume. Extension of the time of dough kneading, up to a limit, permits obtainment of bread with large volume, while excessively long kneading will cause the bread produced to be of unsatisfactory quality.

Porosity is defined as the ratio of bread volume occupied by pores to the total bread volume. Determination of bread porosity can be performed with the help of so-called Dallman Tables (Błaszcak et al., 2004). Another method is based on determination of the difference in volume between undisturbed crumb and crumb with the pores eliminated through compression. Bread porosity can also be measured without destroying the bread structure, through the use of a gas multipycnometer in helium or toluene atmosphere.

Another tool for the estimation of bread porosity may be digital analysis of scanned image of bread crumb (Digital image analysis system) (McCarthy et al., 2005; Carr et al., 2006). (See [Image Analysis in Agrophysics](#)).

Porosity is a characteristic index of bread quality and it is related with bread volume. Porosity reflects the course of all stages of bread production, with special emphasis

on the process of dough fermentation and on the quality of materials used for baking (Bloksma, 1990).

Observation of crumb structure is performed with the use of various types of microscopes, including optical microscopes, scanning electron microscopes, cryogenic electron microscopes, confocal-laser scanning microscopes, as well as ultrasonic techniques.

The cellular structure of bread crumb has a considerable effect on its mechanical properties. Scanlon et al. (2000) observed that the microstructure features of bread crumb were related with the estimation of its texture.

Moisture of bread crumb, another important index of bread quality, is determined by drying a sample of bread to a constant weight. Apart from bread moisture measurement, water activity measurements are also made, with the help of special automatic gauges.

The mechanical properties of bread crumb are commonly determined in single or dual compression test (TPA test). Bread texture determinations, including the TPA test (Texture Profile Analysis), are very often based on earlier works by Szcześniak (1972) and Bourne (1978). Moreover, there is a number of various other methods for making such determinations. The measurements are made with the help of many different instruments – the TA-XT texture analyzer, the Instron apparatus, the Zwick strength tester, and the Stevens texture analyser. In the course of such measurements, a sample of bread crumb is compressed to various depths depending on the test method. The result of single compression tests is the value of firmness, and in dual compression tests the additional values obtained are those of cohesiveness, resilience, gumminess and chewiness. Additionally it is possible to determine the values of springiness and adhesiveness.

Apart from the bread crumb compression tests, also other tests are used, such as the shearing test (Fik and Surówka, 2002), tensile test (Zghal et al., 2002), penetration test (Fiszman et al., 2005), and indentation test (Liu and Scanlon, 2002). Bread crumb samples are also used for performing the relaxation tests (Mandala and Sotirakoglou, 2005), cracking tests, and hysteresis test (Scanlon et al., 2000). The measurements of flat extruded bread are made with the help of acoustic methods (Marzec et al., 2007).

The mechanical properties of bread crumb are related with those of the dough (Scanlon et al., 2000). Bread baked of dough characterized by high strength have crumb that is more compacted than bread baked of weak dough. A number of correlations between the alveographic properties of dough and the mechanical properties of bread crumb have been demonstrated by Dziki and Laskowski (2005).

Next to the raw material quality, the changes in recipe and the process parameters play an important role in the formation of the textural features of bread. For example it was demonstrated that the different water level (Rózyło et al., 2009) and the conditions of the fermentation process effect on breadcrumb texture (Gómez et al., 2008).

The textural features of bread may be modified through the application of natural additives – e.g., other cereals or

flours. Changes in textural features may also be caused by artificial additives.

Staling causes especially intensive changes in textural properties of bread. When gluten-free bread is kept in storage, there is an increase in crumb firmness, with simultaneous drop in crumb moisture and crust firmness (McCarthy et al., 2005). After 2 days of storage, such bread becomes brittle and crumbling, and its springiness, cohesiveness and resilience decreases (Moore et al., 2004). Storage causes a change in the textural properties of bread, crumb firmness being characterized by the highest percentage change as compared to resilience, cohesiveness, gumminess and chewiness, and therefore it can be accepted that firmness is that feature which reflects the degree of bread staleness the best (Rózyło et al., 2009).

Determination of crust coloring is an important parameter in the estimation of bread crust and can be performed with the use of a chromameter, spectrophotometer or calorimeter.

Estimation of the mechanical parameters of bread crust is highly significant in the determination of crust quality. Methods used for the determination include the penetration test (McCarthy et al., 2005), the crust puncture test (Mandala and Sotirakoglou, 2005), and the crust shear test (Fik and Surówka, 2002).

Conclusions

In view of the significant role of bread in the human diet, special attention should be paid to its quality features, and the physical properties – due to their relations with sensory assessment – appear to be the best indicators of bread quality. There are many factors that have a significant effect on the quality of bread. The qualities of raw materials, the recipe applied, production process parameters and storage conditions significantly affect the physical properties of bread. Therefore, knowledge of the physical properties of bread has a notable utility significance, permitting optimization of production in modification of existing products and processes as well as when introducing new ones.

Bibliography

- Błaszcak, W., Sadowska, J., Rosell, C. M., and Fornal, J., 2004. Structural changes in the wheat dough and bread with the addition of alpha-amylases. *European Food Research and Technology*, **219**, 348–354.
- Bloksma, A. H., 1990. Dough structure, dough rheology and baking quality. *Cereal Foods World*, **35**, 237–244.
- Bourne, M. C., 1978. Texture profile analysis. *Food Technology*, **32**, 62–66.
- Carr, L. G., Rodas, M. A. B., Della Tore, J. C. M., and Tadini, C. C., 2006. Physical, textural and sensory characteristics of 7-day frozen part-baked French bread. *LWT Food Science and Technology*, **39**, 540–547.
- Dziki, D., and Laskowski, J., 2005. The influence on buckwheat flour addition on selected properties of wheat dough and bread crumb (in Polish). *Acta Agrophysica*, **6**, 617–624.
- Esteller, M. S., Zancanaro, O. Jr., Santos Palmeira, C. N., and da Silva Lannes, S. Z., 2006. The effect of kefir addition on microstructure parameters and physical properties of porous white bread. *European Food Research and Technology*, **222**, 26–31.

- Fik, M., and Surówka, K., 2002. Effect of prebaking and frozen storage on the sensory quality and instrumental texture of bread. *Journal of the Science of Food and Agriculture*, **82**, 1268–1275.
- Fiszman, S. M., Salvador, A., and Varela, P., 2005. Methodological developments in bread staling assessment: application to enzyme-supplemented brown pan bread. *European Food Research and Technology*, **221**, 616–623.
- Gómez, M., Oliete, B., Pando, V., Ronda, F., and Caballero, P. A., 2008. Effect of fermentation conditions on bread staling kinetics. *European Food Research and Technology*, **226**, 1379–1387.
- Liu, Z., and Scanlon, M. G., 2002. Understanding and modeling the processing - mechanical property relationship of bread crumb assessed by indentation. *Cereal Chemistry*, **79**, 763–767.
- Mandala, I. G., and Sotirakoglou, K., 2005. Effect of frozen storage and microwave reheating on some physical attributes of fresh bread containing hydrocolloids. *Food Hydrocolloids*, **19**, 709–719.
- Marzec, A., Lewicki, P. P., and Rachanowski, Z., 2007. Influence of water activity on acoustic emission of flat extruded bread. *Journal of Food Engineering*, **79**(2), 410–422.
- McCarthy, D. F., Gallagher, E., Gormley, T. R., Schober, T. J., and Arendt, E. K., 2005. Application of response surface methodology in the development of gluten-free bread. *Cereal Chemistry*, **82**, 609–615.
- Moore, M. M., Schober, T. J., Dockery, P., and Arendt, E. K., 2004. Textural comparisons of gluten-free and wheat-based doughs, batters, and breads. *Cereal Chemistry*, **81**, 567–575.
- Różyło, R., Dziki, D., and Laskowski, J., 2009. Effect of different levels of water addition on wheat bread crumb texture (in Polish). *Acta Agrophysica*, **13**, 761–769.
- Sadowska, J., Błaszczałk, W., Fornal, J., Vidal-Valverde, C., and Frias, J., 2003. Changes of wheat dough and bread quality and structure as a result of germinated pea flour addition. *European Food Research Technology*, **216**, 46–50.
- Scanlon, M. G., Sapirstein, H. D., and Fahloul, D., 2000. Mechanical properties of bread crumb prepared from flours of different dough strength. *Journal of Cereal Science*, **32**, 235–243.
- Szczęśniak, A., 1972. Instrumental methods of texture measurements. *Food Technology*, **26**, 51–56.
- Tamba-Berehoiu, R., Popa, N. C., Balan, D., Popescu, S., and Iancu, A., 2004. Testing of some enzymatic mixtures used for the improvement of wheat flours. *Roumanian Biotechnological Letters*, **9**(5), 1871–1878.
- Zghal, M. C., Scanlon, M. G., and Sapirstein, H. D., 2002. Cellular structure of bread crumb and its influence on mechanical properties. *Journal of Cereal Science*, **36**, 167–176.

Cross-references

- [Cereals, Evaluation of Utility Values](#)
[Image Analysis in Agrophysics](#)
[Physical Properties as Indicators of Food Quality](#)
[Physical Properties of Raw Materials and Agricultural Products](#)

BRIGHTNESS TEMPERATURE IN MONITORING OF SOIL WETNESS

Jerzy Usowicz
 Toruń Centre for Astronomy, Nicolaus Copernicus University, Toruń, Poland

Introduction

All bodies, including soil, consist of atoms and molecules. Any body at a final absolute temperature radiates

electromagnetic energy. This electromagnetic radiation is termed as a thermal radiation. According to quantum theory, the thermal radiation is always emitted when the atoms or molecules undergo transitions from higher to lower energy levels. The frequency of the emitted photon is given by the Planck's equation $\Delta E = h\nu$. There are three different kinds of energetic transitions: electron, vibrational, and rotational. Any system which contains a huge number of molecules is characterized by a large number of degrees of freedom. Molecules collide with each other due to their random motion. Every collision causes a change of their energy levels. Spectral lines emitted by such a system are very close to each other which results in a continuous spectrum of radiation. The collision rate depends on the kinetic energy of the random motion. It increases with the absolute temperature of the substance.

In 1900, Max Planck derived a new formula for the thermal radiation of a black body. It was a significant event for the birth and subsequent development of quantum mechanics. The Planck's law describes the relation between the temperature of a black body and its radiated power. It is given by the following formula:

$$I = \frac{2hv^3}{c^2} \frac{1}{e^{\frac{hv}{kT}} - 1}$$

where

T is the temperature, K

c is the speed of light, 2.99×10^8 m s⁻¹

h is the Planck's constant, 6.63×10^{-34} J s

k is the Boltzmann's constant, 1.38×10^{-23} JK⁻¹

I is the specific intensity, W m⁻² Hz⁻¹ Sr⁻¹

The specific intensity is expressed as a power per unit area per unit frequency interval and per unit solid angle.

The Rayleigh–Jeans law is a convenient and accurate approximation of the Planck's formula for $\frac{hv}{kT} \ll 1$. Expanding the exponential in the denominator of Planck's law in a Taylor series about zero argument, we obtain the following formula

$$I = \frac{2kTv^2}{c^2}$$

At this point, we have to invoke the Kirchoff's law which says that the emissivity ε of a body is equal to its absorptivity α . The absorptivity of a body is defined as the ratio of the total thermal energy absorbed by the surface to the total thermal energy incident upon it. By the definition, a black body has absorptivity $\alpha = 1$. Thus, a black body is also the most efficient radiator and has $\varepsilon = 1$.

In reality, bodies or substances emit less than a black body and the specific intensity emitted generally depends on the direction and the polarization. In passive remote sensing, microwave receiver measures the specific intensity $I_\beta(\theta, \phi)$ emitted by the given object, where β denotes

the polarization and $I_\beta(\theta, \phi)$ denotes the angular dependence. An equivalent radiometer temperature called the brightness temperature $T_{B\beta}(\theta, \phi)$ can be derived simply from the Rayleigh–Jeans law as follows:

$$T_{B\beta}(\theta, \phi) = \frac{I_\beta(\theta, \phi)c^2}{kv^2}$$

Assuming that the body has a uniform physical temperature T , the emissivity $\varepsilon_\beta(\theta, \phi)$ is defined as a ratio:

$$\varepsilon_\beta(\theta, \phi) = \frac{T_{B\beta}(\theta, \phi)}{T}$$

From this definition one obtains the fundamental equation used in passive remote sensing:

$$T_{B\beta}(\theta, \phi) = \varepsilon_\beta(\theta, \phi)T$$

According to this equation, the brightness temperature of a body depends on its emissivity and its physical temperature.

Soil can be regarded as a mixture of water and the bulk material which includes sand, silt and clay. The emissivity of soil depends on the effective dielectric constant of this medium (Monerris, 2009). The relationship between brightness temperature and soil emissivity is linear in general; however, the emissivity of water depends nonlinearly on its dielectric constant (Behari, 2005). The theory of microwave remote sensing of soil moisture is based on the large contrast between dielectric properties of liquid water (~ 80) and dry soil (~ 4). As the water content in soil increases, the dielectric constant of the soil–water mixture increases as well. Such changes are detectable by microwave radiometers in surface soil layer of 5 cm depth.

Bibliography

- Behari, J., 2005. *Microwave Dielectric Behavior of Wet Soils*. Berlin: Springer.
 Monerris, A., 2009. *Experimental Estimation of Soil Emissivity and Its Application to Soil Moisture Retrieval in the SMOS Mission*. Ph.D. thesis, Universitat Politècnica de Catalunya, Barcelona, Spain.

Cross-references

- Backscattering
 Remote Sensing of Soils and Plants Imagery
 Soil Physical Degradation: Assessment with the Use of Remote Sensing and GIS

BRUISE

See *Fruits, Mechanical Properties and Bruise Susceptibility*

BUFFER CAPACITY OF SOILS

Mieczysław Hajnos

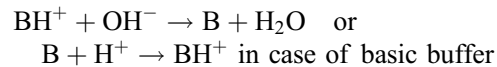
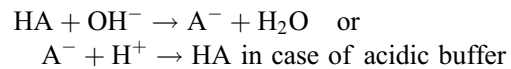
Institute of Agrophysics, Polish Academy of Science,
 Lublin, Poland

Definition

Buffer capacity of soil is defined as a soil's ability to maintain a constant pH level during action on it by an acidifier or alkalescent agent. A soil, considered a mixture of buffered systems, contains components, which have the ability to neutralize acids by bonding H^+ ions as well as bases by the release of hydrogen ions (Federer and Hornbeck, 1985). The effectiveness of soil buffering systems depends on numerous physical, chemical, and biological properties of soils.

Buffer capacity

A buffer solution is an aqueous solution consisting of a mixture of a weak acid and its conjugate base ($HA + A^-$) or a weak base and its conjugate acid ($B + BH^+$). It has the property that the pH of the solution changes very little when a small amount of acid or base is added to it because of the following reactions:



Buffer capacity is a quantitative measure of the resistance of a buffer solution to pH change on addition of hydrogen or hydroxide ions. It can be defined as follows:

$$\text{Buffer capacity} = \frac{dn}{d(pH)} \quad (1)$$

where dn is an infinitesimal amount (in moles) of added base or acid and $d(pH)$ is the resulting infinitesimal change in pH.

The capacity of soils to oppose an acid/alkaline reaction is called buffer properties of soils or soil buffer capacity. Buffer properties of soils are determined by their sorption capacity. The higher the sorption capacity of soil colloids the higher the buffer capacity of soil. Humus colloid fraction exhibits the strongest buffer activity among the soil colloids.

Buffer properties of soils are connected with the following processes: reactions of dissolution of calcium carbonate in weak acids or its total decomposition by strong acids; with weathering of primary silicates resulting in the release of basic cations; ion-exchange process in result of adsorption of hydrogen cations by organic and mineral components of sorption complex; bonding of H^+ by clay minerals' lattices, by hydroxyaluminium complexes or hydrated alumina; reactions of ferrous oxides and

hydroxides in result of which H⁺ cations are neutralized (Ulrich, 1986).

Buffering reactions with bonding or release of protons occur in soils also in the following processes: organic matter mineralization, mineralization and nitrification of organic nitrogen, mineralization and oxidation of organic sulfur, mineralization of organic phosphorous, complexing or releasing of metal cations, etc. (van Breemen et al., 1984).

Knowledge of buffering properties of soils is of great importance in respect to the estimation of a liming effect or influence of degrading factors on the soil environment (Jaworska et al., 2005).

Bibliography

- van Breemen, N., Driscoll, C. T., and Mulder, J., 1984. Acidic deposition and internal proton sources in acidification of soils and waters. *Nature*, **307**, 599–604.
- Federer, C. A., and Hornbeck, J. W., 1985. The buffer capacity of forest soils in New England. *Water, Air, and Soil Pollution*, **26**, 163–173.
- Jaworska, H., Dąbkowska-Naskret, H., and Malczyk, P., 2005. Buffer properties of soils with regard to their vulnerability to degradation. *Ecological Chemistry and Engineering*, **12**, 231–239.
- Ulrich, B., 1986. Natural and anthropogenic components of soil acidification. *Zeitschrift für Pflanzenernährung und Bodenkunde*, **149**, 702–717.

Cross-references

- Alkalinity, Physical Effects on Soils
Electrochemical Measurements in Soils
Liming, Effects on Soil Properties

BULK DENSITY OF SOILS AND IMPACT ON THEIR HYDRAULIC PROPERTIES

Shmuel Assouline

Environmental Physics and Irrigation, Institute of Soil, Water and Environmental Sciences, Agricultural Research Organization – Volcani Center, Bet Dagan, Israel

Definition

Density is the ratio of mass to volume, with a dimension of (ML⁻³). A soil sample at natural conditions consists, in most of the cases, in three phases, solid, gas, and liquid. The bulk density of a soil sample, generally represented by ρ_b , is a physical property defined as the ratio of the total mass of solids (M_s) to the total volume of the sample (V_t):

$$\rho_b = \frac{M_s}{V_t} \quad (1)$$

The bulk density of soils is generally expressed in units of g cm⁻³ or Mg m⁻³.

The bulk density of soils is related to additional physical properties, such as porosity, n , and void ratio, e :

$$\rho_b = \rho_s(1 - n) \quad (2)$$

$$\rho_b = \frac{\rho_s}{e + 1} \quad (3)$$

where ρ_s is the soil particle density defined as the ratio of the total mass of solids (M_s) to the volume of solids (V_s).

The bulk density is required to transform gravimetric water content, θ_g , into volumetric water content, θ_v :

$$\theta_v = \rho_b \theta_g \quad (4)$$

The normal range of ρ_b in natural undisturbed soils varies between 0.7 and 1.8 Mg m⁻³.

The bulk density: an integrative soil physical property

The definition of the bulk density in Equation 1, addressing explicitly the total mass of solids and the total volume it occupies, indicates that it is a physical macro-property related to both soil texture and structure. Soil texture corresponds to the relative amount of sand, silt, and clay components of the solid phase. These components affect the nature of the arrangement of the soil particles, and play a role in determining numerous soil physical, chemical, and biological properties, including porosity and bulk density (Rawls, 1983; Gupta and Larson, 2001; Martin et al., 2009). The nature of the specific relationships depends on the clay type, the presence of organic matter and cementing agents, and the ionic strength of the liquid phase. A special interest was given to the effect of organic matter content on ρ_b (Rawls, 1983; Soane, 1990; Arvidsson, 1998; Ruehlmann and Korschens, 2009).

Soil structure characterizes the spatial arrangement of the solid particles within the total volume, and will thus determine ρ_b . However, soil structure addresses also the specific void size distribution, and related state variables such as tortuosity and connectivity, within the soil sample under interest. It therefore affects basic hydraulic, electrical, mechanical, and thermal soil properties. Consequently, ρ_b is expected to be related to these important soil properties, and to affect water, heat, and gas exchange (Warkentin, 1971; Stepniewski et al., 1994), root growth (Voorhees et al., 1975; Dexter, 1987; Lipiec and Hatano, 2003), and crop production and environment quality (Håkansson et al., 1988; Soane and van Ouwerkerk, 1995; Dexter, 2004). In various regression equations aiming to predict hydraulic properties from available basic soil data, generally addressed as pedotransfer functions, bulk density is a key element of the input dataset (Gupta and Larson, 1979; Rawls et al., 1983; Pachepsky et al., 1998).

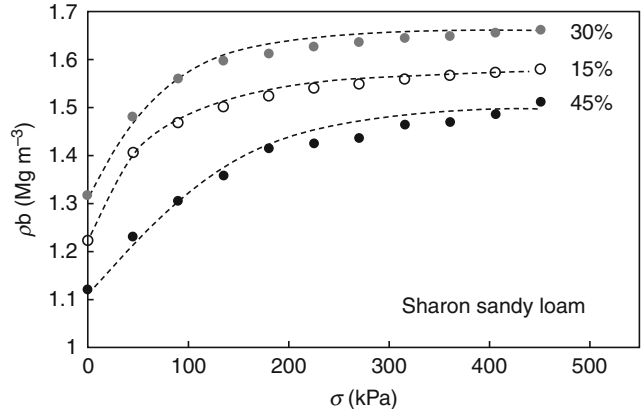
Soil bulk density can be measured using direct or indirect methods. The direct method consists in measuring the mass of the oven-dried soil sample and the volume it occupies (Equation 1). This measurement may be carried out using cylinders of a known volume (Blake and Hartge, 1986;

Campbell and Henshall, 1991). Although being quite simple and straightforward, the direct methods are prone to errors during sample extraction, transport, and handling in the laboratory. Indirect methods are based on measuring the attenuation in the intensity of gamma radiation emitted by a radioactive isotope due to the presence of the soil between the source and the receiver (Vomocil, 1954; Van Bavel et al., 1957; Freitag, 1971; Soane and Henshall, 1979). The attenuation in radiation intensity is related to soil bulk density and water content. Consequently, calibration is required to empirically relate the attenuation to ρ_b , and the soil moisture content has to be known. The disadvantages of the gamma-ray method are that devices are expensive and that their operations require nuclear safety-trained personnel. An additional indirect method relies on the correlation between soil penetration resistance, soil water content, and ρ_b . Soil penetration resistance can be estimated by means of cone penetration tests using penetrometers. Soil penetration resistance was found to increase with increasing ρ_b and to decrease with increasing soil water content. A combined penetrometer–moisture probe aiming to provide simultaneous soil moisture and penetration resistance measurements was developed by Vaz and Hopmans (2001). Penetrometer readings may be empirically related to ρ_b and θ_v . However, these relationships are specific to the soil type and the characteristics of penetrometers. A large number of models are available that relate penetrometers data to ρ_b estimates (Wells and Treesuwant, 1978; Jakobsen and Dexter, 1987; Ayers and Bowen, 1987).

Bulk density is not an intrinsic property of the soil but rather depends on external conditions. Increase in ρ_b occurs at a variety of scales and may result from various natural as well as artificial processes. It can occur around a growing root (Dexter, 1987; Bruand et al., 1996), during rainfall (Tackett and Pearson, 1965; Baumhardt et al., 1990; Bresson et al., 2004; Assouline, 2004), or during the passage of loaded wheels (Lindstrom and Voorhees, 1995; van Dijck and van Asch, 2002). Cycles of wetting and drying, and freezing and thawing, after tillage may also cause the soil bulk density to increase because of natural soil reconsolidation, thereby affecting the hydraulic properties of the soil profile (Mapa et al., 1986; Rousseva et al., 1988; Or et al., 2000).

Soil bulk density and compaction

Compaction is the process of reducing the volume of voids in a soil, mainly those filled with air, by packing the soil particles closer together. Consequently, ρ_b increases during compaction. Figure 1 depicts the increase in ρ_b resulting from the increase in the applied stress, σ , of three sandy loam soil samples at different initial saturation degrees during uniaxial drained compaction tests. Therefore, ρ_b is often used as an indicator to evaluate the impact of vehicular traffic or of tillage systems on the soil physical condition (Gupta and Larson, 1982;



Bulk Density of Soils and Impact on Their Hydraulic Properties, Figure 1 Compaction curves from uniaxial compression test on the Sharon sandy loam at three different initial saturation degrees, and the corresponding fitted model in Equation 5 (dashed lines).

Or and Ghezzehei, 2002). A degree of compactness, defined as the dry bulk density of a soil as a percent of a reference bulk density obtained by a standardized uniaxial compression test, was introduced to allow directly comparable values for all soil types (Håkansson and Lipiec, 2000).

A logarithmic model was generally used to mathematically describe the increase of ρ_b with the applied stress, σ (Bailey and Vanden Berg, 1967; Larson et al., 1980; Gupta and Larson, 1982). In the logarithmic model, ρ_b is undefined for $\sigma = 0$ and it continues to increase as σ increases (Assouline et al., 1997). Furthermore, it is not flexible enough to represent the variability of the compression curve shapes, which can range from nearly linear to sigmoidal curves (Fritton, 2001). Therefore, additional models involving exponential and power functions were developed to provide a reliable mathematical representation of the mechanical compaction process (Bailey et al., 1986; Assouline et al., 1997; Fritton, 2001). Assouline (2002) has generalized the model of Assouline et al. (1997) to account for preconsolidation effect:

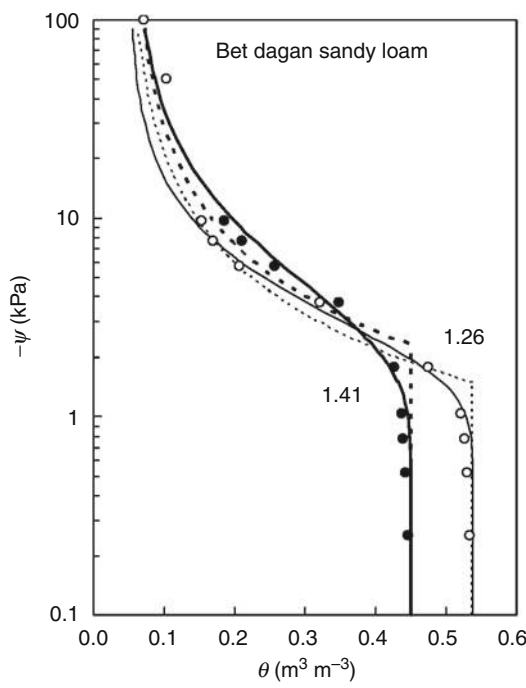
$$\rho = \rho_o + (\rho_{\max} - \rho_o)[1 - e^{-(\kappa\sigma)^{\omega}}]; \quad \omega > 0 \quad (5)$$

where ρ_{\max} , ω , and κ are considered as fitting parameters that depend on the initial soil water content, although ρ_{\max} could be fairly predicted by means of compression tests under laboratory conditions (Hartge, 1986; O'Sullivan, 1992). The model in Equation 5 fulfills the boundary conditions ($\sigma = 0$; $\rho = \rho_o$) and ($\sigma \rightarrow \infty$; $\rho \rightarrow \rho_{\max}$). The ability of the model in Equation 5 to describe compaction curves is illustrated in Figure 1. The expression in Equation 5 was fitted to the data in Figure 1, and reproduces quite accurately the different shapes as well as the effect of the initial water content. It can be seen also that maximum compaction is obtained for some optimal water content.

Effect of ρ_b on soil hydraulic properties

Soil bulk density affects many aspects of the soil–water–plant–atmosphere system. Appropriate quantitative tools with predictive ability are therefore essential to account for compaction effects on agricultural, hydrological, and environmental aspects. Change in ρ_b due to compaction represents the total change in the voids volume of the soil. Small changes in the voids volume distribution, tortuosity, or connectivity could still occur during compaction, especially during elastic deformation, without reflecting on measurable changes in ρ_b (Lenhard, 1986). Nevertheless, different studies have suggested that ρ_b is an appropriate independent variable to express the main effects of compaction on the soil hydraulic properties, that is, the water retention curve (WRC) and the hydraulic conductivity function (HCF) (Assouline et al., 1997; Ahuja et al., 1998; Stange and Horn, 2005; Assouline, 2006a, b).

The study of Assouline (2006a) has proposed quantitative expressions that relate the relative changes in the parameters for the WRC models of Brooks and Corey (1964) and Assouline et al. (1998) to the relative change in ρ_b . Consequently, the effect of the increase in ρ_b on the WRC could be predicted, given that the WRC for a reference bulk density is known. Figure 2 depicts measured WRCs for a sandy loam soil corresponding to

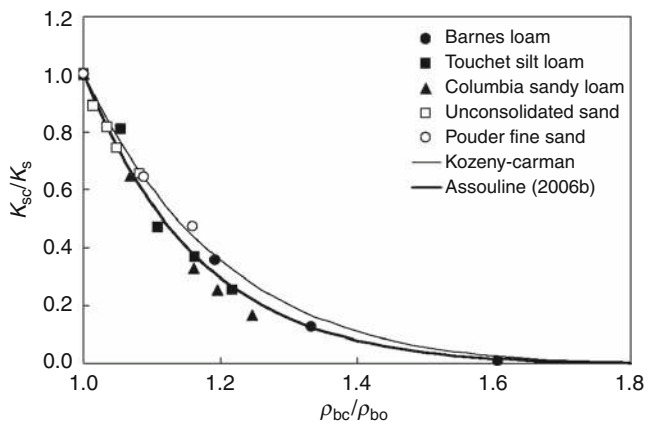


Bulk Density of Soils and Impact on Their Hydraulic Properties, Figure 2 Measured WRCs for a sandy loam soil at two bulk densities and the corresponding modeled curves following Assouline (2006a). The dashed lines correspond to the model of Brooks and Corey (1964) and the solid lines to the model of Assouline et al. (1998).

two bulk densities, 1.26 g cm^{-3} and 1.41 g cm^{-3} . Increase in ρ_b reduces the saturated water content, increases the air entry value, and increases the pore size distribution index. The thin dashed line represent the fitted model of Brooks and Corey (1964) and the solid one, that of Assouline et al. (1998), to the WRC at the reference state $\rho_{bo} = 1.26 \text{ g cm}^{-3}$. The thick dashed and solid lines represent the corresponding predicted curves according to the model of Assouline (2006a).

The impact of ρ_b on the HCF addresses the saturated state, and its corresponding saturated hydraulic conductivity, K_s , and the unsaturated one. The reduced relative part of the large pores in the soil when ρ_b increases (Lipiec et al., 1998; Häkansson and Lipiec, 2000), mostly determine the resulting reduction in K_s (Laliberte et al., 1966; Dawidowski and Koolen, 1987; Dębicki et al., 1993). A large body of studies has suggested quantitative relationships between K_s and ρ_b (Carman, 1937; Laliberte et al., 1966; Mualem and Assouline, 1989; Or et al., 2000; Green et al., 2003; Assouline, 2006b). A concise review of the different approaches developed to relate the permeability of porous media to porosity can be found in Assouline and Or (2008). Figure 3 presents the relative decrease in K_s versus the relative increase in ρ_b for various soil types, as well as the predicted relationship resulting from the Kozeny–Carman expression (Carman, 1937; Or et al., 2000; thin solid line) and from the model of Assouline (2006b, bold solid line).

Studies dealing with the unsaturated case are scarce. Most of these studies apply Mualem's (1976) model of the HCF (Or et al., 2000; Lipiec and Hatano, 2003; Morozumi and Horino, 2004). Assouline (2006b) has extended the HCF model of Assouline (2001) to account for changes in ρ_b . An interesting result of this study is that the relationship between the power parameter of the HCF model and the coefficient of variation of the WRC, which



Bulk Density of Soils and Impact on Their Hydraulic Properties, Figure 3 Measured and modeled relative decrease in K_s versus the relative increase in ρ_b for various soil types (the thin solid line corresponds to Kozeny–Carman expression and the bold solid line, to the model of Assouline (2006b)).

was found to be valid for a large range of soil types, still remain valid when these soils are compacted.

Soil bulk density generally presents some variation with depth within the soil profile under natural conditions as well as under tilled agricultural fields. This behavior, coupled with the relationship between ρ_b and HCF, induces a specific level of anisotropy to the soil profile. Assouline and Or (2006) have analyzed the saturated and the unsaturated anisotropy factors induced by ρ_b distribution with depth. The results indicated that the anisotropy factors can be related to soil texture, especially for fine-textured soils.

Summary

Soil bulk density is an integrative soil physical property containing valuable information on its porosity, level of compactness, and strength. It is a key state variable in the estimates of soil hydraulic properties, thus playing an important role in the definition of rainfall–infiltration–runoff–erosion relationships, heat and gas exchanges, seedling emergence, root growth, crop yields, and soil quality.

Bibliography

- Ahuja, L. R., Fiedler, F., Dunn, G. H., Benjamin, J. G., and Garrison, A., 1998. Changes in soil water retention curves due to tillage and natural reconsolidation. *Soil Science Society of America Journal*, **62**, 1228–1233.
- Arvidsson, J., 1998. Influence of soil texture and organic matter content on bulk density, air content, compression index and crop yield in field and laboratory compression experiments. *Soil and Tillage Research*, **49**, 159–170.
- Assouline, S., and Or, D., 2006. Anisotropy of saturated and unsaturated soils. *Water Resources Research*, **42**, W12403, doi:10.1029/2006WR005001.
- Assouline, S., and Or, D., 2008. Air entry-based characteristic length for estimation of permeability of variably compacted earth materials. *Water Resources Research*, **44**, W11403, doi:10.1029/2008WR006937.
- Assouline, S., Tavares-Filho, J., and Tessier, D., 1997. Effect of compaction on soil physical and hydraulic properties: Experimental results and modeling. *Soil Science Society of America Journal*, **61**, 390–398.
- Assouline, S., Tessier, D., and Bruand, A., 1998. A conceptual model of the soil water retention curve. *Water Resources Research*, **34**, 223–231.
- Assouline, S., 2001. A model of soil relative hydraulic conductivity based on water retention curve characteristics. *Water Resources Research*, **37**, 265–271.
- Assouline, S., 2002. Modeling soil compaction under uniaxial compression. *Soil Science Society of America Journal*, **66**, 1784–1787.
- Assouline, S., 2004. Rainfall-induced soil surface sealing: a critical review of observations, conceptual models and solutions. *Vadose Zone Journal*, **3**, 570–591.
- Assouline, S., 2006a. Modeling the relationship between soil bulk density and water retention curve. *Vadose Zone Journal*, **5**, 554–563.
- Assouline, S., 2006b. Modeling the relationship between soil bulk density and hydraulic conductivity function. *Vadose Zone Journal*, **5**, 697–705.
- Ayers, P. D., and Bowen, H. D., 1987. Predicting soil density using cone penetration resistance and moisture profiles. *Transactions of the ASAE*, **30**, 13311336.
- Bailey, A. C., and Vanden Berg, G. E., 1967. Yielding by compaction and shear in unsaturated soils. *Transactions of the American Society of Agricultural Engineers*, **11**(307–311), 317.
- Bailey, A. C., Johnson, C. E., and Schafer, R. L., 1986. A model for agricultural soil compaction. *Journal of Agricultural Engineering Research*, **33**, 257–262.
- Baumhardt, R. L., Römkens, M. J. M., Whisler, F. D., and Parlange, J. Y., 1990. Modeling infiltration into a sealing soil. *Water Resources Research*, **26**, 2497–2505.
- Blake, G. R., and Hartge, K. H., 1986. Bulk density. In Klute, A. (ed.), *Methods of Soil Analysis. Part I: Physical and Mineralogical Methods*, 2nd edn. Madison: American Society of Agronomy, Soil Science Society of America, p. 1188.
- Bresson, L. M., Moran, C. J., and Assouline, S., 2004. Use of bulk density profiles from X-radiography to examine structural crusts models. *Soil Science Society of America Journal*, **68**, 1169–1176.
- Brooks, R. H., and Corey, A. T., 1964. Hydraulic properties of porous media. Hydrology Paper 3, Fort Collins: Colorado State University, 27pp.
- Bruand, A., Cousin, I., Nicoullaud, B., Duval, O., and Begon, J. C., 1996. Backscattered electron scanning images of soil porosity for analyzing soil compaction around roots. *Soil Science Society of America Journal*, **60**, 895–901.
- Campbell, D. J., and Henshall, K., 1991. Soil analysis. In Smith, K. A., and Mullins, C. E. (eds.), *Soil Analysis: Physical Methods*. New York: Marcel Dekker, p. 620.
- Carman, P. C., 1937. Fluid flow through granular beds. *Transactions of the Institute of Chemical Engineers (London)*, **15**, 150–156.
- Dawidowski, J. B., and Koolen, A. J., 1987. Changes of soil water suction, conductivity, and dry strength during deformation of wet undisturbed samples. *Soil and Tillage Research*, **9**, 169–180.
- Dębicki, R., Glinski, J., Lipiec, J., Pukos, A., and Turski, R., 1993. Soil strength, stability and structural state of orthic Luvisols under different land use. *International Agrophysics*, **7**, 155–161.
- Dexter, A. R., 1987. Compression of soil around roots. *Plant and Soil*, **97**, 401–406.
- Dexter, A. R., 2004. Soil physical quality – Part I. Theory, effects of soil texture, density, and organic matter, and effects on root growth. *Geoderma*, **120**, 201, doi:10.1016/j.geoderma.2003.09.005.
- Freitag, D. R., 1971. Methods of measuring soil compaction. In: Barnes, K. K., et al. (eds.), *Compaction of agricultural soils*. St. Joseph: ASAE Monograph, pp. 45–103.
- Fritton, D. D., 2001. An improved empirical equation for uniaxial soil compression for a wide range of applied stresses. *Soil Science Society of America Journal*, **65**, 678–684.
- Green, T. R., Ahuja, L. R., and Benjamin, J. G., 2003. Advances and challenges in predicting agricultural management effects on soil hydraulic properties. *Geoderma*, **116**, 3–27.
- Gupta, S. C., and Larson, W. E., 1979. Estimating soil water retention characteristics from particle size distribution, organic matter percent and bulk density. *Water Resources Research*, **15**, 1633–1635.
- Gupta, S. C., and Larson, W. E., 1982. Modeling soil mechanical behavior during tillage. In: van Doren et al. (ed.) *Predicting Tillage Effects on Soil Physical Properties and Processes*. ASA Special Publication 44. Madison: ASA, pp. 151–178.
- Gupta, S. C., and Larson, W. E., 2001. A model for predicting packing density of soils using particle-size distribution. *Soil Science Society of America Journal*, **65**, 1787–1795.
- Håkansson, I., and Lipiec, J., 2000. A review of the usefulness of relative bulk density values in studies of soil structure and compaction. *Soil and Tillage Research*, **53**, 71–85.

- Håkansson, I., Voorhees, W. B., and Riley, H., 1988. Vehicle and wheel factors influencing soil compaction and crop response in different traffic regimes. *Soil and Tillage Research*, **11**, 239–282.
- Hartge, K. H., 1986. A concept of compaction. *Zeitschrift für Pflanzenernährung und Bodenkund*, **149**, 361–370.
- Jakobsen, B. F., and Dexter, A. R., 1987. Effect of soil structure on wheat growth, water uptake and grain yield. A computed simulated model. *Soil and Tillage Research*, **10**, 331–345.
- Laliberte, G. E., Corey, A. T., and Brooks, R. H., 1966. Properties of unsaturated porous media. Hydrology papers 17. Fort Collins: Colorado State University.
- Larson, W. E., Gupta, S. C., and Useche, R. A., 1980. Compression of agricultural soils from eight soils order. *Soil Science Society of America Journal*, **44**, 450–457.
- Lenhard, R. J., 1986. Changes in void distribution and volume during compaction of a forest soil. *Soil Science Society of America Journal*, **50**, 1001–1006.
- Lindstrom, M. J., and Voorhees, W. B., 1995. Soil properties across a landscape continuum as affected by planting wheel traffic. In: Robert, P. C., Rust, R. H., and Larson, W. E. (eds.), *Site-Specific Management for Agricultural Systems*. Madison: ASA-SSSA, pp. 351–363.
- Lipiec, J., and Hatano, R., 2003. Quantification of compaction effects on soil physical properties and crop growth. *Geoderma*, **116**, 107–136.
- Lipiec, J., Hatano, R., and Slowinska-Jurkiewicz, A., 1998. The fractal dimension of pore distribution patterns in variously-compacted soil. *Soil and Tillage Research*, **47**, 61–66.
- Mapa, R. B., Green, R. E., and Santo, L., 1986. Temporal variability of soil hydraulic properties with wetting and drying subsequent to tillage. *Soil Science Society of America Journal*, **50**, 1133–1138.
- Martin, M. P., Lo Seen, D., Boulonne, L., Jolivet, C., Nair, K. M., Bourgeon, G., and Arrouays, D., 2009. Optimizing pedotransfer functions for estimating soil bulk density using boosted regression trees. *Soil Science Society of America Journal*, **73**, 485–493.
- Moroizumi, T., and Horino, H., 2004. Tillage effects on subsurface drainage. *Soil Science Society of America Journal*, **68**, 1138–1144.
- Mualem, Y., and Assouline, S., 1989. Modeling soil seal as a nonuniform layer. *Water Resources Research*, **25**, 2101–2108.
- Mualem, Y., 1976. A new model for predicting the hydraulic conductivity of unsaturated porous media. *Water Resources Research*, **12**, 513–522.
- O'Sullivan, M. F., 1992. Uniaxial compaction effects on soil physical properties in relation to soil type and cultivation. *Soil and Tillage Research*, **24**, 257–269.
- Or, D., and Ghezzehei, T. A., 2002. Modeling post-tillage soil structure dynamics: a review. *Soil and Tillage Research*, **64**, 41–59.
- Or, D., Leij, F. J., Snyder, V., and Ghezzehei, T. A., 2000. Stochastic model of posttillage soil pore space evolution. *Water Resources Research*, **36**, 1641–1652.
- Pachepsky, Ya. A., Rawls, W. J., Gimenez, D., and Watt, J. P. C., 1998. Use of soil penetration resistance and group method of data handling to improve soil water retention estimates. *Soil and Tillage Reserach*, **49**, 117–126.
- Rawls, W. J., Brakensiek, D. L., and Soni, B., 1983. Agricultural management effects on soil water processes. Part I: Soil water retention and Green and Ampt infiltration parameters. *Transactions of the ASAE*, **26**, 1747–1752.
- Rawls, W. J., 1983. Estimating soil bulk density from particle and analysis and organic matter content. *Soil Scence*, **135**, 123–125.
- Rousseva, S. S., Ahuja, L. R., and Heathman, G. C., 1988. Use of a surface gamma-neutron gauge for in-situ measurements of changes in bulk density of the tilled zone. *Soil and Tillage Research*, **12**, 235–251.
- Ruehlmann, J., and Korschens, M., 2009. Calculating the effect of soil organic matter concentration on soil bulk density. *Soil Science Society of America Journal*, **73**, 876–885.
- Soane, B. D., and Henshall, J. K., 1979. Spatial resolution and calibration characteristics of two narrow probe gamma-ray transmission systems for the measurement of soil bulk density in situ. *Soil Science*, **30**, 517–528.
- Soane, B. D., and van Ouwerkerk, C., 1995. Implications of soil compaction in crop production for the quality of the environment. *Soil and Tillage Research*, **35**, 5–22.
- Soane, B. D., 1990. The role of organic matter in soil compactability: A review of some practical aspects. *Soil and Tillage Research*, **16**, 179–201.
- Stange, F. C., and Horn, R., 2005. Modeling the soil water retention curve for conditions of variable porosity. *Vadose Zone Journal*, **4**, 602–613.
- Stepniewski, W., Gliński, J., and Ball, B. C., 1994. Effects of compaction on soil aeration properties. In Soane, B. D., and van Ouwerkerk, C. (eds.), *Soil Compaction in Crop Production*. Amsterdam: Elsevier, pp. 167–190.
- Tackett, J. L., and Pearson, R. W., 1965. Some characteristics of soil crusts formed by simulated rainfall. *Soil Science*, **99**, 407–413.
- Van Bavel, C. H. M., Underwood, N., and Rager, S. R., 1957. Transmission of gamma radiation by soils and soil densitometry. *Soil Science Society of America Journal*, **21**, 588–591.
- van Dijk, S. J. E., and van Asch, Th. W. J., 2002. Compaction of loamy soils due to tractor traffic in vineyards and orchards and its effect on infiltration in southern France. *Soil and Tillage Research*, **63**, 141–153.
- Vaz, C. M. P., and Hopmans, J. W., 2001. Simultaneous measurement of soil penetration resistance and water content with a combined penetrometer–TDR moisture probe. *Soil Science Society of America Journal*, **65**, 4–12.
- Vomocil, J. A., 1954. In situ measurement of soil bulk density. *Agricultural Engineering*, **35**, 651–654.
- Voorhees, W. B., Farrell, D. A., and Larson, W. E., 1975. Soil strength and aeration effects on root elongation. *Soil Science Society of America Journal*, **39**, 948–953.
- Warkentin, B. P., 1971. Effects of compaction on content and transmission of water in soils. In Barnes, K. K., et al. (eds.), *Compaction of Agricultural Soils*. St. Joseph: American Society of Agricultural Engineers, pp. 126–153.
- Wells, L. G., and Treewawan, O., 1978. The response of various soil strength indices to changing water content and bulk density. *Transactions of the ASAE*, **16**, 854–861.

Cross-references

- Agrophysics: Physics Applied to Agriculture
 Compaction of Soil
 Compression Index
 Compression Point
 Databases of Soil Physical and Hydraulic Properties
 Hardsetting Soils: Physical Properties
 Hydraulic Properties of Unsaturated Soils
 Infiltration in Soils
 Management Effects on Soil Properties and Functions
 Plant Roots and Soil Structure
 Pore Size Distribution
 Pre-Compression Stress
 Soil Aggregates, Structure, and Stability
 Soil Compactability and Compressibility
 Soil Penetrometers and Penetrability
 Soil Physical Quality

[Soil Surface Sealing and Crusting](#)
[Soil–Wheel Interactions](#)
[Spatial Variability of Soil Physical Properties](#)
[Stress–Strain Relations](#)
[Tillage, Impacts on Soil and Environment](#)
[Trafficability and Workability of Soils](#)

BURROW

See [Soil Penetrability, Effect on Animal Burrowing](#)

BYPASS FLOW IN SOIL

Horst H. Gerke
 Institute of Soil Landscape Research, Leibniz-Centre for Agricultural Landscape Research (ZALF) Müncheberg, Müncheberg, Germany

Synonyms

Funnel flow; Macropore flow; Preferential flow

Definition

Bypass flow. This phenomenon has been described also as short circuiting flow of water in soil, indicating a situation in which surface water is connected with water in the subsurface due to rapid infiltration. Here, infiltrating water is percolating along preferential pathways (i.e., macropores, cracks, fissures, decayed-root channels, or worm burrows) thereby bypassing most of the bulk soil volume.

Preferential flow. This is a general expression to describe water movement along preferred flow paths in soil.

Macropore flow. Preferential flow in structured soil along (large capillary- and) non capillary-sized macropores (i.e., cracks or biopores). The expression *macropore flow* is mostly used to indicate preferential flow in continuous root channels, earthworm burrows, structural fissures, or in shrinkage cracks in well-structured finer-textured soils. Here, flow paths are varying in type from individual macropores to a highly connected pore network. Pore geometries may range from cylindrical to platy and dimensions may vary from over-capillary-sized “macropores” to capillary-sized “mesopores” (for a definition of macro porosity in terms of a specific pore radius see, e.g., Luxmoore, 1981).

Funnel flow. This type refers to the lateral redirection or “funneling” of water in heterogeneously layered soil where water moves along the least resistance layer boundary to bypass less permeable layers.

Introduction

Bypass flow in soil describes the process of preferential water movement through a relatively small fraction of continuous macropores or highly permeable pore regions while most of the surrounding soil volume (i.e., the porous

matrix) is excluded. Nonuniform flow leads to spatially irregular wetting of the soil profile. This is in contrast to the standard uniform flow (e.g., Green and Ampt, 1911), which assumes stable homogeneous wetting fronts that move basically parallel to the infiltration soil surface. Nonuniform soil water flow has been recognized for a long time (e.g., Lawes et al., 1881, see Hendrickx and Flury, 2001). The phenomenon has increasingly gained attention beginning around the 1980s (e.g., see the review of Jarvis, 2007) mainly in the context of soil conservation and water pollution; this is because bypass flow creates highly nonuniform water infiltration and percolation fronts with characteristically differing flow velocities that allow infiltrating water and dissolved chemicals to reach the deeper subsurface environment nearly without any interaction with the bulk soil. In contrast to uniform flow, where water infiltration begins by filling first the smaller, and then successively the larger pores according to capillary forces, the larger pores start filling during bypass flow and conducting water (e.g., Youngs and Leeds-Harrison, 1990). It means that infiltrating water does not have sufficient time to equilibrate with resident water in the matrix during bypass flow. Such transient nonequilibrium condition in the pressure head between flow paths and bulk porous matrix is considered one of the most important features of preferential flow (e.g., Flühler et al., 1996).

Terminology

The term “bypass flow” reflects that large parts of the soil volume are simply bypassed through flow along preferred pathways (i.e., vertically continuous macropores or highly permeable pore networks). The synonymously used term “short-circuiting” (Bouma and Dekker, 1978; Beven and Germann, 1982) indicates that infiltrating water can immediately connect the surface hydrology with that of the subsurface. It is obvious that in this case, not only water but also dissolved chemical and colloids can directly be transported from the soil surface to the groundwater; it may reach the drainage system and eventually surface water bodies practically without any buffering by the soil matrix.

The occurrence of bypass flow requires a concurrence of several effects including sufficiently high infiltration rates (e.g., rainstorms, surface water ponding), a cracked or macroporous soil with proper vertically continuous larger pore system, a certain initial soil moisture regime, and other liquid and solid phase properties. Since myriad combinations are possible in natural soil, the complexity resulted in many different descriptions of observations of nonuniform flow and definitions for basically the same phenomenon.

Thus, the more general term “preferential flow” (Beven, 1991; Hendrickx and Flury, 2001) is frequently used that includes all different types of bypass flow such as *macropore flow* (i.e., preferential flow along continuous decayed-root channels, earthworm burrows, fissures, or cracks for well-structured mostly fine-textured soils), *unstable flow* (i.e., in mostly coarse-textured sandy soils

due to instabilities of the wetting front at fine-over-coarse textural layers (e.g., Dekker and Ritsema, 1994), and *funnel flow* (i.e., the lateral redirection and funneling caused by textural boundaries (e.g., Kung, 1990) along which water bypasses lower-permeable regions). Finger-like unstable flow patterns can result from soil water repellence (Bauters et al., 1998) or air entrapment (e.g., Ritsema and Dekker, 1994), and may lead to *distribution flow* (Ritsema and Dekker, 1995).

Experimental observations

Bypass or preferential flow has been observed in so many different soils that it seems to be the rule rather than the exception (Flury et al., 1994). Many reports are from arable field soils (e.g., Beven and Germann, 1982; Gish and Shirmohammadi, 1991) or unsaturated fractured rocks (e.g., Wang, 1991). *Fingering* has been observed in arable (e.g., Dekker and Ritsema, 2000) as well as in sandy forest soils under pines (*Pinus sylvestris*) (e.g., Ehwald et al., 1961) and in forest-reclaimed mine soils (Hangen et al., 2004). Bypass flow has even been observed in paddy soils (Wopereis et al., 1994; Sander and Gerke, 2007; Janssen and Lennartz, 2008) where surface water during ponding conditions can bypass the compacted plow pan through cracks and biopores thereby leading to water and nutrient losses.

Bypass flow has previously been defined as the flow of “free” (i.e., non- or over-capillary) water along macropores into and through an unsaturated soil matrix (Bouma, 1981; van Stiphout et al., 1987); in the field bypass flow often starts when water infiltrates into open macropores (e.g., Beven and Germann, 1982; White, 1985) at the surface or commences at the boundary between tilled subsoil and untilled subsoil (Quisenberry and Phillips, 1976). More recent tracer studies similarly indicate that the initiation and the degree of preferential flow depends either on deep penetrating macropores that are connected to the soil surface (Zehe and Flühler, 2001) or on the buildup of hydraulic pressure at the plow pan and subsequent infiltration into subsoil macropores (e.g., Kasteel, 1997). Bypass flow was spatially more variable when initiated at the soil surface than when initiated at the plow pan (Weiler and Naef, 2003) and was observed for relatively high (e.g., Granovsky et al., 1993) as well as for relatively low (e.g., Shipitalo and Edwards, 1996) initial water contents. An extensive review of the principles and controls on preferential flow and transport in soil has recently been published by Jarvis (2007).

The fraction of preferential flow increased with irrigation intensity (e.g., Kasteel, 1997) and was larger for ponded than for sprinkling irrigation (e.g., Hamdi et al., 1994). Liu et al. (1994) could demonstrate by means of nuclear magnetic resonance (NMR) technique that in a structured soil the water flow velocity in root pore channels was about 100 times larger than in the surrounding porous soil matrix. Velocities in macropores reached the transition between laminar and turbulent flow (e.g., Mori

et al., 1999; Maruyama et al., 2003). In other studies, bypass-flow velocities of $>500 \text{ mm day}^{-1}$ were determined using an isotope tracer (Deuterium) (Seiler et al., 2002) while matrix-flow velocities ranged between 0.7 m year^{-1} (Loess) and 1.2 m year^{-1} (tertiary gravels and sands) (i.e., $2\text{--}4 \text{ mm day}^{-1}$).

Soil structure

Structured soil consists of a diverse mixture of different and dynamically changing pores of differing sizes, shapes, and continuity, which serve as flow paths under certain initial and boundary conditions. Shrinkage cracks at the soil surface and worm burrows in the subsoil as two main types of relatively large macropores (Figure 1) are highly dynamical pore structures. Cracks appear after extensive drying (Figure 1a) and close during wet periods due to swelling; also, they are being destroyed due to soil cultivation. Although these cracks are clearly over-capillary in size, significant amounts of water are only able to enter the cracks after surface ponding of the soil matrix. In contrast, worm burrows are relatively permanent and mechanically stable macropores, at least those larger ones that extend into the subsoil. The picture (Figure 1b) indicates, however, that also the worm burrows can undergo alterations, for instance, by soil biological activities. Here the abandoned burrow was used as preferred channel for plant roots, and in some parts, it was loosely refilled with soil material. Such alteration, in turn, can drastically change the hydraulic properties of the macropores.

Besides the large macropores, which act as preferential flow paths when infiltration rates are high enough to produce ponding, in many soils, there exists a hierarchy of relatively fine-structured inter-aggregate networks, which form a system of different pore sizes where water retention functions could be determined. Continuous pores of the hierarchical crack network are still highly conductive but may not be denoted as macropores. Embedded within fine-textured soils, these “mesopores” (e.g., Luxmoore, 1981) may possibly form a secondary pore system and may act as preferential flow paths as well as larger macropores.

Basic model approaches

Obviously, there is no universal type of model that allows the quantitative description of bypass flow in soil. The applicability of the different models depends on the specific flow problem and the soil structure (a more detailed overview can be found in Gerke, 2006).

For flow in the above described structured soil, dual-permeability models assuming gravity flow in the macropore domain (MACRO, Jarvis, 1994) or a coupled set of Richards' equations (DUAL, Gerke and van Genuchten, 1993a) are currently applicable. The two “dual-permeability” models assume that water can flow in two separate but interacting porous domains. The models differ mainly in the descriptions of flow in the



Bypass Flow in Soil, Figure 1 (a) Shrinkage cracks of up to 5-cm width at the surface of a clay-loam soil in a wheat field and (b) cross section of a large vertical cylindrical macropore from a worm burrow of *Lumbricus terrestris* of about 0.7 cm in diameter in a silty loam gleyic Luvisol derived from Loess. Both pictures are from arable field soils located near the village of Neuenkirchen, near Schladen, south of the city of Braunschweig, Germany. The burrow section was from the B-horizon (about 55–95 cm soil depth). The abandoned worm burrow contained roots and some soil material, and showed darker-looking coatings along the surrounding matrix.

macropore domain and in the formulation of the inter-domain mass transfer terms.

Germann (1985) and Germann and Beven (1985) suggested using a kinematic wave equation to describe gravitational movement of water in macropores as follows:

$$\frac{\partial q}{\partial t} + v \frac{\partial q}{\partial z} + vr\theta_f = 0 \quad (1)$$

where r is the macropore “sorbance,” z is depth (L), t is time (T), and θ_f is the volumetric water content ($L^3 L^{-3}$) of the macropores, and where the volumetric flux density, q ($L T^{-1}$), and the kinematic wave velocity, v ($L T^{-1}$), are defined by

$$q = b\theta_f^a, v = \frac{\partial q}{\partial \theta_f} \quad (2)$$

in which a is a “kinematic” exponent and b a macropore conductance parameter ($L T^{-1}$). This approach neglects any capillarity (and water retention function) in the macropore domain.

This concept was utilized for the MACRO model, in which a unit hydraulic gradient for flow in the macropore domain (Jarvis, 1994) and an expression similar to the kinematic wave Equation 2 are used to describe gravitational movement of water as

$$q = b \left(\frac{\theta_f}{\theta_{sf}} \right)^a = b(S_{fe})^a \quad (3)$$

where θ_{sf} is the saturated water content ($L^3 L^{-3}$) of the macropores (i.e., macroporosity) and S_{fe} is the relative saturation (–) of the macropore domain. Since θ_f is scaled by θ_{sf} , the fracture conductance parameter b has the physical meaning of a hydraulic conductivity of macropores, K_{sf} ($L T^{-1}$), at full saturation. By assuming that the porosity of the macropore system, ϵ_f , is identical with θ_{sf} , a balance equation for flow in macropores is obtained:

$$\frac{\partial \theta_f}{\partial t} = -\frac{\partial}{\partial z} \left[K_{sf} \left(\frac{\theta_f}{\epsilon_f} \right)^a \right] - S_w \quad (4)$$

where S_w (T^{-1}) denotes water transfer from the macropores into the soil matrix. In the soil matrix domain (subscript m), flow and transport is described using the Richards equation as

$$\frac{\partial \theta}{\partial t} = \frac{\partial}{\partial z} \left(K_m(\theta) \left(\frac{\partial h}{\partial z} - 1 \right) \right) + S_w. \quad (5)$$

where h is matric potential or soil water pressure head (L). Water flow between the two regions was described with a quasi-empirical equation using relative saturation as a driving force. An empirical threshold matric potential value, h_b (L), defines the matrix water content that is required for initiation of flow into the macropore domain. A threshold value of $h_b = -50$ hPa was calibrated to describe the measured preferential chloride transport using MACRO (e.g., Saxena et al., 1994).

A number of applications of the MACRO model revealed the usefulness of the approach for analyzing bypass flow in structured soil (e.g., Larsson and Jarvis, 1999). The MACRO model was further extended toward pesticide and particle transport (e.g., Jarvis et al., 1999) and improved identification of model parameters (Larsbo et al., 2005) among other aspects.

The numerical dual-permeability model (DUAL) of Gerke and van Genuchten (1993a) assumes that the properties of the total soil volume can be characterized by two local properties for porosity, water content, fluid flux density, q ($L T^{-1}$), by the relative volumetric proportion of the fracture pore system $w_f = 1 - w_m$, ($0 < w_f < 1$). Assuming applicability of Darcy's law, water flow in the fracture and matrix pore regions are described by a coupled pair of Richards' equations:

$$C_f \frac{\partial h_f}{\partial t} = \frac{\partial}{\partial z} \left(K_f \frac{\partial h_f}{\partial z} - K_f \right) - \frac{\Gamma_w}{w_f} \quad (6)$$

$$C_m \frac{\partial h_m}{\partial t} = \frac{\partial}{\partial z} \left(K_m \frac{\partial h_m}{\partial z} - K_m \right) + \frac{\Gamma_w}{1 - w_f} \quad (7)$$

where C is the specific water capacity $d\theta/dh$ (L^{-1}), z is depth taken to be positive downward (L), t is time (T), and Γ_w is the water transfer term (T^{-1}). Analogously to flow, coupled sets of convections-dispersion equations are used to describe preferential solute transport in structure soil (Gerke and van Genuchten, 1993a). The mass transfer term has been evaluated to include in a simplistic way the basic soil structural features (Gerke and van Genuchten, 1993b; Gerke and van Genuchten, 1996) such as structural geometries and a locally reduced permeability of clay coating. In this 1D model (DUAL) both, the coupled dual-permeability equation for flow and solute transport, are solved simultaneously using mass-lumped linear Galerkin finite element scheme with Picard iteration and adjustable time steps (Gerke and van Genuchten, 1993a). An alternative partitioned numerical solution treats each pore system separately followed by a sequential execution of the single-domain numerical schemes (Tseng et al., 1995). The DUAL model has been applied in 1D (e.g., Gerke and Köhne, 2004) and extended toward flow and transport in two spatial dimensions (e.g., Gerke et al., 2007) as well as used to analyze nonequilibrium flow conditions (e.g., Šimůnek et al., 2003).

The model approach VIMAC (i.e., Vertical Infiltration through swelling and shrinking MACroporous Clay soils) (Greco, 2002) for preferential flow in macroporous swelling soil considers three different pore domains. Besides the soil matrix, these are the dynamically changing shrinkage cracks and the permanent macropores, both regarded as separate flow domains in which over-capillary flow is described using a kinematic wave equation. This approach more realistically mimics basic soil conditions (cf., Figure 1) of natural field soils, while most of the model parameters can be derived from soil structural

information. It is still unresolved, whether the larger cracks can conceptually be regarded as a pore domain, and whether flow in the permanent macropore domain should always be treated as non-capillary.

Summary

Bypass flow in soil is a frequently observed phenomenon that describes rapid and nonuniform downward water movement along highly conductive pathways through the unsaturated soil. Such preferential flow is caused by a number of different mechanisms that originate primarily from local heterogeneities. In structured soils, vertically continuous earthworm burrows and root channels, or cracks and fissures of an inter-aggregate pore network mainly serve as preferential flow paths. The interrelations between flow and transport processes and soil structural properties under varying initial and boundary conditions are complex and process-based models need to be improved.

Current approaches for a quantitative description of preferential flow mostly assume that the structured soil consists of separate but interacting porous domains. The dual-permeability models assume two mobile flow domains. These models mainly differ in the description of flow in the preferential flow domain (i.e., either Richards' equation assuming capillarity or kinematic wave approach for gravity flow) and with respect to the mass transfer formulation (i.e., from pressure head or saturation-based first-order type formulations to more complex nonlinear formulations or numerical solutions of the local flow equation). Many challenges remain, in particular, how to capture dynamic soil structure effects and to improve quantitative descriptions of bypass flow.

A better understanding of the susceptibility of soils to preferential flow is of importance when studying problems related with unintended contaminations of ground and surface waters. At the same time, the quantitative analyses of water and element balances of ecosystems are methodologically problematic as long as preferential leaching rates cannot adequately be measured or calculated.

Bibliography

- Bauters, T. W. J., DiCarlo, D. A., Steenhuis, T. S., and Parlange, J.-Y., 1998. Preferential flow in water repellent sands. *Soil Science Society of America Journal*, **62**, 1185–1190.
- Beven, K. J., 1991. Modeling preferential flow: an uncertain future? In Gish, T. J., and Shirmohammadi, A. (eds.), *Preferential Flow*. St. Joseph: American Society of Agricultural Engineers, pp. 1–11.
- Beven, K. J., and Germann, P. F., 1982. Macropores and water flow in soils. *Water Resources Research*, **18**, 1311–1325.
- Bouma, J., 1981. Soil morphology and preferential flow along macropores. *Agricultural Water Management*, **3**, 235–250.
- Bouma, J., and Dekker, L. W., 1978. Case-study on infiltration into dry clay soil. 1. morphological observations. *Geoderma*, **20**, 27–40.

- Dekker, L., and Ritsema, C., 1994. How water moves in a water repellent sandy soil: 1. Potential and actual water repellency. *Water Resources Research*, **30**, 2507–2517.
- Dekker, L., and Ritsema, C., 2000. Wetting patterns and moisture variability in water repellent Dutch soils. *Journal of Hydrology*, **231**, 148–164.
- Ehwald, E., Vetterlein, E., and Buchholz, F., 1961. Das Eindringen von Niederschlägen und Wasserbewegungen in sandigen Waldböden. *Journal of Plant Nutrition and Soil Science*, **93**, 202–209.
- Flühler, H., Durner, W., and Flury, M., 1996. Lateral solute mixing processes – a key for understanding field-scale transport of water and solutes. *Geoderma*, **70**(2–4), 165–183.
- Flury, M., Flühler, M., Jury, W. A., and Leuenberger, J., 1994. Susceptibility of soils to preferential flow of water: a field study. *Water Resources Research*, **30**, 1945–1954.
- Gerke, H. H., 2006. Review Article: Preferential flow descriptions for structured soils. *Journal of Plant Nutrition and Soil Science*, **169**, 382–400.
- Gerke, H. H., and van Genuchten, M. T., 1993a. A dual-porosity model for simulating the preferential movement of water and solutes in structured porous media. *Water Resources Research*, **29**, 305–319.
- Gerke, H. H., and van Genuchten, M. T., 1993b. Evaluation of a first-order water transfer term for variably saturated dual-porosity flow models. *Water Resources Research*, **29**, 1225–1238.
- Gerke, H. H., and van Genuchten, M. T., 1996. Macroscopic representation of structural geometry for simulating water and solute movement in dual-porosity media. *Advances in Water Resources*, **19**, 343–357.
- Gerke, H. H., and Köhne, J. M., 2004. Dual-permeability modeling of preferential bromide leaching from a tile drained glacial till agricultural field. *Journal of Hydrology*, **289**, 239–257.
- Gerke, H. H., Dušek, J., Vogel, T., and Köhne, J. M., 2007. Two-dimensional dual-permeability analyses of a bromide tracer experiment on a tile-drained field. *Vadose Zone Journal*, **6**, 651–667.
- Germann, P., 1985. Kinematic wave approach to infiltration and drainage into and from soil macropores. *Transactions of the American Society of Agricultural Engineers*, **28**, 745–749.
- Germann, P., and Beven, K. J., 1985. Kinematic wave approximation to infiltration into soils with sorbing macropores. *Water Resources Research*, **21**, 990–996.
- Gish, T. J., and Shirmohammadi, A. (eds.), 1991. Preferential flow. Chicago: Proceedings of the National Symposium, 16–17 December 1991; St. Joseph: American Society of Agricultural Engineering, p. 408.
- Granovsky, A. V., McCoy, E. L., Dick, W. A., Shipitalo, M. J., and White, W. M., 1993. Water and chemical transport through long-term no-till and plowed soils. *Soil Science Society of America Journal*, **57**, 1560–1567.
- Greco, R., 2002. Preferential flow in macroporous swelling soil with internal catchment: model development and applications. *Journal of Hydrology*, **269**(3–4), 150–168.
- Green, W. H., and Ampt, G. A., 1911. Studies on soil physics. I. The flow of water and air through soils. *Journal of Agricultural Science*, **4**, 1–24.
- Hamdi, M., Durnford, D., and Loftis, J., 1994. Bromide transport under sprinkler and ponded irrigation. *Journal of Irrigation and Drainage Engineering*, **120**, 1086–1097.
- Hangen, E., Gerke, H. H., Schaaf, W., and Hüttl, R. F., 2004. Flow path visualization at a lignitic mine soil using iodine-starch staining. *Geoderma*, **120**, 121–135.
- Hendrickx, J. M. H., and Flury, M., 2001. Uniform and preferential flow mechanisms in the vadose zone. In *Conceptual Models of Flow and Transport in the Fractured Vadose Zone*. Washington, DC: National Research Council, National Academy Press, pp. 149–187.
- Janssen, M., and Lennartz, B., 2008. Characterization of preferential flow pathways through paddy bunds with dye tracer tests. *Soil Science Society of America Journal*, **72**(6), 1756–1766.
- Jarvis, N., 1994. The MACRO model (version 3.1) – Technical description and sample simulations. Ph.D thesis 19, Uppsala: Swedish University of Agricultural Sciences, p. 51.
- Jarvis, N. J., Villholth, K. G., and Ulen, B., 1999. Modelling particle mobilization and leaching in macroporous soil. *European Journal of Soil Sciences*, **50**, 621–632.
- Jarvis, N. J., 2007. A review of non-equilibrium water flow and solute transport in soil macropores: Principles, controlling factors and consequences for water quality. *European Journal of Soil Sciences*, **58**, 523–546.
- Kasteel, R., 1997. Solute transport in an unsaturated field soil: describing heterogeneous flow fields using spatial distribution of hydraulic properties. PhD dissertation thesis 12477, Zürich: ETH Zürich, 108pp.
- Kung, K.-J. S., 1990. Preferential flow in a sandy vadose zone: 1. Field observation. *Geoderma*, **46**, 51–58.
- Larsbo, M., Roulier, S., Semo, F., Kasteel, R., and Jarvis, N., 2005. An improved dual-permeability model of water flow and solute transport in the vadose zone. *Vadose Zone Journal*, **4**, 398–406.
- Larsson, M. H., and Jarvis, N. J., 1999. Evaluation of a dual-porosity model to predict field-scale solute transport in a macroporous soil. *Journal of Hydrology*, **215**, 153–171.
- Lawes, J. B., Gilbert, J. H., and Warington, R., 1881. On the amount and composition of the rain and drainage-waters collected at Rothamsted, Part I and II. *Journal of the Royal Agricultural Society of England, London*, **17**, 241–279.
- Liu, I. Y., Waldron, L. J., Wong, S. T. S., Anderson, S. H., and Hopmans, J. W., 1994. Application of nuclear magnetic resonance imaging to study preferential water flow through root channels. *Soil Science Society America Special Publication*, **36**, pp. 135–148, Madison: American Society of Agronomy.
- Luxmoore, R. J., 1981. Micro-, meso-, and macroporosity of soil. *Soil Science Society of America Journal*, **45**, 671–672.
- Maruyama, T., Tada, A., Iwama, K., and Horino, H., 2003. Direct observation of soil water movement through soil macropores using soft X-rays and stereographing. *Soil Science*, **168**(2), 119–127.
- Mori, Y., Maruyama, T., and Mitsuno, T., 1999. Soft x-ray radiography of drainage patterns of structured soils. *Soil Science Society of America Journal*, **63**(4), 733–740.
- Quisenberry, V. L., and Phillips, R. E., 1976. Percolation of surface-applied water in the field. *Soil Science Society of America Journal*, **40**, 484–489.
- Ritsema, C. J., and Dekker, L. W., 1994. How water moves in a water-repellent sandy soil. 2. Dynamics of fingered flow. *Water Resources Research*, **30**, 2517–2531.
- Ritsema, C. J., and Dekker, L. W., 1995. Distribution flow – a general process in the top layer of water repellent soils. *Water Resources Research*, **31**, 1187–1200.
- Sander, T., and Gerke, H. H., 2007. Preferential flow patterns in paddy fields using a dye tracer. *Vadose Zone Journal*, **6**, 105–115, doi:10.2136/vzj2006.0035.
- Saxena, R. K., Jarvis, N. J., and Bergstrom, L., 1994. Interpreting non-steady state tracer breakthrough experiments in sand and clay soils using a dual-porosity model. *Journal of Hydrology*, **162**, 279–298.
- Seiler, K.-P., von Löwenstern, S., and Schneider, S., 2002. Matrix and bypass-flow in quaternary and tertiary sediments of agricultural areas in south Germany. *Geoderma*, **105**, 299–306.
- Shipitalo, M. J., and Edwards, W. M., 1996. Effects of initial water content on macropore / matrix flow and transport of surface-applied chemicals. *Journal of Environmental Quality*, **25**(4), 662–670.

- Šimunek, J., Jarvis, N. J., van Genuchten, M. T., and Gärdenäs, A., 2003. Review and comparison of models for describing nonequilibrium and preferential flow and transport in the vadose zone. *Journal of Hydrology*, **272**, 14–35.
- Tseng, P.-H., Sciortino, A., and van Genuchten, M Th, 1995. A partitioned solution procedure for simulating water flow in a variable saturated dual-porosity medium. *Advances in Water Resources*, **18**, 335–343.
- Van Stiphout, T. P. J., van Lanen, H. A. J., Boersma, O. H., and Bouma, J., 1987. The effect of bypass flow and internal catchment of rain on the water regime in a clay loam grassland soil. *Journal of Hydrology*, **95**(1–2), 1–11.
- Wang, J. S. Y., 1991. Flow and transport in fractured rocks. *Reviews in Geophysics*, **29**(Suppl), 254–262.
- Weiler, M., and Naef, F., 2003. An experimental tracer study of the role of macropores in infiltration in grassland soils. *Hydrological Processes*, **17**(2), 477–493.
- White, R. E., 1985. The influence of macropores on the transport of dissolved and suspended matter through soil. *Advances in Soil Science*, **3**, 95–120.
- Wopereis, M. C. S., Bouma, J., Kropff, M. J., and Sanidad, W. B., 1994. Reducing bypass flow through a dry, cracked and previously puddled rice soil. *Soil and Tillage Research*, **29**, 1–11.
- Youngs, E. G., and Leeds-Harrison, P. B., 1990. Aspects of transport processes in aggregated soils. *Journal of Soil Science*, **41** (665), 675.
- Zehe, E., and Flühler, H., 2001. Preferential transport of isoproturon at a plot scale and a field-scale tile-drained site. *Journal of Hydrology*, **247**, 100–115.

Cross-references

- Diffusion in Soils
Earthworms as Ecosystem Engineers
Hydraulic Properties of Unsaturated Soils
Hydropedological Processes in Soils
Infiltration in Soils
Laminar and Turbulent Flow in Soils
Layered Soils, Water and Solute Transport
Leaching of Chemicals in Relation to Soil Structure
Microbes and Soil Structure
Nondestructive Measurements in Soil
Noninvasive Quantification of 3D Pore Space Structures in Soils
Organic Matter, Effects on Soil Physical Properties and Processes
Pore Morphology and Soil Functions
Pore Size Distribution
Shrinkage and Swelling Phenomena in Soils
Soil Hydrophobicity and Hydraulic Fluxes
Soil Water Flow
Solute Transport in Soils
Spatial Variability of Soil Physical Properties
Water Budget in Soil
Wetting and Drying, Effect on Soil Physical Properties

C

CAKING

Changing of a powder into a solid mass by heat, pressure, or water.

CALICHE (LIME-PAN)

(I) A zone near the surface, more or less cemented by secondary carbonates of Ca or Mg precipitated from the soil solution. It may occur as a soft thin soil horizon, as a hard thick bed, or as a surface layer exposed by erosion.
(II) Alluvium cemented with NaNO_3 , NaCl and/or other soluble salts in the nitrate deposits of Chile and Peru.

Bibliography

Glossary of Soil Science Terms. Soil Science Society of America. 2010. <https://www.soils.org/publications/soils-glossary>

CANOPY STRUCTURE

Plant canopy structure is the spatial arrangement of the above-ground organs of plants in a plant community.

Bibliography

Russel, G., Marshall, B., and Gordon Jarvis, P. 1990. Plant Canopies: Their Growth, Form and Function. Cambridge University Press.

CAPILLARITY

The tendency of a liquid to enter into the narrow pores within a porous body, due to the combination of the cohesive forces within the liquid (expressed in its surface tension) and the adhesive forces between the liquid and the solid (expressed in their contact angle).

Bibliography

Introduction to Environmental Soil Physics. (First Edition). 2003. Elsevier Inc. Daniel Hillel (ed.) <http://www.sciencedirect.com/science/book/9780123486554>

Cross-references

[Sorptivity of Soils](#)

CAPILLARY FRINGE

The thin zone just above the water table that is still saturated, though under sub-atmospheric pressure (tension). The thickness of this zone (typically a few centimeters or decimeters) represents the suction of air entry for the particular soil.

Bibliography

Introduction to Environmental Soil Physics. (First Edition). 2003. Elsevier Inc. Daniel Hillel (ed.) <http://www.sciencedirect.com/science/book/9780123486554>

Cross-references

[Sorptivity of Soils](#)

CARBON LOSSES UNDER DRYLAND CONDITIONS, TILLAGE EFFECTS

Félix Moreno, José M. Murillo, Engracia Madejón
Instituto de Recursos Naturales y Agrobiología de Sevilla
(IRNAS-CSIC), Sevilla, Spain

Definition

CO_2 emissions are mainly produced by inadequate soil tillage combined with intensive cropping systems and climatic conditions.

Introduction

Losses of soil organic carbon (SOC) are associated with reductions in soil productivity and with increases in CO_2 emissions from soil to the atmosphere (Lal et al., 1989; Bauer et al., 2006; Ventera et al., 2006; Conant et al., 2007). Gas exchange between soils and the atmosphere may be an important contributing factor to global change due to release of greenhouse gases (Ball et al., 1999). Intensive agriculture frequently causes important losses of soil carbon. Conservation tillage (CT) agriculture (reduced tillage) has been promoted since approximately 1960 as a means to counteract all these constraints (Gajri et al., 2002). Moreover, CT improves soil quality and crop performance, especially under semiarid conditions (Moreno et al., 1997; Franzluebbers, 2004; Muñoz et al., 2007).

Tillage effects on carbon losses

Degradative effects of tillage on soil include rapid decline of soil organic carbon due to mineralization rate increase (Lal, 1993). This is particularly important under semiarid conditions using conventional tillage in which moldboard plowing with soil inversion is the main operation (López-Garrido et al., 2009). Moldboard plowing is one of the most important factors increasing CO_2 emissions by soil microbial activity stimulation due to greater soil aeration and breakdown of soil macroaggregates that conduces to a greater release of labile organic matter previously microbial protected. There are studies that suggest that the greenhouse gases contribution of agriculture, such as CO_2 , can be mitigated by widespread adoption of conservation tillage (Lal, 1997; Lal, 2000).

Conservation tillage (CT) is any tillage and planting system that maintains at least 30% of the soil surface covered by residue after planting to reduce soil erosion by water. Where soil erosion by wind is a primary concern, the system must maintain at least 1.1 Mg ha^{-1} flat small grain residue equivalent on the surface during the critical wind erosion period (Gajri et al., 2002). This system reduces the number of operations and trips across the field, and of course, avoids the soil inversion that buries most crop residues into the soil.

The effectiveness of CT in mitigating the greenhouse gas impact of individual agroecosystems could vary

substantially. Studies under different conditions are required to assess the broader of the greenhouse gas impacts of CT (Ventera et al., 2006). Tillage often increases short-term CO_2 flux from the soil due to a rapid physical release of CO_2 trapped in the soil air spaces (Bauer et al., 2006; Álvaro-Fuentes et al., 2008; Reicosky and Archer, 2007; López-Garrido et al., 2009). This rapid flux of CO_2 is influenced by the tillage system and the amount of soil disturbance (Reicosky and Archer, 2007).

Root and microbial activity together constitute soil respiration. Root and rhizosphere respiration can account for as little as 10% to greater than 90% of total “in situ” soil respiration depending on vegetation type and season of the year (Hanson et al., 2000). Nevertheless, only soil organic matter (SOM)-derived CO_2 contributes to changes in atmospheric CO_2 concentration. Long residence time of soil organic matter (SOM) results in very slow turnover rates relative to other less-recalcitrant respiratory substrates. This implies that SOM is the only C pool that can be a real, long-term sink for C in soils. Despite long residence times in steady state, if decomposition exceeds humification, the pool of C in SOM becomes a very large potential source of CO_2 (Kuzyakov, 2006).

Long-term adoption of conservation tillage (reduced and no tillage) in Mediterranean Spanish areas has proven to be an effective way to increase soil organic matter and, especially, to improve biochemical quality at the soil surface (Madejón et al., 2009). However, as the climatic conditions of the semiarid areas are an important limiting factor for the accumulation of organic carbon in the top soil layers, the simple determination of total organic carbon (TOC) is not always the best indicator of the improvement caused by conservation tillage. Under these conditions, it may be more interesting to study the stratification ratio of TOC calculated by the division of TOC content at surface between TOC content at deeper layers (Franzluebbers, 2002). This approach could also be applied to other variables related to soil biology, such as MBC (microbial biomass carbon) and enzymatic activities (Madejón et al., 2009), which are normally significantly correlated with TOC. Changes in soil biochemical properties with conservation tillage and in their stratification ratios should provide practical tools to complement physical and chemical test and, thus, evaluate the effect of conservation tillage in dryland conditions. Despite some studies have reported similar or even greater TOC accumulation in the total profile (1 m and more) under conventional tillage than under CT (Baker et al., 2007), the improvements made by CT surface are very important for the soil functions.

These processes are very influenced by the local conditions and management. Franzluebbers (2004) reported that low benefit of no tillage on TOC storage could be expected in dry, cold regions, in which low precipitation would limit C fixation by plants and decomposition, even when crop residues are mixed with soil by tillage.

However, for most soils, the potential of carbon (C) sequestration upon conversion of plow tillage to no-tillage farming with the use of crop residue mulch and other recommended practices is 0.6–1.2 Pg C year⁻¹ (Lal, 2004). The important ecological and agronomic benefits that can derive from these practices could be limited not only by plowing but also by using crop residues for other purposes. Numerous competing uses of crop residues under arid and semiarid conditions (Bationo et al., 2007) can be a constraint for CT establishment (e.g., grazing and feed livestock). Biofuel production may be another destination (Lal and Pimentel, 2007). There is at present an imperious necessity of using cellulosic biomass instead of crop grain for producing biofuel (mainly ethanol) and, currently, few sources are supposed to be available in sufficient quantity and quality to support development of an economically sized processing facility, except crop residues (Wilhelm et al., 2004).

Despite the suitability of CT to avoid C losses, this system may also have some drawbacks, such as the greater dependence of herbicides, higher level of residue management than conventional tillage, and it could not be adequate to all soils, climates, or crops. Moreover, the no-till system may lead to soil compaction. All these issues require experimentation in each particular scenario. However as a rule, CT does not cause yield losses when adequately established. Particularly, under arid and semiarid conditions in dry years, yields may be greater than under traditional tillage due to water savings resulting from conservation tillage.

Conclusions

Several studies have shown that the potential reduction for CO₂ emission from the adoption of conservation tillage under dryland conditions could be substantial. However, further investigation should be necessary to validate, under different scenarios, the potential effect of soil to sequester carbon in these conditions.

In any case, the adoption of conservation tillage, if adequately established, has a potential effect to increase organic carbon, and thus, soil quality especially at soil surface, essential for the soil functions.

Bibliography

- Álvaro-Fuentes, J., López, M. V., Arrué, J. L., and Cantero-Martínez, C., 2008. Management effects on soil carbon dioxide fluxes under semiarid Mediterranean conditions. *Soil Science Society of America Journal*, **72**, 194–200.
- Baker, J. M., Ochsner, T., Venterea, R. T., and Griffis, T. J., 2007. Tillage and soil carbon sequestration – what do we really know? *Agriculture, Ecosystems and Environment*, **118**, 1–5.
- Ball, B. C., Scott, A., and Parker, J. P., 1999. Field N₂O, CO₂ and CH₄ fluxes in relation to tillage, compaction and soil quality in Scotland. *Soil and Tillage Research*, **53**, 29–39.
- Bationo, A., Kihara, J., Vanlauwe, B., Wasawa, B., and Kimetu, J., 2007. Soil organic carbon dynamics, functions and management in West African agro-ecosystems. *Agricultural Systems*, **94**, 13–25.
- Bauer, P. J., Frederick, J. R., Novak, J. M., and Hunt, P. G., 2006. Soil CO₂ flux from a Norfolk loamy sand after 25 years of conventional and conservation tillage. *Soil and Tillage Research*, **90**, 205–211.
- Conant, R. T., Easter, M., Paustian, K., Swan, A., and Williams, S., 2007. Impacts of periodic tillage on soil C stocks: a synthesis. *Soil and Tillage Research*, **95**, 1–10.
- Franzluebbers, A. J., 2002. Soil organic matter stratification ratio as an indicator of soil quality. *Soil and Tillage Research*, **66**, 95–106.
- Franzluebbers, A. J., 2004. Tillage and residue management effects on soil organic matter. In Magdoff, F., and Weil, R. R. (eds.), *Soil Organic Matter in Sustainable Agriculture*. Boca Raton: CRC Press, pp. 227–268.
- Gajri, P. R., Arora, V. K., and Prihar, S. S., 2002. *Tillage for Sustainable Cropping*. Lucknow: International Book Distributing.
- Hanson, P. J., Edwards, N. T., Garten, C. T., and Andrews, J. A., 2000. Separating root and soil microbial contributions to soil respiration: a review of methods and observations. *Biogeochemistry*, **48**, 115–146.
- Kuzakov, Y., 2006. Sources of CO₂ efflux from soil and review of partitioning methods. *Soil Biology and Biochemistry*, **38**, 425–448.
- Lal, R., 1993. Tillage effects on soil degradation, soil resilience, soil quality and sustainability. *Soil and Tillage Research*, **27**, 1–8.
- Lal, R., 1997. Residue management, conservation tillage and soil restoration for mitigating the greenhouse effect. *Soil and Tillage Research*, **43**, 81–107.
- Lal, R., 2000. Soil conservation and restoration to sequester carbon and mitigate the greenhouse effect. Third International Congress of the European Society for Soil Conservation (ESSC). Valencia (Spain): Key Notes, pp. 5–20.
- Lal, R., 2004. Soil carbon sequestration to mitigate climate change. *Geoderma*, **123**, 1–22.
- Lal, R., and Pimentel, D., 2007. Biofuels from crop residues. *Soil and Tillage Research*, **93**, 237–238.
- Lal, R., Hall, G. F., and Miller, F. P., 1989. Soil degradation. I. basic principles. *Land Degradation and Rehabilitation*, **1**, 51–69.
- López-Garrido, R., Díaz-Espejo, A., Madejón, E., Murillo, J. M., and Moreno, F., 2009. Carbon losses by tillage under semi-arid Mediterranean rainfed agriculture (SW Spain). *Spanish Journal of Agricultural Research*, **7**, 706–716.
- Madejón, E., Murillo, J. M., Moreno, F., López, M. V., Arrué, J. L., Álvaro-Fuentes, J., and Cantero-Martínez, C., 2009. Effect of long-term conservation tillage on soil biochemical properties in Mediterranean Spanish areas. *Soil and Tillage Research*, **105**, 55–62.
- Moreno, F., Pelegrín, F., Fernández, J. E., and Murillo, J. M., 1997. Soil physical properties, water depletion and crop development under traditional and conservation tillage in southern Spain. *Soil and Tillage Research*, **41**, 25–42.
- Muñoz, A., López-Piñeiro, A., and Ramírez, M., 2007. Soil quality attributes of conservation management regimes in a semi-arid region of south western Spain. *Soil and Tillage Research*, **95**, 255–265.
- Reicosky, D. C., and Archer, D. W., 2007. Moldboard plow tillage depth and short-term carbon dioxide release. *Soil and Tillage Research*, **94**, 109–121.
- Venterea, R. T., Baker, J. M., Dolan, M. S., and Spokas, K. A., 2006. Carbon and nitrogen storage are greater under biennial tillage in a Minnesota corn-soybean rotation. *Soil Science Society of America Journal*, **70**, 1752–1762.
- Wilhelm, W. W., Johnson, J. M. F., Hatfield, J. L., Voorhees, W. B., and Linden, D. R., 2004. Crop and soil productivity response to corn residue removal: a literature review. *Agronomy Journal*, **96**, 1–17.

Cross-references

Biochemical Responses to Soil Management Practices
 Greenhouse Gases Sink in Soils
 Hydrophobicity of Soil
 Organic Matter, Effects on Soil Physical Properties and Processes
 Physical Protection of Organic Carbon in Soil Aggregates
 Stratification of Soil Porosity and Organic Matter
 Tillage, Impacts on Soil and Environment

CARBON NANOTUBE

See *Nanomaterials in Soil and Food Analysis*

CATCHMENT (CATCHMENT BASIN)

See *Water Reservoirs, Effects on Soil and Groundwater*

CATION EXCHANGE CAPACITY

See *Surface Properties and Related Phenomena in Soils and Plants*

CEMENTATION

The process by which calcareous, siliceous, or ferruginous compounds tend to dissolve and then re-precipitate in certain horizons within the soil profile, thus binding the particles into a hardened mass.

Bibliography

Introduction to Environmental Soil Physics. (First Edition). 2003.
 Elsevier Inc. Daniel Hillel (ed.) <http://www.sciencedirect.com/science/book/9780123486554>

Cross-references

Orstein, Physical Properties

CEREALS, EVALUATION OF UTILITY VALUES

Dariusz Dziki, Janusz Laskowski
 Department of Equipment Operation and Maintenance in the Food Industry, University of Life Sciences, Lublin, Poland

Definition

Utility values of cereals – feature or features of grains that characterize the properties of kernels in the aspect of

specific utilization. In the most cases, the utility value of cereals concerns using of grains to food production.

Introduction

The assessment of cereal utility value is made from the beginning of the food processing. The utility value of cereal grain depends mainly on species and cultivar properties, climatic conditions, and agricultural treatments. Moreover, the storage conditions of the cereals, the preparing conditions for processing, and the manufacturing process, all have an influence on the utility values of cereals.

The utility values of cereal is widely more significant than the technological value. The cereal utility value does not indicate only the utility of cereal grain to foodstuff production, but also takes into consideration other uses of cereals (e.g., seed production, and utilization in pharmaceutical or chemical industry) However, the technological value of the cereal grains for food production is the most often determined.

Methods of evaluation of cereal grains utility values

The methods of evaluation of the utility values of cereals can be divided into two groups: indirect and direct methods. The most commonly used indirect methods are selected physical and chemical properties of grain, specialist technological indices (such as falling number or sedimentation value), and rheological properties of dough. The results obtained from these tests indirectly provide information about the utility value of cereal grains.

Direct methods, on the other hand, are more suitable for examining the full characteristic of utility values of cereals; however, they are often time consuming and require more expensive equipment. These methods depend on processing grain or flour and imitated industry conditions. Subsequently, the quality of the product is evaluated. Examples of the direct methods are laboratory milling tests and laboratory baking tests.

Indirect methods

The basic assessment of the cereal grain includes such properties as appearance, smell, color, amount and the kind of impurities, the broken grains, and the presence of pests. A more detailed assessment includes the following *physical properties of grains*: density, test weight, 1,000 kernel weight, shape and size of grain, vitreousness (especially for wheat, rice, barley, and corn), mechanical properties (hardness, shear strength, rapture force and rapture energy, crushing strength, etc.) The research conducted on the endosperm structure (electron microscopy and X-ray methods) can also be used for the evaluation of the quality of cereals. Test weight (grain weight in a given volume) is the oldest and the most commonly used quality index of cereal grain. As a general rule, the higher the test weight, the better grain quality. Test weight is influenced by various factors, including fungal infection,

insect damage, kernel shape and density, foreign materials, broken and shriveled kernels, agronomic practice, and the climatic and weather conditions (Czarnecki and Evans, 1986). Tkachuk et al. (1990) have shown a positive correlation between wheat test weight and wheat flour yield and bread-baking usefulness. The test weight shows positive correlation with the grain density. The research of wheat grain density has revealed that the type of grain significantly affects the mean density; healthy kernels averaged $1,280 \text{ kg m}^{-3}$, sprout-damaged kernels averaged $1,190 \text{ kg m}^{-3}$, and scab-damaged kernels averaged $1,080 \text{ kg m}^{-3}$ (Martin et al., 1998).

Thousand kernel weight (TKW) is used by wheat breeders and flour millers as a complement to test weight to better describe cereal kernel composition and potential flour extraction. Generally, grain with a higher TKW can be expected to have a greater potential flour yield.

The parameter that is commonly used for the evaluation of utility values of wheat, barley, rice, and corn is vitreousness. Vitreousness indicates natural kernel translucence, which is a means of description of kernel appearance. Vitreous kernels have a translucent, glassy appearance, as opposed to mealy kernels, which have a light, opaque appearance. Vitreous grains are usually harder and denser, and have higher protein content than mealy grains. Vitreousness is usually described by a visual assessment of grain cross section. This parameter has a significant influence on the milling process (grain cleaning and tempering, passage and total flour extraction, and semolina yield).

The size and shape of grains are often useful parameters to evaluate the cereal utility value. The larger and more spherical grains are characterized by higher yield and endosperm. Small grain screenings are often separated to form sound grains and can be used as a feed component. Also, small grains have a higher level of microbiological contamination. Gaines et al. (1997) evaluated the influence of kernel size on soft wheat quality. It was found that besides kernel size, kernel shriveling should also be taken into consideration. Shriveling greatly reduced the test weight and decreased the amount of flour produced during milling. Compared to sound kernels, shriveled kernels had greater flour protein content, and increased flour ash and kernel softness. Small, non-shriveled kernels had slightly better baking quality than large non-shriveled kernels. In addition to the above mentioned parameters, the kernel size uniformity is very important to the wheat milling industry, especially in such processing as cleaning, conditioning, debranning, or grinding. Kernel size and shape can be precisely described using *Digital Image Analysis* (DIA). This method can be used for the evaluation of milling properties of cereals (flour or semolina yield) (Berman et al., 1996; Novaro et al., 2001).

The mechanical properties of cereals play a significant role in the evaluation of quality of cereals, especially the grain hardness, which is often evaluated. This parameter is one of the most important indices in the evaluation of

the utility value of wheat. The hardest wheat varieties are commonly used for semolina, cuscus, or bulgur production. Varieties having medium hardness are used as a main source for bread flour production, while soft wheat varieties are the good raw material for cookies or cakes flour production (Seibel, 1996).

Grain hardness has the greatest influence on the milling process. Particularly for wheat, this parameter should be taken into consideration both during wheat cleaning and conditioning and during flour milling. The denser structure of hard wheat endosperm does not allow tempering water to be absorbed by hard wheat at a rate faster than that for soft wheat, and therefore, the time of tempering is longer for hard wheat. In general, hard wheat cultivars are tempered to about 16–16.5% moisture whereas soft wheat cultivars are tempered to 15–15.5% (wet basis) (Fang and Campbell, 2003).

The endosperm of hard wheat during grinding tends to grind down to the coarser particles referred to as semolina whereas soft varieties give more flour particles directly. The bran layer of hard wheat is usually more susceptible to grinding than the bran layer of soft wheat. It is found that hard wheat kernels grind better during the reduction stage than soft kernels, and bran includes little endosperm (Gaśiorowski et al., 1999).

The flour particle size distribution also depends on the wheat grain hardness. Testing of the total percentage of flour with particle size of less than $50 \mu\text{m}$ shows considerable differences between soft wheat and hard wheat. Approximately 50% of total flour produced from soft wheat is smaller than $50 \mu\text{m}$ whereas it is only 25% in hard wheat. In fact, hard wheat cultivars display single-mode particle size distribution whereas soft wheat cultivars have bimodal distribution with the first mode at about $25 \mu\text{m}$ (Haddad et al., 1999). Moreover, the flour obtained from hard wheat is easy to sieve whereas soft wheat flour particles tend to stick to other surfaces and to other flour particles, causing sifting problems.

Several tests are available for the determination of cereal grain hardness. These methods often rely on the classic method commonly used for constructional materials (e.g., the Vickers or Brinnel hardness test). However, the most practical application for the evaluation of the utility value of cereals includes tests that indirectly express grain hardness. Especially for wheat, several methods of grain hardness determination have been proposed, such as wheat hardness index (WHI), particle size index (PSI), pearling resistance index (PRI), and a modern method called single kernel characterization system (SKCS). This system is especially useful for a rapid analysis of cereal grain physical properties (Grundas, 2004). The SKCS instrument analyzes 300 kernels individually and determines kernel weight by load cell, kernel diameter and moisture content by electrical current, and kernel hardness (HI) by pressure force. A number of researchers have shown the usefulness of SKCS for the evaluation of wheat utility value, especially milling value. This instrument can be used to evaluate the time of tempering wheat

grain before milling. The SKCS instrument can also be used to determine the physical properties of other cereal species.

Grain hardness is also related to important baking properties of flour. The flour obtained from hard wheat is characterized by higher content on starch damaged. As a result, this flour has higher water absorption and higher gas generation ability and thus bread yield is usually increased.

The chemical properties of cereal grain are also commonly used for the evaluation of cereal utility value. For example, the wheat protein content is one of the most important parameters taken into consideration for wheat grain technological value assessment.

Several tests are available for characterizing the utility value of cereals. For example, the sedimentation test is the basis parameter used for evaluating the baking value of ground wheat or flour sample. The sedimentation test provides information on the protein quantity and the quality. This test is conducted by holding the ground wheat or flour sample in an acid solution. During the sedimentation test, gluten proteins swell and precipitate as a sediment. The sedimentation values can be in the range of 7 for low-protein wheat with weak gluten to as high as 75 or more for high-protein wheat with strong gluten. Positive correlation is observed between sedimentation volume and gluten strength or loaf volume attributes. The sedimentation value depends, among other things, on the flour extraction during milling and the wheat variety (Kruger and Hatcher, 1995).

Another very important parameter is the falling number. This test informs about the enzyme activity (mainly α -amylase) of ground wheat or flour sample. The falling number instrument analyzes the viscosity of flour-and-water paste by measuring the time of mixing and falling stirrer. If the falling number is too high, enzymes can be added to the flour in various ways to compensate. However, on the other hand, if the falling number is too low, enzymes cannot be removed from the flour or wheat, which results in a serious problem that often makes the flour unusable for baking. High α -amylase activity could be caused by immature grain or low resistance to sprouting (Abdel-Aal et al., 1997).

Some methods characterize the cereal utility value on the basis of dough rheological properties. Apparatuses such as alevograph, farinograph, extensigraph, mixograph, and rapid visco analyzer are the most commonly used in the industry practice. Parameters obtained on the basis of these methods are very useful for evaluating the baking value of flour.

Direct methods

The two direct methods most often used to evaluate the cereal utility value are the laboratory flour milling tests and the laboratory baking tests. These methods indicate the milling and baking properties of small cereals and flour samples.

The laboratory flour milling test is used to evaluate the milling performance of wheat and other cereals and to produce flour for other laboratory tests. Various kinds of laboratory automated or semi-automated mills are used to determine the cereal milling value. The most common laboratory mills are the Brabender Quadramat Flour Mills, the Buhler Laboratory Flour Mill, and the Chopin CD1 and CD2 mills. Information obtained on the basis of laboratory flour milling is useful to adjust the mill settings of commercial mills.

The laboratory flour mill results are expressed as flour extraction and flour ash content. Also, parameters such as bran and shorts yield are determined (Posner, 1991). For example, the effectiveness of wheat flour milling can be expressed by the following equation, called Brabender index:

$$W_B = \frac{0.5w}{82z} \quad (1)$$

where, w represents flour extraction (%); z , is the flour ash content (%); 0.5, is the average ash content in wheat endosperm, and 82 represents the average endosperm content in wheat. The higher the value of this index, the better is the cereal utility value (Jurga, 2006).

The laboratory baking test is the best method to evaluate the baking value of cereals and flour. The baking tests can be divided as standard and optimum. The standard baking tests depend on the constant conditions of dough kneading and baking parameters, whereas the optimum methods recommend adjusting the baking recipe and baking parameters to the properties of the flour. Thus, this method allows for the optimum use of flour.

The laboratory baking tests can be realized in two ways:

- By the direct method (the dough is produced from all the ingredients)
- By the indirect method (at the beginning the leaven is prepared and after fermentation dough is produced)

It should be noted that on the basis of the baking tests the sensory assessment of bread is made. Also, the *bread's physical and chemical properties* are determined. The parameters of texture are commonly evaluated.

Summary

The methods of evaluation of cereal utility value are consequently improved for many years and allow to quickly evaluate the quality of grain. The full characteristics of cereal includes evaluation of many parameters, which decide about utility. The described physical properties of grain are the basis in cereal utility evaluation. However, the fully characteristic of cereal must include other parameters.

Bibliography

- Abdel-Aal, E.-S. M., Hulc, P., Mosulski, W., and Bhirud, P. R., 1997. Kernel, milling and baking properties of spring-type spelt and Einkorn Wheats. *Journal of Cereal Science*, **26**, 362–370.

- Berman, M., Bason, M. I., Ellison, F., Peden, G., and Wrigley, C. W., 1996. Image analysis in whole grains using single kernel measurements and whole grain protein analysis. *Cereal Chemistry*, **73**, 323–327.
- Czarnecki, E., and Evans, L. E., 1986. Effect of weathering during delayed harvest on test weight, seed size and grain hardness of wheat. *Canadian Journal of Plant Science*, **66**, 473–482.
- Fang, Ch., and Campbell, G. M., 2003. On predicting roller milling performance V: effect of moisture content on the particle size distribution from first break milling of wheat. *Journal of Cereal Science*, **37**, 31–41.
- Gaines, C. S., Finney, P. L., and Andrews, C., 1997. Influence of kernel size and shriveling on soft wheat milling and baking quality. *Cereal Chemistry*, **74**, 700–704.
- Gąsiorowski, H., Kłodziejczyk, P., and Obuchowski, W., 1999. Wheat kernel hardness (in Polish). *Przegląd Zbożowo-Młyński*, **43**, 6–8.
- Grundas, S., 2004. The characteristic of physical properties of kernels in heads of common wheat *Triticum aestivum* L. (in Polish). *Acta Agrophysica*, **102**, 27–30.
- Haddad, Y., Mabille, F., Mermet, A., Abecassis, J., and Benet, J. C., 1999. Rheological properties of wheat endosperm and grinding behaviour. *Powder Technology*, **105**, 89–94.
- Jurga, R., 2006. The assessment of milling efficiency (in Polish). *Przegląd Zbożowo-Młyński*, **50**, 37–39.
- Kruger, J. E., and Hatcher, D. W., 1995. FY Sedimentation test for evaluation of flour quality of Canadian wheats. *Cereal Chemistry*, **72**, 33–37.
- Martin, C., Herrman, T. J., Loughin, T., and Oentong, S., 1998. Micropycnometer measurement of single kernel density of healthy, sprouted and scab damaged wheats. *Cereal Chemistry*, **75**, 177–180.
- Novaro, P., Colicci, F., Venora, G., and D'Edigio, M. G., 2001. Image analysis of whole grains: a noninvasive method to predict semolina yield in durum wheat. *Cereal Chemistry*, **78**, 217–221.
- Posner, E. S., 1991. Wheat and flour ash as a measure of millability. *Cereal Foods World*, **36**, 626–629.
- Seibel, W., 1996. Weizenmehlqualität und produktvielfalt in Westeuropa Getreide. *Mehl und Brot*, **50**, 316–319.
- Tkachuk, R., Dexter, J. E., and Tipples, K. H., 1990. Wheat fractionation on a specific gravity table. *Journal of Cereal Science*, **11**, 213–223.

Cross-references

- [Breads: Physical Properties](#)
[Grain Physics](#)
[Image Analysis in Agrophysics](#)
[Physical Properties of Raw Materials and Agricultural Products](#)

CHEMICAL IMAGING IN AGRICULTURE

Adam Paweł Kuczyński
 Institute of Agrophysics, Polish Academy of Sciences,
 Lublin, Poland

Synonyms

Chemical mapping; Hyperspectral imaging; Microspectroscopy imaging; Multispectral imaging; Spectral analysis; Spectral imaging; Spectroscopic imaging; Visualizing chemistry

Definition

Chemical imaging in agriculture is a discipline at the intersection of statistics and biophysical chemistry (chemometrics), applied in agriculture, food science, and in agrobiotechnology. It is a discipline whose analytical capability consists in creating visual images (spectral images) of the composition, structure or dynamics of chemical samples (qualitative or quantitative – mapping) from simultaneous measurement of spatial and valid time-dependent spectroscopy variables, and quantitative interpretation of the images also provides answers to the questions “when”, “where”, “what” and “how much”.

Chemical imaging methods (without dyeing) can be used for gaining information about agriculture systems of all sizes, from the single molecule to the cellular level and to the ecosystem in agriculture. Diverse instrumentation, ultra-sensitive and selective techniques of interaction radiation with the sample are employed for making observations on such widely different systems. However, what is the most important in the discipline is the fact that several different physical phenomena and types of signal acquisition can be used in similar, but highly advanced chemometrics algorithms, and that created huge data sets will be processed by one software and computer, permitting multiple potentialities of field application for diagnosis.

Introduction

Many applications of chemical imaging touch our daily lives, for example in subjective (sensory) tests, in the human recognition of nutrient and pigment content in foods; it works as a non-invasive method of diagnosing, understanding and control of plant growth, harvest and post-harvest or simple preservation processes. In such aspects of human perception, the imaging is limited to the life experience, the power of human brain, and simple eye detectors of red, green and blue light data, and that set of human attributes combined permits the recognition of a sample as the chemical fingerprint method (Francis, 1995). In such applications, the present wide range of bio-spectroscopy techniques permits more quantitative analysis of bioactive ingredients, but it will not provide full and complete information on the spatial distribution of chemical components.

The idea that drives the analytical power of chemical imaging is that data scanning draws information from such a large portion of the spectrum of absorption, emission, mass, energy, power etc. that any given object should have a unique spectral signature – a “fingerprint” in at least a few of the many bands that can be scanned and exactly statistically processed.

Image processing

In a standard mapping experiment, i.e., univariate data analysis, an image of the sample will be made based on single value variation as is from data values (intensity at

point, signal to baseline, signal to axis), from the parameters of a curve model fitted to the data (peak area, position, width, intensity), or others (Chi-squared, percent Gaussian). For example, an anthocyanins map could be made from a strawberry sample, in which one band of anthocyanins absorbance is used for the intensity greyscale of the image. Dark areas in the image would indicate non-anthocyanins-bearing compounds. This mapping could potentially give misleading results with more interactive surroundings or color reactant.

By spectral mapping almost the entire spectrum at each mapping point is acquired, and a quantitative analysis can be performed by computer post-processing of the data. The main and increasingly important role of chemometrics is the analysis of multivariate data for many different application areas. Multivariate methods can analyze the whole data set simultaneously and directly related to chemical properties. It allows the potential qualification and quantification of very complex systems such as biological materials.

Packages of software designed for the visualization and analysis of large 3 or 4-dimensional hyperspectral image cubes offer extensive spectral and spatial pre-processing capabilities and support statistical pattern recognition, multivariate classification and quantitative analysis algorithms as well as standard image analysis. Software developed for laboratory imaging and mapping experiments identifies materials using reference spectra (direct classical least squares (DCLS) and partial least squares (PLS), principal component regression (PCAR), multilinear regression) or identifies materials even when no reference data is available (principal component analysis (PCA), multivariate curves resolution (MCR-ALS) or factor analysis). The standard image analysis and visualization post-processing tools, such as particle size and distribution analysis, transform qualitative information contained within an image into quantitative metrics that deliver objective answers.

Multivariate algorithms are constantly being developed, like a life experience, so there is a continuous supply of new and improved methods. The order follows a typical workflow consisting of loading or importing a data set, visualizing and pre-processing the data, analyzing to obtain qualitative or quantitative results, and finally visualizing. The true value of all data registration techniques of chemical imaging are exploited only with access to very advanced statistics and image analysis capabilities.

Techniques of chemical imaging

Many imaging techniques are used, and often used simultaneously in combination for exacting applications. They are significantly differing in their ability to capture lateral dimensions, ranges of penetration depths, or time scales. The bio-spectroscopy techniques, this umbrella term integrates both – are divided into the three main groups (Jackson et al., 2006).

1. Optical imaging and magnetic resonance

The techniques interact with samples using resonance of low-energy (electronic, vibrational, or nuclear). They are non-destructive and can be performed in the body (*in vivo*). Examples include:

- Vibrational imaging – identifies specific molecules by their chemical bonds and use vibrational spectrum like a “fingerprint” of matter (Himmelsbach et al., 2001; Thygesen et al., 2003; Gierlinger and Schwanninger, 2007).
- Fluorescence techniques – rely on fluorescent proteins that are genetically expressed in biological systems or can bind to targets as spectroscopic markers (Xiao et al., 1999; Roos, 2000; Lai et al., 2007).
- Ultrafast spectroscopy – uses ultrafast pulsed light sources that provide peak power needed to measure excited states useful in dynamics reaction (Lichtenthaler and Babani, 2000).
- Nuclear Magnetic Resonance and Magnetic Resonance – technologies that use magnetic fields to provide spatial information on molecules (Glidewell, 2006; Lambert et al., 2006).

2. Electron, x-ray, ion and neutron spectroscopy

The techniques interact with samples using high-energy radiation which provides high-resolution chemical and structural information below surfaces of materials. Examples include:

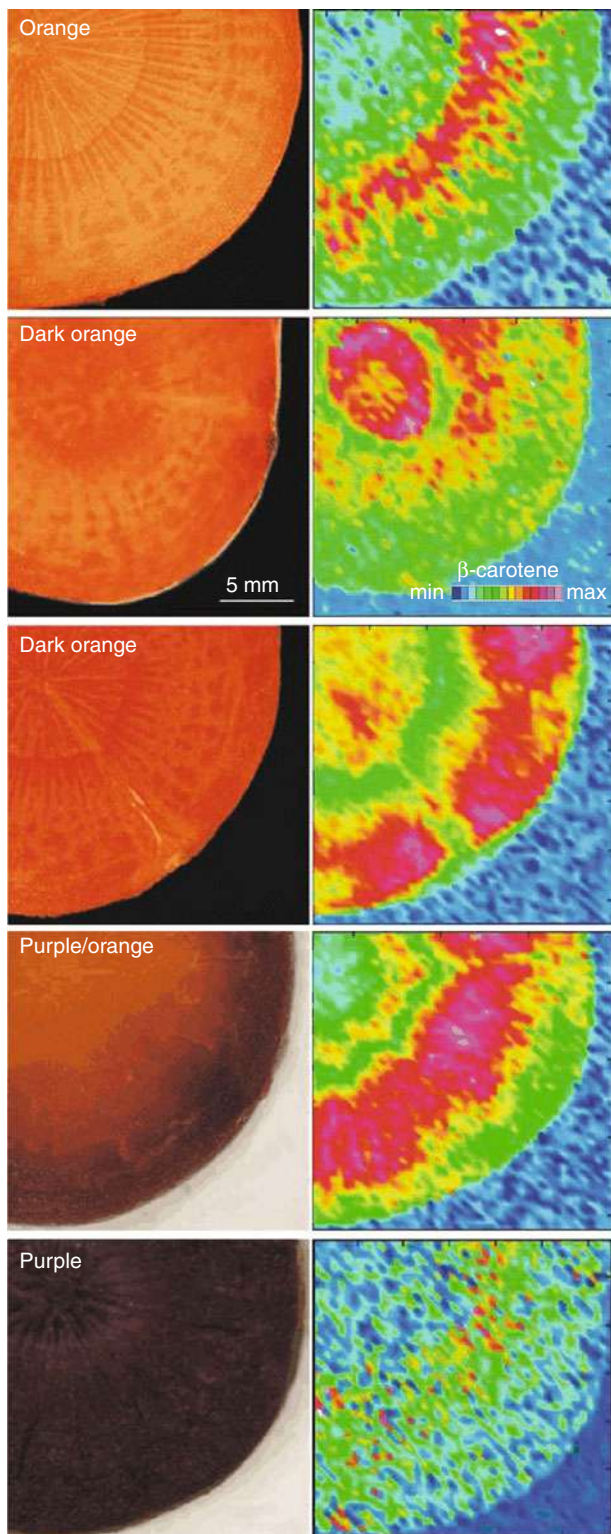
- Electron microscopy – takes advantage of the fact that an electron provides a much higher-resolution of probing than optical and can penetrate deep below the surfaces of materials.
- X-ray spectroscopy – uses high-energy photons to penetrate more deeply than electrons.
- Mass spectrometry – moving a point of ionization over a sample surface and is used for mapping biological samples (Mangabeira et al., 2006; Burrell et al., 2007; Sangwon Cha et al., 2008).

3. Proximal probe

The techniques use small probes very close to the sample. There is a wide variety of tips used in tunneling, force and near-field optical microscopes. For the purposes of recording images, that is an optical-fibre, a semiconducting, or a metallic probe positioned in close proximity to a sample. These methods are especially useful for understanding the chemistry of surfaces (Ding et al., 2008).

The challenge in agriculture

Chemical imaging in agriculture includes the biochemistry which is important in the processing effects on postharvest products, on the composition and safety of foods, feeds, beverages, and other products from agriculture, including wood, fiber and bio-based materials, by-products, and wastes. It covers the chemistry of pesticides, herbicides (Hake et al., 2007; Perkins et al., 2008), veterinary drugs, plant growth regulators, phytonutrients, flavours and aromas, fertilizers, together



Chemical Imaging in Agriculture, Figure 1 Classification of carrot roots by visual images of transversely cut roots and their Raman maps colored according to the band intensity related to β -carotene content. (Modified figure of Baranska et al., 2006.)

with their metabolism, toxicology, and environmental monitoring and remediation. These spectral analyses in agriculture emphasize the relationships between plants, animals and bacteria, and their environment and must be considered within the context of the soil, water, air – within the agro-ecosystem in which living and nonliving components interact in complicated cycles that are critical to a wide variety of organisms.

Chemical imaging in Agriculture can perform qualitative and quantitative analysis of the ingredient distribution (Figure 1), use the science of sampling, set error limits, validate and verify results through calibration and standardization, create new ways to make measurements based on differential spectroscopy properties, and interpret data in proper context and communicate results (Salzer et al., 2000). Finally, the goal for chemical imaging in agro-environment is to recognize and understand chemical structures and processes, and to use that knowledge to control, classify, or eventually create biological structures on demand. Our ability to domesticate crops and eliminate the need for hunting and gathering that allowed for the establishment of permanent settlements and the development of technologically advanced societies has led to a greater overall availability of food, both animal and plant.

Chemical imaging together with biotechnology (Schmidt et al., 2009) is a source of great promise for innovations ranging from improving the diagnosis and treatment of hereditary diseases, to safer drugs, to more environmentally friendly herbicides and pesticides to microbial processes to clean up the environment (Gowen et al., 2007). Making these promises a reality requires rethinking some fundamental assumptions.

Conclusions

In general, all chemical imaging in Agriculture could benefit from the development of higher data acquisition speeds, better data storage and management, new chemical probes and markers, ultrafast optical detectors, possibility of measuring multiple dimensions in parallel and further miniaturisation of instrumentation. As chemical imaging involves the use of a relatively new analytical technique and high cost of instrumentation, the full potential of chemical imaging in Agriculture cannot yet be fully realized, and that potential, should such analytical techniques be implemented on a large scale for the control of intensive agricultural and food production, may bring enormous benefits for health and prophylactic interventions.

Bibliography

- Baranska, M., Baranski, R., Schulz, H., and Nothnagel, T., 2006. Tissue-specific accumulation of carotenoids in carrot roots. *Planta*, **224**, 1028–1037.
- Burrell, M. M., Earnshaw, C. J., and Clench, M. R., 2007. Imaging Matrix Assisted Laser Desorption Ionization Mass Spectrometry: a technique to map plant metabolites within tissues at high spatial resolution. *Journal of Experimental Botany*, **58**, 757–763.

- Cha, S., Zhang, H., Ilarslan, H. I., Wurtele, E. S., Brachova, L., Nikolau, B. J., and Yeung, E. S., 2008. Direct profiling and imaging of plant metabolites in intact tissues by using colloidal graphite-assisted laser desorption ionization mass spectrometry. *The Plant Journal*, **55**, 348–360.
- Ding, S.-Y., Xu, Q., Crowley, M., Zeng, Y., Nimlos, M., Lamed, R., Bayer, E. A., and Himmel, 2008. A biophysical perspective on the cellulosome: new opportunities for biomass conversion. *Current Opinion in Biotechnology*, **19**, 218–227.
- Francis, F. J., 1995. Quality as influenced by color. *Food Quality and Preference*, **6**, 149–155.
- Gierlinger, N., and Schwanninger, M., 2007. Review – The potential of Raman microscopy and Raman imaging in plant research. *Spectroscopy*, **21**, 69–89.
- Glidewell, S. M., 2006. NMR imaging of developing barley grains. *Journal of Cereal Science*, **43**, 70–78.
- Gowen, A. A., O'Donnell, C. P., Cullen, P. J., Downey, G., and Frias, J. M., 2007. Hyperspectral imaging an emerging process analytical tool for food quality and safety control. *Trends in Food Science and Technology*, **18**, 590–598.
- Hake, H., Ben-Zur, R., Schechter, I., and Anders, A., 2007. Fast optical assessment of pesticide coverage on plants. *Analytica Chimica Acta*, **596**, 1–8.
- Himmelsbach, D. S., Barton, F. E., McClung, A. M., and Champagne, E. T., 2001. Protein and apparent amylose contents of milled rice by NIR-FT/Raman spectroscopy. *Cereal Chemistry*, **78**, 488–492.
- Jackson, N. B., Chaurand, P. R., Fulghum, J. E., Hernandez, R., Higgins, D. A., Hwang, R., Kneipp, K., Koretsky, A. P., Larabell, C. A., Stranick, S. J., et al., 2006. *Visualizing Chemistry: The Progress and Promise of Advanced Chemical Imaging*. Washington, DC: National Academies Press.
- Lai, A., Santangelo, E., Soressi, G. P., and Fantoni, R., 2007. Analysis of the main secondary metabolites produced in tomato (*Lycopersicon esculentum*, Mill.) epicarp tissue during fruit ripening using fluorescence techniques. *Postharvest Biology and Technology*, **43**, 335–342.
- Lambert, J., Lampen, P., von Bohlen, A., and Hergenröder, R., 2006. Two- and three-dimensional mapping of the iron distribution in the apoplastic fluid of plant leaf tissue by means of magnetic resonance imaging. *Analytical and Bioanalytical Chemistry*, **384**, 231–236.
- Lichtenthaler, H. K., and Babani, F., 2000. Detection of photosynthetic activity and water stress by imaging the red chlorophyll fluorescence. *Plant Physiology and Biochemistry*, **38**, 889–895.
- Mangabeira, P. A., Gavrilov, K. L., de Almeida, A.-A. F., Oliveira, A. H., Severo, M. I., Rosa, T. S., da Costa Silva, D., Labejof, L., Escaig, F., Levi-Setti, R., Mielke, M. S., Loustalot, F. G., and Galle, P., 2006. Chromium localization in plant tissues of *Lycopersicum esculentum* Mill using ICP-MS and ion microscopy (SIMS). *Applied Surface Science*, **252**, 3488–3501.
- Perkins, M. C., Bell, G., Briggs, D., Davies, M. C., Friedmann, A., Hartb, C. A., Roberts, C. J., and Ruttena, F. J. M., 2008. The application of ToF-SIMS to the analysis of herbicide formulation penetration into and through leaf cuticles. *Colloids and Surfaces B: Biointerfaces*, **67**, 1–13.
- Roos, W., 2000. Review – Ion mapping in plant cells – methods and applications in signal transduction research. *Planta*, **210**, 347–370.
- Salzer, R., Steiner, G., Mantsch, H. H., Mansfield, J., and Lewis, E. N., 2000. Infrared and Raman imaging of biological and biomimetic samples. *Fresenius' Journal of Analytical Chemistry*, **366**, 712–726.
- Schmidt, M., Schwartzberg, A. M., Perera, P. N., Weber-Bargioni, A., Carroll, A., Sarkar, P., Bosneaga, E., Urban, J. J., Song, J., Balakshin, M. Y., Capanema, E. A., Auer, M., Adams, P. D., Chiang, V. L., and James Schuck, P., 2009. Label-free in situ imaging of lignification in the cell wall of low lignin transgenic *Populus trichocarpa*. *Planta*, **230**, 589–597.
- Thygesen, L. G., Lokke, M. M., Micklander, E., and Engelsen, S. B., 2003. Vibrational microspectroscopy of food. Raman vs. FT-IR. *Trends in Food Science and Technology*, **14**, 50–57.
- Xiao, Y., Kreber, B., and Breuil, C., 1999. Localisation of fungal hyphae in wood using immunofluorescence labelling and confocal laser scanning microscopy. *International Biodeterioration and Biodegradation*, **44**, 185–190.

Cross-references

- [Anisotropy of Soil Physical Properties](#)
[Biotechnology, Physical and Chemical Aspects](#)
[Image Analysis in Agrophysics](#)
[Isotropy and Anisotropy in Agricultural Products and Foods](#)
[Mapping of Soil Physical Properties](#)
[Plant Disease Symptoms, Identification from Colored Images](#)
[Spatial Variability of Soil Physical Properties](#)
[Surface Properties and Related Phenomena in Soils and Plants](#)
[X-Ray Method to Evaluate Grain Quality](#)

CHEMICAL TIME BOMB, RELATION TO SOIL PHYSICAL CONDITIONS

Halina Smal

Institute of Soil Science and Environment Management,
University of Life Sciences, Lublin, Poland

Definition

Chemical time bomb (CTB), originally formulated by Stigliani in the late 1980s is defined as

an unforeseen chain of events resulting in the delayed and sudden occurrence of harmful effects due to the mobilization or chemical transformation of chemicals stored in soils and sediments in response to saturation or alteration in certain environmental conditions. (Stigliani, 2002, 99)

The CTB concept refers to the following: (1) soil/sediment ability to store and immobilize toxic chemicals (e.g., heavy metals such as Cd, Cu, Pb, and Ni; persistent organic compounds such as PCBs - polychlorinated biphenyls widely used in the past in many products mainly in electrical equipment, and some pesticides like DDT- dichloro-diphenyl-trichloroethane) in “chemical sinks” having limited capacity, (2) that harmful effects of pollution may not be observed directly but long after (e.g., decades) loading of the chemical to the environment (hence, CTB term). CTB may emerge when a retained, inert chemical is mobilized and released because the capacity of the sink is either exceeded by an excess of the chemical input, or diminished due to changes in “capacity-controlling properties” (CCPs), that determine the sink storage capacity. In the long term, CCPs are not constant and vary as affected by environmental changes (e.g., in land use and climate, hydrology). When any of CCPs passes a threshold, the system may reverse the role from a sink into a source of the chemical, for example, in

crops and vegetation, ground and surface waters. Such a reversal is usually unpredictable, unexpected and sudden (the “explosion”) – on a timescale that is relatively short in comparison with the time between the initial accumulation and the manifestation of detrimental effects.

With respect to heavy metals, particularly important soil CCPs are the following: cation exchange capacity (CEC), pH, redox potential (Eh), organic matter content, salinity, and microbial activity. They are interdependent and directly or indirectly related to the soil physical conditions; in case of CEC and Eh to the following:

CEC – soils with a low value have low capacities to retain heavy metals by sorption. It depends on clay minerals and organic matter content (decreasing reduces CEC) and is reflected in *soil texture* (clay fraction content).

Eh – decreasing (more reducing conditions) dissolves iron and manganese oxides, which mobilizes oxide-sorbed toxic chemicals. Its increasing (more oxidizing conditions) mobilizes heavy metals by dissolving insoluble metal sulfides. Eh is directly influenced by *soil moisture* and may be changed by flooding (Eh decreasing) or drainage (Eh increasing) of lands.

In CTB phenomena, also important are soil physical properties influencing leaching and transport of chemicals – *water retention* and *water flow, erosion*.

Water flow – depends on soil *hydraulic properties*. Among them, a *hydraulic conductivity*, which is a measure of the ability of a soil to transmit water and dissolved solutes and is strongly related to *soil texture, structure, and water content*.

Soil erodibility – erosion increases the risk of runoff and concentrations of toxic substances at locations where transported material is deposited. It reflects among other properties, *soil texture, structure, moisture*, and organic matter content. It is related to farming activities that influence these properties and to changes in land use (e.g., it increases with deforestation).

CTBs example – draining of wetlands in a coastal area of Sweden in the 1900s and in the 1940s, resulting in oxidation of sulfides to H_2SO_4 and strong acidification of nearby lakes; the Minamata (Japan) catastrophe (for details and more examples see Stigliani, 2002).

Bibliography

- Salomons, W., and Stigliani, W. M. (eds.), 1995. *Biogeodynamics of pollutants in soil and sediments, risk assessment of delayed and non-linear responses*. Springer: Berlin Heidelberg. 352 pp.
 Stigliani, W. M., 1988. Changes in valued capacities of soils and sediments as indicators of nonlinear and time-delayed environmental effects. *Environmental Monitoring and Assessment*, **10**, 245–307.
 Stigliani, W. M., 2002. Contaminated lands and sediments: chemical time bombs? In Douglas, I. (ed.), *Causes and Consequences of Global Environmental Change*, Vol. 3. In Munn, T. (ed-in-chief), *Encyclopedia of Global Environmental Change*. Chichester/New York: Wiley, pp. 98–115.

CHISEL

An edge tool with a flat steel blade with a cutting edge used in soil chiselling (loosening by chisel implements).

CLAY MINERALS AND ORGANO-MINERAL ASSOCIATES

Tatiana Victorovna Alekseeva

Laboratory Geochemistry and Soil Mineralogy, Institute of Physicochemical and Biological Problems of Soil Science, Russian Academy of Sciences, Pushchino, Moscow region, Russia

Synonyms

Phyllosilicates

Definition

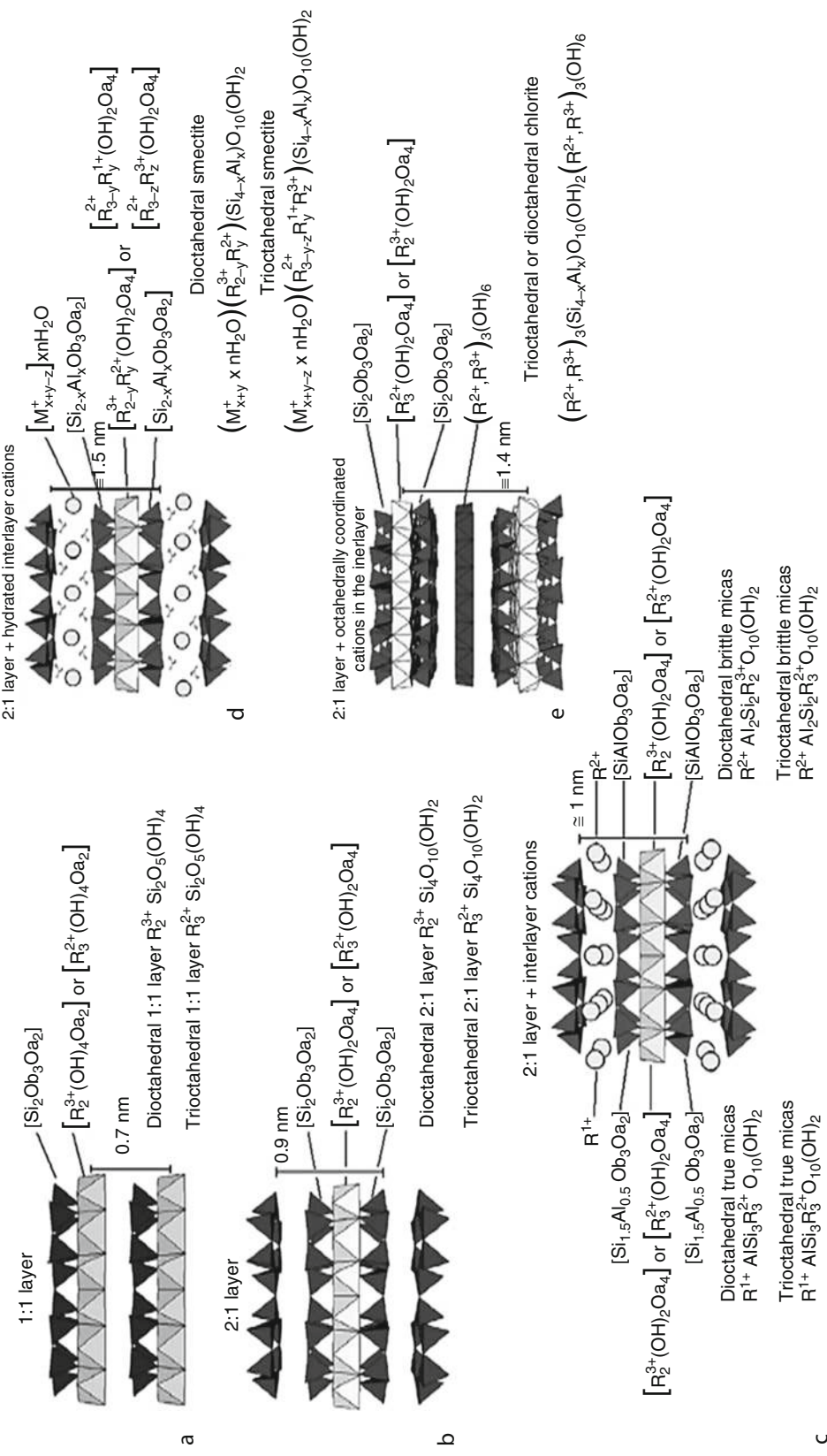
Clay minerals belong to the family of hydrous aluminum phyllosilicates. They make up the fine-grained fraction of rocks, sediments, and soils.

Introduction

Clay minerals are the most important constituents of so-called clay-size fraction (particles are less than 2 micrometers [μm] in equivalent spherical diameter) of soils. Commonly referred to as “fine-grained,” “submicron,” or “ultrafine” particles, recently the term “soil nanoparticles” is coming into usage. The clay size fraction in soils is seldom composed of a single mineral. Typically, it includes mixtures of phyllosilicates, oxides, and hydroxides of Fe, Al, and Mn, occasionally quartz and feldspars and organic materials – humic substances, enzymes, viruses, etc. (Theng and Yuan, 2008) (see *Nanomaterials in Soil and Food Analysis*). Soils’ clay fractions are typically enriched in organic C and P, total N, S, and P, inorganic P, Al, Fe, Ca, Mg; they have higher cation exchange capacity (CEC) in a comparison with bulk soils and coarser fractions. Many soils’ basic physical and chemical characteristics: *buffer capacity, bulk density, cracking and creeping, flocculation and dispersion phenomena, hydrophobicity, infiltration, shrinkage and swelling phenomena, soil aggregation* (see *Soil Aggregates, Structure, and Stability*), *soil structure and compaction limits*, and surface properties (see *Adsorption Energy and Surface Heterogeneity in Soils, Specific Surface Area of Soils and Plants*) (see, e.g., Alekseeva et al., 1999) are influenced by molecular-scale differences in soil clay minerals and/or their concentrations.

Phyllosilicate minerals in soils

The structures of phyllosilicates basically consist of sheets of SiO_4 tetrahedra and sheets of Al or Mg octahedra (as in gibbsite and brucite). Common tetrahedral cations are Si^{4+} , Al^{3+} , and Fe^{3+} . Octahedral cations are usually Al^{3+} , Fe^{3+} ,



Clay Minerals and Organo-Mineral Associates. **Figure 1** Different layer structures: (a) 1:1 layer (i.e., kaolinite- and serpentine-like layer), (b) 2:1 layer with anhydrous interlayer cations (i.e., the mica-like layer), (c) 2:1 layer with hydrated interlayer cations (i.e., smectite- and vermiculite-like layer), (d) 2:1 layer with octahedrally coordinated interlayer cations (i.e., chlorite-like layer). (After Brigatti et al., 2006. With permission from Elsevier.)

Mg^{2+} , and Fe^{2+} . Octahedra show two different topologies related to OH-groups position, i.e., the cis- and the trans-orientation. The 1:1 layer structure consists of the repetition of one tetrahedral and one octahedral sheet, and examples would be kaolinite and serpentine (Figure 1).

A 2:1 layer structure consists of an octahedral sheet sandwiched between two tetrahedral sheets, and examples are micas, smectites, vermiculites, and chlorites. In the 1:1 layer structure, the unit cell includes six octahedral sites (i.e., four cis- and two trans-oriented octahedral) and four tetrahedral sites. Six octahedral sites and eight tetrahedral sites characterize the 2:1 layer unit cell. Structures with all the six octahedral sites occupied are known as trioctahedral. If only four of the six octahedra are occupied, the structure is referred to as dioctahedral. Depending on the composition of the tetrahedral and octahedral sheets, the layer will have no charge or will have a net negative charge. If the layers are charged, this charge is balanced by interlayer cations (Na^+ , K^+ , or others). In each case, the interlayer can also contain water. The crystal structure is formed from a stack of layers interspersed with the interlayers. The periodicity along the c-axis varies from 0.91 to 0.95 nm in talc and pyrophyllite to 1.40–1.45 nm in chlorite. In talc, the interlayer space is empty, whereas in mica and illite it is occupied by anhydrous alkaline and alkaline-earth cations (layer periodicity about 1 nm). The interlayer space of smectite and vermiculite contains alkaline or alkaline-earth cations together with water molecules (layer periodicity is about 1.2 nm when the interlayer position is occupied by cations with low-field strength and water molecules, about 1.5 nm when the interlayer is occupied by high-field strength cations and water molecules, and more than 1.5 nm when water molecules are exchanged by different polar molecules) (Brigatti et al., 2006, p. 21). Table 1 gives the classification scheme for phyllosilicates with typical layer

structures and some basic properties (for detail reading see also Dixon and Weed, 1989).

Additionally to these main groups, chain minerals – palygorskite (attapulgite) and sepiolite are considered 2:1 phyllosilicates and these are important constituents in soils of arid and semiarid climates. They contain a continuous two-dimensional tetrahedral sheet; however, they differ from other layer silicates in that they lack continuous octahedral sheets. Thus, the structures consist of ribbons of 2:1 sheets 4 or 6 SiO_4 tetrahedra (in palygorskite and sepiolite, respectively) wide connected in a “net” structure with holes, which contain a variable amount of zeolitic water. Sepiolite is trioctahedral, whereas palygorskite is intermediate between di- and trioctahedral. Chain phyllosilicates have a fibrous habit with channels running parallel to the fiber length. Fiber sizes vary widely but generally range from about 10 to about 30 nm in width, and from about 5 to about 10 nm in thickness. The CEC of these minerals is low – 3–20 meq 100 g^{-1} . At the same time, anion exchange capacity exceeds 70 meq 100 g^{-1} which together with large external surface (up to $200\text{ m}^2\text{ g}^{-1}$) and even larger internal pore surface (up to $600\text{ m}^2\text{ g}^{-1}$) provides high adsorption capacity for cations, anions, and neutral molecules, and good suspending or gelling characteristics (Mackenzie, 1975; Raussell-Colom and Serratosa, 1987; Brigatti et al., 2006).

Besides monomineralic clay samples and mixtures of discreet clay minerals, one more type of mixtures exists – interstratified or mixed layer minerals or structures. Mixed layers are usually built up by layers of two mineral types but may be the combination of more different components. Interstratified clay minerals can have ordered or regular mixed-layer structures if different layers alternate along the c-direction in a periodic pattern (e.g., the stacking of A and type B layers can be ABABAB or AABAAB etc.) or disordered (irregular) mixed-layer structures, if the

Clay Minerals and Organo-Mineral Associates, Table 1 Classification scheme for phyllosilicates with typical layer structures and their major properties. (Modified after Thorez, 1976.)

Layer type	Interlayer	Net layer charge per formula unit (x)	CEC (meq 100 g^{-1})	SSA ($\text{m}^2\text{ g}^{-1}$)	Group names	Subgroups names (octahedral layer)
1:1	Without	$x \sim 0$	3–15	5–40	Kaolinite-serpentine (Kandites)	Di: Kaolinites Tri: Serpentines
2:1	Without	$x \sim 0$	Up to 5	Up to 5	Pyrophyllite-talc	Di: Pyrophyllites Tri: Talc
	Exchangeable cations, anions, molecules, etc.	$x \sim 0.2\text{--}0.6$	80–120	40–800	Smectites	Di: Montmorillonites Tri: Saponites
	Dry or hydrates cations	$x \sim 0.6\text{--}0.9$	100–150	100–400	Vermiculites	Di: Vermiculites Tri: Vermiculites
		$x \sim 0.6\text{--}2$	10–40	10–100	Micas and illites	Di: Muscovites Tri: Biotites
	Hydroxide layers	x variable	10–40	10–55	Chlorites	Di: Sudoites Di-Tri: Donbassite Tri: Chlorites

stacking along the c-direction of type A and B layers is random (e.g., ABBABAA or AAABABAAAAABABA etc.). Regular sequences are identified by special names. For example, the name “rectorite” is attributed to a regular interstratification of dioctahedral mica and dioctahedral smectite; “tosudite” is a regular interstratification of dioctahedral chlorite and dioctahedral smectite. Interstratified minerals have been mostly recognized in soils but also in sediments and as the hydrothermal and weathering products (MacEwan and Ruiz-Amil, 1975; Thorez, 1976; Brigatti et al., 2006, p. 25).

Three models of origin of soil clay minerals are: (1) inheritance directly from parent materials, (2) transformation when the original structure is usually retained but the interlayer region is visibly altered, and (3) neoformation by the synthesis from the dissolved and amorphous products of weathering; here, the structures may have no relationship to those of the parent material. The soil clay mineral predominance is correlated with climate factors (temperature and water availability in the soil), because these factors strongly affect the chemical weathering in the soil profile. The correlation of soil clay mineralogy with climate conditions has been reviewed extensively. It was suggested that clay mineralogy follows a weathering pattern, from hot and humid to cool and dry, in the order kaolinite→smectite→vermiculite→chlorite and mixed-layer phyllosilicates→Illite and mica (for details see Dixon and Weed, 1989; Wilson, 1999).

Previously neoformation of clays regarded mostly as abiotic processes. Recent findings show that different clay minerals can be synthesized with the participation of microorganisms (Tazaki, 2006). Konhauser and Urrutia (1999) concluded that bacterial clay authigenesis is a common biogeochemical process. Like a biomineratization process, biochemical weathering of clays also meets more interest (Robert and Berthelin, 1986).

Clay minerals are ultrafine particles and their characterization requires special analytical techniques. Standard set includes x-ray diffraction, various spectroscopic methods such as Mossbauer spectroscopy, infrared spectroscopy, NMR spectroscopy, thermal analysis, and electron microscopy (for detail reading see Thorez, 1976; Bergaya et al., 2006).

Organomineral associates in soils

In temperate cultivated soils 50–75% of soil organic matter (OM) exists within clay-sized organo-mineral particles (Kleber et al., 2007). The interactions of clay minerals and OM play the important role in the formation and stabilization of soil aggregates and the behavior of nutrients and pollutants (Six et al., 2002; Alekseeva et al., 2006; Besse-Hoggan et al., 2009).

The ability of minerals to preserve OM results from the combined influence of reactive surface sites and a large specific surface area (SSA). These properties result from heterogeneity and imperfection of the natural mineral

surfaces and small size of clays and soil oxides (Kogel-Knabner et al., 2008).

The interactions of humic substances with soil clay minerals may have a variety of mechanisms which mainly depends upon the nature and properties of the organic species, the properties of the clay mineral and the kind of exchangeable cation at the clay surface, the water content of the system, and the pH of the surrounding medium. The type of clay becomes increasingly important when the soil OM content is low (Cornejo and Harmosin, 1996).

The interactions of OM with mineral surfaces (phyllosilicates and Fe-, Al-, Mn-oxides) and metal ions is one of the mechanisms of OM stabilization. Evidence comes from the fact that soil OM in fine silt and clay fractions is older or has a longer turnover time than OM in other soil OM fractions. Adsorption of OM to mineral surfaces effects the OM decomposition mechanisms and rates. Main chemical mechanisms of interactions are: (1) ligand exchange, (2) polyvalent cation bridges, (3) weak interactions such as hydrophobic interactions, van der Waals forces, and H-bonding (Mineral Organic Microbial Interactions) (Luetzow et al., 2006).

OM bound to minerals mainly by ligand exchange is more resistant against mineralization than OM held by van der Waals forces. Ca-bridges enhanced the stability of sorbed OM but less than by the binding via ligand exchange (Kogel-Knabner et al., 2008).

For each mechanism, only certain amount of OM can be protected and each soil has its own protective capacity. The mineralogy of soil particles controls the protection of OM via the effect of the type and density of active sites capable of adsorbing organic materials. The presence of Fe-Al oxides – hydroxides increases the surface charge density which increases the reactivity of mineral surfaces. Kleber et al. (2007) showed that singly coordinated, reactive OH groups on Fe and Al oxides and at edge sites of phyllosilicates, which are able to form strong bonds by ligand exchange, are a measure of the amount of OM stabilized in soils in organo-mineral associations.

Preferential binding at reactive sorption sites favors typically discontinuous surface accumulation of OM rather than in a continuous coating. Thus, OM is not distributed over the available mineral surfaces but clustered ([Clusters in Soils](#)) in small patches with some vertical extension (Kaiser and Guggenberger, 2003; Kleber et al., 2007). Recently, Kleber et al. (2007) came to the conclusion that adsorbed OM creates the zonal organo-mineral architecture with regular features: contact zone, hydrophobic zone, and kinetic zone. The molecules of the inner zone are the most stable, and molecules of the outer zone have the faster exchange with soil solution. It is suggested that proteins (*N*-containing materials) play a prominent role in the formation of organo-mineral complexes due to both the relatively high abundances of these compounds in soils and the ability of these materials to adsorb irreversibly to mineral surfaces. Proteins can bind particularly strongly and create a basal layer with further opportunities for more numerous interactions. The affinity of proteins

for all types of interfaces found in soils originates in the flexibility of the polypeptide chain and in the diversity of the 2-amino acids that can be classified as positively, neutrally, or negatively charged and on a hydrophobic scale from polar (hydrophilic) to non-polar (Quiquampoix and Burns, 2007).

Additionally to chemical stabilization of OM in soils, its physical protection in soil microaggregates influences OM accumulation ([Physical Protection of Organic Carbon in Soil Aggregates](#)).

Summary

Interactions of clay minerals with OM (soil natural organic polymers) modify properties of both partners and have the large-scale effect on the physical, chemical, and biological properties of soils. Fractionation of soil organic substances due to the properties of a mineral matrix is the other aspect of these interactions. Up to now limited information is available on the relationships between mineralogy and the chemistry of bound OM. Solid state NMR spectroscopy (^{13}C , ^{15}N , ^{31}P , ^1H , etc.) is a promising tool for solving this problem. Kogel-Knabner et al. (2008) showed that mineral-bound OM is depleted in lignin and phenolic components. Clay fractions generally show a higher content alkyl-C groups than whole soils and higher proportions of carboxyl-C than plant residues, indicative of the more oxidized stage of the stabilized OM. Laird et al. (2001) postulated that existing relationships between clay mineralogy and the chemical nature of the associated humic substances indicate that either soil clay mineralogy strongly influences the humification process or that humic substances with different properties are selectively adsorbed on different clay mineral species. Further investigations of the OM associated with different clay minerals are needed before the role of clay–organic interactions on OM constitution, stabilization and turnover times, diagenetic transformations, and other aspects will be clear.

Bibliography

- Alekseeva, T. V., Alekseev, A. O., Sokolowska, Z., and Hajnos, M., 1999. Relationship between mineralogical composition and physical properties of soils. *Eurasian Soil Science*, **32**, 548–557.
- Alekseeva, T., Besse, P., Binet, F., Delort, A. M., Forano, C., Josselin, N., Sancelme, M., and Tixier, C., 2006. Effect of earthworm activity (*Aporrectodea giardi*) on atrazine adsorption and biodegradation. *European Journal of Soil Science*, **57**, 295–307.
- Bergaya, F., Theng, B. K. G., and Lagaly, G. (eds.), 2006. *Handbook of Clay Science*. Amsterdam: Elsevier.
- Besse-Hoggan, P., Alekseeva, T., Sancelme, M., Delort, A. M., and Forano, C., 2009. Atrazine biodegradation modulated by clays and clay/humic acid complexes. *Environment Pollution*, **157**, 2837–2844.
- Brigatti, M. F., Galan, E., and Theng, B. K. G., 2006. Structures and Mineralogy of Clay Minerals. In Bergaya, F., Theng, B. K. G., and Lagaly, G. (eds.), *Handbook of Clay Science*. Amsterdam: Elsevier.
- Cornejo, J., and Harmosin, M. C., 1996. Interactions of humic substances and soil clays. In Piccolo, A. (ed.), *Humic Substances in Terrestrial Ecosystems*. Amsterdam: Elsevier, pp. 595–624.
- Dixon, J. B., and Weed, S. B. (eds.), 1989. *Minerals in Soil Environments*, 2nd edn. Madison: Soil Science Society of America. SSSA Book Series 1.
- Kaiser, K., and Guggenberger, G., 2003. Mineral surfaces and soil organic matter. *European Journal of Soil Science*, **54**, 219–236.
- Kleber, M., Sollins, P., and Sutton, R., 2007. A conceptual model of organo-mineral interactions in soils: self-assembly of organic molecules fragments into zonal structures on mineral surfaces. *Biogeochemistry*, **85**, 9–24.
- Kogel-Knabner, I., Guggenberger, G., Kleber, M., Kandeler, E., Kalbitz, K., Scheu, S., Eusterhues, K., and Leinweber, P., 2008. Organo-mineral associations in temperate soils: integrating biology, mineralogy, and organic matter chemistry. *Journal of Plant Nutrition and Soil Science*, **171**, 61–82.
- Konhauser, K. O., and Urrutia, M. M., 1999. Bacterial clay authigenesis: a common biogeochemical process. *Chemical Geology*, **161**, 399–413.
- Laird, D. A., Martens, D. A., and Kingery, W. L., 2001. Nature of clay-humic complexes in an agricultural soil: I. chemical, biochemical, and spectroscopic analyses. *Soil Science Society of America Journal*, **65**, 1413–1418.
- Luetzow, M. V., Kogel-Knabner, I., Ekschmitt, K., Matzner, E., Guggenberger, G., Marshner, B., and Flessa, H., 2006. Stabilization of organic matter in temperate soils: mechanisms and their relevance under different soil conditions – a review. *European Journal of Soil Science*, **57**, 426–445.
- MacEwan, D. M. C., and Ruiz-Amil, A., 1975. Interstratified Clay Minerals. In Gieseking, J. E. (ed.), *Inorganic Components, Soil Components*. New York: Springer, Vol. 2, pp. 267–334.
- Mackenzie, R. C., 1975. The classification of soil silicates and oxides. In Gieseking, J. E. (ed.), *Soil Components. Vol. 2: Inorganic Components*. New York: Springer, pp. 1–26.
- Quiquampoix, H., and Burns, R. G., 2007. Interactions between proteins and soil mineral surfaces: environmental and health consequences. *Elements*, **3**(6), 401–406.
- Raussell-Colom, J. A., and Serratosa, J. M., 1987. Reactions of clays with organic substances. In Newman, A. C. D. (ed.), *Chemistry of Clays and Clay Minerals*. London: Longman Scientific & Technical, pp. 371–422. Mineralogical Society Monograph No. 6.
- Robert, M., and Berthelin, J., 1986. Role of biological and biochemical factors in soil mineral weathering. In Huang, P. M., and Schnitzer, M. (eds.), *Interactions of Soil Minerals with Natural Organics and Microbes*. Madison: Soil Science Society of America, pp. 453–495. SSSA special publication 17.
- Six, J., Conant, R. T., Paul, E. A., and Paustian, K., 2002. Stabilization mechanisms of soil organic matter: implications for C-saturation of soils. *Plant and Soil*, **241**, 155–176.
- Tazaki, K., 2006. Clays, microorganisms, and biomineratization. In Bergaya, F., Theng, B. K. G., and Lagaly, G. (eds.), *Handbook of Clay Science*. Amsterdam: Elsevier, pp. 477–498.
- Theng, B. K. G., and Yuan, G., 2008. Nanoparticles in the Soil Environment. *Elements*, **4**, 395–399.
- Thorez, J., 1976. *Practical Identification of Clay Minerals*. Belgium: Liege State University, Institute of Mineralogy.
- Wilson, J. J., 1999. The origin and formation of clay minerals in soil; past, present and future perspectives. *Clay Minerals*, **34**, 7–25.

Cross-references

- [Adsorption Energy and Surface Heterogeneity in Soils](#)
[Buffer Capacity of Soils](#)
[Bulk Density of Soils and Impact on Their Hydraulic Properties](#)
[Clusters in Soils](#)
[Compaction of Soil](#)
[Cracking in Soils](#)

Flocculation and Dispersion Phenomena in Soils
 Hydrophobicity of Soil
 Infiltration in Soils
 Nanomaterials in Soil and Food Analysis
 Physical Protection of Organic Carbon in Soil Aggregates
 Shrinkage and Swelling Phenomena in Soils
 Soil Aggregates, Structure, and Stability
 Specific Surface Area of Soils and Plants

CLAYPAN AND ITS ENVIRONMENTAL EFFECTS

Stephen H. Anderson
 Department of Soil, Environmental, and Atmospheric Sciences, University of Missouri, Columbia, MO, USA

Synonyms
 Argillic horizon; Pseudogley; Stagnic properties

Definition

Claypan refers to a subsoil layer, having a much higher clay content than the surface horizons. This layer is slowly permeable and is separated by a sharply defined boundary from overlying horizons. Claypans are dense and hard when dry but plastic and sticky when wet. (Soil Science Society of America, 2008). These soils often have a perched water table present above the claypan during a portion of the year.

Pan. A pan can be genetic or induced. A genetic pan is a natural subsurface soil layer with low or very low hydraulic conductivity. The layer differs in physical and chemical properties from the soil layers immediately above and below the pan. Some genetic pans include claypans, fragipans, and hardpans. An induced pan is a subsurface layer having a higher bulk density and lower total porosity than the soil layers immediately above and below the pan and is a result of pressure that has been applied by normal tillage operations or other artificial means. Synonyms for these induced pans include plowpans, plowsoles, pressure pans, or traffic pans (Soil Science Society of America, 2008).

Introduction

Soils with claypans include significant areas throughout the world. In the Midwestern USA, these soils are included in Major Land Resource Area (MLRA) 113 Central Claypan Area (2.9 million hectares), with most soils classified as Aqualfs and some Udalfs. The United Nations FAO system classifies these soils as Eutric Planosols (Food and Agriculture Organization of the United Nations, 2001). Eutric Planosols have a global extent of 47.53 million hectares. Planosols include 130 million hectares and are extensive in southern Brazil, northern Argentina, Paraguay, eastern Africa, South Africa, eastern Australia, eastern United States, and in southeast Asia from Bangladesh to Thailand (Food and Agriculture Organization of the United Nations, 2001).

The US Soil Classification System of 1938 used the name Planosols for claypan soils. The subsequent US classification system, USDA Soil Taxonomy, includes Planosols in the Great Groups Albaqualfs, Albaquults, and Arialbolls. Claypan soils are in the Great Group Albaqualfs.

Claypan soils include a significant amount of area within the Midwestern USA (Blanco-Canqui et al., 2002). Soils in this area are characterized by a subsoil horizon with an abrupt and significant increase in clay content within a short vertical distance in the soil profile (Soil Science Society of America, 2008). The Midwestern US claypan region and similar soils encompass an area of about 4 million hectares within Missouri, Illinois, and Kansas (Anderson et al., 1990). The depth to the claypan varies from 0.10 to 0.50 m with clay content ranging from 350 to 600 g/kg (35–60%; Blanco-Canqui et al., 2002). Dominant clay minerals include smectites with high shrink swell potential.

Throughout the year, these clays swell during the winter and spring periods and often shrink during the late summer and early autumn periods. When the clays are swollen, their low saturated hydraulic conductivity impedes infiltration and perches water above the claypan, causing a high probability of runoff (Blanco-Canqui et al., 2002). When the clays shrink, preferential flow through these cracks is significant (Baer and Anderson, 1997).

Most claypan soils are classified in high runoff hydrologic groups (Lerch et al., 2008). Soils primarily on hillslopes in dissected till have a slow infiltration rate and moderate runoff potential due to argillic horizons or paleosols that impede downward movement of water. Soils occurring at summit landscape positions have a very slow infiltration rate and high runoff potential due to claypans.

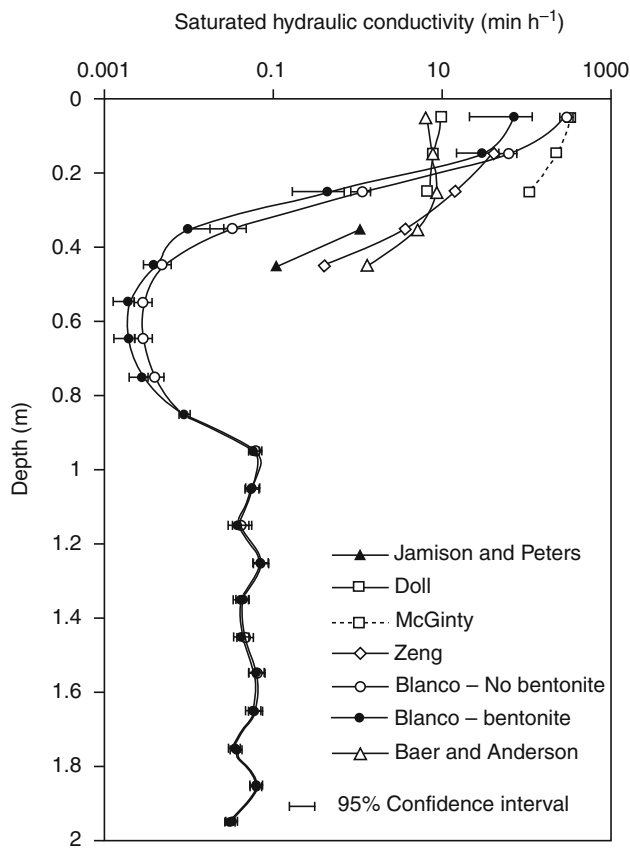
Hydrology

Soil texture and structure have strong effects on saturated hydraulic conductivity, K_{sat} (Blanco-Canqui et al., 2002). Clay-textured soils typically have low to very low K_{sat} values. Due to their low subsoil permeability, claypan soils perch water and create lateral flow and surface runoff. Field work on claypan hydrology suggests that runoff rates may be equal to rainfall under saturated conditions (Saxton and Whitaker, 1970). Long-term studies of runoff and rainfall with the McCredie rainfall-erosion plots at Kingdom City, Missouri, USA indicate that lateral flow known as interflow is a significant component of the total runoff during springtime when precipitation is usually the most intense and erosion rates are highest (Minshall and Jamison, 1965; Ghidley and Alberts, 1998). Claypan soils have enhanced runoff during winter and spring periods due to very low infiltration rates.

In situ lateral K_{sat} has been estimated for claypan soils in monoliths 0.25-m wide by 0.50-m long by 0.23-m deep (Blanco-Canqui et al., 2002). Field measurements of lateral K_{sat} provided a value of 72 mm h^{-1} . This value corresponds well to soil core (76-mm diameter by 76-mm

length) estimates of 71 mm h^{-1} through the silt loam surface horizon (Figure 1). The field estimate of K_{sat} for the claypan was $0.9 \mu\text{m h}^{-1}$. The lowest K_{sat} of the profile measured with soil cores was $2 \mu\text{m h}^{-1}$, which occurred within the 0.50–0.75-m depth (Figure 1), just below the claypan (depth of maximum clay concentration; Blanco-Canqui et al., 2002). The physical nature of this layer was weakly developed, compact, with a firm structure.

A high probability of interflow occurs within these soils (Jamison et al., 1968; Wilkinson and Blevins, 1999). Information on in situ lateral K_{sat} through the horizons above the claypan is important for determining their ability to conduct water laterally and assessing runoff and erosion. Because of their hydrologic attributes, claypan soils have quite different effective K_{sat} values with depth from other Alfisols. Information on K_{sat} depth distribution is valuable in explaining claypan hydrology and for the characterization of variability in horizons of low and high permeability required for accurate flow studies (Blanco-Canqui et al., 2002).



Claypan and its Environmental Effects, Figure 1 Comparison of saturated hydraulic conductivity (K_{sat}) data for claypan soils (Blanco-Canqui et al., 2002). Error bars represent 95% confidence intervals of mean K_{sat} values ($n = 9$). Data obtained with bentonite (Blanco-Bentonite) to plug visible pores represent K_{sat} data for claypan soils. (Reprinted with permission from the Soil Science Society of America.)

Claypan soils under native vegetation have significantly different hydraulic properties compared to soils under long-term grain crop management (Udawatta et al., 2008). Differences can be attributed to better structure as well as preserved pore networks. Soils under native vegetation have enhanced macropore flow, permanent roots, and higher organic matter content. Native permanent vegetation prevents water erosion, which increases the thickness of surface horizons; eroded soils have about 0.25 m thinner silt loam surface horizons than soils with native vegetation. Thicker surface horizons with coarser soil textures have higher hydraulic conductivity values. Under long-term grain crop management, soil hydraulic properties for claypan soils can significantly change due to a reduction in surface layer thickness above the clay layer through erosion as well as from the traffic by agricultural equipment. Improvements in these properties have been observed when using permanent vegetative buffers such as cool season grass buffers and agroforestry tree buffers (Seobi et al., 2005). Although the claypan horizon dominates the surface hydrology for these soils, buffers often provide benefits by slightly reducing runoff from soils under row crop management.

Conservation Reserve Program (CRP) and hay management systems increased field-measured infiltration rates in a summit landscape position compared to grain crop systems (Jung et al., 2007). Hydraulic conductivity measured in a backslope position for CRP and hay cropping systems was 16 and 10 times higher, respectively, than for a mulch-tilled grain cropping system (Jiang et al., 2007a). This was attributed in part to perennial grasses improving aggregate stability and soil organic carbon. Backslope landscape positions are more vulnerable to soil degradation with grain cropping systems compared to other landscape positions.

Soil erosion and agrichemical runoff

Due to enhanced runoff on claypan soils, soil erosion and sediment transport can be a concern. Minimum tillage as well as no-till systems are recommended to reduce this problem. Some studies have shown that no-till management can slightly enhance runoff on claypan soils relative to conventional tillage systems (Ghidley and Alberts, 1998; Ghidley et al., 2005); however, other studies have shown no differences in runoff among tillage systems (Lerch et al., 2008). No-till systems with corn (*Zea mays*) and soybean (*Glycine max*) cropping systems have significantly reduced sediment transport. Most annual soil loss (80% of annual loss) occurs during the rough fallow and seedbed preparation periods, with soil loss under no-till management five to seven times lower compared to other tillage systems (Ghidley and Alberts, 1998).

Vegetative filter strips have been used on claypan soils to mitigate surface runoff, sediment, and nutrient losses (Blanco-Canqui et al., 2004). Narrow, 1-m-long native switchgrass (*Panicum virgatum*) barriers in combination with 8-m-long fescue (*Festuca arundinacea*) filter strips

significantly reduced sediment transport as well as organic N, nitrate, ammonium, particulate P, and phosphate runoff compared to traditional fescue filter strips.

These vegetative filter systems have also been shown to reduce dissolved and sediment-bound herbicide losses in runoff (Lerch et al., 2008). Studies evaluated the transport of glyphosate [*N*-(phosphonomethyl)glycine], atrazine [6-chloro-*N*²-ethyl-*N*⁴-isopropyl-1,3,5-triazine-2,4-diamine], and metolachlor [2-chloro-*N*-(6-ethyl-*o*-tolyl)-*N*-(1*R,S*)-2-methoxy-1-methylethyl]acetamide]. Four meters of native vegetation buffers (mostly eastern gamagrass [*Tripsacum dactyloides*] and switchgrass) reduced herbicides about 75–80% in runoff. Four meters of native species resulted in greater reductions in herbicide transport compared to 8 m of fescue. Buffers enhance plant transpiration which enhances infiltration to reduce surface runoff in these high runoff potential claypan soils. As a general pattern, herbicide concentration or mass loss was greatest for the first runoff event and decreased rapidly as the season progressed.

Contour buffer strips have been demonstrated to reduce runoff, sediment, and nutrient losses in cropped watersheds (Udwatta et al., 2002). Paired watersheds were used to make an assessment of the degree of benefit from these contour buffers. Agroforestry buffers (trees and grasses) and contour grass buffers were found to reduce runoff (1% and 10%), sediment (0% and 19%), total phosphorus (17% and 8%), and nitrate (37% and 24%) losses. Most runoff reductions occurred during the second and third years after treatment establishment.

Management of runoff and associated effects on surface sediment, nutrient, and herbicide transport is an important challenge when using claypan soils for grain crop production. No-till management has been shown to enhance herbicide runoff relative to conventional tillage systems due to lack of herbicide incorporation and slightly increased runoff with no-till systems (Ghidey et al., 2005).

Agrichemical leaching

The claypan soils of the Midwestern USA contain silt loam surface textures and silty clay subsoils (Blanco-Canqui et al., 2002). The subsoil contains a high proportion of montmorillonitic clay, which results in a relatively impermeable soil horizon when wet. Since the claypan is highly impermeable, the assumption is often made that water and solutes cannot move through the claypan to reach groundwater. However, cracks often occur in these soils when they are cropped and their water content is low (Baer and Anderson, 1997). These cracks can allow preferential flow of water and chemicals. In addition, soils have natural features such as interpedal planar voids and biologically induced, highly conductive macropores, which may act as channels for water and chemical transport. In one study, claypans were hypothesized to restrict the movement of agrichemicals to groundwater; however, N fertilizer moved rapidly through preferential flow paths in the soil into the underlying glacial till aquifer (Blevins

et al., 1996; Wilkinson and Blevins, 1999). About one third of the N fertilizer migrated to the groundwater, while another one third was lost due to denitrification which can be a challenge for these soils since they have high soil water content in the spring.

Although enhanced annual runoff occurs from claypan soils, vertical transport can occur after periods of infrequent precipitation. Kazemi et al. (2008) found enhanced herbicide leaching in soils which had antecedent water content near the permanent wilting point (dry treatment). Atrazine, alachlor [2-chloro-2',6'-diethyl-*N*-methoxymethylacetanilide], and the bromide tracer were detected significantly deeper (0.15–0.30 m) when applied to a dry treatment compared to the wet treatment (water content near field capacity). Herbicide retardation coefficients estimated using soil properties were substantially higher compared to estimates from herbicide and bromide profile concentrations, suggesting evidence of nonequilibrium adsorption of atrazine and alachlor probably due to less surface area available for adsorption when transport occurs in shrinkage cracks. Preferential flow of atrazine and alachlor herbicides was found when applications occurred on initially dry claypan soils. The deeper movement of herbicides in initially dry plots was attributed to the presence of shrinkage cracks resulting from low soil water content.

Herbicide degradation has been found to decrease with dry soil water conditions (Kazemi et al., 2008). Degradation was found to be lower for initially dry conditions compared to initially wet conditions. This was attributed to better microbial growth in soils under initially moist conditions. Thus, dry claypan soils enhance preferential transport of herbicides and also decrease their rate of degradation.

Plant productivity

Variable claypan properties across the landscape affect grain yield due to soil property effects on root growth (Myers et al., 2007). Soybean roots were inhibited in E horizons above the claypan; however, roots were stimulated 20–40 cm below the initial claypan depth. Depth to claypan can be used to predict soybean root distributions in claypan landscapes. The depth to the claypan can be rapidly assessed using the apparent bulk electrical conductivity measured using electromagnetic induction (Kitchen et al., 1999). The topsoil thickness above the claypan layer is highly related to the plant available water capacity (Jiang et al., 2007b) and the crop yield (Kitchen et al., 1999). Apparent bulk electrical conductivity from these sensors can be correlated with crop yield due to the effect of the depth to the high charge claypan layer affecting the sensor signal (Kitchen et al., 1999).

Summary

Crop productivity is highly sensitive to topsoil thickness in claypan soils. Prevention of soil erosion is critical in maintaining grain production as well as enhancing water

infiltration in these soils. Conservation best management practices (BMPs) are important to reduce and prevent soil erosion. In some cases, selection of a BMP for one desired outcome may be opposite to another desired outcome (e.g., no-till may be good for erosion control but can increase herbicide loss). When this is the case, priorities will need to be established in order to select the appropriate BMP (Lerch et al., 2008).

Bibliography

- Anderson, S. H., Gantzer, C. J., and Brown, J. R., 1990. Soil physical properties after 100 years of continuous cultivation. *Journal of Soil and Water Conservation*, **45**, 117–121.
- Baer, J. U., and Anderson, S. H., 1997. Landscape effects on desiccation cracking in an Aqualf. *Soil Science Society of America Journal*, **61**, 1497–1502.
- Blanco-Canqui, H., Gantzer, C. J., Anderson, S. H., Alberts, E. E., and Ghidley, F., 2002. Saturated hydraulic conductivity and its impact on simulated runoff for claypan soils. *Soil Science Society of America Journal*, **66**, 1596–1602.
- Blanco-Canqui, H., Gantzer, C. J., Anderson, S. H., Alberts, E. E., and Thompson, A. L., 2004. Grass barrier and vegetative filter strip effectiveness in reducing runoff, sediment, nitrogen, and phosphorous loss. *Soil Science Society of America Journal*, **68**, 1670–1678.
- Blevins, D. W., Wilkison, D. H., Kelly, B. P., and Silva, S. R., 1996. Movement of nitrate fertilizer to glacial till and runoff from a claypan soil. *Journal of Environmental Quality*, **25**, 584–593.
- Food and Agriculture Organization of the United Nations, 2001. Lecture notes on the major soils of the world. FAO Corporate Document Repository. Available from World Wide Web: http://www.fao.org/DOCREP/003/Y1899E/y1899e12.htm#P158_22451.
- Ghidley, F., and Alberts, E. E., 1998. Runoff and soil losses as affected by corn and soybean tillage systems. *Journal of Soil and Water Conservation*, **53**, 64–70.
- Ghidley, F., Blanchard, P. E., Lerch, R. N., Kitchen, N. R., Alberts, E. E., and Sadler, E. J., 2005. Measurement and simulation of herbicide transport from the corn phase of three cropping systems. *Journal of Soil and Water Conservation*, **60**, 260–273.
- Jamison, V. C., Smith, D. D., and Thornton, J. F., 1968. *Soil and Water Research on a Claypan Soil*. USDA Technical Bulletin 1379. Washington: US Government Print Office.
- Jiang, P., Anderson, S. H., Kitchen, N. R., Sadler, E. J., and Sudduth, K. A., 2007a. Landscape and conservation management effects on hydraulic properties of a claypan-soil toposequence. *Soil Science Society of America Journal*, **71**, 803–811.
- Jiang, P., Anderson, S. H., Kitchen, N. R., Sudduth, K. A., and Sadler, E. J., 2007b. Estimating plant-available water capacity for claypan landscapes using apparent electrical conductivity. *Soil Science Society of America Journal*, **71**, 1902–1908.
- Jung, W. K., Kitchen, N. R., Anderson, S. H., and Sadler, E. J., 2007. Crop management effects on water infiltration for claypan soils. *Journal of Soil and Water Conservation*, **62**, 55–63.
- Kazemi, H. V., Anderson, S. H., Goyne, K. W., and Gantzer, C. J., 2008. Atrazine and alachlor transport in claypan soils as influenced by differential antecedent soil water content. *Journal of Environmental Quality*, **37**, 1599–1607.
- Kitchen, N. R., Sudduth, K. A., and Drummond, S. T., 1999. Soil electrical conductivity as a crop productivity measure for claypan soil. *Journal of Production Agriculture*, **12**, 607–617.
- Lerch, R. N., Sadler, E. J., Kitchen, N. R., Sudduth, K. A., Kremer, R. J., Myers, D. B., Baffaut, C., Anderson, S. H., and Lin, C. H., 2008. Overview of the mark Twain/Salt river basin conservation effects assessment project. *Journal of Soil and Water Conservation*, **63**, 345–359.
- Minshall, N. E., and Jamison, V. C., 1965. Interflow in claypan soils. *Water Resources Research*, **1**, 381–390.
- Myers, D. B., Kitchen, N. R., Sudduth, K. A., Sharp, R. E., and Miles, R. J., 2007. Soybean root distribution related to claypan soil properties and apparent soil electrical conductivity. *Crop Science*, **47**, 1498–1509.
- Saxton, K. E., and Whitaker, F. D., 1970. *Hydrology of a Claypan Watershed*. Research Bulletin 974. Columbia: Missouri Agricultural Experiment Station.
- Seobi, T., Anderson, S. H., Udawatta, R. P., and Gantzer, C. J., 2005. Influence of grass and agroforestry buffer strips on soil hydraulic properties for an Albaqualf. *Soil Science Society of America Journal*, **69**, 893–901.
- Soil Science Society of America, 2008. Glossary of soil science terms, 2008 edition. Soil Science Society of America, Madison (available online at <https://www.soils.org/publications/soils-glossary>).
- Udawatta, R. P., Krstansky, J. J., Henderson, G. S., and Garrett, H. E., 2002. Agroforestry practices, runoff, and nutrient loss: a paired watershed comparison. *Journal of Environmental Quality*, **31**, 1214–1225.
- Udawatta, R. P., Anderson, S. H., Gantzer, C. J., and Garrett, H. E., 2008. Influence of prairie restoration on CT-measured soil pore characteristics. *Journal of Environmental Quality*, **37**, 219–228.
- Wilkison, D. H., and Blevins, D. W., 1999. Observations on preferential flow and horizontal transport of nitrogen fertilizer in the unsaturated zone. *Journal of Environmental Quality*, **28**, 1568–1580.

Cross-references

- [Cracking in Soils](#)
[Electrical Resistivity to Assess Soil Properties](#)
[Layered Soils, Water and Solute Transport](#)
[Shrinkage and Swelling Phenomena in Soils](#)
[Wetting and Drying, Effect on Soil Physical Properties](#)

CLEAVAGE PLANE

The smooth, flat surface along which a mineral (also soil clay mineral) readily breaks.

Bibliography

- Glossary of Soil Science Terms. Soil Science Society of America. 2010. <https://www.soils.org/publications/soils-glossary>

CLIMATE CHANGE: ENVIRONMENTAL EFFECTS

Miroslav Kutílek
 Prague, Czech Republic

Synonyms

Global warming

Definition

Climate is defined as the statistical evaluation of meteorological data. They are air temperature, humidity, rainfall, wind, and eventually other observed elements in a given region over a long time period; the World Meteorological Organisation recommends 30 years, but longer periods may be used depending upon the purpose. The obtained results are applied in climate classification; the oldest and well known is the Köppen classification. Several other classifications are used, too, again according to the purpose. Climate should not be confused with weather, which is the set of meteorological data valid at time of observation, usually on scale of days.

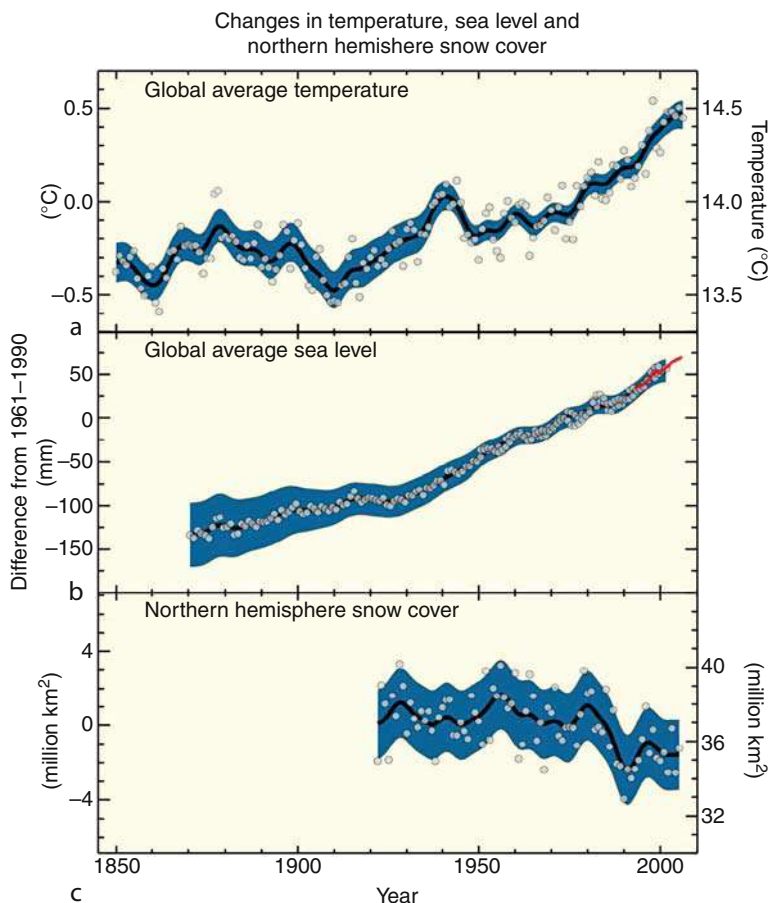
Recent climate change

Introduction

The recent climate change started about 1850. Actually the estimation of the year is a matter of general agreement and it is not strictly equal to local or regional observations.

The climate change is usually characterized by the global temperature in recent studies; other climate characteristics are only sometimes mentioned, too. The temperature increase in the twentieth century was estimated as 0.74°C and the rate of its rise is increasing. Eleven of the last 12 years (1995–2006) rank among the 12 warmest years in the instrumental record of global surface temperature (since 1850). The warmest years in the instrumental record of global surface temperatures are 1998 and 2005 (Trenberth et al., 2007), with 1998 frequently considered as the first one in the rank. Measured temperature of the global ocean has increased to depths of at least 3,000 m in the last 40 years. The energy balance shows that the ocean absorbs more than 80% of the heat added to the climate system. The global warming caused the rate of rise of seawater level by $1.8 \pm 0.3 \text{ mm/year}$ in the second half of the twentieth century (White et al., 2005) (Figure 1).

The reported rise of the global temperature by 0.74°C does not mean that the temperature rose uniformly over the Earth. This same value would not have been obtained



Climate Change: Environmental Effects, Figure 1 Change of the surface global average temperature for the time period 1850–2007 (top); change of the global seawater level elevation (center); change of the northern hemisphere snow covered area in March–April (bottom). Smoothed curves represent decadal averaged values, while circles show yearly values. (According to Fig. SPM-3, IPCC, 2007; Summary for Policymakers.)

everywhere that the temperature was measured locally during the past 100 years. The observed warming has been greater over land than that over the oceans, owing to the smaller thermal capacity of the land. Since the continents occupy larger area on the northern hemisphere, there was a tendency for a higher temperature rise in the northern than in the southern hemisphere (Trenberth et al., 2007). Values of average temperature rise also differ according to differences in climate of various regions. The rise is very small in the equatorial regions and increases with the latitudes, both north and south. The latitude dependence is only one of the many factors that play a role and the local average temperature rise depends upon its particular geographical position on a continent. Values differ for inland climates compared with lands close to the ocean. In Central Europe, the average temperature increased between 1.1°C and 1.3°C in 100 years (Czech Meteorological Institution, 2007), while in Northern Ireland at Armagh Observatory the increase was only 1.2°C in 200 years, that is, from 1796 to 2002. Within the Arctic Circle at latitudes between 70° and 90°, the average temperature rise was 2.1°C in the period 1880–2004 (Trenberth et al., 2007, Figure 3.7). During the first 60 years of that 124-year period, the average temperature increased, then decreased for the next 20 years, and again increased for the following 44 years. In that 124-year period, the average temperature rises were there higher in the period 1920–1940 than they are today.

Warming is strongest over the continental interiors of Asia and northwestern North America and over some mid-latitude ocean regions of the southern hemisphere as well as southeastern Brazil. In the recent period, some regions have warmed substantially while a few have cooled slightly on an annual basis. (Trenberth et al., 2007, p. 250)

These few examples enable us to imagine how difficult it is to estimate the global temperature and its rise merely from the data obtained from any number or all meteorological stations. “No single location follows the global average, and the only way to monitor the globe with any confidence is to include observations from as many diverse places as possible (Trenberth et al., 2007, p. 250).” The estimation of the global temperature from the surface meteorological stations was therefore a difficult task. During the last 28 years, the instrumentation in satellites was applied to measure the Earth’s global surface temperature. These methods of measurement are considered by meteorologists to be the most objective proof of global warming. It was just by these methods that the temperature was found as no more rising in the last decade (Solomon et al., 2007; Easterling and Wehner, 2009).

Measuring methods

In 1653, organized measurements of air temperature began in northern Italy with the first meteorological network initiated in Tuscany, however, without standardized thermometers. In 1714, the mercury thermometer was

provided with a reliable, physically based scale named after its German inventor Gabriel Daniel Fahrenheit (1686–1736). In 1742, another scale established by the Swedish astronomer and physicist Anders Celsius (1701–1744) was proposed and gradually accepted as the standard in meteorology. Then the international meteorological network could start and first networks were realized in the second half of the eighteenth century. Even now with the dense internationally interconnected observation nets, the estimation of the global temperature requires application of sophisticated statistical methods and the results obtained by various institutions and authors may differ. Starting in 1978, the use of satellites to measure the temperature in the troposphere simplified the assessment of the global temperature. The measurements are not performed by classical thermometers. Values of temperature, derived from an analysis of the wavelengths of radiation data, are evaluated and checked by two independent procedures. The most frequently, but not universally used procedures are the remote sensing system, RSS, and that developed by the University of Alabama, Huntsville, UAH. The UAH procedure indicates a slightly smaller global warming than RSS. Because directly measured temperatures during the last 2 and eventually 3 centuries cover very short period, other methods must be used when we study ancient climates. The temperature is ascertained from other measured data, and since temperature is indirectly and approximately estimated, we use the word *proxy* from the Latin *propis, proprius, proximus* – near, nearer, nearest, or very similar. Following proxies are applied: (1) The analysis of concentration changes of isotopes of oxygen and hydrogen in glacier deep core drilling provides estimates of temperature. (2) The concentration change of the isotope beryllium 10 (^{10}Be) in either sediments or ice indicates temperature as well as solar activity. (3) Pollen analysis (palynology) offers information on the dominant plants, which infer past climatic conditions. (4) Tree-ring width and density records (dendrochronology) estimate temperature change and age. (5) Isotopic ratios and chemical composition of corals estimate surface sea temperature. (6) Change found in annual lake sediments called varves provides information on temperature and age. (7) Change in growth of stalagmites in karst caverns and isotopic ratios indicate climatic change. (8) The size of lichens offers information on age and climate. (9) The pedogenesis of fossil and buried soils reflects the climate at the time of their origin.

Factors influencing climate change

Climate change is caused by the action of several factors, which may mutually influence each other. Their forcing varies with geologic time, too, and generally their variability is one of the greatest problems in modeling their role upon the climate change. Another important problem in estimation of the influence of the factors upon the studied meteorological element – the temperature – is the nonlinearity of the relationships.

Astronomic factors: Milankovich cycles

The change of the solar radiation reaching the planet Earth is due to the regular periodic repetition of the change of the Earth's orbital geometry. There are three orbital parameters that change in cycles named Milankovich cycles (Milankovitch, 1920, 1941):

1. The eccentricity of the Earth's orbit around the Sun changes from nearly circular (eccentricity of 0.005) to elliptical (eccentricity 0.058). One complete cycle lasts almost exactly 100,000 years. The combined gravitational field of Jupiter and Saturn is the primary cause of eccentricity change. Earth's orbital eccentricity is now close to its minimal value indicative of a nearly circular path.
2. Axial tilt (obliquity) is the inclination of the Earth's axis in relation to its plane of orbit around the Sun. Oscillations of Earth's axial tilt ranging from 21.5° to 24.5° occurs during a periodicity of 41,000 years. At present, the axial tilt is roughly in the middle of its range.
3. Precession is the Earth's slow wobble as it spins on its axis. It has a periodicity of 21,000 years, while some authors assume it to be closer to 23,000 years. It is primarily caused by the gravitational forces of the Sun and the moon with Saturn and Jupiter also secondarily involved. These cycles and variations of incoming solar radiation are important because the Earth has an asymmetric distribution of continents. They are mainly located in the northern hemisphere. When northern hemisphere summers are coolest since they are farthest from the Sun (aphelion position) due to precession and greater orbital eccentricity and when winters are relatively mild with minimum tilt, snow does not melt in summer and accumulates. In thousands of years, it is transformed into ice and glaciation occurs. A high albedo (reflection of solar radiation) of snow and ice contributes to the cooling during glacial period.

Astronomic factors: solar activity

Solar activity is not constant; it manifests cycles of various lengths and fluctuates periodically around a value of $1,365 \text{ W/m}^2$ (Eichler et al., 2009). Solar activity is accompanied by the existence of the sunspots. When sunspots are abundant during the cycle, it is called the solar maximum and when there are only a few sunspots, it is considered to be the solar minimum. Solar activity is more or less correlated to climatic oscillations with higher solar activity being accompanied by globally warm climate (Lane et al., 1994). The high solar activity and a strong solar wind including the rise of the Sun's magnetic field cause a weakening of the galactic cosmic ray flux – commonly referred to as the shadowing of cosmic rays. The stronger the galactic cosmic ray flux, the greater is the ionized part of the atmosphere having a greater density of nuclei on which water vapor will condense, forming clouds primarily in the lower part of the troposphere (Svensmark, 1998; Marsh and Svensmark, 2000). The clouds reduce the solar

radiation penetrating to the Earth surface and thus cause a relative cooling of the Earth. A 2% decrease in low cloud cover during the solar activity cycle is equivalent to the Earth accepting radiation increased by 1.2 W m^{-2} (Svensmark, 2007). The solar activity had a peak in the time interval 1985–1987 and now it is slightly decreasing, but it is still high above the average of the last 150 years.

Continental drift

Continental drift is a shift of plate carrying the continents and bottom of oceans as a result of plate tectonics. The plates slide very slowly with a speed of 1 to about 15 cm/year on the asthenosphere that is visco-elastic solid. They are associated with geological events such as earthquake, volcanoes, uplift of mountains, mid-ocean rift, and oceanic trench. Where the oceanic plates are moving away from each other, the magma from the asthenosphere fills in the gap and a new oceanic crust is formed (the sea-floor spreading). When two continental plates collide, mountain ranges are created as the colliding crust is compressed and pushed upward. Such collisions may be accompanied with the rise of magma to form volcanoes. Due to the collisions, new supercontinents were formed several times in the geologic history (Rodinia, Pangea, Gondwana). When a thin oceanic plate collides with a thick continental plate and is forced under the continental plate, this process is called subduction. It is responsible for transporting mainly sedimentary rocks rich in CaCO_3 . Hence, great amounts of carbon are conserved below the lithosphere. This gigantic dynamic process influences the entire topography and climate of the “floating” continents. At the same time, continents are shifted from the polar to the equatorial regions and vice versa. An additional consequence of this relocation and of the disruption and fusion of continents is the change of the sea streams and of the direction and strength of blowing winds. All these continually contributed to substantial climate changes during the geologic history of the Earth. Continental drift was discovered by Alfred Wegener (1912, 1920), who related it to climate changes, too.

Greenhouse gases

Radiation from the sun is the source of energy that warms planet Earth. The solar radiation has a value of about $1,366 \text{ watts per square meter (W/m}^2)$ on the outer surface of the Earth's atmosphere (solar constant). It oscillates by about 6.9%, owing to Earth's elliptical path around the Sun. Because the Earth rotates daily, only one-half of our planet receives solar radiation at any one moment. And, taking into account the varying angles at which the radiation is received by the spherical surface of the planet, the average incoming solar irradiance on the Earth's surface is about 342 W/m^2 – approximately four times less than the value of the solar constant. The seasonal and latitudinal distribution and intensity of solar radiation received at the Earth's surface varies substantially. For example, at latitudes of 65° the change in solar energy between summer and

winter can vary by more than 25%. The ratio of incoming and reflected electromagnetic radiation is called albedo. The range of possible values is from 0 (complete absorption and no radiation reflected) to 1 (no absorption at all, the entire incoming radiation is reflected without change). The average albedo is 0.37; therefore, 63% of incoming solar energy contributes not only to the warmth of our planet but also is used in many processes as, for example, the production of green matter, in climatologic processes, etc. The heated surface emanates long-wave infrared radiation (IR). The Earth's atmospheric envelope contains gases that absorb IR from the heated Earth's surface. They are called greenhouse gases. Water vapor, methane (CH_4), carbon dioxide (CO_2), nitrous oxide (N_2O) and ozone (O_3) are the primary greenhouse gases. Without the atmosphere and greenhouse effect, the Earth temperature would be -18°C . Some man-made gases belong to greenhouse gases, too, like fire fighting materials, aerosol spray propellants or solvents, some of the other greenhouse gases are human made, like chlorofluorocarbons (CFC) known under the trade name freon, hydrofluorocarbons (HFC), hydrochlorofluorocarbons (HCFC), sulfur hexafluoride (SF_6), but their use is restricted or they are prohibited due to their very strong greenhouse effect. Earth temperature due to the greenhouse effect is mainly caused by water vapor in the atmosphere; it is 80–90% of the total greenhouse effect. It means that without water vapor the Earth would be cooler by about $29\text{--}30^\circ\text{C}$. The cooling effect of clouds is roughly equivalent to 30 W/m^2 , while the greenhouse effect of CO_2 is about 1.5 W/m^2 , contributing to warming. The concentration of CO_2 in the atmosphere has been fluctuating in ranges from 180 to 300 ppm (parts per million) during the last 2 million years. Only in the industrial era during the last 150 years has there been an increase from 280 ppm to today's CO_2 concentration of about 387 ppm. The authors of Assessments of the Intergovernmental Panel on Climate Change (IPCC) assume that this increase of atmospheric CO_2 concentration is mainly responsible for the recent global warming. Considering Earth's climate system as a balance between incoming short-wave (solar) radiation and outgoing long-wave (thermal infrared) radiation and the increasing greenhouse effect, they made the prognosis on the temperature rise by $3 \pm 1.5^\circ\text{C}$ as the range of uncertainties provided that the CO_2 is doubled to 560 ppm. However, Schwartz (2007) used a detailed balance model to estimate climate sensitivity and obtained the increase of temperature by $1.1 \pm 0.3^\circ\text{C}$ for 560 ppm CO_2 concentration. In addition, he derived a much shorter time constant characterizing the climate response to the atmospheric change of CO_2 when compared to some predictions on the extension of global warming by decades or centuries after CO_2 concentration is lowered. Predictive procedures are not fully acceptable with the simplified assumptions on the sole or dominant greenhouse effect as acting agent in the climate change and if the feedbacks are not fully appreciated in the models.

Thermohaline circulation

Oceanic waters are great regulators of Earth temperature. The heat capacity of water is 4.18 J/g-K , of air it is 1 J/g-K , and of soil and rocks around 0.8 J/g-K . The heat uptake of the world ocean constitutes 84% of the total heat uptake by the climate system. Other major components are heating of continental landmasses, 5%; melting of continental glaciers, 5%, and heating of the atmosphere, 4% (Levitus et al., 2005). When ocean waters flow, they transport huge amounts of energy from the equatorial to the polar regions. With this, transport of energy influencing not only the weather but also the climate, oceanic streams are one of the important factors influencing the climate. There are two main causes of oceanic streams – temperature gradients and differences in seawater density. Due to the temperature gradient, the water flows from the equator to cool poles, as a stream at the ocean surface with the depth about 8001,200 m, and the width of the current is 80–150 km. The discharge is between 20 and 150 Sv (Sverdrups, $1 \text{ Sv} = 10^6 \text{ m}^3/\text{s}$). Just for comparing, the Amazon River has an annual average discharge of 0.2 Sv. When the salt waters of the ocean stream reach the cool regions of high latitudes, they cool also and mix with fresh water of melting ice. Their density increases and the oceanic surface water flows downward. The surface stream changes to the deep ocean stream and flows in opposite direction to the equator. Due to the Earth rotation, the ocean streams direction is deviated by the Coriolis force from the straight path (normal to equator) and the surface and deep streams have not identical paths. For the inhabitants of the northern hemisphere, the Gulf Stream is the best-known ocean current. It is a connected part of all other ocean streams. The whole Earth is encircled by them and since the main cause of their existence is the differences in temperature and in salt content, the term thermohaline circulation is used. Its existence depends upon the configuration of continents. Generally speaking, the form of one supercontinent is less favorable for the thermohaline circulation and the more continents mutually separated exist the better conditions for circulation. It was an important factor of climate change in the geologic past due to the continental drift.

Aerosols volcanoes, asteroids

The term aerosol denotes generally a suspension of fine solid particles or small liquid droplets in a gas. Although their dimensions range from 0.01 to $10 \mu\text{m}$, their maximum occurrence is from 0.6 to $1 \mu\text{m}$. Particles greater than $0.2 \mu\text{m}$ can be detected with an ordinary optical microscope. Particles with diameters less than $0.05 \mu\text{m}$ disappear quickly because they are caught by other particles and lost by aggregation. Particles greater than $15 \mu\text{m}$ are relatively quickly deposited by gravitation. Particles between 0.1 and $2 \mu\text{m}$ remain suspended from 1 to 2 weeks or even more, depending on the winds, keeping them in the atmosphere. Although aerosols can be transported for thousands of kilometers, occurrences of their global

transport is extraordinary, for example, by eruption of large volcanoes. Water vapor condenses on the surface solid particles, which are called condensation nuclei and clouds are formed. The majority of solid aerosol particles occur naturally, originating from volcanoes, dust storms, forest fires, living vegetation, and sea, where water evaporates from droplets leaving salt particles suspended in the air. Human activities, such as burning of fossil fuels and alteration of natural vegetation, also generate aerosols but it accounts for only about 10% of all solid particles. Aerosol particles act mainly as an obstacle to the solar irradiation of the Earth. Their reflection of solar radiation depends primarily upon their size distribution. Incoming solar radiation with the maximum energy at wavelengths between 0.4 and 1 mm is reflected to the outer space by particles in the size range of 0.1–2 μm . The effect is increased if the solid particles are covered with a liquid water film. Since the Earth surface is deprived of its source of heating in this way, an increase of aerosol concentration causes cooling of the Earth, and the opposite, its decrease leads to relative warming. Aerosols greenhouse effect exists, too, but it has low importance in the heat balance. When we deal with the influence of aerosols upon the climate, we purposely measure the concentration (number of aerosol particles) and not the mass (weight) of particles in a volumetric unit of air. The radiometric measurement of solar radiation transmission through an aerosol layer is expressed as the aerosol optical thickness AOT. These types of data have only been available during the last 30 years. The quantitative evaluation of the aerosol influence on the energy balance of the Earth is one of the most difficult parts of climate modeling. For example, models and direct measurements indicate that the cooling effect caused by aerosol scattering could be two times larger than that modeled by IPCC – on the order of 1.5 W/m^2 . Generally, the aerosol effect belongs to the worst quantified parts of models. Regionally, it could even be much larger than the warming effects of greenhouse gases. An intensive increase of aerosol concentration occurred several times in the geological past of the Earth after the impact of an asteroid. The abrupt climate change led to the partial extinction of living organisms. The impact of volcanic eruptions had year's duration because the emitted ashes spread over the entire Earth in an atmospheric aerosol envelope layer. There are many examples on it in Holocene.

Vegetation cover

The incoming solar radiation is absorbed and partially reflected in different ways as the vegetation changes naturally or due to human action. Examples of albedo of various kinds of soil cover are shown in [Table 1](#). They indicate that the entire radiation balance is changing when the vegetation is changed. The most drastic change in the radiation balance occurs when the original forest is lumbered and the soil surface is left without vegetation. In addition to the heating effect due to radiation balance, there is a loss of soil water due to the evaporation. Since there is

Climate Change: Environmental Effects, Table 1 Albedo

Conifer forest	0.08–0.15
Deciduous forest	0.15–0.19
Bare soil	0.17
Grass	0.25
Sand of desert	0.40
Ice	0.6–0.7
Snow	0.8–0.9

a difference between simple evaporation and evapotranspiration from the soil covered by vegetation, the cooling effect differs, too. Deforestation causes changes in the carbon cycle. A forest together with the soil stores more carbon in organic compounds for a much longer time than does an arable soil cultivated for annual crop production. Deforestation results in an abrupt and rapid release of CO_2 from the soil into the atmosphere. Large forested areas differ in clouds regime from the agricultural soil. All these indirectly acting factors contribute to the change of the climate after deforestation of large regions.

Earth's magnetic field

Earth's magnetic field is generated by the so-called geodynamo. The iron in its outer core is a conductor and the geomagnetic field induces electric current in the slowly flowing material surrounding the solid inner core. The Earth rotation plays an important role in it. The feedback process is the generation of a magnetic field by the electrical current and convective flow. The reversal of magnetic poles occurred several times in the geologic history and it has a high probability when the field is very weak. Recent average values in Holocene remain high compared to earlier values. Its last reversal was some 780,000 years ago. Moreover, the magnetic pole position is also not constant – it moves up to 15 km/year. The geomagnetic intensity, measured in Tesla, varies from slightly less than 30,000 nanotesla (nT) to about 60,000 nT at the Earth's surface. Another unit of geomagnetic intensity is 1 Gauss equivalent to 100,000 nT. As the Earth's magnetic field changes, instabilities in the ozone layer occur in both vertical and horizontal directions. They lead to modified temperature gradients and atmospheric circulation. These changes influence the solar wind in the atmosphere and modulate cosmic ray particles. When the geomagnetic field changes its shape and intensity, distinct changes of the climate are expected ([Knudsen and Riisager, 2009](#)). The general increase in precipitation observed over the past 1,500 years correlates with the rapid decrease in dipole moment observed during this period.

Climate change in geologic history

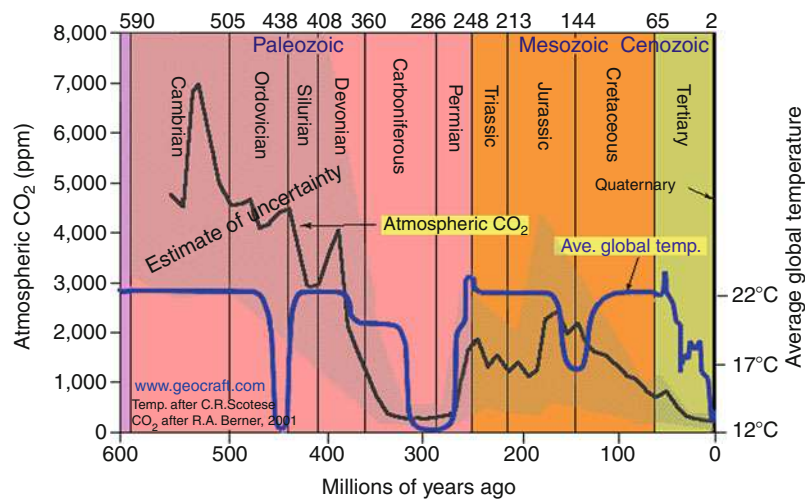
All imaginable forms of climate existed in the past: there were several glacial periods even with Earth existing as a huge snowball, there were also humid tropical periods on all continents without a trace of ice even on the poles, and there were periods when the majority of continents

were occupied by deserts (Kutílek, 2008). In the Precambrian period strong glaciation occurred (Snowball Earth). The supercontinent existed at that time shifted to the southern polar region, the great albedo of snow and ice reduced the absorption of the solar radiation, and the thermohaline circulation was very weak, if even existing. Due to plate tectonic, breaking of the supercontinent, and volcanic activities, greenhouse gases escaped into the atmosphere at the end of Neoproterozoic Era and increased the temperature. Then the climate of the Cambrian Period (540–488 million years before present [Myr BP]) is typically mild without polar ice caps and without substantial climate differences between individual climatic zones. The environmental conditions were completely favorable for the Cambrian life explosion in seawaters. At the end of the Cambrian, the first extinction of life organisms in the Paleozoic Era occurred probably due to the depletion of oxygen by excessive number of various organisms and due to their decay in seawaters. With this extinction, the Ordovician Period (488–445 Myr BP) started. The climate of the Ordovician up to its middle epoch was mild and conditions for life development were favorable. The abrupt cooling in the middle of the period cannot be caused by the change of atmospheric CO₂ concentration since it was 10–15 times higher than that occurring today. One important cause of the glaciation was the shift of a new supercontinent Gondwana to the South Pole. Additive influence had a combination of some not yet well-defined terrestrial, atmospheric, and astronomic factors. The Silurian period (445–410 Myr BP) started as a relative stable greenhouse climate following the Ordovician glaciation. The sea level rising and flooding large, flat, continental coastal belts was a significant impulse for further life evolution and adaptation of life outside of the waters. Climate was diversified according to latitude positions. During the second part of the Silurian period distinct climate oscillations existed. At the Devonian period (410–362 Myr BP), Gondwana shifted from its southern position to the north and the formation of Euramerica, another supercontinent, was completed. With the shifting of great continents, oceanic streams changed their patterns, and the circulation of air modified by strong volcanic activity and plate tectonics changed the distribution of rainfall. Arid regions of rain shadows started to exist while other regions received extremely large amounts of precipitation. Cooling started during the second part of the Devonian, and it was not caused by CO₂ since its atmospheric concentration had risen to about 4,000 ppm. Main factors contributing to cooling were the changes of ocean streams and prevailing major winds. The Carboniferous period (362–299 Myr BP) started with a warming of climate. Collision and subduction of the continents on a great scale led to the gradual, yet strong decrease in atmospheric CO₂ concentration. The second factor playing an important role for CO₂ consumption was a rich abundance of plant life, described frequently as an explosion of terrestrial life. The eastern part of Gondwana began to drift toward the South Pole during

the second half of the period and the development of southern polar ice cap started with subsequent icing of the part of the continent. The very low level of atmospheric CO₂ concentration of the Late Carboniferous continued together with relatively high O₂ concentration during the early Permian (299–251 Myr BP). The climate was influenced by Carboniferous glaciation at the start. Warming gradually followed and glaciers receded. As the majority of land in the large supercontinent was away from the sea and in the rain shadow, its interior was hot and dry. Volcanic activity together with the release of greenhouse gases during large lava eruptions contributed to general warming. In the late Permian and during the transition to the Triassic, a massive extinction dominated (P-Tr extinction), and with about 95% of all-marine taxa and 70% of terrestrial vertebrate disappearing, it was the most severe extinction in the whole geologic history of the Earth. Several mechanisms are discussed in the literature. It probably proceeded in several steps starting with a gradual change of the environment as the sea level changed, increased aridity, and ended owing to catastrophic events of one or multiple impacts of bolides events accompanied by an increased volcanism and the release of methane hydrate from the ocean floor. The first period in the next Mesozoic Era was the Triassic (251–200 Myr BP). Following the catastrophic events of the Permian, a hot and dry climate dominated the majority of the supercontinent Pangea with no evidence of glaciation at or near poles. The Triassic period ended with extinction being restricted primarily to sea life caused by huge volcanic activity accompanying the breaking of Pangea. Bolide impact also contributed to climate change, but with a substantially smaller force than that compared to the Carboniferous, and all changes caused strong climate oscillations. In the Jurassic period (200–146 Myr BP), the breaking up of the supercontinent continued. Today's Greenland was separated and North America divided from Europe and Africa to open the new Atlantic Ocean. India started separating from Antarctica. Before the separation process became intensive, a warm humid climate dominated even in those zones where a mild climate would have been expected, and strong ocean streams contributed to the distribution of warmth far to the high latitudes. Even the poles had mild climates without ice caps. The consequence was the rise of atmospheric CO₂ content up to 2,000 ppm. The climate changed to form distinct climatic zones, some of them with regularly changing wet and dry seasons. All of these conditions are assumed to be the key moment in the evolution of big dinosaurs. The last period of the Mesozoic era was the Cretaceous (146–65.5 Myr). The favorite conditions for a warm and balanced climate continued from the preceding period. The atmospheric CO₂ concentration decreased substantially probably due to the continuing subduction and plants extension while the temperature first remained constant and then even increased. On the boundary with the next time period, the Tertiary, the asteroid impact caused a catastrophic event (the K/T event). The climate change

due to multiple effects ending with aerosols over the entire Earth led to the extinction of dinosaurs. The Paleogene period started with the Paleocene epoch (65.5–55.8 Myr). New fauna together with the evolution of mammals started to develop after the extinction of dinosaurs. The climate was first renewed as it was before the K/T event with only a slight cooling. Even the high latitude kept a mild climate favorable for subtropical vegetation. Later on, close to the transition to the Eocene, the temperature suddenly rose to form the Paleocene/Eocene Thermal Maximum (PETM) lasting for about 100,000 years. The global average temperature rose by 5–8°C within about 10,000 years. It was hypothetically due to the greenhouse effect when closed methane hydrate clusters below the ocean floor were released after the first temperature pulse. Volcanic activity could contribute to it, too. The Eocene epoch (55.8–33.9 Myr BP) was characterized by mild warm climate on all continents – tropical and subtropical vegetation reached up to high latitudes. The warm regime was probably the consequence of the Paleocene/Eocene Thermal Maximum and the very active function of ocean currents carrying warmth from the equator to the Polar Regions. Mammals started to be dominant among the fauna. CO₂ values were distinctly decreasing without causing a decrease of temperature. The bolide impact at the end (“Grande Coupure”) caused the climate change and a limited extinction of some flora and fauna. Oligocene (33.9–23.1 Myr BP) was the end of the Paleogene period (Figure 2). The increased plate dynamics characterized by collision of India with Asia, the separation of Australia from Antarctica, and the increased volcanic activity changed the ocean currents, intensity of monsoons, and resulted in the climate cooling with the initiation of

Antarctic glaciation. The consequence of this climate was that the grassland occupied large areas, and that tropical forests receded from the mild zones of Europe and North America and was restricted to the equatorial belt. At the end of Oligocene, a mild warming caused Antarctic thawing without the influence of CO₂ change. Slight increases of temperature continued into the start of Neogene’s first epoch, the Miocene (23.1–5.3). The increase was monotonic up to the Miocene Climate Optimum (MCO). The continents reached their greatest separation from each other during the entire history of the Earth. This maximum separation brought intensive ocean streaming from the equatorial region to the poles, transporting energy from the warmed belt to originally cool regions. In this geologically most recent warming event, the temperature raised by 3–5°C higher than today, but with atmospheric CO₂ only about half or eventually equal to its present value. The forest cover was large and extended far toward the Polar Regions. At about 14 Myr BP, a strong change of the climate occurred – an initial rapid cooling started a long-time lasting cool climate with significant temperature oscillations. The cool climate brought fluctuating glacial conditions and the beginning of large, continuous continental ice sheets. The global albedo increased, allowing ice sheets to exist at higher CO₂ atmospheric concentrations than that required for glaciation. The start of the event was caused by complex relationships between orbital forcing, carbon burial in ocean and sediments, a major reorganization of ocean circulation patterns and the change in sun activity. The global cooling resulted in the increased aridity. One of the consequences of the decrease of atmospheric CO₂ concentration and of the aridity was the expansion of C4 plants and grassland



Climate Change: Environmental Effects, Figure 2 Throughout the past 600 million years, almost one-seventh of the age of the Earth, the mode of global surface temperatures was ~22°C, even when carbon dioxide concentration peaked at 7,000 ppmv, almost 20 times today's near-record low concentration. If so, then the instability inherent in the IPCC's high-end values for the principal temperature feedbacks has not occurred in reality, implying that the high-end estimates, and by implication, the central estimates, for the magnitude of individual temperature feedbacks may be substantial exaggerations. (Temperature reconstruction by C. R. Scotese; CO₂ reconstruction after R. A. Berner; see also IPCC, 2007; according to Monckton, 2008.)

ecosystems became gradually more important. The next epoch, the Pliocene (5.3–1.8 Myr BP), is the second and last one during Neogene period. The climate became cooler and drier with great zonal differences. Antarctica started to be covered with ice sheet and Arctic icing appeared as a constant ice cap from the mid-Pliocene. The cooling was caused primarily by continental drift. For example, the formation of the narrow strip of Panama completely changed the system of ocean currents in both the Atlantic and Pacific Oceans. The next Pleistocene epoch (1.8–0.0115 Myr BP) is characterized by the existence of long-lasting (about 100,000 years) glacials and short (12,000 years) interglacials. The principle change of climate in the Pleistocene was predominantly caused by Milankovitch cycles, while the relatively short-term warm episodes during glacials were influenced by other factors such as solar activity, thermohaline circulation, aerosols, and volcanoes, with possible role of the change of the Earth's magnetic field. The concentration of atmospheric CO₂ was changing as the consequence of glacials and interglacials. It rose by 80–100 ppm with the total value not exceeding 300 ppm. The change had a time delay up to 600 ± 300 years during the last four interglacials. A similar delay was in the decrease of CO₂ concentration after the start of the glacials. The maximum average temperature lasting for 1,000 years in the last four interglacials was by 2–4°C higher than the recent average. If the whole Pleistocene is characterized by large and intensive glaciations interrupted only by short interglacials, we have to assume that our recent epoch Holocene starting 11,500 years ago is also an interglacial. The warming of the last glacial started already about 16,000 BP but it was twice interrupted by Older and Younger Dryas. The rate of each next warming was roughly the same as the recent one. The retreat of glaciers was slow up to 9 kyr BP, then increasing for 3,000 years. Their melting caused the sea-water level to rise with the average rate about 1.2 m/100 years. It was seven times faster than the recent seawater level rise. During the Würm glaciation (115–11.5 kyr BP), the Sahara desert was larger than it is today and its southern boundary reached several hundred kilometers further south than at the early Holocene (Roberts, 2004). From about 10 kyr BP up to 6 or 5.5 kyr BP, it was basically transformed into a savanna since the whole region was under the influence of the pluvial with frequent and abundant strong rains. The time period between 9,000–5,500 years BP, denoted as the Global Thermal Optimum, is explained by the special position of the Earth axis in the Milankovitch cycle precession, causing a shift of the Intertropical Zone of Convergence (ITZC). The accompanying growth of vegetation changed the albedo resulting in general warming with increased humidity. ITZC moved several times to the north and back and brought differences in rains to the region known as climatic oscillations. A similar situation developed in Mesopotamia and in the Indian subcontinent. The climate in Holocene was never monotoneous. The first short but very intensive cooling arrived at 8,200 BP and lasted only about 400 years. The

main cause was the abrupt drainage of the North American large sea Agassiz, which originated due to melting of the continental glacier. The freshwater drained into the Atlantic Ocean and interrupted the thermohaline circulation. The proxies in Europe indicate a thermal maximum about 6 kyr BP with the temperature by roughly 2°C higher than we have now. Just after the Holocene Thermal Optimum, a global cooling occurred at about 5.5 kyr BP. The vegetation zones shifted to the south of Europe and their composition gradually changed. Global cooling was revealed by a rapid aridization and extension of vast deserts of the Sahara, Arabia, India, and Pakistan. Another strong climate change (about 4.3 to 4.2 kyr BP) accompanied by the reduction of precipitation and by aridity caused strong social and political crises, leading even to the decline of some civilization and cultural centers. Two further rapid climate changes occurred in the BC time period (Mayewski et al., 2004). The Roman Warm Period was detected in the time range between 200 BC and AD 300, where the end is locally shifted in some regions to about AD 100. After that, the Dark Ages Period had the minimum temperature around AD 600. Then the Medieval Warm Period started about AD 850, even though its start could be shifted to a later time in some regions. It lasted as a stable climate up to about AD 1200 with temperatures higher than the recent ones by 1–3°C. In some regions, it ended later about AD 1350. The stable climate of the Medieval Warm Period ended after AD 1350 and the era of unpredictable weather changes began. The first frosty attack came in the first third of the fifteenth century and between 1630 and 1730 the extreme frosty cycle of the Little Ice Period arrived. The main factor causing the oscillation named Little Ice Age was the solar minimum activity detected in three separated waves. The best known Maunder minimum is known, too, by minimal to zero number of sunspots (AD 1645–1715). The lowering of the thermal gradient was another acting factor causing the reduction of the thermohaline circulation. The negligibly small change of CO₂ concentration in the atmosphere, if any, could not have caused such Holocene climate oscillation.

Summarizing remarks

The atmospheric CO₂ concentration is only one of the many factors influencing climate change on the geologic time scale. In some instances it was the dominant agent of warming or cooling. However, there were other geologic periods when the climate changed, but CO₂ concentration remained either constant or the increase of temperature was accompanied by the decrease of CO₂ concentration. This conclusion is valid even for short time climate oscillations detected starting from the Miocene up to Pleistocene. In Holocene, the climate oscillations are typical with the existence of warm and cool periods even on the century scale in the second half of the epoch. The main factors of their occurrence are solar activity, thermohaline circulation, aerosol concentration, and volcanic activity with changes in vegetative cover being less

important. Changes of atmospheric CO₂ concentration were so small that their influence was negligible up to and including the Little Ice Age. Considering earlier interglacials and Holocene climate oscillations, the recent increase of CO₂ atmospheric concentration contributes only to the action of two factors, the solar activity and the change of vegetation cover. The quantification of the role of the acting factors and forces has not yet been estimated by testing the models on the oscillation events in Holocene. The prediction of global warming cannot be therefore based upon the results of models where the greenhouse effect plays a dominant role (IPCC Fourth Assessment, 2007). The environmental effect of the observed global warming can be deduced from the environmental change documented on proxies of the Medieval Warm Period (MWP). A lower intensity of recent warming compared to MWP has to be considered. The mountain glaciers are receding; the polar Arctic glacier shrinks, while the Antarctic glacier does not change substantially. The biota shows the tendency of shifting to the north in the northern hemisphere, but there are no notes of extinction of numerous taxa. Even the further warming will not cause global aridization, desertification, or extension of area of deserts and catastrophic events for the life on the planet (Kutílek, 2008 and the detailed literature quotations there). Quite opposite, the warming if it lasts enough long could bring stronger monsoon in Sahelian part of Africa (Zhang and Delworth, 2006). The increase of CO₂ concentration up to doubling the 1,850-year data does not have catastrophic consequences, the yields will have a rising tendency, and famine is not expected due to the climate change (Kirkham, 2007). On the other hand, the human disturbances may not produce a whole ecosystem breakdown as a single acting force. However, this type of weakening of the resistance of the whole ecosystem can have some not expected consequences, if another impact like global warming acts at the same time (Roberts, 2004).

Bibliography

- Czech Hydro-Meteorological Institution, 2007. *Climate Change at the Start of 21st Century and Its Further Evolution*. 21 February 2007. Prague.
- Easterling, D. R., and Wehner, M. F., 2009. Is the climate warming or cooling? *Geophysical Research Letters*, **36**, L08706.
- Eichler, A., Olivier, S., Henderson, K., Laube, A., Beer, J., Papina, T., Gäggeler, H. W., and Schwikowski, M., 2009. Temperature response in the Altai region lags solar forcing. *Geophysical Research Letters*, **36**, L01808.
- IPCC Fourth Assessment, 2007. See Solomon et al. (2007).
- IPCC, 2007. *Climate change: the physical science basis. Summary for policymakers*. Cambridge, New York: Cambridge University Press.
- Kirkham, M. B., 2007. *Agronomy lectures 820. Elevated CO₂ and drought: plant Water Relations*. Kansas: Kansas State University.
- Knudsen, M. F., and Riisager, P., 2009. Is there a link between Earth's magnetic field and low-latitude precipitation? *Geology*, **37**(1), 71–74.
- Kutílek, M., 2008. *Rationally on Global Warming (in Czech: Racionálně o globálním oteplování)*. Prague: Dokořán.
- Lane, L. J., Nichols, M. H., and Osborn, H. B., 1994. Time series analyses of global change data. *Environmental Pollution*, **83**, 63–68.
- Levitus, S., Antonov, J., and Boyer, T., 2005. Warming of the world ocean, 1955–2003. *Geophysical Research Letters*, **32**, L02604.
- Marsh, N. D., and Svensmark, H., 2000. Low cloud properties influenced by cosmic rays. *Physical Review Letters*, **85**, 5004–5007.
- Mayewski, P. A., Rohling, E. E., Stager, J. C., Karlén, W., Maasch, K. A., Meeker, L. D., Meyerson, E. A., Gasse, F., van Kreveld, S., Holmgren, K., and Thorp, J. L., 2004. Holocene climate variability. *Quaternary Research*, **62**, 243–255.
- Milankovitch, M., 1920. *Théorie Mathématique des Phénomènes Thermiques Produits par la Radiation Solaire*. Paris: Gauthier-Villars.
- Milankovitch, M., 1941. *Kanon der Erdbeleuchtungen und seine Anwendung auf das Eiszeitenproblem*. Belgrade: Zavod za Udzbenike i Nastavna Sredstva (English trans: Pantic, N., 1998. *Canon of Insolation and the Ice Age Problem*. New York: Alven Global).
- Monckton, C., 2008. *Climate sensitivity reconsidered*. APS Forum for Physics and Society, July 2008. <http://www.aps.org/units/fps/newsletters/200807/index.cfm>
- Roberts, N., 2004. *The Holocene. An Environmental History*. Malden: Blackwell Publishing.
- Schwartz, S. E., 2007. Heat capacity, time constant, and sensitivity of Earth's climate system. *Journal Geophysical Research*, **112**, D24S05.
- Solomon, S., Qin, D., Manning, M., Chen, Z., Marquis, M., Averyt, K. B., Tignor, M., and Miller, H. L. (eds.), 2007. *Climate change 2007: the physical science basis. Contribution of Working Group I to the Fourth Assessment Report of the Intergovernmental Panel on Climate Change*. Cambridge, New York: Cambridge University Press.
- Svensmark, H., 1998. Influence of cosmic rays on Earth's climate. *Physical Review Letters*, **81**(22), 5027–5030.
- Svensmark, H., 2007. Cosmoclimatology: a new theory emerges. *Astronomy & Geophysics*, **48**, 118–124.
- Trenberth, K. E., Jones, P. D., Ambenje, P., Bojariu, R., Easterling, D., Klein Tank, A., Parker, D., Rahimzadeh, F., Renwick, J. A., Rusticucci, M., Soden, B., and Zhai, P., 2007. Observations: surface and atmospheric climate change. In *IPCC Climate Change 2007: the physical science basis*. Cambridge, New York: Cambridge University Press.
- Wegener, A., 1912. Die Entstehung der Kontinente. Vortrag gehalten auf der Hauptversammlung zu Frankfurt a. M. am 6. 1. 1912. *Geologische Rundschau*, **3**, 276–292.
- Wegener, A., 1920. *Die Entstehung der Kontinente und Ozeane*. E. Wiedemann.
- White, N. J., Church, J. A., and Gregory, J. M., 2005. Coastal and global averaged sea level rise for 1950 to 2000. *Geophysical Research Letters*, **32**, L01601.
- Zhang, R., and Delworth, T. L., 2006. Impact of Atlantic multidecadal oscillations on India/Sahel rainfall and Atlantic hurricanes. *Geophysical Research Letters*, **33**, L17712.

Cross-references

- Desertification: Indicators and Thresholds
Drought Stress, Effect on Soil Mechanical Impedance and Root (Crop) Growth
Evapotranspiration
Flooding, Effects on Soil Structure
Greenhouse Effect
Remote Sensing of Soils and Plants Imagery
Weather, Effects on Plants

CLIMATE RISK

See *Tillage, Impacts on Soil and Environment*

CLIMATE STRESS MITIGATION TILLAGE

See *Tillage, Impacts on Soil and Environment*

CLOD

A compact, coherent mass of soil varying in size, usually produced by plowing, digging, etc., especially when these operations are performed on soils that are either too wet or too dry and usually formed by compression, or breaking off from a larger unit, as opposed to a building-up action as in aggregation

Bibliography

Glossary of Soil Science Terms. Soil Science Society of America. 2010. <https://www.soils.org/publications/soils-glossary>

CLUSTERS IN SOILS

David L. Pinskiy

Institute of Physico-Chemical and Biological Problems in Soil Science, Laboratory of Physical-Chemistry of Soils, Moscow Region, Russia

Synonyms

Adsorptive cluster; Aggregation; Cluster structure; Fluctuating associations

Definition

Cluster is an association of a limited number of interacted uniform elements (atoms, molecules, ions, superdispersed particles), which generate a new property or a sum of properties.

Introduction

The term “cluster” is widely used in the modern science and technique, however, the precise time of its entry in the science is impossible to define, because it has an especially wide everyday use. Depending on the field of application it attaches different meanings. Kipnis (1981) considers that the term “cluster” for the first time appeared in the manuscript of G. E. Meyer on the statistical mechanics of nonideal gases in 1937. Booming development of studies on the cluster formation is timed to the second half of the twentieth century and is connected to the synthesis of artificial clusters widely applied in the industry. By

the 1980s, a new approach – cluster chemistry – arose as a cross-disciplinary science based on chemistry, physics, and material science. The processes of cluster formation in soils and agrosystems are practically unstudied. There are scarce publications, where the process of cluster formation is mentioned. Yet it is evident that in soils, these processes are important due to the presence of large number of components and heterogeneous phases interacted and permanent changes of the state under external factors.

Cluster formation is possible in different soil phases: solid, liquid, gaseous, and alive, and on the boundaries of their interfaces. Minimal number of cluster elements equals two (Cotton and Walton, 1993). Maximal number corresponds to a value when addition of the next one already does not change the properties of the cluster. Approximate estimates carried out by the chemists for molecular clusters are 10^3 elements (Kipnis, 1981).

Cluster groups form superstructure or supramolecular structures where clusters stand as individual elements.

Formation of cluster structure in soils

Apparently the first studies are that by Bleam and McBride (1985) and Bleam and Bridge (1986), where they describe cluster formation during adsorption of Cu(II) and Mn(II), Mn(II) and Mg(II) cations on titanium dioxides, boehmite, and goethite. The formation of adsorptive clusters $(H_3SiO)_3SiR$ ($R=OH, Cl$) is a simultaneous process at interactions of nucleophilic reagent on silica surface (Chuiko et al., 2007). Numerous studies indirectly confirm the formation of cluster structures at interactions of organic and mineral (mainly clay minerals) soil components. It was demonstrated that the distribution of organic material on mineral surfaces of soil particles has fragmentary (discrete) mode (Mayer and Xing, 2001; Kahle et al., 2002; Kurochkina and Pinskii, 2002; Kaiser and Guggenberger, 2003). Aluminum silicate sediments with low and moderate loadings of organic matter (<3 mg organic C m^{-2}) generally have less than 15% of their surface coated, with organic materials existing in discrete spots on the mineral surface (Arnanson and Keil, 2001). This indicates that the organic material must instead be clustered in small patches with some vertical extension (Kleber et al., 2007).

The formation of solid soil phases passes through the clustering step as well. In particular, it was shown that the formation of new phases from supersaturated water solutions of silica acids is accompanied by clustering of basic (starting, initial) elements (“fluctuating association”). Heterophase fluctuations of the material characterizing pre-transitional state of the system are also probable (Chuiko et al., 2007). On the whole, the formation of a new phase occurs within a common scheme: (1) nucleation, (2) clusterization, (3) formation of grain structure, and (4) formation of crystallites. Evidently, similar processes occur within the formation of other new phases in soil, including the formation of clay mineral during the weathering of *parent rocks*.

Application of new instrumental methods (EAXFS, HRAF) for studying of soils *in situ* made it possible to find out the phenomenon of surface precipitation with participation of heavy metal cations. One of the mechanisms of this phenomenon supposes a range of sequential stages distributed over the time: (1) adsorption, (2) nucleation, (3) precipitation, (4) nucleation, and (5) re-precipitation (Scheidegger et al., 1997; Borda and Sparks, 2007). Another mechanism of the formation of surface-precipitated structures may be connected with micro-heterogeneity of the pH in the vicinity of clay minerals or soil particles. In this case in the solution volume in the close vicinity to the protonated part of the surface, the increase of OH^- ion concentration takes place. It is resulted from H_2O dissociation and binding of H^+ during the surface protonation. The pH values within this part of solution become essentially higher compared to those of the whole solution volume. Therefore, in the close vicinity of the protonated surface the conditions for precipitation of hydroxides or metal carbonates arise, in contrast to the lack of such conditions in the whole volume (Pinsky and Kurochkina, 2006).

Cluster structures are formed in a result of partial hydration of the surface of non-hydrated sparingly soluble salts and minerals as well. The hydration process involves several steps: (1) adsorption and capillary condensation of water in the pore space, (2) dissolving of a part of sparingly soluble salt in the capillary moisture, (3) formation of hydrated structures in solution volume (through clustering of dissolved hydrated elements), and (4) formation of films of hydrated compounds on the surface of unhydrated salt (Kurochkina and Sokolov, 1997).

In general, the processes of cluster formation may be combined by terms of aggregation and disaggregation. In doing so, the mechanisms of their formation differ and are determined by the character of cluster elements, the formation conditions, and the environment. The processes of aggregation take place at the formation of cluster from single elements, distributed within the space or at the formation of larger clusters from the ones of less size. In soils, this group covers the compounds, which are formed in the soil air, during the solvation process and association of ions and molecules in soil solution, including clustering of the solvent – the water (Kipnis, 1981). The existence of such clusters does not result in the new phase formation. They exist in dynamic equilibrium with the environment and, hence, their composition is inconstant. An example of the formation of cluster structures due to disaggregation is generation of secondary minerals from the components of weathering of the parent rocks.

Life time, properties, and functions of clusters

One of the important properties of clusters is their lifetime. It is determined by the properties of the elements forming the cluster, the type of cluster compounds, and the environment, where the formation takes place. We should distinguish free and stabilized by certain factor clusters. Free

clusters more often occur in uncondensed phases – in the soil air, more seldom – in the condensed ones (associates in solutions). Their minimal lifetime evidently is close to the duration of the collision of particles in the gaseous phase – $10^{-12} - 10^{-13}$ s.

Stabilized clusters have more complex structure and composition. The “body” of cluster (the group of interacting elements of a certain type) and stabilizing elements (the ligand cover, central particle, around which the cluster is formed (Kipnis, 1981; Chenu and Plante, 2006), or the matrix may be discriminated. The lifetime of stabilized clusters is comparable with the duration of the existence of molecules or their compounds. For soil science and agrophysics, the most important are the clusters with a lifetime long enough to participate in various physical, chemical, and physicochemical soil processes. A typical example of stabilized clusters is adsorptive clusters and surface precipitates. The existence of matrix, which is parts of the surface of soil particle, is the most vigorous stabilizing factor.

The most important common features of clusters are the following: (1) limited number of interacting elements; (2) transitional (intermediate) form of organization of the matter with elevated (maximal) specific activity compared to that of the elements and providing the transition of the system from one state to another; (3) solid-bodied clusters, which are somewhat intermediate state of the material – in between amorphous and crystalline, when the material exists neither as atoms and molecules, nor in the crystalline frame (Kipnis, 1981).

The formation of clusters requires the overcoming of a certain activation barrier by cluster-forming particles (Suzdalev and Suzdalev, 2001).

Cluster organization of soil matrixes

Soil matrix is an active part of surface layer of solid particles, which induces certain properties of the surface, composition of cations, thickness of water film, organic humus and organo-mineral matrixes, and by that creates relatively constant properties of soils (Zubkova and Karpachevskii, 2001). The basis for soil matrix is the mineral matrix, which comprise mainly clay minerals, amorphous compounds, metal oxides, and talus. In contrast to cluster, the matrix has no limitations by maximal size.

The terms “matrix” and “cluster” are tightly bound. The matrix is one the strongest factors, which stabilizes cluster in soils, and a basement for generation of surface cluster structures. In the information transfer of structure from mineral base to interacting compounds, the key role belongs to active sites and electric heterogeneity of surface elements rather than the geometrical structure of the surface (Distler, 1972).

Studies of adsorption of organic matter on mineral soils, oxides, gibbsite, ferrihidrite, goethite, hematite, kaolin, and illite have demonstrated that the interaction occurs mainly with active (“reactive”) sites on the surface of solid particles (Kaiser and Guggenberger, 2003). The existence

of different types of surface of soil particles with different functional peculiarities was mentioned by Pinskii (1997) and Kleber et al. (2007). Carboxyl-containing organic molecules form firm organo-mineral compounds on positively charged sites of amorphous aluminum silicates via the mechanism of activated chemosorption (Kurochkina and Pinskii, 2002). The distribution of such sites has fragmentary insular character and includes not only tops of angles, edges, or defects of the crystal surface but also the mouths of micropores (Kaiser and Guggenberger, 2003). Uncompensated defects within the volume of the solid body also induce special groups of atoms on the planar crystal surface, which should be considered as peculiar surface clusters (Kipnis, 1981). Thereby, in soils cluster-matrix structures are formed, and they may be designated as active matrixes.

The formation of cluster-matrix structures on the surface of soil particles conditions its *heterogeneity* by composition and properties, affects *adsorption energy*, *structure and stability of aggregates*, soil *hydrophobic-hydrophilic* properties, *sorptivity*, *buffer capacity of soils*, and other *properties and functions*. In particular, the formation of organo-mineral compounds in soils makes *organic matter* much more persistent to biodegradation.

Methods of study of cluster-matrix structures in soils

Current progress in the experimental studies of cluster and matrix structures was provided by application of high-resolution transmission electron and atomic-force microscopy (HRTEM and HRAFM), extended X-ray absorption fine structure spectroscopy (EXAFS), and Fourier transfer infrared (FTIR) spectroscopy. EXAFS has provided the studies of bonding environments of adsorbed and structural species to ascertain the geometry of complexes at mineral surfaces as well as the structure of three-dimensional phases such as precipitates. The recent push to investigate reactivity of critical zone illustrates the need for scientists working in the Earth and environmental sciences to adopt techniques that allow them to gain insight about reactivity, and the changes in the reactivity, on very small scales.

Summary

The term of cluster is defined. The formation of clusters occurs during the adsorption of heavy metals by soils and their further transformation in layered double hydroxides and more persistent compounds. The adsorption of organic matter by the surface of soil mineral particles is accompanied by the formation of cluster compounds as well. As a result, the distribution of organo-mineral compounds within the surface of solid phases has fragmentary character. The processes of clusterizing are followed by the formation of solid phases from the products of parent rock weathering and are accompanied by the formation of hydrated films on the surface of non-hydrated salts

and minerals. Common properties of cluster structures are described. The cluster character of active soil matrixes and their role in the formation of soil properties is demonstrated.

Bibliography

- Arnanson, T. S., and Keil, R. G., 2001. Organic-mineral interactions in marine sediments studied using density fractionation and X-ray photoelectron spectroscopy. *Organic Geochemistry*, **32**, 1401–1415.
- Bleam, W. F., and McBride, M. B., 1985. Cluster formation versus isolated-site adsorption. A study of Mn(II) and Mg(II) adsorption on boehmite and goethite. *Journal of Colloid and Interface Science*, **103**, 124–132.
- Bleam, W. F., and McBride, M. B., 1986. The chemistry of adsorbed Cu(II) and Mg(II) in aqueous titanium dioxide suspensions. *Journal of Colloid and Interface Science*, **110**, 335–346.
- Borda, M. J., and Sparks, D. L., 2007. Kinetics and mechanisms of sorption-desorption in soils: a multiscale assessment. In Violante, A., Huang, P. M., and Gadd, G. M. (eds.), *Biophysico-Chemical Processes of Heavy Metals and Metalloids in Soil Environment*. New York: Wiley, pp. 97–124.
- Chenu, C., and Plante, A. F., 2006. Clay-sized organo-mineral complexes in a cultivation chronosequence: revisiting the concept of the “primary organo-mineral complex”. *European Journal of Soil Science*, **57**, 596–607.
- Chuiko, A. A., Gorlov, Yu I, and Lobanov, V. V., 2007. *Structure and Chemistry of Silica Surface*. Kiev: Naukova Dumka.
- Cotton, F. A., and Walton, R. A., 1993. *Multiple Bonds Between Metal Atoms*. Oxford: Oxford.
- Distler, G. I., 1972. *Information Properties of Solid and Liquid Layers. Surface Forces in Thin Films and Dispersed Systems*. Moscow: Nauka.
- Kahle, M., Kleber, M., and Jahn, R., 2002. Carbon storage in loess derived surface soils from Central Germany: influence of mineral phase variables. *Journal Plant Nutrition Soil Science*, **165**, 141–149.
- Kaiser, K., and Guggenberger, G., 2003. Mineral surface and soil organic matter. *European Journal of Soil Science*, **54**, 219–236.
- Kipnis, A. Ya, 1981. *Clusters in Chemistry*. Moscow: Nauka.
- Kleber, M., Sollins, P., and Sutton, R., 2007. A conceptual model of organo-mineral interaction in soils: self-assembly of organic molecular fragments into zonal structure on mineral surfaces. *Biogeochemistry*, **85**, 9–24.
- Kurochkina, G. N., and Pinskii, D. L., 2002. Mechanism of adsorption of high-molecular surfactants on synthetic analogues of soil aluminosilicates. *Eurasian Soil Science*, **35**(10), 1046–1051.
- Kurochkina, G. N., and Sokolov, O. A., 1997. On the possibility of application of water vapor sorption method for studying the mechanism of chemical hydration of mineral components in soils. *Eurasian Soil Science*, **1**, 49–56.
- Mayer, L. M., and Xing, B., 2001. Organic matter – surface area relationship in acid soils. *Soil Science Society of America Journal*, **65**, 250–258.
- Pinskii, D. L., 1997. *Ion-Exchange Processes in Soils*. Pushchino: ONTI.
- Pinsky, D. L., and Kurochkina, G. N., 2006. Evolution of studies on the physico-chemical adsorbing capacity of soils. In Kudreyarov, V. N. (ed.), *Soil Processes and Spatio-Temporal Organization of Soils*. Moscow: Nauka, pp. 295–311.
- Scheidegger, A. M., Lamble, G. M., and Sparks, D. L., 1997. The kinetics of nickel sorption on pyrophyllite as monitored by x-ray absorption fine structure (XAFS) spectroscopy. *Journal of Physics*, IV (France), **7**, C2-773–C2-775.

- Suzdalev, I. P., and Suzdalev, P. I., 2001. Nanoclusters and nanocluster systems. Assembling, interactions, properties. *Uspekhi Khimii (Russian Chemical Reviews)*, **70**, 203–240.
- Zubkova, T. A., and Karpachevskii, L. O., 2001. *Matrix Organization of Soils*. Moscow: Rusak.

Cross-references

- [Adsorption Energy and Surface Heterogeneity in Soils](#)
[Organic Matter, Effects on Soil Physical Properties and Processes](#)
[Parent Material and Soil Physical Properties](#)
[Physical \(Mechanical\) Weathering of Soil Parent Material](#)
[Physical Protection of Organic Carbon in Soil Aggregates](#)
[Soil Aggregates, Structure, and Stability](#)
[Soil Functions](#)
[Soil Hydropobicity and Hydraulic Fluxes](#)
[Soil Phases](#)
[Sorptivity of Soils](#)
[Specific Surface Area of Soils and Plants](#)
[Surface Properties and Related Phenomena in Soils and Plants](#)

COAGULATION

See [Flocculation and Dispersion Phenomena in Soils](#)

COHESION

The internal mutual bonding of like molecules or particles of a particular substance, imparting strength to a body composed of that substance.

Bibliography

- Introduction to Environmental Soil Physics. (First Edition). 2003. Elsevier Inc. Daniel Hillel (ed.) <http://www.sciencedirect.com/science/book/9780123486554>

Cross-references

- [Friction Phenomena in Soils](#)
[Hardsetting Soils: Physical Properties](#)

COLLOIDS

See [Biocolloids: Transport and Retention in Soils; Electrokinetic \(Zeta\) Potential of Soils](#)

COLOR COMPOSITE (MULTIBAND PHOTOGRAPHY)

A color picture produced by assigning a color to a particular spectral band. Ordinarily blue is assigned to band 1 or 4 (~ 500 to 600 nm), green to band 2 or 5 (~ 600 to 700 nm), and red to band 3 (~ 700 nm to 1 μm) or

7 (~ 800 nm to 1.1 μm), to form a picture closely approximating a color-infrared photograph.

Bibliography

- Glossary of Soil Science Terms. Soil Science Society of America. 2010. <https://www.soils.org/publications/soils-glossary>

Cross-references

- [Color in Food Evaluation](#)
[Color Indices, Relationship with Soil Characteristics](#)

COLOR IN FOOD EVALUATION

Seong Pal Kang

Cognitive Robot Research Center, Korea Institute of Science and Technology, Sung-Buk-gu, Seoul-si, Republic of Korea

Synonyms

Food color measurement

Definition

Color ordering system. A series of standardized color boards or cards used in colorimetric and photometric calibration.

Color space. A color system that consists of color components represents the image values of a color image as numbers.

Color temperature. A characteristic of a visible light that is determined by comparing the chromaticity of a light source with that of an ideal black-body radiator.

Segmentation. A process of partitioning a digital image into multiple segments in order to detect the region of interest.

Introduction

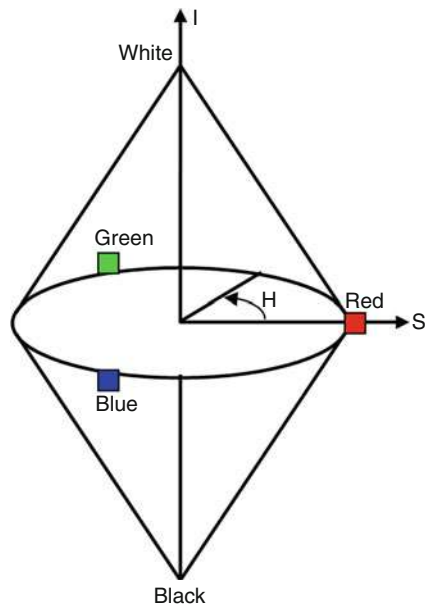
Color has been one of the important factors in food quality measurement. The quality of some food is estimated by its external or internal color. For example, ripeness of fruits could be judged by the external color. This kind of color evaluation could be performed by human visual perception. The color measurement by human perception could vary by persons and the environment-like lighting condition at the place. Thus, color measurement for food evaluation must be carried out by taking into account the color to be measured and the instruments used. There are two important points to consider for color measurement in food evaluation. First, the proper *color space* must be chosen for the specific purpose of the measurement. Second, the equipment setup is also important, because color measurement could be easily affected by any environment change such as lighting devices and color sensors.

Color spaces in food evaluation

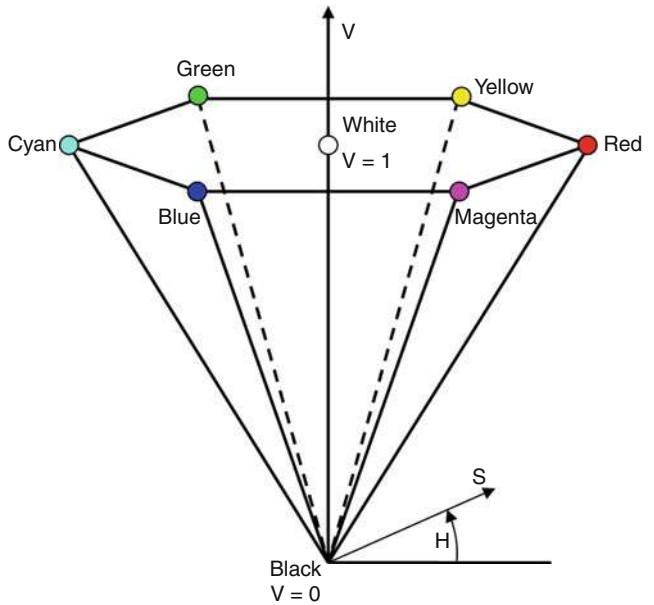
There are various color spaces for various purposes, and four of them are mainly used in food evaluation. The most common color space in digital image processing is RGB. The RGB color space is based on the international standardized wavelengths of the primary colors that are red, green, and blue. This color space is intended to provide description of the standardized primary colors, like long (red), middle (green), and short (blue) wavelengths of the visible light. Image data of CCD (Charge-Coupled Device) sensors of digital cameras are based on this RGB color space. It is easy to use for analysis without color conversion process. However, the wavelength range of each component of the RGB color space is not clearly separated from other components – the ranges overlap with one another. Thus, when a long-medium color (yellow or orange) is represented using the RGB color space, not only the red and green components are used but also the blue component is used because the green component overlaps with the blue. This property of the RGB makes difficult to reproduce real colors. It means that visible colors in real world cannot be equivalent to the combination of the wavelengths of the RGB color space. Many of the research projects in food analysis, like Gökmen et al. (2008), Kılıç et al. (2007), Sun and Brosnan (2003), and so on, employed RGB color space for food color analysis.

HSV (hue, saturation, and value) and HSI (hue, saturation, and intensity) color spaces are used in many food research papers in Du and Sun (2005) and Riquelme et al. (2008). Both color spaces are based on human color perception and generally used in the fields of computer vision and computer graphics (Koschan and Abidi, 2008). These color spaces are based on the RGB color space. In the HSI color space, the three color components are used as coordinate axes as shown Figure 1. The hue H describes the color itself as a value between 0° (at the centre) and 360° (at the edge). The saturation S is a measurement of color purity that represents how much the color is affected by white color. The range of the saturation component is between 0 (black) and 1 (white). The intensity I represents the brightness, having a value between 0 and 1. Thus, all of the three components are calculated from the RGB color components. In the HSV color space, the hue H has a value between 0° and 360° , but the plane represented by H is like a hexagon with different color at each vertex as shown in Figure 2. The value V represents the brightness of the color. V is 0 at the apex in Figure 2.

The common color space in food research has been $L^*a^*b^*$ (CIELab). The CIELab color space is the international standard color space, recommended by the Commission Internationale d'Eclairage (CIE) in 1979 (León et al., 2006). CIELab is a uniform color space that same-size changes in the color coordinates correspond to the changes in the visible space (Koschan and Abidi, 2008). Thus, the color measurement using CIELab could be



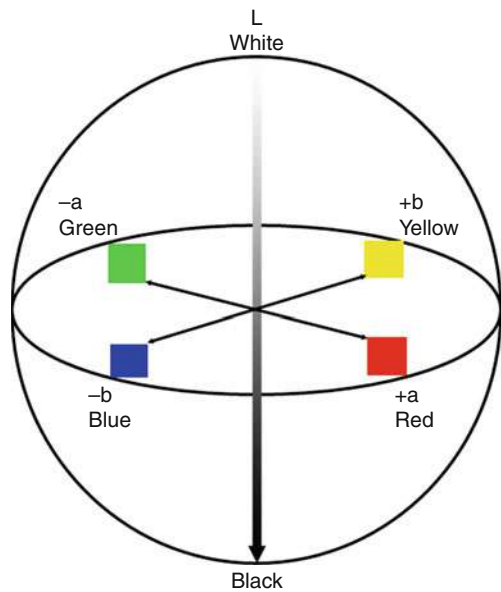
Color in Food Evaluation, Figure 1 Representation of the HSI color space.



Color in Food Evaluation, Figure 2 Representation of the HSV color space.

absolute measurement that detects the color changes and differences between objects. The CIELab space could be expressed as shown in Figure 3.

- L^* represents the lightness, having a value in the range of 0–100, where 0 is black and 100 is white.



Color in Food Evaluation, Figure 3 Representation of the CIELab color space.

- a^* represents variation from green to red in the range of -100 to $+100$.
- b^* represents variation from blue to yellow in the range of -100 to $+100$.

An example of using this uniform color space CIELab is in that the maturity of some fruit could be evaluated without destroying the fruit. If the color changes were modeled and the fruit color is changed as it ripens, the maturity of the food could be estimated. Jha et al. (2007) carried out such experiment and modeled the maturity of mango based on its external color. If the color of the fruit is changed from green to yellow as it ripens, the value of a^* will be changed from negative value to positive or nearly zero, and the value of b^* will be increased. In addition, the values of a^* and b^* components are not affected by the lightness on the curved surface of the objects as reported by Mendoza et al. (2006). Thus, the color changes could be plotted in two-dimensional (2D) plane (a^* vs. b^*). Then the trend of the color variation will be clearly shown on the plots. For such applications, *hue* and *chroma* could be useful, and these are computed from CIELab as below in Equation 1:

$$\text{Hue} = \tan^{-1} \left(\frac{b^*}{a^*} \right), \quad (1)$$

$$\text{Chroma} = \sqrt{a^{*2} + b^{*2}}.$$

There is an example of this kind of experiment using mango carried out by Kang et al. (2008). The green surface color of a fresh mango gradually changed to yellow as it ripened by in a certain storage condition. Then the hue of the green region is gradually decreased as the color

turns into yellow. There is another example using this property of the CIELab color space. Kang and Sabarez (2009) developed a very simple color *segmentation* that obtains a polynomial equation from plots of a^* and b^* on 2D plane and found points close to the equation. Thus, the property of the CIELab color space as a uniform color space could be useful if the food to be examined is affected by the lighting, and the color on the surface must be measured regardless of illumination effect.

The hue components of the HSI and the HSV color spaces are also not affected by lightness of curved surfaces, and other components are reliable only if the object is flat. All the components of the RGB color space are affected by lightness on curved surfaces. The results are presented in Mendoza et al. (2006). If the external surface of the food is not flat, the color values at different height but same color would have different color values. Thus, these color spaces are nonuniform color spaces. The changes of the color components do not correspond to the changes of the visible color. If the color measurement system is based on computer vision system (CVS) and the area to be measured is not flat, the result could not be accurate.

Color values in other color spaces like RGB, HSI, and HSV can be converted into CIELab, and the procedures were explained in Mendoza et al. (2006), Kang et al. (2008), and Koschan and Abidi (2008). Other color conversions are explained in Koschan and Abidi (2008).

Vision system setup in color measurement

In color measurement, the consistency of the measurement is extremely important. If any condition like sensor setting or lighting condition is changed since the previous measurement, the new color measurement cannot be compared with the previous one. Thus, the conditions of the measurement setup such as illumination and sensor calibration must be consistent.

The most common illumination is D65 (i.e., known as “daylight,” corresponding to the *color temperature* at 6,500 K). There is another standard illumination called as illuminant C used as “daylight” likewise 6,500 K. However, the property of the illuminant C is lack of UV radiation if compared to the real daylight, thus D65 is commonly used at present (Koschan and Abidi, 2008). In food evaluation, using the illuminant C can cause wrong color measurement result if the used material has the property affected by UV radiation. On the other hand, D65 has a disadvantage in that it is difficult to manufacture. Thus, fluorescence tube lamps (TL-D Delux, 18 W/965, 6,500 K, Philips) are used as the D65 standard lighting source by Mendoza et al. (2006) and Kang et al. (2008).

Moreover, the color measurement sensors must be selected with consideration of the purpose of the measurement. Colorimeters and digital cameras are generally used as the color measurement sensors. Both sensors could be used to measure absolute colors of food. The advantage

of the colorimeter is easy to use and reliable, but this device has a disadvantage that the sensing area is very small. This device only gives the average value of the small area. Thus, the demand of CVS using digital cameras is rising because of the wide sensing area upto 10° observation angle. However, digital camera-based systems are not simple to use like colorimeters. The digital camera-based systems require analysis software and color calibration under the circumstance to be measured. The digital camera calibration process is explained in Mendoza et al. (2006) and Kang et al. (2008). The brief process is as follows: First, the color measurement system must be decided. Then, images of a set of *color ordering system* must be taken. The actual color values of the color ordering system must be known. The color values in the images should be compared and repeated until the closest camera setting, such as aperture, shutter speed, ISO, and so on, to the color ordering system is found.

Summary

Color spaces and equipment used in food evaluation have been discussed. There are various color spaces, and the right color space must be chosen for the purpose of the evaluation. The CIELab color space has widely been used for color measurement and analysis in food engineering because this is a uniform color space. On the other hand, two color measurement sensors (i.e., colorimeter and CVS) have been discussed. The demand of CVS has been increasing because of wide sensing area. However, when using CVS, the vision system must be designed by taking into consideration about the consistency while the measurement is carried out.

Bibliography

- Du, C. J., and Sun, D. W., 2005. Comparison of three methods for classification of pizza topping using different colour space transformations. *Journal of Food Engineering*, **68**, 277–287.
- Gökmen, V., Açıar, Ö. C., Arribas-Lorenzo, G., and Morales, F. J., 2008. Investigating the correlation between acrylamide content and browning ratio of model cookies. *Journal of Food Engineering*, **87**, 380–385.
- Jha, S. N., Chopra, S., and Kingsly, A. R. P., 2007. Modelling of color values for nondestructive evaluation of maturity of mango. *Journal of Food Engineering*, **78**, 22–26.
- Kang, S. P., East, A. R., and Trujillo, F. J., 2008. Colour vision system evaluation of bicolour fruit: A case study with “B74” mango. *Postharvest Biology and Technology*, **49**, 77–85.
- Kang, S. P., and Sabarez, H. T., 2009. Simple colour image segmentation of bicolour food products for quality measurement. *Journal of Food Engineering*, **94**, 21–25.
- Kılıç, K., Hakki-Boyaci, I., Köksel, H., and Küsmenoğlu, I., 2007. A classification system for beans using computer vision system and artificial neural networks. *Journal of Food Engineering*, **78**, 897–904.
- Koschan, A., and Abidi, M., 2008. *Digital Colour Image Processing*. New Jersey: John Wiley & Sons, Chapters 3 and 4.
- León, K., Mery, D., Pedreschi, F., and León, J., 2006. Color measurement in L*a*b* units from RGB digital images. *Food Research International*, **39**, 1084–1091.
- Mendoza, F., Dejmek, P., and Aguilera, J., 2006. Calibrated color measurement of agricultural foods using image analysis. *Postharvest Biology and Technology*, **41**, 285–295.
- Riquelme, M. T., Barreiro, P., Ruiz-Altsent, M., and Valero, C., 2008. Olive classification according to external damage using image analysis. *Journal of Food Engineering*, **87**, 371–379.
- Sun, D. W., and Brosnan, T., 2003. Pizza quality evaluation using computer vision-part1 Pizza base and sauce spread. *Journal of Food Engineering*, **57**, 81–89.

Cross-references

- Brightness Temperature in Monitoring of Soil Wetness
 Chemical Imaging in Agriculture
 Color Indices, Relationship with Soil Characteristics
 Horticulture Substrates, Structure and Physical Properties
 Image Analysis in Agrophysics
 Machine Vision in Agriculture
 Physical Properties as Indicators of Food Quality
 Plant Disease Symptoms, Identification from Colored Images
 Visible and Thermal Images for Fruit Detection

COLOR INDICES, RELATIONSHIP WITH SOIL CHARACTERISTICS

Manuel Sánchez-Marañón
 Departamento de Edafología y Química Agrícola,
 Universidad de Granada, Granada, Spain

Synonyms

Color indicators, descriptors or parameters

Definition

Soil. Unconsolidated material at the earth surface that serves as a medium for plant growth (see *Agrophysical Objects (Soils, Plants, Agricultural Products, and Foods)*).

Color. Perceptive attributes of a light emitted by a source of visible radiation and diffused by an object such as the soil.

Index. Something that reveals or indicates; a sign; a number used to characterize a set of data.

Soil-color index. Quantitative expression of soil color and indirect indicator of characteristics for the soil.

Introduction

Color has hardly any direct influence on the soil behavior, except for the albedo and the amount of heat absorbed (see *Adsorption Energy and Surface Heterogeneity in Soils*). Most soil processes, however, have color consequences, which can be used as traces of the quality and soil conditions. Early soil scientists such as Dokuchaiev, Sibirtsev, and Hilgard considered the soil color to be a straight-line function of the amount of humus and ferric oxides, and they discussed the significance of black, red, and white colors to soil productivity, age, and drainage (Bigham and Ciolkosz, 1993). Since the 1940s, the visual color

determination by standard Munsell soil-color charts has been widely employed worldwide for soil description. Some workers in the 1960s used the Munsell notation as index for several soil characteristics, but it was chiefly after 1980 when the color indices were supported by instrumental measurements and quantification in uniform color-space models. The present article focuses on the merit of color indices as sources of soil information. It describes (1) the soil-coloring process, (2) the numerical expression of soil color, and (3) the relationship of soil color with soil characteristics. For simplicity, no index of remote sensing is described here (see *Remote Sensing of Soils and Plants Imagery*).

Soil-coloring process

The soil has multiple solid particles surrounded by water and/or air. When light strikes a soil, some light is always directly reflected as if from a mirror (specular reflection). Light may be also partly transmitted through the particles, undergoing refraction, being partly absorbed as heat, and ultimately scattered. Scattering means that light is reemitted traveling in many different directions (Berns, 2000). Most soil particles are opaque or translucent and cause enough scattering so that light is diffusely reflected by them. The color of soil depends on the diffuse reflection of light after interacting with all particles in its way. The final soil color is an additive function of the color of particles weighted in accordance with their proportions (Sánchez-Marañón et al., 2004). A yellowish soil, for example, is due to a majority presence of yellowish particles; they selectively absorb more amount of blue (380–480 nm) and green (480–560 nm) light, while diffusely reflect the remainder light spectrum (yellow, 560–590 nm; orange, 590–630 nm; and red, 630–780 nm).

Silicates, carbonates, sulfates, and other salts are gray, white, or colorless. Soil pigmentation comes from Fe (hydr)oxides such as goethite (α -FeOOH), hematite (α -Fe₂O₃), maghemite (γ -Fe₂O₃), ferrihydrite (Fe₅HO₈·4H₂O), and lepidocrocite (γ -FeOOH). Their yellowish, brown, or reddish colors result from selective absorptions by electronic transitions in the metal, between the metal and ligands, or between adjacent metal ions in different oxidation states. Organic matter is also a usual colorant, causing strong absorption in all wavelengths of the visible range and darkening the soil. Less common are the Fe (II, III) hydroxy salts such as jarosite (KFe₃(SO₄)₂(OH)₆) and vivianite (Fe₃(PO₄)₂·8H₂O) having yellow, green, or blue tints of limited saturation, and black monosulfides, pyrite, and Mn oxides (Bigham and Ciolkosz, 1993). Particle size and arrangement as well as water content also influence soil color. The smaller soil particles (clay fraction) often exert greater influence because they (1) exhibit more surface area for altering the light, (2) contain the majority of pigmenting compounds, and (3) favor physicochemical interactions with colorants due to their charge and surface area. In addition,

scattering decreases as the soil particles become coarser. On the other hand, aggregation involves (1) particle arrangement and the consequent anisotropic distribution of compounds, occluding some and exposing others to the light; (2) increased size of soil units; and (3) generation of pores, trapping light. Finally, upon wetting, the refractive index of pores filled with water increases and a large amount of light is absorbed (Sánchez-Marañón et al., 2007).

Quantifying the soil color

Color can be measured with our own visual system, spectrometers, and colorimeters, following numerical specifications in a color system. The visual determination needs standard soil-color charts made with artificially colored papers and organized in the Munsell system. An observer seeks the closest match between a soil sample and one of the standard colors, for which the notation is: hue H , value V , and chroma C . Spectrometers record the amount of light reflected (R_{λ}) by the soil with respect to that of a perfectly reflecting diffuser (reference white) about each wavelength (λ). Color specification also requires the spectral distribution of a standard illuminant (S_{λ}) and three standard spectral curves ($\bar{x}_{\lambda}\bar{y}_{\lambda}\bar{z}_{\lambda}$) created by the Commission Internationale de l'Éclairage such as the Standard Observer for converting a reflectance spectrum to three perceptive stimuli (Berns, 2000). Tristimulus values represent the amount of red (X), green (Y), and blue (Z) of any color and are given by the following equations:

$$X = \frac{\int_{380}^{780} S_{\lambda} R_{\lambda} \bar{x}_{\lambda} d\lambda}{\int_{380}^{780} S_{\lambda} \bar{y}_{\lambda} d\lambda} \quad Y = \frac{\int_{380}^{780} S_{\lambda} R_{\lambda} \bar{y}_{\lambda} d\lambda}{\int_{380}^{780} S_{\lambda} \bar{y}_{\lambda} d\lambda} \quad Z = \frac{\int_{380}^{780} S_{\lambda} R_{\lambda} \bar{z}_{\lambda} d\lambda}{\int_{380}^{780} S_{\lambda} \bar{y}_{\lambda} d\lambda}$$

Colorimeters directly measure tristimulus values using filtered detectors combined to have responsive matching as closely as possible to $\bar{x}_{\lambda}\bar{y}_{\lambda}\bar{z}_{\lambda}$. Several color-space models have been derived from tristimulus values, with the aim of more closely correlating color parameters with the visual perception and having more uniform steps and spacing. The CIE and CIELAB systems are two outstanding examples. CIE system uses chromaticity coordinates x , y , and tristimulus Y , drawing a horseshoe-shaped spectrum locus by connecting the chromaticity points of the spectrum colors, which define the dominant wavelength (λ_d) and excitation purity (P_c) of the Helmholtz coordinates. CIELAB system considers a three-dimensional space defined by rectangular coordinates a^* b^* L^* or cylindrical polar coordinates L^* C_{ab}^* h_{ab} . Munsell HVC , by far the most familiar to soil scientists, may also be inferred from tristimulus values. Calculations and conversions CIE \leftrightarrow CIELAB \leftrightarrow Munsell are available in the modern measurement equipment and their formulation has been summarized by Viscarra Rossel et al. (2006).

Munsell H has long been used as soil-redness index. Because redness increases as the hue goes from

Y (yellow) to YR (brown) and R (red) and the range of Y and YR decreases from 10 to 0 (e.g., 3.7Y, 0.9Y, 9YR, 5YR, 2.5YR, 10R), it is usual to assign a single number to each hue (e.g., 23.7, 20.9, 19, 15, 12.5, 10). The CIELAB coordinates a^* and b^* , respectively, scalar quantities of red and yellow, are increasingly common in soil studies. CIELAB hue angle h_{ab} , an angular expression of the value of b^* respect to a^* , more accurately indicates the redness degree, which intensifies toward the lower values (usually in soils from 90° to 40°). In the CIE chromaticity diagram, the relative increase of x with respect to y signifies redder λ_d . Munsell V (0–10), CIELAB L^* (0–100), and CIE Y (luminance) provide accurate lightness values serving as soil-darkness indices; the lower the values are, the darker is the soil. Finally, Munsell C or the degree of departure (0–8) of the color from a gray of the same lightness, as well as CIELAB C^*_{ab} and Helmholtz P_c , both measured as the length of the line from the neutral point to the sample point, are used as soil-chromaticity indices. Besides these general indices, many other specific ones have been designed by researchers to incorporate various data into one value (Table 1).

Quantitative relationships between color indices and soil characteristics

Redness indices correlate with free Fe forms. There is a progressive increase of soil redness with an increased amount of free Fe (Figure 1a). The correlation, positive or negative, depending on each index, usually has a significant coefficient r not exceeding 0.7 ($P < 0.05$). The relationship is complicated not only by the combined presence of different pedogenic Fe minerals overlapping colors or by the size, arrangement, isomorphous substitutions, and crystallinity of these minerals, causing variation in their colors, but also by organic matter and Mn oxides,

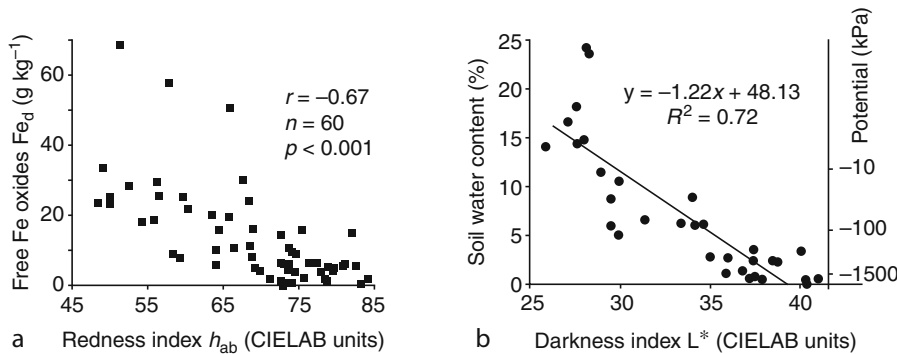
Color Indices, Relationship with Soil Characteristics, Table 1
Some specific color indices for assessing soil characteristics

Index	System	Characteristic	Author
$H \cdot C$	Munsell	Development	Buntley and Westin (1965)
$10(\Delta H + \Delta C)_{\text{dry}} + 10(\Delta H + \Delta C)_{\text{moist}}$	Munsell	Development	Harden (1982)
$\frac{(10 - H)^3 C 10^3}{V^6}$	Munsell	Hematite	Barrón and Torrent (1986)
$\frac{(x - 0.34)^2 10^4}{(y - 0.34) Y^2}$	CIE	Hematite	Barrón and Torrent (1986)
$\frac{a^*(a^{*2} - b^{*2})^{\frac{1}{2}} 10^{10}}{b^* L^{*6}}$	CIELAB	Hematite	Barrón and Torrent (1986)
$\sum \frac{A \text{ thickness}}{(V \cdot C) + 1}$	Munsell	Organic C	Thompson and Bell (1996)
Redox depletions	Munsell	Water saturation	He et al. (2003)

which mask the color of Fe-oxides. Redness indices specifically devised for predicting hematite content (Table 1) consider that dry ground soil samples gain redness as well as chromaticity and darkening with increasing hematite until reaching 15%, the threshold for color saturation. The regression equations fit linear models reaching R^2 coefficients 0.9, especially for the index designed from CIELAB parameters. The regression, however, varies for different sets of soils and is consistent only for soils with very low amounts of organic matter and amorphous Fe forms. Other specific indices related with hematite and goethite are based on the height of selected peaks in the second derivative of the reflectance spectrum, and coefficient K_λ (absorption) and S_λ (scattering) of the Kubelka–Munk theory, but they have been rarely used.

Aerobic weathering generates oxidized (often hydrated) free Fe forms for the soil; as a result, the soil development also correlates with soil redness. Redder hues signify increased weathering and development, which also explains the relation between redness indices, the content in clay and neoformed kaolinite, and soil age. To avoid the influence of the geological substrate on the redness indices, some authors (e.g., Harden, Table 1) subtract the color of parent material from that of the soil horizon. The redness-development relationships are usually fitted to curvilinear models because redness progresses slowly in the first steps of soil development and faster when Fe forms become matured by dehydration and recrystallization. High soil temperatures and dry seasons favor the maturity of Fe forms, and therefore redness indices are also related to climatic factors. Even under the same climatic conditions, somewhat warmer and drier soils are redder because the first weathering product (poorly crystalline Fe hydroxides) rapidly changes to hematite, while appears goethite in colder and damper soils (Singer et al., 1998). Other soil characteristics influenced by the type and amount of Fe oxides such as aggregate stability, porosity, drainage, and phosphate sorption are also connected to the redness indices. The *Soil Physical Quality* (qv) often improves with soil redness, while the yellowness component b^* was found to be positively related to P sorption (Scheinost and Schwertmann, 1995).

Although all color parameters can change depending on organic matter and soil wetness, stepwise multiple-regression analyses usually select Munsell V or CIELAB L^* as more informative (greater explained variability) of both soil characteristics (negative relationship). Strong relations, however, depend on a homogeneous soil landscape if soil textures and parent materials do not vary widely. This guarantees that the quality of organic matter, the way of epitaxial covering, and the lithogenic color baseline do not confuse the relationships. Soils with high organic C content consisting of aliphatic humus can display a similar darkness index as those having comparatively low amounts of organic matter but high aromaticity. Fine particles are better supports for humic pigments, encouraged by their superficial activity, and



Color Indices, Relationship with Soil Characteristics, Figure 1 Relation between redness index h_{ab} and dithionite-soluble iron Fe_d (a), and between darkness index L^* and water content (b) using samples from Mediterranean soils (Sánchez-Marañón et al., 2004, 2007).

the same soil color can be achieved with different organic C contents if the geological substrate also varies. Curvilinear relationships could point to variations in some of these factors in the datasets. The decrease of L^* with increased soil-water content and potential is also similar for soils with the same forming factors and characteristics. The calibration curve in a soil is frequently stepped (ladder shaped) with changes pronounced at certain potentials (-100 and -10 kPa in Figure 1b). There is weak correlation at intermediate potentials, and above -10 kPa, the water effect on L^* is hardly noted or the relation becomes positive. Therefore, a regression model applied to soils with the same color and origin predicts from L^* if the soils are dry, contain plant-available water, or move closer to **Field Water Capacity** (qv). Many other soil-fertility characteristics that depend on organic matter and soil wetness may be related to darkness indices, and some specific index combining thickness of A-horizons and Munsell VC (Table 1) was proved useful to differentiate soil conditions in Mollisols.

Soils in which water saturation occurs in normal years are said to have aquic conditions, and chroma indices usually describe their significance, duration, and water-table fluctuation. Soil-water saturation causes oxygen depletion and chemical reduction of polyvalent metallic elements. This process, called gleization, implies the presence of redoximorphic color features, including bluish- to greenish-gray matrix colors and colored mottles (sometimes, nodules and concretions). The $Fe(II)$ is removed during the reduction time, causing low chromaticity to the soil (Munsell $C \leq 2$), while $Fe(III)$ re-precipitates as hydroxides (often lepidocrocite) in mottles of higher chroma when the saturation event disappears. Low chroma indicates soil areas with redox depletion, while high chromas are redox concentrations. Low chroma colors increase in abundance, the longer a soil is saturated and chemically reduced. Authors that work in this field usually combine the chroma values and abundance of redox depletions into one index.

Conclusions

Soil color can be described by scalar quantities, called color indices, that are related to soil components and, by extension, properties depending on them or conditions for their formation. Accordingly, such color indices provide an integrative way of comparing soils, including evolution, pedoclimate, and fertility. Several circumstances involved in the color of soil materials and their interaction, however, alter the quantitative relationships. For predictive purposes, the relationships should be calibrated in a homogeneous soilscape, using the index and sample type best adapted to the soils and characteristics under study.

Bibliography

- Barrón, V., and Torrent, J., 1986. Use of the Kubelka-Munk theory to study the influence of iron oxides on soil color. *Journal of Soil Science*, **37**, 499–510.
- Berns, R. S., 2000. *Billmeyer and Saltzman's Principles of Color Technology*. New York: Wiley.
- Bigham, J. M., and Ciolkosz, E. J. (eds.), 1993. *Soil Color*. Madison: Soil Science Society of America.
- Buntley, G. J., and Westin, F. C., 1965. A comparative study of developmental color in a Chestnut-Chernozem-Brunizem soil climosequence. *Soil Science Society of America Proceeding*, **29**, 579–582.
- Harden, J. W., 1982. A quantitative index of soil development from field description: examples from a chronosequence in central California. *Geoderma*, **28**, 1–28.
- He, X., Vepraskas, M. J., Lindbo, D. L., and Skaggs, R. S., 2003. A method to predict soil saturation frequency and duration from soil color. *Soil Science Society of America Journal*, **67**, 961–969.
- Sánchez-Marañón, M., Soriano, M., Melgosa, M., Delgado, G., and Delgado, R., 2004. Quantifying the effects of aggregation, particle size and components on the colour of Mediterranean soils. *European Journal of Soil Science*, **55**, 551–565.
- Sánchez-Marañón, M., Ortega, R., Miralles, I., and Soriano, M., 2007. Estimating the mass wetness of Spanish arid soils from lightness measurements. *Geoderma*, **141**, 397–406.
- Scheinost, A. C., and Schwertmann, U., 1995. Predicting phosphate adsorption-desorption on a soilscape. *Soil Science Society of America Journal*, **59**, 1575–1580.

- Singer, A., Schwertmann, U., and Friedl, J., 1998. Iron oxide mineralogy of Terre Rosse and Rendzinas in relation to their moisture and temperature regimes. *European Journal of Soil Science*, **49**, 385–395.
- Thompson, J. A., and Bell, J. C., 1996. Color index for identifying hydric conditions for seasonally saturated Mollisols in Minnesota. *Soil Science Society of America Journal*, **60**, 1979–1988.
- Viscarra Rossel, R. A., Minasny, B., Roudier, P., and McBratney, A. B., 2006. Colour space models for soil science. *Geoderma*, **133**, 320–337.

Cross-references

- Adsorption Energy and Surface Heterogeneity in Soils
Agrophysical Objects (Soils, Plants, Agricultural Products, and Foods)
Field Water Capacity
Remote Sensing of Soils and Plants Imagery
Soil Physical Quality

COMPACTIBILITY

See *Soil Compactibility and Compressibility*

COMPACTION OF SOIL

Densification of an unsaturated soil by the reduction of fractional air volume. Compaction can take place either under a static load or transient vibration or trampling by animals and machines.

Bibliography

Introduction to Environmental Soil Physics. (First Edition). 2003. Elsevier Inc. Daniel Hillel (ed.): <http://www.sciencedirect.com/science/book/9780123486554>

Cross-references

- Grazing-Induced Changes of Soil Mechanical and Hydraulic Properties
Subsoil Compaction

COMPENSATORY UPTAKE

See *Soil Hydraulic Properties Affecting Root Water Uptake*

COMPRESSIBILITY

See *Soil Compactibility and Compressibility*

COMPRESSION INDEX

See *Soil Compactibility and Compressibility*

COMPRESSION POINT

See *Soil Compactibility and Compressibility*

COMPRESSION TEST, TRIAXIAL

See *Triaxial Compression Test*

CONDITIONERS, EFFECT ON SOIL PHYSICAL PROPERTIES

Ryszard Dębicki
Department of Soil Science, Maria Curie-Skłodowska University, Lublin, Poland

Definition and introduction

The search for new effective means of improving the physical, physical-chemical, and chemical properties of soils, which enhance soil fertility, used to and still does arouse interest in many regions of the world for a number of reasons:

1. Classic methods of improving soil fertility require prolonged periods of use and are work-, cost-, and energy-intensive.
2. In contemporary agriculture, there is a lack of sufficient amounts of organic fertilizers, which could eliminate the deficit of humic compounds and prevent the physical degradation of soils.
3. Discovered synthetic structure-forming agents can also be used for such a utilization of some industrial and agricultural waste materials, so that they can be more effectively used for soil fertility enhancement.

Improving the physical properties of soils is directly related to the soil structure (see *Soil Aggregates, Structure, and Stability*). Thus, investigating the phenomena that accompany the creation and sustaining of the soil crumbs allowed to formulate the following hypothesis: The activity of natural binding agents occurring in the soil can be strengthened by introducing synthetic substances, which are more effective and more resistant to microbiological decomposition, and which, during their transition from the soluble into the non-soluble state, will create durable soil aggregates. It has been stated that, beside the mineral colloids (clay minerals, among others), the high molecular organic substances of the linear polymer character, lignin, proteins, nucleic acids, and other substances play a primary role in such processes in soils. Together, these substances create the compounds that are not water-soluble in the soil. All these compounds contain a sufficient number of polar groups to ensure their adsorption on the colloidal soil particles. The cross-bindings and van der Waals' forces between the chains ensure good cohesion of the soil particles (Dechnik and Dębicki, 1977).

Research on the utilization of synthetic, structure-forming agents began as early as in the 1950s (Martin, 1953; Wallace and Terry, 1998). However, despite the investigation of numerous compounds of various chemical characters and of different origin, to date, no agent has been found whose use would be economically justified in broad agricultural practice and environmental protection. Based on extensive studies, it has been concluded that effective structure-forming agents should have good binding properties, be easy to use, durable in the soil environment, nontoxic, and inexpensive. Although an agent that would satisfy all of the above conditions has not yet been found, some of the investigated compounds have been widely used in several measures. For instance, they have been used in the moderate climates; in plant cultivation – to improve the sprouting conditions and germination of industrial or highly marketable plants (Dechnik and Dębicki, 1977); in amelioration – to combat water and wind erosion on terrains susceptible to such phenomena (Fullen et al., 1993; Bjornberg and Aase, 2000) (see *Water Erosion: Environmental and Economic Hazard*); in engineering – to secure road shoulders and road edges, canals and rivers; in the dry climate – to prevent the soil from water evaporating from the bared surfaces or to prepare the ground for tree and bush cultivation in sandy terrain (De Boodt, 1972). Moreover, many of synthetic soil conditioners (e.g., polyelectrolytes) are used for transforming some waste products from various branches of economy (agriculture, forestry, food processing industry, wastewater treatment plants, etc.) or for manufacturing of polymer-coated urea in order to control the release of nitrogen, e.g., polyurethane (Golden et al., 2009). Today, according to Sojka et al. (2005), all synthetic and natural agents, including fertilizers in all stages of modification or unmodified, which are introduced into the soil for the purpose of improving its natural, agronomic, technological, preventive, and other properties, are considered among soil conditioners. In this paper, special consideration is given to the synthetic agents of soil enhancement and to natural wastes transformed through addition of synthetic agents.

Classification, characteristics, and the influence mechanism of synthetic agents used to enhance the physical properties of soils

Numerous patented synthetic and natural soil improvement agents exist. Known are several of their classifications in which the main criterion is either the chemical composition or mode of action, technology, method and area of use, their origin, etc. One characteristic feature of all the soil improvement agents is their ability to create or stabilize the aggregates or the ability to alter other physical and chemical soil properties (such as the size and durability of the soil aggregates, ability to retain water and mineral nutrients, wettability and sorptivity, rate of filtration, cation exchange capacity, and others). The dominant and most widely investigated groups are the organic, water-soluble,

high molecular linear polymers (polyelectrolytes). They were the first synthetic, structure-forming agents introduced in the market by the Monsanto Chemical Co. (USA) under the commercial name "Krilium" (Martin, 1953).

To date, the described synthetic agents are classified by researchers in a variety of ways. Schamp (1976) distinguished between the following groups: polyelectrolytes; emulsions of homopolymers and copolymers of polyvinyl and polybutadien esters; cellulose derivatives; crude oil derivatives; resin substances of various origin; substances derived from fermentation and processing of various wastes (saw dust, industrial plants, municipal wastes, paper wastes, agricultural wastes, etc.).

De Boodt (1972) classified the synthetic agents of soil improvement according to the mode of influence on various soil properties: agents stimulating the hydrophilic phenomena (polyelectrolytes); agents causing hydrophobization of the soil (selected bituminous emulsions); agents increasing the surface horizon temperature of the soil (some bituminous emulsions); agents sustaining only the arable soil structure which loosens the soil and does not impede the development of the plant root system; agents aimed at increasing the cation exchange capacity of the soil (e.g., emulsions of strong acidic character, Al and Mg silica solutions, ion exchange resins, etc.).

Kullman (1972) divided the synthetic agents of soil enhancement into three groups: (1) agents of indirect influence on soil enhancement, i.e., substances, which when introduced in the soil, sustain its looser structure, improve its structural state, increase its resistance to thermal and mechanical factors, but do not directly impact the water and air content in the soil (e.g., flocculants, surface-active substances, some detergents, fat alcohols); (2) direct influence agents, whose introduction in the soil is directly related to the improvement of the water-air relations due to their specific composition (synthetic substances which can fix and store water and nutrients, have the ability to transfer them to plants, create a nonuniform mixture with the soil, improve the structural character of the soils, loosen the soils, and simultaneously increase their water capacity) (Styromull, Hygromull, Pianizol, among others); and (3) agents of indirect and direct influence (all bituminous emulsions, nonorganic gels, ion exchange resins, and others). Using emulsions enables the surface stabilization of the soil, increases the temperature, decreases evaporation, and thus increases the water content in the soil.

The impact of synthetic agents on the physical properties of soils

The wide interest in the possibility of using synthetic and waste-related agents to enhance the soil properties resulted in the fact that today the literature on this topic is extensive. The majority of the research was concerned with investigating the direct impact of the synthetic agents on the soil structure (its aggregation and durability, both in water and

mechanical) (Kullman, 1972; Dechnik and Dębicki, 1977; Wallace and Terry, 1998; Sojka et al., 2005).

Among the presented groups of enhancing agents, the most recognized is the influence of polyelectrolytes and polymer emulsions. Research points to a clear improvement of both the aggregation and the water resistance of various soils with the use of these agents in amounts as small as 0.05–0.1% of the soil mass. Observed is also a significant change in the distribution of the size of the aggregates. Along with the increased content of higher diameter crumbs, the soil loosens, which is indicated by the results of porosity, strength, and micromorphology tests. The scale of these changes depends on the kind and dose of the substance, means of use, state of soil matrix and texture, and level of the soil moisture during the procedure. Optimum structure-forming results were obtained at the level of soil moisture of 60% FWC (field water capacity).

Using the agents with different chemical composition also results in changes of other soil features, for example, the conductivity abilities, which occur not only due to the loosening of the soil, but also because of the changes in its wettability. The presence of the hydrophilic and hydrophobic substances leads to the change in the contact angle between soil particles and the soil solution. This results in the increase or decrease in the rate of water filtration in the soil, its retention, and the rate of evaporation (De Boodt and Dębicki, 1988). Lately again, polyacrylamide was used to reduce saturated water hydraulic conductivity in sandy soils (Young et al., 2009). Research showed that water-soluble polymers had hydrophilic characteristics, while polymer and bituminous emulsions had hydrophobic features. Still others, for example, the foamy substances of the Hygromull, Pianizol, and Polystyrene type, were neutral. They did, however, significantly increase the sorptive capacity of the soil in relation to water and nutrients. Included in this group are urea-formaldehyde resins, zeoliths, and others.

Discovery of the properties of a specific agent and the mechanisms of its influence in the soil allowed steering the physical processes in the soil. It has been shown that due to the use of hydrophobic substances, one could limit the evaporation-related water loss by 40–90%, depending on the procedure used (for instance, mulch or inserting the agent up to the depth of 10 cm or at a specified depth in the soil profile). The use of surface mulch from the hydrophobic substance increases the reserve of plant-available water within the season of germination and sprouting by 5 days.

Introducing the structure-forming agents into the soil results also in significant changes in the physical-chemical and chemical properties of the environment. The use of polyelectrolytes or polymer emulsions leads to the changes in the sorptive capacities of the soil. The kinetics of the ion sorption, the size and energy of the sorption, and the exchange capacity of the soil also change. The agents also influence the soil reaction, mobilization, and the uptake of nutrients, which is related to the biological life of the soil.

Summary

Literature data indicate that the doses of the investigated synthetic agents had a wide range from 0.001% to 1% in relation to the soil mass, depending on the type of the agent, purpose, and the procedure used. These amounts are significant, which led to the idea of using the most effective synthetic agents for such preparation of selected organic and mineral wastes from the industry and agriculture, that they can be further used in the process of improving the soil fertility on a much wider scale than has been used to date. Literature points to the great importance of such research not only in the aspect of reclaiming the soil fertility, but also for the purposes of environmental protection. During the utilization of the wastes with the use of synthetic, structure-forming agents, the doses of these agents substantially decrease and the created substances can be used as means of increasing the fertility of the soil. From the agricultural and economic point of view, it is desirable that synthetic, structure-forming agents and the agents derived from waste processing are characterized by high resistance to microbiological decomposition in the soils. However, from the environmental protection point of view, it is essential that these agents are biodegradable and the products of their decomposition are not toxic to the soil flora and fauna. Therefore, the knowledge of the speed of decomposition of these products and their impact on the microbiological processes in the soils is critical for the wider utilization of these agents in agriculture and environmental protection. The literature on biodegradation of the synthetic, structure-forming agents is scarce. However, research has shown that both the high molecular linear polymers and other agents (used in doses up to 0.1% of the soil mass) have not negatively influenced the biological activity of the soil and were not toxic to the soil microflora.

Bibliography

- Bjornberg, D. L., and Aase, J. K., 2000. Multiple polyacrylamide applications for controlling sprinkler irrigation runoff and erosion. *Applied Engineering in Agriculture*, **16**, 501–504.
- De Boodt, M., 1972. Improvement of soil structure by chemical means. In Hillel, D. (ed.), *Optimizing the Soil; Physical Environment Towards Greater Crop Yields*. New York: Academic, pp. 45–55.
- De Boodt, M., and Dębicki, R., 1988. The effect of polyelectrolytes on water transmission properties of soils. *Polish Journal of Soil Science*, **21**, 7–14.
- Dechnik, I., and Dębicki, R., 1977. The use of synthetic conditioners for soil improvement (In Polish). *Problemy Agrofitzyki*, **23**, 5–201.
- Fullen, M. A., Tye, A. M., Pritchard, D. A., and Reynolds, H. A., 1993. Effects of 'Agri-SC' soil conditioner on the erodibility of loamy sand soils in Eastern Shropshire, UK. *Soil Use and Management*, **9**, 21–24.
- Golden, B. R., Slaton, N. A., Norman, R. J., Wilson, C. E., Jr., and De Long, R. E., 2009. Evaluation of polymer-coated urea for direct-seeded, delayed-flood rice production. *Soil Science Society of America Journal*, **73**, 375–383.
- Kullman, A., 1972. Synthetische Bodenverbesserungsmittel. Veb. Dtsch. Landwirtsch. Berlin, pp. 1–132.

- Martin, W. P., 1953. Status report on soil conditioning chemicals. *Soil Science Society of America Journal*, **17**, 1–9.
- Schamp, N., 1976. Chemicals used in soil conditioning. *Mededelingen Fakulteit Landbouwwetenschappen Rijksuniversiteit Gent*, **41**, 13–18.
- Sojka, R. E., Entry, J. A., and Orts, W. J., 2005. Conditioners. In Hillel, D., et al. (eds.), *Encyclopedic of Soils in the Environment*. Oxford: Elsevier, pp. 301–306.
- Wallace, A., and Terry, R. E. (eds.), 1998. *Handbook of Soil Conditioners; Substances that Enhance the Physical Properties of Soils*. New York: Marcel Dekker.
- Young, M. H., Moran, E. A., Yu, Z., Zhu, J., and Smith, D. M., 2009. Reducing saturated hydraulic conductivity of sandy soils with polyacrylamide. *Soil Science Society of America Journal*, **73**, 13–20.

Cross-references

- [Soil Aggregates, Structure, and Stability](#)
[Water Erosion: Environmental and Economical Hazard](#)

CONDUCTIVITY

The ability of matter to conduct or transmit water, heat, electricity, or sound.

CONE INDEX

See [Soil Penetrometers and Penetrability](#)

CONFINED COMPRESSION TEST

See [Soil Compaction and Compressibility](#)

CONSISTENCY

The manifestations of the forces of cohesion and adhesion acting within the soil at various water contents, as expressed by the relative ease with which a soil can be deformed or ruptured. Engineering descriptions include: (i) the designation of five categories (soft, firm or medium, stiff, very stiff, and hard) as assessed by thumb and thumbnail penetrability and indentability; and (ii) characterization by the Atterberg limits (i.e., liquid limit, plastic limit, and plasticity number). See also [Atterberg Limits](#); [Liquid Limit \(Upper Plastic Limit, Atterberg Limit\)](#); [Plastic Limit](#) and [Plasticity Number](#).

Bibliography

Glossary of Soil Science Terms. Soil Science Society of America. 2010. <https://www.soils.org/publications/soils-glossary>

CONSOLIDATION

The action of producing a solid or compact mass, in the case of soil by compaction. It involves a decrease in the volume of void space.

Cross-references

- [Soil Structure and Mechanical Strength](#)
[Subsoil Compaction](#)

CONTACT AREA OF AGRICULTURAL TYRES, ESTIMATION

Etienne Diserens¹, Abdallah Alaoui²

¹Agricultural Engineering Systems Group, Department of Agricultural Economics and Engineering, Agroscope Reckenholz-Tänikon ART, Ettenhausen, Switzerland

²Hydrology Group, Department of Geography, University of Bern, Bern, Switzerland

Synonyms

Interface soil-tyre

Definition

Contact area. Surface of the soil which is closely connected with the wheels or tracks of the agricultural engine.

Introduction

The main dangers threatening agricultural land in the industrialized world in recent decades are erosion, loss of organic material, and compaction (Jones, 2002). Field driving and field tilling with heavy machines contribute to soil compaction and soil shearing and reduce the storage, and hence availability of oxygen, water nutrients, and heat to the soil with a resulting crop yield decrease (Coehlo et al., 2000; Heinonen et al., 2002; Gregory et al., 2007). This affects the environment by increasing N₂O, CH₄ and CO₂ emission from soils (Horn et al., 1995). It is therefore essential to estimate the contact area *A* of agricultural tyres, since this parameter appears in: (1) the calculation of surface pressures (Keller, 2005; SchjØnning et al., 2008), (2) the models of strain stress propagation in soil (Söhne, 1953; Smith, 1985; Bastgen and Diserens, 2009), and (3) the prediction of severe risks of compaction (van den Akker, 1998; O'Sullivan et al., 1999; Defossez and Richard, 2002; Diserens et al., 2010). Moreover, on farmland or on the road, *A* is also related to the forces acting on the wheel (traction force, rolling resistance, braking force), determining vehicle grip, wear on tread, and road safety (Eichhorn, 1999). As *A* increases due to the use of broad tyre or twin tyre and the correct setting of the inflation pressure, not just the soil loading but also the rolling resistance is reduced, and this saves fuel consumption too (Döll, 1999). The contact area

also depends on the rolling resistance. Rempfer (1998) differentiated between internal and external rolling resistance. The internal resistance relates here to the dissipated energy within the tyre that is mainly dependant on the hysteresis of the material used and therefore the tyre deformation. The external rolling resistance, however, results on the one hand from the soil compaction caused by the tyre and on the other from the so-called "bulldozing effect." Here, it should be said that the internal rolling resistance of trailer is lower than that of traction tyres. Due to the stronger carcass, in particular at the flanks, the implement can be operated at higher inflation pressures to carry higher loads. The higher net-to-gross of the implement tyre tread pattern is designed for a free-rolling application.

The most common relationships between tyre size TS (width $W \times$ outer diameter D), wheel load F , inflation pressure P_i , and contact area A of traction and trailer tyres will be presented here. Influences of loading and of soil resistance on contact area A will be also discussed.

Measurement of the contact area A of tyres

The measurement of A is carried out using the photometry method (two-dimensional projection of the actual static surface area when the tyre is stationary). On meadow, the plant cover is first cut using a mower, followed if necessary by a second cut with a grass mowing machine. The print circumference of the tyre on the ground is first sprinkled with calcium oxide powder. For reference, a rule is placed on the edge of the print area once the load has been removed (Figure 1a and b). The contours are photographed with a digital camera. Print area or contact area A is analyzed by photometry (Diserens and Steinmann, 2002).

Coefficients of variation lower than 5% were found by examining the repeatability of the measurements by the sprinkling method.

To consider also the soil hardness on the surface, the penetration resistance of topsoil is measured with the aid of a Pesol penetrometer (20 daN or 33 MPa, a screwdriver head, bar width $6 \cdot 10^{-3}$ m, bar thickness $1 \cdot 10^{-3}$ m, stem

length $20 \cdot 10^{-2}$ m, stem diameter $4 \cdot 10^{-3}$ m) (Diserens, 2009).

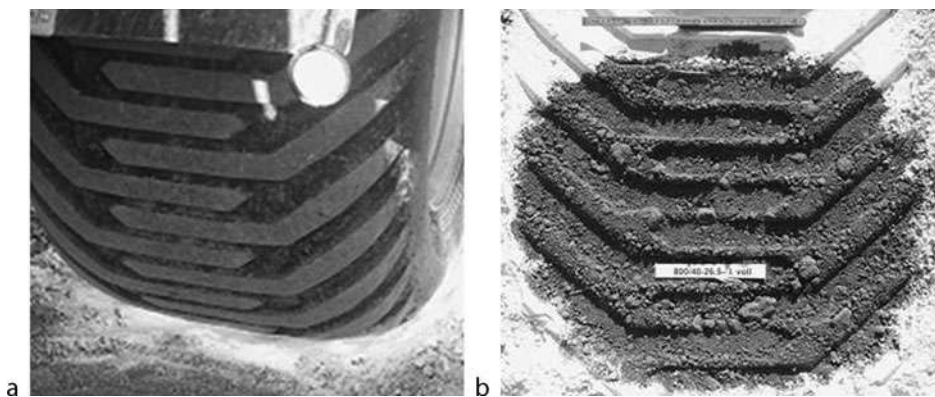
Contact area for traction tyres

There are numerous algorithms for estimating A of traction tyres on agricultural ground. Previous studies have described A strictly on the basis of the measured contact dimensions and the unladen tyre radius (Schwieger, 1996), or the depth of the rut (Bolling, 1987).

The equations developed for a wide range of tyres are characterized by the small number of variables. For high and low bearing capacity, simple formulae are used that take into account the diameter (D) and the width (W) of the tyre (McKyes, 1985). These equations are used to compare different tyre sizes. Similar formulae on soft soils considering the ratio q between tyre height and section width for normal profile ($q \geq 0.8$) and for low size profile ($0.8 < q < 0.6$) are also given (Diserens, 2002).

For hard surface, Steiner (1979) developed two algorithms for cross ply and radial tyres, both for normal profile with inflation pressure ranging between 80 and 220 kPa and wheel load between 5 and 25 kN, taking into account the wheel load, tyre diameter, and inflation pressure. In their Compsoil model, O'Sullivan et al. (1999) used the same independent variables (overall width and diameter of tyre, static wheel load and inflation pressure). In addition, they introduced a proportionality factor according to the soil hardness, which requires information on the soil bulk density of the soil surface. Comparing the shape of A to an ellipse, Grecenko (1995) suggested multiplying the product of the length and the section width of A by a coefficient c varying between 0.8 and 0.9 (1 for a rectangle). From measurements of rather soft ground, Keller (2005) considered A as a super ellipse described by the width of the tyre and the length of the ellipse. The length is correlated with the diameter of the tyre and the pressure ratio (measured tyre pressure divided by recommended pressure for a given load and speed).

The most common relationships given A for traction tyres on soft and hard soils are reported in the Appendix.



Contact Area of Agricultural Tyres, Estimation, Figure 1 Trailer tyre 800/40-26.5. (a) Marking on the field by means of a bellow, (b) Digital recording with reference rule for picture analysis.

Based on field measurements on soft and semi-firm arable soils (penetration resistance $PR < 13$ MPa) for a wide range of radial traction tyres (15 tyre types, rim diameter 24–42), relationships between contact area A (m^2) and easily accessible variables such as tyre size TS (in m^2), wheel load F (kN), and inflation pressure P_i (kPa) are given by means of regression analyses after selecting the tyres in three classes:

For small traction tyres ($TS < 0.6 \text{ m}^2$, $F \leq 25 \text{ kN}$) on soft soils (Equation 1):

$$A = 0.247[TS] + 5.821 \cdot 10^{-3}[F] - 1.933 \cdot 10^{-4}[P_i] \quad R^2 = 0.949 \quad (1)$$

For medium tyres ($0.6 \text{ m}^2 \leq TS < 1.2 \text{ m}^2$, $F \leq 65 \text{ kN}$) on soft soils (Equation 2):

$$A = 0.327[TS] + 3.333 \cdot 10^{-3}[F] - 5.386 \cdot 10^{-4}[P_i] \quad R^2 = 0.970 \quad (2)$$

For large tyres ($TS \geq 1.2 \text{ m}^2$, $F \geq 35 \text{ kN}$) on soft soils (Equation 3):

$$A = 0.230[TS] + 6.014 \cdot 10^{-3}[F] - 11.604 \cdot 10^{-4}[P_i] \quad R^2 = 0.985 \quad (3)$$

Reliable results can be obtained on soft soils after setting also the limit of the wheel load within each class (Equations 1–3). For traction tyres, the dynamic contact area can be deduced by taking into account, respectively, the dynamic load.

Contact area for trailer tyres

Because of the various functions of the farming trailer tyre, taking into account raised load-bearing, adherence

at high speed, lateral stability on wet roads, increased contact area, self-cleaning profile with respect to the traction tyre with raised traction force, raised working speed, the farming trailer tyre has a different composition. Its carcass (heavier cable) on the side transmitting the braking forces and change of direction forces of the wheel on the ground is reinforced. A belt with thicker textile layers and steel layers on the tread exerts a further stabilizing effect when the tyre is subject to heavy loads.

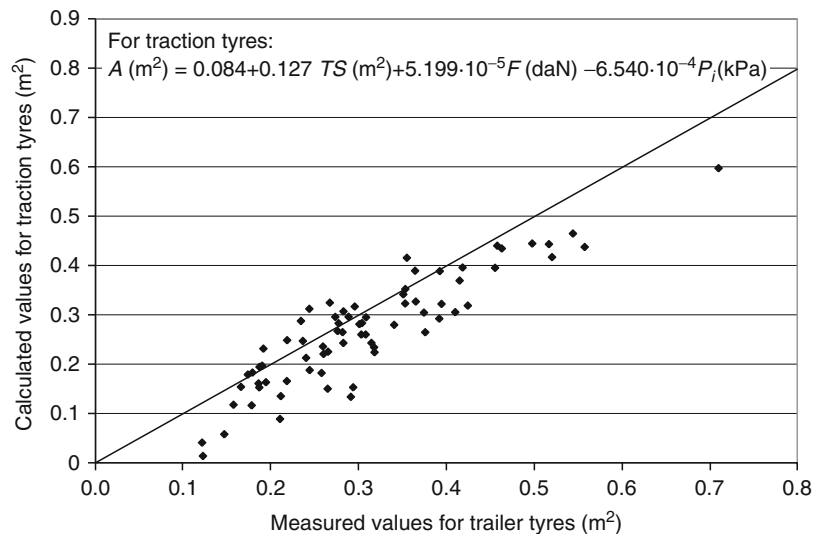
Figure 2 gives a comparison of A values, measured on the ground for farming trailer tyres with the corresponding values calculated from an equation derived from a data sheet of traction tyres with the same soil condition ($PR > 8$ MPa). Most of the points are below the line 1:1 (Figure 2). At similar loading, the diameters are generally smaller and the maximal loads lower (comparing the full loads from self-propelled harvester), thus the values for the trailer tyres will be underestimated after introducing the data in the equation calibrated for traction tyres with higher loads (Figure 2).

Based on field measurements on semi-firm and firm soils, representative conditions in fodder farming ($PR > 8$ MPa) for a wide range of trailer tyres (24 tyre types, rim diameter 15.3–30.5), relationships between A (m^2), tyre size TS (in m^2), wheel load F (kN), and inflation pressure P_i (kPa) are presented by means of regression analyses after representing the tyres by four classes (Diserens, 2009):

For cross-ply trailer tyres ($W < 0.5 \text{ m}$, $F \leq 25 \text{ kN}$) on hard soils (Equation 4):

$$A = 0.208[TS] + 3.176 \cdot 10^{-3}[F] - 0.679 \cdot 10^{-4}[P_i] \quad R^2 = 0.988 \quad (4)$$

For cross-ply trailer tyres ($W \geq 0.5 \text{ m}$, $F \leq 90 \text{ kN}$) on hard soils (Equation 5):



Contact Area of Agricultural Tyres, Estimation, Figure 2 Calculated values for contact area A of traction tyres and measured values for contact area of trailer tyres with a line 1:1 on comparable soil conditions according to Diserens (2009).

$$A = 0.132[TS] + 7.034 \cdot 10^{-3}[F] - 3.725 \cdot 10^{-4}[P_i] \quad R^2 = 0.985 \quad (5)$$

For radial low size ($0.8 < q < 0.6$) trailer tyres ($F \leq 70$ kN) on hard soils (Equation 6):

$$A = 0.069[TS] + 3.140 \cdot 10^{-3}[F] - 1.935 \cdot 10^{-4}[P_i] + 0.092 \quad R^2 = 0.859 \quad (6)$$

For radial terra ($q \leq 0.6$) trailer tyres ($F \leq 70$ kN) on hard soils (Equation 7):

$$A = 0.178[TS] + 4.169 \cdot 10^{-3}[F] - 4.240 \cdot 10^{-4}[P_i] + 0.063 \quad R^2 = 0.830 \quad (7)$$

Reliable results can be obtained on semi-firm and firm soils after setting also the limit of the tyre width W and the wheel load within cross-ply classes (Equations 4 and 5), respectively, within each class (Equations 4–7).

Influences of the loading and the inflation pressure on the contact area A

Several authors note an increase in A when inflation pressure falls for traction tyres (Steiner, 1979; O'Sullivan et al., 1999; Keller, 2005). However, a variation in inflation pressure alone is in fact not always enough to determine whether A increases or decreases (Diserens, 2009). Tyre loading could also play an important role (Table 1). When the tyre is under a light load, the volume of the tyre subject to increased inflation pressure increases (balloon effect) or, in a other way, when the distortion of the tyre decreases after increasing the inflation pressure, the contact pressure increases causing additional deformation of the soil. A could increase in both cases. Above a particular load threshold, the inflation pressure is insufficient to counter the load, so the tyre distorts under the weight and A increases.

Contact Area of Agricultural Tyres, Estimation,
Table 1 Influence of loading on farming trailer contact area assessment. Two examples

Loading [%]	Wheel load [kN]	Inflation pressure [kPa]	Contact area [m ²]
28L-26			
22	9.8	150	0.179
22	9.8	180	0.194
72	32.4	150	0.308
72	32.4	180	0.277
100	45.1	190	—
340/65R18			
31	6.9	450	0.060
31	6.9	500	0.067
98	22.1	460	0.102
98	22.1	510	0.098
100	22.6	540	—

The influence of the load on the inflation pressure depends on the initial inflation pressure and on the volume of the tyre too. The greater the tyre volume and initial inflation pressure, the smaller the inflation pressure variation for loads will be. In comparison with the variations of A or of the mean contact pressure, the variation of the inflation pressure following the loads remains negligible (Diserens, 2009).

Influence of the soil resistance on the contact area A

Several authors note an increase in A when PR of the top-soil decreases (Söhne, 1953; Mc Kyes, 1985; O'Sullivan et al., 1999). However, the opposite can occur (Diserens, 2009). At the same loads and inflation pressures, A values of the farming trailer tyres and traction tyres were measured for two different soils: one on natural grassland ($PR = 15.5$ MPa) and one on winter barley stubble ($PR = 11.7$ MPa) (Figure 3).

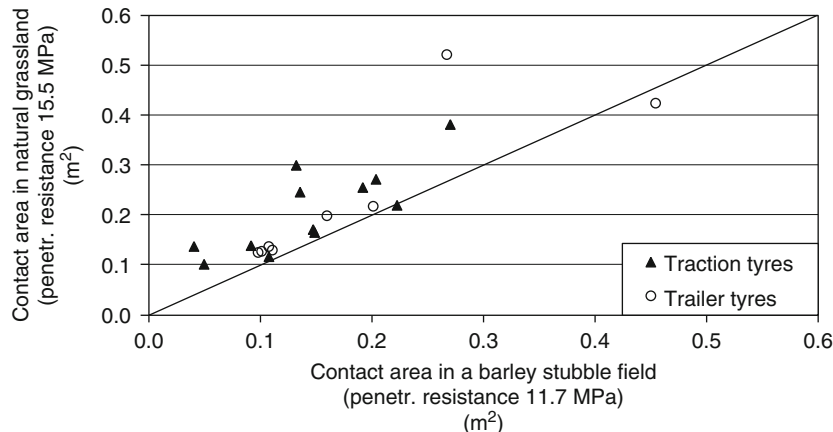
On harder, natural grassland, higher A values were measured. Comparing distortion of the internal contour of a traction tyre 520/70R34 on concrete and on a sandy silt soil, using a laser device placed inside the tyre, Schlotter and Kutzbach (2001) note greater flattening of the tyre on concrete; on a flexible soil, tyre distortion is less marked. On a hard soil, A mainly depends on tyre stiffness, while in the open field, the plasticity and elasticity of the soil combine with that of the tyre, and as the two elements adapt to each other, the distortion of the tyre is reduced. Results on the field and in laboratory show that there is no necessarily linear relationship between soil hardness and contact area.

Summary

- All the measurements for the contact area A occurred are carried out for stationary tyres. For an estimation of the dynamic contact area, it is recommended that the dynamic load for traction tyres be taken into account.
- The connection between the wheel load and the tyre size of a traction tyre and of a trailer tyre is not similar. Consequently it is necessary to develop and use distinct relationships to evaluate A of farming tyres.
- By low loading, A can increase with an increase of inflation pressure. For reliable estimations, loading values above 50% of the maximum permissible load are recommended.
- By estimating A , the aim is henceforth to provide a parameterization of soil hardness while also considering tyre stiffness.

Appendix

Formulae for calculating the contact area for farming traction tyres and their range of application – A (m²): contact area, W (m): width of tyre, D (m): total diameter of tyre, F (kN): tyre load, P_i (kPa): inflation pressure, P_{rec} (kPa): recommended inflation pressure, PR (MPa): Penetration resistance static penetrometer, k : constant, dependent on



Contact Area of Agricultural Tyres, Estimation, Figure 3 Influence of penetration resistance PR with values above 10 MPa on contact area A (Diserens, 2009).

Tyre structure	Hardness of topsoil (0.00–0.10 m) Soft and semi-firm soil with $PR < 13$ MPa	Hardness of topsoil (0.00–0.10 m) Firm soil with $PR \geq 13$ MPa	Authors
$A = (a WD)$ Undifferentiated	$A = 0.50WD$	$A = 0.25WD$ $A = 0.87 W \cdot 0.31D$	McKyes (1985) Inns and Kilgour (1978)
Normal profile ^a Low profile ^b	$A = 0.3360WD$ $A = 0.4420WD$		Diserens (2002) Diserens (2002)
$A = (aWD) + (bF) + (cP_i)$ Undifferentiated	$A = (0.428WD) + (2.25 \cdot 10^{-3} F) - (65.0 \cdot 10^{-5} P_i)$ $A = k W [0.47 + (0.11D^2) - (0.16 \ln(P_i/P_{rec}))]$ $A = (0.310 WD) + (0.00263 F) + (0.239 F/P_i) (8)^c$	$A = (0.041 WD) + (0.613 F/P_i)^d$ $A = 0.01 F [2.677 + (5.75 \cdot 10^{-3} P_i) + (0.011F) - (1.6D)]^e$	Diserens (2002) Keller (2005) O'Sullivan et al. (1999) Steiner (1979)

^aNormal profile: tyre profile with q ratio between height and width ≥ 0.8

^b Low profile: tyre profile with q ratio between height and width $0.6 < q < 0.8$

^cWith bulk density ≤ 1.0 Mg m⁻³

^dWith bulk density ≥ 1.8 Mg m⁻³

^eRadial tyres, validated by an inflation pressure ≥ 80 kPa and width < 0.7 m

real number n that determines the shape of the ellipse (Keller, 2005)

Bibliography

- Bastgen, H. M., and Diserens, E., 2009. q value for calculation of pressure propagation in arable soils taking topsoil stability into account. *Soil & Tillage Research*, **102**, 138–143.
- Bolling, I., 1987. Bodenverdichtung und Triebkraftverhalten bei Reifen – Neue Mess- und Rechenmethoden – *Forschungsbericht Agrartechnik des Arbeitskreises Forschung und Lehre der Max-Eyth-Gesellschaft (MEG)* 133. Dissertation, München.
- Cochlo, M. B., Mateos, L., and Villalobos, F. J., 2000. Influence of a compacted loam subsoil layer on growth and yield of irrigated cotton in Southern Spain. *Soil & Tillage Research*, **57**, 129–142.
- Defossez, P., and Richard, G., 2002. Models of soil compaction due to traffic and their evaluation. *Soil & Tillage Research*, **67**, 41–64.
- Diserens, E., 2002. Ermittlung der Reifen-Kontaktfläche im Feld mittels Rechenmodell. *FAT-Berichte Nr.*, **582**, 12.
- Diserens, E., 2009. Calculating the A of trailer tyres in the field. *Soil & Tillage Research*, **103**, 302–309.
- Diserens, E., and Steinmann, G., 2002. Calculation of pressure distribution in moist arable soils in eastern Switzerland: a simple model approach for the practice. In Vulliet, L., Laloui, L., and Schrefler, B. (eds.), *Environmental Geomechanics*. Monte Verita: EPFL Press, pp. 413–421.
- Diserens, E., Chanet, M., and Marionneau, A., 2010. Machine Weight and Soil Compaction: TASC V2.0.xls – a Practical Tool for Decision-Making in Farming. AgEng2010 – Clermont-Ferrand, 6–8 of september, Proceedings, Ref: 239, 1–10.
- Döll, H., 1999. Lohnen Zwillingsräder an Mähdreschern? *Landwirtschaft ohne Pflug*, Sonderaufgabe Agritechnica, 6–8.
- Eichhorn, H., 1999. *Landtechnik* 7. Auflage Ulmer Verlag, 688 pp.

- Grecenko, A., 1995. Tyre footprint area on hard ground computed from catalogue value. *Journal of Terramechanics*, **32**(6), 325–333.
- Gregory, A. S., Watts, C. W., Whalley, W. R., Kuan, H. L., Griffiths, B. S., Hallett, P. D., and Whitmore, A. P., 2007. Physical resilience of soil to field compaction and the interactions with plant growth and microbial community structure. *European Journal of Soil Science*, **58**, 1221–1232.
- Heinonen, M., Alakukku, L., and Erkki, A., 2002. Effects of reduced tillage and light tractor traffic on the growth and yield of oats. In Pagliai, M., and Jones, R. (eds.), *Sustainable Land Management-Environmental Protection*. Reiskirchen: Catena Verlag. Advances in Geocology, Vol. 35, pp. 367–378.
- Horn, R., Domzal, H., Slowinska-Jurkiewicz, A., and van Ouverkerk, C., 1995. Soil compaction processes and their effects on the structure of arable soils and the environment. *Soil & Tillage Research*, **35**(2–3), 277–304.
- Inns, F. M., and Kilgour, J., 1978. *Agricultural tyres*. Dunlop: London, 69 p.
- Jones, R. J. A., 2002. Assessing the Vulnerability of Soils to Degradation. In Pagliai, M., and Jones, R. (eds.), *Sustainable Land Management-Environmental Protection*. Reiskirchen: Catena Verlag. Advances in Geocology, Vol. 35, pp. 33–44.
- Keller, T., 2005. A model for the Prediction of the A and the Distribution of Vertical Stress below Agricultural Tyres from Readily Available Tyre Parameters. *Biosystems Engineering*, **92**(1), 85–96.
- McKyes, E., 1985. Soil cutting and tillage. *Developments in Agricultural Science*, Amsterdam, Netherlands: Elsevier, 7, pp. 217.
- O'Sullivan, M. F., Henshall, J. K., and Dickson, J. W., 1999. A simplified method for estimating soil compaction. *Soil & Tillage Research*, **49**, 325–335.
- Rempfer, M., 1998. Grundlagen der automatischen Reifenluftdruckverstellung bei landwirtschaftlichen Fahrzeugen. *Agrartechnische Forschung*, **4**(1), 46–55.
- SchjØnning, P., Lamandé, M., TØgeersen, F. A., Arvidsson, J., and Keller, T., 2008. Modelling effects of tyre inflation pressure on the stress distribution near the soil-tyre interface. *Biosystems Engineering*, **99**, 119–133.
- Schlotter, V., and Kutzbach, H. D., 2001. Innenkontour eines Traktorreifens auf festem und nachgiebigem Boden. *Agrartechnische Forschung*, **7**, 23–27.
- Schwieger, H., 1996. Untersuchung neuartiger Laufwerke und lasergestützte Erfassung der Reifen-/Bodenverformung. Forschungsbericht Agrartechnik des Arbeitskreises Forschung und Lehre der Max-Eyth-Gesellschaft Agrartechnik (VDI-MEG) Dissertation Kiel, 165 p.
- Smith, D. L. O., 1985. Compaction by wheels: a numerical model for agricultural soils. *Journal of Soil Science*, **36**, 621–632.
- Söhne, W., 1953. Druckverteilung im Boden und Bodenverformung unter Schlepperreifen. *Grundlagen der Landtechnik*, **5**, 49–62.
- Steiner, M., 1979. Analyse, Synthese und Berechnungsmethoden der Triebkraft-Schlupf-Kurve von Luftreifen auf nachgiebigem Boden. Forschungsbericht Agrartechnik des Arbeitskreises Forschung und Lehre der Max-Eyth-Gesellschaft (MEG) 33. Dissertation München, 190 p.
- van den Akker, J. J. H., 1998. Development, verification and use of the subsoil compaction model Socomo. In *Proceedings of the 1st Workshop of the Concerted Action on Subsoil Compaction*, May 28–30, Wageningen, the Netherlands, 17 p.

Cross-references

- Controlled Traffic Farming
 Hardpan Soils: Management
 Machine Vision in Agriculture
 Mechanical Resilience of Degraded Soils
 Physical Degradation of Soils, Risks and Threats

Rheology in Soils
 Soil Compatability and Compressibility
 Soil Penetrometers and Penetrability
 Soil-Wheel Interactions
 Stress–Strain Relations
 Stress–Strain Relationships: A Possibility to Quantify Soil Strength Defined as the Precompression Stress
 Subsoil Compaction
 Tillage, Impacts on Soil and Environment
 Trafficality and Workability of Soils

CONTINUITY EQUATION

A statement, in mathematical form, that for a conserved substance (i.e., one, such as water, that is neither created nor destroyed in the soil), the time rate of change of content must equal the negative rate of the change of flux with distance (i.e., the amount per unit time entering minus the amount exiting a volume element of soil).

Bibliography

Introduction to Environmental Soil Physics. (First Edition). 2003. Elsevier Inc. Daniel Hillel (ed.) <http://www.sciencedirect.com/science/book/9780123486554>

CONTOUR-FURROW IRRIGATION

Applying irrigation water in furrows that run across the slope with a forward grade in the furrows.

Cross-references

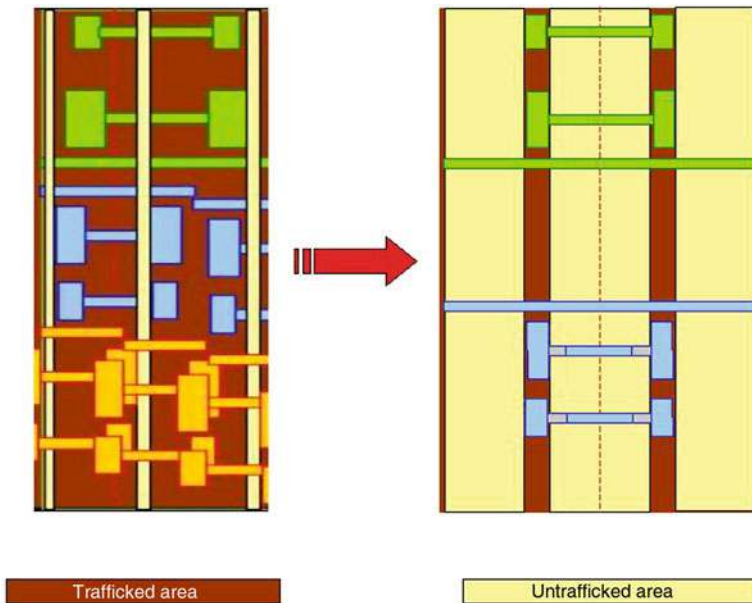
- Irrigation and Drainage, Advantages and Disadvantages
 Irrigation with Treated Wastewater, Effects on Soil Structure

CONTROLLED TRAFFIC FARMING

Thomas Anken, Martin Holpp
 Federal Department of Economic Affairs, Agroscope Reckenholz-Tänikon Research Station ART, Ettenhausen, Switzerland

Definition

Controlled traffic farming (CTF) is a farming system where all field traffic is restricted to permanent, distinct parallel traffic lanes (Figure 1). These traffic lanes are normally untilled and not planted to optimize traction and traffic ability. Soil in the intervening beds is managed to provide the most favorable conditions for crop performance uncompromised by traffic and associated compaction (Tullberg, 2001).



Controlled Traffic Farming, Figure 1 In contrast to random traffic system where the working widths are not adjusted, all the machines are running on the same tracks with a controlled traffic farming system.



Controlled Traffic Farming, Figure 2 In 1983, the first trials have been started with a widespan Gantry vehicle at the Silsoe Research Institute in the UK.

History

The first CTF research projects started with a widespan Gantry in 1983 at the Silsoe Research Institute in the United Kingdom (Chamen et al., 1992). This vehicle had a 12-m-wide track. In the field, the drive wheels were positioned

at right angles to the lateral axis of the frame. On the road, the wheels were positioned parallel to the frame (Figure 2). Compared to the tracked surfaces, Chamen et al. (1992) already observed in these first experiments increased yields and an important decrease in fuel consumption for the

tillage operation and an improvement of the soil structure on the untrafficked area. In spite of good results, the gantry system did not make the breakthrough. This changed in the 1990s in Australia, where CTF was applied with conventional machinery. The increased working widths of the machines and satellite guidance systems made it possible to practice CTF without wide-span vehicles. Yule (2000) estimated for Australia in 1995 a surface of 3,000 ha and already 300,000 ha in year 2000. In 2009, about 3 million hectares were estimated in Australia (Tullberg, 2009). This shows that Australia is by far the leading nation. First initiatives in Europe have been started by Great Britain, Denmark, the Netherlands, Switzerland, Germany, Czech Republic, and Slovak Republic. In contrast to the overseas countries where track width of 3 m are very common, the European countries are practicing CTF mostly with smaller track width. This is due to road regulations which are not allowing vehicles wider than 2.55 m to run on the roads.

Advantages of CTF

- Better soil structure which leads to less fuel consumption for tillage operations. As less power is needed, it is possible to decrease the tractor sizes.
- Increased yields due to the improved soil conditions.
- Better water infiltration and decreased soil erosion due to undestroyed open soil pores (earthworm burrows, cracks).
- Better traffic ability on the consolidated tracks what widens the possibilities for plant protection interventions under wet soil conditions.
- Better nutrient availability due to the better soil structure and improved gas exchange. First results are showing that also the emission of nitrous oxide (Ball et al., 1999) might be reduced.

Inconveniences of CTF

- Field operations can only be executed with adapted equipment.
- Once a track system has been chosen, this system has to be applied during the following years. All the machines have to fit into this system.
- In case of a damaged machine, the exchange with another machine may cause a problem as the replaced machine has to fit into the chosen working and track width.
- Auto steering systems are causing extra costs.
- As traffic over the field is only possible on the defined tracks, the transportation of harvested crops is more time consuming (no shortcuts across the field are possible anymore).
- Sugar beet and potato harvester are not easy to fit into a CTF pattern as their working widths are small and the weights are extremely high. Machineries like the multiphase system for the sugar beet harvest have to be adapted.

Web sites

- www.ctfeurope.com
www.controlledtrafficfarming.com
<http://www.ctf-swiss.ch/>

Bibliography

- Ball, B. C., Parker, J. P., and Scott, A., 1999. Soil and residue management effects on cropping conditions and nitrous oxide fluxes under controlled traffic in Scotland. 2. Nitrous oxide, soil N status and weather. *Soil and Tillage Research*, **52**, 191–201.
- Chamen, W. C. T., Watts, C. W., Leede, P. R. u., and Lonstaff, D. J., 1992. Assessment of a wide span vehicle (gantry), and soil cereal crop responses to its use in a zero traffic regime. *Soil and Tillage Research*, **24**, 359–380.
- Tullberg, J., 2001. Controlled traffic for sustainable cropping. In *Proceedings of the 10th Australian Agronomy Conference*, 28.01–01.02., Hobart, Tasmania, 10 p.
- Tullberg, J., 2009. Brisbane, Oral information.
- Yule, D., 2000. Controlled traffic farming - technology for sustainability. *Proceedings of the 15th Conference of the International Soil Tillage Research Organization*, 2–7 July, Fort Worth, Texas, USA, 8 p.

Cross-references

- [Bypass Flow in Soil](#)
[Crop Responses to Soil Physical Conditions](#)
[Earthworms as Ecosystem Engineers](#)
[Infiltration in Soils](#)
[Root Responses to Soil Physical Limitations](#)
[Soil–Wheel Interactions](#)
[Water Erosion: Environmental and Economical Hazard](#)

CONVENTIONAL TILLAGE

See [Tillage, Impacts on Soil and Environment](#)

COULOMB'S LAW

The frictional resistance toward a tangential stress tending to slide one surface against another is proportional to the normal stress pressing the bodies together.

COUPLED HEAT AND WATER TRANSFER IN SOIL

Joshua L. Heitman¹, Robert Horton²

¹Soil Science Department, North Carolina State University, Raleigh, NC, USA

²Agronomy Department, Iowa State University, Ames, IA, USA

Synonyms

Coupled heat and water transfer in soil is sometimes referred to more generically as coupled heat and mass transfer or coupled energy and mass transfer.

Definition

Coupled heat and water transfer in soil refers to the connected processes of heat and water flow in and through the three-phase (i.e., solid, liquid, and gas) soil system, where heat may be latent and/or sensible and water may be liquid and/or vapor. The processes are coupled because water moving through the soil system always carries with it heat, i.e., convective heat transfer, and temperature differences in the soil system, which also drive heat transfer and water flow. Furthermore, soil water content influences soil thermal properties (e.g., heat capacity, thermal conductivity, and thermal diffusivity), and even the extent to which the soil surface absorbs radiant energy (i.e., albedo) for radiative heat transfer. The soil thermal environment, in turn, influences the extent to which water partitions between liquid and vapor phases.

Coupled heat and water transfer in soil

Background and applications

Coupled heat and water transfer is commonplace in nature and has long been recognized (e.g., Bouyoucos, 1915). When it rains both water and heat enter the soil. As the sun rises and warms the soil surface, the resultant water vapor pressure deficit drives water vapor movement in the soil. This water vapor carries with it both sensible and latent heats, which are transferred through the soil to the atmosphere. As the sun begins to set, the soil surface cools and water vapor from the atmosphere condenses on the soil, losing latent heat through phase change. This liquid water is adsorbed on surfaces due to affinity between solid and liquid or liquid and liquid, and the water may move deeper into the soil profile. In either case, the water carries heat into the soil system by replacing soil air with lower enthalpy per unit volume. This diurnal cycle is present to greater and lesser extents in terrestrial environments worldwide. Annual seasonal cycles occur as well.

Temperature gradients exist in soil due to periodicity of insolation, geothermal temperature distributions, functioning of buried cables, heating and cooling pipes, etc. Existence of temperature gradients causes fluxes of heat and water in soil. All soil biological, chemical, and physical processes are influenced by the fluctuations of soil water content and soil temperature that result from coupled heat and water transfer processes. Coupled heat and water processes occurring in shallow surface soil also exert critical influences on land–atmosphere exchange and drive climate dynamics. Yet, because surface soil is the most dynamic portion of the geosphere, full understanding of these processes remains elusive. Early field experiments provided the first opportunity to observe temporal patterns in near-surface soil moisture and temperature (e.g., Jackson, 1978). Since then, soil-coupled heat and water processes have been parameterized in large-scale models, often with limited appreciation for ubiquitous order-of-magnitude variations in hydrologic and thermal properties within the surface few centimeters of

soil. Routine measurements are also unable to capture rapidly shifting near-surface soil heat and water processes. Still, soil remains so central to understanding life that the 2007 Phoenix Mars Mission included devices specifically designed to measure soil temperature, thermal properties, and water content (Cobos et al., 2006).

Improved insight into coupled heat and water transfer is needed as a basis for more complete understanding of soil water and temperature conditions, soil water evaporation, crop and weed seed germination, nutrient cycling, pesticide volatilization, surface fluxes of carbon dioxide, and trace gas emissions from soil. Improved understanding of coupled heat and water transfer is also fundamental to understanding of the interaction between climate and the near-surface soil environment, as well as the implications of climate change.

Transfer mechanisms

Three principal mechanisms, radiation, convection, and conduction, are responsible, simultaneously, for the transfer of heat in soil. Radiative energy transfer includes incoming direct and diffuse solar (shortwave) radiation as well as longwave sky radiation to the soil surface and longwave radiation emitted outward from the soil surface. Radiative transfer is a significant component of heat transfer at the soil surface, but its significance decreases below the soil surface. Convective heat transfer in soil is associated with a net flux of fluids (liquid and gas). Convection may be responsible for a major portion of the soil heat transfer during periods of large water flux (e.g., during rainfall or irrigation). Convection is also important via vapor fluxes in shallow unsaturated soil layers when large thermal gradients occur. Conduction heat transfer involves the transfer of heat at a molecular scale from positions of large kinetic energy (high temperature) to positions of small kinetic energy (low temperature). Generally, radiative heat transfer primarily occurs at the surface. Convection and conduction occur within soil. In soil, conduction and convection often occur together.

For isothermal water transfer, we typically consider two driving forces: the chemio-potential gradient of soil water and gravity. Refer to [Water Flow](#) for further description. For non-isothermal water transfer, temperature gradients also act as a driving force. Soil moisture transfer induced by a temperature gradient is called thermal moisture transfer (TMT). The flow resulting due to interaction of TMT with moisture flow induced by factors other than temperature gradient is called *non-isothermal moisture transfer* (NIMT) (Globus, 1983). TMT can be vapor, liquid, and combined (series-parallel). For unsaturated conditions, where we have both liquid and vapor components of water, this leads to two additional components of flow, thermal vapor transfer and thermal liquid transfer.

Thermal vapor transfer results mainly from the dependence of water vapor pressure (or concentration) on temperature. As temperature increases, water vapor pressure increases. Thus, a temperature gradient leads to a water

vapor gradient. Treated as diffusion, this temperature gradient drives thermal vapor transfer toward cooler temperature. Like diffusion, thermal vapor transfer depends on the diffusion path and therefore liquid-free porosity and tortuosity, which are in turn related to soil texture, structure, and bulk density.

Liquid TMT can occur by several mechanisms: (1) Expansion and contraction of entrapped air due to temperature change pushes liquid back and forth in nearly saturated soil, for example, in the capillary fringe and near the groundwater table. This is called the *thermomeric effect*, and it is transient. (2) Due to temperature dependence of surface tension at a liquid–air interface, a temperature gradient induces a gradient of surface tension and a respective gradient of capillary pressure of menisci. This can induce hydrodynamic flow just the same as under the influence of a pressure difference of any other origin. This is called the *thermo-capillary meniscous* flow. (3) When a thermal gradient exists along the liquid–air interface of a liquid film covering solid particle(s), the induced surface tension gradient produces *thermocapillary film* flow. The velocity profile of this flow (as a function of distance to solid phase) differs from that of hydraulic flow, since the moving force is applied only to the interface. Both thermocapillary flows are directed toward lower temperature. (4) When enthalpy of pore liquid differs from that of bulk liquid, and, particularly, when there exists some distribution of enthalpy as a function of distance to the solid phase, *thermoosmotic* flow can occur. Thermoosmotic flow directs toward higher temperature. (5) In unsaturated soil, there exists a special *vapor–liquid series-parallel* (or *combined*) TMT, consisting of thermal vapor micro-diffusion inside air space of a pore, combined with liquid flow in capillary and film elements of soil matrix. Because of its dual nature, this flow bears features appropriate both to vapor diffusion as well to liquid flow. For example, it depends upon ambient gas pressure P as vapor diffusion (diminishing with rise of P) and on wettability of a medium (liquid flow diminishes in hydrophobic media).

One particular case of moisture migration in soil under the influence of a temperature gradient is the movement of moisture in soils induced by freezing. This process is often described as TMT, where the driving force is formally represented by the temperature gradient. However, actual water flow in this case is caused by the gradient of chemical potential of water, which arises due to locally reduced liquid water content at and behind the freezing front after soil water freezes. Differences in unfrozen water content create differences in matric potentials. So in this case, it would be proper to substitute temperature gradient by hydrostatic pressure gradient.

Transfer theory

Much of the current theory for describing coupled soil heat and water transfer is rooted in the diffusion-based formulation of Philip and de Vries from the 1950s and 1960s

(Philip and de Vries, 1957; de Vries, 1958), which treats gradients in soil water content and temperature (as well as gravity) as the drivers for liquid flow. This theory has since been modified by others to include the chemopotential gradient in water as a driver for water flow (in place of the water content gradient) (Sohocleous, 1979; Milly, 1982). Alternate theory rooted in irreversible thermodynamics has also been developed (Cary, 1963; Taylor and Cary, 1964) but has mostly been applied treating soil water as a single-component fluid.

Here, we present a mechanistic framework following Philip and de Vries (1957), Milly (1982), and Nassar et al. (1992). The following theory assumes (1) the soil is rigid and inert; (2) hysteresis of water retention curves and transport coefficients can be neglected; (3) transfer of mass and energy occurs only in the vertical direction; (4) the driving forces for water are temperature and matric pressure head gradients and gravity; (5) osmotic potential is negligible; (6) there is local thermodynamic equilibrium within the soil; and (7) heat transfer occurs by conduction and by convection of latent heat and sensible heat.

Water flow

The total flux of water in the soil is the sum of liquid and vapor components

$$q_w = q_l + q_v, \quad (1)$$

where q_w , q_l , and q_v ($\text{kg m}^{-2} \text{s}^{-1}$) are the mass flux of water (total), liquid, and vapor, respectively. In saturated soil, q_v becomes negligible, whereas in relatively dry systems, q_v may be the dominant flux.

The liquid water flux q_l can be described as

$$q_l/\rho_l = -K \frac{\partial \psi}{\partial z} - K \mathbf{k} - D_{Tl} \frac{\partial T}{\partial z}, \quad (2)$$

where ρ_l (kg m^{-3}) is the liquid water density, K (m s^{-1}) is hydraulic conductivity, ψ (m) is the matric potential, z (m) is the vertical space coordinate, \mathbf{k} is a unit vector positive downward, D_{Tl} ($\text{m}^2 \text{s}^{-1} \text{K}^{-1}$) is the thermal liquid diffusivity, and T (K) is temperature. The first two terms on the right represent the classical Darcy–Buckingham flow, driven by the matric potential and elevation (viz. gravity) gradients. See Water Flow for further discussion. The third term on the right represents liquid flux driven by a thermal gradient. A consensus on the formulation of D_{Tl} has not arisen in the literature (Prunty, 2009), but it can be loosely defined according to the mechanisms described in the previous section (viz. temperature effects on liquid water properties). Note also that the temperature effects on liquid flux are sometimes included in the formulation of K via fluid properties (e.g., viscosity).

The water vapor flux q_v is treated as simple diffusion

$$q_v = -D \frac{\partial \rho_v}{\partial z} \quad (3)$$

where ρ_v (kg m^{-3}) is the water vapor density and D ($\text{m}^2 \text{s}^{-1}$) is an effective molecular diffusivity.

In order to express q_v in terms of the same drivers given in [Equation 2](#), ρ_v is appropriately treated as a function of ψ and T . Note that gravity influences on q_v are generally ignored. Expanding ρ_v with respect to ψ and T gives

$$\frac{\partial \rho_v}{\partial z} = \frac{\partial \rho_v}{\partial \psi} \frac{\partial \psi}{\partial z} + \frac{\partial \rho_v}{\partial T} \frac{\partial T}{\partial z}. \quad (4)$$

Combining this expression with [Equation 3](#) then gives

$$q_v = -D \frac{\partial \rho_v}{\partial \psi} \frac{\partial \psi}{\partial z} - D \eta \frac{\partial \rho_v}{\partial T} \frac{\partial T}{\partial z}. \quad (5)$$

Here, consistent with many formulations in the literature, we add an additional term η , which has been proposed to account for increased vapor flux due to locally enhanced thermal gradients across air gaps (viz. air-filled pores) within the three-phase medium (Cass et al., 1984). [Equation 5](#) can then be simplified to

$$q_v / \rho_l = -D_{\psi v} \frac{\partial \psi}{\partial z} - D_{T v} \frac{\partial T}{\partial z}, \quad (6)$$

where $D_{\psi v}$ ($\text{m}^2 \text{s}^{-1}$) and $D_{T v}$ ($\text{m}^2 \text{s}^{-1} \text{K}^{-1}$) are termed the matric vapor and thermal vapor diffusivities, respectively, defined implicitly by [Equation 5](#). We divide here by ρ_l so that $D_{\psi v}$ and $D_{T v}$ provide volume fluxes equivalent to transport terms defined in [Equation 2](#) for liquid water.

Total mass of water in the soil system is the sum of the liquid and vapor mass components

$$\theta_l \rho_l + \theta_v \rho_v,$$

where θ ($\text{m}^3 \text{m}^{-3}$) is the volume fraction of the total soil volume occupied by a given component and subscripts are as defined previously. We assume all soil pore space is occupied either by liquid water or water vapor such that $\theta_l + \theta_v =$ the pore (or void) fraction of the total soil volume. Therefore, as θ_l increases, θ_v must proportionately decrease.

Using conservation of mass, the continuity equation can be expressed as

$$\frac{\partial}{\partial t} (\theta_l \rho_l + \theta_v \rho_v) = \nabla q_w, \quad (7)$$

where t (s) is time. In words, the change in water mass per soil volume with time is equal to the gradient in water mass flux. Expanding the left side of [Equation 7](#), using the dependency of ρ_v on ψ and T noted above and also the functional relationship between θ and ψ , we have

$$\begin{aligned} \rho_l \frac{\partial \theta_l}{\partial t} + \rho_v \frac{\partial \theta_v}{\partial t} + \theta_v \frac{\partial \rho_v}{\partial \psi} \frac{\partial \psi}{\partial \theta_l} \frac{\partial \theta_l}{\partial t} \\ + \theta_v \frac{\partial \rho_v}{\partial T} \frac{\partial T}{\partial t} = \nabla q_w. \end{aligned} \quad (8)$$

Finally, incorporating [Equations 1](#), [2](#), and [6](#), we have a general partial differential equation to describe transient water flow for unsaturated, nonisothermal conditions:

$$\begin{aligned} & \left(1 + \frac{\theta_v}{\rho_l} \frac{\partial \rho_v}{\partial \psi} \frac{\partial \psi}{\partial \theta_l} - \frac{\rho_v}{\rho_l} \right) \frac{\partial \theta_l}{\partial t} + \frac{\theta_v}{\rho_l} \frac{\partial \rho_v}{\partial T} \frac{\partial T}{\partial t} \\ &= \nabla \left[(K + D_{\psi v}) \frac{\partial \psi}{\partial z} + (D_{T l} + D_{T v}) \frac{\partial T}{\partial z} + Kk \right]. \end{aligned} \quad (9)$$

Note that we have divided all terms by ρ_l and used the relationship between θ_l and θ_v to replace $\partial \theta_v / \partial t$ with $-(\partial \theta_l / \partial t)$ in order to simplify the expression.

Heat flow

Ignoring radiation within the soil, the total flux of heat in the soil system is the sum of conduction heat transfer and both latent and sensible heat transfer via convection:

$$q_h = -\lambda \frac{\partial T}{\partial z} - \rho_l L D_{\psi v} \frac{\partial \psi}{\partial z} + c_l (T - T_0) q_w, \quad (10)$$

where q_h (W m^{-2}) is the total heat flux, λ ($\text{W m}^{-1} \text{K}^{-1}$) is the thermal conductivity of the soil, L (J kg^{-1}) is latent heat of vaporization, c_l ($\text{J kg}^{-1} \text{K}^{-1}$) is the specific heat of liquid water, and T_0 (K) is an arbitrary reference temperature. The first term on the right is simple Fourier conduction heat transfer, and λ is dependent on water content and temperature. The remaining terms on the right represent heat carried with the nonstationary component of the soil system – water. The first of these terms is diffusion of water vapor, with associated latent heat from phase change, according to the matric potential gradient. The diffusion vapor flux is a component of the flux given in [Equation 6](#). The rightmost term in [Equation 10](#) is the convective transfer of sensible heat associated with the mass water flux. Because the water flux is on a mass rather than a volume basis, it is appropriate to consider the specific heat of the liquid to determine the associated heat transfer. However, the quantity of heat must be determined by specifying some reference state $c_l T_0$.

The total heat stored (relative to the reference state) in the three-phase soil system includes both sensible and latent components:

$$(c_s \rho_b + c_l \rho_l \theta_l + c_v \rho_v \theta_v) (T - T_0) + L \rho_v \theta_v,$$

where c_s ($\text{J kg}^{-1} \text{K}^{-1}$) is the specific heat of the solid, ρ_b (kg m^{-3}) is the soil bulk density (mass of solid per total soil volume), and c_v ($\text{J kg}^{-1} \text{K}^{-1}$) is the specific heat of the vapor.

Using conservation of energy

$$\begin{aligned} \frac{\partial}{\partial t} [(c_s \rho_b + c_l \rho_l \theta_l + c_v \rho_v \theta_v) (T - T_0) \\ + L \rho_v \theta_v] = \nabla q_h. \end{aligned} \quad (11)$$

This is to say, the change in the quantity of heat stored per volume with time is equal to the gradient in total heat flux. The left side of this expression can be expanded in terms T and θ_l using previously discussed relationships for ρ_v and ψ with T and between θ and ψ

$$H_1 \frac{\partial T}{\partial t} + H_2 \frac{\partial \theta_l}{\partial t} = \nabla q_h, \quad (12)$$

where

$$\begin{aligned} H_1 &= C_b + [L + c_v(T - T_0)] \theta_v \frac{\partial \rho_v}{\partial T}, \\ H_2 &= [L + c_v(T - T_0)] \theta_v \frac{\partial \rho_v}{\partial \psi} \frac{\partial \psi}{\partial \theta} \\ &\quad + c_l \rho_l (T - T_0) - \rho_v [L + c_v(T - T_0)] - W \rho_l. \end{aligned}$$

The expression is simplified by considering a bulk volumetric heat capacity C_b ($\text{J m}^{-3} \text{K}^{-1}$) in place of the sum $c_s \rho_v + c_l \rho_l \theta_l + c_v \rho_v \theta_v$. We here also add an additional term W (J kg^{-1}) to account for the exothermic process of wetting the porous medium with changes in water content (Prunty, 2002).

Finally, combining Equations 10 and 12, we can describe transient heat flow in unsaturated, nonisothermal soil:

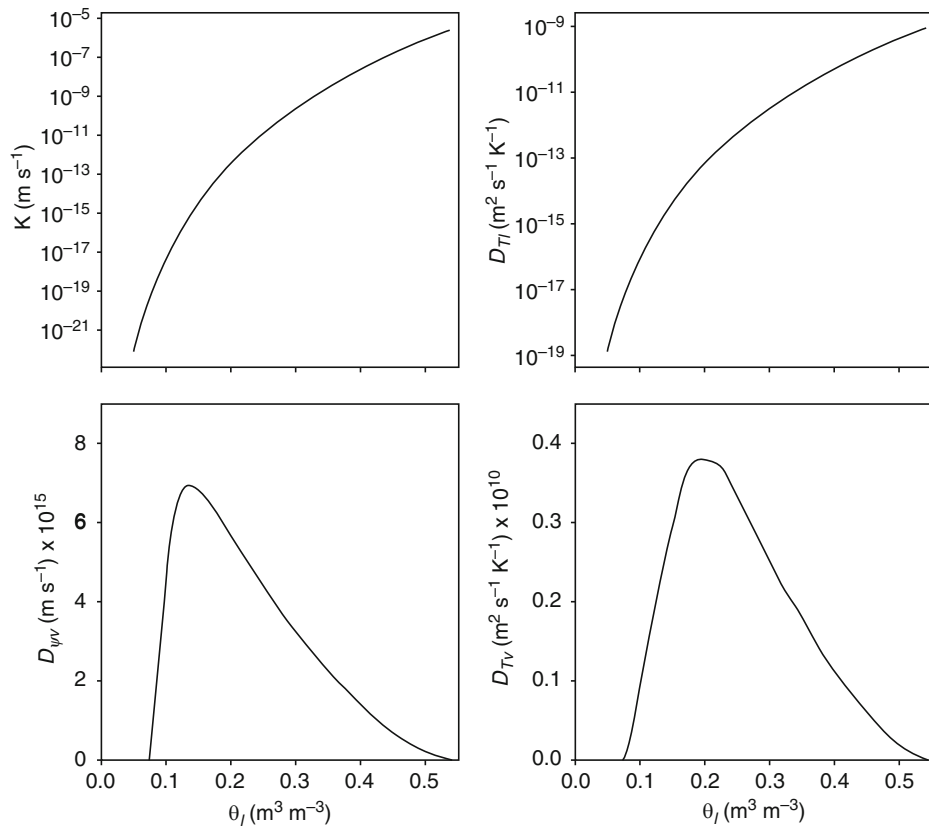
$$\begin{aligned} H_1 \frac{\partial T}{\partial t} + H_2 \frac{\partial \theta_l}{\partial t} &= \nabla \left[\lambda \frac{\partial T}{\partial z} + \rho_l L D_{\psi v} \frac{\partial \psi}{\partial z} \right. \\ &\quad \left. - c_l (T - T_0) q_w \right]. \end{aligned} \quad (13)$$

The q_w term in Equation 13 can be further expanded using Equations 1, 2, and 6.

Transfer coefficients for convective heat transfer

Insight about the relative magnitudes of liquid and vapor flux components for convective heat transfer is critical to understanding coupled heat and water transfer. Theory presented above provides a way to envision ψ and T gradients as drivers for these flux components. It is also important to recognize how the magnitudes of liquid and vapor fluxes vary with associated transfer coefficients, which greatly depend on, among other things, the soil water content (Nassar and Horton, 1997).

Figure 1 presents moisture transfer coefficients K , D_{Tl} , $D_{\psi v}$, and D_{Tv} as a function of θ_l for a silt loam soil over the range from completely dry to saturation (after Heitman



Coupled Heat and Water Transfer in Soil, Figure 1 Hydraulic conductivity (K), thermal liquid diffusivity (D_{Tl}), isothermal vapor diffusivity ($D_{\psi v}$), and thermal vapor diffusivity (D_{Tv}) as a function of soil liquid water content (θ_l). Transfer coefficients are based on the properties of a silt loam soil.

et al., 2008a). Several points are readily apparent: at very low water contents, convection through either liquid or vapor is minimal, as evidenced by the small magnitudes of all four transfer coefficients. When liquid water is absent or water content is very small, conduction must be the dominant mechanism for heat transfer. As water content begins to increase, all transfer coefficients increase, but the most pronounced increase is for vapor coefficients $D_{\psi v}$, and D_{Tv} . In this range, air-filled porosity remains high so as to readily allow diffusion (with rate also depending on drivers). Hence, while conduction may remain important, heat transfer may also occur with convection via vapor, particularly latent heat. As liquid water content continues to increase and air-filled porosity is diminished, $D_{\psi v}$, and D_{Tv} then decline. However, liquid transfer coefficients K and D_{Tl} continue to increase over the whole range in θ_l . Because liquid water carries with it only sensible heat, and because the vapor flux is limited, convection in wet soil occurs primarily as sensible heat alone.

Recent developments in measurement of latent heat fluxes

Measurement of all component fluxes for fully coupled heat and water transfer remains a challenging task (Jury and Lettley, 1979; Cahill and Parlange, 1998; Heitman et al., 2007). Soil heat flux measurement is typically limited to conduction heat flux via soil heat flux plates or other methods. See *Energy Balance of Ecosystems*. Liquid water flux has routinely been estimated from mass balance or by utilizing measured soil water potential and knowledge of the soil hydraulic conductivity function. See *Soil Water Flow*. Measurement of water vapor and latent heat flux has mostly been limited to above-ground approaches or gross estimates from weighing lysimeters. See *Lysimeters: A Tool for Measurements of Soil Fluxes*. However, a new technique has recently been developed to provide measurements of latent heat fluxes within the soil (Heitman et al., 2008b, c). This technique involves measuring the balance of sensible heat terms included in coupled heat and water transfer.

The basis for this approach begins with an approximation of [Equation 13](#) for a finite size soil volume and finite time increment. For short time steps (e.g., a few hours), we assume that only temperature T changes with time t on the left side of [Equation 13](#). We then take a single, measured heat capacity C_b to represent the soil. In making this assumption, we treat liquid and vapor concentrations as constant. While origination of the latent heat flux (viz. evaporation) within the soil volume does mean that liquid water is being changed to vapor, the net change in liquid and vapor content has a small influence on sensible heat storage. Exiting water vapor from within the soil volume is readily replaced by evaporation of small quantities of liquid water so that for a small time step, there is little net change in either vapor or liquid water contents in terms of their impact on C_b (for either component) or latent heat storage (for water vapor).

To complete the heat balance, we also must approximate the heat flux terms included in the right side of [Equation 13](#). It is possible to measure the conduction heat flux $-\lambda \partial T / \partial z$ by standard approaches. To approximate the gradient in conduction heat flux $\nabla(\lambda \partial T / \partial z)$ across the soil volume, $-\lambda \partial T / \partial z$ must be measured at multiple depths (the vertical boundaries for the soil volume of interest). In unsaturated conditions, where the soil latent heat flux is of significant magnitude, liquid mass flux and associated convective sensible heat transfer are relatively minor (as discussed in the previous section). The mass flux and thereby associated convective sensible heat flux with water vapor is also small, because of water vapor's relatively low heat capacity. Thus, the rightmost term of [Equation 13](#) is neglected. These assumptions lead to an approximate heat balance for the soil:

$$C_b \frac{\partial T}{\partial t} \simeq \nabla \left[\lambda \frac{\partial T}{\partial z} + \rho_l L D_{\psi v} \frac{\partial \psi}{\partial z} \right]. \quad (14)$$

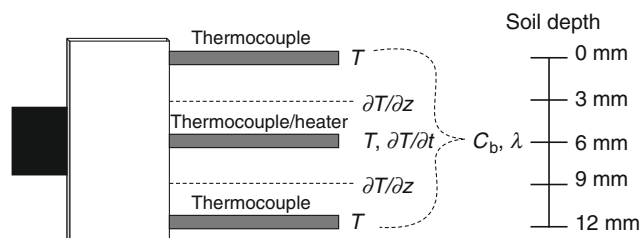
In this balance, only the latent heat flux associated with diffusion of water vapor is not directly measurable. However, by knowing the change in sensible heat storage and the gradient in conductive heat flux, this term can be determined as a residual to the heat balance. In practice, we represent this balance as

$$(G_0 - G_1) - \Delta S = LE, \quad (15)$$

where G_0 and G_1 (W m^{-2}) represent the heat fluxes ($-\lambda \partial T / \partial z$) at the upper and lower boundaries of our finite depth increment dz , respectively, ΔS (W m^{-2}) represents the change in sensible heat storage ($C_b \partial T / \partial t$) within dz , and E ($\text{kg m}^{-2} \text{s}^{-1}$) is the evaporation rate corresponding to the diffusion of water vapor within dz .

Changes in T and thermal properties (C_b and λ) with t and z form the basis of this approach. This information is required at the millimeter scale in order to account for penetration of the drying front and associated latent heat fluxes within the soil. The recent development of heat-pulse sensors ([Figure 2](#)) makes it possible to measure all of the required terms at a fine depth scale.

Heat-pulse sensors consist of three small (1.3-mm-diameter) needles. One needle contains a resistance heater



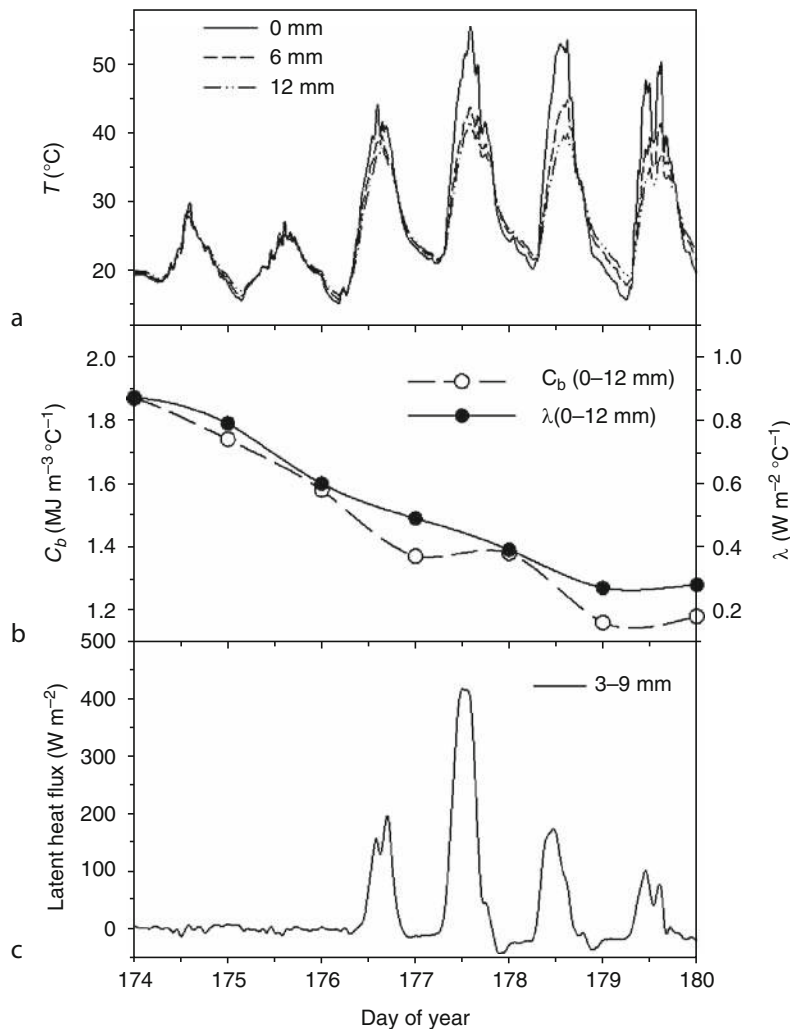
Coupled Heat and Water Transfer in Soil, Figure 2 Heat-pulse sensor as used for measurement of the soil sensible heat balance. Abbreviations are temperature (T), distance (z), time (t), volumetric heat capacity (C_b), and thermal conductivity (λ). The diagram is not to scale.

for applying a small heat input, while the remaining needles contain thermocouples (or thermistors) for measuring temperature response at a fixed distance (typically 6 mm) from the heater. The temperature response can be evaluated to determine C_b and λ . The temperature sensing needles can also be used to passively determine ambient temperature conditions within the soil in order to track temperature changes with time and depth ($\partial T/\partial t$ and $\partial T/\partial z$). [Figure 2](#) illustrates how parameters are collected by the sensor for calculation of the sensible components of [Equation 15](#).

Data (T , C_b , and λ) from a field experiment are shown in [Figure 3](#). These data illustrate a drying event following rainfall on day of year (DOY) 172. Here, the inter-diurnal trend in ambient T is upward at all depths as the soil dries. Drying also produces first rapid and then more gradual declines in soil water content-dependent C_b and λ .

Following the approach outlined above, these data are used for calculation of G_0 and G_1 at depths of 3 and 9 mm, respectively, and ΔS for the 3–9 mm depth increment. Then, from [Equation 15](#), we estimate the net latent heat flux LE for the 3–9 mm depth increment ([Figure 3c](#)).

Results show how the latent heat flux varies diurnally and also shifts in magnitude during the drying event ([Figure 3c](#)). The net latent heat flux for the 3–9 mm depth increment is near zero through DOY 176 with most of the latent heat flux originating in the 0–3 mm soil layer (classic Stage 1 evaporation). Thereafter, the net latent heat flux begins to grow in daily magnitude, illustrating the penetration of the drying front below the 3 mm depth. Summed over multiple depth increments, the net latent flux observed here is equivalent to the total net latent heat flux associated with water evaporation from the soil profile. Comparison of data collected with the sensible heat



Coupled Heat and Water Transfer in Soil, Figure 3 Measurements obtained with a heat-pulse sensor for computing [Equation 14](#): (a) soil temperature (T), (b) volumetric heat capacity (C_b) and thermal conductivity (λ), and (c) Latent heat flux. Data were collected in a bare soil field plot, following rainfall on day of year 172. The legends indicate distance below the soil surface.

balance method for determining the latent heat flux to lysimeters and above-ground approaches for total latent heat flux has generally been favorable.

Summary

Coupled heat and water transfer refers to the interconnectedness of heat and water transfer processes in soil. Water moving through soil carries with it heat, and soil water content influences soil thermal properties. Soil temperature gradients also drive water flow. Thus, coupling of soil heat and water transfer is a normal phenomenon in all natural and managed environments. By influencing microbial activity, plant water use, land-atmosphere exchange, and many other agrophysical processes, coupled soil heat and water transfer has implications at scales ranging from sub-millimeter to continental. These implications warrant careful consideration and study of coupled soil heat and water transfer. Coupled soil heat and water flow can be attributed to a variety of mechanisms. Convection of both sensible and latent heat serves as a primary linkage. Theory has been developed to describe mechanisms of flow. Yet, direct evaluation of the theory from measurements remains challenging, particularly evaluation of vapor flow components. Recent approaches developed to quantify latent heat fluxes within soil through use of a soil sensible heat balance offer some promise for assessing and refining theory. With new developments in measurement and continued interest from a range of scientific applications, coupled soil heat and water transfer will remain a challenging and important topic for study.

Bibliography

- Bouyoucos, G. T., 1915. Effect of temperature on the movement of water vapor and capillary moisture in soils. *Journal of Agricultural Research*, **5**, 141–172.
- Cahill, A. T., and Parlange, M. B., 1998. On water vapor transport in field soils. *Water Resources Research*, **34**, 731–739.
- Cary, J. W., 1963. An evaporation experiment and its irreversible thermodynamics. *International Journal of Heat and Mass Transfer*, **7**, 531–538.
- Cass, A., Campbell, G. S., and Jones, T. L., 1984. Enhancement of thermal water vapor diffusion in soil. *Soil Science Society of America Journal*, **48**, 25–32.
- Cobos, D. R., Campbell, G., and Campbell, C. S., 2006. Taking soil science to outer space: the thermal and electrical conductivity probe (TECP) for the Phoenix 2007 Scout Mission to Mars. Extended Abstracts, 18th World Congress of Soil Science, Philadelphia: Soil Science Society of America, CDROM.
- de Vries, D. A., 1958. Simultaneous transfer of heat and moisture in porous media. *Transactions of the American Geophysical Union*, **35**, 909–916.
- Globus, A. M., 1983. *Physics of non-isothermal soil moisture transfer*. Leningrad: Gidrometeoizdat (in Russian).
- Heitman, J. L., Horton, R., Ren, T., and Ochsner, T. E., 2007. An improved approach for measurement of coupled heat and water transfer in soil cells. *Soil Science Society of America Journal*, **71**, 872–880.
- Heitman, J. L., Horton, R., Ren, T., Nassar, I. N., and Davis, D., 2008a. Test of coupled soil heat and water transfer prediction under transient boundary conditions. *Soil Science Society of America Journal*, **72**, 1197–1207.
- Heitman, J. L., Horton, R., Sauer, T. J., and DeSutter, T. M., 2008b. Sensible heat observations reveal soil–water evaporation dynamics. *Journal of Hydrometeorology*, **9**, 165–171.
- Heitman, J. L., Xiao, X., Horton, R., and Sauer, T. J., 2008c. Sensible heat measurements indicating depth and magnitude of subsurface soil water evaporation. *Water Resources Research*, **44**, W00D05.
- Jackson, R. D., 1978. Diurnal changes in soil water content during drying. In Bruce, R., Flach, K., and Taylor, H. (eds.), *Field Soil Water Regime*. Soil Science Society of America, pp. 37–76.
- Jury, W. A., and Lettey, J., 1979. Water vapor movement in soil: Reconciliation of theory and experiment. *Soil Science Society of America Journal*, **43**, 823–827.
- Milly, P. C. D., 1982. Moisture and heat transport in hysteretic, inhomogeneous porous media: a matrix head-based formulation and a numerical model. *Water Resources Research*, **18**, 489–498.
- Nassar, I. N., and Horton, R., 1997. Heat, water, and solute transfer in unsaturated porous media: I. Theory development and transport coefficient evaluation. *Transport in Porous Media*, **27**, 17–38.
- Nassar, I. N., Globus, A. M., and Horton, R., 1992. Simultaneous soil heat and water transfer. *Soil Science*, **154**, 465–472.
- Philip, J. R., and de Vries, D. A., 1957. Moisture movement in porous materials under temperature gradients. *Transactions of the American Geophysical Union*, **38**, 222–232.
- Prunty, L., 2002. Soil water heat of transport. *Journal of Hydraulic Engineering*, **7**, 435–440.
- Prunty, L., 2009. Soil water thermal liquid diffusivity. *Soil Science Society of America Journal*, **73**, 704–706.
- Sophocleous, M., 1979. Analysis of water and heat flow in unsaturated-saturated porous media. *Water Resources Research*, **15**, 1195–1206.
- Taylor, S. A., and Cary, J. W., 1964. Linear equations for the simultaneous flow of matter and energy in a continuous soil system. *Soil Science Society of America Journal*, **28**, 167–172.

Cross-references

- [Bulk Density of Soils and Impact on Their Hydraulic Properties](#)
[Energy Balance of Ecosystems](#)
[Evapotranspiration](#)
[Hydraulic Properties of Unsaturated Soils](#)
[Lysimeters: A Tool for Measurements of Soil Fluxes](#)
[Physics of Near Ground Atmosphere](#)
[Soil Aggregation and Evaporation](#)
[Soil Hydrophobicity and Hydraulic Fluxes](#)
[Soil Phases](#)
[Soil Water Flow](#)
[Soil Water Management](#)
[Temperature Effects in Soil](#)
[Water Balance in Terrestrial Ecosystems](#)
[Water Budget in Soil](#)

CRACKING IN SOILS

Pascal Boivin
 University of Applied Sciences of Western Switzerland (HES-SO), Geneva, Switzerland

Definition

Cracking refers to the forming of cracks in soils, due to soil shrinkage upon drying. This is considered at two

different scales, namely metric scale for soil horizon or profile, and infra millimetric scale for soil matrix, respectively.

Cracks

Cracks form in soils due to the shrink–swell movements of the soil plasma occurring with changes in water content. (The plasma was first defined by Brewer (1964). According to the SSSA glossary it is: “material, mineral or organic, of colloidal size and relatively soluble material that is not contained in the skeleton grains”). The swelling factors in the plasma are the phyllosilicates and the organic matter. Hence, cracking depends of the content in these constituents. Organic matter, however, also acts as a binding element, which stabilizes the soil structure (Kay, 1998).

At microscopic scale (thin soil sections), cracking was long ago observed as a consequence of soil drying (Brewer, 1964). Cracking is one of the processes generating soil structure and allowing its resilience (Kay, 1998). Micro cracks are structural pores according to Brewer’s classification. An increase in organic carbon content of the soil may result in an increase in plasma swelling and a decrease in bulk soil swelling (Boivin et al., 2009), thus an increase in micro cracking. Microscale cracking shows no preferential orientation.

At metric scale, large cracks (up to several centimeters wide) may open in soil horizons or profiles when the shrinkage is large enough to break the horizontal continuity of the soil. The volume of cracks can be easily estimated in the field (Abidine el and Robinson, 1971). This is generally observed with clayey soils containing phyllosilicates such as vertisols. Cracking causes soil subsidence and may induce preferential flow. Soil subsidence is an anisotropic shrinkage due to vertical collapse and horizontal cracking, which was described by Bronswijk (1991). Crack preferential flow was observed in the case of irrigated cracked soils (Tuong et al., 1996) and its characterization is reviewed by (Simunek et al., 2003; Allaire et al., 2009). The closure of cracks with time upon rewetting was poorly described. However, Favre et al. (1997) showed a complete crack closure after 2.5 h of irrigation in a vertisol.

Summary and conclusions

Cracking is induced by soil plasma volume change with water content and is a major soil structure resilience factor. Microscopic cracks are not preferentially oriented and represent a large part of the structural porosity. Macroscopic cracking is a particular case corresponding to clay phyllosilicate-rich soils. These cracks show a vertical preferential orientation, which may cause preferential flow.

Bibliography

Abidine el, A. Z., and Robinson, G. H., 1971. A study on cracking in some vertisols of the Sudan. *Geoderma*, **5**, 229–241.

- Allaire, S. E., Roulier, S., and Cessna, A. J., 2009. Quantifying preferential flow in soils: A review of different techniques. *Journal of Hydrology*, **378**, 179–204.
- Boivin, P., Schaeffer, B., and Sturmy, W., 2009. Quantifying the relationship between soil organic carbon and soil physical properties using shrinkage modelling. *European Journal of Soil Science*, **60**, 265–275.
- Brewer, R., 1964. *Fabric and Mineral Analysis of Soils*. New York: Wiley.
- Bronswijk, J. J. B., 1991. Drying, cracking, and subsidence of a clay soil in a lysimeter. *Soil Science*, **152**, 92–99.
- Favre, F., Boivin, P., and Wopereis, M. C. S., 1997. Water movement and soil swelling in a dry, cracked vertisol. *Geoderma*, **78**, 113–123.
- Kay, B. D., 1998. Soil structure and organic carbon: a review. In Lal, R., Kimble, J. M., Follett, R. F., and Stewart, A. (eds.), *Soil Processes and the Carbon Cycle*. Boca Raton: CRC Press, pp. 169–197.
- Simunek, J., Jarvis, N. J., van Genuchten, M. T., and Gärdenäs, A., 2003. Review and comparison of models for describing non-equilibrium and preferential flow and transport in the vadose zone. *Journal of Hydrology*, **272**, 14–35.
- Tuong, T. P., Cabangon, R. G., and Wopereis, M. C. S., 1996. Quantifying flow processes during Land soaking of cracked rice soils. *Soil Science Society of America Journal*, **60**, 872–879.

Cross-references

- [Anisotropy of Soil Physical Properties](#)
[Bypass Flow in Soil](#)
[Shrinkage and Swelling Phenomena in Soils](#)
[Wetting and Drying, Effect on Soil Physical Properties](#)

CROP EMERGENCE, THE IMPACT OF MECHANICAL IMPEDANCE

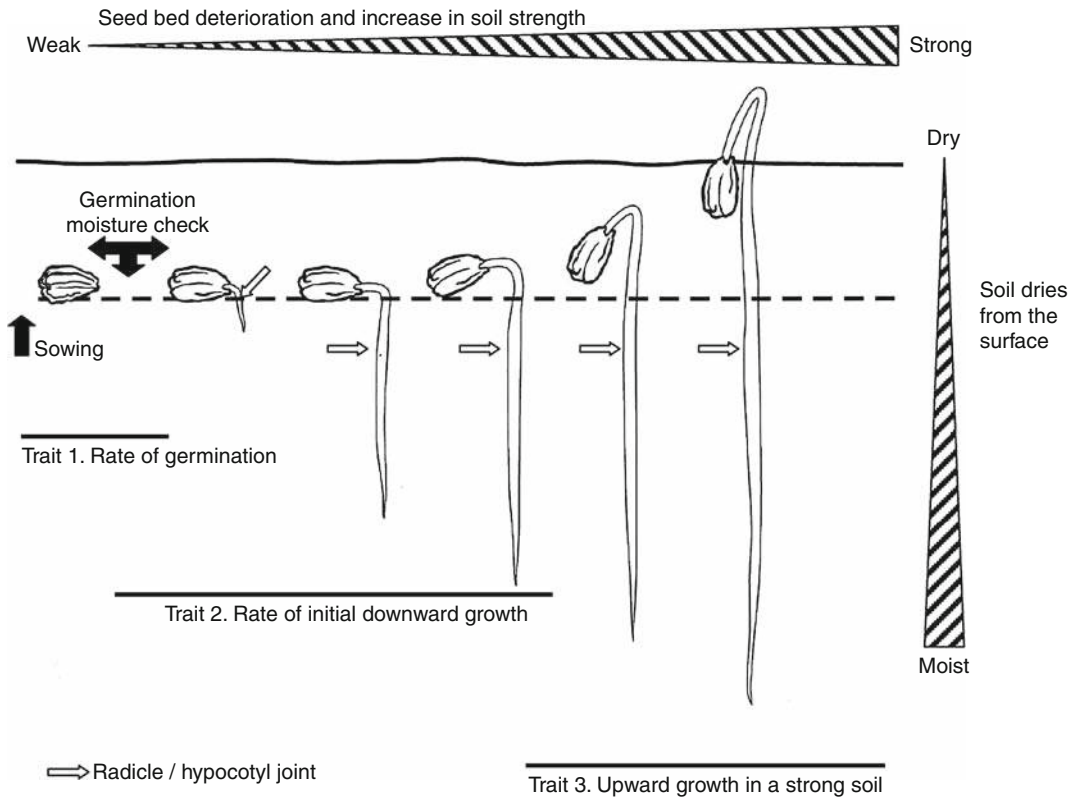
W. R. Whalley¹, W. E. Finch-Savage²

¹Department of Soil Science, Rothamsted Research, Harpenden, West Common, Hertfordshire, UK

²Warwick HRI, Warwick University, Wellesbourne, Warwick, UK

Definition and introduction

To emerge from a germinated seed, the shoot has to be capable of reaching the soil surface, while continued root growth is required to gain access to water in drying seedbeds. This is illustrated in Figure 1 where the seed must first germinate rapidly, then have rapid initial downward growth, and finally have high potential for upward shoot growth in soil of increasing impedance (Figure 1). Once a seed has germinated, seedling growth depends on temperature, water potential, and the mechanical strength of the seedbed (Collis-George and Yoganathan, 1985a, b; Finch-Savage et al., 1998; Townend et al., 1996; Whalley et al., 1999, 2001). Root and shoot elongation rate decrease with water potential in vermiculite (Sharp et al., 1988), but as soil dries it also tends to become stronger and mechanical impedance rather than water stress can become limiting (Weaich et al., 1992). Understanding the impact of mechanical impedance on seedling



Crop Emergence, the Impact of Mechanical Impedance, Figure 1 The phases of emergence in a drying seedbed of increasing mechanical impedance (Redrawn from Finch-Savage et al., 2010).

emergence can be difficult because soil strength and soil water status vary together. There is a need to disentangle the effects of water stress and mechanical impedance on emergence.

Soil strength and water status

The relationship between soil strength and water status is reasonably well understood (Whalley et al., 2007). In a seedbed, soil tends to be loose and its strength tends to result from capillary forces in the water menisci between soil particles. Whalley et al. (2007) showed that penetrometer resistance of loose soils is directly proportional to the effective stress, which in this case is the product of the degree of saturation and the matric potential. Penetrometer pressure of a soil can be greater than 1 MPa at a matric potential of -0.1 MPa (Mullins et al., 1992). Whalley et al. (1999) found that the penetrometer pressure of a sandy soil was 0.57 MPa at a matric potential of only -0.02 MPa. It is important to realize that matric potentials of -0.1 MPa or greater (i.e., in wetter soil) would have little effect on germination or seedling growth in the absence of mechanical impedance. Base water potentials for germination (i.e., the smallest water potential at which

germination can progress to completion (radical emergence)) are typically -1 MPa or less.

Soil strength and shoot elongation

In wheat (Collis-George and Yoganathan, 1985a, b), maize (Weaich et al., 1994), onion, and carrot (Whalley et al., 1999), elongation rate has a nonlinear dependence on mechanical impedance, so a small increase in strength of an initially weak seedbed is likely to have a large effect on emergence. For example, in onion and carrot, small differences in mechanical impedance result in a large reduction in shoot development. This behavior is similar to that observed in wheat (Collis-George and Yoganathan, 1985b) and maize (Weaich et al., 1996) coleoptiles, where small differences in the mechanical impedance of weak soils resulted in large differences in coleoptile elongation rate. Carrot shoots elongate from the tip shoots and increased in diameter in response to mechanical impedance, which is a trait associated with roots that elongate in strong soil (Atwell, 1990). Materechera et al. (1991) have suggested that the degree of thickening in seedling roots growing in strong soil can be used as a predictor of their ability to grow through strong soil. However, the thicker carrot shoots were less effective than their fine roots at

penetrating the strong sand, despite the observation that carrot shoots became even thicker in strong sand (Whalley et al., 1999).

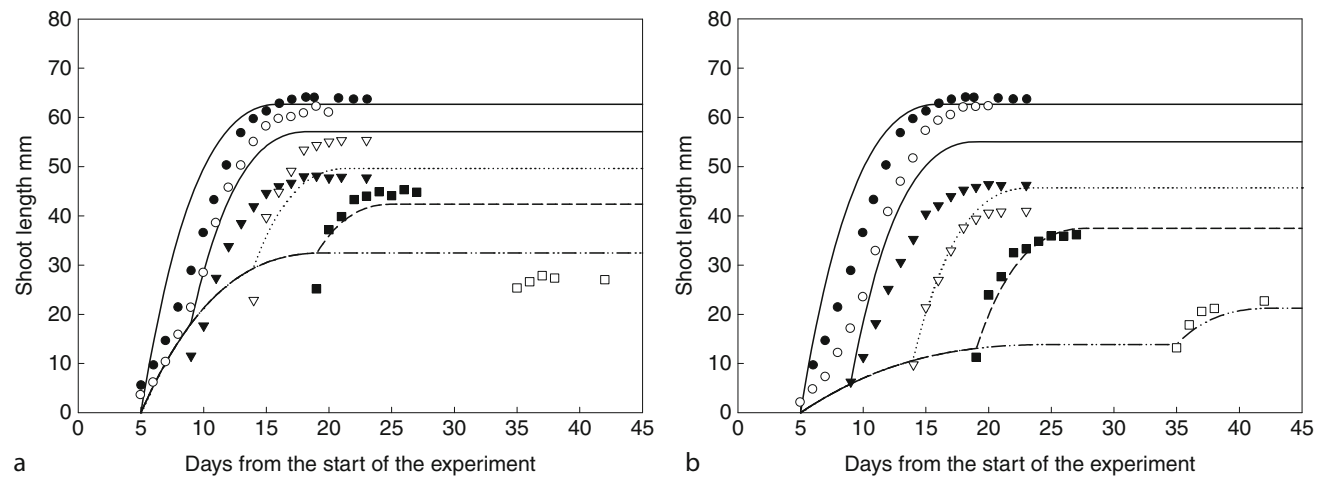
Temporal effects

The relationship between soil strength and water content in the seedbed is not constant in time. In comparison with carrot, onion shoots appear to be more effective at recovering following the removal of mechanical impedance (compare Figures 2 and 3). However, this recovery trait is not that well studied. When impedance is removed onion shoots elongate rapidly, whereas the initial recovery for carrot shoots is small. The differences between species in Figures 2 and 3 are likely to be due to the different elongation mechanisms. Removal of impedance and recovery is equivalent to soil weakening following rainfall. Flushes of emergence are often seen soon after rainfall and the recovery in shoot length in Figures 2 and 3 is a partial explanation.

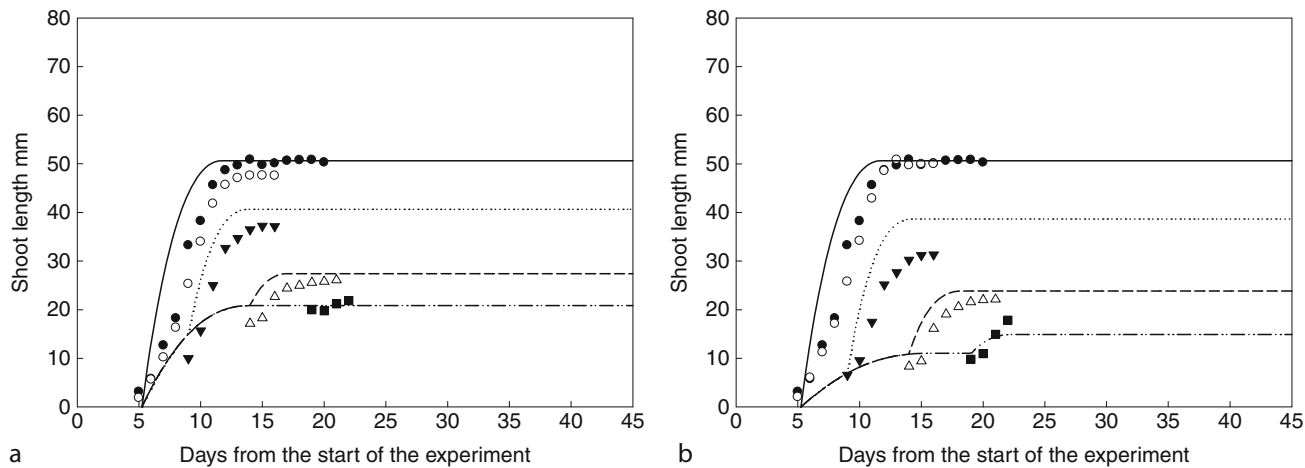
Critical stresses controlling emergence

It will be useful to explore the combinations of stress that are most important in an emerging crop. To do this a model will be of great value. The curves in Figures 2 and 3 were obtained from a shoot elongation model that predicts elongation rate depending on the particular combination of water stress, mechanical impedance, and temperature (see Whalley et al., 1999). Clearly, it is possible to have any combination is possible, but some combinations are likely to be more commonly associated with emergence problems. Even relatively wet soils can have high soil strength, for example, we have measured mean penetrometer pressures of 0.57 MPa and a range from 0.3 to

1.8 MPa in a sandy soil which was equilibrated to a water potential of -0.02 MPa. Under these conditions the model predicts that the effect of mechanical impedance will reduce shoot elongation in both carrot and onion so that the mean final shoot length is equal to a typical sowing depth of approximately 15 mm (i.e., 50% emergence). However, a water potential of -0.02 MPa will have a negligible effect on the numbers of both carrot (Finch-Savage et al., 1998) and onion (Finch-Savage and Phelps, 1993) seeds that would germinate and this is likely to be true for all crop seeds. There is a moisture sensitive block to germination (Finch-Savage and Phelps, 1993; Finch-Savage et al., 1998) that is likely to prevent germination in dry soils, so that seeds tend to germinate following rain or irrigation. As water evaporates from the surface of a wet and bare seedbed the hydraulic conductivity quickly falls to a very low value with decreasing surface water content. The low hydraulic conductivity of the dry surface will tend to reduce the rate of water loss from deeper layers, as, for example, in the results of Lascano and van Bavel (1986). Therefore after germination, the root will grow downward into increasingly wet soil and even when the soil surface becomes dry the seedling may not be water stressed, because the root is likely to be in contact with moist soil. Thus, in practice, for crop emergence in the post-germination phase, water stress may be less important than the effects of high soil strength due to the soil surface drying. This argument justifies placing a greater emphasis on mechanical impedance than water stress when developing models for pre-emergence seedling development. The seedling is only likely to experience very low water potentials in the early stages of development when the root is short or in arid climates.



Crop Emergence, the Impact of Mechanical Impedance, Figure 2 Recovery of onion shoots on sloping filter boards following exposure to mechanical impedance in sand cultures equivalent to penetrometer pressures of 0.19 MPa (a) or 0.53 (b) for 5 days \circ , 9 days ∇ , 14 days $_$, 19 days \blacksquare and 35 days \square . Data for seedlings which have never been impeded are also shown \bullet for purpose of reference. The curves shown were obtained using model for shoot elongation as a function of soil strength, water stress, and temperature (Whalley et al., 1999). Only one curve is shown for both the seedlings which were never impeded and the seedlings which were recovered from the impeding environment after 5 days because the time to germination is 5 days at 20°C (t_g). At time zero the experiment was started with ungerminated seeds.



Crop Emergence, the Impact of Mechanical Impedance, Figure 3 Recovery of carrot shoots on sloping filter boards following exposure to mechanical impedance in sand cultures equivalent to penetrometer pressures of 0.19 MPa (a) or 0.53 MPa (b) for 5 days ○, 9 days ▽, 14 days —, and 19 days ■. Data for seedlings which have never been impeded are also shown, ●, for reference. The curves shown were obtained using model for shoot elongation as a function of soil strength, water stress and temperature (Whalley et al., 1999). Only one curve is shown for both the seedlings which were never impeded and the seedlings which were recovered from the impeding environment after 5 days because the time to germination is 5.25 days at 20°C (t_g). At time zero the experiment was started with ungerminated seeds.

The effects of high soil strength in the surface of the seedbed can also affect the distribution of crop emergence times. For example, in Figures 2 and 3 the recovery in shoot length following the removal of mechanical impedance (e.g., after rain on a dry seedbed) appears to be possible for 20 or more days following germination. Variability in emergence times can be particularly important in vegetable crops where the proportion of the crop in high-value size grades (e.g., diameter of carrot) at harvest depends in large part on uniform emergence of the desired number of seedlings.

Conclusion

In summary soil strengths high enough to decrease emergence can occur from soil drying to matric potentials too high (i.e., soil too wet) to directly affect elongation. In temperate regions, soil strength is the critical stress that determines emergence in the seedbed. In much drier regions emergence may be more limited by germination.

Bibliography

- Atwell, B. J., 1990. The effect of soil compaction on wheat during early tillering I. Growth, development and root structure. *New Phytologist*, **115**, 19–35.
- Collis-George, N., and Yoganathan, P., 1985a. The effect of soil strength on germination and emergence of wheat (*Triticum aestivum* L.) I. Low shear-strength conditions. *Australian Journal of Soil Research*, **23**, 577–587.
- Collis-George, N., and Yoganathan, P., 1985b. The effect of soil strength on germination and emergence of wheat (*Triticum aestivum* L.) II. High shear-strength conditions. *Australian Journal of Soil Research*, **23**, 589–601.
- Finch-Savage, W. E., and Phelps, K., 1993. Onion (*Allium cepa* L.) seedling emergence patterns can be explained by the influence of soil temperature and water potential on seed germination. *Journal of Experimental Botany*, **44**, 407–417.
- Finch-Savage, W. E., Steckel, J. R. A., and Phelps, K., 1998. Germination and post – germination growth to carrot seedling emergence: predictive threshold models and sources of variation between sowing occasions. *New Phytologist*, **139**, 505–516.
- Finch-Savage, W. E., Clay, H. A., Lynn, J., and Morris, K., 2010. Towards a genetic understanding of seed vigour in small-seeded vegetable crops using natural variation in *Brassica oleracea*. *Plant Science*, **179**, 582–589.
- Lascano, R. J., and van Bavel, C. H. M., 1986. Simulation and measurement of evaporation from bare soil. *Soil Science Society of America Journal*, **50**, 1127–1132.
- Materechera, S. A., Dexter, A. R., and Alston, A. M., 1991. Penetration of very strong soils by seedling roots of different plant species. *Plant and Soil*, **135**, 31–41.
- Mullins, C. E., Cass, A., MacLeod, D. A., Hall, D. J. M., and Blackwell, P. S., 1992. Strength development during drying of cultivated, flood-irrigated hardsetting soil. II. Trangie soil, and comparison with theoretical predictions. *Soil and Tillage Research*, **25**, 129–147.
- Sharp, R. E., Silk, W. K., and Hsiao, T. C., 1988. Growth of the maize primary root at low water potentials I. Spatial distribution of expansive growth. *Plant Physiology*, **87**, 50–57.
- Townend, J., Mtakwa, P. W., Mullins, C. E., and Simmonds, L. P., 1996. Soil physical factors limiting establishment of sorghum and cowpea in two contrasting soil types in the semi-arid tropics. *Soil and Tillage Research*, **40**, 89–116.
- Weaich, K., Bristow, K. L., and Cass, A., 1992. Preemergent shoot growth of maize under different drying conditions. *Soil Science Society of America Journal*, **56**, 1272–1278.
- Weaich, K., Bristow, K. L., and Cass, A., 1994. A compression-suction-temperature (CST) cell for simulating the physical environment of preemergent seedlings. *Agronomy Journal*, **86**, 212–216.
- Weaich, K., Bristow, K. L., and Cass, A., 1996. Modelling preemergent maize shoot growth: I. Physiological temperature conditions. *Agronomy Journal*, **88**, 391–397.

- Whalley, W. R., Finch-Savage, W. E., Cope, R. E., Rowse, H. R., and Bird, N. R. A., 1999. The response of carrot (*Daucus carota* L.) and onion (*Allium cepa* L.) seedlings to mechanical impedance and water stress at sub-optimal temperatures. *Plant Cell and Environment*, **22**, 229–242.
- Whalley, W. R., Lipiec, J., Finch-Savage, W. E., Cope, R. E., Clark, L. J., and Rowse, H. R., 2001. Water stress can induce quiescence in newly-germinated onion (*Allium cepa* L.) seedlings. *Journal of Experimental Botany*, **52**, 1129–1133.
- Whalley, W. R., To, J., Kay, B. D., and Whitmore, A. P., 2007. Prediction of the penetrometer resistance of agricultural soils with models with few parameters. *Geoderma*, **137**, 370–377.

Cross-references

- [Hardpan Soils: Management](#)
- [Management Effects on Soil Properties and Functions](#)
- [Pedotransfer Functions](#)
- [Plant Biomechanics](#)
- [Plant–Soil Interactions, Modeling](#)
- [Rhizosphere](#)
- [Root Responses to Soil Physical Limitations](#)
- [Soil Hydraulic Properties Affecting Root Water Uptake](#)
- [Soil Penetrometers and Penetrability](#)
- [Soil Physical Quality](#)

CROP RESPONSES TO SOIL PHYSICAL CONDITIONS

Jerzy Lipiec¹, Artur Nosalewicz¹, Jacek Pietrusiewicz²

¹Institute of Agrophysics, Polish Academy of Sciences, Lublin, Poland

²Department of Plant Anatomy and Cytology, Maria Curie-Skłodowska University, Lublin, Poland

Definitions

Crop responses: changes in the growth and functions of roots and shoots within a growing season and in the final crop yield.

Physical characteristics of soils: the characteristics, processes, or reactions of a soil that are caused by physical forces and are described by, or expressed in, physical terms or equations. Examples of physical properties are bulk density, water holding capacity, hydraulic conductivity, porosity, pore size distribution (Gregory et al., 2002) (see [Cropping Systems, Effects on Soil Physical Properties](#)).

Introduction

When climax vegetation has been on a site for many years, the soil usually is very heterogeneous and is considered to have a good structure for plant growth (Taylor and Brar, 1991). However, after a soil with climax vegetation is brought under cultivation, its heterogeneity usually is reduced. This reduction is mostly due to soil stirring by tillage and pressures from tires of tractors pulling the tillage implements or from the hooves of animals. The changes in soil structure will impose physical conditions influencing root growth and fluxes and thereby essential plant requirements as adequate quantities of

water, oxygen for aerobic respiration, and nutritive elements (Gliński and Lipiec, 1990; Bengough et al., 2006). Crop responses to soil physical conditions depend on the growing stage.

Germination, emergence, and crop establishment

Germination is the process in which a seed or spore emerges from a period of dormancy and is completed when the radicle (embryonic root) emerges from the seed covering structure; emergence is completed when the young shoot emerges through the soil surface. Soil physical conditions at and above planting depth (seedbed layer) are related most closely to the germination, and emergence (e.g., Tamet et al., 1996; Håkansson, 2005). Rapid germination, emergence, and root growth to the subsoil allows early crop establishment (Tisdall, 1996; Atkinson et al., 2009) that enables the plant to use the nitrogen released in the soil, resist fungal disease and pest attack, competition from weeds and roots in the subsoil to avoid waterlogging (Tisdall, 1996; Harris, 1996), increase solar radiation by the growing canopy, and hence is the key to high crop productivity (Cornish, 1984). The main soil physical requirements for germination and emergence include temperature, water content, oxygen availability, and soil strength (see [Root Responses to Soil Physical Limitations](#)).

Temperature

In cold climates, the rate of germination, emergence, and final stand establishment is slowed greatly by low seedbed temperatures. The minimum temperatures for root growth are about 5°C. Cold soil reduces the water uptake due to increased viscosity and cell membrane permeability, metabolic activity resulting in decreased nutrient uptake (Gliński and Lipiec, 1990). Low temperatures are most likely to reduce or stop final emergence when other adverse factors also operate (Hodges et al., 1994). Optimum seed zone temperature for a wide range of seedbed matric potentials (from –10 kPa to –500 kPa) and aggregate size distributions vary from 20°C to 30°C (Schneider and Gupta, 1985).

In hot regions, however, emergence can be hindered by adversely high seedbed temperatures. The maximum temperatures for root growth are from 35°C to 40°C. The mulching can promote the emergence by reducing soil temperatures near the surface and evaporation and hence delaying the onset of water stress and high mechanical impedance (Harris, 1996; Townend et al., 1996).

Root length compared to root weight is a more sensitive indicator of effects of soil temperature. In general, the optimum temperature for roots is somewhat lower than for shoots (Gliński and Lipiec, 1990). To characterize thermal conditions during the early crop growth, the temperature can be expressed in degree-days (one DD is a day with an average daily temperature of 1°C above a base temperature) (Whalley et al., 2000). Base temperatures of 5°C or 10°C are frequently used to calculate accumulated thermal

time and relate it with early plant growth and the development and proliferation of the root system. It helps farmers select the hybrids and varieties that are best suited to their climatic region.

Water

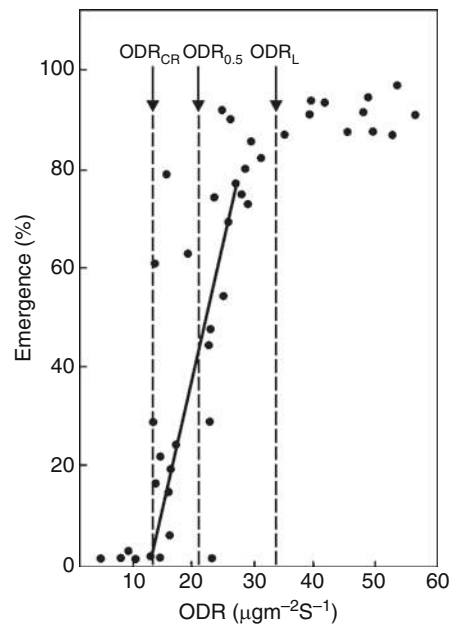
Most seeds must absorb about their own weight in water before they germinate. The water availability depends on soil characteristics, which control how tightly water is held, seed–soil contact areas, and evaporation. Finer-textured and well-structured soils hold water more tightly than coarse-textured soils with the same water content (Cornish, 1984). Irrespective of soil type, the plant-available water is between in situ field capacity and the permanent wilting point (water content at soil matric potential of -1.5 MPa). The seed–soil contact area decreases as soil aggregate size increases and when much undecomposed surface crop residue is present in the soil (Cornish, 1984; Atkinson et al., 2009). Moreover, a seedbed with finer aggregates compared with coarser aggregates results in lower evaporation. In moist soil, however, relative humidity around the seed can be sufficiently high due to vapor transport and then imbibition and germination can occur in the absence of seed–soil contact (Wuest et al., 1999). In dry surface seedbed layer, good crop emergence of small grain crops can be achieved, when the seed was placed directly onto a firm seedbed base and was covered by a 4-cm deep seedbed with $>50\%$ aggregates $<5\text{ mm}$ (Håkansson et al., 2002).

Aeration

Insufficient aeration for germination and emergence is usually caused by poor drainage and by a surface crust that can prevent gas exchange between the soil atmosphere and the air above. In case of direct seeding, insufficient aeration can occur, if the seed is pressed firmly into the wall or bottom of a slot, which is cut by the machine and simultaneously compacted. In the poorly aerated soil, biological activity can consume the limited supply of oxygen, in competition with seeds or seedling roots. From the review of Gliński and Stępniewski (1985) results that many plants as wheat, lettuce, carrot, and onion germinate well even at low oxygen concentration. Some plants, for example, rice, cucumber, and cockscomb preserve their germination ability even in completely anoxic conditions. The emergence of plants is preceded by a considerable development of the root system that needs oxygen supply. The effects of soil oxygen on seedling emergence are better described in terms of oxygen diffusion rate (ODR) than in terms of the oxygen concentration in the soil air. Figure 1 presents an example of the relationship between plant emergence of oats and ODR.

Strength

Soil strength is a measure of deformation resistance (mechanical impedance) and increases with increased soil bulk density or with decreased soil water content or matric



Crop Responses to Soil Physical Conditions, Figure 1 Final emergence of oats vs. oxygen diffusion rate: ODR_{cr} (the level making emergence impossible); $\text{ODR}_{0.5}$ (the value at which the number of emerging seedlings reaches 50% of the seed germination capacity), and ODR_L (causing a significant decrease in emergence relative to germination capacity) (after Gliński and Stępniewski, 1985).

potential. High soil strength is an important constraint to seedling emergence (see *Crop Emergence, the Impact of Mechanical Impedance*) and crop establishment failure. Soil strength of the preemergent shoot environment is more dynamic than that of the root environment and may increase exponentially with time (Weaich et al., 1996). Roots and shoots have to work very hard in strong soil to overcome mechanical impedance (Cornish, 1984). It was shown that germination, root elongation, coleoptile elongation, and emergence of wheat were not affected by soil strengths below 3.0, 2.3, 1.7, and 0.8 MPa, respectively (Jakobsen and Dexter, 1987). However, at strengths exceeding 5 MPa root growth will be nonexistent (Bengough et al., 2006).

Excessive soil strength above developing seedlings can be induced by soil compaction due to machinery traffic at seedbed preparation and sowing, the presence of large clods and crust (surface hard layer) (Håkansson et al., 2002). Large clods often occur in clay soils and their contribution can increase in compacted soil. Soil crusts are formed mostly in soils with low aggregate stability (e.g., silt soils) during irrigation or intense natural rainstorms shortly after planting followed by dry weather (see *Soil Surface Sealing and Crusting*). Impact of the crusts on crop emergence varies with the seed size. In general small seedlings from small seeds are more crust susceptible (e.g., alfalfa) than those from large seeds (e.g., maize).

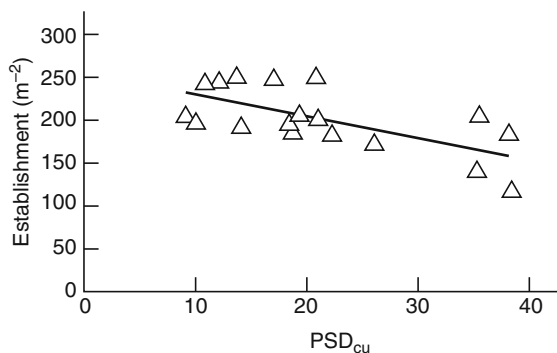
Also heavier seed of the same crop type, as observed for carrot, emerged better from deep sowing in crusted soil due to longer hypocotyls (part of a plant embryo or seedling plant that is below the cotyledons) and greater growth forces (Tamet et al., 1996). Mulches and conservation tillage practices with crop residues on the soil surface and liming of acid soils reduce soil crusting by decreasing raindrop impact and postponing surface drying.

The effect of soil strength on crop emergence depends on sowing depth. The negative effects of increasing soil strength on the emergence are greater at greater sowing depth (Lipiec and Simota, 1994). The risk of poor emergence due to surface layer hardening depended much more on the sowing depth than on the aggregate sizes of the seedbed (Håkansson et al., 2002).

Structure

The influence of a seedbed structure on crop establishment can vary greatly in terms of soil aggregation and subsequent pore size distribution that are largely influenced by cultivation. As shown by Atkinson et al. (2009) soil structures with larger pores are responsible for reducing establishment (Figure 2) due to mostly poor soil–seed contact and lack of water and nutrient capture from large pores. Therefore, press wheels and rolling are used to increase soil–seed contact and final emergence (Cornish, 1984; Håkansson et al., 2002). Incorporating the structural measurements of pore space of soil macrostructure improved predicting crop establishment based on bulk density and cultivation techniques (assigning lower value to less intensive cultivation) (Atkinson et al., 2009). Optimum structural conditions for establishment occurred between ranges for macroporosity of 10–19% and average pore size of 8–12 mm².

It is clear that the fine seedbed structures (<5 mm size) produce the greatest establishment (Håkansson et al., 2002; Atkinson et al., 2009). In particular it refers to sugar beet, cruciferous crops, and clover that have small seeds (1–5 mg seed⁻¹) and should be placed shallow (usually



Crop Responses to Soil Physical Conditions, Figure 2 Relation between wheat establishment and PSDcu (ratio of the size of pores at a 10% and 60% total macropore distribution, the larger the ratio, the greater the number of larger pores) (after Atkinson et al., 2009).

<3.5 cm). Large seed crops are less sensitive to sowing depth. Fine seedbed structures can be achieved through power harrowing and plowing. The poorest soil structure and seedbed performance were produced by disking and rolling (Cornish, 1984; Atkinson et al., 2009).

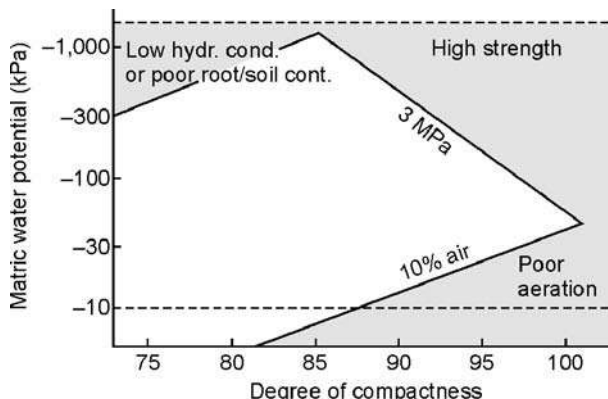
One important factor influencing emergence is soil puddling due to tillage when wet. This traditional practice for rice destroys soil aggregates in the seedbed layer and thereby disturbs emergence of wheat, which is often planted after rice (Tripathi et al., 2007). This study showed that incorporation of crop residue reduced change in soil physical properties and improved germination and yields.

The emergence may be limited by different physical factors depending on site conditions. In the semiarid tropics, it was primarily the large mechanical impedance in the sandy clay loam, whereas in the sandy loam – a combination of high temperature, water stress, and mechanical impedance. Cowpea compared to sorghum emergence was higher due to greater initial rates of root and shoot growth, which allowed it to avoid the greater stresses caused by temperature, drought, and mechanical impedance. The larger cowpea shoots were able to overcome greater mechanical impedance when they approached the soil surface. This aspect is of particular importance in hardsetting soils (Townend et al., 1996). Emergent seedlings of sorghum were often surviving on water taken up by the primary root alone, from moist soil at depth, because all other root initials at the base of the stem were surrounded by hot, dry soil (Harris, 1996). Low temperature and oxygen deficiency in the seedbed layer in cold and wet climate can be main factors limiting the early root and shoot growth.

Early crop growth can be influenced by soil physical characteristics acting independently or in combination. Due to this, it is often difficult to determine their relative contributions. Example would be supra-maximum temperatures ($>40^{\circ}\text{C}$) and high soil strengths experienced by the preemergent shoot in the semiarid tropics (Weaich et al., 1996).

Growth of established crops

Most important soil physical factors influencing growth of roots and shoots of established crops include water status, penetration resistance, and aeration. They are largely affected by alterations in soil structure due to compaction (e.g., Czyż, 2004; Usowicz and Lipiec, 2009) by agricultural machinery and tillage (e.g., Birkás, 2008). The penetration resistance of 3 MPa and air-filled porosity of 10% v/v are usually regarded as critical for plant growth. The results from Figure 3 indicate that as degree of compactness (i.e., ratio of the actual bulk density to a specified reference bulk density for the same soil, obtained by static load of 200 kPa when the soil is wet, Håkansson, 1990) increases, the range of matric potential, in which aeration and mechanical impedance do not limit root growth becomes narrower. The range is termed as least limiting water range (LLWR) and combines main soil



Crop Responses to Soil Physical Conditions,

Figure 3 Relationship between soil strength of 3 MPa and air-filled porosity 10% (v/v) in relation to degree of compactness and matric potential of the plow layer excluding the seedbed (0–5 cm). Problems for crop growth in the upper left corner of the diagram are likely due to mainly low unsaturated hydraulic conductivity and/or poor root-to-soil contact (after Håkansson and Lipiec, 2000).

physical characteristics to describe soil suitability for crop growth (Da Silva et al., 1997). The use of the degree of compactness instead of bulk density enhances the performance and applicability of the LLWR by reducing differences in its values between different soil types (Da Silva et al., 1997). In coarse-textured soils, root growth may be further restricted by rough surface of the sand particles, which resist particle displacement by slippage (Gliński and Lipiec, 1990).

In case of legume plants, soil compaction can decrease nodulation efficiency of the nodules in fixing nitrogen, N uptake, subsequent yield, and protein content of seed (Sweeney et al., 2006; Siczek, 2009). The quantity and distribution of nodules can be altered by controlling the wheel traffic (compaction) in ways, which have implications for increasing nitrogen fixation. Also colonization of dry edible beans by mycorrhizal fungi and the incidence of *Phytophtora* root rot of soybeans are influenced by soil physical properties induced by secondary tillage and traffic (Gliński and Lipiec, 1990).

Effect of soil structural discontinuity

Vertical

An important factor affecting root growth and water use in the field is vertical strength discontinuity. A sharp discontinuity occurs between aggregated seedbed layer and firm soil below (Lipiec et al., 2003b). Soil column experiment showed that root length of maize below the seedbed layer relative to total root length was less than 38% while water use was up to 74%. Total water use from the deeper soil and root water use efficiency were greater for the fine-than coarse-textured soils (Lipiec and Hatano, 2003).

Another discontinuity in soil profile is due to the presence of dense layers such as plow pans, fragipans,

duripans, fine-textured B-horizons, claypans, and high clay horizons developing in a relatively long time span (Lipiec et al., 2003b). They lead to a higher concentration of roots in upper part of the subsoil layer and lower – in deeper soil. Restricted root growth by the dense layers can be a consequence of too low porosity accompanied by insufficient oxygen supply, excessive mechanical impedance, and the absence of pores of diameters greater than root tips (Lipiec et al., 2003b). These parameters are used in modeling root growth and function (Lipiec et al., 2003a). In general, the effect of the dense layers on root growth increases with decreasing depth and thickness of the dense layer (Birkás, 2008). Under droughty conditions, limited root growth results in scarce water supply and consequently plant death (Cornish, 1984). In some soils, the physical constraints to root growth are accompanied by high soil acidity (Lipiec et al., 2003b).

The hindering effects of the subsoil dense layers can be enhanced by traffic of heavy machinery and remain many years or are even permanent, especially in non-swelling and shrinking coarse-textured soils and warm climates with shallow or without annual freezing (Sweeney et al., 2006; Håkansson, 2005) (see *Subsoil Compaction* and *Compaction of Soil*). Usually, dense layers can be localized in the soil profile by maxima of bulk density and soil strength (Lipiec and Hatano, 2003) or reduced aeration in wet soil (Gliński and Stępniewski, 1985). In well-structured and finer-textured soils, the increase in soil compactness can be partly compensated for by the development of a continuous macropore system (Lipiec and Hatano, 2003).

The separate the effect of subsoil dense layers on root growth and uptake functions can be quantified in the field by removing topsoil (Ishaq et al., 2001). Such approach is, however, expensive and difficult to perform. Therefore, column experiments with variously compacted soil layers are used to separate depth effects from strength effects (Busscher et al., 2000). Soil columns can be useful tool for measuring water uptake from particular depths after separation of the layers by, for example, thin perlite or wax-paraffin mixture layer (impermeable for water and allowing root growth) (Nosalewicz and Lipiec, 2002).

Horizontal

Horizontal soil strength discontinuity in cropfields results from mostly uneven distribution of wheel tracks (Raper, 2005; Sweeney et al., 2006) and affects root growth and function (see *Spatial Variability of Soil Physical Properties*). Reduced root growth of plants and associated water use in strong soil were partly compensated for in loose soil of the same plant (Figure 4).

Also water deficits in a soil surrounding part of a one plant root system induces increased water uptake from soil with better soil–water conditions (Šimůnek and Hopmans, 2009; Hu et al., 2009). In studying the effect of spatial distribution of mechanical impedance and aeration on root growth and function approaches with split root systems

in soil of varying bulk density and matric potential were useful (Whalley et al., 2000; Lipiec and Hatano, 2003).

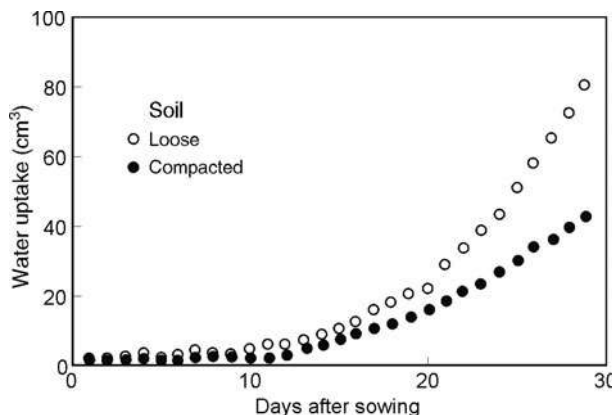
A survey of root growth functions showed that a greater bulk density led to increased water uptake rate (per unit of root) for bean, maize, barley, and rice (Lipiec and Hatano, 2003). This increase was mostly attributed to a greater root–soil contact and to a higher unsaturated hydraulic conductivity and a greater water movement toward the roots. However, increased water uptake rate was not sufficient to compensate entirely for the reduction in total root length and resulted in reduced total water uptake. Similarly, greater nutrient inflow rate per unit length and root–soil contact area without additional nutrient application were not sufficient to compensate for reduced root

size (Lipiec et al., 2003b). The above studies indicate a wide plasticity in root growth and water absorption in response to localized unfavorable soil physical conditions. Including the compensatory water uptake in models improves prediction of soil water content as compared to models accounting only for root distribution (Šimůnek and Hopmans, 2009).

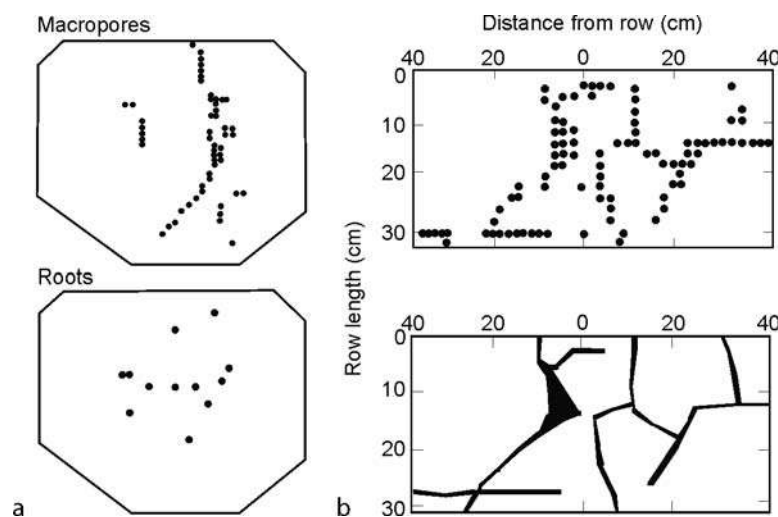
Role of pores

Root response to high soil strength depends on the presence and distribution patterns of pores having diameter equal to or greater than the root tip (approximately 200 µm). A soil matrix with a larger pore size, structural cracks, macropores, and wormholes will offer greater potential for undisturbed root growth because the roots can bypass the zones of high mechanical impedance (Gliński and Lipiec, 1990; Lipiec et al., 2003b).

Figure 5 illustrates similar distribution patterns of macropores and roots. The percentage of roots grown into existing pores and channels increases in deeper and stronger layers where they can be the only possible pathways for root growth. This preferential growth into macropores will lead to increasing critical limits of soil strength for root growth (2.5–3.0 MPa) (Håkansson and Lipiec, 2000). Larger pores can also benefit in poorly aerated soils since they drain at higher matric potential and remain air filled for longer compared to smaller pores (Whalley et al., 2000). This process results in decreasing critical values of air-filled porosity (10%) although part of the soil matrix can be anoxic (Håkansson and Lipiec, 2000). McQueen and Shepherd (2002) suggested the critical lower limit set of macropore volume ($>60 \mu\text{m}$) at 5% for cropped sites on poorly drained soil. An important property of the vertical biopores (made by soil fauna and plant roots) in deeper soil is that they are able to resist vertical



Crop Responses to Soil Physical Conditions,
Figure 4 Cumulative water uptake by split root system of wheat, halves of the same plant grown in loose silt loam (bulk density 1.28 Mg m^{-3}) and compacted (bulk density 1.58 Mg m^{-3}) at matric water potential -35 kPa (after Nosalewicz and Lipiec, 2002).



Crop Responses to Soil Physical Conditions, Figure 5 Distribution patterns of macropores and roots of maize: (a) pot experiment (after Hatano et al., 1988); (b) field experiment (after Tardieu and Manichon, 1986).

compression and they remain stable as the soil swells (Lipiec and Hatano, 2003).

Optimum root size

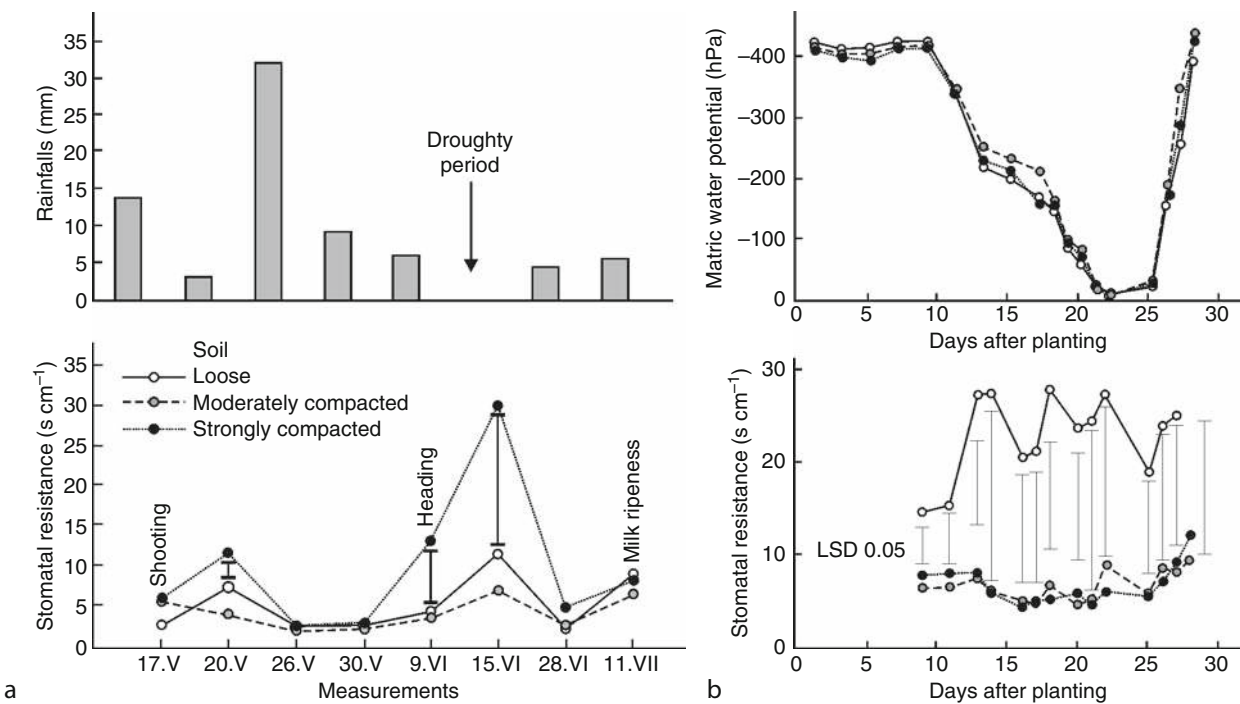
Optimum root size is not always the largest one and depends on the work to be done. For water uptake, the optimum root length density is of $1\text{--}6 \text{ cm cm}^{-3}$ of soil depending on soil type, crop type, and water status in a plant (Gliński and Lipiec, 1990). A relatively small root length density of 1 cm cm^{-3} of soil in winter wheat was capable of extracting most of the available water and for sorghum it was more than 2 cm cm^{-3} (Gliński and Lipiec, 1990), but complete uptake of soil P requires at least $10\text{--}20 \text{ cm cm}^{-3}$ depending upon plant species (Cornish, 1984). Lengths of $5\text{--}10 \text{ cm cm}^{-3}$ are common in surface soils. Root growth in excess of that needed to meet water and nutrient requirements can lead to dissipation of the products of photosynthesis. Therefore, under favorable conditions with a good supply of water (e.g., irrigated areas) and nutrients cultivars with less extensive and shallow root systems can be used whereas in dry areas – those with more extensive and deep root systems.

Root-to-shoot signaling

When soil physical properties suppress root growth and change root distribution, shoot growth, and functions may also be reduced (Sweeney et al., 2006) as an effect of

root-to-shoot signaling (Lipiec and Hatano, 2003; Dodd, 2005). Main shoot functions include photosynthesis and transpiration that are related to the leaf stomatal diffusive resistance. Figure 6a indicates the greater stomatal resistance of spring wheat in compacted than non-compacted soil, particularly in droughty periods. A substantial increase in the stomatal resistance of plants grown in most compacted soil also occurred with transient wetting (Figure 6b) and associated low air-filled porosity in laboratory experiment (Lipiec et al., 1996). Ali et al. (1999) reported that the increased leaf stomata resistance occurred even before a measurable change in leaf water potential.

Several mechanisms are suggested for stomata closure. One mechanism under poor aeration is reduced water flow through roots (Gliński and Stępniewski, 1985; Lipiec et al., 2003b). Accumulation of abscisic acid (ABA) in leaves seems to induce stomata closure through its effect on the potassium ion regulation of guard cell turgor (Tardieu, 1994). The stomata resistance of maize grown in poorly aerated soil was considerably higher in lower than upper leaves (Lipiec and Hatano, 2003) and may imply the upward movement of plant hormones or other substances to the shoots (Tardieu, 1994). This can be supported by study (Bennicelli et al., 1998) indicating that superoxide dismutase (SOD, metalloenzyme, protects aerobic organisms against oxygen-activated toxicity) activity in roots increased earlier (after 2 days of oxygen stress) while that one in the leaves started to increase later (after 8 days).



Crop Responses to Soil Physical Conditions, Figure 6 Stomatal resistance of spring wheat grown in field in relation to soil compaction and rainfalls (a) (after Lipiec and Gliński, 1997) and of maize grown in growth chamber (b) in relation to soil compaction and matric water potential (after Lipiec et al., 1996).

However, there were no detectable root-sourced signals of xylem-sap ABA concentration in wheat due to soil strength, despite changes in stomatal conductance (Whalley et al., 2006). Some authors (e.g., Tardieu, 1994) point out that ABA increase in plants grown in strong soil is a result of root dehydration due to a limited water supply to the roots. Horn (1994) indicates that ABA concentration in plants generally increased proportionally to previous maximum reduction of plant-available water. Although progress has been made toward description of root-to-shoot signaling in recent years still further research is needed to explain perception of soil physical stress by plants and the conversion of physical phenomena such as water and oxygen scarcity or temperature extremes into physiological responses (Lipiec et al., 2003b; Dodd, 2005; Whalley et al., 2006).

Yields

Compaction, tillage, and irrigation were applied in many experiments to get a wide range of soil physical conditions affecting crop yields. Response of crop yield to compaction is most often parabolic with the highest yield obtained on moderately compacted soil (Figure 7) (e.g., Håkansson, 2005; Czyż, 2004). However, in soil of relatively high initial soil compactness under droughty climatic conditions, the yield can decrease with increasing soil compaction (Lipiec and Hatano, 2003). The effects of soil and subsoil compaction by vehicles with high axle load (≥ 10 Mg) on crop yield remained for a number of years in spite of annual winter soil freezing (Håkansson, 2005).

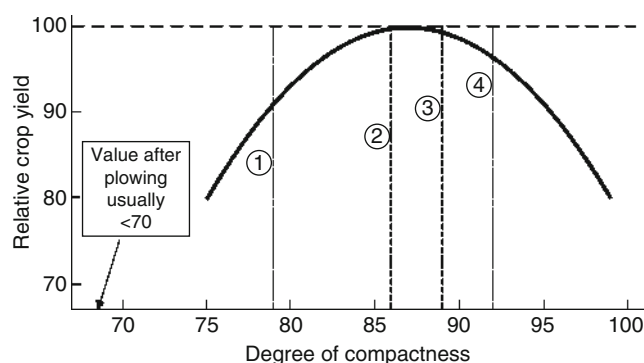
In study of Whalley et al. (2006) the yield of wheat was linearly related with soil strength (as manipulated by compaction and irrigation) and accumulated soil moisture data during growing season. Negative effect of excessive soil strength on barley yield was mostly reflected in years with

unfavorable sowing–shooting weather conditions (scarce rainfalls, high sunshine, and air temperature) (Lipiec et al., 2003b). This interactive effect is primarily important in predicting crop yield of coarse-textured soils where strength problems are enhanced by low available soil water content and rate of the soil water movement deeper in the soil profile (Busscher et al., 2001). In wet and compacted soil, crop yield can be reduced due to deficient soil aeration (Czyż, 2004) and associated low transpiration, shoot growth rates, wilting, leaf epinasty and senescence, and premature termination of growth (Gliński and Stepniewski, 1985). Regarding plant tolerance to deficient soil aeration, there is a wide spectrum of plants from entirely adapted hydrophytes (aquatic plants) to very sensitive crop species severely damaged after short periods (1–2 days) of deficient soil aeration.

Root crops are traditionally regarded as particularly sensitive to excessive strength because their harvestable products grow underground (Lipiec and Simota, 1994). A characteristic morphological response of sugar beets and carrots to mechanical impedance in compacted soil is their forking and fanging (Lipiec et al., 2003b) and decreased marketable yield (tubers > 35 mm) with potatoes. The reduction in root yield of the sugar beets was accompanied by a decrease in sugar content (Lipiec et al., 2003b) and increase in more harmful nonsugars (Gliński and Lipiec, 1990). The response of sugar beets yield to strength was less in dry season compared to wet season that implies the effect of excessive soil strength was masked by moisture deficit (Birkás, 2008). The yield of carrot and potatoes and the proportion of small and deformed roots and tubers that were unsuitable for processing grown in mechanically impeded soil decreased and increased, respectively (Lipiec and Simota, 1994; Dumitru et al., 2000).

The effect of tillage systems on crop performance is not uniform and depends on crop species, soils, climates and agro-ecological conditions (Alvarez and Steinbach, 2009). Under semiarid conditions conventional tillage and deep plowing are superior to conservation tillage (at least 30% of the soil covered by crop residues). The tillage effect is either closely linked to soil aggregation, hence water infiltration rate and water storage capacity, or indirectly related to soil and water conservation. In general, crop yield differences between tillage treatments were diminished when fertilizers were applied. Although conservation tillage is most cost effective farming practice thereby widely adopted, for example, in the USA, generalization should be avoided. Irrespective of management practices, crop yields are highly dependent on soil texture and associated soil water and nutrients storage during growing season.

Mathematical modeling of crop growth responses to soil physical conditions contributes to the better understanding of the complex and variable effects. Many authors indicate that under most conditions the soil water content or the soil water potential comes out to be of particular importance because they directly affect crop



Crop Responses to Soil Physical Conditions, Figure 7 Relative crop yield as related to the degree of compactness of the plow layer (5–25 cm) based on about 100 field trials in Sweden. The treatments were the following: (1) no compaction, (2) one pass, track by track, by a 2-Mg tractor with tire inflation pressure 70 kPa, (3) one pass, track by track, by a 3–3.5-Mg tractor with tire inflation pressure 140 kPa, (4) four passes by a 3–3.5-Mg tractor with tire inflation pressure 180 kPa (after Håkansson, 2005).

growth and yield and indirectly affect significant factors, such as aeration, mechanical impedance, and soil temperature. For this reason, crop yield is frequently predicted from interactions of soil water and plant transpiration and assimilation (Lipiec et al., 2003a).

Modifying soil physical conditions toward crop growth

Tillage, compaction, and crop residue management mostly influence soil physical conditions of the root zone.

Tillage and deep loosening

Moldboard plowing or other deep primary tillage is often used to loosen the topsoil. Because of the high cost of tillage, different limited (plowless) tillage managements are also used. Research indicates that effects of tillage systems on soil physical properties are not consistent (Håkansson, 2005; Strudley et al., 2008; Alvarez and Steinbach, 2009). More studies indicate greater soil bulk density and penetration resistance under limited tillage managements, particularly in the surface layer. In general, the soils under no-till compared to plowed are characterized by a greater number of longitudinally continuous earthworm channels utilized preferentially by roots as passages of comparatively low soil strength and good aeration.

Although deep soil loosening have consistently indicated decreased bulk density and penetration resistance along with increased infiltration and crop rooting its effects on soil structure and crop yield are not always positive (Håkansson, 2005; Raper, 2005). This is due to the limited reversibility since subsoiling or ripping may produce large voids between fairly large soil structure units (>2 mm), but compaction may alter smaller units (<1 mm). Moreover, once soil is deeply loosened, it will easily recompact if traffic is applied in the same area (Raper, 2005). The coarse-textured soils are less responsive to subsoiling than the fine-textured soils because of the low content of finer soil materials or organic matter to stabilize the pore system in the former (see *Hardpan Soils: Management*). Crop yields may not respond positively to deep loosening even though they may appear to be compacted when good fertilization and management practices are used on the plow layer (Håkansson, 2005) or due to the presence of old root channels and earthworm channels (Raper, 2005) (see *Earthworms as Ecosystem Engineers*).

Since deep loosening is expensive, it is often recommendable in case of very severe subsoil compaction (e.g., Munkholm et al., 2005; Håkansson, 2005) and only in a compacted wheel-track zone (Sweeney et al., 2006) or under the crop row, called “precision tillage” or “in-row subsoiling” (see *Precision Agriculture: Proximal Soil Sensing*). The cost of operation can be markedly diminished with crops grown in wide rows. Various aspects of profile modification and other ways to soften hard layers including water/crop management and soil amendments

are discussed in detail by Busscher et al. (2007) and Baumhardt et al. (2008).

Because of costly and limited reversibility of deep loosening and other solutions, the opportunities to minimize subsoil compaction are recommended. They include reduction of axle loads, ground contact pressure and traffic intensity, especially when soils are wet (Håkansson, 2005; Hamza and Anderson, 2005). On the base of measurements of soil displacement under the wheels of heavy vehicles in Sweden a limitation of the load to 6 Mg on a single axle load and 10 Mg on a tandem axle unit was recommended to minimize ground pressure (Håkansson, 2005). Soil compaction depends on the internal soil strength that is described by “precompression stress P_c .” To prevent soil against harmful compaction the concept of critical P_c values can be used as precaution to avoid soil compaction (Horn and Fleige, 2009) (see *Subsoil Compaction* and *Compaction of Soil*).

The area and volume of compacted soil can be considerably reduced by confining heavy field transport to permanent traffic lanes and by controlled traffic in which all traffic throughout the growing season is restricted to permanent, parallel tracks or by restricting traffic for all field operations carried out after crop establishment to the interrow zones (Håkansson, 2005).

Summary

The main soil physical conditions influencing crop growth include temperature, water content, oxygen availability, soil strength of seedbed layer at emergence, and soil below during later growth. Their effects are related to site conditions. For example, in cold climates low seedbed temperatures and/or oxygen deficiency while in hot climates by high temperatures and/or high soil strengths can slow emergence and final stand establishment greatly. An important factor affecting root growth and distribution in tilled soils is vertical and horizontal strength discontinuity. The vertical discontinuity occurs between aggregated seedbed layer and firm soil below and between the plow layer and plow pans. The horizontal discontinuity is mostly caused by a greater strength under machinery tracks. Root response to soil physical conditions depends on the presence and distribution patterns of pores larger than roots that allow bypass the zones of high mechanical impedance and low aeration. When soil physical properties suppress root size, shoot growth and functions are influenced due to root-to-shoot signaling. Main shoot functions include photosynthesis and transpiration that are related to the leaf stomatal diffusive resistance. Usually crop growth is influenced by soil physical characteristics acting in combination and thereby it is often difficult to determine their relative contributions. The soil water status plays a very important role since it affects other significant soil physical factors such as aeration, strength, and temperature. The soil physical conditions are mostly influenced by tillage, compaction, and crop residue management. Further research is needed to explain the

perception of soil physical stress by plants and the conversion of physical phenomena into physiological responses.

Bibliography

- Ali, M., Jensen, C. R., Mogensen, V. O., Andersen, M. N., and Henson, I. E., 1999. Root signalling and osmotic adjustment during intermittent soil drying sustain grain yield of field grown wheat. *Field Crops Research*, **62**, 35–52.
- Alvarez, R., and Steinbach, H. S., 2009. A review of the effects of tillage systems on some soil physical properties, water content, nitrate availability and crops yield in the Argentine Pampas. *Soil and Tillage Research*, **104**, 1–15.
- Atkinson, B. S., Sparkes, D. L., and Mooney, S. J., 2009. Effect of seedbed cultivation and soil macrostructure on the establishment of winter wheat (*Triticum aestivum*). *Soil and Tillage Research*, **103**, 291–301.
- Baumhardt, R. L., Jones, O. R., and Schwartz, R. C., 2008. Long-term effects of profile-modifying deep plowing on soil properties and crop yield. *Soil Science Society of America Journal*, **72**, 677–682.
- Bengough, A. G., Bransby, M. F., Hans, J., McKenna, S. J., Roberts, T. J., and Valentine, T. A., 2006. Root responses to soil physical conditions; growth dynamics from field to cell. *Journal of Experimental Botany*, **57**, 437–447.
- Bennicelli, R. P., Stepniewski, W., Zakrzhevsky, D. A., Balakhnina, T. I., Stepniewska, Z., and Lipiec, J., 1998. The effect of soil aeration on superoxide dismutase activity, malondialdehyde level, pigment content and stomatal diffusive resistance in maize seedlings. *Environmental and Experimental Botany*, **39**, 203–211.
- Birkás, M., 2008. *Environmentally-sound adaptable tillage*. Budapest, Hungary: Akadémia Kiado.
- Busscher, W. J., Lipiec, J., Bauer, P. J., and Carter, T. E., Jr., 2000. Improved root penetration of soil hard layers by a selected genotype. *Communications in Soil Science and Plant Analysis*, **31**, 3089–3101.
- Busscher, W. J., Frederick, J. R., and Bauer, P. J., 2001. Effect of penetration resistance and timing of rain on grain yield of narrow-row corn in a coastal plain loamy sand. *Soil and Tillage Research*, **63**, 15–24.
- Busscher, W. J., Novak, J. M., and Caesar-TonThat, T. C., 2007. Organic matter and polyacrylamide amendment of Norfolk loamy sand. *Soil and Tillage Research*, **93**, 171–178.
- Cornish, P., 1984. Soil physical requirements for germination, root development, plant production and survival. 25 years of the Riverina Outlook Conference, Wagga Wagga, pp. 1973–1998.
- Czyż, E. A., 2004. Effects of traffic on soil aeration, bulk density and growth of spring barley. *Soil and Tillage Research*, **79**, 153–166.
- Da Silva, A. P., Kay, B. D., and Perfect, E., 1997. Management versus inherent soil properties effects on bulk density and relative compaction. *Soil and Tillage Research*, **44**, 81–93.
- Dodd, I. C., 2005. Root-to-shoot signalling: assessing the roles of “up” in the up and down world of long-distance signalling in plants. *Plant and Soil*, **274**, 251–270.
- Dumitru, E., Canarache, A., and Dumitru, S., 2000. Research on soil compaction on arable land in Romania: a review. In *Proceedings 2nd International Conference on Subsoil Compaction*. Hungary: Gödöllő, pp. 44–49.
- Gliński, J., and Lipiec, J., 1990. *Soil physical conditions and plant roots*. Boca Raton, FL: CRC Press.
- Gliński, J., and Stepniewski, W., 1985. *Soil aeration and its role for plants*. Boca Raton, FL: CRC Press.
- Gregory, E. G., Turchenek, L. W., Carter, M. R., and Angers, D. A. (eds.), 2002. *Soil and environmental science dictionary*. Boca Raton, FL: CRC Press LLC.
- Håkansson, I., 1990. A method for characterizing the state of compactness of the plough layer. *Soil and Tillage Research*, **16**, 105–120.
- Håkansson, I., 2005. Machinery-induced compaction of arable soils, incidence – consequences – counter-measures. Swedish University of Agricultural Sciences, Reports from the Division of Soil Management, No. 109.
- Håkansson, I., and Lipiec, J., 2000. A review of the usefulness of relative bulk density values in studies of soil structure and compaction. *Soil and Tillage Research*, **53**, 71–85.
- Håkansson, I., Myrbeck, Å., and Etana, A., 2002. A review of research on seedbed preparation for small grains in Sweden. *Soil and Tillage Research*, **64**, 23–40.
- Hamza, M. A., and Anderson, W. K., 2005. Soil compaction in cropping systems: a review of the nature, causes and possible solutions. *Soil and Tillage Research*, **82**, 121–145.
- Harris, D., 1996. The effects of manure, genotype, seed priming, depth and date of sowing on the emergence and early growth of Sorghum bicolor (L.) Moench in semi-arid Botswana. *Soil and Tillage Research*, **40**, 73–88.
- Hatano, R., Iwanaga, K., Okajima, H., and Sakuma, T., 1988. Relationship between the distribution of soil macropores and root elongation. *Soil Science and Plant Nutrition*, **34**, 535–546.
- Hodges, D., Hamilton, R. I., and Charest, C., 1994. A chilling resistance test for inbred maize lines. *Canadian Journal of Plant Science*, **74**, 687–691.
- Horn, R., 1994. The effect of aggregation of soils on water, gas and heat transport. In Schulze, E. (ed.), *Flux control in biological systems*. San Diego, CA: Academic, pp. 335–361.
- Horn, R., and Fleige, H., 2009. Risk assessment of subsoil compaction for arable soils in Northwest Germany at farm scale. *Soil and Tillage Research*, **102**, 201–208.
- Hu, T., Kang, S., Li, F., and Zhang, J., 2009. Effects of partial root-zone irrigation on the nitrogen absorption and utilization of maize. *Agricultural Water Management*, **96**, 208–214.
- Ishaq, M., Ibrahim, M., Hassan, A., Saeed, M., and Lal, R., 2001. Subsoil compaction effects on crops in Punjab, Pakistan: II. Root growth and nutrient uptake of wheat and sorghum. *Soil and Tillage Research*, **60**, 153–161.
- Jakobsen, F. R., and Dexter, A. R., 1987. Effect of soil structure on wheat root growth, water uptake and grain yield. A computer simulated model. *Soil and Tillage Research*, **10**, 331–345.
- Lipiec, J., and Gliński, J., 1997. Field soil compaction: effects on soil physical properties and stomatal resistance of wheat. In *Proceedings International Symposium “Soil, Human and Environment Interactions”*. Beijing: China Science and Technology Press, pp. 422–427.
- Lipiec, J., and Hatano, R., 2003. Quantification of compaction effects on soil physical properties and crop growth. *Geoderma*, **116**, 107–136.
- Lipiec, J., and Simota, C., 1994. Role of soil and climate factors influencing crop responses to compaction in Central and Eastern Europe. In Soane, B. D., and van Ouwerkerk, C. (eds.), *Soil compaction in crop production*. Amsterdam, Netherlands: Elsevier, pp. 365–390.
- Lipiec, J., Ishioka, T., Szustak, A., Pietrusiewicz, J., and Stepniewski, W., 1996. Effects of soil compaction and transient oxygen deficiency on growth, water use and stomatal resistance of maize. *Acta Agriculturae Scandinavica, Section B, Soil and Plant Science*, **46**, 186–191.
- Lipiec, J., Arvidsson, J., and Murer, E., 2003a. Review of modelling crop growth, movement of water and chemicals in relation to topsoil and subsoil compaction. *Soil and Tillage Research*, **73**, 15–29.
- Lipiec, J., Medvedev, V. V., Birkás, M., Dumitru, E., Lyndina, T. E., Rousseva, S., and Fulajtár, E., 2003b. Effect of soil compaction on root growth and crop yield in Central and Eastern Europe. *International Agrophysics*, **17**, 61–69.

- McQueen, D. J., and Shepherd, T. G., 2002. Physical changes and compaction sensitivity of a fine-textured, poorly drained soil (Typic Endoaquept) under varying durations of cropping Manawatu Region, New Zealand. *Soil and Tillage Research*, **63**, 93–107.
- Munkholm, L. J., Schjønning, P., Jørgensen, M. H., and Thorup-Kristensen, K., 2005. Mitigation of subsoil recompaction by light traffic and on-land ploughing: II. Root and yield response. *Soil and Tillage Research*, **80**, 159–170.
- Nosaliewicz, A., and Lipiec, J., 2002. Effect of localised soil compaction and wetness on early root growth and functions. *Acta Agrophysica*, **78**, 199–208 (in Polish with English summary).
- Raper, R. L., 2005. Subsoiling. In Hillel, D. (ed.), *Encyclopedia of soils in the environment*. Oxford, UK: Elsevier, Vol. 4, pp. 69–76.
- Schneider, E. C., and Gupta, S. C., 1985. Corn emergence as influenced by soil temperature, matric potential and aggregate size distribution. *Soil Science Society of America Journal*, **49**, 415–422.
- Siczek, A., 2009. Effect of bulk density and mulching on root and shoot growth of soybean. PhD Dissertation, Lublin, Poland: Institute of Agrophysics.
- Šimůnek, J., and Hopmans, W., 2009. Modeling compensated root water and nutrient uptake. *Ecological Modelling*, **220**, 505–521.
- Strudley, M. W., Green, T. R., and Ascough, J. C., 2008. Tillage effects on soil hydraulic properties in space and time: State of the science. *Soil and Tillage Research*, **99**, 4–48.
- Sweeney, D. W., Kirkham, M. B., and Sisson, J. B., 2006. Crop and soil response to wheel-track compaction of a caypan soil. *Agronomy Journal*, **98**, 637–643.
- Tamet, V., Boiffin, J., Dürr, C., and Souty, N., 1996. Emergence and early growth of an epigeal seedling (*Daucus carota* L.): influence of soil temperature, sowing depth, soil crusting and seed weight. *Soil and Tillage Research*, **40**, 25–38.
- Tardieu, F., 1994. Growth and functioning of roots and root systems subjected to soil compaction. Towards a system with multiple signalling? *Soil and Tillage Research*, **30**, 217–234.
- Tardieu, F., and Manichon, H., 1986. Characterization en taut que capteur d'eau de l'enracinement du maïs en parcelle cultivee. *Agronomie*, **6**, 18–37.
- Taylor, H. M., and Brar, G. S., 1991. Effect of soil compaction on root development. *Soil and Tillage Research*, **19**, 111–119.
- Tisdall, J. M., 1996. Crop establishment – a serious limitation to high productivity. *Guest editorial. Soil and Tillage Research*, **40**, 1–2.
- Townend, J., Mtakwa, P. W., Mullins, C. E., and Simmonds, L. P., 1996. Soil physical factors limiting establishment of sorghum and cowpea in two contrasting soil types in the semi-arid tropics. *Soil and Tillage Research*, **40**, 89–106.
- Tripathi, R. P., Sharma, P., and Singh, S., 2007. Influence of tillage and crop residue on soil physical properties and yields of rice and wheat under shallow water table conditions. *Soil and Tillage Research*, **92**, 221–226.
- Usowicz, B., and Lipiec, J., 2009. Spatial distribution of soil penetration resistance as affected by soil compaction: The fractal approach. *Ecological Complexity*, **6**, 263–271.
- Weaich, K., Cass, A., and Bristow, K. L., 1996. Pre-emergent shoot growth of maize (*Zea mays*, L.) as a function of soil strength. *Soil and Tillage Research*, **40**, 3–23.
- Whalley, W. R., Lipiec, J., Stepniewski, W., and Tardieu, F., 2000. Control and measurement of the physical environment in root growth experiments. In Smit, A. L., Bengough, A. G., Engels, C., van Noordwijk, M., Pellerin, S., and van de Geijn, S. C. (eds.), *Root methods, a handbook*. Berlin: Springer, pp. 76–112.
- Whalley, W. R., Clark, L. J., Gowing, D. J. G., Cope, R. E., Lodge, R. J., and Leeds-Harrison, P. B., 2006. Does soil strength play a role in wheat yield losses caused by soil drying? *Plant and Soil*, **280**, 279–290.
- Wuest, S. B., Albrecht, S. L., and Skirvin, K. W., 1999. Vapor transport vs. seed–soil contact in wheat germination. *Agronomy Journal*, **91**, 783–787.

Cross-references

- [Controlled Traffic Farming](#)
- [Crop Emergence, the Impact of Mechanical Impedance](#)
- [Earthworms as Ecosystem Engineers](#)
- [Hardpan Soils: Management](#)
- [Hardsetting Soils: Physical Properties](#)
- [Management Effects on Soil Properties and Functions](#)
- [Physics of Plant Nutrition](#)
- [Plant Drought Stress: Detection by Image Analysis](#)
- [Plant Roots and Soil Structure](#)
- [Precision Agriculture: Proximal Soil Sensing](#)
- [Pre-Compression Stress](#)
- [Soil Aggregates, Structure, and Stability](#)
- [Soil Physical Quality](#)
- [Soil Surface Sealing and Crusting](#)
- [Spatial Variability of Soil Physical Properties](#)

CROP ROTATION

See [Cropping Systems, Effects on Soil Physical Properties](#)

CROP WATER USE EFFICIENCY

See [Water Use Efficiency in Agriculture: Opportunities for Improvement](#)

CROP YIELD LOSSES REDUCTION AT HARVEST, FROM RESEARCH TO ADOPTION

Bogusław Szot¹, Mieczysław Szpryngiel², Jerzy Tys¹

¹Institute of Agrophysics, Polish Academy of Sciences, Lublin, Lublin, Poland

²University of Life Sciences, Lublin, Poland

Definition

Interdisciplinary agrophysics, on the basis of fundamental studies on physical properties of plants and agricultural crops, provides other disciplines of agricultural sciences with methods and spectacular research results that are applied in the design and production of agricultural machinery and in its operation during the harvest and postharvest processing of agricultural products. During this operation, *Crop yield losses* appear and they often drastically decrease total yield. Comprehensive agrophysical studies on plants and agricultural products conducted in the aspect of implementation of their results in agricultural practice are able to mitigate crop yield losses.

Introduction

Almost all crop plants have retained, to a lesser or greater extent, atavistic features and tend to shed their seeds as soon as they have attained full ripeness, in order to ensure continuation of the species. Breeders of new cultivars have long observed that phenomenon and undertake efforts aimed at its limitation, though with varying degree of success. Seed losses at the stage of ripening and harvest reach the level of over a dozen, and often several dozen percent of the total yield, which on the global scale gives a hard to estimate reduction of yields actually obtained compared to those predicted during the vegetation of crops.

One of the highly important elements leading to the limitation of those losses is acquisition of in-depth knowledge of the physical properties of such crop plants at various stages of seed ripeness, and proper utilization of the results of such studies in the selection of the time of harvest and in the adaptation of harvesting machines to the specific character of the crop plants and to the structure of the plant canopy.

Cereals and grasses

In the production of cereals and seed grasses, the most important traits include the mechanical properties of stems (significant for the limitation of lodging) and the bond force between the kernel and the spike or the panicle. Highly susceptible to cracking and seed shedding are the fruits of cruciferous plants (siliques) and of large-seed leguminous plants (pods). Similar phenomena occur in seed production of vegetables, medicinal plants, and industrial plants.

The utilization of results of agrophysical studies for the limitation of quantitative losses of seeds cannot be accepted as a success in itself, as there remains another element, no less important, i.e., qualitative losses defined

as damage of various kinds. Damage to seeds is caused by the particular subassemblies of harvesting machinery whose operating parameters are not adapted to the mechanical strength of seeds of various plant species or cultivars. In this respect, the results of agrophysical studies provide information on the values of forces characterizing the mechanical strength of the seeds that cannot be exceeded in the course of harvesting, transport, drying, and storage to obtain material of high quality, both with respect of raw material and of the end product.

Agrophysical studies conducted so far at various research centers have demonstrated that knowledge of the physical properties of plants and agricultural products may constitute the basis for the development of new technologies of seed production with maximum limitation of quantitative and qualitative losses. Some of such solutions have been implemented at full-scale production, bringing measurable economic advantages.

Such a final effect can be achieved through highly detailed laboratory examinations of plant material, taking into account the agricultural techniques applied, the anatomical-morphological features, variety-related traits, stage of ripeness, various levels of moisture, plant protection agents, and preparations applied at the final phase of ripening. Once the results of such comprehensive studies are known, they are tested on the micro-scale on experimental lots, and then on larger field areas, using harvesting machines in order to identify the required settings of their subassemblies or implementing required adaptations. After applying necessary corrections and repeated testing, the results of agrophysical studies can be made available to producers as a new and proven technology of seed acquisition ([Table 1](#)).

Optimization of production of cereals and seed grasses is practically impossible without knowledge of the

Crop Yield Losses Reduction at Harvest, from Research to Adoption, Table 1 Some mechanical properties of cereal plants and seed grasses

Plant	Kernel-spike bond force (N)	Coefficient of variation V(%)	Susceptibility to seed shedding	Resistance to static loads (N)	Deformation (%)	Energy (mJ)
Winter wheat	0.91–2.09	27.0–40.08	Medium	51.0–73.6	11.2–13.0	8.1–14.1
Spring wheat	1.19–1.56	30.09–35.08	Low	46.1–59.8	12.4–13.6	4.5–12.9
Rye	0.98–1.34	22.5–32.9	Medium	78.3–130.5	16.8–19.7	9.8–14.7
Barley	1.80–2.90	20.7–38.1	Very low	147.2–235.9	11.6–12.8	10.2–19.3
Triticale	1.06–1.81	23.3–39.2	Medium	65.7–107.9	10.3–20.6	7.7–16.6
Amaranth	—	—	Low	11.9–70.7	12.1–43.2	0.9–14.7
Cocksfoot grass	0.32–0.48	19.1–33.2	Low	—	—	0.14–0.39
<i>Dactylis glomerata L.</i>						
Fescue grass	0.22–0.25	17.3–26.4	High	—	—	0.32–0.36
<i>Festuca pratensis Huds.</i>						
Dutch rye-grass	0.42–0.47	21.7–32.3	High	—	—	0.05–0.21
<i>Lolium multiflorum Lam.</i> var. <i>westerwoldicum</i>						
Timothy grass	—	—	Medium	—	—	—
<i>Phleum pratense L.</i>						
Brome grass	0.36–0.46	23.4–41.0	Low	—	—	0.04–0.15
<i>Bromus intermis Leyss.</i>						

physical properties of the plants during their ripening and harvest. Knowledge of the limit values of particular traits permits such preparation of agricultural machinery and tools that, in spite of the highly complex interrelations of numerous factors, will permit maximum limitation of quantitative losses while ensuring high quality of sowing material (Arnold et al., 1958; Zoerb, 1960; Hill, 1975).

The susceptibility of cereal and grass kernels to shedding with relation to moisture, i.e., with progressing ripening, varies greatly for the particular species, which is reflected in the values of the kernel-ear bond force (Szot and Reznicek, 1984). That value varies within the range of 0.91–2.90 N for cereals, while for grasses the corresponding range is 0.22–0.48 N (Szpryngiel, 1991). Those values are characterized by notable variability resulting from the genetic traits, cultivation environment, moisture, and phases of ripeness of the plants (Debrand, 1980). Therefore, during the period of ripening the unfavorable phenomenon of seed shedding takes place under the effect of atmospheric factors. In this respect, cereals are notably less susceptible to seed shedding when compared with seed grasses. With a drop in seed moisture, all grass species distinctly weaken the bond between the kernel and the torus within a very short time (even just a few hours), which may cause seed losses of even up to several dozen percent of the yield (Szpryngiel, 1976; Szpryngiel, 1983). Hence, the selection of the date of harvest requires constant monitoring of both the level of seed moisture and of the stage of ripeness. Amaranth can be classified as a specific cereal plant. It provides high yields, but on the condition that its combine harvest is performed when the leaves have been frost bitten or dried, i.e., in late autumn. If such conditions do not occur, two-stage harvesting is applied, consisting in cutting off the panicles for drying and subsequent threshing (Szot, 1999).

The harvest of cereal plants often involves damage to the grain, lowering the quality of the yield. This is related with the resistance of seeds to mechanical loads occurring in the combine harvester (Arnold and Roberts, 1969; Szot, 1984). Apart from the genetic traits, that resistance is affected by moisture and by the environmental conditions under which the crops are cultivated. Hence the significance of proper selection of operating parameters of harvester subassemblies.

Very dry seeds are brittle and crack easily, while wet seeds display plastic properties and a subject to permanent deformations. The lowest level of damage to seeds is observed when the seeds are in the elastic or elasto-plastic state.

Leguminous Plants

Information significant for the limitation of quantitative losses in the production of leguminous plants includes the force and energy of pod cracking (Table 2).

The values of those traits form broad ranges, which differentiates the particular species in terms of the level of seed losses in the course of ripening and harvest. Species characterized by the highest susceptibility to pod cracking

Crop Yield Losses Reduction at Harvest, from Research to Adoption, Table 2 Mechanical properties of some leguminous plants and rapeseed pods

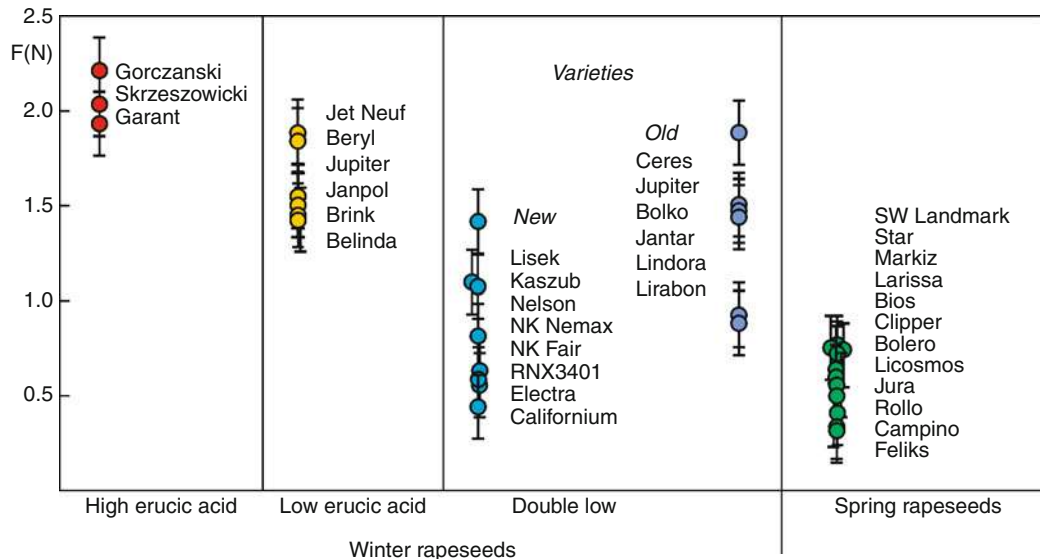
Plant	Cracking force (N)	Cracking energy (mJ)
Broad bean	1.40–1.60	0.72–0.89
Peas	0.32–1.23	0.15–0.40
Beans	0.81–1.24	0.41–0.52
Lupine	1.40–1.80	1.50–1.65
Soybean	1.43–2.02	0.80–1.85
Lentil	0.71–1.21	0.51–1.00
Winter rapeseed	0.42–2.21	6.01–16.03
Spring rapeseed	0.41–0.83	6.02–9.45

and seed shedding include pea, lentil, and beans. More resistant species include broad bean and some lupine cultivars. Choosing suitable parameters of operation of machines used for harvesting those crops will permit considerable limitation of seed losses (Sosnowski, 1991; Dobrzański and Szot, 1997; Szot et al., 2005).

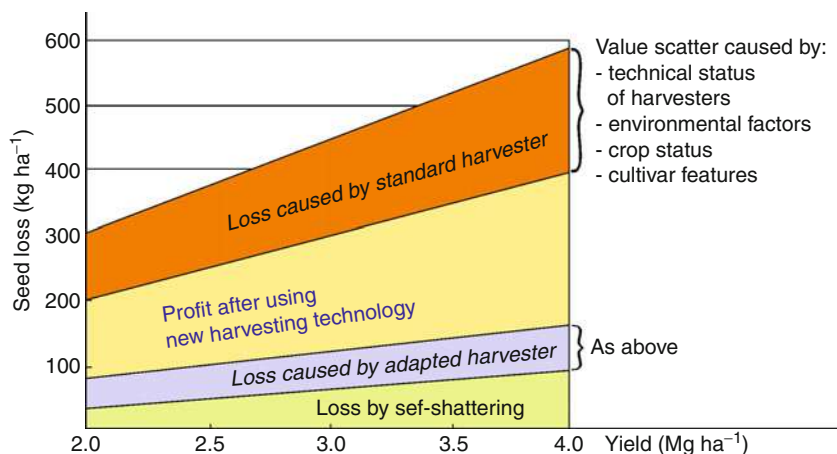
Rapeseed

Rapeseed is a crop that has an increasing economic importance. One of the unfavorable features of that plant, often of fundamental importance in determining the profitability of its cultivation, is the susceptibility of its pods to cracking and seed shedding (Josefsson, 1968; Loof and Jonsson, 1970; Kadkol et al., 1986). The primary factors causing the variability of rapeseed pod strength are the genetic traits, moisture, stage of ripeness, physical condition of the canopy, and atmospheric conditions. Hence, a considerable variability of the mechanical properties of rapeseed pods can be observed even within individual cultivars (Reznicek, 1978; Szot et al., 1991). The lowest values of force causing pod cracking, both for the winter and spring forms of rapeseed, are on average equal to 0.4 N. Whereas, the range of those values for winter rapeseed reaches up to 2.2 N, while for spring rapeseed only to 0.8 N. The values of pod cracking energy correspond to those ranges of force variability. The broader range of values for the winter forms of rapeseed is related with the large numbers of cultivars, including ones that are much more resistant to pod cracking. High erucic acid varieties of rapeseed were cultivated first, then improved varieties with low erucic acid, and nowadays there are so-called double low varieties, i.e., seeds with low erucic and low glucosinolate content. Significant variability of force values causing cracking of pods was observed within these varieties (Figure 1).

A comprehensive study on the physical properties of rapeseed, taking into account all the factors and numerous cultivars, has been conducted within the territory of Poland (Szot et al., 1991). The results obtained were used for the development of a new technology for the acquisition of rapeseeds. That technology provided for the application of suitable settings and adaptations of the particular



Crop Yield Losses Reduction at Harvest, from Research to Adoption, Figure 1 Mean values of force causing cracking of rape pods.



Crop Yield Losses Reduction at Harvest, from Research to Adoption, Figure 2 Relations between rapeseed seed losses and seed yields in combine harvest based on agrophysical research and effects of implementations at rapeseed producing farms.

subassemblies of the combine harvester, taking into account the inter-variety variability of plants and all external factors on the day of the harvest. As a result, based on the fundamental studies of the physical properties of rapeseed and the modification of the operating parameters of the harvester, an economic effect was achieved in the form of maximum limitation of qualitative and quantitative losses of seeds without any additional financial outlays (Szpryngiel et al., 2004). An illustration of those comprehensive studies and the test implementations is given in Figure 2.

Conclusion

Summing up, it should be stated that the application of results of agrophysical research on cereal plants, seed grasses, large-seed leguminous plants, and rapeseed in

agricultural production brings or may bring measurable economic effects. The most visible effects of such activities are observable in relation to rapeseed, as fundamental research and test implementations have resulted in the development of a new technology for the harvest of that crop, ensuring maximum limitation of qualitative and quantitative losses of seeds without any additional financial outlays. Prior to the implementation of that technology, proven and irreversible quantitative losses of seeds were up to, or even above 20% of seed yield, and damage to the seeds often disqualified the material harvested as consumption or sowing material. Therefore, comprehensive agrophysical studies on plants and agricultural products conducted in the aspect of implementation of their results in agricultural practice should be considered as useful and profitable.

Bibliography

- Arnold, P. C., and Roberts, A. W., 1969. Fundamental aspects of load-deformation behavior of wheat grain. *Transactions of the American Society of Agricultural Engineers*, **12**, 104–108.
- Arnold, R. E., Caldwell, F., and Davies, A. C., 1958. The effect of moisture content of the grain and the drum setting of the combine harvester on the quality of oats. *Journal of Agricultural Engineering Research*, **3**, 336–345.
- Debrand, M., 1980. A quel moment recolter les graminées porte-graine? *Bulletin de la Federation Nationale des Agriculteurs Multiplicateurs de Semences (France)*, **18**, 9–15.
- Dobrzański, B., and Szot, B., 1997. Mechanical properties of pea seed coat. *International Agrophysics*, **11**, 301–306.
- Hill, L. D., 1975. Corn quality as influenced by harvest and drying conditions. *Cereal Foods Word*, **20**, 333–335.
- Josefsson, E., 1968. Investigations on Shattering Resistance of Eruciferous Oil Crops. *Zeitschrift fur Pflanzenzuchtung*, **59**, 384–395.
- Kadkol, G. P., Beilharz, V. C., Halloran, G. M., and MacMillan, R. H., 1986. Anatomical basis of shatter-resistance in the oilseed brassicas. *Australian Journal of Botany*, **34**, 595–601.
- Loof, B., and Jonsson, R., 1970. Resultat av undersökningar rörande drasfastheten hos raps. *Sartryck ur Sveriges Utsadesforeningens Tidskrift*, **80**, 193–205.
- Reznicek, R., 1978. Examination of agrophysical properties of rape. *Zeszyty Problemowe Postępów Nauk Rolniczych*, **203**, 253–261.
- Sosnowski, S., 1991. Evaluation of the effect of some threshing assemblies on the level of bean damage (in Polish). *Zeszyty Naukowe AR Kraków*, **162**, 1–63.
- Szot, B., 1984. An evaluation of the influence of agrotechnical factors on the variability of the mechanical properties of winter wheat grain. *Zeszyty Problemowe Postępów Nauk Rolniczych*, **245**, 147–154.
- Szot, B., 1999. Agrophysical properties of amaranth (*Amaranthus cruentus* L) (in Polish). *Acta Agrophysica*, **18**, 1–73.
- Szot, B., and Reznicek, R., 1984. Variability of the grain-to-ear binding force of wheat and rye. *Zeszyty Problemowe Postępów Nauk Rolniczych*, **245**, 111–126.
- Szot, B., Tys, J., Szpryngiel, M., and Grochowicz, M., 1991. Determination of the reasons for rapeseed losses at combine harvesting and some methods of their limitation. *Zeszyty Problemowe Postępów Nauk Rolniczych*, **389**, 221–232.
- Szot, B., Stepniewski, A., and Rudko, T., 2005. Agrophysical properties of lentil (*Lens culinaris* Medik.). Centre of Excellence AGROPHYSICS, IA PAN, EU 5th Framework Program QLAM-2001-00428, pp. 1–77.
- Szpryngiel, M., 1976. Determination of the optimal term of grass seed harvesting (in Polish). *Hodowla Roślin*, **4**, 8–11.
- Szpryngiel, M., 1983. Effect of the combine harvest on grass seed injuries (in Polish). *Zeszyty Problemowe Postępów Nauk Rolniczych*, **258**, 369–376.
- Szpryngiel, M., 1991. Estimation of the Physical Properties of Grass Seed at Combine Harvest (in Polish). Agriculture University in Lublin. *Monograph*, 1–92.
- Szpryngiel, M., Wesołowski, M., and Szot, B., 2004. Economical technology of rape seed harvest. *TEKA Komisji Motoryzacji i Energetyki Rolnictwa O.L. PAN w Lublinie*, **4**, 185–195.
- Zoerb, C. C., 1960. Some mechanical and rheological properties of grain. *Journal of Agricultural Engineering Research*, **1**, 83–93.

Cross-references

Agrophysical Properties and Processes

Agrophysics: Physics Applied to Agriculture

Plant Physical Characteristics in Breeding and Varietal Evaluation

CROPPING SYSTEMS, EFFECTS ON SOIL PHYSICAL PROPERTIES

Stephen H. Anderson

Department of Soil, Environmental and Atmospheric Sciences, University of Missouri, Columbia, MO, USA

Synonyms

Crop rotations; Farming systems; Soil management; Soil productivity; Sustainable cropping systems

Definition

Aggregate stability: The proportion of aggregates in soil that do not easily crumble, disintegrate, or slake (Soil Science Society of America, 2008).

Bulk density: Mass of dry soil per unit volume.

Crop rotation: A land management system in which a sequence of crops is grown in a recurring succession (Soil Science Society of America, 2008).

Hydraulic conductivity: The parameter that represents the ability of soil to conduct water; a proportionality factor in Darcy's Law. It is equivalent to the flux of water per unit gradient of hydraulic potential (Soil Science Society of America, 2008).

Infiltration rate: The amount of water entering a specified area of soil per unit time (Soil Science Society of America, 2008).

Penetration resistance: Force per unit area for penetration of soil by a cone (Soil Science Society of America, 2008).

Physical properties: Those characteristic properties and processes of a soil caused by physical forces. Examples of physical properties include porosity, bulk density, hydraulic conductivity, pore-size distribution, and aggregate stability (Soil Science Society of America, 2008).

Pore-size distribution: Volume fractions of various pore sizes in a soil, includes various size ranges (Soil Science Society of America, 2008).

Porosity: Volume of pores divided by the bulk volume of the soil sample.

Soil water characteristic: Relationship between soil-water content and soil-water matric potential. Also referred to as the water retention curve or the water release curve (Soil Science Society of America, 2008).

Introduction

Development of tillage devices was critically important for early crop production systems because shallow placement of seeds helps to protect them and enhances germination (Hillel, 1998). Human-pulled traction spades evolved to animal-drawn plows, and eventually to modern mechanical tractor-drawn tillage equipment. Tillage systems include the mechanical manipulation of soil for any purpose, but agricultural tillage usually refers to modifying soil conditions, crop residues and/or weeds, and/or incorporating agrichemicals for crop production (Soil Science Society of America, 2008).

A significant challenge of these tillage systems was accelerated soil erosion (Gantzer et al., 1991), which encouraged the development of conservation tillage systems such as no-till to reduce soil disturbance and enhance residue cover. Modern cropping systems include conservation tillage for residue management to minimize soil erosion. Deep tillage systems for crop production have been developed to remove the effects of subsoil compaction or hardpans (Hamza and Anderson, 2005).

Cropping system practices known to influence soil physical properties include crop type (Scott et al., 1994), cultivation (Gantzer and Blake, 1978), and application of organic residues (Gantzer et al., 1987). Tillage systems have long been evaluated as a method to improve cropping systems and their associated soil physical properties.

Cropping systems affect soil organic matter content, which in turn strongly influences soil physical properties. Cropping systems that take land out of native vegetation reduce soil organic matter. Turnover of organic matter from an Alfisol developed under prairie vegetation by cropping was primarily from the rapid fraction with a half-life of 10–15 years (Balesdent et al., 1988). The slow or stable fraction, which constituted about 50% of the current level of organic matter, had nearly a complete turnover period of 600 years.

Changing tillage systems or crop rotations can enhance the accumulation of soil organic carbon. Evaluating a global database of 67 long-term experiments, West and Post (2002) found that a change from conventional tillage to no-till can sequester an average of $57 \text{ g C m}^{-2} \text{ year}^{-1}$. Changing to a more complex rotation can sequester an average of $20 \text{ g C m}^{-2} \text{ year}^{-1}$ excluding corn–soybean (*Glycine max* L.) rotations.

Addition of organic manures as part of cropping systems has been shown to result in increased soil organic matter content. Many reports have shown that these organic manure additions increase water-holding capacity (Hudson, 1994), porosity, hydraulic conductivity, infiltration capacity, and water-stable aggregates while decreasing soil bulk density and surface crusting (Haynes and Naidu, 1998).

Aggregates and aggregate stability

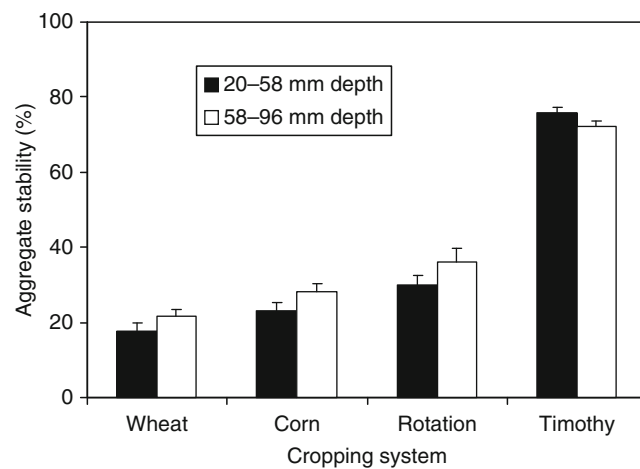
Comparing no-till dryland cropping systems after 12 years in eastern Colorado, USA, Shaver et al. (2002) found that macroaggregates ($>0.25 \text{ mm}$) made up a higher percentage of total aggregates in continuous cropping, wheat–corn–fallow, or wheat–sorghum (*Sorghum bicolor* L.)–fallow cropping systems compared to a traditional wheat fallow system (Shaver et al., 2002). More soil macroaggregates were attributed to greater levels of crop residue and subsequent soil organic matter production. Greater proportions of macroaggregates provided a greater opportunity to capture a higher proportion of precipitation and a more rapid capture of precipitation, which should improve long-term grain productivity of these cropping systems.

The influence of long-term cropping systems on soil aggregate stability was evaluated in Sanborn Field in central Missouri, USA by Rachman et al. (2003). Over 100 years of continuous cropping to timothy (*Phleum pratense* L.) produced higher aggregate stability compared to continuous corn (*Zea mays* L.) or continuous wheat (*Triticum aestivum* L.; Figure 1). This effect was observed in both the 2- to 6-cm (three to four times) and 6- to 10-cm (two to three times) depths. Rachman et al. (2003) speculated that more development of root binding in the timothy plots without annual tillage helped enhance aggregate stability. Annual tillage and exposure to raindrop impact during fallow periods for the corn and wheat plots decreased aggregate stability.

In the same study (Rachman et al., 2003), changing cropping systems from continuous corn or wheat to a three rotation of corn–wheat–red clover (*Trifolium pratense* L.) increased aggregate stability by 29% and 67%, respectively (Figure 1). Possible reasons for the increase in aggregate stability for the rotation plots include bonding material produced by red clover and canopy protection during the fallow period. Organic matter decomposition can be increased with red clover since it fixes nitrogen. The microbially mediated activity of decomposing organic matter produces polymers that bind soil particles together, which slows the rate of aggregate wetting and decreases the extent of slaking (Rachman et al., 2003).

Soil strength

Soil strength measured using a fall-cone penetrometer was found to be nearly five times greater for no-till management compared to conventional tillage management for coastal plain soils in Maryland, USA (Hill, 1990). These



Cropping Systems, Effects on Soil Physical Properties,

Figure 1 Aggregate stability values of two soil depths, 20–58 mm and 58–96 mm, for selected cropping systems in Sanborn Field, Missouri, USA ($n = 8$; Rachman et al., 2003). Bars represent the standard error of the mean. (Reprinted with permission from the Soil Science Society of America.)

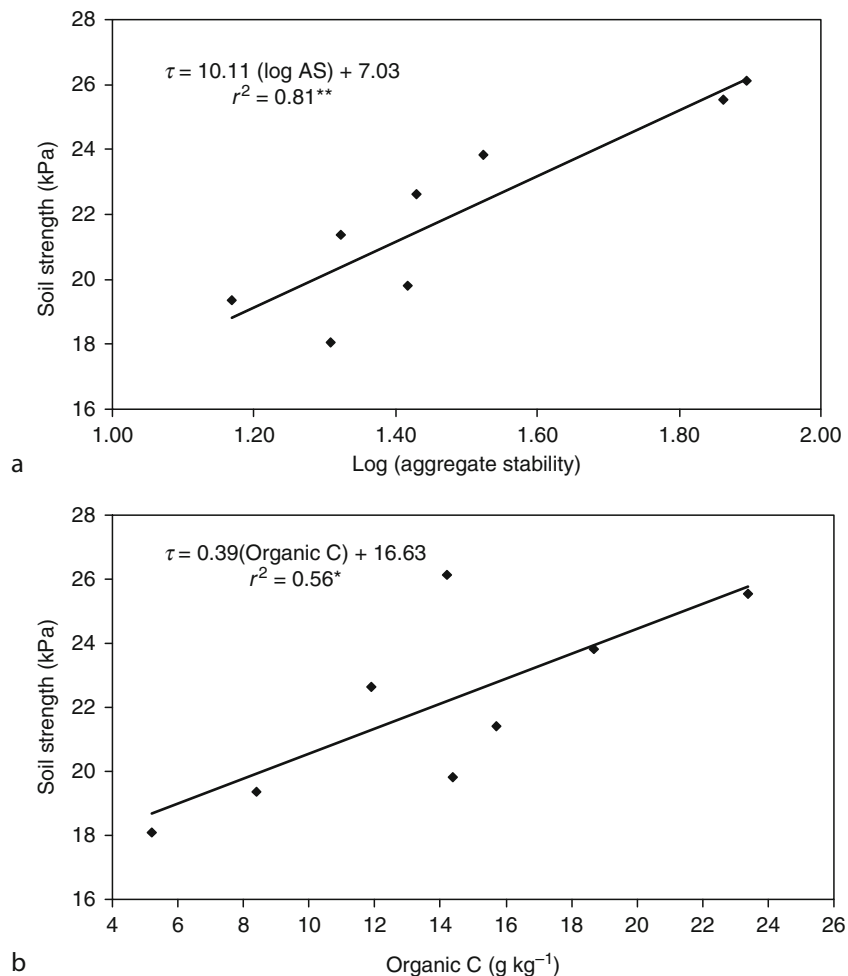
differences were attributed to higher soil bulk density for this treatment since no-till did not receive tillage compared to the conventionally tilled treatments.

The effect of long-term (100 year) cropping systems for Sanborn Field on soil shear strength was also evaluated using a fall-cone device (Rachman et al., 2003). Continuous cropping to timothy produced 27–33% greater soil strength compared to continuous wheat or continuous corn. The 3-year rotation of corn–wheat–red clover was also 14–19% higher compared to the wheat and corn plots. Rachman et al. (2003) speculated that higher organic carbon may have enhanced soil strength; strength was linearly related to organic carbon ($r = 0.75$; Figure 2). Soil strength was also linearly correlated with the log of aggregate stability ($r = 0.90$; Figure 2). Annual tillage for the continuous wheat and corn plots resulted in lower organic carbon, aggregate stability, and soil shear strength.

Bulk density and porosity

Alegre and Cassel (1996) found in the humid tropics that land cleared with bulldozers for continuous cropping systems (1.63 g cm^{-3}) significantly increased bulk density by 12% compared to traditional slash-and-burn systems (1.46 g cm^{-3}). If land is cleared with bulldozers, additional soil management is needed to remove the negative effects of mechanical land clearing. Use of agroforestry systems with cover crops and trees may actually improve soil physical properties (Alegre and Cassel, 1996).

Comparing 6-year old agroforestry (pin oak, *Quercus palustris* Muenchh.) and grass-legume buffers to a corn–soybean rotation under no-till management, Seobi et al. (2005) found that buffers decreased soil bulk density by 2.3%. However, coarse macroporosity (60- to 1,000- μm diam.) increased by 33% for the buffer treatments. Comparing land under row crop management to



Cropping Systems, Effects on Soil Physical Properties, Figure 2 Fall-cone soil shear strength vs. (a) the logarithm of aggregate stability (20–58 mm depth) and (b) organic C ($n = 4$; Rachman et al., 2003). * and ** Significant at the 0.05 and 0.01 probability levels, respectively. (Reprinted with permission from the Soil Science Society of America.)

native and restored prairie sites, Udwatta et al. (2008) found a 19% increase in bulk density throughout the surface 40 cm for a corn–soybean rotation compared to a native prairie site. These differences were attributed to five times lower macroporosity ($>1,000 \mu\text{m}$ diam.) for the cultivated site.

Shaver et al. (2002), in comparing no-till dryland cropping systems after 12 years, found that soil bulk density decreased and soil total porosity and effective porosity (total porosity minus water content at -10 kPa) increased for continuous cropping and wheat–corn–fallow cropping systems compared to a traditional wheat fallow system. These changes in physical properties were attributed to the continuous cropping and wheat–corn–fallow cropping systems returning more residue to the soil. The effects of these cropping systems on soil physical properties may often only be observed after several years.

Water retention and pore-size distribution

Evaluation of soil water retention can be used to determine soil pore-size distributions (Anderson et al., 1990). Crop management and landscape effects on water retention and pore-size distributions were evaluated by Jiang et al. (2007). After 14 years of management, they found significantly higher soil water retention for the Conservation Reserve Program system and hay crop management sites compared to a mulch till corn–soybean rotation from saturation to -1.0 kPa within the upper 10-cm soil depth. Jiang et al. (2007) also found 50% higher macroporosity ($>1,000 \mu\text{m}$ diam.) plus coarse mesoporosity (60- to $1,000\text{-}\mu\text{m}$ diam.) for the 10-cm soil depth in the Conservation Research Program treatment compared to the hay, no-till corn–soybean–wheat rotation, and the mulch till corn–soybean rotation treatments.

Assessing piedmont and coastal plain soils in Maryland, USA, Hill (1990) compared pore-size distributions between conventional tillage and no-till treatments after 11–12 years of management. A significantly larger volume of total pores and pores $>3.0 \mu\text{m}$ in diameter were found for the conventional tillage compared to no-till management for the coastal plain sites. Even though the no-till treatment had less volume for plant available water storage compared to conventionally tilled plots, corn production was higher with no-till probably due to better infiltration, less runoff, and less evaporation (Hill, 1990).

Hydraulic conductivity and infiltration

Evaluating historic crop management plots on Sanborn Field, Anderson et al. (1990) found that annual additions of manure (13.5 Mg ha^{-1}) for 100 years increased saturated hydraulic conductivity by about nine times. These differences were attributed to higher numbers of earthworms, which increased due to the higher amounts of organic matter in these plots.

Crop management and landscape effects on soil saturated hydraulic conductivity were evaluated for claypan

soils in Missouri, USA by Jiang et al. (2007). They found that hydraulic conductivity was 16 and 10 times higher under a Conservation Reserve Program system and hay crop management compared to a mulch till corn–soybean rotation at the backslope position, where the argillic clay subsoil horizon was closest to the surface. At the same site, infiltration was higher for perennial cropping systems such as Conservation Reserve Program and hay crop management compared to annual cropping systems such as mulch till and no-till corn–soybean rotations and a no-till soybean–corn–wheat rotation (Jung et al., 2007). Differences were attributed to lower antecedent soil water content in the spring for the perennial cropping systems.

After 13 years, Blanco-Canqui et al. (2004) evaluated saturated hydraulic conductivity for three tillage systems (no-till, chisel plow, moldboard plow) for two crops (corn, soybean) compared to continuous fallow plots. Crop had a greater effect on hydraulic conductivity compared to tillage with corn management decreasing conductivity compared to soybean management. All tillage and crop management systems had greater hydraulic conductivity compared to fallow management.

No-till management systems have been found to decrease runoff and increase infiltration compared to conventional tillage systems. Edwards (1982) found that no-till, with its increased number of macropores, decreased runoff by 20 times compared to conventional tillage in Ohio, USA. In western Nigeria, Lal (1997) found that tillage management significantly affected infiltration. In an 8-year experiment, no-till management significantly increased infiltration compared to a moldboard plow–harrow–ridge till treatment. In the humid tropics, Alegre and Cassel (1996) found reduced infiltration (35 mm h^{-1}) for mechanically cleared land for continuous cropping systems compared to traditional slash-and-burn systems (420 mm h^{-1}). They suggest use of agroforestry systems with cover crops and trees to improve soil physical properties.

Rachman et al. (2004) found that narrow, stiff-stemmed perennial grass hedges used as vegetative terraces significantly improved water infiltration compared to a traditional corn–soybean rotation on soils formed in deep loess. They found stiff-stemmed hedges had six times higher quasi-steady infiltration rates compared to row crop areas. These differences were attributed to significantly higher macroporosity under grass hedges.

Summary

Soil physical properties are significantly affected by cropping systems, especially tillage management. Tillage usually reduces soil bulk density and increases soil porosity initially; however, tillage decreases soil organic matter, which can also affect bulk density and porosity. Less frequent tillage and crop rotations with legumes enhance aggregate stability. No-till management tends to increase soil bulk density, increase soil strength, decrease total porosity, increase saturated hydraulic conductivity, and

increase infiltration (for well-drained soils). Enhancing residue cover is an important issue for modern conservation crop management systems in order to minimize soil erosion caused by tillage.

Bibliography

- Alegre, J. C., and Cassel, D. K., 1996. Dynamics of soil physical properties under alternative systems to slash-and-burn. *Agriculture, Ecosystems and Environment*, **58**, 39–48.
- Anderson, S. H., Gantzer, C. J., and Brown, J. R., 1990. Soil physical properties after 100 years of continuous cultivation. *Journal of Soil and Water Conservation*, **45**, 117–121.
- Balesdent, J., Wagner, G. H., and Mariotti, A., 1988. Soil organic matter turnover in long-term field experiments as revealed by carbon-13 natural abundance. *Soil Science Society of America Journal*, **52**, 118–124.
- Blanco-Canqui, H., Gantzer, C. J., Anderson, S. H., and Alberts, E. E., 2004. Tillage and crop influences on physical properties for an Epiaqualf. *Soil Science Society of America Journal*, **68**, 567–576.
- Edwards, W. M., 1982. Predicting tillage effects on infiltration. In Unger, P. W., et al. (eds.), *Predicting Tillage Effects on Soil Physical Properties and Processes*. Madison: American Society of Agronomy Special Publication 44, pp. 105–115.
- Gantzer, C. J., and Blake, G. R., 1978. Physical characteristics of Le Suerur clay loam soil following no-till and conventional tillage. *Agronomy Journal*, **70**, 853–857.
- Gantzer, C. J., Buyanovsky, G. A., Alberts, E. E., and Remley, P. A., 1987. Effects of soybean and corn residue decomposition on soil strength and splash detachment. *Soil Science Society of America Journal*, **51**, 202–206.
- Gantzer, C. J., Anderson, S. H., Thompson, A. L., and Brown, J. R., 1991. Evaluation of soil loss after 100 years of soil and crop management. *Agronomy Journal*, **83**, 74–77.
- Hamza, M. A., and Anderson, W. K., 2005. Soil compaction in cropping systems: A review of the nature, causes and possible solutions. *Soil and Tillage Research*, **81**, 121–145.
- Haynes, R. J., and Naidu, R., 1998. Influence of lime, fertilizer and manure applications on soil organic matter content and soil physical conditions: a review. *Nutrient Cycling in Agroecosystems*, **51**, 123–127.
- Hill, R. L., 1990. Long-term conventional and no-tillage effects on selected soil physical properties. *Soil Science Society of America Journal*, **54**, 161–166.
- Hillel, D., 1998. *Environmental Soil Physics*. San Diego: Academic, p. 368.
- Hudson, B. D., 1994. Soil organic matter and available water capacity. *Journal of Soil and Water Conservation*, **49**, 189–194.
- Jiang, P., Anderson, S. H., Kitchen, N. R., Sadler, E. J., and Sudduth, K. A., 2007. Landscape and conservation management effects on hydraulic properties of a claypan-soil toposequence. *Soil Science Society of America Journal*, **71**, 803–811.
- Jung, W. K., Kitchen, N. R., Anderson, S. H., and Sadler, E. J., 2007. Crop management effects on water infiltration for claypan soils. *Journal of Soil and Water Conservation*, **62**, 55–63.
- Lal, R., 1997. Long-term tillage and maize monoculture effects on a tropical Alfisol in western Nigeria. I. Crop yield and soil physical properties. *Soil and Tillage Research*, **42**, 145–160.
- Rachman, A., Anderson, S. H., Gantzer, C. J., and Thompson, A. L., 2003. Influence of long-term cropping systems on soil physical properties related to soil erodibility. *Soil Science Society of America Journal*, **67**, 637–644.
- Rachman, A., Anderson, S. H., Gantzer, C. J., and Thompson, A. L., 2004. Influence of stiff-stemmed grass hedge systems on infiltration. *Soil Science Society of America Journal*, **68**, 2000–2006.
- Scott, H. D., Mauromoustakos, A., Handayani, I. P., and Miller, D. M., 1994. Temporal variability of selected properties of loessial soil as affected by cropping. *Soil Science Society of America Journal*, **58**, 1531–1538.
- Seobi, T., Anderson, S. H., Udawatta, R. P., and Gantzer, C. J., 2005. Influence of grass and agroforestry buffer strips on soil hydraulic properties for an Albaqualf. *Soil Science Society of America Journal*, **69**, 893–901.
- Shaver, T. M., Peterson, G. A., Ahuja, L. R., Westfall, D. G., Sherrod, L. A., and Dunn, G., 2002. Surface soil physical properties after twelve years of dryland no-till management. *Soil Science Society of America Journal*, **66**, 1296–1303.
- Soil Science Society of America, 2008. Glossary of soil science terms, 2008 edition. Soil Science Society of America, Madison, WI, (Online). Available from World Wide Web: <https://www.soils.org/publications/soils-glossary>.
- Udawatta, R. P., Anderson, S. H., Gantzer, C. J., and Garrett, H. E., 2008. Influence of prairie restoration on CT-measured soil pore characteristics. *Journal of Environmental Quality*, **37**, 219–228.
- West, R. O., and Post, W. M., 2002. Soil organic carbon sequestration rates by tillage and crop rotation: a global data analysis. *Soil Science Society of America Journal*, **66**, 1930–1946.

Cross-references

- [Agrophysical Properties and Processes](#)
- [Bulk Density of Soils and Impact on Their Hydraulic Properties](#)
- [Compaction of Soil](#)
- [Controlled Traffic Farming](#)
- [Crop Responses to Soil Physical Conditions](#)
- [Hardpan Soils: Management](#)
- [Infiltration in Soils](#)
- [Management Effects on Soil Properties and Functions](#)
- [Organic Matter, Effects on Soil Physical Properties and Processes](#)
- [Pore Size Distribution](#)
- [Puddling: Effect on Soil Physical Properties and Crops](#)
- [Root Responses to Soil Physical Limitations](#)
- [Soil Aggregates, Structure, and Stability](#)
- [Soil Penetrometers and Penetrability](#)
- [Soil Tilth: What Every Farmer Understands but no Researcher can Define](#)
- [Subsoil Compaction](#)

CRUSHING STRENGTH

The force required to crush a mass of dry soil or, conversely, the resistance of the dry soil mass to crushing. Expressed in units of force per unit area (pressure).

Bibliography

- Glossary of Soil Science Terms. Soil Science Society of America. 2010. <https://www.soils.org/publications/soils-glossary>

CRUST

See [Soil Surface Sealing and Crusting](#)

CULTIVATION UNDER SCREENS, AERODYNAMICS OF BOUNDARY LAYERS

Josef Tanny

Institute of Soil, Water, and Environmental Sciences,
Agricultural Research Organization, The Volcani Center,
Bet Dagan, Israel

Definitions

Cultivation. The process of growing agricultural plants.

Screen. A porous material made of knitted or woven plastic threads. Screens are usually deployed above crops to protect them from various external hazards.

Aerodynamics. Study of air motion and its interaction with bodies in the flow.

Boundary layer. The layer of air adjacent to a bounding surface.

Introduction

The area of agricultural crops grown under screens and within screenhouses is constantly increasing. This is especially true in regions where climatic and environmental conditions, such as high radiation loads during certain seasons, water scarcity, wind and hail storms, and environmental pressure of insects, adversely affect competitive year-round production. The increased use of screenhouses by growers triggered the expansion of research on the effects of various screens on microclimate and on crop water use, as well as on produce quality and quantity. The ultimate goal is to optimize the design and use of screens to obtain high-quality yields. Research on screenhouse microclimate can be traced back to the beginning and middle of the twentieth century (Jenkins, 1900; Stewart, 1907; Waggoner et al., 1959), but only during the past few decades, with the progress of electronic measurement systems and data-processing capabilities, has a much better understanding of the screenhouse environment been achieved.

Screen constructions used to protect crops can be divided into two major categories: (1) horizontal screen covers without sidewalls, deployed at some height above the canopy top; (2) screenhouses consisting of a horizontal screen cover and screened sidewalls. Both types partially isolate the crop system from the outside environment. One major isolating factor is the resistance to transport of momentum, heat, and matter through the screen; this may impair proper ventilation and cause excessive temperature and humidity under the screen. Limited ventilation can also reduce the supply of CO₂ below adequate levels, thus inhibiting photosynthesis and consequently reducing production. On the other hand, reduced wind speed and temperature and increased humidity (or lower vapor pressure deficit) reduce the drying power of the air boundary layer near the plants, and may contribute to water saving. Thus, knowledge of aerodynamic properties of boundary layers along screens covering plant canopies is required for proper performance of the crop system.

The air flow along horizontal screens can be divided into two regions: above and below the screen. Above the screen, a boundary layer flow is established adjacent to the porous surface below, with the far edge of the boundary layer being the free atmosphere above. In this region, we anticipate the prevalence of the logarithmic wind profile, typical of turbulent flows along flat surfaces. Below the screen, the flow may be more complex and may strongly depend on the thickness of the air gap between the canopy top and the screen cover. The close proximity of the canopy elements may also influence the air flow characteristics. For open, uncovered canopies, this region is known as the “roughness sub-layer” where the roughness elements of the canopy (e.g., leaves and stems) control the flow properties. In this region, either logarithmic profile or channel flow profile or some combination of both is possible.

Other parameters influencing the flow properties along screens are the canopy morphology, the crop leaf area index, and the screen porosity, i.e., the ratio of open area to total screen area. Obviously, screens with higher porosity will have a smaller effect on the wind profile as compared with an uncovered canopy.

Theory and methods

The literature on cultivation under screens is focused on quantifying the effect of screens on micro-climate, air flow, and transport above the protected canopy. Hence, this section will briefly review the principles of boundary layer flows above plant canopies.

The wind speed profile in the surface layer above a canopy or a horizontal screen cover can be described (Stull, 1988) by

$$u(z) = \frac{u_*}{k} \left[\ln\left(\frac{z-d}{z_0}\right) + \Psi_M \right], \quad (1)$$

where u is the mean horizontal wind speed, z is the height above the ground, and k is the von-Karman constant ($= 0.41$).

The aerodynamic properties of the boundary layer flow are u_* , the friction velocity which represents the vertical transport of momentum by the turbulent flow; d , the zero-plane displacement which represents the vertical displacement of the wind profile by the canopy elements; z_0 , the roughness length, representing the surface roughness due to the canopy.

The function Ψ_M represents the stability of the air layer above the surface, either the canopy or the screen cover. Under neutral conditions, $\Psi_M = 0$ and the well-known logarithmic wind profile is resumed. Under such conditions, zero wind speed is achieved at $z = d + z_0$. Under stable conditions, $\Psi_M > 0$ and vertical transport is inhibited. Stable flow takes place when cooler (and heavier) air underlies warmer (and lighter) air. Over soil or vegetated surfaces such a situation may occur during clear nights where radiation to the sky cools down the earth's surface. Under unstable conditions, $\Psi_M < 0$ and vertical transport

may be enhanced. Unstable conditions prevail when warmer air underlies cooler one. This usually occurs due to daytime heating of surfaces by solar radiation. Under both non-neutral conditions the log-linear wind profile ([Equation 1](#)) prevails.

Usually, the aerodynamic properties for a specific crop system (e.g., a given crop, a forest canopy, or an orchard covered by a screen) are determined by fitting the wind speed profile equation ([Equation 1](#)), to the wind profile actually measured by anemometers at several levels above the crop or the screen cover. The aerodynamic properties are then used to calculate the aerodynamic resistance which controls vertical transport across the boundary layer. Different expressions are given in the literature for the aerodynamic resistance under unstable, neutral, and stable conditions (Monteith and Unsworth, [2008](#); Stull, [1988](#); Tanny et al., [2009](#)).

Aerodynamic properties of boundary layers above screens

Literature studies were mainly aimed at investigating the effect of screens on the aerodynamic properties (Tanny and Cohen, [2003](#)) and comparing the properties obtained under different crop systems and screens' dimensions (Tanny et al., [2009](#)).

A comparison between aerodynamic properties of boundary layers over covered and uncovered citrus trees was conducted under stable conditions (Tanny and Cohen, [2003](#)). A relatively small shading screen covered few citrus trees and was surrounded by a large uncovered orchard. The screen inhibited the turbulent transport by reducing the friction velocity, u_* . The screen cover reduced the roughness length z_0 , reflecting the difference between the flat and relatively smooth screen surface and the irregular rough surface of the exposed canopy. Over the covered trees, the zero-plane displacement d was larger than over uncovered ones. This was due to the effect of the screen in displacing the wind profile upward. All these effects caused the aerodynamic resistance to be significantly higher over the covered trees as compared to the exposed ones. The increased resistance may be one of the reasons for the reduced crop water consumption observed over covered crops. See, for example, Tanny et al. ([2006](#)) for a banana plantation.

The effect of stability was considered only for the covered citrus trees (Tanny and Cohen, [2003](#)). As expected, stable conditions inhibited the turbulent transport in comparison to unstable conditions. The roughness length decreased and zero-plane displacement increased with increasing stability. Corresponding values of aerodynamic resistance increased with stability. These results showed that roughness length and zero-plane displacement are stability-sensitive properties and do not depend only on geometric surface properties. Unstable flows induce more intense motion in the leaves and the canopy, and a more wave-like motion of the screen than stable flows, thereby increasing the surface roughness. Unstable conditions

enhance the vertical motion of air, which may also contribute to the larger friction velocity and lower values of the zero-plane displacement and aerodynamic resistance.

Different crop-screen systems are characterized by different aerodynamic properties. Properties over a small shade net, covering several citrus trees, were compared with those over a large screenhouse covering a pepper plantation (Tanny et al., [2009](#)). Under stable conditions, normalized aerodynamic properties, including the aerodynamic resistance, were the same at both settings. Under unstable conditions, the boundary layer over the large screenhouse was characterized by a lower aerodynamic resistance and a more intense turbulent transport. Tanny et al. ([2009](#)) suggested that the main reason for this difference is the different interaction of the screen and crop elements in the two settings with the vortices characterizing unstable winds.

Properties of the flow below the screen

The flow below the screen may be more complex than the flow above. Screen, canopy, and the distance between them may influence the flow structure and properties.

Measurements within an insect-proof screenhouse in which pepper was grown (Tanny et al., [2003](#); Möller et al., [2003](#)) have shown that at the leeward half of the screenhouse, airflow direction was essentially opposite to the external wind. On the other hand, in a banana plantation, covered with a much more porous screen, air flow directions inside (at the center) and outside were nearly the same (Tanny et al., [2006](#)). The difference can be attributed to the effect of the screen porosity on air flow patterns. Denser screens may induce larger resistance to the wind, thus causing a more significant deflection of wind streamlines around the screenhouse. Streamline deflections are associated with pressure gradients which may cause counter flow within the structure.

Turbulence characterization was reported for a banana screenhouse, in the air gap between the crop and the screen (Tanny et al., [2006](#)). Mean value of the turbulence intensity was 0.49 ± 0.12 . This suggested that Taylor's hypothesis of frozen turbulence was marginally satisfied (Willis and Deardorf, [1976](#)). Spectral energy density was plotted against frequency; slopes of regression lines were very close to the well-known slope of $-\frac{5}{3}$, typical of the inertial sub-range in steady state boundary layers (Stull, [1988](#)).

During the past 2 decades a new view of canopy flow has emerged, namely, the mixing layer analogy (Raupach et al., [1996](#)), suggesting that the flow above canopies resembles that of a mixing layer rather than a surface layer. This type of flow is associated with well-organized eddies of whole canopy scale resulting from Kelvin–Helmholtz hydrodynamic instabilities. To distinguish between surface layer and mixing layer flows, Raupach et al. ([1996](#)) presented a comparison between several statistic flow properties in the two flow configurations. For example, their Table II shows that in the surface layer

$\sigma_u/u_* = 2.5$, whereas in the mixing layer $\sigma_u/u_* = 1.7$, where σ_u is the standard deviation of the horizontal velocity. Corresponding average values within a large banana screenhouse measured by the present author were: $\sigma_u/u_* = 2.8 \pm 0.67$ at 5 m height and $\sigma_u/u_* = 2.65 \pm 0.65$ at 3.55 m height (where \pm is standard deviation) with trees' height of 3.1 m. These values are much closer to those of a surface layer than a mixing layer, suggesting that this type of flow prevails within the screenhouse.

Summary

Cultivation under screens is becoming more and more popular among growers due to its favorable effects on yield quality, production scheduling, and relatively low cost, as compared to plastic greenhouses. The screens inhibit the exchange of momentum, heat, matter, and radiation between the crop and the atmosphere. Scientific literature demonstrates the increased aerodynamic resistance over covered crops as compared to exposed ones. The higher resistance modifies the crop microclimate under the screen and thus may be partially associated with water saving and increased water use efficiency. Further research is needed to optimize screenhouse design for specific crops in given climatic regions.

Bibliography

- Jenkins, E. H., 1900. *Can wrapper leaf tobacco of the Sumatra type be raised in Connecticut?* Connecticut Agricultural Experimental Station, 24th Annual Report, pp. 322–329.
- Möller, M., Tanny, J., Cohen, S., and Teitel, M., 2003. Micrometeorological characterization in a screenhouse. *Acta Horticulturae*, **614**, 445–451.
- Monteith, J. L., and Unsworth, M., 2008. *Principles of Environmental Physics*, 3rd edn. New York: Elsevier/Academic.
- Raupach, M. R., Finnigan, J. J., and Brunet, Y., 1996. Coherent eddies and turbulence in vegetation canopies: the mixing layer analogy. *Boundary-Layer Meteorology*, **78**, 351–382.
- Stewart, J. B., 1907. *Effects of shading on soil conditions*. Soils Bureau Bulletin, No. 39. Washington, DC: U.S.G.P.O.
- Stull, R. B., 1988. *An Introduction to Boundary Layer Meteorology*. The Netherlands: Kluwer Academic.
- Tanny, J., and Cohen, S., 2003. The effect of a small shade net on the properties of wind and selected boundary layer parameters above and within a citrus orchard. *Biosystems Engineering*, **84**, 57–67.
- Tanny, J., Cohen, S., and Teitel, M., 2003. Screenhouse microclimate and ventilation: an experimental study. *Biosystems Engineering*, **84**, 331–341.
- Tanny, J., Haijun, L., and Cohen, S., 2006. Airflow characteristics, energy balance and eddy covariance measurements in a banana screenhouse. *Agricultural and Forest Meteorology*, **139**, 105–118.

Tanny, J., Möller, M., and Cohen, S., 2009. Aerodynamic properties of boundary layers along screens. *Biosystems Engineering*, **102**, 171–179.

Waggoner, P., Pack, A., and Reifsnyder, W., 1959. The climate of shade. A tobacco tent and a forest stand compared to open fields.

The Connecticut Agricultural Experiment Station, Bulletin, 626.

Willis, G. E., and Deardorff, J. W., 1976. On the use of Taylor's translation hypothesis for diffusion in the mixed layer. *Quarterly Journal Royal Meteorological Society*, **102**, 817–822.

Cross-references

- [Air Flux \(Resistance\) in Plants and Agricultural Products](#)
[Evapotranspiration](#)
[Greenhouse, Climate Control](#)
[Physics of Near Ground Atmosphere](#)
[Soil–Plant–Atmosphere Continuum](#)
[Windbreak and Shelterbelt Functions](#)

CUMULATIVE INFILTRATION

Total volume of water infiltrated per unit area of soil surface during a specified time period. Contrast with infiltration flux (or rate).

Bibliography

- Glossary of Soil Science Terms. Soil Science Society of America. 2010. <https://www.soils.org/publications/soils-glossary>

CUTAN

A microscopic surface layer or skin lining a void or mineral particle in a soil due to concentration of particular soil constituents or in situ modification of the plasma.

Bibliography

- Chesworth, W. (ed.). 2008. *Encyclopedia of Soil Science*, Springer, p.182.
- Glossary of Soil Science Terms. Soil Science Society of America. 2010. <https://www.soils.org/publications/soils-glossary>

CYCLIC COMPRESSIBILITY

See [Soil Compactibility and Compressibility](#)

D

DARCY'S LAW

The basic law describes the flow of water or other liquids in permeable materials (e.g., soil, porous rock, concrete, timber, or other porous material). Darcy's law tells that the water flux q (m s^{-1}) at any point is proportional to the gradient of the water potential at that point and the coefficient of proportionality is the water conductivity coefficient:

$$\vec{q} = K(\psi) \cdot \text{grad}\psi$$

where: q is the water flux [m s^{-1}], $K(\psi)$ is the water conductivity coefficient [m s^{-1}] and ψ is the soil water potential [m].

Cross-references

[Soil Water Flow](#)
[Water Budget in Soil](#)

DATABASES ON PHYSICAL PROPERTIES OF PLANTS AND AGRICULTURAL PRODUCTS

Agnieszka Kaleta, Krzysztof Górnicki
University of Life Sciences (SGGW), Warszawa, Poland

Definition

Physical properties of plants and agricultural products can be defined as the characteristics of described materials that are independent of the observer, measurable, can be quantified, and define the state of the material but not how it attained that state.

Introduction

Physical properties describe the unique, characteristic way a plant or agricultural product responds to physical treatments, for example, thermal, mechanical, or electrical processes. Knowledge of physical properties of described materials is essential for the design of equipment for their handling, storage, and processing. Data on physical properties of plants and agricultural products are needed as input to models predicting the quality and behavior of produce in preharvest, harvest, and postharvest situations. The properties of discussed materials are affected by many factors such as moisture content, growing location, growing year, and cultivar. Many properties also depend on other properties. Physical properties can change during processing operations.

Physical characteristics

The size of spherical particles like peas is easily defined by a single characteristic (its diameter). Complete specification of the form of the objects irregular in shape theoretically requires an infinite number of measurements. However, three mutually perpendicular axes account for some 93% of variation in volume (Mohsenin, 1986). Length, width, and thickness (m) are commonly used that correspond to major, intermediate, and minor axes, respectively. The dimensions increase linearly with increasing moisture content. The dimensions range approximately: (1) length: 0.8×10^{-3} – 18.5×10^{-3} m for seeds and grains, 8.6×10^{-3} – 26.3×10^{-3} m for fresh blueberries, cherries, cranberries, grapes and pistachio nuts, 43.2×10^{-3} – 94×10^{-3} m for fresh apples, peaches, pears, plums, potatoes, and tomatoes, (2) width: 0.6×10^{-3} – 11×10^{-3} m for seeds and grains, 11.4×10^{-3} – 17.8×10^{-3} m for fresh blueberries and cherries, 40.6×10^{-3} – 83.8×10^{-3} m for fresh apples, peaches, pears,

plums, potatoes, and tomatoes, (3) thickness: 0.4×10^{-3} – 10.0×10^{-3} m for seeds and grains, 6.35×10^{-3} – 17.8×10^{-3} m for fresh blueberries, cherries, and cranberries, 38.1×10^{-3} – 76.2×10^{-3} m for fresh apples, peaches, pears, plums, potatoes, and tomatoes. The size of irregularly shaped non-isometric object is a statistical parameter that depends on the direction of measurement. To reduce the resultant scatter in measured diameters, the size of object is expressed in a standardized form. An *equivalent diameter* is one of these forms. The volume diameter (diameter of the sphere having the same volume as object) is the most frequently used definition. For grains, the volume occupied by 1,000 kernels is commonly measured. The *geometric mean diameter* ($d_{eg} = (abc)^{1/3}$, where a is the longest intercept, b is the longest intercept normal to a , c is the longest intercept normal to a and b) is used sometimes. Both diameters increase slightly with the increase of moisture content (linear function). The equivalent diameter for seeds and grains ranges approximately from 0.99×10^{-3} to 9.81×10^{-3} m. The geometric mean diameter ranges approximately: for seeds and grains: 2.93×10^{-3} – 8.33×10^{-3} m, for fresh blueberries and cherries: 10.4×10^{-3} – 17×10^{-3} m, for fresh apples, peaches, plums, pears, potatoes, and tomatoes: 43.4×10^{-3} – 73.7×10^{-3} m. A monodisperse material is characterized uniquely by the size of individual particles. A polydisperse material is characterized by a *particle size distribution* and by a *mean particle size*. Particle size distribution represents the relative amount of material defined either by the number of particles, their surface area, volume, or mass as a function of the particle size. The mean particle size represents the average value for the whole population of particles. *Roundness (angularity)* of an object is most commonly defined as the ratio of: (1) the largest projected area of object in natural rest position to the area of the smallest circumscribing circle, or (2) an average radius of corners or edges to the radius of the largest inscribed sphere. Roundness values differ for both of the above methods. *Sphericity* is most commonly defined as the ratio of: (1) the volume of an object to the volume of the smallest circumscribing sphere, or (2) the equivalent diameter (or the geometric mean diameter) of the object to the diameter of the smallest circumscribing sphere. Sphericity values differ for each of the above methods. Higher values of sphericity and roundness indicate that the object's shape is closer being spherical. Sphericity increases linearly with increasing moisture content. Sphericity ranges approximately: for seeds and grains: 0.58–0.93, for fresh apples, apricots, blueberries, cherries, peaches, and pears: 0.90–0.99. *Surface area* is the area of the outer surface of an object (m^2). *Specific surface area* is defined as the ratio of the surface area of an object to the volume of an object (m^{-1}). Both characteristics depend on linear dimensions of solids and on their moisture content. Surface area of fruits increases linearly with their increasing mass. For seeds and grains, surface area ranges approximately from 3×10^{-6} to 240×10^{-6} m^2 and specific surface area ranges approximately from

500 to $6,060 \text{ m}^{-1}$. *Volume* is defined as the amount of three-dimensional space occupied by an object (m^3). Volume of the solid depends on its linear dimensions, surface area, moisture content, and temperature. Volume ranges approximately: for seeds and grains: 0.5×10^{-9} – 369×10^{-9} m^3 , for fresh blueberries, coffee beans, cherries, and pistachio nuts: 0.3×10^{-6} – 4.5×10^{-6} m^3 , for fresh apples, peaches, pears, plums, potatoes, and tomatoes: 44.2×10^{-6} – 349×10^{-6} m^3 . For grains, the *mass* of 1,000 kernels is commonly measured (kg). Its value is an indicator of the grain size, which can vary relative to growing conditions and maturity, even for the same variety of a given crop. The 1,000-grain mass increases linearly with increasing moisture content and it ranges approximately from 3×10^{-3} to 440×10^{-3} kg. The mass ranges approximately: for fresh blueberries, cherries, cranberries, grapes, pistachio nuts, coffee beans, and walnuts: 0.15×10^{-3} – 7.5×10^{-3} kg, for fresh apples, apricots, peaches, pears, plums, potatoes, and tomatoes: 18.1×10^{-3} – 286×10^{-3} kg. The *solid (true) density* is the mass of solid divided by the volume occupied by the solid excluding the intergranular spaces (kg m^{-3}). True density of grains decreases linearly with increasing moisture content (the changes are not significant). True density can be treated as a measure of, among others, maturity (blueberries, peas, peaches, tomatoes), starch content (potatoes), and peel thickness (grapefruits). True densities range approximately: for seeds and grains: 700 – $2,000 \text{ kg m}^{-3}$, for fruits and vegetables: 700 – $1,200 \text{ kg m}^{-3}$, for wood: 400 – $1,300 \text{ kg m}^{-3}$. *Bulk density* is the mass of a group of individual particles divided by the space occupied by the entire mass, including the air space (kg m^{-3}). The bulk density gives an idea of the storage space required for a known quantity of a particular, for example, grain. The bulk density can be affected by the following factors: mass of particles, their shape and dimensions, particle size distribution, the method used for filling the container, moisture content of particles, the amount and size distribution of foreign materials (chaff, fines, broken grains, and weed seeds). For example, a container filled using a spreader gives a higher bulk density than a container filled using a spout, the presence of foreign materials that are finer and heavier than grain kernels increases bulk density. The bulk density of some grains increase with an increasing moisture content whereas it decreases for some other grains. The bulk densities range approximately: for clean seeds and grains: 240 – 910 kg m^{-3} , for fruits and vegetables: 220 – 830 kg m^{-3} . The *porosity (decimal)* is defined as the ratio of the intergranular volume to the total volume occupied by the particles (i.e., the volume of particles plus the intergranular volume). Porosity depends on true and bulk density of material. Porosity allows fluids to flow through a mass of particles referred to as a packed bed. Beds with low porosity are more resistant to fluid flow and thus are more difficult to dry, heat, or cool. The porosity for clean seeds and grains ranges approximately from 0.26 to 0.80. *Shrinkage* is the decrease in volume of the material during processing such as drying. When moisture

is removed from material, there is a pressure imbalance between inside and outside of the material. This causes contracting stresses leading to material shrinkage or collapse. Shrinkage is defined as the ratio of the volume at a given moisture content to the initial volume of material before processing. Shrinkage depends mainly on moisture reduction (in the empirical formulas linear dependence is mostly assumed) and composition and structure of the material. Data on physical characteristics of plants and agricultural products have been compiled and further details can be taken from Mohsenin (1986), Cenkowski and Zhang (1995), Kaleta (1996), Kudra (1998), Pabis et al. (1998), Sablani and Ramaswamy (2003), Wilhelm et al. (2004), and Jayas and Cenkowski (2006).

Aerodynamic properties

The drag force, F_r ($F_r = C\rho_f A_p v^2$, where ρ_f is the fluid density, A_p is the projected area normal to direction of motion, v is the relative velocity between main body of fluid and object), exerted on an object held in a free stream depends on dimensionless *drag coefficient* C . Drag coefficient depends on the shape of the particle and the state of its surface, and on the Reynolds number Re . The drag coefficients for particles with regular geometric shapes are usually shown on log–log plot, as a function of Re . For turbulent flow and for the values of Re characteristic for the processes of cleaning, separating, and pneumatic transporting, the dependence of drag coefficient on Re can be neglected. The drag coefficients for agricultural products range approximately from 0.16 to 0.44 (Mohsenin, 1986; Kaleta, 1996; Jayas and Cenkowski, 2006). A free-falling body ceases to accelerate after some time and the body reaches a constant *terminal velocity*, at which the net gravitational accelerating force equals the resisting upward drag force. This velocity can be calculated theoretically for particles with regular geometric shapes. For irregularly shaped particles, the terminal velocity is determined experimentally. The terminal velocities range approximately (Mohsenin, 1986; Kaleta, 1996; Jayas and Cenkowski, 2006): for seeds and grains: 4.0–18.3 $m s^{-1}$, for fresh blueberries, cherries, cranberries, grapes, and pistachio nuts: 9.7–22.6 $m s^{-1}$, for fresh apples, apricots, peaches, plums, and potatoes: 22.9–41.5 $m s^{-1}$.

Thermal properties

Specific heat (heat capacity) is the heat required to increase the temperature of one unit of mass by 1° ($J kg^{-1} K^{-1}$). The specific heat depends on: composition of the material, moisture content, and temperature (in heat transfer problems of biological materials usually constant pressure prevails). Specific heat can be computed from the following equations: (1) for temperature above freezing: $c = 837 + 33.5M_w$ (Siebel, 1892), $c = 1424X_c + 1549X_p + 1675X_f + 837X_a + 4187X_w$ (Heldman and Singh, 1981), $c = c_s + 4186M_d$, (2) for temperature below freezing $c = 837 + 12.56M_w$ (Siebel, 1892),

where M_w is the moisture content, % w.b., M_d is the moisture content, d.b., X is the mass fraction of each constituent: carbohydrate (c); protein (p); fat (f); ash (a); water (w), c_s is the specific heat of the dry solid. The specific heat is most commonly calculated from regression equations obtained from empirical data (linearly increasing trend with increasing moisture content and increasing temperature is generally reported). Its value ranges approximately: for wood: 1,880–2,970 $J kg^{-1} K^{-1}$, for dry mass of plants, seeds, and grains: 990–2,050 $J kg^{-1} K^{-1}$, for fresh fruits and vegetables: above freezing: 3,140–4,100 $J kg^{-1} K^{-1}$, below freezing: 1,670–2,390 $J kg^{-1} K^{-1}$. The *thermal conductivity* ($W m^{-1} K^{-1}$) of a material is a measure of its ability to conduct heat. It defines the amount of thermal energy that is transmitted within a unit time and through a unit cross-sectional area when the temperature gradient across a body is a unit degree ($q = -k\nabla T$, where q is the heat flux, k is the thermal conductivity, ∇T is the temperature gradient). The thermal conductivity depends on the composition of the material, moisture content, temperature, and structure of the material including any factor that affects the heat flow path through the material (percent void spaces, shape, size, and arrangement of void spaces, heterogeneity, impurities, particle to particle contact, and fiber orientation). Theoretical models for the prediction of thermal conductivity of plants and agricultural products are based on the composition of material or on the arrangement and geometry of phases present in the material, but they lack accuracy (Sweat, 1992; Kudra, 1998; Saravacos and Maroulis, 2001; Sahin and Sumnu, 2006). Therefore, the thermal conductivity is most commonly calculated from regression equation (linearly increasing trend with increasing moisture content, increasing temperature, and increasing bulk density is generally observed). For high moisture materials below freezing, thermal conductivity increases with a decrease in temperature and a sudden jump in its value can be observed at freezing point. The thermal conductivity ranges approximately from 0.110 to 0.720 $W m^{-1} K^{-1}$ for wood and from 0.280 to 0.640 $W m^{-1} K^{-1}$ for fresh fruits and vegetables (above freezing). The *thermal diffusivity* ($m^2 s^{-1}$) is defined as the ratio of thermal conductivity to the product of density and specific heat. It relates the ability of material to conduct the heat to its ability to store the heat. Thermal diffusivity may be considered as the rate at which heat propagates (diffuses) through a material. The relationship between the moisture content and the thermal diffusivity is rather not a linear function (in the narrow range of moisture content, however, most commonly linear regression is applied). The thermal diffusivity ranges approximately: for wood: 0.94×10^{-7} – $2.2 \times 10^{-7} m^2 s^{-1}$, for seeds and grains: 0.81×10^{-7} – $1.64 \times 10^{-7} m^2 s^{-1}$, for fresh fruits and vegetables: 0.78×10^{-7} – $2.69 \times 10^{-7} m^2 s^{-1}$. Data for specific heat, thermal conductivity, and thermal diffusivity of plants and agricultural products have been compiled from Mohsenin (1980), Sweat (1992), Pabis et al. (1998), Kaleta (1999), Sablani and Ramaswamy (2003), and Jayas

and Cenkowski (2006). Regression equations for the prediction of these thermal properties can be found in the same bibliography. If the temperature of an object changes due to the heat transfer, then the heat transfer involves a transfer of sensible heat. The exchange of energy that occurs during a change in phase (without a temperature change) is called the latent heat. The *heat of fusion (solidification)* is the heat exchange during the phase change from liquid to solid. *Latent heat of vaporization* is the energy to change a liquid to vapor. The heat of vaporization is about seven times more than the heat of fusion, which is five times more than raising the temperature (sensible heating) by 100 K (Wilhelm et al., 2004). For materials of moisture content below approximately 0.14 d.b., to overcome the attractive forces between the adsorbed water molecules and the internal surfaces of material extra energy is needed in addition to the heat required to change the water from liquid to vapor (Pabis et al., 1998). Plants and agricultural products freeze at lower temperatures than pure water (approximately 269.5–272.8 K) due to the presence of solutes and solids in the water (*freezing point depression*) (Kaleta, 1999). Plants and agricultural products are living organisms and they must consume energy to maintain their life processes. They do this by a process of combustion that burns sugar to produce CO₂ and *heat of respiration*. Heat of respiration depends on product, its maturity, storage time (either an increase or a decrease) and increases exponentially with temperature. High respiration rate causes rapid deterioration in product quality (Mohsenin, 1980; Wilhelm et al., 2004).

Hygroscopic properties

The relation between material moisture content and air humidity is described by the drying equilibrium, which results from the fact that liquid moisture trapped in fine capillaries exerts a vapor pressure lower than that of liquid with a free surface. Drying equilibrium is determined experimentally by allowing sufficiently long contact of the bone dry material with air at a given humidity. Points obtained for various air humidities at the same temperature form the isotherm called the *equilibrium moisture content* (EMC) – equilibrium relative humidity (ERH) relationship (EMC represents the moisture content that the material will attain if dried for an infinite time at a particular relative humidity and temperature). The thermodynamic equilibrium can be obtained by moisture desorption (drying) or adsorption, therefore, the respective isotherm is strictly called either a desorption, or adsorption (Kudra and Strumillo, 1998). Desorption isotherms usually give higher moisture content than adsorption isotherms, which results in a hysteresis loop. The composition of the product, its temperature, storage time, drying temperature, and the number of successive adsorption and desorption affects hysteresis. Typical plants and agricultural products desorption/adsorption isotherms are S-shaped and they may be described by a number (~80) of mathematical relations (most of them are semiempirical or empirical equations with two or three fitting parameters).

The commonly used equations are: the Langmuir, Brunauer–Emmett–Teller (BET), Iglesias–Chirife, the modified Henderson, Chen, Chung–Pfost, Halsey, Oswin, and Guggenheim–Anderson–de Boer (GAB) (Rizvi, 1992). Constants of selected equations for the isotherm of various grains and seeds are given by Kaleta (1996), Pabis et al. (1998), and Jayas and Cenkowski (2006). The mechanism of moisture movement during the falling rate period of plants and agricultural products drying is mainly by diffusion. This can be described by Fick's law. Water can move in a solid in the form of liquid and/or vapor. The overall (total) *coefficient of water diffusion* is the sum of the liquid and vapor diffusion coefficients. Water diffusivity in solids depends on their temperature, moisture content, and structure. The overall coefficient of water diffusion (m² s⁻¹) is described by a number of semiempirical or empirical equations (Cenkowski and Zhang, 1995; Pabis et al., 1998; Saravacos and Maroulis, 2001). The Arrhenius-type equation to describe the relationship between diffusion coefficient and temperature and exponential relationship between coefficient and moisture content is mostly used. Shrinkage influences the water diffusion coefficient.

Mechanical properties

The coefficient of friction of the plants and agricultural products is necessary in designing of conveying, transporting, and storing structures. The *friction coefficient* is defined as the ratio between the friction force (force due to the resistance of movement) and the normal force on surface of contact (e.g., wall of the silo). Two types of friction coefficients are considered, the *static coefficient* determined by the force capable to initiate the movement and the *dynamic coefficient* determined by the force needed to maintain the movement of products in contact with the surface, which depends on the type and nature of the material in contact. An increase in coefficients of static and dynamic friction for various grains with increase in moisture content (mostly linear) is mostly observed. Both coefficients depend on the product and surface material. The friction coefficient ranges approximately (Mohsenin, 1986; Sablani and Ramaswamy, 2003; Jayas and Cenkowski, 2006): for seeds and grains: 0.11–0.76, for fresh apples and tomatoes: 0.24–0.88, for wood shavings and chopped grass, straw, and hay: 0.20–0.80. The *angle of natural repose* is the angle formed between the element of a cone and the base of piled cone (the angle with the horizontal at which the product will stand when piled). The properties of the particles forming medium (dimensions, shape, surface frictional properties, deformation ability) influence the value of this angle. The angle of repose increases with an increase in moisture content. Its value for grains ranges approximately from 17° to 45° (Mohsenin, 1986; Sablani and Ramaswamy, 2003). The other mechanical properties of plants and agricultural products can be measured by uniaxial compression, uniaxial tension, shear, and bending. The type of loading, preparation of the specimen,

loading rate, strain (deformation) rate, and other factors are dependent upon the product and desired use of the data (details are given by Mohsenin (1986), Cenkowski and Zhang (1995), and Wilhelm et al. (2004)).

Electromagnetic properties

Electromagnetic radiation is transmitted in the form of waves and it can be classified according to wavelength and frequency. The electromagnetic spectrum is very broad (from the shortest cosmic rays to the longest electric waves). Only a few specialized, narrow regions are utilized in plants and agricultural products applications. These include visible light, infrared, and microwave frequencies. When radiation of a specific wavelength strikes an object, it may be reflected, transmitted, or absorbed. The interaction of visible light and matter is referred to as a *color*. Most of the plants and agricultural products are opaque, they do not allow any transmission of light but absorb and/or reflect all the light striking. If all the visible light is absorbed, the object appears black. If all the visible light is reflected, the object appears white. The selective absorption of different amounts of the wavelength in the visible region determines the color of the object because reflected wavelengths are visible to the observer (e.g., green object reflects the green light spectrum but absorbs violet, blue, yellow, orange, and red). The color of a product is affected by the surrounding lighting intensity and wavelength. Thus, the color an observer perceives of an object can be influenced by changing the ambient light. For this reason, optical properties of product are considered as they interact with light. The human perception of color is highly subjective. Therefore, instrumental methods for color measurement have been developed (Munsell, CIE, CIE $L^*a^*b^*$ (CIELAB), Hunter Lab, and Lovibond). The color of an object is measured and represented by spectrophotometric curves, which are plots of fractions of incident light (reflected or transmitted) as a function of wavelength throughout the visible spectrum. Further details about color are given by Wilhelm et al. (2004) and Sahin and Sumnu (2006). In microwave heating, the dielectric properties of interest are the dielectric constant and the dielectric loss factor. *Dielectric constant* is the ability of a material to store microwave energy. *Dielectric loss factor* is the ability of a material to dissipate microwave energy into heat and this parameter is a measure of microwave absorptivity. As microwaves move through the object, the rate of heat generated per unit volume decreases. For materials having a high loss factor, the rate of heat generated decreases rapidly and the penetration depth of energy decreases. *Power penetration depth* (m) is the depth at which power decreases to e^{-1} of its original value. It depends on both dielectric constant and dielectric loss factor. Dielectric properties of plants and agricultural products depend on moisture content, temperature, composition and physical structure of the material, and the frequency of the oven. At low moisture content, variation of dielectric constant

and dielectric loss factor with moisture content is small. The increase in moisture content increases dipolar rotation and therefore both dielectric properties increase. The temperature dependence of dielectric properties depends on the ratio of bound to free moisture content. If the water is in bound form, the dielectric properties increase with increasing temperature. For the free water, the dependence on the temperature is opposite. At frequencies of home type microwave oven and at ambient temperature, the dielectric constant ranges approximately from 45 to 75 and the dielectric loss factor ranges approximately from 15 to 20 for seeds, grains, and fresh fruits and vegetables (Sahin and Sumnu, 2006).

Conclusions

Physical properties describe the unique, characteristic way a plant or agricultural product responds to physical treatments. Knowledge of these properties constitutes important engineering data in design of machines, processes, and controls and it is necessary for determining the efficiency of a machine and an operation and for evaluating the quality of the final product. Much of the data in the literature is of limited value because not enough supporting data are included, such as detailed product description, temperature, and error in measurement. The product description should include the cultivar, moisture content, maturity, and any pretreatment. Details of the experiment should include sample size, surface conditions, porosity, fiber orientation, sampling procedure, and process variables. The description should provide sufficient detail so that the reader can duplicate exactly the entire experiment. Insufficient description of product and process variables causes very often that data taken from several published sources differ a lot.

Data on physical properties of plants and agricultural products are scattered in an enormous number of scientific papers. Therefore, there is an urgent need to set all the data in order. This may enable some kind of systematization and generalization. Up to now, such extensive, well elaborated databases on all physical properties of plants and agricultural products do not exist and therefore the most important data available in the literature have been summarized in this contribution to give a good start point for such a database for future.

Bibliography

- Cenkowski, S., and Zhang, Q., 1995. Engineering properties of grains and oilseeds. In Jayas, D. S., White, N. D. G., and Muir, W. E. (eds.), *Stored-Grain Ecosystems*. New York: Marcel Dekker, pp. 411–463.
- Heldman, D. R., and Singh, R. P., 1981. *Food Process Engineering*, 2nd edn. Westport: AVI.
- Jayas, D. S., and Cenkowski, S., 2006. Grain property values and their measurement. In Mujumdar, A. S. (ed.), *Handbook of Industrial Drying*, 3rd edn. Philadelphia: Taylor & Francis Group, LLC., pp. 575–603.
- Kaleta, A., 1996. *Modelling of Grain Drying in Silos*. Warszawa: Fundacja Rozwój SGGW (in Polish).

- Kaleta, A., 1999. *Thermal Properties of Plant Materials*. Warsaw: Warsaw Agricultural University Press.
- Kudra, T., 1998. Properties of bio-materials. In Kudra, T., and Strumillo, C. (eds.), *Thermal Processing of Bio-materials*. Amsterdam: Gordon and Breach Science, pp. 49–83, 92–98.
- Kudra, T., and Strumillo, C., 1998. Bio-materials as drying object. In Kudra, T., and Strumillo, C. (eds.), *Thermal Processing of Bio-materials*. Amsterdam: Gordon and Breach Science, pp. 295–320.
- Mohsenin, N. N., 1980. *Thermal Properties of Foods and Agricultural Materials*. New York: Gordon and Breach Science.
- Mohsenin, N. N., 1986. *Physical Properties of Plant and Animal Materials*. New York: Gordon and Breach Science.
- Pabis, S., Jayas, D. S., and Cenkowski, S., 1998. *Grain Drying Theory and Practice*. New York: Wiley.
- Rizvi, S. S. H., 1992. Thermodynamic properties of foods in dehydration. In Rao, M. A., and Rizvi, S. S. H. (eds.), *Engineering Properties of Foods*. New York: Marcel Dekker, pp. 133–214.
- Sablani, S. S., and Ramaswamy, H. S., 2003. Physical and thermal properties of cereal grains. In Chakraverty, A., Mujumdar, A. S., Raghavan, G. S. V., and Ramaswamy, H. S. (eds.), *Handbook of Postharvest Technology. Cereals, Fruits, Vegetables, Tea, and Spices*. New York: Marcel Dekker, pp. 17–40.
- Sahin, S., and Sumnu, S. G., 2006. *Physical Properties of Foods*. New York: Springer Science + Business Media, LLC.
- Saravacos, G. D., and Maroulis, Z. B., 2001. *Transport Properties of Foods*. New York: Marcel Dekker.
- Siebel, E., 1892. Specific heats of various products. *Ice and Refrigeration*, 2, 256–257.
- Sweat, V. E., 1992. Thermal properties of foods. In Rao, M. A., and Rizvi, S. S. H. (eds.), *Engineering Properties of Foods*. New York: Marcel Dekker, pp. 49–87.
- Wilhelm, L. R., Suter, D. A., and Brusewitz, G. H., 2004. *Food and Process Engineering Technology*. St. Joseph: ASAE.

Cross-references

- [Dielectric Properties of Agricultural Products](#)
[Electrical Properties of Agricultural Products](#)
[Fruits, Mechanical Properties and Bruise Susceptibility](#)
[Grains, Aerodynamic and Geometric Features](#)
[Modeling the Thermal Conductivity of Frozen Foods](#)
[Physical Properties as Indicators of Food Quality](#)
[Physical Properties of Raw Materials and Agricultural Products](#)
[Rheology in Agricultural Products and Foods](#)
[Shrinkage and Swelling Phenomena in Agricultural Products](#)
[Water Effects on Physical Properties of Raw Materials and Foods](#)

DATABASES OF SOIL PHYSICAL AND HYDRAULIC PROPERTIES

Attila Nemes
Crop Systems and Global Change Laboratory,
USDA-ARS, Beltsville, MD, USA

Definition

In this chapter, we review databases of international interest that contain significant quality and quantity of soil physical and hydraulic information – with a special emphasis given to soil hydraulic properties.

Introduction

Soil–plant–atmosphere modeling, weather and climate prediction, erosion modeling, and nutrient management advisory are examples for studies that require knowledge of soil physical and hydraulic properties. However, many such properties are costly and tedious to measure both in the field and in the laboratory. For this reason, the number of samples for which soil physical properties are determined in a particular laboratory or institute is usually limited. It has been recognized that collecting such fragmented data into larger databases can benefit all contributors and beyond. By establishing larger, national, or international scale databases, access to larger quantity and variety of data is facilitated; a wider range of methods can be examined and compared, and the user can derive conclusions that may be more widely applicable. In this chapter, the history, structure, contents, and availability of international databases of soil physical and hydraulic properties are summarized; certain data standardization issues are discussed; and a few challenges and database limitations are highlighted.

History of soil physical and hydraulic databases

Storage and retrieval of soil physical data developed with the advances made in (computerized) storage of information; first ASCII files replaced laboratory notebooks, but spreadsheets soon followed. Searchable relational database programs are the platform of choice today for modern databases.

For some countries, data collections at the national or regional scales have existed for decades. Examples for data collections of soil physical properties in particular countries, of which extensive research has been reported, include the databases of Australia (McKenzie et al., 2008), Belgium (Vereecken et al., 1989; Cornelis et al., 2001), Brazil (e.g., Tomassella et al., 2000, 2003), France (Bruand et al., 2004), Germany (Horn et al., 1991; Krahmer et al., 1995), Hungary (Rajkai et al., 1981; Nemes, 2002), the Netherlands (Wösten et al., 2001), Poland (Gliński et al., 1991), and the USA (Rawls et al., 1982; Soil Survey Staff, 1997). Some of these data collections, however, represent only certain region(s) of the listed countries.

Upon recognition of the strengths of and need for combining available data, some data collections were formed by individual scientists following an extensive literature search for the desired data (e.g., Rawls et al., 1982, 1998). Other data collections were formed by an open call and volunteered data by scientists from various parts of the World. The resulting Unsaturated Soil Hydraulic Database (UNSDODA) (Leij et al., 1996) and Grenoble Catalogue of Soils (GRIZZLY) (Haverkamp et al., 1998) were the first two truly international soil hydraulic databases. Different funding agencies also recognized the need for joint efforts and provided funds to support collection and analyses of data of different contributors (e.g., Hydraulic Properties of European Soils (HYPRES), Wösten et al., 1999). The International Soil Reference and Information Centre

(ISRIC) has assembled two databases that contain soil hydraulic properties and that are of international use. At the request of the Global Soil Data Task (GSDT) of the Data and Information System of the International Geosphere Biosphere Programme (IGBP-DIS), ISRIC prepared a uniform soil data set for the development of pedotransfer functions, which we will call the IGBP-DIS database (Tempel et al., 1996). Staff at ISRIC has also made available different versions of a global soil profile database that was developed in the framework of a project entitled “World Inventory of Soil Emission Potentials” (WISE, Batjes, 2002a, b, 2008). The WISE and IGBP-DIS databases contain, among many other attributes, soil physical and hydraulic data that originate from other independent international data sources like the Food and Agriculture Organization (FAO) (Food and Agriculture Organization, 1989) and the ISRIC Soil Information System. However, the majority of the IGBP-DIS database, and a lesser part of the WISE database originate from the National Soil Survey Characterization database (NSSC) of the U.S. Department of Agriculture Natural Resources Conservation Service (USDA-NRCS) (Soil Survey Staff, 1997) that holds data primarily of U.S. soils. While the NRCS-NSSC database is mostly a national scale database for the USA, it is discussed together with the above international databases due to its sheer size ($>100,000$ samples), the wide variety of soil types it covers, and the variety of measured and derived data that are available. Despite being a U.S. national database, the NRCS-NSSC database still includes a limited amount of data from other countries.

It is commonly seen that tropical countries, emerging market countries, and newly industrialized countries are underrepresented either in such international databases or only limited amount of detailed soil physical and hydraulic data are available for them – with only a few countries as exceptions. This has been recognized by several authors (e.g., Nemes et al., 2001; Batjes, 2002a) and some of the implications have been discussed by Tomasella et al. (2003) or De Condappa et al. (2008). Differences in environmental factors that influence soil development are such between the tropical and temperate climate zones that conclusions resulting from soils research may not always be applicable across climate zones. However, projects are increasingly being initiated to expand knowledge on soil hydraulic characteristics of soils in tropical and subtropical countries. The Soil Physics Research Unit of the University of Ghent, for example, is in collaboration with several local scientists to assemble data collections for Chile, Congo, Kenya, Syria, and Tanzania and aims to extend such collaboration to additional countries (Dr. W. Cornelis, 2009, personal communication). Similar projects are in progress – or data collections exist – in Burundi (Bagarello et al., 2009), Cuba (Dr. M.E. Ruiz Perez, 2009, personal communication) or Iran (B. Ghanbarian, 2009, personal communication).

The WISE and IGBP-DIS databases also contain data for tropical and subtropical countries. The amount and detail of physical and hydraulic properties for these soils

vary greatly, but WISE (version 1.1) has such data for ~1,000 soil horizons from 17 countries and IGBP-DIS contains such data for ~900 horizons from 24 countries. India, Israel, China, Brazil, Peru, Botswana, Indonesia, Thailand, Turkey, Columbia, Cuba, and Kenya are best represented in one or both of these two databases. Upgraded versions of WISE (versions 2.1 and 3.1) tend to contain soil hydraulic data for more samples from tropical and subtropical countries; however, information on the water retention curve is limited to fewer points.

In many cases, however, data collected by different scientists or institutions remain fragmented. For example, large amounts of soil physical data have already been collected in Iran, but the data appear to remain stored and utilized by individual research groups locally (B. Ghanbarian, 2009, personal communication). The situation appears to be similar in Indonesia as well (Suprayogo et al., 2003); but this phenomenon is not unique for these countries.

Database structure, contents, and limitations

International databases of soil physical and hydraulic properties typically comprise of multiple interconnected tables, linked by identifiers that are either a unique number or a unique combination of information on the sampled location, and the soil horizon/layer. The complexity of the cited databases differs greatly. Some database properties, advantages, and disadvantages are listed in Table 1.

The range of properties that they cover varies; some of the databases are rich in information about the environment of the sampled location, the methodology used at sampling and measurements, while others contain less information. Some of the databases contain measurements of the same property or characteristic measured under different conditions. Examples are the NRCS-NSSC database with some properties determined under different conditions (e.g., bulk density of oven dried soil vs. wet soil at -33 kPa pressure) or calculated for different fractions of the soil; or the UNSODA database in which hydraulic characteristics are determined for many samples under both wetting and drying conditions and/or in situ (field) or in the laboratory. The location of the reported soils may or may not be spatially referenced, it varies from database to database. The UNSODA database, for example, is not spatially referenced, while the HYPRES database contains the originally available spatial coordinates for most samples. It is also of concern what areas and types of soil the databases actually represent. Users of databases often equate the represented area or soil types with the named source area (e.g., HYPRES – European, Rawls et al. (1982) – U.S.). However, inhomogeneity is often seen in databases in terms of geographical distribution or the representation of soil types, which both can have potentially significant consequences (cf. Nemes et al., 2009). Local experimental preferences can also bring, for example, textural or geographical imbalances to databases. One such example is cited by Nemes et al. (2009): fine-textured salt-affected soils are typically

Databases of Soil Physical and Hydraulic Properties, Table 1 Selected characteristics of international soil physical and hydraulic databases

	UNSODA	GRIZZLY	NRCS-NSSC	HYPRES	IGBP-DIS	WISE (version 3.1)
Reference	Leij et al., 1996, Nemes et al., 2001	Haverkamp et al., 1998	Soil Survey Staff, 1997	Wösten et al., 1999	Tempel et al., 1996	Batjes, 2008
Approx. database size	790	660	>100,000	5,521	>100,000	>48,000
Number of tables	36	4	23 (varies with issuance)	6	1	7
Resource area	Worldwide	Mostly Europe, USA	Mostly USA	Europe (West)	Worldwide	Worldwide
Tropical soils	Very few	Very few	Few	No	Yes	Yes
Methodology	Mixed	Mixed	Uniform	Mixed	Mixed	Mixed
Water retention [$\theta(h)$]	Yes	Yes	Yes (limited points)	Yes	Yes	Yes
Saturated conductivity [$K(s)$]	Yes	Some	No	Yes	No	No (some in version 1.1)
Unsaturated conductivity [$K(\theta)$]	Yes	Some	No	Yes	No	No
Field soil hydraulic data	Yes	No	No	No	No	No
Availability of database strength	Free	Free	Free	Limited	Free	Free
Weakness	Field hydraulic data available	Detailed $\theta(h)$ data	Database size, uniform methodology	Most $K(s)$ and $K(\theta)$	Tropical data	Tropical data
	Database size	Database size, ease of availability	Limited $q(h)$ points, no $K(s)$, $K(\theta)$	Limited access/availability	Limited $\theta(h)$ points, no $K(s)$, $K(\theta)$	Limited $\theta(h)$ points, no $K(s)$, $K(\theta)$
Notes	Built-in reporting with graphics	Three countries and one U.S. state dominate	Different measurement conditions exist	Sample geographic distribution varies	Includes much of NRCS-NSSC	Earlier versions stored $\theta(h)$ at more pressures

overrepresented in Hungarian data collections due to special interest by generations of scientists, despite the fact that such soils represent only a fraction of the area of Hungary.

In terms of hydraulic properties, the range and detail of data that each international database covers varies. The NRCS-NSSC database is the largest original data collection that contains soil hydraulic data. Those are, however, typically limited to two or three water retention points (-10 , -33 , and $-1,500$ kPa) and no hydraulic conductivity data is available. For some of the samples more water retention points exist. On the contrary, the UNSODA and HYPRES databases contain, for most soils, water retention measured at least at 4–8 pressures. More than half the samples in HYPRES and UNSODA also have information on saturated hydraulic conductivity – and fewer on unsaturated hydraulic conductivity. Since most of the soils in IGBP-DIS and some in WISE originate from the NRCS-NSSC database, the availability of water retention data resembles that of NRCS-NSSC. However, a significant portion of the non-U.S. soils in these two databases has four to eight points of the water retention curve measured and available. WISE (version 3.1) contains water retention data at only 3 pressures; which are standard pressures, however. The HYPRES database appears to be the largest international collection of detailed soil water retention and hydraulic conductivity measurements on undisturbed samples. The availability of field measurements of soil hydraulic properties is typically very limited; the UNSODA database holds probably the only substantial collection of field measured soil hydraulic data. Users of the original measured data need to be aware that replicate measurements are often stored for the soil samples.

Data compatibility and standardization

All the listed international databases of soil physical properties are being frequently used in transnational research. Due to the history of international data collections and the existence of various measurement methods and standards worldwide, compatibility of data between databases has always been a concern. Often, even within a database it is of concern. In the simplest cases, conversion is simply a matter of unit conversions (e.g., K(s) expressed in cm/day or in mm/h); in other cases, it requires the use of an empirically developed conversion factor to achieve compatibility (e.g., organic carbon vs. organic matter content). A more difficult task is to convert information that is based on, for example, a complex set of criteria (e.g., national soil classification into World Reference Base for Soil Resources (WRB) or Soil Taxonomy classifications). The availability of multiple methods that seemingly determine the same property warrants that the measurement results are often difficult to compare. Often such methods (1) apply different sampling techniques (e.g., disturbed or undisturbed sample; soil core or soil clod); (2) are used under different environmental conditions (field or

laboratory measurements; different states of wetness at measurement); or (3) are based on entirely different theoretical backgrounds (e.g., soil particle-size measurements by pipette/hydrometer methods vs. the laser diffraction method). Even if the same measurement technique is used, the use of different standards in different countries or laboratories can make data conversion a daunting task, as witnessed by, for example, the rich literature on converting and/or standardizing particle-size distribution (e.g., Nemes and Rawls, 2004 and therein).

Standardization of data has been handled differently in the different international databases. In the NSSC database, standardization took place at the measurement level, since measurements were typically taken according to one set of standards (Soil Survey Staff, 2004). In other cases, data have been assembled from various sources and have either been standardized by the managers of the database (HYPRES, Wösten et al., 1999; Nemes et al., 1999) or such standardization has not taken place (UNSDA, WISE, IGBP-DIS). However, in HYPRES, the original data format and description has also been conserved to allow any future reassessment or reclassification of the data. Documentation of the original data source(s) and of the actual database should be consulted carefully for a better understanding of applied data standards.

Water retention and hydraulic conductivity data that originate from different countries/institutions were typically not measured at standard pressure values. Some projects require that such data are standardized (e.g., Wösten et al., 1999). Their standardization usually takes place by applying one of the continuous water retention and hydraulic conductivity models, most frequently the coupled Mualem–van Genuchten model (Mualem, 1976; van Genuchten, 1980). When any such standardized data are used, it needs to be considered that even such advanced equations do not always fit perfectly to the measured data.

Database availability

While their documentation is publicly available, availability of data of some of the listed databases is limited by license agreements or the need for an agreement with the author(s) or owners (e.g., Rawls et al., 1982 data; HYPRES). Others are free to obtain from the authors or are readily available online for running queries or downloading data (e.g., GRIZZLY; NRCS-NSSC, <http://ssldata.nrcs.usda.gov/>; UNSODA, <http://www.ars.usda.gov/Services/docs.htm?docid=8967>; WISE, <http://www.isric.org/>; IGBP-DIS, <http://www.isric.org/>). Regardless of which data source is being used, source organizations require the user to cite the source of data in their works.

Additional challenges, future needs

Existing databases provide invaluable information to many environment-related studies, but future data collections should address particular needs in order to advance further. One of the concerns is of course the completeness

of data sets. While additional properties of historic data are unlikely to be recovered, new data collections should put emphasis on completeness in terms of frequently used information. This does not only cover laboratory measurements but also information collected in the field upon profile description and sampling.

With the emergence of global positioning devices, spatial referencing should present only a small challenge in the future. Knowing the spatial location of sampled profiles will help in improving the accuracy of new maps. Improving the distribution of samples in sparsely sampled areas could also help in drawing more reliable conclusions for many areas. Hence, related studies that visit and explore previously un-surveyed areas are strongly encouraged. Along with the spatial expansion, a temporal expansion should also be explored. It is known that some soil properties change temporally on a human timescale; sometimes even within days or weeks (e.g., by tillage practices). Often there is an annual cycle involved. Such changes are typically seen in cultivated areas and in areas with cyclic freeze–thaw conditions. A one-time measurement will not represent local conditions well throughout the year. So far, only a limited number of studies explored such variable soil hydraulic conditions via periodic sampling of the same soils. Many modeling-based studies rely on information from large databases, and such temporally variable properties are not currently represented in such databases. Measurement and documentation of temporally variable soil physical and hydraulic properties is encouraged.

Structural development influences the physical behavior of the soil through influencing the characteristics of the void space. Therefore, information on soil structure should be logged for the benefit of future users. Characterization of the void space in soils using modern imaging techniques is also gaining popularity. Once these techniques will become more affordable and more widely applicable, such information could be stored along with other soil physical data. Knowing the architecture of void space in the soil is essential in advancing our knowledge about solute transport; but such knowledge has long been only inferred indirectly from the characteristics of the solid phase of soils.

It has been recognized in the past that while laboratory measurements give us an understanding of characteristics and processes in the soil, they do not always provide full and unbiased information about soil conditions in the field. Hence, studies that involve *in situ* measurements are of special interest, since they may provide more insight into true field conditions and our understanding about the differences in field and laboratory conditions. It has also been recognized that the use of different techniques to determine a particular property or characteristic can pose a challenge while forming conclusions from such data. However, it also provides a great opportunity to examine differences among such techniques and to explore pathways and interpretations between them.

Hence, documentation on how data were collected should always be passed along with the data itself.

Summary and conclusions

We attempted to give a summary of significant – primarily international – sources of soil physical and hydraulic data. Historic soil physical and hydraulic data are being used in a variety of ways worldwide. Their advanced, well-documented, and searchable storage and management is therefore essential for the success of future applications. Though soil hydraulic properties are time consuming to measure, decades of research yielded a wealth of such information that are stored in national/provincial and international databases. The presented databases differ in their source area, extent, structure, applied methodology, level of detail, and in many additional factors. Completeness of data records is also a great challenge; and so is an equal representation of different areas and soil types. Regardless, whether used alone or combined with other data sources such data collections present great opportunities and an invaluable resource for many researchers, educators, practitioners, and policy makers worldwide. Use of these and other databases however, requires caution; interpretations and conclusions have to be drawn with care.

Bibliography

- Bagarello, V., Provenzano, G., and Sgroi, A., 2009. Fitting particle size distribution models to data from Burundian soils for the BEST procedure and other purposes. *Biosystems Engineering*, **104**(3), 435–441.
- Batjes, N. H., 2002a. A homogenized soil profile data set for global and regional environmental research (WISE, Version 1.1) (available online at <http://www.isric.org>). Report 2002/01. Wageningen: International Soil Reference and Information Centre.
- Batjes, N. H., 2002b. Soil parameter estimates for the soil types of the world for use in global and regional modeling (Version 2.1; July 2002). ISRIC Report 2002/02c (Available online at <http://www.isric.org>). Wageningen: International Food Policy Research Institute (IFPRI) and International Soil Reference and Information Centre (ISRIC).
- Batjes, N. H., 2008. ISRIC-WISE Harmonized Global Soil Profile Dataset (Version 3.1). Report 2008/2. Wageningen: ISRIC – World Soil Information (with dataset).
- Bruand, A., Duval, O., and Cousin, I., 2004. Estimation des propriétés de rétention en eau des sols à partir de la base de données SOLHYDRO. *Étude et Gestion des Sols*, **11**(3), 323–332.
- Cornelis, W. M., Ronsyn, J., Van Meirvenne, M., and Hartmann, R., 2001. Evaluation of pedotransfer functions for predicting the soil moisture retention curve. *Soil Science Society of America Journal*, **65**, 638–648.
- De Condappa, D., Galle, S., Dewandel, B., and Havercamp, R., 2008. Bimodal zone of the soil textural triangle: common in tropical and subtropical regions. *Soil Science Society of America Journal*, **72**, 33–40.
- Food and Agriculture Organization (FAO), 1989. FAO-ISRIC Soil Database (SDB). World Soil Resources Report 60 (Reprinted). Rome: Food and Agriculture Organization of the United Nations.

- Gliński, J., Ostrowski, J., Stepniewska, Z., and Stepniewski, W., 1991. Soil sample bank representing mineral soils of Poland (in Polish). *Problemy Agrofizyki*, **66**, 1–61.
- Haverkamp, R., Zammit, C., Bouraoui, F., Rajkai, K., Arrué, J. L., and Heckmann, N., 1998. GRIZZLY, Grenoble Catalogue of Soils: Survey of soil field data and description of particle-size, soil water retention and hydraulic conductivity functions. Laboratoire d'Etude des Transferts en Hydrologie et Environnement (LTHE). France: Grenoble Cedex 9.
- Horn, A., Stumpfe, A., Kues, J., Zinner, H.-J., and Fleige, H., 1991. Die Labordatenbank des Niedersächsischen Bodeninformationssystems (NIBIS), In: Fachinformationssystem Bodenkunde. *Geologisches Jahrbuch*, **A126**, 59–97.
- Krahmer, U., Hennings, V., Müller, U., and Schrey, H.-P., 1995. Ermittlung bodenphysikalischer Kennwerte in Abhängigkeit von Bodenart, Lagerungsdichte und Humusgehalt. *Zeitschrift für Pflanzenernährung und Bodenkunde*, **158**, 323–331.
- Leij, F. J., Alves, W. J., van Genuchten, M. Th., and Williams, J. R., 1996. Unsaturated Soil Hydraulic Database, UNSODA 1.0 User's Manual. Report EPA/600/R96/095. Ada, Oklahoma: US Environmental Agency, 103 pp.
- McKenzie, N. J., Jacquier, D. W., and Gregory, L. J., 2008. Online soil information systems – recent Australian experience. In Hartemink, A. E., McBratney, A. B., de Loures Mendonça-Santos, M. (eds.), Digital soil mapping with limited data. Berlin: Springer Science+Business Media B.V. ISBN: 978-1-4020-8591-8. pp. 283–290.
- Mualem, Y., 1976. New model for predicting the hydraulic conductivity of unsaturated porous media. *Water Resources Research*, **12**(3), 513–522.
- Nemes, A., 2002. Unsaturated soil hydraulic database of Hungary: HUNSODA. *Agrokémia és Talajtan*, **51**(1–2), 17–26.
- Nemes, A., and Rawls, W. J., 2004. Soil texture and particle-size distribution as input to the estimation of soil hydraulic properties. In Pachepsky, Ya A., and Rawls, W. J. (eds.), *Development of pedotransfer functions in Soil Hydrology. Developments in Soil Science*, Vol 30th edn. Amsterdam: Elsevier, pp. 47–70. ISBN 0-444-51705-7.
- Nemes, A., Wösten, J. H. M., Lilly, A., and Oude Voshaar, J. H., 1999. Evaluation of different procedures to interpolate the cumulative particle-size distribution to achieve compatibility within a soil database. *Geoderma*, **90**, 187–202.
- Nemes, A., Schaap, M. G., Leij, F. J., and Wösten, J. H. M., 2001. Description of the unsaturated soil hydraulic database UNSODA version 2.0. *Journal of Hydrology*, **251**(3–4), 151–162.
- Nemes, A., Timlin, D. J., Pachepsky, Ya A., and Rawls, W. J., 2009. Evaluation of the Rawls et al. (1982) Pedotransfer Functions for their Applicability at the U.S. National Scale. *Soil Science Society of America Journal*, **73**, 1638–1645.
- Rajkai, K., Várallyay, G., Pachepsky, Ya. A., and Scherbakov, R. A., 1981. Calculation of waterretention data from the texture and the bulk density of soils. (In Hungarian) *Agrokémia és Talajtan*, **30**, 409–438.
- Rawls, W. J., Brakensiek, D. L., and Saxton, K. E., 1982. Estimation of soil water properties. *Transactions of the American Society of Agricultural Engineers*, **25**(5), 1316–1320, 1328.
- Rawls, W. J., Gimenez, D., and Grossman, R., 1998. Use of soil texture, bulk density, and the slope of the water retention curve to predict saturated hydraulic conductivity. *Transactions of the American Society of Agricultural Engineers*, **41**(4), 983–988.
- Soil Survey Staff, 1997. Soil characterization data. Lincoln, NE: [CD-ROM] Soil Survey Laboratory, National Soil Survey Center, Natural Resources Conservation Service.
- Soil Survey Staff, 2004. Soil survey laboratory methods manual. Version No. 4.0. USDA-NRCS. Soil Survey Investigations Report No. 42. Washington, DC: U.S. Government Printing Office.
- Suprayogo, D., Widianto, C. G., and van Noordwijk, M., 2003. A Pedotransfer Resource Database (PtfrDB) for tropical soils: test with the water balance of WaNuLCAS. In Post, D. (ed.), *MODSIM Proceedings*, Townsville, Australia, July 2003.
- Tempel, P., Batjes, N. H., and van Engelen, V. W. P., 1996. IGBP-DIS soil data set for pedotransfer function development. Working paper and Preprint 96/05. Wageningen, The Netherlands: International Soil Reference and Information Centre (ISRIC).
- Tomasella, J., Hodnett, M. G., and Rossato, L., 2000. Pedotransfer functions for the estimation of soil water retention in Brazilian soils. *Soil Science Society of America Journal*, **64**, 327–338.
- Tomasella, J., Pachepsky, Ya A., Crestana, S., and Rawls, W. J., 2003. Comparison of two techniques to develop pedotransfer functions for water retention. *Soil Science Society of America Journal*, **67**, 1085–1092.
- van Genuchten, M Th, 1980. A closed form equation for predicting the hydraulic conductivity of unsaturated soils. *Soil Science Society of America Journal*, **44**, 892–898.
- Vereecken, H., Maes, J., Feyen, J., and Darius, P., 1989. Estimating the soil moisture retention characteristic from texture, bulk-density, and carbon content. *Soil Science*, **148**, 389–403.
- Wösten, J. H. M., Lilly, A., Nemes, A., and Le Bas, C., 1999. Development and use of a database of hydraulic properties of European soils. *Geoderma*, **90**, 169–185.
- Wösten, J. H. M., Veerman, G. J., de Groot, W. J. M., and Stolte, J., 2001. Water retention and hydraulic conductivity characteristics of top and subsoils in the Netherlands: the Staring Series. Updated version 2001. Alterra report 153. Wageningen, The Netherlands. (in Dutch)

Cross-references

- [Aeration of Soils and Plants](#)
- [Bulk Density of Soils and Impact on Their Hydraulic Properties](#)
- [Coupled Heat and Water Transfer in Soil](#)
- [Field Water Capacity](#)
- [Hydraulic Properties of Unsaturated Soils](#)
- [Hydropedological Processes in Soils](#)
- [Hysteresis in Soil](#)
- [Infiltration in Soils](#)
- [Layered Soils, Water and Solute Transport](#)
- [Leaching of Chemicals in Relation to Soil Structure](#)
- [Mapping of Soil Physical Properties](#)
- [Neural Networks in Agrophysics](#)
- [Online Measurement of Selected Soil Physical Properties](#)
- [Organic Matter, Effects on Soil Physical Properties and Processes](#)
- [Peats and Peatlands, Physical Properties](#)
- [Pedotransfer Functions](#)
- [Physical Properties for Soil Classification](#)
- [Pore Size Distribution](#)
- [Shrinkage and Swelling Phenomena in Soils](#)
- [Soil Aggregates, Structure, and Stability](#)
- [Soil Hydraulic Properties Affecting Root Water Uptake](#)
- [Soil Physical Quality](#)
- [Soil Structure, Visual Assessment](#)
- [Soil Texture: Measurement Methods](#)
- [Soil Water Flow](#)
- [Soil Water Management](#)
- [Solute Transport in Soils](#)
- [Spatial Variability of Soil Physical Properties](#)
- [Standardization in Agrophysics](#)
- [Trafficability and Workability of Soils](#)
- [Water Budget in Soil](#)
- [Water Use Efficiency in Agriculture: Opportunities for Improvement](#)

DEFLATION

A process of wind erosion, by which the loose top layer of the soil is blown away, generally following the denudation and pulverization of the soil in arid regions.

Bibliography

Introduction to Environmental Soil Physics. (First Edition). 2003. Elsevier Inc. Daniel Hillel (ed.) <http://www.sciencedirect.com/science/book/9780123486554>

Cross-references

[Wind Erosion](#)

DEFLOCCULATION

The inverse of flocculation. At low ionic strength of soil solution and domination of alkali metal cations, especially at higher pH values, soil colloidal particles can be dispersed.

Cross-references

[Conditioners, Effect on Soil Physical Properties](#)
[Flocculation and Dispersion Phenomena in Soils](#)

DEGRADATION OF SOIL

The deterioration of soil productivity by such processes as erosion, organic matter depletion, leaching of nutrients, compaction, breakdown of aggregates, waterlogging, and/or salinization.

Bibliography

Introduction to Environmental Soil Physics. (First Edition). 2003. Elsevier Inc. Daniel Hillel (ed.) <http://www.sciencedirect.com/science/book/9780123486554>

Cross-references

[Physical Degradation of Soils, Risks and Threats](#)
[Soil Physical Degradation: Assessment with the Use of Remote Sensing and GIS](#)

DENITRIFICATION

Reduction of nitrogen oxides (usually nitrate and nitrite) to molecular nitrogen or nitrogen oxides with a lower oxidation state of nitrogen by bacteria activity (denitrification) or by chemical reaction involving nitrite (chemodenitrification). Nitrogen oxides are used by

bacteria as terminal electron acceptors in place of oxygen in anaerobic or microaerobic respiratory metabolism.

Bibliography

Glossary of Soil Science Terms. Soil Science Society of America. 2010. <https://www.soils.org/publications/soils-glossary>

Cross-references

[Greenhouse Gas Fluxes: Effects of Physical Conditions](#)
[Greenhouse Gases Sink in Soils](#)
[Oxidation-Reduction Reactions in the Environment](#)

DENSITY

See [*Bulk Density of Soils and Impact on their Hydraulic Properties*](#)

DESERTIFICATION: INDICATORS AND THRESHOLDS

Max Kuderna¹, Adam Zsolnay²

¹wpa Beratende Ingenieure GmbH, Vienna, Austria

²German Research HelmHoltz Zentrum, Center for Environmental Health, München, Germany

Synonyms

Land degradation; Soil degradation

Definition

Desertification is a process by which susceptible areas lose their productive capacity. Desertification means land degradation in arid, semiarid and dry subhumid areas resulting from various factors, including climatic variations and human activities. While land degradation occurs everywhere, it is only defined as “desertification” when it occurs in dry lands.

Introduction

Land degradation and desertification is a paramount international problem, and indicators have been developed to follow it (Doran and Parkin, 1996; Middleton et al., 1997; Dregne, 1986). Many are based on plant communities, or soil loss or salinity.

However, indicators they tend to monitor the status quo over large time periods and are more suitable for crisis assessment than for risk prevention. They are also poorly suited for the sensitive monitoring of the success of remediation efforts.

Therefore, the UN Convention to Combat Desertification (UNCCD) and other organizations have emphasized the continuing need for indicator development based on the mechanisms of land degradation, which are known and have been the object of many studies. In view of

global change, such indicators are especially needed. Changes will often be slow and subtle. An early warning system is required to indicate the need for countermeasures, while they are still economical.

In response to this need, INDEX (acronym for Indicators and Thresholds for Desertification, Soil Quality, and Remediation), a specific targeted research project (STREP) dealing with “Research on mechanisms of desertification and soil quality” was initiated and carried out within the Sixth Framework of the European Commission.

Indicator development: a methodological outline

Indicators for desertification can be applied at different spatial and temporal scales (Figure 1). The goal within INDEX was to investigate the possibility of developing indicators, which reflect ecological quality at the soil level rather than at the more traditional field and catchment levels.

The indicator development was attained in five steps, which narrowed down an initial list of 100 soil parameters to finally three indices, using the following procedure:

1. Analysis of a broad range of parameters on various degraded soils
2. Testing the parameters on a variation of pressure levels
3. Temporal and spatial verification
4. Practical aspects of parameter application as an indicator
5. Combining the remaining parameters into indices using factorial analysis.

Step 1: Tested soil parameters included

- Soil microbiological parameters (bulk functions such as microbial biomass carbon and soil respiration, as well as enzymatic activities and molecular biological parameters)
- Humus parameters (bulk humus, humo-enzymes, and available humus)
- Physical parameters (such as particle size stability, hydraulic parameters, and pore size distribution)

A complete list of all performed analysis is given in [Appendix A](#).

Step 2: The testing was performed on soils from sites across Europe (listed in [Appendix B](#)), where a variation of influencing factors (“pressures” according to the European Environmental Agency’s DPSIR concept – see [Figure 2](#)) related to soil deterioration and desertification could be observed either because of a natural variation along a catena or because of different experimental treatments. The following types of pressures were taken into consideration:

Type I: lack of vegetation as the result of desertification processes

Type II: soil erosion

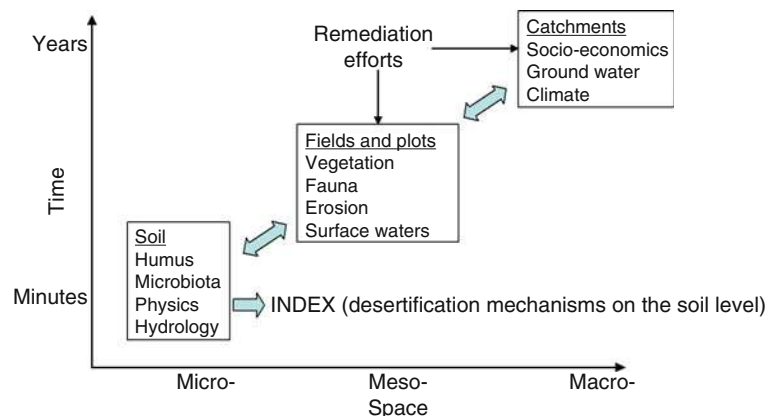
Type III: agricultural management

Only those soil parameters were selected as potential indicators, which reacted logically according to a change of the pressure level.

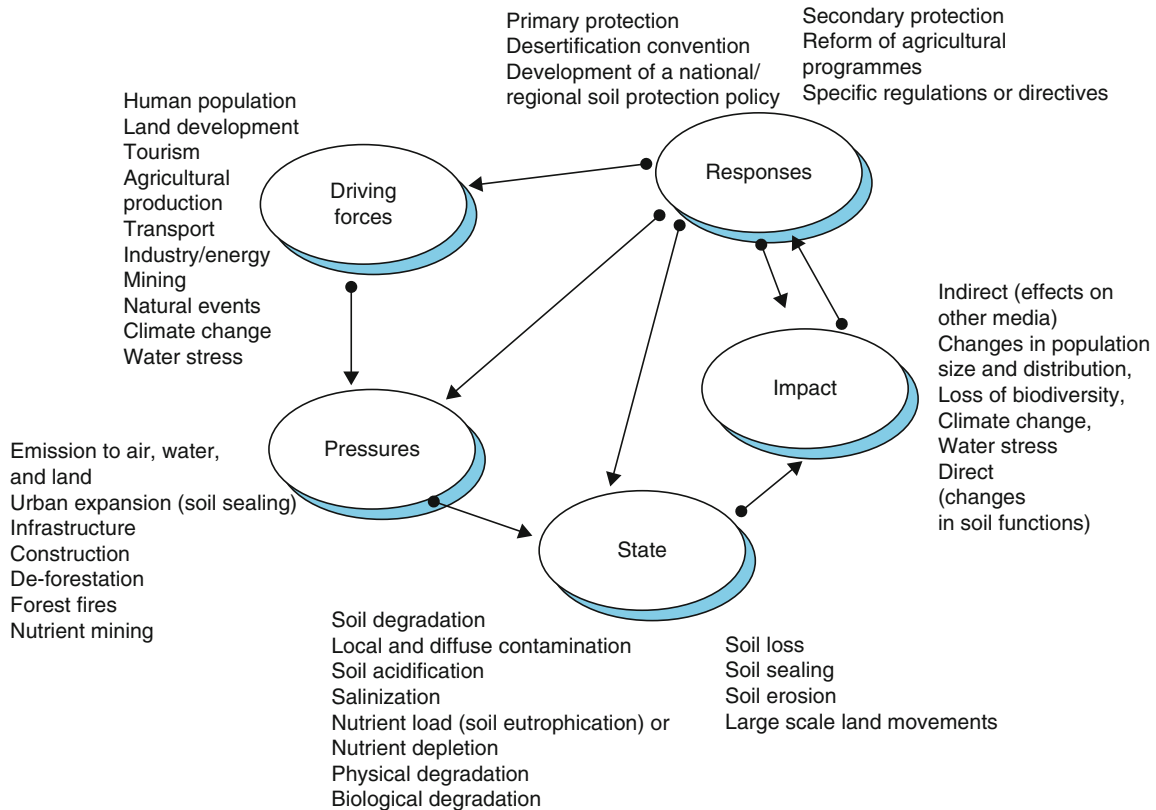
Step 3: Only those parameters, which gave reproducible results from subsequently taken soil samples over the period of 1½ years and on verification sites, which have not been used for *step 2* were considered sufficiently robust and were retained.

Step 4: This was used to eliminate such parameters, which caused experimental difficulties or required very complicated analytical procedures. [Table 1](#) shows the remaining parameters after *step 4*.

Step 5: This step combined these parameters ([Table 1](#)) to three indices (one for each pressure type), applying a factor analysis for *type I* and *type III* sites in order to reduce dimensionality. For pressure *type II*, a single parameter remained from *step 4*, so no factor analysis was required. At sites of *type I* the first factor accounted for 65–92% of the variation according to the sampling site and date. In most cases, however, only one factor was extracted, and this was used as the appropriate index. At sites of *type III* only one factor was extracted, which explained 57–99% of the variation according to the site and the sampling date.



Desertification: Indicators and Thresholds, **Figure 1** The various temporal and spatial scales of possible indicators of soil quality.



Desertification: Indicators and Thresholds, Figure 2 The European Environmental Agency's (EEA's) DPSIR concept as applied to soil degradation processes. Indicators as investigated in the Indicators and Thresholds for Desertification, Soil Quality, and Remediation (INDEX) project reflect the soil state and pressure state relationships.

Desertification: Indicators and Thresholds, Table 1 Selected soil parameters according to pressure type

I: Lack of vegetation as the result of desertification processes	II: Soil erosion	III: Agricultural management
Basal respiration	% particles <0.01 mm in pyrophosphate	β -Glucosidase activity
Microbial biomass carbon		Urease activity
ATP		
Basic phosphatase activity		
Proteins		
β -Glucosidase activity		
Fluorescence efficiency		

A brief explanation on selected parameters

Microbial biomass carbon. This indicates the amount of living microorganisms in soil and reacts to soil degradation processes (Smith et al., 1993; Garcia et al., 2002). It is determined by a fumigation-extraction procedure (Sims and Haby, 1971).

Basal respiration in soil. This parameter indicates the activity of heterotrophic microorganisms and was frequently used to indicate the biological state of soils

(Nannipieri et al., 1990; Pascual et al., 2000). The basal respiration was determined for incubated samples by measuring CO₂ release with a CO₂ IR detector.

ATP. Adenosine triphosphate (ATP) is used by living organisms as a transmitter of energy. It therefore indicates microbial activity on a general level. ATP was extracted by a method described by Webster et al. (1984).

Proteins. Water-soluble proteins (albumin was measured as a representative) are an important labile N-source for living organisms. They were determined according to Lerch et al. (1992).

Urease activity. Under the umbrella term "urease," we include all those hydrolases capable of acting on the C–N (non-peptide) bonds of linear amides. They are exocellular enzymes of a basically microbial origin, as has been demonstrated by several researchers (Ceccanti and Garcia, 1994).

Phosphatase activity. The agronomic and biotechnological importance of phosphatase is that it activates the transformation of organic into inorganic phosphorous, thus making it available to plants. The phosphatase detected in acid soils is normally acidic, while in basic soils it is usually alkaline (Dick and Tabatabai, 1993).

Glucosidase activity. Glucosidase is an enzyme acting the hydrolysis of the glucosidase bonds of the long

carbohydrate chains. The hydrolysis of these substrates play an important role in the microorganisms' attainment of energy from the soil and has shown to perform as a biomarker for degradation processes (Pascual et al., 2000).

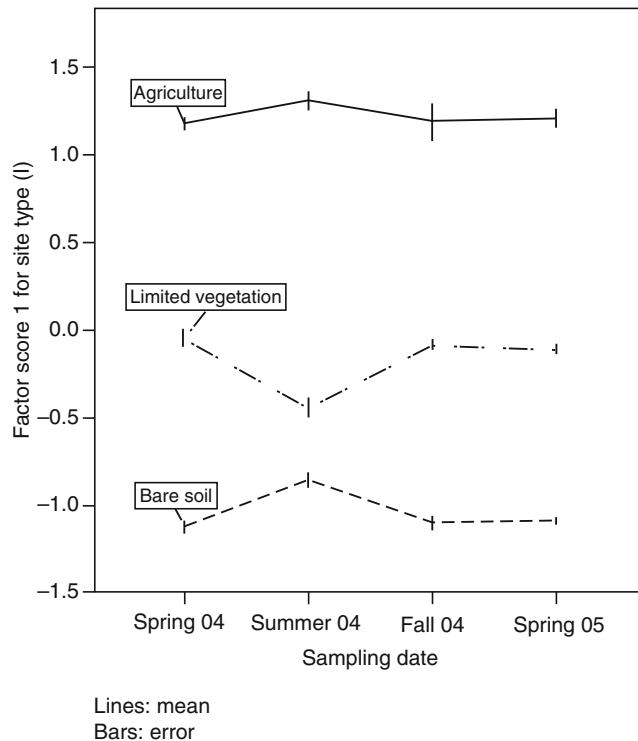
Fluorescence efficiency. Mobile humus in the humus fraction will react more sensitively than other components such as the humic acids. It is also known as dissolved organic matter (DOM) and is a poorly defined pool of compounds, which are available for biogeochemical processes (Zsolnay, 2003). One simple way to obtain it is by aqueous extractions. Its organic carbon content can be quantified, and qualitatively characterized with its UV absorption and fluorescence emission spectra. An interesting parameter is the fluorescence efficiency, which is proportional to the quantum yield (Ewald et al., 1988).

Applications of the indices

Sites with a lack of vegetation as the result of desertification processes (site type I)

Figure 3 gives an example from the Puch experimental site (Germany), where the highest values were found at the agricultural plot, the lowest values at the bare soil and the plot with limited vegetation in between. Although the variation of vegetation has been induced artificially at this site, the index developed gives a clear pattern showing how the soil quality reflects the differences in plant cover.

Very similar results were obtained at various catenae in Spain. Figure 4 gives an example of the application of the



Desertification: Indicators and Thresholds,
Figure 3 Differentiation of treatments at Puch by the first factor.

first factor to the Santomera catena: highest values were found at the forest site, lowest at the bare site, while the site with shrub had values in between them.

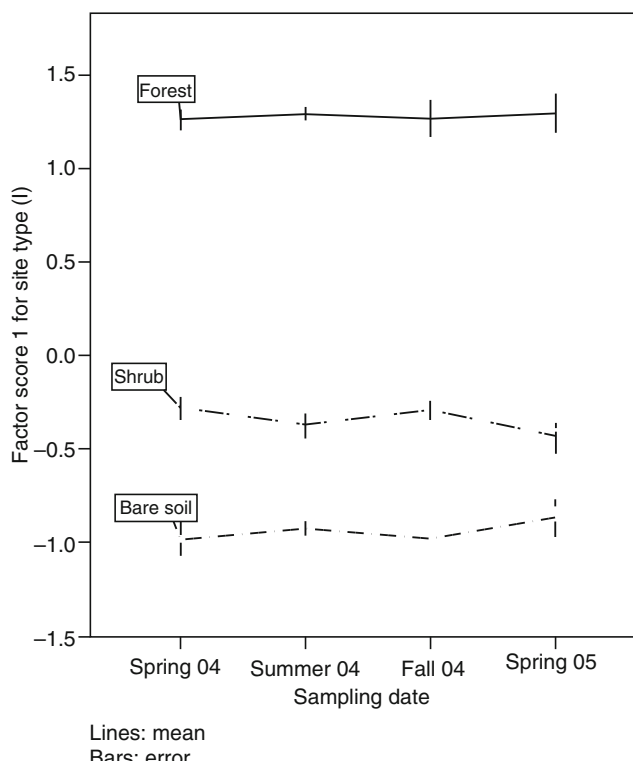
At the Carcavo catena (Spain) the index differentiated between (1) a revegetated site, (2) an abandoned site with natural vegetation, and (3) a degraded soil located in a very barren part of that landscape. Furthermore, the effect of exposition could clearly be seen. The indicator showed that the soil from a north slope had distinctly higher values than that from a south slope. Figure 5 displays the first factor scores for this site.

Sites with soil erosion (type II)

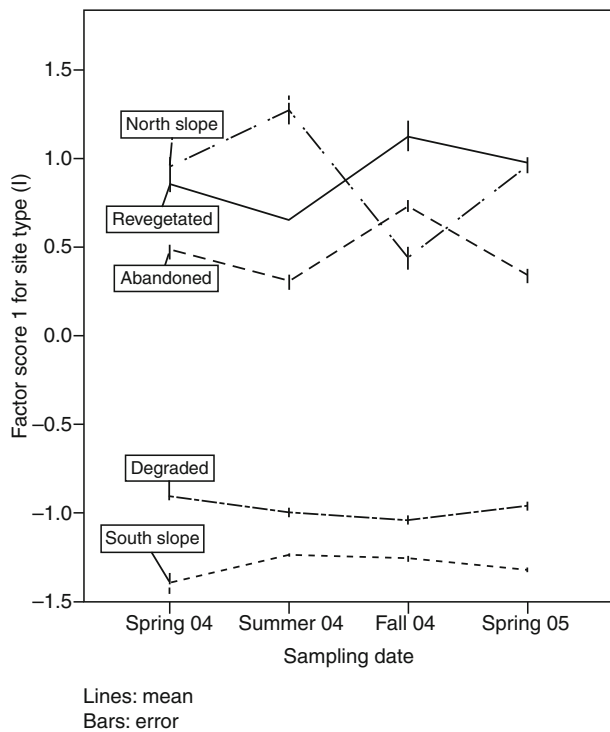
Figure 6 illustrates the application of the indicator to a catena near Gödöllő (Hungary). At sites of type II, soil erosion is not linked to a major variation of plant cover. At the Gödöllő catena, all three locations have been used for agriculture. As the indicator was only measured once in 2004 and in 2005, time series were not possible, but Figure 6 displays box plots of the values obtained during the 2 years.

Sites with different types of agriculture (type III)

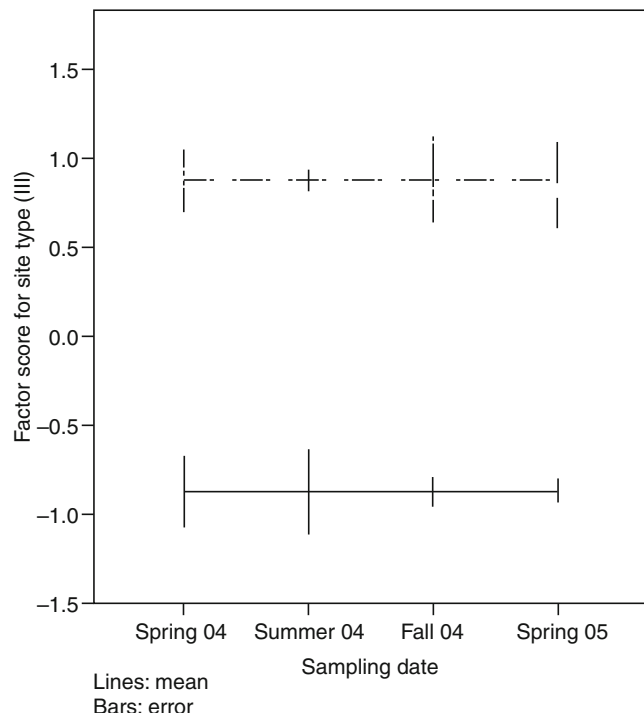
The type of agriculture (organic vs. conventional) was clearly distinguished at the soil level by the applied indicator. Figure 7 shows the results for the sites in Tuscany (Italy) as an example.



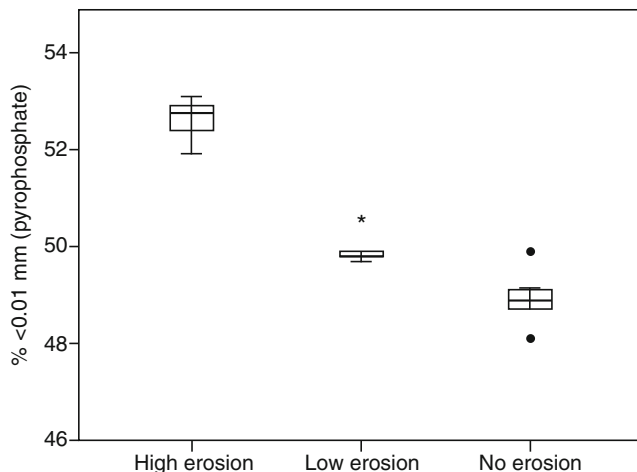
Desertification: Indicators and Thresholds,
Figure 4 Differentiation of different vegetation types along the Santomera catena by the first factor.



Desertification: Indicators and Thresholds,
Figure 5 Differentiation of sites along the Carcavo catena by the first factor.



Desertification: Indicators and Thresholds,
Figure 7 Differentiation of organic farming and conventional agriculture at sites in Tuscany.



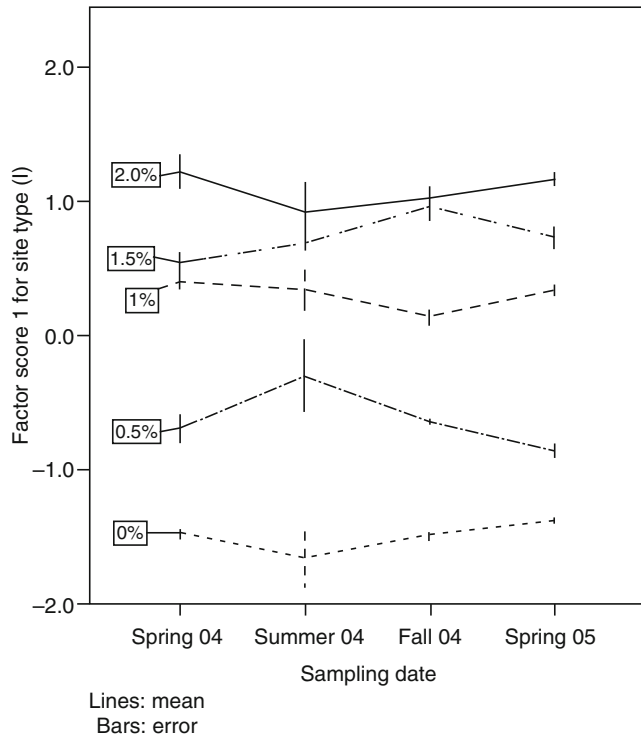
Desertification: Indicators and Thresholds,
Figure 6 Differentiation of soils with different degrees of soil erosion along a Catena near Gödöllö.

Effects of soil remediation

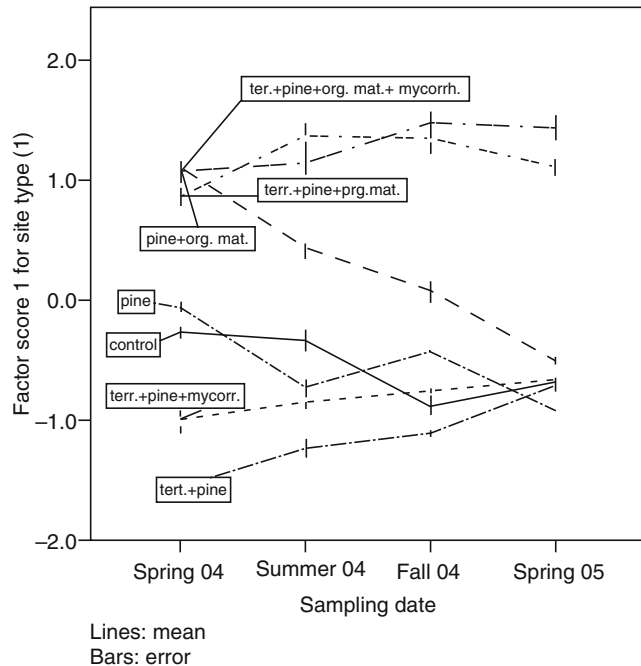
The index developed for sites where desertification was linked to the density of vegetation (sites of *type I*), proved to be very suitable for monitoring the effects of soil remediation. In the case of the Abanilla experimental site,

different amounts of organic matter (municipal solid waste) were added 18 years ago (percentages in [Figure 8](#) give the quantities incorporated into the upper 15 cm of the soil). No further remediation action has taken place since. The application of the index leads to the conclusion that an addition of up to 1.5% of organic matter had a strong lasting effect. However, a further increase of organic matter addition did not cause additional major soil improvements over a long time period and could therefore be avoided for economical reasons.

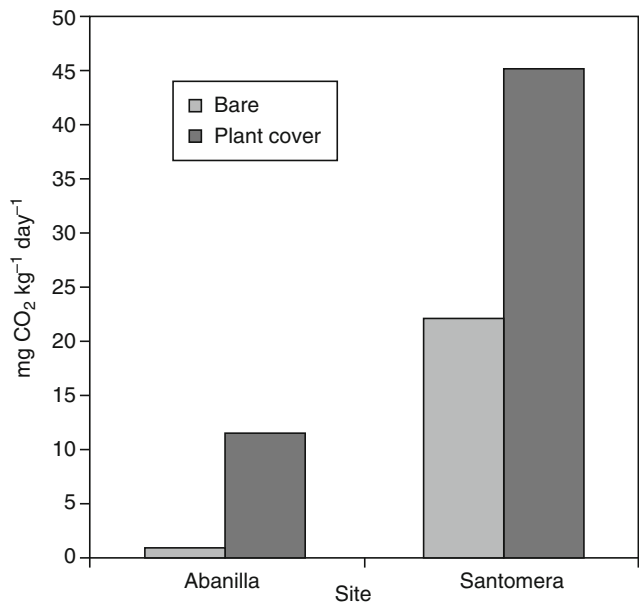
At the Aguilicho experimental site, the effects of reforestation, terracing, application of mycorrhiza, and the addition of organic matter have been tested in various combinations. The index shows ([Figure 9](#)), that only the combination of reforestation (pine), organic matter addition, and terracing had a lasting effect. Terracing and reforestation alone or together did not yield better results than the control, indicating the need for organic matter addition. However, without terracing, organic matter addition and reforestation did not have a positive effect. This inference may be attributed to erosion effects on the steep terrain, which are prevented by the terraces, which also improve water retention. Addition of mycorrhiza had no major effect as compared to treatments with no mycorrhiza. Again, this example demonstrates that the index is a sensitive tool to monitor if and how soil quality is improved by remediation measures in a region with a threat of desertification.



Desertification: Indicators and Thresholds, Figure 8 Effect of different levels of organic matter addition on the soil index at Abanilla experimental site.



Desertification: Indicators and Thresholds, Figure 9 Effect of reforestation, organic matter addition, mycorrhiza application, and terracing on the soil index at Aguiluco experimental site.



Desertification: Indicators and Thresholds, Figure 10 Soil respiration increases with plant cover density. Bare soils at one site, however, may have higher values than locations with plant cover at another.

Limitations

A universal approach comparing soil degradation across all sites was not tenable. Figure 10 gives an example: soil respiration values increased with plant density at each site, but for example, the bare location at Santomera had higher respiration values than the location with high plant coverage at Abanilla, which is only a few kilometers away.

For this same reason, no universal thresholds for the indices here can be established, but measurements have to be made relative to those local reference plots. In case of a soil remediation, this would imply for instance that the success of any remediation has to be proven against control plots. If the degree of soil degradation or desertification needs to be monitored, the index may be used for indicating different degrees of degradation along a catena or within a landscape. It can also be used to follow temporal changes at a given location.

Summary

The developed indices are well suited to indicate differences of soil degradation as related to desertification processes and the effects of remediation. They are sensitive and react quickly to changes in soil management. Although they are relatively robust to seasonal influences, repeated measurements in time are recommended. Fortunately, the indices are relatively inexpensive and can be done without great effort. Threshold values, however, need to be deduced from local reference sites, as the indices only work on a relative scale.

Acknowledgment

The following institutions participated in the described research: GSF (HelmholtzZentrum münchen), CSIC – Consejo Superior de Investigaciones Científicas, I.S.E. – Consiglio Nazionale delle Ricerche, University of Szeged, Szent Istvan University, University of Warwick, wpa Beratende Ingenieure GmbH.

Appendix A: List of tested parameters

Microbial parameters

Total organic carbon, humic substances, carbon, water-soluble carbohydrates, proteins, biomass carbon, accumulative respiration, basal respiration, qCO₂, ATP, dehydrogenase activity, urease activity, BAA protease activity, β-glucosidase activity, basic phosphatase activity, Shannon–Weaver index of diversity.

Humus parameters

Bulk: Total organic carbon, total inorganic carbon, total pyrophosphate extractable carbon, total pyrophosphate extractable carbon > 10,000 Da, total nitrogen

Enzyme activities in pyrophosphate soil extracts: β-glucosidase, phosphatase, urease, protease BAA

Pyrolytic indices of soil: Mineralization index: furfural/pyrrole, humification index: benzene/toluene, mineralization index: pyrrole/phenol, energetic index: aliphatic/aromatic

Pyrolytic Indices of pyrophosphate extracts: Mineralization index: furfural/pyrrole, humification index: benzene/toluene, mineralization index: pyrrole/phenol, energetic index: aliphatic/aromatic, β-glucosidase activity in the stable humic complex after IEF (isoelectric focusing), carbon percentage of the stable humic complex (bands 3 and 4) after IEF, with respect to the total IEF located carbon, relative content of β-glucosidase activity of the stable humic complex (bands 3 and 4) with respect to the total carbon content in the soil extract (fraction > 104 Dalton)*1,000, β-glucosidase: specific enzyme activity in dialyzed soil extracts (fraction > 104 Dalton) *1,000

Aqueous (0.1 N CaCl₂) extracts: WEOC (water extractable organic carbon) in extraction solution, WEOC per gram dry soil, UV absorption of solution ($\lambda = 254$ nm), summed emission fluorescence ($\lambda_{\text{ex}} = 254$ nm; $\lambda_{\text{em}} = 300$ –480 nm), lower emission fluorescence ($\lambda_{\text{ex}} = 254$ nm; $\lambda_{\text{em}} = 300$ –345 nm), higher emission fluorescence ($\lambda_{\text{ex}} = 254$ nm; $\lambda_{\text{em}} = 435$ –480 nm), absorptivity (UV/DOC), relative summed emission fluorescence (SF/DOC), relative lower emission fluorescence (L/DOC), relative higher emission fluorescence (H/DOC), humification Index (H/L), and fluorescence efficiency (SF/UV)

Physical soil parameters

Pore volume, total cumulative volume, specific surface area, pore radius average, moisture retained by disturbed samples, particle size (0.01 mm) in water (A), particle size (0.01 mm) in pyrophosphate (B), dispersion factor short = A/B, aggregate stability (Sekera optical method).

Rheological parameters

Water content of soil suspension, maximum of shear stress vs. time function, initial shear stress, area of thixotropic loop in low shear region from 0.1 to 10 s⁻¹, extrapolated yield value from shear stress vs. shear rate function, slope of the linear part of down flow curve (shear stress vs. shear rate function).

Appendix B: List of testing and verification sites

Sites for parameter testing (step 2)

Country	Location	Variation of treatments (pressures)	Type of site
Germany	Puch	Agricultural mismanagement and absence of vegetation	Agricultural field
Hungary	near Gödöllö	Soil erosion	Agricultural catena
Italy	Basilicata	Different agricultural practices under arid climate	Agricultural field
	Tuscany	Different agricultural practices under moderate climate	Agricultural field
Spain	Abanilla	Erosion and mismanagement	Catena
	Carcavo	Revegetation of a degraded forest	Degraded forest catena
	Santomera	Deforestation	Forest plots
	Santomera	Erosion and mismanagement	Catena

Sites for spatial verification (step 3)

Country	Location	Variation of treatments (pressures)	Type of site
Cyprus	Zygi	Different agricultural practices under arid climate	Agricultural field
Austria	Mistelbach	Soil erosion	Agricultural catena
Italy	Agri Basin	Erosion and mismanagement	Catena

Sites with specific soil remediation measures

Country	Location	Tested remediation measures
Spain	Abanilla	Addition of various amounts of organic matter Aguilucho Terracing, reforestation, organic matter addition, mycorrhiza

Bibliography

- Ceccanti, B., and Garcia, C., 1994. Coupled chemical and biochemical methodologies to characterize a composting process and the humic substances. In Senesi, N., and Miano, T. M. (eds.), *Humic Substances in the Global Environment and Implications on Human Health*. Amsterdam: Elsevier, pp. 1279–1284.

- Dick, W. A., and Tabatabai, M. A., 1993. Significance and potential uses of soil enzymes. In Blaine, F. (ed.), *Soil Microbial Ecology*. New York: Marcel Dekker, pp. 95–127.
- Doran, J. W., and Parkin, T. B., 1996. Defining and assessing soil quality. In Doran, J. W., Coleman, D. C., Bezdisk, D. F., and Steward, B. A. (eds.), *Defining Soil Quality for a Sustainable Environment*. Madison: Soil Science Society Special Publication, N°35.
- Dregne, H. E., 1986. Desertification of arid lands. In El-Baz, F., and Hassan, M. H. A. (eds.), *Physics of Desertification*. Dordrecht: Martinus.
- Ewald, M., Berger, P., and Visser, S. A., 1988. UV-visible absorption and fluorescence properties of fulvic acids of microbial origin as functions of their molecular weights. *Geoderma*, **43**, 11–20.
- Garcia, C., Hernandez, T., Roldan, A., and Martin, A., 2002. Effect of plant cover decline on chemical and microbiological parameters under Mediterranean climate. *Soil Biology and Biochemistry*, **34**, 635–642.
- Lerch, R. N., Barbarick, K. A., Sommers, L. E., and Wastfall, D. G., 1992. Sewage sludge proteins as labile carbon and nitrogen sources. *Soil Science Society of America Journal*, **45**, 1470–1476.
- Middleton, N., Thomas, D., and United Nations Environment Programm, 1997. World Atlas of Desertification. London: Hodder Arnold.
- Nannipieri, P., Grego, S., and Ceccanti, B., 1990. Ecological significance of the biological activity in soils. In Bollag, J. M., and Stotzky, G. (eds.), *Soil Biochemistry*. New York: Marcel Dekker, Vol. 6, pp. 203–355.
- Pascual, J. A., Garcia, C., Hernandez, T., Moreno, J. L., and Ros, M., 2000. Soil microbial activity as a biomarker of degradation and remediation processes. *Soil Biology and Biochemistry*, **32**, 1877–1883.
- Sims, J. R., and Haby, V. A., 1971. Simplified colorimetric determination of soil organic matter. *Soil Science*, **112**, 137–141.
- Smith, J. L., Papendick, R. I., Bezdicek, D. F., and Lynch, J. M., 1993. Soil organic matter dynamics and crop residue management. In Meeting, B. (ed.), *Soil Microbial Ecology*. New York: Marcel Dekker.
- Webster, J., Hampton, G., and Leach, F., 1984. ATP in soil: a new extractant and extraction procedure. *Soil Biology and Biochemistry*, **19**, 703–707.
- Zsolnay, Á., 2003. Dissolved organic matter: artefacts, definitions, and function. *Geoderma*, **113**, 187–209.

Cross-references

- [Biochemical Responses to Soil Management Practices](#)
[Climate Change: Environmental Effects](#)
[Enzymes in Soils](#)
[Management Effects on Soil Properties and Functions](#)
[Microbes, Habitat Space, and Transport in Soil](#)

DETACHMENT

Erosion process begins with detachment of a particle from surrounding material. This process sometimes requires breaking of bonds which hold particles together.

Cross-references

- [Water Erosion: Environmental and Economical Hazard](#)

DETERMINISTIC MODEL

Model based upon the concept that a discrete value exist for the variable of interest at each point in space and given a set of input values, a unique output can be determined.

Bibliography

Glossary of Soil Science Terms. Soil Science Society of America. 2010. <https://www.soils.org/publications/soils-glossary>

Cross-references

- [Agrophysics: Physics Applied to Agriculture](#)

DEW POINT

The temperature at which the vapor pressure of the atmosphere reaches a point of saturation and the vapor begins to condense into droplets of liquid water.

Bibliography

Introduction to Environmental Soil Physics (First Edition) 2003 Elsevier Inc. Daniel Hillel (ed.) <http://www.sciencedirect.com/science/book/9780123486554>

DIELECTRIC LOSS TANGENT

See [Organic Dusts, Electrostatic Properties](#)

DIELECTRIC PROPERTIES OF AGRICULTURAL PRODUCTS

Stuart O. Nelson, Samir Trabelsi
U.S. Department of Agriculture, Agricultural Research Service, Russell Research Center, Athens, GA, USA

Synonyms

Electric permittivity

Definition

Dielectric properties. Those characteristics of poorly conducting materials that determine their interaction with electric fields.

Introduction

Dielectrics are a class of materials that are poor conductors of electricity, in contrast to materials such as metals that are generally good electrical conductors. Many materials, including living organisms and most agricultural products, conduct electric currents to some degree, but are still classified as dielectrics. The electrical nature of these

materials can be described by their dielectric properties, which influence the distribution of electromagnetic fields and currents in the region occupied by the materials, and which determine the behavior of the materials in electric fields. Thus, the dielectric properties determine how rapidly a material will warm up in radio frequency or microwave dielectric heating applications. Their influence on electric fields also provides a means for sensing certain other properties of materials that may be correlated with the dielectric properties, by nondestructive electrical measurements. Therefore, dielectric properties of agricultural products may be important for applications in the agricultural industry that will benefit consumers in general.

Further definitions

A few simplified definitions of dielectric properties are necessary for meaningful discussion of their applications. A fundamental characteristic of all forms of electromagnetic energy is their propagation through free space at the velocity of light, c . The velocity of propagation v of electromagnetic energy in a material other than free space depends on the electromagnetic characteristics of that material and is given as

$$v = \frac{1}{\sqrt{\mu \epsilon}} \quad (1)$$

where μ is the magnetic permeability of the material and ϵ is the electric permittivity. For free space, this becomes

$$c = \frac{1}{\sqrt{\mu_0 \epsilon_0}} \quad (2)$$

where μ_0 and ϵ_0 are the permeability and permittivity of free space. Most agricultural products are nonmagnetic, so their magnetic permeability has the same value as μ_0 . These materials, however, have different permittivities than free space. The permittivity can be represented as a complex quantity

$$\epsilon = \epsilon' - j\epsilon'' \quad (3)$$

where $j = \sqrt{-1}$. The complex permittivity relative to free space is then given as

$$\epsilon_r = \frac{\epsilon}{\epsilon_0} = \epsilon'_r - j\epsilon''_r \quad (4)$$

where ϵ_0 is the permittivity of free space, the real part ϵ'_r is called the dielectric constant, and the imaginary part ϵ''_r is the dielectric loss factor. These latter two quantities are the dielectric properties of practical interest, and the subscript r will be dropped for simplification in the remainder of this article. The dielectric constant ϵ' is associated with the ability of a material to store energy in the electric field in the material, and the loss factor ϵ'' is associated with the ability of the material to absorb or dissipate energy, that is, to convert electric energy into heat energy. The dielectric loss factor, for example, is an index of

a material's tendency to warm up in a microwave oven. The dielectric constant is also important because of its influence on the distribution of electric fields. For example, the electric capacitance of two parallel conducting plates separated by free space or air will be multiplied by the value of the dielectric constant of a material if the space between the plates is filled with that material.

It should also be noted that $\epsilon = \epsilon' - j\epsilon'' = |\epsilon| e^{-j\delta}$ where δ is the loss angle of the dielectric. Often, the loss tangent, $\tan \delta = \epsilon''/\epsilon'$, or dissipation factor, is also used as a descriptive dielectric parameter, and sometimes the power factor, $\tan \delta / \sqrt{1 + \tan^2 \delta}$, is used. The ac conductivity of the dielectric σ in S/m is $\sigma = \omega \epsilon_0 \epsilon''$, where $\omega = 2\pi f$ is the angular frequency, with frequency f in Hz. In this article, ϵ'' is interpreted to include the energy losses in the dielectric due to all operating dielectric relaxation mechanisms and ionic conduction.

Agricultural products

Dielectric properties of agricultural products have been of interest for many years (Nelson, 2006). One of the earliest applications of such electrical properties was the study of dc electrical resistance of grain for rapidly determining its moisture content. In later work with radio-frequency (RF) measurements, changes in the capacitance of sample-holding capacitors, when grain samples were introduced between the capacitor plates, were correlated with grain moisture content and used for grain moisture measurement. The subsequent development of electrical grain moisture meters has been described in earlier reviews (Nelson, 2006).

The use of the dielectric properties of grain for moisture measurement has been the most prominent agricultural application for such data. In the early work, no quantitative data on the dielectric properties of the grain were reported. Interest generally focused on the influence of a grain sample on the response of an electrical circuit, and the instrument readings were calibrated with values measured by standard procedures for moisture determination. The need for quantitative values of the dielectric properties arose from research on the application of RF dielectric heating to agricultural problems. The first quantitative data on the dielectric properties of grain were reported for barley along with a method for reliable measurement of those properties in the 1-MHz to 50-MHz frequency range (Nelson et al., 1953). Quantitative dielectric properties data, obtained for similar reasons, were soon reported in Russia for wheat and other grain and crop seeds (Knipper, 1959). Extensive measurements on grain and crop seed in the 1-MHz to 50-MHz range, taken over a decade of research on RF dielectric heating applications, were summarized and made available for use in electric moisture meter design and other applications (Nelson, 1965).

The other principle application for dielectric properties of agricultural materials has been for use in research on potential dielectric heating applications. One of these applications was the possible selective dielectric heating

for control of insects that infest stored grain (Nelson and Whitney, 1960; Nelson, 1996).

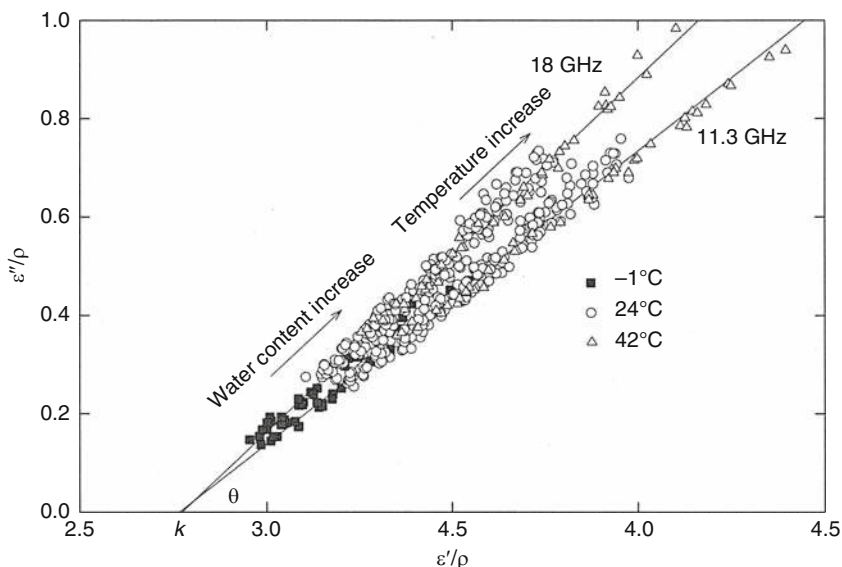
The principles governing the interaction between materials and RF and microwave electric fields, as influenced by the dielectric properties, have been detailed in a recent review article (Nelson, 2006). The same article included a review of principles and techniques for dielectric properties measurements at frequencies ranging from audio frequencies through radio frequencies well into the microwave region. Sources of dielectric properties data for a number of agricultural products will be identified in this article, and some typical data for such dielectric properties will be presented here.

Cereal grains and oilseeds

Dielectric properties of grain and seed over wide ranges of frequency and moisture content have been summarized previously, and graphical and tabular data are available for reference (ASAE, 2000). Models for calculating dielectric constants of many cereal grains and soybeans as functions of frequency, moisture content, and bulk density have been reported (Nelson, 1987; Kraszewski and Nelson, 1989; ASAE, 2000). Some recent dielectric spectroscopy measurements (Nelson and Trabelsi, 2006) on ground hard red winter wheat at frequencies from 10 MHz to 1,800 MHz over the temperature range from 25°C to 95°C were reported (Nelson and Trabelsi, 2006). The earlier reported data were useful to those developing improved grain and seed moisture meters. The recent measurements were part of a study to improve understanding of the temperature dependence of grain permittivity.

Although grain moisture meters, which sense the moisture content through correlations between the RF dielectric properties of the grain and its moisture content, have been in common use for more than 60 years, more recent advances have been reported in use of higher frequencies in the microwave range for grain and seed moisture sensing (Trabelsi et al., 1998). The basis for one such application is illustrated in Figure 1. Here, the dielectric constant and loss factor of hard red winter wheat, each divided by bulk density ρ of the grain, are plotted in an Argand diagram in the complex plane. Note that, at a given frequency, all of the points, regardless of moisture content and temperature, lie along a straight line. The slope of the line increases with frequency and pivots about a point on the $\epsilon''/\rho = 0$ axis that represents the ϵ'/ρ value for completely dry or very cold grain. The equation of the straight line provides a means for determining the bulk density of the grain independent of moisture content and temperature and also provides a basis for sensing moisture content independent of density from the measured permittivity at a single frequency (Trabelsi et al., 1998). This microwave-sensing technique should be useful for monitoring moisture content in moving grain and other particulate materials, since it offers a density-independent method for sensing moisture content in granular and particulate materials.

Another application for dielectric properties of grain was involved in the study of high-frequency dielectric heating for the selective heating of stored-grain insects (Nelson, 1996). In this instance, the dielectric properties of hard red winter wheat and a common stored-grain insect, the rice weevil, *Sitophylus oryzae* L., were measured over a broad range of frequencies and compared to



Dielectric Properties of Agricultural Products, Figure 1 Complex-plane plot of the dielectric constant and loss factor, divided by bulk density, for hard red winter wheat of various moisture contents and bulk densities at indicated temperatures for two frequencies, 11.3 GHz and 18.0 GHz (Trabelsi et al., 1998).

determine the frequencies for optimally heating the insects. Results of that study are summarized in [Figure 2](#). Because the loss factor is the dominant characteristic determining the energy absorption and heating, the frequency range between about 10 MHz and 100 MHz provides the best opportunity for selective heating of the insects.

Fruits and vegetables

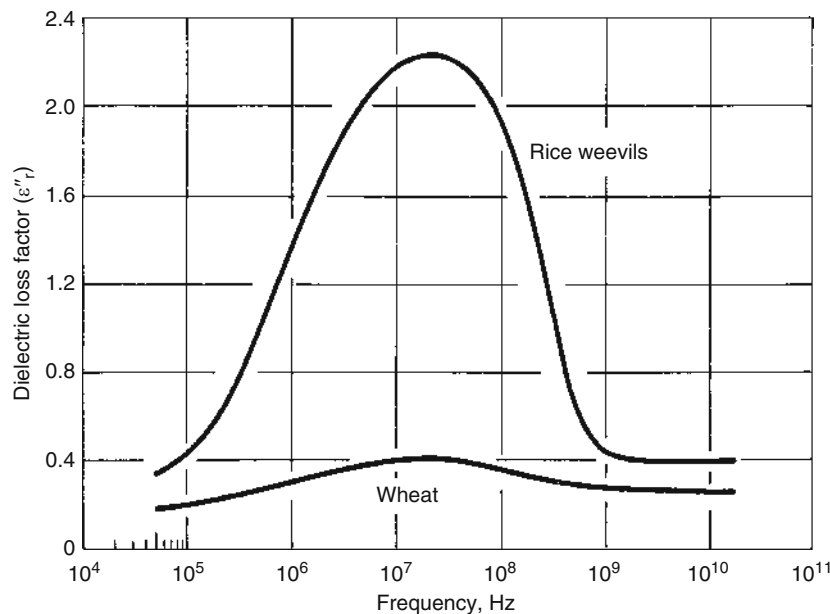
Because of the need for rapid nondestructive quality measurements for fresh fruits and vegetables, the dielectric properties of a few products were measured at microwave frequencies (Nelson, 1980; Nelson, 1983; Nelson, 1992). Although these studies provided background data on dielectric properties of several fruits and vegetables, the measurements did not show any promise for detecting peach maturity or hardcore condition in sweet potatoes by measurements at single frequencies (Nelson, 1980). Therefore, broadband permittivity measurements were initiated to study the dielectric properties of several fruits and vegetables over the frequency range from 200 MHz to 20 GHz (Nelson et al., 1994). Measurements over the same frequency range were obtained for tree-ripened peaches, *Prunus persica* (L.) Batsch., of different maturities (Nelson et al., 1995). Differences in the dielectric properties for different stages of maturity were noted at particular frequencies, and permittivity-based maturity indices, which combined the dielectric constant values at 200 MHz and the loss factor values at 10 GHz, were suggested, but it was noted that much more work was needed to establish their practicability.

Because the dielectric constants of peaches at different maturities diverged at the lower end of the frequency range, it appeared worthwhile to explore the dielectric

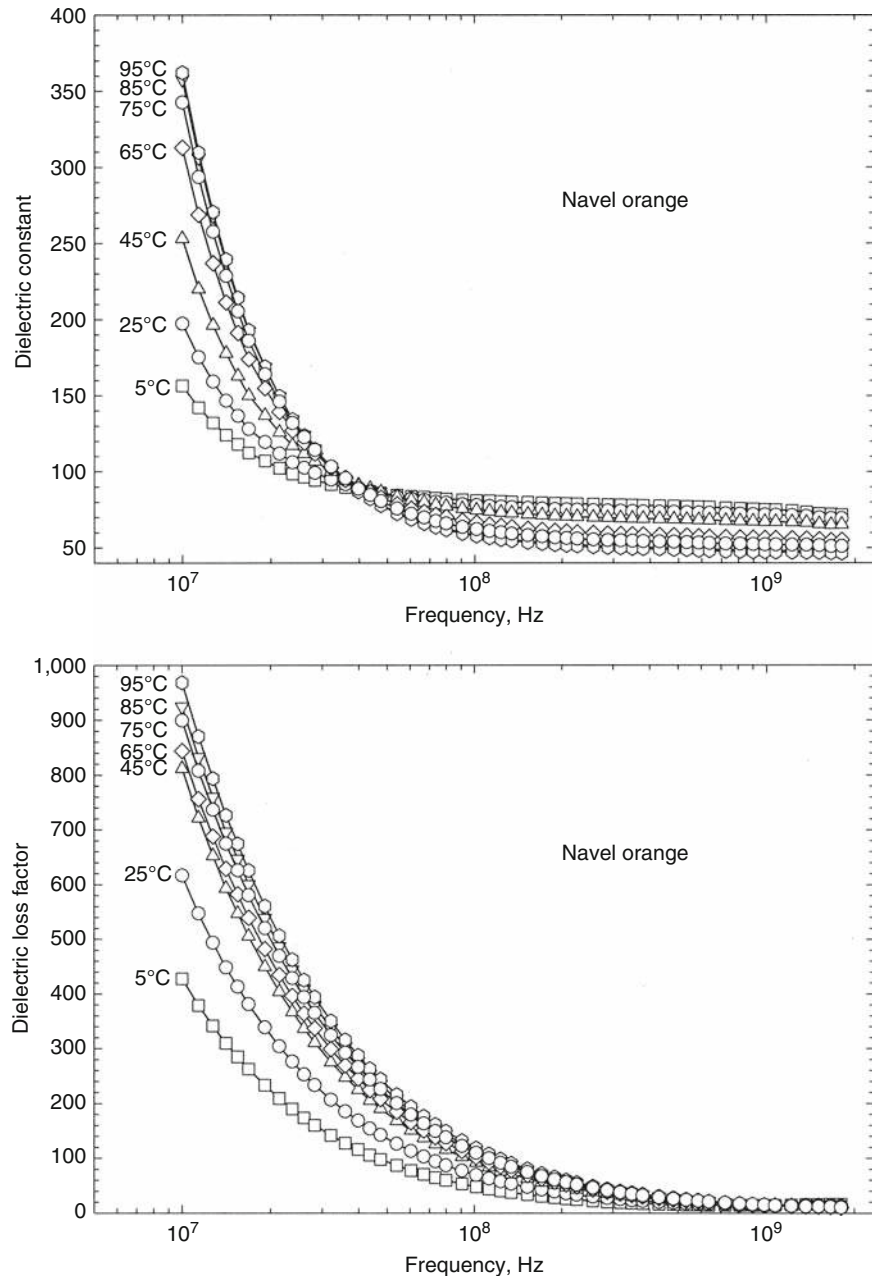
behavior of some fruits and vegetables at frequencies somewhat below this range (Nelson, 2003). Also, because changes in the dielectric properties of materials are important in RF and microwave heating, temperature-dependent data were obtained. An example of permittivity data obtained in the frequency range from 10 MHz to 1.8 GHz over the temperature range from 5°C to 95°C is shown in [Figure 3](#) for navel orange, *Citrus aurantium* subsp. *bergamia*, tissue (Nelson, 2006). In [Figure 3](#), the temperature dependence of the dielectric constant disappears at about 40 MHz. Above that frequency, the temperature coefficient for the dielectric constant is negative, but below that frequency the temperature coefficient is positive. This is most likely the frequency above which dipole relaxation accounts for most of the energy loss and below which ionic conduction is the dominant loss mechanism. That frequency varied for different fresh fruits and vegetables, but generally ranged between about 20 MHz and 120 MHz (Nelson, 2005).

Dielectric properties of freshly harvested melons have been studied to determine whether useful correlations exist between their dielectric properties and sweetness, as measured by soluble solids content (Nelson et al., 2006; Nelson et al., 2007). Although interesting correlations were obtained relating dielectric properties and soluble solids in complex-plane plots, correlations for predicting melon sweetness from the dielectric properties have so far not been successful (Nelson et al., 2007).

Dielectric properties of apples were recently measured and studied to determine whether they might be useful in sensing quality of stored apples (Guo et al., 2007a). Dielectric properties of the apples remained relatively constant during the 10-week refrigerated storage period.



Dielectric Properties of Agricultural Products, Figure 2 Variation with frequency of the dielectric loss factor of bulk samples of adult rice weevils and wheat at 24°C from 50 kHz to 12 Ghz (Nelson, 1996).

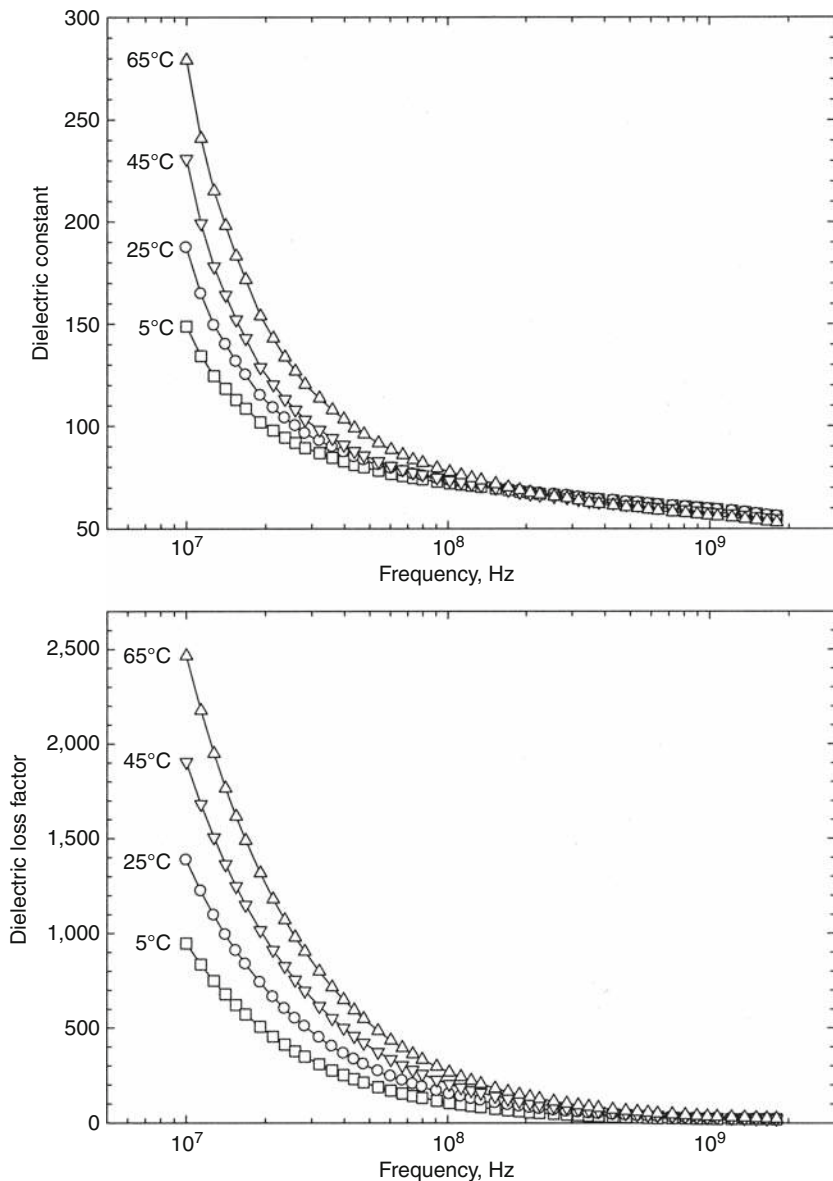


Dielectric Properties of Agricultural Products, Figure 3 Frequency and temperature dependence of the permittivity of navel orange, *Citrus aurantium* subsp. *bergamia*, at indicated temperatures (Nelson, 2003).

Dielectric properties of a commercial apple juice product were measured over the 200-MHz to 20-GHz frequency range (Nelson and Bartley, 2002). Because of the high water content of the apple juice, the dielectric relaxation of liquid water was clearly evident in resulting data. The temperature dependence of the dielectric properties of the apple juice is also very similar to that of pure liquid water, with the relaxation frequency for pure water shifting from below 20 GHz to higher frequencies as temperature increases (Hasted, 1973).

Poultry products

Some dielectric spectroscopy measurements have been taken recently on poultry products in exploratory work on quality sensing (Zhuang et al., 2007). Dielectric properties values for fresh chicken breast meat in the 10–1,800-MHz frequency range at temperatures from 5°C to 65°C are shown in Figure 4. These curves show frequency dependence of the dielectric properties similar to those for tissues of fruits and vegetables. Probable



Dielectric Properties of Agricultural Products, Figure 4 Frequency and temperature dependence of the dielectric properties of fresh chicken breast meat, *Pectoris major*, deboned at 2-h postmortem (Zhuang et al., 2007).

potential was indicated for using dielectric properties to assess meat quality characteristics.

Dielectric spectroscopy measurements were also taken on the albumen and yolk of fresh chicken eggs and at weekly intervals during 5 weeks of storage (Guo et al., 2007b). Dielectric properties changed during the storage period, but they did not correlate well with traditional quality factors for eggs.

Summary

Dielectric properties of materials are defined, and the importance and usefulness of the dielectric properties of agricultural products are discussed briefly, pointing out

their use in the rapid sensing and measurement of moisture content in grain and seed and in governing the behavior of materials subjected to RF and microwave electric fields for dielectric heating applications. Sources of information on the dielectric properties of such products are provided, and values of the dielectric constants and loss factors are presented graphically for a few products, including grain, fruit, and poultry products. These examples provide information not only on typical values of the dielectric properties, but also on their dependence on such variables as frequency of the alternating electric fields applied, moisture content, and temperature of the products.

Bibliography

- ASAE, 2000. *ASAE D293.2 Dielectric properties of grain and seed, ASAE Standards 2000*. St. Joseph: American Society of Agricultural Engineers, pp. 549–558.
- Guo, W., Nelson, S. O., Trabelsi, S., and Kays, S. J., 2007a. 10–1800-MHz dielectric properties of fresh apples during storage. *Journal of Food Engineering*, **83**, 562–569.
- Guo, W., Trabelsi, S., Nelson, S. O., and Jones, D. R., 2007b. Storage effects on dielectric properties of eggs from 10 to 1800 MHz. *Journal of Food Science*, **72**(5), E335–E340.
- Hasted, J. B., 1973. *Aqueous Dielectrics*. London: Chapman and Hall.
- Knipper, N. V., 1959. Use of high-frequency currents for grain drying. *Journal of Agricultural Engineering Research*, **4**(4), 349–360.
- Kraszewski, A. W., and Nelson, S. O., 1989. Composite model of the complex permittivity of cereal grain. *Journal of Agricultural Engineering Research*, **43**, 211–219.
- Nelson, S. O., 1965. Dielectric properties of grain and seed in the 1 to 50-mc range. *Transactions of the ASAE*, **8**, 38–48.
- Nelson, S. O., 1980. Microwave dielectric properties of fresh fruits and vegetables. *Transactions of the ASAE*, **23**, 1314–1317.
- Nelson, S. O., 1983. Dielectric properties of some fresh fruits and vegetables at frequencies of 2.45 to 22 GHz. *Transactions of the ASAE*, **26**, 613–616.
- Nelson, S. O., 1987. Models for the dielectric constants of cereal grains and soybeans. *The Journal of Microwave Power and Electromagnetic Energy*, **22**, 35–39.
- Nelson, S. O., 1992. Microwave dielectric properties of fresh onions. *Transactions of the ASAE*, **35**, 963–966.
- Nelson, S. O., 1996. Review and assessment of radio-frequency and microwave energy for stored-grain insect control. *Transactions of the ASAE*, **39**, 1475–1484.
- Nelson, S. O., 2003. Frequency- and temperature-dependent permittivities of fresh fruits and vegetables from 0.01 to 1.8 GHz. *Transactions of the ASAE*, **46**, 567–574.
- Nelson, S. O., 2005. Dielectric spectroscopy of fresh fruit and vegetable tissues from 10 to 1800 MHz. *The Journal of Microwave Power and Electromagnetic Energy*, **40**, 31–47.
- Nelson, S. O., 2006. Agricultural applications of dielectric measurements. *IEEE Transactions on Dielectrics and Electrical Insulation*, **13**, 688–702.
- Nelson, S. O., and Bartley, P. G. Jr., 2002. Frequency and temperature dependence of the dielectric properties of food materials. *Transactions of the ASAE*, **45**, 1223–1227.
- Nelson, S. O., and Trabelsi, S., 2006. Dielectric spectroscopy of wheat from 10 MHz to 1.8 GHz. *Measurement Science and Technology*, **17**, 2294–2298.
- Nelson, S. O., and Whitney, W. K., 1960. Radio-frequency electric fields for stored-grain insect control. *Transactions of the ASAE*, **3**, 133–137.
- Nelson, S. O., Soderholm, L. H., and Yung, F. D., 1953. Determining the dielectric properties of grain. *Agricultural Engineering*, **34**, 608–610.
- Nelson, S. O., Forbus, W. R. Jr., and Lawrence, K. C., 1994. Permittivities of fresh fruits and vegetables at 0.2 to 20 GHz. *The Journal of Microwave Power and Electromagnetic Energy*, **29**, 81–93.
- Nelson, S. O., Forbus, W. R. Jr., and Lawrence, K. C., 1995. Assessment of microwave permittivity for sensing peach maturity. *Transactions of the ASAE*, **38**, 579–585.
- Nelson, S. O., Trabelsi, S., and Kays, S. J., 2006. Dielectric spectroscopy of honeydew melons from 10 MHz to 1.8 GHz for quality sensing. *Transactions of the ASABE*, **49**, 1977–1981.
- Nelson, S. O., Guo, W., Trabelsi, S., and Kays, S. J., 2007. Dielectric spectroscopy of watermelons for quality sensing. *Measurement Science and Technology*, **18**, 1887–1892.
- Trabelsi, S., Kraszewski, A., and Nelson, S. O., 1998. New density-independent calibration function for microwave sensing of moisture content in particulate materials. *IEEE Transactions on Instrumentation and Measurement*, **47**, 613–622.
- Zhuang, H., Nelson, S. O., Trabelsi, S., and Savage, E. M., 2007. Dielectric properties of uncooked chicken breast muscles from ten to one thousand eight hundred megahertz. *Poultry Science*, **86**, 2433–2440.

Cross-references

- Databases on Physical Properties of Plants and Agricultural Products
 Electrical Properties of Agricultural Products
 Grain Physics
 Nondestructive Measurements in Fruits
 Physical Properties as Indicators of Food Quality
 Physical Properties of Raw Materials and Agricultural Products

DIFFUSE DOUBLE LAYER (DDL)

Md. Abdul Mojid

Irrigation and Water Management, Agricultural University, Mymensingh, Bangladesh

Synonyms

Electrical double layer (EDL); Electrical triple layer (ETL)

Definition

Diffuse double layer (DDL) is an ionic structure that describes the variation of electric potential near a charged surface, such as clay, and behaves as a capacitor.

Formation: Clays are aluminosilicates in which some of the aluminum and silicon ions are replaced by elements with different charge. For example, aluminum (Al^{3+}) may be replaced by iron (Fe^{2+}) or magnesium (Mg^{2+}), leading to a net negative charge. When suspended in an electrolyte, clay particles are surrounded by a hydrosphere of adsorbed water that contains a thin layer of adsorbed cations. Outside this layer, ions of opposite polarities form an electrically neutral diffuse layer. The adsorbed cations are influenced by electrostatic attraction, but those in the diffuse layer are influenced by two equal but opposing forces: electrostatic attraction and diffusive forces. This ionic structure consisting of the negative surface charges, adsorbed cations, and diffuse layer is known as the diffuse double layer, DDL. The thickness of the DDL is $<10^{-6}$ cm (Pamukcu, 1997).

Models: The Helmholtz, Gouy–Chapman, and Gouy–Chapman–Stern models describe the structure of a DDL. The first model states that the surface charge is neutralized by cations placed rigidly at an increment of their radius from the surface. The surface charge potential is dissipated linearly from the surface to the cations. The hypothesis of the rigid layers of cations is, however, questionable. The loosely held cations diffuse into the

liquid phase until the counter potential restricts this process – is the assumption of the second model. This assumption, also questionable, treats ions as point charges and physically limitless approach of the ions to the surface. The third model postulates that ions have finite size and the first layer of ions is at a distance equal to the radius of the ion from the surface. Also, some of the ions are adsorbed by the surface in the plane, and this layer is called the Stern layer.

Main features: Clay particles are surface-active materials and many of their properties depend on the activity of surface phenomena. The cations in the Stern layer can be replaced by other cations; thus, they are exchangeable and become available to plants. The capacity of a soil for exchange of cations between the soil and the surrounding solution is its cation exchange capacity, CEC. The cations in the DDL move along the clay–water surface under the influence of an electrical field (Revil and Glover, 1997) resulting in the surface electrical conduction. Increasing electrolyte concentration or decreasing water content reduces the thickness of DDLs and hence the mobility of cations within them. The cations in the Stern layer, although once assumed immobile, are now found mobile (Leroy and Revil, 2004) leading to the assumption of a dynamic Stern layer.

Bibliography

- Leroy, P., and Revil, A., 2004. A triple-layer model of the surface electrochemical properties of clay minerals. *Journal of Colloid and Interface Science*, **270**, 371–380.
- Pamukcu, S., 1997. Electro-chemical technologies for in-situ restoration of contaminated subsurface soils (invited paper). *Electronic Journal of Geotechnical Engineering* (Online). Available from World Wide Web: <http://www.ejge.com/1997/Ppr9704/Ppr9704.htm>.
- Revil, A., and Glover, P. W. J., 1997. Theory of ionic surface electrical conduction in porous media. *Physical Review B*, **55**, 1757–1773.

DIFFUSION IN SOILS

Witold Stępniewski¹, Henryk Sobczuk²,
Marcin Widomski¹

¹Department of Land Surface Protection Engineering,
Lublin University of Technology, Lublin, Poland

²Department of Thermal Techniques, Lublin University of
Technology, Lublin, Poland

Synonyms

Gas diffusion in soil; Heat diffusion in soil; Soil water dispersion; Solute diffusion in soil; Water diffusion in soil; Water transport in unsaturated soil

Definition

Diffusion is a process that causes the spread of a constituent mass within the medium under gradient of

concentration. It originates from the random motion of particles (molecular diffusion). Diffusion equation describes well various spread processes of water, gases, solutes, and heat in porous media. In case of a porous material, diffusion coefficient is interpreted as dispersion coefficient with the value dependent on porous material structure. Diffusion equation allows to describe, in a simple manner, the transfer of mass or heat in porous media by inclusion of various effects into one parameter – dispersion coefficient.

Introduction

In soil, various diffusion processes occur. They comprise diffusive transport of heat energy, of gases, of solutes, as well as of water under unsaturated conditions. These processes are important for plant biomass production and for the state of the environment.

Equation of motion based on Newton's Laws connects acceleration and force into simple equation:

$$\vec{F} = m\vec{a} \quad (1)$$

where \vec{F} is vector of force m is mass \vec{a} is vector of acceleration.

Analyzing transport processes in microscale, one should consider various forces acting on each part of the system and forces acting among particular parts of the system:

$$\frac{d(m\vec{v})}{dt} = \sum \vec{F}_i \quad (2)$$

where \vec{v} is vector of flow velocity t is time.

This in fact leads to a partial differential equation of the second order in three-dimensional space. In case of porous material, it gives complicated equations that are not tractable in a practical way.

While considering the porous medium such as soil in a macroscopic scale one should take into account a representative volume of the medium to perform homogenization of its properties.

All factors that influence flow can be combined into one parameter that governs water movement. Describing water flow in the soil medium, one should consider water interaction with solid phase, gravity forces influence on flux, water internal friction, etc. Instead, all those effects are lumped into one parameter called diffusivity function or diffusion coefficient.

Moisture diffusivity in soil

This kind of reasoning lead to the Darcy's equation (1856) giving connection between macroscopic, saturated water flow velocity v , and pressure drop Δh over the sample length Δx :

$$v = K_{sat} \frac{\Delta h}{\Delta x} \quad (3)$$

Coefficient K_{sat} , called today saturated hydraulic conductivity, is a parameter that depends on the soil type and bulk density.

For unsaturated conditions, this equation is applicable in a modified form:

$$f_w = -K \frac{\partial \Phi}{\partial x} \quad (4)$$

where f_w is water flux K is hydraulic conductivity function Φ is pressure potential in the samplex is spatial coordinate.

In this equation, hydraulic conductivity function K is highly moisture dependent and is specific for a soil sample.

Above equations are based on the assumption that water potential gradient is a driving force causing water flow in the sample. Often, it is useful to consider water content gradient as a factor causing water flow. In such a case, the previous equation reads:

$$f_w = -K \frac{d\Phi}{d\Theta} \frac{\partial \Theta}{\partial x} \quad (5)$$

where Θ is a volumetric moisture content of the soil sample.

In this picture, new characteristic of the flux can be introduced, namely, diffusivity function D_w :

$$f_w = -D_w \frac{\partial \Theta}{\partial x} \quad (6)$$

It is visible from the comparison of above equations that:

$$D_w = K \frac{d\Phi}{d\Theta} \quad (7)$$

what means that the diffusivity is equal to water permeability K multiplied by the slope of the water retention curve $d\Phi/d\Theta$.

Moisture potential is usually considered as consisting of two different parts:

$$\Phi = h + z. \quad (8)$$

In this equation, h is a pressure part of the potential and z is gravitational part of the potential, represented in the equation by the elevation z over a chosen reference level. Pressure potential is dependent on moisture content, soil type and structure, while gravitational potential depends on gravitational forces.

In three dimensions, the equation for flux of water reads as follows:

$$\bar{f}_w = -K \left(\vec{i} \frac{\partial \Phi}{\partial x} + \vec{j} \frac{\partial \Phi}{\partial y} + \vec{k} \frac{\partial \Phi}{\partial z} \right). \quad (9)$$

Flux \bar{f}_w is treated here as a vector in three-dimensional space. Application of the equation for moisture potential leads to the equation:

$$\bar{f}_w = -K \left(\vec{i} \frac{\partial h}{\partial x} + \vec{j} \frac{\partial h}{\partial y} + \vec{k} \left(\frac{\partial h}{\partial z} + 1 \right) \right). \quad (10)$$

which shows clearly the influence of gravity force on the flux in vertical (z) direction.

When applying change of the variables to the diffusivity, the above equation reads:

$$\bar{f}_w = -K \frac{dh}{d\Theta} \left(\vec{i} \frac{\partial \Theta}{\partial x} + \vec{j} \frac{\partial \Theta}{\partial y} + \vec{k} \left(\frac{\partial \Theta}{\partial z} + \frac{d\Theta}{dh} \right) \right) \quad (11)$$

and the coefficient D_w :

$$D_w = K \frac{dh}{d\Theta} \quad (12)$$

is a moisture diffusivity function.

Application of the mass conservation law:

$$\frac{\partial \Theta}{\partial t} = -\operatorname{div} \bar{q} \quad (13)$$

to the flux \bar{q} leads to the water diffusion equation:

$$\begin{aligned} \frac{\partial \Theta}{\partial t} &= \frac{\partial}{\partial x} \left(D_w \frac{\partial \Theta}{\partial x} \right) + \frac{\partial}{\partial y} \left(D_w \frac{\partial \Theta}{\partial y} \right) \\ &\quad + \frac{\partial}{\partial z} \left(D_w \frac{\partial \Theta}{\partial z} \right) + \frac{dK}{d\Theta} \frac{\partial \Theta}{\partial z} \end{aligned} \quad (14)$$

with gravitational term $\frac{dK}{d\Theta} \frac{\partial \Theta}{\partial z}$.

In practice, diffusion coefficient depends on the moisture content and often, due to the spatial variability of the soil, is position dependent. This causes certain problems in the application of this model to real conditions.

This equation together with initial and boundary conditions form a complete system that describes fate of moisture content in a certain volume. Initial condition function defines initial values of the moisture content in each point of the volume under consideration, while boundary conditions define values of moisture and/or flux of water at the boundaries of considered volume at the time when moisture movement is calculated.

To determine the moisture content distribution in a medium in a certain time, it is necessary to solve the water flow equation.

The solution depends on the actual moisture conditions existing at the boundaries of the considered region and, on initial moisture conditions inside the considered region. Moisture flow equation is the second-order equation in spatial coordinates. One has to provide the value of moisture content and of moisture gradient at the boundary.

The factor containing the water hydraulic conductivity K in the equation origins from the gravity forces and is present only in the equation where vertical flow is applicable.

Solution of the diffusion equations

Usually, when diffusion coefficient depends on the moisture content, one has to solve the diffusion equation numerically due to complicated form of this function. In some cases, for simple diffusivity functions analytical solution is known. This is the situation for constant diffusion coefficient and for various geometries of modeled volume.

Dependence of water diffusion on moisture content
Diffusion coefficient of water in the soil is specific for a given soil. It depends on the status and moisture content. In order to be able to model various shapes of diffusion functions, many mathematical functions presenting empirical models have been used ([Table 1](#)).

Importance of gravity forces

Gravity forces are especially important under the conditions close to saturation when pressure head gradient is low. When pressure head gradient has a large value in comparison to unity, the gravity forces do not play a significant role in water flow. In such a situation, water can easily flow against the gravity from the deeper layers of the soil to the surface.

Calculation of moisture diffusivity

Moisture diffusivity can be calculated from the measurement results of transient moisture profiles of isothermal, horizontal water flow. Inverse analysis with the application of Boltzmann–Matano transformation is possible (e.g., Pachepsky et al., [2003](#)). One dimensional diffusion equation for such a case has a form (e.g., Black et al., [1969](#); Lisle et al., [1987](#); Parlange et al., [1993](#)):

$$\frac{\partial \Theta}{\partial t} = \frac{\partial}{\partial x} \left(D_w(\Theta) \frac{\partial \Theta}{\partial x} \right), \quad (15)$$

where Θ is volumetric water content, t is time of water absorption, and x is distance of monitored moisture content from the water exposed surface of the sample. Boundary conditions are constant with a step at the beginning of the process:

Diffusion in Soils, Table 1 Empirical equations relating water diffusivity to volumetric water content

Equation	Symbols meaning	Source
$D_w = a \frac{\Theta^b}{(\Theta_s - \Theta)^a}$	D_w – diffusion coefficient Θ_s – saturated volumetric water content	Ahuja and Swartzendruber (1972)
$D_w = \frac{K_s}{\lambda z (\Theta_s - \Theta)} s^{3/2+1/\lambda}$	Θ – actual volumetric water content s – saturation of the soil K_s – saturated hydraulic conductivity	Mualem (1976)
$D_w = a \frac{\Theta^b}{(\Theta_s - \Theta)^a}$	α, a, b, λ – fitting parameters	van Genuchten (1980)

$$\Theta(0, t) = \Theta_1, \quad (16)$$

initial moisture in the sample is constant with a value:

$$\Theta(x, 0) = \Theta_2. \quad (17)$$

Application of Boltzmann transformation of variables that introduces variable:

$$\Theta(x, t) = \Theta(\eta) \quad (18)$$

with

$$\eta = \frac{x}{2\sqrt{t}}, \quad (19)$$

converts the partial differential equation into ordinary equation in a new variable:

$$\frac{d}{d\eta} \left(D_w(\Theta) \frac{d\Theta}{d\eta} \right) + 2\eta \frac{d\Theta}{d\eta} = 0 \quad (20)$$

with the boundary conditions

$$\omega(0) = \Theta_1, \quad (21)$$

$$\omega(\infty) = \Theta_2. \quad (22)$$

This equation can be solved by integration giving:

$$D_w(\Theta) = \frac{1}{2t_0(d\Theta/d\eta)\eta_0} \int_{\eta_0}^{\infty} \eta \frac{d\Theta}{d\eta} d\eta. \quad (23)$$

One should know the variability of moisture content in space and time $\Theta(x, t) = \Theta(\eta)$ from the experiment in order to apply this method.

Diffusion processes in soil, beyond the diffusion of water under unsaturated conditions, as described above, comprise diffusion of heat, of gases, and of solutes. The diffusion equations for these agents are in all the cases similar (cf. [Tables 2](#) and [3](#)). In each case, the flux of the agent under consideration is proportional to the driving force of the process and to a coefficient characterizing the transport properties of the given material.

The driving force of water movement is the gradient of water potential (Darcy's law). The heat flux is driven by the temperature gradient (Fourier's equation). In case of diffusion of gases and solutes, the driving forces are the concentration gradients of the gases or of the solutes (First Fick's equation).

Diffusion in Soils, Table 2 Equations for water movement under unsaturated conditions in soil and heat transfer both under saturated and unsaturated conditions (modified from Bolt et al., 1966)

General notion	Water	Heat	Symbols
Flux	$f_w = -K(\partial\Phi/\partial x)$, Darcy (1856)	$f_h = -\lambda(\partial T/\partial x)$, Fourier (1822)	f_w – unit flux of water
Conservation equation	$\partial\Theta/\partial t = -(\partial f_w/\partial x) \pm q_w$	$\partial(c_v T)/\partial t = -(\partial f_h/\partial x) \pm q_h$	f_h – unit heat flux K – water permeability
Movement equation for soil profile	$\partial\Theta/\partial t = (\partial/\partial x)(D_w(\partial\Phi/\partial x)) \pm q_w$	$\partial T/\partial t = (\partial/\partial x)(D_h(\partial T/\partial x)) \pm q_h$	λ – heat conductivity Φ – water potential T – temperature x – distance t – time Θ – volumetric water content c_v – heat capacity q_w, q_h – source/sink terms $D_w = K_h(\partial\Phi/\partial\Theta)$ $D_h = \lambda/c_v$

Diffusion in Soils, Table 3 Equations for gas and solute diffusion in soil (modified from Bolt et al., 1966)

General notion	Gas	Solute	Symbols
Flux	$f_g = -D_g(\partial C/\partial x)$, Fick (1855)	$f_s = -D_s(\partial C/\partial x)$, Fick (1855)	f_g – unit flux of gas
Conservation equation	$\partial[C(\varepsilon_g + B\Theta)]/\partial t = -(\partial f_g/\partial x) \pm q_g$	$\partial(\Theta C)/\partial t = -(\partial f_s/\partial x) \pm q_s$	f_s – unit solute flux B – Bunsen's coefficient of solubility
Movement equation for soil profile	$\partial C/\partial t = (\partial/\partial x)(D_g^*(\partial C/\partial x)) \pm q_g^*$	$\partial C/\partial t = (\partial/\partial x)(D_s^*(\partial C/\partial x)) \pm q_s^*$	C – concentration of the gas or solute Θ – volumetric water content x – distance t – time D_g – gas diffusion coefficient D_s – solute diffusion coefficient ε_g – air-filled porosity $D_{g*} = D_g/(\varepsilon_g + B\Theta)$ $D_{s*} = D_s/\Theta$ ΘC – amount of solute in a unit soil volume $[C(\varepsilon_g + B\Theta)]$ – amount of gas in unit soil volume q_g, q_g^*, q_s, q_s^* – source/sink terms

The properties of the diffusion medium are characterized by water permeability in case of water movement. In case of heat flux, it is the heat conductivity, while in case of gas and solute diffusion, it is the diffusion coefficient.

The similarities among the above processes become more evident after combination with the conservation equation. Then the equation gets the form of the second Fick's equation (Table 3) and material constant characterizing the properties of the medium acquires the dimension of square unit of length per unit of time (most often $m^2 s^{-1}$).

Thermal diffusivity in soil

The flow of heat in a soil is connected with many processes. Usually, it is not a simple heat conduction but involves also radiation heat transport, vapor transport with latent heat movement. In the simplest case, it is assumed that heat transfer undergoes conduction and can be

described with the diffusion equation. It is in fact the flow of thermal energy in the stable soil caused by temperature gradient.

Heat conduction equation comes out from the application of constitutive equation for the heat conduction in a matter, i.e., Fourier's law, $\vec{q}_h = -\lambda\nabla T$, that combines temperature gradient and heat flux in a linear manner with energy balance equation $dE/dt = \dot{Q} + \dot{W}$ that expresses energy conservation in the flow process, where \dot{Q} denotes heat flux term, \dot{W} represents work flux, and λ is the heat conductivity.

The application of both equations leads in the simplest case to (Hillel, 1982; Marshall and Holmes, 1988):

$$\frac{\partial T}{\partial t} = D_h \frac{\partial^2 T}{\partial x^2} \quad (24)$$

which has the form of diffusion equation for temperature distribution. The coefficient D_h is a thermal diffusivity

coefficient. One should keep in mind that despite of the form, this equation describes heat transport and not temperature transport.

Thermal diffusivity D_h can be calculated from the formula:

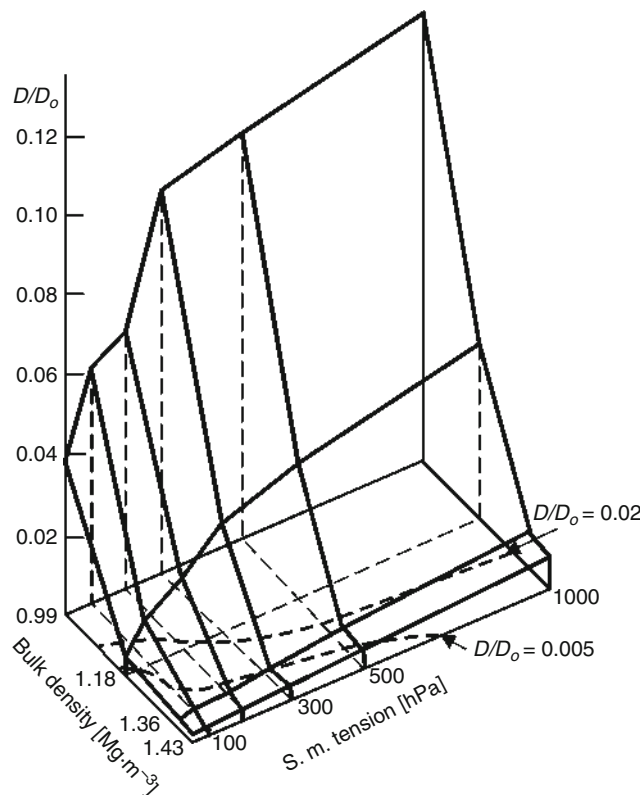
$$D_h = \frac{\lambda}{c_v} \quad (25)$$

where c_v is its heat capacity.

Thermal diffusivity of soils varies due to soil parameters variation. Moisture content is one of most important factors that change thermal diffusivity. Heat capacity of the soil is almost a linear function of moisture content, while thermal conductivity depends on moisture content nonlinearly (Figure 1). Thermal diffusivity has a maximum for certain moisture content, what is of high practical importance. Soil with the moisture content around this value will heat much quicker than soil with moisture far from that value. Optimal moisture allows to germinate seeds in spring significantly earlier.

Diffusion of gases

Concentration diffusion plays an essential role in the gas exchange within soil. The diffusive flow f_g of a gas within a porous medium is described by the first Fick's law.



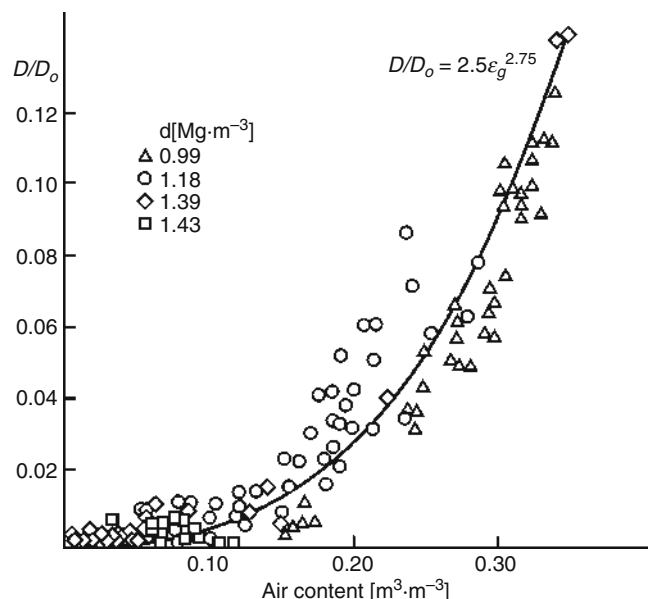
Diffusion in Soils, Figure 1 Dependence of relative gas diffusion coefficient in a loamy textured Chernozem Rendzina (Bezek, Poland) on soil moisture tension and bulk density (modified from Stępniewski, 1981).

$$f_g = -D_g \frac{\partial C}{\partial x} \quad (26)$$

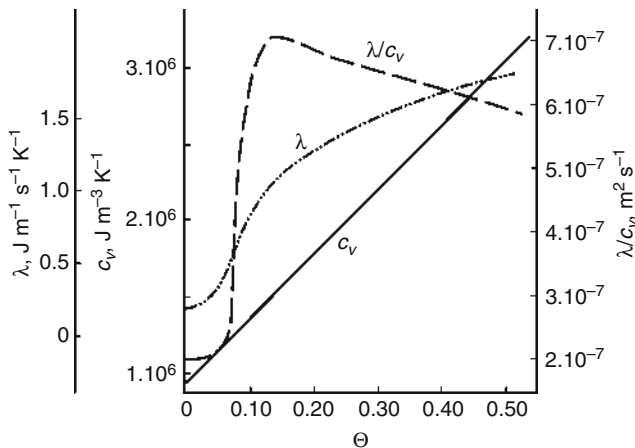
The change of the concentration of gases with time is described by the second Fick's law, containing also the sink/source term (Table 3).

Coefficient of gas diffusion in soil D_g depends on the kind of the diffusing gas, on the temperature and pressure, as well as on the content of air-filled pores, and their tortuosity, continuity, and shape. These, in turn, depend on the spatial arrangement of soil particles and distribution of water. The diffusive properties of soil medium usually are characterized by relative diffusion coefficient D_g/D_o , where D_o is the diffusion coefficient of the same gas in free atmospheric air under the same temperature and pressure conditions. The D_g/D_o value does not depend on the temperature, pressure, or the kind of the diffusing gas (e.g., Kristensen et al., 2010).

The dependence of relative gas diffusion coefficient on *soil bulk density* and on soil moisture tension is presented in Figure 2, and that on air-filled porosity ε_g – in Figure 3. The value of D_g/D_o in soil is usually below 0.2. As it can be noticed, it increases with soil moisture tension, and rapidly decreases with soil bulk density. It should be emphasized that gas diffusion coefficient in porous media does not depend on the size of the pores, as long as the pore diameters are greater than the mean free path of the molecules of the gas under consideration (Glinski and Stępniewski, 1985). This limit is the pore diameter of 0.10 µm. In the case of soil, pores of that size are emptied of water at soil moisture tension above 3 MPa ($pF > 4.5$),



Diffusion in Soils, Figure 2 Relationship of D/D_o to air-filled porosity ε_g , of the same as in Figure 1 loamy textured Chernozem Rendzina at different bulk densities d (modified from Stępniewski, 1981).



Diffusion in Soils, Figure 3 Thermal conductivity λ , heat capacity c_v , and thermal diffusivity $D_h = \lambda/c_v$ versus volumetric water content for a sandy soil of 50% total porosity and 3.5% organic matter content (modified from Van Duin, 1956).

i.e., at moisture contents below the permanent wilting point. It means that diffusion of gases within macropores ($>30\text{ }\mu\text{m}$) and mezopores ($30\text{--}0.2\text{ }\mu\text{m}$) usually containing plant available water does not depend on the pore size. It was demonstrated that the magnitude of gas diffusivity (as well as that of thermal diffusivity) is more sensitive to the porosity than to the scale dependency inherent in fractal structures (Anderson et al., 2000).

D_g/D_o usually shows a curvilinear relationship versus ε_g , as shown in Figure 3. It can be described by an empirical power model in the form:

$$\frac{D_g}{D_o} = \gamma \varepsilon_g^\mu \quad (27)$$

where γ and μ are empirical coefficients characterizing the diffusion medium.

It should be kept in mind that gas diffusion in soil comprises not only the macroscale diffusion within the entire soil profile, but also microscale and approximately spherical diffusion within particular aggregates, as well as longitudinal and radial diffusion within the plant root tissues (e.g., Gliński and Stępniewski, 1985; Cook and Knight, 2003). Due to soil heterogeneity and importance of microscale diffusion processes, the composition of air within the intra-aggregate pores may differ from that in the inter-aggregate pores. The former pores contain less oxygen and more carbon dioxide compared to the inter-aggregate pores (e.g., Zausig et al., 1993; Højberg et al., 1994; Horn, 1994; Horn and Smucker, 2005).

Diffusion of solutes

Diffusion of inert, nonreactive solutes in soil can be described by the first and the second Fick's equations presented in Table 3. Unlike the diffusion of gases, the diffusion of solutes takes place in the liquid phase of the soil.

Due to this, the diffusion coefficient depends on the continuity and tortuosity of the pores filled with water and increases with the degree of saturation with waters.

In case of reactive solutes which can undergo processes of adsorption, dissociation, ion exchange, and chemical reactions, these processes have to be taken into consideration within the sink/source term.

Summary

Diffusion processes in soil comprise transport of water under unsaturated conditions, transport of gases in liquid and gaseous phase, transport of heat in all the three phases, as well as transport of solutes within liquid phase. The flux per unit cross-sectional area and per unit time is proportional to driving forces of these processes which are the gradients of water content, of gas concentration, of temperature, and of solute concentration, respectively, as well as to the parameter called diffusion coefficient (dimension $\text{m}^2\text{ s}^{-1}$), characterizing properties of the medium in which the diffusion process takes place. Combination of these equations with the conservation law gives the formulas of the second Fick's equation type for all the fluxes with the source/sink term. It should be underlined that under field conditions diffusion processes are usually coupled one with other or with mass flow processes caused by infiltration and lateral flow of water as well as by gas movement due to pressure gradient.

Bibliography

- Ahuja, L. R., and Swartzendruber, D., 1972. An improved form of soil-water diffusivity function. *Soil Science Society of America Proceedings*, **36**, 9–14.
- Anderson, A. N., Crawford, J. W., and McBratney, A. B., 2000. On diffusion in fractal soil structures. *Soil Science Society of America Journal*, **64**, 19–24.
- Black, T. A., Gardner, W. R., and Thurthell, G. W., 1969. Prediction of evaporation, drainage and soil water storage for a bare soil. *Soil Science Society of America Journal*, **33**, 655–660.
- Bolt, G. A., Jans, A. R. P., and Koenigs, F. F. R., 1966. *Basic Elements of Soil Chemistry and Physics*. Wageningen: Agricultural University.
- Cook, F. J., and Knight, J. H., 2003. Oxygen transport to plant roots. Modeling for physical understanding of soil aeration. *Soil Science Society of America Journal*, **67**, 20–31.
- Darcy, H., 1856. *Les fontaines publiques de la ville de Dijon*. Paris: Dalmont.
- Fick, A., 1855. On liquid diffusion. *Philosophical Magazine and Science Journal*, **10**, 31–39.
- Fourier, J., 1822. *Theorie Analytique de la Chaleur*. Firmin Didot.
- Gliński, J., and Stępniewski, W., 1985. *Soil Aeration and Its Role for Plants*. Boca Raton: CRC.
- Hillel, D., 1982. *Introduction to Soil Physics*. San Diego: Academic.
- Højberg, O., Revsbech, N. P., and Tiedje, J. M., 1994. Denitrification in soil aggregates analyzed with microsensors for nitrous oxide and oxygen. *Soil Science Society of America Journal*, **58**, 1691–1698.
- Horn, R., 1994. Effect of aggregation of soils on water, gas and heat transport. In Schulze, E. E. (ed.), *Flux Control in Biological Systems*. San Diego: Academic, Vol. 10, pp. 335–361.
- Horn, R., and Smucker, A., 2005. Structure formation and its consequences for gas and water transport in unsaturated arable and forest soils. *Soil and Tillage Research*, **82**, 5–14.

- Kristensen, A. H., Thorbjørn, A., Jensen, M. P., Pedersen, M., and Moldrup, P., 2010. Gas-phase diffusivity and tortuosity of structured soils. *Journal of Contaminant Hydrology*, **115**, 26–33.
- Lisle, I. G., Parlange, J. Y., and Haverkamp, R., 1987. Exact desorptives for power law and exponential diffusivities. *Soil Science Society of America Journal*, **51**, 867–869.
- Marshall, T. J., and Holmes, J. W., 1988. *Soil Physics*, 2nd edn. New York: Cambridge University Press.
- Mualem, Y., 1976. A new method for predicting the hydraulic conductivity of unsaturated porous media. *Water Resources Research*, **12**, 513–522.
- Pachepsky, Y., Timlin, D., and Rawls, W., 2003. Generalized Richards' equation to simulate water transport in unsaturated soils. *Journal of Hydrology*, **272**, 3–13.
- Parlange, M. B., Katul, G. G., Folegati, M. V., and Nielsen, R. D., 1993. Evaporation and the field scale soil water diffusivity function. *Water Resources Research*, **29**(4), 1279–1286.
- Stepniewski, W., 1981. Oxygen diffusion and strength as related to soil compaction II. Oxygen diffusion coefficient. *Polish Journal of Soil Science*, **14**, 3–13.
- van Duin, R. H. A., 1956. *On the Influence of Tillage on Conduction of Heat, Diffusion of Air, and Infiltration of Water in Soil*. Wageningen: Versl. Landbouwk. Onderz.
- van Genuchten, M. Th., 1980. A closed form equation for predicting the hydraulic conductivity of unsaturated soil. *Soil Science Society of America Journal*, **44**, 892–898.
- Zausig, J., Stepniewski, W., and Horn, R., 1993. Oxygen concentration and redox potential gradients in different model soil aggregates at a range of low moisture tensions. *Soil Science Society of America Journal*, **57**, 906–916.

Cross-references

- Air Flux (Resistance) in Plants and Agricultural Products
 Bulk Density of Soils and Impact on Their Hydraulic Properties
 Climate Change: Environmental Effects
 Coupled Heat and Water Transfer in Soil
 Greenhouse Gas Fluxes: Effects of Physical Conditions
 Greenhouse Gases Sink in Soils
 Hydraulic Properties of Unsaturated Soils
 Hydrometeorological Processes in Soils
 Layered Soils, Water and Solute Transport
 Soil Hydrophobicity and Hydraulic Fluxes
 Soil Water Flow
 Solute Transport in Soils
 Temperature Effects in Soil

DILATANCY

The tendency of a body under shearing stress to expand as it deforms. This property is typical of sandy soils and powders, as a result of the sliding and rolling of particles over one another along the shearing plane.

DISCHARGE

The volume of water flow through the stream or open channel past a point in a given time period.

Bibliography

Glossary of Soil Science Terms. Soil Science Society of America. 2010. <https://www.soils.org/publications/soils-glossary>

Cross-references

- Water Balance in Terrestrial Ecosystems

DISPERSION

The tendency of clay particles in an aqueous suspension to either clump together into flocs or to separate from one another and thus disperse in the fluid medium, depending on the composition and concentration of the electrolytes in the ambient solution.

Bibliography

Introduction to Environmental Soil Physics. (First Edition). 2003. Elsevier Inc. Daniel Hillel (ed.) <http://www.sciencedirect.com/science/book/9780123486554>

Cross-references

- Flocculation and Dispersion Phenomena in Soils

DISPERSIVITY

The ratio of the hydrodynamic dispersion coefficient (d) divided by the pore water velocity (v); thus $D = d/v$.

Bibliography

Glossary of Soil Science Terms. Soil Science Society of America. 2010. <https://www.soils.org/publications/soils-glossary>

DIURNAL STRAINS IN PLANTS

Paweł Kojas¹, Tomasz Rusin²

¹Polish Academy of Sciences, Botanical Garden – Center for Biological Diversity Conservation, Warsaw, Poland

²MTS Systems Corporation, Warsaw, Poland

Synonyms

Circadian rhythm in fluctuations of diameter; Daily plant organ radius variations; Diurnal changes in plant organ diameter; Diurnal fluctuations in size

Definition

Diurnal strains in plants:

- Diurnal – having a daily cycle
- Strain – a deformation produced by stress

Periodic reversible shrinkage and irreversible and/or reversible swelling of plant tissues. This process is a function of the changing levels of tissue hydration. Tissue hydration during natural day/night cycles in plants which have lost their leaves (late autumn, winter and early spring) depends on water accessibility and temperature, whereas in plants with leaf, tissue hydration additionally depends on the transpiration rate which is connected with air humidity, wind speed, CO₂ concentration, etc. Swelling of tissues is caused by hydrostatic pressure and mainly occurs at night. In contrast, during the day tissues shrink because of decrease in turgidity caused by transpiration. The measurable effect of this process is the decrease in the tangential strain. The strain is a response to the mechanical stress imposed on the plant cell walls by changing water pressure. The nature of the strain generated by changes in water pressure depends on the properties of the cell wall and it can be elastic, viscoelastic, and plastic. There are different phenomena which generate tangential strains in plant organs: variations in hydrostatic pressure, variations in osmotic pressure, variations in temperature, and growth of the tissues.

Historical perspective

Reversible shrinkage of plant organs was first reported during periods of temperatures below the freezing point (Hoffmann, 1857; Sachs, 1860). Wiegand (1906) described the swelling of tree branches during thawing and described a much bigger extension of the bark than of the xylem. This reversible seasonal deformation was attributed to the elastic properties of plant tissues. One of the first pieces of information concerning diurnal decrease in the size of a plant organ (orange fruit) was reported by (Bartholomew, 1923). However, initially the mainstream research in diurnal strains was connected with systematic observations of the radial growth of trees. Development of new tools and methods of observation helped to identify a daily rhythm of shrinkage and swelling of tree trunks (MacDougal, 1924; Reineke, 1932).

The first rapid increase in research on this phenomenon started in the late 1950s and lasted till the middle of the 1970s of the last century (Ninokata and Miyazato, 1959; Kozlowski and Winget, 1964; Klepper, 1968; Klepper et al., 1971; Molz and Klepper, 1973; Pereira and Kozlowski, 1976). During this time, the mechanism of diurnal variations in size of different plant organs was identified and described. However, the phenomenon was seen as a side effect of transpiration and water accessibility without any significant function. Since that time, both the recognition of the mechanism as well as the understanding of the role of diurnal strains in plant organs has expanded considerably.

Mechanism of diurnal strains fluctuation

During the early evolution of land plants, the problem of water loss due to direct exposure to dry air had to be solved (water stress). It was resolved on the physiological level by enhancement of osmotic adjustment and on the

structural level by the development of epidermis. However, evolution of a non-permeable epidermis would create new problem with gas exchange. The compromise which was achieved and enabled adaptive radiation of land plants was the evolution of stomata.

Although water is lost during the day, osmotic adaptation helps the plant to survive a short period of water stress. During the night, water is replenished in greater quantity than the amount lost, which generates a mechanical stress. The side effect of these two consecutive stresses is cyclic deformation of plant organs.

During the vegetative season when the sun is rising (1) stomata open (2) (Wronski et al., 1985; Herzog et al., 1995). Temperature steadily increases afterward (3), whereas the relative humidity of the air decreases (4). In this way, preferable conditions for high rate of water transpiration (5) are established (Lövdahl and Odin, 1992). Transpiration causes a decrease in water potential in water conduits (6) and eventually leads to water tension (7) in Soil-Plant-Atmosphere Continuum (SPAC). Water tension is a reason for the decrease in hydration of an apoplast (8), which actually means decrease in water potential of the apoplast and ultimately measurable shrinkage of the xylem (9). In this way, a steep gradient of water potential between apoplast and symplast (10) is created (Molz and Klepper, 1972) and in consequence, water flows from turgid cells (living cells of the symplast with high water potential) toward apoplast and water conduits (11) (with lower water potential). Cell-wall pressure (turgidity) pushes water outward in the living cells, effectively decreasing cells' water potential. Loss of water causes a decrease in turgidity (12) and stabilizes the water potential inside the cell at the apoplast water potential level. Loss of turgidity causes shrinkage of living tissues (13) (Yoshida et al., 2000; Tyree and Zimmerman, 2002; Alméras et al., 2006), and the below-threshold value is recognized by a living system as a water stress (14) (Molz and Klepper, 1973). During the day, the mechanism of restoration of the initial water status in cells leads to osmotic adjustment (15). This means that the water stress turns on an adaptational reaction, which decreases osmotic potential, lowering cell water potential (16), and thus preventing outward water movement. Osmotic adjustment allows for maintenance of relatively greater volume at low water potential and it helps to stop decline in turgidity.

As a rule, the process of adaptation toward water stress is overshoot (17) (Belousov and Grabovsky, 2006) – excessive decrease of water potential in the symplast causes water movement into living cells, though in plant conduits water tension has a very low water potential (refilling under water stress due to osmotic adaptation [18]). It happens when the day is very long and the osmotic adaptation passes through the constraints of water tension.

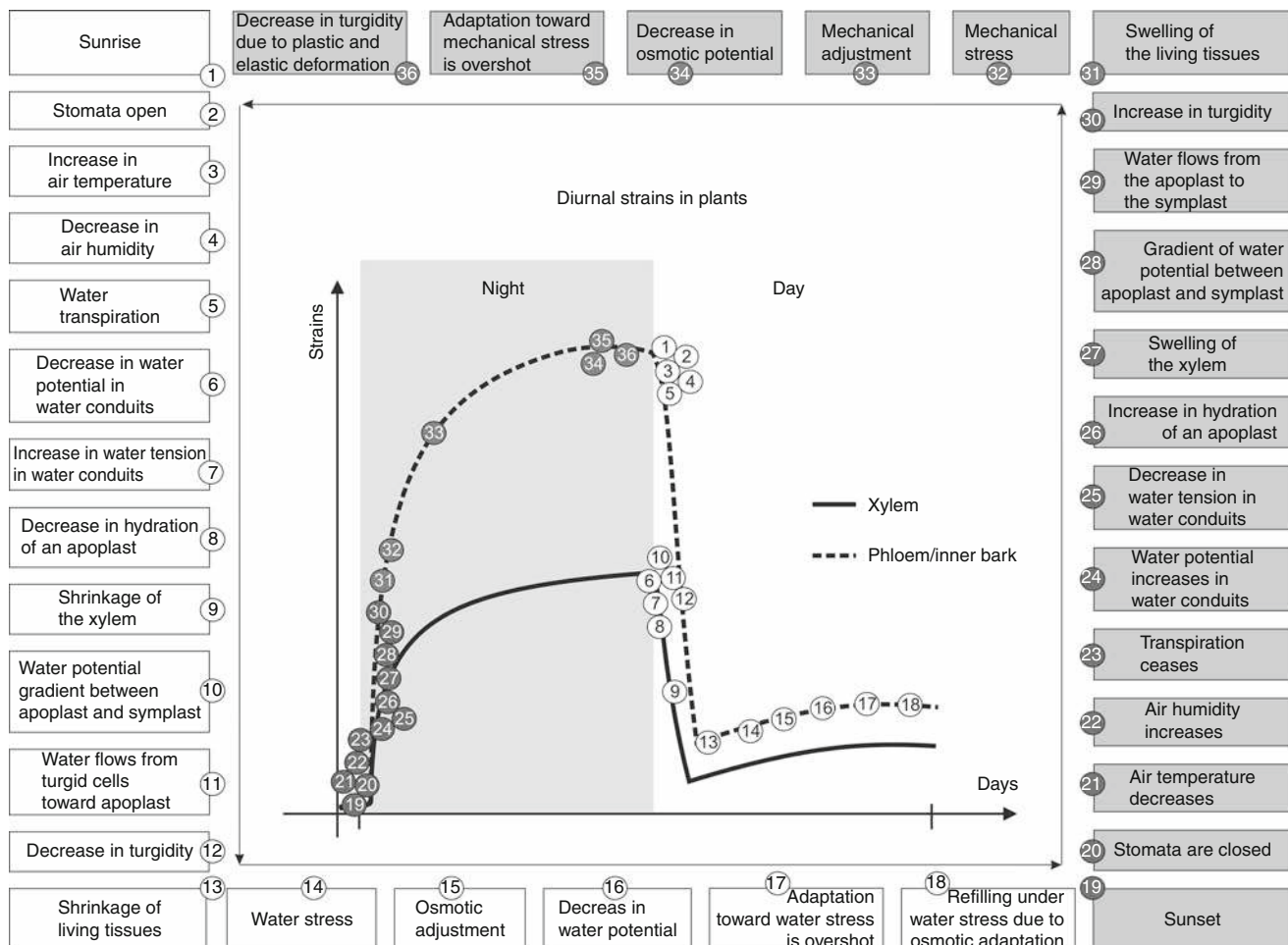
This adaptation to water stress is ended sharply at sunset (19) when stomata are closed (20) (Wang et al., 2008). During the night, air temperature decreases (21) and air humidity increases (22) (Lövdahl and Odin, 1992). In such circumstances transpiration ceases (23). In plant

water conduits water potential increases (24), causing a decrease in the water tension (25). This means rehydration of the apoplast (26). In consequence, swelling of the xylem elements (27) occurs (Mengel and Kirkby, 2001). Higher water potential in water conduits and lower water potential of living cells produce water potential gradient (28) and causes water flow from the apoplast to the symplast (29) (Molz and Klepper, 1972). Rehydration of living cells causes increase in turgidity (30), which at the tissue level is a basis for swelling (elastic and plastic deformation) of living tissues (31) (Yoshida et al., 2000; Tyree and Zimmermann, 2002; Alméras et al., 2006). The water recharging mainly occurs from sunset to midnight (Wang et al., 2008). In this way, during the first few hours of the night, mechanical stress inside the plant is generated (32) (Stankovic et al., 1998). One of the adaptive mechanisms to this stress is mechanical adjustment (33) (cell growth, cell-wall relaxation, schizogenous space formation, or schizolisisogenous space formation [Evert and Eichhorn, 2006]). The second adaptive mechanism to this stress is decrease in osmotic potential (34) (osmotic

adjustment). In consequence, adaptation to mechanical stress prevents an uptake of water into living cells, but again this adaptation process is overshoot (35) (Belousov and Grabovsky, 2006) at the end of the night and a small decrease in turgidity can be observed due to mechanical adaptation (i.e., plastic deformation) (36). This happens when the night is very long and mechanical adaptation relaxes tensile stress. Living tissues are vulnerable toward incoming daily water imbalance. On the next day, the whole process starts from the beginning (1) (Figure 1).

Measurements and applications

Diurnal strain measurements are nondestructive and can be monitored continuously with different types of dendrometers. The simplest technique is application of a caliper or one of the linear variable differential transformers (LVDT sensors) based on strain gauges (Ninokata and Miyazato, 1959; Klepper et al., 1971; Okuyama et al., 1995; Yoshida et al., 2000; Daudet et al., 2005). New noninvasive techniques are still developing. One of



Diurnal Strains in Plants, Figure 1 Mechanism of diurnal strains fluctuation. Numbers between 1 and 18 represent processes and events during the day and numbers from 19 to 36 symbolize processes and events during the night.

the most promising techniques which allows truly noninvasive measurements is digital image correlation (DIC) (Sutton et al., 2000). A second new technique is Electronic Speckle Pattern Interferometry (ESPI) (Jones and Wykes, 1989). Optical methods are inherently nonintrusive and noncontacting. They are highly also sensitive and provide full-field measurement data.

Diurnal strain measurements are potentially a powerful tool for studying (Alméras, 2008):

1. Tree physiology, i.e., helps to obtain information about:
 - (a) Tree water status (Klepper et al., 1971; So et al., 1979; Ueda and Shibata, 2001)
 - (b) Water transport (Zweifel et al., 2000; Sevanto et al., 2002)
 - (c) Transpiration rate (Herzog et al., 1995)
 - (d) Spatial and temporal patterns of physiological activity (Sevanto et al., 2002)
 - (e) Cambial growth dynamics (Kozlowski and Winget, 1964; Deslauriers et al., 2003)
 - (f) Wood morphogenesis (Okuyama et al., 1995; Abe and Nakai, 1999)
 - (g) The transport of sugar in phloem (Sevanto et al., 2003; Daudet et al., 2005)
 - (h) The rate of embolism in a stem (Hölttä et al., 2002)
 - (i) Embolism removal (Zwieniecki and Holbrook, 1998)
 - (j) The reduction in wood conductivity in senescent trees (Ueda and Shibata, 2002)
2. Practical applications, such as:
 - (a) Correcting continuously recorded dendrometric data (Kozlowski and Winget, 1964; Deslauriers et al., 2003)
 - (b) Estimating transpiration (Herzog et al., 1995)
 - (c) Establishing irrigation scheduling (Goldhammer and Fereres, 2001; Remorini and Massai, 2003)
 - (d) Detecting the effects of pathogens on plant water status (Cohen et al., 1997)

Summary

Daily shrinkage in plant organs is generally related to the variation in water potential. Plant organs shrink during the day because plants lose more water by transpiration than they can take up. The higher the water stress, the more the water lost during the day. At night, when there is little loss of water, plant organs will increase in diameter because of the uptake and storage of water. Since the living cells are much more elastic than wood cells, diurnal plant organ fluctuations are mainly influenced by changes of the thickness of living tissues. Therefore in stems of woody plants, the shrinking and swelling take place mainly in a ring of phloem outside the xylem. Both the shrinkage and swelling of the cells, tissues, or organs are the effects of stress. Shrinkage is caused by daily water stress, whereas swelling is caused by nocturnal mechanical stress. Whenever a change of local stress is applied to cells or tissue, they respond by actively generating forces

directed toward the restoration of the initial stress value (adaptation), but by overshooting it. This causes cyclic deformations which partly are irreversible. The irreversible part of deformation is called growth.

Bibliography

- Abe, H., and Nakai, T., 1999. Effect of the water status within a tree on tracheid morphogenesis in *Cryptomeria japonica* D. Don. *Trees*, **14**, 124–129.
- Alméras, T., 2008. Mechanical analysis of the strains generated by water tension in plant stems. Part II: strains in wood and bark and apparent compliance. *Tree Physiology*, **28**, 1513–1523.
- Alméras, T., Yoshida, M., and Okuyama, T., 2006. Strains inside xylem and inner bark of a stem submitted to a change in hydrostatic pressure. *Trees*, **20**, 460–467.
- Bartholomew, E. T., 1923. Internal decline of lemons. II. Growth rate, water content, and acidity of lemons at different stages of maturity. *American Journal of Botany*, **10**, 117–126.
- Belousov, L. V., and Grabovsky, V. I., 2006. Morphomechanics: goals, basic experiments and models. *The International Journal of Developmental Biology*, **50**, 81–92.
- Cohen, M., Luque, J., and Alvarez, I. F., 1997. Use of stem diameter variations for detecting the effects of pathogens on plant water status. *Annales des Sciences Forestières*, **54**, 463–472.
- Daudet, F. A., Améglio, T., Cochard, H., Archilla, O., and Lacointe, A., 2005. Experimental analysis of the role of water and carbon in tree stem diameter variations. *Journal of Experimental Botany*, **56**, 135–144.
- Deslauriers, A., Morin, H., Urbinati, C., and Carrer, M., 2003. Daily weather response of balsam fir (*Abies balsamea* (L.) Mill.) stem radius increment from dendrometer analysis in the boreal forests of Québec (Canada). *Trees*, **17**, 477–484.
- Evert, R. F., and Eichhorn, S. E., 2006. *Esau's Plant Anatomy: Meristems, Cells, and Tissues of the Plant Body: Their Structure, Function, and Development*, 3rd edn. Hoboken: Wiley.
- Goldhammer, D. A., and Fereres, E., 2001. Irrigation scheduling protocols using continuously recorded trunk diameter measurements. *Irrigation Science*, **20**, 115–125.
- Herzog, K. M., Hässler, R., and Thum, R., 1995. Diurnal changes in the radius of a subalpine Norway spruce stem: their relation to the sap flow and their use to estimate transpiration. *Trees*, **10**, 94–101.
- Hoffmann, H., 1857. *Witterung und Wachstum, oder Grundzüge der Pflanzenklimatologie*. A. Leipzig: Förster'sche Buchhld.
- Hölttä, T., Vesala, T., Perämäki, M., and Nikinmaa, E., 2002. Relationships between embolism, stem water tension and diameter changes. *Journal of Theoretical Biology*, **215**, 23–38.
- Jones, R., and Wykes, C., 1989. *Holographic and Speckle Interferometry*. Cambridge: Cambridge University Press.
- Klepper, B., 1968. Diurnal pattern of water potential in woody plants. *Plant Physiology*, **43**, 1931–1934.
- Klepper, B., Browning, V. D., and Taylor, H. M., 1971. Stem diameter in relation to plant water status. *Plant Physiology*, **48**, 683–685.
- Kozlowski, T. T., and Winget, C. H., 1964. Diurnal and seasonal variations in radii of tree stems. *Ecology*, **45**, 149–155.
- Lövdahl, L., and Odin, H., 1992. Diurnal changes in the stem diameter of Norway spruce in relation to relative humidity and air temperature. *Trees*, **6**, 245–251.
- MacDougal, D. T., 1924. Dendrographic measurements. In MacDougal, D. T., and Shreve, F. (eds.), *Growth in Trees and Massive Organs of Plants*. Washington, DC: Carnegie Institute, pp. 3–88.
- Molz, F. J., and Klepper, B., 1972. Radial propagation of water potential in stems. *Agronomy Journal*, **64**, 467–473.

- Molz, F. J., and Klepper, B., 1973. On the mechanism of water-stress induced stem deformation. *Agronomy Journal*, **65**, 304–306.
- Ninokata, K., and Miyazato, M., 1959. Measurement of daily variations of diameter of trunk by the electrical strain gauge. *Bulletin of the Faculty of Agriculture, Kagoshima University*, **8**, 76–88.
- Mengel, K., and Kirkby, E. A., 2001. *Principles of Plant Nutrition*, 5th edn. Dordrecht: Kluwer Academic.
- Okuyama, T., Yoshida, M., and Yamamoto, H., 1995. An estimation of turgor pressure change as one of the factors of growth stress generation in cell walls. *Mokuzai Gakkaishi*, **41**, 1070–1078.
- Pereira, J. S., and Kozlowski, T. T., 1976. Diurnal and seasonal changes in water balance of *Abies balsamea* and *Pinus resinosa*. *Oecologia Plantarum*, **11**, 397–412.
- Reineke, L. H., 1932. A precision dendrometer. *Journal of Forestry*, **30**, 692–697.
- Remorini, D., and Massai, R., 2003. Comparison of water status indicators for young peach trees. *Irrigation Science*, **22**, 39–46.
- Sachs, J., 1860. Kristallbildung beim gefreien und auftauen saftiger pflanzenteile, mitgeteilt von W. Hofmeister. Berichte Verhandlung Sächs. Akademie der Wissenschaften, **12**, 1–50.
- Sevanto, S., Vesala, T., Perämäki, M., and Nikinmaa, E., 2002. Time lags for xylem and stem diameter variations in a Scots pine tree. *Plant, Cell and Environment*, **25**, 1071–1077.
- Sevanto, S., Vesala, T., Perämäki, M., and Nikinmaa, E., 2003. Suger transport together with environmental conditions controls time lags between xylem and stem diameter changes. *Plant, Cell and Environment*, **26**, 1257–1265.
- So, H. B., Reicosky, D. C., and Taylor, H. M., 1979. Utility of stem diameter changes as predictors of plant canopy water potential. *Agronomy Journal*, **71**, 707–713.
- Stankovic, B., Witters, D. L., Zawadzki, T., and Davies, E., 1998. Action potentials and variation potentials in sunflower: an analysis of their relationships and distinguishing characteristics. *Physiologia Plantarum*, **103**, 51–58.
- Sutton, M. A., McNeill, S. R., Helm, J. D., and Chao, Y. J., 2000. Advances in two-dimensional and three-dimensional computer vision. In Rastogi, P. K. (ed.), *Photomechanics*. Berlin: Springer, pp. 323–372.
- Tyree, M. T., and Zimmermann, M. H., 2002. *Xylem Structure and the Ascent of Sap*. Berlin: Springer.
- Ueda, M., and Shibata, E., 2001. Diurnal changes in branch diameter as indicator of water status of Hinoki cypress *Chamaecyparis obtusa*. *Trees*, **15**, 315–318.
- Ueda, M., and Shibata, E., 2002. Water status of Hinoki cypress (*Chamaecyparis obtusa*) under reduced hydraulic conductance estimated from diurnal changes in trunk diameter. *Trees*, **16**, 523–528.
- Wang, H., Zhao, P., Wang, Q., Cai, X., Ma, L., Rao, X., and Zeng, X., 2008. Nocturnal sap flow characteristics and stem water recharge of *Acacia mangium*. *Frontiers of Forestry in China*, **3**, 72–78.
- Wiegand, K. M., 1906. Pressure and flow of sap in the maple. *The American Naturalist*, **40**, 409–453.
- Wronski, E. B., Holmes, J. W., and Turner, N. C., 1985. Phase and amplitude relations between transpiration, water potential and stem shrinkage. *Plant, Cell and Environment*, **8**, 613–622.
- Yoshida, M., Yamamoto, O., and Okuyama, T., 2000. Strain changes on the inner bark surface of an inclined coniferous sapling producing compression wood. *Holzforschung*, **54**, 664–668.
- Zweifel, R., Item, H., and Häslер, R., 2000. Stem radius changes and their relation to stored water in stems of young Norway spruce. *Trees*, **15**, 50–57.
- Zwieniecki, M. A., and Holbrook, N. M., 1998. Diurnal variation in xylem hydraulic conductivity in white ash (*Fraxinus americana* L.), red maple (*Acer rubrum* L.) and red spruce (*Picea rubens* Sarg.). *Plant, Cell and Environment*, **21**, 1173–1180.

Cross-references

- Biospeckle
Evapotranspiration
Mycorrhizal Symbiosis and Osmotic Stress
Plant Biomechanics
Shrinkage and Swelling Phenomena in Soils
Stomatal Conductance, Photosynthesis, and Transpiration, Modeling
Stress–Strain Relations
Tensiometry
Water Uptake and Transports in Plants Over Long Distances
Weather, Effects on Plants

DNA IN SOILS: MOBILITY BY CAPILLARITY

Maria Teresa Ceccherini, Giacomo Pietramellara
Dipartimento Scienza del Suolo e Nutrizione della Pianta,
Università degli Studi di Firenze, Firenze, Italy

Synonyms

Vertical advection

Definitions

DNA. Deoxyribonucleic acid that carries the genetic information in the cell and is capable of self-replication and synthesis of RNA (ribonucleic acid) in a process called transcription. DNA consists of two long chains of nucleotides twisted into a double helix and joined by hydrogen bonds between the complementary bases adenine and thymine or cytosine and guanine.

Soil. The top layer of the Earth's surface, consisting of rock and mineral particles mixed with organic matter. It plays an irreplaceable role in the biosphere because it governs plant productivity of terrestrial ecosystem and allows the completion of the biogeochemical cycles through its inhabiting microorganisms. The main characteristics are the domination of the solid phase, the presence of aqueous and gaseous phases, and its capacity of reactions by surface-active particles.

Vadose zone. Also termed the unsaturated zone, it is the portion of Earth between the land surface and the phreatic zone or zone of saturation ("vadose" is Latin for "shallow"). Water in the vadose zone has a pressure head less than atmospheric pressure, and is retained by a combination of adhesion (*funicular groundwater*) and capillary action (*capillary groundwater*).

Advection. A transport mechanism of a substance with a fluid in motion. An example of advection is the transport of solutes (DNA, pollutants) in the soil water flow.

Capillarity. The flow of liquids through porous media, such as the flow of water through soil. The capillary fringe is the subsurface layer in which groundwater seeps up from a water table by capillary action to fill pores. If pore size is small and relatively uniform, it is possible that soils can be completely saturated with water for several feet above the water table. Alternately, the saturated portion

will extend only a few inches above the water table when pore size is large. In smaller pores of the soil, water is held against the force of gravity by capillary forces and is called capillary water. This constitutes the only available source of water to plants.

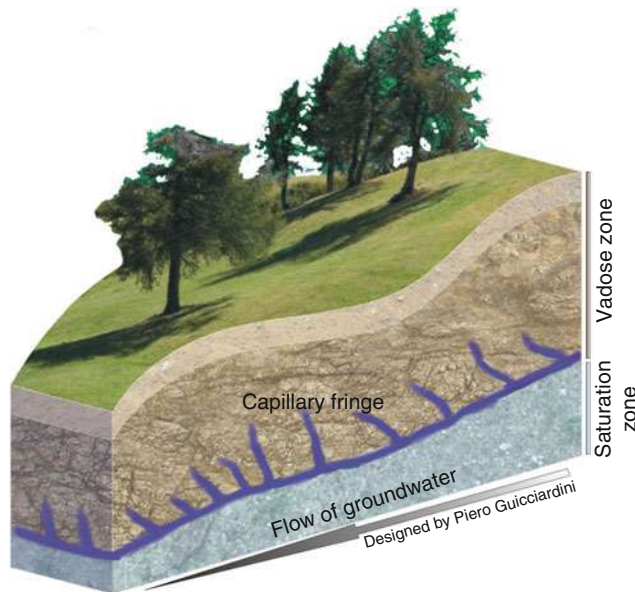
Real-time PCR. It allows for the detection of PCR (Polymerase chain reaction) amplification during the early phases of the reaction and this provides a distinct advantage over traditional PCR detection. Traditional methods use agarose gels for detection of amplicons at the final phase of the PCR reaction. Real-time PCR detects the accumulation of amplicons during the reaction and the data is measured at the exponential phase.

Introduction

The total soil DNA (tDNA) includes both intracellular (iDNA) and extracellular DNA (eDNA), with the latter originated from the former by active or passive extrusion mechanisms or by cell lysis. The eDNA can represent a relevant fraction of tDNA and thus a significant portion of the entire soil metagenome. Studies on the ecological relevance of eDNA in soils have concerned the gene transfer through transformation and interaction between eDNA molecules with the reactive surface of clay minerals, humic substances, and sand particles (Nielsen et al., 2006). Only recently has the attention been directed at the role of eDNA in the formation of bacterial biofilm in soil (Böckelmann et al., 2006) and at the possibility that eDNA can be transported by water through the soil profile (Agnelli et al., 2004). The key role of transformation in evolutionary terms justifies to continue the investigation on the fate of extracellular DNA in soil (Pietramellara et al., 2007). Extracellular DNA is also an important source of nitrogen and phosphorous, which are recycled by bacteria for the synthesis of new DNA; it might participate in gene transfer and, thus, in microbial evolution (de Vries and Wackernagel, 2004). Researches demonstrate that transgenes can move beyond the intended organism and into the surrounding environment, and it can be subjected to vertical advection if in the water solution (Dighton et al., 1997; Poté et al., 2003; Ceccherini et al., 2009b) that is in the vadose zone (Figure 1) of soil (Arias-Estévez et al., 2008). The extracellular DNA can be transported in the soil water flow also by horizontal movements, in fact, using soil column systems, the vertical and horizontal movements of a target sequence were monitored and quantified via real-time PCR in microcosm (Ascher et al., 2009) and *in field* experiments (Ceccherini et al., 2009a).

The extracellular DNA in soil

The release of DNA in soil is still poorly known and, for this reason, it is interesting to briefly discuss on what is known on the release of DNA from bacteria, fungal cells, and plant cells in soil. Conditions causing cell death are important for the release of DNA molecules; in prokaryotic and eukaryotic cells, the release can occur by physical



DNA in Soils: Mobility by Capillarity, Figure 1 Some different forms of soil water.

or spontaneous damage of the cell, by pathogen-induced cell lysis and necrosis or by active extrusion (Levy-Booth et al., 2007). Many genera of environmental bacteria, such as *Acinetobacter*, *Bacillus*, *Micrococcus*, release DNA during growth in liquid media (Lorenz and Wackernagel, 1994; Paget and Simonet, 1994), and this release can be stimulated by the presence of other organisms (Matsui et al., 2003). Here some examples are reported to give concise information to the readers. During biofilm formation by *Pseudomonas aeruginosa*, active DNA extrusion involved acylated homoserine lactone signaling molecules and was inhibited by halogenated furanone (HF). The DNA extrusion can also occur by membrane vesicle lysis, a process regulated by quorum sensing (Allesen-Holm et al., 2006). The breaking of bacterial cell walls and membranes can also occur by autolysis with release of DNA and RNA (Nishimura et al., 2003).

The release of DNA from fungal cells has been less investigated than that from bacterial cells despite 70% of the DNA in soil being of fungal origin (Borneman and Hartin, 2000).

Several studies have investigated the persistence of plant DNA in the terrestrial environments (Widmer et al., 1996; Lynch et al., 2004) but the release of DNA from plant roots and plant debris is still poorly understood. This release can occur after autolysis and decomposition of wilting tissues, by mechanical disruption of tissues or by enzymatic degradation of cell structures by plant pathogens. It is well known that chlorophyll, proteins, and RNA molecules are enzymatically degraded during leaf senescence (Green, 1994), and this probably also occurs for the DNA molecules.

Only few reports have studied the release of DNA from plastids or mitochondria. Probably, their DNA is more protected than the chromosomal one against degradation by cytoplasmic nuclelease activity, due to the presence of the organellar membranes (Nielsen et al., 2006). However, some authors (Ceccherini et al., 2003) reported a 98% loss of a chloroplast *aadA* gene in ground tobacco leaf material after 72 h as compared to a 56% loss of total DNA. Finally, during the decomposition of dead cells and tissues, conditions such as rapid desiccation, low temperatures, high salt concentrations, or low pH values, can affect the activity of the endoenzymes, increasing the persistence of both cells or tissues and their DNA (Hofreiter et al., 2001).

However, DNA released into the soil environment, both after cell death and by active extrusion, rarely is present as a pure molecule. Generally the DNA is released in the extracellular environment together with proteins, glucides, lipids, which could be considered as constitutional organic components (COC), and with RNA and cellular wall debris (CWD); this kind of DNA was termed “dirty eDNA” (Tamayo et al., 1999; Pietramellara et al., 2007).

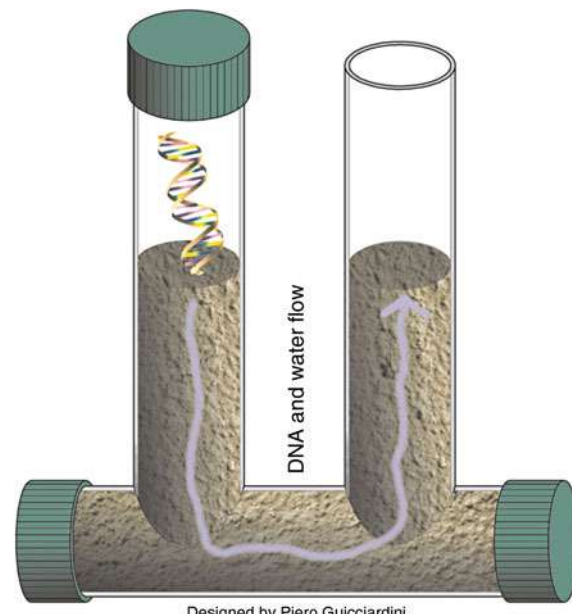
The capillarity

Soil capillaries are characterized by a rapid transport of water and solutes through the soil. These flows occur in macropores such as root and earthworm channels, mouse burrows, fissures, and cracks. Through preferential flow, there is transport of dissolved organic matter, like extracellular DNA, following vertical advection movements, and this soil area shows higher microbial biomass than the soil matrix, with an enhanced turnover of soil organic matter and nutrients (DiCarlo et al., 1999). A significant aspect of the majority of the studies on soil ecology is the lack of a dynamic soil system with water movement. Therefore, information on the transport of eDNA and on its potential transforming ability in subsurface soil is lacking. Moreover, plants get most of their water from capillary water retained in soil pores after gravitational water has drained and surface tension (suction) holds capillary water around the soil particles. As water is removed by plants or by evaporation from the soil surface, the films of water remaining around the soil particles become thinner and are held by the soil particles more tightly. This underlines the interest of some authors to monitor the movements and thus the fate of eDNA, using simulating or natural soil systems.

One of this kind of studies, addressing the possibility that DNA could move vertically in the capillary fringe, monitored the 35S-*nptII* sequence by PCR. DNA was added as a water solution at the bottom of the unsaturated soil column. After the addition, capillary water rose 4 cm within the soil column and the target DNA was detected up to that height. After a second wetting (12 h later), the target sequence was detected up to the top of the soil column (10 cm). However, after a third wetting

(24 h later), the marker sequence was only found at heights from 0.5 cm to 4 cm. Results clearly showed the vertical movement of DNA due the capillary rise and suggested the possibility of DNA degradation within the soil column (Ceccherini et al., 2007). Moreover, using simulating systems, the movements of a target sequence, belonging to *bt-maize MON810*, were quantified via real-time PCR. The genomic DNA was added at the top of unsaturated soil columns (Figure 2). The presence of the sequence in the eDNA fraction extracted from representative parts of the soil columns, demonstrated the DNA drifts in vertical and horizontal directions following the water solution motions. The high yields of the target sequence quantified in the eDNA also pointed out the efficiency of the eDNA extraction method (Ascher et al., 2009).

To complete this brief description, it is interesting to report some studies about solute movements by the gravitational pathway in soil. In a first case, unsaturated soil columns were used to examine the release and transport of DNA content of a tomato leaf, which was introduced into a column system after being dried at 35°C for 3 days. DNA from column leachate water was extracted and analyzed and tomato sequences detected by specific PCR amplification. Analysis using agarose gel electrophoresis showed degradation of DNA after its passage through unsaturated soil columns. The presence of tomato genes in the leachate water suggested a potential release of DNA from leaves and a potential transport of DNA over considerable distances in water-unsaturated soil. Consequently, transport of plant DNA in the vadose zone is



DNA in Soils: Mobility by Capillarity, Figure 2 Representation of a column system used to show the vertical and horizontal fluxes of a DNA solution in soil.

indicated, and also the risk that the DNA may reach the groundwater (Poté et al., 2007). In a second case, the study addressed the possibility that a target sequence of transgenic *bt*-maize could be detected *in field* where the crop was growing. The rhizosphere eDNA was extracted at different times, representative of maize growing stages and the target sequence was quantified via real-time PCR. This molecular approach revealed to be suitable for specific detection of target DNA, supporting the persistence of DNA *in field* (Ceccherini et al., 2009a).

Conclusions

The importance of natural transformation in evolutionary terms represents a valid reason to improve the investigation on the fate of extracellular DNA in soil. Several authors have demonstrated that there is a sharp discrepancy between its biological efficiency and its persistence; fragments of target DNA were detected after a long time in soil but no transformations were determined, probably because the genetic information originally present in the complete DNA molecule could be lost by degradation. Availability of water in soil is an important factor driving microbial activity. In bulk soil, bacterial cells occur mainly adsorbed to surfaces, refractory to movement, interacting only with partners in their immediate vicinity, unless they are transported by the soil water solution. Thus, water flow by capillarity induced by plant uptake and evaporation from soil surface, enhancing microbial and eDNA movements, can promote cellular activities with possibilities of horizontal gene transfer.

Bibliography

- Agnelli, A., Ascher, J., Corti, G., Ceccherini, M. T., Nannipieri, P., and Pietramellara, G., 2004. Distribution of microbial communities in a forest soil profile investigated by microbial biomass, soil respiration and DGGE of total and extracellular DNA. *Soil Biology and Biochemistry*, **36**, 859–868.
- Allesen-Holm, M., Barken Bundvik, K., Yang, L., Klausen, M., Webb, J., Kejelleberg, S., Molin, S., Givskov, M., and Tolker-Nielsen, T., 2006. A characterization of DNA release in *Pseudomonas aeruginosa* cultures and biofilms. *Molecular Microbiology*, **59**, 1114–1128.
- Arias-Estévez, M., López-Periago, E., Martínez-Carballo, E., Simal-Gándara, J., Mejuto, J.-C., and García-Río, L., 2008. The mobility and degradation of pesticides in soils and the pollution of groundwater resources. *Agriculture, Ecosystems and Environment*, **123**, 247–260.
- Ascher, J., Ceccherini, M. T., Guerri, G., Nannipieri, P., and Pietramellara, G., 2009. “E-motion” of extracellular DNA (e-DNA) in soil. *FEB*, **18**, 1764–1767.
- Böckelmann, U., Janke, A., Kuhn, R., Neu, T. R., Wecke, J., Lawrence, J. R., and Szewzyk, U., 2006. Bacterial extracellular DNA forming a defined network-like structure. *FEMS Microbiology Letters*, **262**, 31–38.
- Borneman, J., and Hartin, J., 2000. PCR primers that amplify fungal rRNA genes from environmental samples. *Applied and Environmental Microbiology*, **66**, 4356–4360.
- Ceccherini, M. T., Ascher, J., Agnelli, A., Borgogni, F., Pantani, O. L., and Pietramellara, G., 2009a. Experimental discrimination and molecular characterization of the extracellular soil DNA fraction. *Antonie van Leeuwenhoek*, **96**, 653–657, doi:10.1007/s10482-10009-19354-10483.
- Ceccherini, M. T., Ascher, J., Guerri, G., and Pietramellara, G., 2009b. In-field detection and quantification of extracellular DNA. *Journal of Plant Nutrition and Soil Science*, **172**, 626–629, doi:10.1002/jpln.200900081.
- Ceccherini, M. T., Ascher, J., Pietramellara, G., Vogel, T. M., and Nannipieri, P., 2007. Vertical advection of extracellular DNA by water capillarity in soil columns. *Soil Biology and Biochemistry*, **39**, 158–163.
- Ceccherini, M. T., Potè, J., Kay, E., Van Tran, V., Maréchal, J., Pietramellara, G., Nannipieri, P., Vogel, T. M., and Simonet, P., 2003. Degradation and transformability of DNA from transgenic leaves. *Applied and Environmental Microbiology*, **69**, 673–678.
- de Vries, J., and Wackernagel, W., 2004. Microbial horizontal gene transfer and the DNA release from transgenic crop plants. *Plant and Soil*, **266**, 91–104.
- DiCarlo, D. A., Bauters, T. W. G. J., Darnault, C. J. G., Steenhuis, T., and Parlange, J.-Y., 1999. Lateral expansion of preferential flow paths in sands. *Water Resources Research*, **35**, 427–434.
- Dighton, J., Jones, H. E., Robinson, C. H., and Beckett, J., 1997. The role of abiotic factors, cultivation practices and soil fauna in the dispersal of genetically modified microorganisms in soils. *Applied Soil Ecology*, **5**, 109–131.
- Green, P., 1994. The ribonucleases of higher plants. *Annual Review of Plant Physiology and Plant Molecular Biology*, **45**, 421–445.
- Hofreiter, M., Serre, D., Poniar, H., Kuch, M., and Pääbo, S., 2001. Ancient DNA. *Nature Reviews Genetics*, **2**, 353–360.
- Levy-Booth, D. J., Campbell, R. G., Gulden, R. H., Hart, M. M., Powell, J. R., Klironomos, J. N., Pauls, K. P., Swanton, C. J., Trevors, J. T., and Dunfield, K. E., 2007. Cycling of extracellular DNA in the soil environment. *Soil Biology and Biochemistry*, **39**, 2977–2991.
- Lorenz, M. G., and Wackernagel, W., 1994. Bacterial gene transfer by natural genetic transformation in the environment. *Microbiological Reviews*, **58**, 563–602.
- Lynch, J. M., Benedetti, A., Insam, H., Nuti, M. P., Smalla, K., Torsvik, V., and Nannipieri, P., 2004. Microbial diversity in soil: ecological theories, the contribution of molecular techniques and the impact of transgenic plants and transgenic microorganisms. *Biology and Fertility of Soils*, **40**, 363–385.
- Matsui, K., Ishii, N., and Kawabata, Z., 2003. Release of extracellular transformable plasmid DNA from *Escherichia coli* cocultivated with algae. *Applied and Environmental Microbiology*, **69**, 2399–2404.
- Nielsen, K. M., Calamai, L., and Pietramellara, G., 2006. Stabilization of extracellular DNA by transient binding to various soil surfaces. In Nannipieri, P., and Smalla, K. (eds.), *Nucleic Acids and Proteins in Soil*. Springer, Berlin, Vol. 8, pp. 141–158.
- Nishimura, S., Tanakal, T., Fujita, K., Itaya, M., Hiraishil, A., and Kikuchil, Y., 2003. Extracellular DNA and RNA produced by a marine photosynthetic bacterium *Rhodovulum sulfidophilum*. *NAR Supplement*, **3**, 279–280.
- Paget, E., and Simonet, P., 1994. On track of natural transformation in soil. *FEMS Microbiology Ecology*, **15**, 109–118.
- Pietramellara, G., Ascher, J., Ceccherini, M. T., Wenderoth, D. F., and Nannipieri, P., 2007. Adsorption of dirty DNA on clay minerals and its transformation efficiency. *Biology and Fertility of Soils*, **43**, 731–739.
- Poté, J., Ceccherini, M. T., Van Tran, V., Rosselli, W., Wildi, W., Simonet, P., and Vogel, T., 2003. Fate and transfer of antibiotic resistance genes in saturated soil columns. *European Journal of Soil Biology*, **39**, 65–71.

- Poté, J., Rosselli, W., Wigger, A., and Wildi, W., 2007. Release and leaching of plant DNA in unsaturated soil column. *Ecotoxicology and Environmental Safety*, **68**, 293–298.
- Tamayo, J., Miles, M., Thein, A., and Soothill, P., 1999. Selective cleaning of the cell debris in human chromosome preparations studied by Scanning Force Microscopy. *Journal of Structural Biology*, **128**, 200–210.
- Widmer, F., Seidler, R., and Watrud, L., 1996. Sensitive detection of transgenic plant marker gene persistence in soil microcosms. *Molecular Ecology*, **5**, 603–613.

Cross-references

- [Biofilms in Soil](#)
[Microbes and Soil Structure](#)
[Microbes, Habitat Space, and Transport in Soil](#)
[Soil Functions](#)
[Soil Water Flow](#)
[Surface and Subsurface Waters](#)

DOUBLE LAYER

See [Electrical Double Layer \(Diffuse Layer, Double Layer\)](#)

DRAINAGE

Outflow of water from the soil, either naturally or artificially. Surface drainage refers to the downslope flow of excess water from the soil surface. Subsurface (groundwater) drainage refers to the removal of water from within or below the soil, generally involving the lowering of the water table.

Bibliography

Introduction to Environmental Soil Physics. (First Edition). 2003. Elsevier Inc. Daniel Hillel (ed.) <http://www.sciencedirect.com/science/book/9780123486554>

Cross-references

- [Irrigation and Drainage, Advantages and Disadvantages](#)

DRIP IRRIGATION

An irrigation method which allows water and fertilizers to drip slowly to the root system of plants. Either onto the soil surface or directly onto the roots. This method provides farms the most efficient way to grow crops in water scarce areas.

Cross-references

- [Irrigation and Drainage, Advantages and Disadvantages](#)
[Irrigation with Treated Wastewater, Effects on Soil Structure](#)

DROUGHT

An extended period of dry weather which, as a minimum, can result in a partial crop failure or an inability to meet normal water demands.

Bibliography

Library of Congress Cataloging-in-Publication Data Environmental engineering dictionary and directory/Thomas M. Pankratz <http://www.docstoc.com/docs/2845196/CRC-Press>

Cross-references

- [Drought Stress, Effect on Soil Mechanical Impedance and Root \(Crop\) Growth](#)

DROUGHT STRESS, EFFECT ON SOIL MECHANICAL IMPEDANCE AND ROOT (CROP) GROWTH

W. R. Whalley, L. J. Clark
 Department of Soil Science, Rothamsted Research,
 Harpenden, West Common, Hertfordshire, UK

Definition and introduction

While there is no doubt that limited water availability decreases root growth, it is often assumed that this is the main cause of decreased growth in drying soil. However, this may not always be the case. Many laboratory experiments on water stress use growth media where the mechanical impedance remains low and constant as its matric potential becomes more negative. For example, roots are often grown in vermiculite, where water content is adjusted to give a required matric potential, or in solutions such as PEG that are adjusted to a required osmotic potential (Whalley et al., 2000). However, as the water potential of the root environment becomes more negative, not only does the elongation rate decrease but also the pressure that roots are able to exert on their surroundings (Whalley et al., 1998). While this effect on root growth pressure may not be relevant to elongation through media with negligible impedance, it is relevant to elongation through strong soil. In fact, root growth pressure is far more sensitive than the rate of elongation (through low-impedance media) to water potential. As the matric potential of most soils becomes more negative, its strength increases greatly. There are relatively few studies that consider both soil strength and water potential, but those that do conclude that soil strength has a greater effect on root growth and penetration than soil water potential (e.g., Mirreh and Ketcheson, 1973; Yapa et al., 1988; Whalley et al., 1999). A difficulty of such experiments is that it is difficult to control soil water status and mechanical impedance independently (Whalley et al., 2000). To fully understand the effects of high soil strength on root elongation,

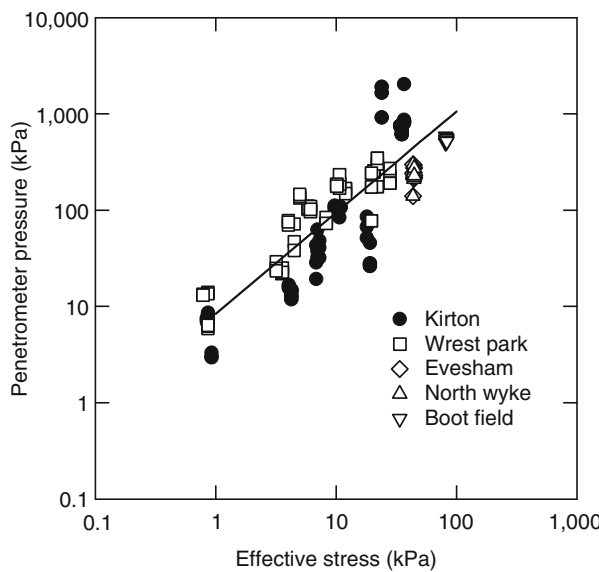
the relationship between soil water status and soil strength must be understood.

Soil strength and soil water status

For loose soil, with a bulk density less than about 1.4 g cm^{-3} , effective stress (product of degree of saturation and matric potential) gives a common relationship between penetrometer pressure and soil water status for a wide range of soils (Figure 1). Soil strength increases rapidly with soil drying, and even relatively wet soils are found to be strong even though they had not been compacted. In denser soils, however, empirical models that predict penetrometer resistance depend on soil type (e.g., Hernanz et al., 2000). Although good models to predict the penetration resistance of soil exist (Farrell and Greacen, 1966), in practice they are difficult to use because they need such extensive soil characterization. The following pedotransfer function to predict soil penetrometer resistance, Q , from soil density, ρ , degree of saturation, S , and matric potential Ψ

$$\log_{10}Q = 0.35\log_{10}(|\Psi S|) + 0.93\rho + 1.26 \quad (1)$$

was developed for a large number of Canadian soils (Whalley et al., 2007). This has the advantage that details of particle size distribution and organic matter content are not needed and data from moisture sensors can be used to predict penetrometer resistance, provided bulk density is known. An anomalous prediction of Equation 1 is that, as soil becomes increasingly dry and S approaches zero, the soil is predicted to become weaker, decreasing from

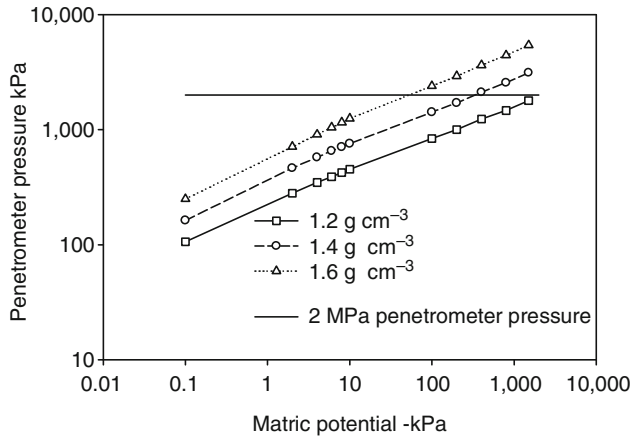


Drought Stress, Effect on Soil Mechanical Impedance and Root (Crop) Growth, Figure 1 Resistance to a rotating penetrometer plotted against effective stress for five different soils. (From Whalley et al., 2005). Resistance to a rotating penetrometer is considered to be a good approximation to the resistance to root penetration.

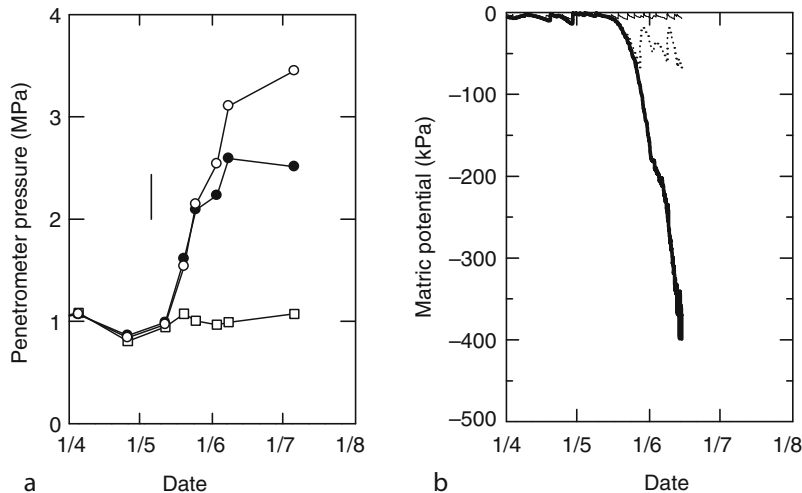
a maximum. For sand-kaolinite mixtures, this has been shown to be the case (Mullins and Panayiotopoulos, 1984) and beach sand also behaves in a similar manner. However, in agricultural soils strength does not decrease from the maximum, probably because of cementation by biological exudates and mineral precipitation as soil dries. Since Equation 1 was fitted to data from agricultural soils for $\Psi > -1.5 \text{ MPa}$, this anomalous behavior has been taken into account empirically. One of the implications of Equation 1 is that when soil is dense, high penetrometer pressures will be reached in much wetter soils than is the case for loose soil (Figure 2). Field data from Whalley et al. (2006) confirms that in the field, high soil strength occurs in relatively well-watered environments (see Figure 3). Penetrometer pressures in excess of 2 MPa were found in soil maintained at matric potentials of approximately -80 kPa .

Root elongation rate and soil strength

Penetrometer pressures between 2 and 3 MPa are commonly cited as a threshold to root elongation. However, root elongation rate decreases approximately linearly as soil strength increases (Bengough and Mullins, 1991). There has been a considerable research effort directed at understanding the elongation rate of roots growing in soils of various strengths. A seminal paper is that of Greacen and Oh (1972), who set out how the difference in pressure due to soil strength and cell turgor was accommodated by the cell wall. This model is appealing in its simplicity, but unfortunately it is inconsistent with physiological measurements. Passioura and Fry (1992) proposed a solution to allow ephemeral changes to elongation rate, due to set increases in turgor, as observed experimentally in algal



Drought Stress, Effect on Soil Mechanical Impedance and Root (Crop) Growth, Figure 2 Relationships between penetrometer pressure and matric potential calculated with Equation 1 using water release characteristic data for a silt soil. The horizontal line indicates a penetrometer resistance that is becoming too high for root elongation. As a dense soil dries, this penetrometer resistance is reached at a much higher value (i.e., in a wetter soil) in comparison with the loose soil. (Redrawn from Whitmore and Whalley, 2009.)



Drought Stress, Effect on Soil Mechanical Impedance and Root (Crop) Growth, Figure 3 The mean penetrometer resistance at a depth of 20 cm (a), the matric potential at a depth of 20 cm plotted against time (b) due to soil drying by wheat. The effects of three treatments are shown. These were well watered (open squares on the left panel and faint black line in right panel), drying limited to -80 kPa (closed circles on the left panel and dotted line in right panel), and finally rain fed (open circles on the left panel and heavy black line in right panel). The vertical line on the panel (a) is the SED (standard error for the difference). Note that when soil dries to -80 kPa, the penetrometer resistance exceeds 2 MPa. (Redrawn from Whalley et al., 2006.)

cells. To our knowledge this model has never been applied to root elongation which is probably because too much detailed information on cell-wall stiffening as a response to external stresses is needed.

Root penetration at boundaries

Roots can grow into rigid pores smaller than their nominal diameter (Bengough et al., 1997; Scholefield and Hall, 1985). In ryegrass, Scholefield and Hall (1985) found that this ability was limited by the size of the root cap and the stele, but Bengough et al. (1997) reported that the stele of maize roots did narrow in response to radial constriction. In soil, roots will often exploit cracks, voids, and large pores, or enlarge smaller pores by displacing soil particles. On encountering strong soil, root cell division and elongation are decreased (Eavis, 1967). Root diameter just behind the apex increases, and the production of lateral roots can be increased and also commences closer to the apex (Atwell, 1988). The increase in root diameter in response to impedance is caused by cortical cells enlarging radially rather than axially, with a corresponding change in the orientation of the cellulose microfibrils in the cell walls (Veen, 1982).

Thicker dicot roots have been observed to penetrate compacted subsoil in the field better than thinner monocot roots (Materechera et al., 1991, 1992). In both pea and lupin, 59% of the roots that reached the compacted layer were able to penetrate it, whereas in wheat and barley the root penetration was only 33% and 36%, respectively. The same authors found that species with thicker roots had better penetration of the subsoil, and particularly that the extent of thickening in the high-impedance treatment

Drought Stress, Effect on Soil Mechanical Impedance and Root (Crop) Growth, Table 1 Bending stiffness of roots of Azucena and Bala which had been grown either in strong (Impeded) or in weak (control) sand. The data was Log transformed before REML (analysis using the method of residual maximum likelihood) and the SED (standard error for the difference) is 0.1359. The back transformed bending stiffness in N mm $^{-1}$ is shown in brackets. (Taken from Clark et al., 2008a.)

	Control roots	Impeded roots
Azucena	-1.606 (0.2000)	-1.765 (0.1712)
Bala	-2.698 (0.0673)	-3.607 (0.0271)

relative to the control was important. It was also suggested that thicker roots gave better penetration because they would be more resistant to buckling (Barley and Greacen, 1967). In rice, genetic variability in root penetration into strong layers has been associated with genetic control of root diameter (Clark et al., 2008a). Although, greater bending stiffness in rice was associated with better penetration of strong layers, Clark et al. (2008a) noted that the process of penetration of a strong soil reduced bending stiffness (Table 1). This was thought to be due to cell-wall relaxation, which is implicated in the development of growth pressure (Clark et al., 1996).

An important observation by Clark et al. (2008b) is that the penetration of roots into a strong layer can be increased if there is a spatial gradient in soil strength. When there was a spatial gradient in strength, the penetration ability of Bala (a poor performing rice line) to penetrate a wax layer was similar to the better-performing Azucena in the absence spatial gradient in soil strength.

Summary

The most important message to take is that increases in soil strength sufficiently large to impede root elongation can occur after only a moderate degree of soil drying. In Figure 3, it can be seen that at matric potentials of around -80 kPa, which would normally be considered well watered for field-grown crops, penetrometer pressures in excess of 2 MPa were recorded. In such conditions root elongation is limited by high soil strength and not by the lack of water availability.

Bibliography

- Atwell, B. J., 1988. Physiological responses of lupin roots to soil compaction. *Plant and Soil*, **111**, 277–281.
- Barley, K. P., and Greacen, E. L., 1967. Mechanical resistance as a soil factor influencing the growth of roots and underground shoots. *Advances in Agronomy*, **19**, 1–40.
- Bengough, A. G., and Mullins, C. E., 1991. Penetrometer resistance, root penetration resistance and root elongation rate in two sandy loam soils. *Plant and Soil*, **131**, 59–66.
- Bengough, A. G., Croser, C., and Pritchard, J., 1997. A biophysical analysis of root growth under mechanical stress. *Plant and Soil*, **189**, 155–164.
- Clark, L. J., Whalley, W. R., Dexter, A. R., Barraclough, P. B., and Leigh, R. A., 1996. Complete mechanical impedance increases the turgor of cells in the apex of pea roots. *Plant Cell and Environment*, **19**, 1099–1102.
- Clark, L. J., Price, A. H., Steele, K. A., and Whalley, W. R., 2008a. Evidence from near-isogenic lines that root penetration increases with root diameter and bending stiffness in rice. *Functional Plant Biology*, **35**, 1163–1171.
- Clark, L. J., Ferraris, S., Price, A. H., and Whalley, W. R., 2008b. A gradual rather than abrupt increase in strength gives better root penetration of strong layers. *Plant and Soil*, **307**, 235–242.
- Eavis, B. W., 1967. Mechanical impedance and root growth. *Symposium of the Institute of Agricultural Engineering*, Silsoe, UK, 4/F/39, 1–11.
- Farrell, D. A., and Greacen, E. L., 1966. Resistance to penetration of fine probes in compressible soil. *Australian Journal of Soil Research*, **4**, 1–17.
- Greacen, E. L., and Oh, J. S., 1972. Physics of root growth. *Nature New Biology*, **235**, 24–25.
- Hernanz, J. L., Peixoto, H., Cerisola, C., and Sanchez-Geron, V., 2000. An empirical model to predict soil bulk density profiles in field conditions using penetration resistance, moisture content and soil depth. *Journal of Terramechanics*, **37**, 167–184.
- Materechera, S. A., Dexter, A. R., and Alston, A. M., 1991. Penetration of very strong soils by seedling roots of different plant species. *Plant and Soil*, **135**, 31–41.
- Materechera, S. A., Alston, A. M., Kirby, J. M., and Dexter, A. R., 1992. Influence of root diameter on the penetration of seminal roots into a compacted subsoil. *Plant and Soil*, **144**, 297–303.
- Mirreh, H. F., and Ketcheson, J. W., 1973. Influence of soil water matric potential and the resistance to penetration on corn root elongation. *Canadian Journal of Soil Science*, **53**, 383–388.
- Mullins, C. E., and Panayiotopoulos, K. P., 1984. The strength of unsaturated mixtures of sand and kaolin and the concept of effective stress. *Journal of Soil Science*, **35**, 459–468.
- Passioura, J. B., and Fry, S. C., 1992. Turgor and cell expansion – beyond the lockhart equation. *Australian Journal of Plant Physiology*, **19**, 565–576.
- Scholefield, D., and Hall, D. M., 1985. Constricted growth of grass roots through rigid pores. *Plant and Soil*, **85**, 153–162.
- Veen, B. W., 1982. The influence of mechanical impedance on the growth of maize roots. *Plant and Soil*, **66**, 101–109.
- Whalley, W. R., Bengough, A. G., and Dexter, A. R., 1998. Water stress induced by PEG decreases the maximum growth pressure of the roots of pea seedlings. *Journal of Experimental Botany*, **49**, 1689–1694.
- Whalley, W. R., Finch-Savage, W. E., Cope, R. E., Rowse, H. R., and Bird, N. R. A., 1999. The response of carrot (*Daucus carota* L.) and onion (*Allium cepa* L.) seedlings to mechanical impedance and water stress at sub-optimal temperatures. *Plant Cell Environment*, **22**, 229–242.
- Whalley, W. R., Lipiec, J., Stepniewski, W., Tardieu, F., et al., 2000. Control and measurement of the physical environment in root growth experiments. In Smit (ed.), *Root Methods – A Handbook*. Hiedelberg: Springer-Verlag, pp. 75–112.
- Whalley, W. R., Leeds-Harrison, P. B., Clark, L. J., and Gowing, D. J. G., 2005. The use of effective stress to predict the penetrometer resistance of unsaturated agricultural soils. *Soil and Tillage Research*, **84**, 18–27.
- Whalley, W. R., Clark, L. J., Gowing, D. J. G., Cope, R. E., Lodge, R. J., and Leeds-Harrison, P. B., 2006. Does soil strength play a role in wheat yield losses caused by soil drying? *Plant and Soil*, **280**, 279–290.
- Whalley, W. R., To, J., Kay, B. D., and Whitmore, A. P., 2007. Prediction of the penetrometer resistance of agricultural soils with models with few parameters. *Geoderma*, **137**, 370–377.
- Whitmore, A. P., and Whalley, W. R., 2009. Physical effects of soil drying on roots and crop growth. *Journal of Experimental Botany*, **60**, 2845–2857.
- Yapa, L. G. G., Fritton, D. D., and Willatt, S. T., 1988. Effect of soil strength on root growth under different water conditions. *Plant and Soil*, **109**, 9–16.

Cross-references

- [Hardpan Soils: Management](#)
[Management Effects on Soil Properties and Functions](#)
[Pedotransfer Functions](#)
[Plant Biomechanics](#)
[Plant Drought Stress: Detection by Image Analysis](#)
[Plant Roots and Soil Structure](#)
[Plant–Soil Interactions, Modeling](#)
[Rhizosphere](#)
[Root Responses to Soil Physical Limitations](#)
[Soil Compaction and Compressibility](#)
[Soil Hydraulic Properties Affecting Root Water Uptake](#)
[Soil Penetrometers and Penetrability](#)
[Soil Physical Quality](#)
[Subsoil Compaction](#)

DRYING OF AGRICULTURAL PRODUCTS

Digvir S. Jayas, Chandra B. Singh
 Department of Biosystems Engineering, University of Manitoba, Winnipeg, MB, Canada

Definition

Drying is the process of the removal of water (moisture) from hygroscopic materials at low to medium moisture contents (normally $<30\%$ wet basis) by means of evaporation. When the moisture content of the agricultural products is high (usually $>50\%$ wet basis) the process of

removal of moisture is referred to as dehydration. The examples of the products that are dried include cereals, oilseeds, legumes, and some processed foods; and examples of the products that are dehydrated include fruits, meats, and vegetables (Pabis et al., 1998; Sokhansanj and Jayas, 2006).

Process

Drying/dehydration is one of the most important postharvest treatments being adopted worldwide to reduce the spoilage and increase the shelf life or storage durability of agricultural products. Removal of moisture is a complex simultaneous heat and mass transfer process but treating it as such is not sufficient because end use characteristics or quality of the product cannot be handled this way. Moisture from inside the hygroscopic materials moves to the surface and then it evaporates to the surrounding atmosphere. This movement in moisture is caused by the gradient of water vapor pressure being high inside the materials to being low outside the materials. The movement of moisture could be by liquid diffusion, vapor diffusion, capillary flow, or a combination of these features. Usually the moisture gradient is established by application of heat from external sources. The process can be done at atmospheric pressures but can also be done under vacuum, and similarly the process can be done at a range of temperatures. The selection of the process temperature and pressure depends on the end use quality of the dried/dehydrated products. Heat is transferred to the product by a heating medium usually hot air or superheated steam, this heating medium also carries the moisture away from the product. Sometimes heat can be applied by contact such as by mixing hot sand with granular material or by coating a liquid product on a rotating drum whereas at other times heat could be applied through radiation, for example, in infrared dryers or through volumetric heating, for example, in microwave dryers. Drying of products using solar radiation (sun drying) is the simplest and oldest form of drying; however, sun drying is weather dependent and is slow, therefore other sources of heat are used. Depending on the heat source, operating pressure, and operating mechanism, dryers are classified as hot air, infrared, microwave, vacuum, freeze, flash, superheated steam, spouted bed, fluidized bed, and spray. The dryers are also classified based on the relative flow of material and the heating medium as concurrent flow, counter flow, cross flow, or mixed flow.

Challenges in drying agricultural products

Most dehydrated products are rehydrated prior to consumption; therefore, the texture and taste of the product

after rehydration are important quality parameters. Since agricultural products are sensitive to the heat (temperature), improper drying may cause the thermal damage to the product and the product may be spoiled or quality of end product may be poor. Under-drying will reduce the shelf life and over-drying will result in loss of mass, more power consumption, and thus economical losses. Drying characteristics of various agricultural and biomaterials are different and are also influenced by growing region, growing season, and weather conditions; therefore, it becomes necessary to study drying characteristics of the specific product for design of proper and efficient dryers.

Bibliography

- Pabis, S., Jayas, D. S., and Cenkowski, S., 1998. *Grain Drying Theory and Practice*. New York: Wiley.
Sokhansanj, S., and Jayas, D. S., 2006. Drying of foodstuffs. In Mujumdar, A. S. (ed.), *Handbook of Industrial Drying*, Vols. I-II. New York: Marcel Dekker.

Cross-references

- [Aeration of Agricultural Products](#)
[Hysteresis in Foods](#)
[Solar Drying of Biological Materials](#)
[Water Effects on Physical Properties of Raw Materials and Foods](#)

DURIPAN

A subsurface soil horizon that is cemented by illuvial silica, usually opal or microcrystalline forms of silica, to the degree that less than 50 percent of the volume of air-dry fragments will slake in water or HCl.

Bibliography

- Glossary of Soil Science Terms. Soil Science Society of America. 2010. <https://www.soils.org/publications/soils-glossary>

Cross-references

- [Claypan and its Environmental Effects](#)

DYNAMIC LOAD

A load connected with the elastic deformations of a body (e.g., soil, grains, fruits) subjected to time-dependent external forces.

E

EARTHWORMS AS ECOSYSTEM ENGINEERS

Patrick Lavelle
IRD/UPMC Université Paris 6, CIAT, Cali, Colombia

Definition

Earthworms probably are the most common animals on Earth. Appeared some 10 M years ago, they have coevolved with their environment and developed intimate mutualistic relationships with microorganisms and other soil inhabitants through ecosystem engineering.

What does an earthworm life look like? Adaptive strategies

Organisms that live in soils have adapted to three major limitations: moving in a compact environment, respiring in a porous space that is alternatively filled of water or air, and feeding on generally poor quality resources.

Earthworms can move in the soil thanks to a hydrostatic skeleton that allows to concentrate strength at the fore part of the animal and drill into the soil compact structure, or pull soil particles and detach them from the soil matrix before ingesting them. Their gut is a simple elongated tube in which the greatest part of digestion is performed by ingested microflora in a rather elaborated digestion partnership.

Respiration is cutaneous, which requires a constantly humid skin. High molecular weight hemoglobin in blood allows earthworms to make use of low concentrations of oxygen in the environment.

Earthworms feed on and live in leaf litter (epigeic functional category), live in subvertical galleries and feed on a mixture of litter and soil (anecics), or live and feed in soil (endogeics).

Active soil and litter movers and conductors of most soil organisms activities, earthworms are both dominant biological and physical engineers.

The earthworm engine: what makes earthworms such powerful bioturbators?

How to find energy to move each day 1–20 times its own weight of soil. An energy balance on the razor edge

Microbial communities that are mostly dormant in soil are selectively activated in earthworm guts through the addition of intestinal mucus (6–40% of ingested soil dry weight) and water (1 v/v soil). Although little is known of which functions are activated, we know that this mostly concerns bacterial communities as opposed to fungal, and that most enzymatic activities developed in earthworm guts actually come from these activated bacteria. Especially remarkable, as regards soil function are the occurrence of N fixing bacteria, P and N mineralization, and occasional Ca excretion.

Mutualist relationships with microflora allow earthworms to assimilate large amounts of energy, estimated at 5–10% of the energetic value of digested litter and organic matter, a rather high proportion considering the relatively low quality of the food that is, in the case of soil organic matter, dispersed in a rather compact mineral matrix.

The very scarce examples of energy budget available for earthworms show a very large investment in mechanical activities. In case of the endogeic tropical earthworm *Reginaldia omodeoi* (formerly known as *Millsonia anomala*), they represent over 96% of assimilated energy and allow the worms to ingest and egest daily from 10 to 25 times their own weight of soil depending on the age and general soil conditions (moisture, temperature, and

organic matter content). At the scale of a population and landscape scale, several 100 t ha⁻¹ (up to 1,250 t in moist savannas of Ivory Coast) casts may be deposited each year, mainly concentrated in the 20 upper cm of soil.

The value of earthworm-made habitats for soil inhabitants

Earthworms build three kinds of biogenic structures: galleries, middens, and casts.

Galleries may represent rather extended and connected networks of tubular pores that develop mainly in the upper 20 cm of soil, although they may occasionally reach several meters in depth. Total length of galleries may reach 890 m m⁻², which represents a total volume of 9.2 l.

Middens are specific structures made by anecic earthworms when they collect litter close to the mouth of their gallery and favor its preliminary decomposition by micro-organisms (mainly bacteria) and smaller fauna before ingesting it.

Casts may be rather diverse in their shapes, sizes, and compositions depending on soil quality and the feeding regime of the worm.

They are in any case very special microsites in soils, with high organic contents resulting from selective ingestion of organic particles and high concentrations in mineral N (20 to >200 ppm NH₄⁺ depending on the initial soil N content) and P (2–43.3 µg g⁻¹).

Earthworm structures are thus suitable habitats for a wide range of microorganisms (mainly bacteria), micro- and meso-fauna that take advantage of the generally improved conditions, and shelter provided. Earthworms may, however, sometimes have adverse effects on some litter arthropods affected by surface litter removal. Nematodes communities, especially of plant parasitic nematodes, have also been reported to be depressed in the presence of earthworms. Several mechanisms seem to be involved, such as provoked hatching of larvae that further die trapped into compact cast structures, or destruction of chemo receptors by specific proteolytic enzymes produced by bacteria in the earthworm gut.

Earthworms and ecosystem services: the landscape scale

For their intense effects as biological engineers that shape and regulate activities of microorganisms and smaller invertebrates, and physical engineers that construct porosity and soil macro aggregation, earthworms have significant effects on the provision of ecosystem services by soils.

Earthworms and climate regulation: C sequestration and green house gasses

Earthworms participate in climate regulation effects of soil through C sequestration and green house gasses

emissions. The overall effect of earthworms is not yet fully understood, since they have highly contrasted effects depending on the scale of measurement: great enhancement of C mineralization and greenhouse gas (GHG) emissions at small scales of time and space (gut content and freshly deposited casts) followed by inhibition in the compact structure of casts where microbial activity is progressively reduced to zero. It seems that a key element to determine whether the long-term effect of earthworms on soil C sequestration is positive or negative is the life span of earthworm casts. Very scarce experimental work show that casts once stabilized by a drying cycle, may resist for very long periods of time (several years) unless they are broken down by other ecosystem engineers or natural physical processes.

Earthworms and water supply: infiltration, storage, and transfer

Bioturbation and tunneling effected by earthworms significantly influence soil hydraulic properties. The result is mostly an enhanced water infiltration and transfer toward deeper soil strata although the overall effect of an earthworm community may greatly depend on the relative proportion of functional groups with contrasted effects. The so-called compacting species accumulate in soil large amounts of compact casts that form the stable macro aggregates that provide soils with structural stability and favorable hydraulic properties. However, when alone, these worms rapidly compact the soil, and in extreme cases create an impermeable crust of coalescent casts that may have catastrophic effects on plant communities. De-compacting species are much smaller worms that may feed on casts of compacting species thus regulating their impact on soil hydraulic properties; an adequate balance between effects of both types seems to be necessary to maintain optimal hydraulic conditions in the upper centimeters of soil where earthworm activity is mainly concentrated.

Earthworms and primary production: the five processes

The most spectacular effect of earthworms is observed on plants. Five different mechanisms are known to alternate or add their effects to stimulate plant growth and vigor: (1) nutrient release in the plant rhizosphere, (2) stimulation of microbial mutualists (especially mycorrhizae), (3) organization of soil structure that improves water supply, (4) control of pests and diseases, and (5) pseudo hormonal effects with a stimulation of Plant Growth promoters in the rhizosphere. Although the relative contribution of each single process is not known in most cases, there is some evidence that pseudo hormonal effects may be a rather constant effect while nutrient release and pest control occasionally have determinant impacts.

Do earthworms benefit from their own activities?

Are earthworms accidental engineers or do the structures that they create represent an extension of their phenotype improving their adaptive value? Since earthworms from a given species do not reingest their own casts, they have been said to be accidental engineers. However, at a larger scale, there is some evidence that soils comprise mosaics of functional domains with different species of soil engineers, earthworms, roots, termites, or ants. Most engineers affect soil structure, the composition of communities of smaller organisms, and soil processes in different ways; there is some evidence that each such activity is limited in time and the mosaic represented by the physical domains of all these ecosystem engineers might represent the spatial consequence of a process of ecosystem succession at their respective scales of dm^2 to m^2 . If this is true, each species would be part of an auto organized system in which species engineering activities are part of an auto organized system that ultimately has positive feedback on their fitness. The community composed by the different ecosystem engineers as a whole may thus be considered having an extended phenotype strategy.

Earthworm management

Earthworms are rather sensitive to ecosystem changes associated with most land use strategies. They are especially vulnerable to tillage, pesticides, and bare soil conditions. In most cases, active communities may be maintained even in relatively intensive practices provided (1) soil is covered all the time and fertilizer inputs comprise a minimum proportion of organic elements; (2) tillage is limited at a minimum or simply avoided; and (3) if pesticides are to be used, their inotoxicity toward earthworms must have been demonstrated in field conditions.

Bibliography

- Edwards, C. A., and Bohlen, P. J., 1996. *Biology and Ecology of earthworms*, 3rd edn. London: Chapman and Hall.
 Lavelle, P., and Spain, A. V., 2001. *Soil Ecology*. Amsterdam: Kluwer Scientific.
 Lavelle, P., Bignell, D., and Lepage, M., 1997. Soil function in a changing world: the role of invertebrate ecosystem engineers. *European Journal of Soil Biology*, **33**, 159–193.
 Lavelle, P., Barot, S., Blouin, M., Decaëns, T., Jimenez, J. J., and Jouquet, P., 2007. In Cuddington, K., Byers, J. E., Wilson, W. G., and Hastings, A. (eds.), *Ecosystem Engineers: From Protists to Plants*. Academic, Theoretical Ecology Series, pp. 77–106.

Cross-references

- [Bypass Flow in Soil](#)
[Infiltration in Soils](#)
[Soil Aggregates, Structure, and Stability](#)
[Soil Structure, Visual Assessment](#)

ECOHYDROLOGY

Maciej Zalewski

International Institute of Polish Academy of Sciences,
 European Regional Centre for Ecohydrology under the
 auspices of UNESCO, Łódź, Poland
 Department of Applied Ecology, University of Łódź,
 Łódź, Poland

Definition

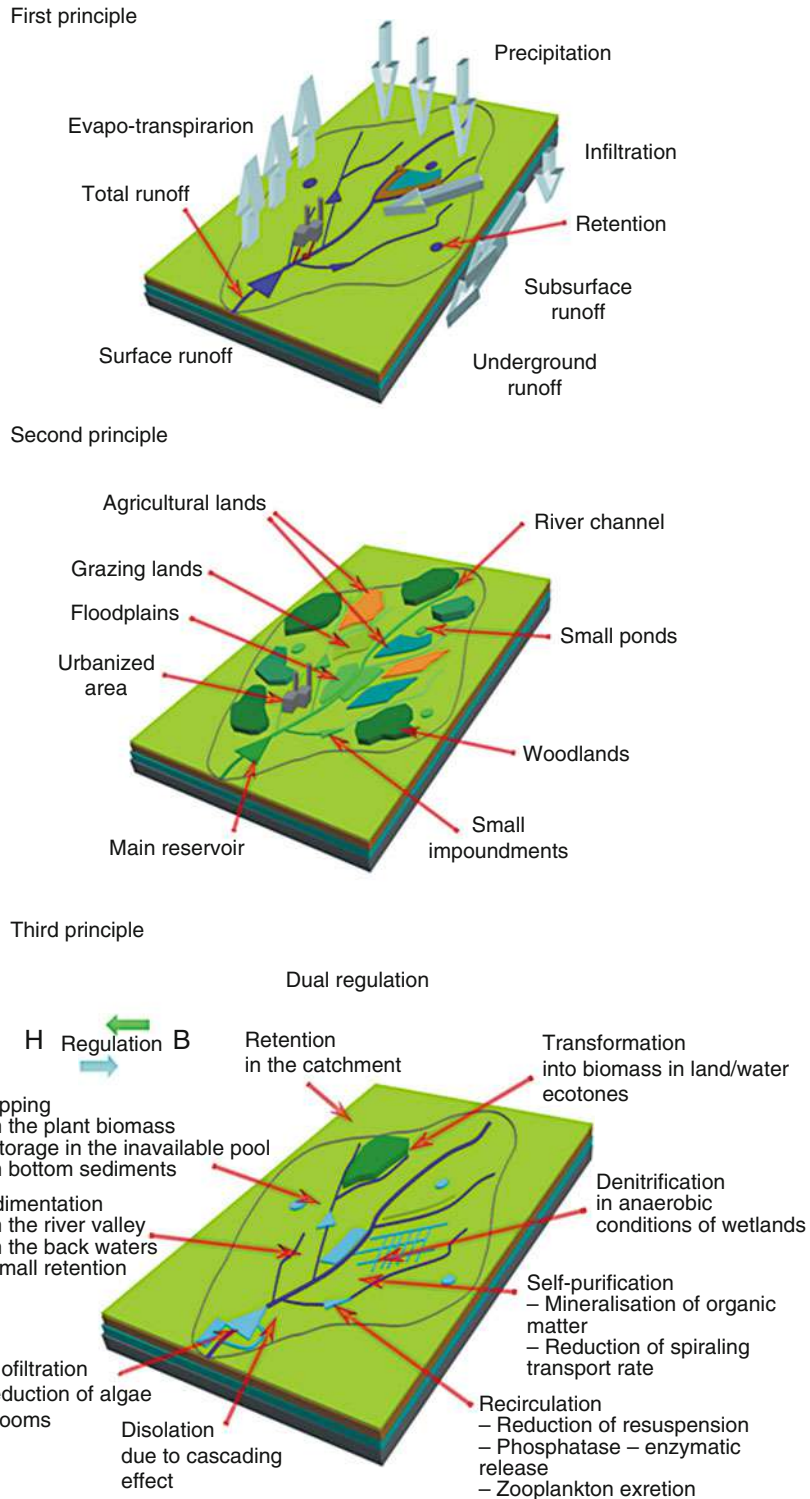
Ecohydrology (EH) a subdiscipline of hydrology that focuses on ecological processes occurring within the hydrological cycle and strives to utilize such processes for enhancing environmental sustainability. Has been developed under the International Hydrological Programme of UNESCO.

The general assumption of EH is to reverse degradation and achieve sustainable water and ecosystems in anthropogenically modified basins. In addition to the reduction of erosion, nutrients, and pollutant emissions there is a necessity to regulate ecological processes based on understanding “water – biota interactions,” from molecular (e.g., microbial loop) to ecosystem (biomanipulation) and to landscape scales (reforestation, creation land/water ecotone zones).

Two halves of ecohydrology can be distinguished: (1) Terrestrial (EHT), where the major question is how plant cover in given geomorphology and soil conditions changes the dynamic water balance and nutrients/pollutants transfer in to aquatic ecosystems and (2) Aquatic (EHA), where hydrology–biota interactions may change nutrients/pollutants allocation from dynamic to non-available pools, such as changing the intensity of eutrophication (up to an order of magnitude).

The following principles of EH provide a framework for its implementation ([Figure 1](#)):

1. Hydrological: The quantification of the hydrological cycle of a basin, should be the template for functional integration of hydrological and biological processes.
2. Ecological: Integrated processes at a river basin scale can be steered in such a way as to enhance the basin's carrying capacity (resilience, biodiversity, and ecosystem services).
3. Ecological engineering: The “key element of EH as a new tool for Integrated Water Resources Management (IWRM) is “dual regulation” – use of the understanding of terrestrial and aquatic organisms’ adaptation to water quality and dynamics. It can be expressed by testable hypotheses, as follows (1) Hydrological processes generally regulate biota; (2) Biota can be shaped as a tool to regulate hydrological processes; (3) These two types of regulations can be harmonized with hydrotechnical infrastructure to achieve sustainable water and ecosystem services.



Ecohydrology, Figure 1 Three ecological principles. Hydrological (upper), ecological (middle), and ecotechnological (lower).

Methodology of science – EH is integrative – a transdisciplinary, problem-solving science based upon the deductive concept, formulated from the general theory of physics, hydrology, and ecology. As a transdisciplinary science, the implicit goal of which is to achieve sustainability, EH integrates not only hydrology and ecology but also considers geophysics, geology, molecular biology, genetics, geo-information techniques, mathematical modeling with socioeconomic (e.g., foresight) and legal aspects.

EH goals as a problem-solving science

1. Slowing down the transfer of water from the atmosphere to the sea (considering flood and drought control as priorities)
2. Reduce input and regulate the allocation of excess nutrients and pollutants in aquatic ecosystems to improve water quality, biodiversity, and human health
3. Enhancement of ecosystem carrying capacity (resilience, biodiversity, ecosystem services for society) in harmonization with the societal needs within the framework of Integrated Water Resources Management (IWRM)

ECOSYSTEM

See [Water Balance in Terrestrial Ecosystems](#)

EFFECTIVE RAINFALL

A rainfall that produces surface runoff.

Bibliography

Library of Congress Cataloging-in-Publication Data Environmental engineering dictionary and directory/Thomas M. Pankratz <http://www.docstoc.com/docs/2845196/CRC-Press>

ELASTICITY

The property of a body to deform instantaneously under an applied stress and in proportion to it, to retain the new form as long as the stress is maintained, then to regain the original dimensions when the stress is released.

Bibliography

Introduction to Environmental Soil Physics (First Edition) 2003 Elsevier Inc. Daniel Hillel (ed.) <http://www.sciencedirect.com/science/book/9780123486554>

ELASTOPLASTICITY

State of a matter (e.g., soil, grains, fruits) subjected to a stress greater than its elastic limit but not so great as to cause it to rupture, in which it exhibits both elastic and plastic properties.

ELECTRICAL CONDUCTIVITY

The ability of a body (e.g., soil, grains, fruits) to conduct electricity.

ELECTRICAL DOUBLE LAYER (DIFFUSE LAYER, DOUBLE LAYER)

An idealized model to describe the electrical state of a surface, and commonly used to describe the physical behaviour of clay particles in soil. The clay surface and its surface charge constitute one layer, while aqueous solution in contact with the solid is a second (Stern) layer. The latter is held in place by counterions to the ions on the charged surface, the two together forming a kind of molecular capacitor. Ions further from the surface, and less strongly held, form a more diffuse (or Gouy) layer.

Bibliography

Chesworth, W. (ed.). 2008. Encyclopedia of Soil Science, Springer, p. 207.

Cross-references

[Diffuse Double Layer \(DDL\)](#)
[Electrokinetic \(Zeta\) Potential of Soils](#)
[Surface Properties and Related Phenomena in Soils and Plants](#)

ELECTRICAL PERMEABILITY

See [Organic Dusts, Electrostatic Properties](#)

ELECTRICAL PROPERTIES OF AGRICULTURAL PRODUCTS

Zuzana Hlaváčová
 Department of Physics, Slovak University of Agriculture in Nitra, Nitra, Slovakia

Synonyms

Dielectric properties; Electric characteristics; Electrical properties

Definition

Electric properties – electric conductance, conductivity, electric resistance, resistivity, impedance, admittance, permittivity, relative permittivity, complex permittivity with the components – real part that is equal to permittivity and imaginary part characterizing dielectric losses in material, further we can mention dielectric loss angle, loss tangent, Maxwell relaxation constant.

Electric properties are the properties that characterize transport of charge carriers in the material or propagation of electromagnetic waves in material. Conductance – G (siemens – S) is an ability of the material to conduct the electric current. Four types of conduction can be mentioned. The charge carriers are electrons related to the electron conductance. Ions are charge carriers related to the ionic conductance. If the charge carriers are positively charged particles, it is called hole conductance (P-type), and in the case of macromolecules or particles aggregation it is electroforetic conductance.

Resistance – R (ohm – Ω) is the reciprocal value of the conductance. Conductivity – σ (S m^{-1}) is the conductance of material related to its proportions. Resistivity – ρ (Ωm) is reciprocal value of the conductivity. Impedance – Z (Ω) is material resistance at the alternate current. Admittance – Y (S) is reciprocal value of the impedance.

Introduction

It is necessary to consider the change of the electric conductivity type at transition of the electric current through the biological material. The inside of the cell has the ionic conductivity. The electric current in a cellular membrane (insulator) passes as displacement current. The density of the electric current i is defined as

$$i = \frac{1}{S} \frac{dQ}{d\tau} \quad (1)$$

where: Q – charge (coulomb – C), τ – time (s), S – surface (m^2).

The relationship between the density of the current and electric field intensity is

$$\vec{i} = \sigma \vec{E} = -\sigma \text{grad} U \quad (2)$$

where: σ – electric conductivity (S m^{-1}), $\text{grad } U$ – gradient of the electric voltage (V m^{-1}), \vec{E} – intensity of the electric field (V m^{-1}). This equation is also valid for electrolyte at low values of electric field intensity. Wien has shown in 1927 that some anomalies occur from the presented equation at intensity of 10^7 V m^{-1} .

Berliner (1973) declared that it is necessary to consider three components of direct electric current, when it is transiting through the material: conduction component, which is invariable in the time; absorption component i_a due to polarization effects and it can be described as follows

$$i_a = A\tau^{-k} \quad (3)$$

where: A – constant (amper – A), k – constant (1), and if the time τ is equal 0, then i_a is equal 0 too; and finally, the charging component i_n , which can be described as a flow passing through the capacitor with a capacity C by relation

$$i_n = \frac{U}{R} e^{-\frac{\tau}{RC}} \quad (4)$$

where: R – resistance of the circuit (Ω), U – source voltage (V). If the time τ is approaching to 0, charging component is approaching to ratio $\frac{U}{R}$. The line current decreases with the time and its value is approaching to the conduction component. Electric measurements by direct current are strongly influenced by the polarization effects at high moisture content of the material.

If the current passing through the material is unsteady, for the electric current density is valid

$$i = \sigma E + \frac{d(\varepsilon E)}{d\tau} \quad (5)$$

where: ε – permittivity of material (F m^{-1}) (*Dielectric Properties of Agricultural Products*). Complex value of current density is valid in the case of alternating electric field in the form

$$\hat{i} = (\sigma + j\omega \varepsilon) \hat{E} \quad (6)$$

where: \hat{E} – complex value of electric field intensity, j – imaginary unit (1), ω – angular frequency (s^{-1}).

Permittivity of moist material must be considered to be complex. It has a real part ε' and an imaginary part ε''

$$\hat{\varepsilon} = \varepsilon' - j\varepsilon'' = \varepsilon - j\frac{\sigma}{\omega} = \varepsilon (1 - j \operatorname{tg} \delta_\varepsilon) \quad (7)$$

where δ_ε is the loss angle (1) of the dielectric and

$$\operatorname{tg} \delta_\varepsilon = \frac{\sigma}{\omega \varepsilon} \quad (8)$$

where: $\operatorname{tg} \delta_\varepsilon$ – loss tangent (1).

ε'' is interpreted to include the energy losses in the dielectric arising from all dielectric relaxation mechanisms and ionic conduction. Materials, such as agricultural products and foods, generally show significant loss factors, and the dielectric properties are therefore dependent on both temperature and frequency, as well as the chemical and physical characteristics of the material including composition and density (Topp and Ferré, 2001).

Electric current passes as a displacement current in the nonconductors. Maxwell named the quantity

$$\vec{i} = \varepsilon \frac{\partial \vec{E}}{\partial \tau} \quad (9)$$

as the displacement current density. If the alternating currents are used at the measurements, then the Maxwell relaxation constant places an important role. It is defined by the equation

$$\tau_M = \frac{\varepsilon}{\sigma} \quad (10)$$

τ_M presents the time (s), after which the space charge density falls e -times in the material. Maxwell relaxation constant is the criterion of material return to equilibrium state, that is, to state without space charge. This time with values for conductor from 10^{-15} to 10^{-13} s and for non-conductors achieves up to 10^6 s (Hlaváčová, 2003).

Electrical properties of agricultural products

Electric properties of the agricultural products of biological origin have been of interest for many years. When studying the physical properties of tissue, it is necessary to consider its non-homogeneity from the macroscopic and microscopic points of view. When testing the electric properties from the microscopic point of view, it is evident that the inside of the cell is conductive because there is a conductivity of ion type in the content of the organic and inorganic matter solutions. The cell membranes are not conductors. From the macroscopic point of view, the agricultural products can be regarded as non-homogeneous semiconductors or dielectrics. The density and structural arrangement of the cells as well as the properties of each type of tissue can influence the electrical properties of these materials. The characteristics of loose and porous materials are also influenced by the properties of air, which is trapped between the parts or in the pores, especially by its relative humidity and temperature. The deployment of the parts in the pack, the size of parts, gappiness, contact surface, and bulk density also influence the electric properties of loose materials. Among the influential factors for porous materials, the following can be involved: size and distribution of pores, porosity, and bulk density. A further factor is the temperature of the material, but the most significant is the influence of the presence of water (see *Water in Forming Agricultural Products*), its uneven deployment in the material, different binding energy in each water bond in the material (see *Adsorption Energy of Water on Biological Materials*), and sorption properties (Hlaváčová, 2003).

The resistivity of some materials at temperature of 20°C is given in Table 1 (Physical properties of food – http://www.tf.uniag.sk/e_sources/katfyz/fvp/uvod.htm; Blahovec, 2008; See also *Physical Properties as Indicators of Food Quality*).

The influence of water presence in agricultural products on electric properties is shown for example on Figure 1.

The resistivity is decreased from value 10^8 to $10^4 \Omega\text{m}$. The dependency of agricultural products resistivity has the decreasing power function character whose regression equation is

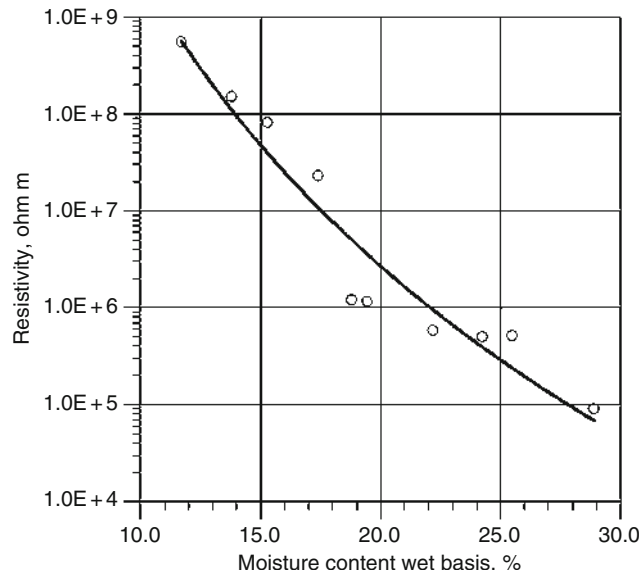
$$\rho = \rho_o \omega^{-d} \quad (11)$$

where ρ is resistivity, ρ_o is resistivity at the reference moisture content, ω – moisture content wet basis, and d a constant.

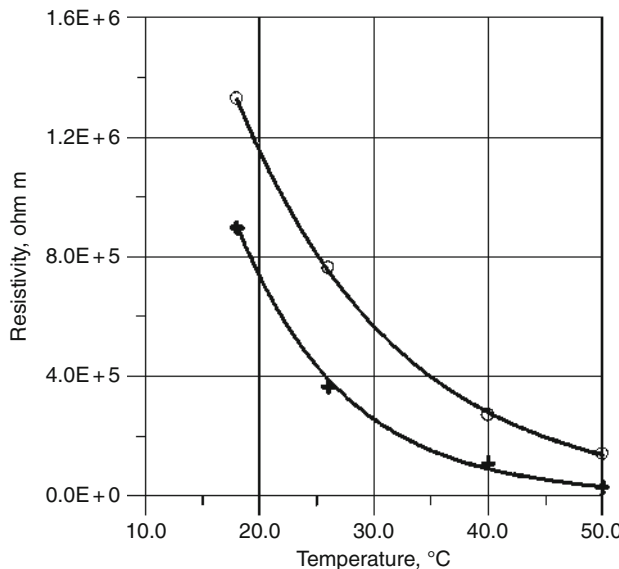
Electrical Properties of Agricultural Products, Table 1 Resistivity of some materials

Material	$\rho (\Omega\text{m})$
Gold	2.04×10^{-8}
Silver	1.505×10^{-8}
Copper	1.555×10^{-8}
Silicon	3×10^3
NaCl solution concentration $\leq 0.5 \text{ kg m}^{-3}$	13.3
Concentration (2–5) kg m^{-3}	1.33–3.33
Saturated solution	0.15
Milk, milk products	1.67–2.75
Sour milk	1.25–1.6
Beer	5.56–7.7
Juice	2.63–2.86
Syrups	16.7–25
Mineral water	1.25–7.7
Fresh fruit juice	2.5–5
Water	39
Tomatoes ($\omega = 95\%$)	35.7
Cucumbers ($\omega = 95\%$)	43.5
Potatoes ($\omega = 75\%$)	26.3–27
Root vegetables	24.4–66.7
Pears	37–71.4
Apples	17.9–26.3
Wheat ($\omega = 24\%$) ($\omega = 10\%$)	$\sim 10^4$ $\sim 10^8$
Butter	~ 12.5
Bread crumb	~ 57

ω – moisture content wet basis



Electrical Properties of Agricultural Products, Figure 1 The dependency of the resistivity on moisture content wet basis for *Amaranthus hypochondriacus* at an average bulk density of 760.4 kg m^{-3} (Hlaváčová, 2003).



Electrical Properties of Agricultural Products, Figure 2 The temperature dependencies of resistivity for corn (*Zea Mays*) grain hybrids of *Fabullis* (○) at the moisture content wet basis of 16.9% and of *Raissa* (+) at 17.34%.

On Figure 2, temperature dependencies of the resistivity of two hybrids of corn are presented to illustrate the influence of temperature on electric properties.

Information on the temperature distributions and electric properties dependency on temperature of a treated material are necessary in the case of thermal treatment (e.g., ohmic heating). We found out that the conductivity of seeds or grains increases and the resistivity decreases with temperature exponentially for all samples at all moisture contents (Hlaváčová, 2003). Displacement of the curves on Figure 2 can be caused by various properties of two hybrids.

The regression equation for resistivity has the form

$$\rho = \rho_o e^{-k\frac{t}{t_o}} \quad (12)$$

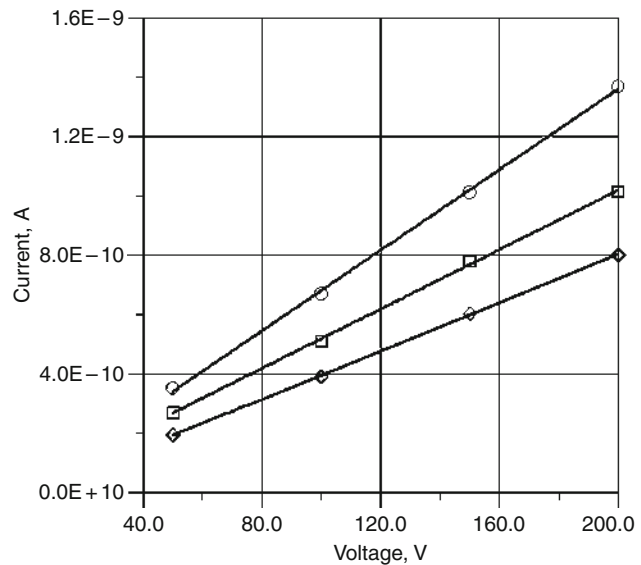
where: ρ_o – resistivity at the reference temperature, t – temperature, k – constant, $t_o = 1^\circ\text{C}$.

This equation is in a good relation with Arrhenius formula for the conductivity in the case of agricultural products

$$\sigma = \sigma_o e^{\frac{E_a}{kT}} \quad (13)$$

where: E_a – activation energy for conductivity, k – Boltzman constant, T – thermodynamic temperature.

Other influence on electric properties is shown on Figure 3. The measurements were made with variously treated seeds (rubbed, coated, and encrusted) of nine sugar beet cultivars (Hlaváčová, 2003). It was found that the electrical conductivity of seeds is affected by their surface treatment. The current passing through the pack of seeds



Electrical Properties of Agricultural Products, Figure 3 Voltage dependencies of the current passing through the sample of sugar beet (*Beta vulgaris L.*) seeds, cultivars *Intera* (rubbed seeds, ○), *Polina* (coated seeds, □) and *Remona* (encrusted seeds, ◇) at average moisture content of 9.39%.

was measured. The current increases linearly with the voltage (in the measured voltage range to 200 V). The current was highest when flowing through a sample of rubbed seeds and lowest when passing through a sample of encrusted seeds.

Average conductivity at the moisture content of 9.39% for cultivar *Remona* (encrusted seeds) was $1.741 \times 10^{-10} \text{ S m}^{-1}$, for cultivar *Polina* (coated seeds) $2.285 \times 10^{-10} \text{ S m}^{-1}$, and for *Intera* (rubbed seeds) $3.006 \times 10^{-10} \text{ S m}^{-1}$. It results that coating and encrusting of seeds decrease their conductivity. The mode of sugar beet seeds surface treatment could be estimated by the measurements of their electric properties.

Kuang and Nelson (1998) described low-frequency dielectric properties (see *Dielectric Properties of Agricultural Products*) of biological tissues, characterized by α - and β -dispersions. There are included ion activities, tissue microstructure, electrode polarization, which always cause problems at the measurement.

Electrical properties utilization

Electrical properties are utilized in many areas of human activities. They have the biggest application at moisture content measurements. The material investigation and moisture measuring using electromagnetic waves in wide spectrum serve for quality control and improvement in many branches like industry, forest and wood-working industry, civil engineering, agriculture, and commerce (Nelson, 2005).

Agricultural products properties are determined from their leachates too. Couto et al. (1998) utilized conductivity measurement of leachates for quantitative mechanical damage evaluation in soybeans. For example, Maezawa and Akimoto (1996) utilized electrical conductivity to determine the characteristics of low-temperature sensitive vegetables. Other types of electric properties utilization were collected in the paper of Kuang and Nelson (1998), as well as in the paper of Hlaváčová (2003). We can use electrical properties on microscopic levels, for instance for the cell turgor pressure determination. On the macroscopic level, electric properties are exploited at the determination of agricultural products' moisture content (seeds, grains, vegetables, cotton lint, etc.), at determination of seeds or grain deterioration, of seeds germination (see *Electromagnetic Fields, Impact on Seed Germination and Plant Growth*), of frost sensitivity or chilling and freezing tolerance, at determination of seeds vigor, of soybean seed coat lignin content, and for selection of seeds with high viability. The electrical measurements are utilized in many works to determine the properties of the fruit; the electrical conductivity of intact fruits was utilized for finding the relationship between the electrical parameters of the tissue and quality indices, including the probability of occurrence of sound, diseased, and damaged fruit for different storage periods (*Nondestructive Measurements in Fruits*). The electric conductivity or resistivity measurement can be used at the quality of food indication (*Physical Properties as Indicators of Food Quality*), for example, determination of chloride in milk or clinical mastitis detection, the inactivation of *Escherichia coli* in skim milk or meat by high intensity pulsed electric fields. Electrical heating is utilized for the food treatment, for instance the direct ohmic heating, sterilization, or pasteurization.

Electromagnetic heating, such as microwave and radiofrequency heating, is used in many processes such as reheating, precooking, tempering, baking, drying, together with pasteurization, and sterilization in industry and at home, as well as including electromagnetic heating processes related to dielectric properties (see *Dielectric Properties of Agricultural Products*) of the material. Since microwave heating is common in many food processes, determination of dielectric properties becomes significant to understand the heating profiles of foods in a microwave oven, and to develop equipment and microwaveable foods (Sahin and Sumnu, 2006).

Conclusions

Electric properties of the agricultural products are influenced by the internal structure and from the macroscopic point of view by the properties of air, which is trapped between the parts or in the pores in the case of loose and porous materials, most especially its relative humidity and temperature. The deployment of the parts

in the pack, the size of parts, gappiness, contact surface, and bulk density also influence the electrical properties of loose materials. Among the influential factors related to porous materials, the following can be involved: size and distribution of pores, porosity, and bulk density. A further factor is the temperature of the material, but the most significant is the influence of presence of water (see *Water in Forming Agricultural Products*), its uneven deployment in the material, different binding energy in each water bond in the material (see *Adsorption Energy of Water on Biological Materials*), and sorption properties. Electric properties are utilized in many areas of human activities. They have the biggest application at moisture content measurements.

Electric properties data on agricultural products and foods have been compiled for reference in several publications. However, these materials are so complex in their composition and in their electric behavior that it is necessary to measure the electric properties under the particular conditions of interest to obtain reliable data.

Bibliography

- Berliner, M. A., 1973. *Moisture Measurement (in Russian)*. Moskva: Energia.
- Blahovec, J., 2008. *Agromaterials*. Prague: Czech University of Life Sciences.
- Couto, S. M., et al., 1998. An electrical conductivity method suitable for quantitative mechanical damage evaluation. *Transaction of the ASAE*, **2**, 421–426.
- Hlaváčová, Z., 2003. Low-frequency electric properties utilization in agriculture and food treatment. *Research in Agricultural Engineering*, **4**, 125–136.
- Kuang, W., and Nelson, S. O., 1998. Low-frequency dielectric properties of biological tissues: a review with some new insights. *Transaction of the ASAE*, **1**, 173–184.
- Maezawa, S., and Akimoto, K., 1996. Characteristics of electrical conductivity of low-temperature sensitive vegetables. *Research Bulletin of the Faculty of Agriculture, Gifu University, Japan*, **61**, 81–86.
- Nelson, S. O., 2005. *Dielectric properties measurement for agricultural applications*. 2005 ASABE Annual Meeting, Milwaukee, Wisconsin, USA, ASABE paper No. 053134.
- Physical Properties of Food – http://www.tf.uniag.sk/e_sources/katfyz/fvp/uvod.htm.
- Sahin, S., and Sumnu, S. G., 2006. *Physical Properties of Foods*. New York: Springer Science + Business Media.
- Topp, G. C., and Ferré, P. A., 2001. Electromagnetic wave measurements of soil water content: a state-of-the-art. In *Proceedings of Fourth International Conference on Electromagnetic Wave Interaction with Water and Moist Substances*. Weimar, pp. 327–335.

Cross-references

- [Adsorption Energy of Water on Biological Materials](#)
[Dielectric Properties of Agricultural Products](#)
[Electromagnetic Fields, Impact on Seed Germination and Plant Growth](#)
[Nondestructive Measurements in Fruits](#)
[Physical Properties as Indicators of Food Quality](#)
[Water in Forming Agricultural Products](#)

ELECTRICAL PROPERTIES OF SOILS

Shmulik P. Friedman

Environmental Physics and Irrigation, Institute of Soil, Water and Environmental Sciences, The Volcani Center, Agricultural Research Organization, Bet Dagan, Israel

Definitions and terminology

Electrical conductivity (σ) [$\text{Q}^2\text{T}^1\text{M}^{-1}\text{L}^{-3}$, Sm^{-1}] is defined as the ratio of the electrical current density (J) [$\text{QT}^{-1}\text{L}^{-2}$] to the electric field strength (E) [$\text{MLQ}^{-1}\text{T}^{-2}$]:

$$J = \sigma E \quad (1)$$

and describes a material's ability to conduct an electrical current. The *dielectric permittivity* (ϵ) [$\text{Q}^2\text{T}^2\text{M}^{-1}\text{L}^{-3}$, Fm^{-1}] is the ratio of the electrical flux density, D [QL^{-2}] (electrical displacement) to the electrical field strength:

$$D = \epsilon E \quad (2)$$

and as such it is a macroscopic measure of the ability of the medium to polarize in response to an applied electrical field. In other words, the permittivity relates to a material's ability to transmit (or "permit") an electrical field. In terms of a parallel-plate capacitor, the electrical flux density (D) relates to the total (true) charge density on its surfaces, to the electrical field (E), to the free charge density, and to the bound (neutralized by the medium's polarization) surface charge density that represents a new defined vector of the same physical dimensions as D named polarization (P) [QL^{-2}] (von Hippel, 1954). In vacuum, D and E are related through $D = \epsilon_0 E$, where ϵ_0 is the permittivity of vacuum, equal to $8.854 \times 10^{-12} \text{ F m}^{-1}$. In the general case, Equation 2 holds and the interrelation between the three field vectors is:

$$D = \epsilon E = \epsilon_0 E + P \quad (3)$$

The ratio, $P/\epsilon_0 E$, namely, the bound to free charge density ratio, is termed *dielectric susceptibility* ($\chi \equiv \epsilon/\epsilon_0 - 1$), and it can be alternatively used for relating the polarization (of an isotropic, linear dielectric material) to the electrical field: $P = \chi \epsilon_0 E$.

The conductive and capacitive properties of soils can be represented by either a *complex conductivity* (σ^*) (/its reciprocal *complex resistivity*, ρ^*) or a *complex permittivity* (ϵ^*), related through

$$\sigma^* = \frac{1}{\rho^*} = i2\pi f \epsilon^* \quad (4)$$

where f is the frequency and $i = \sqrt{-1}$. The complex conductivity is expressed by its *real* (σ') and *imaginary* (σ'') components:

$$\sigma^* = \sigma' + i\sigma'' \quad (5)$$

and the common terminology is to express the complex permittivity with two positive permittivity entities. The

real part (ϵ') represents energy storage and the imaginary part (ϵ'') represents energy dissipation, assumed to stem from two contributions: dielectric relaxation (ϵ_d'') and low-frequency ("direct current," DC) conductivity ($\sigma_{DC}/2\pi\epsilon_0 f$)

$$\epsilon^* = \epsilon' - i\epsilon''; \epsilon''(f) = \epsilon_d''(f) + \sigma_{DC}/2\pi\epsilon_0 f \quad (6)$$

The ratio between the dissipative and conservative permittivities is called the *loss tangent*: $\tan \delta = \epsilon''/\epsilon'$.

The *dielectric constant*, also termed *relative permittivity* (ϵ_r), is the ratio of the real permittivity of the material (ϵ') to the permittivity of vacuum (ϵ_0), and it is proportional to the imaginary component of the complex conductivity

$$\epsilon_r = \frac{\epsilon'}{\epsilon_0} = \frac{\sigma''}{2\pi f \epsilon_0} \quad (7)$$

In the following we will refer to only the dimensionless, real high-frequency relative permittivity (ϵ_r), denoting it as ϵ (omitting the r and ∞ subscripts and the ' r ' superscript), and to only the low-frequency real conductivity (σ_{DC}) denoting it as σ (omitting the DC subscript and the ' r ' superscript).

The *effective* (also termed *apparent* (σ_a) or *bulk* (σ_b)) *electrical conductivity* of the soil (σ_{eff} , Sm^{-1}) can be defined in more than one way: Torquato (2002, p. 359), for example, defines it as the relation between the volume-averaged electrical field ($\langle E \rangle$, Vm^{-1}) and the volume-averaged electrical current density ($\langle J \rangle$, Am^{-2})

$$\langle J \rangle = \sigma_{eff} \langle E \rangle \quad (8)$$

Here we will adopt a more general and practical approach to defining σ_{eff} (and similarly the *effective permittivity*, ϵ_{eff}): the conductivity (/permittivity) of a homogeneous, single-phase material that elicits the same response in a measuring device.

Introduction

Measurements of electrical properties of soils began at the end of nineteenth century (e.g., Briggs, 1899; Wenner, 1915; Smith-Rose, 1933; Archie, 1942). The low-frequency (Hz to kHz) electrical conductivities of soils (σ_{DC}) are in the range of $0.001\text{--}2 \text{ dSm}^{-1}$ and their high-frequency (MHz to GHz) dielectric constants (ϵ_∞) possess values of $3\text{--}50$. As such, soils can be classified as good conductors ($\sigma/(2\pi f\epsilon) >> 1$), inhibiting the propagation of electromagnetic (EM) waves at low frequencies (adequately described mathematically by the diffusion equation), and as low-loss dielectrics ($\sigma/(2\pi f\epsilon) << 1$) at high frequencies (where EM wave propagation is adequately described by the wave equation). The low-frequency (LF) electrical conductivity (σ_{DC}) and the high-frequency (HF) dielectric constant (ϵ_∞) are the more commonly measured and modelled electrical properties, as they serve for evaluating the soil water content and soil solution salinity. Thus, the scope of this entry is limited to the "static" (frequency-invariant) features of these two properties. The reader interested in the

frequency response (dispersion, relaxation) of the soil conductivity and permittivity is referred to other manuscripts (Dukhin, 1971; Santamarina et al., 2001). The following entries list the common methods for measuring the soil's LF σ_{eff} and HF ϵ_{eff} , discuss in brief their dependence on the various compositional, geometrical, and interfacial soil attributes, and review major empirical and physical models for describing σ_{eff} and ϵ_{eff} .

Electrical conductivity (EC)

Methods of measurement of low-frequency σ_{eff}

The three common methods for measuring the soil LF (Hz to kHz) electrical conductivity are: (1) Direct (contact) electrical resistivity, ER, based on injecting current through two electrodes and measuring the voltage drop in two other electrodes via four-probe arrays (Rhoades and van Schilfgaarde, 1976; Binley and Kemna, 2005); (2) Electromagnetic induction (EMI) based on inducing a magnetic field in the soil via a transmitter and measuring the secondary magnetic field via a receiver antenna (Everett and Meju, 2005); and (3) Time Domain Reflectometry (TDR) based on measuring the attenuation of an electromagnetic wave travelling through a waveguide inserted in the soil (Dalton et al., 1984; Robinson et al., 2003). ER operates at various modes, for example, shaft-mounted four-electrode inserted after pre-augering and surface arrays and between boreholes, and in a broad range of spatial scales from millimeters to kilometers, EMI devices usually measure to depths from 1 m to tens of meters and the TDR probes are usually about 10 cm long. The commonly used frequency range for the soil σ_{DC} determination in the field is about 100 Hz to several kHz, because at lower frequencies electrode polarization interferes with the readings and at higher frequencies (kilo- to megahertz) the EC is no longer constant at the DC value, but increases with frequency.

Soil attributes affecting σ_{eff} and its modelling

An unsaturated soil is considered to be a three-phase, solid–water–air system. The minerals constituting the solid phase of soils are nonconducting ($\sigma_s = 0$), as, of course, is the air ($\sigma_A = 0$), so that the only conducting phase is the aqueous solution, which has an intrinsic specific electrical conductivity of σ_W (Sm^{-1}). For these reasons, in certain circumstances, especially when σ_W can be reliably evaluated, measurements of the soil effective EC (σ_{eff}) can be used for evaluating volumetric water contents (θ) and, as a special, two-phase case, the porosity (n) of water-saturated soils.

The *major factors that affect σ_{eff}* can be grouped into three categories: Those in the first category describe the *bulk soil* and define the respective volumetric fractions occupied by the three phases and possible secondary structural configurations (aggregation): porosity (n), water content (θ), and structure. Factors in the second category are the important *solid particle* quantifiers, which are relatively time invariable: particle shape and orientation, particle-size

distribution, cation-exchange capacity, and wettability. Factors in the third category are the relevant *soil solution* attributes, and as these change quickly in response to alterations in management and environmental conditions, we may also call them *environmental* factors: ionic strength (σ_W), cation composition (SAR, Sodium Adsorption Ratio $\equiv (\text{Na}^+)/((\text{Ca}^{2+} + \text{Mg}^{2+})/2)^{1/2}$), and temperature. As stated above, the soil solution is the only conducting phase, which is why its volumetric fraction (n in a water-saturated soil and θ in unsaturated soils) and conductivity (σ_W) are the two dominant factors in determining σ_{eff} . Nevertheless, the geometry and topology of the aqueous phase is determined by the solid-phase attributes. Furthermore, the contribution of the adsorbed cations to the overall soil σ_{eff} , significant for medium- and fine-textured soils, is also determined mostly by the soil's cation-exchange capacity, which is a solid-phase attribute.

Archie's empirical law (Archie, 1942) is the most widely used relationship to relate σ_{eff} of water-saturated rocks and soils to their porosity (n) and solution EC (σ_W):

$$\sigma_{eff} = \frac{\sigma_W}{F} = \sigma_W n^m \quad (9)$$

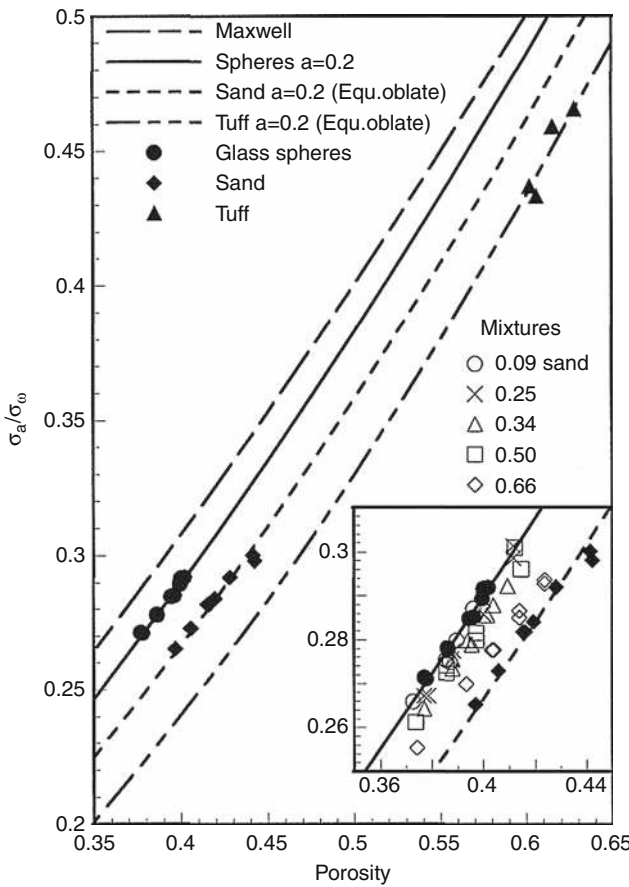
The electrical formation factor $F (= n^{-m})$ is an intrinsic measure of the microgeometry of the soil. Archie found that the exponent m ranged from 1.3 for unconsolidated sands to approximately 2.0 for consolidated sandstones, and a broader range from 1.2 to 4.4 for other granular materials is tabulated elsewhere (Lesmes and Friedman, 2005). As m increases with cementation, Archie termed it the cementation index. For granular, unconsolidated media such soils m increases as the grains become less spherical while variations in grain size and sorting has little effect on m (Jackson et al., 1978). For packings of mono-size glass spheres, sand particles, and tuff particles, characterized as oblate particles of aspect ratios of 1, 0.48, and 0.33, for example, the best-fitted m values were 1.35, 1.45, and 1.66 (Friedman and Robinson, 2002).

One possible constructive physical approach for describing the $\sigma_{eff}/\sigma_W(n)$ relationship of coarse-textured soils is to adopt *mean field theories* (also termed "mixing laws" or "mixing models") (Sihvola, 1999; Torquato, 2002; Wang and Pan, 2008). These theories deal with the actual three-dimensional structure of the multiphase medium or with its idealized geometrical description, referring to one phase as inclusions immersed in a host material representing the second phase. The universal expression of Sihvola and Kong (1988) for the effective conductivity (σ_{eff}) of spherical, nonconducting ($\sigma_s = 0$) particles, for example, is

$$\sigma_{eff} = \sigma_W + \left\{ \left[\frac{(n-1)\sigma_W [\sigma_W + v(\sigma_{eff} - \sigma_W)]}{\frac{2}{3}\sigma_W + v(\sigma_{eff} - \sigma_W)} \right] \cdot \left[1 - \frac{\frac{1}{3}(n-1)\sigma_W}{\frac{2}{3}\sigma_W + v(\sigma_{eff} - \sigma_W)} \right]^{-1} \right\} \quad (10)$$

which contains a heuristic parameter, v , that accepts values between 0 and 1 and accounts for the effect of neighboring particles on the internal electrical field of a reference particle. Best-fitting the heuristic mixing parameter v of [Equation 10](#) to the measured $\sigma_{\text{eff}}/\sigma_W(n)$ relationship for packings of glass spheres ([Figure 1](#)) resulted in $v = 0.2$ ([Friedman and Robinson, 2002](#)).

[Equation 10](#) applies to spherical particles, but the most important geometrical soil attribute with regard to its $\sigma_{\text{eff}}/\sigma_W(n)$ relationship is probably *particle shape*, which varies from almost spherical sand grains to flat, disklike and long, needlelike clay tactoids. It is practically impossible to calculate the effective conductivity of packings of angular and rough-surfaced particles, but these features were found to be of secondary importance in their effects on σ_{eff} ([Friedman and Robinson, 2002](#)). Representing the



Electrical Properties of Soils, Figure 1 Ratio of the effective (apparent) electrical conductivity (σ_{eff}) to that of the solution (σ_W) as a function of the porosity. Lines represent [Equation 28](#) with the value of $v = 0.2$ (denoted a in the legend) fitted to the glass spheres data. The main graph shows the glass spheres, sand (aspect ratio of $a/b = 0.46$), and tuff ($a/b = 0.35$) particles, where the aspect ratios have been adjusted to fit the data. The inset graph shows data for sand mixed in glass spheres ([From Friedman and Robinson \(2002\)](#). Reproduced by permission of the American Geophysical Union, Copyright (2002) AGU).

particle geometry as an ellipsoid of revolution (spheroid) provides both convenient analytical expressions and sufficient flexibility for transformation into a variety of shapes by altering the aspect ratio ([Sihvola and Kong, 1988](#); [Sareni et al., 1997](#); [Jones and Friedman, 2000](#)). By extending or contracting the b and c axes while keeping a constant, one can transform a sphere into either a disklike (oblate) or needle-shaped (prolate) particle, such as are often encountered in the natural environment. Particle shape is then incorporated in σ_{eff} modelling through a parameter named the depolarization factor (N^i), which describes the extent to which the inclusion polarization is reduced according to its shape and orientation with respect to the applied electrical field. For the special cases of ellipsoids of revolution ($a \neq b = c$), [Jones and Friedman \(2000\)](#) found that $N^a(a/b)$ can be satisfactorily approximated ($r^2 = 0.9999$) by a single empirical expression,

$$N^a = \frac{1}{1 + 1.6(a/b) + 0.4(a/b)^2}; \quad (11)$$

$$N^b = N^c = \frac{1}{2}(1 - N^a)$$

through the whole range of aspect ratios, a/b , from thin disks to long needles. The depolarization factors are: for a sphere, in which a , b , and c are all equal in length $N^{a,b,c} = 1/3, 1/3, 1/3$; for a thin disk (extreme oblate), 1, 0, 0, respectively; and for a long needle (extreme prolate), 0, $1/2$, $1/2$, respectively. The particle aspect ratio, a/b , of coarse-textured soils can be retrieved from databases, evaluated directly by visual inspection under magnification, or determined indirectly by the simple angle of repose measurement ([Friedman and Robinson, 2002](#)).

Nonspherical particles can form either *anisotropic* or *isotropic* packings, depending on whether they are preferentially aligned in the same direction or are randomly oriented. The effective conductivity of nonspherical particles, aligned to form a uniaxial–anisotropic medium, is no longer a scalar, but is a second-order tensor, defined by its diagonal components $\sigma_{\text{eff}}^a \neq \sigma_{\text{eff}}^b = \sigma_{\text{eff}}^c$ ([Sihvola and Kong, 1988](#)), and horizontal σ_{eff} (parallel to bedding planes) are usually larger than vertical σ_{eff} (perpendicular bedding planes) for both water-saturated and unsaturated media ([Friedman and Jones, 2001](#)). However, slightly nonspherical particles can be oriented almost randomly and form an approximately isotropic medium with a scalar σ_{eff} modelled as ([Sihvola and Kong, 1988](#)):

$$\sigma_{\text{eff}} = \sigma_W + \left\{ \left[\sum_{i=a,b,c} \frac{(n-1)[\sigma_W + v(\sigma_{\text{eff}} - \sigma_W)]\sigma_W}{3[\sigma_W + v(\sigma_{\text{eff}} - \sigma_W) - N^i \sigma_W]} \right] \cdot \left[1 - \sum_{i=a,b,c} \frac{(n-1)N^i \sigma_W}{3[\sigma_W + v(\sigma_{\text{eff}} - \sigma_W) - N^i \sigma_W]} \right]^{-1} \right\} \quad (12)$$

Friedman and Robinson (2002) measured the $\sigma_{eff}/\sigma_W(n)$ relationships of also packings of sand and tuff particles (and sand–glass spheres mixtures) (Figure 1). Keeping $v = 0.2$ (fitted for the spherical glass spheres), and adjusting the aspect ratios of the sand and tuff particles to provide a best fit to their $\sigma_{eff}/\sigma_W(n)$ measurements gave a/b values of 0.46 and 0.35 (oblate shaped: $a < b = c$), respectively, which are remarkably similar to those determined from the repose angle measurements (i.e., 0.48 and 0.33, and also to particle shape factors, $4\pi Area/Perimeter^2$, determined by image analysis of two-dimensional particle micrographs) and to those predicting the $\varepsilon_{eff}(n)$ relationships of these packings (Figure 5).

The effect of the soil's *particle-size distribution (PSD)* on its σ_{eff} is expected to be less pronounced than those of particle shape and orientation (similarly to its effect on ε_{eff} , discussed below), slightly decreasing the $\sigma_{eff}/\sigma_W(n)$ relationships as the width of the PSD increases (Robinson and Friedman, 2005).

Archie's (1942) law for describing the dependence of σ_{eff} of *unsaturated* soils and rocks on their saturation degree ($S \equiv \theta/n$) is

$$\sigma_{eff}(S) = \sigma_{sat} S^d \quad (13)$$

where σ_{sat} is the effective conductivity of the fully saturated soil. The saturation index (d) was observed to be about 2 for consolidated rocks and to range from 1.3 to 2 for unconsolidated sands (e.g., Schön, 1996). This power law was observed to hold down to saturations of about 0.15–0.20. At lower saturations, the power law breaks down, especially in fine-textured soils, as surface effects become dominant. In the absence of surface conductivity, the extended form of Archie's law can be used to predict the effective conductivity of partially saturated soils:

$$\sigma_{eff} = \sigma_W n^m S^d \quad (14)$$

The saturation index is usually larger than the cementation index ($d > m$), because as saturation decreases, the water films surrounding the grains become thinner and the conducting paths become more tortuous. Gorman and Kelly (1990), for example, obtained average best-fitted values of $m = 1.30$ and $d = 1.53$ for various Ottawa sand mixtures. Ament et al. (2000) assumed for simplicity that $m = d$ in Archie's model, and obtained an average, best-fitted exponent of $m = 1.58$ for sandy loam soils. The commonly used semiempirical model of Mualem and Friedman (1991) relating σ_{eff} to the soil pore-size distribution (as inferred from its water retention characteristics, $\psi(S_e)$, ψ (m) being the matric head), and a tortuosity factor, θ^λ

$$\sigma_{eff}/\sigma_W = \theta^\lambda \left[\int_0^{S_e} \frac{dS_e}{\psi} \right]^2 / \int_0^{S_e} \frac{dS_e}{\psi^2} \quad (15)$$

predicts that $m = 1 + \lambda$ and $d = 2 + \lambda$, where λ is a tortuosity exponent that for coarse-textured soils can be taken as 0.5,

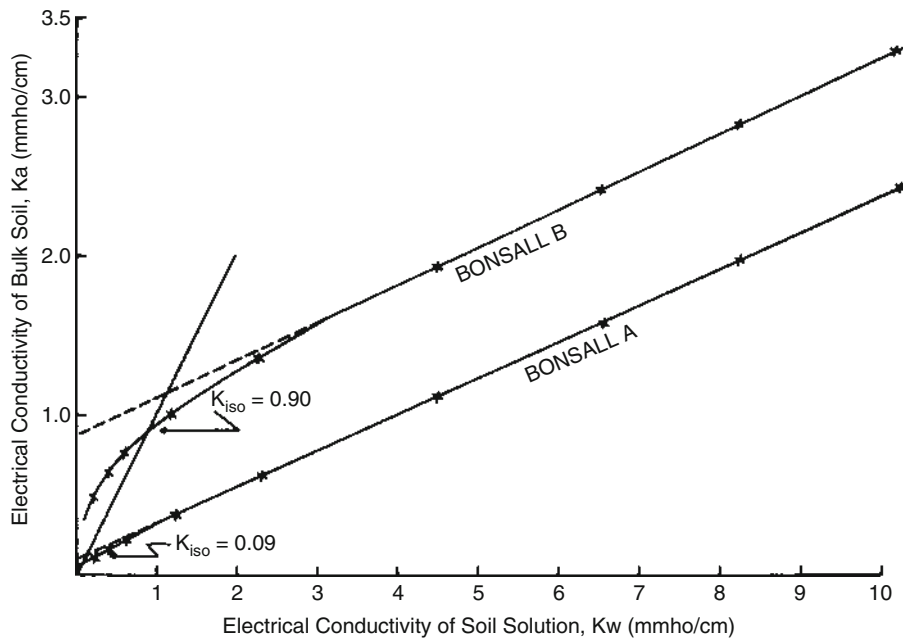
making $m = 1.5$ and $d = 2.5$. In general, λ can be best-fitted to the $\sigma_{eff}/\sigma_W(\theta)$ and $\psi(S_e)$ measurements (Weerts et al., 1999). Mualem and Friedman's (1991) model does not refer to the whole liquid phase volume but subtracts from both n and θ a noncontributing volume (θ_0) close to the solid surfaces, which they proposed to estimate as the water content at wilting point (matric pressure of -1.5 MPa) that correlates well with the specific surface area and clay fraction of the soil. The effective degree of saturation in Equation 15 is then defined as $S_e \equiv (\theta - \theta_0)/(n - \theta_0)$. Equation 15 can also be written as $\sigma_{eff}/\sigma_W = \theta^{2+\lambda}/n$, and Persson (1997), for example, best-fitted a λ value of about 0.2 to $\sigma_{eff}/\sigma_W(\theta)$ measurements in a sand ($n = 0.38$), homogeneously packed into short ($\lambda = 0.25$) or long ($\lambda = 0.16$) columns. An earlier attempt to relate the $\sigma_{eff}/\sigma_W(\theta)$ relationship to the soil's pore-size distribution was made by Nadler (1982) who noticed that the formation factor–water content function, $F(\theta)$, resembles the shape of the soil water retention curve, $\psi(\theta)$. Therefore, he suggested the use of an expression of the form $F(\theta) = a\psi$ in which a is an empirically determined proportionality constant for the relatively dry region, while for the relatively wet region he suggested using Burger's (1919) two-phase mixing law, arbitrarily extended to an unsaturated soil: $F(\theta) = 1 + k(1-\theta)/(\theta)$ in which k is an empirically determined, S -independent particle shape factor.

In fine-grained soils or in nonsaline (low σ_W) conditions, the *contribution of adsorbed ions (surface conduction)* to σ_{eff} can be significant and the $\sigma_{eff}(\sigma_W)$ relationship is nonlinear (Figure 3). The most frequently applied simplifying assumption is that σ_{eff} can be regarded as being replaced by two conductors in parallel, one representing the free-solution ions (σ_W/F) and the other the adsorbed ones ($\sigma_{surface}$) (Waxman and Smits, 1968; Rhoades et al., 1976; Shainberg et al., 1980; Nadler, 1982; Mualem and Friedman, 1991):

$$\sigma_{eff} = \frac{\sigma_W}{F} + \sigma_{surface} \quad (16)$$

The solution and surface conduction mechanisms do not strictly act in parallel in the macroscopic, soil sample scale, but only in the single-pore scale.

The decoupling assumption embedded in Equation 16 is thus physically inappropriate for application to a locally heterogeneous medium and its use can lead to a significant overestimation of σ_W/F , especially for media of high cation-exchange capacity, broad pore-size distribution, and low connectivity (Friedman, 1998b). Yet, this simple parallel-conduction model has several practical advantages. One major advantage is that F and $\sigma_{surface}$ (if assumed to be σ_W -independent) can be easily estimated by plotting on a linear scale σ_{eff} versus σ_W (Figure 2). The formation factor can be then estimated from the slope of the linear portion of the $\sigma_{eff}(\sigma_W)$ plot at high σ_W , and the σ_W -independent assumed $\sigma_{surface}$ (for high enough σ_W ; e.g., $\sigma_W > 4$ dSm $^{-1}$ in Figure 2) can be estimated from the extrapolated y -intercept at $\sigma_W = 0$. At relatively saline solutions, both $\sigma_{eff}(\sigma_W)$ functions are linear with similar



Electrical Properties of Soils, Figure 2 The effective electrical conductivity, σ_{eff} (denoted here K_a) of water-saturated Bonsall soil from the A and B horizons as a function of the electrical conductivity of the soil solution, σ_w (denoted here K_w). K_{iso} is the isoconductivity point where $\sigma_{eff} = \sigma_w$ (From Shainberg et al., 1980. Reproduced by permission of the Soil Science Society of America).

slopes (0.225 and 0.235 for the A and B horizons, respectively) regardless of the different clay percentage of the two soil horizons. At low σ_w , the two $\sigma_{eff}(\sigma_w)$ relationships are nonlinear, especially that of the clayey B horizon (35% clay versus 8% of the A horizon). Shainberg et al. (1980) studied the effects of CEC (*cation-exchange capacity*) and ESP (*exchangeable sodium percentage*) in conditions of nonlinear $\sigma_{eff}(\sigma_w)$ relationships and found that the contribution of the surface conductance to σ_{eff} (as indicated by the intercept of the tangent line at $\sigma_w=0$) increases with increasing CEC (/clay content). Although less conclusive, the surface conductivity was also found to increase with the ESP (or corresponding SAR) levels, probably because of the higher electrical mobility of the adsorbed sodium ions as compared to calcium. Based on other studies, Rhoades et al. (1999) concluded that the $\sigma_{eff}(\sigma_w)$ relationship does not depend on the soil ESP(SAR), provided soil structure and porosity have not been seriously degraded by the sodicity.

Among *empirical functions* proposed by soil scientists for describing the $\sigma_{eff}(\sigma_w, \theta)$ relationship, the most commonly used is that of Rhoades et al. (1976) who referred to $\sigma_{surface}$ as essentially independent of θ and σ_w and wrote Equation 16 as:

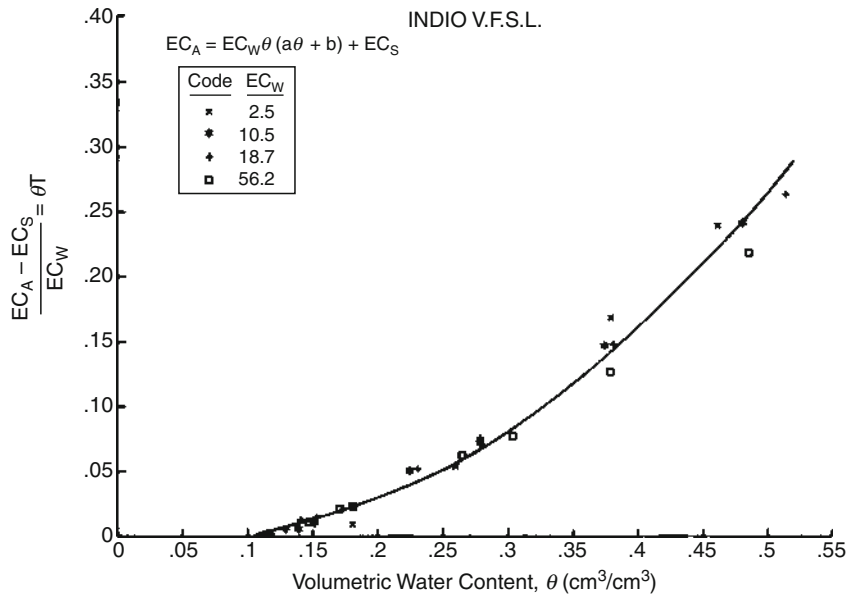
$$\sigma_{eff} = T(\theta)\theta\sigma_w + \sigma_{surface}; T(\theta) = a\theta + b \quad (17)$$

The transmission coefficient (T) is assumed to be a linear function of θ . The empirical parameters a and b

varied among different soils: $a = 2.1, b = -0.25$ for clay soils; and $a = 1.3-1.4, b = -0.11 - , -0.06$ for the other three loam soils discussed in their 1976 article. An example of a transmission coefficient best-fitted to $\sigma_{eff}(\sigma_w, \theta)$ measurements at 4 σ_w levels in a very fine sandy loam (6% clay, 52% silt) is presented in Figure 3 with $T(\theta)\theta = 1.2867\theta^2 - 0.1158\theta$ plotted. It is seen that $T(\theta)\theta$ is indeed a parabolic function of θ , virtually independent of σ_w , validating the applicability of the simplified, two-conductor model (Equations 16 and 17) for saline conditions.

The surface conductivity term should increase with the solution EC which was addressed by various empirical expressions, with parameters accounting for the cation-exchange capacity (surface charge density) and electrical mobility of exchangeable cations (Waxman and Smits, 1968; Nadler et al., 1984; Sen et al., 1988), that were also correlated to easily measured textural characteristics, for example, the hygroscopic water content (Nadler et al., 1984) or Archie's cementation exponent (Sen et al., 1988).

The effects of soil microgeometry, mineralogy, and solution chemistry on the *surface conductivity term* ($\sigma_{surface}, \text{Sm}^{-1}$) of Equations 16 and 17 should reflect the interfacial electrical charge density, the equivalent counterions mobility, and the tortuosity of the surface paths, which is similar to, but not necessarily equal to, the tortuosity of the pore paths. Toward this end, it is required to model the electrical double layer (EDL) that forms on the surface of the mineral grains and to evaluate the intrinsic (specific) surface conductance, $Z_{surface}$ (S), which usually possesses values in the range of



Electrical Properties of Soils, Figure 3 Plot of $(\sigma_{eff} - \sigma_{surface})/\sigma_W = T(\theta)\theta$ according to Equation 17 of measured $\sigma_{eff}(\sigma_W, \theta)$ data for Indio very fine sandy loam equilibrated with solutions of different σ_W (given in $dS m^{-1}$). The solid line represents Equation 17 with the best-fitted transmission coefficient: $T(\theta) = 1.2867\theta - 0.1158$ (From Rhoades et al., 1976. Reproduced by permission of the Soil Science Society of America).

10^{-9} – 10^{-8} S. The specific surface conductance represents the conduction in the fixed (Stern), usually assumed negligible for σ_{DC} , and diffuse parts of the EDL.

A comprehensive, rigorous discussion of the effect of surface conductance on $\sigma_{eff}(\sigma_W, \theta)$ would be too long for this entry and is also not relevant for most practical applications because there are too many unknown parameters involved. The interested reader is, therefore, referred to other publications using single-grain σ_{eff} models for incorporating the contribution of $Z_{surface}$ (e.g., Kan and Sen, 1987; Johnson and Sen, 1988; Schwartz et al., 1989; Lyklema, 1995; Revil and Glover, 1997, 1998; Revil et al., 1998). Also three-dimensional networks of conductors can be used to model the interactions between the bulk and surface conduction mechanisms (e.g., Bernabe and Revil, 1995; Friedman, 1998b). However, these network models are not very applicable in practical applications. From the practical point of view, it should be noted that measuring methods such as induced polarization (Lesmes and Frye, 2001) can be applied in the field and have the potential merit of assisting in differentiating the contributions of surface and bulk fluid conductivities to the measured σ_{eff} .

The electrical conductivity of free solution (σ_w) increases by about 2% per $1^\circ C$ (around $25^\circ C$, corresponding to the decrease of the free water viscosity) and a similar $temperature(T)$ -dependence effect is to be expected for σ_{eff} of coarse-textured soils so that the reduced conductivity, σ_{eff}/σ_w , is temperature independent. However, in clayey soils that exhibit significant surface

conduction, the counterion mobility increases more sharply with temperature and the $\sigma_{eff}(T)$ relationship is more complex (Clavier et al., 1984; Sen and Goode, 1992; Wraith and Or, 1999). Sen and Goode (1992), for example, present slopes from 0.02, corresponding to the slope of free solution, to 0.12 of $\sigma_{eff}(T)$ measurements at high σ_w for shaly sands containing varying amounts of clay.

Dielectric permittivity

Methods of measurement of high-frequency ϵ_{eff}

The common methods for measuring the soil high-frequency (MHz to GHz) permittivity are (in order of increasing frequencies with some overlaps): (1) Capacitance probes, based on measuring the operating frequency in an oscillator circuit (Blonquist et al., 2005; Skierucha and Wilczek, 2010); (2) Impedance probes, based on measuring the reflection coefficient of a standing wave (Gaskin and Miller, 1996; Blonquist et al., 2005); (3) Ground Penetrating Radar (GPR) based on measuring the propagation velocity of transmitted, free electromagnetic (EM) waves (Annan, 2005); and (4) TDR based on measuring the propagation velocity of EM waves travelling through waveguides (Topp et al., 1980; Robinson et al., 2003). The in situ capacitance, impedance, and TDR probes are all few centimeters long, and GPR can operate in resolutions of few centimeters to tens of meters for GHz to MHz frequencies, from either above the soil surface or between boreholes.

Soil attributes affecting ε_{eff} and its modelling

The problems of determining the effective electrical conductivity and the effective dielectric permittivity, based on the volumetric fractions and geometrical attributes of the three soil phases, $\sigma_{eff}(\sigma_S, \sigma_W, \sigma_A, n, \theta)$ and $\varepsilon_{eff}(\varepsilon_S, \varepsilon_W, \varepsilon_A, n, \theta)$, are mathematically analogous: Both involve solving the Laplace equation for the potential while preserving the continuity of the potentials and normal fluxes at the interfaces between the phases. The major difference is that while for EC only one phase is conducting ($\sigma_W > 0, \sigma_S = \sigma_A = 0$), for the permittivity all three solid, water, and air phases are “conductive” (in the mathematical sense) and possess intrinsic, single-phase, 100 MHz-GHz permittivities of approximately 5, 80, and 1, respectively. Although the *permittivity contrasts* are finite (as opposed to $\sigma_W/\sigma_S = \sigma_W/\sigma_A = \infty$), as the permittivity of water, stemming from orientation polarization, is much higher than those of the other two phases ($\varepsilon_W/\varepsilon_S \approx 16; \varepsilon_W/\varepsilon_A \approx 80$), the soil’s ε_{eff} is very sensitive to its volumetric water content, which explains the merit of the dielectric methods for determining the volumetric water content (θ) of partially saturated and the porosity (n) of water-saturated soils and rocks. The large enough contrast between the permittivities of earth minerals and air ($\varepsilon_S/\varepsilon_A \approx 5$) is also usually sufficient for determining the porosity of dry soils and rocks, but the measured ε_{eff} is less sensitive to n than that of water-saturated media. For real multiphase media such as wet soils, the Laplace equation can be solved by numerical methods if their complex geometry can be reliably characterized and discretized. Another option is to refer to a simplified geometry of some common representative quantifiers and to solve the electrostatic problem for the transformed medium. An exact analytical solution to the Laplace equation does not exist even for the most simplified mixture geometry one can conceive (Robinson and Friedman, 2005; Doyle et al., 2007). Therefore, the common practice is to apply some approximating assumptions regarding the spatial structure of the electrical fields in the different phases, a concept which we term here mean field theories.

The *major factors determining the effective permittivity of soils* are volumetric water content, porosity, particle shape and orientation, particle-size distribution, mineralogy, and temperature.

The three components version of the refractive index (RI) model (Birchak et al., 1974), which accounts for only the *volumetric fractions of the three phases*, is (Alharthi and Lange, 1987; Whalley, 1993; Robinson et al., 1999)

$$\varepsilon_{eff}^{\frac{1}{2}} = \theta \varepsilon_W^{\frac{1}{2}} + (n - \theta) \varepsilon_A^{\frac{1}{2}} + (1 - n) \varepsilon_S^{\frac{1}{2}} \quad (18)$$

The physical assumption behind Equation 18 (sometimes referred to as time propagation equation (Wharton et al., 1980) or ray theory (Chan and Knight, 2001)) is that the travel time of an EM wave in a two-phase medium is a summation of three travel times: in the solids, water, and air, as if propagating in a direction perpendicular to the layering of these phases. Each single-phase travel

time is proportional to the layer thickness, namely, to the volumetric fraction of the phase, and to its propagation velocity, which is proportional to $1/\sqrt{\varepsilon_i}$ of that phase. This three-phase layers arrangement is, of course, a very poor description of the real geometry of the soil’s mineral skeleton, and the water-phase configuration in the compliant pore system. In addition, when the wavelength (centimeters for GHz frequencies) is much larger than the solid particles (usually from micrometers to fractions of millimeters), the EM wave “does not see” the solid inclusions, but rather a single homogeneous mixture of a given permittivity, which we term here effective permittivity. The ε_{eff} depends on the single-phase permittivities and volumetric fractions according to a different physics, which allows for the concentration of the conducting paths in the more conducting phases and for the circumventing of the isolating objects.

The most commonly used *empirical $\varepsilon_{eff}(\theta)$ relationship* nowadays, rightly, is the “universal” formula of Topp et al. (1980):

$$\varepsilon_{eff} = 3.03 + 9.3\theta + 146\theta^2 - 76.7\theta^3 \quad (19)$$

which was best-fitted to careful measurements made on four soil types and was suggested to hold approximately for all types of mineral soils. This relationship was found to give good predictions, mostly for coarse- and medium-textured soils (Dirksen and Dasberg, 1993; Friedman, 1998a), and was also found close to relationships resulting from different theoretical approaches (Van Loon et al., 1991; Friedman, 1997, 1998a). Comparing the $\varepsilon_{eff}(\theta)$ relationships of various soils to the functional water content dependencies of other transport properties (electrical and thermal conductivities, solute and gas molecules diffusivities, and hydraulic conductivity) reveals that the $\varepsilon_{eff}(\theta)$ relationship is indeed less strongly dependent on soil type as compared to the other transport parameters. Yet, as expected on physical grounds and observed in many experimental studies, the $\varepsilon_{eff}(\theta)$ relationship does depend on the soil textural and mineralogical properties (Hoekstra and Delaney, 1974; Wang and Schmugge, 1980; Dobson et al., 1984; Dirksen and Dasberg, 1993; Heimovaara et al., 1994; Friedman, 1998a) in a complicated manner and in some cases to a significant extent.

Various other empirical equations have been suggested for the relationship between the MHz-GHz ε_{eff} and θ (Wang and Schmugge, 1980; Hallikainen et al., 1985; Roth et al., 1992; Malicki et al., 1996), mostly polynomial functions, in some cases describing the relationships reliability by allowing their coefficients to be dependent on, for example, the clay and sand percentage (Dobson et al., 1984) or on the bulk density and clay and organic matter contents (Jacobsen and Schjønning, 1993). Another empirical approach is to replace the $1/2$ exponent of the RI model with a free parameter, which is supposed to account for some of the determining factors. Roth et al. (1990), for example, found an optimal exponent of 0.46, which is another support for the empirical merit of the RI model.

Replacing the $\frac{1}{2}$ exponent of [Equation 18](#) with $\frac{1}{3}$ results in the Loyenga's ([1965](#)) mixing model, which is not superior to the RI model from both theoretical and empirical aspects ([Robinson and Friedman, 2003](#)). The only explainable exponents of the RI-type model are the two extreme values of 1 (arithmetic mean) and -1 (harmonic mean), which refer to the three phases arranged unrealistically in parallel layers with the applied electrical field directed parallel (1) or perpendicular (-1) to the layering. These two relationships constitute the most extreme theoretical upper and lower bounds (known as Wiener bounds, [Sihvola, 1999](#)) to the $\epsilon_{eff}(\theta)$ relationship, and any outside measurements or theoretical results should be doubted.

Most of the theoretical approaches for relating ϵ_{eff} of dielectric mixtures to their constituents volumetric fractions and single-phase permittivities fall into one of the two major conceptual categories of discrete capacitor network models ([Ansoult et al., 1985](#); [Friedman, 1997](#); [Tabbagh et al., 2000](#)), which will not be discussed here and continuum *mean field theories* or “*mixing models*” ([Sihvola, 1999](#)). One example is the Maxwell–De Loor mixing model, which assumes the solid phase to be a host medium for randomly distributed and oriented disk-shaped inclusions of the other phases ([De Loor, 1968](#)). The assumption of a continuous solid phase may be adequate for some low-porosity rocks, but not for soils. A more realistic description of the soil aqueous phase, at least at intermediate and high water contents, is probably not that of disconnected inclusions, but of a continuous background phase. [Friedman \(1998a\)](#) studied the role of the configuration of the three soil phases by extending the two-phase Maxwell-Garnett ([1904](#)) formula (MG) to two-phase composite spherical inclusions (a core of ϵ_2 surrounded by a concentric shell of ϵ_1) immersed in the third phase (of ϵ_0) serving as the background. The resulting MG-type mixing model for the effective permittivity of a three-phase mixture, $\epsilon_{eff}(\epsilon_0, \epsilon_1, \epsilon_2, f_1, f_2)$, of volumetric fractions f_1, f_2 , and $f_0 (= 1 - (f_1 + f_2))$ is ([Tinga et al., 1973](#); [Friedman, 1998a](#)):

$$\epsilon_{eff} = \epsilon_0 + \frac{3[(f_2 + f_1)(\epsilon_1 - \epsilon_0)(2\epsilon_1 - \epsilon_2) - f_2(\epsilon_1 - \epsilon_2)(2\epsilon_1 + \epsilon_0)]\epsilon_0}{\left[(2\epsilon_0 + \epsilon_1)(2\epsilon_1 + \epsilon_2) - 2\frac{f_2}{f_2 + f_1}(\epsilon_1 - \epsilon_0)(\epsilon_1 - \epsilon_2) \right]} \\ - \frac{[(f_2 + f_1)(\epsilon_1 - \epsilon_0)(2\epsilon_1 + \epsilon_2) + f_1(\epsilon_1 - \epsilon_2)(2\epsilon_1 + \epsilon_0)]}{(f_2 + f_1)} \quad (20)$$

There are six possible concentric arrangements of the three phases (attributing ϵ_S , ϵ_W , and ϵ_A to either ϵ_0 , ϵ_1 , or ϵ_2), and as the permittivity of water is much higher than that of the other components, it is especially the location of the water phase which dictates the resulting ϵ_{eff} . The minimal $\epsilon_{eff}(\theta)$ relationships correspond to configurations in which the water, with its significantly higher dielectric constant is encapsulated within the solid and gaseous phases (*WSA*). The maximal ϵ_{eff} values stem from an arrangement with permittivities increasing radially outward (*ASW*). The real configuration of the solid, water, and gaseous phases in soil is not a constant one, but varies

with the saturation degree. For low water contents, it is reasonable to assume that the gaseous phase is continuous and surrounding the solid and liquid phases. As the water content increases, the gaseous phase develops discontinuities and a better description is that of a continuous liquid phase surrounding the solid and gaseous phases. Thus, [Friedman \(1998a\)](#) proposed saturation-degree-dependent weight functions for two chosen dry (*SWA*) and wet (*ASW*) configurations:

$$f_w^{SWA} = 1 - S; f_w^{ASW} = S; S = \frac{\theta}{n} \quad (21)$$

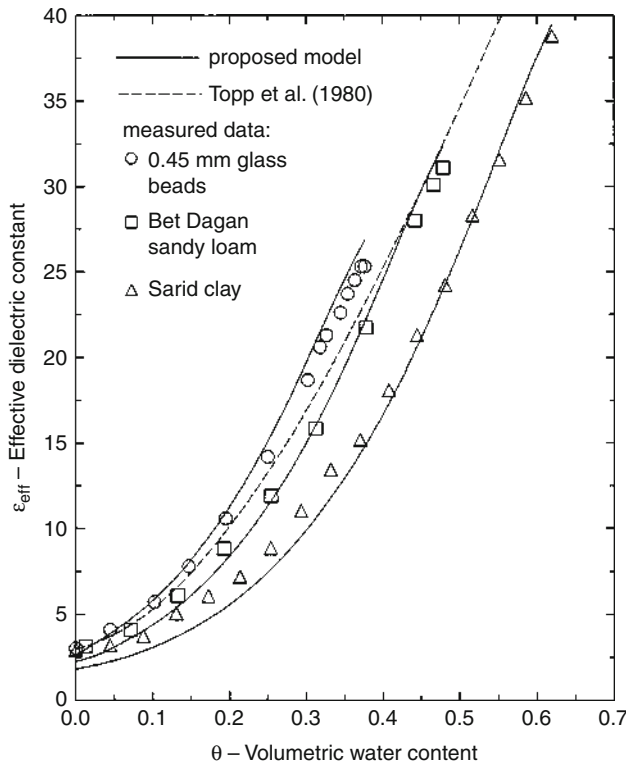
and representing their mutual contribution by the Effective Medium Approximation (EMA) ([Bruggeman, 1935](#)), which treats both components symmetrically. Applying the EMA equation to the dual *SWA-ASW* system (with $f_w^{SWA} + f_w^{ASW} = 1$) results in the following quadratic equation for ϵ_{eff} :

$$\epsilon_{eff} = \left\{ \frac{[f_w^{SWA}(\epsilon_{ASW} - 2\epsilon_{SWA}) + f_w^{ASW}(\epsilon_{SWA} - 2\epsilon_{ASW})]^2}{16} \right. \\ \left. + \frac{\epsilon_{SWA}\epsilon_{ASW}}{2} \right\}^{1/2} \\ - \frac{[f_w^{SWA}(\epsilon_{ASW} - 2\epsilon_{SWA}) + f_w^{ASW}(\epsilon_{SWA} - 2\epsilon_{ASW})]}{4} \quad (22)$$

This approach of macroscopic mixing of “percolating” (*ASW*, continuous water phase) and “non-percolating” (*SWA*, discontinuous water phase) configurations resembles (in this sense) the local porosity theory of [Hilfer \(1991\)](#), which refers to the local, microscopic porosities and percolation probabilities of the real, detailed structure of the porous medium. Replacing [Equation 20](#) with the corresponding expressions for confocal composite ellipsoidal inclusions ([Sihvola and Lindell, 1990](#)) applies it to nonspherical particles.

[Jones and Friedman \(2000\)](#) extended this approach to nonspherical particles and demonstrated reasonable agreements with directional ϵ_{eff} and ϵ_{eff} measurements in partially saturated anisotropic packings of mica particles. Extension of this approach for aggregated media, characterized by a bimodal pore-size distribution is provided in [Miyamoto et al. \(2005\)](#) and [Blonquist et al. \(2006\)](#).

The composite sphere model presented above ([Equations 20–22, Figure 4](#)) with $\epsilon_W \approx 80$ generally gives higher ϵ_{eff} values than the measured ones, especially for fine-textured soils of high specific surface area (usually associated with high porosity) and at low- and mid-range water contents. One main reason for this discrepancy is the inadequate attribution of an $\epsilon_W \approx 80$ value to the whole aqueous phase volumetric fraction. There is much experimental evidence ([Hoekstra and Delaney, 1974](#); [Dobson et al., 1985](#); [Dirksen and Dasberg, 1993](#); [Heimovaara et al., 1994](#); [Wraith and Or, 1999](#)), as well as theoretical arguments



Electrical Properties of Soils, Figure 4 Measured effective permittivities as a function of volumetric water content for three granular media (symbols), and their prediction according Friedman (1998a) composite sphere model (solid lines, Equations 20–22 and 24–26). Also shown is the universal function of Topp et al. (1980) (dashed line) (From Friedman (1998a). Reproduced by permission of the American Geophysical Union, Copyright (1998) AGU).

(Or and Wraith, 1999) to indicate that the GHz permittivities of the thin water films surrounding the soil particles are much lower than that of free water at the same temperature, frequency, and ionic strength (Kaatze, 1996). The presence of soil minerals affects the dielectric properties of the water molecules adjacent to their surfaces by restricting their rotational movements, thus reducing their polarizability and permittivity. This phenomenon can be very significant in fine-textured soils and is usually incorporated in $\epsilon_{eff}(\theta)$ modelling by adding a fourth, *bound water* phase of a lower permittivity (Dobson et al., 1985; Dirksen and Dasberg, 1993; Robinson et al., 2002). Dobson et al. (1985) added it as a fourth component, having volumetric fraction θ_{BW} and permittivity ϵ_{BW} , while extending the Maxwell–De Loor mixing model (De Loor, 1968) giving:

$$\epsilon_{eff} = \frac{3\epsilon_S + 2(\theta - \theta_{BW})(\epsilon_W - \epsilon_{BW}) + 2\theta_{BW}(\epsilon_{BW} - \epsilon_S) + 2(n - \theta)(\epsilon_A - \epsilon_S)}{3 + (\epsilon_S/\epsilon_{BW} - 1) + \theta_{BW}(\epsilon_S/\epsilon_{BW} - 1) + (n - \theta)(\epsilon_S/\epsilon_A - 1)} \quad (23)$$

Dirksen and Dasberg (1993) adopted this model and assumed that the soil minerals are surrounded by a single monomolecular layer of bound water of a GHz permittivity of 3.2, as that of ice, and that the rest of water are free water. One severe limitation of this approach is that the free and “bound” water are treated as two separate phases, randomly dispersed in the mixture and without any spatial correlation. This limitation can be overcome within, for example, the framework of the above-presented composite sphere model, by treating the neighboring free and “bound” water phases as two adjacent spherical shells. Robinson et al. (2002) suggested to evaluate the amount of bound water by the easily measurable hygroscopic water content of the soil, in agreement with the high correlation between the amount of hygroscopic water at 50% relative humidity and a single monomolecular layer found by Dirksen and Dasberg (1993), and to add a fourth, bound water phase to the RI model (Equation 18). Dobson et al. (1985) also tested the four-phase RI mixing model (with high bound water permittivities of 20–40) and found an optimal exponent of 0.65 for a variety of soil textures and several GHz frequencies.

A more physical treatment of the bound water phenomena was provided by Or and Wraith (1999) relating the dielectric relaxation frequency of the bound water to their viscosity according to the Debye (1929) model and incorporating the dependence of the water viscosity on its distance from clay surfaces according to Low's (1976) findings. For practical purposes, Or and Wraith (1999) proposed to characterize the bound water as a single layer with a temperature-independent permittivity of 12 and thickness determined by letting the relaxation frequencies of its water molecules be lower than a cutoff frequency of the measuring device (e.g., 1 GHz for a Tektronix 1502B Time Domain Reflectometer).

An alternative approach to incorporate bound water effects is to refer to a single water phase, its permittivity being dependent on the soil texture and water content. Friedman (1998a) suggested a pragmatic approach, assuming that the GHz permittivities of the soil solution grow in an exponential mode with the distance from the solid surface, x , from their minimal value at $x = 0$ (ϵ_{min}) to a maximum value corresponding to that of free water (at the given temperature, frequency, and solutes concentration, ϵ_{max}) according to a general scaling length, $1/\lambda$, common to all soil minerals:

$$\epsilon(x) = \epsilon_{min} + (\epsilon_{max} - \epsilon_{min})(1 - e^{-\lambda x}); \quad (24)$$

$$\epsilon_{min} = 5.5; \lambda = 10^8 \text{ cm}^{-1}$$

For evaluating the average, single-phase water permittivity (ϵ_W), Friedman (1998a) proposed to take the harmonic mean of $\epsilon(x)$ (Equation 24) resulting in

$$\epsilon_W(d_W) = \frac{d_W \epsilon_{max}}{d_W + \frac{1}{\lambda} \ln \left[\frac{\epsilon_{max} - (\epsilon_{max} - \epsilon_{min})e^{-\lambda d_W}}{\epsilon_{min}} \right]} \quad (25)$$

where the average thickness of the water shell (d_w) is calculated by dividing the volume of water contained in a volume of the bulk soil by the wettable surface areas of its solid phase, which for a unit soil volume means dividing the volumetric water content by the product of the soil bulk density (ρ_b , ML^{-3}) and specific surface area (S_{SA} , L^2M^{-1})

$$d_w = \frac{\theta}{\rho_b S_{SA}} \quad (26)$$

Figure 4 presents a test of the Friedman's (1998a) $\epsilon_{eff}(\theta)$ model against measurements with three granular materials, together with the Topp et al.'s universal function (Equation 19). It seems that the composite sphere model prediction is reasonable for all three media – coarse, medium, and fine textured – whereas Topp et al.'s function adequately describes only the $\epsilon_{eff}(\theta)$ curve of the medium-textured Bet Dagan sandy loam. The predictability of the Friedman's (1998a) composite sphere model, a capacitor-network model (Friedman, 1997), and other three empirical models (Topp et al., 1980; Dobson et al., 1984; Roth et al., 1992) was further tested against 19 additional measured $\epsilon_{eff}(\theta)$ curves of mineral porous media of a broad textural range, taken from published reports of measurements under controlled conditions (n , temperature) and which provide information on the ρ_b (/n) of the packed samples, on the S_{SA} or on the soil texture, from which S_{SA} can be estimated. Based on a root-mean-square-deviation test, it can be generally stated that the performance of all those five models is quite similar, with the composite-sphere model yielding the best predictability for the whole set of 22 media as well as for just the 18 natural soils. Therefore, if the soil porosity and specific surface area can be reasonably evaluated, and there is readiness to perform the simple spreadsheet calculations (Equations 20–22 and 24–26), it is recommended to use this physical model, bearing in mind its main strengths and weaknesses: it takes into account the saturation degree-dependent phase configurations and bound water (soil texture) effects, but it ignores *particle shape* effects, which are probably responsible for some of the differences among the $\epsilon_{eff}(\theta)$ relationships of the three media presented in **Figure 4**, which we are going to discuss next, referring to the two extremes of water-saturated and oven-dry media.

Firstly, we present the universal mixing law for the two-phase effective permittivity, $\epsilon_{eff}(n, \epsilon_s, \epsilon_0)$, of spherical inclusions (the solid particles with permittivity ϵ_s) immersed in a background of permittivity ϵ_0 (either ϵ_w for water-saturated soils or ϵ_a for oven-dry soils) (Sihvola and Kong, 1988)

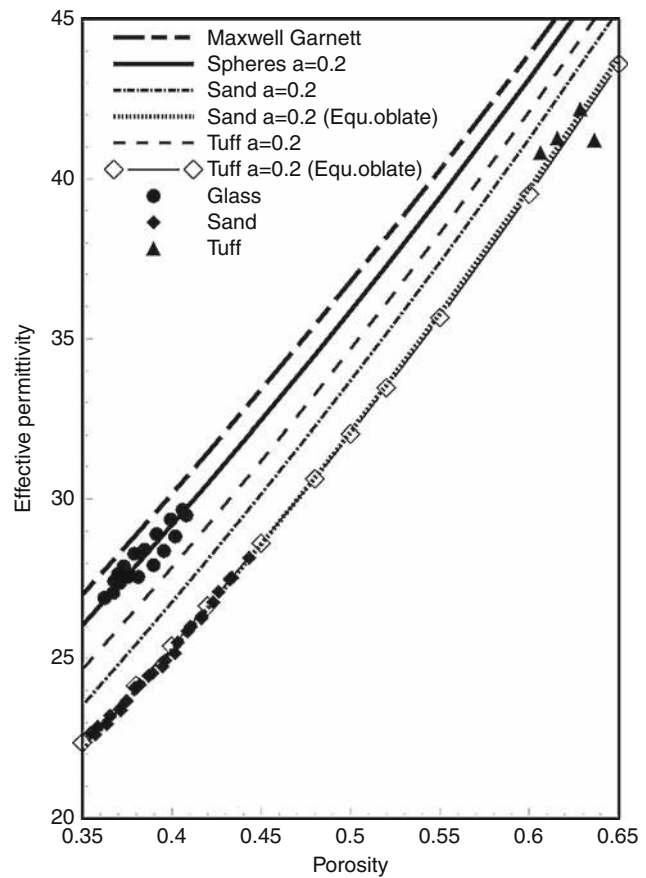
$$\epsilon_{eff} = \epsilon_0 + \left\{ \left[\frac{(1-n)(\epsilon_s - \epsilon_0)[\epsilon_0 + v(\epsilon_{eff} - \epsilon_0)]}{3[\epsilon_0 + v(\epsilon_{eff} - \epsilon_0) + (\epsilon_s - \epsilon_0)]} \right] \cdot \left[1 - \frac{(1-n)(\epsilon_s - \epsilon_0)}{3[\epsilon_0 + v(\epsilon_{eff} - \epsilon_0) + (\epsilon_s - \epsilon_0)]} \right]^{-1} \right\} \quad (27)$$

which is the analogue to the effective conductivity, $\sigma_{eff}(n, \sigma_w, \sigma_s = 0)$ expression (Equation 12), except for the solid phase being “conductive” ($\epsilon_s > 0$) for the $\epsilon_{eff}(n, \epsilon_s, \epsilon_0)$ problem. Keeping $v = 0.2$ (as for the $\sigma_{eff}(n)$ of glass spheres packings, **Figure 1**) results in a good prediction of the $\epsilon_{eff}(n)$ of water-saturated packings of glass spheres (**Figure 5**; Friedman and Robinson, 2002).

The extension of Equation 27 to randomly oriented spheroidal particles (the analogue to Equation 12) is (Sihvola and Kong, 1988).

$$\epsilon_{eff} = \epsilon_0 + \frac{\sum_{i=a,b,c} \frac{(1-n)[\epsilon_0 + v(\epsilon_{eff} - \epsilon_0)][\epsilon_s - \epsilon_0]}{3[\epsilon_0 + v(\epsilon_{eff} - \epsilon_0) + N^i(\epsilon_s - \epsilon_0)]}}{1 - \sum_{i=a,b,c} \frac{(1-n)N^i(\epsilon_s - \epsilon_0)}{3[\epsilon_0 + v(\epsilon_{eff} - \epsilon_0) + N^i(\epsilon_s - \epsilon_0)]}} \quad (28)$$

Measured $\epsilon_{eff}(n)$ relationships of the water-saturated glass spheres, sand particles, and tuff particles along with



Electrical Properties of Soils, Figure 5 Effective permittivity as a function of porosity for glass spheres ($\epsilon_s = 7.6$), quartz sand ($\epsilon_s = 4.7$), and tuff grains ($\epsilon_s = 6.0$). Predictions of permittivity are presented for equivalent oblates of $a/b = 0.465$ for sand and 0.364 for tuff. Note that the sand and tuff lie on lines close together due to the difference in the permittivity of the solid grains (From Friedman and Robinson, 2002. Reproduced by permission of the American Geophysical Union, Copyright (2002) (AGU)).

those evaluated by [Equation 28](#) are presented in [Figure 5](#), demonstrating remarkable prediction capability of the mixing model. This closure is also indicative of the merits and physical significance of the empirical relationship between the slope angle and the shape factor, of the choice of an oblate-spheroid geometry to represent the particle shape, and of the heuristic mixing models ([Equations 12](#) and [28](#)) with $v = 0.2$ for predicting the $\epsilon_{eff}(n)$ and $\sigma_{eff}(n)$ relationships of isotropic granular media made of nonspherical particles. Here, as opposed to $\sigma_{eff}(n)$ ([Figure 1](#)), the relationships vary not only because of particle shape, but also due to different solid (independently determined) permittivities of $\epsilon_S = 7.6$, 4.7, and 6.0 for the glass spheres, sand, and tuff, respectively. The significance of the particle shape effects is demonstrated by the $\epsilon_{eff}(n)$ lines for spherical particles ([Equation 27](#), or assuming an aspect ratio of $a/b/c = 1$ for the polarization factors of [Equation 28](#)), which are higher than the corresponding $\epsilon_{eff}(n)$ relationships for the actual oblate ($a < b = c$) particles.

As to the effect of the soil's *particle-size distribution* (*PSD*) on its ϵ_{eff} : Similarly to σ_{eff} , the mean particle size does not affect ϵ_{eff} and it is only the broadness (variance) of the PSD which is expected to affect the $\epsilon_{eff}(n, \theta)$ relationship. The MG model (two-phase version of [27](#)) formed the basis of a self-similar model derived by Sen et al. ([1981](#)), its main modification was of sequential additions of the inclusion solid phase into the host water phase, while the background pore system remains intact to low values of porosity. The resulting formula is impressively simple (Sen et al., [1981](#)):

$$\left(\frac{\epsilon_S - \epsilon_{eff}}{\epsilon_S - \epsilon_0}\right) \left(\frac{\epsilon_0}{\epsilon_{eff}}\right)^{1/3} = n \quad (29)$$

Nevertheless, this model should apply, in principle, to a fractal medium of infinitely wide PSD and should therefore form a lower (/upper) bound for the estimate of ϵ_{eff} of real water-saturated ($\epsilon_0 = \sigma_W$) (/oven-dry, $\epsilon_0 = \sigma_A$) granular media made of spherical particles of bounded particle-size distribution, as indeed proven by Robinson and Friedman ([2001](#)). Using mixtures of mono-size fractions of glass spheres and mixture of mono-size sand grains, Robinson and Friedman ([2001](#)) demonstrated how an increased broadness of the PSD reduces the ϵ_{eff} of water-saturated packings (and how it is expected to increase the ϵ_{eff} of oven-dry soil, thus, practically not affecting it for wet soils). It should be noted that the increasing width of PSD and particle asphericity tend to reduce the medium porosity. However, the effects on ϵ_{eff} and σ_{eff} discussed here are beyond this indirect effect, namely, referring to how these geometrical attributes affect ϵ_{eff} for a given porosity.

Knowing nothing on the soil mineralogy it is recommended to use a value of $\epsilon_S = 5$ for the *solid phase permittivity* when evaluating ϵ_{eff} (Dirksen and Dasberg, [1993](#); Friedman, [1998a](#)). A value of $\epsilon_S = 5.1$, for example, was determined for a sandy loam soil by Robinson and

Friedman ([2003](#)). If the mineralogical composition (and the corresponding mineral permittivities) is known then the appropriate modelling approach would be to extend the summations in, for example, [Equation 27](#) or [28](#) to several kinds of solid inclusions. Nevertheless, referring to a single type of solid inclusion with a permittivity equal to the arithmetic mean of the known composition introduces a negligible error, as demonstrated by Robinson and Friedman ([2002](#)) using mixtures of glass spheres ($\epsilon_S = 7.6$) and quartz sand grains ($\epsilon_S = 4.7$). Therefore, using a single mean ϵ_S value is satisfactory. ϵ_S of soil minerals range in general in 4–9 (Olhoeft, [1981](#); Robinson and Friedman, [2003](#); Robinson, [2004](#)) and that of soil organic matter is slightly lower. ϵ_S can be measured by the immersion method (Robinson and Friedman, [2003](#)), namely, by measuring the effective permittivity of packings of the same porosity, $\epsilon_{eff}(\epsilon_S, \epsilon_0, n = \text{const.})$, immersed in background fluids of different permittivities, ϵ_0 (higher and lower than ϵ_S), interpolating $\epsilon_{eff}(\epsilon_0)$ with a mixing model, and determining ϵ_S by the interception of $\epsilon_{eff}(\epsilon_0)$ and the 1:1 line.

The data and modelling (using $\epsilon_S = 5$) in this entry refers to only mineral soils. For the $\epsilon_{eff}(\theta)$ relationships of peat or soils of *high organic matter contents*, it is recommended to use different empirical equations best-fitted to these organic soils (Topp et al., [1980](#); Roth et al., [1992](#); Pepin et al., [1992](#)).

The permittivity of free water decreases by about $^{1/3}\%$ per 1°C increase due to random thermal motion enhancement and diminished directional polarization. Thus, ϵ_{eff} of coarse-textured soils slightly decrease with increasing *temperature* (T). However, in clayey soils with appreciable bound water increasing temperature causes release of low-permittivity bound water, which results in an overall increase of ϵ_{eff} (Hoekstra and Delaney, [1974](#); Wraith and Or, [1999](#); Or and Wraith, [1999](#)), a phenomenon Or and Wraith ([1999](#)) termed "thermo-dielectric effect," and proposed to utilize for evaluating the soil-specific surface area from $\epsilon_{eff}(T)$ measurements.

The MG ([Equation 27](#), assuming $v = 0$) prediction of, for example, $\epsilon_{eff} = 35.6$ for $n = 0.5$, $\epsilon_S = 5$, and $\epsilon_W = 80$ is close to the value of $\epsilon_{eff} = 34.6$ resulting from the frequently used empirical relationship of Topp et al. ([1980](#)) for a volumetric water content of 0.5. As opposed to it, the refractive index model ([Equation 18](#)) results in a much lower value of $\epsilon_{eff} = 31.25$. Robinson et al. ([2005](#)) demonstrated good predictability and proposed to use for practical purposes of water content determinations in coarse-textured soils the following hybrid, RI – two-phase mixing model

$$\epsilon_{eff}^{\frac{1}{2}} = \left(\frac{\theta}{n}\right) \epsilon_{sat}^{\frac{1}{2}} + \left(1 - \frac{\theta}{n}\right) \epsilon_{dry}^{\frac{1}{2}} \quad (30)$$

with the effective permittivities of the water-saturated (ϵ_{sat}) and oven-dry (ϵ_{dry}) soil determined by measurements or by the more reliable (compared to three-phase) two-phase mixing models (e.g., [Equation 27](#) or [28](#)).

Summary

The soil's electrical conductivity (σ_{eff}) and dielectric permittivity (ϵ_{eff}) are two macroscopic properties determined by the volumetric fractions and by the intrinsic properties of the soil's solid, liquid, and gaseous phases and their geometrical and interfacial features. Measurements of high-frequency ϵ_{eff} serve for the evaluation of the soil's porosity and volumetric water contents, and additional, simultaneous measurements of the low-frequency σ_{eff} allow evaluating the salinity of the soil's solution. Thus, measurements of σ_{eff} and ϵ_{eff} are useful for monitoring the flow and retention of water and electrolytes in the soil profile.

Bibliography

- Alharthi, A., and Lange, J., 1987. Soil water saturation: dielectric determination. *Water Resources Research*, **23**, 591–595.
- Amente, G., Baker, J. M., and Reece, C. F., 2000. Estimation of soil solution electrical conductivity from bulk soil electrical conductivity in sandy soils. *Soil Science Society of America Journal*, **64**, 1931–1939.
- Annan, P., 2005. GPR methods for hydrogeological studies. In Rubin, Y., and Hubbard, S. S. (eds.), *Hydrogeophysics*. Dordrecht: Springer, pp. 185–213. Chapter 7.
- Ansoult, M., De Backer, L. W., and Declercq, M., 1985. Statistical relationship between apparent dielectric constant and water content in porous media. *Soil Science Society of America Journal*, **49**, 47–50.
- Archie, G. E., 1942. The electrical resistivity log as an aid in determining some reservoir characteristics. *Transactions of the American Institute of Mining, Metallurgical and Petroleum Engineers*, **146**, 54–62.
- Bernabé, Y., and Revil, A., 1995. Pore-scale heterogeneity, energy dissipation and the transport properties of rocks. *Geophysical Research Letters*, **22**, 1529–1232.
- Binley, A., and Kemna, A., 2005. DC resistivity and induced polarization methods. In Rubin, Y., and Hubbard, S. S. (eds.), *Hydrogeophysics*. Dordrecht: Springer, pp. 129–156. Chapter 5.
- Birchack, J. R., Gardner, C. Z. G., Hipp, J. E., and Victor, J. M., 1974. High dielectric constant microwave probes for sensing soil moisture. *Proceedings of Institute of Electrical and Electronics Engineers*, **62**, 93–98.
- Blonquist, J. M., Jones, S. B., and Robinson, D. A., 2005. Standardizing characterization of electromagnetic water content sensors: Part 2. Evaluation of seven sensing systems. *Vadose Zone Journal*, **4**, 1059–1069.
- Blonquist, J. M., Jr., Jones, S. B., Lebron, I., and Robinson, D. A., 2006. Microstructural and phase configurational effects determining water content: dielectric relationships of aggregated porous media. *Water Resources Research*, **42**, W05424, doi:10.1029/2005WR004418.
- Briggs, L. J., 1899. *Electrical instruments for determining the moisture, temperature, and soluble salts content of soils*. USDA Division of Soils Bull. 10, U.S. Government Printing Office, Washington, DC.
- Bruggeman, D. A. G., 1935. The calculation of various physical constants of heterogeneous substances: I. The dielectric constants and conductivities of mixtures composed of isotropic substances. *Annals of Physics*, **24**, 636–664 (in German).
- Burger, H. C., 1919. Das leitvermögen verdünnter mischkristallfreien Legierungen. *Physikalische Zeitschrift*, **20**, 73–75 (in German).
- Chan, C. Y., and Knight, R., 2001. Laboratory measurements of electromagnetic wave velocity in layered sands. *Water Resources Research*, **37**, 1099–1105.
- Clavier, C., Coates, G., and Dumanoir, J., 1984. Theoretical and experimental bases for the dual-water model for interpretation of shaly sands. *Society of Petroleum Engineers. Journal*, **24**, 153–168.
- Dalton, F. N., Herkelrath, W. N., Rawlins, D. S., and Rhoades, J. D., 1984. Time domain reflectometry: simultaneous measurement of soil water content and electrical conductivity with a single probe. *Science*, **224**, 989–990.
- de Loor, G. P., 1968. Dielectric properties of heterogeneous mixtures containing water. *The Journal of Microwave Power*, **3**, 7–73.
- Debye, P., 1929. *Polar Molecules*. New York: Dover.
- Dirksen, C., and Dasberg, S., 1993. Improved calibration of time domain reflectometry soil water content measurements. *Soil Science Society of America Journal*, **57**, 660–667.
- Dobson, M. C., Kouyate, F., and Ulaby, F. T., 1984. A reexamination of soil textural effects on microwave emission and backscattering. *IEEE Transactions on Geoscience and Remote Sensing*, **GE-22**, 530–536.
- Dobson, M. C., Ulaby, F. T., Hallikainen, M. T., and El-Rayes, M. A., 1985. Microwave dielectric behavior of wet soil: II. Dielectric mixing models. *IEEE Transactions on Geoscience and Remote Sensing*, **GE-23**, 35–46.
- Doyle, T. E., Robinson, D. A., Jones, S. B., Warnick, K. H., and Carruth, B. L., 2007. Modeling the permittivity of two-phase media containing monodisperse spheres: effects of microstructure and multiple scattering. *Physical Review B*, **76**, 054203.
- Dukhin, S. S., 1971. Dielectric properties of disperse systems. In Matijevic, E. (ed.), *Surface and Colloid Science*. New York: Wiley, Vol. 3, pp. 83–165.
- Everett, M. E., and Meju, M. A., 2005. Near-surface controlled-source electromagnetic induction: Background and recent advances. In Rubin, Y., and Hubbard, S. S. (eds.), *Hydrogeophysics*. Dordrecht: Springer, pp. 157–183. Chapter 6.
- Friedman, S. P., 1997. Statistical mixing model for the apparent dielectric constant of unsaturated porous media. *Soil Science Society of America Journal*, **61**, 742–745.
- Friedman, S. P., 1998a. A saturation degree-dependent composite spheres model for describing the effective dielectric constant of unsaturated porous media. *Water Resources Research*, **34**, 2949–2961.
- Friedman, S. P., 1998b. Simulation of a potential error in determining soil salinity from measured apparent electrical conductivity. *Soil Science Society of America Journal*, **62**, 593–599.
- Friedman, S. P., and Jones, S. B., 2001. Measurement and approximate critical path analysis of the pore scale-induced anisotropy factor of an unsaturated porous medium. *Water Resources Research*, **37**, 2929–2942.
- Friedman, S. P., and Robinson, D. A., 2002. Particle shape characterization using angle of repose measurements for predicting the effective permittivity and electrical conductivity of saturated granular media. *Water Resources Research*, **38**(11), 1236, doi:10.1029/2001WR000746.
- Gaskin, G. J., and Miller, J. D., 1996. Measurement of soil water content using a simplified impedance measuring technique. *Journal of Agricultural Engineering Research*, **63**, 163–160.
- Gorman, T., and Kelly, W. E., 1990. Electrical-hydraulic properties of unsaturated Ottawa sands. *Journal of Hydrology*, **118**, 1–18.
- Hallikainen, M. T., Ulaby, F. T., Dobson, M. C., El-Rayes, M. A., and Wu, L. K., 1985. Microwave dielectric behavior of wet soil: I. Empirical models and experimental observations. *IEEE Transactions of Geoscience and Remote Sensing*, **GE-23**, 25–34.
- Heimovaara, T. J., Bouting, W., and Verstraten, J. M., 1994. Frequency domain analysis of time domain reflectometry waveforms: 2. A four-component complex dielectric mixing model for soils. *Water Resources Research*, **30**, 201–209.
- Hilfer, R., 1991. Geometric and dielectric characterization of porous media. *Physical Review B*, **44**, 60–75.

- Hoekstra, P., and Delaney, A., 1974. Dielectric properties of soil at UHF and microwave frequencies. *Journal of Geophysical Research*, **79**, 1699–1708.
- Jackson, P. D., Smith, D. T., and Stanford, P. N., 1978. Resistivity-porosity-particle shape relationships for marine sands. *Geophysics*, **43**, 1250–1268.
- Jacobsen, O. H., and Schjønning, P., 1993. A laboratory calibration of time domain reflectometry for soil water measurement including effects of bulk density and texture. *Journal of Hydrology*, **151**, 147–157.
- Johnson, D. L., and Sen, P. N., 1988. Dependence of the conductivity of a porous medium on electrolyte conductivity. *Physical Review B*, **37**, 3502–3510.
- Jones, S. B., and Friedman, S. P., 2000. Particle shape effects on the effective permittivity of anisotropic or isotropic media consisting of aligned or randomly oriented ellipsoidal particles. *Water Resources Research*, **36**, 2821–2833.
- Kaatze, U., 1996. Microwave dielectric properties of water. In Kraszewski, A. W. (ed.), *Microwave Aquametry Electromagnetic Wave Interaction with Water-Containing Materials*. Piscataway: IEEE Press, pp. 37–53. Chapter 2.
- Kan, R., and Sen, P. N., 1987. Electrolyte conduction in periodic arrays of insulators with charges. *The Journal of Chemical Physics*, **86**, 5748–5756.
- Lesmes, D. P., and Friedman, S. P., 2005. Relationships between the electrical and hydrogeological properties of rocks and soils. In Rubin, Y., and Hubbard, S. S. (eds.), *Hydrogeophysics*. Dordrecht: Springer, pp. 87–128. Chapter 4.
- Lesmes, D. P., and Frye, K. M., 2001. The influence of pore fluid chemistry on the complex conductivity and induced polarization responses of Berea sandstone. *Journal of Geophysical Research*, **106**, 4079–4090.
- Looyenga, H., 1965. Dielectric constants of mixtures. *Physica*, **31**, 401–406.
- Low, P. F., 1976. Viscosity of interlayer water in montmorillonite. *Soil Science Society of America Journal*, **40**, 500–505.
- Lyklema, J., 1995. *Fundamentals of Interface and Colloid Science*. London: Academic. Solid-Liquid Interfaces, Vol. II.
- Malicki, M. A., Plagge, R., and Roth, C. H., 1996. Improving the calibration of dielectric TDR soil moisture determination taking into account the solid soil. *European Journal of Soil Science*, **47**, 357–366.
- Maxwell-Garnett, J. C., 1904. Colours in metal glasses and in metal films. *Philosophical Transactions of the Royal Society of London*, **203**, 385–420.
- Miyamoto, T., Annaka, T., and Chikushi, J., 2005. Extended dual composite sphere model for determining dielectric permittivity of andisols. *Soil Science Society of America Journal*, **69**, 23–29.
- Mualem, Y., and Friedman, S. P., 1991. Theoretical prediction of electrical conductivity in saturated and unsaturated soil. *Water Resources Research*, **27**, 2771–2777.
- Nadler, A., 1982. Estimating the soil water dependence of the electrical conductivity soil solution/electrical conductivity bulk soil ratio. *Soil Science Society of America Journal*, **46**, 722–726.
- Nadler, A., Frenkel, H., and Mantell, A., 1984. Applicability of the four-probe technique under extremely variable water contents and salinity distributions. *Soil Science Society of America Journal*, **48**, 1258–1261.
- Olhoeft, G. R., 1981. Electrical properties of rocks. In Touhoukian, Y. S., and Ho, C. Y. (eds.), *Physical Properties of Rocks and Minerals*. New York: McGraw-Hill. McGraw-Hill/CINDAS Data Series on material properties, Vol. II-2, pp. 298–329.
- Or, D., and Wraith, J. M., 1999. Temperature effects on soil bulk dielectric permittivity measured by time domain reflectometry: a physical model. *Water Resources Research*, **35**, 371–383.
- Pepin, S., Plamondon, A. P., and Stein, J., 1992. Peat water content measurement using time domain reflectometry. *Canadian Journal of Forest Research*, **22**, 534–540.
- Persson, M., 1997. Soil solution electrical conductivity measurements under transient conditions using time domain reflectometry. *Soil Science Society of America Journal*, **61**, 997–1003.
- Revil, A., and Glover, P. W. J., 1997. Theory of ionic-surface electrical conduction in porous media. *Physical Review B*, **55**, 1757–1773.
- Revil, A., and Glover, P. W. J., 1998. Nature and surface electrical conductivity in natural sands, sandstones, and clays. *Geophysical Research Letters*, **25**, 691–694.
- Revil, A., Cathles, L. M., III, Losh, S., and Nunn, J. A., 1998. Electrical conductivity in shaly sands with geophysical applications. *Journal of Geophysical Research*, **103**(B10), 23925–23936.
- Rhoades, J. D., and van Schilfgaarde, J., 1976. An electrical conductivity probe for determining soil salinity. *Soil Science Society of America Journal*, **40**, 647–650.
- Rhoades, J. D., Ratts, P. A. C., and Prather, R. J., 1976. Effects of liquid-phase electrical conductivity, water content, and surface conductivity on bulk soil electrical conductivity. *Soil Science Society of America Journal*, **40**, 651–655.
- Rhoades, J. D., Manteghi, N. A., Shouse, P. J., and Alves, W. J., 1989. Soil electrical conductivity and soil salinity: new formulations and calibrations. *Soil Science Society of America Journal*, **53**, 433–439.
- Rhoades, J. D., Chanduvi, F., Lesch, S., 1999. *Soil salinity assessment: methods and interpretation of electrical conductivity measurements*. Rome, Italy: Food and Agriculture Organization of the United Nations. FAO Irrigation and Drainage paper No. 57.
- Robinson, D. A., 2004. Measurement of the solid dielectric permittivity of clay minerals and granular samples using time domain reflectometry immersion method. *Vadose Zone Journal*, **3**, 705–713.
- Robinson, D. A., and Friedman, S. P., 2001. The effect of particle size distribution on the effective dielectric permittivity of saturated granular media. *Water Resources Research*, **37**, 33–40.
- Robinson, D. A., and Friedman, S. P., 2002. The effective permittivity of dense packings of glass beads, quartz sand and their mixtures immersed in different dielectric background. *Journal of Non-Crystalline Solids*, **305**, 261–267.
- Robinson, D. A., and Friedman, S. P., 2003. A method for measuring the solid particle permittivity or electrical conductivity of rocks, sediments, and granular materials. *Journal of Geophysical Research*, **108**(B2), 2075, doi:10.1029/2001JB000691.
- Robinson, D. A., and Friedman, S. P., 2005. Electrical conductivity and dielectric permittivity of sphere packing: measurements and modelling of cubic lattices, randomly packed monosize spheres and multi-size mixtures. *Physica A: Statistical Mechanics and its Applications*, **358**, 447–465.
- Robinson, D. A., Cooper, J. D., and Gardner, C. M. K., 2002. Modelling the relative permittivity of soil hygroscopic water content. *Journal of Hydrology*, **255**, 39–49.
- Robinson, D. A., Jones, S. B., Wraith, J. M., Or, D., and Friedman, S. P., 2003. A review of advances in dielectric and electrical conductivity measurement using time domain reflectometry: simultaneous measurement of water content and bulk electrical conductivity in soils and porous media. *Vadose Zone Journal*, **2**, 444–475.
- Robinson, D. A., Jones, S. B., Blonquist, J. M., Jr., and Friedman, S. P., 2005. A physically derived water content/permittivity calibration model for coarse-textured, layered soils. *Soil Science Society of America Journal*, **69**, 1372–1378.

- Roth, K., Schulin, R., Fluhler, H., and Attinger, W., 1990. Calibration of time domain reflectometry for water content measurement using a composite dielectric approach. *Water Resources Research*, **26**, 2267–2273.
- Roth, C. H., Malicki, M. A., and Plagge, R., 1992. Empirical evaluation of the relationship between soil dielectric constant and volumetric water content as the basis for calibrating soil moisture measurements by TDR. *Journal of Soil Science*, **43**, 1–13.
- Santamarina, J. C., Klein, K. A., and Fam, M. A., 2001. *Soils and Waves*. Chichester: Wiley.
- Sareni, B., Krähenbühl, L., Beroual, A., and Brosseau, C., 1997. Effective dielectric constant of random composite materials. *Journal of Applied Physics*, **81**, 2375–2383.
- Schön, J. H., 1996. Physical properties of rocks – fundamentals and principles of petrophysics, Handbook of Geophysical Exploration, Seismic Exploration. *Elsevier Science*, **18**, 379–478.
- Schwartz, L. M., Sen, P. N., and Johnson, D. L., 1989. Influence of rough surfaces on electrolyte conduction in porous media. *Physical Review B*, **40**, 2450–2458.
- Sen, P. N., and Goode, P. A., 1992. Influence of temperature on electrical conductivity of shaly sands. *Geophysics*, **57**, 89–96.
- Sen, P. N., Scala, C., and Cohen, M. H., 1981. A self-similar model for sedimentary rocks with application to the dielectric constant of fused glass beads. *Geophysics*, **46**, 781–795.
- Sen, P. N., Goode, P. A., and Sibbit, A., 1988. Electrical conduction in clay bearing sandstones at low and high salinities. *Journal of Applied Physics*, **63**, 4832–4840.
- Shainberg, I., Rhoades, J. D., and Prather, R. J., 1980. Effect of ESP, cation exchange capacity, and soil solution concentration on soil electrical conductivity. *Soil Science Society of America Journal*, **44**, 469–473.
- Sihvola, A., 1999. *Electromagnetic mixing formulas and applications*. Stevenage: Institution of Electrical Engineers. Electromagnetic Waves Series, Vol. 47.
- Sihvola, A., and Kong, J. A., 1988. Effective permittivity of dielectric mixtures. *IEEE Transactions on Geoscience and Remote Sensing*, **26**, 420–429.
- Sihvola, A., and Kong, J. A., 1989. Correction to “Effective permittivity of dielectric mixtures”. *IEEE Transactions on Geoscience and Remote Sensing*, **21**, 101–102.
- Sihvola, A., and Lindell, I. V., 1990. Polarizability and effective permittivity of layered and continuously inhomogeneous dielectric ellipsoids. *Journal of Electromagnetic Waves and Applications*, **4**, 1–26.
- Skierucha, V., and Wilczek, A., 2010. A FDR Sensor for measuring complex soil dielectric permittivity in the 10–500 MHz frequency range. *Sensors*, **10**, 3314–3329, doi:10.3390/s100403314.
- Smith-Rose, R. L., 1933. The electrical properties of soil for alternating currents at radio frequencies. *Proceedings of the Royal Society of London*, **140**, 359–377.
- Tabbagh, A., Camerlynk, C., and Cosenza, P., 2000. Numerical modeling for investigating the physical meaning of the relationship between relative dielectric permittivity and water content of soils. *Water Resources Research*, **36**, 2771–2776.
- Tinga, W. R., Voss, W. A. G., and Blossey, D. F., 1973. Generalized approach to multiphase dielectric theory. *Journal of Applied Physics*, **44**, 3897–3902.
- Topp, G. C., Davis, J. L., and Annan, A. P., 1980. Electromagnetic determination of soil water content: measurements in coaxial transmission lines. *Water Resources Research*, **16**, 574–582.
- Torquato, S., 2002. *Random Heterogeneous Materials: Microstructure and Macroscopic Properties*. New York: Springer.
- Van Loon, W. K. P., Perfect, E., Groenevelt, P. H., and Kay, B. D., 1991. Application of dispersion theory to time domain reflectometry in soils. *Transport in Porous Media*, **6**, 391–406.
- von Hippel, A. R. (ed.), 1954. *Dielectrics Materials and Applications*. Cambridge/New York: The Technology press of MIT/Wiley.
- Wang, M., and Pan, N., 2008. Predictions of effective properties of complex multiphase materials. *Materials Science and Engineering Reports*, **63**, 1–30.
- Wang, J. R., and Schmugge, T. J., 1980. An empirical model for the complex dielectric constant of soils as a function of water content. *IEEE Transactions on Geoscience and Remote Sensing*, **GE-18**, 288–295.
- Waxman, M. H., and Smits, L. J. M., 1968. Electrical conductivities in oil-bearing shaly sands. *Society of Petroleum Engineers Journal*, **8**, 107–122.
- Weerts, A. H., Boutingen, W., and Verstraten, J. M., 1999. Simultaneous measurement of water retention and electrical conductivity in soils: testing the Mualem-Friedman tortuosity model. *Water Resources Research*, **35**, 1781–1787.
- Wenner, F., 1915. A method of measuring earth resistivity, U. S. Department of Com. Bureau of Standards Science Paper No. 258, NIST, Gaithersburg, MD.
- Whalley, W. R., 1993. Considerations on the use of time-domain reflectometry (TDR) for measuring soil water content. *Journal of Soil Science*, **44**, 1–9.
- Wharton, R. P., Hazen, G. A., Rau, R. N., and Best, D. L., 1980. Electromagnetic propagation logging: Advances in technique and interpretation. *Society of Petroleum Engineers*, Paper No. 9267.
- Wraith, J. M., and Or, D., 1999. Temperature effects on soil bulk dielectric permittivity measured by on time domain reflectometry: experimental evidence and hypothesis. *Water Resources Research*, **35**, 361–369.

Cross-references

- [Dielectric Properties of Agricultural Products](#)
[Diffuse Double Layer \(DDL\)](#)
[Diffusion in Soils](#)
[Electrical Properties of Agricultural Products](#)
[Electrical Resistivity to Assess Soil Properties](#)
[Electrochemical Measurements in Soils](#)
[Electrokinetic \(Zeta\) Potential of Soils](#)
[Electromagnetic Fields, Impact on Seed Germination and Plant Growth](#)
[Fractal Analysis in Agrophysics](#)
[Ground-Penetrating Radar, Soil Exploration](#)
[Hydraulic Properties of Unsaturated Soils](#)
[Isotropy and Anisotropy in Agricultural Products and Foods](#)
[Magnetic Properties of Soils](#)
[Mapping of Soil Physical Properties](#)
[Nondestructive Measurements in Soil](#)
[Online Measurement of Selected Soil Physical Properties](#)
[Physico-Chemical Methods for Remediation of Contaminated Soils](#)
[Pore Size Distribution](#)
[Scaling of Soil Physical Properties](#)

ELECTRICAL RESISTIVITY

A measure indicating how strongly a body resists the flow of electric current.

ELECTRICAL RESISTIVITY TO ASSESS SOIL PROPERTIES

Guy Richard, Maud Séger, Arlène Besson,
Isabelle Cousin
Institut National de la Recherche Agronomique (INRA)
Unité de Science du Sol, Centre de Recherche d'Orléans,
Olivet cedex, Orléans, France

Definitions

Soil electrical resistivity. Resistance of soils to electrical current flow for a given electrical potential across the soil material. The SI unit is ohm meter (Ωm).

Soil structure. Spatial arrangement of soil particles at various scales, typically from clay particles (μm) to soil profile (m).

Introduction

Soil structure, that is, the arrangement of soil particles in space (Guérif, 1987; Dexter, 1988) is one of the factors of physical quality of soils. In the agricultural context, this structure is modified at several space and time scales by different factors: plants growth, earthworm's activity, traffic, tillage, and climate. Because the mechanical stresses applied to the soil by these factors do not affect the whole soil volume, soil structure of agricultural fields is generally very heterogeneous. Several methods for the characterization of soil structure at the profile scale (i.e., the macrostructure) already exist. These are based on the visual description of a soil pit (Roger-Estrade et al., 2004), on measurements of soil properties such as bulk density, porosity, water retention, and penetration resistance, or on characterization of the water infiltration.

One of the main problems of these methods for soil structure analysis in field conditions is that they are destructive and cannot easily be used to obtain a spatial and temporal monitoring of the soil structural heterogeneity. Geophysical nondestructive methods such as electrical resistivity have already been demonstrated as useful quantitative methods for soil mapping at farmer scale (Bourennane et al., 1998), monitoring of water content or solute transfer (Michot et al., 2003), and description of porosity evolution (Dannowski and Yaramancı, 1999). Electrical resistivity of soils depends on volumetric clay and water contents because the electrical flow occurs within the pores filled in water and at the surface of clayed particles. Consequently, electrical resistivity would depend on soil bulk density and more generally on soil structure.

The aim of the study conducted from several years at INRA in France is to examine the feasibility of using electrical resistivity in describing the structure of tilled layers in agricultural fields, that is, the change in soil macrostructure due to traffic (compaction), tillage (fragmentation), and climate (crack formation).

Electrical resistivity measurements

The electrical resistivity of a soil volume is calculated from the potential difference due to the continuous and low frequency artificial current injected by electrodes into the soil. There are different electrode configurations, called electrodes arrays where the electrical current (I) is injected by two electrodes conventionally named A and B and the potential difference (ΔV) is measured by two other electrodes M and N. The measured electrical resistivity of the prospected medium is called apparent resistivity (ρ_a) and is calculated by Eq. 1:

$$\rho_a = \left[\frac{2\pi}{(1/AM) - (1/BM) - (1/AN) + (1/BN)} \right] \frac{\Delta V}{I} \quad (1)$$

where AM (resp. BM , AN , BN) represents the distance between electrodes A and M (resp. B and M, A and N, B and N).

The electrode configuration used in our experiments is the Wenner array. Four electrodes are arranged in line, with A and B electrodes at the external positions and M and N electrodes in between. The distances AM , MN , NB are equal (0.10 m in our case). We measured soil electrical resistivity and analyzed its spatial distribution in 2D from the tomography technique (ERT). For that, the Wenner array is moved on a line from one point to another to measure the electrical resistivity of adjacent locations. By increasing the distance between all the four electrodes, the depth of investigation increases and deeper zones in the soil profile can be characterized. The measured resistivities can thus be quickly obtained. They are called "apparent resistivities" because each value corresponds to an integrated volume.

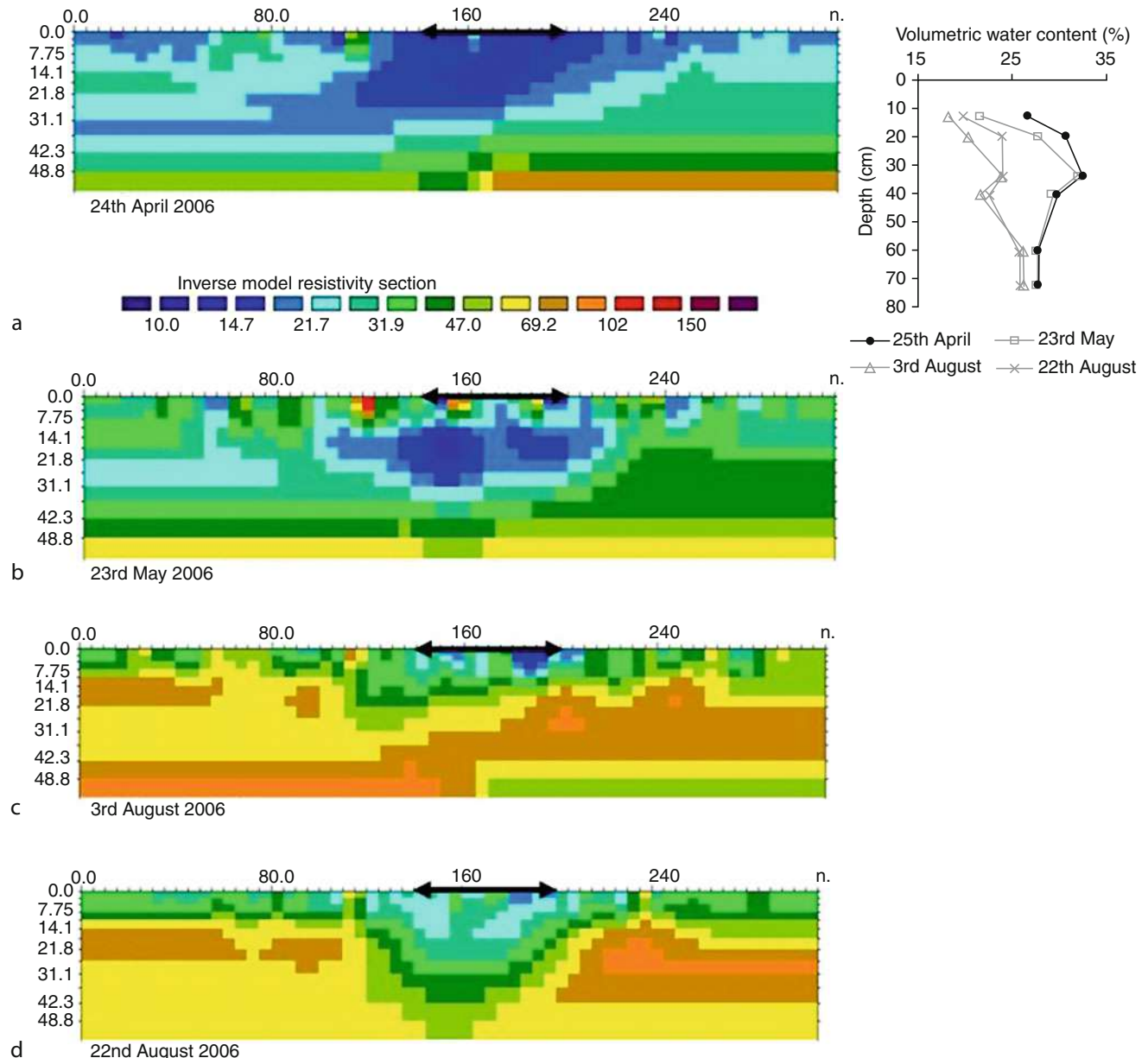
Raw resistivity data are so-called "bulk or volume" resistivity for which a soil volume is measured. To be accurately analyzed in space, the spatial distribution of bulk resistivity is determined by inverse modeling. Resulting resistivity, that is, resistivity forward solution, is then called "inverted resistivity," calculated at each block of structured grid. The inverse resistivity problem is nonlinear, nonunique, and ill-posed with respect to data errors and incomplete data sets. It is usually solved in an iterative process that applies a forward modeling routine for nearly arbitrary resistivity distributions in every inversion step. For a thorough presentation of goelectrical inverse process, the reader could refer to books on the subject, such as those by Aster et al. (2005) or Tarantola (2005).

We used the Res2Dinv program with the smoothness-constrained least-squares method based on the quasi-Newton optimization technique (Loke and Barker, 1996). An estimation of the difference between measured and inverted resistivity is given by the Root Mean Square error (RMS). Because of the solution nonuniqueness, we assumed that the most reliable and realistic inverted resistivity distribution was obtained for a RMS lower than 10% (Delapierre, 1998).

Inverted data were then represented on a regular and refined grid with an increasing cell size toward the spatial boundaries (e.g., see Figure 1).

Temperature influences electrical resistivity values and it is very important to correct the temperature effect (Besson et al., 2008). The Campbell equation is the most commonly used (Campbell et al., 1948):

$$\frac{1}{\rho_T} = \frac{1}{\rho_{ref}} [1 + \alpha(T - T_{ref})] \quad (2)$$



Electrical Resistivity to Assess Soil Properties, Figure 1 2D electrical resistivity profiles (depth and width in centimeters) in Villamblain immediately at compaction (a) 1 month; (b) 3 months; (c) and 4 months; (d) after compaction. The *black arrow* represents the position of the wheel (tire with a 65 cm width).

where T represents the temperature of the measurement, T_{ref} the electrical resistivity measured at the reference temperature (usually taken equal to 25°C), ρ the electrical resistivity at T , ρ_{ref} the electrical resistivity at T_{ref} , and α a correction factor equal to 0.02.

Field experiments

Field experiments were performed in two plots with a loamy soil – typical Luvisol (FAO, 2006) in Estrées-Mons, Picardie Region – and a loamy-clay soil – haplic

Cambisol (FAO, 2006) in Villamblain, Beauce Region. For both sites, we created a compacted band by wheeling at field capacity with a heavy tractor.

For the Estrées-Mons site, a sub-plot was tilled with a mouldboard plow (in the direction of wheeling). The objective was to fragment the compacted band and to create a complex arrangement of compacted blocks, loose material, and large voids. For the Villamblain site, the compacted band was not disturbed, subject only in time to the climate and biological activities.

Soil structure was characterized from the visual observation of a soil pit dug perpendicularly to the tillage direction. Macroscopic features were classified with a particular attention to zones with massive structure and no visible macroporosity. These zones, called Δ zones (Manichon, 1982), resulted from the maximum intensity of soil

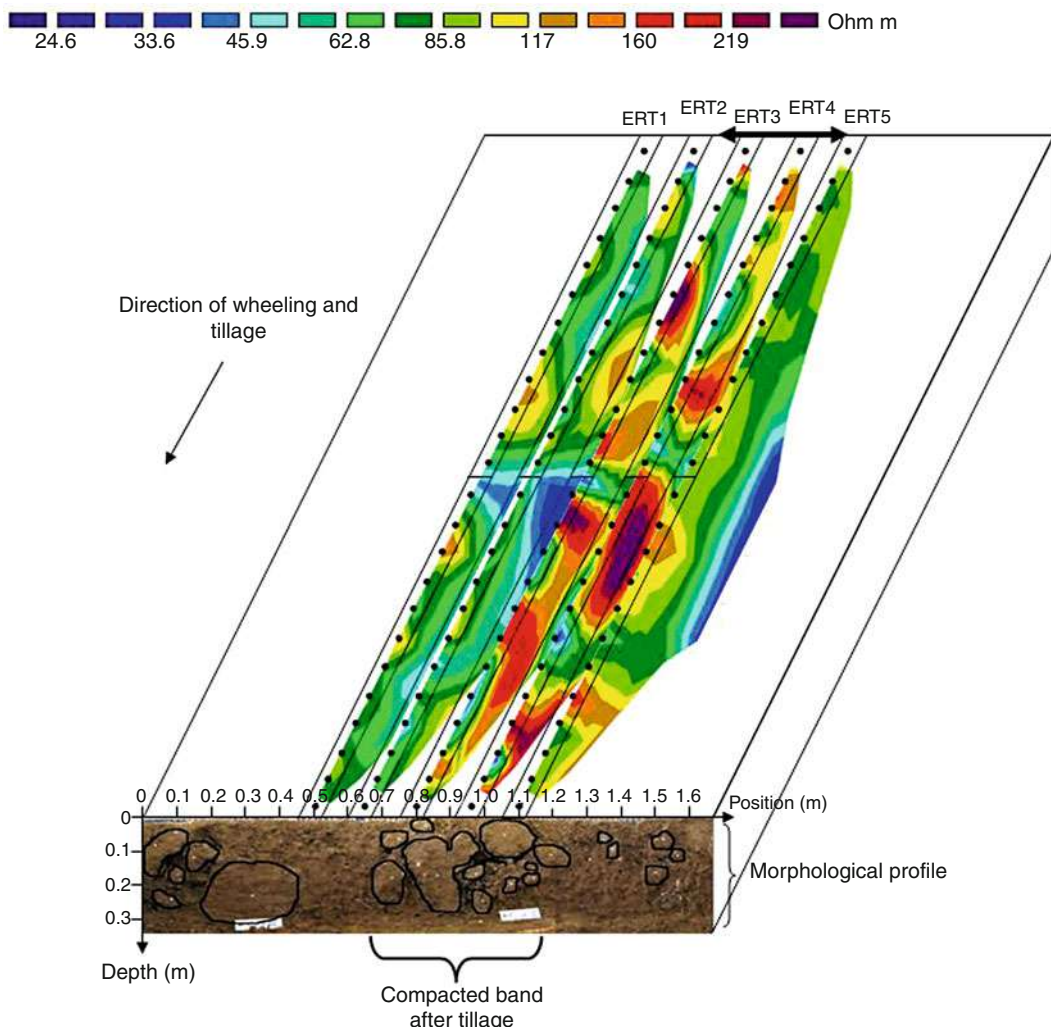
compaction in field conditions. The Δ zones had a massive structure, no visible macropore, high cohesion, and a clean breaking surface. Bulk densities were also measured on undisturbed soil cores sampled in both soil profiles.

ERT measurements were measured as described above before each dug pit. Multielectrode lines were perpendicular (Villamblain) or parallel (Estrées-Mons) to the traffic direction. We used resistivimeter (Syscal R1) from the Iris technology (Iris Instrument, France).

Results

Compaction after traffic (Estrées-Mons and Villamblain sites)

Soil compaction was characterized by an increase in bulk density of the topsoil from 1.36 to 1.47 Mg m^{-3} in the haplic Cambisol soil (Villamblain site) and from 1.39 to



Electrical Resistivity to Assess Soil Properties, Figure 2 2D electrical resistivity profiles in Estrées-Mons after tillage. The five electrical profiles (ERT1 to ERT5) were performed in the direction of the wheeling and tillage and the distance between the profiles was 15 cm. The black lines on the morphological profile correspond to the contours of the compacted blocks and the black arrow corresponds to the position of the wheel.

1.59 Mg m^{-3} in the loamy soil (Estrées-Mons site). The structure of bands under wheel tracks was Δ type, that is, cohesive and massive. For non-trafficked zones, the soil structure was more porous and aggregated, which is consistent with less compaction and disturbance.

Results of ERT are illustrated on Figure 1a (Villamblain site). For the soil layer 0–30 cm depth, resistivity was approximately equal to $10 \Omega\text{m}$ under the wheel tracks and $25 \Omega\text{m}$ outside the wheel tracks. The smallest value of resistivity was attributed to compaction. Besson et al. (2004) observed similar results in Estrées-Mons site, with a decrease in resistivity of $15 \Omega\text{m}$ (i.e., from 40 to $25 \Omega\text{m}$) due to compaction. This effect on resistivity was measured just after traffic and when the soil was wet, that is, close to field capacity. Indeed, resistivity variation due to compaction is generally exacerbated for dry soils.

Fragmentation after tillage (Estrées-Mons site)

Five electrical profiles called ERT1 to ERT5 were performed from the top of the plot, parallel to the traffic direction (Figure 2). The fragmentation of compacted band by tillage induced heterogeneous macrostructure with a mix of dense Δ clods embedded by large voids and porous matrix as shown on the morphological profile on Figure 2. Ten morphological profiles (not showed here) were performed perpendicular to the traffic line and this complex structure remained the same on each profile. The structural heterogeneity of the tilled layer greatly altered resistivity that varied then from ~ 25 to $\sim 250 \Omega\text{m}$ and the electrical resistivity was highly variable in the first 10 cm for each electrical profile. For the electrical profiles positioned outside the compacted band (ERT1, ERT2, and ERT5), resistivity was approximately equal to 50 – $70 \Omega\text{m}$. For the electrical profiles located in the position of the initial compacted band (ERT3 and ERT4), resistivity exceeded largely $70 \Omega\text{m}$ despite the presence of dense Δ clods. This last result was explained by void-surrounded clods. Even relatively small ones, voids generated noise in resistivity data, restricting the interpretation of ERT in terms of soil structure.

The high sensitivity of electrical resistivity to voids is then complementary to the morphological profiles that are, in turn, more efficient to describe the organization of Δ clods and loose material (Séger et al., 2009).

Cracks after drying (Villamblain site)

Samouëlian et al. (2004) have demonstrated, in laboratory conditions (on a soil block of 0.3 m^3), that the detection of cracks during a drying period was feasible through electrical resistivity measurements. Figure 1a–d shows the change in ERT in the field under natural conditions during several months after compaction (Villamblain site), not only due to moisture evolution but also due to structural evolution of the dense band.

First, the contrast in resistivity between compacted and non-compacted zones increased, as already mentioned (Figure 1a–c). It seems that the non-compacted zone dried out more rapidly in time than the compacted zone. This is consistent with a higher unsaturated hydraulic

conductivity expected for dense zones as suggested by Richard et al. (2001). Second, we observed high values of resistivity ($>100 \Omega\text{m}$) at three locations up to the dense band, that is, in the near soil surface (Figure 1b). These resistant zones extend during the drying period till beginning of August (Figure 1c). Anyhow, after a storm in August, the water content significantly increased in tilled layer and these zones had again a small resistivity (Figure 1d).

It seems that the cracks, as consequences of the severe drying that occurred in summer in the soil surface, enhanced resistivity values as previously shown in the laboratory. Cracks became preferential pores for water flows and therefore could again be characterized by a low electrical resistivity after a rainfall event.

Conclusions

Our results enhanced the feasibility of electrical resistivity measurements to characterize the heterogeneity of the soil structure at the profile scale without any soil sampling and soil pit. The geophysical method enables to define geometry of compacted band generated by traffic, to characterize the degree of fragmentation of the tilled layer with a decimetric resolution. Electrical Resistivity Tomography constitutes an alternative tool to the X-ray tomography for studies in the field. Further research is needed to improve quantification of the soil structure heterogeneity by geophysical methods and to elucidate the mechanisms responsible for the control of tillage on flow and transport.

Bibliography

- Aster, R. C., Borchers, B., and Thurber, C. H., 2005. *Parameter Estimation and Inverse Problems*. London: Elsevier Academic.
- Besson, A., Cousin, I., Samouëlian, A., Boizard, H., and Richard, G., 2004. Structural heterogeneity of the soil tilled layer as characterized by 2D electrical resistivity surveying. *Soil and Tillage Research*, **79**, 239–249.
- Besson, A., Cousin, I., Dorigny, A., Dabas, M., and King, D., 2008. The temperature correction for the electrical resistivity measurements in undisturbed soil samples: analysis of the existing models and proposal of a new model. *Soil Science*, **173**(10), 707–720.
- Bourennane, H., King, D., Le Parco, R., Isambert, M., and Tabbagh, A., 1998. Three-dimensional analysis of soils and surface materials by electrical resistivity survey. *European Journal of Environmental Engineering Geophysics*, **3**, 5–23.
- Campbell, R. B., Bower, C. A., and Richard, L. A., 1948. Change in electrical conductivity with temperature and the relation with osmotic pressure to electrical conductivity and ion concentration for soil extracts. *Soil Science Society of America Proceedings*, **13**, 33–69.
- Dannowski, G., and Yaramancı, U., 1999. Estimation of water content and porosity using radar and geoelectrical measurements. *European Journal of Environmental and Engineering Geophysics*, **4**, 71–85.
- Delapierre, A., 1998. Représentation en 3D d'une partie des vestiges d'une villa gallo-romaine à l'aide des méthodes électriques (Site gallo-romain d'Orbe-Boscéaz, Vaud, Suisse). PhD Thesis, University of Lausanne, Switzerland.
- Dexter, A. R., 1988. Advances in characterization of soil structure. *Soil and Tillage Research*, **11**, 199–238.

- FAO, 2006. *World Reference Base for Soil Resources*. Rome: FAO, ISRIC, ISSS.
- Guérif, J., 1987. L'analyse de la porosité: application à l'étude du compactage des sols. In Monnier, G., and Goss, M. J. (eds.), *Soil Compaction and Regeneration*. Rotterdam: A.A. Balkema, pp. 1–13.
- Loke, M. H., and Barker, R. D., 1996. Rapid least-squares inversion of apparent resistivity pseudo-sections using a quasi-Newton method. *Geophysical Prospecting*, **44**, 131–152.
- Manichon, H., 1982. Observation morphologique de l'état structural et mise en évidence d'effets de compactage des horizons travaillés. In Monnier, G., and Goss, M. J. (eds.), *Soil Compaction and Regeneration*. Rotterdam: A.A. Balkema, pp. 39–52.
- Michot, D., Benderitter, Y., Dorigny, A., Nicoulaud, B., King, D., and Tabbagh, A., 2003. Spatial and temporal monitoring of soil water content with an irrigated corn crop cover using electrical resistivity tomography. *Water Resources Research*, **39**, 1138–1160.
- Richard, G., Cousin, I., Sillon, J. F., Bruand, A., and Guérif, J., 2001. Effect of compaction on the porosity of a silty soil: influence on unsaturated hydraulic properties. *European Journal of Soil Science*, **52**, 49–58.
- Roger-Estrade, J., Richard, G., Caneill, J., Boizard, H., Coquet, Y., Defossez, P., and Manichon, H., 2004. Morphological characterisation of soil structure in tilled fields: from a diagnosis method to the modelling of structural changes over time. *Soil and Tillage Research*, **79**, 33–49.
- Samouélian, A., Richard, G., Cousin, I., Guérin, R., Bruand, A., and Tabbagh, A., 2004. Three-dimensional crack monitoring by electrical resistivity measurement. *European Journal of Soil Science*, **55**, 751–762.
- Séger, M., Cousin, I., Frison, A., Boizard, H., and Richard, G., 2009. Characterisation of the structural heterogeneity of the soil tilled layer by using in situ 2D and 3D electrical resistivity measurements. *Soil and Tillage Research*, **103**, 387–398.
- Tarantola, A., 2005. *Inverse Problem Theory and Methods for Model Parameter Estimation*. Philadelphia: Society for Industrial and Applied Mathematics.

Cross-references

- [Electrical Properties of Soils](#)
[Proton Nuclear Magnetic Resonance \(NMR\) Relaxometry in Soil Science](#)
[Soil Aggregates, Structure, and Stability](#)
[Soil Structure, Intersecting Surface Approach, and its Applications](#)
[Soil Structure, Visual Assessment](#)
[Spatial Variability of Soil Physical Properties](#)

ELECTRICAL SUSCEPTIBILITY

See [Organic Dusts, Electrostatic Properties](#)

ELECTROCHEMICAL MEASUREMENTS IN SOILS

Andrzej Bieganowski, Jolanta Cieśla
 Institute of Agrophysics, Polish Academy of Sciences,
 Lublin, Poland

Definition

Electrochemistry is a science (branch of chemistry) that deals with the electrical aspects of chemical reactions.

The main division of electrochemical methods used for testing of solutions is the following:

- Potentiometric methods – the potential of electrode is measured that depends on the ion activity of tested substance in the solution.
- Coulometric methods – the electrical charge transferred in redox (reduction/oxidation) reaction is measured (see [Oxidation–Reduction Reactions in the Environment](#)).
- Conductometric methods – the electric conductivity of tested solution is measured (see [Electrical Properties of Soils](#)).
- Voltammetric methods – the current–voltage characteristics of tested solutions are determined.
- Electrolytic methods – the mass of electrolysis products is measured.

Introduction

The use of electrochemical methods in soils encounters methodological problems that are not met in “solution” chemistry, which results from the fact that the soil is a three-phase and even a living (containing a huge number of living organisms) system (see [Agrophysical Objects \(Soils, Plants, Agricultural Products, and Foods\)](#)). The consequence of it is heterogeneity of the soil and variation of its properties in space and time. Moreover, what is very important in electrochemical measurements, it is very difficult to characterize the measurement conditions. Below soil water saturation state it is very difficult (and sometimes impossible) to describe the distribution of the liquid phase in the soil (see [Solute Transport in Soils](#) and [Hydraulic Properties of Unsaturated Soils](#)). A separate problem is the presence, practically always, of interfering substances in the soil.

Methodological problems cause different approaches to investigations in the soil. The easiest, and sometimes completely sufficient, are the measurements of soil extracts. These measurements do not practically differ from “pure” chemistry measurements.

The completely different approach of electrochemical measurements must be applied to measurements conducted directly in the soil (*in situ*). Most of the electrochemical methods can be applied in the laboratory as well in the field, but frequently the equipment must be different.

The specificity of tests in the soil causes that only a few methods can be applied for the measurement of this object. The most popular methods are (Brett, 2001) the following:

Potentiometric
 Voltammetric
 Conductometric

Potentiometric method

This method is based on measurement of the potential difference, which is created in an electrochemical cell composed of two electrodes (indicator electrode and reference electrode) immersed in the analyzed sample (Yu and Ji, 1993).

The measurement is made using a high-impedance voltmeter at zero current. Potentiometric signal is proportional to the logarithm of the investigated ion activity. However, the range of linear response of the electrode system is limited by many factors such as measurement conditions, sample composition, as well as electrode properties. The potentiometric method is simple, fast, and relatively cheap. The sensors are easily miniaturized.

Electrodes, which are used for potentiometric measurements, should give a stable and reproducible signal, have short recovery time, long lifetime, and strong mechanical construction.

The indicator electrode should be sensitive and selective enough to make analysis in the presence of other (interfering) ions. The signal of the reference electrode should be stable and independent of the ion activity of the analyzed component (Brzózka and Wróblewski, 1999). The calomel ($\text{Hg}/\text{Hg}_2\text{Cl}_2/\text{Cl}^-$) and silver/silver chloride (Ag/AgCl) electrodes are the most often used as the reference electrodes in potentiometric analysis of soil samples (Yu and Ji, 1993).

The most often used potentiometric sensors are the ion-selective electrodes. These electrodes consist of an ion-selective membrane, one side of which is in contact with the measured solution and the second side with the inner electrolyte solution. The permselective mass transfer (by the ion-exchange mechanism or other mechanism) across a phase boundary causes the Gibbs energy change and the potentiometric signal change in a consequence (Buck and Lindner, 1994).

An example of an ion-selective electrode is the pH glass electrode, which is built of aluminosilicate glass bubble containing an inert pH buffer solution and an inert reference electrode. At the sample solution/outside part of the glass membrane interface the thermodynamic equilibrium of hydrogen ions is obtained. If the hydrogen ions activity in both phases (sample and membrane) is different, then the ions are carried out. The resultant potential (E_1) depends on the activity of the hydrogen ions in the sample solution and the outside part of the glass membrane. The potential at the inside part of the glass membrane/inert pH buffer interface (E_2) depends on the hydrogen ions activity in the buffer solution and the inside part of glass. The total potential is equal to the difference between E_1 and E_2 . If the hydrogen ions activity in both parts of the glass membrane is the same and this activity in the buffer solution is constant, the potential of glass electrode depends only on the hydrogen ions activity in the sample solution (Brzózka and Wróblewski, 1999).

In the presence of interfering ions in the sample, the potential of the ion-selective electrode depends also on the activity of these ions and on the selectivity coefficient of the electrode.

According to IUPAC (International Union of Pure and Applied Chemistry) recommendation, there are three main types of ion-selective electrodes classified as (Buck and Lindner, 1994):

1. Primary ion-selective electrodes:

- (a) *Crystalline electrodes* (with *homogenous* or *heterogeneous* membrane). Homogenous membrane is prepared from a single compound or a homogenous mixture of compounds. In the heterogeneous type of electrodes, an active substance or mixture of substances is placed in a matrix of the ion-selective membrane.
 - (b) *Noncrystalline electrodes*, whose ion-selective membrane placed between two aqueous solutions is composed of an ion exchanger, a plasticizer solvent, and some selectivity-enhancing species. This type of electrodes can be divided into two groups:
 - *Rigid, self-supporting, matrix electrodes*, where the thin polymer with charged sites or a thin piece of glass is a sensing membrane. Selectivity of these membranes is determined by the polymer or glass composition.
 - *Electrode with mobile-charged sites* on the membrane (positively charged, hydrophobic cations on the membranes, which are sensitive to changes of the anions activity; negatively charged hydrophobic anions on the cation-selective membranes; uncharged ion carrier, which creates complexes with the anions or cations; hydrophobic ion pair electrodes of plasticized polymers containing a dissolved hydrophobic ion pair).
2. Compound or multiple (multi layer) ion-selective electrodes (gas-sensing electrodes and enzyme-substrate electrodes).
3. *Metal contact or all-solid-state ion-selective electrodes*, which do not have an inner electrolyte solution and the selective constituent is placed on the electronic conductor.

The potentiometric method can be used in different ways (Yu and Ji, 1993):

- *Direct indication* of ion activity basing on linear part of calibration curve. Some limitation is that the composition and ionic strength of calibration solutions and the sample should be nearly the same.
- *Known addition method*, when a small volume of standard solution is added to the sample and the potential is measured before and after the addition.
- *Known subtraction method*, when a small volume of precipitating or complexing agent solution is added to the sample to decrease the determined ion activity by about 50%. The potential is measured before and after the addition.

Most potentiometric measurements are carried out in solutions and/or in soil extracts, because solid phase affects the results due to the suspension effect. This effect is connected with an additional change of ion-selective electrode potential (*suspension effect of the first kind*) and reference electrode potential (*suspension effect of the second kind*) when they are immersed in the suspension. When

the ion-selective electrode is placed in a sediment or suspension, an additional potential is created due to the overlapping of the electrode diffuse double layer with the particle diffuse layers (see [Diffuse Double Layer \(DDL\)](#)). The second kind suspension effect is connected with changing the transference numbers of the cations and anions flowing out from the salt bridge solution of the reference electrode to the vicinity of surface-charged particles in the sample. The anomalous values of liquid junction potential are the results of the above (Oman et al., 2007a, b).

The potentiometric method is most often used in pH determination. The analyses are made by means of a glass electrode in a 1:5 (volume fraction) suspension of soil in water (pH in H_2O), in 1 mol/dm³ potassium chloride solution (pH in KCl), or in 0.01 mol/dm³ calcium chloride solution (pH in CaCl₂), according to the procedure of ISO 10390:2005 (Black, 1965; ISO 10390, 2005).

Potentiometric sensors are used mostly for analysis of liquid samples in laboratory conditions, according to the mentioned limitations of the method. However, some investigation are undertaken to apply the sensors in automatic mobile systems of soil monitoring. The ion-selective electrodes or ion-selective field effect transistors, due to the possibility of their miniaturization, are placed on machines, which are moving across the field and taking soil samples in combination with the geographical position registration. Some of the proposed equipment can extract soil solution in the field for making potentiometric analysis just after, and the other make ionometric measurements directly in moist soil (Adamchuk et al., 2004). However, it should be marked that the last method gives unreliable data due to unknown value of the suspension effect.

In soil research, the potentiometric titration is used also for characterization of the soil buffer capacity ([Buffer Capacity of Soils](#)) by acid-base titration and for surface charge of solid phase (minerals) by back-titration: subtraction of solution titration curve from the suspension titration curve gives solid phase variable charge vs. pH dependence.

Voltammetric methods

Voltammetric methods measure the electric current as a function of the applied electric potential and interpret the current–voltage relationship ([Figure 1](#)).

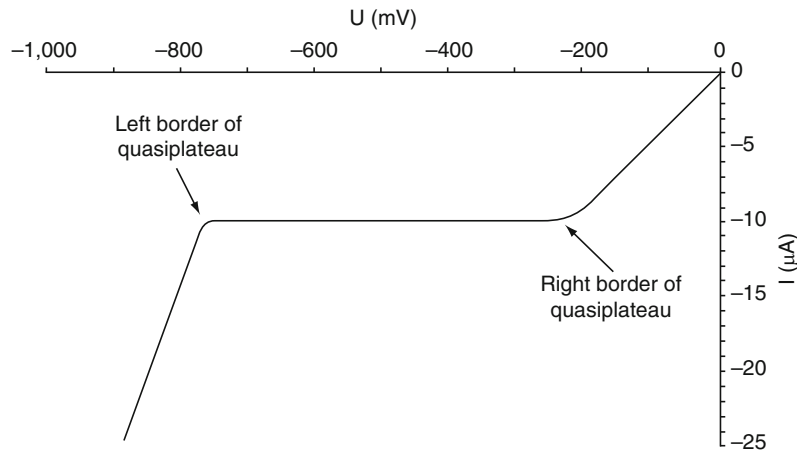
Common in soil science simplification of voltammetric methods is the amperometric one measuring the electric current in the system at an electric potential that is fixed at a constant value.

Oxygen diffusion rate (ODR) measured by amperometric method and oxygen flux density (OFD) measured by voltammetric method are important soil parameters.

The ODR describes the potential oxygen flux density in the soil. The measurement unit of ODR is g cm⁻² s⁻¹. The measurement can be realized in two ways:

1. The first proposition of Lemon and Erickson was based on a two-electrode setup. The cathode was made of platinum wire melted into the glass. The anode was a saturated calomel electrode (SCE) or a silver/silver chloride electrode. The potential, which was applied, had to be high enough to reduce the molecules of oxygen on the electrode but smaller than the potential of water electrolysis (usually -0.65 V). Due to the ambiguous determination of the real potential of platinum cathode in relation to the soil solute under a specific voltage applied to the electrodes, this method became a subject of criticism (Bieganowski, 2004).
2. The problem of precise controlling of the cathode potential was solved by Malicki and Walczak (1983) by incorporation into the measuring system a third electrode (a reference electrode) which, by the system of potentiostat, made it possible to arrange the potential of the platinum cathode (Bieganowski, 2004).

For determination of the OFD (g cm⁻² s⁻¹) the full current–voltage curve is registered (the potential of the cathode is linearly changed) and the values of the current at the plateau range ([Figure 1](#)) are used to calculate the oxygen flux density. The advantage of using the



Electrochemical Measurements in Soils, Figure 1 Idealized current–voltage curve (Bieganowski, 2004).

voltammetric method is the possibility of rejection of non-interpretable measurements (for instance when the soil moisture content is too small there is the lack of the plateau on the current–voltage curve and such a measurement should be rejected).

Both the ODR and OFD methods have the same assumptions:

- The only substance, which is reduced on the cathode (at established or changing potential) is oxygen.
- The concentration of oxygen on the cathode surface is equal to zero.
- The only way of oxygen transport to the electrode surface is diffusion (when this assumption is not valid there is a lack of plateau on the current–voltage curve).

In a real situation, the ODR and OFD methods can be used in saturated or nearly saturated mineral soils (organic substances can be reduced simultaneously with oxygen, which can be the source of the method error).

Applications of voltammetric methods in the soil solution and extracts measurements have less significance.

Conductometric method

Conductometric methods are based on the relation between the composition of a reference solution and the electrical conductance of tested solution/suspension. These methods are simple, rapid, nondestructive, and possible to use directly in the soil. The conductometric measurements characterize only the total amount of ions and not individual ions; however, the popularity of conductometric methods in the soil sciences lies in that the bulk conductivity of the soil solution is well correlated with soil total salt content. Therefore, the method is frequently used for saline soils and mineral fertilization status studies.

The interpretation of conductometric measurements in the soils is more complicated than in “pure” solutions because soil is a more complicated medium. The electric conductivity of soil as a whole can markedly differ from the conductivity of its equilibrium solution due to

- Additional electric current caused by movement of surface-charged soil colloids in the electric field together with ions.
- Input of surface conductance (the adsorbed ions in the electrical double layer can migrate in the electric field).
- Uneven and elongated paths of the ions and charged mineral/soil particles in complex soil pore system.
- Increased electrical resistance of air-filled soil pores.

The conductometric methods can be divided into two groups:

- AC methods – the alternating-current (AC) is used.
- DC methods – the direct-current (DC) is used.

Both groups of methods have specific advantages and limitations. The most important problems are the capacitance, inductance, and polarization. These phenomena

can be under control depending on the electrode construction, for instance. For details one can be referred to the very good study by Yu and Ji (1993).

Conductometric titration, a useful method in soil investigations (for instance for estimation of *Cation–Exchange Capacity, CEC*), must be carried out in soil extracts and therefore is beyond the scope of this entry.

In the second half of the twentieth century, there were attempts at using conductometric (or resistance – see *Electrical Resistivity to Assess Soil Properties*) methods for determination of soil moisture content. As it turned out, this approach failed because these methods are not selective, not stable, and highly dependent on the temperature, salinity, texture, density, and pH of the soil (Malicki, 1993).

Summary

Some of the electrochemical methods are very important in the measurements of soil properties. The most often used of them are potentiometric (in pH measurements and ion-selective electrodes for some soil solution ions) and conductometric (in soil solution conductivity measurements) ones. The electrochemical methods are comparatively simple, cheap, and reliable. The measuring procedures and equipment are continuously improved and developed.

Bibliography

- Adamchuk, V. I., Hummel, J. W., Morgan, M. T., and Upadhyaya, S. K., 2004. On-the-go sensors for precision agriculture. *Computers and Electronics in Agriculture*, **44**, 71–91.
- Bięganowski, A., 2004. Comparison of two- and three-electrode systems in measurements of potential flux density of oxygen in soil. *International Agrophysics*, **18**, 111–120.
- Black, C. A. (ed.), 1965. *Methods of Soil Analysis, Part 1. Physical and Mineralogical Properties. Including Statistics of Measurement and Sampling*. Madison: American Society of Agronomy.
- Brett, C. M. A., 2001. Electrochemical sensors for environmental monitoring. Strategy and examples. *Pure and Applied Chemistry*, **73**, 1969–1977.
- Brzózka, Z., and Wróblewski, W., 1999. *Chemical Sensors (in Polish)*. Warsaw: OWPW.
- Buck, R. P., and Lindner, E., 1994. Recommendation for nomenclature of ion-selective electrodes. IUPAC Recommendations 1994. *Pure and Applied Chemistry*, **66**, 2527–2538.
- ISO 10390, 2005. Soil quality. Determination of pH.
- Malicki, M., and Walczak, R., 1983. A gauge of the redox potential and the Oxygen diffusion rate in the soil, with an automatic regulation of cathode potential. *Zesz. Probl. Post. Nauk. Raln.*, **220**, 447–451.
- Malicki, M., 1993. Influence of soil physical properties on electrical parameters of electrode soil system in the aspect of determination of soil moisture and salinity (in Polish). *Acta Agrophysica (Series Monographs)*.
- Oman, S. F., Camoes, M. F., Powell, K. J., Rajagopalan, R., and Spitzer, P., 2007a. Guidelines for potentiometric measurements in suspensions. Part A. The suspension effect. IUPAC Technical report. *Pure and Applied Chemistry*, **79**, 67–79.
- Oman, S. F., Camoes, M. F., Powell, K. J., Rajagopalan, R., and Spitzer, P., 2007b. Guidelines for potentiometric measurements in suspensions. Part B. Guidelines for practical pH

measurements in soil suspension. IUPAC Recommendations 2006. *Pure and Applied Chemistry*, **79**, 81–86.
 Yu, T. R., and Ji, G. L., 1993. *Electrochemical Methods in Soil and Water Research*. Oxford: Pergamon.

Cross-references

- [Agophysical Objects \(Soils, Plants, Agricultural Products, and Foods\)](#)
- [Buffer Capacity of Soils](#)
- [Diffuse Double Layer \(DDL\)](#)
- [Electrical Properties of Soils](#)
- [Electrical Resistivity to Assess Soil Properties](#)
- [Hydraulic Properties of Unsaturated Soils](#)
- [Oxidation–Reduction Reactions in the Environment](#)
- [Solute Transport in Soils](#)

ELECTROKINETIC (ZETA) POTENTIAL OF SOILS

Mieczysław Hajnos, Jolanta Cieśla

Institute of Agrophysics, Polish Academy of Sciences,
 Lublin, Poland

Definition

From a theoretical viewpoint, *zeta potential* is electric potential in the interfacial double layer (DL) at the location of the slipping plane versus a point in the bulk fluid away from the interface. Electrokinetic potential in colloidal systems is called zeta potential. In the colloidal chemistry literature, it is usually denoted using the Greek letter zeta, hence ζ -potential. Thus, zeta potential is the potential difference between the dispersion medium and the stationary layer of fluid attached to the dispersed particle.

Introduction

Soil colloids are particles of diameter below 0.002 mm. They are formed by clay minerals (crystalline aluminum silicates of kaolin, montmorillonite, and illite groups, crystalline hydrated aluminum and iron oxides, amorphous minerals, humus as well as clay – humus complexes).

Colloid is composed of (Delgado et al., 2005) the following:

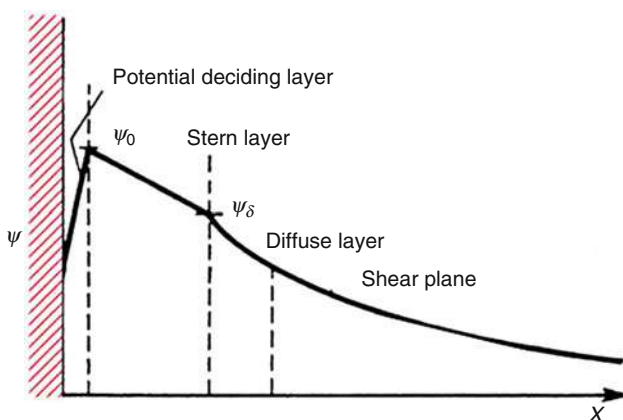
- (a) Kernel (micelle) of crystalline or amorphous structure and porous or dense construction
- (b) Internal layer of cations or anions, which constitutes a component of the kernel
- (c) External layer of compensating ions of opposite charge to the ions of internal layer

The most important colloid properties are determined by their electric charge occurred on the surface of colloid particles. Soil colloids are most often negatively charged (Sequaris and Lewandowski, 2003; Delgado et al., 2005).

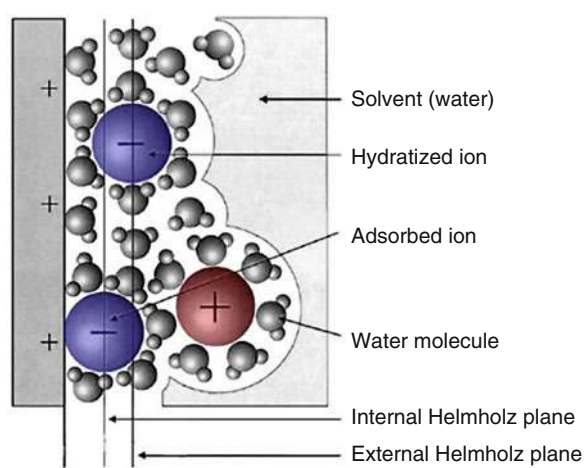
The value of electric charge depends on the composition of colloid kernel and sources of the charge are the following:

- (a) Unsaturated valencies occurring on the edges of silicate alumina layers, on the internal mineral surfaces as well as on the humus particles.
- (b) Interlayer exchange in crystals of minerals.

Electric charge of one symbol formed on the surface of colloid particles creates from the side of liquid, as a result of electrostatic interactions, the layer of opposite ions composed of exchangeable ions (dynamic Stern layer) (Figure 1) (Delgado et al., 2005). In the layer, ions are permanently connected with the micelle and can be taken into account as its component. Around the Stern layer are situated ions of the same charged sign as in Stern layer but there are hydrated ones. This layer is called as external Helmholtz layer (Figure 2). Next is situated the layer of heteronymous charged ions (diffusive layer). There are mobile ions, in which concentration decrease directly proportionally with the increase of distance from the micelle



Electrokinetic (Zeta) Potential of Soils, Figure 1 Dependence of potential against an interface distance.



Electrokinetic (Zeta) Potential of Soils, Figure 2 Structure of a double layer (DL).

surface, reaching ion equilibrium state with the solution. Ions of Stern layer and external Helmholtz layer hold on the colloid surface, whereas ions of diffusive layer are moving freely with the movement of solution in relation to solid. On the border of these two layers (mobile and immobile) called sliding layer, is found electric potential called electrokinetic potential or zeta potential.

The consequence of existence of electric double layer is electrokinetic phenomena (EKP).

Electrokinetic phenomena (EKP)

Electrokinetic phenomena (EKP) can be defined as all those phenomena involving tangential fluid motion adjacent to a charged surface. They are manifestations of the electrical properties of interfaces under steady-state condition and isothermal condition. In practice, they are often the only source of information available on those properties. For this reason, their study constitutes one of the classical branches of colloid science, electrokinetics, which has been developed in close connection with the theories of the electrical double layer (EDL) and of electrostatic surface forces (Dukhin and Derjaguin, 1974; Hunter, 1981; Lyclema, 1995; Hunter, 2001). From the point of view of nonequilibrium thermodynamics, EKP are typically cross-phenomena, because thermodynamic forces of a certain kind create fluxes of another type. For instance, in electroosmosis and electrophoresis, an electric force leads to a mechanical motion, and in streaming current (potential), an applied mechanical force produces an electric current (potential). First-order phenomena may also provide valuable information about the electrical state of the interface: for instance, an external electric field causes the appearance of a surface current, which flows along the interfacial region and is controlled by the surface conductivity of the latter. If the applied field is alternating, the electric permittivity of the system as a function of frequency will display one or more relaxations. The characteristic frequency and amplitude of these relaxations may yield additional information about the electrical state of the interface.

A brief description of the main and related EKP (Buckman and Brady, 1969; Dukhin and Derjaguin, 1974; Hunter, 1981; Lyclema, 1995; Hunter, 2001, Delgado et al., 2005):

Electrophoresis is the movement of charged colloidal particles or polyelectrolytes, immersed in a liquid, under the influence of an external electric field. The electrophoretic velocity, v_e (m s^{-1}), is the velocity during electrophoresis. The electrophoretic mobility, u_e ($\text{m}^2 \text{V}^{-1} \text{s}^{-1}$), is the magnitude of the velocity divided by the magnitude of the electric field strength. The mobility is counted positive if the particles move toward lower potential (negative electrode) and negative in the opposite case.

Electroosmosis is the motion of a liquid through an immobilized set of particles, a porous plug, a capillary, or a membrane, in response to an applied electric field. It is the result of the force exerted by the field on the

countercharge in the liquid inside the charged capillaries, pores, etc. The moving ions drag the liquid in which they are embedded along. The electroosmotic velocity, v_{eo} (m s^{-1}), is the uniform velocity of the liquid far from the charged interface. Usually, the measured quantity is the volume flow rate of liquid ($\text{m}^3 \text{s}^{-1}$) through the capillary, plug, or membrane, divided by the electric field strength, $Q_{eo,E}$ ($\text{m}^4 \text{V}^{-1} \text{s}^{-1}$), or divided by the electric current, $Q_{eo,I}$ ($\text{m}^3 \text{C}^{-1}$). A related concept is the electroosmotic counterpressure, Δp_{eo} (Pa), the pressure difference that must be applied across the system to stop the electroosmotic volume flow. The value Δp_{eo} is considered to be positive if the high pressure is on the higher electric potential side.

Streaming potential, U_{str} (V), is the potential difference at zero electric current, caused by the flow of liquid under a pressure gradient through a capillary, plug, diaphragm, or membrane. The difference is measured across the plug or between the ends of the capillary. Streaming potentials are created by charge accumulation caused by the flow of countercharges inside capillaries or pores.

Sedimentation potential, U_{sed} (V), is the potential difference sensed by two identical electrodes placed some vertical distance L apart in a suspension in which particles are sedimenting under the effect of gravity. The electric field generated, U_{sed}/L , is known as the sedimentation field, E_{sed} (V m^{-1}). When the sedimentation is produced by a centrifugal field, the phenomenon is called centrifugation potential.

Measurement of the zeta potential of soil material

For the measurement of the zeta potential of soil material, two groups of methods are most frequently used. The first group consists of methods based on the electrophoretic phenomenon, and the second based on electroosmosis. The application of the electrophoretic methods in soil material, however, is limited because they allow the measurement to be carried out only on the colloidal fraction (Delgado et al., 2005).

The *electroosmotic methods* are more suitable for soil material because they make possible the carrying out of measurements in soils of natural granulometric composition.

The value of the zeta potential can be calculated by substituting the experimental data for the Smoluchowski equation (Smoluchowski, 1921)

$$\zeta = -\frac{\eta \chi V}{\varepsilon E} \quad (1)$$

where χ – proper conductance of solution; V – velocity of liquid transportation – electroosmotic velocity; E – current intensity; η – dynamic viscosity of liquid; ε is the dielectric constant of the medium.

In the *electrophoresis method* (Buckman and Brady, 1969; Hunter, 2001), the ζ -potential can be determined by placing fine particles in an electric field and measuring their mobility, V_E , using a suitable microscopic technique.

The mobility is then related to the ζ -potential at the interface using the Smoluchowski equation

$$\zeta = \frac{V_E \eta}{\varepsilon} \quad (2)$$

where η is liquid viscosity, ε is the dielectric constant of the medium.

The *streaming potential technique* has been extensively applied to flat surfaces to study solid–liquid interface electrical properties (Delgado et al., 2005) in a parallel plate microchannel. In this technique, the downstream convection of ions via pressure-driven flow induces a streaming potential which, for steady incompressible and laminar flow, can be related to the ζ – potential:

$$\zeta = \frac{\eta \chi V_{str}}{\varepsilon P} \quad (3)$$

where η is liquid viscosity, ε is the dielectric constant of the medium, P is the pressure causing flow, V_{str} is the streaming potential measured, and χ is the proper conductance of solution.

Other techniques for determination of electrophoretic mobility or zeta potential of minerals as well as soil particles in suspension are electrophoretic light scattering (ELS), known as laser Doppler velocimetry method (Chip et al., 2003; Delgado et al., 2005) and electroacoustics – especially the electrokinetic sonic amplitude (ESA) measurement (Chip et al., 2003; Greenwood et al., 2007).

Laser Doppler velocimetry is the optical method based on the phase analysis light scattered by charged colloidal particles, which are immersed in liquid and moved in external electric field (Delgado et al., 2005). The frequency of the light scattered by the moving particles is shifted in comparison with the light emitted from the source (Doppler effect). If the directions of the incident light, the scattered light and particles movement are known, this shift is proportional to the particles' speed. As a monochromatic coherent light source in the measurement systems, the Helium–Neon or Argon–Ion lasers are very often used. Application of alternating electric field during measurement, whereas the particles are still able to move according to their electrophoretic mobility, reduces the polarization of electrodes and eliminates the influence of electroosmotic effect on the results. Laser method is automated, quick, and it needs only small volume of soil suspension (a few milliliters). On the other hand, there are some requirements for the analyzed samples (Delgado et al., 2005):

- (a) The continuous phase should be transparent liquid with refractive index different from that of dispersed particles.
- (b) The upper size of charged particles should be rather lower than 30 μm (diameter), because of sedimentation occurrence.
- (c) Dilution must be enough for particles not to interfere with each other.

- (d) Fluorescence of sample may inhibit measurement by reduction in the signal-to-noise ratio.

Electrokinetic sonic amplitude (ESA) is connected with the application of alternating electric field to a suspension where particles density differs from that of continuous phase. Electrophoretic motion of particles in this electric field causes the increase of a sound wave (Delgado et al., 2005).

It should be noticed that the used method affects in some way the obtained results, and even by the same measurement conditions as well as sample preparation techniques, the values of electrophoretic mobility or zeta potential may be different.

Zeta potential effects on soil

Zeta potential decides on surface phenomena occurring on solid–liquid interface. Such phenomena are processes of aggregation and peptization of soil colloids. The phenomena follow from the occurrence of opposite forces, which result from the distribution of ions surrounding the colloid kernel. Sphere of ions (ion layers) around the micelle leads to rise repulsing and attraction forces. Repulsion forces appear in moment of approach of two particles, when their double electrical layers begin to overlap. For connection of two particles, the energy is needed of higher level than repulsion forces. The level of indispensable energy markedly increases when particles are closer and closer. Maximum electrostatic repulsion force describes surface potential of particles.

Van der Waals attraction forces are the result of interaction of individual molecules of every colloid particle in such a way that every molecule of first particle attracts every molecule of the second one. Total attraction force is a sum of interaction of all molecules. The theory interpreting surface interactions (balance of repulsion and attraction forces) is elaborated by Derjaguin, Landau, Verwey, and Overbeek and in short called DLVO theory. The theory interprets phenomena such as aggregation, coagulation, flocculation, and peptization of colloids.

Aggregation consists in joining of individual colloid particles in larger agglomerations called aggregates. Run of the process can perform in double manner: coagulation and flocculation, that is, joining of colloids by hydration layers, without previous decrease of electrokinetic potential

Coagulation, that is, joining of colloids as a result of decrease of electrokinetic potential, can happen in soils under the influence of electrolytes (mineral fertilizers) introduced to soils. Strong concentration of ions in internal micelle layers and decrease of their electrokinetic potential takes place as the result of it. Moreover, the degree of coagulation interaction of ions on negatively charged colloid particles is the greater, the higher diameter and valency as well as lower hydration of ion. Especially strong influence on soil colloids is exhibited by hydrogen and aluminum ions.

Flocculation, that is, joining of colloids by hydration layers, without previous decrease of electrokinetic

potential, in soils can run spontaneously or under influence of flocculants. Often flocculation occurs during desiccation of soils or during consecutive periods of their freezing and defreezing when dehydration of soil colloids occurs. Synthetic flocculants are organic substances (ionic and nonionic polymers), which bind colloids together with the aid of hydrogen bonds.

Peptization is the process responsible for the formation of stable dispersion of colloidal particles of soil in water.

Summary

Potential zeta or electrokinetic potential is a property of charged interfaces, for example, soil surface/soil solution. The consequence of existence of electric double layer is electrokinetic phenomena such as electrophoresis, electroosmosis, streaming potential, and sedimentation potential. Zeta potential can be measured mainly by electroosmotic and electrophoretic methods. Zeta potential decides on surface phenomena occurring on solid–liquid interface. Such phenomena for example are processes of aggregation and peptization of soil colloids.

Bibliography

- Buckman, H. C., and Brady, N. S., 1969. *The Nature and Properties of Soils*. London: Macmillan.
- Chip, A., Ma, L. Q., Rhue, R. D., and Kellenley, E., 2003. Point of zero charge determination in soils and minerals via traditional methods and detection of electroacoustic mobility. *Geoderma*, **113**, 77–93.
- Delgado, A. V., Gonzales-Caballero, F., Hunter, R. J., Koopal, L. K., and Lyklema, J., 2005. Measurement and interpretation of electrokinetic phenomena. *Pure and Applied Chemistry*, **77**, 1753–1805.
- Dukhin, S. S., and Derjaguin, B. V., 1974. Electrokinetic Phenomena. In Matijevic, E. (ed.), *Surface and Colloid Science*. New York: Wiley, Vol. 7, Chap. 2.
- Greenwood, R., Lapcikova, B., Surynek, M., Waters, K., and Lapcik, L., Jr., 2007. The zeta potential of kaolin suspension measured by electrophoresis and electroacoustics. *Chemical Papers*, **61**, 83–92.
- Hunter, R. J., 1981. *Zeta Potential in Colloid Science*. New York: Academic.
- Hunter, R. J., 2001. *Foundations of Colloid Science*. Oxford: Oxford University Press, Chap. 8.
- Lyklema, J., 1995. *Fundamentals of Interfaces and Colloid Science*. New York: Academic, Vol. II, Chaps. 3 and 4.
- Sequaris, J.-M., and Lewandowski, H., 2003. Physicochemical characterization of potential colloids from agricultural topsoils. *Colloids and Surfaces A: Physicochemical and Engineering Aspects*, **217**, 93–99.
- Smoluchowski, M., 1921. Elektrische endosmose und strömungsströme. In Graetz, L. (ed.), *Handbuch der Electrizität und des Magnetismus*. Leipzig: Barth, Vol. 2, p. 366.

Cross-references

- [Diffuse Double Layer \(DDL\)](#)
- [Electrical Properties of Soils](#)
- [Flocculation and Dispersion Phenomena in Soils](#)
- [Soil aggregates, Structure, and Stability](#)
- [Soil Phases](#)
- [Soil Water Flow](#)
- [Solute Transport in Soils](#)
- [Surface Properties and Related Phenomena in Soils and Plants](#)

ELECTROMAGNETIC FIELD

See [Magnetic Treatment of Irrigation Water, Effects on Crops](#)

ELECTROMAGNETIC FIELDS, IMPACT ON SEED GERMINATION AND PLANT GROWTH

Stanisław Pietruszewski

Department of Physics, University of Life Sciences,
Lublin, Poland

Introduction

The germination, growth, yield, and quality of crops are determined by the properties of seed material, which can be improved by pre-sowing treatment with the involvement of various physical factors such as the electric field, magnetic field, laser radiation, and microwave radiation. Physical methods applied in the treatment of greenhouse plants include also the use of magnetically treated water.

The first experiments investigating the effect of magnetic fields on biological organisms, including plants, were carried out in the second half of the nineteenth century. The first publication on the subject was the study by J. Reinke dating back to 1876, which discussed the results of experiments into the magnetic field's effect on plant development (Reinke, 1876). This study did not report a relationship between the magnetic field and seed germination and plant growth. Similarly D'Aste (1882) did not find any links between the magnetic field and seed germination, while Tolomei (1893) observed that the magnetic field speeded up germination. Tolomei was also the first scientist to discover the effect of magnetotropism. This phenomenon was further investigated by Audus (1960). Volume 1 and Volume 2 monograph by W. J. Danilewski (1901) in which the author discussed the experimental and theoretical grounds of the effect of magnetic fields on various biological structures, ranging from cells to entire organisms.

Another classic and historical publication is a study of Eward (1903). Eward observed that when aquatic plants (*Valisneria* and *Chara*) were placed in a magnetic field, their cytoplasmic motion ceased when magnetic field lines were perpendicular to the direction of that motion. This effect was not observed in a parallel magnetic field. Thirty years later, this phenomenon was validated by Sawostin (1930). He noted that cytoplasmic motion was reduced by 15–30% in a parallel magnetic field with the intensity of 7,000 Oe (0.7 T). Cytoplasmic motion was speeded up in a perpendicular magnetic field with the same intensity. Sawostin also observed that the magnetic field accelerated root growth and increased cell membrane permeability. The above findings enabled the researcher to grow wheat germs 100% longer than average (Presman, 1971). Biomagnetic research flourished only in the 1960s

when a number of breakthrough publications reporting on the magnetic field's effect on live biological organisms were published in the USA (Barnothy, 1964, 1969) and the former USSR (Presman, 1971).

The pre-sowing effect of magnetic fields on seed material

The pre-sowing stimulation of seeds with a magnetic field may involve a constant magnetic field produced by permanent magnets and electromagnets as well as a variable magnetic field. A variable magnetic field is produced by specially designed electromagnets. In general, magnetic fields speed up seed germination and plant growth. The intensity of the applied magnetic fields and the time of seed exposure vary greatly.

In an experiment involving a very weak constant magnetic field of 0.5 mT, Nowitzky et al. (2001) noted an increase in leaf size as well as higher protein and chlorophyll levels in onion sets. Aladjadjiyan (2002) observed the effect of lengthening of monopodiums of sweet corn cultivated under 150 mT constant magnetic fields and in the case of alternating magnetic fields of 60–200 mT also the growth in the crop yield. Carbonell et al. (2000) noted higher rice seed germination rates under the influence of 150 and 200 mT magnetic fields as well as faster growth rates of barley subjected to a magnetic field with the intensity of 125 mT with exposure time of 24 h (Martinez et al., 2000). Atak et al. (2003) subjected soybean seeds to magnetic fields of 2.9–4.6 mT and noted accelerated root growth as well as an increase in the levels of chlorophyll *a* and *b*.

Rochalska and Grabowska (2007) demonstrated that a variable magnetic field of 16 Hz, 5 mT, lowers the activity of alpha-amylase and beta-amylase enzymes in wheat. Aksenov et al. (2001) noted an increase in the growth rates of wheat roots and germs under the influence of a 50 Hz, 30 mT magnetic field. The effect of a weak magnetic field with the intensity of 20 µT and frequency of 16% Hz increased the weight and height of sunflower plants and enhanced wheat germination rates (Fischer et al., 2004). Ratusnyak et al. (2008) demonstrated that high-frequency magnetic fields of 30–60 GHz with a stream from 10^{-16} to 10^{-10} W cm⁻² and exposure time of 5–15 min stimulated the growth of microflora in pine seeds.

The above data indicate that the results noted at various research centers are difficult to compare. Difficulties are also encountered when interpreting the results of pre-sowing stimulation of seeds with an electric field. This is related to a very broad range of intensity of magnetic fields and varied exposure times. To facilitate the comparison of results from various studies a common unit, being the product of magnetic (electric) field density and exposure time, has been proposed (Pietruszewski, 1999; Pietruszewski et al., 2007). The density of a magnetic field or an electric field is determined with the use of the following formula:

$$\rho = \frac{1}{2} \varepsilon_0 E^2 = \frac{1}{2} \mu_0 H^2 = \frac{1}{2\mu_0} B^2 \quad (1)$$

where ε_0 – vacuum permittivity, μ_0 – vacuum permeability, E – electric field intensity, H – magnetic field intensity, B – magnetic induction.

The exposure dose is described by the following dependence:

$$D = \rho \cdot t \quad (2)$$

where t – exposure time.

The magnetic exposure dose dependencies of germination kinetic and the wheat crop yield were previously by Pietruszewski and Kania (2010).

Mechanism of interaction

The discovery that an external magnetic or an electromagnetic field affects the development of living organisms prompted scientists to postulate various hypotheses explaining this phenomenon. They attempted to develop a scientific model based on the classical laws of electrodynamics. Researchers assumed that an external magnetic field should affect the permeability of the cell membrane and, consequently, the diffusion of ions, mainly sodium Na⁺ and potassium K⁺ ions and hypothesized that:

1. Changes in the rate and mechanism of diffusion and in the biological orientation of macromolecules with a magnetic susceptibility
2. Changes in the probability of mutual interactions in biochemical reactions owing to the magnetic field's effect on the electron structures of molecules

Although the above hypotheses offer some fascinating insights, they are difficult to validate experimentally due to a very broad range of the applied intensity levels as well as the characteristic attributes of fields (constant and variable fields). Constant magnetic fields exert a different effect on organic structures than variable fields. According to Wadas (1991), a magnetic field's effect on living organisms can be through the effects on: non-compensated electron spins, liquid crystals in the organisms, and moving positive and negative charges.

The generation of induction microcurrents is yet another effect that can be attributed to a variable (alternating) magnetic field. Wadas (1991) argued that a magnetic field whose intensity falls below a given threshold level, which is difficult to determine and which varies between organisms, stimulates enzymatic activity and speeds up metabolism. An increase in enzymatic activity under the influence of a magnetic field is also observed in animal organisms. This observation prompted Wadas to formulate a hypothesis that the above is a general law of nature. It should also be noted that magnetic field does not exert a selective effect on living organisms, but impacts all molecules, including those that do not need it.

In his work entitled *Magneto-Biophysics – A New Dimension in Research*, Weiss (1989) writes that although the effect of magnetic fields on living organisms (humans, animals, plants) had fascinated scientists for centuries, magneto-biophysics is still in its infancy as a science. Weiss believes that magnetic fields will have numerous applications in biology, medicine, agriculture, and food economics in the nearest future. Magnetic ions and molecules are found in an excited state only in living organisms. Such states are ascribed to the effect of electrostatic, magnetostatic, electromagnetic, and gravitational fields. The mutual interactions between those fields and their effect on cells and living organisms continue to pose new challenges for physicists and biologists (Wadas, 1991).

Conclusion

Pre-sowing treatment involving the exposure of seed material to a magnetic or an electromagnetic field improves germination rates, seedling growth and yield. This effect is determined by seed type, magnetic field, and the time of exposure. Owing to a high variety of the applied fields, a unit of measure that best describes the pre-sowing stimulation of seeds is the magnetic exposure dose that accounts for both field intensity and exposure time. The mechanism of magnetic and electromagnetic fields' interaction with biological structures has not been fully elucidated to date. The presented hypotheses describe a specific phenomenon, and they do not propose a general theory. The discussed methods of pre-sowing treatment of seeds are environmentally friendly, and they should find a broad range of applications.

Bibliography

- Aksenov, S. I., Gruzina, T. I., and Goriachev, S. N., 2001. Characteristics of low frequency magnetic field effect on swelling of wheat seeds at various stages. *Biofizika*, **46**, 1127–1132.
- Aladjadijyan, A., 2002. The use of physical method for plant growing stimulation in Bulgaria. *Journal of Central European Agriculture*, **8**, 369–380.
- Atak, C., Emiroğlu, Ö., Alikamençlu, S., and Rzakoulieva, A., 2003. Stimulation of regeneration by magnetic field in soybean (*Glycine max* L. Merrill) tissue cultures. *Journal of Cell and Molecular Biology*, **2**, 113–119.
- Audus, L. J., 1960. Magnetotropism: a new plant growth response. *Nature*, **185**, 132–134.
- Barnothy, M. F. (ed.), 1964. *Biological Effect on Magnetic Fields*. New York: Plenum, Vol. 1.
- Barnothy, M. F. (ed.), 1969. *Biological Effect on Magnetic Fields*. New York: Plenum, Vol. 2.
- Carbonell, M. E., Martinez, E., and Amaya, J. M., 2000. Stimulation of germination in rice (*Oryza sativa* L.) by a static magnetic field. *Electro- and Magnetobiology*, **19**, 121–128.
- D'Aste (1882) Influence physiologique de l'état magnétique. Comptes Rendus de la Société de Biologie (Paris) 4:278 (Barnothy, M. F. *Biological Effect on Magnetic Fields*, Vol. 1, pp. 183–195).
- Danilewski, W. J., 1901. Studies on the influence of electricity on physiology of plants. Kharkov. In Presman, A. J. (ed.), *Electromagnetic Fields and Live Nature*, 1971. Warszawa: PWN.
- Eward, A., 1903. On the physics and physiology of protoplasmic streaming in plants. Oxford. In Presman, A. J. (ed.), *Electromagnetic Fields and Live Nature*, 1971. Warszawa: PWN.
- Fischer, G., Tausz, M., and Gill, D., 2004. Effect of weak 16% Hz magnetic field on growth parameters of young sunflower and wheat seedling. *Bioelectromagnetics*, **25**, 638–641.
- Martinez, E., Carbonell, M. V., and Amaya, J. M., 2000. A static magnetic field of 125 mT stimulates the initial growth stages of barley (*Hordeum vulgare* L.). *Electro- and Magnetobiology*, **19**, 271–277.
- Nowitzky, I., Novitskaya, G. V., Kosheshova, T. K., Nechiporenko, G. A., and Dobrovols'kiy, M. V., 2001. Growth of green onions in a weak permanent magnetic field. *Journal of Plant Physiology*, **48**, 709–715.
- Pietruszewski, S., 1999. *Magnetic Treatment of Spring Wheat Seeds*. The Scientific Trials of Agricultural University in Lublin.
- Pietruszewski, S., and Kania, K., 2010. Effect of magnetic field on germination and yield of wheat. *International Agrophysics*, **24**, 297–302.
- Pietruszewski, S., Muszyński, S., and Dziwulska, A., 2007. Electromagnetic fields and electromagnetic radiation as non-invasive external stimulants for seeds (selected methods and responses). *International Agrophysics*, **21**, 95–100.
- Presman, A. J., 1971. *Electromagnetic Fields and Live Nature*. Warszawa: PWN.
- Ratushnyak, A. A., Andreeva, M. G., Morozova, G. A., and Trushin, M. V., 2008. Effect of extremely high frequency electromagnetic fields on microbiological community in rhizosphere of plants. *International Agrophysics*, **22**, 71–74.
- Reinke, J., 1876. Untersuchungen der Wachstrum. Botan. Ztg. **34**, 129 (Barnothy, M. F. *Biological Effect on Magnetic Fields*, Vol. 1, pp. 183–195).
- Rochalska, M., and Grabowska, K., 2007. Influence of magnetic fields on activity of enzyme: α - and β -amylase and glutathione S-transferase (GST) in wheat plants. *International Agrophysics*, **21**, 185–188.
- Sawostin, P. W., 1930. Magnetic growth reaction in plants. *Planta*, **12**, 327–333.
- Tolomei, G., 1893. Anzione del magnetismo sulla germinazione. *Malpighia*, **7**, 470 (Barnothy, M. F. *Biological Effect on Magnetic Fields*, Vol. 1, pp. 183–195).
- Wadas, R., 1991. *Biomagnetism*. Warszawa: PWN.
- Weiss, H., 1989. Magnetobiophysics – a new research line? In *Proceedings of the Fourth ICPPAM*. Rostock, pp. 885–891.

Cross-references

- Agrophysics: Physics Applied to Agriculture*
Magnetic Treatment of Irrigation Water, Effects on Crops

ELUTRIATION

Separating lighter from heavier particles in a granular mixture, by washing in water.

Bibliography

- Chesworth, W. (ed.). 2008. *Encyclopedia of Soil Science*, Springer, p 207.

ELUVIATION

The removal of soil material in solution (described by the term “leaching”) or suspension through the soil. The direction of displacement depends on the direction of water movement.

Bibliography

- Chesworth, W. (ed.). 2008. Encyclopedia of Soil Science, Springer, p.207.
 Glossary of Soil Science Terms. Soil Science Society of America. 2010. <https://www.soils.org/publications/soils-glossary>

Cross-references

[Leaching of Chemicals in Relation to Soil Structure](#)

EMISSIVITY

Energy emitted from the surface/energy emitted by a black surface at same temperature.

EMPIRICAL MODEL

Simple mathematical relationships derived from observations for describing more complex processes.

Bibliography

- Glossary of Soil Science Terms. Soil Science Society of America. 2010. <https://www.soils.org/publications/soils-glossary>

Cross-references

[Agrophysics: Physics Applied to Agriculture](#)

ENERGETICALLY HOMOGENOUS (HETEROGENOUS) SURFACE

See [Adsorption Energy and Surface Heterogeneity in Soils](#)

ENERGY BALANCE OF ECOSYSTEMS

Andrzej Kędziora
 Institute for Agricultural and Forest Environment, Polish Academy of Sciences, Poznań, Poland

Definition

The set of all energy fluxes incoming and outgoing from any active surface or layer of any object are called energy

balance. Usually fluxes incoming to the system are taken as positive, while the outgoing as negative.

Introduction

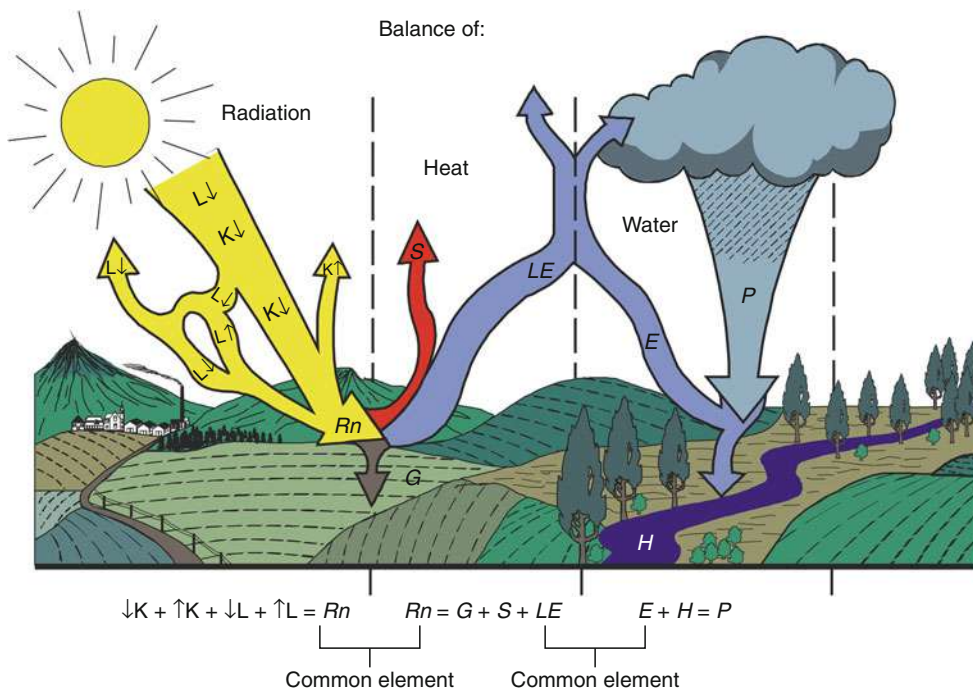
On a global scale, there are two processes that form the basis for all other processes occurring in nature. These are energy flow and matter cycling (Ryszkowski and Kędziora, 1987, 2004). Energy supply, at least, from the theoretical point of view is not limited (because of the sun activity), but water supplies are limited and not restored. These two processes are strongly linked and their quantitative characteristics are best accomplished by water and energy balances.

Electromagnetic radiation coming from the sun is the main input of energy for the earth ecosystems. Incoming solar radiation is composed predominantly of visible and near infrared shortwave radiation characterized by the high capacity to perform works during its transformations (Rosenberg, 1974). The output of energy into the cosmic space is mainly in the form of long infrared radiation of which intensity depends on temperature of the body surface, showing lower capability for performing work (higher entropy).

The conversion of solar energy is the driving force for processes in the majority of ecosystems or landscapes under normal conditions (Frangopoulos, 2003; Ryszkowski and Kędziora, 2004). The influx of solar energy can be partitioned mainly into fluxes used for evapotranspiration – ensuring water cycling, then for air heating – determining local temperatures and air mass transfers and for soil and water heating. In addition to these four main (from the quantitative point of view) fluxes, there are much smaller fluxes, but very important from the functionality point of view. They are the flux of advection, photosynthesis, and flux stored in the biomass.

Energy balance

There are three balances that should be considered together if anyone would like to characterize the energy balance in the ecosystem fully. They are radiation balance, heat balance, and water balance (Figure 1). Radiation balance determines the energy (leaving out nuclear and geothermal energy) being the moving force of all processes and support of life, as well as the source of energy used by human community. The set of all energy fluxes is called the heat balance equation. In the same way, the set of all water fluxes incoming into the system or outgoing is called the water balance equation (Kędziora and Olejnik, 1996; Piccolo, 2009). All energy fluxes incoming into the system and outgoing must be balanced to keep the system in equilibrium. The heat balance and the water balance are joined by latent heat flux (heat balance) and evaporating water (water balance). It means that the heat balance determines the energy, which can be used for evapotranspiration, but on the other hand, the water balance affects the structure of heat balance. In the nature some kind of “rule of evapotranspiration priority” exists,



Energy Balance of Ecosystems, Figure 1 Radiation, heat, and water balances of an agricultural landscape.

which says that if in the system there is enough available water for evaporation, the system directs all energy fluxes toward evaporating surface to cover the energetic cost of this process, using not only whole net radiation but also changing the direction of sensible and soil heat fluxes (Monteith, 1975; Kędziora and Ryszkowski, 1999; Olejnik et al., 2002).

This phenomenon can be explained as follows. Intensive evapotranspiration of plant cover occurs in relatively lower temperature, because most of the net radiation is used for this process, so much less energy can heat leaves and air. Thus, during the process of evapotranspiration the entropy production is higher than in the other processes (entropy is equal to the useful energy divided by temperature in which the process occurs). According to thermodynamics laws, this process is realized first, which produces the highest amount of entropy.

Taking into account the impact of ecosystems on energetic effect of solar energy point of view, intensively evaporating surface can be called “coolers of environment” while the dry surfaces, like the field after harvesting, can be called “heaters of environment.”

Radiation balance of a system

Radiation balance is usually written down in the form:

$$Rn = Rs(i) + Rs(o) + Rl(i) + Rl(o)$$

The net radiation (Rn) is the result of incoming and outgoing shortwave and longwave radiation fluxes and the reflection coefficient (albedo) of the ecosystem surface.

Incoming shortwave radiation flux, $Rs(i)$, depends mainly on sky cloudiness and solar elevation, which is a function of a day in a year and latitude. Outgoing shortwave radiation flux, $Rs(o)$, depends on albedo (α) of an ecosystem $Rs(o) = \alpha \cdot Rs(i)$. Incoming longwave radiation flux, $Rl(i)$, depends only on temperature of upper atmosphere during sunny days and on temperature of cloud bottom during cloudy days, while outgoing longwave radiation flux, $Rl(o)$, depends on the earth surface temperature. Solar energy reaching the earth system is determined by “solar constant,” which is defined as “solar radiation flux density measured at the earth orbit.”

Heat balance of a system

As it was said in the “Introduction” that the heat balance and the water balance are strongly linked, so the further description will relate to these two balances.

Heat balance equation is usually written in the form:

$$Rn + S + G + LE + A + F + M = 0,$$

where Rn , net radiation; LE , latent heat of evapotranspiration; S , sensible heat of air heating; G , soil heat; A , heat of advection; F , heat of biogeochemical processes; and M , heat stored by plant cover (all expressed in $\text{W} \cdot \text{m}^{-2}$). Usually the last three components are omitted because their values do not exceed a few $\text{W} \cdot \text{m}^{-2}$. But in some cases the advection must be included into equation. For example, when intensively evaporating ecosystem is surrounded by dry areas (forest island located between

grain crop fields after harvesting) the advection flux density can reach as much as 40% of net radiation.

The water balance equation is usually written in form:

$$P + E + H \pm \Delta R = 0,$$

where P , precipitation; E , evapotranspiration; H , run-off; ΔR , changes in soil water retention (all expressed in mm). There are many factors that determine the value of particular components of the heat and water balances. The main factors are as follows:

Net radiation is a function of:

- Solar radiation determining the density of energy flowing toward active surface and depending on season and latitude
- Relative sunshine expressing the time of full solar radiation
- Temperature of evaporating surface determining the energy flux density emitted from the surface
- Temperature of the atmosphere
- Water vapor pressure in the atmosphere, which is main factor determining the atmospheric ability for absorption of the energy emitted by the earth surface, and the same determining amount of energy reemitted by the sky toward earth surface
- Albedo of evaporating surface determining the amount of solar energy reflected by the active surface

Sensible heat flux is a function of:

- Plant cover
- Net radiation
- Surface temperature
- Vertical gradients of wind speed and air temperature
- Aerodynamic characteristic of active surface
- Habitat moisture
- Stability of the atmosphere

Soil heat flux depends mainly on:

- Plant cover
- Temperature gradient in the soil, which is the driving force of energy flow into the soil
- Thermal diffusivity of soil determining the rate of heat flux inflowing into the soil
- Soil moisture and porosity

Latent heat of evapotranspiration and *evapotranspiration* mainly depend on:

- Plant cover
- Habitat moisture
- Energy available for evapotranspiration processes
- Evaporation demands of the atmosphere
- Stability of the atmosphere

Heat advection is a function of:

- Horizontal gradient of air temperature, which is the driving force of horizontal flow of heat
- Aerodynamic parameters of active surface determining the coefficient of turbulent exchange

- Wind speed determining the intensity of horizontal flow of air mass

Energy available for evapotranspiration is a sum of net radiation and heat advection.

Habitat moisture depends mainly on:

- Precipitation
- Soil water retention

Atmospheric demand of evaporation is a function of:

- Wind speed
- Saturation water vapor pressure deficit

Surface runoff depends mainly on:

- Intensity of rainfall,
- Coefficient of water infiltration of the soil
- Physiography

Most of these factors are controlled by plant cover (Jaeger and Kessler, 1997; Kędziora et al., 1989; Olejnik et al., 2002). The well-developed plant cover the higher intensity of evapotranspiration and in turn the lower temperature of the active surface and the higher pressure of water vapor in the atmosphere. Cooling of the active surface caused by the intensively evaporating plant cover causes the horizontal temperature gradient. Plant cover impacts on micrometeorological condition of the landscape as well as condition of surface runoff and water infiltration rate. The higher plant covers the higher roughness parameter of the surface and the intensive turbulent exchange of energy and matter between earth surface and atmosphere.

Structure of heat balance of ecosystems

Structure of heat balance of ecosystem or landscape depends on many factors from which the most important are:

- Plant cover (leaf area index and development phase)
- Moisture condition of habitat (water availability for evapotranspiration)
- General climatic conditions (climatic zone)
- Landscape structure

Plant cover affects the heat balance structure by changing net radiation, increasing evapotranspiration, decreasing sensible and soil heat fluxes, and generating advection heat. An ecosystem having high leaf area index (ratio of total one side leaves area to the area on which plants are growing), usually has lower albedo than areas covered by poor vegetation or bare soil (excluding black soil), which have higher net radiation. Such an ecosystem decreases the solar radiation flux reaching soil surface, and the same decreases the soil heat fluxes. The ecosystems of plants having deep root systems are able to use water from deeper soil layers and, as a result, they can evaporate very intensively. This process cooling the canopy of the plants causes decrease of sensible heat flux (smaller vertical gradient of air temperature) and origin

of advection process (increasing horizontal gradient of air temperature).

Seasonal course of heat balance components in an agricultural landscape

The annual course of heat balance components depends mainly on seasonal changes of plant biomass, precipitation, and solar radiation. From this point of view, in temperate zone, ecosystems can be divided into four types:

- Forests and other ecosystem growing continuously from spring to autumn
- Meadows and other perennial crops (alfalfa for instance) having two or more periods of growth interrupted by harvest
- Winter crops (wheat or rape seed for example) having growth period in the spring and early summer
- Ecosystems having growth period in the late spring and in summer (row crop, spring crops, maize)

In the first type of ecosystem, always the latent heat flux prevails and consists about 80–90% of net radiation, depending on habitat moisture. Well-developed forest growing on very moist area can use for evapotranspiration the whole net radiation flux or even more. Sensible heat consists about 10–25% while the soil heat does not exceed a few percent.

In the second type of ecosystem during the majority of each growth period, latent heat prevails, especially in the period of fully developed stage. In this time, latent heat consists about 60–80% of net radiation, sensible heat consists about 20–30% while soil heat about 10–20%. Only in the summer period when moisture of habitat is very low, after harvesting, sensible heat flux can for the short time overcomes latent heat.

In the third type of ecosystems, in the spring, when soil moisture is high, the latent heat is much higher than sensible heat flux reaching up to 90% of net radiation. As water supplies run low the proportion of sensible to latent heat (Bowen ratio) increases reaching in the mature period values equal 1. After harvest (and of August and September) sensible heat flux can be higher than latent heat, depending on soil moisture.

In the last type of ecosystems the situation is quite different. In the early spring (time before germination) when soil moisture is very high, the evaporation of bare soil is intensive and latent heat flux is higher than sensible heat flux. During sunny days, when solar radiation is very intensive, the soil heat can be the biggest component of heat balance (Stohlgren et al., 1998; Pielke and Avissar, 1990; Kimura et al., 2005). As soil heat runs low, evapotranspiration decreases, and for the short time (two 10-days) the sensible heat flux prevails over latent heat flux. Then, as plant development increases, latent heat flux also increases and latent heat flux becomes higher than sensible heat, and soil heat is very small. Such a situation exists up to the end of vegetation period.

Conclusion

The heat balance is the best energetic characteristic of ecosystem or landscape that enables us to understand the processes of energy flow and matter cycling in the agricultural areas. It should be kept on mind that plant cover is the most important factor controlling heat and water balances of the landscape. Thus, it allow us, through the proper management of landscape structure, to control the structure of heat and water balance and microclimatic condition of the agricultural areas, and the same to optimize the use of solar energy toward maximizing the use of the environment potential for production of the food and to ensure the sustainable development of rural areas.

Bibliography

- Frangopoulos, C., 2003. Exergy, energy system analysis, and optimization. In Tolba, M. K. (ed.), *Our Fragile World*. Oxford: Eolss, pp. 454–470.
- Jaeger, L., and Kessler, A., 1997. Twenty years of heat and water balance climatology at the Hartheim pine forest, Germany. *Agricultural and Forest Meteorology*, **84**(1), 25–36.
- Kędziora, A., and Olejnik, J., 1996. Heat balance structure in agroecosystems. In Ryszkowski, L., French, N. R., and Kędziora, A. (eds.), *Dynamics of an Agricultural Landscape*. Poznań: PWRIŁ.
- Kędziora, A., and Ryszkowski, L., 1999. Does plant cover structure in rural areas modify climate change effects? *Geographia Polonica*, **72**, 63–85.
- Kędziora, A., Olejnik, J., and Kapuściński, J., 1989. Impact of landscape structure on heat and water balance. *Ecology International Bulletin*, **17**, 1–17.
- Kimura, R., Liu, Y., Takayama, N., Zhang, X., Kamichika, M., and Matsuoka, N., 2005. Heat and water balances of the bare soil surface and the potential distribution of vegetation in the Loess Plateau, China. *Journal of Arid Environments*, **63**(2), 439–457.
- Monteith, J. L., 1975. *Vegetation and the Atmosphere, Vol. 1: Principles*. London: Academic, Vol. 1. 278.
- Olejnik, J., Kędziora, A., and Eulensteine, F., 2002. Mitigation of radiation and heat balance structure by plant cover structure. In Ryszkowski, L. (ed.), *Landscape ecology in agroecosystems management*. Boca Raton: CRC Press, pp. 29–55.
- Piccolo, M. C., 2009. Heat energy balance in coastal wetlands. In Perillo, G. M. E., Wolanski, E., Cahoon, D. D. R., and Brinson, M. M. (eds.), *Coastal Wetlands: An Integrated Ecosystem Approach*. Amsterdam: Elsevier, pp. 221–230.
- Pielke, R. A., and Avissar, R., 1990. Influence of landscape structure on local and regional climate. *Landscape Ecology*, **4**, 133–155.
- Rosenberg, N. J., 1974. *Microclimate: The Biological Environment*. New York: Wiley. 315 pp.
- Ryszkowski, L., and Kędziora, A., 1987. Impact of agricultural landscape structure on energy flow and water cycling. *Landscape Ecology*, **1**(2), 85–94.
- Ryszkowski, L., and Kędziora, A., 2004. Energetics of ecosystem and landscape changes. *Ecological Questions*, **5**, 9–22.
- Ryszkowski, L., and Kędziora, A. 2008. The influence of plant cover structures on water fluxes in agricultural landscapes. In Bossio, D., and Geheb, K. (eds.), *Conserving Land, Protecting Water*. UK: CAB International. Vol. 6, pp. 163–177.
- Stohlgren, T. J., Chose, T. N., Pielke, R. A., Kittels, G. F., and Baron, J. S., 1998. Evidence that local land use practices influence regional climate, vegetation and stream flow patterns in adjacent natural areas. *Global Change Biology*, **4**, 495–504.

Cross-references

[Adsorption Energy and Surface Heterogeneity in Soils](#)
[Adsorption Energy of Water on Biological Materials](#)
[Soil–Plant–Atmosphere Continuum](#)
[Water Balance in Terrestrial Ecosystems](#)

ENERGY BALANCE OF A FIELD

An expression of the classical law of energy conservation, stating that the sum of the energy inputs minus the energy outputs of a field (including radiant energy, sensible heat, latent heat) over a specified period must equal the change in energy content (both thermal and chemical)

Bibliography

Introduction to Environmental Soil Physics (First Edition) 2003
 Elsevier Inc. Daniel Hillel (ed.) <http://www.sciencedirect.com/science/book/9780123486554>

Cross-references

[Coupled Heat and Water Transfer in Soil](#)
[Energy Balance of Ecosystems](#)

ENTHALPY

A measure of the total energy of a thermodynamic system (e.g., solid, liquid or vapor).

ENTROPY

A measure of unavailable energy of an isolated thermodynamic system.

Cross-references

[Energy Balance of Ecosystems](#)

ENVIRONMENTAL CONSERVING TILLAGE

See [Tillage, Impacts on Soil and Environment](#)

ENZYME

Organic catalysts that convert a substrate or nutrient to a form which can be transported into a cell.

ENZYMES IN SOILS

Małgorzata Brzezińska
 Institute of Agrophysics, Polish Academy of Sciences,
 Lublin, Poland

Definition

Soil enzymes. Enzymes in any of the states of occurrence in soils (Ladd et al., 1996).

Numerous processes in soil depend on enzymatic catalysis, including organic matter decomposition, gas emission and sink, pollutants breakdown, energy flow, and nutrient cycling in ecosystem.

Enzymes in soils are associated with different soil constituents. Intracellular enzymes are present in proliferating microorganisms (primarily bacteria and fungi), plant roots, and soil microfauna, or attached to dead cells and cell debris. Numerous extracellular enzymes usually operate at a distance from the parent cell; the capacity to produce and secrete biocatalysts is of survival importance for soil microorganisms and plants. Enzymes in the liquid phase (extracellular as well as released from lysed cells) have generally a short half-life due to rapid denaturation and degradation. However, when complexed with clay minerals or humic colloids, enzymes retain their catalytic properties for a long time, usually at the cost of some loss of the activity. Thus, enzymes may persist and may be active in soil in which no proliferation takes place (*accumulated* or *abiotic* enzymes). While some enzymes (e.g., polysaccharidases) as a rule are extracellular, others are considered to act only intracellularly, hereby reflecting the actual activity of the soil biota (e.g., dehydrogenases) (Burns, 1978; Nannipieri et al., 2002; Skujins, 1967).

Many enzymes are measured in soils, predominantly of the classes of hydrolases and oxidoreductases. The assays are generally simple, sensitive, and relatively rapid. The standard methods determine an overall enzyme activity in soil, and combined with molecular techniques can elucidate many aspects of microbial activity in soil (Bastida et al., 2008).

Soil enzymes are sensitive to variations induced by environmental factors and anthropogenic disturbances, are strongly affected by physical conditions, soil type, and vegetation, and respond to changes in soil management more quickly than other soil variables. Numerous studies confirm that soil enzymes correlate with other indices of fertility and biological activity and are useful in making predictions about the soil environment. There is growing interest in the applications of soil enzymes as the early and sensitive indicators of soil ecological stress and soil quality change in agroecosystem and natural or contaminated soils.

Bibliography

Bastida, F., Zsolnay, A., Hernández, T., and García, C., 2008. Past, present and future of soil quality indices: a biological perspective. *Geoderma*, **147**, 159–171.

- Burns, R. G., 1978. *Soil Enzymes*. London: Academic Press.
- Ladd, J. N., Foster, R. C., Nannipieri, P., and Oades, J. M., 1996. Soil structure and biological activity. In Stotzky, G., and Bollag, J. M. (eds.), *Soil Biochemistry*. New York: Marcel Dekker, Vol. 9, pp. 23–77.
- Nannipieri, P., Kandeler, E., and Ruggiero, P., 2002. Enzyme activities and microbiological and biochemical processes in soil. In Burns, R. G., and Dick, R. P. (eds.), *Enzymes in the Environment: Activity, Ecology, and Applications*. New York: Marcel Dekker, pp. 1–33.
- Skujins, J. J., 1967. Enzymes in soils. In McLaren, A. D., and Peterson, G. H. (eds.), *Soil Biochemistry*. New York: Marcel Dekker, Vol. 1, pp. 371–414.

Cross-references

- [Biochemical Responses to Soil Management Practices](#)
[Biofilms in Soil](#)
[Microbes and Soil Structure](#)
[Soil Biota, Impact on Physical Properties](#)

ERODIBILITY OF SOIL

See [Organic Matter, Effects on Soil Physical Properties and Processes](#)

EROSION

(i) The wearing away of the land surface by rain or irrigation water, wind, ice, or other natural or anthropogenic agents that abrade, detach and remove geologic parent material or soil from one point on the earth's surface and deposit it elsewhere, including such processes as gravitational creep and so-called tillage erosion; (ii) The detachment and movement of soil or rock by water, wind, ice, or gravity. The following terms are used to describe different erosion types, processes, and mechanisms.

Bibliography

- Chesworth, W. (ed.). 2008. *Encyclopedia of Soil Science*, Springer, p.207.
 Glossary of Soil Science Terms. Soil Science Society of America. 2010. <https://www.soils.org/publications/soils-glossary>

Cross-references

- [Furrow Erosion](#)
[Gully \(Linear\) Erosion](#)
[Ice Erosion \(Glacial Erosion, Thermal Erosion\)](#)
[Rill Erosion](#)
[Sheet Erosion](#)
[Tillage Erosion](#)
[Water Erosion: Environmental and Economical Hazard](#)
[Wind Erosion](#)

EROSIVITY

See [Organic Matter, Effects on Soil Physical Properties and Processes](#)

ESTIMATION OF QUARTZ CONTENT IN MINERAL SOILS

Vlodek R. Tarnawski¹, Toshihiko Momose²
 Wey H. Leong³, David J. W. Piper⁴

¹Division of Engineering, Saint Mary's University, Halifax, NS, Canada

²Bavarian Environment Agency, Hof/Saale, Germany

³Department of Mechanical and Industrial Engineering, Ryerson University, Toronto, ON, Canada

⁴Geological Survey of Canada, Bedford Institute of Oceanography, Dartmouth, Canada

Definition

Mineral soils. Soils composed predominantly of minerals. **Quartz.** One of the most common constituents of the Earth's crust, abundant in sandstones, granite, and soils. It is made up of silica (SiO_2) having a superior ability to conduct heat.

Thermal conductivity of soils. The bulk property of soils describing their ability to conduct heat. It is measured in Watts per Kelvin per meter (W/K/m).

Introduction

Thermal conductivity of soil solids (λ_s) is an essential parameter required by a majority of models in the prediction of soil thermal conductivity (λ). The value of λ_s depends strongly on the fraction of quartz (Θ_q) in soil solids and its thermal conductivity (λ_q), whose value is considerably higher than the remaining soil minerals. For that reason, Θ_q is a key parameter for assessing λ_s , but data on Θ_q is very scarce and often contradictory with soil texture. Quartz (SiO_2) occurs mainly in coarse soil fractions (i.e., sands and gravels) as it does not break up easily and is more water and weather resistant than other soil minerals. Up to this date, the only available set of mineral composition data is that for 19 soils by Kersten (1949), and it shows considerable Θ_q inconsistency with respect to soil texture; for that reason, it cannot be successfully applied to other soils. Many of the soils studied by Kersten are not fully formed due to their young origin (post-glacial time) and the volcanic environment of Alaska. Peters-Lidard et al. (1998) published rough Θ_q estimates for 12 standard soils by the United States Department of Agriculture (USDA), assuming that Θ_q was roughly equivalent to mass fractions of sand. These estimates, however, were never verified by laboratory measurements. As a result, λ_s was assumed as a fitting parameter in a large majority of predictive models (de Vries, 1963; Johansen, 1975; Gori, 1983, etc.). Purushothamaraj and Judge (1977) presented the λ_s from the measured λ data of various soils. Values of λ_s varied from 3.2 to 9 W/m K for sand solids, 2.4–5.9 W/m K for silt solids, and 2.8–4.8 W/m K for clay solids; due to large λ_s variation, this data is hard to apply. There are several instrumental techniques that could be potentially applied

to the determination of minerals in soils: the most frequently used are chemical analysis, differential thermal analysis (DTA), and X-ray diffraction (XRD) (Rowse and Jepson, 1972; Hardy, 1992). The chemical methods, however, often produce problematic Θ_q due to the presence of SiO_2 in other minerals. The DTA technique is based on the analysis of temperature difference between the soil sample and temperature stable reference material, both being heated in an oven at a constant temperature and compared to that of pure minerals tested separately as references of similar size, origin, and crystallinity (Karathanasis and Harris, 1994). The method is error prone due to sample packing, peak height, and instrument reproducibility (Rowse and Jepson, 1972). According to Hardy (1992) and Bish (1994), the XRD technique is in general less accurate than the chemical methods but recent design advances in XRD equipment makes this technique fast and reliable for regular mineral recognition. Recently, Tarnawski et al. (2009a) proposed a new way of assessing quartz content using inverse modeling of soil thermal conductivity at full saturation (λ_{sat}). This modeling approach produced reasonable results to experimental Θ_q data of ten soils studied by Kersten (1949). This approach, however, requires further verification against XRD data which represent a broad variety of mineral soils.

Quantitative X-ray diffraction method

Theoretical background

The majority of soil minerals, with the exception of poorly crystalline clays, can be described as a crystal lattice made of repeating planes of atoms. When the X-ray beam confronts the crystal lattice, it can pass through, be absorbed, refracted and scattered, and diffracted. Each mineral diffracts X-rays in its own unique pattern that depends on the crystal lattice structure. The X-ray beam is generated by a high energy source (15–60 kV) within a sealed vacuum tube (XRD apparatus). The X-ray beam is directed on a slide containing a finely powdered soil, usually ground to particle sizes less than 10 μm . The resulting diffraction is recorded at specific angles by a rotating detector and then converted into quantifiable images

by specialized software. A typical X-ray powder diffractogram is obtained by changing the angle of glancing diffraction (θ) between the X-ray source, the powder slide, and the detector. The diffractogram peaks indicate positions where the X-ray beam has been diffracted by the crystal lattice. A peak area or peak height is usually considered as a measure of diffracted intensity (I). The wavelength of the incident X-ray beam (λ) is a characteristic constant of the X-ray tube target. Then, the distance between adjacent planes of crystal lattice structure (d) and θ obey the Bragg law.

$$N \cdot \lambda = 2 \cdot d \cdot \sin \theta \quad (1)$$

where N is the order of reflection (integer).

A proper examination of mineral specific peaks (area or height) leads to quantitative assessment for a particular mineral. The XRD technique has two main sources of error, namely: interference from other minerals and peak height reproducibility (Rowse and Jepson, 1972).

Experimental procedure and results

Samples of ten natural soils (Table 1) were analyzed by X-ray diffraction (Siemens D 500). A small amount of soil sample was required to fill in a small disk. In order to have clearly interpretable diffraction patterns for natural soils, fine grains are advantageous as they produce a very large number of crystal orientations exposed to the X-ray beam. According to Hardy (1992), a slope of the calibration curve varies insignificantly within 5–20 μm . A large majority of tested soils have a very small fraction of clay, therefore, soil grains were pulverized, in a tungsten carbide grinding mill, to a particle size <20 μm . The grain size distribution was checked using a particle size analyzer. Then, slides containing pulverized soil grains were exposed to X-ray beam. A working calibration curve (Equation 2) was established from six standard samples, a mixture of known quartz fraction (0, 0.1, 0.5, 0.7, 0.9, 1.0) and talc. In the obtained calibration curve, the intensity of quartz reflection (I_q) with respect to Θ_q obeys the following relation:

Estimation of Quartz Content in Mineral Soils, Table 1 Physical characteristics of ten fully saturated soils with XRD and TCP analyses

Soil name	n	m_{cl}	m_{si}	m_{sa}	$\lambda_{\text{s-cal}}$	λ_{sat}	$\theta_{q-\text{XRD}}$	$\theta_{q-\text{cal}}$
Ottawa sand (C109)	0.40	0.00	0.00	1.00	8.3	2.9	1.0	1.0
Ottawa sand (C190)	0.40	0.00	0.00	1.00	8.1	2.9	1.0	1.0
Acadia	0.55	0.10	0.57	0.33	4.2	1.5	0.5	0.6
Alberta	0.55	0.10	0.52	0.38	3.8	1.4	0.6	0.5
Cumberland	0.45	0.05	0.34	0.61	5.0	1.9	0.7	0.7
PEI	0.41	0.03	0.14	0.84	4.5	2.0	0.6	0.6
Pugwash	0.40	0.05	0.37	0.57	5.1	2.1	0.6	0.7
Toyoura	0.40	0.00	0.00	1.00	6.9	2.6	0.8	0.9
Red Y	0.60	0.43	0.23	0.34	3.0	1.2	0.4	0.3
Tottori Sand	0.42	0.03	0.05	0.92	4.5	1.9	0.5	0.6

Note: $\lambda_w \approx 0.61 \text{ W/m K}$ at 25°C; $\lambda_q \approx 7.60 \text{ W/m K}$ at 25°C

$$I_q = 117.46 \cdot \Theta_q + 0.515(nm) \quad r^2 = 0.99. \quad (2)$$

The calibration curve (Equation 2) was used to convert the peak intensity values in the powdered soils to quartz content. The precision of Θ_{q-XRD} estimates was usually better than $\pm 10\%$ (Table 1). The advantages of the XRD technique are, among others, simple sample slide preparation and rapid measurements. The XRD technique requires, however, expensive laboratory equipment (XRD apparatus, tungsten carbide grinders, etc.) and highly trained personnel. Therefore, recently more research attention is focused on indirect estimation of Θ_q from measured soil λ at full saturation.

Modeling quartz content from measured λ_{sat}

Theoretical background

The content of quartz (Θ_q) can also be assessed from λ_{sat} using a weighted geometric mean model (Tarnawski et al., 2009a).

$$\lambda_{sat-cal} = \lambda_s^{1-n} \cdot \lambda_w^n \quad (3)$$

where, λ_w is the thermal conductivity of water; $\lambda_{sat-cal}$ is a calculated λ_{sat} ; n is soil porosity.

Due to its simplicity and good predictions, this model has been frequently used for assessing λ of saturated two-component porous media (Woodside and Messmer, 1961; Johansen, 1975). For saturated soils, the model gives good estimates of λ_{sat} . This model has also been successfully applied to evaluating λ_s .

$$\lambda_s = \lambda_q^{\Theta_q} \cdot \lambda_{o-min}^{1-\Theta_q}, \quad (4)$$

where λ_{o-min} is a lump thermal conductivity of all soil minerals without quartz.

A lumped λ value of the remaining minerals (λ_{o-min}), other than quartz, is usually assumed to be about 2 W/m K (Farouki, 1986).

In spite of simplicity, the above equations (Equations 3 and 4) are difficult to use due to a lack of Θ_q and λ_q data. Accurate estimates of these parameters do not exist and, therefore, they are usually chosen subjectively to artificially enhance the λ model predictions.

Both parameters, however, can be assessed indirectly from the λ_{sat} measured data. By combining Equations 3 and 4, λ_s and Θ_q can be calculated from the following relations:

$$\lambda_{s-cal} = \left(\frac{\lambda_{sat-exp}}{\lambda_w^n} \right)^{1/(1-n)} \quad (5)$$

$$\Theta_{q-cal} = \frac{\ln(\lambda_{s-cal}/\lambda_{o-min})}{\ln(\lambda_q/\lambda_{o-min})}. \quad (6)$$

Quartz is a dominant component of many rocks and natural soils, and its λ is notably higher than other soil minerals. The quartz itself is an anisotropic mineral, whose ability to conduct heat depends on heat flow

direction; along the direction perpendicular to the c-axis (threefold crystallographic axis) $\lambda_{q-\perp}$ is 6.5 W/m K, while along the c-axis the $\lambda_{q-\parallel}$ is 11.3 W/m K (Farouki, 1986). A further modeling complication is due to a fact that quartz grain orientation in a soil system with respect to the flow of heat is usually unknown. Therefore, a lumped thermal conductivity of randomly oriented quartz crystals is used. Its value is usually assessed by a weighted arithmetic mean (de Vries, 1952)

$$\lambda_q = \frac{1}{3} \cdot (2 \cdot \lambda_{q-\perp} + \lambda_{q-\parallel}) \quad (7a)$$

or by a weighted geometric mean (Farouki, 1986)

$$\lambda_q = \lambda_{q-\perp}^{2/3} \cdot \lambda_{q-\parallel}^{1/3}. \quad (7b)$$

The large majority of predictive λ models assume λ_q as temperature (T) independent, but in reality λ_q declines with T . A fitted λ_q vs. T relation, based on data published by Clauser and Huenges (1995) and Equation 7b, has the following form ($r^2 = 0.99$):

$$\lambda_q = 8.128 - 0.021T(0^\circ C < T < 100^\circ C). \quad (8)$$

The thermal conductivity of water was obtained from experimental data published by Sengers and Watson (1986).

$$\lambda_w = 0.57109 + 0.0017625T - 0.0000067036T^2. \quad (9)$$

Measurement of λ_{sat}

Fully saturated soil samples are not easy to prepare due to difficulty in removing trapped air between soil particles. A calculated mass of soil, equivalent to the assumed dry bulk density, was added to a known volume of a sampler. Soil compaction was accomplished by repeatedly tapping the lateral surface of the cylinder. For coarse soils (e.g., C109, C190), water, free of dissolved oxygen, was gradually added along the cylinder's perimeter until the total weight of added water was equal to calculated mass of water corresponding to the relative volume of the tested soil. For fine soils, the saturated soil sample was placed in a laboratory exicator and exposed to $p_{vacuum} = 1-10$ mmHg, thus speeding up the removal of trapped air. The value of λ_{sat} for ten soils was determined using a thermal conductivity probe (TCP) that consists of a stainless steel tubular sheath, containing a constantan heater wire and a T-type thermocouple. The internal space of the sheath was filled in with a low-viscosity epoxy. To simulate a line heat source, the ratio of the probe length to the probe diameter should be at least 50. The time of λ_{sat} measurements was approximately 120 s. More details about the theoretical and practical considerations regarding the probe design and operation, as well as the experimental set-up, can be obtained from Tarnawski et al. (2009b). For λ_{sat} measurements, the temperature rise of the probe was kept below 4°C by maintaining a constant

current of 0.21 A (supplied to the probe heater), resulting in a TCP source strength of 9.9 W/m. Uncertainties of λ measurements for saturated soils were from 3% to 6%. A summary of soil physical characteristics such as clay, silt, sand, and gravel mass fractions, soil porosity (n), λ_{sat} , and Θ_q data (rounded to decimal point) are given in [Table 1](#).

The inverse modeling of quartz content from measured λ_{sat} is a very promising and inexpensive method producing very close results to $\Theta_{q-\text{XRD}}$ data. However, this approach requires accurate λ_{sat} data.

Assessment of quartz content from available λ data
The available λ data of soils is often incomplete and without λ_{sat} data. Therefore, λ data was carefully scrutinized in terms of soil origin, limited dispersion of λ data, and wide coverage of the degree of saturation (S_r). Only soils with extensive λ data spread over a wide range of wetness were selected for inverse modeling, i.e., $S_{r-\min} < 0.07$ and $S_{r-\max} > 0.5$. The soils studied by Kersten (1949) and Lu et al. (2007) were considered for comparison purposes only. The Alaskan soils tested by Kersten (1949) were not fully formed due to their young post-glacial and volcanic origin. Those investigated by Lu et al. (2007) show a considerable diversity of quartz occurrence. Finally, 11 soils were selected and their physical characteristics were

summarized in [Table 2](#). A prevailing number of soils have λ data in a very close vicinity to the dry condition, while λ_{sat} records are very rare. Missing λ_{sat} values were obtained by fitting existing experimental λ data of a particular soil to a three-parameter function given by Lu et al. (2007). Among five normalized conductivity functions tested by Tarnawski et al. (2009a), the exponential function in [Equation 10](#) is the most suitable for modeling thermal conductivity of soils.

$$\lambda = \lambda_{\text{dry}} + \exp\{\alpha \cdot (1 - S_r^{\alpha-\beta})\} \cdot (\lambda_{\text{sat}} - \lambda_{\text{dry}}), \quad (10)$$

where α , β , and λ_{sat} are fitting parameters.

The λ data at $S_r < 0.02$ was assumed to represent λ at dryness (λ_{dry}). In a case when λ_{dry} and λ_{sat} were not available, a four-parameter fitting was applied.

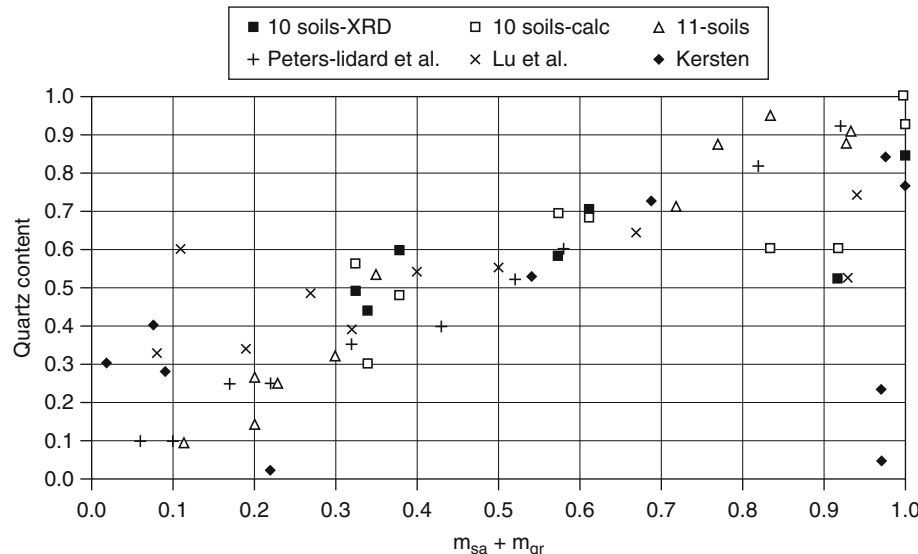
A similar reverse modeling of λ_{sat} , based on an iterative approach, was described by Tarnawski et al. (2009a). Once an experimental or fitted λ_{sat} is obtained, the lumped λ_s can be evaluated using [Equation 5](#). The average λ_s (4.61 W/m K) of the 11 soils is higher than the average λ_s used by Johansen (3 W/m K). Taking into account newly confirmed $\lambda_{\text{sat-exp/fit}}$ given by [Equation 10](#), the $\Theta_{q-\text{cal}}$ can be evaluated by [Equation 6](#), considering $\lambda_{o-\min} \approx 2$ W/m K and $\lambda_q \approx 7.60$ W/m K. A summary of fitting results such as α , β , $\lambda_{\text{dry-exp/fit}}$, $\lambda_{\text{sat-exp/fit}}$, and $\Theta_{q-\text{cal}}$ for 11 soils under consideration is given in [Table 3](#).

Estimation of Quartz Content in Mineral Soils, Table 2 Physical properties of 11 soils from literature

Soil name	Reference	m_{clay}	m_{silt}	m_{sand}	m_{gravel}	n
Berino sand	Horton and Wierenga (1984)	0.05	0.03	0.93	0.00	0.39
Mississippi river sand	Tehrani (1978)	0.01	0.05	0.84	0.09	0.38
Loamy sand	Noborio et al. (1996)	0.09	0.07	0.84	0.00	0.41
BigHorn sandy loam	Deru (2003)	0.13	0.10	0.77	0.00	0.38
Volkmar	Campbell et al. (1994)	0.12	0.16	0.72	0.00	0.47
Moon valley	Tehrani (1978)	0.04	0.60	0.35	0.00	0.45
Ritzville (silt loam)	McInnes (1981)	0.05	0.65	0.30	0.00	0.58
Walla-Walla	Campbell et al. (1994)	0.14	0.63	0.23	0.00	0.54
Mokins	Campbell et al. (1994)	0.25	0.55	0.20	0.00	0.56
Portneuf silt loam	Cass et al. (1984)	0.19	0.61	0.20	0.00	0.52
Palouse-A	Campbell et al. (1994)	0.21	0.68	0.11	0.00	0.53

Estimation of Quartz Content in Mineral Soils, Table 3 Details of indirect estimation of $\lambda_{\text{dry-exp/fit}}$, $\lambda_{\text{sat-exp/fit}}$, and $\Theta_{q-\text{cal}}$

Soil name	$S_{r-\min}$	$S_{r-\max}$	α	β	r^2	$\lambda_{\text{dry-exp/fit}}$	$\lambda_{\text{sat-exp/fit}}$	$\Theta_{q-\text{cal}}$
Berino sand	0.00	1.00	1.00	1.39	0.90	0.26	2.8	0.9
Mississippi river sand	0.02	1.00	0.85	1.24	0.95	0.26	2.8	0.9
Loamy sand	0.00	0.97	0.69	1.05	1.00	0.26	2.5	0.9
BigHorn sandy loam	0.00	1.00	1.00	1.30	0.99	0.31	2.6	0.9
Volkmar	0.04	0.61	0.48	1.10	0.98	0.23	2.0	0.7
Moon valley	0.02	0.64	0.16	1.21	0.98	0.21	1.7	0.5
Ritzville (silt loam)	0.00	0.61	0.92	1.43	0.90	0.14	1.3	0.3
Walla-Walla	0.07	0.67	0.79	1.51	0.97	0.18	1.3	0.2
Mokins	0.05	0.69	0.17	1.60	0.97	0.25	1.2	0.3
Portneuf silt loam	0.00	0.85	0.09	1.52	0.93	0.22	1.3	0.1
Palouse-A	0.04	0.70	0.09	1.66	0.99	0.22	1.1	0.1



Estimation of Quartz Content in Mineral Soils, Figure 1 Predicted and experimental Θ_q data vs. m_{co} .

Summary of results and discussion

Quartz is a very hard and weather resistant mineral, therefore, its dominant occurrence is mainly in coarse soils. Figure 1 displays the estimated Θ_q , as a function of soil coarse mass fraction ($m_{co} = m_{sa} + m_{gr}$), for the 11 soils under investigation, together with Θ_q data from Lu et al. (2007), Kersten (1949), and Peters-Lidard et al. (1998) as default Θ_q for 12 USDA standard soils, and Θ_{q-XRD} values from Table 1. Figure 1 shows a relatively close match between some of the 11 soils' Θ_q (Table 3) and the XRD data of 10 soils (Table 1). In turn, the Θ_q data by Peters-Lidard et al. (1998) fairly agrees with that of the 11 soils and Θ_{q-XRD} of 10 tested soils. The values of Θ_q by Lu et al. (2007) fairly agree with the Θ_q of the 11 soils, with the exception of two coarse and a silty-loam soil. In turn, quartz fractions given by Kersten (1949) often show erratic variation with soil texture that could be caused by a completely different soil origin.

Conclusions

Predictions of soil thermal conductivity are strongly influenced by the content of quartz, for which data is very scarce. Inverse modeling of quartz content from measured thermal conductivity at saturation is a very promising and relatively inexpensive approach that may partially resolve this issue. This approach, however, requires accurate thermal conductivity data at full saturation, which can be either measured directly using, for example, a TCP or obtained by fitting λ data over a wide range of wetness. However, it has to be kept in mind that soil mineralogy is strongly influenced by the parent material from which soils were formed. Therefore,

a wide range of variation of quartz content may occur in soils having very similar texture, but coming from different places of dissimilar genesis history. For example, some of Kersten's natural soils have a relatively young origin, dating the post-glacial time of Alaska, and therefore show very deviant records of quartz content with respect to soil texture. More reliable data from XRD, on soil thermal conductivity in full range of wetness, and on mineralogical composition of soils from different origins are needed to further confirm this inverse modeling approach.

Bibliography

- Bish, D. L., 1994. Quantitative X-ray diffraction analysis of soils, pp. 267–295. In Amonette, J. E., and Zelazny, L. W. (eds.), *Quantitative Methods in Soil Mineralogy*. Madison: SSSA Misc. Publ. SSSA.
- Campbell, G. S., Jungbauer, J. D., Bidlake, W. R., and Hungerford, R. D., 1994. Predicting the effect of temperature on soil thermal conductivity. *Soil Science*, **158**(5), 307–313.
- Cass, A., Campbell, G. S., and Jones, T. L., 1984. Enhancement of thermal water vapor diffusion in soil. *Soil Science Society of America Journal*, **48**, 25–32.
- Clauser, C., and Huenges, E., 1995. Thermal conductivity of rocks and minerals. In Ahrens, T. J. (ed.), *Rock Physics and Phase Relations – A Handbook of Physical Constants*. Washington: AGU Reference Shelf. American Geophysical Union, Vol. 3, pp. 105–126.
- Deru, M., 2003. *A Model for Ground-Coupled and Moisture Transfer from Buildings*. National Renewable Energy Laboratory, NREL/TP-550-33954, Contract No. DE-AC36-99-GO10337, <http://www.nrel.gov/docs/fy03osti/33954.pdf> (accessed 5 June 2006).
- de Vries, D. A., 1952. Thermal conductivity of soil. *Mededelingen van de Landbouwhogeschool te Wageningen*, **52**(1), 1–73; Trans: Building Research Station (Library Communication no. 759), England.

- de Vries, D. A., 1963. Thermal properties of soils. In van Wijk, W. R. (ed.), *Physics of the Plant Environment*. New York: John Wiley, pp. 210–235.
- Farouki, O. T., 1986. *Thermal Properties of Soils. Series on Rock and Soil Mechanics*. Clausthal-Zellerfeld: Trans Tech Publications, Vol. 11.
- Gori, F., 1983. A theoretical model for predicting the effective thermal conductivity of unsaturated frozen soils. In *Proceedings of the 4th International Conference on Permafrost. Fairbanks, Alaska*, Washington, National Academy Press, pp. 363–368.
- Hardy, M., 1992. X-ray diffraction measurement of the quartz content of clay and silt fractions in soils. *Clay Minerals*, **27**, 47–55.
- Horton, R., and Wierenga, P. J., 1984. The effect of column wetting on soil thermal conductivity. *Soil Science*, **138**(2), 102–108.
- Johansen, O., 1975. *Thermal Conductivity of Soils*, Ph.D. thesis, Trondheim, Norway (CRREL Draft Translation 637, 1977, ADA 044002).
- Karathanasis, A. D., and Harris, W. G., 1994. Quantitative thermal analysis of soil materials. In Amonette, J. E., and Zelazny, L. W. (eds.), *Quantitative Methods in Soil Mineralogy*. Madison: SSSA Misc. Publ. SSSA, pp. 360–429.
- Kersten, M. S., 1949. *Thermal Properties of Soils*. Bulletin No. 28, University of Minnesota Engineering Experiment Station, **LII** (21).
- Lu, S., Ren, T., Gong, Y., and Horton, R., 2007. An improved model for predicting thermal conductivity from water content at room temperature. *Soil Science Society of America Journal*, **71**(1), 8–14.
- McInnes, K., 1981. *Thermal Conductivities of Soils from Dry Land Wheat Regions in Eastern Washington*. MS thesis, Pullman, WA, Washington State University.
- Noborio, K., McInnes, K. J., and Heilman, J. L., 1996. Two-dimensional model for water heat, and solute transport in furrow-irrigated soil: II. Field evaluation. *Soil Science Society of America Journal*, **60**, 1001–1009.
- Peters-Lidard, C. D., Blackburn, E., Liang, X., and Wood, E. F., 1998. The effect of soil thermal conductivity parameterization on surface energy fluxes and temperatures. *Journal of Atmospheric Science*, **55**(7), 1209–1224.
- Purushothamaraj, P., and Judge, A., 1977. *Thermal Conductivity of Soil Solids*. Unpublished paper from the Earth Physics Branch, Canada, National Research Council.
- Rowse, J. B., and Jepson, W. B., 1972. The determination of quartz in clay minerals. *Journal of Thermal Analysis*, **4**, 1969–1975.
- Sengers, J. V., and Watson, J. T. R., 1986. Improved international formulations for the viscosity and thermal conductivity of water and steam. *Journal of Physical and Chemical Reference Data*, **15**, 1291–1314.
- Tarnawski, V. R., Momose, T., and Leong, W. H., 2009a. Assessing the impact of quartz content on the prediction of soil thermal conductivity. *Géotechnique*, **59**(4), 331–338.
- Tarnawski, V. R., Momose, T., Leong, W. H., Bovesecchi, G., and Coppa, P., 2009b. Thermal conductivity of standard sands. Part I. Dry state conditions. *International Journal of Thermophysics*, **30**, 949–968.
- Tehrani, J. M., 1978. *Measurement of Thermal Conductivity of Soils*. MS thesis, Minneapolis, MN, University of Minnesota.
- Woodside, M., and Messmer, J. M., 1961. Thermal conductivity of porous media. *Journal of Applied Physics*, **32**(9), 1688–1706.

Cross-references

- [Coupled Heat and Water Transfer in Soil](#)
[Databases of Soil Physical and Hydraulic Properties](#)
[Mapping of Soil Physical Properties](#)
[Mineral–Organic–Microbial Interactions](#)
[Temperature Effects in Soil](#)

EVAPORATION

The process in which water is converted to a vapor that can be condensed.

Cross-references

- [Conditioners, Effect on Soil Physical Properties](#)
[Evapotranspiration](#)
[Soil Aggregation and Evaporation](#)

EVAPOTRANSPIRATION

Viliam Novák

Institute of Hydrology, Slovak Academy of Sciences, Bratislava, Slovakia

Definition

Evapotranspiration as a process is referred to simultaneous losses of water from plants and soil surfaces to the atmosphere. It consists of two particular processes: transpiration and evaporation. Transpiration is referred to water losses from the plant; evaporation is water loss directly from the soil surface, or from evaporating surfaces other than the plants. The precondition of transpiration is transport of the water from soil through plant to the atmosphere. Therefore, evaporation of water previously intercepted by the plant canopy surface from rain (intercepted water), is treated as evaporation too. Physically, evapotranspiration is phase change of the liquid water to water vapor and its transfer to the atmosphere. The evaporation surfaces during transpiration are mostly internal stomata surfaces.

Introduction

Evapotranspiration role in an environment can be characterized by

1. Evapotranspiration as a part of the earth's water balance
2. Evapotranspiration as a part of energy balance of the earth
3. Transpiration participates in biomass production process

The role of evapotranspiration in a root zone water balance can be expressed by the water balance equation; this equation is relating gains and losses of water in the soil root zone in the defined time interval Δt as

$$P + I_r = I + O + (E_e + E_t) + I_d + \Delta W \quad (1)$$

where P and I_r are precipitation and irrigation, I is infiltration to the soil, O is surface runoff, E_e and E_t are evaporation and transpiration, I_d is rate of water movement through bottom of the root zone, which can be capillary rise or deep percolation, and ΔW is the soil root zone water

content change during the period under consideration. All the terms are expressed in mm of water layer over the soil surface (or in kg m^{-2}), during the time interval Δt (usually in hours or more frequently in days).

Evapotranspiration $E = E_e + E_t$ is usually the most important term of the right side of the [Equation 1](#). Expressing the water balance of Central European countries during the hydrological year, the ratio of evapotranspiration and precipitation annual sums is 0.65 for Slovakia, 0.77 for Poland, but 0.91 for Hungary, in the average. It depends on characteristics of the landscape, prevailing in particular country, but it can be seen that “hilly” landscape of Slovakia is utilizing smaller part of precipitation for evapotranspiration than Hungary, with flat landscape and higher air temperature and thus higher potential (maximum possible) evapotranspiration. Analyzing agricultural cropped field, during the vegetation period, the ratio E/P is usually 0.8; during the periods with higher evapotranspiration than precipitation, the soil water content is depleting, or capillary rise from groundwater can take place.

The water movement and its balance are intimately connected with the energy balance, since it involves processes that require energy. Evaporation and transpiration are those processes through which both water and energy balance are connected.

The important feature of evapotranspiration is the high consumption of energy during the evaporating process. As it is known, evaporation of 1 g of water (and transpiration as well), needs 2,450 J of energy (at 20°C). It is 5.8 times more than it is used for heating of 1 g of water from 0°C to 100°C. During the sunny day in Central Europe, the part of energy consumed as latent heat of evaporation is about 0.8 of the net radiation, R_n . It is the energy at the evaporating surface level, which can be utilized for processes performing at that level. The annual portion of energy consumed as latent heat of evapotranspiration over the Earth is 0.56 R_n , transpiration consumes 0.4 R_n (Baumgartner and Reichel, [1975](#)). Over Slovakia, it is about 0.53 R_n and 0.42 R_n , respectively, close to the Earth's averages.

Therefore, evapotranspiration is an important process, strongly influencing the energy balance structure of the landscape and of the field. The lack of evapotranspiration due to absence of water or plants should lead to overheating of the land, and thus increasing its air temperature as well. The energy balance of the evaporating surface can be written as

$$R_n = G + H + LE \quad (2)$$

R_n is the net radiation flux density, G is the soil heat flux, H is the sensible heat flux; it is heat flux from the soil (and canopy) to the atmosphere, and LE is the latent heat flux, determining the energy consumed by evaporation, i.e., for transition of water from the liquid to the gas phase. (Dimension of all terms is $\text{J m}^{-2}\text{s}^{-1}$.) Here L is the latent heat of vaporization ($L = 2.45 \cdot 10^6 \text{ J kg}^{-1}$). The consumption of energy by photosynthesis is small (usually less than 0.02 R_n) and in the above equation is neglected.

Transpiration and biomass production

The aim of soil and water management is to maximize the biomass production by soil and water management. As it was found from numerous measurements (Hanks and Hill, [1980](#)), dry matter production Y_d is proportional to the seasonal transpiration total E_t :

$$Y_d = n \cdot E_t \quad (3)$$

where n is the water efficiency coefficient. It is related to the plant and environmental properties, and for particular canopy and soil, can be treated as a constant. The value of this constant, which represents dry biomass production in kg m^{-2} per unit transpiration rate (expressed in kg m^{-2} or in mm of the water layer), ranges between 0.002 and 0.006, depending on the site conditions. From [Equation 3](#) it follows that the maximum (potential) yield Y_{dp} can be reached at the potential transpiration rate E_{tp} :

$$Y_{dp} = n \cdot E_{tp} \quad (4)$$

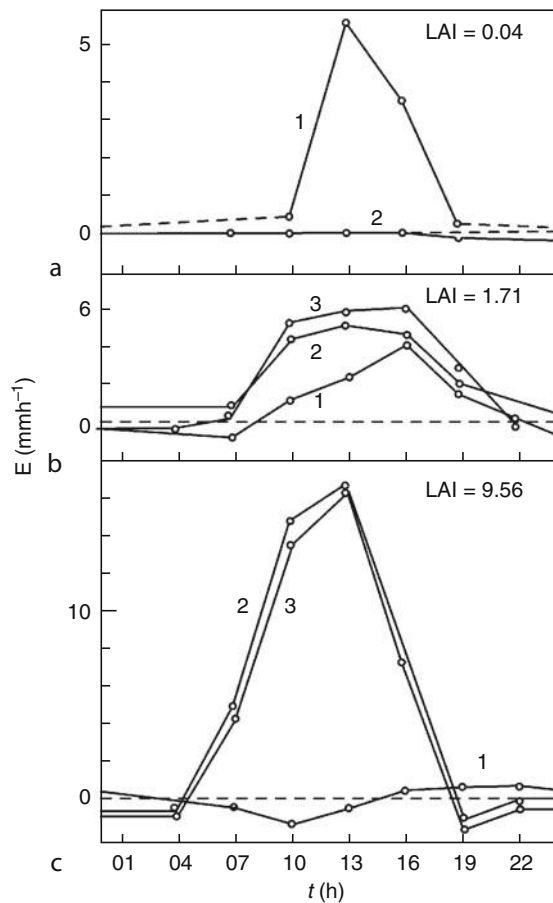
Therefore, precondition of the maximum yield at given conditions is to manage soil irrigation to ensure the potential transpiration.

Daily courses and totals of evapotranspiration

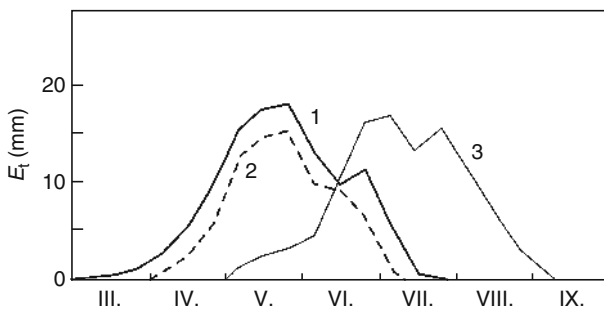
Daily courses of potential evapotranspiration and of its components (transpiration and evaporation), usually follow the most important atmospheric characteristics of an atmosphere: net radiation, air temperature, air humidity, and wind velocity (Novák et al., [1997](#)). Actual evapotranspiration (and its components) are strongly influenced by the soil water, which can limit the root extraction rate. [Figure 1](#) presents daily courses of the potential evapotranspiration, transpiration, and evaporation, during sunny days for winter wheat and different leaf area index (LAI), strongly influencing the evapotranspiration structure. The higher the LAI, the smaller is the evaporation, the higher is the transpiration and the biomass production. Daily evapotranspiration rates of canopies grown in Central Europe are less than 7 mm day^{-1} , but rates between 2 mm day^{-1} and 4 mm day^{-1} are the most common during the summer. Even in tropical conditions, maximum daily rates of E are usually less than 10 mm day^{-1} .

Seasonal courses of evapotranspiration

Seasonal courses of evapotranspiration depend mostly on characteristics of the atmosphere, and on the soil water content seasonal courses. The transpiration–evaporation ratio depends mostly on LAI seasonal courses. [Figure 2](#) presents annual courses of the decade transpiration sums during the vegetation period, of the winter wheat, the spring barley, and the maize. Different positions of curves depend on the beginning of the vegetation period of the particular plant and on its duration. Transpiration totals during the vegetation period were estimated as 120 mm for winter wheat, 105 mm for maize, and 80 mm for spring barley. The ratios of $E_t/E = 0.8$, $E_e/E = 0.2$, and $E_t/E_p = 0.8$, respectively,



Evapotranspiration, Figure 1 Evaporation from soil surface (1), transpiration (2), and evapotranspiration (3) of winter wheat daily courses for different leaf area index (LAI). May 4, 1978, Cerhovice site, Czech Republic.



Evapotranspiration, Figure 2 Ten day transpiration totals of winter wheat (1), spring barley (2), and maize (3) seasonal course, calculated by Penman-Monteith (PM) approach. 1981, Trnava site, South Slovakia.

were estimated for winter wheat canopy in year with average precipitation total in Central Slovakia; E_p is potential evapotranspiration total during the whole vegetation period.

Determination methods of the evapotranspiration and of its components

The oldest, but still reliable method of evapotranspiration determination is the use of lysimeters. Lysimeters are impermeable vessels big enough to allow for non-limited growth of plants. They are located in the field, not disturbing the canopy height and density. Evapotranspiration is usually evaluated from differences in lysimeter weight during the rain-free periods. Other, but less accurate method is estimation of the evapotranspiration, by using water balance equation from the soil water content profiles during precipitation-free time intervals, which should be not shorter than 2 weeks, because of the standard measurement errors.

Another, contemporary method of evapotranspiration measurement is the eddy correlation technique (Dyer, 1961). This method allows for evaluation of the instantaneous evapotranspiration fluxes using observed data of the air temperature, air humidity, and wind velocity fluctuations.

Energy balance method is a reliable one for evapotranspiration rate estimates. This method is based on evaluation of the term E from the [Equation 2](#), when other terms are estimated independently. As this method needs nonstandard data, it is used only seldom. There is a wide family of empirical methods for estimation of the evapotranspiration and of its components. The equations of Thornthwaite, Blaney-Criddle, Hargreaves, Priestley-Taylor, Türc, and others are frequently used (Novák, 1995).

Evapotranspiration is often evaluated as proportional to some meteorological characteristics (net radiation, air temperature, and air humidity). Such approaches are used for approximative estimation of the average evapotranspiration rates, for weeks and months. Their use is limited, they are valid usually only for the regions where they were developed and calibrated.

Generally accepted and widely used are the methods of evapotranspiration calculation, using the (Penman's 1948) approach. Penman combines energy balance equation ([Equation 2](#)) and heat and mass transfer equations

$$H = \rho_a c_p D(T_s - T_2) \quad (5)$$

$$E = \rho_a D(q_s - q_2) \quad (6)$$

where E is the water vapor (evaporation) flux ($\text{kg m}^{-2} \text{s}^{-1}$), H is the sensible heat flux ($\text{J m}^{-2} \text{s}^{-1}$), ρ_a is air density (kg m^{-3}), c_p is heat capacity of air at constant pressure (J kg^{-1}), D is the eddy coefficient of turbulent diffusion (m s^{-1}), T_s and q_s are air temperature and specific air humidity at the evaporating surface, T_2 and q_2 are the same as above, but at standard height, 2 m above the soil surface.

The problem complicating the use of such approach is estimation of the air humidity and of the temperature at the evaporating surface. To eliminate this need, Penman (1948) introduced linear relationship between the surface temperature and the temperature at standard height. This

approach allows to evaluate surface temperature using standard temperature measured at the 2-m height. Other necessary data, needed in Penman's equation can be measured easily. Penman's formula made possible to estimate the potential evapotranspiration. It is used to calculate evapotranspiration from the bare soil, from the dense canopies well supplied with water, and from the water table, generally from evaporating surfaces under not limiting water conditions.

The next important step put forward to calculate different canopies transpiration rate E_t was made by Monteith (1965) by proposing the bulk canopy resistance r_c , characterizing the effect of particular canopy as a whole. This is the famous, "big leaf" approach, which represents canopy as one homogeneous evaporating layer. This approach was proved very useful and this, so-called Penman–Monteith (PM) equation is the most widely used evapotranspiration model:

$$LE_t = \frac{\Delta (R - G) + \rho c_p \frac{d}{r_a}}{\Delta + \gamma \left(1 + \frac{r_c}{r_a}\right)} \quad (7)$$

where E_t is the transpiration rate ($\text{kg m}^{-2}\text{s}^{-1}$), ρ is the dry air density (kg m^{-3}), c_p is the specific heat of the air at constant pressure ($\text{J kg}^{-1}\text{K}^{-1}$), d is the air saturation deficit (Pa), r_a is the bulk aerodynamic resistance (s m^{-1}), r_c is the bulk canopy resistance (s m^{-1}), γ is the psychrometric constant (Pa K^{-1}), and Δ is the temperature derivative of the saturated vapor pressure curve (Pa K^{-1}).

The specific features of different canopies transpiration in the above mentioned equation can be expressed by the net radiation term R_n , soil heat flux G , by the canopy resistance r_c , and by the value of aerodynamic resistance r_a . The daily courses of R_n should be measured, the daily totals or daily averages of R_n can be calculated using procedure described by Novák (1995), in which albedo of the evaporating surface plays an important role. The daily courses of G should be measured when calculating daily courses of evapotranspiration. Calculating daily totals of E_t , G can be neglected. The aerodynamic term r_a depends on wind speed and dynamic roughness parameter z_0 , d is the air saturation deficit, and Δ is the same as mentioned above. A specific form of the Penman–Monteith equation, in which the aerodynamic resistance and bulk canopy resistance are specified, is recommended by FAO for calculating reference crop evaporation, i.e., evaporation from dense crop, well supplied with water (Allen et al., 1998).

A crucial problem of using this equation to calculate transpiration is in estimation of the canopy resistance r_c , which depends on a variety of environmental parameters, mainly R_n and the leaf water potential. Leaf water potential depends on the soil water potential. The higher the soil water content, the smaller is the r_c (Jarvis, 1976; Choudhury and Monteith, 1988). Canopy resistance r_c is changing during the day and season and is specific for particular plants. To overcome this, the simplified versions of PM equation are used to calculate the potential evapotranspiration, and

then the empirical relationship between the relative transpiration and soil water content is used. (Ritchie and Burnett, 1971; Novák, 1995; Feddes and Raats, 2004).

Conclusions

Evapotranspiration is a key process in water and energy balance of the Earth. Energy utilized for evapotranspiration is 0.53 of the net radiation (transpiration consumes 0.42 part of the net radiation); only the rest is used for all the energy-consuming processes. Transpiration as a part of evapotranspiration is vital for biomass production, stomata are entrance for CO_2 , and exit for water vapor, both processes occur simultaneously. Evapotranspiration is also vital for air temperature stabilization of the Earth.

Bibliography

- Allen, R., Pereira, L., Raes, D., and Smith, M., 1998. *Crop Evapotranspiration, Guidelines for computing crop water requirements*. FAO Irrigation and Drainage Paper 56, FAO Rome, 300pp.
- Baumgartner, A., and Reichel, N., 1975. *The World Water Balance*. Amsterdam/New York: Elsevier.
- Choudhury, B. J., and Monteith, J. L., 1988. A four-layer model for the heat budget of homogeneous land surface. *Quarterly Journal Royal Meteorological Society*, **114**, 373–398.
- Dyer, A. J., 1961. Measurement of evaporation and heat transfer in the lower atmosphere by an automatic eddy correlation technique. *Quarterly Journal Royal Meteorological Society*, **87**, 401–412.
- Feddes, R. A., and Raats, P. A. C., 2004. Parametrising the soil–water–plant root system. In Feddes, R., de Rooij, G. H., and van Dam, J. C. (eds.), *Unsaturated Zone Modeling, Progress, Challenges and Applications*. Dordrecht: Kluwer Academic.
- Hanks, R. J., and Hill, R. V., 1980. *Modeling Crop Responses to Irrigation in Relation to Soils, Climate and Salinity*. IIIC publication number 6.
- Jarvis, P. G., 1976. The interpretations of the variations in leaf water potential and stomatal conductance found in the canopies in the field. *Philosophical Transactions of the Royal Society. London B*, **273**, 593–610.
- Monteith, J. L., 1965. Evaporation and environment. In Fogg, G. E. (ed.), *The State and Movement of Water in Living Organisms*. Cambridge: Cambridge University Press, pp. 205–234.
- Novák, V., 1995. *Evapotranspiration and Its Estimation (in Slovak)*. Bratislava: Veda.
- Novák, V., Hurtalová, T., and Matejka, F., 1997. Sensitivity analysis of the Penman type equation for calculation of potential evapotranspiration. *Journal of Hydrology and Hydromechanics*, **45**, 173–186.
- Penman, H. L., 1948. Natural evaporation from open water, bare soil and grass. *Proceedings of the Royal Society of London A*, **193**, 120–145.
- Ritchie, J. T., and Burnett, E., 1971. Dryland evaporative flux in subhumid climate. II. Plant influences. *Agronomy Journal*, **63**, 56–62.

Cross-references

- Ecohydrology
- Physics of Near Ground Atmosphere
- Soil Water Flow
- Stomatal Conductance, Photosynthesis, and Transpiration, Modeling Water Balance in Terrestrial Ecosystems
- Water Budget in Soil

EXCHANGE COMPLEX

Soil mineral and organic surfaces capable of holding easily exchangeable cations.

EXCHANGEABLE IONS

(i) Anion. A negatively charged ion held on or near the surface of a solid particle by a positive surface charge and which may be easily replaced by other negatively charged ions. (ii) Cation. A positively charged ion held on or near the surface of a solid particle by a negative surface charge and which may be replaced by other positively charged ions in the soil solution.

Bibliography

Glossary of Soil Science Terms. Soil Science Society of America. 2010. <https://www.soils.org/publications/soils-glossary>

Cross-references

Surface Properties and Related Phenomena in Soils and Plants

EXTRUSION, EFFECT ON PHYSICAL AND CHEMICAL PROPERTIES

Leszek Mościcki

Department of Food Process Engineering, University of Life Sciences, Lublin, Poland

Synonyms

Extrusion-cooking of vegetable raw materials; Food extrusion

Definition

Extrusion-cooking. HTST processing of grinded vegetable raw materials at relatively high pressure (up to 20 MPa) and temperature (up to 200°C) to achieve new generation food and feed products of different/engineered physical and chemical properties.

Extrusion-cooker or food extruder. A processing machine unit, specially designed for.

Extrudates. Products of extrusion-cooking.

Introduction

The extrusion technology, well-known in the plastic industry, has recently become widely used in agri-food industry, where it is referred to as *extrusion-cooking*. It has been employed for the production of so-called engineered food and special feed. Generally speaking, extrusion-cooking of vegetable raw materials consists in the extrusion of grinded material at barothermal conditions. With the help of shear energy, exerted by the rotating screw, and

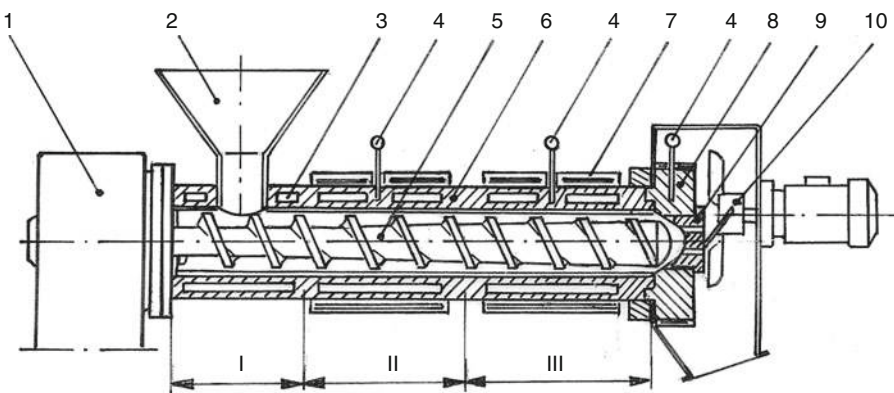
additional heating by the barrel, the food material is heated to its melting point or plasticating point (Harper, 1981; Mercier et al., 1998; Mościcki et al., 2007; van Zuilichem, 1992). In this changed rheological status the food is conveyed under high pressure through a die or a series of dies and the product expands to its final shape. That results in much different physical and chemical properties of the extrudates in comparison to raw materials used.

Food extruders (Figure 1 presents a design of single-screw extrusion-cooker) belong to the family of HTST (High Temperature Short Time)-equipment, with a capability to perform cooking tasks under high pressure. This aspect may be explained for vulnerable food and feed as an advantageous process since small time span exposures to high temperatures will restrict unwanted denaturation effects on, e.g., proteins, amino acids, vitamins, starches, and enzymes. Physical technological aspects like heat transfer, mass transfer, momentum transfer, residence time, and residence time distribution have a strong impact on the food and feed properties during extrusion-cooking and can drastically influence the final product quality. An extrusion-cooker is a process reactor (van Zuilichem, 1992), in which the designer has created the prerequisites in the presence of a certain screw lay-out, the use of mixing elements, the clearances in the gaps, the installed motor power, and barrel heating and cooking capacity, to control a food and feed reaction. This can be a reason “in itself,” when only mass is transferred in wanted and unwanted reaction products due to heating, e.g., the denaturation of proteins under presence of water and the rupture of starches, both affected by the combined effects of heat and shear. The reaction can also be provoked by the presence of a distinct biochemical or chemical component like an enzyme or a pH controlling agent. When we consider the cooking extruder to be more than was mentioned originally, a thorough investigation of the different physical technological aspects is more than desirable.

Application

Currently, extrusion-cooking as a method is used for the manufacture of many foodstuffs, ranging from the simplest expanded snacks to the highly processed meat analogues (Figure 2). The most popular extrusion-cooked products are the following:

- Direct extrusion snacks, RTE (ready-to-eat) cereal flakes, and diverse breakfast foods produced from cereal material and differing in shape, color, and taste and easiest to implement in terms of production
- Snack pellets: half products suitable for fried or hot air expanded snacks, pre-cooked pasta
- Baby food, pre-cooked flours, instant concentrates, functional components
- Pet food, aquafeed, feed concentrates, and calf-milk replacers
- Textured vegetable protein (mainly from soybeans, though not always) used in the production of meat analogues



Extrusion, Effect on Physical and Chemical Properties, Figure 1 A cross-section of a single-screw food extruder: 1 – engine, 2 – feeder, 3 – cooling jacket, 4 – thermocouple, 5 – screw, 6 – barrel, 7 – heating jacket, 8 – head, 9 – die, 10 – cutter, I – transport section, II – compression section, III – melting and plasticization section.



Extrusion, Effect on Physical and Chemical Properties, Figure 2 Various assortments of popular extrudates.

- Crispy bread, bread crumbs, emulsions, and pastes
- Barothermally processed vegetable components for the pharmaceutical, chemical, paper, and brewing industry
- Confectionery: different kinds of sweets, chewing gum

Effects of extrusion-cooking

Extrusion-cooking is accompanied by the process of starch gelatinization, involving the cleavage of intermolecular hydrogen bonds. It causes a significant increase in water absorption, including the breakage of starch granules. Gelatinized starch increases the dough viscosity, and high protein content in the processed material facilitates higher flexibility and dough aeration (Mercier et al., 1998; Mościcki et al., 2007). After leaving the die hot material rapidly expands as a result of immediate vaporization and takes on a porous structure. In the extruded dough protein membranes, closing occurs creating cell-like spaces, and starch, owing to dehydration,

loses its plasticity and fixes the porous nature of the material. Rapid cooling causes the stiffening of the mass, which is typical for carbohydrate complexes embedded in a protein matrix and their total enclosure by the membrane of hydrated protein. The resulting product is structurally similar to a honeycomb shaped by the clusters of molten protein fibers.

Starch occurs primarily in cereal grains and potatoes. It takes the form of granules of different and characteristic shape, depending on the origin as well as on the variety and type of fertilization. As commonly known, two main components of starch are amylose and amylopectin displaying different physical and chemical properties, for example, chemical structure. The technological assessment of extrudates takes two factors into account: the water solubility index (WSI) and the water absorption index (WAI). These properties were studied in many laboratories and the conclusions were that WAI of many starch products increases together with the temperature rising in the extruder's barrel. It has been assumed that the maximum value is obtained around the temperature ranges from 180°C to 200°C (Mercier et al., 1998). When these temperatures are exceeded, WAI drops and causes the WSI increase. The lower the material initial moisture content used in extrusion, the higher the extrudate's WSI rate that can be obtained. A noticeable influence on the product properties has the percentage of amylose and amylopectin and its ratio in the processed material (Camire et al., 1990; Cheftel, 1986; Mercier et al., 1998).

The extrusion processing of starchy materials certainly impacts the changes in product viscosity (pasting characteristic) after dissolving in water. This feature is very important for the technological point of view. Using Brabender viscometer we can see that the characteristic viscosity curve for starch is clearly reduced through extrusion; at the same time, the decrease of viscosity is greater if higher temperatures were applied during the extrusion-cooking. The application of higher pressure during the extrusion (compression changing) does not affect the extrudate viscosity; however, it affects on viscosity

stability of products retained at a temperature of 95°C. In some cases, the properties of extrudate may be arranged by amylose bounding with fatty acids or monoglycerides.

Another factor determining changes in the starch molecules during the extrusion-cooking process is the pressure and the values of existing shearing forces (Meuser et al., 1987). In order to obtain certain technological properties of extrudates, which are often semi-finished products intended for further processing, it is necessary to set proper parameters of the extrusion process. This is achieved by the use of screws with varying compression degrees, relevant rpm of the working screw, appropriate die size, SME input, etc.

An interesting and important extrudate feature is the digestion rate of starch. Research on starch digestibility processed by extrusion-cooking has shown (Anderson et al., 1970; Cheftel, 1986) that it mostly depends on the generated structure. The researchers concluded that maize starch extruded at a temperature of 135°C was significantly less digestible if coarse. Fine ground extrudate treated with α -amylase displayed a 20% higher degree of enzymatic hydrolysis than non-ground material, and after grinding it into flour, the hydrolysis degree reached 80%. Such differences in digestion were not present with extrudates obtained after the application of process temperature of 225°C. In addition, with such thermal treatment, the highest expansion of extruded maize was observed.

Thermoplastic processing of vegetable materials by the extrusion-cooking also causes significant changes in protein substances, which can be found in vegetable materials. Mercier et al. (1998) demonstrated, for properly setting the parameters of thermoplastic processing, that it is possible to obtain cereal extrudate of a relatively high amyloytic activity. Nevertheless, the influence of extrusion on the enzymatic activity must be taken into account, particularly when it is important from the technological point of view (the purpose of the product), or when these processes are carried out in order to explore the mechanism of starch dextrinization that occurs during extrusion.

Polysaccharides and lignins – the basic fiber components – perform differently during barothermal treatment such as extrusion. The degree of fiber degradation depends on the size of shear stresses. Björck and Asp (1984) found that extrusion processing almost twice increased the content of water-soluble fiber in processed wheat grain. It was simultaneously confirmed by Varo et al. (1983) who used many different analytical methods during the cereal extrudates testing. There were no statistically significant changes in the quantity of fiber in relation to the input material before extrusion.

The decomposition of fiber to glucose and lignin, combined with the use of urea during the extrusion of pine sawdust for the purpose of feed, was measured by Mościcki and Van Zuilichem (1986). The obtained results confirmed the usefulness and effectiveness of extrusion technique in the process of cellulose degradation, and the final product, energy and protein-rich, has proved to

be a good alternative as a valuable feed component for ruminants which have the capacity to absorb inorganic origin proteins.

Vitamins can be destroyed through the action of temperature or by oxidation. Since extrusion mostly involves thermal treatment at temperatures of 100°C or higher, some loss of vitamins in the processed material is expected, especially of the temperature-sensitive ones, such as vitamin C. Many authors presented some works on these matters and confirmed the occurrence of this phenomenon, but because of the HTST-type shock treatment, they found that the extent of losses was much less compared with conventional methods such as static, long-term cooking. Since the basic raw materials used in the processing of extruded products are cereals, much attention was attached to the changes in B-group vitamins, particularly thiamine B₁, riboflavin B₂, and niacin (Beetner et al., 1976; Harper et al., 1977; Mustakas et al., 1970). Thiamine being the most sensitive to temperature is damaged during extrusion, depending on the processing conditions, temperature rise, and screw speed. Riboflavin losses are much lower (retention post-extrusion was 92%) and decrease with the increasing water content in the mixture (Camire et al., 1990).

Starch extrudates, due to a high stability of viscosity, are widely used in the manufacture of starch modifiers and functional substances. In bakery, extruded maize is used as a binding agent for meat fillings and as a raising agent in baking cakes. It improves their texture (crispiness) and taste. Physicochemical properties of starch extrudates (low solubility and viscosity) make such products very competitive if compared with those obtained through chemical modifications. Extrusion of lipid-free starch increases its digestibility as a result of the oligosaccharides formation – this determines the usefulness of this technique in the baby food manufacture (Mercier et al., 1998).

The greatest interest of extrusion-cooking technique is in production of snacks, breakfast cereals, and textured proteins obtained from soybeans and used as animal protein replacements in food processing. Although soy proteins play a key role, there are experiments performed with other vegetable materials such as broad bean or faba bean, which can substitute this plant.

It is also worth noting that extruded products demonstrated long shelf life. Partial lipids binding by the processed mass increases their resistance to oxidation processes, while lipases and lipoxygenase are almost completely inactivated. In addition, thermal processes cause deep sterilization, therefore microbiological contamination of the obtained products is limited. If in proper storage conditions, these products can be stored for more than a year.

Summary

A utilitarian importance of the extrusion-cooking of vegetable raw materials has made it widely implemented for the food and feed manufacture all over the world. The manufacturers adapted twin-screw extruders report significant economic benefits. These machines are more

efficient and less energy consuming than single-screw extruders. The extrusion reveals great potential for further expansion in the domestic food and feed industry. It is not only on account of its growing application abroad, especially in developed countries. Extrusion is a giant step in the use and marketing of those products which are regarded as having little or no economic value, such as the seeds of leguminous plants.

Bibliography

- Anderson, R. A., Conway, H. F., and Pepliński, A. J., 1970. Gelatinization of corn grits by roll cooking, extrusion cooking and steaming. *Die Starke*, **22**, 130–135.
- Beetner, G., Tsao, T., Frey, A., and Lorenz, K., 1976. Stability of thiamine and riboflavin during extrusion processing of triticale. *Journal of Milk Food Technology*, **39**, 244–245.
- Björck, I., and Asp, N.-G., 1984. *Effects of Extrusion Cooking On The Nutritional Value, Extrusion-Cooking Technology*. London: Elsevier.
- Camire, M. E., Camire, A., and Krumhar, K., 1990. Chemical and nutritional changes in foods during extrusion. *Food Science and Nutrition*, **29**, 35–57.
- Cheftel, J. C., 1986. Nutritional effects of extrusion cooking. *Food Chemistry*, **20**, 263–283.
- Harper, J. M., 1981. *Extrusion of Foods*. Boca Raton, FL: CRC Press.
- Harper, J. M., 1986. Extrusion texturization of foods. *Food Technology*, **40**, 70–76.
- Harper, J. M., Stone, M. L., Tribelhorn, R. E., Jansen, G. R., Lorenz, K. J., and Maga, J. A., 1977. *LEC Report 2*. Colorado State University, Fort Collins, CO.
- Mercier, C., Linko, P., and Harper, J. M., 1998. *Extrusion Cooking*. St. Paul, MN: American Association of Cereal Chemists Inc.
- Meuser, F., Pfaller, W., and Van Lengerich, B., 1987. Technological aspects regarding specific changes to the characteristic properties of extrudates by HTST-extrusion cooking. In *Extrusion Technology for the Food Industry*. London: Elsevier Applied Science Publishers Ltd., pp. 35–54.
- Mościcki, L., Mitrus, M., and Wojtowicz, A., 2007. *Extrusion Technique in Food Industry* (in Polish). Warsaw, Poland: PWRiL.
- Mościcki, L., and Van Zuilichem, D. J., 1986. Extruded saw dust for Ruminants (in Polish). *Biuletyn Informacyjny Przemysłu Paszowego*, 51–56.
- Mustakas, G. C., Albrecht, W. J., Bookwalter, G. N., McGhee, J. E., Kwolek, W. F., and Griffin, E. L., 1970. Extruder processing to improve nutritional quality, flavor and keeping quality of full-fat soya flour. *Food Technology*, **24**, 1290–1296.
- Varo, P., Laine, R., and Koivistoinen, P., 1983. The effect of heat treatment on dietary fibre: Interlaboratory study. *J. AOAC*, **66**, 933–938.
- Van Zuilichem, D. J., 1992. *Extrusion Cooking. Craft or Science?* PhD thesis, the Netherlands, Wageningen University.

Cross-references

- [Agriculture and Food Machinery, Application of Physics for Improving](#)
[Cereals, Evaluation of Utility Values](#)
[Physical Properties of Raw Materials and Agricultural Products](#)
[Quality of Agricultural Products in Relation to Physical Conditions](#)
[Thermal Technologies in Food Processing](#)

EXUDATE, ROOT

Low molecular weight metabolites that enter the soil from plant roots.

See [Plant Roots and Soil Structure; Rhizosphere](#)

F

FABRIC

The physical constitution of soil material and granular solids as expressed by the spatial arrangement of the solid particles and associated voids.

FAILURE

The reaction of a body to stresses that exceed its strength, generally leading to loss of cohesion or structural integrity by such modes as fracturing, slumping, plastic yielding or apparent liquefaction.

Bibliography

Introduction to Environmental Soil Physics. (First Edition). 2003. Elsevier Inc. Daniel Hillel (ed.) <http://www.sciencedirect.com/science/book/9780123486554>

FATIGUE STRENGTH

The maximum stress a body can withstand for a specific number of repeated applications prior to its failure.

FATS: RHEOLOGICAL CHARACTERISTICS

Fernanda Peyronel, Thamara Laredo,
Alejandro G. Marangoni
Department of Food Science, University of Guelph Food
and Soft Materials Science, Guelph, ON, Canada

Definition

Rheology is the study of the way that materials flow or deform under an applied stress.

Jan Gliński, Józef Horabik & Jerzy Lipiec (eds.), *Encyclopedia of Agrophysics*, DOI 10.1007/978-90-481-3585-1,
© Springer Science+Business Media B.V. 2011

Introduction

Rheology tries to explain the relationship between stress and strain (deformation) or strain rate (flow) in a material by giving information as to whether the material is elastic, viscous, or plastic (Steffe, 1996; McClements, 2005). Fats are known to behave like rigid solids until a deforming stress exceeds the yield value at which point the product starts to flow like a viscous liquid (de Man and Beers, 1987). This plasticity arises from the fact that the crystallized material forms a fat crystal network that entraps liquid oil (Marangoni, 2005). This characteristic of fats makes rheology an excellent technique to study them. Some of the textural properties that humans perceive when consuming fat products, like hardness, creaminess, brittleness, and tenderness, are largely rheological in nature. It is common in rheology to work with the so-called “constitutive relations” or rheological equation of state. The basic equations are: Modulus = Stress/Strain and Viscosity = Stress/Shear rate, both of which describe the relationship between a “driving” force and the effect upon the system. When studying viscoelastic materials, two moduli are always calculated, the storage modulus (G') that reflects the energy-conserving or elastic characteristics, and the loss modulus (G'') that describes the energy dissipated as heat.

For example, G' has been found to be a suitable indicator of the hardness for milk fat and butter (Wright et al., 2001) and many other fats (Narine and Marangoni, 1999, 2001), as well as giving information regarding spreadability and mouth feel (Rousseau and Marangoni, 1999).

This entry focuses first on developing a mathematical formulation of some of the basic concepts used in rheology, followed by a section that explains the rheometer used in our laboratory.

Basic concepts: strain and stress

A body of matter can be thought as composed of interacting point masses. Each point mass is defined by

a pair (m, P) , which defines the mass, m , and the position P in space. Deformation is the process through which these point masses change their relative position with respect to the center of mass of the body.

Strain, s , is a displacement defined as a relative change in length. It is a dimensionless quantity. Stress, σ , is the acting force per unit area responsible for deformation. It is composed of a normal (tensile or compressive) and a tangential (shear) component. The SI units of stress are Pascals (Pa) which is equivalent to one Newton per square meter.

What follows is an overview of the mathematical description of both tensile and shear strain. Consider a rectangular bar, of a given material, to which a tensile stress has been applied. The bar will elongate as a result, as shown in [Figure 1](#). The resulting length, L , of the bar will be:

$$L = L_0 + \delta L \quad (1)$$

where L_0 is the initial length of the bar and δL is the increase in length. This deformation can be expressed in terms of the strain, s ,

$$s_c = \frac{\delta L}{L_0} = \frac{L - L_0}{L_0} = \frac{L}{L_0} - 1 \quad (2)$$

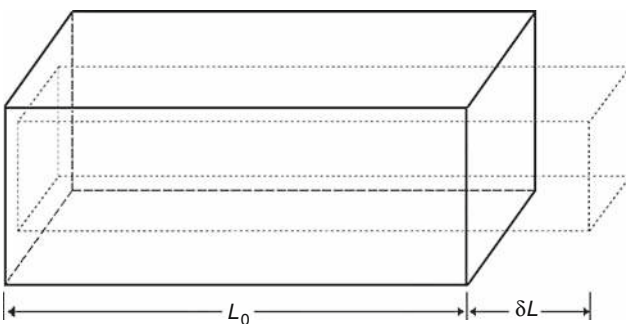
This is known as the Cauchy strain, s_c .

The Hencky strain s_h (or true strain) is obtained by integrating over an infinitesimally small incremental strain dL/L_0 from L_0 to L :

$$s_h = \int_{L_0}^L \frac{dL}{L} = \ln \frac{L}{L_0} \quad (3)$$

The Hencky strain or logarithmic strain is used when deformation takes place in a series of increments, taking into account the influence of the strain path (Rees, [2006](#)).

Consider the same rectangular bar, but now the force applied is tangential, such that the upper surface has been displaced by δL and the bottom surface is stationary, as seen in [Figure 2](#). This type of strain is called simple shear. In this case the angle of shear, or shear strain, γ , may be calculated as:



Fats: Rheological Characteristics, Figure 1 Linear elongation of a rectangular bar (Adapted from Steffe ([1996](#))).

$$\tan \gamma = \frac{\delta L}{h} \quad (4)$$

where h is the height of the bar. For small deformations, $\tan \gamma$ is approximately equal to γ in radians.

Ideal and nonideal matter

Food can have a wide range of rheological properties which usually give way to very complex behaviors. However, it is possible to characterize many types of foods in terms of the simpler *ideal* solid, liquid, or plastic. Complex systems can then be explained by combining two or more of these simpler models.

Solids

In an ideal or Hookean solid the deformation is strictly proportional to the applied force. Hence, the behavior of an ideal solid with respect to an applied external force can be expressed in terms of a single parameter: the proportionality constant between the deformation and the force producing it, such that,

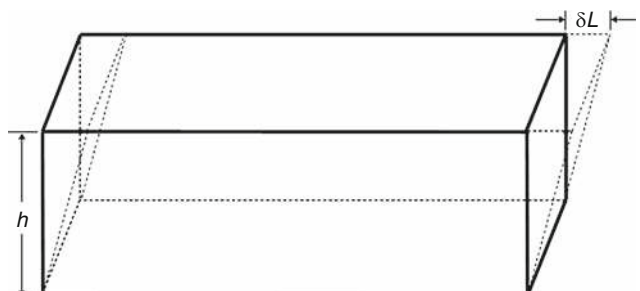
$$\sigma = G\gamma \quad (5)$$

where G is known as the shear modulus and σ and γ are the stress and the deformation, respectively.

Only elastic solids display Hookean behavior. Some solid materials in food behave as an ideal solid only for small deformations. At strains above this hookean region, the stress is no longer proportional to the strain and an apparent modulus (which is a function of the strain) is defined. Even though the material does not obey Hooke's law it will still return to its original shape once the force is removed. However, there is a point above which the solid does not return back to its original shape once the force is removed. This occurs because the forces that hold together the structural units, at the appropriate length scale, are exceeded, making the solid either break or flow (Prentice, [1984](#)).

Fluids

A fluid is distinguished from a solid in that it does not possess a rigid structure. Upon the application of an external



Fats: Rheological Characteristics, Figure 2 Shear deformation of a rectangular bar (Adapted from Steffe ([1996](#))).

force, and because an ideal liquid is isotropic, the elements will move without modification of the structure for as long as the force is applied. The characteristic property in this case is that the rate at which the material deforms is proportional to the applied force. The proportionality constant in this case is the viscosity, η :

$$\sigma = \eta \dot{\gamma} \quad (6)$$

where σ is the applied stress and $\dot{\gamma}$ is the strain rate. Under certain conditions, a number of fluids such as water, tea, honey, or syrups will exhibit ideal Newtonian behavior.

The rheological properties of Newtonian liquids are independent of the shear rate and the previous shear histories, and are dependent only on the temperature and composition.

The viscosity of non-Newtonian liquids is not constant and can be dependent on the rate and/or the time over which the shear force is applied. The word viscosity is generally reserved for Newtonian liquids; for non-Newtonian liquids the viscosity at a given shear rate is called the apparent viscosity. Usually, the symbols η and η_a are used for the viscosity and apparent viscosity, respectively. When the behavior of a non-Newtonian liquid under a shear force is dependent on the shear rate but independent on the time, the system is under such stress that the fluid is said to have a nonideal shear rate-dependent behavior. In particular, if the apparent viscosity decreases when the shear rate is increased, the fluid is a shear-thinning or a pseudoplastic fluid. If the apparent viscosity increases as the shear rate is increased, the fluid is a shear-thickening, or dilatant, fluid. Non-Newtonian liquids that are also dependent on the time over which they are under shear, are said to have a nonideal time-dependent behavior. They are subdivided into two categories. At a constant temperature and shear rate, if the viscosity decreases as a function of time, then the fluid is thixotropic; however, if the viscosity increases with time, the fluid is rheopectic.

Plastics

The rheological behavior of an ideal (or Bingham) plastic is described by two equations:

$$\sigma = G\gamma \quad (\text{for } \sigma < \sigma_0) \quad (7)$$

$$\sigma - \sigma_0 = \eta \dot{\gamma} \quad (\text{for } \sigma > \sigma_0) \quad (8)$$

where σ_0 is defined as the yield stress and all other symbols are as previously defined. Below the critical yield stress, application of a stress leads to elastic deformation of the sample. Above σ_0 some bonds in the sample break, leading to its plastic deformation or to the flow of the sample. Whereas in ideal plastics there is a clear definition between elastic and viscous behavior, nonideal plastics exhibit these two behaviors simultaneously. These are said to be viscoelastic materials (Prentice, 1984).

Solid fats have a plastic behavior that results from the presence of a certain percentage of crystallized fat within

a lipid matrix. This crystal network consist of a three-dimensional array of interlaced particles, arranged as branched and interlinked chains, formed by separate crystals or preformed aggregates. Before discussing the rheology of fats, it is convenient to define a few concepts usually used to describe the rheological behavior of matter.

Definitions of moduli

The tendency of a sample to be deformed is a measure of its elastic modulus, which is defined as the slope of its strain–stress curve in the linear (elastic) region. Depending on what stress is applied and how the strain is measured, different moduli can be determined. For example, when shear stress is applied, the shear modulus, G , is:

$$G = \frac{\sigma}{\gamma} \quad (9)$$

which is [Equation 5](#) rearranged.

For tensile and compressive stresses, the Young's modulus of elasticity, E , is defined as

$$E = \frac{\sigma}{s} \quad (10)$$

The bulk modulus, K , is used when there is a change in the volume of the sample upon the application of a three-dimensional stress:

$$K = \frac{\Delta P}{\Delta V/V_0} \quad (11)$$

where ΔP is the change in pressure and $\Delta V/V_0$, the relative change in volume of the solid (Eirich, 1956).

Basic concepts in dynamic measurements

Two types of experiments can be carried out to characterize the viscoelastic properties of food materials: transient ones and dynamic ones. In transient experiments, a simple shear stress is applied on a sample and the corresponding strain observed during the time of the load and as it relaxes.

The dynamic method consist of the application of a continuous stress or strain in an oscillatory fashion, where the material is subjected to a sinusoidal perturbation, either in the form of deformation (for controlled rate instruments) or stress (for controlled stress equipment). In a controlled rate experiment, the time dependence of the amplitude of the input strain wave is given by:

$$\gamma = \gamma_0 \sin(\omega t) \quad (12)$$

where γ_0 is the maximum amplitude of the strain and ω is the frequency expressed in rad/s, which is equivalent to $\omega/(2\pi)$ hertz. The periodic shear rate can then be found by taking the derivative of [Equation 12](#),

$$\dot{\gamma} = \gamma_0 \omega \cos(\omega t) \quad (13)$$

For a Kelvin–Voigt viscoelastic solid, the total stress (Δ) on the system corresponds to the sum of the elastic (Δ_e) and viscous (Δ_v) stresses, and thus

$$\Delta = \Delta_e + \Delta_v = G \cdot \gamma + \eta \dot{\gamma} \quad (14)$$

where η is the viscosity. Substituting Equations 12 and 13 into 14 results in

$$\Delta = G' \cdot \gamma_0 \sin(\omega t) + G'' \gamma_0 \cos(\omega t) \quad (15)$$

where G' is the shear storage modulus and G'' is the shear loss modulus ($G'' = \eta \cdot \omega$). Both of these are functions of frequency that can be expressed in terms of the phase shift and the amplitude ratio between the shear stress and strain

$$\Delta = \Delta_0 \sin(\omega t + \delta) \quad (16)$$

where Δ_0 is the maximum amplitude of the shear stress and δ is the phase lag or shift angle relative to the strain wave. The ratio of these two moduli is a common material function used to describe viscoelastic behavior:

$$\tan(\delta) = \frac{G''}{G'} \quad (17)$$

$\tan(\delta)$ is directly related to the energy lost per cycle divided by the energy stored per cycle. Additional frequency-dependent material functions include the complex modulus (G^*), complex viscosity (η^*), dynamic viscosity (η'), complex compliance (J^*), storage compliance (J') and loss compliance (J''), among others.

When the sample is an ideal (or purely elastic) solid, the maximum strain occurs when the maximum stress is applied. The stress and strain are said to be in phase. If the material is purely viscous, the stress and strain are out-of-phase by 90° . Viscoelastic materials exhibit a behavior that lays somewhere in between these two extremes, where the phase shift δ is $0^\circ < \delta < 90^\circ$ (Steffe, 1996).

Dynamic measurements allow for the study of the viscoelastic behavior of materials. This is performed by applying an oscillatory stress or strain to the sample. Typically, a sinusoidal strain is applied to the sample causing some level of stress to be transmitted through the material. The magnitude and time lag of the transmission depend on the viscoelastic nature of the test substance. If the material is more liquid-like, much of the stress is dissipated in frictional losses; in more elastic materials the stress is mostly transmitted. Likewise, the phase shift (or lag) is large for highly viscous materials but small for materials that exhibit a high degree of elasticity. Oscillatory testing is referred to as “small amplitude oscillatory testing” because small deformations must be employed to maintain linear viscoelastic behavior.

Experimental aspects of fat rheology

One aspect of fat rheology is that the variables and parameters over which the user has control on a rheometer are dependent on the type of rheometer used. Another aspect

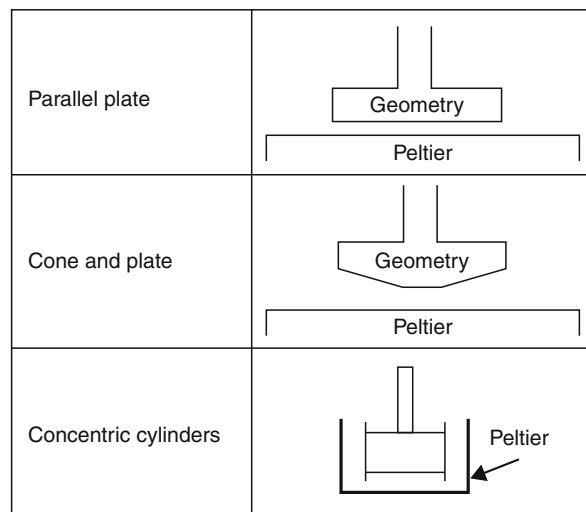
is the sample preparation, which ideally has to be, highly reproducible and simple. What follows, is a discussion of these two aspects together with a brief interpretation of data obtained on cocoa butter.

Rotational rheometers

Fats are commonly studied under the dynamic method with an oscillatory rheometer. In this kind of rheometer, the material is placed between two surfaces: the bottom surface, which is usually fixed, and the top surface, called *the geometry* that rotates. The instrument can be operated in steady shear mode (constant angular velocity) or oscillatory mode (dynamic). In the dynamic mode, samples are subjected to sinusoidal stress and the resulting sinusoidal strain is measured, or vice versa. Typical geometries include parallel plate, cone-and-plate, and concentric cylinders type (Figure 3).

The geometry is chosen based on the prior knowledge of the material under study, which involves some knowledge of its viscosity and/or flow. Usually concentric cylinders are used for low viscosity liquids, cone-and-plate are used for liquids and dispersion with particles smaller than $5 \mu\text{m}$, and parallel plates are used for gels, pastes, soft solids, and polymer melts.

Since the top geometry comes in different physical sizes, it can accommodate the study of a variety of materials. Large diameter geometries (60 mm, 40 mm) are used for low viscosity materials, while smaller diameters (20 mm, 15 mm, 10 mm) are used for high viscosity materials. The rheometer uses the geometry specifications to give a result that is independent of the geometry used. This makes the design and loading of the sample an important aspect in the measurement. In a controlled stress rheometer, a shear stress is applied to the material and the resulting strain or strain rate is measured. In contrast, in



Fats: Rheological Characteristics, Figure 3 Three different geometries and their corresponding base plates, commonly used in rotational rheometers.

a controlled strain rheometer a strain or strain rate is applied, and stress is measured. In most materials, the relationship between stress and strain can be understood using either rheometer design. However, the focus of next section is on stress control rheometers, as this is the instrument used in our laboratory.

Controlled stress rheometer

Figure 4 shows a rotational controlled stress Rheometer. It consists of a main unit mounted on a cast metal stand [1], with the electronic control circuitry contained within a separate electronics control box [2] and the sample holder [3].

The sample holder includes the temperature control system which uses the Peltier effect to rapidly and accurately control heating and cooling. Since the Peltier system operates as a heat pump, it is necessary to have the system hooked to a water pump or waterbath, to provide sufficient fluid flow through the Peltier heat exchange jacket built into the plate.

This controlled stress instrument uses an air bearing to provide “frictionless” movement of the upper fixture (**Figure 5**) and a noncontact drag cup motor to generate controlled torque on the shaft. A position indicator is used to measure displacement.

In this kind of rheometer, torque is applied to either control the stress at a desired level or to drive the strain

to a desired amount (Steffe, 1996). In some cases the applied motor torque and the measured amplitude are coupled.

Rheological parameters

Fundamentally, a rotational rheometer applies or measures torque, angular displacement, or rotational speed. The relationship between stress and deformation is a property of the material. Hence, rheology is a powerful technique that allows for the understanding of the material at the microscale level.

The information commonly obtained for fats from a rheometric measurement comes from the values of G' , G'' , and $\tan \delta$, which can be expressed as a function of time, temperature, frequency, stress, or strain. **Table 1** summarizes the physical parameters used in rheometry as well as the rheological parameters obtained from the measurement, for both stress- and strain-controlled instruments.

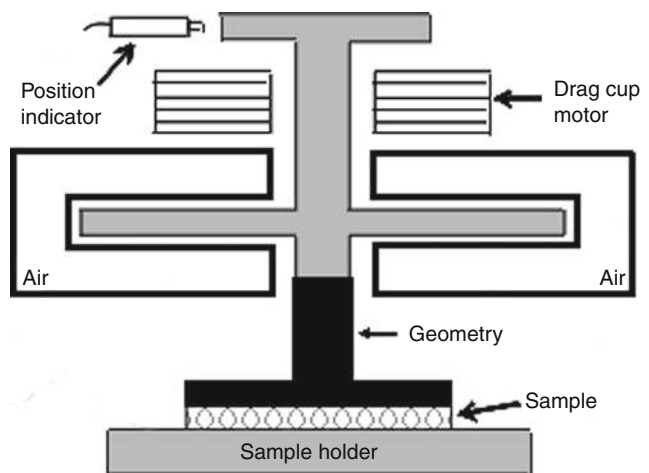
The advantages of using dynamic mechanical testing are that the shear rates involved are low, that only a small sample is required, and that both the elastic and viscous components of a material are probed simultaneously (Ferry, 1980).

Fats are usually analyzed in the so-called linear viscoelastic region, LVR (**Figure 6**), which is the region where the material's properties do not depend on the magnitude of the stress, the magnitude of the deforming strain, or the strain rate.

The yield stress or yield point, is the point that signals the beginning of structural breakdown and it is determined by a change in the slope of both G' and G'' curves. G' and G'' are used to characterize the system only when the samples are measured in the linear viscoelastic region. The LVR is determined from experimental data, usually running a stress sweep at a frequency of 1 Hz. Once the LVR is found, it is recommended that a frequency sweep



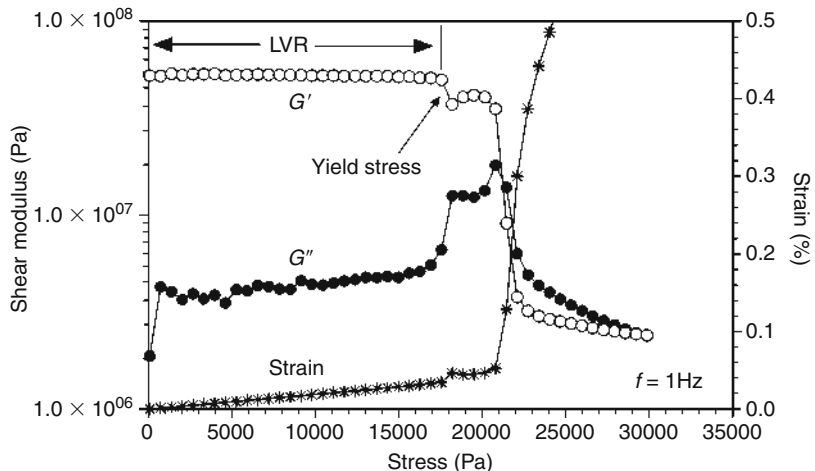
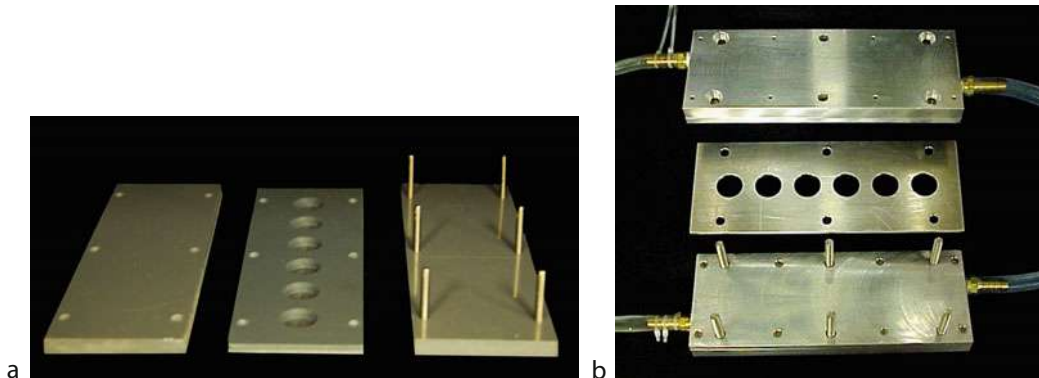
Fats: Rheological Characteristics, Figure 4 TA Rheometer AR2000 Controlled Stress Dynamic Shear Rheometer.



Fats: Rheological Characteristics, Figure 5 A schematic of a controlled stress instrument (Adapted from Steffe (1996)).

Fats: Rheological Characteristics, Table 1 Controlled and calculated variables in a rheometer

Type of rheometer	Physical parameter controlled	Rheological parameter controlled	Physical parameter result	Calculated rheological result	Rheological parameter
Stress controlled	Torque	Shear stress	Rotational speed	Shear strain	$G', G'', \tan \delta$
Strain controlled	Angular displacement	Shear strain	Torque	Shear stress	$G', G'', \tan \delta$

**Fats: Rheological Characteristics, Figure 6** Typical responses to strain or stress showing the Linear viscoelastic region (LVR) and the strain or stress at the limit of linearity (yield stress) for cocoa butter crystallized at 22°C.**Fats: Rheological Characteristics, Figure 7** Plastic (a) and aluminum (b) molds used to make fat samples to be used in the rheometer.

be performed using the appropriate values of stress obtained in the LVR region.

Fat sample preparation

Specific molds to make fat samples were designed and built in our laboratory. The molds have three distinctive parts: a flat bottom, an intermediate template with holes of 10 mm in radius and either 1 mm or 3.2 mm in height, and a flat cover. The cover can be screwed in place with

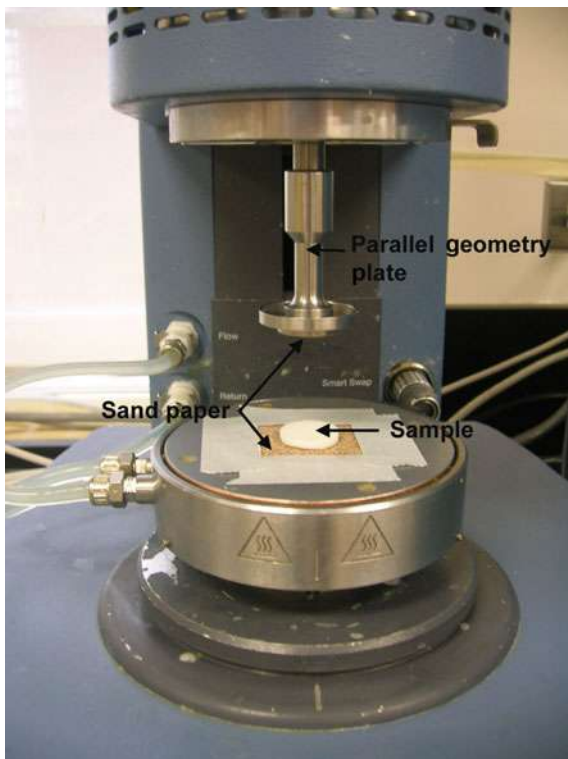
butterfly screws, as shown in Figure 7. Plastic molds (Figure 7a) are the standard ones that can be used at room temperature or at a specific temperature in an incubator. The aluminum mold (Figure 7b) has the extra advantage that allows the control of the cooling rate via a waterbath.

The typical procedure followed in our laboratory for sample preparation consists of the following steps:

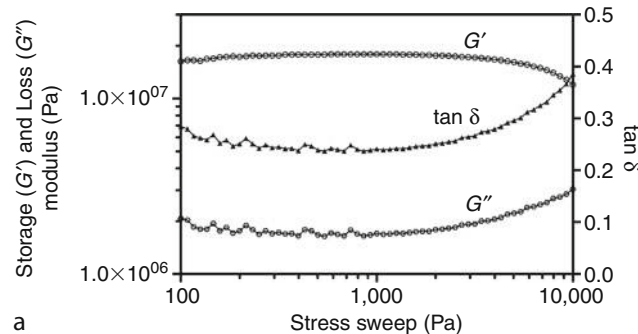
1. Melt the desired material in the oven, at a high enough temperature to erase all crystal history. In general, 60°C

- for 30 min or 80°C for 15 min are typical values used in our laboratory.
2. Place molds, a piece of parafilm, and a piece of aluminum foil in the oven at 60°C to equilibrate them. Parafilm does not withstand temperatures higher than 60°.
 3. Assemble the bottom part of the molds by placing first a piece of aluminum foil and then a piece of parafilm. Assemble the middle template and pour the molten material into the holes.

4. Cover the holes with a layer of parafilm and a layer of aluminum paper before screwing in place the cover of the mold. The parafilm and aluminum paper help in creating a smooth surface on the fat and on the removal of the fat samples once they are crystallized.
5. Crystallize samples inside the mold under the desired conditions and de-mold when ready.
6. In order to prevent slippage it is necessary to glue sandpaper on the geometry of the rheometer and on the Peltier plate, to prevent slippage. Usually a 50 grit sandpaper is attached with Krazy Glue™ as seen in Figure 8.



Fats: Rheological Characteristics, Figure 8 Position of the sample, the sand paper, and the geometry on the rheometer.



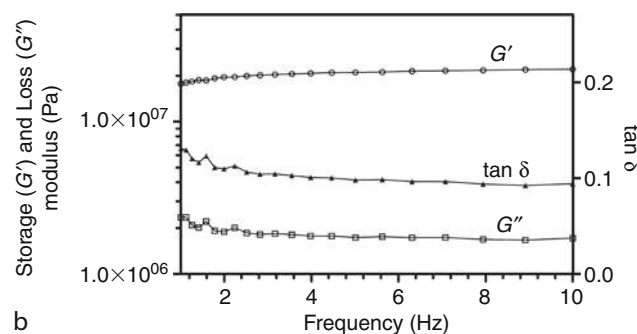
Fats: Rheological Characteristics, Figure 9 G' , G'' , and $\tan \delta$ obtained with our rheometer for Cocoa Butter. Figure (a) is a stress sweep at a constant frequency of 1 Hz, while Figure (b) is a frequency sweep at a constant stress of 1,000 Pa.

Cocoa butter example

Fats are complex systems made of many different molecules, and a complex structural hierarchy at the nano, micro, and macro scales, which make the rheological testing very complex. Preliminary measurements are usually needed to find the optimal conditions under which the rheological analysis should be performed for the sample under study. An oscillatory test using stress as the variable provides information regarding the LVR region, as well as optimal values for the frequency that can then be used to do an oscillatory frequency test. It is common to report results of G' and G'' as a function of either stress or strain. Figure 9 shows values of G' , G'' , and $\tan \delta$ for cocoa butter using: (a) shear stress and (b) frequency, as the controlled variables.

Conclusions

Rheology is a powerful analytical method for the study of fats. It provides insight on the molecular interactions that give rise to the specific properties of the sample. However, the choice of the experimental conditions is crucial for obtaining results that represent the behavior of the sample. In this sense, the use of controlled stress rheometers working in a dynamic mode has proven to be a reliable method for the measurement of rheological properties in fats. The small oscillation amplitude and stresses achievable with these instruments allow for the interpretation of the fat



behavior at different length scales, which in turn is what is needed to fully understand the properties of the material.

Bibliography

- De Man, J. M., and Beers, A. M., 1987. Fat crystal networks: Structure and rheological properties. *Journal of Textural Studies*, **18**, 303–318.
- Eirich, F. R., 1956. *Rheology: theory and applications*. New York: Academic.
- Ferry, J. D., 1980. *Viscoelastic Properties of Polymers*, 3rd edn. New York: Wiley.
- Marangoni, A. G., 2005. *Fat Crystal Networks*. New York: Marcel Dekker.
- McClements, D. J., 2005. *Food emulsions, Principles, practices, and techniques*, 2nd edn. Boca Raton: CRC.
- Narine, S. S., and Marangoni, A. G., 1999. Microscopic and rheological studies of fat crystal networks. *Journal of Crystal Growth*, **198**, 1315–1319.
- Narine, S. S., and Marangoni, A. G., 2001. Elastic modulus as an indicator of macroscopic hardness of fat crystal networks. *Lebensmittel – Wissenschaft und Technologie*, **34**, 33–40.
- Prentice, J. H., 1984. *Measurements in the Rheology of Food Stuffs*. London: Elsevier Applied Science.
- Rees, D., 2006. *Basic Engineering Plasticity: An Introduction with Engineering and Manufacturing Applications*. Burlington: Butterworth-Heinemann.
- Rousseau, D., and Marangoni, A. G., 1999. The effects of interesterification on physical and sensory attributes of butterfat and butter-fat-canola oil spreads. *Food Research International*, **31**, 381–388.
- Steffe, J. F., 1996. *Rheological methods in food process engineering*, 2nd edn. MI: Freeman Press.
- Wright, A. J., Scanlon, M. G., Hartel, R. W., and Marangoni, A. G., 2001. Rheological properties of milk fat and butter. *Journal of Food Science*, **66**, 1056–1071.

Cross-references

[Rheology in Agricultural Products and Foods](#)

[Rheology in Soils](#)

[Stress–Strain Relations](#)

FERTILIZERS (MINERAL, ORGANIC), EFFECT ON SOIL PHYSICAL PROPERTIES

Kuntal Hati¹, Kalikinkar Bandyopadhyay²

¹Division of Soil Physics, Indian Institute of Soil Science, Bhopal, Madhya Pradesh, India

²Central Institute for Cotton Research, Coimbatore, Tamil Nadu, India

Definition

Fertilizer. Any organic or inorganic material of natural or synthetic origin (other than liming materials) that is added to a soil to supply one or more plant nutrients essential to the growth of plants.

Mineral fertilizer: A fertilizer material in which carbon is not an essential component of its basic chemical structure. They are also called as inorganic or chemical fertilizer.

Organic fertilizer. A material containing carbon and one or more plant nutrients in addition to hydrogen and/or

oxygen is called organic fertilizer. This generally means that the nutrients contained in the product that are derived solely from the remains or a by-product of an organism.

Physical properties (of soils). Those characteristics, processes, or reactions of a soil that are caused by physical forces and that can be described by, or expressed in, physical terms or equations. For example, size, density, temperature, water, hydraulic conductivity, porosity, and pore-size distribution are physical properties.

Introduction

Fertilizers are common amendments that are routinely applied to agricultural soils for sustaining or improving productivity of crops by supplying mineral nutrients to plant. Fertilizer technologies developed significantly as the chemical needs of growing plants were discovered. Commercial fertilizers are used in modern agriculture to correct known plant-nutrient deficiencies; to maintain optimum soil fertility conditions; to provide nutrition, which aid plants in withstanding stress conditions; and to improve crop quality. The use of modern synthetic fertilizers has significantly improved the quality and quantity of the food available today, although environmentalists debate over their long-term use. The main nutrients supplied routinely as fertilizers to agricultural soils are nitrogen, phosphorus, and potassium. In addition to this, fertilizers containing secondary nutrients (Ca, Mg, S) and micronutrients (Fe, Mn, Zn, Cu, Mo, B) are also applied by farmers as per the deficiency of these nutrients in soil and crop requirement. Fertilizers are generally placed into two categories namely, organic fertilizer and mineral or inorganic fertilizer. Organic fertilizers are composed of naturally occurring compounds such as peat or compounds manufactured through natural processes (such as composting). The word organic fertilizer generally means that the nutrients contained in the product are derived solely from the remains or a by-product of an organism. Cottonseed meal, blood meal, fish emulsion, manures, slurry, worm castings, peat, seaweed, guano, different types of composts, and sewage sludge are examples of organic fertilizers. Green manure crops, grown to add nutrients to the soil, are also considered as organic fertilizer. Microorganisms in the soil decompose the organic fertilizers, making its elements available for use by plants. Mineral fertilizers are compounds occurring either as natural deposits (Chilean sodium nitrate, mined rock phosphate) or are synthesized in a chemical factory (diammonium phosphate, ammonium nitrate, ammonium sulfate, single super phosphate, muriate of potash). Inorganic fertilizers upon application to soil dissolve fully or sparingly in the soil–water system and release the nutrient(s) in the ionic form, which are absorbed by the plants. However, some fertilizers like urea, after application to soil undergo chemical transformation before releasing the nutrients in plant available form. Urea is a synthetic organic fertilizer, an organic substance manufactured from inorganic materials but it is generally categorized as an

inorganic fertilizer because of its rapid hydrolysis to form ammonium ions in soils. Inorganic (or mineral) fertilizers vary in appearance depending on the process of manufacture. The fertilizer particles are available in many different sizes and shapes like crystals, pellets, granules, or dust, and the fertilizer grades can include straight fertilizers (containing one nutrient element only, e.g., urea, single super phosphate, muriate of potash), compound fertilizers (containing two or more nutrients usually combined in a homogeneous mixture by chemical interaction, e.g., diammonium phosphate, ammonium sulfate), and fertilizer blends (formed by physically blending mineral fertilizers to obtain desired nutrient ratios).

The organic fertilizers are usually low in nutrient content and thus required in high volume or bulk to supply a desired amount of nutrient to the crops. Many governments and agricultural departments particularly in developing countries go to great lengths to increase the supply of organic fertilizers, such as organic manures and composting materials, but not enough of these fertilizers are available to meet the existing and ever increasing future fertilizer needs. Compared to organic compost, mineral or inorganic fertilizers have the added advantage of being less bulky. Being less bulky makes chemical fertilizer easier to transport, both overland and from the soil into the plants itself, because they get to be available to the plant relatively quickly when incorporated as part of the plant-food constituents. There has been much controversy over whether organic or mineral fertilizers are a better source of nutrients for plants. Here it is important to note that plants do not recognize the difference between the nutrients derived from organic and inorganic fertilizers. Their tiny root hairs can absorb only nutrients that have been broken down into inorganic, water-soluble forms. That means the plant makes no difference between the nutrient ions coming from a compost pile or a fertilizer factory. However, to obtain optimum crop yield it is essential for integrated application of both organic and inorganic fertilizers containing all the nutrients in balanced proportion as per crop demand. There are, however, advantages and disadvantages to each type of fertilizer material, organic or mineral.

Organic fertilizer

Advantages – There is less danger of overfertilization by adding decomposed organic material to a crop. It provides a slow release of nutrients as microorganisms in the soil break the organic material down into an inorganic, water-soluble form, which the plants can use. The addition of organic material generally increases the organic carbon content of the soil and improves soil structure or “workability.” It also improves the chemical and biological properties of the soil. Continued use of organic fertilizers results in increased soil organic matter, reduced erosion, better water infiltration and aeration, higher soil biological activity as the materials decompose in soil, and increased yields after the year of application (residual effects).

Limitations – For the most part, the nutrients in organic fertilizer are not immediately available to the plants due to their slow-release nature. Thus, if there is an immediate need for nutrients to crop, organic fertilizer cannot supply them in a hurry. Furthermore, information on the amount of nutrients and the exact elements in an organic fertilizer such as manure is not readily available to the crop growers. The organic fertilizers are usually required in high quantity to have desired effects as they are low in nutrient content. This condition makes them uneconomical to transport them far from their point of production. The possibility of nitrogen depletion is another drawback of organic fertilizers. Because of complex bacterial action, the addition of a large amount of organic material with high C/N ratio can cause a temporary nitrogen depletion in the soil and therefore in the plants because of immobilization process. Indiscriminate use of animal manures and human waste (sewage sludge), as has been practiced for their disposal in some areas, can create human health hazards through the accumulation of nitrates, phosphates, heavy metals, and pathogens in the soil. Other than this use, there are other competing uses of organic residues like fuel and animal feed in developing countries, which makes them unavailable for agricultural purpose.

Mineral fertilizer

Advantages – The primary advantage of using packaged mineral fertilizer is that nutrients are immediately available to the plants. As mineral fertilizers contain precise and guaranteed levels of nutrients, in forms that are readily available for plant uptake and use, the exact amounts of a given element can be calculated and given to plants. Because of their high nutrient content, mineral fertilizers are easy and economical to ship to great distances from their point of production.

Limitations – Commercial fertilizer, especially nitrogen, is easily washed below the level of the plant's root system through the leaching of rain or irrigation, which may pollute the ground water or may cause eutrophication in lakes and water bodies. Improper use of these fertilizers can lead to volatilization loss of ammonia under high soil pH and also emission of nitrous oxide because of denitrification under anaerobic condition. An application of too heavy dose of fertilizers close to the roots of the plants may cause “burning” (actually a process of desiccation by the chemical salts in the fertilizer). As well, overly heavy applications of commercial fertilizers can build up toxic concentrations of salts in the soil, thus creating chemical imbalances. Excessive use of straight fertilizers leads to soil mining of essential nutrients causing multi-nutrient deficiencies and unsustainable crop yield.

Fertilizer effect on soil physical properties

Favorable effects

Fertilizers are applied to soils in order to maintain or improve crop or pasture yield. The increased plant biomass produced by fertilizer results in increased return of

organic material to the soil in the form of decaying roots, litter, and crop residues. Mineral fertilizers indirectly influence soil organic matter content by increasing crop productivity and thereby the amount of organic matter returned to the soil in various crop residues. The effect of mineral fertilizers may therefore be compared to that of straw incorporation. But when animal manure with a plant nutrient content equivalent to that of the mineral fertilizer dressing is applied, the soil receives an additional input of organic material, which contributes to the soil organic matter pool. The increase in organic matter formed due to mineral fertilizer-induced crop yield increases is generally of a more aromatic nature and thus has a higher Cation Exchange Capacity (CEC) than that formed due to organic fertilizer (farmyard manure) addition (Schjonning et al., 1994). Increased organic matter inputs stimulate the microbial and faunal activity of the soil and consequently favor improved soil physical conditions. Increasing soil organic matter content characteristically leads to a decrease in bulk density and surface crusting and an increase in water holding capacity, macroporosity, infiltration capacity, hydraulic conductivity, and aggregation. These aspects are discussed below in detail:

1. Structure and aggregation: Soil aggregates are the basic unit of soil structure and are composed of primary particles and binding agents (Tisdall and Oades, 1982; Haynes et al., 1991). Soil aggregation is the process by which aggregates of different sizes are joined and held together by different organic and inorganic binding agents. In surface soils, organic matter is the main binding agent responsible for the water stability of soil aggregates by the formation of clay humus complex. The aggregate stability is positively correlated with the soil organic carbon content (Hati et al., 2008). Therefore, it is expected that addition of organic-fertilizers or materials rich in organic carbon such as manure or sludge will lead to an improvement of the aggregation status of soil. Long-term fertilizer studies have shown that application of fertilizers to soil induces an increase in number and size of water stable aggregates. Inorganic fertilizer additions can have physicochemical effects on soil, which influence soil aggregation. Phosphatic fertilizers and phosphoric acid can favor aggregation by the formation of Al or Ca phosphate-binding agents while where fertilizer NH_4^+ accumulates in the soil at high concentrations, it behaves like Na^+ and causes dispersion of clay colloids.
2. Bulk density and porosity: Application of organic-fertilizer in long-term normally reduces the bulk density of the soil due to higher organic matter content of the soil, better aggregation and a consequent increase in volume of pores and increased root growth. Furthermore, addition of large quantity of organic manure or wastes reduces the bulk density of the soil due to a dilution effect caused by mixing of the added organic
- material with the denser mineral fraction of the soil (Khaleel et al., 1981). Organic fertilizer addition leads to an increase in total pore volume of the soil. Besides total pore volume, pore-size distribution also changes with fertilization. Organic matter addition through sludge and compost increases the percentage of transmission (50–500 μm) and storage (0.5–50 μm) pores while reduces the percentages of fissure ($>500 \mu\text{m}$) (Metzger and Yaron, 1987).
3. Water retention properties: Water retention by soils is controlled primarily by the following: (1) the number of pores and pore-size distribution of soils; and (2) the specific surface area of soils. Because of increased aggregation with application of organic-fertilizers, total pore space in soil is increased. Furthermore, as a result of decreased bulk density, the pore-size distribution is altered and the relative number of small pores increases, especially for coarse-textured soils. Organic-fertilizer application improves water retention properties of soil through its effect on pore-size distribution and soil structure. Organic-fertilization increases soil–water retention more at lower suctions due to increase in micropores and inter-aggregate pores caused by enhanced soil organic matter content and higher activity of soil fauna, e.g., earthworms and termites. At higher tensions close to the wilting point (1.5 MPa), nearly all pores are filled with air and the surface area and the thickness of water films on soil particle surfaces determine moisture retention. Following an addition of organic matter, specific surface area increases resulting in increased water holding capacity at higher tensions.
4. Water transmission properties: Fertilization indirectly influences the water transmission properties of the soil through their influence on aggregation status and on porosity. As good structural conditions are usually associated with adequate water transmission properties, it can be inferred that fertilization will generally improve the water transmission properties.
 - (a) Hydraulic conductivity: Addition of organic manure and mineral fertilizer results better aggregation, increase in effective pore volume and an increase in continuity of pores due to enhanced root growth and formation of bio-pores, increased faunal activity and earthworm population and burrows. As soil permeability is a function of effective pore volume, increased pore volume has a positive influence on the saturated hydraulic conductivity of the soil (Hati et al., 2006).
 - (b) Infiltration: Infiltration through the soil surface depends on the soil surface features and the hydraulic conductivity in the underlying soil. The application of organic fertilizer generally improves both the initial and steady-state infiltration rate due to the beneficial effect of fertilization on the water stability of soil aggregates, consequent reduction in crust formation, and increase in hydraulic conductivity.

Detrimental effects

Excess or imbalanced application of fertilizers to soil can have some negative effect on soil physical properties. An application of ammonium containing or forming fertilizers sometimes shows adverse effect on soil aggregation. When the monovalent NH_4^+ ion accumulates in soils in large amount it becomes a dominant exchangeable cation and like Na^+ it favors dispersion of soil colloids (Haynes and Naidu, 1998). In many cases, application of fertilizer K alone particularly in humid temperate region decreases the aggregate stability of the soil owing to an increase in the proportion of exchangeable cations present in monovalent form and leaching of Ca and Mg. Long-term application of N-containing mineral fertilizer alone in Alfisols of humid tropics can deteriorate the physical properties of the soil due to reduction in pH and yield of crops (Hati et al., 2008).

Application of organic fertilizers to soil at rates far in excess of traditional rates for the purpose of disposal of wastes (e.g., animal manure from feed lots, composted municipal wastes, and sewage sludge) also have detrimental effects on soil physical properties like surface crusting, increased detachment of soil particles by raindrops, and decreased hydraulic conductivity. The primary reason for this soil structural breakdown is the high content of monovalent cations (Na^+ and K^+) in animal waste materials and accumulation of high concentration of NH_4^+ through mineralization of N in organic wastes. Sometimes excessive NO_3^- formed in the animal manure feedlot can leach down the profile and pollute the ground water. Besides this, at a high rate of organic matter application to soil, the soil tends to become water repellent due to production of water-repellent substances by fungi involved in the decomposition of the manure (Weil and Kroontje, 1979).

Summary

Fertilizers, both organic and mineral, are essential for sustainable crop production. Organic fertilizers play a significant role in improving the soil physical properties like soil aggregation, pore-size distribution reduction in soil compaction and crusting, and also improving the soil water retention and transmission characteristics. However, there is limitation in availability of the organic fertilizers sufficient enough to meet the crop demand to produce food, feed, and fiber for the growing population. The role of inorganic fertilizers cannot be ignored to meet the immediate crop demand. Besides this condition, the inorganic fertilizers also help in addition of organic residues to soil through enhanced biomass production and root growth. Therefore, both organic and inorganic fertilizers should be applied in integrated manner and in balanced proportion to improve soil health, minimize environmental pollution, and sustain crop yield at higher level.

Bibliography

Hati, K. M., Mandal, K. G., Misra, A. K., Ghosh, P. K., and Bandyopadhyay, K. K., 2006. Effect of inorganic fertilizer and

- farmyard manure on soil physical properties, root distribution, water-use efficiency and seed yield of soybean in Vertisols of central India. *Bioresource Technology*, **97**, 2182–2188.
- Hati, K. M., Swarup, A., Mishra, B., Manna, M. C., Wanjari, R. H., Mandal, K. G., and Misra, A. K., 2008. Impact of long-term application of fertilizer, manure and lime under intensive cropping on physical properties and organic carbon content of an Alfisol. *Geoderma*, **148**, 173–179.
- Haynes, R. J., and Naidu, R., 1998. Influence of lime, fertilizer and manure applications on soil organic matter content and soil physical conditions: a review. *Nutrient Cycling in Agroecosystems*, **51**, 123–137.
- Haynes, R. J., Swift, R. S., and Stephen, R. C., 1991. Influence of mixed cropping rotations (pasture-arable) on organic matter content, water stable aggregation and clod porosity in a group of soils. *Soil and Tillage Research*, **19**, 77–87.
- Khaleel, R., Reddy, K. R., and Overcash, M. R., 1981. Changes in soil physical properties due to organic waste application: a review. *Journal of Environmental Quality*, **10**, 133–141.
- Metzger, L., and Yaron, B., 1987. Influence of sludge organic matter on soil physical properties. *Advances in Soil Science*, **7**, 141–163.
- Schjonning, P., Christensen, B. T., and Carstensen, B., 1994. Physical and chemical properties of a sandy loam receiving animal manure, mineral fertilizer or no fertilizer for 90 years. *European Journal of Soil Science*, **45**, 257–268.
- Tisdall, J. M., and Oades, J. M., 1982. Organic matter and water-stable aggregates in soil. *European Journal of Soil Science*, **33**, 141–163.
- Weil, R. R., and Kroontje, W., 1979. Physical condition of a Davidson clay loam after five years of heavy poultry manure applications. *Journal of Environmental Quality*, **8**, 387–392.

Cross-references

- [Bulk Density of Soils and Impact on Their Hydraulic Properties](#)
[Liming, Effects on Soil Properties](#)
[Organic Matter, Effects on Soil Physical Properties and Processes](#)
[Soil Aggregates, Structure, and Stability](#)
[Soil Biota, Impact on Physical Properties](#)
[Soil Physical Quality](#)

FICK'S LAW

The law describing the movement of ions or molecules by diffusion due to a concentration gradient.

Cross-references

- [Diffusion in Soils](#)

FIELD WATER CAPACITY

Karl Vanderlinden¹, Juan V. Giráldez²

¹Centro Las Torres-Tomejil, IFAPA,
Alcalá del Río (Seville), Spain

²Department of Agronomy, University of Córdoba,
Córdoba, Spain

Synonyms

Field capacity; In situ field capacity

Definition

Field water capacity is defined by the Soil Science Glossary Terms Committee (2008) as the content of water, on a mass or volume basis, remaining in a soil 2 or 3 days after having been wetted with water and after free drainage is negligible.

Field water capacity or *field capacity* (FC) is the upper limit of the *available soil water* (AW) reservoir, from which water can be released but not necessarily absorbed by plants, until the *permanent wilting point* (PWP) is reached. An earlier definition of the concept by Veihmeyer and Hendrickson (1931, p. 181), “the amount of water held in soil after the excess gravitational water has drained away and after the rate of downward movement of water has materially decreased,” is rather subjective. The water content at FC has been operatively approximated as the equilibrium volumetric soil water content at values of the matric potential ranging from -1 to -50 kPa, with -33 kPa as a generally accepted reference value. Since FC depends on field conditions (e.g., porosity, structure), in situ determination is considered more accurate (Ritchie, 1981). The dynamic aspect, implicit in the definition of FC, was not considered until Nachabe (1998) and Meyer and Gee (1999) proposed to estimate the water content at FC, θ_{FC} , as the value at which the hydraulic conductivity of the soil reaches a fixed low value, $q_{FC} = k(\theta_{FC})$, considering that the free drainage flow is essentially gravity driven, with unit potential gradient, and that the flux density of the water, q , equals the hydraulic conductivity, $q = k(\theta)$. Nachabe (1998) suggested a value of $q_{FC} = 0.05$ mm/day = $5.8 \cdot 10^{-10}$ m/s, and Meyer and Gee (1999) chose a range (10^{-8} – 10^{-10} m/s) to include soils with different textural classes. In both cases, the conductivity-derived water contents at field capacity were very close to the field estimated data of Ratliff et al. (1983) and to some of the retention-curve-derived values for a matric potential of -33 kPa. Nachabe (1998) used a simplified model to describe the soil water redistribution process, adopting the Brooks and Corey hydraulic conductivity expression, $k = k_s \cdot \Theta^n$, with k_s , the saturated conductivity, Θ , the effective saturation, and n , a coefficient to determine the time required to reach FC:

$$t_{FC} = \frac{I}{n} \left(\frac{1}{q_{FC}} - \frac{1}{k_s \Theta_i^n} \right) \quad (1)$$

Equation (1) indicates the influence of the initial infiltration depth, I , and effective saturation, Θ_i on the drainage time, yielding larger values than 2 or 3 days of the original definition. Minasny and McBratney (2003) introduced a physical estimation of the PWP by introducing the integral energy or the integral of the water retention curve as a measure of the energy required to extract the water of the soil to a certain level. These approaches allow a more precise estimation of the ill-defined and commonly used concepts of FC, PWP, and AW.

Bibliography

- Meyer, P. D., and Gee, G. W., 1999. Flux-based estimation of field capacity. *Journal of Geotechnical and Geoenvironmental Engineering*, **125**, 595–599.
- Minasny, B., and McBratney, A. B., 2003. Integral energy as a measure of soil-water availability. *Plant and Soil*, **249**, 253–262.
- Nachabe, M. H., 1998. Refining the definition of field capacity in the literature. *Journal of Irrigation and Drainage Engineering*, **124**, 230–232.
- Ratliff, L. F., Ritchie, J. T., and Cassel, D. K., 1983. Field-measured limits of soil water availability as related to laboratory-measured properties. *Soil Science Society of America Journal*, **47**, 770–775.
- Ritchie, J. T., 1981. Soil water availability. *Plant and Soil*, **58**, 327–338.
- Soil Science Glossary Terms Committee, 2008. *Glossary of Soil Science Terms 2008*. Madison: SSSA, p. 92.
- Veihmeyer, F. J., and Hendrickson, A. H., 1931. The moisture equivalent as a measure of the field capacity of soils. *Soil Science*, **32**, 181–194.

Cross-references

- [Water Balance in Terrestrial Ecosystems](#)
[Water Budget in Soil](#)

FINGERING

The appearance of protrusions in the normally smooth wetting front during infiltration. Such “fingers” may propagate downward into the subsoil and carry plumes of water and solutes while bypassing the greater volume of the soil matrix. The phenomenon is also called “wetting-front instability” and “unstable flow.”

Bibliography

- Introduction to Environmental Soil Physics. (First Edition). 2003. Elsevier Inc. Daniel Hillel (ed.) <http://www.sciencedirect.com/science/book/9780123486554> GLOSSARY

FIRMNESS

Resistance to externally applied load.

FISSURES

Fissures in soils are cracks at or near the soil surface resulting e.g., from soil compaction or lowering of the water table by excessive groundwater pumping.

FLEXURAL STRENGTH

Strength of a material in blending, that is, resistance to fracture.

FLOCCULATION AND DISPERSION PHENOMENA IN SOILS

Emil Chibowski

Maria Curie-Skłodowska University, Lublin, Poland

Synonyms

Agglomeration; Aggregation; Coagulation; Peptization; Suspension

Definition

Flocculation – process during which particles, for example, of a soil, dispersed in a solution contact and adhere each other, forming clusters, flocks, flakes, or clumps of a larger size. The term originates from the word “floc,” which is the flake of precipitate that comes out of solution. The floc may float to the top or settle to the bottom of the liquid, as well can be readily filtered from the liquid. Flocculation is synonymous with agglomeration and coagulation.

Dispersion – a system in which solid or liquid particles are dispersed in a continuous phase (liquid, gas, or even solid) of different composition. In soils dispersion occurs when a soil contains clays. When such a soil is wetted the clay particles are detached from each other and form dispersion, that is, separation of the soil into single particles occurs.

Introduction

Various physicochemical processes take place in soil–water systems, among others flocculation and dispersion. Usually they are complicated because of very complex character of soils, their mineralogy, content of clay minerals, organic substances, etc. Many factors affect course of the processes, that is, type of ions present, the ionic strength, adsorption of the ions, pH, and temperature (Pils et al., 2007 and the references therein). Taking into account the content of clay fraction natural soils can be classified as: sand (<10 wt%), loamy sand (<15 wt%), sandy loam (<20 wt%), sandy clay loam (<30 wt%), sandy clay (<55 wt%), and clay (Pivovarov, 2006). Soils can be also classified with respect to the soluble salts (EC) and sodium adsorption ratio (SAR) amounts and these two parameters indicate somehow the soil structure. In this way four types of soils can be distinguished, as shown below (Walworth, 2006).

Soil	EC	SAR	Soil status
Normal	<4	<13	Flocculated
Saline	>4	<13	Flocculated
Sodic	<4	>13	Dispersed
Saline-sodic	>4	>13	Flocculated

In soils, the flocculation process concerns mostly the clay particles present. Clay particles usually possess net negative charge and therefore they electrostatically attract positively charged ions, such as Ca^{2+} cations, which form bridges, holding the particles together. Therefore, these cations can induce flocculation of clay particles. Three main types of clay can be distinguished: illite (muscovite), kaolinite, and montmorillonite (Pivovarov, 2006). In the clay fraction, an average content of Al amounts about 20 wt%. These silicate minerals have different lattice structure and hence different affinity to bind sodium cations. They consist of layer platelets and in case of kaolinite, the platelets are formed of octahedral alumina layer on one side of which there is tetrahedral silicate layer and no cations can be exchanged between the kaolinite plates. Hence, kaolinite possesses exchangeable cations on its surface. In case of muscovite on both sides of alumina platelet there are tetrahedral silicate layers. There is electric charge on the muscovite surface because each fourth Si atom is replaced by Al atom and the exchangeable cations are placed in the lattice (Pivovarov, 2006). In montmorillonite clays, the platelets are weakly bound and are affected by sodium ions the most, while in the kaolinite the least. The same trend is also true as for their swelling and dispersion. Dispersion being the process of separation of soil into single particles is governed by soil texture, clay type, soil organic matter content, soil salinity, and the exchangeable cations present. Dispersion and slaking have a large effect on the soil behavior. The dispersed clay particles may plug in the soil pore structure and thus decrease water penetration. Occurrence of dispersion process is generally a major cause of the soil erosion, as well as after such soil repeated wetting and drying its structure may become cemented. These two processes will be described in some detail below.

Flocculation

Generally flocculation process is applied to remove solid particles from a solution. It can occur naturally, but in practical industrial applications more efficient process needs addition of some flocculants. It is used to a large scale, for example, in waste water treatment. Flocculation may be desired process (e.g., sedimentation of the particles from waste waters) or undesired (e.g., in some dairy processes) (Smith, 2009). Flocculated soil particles form aggregates which may also form cemented clusters of clay, silt, and sand particles (Walworth, 2006). In dispersed

clay, suspension being in quiescent conditions, flocculation of its particles may occur spontaneously because negative charges present on the platelets faces attract positive charges on their edges thus forming flakes. Such aggregates facilitate water penetration between them as well as growth of plant roots. In soil, most common cations are sodium Na^+ , potassium K^+ , magnesium Mg^{2+} , and calcium Ca^{2+} . The bivalent cations are good flocculants while the monovalent are good dispersants. The relative flocculating power of the above-mentioned cations is: 1.0, 1.7, 27.0, and 43.0, respectively (Walworth, 2006). All cations in water are hydrated and the smaller charge and the larger hydrated radius, the cation is the poorer flocculant. The flocculation power is determined as the Sodium Adsorption Ratio (SAR) expressed by the cation molar concentrations:

$$\text{SAR} = \frac{[\text{Na}^+]}{\sqrt{[\text{Ca}^{2+}] + [\text{Mg}^{2+}]}} \quad (1)$$

The lower the value of SAR (i.e., larger bivalent cation concentration), the more flocculated is the soil. Also, if the content of soluble salt is high (high ionic strength) the soil will flocculate, even at an elevated content of sodium ions (Walworth, 2006). Fine particles of soil (clay minerals), say less than 0.1 μm (100 nm), usually possess electric charge (typically negative one) and in aqueous solution repel each other and remain suspended. Once their electrostatic charge is neutralized by the addition of an electrolyte or other chemical compound (flocculant), the particles start to collide and due to attractive van der Waals forces flocculate forming agglomerates. Generally, stability of colloidal particles including soil colloids can be evaluated using the Derjaguin–Landau–Verwey–Overbeek (DLVO) theory of colloid stability, which balances the electrostatic repulsive forces, resulting from the presence of electrical double layer at the particle surface and the attractive van der Waals forces between them (Israelachvili, 1985). It explains the effect of increasing ionic strength and the ion charge on flocculation of the particles, which is caused by the compression of thickness of the diffuse part of the double layer. However, the theory fails in case of very hydrophilic particles, because it does not consider hydration force and/or the Lewis acid–base interactions, which in most cases are the hydrogen bonding. This is taken into account in the extended DLVO theory proposed by van Oss et al. (1990) (Wiacek and Chibowski, 1999). Classical DLVO theory also does not predict formation and destruction of smectite quasicrystals (Pils and Laird, 2003). From kinetics point of view, flocculation may be classified as transport-controlled or surface reaction-controlled process. The transport-controlled flocculation is termed if the process rate is determined by the movement of two or more particles toward one another prior to their close encounter and immediate coalesce to form a large particle. The surface-controlled flocculation occurs if it is particle coalesce instead of particle movement toward collision that limits the rate of flocculation

(Sposito, 2008, p. 244). Then, three mechanisms of transport-controlled flocculation are possible, that is, (1) the Brownian motion or *perikinetic flocculation*, which occurs in case of diffusing particles in a question suspension (smaller than 1 μm), (2) *orthokinetic flocculation* caused by stirring, (3) *differential sedimentation* due to gravitational or centrifugal forces. These later two mechanisms involve also particles larger than 1 μm . The details on the flocculation kinetics can be found in Sposito (2008) monograph, *The Chemistry of Soils*. As was mentioned above flocculated/dispersed state of soil colloidal particles largely depends on the amount of electrolyte concentration (EC) and the cations valency, and when the attractive van der Waals forces overcome repulsive electrostatic ones the rapid flocculation (coagulation) process should take place. The concentration at which it happens is termed *critical flocculation concentration* (CFC) (Zhang, 2002). It should be also mentioned that synthetic polymers have been also applied in practice to enhance flocculation in soil (Zhang, 2002; Pivovarov, 2006). The presence of humic substances in soil may enhance clay particles flocculation by binding the particles together (Pils et al., 2007). On the other hand, Heil and Sposito (1993) investigated the influence of organic matter on flocculation of soil colloidal particles depending on the electrolyte concentration, pH, and exchangeable or dissolved bivalent cations. They found that the flocculation increased with increasing content of organic matter. With increasing pH flocculated amount also increased, but this relationship reversed if the organic matter had been removed. Generally, they stated that the electrolyte concentration needed to flocculate the soil, effect of pH, and effectiveness of calcium versus magnesium cations – all these factors depend on the organic substances content in the soil (Heil and Sposito, 1993).

Dispersion

The dispersion and slaking processes, like flocculation, affect greatly soil properties. As a result of their occurrence, the individual particles are liberated and the structure and/or aggregation of the soil is destroyed. It has fundamental meaning for water infiltration, redistribution, and evaporation in the subsoil (Khan and So, 2006). The 7–10% content of dispersion Khan and So (2006) denoted as “critical dispersion,” then at 10–13% rapid water blockade takes place, and at a level of 15% and more extremely low rate of water infiltration will be observed. The suspension is a heterogeneous system consisting of solid particles (the internal phase) and a liquid (external phase). The dispersed soil colloidal particles among others cause the soil erosion, the siltation in rivers, ponds, lakes, and other reservoirs, the transportation of nutrients, and the crusting of surface soils. The suspended in runoff water clay particles will not sediment as long as the water velocity is sufficient to cause turbulence, which churns and mixes the flow. If the particles are sufficiently large (larger than 1 μm), due to gravity they will finally sediment if left in quiescent conditions. During a longer time period the sediment

forms large deposits. Such processes cause the largest pollution in stormwater runoff and may have serious destroying impact on ecosystems (Web page 2, 2008). However, to sediment in water particles smaller than 0.1 μm , even in quiescent conditions, some flocculant agent has to be used, and in some systems a multivalent cation like Ca, Al, Fe, Mg (see above) might be sufficient, or a suitable polymer can be added. Here pH and temperature may play an essential role too. As was mentioned above, appropriate concentration of sodium cations in soil is very important for its dispersiveness. Moreover, some investigations have shown that in the absence of montmorillonite, dispersion did not occur even at high amount of Na^+ present in the soil pore water (Bhuvaneshwari et al., 2009). Generally, dispersion may result of two processes occurring simultaneously, that is, mechanical and physicochemical (Alvarez-Benedi et al., 2004), and the dispersion phenomena can be studied on local, fluid, and macroscopic levels, depending on how big volume element is taken into account (Fried and Combarnous, 1971). The macroscopic level is considered in case of porous media with a solid matrix and here, the averaged parameters characterizing the dispersed system are obtained. Mechanical dispersion is obtained when liquid flows through a porous system and originates from boundary and geometrical effects and increases with the liquid velocity (Álvarez-Benedi et al., 2004). Physicochemical dispersion originates from the molecular diffusion caused by gradient in chemical potential. This mechanism is not dependent on the fluid velocity flow and takes place even in quiescent conditions. In this case, an increase in the temperature will affect (increase) the diffusion coefficient too, and thus the dispersion occurrence (Álvarez-Benedi et al., 2004). In studies of dispersion phenomena in soils often the term *dispersion coefficient* appears, which is defined in different ways. For example, it was defined as percentage of clay matter present in the soil that could be dispersed by contact with water, hence its value might range from 0% to 100%, depending on the degree of the soil flocculation (0%) or dispersion (100%) (Web page 1). But, the same term is also used to describe the displacement of solution (solute) in a porous soil, and hence can be termed as coefficient of proportionality between the dispersive flux of a solute and the gradient of its concentration. Then the equation describing the solute displacement involving also adsorption of the solute components is following:

$$\frac{\partial C}{\partial t} + \frac{\rho \partial s}{\theta \partial t} = D \frac{\partial^2 C}{\partial x^2} - V \frac{\partial C}{\partial x}, \quad (2)$$

where C is the solute concentration, ρ is the bulk density, s is the adsorbed concentration, D is the *dispersion coefficient* ($\text{cm}^2 \text{s}^{-1}$), V is the velocity of water in the pores, t is the time, x is the distance, and θ is the volume content of water. Here, the dispersion coefficient expresses the dispersion of solute during its movement and involves its mechanical dispersion and molecular diffusion

(Ahmad, 2002). Moreover, notations *unsaturated dispersion coefficient* and the *saturated dispersion coefficient* are also met. The dispersion coefficient is also expressed as:

$$D = D_o + \alpha v \quad (3)$$

where D is the dispersion coefficient (cm^2/s) and D_o is the effective molecular diffusion in a porous medium (cm^2/s), while α is the *dispersivity* (cm), and v is the mean pore water velocity (cm/s) (Matsubayashi et al., 1997). These authors found that according to the above equation under saturated conditions, the dispersion coefficient increases linearly with increasing pore water velocity. The same was true under unsaturated conditions but only to defined rate of the velocity. Moreover, at the same pore water velocity the coefficient was larger in unsaturated solution than in saturated. For more advanced models of the solute dispersion and the solute transport see Chap. 3.4.3 in Alvarez-Benedi et al. (2004). Field experiments showed that the dispersion coefficient depends on the ground water velocity and it is practically constant at low velocities (when molecular diffusion is the principal factor), but it increases linearly with the ground water velocity increase, when the hydraulic dispersion is dominating. Hence the dispersion coefficient D can be expressed as a sum of two components: effective molecular diffusion coefficient D_d and hydraulic dispersion coefficient D_h (Kuo, 1999). Similar studies on field soils showed that the dispersivity lies between 0.7 cm (sand) and 16–38 cm (clay loam) (Lal and Shukla, 2004). The nature of organic carbon, cations, electrolytes, and pH present in soil, all of them influence dispersivity of soil aggregates (Bronick and Lal, 2005 and the references there in). Also, larger amounts of ammonium cation originating from a fertilizer can disperse the soil clay. Contrary, an amount of added gypsum reduces the dispersivity by affecting the electrolyte concentration and its composition. Moreover, manuring usually increases the dispersion of soil aggregates (Bronick and Lal, 2005).

Summary

Good wettability (hydrophilicity) of a soil (Reddi and Inyang 2000; Ritsema and Dekker, 2003) is of crucial importance for water infiltration and plants vegetation. Flocculation and dispersion phenomena occurring in the soil play a very essential role for water transport, too. While the flocculation processes usually lead to the soil aggregates formation and hence an easier water penetration and fertilizers delivery to the plant roots, so the dispersion processes may cause blockade of soil pores and thus hinder the water flow and fertilizers transport. Because of very complex nature of composition and structure of soils, a general detailed forecast of these processes run is difficult. Nevertheless, some their general features can be described and they were briefly described above.

Bibliography

Ahmad, A. M., 2002. *Development of an Equivalent Dispersion Coefficient for a Complex Contaminant Transport Model*.

- M.Sc. thesis, Dhahran, Saudi Arabia, King Fahd University of Petroleum & Minerals (available online at <https://eprints.kfupm.edu.sa/9681/1/9681.pdf>).
- Alvarez-Benedi, J., Munoz Carpena, R., and Vanclooster, M., 2004. Modeling as a tool for the characterization of soil water and chemical fate and transport. In Alvarez-Benedi, J., and Munoz Carpena, R. (eds.), *Soil-Water-Solute Process Characterization: An Integrated Approach*. Boca Raton: CRC Press, pp. 104–121.
- Bhuvaneswari, S., Soundara, B., Robinson, R. G., and Gandhi, S. R., 2009. *Stabilization and Microstructural Modification of Dispersive Clayey Soils* (available online at <http://www.civil.iitm.ac.in/people/faculty/srgandhi/International%20%20Conferences/Bhuvneswari.pdf>).
- Bronick, C. J., and Lal, R., 2005. Soil structure and management: a review. *Geoderma*, **124**, 3–22.
- Fried, J. J., and Combarous, M. A., 1971. Dispersion in porous media. In Chow, V. T. (ed.), *Advances in Hydroscience*. New York: Academic, pp. 169–282.
- Heil, D., and Sposito, G., 1993. Organic matter role in illitic soil colloids flocculation: I. Counter ions and pH. *Soil Science Society of America Journal*, **57**, 1241–1246.
- Israelachvili, J. N., 1985. *Intermolecular and Surface Forces*. New York: Academic, pp. 187–193.
- Khan, T., and So, B., 2006. *Effect of Soil Dispersion on the Processes of Infiltration, Redistribution and Evaporation* (available online at <http://www.ucalgary.ca/~cguconf/2006webs/Abstracts/Khan.pdf>).
- Kuo, J.-F. (Jeff), 1999. *Practical Design Calculations for Groundwater and Soil Remediation*. New York: CRC Press, pp. 57–102.
- Lal, R., and Shukla, M. K., 2004. *Principles of Soil Physics Series: Books in Soils, Plants, and the Environment*. Marcel Dekker: New York, pp. 477–486.
- Matsubayashi, U., Devkota, L. P., and Takagi, F., 1997. Characteristics of the dispersion coefficient in miscible displacement through a glass beads medium. *Journal of Hydrology*, **192**, 51–64.
- Pils, J., and Laird, D., 2003. *Mechanisms Governing Flocculation and Dispersion of Smectic Colloids*. *Soil and Water Quality Research, Clay Minerals Society Meeting*, Athens, p. 123 (available online at http://www.ars.usda.gov/research/publications/publications.htm?seq_no_115=150717).
- Pils, J. R. V., Laird, D. A., and Evangelou, V. P., 2007. Role of cation demixing and quasicrystal formation and breakup on the stability of smectitic colloids. *Applied Clay Science*, **35**, 201–211.
- Pivovarov, S., 2006. Physico-chemical modelling of heavy metals (Cd, Zn, Cu) in natural environments. In Somasundaran, P., and Hubbard, A. T. (eds.), *Encyclopedia of Surface and Colloid Science*, V.7th edn. New York: Taylor & Francis, pp. 4621–4634.
- Reddi, L. N., and Inyang, H. J., 2000. *Geoenvironmental Engineering Principles and Applications*. New York: Marcel Dekker. Part I, Chaps. 3 and 5.
- Ritsema, C. J., and Dekker, L. W., 2003. *Soil Water Repellency*. Amsterdam: Elsevier Science B.V.
- Smith, S. E., 2009. <http://www.wisegeek.com/what-is-flocculation.htm>.
- Sposito, G., 2008. *Chemistry of Soils*. New York: Oxford University Press.
- Van Oss, C. J., Giese, R. F., and Conztanzo, P. M., 1990. DLVO and non-DLVO interactions in hectorite. *Clays and Clay Minerals*, **38**, 151–159.
- Walworth, J., 2006. *Soil Structure: The Roles of Sodium and Salts* (available online at <http://www.ag.arizona.edu/pubs/crops/az1414.ppt>).
- Web page 1, <http://prr.hec.gov.pk/Chapters/1900-3.pdf>.
- Web page 2, 2008. Iowa Statewide Urban Design Standards Manual, 7C-1. The Erosion and Sedimentation Process. [www.iowasudas.org/design.cfm](http://iowasudas.org/design.cfm).
- Wiacek, A., and Chibowski, E., 1999. Application of an extended DLVO theory for the calculation of the interactions between emulsified oil droplets in alcohol solutions. *Colloids and Surfaces B*, **14**, 19–26.
- Zhang, X.-C. J., 2002. Erosion and sedimentation control: amendment techniques. In Lal, R. (ed.), *Encyclopedia of Soil Science*, 2nd edn. New York: Marcel Dekker, Vol. 1.

Cross-references

- [Clay Minerals and Organo-Mineral Associates](#)
[Coupled Heat and Water Transfer in Soil](#)
[Diffuse Double Layer \(DDL\)](#)
[Electrokinetic \(Zeta\) Potential of Soils](#)
[Field Water Capacity](#)
[Hydraulic Properties of Unsaturated Soils](#)
[Hydrophobicity of Soil](#)
[Infiltration in Soils](#)

FLOODING, EFFECTS ON SOIL STRUCTURE

Miguel A. Taboada^{1,2,3}, Patricia L. Fernández³,
 Maria F. Varela^{2,3}

¹INTA, CIRN – CONICET, Instituto de Suelos, Villa Udaondo- Castelar, Provincia de Buenos Aires, Argentina

²CONICET, Ciudad Autónoma de Buenos Aires, Argentina

³Universidad de Buenos Aires, Ciudad Autónoma de Buenos Aires, Argentina

Synonyms

Ponding; Submerged soils

Definition

Flooding soils: They are those in which water covers the soil, or is present either at or near the surface of the soil all year or for varying periods of time during the year. Flooding soils are classified as Fluvisols, Planosols, and Gleysols in the FAO-UNESCO Soil Map (2000). Fluvisols are covered part of the year by surface water from river overflows; Planosols are soils having an impervious Bt horizon, supporting perched water during short periods; and Gleysols are soils affected by stagnant water tables during long periods.

Soil structure: It is concerned with the organization of soil constituents into larger aggregates and arrangement of porosity and pore size distribution.

Introduction

Soil structural behavior of flooded soils received considerable less attention, as compared with agricultural, dryland soils. A key factor determining soil structural behavior is the quality of flooding water, which depends on soil profile characteristics. Soils without a tough Bt horizon have no limitations for free down- and upward water movements throughout the profile. In them, water table rises can reach their top horizons and deposit soluble salts in them. In soils with a tough, impervious Bt horizon, water

table rises are controlled by this horizon and cannot reach the topsoil (Lavado and Taboada, 1988). Flooding water in them is typically of rain origin and does not cause severe consequences on soil properties and vegetation (Taboada et al., 2001; Insausti et al., 2008).

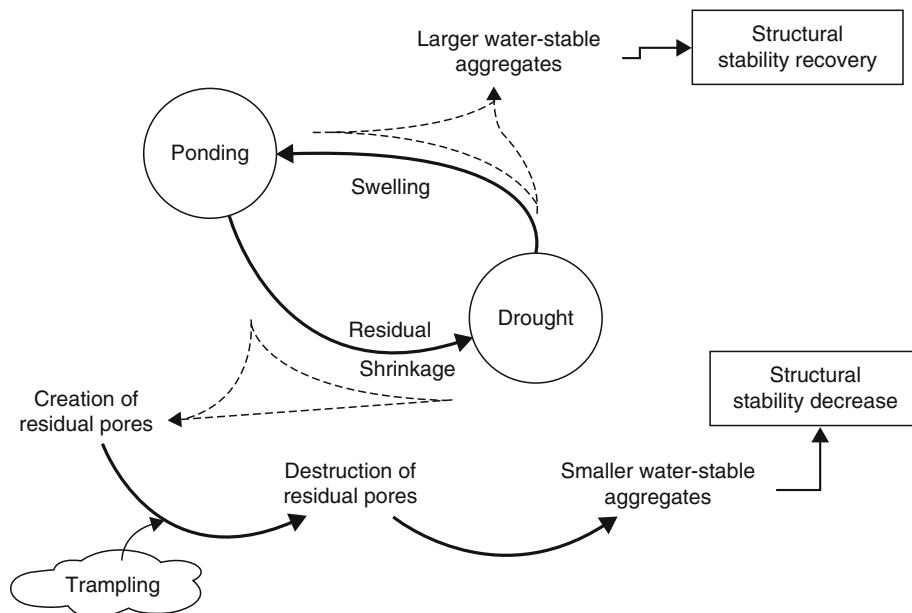
Soil structural behavior in flooding soils

Flooding soils are subjected to seasonal flooding and subsequent dry periods. They undergo drastic structural changes due to alternate wetting and drying (W/D), which

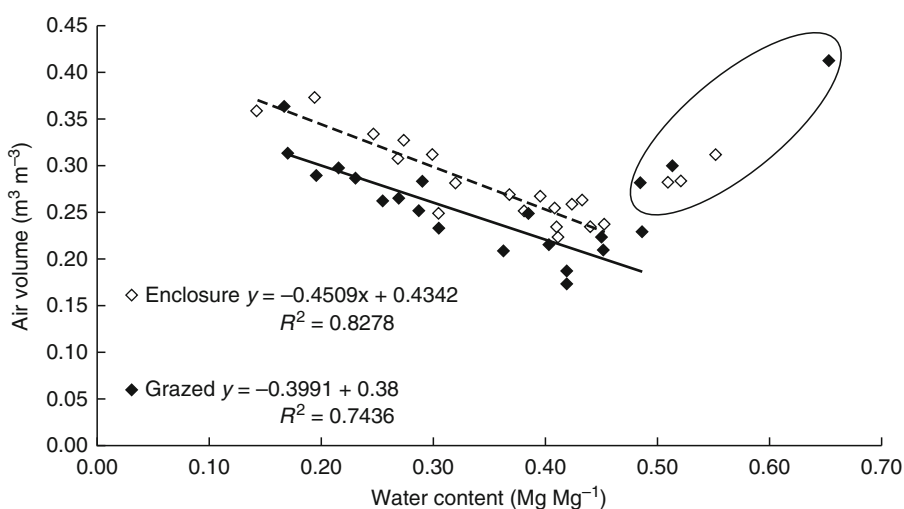
exert strong influences on: (1) soil structural stability, (2) soil mechanical properties, and (3) trapped air volumes.

Soil structural stability

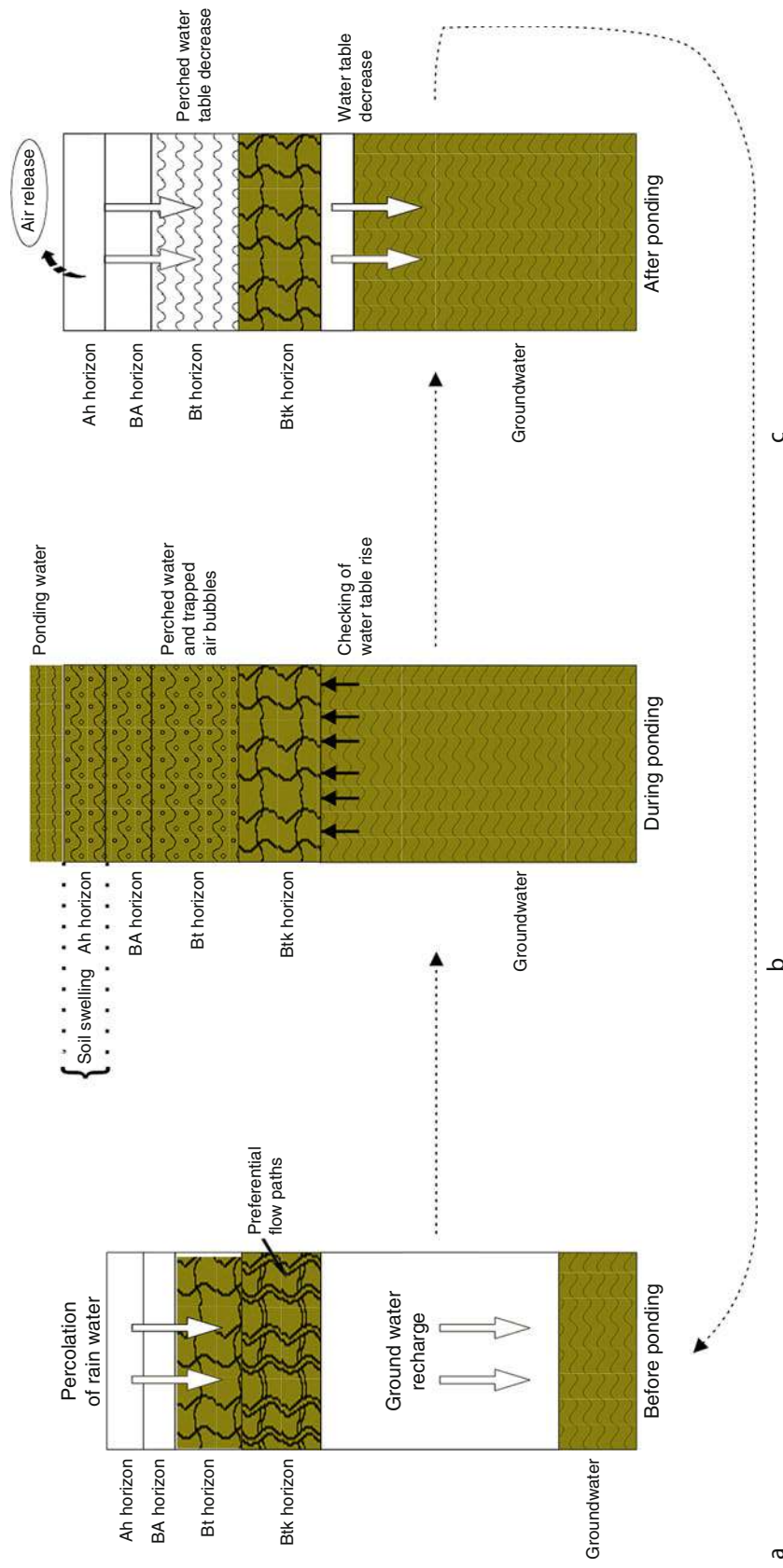
Soil aggregates are biologically stabilized either by bonding between organic compounds and soil mineral particles or physical binding due to fine grass roots and fungal hyphae (Tisdall and Oades, 1982; Oades, 1993). The abiotic stabilization of soil structure depends on soil chemical



Flooding, Effects on Soil Structure, Figure 1 Conceptual model showing the process of soil structural destabilization when the soil dries and the process of structural recovery when the soil wets. (Adapted from Taboada et al., 1999).



Flooding, Effects on Soil Structure, Figure 2 Soil air volume calculated in enclosed and grazed situations in Typic Natraquoll from the Flooding Pampa of Argentina. (Adapted from Taboada et al., 2001).



Flooding, Effects on Soil Structure, Figure 3 Conceptual model describing the process of soil swelling because of air entrapment. (a) Before ponding; free water and air movements throughout the profile (bio-opened system); (b) during ponding: soil swelling by air trapped within water table perched over the impervious Btk horizon (air-occluded system); (c) after ponding: soil shrinkage after perched water and water table decreases and rapid air escapes to the atmosphere. (Adapted from Taboada et al., 2001).

composition, and also swell–shrink soil capacity during W/D cycles (Dexter, 1988; Oades, 1993). The role of polyvalent cations in the aggregate stability of flooding soils is great and it masks the contribution of other aggregating agents. The Fe, Al, and Mn dynamics of these soils and the prevailing condition of seasonal waterlogging encourage soil aggregate stability. These polyvalent metals may form bridges between clay and organic matter in the formation of aggregates (Igwe and Stahr, 2004). Caron et al. (1992) observed that the extreme W/D cycles of flooded soils might lead to breakdown of aggregate stability of soils, due to the extinction of interparticle cohesion, which is also known as the “antecedent soil moisture effect” (Gerard, 1987; Perfect et al., 1990). Soil mellowing, which consists in their partial slaking by trapped air pressures, often results when soils are carried to high water contents (Grant and Dexter, 1990).

Results obtained in grazed grassland soils of the flooding Pampa (Taboada and Lavado, 1993; Taboada et al., 1999) show that flooding by rainwater does not destabilize topsoil structure. In this region, soil water content was the primary cause of changes in total porosity, because of shrink–swell processes. The periods when trampling affected topsoil porosity and aggregate stability were in summer when soil is dry. A conceptual model shows the process of soil structural destabilization when the soil dries and the process of structural recovery when the soil wets (Figure 1).

The conceptual model postulates that decreases in structural stability result from crushing air-filled pores by cattle hooves. Only at low water contents was the structure of the topsoil destabilized by grazing. The recovery of structural stability began in the fall and was completed in the winter, when the soil was flooded. The structural recovery results from swelling, when the smaller aggregates created by trampling of dry soil are bound again into larger structural units. Soil swelling as a result of trampling was also found by Mulholland and Fullen (1991), Mullins and Fraser (1980), and Scholefield et al. (1985).

Soil mechanical properties

According to soil rheology, soil undergoes elastic deformation and shallow compaction when loaded at a moist condition (Lal and Shukla, 2004). Flooding soils are typically devoted to livestock production on native grazed grasslands. Soil water content determines the magnitude of the stress caused by animal hoof impact mainly (Warren et al., 1986; Mulholland and Fullen, 1991). When a wet soil is trampled, there is plastic flow around the hoof (Mullins and Fraser, 1980; Scholefield et al., 1985). Repeated treading in these conditions produces deep hoofprints, this process is called poaching, and leads to damage the sward (Mullins and Fraser, 1980; Scholefield et al., 1985; Greenwood and Mc. Kenzie, 2001). This effect, generally, coincides with the presence of free surface water (Mulholland and Fullen, 1991), with a progressive loss of soil strength, and creates dense, unstable surface clods (Warren et al., 1986). At our site, the low stocking

rate was probably insufficient to create this repeated stress. Previously damaged soil pores can be regenerated, however, during W/D cycles. This depends on soil shrink–swell (Dexter, 1988; Drewry, 2006), provided the externally applied stress is decreased or removed. The regeneration mechanism depends on the formation of microcracks, as a compacted soil layer dries (Dexter, 1988).

Trapped air volumes

Seasonally flooded soils could present trapped air due to influence of soil wetting fronts (Taboada et al., 2001). Their influence is shown by air volume–water content relationships, determined in a flooding Pampa soil (Typic Natraquoll) in grazed and enclosed field situations (Figure 2). Straight negative lines show the expected air volume increases on drying. A group of points departed from the fitted lines, showing the occurrence of air entrapment when the soil is wet. Trapped air volumes cause the soil swelled by “inflation” (Gäth and Frede, 1995), which contributes to soil structural recovery found during flooding in this region (Taboada et al., 2001).

A conceptual model describes how the soil evolves from a “bio-opened” system when desiccation cracks are opened in the Bt horizon, to an “air-occluded” system when air becomes trapped within water table perched over the impervious Btk horizon (Figure 3).

Interesting to note, a similar “air inflation” process was recently found in agricultural soils from the North Pampas region (Fernández et al., 2010). In this case, trapped air volumes resulted from livestock trampling at waterlogged conditions at low stocking rates. These processes of air inflation can be pointed out as the main reason why the predictions based on soil rheology are not always accomplished in flooding and waterlogged soils.

Conclusions

Soil structural behavior of flooding soils cannot be easily explained, following the criteria established for agricultural, unsaturated soils. Despite they often sustain grassland vegetation, whose roots are permanent stabilizing agents, the stabilization of topsoil structure seems to be mainly abiotic, based on the drastic W/D cycles.

Grassland soils of the flooding Pampa of Argentina can be considered a good study case, which shows positive effect of flooding with rainwater in topsoil structure. In this region, structural damages occur in dry summer when livestock hooves crush surface aggregates.

The build-up of trapped air pressures is an important fact in flooded soils. It results in soil swelling by air inflation. The influence of this process on soil structural recovery during flooding needs further investigation.

Bibliography

- Caron, J., Kay, B. D., and Stone, J. A., 1992. Improvement of structural stability of a clay loam with drying. *Soil Science Society of America Journal*, **56**, 1583–1590.

- Dexter, A. R., 1988. Advances in characterization of soil structure. *Soil and Tillage Research*, **11**, 199–235.
- Drewry, J. J., 2006. Natural recovery of soil physical properties from treading damage of pastoral soils in New Zealand and Australia: a review. *Agriculture, Ecosystems and Environment*, **114**, 159–169.
- FAO-UNESCO, 2000. *The FAO/UNESCO Digital Soil Map of the World and derived Soil Properties on CD-Rom*. Roma: FAO-AGL.
- Fernández, P. L., Álvarez, C. R., Schindler, V., and Taboada, M. A., 2010. Changes in topsoil bulk density after grazing crop residues under no-till farming. *Geoderma*, **159**, 24–30.
- Gäth, S., and Frede, H. G., 1995. Mechanisms of air slaking. In Hartge, K. H., and Stewart, B. A. (eds.), *Soil Structure: Its Development and Function*. Boca Raton: CRC Lewis, pp. 159–173.
- Gerard, C. J., 1987. Laboratory experiments on the effects of antecedent moisture and residue application on aggregation of different soils. *Soil and Tillage Research*, **9**, 21–32.
- Grant, C. D., and Dexter, A. R., 1990. Air entrapment and differential swelling as factors in the mellowing of moulded soil during rapid wetting. *Australian Journal of Soil Research*, **28**, 361–369.
- Greenwood, K. L., and Mc. Kenzie, B. M., 2001. Grazing effects on soil physical properties and the consequences for pastures: a review. *Australian Journal of Experimental Agriculture*, **41**, 1231–1250.
- Igwe, C. A., and Stahr, K., 2004. Water-stable aggregates of flooded Inceptisols from south-eastern Nigeria in relation to mineralogic and chemical properties. *Australian Journal of Soils Research*, **42**, 171–179.
- Insausti, P., Taboada, M. A., and Lavado, R. S., 2008. Floods recover the deterioration of grasslands and soils caused by cattle in the Flooding Pampas of Argentina. In Schröder, H. G. (ed.), *Grasslands: Ecology, Management and Restoration*. New York: Nova Science, pp. 93–107.
- Lal, R., and Shukla, M. K., 2004. *Principles of Soil Physics*. New York/Basel: Marcel Dekker.
- Lavado, R. S., and Taboada, M. A., 1988. Soil water, salts, and sodium dynamics in a Natraquoll of Argentina. *Catena*, **15**, 577.
- Mullins, C. E., and Fraser, A., 1980. Use of the drop penetrometer on undisturbed and remolded soils at a range of soil water tensions. *Journal of Soil Science*, **31**, 25–32.
- Mulholland, B., and Fullen, M. A., 1991. Cattle trampling and soil compaction on loamy sands. *Soil Use and Management*, **7**, 189–193.
- Oades, J. M., 1993. The role of biology in the formation, stabilization and degradation of soil structure. *Geoderma*, **56**, 377–400.
- Perfect, E., Kay, B. D., Van Loon, W. K. P., Sheard, R. W., and Pojasok, T., 1990. Factors influencing soil structural stability within a growing season. *Soil Science Society of America Journal*, **54**, 173–179.
- Scholefield, D., Patto, P. M., and Hall, D. M., 1985. Laboratory research on the compressibility of four topsoils from grassland. *Soil and Tillage Research*, **6**, 1–16.
- Taboada, M. A., and Lavado, R. S., 1993. Influence of trampling on soil porosity under alternate dry and ponded conditions. *Soil Use and Management*, **9**, 139–143.
- Taboada, M. A., Lavado, R. S., Svartz, H., and Segat, A. M. L., 1999. Structural stability changes in a grazed grassland Natraquoll of the Flooding Pampa of Argentina. *Wetlands*, **19**, 50–55.
- Taboada, M. A., Lavado, R. S., Rubio, G., and Cosentino, D. J., 2001. Soil volumetric changes in natric soils caused by air entrapment following seasonal ponding and water table. *Geodema*, **101**, 49–64.
- Tisdall, J. M., and Oades, J. M., 1982. Organic matter and water-stable aggregates in soils. *Journal of Soil Science*, **62**, 141–163.
- Warren, S. D., Nevill, M. B., Blackburn, W. H., and Garza, N. E., 1986. Soil response to trampling under intensive rotation grazing. *Soil Science Society of America Journal*, **50**, 1136–1340.

Cross-references

- [Claypan and its Environmental Effects](#)
[Grazing-Induced Changes of Soil Mechanical and Hydraulic Properties](#)
[Puddling: Effect on Soil Physical Properties and Crops](#)
[Rheology in Soils](#)
[Shrinkage and Swelling Phenomena in Soils](#)
[Soil Aggregates, Structure, and Stability](#)
[Traficability and Workability of Soils](#)
[Wetlands, Management, Degradation and Restoration](#)
[Wetting and Drying, Effect on Soil Physical Properties](#)

FLOW

See [Laminar and Turbulent Flow in Soils](#)

FLOWABILITY

Capability of particulate solids, powders and liquid to move by flow.

FLUVIAL EROSION

Erosion produced by the action of a river or stream.

FLUX

See [Soil Hydrophobicity and Hydraulic Fluxes](#)

FOOD FREEZING

Food preservation method in which a water-based item is flash-frozen to deactivate the microorganisms present in it without killing them.

FOOD MACHINERY

See [Agriculture and Food Machinery, Application of Physics for Improving](#)

FOURIER'S LAW

The law governing heat conduction, stating that the flux of heat in a homogeneous body is in the direction of, and

proportional to, the temperature gradient, with a coefficient of proportionality known as “thermal conductivity”.

Bibliography

Introduction to Environmental Soil Physics. (First Edition). 2003. Elsevier Inc. Daniel Hillel (Ed.) <http://www.sciencedirect.com/science/book/9780123486554>

FRACTAL ANALYSIS IN AGROPHYSICS

Yakov A. Pachepsky¹, Fernando San José Martínez², Miguel Angel Martín²

¹Environmental Microbial and Food Safety Laboratory, Animal and Natural Resource Institute, Beltsville Agricultural Research Center, USDA-ARS, Beltsville, MD, USA

²Department of Applied Mathematics in Agricultural Engineering, Technical University of Madrid (UPM), Madrid, Spain

Synonyms

Fractal modeling

Definition

Fractal. Rough or fragmented geometric shape that can be subdivided into parts, each of which is (at least approximately) a reduced-size copy of the whole.

Fractal analysis. Using fractals to approximate observed geometric shapes or shapes at graphs, depicting spatial or temporal distributions of nongeometric properties.

Introduction

The geometric irregularity is an intrinsic property of soils and plants. Soil pores and particles, organisms living in soils, as well plant roots and shoots, have a wide range of sizes and shapes. Soil and crop canopy surfaces are rough, and patterns on soil and yield maps have complex shapes. This geometric irregularity is easy to perceive and observe, but quantifying it has long presented a daunting challenge. Such quantifying is imperative because the geometric irregularity is the cause and the reflection of spatial and temporal variability that in turn strongly affects soil and crop management.

Geometric measurements in agrophysics are done at different measurement scales. *Measurement, or observation, scales* are lengths, areas, or volumes within which the shape irregularity is ignored and curves or surfaces are assumed to have a simple geometric shape, e.g., line segment or part of a plane. Measurement scale is often called support, resolution, or simply scale. There is ample empirical evidence that total length, total area, or total volume does not stay constant as the measurement scale changes. A decrease in measurement scale usually causes an increase in total length, area, or volume. Thus,

geometric properties of soil and soil cover as well as plants and crop canopies appear to be scale dependent.

One class of geometrical objects whose total length, area, or volume depends on the measurement scale consists of objects that reveal similar geometrical shapes when observed at different measurement scales. Such objects were termed *fractals* by Mandelbrot (1983), who suggested that fractals rather than regular geometrical shapes like segments are more appropriate to approximate irregular natural shapes that have hierarchies of ever-finer detail.

Fractals are rough or fragmented geometric shapes that can be subdivided into parts, each of which is (at least approximately) a reduced-size copy of the whole. Examples of geometrical fractals and their natural counterparts are shown in Figure 1. These examples illustrate that although fractals cannot represent each and every detail of the hierarchy of ever-finer detail in the real world, they can represent the shape similarity at different scales. Applications of fractal geometry in environmental sciences became very popular during the last 30 years because of its promise to relate features of natural objects observed at different scales.

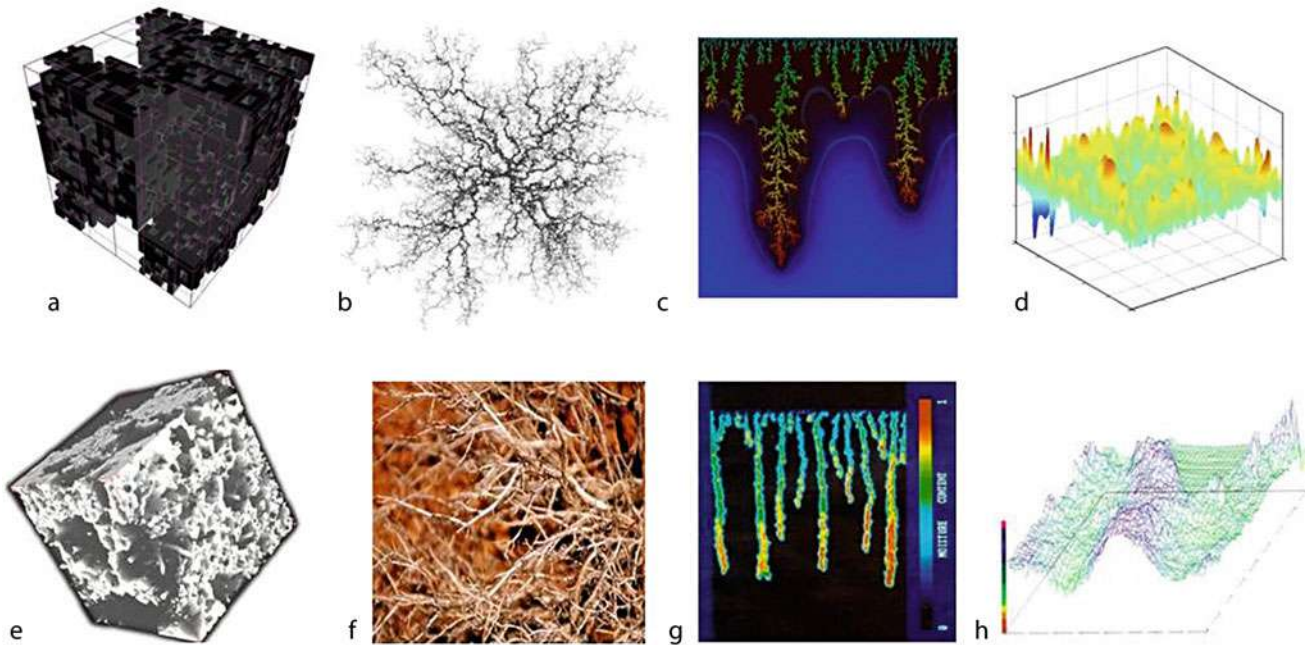
Although fractals are purely geometrical objects, fractal representations of nongeometrical properties, e.g., mass, concentration, or population density, have become ubiquitous. Such representations are possible because measurements of nongeometric quantities can be expressed as a graph which is already a geometric object and can be analyzed as such using the fractal concepts. Similarly, graphs of temporal dependencies have been analyzed to reveal fractal behavior in time, rather than in space.

Observations of natural objects at different scales have shown that not only the total amount of the observed property (length, area, or volume) depends on the measurement scale but also the distribution of this total amount among different measurement cells at this scale appears to depend on the cell size, i.e., scale. Analysis of the distribution change with scale reveals the degree of heterogeneity within the system. The more asymmetric the distributions become as the scale decreases, the more heterogeneous is the system. The class of geometric objects having such a property has been termed *multifractals* (Evertsz and Mandelbrot, 1992). Applicability of multifractal mathematical model has been demonstrated for many environmental systems. For example, soil porosity, organic matter content, bacteria populations, or chemical concentrations show large variability when measured at one specific observation scale, i.e., with the same support. The variability changes with support, and the multifractal model appears to be a plausible mathematical tool to simulate these changes.

The types of fractal objects used in agrophysics are manifold. This entry provides a brief introduction in concepts and techniques behind those applications.

Fractal objects and models

Geometrical fractal objects reveal similar features at different scales because they are constructed iteratively, by



Fractal Analysis in Agrophysics, Figure 1 Examples of geometric fractals (a–d) and natural objects exhibiting fractal properties (e–h); (a) Menger sponge, (b) diffusion-limited aggregation structure in three dimensions (From Bourke, 2006. With permission), (c) diffusion-limited aggregation structure in two dimensions (From Prusinkiewicz et al., 1997. With permission), (d) self-affine surface (From Zou et al., 2007. With permission), (e) visualized inter-aggregate pore inferred from the computer tomography (From Helmholtz Center for Environmental Research, Soil Physics, <http://www.ufz.de/index.php?en=12359>. With permission), (f) root system (From Center for Polymer Studies, Boston university, <http://polymer.bu.edu/ogaf/html/chp53.htm>. With permission), (g) infiltration in layered sand (From Soil and Water Laboratory, Cornell University, <http://soilandwater.bee.cornell.edu/>. With permission), (h) microtopography of the measured apple surface after storage. (From Fekete et al., 2007. With permission.)

repetition of the same form- or shape-changing operation at different measurement scales. An example of such construction is given in Figure 1a for the fractal object called Menger sponge. The *initial shape*, or *initiator*, is a cube. The shape-changing operation, or *generator*, is dividing the cube into 27 smaller equal cubes and extracting seven cubes, six from each facet and one from the center. Menger sponge is self-similar because it can be broken down into arbitrary small pieces, each of which is a small replica of the entire structure. If the Menger sponge is reduced by a factor of 1/3 and 20 copies are made, then these copies can be pasted together to give back the Menger sponge; 1/9 reduction requires 400 copies, 1/27 reduction requires 8,000 copies, etc. In all self-similar objects, there is a relationship between the reduction factor R and the number of pieces N into which the object is divided. Those relationships follow a power law:

$$N = R^{-D_{ss}}, \quad (1)$$

where D_{ss} is called the *self-similarity dimension*. The value of D_{ss} can be found by equating logarithms of both parts in Equation (1), i.e., $D_{ss} = -\log(N)/\log(R)$. For the Menger sponge, the reduction factor is 1/3, $D_{ss} = -\log(20)/\log(1/3) = -\log(400)/\log(1/9) = -\log(8000)/\log(1/27) = 2.727$.

Figure 1b provides another example of an iteratively built geometric fractal generated by the diffusion-limited aggregation (DLA) process (Feder, 1988). A sticky particle is randomly introduced on a “launching” circle and is allowed to follow a random path until: (1) it sticks to the growing cluster of particles by entering a grid adjacent to the cluster or (2) until it wanders across a larger “killing” circle. The resulting sparse, tree-like structure has been taken as an excellent representation of the dendritic growth patterns of roots and fungi (Turcotte, 2007).

The self-similarity dimension receives the physical meaning of fractal dimension when the fractal object is used as the model of the real system, and the geometric measures of this object are equated to geometric measures of the system. For example, let empty parts of the Menger sponge be used to simulate pores in soil at different measurement scales. Let V_0 be the volume of the initiator. The measurement scale is V_0R^3 , the number of similar pieces at this scale is N , and their total volume is:

$$V = NV_0R^3 = V_0R^{3-D_{ss}} \quad (2)$$

Because the fractal object represents remaining mass in this case, the dimension D_{ss} is interpreted as the *mass fractal dimension*.

Relationships (1), (2), and likes hold over a range of scales, i.e., they are scale invariant within this range. They are interchangeably referred to as scaling relationships, or fractal scaling laws, or simply scaling.

The iterative construction of ideal fractals continues ad infinitum, whereas natural objects have the minimum and the maximum observation scales, or *lower and upper cut-off scales* beyond which the relationship (1) usually breaks. The value of the measure for the initiator, for example, the V_0 value in (2), is not known if the fractal scaling is valid only within a specific scale range. Thus, four values – fractal dimension, upper-, and lower-scale cutoff, and the initiator measure – are parameters of a fractal model in agrophysical studies.

Ideal shapes as in Figure 1a–d cannot be found in real porous media in the same way as ideal geometric lines, spheres, cylinders, etc. cannot be found. Applying random changes in the generator procedure results in constructing stochastic fractals that look much more like fractals in nature (Peitgen et al. 2004). Because random changes are applied, realizations of stochastic fractals with the same initiator and generator differ. Stochastic fractals retain the important feature of dependence of geometric properties on measurement scale, only this feature is preserved in *statistical sense*. This means that Equation (1) will not hold exactly for any realization of stochastic fractals at any measurement scale. Nevertheless, the dependence measurement scale on the property of interest in log–log scale for each realization is close to the same power law dependence.

Data on surface roughness or topography along spatial transects do not follow the self-similarity law (1), but demonstrate another, anisotropic type of scale dependence, called self-affinity. If surface is self-affine then, to reveal the statistical similarity in this the surface, the change of the horizontal measurement scale λ times has to correspond to changing the vertical measurement scale λ^H times. The value H is called the Hurst exponent, $0 \leq H \leq 1$. Value of H is equal to one in isotropic, self-similar fractals such as Menger sponge in Figure 1a. Self-affine one-dimensional lines represent the type of geometric irregularity known as fractal *Brownian noise* (Mandelbrot and Van Ness, 1968). An example of such

noise is shown in Figure 2. When the self-affine curves are analyzed, high values of the Hurst exponent indicate some degree of memory, persistence, or autocorrelation in the data. Low values of H suggest an anti-correlation or self-correcting response in the observed process.

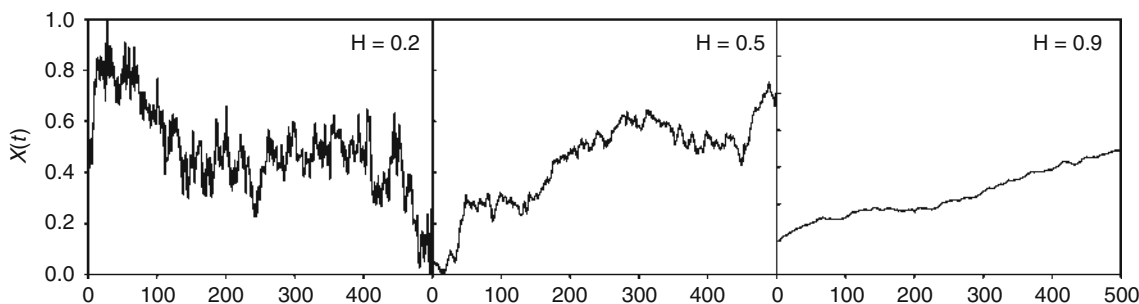
Multifractals present yet another example of scale-invariant object, where the dependence of statistical distributions on the measurement scale holds through certain range of scales, and therefore is scale invariant. If a property is measured at a particular measurement scale in many measurement cells (grid intervals in one-dimensional, grid cells in two-dimensional systems, or in 3D voxels in three dimensions), then the probability distribution function is obtained for so-called mass fractions μ that are measurements in each cell divided by the total value of the property measured in all cells at this scale. Changes in mass fraction distributions with scale are shown to characterize the inherent heterogeneity of the system.

One process of constructing the multifractal object is known as the multiplicative cascade (Figure 3). The cascade starts at the scale S (level 0) with an initial amount $\mu_0 = 1$. At the next scale, $S/4$, the measures in four measurement cells are obtained by multiplying μ_0 by the random factor $w_i < 1$, $i = 1,2,3,4$, and w_i are selected so that $\sum \mu(S_i) = \mu(S)$. The resulting mass distribution is a multifractal when this process continues *at infinitum*. The selection of the statistical distribution for the factor w_i values controls properties of the resulting multifractal.

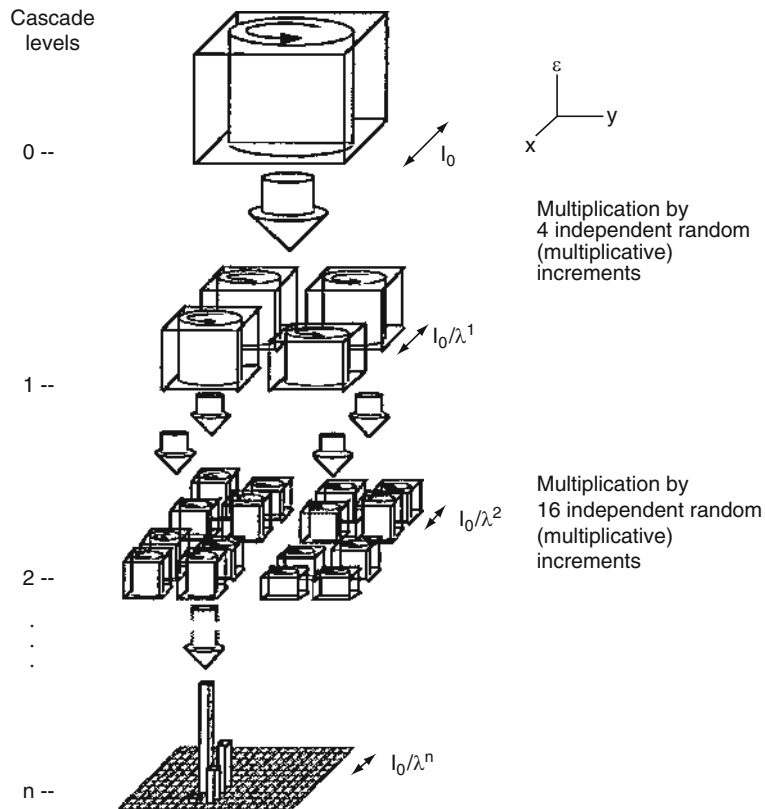
Physical processes resulting in fractal scaling in agrophysics

Many physical processes have been shown to generate fractal scaling (Pachepsky et al., 2000; Senesi and Wilkinson, 2008). Some of them are relevant to soil and biota development and functioning, and the correspondent fractal models are being applied in agrophysics. One example is the scale-invariant fragmentation (Turcotte, 1986) that leads to dependence between the number of fragments and their size:

$$N_r = kr^{-D_F} \quad (3)$$



Fractal Analysis in Agrophysics, Figure 2 Examples of fractal Brownian noises for three values of the Hurst exponent H . (From Kravchenko and Pachepsky, 2004. With permission.)



Fractal Analysis in Agrophysics, Figure 3 Schematic diagram of a multiplicative cascade. (From Schertzer and Lovejoy, 1991, p. 49. With permission.)

where r is the fragment radius, N_r is the number of fragments having radii less than r , k is a constant, and D_F is the fragmentation fractal dimension. The incomplete fragmentation process has the fractal dimension that can be related to density-size scaling of soil aggregates and appears to be the mass fractal dimension.

Agglomeration on a substrate can generate fractal structures (Witten and Sanders, 1981; Chen and Wilkinson, 1985). Particles may arrive to the surface by random diffusion or with ballistic energy. They may either just stick together or there is a chemical reaction involved which may change the local concentration gradient and sticking probability. Allowing particles to walk randomly until they strike the surface or another particle, which is already motionless, builds the fractal coating.

Various mechanisms were proposed to explain fractal branching networks that are omnipresent in nature. Such networks in living organisms have been suggested to evolve as the means of maximizing metabolic capacity, namely, the rate at which energy and material resources are taken up from the environment and allocated to some combination of survival and reproduction. On the other hand, it was argued that inherent randomness is a sufficient condition for the generation of tree patterns under evolutionary dynamics, and the decrease of energy

expenditure is not the cause but a consequent signature (West et al., 1999; Paik and Kumar, 2008).

Instability and chaotic behavior were shown to generate fractal structures. For example, the finger flow in soils can evolve as the result of soil layering, causing the instability in the wetting front boundary (Posadas et al., 2009). Atmospheric turbulence within canopies can cause fractal scaling of micrometeorological parameters (Chester et al., 2007). The superposition of processes of different nature acting simultaneously over a range of scales can generate multifractal patterns revealed in spatial and temporal variability of soil properties (Burrough, 1983).

Purposes and methods of fractal analysis

Fractal analysis aims to see if the data obtained at different scales can be related with scale-independent relationship consistent with one of the fractal models.

Purposes of fractal analysis depend on the overall goal of the research where such analysis is applied. Here are some of the purposes:

1. Find the relationships between system properties obtained at different scales; this is useful if measurements on some scales are more difficult than at others. This type of analysis has been used, for example, to

- estimate soil hydraulic properties that are difficult to measure.
2. Compress data obtained at different scales; fractal models have relatively smaller number of parameters and allow relating parameters of irregularity at different scales with simple relationships.
 3. Use fractal parameters as the indicator of change in environmental conditions or management.
 4. Infer the underlying physical and biological processes that cause the observed scale independence.
 5. Determine cutoffs in fractal scaling. Cutoffs can serve as indicators of the change in control processes at some scale.
 6. Generate synthetic examples of fractal media. Such examples provide a realistic representation of multiscale hierarchy in conduits and storages and are used in simulation of transport processes.
 7. Identify scale-related changes in relationships between soil properties that show fractal and multifractal features.
 8. Select an appropriate interpolation method for the development of soil property distribution maps.

Fractal analysis is applied to geometric objects – lines, surfaces, and three-dimensional shapes. These objects are either actually observed or obtained from other measurements by graphing observations or presenting them as an image.

Fractal analysis consists of:

1. Measuring the property of interest on an observed geometric shape or on a graphic representation of spatial or temporal series or imagery
2. Fitting a fractal model to the observed dependence of a property on scale

Measurement of scale dependence

Both direct and indirect measurements of geometric quantities are in use in agrophysics. Indirect, or proxy, geometrical measurements are very common. Nongeometrical values are converted into a geometrical value using a physical model. For example, capillary pressures in soils are converted in radii using capillary models. Then, different pressures correspond to different scales of measurement, and the dependence of filled pore volume on the scale can be investigated to reveal fractal pore structure. Similarly, masses of adsorbed molecules are converted in area values using molecular monolayer model, then the change in molecule size is equivalent to change in the measurement scale, and the dependence of monolayer area on the scale can be researched to establish fractal scaling of the adsorbing surface. X-ray computed tomography data provides information about the density differences of the soil components based on the radiation attenuation. Remote sensing of canopies presents spatial distribution of soil–plant–atmosphere systems as reflected in the images of radiance or irradiance. [Table 1](#) presents some

examples of measurements and relationships used in agrophysical studies to reveal fractal scaling.

Fitting a fractal model to data

A common way to reveal a fractal scaling law is to plot the measurement scale versus the property of interest in double logarithmic, or log–log, scale. The presence of a linear relationship indicates that fractal model may be appropriate to simulate the scale dependence in the property. The fractal dimension then can be found from the slope of the regression line. For example, the relationship (2) in log–log scale can be transformed into:

$$\log V = \log V_0 + (3 - D_{ss}) \log R \quad (4)$$

and the fractal dimension D_{ss} equals three minus slope. A similar transformation is applicable to all scaling relationships in [Table 1](#).

While it is true that natural objects are not made up of spheres and straight lines, it is also true that soil, plant, or atmospheric fields are far from being precisely fractal. Therefore, relationships of fractal geometry can be only approximately true in agrophysics. Different measurement methods lead to different results even for ideal geometric fractals. Values of fractal parameters obtained by different methods should never be compared for soils. Using proxy measurements creates additional uncertainty, since ideal shapes are assumed to convert nongeometrical to geometrical measures.

Uncertainty also exists in selecting the range of measurement scales in which the fractal scaling is valid. One way to decrease this uncertainty is to include cutoff values in the list of estimated parameters along with the slope and the intercept of the linear regression used to estimate the fractal dimension and the initiator measure.

To find parameters of the multifractal model, the mass fractions μ_i have to be defined at each available measurement scale ε , which is usually defined by the size of measurement cell in one, two, or three dimensions. Mass fractions have to be skewed using the series of values of q that typically range from -10 to 10 according to the equation:

$$\mu_i(q, \varepsilon) = \frac{\mu_i(\varepsilon)^q}{\sum_{i=1}^{n(\varepsilon)} \mu_i(\varepsilon)^q}. \quad (5)$$

Finally, values

$$\alpha_q = \frac{\sum_{i=1}^{n(\varepsilon)} \mu_i(q, \varepsilon) \log \mu_i(\varepsilon)}{\log \varepsilon} \quad (6)$$

and

$$f(\alpha_q) = \frac{\sum_{i=1}^{n(\varepsilon)} \mu_i(q, \varepsilon) \log \mu_i(q, \varepsilon)}{\log \varepsilon} \quad (7)$$

are computed for each q . Values α_q are the Hölder exponents and values $f(\alpha_q)$ form the singularity spectrum.

Fractal Analysis in Agrophysics, Table 1 Examples of measurements and relationships to perform fractal analysis in agrophysics

Method, reference to an example of application	Measurement scale or proxy measurement	Measured value	Scaling relationship	Fractal dimension
Box counting (Feder, 1988)	Δ – mesh size of a grid covering a line	N_L – number of grid cells where the line is present	$N_L \propto \Delta^{-D_K}$	D_K – Kolmogorov dimension ^a
Erosion-dilation (Russ, 1994)	M – number of times when erosion or dilation are applied	N_a – number of pixels that are affected by the erosion and dilation	$N_a \propto M^{-D_M}$	D_M – Minkowski dimension
Image coarsening (Stoyan and Stoyan 1994)	Δ – Pixel size	N_L – Number of cells where the line is present	$N_L \propto \Delta^{-D_K}$	D_K – Kolmogorov dimension ^a
Semivariogram (Burrough, 1983)	h – Distance between observation points	Semivariogram $\gamma(h) = \frac{1}{2m_h} \sum [Z(x) - Z(x+h)]^2$ Z is the observed point on the self-affine line, m_h is the total number of points separated by the distance h .	$\gamma \propto h^{2(2-D_L)}$	Fractal dimension of the self-affine line
Power spectrum (Turcotte, 1992)	f – Frequencies in Fourier expansion of the data series	a^2 – squared coefficients of the Fourier expansion	$a^2 \propto f^\beta$	$D_L = 2 + \beta/2$ – Fractal dimension of the self-affine line; $D_S = 3 + \beta/2$ – Fractal dimension of the self-affine surface
Roughness based (Pachepsky et al., 1997)	w – Size of windows over the data series	Root-mean squared deviations from the linear trend within the window $RMS = \frac{1}{n_w} \sum_{i=1}^{n_w} \sqrt{\frac{1}{m_i-2} \sum_{j=1}^{m_i} \varepsilon_{ij}^2}$ where n_w is the total number of windows of length w in the data, m_i is the number of points in the i th window, ε_{ij} is the residual of the linear regression in the j th data point in the i th window	$RMS \propto w^q$	$D_L = 2 + q$ – Fractal dimension of the self-affine line; $D_L = 3 + q$ – Fractal dimension of the self-affine surface
Area-perimeter (Lovejoy, 1982)	A – Outline area	P – Outline perimeter	$P \propto A^{\frac{D_L}{2}}$	D_L – Fractal dimension of the outline
Circle counting (Feder, 1988)	r – Pore radius	N_c – Number of circles with radii larger than r	$N_m \propto r^{-D_m}$	D_m – Mass fractal dimension
Adsorption of molecules of different sizes (Avnir et al., 1985)	r – Molecule radius	N_m – Number of molecules in monomolecular coverage	$N_m \propto r^{-D_s}$	D_s – Surface fractal dimension
Single adsorbate isotherm (Sokolowska, 1989)	$\frac{p}{p_0}$ – Relative pressure	n – Adsorption	$n \propto \left(-\ln \frac{p}{p_0}\right)^{D_s-3}$	D_s – Surface fractal dimension
Single adsorbate isotherm (Hajnos et al., 2000)	$\frac{p}{p_0}$ – Relative pressure	A_e – Area of the condensed adsorbate–vapor interface	$A_e \propto \left(-\ln \frac{p}{p_0}\right)^{D_s-2}$	D_s – Surface fractal dimension
Mercury or water porosimetry (Bartoli et al. 1999)	p – Capillary pressure	$\frac{dV}{dr}$ – Rate of the volume change at the pore radius obtained from the capillary law $r = \frac{\text{const}}{p}$	$\frac{dV}{dr} \propto r^{2-D}$	D is the mass fractal dimension D_m if the object is the mass fractal, the surface fractal dimension if the object of the study is the surface fractal
Light scattering (Gouyet, 1994)	I – Intensity of the scattered radiation	Q – Scattering vector	$I \propto Q^{-s}$	s is the mass fractal dimension D_m if the object is the mass fractal, and $s = 6 - D_s$ if the object of the study is the surface fractal

^aApproximates the fractal dimension of line

In general, this spectrum has a parabolically shaped concave down shape. The degree on concaveness and the asymmetry of the parabolic shape provide information about the heterogeneity in the system under study (e.g., Caniego et al., 2005).

Conclusions

The major contribution that fractal geometry makes in agrophysics is a general, simple, and succinct representation of complex structures by a small number of fractal parameters. Fractal parameters are complementary to other agrophysical parameters.

Fractals should never be considered an ultimate model of heterogeneity in the soil-plant-atmosphere system. Rather, they provide a balance between accuracy and clarity that may aid us in gaining insight into sources and consequences of the observed complexity. Eventually, once a greater insight into key processes is obtained, we expect causes of the apparent fractal scaling to be revealed and quantified.

Bibliography

- Avnir, D., Farin, D., and Pfeifer, P., 1985. Surface geometric irregularity of particulate materials: the fractal approach. *Journal of Colloid and Interface Science*, **103**, 112–123.
- Bartoli, F., Gomedy, V., Vivier, H., and Niquet, S., 1999. The relation between silty soil structures and their mercury porosimetry curve counterparts: fractals and percolation. *European Journal of Soil Science*, **50**, 9–22.
- Bourke, P., 2006. Constrained diffusion-limited aggregation in 3 dimensions. *Computers & Graphics*, **30**, 646–649.
- Burrough, P. A., 1983. Multiscale sources of spatial variation in soil. I. The application of fractal concepts to nested levels of soil variation. *Journal of Soil Science*, **34**, 577–597.
- Caniego, F. J., Espejo, R., Martín, M. A., and San José Martínez, F., 2005. Multifractal scaling of soil spatial variability. *Ecological Modelling*, **182**, 291–303.
- Chen, J. D., and Wilkinson, D., 1985. Pore-scale viscous fingering in porous media. *Physical Review Letters*, **58**, 1892–1895.
- Chester, S., Meneveau, C., and Parlange, M. B., 2007. Modeling turbulent flow over fractal trees with renormalized numerical simulation. *Journal of Computational Physics*, **225**, 427–448.
- Evertsz, C. J. G., and Mandelbrot, B. B., 1992. Multifractal measures. In Peitgen, H., Jürgens, H., and Saupe, D. (eds.), *Chaos and Fractals*. Berlin: Springer, p. 921.
- Feder, J., 1988. *Fractals*. New York: Plenum.
- Fekete, A., Nagy, M., and Kaszab, T., 2007. Estimation of fruit mass loss by optical method. ASABE Annual International Meeting, Paper No. 076110.
- Gouyet, J. F., 1996. *Physics and Fractal Structures*. Paris: Mason.
- Hajnos, M., Korsunkaia, L. P., and Pachepsky, Y. A., 2000. Fractal dimensions of soil pore surfaces in managed grassland. *Soil and Tillage Research*, **55**, 63–70.
- Kravchenko, A. N., and Pachepsky, Y. A., 2004. Fractal techniques to assess spatial variability in soil processes. In Álvarez-Benedí, J., and Muñoz-Carpena, R. (eds.), *Soil-Water-Solute Process Characterization: An Integrated Approach*. Boca Raton: CRC Press, pp. 617–638.
- Lovejoy, S., 1982. The area-perimeter relation for rain and cloud areas. *Science*, **216**, 185.
- Mandelbrot, B. B., 1983. *The Fractal Geometry of Nature*. New York: Freeman.
- Mandelbrot, B. B., and Van Ness, J. W., 1968. Fractional Brownian motions, fractional noises and applications. *SIAM Reviews*, **10**, 422–437.
- Pachepsky, Ya A., Crawford, J. W., and Rawls, W. J. (eds.), 2000. *Fractals in Soil Science*. Amsterdam: Elsevier.
- Pachepsky, Ya A., Ritchie, J. C., and Gimenez, D., 1997. Fractal modeling of airborne laser altimetry data. *Remote Sensing of Environment*, **61**, 150–161.
- Paik, K., and Kumar, P., 2008. Emergence of self-similar tree network organization. *Complexity*, **13**, 30–37.
- Peitgen, H. O., Jürgens, H., and Saupe, D., 2004. *Chaos and Fractals. Frontiers of Science*. New York: Springer.
- Posadas, A., Quiroz, R., Tannus, A., Crestana, S., and Vaz, C. M., 2009. Characterizing water fingering phenomena in soils using magnetic resonance imaging and multifractal theory. *Nonlinear Processes in Geophysics*, **16**, 159–168.
- Prusinkiewicz, P., Hammel, M., and Mech, R., 1997. *Visual Models of Morphogenesis: A Guided Tour*. Canada: University of Calgary. Available from World Wide Web: <http://algorithmicbotany.org/vmm-deluxe>.
- Russ, J. C., 1994. *Fractal Surfaces*. New York: Plenum.
- Schertzer, D., and Lovejoy, S., 1991. Scaling nonlinear variability in geodynamics: multiple singularities, observables, universality classes. In Schertzer, D., and Lovejoy, S. (eds.), *Non-linear Variability in Geophysics. Scaling and Fractals*. Dordrecht: Kluwer.
- Senesi, N., and Wilkinson, K. J. (eds.), 2008. *Biophysical chemistry of fractal structures and processes in environmental systems*. Hoboken: Wiley.
- Sokołowska, Z., 1989. On the role of energetic and geometric heterogeneity in sorption of water vapor by soils. *Geoderma*, **45**, 251–265.
- Stoyan, D., and Stoyan, H., 1994. *Fractals Random Shapes and Point Fields*. Chichester: Wiley.
- Turcotte, D. L., 1986. Fractals and fragmentation. *Journal of Geophysical Research*, **91**, 1921–1926.
- Turcotte, D. L., 1992. *Fractals and Chaos in Geology and Geophysics*. New York: Cambridge University Press.
- Turcotte, D. L., 2007. Self-organized complexity in geomorphology: observations and models. *Geomorphology*, **91**, 302–310.
- West, G. B., Brown, J. H., and Enquist, B. J., 1999. The fourth dimension of life: fractal geometry and allometric scaling of organisms. *Science*, **284**, 1677–1679.
- Witten, T. A., and Sander, L. M., 1981. Diffusion-limited aggregation, a kinetic critical phenomenon. *Physical Review Letters*, **47**, 1400–1403.
- Zou, M., Yu, B., Feng, Y., and Xu, P., 2007. A Monte Carlo method for simulating fractal surfaces. *Physica A*, **386**, 176–186.

FRACTURE

The characteristic appearance of the surface of a broken material (e.g., minerals, grains).

FRAGIPAN

A dense, natural subsurface layer of hard soil with relatively slow permeability to water, mostly because of its extreme density or compactness rather than its high clay content or cementation <http://encyclopedia2.thefreedictionary.com/fragipan>.

Cross-references

[Claypan and its Environmental Effects](#)
[Subsoil Compaction](#)

FRICTION

The resistive force that occurs when two surfaces move along each other when forced together. It results in physical deformation and heat buildup.

FRICTION PHENOMENA IN SOILS

Rainer Horn
 Institute for Plant Nutrition and Soil Science, Christian-Albrechts-University zu Kiel, Kiel, Germany

Introduction

The determination of interparticle, inter-aggregate, or intra-aggregate forces allows a more complete insight in the soil strength and the bindings forces and can be also applied to even predict the soil strength on various scales using PDF or related equations (as shown in ID 00144). The values for the cohesion and angle of internal friction strongly depend not only on soil texture but also to a much greater extent on soil structure apart from a slight increase of the cohesive forces with bulk density. The values strongly depend on the matric potential and can be quantified both under laboratory and also under in situ conditions.

Definition

In between single particles, aggregates, or at the root soil interface frictional forces occur, which prevent the particles from direct sliding. The coarser the particles or aggregates, the rougher the surfaces; the denser these particles are packed, the higher is the strength which must be exceeded by the applied stresses in order to rearrange or to move them. In general, the shear strength parameters:

cohesion (c) and angle of internal friction (φ) are defined by the Mohr–Coulomb failure line and described by:

$$\tau = \sigma_n \tan \varphi + c,$$

whereby

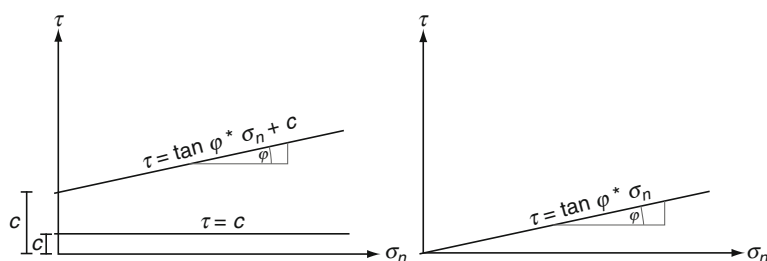
φ is the angle of internal friction, c defines the cohesion, and σ_n is the applied vertical stress.

Cohesion and angle of internal friction are additionally influenced by shear speed and drainage conditions for a given soil. The shear test can be carried out by the direct shear approach, whereby the type and direction of the shear plane, which is assumed to be affected only by normal and shear stresses, are fixed. Normal stress is applied to the specimen in the vertical and shear stress in the horizontal direction. To determine the Mohr–Coulomb failure line, at least four to five samples need to be tested, each with a different normal stress. The maximum shear resistance (τ_{\max}) is determined from a shear stress-displacement curve and plotted against the corresponding normal stress (σ_n) (Figure 1).

The determination of the shear strength of single aggregates or even only of soil crust surfaces (against the wind erosion) requires more sensitive and smaller shear devices like the crushing test (in order to determine the aggregate strength) or rheometrical approaches (like oscillation rheometer). For both tests approximately 20–30 aggregates or soil specimen must be measured at a given predrying intensity (matric potential) in order to get statistically reliable results (Horn and Baumgartl, 2002; Horn and Dexter, 1989; Markgraf and Horn, 2006).

The third approach is triaxial tests, where the stress path applied resembles more the in situ conditions (For more details see Hartge and Horn, 1999, 2009; McCarthy, 2007; Zhang et al., 2001).

Table 1 sums up the texture and structure-dependent values for φ and c as a function of the predrying intensity Ψ_m . At a given texture, the more rigid the soil, the more pronounced the aggregation and the drier the soil samples. Values for the angle of internal friction for a single aggregate ($>45^\circ$) are even higher than for the bulk soils. However, aggregated bulk soil reveals higher friction angles than the homogenized soil at the same bulk density (Figure 2). This shear strength gain is, however, lost again

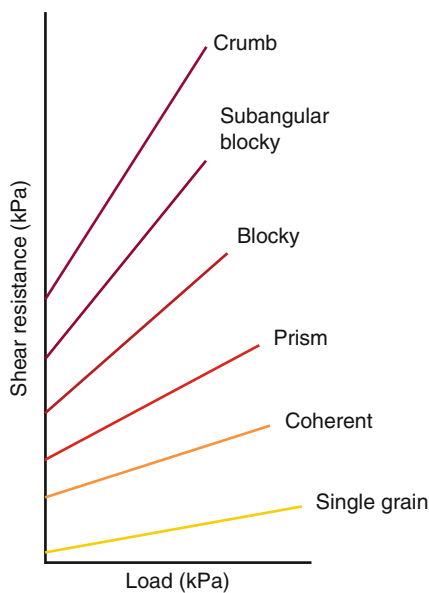


Friction Phenomena in Soils, Figure 1 The Mohr–Coulomb failure line for water saturated systems ($\tau = c$), structured unsaturated soils ($\tau = \tan \varphi * \sigma_n + c$; left) and dry sand ($\tau = \tan \varphi * \sigma_n$; right).

Friction Phenomena in Soils, Table 1 Cohesion c and angle of internal friction φ values as a function of soil texture, structure, and matric potential (defined as pF) (Taken from Horn and Fleige, 2003)

Soil texture classes	Soil structure	pF 1.8		pF 2.5	
		c (kPa)	φ ($^{\circ}$)	c (kPa)	φ ($^{\circ}$)
X	sin	0	25	0	26
Ss, Su 2-4	sin	8	26	12	28
Sl 2-4	sin	8	30	10	32
Slu	coh/pri	12	34	14	37
	pol	15	39	18	41
St 2-3	coh/pri	13	38	15	40
	pol	20	41	23	43
Uu, Us	sin	2	29	4	30
Us	coh/pri	10	35	15	39
	cru	8	37	12	40
Ut 2-4	coh/pri	12	35	26	37
Uls	pol	18	35	20	38
	sub/cru	44/40	40/43	50/45	42/45
Lu	coh/pri	10/12	30/35	15	32/36
	pol	16	35	18	37
	sub/cru	34	38/39	44	40/46
Ls 2-4	coh/pri	10	22/25	14	31/33
Lts	pol	19	30	26	35
	sub/cru	26/22	36/38	38/33	39/42
Lt 2-3	sin	1	19	2	23
	coh/pri	15	28/32	26/34	36/38
	pol	30	36	41	40
	sub	46	39	66	43
Tu	coh/pri	32	22/28	45	30/32
	pol	40	30	70	34
	sub	45	36	40	42
Tt	sin	0	16	0	20
Tl, Tt	coh/pri	30/40	24/32	34/45	38/42
Ts 2-4	pol	50	44	60	48
	sub	50	48	70	56

X = coarse fragment (>80 wt%), sin = single grain, coh = coherent, pri = prismatic, pol = blocky, sub = subangular, cru = crumb



Friction Phenomena in Soils, Figure 2 Mohr–Coulomb failure line as a function of soil aggregation.

when stresses exceed the overall stability of the aggregated sample, leading to a reduction of the angle of internal friction to values similar for homogenized soil. When the maximum value of stress exceeds the maximum strength such that structure is homogenized only texture-dependent properties remain.

Conclusions

The analysis of the shear resistance parameters: angle of internal friction and cohesion allows the quantification of the soil strength and can be also applied to define the various processes and physical, chemical, and biological reasons of soil strengthening.

Bibliography

- Hartge, K. H., and Horn, R., 1999. *Einführung in die Bodenphysik, 3 Auflage*. Heidelberg: Spektrum Verlag.
- Hartge, K. H., and Horn, R., 2009. *Bodenphysikalisches Praktikum, 4 Auflage*. Stuttgart: Schweizerbart Verlag.
- Horn, R., and Baumgartl, T., 2002. Dynamic properties of soils. In Warrick, A. W. (ed.), *Soil Physics Companion*. Boca Raton: CRC Press, pp. 17–48.

- Horn, R., and Dexter, A. R., 1989. Dynamics of soil aggregation in an irrigated desert loess. *Soil and Tillage Research*, **13**, 253–266.
- Horn, R., and Fleige, H., 2003. A method of assessing the impact of load on mechanical stability and on physical properties of soils. *Soil and Tillage Research*, **73**, 89–100.
- Markgraf, W., and Horn, R., 2006. Rheological-stiffness analysis of K-treated and CaCO₃-rich soils. *Journal of Plant Nutrition and Soil Science*, **169**, 411–420.
- McCarthy, D. F., 2007. *Essentials of Soil Mechanics and Foundations*, 7 Auflage. New York: Pearson.
- Zhang, B., Zhao, Q., Horn, R., and Baumgartl, T., 2001. Shear strength of surface soil as affected by soil bulk density and soil water content. *Soil and Tillage Research*, **59**, 97–106.

Cross-references

- Agophysical Properties and Processes
 Soil Aggregates, Structure, and Stability
 Soil Aggregation and Evaporation
 Trafficability and Workability of Soils
 Triaxial Compression Test

FROZEN FOODS

See *Modeling the Thermal Conductivity of Frozen Foods*

FRUITS, MECHANICAL PROPERTIES AND BRUISE SUSCEPTIBILITY

Margarita Ruiz-Altisent, Guillermo P. Moreda
 Laboratorio de Propiedades Físicas y Tecnologías Avanzadas en Agro-Alimentación (LPF-TAGRALIA), Universidad Politécnica de Madrid, Madrid, Spain

Definitions

Bruise. Subcutaneous mechanical damage without rupture of the skin caused to a fruit by an impact, a quasi-static compression, or a vibration. It consists of the local degradation of the flesh tissue, combined with intracellular water extravasation and browning (oxidation) of phenolic compounds from released intracellular water.

Bruise Susceptibility. Degree of ease or difficulty by which a fruit bruises. Besides of species and cultivar, bruise susceptibility depends on the physical condition or physiological status of each individual fruit, which can be assessed, among others, based on *mechanical properties*. The point at which fruits start to show symptoms of bruising is called *bruise threshold*. When this threshold is exceeded, mechanical load-induced stress exceeds flesh tissue failure stress, and a bruise results.

Mechanical Properties of Fruits. Properties related to the response of the fruit to mechanical loads such as impacts and quasi-static compressions. A major aim of determining the mechanical properties of a given specimen is to assess its physical condition. This includes aspects like firmness and turgidity. Another objective of quasi-static

compression testing is to determine maximum allowable static load for minimizing mechanical damage. Mechanical properties can be measured as stresses and deformations (strains), using appropriate instruments (see *Stress–Strain Relations*). For example, elastic modulus (Young's modulus) is often used by engineers as an index of product firmness. Another index relating stress and strain, considered a reference measurement of fruit firmness, is obtained through the Magness-Taylor test. This is an invasive or destructive procedure consisting of penetrating the flesh of a fruit with an 8 mm diameter cylindrical plunger at a constant loading rate, typically 20 mm min⁻¹, with the purpose of measuring the so-called Magness-Taylor firmness.

Introduction

Texture is one of the primary quality attributes of fruits and vegetables. It is determined by the mechanical properties of the tissue, which are affected by factors such as ripening stage and water status (Oey et al., 2007). Serious textural damage can occur to fruit pulp tissue on slow or quasi-static compression (as in bulk storage) or impact compression (as in drop on handling). Tissue failure leading to textural damage can occur as cleavage (i.e., cracking) caused by normal stresses and as slip or bruising caused by shear stress (Taub and Singh, 1998).

Bruising lowers the fruit grade (see *Quality of Agricultural Products in Relation to Physical Conditions*), increases decay, and ultimately results in lost revenue which affects packers, producers, and the industry as a whole (Guyer et al., 1991). In most fruit species, paradigmatically apples, flesh tissue is more easily bruised by impact compression than by slow compression; however, for strawberries the opposite applies (Holt and Schoorl, 1982). The amount of impact bruising that occurs to a fruit depends upon the number and severity of impacts that it experiences (see *Mechanical Impacts at Harvest and After Harvest Technologies*), and upon the *bruise susceptibility* of the fruit.

Susceptibility of fruits to mechanical damage

It is important to determine to what extent fruits are damaged when static or quasi-static (slow compression) and dynamic (impact compression, vibration) loads are applied on them. According to Stroshine and Hamann (1996), the mechanical properties of fruits determine the distribution of applied forces within them. Fruit bruises generally develop somewhere below the skin surface, where the shear stress is maximum (Schulte et al., 1994). Bruises are caused by three types of loading: impact, compression, and vibration. Bruising can result from a short sudden force: impact onto another fruit, tree, ground, or hard surface (Mohsenin, 1986). It can also result from vibration during transportation and handling, or a long term steady force such as packing box pressure.

The knowledge of how, why, and in what measure fruits are damaged when mechanical loads are applied on them is of big interest in order to:

- Determine optimum harvest time
- Select and breed cultivars according to their intended use: fresh consumption, processing
- Study ways to reduce or avoid the incidence of mechanical damage at harvest and postharvest

Damage susceptibility studies provide a useful experimental tool in this subject. The general objective of any susceptibility test is to determine how fruits respond to application of loads of different nature and intensity. The particular objective is to determine the point at which fruits start to show symptoms of mechanical damage. This point is called *bruise threshold*. According to García (2000), most susceptibility tests consist of the following stages:

1. Application of a controlled load on homogeneous samples of fruits of one or more cultivars, along with measurement and registration of load intensity.
2. Visual inspection of the fruit zone where the load has been applied. If damage is observed, measurement of the affected zone's size.
3. Analysis of results. Determination of the relationship between load applied and damage inflicted to the fruit. Identification of the bruise threshold.

When bruise appears, the variables measured to quantify it are the bruise diameter and depth, as well as the contact area corresponding to the load application. From these variables, some researchers adopt the *bruise area* as the main indicator of damage, whereas others use the *bruise volume* (V).

There are two traditional ways of applying an impact load on a fruit: to strike the fruit with a pendulum, or to drop the fruit from a given height onto a flat surface called *impact surface*. Hereinafter we refer to the second possibility. Bruise severity depends on the amount of energy absorbed or dissipated by the fruit. For an impact surface of a given hardness, the *absorbed energy* (E') increases with *impact energy* (E). In the case of a fruit dropped from a given height, [Equation 1](#) yields the value of E :

$$E = mgh \quad (1)$$

where E , impact energy (J); m , fruit mass (kg); g , acceleration of gravity (m s^{-2}); h , drop height (m).

An interesting index to quantify bruise susceptibility is the ratio of V to E (Bollen, 2005). This index makes comparisons among results obtained by different researchers easier. Nevertheless, for fully comparable results, the hardness of the impact surface should be constant among the different research works. Otherwise a same E can translate into different values of E' , which is ultimately the energy determining the severity of the bruise. In regards to the characteristics of the impact surface, Hyde (1997) reported that cushioning reduces the effective

severity of an impact in two ways: by absorbing energy and by spreading the load.

Although the ideal form of determining the bruise threshold is through direct ad hoc testing (susceptibility study), if circumstances recommend it, an analytic approach may be adopted. Thus, Baritelle and Hyde (2001) proposed an equation for estimating impact bruise threshold in apples, pears, and potatoes, based on tissue failure properties (see [Stress–Strain Relations](#)), Poisson's ratio, and specimen mass and radius of curvature, [Equation 2](#):

$$h = \frac{C\sigma_f(\varepsilon_f)^4(1 - \mu^2)^4 R^3}{mg} \quad (2)$$

where h , bruise threshold drop height (mm); C , constant (dimensionless); σ_f , failure stress (Pa); ε_f , failure strain (dimensionless); μ , Poisson's ratio (dimensionless); R , radius of curvature (m); m , mass (kg); g , acceleration of gravity (m s^{-2}).

For using [Equation 2](#) on a given fruit species and cultivar, it is necessary to know parameters such as σ_f , ε_f , or μ , which can be eventually found in literature; otherwise they would have to be measured. The value of C depends on the hardness of the impact surface.

Bruise susceptibility of pome fruit

Bruise damage is a major cause of quality loss for apples, and many studies have identified factors that have an effect on bruise susceptibility (Bollen, 2005; Pang et al., 1996; García et al., 1995). Most bruising occurs as a result of impacts, and several researchers have shown that bruising is linearly related to E (E') (Chen and Sun, 1981; Pang et al., 1992).

Fruit turgidity has an effect on impact bruise susceptibility in apples and pears. García et al. (1995) concluded that fruits with high turgidity are more susceptible to bruising. On the other hand, these authors submitted that deformation at skin puncture was shown to be the physical parameter most related to fruit turgidity.

With regard to the relation between bruise susceptibility and fruit firmness, García et al. (1995) found that fruits harvested early in the season, i.e., firmer fruit, were less susceptible to bruising than those harvested later in the season, i.e., softer fruit.

For apples, the risk of bruising is generally accepted to be higher at lower temperatures (Donati et al., 2005), but Saltveit (1984) also noted an increased tendency to bruising at higher than ambient temperatures (30°C).

Finally, bruise susceptibility depends on the cultivar. For example, *Stark Delicious* apples are more susceptible to bruise than *Golden Delicious* apples (Ragni and Berardinelli, 2001).

Bruise susceptibility of stone fruit

Brusewitz et al. (1991) investigated the impact bruise resistance of peaches. They concluded that ripeness was highly correlated with the percentage of fruit bruised and

bruise volume. Schulte et al. (1994) dropped peaches onto several impact surfaces to determine impact conditions that initiated bruising. After impact, the peaches were tested for flesh firmness and sorted into firm, soft, and very soft groups for bruise analysis. They obtained that the drop height that did not bruise decreased as fruit softened. This result agrees with that obtained by Brusewitz et al. (1991), since ripe peaches are softer than unripe ones.

Blahovec (1999) compressed individual cherries between two plates in the quasi-static compression test of *loading-unloading* (see *Rheology in Agricultural Products and Foods*), to determine the energy absorbed (E'') by the fruit during the test. After compression, he determined the bruise volume of the deformed fruit. He obtained that the index V/E'' increased with increasing values of E'' , as it occurs on apples, although for the cherries, up from a given value of E'' , the index V/E'' decreased.

Susceptibility of citrus fruits to mechanical damage

Mechanical damage in citrus fruits does not become visible after a few hours as it occurs with apples; instead several days must elapse to detect affected areas. The critical aspect in citrus fruits is not the mechanical damage itself, but its consequences. Any injury on the fruit, regardless of its size, is an invitation for pathogens, mainly fungi, to colonize the whole fruit.

Oleocellosis, also known as “oil spotting,” is an unattractive surface blemish on citrus fruits, directly related to mechanical damage. According to Wardowski et al. (1976), spots of oleocellosis are the result of the rupture of glands in the flavedo – the outermost layer of the citrus peel – which provokes the extravasation of the essential oils in the glands. This extravasation collapses the subcuticular cells, due to phytotoxicity, and gradually begins to darken and depress the affected tissue, finally turning it brown. The rupture of the glands containing the essential oils can be provoked by impacts, quasi-static compressions and abrasions. According to Ahmed et al. (1973), the resistance to rupture of lemon glands is approximately three times that of orange or tangerine. Susceptibility to oleocellosis damage depends on:

- The degree of turgidity of the fruit: Susceptibility increases with increasing turgidity.
- Environmental conditions: For example, susceptibility increases with increasing air relative humidity.
- Ripeness degree of the fruit: Susceptibility decreases with increasing ripeness. This effect is different to what happens in products such as pome or stone fruit. Pears, peaches, and many other fruits are harvested early in the season, partly because the bruise susceptibility of these products increases with maturity. Therefore, from this point of view, it is preferable to harvest citruses late in the season – and more considering their condition of non-climacteric fruits. However, it is reasonable to harvest stone and pome fruits early, because being climacteric fruits they will continue their ripening after harvest. On the other hand, optimum organoleptic

features are achieved when the fruit, whatever its type, is left to ripe in the tree. In conclusion, for climacteric fruits such as stone or pome fruit, a trade-off must be adopted between bruise susceptibility and flavor.

Bruise susceptibility of tomato and kiwifruit

In the case of tomato, it is almost impossible to measure the diameter and length of the bruise. Therefore, the only way to quantify bruise damage is through E' . The results obtained by Van Zeebroeck et al. (2007) suggest a lower bruise susceptibility of warmer tomatoes (tomatoes at 20°C vs. tomatoes at 15°C). These authors also found that E' , hence V , increases with increasing ripeness of tomato.

Hasey (1994), studying the bruising of kiwifruit during transport, reported that softer fruits were more easily damaged by vibration than firmer fruits. She also obtained that vibration bruising of kiwifruit usually results in only minor signs of surface injury, but can cause severe internal flesh injury.

Summary

Loss of commercially valuable fruits as a result of mechanical damage continues to be an issue for postharvest operators. For most fruit types, bruising is the most common type of postharvest mechanical injury, other types of mechanical damage being abrasions and open injuries (e.g., punctures). Not only a direct effect of fruit bruising affecting the quality appreciation by the consumer exists, but bruises, even small ones, can open the way for pathogen attack (Van Zeebroeck et al., 2006). By understanding the fruit susceptibility to bruising it is possible to identify when to adopt techniques which will reduce the chances of sustaining high levels of damage, or identify cultivars that require additional care when handling (Bollen, 2005). Baritelle and Hyde (2001) suggested that reducing relative turgor through slight dehydration can reduce tissue elastic modulus, which can in turn make the fruit more “self-cushioning,” by distributing a given force over a larger area of the fruit’s curved surface. This distribution effect also occurs in padding materials for reducing the aggressiveness of packing-line machinery (see *Mechanical Impacts at Harvest and After Harvest Technologies*). The result is reduced impact-induced stress, and thereby reduced probability of bruise occurrence. For most fruits, bruise susceptibility increases with maturity. This is partly responsible for the early-harvesting typical of our days often criticized by many consumers. Consumers argue that nowadays a fruit is not as tasty as it was some decades ago, when it was harvested later in the season. But this is a side effect of our days, when fruits have to travel long distances from the production to the consumption centers.

Bibliography

- Ahmed, E. M., Martin, F. G., and Fluck, R. C., 1973. Damaging stresses to fresh and irradiated citrus fruits. *Journal of Food Science*, **38**, 230–233.

- Baritelle, A. L., and Hyde, G. M., 2001. Commodity conditioning to reduce impact bruising. *Postharvest Biology and Technology*, **21**, 331–339.
- Blahovec, J., 1999. Bruise resistance coefficient and bruise sensitivity of apples and cherries. *International Agrophysics*, **13**, 315–321.
- Bollen, A. F., 2005. Major factors causing variation in bruise susceptibility of apples (*Malus domestica*) grown in New Zealand. *New Zealand Journal of Crop and Horticultural Science*, **33**, 201–210.
- Brusewitz, G. H., Mc Collum, T. G., and Zhang, X., 1991. Impact bruise resistance of peaches. *Transactions of the American Society of Agricultural Engineers*, **34**, 962–965.
- Chen, P., and Sun, Z., 1981. Impact parameters related to bruise injury in apples. ASAE Paper No. 81-3041.
- Donati, V., Mawson, A. J., and Schotsmans, W. C., 2005. Bruise susceptibility of heat treated apples. *Acta Horticulturae (ISHS)*, **687**, 405–408.
- García, F., 2000. Quality of postharvest processes and handling equipment for citrus and stone fruit, with reference to mechanical damage. Models of damage prediction (in Spanish). Ph.D. Dissertation. Universidad Politécnica de Madrid.
- García, J. L., Ruiz-Alsitent, M., and Barreiro, P., 1995. Factors influencing mechanical properties and bruise susceptibility of apples and pears. *Journal of Agricultural Engineering Research*, **61**, 11–18.
- Guyer, D. E., Schulte, N. L., Timm, E. J., and Brown, G. K., 1991. Minimizing apple bruising in the packingline. *Tree Fruit Postharvest Journal*, **2**, 14–20.
- Hasey, J. K., 1994. *Kiwifruit Growing and Handling*. Oakland: ANR.
- Holt, J. E., and Schoorl, D., 1982. Strawberry bruising and energy dissipation. *Journal of Texture Studies*, **13**, 349–357.
- Hyde, G. M., 1997. Bruising-impacts, why apples bruise, and what you can do to minimize bruising. *Tree Fruit Postharvest Journal*, **8**, 9–12. (Online). Available from World Wide Web: <http://postharvest.tfrec.wsu.edu/pgDisplay.php?article=J8I4A>. Accessed January 10th 2010.
- Mohsenin, N. N., 1986. *Physical Properties of Plant and Animal Materials*. New York: Gordon & Breach.
- Oey, M. L., Vanstreels, E., De Baerdemaeker, J., Tijskens, E., Ramon, H., Hertog, M. L. A. T. M., and Nicolaï, B., 2007. Effect of turgor on micromechanical and structural properties of apple tissue: a quantitative analysis. *Postharvest Biology and Technology*, **44**, 240–247.
- Pang, D. W., Studman, C. J., and Ward, G. T., 1992. Bruising damage in apple-to-apple impact. *Journal of Agricultural Engineering Research*, **52**, 229–240.
- Pang, D. W., Studman, C. J., Banks, N. H., and Baas, P. H., 1996. Rapid assessment of the susceptibility of apples to bruising. *Journal of Agricultural Engineering Research*, **64**, 37–48.
- Ragni, L., and Berardinelli, A., 2001. Mechanical behaviour of apples, and damage during sorting and packing. *Journal of Agricultural Engineering Research*, **78**, 273–279.
- Saltveit, M. E., 1984. Effects of temperature on firmness and bruising of Starkrimson Delicious and Golden Delicious apples. *HortScience*, **19**, 550–551.
- Schulte, N. L., Timm, E. J., and Brown, G. K., 1994. ‘Redhaven’ peach impact damage thresholds. *HortScience*, **29**, 1052–1055.
- Stroshine, R., and Hamann, D., 1996. *Physical Properties of Agricultural Materials and Food Products*. West Lafayette: Copy Cat.
- Taub, I. A., and Singh, R. P. (eds.), 1998. *Food Storage Stability*. Boca Raton: CRC Press.
- Van Zeebroeck, M., Tijskens, E., Dintura, E., Kafashan, J., Loots, J., De Baerdemaeker, J., and Ramon, H., 2006. The discrete element method (DEM) to simulate fruit impact damage during transport and handling: model building and validation of DEM to predict bruise damage of apples. *Postharvest Biology and Technology*, **41**, 85–91.
- Van Zeebroeck, M., Van linden, V., Darius, P., De Ketelaere, B., Ramon, H., and Tijskens, E., 2007. The effect of fruit properties on the bruise susceptibility of tomatoes. *Postharvest Biology and Technology*, **45**, 168–175.
- Wardowski, W. F., Mc Cormack, A. A., and Grierson, W., 1976. Oil spotting (oleocellosis) of citrus fruit. *Florida Cooperative Extension Service Circular* 410. University of Florida.

Cross-references

- [Mechanical Impacts at Harvest and After Harvest Technologies](#)
[Quality of Agricultural Products in Relation to Physical Conditions](#)
[Rheology in Agricultural Products and Foods](#)
[Stress–Strain Relations](#)

FUNNEL FLOW

Synonyms

Macropore flow; Preferential flow

See [Bypass Flow in Soil](#)

FURROW

A channel cut into soil by plow or disc, for the purpose of cultivation or drainage.

FURROW EROSION

The erosion that occurs with the process of furrow irrigation.

Cross-references

- [Water Erosion: Environmental and Economical Hazard](#)

FURROW IRRIGATION

Irrigation in which the water is applied between crop rows in furrows made by tillage implements.

Cross-references

- [Irrigation and Drainage, Advantages and Disadvantages](#)
[Irrigation with Treated Wastewater, Effects on Soil Structure](#)

G

GAS EXCHANGE IN SOILS

See [Aeration of Soils and Plants](#)

GASES SINK

See [Greenhouse Gases Sink in Soils](#)

GEOLOGIC EROSION

A process that changes soil into sediment. It relates to movement and resistance of soil to the forces of water and wind that lead to detachment and transportation of soil particles, sedimentary rocks and various land formations.

GEOSTATISTICS

Applies the theories of stochastic processes and statistical inference to geographic phenomena. Geostatistics is a branch of statistics focusing on spatial or spatiotemporal datasets. Developed originally to predict probability distributions of ore grades for mining operations, it is currently applied in diverse disciplines including petroleum geology, hydrogeology, hydrology, meteorology, oceanography, geochemistry, metallurgy, geography, forestry, environmental control, landscape ecology, soil science, and agriculture (esp. in precision farming).

GIBBS FREE ENERGY

The thermodynamic potential for a system whose independent variables are the absolute temperature, applied pressure, mass variables, and other independent, extensive variables. The change in Gibbs free energy, as a system passes reversibly from one state to another at constant temperature and pressure, is a measure of the work available in that change of state.

Bibliography

Glossary of Soil Science Terms. Soil Science Society of America. 2010. <https://www.soils.org/publications/soils-glossary>

GRAIN PHYSICS

Stanisław Grundas¹, Agnieszka Nawrocka², Josef Pecen³

¹Institute of Agrophysics, Polish Academy of Sciences, Lublin, Poland

²Institute of Agrophysics, Lublin, Poland

³Department of Sustainable Technologies, Institute of Tropics and Subtropics, University of Life Sciences Prague, Prague 6 - Suchdol, Czech Republic

Synonyms

Grains; Kernel; Seeds

Definitions

Kernel. Kernel is the cereal fruit (botanically called *caryopsis*). It consists of three components: bran, germ,

and endosperm. The fruit can play role as a grain or a seed depending on its utilization.

Grain. This term includes cereals, pulses, and oilseeds. Grain, according to its economical utilization, is divided into food grain crops, feed (fodder) crops, and industrial crops. Grains are also divided on three groups depending on type of main component: cereal fruits (polysaccharides), legumes (proteins), and oil plants (lipids).

Seed. Seed is a reproductive material of the cultivated plants. It is applied to obtain a new plant generation on a generative way.

Introduction

Crops cultivation started ages ago at the time when *Homo sapiens*, who lived in tropical and subtropical forests, changed gathering the gifts of nature (leaves, fruits, and roots) for primitive hoeing. Archeologists found fossils from the first cultivated plants dated back to Early Neolithic Period (10,000–12,000 years ago). A hypothesis that people had started plowing in the Upper Paleolithic Period (40,000–50,000 years ago) was proven by the recent archeological studies (Gordeev and Butkovsky, 2005).

Wide range of cultivated grain species including cereals, pulses (grain legumes), and oil plants (oilseeds) are exploited all over the world. Among different types of cultivated plants cereals are basic part of the human diet from ages. The word “daily bread,” the most common product obtained from grain, has become synonymous with food. Grain and grain products are vital for human activities since the proverb says: “Bread is beyond everything.” One of the grain products is a whole grain which is usually called “kernel.” If the kernel has been cracked, crushed, or flaked, then in order to be called whole grain, it must retain nearly the same relative proportions of bran, germ, and endosperm as the original grain.

Wrigley et al. (2004) describe a lot of cultivated plant species, especially cereals and pseudocereals. The cereal group consists of a few species such as wheat, rye, triticale, barley, oats, and corn, whereas buckwheat, millet, rice, and sorghum are included to pseudocereals. This division is connected with the fact that pseudocereal kernels are gluminous. It means that the buckwheat grain is covered with fruit glumes, while wheat grain is covered with flower glumes. Another group of cultivated plants are legumes that consist of ten crop species depending on specification. In Europe large-seeded annual plants (pea, soy, broad beans, lentil, pea-vine, haricot, chick-pea, spring vetch, feed lupine, etc.) are grown. Soy is referred both to leguminous and oil grain. Oil-bearing crops as a canola, sunflower, flax, etc., from which oils are produced and used mainly as oil for food and industrial purposes.

Physical properties of grain

Physical properties of grain are considered as features that are measured by instrumental methods. The properties are applying for estimation of grain quality depending on its destination. Using methods cannot change structure of

the grain, thus they must be nondestructive. Grain physical properties depend on size and structure of a studied object or amount of matter in it. Grain is regarded as an anisotropic center since some of its physical properties are linked with the direction of observation.

Grain is also considered to be viscoelastic material as many other biological materials. This kind of materials has interesting properties that exhibit viscous behavior as the gradual deformation of molasses and latex. For example, wheat with 9.3% moisture showed high elastic behavior compared with wheat tempered at 22.5% moisture that showed a plastic behavior (Ponce-Garcia et al., 2008) as well as elasticity (like a rubber band or monocrystal that stretches instantaneously and quickly returns to its original state once a load is removed). Various materials exhibit viscoelasticity with the deformation depending on load, time, temperature, and humidity.

Since there is a necessity for continuous estimation of grain quality, the physical properties are divided into the following groups:

- Mechanical: Young's modulus, ductility, moment of inertia, weight, specific gravity, hardness, density, mass, porosity, viscosity, volume, moisture, etc.
- Thermal: thermal transfer, heat conductivity, etc.
- Acoustic: velocity, emission, damping, etc.
- Optical: reflectance, refraction, luminance, refractive index, chromaticity, absorption, color, etc.
- Electrical: electric potential, capacitance, resistance, conductance, impedance, permeability of storage grain, etc.
- Magnetic: magnetic permeability, inductance

The grain has undergone handling and processing by using various means such as mechanical, thermal, electrical, spectral, and sonic techniques. For this reason, some information about basic physical properties of grain will be presented. Knowledge of these properties should construct the base of essential engineering data for designing of machines, determining of its efficiency control of processes or operation during food or feed production. Such basic information should have a sufficient meaning not only to engineers but also to other scientists who may exploit these properties and find new applications for final grain products.

To better understand some terms a few examples are given below. Grain mechanical damage that has not resulted from damage during development of the crop may be due to problems encountered at harvest, transport, subsequent storage, and processing. Grain mechanical damage is considered as a state of interruption of tissue continuity. It can be caused by external static, impact loading, or internal strain during intensive drying of wet grain or intensive wetting of dry ones. Mechanical damage of grain, which occurs in harvesting, threshing, and handling, can seriously affect viability and germination power of seeds, growth vigor, insect and fungi attack, and utility value of the final product. Decrease of viability is due to mechanical damage of the seed embryo,

especially during harvesting of cereals in the wetted region of cultivation, for example, in Scandinavian Countries.

Grain damage can be also caused by insect and/or fungus activity. Therefore, it is important to be familiar with normal, healthy cereal grains before trying to recognize physical defects of damaged ones. Causes of physical defects are not always obvious. Many of them result from pest infestation or disease infection that appeared earlier in the growing season.

All physical properties of grains/seeds originating from cultivated plants depend mainly on their humidity and temperature, which are very important. In fact, each biological material and the majority of its properties depend on temperature and water content inside the object and in its surrounding. Having acquaintance with the above-mentioned features provides insights into the physical structure of the cereal at both macroscopic and microscopic levels. Mechanical damage occurs wherever grain is subjected to the destructive action of internal or external forces, commonly in the form of impact, causing internal or surface cracks. One of the most often used properties of grain is hardness. Hardness of grain has been a subject of interest to millers, livestock feeders, breeders, and other agricultural scientists. According to literature (Mohsenin, 1978) biting and cutting the grain has provided a qualitative evaluation of grain hardness. A number of attempts have been made to find an objective and a qualitative method of the individual kernel hardness determination. One of these methods can be the SKCS apparatus (Single Kernel Characterization System, type 4100) made by Perten Instruments in Illinois (USA).

Mechanical properties such as strength, impact, and shear resistance are crucial for agricultural engineering to become acquainted with seed resistance to cracking during harvesting and handling conditions. The internal cracks in grain are caused very often by external forces (as impact), acting on grains during harvesting or handling processes. The second main reason of internal cracks originating are internal forces arising inside kernel as consequence of the fast changes of field conditions, temperature, and humidity of climate mainly, not the grains. The internal cracks are studied using soft X-ray and/or colorimetric techniques. X-ray investigations are carried out mainly in the Institute of Agrophysics of Polish Academy of Science (PAS) in Lublin, Poland, in Agrophysical Research Institute of Russian Academy of Agricultural Sciences (RAAS), St Petersburg, Russia, and in Czech University of Life Science (CULS) in Prague, Czech Republic. X-ray detection makes it possible to analyze position of cracks and also to quantify them inside the kernel. This method allows evaluating the physical state of the grain endosperm (Grundas et al., 1999). Studies, carried out in the above-mentioned institutes, have shown that moisture content influences on grain resistance to cracking. Natural processes like rain or dew cause sudden increase of grain moisture and it is a main reason of cracks formation in the endosperm.

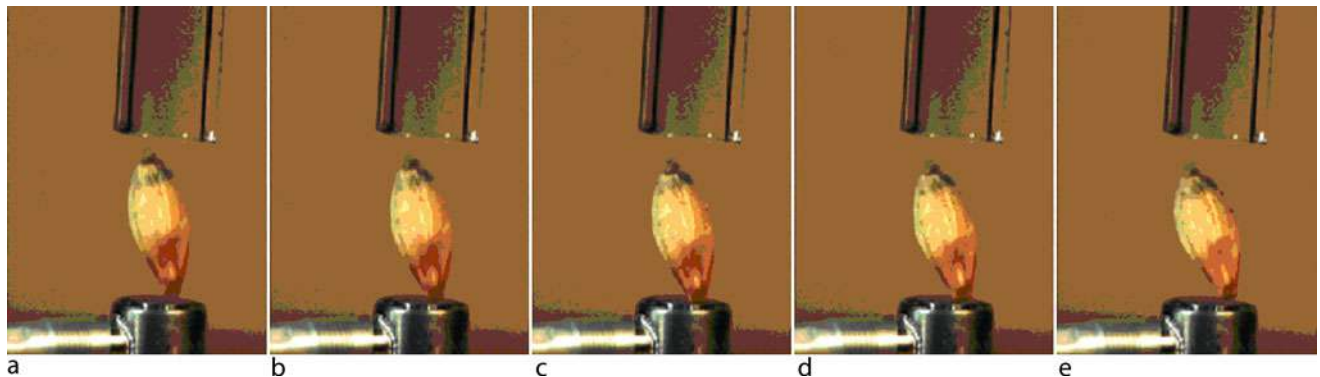
Results of research carried out by using X-ray methods showed also a significant difference in grain endosperm cracks between common wheat varieties. Natural wetting of dry grain (below 14% of moisture content) during rainfall, when wheat is standing in the field, is one of the reasons of cracking. Intensive drying of wet grain (above 15% of moisture content) in field or industry or in laboratory conditions is also the reason of cracking. In drier climate, premature ripening may occur due to stress connected with drought. In these conditions, grains are unlikely to reach full potential. The susceptibility of grain to mechanical damage is determined by genetic factors (e.g., grain hardness), environmental effects (climatic condition during pre-harvest period), and by the condition of grain storage (especially excessive humidity). The combination of these properties determines the utility value of grain material. The big effect of kernel humidity on its behavior is shown in next two literature examples: Al-Mahasneh and Rababah (2007) and Mohoric et al. (2009). Furthermore, mechanical properties of grain also change under biological factors, for example, insect pest infestation (Nawrocka et al., 2010) and fungi.

Shape, size, volume, surface area, density, porosity, color, and appearance are some of the physical characteristics of grain that are important in some problems connected with design of specific machines for harvesting and processing of raw materials or analysis of grain behavior during handling. What shape should be assumed for single grain in bulk material and which dimension should be employed in calculations are basic questions that have to be answered before selection of healthy grain or seeds from undesirable materials by preferred pneumatic or electrostatic devices. Knowledge about shape and size is also important for stress distribution in bulk material under load. Contact area is also vital for effective and safety transport of bulk material.

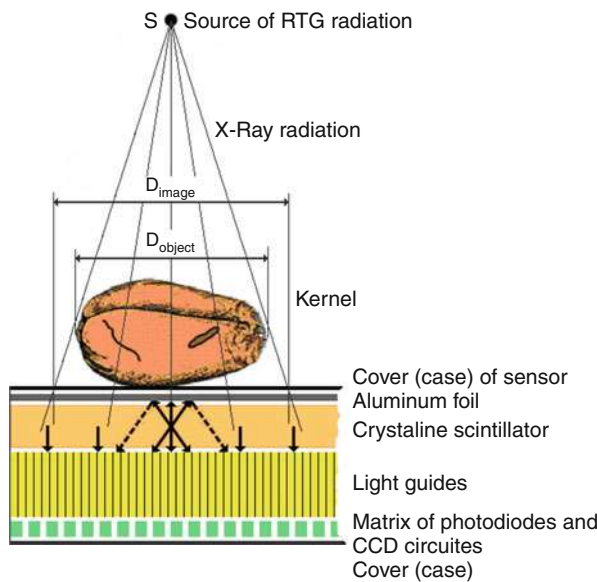
Knowledge of density and specific gravity of grains or seeds is needed, for example, in calculation of thermal diffusivity, in heat transfer, and in pneumatic and hydraulic handling. The irregular shape and porous nature of grains make problems in volume and density measurements.

Figure 1 shows the examples of grain impact. From a mechanical point of view, mechanism and the conditions of the running impact on grain play a big role in its damage (Stronge, 2000). The velocity of impact is not too high and the collision objects are rigid or viscoelastic bodies and very often is running noncollinear configuration of acting bodies. After rebound the kernel starts its rotation. An incidence of kernel is not on the center of the force transducer. This fact and the inclination of longitudinal axis of kernel are main reasons of a kernel rotation about a perpendicular axis.

Figure 2 shows the principle of scintillation sensor work, which is used for direct making of digital roentgenograms (Del Guera, 2004). The figure explains simultaneously a reason of “fuzzy contours” of roentgenogram. This phenomenon is caused by the difference in dimensions of image (D_{image}) and object (D_{object}), which depend



Grain Physics, Figure 1 A visualization of kernel deformation during its acting onto the force transducer is shown. The periodicity of the snaps is 200 μ s. The kernel of barley is falling onto the force transducer. The snaps (a) and (b) are before the impact, (c) during the impact and (d) and (e) are after the impact of kernel (Pecen et al., 2007).



Grain Physics, Figure 2 A basic principle and structure of scintillation sensor for direct making of digital roentgenograms.



Grain Physics, Figure 3 The example of real scintillation sensor (on the left) with active field of 9 cm^2 and dimensions 2.6 \times 3.5 cm. Matrix consists of two billion photodiodes with pitch about 25 μm . There is also X-ray image of *Ricin Castor* on the right.

on the geometrical arrangement of X-ray apparatus. A strong influence on “fuzzy contours” and X-ray image resolution has thickness and properties of the sensor scintillation layer. This type of sensor is widely used in practice and its properties depend mainly on properties of the sensor scintillation layer. This type of sensor is used in the laboratory of CULS, Prague. An image of this kind of sensor and a roentgenogram made by it are depicted on Figure 3.

Near-infrared hyperspectral imaging (NIR HSI) is another method used to determine the physical properties of grain. It integrates conventional imaging and spectroscopy to attain both spatial and spectral information from an object. Hyperspectral images (hypercubes) are three-dimensional blocks of data, comprising two spatial and one wavelength dimension. It allows for the visualization of biochemical constituents of a sample, separated into particular areas of the image, since regions of a sample with similar spectral properties have similar chemical composition. It is currently unfeasible to obtain information in all three dimensions of a hypercube simultaneously (Gowen et al., 2007).

The NIR technique can be applied to determine moisture, protein, lipid and starch content, wet and dry gluten, and alveograph parameters of whole wheat in the laboratory (Miralbes, 2003) as well as on the field during harvesting (Maertens et al., 2004). It also allows for detection of single wheat kernels containing insects (Maghirang et al., 2003) and classification of healthy and fungal-damaged soybean seeds (Wang et al., 2003).

TD-NMR technology (time-domain nuclear magnetic resonance) is widely used for various process and quality control, and R&D applications. Moisture and protein content of bulk cereal grain samples can be measured very quickly by a TD-NMR benchtop instrument at the harvest point. The same technique can be used to implement rapid quality control of incoming cereal grains at the food processing plant. TD-NMR can contribute significantly

toward quality improvement and can be a powerful tool for rapid analysis (Ghosh and Tombokan, 2009).

Conclusions

Physical measures to prevent some of the main causes for rejected grain samples are suggested. The physical condition of grain, which travels from field crop to commodity, is described. The simple method, used in the past to measure these quantities, have improved over time and nowadays that measure methods provide more information about studied objects. These methods are often noninvasive. Development of field measurement was caused mainly by a progress in information technologies and by the use of new physical principles. Nowadays more sophisticated and very sensitive methods for measuring individual properties of grain and seed are used. Very often optical properties of studied materials are preferred for their better characterization. These methods bring better knowledge about a material behavior on a cell level, and obtained results allow better utilization of studied materials.

Bibliography

- Al-Mahasneh, M. A., and Rababah, T. M., 2007. Effect of moisture content on some physical properties of green wheat. *Journal of Food Engineering*, **79**, 1467–1473.
- Del Guera, A., 2004. *Ionizing Radiation Detector for Medical Imaging*. World Scientific Publishing Company, pp. 524, ISBN-10: 981238674242, ISBN-13: 978-98112386748.
- Ghosh, S., and Tombokan, X., 2009. TD-NMR technology: a noninvasive tool for high-throughput QC and rapid cereal product improvement. *Cereal Foods World*, **July-August**, 152–157.
- Gordeev, A. V., and Butkovsky, V. A., 2005. *Russia-Grain Power*. Moscow: Publishing House “Food Industry”.
- Gowen, A. A., O’Donnell, C. P., Cullen, P. J., Downey, G., and Frias, J. M., 2007. Hyperspectral imaging – an emerging process analytical tool for food quality and safety control. *Trends in Food Science and Technology*, **18**, 590–598.
- Grundas, S., Velikanov, L., and Archipov, M., 1999. Importance of wheat grain orientation for the detection of internal mechanical damage by the x-ray method. *International Agrophysics*, **13**, 355–361.
- Maertens, K., Reynolds, P., and De Baerdemaeker, J., 2004. On-line measurement of grain quality with NIR technology. *Transactions of the American Society of Agricultural Engineers*, **47**, 1135–1140.
- Maghirang, E. B., Dowell, F. E., Baker, J. E., and Throne, J. E., 2003. Automated detection of single wheat kernels containing live or dead insects using near-infrared reflectance spectroscopy. *Transactions of the American Society of Agricultural Engineers*, **46**, 1277–1282.
- Miralbes, C., 2003. Prediction chemical composition and alveograph parameters on wheat by near-infrared transmittance spectroscopy. *Journal of Agricultural and Food Chemistry*, **51**, 6335–6339.
- Mohoric, A., Vergeldt, F., Gerkema, E., van Dalen, G., van den Doel, L. R., van Vliet, L. J., van As, H., and van Duynhoven, J., 2009. The effect of rice kernel microstructure on cooking behavior: a combined μ -CT and MRI study. *Food Chemistry*, **115**, 1491–1499.
- Mohsenin, N. N., 1978. *Physical Properties of Plant and Animal Material. Structure, Physical Characteristics and Mechanical Properties*. New York: Gordon and Breach. 758 pp. ISBN 0677023006.
- Nawrocka, A., Grundas, S., and Grodek, J., 2010. Losses caused by granary weevil larva in wheat grain using digital analysis of x-ray image. *International Agrophysics*, **24**, 63–68.
- Pecen, J., Szwed, G., Nasef, D., Grundas, S., 2007. The different in impact records on varieties of barley kernel. In *Proceedings of the Third International Conference on Trends in Agricultural Engineering (TAE2007)*, Czech University of Life Science, Prague, Czech Republic, September 12–14, 2007, pp. 355–359.
- Ponce-Garcia, N., Figueroza, J. D. C., Lopez-Huape, G. A., Martinez, H. E., and Martinez-Periche, R., 2008. Study of viscoelastic properties of wheat kernels using compression load methods. *Cereal Chemistry*, **85**, 667–672.
- Stronge, W. J., 2000. *Impact Mechanics*. Cambridge: The University Press. ISBN 0-5216-3286-2.
- Wang, D., Dowell, F. E., Ram, M. S., and Schapaugh, W. T., 2003. Classification of fungal-damaged soybean seeds using near-infrared spectroscopy. *International Journal of Food Properties*, **7**, 75–82.
- Wrigley, C., Walker, C., and Corke, H., 2004. *Encyclopedia of Grain Science*. Oxford: Elsevier Academic, Vol. 3. ISBN 0-12-765490-9.

Cross-references

- [Agrophysical Objects \(Soils, Plants, Agricultural Products, and Foods\)](#)
[Cereals, Evaluation of Utility Values](#)
[Grains, Aerodynamic and Geometric Features](#)
[Image Analysis in Agrophysics](#)
[Microstructure of Plant Tissue](#)
[Physical Properties as Indicators of Food Quality](#)
[Proton Nuclear Magnetic Resonance \(NMR\) Relaxometry in Soil Science](#)
[X-ray Method to Evaluate Grain Quality](#)

GRAINS, AERODYNAMIC AND GEOMETRIC FEATURES

Bronisława Barbara Kram
Institute of Agricultural Engineering, University of Environmental and Life Sciences, Wrocław, Poland

Definition

Grains include cereals, pulses, and oilseeds. They are often referred to seeds that are reproductive materials of the cultivated plants (see [Grain Physics](#)).

Aerodynamics is a field of dynamics that deals with the problems of gas flow and forces produced by the phenomena.

Introduction

The forces affect a solid during its movement in gaseous environment. The magnitude of the force is affected by the parameters of the solid (length l [m], air density ρ [kg m^{-3}], coefficient of internal friction μ [$\text{kg m}^{-1} \text{s}^{-1}$]) as well as air stream velocity v [m s^{-1}]. Combination of above-mentioned components yields the Reynolds number

$Re = (v \cdot l) = (\mu/\rho)[-]$ which is very important in the theoretical aerodynamic calculations.

In practice, air acts as a carrier both during transport, classification, as well as cleaning. The most usual is a system, where particles (grains) are transferred in a moving stream of air. Grain parameters like weight, size, and shape as well as moisture have an essential influence on its aerodynamic characteristics like critical velocity v_k , coefficient of aerodynamic resistance k_x , and coefficient of fineness k_0 .

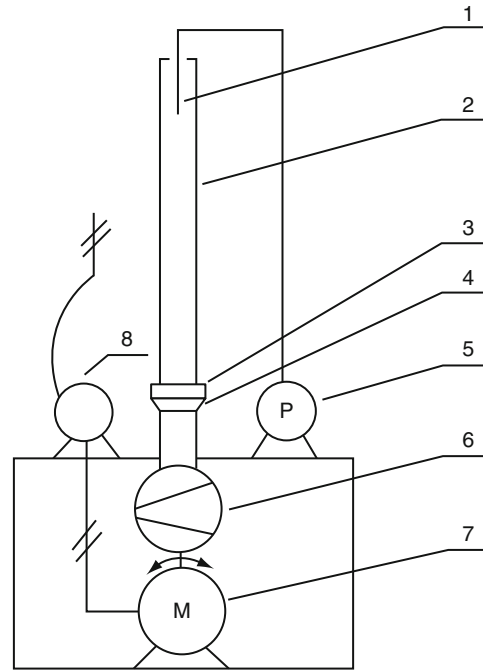
Survey of literature

Agricultural engineering has forced the investigation on the aerodynamic properties of the vegetables. Letoshnev (1949) considered in detail the problem of the aerodynamic properties in his textbook on the construction of agricultural machines. He referred there to Bezruckin (1936), who as early as in the 1930s, reported the numerical values of the properties for the basic seeds. In his very important for agricultural physicists textbook, Mohsenin (1970) devoted a lot of attention to the problem of aerodynamics; he presented two methods of estimation of the aerodynamic properties of agricultural products: in a vertical air tunnel for terminal velocity determination in air and in vertical water tunnel for determining terminal velocity in water. He included also the results of investigations of the aerodynamic properties by Bilanski et al. (1962). The method of critical velocity estimation in the vertical air tunnel is commonly employed with various constructional modifications. Bogaczyński (1975) measured a dynamic pressure in a vertical air tunnel and estimated the coefficient of resistance and then the critical velocity for wheat, barley, and rye. Coates and Yazici (1990) announced the aerodynamic properties of sorghum and jojoba seeds, respectively. Tabak and Wolf (1998) described in detail a vertical wind tunnel used to determine the critical velocity and coefficient of resistance of cotton-seeds. The aerodynamic properties of grain and straw materials were examined by Gorial and O'Callaghan (1990) and Zewdu (2007); weed seeds were investigated by Kahrs (1994). Jha and Kachru (1998) dealt with testing of the properties of makhana while Omobuwajo et al. (1999) examined African breadfruit seeds. In the following years the aerodynamic properties of pine nuts were studied by Faruk Ozguven and Kubilay Vursavus (2005), sunflower seeds were investigated by Gupta et al. (2007). A test stand and results of investigations on various coffee beans were presented in detail by Alfonso Junior et al. (2007).

Methodology

The method of estimation of a particle (grain) critical velocity v_k consists in a placement of the particle in a vertical air stream (Figure 1) and keeping it in an equilibrium state.

A glass pipe 2 equipped with a charging mechanism 3.4 for grain supply at its bottom part, a supporting sieve and air inlet is used for observation of the grain behavior. The



Grains, Aerodynamic and Geometric Features,

Figure 1 Scheme of the stand for determination of the grain aerodynamic properties: 1, Pitot tube; 2, glass tube; 3, charging mechanism; 4, screen; 5, compensating micromanometer; 6, fan; 7, electric motor; 8, autotransformer.

air stream is generated by a fan 6, driven by an electric motor 7. The yield of the fan is controlled by the change of rotational speed of the motor (by autotransformer 8). Pitot tube 1, arranged in the upper part of the glass pipe 2, is connected with a compensating micromanometer 5, measuring dynamic pressure in H_2O . The system composed of the devices (Figure 1) is employed for the measurement of pressure of the flowing air within accuracy $h = 0.01 \text{ mmH}_2\text{O}$. When the tested grain is in an equilibrium state, dynamic pressure p_{dyn} , described by Equation 1 can be measured:

$$p_{dyn} = \frac{v^2 \cdot \gamma}{2 \cdot g} \quad [\text{Pa}], \quad (1)$$

where

- v , air velocity $[\text{ms}^{-1}]$,
- γ , specific gravity of air $[\text{Nm}^{-3}]$,
- g , acceleration gravity $[\text{ms}^{-2}]$.

After transformation of the equation, critical velocity v_k may be evaluated:

$$v_k = \sqrt{\frac{2 \cdot g \cdot p_{dyn}}{\gamma}} \quad [\text{m s}^{-1}]. \quad (2)$$

In the equilibrium state, the weight of grain G [N] located in the vertical air stream is compensated by the resistance force R [N], expressed by Newton equation:

$$R = k_x \cdot S \cdot p_{dyn} \quad [N], \quad (3)$$

where

k_x coefficient of aerodynamic resistance [—],
 S lifting surface [mm^2].

From the equation, the coefficient of aerodynamic resistance k_x can be assessed:

$$k_x = \frac{G}{S \cdot p_{dyn}}. \quad (4)$$

The ability of a particle to resist against air stream is defined by the coefficient of fineness. It can be derived from the dependence between the resistance force, weight of particle, and its acceleration:

$$a = \frac{R}{m} = \frac{k_x \cdot S \cdot p_{dyn}}{m} = \frac{k_x \cdot S \cdot \rho}{2 \cdot m} \cdot v_k^2 \quad [\text{m s}^{-2}], \quad (5)$$

where

a , acceleration [m s^{-2}],
 m , mass of grain [mg],
 ρ , air density [kg m^{-3}].

The quantity $k_x \cdot S \cdot \rho / 2 \cdot m$ is called a coefficient of fineness k_0 :

$$k_0 = \frac{k_x \cdot S \cdot \rho}{2 \cdot m} \quad [\text{m}^{-1}]. \quad (6)$$

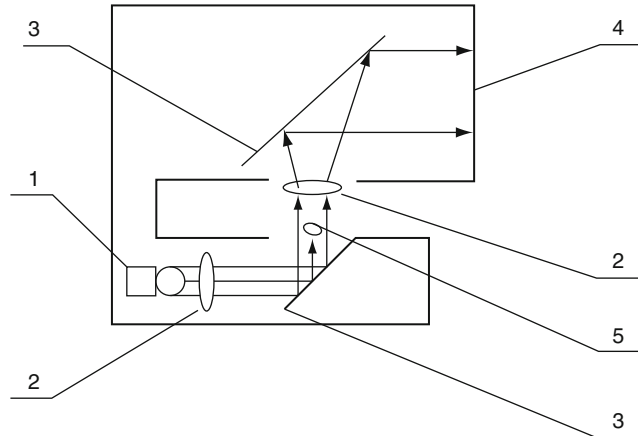
A lifting surface, necessary for the calculations is determined with an optical device (Figure 2) consisting of light sources (1), set of lenses (2), set of flat mirrors (3), screen with scale (4) enabling magnification of perpendicular projection of a tested grain (5) by the factor of 29.7. When we have the outlines of three perpendicular projections, we can measure and estimate the length, width, and thickness of a grain.

The method of setting of grain and the exemplary contours of three orthogonal projections presents Figure 3.

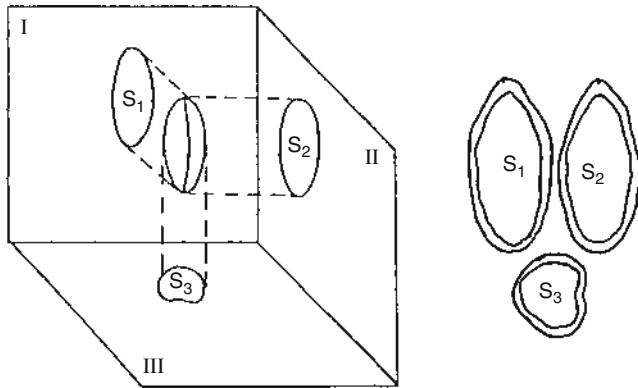
The largest of the three perpendicular projections is assumed as the lifting surface. After planimetry of the obtained outline of measured surface, its size can be estimated with a high accuracy. Size and shape of the lifting surface depend on the species and variety of tested grain. Some examples of lifting surfaces of tested grains are shown in Figure 4.

Aerodynamic characteristics

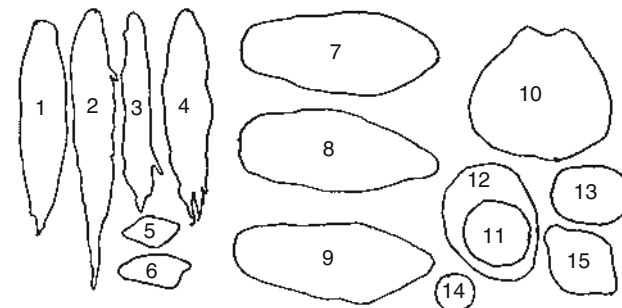
Aerodynamic characteristics were developed for the basic grains including: rape, seeds of chosen leguminous plants, maize, buckwheat, amaranth, and grass seeds.



Grains, Aerodynamic and Geometric Features,
Figure 2 Optical system of the device for determination of the grain lifting surface: 1, light sources; 2, set of lenses; 3, set of flat mirrors; 4, screen with scale; 5, grain.



Grains, Aerodynamic and Geometric Features,
Figure 3 Importing grain during determination of orthogonal projections, example contours of three orthogonal projections.



Grains, Aerodynamic and Geometric Features,
Figure 4 Lifting surface of seeds and grains: 1, Meadow Fescue; 2, Cocksfoot; 3, Smooth Brome-grass; 4, Westerwolds Ryegrass; 5, Timothy grass without glume; 6, Timothy grass with glume; 7, wheat; 8, rye; 9, triticale; 10, maize; 11, soya bean (dry); 12, soya bean of moistening; 13, horse bean; 14, amaranth; 15, buckwheat.

Lifting surface, weight, and length of a tested dry grain affect both critical velocity and coefficient of fineness. In all investigated cases high regularity has occurred. The critical velocity increased with growing weight, lifting surface and length of tested grain according to power or exponential relationship. On the other hand, the coefficient of aerodynamic resistance did not depend on any property of tested grain and therefore its average value was assumed as a characteristic property for a considered variety ([Table 1](#)).

Additionally, the investigation of horse bean and buckwheat was carried out for grain without seed cover due to technological requirements ([Table 2](#)).

In the case of maize, the grains for investigation were collected from three different zones of the cob. The first part of the cob (ca. one third of cob length from its rachis) called later A zone has the grains in the shape resembling a cone; the middle part, called B zone, has the grains in shape of disks with extended lifting surface; and the shape of grains from C zone (upper part of the cob) resembles spheres. The obtained results confirmed the influence of the shape of tested grains on their aerodynamic characteristics ([Table 2](#)).

To determine the effect of humidity on the aerodynamic characteristics, individual grains should be artificially moisturized. From dry grains with a defined humidity, one grain with a weight m is selected. When the weight m and humidity W of the grain are known, its dry matter m_s can be evaluated.

After immersing the grain in distilled water (for the time following from previously considered moisturizing dynamics), its weight rises to m_1 and humidity to W_1 , which can be easily estimated from the following equations:

$$W = \frac{m - m_s}{m} \cdot 100\%, \quad (7)$$

$$m_s = \frac{m(100 - W)}{100}, \quad (8)$$

$$W_1 = \frac{m_1 - m_s}{m_1} 100\% \quad [\%] \quad (9)$$

where:

W , moisture of grain [%],

m , mass of grain [mg],

m_1 , mass of moisturizing grain [mg],

m_s , dry substance [mg],

W_1 , moisture of moisturizing grain [%].

After the first moisturizing, the lifting surface is evaluated and the grain is placed in the vertical air stream. When the grain is in an equilibrium state, the dynamic pressure is measured. The procedure is repeated several times for an individual grain.

After numerical elaboration of the experiment it has been stated that the humidity affects critical velocity in a

Grains, Aerodynamic and Geometric Features, Table 1 Basic geometry and aerodynamic properties of seeds (Szpryngiel and Kram, 1994; Kram and Szot, 1999; Kram et al., 2007a, b)

Plant species	Mass, m [mg]	Length, l [mm]	Lifting surface, S [mm^2]	Critical velocity, v_k [$\text{m}\cdot\text{s}^{-1}$]	Coefficient of fineness, k_0 [m^{-1}]	Coefficient of aerodynamic resistance, k_x [-]
Westerwolds Ryegrass seeds without glume	1.35–6.35	4.24–7.74	3.85–10.88	3.22–10.88	0.946–0.352	0.375
Meadow Fescue seeds without glume	1.0–3.85	4.88–9.76	3.31–7.75	2.68–5.34	1.366–0.344	0.301
Smooth Brome-grass seeds without glume	1.55–6.35	3.54–7.58	2.64–7.65	2.83–5.29	1.225–0.351	0.567
Cocksfoot seeds without glume	0.85–2.55	4.11–8.08	2.45–7.65	3.17–5.61	0.976–0.312	0.443
Timothy Grass seeds without glume	0.20–1.05	1.10–2.00	0.50–1.34	4.44–6.17	0.498–0.258	0.404
Timothy Grass seeds with glume	0.25–0.90	1.60–2.35	0.76–1.49	3.46–5.44	0.819–0.331	0.399
Amaranth	0.46–1.11	1.00–1.50	0.81–1.47	3.10–4.25	1.021–0.543	0.814
Buckwheat Red-Corolla nutlets with cover	10.7–40.8	4.53–8.30	13.85–29.55	4.10–7.95	0.584–0.155	0.427
Buckwheat Red-Corolla nutlets without cover	6.6–31.8	3.60–5.73	6.35–14.67	5.66–9.64	0.306–0.106	0.497
Lupine Bar	34.8–182.9	4.6–7.8	12.88–15.66	12.26–15.61	0.065–0.040	0.321
Lupine Radames	59.5–332.2	6.0–10.3	21.52–68.04	11.88–14.43	0.070–0.047	0.331
Soya bean Polan	82.0–221.0	5.8–12.1	24.19–49.39	12.09–14.27	0.067–0.048	0.354
Horse bean Tom with seed cover	351.4–640.5	9.0–12.1	51.83–84.36	11.9–14.76	0.069–0.045	0.672
Horse bean Tom without seed cover	287.2–537.1	8.0–11.9	41.40–69.40	9.19–11.88	0.116–0.070	1.001

Grains, Aerodynamic and Geometric Features, Table 2 Basic aerodynamic properties of grains

Plant species	Mass, m [mg]	Lifting surface, S [mm^2]	Critical velocity, v_k [$\text{m}\cdot\text{s}^{-1}$]	Coefficient of fineness, k_0 [m^{-1}]	Coefficient of aerodynamic resistance, k_x [-]
Wheat Gama	31.9–67.8	13.25–24.00	9.30–11.28	0.113–0.077	0.371
Wheat Henika	27.3–59.0	13.69–22.26	9.48–10.94	0.109–0.082	0.360
Wheat Almari	20.2–66.4	11.44–24.57	7.28–10.43	0.185–0.090	0.454
Wheat Jawa	21.8–61.7	12.00–23.94	8.44–10.12	0.138–0.096	0.416
Rye Motto	18.8–63.9	9.77–29.57	8.19–9.90	0.146–0.100	0.431
Rye Dańskowskie Złote	26.3–54.9	12.79–22.20	8.78–10.32	0.127–0.092	0.405
Triticale Presto	23.5–62.0	13.29–24.94	7.22–9.85	0.188–0.101	0.464
Triticale Ugo	24.7–66.3	13.23–26.44	7.50–9.97	0.174–0.099	0.437
Barley Rastik	18.0–61.0	13.10–25.42	7.33–10.22	0.183–0.094	0.370
Barley Rataj	10.3–60.4	12.99–25.90	4.94–9.20	0.402–0.116	0.463
Maize K0042270					
A	286	63.51	17.51	0.032	0.235
B	286	74.12	16.79	0.035	0.219
C	286	66.45	17.59	0.032	0.223
Maize BEKO210					
A	282	61.07	17.26	0.033	0.248
B	282	68.83	16.99	0.034	0.227
C	282	53.20	18.01	0.030	0.261

Grains, Aerodynamic and Geometric Features, Table 3 Basic aerodynamic properties of moisturized grains

Plant species	Mass, m [mg]	Moisture, W [%]	Lifting surface, S [mm^2]	Critical velocity, v_k [$\text{m}\cdot\text{s}^{-1}$]	Coefficient of fineness, k_0 [m^{-1}]	Coefficient of aerodynamic resistance, k_x [-]
Wheat Gama	30	8.6–34.3	13.25–20.06	9.30–10.47	0.113–0.090	0.460–0.340
	55	8.6–35.6	19.56–29.69	10.46–11.73	0.090–0.071	0.397–0.331
Wheat Henika	30	9.3–32.7	13.69–19.50	9.82–10.99	0.102–0.081	0.377–0.306
	55	9.3–31.6	20.14–27.66	9.75–11.10	0.103–0.080	0.448–0.367
Wheat Almari	30	10.6–40.0	14.26–19.38	9.21–10.04	0.116–0.097	0.409–0.345
	60	10.6–41.0	22.53–29.92	9.91–10.84	0.100–0.084	0.426–0.382
Wheat Jawa	30	11.1–40.9	13.29–19.27	8.99–10.12	0.121–0.096	0.439–0.387
	60	11.1–39.0	23.17–31.74	9.87–10.88	0.101–0.083	0.417–0.354
Rye Motto	30	12.5–32.8	12.34–17.78	8.49–9.33	0.136–0.113	0.465–0.389
	60	12.5–36.9	23.08–34.47	8.91–10.21	0.124–0.094	0.482–0.377
Rye Dańskowskie Złote	30	8.8–40.2	12.79–20.32	8.49–9.8	0.136–0.102	0.432–0.357
	60	8.8–43.8	20.29–30.43	9.11–10.32	0.118–0.092	0.490–0.377
Triticale Presto	30	11.2–42.4	15.30–21.06	8.42–9.46	0.138–0.110	0.432–0.388
	60	11.2–44.9	24.26–35.67	9.20–10.58	0.116–0.088	0.453–0.375
Triticale Ugo	30	10.9–42.5	15.62–20.06	8.43–9.38	0.138–0.112	0.442–0.385
	60	10.9–44.0	25.07–34.92	9.78–10.62	0.103–0.087	0.452–0.406
Maize KB270	286	5.8–40.0	66.45–85.17	17.60–19.77	0.032–0.025	0.222–0.216
Maize BEKO210	282	8.5–41.8	53.20–75.40	18.28–19.59	0.030–0.026	0.254–0.245
Lupine Bar	97	7.3–65.2	21.24–53.72	11.58–14.92	0.073–0.044	0.390–0.293
Lupine Radames	146	9.5–57.4	35.36–81.08	11.45–14.25	0.075–0.048	0.444–0.321
Soya bean Polan	122	9.9–61.3	32.32–78.52	11.95–13.52	0.069–0.054	0.412–0.329
Horse bean Tom	400	12.6–60.9	66.84–145.40	13.08–15.88	0.057–0.039	0.684–0.401
	620	12.6–55.3	93.04–173.96	13.33–16.07	0.055–0.038	0.569–0.406

high degree (Table 3). Generally, with an increase in grain humidity, its weight and lifting surface as well as critical velocity increase. Consequently, with the increase in critical velocity, both the coefficient of fineness and coefficient of aerodynamic resistance decrease (in case of moisturized

grain, its coefficient of aerodynamic resistance also depends on humidity). There is however one exception. It is the soya bean (Table 3). With an increase in the grain humidity the critical velocity decreases and in consequence the other coefficients rise. It follows probably from the fact

Grains, Aerodynamic and Geometric Features, Table 4 The values of critical velocity for various plant species

Plant species	Critical velocity, v_k [m·s ⁻¹]	Authors
Wheat	8.90–11.50	Bezruckzin (1936)
	8.99	Bilanski et al. (1962) ^a
Rye	6.38–9.29	Bogaczyński (1975)
	8.36–9.89	Bezruckzin (1936)
Oats	5.41–8.65	Bogaczyński (1975)
	8.08–9.11	Bezruckzin (1936)
Barley	5.88–6.34	Bilanski et al. (1962) ^a
	8.41–10.77	Bezruckzin (1936)
Pea	7.01	Bilanski et al. (1962) ^a
	6.50–8.65	Bogaczyński (1975)
Vetch	15.50–17.50	Bezruckzin (1936)
Lentil	13.23–17.00	Bezruckzin (1936)
Corn	8.34–9.75	Bezruckzin (1936)
Millet	12.48–14.03	Bezruckzin (1936)
Flax	10.64	Bilanski et al. (1962) ^a
Alfalfa	9.83–11.80	Bezruckzin (1936)
Soybeans	4.66	Bilanski et al. (1962) ^a
Jojoba seed	5.46	Bilanski et al. (1962) ^a
Cotton seeds	13.50	Bilanski et al. (1962) ^a
Makhana	11.90–14.76	Kram (2010)
African breadfruit	13.90	Coates and Yazici (1990)
Seeds	6.20–10.20	Tabak and Wolf (1998)
Kernel	4.48–6.10	Jha and Kachru (1998)
Hull	8.02	Omobuwajo et al. (1999)
Pine nuts	7.71	
Nut	2.90	
Kernel	7.01–8.86	Faruk Ozguven and Kubilay Vursavus (2005)
Hull	6.21–8.10	
Sunflower seed	3.18–4.40	
Conilon coffee cherries (moisture content 8.7–56.1%)	2.54–3.53	Gupta et al. (2007)
Conilon coffee beans (moisture content 10.5–41.5%)	11.03–15.47	Alfonso Junior et al. (2007)
	9.00–11.44	

^aIn the original textbook by the author, the critical velocity is presented in feet per second (v [fps]), to simplify the considerations it has been recalculated in meters per second (v [m/s]), assuming 1 ft = 0.3048 m.

that a dry soya bean is almost a regular sphere which changes its shape after moisturizing into the shape of flat bean with an extended lifting surface. However, all considered aerodynamic characteristics versus humidity can be described by the simple power or exponential equations.

Summary

The investigations on aerodynamic properties are very time consuming and laborious, thus they require numerous repetitions. For the estimation of the coefficient of aerodynamic resistance the value of lifting surface

is necessary. The last can be assessed in several ways. The measurements of critical velocity are carried out in various measuring stands but since the main idea consisting in keeping the grain in a vertical air stream is maintained, their results are comparable. The values of critical velocity for various seeds, obtained over several years by different authors are collected in Table 4.

Bibliography

- Alfonso Junior, P. C., Correa, P. C., Pinto, F. A. C., and Queiroz, D. M., 2007. Aerodynamic properties of coffee cherries and beans. *Biosystems Engineering*, **98**, 39–46.
- Bezruckzin, I. P., 1936. *Farm Machine*, No. 3.
- Bilanski, W. K., Collins, S. H., and Chu, P., 1962. Aerodynamic properties of seed grains. *Agricultural Engineering*, **43**, 216–219.
- Bogaczyński, K., 1975. Some aerodynamic properties of selected samples of wheat, rye, and barley seeds. *Acta Alimentaria Polonica*, **1**, 165–175.
- Coates, W., and Yazici, E., 1990. Aerodynamic characteristics of jojoba seeds and like-sized stones. *Transactions of the ASABE*, **33**, 1449–1456.
- Gorial, B. Y., and O'Callaghan, J. R., 1990. Aerodynamic properties of grain/staw materials. *Journal of Agricultural Engineering Research*, **46**, 275–290.
- Gupta, R. K., Arora, G., and Sharma, R., 2007. Aerodynamic properties of sunflower seed (*Helianthus annuus* L.). *Journal of Food Engineering*, **79**, 899–904.
- Jha, S. N., and Kachru, R. P., 1998. Physical and aerodynamic properties of makhana. *Journal of Food Process Engineering*, **21**, 301–316.
- Kahrs, J., 1994. Aerodynamic properties of weed seeds. *International Agrophysics*, **8**, 259–262.
- Kram, B., 2010. Aerodynamic properties of soybean seeds (in Polish). *Inżynieria Rolnicza*, **1**, 265–271.
- Kram, B., and Szot, B., 1999. Aerodynamic and geometric properties of amaranth seeds. *International Agrophysics*, **13**, 227–232.
- Kram, B., Woliński, J., and Wolińska, J., 2007a. Aerodynamic properties of nutlets of Red Corolla buckwheat. *Acta Agrophysica*, **9**, 399–406.
- Kram, B., Woliński, J., and Wolińska, J., 2007b. Comparative studies on geometric traits of nutlets with and without seeds cover in Red-Corolla buckwheat. *Acta Agrophysica*, **9**, 657–664.
- Letoshnev, M. N., 1949. *Farm Machinery*. Moscow.
- Mohsenin, N. N., 1970. *Physical Properties of Plant and Animal Materials*. New York: Gordon & Breach Science.
- Omobuwajo, T. O., Akande, E. A., and Sanni, L. A., 1999. Selected physical, mechanical and aerodynamic properties of African breadfruit (*Treculia africana*) seeds. *Journal of Food Engineering*, **40**, 241–244.
- Ozguven, F., and Vursavus, K., 2005. Some physical, mechanical and aerodynamic properties of pine (*Pinus pinea*) nuts. *Journal of Food Engineering*, **68**, 191–196.
- Szpryngiel, M., and Kram, B., 1994. Rye-grass seeds aerodynamic properties vs seed weight and dimensions. *International Agrophysics*, **8**, 343–347.
- Tabak, S., and Wolf, D., 1998. Aerodynamic properties of cotton seeds. *Journal of Agricultural Engineering Research*, **70**, 257–265.
- Zewdu, A. D., 2007. Aerodynamic properties of grain and straw material. *Biosystems Engineering*, **98**, 304–309.

Cross-references

- Agophysical Properties and Processes*
Grain Physics

GRASS FIBERS, PHYSICAL PROPERTIES

Majda Sfiligoj Smole, Silvo Hribenik

Department of Textile Materials and Design, University of Maribor, Maribor, Slovenia

Definition

Grass fibers are sclerenchyma elongated cells which occur in different parts of plants, mainly in the stems and leaves. They can be found in ground and vascular tissues for mechanical support, but sometimes they occur in dermal tissues as well (Langer et al., 1991; Pazourek et al., 1997). This type of cell is of particular importance for the production of bast textile fibers as flax, hemp, etc.

Origin

Grasses (Poaceae) form one of the largest plant families consisting of some 650–785 genera and about 10,000 species (Petersen, 1981; Holmes, 1989; Leslie et al., 1992; Moser et al., 1996). Members of this family occur abundantly in every climatic region and certain possibilities for their nontraditional application are evident, e.g., production of pulp and paper (e.g., Pahkala, 2001). Perennial Ryegrass (*Lolium perenne*), Italian Ryegrass (*L. multiflorum*), Hybrid Ryegrasses (*L. perenne* × *multiflorum*), Timothy (*Phleum pratense*), Fescues (Meadow fescue – *Festuca pratensis*, Tall Fescue – *F. arundinacea*) are some of the most important representatives in this group of grasses, while legumes are presented by white clover (*Trifolium repens*), red clover (*Trifolium pratense*), and lucerne (*Medicago sativa*).

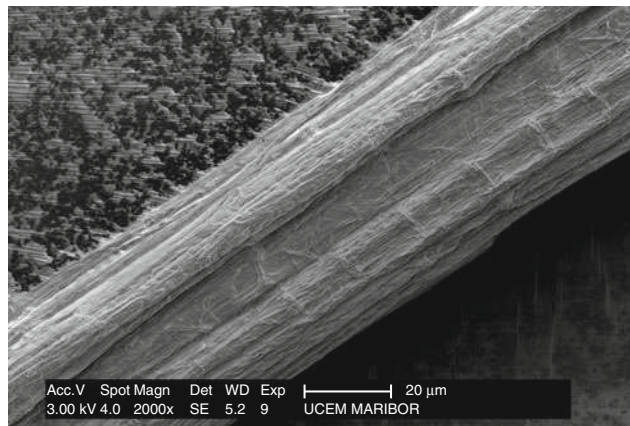
Isolation: The biological and chemical procedures for leaves and stems retting (i.e., separation of the fibers from the rest of the plant), respectively can be used to obtain technical grass fibers in the form of fiber bundles. However, mechanical separation of the fiber bundles is additionally needed (Sfiligoj Smole et al., 2004). The fiber bundles are mainly inhomogeneous and sclerenchyma cells are often accompanied by tracheary elements. Fiber content in stems is higher when compared to that in leaves (e.g., fiber content in hybrid ryegrass stems is 39.5% and in leaves it is 7.9%).

Fibers morphology

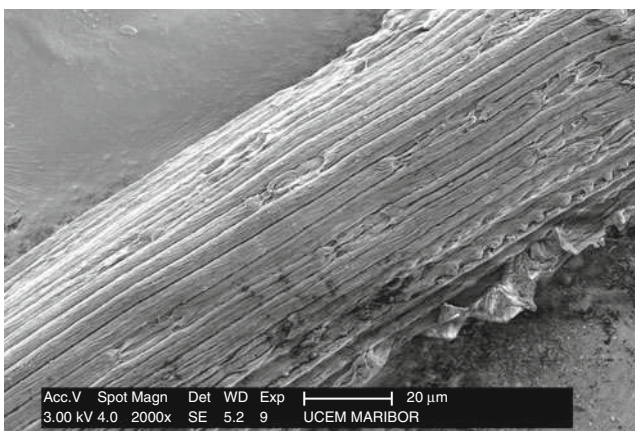
Scanning electron microscope images of the longitudinal views of the fibers isolated from hybrid ryegrasses by alkaline procedure are given in Figures 1 and 2.

Properties

The length of the elementary cells in grasses and legumes is between 0.5 and 3 mm; slightly shorter fiber cells are present in leaves when compared to the cells from stems. The diameter of the isolated cells is approximately 10–18 µm. Due to the history of the grasses (deformation and damage caused by the treatment of grasses, maturity grade, and conditions during grass growth), the plant



Grass Fibers, Physical Properties, Figure 1 Longitudinal view of fibers from a leaf of an ensiled ryegrass.



Grass Fibers, Physical Properties, Figure 2 Longitudinal view of fibers from a stem of an ensiled ryegrass.

structures vary considerably in their properties. Nevertheless, the mechanical properties of fiber bundles of the grass leaves in the axial direction are lower in comparison to the mechanical properties of fiber bundles of the stems, although the differences are insignificant. The stress-strain behavior of fiber structures indicates a rigid character. Elongations of samples at break are rather low, but higher than in the case of whole stems or leaves. The elongations vary between 1.5% and 5.5% and tenacities from 7.5 to 21 cN tex⁻¹. The obtained values are comparable with the mechanical properties of some textile bast fibers, e.g., jute, hemp, or coir.

Bibliography

- Holmes, W., 1989. *Grass, Its Production and Utilization*. Oxford: The British Grassland Society, Blackwell Scientific.
- Langer, R. H. M., and Hill, G. D., 1991. *Agricultural Plants*. Cambridge: Cambridge University Press.
- Leslie, W., and Dallwitz, J. M., 1992. *The Grass Genera of the World*. Wallingford: CAB International.

- Moser, L. E., Buxton, D. R., and Casler, M. D., 1996. *Cool-Season Forage Grasses*. Madison: American Society of Agronomy, Wisconsin USA.
- Pahkala, K. S., 2001. *Non-wood plants as raw material for pulp and paper*. Dissertation, Helsinki: Faculty of Agriculture and Forestry, University of Helsinki.
- Petersen, A., 1981. *Die Gräser als Kulturpflanzen und Unkräuter auf Wiese, Weide und Acker*. Berlin: Akademie.
- Pazourek, J., and Votrubova, O., 1997. *Atlas of Plant Anatomy*. Prague: Peres.
- Sfiligoj Smole, M., Stana Kleinschek, K., Kreže, T., Strnad, S., Mandl, M., and Wachter, B., 2004. Physical properties of grass fibres. *Chemical and Biochemical Engineering Quarterly*, **18**(1), 47–53.

GRAVIMETRIC WATER CONTENT

The ratio of water mass to dry matter mass.

GRAVITATIONAL POTENTIAL

The gravitational potential at a point is equal to the work by the exterior force as a particle of unit mass is brought from infinity to its position in the gravitational field.

GRAVITY HEAD (GRAVITY POTENTIAL)

The amount of work required to raise a body a specified height in a gravity field. Gravity head is expressed as energy per weight and is equal to the distance Z , of a measurement point in the soil above an arbitrary reference height (z). Gravity potential is expressed as energy per volume and is equal to the product of the distance raised, Z , the water density, ρ and the gravitation constant, g ($\rho g Z$).

GRAZING-INDUCED CHANGES OF SOIL MECHANICAL AND HYDRAULIC PROPERTIES

Julia Krümmelbein
Soil Protection and Recultivation, Brandenburg
University of Technology, Cottbus, Germany

Synonyms

The influence of grazing on soil physical properties

Definition

Grazing. The activity of wild or domestic herbivores (e.g., deer, sheep, cattle) walking around and feeding on plants (mainly grasses and herbs).

Introduction

Soils that are grazed by animals undergo mechanical stresses, partly normal forces (load) and partly shearing forces (slip). The amount of loads and shearing forces depends on the kind of grazing animals and is sometimes comparable to agricultural machinery (Greenwood and McKenzie, 2001). Grazing and treading animals affect the (top) soil due to mechanical damage of the sod and the uppermost soil layers and due to soil deformation (Greenwood and McKenzie, 2001; Krümmelbein et al., 2006). Trampling by grazing animals results in the deformation and compaction of particularly the top soil (Zhang and Horn, 1996; Villamil et al., 2001; Greenwood and McKenzie, 2001; Martinez and Zinck, 2004; Krümmelbein et al., 2006; Tian et al., 2007). Grazing also influences the amount and composition of soil organic matter by the export of biomass and its return as excrements. This in turn influences biological activity and thus natural regeneration of soil structure by root activity (Angers and Caron, 1998; Greenwood and McKenzie, 2001).

Compressive and shearing soil deformation by grazing animals

The intensity and amount of deformation depends on the soil water content and the amount of pressure exerted on the soil; it becomes more distinct and more visible the higher the water content, and the stress exerted on the soil is, in comparison to the internal soil strength (Horn and Rostek, 2000; Arvidsson et al., 2003). The trampling effect of grazing animals is depending on their weight, hoof size, and kinetic energy. The pressure exerted on the soil becomes higher when the grazing animal is moving. While an animal is moving, only three or two and in extreme situations (e.g., while escaping) only one hoof touches the ground, meaning that the whole body mass is transferred by a reduced hoof area. Scholefield et al. (1985) measured that the pressure of a walking cow is twice as high as the pressure of a standing cow. Shearing forces due to grazing have widely been ignored although they are transmitted on the soil surface by all moving and scrabbling animals. We have to consider that such dynamic shearing movements modify soil structure and thus decrease soil stability (Peth, 2004; Krümmelbein et al., 2006). With increasing soil water content this effect becomes more pronounced, shearing occurs more frequently and it particularly occurs in the upper soil layer. Grazing leads to increasing values of precompression stress. This indicates a grazing-induced compaction of the soil, along with increasing soil strength against compressive forces and an increasing bulk density (Peth, 2004; Krümmelbein et al., 2006). Cyclic loading experiments have shown that with increasing grazing intensity the soil becomes less sensitive to repeated loading (Krümmelbein, 2007). The soil structure deterioration due to grazing is not only pointed out by increasing strength against compressive forces but also by decreasing

angles of internal friction with increasing grazing intensity (Krümmelbein et al., 2006; Krümmelbein, 2007). The angle of internal friction is one component of shear strength and a measure for the structural development of a soil; the greater the angle of internal friction, the further advanced is the structural formation of the soil (Silva et al., 2004).

Effects of soil deformation

Pore system

Soil compaction is characterized by a volume decrease, particularly of the coarse pore volume, accompanied by an increase of the fraction of smaller pores. The structural change due to grazing is also reflected by decreasing values of vertically oriented saturated hydraulic conductivity with increasing grazing intensity and particularly by the anisotropy of the saturated hydraulic conductivity (Krümmelbein et al., 2006). The total pore volume decreases, the pore size distribution shifts showing a decrease of coarse pores and an increase of medium and fine pores (Greenwood and McKenzie, 2001; Peth, 2004; Krümmelbein, 2007). Due to grazing, there is not only a modification in the total pore volume and the pore size distribution, but also a decrease in the pore continuity. The decrease of pore volume and pore continuity and the changed pore size distribution affect soil functions, e.g., air and water conductivity, which are decreased in deformed soils (Vogeler et al., 2006; Krümmelbein et al., 2006), water retention (Kutílek et al., 2006; Krümmelbein, 2007), and soil biological processes (Whalley et al., 1995).

Infiltration and saturated hydraulic conductivity and its anisotropy

Even more sensitive to compaction than the pore volume is the pore continuity (Ball and Robertson, 1994). Pore continuity in turn determines saturated hydraulic conductivity and air permeability. In general, the saturated hydraulic conductivity is not only decreased due to a grazing-induced formation of a platy structure, but also becomes higher in the horizontal compared to the vertical direction and results in anisotropic flow conditions (Dörner Fernández, 2005; Krümmelbein et al., 2006).

The alterations in flow direction and pore continuity by grazing also reduce the water infiltration into the soil because of the loss of macropores open to the surface. Removal of vegetation also decreases the number of root channels that are important for water infiltration into the soil (Pietola et al., 2005; Kennedy and Schillinger, 2006).

Water repellency

Infiltration can also be decreased by changes in water repellency. Soils of higher grazing intensities mostly show decreased water repellency at comparable soil water contents because less soil organic matter accumulates which enhances the potential water repellency (Krümmelbein, 2007). Because of the high amounts of living and dead

biomass on ungrazed sites, the soil water content of those sites mostly is higher than on grazed sites (Zhao et al., 2007). In turn, water repellency increases with decreasing water contents, accordingly the actual water repellency is often higher on grazed than on ungrazed sites (Zhao et al., 2007). The higher the water repellency, the lower is the amount of water infiltrating into the soil (Lamparter et al., 2006). Water repellency also affects capillary rise negatively (Bachmann et al., 2001). The combination of effects of soil compaction, shearing, water repellency, etc. leads to higher runoff rates on grazed compared to ungrazed sites (Greenwood and McKenzie, 2001).

Interrelation between mechanical and hydraulic properties

The mechanical and hydraulic changes described above are interlinked with each other. They commonly have negative effects for the productivity of grassland soils and their ecological functioning (Greenwood and McKenzie, 2001). Poor physical quality of soils due to soil compaction can, apart from the negative economical impact due to productivity losses, sometimes lead to drastic environmental consequences, such as flood disasters as, e.g., encountered lately in areas of Central Europe(Akkermann, 2004) and landslides in hilly or mountainous areas. Soil compaction deteriorates the pore system and induces increasing intra-aggregate bulk density and a reduced interaggregate macropore system, followed by an even more intense shear-induced deterioration of soil structure. Thus, as the final stage even a complete aggregate homogenization due to shear forces can occur on grazed soils, which results in lower infiltration rates, higher run off and greater probability for water erosion events (Pietola et al., 2005; Peth and Horn, 2006). Thus, structure degradation and sparse vegetation enhance not only water but also wind erosion (Hesse and Simpson, 2006; Zhao et al., 2007). In many semiarid areas, compaction and structural degradation of the top soil resulting from intense grazing has led to widespread degradation processes (Krümmelbein et al., 2006; Krümmelbein, 2007), such as wind erosion resulting in heavy dust emissions (Li et al., 2003). It is well known that on intensely grazed grassland soils also water erosion is a common phenomenon during strong rainfall events, partly accompanied by severe gully development (Arnaez et al., 2007; Wei et al., 2007).

Soil recovery from structure degradation

Soils have a limited ability to structurally recover from former mechanical deterioration such as compaction (Drewry, 2006; Krümmelbein, 2007). In general it is known that due to wetting and drying cycles and, consequently, swelling and shrinkage, soil structure is able to recover from a compacted or even homogenized state by forming new aggregates. Because these aggregates are surrounded by the interaggregate pore space, wetting and drying may also be able to improve the aeration and water

infiltration as well as the thermal properties of the soil in dependence of the number and intensity of these swell-shrink processes (Horn, 1994). Especially, soils with a clay content of more than 12% show intense swelling and shrinkage processes (Horn, 2002). Structure homogenizing processes, e.g., mechanical disturbance of the soil, lead to normal shrinkage accompanied by crack formation and separation of the soil into smaller parts (Janssen et al., 2006). Wetting and drying of homogenized soils create planes of weakness, along which the soil breaks into aggregates (Utomo and Dexter, 1982). A formerly disturbed soil can partly regain its strength over a period of time. When the original strength is regained, it is called thixotropy (Utomo and Dexter, 1982; Markgraf et al., 2006).

Wiermann and Horn (2000) showed that a loess-derived Luvisol exhibited distinct signs of regeneration after a single compaction event, e.g., in terms of increasing macroporosity and gas permeability at 10 cm depth. North Ethiopian soils degraded by grazing show distinct signs of regeneration after 5 years (Mekuria et al., 2007). Biological activity of soil fauna and flora can further enhance structure formation and remediation due to various mechanisms (Horn and Dexter, 1989). Soil fauna influences structure due to its grubbing and digging actions in the soil, leaving loosened zones (channels) surrounded by compacted areas (channel walls) (Schrader et al., 2007). Bossuyt et al. (2006) and Pulleman et al. (2005) describe the important contribution of earthworms to microaggregate formation and incorporation and protection of organic matter in these aggregates. The saprophagous macrofauna can furthermore enhance microbial respiration and biomass and increase the water retention of the soil due to litter fragmentation and soil mixing, thus increasing organic matter accumulation and relocation (Frouz et al., 2007).

Plant roots can also influence the recovery of soil structure in various ways. They form continuous vertical pores and therefore disrupt and reaggregate homogenous soils into smaller units. This is due not only to the shearing and compressive forces roots exert on the soil, but also to the water uptake of the roots, followed by more intense and frequent wetting and drying cycles close to the roots, creating more negative pore water pressure, which induces crack formation and age hardening of existing soil aggregates as mentioned above. Roots furthermore increase the structural soil stability with fine roots and root hairs growing around soil aggregates; fungal hyphae can be associated to plant roots and further enhance the binding of soil aggregates as well as plant residues (Greenwood and McKenzie, 2001). Former studies revealed a positive correlation between root mass and porosity in pastures and an increased infiltration due to macropores created by living roots (Greenwood and McKenzie, 2001). Even when the roots are dead, the continuity of the old root channels and the cracks induced by shrinkage due to root water uptake persisted and kept the infiltration rate at a high level (Priksat et al., 1994). Czarnes et al. (2005) showed

that the exudates of plant roots and microbes in the rhizosphere together with intense wetting and drying cycles improve soil structure. Recently advanced x-ray microtomographies of soil aggregates allow to show the complexity of intra-aggregate pore systems (Schrader et al., 2007; Peth et al., 2008) and prove that soil micro organisms significantly contribute to the processes of aggregate formation by improving their habitat (Feeney et al., 2006), inducing crack formation in the soil (Preston et al., 2001) and by rearranging clay particles adjacent to them (Chenu, 1993, 2001). Micro organisms can also influence the amount and distribution of water repellency; carbon in turn influences soil wettability (Hallett et al., 2004) and mechanical stability (Horn, 1994; Chenu et al., 2000; Mataix-Solera and Doerr, 2003). Herrick and Lal (1995) pointed out the importance of excretal return to tropical pastures to keep soil organisms active and maintain good physical pasture properties. Recapitulating it can be stated that soil flora and fauna, including micro organisms and, accordingly, carbon content and composition and mechanical as well as hydraulic processes are closely interlinked with each other and with external factors such as climate and management.

Summary and conclusions

Grazing affects the physical conditions of soils. The effects which can be attributed to grazing are limited to the upper 10–15 cm below surface. Most of the changes are unfavorable in terms of productivity and ecosystem services of grassland ecosystems. Grazing induced changes of soil mechanical and hydraulic properties are strongly interrelated with each other and lead to an increased sensitivity to wind and water erosion. The susceptibility of soils to structural deterioration increases with increasing water content. Repeated mechanical loading combined with shearing forces as applied by grazing animals adversely affect soil structure along with diminishing angles of internal friction and a decrease of the total and coarse pore volume. This in turn affects the pore water pressure and the occurrence and orientation of water menisci, which in dry states are concave, thus stabilizing. If due to the compression of coarse pores the hydraulic conductivity of the soil becomes too low to remove excess soil water from the pore system during loading, soil compaction leads to less negative and sometimes even positive pore water pressure during loading, resulting in convex, thus mechanically destabilizing menisci according to the effective stress equation (Nuth and Laloui, 2008). With incomplete drainage of excess soil water, soil strength can be severely decreased. Soil mechanical changes are interconnected with changes in the pore system; accordingly, soil functions such as hydraulic conductivity and air conductivity are influenced by grazing. Water infiltration and saturated hydraulic conductivity, which are highly depending on the pore diameter and pore continuity, are also highly sensitive to deformations induced by mechanical stresses exerted by grazing animals.

Natural soil recovery due to wetting and drying cycles, soil fauna, root growth, and decay occurs but takes several years to decades. It is also not proofed that recovery will ever lead back to the state before being influenced by grazing.

Bibliography

- Akkermann, M., 2004. *Beurteilung des Einflusses einer angepassten Ackernutzung auf den Hochwasserabfluss*. Dissertation Geowissenschaften und Geographie, Universität Hannover.
- Angers, D. A., and Caron, J., 1998. Plant-induced changes in soil structure: processes and feedbacks. *Biogeochemistry*, **42**(1/2), 55–72.
- Arnaez, J., Lasanta, T., Ruiz-Flaño, P., and Ortigosa, L., 2007. Factors affecting runoff and erosion under simulated rainfall in Mediterranean vineyards. *Soil and Tillage Research*, **92**(2), 324–334.
- Arvidsson, J., Sjöberg, E., and Van Den Akker, J. J. H., 2003. Subsoil compaction by heavy sugarbeet harvesters in southern Sweden III. Risk assessment using a soil water model. *Soil and Tillage Research*, **73**(1–2), 77–87.
- Bachmann, J., Horton, R., and Van der Ploeg, R. R., 2001. Isothermal and nonisothermal evaporation from four sandy soils of different water repellency. *Soil Science Society of America Journal*, **65**(6), 1599–1607.
- Ball, B. C., and Robertson, E. A. G., 1994. Effects of uniaxial compaction on aeration and structure of ploughed or direct drilled soils. *Soil and Tillage Research*, **31**, 135–148.
- Bossuyt, H. S. J., and Hendrix, P. F., 2006. Interactive effects of functionally different earthworm species on aggregation and incorporation and decomposition of newly added residue carbon. *Geoderma*, **130**, 14–25.
- Chenu, C., 1993. Clay- or sand-polysaccharides associations as models for the interface between microorganisms and soil: water-related properties and microstructure. *Geoderma*, **56**, 143–156.
- Chenu, C., Le Bissonnais, Y., and Arrouays, D., 2000. Organic matter influence on clay wettability and soil aggregate stability. *Soil Science Society of America Journal*, **64**, 1479–1486.
- Chenu, C., Hassink, J., and Bloem, J., 2001. Short term changes in the spatial distribution of microorganisms in soil aggregates as affected by glucose addition. *Biology and Fertility of Soils*, **34**, 349–356.
- Czarnes, S., Hallett, P. D., Bengough, A. G., and Young, I. M., 2005. Root- and microbial-derived mucilages affect soil structure and water transport. *European Journal of Soil Science*, **51**, 435–443.
- Dörner Fernández, J. M., 2005. *Anisotropie von Bodenstrukturen und Porenfunktionen in Böden und deren Auswirkungen auf Transportprozesse im gesättigten und ungesättigten Zustand*. Universität Kiel: Schriftenreihe Institut für Pflanzenernährung und Bodenkunde. 68.
- Drewry, J. J., 2006. Natural recovery of soil physical properties from treading damage of pastoral soils in New Zealand and Australia: a review. *Agriculture, Ecosystems and Environment*, **114**(2–4), 159–169.
- Feeley, D. S., Crawford, J. W., Daniell, T., Hallett, P. D., Nunan, N., Ritz, K., Rivers, M., and Young, I. M., 2006. Three-dimensional microorganization of the soil-root-microbe system. *Microbial Ecology*, **52**, 151–158.
- Frouz, J., Elhottová, D., Kuráž, V., and Šourková, M., 2007. Effects of soil macrofauna on other soil biota and soil formation in reclaimed and unreclaimed post mining sites: results of a field microcosm experiment. *Applied Soil Ecology*, **33**(3), 308–320.
- Greenwood, K. L., and McKenzie, B. M., 2001. Grazing effects on soil physical properties and the consequences for pastures: a review. *Australian Journal of Experimental Agriculture*, **41**(12), 1231–1250.
- Hallett, P. D., Nunan, N., Douglas, J. T., and Young, I. M., 2004. Millimeter-scale spatial variability in soil water sorptivity: scale, surface elevation and subcritical repellency effects. *Soil Science Society of America Journal*, **68**, 352–358.
- Herrick, J. E., and Lal, R., 1995. Soil physical property changes during dung composition in a tropical pasture. *Soil Science Society of America Journal*, **59**, 908–912.
- Hesse, P. P., and Simpson, R. L., 2006. Variable vegetation cover and episodic sand movement on longitudinal desert sand dunes. *Geomorphology*, **81**(3–4), 29, 276–291.
- Horn, R., 1994. The effect of aggregation of soils on water, gas, and heat transport. In Schulze, E.-D. (ed.), *Flux Control in Biological Systems: From Enzymes to Populations and Ecosystems*. London: Academic, pp. 335–361.
- Horn, R., 2002. Soil mechanical properties and processes in structured unsaturated soils under various landuse and management systems. *Advances in GeoEcology*, **35**, 305–318.
- Horn, R., and Dexter, A., 1989. Dynamics of soil aggregation in an irrigated desert loess. *Soil and Tillage Research*, **13**, 253–266.
- Horn, R., and Rostek, J., 2000. *Subsoil compaction processes – state of knowledge*. *Advances in GeoEcology*. Reiskirchen: Catena, Vol. 32.
- Janssen, I., Peng, X., and Horn, R., 2006. Physical Properties of Paddy fields as a Function of Cultivation History and Texture. *Advances in GeoEcology*, **38**, 93–101.
- Kennedy, A. C., and Schillinger, W. F., 2006. Soil quality and water intake in traditional-till vs. no-till paired farms in Washington's Palouse region. *Soil Science Society of America Journal*, **70**(3), 940–949.
- Krümmelbein, J., 2007. Influence of various grazing intensities on soil stability and water balance of a steppe soil in inner Mongolia, P.R. China. Schriftenreihe Inst. für Pflanzenernährung und Bodenkunde, Universität Kiel, 74.
- Krümmelbein, J., Wang, Z., Zhao, Y., Peth, S., and Horn, R., 2006. Influence of various grazing intensities on soil stability, soil structure and water balance of grassland soils in Inner Mongolia, P.R. China. *Advances in GeoEcology*, **38**, 93–101 (ISBN 3-923381-52-2).
- Kutílek, M., Jendele, L., and Panayiotopoulos, K. P., 2006. The influence of uniaxial compression upon pore size distribution in bi-modal soils. *Soil and Tillage Research*, **86**(1), 27–37.
- Lamarter, A., Deurer, M., Bachmann, J., and Duijnvisveld, W. H. M., 2006. Effect of subcritical hydrophobicity in a sandy soil on water infiltration and mobile water content. *Journal of Plant Nutrition and Soil Science*, **169**(1), 38–46.
- Li, F.-R., Zhao, L.-Y., Zhang, H., Zhang, T.-H., and Shirato, Y., 2003. Wind erosion and airborne dust deposition in farmland during spring in the Horqin Sandy Land of eastern Inner Mongolia. *Soil and Tillage Research*, **75**, 121–130.
- Markgraf, W., Horn, R., and Peth, S., 2006. An approach to rheometry in soil mechanics-Structural changes in bentonite, clayey and silty soils. *Soil and Tillage Research*, **91**(1–2), 1–14.
- Martinez, L. J., and Zinck, J. A., 2004. Temporal variation of soil compaction and deterioration of soil quality in pasture areas of Colombian Amazonia. *Soil and Tillage Research*, **75**, 3–17.
- Mataix-Solera, J., and Doerr, S. H., 2003. Hydrophobicity and aggregate stability in calcareous topsoils from fire-affected pine forests in south eastern Spain. *Geoderma*, **118**, 77–88.
- Mekuria, W., Veldkamp, E., Haile, M., Nyssen, J., Muys, B., and Gebrehiwot, K., 2007. Effectiveness of exclosures to restore degraded soils as a result of overgrazing in Tigray, Ethiopia. *Journal of Arid Environments*, **69**(2), 270–284.
- Nuth, M., and Laloui, L., 2008. Effective stress concept in unsaturated soils: clarification and validation of a unified framework.

- International Journal for Numerical and Analytical Methods in Geomechanics*, **32**, 771–801.
- Peth, S., 2004. Bodenphysikalische Untersuchungen zur Trittbelaustung von Böden bei der Rentierweidewirtschaft an borealen Wald- und subarktisch-alpinen Tundrenstandorten – Auswirkungen auf thermische, hydraulische und mechanische Bodeneigenschaften. Schriftenreihe Inst. für Pflanzenernährung und Bodenkunde, Universität Kiel, 64.
- Peth, S., and Horn, R., 2006. Consequences of grazing on soil physical and mechanical properties in forest and tundra environments. *Ecological studies*, **184**, 217–243.
- Peth, S., Horn, R., Beckmann, F., Donath, T., Fischer, J., and Smucker, A. J. M., 2008. 3D Quantification of intra-aggregate pore space features using synchrotron-radiation-based microtomography. *Soil Science Society of America Journal*, **72**, 897–907.
- Pietola, L., Horn, R., and Yli-Halla, M., 2005. Effects of trampling by cattle on the hydraulic and mechanical properties of soil. *Soil and Tillage Research*, **82**, 99–108.
- Preston, S., Wirth, S., Ritz, K., Griffiths, B. S., and Young, L. M., 2001. The role played by microorganisms in the biogenesis of soil cracks: importance of substrate quantity and quality. *Soil Biology and Biochemistry*, **33**, 1851–1858.
- Priksat, M. A., Kaspar, T. C., and Ankeny, M. D., 1994. Positional and temporal changes in ponded infiltration in a corn field. *Soil Science Society of America Journal*, **58**, 181–184.
- Pulleman, M. M., Six, J., van Breemen, N., and Jongmans, A. G., 2005. Soil organic matter distribution and microaggregate characteristics as affected by agricultural management and earthworm activity. *European Journal of Soil Science*, **56**, 453–467.
- Scholefield, D., Patto, P. M., and Hall, D. M., 1985. Laboratory research on the compressibility of four topsoils from grassland. *Soil and Tillage Research*, **6**, 1–16.
- Schrader, S., Rogasik, H., Onasch, I., and Jégou, D., 2007. Assessment of soil structural differentiation around earthworm burrows by means of X-ray computed tomography and scanning electron microscopy. *Geoderma*, **137**(3–4), 378–387.
- Silva, R. B., Dias Junior, M. S., Santos, F. L., and Franz, C. A. B., 2004. Resistência ao cisalhamento de um latossolo sob diferentes uso e manejo (Shear strength of a Eutroorthox under different use and management). *Brazilian Journal of Soil Science*, **28**, 165–173.
- Sridharan, A., and Gurtug, Y., 2007. Compressibility characteristics of soils. *Geotechnical and Geological Engineering*, **23**(5), 615–634.
- Tian, Y. Q., McDowell, R., Yu, Q., Sheath, G. W., Carlson, W. T., and Gong, P., 2007. Modelling to analyse the impacts of animal treading effects on soil infiltration. *Hydrological Processes*, **1**(8), 1106–1114.
- Utomo, W. H., and Dexter, A., 1982. Changes in soil aggregate water stability induced by wetting and drying cycles in non-saturated soil. *Journal of Soil Science*, **33**, 623–637.
- Villamil, M. B., Amiotti, N. M., and Peinemann, N., 2001. Soil degradation related to overgrazing in the semi-arid Southern Caldenal area of Argentina. *Soil Science*, **166**(7), 441–452.
- Vogeler, I., Cichota, R., Sivakumaran, S., Deurer, M., and McIvor, I., 2006. Soil assessment of apple orchards under conventional and organic management. *Australian Journal of Soil Research*, **44**, 745–752.
- Wei, W., Chen, L., Fu, B., Huang, Z., Wu, D., and Gui, L., 2007. The effect of land uses and rainfall regimes on runoff and soil erosion in the semi-arid loess hilly area, China. *Journal of Hydrology*, **335**(3–4), 247–258.
- Whalley, W. R., Dumitru, E., and Dexter, A. R., 1995. Biological effects of soil compaction. *Soil and Tillage Research*, **35**, 23–36.
- Wiermann, C., and Horn, R., 2000. Effect of different tillage systems on the recovery of soil structure following a single compaction event. In Horn, R., van den Akker, J. J. H., and Arvidsson, J. (eds.), *Subsoil Compaction: Distribution, Processes and Consequences. Advances in Geoeology* 32. Reiskirchen: Catena Verlag, pp. 339–350.
- Zhang, H. Q., and Horn, R., 1996. Einfluss der Beweidung auf die physikalischen Eigenschaften einer Salzmarsch im Deichvorland (I): die gesättigte Wasserleitfähigkeit und das Bodengefüge. *Zeitschrift für Kulturtechnik und Landentwicklung*, **37**, 24–31.
- Zhao, Y., Peth, S., Krümmelbein, J., Horn, R., Wang, Z., Steffens, M., Hoffmann, C., and Peng, X. H., 2007. Spatial variability of soil properties affected by grazing intensity in Inner Mongolia grassland. *Ecological Modelling*, **205**, 241–254.

Cross-references

- [Anisotropy of Soil Physical Properties](#)
- [Bulk Density of Soils and Impact on Their Hydraulic Properties](#)
- [Compaction of Soil](#)
- [Desertification: Indicators and Thresholds](#)
- [Field Water Capacity](#)
- [Hydraulic Properties of Unsaturated Soils](#)
- [Hydrophobicity of Soil](#)
- [Infiltration in Soils](#)
- [Mechanical Resilience of Degraded Soils](#)
- [Physical Degradation of Soils, Risks and Threats](#)
- [Plant Roots and Soil Structure](#)
- [Pre-Compression Stress](#)
- [Pre-Compression Test](#)
- [Shrinkage and Swelling Phenomena in Soils](#)
- [Soil Compactability and Compressibility](#)
- [Soil Functions](#)
- [Spatial Variability of Soil Physical Properties](#)
- [Stress–Strain Relations](#)
- [Subsoil Compaction](#)
- [Wind Erosion](#)

GREENHOUSE, CLIMATE CONTROL

Istvan Farkas

Department of Physics and Process Control, Szent Istvan University, Gödöllő, Hungary

Synonyms

Optimization of greenhouse parameters

Definition

Climate control refers to keep the desired value of the greenhouse inside parameters as temperature, light, humidity, and CO₂ concentration in order to provide optimal conditions for the plants.

With respect to the energy cost, the temperature in greenhouse should keep around a desired level. Lower accuracy requires higher set point in temperature, which results in more energy consumption (Tantau, 1997). The temperature can be increased by heating of the air and, at the same time, the use of thermal screens may decrease the energy consumption during nighttime periods.

The light control is mainly based on the requirement of the plant growing age.

The control of humidity provides to avoid the extremely high or low air humidity values. Concerning to energy saving avoiding the high humidity is more important. The control of humidity can be achieved by heating and/or by ventilation.

CO_2 concentration can be controlled by opening the top window in the greenhouse.

In order to assess appropriate control strategies, the productivity and quality of the plant should be provided duration of growing. The set-points are based on the practical experiments, but it is aimed to modify them according to the plant responses, which can be reached via leaf conductivity, CO_2 consumption, or nutrient uptake. The set-point for control variables has a strong influence on the energy consumption of greenhouses. The climate control computer has got a feeding control extension, which provides nutrients in solution to plants (van Henten, 1994).

Bibliography

- Tantau, H.-J., 1997. Energy saving potential of greenhouse climate control, M²SABI'97 IMACS/IFAC Symposium, Hungary: Budapest, pp. 245–251.
van Henten, E. J., 1994. Greenhouse climate management: an optimal control approach, Thesis, Wageningen, The Netherlands.

Cross-references

- Agrophysical Objects (Soils, Plants, Agricultural Products, and Foods)
Coupled Heat and Water Transfer in Soil
Drought Stress, Effect on Soil Mechanical Impedance and Root (Crop) Growth
Evapotranspiration
Greenhouse Gas Fluxes: Effects of Physical Conditions
Plant Drought Stress: Detection by Image Analysis
Plant Wellness

GREENHOUSE EFFECT

Inhibition of the atmospheric transmission of outgoing thermal radiation from the earth, due to the presence of certain gases in the atmosphere. The principal “greenhouse gas” is water vapor. Another important one is carbon dioxide, the concentration of which has been increasing due to forest clearing, cultivation of formerly virgin soils, and – especially – the burning of fossil fuels (coal, petroleum, natural gas).

Bibliography

- Introduction to Environmental Soil Physics. (First Edition). 2003. Elsevier Inc. Daniel Hillel (ed.) <http://www.sciencedirect.com/science/book/9780123486554>

Cross-references

- Greenhouse Gas Fluxes: Effects of Physical Conditions
Greenhouse Gases Sink in Soils
Greenhouse, Climate Control

GREENHOUSE GAS FLUXES: EFFECTS OF PHYSICAL CONDITIONS

Ryusuke Hatano

Laboratory of Soil Science, Graduate School of Agriculture, Hokkaido University Kita-Ku, Sapporo, Hokkaido, Japan

Definition

Physical conditions: Soil moisture, soil temperature, air pressure, rainfall, snowfall, flooding, drainage, aeration, freezing, and thawing affecting plant roots, soil fauna, and soil microbial activities, producing and consuming greenhouse gases in soil.

Greenhouse gases: Including carbon dioxide (CO_2), methane (CH_4), and nitrous oxide (N_2O) produced and consumed in soil and absorbing and emitting radiation within the thermal infrared range in the atmosphere.

Carbon dioxide (CO_2): Colorless and odorless gas (mol weight 44.010 g mol⁻¹; density 1.977 g L⁻¹ at 1 atm and 0°C; solubility in water 0.47 g CO_2 –C L⁻¹ at 1 atm and 20°C), consumed by plants during photosynthesis to make organic matter, and produced by respiration of animals, plants, and microorganisms to obtain energy through decomposition of organic matter.

Methane (CH_4): Colorless, odorless gas (mol weight 16.042 g mol⁻¹; density 0.717 g L⁻¹ at 1 atm and 0°C; solubility in water 0.018 g CH_4 –C L⁻¹ at 1 atm and 20°C), oxidized by photochemical reaction in the atmosphere and consumed by methanotrophic bacteria in dry soil, and produced by methanogenic bacteria in wet soil.

Nitrous oxide (N_2O): Colorless and odorless gas (mol weight 44.013 g mol⁻¹; density 1.977 g L⁻¹ at 1 atm and 0°C; solubility in water 0.79 g N_2O –NL⁻¹ at 1 atm and 20°C), consumed by denitrifying bacteria and produced by nitrifying and denitrifying bacteria.

Gas flux: Amount of gas flowing through a unit area per unit time.

Introduction

An increase in the concentrations of greenhouse gases (GHG; carbon dioxide [CO_2], methane [CH_4] and nitrous oxide [N_2O]) in the troposphere causes global warming (Prather et al., 2001). The global atmospheric concentrations of CO_2 , CH_4 , and N_2O have increased from a pre-industrial value of about 280 ppm, 715 ppb, and 270 ppb, respectively, to 379 ppm, 1,774 ppb, and 319 ppb in 2005 (Forster et al., 2007). Increase of GHG emissions increases radiative forcing warming the earth. Contribution of CO_2 , CH_4 , and N_2O to total radiative forcing in 2005 is 63%, 18%, and 6%, respectively, and chlorofluorocarbons (CFCs) and others account for the rest of 13% (Forster et al., 2007). Global warming potential (GWP), which is the index in order to compare the relative radiative forcing of different GHGs and GWP in 100-year

time horizon is 1 for CO₂, 25 for CH₄, and 298 for N₂O (Forster et al., 2007). N₂O is a long-lived gas and contributes to stratospheric ozone destruction (Cicerone, 1987).

Soil is the major source of GHG emissions into the atmosphere. Land use change contributes 20% of total CO₂ emission into the atmosphere (7.9 Gt C year⁻¹ in the 1990s); rice paddy, and wetland soils contribute 34% of total CH₄ emission (515 Mt CH₄ year⁻¹); and agricultural soils contribute 24% of total N₂O emission (16.2 Mt N year⁻¹) (Prather et al., 2001).

CO₂, CH₄, and N₂O are produced and consumed in soil by mainly microbial activities, which changes the concentrations of these gases in soil. Soil microbial activities are influenced by soil environment factors, which are soil temperature; soil moisture; available carbon; nutrients; acidity; redox potential, which are affected by the factors of climate, topography, soil texture, soil structure, vegetation, and land use. Change in soil gas concentration varies concentration gradients between the soil and the atmosphere, regulating gas diffusion fluxes through the soil. Slower flux provides the opportunity for further microbial reaction in the soil. Also, the gas flux is influenced by the pressure gradient. Some of the gases dissolved in soil water leach into groundwater and secondarily emitted after drainage water is discharged to the ground surface. The rates of production and consumption of GHGs, diffusion, mass flow, and dissolved gas leaching in soil are the main factors controlling GHG exchange between the soil and the atmosphere. This paper provides the information about the effect of soil physical conditions on the controlling factors for soil CO₂, CH₄, and N₂O fluxes.

CO₂

CO₂ is produced in soil through heterotrophic respiration (organic matter decomposition by heterotrophic organisms) and plant root respiration. The emission of CO₂ is called soil respiration (Raich and Schlesinger, 1992). Increase of heterotrophic respiration in soil decreases soil

organic carbon. Supplying oxygen molecule from the atmosphere into soil through aeration proceeds soil heterotrophic respiration. Tillage stimulates the heterotrophic respiration and reduces soil organic carbon (Jarecki and Lal, 2003). Increase of soil temperature increases soil microbial activity. There is a relationship between soil temperature (*T*) and CO₂ emission (*F_c*) from soil as follows:

$$F_c = a \exp(b T) \quad (1)$$

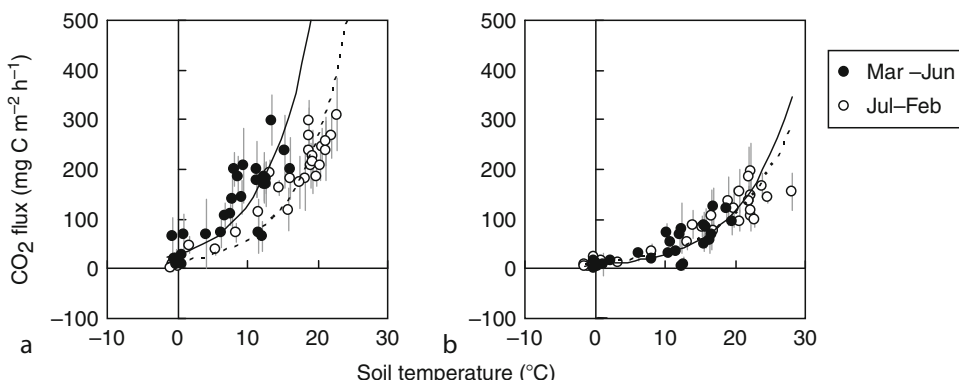
where *a* and *b* are fitted constants.

Figure 1 shows an example of the relationship between soil temperature at a depth of 5 cm and CO₂ fluxes measured by chamber method at the root-included plot and root-excluded plot in a Japanese grassland (Shimizu et al., 2009). The CO₂ fluxes were higher in spring (beginning of March to end of June) than in other seasons (beginning of July to end of February) at the same temperature due to the decomposition of litter supplied into soil during the winter, resulting in being divided into two groups at each plot. The relationship between the CO₂ flux and the soil temperature in each plot was well explained by Equation 1 for each season. There was a significant difference in the regression between the seasons (*P* < .001) in root-included plot, while there was no significant difference between the season in the regressions for the root-excluded plot (Table 1).

The *Q*₁₀ value is the rate of increase in CO₂ emission with 10°C of increase in soil temperature along with the exponential relationship between them. It was calculated by applying the fitted constant (*b*) obtained from Equation 1 to Equation 2.

$$Q_{10} = \exp(10 b) \quad (2)$$

The *Q*₁₀ value of CO₂ fluxes of the Japanese grassland was higher in root-included plot (4.50) than in root-excluded plot (3.61) (Table 1). The *Q*₁₀ values of CO₂ fluxes derived from plant root respiration and soil organic



Greenhouse Gas Fluxes: Effects of Physical Conditions, Figure 1 Relationship between CO₂ flux and soil temperature in root-included plot (a) and root-excluded plot (b) (From Shimizu et al., 2009). Data represent mean \pm SD (*n*=6). The lines indicate the exponential regression models for each season (solid line, from the beginning of March to the end of June; dashed line, from the beginning of July to the end of February), and the models are described in Table 1.

Greenhouse Gas Fluxes: Effects of Physical Conditions,
Table 1 The exponential regression models using soil
 temperature at 5 cm depth to predict the CO₂ flux and Q₁₀
 (From Shimizu et al., 2009)

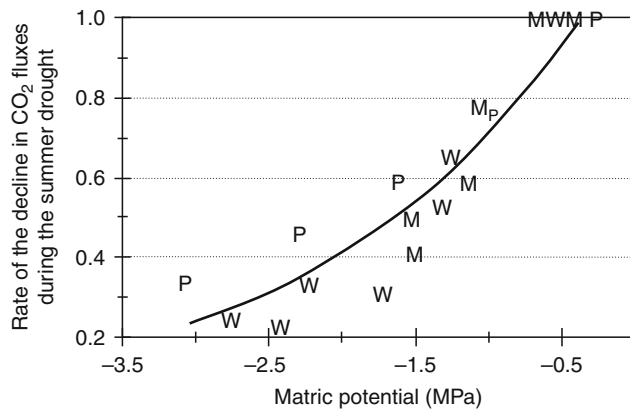
Treatment	Equation	R ²	P value	Q ₁₀
Root-included fertilizer plot				
March–June	F=27.6 exp (0.151 T)	0.65	<.001	4.53
July–February	F=12.8 exp (0.150 T)	0.85	<.001	4.50
Root-excluded control plot				
March–June	F=7.6 exp (0.136 T)	0.61	<.001	3.90
July–February	F=10.0 exp (0.120 T)	0.90	<.001	3.31

The model is $F=a \exp (bT)$, where F is the CO₂ flux (mg C m⁻² h⁻¹) and T is the soil temperature at 5 cm depth (°C)

matter decomposition in mixed-hardwood forest soil of temperate zone were 4.6 and 2.5, respectively (Boone et al., 1998). Also, the Q_{10} value of CO₂ fluxes at an intact site of Siberian larch forest was 4.35, while it decreased to 1.69 and 2.09 at the burnt and cutover sites, respectively (Takakai et al., 2008a). These findings suggest that Q_{10} value of CO₂ flux is higher in root respiration than in soil organic matter decomposition.

There is an optimal water filled pore space (WFPS) for soil CO₂ production, which is around 60% (Linn and Doran, 1984). However, in actual field there is an interaction between soil moisture and soil temperature, and there is a tendency that temperature increases with decreases of soil moisture. Therefore, sometimes CO₂ fluxes correlated with not only soil temperature positively but also soil moisture negatively. Soil temperature is a better predictor for CO₂ fluxes, and a Q_{10} function can predict reasonably annual CO₂ fluxes. However, rapid decline in CO₂ fluxes caused by significant drought was found in the Harvard Forest in central Massachusetts. Figure 2 shows that the rate of the decline in CO₂ fluxes correlated exponentially with decreasing soil matric potential (the rate of the decline in CO₂ fluxes = $1.21 \times e^{(0.553 \times \text{matric potential})}$, $R^2=0.83$, $P<.01$). Combining this function of the decline in CO₂ fluxes to the soil matric potential and Q_{10} function can provide better prediction of CO₂ fluxes (Davidson et al., 1998). However, CO₂ fluxes in crop fields in tropical dryland correlated better with soil moisture content than with soil temperature (Singh et al., 2009).

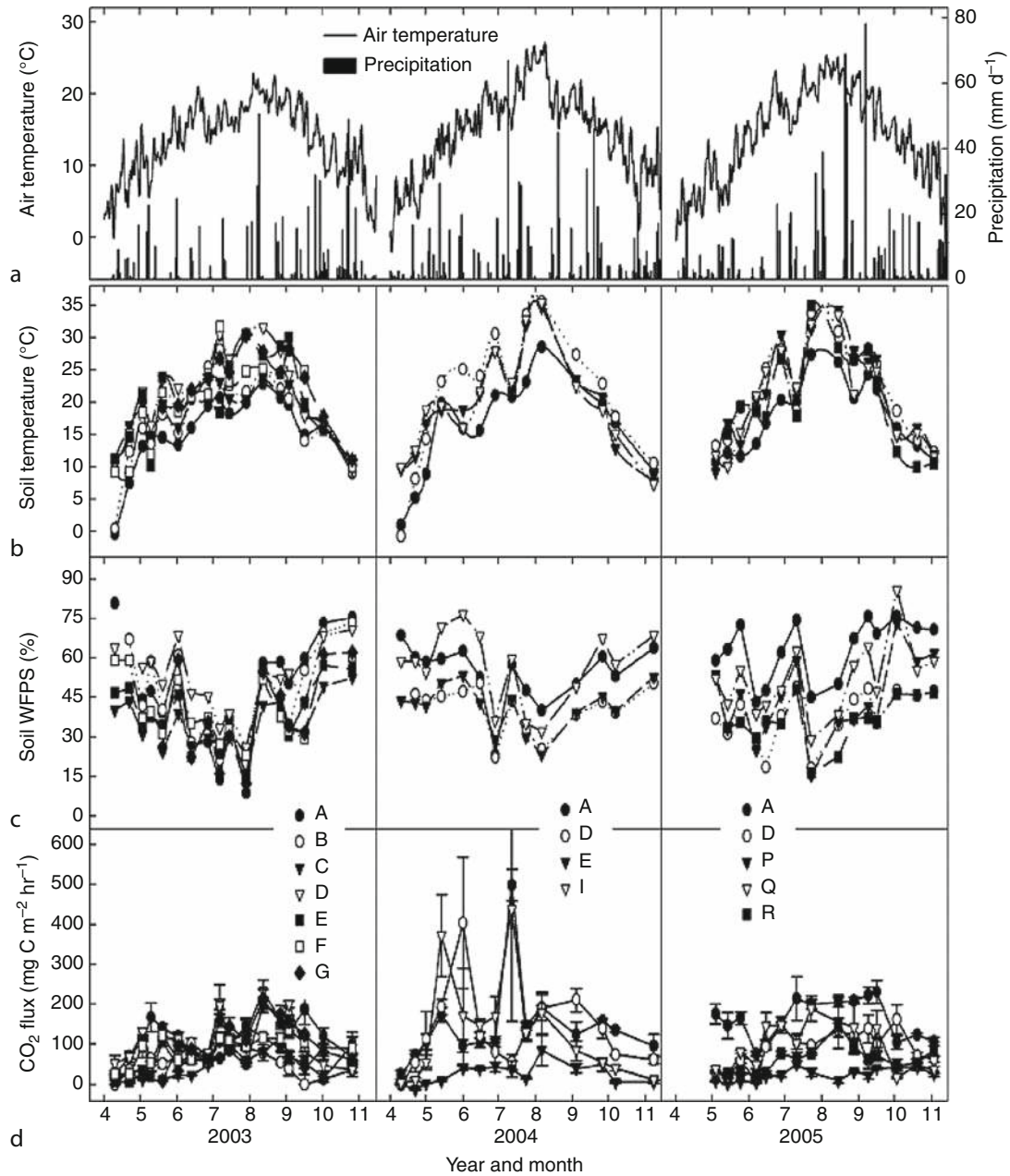
Figure 3 shows the CO₂ fluxes derived from soil organic matter decomposition measured at the root-excluded plots established in the 11 upland crop fields with different types of soil (Brown Forest soils, Brown Lowland soils, Gray Lowland soils, Psedogleys) with various texture (18.4–51.6% of sand content) in Mikasa city, central Hokkaido, Japan, over the no snow cover months (mid-April to early November) from 2003 to 2005 (Mu et al., 2008). The seasonal pattern of soil CO₂ fluxes mainly followed the seasonal changes in soil temperature but was occasionally interrupted by soil moisture



Greenhouse Gas Fluxes: Effects of Physical Conditions,
Figure 2 Effect of soil matric potential on the rate of decline in CO₂ fluxes (normalized soil respiration) during the summer drought (Davidson et al., 1998). The plotting symbols refer to the site drainage classes (V, very poorly drained, P, poorly drained, M, moderately well drained, W, well drained).

fluctuation. Soil CO₂ fluxes increased with increasing soil temperature prior to June. Large fluctuation in soil CO₂ fluxes was observed from June to August, which was coincided with drying/rewetting events occurring during this period. After August, soil CO₂ fluxes declined with decreasing soil temperature. The instantaneous CO₂ fluxes ranged from 0.1 to 234 mg C m⁻² h⁻¹ for 2003 and from 2.6 to 231 mg C m⁻² h⁻¹ for 2005. Several significantly high emission episodes (300–500 mg C m⁻² h⁻¹) were recorded at the sites investigated following heavy rainfall within the previous week (amounting to 33–82 mm) in 2004.

Multiple regression analysis for correlation of logarithmic value of the CO₂ flux to soil temperature and WFPS showed that soil temperature alone or together with WFPS, clay content, and CN ratio could explain 27–76% of the temporal variation in the instantaneous soil CO₂ fluxes at the sites. Furthermore, there was a significant quadratic relationship between mean CO₂ flux or cumulative CO₂ emission and clay plus silt content (Figure 4). In contrast, mean CO₂ flux and cumulative CO₂ emission had no significant relationship with the mean values of soil temperature and moisture ($P > .2$). This suggests that soil texture is important for explaining spatial variability in soil CO₂ flux between sites within the same climate region. According to the quadratic function in Figure 4, soil mean or cumulative CO₂ flux will increase with increasing clay plus silt content at a clay plus silt content to 63%, but a further increase in clay plus silt content will lead to a decrease in soil CO₂ flux. Soil clay and silt facilitate soil aggregation and increase the stability of soil aggregates, which can reduce fluctuation in temperature and water content and can protect microorganisms from predation by soil fauna (Hassink et al., 1993). As a result, soil microbial biomass and microbial activity appeared to increase with increasing clay and silt content.

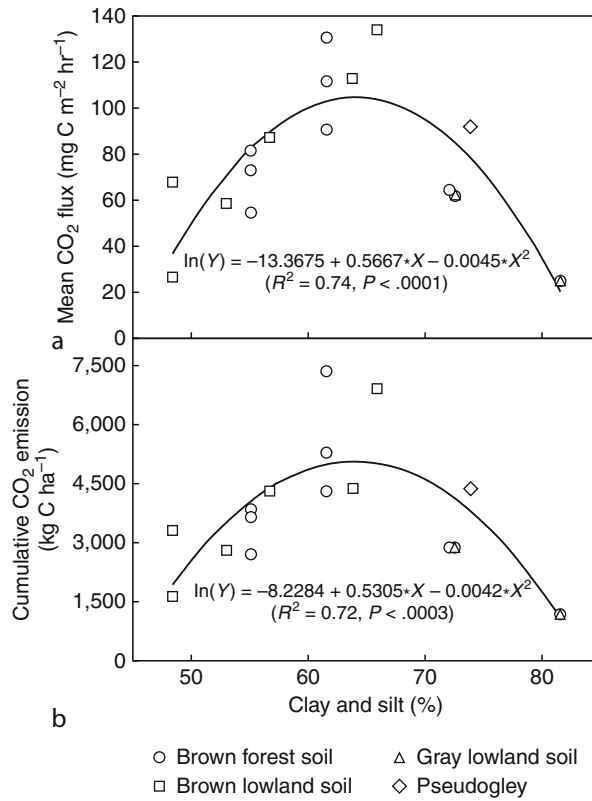


Greenhouse Gas Fluxes: Effects of Physical Conditions, Figure 3 Seasonal patterns in (a) local weather conditions, (b) soil temperature, (c) moisture, and (d) soil CO₂ fluxes derived from soil organic matter decomposition in the 11 upland crop fields with different types of soil in Mikasa city, central Hokkaido, Japan. WFPS, water-filled pore space. Error bars indicate the standard error ($n=3$). A is grassland soil, others are cropland bare soils (Mu et al., 2008).

This might be a reason for the increase in soil CO₂ flux at the lower contents of clay and silt. In contrast, it is well known that soil clay and silt can absorb organic matter and stop it from being decomposed by microorganisms (Hassink et al., 1993). When the content of clay and silt exceeds a certain level (in this case 63%), the organic matter available for the decomposition might become limited and leads to a decrease in soil CO₂ flux. As a consequence

of the negative relationship between soil CO₂ flux and higher fine particle content in soils, soil carbon content might be expected to increase with increasing fine particle content.

Indirect CO₂ emission through the subsurface drainage in an onion field of Gray Lowland soil in central Hokkaido, Japan, increased with increase of discharge rate during snowmelt season and rainfall events, and annual



Greenhouse Gas Fluxes: Effects of Physical Conditions,
Figure 4 Correlation of clay and silt content with (a) annual mean CO_2 flux and (b) cumulative CO_2 emission (Mu et al., 2008).

indirect CO_2 emission was $13.2 \text{ g C m}^{-2} \text{ year}^{-1}$, which corresponds to 2.5% of the direct CO_2 emission from soil to the atmosphere (Sawamoto et al., 2003). Indirect CO_2 emissions observed at different land uses of a well-permeable loamy soil varied with the land use. It was higher in a paddy rice field (33.4 and $36.7 \text{ g C m}^{-2} \text{ year}^{-1}$) than in upland fields (7.62 and $8.01 \text{ g C m}^{-2} \text{ year}^{-1}$ in a soybean field and 11.7 and $10.5 \text{ g C m}^{-2} \text{ year}^{-1}$ in a upland rice field) (Minamikawa et al., 2009). Flooding was the most influential factor determining the indirect emission in the paddy rice plots, because flooding substantially increased the drainage volume and thus increased the indirect emission.

CH_4

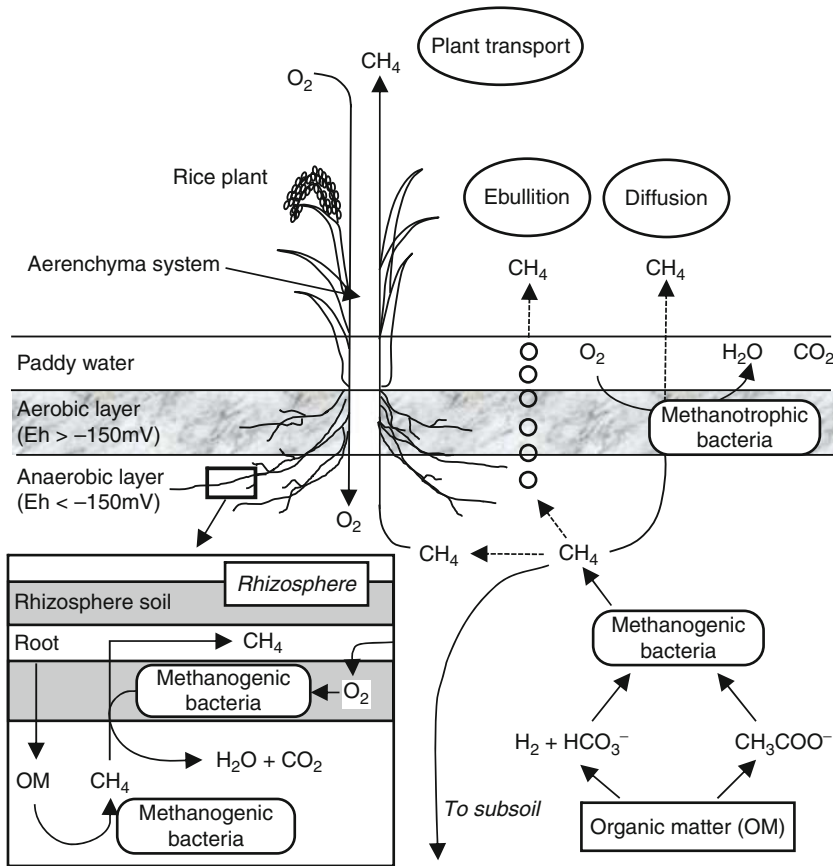
CH_4 is produced by methanogenic bacteria and consumed by methanotrophic bacteria (Mer and Roger, 2001). When the soil redox potential (Eh) is below -200 mV after flooding, methanogenic bacteria produce CH_4 using acetate and $\text{CO}_2 + \text{H}_2$, which are produced by fermenting and syntrophic bacteria under anaerobic condition (Yamane and Sato, 1964; Conrad, 1999). In general, contribution of acetate and $\text{CO}_2 + \text{H}_2$ to CH_4 production is 67% and 33%, respectively. However, excess CO_2 production occurs when some of the soil organic acids act

as electron acceptor (Yao and Conrad, 2000). Most methanogenic bacteria have their optimum pH at 7 (Goodwin and Zeikus, 1987). CH_4 production in soil is influenced by soil temperature. CH_4 production in various wetlands increases with increasing temperature from 2°C to 39°C (Bergman et al., 1998). CH_4 production is also influenced by the substrate. Significantly low CH_4 production was found in ombrotrophic bogs composed of acid and fibric peat in temperate region (Moore and Knowles, 1990).

Methanotrophic bacteria oxidized CH_4 in aerobic spot in soil (Hanson and Hanson, 1996). Measurements in flooded rice fields indicated that 80% of the methane produced was oxidized at the soil surface (Conrad and Rothfus, 1991). CH_4 uptake by aerobic soil decreases with an increase of water-filled pore space (WFPS) (Nesbit and Breitenbeck, 1992; Sitaula et al., 1995). Also, CH_4 uptake rate is decreased by the addition of NH_4^+ (Steudler et al., 1989) due to both a competitive inhibition of the CH_4 mono-oxygenase (MMO) enzyme as well as a noncompetitive (toxic) inhibition by hydroxylamine (NH_2OH) or nitrite (NO_2^-) produced by NH_4^+ oxidation (King and Schnell, 1994). Less temperature dependence of CH_4 consumption was found compared to that of CH_4 production in peat soil (Dunfield et al., 1993).

CH_4 fluxes between the soil and the atmosphere are determined by the balance of CH_4 production and CH_4 consumption in soil (Conrad, 1995) and strongly influenced by water table position (Moore and Knowles, 1990). Measurements in three ecosystems of forest, oil palm and sago plum in tropical peatland, Sarawak, Malaysia, showed that CH_4 was emitted at forest and sago plum with high groundwater table and it was taken up at oil palm with low groundwater table (Melling et al., 2005). CH_4 emission from the grassland of permafrost in Yakutsk was observed when the grassland was flooded with snow melting and permafrost thawing (Takakai et al., 2008b).

Figure 5 shows the processes involving CH_4 emission from rice paddy field. CH_4 is emitted mostly through rice aerenchyma and, at a lower level, through diffusion and ebullition after CH_4 was produced by methanogenic bacteria in anaerobic soil through organic matter decomposition, and CH_4 was consumed by methanotrophs in oxidized zones (rhizosphere, lower part of culms, soil–water interface, and submersion water) (Schütz et al., 1989). Once soil is flooded and water logged, anoxic and anaerobic conditions quickly develop in rice paddy soils due to decreasing aeration, resulting in the sequential utilization of a series of electron acceptors such as oxygen, NO_3^- , Mn(IV), Fe(III), and SO_4^{2-} . CH_4 production starts under highly reductive conditions after alternative electron acceptors have been depleted (Takai, 1970). CH_4 produced in rice paddy soils is emitted to the atmosphere by three pathways: molecular diffusion, ebullition as gas bubbles, and rice aerenchyma transport. Contributions from individual pathways vary over time and space, and rice aerenchyma is the major pathway accounting for more than 90% of the total CH_4 emitted from soils over the



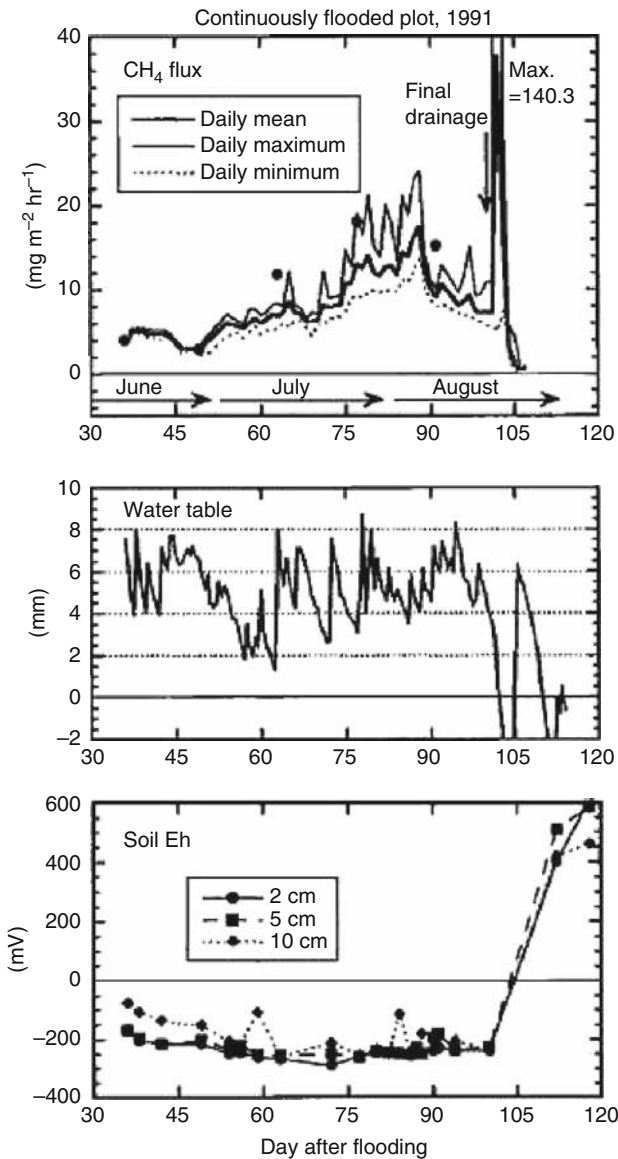
Greenhouse Gas Fluxes: Effects of Physical Conditions, Figure 5 Scheme of production, reoxidation, and emission of CH_4 in a paddy field. (Modified from Schütz et al., 1989 by Yagi, 1994.)

growing season due to inhibition of upward gas diffusion by flooding. A fraction of CH_4 produced in soils is oxidized in the rhizosphere, either aerobically by oxygen released from plant roots or anaerobically by other electron acceptors such as $\text{Fe}(\text{III})$ and SO_4^{2-} .

Figure 6 shows an example of CH_4 flux from the continuous flooded rice paddy field in Japan (Yagi et al., 1996). The CH_4 flux gradually increased until the beginning of August and decreased thereafter until the final drainage, with minimum flux occurring in the early morning and the maximum flux in the early afternoon. The mean CH_4 flux ranged from 2 to 16 $\text{mg CH}_4 \text{ m}^{-2} \text{ h}^{-1}$ during the period of flooding, but the CH_4 flush of 140 $\text{mg CH}_4 \text{ m}^{-2} \text{ h}^{-1}$ in maximum was observed at 8 h after water table dropped below the soil surface associated with final drainage for harvest. The CH_4 emission decreased below 1 $\text{mg CH}_4 \text{ m}^{-2} \text{ h}^{-1}$ at 3 days after the final drainage. Soil Eh at 2 and 5 cm depths were between -288 and -165 mV during the flooding period, indicating that the redox potential in the surface layer of the paddy soil was low enough for active methanogenesis. However, after final drainage, the soil Eh increased significantly. The large CH_4 flush after final drainage was possibly caused by a direct diffusion of CH_4 entrapped in soil through

macropores and cracks in soil after the removal of the water seal by final drainage, followed by a rapid decrease in the CH_4 emission. Total CH_4 emission during the cultivation period was 14.8 $\text{g CH}_4 \text{ m}^{-2}$, and the CH_4 flush after final drainage accounted for 7% of the total CH_4 emission.

CH_4 emissions from paddy fields are also influenced by agricultural management practices, mainly drainage practices and residue incorporation into soil. Total CH_4 emission during a rice cultivation period was reduced from 42% to 45% by two 3-day and 6-day short-term draining practices in the midseason of rice cultivation compared to the CH_4 emissions in a continuous flooded field (Yagi et al., 1996). In a Texas rice paddy field, a 6-day draining practice and three 2- to 3-day draining practices reduced total CH_4 emission by 48% and 88%, respectively (Sass et al., 1992). There was a significant correlation between rice straw carbon application rate (0–219 g C m^{-2}) and total CH_4 emission during cultivation period (4.04–40.8 g C m^{-2} per cultivation period) in continuously flooded paddy fields in central Hokkaido, Japan (Naser et al., 2007). Similar trends have also been observed in rice paddy fields in Italy (Schütz et al., 1989), Texas, USA (Sass et al., 1990), Japan (Yagi and Minami, 1990), the Philippines (Wassmann et al., 1996),



Greenhouse Gas Fluxes: Effects of Physical Conditions,
Figure 6 Seasonal variation of CH_4 flux, water table, and soil redox potential (Eh) at depths of 2, 5, and 10 cm measured at the continuous flooded plot in a Japanese rice paddy field. Solid dot indicates the flux data obtained by the manual measurements (Yagi et al., 1996).

and Louisiana, USA (Kongchum et al., 2006). However, CH_4 emission per unit dry matter of rice straw applied during the rice growing period season was significantly higher in the snowy temperate region than in other regions because of deep snow cover, low temperature, and unplowed conditions which might have retarded the decomposition of rice straw over the winter fallow (Naser et al., 2007).

Contribution of ebullition with falling atmospheric pressure has been less than 10% of total annual CH_4

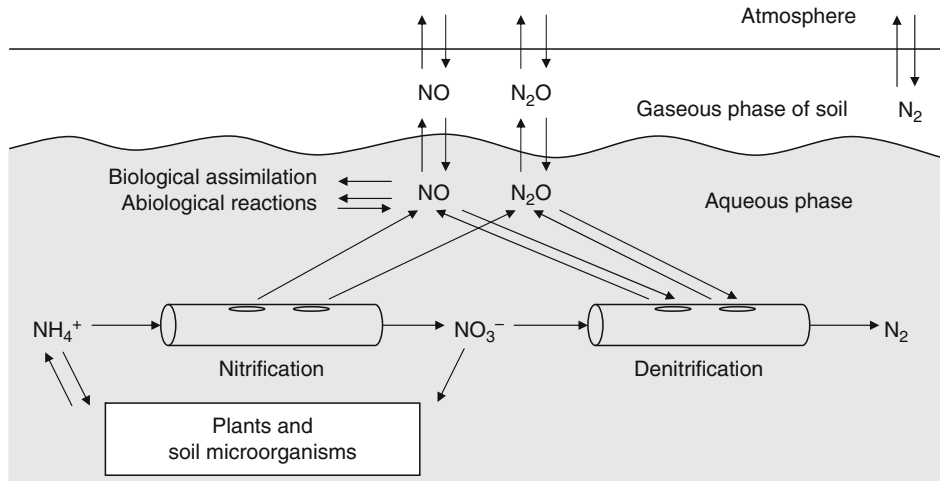
emission (Schütz et al., 1989), but abrupt CH_4 flux from a Japanese wetland, which can change by two orders of magnitude within several tens of minutes was recently found due to the release of free-phase CH_4 triggered by a drop in air pressure (Tokida et al., 2007).

Indirect CH_4 emission through subsurface drainage in an onion field of Gray Lowland soil in central Hokkaido, Japan, increased with increase of drainage rate during snowmelt season and rainfall events (Sawamoto et al., 2003). Annual indirect CH_4 emission was $11.5 \text{ mg C m}^{-2} \text{ year}^{-1}$, which corresponds to 58% of the direct CH_4 emission from soil to the atmosphere. This high contribution suggests subsoil CH_4 production. On the other hand, in a well-permeable loamy soil, indirect CH_4 emissions were considerably low even in paddy field (Minamikawa et al., 2009). The values were 2.20 and $0.964 \text{ mg C m}^{-2} \text{ year}^{-1}$ in a paddy rice field, 0.145 and $0.159 \text{ mg C m}^{-2} \text{ year}^{-1}$ in a soybean field, 0.238 and $1.28 \text{ mg C m}^{-2} \text{ year}^{-1}$ in an upland rice field, and the proportion of the indirect CH_4 emission to the direct CH_4 emission from the soil to the atmosphere was only 0.05% and 0.03% , $0.30\text{--}0.22\%$ and $0.46\text{--}2.64\%$, respectively.

N₂O

N_2O is mainly formed as a by-product of nitrification and as an intermediary of denitrification (Bremner, 1997). In aerobic condition, autotrophic nitrification is the main source of N_2O , but heterotrophic nitrification is generally regarded as a minor source of N_2O (Inubushi et al., 1996; Wrage et al., 2001). However, at low pH, N_2O is formed by chemodenitrification, which is the chemical decomposition of HNO_2 , following reaction with organic (e.g., amines) or inorganic (e.g., Fe^{2+}) compounds (van Cleempunt, 1998). At low O_2 concentration around 1 kPa dissolved O_2 , N_2O is produced through nitrifier-denitrification process, which is a biological process proceeding NH_4^+ oxidation using NO_2^- reduction simultaneously (Muller et al., 1995). Under anaerobic condition, N_2O is produced as an intermediary mainly through denitrification and anaerobic ammonium oxidation (Anammox). Heterotrophic denitrification, in which NO_3^- is converted to N_2 with organic matter decomposition, is the significant process for N_2O production. Autotrophic denitrification in which NO_3^- is converted to N_2 with the oxidation of sulfide (Cardoso et al., 2006) or ion oxidation (Till et al., 1998). Anammox is also a biological process in which NH_4^+ is converted to N_2 gas with NO_2^- reduction as the electron acceptor (Strous et al., 1997; Kampschreur et al., 2008).

During nitrification and denitrification which are the major processes producing N_2O in soil, NO is also produced. **Figure 7** shows a conceptual “hole-in-the-pipe” model, using the analogy of a leaky pipe, which suggests three levels regulating N_2O and NO emission from the soil to the atmosphere (Firestone and Davidson, 1989; Davidson and Verchot, 2000). At first level, there are



Greenhouse Gas Fluxes: Effects of Physical Conditions, Figure 7 Diagram of the hole-in-the-pipe conceptual model (Davidson et al., 2000).

factors controlling the rates of nitrification and denitrification (the “flow through the pipe”), which are the amounts of raw material (soil mineral N), soil temperature, and soil moisture; at second level, there are factors regulating the proportions of N₂O and NO productions in nitrification and denitrification (the “size of the holes in the pipe”), which are acidity, concentrations of NO₃⁻, and available carbon in soil; and at third level, there are factors controlling the consumption of N₂O and NO within the soil matrix, which are diffusion and mass flow in soil depending on soil texture, soil structure, air-filled pore space, temperature, and air pressure. Increase of soil moisture decreases air-filled pore space, which decreases gas diffusivity in soil, increasing the opportunities for further microbial reaction in soil.

Optimal moisture condition for organic matter decomposition (mineralization) and nitrification is around 60% of water-filled pore space (WFPS), while the optimal condition for denitrification is at saturation of the WFPS, with sufficient presence of nitrate and available organic carbon (Linn and Doran, 1984). The ratio of N₂O–N/NO–N ranges from 0.2 to 1 during nitrification and is approximately 100 during denitrification (Lipschultz et al., 1981).

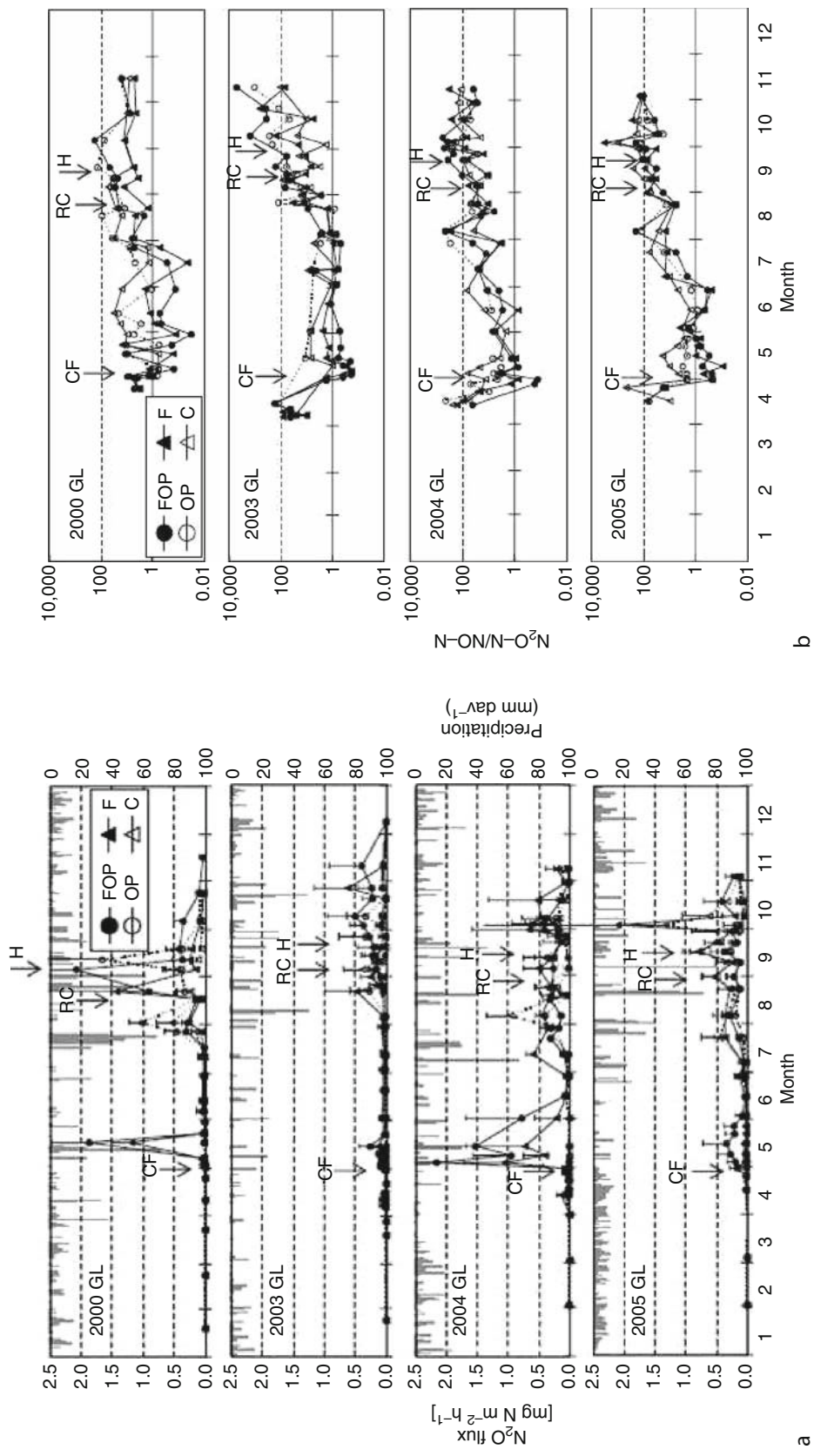
Figure 8 shows examples of the seasonal and yearly variation in N₂O fluxes (a) and N₂O–N/NO–N ratio (b) measured in an Onion field of Gray Lowland soil in central Hokkaido, Japan (Toma et al., 2007). The measurements were conducted in four treatments; chemical N fertilization and organic matter application, with plants (FOP); chemical N fertilization only, without plants (F); organic matter application only, with plants (OP); and control, no fertilization, or organic matter application, without plants (C). In chemical N fertilizer–applied treatments (FOP and F), there were two peaks in the periods from May to June and from late August to October (Figure 8a), and the N₂O–N/NO–N ratio decreased to less than 1 from May to June and increased to approximately

100 from September to October (Figure 8b). These indicate nitrification after spring N fertilization and denitrification with increase of rainfall. On the other hand, in no chemical N fertilizer–applied treatments (OP and C), only one peak was found in the period from August to October (Figure 8a), and the N₂O–N/NO–N remained above 1 from May to June (Figure 8b). There was a significant correlation between 2-month N₂O emission from May to June and mean temperature during these months ($n=8$, $r^2=0.53$, $P < .05$; Figure 9a). The N₂O production after spring fertilization resulting from the nitrification process may be affected by temperature. The 2-month N₂O emissions from September to October in the FOP and OP treatments, however, were positively correlated with the precipitation during these months ($n=8$, $r^2=0.39$, $P < .1$; Figure 9b).

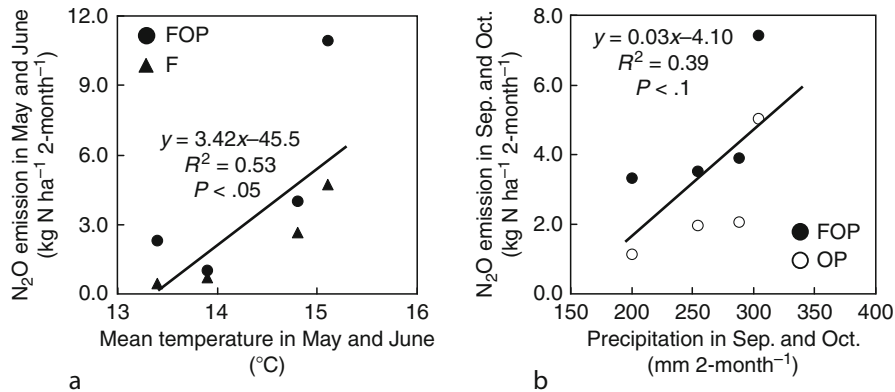
Figure 10 shows the relationship between total N application rate and N₂O emission from Japanese upland fields, with measurement period more than 90 days. N₂O emission increased with increase of N application rate and was generally higher in poorly drained soil than that in well-drained soil (Akiyama et al., 2006).

Huge amount of annual N₂O emission of 259 kg N ha⁻¹ year⁻¹ in maximum was found at the croplands of tropical peatland in Palangka Raya, central Kalimantan, Indonesia. During the rainy season, N₂O fluxes from the soil surface of the croplands increased with increase of NO₃⁻ content in the soil when water-filled pore space in the top soil exceeded 60–70% (Takakai et al., 2006). Acid-tolerant *Janthinobacterium* sp. as an N₂O emitter isolated from the cropland peat soil showed high ability of denitrification (NO₃⁻ reduction) but low activity of N₂O reductase (Hashidoko et al., 2008).

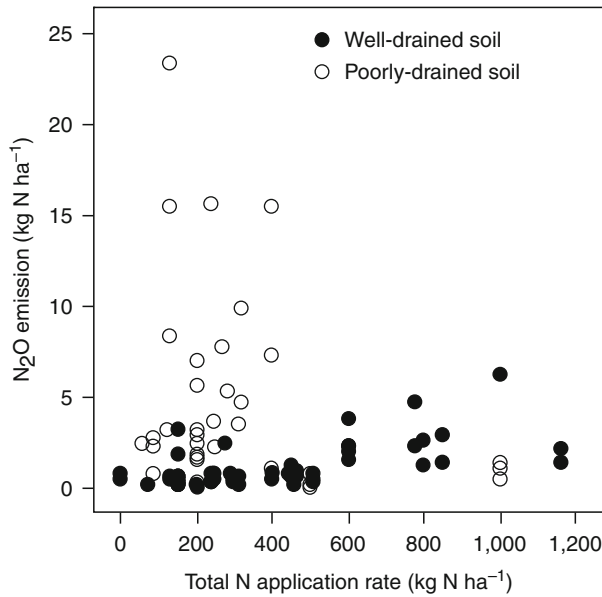
In temperate and boreal climates with periodic soil freezing and thawing, high N₂O emission from soil in the winter and early spring is usually observed (Christensen and Tiedje, 1990; Flessa et al., 1995).



Greenhouse Gas Fluxes: Effects of Physical Conditions. **Figure 8** Seasonal variation in N_2O flux (a) and $\text{N}_2\text{O-N}/\text{NO-N}$ ratio (b) at the onion fields of Gray Lowland soil (GL) in central Hokkaido, Japan (From Toma et al., 2007). The arrows indicate the time of chemical fertilizer application (CF), root cutting (RC), and harvest and residue application (H). The four treatments were: chemical nitrogen fertilization, with plants (FOP); chemical nitrogen fertilization only, without plants (F); organic matter application, with plants (OP); no fertilization or organic matter, and no plants (C). Error bars indicate standard deviation.



Greenhouse Gas Fluxes: Effects of Physical Conditions, Figure 9 Relationship between N_2O emission and mean temperature and precipitation at the onion field of Gray Lowland soil in central Hokkaido, Japan (From Toma et al., 2007). (a) Relationship between the 2-month N_2O emission and mean air temperature from May to June in 2000 and 2003–2005 in the chemical nitrogen fertilization and organic matter application, with plants (FOP) and the chemical nitrogen fertilization only, without plants (F) treatments; (b) relationship between the 2-month N_2O emission and precipitation from September to October in those years in the FOP and the organic matter application, with plants (OP) treatments.



Greenhouse Gas Fluxes: Effects of Physical Conditions, Figure 10 Relationship between total N input (kg N ha^{-1}) and N_2O emission (kg N ha^{-1}) from upland fields; measurement period more than 90 days (Akiyama et al., 2006).

Biological denitrification is the main process in N_2O production when soil is undergoing the process of freezing and thawing (Müller et al., 2002; Öquist et al., 2004). This might be caused by an imbalance of N_2O -producing and N_2O -reducing activities of denitrifying communities enhanced by the freeze–thaw cycles (Yanai et al., 2007).

Indirect N_2O emission through subsurface drainage in an Onion field of Gray Lowland soil in central Hokkaido, Japan, increased with increase of drainage rate during snowmelt season and rainfall events

(Sawamoto et al., 2003). Direct N_2O emission from the field increased significantly with increase in precipitation in the growing seasons (Kusa et al., 2002), and NO_3^- leaching increased with increase of precipitation in the same field (Hayashi and Hatano, 1999). Annual indirect N_2O emission was $74.7 \text{ mg N m}^{-2} \text{ year}^{-1}$ which corresponds to 4.6% of the direct N_2O emission from the soil to the atmosphere. The NO_3^- concentration in the drainage ranged from 8.5 to 25.5 mg N L^{-1} and the dissolved N_2O concentration ranged from 19.3 to $189 \mu\text{g N L}^{-1}$. But, there was no significant relationship between $\text{N}_2\text{O}-\text{N}$ and NO_3^--N concentration. The ratio of $\text{N}_2\text{O}-\text{N}/\text{NO}_3^--\text{N}$ (kg kg^{-1}) ranged from 0.00076 to 0.0105 (Sawamoto et al., 2003). The ratio has been estimated to be 0.0024 using 15 data sets of N_2O and NO_3^- concentrations in drainage water (Sawamoto et al., 2005). In a well-permeable loamy soil in Tsukuba, Japan, considerably different tendency in indirect N_2O emission was found.

Summary

Soil is the major source of CO_2 , CH_4 , and N_2O emissions into the atmosphere. Those gases are produced and consumed in soil by mainly microbial activities which are strongly influenced by soil environmental factors. This paper reviewed the relationship between the fluxes of those gases and soil environmental factors.

Soil temperature is the most important soil environmental factor for CO_2 flux from soil. However, significant drought declined soil CO_2 flux rapidly and heavy rain event induced episodic CO_2 flux from soil. Different soils within a watershed have different relationships between CO_2 flux and soil temperature and soil moisture. However, soil texture significantly influenced CO_2 emission from the soil during a growing season, and there was a critical clay and silt content for the CO_2 emission.

Soil moisture is the most important soil environmental factor for CH₄ flux from soil, because CH₄ is produced by methanogenic bacteria in anaerobic soil and consumed by methanotrophic bacteria in aerobic soil. In paddy field, rice aerenchyma is the major pathway during the growing season due to inhibition of upward gas diffusion by flooding. Final drainage at the end of growing season in paddy field often induced large CH₄ flush due to a direct diffusion of CH₄ entrapped in soil after the removal of the water seal by drainage. Short-term drainage practice during the growing season in paddy field reduced the CH₄ emission, but the increase of rice straw incorporation significantly increased CH₄ emissions.

Soil temperature and soil moisture are significant soil environmental factors for N₂O flux from soil, because N₂O is mainly formed as a by-product of nitrification and as an intermediary of denitrification. Long-term observation in an upland field indicated that N₂O emission induced by nitrification increases by the increase of soil temperature, and N₂O emission induced by denitrification increases by the increase of precipitation. Very high N₂O flux was found at the croplands of tropical peatland in Indonesia when water-filled pore space in the top soil exceeded 60–70%. This was ascribed to acid-tolerant bacterium with low activity of N₂O reductase. On the other hand, soil freezing and thawing in temperate and boreal climates enhances high N₂O flux from soil in the winter and early spring.

Bibliography

- Akiyama, H., Yan, X., and Yagi, K., 2006. Estimations of emission factors for fertilizer-induced direct N₂O emissions from agricultural soils in Japan: summary of available data. *Soil Science and Plant Nutrition*, **52**, 774–787.
- Bergman, I., Svensson, B. O. H., and Nilsson, M., 1998. Regulation of methane production in Swedish acid mire by pH, temperature, and substrate. *Soil Biology and Biochemistry*, **30**, 729–741.
- Boone, R. D., Nadlhofer, K. J., Canary, J. D., and Kaye, J. P., 1998. Roots exert a strong influence on the temperature sensitivity of soil respiration. *Nature*, **396**, 570–572.
- Bremner, J. M., 1997. Source of nitrous oxide in soils. *Nutrient Cycling in Agroecosystems*, **49**, 7–16.
- Cardoso, R. B., Sierra-Alvarez, R., Rowlette, P., Flores, E. R., Gomez, J., and Field, J. A., 2006. Sulfide oxidation under chemolithoautotrophic denitrifying conditions. *Biotechnology and Bioengineering*, **95**, 1148–1157.
- Christensen, S., and Tiedje, J. M., 1990. Brief and vigorous N₂O production by soil at spring thaw. *Journal of Soil Science*, **41**, 1–4.
- Cicerone, R. J., 1987. Changes in stratospheric ozone. *Science*, **237**, 35–42.
- Conrad, R., 1995. Soil microbial process involved in production and consumption of atmospheric trace gases. *Advances in Microbial Ecology*, **14**, 207–238.
- Conrad, R., 1999. Contribution of hydrogen to methane production and control of hydrogen concentrations in methanogenic soils and sediments. *FEMS Microbiology Ecology*, **28**, 193–202.
- Conrad, R., and Rothfus, F., 1991. Methane oxidation in the soil surface layer of a flooded rice field and the effect of ammonium. *Biology and Fertility of Soils*, **12**, 28–32.
- Davidson, E. A., and Verchot, L. V., 2000. Testing the hole-in-the-pipe model of nitric and nitrous oxide emissions from soils using the TRAGNET database. *Global Biogeochemical Cycles*, **14**, 1035–1043.
- Davidson, E. A., Belk, E., and Boone, R. D., 1998. Soil water content and temperature as independent or confounded factors controlling soil respiration in a temperate mixed hardwood forest. *Global Change Biology*, **4**, 217–227.
- Davidson, E. A., Keller, M., Erickson, H. E., Verchot, L. V., and Veldkamp, E., 2000. Testing a conceptual model of soil emissions of nitrous and nitric oxides. *Bioscience*, **50**, 667–680.
- Dunfield, P., Knowles, R., and Moore, T. R., 1993. Methane production and consumption in temperate and subarctic peat soils: response to temperature and pH. *Soil Biology and Biochemistry*, **25**, 321–326.
- Firestone, M. K., and Davidson, E. A., 1989. Microbiological basis of NO and N₂O production and consumption in soil. In Andreae, M. O., and Schimel, D. S. (eds.), *Exchange of Trace Gases between Terrestrial Ecosystems and the Atmosphere*. New York: Wiley, pp. 7–21.
- Flessa, H., Dörsch, P., and Beese, F., 1995. Seasonal variation of nitrous oxide and methane fluxes in differently managed arable soils in southern Germany. *Journal of Geophysical Research*, **100**, 23115–23124.
- Forster, P., Ramaswamy, V., Artaxo, P., Berntsen, T., Betts, R., Fahey, D. W., Haywood, J., Lean, J., Lowe, D. C., Myhre, G., Nganga, J., Prinn, R., Raga, G., Schulz, M., and Van Dorland, R., 2007. Changes in atmospheric constituents and in radiative forcing. In Solomon, S., Qin, D., Manning, M., Chen, Z., Marquis, M., Averyt, K. B., Tignor, M., and Miller, H. L. (eds.), *Climate Change 2007: The Physical Science Basis. Contribution of Working Group I to the Fourth Assessment Report of the Intergovernmental Panel on Climate Change*. Cambridge: Cambridge University Press.
- Goodwin, S., and Zeikus, J. G., 1987. Ecophysiological adaptations of anaerobic bacteria to low pH: analysis of anaerobic digestion in acid bog sediments. *Applied and Environmental Microbiology*, **53**, 57–64.
- Hanson, R. S., and Hanson, T. E., 1996. Methanotrophic bacteria. *Microbiological Reviews*, **60**, 439–471.
- Hashidoko, Y., Takakai, F., Toma, Y., Darung, U., Melling, L., Tahara, S., and Hatano, R., 2008. Emergence and behaviors of acid-tolerant *Janthinobacterium* sp. that evolves N₂O from deforested tropical peatland. *Soil Biology and Biochemistry*, **40**, 116–125.
- Hassink, J., Bouwman, L. A., Zwart, K. B., Bloom, J., and Brussard, L., 1993. Relationships between soil texture, physical protection of soil organic matter, soil biota and C and N mineralization in grassland soils. *Geoderma*, **57**, 105–128.
- Hayashi, Y., and Hatano, R., 1999. Annual nitrogen leaching in subsurface-drained water from a clayey aquic soil growing onions in Hokkaido, Japan. *Soil Science and Plant Nutrition*, **45**, 451–459.
- Inubushi, K., Naganuma, H., and Kitahara, S., 1996. Contribution of denitrification and autotrophic and heterotrophic nitrification to nitrous oxide production in andosols. *Biology and Fertility of Soils*, **23**, 292–298.
- Jarecki, M. K., and Lal, R., 2003. Crop management for soil carbon sequestration. *Critical Reviews in Plant Sciences*, **22**, 471–502.
- Kampschreur, M. J., van der Star, W. R. L., Wielders, H. A., Mulder, J. W., Jetten, M. S. M., and van Loosdrecht, M. C. M., 2008. Dynamics of nitric oxide and nitrous oxide emission during full-scale reject water treatment. *Water Research*, **42**, 812–826.
- King, G. M., and Schnell, S., 1994. Effect of increasing atmospheric methane concentration on ammonium inhibition of soil methane consumption. *Nature*, **370**, 282–284.
- Kongchum, M., Bollich, P. K., Hunnall, W. H., DeLaune, R. D., and Lindau, C. W., 2006. Decreasing methane emission of rice by better crop management. *Agronomy for Sustainable Development*, **26**, 1–10.

- Kusa, K., Sawamoto, T., and Hatano, R., 2002. Nitrous oxide emissions for six years from a gray lowland soil cultivated with onions in Hokkaido, Japan. *Nutrient Cycling in Agroecosystems*, **63**, 239–247.
- Linn, D. M., and Doran, J. W., 1984. Effect of water-filled pore space on carbon dioxide and nitrous oxide production in tilled and nontilled soils. *Soil Science Society of America Journal*, **48**, 1267–1272.
- Lipschultz, F., Zafiriou, O. C., Wofsy, S. C., McElroy, M. B., Valois, F. W., and Watson, S. W., 1981. Production of NO and N₂O by soil nitrifying bacteria. *Nature*, **294**, 641–643.
- Melling, L., Hatano, R., and Goh, K. J., 2005. Methane emission from three ecosystems in tropical peatland of Sarawak, Malaysia. *Soil Biology and Biochemistry*, **37**, 1445–1453.
- Mer, J. L., and Roger, P., 2001. Production, oxidation, emission and consumption of methane by soils: a review. *European Journal of Soil Biology*, **37**, 25–50.
- Minamikawa, K., Nishimura, S., Sawamoto, T., Nakajima, Y., and Yagi, K., 2009. Annual emissions of dissolved CO₂, CH₄, and N₂O in the subsurface drainage from three cropping systems. *Global Change Biology*, doi:10.1111/j.1365-2486.2009.01931.x.
- Moore, T. R., and Knowles, R., 1990. Methane emissions from fen, bog and swamp peatlands in Quebec. *Biogeochemistry*, **11**, 45–61.
- Mu, Z. J., Kimura, S. D., Toma, Y., and Hatano, R., 2008. Evaluation of the soil carbon budget under different upland cropping systems in central Hokkaido, Japan. *Soil Science and Plant Nutrition*, **52**, 371–377.
- Müller, E. B., Stouthamer, A. H., and van Verseveld, H. W., 1995. Simultaneous NH₃ oxidation and N₂ production at reduced O₂ tensions by sewage sludge subcultured with chemolithotrophic medium. *Biodegradation*, **6**, 339–349.
- Müller, C., Martin, M., Stevens, R. J., Laughlin, R. J., Kammann, C., Ottow, J. C. G., and Jäger, H.-J., 2002. Processes leading to nitrous oxide emissions in grassland soil during freezing and thawing. *Soil Biology and Biochemistry*, **34**, 1325–1331.
- Naser, H. M., Nagata, O., Tamura, S., and Hatano, R., 2007. Methane emissions from five paddy fields with different amount of rice straw application in central Hokkaido, Japan. *Soil Science and Plant Nutrition*, **53**, 95–101.
- Nesbit, S. P., and Breitenbeck, G. A., 1992. A laboratory study of factors influencing methane uptake by soils. *Agriculture, Ecosystems and Environment*, **41**, 39–54.
- Öquist, M. G., Nilsson, M., Sörensson, F., Kaisimir-Klemmedtsson, Å., Persson, T., Weslien, P., and Klemmedtsson, L., 2004. Nitrous oxide production in a forest soil at low temperatures – processes and environmental controls. *FEMS Microbiology Ecology*, **49**, 371–378.
- Prather, M., Ehhalt, D., Dentener, F., Derwent, R., Dlugokencky, E., Holland, E., Isaksen, I., Katima, J., Kirchhoff, V., Matson, P., Midgley, P., and Wang, M., 2001. Atmospheric chemistry and greenhouse gases. In Houghton, J. T., Ding, Y., Griggs, D. J., Noguer, M., van der Linden, P. J., Dai, X., Maskell, K., and Johnson, C. A. (eds.), *Climate Change 2001: The Scientific Basis. Contribution of Working Group I to the Third Assessment Report of the Intergovernmental Panel on Climate Change*. Cambridge: Cambridge University Press, pp. 243–253.
- Raich, J. W., and Schelesinger, W. H., 1992. The global carbon dioxide flux in soil respiration and relationship to vegetation and climate. *Tellus*, **44B**, 81–99.
- Sass, R. L., Fisher, F. M., Harcombe, P. A., and Turner, F. T., 1990. Methane production and emission in a Texas rice field. *Global Biogeochemical Cycles*, **4**, 47–68.
- Sass, R. L., Fisher, F. M., Wang, Y. B., Turner, F. T., and Jund, M. F., 1992. Methane emission from rice fields: the effect of floodwater management. *Global Biogeochemical Cycles*, **6**, 249–262.
- Sawamoto, T., Kusa, K., Hu, R., and Hatano, R., 2003. Dissolved N₂O, CH₄ and CO₂ emissions from subsurface-drainage in a structured clay soil cultivated with onion in Central Hokkaido, Japan. *Soil Science and Plant Nutrition*, **49**, 31–38.
- Sawamoto, T., Nakajima, Y., Kasuya, M., Tsuruta, H., and Yagi, K., 2005. Evaluation of emission factors for indirect N₂O emission due to nitrogen leaching in agro-ecosystems. *Geophysical Research Letter*, **32**, L03403, doi:10.1029/2004GL021625.
- Schütz, H., Seiler, W., and Conrad, R., 1989. Processes involved in formation and emission of methane in rice paddies. *Biogeochemistry*, **7**, 33–53.
- Shimizu, M., Marutani, S., Ar, D., Jin, T., Hata, H., and Hatano, R., 2009. The effect of manure application on carbon dynamics and budgets in a managed grassland of Southern Hokkaido, Japan. *Agriculture, Ecosystems and Environment*, **130**, 31–40.
- Singh, K. P., Ghoshal, N., and Sonu Singh, S., 2009. Soil carbon dioxide flux, carbon sequestration and crop productivity in a tropical dryland agroecosystem: influence of organic inputs of varying resource quality. *Applied Soil Ecology*, **42**, 243–253.
- Sitaula, B. K., Bakken, L. R., and Abrahamsen, G., 1995. CH₄ uptake by temperate forest soil: effect of N input and soil acidification. *Soil Biology and Biochemistry*, **27**, 871–880.
- Steudler, P. A., Bowden, R. D., Melillo, J. M., and Aber, J. D., 1989. Influence of nitrogen fertilization on methane uptake in temperate forest soils. *Nature*, **341**, 314–316.
- Strous, M., van Gerven, E., Kuenen, J. G., and Jetten, M., 1997. Effects of aerobic and microaerobic conditions on anaerobic ammonium-oxidizing (Anammox) sludge. *Applied and Environmental Microbiology*, **63**, 2446–2448.
- Takai, Y., 1970. The mechanism of methane fermentation in flooded paddy soil. *Soil Science and Plant Nutrition*, **16**, 238–244.
- Takakai, F., Morishita, T., Hashidoko, Y., Darung, U., Kuramochi, K., Dohong, S., Limin, S. H., and Hatano, R., 2006. Effects of agricultural land-use change and forest fire on N₂O emission from tropical peatlands, Central Kalimantan, Indonesia. *Soil Science and Plant Nutrition*, **52**, 662–674.
- Takakai, F., Desyatkin, A. R., Lopez, C. M. L., Fedrov, A. N., Desyatkin, R. V., and Hatano, R., 2008a. Influence of forest disturbance on CO₂, CH₄ and N₂O fluxes from larch forest soil of permafrost taiga region in eastern Siberia. *Soil Science and Plant Nutrition*, **54**, 938–949.
- Takakai, F., Desyatkin, A. R., Lopez, C. M. L., Fedorov, A. N., Desyatkin, R. V., and Hatano, R., 2008b. CH₄ and N₂O emissions from a forest-alas ecosystem in the permafrost taiga forest region, eastern Siberia, Russia. *Journal of Geophysical Research*, **113**, G02002, doi:10.1029/2007JG000521.
- Till, B. A., Weathers, L. J., and Alvarez, P. J. J., 1998. Fe(0)-supported autotrophic denitrification. *Environmental Science and Technology*, **32**, 634–639.
- Tokida, T., Miyazaki, T., Mizoguchi, M., Nagata, O., Takakai, F., Kagemoto, A., and Hatano, R., 2007. Falling atmospheric pressure as a trigger for methane ebullition from peatland. *Global Biogeochemical Cycles* 21(2): Art. No. GB2003 APR 18.
- Toma, Y., Kimura, S. D., Hirose, Y., Kusa, K., and Hatano, R., 2007. Variation in the emission factor of N₂O derived from chemical nitrogen fertilizer and organic matter: a case study of onion fields in Mikasa, Hokkaido, Japan. *Soil Science and Plant Nutrition*, **53**, 692–703.
- van Cleemput, O., 1998. Subsoils: chemo- and biological denitrification, N₂O and N₂ emissions. *Nutrient Cycling in Agroecosystems*, **52**, 187–194.
- Wassmann, R., Neue, H. U., Alberto, M. C. R., Lantin, R. S., Bueno, C., Llenaresas, D., Arah, J. R. M., Papen, H., Seiler, W., and Rennenberg, H., 1996. Fluxes, and pools of methane in wetland rice soils with varying organic inputs. *Environmental Monitoring and Assessment*, **42**, 163–173.

- Wrage, N., Velthof, G. L., van Beusichem, M. L., and Oenema, O., 2001. Role of nitrifier denitrification in the production of nitrous oxide. *Soil Biology and Biochemistry*, **33**, 1723–1732.
- Yagi, K., 1994. Methane. In Minami, K. (ed.), *Pedosphere and Atmosphere*. Tokyo: Asakura Syoten, p. 66. in Japanese.
- Yagi, K., and Minami, K., 1990. Effect of organic matter application on methane emission from some Japanese rice fields. *Soil Science and Plant Nutrition*, **36**, 599–610.
- Yagi, K., Tsuruta, H., Kanda, K., and Minami, K., 1996. Effect of water management on methane emission from a Japanese rice paddy field: automated methane monitoring. *Global Biogeochemical Cycles*, **10**, 255–267.
- Yamane, I., and Sato, K., 1964. Decomposition of glucose and gas formation in flooded soil. *Soil Science and Plant Nutrition*, **10**, 127–133.
- Yanai, Y., Toyota, K., and Okazaki, M., 2007. Response of denitrifying communities to successive soil freeze-thaw cycles. *Biology and Fertility of Soils*, **44**, 113–119.
- Yao, H., and Conrad, R., 2000. Electron balance during steady-state production of CH₄ and CO₂ in anoxic rice soil. *European Journal of Soil Science*, **51**, 369–378.

Cross-references

- [Aeration of Soils and Plants](#)
[Carbon Losses Under Dryland Conditions, Tillage Effects](#)
[Climate Change: Environmental Effects](#)
[Diffusion in Soils](#)
[Flooding, Effects on Soil Structure](#)
[Leaching of Chemicals in Relation to Soil Structure](#)
[Tillage, Impacts on Soil and Environment](#)

GREENHOUSE GASES SINK IN SOILS

Teresa Włodarczyk

Institute of Agrophysics, Polish Academy of Sciences,
Lublin, Poland

Synonyms

Consumption; Uptake

Definition

Greenhouse gases sink in soils is defined as reducing their amount in the atmosphere and in the soils atmosphere or solution due to some biological processes. Carbon dioxide (CO₂) is naturally sequestered (sunk) in plants, soils, and in ocean life. Methane is oxidized by methane-oxidizing microorganisms (methanotrophs). A complete denitrification, at which N₂O is reduced to N₂, is assumed to be the main elimination or sink process of N₂O in the soils.

Introduction

The main greenhouse gases in the Earth's atmosphere are water vapor, carbon dioxide (CO₂), methane (CH₄), and nitrous oxide (N₂O), which enhances the greenhouse effect. Since around the time of the Industrial Revolution in Western countries, concentrations of carbon dioxide, methane, and nitrous oxide have increased. Mitigation of greenhouse gases emission leads to minimizing the effects

of global warming. Very important is stabilization of greenhouse gas concentrations in the atmosphere at a level that would prevent dangerous anthropogenic interference with the climate system.

Carbon sink

A carbon sink is a natural or manmade reservoir that accumulates and stores some carbon-containing chemical compound for an indefinite period. The main natural sinks are absorption of carbon dioxide by the oceans and photosynthesis by plants and algae. The main manmade sinks are landfills and carbon capture and storage proposals. Carbon dioxide sequestration (or carbon sequestration) is the term given for locking up CO₂ somewhere other than the atmosphere. In biological sequestration, carbon is naturally sequestered in plants, soils, and in ocean life. Soils represent a short to long-term carbon storage medium, and contain more carbon than all terrestrial vegetation and the atmosphere combined and are a major reservoir of carbon and an important sink. Because of the relatively long period of time that carbon spends within the soil and is thereby withheld from the atmosphere, it is often referred to as being sequestered (Swift, 2001). Plant litter and other biomass are accumulated as organic matter in soils especially in litter and soils of colder regions such as the boreal forests. The carbon sequestration potential of soils (by increasing soil organic matter) is substantial. Improving the humus levels of these soils would both improve soil quality and increase the amount of carbon sequestered in these soils. Decomposition rates can be slowed by reducing tillage and by growing crops with low residue quality that is more difficult for microbes to decompose. No tillage implants seeds without turning the soils reduce the loss of soil organic matter. Natural soils retain carbon in stable micro aggregates for up to hundreds of years unless environmental conditions are changed and the stable soil structure is damaged (Luo and Zhou, 2006). The C sequestration potential of a soil depends on the vegetation it supports, its mineralogical composition, the depth of the soil, soil drainage, the availability of water and air, the temperature of the soil environment, and the chemical characteristics of the soil organic matter and its ability to resist microbial decomposition (Swift, 2001). Conversion of the soil to pastureland, particularly with good management of grazing, can sequester more carbon. Thus, soil restoration and woodland regeneration, no-till farming, cover crops, nutrient management, manuring and sludge application, improved grazing, water conservation and harvesting, efficient irrigation, agroforestry practices, growing energy crops on spare lands, and pyrolyzing the biomass to biochar are recommended management practices to increase the soil carbon sequestration (Lal, 2004). The chemosynthetic autotrophs (chemolithotrophs) take carbon dioxide as their carbon source for growth and derive their energy from oxidation of inorganic materials like iron, sulfur, ammonia, and nitrite. *Grasslands* contribute

huge quantities of soil organic matter over time, mostly in the form of roots, and much of this organic matter can remain unoxidized for long periods. They also deposit carbon directly to the soil in the form of char that does not significantly degrade back to carbon dioxide. No-till pastureland, particularly with good management of grazing, can sequester even more carbon in the soil. The wetlands cover only 3% of land area but store nearly 37% of global terrestrial carbon. As a consequence of anoxic conditions, the rate of organic matter decomposition is slow and carbon tends to accumulate in wetland soils. Wetland soil carbon storage is sensitive to climatic changes, water table fluctuations, and human disturbances. Peat lands cover about 75% of the wetlands by area and are particularly important for storage of soil carbon (Luo and Zhou, 2006). Organic matter in peat bogs undergoes slow anaerobic decomposition below the surface and fixes more carbon from the atmosphere than is released. Peat bogs absorb approximately one-quarter of the carbon stored in land plants and soils. Forests are carbon stores, and they are carbon dioxide sinks when they are increasing in density or area. As part of photosynthesis, trees absorb carbon dioxide from the atmosphere and store it as carbon. Rapidly growing trees absorb a larger amount of carbon dioxide. The sink effect exists only when they grow in size. Mature trees grow less rapidly and thus have a lower intake of carbon dioxide. One ton of dry wood is equivalent to 1.8 tons of carbon dioxide. Upon harvesting, wood can be incorporated into construction or a range of other durable products, thus sequestering its carbon over years or even centuries. Management measures to improve carbon storage in forest include prolonging rotation, changing tree species, continuous cover forestry, fire control, combined water storage with peat swamp afforestation, fertilization, and reducing the rate of deforestation. (Luo and Zhou, 2006).

CH₄ sink

The atmospheric concentration of CH₄ has increased and more than doubled during the past 200 years (Mancinelli, 1995). Aerobic consumption of CH₄ is common in soils and aquatic environments. There are only two important sinks for atmospheric CH₄. The major sink is reaction of CH₄ with hydroxyl radical. Additionally, CH₄ is consumed by aerobic microbial activity in soils. The soil CH₄ sink is sensitive to nitrogen fertilization. Methanotrophs play a major role in the reduction of the release of methane into the atmosphere from environments such as rice paddies, landfills, bogs, and swamps where methane production is relatively high and from aquatic systems, soils, forest, tundra, and agricultural soils.

Aerobic methane oxidation

Methane-oxidizing microorganisms (methanotrophs) are found in variety of soil and aquatic environments and play an important role in regulating atmospheric methane

content. Oxidation of methane to carbon dioxide in soils occurs primarily as part of aerobic metabolism in methanotrophic bacteria. Methanotrophs are able to metabolize methane as their only source of carbon and energy mostly in soils, where methane is produced. Methanotrophs are often concentrated in a narrow band where methane diffusing away from its source (an anaerobic zone) meets oxygen from the air. Although nearly all methane oxidizers are obligate aerobes, they are microaerophilic, preferring oxygen level lower than atmospheric levels. The net reaction of methane oxidation under aerobic conditions can be described as CH₄ + O₂ → CO₂ + H₂O (Mancinelli, 1995).

Methane is oxidized in soil by methanotrophs with the use of a chain of enzymes such as methanol, formaldehyde, formate, and nonspecific aldehyde dehydrogenases (Large, 1983). It was found that during incubation of a Mollic Gleysol with methane in the headspace dehydrogenase activity of the soil significantly increased, compared to the control value, after 2 days to its maximum and decreased slowly during the next days (Brzezińska et al., 1998).

Methanotrophic bacteria possess both dissimilatory and assimilatory pathways of methane oxidation. In dissimilatory pathways, methane is oxidized completely to carbon dioxide, thereby producing cellular energy, and none of the carbon becomes cellular material, or biomass. In assimilatory pathways, methane is oxidized and converted to cellular biomass. In both pathways, methane is first oxidized to methanol by methane monooxygenase (MMO) using molecular oxygen, which is then oxidized to formaldehyde. The formaldehyde can be used as reducing power in the electron transport chain, oxidized to formate, or assimilated by the cell via the ribulose monophosphate pathway and/or the serine pathway. The cell then either oxidized the formate to carbon dioxide or uses it as reducing power to drive the electron-transport chain. Several physicochemical factors influence rates of methane oxidation in soil, including soil diffusivity, water potential, and levels of oxygen, methane, ammonium, nitrate, nitrite, and copper. Most of these factors exert influence through interactions with MMO (Mancinelli, 1995). In general, methanotrophic activity increased with increasing CH₄ addition in the different range of initial methane content. Soils are characterized by different requirements with respect to threshold methane concentration expressed as high- or low-affinity oxidation. The differences in methanotrophic activity mainly depend on differences in organic matter content and availability and methanotrophs existing in the soils (Włodarczyk et al., 2004).

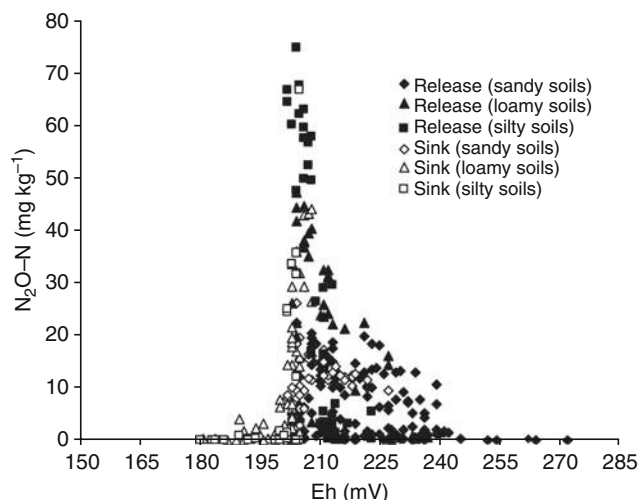
Anaerobic oxidation of methane

Anaerobic oxidation of methane (AOM) is a microbial process occurring mainly in anoxic marine sediments and reducing the emission of methane from the ocean into the atmosphere. During AOM, methane is oxidized with sulfate as the terminal electron acceptor: CH₄ + SO₄²⁻ → HCO₃⁻ + HS- + H₂O. AOM is mediated by

a syntrophic consortium of methanotrophic archaea and sulfate-reducing bacteria. Recent investigations have shown that some consortia of archaea and bacteria are also able to oxidize methane with nitrate instead of sulfate (Raghoebarsing et al., 2006). But recent findings suggest that this nitrate-reducing process coupled to methane oxidation can also be performed by a single bacterium without the need for an archaeal partner.

N₂O sink

Natural production and emission to the atmosphere of nitrous oxide is from microbial activity in soils and in the aquatic systems. N₂O is greenhouse gas that increased by 16% over the last 200 years. N₂O uptake has been observed in soils, aquatic systems, and riparian zones. A complete denitrification, at which N₂O is reduced to N₂, is assumed to be the main elimination or sink process of N₂O in the soils, beside dissolution in water. However, other types of N₂O sink were observed, for example, N₂O fixation with following transforming to NH₃. Only 1% of the microbes in soils have the ability to produce the enzyme N₂O reductase that reduces N₂O to N₂. The production of the enzyme is controlled by environmental influences like oxygen concentration and the concentration of the denitrification intermediate products. The potential of this process depends highly on the N₂O and O₂ concentrations, and aggregate sizes in the soil (Vieten, 2008). Next factors affecting N₂O uptake by soils are nitrogen availability, soil wetness, temperature, soil drainage conditions, and soil pH. Maximum N₂O reduction was measured at pH 6 and 7 (Smith et al., 1983). Agricultural soils are usually fertilized and therefore not likely to be sinks for N₂O, some studies report on N₂O uptake in fertilized fields; several studies report on considerable N₂O uptake in forest soils, which may potentially be important sinks for atmospheric N₂O; riparian zones depending on local conditions may be potential sinks for N₂O; N₂O uptake may occur in the open ocean (Kroeze et al., 2007). Because the N₂O emission at the soil surface is the result of production and consumption processes, some research has concentrated on net N₂O production. However, there are some reports of net negative fluxes of N₂O (i.e., fluxes from the atmosphere to the soil). Low mineral N and large moisture contents have sometimes been found to favor N₂O consumption. Denitrification is the responsible process, reducing N₂O to N₂. However, it has also been reported that nitrifiers consume N₂O in nitrifier denitrification. The wide range of conditions found to allow N₂O consumption, ranging from low to high temperatures, wet to dry soils, and fertilized to unfertilized plots. Generally, conditions interfering with N₂O diffusion in the soil seem to enhance N₂O consumption. Soil sink could help account for the current imbalance in estimated global budgets of N₂O (Chapuis-Lardy et al., 2007). N₂O emission and consumption is regulated within a narrow redox potential range +120 to +250 mV (Yu et al., 2001) and +200 to 230 mV (Włodarczyk et al., 2005).



Greenhouse Gases Sink in Soils, Figure 1 Relationship between the N₂O-N content and the redox potential of the releasing and consumption phases. (From Włodarczyk et al., 2005.)

et al., 2005) due to the balance of N₂O production and its further reduction to N₂. The interval of redox potentials allowing the existence of gaseous nitrous oxide in the equilibrium or “quasi-equilibrium” with the soil is very narrow and does not exceed 50 mV (Figure 1). Soils texture and particle size distribution significantly differentiated soil ability to N₂O consumption. Nitrous oxide sink showed a significant positive correlation with the fraction 0.05–0.002 mm and a negative one with the fractions >0.05 mm (Włodarczyk et al., 2005).

Summary

Sink of the main greenhouse gases in the Earth’s atmosphere such as CO₂, CH₄ and N₂O were viewed. Mitigation of greenhouse gases emission leads to minimizing the effects of global warming. The main natural carbon sinks are absorption of carbon dioxide by the oceans and photosynthesis by plants and algae. The main manmade sinks are landfills and carbon capture and storage proposals. Methanotrophs play a major role in the reduction of the release of methane into the atmosphere from environments such as rice paddies, landfills, bogs, and swamps where methane production is relatively high. Anaerobic oxidation of methane is a microbial process reducing the emission of methane from the ocean into the atmosphere. A complete denitrification, at which N₂O is reduced to N₂, is assumed to be the main elimination or sink process of N₂O in the soils, besides dissolution in water. Forest soils and riparian zones may potentially be important sinks for atmospheric N₂O depending on local conditions.

Bibliography

- Brzezińska, M., Kuzyakow, Y., Włodarczyk, T., Stahr, K., and Stępniewski, W., 1998. Oxidation of methane and

- dehydrogenase activity in a Mollic Gleysol – Short communication. *Journal of Plant Nutrition and Soil Science*, **161**, 697–698.
- Chapuis-Lardy, L., Wrage, N., Metay, A., Chotte, J.-L., and Bernoux, M., 2007. Soils, a sink for N_2O ? A review. *Global Change Biology*, **13**(1), 1–17.
- Kroeze, C., Bouwman, A. F., and Slomp, C. P., 2007. Sinks for nitrous oxide at the earth's surface. In Reay, D., Hewitt, C. N., Smith, K., and Grace, J. (eds.), *Greenhouse Gas Sinks*. Wallingford: CABI International, pp. 227–242.
- Lal, R., 2004. Soil carbon sequestration impacts on global climate changes and food security. *Science*, **304**, 1623–1627.
- Large, J. P., 1983. Methylotrophy and Methanogenesis (vol. 8 in the series Aspects of Microbiology). In Cole, J. A., Knowles, C. J., and Schlessinger, D. (eds.), Wokingham: Van Nostrand-Reinhold.
- Luo, Y., and Zhou, X., 2006. *Soil Respiration and the Environment*. Amsterdam: Elsevier.
- Mancinelli, R. L., 1995. The regulation of methane oxidation in soil. *Annual Review of Microbiology*, **49**, 581–605.
- Raghoebarsing, A. A., Pol, A., van de Pas-Schoonen, K. T., Smolders, A. J., Ettwig, K. F., Rijpstra, W. I., Schouten, S., Damsté, J. S., Op den Camp, H. J., Jetten, M. S., and Strous, M., 2006. A microbial consortium couples anaerobic methane oxidation to denitrification. *Nature*, **440**, 878–879.
- Smith, C. J., Wright, M. F., and Patrick, W. H., Jr., 1983. The effect of soil redox potential and pH on the reduction and production of nitrous oxide. *Journal of Environmental Quality*, **12**, 186–188.
- Swift, R. S., 2001. Sequestration of carbon by soil. *Soil Science*, **166**(11), 858–871.
- Vieten, B., 2008. N_2O reduction in soils. PhD thesis, University of Basel, Faculty of Science. Official URL: http://edoc.unibas.ch/diss/DissB_8389.
- Włodarczyk, T., Stępniewska, Z., Brzezińska, M., Pindelska, E., and Przywara, G., 2004. Influence of methane concentration on methanotrophic activity of Mollic Gleysol and Haplic Podzol. *International Agrophysics*, **18**, 375–379.
- Włodarczyk, T., Stępniewski, W., and Brzezińska, M., 2005. Nitrous oxide production and consumption in Calcaric Regosols as related to soil redox and texture. *International Agrophysics*, **19**, 263–271.
- Yu, K. W., Wang, Z. P., Vermoesen, A., Patrick, W. H., Jr., and Van Cleemput, O., 2001. Nitrous oxide and methane emission from different soil suspensions: effect of soil redox status. *Biology and Fertility of Soils*, **34**, 25–30.

Cross-references

- [Climate Change: Environmental Effects](#)
[Greenhouse Gas Fluxes: Effects of Physical Conditions](#)

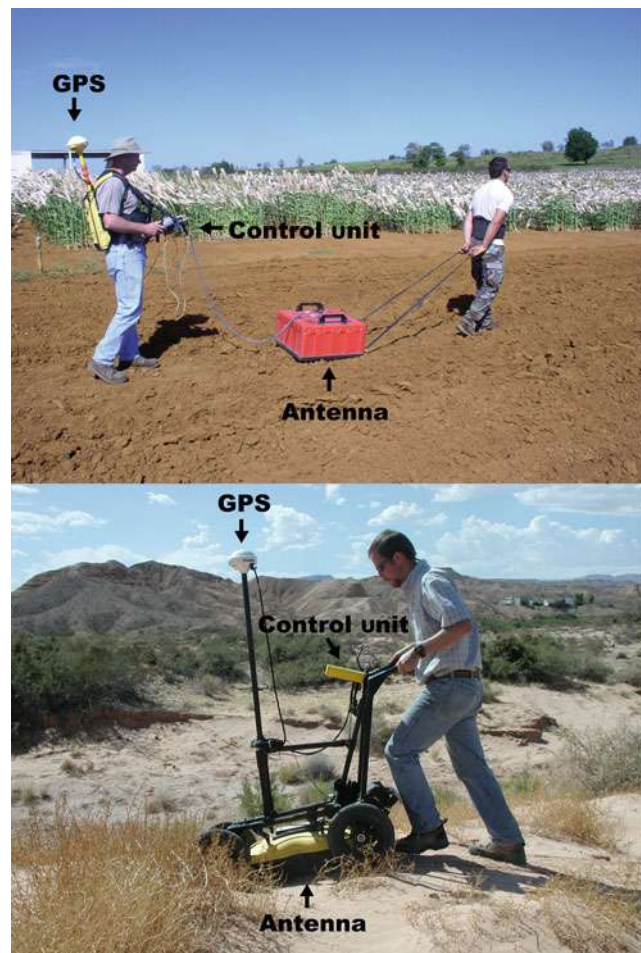
GROUND-PENETRATING RADAR, SOIL EXPLORATION

Jim Doolittle
USDA-NRCS, National Soil Survey Center, Newtown Square, PA, USA

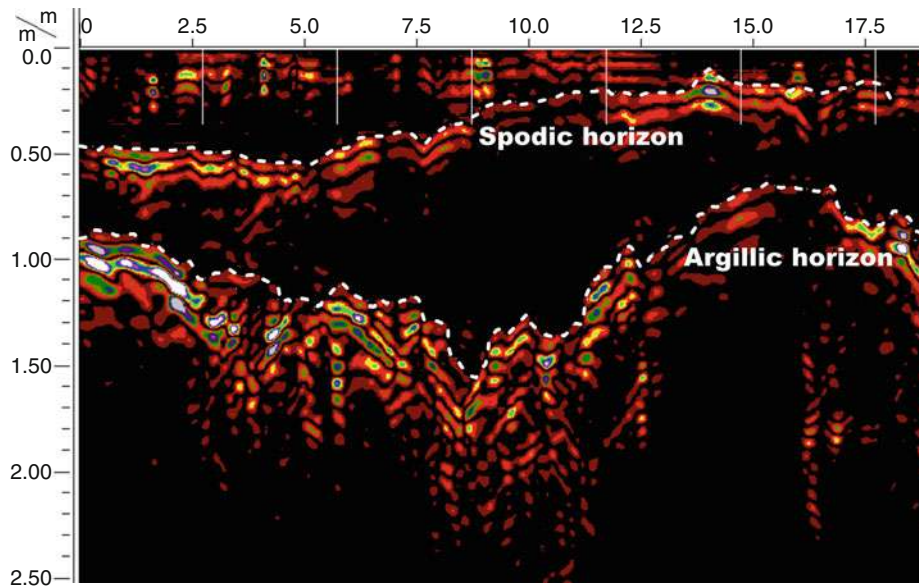
Ground-penetrating radar (GPR) is a noninvasive, high-resolution geophysical method used in soil exploration. Ground-penetrating radars transmit short pulses of high- to ultra-high frequency (center frequencies from 12.5 MHz to 2.6 GHz) electromagnetic energy into the ground to detect subsurface interfaces. A time-scaled system, GPR measures the time that it takes pulses of

electromagnetic energy to travel from an antenna to a subsurface interface and back. Interfaces often correspond to major soil, stratigraphic, and lithologic layers or features. Whenever a pulse contacts an interface separating layers with different relative dielectric permittivity (ϵ_r), a portion of the energy is reflected back to a receiving antenna. The more abrupt and contrasting the permittivity on opposing sides of an interface, the greater the amount of energy that is reflected back to the antenna and the greater the amplitude of the recorded signal. To convert the travel time into a depth scale, the velocity of pulse propagation or the depth to a reflector must be known.

A typical GPR system consists of a radar control unit with antenna (Figure 1). The control unit serves as a user interface and consists of a colored screen, microprocessor, and mass storage device. Choice of antenna is depth, target, and soil dependent. Higher frequency antennas provide greater resolution but do not penetrate as deeply as lower frequency antennas. Soils having high electrical



Ground-Penetrating Radar, Soil Exploration, Figure 1 Modern GPR systems are lightweight, highly mobile, and integrated with global positioning systems (GPS).



Ground-Penetrating Radar, Soil Exploration, Figure 2 Highlighted on this radar record of Pomona soils (sandy, siliceous, hyperthermic Ultic Alaquods) are the upper boundaries of the spodic and argillic horizons.

conductivity rapidly attenuate radar energy, restrict penetration depths, and severely limit the effectiveness of GPR (Daniels, 2004; Jol, 2009). The electrical conductivity of soils increases with increasing water, soluble salt, and/or clay contents.

Ground-penetrating radar provides spatially continuous records of the subsurface. Figure 2 is a representative radar record from an area of Pomona soils, which form in sandy over loamy marine sediments in Florida (USA). In Figure 2, the continuity and depths to both the spodic and argillic horizons are highlighted with segmented lines.

In soil exploration, GPR is principally used to document the presence, depth, lateral extent, and continuity of subsurface soil horizons, stratigraphic layers, and lithologic units (Collins, 2008; Daniels, 2004; Jol, 2009). It has also been used to: identify preferential flow pathways, animal burrows, and buried drainage tiles; assess root biomass and hydrocarbons in soils; study soil moisture dynamics, water table depths, and the movements of agrochemicals; predict groundwater flow patterns; and characterize near-surface hydrologic conditions.

Bibliography

- Collins, M. E., 2008. History of ground-penetrating radar applications in agriculture. In Allred, B. J., Daniels, J. J., and Ehsani, M. R. (eds.), *Handbook of Agricultural Geophysics*. Boca Raton: CRC Press, pp. 45–55.
 Daniels, D. J., 2004. *Ground Penetrating Radar*, 2nd edn. London: The Institute of Electrical Engineers.
 Jol, H., 2009. *Ground Penetrating Radar: Theory and Applications*. Amsterdam: Elsevier Science.

Cross-references

- [Electrical Properties of Soils](#)
[Hydropedological Processes in Soils](#)
[Mapping of Soil Physical Properties](#)
[Nondestructive Measurements in Soil](#)

GROUNDWATER

The water in the saturated portion of the soil or the underlying porous materials.

GULLY (LINEAR) EROSION

The erosion process whereby water accumulates and often recurs in narrow channels and, over short periods, removes the soil from this narrow area to considerable depths, often defined for agricultural land in terms of channels too deep to easily ameliorate with ordinary farm tillage equipment, typically ranging from 0.5 m to as much as 25–30 m.

Bibliography

- Glossary of Soil Science Terms. Soil Science Society of America. 2010 <https://www.soils.org/publications/soils-glossary>

Cross-references

- [Water Erosion: Environmental and Economical Hazard](#)

H

HARDENING

Hardening or induration of a soil takes place by the loss of void space by compaction or filling with fine materials.

Bibliography

Chesworth, W. (ed.). 2008. Encyclopedia of Soil Science, Springer, p. 303.

HARDPAN

A compacted, impermeable layer of soil at or near the surface.

HARDPAN SOILS: MANAGEMENT*

Warren J. Busscher
Agricultural Research Service, US Department of Agriculture, Coastal Plain Soil, Water and Plant Research Center, Florence, SC, USA

Synonyms

Hard-layer soils; Management of hard-layered soils

Definition

Hardpan soil. A soil that has a layer whose physical characteristics limit root penetration and restrict water movement.

Penetration resistance. The penetration resistance (or soil strength) is usually measured as the force exerted on

*All rights reserved

a standardized implement (penetrometer) as it is pushed into the soil divided by the cross-sectional area of its tip.

Introduction

Hardpans, hard layers, or compacted horizons, either surface or subsurface, are widespread problems that limit crop production. Hard layers can be caused by traffic or soil genetic properties that result in horizons with high density or cemented soil particles (Hamza and Anderson, 2005); these horizons have elevated penetration resistances that limit root growth and reduce water and airflow. Limited root growth leads to limited crop water and nutrient uptake. Reduced water flow prevents rainfall or irrigation water from filtering into the soil profile where it can be stored for plant growth. Reduced airflow limits oxygen and carbon dioxide exchange with the atmosphere; exchange is needed for plant and microorganism respiration. These limitations reduce crop productivity.

Improving the hard layer consists of reducing its hardness or penetration resistance. When we reduce the layer's hardness, we assume that it and/or the layers below it have properties conducive to plant growth. As the hard layer softens, water and air are able to move into and/or through it and into the layers below, improving conditions for root growth and with its productivity. There are several ways to improve hard layers; the most common is tillage; but other solutions exist in the forms of water/crop management and soil amendments.

Tillage

Tillage has been and is the common method used to remediate hard-layer problems; it physically breaks up hard layers. Tillage by hand involves digging with a spade, broad fork, or U-fork. In large-scale mechanical agriculture, tillage involves using a tractor to pull any of a number of tines or shanks through the soil. In the mechanical method, shallow hard layers (<5 cm) can be

broken up with tines or cultivators that disrupt the surface soil. Deeper hard layers (>15 cm) can be broken up with shanks. Shanks are sized or adjusted so they are pulled through the soil at the depth of the hard layer shattering it and decreasing its resistance to root growth. Different shank designs that are manufactured by various tillage companies produce different results or work with different efficiencies depending on the type of hard layer and the type of soil. Consider the example seen in [Figure 1](#) where the hard layer was located in loamy sand between 20-cm and 40-cm depths. Tillage in this example was performed with an older 5-cm thick shank that produced wider zones of disruption and used more energy than narrower shanks. Also seen in [Figure 1](#), the process that reduced soil penetration resistance under the row increased it under the trafficked mid row because of the tractor weight.

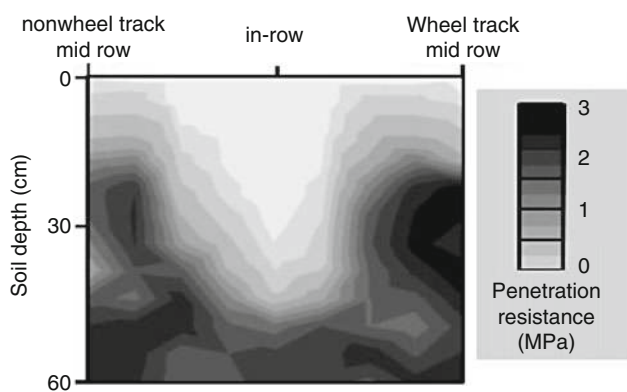
To meet conservation goals, deep tillage such as that shown in [Figure 1](#) can be performed in such a way that it does not invert soil; equipment companies have developed shanks that break up soil with minimal surface disruption. Non-inversion tillage leaves most crop residue on the soil surface protecting it from erosion, surface crusting/compaction, and excessive evaporation ([Raper, 2007](#)). Though early studies with non-inversion and reduced tillage demonstrated little or no yield advantage, improvements in planters, residue management, and soil/crop management practices increased the success of conservation systems by optimizing factors that affected seed germination and vigor.

The problem with tillage is that the reduction of penetration resistance is temporary. For some soils, temporary means a few to several years. For others, it can mean only a few months ([Raper et al., 2005a](#)). Most often it is effective for only months. In either case, over time, soil reconsolidates leading to reduced water/airflow, reduced root growth, and lower crop yields ([Håkansson and Lipiec, 2000](#)). Even if the reconsolidated soil's penetration resistance is not as high as it was originally, it can be high enough to limit growth. As a result, tillage has to be

performed repeatedly at prescribed frequencies, often seasonally or annually. Frequent tillage can be expensive because it often requires large tractors (14–20 kg weight per shank), 20–40 min ha^{-1} of labor, and 20–25 L ha^{-1} of fuel. Eventually, the producer has to make the decision whether or not to till based on the value of increased yield by tillage vs. the cost of tillage ([Bolliger et al., 2006](#)).

In an effort to save time, fuel, and production costs, deep tillage studies have included soil disruption on a multiple-year rotation. In many cases, not tilling every year reduces yield to levels that may (or may not) be acceptable given the increase in fuel costs. Additionally, annual deep tillage may not be needed for some crops, such as cotton, to maintain yields. Deep tilling every 2–3 years may be just as effective as deep tilling annually ([Busscher et al., 2010](#)). This will depend on the crop and variety grown, amount of re-compaction, and other crop management techniques such as row width and traffic/compaction patterns.

Another effort to save fuel and production costs involves varying the tillage depth. Deep tillage is often performed with implements set to a fixed depth. But depth to the compacted layer varies throughout a field. What depth should the implement have? On the one hand, if tillage depth is based on the deeper zones of the compacted layer, the implement disrupts too much soil where the compacted layer is shallow; this wastes fuel. On the other hand, if tillage depth is based on the shallower zones, the implement will not disrupt the whole compacted layer, leaving hard zones that limit root growth. Technologies are now available that allow tillage to vary with the depth of the compacted layer; this can be accomplished by mapping the hard layer of a field or placing sensors on the shanks. Shanks are then raised and lowered as needed. This action can save energy without sacrificing crop yields. Research has shown that this “site-specific tillage” produced yields equivalent to those of uniform deep tillage while reducing tractor draft forces, drawbar power, and fuel used ([Raper et al., 2005b](#)).



Hardpan Soils: Management, Figure 1 Soil penetration resistance for a loamy sand that has a hard layer at 20- to 40-cm depths. The soil was tilled to a depth of about 45 cm with shank that did not invert the soil.

Other solutions

Soil Organic Matter: For the past few decades, soil scientists and producers have been trying to increase organic matter levels in soils ([Carter, 2002](#)). This improves fertility, decreases strength in hard layers (especially those close to the surface), and increases yield ([Soane, 1990](#)). But with the increase in fuel prices comes the need for organic matter/residue in the form of cellulose. The same organic matter that scientists and producers were trying to increase in soils may be removed to produce ethanol. Both increased organic matter and removed cellulose might be attainable; but only after some research. Research on organic matter removal had started during the 1970s fuel crisis; but because the crisis did not continue, the research priority decreased as funding ceased. Results from the 1970s showed that some residue could be removed provided that nutrients were replaced with fertilizers. The problem with this finding is that fertilizer

production requires large amounts of energy. The previously unfinished research has resumed asking questions about the sustainability, economic efficiency, energy efficiency of residue removal, and the effect of the removal on soil properties such as penetration resistance.

To ameliorate hard layers, additions of organic matter need not come from crop residues. Another way to add it, especially to subsurface hard layers, is through root growth (Yunusa and Newton, 2003). In this method, cover crops are grown between growing seasons aimed at penetrating the hard layers with their roots. Cover crop roots are able to penetrate soil where production crops cannot either because conditions between growing seasons are different, for example, cold and wet, or because the cover crop has hearty roots but it is not an economic crop. For example, large rooted crops such as radish are grown to add both large holes and large amounts of organic matter to the hard layer. In another method, rye cover crop roots penetrate compacted layers softened because they are wet in winter; rye roots leave holes behind for summer row crop roots to follow. Success of these methods depends on whether the roots can grow deep enough to affect the hard layer and whether or not the holes left by the roots collapse.

Other management: Another way to soften hard layers that met with some success was to irrigate the soil with drip tubes buried just above the hard layer. In this method, irrigation water keeps the hard layer soft while supplying the crop's needs. However, tubes buried above a hard layer require careful management to avoid overwatering or under watering. Overwatering prevents roots from penetrating a flooded layer while under watering does not loosen the hard layer enough. It is likely that both types of irrigation will occur simultaneously between and at the buried tubes or between and at irrigation ports or emitters along the tubes. Water management needs to find a proper irrigation schedule that can satisfy all needs for each soil. Because water is not at the soil surface, this type of irrigation reduces evaporation saving water but a relatively dry surface can reduce germination and stand establishment during years with early dry seasons.

A long-term solution that reduces both compaction and energy demand is to add amendments to soil. The amendment chosen will have to reduce compaction much like the organic matter does and it should be effective for several years because it will be expensive to incorporate it into the soil. Potential amendments include polyacrylamide (PAM) and biochar. PAM was tried in the 1950s. Older formulations were used to stabilize aggregates in the surface 30-cm to 40-cm depths. Hundreds of kilograms of PAM per hectare were needed, limiting PAM-use to high value crops and nurseries. Since the 1950s, polymer formulations and purity have improved, making them more effective at lower concentrations. In the 1990s, environmentally safe PAM was found to be an effective erosion-preventing and infiltration-enhancing polymer when applied at 1–10 mg L⁻¹ in furrow irrigation water. This can affect the surfaces of irrigated soils; but if the hard layer is deep

in the profile, the amount of PAM and its mixing into the soil will cost several hundred euros per hectare. Given the high cost of fuel, this cost might be feasible if the PAM could last multiple years. Current estimates have the PAM breaking down at a rate of 10% per year.

Another amendment that has attracted attention in the past few years is biochar. Biochar captured the attention of the agricultural community as a result of archeological/agricultural findings of charcoal-amended soils in the Amazon and other historically old areas. Charcoal- or biochar-amended soils were found to have supported larger populations 500–1,000 years ago than previously estimated and today they are still more productive than expected. If biochar can be effective over time and if it improves productivity, it could be economically feasible to use it as a long-term soil amendment to eliminate or reduce hard-layer tillage (Busscher et al., 2010). More research needs to be performed before making a final decision; but preliminary results are favorable. Biochars vary based on their source material and production technique. Current work is underway to match biochar properties to the needs of the soil and its hard layer; then their effectiveness needs to be assessed.

Effects on individuals

Whether or not you work in tillage management or agrophysics, they affect you because of their impact on food, fiber, and energy production. As populations increase and as we make more demands on our resources, we will require tillage management and other areas of agriculture to produce more food for more people with a limited and dwindling soil base (Small, 2009). We can all become involved by being educated and active in conservation efforts to improve the lot of our soils, our environment, and our fellow men.

Bibliography

- Bolliger, A., Magid, J., Amado, J. C. T., Skóra Neto, F., Ribeiro, M., Calegari, A., Ralisch, R., and de Neergaard, A., 2006. Taking stock of the Brazilian "Zero-Till Revolution": a review of landmark research and farmers' practice. *Advances in Agronomy*, **91**, 47–110.
- Busscher, W. J., Schomberg, H. H., and Raper, R. L., 2010. Soil and water conservation in the southeastern United States: a look at conservation practices past, present, and future. In Zobeck, T. M., and Schillinger, W. F. (eds.), *Soil and Water Conservation Advances in the United States*. Madison: Soil Science Society of America, pp. 183–200.
- Carter, M. R., 2002. Soil quality for sustainable land management: organic matter and aggregation interactions that maintain soil functions. *Agronomy Journal*, **94**, 38–47.
- Håkansson, I., and Lipiec, J., 2000. A review of the usefulness of relative bulk density values in studies of soil structure and compaction. *Soil and Tillage Research*, **53**, 71–85.
- Hamza, M. A., and Anderson, W. K., 2005. Soil compaction in cropping systems: A review of the nature, causes and possible solutions. *Soil and Tillage Research*, **82**, 121–145.
- Raper, R. L., 2007. In-row subsoilers that reduce soil compaction and residue disturbance. *Applied Engineering in Agriculture*, **23**, 253–258.

- Raper, R. L., Schwab, E. B., Balkcom, K. S., Burmester, C. H., and Reeves, D. W., 2005a. Effect of annual, biennial, and triennial in-row subsoiling on soil compaction and cotton yield in Southeastern U.S. silt loam soils. *Applied Engineering in Agriculture*, **21**(3), 337–343.
- Raper, R. L., Reeves, D. W., Shaw, J. N., Van Santen, E., and Mask, P. L., 2005b. Using site-specific subsoiling to minimize draft and optimize corn yields. *Transactions of the American Society of Agricultural Engineers*, **48**, 2047–2052.
- Soane, B. D., 1990. The role of organic matter in soil compactibility: a review of some practical aspects. *Soil and Tillage Research*, **16**, 179–201.
- Small, A., 2009. Land degradation on the rise (Online). Available from World Wide Web: <http://www.fao.org/> accessed 21 May 2009.
- Yunusa, I. A. M., and Newton, P. J., 2003. Plants for amelioration of subsoil constraints and hydrological control: the primer-plant concept. *Plant and Soil*, **257**, 261–281.

Cross-references

- Compaction of Soil
- Conditioners, Effect on Soil Physical Properties
- Hardsetting Soils: Physical Properties
- Infiltration in Soils
- Layered Soils, Water and Solute Transport
- Root Responses to Soil Physical Limitations
- Soil Surface Sealing and Crusting
- Soil Penetrometers and Penetrability
- Subsoil Compaction

HARDSETTING SOILS: PHYSICAL PROPERTIES

Neyde Fabíola Balarezo Giarola¹,

Herdjania Veras de Lima², Alvaro Pires da Silva³

¹Departamento de Ciéncia do Solo e Engenharia Agrícola, Universidade Estadual de Ponta Grossa, Ponta Grossa – Paraná, Brazil

²Instituto de Ciéncias Agrárias, Universidade Federal Rural da Amazônia, Belém – Pará, Brazil

³Departamento de Ciéncia do Solo, Escola Superior de Agricultura “Luiz de Queiroz”, Universidade de São Paulo, Piracicaba – São Paulo, Brazil

Synonyms

Cohesive soils or soils with a cohesive character

Definition

Hardsetting soils or soils exhibiting hardsetting behavior. Soils that have horizons that, when dried, harden significantly, constituting a mass without structure (apedal); this soil tilth is more difficult or even impossible. This impediment can be avoided by humidifying the soils (Mullins et al., 1990; Mullins, 1999).

Cohesive soils or soils with cohesive character. Soils with dense pedogenic subsurface horizons, which are very resistant to penetration of the knife or hammer and are very hard to extremely hard when dry, becoming friable or firm when moist. In natural conditions, they have

a weak structural organization, generally appearing solid or with some tendency to form blocks (Fabiola et al., 2003; Lima et al., 2006).

Introduction

Hardsetting is a phenomenon that occurs in many soils around the world in arid tropical, semiarid, and Mediterranean regions (Mullins, 1999) and covers more than 110 million ha of areas of agricultural exploitation. The term hardsetting was introduced by Northcote (1960) in binary textured soils of Western Australia, and was subsequently recognized in Africa, Asia, and South America (Mullins et al., 1987; Mullins et al., 1990; Chartres et al., 1990; Fabiola et al., 2003; Lima et al., 2006).

The Australians were pioneers in identifying and mapping hardsetting soils, as well as in incorporating these characteristics into a soil taxonomic classification system (Harper and Gilkes, 1994; Isbell, 1996). Nevertheless, the ambiguous nature of hardsetting behavior has limited the use of the term in other classification systems outside Australia and Brazil (Harper and Gilkes, 1994).

Many agricultural problems are associated with hardsetting soils, including a more restricted period for soil tillage and an increase in physical impediments to adequate root development (Mullins et al., 1987; Mullins et al., 1990). Hardsetting is normally associated with processes of soil degradation such as erosion, compaction, crusting, and acidification of the soil (Mullins, 1997). In these soils, the agricultural production is frequently frustrating due to low production and a high cost/benefit ratio.

Characteristics of hardsetting soils

Hardsetting soils present a pedogenetic densification in the surface horizons (A and AB) and the subsurface horizons (BA, B, E, EB, BE) (Mullins et al., 1990; Chartres et al., 1990; Fabiola et al., 2003). When dry, they present a lack of visible structural organization (they are massive), elevated resistance to penetration by a knife or auger, and a hard to very hard (at times extremely hard) consistency. The humid soil consistency varies from friable to firm, and a dry sample, when immersed in water, disintegrates rapidly (Mullins, 1997).

Hardsetting characteristics normally occur in deep soils, with a loamy-sandy-clay texture, clay-like or very clay-like, in a plain to gently undulating relief. Hardsetting horizons possess soil bulk density higher than the underlying horizons and tensile strength values ≥ 0.09 MPa (Fabiola et al., 2003). From a chemical point of view, they present a low base saturation ($V < 50\%$), organic material content $< 2.0\%$, Fe_2O_3 content (by H_2SO_4) < 8 g kg^{-1} , and an illitic or kaolinitic mineralogy (Mullins et al., 1990; Giarola et al., 2001).

It is important to distinguish between hardsetting and compacted soils. Soil compaction results from repeated or long-term movement of agricultural machinery and stock compacting the soil profile when it is moist, often remaining hard when wet. In many cases, this compaction

layer occurs at depth. Hardsetting affects the A1 horizon (Mullins et al., 1987), but the soil softens when moist.

The hardsetting horizons should not be confused with fragipan, which also presents high levels of cohesion, but presents diverse pedogenetics (chemical grouting), occurring at greater depths; fragipan has different implications in relation to soil management (Chartres et al., 1990).

Hardsetting processes

The hardsetting character can be associated with the following processes: (1) the precipitation of soluble salts in the contact zone between aggregates and/or soil particles (Mullins and Panayiotopoulos, 1984; Mullins et al., 1987; Mullins, 1999); (2) the dispersion of soil clay, associated or not with the presence of sodium (Mullins, 1999); (3) natural bulk density increases of the soil particles, which increase the effective stress and the water matrix potential in the soil as the soil dries (Fabiola et al., 2003) (Figure 1).

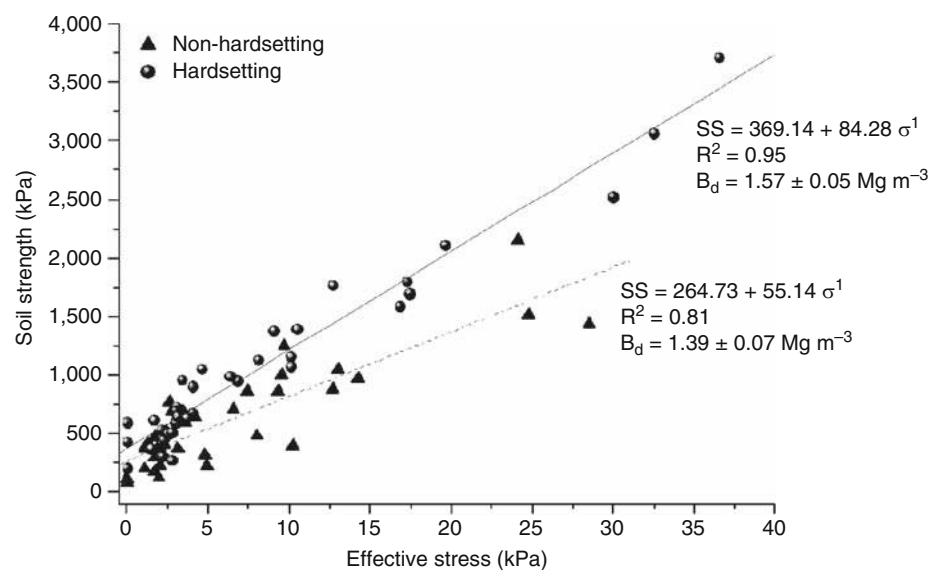
Other types of hardsetting soils have been distinguished in northern Cameroon (Lamotte, et al., 1997): (1) Soils with very hard sandy layers that usually occur under a more or less softer sandy layer. Some indications suggest that these properties could result from the gradual clogging of the pores between sand grains due to newly formed clay. Such a process may be favored by the succession of drying and wetting periods. (2) Soils with a very hard clay layer that are thought to be derived from Vertisols degraded by cultivation. These very hard layers, sandy or clayey, are not necessarily associated with a high sodium content but rather with a low iron content, as reflected by their pale color.

Physical behavior of hardsetting soils

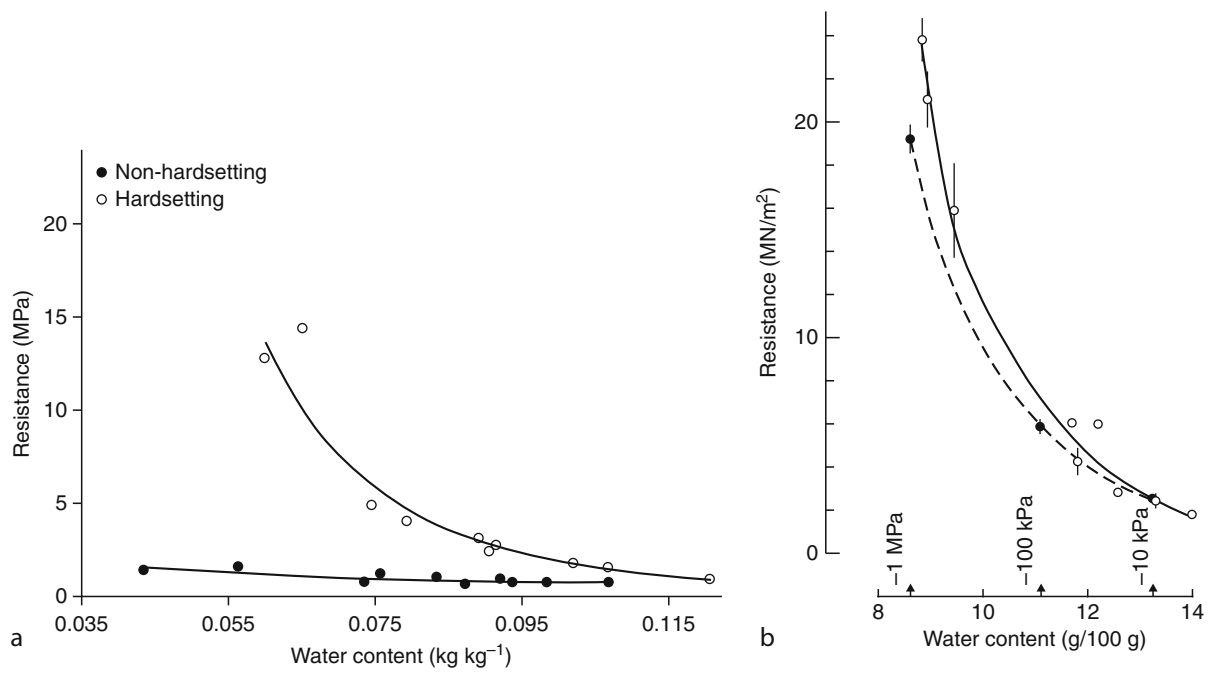
Once wet, the unstable hardsetting soil structure collapses and then shrinks as it dries. This leads to a “massive” soil layer with little or no cracks and greatly reduced pore space (Lima et al., 2006). This hard-set “massive” structure is associated with poor infiltration, a low water holding capacity, and a high soil strength (Figure 1). In many instances, this causes patchy establishment and poor crop and pasture growth. Naturally hardsetting soils are unable to develop water-stable aggregates (Mullins et al., 1990). This means that during wetting, soil aggregates start to swell and become soft. This occurs prior to “slumping” (also referred to as “slaking”) when the aggregates collapse and disintegrate.

Hardsetting can also occur in soil with a high exchangeable sodium percentage (ESP) through the “dispersion” of soil aggregates. This results in clay and silt becoming suspended in the soil solution and causing a breakdown of aggregates (Mullins et al., 1990). Other factors that influence the dispersion of soil aggregates include the soil electrical conductivity (EC), calcium/magnesium ratios, and the organic matter content. Soil types more prone to soil structure decline are sandy loams to clay loams (between 10% to 35% clay), particularly those low in organic matter (<2%) (Giarola et al., 2001).

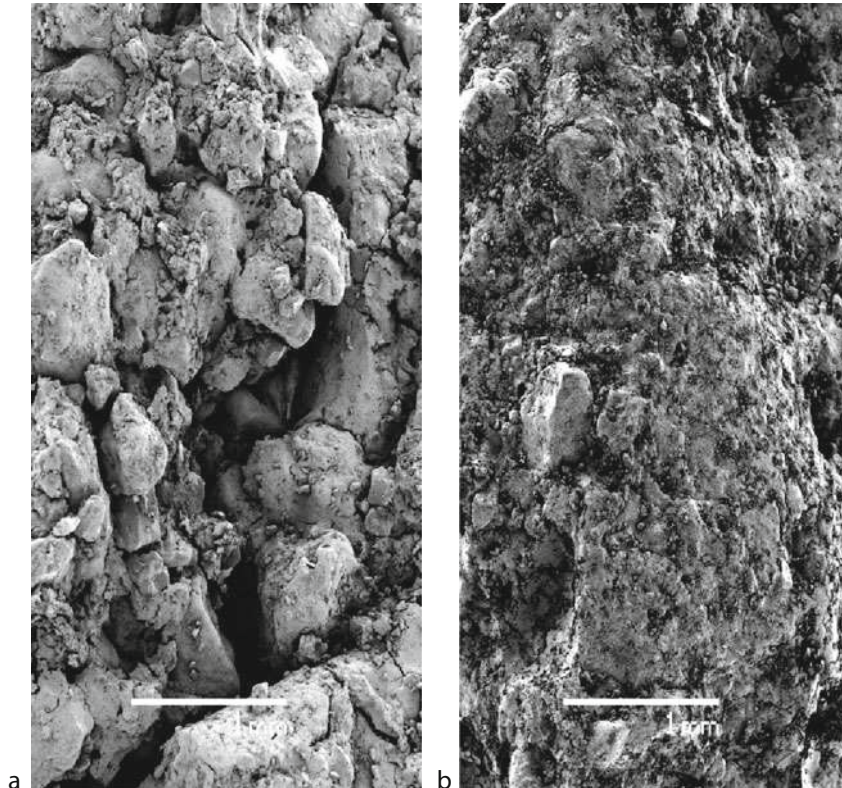
The soil resistance to penetration curve (RP) can be used to differentiate hardsetting from non-hardsetting soils. In soils with hardsetting horizons, in the same moisture range, the variation of soil resistance is much greater than in soils with stable structures (Figure 2). The soil resistance normally exceeds 3 MPa before the soil reaches the permanent wilting point (1,500 kPa of



Hardsetting Soils: Physical Properties, Figure 1 Soil strength (SS) versus effective stress (σ') for non-hardsetting (A1) and hardsetting (AB1) horizons. B_d is the bulk density.



Hardsetting Soils: Physical Properties, Figure 2 Curve of soil resistance to penetration for hardsetting and non-hardsetting soils from Brazil (a) and Australia (b). Source: adapted from (a) Giarola et al. (2001) and (b) Mullins et al. (1987).



Hardsetting Soils: Physical Properties, Figure 3 Structural arrangement of soil particles of (a) non-hardsetting and (b) hardsetting horizons from Cruz das Almas, Bahia, Brazil.

matrix potential). Some soils studied by Mullins et al. (1987) developed a resistance to penetration greater than 3 MN m^{-2} , before being dried to a potential of 100 kPa. Ley et al. (1995) found an RP equal to or greater than 2 MPa in some soils from Nigeria, when these soils were dried at a matrix potential of only 100 kPa. Similar results have been obtained for hardsetting soils from the United Kingdom (Young et al., 1991), Australia (Mullins et al. 1987), Tanzania (Mullins, 1997), and Brazil (Fabiola et al., 2003).

In addition to their high cohesion, the denser layers have higher bulk densities ($1.6\text{--}1.8$ compared to $1.4\text{--}1.5 \text{ Mg m}^{-3}$) and lower permeabilities compared to the softer upper layers (Fabiola et al., 2003; Lima et al., 2006) (Figure 3).

The decrease in total pore volume is another negative consequence of hardsetting behavior, as it affects the biological activity, the movement and capacity of water retention, and the availability of water for plants. The lower pore volume shows a marked effect on the increase of RP during soil drying, which can vary from close to zero to 25 MPa at the point of permanent wilt (matrix potential $[\psi_m] = 1.5 \text{ MPa}$). Values of RP = 3 MPa were also obtained for a dampness close to $0.15 \text{ cm}^3 \text{ cm}^{-3}$, which is sufficient to impede plant growth or emergence (Mullins, 1997).

The tensile strength (TS) of aggregates is another parameter used to recognize hardsetting behavior. Values of TS = 200 kPa were registered in materials from Australian hardsetting soils after air drying (Ley et al., 1989; Gusli et al., 1994). In Brazil, the TS varied from 37 to 76 kPa in hardsetting horizons with a loamy-sandy-clay texture (Fabiola et al., 2003; Lima et al., 2006).

Conclusions

Hardsetting soils are structurally unstable soils common in Oceania, Africa, Asia, and South America. Because of their instability to wetting, cultivated hardsetting soils become almost homogenous masses upon drying and present physical problems such as high soil strength, poor infiltration, and crusting, which tend to adversely affect crop performance and management. The latter includes losses in the timeliness of cultivation, as well as a requirement for more frequent irrigation and tillage, leading to further deterioration in soil structure. The lack of defined parameters that indicate the presence of hardsetting behavior and the different degrees of cohesion make it impossible to accurately and easily recognize this behavior in soils.

Bibliography

- Chartres, C. J., Kirby, J. M., and Raupach, M., 1990. Poorly Ordered Silica and Aluminosilicates as Temporary Cementing Agents in Hard-Setting Soils. *Soil Science Society of America Journal*, **54**, 1060–1067.
- Fabiola, N., Giarola, B., da Silva, A. P., Imhoff, S., and Dexter, A. R., 2003. Contribution of natural soil compaction on hardsetting behavior. *Geoderma*, **113**, 95–108.

- Giarola, N. F. B., da Silva, A. P., Tormena, C. A., Souza, L. S., and Ribeiro, L. P., 2001. Similaridades entre o caráter coeso dos solos e o comportamento hardsetting: estudo de caso. *Revista Brasileira de Ciência do Solo*, **25**, 239–247.
- Giarola, N. F. B., Lima, H. V., Romero, R., Brinatti, A. M., and da Silva, A. P., 2009. Mineralogia e cristalografia da fração argila de horizontes coesos de solos nos tabuleiros costeiros. *Revista Brasileira de Ciência do Solo*, **33**, 33–40.
- Gusli, S., Cass, A., Macleod, D. A., and Blackwell, P. S., 1994. Structural collapse and strength of some Australian soils in relation to hardsetting: II. Tensile strength of collapsed aggregates. *European Journal of Soil Science*, **45**, 23–29.
- Harper, R. J., and Gilkes, R. J., 1994. Hardsetting in the surface horizons of sandy soils and its implications for soil classification and management. *Australian Journal of Soil Research*, **32**, 603–619.
- Isbell, R. F., 1996. *The Australian soil classification*. Melbourne: CSIRO Publishing.
- Lamotte, M., Bruand, A., Ohnenstetter, D., Idelfonse, P., and Pédro, G., 1997. A hard sandy-loam soil from semi-arid Northern Cameroon: II. Geochemistry and mineralogy of bonding agent. *European Journal of Soil Science*, **48**, 227–237.
- Ley, G. J., Mullins, C. A., and Lal, R., 1989. Hard-setting behaviour of some structurally weak tropical soils. *Soil and Tillage Research*, **13**, 365–381.
- Ley, G. J., Mullins, C. A., and Lal, R., 1995. The potential restriction to root growth in structurally weak Tropical soils. *Soil & Tillage Research*, **33**, 133–142.
- Lima, H. V., da Silva, A. P., Santos, M. C., Cooper, M., and Romero, R. E., 2006. Micromorphology and image analysis of a hardsetting ultisol (Argissolo) in the state of Ceará (Brazil). *Geoderma*, **132**, 416–426.
- Mullins, C. E., MacLeod, D. A., Northcote, K. H., Tisdall, J. M., and Young, I. M., 1990. Hardsetting soils: behavior, occurrence and management. *Advances in Soil Science*, **11**, 38–108.
- Mullins, C. E., and Panayiotopoulos, K. P., 1984. The strength of unsaturated mixture of sand and caolin and the concept of effective stress. *Journal of Soil Science*, **35**, 459–468.
- Mullins, C. E., Young, A. G., Bengough, A. G., and Ley, G. J., 1987. Hard-setting soils. *Soil Use and Management*, **3**, 79–83.
- Mullins, C. E., 1997. Hardsetting. In Lal, R., Blum, W. H., Valentine, C., and Stewart, B. A. (eds.), *Methods for assessment of soil degradation*. New York: CRC Press, pp. 109–128. Advances in Soil Science, 19.
- Mullins, C. E., 1999. Hardsetting soils. In Sumner, M. E. (ed.), *Handbook of soil science*. New York: CRC Press, pp. G65–G87.
- Northcote, K. H., 1960. A factual key for the recognition of Australian soils. Division of Soils. Melbourne: CSIRO, 120p. (Divisional Report, 4/60).
- Young, I. M., Mullins, C. E., Costigan, P. A., and Bengough, A. G., 1991. Hardsetting and structural regeneration in two unstable British sandy loams and their influence on crop growth. *Soil and Tillage Research*, **19**, 383–394.

Cross-references

- Aeration of Soils and Plants
Compaction of Soil
Conditioners, Effect on Soil Physical Properties
Crop Emergence, the Impact of Mechanical Impedance
Crop Responses to Soil Physical Conditions
Infiltration in Soils
Layered Soils, Water and Solute Transport
Root Responses to Soil Physical Limitations
Soil Penetrometers and Penetrability
Soil Surface Sealing and Crusting
Subsoil Compaction

HARVEST TECHNOLOGY

See [Mechanical Impacts at Harvest and After Harvest Technologies](#)

HEAT ADVECTION

See [Energy Balance of Ecosystems](#)

HEAT BALANCE

$R_n + M = C + \lambda E + G$, where: R_n - net gain of heat from radiation, M - net gain of heat from metabolism, C – loss of sensible heat by convection, λE - loss of sensible heat by evaporation, G –conductivity to the environment.

Bibliography

Monteith, J. and Unsworth, M., 2007. Principles of Environmental Physics. Academic Press.

Cross-references

[Energy Balance of Ecosystems](#)

HEAT CAPACITY

Synonyms

Thermal capacity

The quantity of heat required to raise a unit volume of the substance 1 degree of temperature.

Cross-references

[Coupled Heat and Water Transfer in Soil](#)
[Thermal Technologies in Food Processing](#)

HEAT DIFFUSION

See [Diffusion in Soils](#)

HEAT OF CONDENSATION

The amount of heat released when a vapor changes state to a liquid.

HEAT OF SUBLIMATION

The amount of energy required to convert ice directly to a vapor.

HEAT OF VAPORIZATION

The amount of heat required to change a volume of liquid to a vapor.

HEAT OF WETTING

The heat released by a unit mass of initially dry soil when immersed in water. It is related to the soil's specific surface (i.e., the content and composition of the clay fraction).

HENRY'S LAW

The weight of any gas that will dissolve in a given volume of a liquid at constant temperature is directly proportional to the pressure that the gas exerts above the liquid.

HOOKE'S LAW

The deformation (strain) of a body under stress is proportional to the stress applied to it. This law pertains to elastic bodies. The constant of proportionality between stress and strain is known as "Young's modulus."

Bibliography

Introduction to Environmental Soil Physics (First Edition) 2003
 Elsevier Inc. Daniel Hillel (ed.) <http://www.sciencedirect.com/science/book/9780123486554>

HORTICULTURE SUBSTRATES, STRUCTURE AND PHYSICAL PROPERTIES

Anna Słowińska-Jurkiewicz,
 Monika Jaroszuk-Sierocińska
 Institute of Soil Science and Environment Management,
 University of Life Sciences, Lublin, Poland

Definition

Horticultural substrate. It is the life environment of the plant roots, isolated from the parent rock.

Structure. Form of spatial arrangement of the solid phase. Structural elements in the horticultural substrate are the primary particles of the solid phase, their complexes, or aggregates and pores, or the space between the solid phase particles and aggregates.

Physical property. Physical property is the attribute of a substance that can be observed and measured without changing one substance into another. The main physical parameters characterizing the physical condition of the

horticultural substrate are bulk density, total porosity, container water capacity, available water retention, air capacity, water, and air permeability.

Introduction

In the second half of the twentieth century, horticultural substrates made mainly from white peat were the most widely used. Now, the assortment of applied materials has increased considerably. Besides the commonly used organic substrates, some other materials are also being used. It is, first of all, the rockwool, produced from the melted diabase or basalt with addition of some dolomite as well as the artificial substrates such as superabsorbents. The physical condition of the applied materials definitely decides on the success of the cultivation. The suitable growth of the plants and their development can be assured, above all, by the proper proportions of the amount of water and air in the substrate (Verdonck et al., 1983). A very important problem in case of the determination of the physical properties of the horticultural substrates is the application of such standard methods, which make possible to receive the comparable results of the measurements (Gabriëls and Verdonck, 1991; Bohne and Günther, 1997).

Classification of the substrates

Taking into the consideration the materials, which can be used as substrates in horticulture, one can classify them, first of all, into the unary and multicomponent substrates. Among the unary substrates, one discerns the organic, mineral, and artificial ones. To the organic substrates belong white peat, black peat, brown coal, straw, coconut fiber and dust, tobacco, and wood waste. Gravel, sand, grit, keramsite, perlite, and rockwool are grouped among the mineral substrates, while the artificial substrates comprise the phenolic ones, the polyurethane, polyethylene, and polyvinylchloride foams as well as the superabsorbents composed of polyvinyl alcohol, polyoxyethylene, or polyacrylates. To the multicomponent substrates belong the traditional horticultural substrates produced from leaves, sod, heather, compost and garden soil; peat substrates, and standard soils. Standard soils are the substrates, prepared from the materials of defined properties and constant composition. To some of the first such universal horticultural substrates belong John Innes Composts, elaborated in the mid-thirties of the twentieth century in Great Britain. They are formed of the loam, peat, and grit-sand, completed by the addition of some mineral fertilizers. A well-known standard soil is "Einheitserde" elaborated by Anton Frühstorfer in Germany. It is made of white peat, black peat, and loam or clay (Turski et al., 1980).

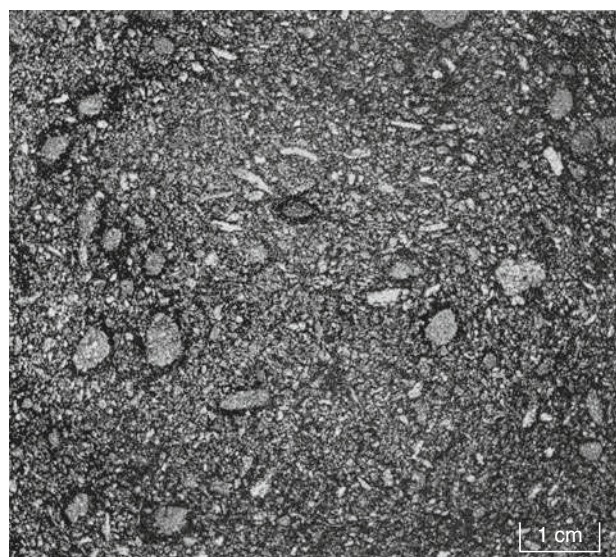
Structure

Structure considerably decides on such conditions of the plant growth and development, as supply in air and water as well as on the temperature in the root area. In the field conditions, the most suitable physical condition of the soil is guaranteed by the aggregate structure. It is characteristic

for the soils, in which there occur the aggregates – the clumps of the particles of the solid substance only in certain points loosely connected. There is air in the large interaggregate spaces, while the small internal pores of the aggregates keep water in them; this ensures that the plant roots have free access both to the water and to the oxygen. In the horticultural substrates, the aggregate structure is not as much essential as in the natural soils. The amount of water and air in the substrate highly depends on the way of hydration, on the regulating the water outflow, on the dimensions, and on the shape of the container, and not on the solid phase geometry, as it takes place in soil (Fonteno, 1989; Argo, 1998). Very good conditions of the growth and development of the plants, in spite of the lack of aggregate structure, is assured by the rockwool, in which the pressed concentrations of the fibers shape a characteristic sponge-like structure. In the horticultural substrates the aggregate structure occurs most often in case of the loosely heaped-up materials of a considerable contribution of the organic substance, while the structure of separated particles is characteristic for the mineral horticultural substrates (Słowińska-Jurkiewicz and Jaroszuk-Sierocińska, 2007). Very advantageous structure of horticultural substrates represents Figure 1.

Physical properties

Traditionally, such substrates were considered to be the most suitable for the cultivation of the garden plants in which one-half of the volume is occupied by the solid phase, and the other by the pores, just as in the mineral



Horticulture Substrates, Structure and Physical Properties,
Figure 1 Structure of the mixture of white peat (50%, v/v) with coconut fiber (50%, v/v). Image in 256 gray degrees of polished opaque block (surface dimensions 8 × 9 cm) developed from this substrate impregnated with polyester resin. Color of the pores is black and of the solid phase – gray (Słowińska-Jurkiewicz and Jaroszuk-Sierocińska, 2007).

soils (Penningsfeld and Kurzman, 1966). De Boodt (1965) stated that an ideal substrate should be characterized by a considerably larger total porosity, about $0.85 \text{ m}^3 \text{ m}^{-3}$ and a low bulk density, 0.215 Mg m^{-3} . Such conditions can be realized, first of all, in the soilless substrates, produced on the base of peat, as well as in the modern substrates, such as rockwool. Pores and their dimensions play an important part in the water and air conditions. In the pores there is either the water or the air. One admits that the large pores contain the air (except the situation of a complete saturation of substrate with water), while the small pores are filled with water. Drzal et al. (1999) introduced a classification on large pores (macropores), of dimensions $>416 \mu\text{m}$, from which the water flows out, quickly, under the influence of the gravitation force, middle-size pores (mesopores), of dimension from 416 up to $10 \mu\text{m}$, in which the water, available for the plants, is retained against the gravitation, as well as the small pores (micropores), covering the range from 10 up to $0.2 \mu\text{m}$. The micropores contain the water which is not used by the plants in case of a normal hydration, and being a reserve in the situation of a water stress. The pores of dimensions below $0.2 \mu\text{m}$ or the ultramicropores, keep the water unavailable for plants. To the dimension of pores $416 \mu\text{m}$ corresponds the water potential of -0.7 kPa , to the dimension $10 \mu\text{m}$, water potential -31 kPa , and to dimension of $0.2 \mu\text{m}$, water potential -1.5 MPa . According to White and Mastalerz (1966), De Boodt and Verdonck (1972), and Fonteno (1989, 1993) in case of characterizing the water properties of the horticultural substrates, as a basic parameter there should be named the container water capacity, defined as the amount of water, remained in the substrate after the free outflow of the gravitational water, but before the beginning of evaporation. This amount depends not only on the character of the substrate but considerably on the dimensions, and also on the shape of the container, in which the plant is

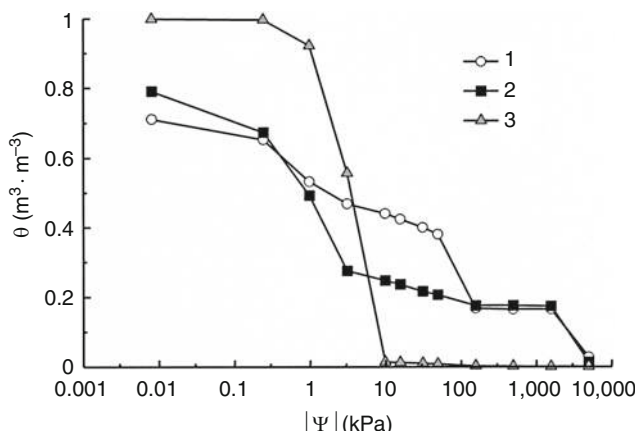
cultivated (Drzal et al., 1999). After the irrigation and outflow, the level of free water occurs on the bottom of the container. For every 1-cm increase of the height above the bottom of the container the water potential decreases by 0.1 kPa , and, this way, decreases the possibility of its keeping. For the container of 20-cm high, the average water potential corresponding to the container water capacity is equal to -1 kPa . In regard to the water retention in the substrates, De Boodt and Verdonck (1972) applied the concept of an easily available water in the range of water potential from -1 to -5 kPa and water buffering capacity from -5 to -10 kPa . Brückner (1997) made a difference between the light available water retention in the range of water potential from -1 to -10 kPa and the heavy available water retention in the range from -10 kPa to -1.5 MPa . Light available water retention is especially important for steering the irrigation. It should begin soon after its consumption by the plants, and thus in the case of water potential being -10 kPa . Aside of the characteristics determining a capability of the material to collecting the water, very important are the parameters determining its capability to water filtration, both in the saturated and in the unsaturated zone (Sławiński et al., 1996). In the condition of the saturation the movement of water is determined by the large pores. With the moisture decrease in the substrate, after the water outflow from the large pores, the movement of water takes place in the smaller pores also, which results in a more tortuous route of water outflow (Fonteno, 1993). In the substrate environment, aside of water, also the air plays an important part (Caron and Nkongolo, 1999). In an ideal environment of root growth of porosity $0.85 \text{ m}^3 \text{ m}^{-3}$ placed in the pot of 15-cm high, in state of container water capacity, the air should occupy $0.25 \text{ m}^3 \text{ m}^{-3}$ and water, $0.60 \text{ m}^3 \text{ m}^{-3}$ (De Boodt and Verdonck, 1972). It should be remembered that the change of the bulk density of substrates, related to their compaction during the transport

Horticulture Substrates, Structure and Physical Properties, Table 1 Basic physical properties of loose horticultural substrates

Type of substrate	Bulk density (Mg m^{-3})	Total porosity ^a ($\text{m}^3 \text{ m}^{-3}$)	Container water capacity at -1 kPa		Available water retention from -1 to -10 kPa		Air capacity at -1 kPa ^b ($\text{m}^3 \text{ m}^{-3}$)
			(kg kg^{-1})	($\text{m}^3 \text{ m}^{-3}$)	(kg kg^{-1})	($\text{m}^3 \text{ m}^{-3}$)	
Wheat peat	0.127	0.911	4.193	0.536	0.718	0.090	0.375
Peat substrate	0.247	0.853	3.211	0.796	0.962	0.238	0.057
Soil with coconut fiber	0.207	0.862	2.960	0.614	0.629	0.129	0.248
Coconut fiber	0.053	0.971	9.290	0.501	4.627	0.250	0.470
Composting bark	0.198	0.874	2.806	0.552	1.190	0.236	0.322
Pine bark	0.143	0.900	1.429	0.204	0.327	0.047	0.696
Sand	1.441	0.453	0.200	0.284	0.096	0.138	0.169
Grit	1.485	0.481	0.046	0.068	0.032	0.047	0.413
Keramsite	0.702	0.710	0.337	0.237	0.024	0.017	0.473
Perlite	0.156	0.943	2.620	0.409	1.166	0.182	0.534
Rockwool	0.082	0.971	11.239	0.922	11.053	0.906	0.049

^aTotal porosity calculated according to the values of particle density and bulk density

^bAir capacity at -1 kPa calculated as a difference between the total porosity and the container water capacity value



Horticulture Substrates, Structure and Physical Properties,
Figure 2 Water retention curves of three horticultural substrates: white peat – 1, coconut fiber – 2, and rockwool – 3. On the horizontal axis there are the absolute values of water potential ($|\Psi|$) in kPa and on vertical axis there are the values of moisture content (θ) in $\text{m}^3 \text{ m}^{-3}$ (Jaroszuk-Sierocińska and Słowińska-Jurkiewicz, 2009).

and performing various cultivating works, can result in a radical decrease in the air capacity (Brückner, 1997; Jaroszuk and Słowińska-Jurkiewicz, 2003). The values of the basic physical properties of most often used substrates are listed in Table 1 (Jaroszuk and Słowińska-Jurkiewicz, 2005).

Conclusions

Horticultural substrates show the most various physical properties, depending on the character of the materials used to their production. Among the actually used substrates, the best physical condition, from the point of view of the horticultural production, is characteristic for rockwool and coconut fiber (Figure 2). These substrates can certainly substitute the white peat in the process of horticultural production, what surely results in protections of the bogs under the menace of the excessive exploitation.

Bibliography

- Argo, W., 1998. Root medium physical properties. *Hort Technology*, **8**, 481–485.
- Bohne, H., and Günther, C., 1997. Physical properties of peat determined with different methods. *Acta Horticulturae*, **450**, 271–276.
- Brückner, U., 1997. Physical properties of different potting media and substrate mixtures – especially air- and water capacity. *Acta Horticulturae*, **450**, 263–270.
- Caron, J., and Nkongolo, V. K. N., 1999. Aeration in growing media: recent developments. *Acta Horticulturae*, **481**, 545–552.
- De Bocht, M., 1965. Vergelijkende studie van de fysische eigenschappen van kunstmatige bodems en de groei van sierplanten. *Pédoologie*, **15**, 159–176.
- De Bocht, M., and Verdonck, O., 1972. The physical properties of the substrates in horticulture. *Acta Horticulturae*, **26**, 37–44.
- Drzal, M. S., Cassel, D. K., and Fonteno, W. C., 1999. Pore fraction analysis: a new tool for substrate testing. *Acta Horticulturae*, **481**, 43–55.
- Fonteno, W. C., 1989. An approach to modeling air and water status of horticultural substrates. *Acta Horticulturae*, **238**, 67–74.
- Fonteno, W. C., 1993. Problems & considerations in determining physical properties of horticultural substrates. *Acta Horticulturae*, **342**, 197–204.
- Gabriëls, R., and Verdonck, O., 1991. Physical and chemical characterization of plant substrates: towards a European standardization. *Acta Horticulturae*, **294**, 249–260.
- Jaroszuk, M., and Słowińska-Jurkiewicz, A., 2003. Comparison of water properties of two horticultural substrates – high moor peat and coconut substrate (in Polish). *Acta Agrophysica*, **89**, 641–645.
- Jaroszuk, M., and Słowińska-Jurkiewicz, A., 2005. Characteristics of basic water-air properties of horticultural substrates used in container cultivation (in Polish). *Zeszyty Problemowe Postępów Nauk Rolniczych*, **504**, 105–110.
- Jaroszuk-Sierocińska, M., and Słowińska-Jurkiewicz, A., 2009. Water potential-moisture content characteristics of horticultural substrates (in Polish). *Zeszyty Problemowe Postępów Nauk Rolniczych*, **535**, 137–144.
- Penningsfeld, F., and Kurzman, P., 1966. *Hydrokultur und Torfkultur*. Stuttgart: Verlag Eugen Ulmer.
- Słowiński, C., Sobczuk, H. A., and Walczak, R. T., 1996. Hydrological characteristics of horticultural substrates: water availability for plant aspect (in Polish). *Zeszyty Problemowe Postępów Nauk Rolniczych*, **429**, 275–278.
- Słowińska-Jurkiewicz, A., and Jaroszuk-Sierocińska, M., 2007. Micromorphographic analysis of the structure of horticultural substrates (in Polish). *Acta Agrophysica*, **151**, 207–217.
- Turski, R., Hetman, J., and Słowińska-Jurkiewicz, A., 1980. The substrates used in greenhouse horticulture (in Polish). *Roczniki Nauk Rolniczych Seria D*, **180**, 1–88.
- Verdonck, O., Penninck, R., and De Bocht, M., 1983. The physical properties of different horticultural substrates. *Acta Horticulturae*, **15**, 155–160.
- White, J. W., and Mastalerz, J. W., 1966. Soil moisture as related to container capacity. *Proceedings of the American Society for Horticultural Science*, **89**, 758–765.

Cross-references

- Pore Size Distribution
Soil Water Management

HUMUS

The well decomposed, more or less stable part of the organic matter in mineral soils.

HYDRAULIC DIFFUSIVITY

The ratio between the flux of water and the gradient of soil wetness. This term is somewhat misleading, since it does not refer to diffusion as such but to convection. The term is taken from the analogy to the diffusion equation (Fick's law), stating that the rate of diffusion is proportional to the concentration gradient.

Bibliography

Introduction to Environmental Soil Physics (First Edition) 2003
Elsevier Inc. Daniel Hillel (ed.) <http://www.sciencedirect.com/science/book/9780123486554>

HYDRAULIC GRADIENT

The slope of the hydraulic grade line which indicates the change in pressure head per unit of distance.

HYDRAULIC HEAD

The sum of the pressure head (hydrostatic pressure relative to atmospheric pressure) and the gravitational head (elevation relative to a reference level). The gradient of the hydraulic head is the driving force for water flow in porous media.

Bibliography

Introduction to Environmental Soil Physics (First Edition) 2003
Elsevier Inc. Daniel Hillel (ed.) <http://www.sciencedirect.com/science/book/9780123486554>

HYDRAULIC PROPERTIES OF UNSATURATED SOILS

Martinus Th. van Genuchten¹, Yakov A. Pachepsky²

¹Department of Mechanical Engineering, COPPE/LTTC, Federal University of Rio de Janeiro, UFRJ, Rio de Janeiro, Brazil

²Environmental Microbial and Food Safety Laboratory, Animal and Natural Resource Institute, Beltsville Agricultural Research Center, USDA-ARS, Beltsville, MD, USA

Definition

Hydraulic Properties of Unsaturated Soils. Properties reflecting the ability of a soil to retain or transmit water and its dissolved constituents.

Introduction

Many agrophysical applications require knowledge of the hydraulic properties of unsaturated soils. These properties reflect the ability of a soil to retain or transmit water and its dissolved constituents. For example, they affect the partitioning of rainfall and irrigation water into infiltration and runoff at the soil surface, the rate and amount of redistribution of water in a soil profile, available water in the soil root zone, and recharge to or capillary rise from the groundwater table, among many other processes in the unsaturated or vadose zone between the soil surface and the groundwater table. The hydraulic properties are also critical components of mathematical models for

studying or predicting site-specific water flow and solute transport processes in the subsurface. This includes using models as tools for designing, testing, or implementing soil, water, and crop management practices that optimize water use efficiency and minimize soil and water pollution by agricultural and other contaminants. Models are equally needed for designing or remediating industrial waste disposal sites and landfills, or assessing the long-term stewardship of nuclear waste repositories.

Predictive models for flow in variably saturated soils are generally based on the Richards equation, which combines the Darcy–Buckingham equation for the fluid flux with a mass conservation equation to give (Richards, 1931):

$$\frac{\partial \theta(h)}{\partial t} = \frac{\partial}{\partial z} \left[K(h) \frac{\partial h}{\partial z} - K(h) \right] \quad (1)$$

in which θ is the volumetric water content ($L^3 L^{-3}$), h is the pressure head (L), t is time (T), z is soil depth (positive down), and K is the hydraulic conductivity ($L T^{-1}$). Equation 1 holds for one-dimensional vertical flow; similar equations can be formulated for multidimensional flow problems. The Richards equation contains two constitutive relationships, the soil water retention curve, $\theta(h)$, and the unsaturated soil hydraulic conductivity function, $K(h)$. These hydraulic functions are both strongly nonlinear functions of h . They are discussed in detail below.

Water retention function

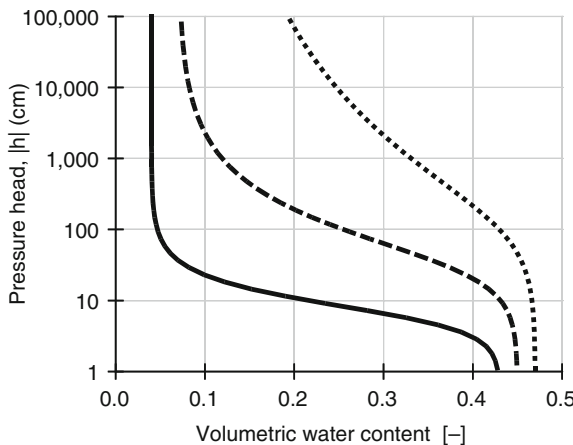
The soil water retention curve, $\theta(h)$, describes the relationship between the water content, θ , and the energy status of water at a given location in the soil. Many other names may be found in the literature, including soil moisture characteristic curve, the capillary pressure–saturation relationship, and the pF curve. The retention curve historically was often given in terms of pF, which is defined as the negative logarithm (base 10) of the absolute value of the pressure head measured in centimeters. In the unsaturated zone, water is subject to both capillary forces in soil pores and adsorption onto solid phase surfaces. This leads to negative values of the pressure head (or matric head) relative to free water, or a positive suction or tension. As opposed to unsaturated soils, the pressure head h is positive in a saturated system. More formally, the pressure head is defined as the difference between the pressures of the air phase and the liquid phase. Capillary forces are the result of a complex set of interactions between the solid and liquid phases involving the surface tension of the liquid phase, the contact angle between the solid and liquid phases, and the diameter of pores.

Knowledge of $\theta(h)$ is essential for the hydraulic characterization of a soil, since it relates an energy density (potential) to a capacity (water content). Rather than using the pressure head (energy per unit weight of water), many agrophysical applications use the pressure or matric potential (energy per unit volume of water, usually measured in Pascal, Pa), $\psi_m = \rho_w g h$, where ρ_w is the density of water (ML^{-3}) and g the acceleration of gravity (LT^{-2}).

Figure 1 shows typical soil water retention curves for relatively coarse-textured (e.g., sand and loamy sand), medium-textured (e.g., loam and sandy loam), and fine-textured (e.g., clay loam, silty loam, and clay) soils. The curves in **Figure 1** may be interpreted as showing the equilibrium water content distribution above a relatively deep water table where the pressure head is zero and the soil fully saturated. The plots in **Figure 1** show that coarse-textured soils lose their water relatively quickly (at small negative pressure heads) and abruptly above the water table, while fine-textured soils lose their water much more gradually. This reflects the particle or pore-size distribution of the medium involved. While the majority of pores in coarse-textured soils have larger diameters and thus drain at relatively small negative pressures, the majority of pores in fine-textured soils do not drain until very large tensions (negative pressures) are applied.

As indicated by the plots in **Figure 1**, the water content varies between some maximum value, the saturated water content, θ_s , and some small value, often referred to as the residual (or irreducible) water content, θ_r . As a first approximation and on intuitive ground, the saturated water content is equal to the porosity, and θ_r equal to zero. In reality, however, the saturated water content, θ_s , of soils is generally smaller than the porosity because of entrapped and dissolved air. The residual water content θ_r is likely to be larger than zero, especially for fine-textured soils with their large surface areas, because of the presence of adsorbed water. Most often θ_s and especially θ_r are treated as fitting parameters without much physical significance.

Soil water retention curves such as shown in **Figure 1** are not unique but depend on the history of wetting and drying. Most often, the soil water retention curve is determined by gradually desaturating an initially saturated soil by applying increasingly higher suctions, thus producing a main drying curve. One could similarly slowly wet an



Hydraulic Properties of Unsaturated Soils, Figure 1 Typical soil water retention curves for relatively coarse- (solid line), medium- (dashed line), and fine-textured (dotted line) soils. The curves were obtained using [Equation 6a](#) assuming hydraulic parameter values as listed in [Table 1](#).

initially very dry sample to produce the main wetting curve, which is generally displaced by a factor of 1.5–2.0 toward higher pressure heads closer to saturation. This phenomenon of having different wetting and drying curves, including primary and secondary scanning curves is referred to hysteresis. Hysteresis is caused by the fact that drainage is determined mostly by the smaller pore in a certain pore sequence, and wetting by the larger pores (this effect is often referred to as the ink bottle effect). Other factors contributing to hysteresis are the presence of different liquid–solid contact angles for advancing and receding water menisci, air entrapment during wetting, and possible shrink–swell phenomena of some soils.

Hydraulic conductivity function

The hydraulic conductivity characterizes the ability of a soil to transmit water. Its value depends on many factors such as the pore-size distribution of the medium, and the tortuosity, shape, roughness, and degree of interconnectedness of the pores. The hydraulic conductivity decreases considerably as soil becomes unsaturated since less pore space is filled with water, the flow paths become increasingly tortuous, and drag forces between the fluid and the solid phases increase.

The unsaturated hydraulic conductivity function gives the dependency of the hydraulic conductivity on the water content, $K(\theta)$, or pressure head, $K(h)$. **Figure 2** presents examples of typical $K(\theta)$ and $K(h)$ functions for relatively coarse-, medium-, and fine-textured soils. Notice that the hydraulic conductivity at saturation is significantly larger for coarse-textured soils than fine-textured soils. This difference is often several orders of magnitude. Also notice that the hydraulic conductivity decreases very significantly as the soil becomes unsaturated. This decrease, when expressed as a function of the pressure head (**Figure 2**; right), is much more dramatic for the coarse-textured soils. The decrease for coarse-textured soils is so large that at a certain pressure head the hydraulic conductivity becomes smaller than the conductivity of the fine-textured soil. The water content where the conductivity asymptotically becomes zero (**Figure 2**; left) is often used as an alternative working definition for the residual water content, θ_r .

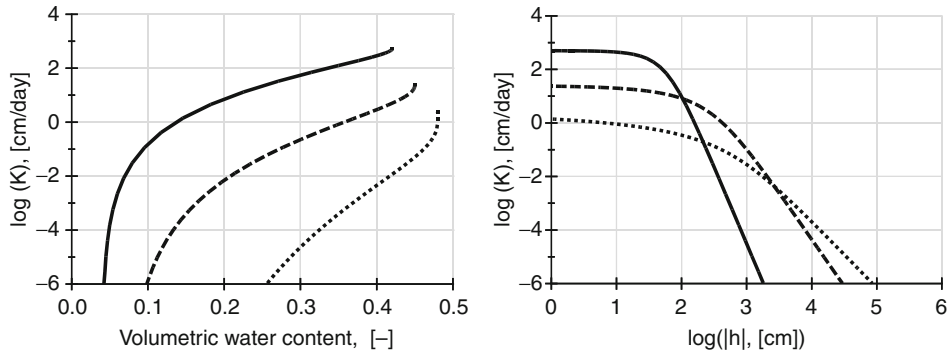
Soil water diffusivity

Another hydraulic function often used in theoretical and management application of unsaturated flow theories is the soil water diffusivity, $D(\theta)$, ($L^2 T^{-1}$), which is defined as

$$D(\theta) = K(\theta) \left| \frac{dh}{d\theta} \right|. \quad (2)$$

This function appears when [Equation 1](#) is transformed into a water-content-based equation in which θ is now the dependent variable:

$$\frac{\partial \theta}{\partial t} = \frac{\partial}{\partial z} \left[D(\theta) \frac{\partial h}{\partial z} - K(\theta) \right]. \quad (3)$$



Hydraulic Properties of Unsaturated Soils, Figure 2 Typical curves of the hydraulic conductivity K , as a function of the pressure head (left) and water content (right) for coarse- (solid line), medium- (dashed line), and fine-textured (dotted line) soils. The curves were obtained using Equation 6b assuming hydraulic parameter values as listed in Table 1.

Equation 3 is very attractive for approximate analytical modeling of unsaturated flow processes, especially for modeling horizontal (without the $K(\theta)$ gravity term) and vertical infiltration (e.g., Philip, 1969; Parlange, 1980). However, the water-content-based equation is less attractive for more comprehensive numerical modeling of flow in layered media, flow in media that are partially saturated and partially unsaturated, and for highly transient flow problems.

Analytical representations

To enable their use in analytical or numerical models for unsaturated flow, the soil hydraulic properties are often expressed in terms of simplified analytical expressions. A large number of functions have been proposed over the years to describe the soil water retention curve, $\theta(h)$, and the hydraulic conductivity function, $K(h)$ or $K(\theta)$. A comprehensive review of the performance of some of many these models is given by Leij et al. (1997). The functions range from completely empirical equations to models based on the simplified conceptual picture that soils are made up of a bundle of equivalent capillary tubes that contain and transmit water.

While extremely simplistic as indicated by Tuller and Or (2001) among others, conceptual models that view a soil as a bundle of capillaries of different radii are still useful for explaining the shape of the water retention curve for different textures, as well as to provide a means for predicting the hydraulic conductivity function from soil water retention information. These models typically assume that pores at a given pressure head are either completely filled with water, or empty, depending upon the applied suction. Flow in each water-filled capillary tube is subsequently calculated using Poiseuille's law for flow in cylindrical pores. By adding the contribution of all capillaries that are still filled with water at a particular pressure head, making some assumption about how small and large capillaries connect to each other in sequence

(using a cut-and-paste concept of a cross-section of the medium containing different-sized pores), and then integrating over all water-filled capillaries leads to the hydraulic conductivity of the complete set of capillaries, and consequently of the soil itself. The approach allows information of the soil water retention curve to be translated in predictive equations for the unsaturated hydraulic conductivity. Many theories of this type, often referred to also as statistical pore-size distribution models, have been proposed in the past, including Childs and Collis-George (1950), Burdine (1953), Millington and Quirk (1961), and Mualem (1976). A review of the different approaches is given by Mualem (1992). Examples of analytical $\theta(h)$ and $K(h)$ equations resulting from this approach are the hydraulic functions of Brooks and Corey (1964), based on the approach by Burdine (1953), and equations by van Genuchten (1980) and Kosugi (1996), based on the theory of Mualem (1976).

The classical equations of Brooks and Corey (1964) for $\theta(h)$, $K(h)$, and $D(\theta)$ are given by

$$\theta = \begin{cases} \theta_r + (\theta_s - \theta_r) \left| \frac{h_e}{h} \right|^{\lambda} & h < h_e \\ \theta_s & h \geq h_e \end{cases} \quad (4a)$$

$$K(h) = K_s S_e^{2/\lambda+l+1} \quad (4b)$$

$$D(\theta) = \frac{K_s}{\alpha(\theta_s - \theta_r)} S_e^{1/\lambda+l} \quad (4c)$$

where, as before, θ_r is the residual water content ($L^3 L^{-3}$), θ_s is the saturated water content ($L^3 L^{-3}$), h_e is often referred to as the air-entry value (L), λ is a pore-size distribution index characterizing the width of the soil pore-size distribution, K_s is the saturated hydraulic conductivity (LT^{-1}), l a pore-connectivity parameter assumed to be 2.0 in the original study of Brooks and Corey (1964), and $S_e = S_e(h)$ is effective saturation given by

$$S_e(h) = \frac{\theta(h) - \theta_r}{\theta_s - \theta_r} \quad (5)$$

For completeness we have given here also the expression for the soil water diffusivity, $D(\theta)$. Note that Equations 4b and 4c contain parameters that are also present in Equation 4a, in particular θ_r and θ_s through Equation 5, as well as h_e and λ . The value of λ in Equation 4a reflects the steepness of the retention function and is relatively large for soils with a relatively uniform pore-size distribution (generally coarse-textured soils such as those shown in Figures 1 and 2), but small for soils having a wide range of pore sizes.

One property of Equation 4a is the presence of a sharp break in the retention curve at the air-entry value, h_e . This break (or discontinuity in the slope of the function) is often visible in retention data for coarse-textured soils, but may not be realistic for fine-textured soils and soils having a relatively broad pore- or particle-size distribution. A sharp break is similarly present in the hydraulic conductivity function when plotted as a function of the pressure head, but not versus the water content. As an alternative, van Genuchten (1980) proposed a set of equations that exhibit a more smooth sigmoidal shape. The van Genuchten equations for $\theta(h)$, $K(h)$, and $D(\theta)$ are given by:

$$\theta(h) = \theta_r + \frac{\theta_s - \theta_r}{(1 + |\alpha h|^n)^m} \quad (m = 1 - 1/n; n > 1) \quad (6a)$$

$$K(h) = K_s S_e^l \left[1 - \left(1 - S_e^{1/m} \right)^m \right]^2 \quad (6b)$$

$$D(\theta) = \frac{(1-m)K_s}{\alpha m(\theta_s - \theta_r)} S_e^{l-1/m} \left[\left(1 - S_e^{1/m} \right)^{-m} + \left(1 - S_e^{1/m} \right)^m - 2 \right] \quad (6c)$$

respectively, where α (L^{-1}), n (–), and m ($= 1 - 1/n$) (–) are shape parameters, and l is the pore-connectivity parameter (–). The parameter n in Equation 6 tends to be large for soils with a relatively uniform pore-size distribution and small for soils having a wide range of pore sizes. The pore-connectivity parameter l in Equation 6b was estimated by Mualem (1976) to be about 0.5 as an average for many soils. However, many other values

for l have been suggested in various studies. Based on an analysis of a large data set from the UNSODA database, Schaap and Leij (2000) recommended using l equal to –1 as a more appropriate value for most soil textures.

Equations 6a, 6b, and 6c assume the restrictive relationship $m = 1 - 1/n$, which simplifies the predictive $K(h)$ expression compared to leaving m and n as independent parameters in Equation 6b. In particular, the convex and concave curvatures at the high and low pressure heads in Figure 1 have then a particular relationship with each other. Other restrictions on Equation 6a have been used also. For example, Haverkamp et al. (2005) used the restriction $m = 1 - 2/n$ in connection with Equation 6a and Burdine's (1953) model to produce a different expression for $K(h)$. The restrictions are not formally needed, since they limit the flexibility of Equation 6a in describing experimental data. However, the predicted $K(h)$ function obtained with the theories of Burdine or Mualem becomes then extremely complicated by containing incomplete beta or hypergeometric functions, thus limiting the practicality of the analytical functions.

Rawls et al. (1982) provided average values of the parameters in the Brooks and Corey (1964) soil hydraulic parameters for 11 soil textural classes of the U.S. Department of Agriculture (USDA) textural triangle. Carsel and Parrish (1988) gave similar values for the van Genuchten (1980) parameters for 12 USDA soil textural classes. In Table 1, we list typical van Genuchten hydraulic parameter values for relative coarse-, medium-, and fine-textured soils. The data in this table were actually used to calculate the water retention and hydraulic conductivity functions, shown in Figures 1 and 2, respectively, with Equations 6a, b. Average values such as those given in Table 1, or provided in more detail by Rawls et al. (1982) and Carsel and Parrish (1988), are often referred to as textural class averaged pedotransfer functions. Pedotransfer functions are relationships that use more easily measured of readily available soil data to estimate the unsaturated soil hydraulic parameters or properties (Bouma and van Lanen, 1987; Leij et al., 2002; Pachepsky and Rawls, 2004).

We note that Equations 4 and 6 provide only two examples in which the hydraulic properties are described analytically. Many other combinations (Leij et al., 1997; Kosugi et al., 2002) are possible and have been used. For example, the combination of Equation 6a for $\theta(h)$ with a simple expression like

Hydraulic Properties of Unsaturated Soils, Table 1 Typical values of the soil hydraulic parameters in the analytical functions of van Genuchten (1980) for relatively coarse-, medium-, and fine-textured soils. The parameters were used to calculate the hydraulic properties plotted in Figures 1 and 2 using Equations 6a and 6b, respectively

Soil texture	θ_r (cm day $^{-1}$)	θ_s (cm 3 cm $^{-3}$)	α (cm 3 cm $^{-3}$)	n (cm $^{-1}$)	K_s (–)
Coarse	0.045	0.430	0.145	2.68	712.8
Medium	0.057	0.410	0.124	2.28	350.2
Fine	0.020	0.540	0.0010	1.2	45.0

$$K(h) = K_s S_e^b \quad (7)$$

which is essentially identical to [Equation 4b](#), for $K(h)$ is also very realistic. Another attractive alternative equation for $K(h)$ is of the form (e.g., Vereecken et al., [1989](#))

$$K(h) = \frac{K_s}{1 + |ah|^b} \quad (8)$$

Many alternative expressions have been used also for the soil water diffusivity function, $D(\theta)$, mostly to facilitate simplified analytical analyses of unsaturated flow problems (e.g., Parlange, [1980](#)).

Experimental procedures

A large number of experimental techniques can be used to estimate the hydraulic properties of unsaturated soils. A direct approach for the water retention function would be to measure a number of water content (θ) and pressure head (h) pairs, and then to fit a particular retention function to the data. Direct measurement techniques include methods using a hanging water column, pressure cells, pressure plate extractors, suction tables, soil freezing, and many other approaches. Comprehensive reviews of various methods are given by Gee and Ward ([1999](#)) and Dane and Hopmans ([2002](#)). Once the pairs of θ and h data are obtained, the data may be analyzed in terms of specific analytical water retention and conductivity functions such as those discussed earlier. Several convenient software packages are available for this purpose (van Genuchten et al., [1991](#); Wraith and Or, [1998](#)). Alternatively, the data can be analyzed without assuming specific analytical functions for $\theta(h)$ and $K(h)$ or $K(\theta)$. This could be done using linear, cubic spline, or other interpolation techniques (Kastanek and Nielsen, [2001](#); Bitterlich et al., [2004](#)).

Similar direct measurement approaches involving pairs of conductivity (or diffusivity) and pressure head (or water content) data are also possible for the $K(h)$ and $D(\theta)$ functions, at least in principle (Dane and Topp, [2002](#)), including for the saturated hydraulic conductivity, K_s . The saturated hydraulic conductivity can be measured in the laboratory using a variety of constant or falling head methods, and in the field using single or double ring infiltrometers, constant head permeameters, and various auger-hole and piezometer methods (Dane and Topp, [2002](#)). Unfortunately, because of the strongly nonlinear nature of the soil hydraulic properties, pairs for the $K(h)$ and $D(\theta)$ data are not easily measured directly, especially at relatively low (negative) pressure heads, unless more specialized techniques are used such as centrifuge methods (Nimmo et al., [2002](#)). Even then, the data are generally not distributed evenly over the entire water content range of interest. Consequently, unsaturated hydraulic conductivity properties are most often estimated using inverse or parameter estimation procedures.

Parameter estimation methods generally involve the measurement during some experiment of one or several

capacity or flow attributes (e.g., water contents, pressure heads, boundary fluxes), which are then used in combination with a mathematical solution (generally numerical) to obtain estimates of the hydraulic parameters such as those that appear in [Equations 4](#) and [6](#), or other functions. Popular methods include one-step and multi-step outflow methods (Kool et al., [1987](#); van Dam et al., [1994](#)), tension infiltrometers methods (Šimůnek et al., [1998a](#)), and evaporation methods (Šimůnek et al., [1998b](#)), although many other laboratory and field methods also exist or can be similarly employed (Hopmans et al., [2002](#)). This also pertains to different approaches for minimizing the objective function, including quantification of parameter uncertainty (Abbaspour et al., [2001](#); Vrugt and Robinson, [2007](#)). Very attractive now also is the use of combined hard (e.g., directly measured) and soft (e.g., indirectly estimated) data, including hydrogeophysical measurements and information derived from pedotransfer functions, to extract the most out of available information (e.g., Kowalski et al., [2004](#); Segal et al., [2008](#)).

Hydraulic properties of structured soils

The Richards [equation 1](#) typically predicts a uniform flow process in the vadose zone. Unfortunately, the vadose zone can be extremely heterogeneous at a range of scales, from the microscopic (e.g., pore scale) to the macroscopic (e.g., field or larger scale). Some of these heterogeneities can lead to a preferential (or bypass) flow process that macroscopically is very difficult to capture with the standard Richards equation. One obvious example of preferential flow is the rapid movement of water and dissolved solutes through soil macropores (e.g., between soil aggregates, or created by earthworms or decayed root channels or rock fractures), with much of the water bypassing (short-circuiting) the soil or rock matrix. However, many other causes of preferential flow exist, such as flow instabilities caused by soil textural changes or water repellency (Hendrickx and Flury, [2001](#); Šimůnek et al., [2003](#); Ritsema and Dekker, [2005](#)), and lateral funneling of water along sloping soil layers (e.g., Kung, [1990](#)).

While uniform flow in granular soils is traditionally described with a single-porosity model such as the Richards equation given by [Equation 1](#), flow in structured media can be described using a variety of dual-porosity, dual-permeability, multi-porosity, and/or multi-permeability models (Šimůnek and van Genuchten, [2008](#); Köhne et al., [2009](#)). While single-porosity models assume that a single pore system exists that is fully accessible to both water and solute, dual-porosity and dual-permeability models both assume that the porous medium consists of two interacting pore regions, one associated with the inter-aggregate, macropore, or fracture system, and one comprising the micropores (or intra-aggregate pores) inside soil aggregates or the rock matrix. Whereas dual-porosity models assume that water in the matrix is stagnant, dual-permeability models allow also for water flow within the soil or rock matrix.

To avoid over-parameterization of the governing equations, one useful simplifying approach is to assume instantaneous hydraulic equilibration between the fracture and matrix regions. In that case, the Richards equation can still be used, but now with composite hydraulic properties of the form (e.g., Peters and Klavetter, 1988)

$$\theta(h) = w_f \theta_f(h) + w_m \theta_m(h) \quad (9a)$$

$$K(h) = w_f K_f(h) + w_m K_m(h) \quad (9b)$$

where the subscripts f and m refer to the fracture (macropore) and matrix (micropore) regions, respectively, and where w_i are volumetric weighting factors for the two overlapping regions such that $w_f + w_m = 1$. Rather than using Equations 6a,b directly in Equations 9a and 9b, Durner (1994) proposed a slightly different set of equations for the composite functions as follows

$$S_e(h) = \frac{\theta(h) - \theta_r}{\theta_s - \theta_r} = \frac{w_f}{[1 + |\alpha_f h|^{n_f}]^{m_f}} + \frac{w_m}{[1 + |\alpha_m h|^{n_m}]^{m_m}} \quad (10a)$$

$$K(S_e) = K_s \frac{(w_f S_{e_f} + w_m S_{e_m})^l \left\{ w_f \alpha_f [1 - (1 - S_{e_f}^{1/m_f})^{m_f}] + w_m \alpha_m [1 - (1 - S_{e_m}^{1/m_m})^{m_m}] \right\}^2}{(w_f \alpha_f + w_m \alpha_m)^2} \quad (10b)$$

where α_i , n_i , and $m_i (=1 - 1/n_i)$ are empirical parameters of the separate hydraulic functions ($i=f,m$). An example of composite retention and hydraulic conductivity functions based on Equations 10a and 10b is shown in Figure 2 for the following set of parameters: $\theta_r=0.00$, $\theta_s=0.50$, $l=0.5$, $K_s=1 \text{ cm d}^{-1}$, $\alpha_m=0.01 \text{ cm}^{-1}$, $n_m=1.50$, $w_m=0.975$, $w_f=0.025$, $\alpha_f=1.00 \text{ cm}^{-1}$, and $n_f=5.00$. The fracture domain in this case represents only 2.5% of the entire pore space, but accounts for almost 90% of the hydraulic conductivity close to saturation (Figure 3).

While still leading to uniform flow, models using such composite media properties do allow for faster flow and transport during conditions near saturation, and as such

provide more realistic simulations of field data than the standard approach using unimodal hydraulic properties of the type shown in Figures 1 and 2. In soils, the two parts of the conductivity curves may be associated with soil structure (near saturation) and soil texture (at lower negative pressure heads).

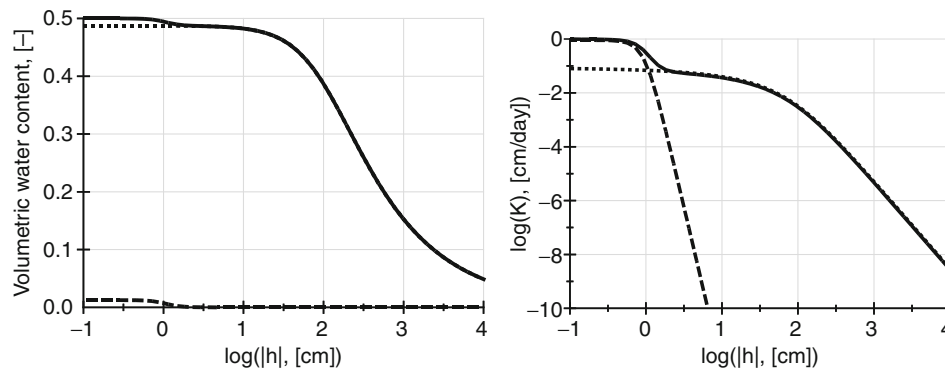
The use of composite hydraulic functions such as those shown in Figure 2 is consistent with field measurements suggesting that the macropore conductivity of soils at saturation is generally about one to two orders of magnitude larger than the matrix conductivity at saturation, depending upon texture. These findings were confirmed by Schaap and van Genuchten (2006) using a detailed neural network analysis of the UNSODA unsaturated soil hydraulic database (Leij et al., 1996). The analysis revealed a relatively sharp decrease in the conductivity away from saturation and a slower decrease afterward. Schaap and van Genuchten (2006) suggested an improved composite function for $K(h)$ to account for the effects of macropores near saturation as follows:

$$K(h) = \left(\frac{K_s}{K_m(h)} \right)^{R(h)} K_m(h) \quad (11a)$$

where

$$R(h) = \begin{cases} 0 & h < -40 \text{ cm.} \\ 0.2778 + 0.00694h & -40 \leq h < -4 \text{ cm} \\ 1 + 0.1875h & -4 \leq h \leq 0 \text{ cm} \end{cases} \quad (11b)$$

and where $K_m(h)$ is the traditional hydraulic conductivity function for the matrix as given by Equation 6b. Equations 11a and 11b were found to produce very small systematic errors between the observed (UNSOADA) and calculated hydraulic conductivities across a wide range of pressure heads between saturation and -150 m . While the macropore contribution was most significant between pressure heads 0 and -4 cm , its influence on the conductivity function extended to pressure heads as low as -40 cm (Equation 11b).



Hydraulic Properties of Unsaturated Soils, Figure 3 Bimodal water retention (left) and hydraulic conductivity (right) functions as described with the composite soil hydraulic model of Durner (1994).

Multiphase constitutive relationships

The use of [Equation 1](#) implies that the air phase has no effect of water flow. This is a realistic assumption for most flow simulations, except near saturation in relatively closed systems where air may not move freely. The resulting situation may need to be described using two flow equations, one for the air phase and one for the liquid phase. The same is true for multiphase air, oil, and water systems in which the fluids are not fully miscible. Flow in such multiphase systems generally require flow equations for each fluid phase involved. Two-phase air-water systems hence could be modeled also using separate equations for air and water. This shows that the standard Richards equation is a simplification of a more complete multiphase (air-water) approach in that the air phase is assumed to have a negligible effect on variably saturated flow, and that the air pressure varies only little in space and time. This assumption appears adequate for most variably saturated flow problems. Similar assumptions, however, are generally not possible when nonaqueous phase liquids (NAPLs) are present. Mathematical descriptions of multiphase flow and transport hence in general require flow equations for each of the fluid phases involved. Assuming applicability of the van Genuchten hydraulic functions and ignoring the presence of residual air and water, the hydraulic conductivity functions for the liquid (wetting) and air phase (non-wetting) phases are given by (e.g., Luckner et al., [1989](#); Lenhard et al., [2002](#)):

$$K_w(S_e) = K_w S_e^l \left[1 - \left(1 - S_e^{1/m} \right)^m \right]^2 \quad (12a)$$

$$K_a(S_e) = K_a (1 - S_e)^l \left[1 - S_e^{1/m} \right]^{2m} \quad (12b)$$

where the subscripts *w* and *a* refer to the water and air phases, respectively, and K_w and K_a are the hydraulic conductivities of the medium to water and air when filled completely with those fluids. A detailed overview of various approaches for measuring and describing the hydraulic properties of multi-fluid systems is given by Lenhard et al. ([2002](#)).

A look ahead

The unsaturated soil hydraulic properties are key factors determining the dynamics and movement of water and its dissolved constituents in the subsurface. Reliable estimates are needed for a broad range of agrophysical applications, including for subsurface contaminant transport studies. A large number of approaches are now available for describing and measuring the hydraulic properties, especially for relatively homogeneous single-porosity soils. This includes direct measurement of discrete $\theta(h)$, and $K(h)$ or $K(\theta)$ data points and fitting appropriate analytical models to the data, and the use of increasingly sophisticated inverse methods.

Considerable challenges remain in the description and measurement of the hydraulic properties of structured

media (macroporous soils and fractured rock). The hydraulic properties of such media may require special provisions to account for the effects of soil texture and soil structure on the shape of the hydraulic functions near saturation, thus leading to dual- or multi-porosity formulations as indicated by Schaap and van Genuchten ([2006](#)) and Jarvis ([2008](#)), among others. Estimation of the effective properties of heterogeneous (including layered) field soil profiles also remains an important challenge. Very promising here is the increased integration of hard (directly measured) data and soft (indirectly estimated) information for improved estimation of field- or larger-scale hydraulic properties, including the use of noninvasive geophysical information. New noninvasive technologies with enormous potential range from neutron and X-ray radiography and magnetic resonance imaging at relatively small (laboratory) scales, to electrical resistivity tomography and ground penetrating radar at intermediate (field) scales, to passive microwave remote sensing at regional or larger scales. Challenges remain on how to optimally integrate, assimilate, or otherwise fuse such information with direct laboratory and field hydraulic measurements (Yeh and Šimunek, [2002](#); Kowalski et al., [2004](#), Looms et al., [2008](#); Ines and Mohanty, [2008](#)), including the optimal and cost-effective use of pedotransfer function and soil texture information, and resultant quantification of uncertainty (Minasny and McBratney, [2002](#); Wang et al., [2003](#)). These various integrated technologies undoubtedly will further advance in the near future, as well as the use of increasingly refined pore-scale modeling approaches (e.g., Tuller and Or, [2001](#)) at the smaller scales for more precise simulation of the basic physical processes governing the retention and movement of water in unsaturated media.

Bibliography

- Abbaspour, K. C., Schulin, R., and Th. van Genuchten, M., 2001. Estimating unsaturated soil hydraulic parameters using ant colony optimization. *Advances in Water Resources*, **24**, 827–841.
- Bitterlich, S., Durner, W., Iden, S. C., and Knabner, P., 2004. Inverse estimation of the unsaturated soil hydraulic properties from column outflow experiments using free-form parameterizations. *Vadose Zone Journal*, **3**, 971–981.
- Bouma, J., and van Lanen, J. A. J., 1987. Transfer functions and threshold values: from soil characteristics to land qualities. In Beek, K. J., et al. (eds.), *Quantified Land Evaluation*. Enschede: Int. Inst. Aerospace Surv. Earth Sci. ITC Publ. No. 6, pp. 106–110.
- Brooks, R. H., and Corey, A. T., 1964. Hydraulic properties of porous media, Hydrol. Paper No. 3, Colorado State Univ., Fort Collins, CO.
- Burdine, N. T., 1953. Relative permeability calculations from pore-size distribution data. *Petr. Trans. Am. Inst. Mining Metall. Eng.*, **198**, 71–77.
- Carsel, R. F., and Parrish, R. S., 1988. Developing joint probability distributions of soil water retention characteristics. *Water Resources Research*, **24**, 755–769.
- Childs, E. C., and Collis-George, N., 1950. The permeability of porous materials. *Proceedings of the Royal Society of London, Series A*, **201**, 392–405.

- Dane, J. H., and Hopmans, J. W., 2002. Water retention and storage. In Dane, J. H., and Topp, G. C. (eds.), *Methods of Soil Analysis, Part 1, Physical Methods*. Chapter 3.3, 3rd edn. Madison, WI: Soil Science Society of America, pp. 671–720.
- Dane, J. H., and Topp, G. C. (eds.), 2002. *Methods of Soil Analysis, Part 1, Physical Methods*, 3rd edn. Madison: Soil Science Society of America.
- Durner, W., 1994. Hydraulic conductivity estimation for soils with heterogeneous pore structure. *Water Resources Research*, **32**(9), 211–223.
- Gee, G. W., and Ward, A. L., 1999. Innovations in two-phase measurements of hydraulic properties. In Th. van Genuchten, M., Leij, F. J., and Wu, L. (eds.), *Proceedings of the International Workshop, Characterization and Measurement of the Hydraulic Properties of Unsaturated Porous Media. Parts 1 and 2*. Riverside: University of California, pp. 241–270.
- Haverkamp, R. F. J., Leij, C. F., Sciotino, A., and Ross, P. J., 2005. Soil water retention: I Introduction of a shape index. *Soil Science Society of America Journal*, **69**, 1881–1890.
- Hopmans, J. W., Šimůnek, J., Romano, N., and Durner, W., 2002. Inverse modeling of transient water flow. In Dane, J. H., and Topp, G. C. (eds.), *Methods of Soil Analysis, Part 1, Physical Methods*, 3rd edn. Madison: SSSA, pp. 963–1008.
- Hendrickx, J. M. H., and Flury, M., 2001. Uniform and preferential flow, mechanisms in the vadose zone. In *Conceptual models of flow and transport in the fractured vadose zone*. Washington, DC: National Research Council, National Academy, pp. 149–187.
- Ines, A. V. M., and Mohanty, B., 2008. Near-Surface soil moisture assimilation for quantifying effective soil hydraulic properties under different hydroclimatic conditions. *Vadose Zone Journal*, **7**, 39–52.
- Jarvis, N., 2008. Near-saturated hydraulic properties of macroporous soils. *Vadose Zone Journal*, **7**, 1256–1264.
- Kastanek, F. J., and Nielsen, D. R., 2001. Description of soil water characteristics using cubic spline interpolation. *Soil Science Society of America Journal*, **65**, 279–283.
- Köhne, J. M., Köhne, S., and Šimůnek, J., 2009. A review of model applications for structured soils: a) Water flow and tracer transport. *Journal of Contaminant Hydrology*, **104**, 4–35.
- Kool, J. B., Parker, J. C., and van Genuchten, M Th., 1987. Parameter estimation for unsaturated flow and transport models – a review. *Journal of Hydrology*, **91**, 255–293.
- Kosugi, K., 1996. Lognormal distribution model for unsaturated soil hydraulic properties. *Water Resources Research*, **32**(9), 2697–2703.
- Kosugi, K., Hopmans, J. W., and Dane, J. H., 2002. Parametric models. In Dane, J. H., and Topp, G. C. (eds.), *Methods of Soil Analysis, Part 1, Physical Methods*, 3rd edn. Madison: SSSA, pp. 739–757.
- Kowalski, M. B., Finsterle, S., and Rubin, Y., 2004. Estimating slow parameter distributions using ground-penetrating radar and hydrological measurements during transient flow in the vadose zone. *Advances in Water Resources*, **27**, 583–599.
- Kung, K.-J. S., 1990. Preferential flow in a sandy vadose zone. 2. Mechanism and implications. *Geoderma*, **46**, 59–71.
- Leij, F. J., Alves, W. J., van Genuchten, M. Th., and Williams, J. R., 1996. The UNSODA-Unsaturated Soil Hydraulic Database. User's manual Version 1.0. Report EPA/600/R-96/095. National Risk Management Research Laboratory, Office of Research and Development, U.S. Environmental Protection Agency, Cincinnati, OH.
- Leij, F. J., Russell, W. B., and Lesch, S. M., 1997. Closed-form expressions for water retention and conductivity data. *Ground Water*, **35**, 848–858.
- Leij, F. J., Schaap, M. G., and Arya, L. R., 2002. Indirect methods. In Dane, J. H., and Topp, G. C. (eds.), *Methods of Soil Analysis*, Part 1, Physical Methods, 3rd edn. Madison: Soil Science Society of America, pp. 1009–1045.
- Lenhard, R. J., Oostrom, M., and Dane, J. H., 2002. Multi-fluid flow. In Dane, J. H., and Topp, G. C. (eds.), *Methods of Soil Analysis, Part 4, Physical Methods*, SSSA Book Series 5, Chapter 7. Madison: Soil Science Society of America, pp. 1537–1619.
- Looms, M. C., Binley, A., Jensen, K. H., Nielsen, L., and Hansen, T. M., 2008. Identifying unsaturated hydraulic properties using an integrated data fusion approach on cross-borehole geophysical data. *Vadose Zone Journal*, **7**, 238–248.
- Luckner, L., van Genuchten, M Th., and Nielsen, D. R., 1989. A consistent set of parametric models for the two-phase flow of immiscible fluids in the subsurface. *Water Resources Research*, **25**(10), 2187–2193.
- Minasny, B., and McBratney, A. B., 2002. The efficiency of various approaches to obtaining estimates of soil hydraulic properties. *Geoderma*, **107**(1–2), 55–70.
- Millington, R. J., and Quirk, J. P., 1961. Permeability of porous materials. *Transactions of the Faraday Society*, **57**, 1200–1206.
- Mualem, Y., 1976. A new model for predicting the hydraulic conductivity of unsaturated porous media. *Water Resources Research*, **12**, 513–522.
- Mualem, Y., 1992. Modeling the hydraulic conductivity of unsaturated porous media. In Th. van Genuchten, M., Leij, F. J., and Lund, L. J. (eds.), *Proceedings of the International Workshop, Indirect Methods for Estimating the Hydraulic Properties of Unsaturated Soils*. Riverside: University of California, pp. 45–52.
- Nimmo, J. R., Perkins, K. S., and Lewis, A. M., 2002. Steady-state centrifuge. In Dane, J. H., and Topp, G. C. (eds.), *Methods of Soil Analysis, Part 4, Physical Methods*, SSSA Book Series 5, Chapter 7. Madison: Soil Science Society of America, pp. 903–916.
- Pachepsky, Y. A., and Rawls, W. J., 2004. Status of pedotransfer functions. In Pachepsky, Y. A., and Rawls, W. J. (eds.), *Development of Pedotransfer Functions in Soil Hydrology*. Amsterdam: Elsevier, pp. vii–xviii.
- Parlange, J.-Y., 1980. Water transport in soils. *Annual Review of Fluid Mechanics*, **12**, 77–102.
- Peters, R. R., and Klavetter, E. A., 1988. A continuum model for water movement in an unsaturated fractured rock mass. *Water Resources Research*, **24**, 416–430.
- Philip, J. R., 1969. Theory of infiltration. In Chow, V. T. (ed.), *Advances in Hydroscience*, **5**, 215–296; New York: Academic, pp. 215–296.
- Rawls, W. J., Brakensiek, D. L., and Saxton, K. E., 1982. Estimation of soil water properties. *Transactions on ASAE*, **25**(5), 1316–1320 and 1328.
- Richards, L. A., 1931. Capillary conduction of fluid through porous mediums. *Physics*, **1**, 318–333.
- Ritsema, C. J., and Dekker, L. W. (eds.), 2005. Behaviour and management of water-repellent soils. *Australian Journal of Soil Research*, **43**(3), i–ii, 1–441.
- Schaap, M. G., and Leij, F. J., 2000. Improved prediction of unsaturated hydraulic conductivity with the Mualem-van Genuchten Model. *Soil Science Society of America Journal*, **64**, 843–851.
- Schaap, M. G., and van Genuchten, M Th., 2006. A modified Mualem-van Genuchten formulation for improved description of the hydraulic conductivity near saturation. *Vadose Zone Journal*, **5**, 27–34.
- Segal, E., Bradford, S. A., Shouse, P., Lazarovitch, N., and Corwin, D., 2008. Integration of hard and soft data to characterize field-scale hydraulic properties for flow and transport studies. *Vadose Zone Journal*, **7**, 878–889.
- Šimůnek, J., and van Genuchten, M Th., 2008. Modeling nonequilibrium flow and transport processes using HYDRUS. *Vadose Zone Journal*, **7**, 782–797.

- Šimůnek, J., Wang, D., Shouse, P. J., and van Genuchten, M. Th., 1998a. Analysis of field tension disc infiltrometer data by parameter estimation. *International Agrophysics*, **12**, 167–180.
- Šimůnek, J., Wendroth, O., and van Genuchten, M. Th., 1998b. A parameter estimation analysis of the evaporation method for determining soil hydraulic properties. *Soil Science Society of America Journal*, **62**(4), 894–905.
- Šimůnek, J., Jarvis, N. J., Th. van Genuchten, M., and Gärdenäs, A., 2003. Nonequilibrium and preferential flow and transport in the vadose zone: review and case study. *Journal of Hydrology*, **272**, 14–35.
- Tuller, M., and Or, D., 2001. Hydraulic conductivity of variably saturated porous media – film and corner flow in angular pore space. *Water Resources Research*, **37**, 1257–1276.
- van Dam, J. C., Stricker, J. N. M., and Droogers, P., 1994. Inverse method for determining soil hydraulic functions from multi-step outflow experiments. *Soil Science Society of America Journal*, **58**, 647–652.
- van Genuchten, M. Th., 1980. A closed-form equation for predicting the hydraulic conductivity of unsaturated soils. *Soil Science Society of America Journal*, **44**, 892–898.
- van Genuchten M. Th., Leij, F. J., and Yates, S. R., 1991. The RETC code for quantifying the hydraulic functions of unsaturated soils. Report EPA/600/2-91/065. U.S. Environmental Protection Agency, Ada, OK.
- Vereecken, H., Maes, J., Feyen, J., and Darius, P., 1989. Estimating the soil moisture retention characteristic from texture, bulk-density, and carbon content. *Soil Science*, **148**, 389–403.
- Vrugt, J. A., and Robinson, B. A., 2007. Improved evolutionary optimization from genetically adaptive multimethod search. *Proceedings of the National Academy of Sciences of the United States of America*, **104**, 708–711.
- Wraith, J. M., and Or, D., 1998. Nonlinear parameter estimation using spreadsheet software. *Journal of Natural Resources and Life Sciences Education*, **27**, 13–19.
- Wang, W., Neuman, S. P., Yao, T., and Wierenga, P. J., 2003. Simulation of large-scale field infiltration experiments using a hierarchy of models based on public, generic, and site data. *Vadose Zone Journal*, **2**, 297–312.
- Yeh, T.-C. J., and Šimůnek, J., 2002. Stochastic fusion of information for characterizing and monitoring the vadose zone. *Vadose Zone Journal*, **1**, 227–241.

Cross-references

- [Bypass Flow in Soil](#)
- [Databases of Soil Physical and Hydraulic Properties](#)
- [Ecohydrology](#)
- [Evapotranspiration](#)
- [Field Water Capacity](#)
- [Hydropedological Processes in Soils](#)
- [Hysteresis in Soil](#)
- [Infiltration in Soils](#)
- [Layered Soils, Water and Solute Transport](#)
- [Pedotransfer Functions](#)
- [Physics of Near Ground Atmosphere](#)
- [Pore Size Distribution](#)
- [Soil Hydrophobicity and Hydraulic Fluxes](#)
- [Soil Water Flow](#)
- [Soil Water Management](#)
- [Sorptivity of Soils](#)
- [Surface and Subsurface Waters](#)
- [Tensiometry](#)
- [Water Balance in Terrestrial Ecosystems](#)
- [Water Budget in Soil](#)
- [Wetting and Drying, Effect on Soil Physical Properties](#)

HYDRODYNAMIC DISPERSION

The tendency of a flowing solution in a porous medium that is permeated with a solution of different composition to disperse, due to the non-uniformity of the flow velocity in the conducting pores. The process is somewhat analogous to diffusion, though it is a consequence of convection.

Bibliography

Introduction to Environmental Soil Physics (First Edition) 2003
Elsevier Inc. Daniel Hillel (ed.) <http://www.sciencedirect.com/science/book/9780123486554>

HYDROPEDOLOGICAL PROCESSES IN SOILS

Svatopluk Matula

Department of Water Resources, Food and Natural Resources, Czech University of Life Sciences, Prague, Czech Republic

Synonyms

Soil hydrophysical processes; Soil physical processes; Soil water processes; Soil water–soil morphology interactions

Definition

The *hydropedological processes* in the broader sense are all soil processes in which flowing or stagnant water acts as the environment or agent or the vehicle of transport. These processes affect the visible or otherwise discernible morphological features of the soil profile and analogous features on the pedon, polypedon, catena, and soil landscape or soil series scales. These features can be distinguished and categorized according to various pedological classification systems (Lal, 2005) and, vice versa, used to identify and semi-quantify the soil water processes (e.g., Stewart and Howell, 2003) that have produced or affected them. In the narrower sense, only those processes in which water itself (its content, energy status, movement, and balance) is in the focus are regarded as hydropedological processes.

Introduction

Pedology is the branch of soil science dealing with soil genesis, morphology, and classification. In some parts of the world, however, the word *pedology* has been or still is used to denote the whole of soil science. Under these conditions, it was quite natural to name that branch of soil science that deals with soil water (e.g., Stewart and Howell, 2003) and is otherwise referred to, for example, as soil physics, soil water physics, physics of soil water, or soil hydrology as *hydropedology*, notwithstanding its relations (or rather the absence of such relations) to soil

genesis, morphology, and classification. This happened in the fifties of the last century in Czechoslovakia, where the word “hydropedology” was used to denote the discipline of applied soil survey for designing irrigation and drainage systems on agricultural lands (ON 73 6950, 1974; Kutílek et al., 2000). Similar usage may have developed in other countries, too. Recently, the term “hydropedology” was redefined with due regard to both parts of the word, i.e., to the water in the soil and the pedology as defined in the first sentence of this paragraph (Lin, 2003; Lin et al., 2005, 2006a). Hydropedology is thus emerging as a new field, formed from the intertwining branches of soil science, hydrology, and some other closely related disciplines (Lin et al., 2006b, 2008a, b; Lin, 2009). As in hydrogeology, hydroclimatology, and ecohydrology, the emphasis is on connections between hydrology and other spheres of the earth (Wikipedia, 2009), in particular on the pedologic controls on hydrologic processes and properties and hydrologic impacts on soil formation, variability, and functions. Hydropedology emphasizes the *in situ* soils in the context of the landscape (Hydropedology, 2009).

Hydropedological processes in the soil

The soil and the living or dead vegetation on it transforms the precipitation and snowmelt water into overland flow, infiltration, and evaporation (e.g., Lal, 2005). All these three processes depend not only on the state and properties of the soil on the spot but also on the surface run on and subsurface inflow of water from the upslope parts of the landscape, on the arrangement and properties of soil horizons (e.g., Lal, 2005) (lithologically or pedogenetically generated), and on the boundary conditions at the bottom of the soil (bearing in mind how difficult it is to define any “bottom” of the soil).

The overland flow is generated (in most cases) only locally, due either to the insufficiency of the soil infiltration capacity, the lack of soil permeability when the soil is frozen or covered with ice crust, or to shallow groundwater exfiltrating from the soil in the downslope parts of the landscape, where the soils are often stigmatized by hydromorphism (gleyization, peat horizons, salinization). The overland flow is a vehicle of soil erosion and a carrier of eroded soil particles. The eroded particles are deposited in the places where the overland flow loses its carrying capacity. In this way, the overland flow contributes substantially to the thinning of the upland soils and thickening of the lowland soils and the submerged soils in streams, reservoirs, lakes, and seas.

The shallow subsurface downslope flow often occurs as perched groundwater accumulated on the top of less permeable soil horizons, produced by technogenic compaction or translocation of clay particles (illuviation) or iron and aluminum (lateritization) or iron and organic matter (podsolization) or simply because of the lack of organic matter or the absence of tillage that would render the top-soil more permeable than the subsoil.

The infiltration capacity of the soil is affected, among other factors, by the aptitude of the surface soil to crusting, the roughness of the soil surface and the presence and openness of macropores (Stewart and Howell, 2003) (biopores, cracks, and tillage-induced pores).

The key role in the pedological control of landscape hydrology is played by the retention capacity of the soil profile (e.g., Dingman, 2002). Although it is not exactly true that the soil is capable of retaining all water until its field capacity is exceeded, this rule is nevertheless approximately valid. A nonlinear process, referred to as the “soil moisture accounting,” has to be included in hydrological models in order to turn the infiltration input into the shallow subsurface and deep groundwater runoff output (e.g., Kachroo, 1992). The available water capacity of the soil (the field capacity minus the wilting point) plays also a crucial role in supporting vegetation growth and evapotranspiration.

The field-capacity rule is sometimes vitiated by various types of preferential flow, i.e., a fast gravitationally driven downward movement of water through the spots that are either more permeable or more wettable than the rest of the soils or appear as random manifestations of the hydraulic instability at the wetting front (fingering). This phenomenon is a zone of active research (e.g., Roulier and Schulin, 2008). However, the question of where, when, and to which extent these phenomena occur in different soils and rocks (so that we can predict them) remains largely unanswered.

The hydraulic properties of the soil (Stewart and Howell, 2003), such as the soil moisture retention curve, the saturated hydraulic conductivity, the unsaturated hydraulic conductivity function, the shrinkage curve, the wettability parameters, and many other properties, sometimes easy to quantify but sometimes still resisting to quantification, are mutually correlated and, which is advantageous, are also correlated to other, more easily determinable soil properties such as the particle size distribution, bulk density, and organic matter content (Pachepsky and Rawls, 2004; Pachepsky et al., 2006). It is not incidental that the traditional Czechoslovak “hydropedology” (see above) turned in practice mainly into the particle size distribution analysis of command areas. One task of modern hydropedology would be, in this respect, to reinvestigate the spatial distribution of soil texture classes in conjunction with other soil features, such as the soil depth, soil horizons, the position in the landscape, the degree of hydromorphism, etc.

Conclusions

The hydropedological processes as a part of soil-water relation processes belong to a new discipline, hydropedology (Lin et al., 2008c). Hydropedology undergoes burgeoning development. Its new topics and subtopics crop up all the time and many existing hot topics can easily accommodate under its wings. In most cases, the acceptance of hydropedological viewpoints is useful and makes the researcher more interdisciplinary and open to new ideas.

Bibliography

- Dingman, S. L., 2002. *Physical Hydrology*. Long Grove: Waveland Press.
- Hydropedology, 2009. Available from World Wide Web: <http://hydropedology.psu.edu/hydropedology.html>. Accessed September 30, 2009.
- Kachroo, R. K., 1992. River flow forecasting. Part 5. Applications of a conceptual model. *Journal of Hydrology*, **133**, 141–178.
- Kutílek, M., Kuráž, V., and Císlervá, M., 2000. *Hydropedologie 10. Textbook*, 2nd edn. Prague: Faculty of Civil Engineering, Czech Technical University (in Czech).
- Lal, R. (ed.), 2005. *Encyclopedia of Soil Science*, 2nd edn. New York: Taylor & Francis.
- Lin, H. S., 2003. Hydropedology: bridging disciplines, scales, and data. *Vadose Zone Journal*, **2**, 1–11.
- Lin, H. S., 2009. Earth's critical zone and hydropedology: concepts, characteristics, and advances. *Hydrology and Earth System Science Discussion*, **6**, 3417–3481.
- Lin, H. S., Bouma, J., Wilding, L., Richardson, J., Kutílek, M., and Nielsen, D., 2005. Advances in hydropedology. *Advances in Agronomy*, **85**, 1–89.
- Lin, H. S., Bouma, J., Pachepsky, Y., Western, A., van Genuchten, M. Th., Thompson, J., Vogel, H., and Lilly, A., 2006a. Hydropedology: synergistic integration of pedology and hydrology. *Water Resource Research*, **42**, W05301, doi:10.1029/2005WR004085.
- Lin, H. S., Bouma, J., and Pachepsky, Y. (eds.), 2006b. Hydropedology: bridging disciplines, scales, and data. *Geoderma*, **131**, 255–406.
- Lin, H. S., Bouma, J., Owens, P., and Vepraskas, M., 2008a. Hydropedology: fundamental issues and practical applications. *Catena*, **73**, 151–152.
- Lin, H. S., Brooks, E., McDaniel, P., and Boll, J., 2008b. Hydropedology and surface/subsurface runoff processes. In Anderson M. G. (ed.), *Encyclopedia of Hydrological Sciences*. Chichester, UK: Wiley. doi:10.1002/0470848944.hsa306.
- Lin, H. S., Chittleborough, D., Singha, K., Vogel, H.-J., and Mooney, S., 2008c. The outcomes of the first international conference on hydropedology. In PES-02, 2008. *The Earth's Critical Zone and Hydropedology*. Symposium PES-02, International Geological Congress, Oslo, August 6–14, 2008. http://www.cprm.gov.br/33IGC/Sess_430.html. Accessed October 30, 2009.
- ON 73 6950, 1974. Hydropedological survey for land improvement purposes. Technical Standard. Prague: Hydropunkt (in Czech).
- Pachepsky, Y., and Rawls, W. J., 2004. *Development of Pedotransfer Functions in Soil Hydrology. Developments in Soil Science*. Amsterdam: Elsevier, Vol. 30.
- Pachepsky, Y. A., Rawls, W. J., and Lin, H. S., 2006. Hydropedology and pedotransfer functions. *Geoderma*, **131**, 308–316.
- Roulier, S., and Schulin, R. (eds.), 2008. A monothematic issue on preferential flow and transport in soil. *European Journal of Soil Science*, **59**, 1–130.
- Stewart, B. A., and Howell, T. A. (eds.), 2003. *Encyclopedia of Water Science*. New York: M. Dekker.
- Wikipedia, 2009. Available from World Wide Web: <http://en.wikipedia.org/wiki/Hydropedology>. Accessed October 30, 2009.

Cross-references

- Bypass Flow in Soil
Ecohydrology
Field Water Capacity
Hydraulic Properties of Unsaturated Soils
Hysteresis in Soil
Infiltration in Soils
Laminar and Turbulent Flow in Soils

Overland Flow
Pedotransfer Functions
Soil Water Flow
Water Budget in Soil

HYDROPHOBICITY

See [Soil Hydrophobicity and Hydraulic Fluxes](#)

Cross-references

- [Conditioners, Effect on Soil Physical Properties](#)

HYDROPHOBICITY OF SOIL

Paul D. Hallett¹, Jörg Bachmann², Henryk Czachor³, Emilia Urbanek⁴, Bin Zhang⁵

¹Scottish Crop Research Institute, Dundee, UK

²Institute of Soil Science, Leibniz University of Hannover, Hannover, Germany

³Institute of Agrophysics, Polish Academy of Sciences, Lublin, Poland

⁴Department of Geography, Swansea University, Swansea, UK

⁵Institute of Agricultural Resources and Regional Planning, Chinese Academy of Agricultural Sciences, Beijing, PR China

Synonyms

Localized dry spot; Soil water repellency

Definition

Hydrophobic – meaning “water fearing” in Greek.

Hydrophobic soils – repel water, generally resulting in water beaded on the surface.

Hydrophobicity – sometimes refers to a soil–water contact angle $>0^\circ$. These soils absorb less water and more slowly than hydrophilic soils.

Introduction

Hydrophobicity impedes the rate and extent of wetting in many soils. It is caused primarily by organic compounds that either coat soil particles or accumulate as particulate organic matter not associated with soil minerals. Sandy textured soils are more prone to hydrophobicity because their smaller surface area is coated more extensively than soils containing appreciable amounts of clay and silt. The most important effect of hydrophobicity is changes to soil water dynamics. Hydrophobicity causes negative effects through reduced infiltration and water retention, leading to enhanced run-off across the soil surface, preferential flow pathways in the unsaturated zone of the soil, and less plant available water. Many soils that appear to readily take in water have small levels of hydrophobicity.

Reduced wetting rates caused by hydrophobicity may also have a positive impact on soil structural stability. Hydrophobicity can be enhanced by soil drying, heating from fires, soil nutrients, and organic inputs.

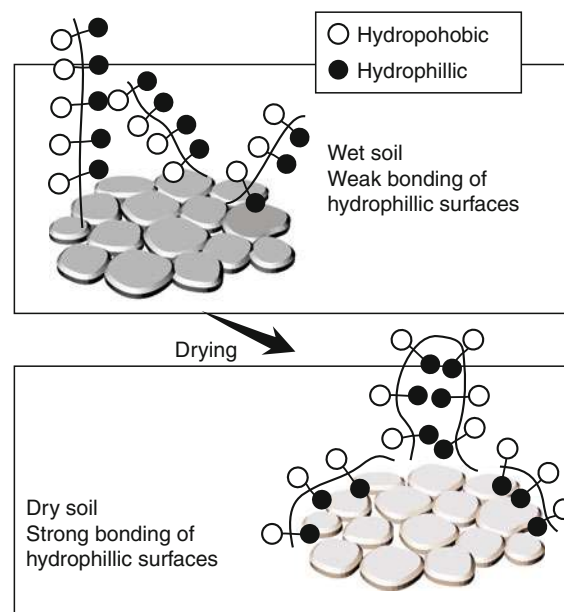
Geographical occurrence of soil hydrophobicity

Before a surge in research beginning in the 1990s, soil hydrophobicity was generally only associated with semi-arid or coastal soils (DeBano, 2000). The hydrophobicity of over 5 million hectares of agricultural soils in Australia can cause production losses of up to 80% (Blackwell, 2000). It is also a known problem of golf course greens and other sports soils (York and Canaway, 2000). Many coniferous forest soils are extremely prone to soil hydrophobicity (Doerr et al., 2009), particularly following wildfires (Mast and Clow, 2008). Since 1990, greater surveying and the development of more sensitive testing techniques identified soil hydrophobicity as a common property of most soils (Tilman et al., 1989; Doerr et al., 2000). It is now known that temperate soils are affected by soil hydrophobicity, including over 75% of land under pasture and cropping in the Netherlands (Dekker and Ritsema, 1994). Soil hydrophobicity has also been found in subtropical soils (Yao et al., 2009) and can be accentuated by hydrocarbon contamination (Roy et al., 1999). Smaller levels of soil hydrophobicity are found in most soils globally, with soil management (Woche et al., 2005), land use, texture (Doerr et al., 2006), and organic matter (Tilman et al., 1989; Capri et al., 1995) known to influence the severity. Hydrophobicity tends to increase with decreasing pH, although it has been found in alkaline soils and peats (Doerr et al., 2006).

Causes of soil hydrophobicity

Long-chain amphiphilic organic compounds produced by a range of biota can induce hydrophobicity in soil (Capri et al., 1995). These compounds can be highly hydrophilic, but drying causes bonding of hydrophilic (polar) ends of the molecules to each other or soil surfaces, resulting in an exposed hydrophobic (nonpolar) organic surface (Figure 1). Exudates and mycelia produced by fungi have been associated with water repellency in many studies (Bond, 1964; White et al., 2000; Feeney et al., 2006). Plant leaves, root mucilage, algae, and bacterial exudates can also cause soil hydrophobicity (Doerr et al., 2000; Ellerbrock et al., 2009; Martinez-Zavala and Jordan-Lopez, 2009; Hallett et al., 2009). The Lotus effect (Barthlott and Neinhuis, 1997) is an example of extreme hydrophobicity (water drops are not attached to the surface) due to specific combination of hydrophobic waxes and roughness on plant leaves of many plant species.

Although soils may have very different amounts of potentially hydrophobic compounds depending on geography, soil type, and management (Piccolo and Mbagwu, 1999), their concentrations are often poorly related to soil hydrophobicity, particularly if grouped as total organic carbon (Doerr et al., 2000). Severe soil hydrophobicity



Hydrophobicity of Soil, Figure 1 The polar hydrophilic ends of amphiphilic organic compounds bond to each other and soil particles when dry, resulting in a hydrophobic surface.
(Reprinted from Hallett, 2008.)

can result if a few grains have a hydrophobic coating in repacked sands (Steenhuis et al., 2005), but in natural soils the effects could be decreased by cracking of the organic surface during drying, relative humidity impacts, and interactions with other organic compounds (Doerr et al., 2000).

The spacing, packing, and roughness of grains also influence soil hydrophobicity. "Superhydrophobicity," where water rests on the tips of particles like a bed of nails, has been shown to be a potential process in soils (McHale et al., 2005).

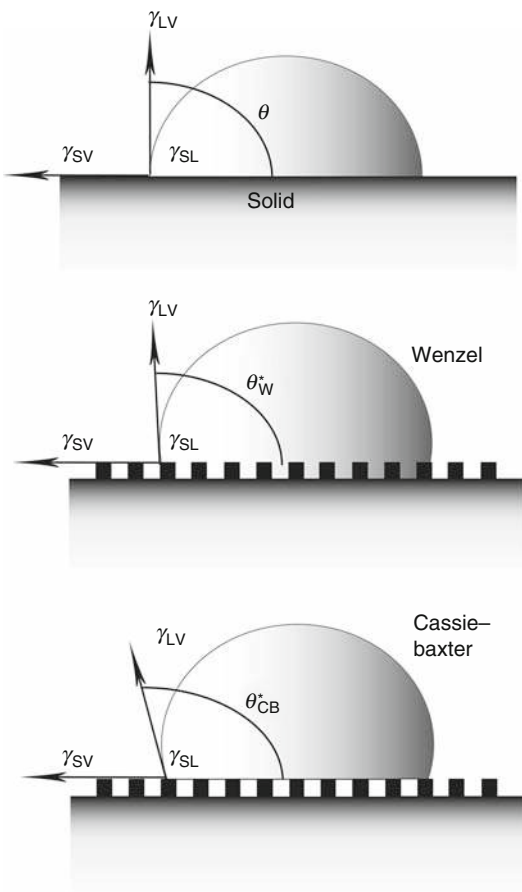
Physics of water repellency

The contact angle, θ , between a drop of water and a solid surface is controlled by the solid–vapor, γ_{sv} , solid–liquid, γ_{SL} and liquid–vapor γ_{LV} interfacial tensions (Figure 2). The Young's equation

$$\cos \theta = (\gamma_{\text{sv}} - \gamma_{\text{SL}})/\gamma_{\text{LV}} \quad (1)$$

describes the relation between the contact angle and the interfacial tensions for perfectly flat solid surfaces.

Although contact angles may vary continuously depending on the surface tension of the solid, it is convenient to think in terms of three different wetting situations. Complete wetting, for which the ideal θ is zero (perfectly wettable) and the liquid forms a very thin film, partial wetting with $0^\circ < \theta \leq 90^\circ$ (subcritical water repellency), and non-wetting (severe water repellency) with $\theta > 90^\circ$. Roughness of soil particles and pore surfaces can increase θ for already hydrophobic soils by either increasing



Hydrophobicity of Soil, Figure 2 Interaction between a drop of water and solid surface. The solid–vapor, γ_{SV} , solid–liquid, γ_{SL} , and liquid–vapor, γ_{LV} interfacial tensions control contact angle, θ . Surface roughness can increase θ through Wenzel or Cassie–Baxter processes.

the solid–liquid contact area (Wenzel) or if air within asperities increases the liquid–vapor area at the solid–liquid interface (Cassie–Baxter) (Bachmann and McHale, 2009). These processes can lead to superhydrophobicity and help explain why dry soils are more hydrophobic than wet soils (McHale et al., 2005).

The rate that soil absorbs water is defined by sorptivity, S and it will be influenced by θ as

$$S = S_i \cdot \cos(\theta), \quad (2)$$

where S_i is the intrinsic sorptivity (Philip, 1957). For a totally non-repellent soil, $S = S_i$ as $\cos(0^\circ)$ is 1. Capillarity is influenced by θ as

$$z\rho g = \frac{2\gamma \cdot \cos(\theta)}{r}, \quad (3)$$

where z is capillary rise, γ is the surface tension of water, ρ is water density, g is gravity, and r is the pore radius. A contact angle of 30–60° is not uncommon in soils that

are not recognized as hydrophobic but are to a certain extent water repellent (Woche et al., 2005) and this represents a greater than sixfold drop in sorptivity. Consequently, the observed capillarity rise may be considerably smaller than theoretically expected from Equation 3 with $\theta = 0$.

Measuring water repellency

Numerous approaches exist to measure water repellency in soil (Table 1). The water drop penetration time test (WDPT) is the most commonly used because of its simplicity, suitability for field measurements, and ability to measure the persistence of water repellency over periods of several hours (Dekker et al., 2009). As water repellency is influenced by the hydration status of soil, Dekker et al. (2001) extended the WDPT approach to measure “potential water repellency” using tests on soils equilibrated to different water contents in the laboratory. Usually soil is most water repellent when it is close to its air-dry water content (Dekker and Ritsema, 1994). Severity classes of water repellency can be determined from the WDPT, although some disagreement of critical thresholds exists in the literature. Table 2 provides the most widely accepted WDPT classifications.

The molarity of an ethanol droplet test (MED) is a suitable method for field measurements and indicates how strongly a water drop is repelled by a soil at the time of application (King, 1981). In the MED test, defined surface tensions of water are achieved by varying the molarity with the addition of different amounts of ethanol. The critical surface tension is taken as the minimum ethanol concentration where infiltration occurs in <5 s (Doerr, 1998).

A direct measurement of the soil–water contact angle based on the Sessile Drop method can be achieved using a Goniometer (Bachmann et al., 2000; Diehl and Schaumann, 2007). The capillary rise method (CRM) compares the infiltration rates of water and a liquid (usually hexane) not influenced by hydrophobicity (Bachmann et al., 2003) and is the standard approach used to measure the wetting of powders. A similar concept forms the basis of the intrinsic sorptivity test, where a water repellency index is assessed by comparing the sorptivity of water and ethanol measured with tension infiltrometers (Tilman et al., 1989). The hydrophobicity of individual soil aggregates can be measured by adapting either the CRM (Goebel et al., 2008) or intrinsic sorptivity (Hallett and Young, 1999) methods to assess wetting over smaller surface areas. The approach used to assess the water repellency index can also evaluate the apparent soil–water contact angle (Czachor, 2006). Error in the calculation of apparent soil–water contact angle by CRM or intrinsic sorptivity methods results because of pore roughness and heterogeneity impacts.

Implications

Soil hydrophobicity is a fundamental physical property of soil that has potentially severe implications to the environment, food security, and land-based industries.

Hydrophobicity of Soil, Table 1 Major approaches used to assess the hydrophobicity of soil

Test	Approach	Advantages	Disadvantages	Reference
Contact angle “Capillary rise”	Compares wetting rate of water and hexane into a packed column of soil	Physically meaningful Quantifies apparent contact angle	Time consuming Soil is disturbed when packed into columns	Bachmann et al. (2003)
Intrinsic sorptivity or repellency index, R	Compares sorptivity of water and ethanol measured with infiltrometer	Physically meaningful Miniature infiltrometers allow measurements of individual soil aggregates	Interaction between ethanol and soil may influence results	Tilman et al. (1989), Hallett and Young (1999)
Molarity of an ethanol droplet (MED)	Different concentrations of ethanol in water applied as drops to soil surface Critical minimum “molarity” where rapid infiltration occurs	Quick and easy (10 s per test)	Physical meaning requires greater investigation Surface roughness influences results	King (1981), Dekker et al. (2001), Roy and McGill (2002)
Sessile drop	Optical measure of contact angle of water drop on soil surface using Goniometer or light microscope	Measures contact angle directly	Affected by surface roughness Difficult to measure on wettable soils	Bachmann et al. (2000), Diehl and Schaumann (2007)
Water drop penetration time (WDPT)	Infiltration time of a drop of water placed on the surface of soil	Easily measures the persistence of hydrophobicity	Affected by pore structure Takes considerable time in repellent soil Not sensitive enough for low levels of hydrophobicity	Dekker et al. (2009)
Wilhelmy plate method (WPM)		Measures both advancing and receding contact angles	Uses a disturbed sample. Impact of adhesive and glass slide	Woche et al. (2005)

Hydrophobicity of Soil, Table 2 Classes of water repellency defined by Dekker et al. (2001) for the water drop penetration time (WDPT) test

Class	Severity	WDPT
0	Wettable, non-repellent	<5 s
1	Slightly water repellent	5–60 s
2	Strongly water repellent	60–600 s
3	Severely water repellent	600–3,600 s
4	Extremely water repellent	1–3 h
5		3–6 h
6		>6 h

The decreased rate of water infiltration and retention caused by hydrophobicity results in greater overland flow, less water retention, and the development of preferential flow paths and patchy dry spots in soil. Conventional soil physics approaches to describe water transport and retention require extensions to be effective in soils exhibiting even small levels of hydrophobicity (Deurer and Bachmann, 2007).

On golf courses, soil hydrophobicity is prominent and exacerbated by nutrient inputs and the small surface area of sand grains used to form putting greens (York and Canaway, 2000). Drought-stressed grass develops over hydrophobic soils as plant available water is reduced severely. In severely water stressed countries, the long-term irrigation of soil with treated effluent (waste water)

can present a serious challenge if hydrophobicity causes poor delivery and retention of water in the root zone (Wallach et al., 2005; Gruber et al., 2006; Vogeler, 2009).

Increased overland flow due to hydrophobicity accentuates soil erosion (Scott and Van Wyk, 1990; Shakesby et al., 2000; Benavides-Solorio and MacDonald, 2005), particularly following forest fires (Osborn et al., 1964). The impact follows seasonal shifts in hydrophobicity, with the impacts greatest during the summer (Witter et al., 1991; Jungerius and ten Harkel, 1994). Raindrops on hydrophobic soils produce fewer, slow-moving ejection droplets compared to wettable soils but remove more sediment (Terry and Shakesby, 1993). With successive drops, the surface of hydrophobic soils remain dry and noncohesive, leading to displacement by rain splash despite the overlying film of water (Doerr et al., 2003; Leighton-Boyce et al., 2007).

There is anecdotal evidence that heavy precipitation following dry periods can lead to flooding due to soil hydrophobicity. With increasing drought and severe weather predicted with climate change, this could have severe implications, particularly if predicted increases in the frequency and severity of soil wetting and drying occur.

Not all implications of soil hydrophobicity are deleterious to the environment or food production. Slower wetting rates of soil caused by hydrophobicity can result in increased soil aggregate stability (Goebel et al., 2005). Evaporation is also decreased by hydrophobic surface soil

(Shokri et al., 2009) and this mechanism is used by microbiotic crusts to conserve water in extremely arid environments (Issa et al., 2009).

Amelioration

Physical, chemical, and biological approaches have been developed to combat problems associated with hydrophobic soils. As soil hydrophobicity is pH dependent, lime application can reduce acidity of soils and is a very common amelioration strategy. Wetting agents are also in widespread use (Oostindie et al., 2008), particularly on amenity soils (Cisar et al., 2000) but also increasingly on agricultural land (Miyamoto, 1985). They can improve water distribution and infiltration rates by either acting as surfactants that decrease the surface tension of water or by altering the contact angle of soil surfaces (Kostka, 2000). A common approach on hydrophobic agricultural soils is the addition of clay to cover hydrophobic surfaces and make them hydrophilic (Blackwell, 2000). Kaolinitic clays are the most effective in reducing repellency (Ma'shum et al., 1989; Ward and Oades, 1993; McKissock et al., 2002; Dlapa et al., 2004), but relatively large quantities of clay are required to achieve the desired effect (100 t ha^{-1}) (Blackwell, 1993), so the approach is only economical if the clays occur naturally on site. Furrows can also help combat the impact of hydrophobicity by harvesting water and diverting it to the root zone (Blackwell, 2000).

Intensive cultivation decreases soil hydrophobicity as organic coatings are abraded and new soil surfaces are exposed. However, the shift in microbial dynamics and carbon mineralization that ensues can lead to hydrophobicity developing again (Feeney et al., 2006). Zero or reduced tillage, on the other hand, can decrease soil hydrophobicity by maintaining greater soil moisture (Blackwell, 2000) and potentially by altering the functional capacity of microbes to degrade hydrophobic compounds (Roper, 2005). Wax degrading bacteria have been isolated that have been demonstrated to reduce soil hydrophobicity (Roper, 2004).

Bibliography

- Bachmann, J., and McHale, G., 2009. Superhydrophobic surfaces: a model approach to predict contact angle and surface energy of soil particles. *European Journal of Soil Science*, **60**, 420–430.
- Bachmann, J., Ellies, A., and Hartge, K. H., 2000. Development and application of a new sessile drop contact angle method to assess soil water repellency. *Journal of Hydrology*, **231–232**, 66–75.
- Bachmann, J., Woche, S. K., Goebel, M. O., Kirkham, M. B., and Horton, R., 2003. Extended methodology for determining wetting properties of porous media. *Water Resources Research*, **39**, 1–14.
- Barthlott, W., and Neinhuis, C., 1997. Purity of the sacred lotus, or escape from contamination in biological surfaces. *Planta*, **202**, 1–8.
- Benavides-Solorio, Jd. D., and MacDonald, L. H., 2005. Measurement and prediction of post-fire erosion at the hillslope scale, Colorado Front Range. *International Journal of Wildland Fire*, **14**, 457–474.
- Blackwell, P., 1993. Improving sustainable production from water repellent sands. *Journal of Agriculture of Western Australia*, **34**, 160–167.
- Blackwell, P. S., 2000. Management of water repellency in Australia, and risks associated with preferential flow, pesticide concentration and leaching. *Journal of Hydrology*, **231–232**, 384–395.
- Bond, R. D., 1964. The influence of the microflora on the physical properties of soils. II. Field studies on water repellent sands. *Australian Journal of Soil Research*, **2**, 123–131.
- Capriel, P., Beck, T., Borchert, H., Gronholz, J., and Zachmann, G., 1995. Hydrophobicity of the organic matter in arable soils. *Soil Biology and Biochemistry*, **27**, 1453–1458.
- Cisar, J. L., Williams, K. E., Vivas, H. E., and Haydu, J. J., 2000. The occurrence and alleviation by surfactants of soil-water repellency on sand-based turfgrass systems. *Journal of Hydrology*, **231–232**, 352–358.
- Czachor, H., 2006. Modelling the effect of pore structure and wetting angles on capillary rise in soils having different wettabilities. *Journal of Hydrology*, **328**, 604–613.
- DeBano, L. F., 2000. Water repellency in soils: a historical overview. *Journal of Hydrology*, **231–232**, 4–32.
- Dekker, L. W., and Ritsema, C. J., 1994. How water moves in a water repellent sandy soil. I. Potential and actual water repellency. *Water Resources Research*, **30**, 2507–2517.
- Dekker, L. W., Doerr, S. H., Oostindie, K., Ziogas, A. K., and Ritsema, C. J., 2001. Water repellency and critical soil water content in a dune sand. *Soil Science Society of America Journal*, **65**, 1667–1674.
- Dekker, L. W., Ritsema, C. J., Oostindie, K., Moore, D., and Wesseling, J. G., 2009. Methods for determining soil water repellency on field-moist samples. *Water Resources Research*, **45**, W00D33.
- Deurer, M., and Bachmann, J., 2007. Modeling water movement in heterogeneous water-repellent soil: 2. A conceptual numerical simulation. *Vadose Zone Journal*, **6**, 446–457.
- Diehl, D., and Schaumann, G. E., 2007. The nature of wetting on urban soil samples: wetting kinetics and evaporation assessed from sessile drop shape. *Hydrological Processes*, **21**, 2255–2265.
- Dlapa, P., Doerr, S. H., Lichner, L., Šír, M., and Tesař, M., 2004. Effect of kaolinite and Ca-montmorillonite on the alleviation of soil water repellency. *Plant and Soil Environment*, **50**, 358–363.
- Doerr, S. H., 1998. On standardising the “water drop penetration time” and the “molarity of an ethanol droplet” techniques to classify soil hydrophobicity: a case study using medium textured soils. *Earth Surface Processes and Landforms*, **23**, 663–668.
- Doerr, S. H., Shakesby, R. A., and Walsh, R. P. D., 2000. Soil water repellency: its causes, characteristics and hydrogeomorphological significance. *Earth Science Reviews*, **51**, 33–65.
- Doerr, S. H., Ferreira, A. J. D., Walsh, R. P. D., Shakesby, R. A., Leighton-Boyce, G., and Coelho, C. O. A., 2003. Soil water repellency as a potential parameter in rainfall-runoff modelling: experimental evidence at point to catchment scales from Portugal. *Hydrological Processes*, **17**, 363–377.
- Doerr, S. H., Shakesby, R. A., Dekker, L. W., and Ritsema, C. J., 2006. Occurrence, prediction and hydrological effects of water repellency amongst major soil and land-use types in a humid temperate climate. *European Journal of Soil Science*, **57**, 741–754.
- Doerr, S. H., Woods, S. W., Martin, D. A., and Casimiro, M., 2009. ‘Natural background’ soil water repellency in conifer forests of the north-western USA: Its prediction and relationship to wildfire occurrence. *Journal of Hydrology*, **371**, 12–21.
- Ellerbrock, R. H., Gerke, H. H., and Bohm, C., 2009. In situ drift characterization of organic matter composition on soil structural surfaces. *Soil Science Society of America Journal*, **73**, 531–540.

- Feeney, D. S., Crawford, J. W., Daniell, T., Hallett, P. D., Nunan, N., Ritz, K., Rivers, M., and Young, I. M., 2006. Three-dimensional microorganization of the soil-root-microbe system. *Microbial Ecology*, **52**, 151–158.
- Goebel, M. O., Bachmann, J., Woche, S. K., and Fischer, W. R., 2005. Soil wettability, aggregate stability, and the decomposition of soil organic matter. *Geoderma*, **128**, 80–93.
- Goebel, M. O., Bachmann, J., and Woche, S. K., 2008. Modified technique to assess the wettability of soil aggregates: comparison with contact angles measured on crushed aggregates and bulk soil. *European Journal of Soil Science*, **59**, 1241–1252.
- Graber, E. R., Ben-Arie, O., and Wallach, R., 2006. Effect of sample disturbance on soil water repellency determination in sandy soils. *Geoderma*, **136**, 11–19.
- Hallett, P. D., 2008. A brief overview of the causes, impacts and amelioration of soil water repellency. *Soil and Water*, **3**, S21–S29.
- Hallett, P. D., and Young, I. M., 1999. Changes to water repellence of soil aggregates caused by substrate-induced microbial activity. *European Journal of Soil Science*, **50**, 35–40.
- Hallett, P., Feeney, D., Bengough, A., Rillig, M., Scrimgeour, C., and Young, I., 2009. Disentangling the impact of AM fungi versus roots on soil structure and water transport. *Plant and Soil*, **314**, 183–196.
- Issa, O. M., Defarge, C., Trichet, J., Valentin, C., and Rajot, J. L., 2009. Microbiotic soil crusts in the Sahel of Western Niger and their influence on soil porosity and water dynamics. *Catena*, **77**, 48–55.
- Jungerius, P. D., and ten Harkel, M. J., 1994. The effect of rainfall intensity on surface runoff and sediment yield in the grey dunes along the Dutch coast under conditions of limited rainfall acceptance. *Catena*, **23**, 269–279.
- King, P. M., 1981. Comparison of methods for measuring severity of water repellence of sandy soils and assessment of some factors that affect its measurement. *Australian Journal of Soil Research*, **19**, 275–285.
- Kostka, S. J., 2000. Amelioration of water repellency in highly managed soils and the enhancement of turfgrass performance through the systematic application of surfactants. *Journal of Hydrology*, **231–232**, 359–368.
- Leighton-Boyce, G., Doerr, S. H., Shakesby, R. A., and Walsh, R. D. P., 2007. Quantifying the impact of soil water repellency on overland flow generation and erosion: a new approach using rainfall simulation and wetting agents on in situ soils. *Hydrological Processes*, **21**, 2337–2345.
- Martinez-Zavalá, L., and Jordan-Lopez, A., 2009. Influence of different plant species on water repellency in Mediterranean heathland soils. *Catena*, **76**, 215–223.
- Ma'shum, M., Oades, J. M., and Tate, M. E., 1989. The use of dispersible clays to reduce water-repellency of sandy soils. *Australian Journal of Soil Research*, **27**, 797–806.
- Mast, M. A., and Clow, D. W., 2008. Effects of 2003 wildfires on stream chemistry in Glacier National Park, Montana. *Hydrological Processes*, **22**, 5013–5023.
- McHale, G., Newton, M. I., and Shirtcliffe, N. J., 2005. Water-repellent soil and its relationship to granularity, surface roughness and hydrophobicity: a materials science view. *European Journal of Soil Science*, **56**, 445–452.
- McKissock, I., Gilkes, R. J., and Walker, E. L., 2002. The reduction of water repellency by added clay is influenced by clay and soil properties. *Applied Clay Science*, **20**, 225–241.
- Miyamoto, S., 1985. Effects of wetting agents on water infiltration into poorly wettable sand, dry sod and wettable soils. *Irrigation Science*, **6**, 271–279.
- Oostindie, K., Dekker, L. W., Wesseling, J. G., and Ritsema, C. J., 2008. Soil surfactant stops water repellency and preferential flow paths. *Soil Use and Management*, **24**, 409–415.
- Osborn, J. F., Pelishek, R. E., Krammes, J. S., and Letey, J., 1964. Soil wettability as a factor in erodibility. *Soil Science Society of America Journal*, **28**, 294–295.
- Philip, J. R., 1957. The theory of infiltration. 1. The infiltration equation and its solution. *Soil Science*, **83**, 345–357.
- Piccolo, A., and Mbagwu, J. S. C., 1999. Role of hydrophobic components of soil organic matter in soil aggregate stability. *Soil Science Society of America Journal*, **63**, 1801–1810.
- Roper, M. M., 2004. The isolation and characterisation of bacteria with the potential to degrade waxes that cause water repellency in sandy soils. *Australian Journal of Soil Research*, **42**, 427–434.
- Roper, M. M., 2005. Managing soils to enhance the potential for bioremediation of water repellency. *Australian Journal of Soil Research*, **43**, 803–810.
- Roy, J. L., and McGill, W. B., 2002. Assessing soil water repellency using the molarity of ethanol droplet (MED) test. *Soil Science*, **167**, 83–97.
- Roy, J. L., McGill, W. B., and Rawluk, M. D., 1999. Petroleum residues as water-repellent substances in weathered nonwettable oil-contaminated soils. *Canadian Journal of Soil Science*, **79**, 367–380.
- Scott, D. F., and Van Wyk, D. B., 1990. The effects of wildfire on soil wettability and hydrological behaviour of an afforested catchment. *Journal of Hydrology*, **121**, 239–256.
- Shakesby, R. A., Doerr, S. H., and Walsh, R. P. D., 2000. The erosional impact of soil hydrophobicity: current problems and future research directions. *Journal of Hydrology*, **231–232**, 178–191.
- Shokri, N., Lehmann, P., and Or, D., 2009. Characteristics of evaporation from partially wettable porous media. *Water Resources Research*, **45**, W02415.
- Steenhuis, T. S., Hunt, A. G., Parlange, J. Y., and Ewing, R. P., 2005. Assessment of the application of percolation theory to a water repellent soil. *Australian Journal of Soil Research*, **43**, 357–360.
- Terry, J. P., and Shakesby, R. A., 1993. Soil hydrophobicity effects on rainsplash: simulated rainfall and photographic evidence. *Earth Surface Processes and Landforms*, **18**, 519–525.
- Tilman, R. W., Scotter, D. R., Wallis, M. G., and Clothier, B. E., 1989. Water-repellency and its measurement by using intrinsic sorptivity. *Australian Journal of Soil Research*, **27**, 637–644.
- Vogeler, I., 2009. Effect of long-term wastewater application on physical soil properties. *Water, Air, and Soil Pollution*, **196**, 385–392.
- Wallach, R., Ben-Arie, O., and Gruber, E. R., 2005. Soil water repellency induced by long-term irrigation with treated sewage effluent. *Journal of Environmental Quality*, **34**, 1910–1920.
- Ward, P. R., and Oades, J. M., 1993. Effect of clay mineralogy and exchangeable cations on water-repellency in clay-amended sandy soils. *Australian Journal of Soil Research*, **31**, 351–364.
- White, N. A., Hallett, P. D., Feeney, D. S., Palfreyman, J. W., and Ritz, K., 2000. Changes to water repellence of soil caused by the growth of white-rot fungi: studies using a novel microcosm system. *FEMS Microbiology Letters*, **184**, 73–77.
- Witter, J. V., Jungerius, P. D., and ten Harkel, M. J., 1991. Modelling water erosion and the impact of water repellency. *Catena*, **18**, 115–124.
- Woche, S. K., Goebel, M. O., Kirkham, M. B., Horton, R., Van der Ploeg, R. R., and Bachmann, J., 2005. Contact angle of soils as affected by depth, texture, and land management. *European Journal of Soil Science*, **56**, 239–251.
- Yao, S., Qin, J., Peng, X., and Zhang, B., 2009. The effects of vegetation on restoration of physical stability of a severely degraded soil in China. *Ecological Engineering*, **35**, 723–734.
- York, C. A., and Canaway, P. M., 2000. Water repellent soils as they occur on UK golf greens. *Journal of Hydrology*, **231–232**, 126–133.

Cross-references

- Bypass Flow in Soil
 Clay Minerals and Organo-Mineral Associates
 Hydraulic Properties of Unsaturated Soils
 Infiltration in Soils
 Microbes, Habitat Space, and Transport in Soil
 Mineral–Organic–Microbial Interactions
 Organic Matter, Effects on Soil Physical Properties and Processes
 Overland Flow
 Physical Degradation of Soils, Risks and Threats
 Soil Hydrophobicity and Hydraulic Fluxes
 Soil Water Flow
 Spatial Variability of Soil Physical Properties
 Wetting and Drying, Effect on Soil Physical Properties
 Wildfires, Impact on Soil Physical Properties

HYPOBARIC STORAGE

Hypobaric storage involves the cold storage of fruit under partial vacuum. Typical conditions include pressures as low as 80 and 40 millimetres of mercury and temperatures of 5° C (40° F). Hypobaric conditions reduce ethylene production and respiration rates; the result is an extraordinarily high-quality fruit even after months.

Bibliography

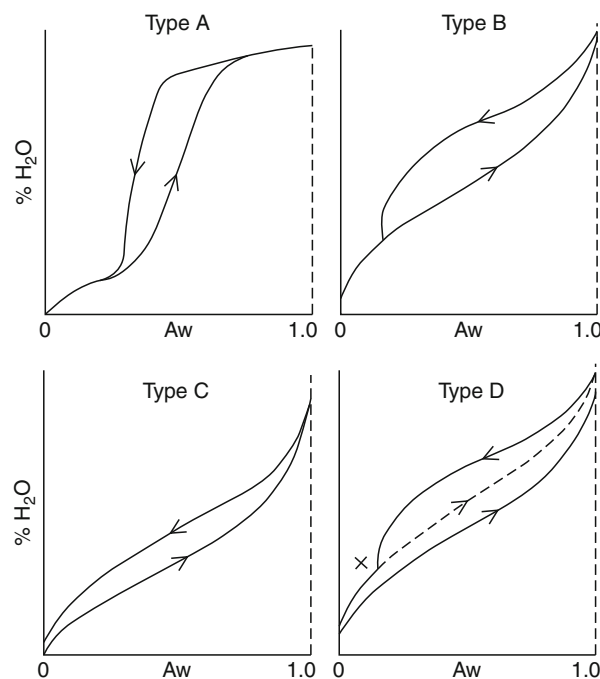
<http://www.britannica.com/EBchecked/topic/279852/hypobaric-storage>

HYSTERESIS IN FOODS

Matthew Caurie

Department of Home Economics Education, University of Education, Winneba, Ghana

Hysteresis in foods is the phenomenon by which at constant water activity (Aw) and temperature, a food adsorbs a smaller amount of water during adsorption than during a subsequent desorption process. Previous hypotheses to explain the phenomenon (Zsigmondy, 1911; Cohan, 1938, 1944; Everett, 1967; McBain, 1935; Kraemer, 1930) have been based on capillary condensation but the phenomenon is exhibited in foods and other substances believed to have negligible capillaries or pores. Current explanation (Caurie, 2007) states that sites adsorb moisture appropriate to their surface energies. During adsorption, micro-cracks and fissures form in the food to expose additional sites. Exposed sites unable to adsorb moisture on the way up to higher water activities (Aws) because of inappropriate surface energies adsorb additional moisture on return to lower Aws at appropriate Aw and surface energies to exhibit a hysteresis loop.



Hysteresis in Foods, Figure 1 Types of hysteresis.

The equation derived to fit the above interpretation of hysteresis has the form (Caurie, 2007)

$$m\left(\frac{1}{a} - 1\right) = K \exp\left(B \frac{Q}{T}\right), \quad (1)$$

where m = percent moisture content at water activity a ; Q = surface energy (keal/mole); T = absolute temperature; K, B = constants.

Bibliography

- Caurie, M., 2007. Hysteresis phenomenon in foods. *International Journal of Food Science & Technology*, **42**, 45–49.
 Cohan, L. H., 1938. Sorption hysteresis and the vapour pressure of concave surfaces. *Journal of the American Chemical Society*, **60**, 433–435.
 Cohan, L. H., 1944. Hysteresis and the capillary theory of adsorption of vapours. *Journal of the American Chemical Society*, **66**, 98–105.
 Everett, B. H., 1967. Adsorption hysteresis. In Flood, E. A. (ed.), *The solid-gas interface, Vol. II*. New York: Marcel Dekker Inc., p. 1055.
 Kraemer, E. O., 1930. The colloidal state and surface chemistry. In Taylor, H. S. (ed.), *Treatise on Physical Chemistry, Vol. II*, 2nd edn. New York: D. Van Nostrand Co. Inc., p. 1661.
 McBain, J. W., 1935. An explanation of hysteresis in the hydration and dehydration of gels. *Journal of the American Chemical Society*, **57**, 699–701.
 Zsigmondy, R., 1911. Structures of gelatinous silicic acid. Theory of dehydration. *Zeitschrift Anorganic Chemistry*, **71**, 356–377.

HYSTERESIS IN SOIL

Cezary Ślawiński

Institute of Agrophysics, Polish Academy of Sciences,
Lublin, Poland

Synonyms

Soil water hysteresis

Definition

Hysteresis in soil is defined as the difference in the relationship between the water content of the soil and the corresponding water potential obtained under wetting and drying process.

The relationship between soil water content and soil water potential is called soil water retention curve (SWRC). This dependency manifests itself through hysteresis. It was shown by Haines in 1930 (Haines, 1930). This means that water content in the drying (or drainage) branch of water potential – water content relationship – is larger than water content in the wetting branch for the same value of water potential. For hygroscopic water, this effect is due to differences of water content at increasing and decreasing vapor tension in soil. During the increase of vapor tension, the water content in soil is lower than during the vapor tension decrease. For capillary water, the hysteresis phenomena result from pore shape irregularity. Irregular soil capillary is characterized by volume V and minimal r and maximal R radiiuses. Empty capillary is filled with water at under pressure corresponding to radius R . After filling with water, the meniscus is created, corresponding to radius r and the same capillary can be emptying at much higher water under pressure. The hysteresis region is called hysteresis loop. The wetting and

drying curves can be of the first or higher orders depending on actual soil water potential at which the wetting or drying process is started. Numerous models describing soil water hysteresis were developed. These models can be categorized into two main groups: the conceptual models and empirical models. The conceptual models are basically based on the domain theory. The independent domain theory of soil water hysteresis assumes that each soil water domain wets and dries at the characteristic water potentials irrespective of neighboring domains. This theory has been developed by Néel (1942, 1943). The modification of this theory takes into account interaction between particular domains and in literature is referred as dependent domain theory (Poulovassilis and Childs, 1971; Topp, 1971; Mualem and Dagan, 1975). Empirical models are mainly related to the analysis of the shape and properties of water retention curves.

Bibliography

- Haines, W. B., 1930. Studies in the physical properties of soil: V. The hysteresis effect in capillary properties, and the modes of moisture associated therewith. *Journal of Agricultural Science*, **20**, 97–116.
- Mualem, Y., and Dagan, G., 1975. A dependence domain model of capillary hysteresis. *Water Resources Research*, **11**, 452–460.
- Néel, L., 1942. Théorie des lois d'aimantation de Lord Rayleigh. 1^{ère} partie: les déplacements d'une paroi isolée. *Cahiers de Physique*, **12**, 1–20.
- Néel, L., 1943. Théorie des lois d'aimantation de Lord Rayleigh. 2^{ème} partie: multiples domaines et champ coercitif. *Cahiers de Physique*, **13**, 18–30.
- Poulovassilis, A., and Childs, E. C., 1971. The hysteresis of pore water: the non-independence of domains. *Soil Science*, **112**, 301–312.
- Topp, G. C., 1971. Soil-water hysteresis: the domain theory extended to pore interaction conditions. *Soil Science American Proceedings*, **35**, 219–225.

ICE EROSION (GLACIAL EROSION, THERMAL EROSION)

Ice erosion occurs in several forms: Glacial, melt, ice movement, and thermal. Glacial erosion is the best known form of ice erosion, in which glaciers crush and shift large amounts of soil, their weight undercutting soil structures and also creating a range of vertical sides to the areas which they pass, which in turn erode through gravity and landslides. Ice melt causes the formation of solutions of materials which wash away, eroding soil and rock. Ice movement is abrasive on other surfaces, creating weak points, a mini glacial action. Thermal erosion is caused by expansion and contraction of soils and rocks affected by ice.

Bibliography

http://www.examplesof.com/science/ice_erosion.html

ILLUVIATION

The deposition in the lower soil horizon of material, particularly clay-sized particles, transported by water (in suspension or in solution) from the upper horizon.

Bibliography

Chesworth, W. (ed.). 2008. Encyclopedia of Soil Science, Springer, p 329.

Cross-references

[Organic Matter, Effects on Soil Physical Properties and Processes](#)

IMAGE ANALYSIS IN AGROPHYSICS

Magnus Persson

Department of Water Resources Engineering,
Lund University, Lund, Sweden

Definition

Image analysis can be defined as extraction of useful information from images by means of digital image processing techniques. In agrophysics, image analysis can be used to measure specific features of the soil or vegetation.

Introduction

An image can be considered as a large data matrix, where each element (often called pixel) contains information about the brightness (in black and white images) or color of a small area of the motif. Features of the image such as color or structures present can be related to physical properties of the motif (or parts of it). Using image analysis, it is possible to find patterns and boundaries, track objects, analyze colors, etc., in an automated way, making image analysis ideal for various applications such as surveillance, robotics, astronomy, remote sensing, and agrophysics.

Images can be captured in several different ways. Nowadays, digital cameras are used in most applications since they instantly produce digital images that directly can be analyzed mathematically. The wavelength of the recorded light can be different, normally cameras record visible light (roughly 400–700 nm), but longer or shorter wavelength are also used (IR, UV, or even X-ray). The scales of images can also vary; microscale images can be obtained through microscopes while satellite images almost can cover entire continents.

There is a great potential of using image analysis application in agrophysics. Both characteristics of the crops and the soil material can be assessed or measured using image analysis. In this article, I will focus on image analysis for determining soil characteristics since image analysis related to crops can be found elsewhere (e.g., Zheng and Moskal, 2009); (see *Plant Disease Symptoms, Identification from Colored Images; Plant Drought Stress: Detection by Image Analysis; Visible and Thermal Images for Fruit Detection*). For X-ray computed tomography imaging and other related methods, see, for example, Taina et al. (2008).

In soil science, image analysis has become increasingly popular during the last decade. There are many interesting applications such as determining the size and shapes of macroporosity (e.g., Czachor and Lipiec, 2004), root mass and root length (Kimura et al., 1999), organic matter content (Chen et al., 2000), soil albedo (Post et al., 2000), water content (Persson, 2005b), and solute concentration (Forrer et al., 2002).

Images are generally analyzed to determine either color of an object or to find and analyze shapes and patterns. There are many more types of analyses that can be done to extract useful information from images related to agrophysics. Some examples are Fourier transforms, fractal dimension analysis, texture analysis, etc. It should be noted that various image enhancing processes are applied in the image analysis process, for example, various kinds of digital filters, etc. One important process often used as one of the first steps in image analysis is segmentation. Segmentation means that the image is partitioned into segments containing multiple pixels corresponding to structural elements or other objects of interest. The purpose of segmentation is to reduce an image to information. One simple example is thresholding of a gray scale image to produce a binary image. Pixels with brightness above a certain threshold are given the value 1, all other pixels are given the value 0.

It should be noted that even if image analysis can be automated, it contains several steps which can be affected by subjectivity. Different operators are likely to come to slightly different conclusions based on the same images. Thompson et al. (1992) discussed this problem and suggested some types of standardization. Unfortunately, very few of his suggestions have been implemented. Therefore, caution should be taken when results from different investigators are compared.

Some applications

Dye tracers have been used for many years by soil scientists investigating the effects of soil heterogeneity as they allow visualization of spatial flow patterns (see, e.g., Flury and Flühler, 1995). This method has proven very useful for detecting preferential flow paths in the soil. Traditionally, image analysis of the dye photographs has only involved separation between stained and non-stained soil.

However, image analysis improved to the extent that the estimation of dye concentration from soil color was possible (e.g., Ewing and Horton, 1999; Forrer et al., 2002).

Physically, the wavelength of light determines its color. The color of an object is determined both by the spectrum of the incident illumination and on the reflectance spectrum of the surface. A color model (color space) is an abstract mathematical model describing the way colors can be represented as tuples of numbers. Some examples are RGB (red, green, and blue), CMYK (cyan, magenta, yellow, and black), and HSV (hue, saturation, and value). In the RGB color space, which is the one used by most digital cameras and computer screens, all colors can be represented by mixing various amounts of red, green, and blue. In most applications, each channel contains 8 bits of data $2^8 = 255$. Thus, $255^3 = 16,581,375$ different colors can be described.

Color consistency means that an image of an object should have the same color regardless of the ambient lighting conditions. Factors affecting the color of an object are inhomogeneous illumination, color temperature, and image noise. Any image can be transferred to a common norm by correcting for color temperature and inhomogeneous illumination (see Persson, 2005a). Image noise, however, is random and cannot be corrected for. Using high-end cameras and a powerful light source will in most cases reduce the image noise sufficiently. Different averaging filters can also be used.

The color as expressed in a specific color space of the corrected images can then be related to dye concentration. In most cases, an empirical polynomial equation is adopted to model the relationship between RGB or HSV values and dye concentration (Ewing and Horton, 1999; Aeby et al., 2001; Persson et al., 2005). Other more complex models like neural networks have also been used (Persson, 2005a).

Different types of dye tracers have been used, from various types of food dye to fluorescent tracers. Multiple tracer experiments have been carried out to study the transport and sorption of different compounds.

The same fundamental principle of color consistency can also be used for determining other physical characteristics of soil material like organic matter content (Chen et al., 2000), soil albedo (Post et al., 2000), or water content (Persson, 2005b).

There are several ways to describing the shape-related features of an object, for example, form factor, roundness, and elongation. Each of these is strictly mathematically described. By defining the limits for these parameters, different kinds of objects can be separated from each other.

Image analysis of the soil pore space is normally done on small-scale samples impregnated with a resin. Different types of resin have been used; usually, the resin contains some sort of dye so that it stands out from the color of the soil grains. Using fluorescent resins and light sources with different wavelengths, even more information can be extracted from the images. After hardening,

the sample is cut into thin sections that are photographed (e.g., Bouma et al., 1977; Protz et al., 1992; Ringrose-Voase, 1996). After segmentation, the pore space can be analyzed to find the shape and size of pores between the grains. Furthermore, characteristics such as connectivity of pores, types of soil material, and identification of earth worm channels, can be determined.

Some studies about automated classification of soils using image analysis have been presented. Marschallinger (1997) showed how image analysis could be used for classifying minerals in rock samples. Maragos et al. (2004) presented an automated system for estimation of the bioecological quality of soils using sophisticated image analysis. Generally, these applications require large computational efforts, but with the development of computers and image analysis software, usage of these applications will likely increase in the near future.

Interesting attempts on relating microscale characteristics of the pore network determined using image analysis to the transport of water and solutes. Pioneering work had been carried out already by Bullock and Thomasson (1979) who compared the characterization of macroporosity and water retention data. Walker and Trudgill (1983) studied the relationship between image analysis of pore network and dispersivity.

Image analysis for determining root length and diameter has received a lot of attention. Previous analysis methods (manual inspection) were very labor intensive and several commercial image analysis software packages have been developed (e.g., Kirchhof, 1992; van der Weele et al., 2003; French et al., 2009).

Conclusion

Image analysis and especially its application to agrophysics is still a young science. Most research within the field has been done during the last decades. Some applications are already routinely used, whereas many potential applications have received little attention yet. Especially interesting is automated image analysis for soil classification and studies, where pore scale soil properties are related to macroscopic features like water retention or soil fertility. Another area where I expect further development is the use of automated image analysis to study dynamic processes, for example, solute transport or root growth.

Last, I have to point out the great potential of using images and image analysis for educational purposes. Learning and understanding complicated processes is greatly enhanced when they can be visualized. Therefore image analysis applications are ideal for teaching or when communicating with the public.

Bibliography

Aebi, P., Schultze, U., Braichotte, D., Bundt, M., Wydler, H., and Flühler, H., 2001. Fluorescence imaging tracer distributions

- in soil profiles. *Environmental Science & Technology*, **35**, 753–760.
- Bouma, J., Jongerium, A., Boersma, O., Jager, A., and Schoonderbreek, D., 1977. The function of different types of macropores during saturated flow through four swelling soil horizons. *Soil Science Society of America Journal*, **41**, 945–950.
- Bullock, P., and Thomasson, A. J., 1979. Rothamsted studies of soil structure, 2 measurement and characterization of macroporosity by image analysis and comparison with data from water-retention measurements. *Journal of Soil Science*, **30**, 391–413.
- Chen, F., Kissel, D. E., West, L. T., and Adkins, W., 2000. Field-scale mapping of surface soil organic carbon using remotely sensed imagery. *Soil Science Society of America Journal*, **64**, 746–753.
- Czachor, H., and Lipiec, J., 2004. Quantification of soil macroporosity with image analysis. *International Agrophysics*, **18**, 217–223.
- Ewing, R. P., and Horton, R., 1999. Discriminating dyes in soil with color image analysis. *Soil Science Society of America Journal*, **63**, 18–24.
- Flury, M., and Flühler, H., 1995. Tracer characteristics of Brilliant Blue FCF. *Soil Science Society of America Journal*, **59**, 22–27.
- Forrer, I., Papritz, A., Kasteel, R., Flühler, H., and Luca, D., 2002. Quantifying dye tracers in soil profiles by image processing. *European Journal of Soil Science*, **51**, 313–322.
- French, A., Ubeda-Tomás, S., Holman, T. J., Bennett, M. J., and Pridmore, T., 2009. High-Throughput quantification of root growth using a novel image-analysis tool. *Plant Physiology*, **150**, 1784–1795.
- Kimura, K., Kikuchi, S., and Yamasaki, S., 1999. Accurate root length measurement by image analysis. *Plant and Soil*, **216**, 117–127.
- Kirchhof, G., 1992. Measurement of root length and thickness using a hand-held computer scanner. *Field Crops Research*, **29**, 79–88.
- Maragos, P., Sofou, A., Stamou, G. B., Tzouvaras, V., Papatheodorou, E., and Stamou, G. P., 2004. Image analysis of soil micromorphology: feature extraction, segmentation, and quality inference. *EURASIP Journal on Applied Signal Processing*, **2004**, 902–912.
- Marschallinger, R., 1997. Automatic mineral classification in the macroscopic scale. *Computers and Geosciences*, **23**, 119–126.
- Persson, M., 2005a. Accurate dye tracer concentration estimations using image analysis. *Soil Science Society of America Journal*, **69**, 967–975.
- Persson, M., 2005b. Estimating surface soil moisture from soil color using image analysis. *Vadose Zone Journal*, **4**, 1119–1122.
- Persson, M., Hardy, S., Olsson, J., and Wendt, J., 2005. Solute transport dynamics by high-resolution dye tracer experiments—image analysis and time moments. *Vadose Zone Journal*, **4**, 856–865.
- Post, D. F., Fimbres, A., Matthias, A. D., Sano, E. E., Accioly, L., Batchily, A. K., and Ferreira, L. G., 2000. Predicting soil albedo from soil color and spectral reflectance data. *Soil Science Society of America Journal*, **64**, 1027–1034.
- Protz, R., Sweeney, S. J., and Fox, C. A., 1992. An application of spectral image analysis to soil micromorphology. I: Methods of analysis. *Geoderma*, **53**, 275–288.
- Ringrose-Voase, A. J., 1996. Measurement of soil macropore geometry by image analysis of sections through impregnated soil. *Plant and Soil*, **183**, 27–47.
- Taina, I. A., Heck, R. J., and Elliot, T. R., 2008. Application of X-ray computed tomography to soil science: A literature review. *Canadian Journal of Soil Science*, **88**, 1–20.
- Thompson, M. L., Singh, P., Corak, S., and Straszheim, W. E., 1992. Cautionary notes for the automated analysis of soil pore-space images. *Geoderma*, **53**, 399–415.

- van der Weele, C. M., Jiang, H. S., Palaniappan, K. K., Ivanov, V. B., Palaniappan, K., and Baskin, T. I., 2003. A new algorithm for computational image analysis of deformable motion at high spatial and temporal resolution applied to root growth. Roughly uniform elongation in the meristem and also, after an abrupt acceleration, in the elongation zone. *Plant Physiology*, **132**, 1138–1148.
- Walker, P. J. C., and Trudgill, S. T., 1983. Quantimet image analysis of soil pore geometry: Comparison with tracer breakthrough curves. *Earth Surface Processes and Landforms*, **8**, 465–472.
- Zheng, G., and Moskal, L. M., 2009. Retrieving leaf area index (LAI) using remote sensing: theories, methods and sensors. *Sensors*, **9**, 2719–2745.

Cross-references

- [Plant Disease Symptoms, Identification from Colored Images](#)
[Plant Drought Stress: Detection by Image Analysis](#)
[Soil Water Flow](#)
[Solute Transport in Soils](#)
[Visible and Thermal Images for Fruit Detection](#)

IMBIBITION

The absorption or adsorption of water by a solid (e.g., grains) or colloid that results in swelling.

INDICATOR PLANTS

Plants characteristically associated with specific soil or site conditions, such as soil acidity, alkalinity, wetness, or a chemical element.

INFILTRABILITY

The flux of infiltration resulting when water at atmospheric pressure is applied and maintained at the soil surface. Infiltrability is relatively high when water is first applied to a dry soil, but diminishes in time and, if the soil is deep, it eventually tends asymptotically toward a constant rate called the soil's "steady infiltrability."

Infiltration: Water entry into the soil, generally by downward flow through all or part of the soil surface.

Bibliography

Introduction to Environmental Soil Physics (First Edition) 2003
 Elsevier Inc. Daniel Hillel (ed.) <http://www.sciencedirect.com/science/book/9780123486554>

INFILTRATION CAPACITY

See [Infiltration in Soils](#)

INFILTRATION IN SOILS

Miroslav Kutílek
 Prague 6, Czech Republic

Definition

Infiltration denotes the entry of water into the soil through its surface. The source of water is either free accumulated water on the surface as, e.g., in lakes, puddles, or it is a rain. We shall restrict our concept just to the vertical flow.

Basic concepts

Considering the water cycle, the infiltration process separates rain into two parts. One part stored within the soil supplies water to the roots of vegetation and recharges ground waters. The other part, which does not penetrate the soil surface, is responsible for surface runoff. Infiltration is therefore a pivotal point within the hydrologic cycle. The flux density of water across a topographical soil surface is the infiltration rate, q , dimensionally $[LT^{-1}]$, in units usually mm/s or cm/h. It was earlier not properly denoted as infiltration velocity, infiltration capacity, or infiltrability. The total amount of water that infiltrated from the start of the process to time t is called cumulative infiltration I , [L], usually in mm, or cm. It is a monotonously increasing function $I(t)$. We shall omit details of a simple and rarely occurring type of steady infiltration of known $q = \text{const.}$, completed by the definition of the position of the ground water level. Since the infiltration rate is given, we solve only the pressure head distribution between the soil surface and the ground water level by solving the Darcy–Buckingham equation. Or, vice versa, we could obtain q when the pressure head distribution $h(z)$ is measured. We shall discuss unsteady infiltration in two sections according to the boundary conditions governing the type of infiltration. When the soil surface is instantaneously and excessively ponded as it is in an infiltration test performed with a ring infiltrometer or after initial ponding of the alluvium, or after flooding the irrigation basin, we have to solve infiltration with the Dirichlet's boundary condition (DBC). When infiltration occurs under natural rainfall or under the sprinkler irrigation, we meet Neuman's boundary condition (NBC) for the full duration of the rain.

Unsteady infiltration with Dirichlet's boundary condition (DBC)

We are assuming that a soil surface is flooded with a constant small depth of water $h = h_o$ at time $t \geq 0$ with $\theta = \theta_S$ at $z = 0$ again at $t \geq 0$, where θ_S denotes the saturated soil water content. Before the soil surface is flooded ($t \leq 0$), the pressure head $h = 0$ with the initial soil water content $\theta = \theta_i$. The vertical axis z is oriented positively downward with $z = 0$ at the soil topographic surface.

Semi-analytical solutions

We assume a homogeneous soil without layering. For a physically based understanding of infiltration, the principles of Philip's (1957 and 1969) semi-analytical solution will be presented. Richards' equation in the diffusivity form

$$\frac{\partial \theta}{\partial t} = \frac{\partial}{\partial z} \left[D(\theta) \frac{\partial \theta}{\partial z} \right] + \frac{dK}{d\theta} \frac{\partial \theta}{\partial z}$$

is solved for the given boundary conditions. Diffusivity D is

$$D(\theta) = K(\theta) \frac{dh}{d\theta}$$

$K(\theta)$ is the unsaturated conductivity; h is the pressure head (soil water potential).

The second term on the right side of the Richards' equation is deleted in the first step of the procedure and thus this first step solution is valid for the horizontal infiltration with space variable x . When solving it, the Boltzmann transformation

$$\eta(\theta) = xt^{-1/2}$$

is introduced in order to transform the partial differential equation into the ordinary one. This procedure transforms many soil water profiles during horizontal infiltration $\theta_n[x(t_n)]$ into single one $\theta(\eta)$. The area below the curve θ/x is the total water content in the wetted part of the soil column [L] and it is the cumulative infiltration, denoted by I . Then with the term sorptivity S [$LT^{-1/2}$] is

$$S = \int_{\theta_i}^{\theta_s} \eta(\theta) d\theta$$

and

$$I = St^{1/2}$$

or for infiltration rate $q = dI/dt$ is

$$q = 1/2 St^{-1/2}$$

and therefore $q(t \rightarrow 0) \rightarrow \infty$. Sorptivity depends not only upon the $D(\theta)$ function but upon θ_i . The value of S decreases with increasing θ_i and as $\theta_i \rightarrow \theta_s$, $S \rightarrow 0$. When S is measured for a particular θ_{i1} , we can linearly interpolate between θ_{i1} and θ_s in order to obtain a first approximation of S for $\theta_{i2} > \theta_{i1}$. Sorptivity is an integral part of most investigations describing vertical infiltration. It is the first approximation of the solution of infiltration if gravity is neglected. In order to include the influence of gravity, i.e., the second term of the basic Richards' equation, we have to correct the approximation (i.e., the horizontal infiltration) by the term y , i.e., $z = z_1 + y$. However, because an exact value of y cannot be obtained, its approximation y_1 defines another correction u , i.e., $y = y_1 + u$. Again, instead of an exact u we can only find still another

estimate u_1 . Hence, Philip (1957) obtained the infinite series solution

$$z(\theta, t) = \eta_1(\theta)t^{1/2} + \eta_2(\theta)t + \eta_3(\theta)t^{3/2} + \dots + \eta_n(\theta)^{n/2}$$

Since except of large times the series converges, the simplified form of Philip's equation is used

$$I = St^{1/2} + At$$

with A an empirical constant, usually $A = mK_S$ with m in ranges between 0.2 to 0.67, and very simplified $m = 2/3$. Since the infiltration rate q is obtained from the cumulative infiltration $q = dI/dt$ then the infiltration rate $q(t)$ is

$$q = \frac{1}{2} St^{-1/2} + A$$

Another approximation by Kutílek and Krejča (1987) is extending the Philip's solution to the form

$$I = St^{1/2} + C_2 t + C_3 t^{3/2}$$

where C_2 and C_3 are determined from the time t_C denoting the time when the infiltration rate q is in field conditions approaching constant. Then

$$C_3 = \frac{S}{3t_C}$$

$$C_2 = K_S - (3SC_3)^{1/2}$$

Brutsaert (1977) also began with the horizontal solution of Philip (1957) and sought a correction for the gravitational force. He obtained

$$I = K_S t + \frac{S^2}{BK_S} \left\{ 1 - \frac{1}{[1 + (BK_S t^{1/2})/S]} \right\}$$

The value of S in previous equations is advantageously obtained using the approximate expression of Parlange (1975)

$$S^2 = \int_{\theta_i}^{\theta_s} (\theta_s + \theta - 2\theta_i) D(\theta) d\theta$$

More semi-analytical solutions were developed; see, e.g., Kutílek and Nielsen (1994). However, the numerical solutions are preferred for field conditions, where we meet the nonhomogeneous soil profiles.

Empirical equations

Empirical equations have been used to describe a decreasing infiltration rate q as a function of time t . The shape of a smooth curve drawn through measured values of $q(t)$ was simply compared with that of an analytic function. Inasmuch as both equations and

experiments were empirical, it is useless to try to physically interpret the coefficients of the equations. The coefficients have the character of fitting parameters only with no scientific merit.

Kostiakov's (1932) equation of $q(t)$ is the hyperbola

$$q = c_1 t^{-\alpha}$$

and

$$I = \frac{c_1}{1 - \alpha} t^{(1-\alpha)}$$

where c_1 and α are empirical coefficients. The value of c_1 should equal q_1 , the infiltration rate at one unit of time (usually 1 min), and $0 < \alpha < 1$. The equation does not describe infiltration at large times in as much as $q \rightarrow 0$ when $t \rightarrow \infty$.

Mezencev (1948) overcame this inconvenience by shifting the q -axis

$$q = c_2 + c_3 t^{-\beta}$$

and

$$I = c_2 t + \frac{1}{1 - \beta} c_3 t^{(1-\beta)}$$

where c_2 , c_3 and β are empirical coefficients. With the shift, as $t \rightarrow s$, $c_2 \rightarrow q_c$, the constant infiltration rate is reached, and hence, $q_c \approx K_s$. The infiltration rate after the first time unit $q_1 = (c_2 + c_3)$.

Horton's equation (1940) represents an exponential decay of $q(t)$

$$q = c_4 + c_5 \exp(-\gamma t)$$

and

$$I = c_4 t + \frac{c_5}{\gamma} [1 - \exp(-\gamma t)]$$

where c_4 , c_5 and γ are empirical coefficients. In contradiction to the theory of infiltration for a DBC, q has a finite value at $t = 0$. As $t \rightarrow \infty$, $c_4 \rightarrow q_c$, which yields a value of $c_4 \approx K_s$. With this approximation for K_s , the value of $c_5 = [q(0) - K_s]$ where $q(0)$ is q at $t = 0$. As Horton derived his equation for infiltration of a high intensity rainfall, the physical objection against a finite value of $q(t=0)$ is largely eliminated

Unsteady infiltration with Neuman's boundary condition (NBC)

When we describe rainfall infiltration, we do not describe individual raindrop events, but consider the rain as a continuous flux with the intensity of the rain q_r , the flux density passing either totally or at least partially through the surface of the soil, i.e., we keep the principle of the representative elementary volume, REV. The boundary

condition at $z = 0$ and $t \geq 0$ is formulated by the Darcy-Buckingham equation

$$q = -K \frac{\partial H}{\partial z}$$

or in the diffusivity form

$$q = K(\theta) - D(\theta) \frac{\partial \theta}{\partial z}$$

Neuman's boundary condition describes not only rainfall infiltration, but infiltration caused by sprinkler irrigation or by rain simulator, or by a special flux controlled technique, e.g., by a peristaltic pump providing a constant flux through a membrane placed upon the soil surface. It does not describe satisfactorily the drip irrigation since it has to be defined as two-dimensional process. The initial condition is kept the same as that for the DBC. We distinguish three types of cases: (1) constant rain intensity $q_r > K_s$, (2) constant rain intensity $q_r < K_s$, and (3) rain intensity $q_r(t)$. In all three categories soil water profiles $\theta(z)$ at intermediate times do not resemble $\theta(z)$ during early stages of infiltration. The distinguishing feature is that the soil water content $\theta_o(t)$ increases at the surface with time.

Constant rain intensity $q_r \geq K_s$. The value of the soil water content of the surface θ_o increases steeply with time until it reaches θ_s . The greater is q_r , the steeper is $\theta_o(t)$. If rain continues, water ponds on the surface; the start of ponding is called ponding time t_p . If surface runoff is prevented, the depth of water on the surface $h_o(t)$ increases with time and $h_o > 0$ for $t > t_p$. With the increase of h_o being time dependent, $dh_o/dt < q_r$. The shape of the soil water profile at $t < t_p$ depends upon both q_r and the hydraulic functions of the soil. Generally, the soil water content is below full saturation for all $t < t_p$. The ponding time t_p decreases with an increase of q_r and $t_p > t_x$ where t_x is the intersection of q_r and q_D . Index D denotes infiltration by DBC. With the assumption that the soil water profiles $\theta(z, t_p)_N$ and $\theta(z, t_x)_D$ are identical and with

$$q_r(t_p) = q_D(t_x)$$

we obtain using the algebraic Philip's equation (Kutilek and Nielsen, 1994)

$$t_p = \left(\frac{S}{A} \right)^2 \frac{2Q - 1}{4Q(Q - 1)^2}$$

where $Q = q_r/A$. At $t \leq t_p$ the infiltration rate $q_o = q_r$. At $t > t_p$ the infiltration rate $q_o < q_r$ and it can be approximated by shifting $q_D(t)$ by $(t_p - t_x)$.

For *constant rain intensity $q_r \leq K_s$* , the flow is governed by NBC and the term t_p does not exist. On the soil surface the value of q_o is always less than that of q_s and therefore $\theta_o < \theta_s$, the surface is never saturated by water.

For nonconstant rain intensity $q_r(t)$, we formulate the functional dependence $q_r(t)$ in the NBC and in the solution. The mathematical steps in the analysis are identical to the steady rain infiltration, but the time dependency has to be defined. For the study of natural rains infiltration, the numerical procedures are applied. The process is usually complicated by the nonconstant values of hydraulic parameters and functions mainly of the surface thin layer, where the soil is puddled, pore size distribution substantially changed causing a change in saturated conductivity in the order of magnitude and a change of all functional relationships.

Summary

The entry of water into the soil through its surface is denoted as infiltration. There are two types of infiltration processes: one is defined with constant pressure head on the surface and it is realized as unsteady flow approaching after large time constant flux. Practical example is the flooding of the surface and the following infiltration from this source. In the second type of infiltration, the flux is defined on the surface. Practical example is the infiltration from rain when the rainwater is not accumulating on the surface.

Bibliography

- Brutsaert, W., 1977. Vertical infiltration in dry soil. *Water Resources Research*, **13**, 363–368.
- Horton, R. E., 1940. An approach towards a physical interpretation of infiltration capacity. *Soil Science Society of America Proceedings*, **5**, 399–417.
- Kostiakov, A. N., 1932. On the dynamics of the coefficient of water-percolation in soils and on the necessity of studying it from a dynamic point of view for purposes of amelioration. In *Transactions of 6th Congress of International Soil Science Society*, Moscow, Part A, pp. 17–21.
- Kutilek, M., and Krejča, M., 1987. A three-parameters infiltration equation of the Philip's type solution (in Czech). *Vodohospodářský Časopis*, **35**, 52–61.
- Kutilek, M. and Nielsen, D.R., 1994. *Soil Hydrology*. Catena, Cremlingen-Destedt, Germany.
- Mezencev, V. J., 1948. Theory of formation of the surface runoff (in Russian). *Meteorologia i Gidrologia*, **3**, 33–40.
- Parlange, J. Y., 1975. On solving the flow equation in unsaturated soils by optimization: Horizontal infiltration. *Soil Science Society of America Proceedings*, **39**, 415–418.
- Philip, J. R., 1957. The theory of infiltration: 1 The infiltration equation and its solution. *Soil Science*, **83**, 345–357.
- Philip, J. R., 1969. Theory of Infiltration. In *Advances of Hydroscience*, 5, Academic Press, New York, pp. 215–305.

Cross-references

- [Hydraulic Properties of Unsaturated Soils](#)
[Pore Size Distribution](#)
[Puddling: Effect on Soil Physical Properties and Crops](#)
[Soil Surface Sealing and Crusting](#)
[Soil Water Flow](#)
[Sorptivity of Soils](#)

INSOLATION

Exposure to the radiation of the sun and the action of the sun's rays on soils or other materials or bodies exposed to such. Applied particularly to the effect of temperature change on mechanical weathering.

Bibliography

- Chesworth, W. (ed.). 2008. Encyclopedia of Soil Science, Springer, p. 362.

Cross-references

- [Physical \(Mechanical\) Weathering of Soil Parent Material](#)

INSTITUTE OF AGROPHYSICS IN LUBLIN: PROGRESS IN AGROPHYSICS

Józef Horabik, Grzegorz Józefaciuk

Institute of Agrophysics, Polish Academy of Sciences,
Lublin, Poland

Introduction

Institute of Agrophysics of Polish Academy of Sciences was created in 1968. It is located almost in the centre of Europe, in Lublin, in southeastern Poland. The Institute was established by Professor Bohdan Dobrzański, Rector of Maria Curie Skłodowska University and of Agricultural Academy in Lublin, who was also the first Director of the Institute. During 40 years activity, the Institute has employed over 150 workers. It promoted over 20 professors, 30 DScs, and 40 PhDs. The Institute has the authorization to confer PhD and DSc degrees in Agronomy–Agrophysics. The Institute promotes knowledge at all levels of education presenting the latest achievements of science to great groups of viewers, organizing classes for students from southeast Poland universities and experimental presentations illustrating natural processes in primary and secondary schools, corresponding to topics of lessons of biology, chemistry, mathematics, and physics. The Institute conducts PhD studies in the field of agronomy–agrophysics and Joint Doctoral Courses with University of Life Sciences in Lublin.

The Institute has longstanding cooperation with over 60 scientific partners all over the world. Continuously new scientific links are created as well. Cooperation with Polish small and medium enterprises, industry, and local administration is additional and important part of the Institute activity. As a result of its activity and cooperation, Institute of Agrophysics realized over 100 national projects and participated in 20 of EU FP5 and FP6 projects, including domestic projects founded by EU, all related to environment and food research. Overall, the Institute researchers published over 4000 scientific papers, 100 monographs, organized over 40 international and

50 domestic conferences, and a number of workshops, seminars, and schools. The Institute has published three journals: International Agrophysics, Acta Agrophysica, and Polish Journal of Soil Science.

Agrophysics, the main area of the Institute activity, concerns applications of physics in agriculture. It places particular attention to sustainable plant production and modern processing technologies.

At present over 60 researchers, representing various disciplines work in six departments, specializing in solving a broad range of agrophysical problems related to properties and processes occurring in soils, plants, and granular materials, including water, salt, and energy exchange in soil environment, physicochemical properties of porous bodies, and related sorption equilibria, soil degradation (organic matter lost, heavy metal pollution, acidification, alkalinization, salinization, structure destruction, erosion, soil translocation, and stresses under machinery wheels), time and spatial variability of soil parameters, soil aeration, stability of nitrogen and carbon in soil, emission of greenhouse gases, soil biological activity, redox potential, mechanical characteristics and damage of cellular structures, plant growth and root functions, plant and soil properties under stress, grain quality at harvest, drying and storage, physical properties of agricultural materials and food powders, diagnosis of mechanical parameters of fruits and vegetables important for storage, handling, and processing, physical processes in granular materials of plant origin, and many others. Special attention is directed to measurements, monitoring and modeling of the early stages of food chain, i.e., all initial subsequent steps of healthy food production starting from recognizing soil conditions and ending on assessment of raw agricultural products quality.

The Institute has elaborated a set of unique measuring methods and equipment for identification and diagnosis of agricultural materials properties, description of parameters, data interpretation, and gathering datasets concerning actual state and history of systems as well as physical-mathematical, phenomenological, and statistical models for simulation and prognosis of environmental and anthropogenic processes in soils, plants, and raw agricultural products.

Department of metrology and modeling of agrophysical processes

The department developed a set of tools to study and control physical, hydrophysical, and thermophysical properties of soils and their relation with mass and energy transport in the soil-plant-atmosphere system. Two basic methods of physical modeling, phenomenological and theoretical physical-mathematical are employed on the basis of physical and physicochemical properties of the soil solid phase to study hydrophysical properties of soils (water retention curve and hydraulic conductivity coefficient) and processes of mass and heat transport in the soil medium with the use of numerical techniques. Soil moisture and its spatiotemporal evolution are studied and the

data are provided for numerical weather and climate models. The department elaborated a reflectometric meter and a probe measuring at the same time and from the same sample of soil its moisture, temperature, and salinity that can work in a field system monitoring of those values and communicating with the user by Internet server where the acquired data are stored. Thermography (remote noncontact evaluation of surface temperature distribution) is used for determination of plant water stress and evapotranspiration in the field, detection of plant cover areas attacked by diseased and insects, evaluation of fruit quality and seed germination capacity, controlling thermal conditions in greenhouses in the aspect of their optimum exploitation. The pulse-phase thermography is used for studies of internal intrusions such as bruises and water core in fruit, or military mines in soil.

Department of natural environment biogeochemistry

This department studies the interlocking roles of biological, chemical, and physical forces in controlling processes vital to sustaining life with special attention placed on the role of microorganisms. The methods were developed to study aeration of soil profile at various environmental conditions, oxygen availability for plant roots, plant response on oxygen stress, and protective mechanisms of plants at low soil oxygen level. Extensive studies are focused on the effect of redox potential on biological activity and emission and sink of greenhouse gases from soils. Soil microbial indicators are used for monitoring soil biological activity and evaluation of impacts of both environmental and anthropogenic factors. Oxygenology, a new scientific discipline within the environmental sciences related to the presence and role of oxygen in nature on Earth has been defined in this department. It comprises issues of storage, transport, generation, absorption, turnover, functions, and measurement of oxygen content in the environment.

Department of microstructure and mechanics of biomaterials

This department developed experimental and theoretical tools to study structural (from nano- to macroscale) determinants of mechanical properties of fruits and vegetables for quality control and optimization of processing. Atomic force, confocal laser scanning, tandem scanning reflected light microscope, transmission optical microscope and macroscope techniques, image analysis, fracture and acoustic emission analysis, physical and numerical models are applied for microstructure quantification of cellular (plants) and granular structures (soil). New method of spatial-temporal reflected laser light scatters correlation (biospeckle) was introduced for monitoring living processes within biomaterials that is used for estimation a state of the fruit or vegetables during vegetation or storage. The structure of real cell walls of fruit and vegetables is simulated by artificial cellulose

produced by bacteria *Gluconacetobacter xylinus*. Its physical dimensions are useful for mechanical testing, thus can be used for investigation of influence of various external factors, like temperature, humidity, and food additives on cell wall properties.

Department of soil and plant system

This department elaborated methods for studies and description of soil management effects on plant growth and functions, and water uptake by roots in relation to soil structure. Field and model studies of soil erosion allowed to construct models for establishing soil susceptibility to erosion, prognosis of water erosion of soils and soil translocation rates under various tillage implements, erosion impact on soil productivity, and pollution of surface waters. Simulations of stresses and strains in soils were used for quantitative estimation of the effect of pore and aggregate structure on soil compaction under varying climate conditions and cropping practices, and under machinery wheels. The laboratory system maintaining constant soil water potential and allowing to measure daily water uptake by plant roots was elaborated to control process of root growth and estimation of crop demands. The system is used to measure water uptake by roots growing within various density horizontal soil layers in split root system.

Department of physical chemistry of porous materials

This department developed methods to apply physicochemical soil properties as surface area, adsorption energy, fractal dimension, pore size distribution, surface charge, surface acidity, and surface free energy as indicators of changes in soil under various environmental conditions. Physicochemical methods of description of soil degradation processes as organic matter lost, heavy metal pollution, acidification, alkalization, salinization, and structure destruction were elaborated and physicochemical methods of soil amelioration and detoxification were established. Surface chemistry methods were introduced as new tools to analyze surface properties of plant roots and their changes under stress conditions. Formation and stability of soil structure and microstructure were described using analysis of surface energetic and geometric heterogeneity, organomineral interactions in soils, soil porosity, wettability, and surface free energy components.

Department of physical and technological properties of agricultural materials

Laboratory of physical bases of grain quality evaluation

This laboratory elaborated methods for establishing susceptibility of cereal grains to emerging of endosperm cracks in preharvest period, and of digital analysis of X-ray images to recognition of growth and develop of grain weevil in wheat grain. Recognition of the growth stage of weevil larvae is used to localize an infection point during grain transport history that is particularly important

to establish responsibility for infection in imported grain. New method in studies of physical properties of gluten via analysis of gluten membranes expansion as a function of temperature was introduced to estimate ability of fixing fermentation gas bubbles within cake that is a key parameter for sponginess and crumb structure fixation of bread in baking technology.

Laboratory of physical properties of crops

This laboratory develops measuring methods and introduces new techniques of the estimation of physical properties of crops and their damages and losses during harvest, handling, and storage, and the effect of injuries on the reproducible and consumption quality of raw material. Factors affecting quality of fruits and vegetables, and seeds of oil and leguminous plants are studied to introduce new technologies enhancing the quality of food materials, products, and fodders. Technology of virgin type rape oil production, online fruit quality control in sorting line, and production of chain saw lubricant from mustard oil are implemented.

Laboratory of physics of granular plant materials

This laboratory performs studies of mechanical parameters of agricultural granular materials and food powders and formulates models of basic mechanisms important for storage, handling, and processing to overcome difficulties originating from grains deformation, variation in flowability, and changes of secondary variables with moisture content of the material. New discrete element method is used to simulate granular flows, granular compaction, segregation, convection, avalanches, surface waves, collisions and friction, inelastic collapse, jamming and fluctuations, energy flows, strength properties, anisotropy of packing, stress fluctuation to understand mechanical behavior of plant granular materials: quasi-static processes observed in experimental testing of grain in bulk; particle-plane impact, uniaxial compression, filling and discharge processes.

Several interdisciplinary topics are realized by several departments together as studies of soil filtering and buffering properties to protect water ecosystems against contamination and purification of wastewaters; role of microorganisms in transformation of organic substances in soil and formation of soil aggregates; enzymatic activity of soil to regulate the availability of nutrients for plants; role of soil components and biota in creation of water repellency in soil to regulate soil water retention; processes of carbon and plant nutrients transformations; gas production and emission to the atmosphere from soils to assess their role in global greenhouse effects causing climate change; fast assessment of complex biochemical composition and nutritive value of fresh fruits and vegetables with multispectral biospectroscopy methods with data acquisition systems, computers and optoelectronic devices to introduce widespread and uniform justification system to practice.



Institute of Agrophysics in Lublin: Progress in Agrophysics, Figure 1 A new agrophysical centre, Lublin-Felin from bird's eye view.

New structure

With the support of the E.U. projects, new buildings with well-equipped modern laboratories were created in 2009–2010 within the Institute (Figure 1). They are focused, among others, to the quality control of plant materials processed for food and nonfood products, implementation of innovative solutions in agricultural and food sector, and increase of the natural environment control, renewable energy and biomass acquiring, methane fermentation, biogas analysis, treatment and utilization of post fermentation sludge by recycling and utilization of sludge solid phase for soil improvement. All these activities may serve in developing and diffusion of innovative solutions between science and economy.

Outlook

Recently the Institute creates close interdisciplinary links with other sciences including plant physiology and genetics, molecular biology, nanotechnology, chemical physics, informatics, mathematics, food technology, animal production, and even architecture, veterinary science, or medicine.

Bibliography

- Horabik, J., and Jozefaciuk, G., (eds.), 2008. *Agrophysics for Quality of Environment and Food*. Printed by Institute of Agrophysics. ISBN978-83-89969-26-2.
 Walczak, R. T., Glinski, J., and Horabik, J., 2003. Agrophysics and its role in development of agricultural sciences (in Polish). *Acta Agrophysica*, 100.

Cross-references

- [Agrophysics: Physics Applied to Agriculture](#)
- [Crop Responses to Soil Physical Conditions](#)
- [Grain Physics](#)
- [Greenhouse Gases Sink in Soils](#)
- [Institute of Agrophysics in Saint-Petersburg: Roots of Agrophysics](#)
- [Microstructure of Plant Tissue](#)
- [Monitoring Physical Conditions in Agriculture and Environment](#)
- [Nondestructive Measurements in Soil](#)
- [Physical Phenomena and Properties Important for Storage of Agricultural Products](#)
- [Physical Properties of Raw Materials and Agricultural Products](#)
- [Soil–Plant–Atmosphere Continuum](#)
- [Specific Surface Area of Soils and Plants](#)

INSTITUTE OF AGROPHYSICS IN SAINT-PETERSBURG: ROOTS OF AGROPHYSICS

Igor B. Uskov, Victor P. Yakushev
 Agrophysical Research Institute, Russian Academy of Agricultural Science, St. Petersburg, Russia

Definition of agrophysics

Agrophysics (or agricultural physics) is a science that studies physical, physicochemical, and biophysical processes in the system “the soil – the plants – the active layer of the atmosphere” as well as main principles of the production process, physical properties of the system

components, and of various agricultural products. This science works out scientific foundations, methods, technical and mathematical tools, as well as agricultural techniques of an expedient use of natural resources and improvement of the agricultural ecosystem, arable farming, and crop production. This is a branch of physics that studies physical components of agroecosystems and agricultural landscapes as well as structural and functional patterns of their interaction. Its aim is agroecological optimization of modern farming systems.

Introduction

One of the founders of modern agrophysics was Academician Abram Feodorovich Ioffe (1880–1960). In his fundamental works *Physics and Agriculture* (Ioffe, 1955), and *Physics for Agriculture* (Ioffe, 1959), he pointed out the principal and important points about the time directions of investigations in this new branch of natural and agricultural sciences. These included development of research and measuring tools for agriculture, biology, and agrochemistry, light-physiology and light-culture of plants, artificial soil structure formation, measures against droughts, frosts, and other unfavorable weather conditions, use of polymers in arable farming and plant growing, study of soil hydrophysics and designing methods of active water and heat regulation in soil and plants, and the creation, in the future, of the so-called electronic agronomist.

Institute of agrophysics, its founders, and their achievements

In 1932, the Institute of Physics and Agriculture, later called the Research Institute of Agrophysics, was organized in Leningrad on the initiative of A.F. Ioffe and with the support of the President of the All-Union Academy of Agricultural Sciences N.I. Vavilov. The Institute started its work dealing with the problems indicated by its founder and first director. One of Ioffe's associates and followers was Professor A.F. Chudnovsky (1910–1985). In his studies *Heat Exchange in Disperse Medium* (Chudnovsky, 1954), *Semiconductor Devices in Agriculture* (Chudnovsky and Shlimovich, 1961), and *Thermophysics of the Soil* (Chudnovsky, 1976), he developed the theory and methods of soil heat regulation, suggested ways of farming optimization, and elaborated automatic systems of technology control for irrigated agriculture. He also stated principles of agrophysical instrumentation that served as a basis for many developments, beginning with the creation of the soil radiation constant detector (A.V. Kurtener). The distinguishing feature of agrophysical engineering at the institute was a particular sequence of devising: starting with a laboratory model for studying physical processes which allowed the utmost completeness and precision of measurements but was not very reliable in practice and carrying on with a technological instrument whose precision made it

possible even to nonspecialists to make measurements in field conditions.

The research of Professor F.E. Koliasev (1898–1958) played a key role in laying the foundations of the agricultural theory in agrophysics and in developing it. He advanced the concept of soil differential moisture and methods of soil water content regulation in various soils and climatic zones of the country in his studies *Methods of Artificial Soil Structuring* (Koliasev and Vershinin, 1935) and *Concerning the Soil Differential Moisture Theory* (Koliasev and Melnikova, 1949). The works of Professor P.V. Vershinin (1909–1978) were also of great importance to the development of the soil structuring theory and the control methods; they include *The Basics of the Physical Chemistry of Artificial Soil Structure* (Vershinin and Konstantynova, 1935) and *Soil Structure and Conditions of Its Formation* (Vershinin, 1958). These works treat such theoretical and practical issues as soil structuring and the use of chemical soil stabilizers for protecting the soil from erosion. Professor I.B. Revut (1909–1978) made a great contribution to the development of soil physics. In his studies *Physics in Agriculture* (Revut, 1960), *How to Work the Soil Properly* (Revut, 1966), and *Physics of the Soil* (Revut, 1972), he explains the essentials of soil treatment in different soils and climatic zones.

The corresponding member of the Academy of Agricultural Sciences S.V. Nerpin (1915–1993) was the originator of two branches of agrophysical soil science: soil hydromechanics and theoretical physicochemical soil mechanics. His main works – *Physics of the Soil* (Nerpin and Chudnovsky, 1967) and *Energy and Mass Exchange in the Plant–Soil–Air System* (Nerpin and Chudnovsky, 1975) – have never been equaled in the world scientific literature on the subject. They discuss the theory and the methods of controlling field moisture regime. S.V. Nerpin founded the school of theoretical and computational agrohydrology and laid the groundwork for mathematical modeling in agrophysics. Professor A.M. Globus' fundamental studies *Experimental Hydrophysics of the Soils* (Globus, 1969) and *Physics of Non-isothermal Intrasoil Moisture Exchange* (Globus, 1983) marked, in essence, the beginning of investigations in soil hydrophysics.

Academician E.I. Ermakov (1929–2006) contributed greatly to working out the theory of soil formation in the plant–soil system. He also developed a new direction in science – the use of similarity principles for physical simulation of processes in these systems with the help of vegetation-climatic installations.

The beginning of large-scale investigations in chemical physics of the soils is connected with the name of Professor M.K. Melnikova (1901–1986), the head of the first radiochemical laboratory created to study unknown behavior of uranium and plutonium fission products in the soil and to develop agrotechnical methods of reducing radioactive contamination of agricultural products. These research areas were highly relevant while nuclear weapon testing was going on. Her works *The Foundations of*

Agrophysics (Vershinin et al., 1959), On the Behaviour of Uranium and Plutonium Fission Products in the Soil and Their Absorption by Plants, and The Use of Radioactive Isotopes and Radiation in Agricultural Investigations introduced the method of isotope tracers into soil science. The works of Professor J.A. Kokotov made a very important contribution to the theory of ion exchange in the soil (in acid soils, in particular). They include *Balance and Kinetics of Ion Exchange* (Kokotov and Pasechnik, 1970), *Ion-Exchange Resins and Ion Exchange* (Kokotov, 1980), *The Ion Exchange Theory (Complicated Ion-Exchange Systems)* (Kokotov, 1986). Professor N.F. Batygin (1928–2000) laid down theoretical foundations of agrophysical studies in radiobiology in his work *The Use of Ionizing Radiation in Plant Life Regulation* (Batygin, 1966).

In 1928, an agroclimatology sector was organized at the Institute of Experimental Agriculture. In 1932, the Main Geophysical Observatory (MGO) named after A.I. Voeikov started investigations in the field of agroclimate zoning and climatic resources estimation in agricultural production. In August 1935, the studies at the MGO were stopped but taken up by the Agrophysical Institute (API) founded by A.F. Ioffe. Scientists of API had concentrated their efforts on the physical process investigation that influences the field's microclimate, unlike the geographical climatic approach of the MGO. The goal was to work out the theory, the agrotechnological approaches as well as effective microclimate resources management within the agroecological system under changing physical conditions of plants' habitat, that is, to develop a meliorative agromicroclimatology. The first collection of scientific works of the Institute of Agrophysics (1935) with the participation of B.P. Alexandrov, A.V. Kurtener, and N.N. Banasevich already included articles on heat and water regimes in the soil; the third collection (1941) contained an entire section devoted to microclimate issues. The monographs *Climatic Factors and Heat Regime in Open and Protected Ground and Agricultural Field Microclimate Control* (Kurtener and Uskov, 1982, 1988) were dedicated to the development of theoretical and practical agroclimatology.

The *Physiological Foundations of Plants Drought Resistance* (1926), a world-renowned monograph of Academician N.A. Maksimov (1880–1952), one of the first plant physiologists of the Institute of Agrophysics, marked the beginning of investigations into plant ecological physiology. Professor V.P. Malchevsky (1906–1942) made a major contribution to the creation of the plant light physiology and light culture theory. He developed light culture and light stimulation methods for use in hothouses and closed chambers with artificial light and suggested light stimulation of seeds and seedling for intensifying photosynthesis and reducing vegetation period. The corresponding member of the Academy of Agricultural Sciences B.S. Moshkov (1904–1997) became world famous for his works *Plant Growing under Artificial Light*

(Moshkov, 1953), *Plant Photoperiodism* (1961), *Plant Growing in the Future* (Moshkov, 1962) and *Plant Actinometry* (Moshkov, 1987); he made a significant contribution to the plant light physiology and ontogeny theory and discovered the specific physiological role of the leaf in the photoperiodism. The study of the cellulose ether film properties led to universal replacement of glass with clear plastic films in the protection of the ground in indoor structures (D.A. Fiodorov, I.N. Kotovich). V.G. Karmanov (1913–1997) put forward the theory of plant biological cybernetics as a branch of science dealing with the cybernetic control of physiological processes in plants. The key points of this line of research became phytomonitoring (S.S. Radchenko) as well as the biophysical concept of the transport and heat exchange systems in a whole plant and in cell membranes (Professor O.O. Lialin, 1932–1994).

The studies of Academician N.F. Bondarenko's (1928–2003) promoted agrophysical scientific development and a wide application of the "harvest programming" method; his investigation initiated the development of information technologies in modern agrophysics employing precision agriculture techniques that realized A.F. Ioffe's idea about the creation of an "electronic farmer" (devised by the corresponding member of the Academy of Agricultural Sciences V.P. Yakushev).

Along with the progress in the related branches of physics, geophysics, biophysics, plant physiology, mathematical physics and computational mathematics, some new areas of interest appeared over the years in the structure of agrophysical investigation. They were mostly focused on devising methods of active intervention in the vegetation processes and their regulation by means of measurement, state diagnostics and management technologies. Among these areas are: mathematical modeling of agricultural production (R.A. Poluektov); simulation of agrophysical systems and processes (B.N. Michurin, A.M. Globus, I.B. Uskov, V.G. Onishchenko); interaction of biological objects with different physical fields (light, gravitational, magnetic, electromagnetic, acoustic, electrostatic) (B.S. Moshkov, N.F. Batygin, N.F. Bondarenko, I.S. Lisker, V.N. Lazutin); information technologies of production management in arable farming and plant growing (V.P. Yakushev, I.M. Mikhailenko); agrophysical instrumentation, elaboration of vegetative systems with controlled climate (V.G. Karmanov, A.F. Chudnovsky, J.P. Baryshnev); a new type of coordinate precision agriculture as the first step to the creation of the "electronic farmer" (V.P. Yakushev).

Conclusions

The above-mentioned founders of the agrophysical science believed that their investigations should first and foremost help with the transition from descriptive agronomical science to that based on measurements and calculations of agricultural methods and factors of plant

growth, development and productivity which would control production processes in the field and the formation of harvests in open and protected ground.

Bibliography

- Arhipov, M. V., 2001. *Radiographic Analysis in Plant Science and Agriculture*. Moscow: Russian Academy of Agriculture (in Russian).
- Batygin, N. F., 1966. *The Use of Ionizing Radiation in Plant Life Regulation*. Leningrad: Kolos (in Russian).
- Batygin, N. F., 1986. *Ontogeny of Higher Plants*. Moscow: Agropromizdat (in Russian).
- Bondarenko, N. F., Zhykovsky, E. E., Mushkin, I. G., Poluektov, R. A., and Uskov, I. B., 1982. *Modelling of Agroecosystem Productivity*. Leningrad: Hydrometeoizdat (in Russian).
- Chudnovsky, A. F., 1954. *Heat Exchange in Disperse Medium*. Moscow: Gostehizdat (in Russian).
- Chudnovsky, A. F., and Shlimovich, B. M., 1961. *Semiconductor in Agriculture*. Moscow: Znanie (in Russian).
- Chudnovsky, A. F., 1976. *Thermophysics of the Soil* (in Russian). Moscow: Nauka.
- Chudnovsky, A. F., and Shlimovich, B. M., 1970. *Semiconductor Devices in Agriculture*. Nauka: Leningrad (in Russian).
- Chudnovsky, A. F., Karmanov, V. G., Savin, V. N., and Riabova, E. P., 1965. *Cybernetics in Agriculture*. Leningrad: Kolos (in Russian).
- Globus, A. M., 1969. *Experimental Hydrophysics of the Soil*. Leningrad: Hydrometeoizdat (in Russian).
- Globus, A. M., 1983. *Physics of Non-isothermal Intrasoil Moisture Exchange*. Leningrad: Hydrometeoizdat (in Russian).
- Globus, A. M., 2007. The Institute of Agrophysics: 75 Years on the Way to Precision Farming. St. Petersburg: Agrophysical Research Institute (in Russian).
- Ioffe, A. F., 1955. *Physics and Agriculture*. Moscow: The Soviet Union Academy of Sciences (in Russian).
- Ioffe, A. F., 1959. *Physics for Agriculture*. Moscow: Znaniye (in Russian).
- Kokotov, J. A., 1980. *Ion-exchange Resins and Ion Exchange*. Leningrad: Himia (in Russian).
- Kokotov, J. A., 1986. *The Ion Exchange Theory (Complicated Ion-Exchange Systems)*. Leningrad: Himia (in Russian).
- Kokotov, J. A., and Pasechnik, B. A., 1970. *Balance and Kinetics of Ion Exchange*. Leningrad: Himia (in Russian).
- Koliasev, F. E., and Vershinin, P. V., 1935. *Methods of Artificial Soil Structuring*. Moscow-Leningrad: Selhosgiz (in Russian).
- Koliasev, F. E., and Melnikova, M. K., 1949. *Concerning the Soil Differential Moisture Theory*. Moscow: Pochvovedenie (in Russian).
- Kotovich, I. N., Masaitis, G. V., and Paschenko, T. E., 1985. *Clear Plastic Film for Growing and Storage of Fruit and Vegetables*. Moscow: Himia (in Russian).
- Kurtener, D. A., and Uskov, I. B., 1982. *Climatic Factors and Heat Regime in Open and Protected Ground*. Leningrad: Hydrometeoizdat (in Russian).
- Kurtener, D. A., and Uskov, I. B., 1988. *Agricultural Field Microclimate Control*. Leningrad: Hydrometeoizdat (in Russian).
- Michurin, B. N., 1975. *Energy of Soil Moisture*. Leningrad: Hydrometeoizdat (in Russian).
- Moshkov, B. S., 1953. *Plant Growing Under Artificial Light*. Moscow-Leningrad: Selhosgiz (in Russian).
- Moshkov, B. S., 1961. *Plant Photoperiodism*. Moscow: Selhozizdat (in Russian).
- Moshkov, B. S., 1962. *Plant Growing in the Future*. Moscow: Znanie (in Russian).
- Moshkov, B. S., 1966. *Plant Growing with Artificial Light*. Moscow, Leningrad: Kolos (in Russian).
- Moshkov, B. S., 1987. *Plant Actinometry*. Moskov: Agropromizdat (in Russian).
- Nerpin, S. V., and Chudnovskii, A. F., 1984a. *Heat and Mass Transfer in the Plant–Soil–Air System*. New Delhi: Oxonian.
- Nerpin, S. V., and Chudnovskii, A. F., 1984b. *Heat and Mass Transfer in the Plant–Soil–Air System*. New Delhi: Oxonian Press, p. 3350.
- Nerpin, S. V., and Chudnovsky, A. F., 1967. *Physics of the Soil*. Moscow: Nauka (in Russian).
- Nerpin, S. V., and Chudnovsky, A. F., 1975. *Energy and Mass Exchange in the Plant–Soil–Air System*. Leningrad: Hydrometeoizdat (in Russian).
- Poluektov, R. A., 1980. *A Dynamic Model of Ecosystems*. Leningrad: Hydrometeoizdat (in Russian).
- Revut, I. B., 1960. *Physics in Agriculture*. Moscow, Leningrad: Fizmatgiz (in Russian).
- Revut, I. B., 1964. *Physics of the Soil*. Leningrad: Kolos (in Russian).
- Revut, I. B., 1966. *How to Work the Soil Properly*. Moscow: Znanie (in Russian).
- Revut, I. B., 1972. *Physics of the Soil*. Leningrad: Kolos (in Russian).
- Uskov, I. B. (ed.), 2002. *Agrophysics from A. F. Ioffe to the Present*. St. Petersburg: Agrophysical Research Institute (in Russian).
- Vershinin, P. V., and Konstantynova, V. P., 1935. *The Basics of the Physical Chemistry of Artificial Soil Structure*. Moscow-Leningrad: Selhosgiz (in Russian).
- Vershinin, P. V., 1958. *Soil Structure and Conditions of its Formation*. Moscow-Leningrad: The Soviet Union Academy of Sciences USSR (in Russian).
- Vershinin, P. V., Melnikova, M. K., and Michurin, B. N., 1959. *The Foundations of Agrophysics*. Moscow: Fizmatgiz (in Russian).
- Vershinin, P. V., Melnikova, M. K., Michurin, B. N., Moshkov, B. S., Poiasov, N. P., and Chudnovsky, A. F., 1960. *Foundations of Agrophysics*. Moscow: Fizmatgiz (in Russian).
- Yakushev, V. P., 2002. *On the Way to Precision Farming*. St. Petersburg: Agrophysical Research Institute (in Russian).
- Yakushev, V. P., and Yakushev, V. V., 2007. *Information Support System of Precision Farming*. St. Petersburg: Nauk (in Russian).

INTEGRATED DRAINAGE

A general term for a drainage pattern in which stream systems have developed to the point where all parts of the landscape drain into some part of a stream system, the initial or original surfaces have essentially disappeared and the region drains to a common base level.

Bibliography

- Glossary of Soil Science Terms. Soil Science Society of America. 2010. <https://www.soils.org/publications/soils-glossary>

INTERCEPTION

See *Rainfall Interception by Cultivated Plants; Light Interception by Plant Canopies*

INTERFLOW

Water that infiltrates into the soil and moves laterally through the upper soil horizons until intercepted by a stream channel.

Bibliography

Glossary of Soil Science Terms. Soil Science Society of America. 2010. <https://www.soils.org/publications/soils-glossary>

INTERNAL DRAINAGE

The post-infiltration movement of soil moisture in an initially deeply wetted or saturated profile, or in the presence of a high water table.

Bibliography

Introduction to Environmental Soil Physics (First Edition) 2003 Elsevier Inc. Daniel Hillel (ed.) <http://www.sciencedirect.com/science/book/9780123486554>

INTERRILL EROSION

The removal of a fairly uniform layer of soil on a multitude relatively small areas by splash due to raindrop impact and by sheet flow.

Bibliography

Glossary of Soil Science Terms. Soil Science Society of America. 2010. <https://www.soils.org/publications/soils-glossary>

Cross-references

Water Erosion: Environmental and Economical Hazard

INTERSECTING SURFACES APPROACH (ISA)

See [Soil Structure, Intersecting Surface Approach, and its Applications](#)

INTRINSIC PERMEABILITY

The property of a porous material that expresses the ease with which gases or liquids flow through it. Often symbolized by $k = Kn/pg$, where K is the Darcy hydraulic conductivity, n is the fluid viscosity, p is the fluid density, and g is the acceleration of gravity. Dimensionally, k is an area [L^2].

Bibliography

Glossary of Soil Science Terms. Soil Science Society of America. 2010. <https://www.soils.org/publications/soils-glossary>

ION EXCHANGE

The adsorption of ions by the surfaces of clay particles, and their exchange with ions in the surrounding aqueous solution.

Cross-references

[Surface Properties and Related Phenomena in Soils and Plants](#)

ION HYDRATION

Orientation and bonding of water molecules to the surface of an ion.

IRRIGATION AND DRAINAGE, ADVANTAGES AND DISADVANTAGES

Lajos Blaskó

Karcag Research Institute of Centre for Agricultural and Technical Sciences, Debrecen University, Karcag, Hungary

Synonyms

Regulation of soil water regime

Definition

Irrigation and drainage – artificial application of water to land and artificial removal of excess water from land ([Encyclopedia Britannica](#)).

Introduction

Most of the material transport processes in soils are closely related to the water movement. The water regime type of a soil depends on the meteorological and hydrological conditions of the region where the soil is located and on the chemical and physical properties of the soil. Soil with leaching characteristic (decreasing water soluble salt content in the top layer) can develop in areas where the natural or natural + artificial water input on the soil surface exceeds the evapotranspiration from the soil surface in a longer period of the year. Soil profiles with accumulation of soluble salts can be found in areas where the amount of natural precipitation is not high enough to leach the weathering products, or the level of salty groundwater

table is high enough to reach the top layer of soil through capillary rise.

Irrigation and drainage are the most important means to modify the water regime properties of soils.

Irrigation

Advantages

Irrigation covers several essential agricultural requirements in the arid areas of the world:

- Water supply for plant growth, nutrient transport
- A flow of water to leach or dilute the salt content of the soil
- It is one of the most effective means of mitigation of wind erosion
 - by maintaining a protective vegetation cover
 - by maintaining a higher moisture content of the soil

Disadvantages

Soil salinization is a major threat to irrigated agriculture. Salt accumulation can be directly caused by the capillary rise from saline groundwater or by the irrigation water itself, because of the high salt content of the water and limited leaching in the soil. The two types of salt accumulation in soils can be distinguished by taking into account the place of the accumulation in most cases. If the salinization or sodication is caused by the irrigation of poor quality water, the increasing salt content can be measured in the surface layer. The salinization caused by the rising saline water table affects the deeper layers and can only be diagnosed by measuring the salt content of the deeper layers. The latent character makes this process even more dangerous. If the rising groundwater contains Na_2CO_3 too, the salt accumulation can hardly be reversed by leaching because – as Várallyay (1981) figured out – the water conductivity is much more limited by Na_2CO_3 in the low suction range (case of leaching) than in the higher suction range (e.g., capillary rise).

Salt accumulation on the soil surface can be prevented by keeping the irrigation water standards. In well-drained soils, where salinity is caused by neutral sodium salts, the accumulated amount can be leached by applying more water than that lost by evaporation and by the consumption of plants. The amount of excess water was defined as the leaching requirement (LR) by the US Salinity Laboratory (Richards, 1954). LR depends on the salinity tolerance of the cultivated plants.

Salinity problems caused by rising groundwater can be controlled by keeping the groundwater table below a critical level at which salt accumulation cannot be expended. A calculation method based on salt balance, ground water quality and water regime properties of the soils was elaborated by Szabolcs et al. (1969).

Recently, several computer models have started being used for predicting the salt accumulation, for example, DRANMOD (Abdel-Dayem and Skaggs, 1990),

LEACHMS (Wagenet and Hutson, 1992), and UNSATCHEM (Simunek and Suarez, 1994).

Field studies (Tóth and Blaskó, 1998) showed that seepage from unlined channels can be one of the main man-made causes of the rising groundwater in an irrigated area.

The possible soil physical disadvantage of sprinkling irrigation with high intensity is surface sealing and crusting. Summer and Stewart (1992) edited a synthetic work about the tendency of dispersion and crusting on the soils pointing out the main causes of structural deterioration. Blaskó et al. (1998) found that dispersion occurred most frequently in soils with unfavorable chemical properties containing swelling clay minerals and high amount of clay fraction with exchangeable sodium. Examining the inclination toward crust formation, it was revealed that soils with the most unfavorable hydraulic conductivity were the most sensitive to become crusty.

Drainage

Advantages

Subsurface and surface drainage systems are the most effective means of soil water regime regulation. The main function of the subsurface drainage is keeping the groundwater level below a critical level and to let the water moving out by gravitation from the top layers to the pipes. The purpose of surface drainage is to let the excess water out from the soil surface. These functions prevent the soil from overwetted state.

Beside the regulation of soil moisture content on areas affected by salty groundwater, drainage systems can control the salt accumulation and leaching processes as well.

In a long-term amelioration experiment on a salt-effected soil with structural B-horizon, the salts leached from the topsoil in case of non-drained variants remained in the layers close to the surface, involving the risk of resalinization due to the rise of groundwater table, while in case of drained soil there was a significant decrease of sodium in the whole layer above the drainage system (Blaskó, 2004).

Disadvantages

In drained areas, the typical characteristic is the accelerated material movement in correlation with a faster water movement.

Studying the chemical composition of drain waters, the nitrogen was proved to be the most threatened material in the order of leaching (Armstrong et al., 1983; Blaskó and Juhász, 1989).

The amount of nitrogen loss depends on the depth of the drainage system, as well.

N leaching has been studied in lysimeters, and it was found (Rézegyi and Heltai, 1984; Nyiri and Karuczka, 1989; Karuczka and Zsembeli, 1999) that N leaching was more severe in soils where a shallow drainage system (1–1.5 m depth) had been applied.

Natural streams or rivers can be the outlets for drainage systems. Nutrients carried in drainage water can cause eutrophysisation of “living” waters.

The nitrogen loss can only be mitigated by split application of the mineral fertilizer, but the loss caused by heavy rains in time of intensive nitrification cannot be avoided (Juhász et al., 1997).

The drainage waters coming from salt-affected areas may increase the salt content of streams, rivers, and lakes, so an excessive drainage of salt-affected areas can cause the export of the salinity problem on other territories.

Summary

Irrigation and drainage are the most effective means of water regime regulation in soil–water systems. In addition to influencing the water supply of plants, they have a strong influence on the accumulation and leaching processes in the soils as well.

The main advantages of drainage and irrigation are the regulation of water regime of soils, maintaining the available moisture content and letting the excess water out from overmoistened soil. Besides, they control the salt accumulation processes. The “leaching requirement” (LR) of irrigation water washes out the salts from the rooting zone until the tolerance level of a given plant. The subsurface drainage system prevents the top layers from salt accumulation which would be caused by capillary rise from the groundwater.

The potential disadvantages of the irrigation are salt accumulation caused by irrigation water of poor quality or by rising groundwater level caused by seepage from unlined irrigation channels. The main disadvantage of a drainage system can be the accelerated leaching out of nitrogen and other salts, causing eutrophysation or the increase of the salt content of streams and rivers. Usually, the disadvantages can be avoided by using proper irrigation methods and keeping the irrigation water standards. The nitrogen loss can only be mitigated by split application of nitrogen fertilizers.

Bibliography

- Abdel-Dayem, S., and Skaggs, R.W., 1990. Extension of DRAINMOD for simulating water management in arid regions. In *Symposium on Land Drainage for Salinity Control in Arid and Semi-Arid Regions*, Cairo, Egypt, February 25–March 2, Vol. 2, pp. 201–212.
- Armstrong, A. C., Show, H., and Wilcocksow, S. J., 1983. Field drainage and nitrogen leaching some experimental results. *Journal of Agricultural Science London*, **1**, 253–255.
- Blaskó, L., 2004. *Salinization and Amelioration Possibilities of Salt Affected Soils on the Great Hungarian Plain*. Eurosoil 2004 (available online at http://www.bodenkunde2.uni-freiburg.de/eurosoil/abstracts/id1049_Blasko_full.pdf).
- Blaskó, L., and Juhász, Cs., 1989. *Examination of Material Movements in Complex Ameliorated Soils Near by the Lake Tisza*. Pollution and Water Resources. Columbia University Seminar Series.
- Blaskó, L., Wafi Mohamed, J. K., and Karuczka A., 1998. Susceptibility to sealing and crusting of the main Hungarian Plain soil types and elaboration of suitable method for its moderation. In *International Congress on Soil Condition and Crop Production*, Gödöllő, Hungary, pp. 33–35.
- Encyclopedia Britannica. Irrigation and drainage. Available from World Wide Web: <http://www.britannica.com/EBchecked/topic/294780/irrigation>.
- Juhász, C., Blaskó, L., Karuczka, A., and Zsembeli, J., 1997. Environmental effect of drain waters from heavy textured soils. *Roslinná Výroba*, **43**, 87–94.
- Karuczka, A., and Zsembeli, J., 1999. *Examination of Water and Nutrient Transport in Compensation Lysimeters*. Stoffflüsse und ihre regionale Bedeutung für die Landwirtschaft. Bericht. 8. Gumpensteiner Lysimetertagung, pp. 111–113.
- Nyiri, L., and Karuczka, A., 1989. The influence of meliorative soil moisture regulations on drained waters NO_3^- content and its dynamics. *A Debreceni Agrártudományi Egyetem Tudományos Közleményei*, **28**, 453–462 (in Hungarian).
- Rézhegyi, P., and Heltai, G., 1984. Investigation by lysimeters of the nitrogen washout with help of n^{15} isotopes. *Melioráció-öntözés és tápanyaggazdálkodás*, **2**, 53–55 (in Hungarian).
- Richards, L. A. (ed.), 1954. *Diagnosis and Improvement of Saline and Alkali Soils USDA. Handbook 60*. Washington: US Government Printing Office.
- Simunek, J., and Suarez, D. L., 1994. Two-dimensional transport model for variably saturated porous media with major ion chemistry. *Water Resources Research*, **30**, 1115–1133.
- Summer, M. E., and Stewart, B. A., 1992. *Soil Crusting, Chemical and Physical Processes*. Boca Raton: Lewis Publisher.
- Szaboles, I., Darab, K., and Várallyay, G., 1969. Methods of predicting salinization and alkalinization processes due to irrigation on the Hungarian Plain. *Agrokémia és Talajtan*, **18**, 351–376.
- Tóth, T., and Blaskó, L., 1998. Secondary salinization caused by irrigation ESSC Meeting, 1995. Tenerife-Fuerteventura-Lanzarote. Abstracts: P56–57. In Rodriguez, A., Jiménez Mendoza, C. C., and Tejedor Salguero, M. I. (eds.), *The Soil as a Strategic Resource: Degradation Processes and Conservation Measures*. Logrono: Geoforma Ediciones, pp. 229–253.
- Várallyay, G., 1981. Extreme moisture regime as the main limiting factors of the fertility of salt affected soils. *Agrokémia és Talajtan.*, **30**, 73–96.
- Wagenet, R. J., and Hutson, J. L., 1992. *LEACHM: A Process Based Model of Water and Solute Movement, Transformation, Plant Uptake and Chemical Reactions in the Unsaturated Zone*. Ithaca: Centre of Environmental Research, Cornell University.

Cross-references

- [Salinity, Physical Effects on Soils](#)
[Shrinkage and Swelling Phenomena in Soils](#)
[Soil Water Flow](#)
[Soil Water Management](#)
[Solute Transport in Soils](#)
[Surface and Subsurface Waters](#)
[Water Budget in Soil](#)

IRRIGATION WATER USE EFFICIENCY

See [Water Use Efficiency in Agriculture: Opportunities for Improvement](#)

IRRIGATION WITH TREATED WASTEWATER, EFFECTS ON SOIL STRUCTURE

Guy J. Levy

Institute of Soil, Water and Environmental Sciences,
The Volcani Center, Agricultural Research Organization,
Bet Dagan, Israel

Definition

Treated waste water (TWW) is referred to in the context of the current presentation as raw sewage water, originating mainly from domestic sources, that has been subjected to a number of treatment processes, making the water suitable for irrigation of arable land.

Introduction

The use of TWW for irrigation of cultivated fields has increased considerably in recent years, especially in areas suffering from shortage of freshwater (e.g., arid and semi-arid regions). With this increased necessity to use TWW for irrigation, farmers are faced with unique and unfamiliar problems among which is the possible degradation in soil structure and stability.

Soil structure is commonly referred to as the size, shape, and arrangement of solids and voids, as well as the continuity of pores and voids. Soil structure directly affects the soil's capacity to retain and transport water, and organic and inorganic constituents, thereby influencing important field-scale phenomena such as soil water movement and retention, erosion, crusting, nutrient recycling, root penetration, and crop yield (Lal, 1991). Hence, favorable soil structure and stable aggregates are important for improving soil quality, increasing agronomic productivity and sustainability, and decreasing soil erodibility.

The current presentation attempts to summarize existing knowledge on the impact of irrigation with TWW on some soil determinants that are closely associated with soil structure and stability.

Characteristics of TWW

Raw sewage water can be subjected to different treatments. Secondary (biological) treatment is generally required when the TWW is intended for irrigation of cultivated land (Feigin et al., 1991). Some typical properties of TWW from Israel after a secondary treatment and those of its freshwater (FW) of origin are presented in Table 1. TWW contains significantly higher levels of beneficial components for agricultural use such as nitrogen, phosphorus, potassium, and possibly some other beneficial elements in minimal concentrations. The concentration of boron (an essential microelement for crops that has a small concentration window between deficiency and toxicity) in TWW may often be in the toxic range.

TWW also exhibits higher loads than FW of suspended solids and dissolved organic matter (DOM), commonly

Irrigation with Treated Wastewater, Effects on Soil Structure, Table 1 Chemical characteristics of secondary treated wastewater (TWW) and freshwater (FW) used for irrigation in the Bet She'an Valley, Israel. Average values for 4 years (2002–2005) (Adapted from Bhardwaj et al., 2007)

Water quality parameter ^a	Irrigation water	
	TWW	FW
SAR	5.12 (0.95) ^b	3.12 (0.37)
EC (dS m ⁻¹)	1.91 (0.23)	1.23 (0.10)
pH	7.58 (0.27)	7.60 (0.32)
N-NH ₄ ⁺ (mg L ⁻¹)	35.1 (11.0)	0.00 (0.00)
N-NO ₃ ⁻ (mg L ⁻¹)	0.14 (0.24)	0.06 (0.12)
P (mg L ⁻¹)	2.34 (3.23)	0.00 (0.00)
K (meq L ⁻¹)	0.97 (0.05)	0.32 (0.26)
Ca + Mg (meq L ⁻¹)	6.80 (0.83)	5.93 (0.70)
Na (meq L ⁻¹)	8.72 (1.44)	5.37 (0.29)
Cl (mg L ⁻¹)	314.4 (24.7)	280.62 (28.01)
B (mg L ⁻¹)	0.28 (0.06)	0.10 (0.005)
TSS (mg L ⁻¹)	170.4 (69.8)	0.00 (0.00)
BOD (mg L ⁻¹)	86.8 (52.7)	0.00 (0.00)
COD (mg L ⁻¹)	136.2 (37.1)	0.00 (0.00)

^aSAR sodium adsorption ratio, EC electrical conductivity, TSS total suspended solids, BOD biochemical oxygen demand, COD chemical oxygen demand

^bNumbers in parenthesis are one standard deviation

expressed in terms of BOD or COD (Table 1). TWW is more saline and has a higher sodium adsorption ratio (SAR) than its FW of origin. TWW may contain some trace elements but generally at concentrations that are suitable for long-term irrigation (Feigin et al., 1991).

Presence of pathogenic microorganisms (e.g., viruses, bacteria, protozoa) in the TWW represents the most common threat to the agricultural use of wastewater, both for workers and end consumers of crops, but not necessarily to the soil.

TWW impact on mechanisms affecting soil structure

Processes that may harm soil structure and stability include clay swelling and dispersion, and aggregate breakdown through slaking or impact of water drops of high kinetic energy (e.g., rain or overhead sprinkler irrigation systems). These processes are expected to occur mainly in winter when the soil is leached with rain water (i.e., water free of electrolytes). Under these conditions, the sensitivity of the soil clay to swelling and dispersion is high (Shainberg and Letey, 1984), as is the susceptibility of aggregates to slaking (Levy et al., 2003).

Irrigation with TWW is likely to enhance the processes of clay swelling and dispersion in comparison to irrigation with FW because of the higher SAR and the presence of DOM in the TWW. Sodic conditions, especially in the absence of electrolytes, render soil clays greater sensitivity to swelling and dispersion (Shainberg and Letey, 1984) and lead to weakening of soil aggregates (Abu Sharar et al., 1987). In addition, the presence of dissolved humic

substances in the TWW may enhance clay dispersivity (e.g., Tarchitzky et al., 1993). This effect is attributed to the interaction of the negatively charged organic molecules with the positively charged edges of the clay, which prevents the edge-to-face association of clay particles responsible for flocculation (Tarchitzky et al., 1993). The presence of DOM in the TWW could have an additional indirect effect on the soil via its effect on the SAR; the effective SAR of the TWW is expected to be greater than that commonly calculated based on the total concentration of cations in the solution (Halliwell et al., 2001). The difference between the commonly calculated SAR and the effective one could reach up to 50% due to the great affinity of the divalent cations to organic ligands (Fotovat et al., 1996).

Aggregate stability

The term soil-structure stability is often considered synonymous with aggregate stability, especially in cases where aggregates break down by water (Kay and Angers, 1999). In general, organic substances are considered as cementing agents that improve aggregate stability (e.g., Bronick and Lal, 2005). However, humic substances have been observed to have a dual role as aggregating and disaggregating agents (Oades, 1984). Some studies have indicated that the aforementioned duality is related to the concentration of humic substances; at low concentrations ($<0.05\text{--}0.10\text{ g kg}^{-1}$) the humic substances stabilize aggregates, while at higher concentrations they have a dispersive effect (Piccolo et al., 1996).

Studies of aggregate slaking (i.e., aggregate breakdown caused by compression of entrapped air during fast wetting) revealed that for soils having *a priori* unstable aggregates (coarse- and medium-textured soils, $<25\%$ clay), sensitivity to slaking of aggregates taken from TWW-irrigated fields was comparable to that of aggregates taken from FW-irrigated fields (Levy and Mamedov, 2002; Levy et al., 2003). In such soils, irrigation with TWW, which induces conditions favoring clay dispersion via increased sodicity, seems to play a minor role in determining aggregate stability. Conversely, in fine-textured soils ($>40\%$ clay) having *a priori* stable aggregates, aggregates from TWW-irrigated soils were more sensitive to slaking (i.e., less stable) than those taken from FW-irrigated soils (Levy and Mamedov, 2002; Levy et al., 2003). Evidently, in clay soils where the clay stabilizes the aggregates (Kemper and Koch, 1966), conditions favoring dispersive behavior of clay (high sodicity and the presence of humic substances in the TWW) adversely affect aggregate resistance to slaking.

The impact of irrigation with TWW on aggregate stability seems to depend also on the intensity of cultivation. In aggregates taken from intensively cultivated fields (e.g., field crops) aggregates from TWW-irrigated land were less stable than those taken from FW-irrigated land (Levy et al., 2006). In samples taken from orchards where soil cultivation is minimal and the aggregates are not subjected

to frequent disturbance, stability of aggregates from TWW- and FW-irrigated samples was comparable (Levy et al., 2006; Bhardwaj et al., 2007).

Saturated hydraulic conductivity

During the irrigation season it is mainly the presence of suspended solids in the TWW, especially in poorly treated wastewater, that could adversely affect soil physical and hydraulic properties. Suspended solids present in the TWW may accumulate and physically block water conducting pores, thereby leading to a sharp decrease in soil HC. Blocking of the pores depends on (1) the load of suspended solids in the wastewater (Rice, 1974), (2) the environmental conditions prevailing in the soil, which determine the rate of breakdown of the suspended solids (DeVries, 1972), and (3) soil texture; the finer the soil texture, the greater the decrease in the HC (Levy et al., 1999; Lado and Ben-Hur, 2009).

In cases where TWW that had been subjected to a high level of treatment is used and a reduction in the HC following irrigation with TWW is observed, the reduction could be ascribed to clay swelling and dispersion that are enhanced by the higher SAR of the TWW (Mace and Amrhein, 2001) and/or the presence of DOM in the TWW (Tarchitzky et al., 1999). In addition, a decrease in HC during leaching with TWW of good quality, but of high C to N ratio, could arise from the growth of microorganisms in the soil, which can partially clog water-conducting pores (Magesan et al., 1999).

The impact of irrigation with TWW on soil HC during the subsequent rainy season, i.e., when the soil is exposed to water nearly free of electrolytes seems to depend on soil texture and conditions prevailing in the soil (e.g., intensity of cultivation, rate of wetting, method of irrigation), and to vary seasonally.

For instance, in a sandy clay, no differences were noted between the HC of TWW- and FW-irrigated samples taken from both intensely and non-intensely cultivated fields. By comparison, in a clay soil, for both types of the aforementioned fields, the HC of the TWW-irrigated samples was significantly lower than that of the FW-irrigated samples (Levy et al., 2006).

Preventing aggregate slaking (i.e., by ensuring aggregate wetting at a slow rate) prior to measuring the HC, significantly reduced the adverse impact of long-term irrigation with TWW on the reduction in HC, compared to conditions where aggregate slaking was allowed (Shainberg et al., 2001; Mandal et al., 2008). However, when the HC of intact cores (i.e., no destruction of soil structure) of a clay soil collected from an orchard at locations in close proximity to micro-sprinklers or dripers was studied, the results showed that the method of irrigation (drip vs. microsprinkler), rather than irrigation water quality (TWW vs. FW), determined the response of the soil to leaching with deionized water (Bhardwaj et al., 2007).

A study that compared the HC of intact cores taken in spring (after the rainy season) to those taken in autumn (at the end of the irrigation season) from a silty clay irrigated with TWW showed that the HC of the spring samples was nearly sixfold higher than that of the autumn samples (Bhardwaj et al., 2008). It was postulated that the lower HC in the autumn samples was associated with the partial blocking of soil pores by suspended solids present in the TWW. It was further suggested that the suspended solids that accumulated in the soil during the irrigation season broke down in the course of the rainy season (DeVries, 1972), leading to the observed increase in the HC of the samples taken in spring (Bhardwaj et al., 2008).

Infiltration rate (IR), runoff, and soil loss

Most studies that evaluated the impact of irrigation with TWW on soil permeability, runoff, and erosion concentrated on soil sensitivity to those determinants under simulated or natural rain conditions.

Laboratory studies with rainfall simulators (where deionized water was used) showed that for TWW-irrigated soils the infiltration rate (IR) values were lower (Mamedov et al., 2000a) and runoff levels were higher (Mamedov et al., 2001b) than those obtained in FW-irrigated samples. However, the reported differences were relatively small, especially for rain with kinetic energy typical of Mediterranean-type rainstorms (15.9 kJ m^{-3}). It appears that, despite the relatively higher ESPs of the TWW-irrigated soils, which enhance clay dispersion, the raindrop impact energy (in the case of the high kinetic energy rain) causes aggregate breakdown and compaction and controls the process of seal formation at the soil surface, resulting in subsequent low IR and high runoff levels.

A field study on two calcareous soils showed that runoff levels from FW- and TWW-irrigated fields were comparable (Agassi et al., 2003). The rapid decrease in the exchangeable sodium percentage (ESP) of the upper soil layer in the TWW-irrigated field (the layer where seal development occurs) during the rainy season, from 5 to 6 at the end of summer to its natural level of ~ 2 , as found in the FW-irrigated field, attributed to the presence of lime in the soil, was held responsible for the observed similarity in the IR and runoff recorded for the soils from the FW- and TWW-irrigated fields (Agassi et al., 2003). These findings also explain the observed adverse effects of irrigation with TWW on soil permeability and runoff production in a non-calcareous sandy soil used in the studies of Mamedov et al. (2001a, b) and Lado et al. (2005).

Soil susceptibility to sealing and runoff production depends on the conditions prevailing at the soil surface prior to exposing the soil to rain. Allowing the surface aggregates to slake (using fast wetting) before exposing the soil to rain enhances the development of a seal with low permeability and subsequently the production of high

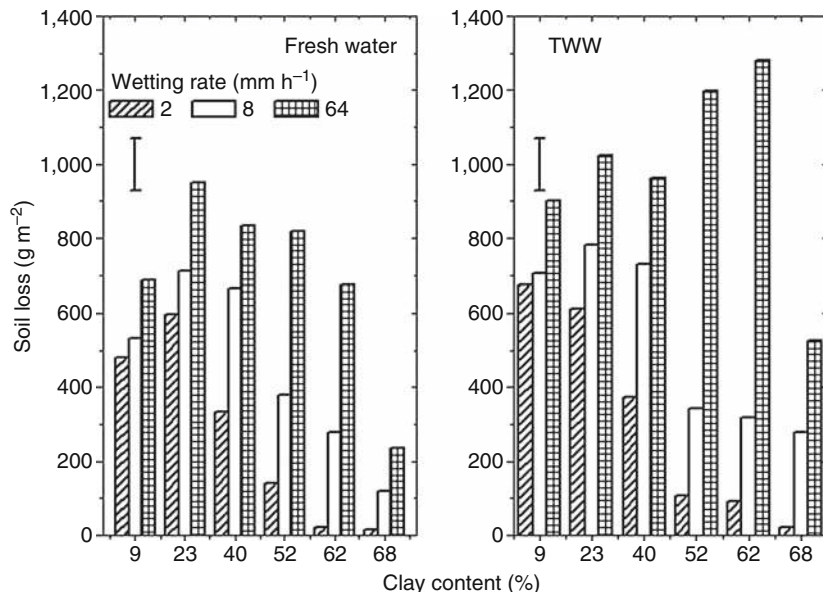
levels of runoff (Levy et al., 1997). However, but for a sandy soil, comparable runoff levels were observed for TWW- and FW-irrigated medium- and fine-textured soils irrespective of the initial conditions (i.e., degree of aggregate slaking) that existed at the soil surface prior to applying rain (Mamedov et al., 2001a; Lado et al., 2005).

Comparison of soil loss from FW- and TWW-irrigated soils, subjected to different levels of rain kinetic energy, showed that soil loss from the TWW-irrigated soils was always significantly higher (Mamedov et al., 2000b), while respective IR levels did not differ significantly between soils irrigated with the two water qualities (Mamedov et al., 2000a).

Under circumstances where soil surface conditions were manipulated by using different wetting rates prior to applying rain, it was observed that under conditions of fast wetting (sever aggregate slaking), the TWW-irrigation soils yielded higher soil loss levels compared with the FW-irrigated samples (Figure 1). This observations for soil loss, combined with the similar level of runoff in the two types of samples (Mamedov et al., 2001a), suggested that once the surface aggregates are slaked by fast wetting, the slaked particles are more readily detached and removed from the soil by the runoff water in the TWW-irrigated samples than in the FW-irrigated ones, resulting in a higher soil loss load. When non-slaked aggregates (i.e., slowly wetted aggregates) were exposed to the impact of rain drops, irrigation with TWW had no additional adverse effect on soil susceptibility to sealing, runoff, and soil loss production beyond that of FW (Mamedov et al., 2001a; Mamedov et al., 2001b). More recently, Lado et al. (2005) suggested that for non-calcareous sandy soils, TWW-irrigated samples are more susceptible to runoff and soil loss production than FW-irrigated ones, irrespective of initial conditions of slaked or non-slaked surface aggregates.

Summary

Examination of numerous studies that evaluated the impact of long-term irrigation with TWW on different indices representing soil structure and stability revealed that the effects of using TWW for irrigation are inconsistent. The observed inconsistencies may stem from (1) the fact that different mechanisms (clay swelling and dispersion, aggregate slaking) control in different ways the response of the determinants tested, (2) variability in soil properties (mainly clay content and presence of lime) affecting soil stability, and (3) disparity in the conditions prevailing in the soil (e.g., intensity of tillage, rate of wetting). It emerges that under conditions where either aggregate slaking is prevented or aggregates are subjected to only minor disturbance (non-intensive tillage), the use of TWW for irrigation has almost no adverse effects on soil structure and stability, especially in calcareous soils. In cases where long-term irrigation with TWW had led to some deterioration in determinants associated with



Irrigation with Treated Wastewater, Effects on Soil Structure, Figure 1 Effects of water quality and rate of wetting on soil loss from soils with different clay content exposed to simulated deionized rain water. Bars indicate a single confidence interval value at $\alpha = 0.001$. (Adapted from Mamedov et al., 2001b.)

soil-structure stability, the magnitude of the deterioration was not severe.

Soils are a valuable resource that, once degraded, would be extremely difficult and costly to reclaim. Irrigation with TWW should, therefore, be accompanied by close monitoring of different indicators of soil structure in order to maintain the soils in a satisfactory state for continued productive use by future generations.

Bibliography

- Abu Sharar, T. M., Bingham, F. T., and Rhoades, J. D., 1987. Stability of soil aggregates as affected by electrolyte concentration and composition. *Soil Science Society of America Journal*, **51**, 309–314.
- Agassi, M., Tarchitzky, J., Keren, R., Chen, Y., Goldstein, D., and Fizik, E., 2003. Effects of prolonged irrigation with treated municipal effluent on runoff rate. *Journal of Environmental Quality*, **32**, 1053–1057.
- Bhardwaj, A. K., Goldstein, D., Azenkot, A., and Levy, G. J., 2007. Irrigation with treated waste water under two irrigation methods: effects on hydraulic conductivity of a clay soil. *Geoderma*, **140**, 199–206.
- Bhardwaj, A. K., Mandal, U. K., Bar-Tal, A., Gilboa, A., and Levy, G. J., 2008. Replacing saline-sodic irrigation water with treated wastewater: effects on saturated hydraulic conductivity, slaking and swelling. *Irrigation Science*, **26**, 139–146.
- Bronick, C. J., and Lal, R., 2005. Soil structure and management: a review. *Geoderma*, **124**, 3–22.
- DeVries, J., 1972. Soil infiltration of waste water effluent and the mechanisms of pore clogging. *Journal of Water Pollution and Contamination*, **44**, 565–573.
- Feigin, A., Ravina, I., and Shalheveth, J., 1991. Irrigation with sewage effluent: management for environmental protection. *Advanced Series in Agricultural Sciences*, vol. 17. Berlin: Springer.
- Fotovat, A., Smith, L., Naidu, R. J., and Oades, J., 1996. Analysis of indigenous zinc in alkaline sodic soil solutions by graphite furnace atomic absorption spectrometry. *Communication in Soil Science and Plant Analyses*, **27**, 2997–3012.
- Hallsworth, D. J., Barlow, K. M., and Nash, D. M., 2001. A review of the effects of wastewater sodium on soil physical properties and their implications for irrigation systems. *Australian Journal of Soil Research*, **39**, 1259–1267.
- Kay, B. D., and Angers, D. A., 1999. Soil Structure. In Sumner, M. E. (ed.), *Handbook of Soil Science*. Boca Raton: CRC Press, pp. A229–A276.
- Kemper, W. D., and Koch, E. J., 1966. Aggregate stability of soils from western USA and Canada. USDA Technical Bulletin No. 1355, Washington, DC: US Government Printing Office.
- Lado, M., and Ben-Hur, M., 2009. Treated domestic sewage irrigation effects on hydraulic properties in arid and semiarid zones: a review. *Soil and Tillage Research*, doi:10.1016/j.still.2009.04.011.
- Lado, M., Ben-Hur, M., and Assouline, S., 2005. Effects of effluent irrigation on seal formation, infiltration and soil loss during rainfall. *Soil Science Society of America Journal*, **69**, 1432–1439.
- Lal, R., 1991. Soil structure and sustainability. *Journal of Sustainable Agriculture*, **1**, 67–92.
- Levy, G. J., and Mamedov, A. I., 2002. High-Energy-Moisture-Characteristics aggregate stability as a predictor for seal formation. *Soil Science Society of America Journal*, **66**, 1603–1609.
- Levy, G. J., Levin, J., and Shainberg, I., 1997. Prewetting rate and aging effects on seal formation and interrill soil erosion. *Soil Science*, **162**, 131–139.
- Levy, G. J., Rosenthal, A., Tarchitzky, J., Shainberg, I., and Chen, Y., 1999. Soil hydraulic conductivity changes caused by irrigation with reclaimed waste water. *Journal of Environmental Quality*, **28**, 1658–1664.

- Levy, G. J., Mamedov, A. I., and Goldstein, D., 2003. Sodicity and water quality effects on slaking of aggregates from semi-arid soils. *Soil Science*, **168**, 552–562.
- Levy, G. J., Goldstein, D., Trachitzky, J., and Chen, Y., 2006. Combined effects of irrigation with treated waste water and tillage on soil structural stability (in Hebrew). Final report submitted to the Chief Scientist, State of Israel: Ministry of Agriculture.
- Mace, J. E., and Amrhein, C., 2001. Leaching and reclamation of a soil irrigated with moderate SAR waters. *Soil Science Society of America Journal*, **65**, 199–204.
- Magesan, G. N., Williamson, J. C., Sparling, G. P., Schipper, L. A., and Lloyd-Jones, A. R. H., 1999. Hydraulic conductivity in soils irrigated with wastewaters of differing strengths: field and laboratory studies. *Australian Journal of Soil Research*, **37**, 391–402.
- Mamedov, A. I., Shainberg, I., and Levy, G. J., 2000a. Irrigation with effluent water: Effect of rainfall energy on soil infiltration. *Soil Science Society of America Journal*, **64**, 732–737.
- Mamedov, A. I., Shainberg, I., and Levy, G. J., 2000b. Rainfall energy effects on runoff and interrill erosion in effluent irrigated soils. *Soil Science*, **165**, 535–544.
- Mamedov, A. I., Levy, G. J., Shainberg, I., and Letey, J., 2001a. Wetting rate, sodicity and soil texture effects on infiltration rate and runoff. *Australian Journal of Soil Research*, **39**, 1293–1305.
- Mamedov, A. I., Shainberg, I., and Levy, G. J., 2001b. Irrigation with effluents: effects of prewetting rate and clay content on runoff and soil loss. *Journal of Environmental Quality*, **30**, 2149–2156.
- Mandal, U. K., Bhardwaj, A. K., Warrington, D. N., Goldstein, D., Bar-Tal, A., and Levy, G. J., 2008. Changes in soil hydraulic conductivity, runoff, and soil loss due to irrigation with different types of saline-sodic water. *Geoderma*, **144**, 509–516.
- Oades, J. M., 1984. Soil organic matter and structural stability: Mechanisms and implications for management. *Plant and Soil*, **76**, 319–337.
- Piccolo, A., Pietramellara, G., and Mbagwu, J. S. C., 1996. Effects of coal derived humic substances on water retention and structural stability of Mediterranean soils. *Soil Use and Management*, **12**, 209–213.
- Rice, R. C., 1974. Soil clogging during infiltration of secondary effluent. *Journal of Water Pollutants Control*, **46**, 708–716.
- Shainberg, I., and Letey, J., 1984. Response of soils to sodic and saline conditions. *Hilgardia*, **52**, 1–57.
- Shainberg, I., Levy, G. J., Goldstein, D., Mamedov, A. I., and Letey, J., 2001. Prewetting rate and sodicity effects on the hydraulic conductivity of soils. *Australian Journal of Soil Research*, **39**, 1279–1291.
- Tarchitzky, J., Chen, Y., and Banin, A., 1993. Humic substances and pH effects on sodium and calcium montmorillonite flocculation and dispersion. *Soil Science Society of America Journal*, **52**, 1449–1452.
- Tarchitzky, J., Golobati, Y., Keren, R., and Chen, Y., 1999. Waste-water effects on montmorillonite suspensions and hydraulic properties of sandy soil. *Soil Science Society of America Journal*, **63**, 554–560.

Cross-references

- Flocculation and Dispersion Phenomena in Soils
Infiltration in Soils
Organic Matter, Effects on Soil Physical Properties and Processes
Physical Degradation of Soils, Risks and Threats
Salinity, Physical Effects on Soils
Soil Aggregates, Structure, and Stability
Soil Physical Quality
Soil Surface Sealing and Crusting

ISOELECTRIC POINT

The activity of potential determining ion in a solution in equilibrium with a variable charge surface whose net electrical charge is zero. For soils it refers to the pH of the isoelectric point of pH dependent charge materials. It applies only to single components, not mixtures.

Bibliography

Glossary of Soil Science Terms. Soil Science Society of America. 2010. <https://www.soils.org/publications/soils-glossary>

Cross-references

Surface Properties and Related Phenomena in Soils and Plants

ISOTOPES

See *Stable Isotopes in Evaluation of Greenhouse Gas Emission; Stable Isotopes, their Use in Soil Hydrology*

ISOTROPY AND ANISOTROPY IN AGRICULTURAL PRODUCTS AND FOODS

Józef Horabik, Marek Molenda

Institute of Agrophysics, Polish Academy of Sciences, Lublin, Poland

Definition

The term isotropy means homogeneity of physical properties in all directions.

The term anisotropy is used to describe direction-dependent physical properties of materials as opposed to isotropy. It can be defined as a difference in a value of property when measured along different axes.

Introduction

Numerous solids can be naturally anisotropic. Anisotropy can be also frequently induced during storage, handling, and processing of materials as a result of specific treatment, portion of fine fraction, or mechanical interactions between particles.

For practice of biomaterials storage, handling and processing anisotropy of the mechanical properties (elasticity, plasticity, viscoelasticity, fracture, and mechanical strength), the diffusion properties responsible for filtration in porous materials, and the thermal properties are the most important.

Natural anisotropy

Inherently anisotropic solids are very common in nature. The typical examples in the microscale are crystals and polycrystals in which the grains are not completely

random but have a preferred orientation. Also in the case of plants, the growth of their cells is not completely random. Preferred directions of plant growth result in an anisotropic behavior of the tissue by introducing oriented directions of structure (Erickson, 1976). Preferred directions of cell division and cell wall expansion in a developing organ lead to anisotropic tissue growth (Bittig et al., 2008). The direction of maximal expansion rate is related to the direction of net alignment among cellulose microfibrils (Baskin, 2005). The behavior of plant tissue is not isotropic and related to its structural composition. The apple tissue has marked anisotropy in its fracture properties: flesh of the apple can be split much more easily along the fruit's radius than in a direction parallel to the fruit's tangent (Khan and Vincent, 1993). On the scale of biological tissue, the preferred orientation of fiber bundles creates very strong anisotropy. Their properties vary widely when measured with the growth direction grain or against it. Wood, carrot, onion, and meat are very illustrative examples of naturally anisotropic biological materials. Fiber tissues are much stronger along the fiber than across it. The fibrous structure of meat products leads to anisotropy of the thermal conductivity, which can be enhanced during freezing by the anisotropic growth of ice crystals in the direction of the temperature gradient (van der Sman, 2008).

Introduced anisotropy

Anisotropic structures of solids can be formatted during processing (extrusion, rolling, chopping, and slicing) due to certain texture patterns obtained in processing or due to some inclusions into isotropic matrix. Extrusion cooking can create anisotropy in the mechanical properties of produced foams, which is important to the consumer-perceived textural characteristics (Hutchinson and Simms, 1988). The application of well-defined flow in processing can result in formation of anisotropic structure of complex materials like foods (Manski et al., 2007). Preferred orientation of protein fibers results in anisotropy of fracture properties of Mozzarella cheese (Ak and Gunasekaran, 1997). The dynamics of capillary flow in porous media depends on microstructure: the hydration rate from cut-edges of leaf tea is a hundred fold faster than that from top to bottom surfaces (Weerts et al., 2006). Inclusions of some microfiber or microparticles into isotropic material during food processing results in that the composite either have the structure of reinforcing fibers in a matrix, with fibers oriented in one direction or in multiple directions, which leads to difference in mechanical strength along different directions (food-grade anisotropic materials lumpy micro-rods with microparticle inclusions (Campbell et al., 2009)).

Anisotropy of granular solids

When a bulk of grains is handled, the individual grains tend to be aligned in the Earth's gravitational field. Anisotropy appears in final stage of slow kernels interactions (impacts, rolling, sliding, and shearing) due to

particles tendency to rest in the most stable position with respect to the gravitational field. An example is slow slipping of particles along the line of the cone of natural repose. The particles tend to rest with the longest axes along the cone generatrix. When a granular assembly is composed of spherical particles, anisotropy results from preferred orientation of normal direction in contact points. When a granular assembly is composed of nonspherical particles, the two types of anisotropy are produced: (1) due to the preferred orientation of nonspherical particles and (2) due to concentration of normal direction in contact points (Oda, 1978). As a result, the shear strength of a granular assemble is anisotropic and the resistance to air flow is also anisotropic. The strength anisotropy leads to nonuniform load distribution on structures and nonuniform flow (Horabik et al., 1988). The pressure drop through a bulk of grains can be different in each direction due to difference in associated pores structure (Łukaszuk et al., 2009).

Description of anisotropic behavior

Description of behavior of anisotropic body is much more difficult than isotropic one. For mathematical modeling, the tensor notation is commonly used. Theory of linear elasticity requires two parameters of elasticity for isotropic body while for the anisotropic body the general Hook's law requires 18 independent elastic parameters (Timoshenko and Goodier, 1970). Similarly, plastic behavior of anisotropic body requires much more material parameters than isotropic one. To explain anisotropic response of granular solids the so-called fabric (spatial arrangement of solids and associated voids) derived from micromechanical approach should be introduced into the stress-strain relationship.

Summary

Anisotropic behavior of agricultural products and foods is frequently observed in nature. Proper designing of technological processes requires precise understanding of physical processes. Very important is to recognize whether behavior of solids is isotropic or anisotropic.

Bibliography

- Ak, M. M., and Gunasekaran, S., 1997. Anisotropy in tensile properties of Mozzarella cheese. *Journal of Food Science*, **62**, 1031–1033.
- Baskin, T. I., 2005. Anisotropic expansion of the plant cell wall. *Annual Review of Cell and Developmental Biology*, **21**, 203–222.
- Bittig, T., Wartlick, O., Kicheva, A., González-Gaitán, M., and Jülicher, F., 2008. Dynamics of anisotropic tissue growth. *New Journal of Physics*, **10**, 063001, doi:10.1088/1367-2630/10/6/063001.
- Campbell, A. L., Stoyanov, S. D., and Paunov, V. N., 2009. Fabrication of functional anisotropic food-grade micro-rods with micro-particle inclusions with potential application for enhanced stability of food foams. *Soft Matter*, **5**, 1019–1023.
- Erickson, R. O., 1976. Modeling of Plant Growth. *Annual Review of Plant Physiology*, **27**, 407–434.

- Horabik, J., Ross, I. J., and Schwab, C. V., 1988. Effects of spatial orientation on grain load distribution. *Transactions of the American Society of Agricultural Engineers*, **31**, 1787–1793.
- Hutchinson, R. J., and Simms, I., 1988. Anisotropy in the mechanical properties of extrusion cooked maize foams. *Journal of Materials Science Letters*, **7**, 666–668.
- Khan, A. A., and Vincent, J. F. V., 1993. Anisotropy in the fracture properties of apple flesh as investigated by crack-opening tests. *Journal of Materials Science*, **28**, 45–51.
- Lukaszuk, J., Molenda, M., Horabik, J., and Montross, M. D., 2009. Variability of pressure drops in grain generated by kernel shape and bedding method. *Journal of Stored Products Research*, **45**, 112–118.
- Oda, M., 1978. Significance of fabric in granular mechanics. *Proceedings of US-Japan Seminar "Continuum Mechanical and Statistical Approaches in the Mechanics of Granular Materials"*, Sendai, Japan, 7–26.
- Manski, J. M., van der Goot, A. J., and Booma, R. M., 2007. Advances in structure formation of anisotropic protein-rich foods through novel processing concepts. *Trends in Food Science & Technology*, **18**, 546–557.
- Timoshenko, S., and Goodier, J. N., 1970. *Theory of Elasticity*, 3rd edn. New York: Hill.
- van der Sman, R. G. M., 2008. Prediction of enthalpy and thermal conductivity of frozen meat and fish products from composition data. *Journal of Food Engineering*, **84**, 400–412.
- Weerts, A. H., Lian, G., and Martin, D., 2006. Modeling rehydration of porous biomaterials: anisotropy effects. *Journal of Food Science*, **68**, 937–942.

Cross-references

[Anisotropy of Soil Physical Properties](#)

[Physical Phenomena and Properties Important for Storage of Agricultural Products](#)

[Physical Properties of Raw Materials and Agricultural Products Stress–Strain Relations](#)

K

KERNEL

See *Grain Physics*

KINEMATIC VISCOSITY

A fluid's absolute viscosity divided by its mass density.

Bibliography

Library of Congress Cataloging-in-Publication Data Environmental engineering dictionary and directory/Thomas M. Pankratz <http://www.docstoc.com/docs/2845196/CRC-Press>

KIRCHHOFF'S LAWS

Basic rules for electric circuits, which state (a) the algebraic sum of the currents at a network node is zero and (b) the algebraic sum of the voltage drops around a closed path is zero.

Cross-references

[Agrophysics: Physics Applied to Agriculture](#)

KRIGING

A method of estimating the unmeasured value of a physical property for any location by means of a geostatistical interpolation procedure in which the known values of surrounding locations are analyzed spatially so as to minimize the overall variance.

Bibliography

Introduction to Environmental Soil Physics (First Edition) 2003 Elsevier Inc. Daniel Hillel (ed.) <http://www.sciencedirect.com/science/book/9780123486554>

Cross-references

[Mapping of Soil Physical Properties](#)

L

LAMINAR AND TURBULENT FLOW IN SOILS

Henryk Czachor

Institute of Agrophysics, Polish Academy of Sciences,
Lublin, Poland

Definitions

Laminar flow is streamlined and directly proportional to the pressure difference.

Turbulent flow is a flow without stable streamlines, and it is not directly proportional to the pressure difference.

Laminar flow in a cylindrical channel can be seen as a set of steady state parallel streamlines of different velocities. Radial velocity profile is described by a parabolic function – zero – at the wall and the maximum value in the center equals twice the mean velocity. Streamlines in a turbulent flux are not stable.

Flow character is determined by means of the Reynolds number Re .

$$Re = \rho u D / \mu; \quad (1)$$

where ρ – fluid density (kg m^{-3}), u – velocity (m s^{-1}), μ – dynamic viscosity (N s m^{-2}), D – channel diameter (m).

Type of flow in a cylindrical channel depends on the Reynolds number Re – for $Re < 2,300$, flow is laminar, if $2,300 < Re < 4,000$ – transition zone, $Re > 4,000$ – turbulent flow.

When liquid flows through a porous medium composed of spherical particle of diameter D , the Reynolds number Re can be estimated as (Rhodes, 1989):

$$Re = \rho V D / (\mu(1 - p)), \quad (2)$$

where V – the mean fluid velocity (m s^{-1}), p – porosity.

Laminar flow through a porous medium occurs for $Re < 10$ and fully turbulent for $Re > 2,000$. For example,

the Reynolds number Re of water flow trough, a mono size sand of grain diameter 2 mm, of velocity $V = 2 \text{ mm s}^{-1}$ and porosity $p = 0.4$ equals $6.7 < 10$ what means that it is a laminar one. One can suppose that the water flux in finer soils is a laminar one.

Turbulent flow in soils may occur in macropores ($D > 2-3 \text{ mm}$) made by fauna, for example, earthworms. When laminar, the water flux is proportional to the water potential gradient described by the Richards equation (Iwata et al., 1988).

Bibliography

- Iwata, S., Tabuchi, T., and Warkentin, B. P., 1988. *Soil-Water Interactions*. New York: Marcel Dekker.
Rhodes, M., 1989. *Introduction to Particle Technology*. Chichester: Wiley. ISBN: 0-471-98482-5.

Cross-references

- Hydraulic Properties of Unsaturated Soils
Infiltration in Soils
Pore Size Distribution
Soil Hydrophobicity and Hydraulic Fluxes
Soil Water Flow

LAMINAR FLOW

The flow of a fluid such that adjacent laminae (layers), moving at different velocities, slide over one another smoothly, without creating eddies.

Bibliography

- Introduction to Environmental Soil Physics (First Edition) 2003
Elsevier Inc. Daniel Hillel (ed.) <http://www.sciencedirect.com/science/book/9780123486554>

LAND RECLAMATION

The process of improving or restoring the condition of land to a better or more useful state.

LANDFILL

A land disposal site that uses an engineering method of solid waste disposal to reduce environmental hazards and protect the quality of surface and subsurface waters.

LANDSLIDE

See *Soil Physical Degradation: Assessment with the Use of Remote Sensing and GIS*

LAPLACE EQUATION

The partial differential equation describing steady-state groundwater flow.

LATENT HEAT

The heat needed to cause a change of state at constant temperature, such as the vaporization of water or the melting of ice.

LAYERED SOILS, WATER AND SOLUTE TRANSPORT

H. M. Selim
School of Plant, Environmental and Soil Sciences (SPESS), Agricultural Center, Louisiana State University, Baton Rouge, LA, USA

Definition

The phenomenon of *layering of the soil profile* is an intrinsic part of soil formation. Soils are naturally made up of several layers or strata having distinct physical and chemical properties. These properties reflect various processes and their soil genesis. Layers are commonly of uniform thicknesses and stratified horizontally. Water and solute movement in soils are naturally occurring processes where the flow must account for the different properties of the various soil layers.

Introduction

Soils are defined as heterogeneous systems that are made up of various constituents having distinct physical and

chemical properties. A major source of soil heterogeneity is soil stratifications or layering. The phenomenon of stratifications or layering of the soil profile is an intrinsic part of soil formation processes and has been documented for several decades by soil survey work.

The transport processes of dissolved chemicals in stratified or layered soils have been studied for several decades by Shamir and Harleman (1967), Selim et al. (1977), Bosma and van der Zee (1992), Wu et al. (1997), among others. Solute transport in layered soils can be investigated through numerical methods as well as approximate analytical solutions. An early analytical method was proposed by Shamir and Harleman (1967) who used a system's analysis approach. They assumed that different layers were independent with regard to solute travel time. Each layer's response served as the boundary condition (BC) for the downstream layer and so on. Later, Selim et al. (1977) discussed the movement of reactive solutes through layered soils using finite difference numerical methods. They considered both equilibrium and kinetic sorption models of the linear and nonlinear types. In the late 1980s, Leij and Dane (1989) developed analytical solutions for the linear sorption type models using Laplace transforms. Their solutions were based on the assumption that each layer was semi-infinite. Bosma and van der Zee (1992) also proposed an approximate analytical solution for reactive solute transport in layered soils using an adaptation of the traveling wave solution. Recently, Wu et al. (1997) developed another analytical model for nonlinear adsorptive transport through layered soils ignoring the effects of dispersion. In addition, Guo et al. (1997) showed that the transfer function approach was a very powerful tool to describe the nonequilibrium transport of reactive solutes through layered soil profiles with depth-dependent adsorption.

When we study transport process of dissolved chemicals in layered soils, it is of interest to investigate whether soil layering affects solute breakthrough. When flow remains one-dimensionally vertical, which is the case when horizontal stratification is dominant, it is of interest whether the layering order affects breakthrough results at the groundwater level (van der Zee, 1994). The early results from Shamir and Harleman (1967) showed that the order of layering did not affect breakthrough significantly. This interesting result was further elaborated upon by Barry and Parker (1987) based on various analytical approaches. Results from various linear and nonlinear numerical simulations for several sorption model types also supported this conclusion (Selim et al., 1977). Furthermore, Selim et al. (1977) concluded that layering order was also unimportant for Freundlich adsorption. Their experimental results also supported this conclusion. However, van der Zee (1994) attributed Selim et al. (1977) results to the small Peclet number assumed for the nonlinear layer, which prevents nonlinearity effects to be clearly manifested. van der Zee (1994) used a hypothetical result to illustrate that layering sequence should have an effect. However, what van der Zee (1994) used to

support his conclusion was the traveling wave, which was the curve of concentration versus depth at different times, i.e., concentration profile. Recently, Zhou and Selim (2001) accounted for several nonlinear and kinetic retention mechanisms for multilayered soils. For individual soil layers, Zhou and Selim (2001) considered solute retention mechanisms of the nonlinear (Freundlich), Langmuir, first- and n th order kinetic, second-order kinetic, and irreversible reactions. For all retention mechanisms used, their simulation results indicated that solute breakthrough curves (BTCs) were similar regardless of the layering sequence in a soil profile. This finding is consistent with earlier finding of Selim et al. (1977) and contrary to that of Bosma and van der Zee (1992) for nonlinear adsorption.

In the subsequent section, we present general equations for solute transport in multilayered systems followed by a discussion of the various choices of boundary conditions at the interface between layers. We further present selected case studies of linear and nonlinear adsorption mechanisms in layered soil systems based on numerical simulations for a range of soil properties and fluxes (or Brenner numbers). Experimental results based on miscible displacements from packed sand-clay soil column for a tracer (tritium) and for reactive solutes (Ca and Mg) BTCs are subsequently presented in support of theoretical findings.

Convection-dispersion equation

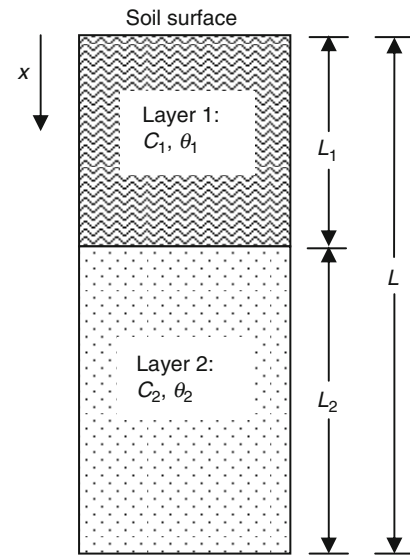
A two-layered soil column of length L is shown in Figure 1. The length of each layer is denoted by L_1 and L_2 , respectively. To show heterogeneity, each soil layer has specific, but not necessarily the same water content, bulk density, and solute retention properties. Only vertical direction steady-state water flow perpendicular to the soil layers (Figure 1) will be considered. The convective-dispersive equation (CDE) governing solute transport in the i th layer (see Figure 1) is given by Equation 1 (Selim et al., 1977):

$$\rho_i \frac{\partial S_i}{\partial t} + \theta_i \frac{\partial C_i}{\partial t} = \frac{\partial}{\partial x} \theta_i D_i \frac{\partial C_i}{\partial x} - q \frac{\partial C_i}{\partial x} - Q_i \quad (1)$$

$$(0 \leq x \leq L_i, i = 1, 2)$$

where (omitting the i) C = resident concentration of solute in soil solution ($\mu\text{g cm}^{-3}$), S = amount of solute adsorbed by the soil matrix ($\mu\text{g g}^{-1}$), ρ = soil bulk density (g cm^{-3}), θ = volumetric soil water content ($\text{cm}^3 \text{cm}^{-3}$), D = solute dispersion coefficient ($\text{cm}^2 \text{day}^{-1}$), q = Darcy soil-water flow velocity (cm day^{-1}), Q = a sink or source for irreversible solute interaction ($\mu\text{g cm}^{-3} \text{day}^{-1}$), x = distance from the soil surface (cm), and t = time (day).

The reversible solute retention from the soil solution is represented by the term $\partial S / \partial t$, on the left side of Equation 1 while the irreversible solute removed from soil solution is expressed by the term Q on the right side of Equation 1.



Layered Soils, Water and Solute Transport,
Figure 1 Schematic diagram of a two-layered soil.

Boundary condition at the interface

An important boundary condition needed in the analysis of multilayered soils is that at the interface between layers. It should be noted that both first-type and third-type boundary conditions are applicable at the interface. Leij et al. (1991) showed that although the principle of solute mass conservation is satisfied, a discontinuity in concentration develops when a third-type interface condition is used. On the other hand, a first-type interface condition will result in a continuous concentration profile across the boundary interface at the expense of solute mass balance. To overcome the limitations of both first- and third-type conditions, a combination of first- and third-type condition was implemented. The first-type condition can be written as

$$C_I|_{x \rightarrow L_1^-} = C_{II}|_{x \rightarrow L_1^+}, \quad t > 0 \quad (2)$$

where $x \rightarrow L_1^-$ and $x \rightarrow L_1^+$ denote that $x = L_1$ is approached from the upper layer and lower layer respectively. Similarly, the third-type condition can be written as

$$\left(qC_I - \theta_I D_I \frac{\partial C_I}{\partial x} \right) \Big|_{x \rightarrow L_1^-} = \left(qC_{II} - \theta_{II} D_{II} \frac{\partial C_{II}}{\partial x} \right) \Big|_{x \rightarrow L_1^+}, \quad t > 0 \quad (3)$$

Incorporation of Equation 6 into Equation 7 yields

$$\theta_I D_I \frac{\partial C_I}{\partial x} \Big|_{x \rightarrow L_1^-} = \theta_{II} D_{II} \frac{\partial C_{II}}{\partial x} \Big|_{x \rightarrow L_1^+}, \quad t > 0 \quad (4)$$

The BC of [Equation 4](#) was first proposed by Zhou and Selim ([2001](#)) and resembles that for a second-type BC as indicated earlier by Leij et al. ([1991](#)).

Equilibrium retention models

The form of solute retention reactions in the soil system must be identified if prediction of the fate of reactive solutes in the soil using the convection-dispersion [Equation 7](#) is sought. The reversible term $(\partial s/\partial t)$ is often used to describe the rate of sorption or exchange reactions with the solid matrix. Sorption or exchange has been described by either instantaneous equilibrium or a kinetic reaction where concentrations in solution and sorbed phases vary with time. Linear, Freundlich, and one- and two-site Langmuir equations are perhaps the most commonly used to describe equilibrium reactions. In the subsequent sections, we discuss Freundlich and Langmuir reactions and their use in describing equilibrium retention. This is followed by kinetic type reactions and their implication for single and multireaction retention and transport models (see [Table 1](#)).

Linear adsorption

[Figure 2](#) shows a comparison of breakthrough curves (BTCs) for a two-layered soil column with reverse layering orders. Here we report results for a layered soil column where one layer is nonreactive ($R = 1$) and the other is linearly adsorptive. For the case of linear adsorption, a dimensionless retardation factor can be obtained from [Equation 1](#) and is given by

$$R = 1 + \frac{\rho K_d}{\theta} \quad (5)$$

Here for the case where $K_d = 0$, the retardation factor R equals 1 and solute is considered nonreactive. The BTC for the case $R1 \rightarrow R2$ where the nonreactive layer was first encountered (top layer) was similar to that when the layering sequence was reversed ($R2 \rightarrow R1$) and the reactive layer ($R2$) was the top layer. Therefore, for the linear adsorption case, one concludes that the order of soil

Layered Soils, Water and Solute Transport, Table 1 Selected equilibrium and kinetic type models for solute retention in soils (Adapted from Selim and Amacher ([1997](#)), with permission)

Model	Formulation ^a
Equilibrium type	
Linear	$S = K_d C$
Freundlich (nonlinear)	$S = K_f C^b$
Langmuir	$S/S_{\max} = \frac{\omega C}{(1+\omega C)}$
Kinetic type	
First order	$dS/dt = k_f (\theta / \rho) C - k_b S$
<i>n</i> th order	$dS/dt = k_f (\theta / \rho) C^n - k_b S$
Irreversible (sink/source)	$dS/dt = k_s (\theta / \rho) (C - C_p)$
Langmuir kinetic	$dS/dt = k_f (\theta / \rho) C (S_{\max} - S) - k_b S$
Second order	$dS/dt = k_f \phi (\theta / \rho) C - k_b S$

^a K_d , K_f , k_b , k_f , k_s , n , S_{\max} , C_p , and ω are adjustable model parameters.

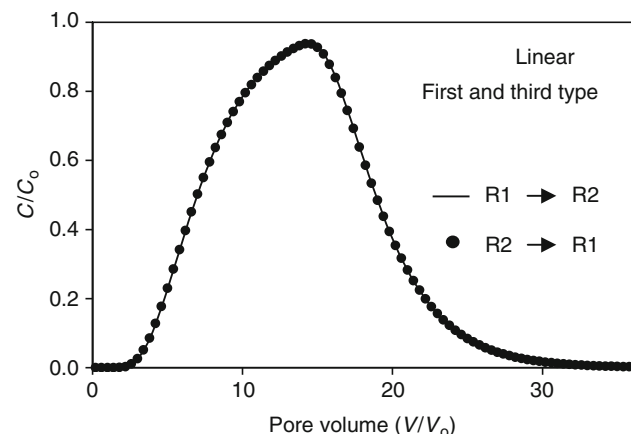
stratification or layering sequence fails to influence solute BTCs and consistent with those reported earlier by Shamir and Harleman ([1967](#)) and Selim et al. ([1977](#)) for systems with two or more layers. Based on these results, a layered soil profile could be regarded as homogeneous with an average retardation factor used to calculate effluent concentration distributions. An average retardation factor \bar{R} for N -layered soil can simply be obtained from

$$\bar{R} = \frac{1}{L} \sum_{i=1}^N R_i L_i \quad (6)$$

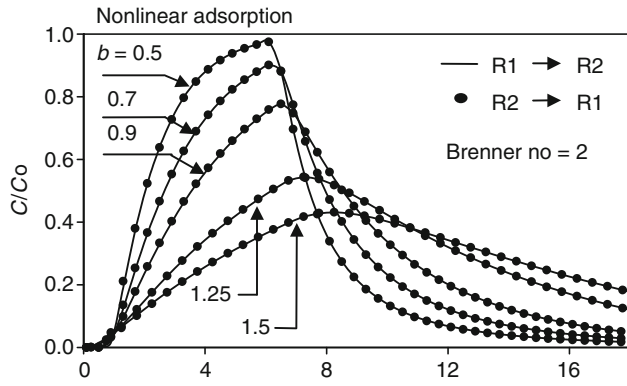
BTCs identical to those in [Figure 2](#) were obtained using the solution to the convection-dispersion [Equation 7](#) presented by van Genuchten and Alves ([1982](#)) and an average retardation factor. This averaging procedure ([Equation 6](#)) can also be used to describe the BTCs from a soil profile composed of three or more layers. However, if solute distribution within the profile is desired, the use of an average retardation factor is no longer valid and the problem must be treated as a multilayered case.

Nonlinear Freundlich adsorption

Simulated BTCs of solutes from a two-layered soil system with one as a nonlinear (Freundlich) adsorptive layer are given in [Figure 3](#). Here, $R1$ represents a nonreactive layer whereas $R2$ stands for a nonlinear (Freundlich) adsorptive layer. Our simulations were carried out for a wide range of the Peclet or Brenner number ($B = qL/\theta D$). We also examined the influence of the nonlinear Freundlich parameter b (see [Table 1](#)) on the shape of the BTCs. For most reactive chemicals, including pesticides and trace elements b is always less than unity (Selim and Amacher, [1997](#)). Based on our simulations, BTCs were not influenced by the layering sequences regardless of the Brenner number B .



Layered Soils, Water and Solute Transport, [Figure 2](#) Simulated breakthrough results for a two-layered soil column under different layering orders ($R1 \rightarrow R2$ and $R2 \rightarrow R1$). Here $R1$ is for a nonreactive layer and $R2$ is for a reactive layer with linear adsorption.



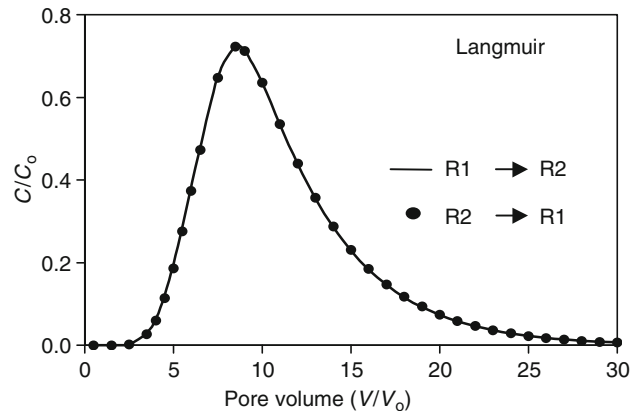
Layered Soils, Water and Solute Transport,

Figure 3 Simulated breakthrough results for a two-layered soil column under different layering orders ($R1 \rightarrow R2$ and $R2 \rightarrow R1$). Here $R1$ is for a nonreactive layer and $R2$ is a reactive layer with nonlinear adsorption with b values (Equation 11) of 0.5, 0.7, 0.9, 1.25, and 1.5. The Brenner numbers B used was 2.

when nonlinear Freundlich adsorption was considered. This result is similar to that of Selim et al. (1977). Dispersion becomes the dominant process in the case where the Brenner number is small whereas convection becomes the dominant process for large B values. The BTCs exhibit increasing retardation or delayed arrival, and excessive tailing of the right-hand side of the BTCs for increasing values of nonlinear adsorption parameter b . In addition, the BTCs become less spread (i.e., a sharp front) with increasing Brenner numbers. All such cases provide similar observations, i.e., the effects of nonlinearity of adsorption are clearly manifested. Nevertheless, for all combinations of b and the Brenner number B used in our simulations, the BTCs under reverse layering orders showed no significant differences. In other words, layering order is not important for solute breakthrough in layered soils with nonlinear adsorptive as the dominant mechanism in one of the layers. Zhou and Selim (2001) arrived at similar conclusions for layered soil profiles when several retention mechanisms of the kinetic reversible and irreversible type were considered.

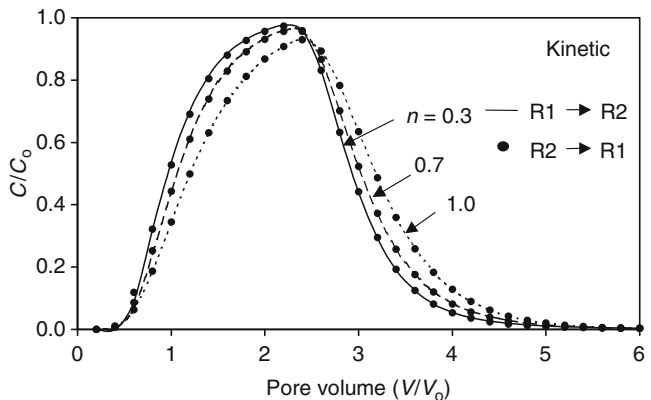
Langmuir

In order to illustrate the universal validity of the above finding, other solute adsorption processes of the nonlinear type were investigated. Langmuir adsorption model is perhaps one of the most commonly used equilibrium formulation for describing various reactive solutes in porous media. We only considered simulated columns consisting of one nonreactive layer and one reactive layer with Langmuir-type adsorption mechanism. The simulation results are shown in Figure 4. The combined first- and third-type BC was used at the interface between the layers. Consistent with the above finding, we found that for all parameters used in this study, the layering sequence has no effect on the BTCs when Langmuir-type adsorption was the dominant mechanism.



Layered Soils, Water and Solute Transport,

Figure 4 Simulated breakthrough results for a two-layered soil column under different layering orders ($R1 \rightarrow R2$ and $R2 \rightarrow R1$). Here $R1$ is for a nonreactive layer and $R2$ is for a reactive layer with Langmuir adsorption.



Layered Soils, Water and Solute Transport,

Figure 5 Simulated breakthrough results for a two-layered soil column under different layering orders ($R1 \rightarrow R2$ and $R2 \rightarrow R1$). Here $R1$ is for a nonreactive layer and $R2$ is for a reactive layer with kinetic adsorption with $n = 0.3, 0.7$, and 1.0, respectively. A second-type boundary condition (BC) was used at the interface.

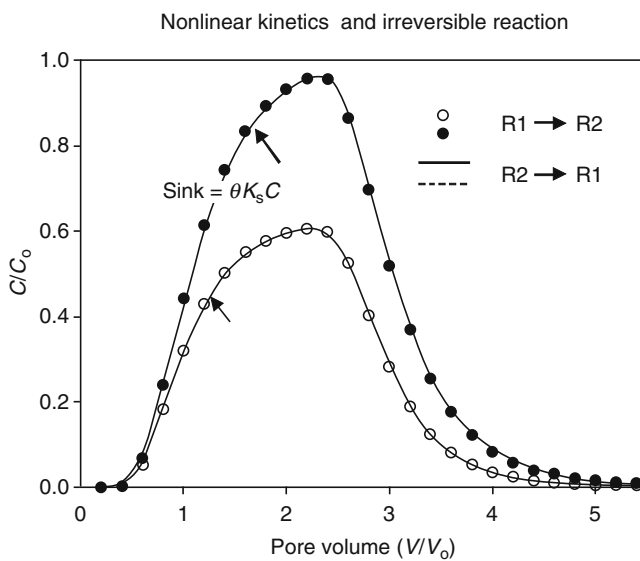
Kinetic retention

In this section, first and n th order reversible kinetics (see Table 1) was considered as the dominant retention mechanism. Values of the reaction order n used were 0.3, 0.7, and 1.0. The BTCs under reverse layering orders showed a very good match regardless of the value of the nonlinear parameter n . For all cases, a good match was also realized (see Figure 5). We also carried out simulations where both layers were assumed reactive. Other retention mechanisms considered included irreversible reaction as well as second-order mechanism. Regardless of the retention mechanism, simulations results indicated that layered soils with reverse layering orders showed BTCs no

significant differences. For example, in the presence of a sink term, the order of soil layers did not influence the shape or the position of the BTCs as illustrated in Figure 6. This finding is consistent with that of Selim et al. (1977) where a similar sink term was implemented.

Water-unsaturated soils

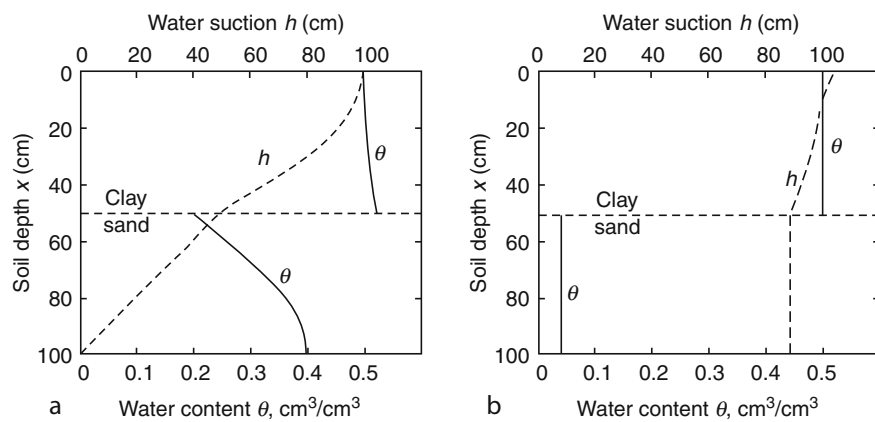
Selim et al. (1977) simulated solute transport through water unsaturated multilayered soil profiles, where a



Layered Soils, Water and Solute Transport, Figure 6 Simulated breakthrough results for a two-layered soil column under different layering orders ($R1 \rightarrow R2$ and $R2 \rightarrow R1$). Here $R1$ is for a nonreactive layer adsorption and $R2$ is a reactive layer with n th order kinetic adsorption and irreversible sink.

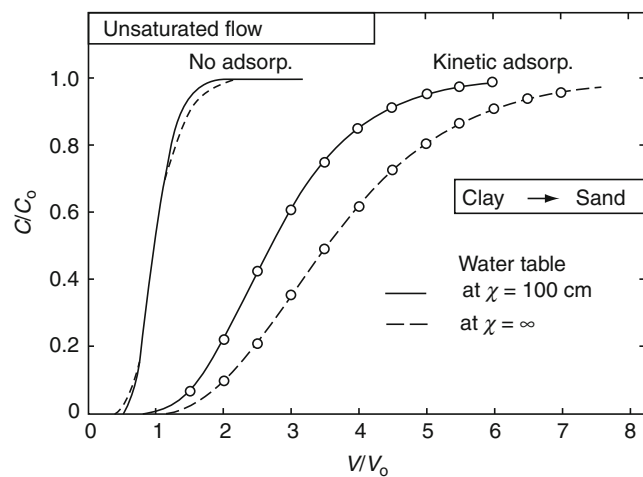
steady vertically downward water flow ($q = \text{constant}$) was considered. A soil profile was assumed to consist of two distinct layers, sand and clay, each having equal lengths and was underlain by a water table at a depth $L = 100 \text{ cm}$. The case where the water table was at great depth ($z \rightarrow \infty$) was also considered. When a constant flux was assumed, the steady-state θ and water suction (h) distributions for a sand–clay and a clay–sand soil profile were calculated (see Figure 7 for the sand–clay case). Solute concentration versus pore volume of effluent (collected at 100-cm depth) for a nonreactive and reactive solute having linear (equilibrium) retention is shown in Figure 7. As expected, similar BTC results for the nonreactive solute for sand–clay or clay–sand soil profiles were obtained. In contrast, BTCs for the reactive solute show a distinct separation, with lower retardation factors for the soil profiles having a water table at $z = 100 \text{ cm}$ than at $z \rightarrow \infty$. This observation is consistent for the sand–clay as well as clay–sand profiles. Due to the higher water contents in the soil profiles where the water table was at $x = 100$, the retardation factor R is less in comparison to the case where the water table was at great depth ($z \rightarrow \infty$).

If the water content distributions were considered uniform, with an average water content within each individual layer (see Figure 8), the problem of solute transport and retention through unsaturated multilayered soil profiles can be significantly simplified as discussed in the previous section. The open circles in Figure 8 are calculated results of concentration distributions for the reactive and nonreactive solutes when an average water content within each layer was used. These results show that, for all unsaturated profiles considered, the use of average water contents (open circles) provided identical concentration distributions to those obtained where the actual water content distributions were used (dashed and solid lines). Thus, when a steady water flux is maintained through the profile, BTCs of reactive and nonreactive solutes at a given



Layered Soils, Water and Solute Transport, Figure 7 Simulated soil–water content θ and water suction h versus depth in a clay–sand profile having a water table (a) at 100-cm depth and (b) great depth.

location in the soil profile can be predicted with average water contents within unsaturated soil layers. Based on the above results, we can conclude that average micro-hydrologic characteristics for a soil layer can be used to describe the movement of solutes leaving a multilayered soil profile. This conclusion supports the assumption made earlier that uniform soil water content can be used to represent each soil layer in order to simplify the solute transport problem. However, such a simplifying approach was not applicable for the general case of transient water-flow conditions of unsaturated multilayered soils. As illustrated by Selim (1978), the transport of reactive, as well as nonreactive, solutes through multilayered soils,

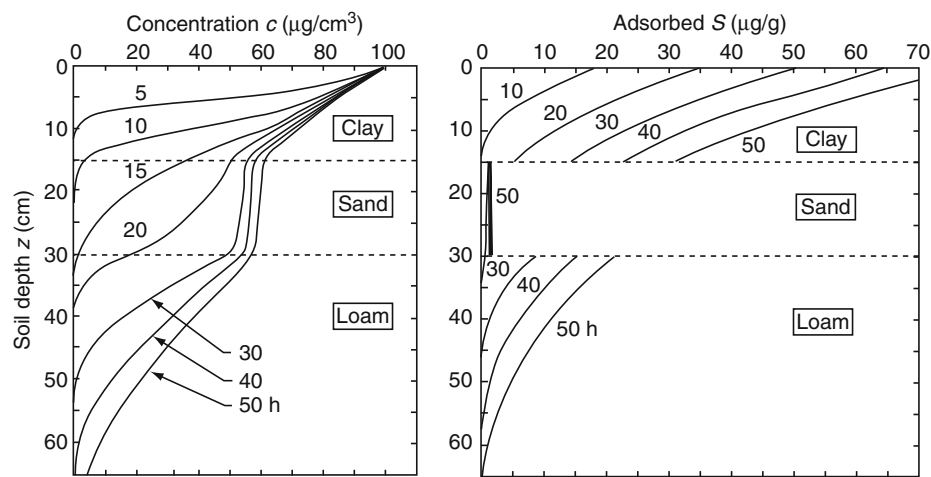


Layered Soils, Water and Solute Transport,
Figure 8 Simulated effluent concentration distribution for reactive and nonreactive solutes in an unsaturated clay–sand profile. Open circles are based on average water content θ for each soil layer.

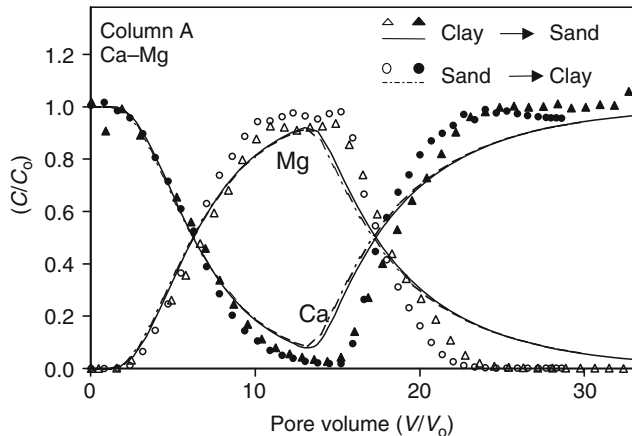
for transient water flow, was significantly influenced by the order in which the soil layers were stratified.

Solute transport in a three-layered soil profile (clay over sand over loam) is shown in Figure 9. In this example, we illustrate solute transport during water infiltration in an unsaturated soil (see Selim, 1978). Here application of a solute solution at the soil surface was assumed for an extended period of time; i.e., continuous application. The reactivity of individual soil layers to the applied solute was assumed to follow first-order kinetics. Because of slow kinetic adsorption, the amount of solute adsorbed S continued to increase with time in the clay layer in comparison to the other two layers. Such a slow adsorption resulted in a decrease of solute concentration with soil depth in the clay layer. In contrast, a somewhat uniform distribution was observed for the sand layer accompanied by an increase in the loam layer. Solute transport during infiltration and water redistribution was investigated for several other combinations of soil layer stratifications and the results indicated that solute transport through multilayered soil was significantly influenced by the order in which the soil layers are stratified.

Examples of experimental and predicted BTC results based on miscible displacements from packed soil columns having two layers are shown in Figures 10 and 11. Predictions and experimental BTC results for tritium are shown in Figure 11 (solid and dashed lines) for a sand–clay and clay–sand sequence and they indicate a good match of the experimental data. All input parameters were directly based on our experimental measurements and support our earlier findings. Zhou and Selim (2001) simulated the breakthroughs of Ca and Mg using a two-layered model for reactive solutes. The simulation results are shown in Figure 10 (solid and dashed lines for different layering arrangements) where the reaction mechanism for the Ca–Mg system was assumed to be governed by simple ion exchange for a binary system:

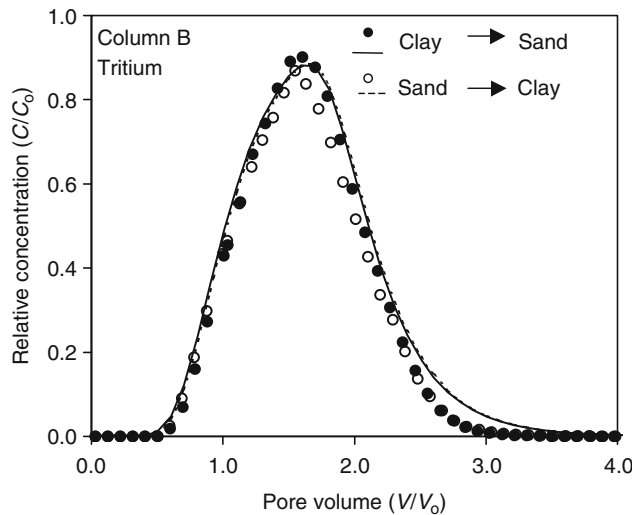


Layered Soils, Water and Solute Transport, Figure 9 Solute concentration and amount of solute absorbed versus soil depth in a three-layered soil profile with first-order kinetic retention reactions.



Layered Soils, Water and Solute Transport,

Figure 10 Experimental (symbols) and simulated (dashed and solid lines) breakthrough results for Ca and Mg in a two-layered soil column (Sharkey clay → sand, column A) under different layering sequences.



Layered Soils, Water and Solute Transport,

Figure 11 Experimental (symbols) and simulated (dashed and solid lines) breakthrough results for tritium in a two-layered soil column (Sharkey clay → sand, column B) under different layering orders.

$$S = \frac{K_{12}cS_T}{1 + (K_{12} - 1)c} \quad (7)$$

where c is relative concentration (C/C_0), K_{12} is the selectivity coefficient (dimensionless), and S_T is the cation exchange capacity (CEC). The simulation curves agree with the experimental data, especially for the adsorption front and also exhibit tailing of the release curve for both Ca and Mg. Such tailing was not observed based on the experimental data, however. Results for nonreactive

tracer solute are shown in Figure 11. Here experimental (symbols) and simulated (dashed and solid lines) breakthrough results for tritium in a two-layered soil column (Sharkey clay → sand, column B) under different layering orders are presented and clearly illustrate that the order of layering does not influence solute transport under steady flow conditions.

Summary and a look ahead

Water and solutes in soils is dependent on the layering of the soil profile. Specifically, physical and chemical properties of individual soil layers as well as the sequence of layering dictate the behavior of water and reactive chemicals in the soil profile. Based on mathematical analyses and laboratory experiments, solute transport is independent of the order of soil layers. This finding is applicable for reversible and irreversible solute reactions of the equilibrium and kinetic types. These reactions include Freundlich, Langmuir, and reversible and irreversible first- and n th order kinetics. Furthermore, simplified approaches can be used to quantify the transport of reactive chemicals in soil profile, if equilibrium type reactions of the linear type are dominant for individual soil layers. Future research should include soil profiles where the layers are not horizontally stratified. Inclined soil layers are common and observed in hilly regions and sloping soils. Areas within delta regions, the soil surface as expected should be nearly flat, however. Preferential flow or flow in fractured media with multiple porosities (macro- and meso-pores) is another area for future research of water and solute transport in layered soils.

Bibliography

- Barry, D. A., and Parker, J. C., 1987. Approximations for solute transport through porous media with flow transverse to layering. *Transport in Porous Media*, **2**, 65–82.
- Bosma, W. J. P., and van der Zee, S. E. A. T. M., 1992. Analytical approximations for nonlinear adsorbing solute transport in layered soils. *Journal of Contaminant Hydrology*, **10**, 99–118.
- Guo, L., Wagenet, R. J., Hutson, J. L., and Boast, C. W., 1997. Nonequilibrium transport of reactive solutes through layered soil profiles with depth-dependent adsorption. *Environmental Science & Technology*, **31**, 2331–2338.
- Leij, F. J., and Dane, J. H., 1989. Analytical and numerical solutions of the transport equation for an exchangeable solute in a layered soil. Agronomy and Soils Departmental Series No. 139. Alabama Agricultural Experimental Station, Alabama: Auburn University.
- Leij, F. J., Dane, J. H., and van Genuchten, M Th., 1991. Mathematical analysis of one-dimensional solute transport in a layered soil profile. *Soil Science Society of America Journal*, **55**, 944–953.
- Selim, H. M., 1978. Transport of reactive solutes during transient unsaturated water flow in multilayered soils. *Soil Science*, **126**, 127–135.
- Selim, H. M., and Amacher, M. C., 1997. *Reactivity and Transport of Heavy Metals in Soils*. Boca Raton: CRC/Lewis.
- Selim, H. M., Davidson, J. M., and Rao, P. S. C., 1977. Transport of reactive solutes through multilayered soils. *Soil Science Society of America Journal*, **41**, 3–10.

- Shamir, U. Y., and Harleman, D. R. F., 1967. Dispersion in layered porous media. *Proceedings of the American Society Civil Engineers, Hydraulic Division*, **93**, 237–260.
- Van der Zee, S. E. A. T. M., 1994. Transport of reactive solute in soil and groundwater. In Adriano, D. C., Iskandar, I. K., and Murarka, I. P. (eds.), *Contamination of Groundwaters*. Boca Raton: St. Lucie, pp. 27–87.
- van Genuchten, M. Th., and Alves, W. J., 1982. Analytical solutions of the one-dimensional convective-dispersive solute transport equation. US Department of Agriculture Bulletin No. 1661.
- Wu, Y. S., Kool, J. B., and Huyakorn, P. S., 1997. An analytical model for nonlinear adsorptive transport through layered soils. *Water Resources Research*, **33**, 21–29.
- Zhou, L., and Selim, H. M., 2001. Solute transport in layered soils: nonlinear kinetic reactivity. *Soil Science Society of America Journal*, **65**, 1056–1064.

Cross-references

- [Leaching of Chemicals in Relation to Soil Structure](#)
[Soil Water Flow](#)
[Solute Transport in Soils](#)

LEACHING OF CHEMICALS IN RELATION TO SOIL STRUCTURE

Tom M. Addiscott
 Soil Science Department, Rothamsted Research,
 Harpenden, Herts, UK

Synonyms

Channelling; Effect of soil structure on leaching; Mobile/immobile transport; Leaching; Lixivation; Ped structure; Short-circuiting; Soil structure; Pore structure; Transport

Definition

Leaching – washing out soluble chemicals or other materials from the soil by water percolating through the soil. This can be strongly influenced by the structure of the soil. The term “leaching” is sometimes used to describe the washing out chemicals sorbed on soil particulate matter from the soil, but the more general term “transport” may be more appropriate.

History of the topic

The *Oxford English Dictionary* suggests that the word “leach” was first used in about 1800 but that it initially referred to the leaching of solutes from ash. The application of the term must have passed readily from ash to soil. The idea that the soil structure had an influence on leaching can be traced back to the studies of Lawes et al. (1882). They deduced the existence of mobile and immobile categories of water in the soil from their measurements of nitrate and water passing through the soil of the Broadbalk Experiment at Rothamsted to the drains.

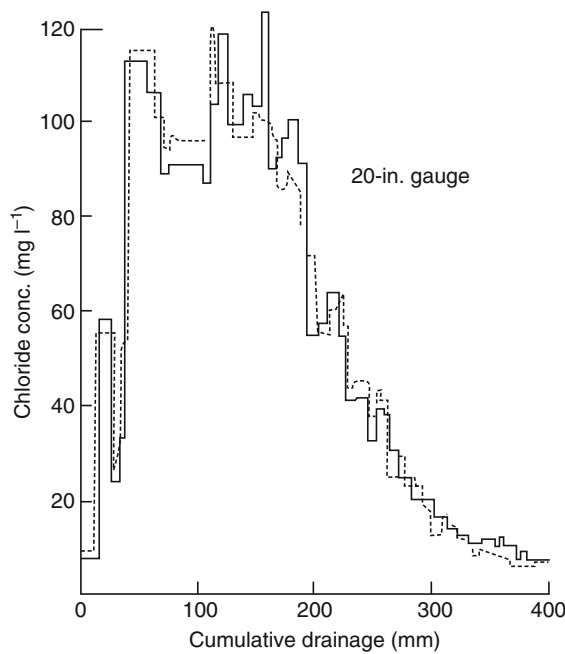
This discovery seems to have remained forgotten for many years, and a number of leaching experiments were made, mainly in the USA in the 1960s, in which the soil

was sieved to a uniform size and leached in a fairly small column (e.g., Nielsen and Biggar, 1961), thereby eliminating the effects of its structure. However, McMahon and Thomas (1974) published an important paper in the USA, showing that the movement of chloride and tritiated water in a column of sieved soil differed very considerably from the movement in a column of the same soil undisturbed, indicating a clear structural influence on leaching. They found the effect in three contrasting soils.

Not long after the McMahon and Thomas paper was published, another of the Rothamsted experiments set up by Lawes and Gilbert provided strong evidence of mobile and immobile water in the soil. The three drain gauges at Rothamsted, constructed in 1870, were designed to measure the quantity of drainage through 20, 40, or 60 in. of soil (0.5, 1, or 1.5 m), their surface area being 1/1,000 acre (4.047 m²). The gauges would be described as lysimeters today. It says much for the scientific foresight of Lawes and Gilbert that they realized that disturbing the structure of the soil would alter the passage of water through the soil, and they constructed the gauges in a way that minimized soil disturbance. Natural blocks of soil were isolated by brick walls and undermined and supported such that collectors for the drainage could be installed. What Lawes and Gilbert do not seem to have realized is that the air–water interface at the base of the soil would have some effect on the pattern of drainage.

Lawes and Gilbert had in effect constructed an almost ideal facility for an experiment on leaching in structured soil, but that experiment was not to be made for more than 100 years. In 1974, D.A. Rose and J. Bolton applied chloride to the 20- and 60-in. gauges and analyzed the drainage for chloride. Plotting the chloride concentration against cumulative drainage for the 20-in. gauge gave the relation shown in Figure 1 (Addiscott et al., 1978), which bore no resemblance at all to the smooth bell-shaped curves obtained in leaching experiments with sieved soil.

The shape of the relation was interpreted by these authors as depending on the changing distribution of chloride within the soil profile and the retention of either chloride or water containing little chloride in the immobile phase. (The term phase is used for convenience and not with the specific meaning given to it by Willard Gibbs.) When most of the chloride was still in the upper part of the profile, large rainfall events tended to cause large concentrations of chloride to “shoot through” into the drainage via the mobile phase. Re-equilibration in the lower part of the profile brings the concentration in the mobile phase back toward the previous concentration in the immobile phase, so that a subsequent small rainfall causes drainage with a small chloride concentration. The situation is reversed when the bulk of the chloride has moved to the lower part of the profile, so that small amounts of rain after large ones give small peaks during the overall decline. In the left-hand side of the diagram, the bulk of the chloride is in the upper part of the profile, whereas in the right-hand side it is in the lower part. Figure 1 thus



Leaching of Chemicals in Relation to Soil Structure,
Figure 1 Relationship between chloride concentration and cumulative drainage in the 20-in. drain gauge. *Solid line:* Measured. *Broken line:* Simulated. Note: By the time drainage had ceased, only 79.5% of the applied chloride had emerged, so the simulation assumes that only 79.5% was applied. (Adapted from Addiscott et al., 1978, Figure 2. Reproduced with the permission of the Ann Arbor Press.)

shows very clearly the kind of effect soil structure can have on leaching.

The Broken line in Figure 1 shows a simulation of the data with Addiscott's (1977) SL3 model. This was a simple layer model in which each layer had a mobile and an immobile phase and it included a routine that enabled incoming rainfall to displace the mobile water down through more than one layer according to the amount of rain. Thus, a 20-mm rainfall event could possibly move mobile water down five or more layers, which would have been about half the depth of the gauge. The fairly good fit of the simulation to the data suggests that the interpretation of the data in the previous paragraph is broadly correct. There can be no doubt that the soil in the drain gauge contains both mobile and immobile water. In fact most soils do.

The relation for the 60-in. drain gauge (not shown here) is even further removed from the bell-shaped leaching curve, with more extreme peaks and troughs. This is because the soil between 20 and 60 in. largely comprises what Lawes and Gilbert called "a rather stiff clay." Water and solute movement through heavy clay soils occurs mainly through cracks and other macro-pores, with little or none passing through the clay matrix. The problem is exacerbated in some clays by the clay-absorbing water and swelling in consequence, thereby diminishing the

water pathways. One consequence of this kind of flow is that the mobile water interacts with only a small proportion of the clay matrix.

Modeling the effects of soil structure on leaching

The SL3 model outlined above can be described as a functional model (Addiscott and Wagenet, 1985). This implies that it incorporates a simplified treatment of the leaching process and makes no claim to fundamentality. In particular, it does not incorporate the convection-dispersion equation (e.g., Wagenet, 1983) in any form. Another simple approach to nonuniform solute displacement is that of Thomas et al. (1978), which uses chromatography theory.

Models based on the convection-dispersion equation are usually described as mechanistic. The first mechanistic approach to leaching in aggregated media was probably that of Passioura (1971), but the best-known mechanistic mobile/immobile leaching model is that of van Genuchten and Wierenga (1976). Indeed, this is probably the most widely known leaching model of all.

Beven and Germann (1981, 1982) were among the first to take up the challenge of modeling solute leaching in heavy clay soils with cracks or macro-pores. Jarvis and Leeds-Harrison (1987) modeled water flow in such soils and their model was adapted to include solutes (Jarvis, 1989; Matthews et al., 1997).

Movement of solutes between the mobile and immobile phases

Most solute movement between the mobile and immobile phases occurs by diffusion. But when water is imbibed by a dry ped in the immobile phase, solutes may be drawn in too. Similarly, solute could be lost from the immobile phase if an oversaturated ped released water and solute into the mobile phase. Nondiffusional movement of this kind between the phases is not discussed further here.

Diffusion

Diffusion of a solute can be measured or modeled most easily when it occurs to or from a sphere or other regular shape immersed in a fixed volume of solution that is not subject to any inputs or removals of the solute. The mathematics of the process is well established (Crank, 1956), but the necessary boundary conditions can only be realized in laboratory experiments. Rao et al. (1980a) made some interesting experiments with porous spheres and successfully simulated the results. They also incorporated their approach into a transport model (Rao et al., 1980b). But one aspect of their diffusion work points to a more general problem. They had to take very small samples of the solution bathing the porous spheres to avoid altering its volume and thence the boundary conditions. The general problem thus highlighted is that the boundary conditions necessary for the application of diffusion theory are virtually never found in the soil. The soil aggregates are neither regular in shape nor uniform in size, and whenever there is an appreciable amount of rain the

water bathing them undergoes a change in concentration, thereby disrupting the diffusion gradient.

Addiscott (1982) avoided some of these problems by developing a simple model for cubic aggregates that could accommodate aggregates of differing sizes in the batch studied as well as changes in the volume or concentration of the bathing solution, but this approach was not mathematically exact. This diffusion model was incorporated in the PEDAL leaching model (Addiscott, 1984).

Diffusion influences leaching by delaying the movement of solute to the surface of the aggregate, where it is vulnerable to leaching and this characteristic is sometimes described as "holdback." Holdback can also be seen as protecting solute-free water against invading solute.

Properties of the aggregates or peds that affect leaching by affecting holdback from diffusion

The property that most determines holdback is the size of the aggregates. According to diffusion theory, the holdback will be proportional to the square of the aggregate radius and, in practice, small aggregates give little holdback. Addiscott et al. (1983) measured diffusion of nitrate from aggregates ranging in size from 0.5–1 mm to 4–5 mm diameter and found in the largest of these categories that it took only 1,600 s, less than half an hour for 93% of the maximum possible diffusion to occur. A theoretical study on cubic aggregates using the PEDAL model (Addiscott, 1984) suggested that aggregates or peds needed to have a side length of at least 15 mm to give any appreciable amount of holdback against leaching. The pattern of rainfall had some influence on this result.

Where there is a distribution of aggregate sizes, the smallest aggregates will release the solute they contain fastest, thereby changing the diffusion gradient for larger aggregates. This implies that the nature of the distribution should be a consideration. As soil aggregates are often produced by a shattering process, their size distribution is likely to be log normal (Epstein, 1948). The PEDAL model suggested that there were appreciable differences in the pattern of leaching from uniform and normally and log-normally distributed aggregates. These patterns were themselves influenced by the pattern of rainfall.

Diffusion in perspective

There can be no doubt that diffusion plays a part in the movement of solutes between the mobile and immobile phases. However, it seems likely that the soil aggregates need to be about 15 mm in size for diffusion to provide appreciable holdback. It is worth noting that neither Addiscott's (1977) SL3 model, which produced the simulation shown in Figure 1 nor the widely used model of van Genuchten and Wierenga (1976) included an explicit treatment of diffusion between the phases. The importance of one factor, however, is emphasized by both the shape of Figure 1 and the simulations with the PEDAL model, and that factor is the pattern of rainfall.

Summary

All soils contain, to a greater or lesser extent, mobile and immobile categories of water. Clay soils show this distinction most because they tend to have the most clearly defined structure. Crumbs, peds, or other aggregates hold back solute against leaching because of the time solute takes to diffuse from the aggregates into the mobile water surrounding them. The involvement of diffusion suggests that the size distribution of the aggregates is an issue, but measurements and modeling studies suggest that aggregate size only matters when it is greater than 15 mm. The pattern of rainfall is more important. At least two computer models for leaching in soils use a "hold-back factor" rather than modeling diffusion explicitly.

Bibliography

- Addiscott, T. M., 1977. A simple computer model for leaching in structured soils. *Journal of Soil Science*, **28**, 554–563.
- Addiscott, T. M., 1982. Simulating diffusion within soil aggregates: a simple model for cubic and other regularly shaped aggregates. *Journal of Soil Science*, **33**, 37–45.
- Addiscott, T. M., 1984. Modelling the interaction between solute leaching and intra-ped diffusion in heavy clay soils. In Bouma, J., and Raats, P. A. C. (eds.), *Proceedings of the ISSS Symposium on Water and Solute Movement in Heavy Clay Soils*. Wageningen: ILRI, pp. 279–292 (ILRI Publication No 37).
- Addiscott, T. M., and Wagenet, R. J., 1985. Concepts of solute leaching in soils: a review of modelling approaches. *Journal of Soil Science*, **36**, 411–424.
- Addiscott, T. M., Rose, D. A., and Bolton, J., 1978. Chloride leaching in the Rothamsted Drain Gauges: Influence of rainfall pattern and soil structure. *Journal of Soil Science*, **29**, 305–314.
- Addiscott, T. M., Thomas, V. H., and Janjua, M. A., 1983. Measurement and simulation of anion diffusion from natural soil aggregates and clods. *Journal of Soil Science*, **34**, 709–721.
- Beven, K., 1981. Micro-, meso- and macro-porosity and channeling phenomena in soils. *Soil Science Society of America Journal*, **45**, 1245.
- Beven, K., and Germann, P. F., 1981. Water flow in macropores, II. A combined flow model. *Journal of Soil Science*, **32**, 115–129.
- Beven, K., and Germann, P. F., 1982. Macropores and water flow in soils. *Water Resources Research*, **18**, 1311–1325.
- Bouma, J., 1981. Soil morphology and preferential flow along macropores. *Agricultural Water Management*, **3**, 235–250.
- Crank, J., 1956. *The Mathematics of Diffusion*. Clarendon: Oxford, pp. 88–91.
- Epstein, B., 1948. Logarithmic-normal distribution in breakage of solids. *Industrial and Engineering Chemistry*, **40**, 2289–2291.
- Jarvis, N. J., 1989. CRACK – a model of water and solute movement. Technical description and user notes. Report 159. Division of Hydrotechnics, Department of Soil Sciences, Swedish University of Agricultural Sciences, Uppsala.
- Jarvis, N. J., and Leeds-Harrison, P. B., 1987. Modelling water movement in drained clay soil. I. Description of the model, sample output and sensitivity analysis. *Journal of Soil Science*, **38**, 487–498.
- Lawes, J. B., Gilbert, J. H., and Warington, R., 1882. On the amount and composition of drainage water collected at Rothamsted. III The quantity of nitrogen lost by drainage. *Journal of the Royal Agricultural Society of England (Series 2)*, **18**, 43–71.
- Matthews, A. M., Portwood, A. M., Armstrong, A. C., Leeds-Harrison, P. B., Harris, G. L., Catt, J. A., and Addiscott, T. M., 1997. Crack-NP. Development of a model for predicting

- pollutant transport at the Brimstone site, Oxfordshire, UK. *Soil Use and Management*, **16**, 279–286.
- McMahon, M. A., and Thomas, G. W., 1974. Chloride and tritiated water flow in disturbed and undisturbed soil cores. *Soil Science Society of America Journal*, **38**, 727–732.
- Nielsen, D. R., and Biggar, J. W., 1961. Miscible displacement I. Experimental information. *Soil Science Society of America Journal*, **25**, 1–5.
- Passioura, J. B., 1971. Hydrodynamic dispersion in porous media. I. Theory. *Soil Science*, **111**, 339–344.
- Rao, P. S. C., Jessup, R. E., Rolston, D. E., Davidson, J. M., and Kilcrease, D. P., 1980a. Experimental and mathematical treatment of nonadsorbed solute transfer by diffusion in spherical aggregates. *Soil Science Society of America Journal*, **44**, 684–688.
- Rao, P. S. C., Rolston, D. E., Jessup, R. E., and Davidson, J. M., 1980b. Solute transport in aggregated porous media. Theoretical and experimental evaluation. *Soil Science Society of America Journal*, **44**, 1139–1146.
- Thomas, G. W., Phillips, R. E., and Quisenberry, V. L., 1978. Characterization of water displacement using simple chromatographic theory. *Journal of Soil Science*, **29**, 32–37.
- Van Genuchten, M. Th., and Wierenga, P. J., 1976. Mass transfer studies in porous sorbing media. I. Analytical solutions. *Soil Science Society of America Journal*, **40**, 473–480.
- Wagenet, R. J., 1983. Principles of salt movement in soils. In Nelson, D. W., Elrick, D. E., Tanji, K. K., Kral, D. M., and Hawkins, S. H. (eds.), *Chemical Mobility and Reactivity in Soil Systems, Special Publication 11*. Madison: American Society of Agronomy.

Cross-references

- [Diffusion in Soils](#)
[Hydraulic Properties of Unsaturated Soils](#)
[Lysimeters: A Tool for Measurements of Soil Fluxes](#)
[Pore Size Distribution](#)
[Shrinkage and Swelling Phenomena in Soils](#)
[Soil Aggregates, Structure, and Stability](#)
[Soil Water Flow](#)
[Solute Transport in Soils](#)

LEAST LIMITING WATER RANGE (LLWR)

See [Soil Physical Quality](#)

LIGHT INTERCEPTION BY PLANT CANOPIES

Pierre Dutilleul
 Department of Plant Science, McGill University,
 Macdonald Campus, Ste-Anne-de-Bellevue, QC, Canada

Synonyms

Light attenuation within the leaf canopy

Definition

Beyond the simple fact that photons hit leaves, several processes must be distinguished in the interception of light

by plant canopies. Some of these processes are established before the interception itself. One is related to the spatial distribution of leaves in the air: (1) whether they are positioned horizontally or vertically, depending on the time of day and the day of the year, (2) whether they are located in the upper layer of the canopy or a lower one, and (3) whether they are small or large in size. Another is of genetic or evolutionary nature and explains why subordinate species are adapted to irradiances lower than the dominant species. A second set of processes become involved after light interception by the leaf canopy has started. Light and carbon dioxide (CO_2) are the major inputs of photosynthesis, which is basically performed at the single leaf level in higher plants. While growing, plants thus contribute to recycling of atmospheric CO_2 .

Light interception by plant canopies can be described at two levels (single leaf, canopy) and from various perspectives (physical, mathematical, statistical).

Single leaf level: Ordinarily (in C_3 plants, where CO_2 is fixed by the enzyme RuBisCo), photosynthesis is performed in the mesophyll cells, which are directly exposed to air spaces inside the leaf, and gas exchange takes place through the stomata, which are pores found in the leaf and stem epidermis.

Canopy level: Treating the canopy as two populations of leaves, sunlit and shaded, and calculating the mean irradiance of these two populations and the corresponding leaf areas provides a canopy model equation in the form of a weighted sum (Norman, 1980). The proportion of sunlit and shaded leaves is determined by the canopy extinction coefficient and the solar zenith angle.

Physical: Average penetration of light through a plant canopy is expected to decrease exponentially with decreasing height following the Beer–Lambert law, which assumes that the plant canopy is a uniform absorber of light in any horizontal layer (Monsi and Saeki, 1953). Hirose (2005) reviews extensions in which the notions of direct versus diffuse light are defined; this has links with Norman's sunlit and shaded leaves.

Mathematical: Fractals possess a non-integer dimension and are characterized by structural similarity at all scales. Fractal geometry elements were applied to study branching pattern structure. In particular, the application of the Beer–Lambert law for light interception by a plant canopy is improved by inclusion of the fractal dimension estimated from the photograph of a leafless plant (Foroutan-pour et al., 2001).

Statistical: With imaging technologies such as computed tomography (CT) scanning, it is possible to collect three-dimensional (3-D) spatial data on developing plant canopies and rebuild them, with leaves distinct from branches, on a computer (Dutilleul et al., 2005). The strong correlation between light interception and the fractal dimension of skeletonized 3-D images of branching patterns constructed from CT scanning data shows that such data contain fundamental information about canopy architecture geometry (Dutilleul et al., 2008).

Bibliography

- Dutilleul, P., Lontoc-Roy, M., and Prasher, S. O., 2005. Branching out with a CT scanner. *Trends in Plant Science*, **10**, 411–412.
- Dutilleul, P., Han, L., and Smith, D. L., 2008. Plant light interception can be explained via computed tomography scanning: demonstration with pyramidal cedar (*Thuja occidentalis*, *Fastigata*). *Annals of Botany*, **101**, 19–23.
- Foroutan-pour, K., Dutilleul, P., and Smith, D. L., 2001. Inclusion of the fractal dimension of leafless plant structure in the Beer-Lambert law. *Agronomy Journal*, **93**, 333–338.
- Hirose, T., 2005. Development of the Monsi-Saeki theory on canopy structure and function. *Annals of Botany*, **95**, 483–494.
- Monsi, M., and Saeki, T., 1953. Über den Lichtfaktor in den Pflanzengesellschaften und seine Bedeutung für die Stoffproduktion. *Japanese Journal of Botany*, **14**, 22–52.
- Norman, J. M., 1980. Interfacing leaf and canopy light interception models. In Hesketh, J. D., and Jones, J. W. (eds.), *Predicting Photosynthesis for Ecosystem Models*. Boca Raton: CRC Press, pp. 49–84.

Cross-references

- [Agrophysical Properties and Processes](#)
[Climate Change: Environmental Effects](#)
[Databases on Physical Properties of Plants and Agricultural Products](#)
[Evapotranspiration](#)
[Fractal Analysis in Agrophysics](#)
[Greenhouse Gas Fluxes: Effects of Physical Conditions](#)
[Image Analysis in Agrophysics](#)
[Microstructure of Plant Tissue](#)
[Physics of Plant Nutrition](#)
[Plant Drought Stress: Detection by Image Analysis](#)
[Remote Sensing of Soils and Plants Imagery](#)
[Soil–Plant–Atmosphere Continuum](#)
[Weather, Effects on Plants](#)

LIMING, EFFECTS ON SOIL PROPERTIES

Tadeusz Filipek

Department of Agricultural and Environmental Chemistry, University of Life Sciences, Lublin, Poland

Definition

Liming is the application of mineral calcium and magnesium compounds, mainly carbonates, oxides, hydroxides, or a mixture of them and, more rarely, silicates into acidic soils to decrease the concentration of protons (McLean, 1971; Miller et al., 1995). To be effective, a liming material must displace hydrogen, aluminum, and manganese ions from exchange sites of soil colloids and then neutralize H^+ and precipitate Al^{3+} and Mn^{2+} in soil solution (Smallidge et al., 1993; Filipek, 1994; Barak et al., 1997).

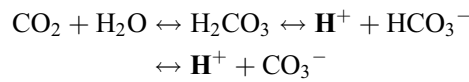
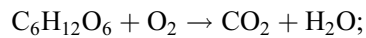
Soil acidification

Acidification of soil is a natural process, one that has a major influence on soil properties and plant growth. During soil acidification, cations of calcium, magnesium, potassium, and sodium are leached out with rainwater and

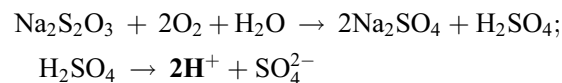
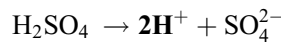
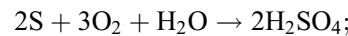
replaced by hydrogen and aluminum. Increasing soil acidity makes some nutrients less readily available, and aluminum and manganese more mobile and toxic. Soils are acidic not only due to natural causes but also due to man-made causes of acidification (Robson, 1989; Dechnik and Kaczor, 1994; Pakpe and Papen, 1998; Filipek et al., 2003; Skowrońska and Filipek, 2007).

Natural causes of acidification

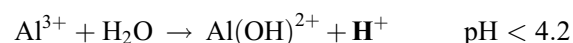
- Leaching of bases (Ca^{2+} , Mg^{2+} , K^+ , Na^+) out of root zone (in humid climate), which intensifies with increasing precipitation and concentration of nitrates as well as chlorides in soil solution; sites of displaced bases are taken up by hydrogen and aluminum ions.
- Organic and inorganic acids formed during decomposition of soil organic matter, plant residues, and soil biota:



- Plant removal of bases from soil and excretion of H^+ to maintain cation ↔ anion balance within the plant
- Microbial and chemical oxidation processes of C, S, N compounds

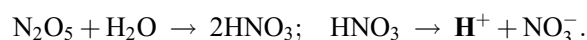
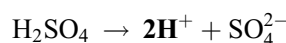


- Hydrolysis of aluminum salts as follows:



Man-made causes of acidification

- Acid precipitation as the effect of gaseous emissions (mainly SO_2 , NO_x) originating from fossil fuel combustion in power plants, industry, and motor vehicles, which return to the Earth's surface as sulfuric and nitric acids as follows:



- Application of ammonium-based fertilizers contributed to acidity since living organisms release H^+ balancing NH_4^+ cation that is taken up and a two-step (*Nitrosomonas*, *Nitrobacter*) nitrification process generates protons as follows:



Problems of very acidic soils concern aluminum toxicity to plant roots, manganese toxicity to plants, calcium and magnesium deficiency, immobilization of phosphorus and molybdenum by mobile Fe and Al, low soil microbial activity, and reduced nitrogen transformation and fixation (Persson, 1988; Robson, 1989; Filipek, 1994; Barak et al., 1997).

Limes

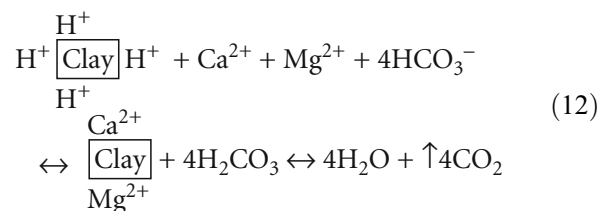
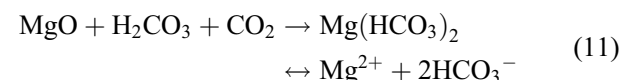
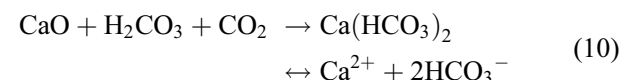
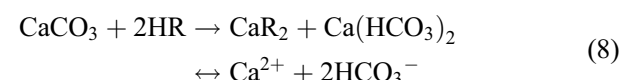
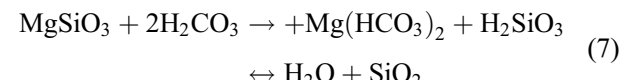
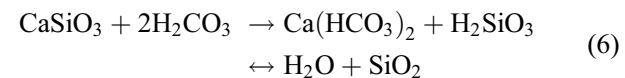
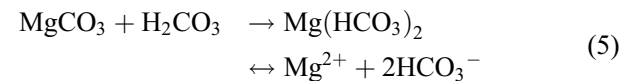
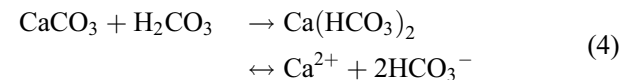
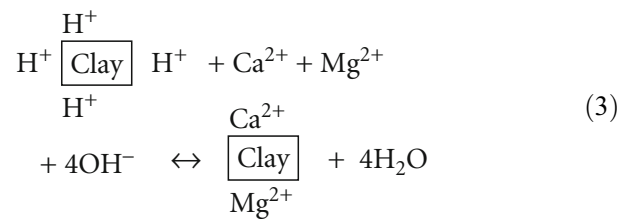
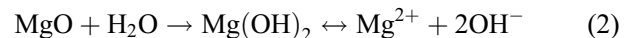
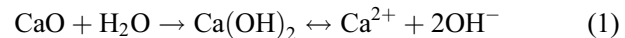
Commonly used materials to raise soil pH are calcitic lime – $CaCO_3$, dolomitic lime – $CaCO_3 \cdot MgCO_3$, manufacturing process products – CaO , MgO , $Ca(OH)_2$, $Mg(OH)_2$, and by-products containing oxides, hydroxides, carbonates, and silicates of Ca, Mg, K, and Na (Erland and Söderström, 1991; Belkacem and Nys, 1995). The quality of liming material is determined by two characteristics: the neutralizing value and fineness (Table 1). The first determines the total power of neutralizing in comparison to pure $CaCO_3$ taken as 1.00 and the second influences the rate of dissolution and neutralization. The fineness of lime determines the efficiency of soil \leftrightarrow lime reactions and, to a large extent, the rate of short-time neutralization.

Liming, Effects on Soil Properties, Table 1 Basic characteristics of limes

Liming material	Neutralizing power expressed as CaO (%)	Relative neutralizing value rate (NV)
Pure $CaCO_3$	56	1.00
Pure CaO	100	1.78
Pure $Ca(OH)_2$	76	1.35
Pure MgO	140	2.50
Pure $MgCO_3$	67	1.20
Pure $CaSiO_3$	48	0.86
Calcareous lime $CaCO_3$	40–56	0.71–1.00
Dolomitic lime $CaCO_3 \cdot MgCO_3$	50–62	0.89–1.11
Burned lime CaO	75–100	1.34–1.78
Hydrated lime, $Ca(OH)_2$	66–80	1.18–1.43
Marls $CaCO_3$ + clay + impurities	28–45	0.50–0.80
Basic slag (oxides, carbonates, silicates)	28–40	0.50–0.71
Wood ash (oxides, carbonates, silicates)	22–40	0.39–0.71
By-products (oxides, carbonates, silicates)	Variable	

Neutralization processes

Calcium or magnesium oxides, carbonates, and silicates applied into the soil reduce soil acidity (increase pH) by changing some of the hydrogen ions into water and carbon dioxide (CO_2) volatilizing into the atmosphere. A Ca^{2+} ion from the lime replaces two H^+ ions from the soil cation exchange sites. The carbon dioxide (CO_2) can react with water to form carbonate acid (H_2CO_3). Protons are neutralized by OH^- and H_2O is formed as follows:



Effect of liming on soil

Liming increases soil pH and removes toxicities of aluminum and manganese associated with acidity, and amends soil physical, physicochemical, chemical, and biological properties (Brown et al., 1959; McLean, 1971; Edmeades et al., 1981; Costa et al., 2004). Calcium cations coagulate soil organic and mineral colloids and can improve soil structure by binding together sand, silt, and clay particles into units called aggregates. Stable aggregates enhance infiltration during heavy rain. On the other hand, liming increases the resistance of the soil to pulverizing when cultivated. Aggregate structure affects other soil physical, physicochemical, and biochemical processes.

Liming affects cation exchange capacity (CEC), which depends on the amount and kind of colloids and base saturation. In general, the more the amount of clay, organic matter, and base cations present, the higher the CEC. Another lime and CEC-related property is soil buffer capacity, that is, the resistance of soil to changes in pH. A high percentage of base saturation of soil (%BS) makes soil more resistant to pH decrease.

Liming promotes the decomposition (mineralization) of soil organic matter (SOM), and consequently, it increases the mobilization of plant nutrients from the organic matter and also decreases the content of organic carbon. The increase in soil pH affects the solubility of most plant nutrients, making most of them more available (N, P, S, Mo, K, Mg, Ca) to the plant and some, less available (B, Mn, Cu, Zn).

In addition, liming a soil can affect its microbial properties. In general, increasing calcium content and pH of the soil stimulate microbial growth and influence nutrient availability and nitrogen fixation. Conversely, the increased microbial growth may result in more rapid loss of soil organic matter, which is usually viewed negatively.

The most important problems of overliming, especially tropical soils, is more physical than chemical because of soil permeability. The structure in many tropical soils is stabilized by iron and aluminum oxides binding particles together with the structure, reaching a high level of stability, accounting for the high infiltration rates, and consequent rapid leaching of bases from these soils. Adding too much lime and a high increase in soil pH can elevate molybdenum content to toxic levels. In addition, plants can become deficient in nutrients, such as P, Mg, Zn, Cu, B. This is both a result of these nutrients being less soluble at higher pH levels and decreased acid weathering of the few nutrient-containing minerals still in the soil.

Conclusions

Because of natural and man-made causes of acidification, a great percentage of natural and agriecosystem soils are acidic. Liming of acidic soils is one of the most effective methods of nutrient, soil, and environment management. The application of mineral calcium and magnesium compounds into acidic soils decreases the concentration of protons. It also removes toxicities of aluminum and

manganese, coagulates soil colloids, and improves soil structure. Liming increases cation exchange capacity (CEC) and base saturation of soil (%BS). The application of Ca and Mg compounds into soil affects mobilization/immobilization of elements and improves nutrient management in ecosystems. It makes soil more resistant to degradation and pH decrease.

Bibliography

- Barak, P., Jobe, B. O., Krueger, A. R., Peterson, L. A., and Laird, D. A., 1997. Effects of long-term soil acidification due to nitrogen fertilizer inputs in Wisconsin. *Plant and Soil*, **197**, 61–69.
- Belkacem, S., and Nys, C., 1995. Consequences of liming and gypsum top-dressing on nitrogen and carbon dynamics in acid soils with different humus forms. *Plant and Soil*, **173**, 79–88.
- Brown, A. L., Nielsen, T. R., and Halevy, E., 1959. Lime effect on soil properties studies made on the effect of massive lime application on physical properties of five types of Sacramento Valley soils. *California Agriculture*, **34**(1), 281–284. August 9–16 (online).
- Costa, F., Albuquerque, J. A., and Fontoura, S. M. V., 2004. Liming effect on electrochemical and physical properties of a no-tilled oxisol. *Ciencia Rural*, **34**(1), 281–284 (online).
- Dechnik, I., and Kaczor, A., 1994. The after-effect of simulated acid rain on some properties of brown soil. *Polish Journal of Soil Science*, **XXVII**(1), 11–18.
- Edmeades, D. C., Judd, M., and Sarathchandra, S. U., 1981. The effect of lime on nitrogen mineralization as measured by grass growth. *Plant and Soil*, **60**, 177–186.
- Erland, S., and Söderström, B., 1991. Effects of lime and ash treatments on ectomycorrhizal infection of *Pinus sylvestris* L. seedlings planted in a pine forest. *Scandinavian Journal of Forestry Research*, **6**, 519–525.
- Filipek, T., 1994. The content of exchangeable aluminium in soils and plant growth. *Journal of Ecological Chemistry*, **4**(3), 367–375. Special issue.
- Filipek, T., Fotyma, M., and Lipiński, W., 2003. Changes of acidification pressure, the use fertilizers and soil reaction in Poland during last 45 years. In *14th International Symposium of Fertilizers “Fertilizers in context with resource management in agriculture,” June 22–25, 2003, Debrecen, Hungary, Proceedings*, I, pp. 255–262.
- McLean, E. O., 1971. Potentially beneficial effects from liming: chemical and physical. *Soil Crop and Science Society of Florida Proceedings*, **31**, 189–196.
- Miller, J. D., Anderson, H. A., Harriman, R., and Collen, P., 1995. The consequences of liming a highly acidified catchment in central Scotland. *Water, Air, and Soil Pollution*, **85**, 1015–1020.
- Pakpe, H., and Papen, H., 1998. Influence of acid rain and liming on fluxes of NO and NO₂ from forest soil. *Plant and Soil*, **199**, 131–139.
- Persson, T., 1988. Effects of acidification and liming on soil biology. In Andersson, F., and Persson, T. (eds.), *Liming as a Measure to Improve Soil and Tree Condition in Areas Affected by Air Pollution*. National Swedish Environment Protection Board, Report 518, pp. 5–71.
- Robson, A. D., 1989. *Soil Acidity and Plant Growth*. Australia: Academic.
- Skowrońska, M., and Filipek, T., 2007. The acidifying potential of gaseous atmospheric pollutants (SO₂, NO_x, NH₃) and nitrogen fertilizers in Poland. *Polish Journal of Environmental Studies*, **16**(3A), 247–250.
- Smallidge, P. J., Brach, A. R., and Mackun, I. R., 1993. Effects of watershed liming on terrestrial ecosystem processes. *Environmental Reviews*, **1**, 157–171.

Cross-references

[Agrophysical Objects \(Soils, Plants, Agricultural Products, and Foods\)](#)
[Buffer Capacity of Soils](#)
[Clay Minerals and Organo-Mineral Associates](#)
[Climate Change: Environmental Effects](#)
[Fertilizers \(Mineral, Organic\), Effect on Soil Physical Properties](#)
[Leaching of Chemicals in Relation to Soil Structure](#)
[Organic Matter](#)
[Oxidation-Reduction Reactions in the Environment](#)
[Soil Aggregates](#)
[Trace Elements in Crops: Effects of Soil Physical and Chemical Properties](#)

LIQUID LIMIT (UPPER PLASTIC LIMIT, ATTERBERG LIMIT)

The water content between the liquid and plastic states of consistence of a soil.

LOADING

See [Soil Compaction and Compressibility](#)

LODGING OF CROPS

The process by which the shoots of cereals are displaced from their vertical stance.

See [Plant Lodging, Effects, and Control](#)

LYSIMETERS: A TOOL FOR MEASUREMENTS OF SOIL FLUXES

Johann Fank
 Department of Water Resources Management
 RESOURCES - Institute of Water, Energy, and
 Sustainability, Joanneum Research, Graz, Styria, Austria

Definition

The term *lysimeter* is a combination of the Greek words “*lusis*” meaning solution and “*metron*” meaning measure. A lysimeter is a device that isolates a volume of soil or earth between the soil surface and a given depth and includes a percolating water sampling system at its base. In general, a lysimeter consists of a container filled with soil and a mechanism to collect and quantify the amount of water that accumulates at the bottom (DVWK, 1980). The DIN 4049–3 (1994) (German Industrial Standard) defines a lysimeter as a device to collect seepage water for mass and solute balances in relation to soil, parent rock, vegetation, local climate, and other site conditions.

Lysimeters have a long history of development, and different designs have been adopted. Therefore, an exact definition of a lysimeter cannot be provided.

Introduction

According to the DVWK (Deutscher Verband für Wasserwirtschaft und Kulturbau) in 1980, the explanation and the use of lysimeters may be extended as follows:

- Soil is hydrologically isolated from the surrounding soil.
- Lysimeters are containers filled with disturbed (= artificially filled) or undisturbed (= monolithic) bare soil or soil covered with natural or cultivated vegetation.
- Seepage water is measured directly; vertical water movement is also to be determined.
- Percolating water is collected either gravimetrically (= gravitation lysimeter) or through suction cups/a suction plate with a negative soil water pressure head, identical to that in the field next to the lysimeter (= suction lysimeter).
- An artificial groundwater level can be simulated.
- Lysimeters are either weighable or non-weighable; weighable lysimeters provide information about the change of water storage for any time period; non-weighable lysimeters collect only the water percolating from the soil column.

Accurate crop evapotranspiration (ET) data are required to improve agricultural water resources management. Lysimeters are still considered to be the standard method to directly measure ET. Non-weighable lysimeters are used to determine ET as a residual by measuring all other components of the soil water balance, including water inputs (rain and irrigation), outputs (drainage and runoff), and change in soil water storage (Garcia et al., 2004). If the lysimeters are weighable, the current evapotranspiration can be deduced from their weight change (Young et al., 1996). The ET calculated from the mass changes, however, needs to be adjusted to account for mass changes caused by factors other than ET, such as drainage or water input (Malone et al., 2000). Meissner et al. (2007) have shown that, beside standard Lysimeter data evaluation, precise measurement of dew, fog, and rime is possible using a high-precision gravitation lysimeter. Due to these characteristics, lysimeters are an excellent tool to derive or calibrate water and solute transport models (Wriedt, 2004) for unsaturated zone simulation.

Lysimeters have been designed in different sizes, which vary significantly, and shapes including square, circular, and rectangular. The shape and the size are chosen according to the intended use and the required or desired resolution. According to method in which the soil inside the lysimeter is collected, lysimeters can be monolithic, repacked (or reconstructed), or a combination of both (Payero and Irmak, 2008).

Accurate information about the soil water balance is needed to quantify solute transfer within the unsaturated

zone. A large weighable lysimeter is the best method for obtaining reliable data about seepage-water quantity and quality. However, this method involves significant investment and additional expenses for maintenance (Meissner et al., 2007). The evaluation of lysimeter data allows a much more reliable calculation of the solute load carried toward the groundwater than any other method (Klocke et al., 1993). However, some shortcomings are assigned to lysimeter measurements, such as the well-known oasis effects, preferential flow paths at the walls of the lysimeter cylinders due to an insufficient fit of soil monoliths inside the lysimeters or the influence of the lower boundary conditions on the outflow rates.

The history of the lysimeter

There have been two distinct but interweaving strands in the use of lysimeters. The history of the lysimeter stems back over almost four centuries to the time of the natural philosophers: the development of our understanding of plant physiology and soil constraints to crop development and the understanding of field and regional hydrology (Goss and Ehlers, 2009). Philipe de la Hire (1640–1718) who was interested in discovering the origin of springs is generally recognized as the instigator of the use of lysimeters for hydrological studies. John Dalton (1766–1844) and Thomas Hoyle built their lysimeter to investigate the evaporative return from land to the atmosphere. In the year 1850, Way reported his fundamental studies on the chemical changes of solutions percolating through soil. He was the first experimenter to carry out extensive lysimeter investigations to clarify the problem of soil fertility. The first lysimeters were constructed in Rothamsted, England (1870), and were designed to retain the natural structure and profile of the soil. John Lawes (1814–1900) applied their monolithic construction to determine the quantity and chemical quality of the deep drainage component of the water balance. Improvements in technology allowed a more exact assessment of changes in the water content of the lysimeter soil by weight. The first weighing lysimeter was put together in Germany (von Seehorst, 1902). Early lysimeter studies did not attempt to differentiate between evaporation from the soil and the water moving from the soil to the atmosphere via the plant transpiration stream. The first systematic investigation of the water requirements of maize took place at the Agricultural Experimental Station of Nebraska. Water use by different crops was studied by Briggs and Shantz at Akron, Colorado, USA, between 1911 and 1913 (Goss and Ehlers, 2009).

In 1940, Kohnke and Dreibelbis conducted a critical review of the literature on lysimeters. They cited 489 findings for the period 1688–1939 and stated that lysimeters had distinct limitations. “But without doubt many questions concerning pedology, soil fertility, and hydrology can be answered by the correct use of lysimeters. Filled-in lysimeters may fulfill useful tasks in fertility investigations if a sound water balance is maintained in the soil; but for pedologic and hydrologic studies carefully designed

monolith lysimeters seem to be indispensable” (Kohnke and Dreibelbis, 1940, p. 30).

The lysimeter facilities at the North Appalachian Experimental Watershed, Coshocton, Ohio were built in 1937 and incorporated many of the essential features for studying the components of the soil water balance. Results for the water balance from the Coshocton lysimeters were compared with those of an adjacent small watershed, and were found to be highly similar (Harrold and Dreibelbis, 1967).

The use of lysimeters of smaller surface area allowed the collection of soil monoliths that could be transported to a central facility, where the weather variables were the same, thereby permitting a greater insight into how the water balance changes over time in different soils (Letcombe Laboratory, Oxfordshire, UK 1973; Brandis, Germany, 1980; German Research Center for Environmental Health, Munich 1996 and others). All the lysimeter installations described above are limited in the fact that agronomic activities associated with soil management (tillage), for example, sowing, crop protection, harvesting, residue management as well as manure management are limited to hand operation. In 1978, a large-scale field lysimeter installation was established in deep clay soil at a field site of Letcombe Laboratory near Faringdon, Oxfordshire, the UK (Cannell et al., 1984).

Lysimeters have been used extensively to determine the crop coefficients of water use, particularly the evapotranspiration relative to a reference crop, or to a standard device for measuring evaporation. In all cases, a key issue is how well the growth and water dynamics associated with the crop in the lysimeter installation accord with those of a crop in the field (Allen et al., 1991).

A survey conducted in 2004 (Lanthaler and Fank, 2005) on lysimeters used in Europe (updated in 2006) found 151 locations in Europe where lysimeter facilities were in operation. The majority of the lysimeter vessels (86.2%) are non-weighable. This strengthens the “disadvantage” of ponderable lysimeters as the weighing equipment is more expensive and in fields, weighable lysimeters are more difficult to use. Approximately 70% of the non-weighable lysimeters are backfilled, whereas 44.4% of all ponderable vessels are filled monolithically. Lysimeters in Europe are predominantly used for agricultural research (approximately 63% of all lysimeters are installed in arable land/field).

Essential concepts and applications

The need for water quality and nutrient management as well as the need for a better understanding of water drainage and chemical leaching through the vadose zone is continuing to grow. Therefore, monitoring and measuring techniques that can determine drainage flux from undisturbed soil profiles is critical for the determination of nutrient budgets and the evaluation of land-use practices on water quality (Masarik et al., 2004). Equilibrium tension lysimeters were developed by Brye et al. (1999) to address the problems associated with zero-tension

lysimeters and fixed-tension lysimeters, and can be installed below a soil profile that is intact. By adjusting lysimeter suction to match soil-water matric potential, equilibrium tension lysimeters maintain an equilibrium between lysimeters and the bulk soil.

The undisturbed extraction of a soil monolith during the filling of a lysimeter vessel is of great importance for all subsequent investigations, especially for establishing flow and transport conditions that mimic natural field conditions. An evaluation of different methods to obtain large undisturbed soil cores is provided by Derby et al. (2002). Substantial progress concerning the collection of cylindrical lysimeter monoliths is achieved by the development of an extraction technology, which cuts the outline of the soil monolith employing a rotary cutting system (Meissner et al., 2007). The new procedure avoids structural damages and substantially reduces the necessary technical expenditure during monolith extraction. The extraction site is only minimally affected, since the force needed to cut the soil monolith is small, due to reduced coat friction.

In connection with the additional recording of the amount of percolating water ($SW [l m^{-2}]$) and precipitation ($P [l m^{-2}]$) a weighing lysimeter permits the quantification of the water balance of the soil column. The change in the amount of water stored in the lysimeter ($\Delta S [l m^{-2}]$) is detected based on measuring the mass change of the soil column. Evapotranspiration ($ET [l m^{-2}]$) can be calculated at any point in time using the water balance equation (Equation 1).

$$ET = P - SW \pm \Delta S \quad (1)$$

If the water balance is calculated correctly, the solute balance can be determined for a defined time interval with sufficient accuracy using Equation 2, where $L (mg m^{-2})$ is equal to the solute load, and C_s represents solute concentration in seepage water ($mg l^{-1}$).

$$L = C_s SW \quad (2)$$

The quantification of soil water balance parameters is hardly possible when using traditional soil hydrological measurement procedures, especially in the event of flooding. Therefore, a weighable outdoor groundwater lysimeter was developed (Bethge-Steffens et al., 2004). This weighable groundwater lysimeter provides the basis for recording the water balance quantities such as precipitation, evapotranspiration, groundwater recharge, capillary rise, and interaction with the watercourse (reflected in the groundwater level). It enables an accurate quantification of the vertical water flow at floodplain sites. The modified water balance equation for groundwater-influenced and temporarily waterlogged sites is

$$P + P_{ond} = ET(R_{out} - R_{in}) \pm \Delta S \quad (3)$$

where $P_{ond} (l m^{-2})$ = surface floodwater, $R_{out} (l m^{-2})$ = groundwater outflow, and $R_{in} (l m^{-2})$ = groundwater inflow (Meissner et al., 2008).

Lysimeters are often located at a special lysimeter station with an access point for functional inspection as well as for the accommodation of measuring, checking, and weighing devices. To reduce costs and secure mobility Meissner et al. (2008) presented a polyethylene lysimeter station as a container, where four lysimeter vessels are located in a clover type arrangement around a central access point.

However there are some arguments against the use of lysimeters for monitoring water balance parameters and measuring solute transport parameters in the soil and unsaturated zone. These include the discussion of some sources of error existing potentially in lysimeter measurements, such as the well-known oasis effects, preferential flow paths at the walls of the lysimeter cylinders due to an insufficient fit of soil monoliths inside the lysimeters or the influence of the lower boundary conditions on the outflow rates. In 2004, monolithic equilibrium tension lysimeters were implemented in the Wagna agricultural test field in southern Austria (Fank and von Unold, 2007). Due to the implementation of the lysimeter directly in the agricultural field, no oasis effect is cognizable. The two scientific field lysimeters (von Unold and Fank, 2008) have a depth of 2 m and a surface area of 1 m². The precision load cells on the concrete fundament measure the lysimeters mass with a resolution of 35 g (0.035 mm water equivalent). The bottom of the lysimeter – the lower boundary condition – is realized as a suction cup rake. The soil water tension measured at 1.8 m below the surface of the undisturbed field is transferred to the suction cups that guarantee the same flow rates in the lysimeter as in the undisturbed soil using an automatically controlled vacuum pump. For tillage purposes, the load cells are lowered to the fundament and the upper ring of the lysimeter is removed. The field and the lysimeter may be cultivated in the same manner as the field. Afterward, the ring is remounted and the lysimeter is lifted onto the load cells. In April 2005, a tracer experiment was performed. Data analysis shows conservative behavior of the bromide. Mass uptake by plants was proportional to the water uptake, and the total mass recovery of bromide was >95%. Based on the evaluation of the tracing experiments, no fringe effects have been found; this finding indicates that the excavation technique done by hand causes no significant disturbance. The comparison of measured soil water parameters between a hydrologic measuring profile close to the lysimeter and the lysimeters monolith have shown that the differences are very small and reflect natural heterogeneity.

Conclusions

Based on the developments of lysimeter techniques – not of too expensive high precision weighable monolithic lysimeters – we get accurately measured water balance and solute transport parameters. Due to these characteristics, lysimeters are an excellent tool to validate the transferability of water and solute transport models, which are

mostly derived on the basis of laboratory experiments for their application on the field scale. Monolithic field lysimeters cover one scale of scientific or applied research working level, which is suited between laboratory scale and field scale. They combine the advantages of true field conditions and laboratory possibilities of varying parameters, handling, and maintenance.

From their inception, lysimeters have allowed the role of the plant in the local hydrological balance to be investigated and established. At the same time, the lysimeter has been a powerful tool in developing a greater understanding of the components of the soil water balance and allowing a detailed quantitative assessment. The ability to integrate information obtained at different levels of investigation, both in terms of scale and intensity, has resulted in a more holistic understanding of soil water dynamics. Lysimeters have allowed the quality of water draining from agricultural land to be determined, and, as exemplified by information from plant nutrient studies, the role of management practices to be evaluated (Goss and Ehlers, 2009).

Bibliography

- Allen, R. G., Pruitt, W. O., and Jensen, M. E., 1991. Environmental requirements of lysimeters. In *Lysimeters for Evapotranspiration and Environmental Measurements*. Proceedings of the International Symposium on Lysimetry Honolulu, Hawaii, July 23–25, 1991, New York: American Society of Civil Engineers, pp. 170–181.
- Bethge-Steffens, D., Meissner, R., and Rupp, H., 2004. Development and practical test of a weighable groundwater Lysimeter at floodplain sites. *Journal of Plant Nutrition and Soil Science*, **167**, 516–524, doi:10.1002/jpln.20032 1304.
- Brye, K. R., Norman, J. M., Bundy, L. G., and Gower, S. T., 1999. An equilibrium tension lysimeter for measuring drainage through soil. *Soil Science Society of America Journal*, **63**, 536–543.
- Cannell, R. Q., Goss, M. J., Harris, G. L., Jarvis, M. G., Douglas, J. T., Howse, K. R., and Le Grice, S., 1984. A study of mole drainage with simplified cultivation for autumn sown crops on a clay soil. 1. Background, experiment and site details, drainage systems, measurement of drainflow and summary of results, 1978–1980. *Journal of Agricultural Science*, **102**, 539–559.
- Derby, N. E., Knighton, R. E., and Montgomery, B. R., 2002. Construction and performance of large soil core lysimeters. *Soil Science Society of America Journal*, **66**, 1446–1453.
- DIN 4049–3 (German Industrial Standard) 1994. *Hydrologie – Begriffe zur quantitativen Hydrologie*. Berlin: Beuth.
- DVWK 1980. (German Association of Water Management, Waste-water and Waste) Empfehlungen zum Bau und Betrieb von Lysimetern. DVWK-Regeln. Heft 114. Hamburg: Parey.
- Fank, J., and von Unold, G., 2007. High-precision weighable field Lysimeter – a tool to measure water and solute balance parameters. *International Water and Irrigation*, **27**(3), 28–32. Tel Aviv.
- Garcia, M., Raes, D., Allen, R. G., and Herbas, C., 2004. Dynamics of reference evapotranspiration in the Bolivian highlands (altiplano). *Agricultural and Forest Meteorology*, **125**, 67–82.
- Goss, M. J., and Ehlers, W., 2009. The role of lysimeters in the development of our understanding of soil water and nutrient dynamics in ecosystems. *Soil Use and Management*, **25**, 213–223, doi:10.1111/j.1475-2743.2009.00230.x.
- Harrold, L. L., and Dreisel, F. R., 1967. Agricultural hydrology as evaluated by monolith lysimeters 1944–1955. U.S.D.A Technical Bulletin No. 1367. Washington, D.C.: U.S. Department of Agriculture.
- Klocke, N. L., Todd, R. W., Hergert, G. W., Watts, D. G., and Parkhurst, A. M., 1993. Design, installation, and performance of percolation lysimeters for water-quality sampling. *Transactions of the American Society of Agricultural Engineers*, **36**, 429–435.
- Kohnke, H., and Dreisel, F. R., 1940. A survey and discussion of lysimeters and a bibliography on their construction and performance. U.S. Department of Agriculture. Miscellaneous publication no. 372, 32 pp.
- Lanthaler, C., and Fank, J., 2005. Lysimeter stations and soil hydrology measuring sites in Europe – Results of a 2004 survey. *Proceedings of the 11th Gumpensteiner Lysimetertagung, Lysimetrie im Netzwerk der Dynamik von Ökosystemen*, 19–24, Irdning.
- Malone, R. W., Bonta, J. V., Stewardson, D. J., and Nelsen, T., 2000. Error analysis and quality improvement of the Coshocton weighing lysimeters. *Transactions of the American Society of Agricultural Engineers*, **43**, 271–280.
- Masarik, K. C., Norman, J. M., Brye, K. R., and Baker, J. M., 2004. Improvements to measuring water flux in the vadose zone. *Journal of Environmental Quality*, **33**, 1152–1158.
- Meissner, R., Seeger, J., Rupp, H., Seyfarth, M., and Borg, H., 2007. Measurement of dew, fog, and rime with a high-precision gravitation Lysimeter. *Journal of Plant Nutrition and Soil Science*, **2007**(170), 335–344.
- Meissner, R., Rupp, H., and Seyfarth, M., 2008. Advances in outdoor lysimeter techniques. *Water, Air, and Soil Pollution: Focus*, **8**, 217–225, doi:10.1007/s11267-007-9166-2.
- Payero, J. O., and Irmak, S., 2008. Construction, installation, and performance of two repacked weighing lysimeters. *Irrigation Science*, **26**, 191–202, doi:10.1007/s00271-007-0085-9.
- Von Seelhorst, C., 1902. Mitteilungen vom landwirtschaftlichen Versuchsfelde der Universität Göttingen. Vegetationskästen zum Studium des Wasserhaushaltes im Boden. *Journal für Landwirtschaft*, **50**, 277–280.
- von Unold, G., and Fank, J., 2008. Modular design of field lysimeters for specific application needs. *Water, Air, and Soil Pollution: Focus*, **8**, 233–242, doi:10.1007/s11267-007-9172-4.
- Wriedt, G., 2004. Modelling of nitrogen transport and turnover during soil and groundwater passage in a small lowland catchment of Northern Germany. PhD thesis, Potsdam: University of Potsdam.
- Young, M. H., Wierenga, P. J., and Mancino, C. F., 1996. Large weighing lysimeters for water use and deep percolation studies. *Soil Science Society of America Journal*, **161**, 491–501.

Cross-references

- [Agroforestry Systems, Effects on Water Balance in Cropping Zone](#)
- [Bypass Flow in Soil](#)
- [Climate Change: Environmental Effects](#)
- [Coupled Heat and Water Transfer in Soil](#)
- [Ecohydrology](#)
- [Evapotranspiration](#)
- [Hydraulic Properties of Unsaturated Soils](#)
- [Layered Soils, Water and Solute Transport](#)
- [Leaching of Chemicals in Relation to Soil Structure](#)
- [Pedotransfer Functions](#)
- [Soil Water Flow](#)
- [Soil Water Management](#)
- [Solute Transport in Soils](#)
- [Surface and Subsurface Waters](#)
- [Tensiometry](#)
- [Water Balance in Terrestrial Ecosystems](#)
- [Water Budget in Soil](#)
- [Water Use Efficiency in Agriculture: Opportunities for Improvement](#)

M

MACHINE VISION

See [Visible and Thermal Images for Fruit Detection](#)

MACHINE VISION IN AGRICULTURE

John Billingsley
University of Southern Queensland, Toowoomba, QLD, Australia

Definition

Machine vision: Visual data that can be processed by a computer, including monochrome, color and infra red imaging, line or spot perception of brightness and color, time-varying optical signals.

Agriculture: Horticulture, arboriculture and other cropping methods, harvesting, post production inspection and processing, livestock breeding, preparation and slaughter.

Introduction

The combination of low-cost computing power and applications that target its use for entertainment has led to a readily available platform for analyzing vision signals in a variety of ways. Applications are many and various, but some of the most potentially significant ones are found in agriculture.

Sorting by color

For some decades, a simplified form of machine vision has been used for sorting produce (Tao et al., 1995). Tomatoes may be picked green for ripening in the shed. When their color is changing, they ride a conveyor that has pockets for individual fruit. These holders can be tripped by a computer signal, to eject the tomato at one of many packing stations corresponding to the degree of ripeness, as defined by color.

A very similar system is used for grading apples, as seen in [Figures 1 and 2](#).

Fragments of nut shell can be detected when pecan nuts are shelled, once again by detection of the color. Kernels fall through the inspection area at a speed of around one meter per second. In an early system, light that was reflected from the kernel was split between two photocells that detected the intensity of different wavelengths. The ratio enabled color to discriminate between nut and shell. More recent versions incorporate laser scanning. As the nut falls further, a jet of air is switched to deflect any detected shell into a separate bin.

Detection of weeds

Color discrimination can also be used in the field to discriminate between plants and weeds for the application of selective spraying (Åstrand and Baerveldt, 2002; Zhang et al., 2008). It is possible for the color channels of the camera to include infra-red wavelengths, something that can be achieved by removing the infra-red blocking filter from a simple webcam. [Figure 3](#) is a low-resolution frame-grab showing one stage in the detection of a grass-like weed, “panic,” during trials in sugar cane. The computer has marked pixels determined to be “weed” in yellow.

Quality assessment

True machine vision concerns shape information. One example is the assessment of fodder quality. From a web-cam image of a sample handful of hay, the stem-widths can be measured and a histogram displayed. Color can also be determined by comparison of the video signal against that from the image of a calibration card. This makes an objective standard possible, to achieve agreement between vendor and purchaser (Dunn and Billingsley, 2007).

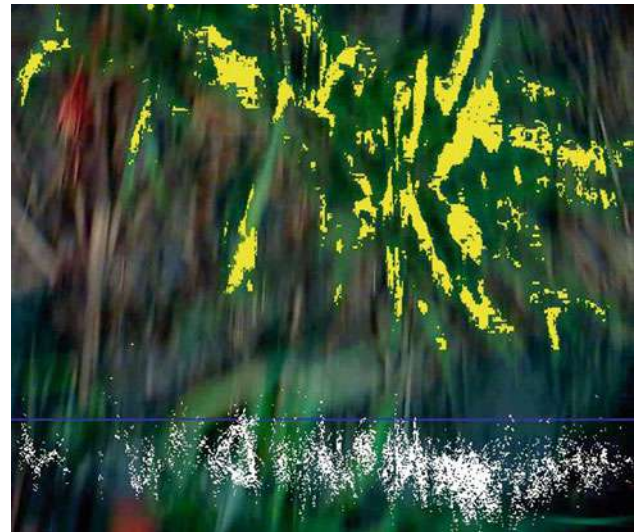
Shape information can also be used to monitor the growth of a crop, measuring stem length between nodes automatically (McCarthy et al., 2008).



Machine Vision in Agriculture, Figure 1 Apples moving towards washing and grading.



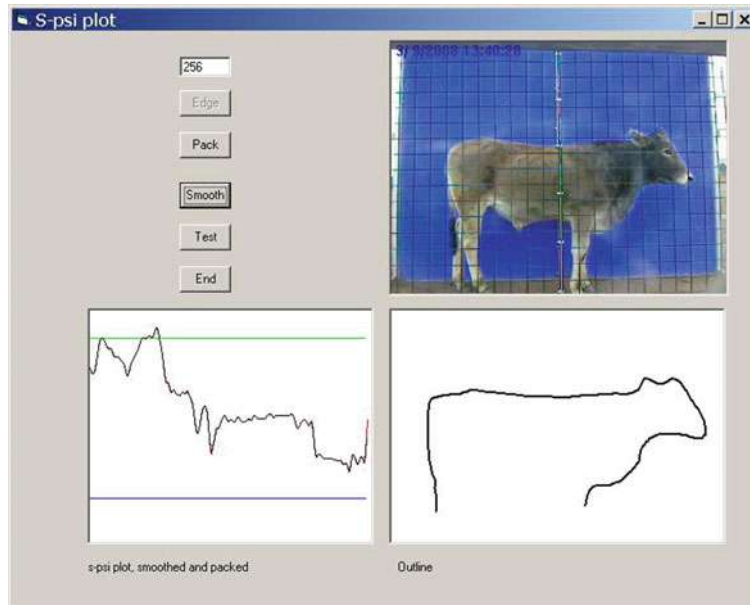
Machine Vision in Agriculture, Figure 2 A conveyor automatically ejects each apple at the correct station.



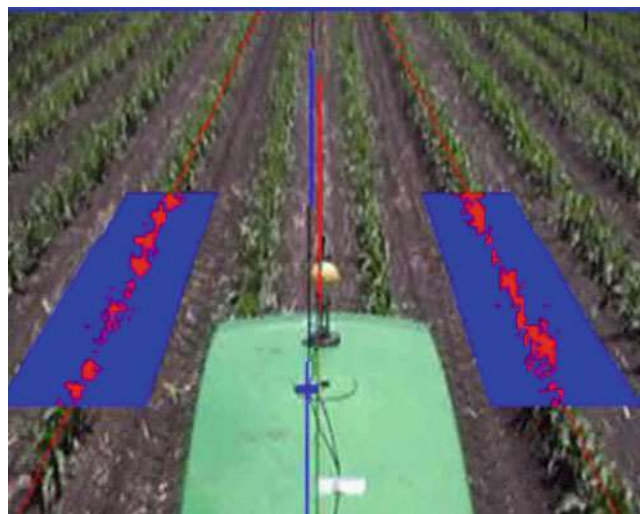
Machine Vision in Agriculture, Figure 3 A frame-grab from the computer-processing of image data to locate weeds.

Livestock identification

A more detailed version of shape information, in the form of an s-psi profile, has been used to discriminate between animals of different species passing a checkpoint while they approach a watering place. Now the image represents the profile of the animal as seen against a background. A blue background simplifies discrimination for producing a silhouette. From this a boundary can be found by edge-tracing, which yields a sequence of incremental



Machine Vision in Agriculture, Figure 4 S-psi plot of the outline of a steer.



Machine Vision in Agriculture, Figure 5 Frame-grab from the video image that is steering a tractor at speed.

vectors that form a “Freeman chain.” These in turn deliver a sequence of tangent angles, to be plotted against the distance travelled around the circumference of the silhouette, as seen in [Figure 4](#).

From the original megabyte image, some 256 bytes of data now define the shape of the animal in view, for correlating against a set of templates to separate sheep from goats or camels from cattle. A gate is then driven to exclude or to draft the animals. This work is being refined to assess the condition of cattle as they pass a point where

their RFID tag can be read, to monitor their progress towards “harvesting.”

Picking

Many attempts have been made over the years to use machine vision to detect and locate fruit for automatic picking. Although positive research results have been reported, operational speeds are generally low and there has been very limited commercial success. It has been suggested that the growing availability of broadband communication can make it possible for “armchair pickers” to tele-operate picking machinery, with the aid of real-time imaging.

Machine guidance

Vision guidance has been applied with great technical success to tractors (Billingsley and Schoenfisch, [1996](#)). Within each received image, the software locates the rows of crop and assesses the control action needed to bring the vehicle back on course. The algorithms were developed in the early 1990s, when computing power was much less plentiful. The result is a robust strategy that can time-share with GPS analysis and other signal processing.

Within the field of view, “keyholes” are defined that will each contain the image of a single row. Within each keyhole, plant images in the form of green pixels are regarded as data points through which to construct a regression line. For the next image, the keyholes are moved to be centered on these regression lines. The set of two or three keyholes move at once to indicate the vanishing point, from which the heading error and the lateral displacement can be deduced. These signals then give a steering command to bring the tractor back on track, to

an accuracy of a centimeter or two. A frame-grab from the steering software is shown in [Figure 5](#).

The method is greatly superior to the use of GPS, satellite navigation, since an operation such as cultivating will cut the ground at a point relative to the actual location of the plants, not relative to where the plants are supposed to have been planted.

It is unfortunate that marketing of the system started when enthusiasm for GPS was reaching fever pitch and success has passed it by. Nevertheless research on vision guidance is widespread (Gottschalk et al., [2008](#)).

Conclusions

As sensors and computing power become ever cheaper, the opportunity for farm robotics increases. It would be unwise to make a large machine autonomous, not least for insurance against the damage it might cause. Small robot machines, however, can already be equipped with vision, navigation, detection and communication systems at a very modest price. We may very soon see teams of “Autonomous Robot Farmhands” at work in the field.

Bibliography

- Astrand, B., and Baerveldt, A.-J., 2002. An agricultural mobile robot with vision-based perception for mechanical weed control. *Journal Autonomous Robots*, **13**(1), 21–35.
- Billingsley, J., and Schoenfisch, M., 1996. The successful development of a vision guidance system for agriculture. *Computers and Electronics in Agriculture*, **16**(2), 147–163.
- Dunn, M., and Billingsley, J., 2007. The use of machine vision for assessment of fodder quality. In *Proceedings of the 14th International Conference on Mechatronics and Machine Vision in Practice*, Xiamen, PRC, 3–5 December 2007, pub IEE ISBN 1-4242-1357-5, pp. 179–184.
- Gottschalk, R., Burgos-Artizru, X. P., Ribeiro, A., Pajares, G., and Sainchez-Miralles, A., 2008. Real-time image processing for the guidance of a small agricultural field inspection vehicle. In *Proceedings Mechatronics and Machine Vision in Practice, 2008*, pp. 493–498.
- McCarthy, C. L., Hancock, N. H., and Raine, S. R., 2008. On-the-go machine vision sensing of cotton plant geometric parameters: first results. In Billingsley, J., and Bradbeer, R. S. (eds.), *Mechatronics and Machine Vision in Practice*. New York: Springer-Verlag, pp. 305–312.
- Tao, Y., Heinemann, P. H., Varghese, Z., Morrow, C. T., and Sommer, H. J., III, 1995. Machine vision for color inspection of potatoes and apples. *Transactions of the ASAE*, **38**(5), 1555–1561.
- Zhang, Z., Kodagoda, S., Ruiz, D., Katupitiya, J., and Dissanayake, G., 2008. Classification of bidens in wheat farms. In *Proceedings of Mechatronics and Machine Vision in Practice, 2008*, pp. 505–510.

MACROPORE FLOW

Synonyms

Funnel flow; Preferential flow

See [Bypass Flow in Soil](#)

MAGNETIC PROPERTIES OF SOILS

Andrey Alekseev

Laboratory Geochemistry and Soil Mineralogy, Institute of Physicochemical and Biological Problems of Soil Science, Russian Academy of Sciences, Pushchino, Moscow Region, Russia

Synonyms

Environmental magnetism; Soil magnetism

Definition

Magnetic properties of soils are dominantly controlled by the presence, volumetric abundance, and oxidation state of iron in soils. Different types of Fe oxides, Fe–Ti oxides, and Fe sulfides are the predominant causes of magnetic soil characteristics. The concentration of magnetic Fe oxides in soils is affected by the parent material and soil-forming factors and processes.

Introduction

Magnetism is a fundamental property of all natural materials. The most important kinds of magnetic properties are those called diamagnetism, paramagnetism, ferromagnetism, ferrimagnetism, and superparamagnetism. The magnetic properties of soils are a subject of investigation started first more than 50 years ago (Le Borgne, [1955](#)). Magnetism of soils have traditionally been investigated in the environmental science and geophysics communities to indicate soil development, paleosols and climate change, pollution, and as tools for archaeological mapping and prospecting (Thompson and Oldfield, [1986](#); Maher and Thompson, [1999](#); Evans and Heller, [2003](#); Maher, [2008](#)).

Soil magnetics

The magnetic characteristics of soil and sediments reflect the amount and quality of ferruginous minerals they contain and are connected with their content, mineralogy, and the grain size. The presence of Fe oxides in different forms and quantities is the predominant cause of the magnetic properties of soils. Iron oxide minerals can be both pedogenic (product of soil formation) and lithogenic (unweathered minerals from the parent material) in origin. Iron is the most common element in the crust of the earth. Iron is not only essential to plant development, but it also participates in the formation of complexes of clay and organic matter, which in turn influence soil structure and fertility. Iron-containing minerals can be found in igneous, metamorphic, and sedimentary rocks. As a rule, clay minerals possess paramagnetic properties. The most widespread minerals of sedimentary rocks and soils quartz, carbonates, feldspars are diamagnetic or weak paramagnetic and also do not bring the appreciable contribution to the magnetic behavior of soils. Hydrated Fe oxides like goethite, which is the most abundant Fe oxide in soils around the world, ferrihydrite, and lepidocrocite play

a minor role in determining the magnetic character of soils. The concentration of (magnetic) Fe oxides in soils is affected by the parent material, soil age, soil-forming processes, biological activity, and soil temperature (Singer et al., 1996). In soils, primary ferromagnetic minerals of detrital origin derive from the disintegration of the bedrock and they reflect its mineralogy. Secondary minerals are formed through complex chemical and biological processes, which also depend on climate and the soil pH, humidity, and organic matter content. These processes operate not only on primary ferromagnetic minerals, but also on the elementary iron contained in many silicates. Depending on the parent material, the physicochemical conditions and the pedogenetic processes, goethite, hematite, maghemite, or magnetite can be formed. Mineralogically, by soil magnetism point of view, the most important ingredients are magnetite (Fe_3O_4), maghemite ($\gamma\text{-Fe}_2\text{O}_3$), and hematite ($\alpha\text{-Fe}_2\text{O}_3$). The main properties and pathway of formation of these minerals are discussed in many books and review papers (Thompson and Oldfield, 1986; Cornell and Schwertmann, 2003; Mullins, 1977; Schwertmann, 1988). The nature, content, and grain size of each magnetic phase reflect the physicochemical conditions of the soil. For example, magnetic susceptibility enhancement in topsoil is found in most temperate soils (Le Borgne, 1955; Babanin, 1973; Maher, 1986; Alekseev et al., 1988), except in acidic, podzolic, and waterlogged conditions (Maher, 1998); it can be related to soil conditions at the surface. Magnetic minerals, which occur in very small concentration in most soils, are as fingerprints of pedological processes. At present, several theories are put forward to explain the concentration and distributions of the ferrimagnetic minerals in soils: burning, biotic transformation of hydrous ferric oxides; abiotic transformation of hydrous ferric oxides; residual primary minerals; magnetotactic bacteria; anaerobic dissimilatory bacteria; and atmospheric contamination and pollution. Environmental magnetic studies have revealed that a range of ferrimagnetic minerals can be formed at Earth surface temperatures and pressures within soils and sediments, rather than merely "inherited" from disintegration and weathering of magnetic mineral-bearing igneous rocks. Notably, trace concentrations of nanoscale magnetite can be precipitated *in situ* in the soil matrix of well-drained, generally oxidizing, near-neutral soils (Maher, 2008). The generally accepted view is that most soils produce secondary nanoscale iron oxides magnetite/maghemite in surface horizons (Maher 1998; Alekseev et al., 2003; Maher et al., 2003; Blundell et al., 2009). The magnetic research techniques are express which allow producing the mass analysis in comparison with other methods. Magnetic methods have many advantages over other techniques: nearly all rocks and soils contain magnetic iron oxides/sulfides, sample preparation and measurement is quick, easy and generally nondestructive, and the methods are sensitive to both concentration and grain-size – particularly for ultrafine grains, which can be difficult to detect by other means.

Magnetic parameter and instrumentation

To describe magnetic properties of soil, different types of magnetization are commonly used.

Magnetic susceptibility – when a low-intensity magnetic field is applied to a material, the net magnetic moment (magnetization, M) is proportional to the applied field strength (H). Therefore, the low-field magnetic susceptibility, which is defined as M/H and expressed per unit volume (κ) or per unit mass (χ), is a material-specific property. Magnetic susceptibility (χ) reflects the total concentration of ferrimagnetic or total concentration of paramagnetic minerals and antiferromagnetic with low content of ferromagnetics. A magnetic susceptibility (χ) is one of most simply obtained magnetization characteristics and rather large set of the data on the application of this parameter for the problems of soil science exists.

Remanent magnetization occurs within ferromagnetic and ferrimagnetic minerals and exists in the absence of an applied field.

Viscous remanent magnetization refers to the delay of the secondary magnetic field relative to the primary magnetic field and has been linked to the presence of superparamagnetic grains of iron oxides.

Four laboratory instruments make up the basic requirements for magnetic characterization of environmental samples and soils: a susceptibility bridge (preferably dual frequency); a magnetometer; magnetizing coils; and a demagnetizer. These magnetic techniques are nondestructive and sensitive to trace amounts of magnetic minerals (Thompson and Oldfield, 1986; Maher and Thompson, 1999; Maher, 2008).

The magnetic properties of soils typically have been studied using the following equipment as example: – magnetic susceptibility (χ) – MS 2 Bartington or Kappameter KT-5-9 (field measurements), Kappabridges (2–4) (laboratory measurements); frequency – dependent magnetic susceptibility (χ_{fd}) – MS 2 Bartington; curves of saturation magnetizations (IRM) in magnetic fields with strength up to 1–4 T – Molspin magnetometer and Molspin pulse magnetizer; anhysteretic remanent magnetization (ARM) – complex of the equipment included Molspin demagnetizer and Molspin magnetometer; complete magnetization curves (hysteresis curve) – vibrating sample magnetometer-VSM Molspin (Table 1).

Soil magnetism applications

Present instruments and methods enable very sensitive determination of low concentrations of strong ferrimagnetic minerals in soils. Possible mechanisms of magnetic enhancement of soils due to increased concentrations of secondary ferrimagnetic minerals are discussed above. Herewith, we will outline some examples of application of magnetic study of the soils. Magnetic properties measurements of soils are mostly used for three purposes: to read the climatic signal recorded by palaeosols, to identify pollution in soils, and as tools for archaeological mapping and prospecting.

Magnetic Properties of Soils, Table 1 Magnetic parameters and their interpretation (Thompson and Oldfield, 1986; Maher and Thompson, 1999; Evans and Heller, 2003; Maher, 2008)

χ ($10^{-8} \text{ m}^3 \text{ kg}^{-1}$)	Magnetic susceptibility (χ or χ_{lf}) – total concentration of ferrimagnetic or total concentration of paramagnetic minerals and antiferromagnetic by low content of ferrimagnetic
χ_{fd} %	Frequency-dependent magnetic susceptibility. Is calculated on a difference of measurements at different frequencies (for MS2 460 Hz and 4,600 Hz χ_{hf} accordingly): $(\chi_{fd})\% = (\chi_{lf} - \chi_{hf})/\chi_{lf} \times 100$
χ_{ARM} ($10^{-8} \text{ m}^3 \text{ kg}^{-1}$)	Reflects the presence of ultrafine ferrimagnetic grains. Is especially sensitive to the size of particles in an interval 0.015–0.025 μm
$\chi_{ARM/SIRM}$ (m A^{-1})	Susceptibility of anhysteretic remanent magnetization (ARM). Maximum intensity of the alternating field used in the instrument Molspin demagnetizer for magnetization –100 mT, with step of decrease of a magnetic field for each cycle 0.016 mT, strength of the constant biasing field –0.08 mT. It is high sensitive to ferrimagnetic with the size of particles in an interval 0.02–0.4 μm . Reflects the presence of fine-grained magnetite (stable single domain grains)
$\text{IRM}_{100\text{mT}}/\text{SIRM}$	The ratio is sensitive to grain-size changes of ferrimagnetics. For superparamagnetic particles the significances in an interval –0.5 to 1.5 are characteristic, for stable single domain particles 1.8–2.0
$\text{SIRM-IRM}_{300\text{mT}}$	Allows evaluating the contents of ferrimagnets (magnetite, maghemite). As the majority of ferrimagnetic is fully saturated in fields of 100 mT
	Can be used for approximating the total concentration of high coercivity minerals (hematite + goethite)
	Remanence acquired in a field of 1 T is referred as SIRM (SIRM = $\text{IRM}_{1,000\text{mT}}$). It is necessary to note that the full saturation for antiferromagnetic phases can be reached at fields strength above 4 T

As example, recently, a quantitative, soil magnetism-based climofunction has been established for the area of the Russian steppe (Maher et al., 2002; Maher et al., 2003). A similar correlation between rainfall and magnetic susceptibility was previously obtained for the Chinese Loess Plateau and explained as a result of pedogenic formation of magnetite and maghemite via oxidation/reduction processes through soil wetness events (Maher and Thompson, 1999).

The pedogenic magnetic response of these well-drained, near-neutral, Russian steppe soils appears strongly correlated with that of the similarly well-drained and buffered modern soils across the Chinese Loess Plateau (and across the wider Northern Hemisphere temperate zone). Such correlation suggests that the rainfall component of the climate system is a key influence on soil magnetic properties in both these regions. This direct coupling of the soil magnetism of modern soils with present-day climate substantiates the use of magnetic climofunctions to make quantitative estimates of past rainfall variations from the magnetic properties of buried palaeosols for both the Russian steppe and the Chinese Loess Plateau.

Applying a soil magnetism climofunction, calculated from a modern-day soil training set, to each set of buried soils enables quantitative estimation of precipitation at each time step when soil burial occurred as for Holocene paleosols or loess-paleosols sequences of Pleistocene (Alekseeva et al., 2007).

Atmospherically deposited ferrimagnetic particles of anthropogenic origin also contribute a great deal to the concentration-dependent magnetic properties of top soils, such as low-field magnetic susceptibility. The highest concentration of anthropogenic ferrimagnetic particles is usually found in humic layers (e.g., Strzyszcz et al., 1996). Practically all industrial fly ashes contain a significant fraction of ferromagnetic particles, the most important sources being fly ashes produced during combustion of fossil fuel (Hanesch and Scholger, 2002; Kapička et al., 2003). Other sources, such as iron and steel works, cement

works; public boilers and road traffic also contribute to contamination by anthropogenic ferrimagnetics (Heller et al., 1998; Scholger, 1998; Hoffmann et al., 1999). In contrast to particles of pedogenic origin, anthropogenic ferrimagnetics are characterized by specific morphology and distinct magnetic properties. They are often observed in the form of spherules, with the magnetic phase frequently sintered on aluminum silicates or amorphous silica. Prevailing ferrimagnetic phases are Fe oxides, namely magnetite and maghemite, with Fe ions very often substituted by other cations (Strzyszcz et al., 1996). Application of the comparatively simple technique of measuring magnetic susceptibility enables delineation of areas with concentrations of deposited anthropogenic ferrimagnetics significantly above background values. Magnetic mapping thus represents a rapid, sensitive, and cheap tool for targeting the areas of interest. These studies showed that in polluted areas, the magnetic susceptibility of surface soil layers is considerably higher. Recently, rock-magnetic methods have been applied to modern soils in several environmental studies (for an overview see, e.g., Petrovský and Ellwood, 1999). Measurements of low-field magnetic susceptibility of surface soils have been applied recently around local pollution sources and at a larger, regional scale, areas in Poland and Great Britain and Austria have been investigated (Strzyszcz et al., 1996; Heller et al., 1998; Hanesch and Scholger, 2002; Magiera et al., 2006).

Summary

In a course of soil formation, the change of magnetic properties of soils in comparison with parent material takes place. The amplitude of these changes depends on the factors of soil formation. Generally, the conditions of transformation of iron-containing minerals result in enhancement of the contents of ferric oxides in soils. The analysis of magnetic properties of zonal soils shows that the behavior of soil magnetics in profile reflects genetic properties of soils at the soil type level and

connected with distribution and state of iron minerals in soils and landscapes. Atmospherically deposited ferrimagnetic particles of anthropogenic origin also contribute a great deal to the concentration-dependent magnetic properties of top soils. Magnetic properties measurements of soils are mostly used for three purposes: to read the climatic signal recorded by palaeosols, to identify pollution in soils, and as tools for archaeological mapping and prospecting. The definition of soil magnetism as a genetic parameter, which is able together with other soil properties to be used for diagnostics of soil looks to be useful and important. Magnetic methods have many advantages over other techniques: sample preparation and measurement is quick, easy and generally nondestructive, and the methods are sensitive to both concentration and grain-size – particularly for ultrafine grains, which can be difficult to detect by other means. Hence, magnetic analyses of soils provide an additional, sensitive window on soil iron.

Bibliography

- Alekseev, A. O., Kovalevskaya, I. S., Morgan, E. G., and Samoylova, E. M., 1988. Magnetic susceptibility of soils in a catena. *Soviet Soil Science (Pochvovedenie)*, **8**, 27–35.
- Alekseev, A. O., Alekseeva, T. V., and Maher, B. A., 2003. Magnetic properties and mineralogy of iron compounds in steppe soils. *Eurasian Soil Science*, **36**, 59–70.
- Alekseeva, T., Alekseev, A., Maher, B. A., and Demkin, V., 2007. Late Holocene climate reconstructions for the Russian steppe, based on mineralogical and magnetic properties of buried palaeosols. *Palaeogeography, Palaeoclimatology, Palaeoecology*, **249**, 103–127.
- Babanin, V. F., 1973. The use of magnetic susceptibility in identifying forms of iron in soils. *Soviet Soil Science (Pochvovedenie)*, **5**, 487–493.
- Blundell, A., Dearing, J. A., Boyle, J. F., and Hannam, J. A., 2009. Controlling factors for the spatial variability of soil magnetic susceptibility across England and Wales. *Earth-Science Reviews*, **95**, 158–188.
- Cornell, R. M., and Schwertmann, U., 2003. *The Iron Oxides*. Weinheim: Wiley-VCH.
- Evans, M. E., and Heller, F., 2003. *Environmental Magnetism: Principles and Applications of Enviromagnetics*. San Diego: Academic.
- Hanesch, M., and Scholger, R., 2002. Mapping of heavy metal loadings in soils by means of magnetic susceptibility measurements. *Environmental Geology*, **42**, 857–870.
- Heller, F., Strzyszcza, Z., and Magiera, T., 1998. Magnetic record of industrial pollution in forest soils of Upper Silesia, Poland. *Journal of geophysical research*, **103**, 17767–17774.
- Hoffmann, V., Knab, M., and Appel, E., 1999. Magnetic susceptibility mapping of roadside pollution. *Journal of Geochemical Exploration*, **66**, 313–326.
- Kapička, A., Jordanova, N., Petrovský, E., and Podrázska, V., 2003. Magnetic study of weakly contaminated forest soils. *Water, Air and Soil Pollution*, **148**, 31–44.
- Le Borgne, E., 1955. Susceptibilité magnétique anormale du sol superficiel. *Annales de Géophysique*, **11**, 399–419.
- Magiera, T., Strzyszcza, Z., Kapička, A., and Petrovský, E., 2006. Discrimination of lithogenic and anthropogenic influences on topsoil magnetic susceptibility in Central Europe. *Geoderma*, **130**, 299–311.
- Maher, B. A., 1986. Characterisation of soils by mineral magnetic measurements. *Physics of the Earth and Planetary Interiors*, **42**, 76–92.
- Maher, B. A., 1998. Magnetic properties of modern soils and Quaternary loessic paleosols: palaeoclimatic implications. *Palaeogeography, Palaeoclimatology, Palaeoecology*, **137**, 25–54.
- Maher, B. A., 2008. Environmental magnetism and climate change. *Contemporary Physics*, **48**, 247–274.
- Maher, B. A., and Thompson, R. (eds.), 1999. *Quaternary Climates, Environments and Magnetism*. Cambridge: Cambridge University Press.
- Maher, B. A., Alekseev, A., and Alekseeva, T., 2002. Variation of soil magnetism across the Russian steppe: its significance for use of soil magnetism as a paleorainfall proxy. *Quaternary Science Reviews*, **21**, 1571–1576.
- Maher, B. A., Alekseev, A., and Alekseeva, T., 2003. Magnetic mineralogy of soils across the Russian steppe: climatic dependence of pedogenic magnetite formation. *Palaeogeography, Palaeoclimatology, Palaeoecology*, **201**, 321–341.
- Mullins, C. E., 1977. Magnetic susceptibility of the soil and its significance in soil science: a review. *Journal of Soil Science*, **28**, 223–246.
- Petrovský, E., and Ellwood, B. B., 1999. Magnetic monitoring of air-land and water-pollution. In Maher, B. A., and Thompson, R. (eds.), *Quaternary Climates, Environments and Magnetism*. Cambridge: Cambridge University Press.
- Scholger, R., 1998. Heavy metal pollution monitoring by magnetic susceptibility measurements applies to sediments of the river Mur (Styria, Austria). *European Journal of Environmental and Engineering Geophysics*, **3**, 25–37.
- Schwertmann, U., 1988. Occurrence and formation of iron oxides in various pedoenvironments. In Stuki, J. W., Goodman, B. A., and Schwertmann, U. (eds.), *Iron Oxides in Soils and Clay Minerals*. Dordrecht: Reidel.
- Singer, M. J., Verosub, K. L., Fine, P., and TenPas, J., 1996. A conceptual model for the enhancement of magnetic susceptibility in soils. *Quaternary International Journal*, **34–36**, 2443–2458.
- Strzyszcza, Z., Magiera, T., and Heller, F., 1996. The influence of industrial immisions on the magnetic susceptibility of soils in Upper Silesia. *Studia Geophysica et Geodaetica*, **40**, 276–286.
- Thompson, R., and Oldfield, F., 1986. *Environmental Magnetism*. London: Allen and Unwin.

Cross-references

- [Clay Minerals and Organo-Mineral Associates](#)
- [Climate Change: Environmental Effects](#)
- [Databases of Soil Physical and Hydraulic Properties](#)
- [Physical Properties for Soil Classification](#)
- [Mapping of Soil Physical Properties](#)
- [Mineral–Organic–Microbial Interactions](#)
- [Nanomaterials in Soil and Food Analysis](#)
- [Oxidation–Reduction Reactions in the Environment](#)
- [Parent Material and Soil Physical Properties](#)
- [Physical \(Mechanical\) Weathering of Soil Parent Material](#)
- [Wildfires, Impact on Soil Physical Properties](#)

MAGNETIC RESONANCE IMAGING IN SOIL SCIENCE

Andreas Pohlmeier
ICG-4, Research Centre, Jülich, Germany

Definition

Magnetic resonance imaging (MRI) or magnetic resonance tomography (MRT) is a noninvasive, three-dimensional

(3D) imaging technique for monitoring water content, water fluxes, and tracer transport in porous media. It uses the effect of nuclear magnetic resonance (NMR) of certain atomic nuclei, mostly ^1H in H_2O , which is modulated by the chemical and physical environment inside the porous medium. The methods yield finally 2D (slices) or 3D (volume graphics) images of the medium under investigation.

Basics

Magnetic resonance imaging is based upon the physical effect of nuclear magnetic resonance (NMR) of spin bearing atomic nuclei (Callaghan, 1991; Blümich, 2000). The most important NMR active nuclei in soil science applications are ^1H , ^{13}C , ^{19}F , ^{31}P , and ^{23}Na , of which mostly ^1H with a spin quantum number of $I = \frac{1}{2}$ (e.g., in H_2O) is used for imaging purposes leading to a nuclear magnetic moment μ . If placed in an external magnetic field \mathbf{B}_0 pointing into z -direction of a Cartesian coordinate system, (The direction of the external magnetic field \mathbf{B}_0 is mostly determined by convention as “ z ”) the nuclear magnetic moment precesses around the axis of \mathbf{B}_0 with the *Larmor frequency* v_0 :

$$v_0 = \omega_0/2\pi = -\gamma|B_0|/2\pi \quad (1)$$

The parameter γ , a proportionality constant termed as gyromagnetic ratio, is a basic property of the respective nucleus. For protons its value is $\gamma_{\text{H}} = 2.68 \times 10^8 \text{ T}^{-1} \text{ s}^{-1}$, leading to typical values of $v_0 = 300 \text{ MHz}$ at $|B_0| = 7 \text{ T}$ in stationary superconducting magnets, and $v_0 = 4.3 \text{ MHz}$ at $|B_0| = 0.1 \text{ T}$ in mobile low-field relaxometers and scanners. Due to the quantum mechanical nature of the nuclear spin for proton magnetic moments, only two states are allowed in an external magnetic field: parallel (\uparrow) and antiparallel orientation (\downarrow). The energy gap between these two states is $\Delta E = h\nu_0$, where h is Planck's constant and the two states are populated according to Boltzmann's law: $n\uparrow/n\downarrow = \exp(-\Delta E/kT)$. In practice, it is more convenient not to regard single spins but ensembles of spins, which may be treated semi-classically. If an ensemble is sufficiently large, the x - and y -components of the nuclear magnetic moments precessing around the z -axis cancel mutually, so only the z -component persists. Since the lower energy state is slightly higher populated than the higher state, a macroscopic magnetic moment \mathbf{M}_0 pointing into z -direction is observable. Now, by absorption of electromagnetic radiation matching exactly the *Larmor frequency*, spins may swap from parallel to antiparallel orientation. Regarding the ensemble, this irradiation by a sufficiently long pulse, termed as 90° pulse, leads to a rotation of \mathbf{M}_0 into the xy -plane, where it precesses again with the Larmor frequency v_0 around the z -axis. Subsequently, the excess energy of the ensemble is lost by two relaxation mechanisms:

Firstly, the coherence of the magnetic moments in the xy -plane decays with the *transverse relaxation time* T_2 , see Equation 2 and radiation is emitted, which is detectable by an external receiver coil. This is the free induction decay (FID).

$$M_{xy} = M_0 \exp(-t/T_2), \quad (2)$$

It is composed of two contributions: coherence loss (dephasing) in static inhomogeneities, which is reversible, and irreversible loss due to stochastic motions. The reversible contribution of dephasing can be restored by the creation of a *spin echo* by means of the application of a 180° pulse after a period of $t_E/2$ (cf. Equation 5) after the 90° pulse. What remains is the irreversible part. For details, see textbooks (Callaghan, 1991; Blümich, 2000).

Secondly, the thermal equilibrium is restored, that is, magnetization in the z -direction is reformed again. This is called *longitudinal relaxation* characterized by the relaxation time T_1 :

$$M_z = M_0(1 - \exp(-t/T_1)) \quad (3)$$

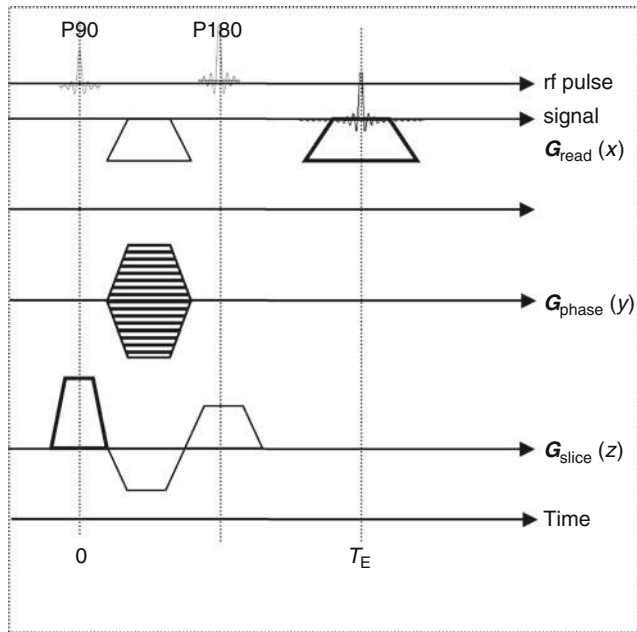
Pure water possesses relaxation times of about 3 s in high field, but the environment, in which the interesting water molecules are located, reduces T_1 and T_2 considerably. Decisive factors are (1) pore size, (2) pore filling factor, (3) pore geometry, (4) chemical nature of pore walls, (5) dissolved paramagnetic substances and, in case of T_2 , (6) diffusive motion in internal magnetic field gradients. By the latter effect T_2 can get much faster than one millisecond, which has implications on imaging capabilities, see below. The investigation of relaxation times is the basis of relaxometric exploration of pore space in geological materials (Dunn et al., 2002), see also the article Proton NMR Relaxometry in Soil Science, Nr of G. Schaumann in the encyclopedia.

Imaging

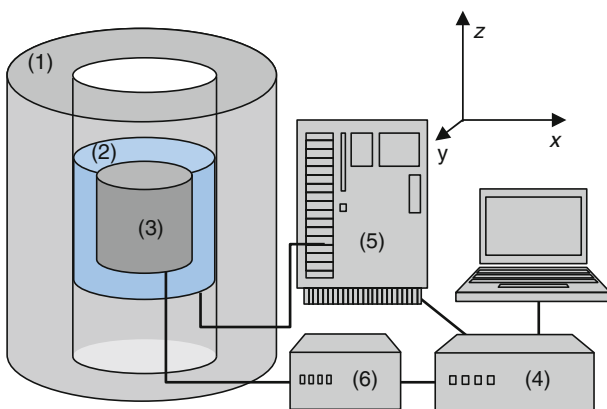
Magnetic resonance imaging (MRI) is the extension of NMR by adding spatial resolution to the observed NMR signal. In the following a basic spin echo imaging method is presented exemplarily (see Figure 1). According to Equation 1, the precession frequency is proportional to the magnetic field \mathbf{B}_0 . If an additional spatially variable magnetic field (a *gradient* $\mathbf{G}_{\text{slice}}$) is added to \mathbf{B}_0 during excitation only one slice is excited according to Equation 4:

$$v_0 = -\gamma|B_0 + \mathbf{G}_{\text{slice}} \cdot \mathbf{z}|/2\pi. \quad (4)$$

All subsequent detectable signals originate only from this slice leading to the family of the so-called multi-slice imaging sequences, see Figure 1. The next dimension (here: x) is addressed by application of a further gradient \mathbf{G}_{read} (orthogonal to $\mathbf{G}_{\text{slice}}$) during the detection of the signal that encodes the frequency of the received signal with respect to the x -direction. The third dimension is finally encoded by the phase-selective $\mathbf{G}_{\text{phase}}$, orthogonal to the other two gradients. After its application, the phase of the signal is turned with respect to a reference, and the phase shift is proportional to the position on the y -axis. The real-space image is finally obtained by two-dimensional Fourier transformation. The signal intensity is given by



Magnetic Resonance Imaging in Soil Science, Figure 1 Basic spin echo imaging pulse sequence. P90 and P180 mean 90° and 180° pulses of electromagnetic irradiation for excitation of the spin ensemble system and creation of the echo, respectively. The gradients in this example are applied in x -, y -, and z -directions, but can also be applied in other orders.



Magnetic Resonance Imaging in Soil Science, Figure 2 Schematic magnetic resonance imaging (MRI) scanner. For details, see text.

$$S(xyz) \propto \rho_0(xyz)(1 - \exp(-t_R/T_1(xyz))) \times \exp(-t_E/T_2(xyz)), \quad (5)$$

where ρ_0 is the spin density, t_R is the repetition time between successive excitation pulses, and t_E is the echo time, that is, twice the period between 90° and 180° pulse, T_1 and T_2 are the longitudinal and transverse relaxation times, respectively. Note that ρ_0 as well as T_1 and T_2 depend on space. The sequence in Figure 1 is only an

example of a basic, but still widespread MRI pulse sequence (Spin echo multi slice sequence, also termed as spin warp sequence). Besides this, many partly very specialized sequences exist, for example, rapid imaging, relaxometric imaging, and motion sensitive imaging (Callaghan, 1991; Blümich, 2000).

Hardware

Schematically, the necessary hardware consists of following components (Figure 2): (1) a cylindrical magnet with a bore, in which the gradient system (2) and the transmitter–receiver coil (3) is placed. Stationary magnets are mostly superconductors, where permanent current flows in a liquid helium cooled coil, which creates a main magnetic field B_0 pointing along the axis of the cylinder (z -direction). The gradient system consists of three additional coils that create orthogonal magnetic field gradients in the x -, y -, and z -directions. These gradients are operated by the spectrometer (4), which creates and controls the pulse sequences via gradient amplifiers (5). The excitation of the spin system and the monitoring of the transmitted signals are performed by the rf-coil (3), which transmits and receives rf-pulses. This is also controlled by the spectrometer (4) and the rf amplifier (6). In order to be able to turn the magnetization M_0 into the xy -plane the direction of the magnetic field B_1 of the rf-pulses must be orthogonal to B_0 . This is performed in conventional superconducting scanners by a so-called birdcage-rf coil. For novel low-field scanners, which are composed of Halbach-rings of permanent magnets (Raich and Blümller, 2004), B_0 points orthogonal to the main axis, and the rf coil can be a simple solenoid coil.

Applications

The application of MRI for soil systems started in the 1980s. A very early example was the unilateral imaging of water content in a natural soil on the field scale, where an electromagnet was positioned on a sledge and pulled across a field by a tractor (Paetzold et al., 1985). The signal created by a radiofrequency irradiation pulse was detected and water content was derived from the signal intensity. Most recently, the imaging of water on the field scale draws again attraction by the further development of magnetic resonance sounding (NMRS) or surface NMR (Roy and Lubczynski, 2005; Mohnke and Yaramanci, 2008; Yaramanci et al., 2008). Originally, this method has been developed for detection of aquifers in geological formations like karsts. But with the advancing technology, especially with respect to noise compensation, the method might get available for the investigation of soils with much less water content and much faster relaxation times (Hertrich et al., 2007).

In the lab, MRI has also been applied for the investigation of water content and dynamics in repacked natural porous media and natural soil cores (Nestle et al., 2002). The general problem for its application in soils is the inherently rapid T_2 relaxation times (Hall et al., 1997;

Votrubova et al., 2000), down to the sub-millisecond range. Also, one must take into consideration that T_2 for a given porous medium is not a constant but depends also on t_E due to diffusional motion in internal gradients (Barrie, 2000; Dunn et al., 2002). The limiting value of t_E is about 1.5 ms at present, so in the past many imaging studies in natural soils failed. However, the group of M. Cislerova was able to apply the method on infiltration processes in natural soil cores (Cislerova et al., 1997; Votrubova et al., 2003), where the infiltrating water followed preferential flow paths in a network of macropores, which are characterized by comparably long T_2 relaxation times. Figure 3 shows an image of a central vertical slice through a soil core after infiltration from top, which was obtained by a spin-echo sequence using $t_E = 5$ ms. Clearly visible are the preferential flow paths.

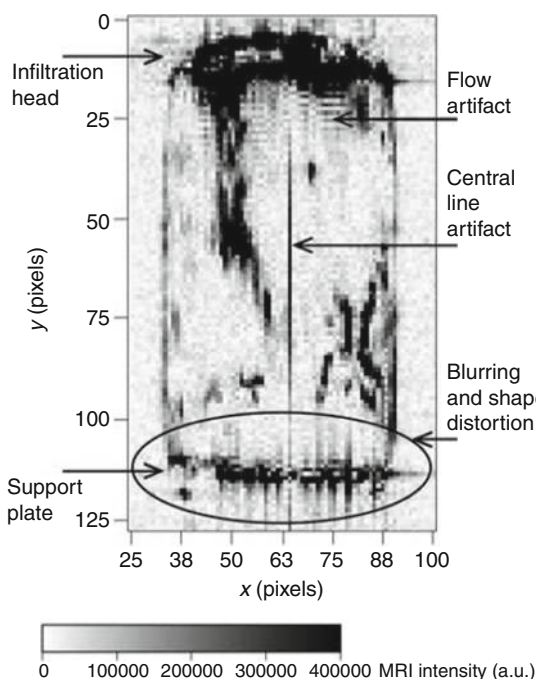
Besides $^1\text{H}_2\text{O}$ imaging, also other nuclei can be used for monitoring soil processes. This method is quite rare, but promising for the quantification of dual phase fluxes. Simpson et al. monitored water and fluorinated compounds (fluorinated benzene, NaF, trifluralin) in four natural soil cores. Since free water possesses longer relaxation times, and it is still visible when imaged at long t_E , the authors varied t_E in the range between 2.5 and 40 ms in order to differentiate between bound water and free water. Then the displacement of water by hexafluorobenzene during infiltration from top was imaged by ^{19}F MRI. This

fluorinated liquid has been chosen as model nonaqueous phase liquid (NAPL), because ^{19}F possesses the same spin like water and a similar gyromagnetic ratio of $\gamma_F = 2.52 \times 10^8 \text{ T}^{-1} \text{ s}^{-1}$.

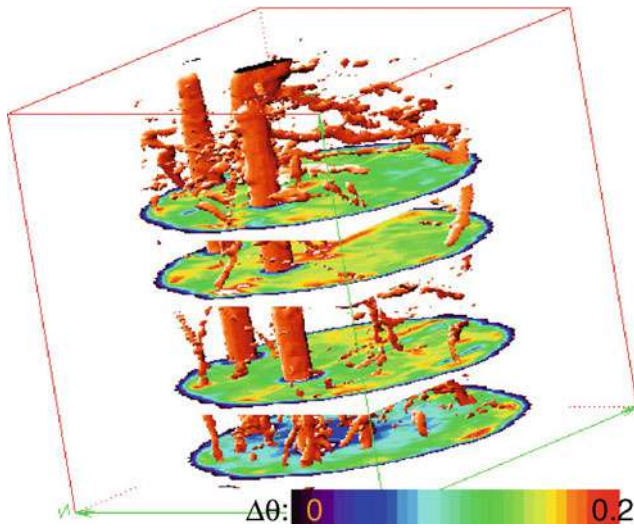
A permanently challenging topic in soil science is the imaging of flow processes. MRI is principally very suitable for such purposes, since it can monitor the motion of water and therefore flow velocities and diffusion coefficients directly (Callaghan et al., 1988; Baumann et al., 2000; Scheenen et al., 2001). This is performed by the introduction of additional motion encoding gradients before the detection of echoes, which prolongates interval between excitation pulse and detection. Therefore, these methods are restricted to the investigation of sediments and model porous media with sufficiently slow transverse relaxation times (Baumann et al., 2000; Herrmann et al., 2002b). For applications in soils, the first difficulty is the short transverse relaxation time, which lets signals vanish after some milliseconds. Secondly, flow processes in soils are mostly slower than the few tenths of mm/s, which is the present limit for flow imaging (Bendel, 2009). So, fluxes should be better visualized indirectly by motion of tracers. Popular tracers are paramagnetic ions like Cu^{2+} , Ni^{2+} , or Mn^{2+} (Greiner et al., 1997; Herrmann et al., 2002a; Oswald et al., 2007), and complexes like GdDTPA^{2-} that are widely used in medicine (Hermann et al., 2008; Haber-Pohlmeier et al., 2009, 2010). The mode of action is predominantly the reduction of the longitudinal relaxation time T_1 . If one sets the experimental parameter T_R in Equation 5 to a sufficiently small value, the signal intensity in regions without tracer is low, whereas signal intensities originating from regions with high tracer concentrations remain high. This technique has been successfully applied for quantifying flux processes in natural porous media and very recently for the first time in a natural soil (Haber-Pohlmeier et al., 2009, 2010).

As already mentioned, soils possess short relaxation times, which can reduce the intensities of echoes considerably or prevent the detection of echoes completely. A family of MRI techniques based on *single point imaging* can overcome this restriction by avoiding the creation of echoes and probe directly the free induction decay, which appears after any exciting pulse (Balcom et al., 1996). Their general drawbacks are long measuring times combined with low resolution. However, such methods are used for the investigation of water in porous rocks (Gingras et al., 2002; Chen et al., 2006) and root–soil systems (Pohlmeier et al., 2008).

The final topic to be addressed here is the investigation of root–water–soil relations by MRI. MRI is especially suitable for this, since such interactions are sensitive for classical invasive methods but possess huge importance for the understanding of plant growth and stress tolerance. The earliest investigations range back to the 1980s (Bottomley et al., 1986; Bacic and Ratkovic, 1987; Brown et al., 1990; Chudek et al., 1997). For imaging of root systems, the short transverse relaxation times of soil material helps, since roots possess relative long relaxation times, so



Magnetic Resonance Imaging in Soil Science,
Figure 3 MR image of a soil core after infiltration of water from top. (Modified from Votrubova et al., 2003. Copyright [2003] American Geophysical Union, Reproduced/modified by permission of American Geophysical Union.)



Magnetic Resonance Imaging in Soil Science, Figure 4 *Ricinus* root-soil system. Water content difference maps $\Delta\theta$ between day-6 and day-1, overlaid by the root system. The long cylinders in the left part are reference tubes. (From Pohlmeier et al., 2010.)

by the choice of long echo times (t_E in Equation 5) the signal from the soil is completely faded out, and only the root system appears in the images (MacFall and van As, 1996; Menzel et al., 2007; Pohlmeier et al., 2008). In contrast, if one intends to measure water content in the vicinity of roots one should use very short echo times or even employ single point imaging techniques (Pohlmeier et al., 2007). Figure 4 shows an example of water content changes during a desiccation experiment over 6 days in a ricinus root system grown in fine sand, where the water content was determined by a multi-slice multi-echo pulse sequence with quite short echo time. The resulting echo-trains are fitted by exponential functions and the water content was obtained from the amplitude of these functions and calibration on reference tubes with known water content. The root system architecture was imaged by a fast spin echo method with longer echo time. The stronger depletion in the top layers of the soil is visible, whereas the bottom regions remain wetter.

Using MRI, several authors stated water depletion zones around roots (MacFall et al., 1990; Segal et al., 2008) while under very dry conditions also hints on opposite trend, that is, increased water contents around roots are found (Carminati et al., 2010). This is still a topic of discussion. Further necessary for the interpretation of such effects is the combination of noninvasive 3D images with model calculations based on soil physical principles (Javaux et al., 2008), see also the article Plant Soil Interactions, Modelling of M. Javaux in this encyclopedia.

Summary and outlook

Summarizing, one can state that MRI is very suitable for monitoring processes in model and natural soils like water content changes, root system architecture, flow processes,

and tracer motion. One should always take into account that transverse relaxation times decrease with decreasing pore size and water content and increasing content of paramagnetic ions like Fe^{3+} and Mn^{2+} . Thus, MRI is generally more sensitive for water in macropores. Therefore, quantitative water content imaging should employ fast echo times in combination with multi-echo sequences and extrapolation to zero time, or even ultrafast pulse sequences like SPRITE (Single Point Imaging with T_1 Enhancement [Balcom et al., 1996; Pohlmeier et al., 2007]). Such sequences abandon the creation of an echo and sample the FID directly on the expense of enhanced overall measuring time. Flux processes can be visualized directly in macropores or indirectly by the usage of contrast agents (tracers).

Bibliography

- Bacic, G., and Ratkovic, S., 1987. NMR Studies of Radial Exchange and Distribution of Water in Maize Roots: The Relevance of Exchange Kinetics. *Journal of Experimental Botany*, **38**, 1284–1297.
- Balcom, B. J., MacGregor, R. P., et al., 1996. Single-point ramped imaging with T_1 enhancement (SPRITE). *Journal of Magnetic Resonance Series A*, **123**(1), 131–134.
- Barrie, P. J., 2000. Characterization of porous media using NMR methods. *Annual Reports on NMR Spectroscopy*, **41**, 265–316.
- Baumann, T., Petsch, R., et al., 2000. Direct 3-d measurement of the flow velocity in porous media using magnetic resonance tomography. *Environmental Science & Technology*, **34**(19), 4242–4248.
- Bendel, P., 2009. Quantification of slow flow using FAIR. *Magnetic Resonance Imaging*, **27**(5), 587–593.
- Blümich, B., 2000. *NMR imaging of materials*. Oxford: Clarendon.
- Bottomley, P. A., Rogers, H. H., et al., 1986. NMR Imaging Shows Water Distribution and Transport in Plant-Root Systems In situ. *Proceedings of the National Academy of Sciences of the United States of America*, **83**(1), 87–89.
- Brown, J. M., Kramer, P. J., et al., 1990. Use of Nuclear Magnetic Resonance Microscopy for Noninvasive Observations of Root-Soil Water Relations. *Theoretical and Applied Climatology*, **42**, 229–236.
- Callaghan, P. T., 1991. *Principles of Nuclear Magnetic Resonance Microscopy*. Oxford: Oxford University Press.
- Callaghan, P. T., Eccles, C. D., et al., 1988. NMR Microscopy of dynamic displacements – k-space and q-space imaging. *Journal of Physics*, **E21**, 820–822.
- Carminati, A., Moradi, A., et al., 2010. Dynamics of soil water content in the rhizosphere. *Plant and Soil*, **332**, 163.
- Chen, Q., Rack, F., et al., 2006. Quantitative magnetic resonance imaging methods for core analysis. New techniques in Sediment Cora Analysis. London. *Geological Society London*, **267**, 193–207.
- Chudek, J. A., Hunter, G., et al., 1997. An application of NMR microimaging to investigate nitrogen fixing root nodules. *Magnetic Resonance Imaging*, **15**, 361–368.
- Cislerova, M., Votrubova, J., et al., 1997. *Magnetic Resonance Imaging and Preferential Flow in Soils. Characterization and Measurement of the Hydraulic Properties of Unsaturated Porous Media*. Riverside: University of California.
- Dunn, K. J., Bergmann, D. J., et al., 2002. *Nuclear Magnetic Resonance, Petrophysical and Logging Applications*. Amsterdam: Pergamon.
- Gingras, M. K., MacMillan, B., et al., 2002. Visualizing the internal physical characteristics of carbinate sediments with magnetic

- resonance imaging and petrography. *Bulletin of Canadian Petroleum Geology*, **50**(3), 363–369.
- Greiner, A., Schreiber, W., et al., 1997. Magnetic resonance imaging of paramagnetic tracers in porous media: quantification of flow and transport parameters. *Water Resources Research*, **33**(6), 1461–1473.
- Haber-Pohlmeier, S., Van Dusschoten, D., et al., 2009. Waterflow visualized by tracer transport in root-soil-systems using MRI. *Geophysical Research Abstracts*, **11**, EGU2009–8096.
- Haber-Pohlmeier, S., Staph, S., et al., 2010. Waterflow monitored by tracer transport in natural porous media using MRI. *Vadose Zone Journal*, **9**, 835–845.
- Hall, L. D., Amin, M. H. G., et al., 1997. MR properties of water in saturated soils and resulting loss of MRI signal in water content detection at 2 tesla. *Geoderma*, **80**(3–4), 431–448.
- Hermann, P., Kotek, J., et al., 2008. Gadolinium (iii)complexes as MRI contrast agents: ligand design and properties of the complexes. *Dalton Transactions*, **June 21**, 3027–3047.
- Hermann, K. H., Pohlmeier, A., et al., 2002a. Three-dimensional imaging of pore water diffusion and motion in porous media by nuclear magnetic resonance imaging. *Journal of Hydrology*, **267**(3–4), 244–257.
- Hermann, K. H., Pohlmeier, A., et al., 2002b. Three-dimensional nickel ion transport through porous media using magnetic resonance Imaging. *Journal of Environmental Quality*, **31**(2), 506–514.
- Hertwich, M., Braun, M., et al., 2007. Surface nuclear magnetic resonance tomography. *IEEE Transactions on Geoscience and Remote Sensing*, **45**, 3752–3759.
- Javaux, M., Schröder, T., et al., 2008. Use of a Three-Dimensional Detailed Modeling Approach for Predicting Root Water Uptake. *Vadose Zone Journal*, **7**(3), 1079–1088.
- MacFall, J. S., and Van As, H., 1996. Magnetic resonance imaging of plants. In Shachar-Hill, Y., and Pfeffer, P. E. (eds.), *Nuclear Magnetic Resonance in Plant Biology*. Rockville: The American Society of Plant Physiologists, pp. 33–76.
- MacFall, J. S., Johnson, G. A., et al., 1990. Observation of a water depletion region surrounding loblolly pine roots by magnetic resonance imaging. *Proceedings of the National Academy of Sciences of the United States of America*, **87**, 1203–1207.
- Menzel, M. I., Oros-Peusquens, A. M., et al., 2007. 1 H-NMR imaging and relaxation mapping – a tool to distinguish the geographical origin of German white asparagus? *Journal of Plant Nutrition and Soil Science*, **170**, 24–38.
- Mohnke, O., and Yaramancı, U., 2008. Pore size distributions and hydraulic conductivities of rocks derived from Magnetic Resonance Sounding relaxation data using multi-exponential decay time inversion. *Journal of Applied Geophysics*, **66**(3–4), 73–81.
- Nestle, N., Baumann, T., et al., 2002. Magnetic resonance imaging in environmental science. *Environmental Science & Technology*, **36**(7), 154A–160A.
- Oswald, S. E., Spiegel, M. A., et al., 2007. Three-dimensional saltwater-freshwater fingering in porous media: contrast agent MRI as basis for numerical simulations. *Magnetic Resonance Imaging*, **25**, 537–540.
- Paetzold, R. F., Matzkanin, G. A., et al., 1985. Surface Soil-Water Content Measurement Using Pulsed Nuclear Magnetic-Resonance Techniques. *Soil Science Society of America Journal*, **49**(3), 537–540.
- Pohlmeier, A., Oros-Peusquens, A. M., et al., 2007. Investigation of water content and dynamics of a Ricinus root system in unsaturated sand by means of SPRITE and CISS: correlation of root architecture and water content change. *Magnetic Resonance Imaging*, **25**, 579–580.
- Pohlmeier, A., Oros-Peusquens, A. M., et al., 2008. Changes in Soil Water Content Resulting from Ricinus Root Uptake Monitored by Magnetic Resonance Imaging. *Vadose Zone Journal*, **7**, 1010–1017.
- Pohlmeier, A., Vergeldt, F., et al., 2010. MRI in Soils: Determination of water content changes due to root water uptake by means of Multi-Slice-Multi-Echo sequence (MSME). *The Open Magnetic Resonance Journal*, **3**, 39–47.
- Raich, H., and Blümler, P., 2004. Design and Construction of a Dipolar Halbach Array with an Homogeneous Field from N * 8 Identical Bar-Magnets - NMR-Mandalas-. *Conc. Magn. Reson. B Magn. Reson. Eng.*, **23B**, 16–25.
- Roy, J., and Lubczynski, M. W., 2005. MRS multi exponential decay analysis: aquifer pore size distribution and vadose zone characterization. *Near Surface Geophysics*, **3**(4), 287–298.
- Scheenen, T. W. J., Vergeldt, F. J., et al., 2001. Microscopic imaging of slow flow and diffusion: a pulsed field gradient stimulated echo sequence combined with turbo spin echo imaging. *Journal of Magnetic Resonance*, **151**(1), 94–100.
- Segal, E., Kushnir, T., et al., 2008. Water uptake and the hydraulics of the root hair rhizosphere. *Vadose Zone Journal*, **7**, 1024–1037.
- Votrubova, J., Sanda, M., et al., 2000. The relationships between MR parameters and the content of water in packed samples of two soils. *Geoderma*, **95**(3–4), 267–282.
- Votrubova, J., Cislerova, M., et al., 2003. Recurrent ponded infiltration into structured soil: A magnetic resonance imaging study. *Water Resources Research*, **39**(12), 1371.
- Yaramancı, U., Legchenko, A., et al., 2008. Magnetic Resonance Sounding Special Issue of Journal of Applied Geophysics, 2008. *Journal of Applied Geophysics*, **66**(3–4), 71–72.

Cross-references

- [Agrophysical Objects \(Soils, Plants, Agricultural Products, and Foods\)](#)
- [Agrophysics: Physics Applied to Agriculture](#)
- [Image Analysis in Agrophysics](#)
- [Infiltration in Soils](#)
- [Magnetic Properties of Soils](#)
- [Nondestructive Measurements in Soil](#)
- [Noninvasive Quantification of 3D Pore Space Structures in Soils](#)
- [Plant Roots and Soil Structure](#)
- [Plant–Soil Interactions, Modeling](#)
- [Pore Size Distribution](#)
- [Proton Nuclear Magnetic Resonance \(NMR\) Relaxometry in Soil Science](#)
- [Root Water Uptake: Toward 3-D Functional Approaches](#)
- [Soil Hydraulic Properties Affecting Root Water Uptake](#)
- [Soil–Plant–Atmosphere Continuum](#)
- [Soil Water Flow](#)
- [Solute Transport in Soils](#)

MAGNETIC TREATMENT OF IRRIGATION WATER, EFFECTS ON CROPS

Basant Maheshwari, Harsharn Grewal
School of Natural Sciences, Hawkesbury Campus,
Building H3, University of Western Sydney, Penrith South
DC, NSW, Australia

Definition

Water productivity: Crop yield per unit volume of water used. Definitions of water productivity differ based on the context. For example, from the point of view of growing

crops, obtaining more kilograms per unit of transpiration is the main aspect productivity of water. In the case of regional or catchment scale, the focus of water productivity is the value derived from the use of water for purposes such as crops, forests, fisheries, ecosystems, and other uses.

Electromagnetic field: A field of force associated with a moving electric charge equivalent to an electric field and a magnetic field at right angles to each other and to the direction of propagation.

Magnetic treatment: Exposure of material such as water to a magnetic field for a short duration (a few seconds) or longer to possibly change some of its properties for beneficial effects.

Introduction

The total volume of fresh water available is limited but the demand for water is growing at a rapid pace. In this context there has been a growing interest to use water more efficiently and effectively, increase reuse of effluent, develop ways to use lower quality water and improve the overall productivity of water used for irrigation. This means we need to develop ways that will increase the productivity and sustainability of water used for irrigation. One of the ways by which we can reduce the total water used for irrigation is to employ practices that improve crop yield per unit volume of water used (i.e., water productivity). There have been claims made that the magnetic treatment of irrigation water can improve water productivity. If those claims are valid there is scope for magnetic treatment of water to save water and assist in coping with the future water scarcity.

Effects of magnetic field

There is very little study reported, with valid scientific experiments, on the effects of magnetic treatment of water on crop yield and water productivity. However, there have been some closely related studies that report on the effects of magnetic field on seed germination, plant physiology, and overall plant growth and, as such, those studies may indirectly help to understand the role of magnetic treatment of irrigation water and plant growth. For example, Lin and Yotvat (1990) reported an increase in water productivity in both livestock and crop farming with magnetically treated water. Some studies have shown that there is an increase in the number of flowers, earliness and total fruit yield of strawberry and tomatoes by using magnetic fields (Esitken and Turan, 2004; Danilov et al., 1994). An increase in nutrient uptake by magnetic treatment was also observed in tomatoes by Duarte Diaz et al. (1997).

External electric and magnetic fields influence both the activation of ions and polarization of dipoles in living cells (Johnson and Guy, 1972; Moon and Chung, 2000). Electromagnetic fields (EMFs) can alter the plasma membrane structure and function (Paradisi et al., 1993; Blank, 1995). Goodman et al. (1983) reported an alteration of the level of some mRNA after exposure to EMFs. Amaya et al. (1996) and Podešný et al. (2004) have shown that an optimal

external electromagnetic field accelerates the plant growth, especially seed germination percentage and speed of emergence.

Some studies focused on how static magnetic field affect chlorophyll and phytohormone levels in some plants. Turker et al. (2007) observed that chlorophyll and phytohormone levels decreased when static magnetic field, parallel either to gravity force (field-down) or anti-parallel (field-up) was applied to maize plants. However, chlorophyll concentration increased in sunflowers by applying magnetic field in either direction.

Magnetic fields can also influence the root growth of some plant species (Belyavskaya, 2001, 2004; Muraji et al., 1992, 1998; Turker et al., 2007). In the case of maize (*Zea mays*) the exposure of maize seedlings to 5 mT magnetic fields at alternating frequencies of 40–160 Hz improved root growth (Muraji et al., 1992). However, there was a reduction in primary root growth of maize plants grown in a magnetic field alternating at 240–320 Hz. The highest growth rate of maize roots was achieved in a magnetic field of 5 mT at 10 Hz. Turker et al. (2007) reported an inhibitory effect of static magnetic field on root dry weight of maize plants but there was a beneficial effect of magnetic fields on root dry weight of sunflower plants.

Belyavskaya (2004) and Turker et al. (2007) reported that a weak magnetic field has an inhibitory effect on the growth of primary roots during early growth. The proliferative activity and cell reproduction in meristem in plant roots are reduced in weak magnetic fields (Belyavskaya, 2004). The cell reproductive cycle slows down due to the expansion of the G1 phase in many plant species and the G2 phase in flax and lentil roots. There was a decrease in the functional activity of genomes at early pre-replicate period in plant cells exposed to weak magnetic fields. In general, these studies conclude that weak magnetic fields cause intensification of protein synthesis and disintegration in plant roots.

Impact of heat stress at 40°C, 42°C, and 45°C for 40 min in cress seedlings (*Lepidium sativum*) was reduced by exposing plants to extremely low-frequency (ELF) magnetic field (50 Hz, 100 µT) (Ruzic and Jerman, 2002). Magnetic fields act on the same cellular metabolic pathways as temperature stress and as such the study suggests that magnetic fields act as a protective factor against heat stress.

Magnetic treatment and seed germination

Magnetic treatment of seed or water used for germination can influence germination and seedling emergence. Reina et al. (2001) reported an increase in germination percentages of lettuce seeds by treating these with 10 mT stationary magnetic fields. They reported that magnetic fields resulted in an increase in water absorption rate of lettuce seeds and may have contributed to increased germination percentages. Some studies reported that the magnetic exposure of seeds, viz., cereals and beans, prior to sowing can improve germination rate and early growth (Pittman 1963a, b;

Pittman and Anstey, 1967). Similarly, the application of stationary magnetic fields before sowing had a significant increase in germination rates and seedling vigor in groundnut, onion, and rice seeds (Vakharia et al., 1991; Alexander and Doijode, 1995). The exposure of broad bean seeds by Podlešny et al. (2004) to variable magnetic strengths before sowing showed some beneficial effects on seed germination and emergence. In particular, they found that seedling emergence was more regular after the use of the magnetic treatment and occurred 2–3 days earlier in comparison to seedlings in the control treatment. In tomatoes, De Souza et al. (2006) observed that the magnetically treated tomato seeds improved the leaf area, leaf dry weight, and yield of tomato crop under field conditions.

The beneficial effects of magnetically treated irrigation water have also been reported on germination percentages of seeds. For example, an increase in germination of *Pinus tropicalis* seeds from 43% in the control to 81% with magnetically treated water was observed by Morejon et al. (2007). For tomatoes, pepper, cucumber and wheat seeds Hilal and Hilal (2000) reported that germination and seedling emergence was improved when magnetically treated water and seeds were used. In particular, germination of pepper seeds was higher with magnetically treated seeds when compared with magnetically treated irrigation water and cucumber seeds had the highest germination percentage when both irrigation water and seeds were magnetically treated.

How do magnetic fields influence?

The mechanisms that influence plant growth and seed germination through magnetic treatment are not well understood. Some beneficial effects of the treatment could be related to the “gas bubble-water interface” (Vallée et al., 2005). Furthermore, these effects may be related to mechanisms such as intramolecular and intra-ionic interactions, effects of Lorentz forces, dissolution of contaminants and interfacial effects (Baker and Simon, 1996). The changes in hydrogen bonding and increased mobility of Na^+ and Cl^- ions with exposure of irrigation water to magnetic fields may also play some role in the plant growth and seed germination (Chang and Weng, 2008). It is also suggested that the magnetic treatment of water may result in changes in physical and chemical properties of water such as hydrogen bonding, polarity, surface tension, conductivity, pH, refractive index and solubility of salts (Smikhina, 1981; Srebrenik et al., 1993; Amiri and Dadkhah, 2006; Otsuka and Ozeki, 2006; Chang and Weng, 2008).

Magnetic treatment and water productivity

Maheshwari and Grewal (2009) investigated the effects of magnetically treated potable water, recycled water and saline water on crop yields and water productivity under controlled environmental conditions in a glasshouse. The main aim of the study was to examine the impact of magnetic treatment of different water sources on water productivity and yield of snow peas, celery, and peas.

The study has provided some preliminary results on how the magnetic treatment influences the key parameters of (1) water – pH and EC; (2) crop – yield, water productivity, total crop water use and crop nutrient composition; and (3) soil – pH, EC, and available N, P, and K. Statistical analysis of the data indicated that the effects of the magnetic treatment varied with crop type and the source of water. There was no statistically significant effect of magnetic treatment on the total water used by the crop during the growing season in any of the three crops. However, the magnetic treatment of water tends to increase (statistically significant) crop yield (fresh weight) and water productivity (kg of fresh or dry produce per kL of water used) of celery and snow peas. On the other hand, the magnetic treatment had no significant effect on both crop yield and water productivity for peas.

In general, the results obtained during this preliminary study on the use of magnetically treated water on celery and snow peas are interesting but the effect of the magnetic treatment on crop yield and water productivity was variable and occurred under some set of conditions and not in others. Therefore, from the glasshouse experimental data, it is difficult to make any recommendation with certainty as to the effectiveness of the magnetic treatment under field conditions.

Summary

The past studies reveal that the magnetic field or treatment can affect plant growth and other related parameters. Similarly, the past studies have indicated that there are some beneficial effects of magnetic treatment on seed germination and seedling emergence. Nevertheless, we have no clear understanding yet as to the mechanisms behind these effects on plant growth, water productivity, and the changes magnetic treatment brings about in nutritional aspects of seed germination and seedling growth.

To assess the potential of the magnetic treatment for practical applications, we need further testing under field conditions to clearly understand and demonstrate the beneficial effects of the magnetically treated irrigation water for crop production under real-world situations. Further research is also warranted to understand how the magnetic treatment affects crop and soil parameters and therefore soil, crop and water quality conditions under which the treatment will be effective to provide water productivity gains.

Bibliography

- Alexander, M. P., and Doijode, S. D., 1995. Electromagnetic field: a novel tool to increase germination and seedling vigour of conserved onion (*Allium cepa* L.) and rice (*Oryza sativa* L.) seeds with low viability. *Plant Genetic Resources Newsletter*, **104**, 1–5.
- Amaya, J. M., Carbonell, M. V., Martinez, E., and Raya, A., 1996. Effects of stationary magnetic fields on germination and growth of seeds. *Horticultural Abstracts*, **68**, 1363.
- Amiri, M. C., and Dadkhah, A. A., 2006. On reduction in the surface tension of water due to magnetic treatment. *Colloids and Surfaces, A: Physicochemical and Engineering Aspects*, **278**, 252–255.

- Baker, J. S., and Simon, J. J., 1996. Magnetic amelioration of scale formation. *Water Research*, **30**, 247–260.
- Belyavskaya, N. A., 2001. Ultrastructure and calcium balance in meristem cells of pea roots exposed to extremely low magnetic fields. *Advances in Space Research*, **28**, 645–650.
- Belyavskaya, N. A., 2004. Biological effects due to weak magnetic field on plants. *Advances in Space Research*, **34**, 1566–1574.
- Blank, M., 1995. Biological effects of environmental electromagnetic fields: molecular mechanisms. *BioSystems*, **35**, 175–178.
- Chang, K. T., and Weng, C. I., 2008. An investigation into structure of aqueous NaCl electrolyte solutions under magnetic fields. *Computational Materials Science*, **43**, 1048–1055.
- Danilov, V., Bas, T., Eltez, M., and Rizakulyeva, A., 1994. Artificial magnetic field effects on yield and quality of tomatoes. *Acta Horticulturae*, **366**, 279–285.
- De Souza, A., Garcí, D., Sueiro, L., Gilart, F., Porras, E., and Licea, L., 2006. Pre-sowing magnetic treatments of tomato seeds increase the growth and yield of plants. *Bioelectromagnetics*, **27**, 247–257.
- Duarte Diaz, C. E., Riquenes, J. A., Sotolongo, B., Portuondo, M. A., Quintana, E. O., and Perez, R., 1997. Effects of magnetic treatment of irrigation water on the tomato crop. *Horticultural Abstracts*, **69**, 494.
- Esitken, A., and Turan, M., 2004. Alternating magnetic field effects on yield and plant nutrient element composition of strawberry (*Fragaria x ananassa* cv. *camarosa*). *Acta Agriculturae Scandinavica. Section B: Soil and Plant Science*, **54**, 135–139.
- Goodman, R., Bassett, C. A., and Henderson, A., 1983. Pulsing electromagnetic fields induce cellular transcription. *Science*, **220**, 1283–1285.
- Hilal, M. H., and Hilal, M. M., 2000. Application of magnetic technologies in desert agriculture. 1 – Seed germination and seedling emergence of some crops in a saline calcareous soil. *Egyptian Journal of Soil Science*, **40**, 413–422.
- Johnson, C. C., and Guy, A. W., 1972. Non-ionizing electrostatic wave effects in biological materials and systems. *Proceedings of Institute of Electrical and Electronics Engineers*, **60**, 692–718.
- Lin, I. J., and Yovvat, J., 1990. Exposure of irrigation and drinking water to a magnetic field with controlled power and direction. *Journal of Magnetism and Magnetic Materials*, **83**, 525–526.
- Maheshwari, B. L., and Grewal, H. S., 2009. Magnetic treatment of irrigation water: its effects on vegetable crop yield and water productivity. *Agricultural Water Management*, **96**, 1229–1236.
- Moon, J., and Chung, H., 2000. Acceleration of germination of tomato seeds by applying AC electric and magnetic fields. *Journal of Electrostatics*, **48**, 103–114.
- Morejon, L. P., Castro Palacio, J. C., Velazquez Abad, L. G., and Govea, A. P., 2007. Simulation of *pinus tropicalis* M. seeds by magnetically treated water. *International Agrophysics*, **21**, 173–177.
- Muraji, M., Nishimura, M., Tatebe, W., and Fujii, T., 1992. Effect of alternating magnetic field on the growth of the primary root of corn. *Institute of Electrical and Electronics Engineers Transaction of Magnetics*, **28**, 1996–2000.
- Muraji, M., Asai, T., and Tatebe, W., 1998. Primary root growth rate of *Zea mays* seedlings grown in an alternating magnetic field of different frequencies. *Biochemistry and Bioenergetics*, **44**, 271–273.
- Otsuka, I., and Ozeki, S., 2006. Does magnetic treatment of water change its properties? *The Journal of Physical Chemistry*, **110**, 1509–1512.
- Paradisi, S., Donelli, G., Santini, M. T., Straface, E., and Malorni, W., 1993. A 50-Hz magnetic field induces structural and biophysical changes in membranes. *Bioelectromagnetics*, **14**, 247–255.
- Pittman, U. J., 1963a. Magnetism and plant growth. 1. Effect on germination and early growth of cereal seeds. *Canadian Journal of Plant Science*, **43**, 512–518.
- Pittman, U. J., 1963b. Magnetism and plant growth. III. Effect on germination and early growth of corn and beans. *Canadian Journal of Plant Science*, **45**, 549–555.
- Pittman, U. J., and Anstey, T. H., 1967. Magnetic treatment of seed orientation of a single harvest snap bean (*Phaseolus vulgaris* L.). *Proceedings of American Society of Horticultural Science*, **91**, 310–314.
- Podleśny, J., Pietruszewski, S., and Podleśna, A., 2004. Efficiency of the magnetic treatment of broad bean seeds cultivated under experimental plot conditions. *International Agrophysics*, **18**, 65–71.
- Reina, F. G., Pascual, L. A., and Fundora, I. A., 2001. Influence of a stationary magnetic field on water relations in lettuce seeds. Part II: experimental results. *Bioelectromagnetics*, **22**, 596–602.
- Ruzic, R., and Jerman, I., 2002. Weak magnetic field decreases heat stress in cress seedlings. *Electromagnetic Biology and Medicine*, **21**, 69–80.
- Smikhina, L. P., 1981. Changes in refractive index of water on magnetic treatment. *Colloid Journal*, **2**, 401–404.
- Srebrenik, S., Nadiv, S., and Lin, L. J., 1993. Magnetic treatment of water – a theoretical quantum model. *Magnetic and Electrical Separation*, **5**, 71–91.
- Turker, M., Temirci, C., Battal, P., and Erez, M. E., 2007. The effects of an artificial and static magnetic field on plant growth, chlorophyll and phytohormone levels in maize and sunflower plants. *Phyton-Annales Rei Botanicae*, **46**(2), 271–284.
- Vakharia, D. N., Davariya, R. L., and Parameswaran, M., 1991. Influence of magnetic treatment on groundnut yield and yield attributes. *Indian Journal of Plant Physiology*, **34**, 131–136.
- Vallée, P., Lafait, J., Mentré, P., Monod, M. O., and Thomas, Y., 2005. Effects of pulsed low frequency electromagnetic fields on water using photoluminescence spectroscopy: role of bubble/water interface. *The Journal of Chemical Physics*, **122**, 114513–8.

Cross-references

- [Irrigation with Treated Wastewater, Effects on Soil Structure](#)
[Magnetic Properties of Soils](#)
[Physics of Plant Nutrition](#)
[Plant Roots and Soil Structure](#)
[Plant–Soil Interactions, Modeling](#)
[Plant Wellness](#)
[Water Use Efficiency in Agriculture: Opportunities for Improvement](#)

MANAGEMENT EFFECTS ON SOIL PROPERTIES AND FUNCTIONS

Rainer Horn

Institute for Plant Nutrition and Soil Science,
Christian-Albrechts-University zu Kiel, Kiel,
Germany

Definition

The introduction and application of agricultural and forestry machinery often result in severe soil compaction and soil deformation with intense decrease in total pore volume, alterations in the pore-size distribution, and especially in their functions concerning gas, water and heat transfer as well as altered accessibility of chemical adsorption sites of clay minerals, organic substances, and further variable exchange places.

Introduction

Soils as three-phase systems fulfill not only the archive function (historical memory of former properties, climates, management practices, land use, etc.), they are essentially needed for plant growth and yield, as reservoir for microbes and they are also responsible for filtering and buffering of soil water in order to get clean drinking- and groundwater, they contribute to the transformation under *in situ* conditions and serve as the resource for raw material. In the following, the process of soil deformation will be shortly summarized in order to derive the interactions between soil structure and chemical as well as physical and biological properties, which are affected by soil deformation. Finally, some conclusions for a sustainable land use and soil management will be given.

Soils: their functions in view of the existing soil protection laws or recommendations

Soils as nonrenewable goods have to be protected and should be only used according to their properties. The European Soil Charta 1972 of the European Assembly was the first, which did underline and support this idea and which in 1998 became the nucleus for the German Soil Protection Law. This law was the first and until now the only one in Europe while, e.g., the European Soil Framework Directive (2006) is still under a very controversial debate. However, there is an urgent need to specify more in detail the requests and limitations but also to quantify the limits of an unprevented or unhindered land use. It has to be pointed out that for a sustainable soil land use their physical, chemical, and biological soil functions must be related to the intensity and function values and have to include the dependent recommendations in order to prevent any irreversible soil degradation.

If we consider the properties for arable horticulture, landscape planning, and in forestry soils, they all require primarily a sufficiently rigid pore system, which guarantees the water, gas and heat exchange, nutrient transport and adsorption as well as an optimal rootability, which also includes a sufficient microbial activity and composition in order to also decompose the plant debris. All these requests must be included in a quantitative way in the Protection law but there is still an urgent need to specify these “optimal” properties. However, it is very difficult for the land user to forecast and to relate their own farming management practices to coming weather conditions, e.g., the storage capacity for water and nutrients in the topsoil sufficient to grow a good crop yield during the following season under dry conditions or are the soils permeable enough to drain off the access rain water and to reaerate the root zone quick enough in order to avoid declining redox potential values and the accumulation of anoxic gases in the pores. Thus, the major challenges are interlinked between soil and weather conditions, which request a more intense analysis of the effect of soil structure on the nutrient, gas, and water fluxes in anthropogenically managed soils under various land uses.

Processes of aggregate formation and persistence

Soils containing more than 12% clay (particle size < 2 µm) or even pure sandy soils with some salts tend to form aggregates. Usually the process occurs when soils dry and swell, and it is further enhanced by biological activity. Aggregates may show great variation in size from crumbs (diameter < 2 mm) to polyhedres or subangular blocks of 0.005–0.02 m, or even to prisms or columns of more than 0.1 m. During the first period of shrinkage, mineral particles are pulled together by capillary forces, which increase the number of points of contact and result in a higher bulk density. The initial aggregates always have rectangular-shaped edges because, under these conditions, stress release would occur perpendicular to the initial crack and stress would remain parallel to the crack (strain-induced fracturing). However, due to the increased mechanical strength the particle mobility declines and results in the formation of nonrectangular shear plains as the following crack generation. They are created after repeated swelling and shrinking processes and result in fractures in which the value of the angle of internal friction determines the deviation from 90° (Or and Ghezzehei, 2002). In newly formed aggregates, the number of contact points depends on the range of water potential and on the distribution of particle sizes as well as on their mobility (i.e., state of dispersion, flocculation, and cementation). Soil shrinkage, including crack formation, increases bulk density of aggregates. The increase in bulk density with the initial wetting and drying of the soil permits the aggregates to withstand structural collapse. The increase of the strength of single aggregates is further enhanced by a particle rearrangement, if the soil is nearly saturated with water increasing the mobility of clay particles due to dispersion and greater menisci forces of water (Horn and Dexter, 1989). Subsequent drying causes enhanced adhesion by capillary forces, which lead to greater cohesion as mineral particles are brought into contact following the evaporatory losses of the capillary water. Thus, the strength of the bigger, i.e., initial aggregates is increased due to a particle mobilization and results both in smaller and stronger aggregates with even a smaller aggregate bulk density. The strongest aggregate type under this aspect is the spherical shape, which has reached the stage of the smallest free entropy. Therefore, aggregate strength depends on (1) capillary forces, (2) intensity of shrinkage (normal/residual), (3) number of swelling and shrinkage cycles, i.e., the shrinkage/swelling history, (4) mineral particle mobility (i.e., rearrangement of particles to achieve arrangements of lowest free energy), and (5) bonding energy between particles in/or between aggregates or in the bulk soil. Generally, aggregates persist as long as the soil strength (defined by the failure line of Mohr–Coulomb) is higher than the given load or shrinkage forces soils remain rigid. If however, additional kinetic energy (which even is more efficient in combination with accessible water) is applied, aggregate deterioration and homogenization occur. Thus, a complete

homogenization of the soil structure due to shearing and/or puddling takes place if kneading (expressed as octahedral shear stresses and mean normal stresses) exceeds the aggregate and structure strength. After a mostly complete homogenization normal shrinkage, processes restart again (Horn et al., 1994). Consequently, a weaker soil structure and finally a pasty structure can be defined by very small cohesion and angle of internal friction values (Horn, 1976; Janssen et al., 2006). Thus, the determination of soil and/or aggregate strength has always to be subdivided into (1) mechanically, hydraulically, or chemically prestressed and (2) virgin conditions, which also ultimately affect the predictability of physical properties. These general ideas have been described in greater detail by Horn and Baumgartl (2002), Groenevelt and Grant (2002), Grant et al. (2002), and Peng and Horn (2005).

In conclusion, it has to be stated, that aggregate formations as well as changes in aggregate strength are directly related also to tillage systems. Conventional tillage especially of the A-horizon annually includes plowing, chiseling, and the seedbed preparation apart from multiple wheeling events depending on the crop management requirements, which ends in mostly homogenized structure conditions annually. Thus, a more complete aggregate formation will not take place. Conservational tillage systems on the other hand causes less disturbance and allow a more complete rearrangement of particles and strengthening of the structure system if preserved throughout several years.

Soil structure and soil use: how to sustain the required and natural soil and site-specific functions

During the last 4 decades, not only the mass of the agricultural and forestry machines but also the frequency of wheeling has increased intensely and resulted in a compression and soil deformation status, which can be suboptimal concerning plant growth and crop yield as well as the uncertainty of getting a predictable yield. At present, the maximum mass of machines exceeds by far 60 Mg and therefore also enhance the probability of subsoil compaction and long-term soil degradation. Not only in agriculture but also in forestry, such enlarged machines are used for tree harvesting and clear cutting and results in an intense subsoil degradation due to shear and vibration induced soil deformation especially if the soil water content in the subsoil is high and the internal soil strength very low (Horn et al., 2007).

Soil processes like the formation of a platy structure, deterioration of a continuous pore system are therefore signs of an intense soil degradation, which also coincides with an increased anisotropy of pore functions and may cause an increased lateral soil movement (= soil water erosion). For more details, see Soane and van Ouwerkerk (1994), Pagliai and Jones (2002), Ehlers et al. (2003), Lipiec and Hatano (2003), and Horn et al. (2005, 2006).

Consequences of soil deformation on changes in soil functions

Cation adsorption capacity, intensity, and accessibility

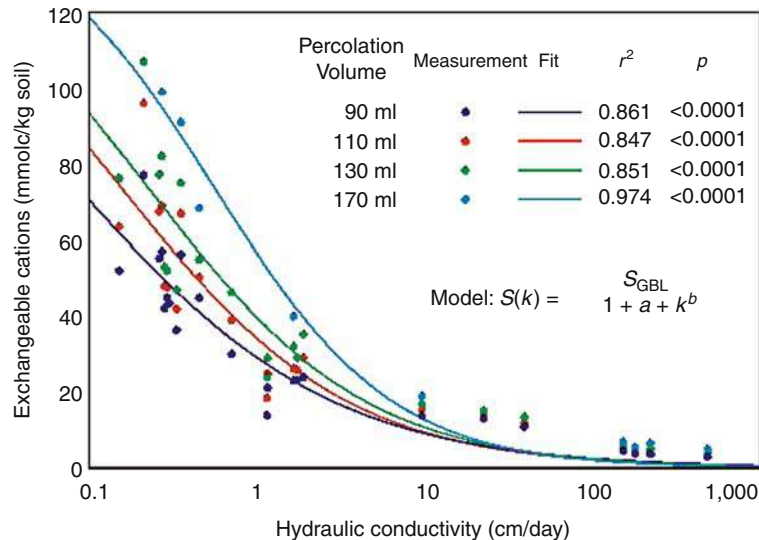
Soil aggregates can be classified by a certain accessibility of the exchange places for cations, which in comparison with that one of the homogenized material may be intensely reduced. We have to differentiate between the capacity and intensity properties. In homogenized soils, capacity (= potential) and intensity (= actual) parameters are identical, which holds true especially for the seedbed where fertilized ions are mostly adsorbed at the exchange places of the soil particles. For soil horizons with a prismatic structure, we can assume a reduction of up to 15% from the potential properties, while soil horizons with blocky or subangular blocky structure will even have a reduction of up to 50–80%.

In this context also soil texture and bulk density of the bulk soil and of the single aggregates further affect these actual conditions. Soils with a crumbly structure have again an improved accessibility due to a macroscopic homogenization of the aggregates themselves by the microbial activity as can be also derived from their particle and organic substance arrangement in the bulk soil. Thus, we can assume a nearly 90% accessibility of the cation exchange capacity values under these conditions. If, however, soils have a platy structure, the intensity (= actual) properties are as small as 30% of the capacity values due to the compressed pores in between singles particles within the plats and because of correspondingly retarded ion mass flow and diffusion within the plats. Thus, plats provide the greatest differences between the capacity and intensity properties and therefore also the most reduced accessibility of the exchange places. These differences can also be derived from the relationship between the exchangeable cations and the actual hydraulic conductivity, which is a measure of the effect of preferential flow processes. Compared to the theoretical CEC of 140 mmol kg⁻¹ soil, the actual values were the smaller the higher was the hydraulic conductivity (Figure 1). The drier the soil the smaller the water fluxes and the more retarded are the exchange processes the higher is the actual value but it will not reach the maximum values under the dominating hydraulic site properties (Figure 2).

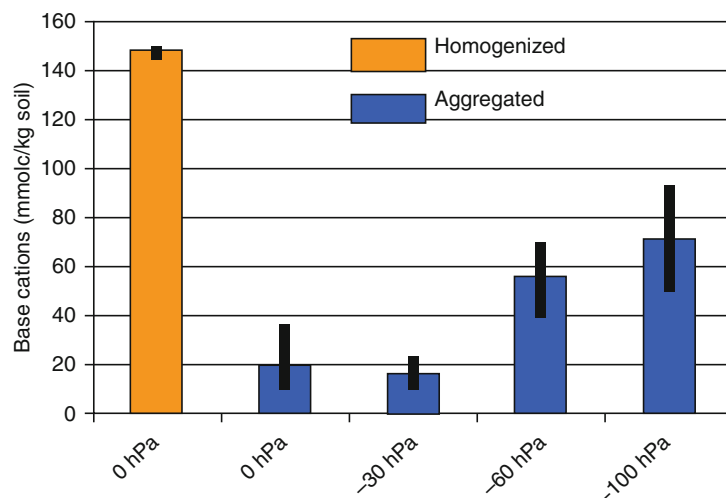
Thus, neither the fertilized nutrients nor the natural ions within the soil can be fully accounted for a good yield, if the aeration, the accessibility, and nutrient availability are not provided.

Soil water and gas

An increased soil volume coincides with a reduced pore volume with the dominance of finer pores and less coarser ones. Thus, the air capacity is reduced with increasing soil deformation but the changes in the pores, which contain the water available for plants depends on the applied stresses as well as the texture and the bulk density.



Management Effects on Soil Properties and Functions, Figure 1 Effect of soil structure on chemical exchange processes (taken from Hartmann et al., 1998).



Management Effects on Soil Properties and Functions, Figure 2 Effect of predrying and of aggregation on the base cation adsorption in comparison to the homogenized conditions (Bt-horizon of a Luvisol derived from loess, blocky structure).

The hydraulic conductivity as a water available for plants depends tensorial function in principle decreases with applied stresses by many orders of magnitude while the unsaturated hydraulic conductivity is even increased at a given matric potential value (Figure 3).

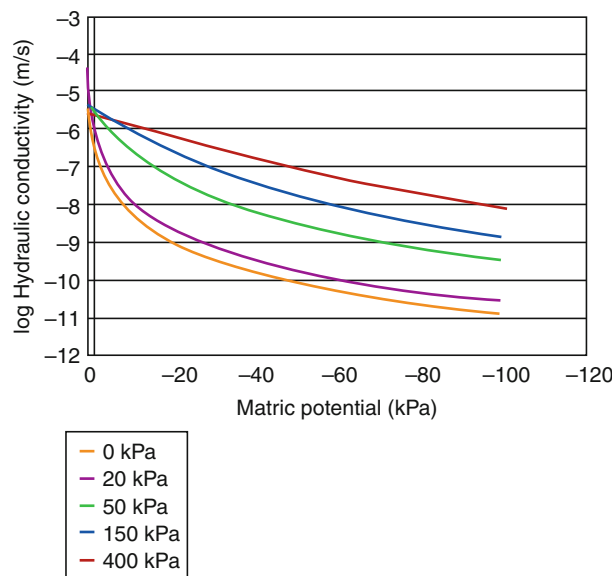
Even more important is the increased relevance of the anisotropy of hydraulic functions. Mualem (1984), Tigges (2000), Doerner (2005), and Doerner and Horn (2009) documented the increasing effect of stress-and shear-affected horizontal anisotropy of the hydraulic and gas permeability, which coincides not only with a retarded gas exchange and an increased proportion of, e.g., CO₂

in the pores but which will also result in an enhanced lateral water flow and soil erosion. Figure 4 documents the stress-and strain-induced changes in hydraulic properties and functions.

Effect of soil management on gas composition

Each reduction in conducting coarse pores also result not only in a prevented CO₂ exchange to the atmosphere and a prevented O₂ flux in the soil but will also lead to anoxic conditions in the soil, which will also affect the quality and quantity of the emitted gas (Glinski and Stepniewski, 1985).

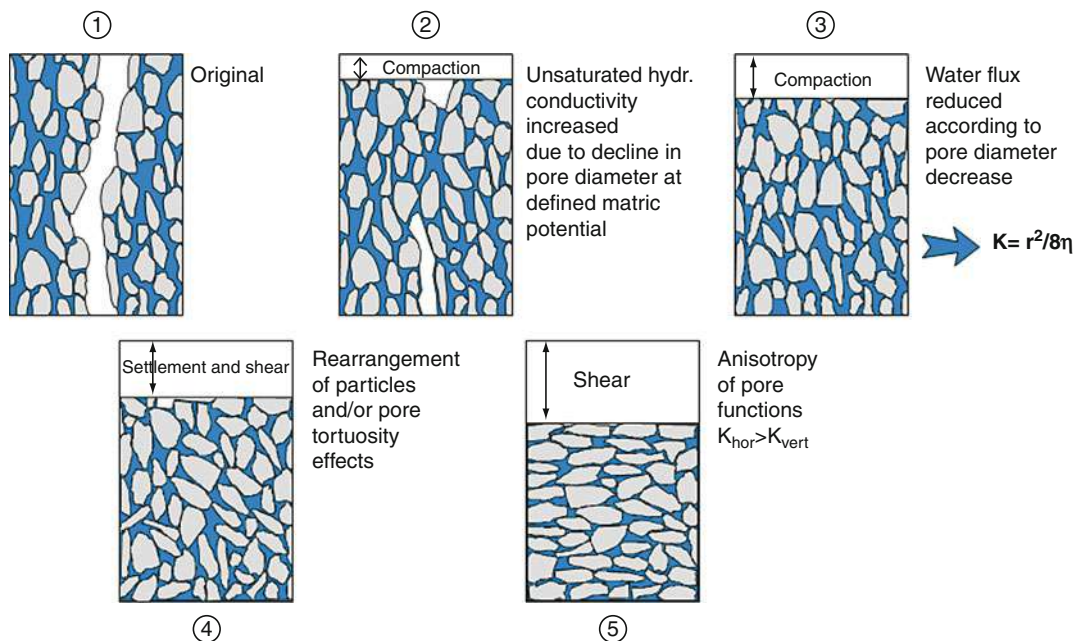
Aeration and gas exchange in soils always depend on the microbial composition and activity, which depending on the pH value and water saturation can lead to an enormous alteration of the gas composition, microbial activity and composition, and redox potential values. As an example of possible stress effects on redox potential changes in dependence of the internal soil strength (expressed as



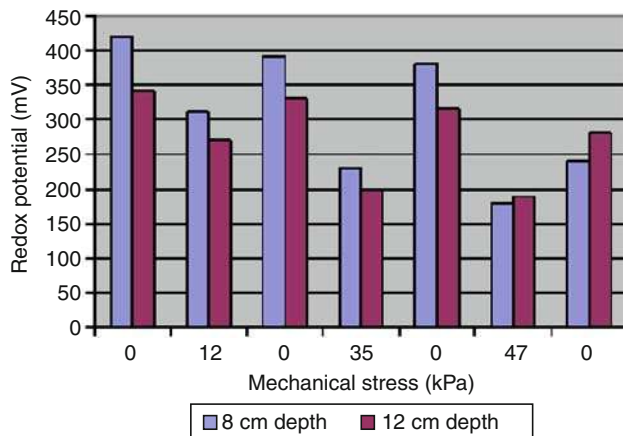
Management Effects on Soil Properties and Functions,
Figure 3 Stress-dependent change of hydraulic properties: hydraulic conductivity as a function of matric potential.

precompression stress) Figure 5 informs stress-dependent Eh value changes in an Ah horizon of a Cambisol. It can be seen that stressing with up to 35 kPa followed by a stress release (0 kPa) at both depths always resulted in a complete recovery. If exceeding the internal soil strength of approximately 42 kPa by a further increase to 47 kPa a significant and irreversible decline was detected with no recovery after stress release. Thus, all chemical elements, which undergo a valence change, depending on the actual Eh value at the given pH may be also mobilized and translocated to the more aerated soil volumes. Amongst the Eh-sensitive elements are under more un-aerated soil conditions, e.g., from the completely aerated condition: NO_3^- (to N_2O or at last NH_4^+) or CO_2 (to CH_4 in case of complete anoxic conditions) as well as Fe^{3+} to 2^+ or Mn^{4+} to 2^+ . Thus, also the chemical compositions of the gas composition in the soil or that of the seepage water are affected.

Ball et al. (2000), e.g., described the effect of N_2O emission due to wheeling throughout the year and also included N-fertilization. In compacted soils, N_2O emission was significantly increased after fertilization and especially if in addition rainfall had re-saturated the soil. Under zero compaction, no intense changes were to be seen, which can be explained by a higher water infiltration rate and a quicker reaeration of the coarse and gas and water-conducting pores. If we further consider the compaction dependent reduction of CH_4 consumption in soils, which is approximately 50%, we can also calculate the CO_2 equivalents from CH_4 consumption are texture dependent (Teepe et al., 2004): 47 kg ha^{-1} a (silty clay loam), 157 (silt), and 249 (sandy loam). Assuming that



Management Effects on Soil Properties and Functions, Figure 4 Stress and strain effects on hydraulic properties.



Management Effects on Soil Properties and Functions,
Figure 5 Redox potential values as a function of applied cyclic mechanical stress. Cambisol Ah horizon, pH: 5.2, -60 hPa (data taken from Horn, 1985).

only 6% of the area was compacted, the reduction of the CH_4 consumption in terms of CO_2 equivalents resulted in 4, 11, and 13 $\text{kg CO}_2 \text{ha}^{-1} \text{a}^{-1}$. In forest soils, the spatial pattern of the depth dependent CO_2 concentration reveals a significant increase directly below the wheel track, which fades off to the side and to the depth (Figure 6).

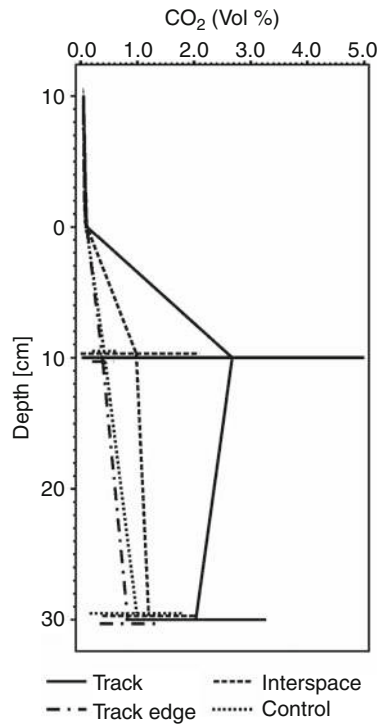
Based on the dataset of Stepniewska et al. (1997), a soil texture-dependent resistivity values for a given redox potential value of 300 mV could be used to quantify the resistance against Eh changes. If 300 mV irrespective of the stress applied at a given texture is still available after 5 days, we could classify the soil as rigid. If, on the other hand, within less than 3 days the critical value is further declined a more severe stress effect has to be considered.

Soil deformation and thermal properties

Denser, less aerated, and more water saturated soils are not only less aerated but they are mostly cold due to the higher specific heat capacity and thermal conductivity.

Additionally, radiation effects are reduced during cold nights but as a negative effect also the often expected freezing effect for structure reamelioration is furthermore reduced.

Under European climatic conditions, such soil amelioration is mostly restricted to the plowed A horizon but does not deeper down. Even if the subsoil gets frozen, the ice lense formation gain would primarily create a horizontal platy structure due to water volume expansion during freezing. Furthermore, we have to evaluate the orientation of newly formed pores, which as soon as they are mostly horizontally oriented would collapse during the following restressing of the topsoil during trafficking.



Management Effects on Soil Properties and Functions,
Figure 6 CO_2 -concentration in the soil air at different depths and distance from the wheel track due to the application of a chain harvester (45 Mg) in the Black Forest. The wheeling was carried out in 2000 (taken with courtesy from J. Schäffer, 2005).

Soil deformation and microbial activity

Soil compaction causes a reduced accessibility for soil microbes, which may be partly not negative because the damages caused by ingestion through collemboles and mollusk are reduced. The activity of earthworms (penetration and formation of new burrows) depends on the internal soil strength. They can apply up to 200 kPa lateral pressure in order to translocate soil particles to the side and even 100 kPa in radial direction. The less intense the tillage treatments the higher are the number of earthworms. Under conservation tillage, more than 100 individuals were counted per meter square, while less than ten were available at the same time under conventional tillage in a luvisol derived from loess. However, even if we consider these 100 individuals/m² their activity results only in the realevation of 30 Mg/ha *a (for year), which is an enormous amount but less than 1% of the strain-affected soil compaction. McKenzie et al. (2009) documented that earthworms like *Lumbricus* and *Allolobophora* species can withstand high external stresses, which is not the fact for mesofauna: acari and collembolae, which will be squeezed under the wheels even within the top 30-cm apart from the fact that soil compaction and deformation result in a retarded aeration and accumulation of CO_2 or even CH_4 in soil pores and hinders the normal population growth.

Consequences of soil deformation on further environmental processes

The effects of soil compaction on plant growth are widespread. They depend not only on the intensity of soil compaction but also on the plant properties themselves.

The closer to the soil surface and the thicker the compacted layer is, the more pronounced negative effect on plant growth and yield. It is essential to analyze whether or not the compacted soil layer is completely impermeable or there are still a few coarse pores, which can help to reach the deeper and less dense soil layers and to overcome such limitations in the topsoil. Oxygen deficiency results in a reduced root growth, increased CO₂ and ethylene concentration and the formation of short-chained fatty acids in the soil. Because the stress propagation with depth is always three-dimensional, we also have to analyze the effects in deeper depth because compacted areas at depth will be mostly surrounded by roots but not penetrated and cause a reduced availability of nutrients and also of oxygen at these depths.

Consequences of soil deformation on soil erosion

It is obvious that stress application always results in the formation of a platy structure and horizontally oriented coarse pores, which increase the horizontal hydraulic conductivity and result in an increased water and solute transport. Among others Fleige (2000) proofed that the soil loss due to water erosion in the slightly sloppy glacial till region of Schleswig Holstein increased ten times compared to non compacted sites and also resulted in a downhill mass transport of more than 35 Mg ha⁻¹ a⁻¹ and the formation of a colluvisol in the flatter region (onsite damage compared to the even worse offsite effects).

Some remarks on crop yield

From the agricultural point of view, crop yield and the net benefit are the main criterion. Thus, yield decline of up to 35% in the first year after soil compaction are to be considered as more than critical. But even if these reductions are only rarely to be seen the uncertainty of getting sufficient yield continuously increased over the years. At present, more than 32 Mio ha of arable soils are irreversibly degraded even only in Europe due to soil compaction the effect is even continuously increasing in recent years. The yield decline due to soil compaction for sugar beets can be derived from the smaller beet weight per ha also because the destruction of the beets during harvest is increased.

Van den Akker et al. (1999) mentioned that a single wheeling with a 38 Mg sugar beet harvester results in an annual yield loss of 0.5%, which sums up to approximately 100 Mio € a⁻¹ loss calculated on the basis of 500,000 ha in Europe.

If the machine mass of the sugar beet harvesters increases with 5 Mg/10 years (as it was the fact in the past), we have to even expect higher yield losses in the future. Concerning the yield losses of corn in the USA

we have to consider approximately 6%/year due to soil compaction while corresponding losses of grain in the former USSR results in 7–8% of the total yield; sugar beets showed a decline by 3% while corn yield was lowered by 4% due to soil compaction effects. Finally, in Germany the often predicted wheat yield increase due to the beneficial climate, soil and genetic properties of the seeds under the improved CO₂ concentration in the atmosphere and the higher temperature only resulted in 0.1 Mg ha⁻¹ a⁻¹ in Schleswig Holstein while in Bavaria the yield remained only constant irrespective of all these improvements because the proportion of the headland increased because of the larger machines, which require more space for turning round in comparison to the total field area.

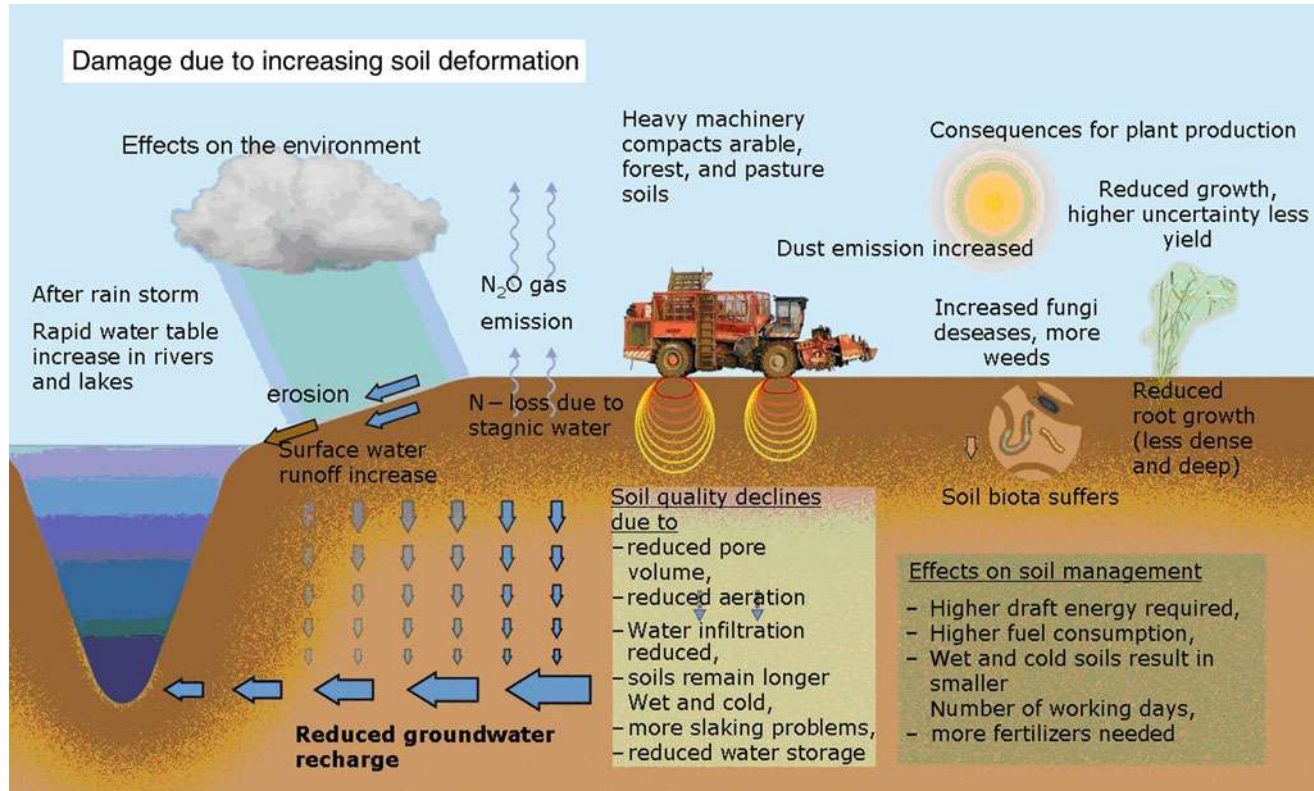
Effect of soil structure degradation on the landscape hydrology

Deep drainage of rainwater requires permeable soils with a continuous and large pore system. As soon as the arable landscapes remain compacted with a reduced water infiltrability (can be reduced up to three orders of magnitude) and storage capacity. Very pronounced are these effects during and after heavy rainstorm events and can result in an increased surface water runoff also in combination with a pronounced nutrient and heavy metal leaching. If during a rain storm most of the pores become water saturated but only the coarse pores (which due to soil compaction are reduced in diameter and total amount) are still aerated but additional rainwater will completely saturate the soil volume, then the storage capacity is quickly filled and all the additional rainwater will result in surface water runoff.

If we further assume that the natural saturated hydraulic conductivity of uncompacted soils in the loess area with approximately 40% pore volume reaches 2.7 cm day⁻¹ on average we can assume a corresponding water infiltration of 2.7 cm day⁻¹ at a hydraulic gradient of 1. If due to soil compaction the hydraulic conductivity is reduced to 1 cm day⁻¹ but the rainfall is the same as before, 1.7 cm day⁻¹ of water contribute to the surface water volume. If we now multiply this amount with the total landscape area, the small value of 17 l m⁻² result in 17,000 m³ km⁻². Thus, the high floods in riverbeds like the Rhine or Elbe in Germany can be easily also related to the negative effects of subsoil compaction. Soil slaking due to the kinetic energy input of the water droplets, which is the more pronounced, the higher is the initial water saturation in combination with the increased shear forces of the water suspensions result in an even higher soil deterioration and soil loss (for more detailed information see Van der Ploeg and Schweigert, 2001 and Gieska et al., 2003).

Protection measures

The worldwide identical tendency of increased machine masses at an identical contact area pressure, which is far beyond the acceptable values for a sustainable land management prevent a natural reamelioration of the



Management Effects on Soil Properties and Functions, Figure 7 Summary of the effects of stress application on soil properties and functions (translated and slightly modified from van der Ploeg et al., 2006).

precompressed (= overcompacted) soils by increasing the pore volume and improved pore continuity. In order to gain better and safer growth conditions, these precompressed (= overcompacted) and deformed soils must be improved by more site-adjusted soil management systems (conservation instead of conventional tillage and a more intense shrinkage due to water uptake by roots followed by a corresponding increased soil shrinkage and stabilization. The consequent application of traffic lanes for all field operations would result in normal compacted seedbeds in between (like in horticulture) with highest yields, the consequent application of machines, which are light and have a contact area pressure smaller than the precompression stress over depth throughout the years/decades will certainly result in a newly arranged and stronger pore system, which guarantees a better aeration and quicker water infiltration linked with a better rootability.

In the past, numerous approaches tried to improve the effectiveness of the machines and to reduce the soil deformation risk but all attempts like reduced tire inflation pressure, belts, larger tires were not as successful as expected because the main problem remains the still increasing machine mass and/or the frequency of wheeling throughout the year. The final concluding picture, which underlines the multidisciplinary effects of soil deformation on site properties is shown in Figure 7.

Summary

The rigidity of soils depends primarily on the internal particle arrangement and thus on the rigidity of the soil structure, which guarantee gas, water, heat, and nutrient transport and exchange processes. If, however, the external stresses applied exceed the internal soil strength, not only the pore system collapse and will be diminished in volume and size but also the pore continuity and the accessibility of surfaces (e.g., for cation exchange) are negatively affected. Consequently, not only the plant growth, yield, and the predictability of them become more undefined but also the emission of green house gases increases or flooding events will occur more often.

Bibliography

- Ball, B. C., Horgan, G. W., and Parker, J. P., 2000. Short range spatial variation of nitrous oxide fluxes in relation to compaction and straw residue. *European Journal of Soil Science*, **51**, 607–616.
- Doerner, J., 2005. *Anisotropie von Bodenstrukturen und Porenfunktionen in Böden und deren Auswirkung auf Transportprozesse im gesättigten und ungesättigten Zustand*. PhD thesis, H. 68, ISBN: 0933-680X.
- Doerner, J., and Horn, R., 2009. Direction-dependent behavior of hydraulic and mechanical properties in structured soils under conventional and conservation tillage. *Soil and Tillage Research*, **102**, 225–233.

- European Soil Framework Directive (2006) Proposal for a directive of the European parliament and of the council establishing a framework for the protection of soil and amending directive. 2004/35/EC, p. 30.
- Ehlers, W., Schmidtke, K., and Rauber, R., 2003. Änderung der Dichte und Gefügefunktion südniedersächsischer Lössböden unter Ackernutzung. *Landnutzung und Landentwicklung*, **44**, 9–18.
- Fleige, H., 2000. *Ökonomische und ökologische Bewertung der Bodenerosion am Beispiel einer Jungmoränenlandschaft Ostholsteins*. PhD thesis, Schriftenreihe des Instituts für Pflanzenernährung und Bodenkunde, H. 53, ISBN: 0933-680X.
- Gieska, M., van der Ploeg, R. R., Schweigert, P., and Pinter, N., 2003. Physikalische Bodendegradierung in der Hildesheimer Börde und das Bundes-Bodenschutzgesetz. *Berichte über Landwirtschaft*, **81**(4), 485–511.
- Glinski, J., and Stepniewski, W., 1985. *Soil Aeration and Its Role for Plants*. Boca Raton: CRC Press. 287 pp.
- Grant, C. D., Groenevelt, P. H., and Bolt, G. H., 2002. On hydrostatics and matrastatics of swelling soils. In Raats, P. A. C. et al. (eds.), *Environmental Mechanics: Water, Mass, and Energy Transfer in the Biosphere*. Geophysical Monograph 129, AGU, pp. 95–105.
- Groenevelt, P. H., and Grant, C. D., 2002. Curvature of shrinkage lines in relation to the consistency and structure of a Norwegian clay soil. *Geoderma*, **106**, 235–247.
- Hartmann, A., Gräsle, W., and Horn, R., 1998. Cation exchange processes in structured soils at hydraulic properties. *Soil and Tillage Research*, **47**, 67–73.
- Horn, R., 1976. Festigkeitsänderungen infolge von Aggregierungsprozessen eines mesozoischen Tones. Diss. TU Hannover.
- Horn, R., 1985. Die Bedeutung der Trittverdichtung durch Tiere auf physikalische Eigenschaften alpiner Böden. *Z.f. Kulturtechnik u. Flurbereinigung* **26**, 42–51.
- Horn, R., and Dexter, A. R., 1989. Dynamics of soil aggregation in an irrigated desert loess. *Soil and Tillage Research*, **13**, 253–266.
- Horn, R., Taubner, H., Wuttke, M., and Baumgartl, T., 1994. Soil physical properties and processes related to soil structure. *Soil and Tillage Research*, **30**(Special Issue), 187–216.
- Horn, R., Van Den Akker, J. J. H., and Arvidsson, J. (eds.), 2000. Subsoil compaction: distribution, processes and consequences. *Advances in GeoEcology*, **32**, 480S, Reiskirchen.
- Horn, R., and Baumgartl, T., 2002. Dynamic properties of soils. In Warrick, A. W. (ed.), *Soil Physics Companion*. Boca Raton: CRC, pp. 17–48.
- Horn, R., Fleige, H., Peth, S., and Peng, X. H. (eds.), 2006. Soil management for sustainability. *Advances in GeoEcology*, **38**, 497 pp. ISBN: 3-923381-52-2.
- Horn, R., Fleige, H., Richter, F.-H., Czyz, E. A., Dexter, A., Diaz-Pereira, E., Dumitru, E., Enache, R., Rajkai, K., De La Rosa, D., and Simota, C., 2005. SIDASS project part 5: prediction of mechanical strength of arable soils and its effects on physical properties at various map scales. *Soil and Tillage Research*, **82**, 47–56.
- Horn, R., Vossbrink, J., Peth, S., and Becker, S., 2007. Impact of modern forest vehicles on soil physical properties. *Forest Ecology and Management*, **248**, 56–63.
- Janssen, I., Peng, X., and Horn, R., 2006. Physical soil properties of paddy fields as a function of cultivation history and texture. *Advances in GeoEcology*, **38**, 446–455, ISBN: 3-923381-52.
- Lipiec, J., and Hatano, R., 2003. Quantification of compaction effects on soil physical properties and crop growth. *Geoderma*, **116**, 107–136.
- McKenzie, B. M., Kühner, S., MacKenzie, K., Peth, S., and Horn, R., 2009. Soil compaction by uniaxial loading and the survival of the earthworm *Aporrectodea caliginosa*. *Soil and Tillage Research*, **104**, 320–323.
- Mualem, Y., 1984. Anisotropy of unsaturated soils. *Soil Science Society of America Journal*, **48**, 505–509.
- Or, D., and Ghezzehei, T. A., 2002. Modeling post-tillage soil structural dynamics: a review. *Soil and Tillage Research*, **64**, 41–59.
- Pagliai, M., and Jones, R. (eds.), 2002. Sustainable Land Management – Environmental Protection – A Soil Physical Approach. *Advances in GeoEcology*, **35**, Catena, Reiskirchen. ISBN: 3-923381-48-4.
- Peng, X., and Horn, R., 2005. Modelling soil shrinkage curve across a wide range of soil types. *Soil Science Society of America Journal*, **69**, 584–592.
- Schäffer, J., 2005. Bodenverformung und Wurzelraum. In Teuffel von, K., Baumgarten, M., Hanewinkel, M., Konold, W., Spiecker, H., Sauter, H.-U., von Wilpert, K. (Hrsg.) (eds.), *Waldumbau für eine zukunftsorientierte Waldwirtschaft*. Springer, Berlin, 422 S, pp. 345–361, ISBN: 3-540-23980-4.
- Soane, B., and van Ouwerkerk, C. (eds.), 1994. *Soil Compaction*. Elsevier Verlag, Amsterdam, ISBN: 0-444-88286-3.
- Stepniewska, Z., Stepniewski, W., Gliński, J., and Ostrowski, J., 1997. *Atlas of Redox Properties of Arable Soils of Poland*. Lublin-Falenty: Institute of Agrophysics PAS and Institute of Land Reclamation and Grassland Farming.
- Teepe, R., Brumme, R., Beese, F., and Ludwig, B., 2004. Nitrous oxide emission and methane consumption following compaction of forest soils. *Soil Science Society of America Journal*, **68**, 605–611.
- Tigges, U., 2000. Untersuchungen zum mehrdimensionalen Wassertransport unter besonderer Berücksichtigung der Anisotropie der hydraulischen Leitfähigkeit. PhD thesis, Schriftenreihe des Instituts für Pflanzenernährung und Bodenkunde, H. 56, ISBN: 0933-680X.
- Van der Ploeg, R. R., and Schweigert, P., 2001. Reduzierte Bodenbearbeitung im Ackerbau – eine Chance für Wasserkulturwirtschaft, Umwelt und Landwirtschaft. *Wasserwirtschaft*, **91**, 9.
- van der Ploeg, R. R., Ehlers, W., and Horn, R., 2006. Schwerlast auf dem Acker. *Spektrum der Wissenschaft*. August 2006, 80–88.
- van den Akker, J. J. H., Arvidsson, J., and Horn, R., (eds.), 1999. Experiences with the impact and prevention in the European Community. Report 168, ISSN: 0927–4499.

Cross-references

- [Agophysical Objects \(Soils, Plants, Agricultural Products, and Foods\)](#)
[Crop Responses to Soil Physical Conditions](#)
[Earthworms as Ecosystem Engineers](#)
[Physical Degradation of Soils, Risks and Threats](#)

MAPPING OF SOIL PHYSICAL PROPERTIES

Jan Gliński¹, Janusz Ostrowski²

¹Institute of Agrophysics, Polish Academy of Sciences, Lublin, Poland

²Institute of Technology and Life Sciences, Raszkow, Poland

Definition

A map is a visual reflection of an area drawn to different scales. To illustrate special purposes thematic maps are designed.

Introduction

Soil physical properties show great variability as well in vertical as horizontal scale. Their significance for

agricultural and environmental purposes requires maps (Várányay, 1989; Várányay, 1994; Stepniewska et al., 1997; Ostrowski et al., 1998; Wösten, 2000; Walczak et al., 2002a; Duffera et al., 2007; Iqbal et al., 2005; Leenhardt et al., 2006; Santra et al., 2008).

One can distinguish two groups of soil physical properties which are mapped:

- Current such as: water content, soil temperature
- Not significantly dependent on time such as soil mineral composition, texture, specific surface area

Maps can reflect:

- Physical short-lasting properties such as soil moisture, soil temperature.
- Physical long-lasting processes such as soil erosion and soil desertification. These maps are continuously repeated.
- Soil physical properties based on their spatial variability.

A variety of different techniques are used for construction of maps of soil physical properties. They are based on: delineation of soil units, which represent areas of determined classes of soil physical property units, remote sensing, digital format, and spatial interpretation of point-based measurements of soil physical properties. The conversion of point data into continuous raster maps allows the survey data to be incorporated into computer and more easily used for decisionmakers (Taylor and Minasny, 2006). Maps can be prepared on the basis of existing data or on data coming from analyses of field soil samples derived from representative places (areas) appointed in advance. Most maps of soil physical properties concern top soil layers, but for modeling of environmental processes mapping of deeper soil layers is also made (Stepniewska et al., 1997; Stawiński et al., 2000; Walczak et al., 2002a; Walczak et al., 2002b). Within soil taxonomic unit areas of some soil maps, the extent and distribution of physical properties such as texture and hydrology are distinguished (Białousz et al., 2005). Now, the general procedure applied in the preparation soil maps is based on the estimation semivariogram parameters of soil properties using geostatistical tools and further applying them to drawing maps using ordinary kriging (Usowicz et al., 1996; Santra et al., 2008).

Computer maps of physical properties of soils

Wösten (2000) elaborated the map of total available water for plants on a European scale. In his work he based on the database of HYdraulic PROPERTIES of European Soils (HYPRES) which contained information on about 4,500 soil horizons representing 95 different soil types of 12 European countries. Computerized manipulation of this database and its derived pedotransfer functions in combination with the 1:1,000,000 scale Soil Map allowed for the generation of the spatial distribution of soil water availability within Europe.

On the smaller, regional (country) scale application, the construction of maps of field water capacity, water conductivity, specific surface area, redox properties, and also potential denitrification in soils is presented on the example of Poland. These maps were prepared in cooperation between two institutes: the Institute of Agrophysics of the Polish Academy of Sciences in Lublin and the Institute of Grassland Farming and Land Reclamation in Falenty.

Construction of maps

Polish soils (mostly mineral arable soils) are very much differentiated in terms of their origin, connected with different parent rocks (mostly sands, loams and silts of glacial and post-glacial formations), location in the landscape (lowlands, uplands, mountains), and influences of climate which has a transition character between the maritime and continental. On the surface of the land, they form a mosaic of various soil taxonomic units which are cartographically presented on maps of different scales. According to the FAO classification they are Rendzinas, Phaeozems, Cambisols, Luvisols, Podzols, Fluvisols, Gleysols, and Histosols (Białyusz et al., 2005). The preparation of maps of physical properties variability and differentiation of Polish arable soils was based on data derived from the existing Bank of Soil Samples (Gliński et al., 1992) stored in the Institute of Agrophysics in Lublin. The samples represent 29 soil units of similar properties concerning homogeneous areas (Table 1), distinguished on the basis of works of the Institute of Soil Science and Plant Cultivation in Puławy (Witek, 1974).

The area of soil units ranges from 380 to 40,980 km² in terms of their appearance in Poland. Each of the unit is represented by a number of soil profiles in proportions appropriate to its area. Soil samples with disturbed and undisturbed structures were taken from topsoils (0–20 cm), upper subsoils (20–40 cm), with predominance of the mineralization processes of the organic matter contained in it, and lower subsoils (below 40 cm) with natural features of the mineral soil substrate. This way a collection was created of soil samples coming from 1,000 soil profiles localized throughout the country, representative of the variability and differentiation of the soil cover. Soil samples collected in the Bank served for the acquisition of point data from measurements and standardized studies on physical properties of soils which were stored in the Soil-Cartographic Database (Ostrowski et al., 1998) and then computer processed to generate color maps of: field water capacity, water hydraulic conductivity, specific surface area, redox properties, and potential denitrification in soils. The maps were obtained through statistical analysis of a set of soil units and of individual measurements of random soil samples. They were plotted using computer technology by combining the results of measurements with the content of the arable land map on a scale of 1:1,000,000 and digitally recorded in the Soil-Cartographic Database. The base consists of a set of files containing the contents of the soil map and the software necessary for the storing and

Mapping of Soil Physical Properties, Table 1 Soil units, their area in Poland, and number of profiles representing particular units

No. of soil unit	Soil unit	Area (km ²)	No. of soil profiles
1	Rendzic Leptosols – pure	1,900	8
2	Rendzic Leptosols – mixed	450	8
3	Haplic Phaeozems	2,360	10
4	Haplic Luvisols and Dystric Cambisols – loose sands	40,980	169
5	Haplic Luvisols and Dystric Cambisols – light loamy sands	1,630	18
6	Haplic Luvisols and Eutric Cambisols – loamy sands	6,050	10
7	Eutric Cambisols – loamy sands over loams		26
7a	Haplic Podzols – loamy sands	18,580 (7 + 7a)	47
8	Eutric Cambisols – light loams		34
8a	Haplic Podzols – light loams	18,970 (8 + 8a)	43
9	Eutric Cambisols – medium loams		27
9a	Haplic Podzols – medium loams	9,370 (9 + 9a)	13
10	Eutric Cambisols and Haplic Luvisols – heavy loams	1,210	9
11	Eutric Cambisols and Haplic Luvisols – loams	5,700	11
12	Haplic Luvisols and Distric Cambisols – gravels	880	23
13	Eutric Cambisols – hydrogenic silts		8
13a	Haplic Podzols – hydrogenic silts	7,980 (13 + 13a)	13
14	Haplic Luvisols and Eutric Cambisols – loess	10,560	23
15	Haplic Luvisols and Eutric Cambisols – clays	500	9
16	Haplic Luvisols and Eutric Cambisols – loams and skeleton loams	1,680	10
17	Haplic Luvisols and Eutric Cambisols – loams	1,920	34
18	Haplic Luvisols and Eutric Cambisols – clays	380	7
19	Haplic Luvisols and Eutric Cambisols – silt	2,010	13
20	Eutric Fluvisols – loams and silts	5,050	10
21	Distric Fluvisols – sands	2,110	13
22	Eutric Fluvisols – light silty loam	700	7
23	Mollic Gleysols – dev. from loams and silts	6,600	31
24	Mollic Gleysols – dev. from sands	3,940	27
25	Terric Histosols	11,400	11
	Total	162,320	672

creating of various sorts of derivative maps relating to the soil cover (Walczak et al., 2002a). The basic file contains a map of soil units distribution. The main function of the processing system is grouping the soils into appropriate classes and then applying an identical color to the contours of all soils belonging to this class. As a result, a color topical map showing class distribution is created. In the mathematical approach, the solution consists in a topological connection of soil contours into one topical contour according to the assumed function of subordination. When working out the topical maps, a preliminary assumption is that a soil map will be introduced to the computer for the automatic generation of topical data by the input of transformation tables of soil units into topical units (expressed for given physical soil property values). The basis for the generation of a computer map image is a procedure based on an algorithm:

$$< J_{g1} \in - O_n, J_{g2} \in O_n \dots \dots , J_{gm} \in O_n > \in TJ_n,$$

where TJ_n – the nth topical unit, O_n – the nth soil evaluation, J_{g1}, \dots, J_{gm} – soil units belonging to the n evaluation.

Due to the character of the generalization of results, it was established that maps would be generated on the scale of 1:2,500,000, so that they can be sized to an A-3 format, ensuring appropriate clarity and legibility of the spatial structure of soil feature carted. It was assumed that soil

contours with a determined property would be signaled with a coloring into which other forms of land use would be incorporated, i.e., grassland, larger housing areas (towns), forests, and inland water reservoirs. Since the distribution of the above elements, supplementing the content of the map gives sufficient information on the spatial location on the country scale, no topographic content was introduced into the maps of physical soil properties such as roads, river nets, names of towns, so as not to disrupt legibility and clarity of their content or diminish their informative value. The contours shown in the color maps group mean physical properties values within the classes of the property determined preserving also individual deviations resulting from detailed studies.

Maps of hydro-physical properties of soils

The hydro-physical properties of soils play a significant role both in agriculture, through biomass production, and in natural environment through water quality. Their knowledge is necessary for the interpretation and forecasting of nearly all physical, chemical, and biological processes which occur in soil environment. Two main hydro-physical properties of soils were mapped, e.g., those concerning field water capacity (Walczak et al., 2002b) and water conductivity (Walczak et al., 2002a). Using the standard method (pressure chamber), the relation between

soil water potential and water content within the range from 0.1 kJ m⁻³ (pF 0) to 1,500 kJ m⁻³ (pF4.2) was determined in soil samples representing the plough layers, subsoils, and deeper layers. The results obtained were subordinated to ten 5% intervals from <5 to 45–50% water capacity (cm cm⁻³) and used to construct color maps for topsoils, upper subsoils, and lower subsoils. An example of one of such maps is shown in Figure 1.

Water conductivity coefficient k was determined in standard 100-cm³ cylinders filled with undisturbed soil in which holes were drilled at heights of 1, 2.5, and 4 cm from the bottom and TDR humidity measuring probes together with micro-tensiometers measuring soil water potential were installed in the holes. The soil samples were saturated with water till full water capacity was reached and then left under cover for 24 h in order to reach a state of thermodynamic equilibrium. Afterward, the samples were uncovered and their humidity level and soil water potentials (at 0.1, 16, and 100 kJ m⁻³) were monitored during evaporation. The TDR gauges were linked to a PC which made automatic measurements possible, and the values of humidity and water potential taken were recorded on the computer. These measurements were used to calculate the coefficient of water conductivity k . Its values were divided into three intervals:

- For 0.1 kJ m⁻³ – above 0.5 cm day⁻¹
- For 16 kJ m⁻³ – from 0.01 to 0.5 cm day⁻¹
- For 100 kJ m⁻³ – below 0.01 cm day⁻¹

and were then related to generalized soil units on color maps for topsoils, upper subsoils, and lower subsoils.

Maps of soil specific surface area

Knowledge of the specific surface area of soils permits joint interpretation of clay and humus content and composition in soil phenomena and processes affecting productive properties of soils and natural environment. This knowledge and cartography of this feature also makes possible better creation of spatial hydro-physical and fertility prognostic models of soil processes. Four color maps of total and external soil surface area expressed in m² g⁻¹ of soil were elaborated for the topsoils and upper subsoils (Stawiński et al., 2000). Soils for mapping were grouped in categories, e.g., eight categories of total specific surface area for topsoils: <12, 12–16, 16–20, 20–30, 30–50, 50–70, 70–90, and >90 m² g⁻¹.

Maps of soil redox properties

Redox status of soils is a base for understanding many soil properties such as composition of soil solution, soil reaction, availability of water and nutrients for plants, gases emission to the atmosphere, stability of metal-organic compounds, electrokinetic soil properties, biological activity, and others. Redox potential (Eh) is a measure of soil aeration status. When analyzing soil properties under oxygen deficit due to an excessive soil moisture, a new term – *redox resistance*

of soil was found purposeful to introduce (Gliński and Stepniewska, 1986). Its measure is a time (in days) after which, in a fixed conditions of moisture (full saturation with water) and temperature, soil Eh drops below 300 or 400 mV. These values, named t_{300} and t_{400} indicators, correspond with the reduction of iron and manganese in soil at 300 mV and nitrate decomposition at 400 mV. For surface layers of Polish soils, at a temperature of +20°C, values of t_{300} range from 0.2 to 4.4 days and t_{400} from 0 to 1.7 days. For deeper layers they are higher. The color maps, in the amount of 33, were gathered in the Atlas of the Redox Properties of Arable Soils in Poland (Stepniewska et al., 1997).

These maps show:

- Soil redox resistance indicators t_{300} and t_{400} of plough layers, subsoils and deeper layers at the temperatures of 4°C, 10°C, 15°C, and 20°C for t_{300} , and 4°C, 7°C, and 20°C for t_{400}
- Standardized redox potential (Eh at pH 7) at two temperatures 4°C and 20°C

The maps may be used for:

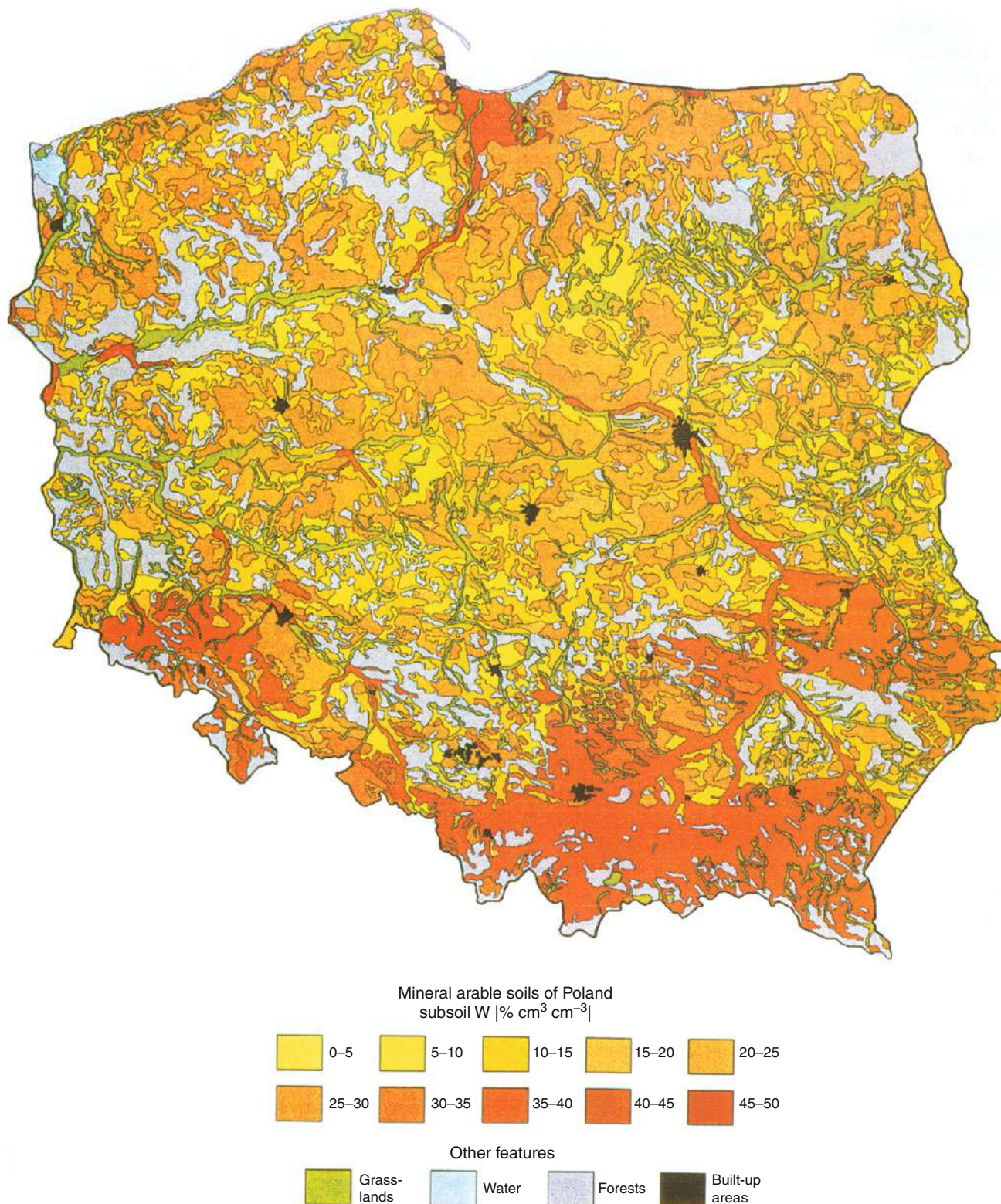
- Evaluation of hazards and agricultural damage (e.g., crop yield losses) connected with temporal water saturation of soil.
- Estimation of ecological damage connected with nitrogen losses due to denitrification and the emission of nitrous oxide (strong greenhouse gas) to the atmosphere.
- Prediction of negative ecological and agricultural effects of climate change.
- Using t_{300} and t_{400} values for land reclamation design and as an environmental parameter for hydrological calculations (admission time of soil waterlogging).

Map of potential denitrification in soils

Denitrification of nitrates (V) is the main mechanism responsible for N₂O production in ecosystems under hypoxic conditions. To show its importance the term *potential denitrification (PD)* was proposed as an important feature in agriculture (efficiency of nitrate fertilization) and natural environment (greenhouse gas emission). The formula used for the calculation of PD (kg ha⁻¹ day⁻¹ N–N₂O) is based on the knowledge of soil redox resistance indicators t_{300} and t_{400} , nitrogen content C_{NO_3-N} (mg (kg soil⁻¹)), soil layer thickness H (m), and soil bulk density d (Mg m⁻³):

$$PD = 10HdC_{NO_3-N}/t_{300} - t_{400}.$$

The analyses carried out on about 700 samples representing topsoils gathered in the Bank of Soil Samples allowed to calculate PD for soil units of the entire territory of Poland. On the basis of homogenous values of potential denitrification six groups of PD were distinguished (<7.5, 7.5–15, 15–30, 30–50, 50–80, and >80) and presented in the form of a map (Gliński et al., 2000).



Mapping of Soil Physical Properties, Figure 1 Map of water retention at field water capacity (pF 2.2) of Polish soils. (From Walczak et al., 2002b.)

Conclusions

Maps constructed on local (plot, field) and regional scale showing distribution of soil physical properties have a definite area of interest, e.g., for irrigation planning, soil water management, land reclamation, precision agriculture (precision farming, precision tillage), drought mitigation, and efficient use of fertilizers. They are also essential for modeling various current and predicted soil physical properties (processes) and are helpful for decisions on application of these management practices to defined soil areas.

Bibliography

- Białyusz, S., Marcinek, J., Stuczyński, T., and Turski, R., 2005. *Soil survey, soil monitoring and soil databases in Poland*. European Soil Bureau – Research Report No. 9 ESB-RR9, pp. 263–273.
- Duffera, M., White, J., and Weisz, R., 2007. Spatial variability of Southeastern U.S. Coastal Plain soil physical properties: implications for site-specific management. *Geoderma*, **137**, 327–339.
- Gliński, J., and Stepniewska, Z., 1986. An evaluation of soil resistance to reduction processes. *Polish Journal of Soil Science*, **19**, 15–19.
- Gliński, J., Ostrowski, J., Stepniewska, Z., and Stepniewski, W., 1992. Soil samples bank representing mineral soils of Poland (in Polish). *Problemy Agrofizyki (Series Monographs)*, **66**, 4–57.
- Gliński, J., Stepniewska, Z., Stepniewski, W., Ostrowski, J., and Szmagara, A., 2000. A contribution to the assessment of potential denitrification in arable mineral soils of Poland. *Journal of Water and Land Development*, **4**, 175–183.
- Iqbal, J., Thomasson, J. A., Jenkins, J. N., Owens, P. R., and Whisler, F. D., 2005. Spatial variability analysis of soil physical properties of alluvial soils. *Soil Science Society of America Journal*, **69**, 1338–1350.
- Leenhardt, D., Voltz, M., Bornand, M., and Webster, R., 2006. Evaluating soil maps for prediction of soil water properties. *European Journal of Soil Science*, **45**, 293–301.
- Ostrowski, J., Stepniewska, Z., Stepniewski, W., and Gliński, J., 1998. Computer maps of the redox properties of arable soils in Poland. *Journal of Water and Land Development*, **2**, 19–29.
- Santra, P., Chopra, U. K., and Chakraborty, D., 2008. Spatial variability of soil properties and its application in predicting surface map of hydraulic parameters in an agricultural farm. *Current Science*, **95**, 937–945.
- Stawiński, J., Gliński, J., Ostrowski, J., Stepniewska, Z., Sokołowska, Z., Bowanko, G., Józefaciuk, G., Książopolska, A., and Matyka-Sarzyńska, D., 2000. Spatial characterization of specific surface area of Arable soils in Poland (in Polish). *Acta Agrophysica (Series Monographs)*, **33**, 1–52.
- Stepniewska, Z., Stepniewski, W., Gliński, J., and Ostrowski, J., 1997. *Atlas of the Redox Properties of Arable Soils of Poland*. Lublin: IA PAN Lublin – IMUZ Falenty.
- Taylor, J. A., and Minasny, B., 2006. A protocol for converting qualitative point soil pit survey data into continuous soil property maps. *Australian Journal of Soil Research*, **44**(5), 543–550.
- Usowicz, B., Kossowski, J., and Baranowski, P., 1996. Spatial variability of soil thermal properties in cultivated fields. *Soil Tillage Research*, **39**, 85–100.
- Várallyay, Gy., 1989. Mapping of hydrophysical properties and moisture regime of soils. *Agrokémia és Talajtan*, **38**, 800–817.
- Várallyay, Gy., 1994. Soil databases, soil mapping, soil information and soil monitoring systems in Hungary. FAO/ECE International Workshop on Harmonization of Soil Conservation Monitoring Systems (Budapest, 14–17 September 1993). Budapest: RISSAC, pp. 107–124.
- Walczak, R., Ostrowski, J., Witkowska-Walczak, B., and Śląwiński, C., 2002a. Spatial characteristics of water conductivity in the surface level of Polish arable soils. *International Agrophysics*, **16**, 239–247.
- Walczak, R., Ostrowski, J., Witkowska-Walczak, B., and Śląwiński, C., 2002b. Spatial characteristic of hydro-physical properties in arable mineral soils in Poland as illustrated by the field water capacity (FWC). *International Agrophysics*, **16**, 151–159.
- Walczak, R., Ostrowski, J., Witkowska-Walczak, B., and Śląwiński, C., 2002c. Hydrophysical Characteristics of Mineral Arable Soils of Poland (in Polish with English summary). *Acta Agrophysica (Series Monographs)*, **79**, 5–98.
- Witek, T., 1974. *An agricultural productive space in numbers* (in Polish). Puławy: Institute of Soil Science and Plant Cultivation.
- Wösten, J. H. M., 2000. The HYDRES database of hydraulic properties of European soils. *Advances in GeoEcology*, **32**, 135–143.

Cross-references

- [Remote Sensing of Soils and Plants Imagery](#)
[Spatial Variability of Soil Physical Properties](#)

MATRIC POTENTIAL

See [Physical Dimensions and Units Use in Agriculture; Water Use Efficiency in Agriculture: Opportunities for Improvement](#)

MATRIX OF THE SOIL

The assemblage and arrangement of the solid phase (mineral and organic components) constituting the body of the soil, and the interstices (pores) contained within it.

Bibliography

Introduction to Environmental Soil Physics (First Edition) 2003 Elsevier Inc. Daniel Hillel (ed.) <http://www.sciencedirect.com/science/book/9780123486554>

MEASUREMENTS NON-DESTRUCTIVE

See [Nondestructive Measurements in Fruits; Nondestructive Measurements in Soil](#)

MECHANICAL IMPACTS AT HARVEST AND AFTER HARVEST TECHNOLOGIES

Zbigniew Ślipek, Jarosław Frączek
 Department of Mechanical Engineering and Agrophysics,
 University of Agriculture, Kraków, Poland

Definition

Mechanical impact. A complex of physical phenomena that takes place at impact of two or more bodies.

Harvest technology. A sequence of activities and operations occurring one after the other, performed by machine or carried out manually in order to gather the ripened crop from the field.

After harvest technology. Operations regarding the handling of harvested crop, including transportation, sorting, cleaning, drying or cooling, storing, and packaging.

Introduction

Each technological system of harvest and post-harvest handling requires the use of machines whose operating elements bring about plant material load, thus permitting the end product to be satisfactory both in terms of quantity and quality (Figure 1). On the one hand mechanical impact is required in order to permit the machine to function according to its purpose, but on the other hand this often causes undesired effects (loss). The desire to increase

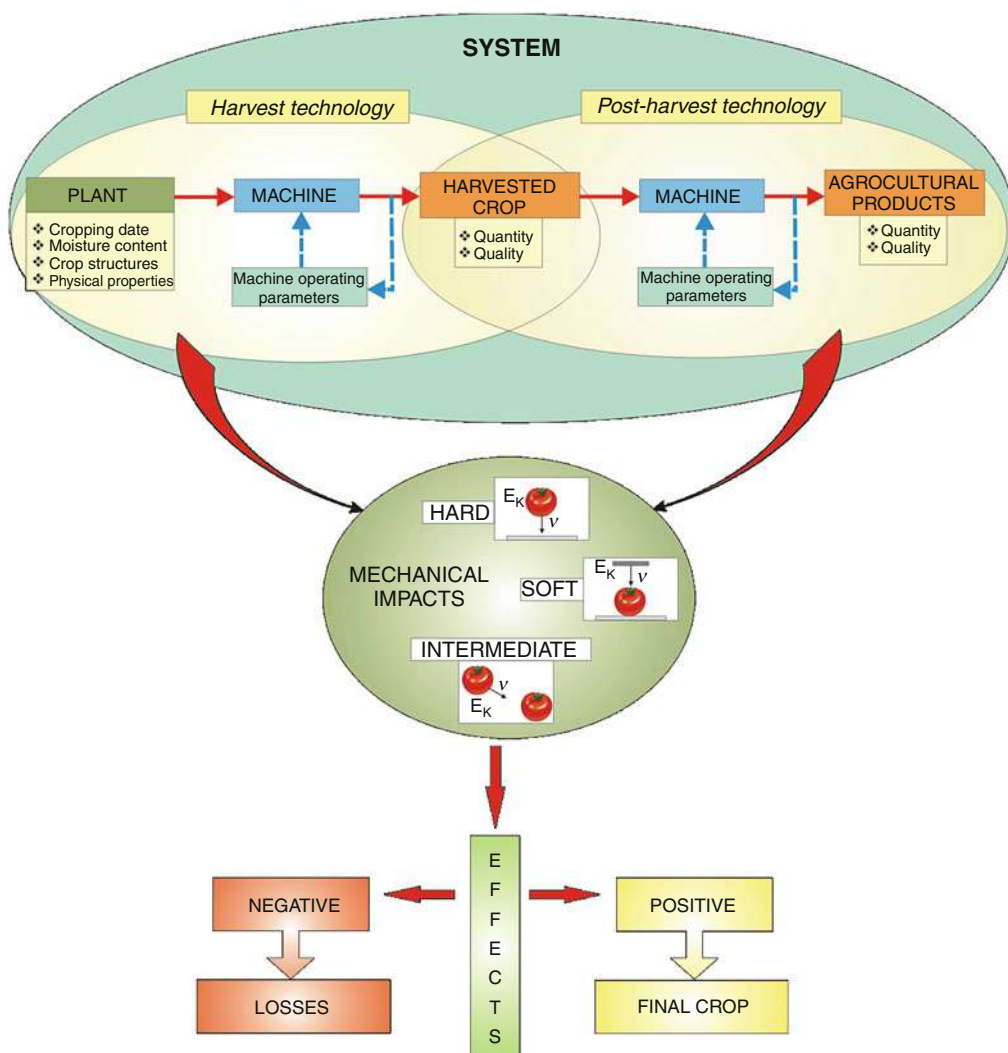
machine output is connected with the ever more aggressive impact of machines on material, which usually leads to greater damage being caused to crops.

There are two ways in which the rational use of machines for harvest and post-harvest handling may take place:

- By appropriate selection and by steering the operating parameters
- By selecting the best time for performing the technological process

Theory

Machine–plant interaction that takes place during the post-harvest collection and handling process is primarily of an impact nature. Concerning the physical description of interaction that occurs in such situations, it is necessary to take into account the mechanics of impact and its implication to plant materials (Mohsenin, 1986).



Mechanical Impacts at Harvest and After Harvest Technologies, Figure 1 Machine–plant material system relations.

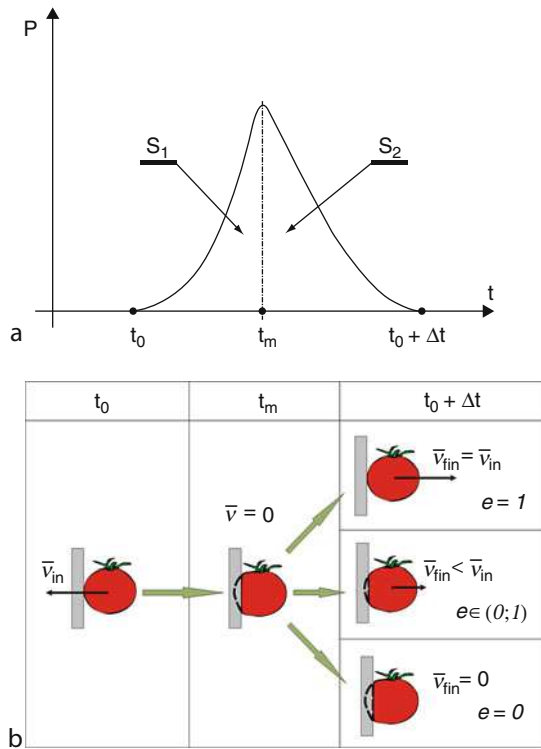
In order to indicate the presence of forces during impact it is necessary to consider the mechanical properties of both the impacting object and the object being impacted. A typical characteristic of impact is the occurrence of so-called instantaneous forces, which act very briefly ($\Delta t \rightarrow 0$) and attain high values in comparison to other forces that occur. The measure for instantaneous forces is the impact pulse:

$$S = \int_{t_0}^{t_0 + \Delta t} P(t) dt \quad (1)$$

where S – impact pulse t_0 – moment of occurrence of the instantaneous force Δt – time of operation of the instantaneous force $P(t)$ – instantaneous force.

The course of impact may be divided into two phases: compression and restitution (Gilardi and Sharf, 2002). The first phase, which involves a sudden increase in force, starts as soon as the bodies encounter each other at t_0 point and end at t_m point when distortion attains maximum value (Figure 2a). The relative velocity of both bodies is then equal to zero. In the second phase instantaneous force decreases. The shape of the $P(t)$ curve depends on:

- The elastic–plastic properties and dimensions of the impacting bodies



Mechanical Impacts at Harvest and After Harvest Technologies, Figure 2 Body impact against a motionless obstacle (a) change of instantaneous force; (b) types of impacts.

- Body surface shape (particularly at the point of contact)
- The direction of the velocity vector
- Impact energy value
- Freedom of distortion

For plant materials this curve is determined empirically. S_1 and S_2 , impact pulse values, respectively in phases one and two of impact, serve the purpose of determining the restitution coefficient:

$$e = \frac{S_1}{S_2} \quad (2)$$

It defines the proportion between elastic and plastic distortion. If $e = 1$ we have to do with ideally elastic impact; however for $e = 0$ impact is ideally plastic. For true plant materials “ e ” belongs to the $(0; 1)$ range and to a very large degree depends on the moisture content of the material (the lower the moisture content the greater the restitution coefficient). It is determined when a body impacts a motionless obstacle (Figure 2b). In such cases normal velocity is defined: initial v_{in} and final v_{fin} , while the restitution coefficient is calculated as the ratio of both velocities.

Total distortion ε that takes place during impact is the sum of elastic distortion ε_s and plastic distortion ε_p . The magnitude of these distortions depends on anatomical and morphological structure and the physical properties of plant material. The anisotropicity of these types of materials hinders any clear definition of mechanical and endurance parameters, which are very strongly correlated with moisture, which has a decisive influence on elastic and plastic properties (and therefore on the type of distortion). Plant materials with large water content are dominated by plastic traits, while dry material contains elastic or brittle characteristics. This is reflected in the effects of impact. Concerning materials with large water content, the energy of elastic distortions constitutes only a small part of overall distortion energy. During harvest and post-harvest handling one may distinguish the following types of load (Figure 2b):

- Hard – these are manifest when the initial value of E_{in} impact kinetic energy is dissipated by the impacting body (e.g., the fall of an apple, tomato, or melon onto the hard surface of a crate leads only to the distortion of the impacting fruit).
- Soft – this is the kind of impact in which distortion of the impacted body is considerably greater than distortion of the impacting body (e.g., the impact of a beater against threshed material leads only to the distortion of the impacted plant mass).
- Intermediate – this is the simultaneous distortion of the impacting body and of the impacted body (e.g., the fall of a single piece of fruit onto a pile of fruit kept in a container leads to all of the impacted bodies being distorted).

In terms of agrophysics the negative effect of impact is plastic distortion, which leads to a permanent deterioration

in the quality of the biological material. The following should be distinguished:

- Local distortion – these cover a relatively small area that focuses immediately on the point of impact and leads to different types of micro-damage (abrasion, skin puncture, etc.). These distortions are the result of instantaneous force and depend on local plant material susceptibility and the shape of the surface at the point of contact.
- Global distortion – these appear in the form of disturbance waves (distortions, stress) covering the entire volume of the impacted body. Under such circumstances permanent distortions appear on a macro scale (grain fragmentation, tomato cracking, apple crushing etc.).

It must be noted that surface and internal stress caused during impact are far greater at the point of contact than beyond that point.

Harvest and after harvest processes – agrophysical aspects

Grain crops

Most frequently the harvesting of these plants takes place in the form of a single phase. The technological process involves the cutting of plants, transport, threshing, separation and cleaning, and the gathering of grain (seed) in a container. In combine-harvesters, the most intensive effect on plant material takes place in the threshing unit which, depending on the construction, threshes by striking, wiping, and vibrating the threshed material. Threshing drum operations considerably distort plant mass (e.g., cereals) by soft impacts, which, depending on instantaneous contact conditions (moisture content in grain, grain orientation in terms of the working element, collision velocity, and friction) could lead to total grain fragmentation or to a variety of damage to the grain. Low intensity threshing which is favorable in terms of mechanical damage (low drum revolutions, large operating slot between the drum and the threshing floor) may, however, cause grain loss through incomplete grain threshing.

Threshing output and effectiveness depends on:

- The properties of the threshed material (type and variety, material threshing capacity, moisture content, the elastic properties of stalks or culms, the ration of grain to straw, and others)
- Technical conditions (the type of threshing unit, regulating parameters, and others)
- Threshing unit feed (the volume of feed, evenness, the arranging of plants in the threshing layer, and others)

The operating parameters of modern combine-harvesters may be steered electronically, on the basis of information on the exit and entry points of harvested material, supplied online. The implementation of information

used for steering purposes is the subject of research. The gauging of the mechanical properties of plant material, including susceptibility to mechanical impact, is carried out at laboratory workstations, which permit the application of precise loads under determined and controlled conditions (Kang et al., 1995).

Transport, cleaning, and drying take place after the harvesting of grain. During these processes the material is subject to a variety of additional mechanical impacts. The danger of damaging the grain during these processes is, admittedly, far smaller; however, mechanical load may overlap and the damage previously caused to grain may become worse (Frączek and Ślipek, 1999). This leads to a reduction in raw material quality during storage (infestation by microorganisms, the settling of pests, increased respiration intensity) and processing. Mechanical damage to grains to be used as seeds (in particular damage to the germ) may reduce their ability to germinate and emerge.

Fruits and vegetables

The market of today requires that fruits and vegetables, in particular those items intended to be eaten directly, be of high quality – this includes the right shape, color and, above all, the absence of any damage. The collection of these products with the use of machines, therefore, requires that extreme care be exerted as a result of load impact. The technological collection of fruit is based on the mechanical effects of vibrating or rotating parts.

Mechanical collection from trees usually takes place by means of vibration (e.g., Mateev and Kostadinov, 2004). The fruit falls on special screens which are spread out beneath the crowns of trees or (when using simplified technologies) directly onto the ground from where it is gathered and loaded onto containers. These types of technologies are primarily used when fruit is collected for processing.

Fruits such as raspberries, currants, gooseberries, and strawberries are collected with the use of harvesters only for processing purposes. Collection for consumption purposes still takes place by hand. That does not mean that with this technology the fruit does not come in direct contact with mechanical elements. During collection various types of devices are used in order to facilitate manual collection and increase output (conveyors, elevators). In recent times, the use of autonomous robots for collecting fruit considerably decreases load impact, which is the reason why fruit gets damaged. Further development of these robots will undoubtedly help reduce the damage caused to fruit, particularly if collected for direct consumption purposes.

During the mechanical collection of fruit it is also important to make sure that machines operate under conditions not permitting any considerable damage to occur to the parent plant because of the need for yielding in the next vegetation season.

The main purpose of post-harvest technologies is to increase the added value of the product. Various technological lines perform the selection, cleaning, washing, sanitation, classification, weighing, and packing of products. While these technologies are in operation, mechanical influence, admittedly, takes place at low mechanical speed, but still the fruits and vegetables are exposed to the danger of damage and bruising (e.g., Ragni and Berardinelli, 2001). When products are subject to gravitational transport or change the direction in which they move they are particularly prone to damage.

The technologies for collecting vegetables usually involve separating the usable part growing above the ground (e.g., cabbage, cucumber, tomato), extracting the root (e.g., carrot, parsley) or tubers (potatoes), separation, gathering the yield, and transporting it. Most frequently machines damage the skin and bruise the harvestable products. During post-harvest handling the products are calibrated, washed, weighed, and packed. Multiple impact events and associated damage result later in greater respiration intensity and loss of storage life.

Conclusion

Originally, research in agrophysics concentrated on assessing various mechanical traits of agricultural plants and was based primarily on destructive methods. In recent years a range of nondestructive methods of assessing the physical condition of plant material has been elaborated (e.g., Ortiz et al., 2001). These methods include image analysis (size, shape, weight, surface morphology, skin color), electrical and optical properties, vibration and acoustic tests and nuclear magnetic resonance techniques. Destructive methods that offer direct information about the mechanical properties of fruits and vegetables (mechanical impact tests) are used less and less frequently when assessing the suitability of plants for collection. These tests, however, are used for verifying the methods of direct assessment, outlining the mechanical characteristics of materials for the purpose of designing machines or for modelling work processes.

Post-harvest collection and handling machines whose designs are based on comprehensive scientific know-how, should meet the requirements on high quality and safety of agricultural products. The implementation of mechatronic systems permits, to an increasingly large degree, the subtle control and steering of technological processes. Comprehensive operations aimed at improving the quality of agricultural products require thorough knowledge of machine and plant systems. It is particularly important to be aware of the physical parameters of plant material, which are quickly and easily gauged in the dynamic technological processes.

Bibliography

Frączek, J., and Ślipek, Z., 1999. Fatigue strength of wheat grains. The analysis of grain deformation at multiple loads. Part 1. *International Agrophysics*, **13**, 93–97.

- Gilardi, G., and Sharf, I., 2002. Literature survey of contact dynamics modelling. *Mechanism and Machine Theory*, **37**, 1213–1239.
- Kang, Y. S., Spillman, C. K., Steele, J. L., and Chung, D. S., 1995. Mechanical properties of wheat. *Transactions of the American Society of Agricultural Engineers*, **38**, 573–578.
- Mateev, L. M., and Kostadinov, G. D., 2004. Probabilistic model of fruit removal during vibratory morello harvesting. *Biosystems Engineering*, **87**, 425–435.
- Mohsenin, N. N., 1986. *Physical Properties of Plant and Animal Materials*, 2nd edn. New York: Gordon and Breach Science.
- Ortiz, C., Barreiro, P., Correa, E. F., Riquelme, F., and Ruiz-Altsentz, M., 2001. Non-destructive identification of woolly peaches using impact response and near-infrared spectroscopy. *Journal of Agricultural Engineering Research*, **78**, 281–289.
- Ragni, L., and Berardinelli, A., 2001. Mechanical behaviour of apples, and damage during sorting and packaging. *Journal of Agricultural Engineering Research*, **78**, 273–279.

Cross-references

[Agophysical Properties and Processes](#)

[Crop Yield Losses Reduction at Harvest, from Research to Adoption](#)

[Nondestructive Measurements in Fruits](#)

MECHANICAL RESILIENCE OF DEGRADED SOILS

Heiner Fleige

Institute for Plant Nutrition and Soil Science, Christian-Albrechts-University zu Kiel, Kiel, Germany

Mechanical resilience of soils can be defined by the value of the precompression stress (P_c), which depends especially on soil texture, soil structure, and water content. P_c is derived from confined compression tests on undisturbed, aggregated, and unsaturated soils. It is assumed that at stresses lower than the P_c , an elastic stress path exists, resulting in no extra soil deformation and thus, no change in the pore system and its function. Stresses beyond the P_c induce changes of pore functions and pore continuity because of plastic soil deformation (= degraded soil). Consequently, not only water infiltration will be reduced but it also causes reduced gas, and water fluxes, as well as water logging, interflow, runoff, and soil erosion. The prediction of the P_c and its effects on physical properties by pedotransfer functions as well as P_c -maps on different scales (e.g., Europe, Germany, farm scale) are demonstrated in Horn et al. (2005) and Horn and Fleige (2009).

Bibliography

- Horn, R., Fleige, H., Richter, F.-H., Czyż, E. A., Dexter, A., Diaz-Pereira, E., Dumitru, E., Enarche, R., Mayol, F., Rajkai, K., De la Rosa, D., and Simota, C., 2005. Prediction of mechanical strength of arable soils and its effects on physical properties at various map scales. *Soil and Tillage Research*, **82**, 47–56.
- Horn, R., and Fleige, H., 2009. Risk assessment of subsoil compaction for arable soils in Northwest Germany at farm scale. *Soil and Tillage Research*, **102**, 201–208.

MEMBRANES, ROLE IN WATER TRANSPORT IN THE SOIL-ROOT-XYLEM SYSTEM

Marian Kargol

Independent Department of Environment Protection and Modelling, The Jan Kochanowski University of Humanities and Sciences, Kielce, Poland

Introduction

This article discusses agrobiophysical aspects of soil water intake by a plant root and water transport along its radial route. In other words, this article presents certain interpretative ideas explaining the mechanisms of water transport in the soil–root–xylem system. In this context, a certain amount of basic information on membranes (cell membranes in particular) and permeability of various substances across them shall be presented first. Next, major membrane theories on the processes of water intake from the soil and its two-way transport across the root (from the soil to the xylem of the vascular cylinder, and in the opposite direction) shall be discussed. The issue of root pressure generation shall also be investigated (Fiscus, 1975, 1986; Ginsburg, 1971; Kargol, 1994, 1995, 2007; Pitman, 1982; Steudle et al., 1987; Taura et al., 1987).

Membranes and mathematical formalisms of their substance transport

Porous membranes

In general, membranes can be divided into *artificial* and *biological*. The former include, for example, cellophane, nephrophan, or collodion membranes. The latter include cell and cellular organelle membranes, as well as tissue membranes.

In research practice, we mostly deal with porous membranes. This also pertains to cell membranes. Porous membranes can be divided into two groups, that is, *homogeneous* and *heterogeneous*. A membrane is homogeneous if its pores do not differ from one another in cross-section radius dimensions. If a membrane's pores do differ from one another in their cross-section radius dimensions, it is to be treated as heterogeneous. Processes of permeability across a variety of membranes have been investigated mainly with the use of the Kedem & Katchalsky (KK) formalism equations (Katchalsky and Curran, 1965). In recent years, equations of the mechanistic formalism (MF) have been developed (Kargol, 2002, 2006, 2007; Kargol and Kargol, 2003, 2006).

Equations of the KK formalism

Transport equations of the KK formalism have been derived on the grounds of linear thermodynamics of irreversible processes, basing on a model of a membrane treated as a “black box.” A practical version of these equations may be thus written:

$$J_v = L_p \Delta P - L_p \sigma \Delta \Pi, \quad (1)$$

$$j_s = \omega \Delta \Pi + (1 - \sigma) \bar{c}_s J_v, \quad (2)$$

where J_v and j_s are density of the solution volume flow (v) and density of the solute flow (s); $\Delta P = P_2 - P_1$ is the mechanical pressure difference between P_2 and P_1 ; $\Delta \Pi = RT(C_2 - C_1)$ is osmotic pressure difference; L_p , σ and ω are coefficients (of filtration, reflection, and permeability); $\bar{c}_s = 0.5 (C_1 + C_2)$ is the mean concentration of concentrations C_1 and C_2 ; R is the gas constant; T is temperature.

Transport parameters occurring therein are given by the formulas

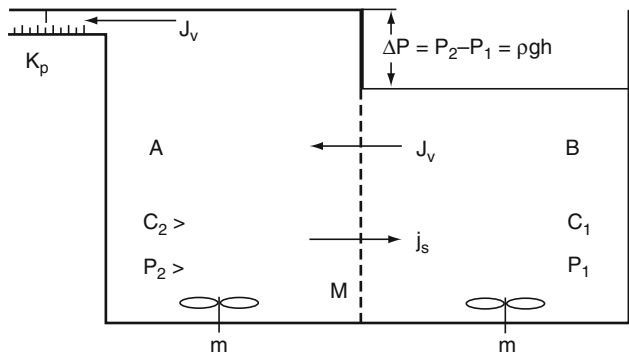
$$L_p = \left(\frac{J_v}{\Delta P} \right)_{\Delta \Pi=0}, \quad (3)$$

$$\sigma = \left(\frac{\Delta P}{\Delta \Pi} \right)_{J_v=0}, \quad (4)$$

$$\omega = \left(\frac{j_s}{\Delta \Pi} \right)_{J_v=0}. \quad (5)$$

The above notation of Equations 1 is adequate to the membrane system as schematically depicted in Figure 1. In this system, the membrane M separates the compartments A and B, filled with solutions, which satisfy the inequality $C_1 < C_2$. They are under mechanical pressures, which satisfy the relation $P_1 < P_2$. Generally speaking, the KK equations are rather difficult in terms of interpretation. This pertains particularly to the parameter ω , which appears in Equation 2. This results from the fact that this parameter, as defined by the Formula 5, is determined at $J_v = 0$, that is, at simultaneous existence on the membrane of two stimuli that satisfy the relation: $|\Delta P| = |-\sigma \Delta \Pi|$.

This means that, in the case of membranes for which σ is found in the interval $0 < \sigma < 1$, the transport of a given solute across the membrane is generated by two stimuli. Hence it follows that ω is not only the coefficient of diffusive solute permeability. The terms $\omega \Delta \Pi$ and $(1 - \sigma) \bar{c}_s J_v$ also pose problems for interpretation. According to this



Membranes, Role in Water Transport in the Soil-Root-Xylem System, Figure 1 Model membrane system with stirrers m,m (description in text).

formalism, membranes can be divided into *semipermeable* (at $\sigma=1$), *selective* (when $0 < \sigma < 1$), and *nonselective* (if $\sigma=0$).

Equations of the mechanistic formalism (MF)

In research work, we mainly deal with porous membranes. This also pertains, as we now know, to cell membranes. Consequently, in recent years, we have developed the so-called mechanistic formalism for membrane substance transport (Kargol, 2002, 2006, 2007; Kargol and Kargol, 2003, 2006). The equations of this formalism take the following forms:

$$J_{vm} = L_p \Delta P - L_p \sigma \Delta \Pi, \quad (6)$$

$$j_{sm} = \omega_d \Delta \Pi + (1 - \sigma) \bar{c}_s L_p \Delta P, \quad (7)$$

where (analogous to the KK equations), J_{vm} is the solution volume flow and j_{sm} is the solute flow. These flows are functions of the pressure difference ΔP and the pressure difference $\Delta \Pi$.

Individual terms of these equations signify filtration, osmosis, diffusion, and convection. The equations have been derived on the basis of a model of the membrane system as shown in Figure 2. In this system, the heterogeneous porous membrane M contains the statistical number of cylindrical pores permeable to water. The membrane separates the compartments A and B, which contain solutions of the concentrations C_1 and C_2 under mechanical pressures P_1 and P_2 .

In a real membrane, pores are arranged randomly. In order to facilitate the present considerations, it has been assumed that pores of that membrane are arranged according to their dimensions in one direction, from the pores with the smallest radii (r_1^{\min}), to the largest ones (r_N^{\max}). With reference to this membrane, it is possible to

find such a solute (s) with such a molecule radius r_s that the following relation will be fulfilled:

$$r_1^{\min} = r_w < r_2 < \dots < r_s < \dots < r_N^{\max},$$

where r_w is the radius of the solvent (water) molecules. Under the circumstances, the membrane M may be divided into Part (a), which contains a certain number n_a of semipermeable pores (with the reflection coefficient $\sigma_a=1$ and filtration coefficient L_{pa}), and Part (b), which contains $n_b=N-n_a$ of permeable pores. This part of the membrane has the filtration coefficient L_{pb} and reflection coefficient $\sigma_b=0$. From the above, it follows that a single pore of the membrane may take values of the reflection coefficient σ_p amounting to either 0 or 1 (Kargol, 2002, 2006; Kargol and Kargol, 2003a, b, 2006).

Having analyzed the membrane system as shown in Figure 2, it is easy to understand that $J_{va}=J_{vwa}$ is the solvent (water, w) volume flow, while J_{vb} is the solution volume flow, which permeates across Part (b) of the membrane. The flow J_{vb} has two components, that is, J_{vwb} (water volume flux) and J_{vsb} (solute volume flux). These flows, in turn, also have two components each, that is, $J_{vwb}^{\Delta P}$ and $J_{vwb}^{\Delta \Pi}$, and J_{vsd} and J_{vsk} (which are solvent (w) and solute (s) volume flows respectively). All these flows are generated by the stimuli ΔP and $\Delta \Pi$ respectively. It must be noted that in the light of this membrane model, the transport situation appears to be absolutely clear in terms of interpretation. On this basis, it also makes sense to say that the mechanistic formalism for membrane transport (MF) offers a more thorough investigation tool than the KK formalism.

On the equivalence of the equations of the KK formalism and the MF formalism

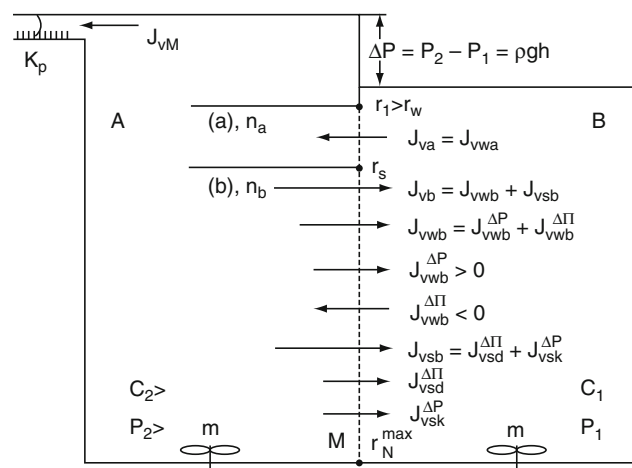
Transport equations of the mechanistic formalism (MF) may in general be treated as alternative to the equations of the KK formalism. This view results mainly from the fact that the equations for the solute flow of these formalisms, that is, Equations 2 and 7, display certain differences. Yet thanks to our introduction of the so-called transport parameter correlations between L_p , σ and ω (KK), and L_p , σ and ω_d (MF), it is easy to observe that these (KK and MF) equations are mutually equivalent (Kargol, 2007; Kargol and Kargol, 2006). The relations are given by the formulas

$$\omega = (1 - \sigma^2) \bar{c}_s L_p, \quad (8)$$

$$\omega_d = (1 - \sigma) \bar{c}_s L_p. \quad (9)$$

On the basis of the above, the following relation is obtained: $\omega = \omega_d (1 + \sigma)$.

Thanks to these relations, it becomes possible to use – for further and more thorough investigations – the enormous experimental potential (related to substance permeation across cell membranes), which has so far been obtained on the basis of the transport equations of the KK formalism.



Membranes, Role in Water Transport in the Soil–Root–Xylem System, Figure 2 Membrane system (M, membrane; A and B, compartments; m, m, stirrers).

Cell membranes as porous structures

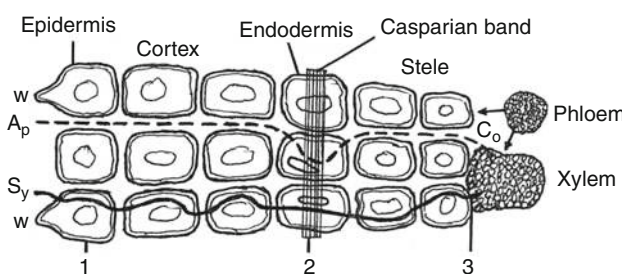
In general, it may be stated that in research practice we mainly deal with porous membranes. As is becoming increasingly well known, cell membranes are porous, too. Suffice it to say that cell membranes have various pores (channels), through which in a controlled manner various substances, including water can penetrate (Kargol, 2007; Stryer, 2000). Speaking about these pores, we also mean water channels, formed by certain transport proteins (called aquaporins). The porous structure of the cell membrane is also formed by ion channels through which (when open) not only ions but also water can pass. These channels have hydrophilic internal walls and are filled with water. Pores formed by some antibiotics, located in the lipid bilayer of the cell membrane, may also be permeable to water. Moreover, certain pores can occur directly in the lipid bilayer of cell membranes. All these pores vary from one to another in terms of their cross-section radius dimensions. They fulfill various specialized transport functions pertaining to permeability of water and various solutes through them.

Membrane ideas for explanation of water transport processes across the root

We shall now consider some basic issues related to agrobiophysical aspects of water intake from the soil by plants, and water transport across the root (Fiscus, 1975, 1986; Ginsburg, 1971; Kargol, 1994, 1995, 2007; Pitman, 1982; Steudle et al., 1987; Taura et al., 1987). The discussion of these issues will be preceded by an outline of the root structure.

Anatomical structure of the root

In the soil, the root must have particular contact with the water found therein. It is also important for the contact to occur mainly in the trichome zone of the root. This zone is the most capable of water intake. With a view to facilitating our discussion of the mechanisms of root water intake (as well as water movement to the xylem of the vascular cylinder), let us look at its main structural features. They have been shown schematically in Figure 3. The protoplasts of



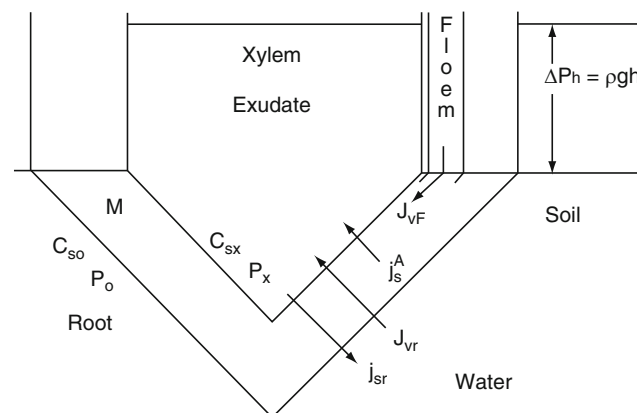
Membranes, Role in Water Transport in the Soil-Root-Xylem System, Figure 3 Fragment of root cross section, trichome zone (S_y , symplastic route; A_p , apoplastic route; w, w , trichomes; 1, 2 and 3, barriers).

primary bark cells are, as we know, joined with one another by means of cytoplasmic bridges (plasmodesmata). With the help of these bridges, they are also linked – on the outside – with epidermis cell protoplasts, and on the inside – with endodermis cell protoplasts. The protoplasts of the parenchyma cells of the vascular cylinder are similarly joined to the endodermis. Thus, the root symplast spreads from the epidermis to the xylem, forming a cytoplasmatic continuum. This continuum provides a symplastic water route. It is illustrated by Line (S_y).

Cell walls and intra-cell voids form the so-called apoplastic water route. This route is shown by the broken line (A_p) in Figure 3. Even though it stretches from the epidermis to the xylem, it still has in the endodermis layer a significant barrier (in connection with the existence of the Casparyan band therein). In general, in the root radial water route, three barriers can be distinguished. They have been marked with Figures 1, 2, and 3.

The Fiscus single-membrane theory of water transport across the root

Ascribing to barriers 1, 2, and 3 (cf. Figure 3) the status of membranes, several membrane models have been developed to emulate the root radial water route. The simplest of these is the single-membrane model, as proposed by Fiscus (Fiscus, 1975, 1986). In this model, shown in Figure 4, all the three above mentioned barriers have been replaced with one membrane M with the filtration coefficient L_{pr} , the reflection coefficient σ_r and the permeability coefficient ω_r . The membrane separates two solutions of the concentrations C_{so} and C_{sx} , that is, the soil solution and the exudate (the xylem solution). These remain under mechanical pressures P_o and P_x respectively. Basing on that model, it has been possible (on the basis of the KK equations) to determine experimentally the values of all



Membranes, Role in Water Transport in the Soil-Root-Xylem System, Figure 4 Single-membrane model of root radial route (M is the membrane; C_{sx} , C_{so} are concentrations; P_x , P_o and ΔP_h are mechanical pressures; J_{vr} and j_{sr} are passive flows; j_s^A is the active solute flow; J_{vf} is the phloem volume flow; ρ is density; g is gravitational acceleration; h is height).

the three transport parameters (L_{pr} , σ_r , and ω_r), for roots of various crop plants and for various solutes. Due to the determination of these parameters, it has been possible to describe transport properties (of the model root) by means of the KK equations thus written

$$\begin{aligned} J_{vr} &= L_{pr}\Delta P - L_{pr}\sigma_r\Delta\Pi \\ &= L_{pr}(P_x - P_o) - L_{pr}\sigma_rRT(C_x - C_o), \end{aligned} \quad (10)$$

$$\begin{aligned} J_{sr} &= \omega_r\Delta\Pi + (1 - \sigma_r)\bar{c}_s J_{vr} \\ &= \omega_rRT(C_{sx} - C_o) + (1 - \sigma_r)\bar{c}_s J_{vr}, \end{aligned} \quad (11)$$

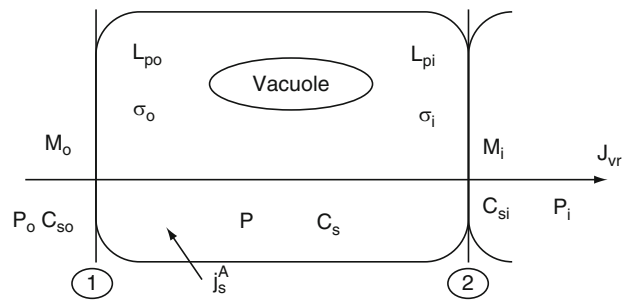
where J_v is the volume flow; j_s is the solute flow; $\Delta\Pi$ and ΔP are (mechanical and osmotic) pressure differences; $\bar{c}_s = 0,5(C_{sx} + C_o)$ is the mean concentration (of the concentrations C_{sx} and C_o); P_x and P_o are mechanical pressures in the xylem and the soil; R and T are the gas constant and temperature.

According to the model described with Equations 13 and 14, the flows J_{vr} and j_{sr} are determined (in their value and direction (sense)) by the values of pressure differences $\Delta\Pi$ and ΔP . This model appears to be rather far removed from the biological reality. Nonetheless, it has played a particularly important role in experimental and theoretical investigations pertaining to determination of transport properties of the root radial transport route in a variety of crop plants (Fiscus, 1975, 1986; Steudle et al., 1987; Kargol, 1994, 2007). Moreover, it explains to a large extent the agrobiophysical water transport mechanisms across the root as well as generation of the so-called root pressure. This pressure is expressed by the formula $\Delta P_\eta = \rho gh$, where ρ is density, g is gravitational acceleration; h is the height to which the root can pump water under that pressure.

According to this model, root pressure is osmosis driven, as the experimentally determined coefficient σ_r pertaining to the membrane M , which emulates the root radial water route takes the value of $\sigma_r > 0$. On the basis of this model (Fiscus, 1975, 1986) as well as Steudle and others (Steudle et al., 1987), experimentally determined the parameters L_{pr} , σ_r , and ω_r for many crop plant roots.

The Ginsburg double-membrane model, which explains radial water transport in the root

Another model, which emulates the radial water route is Ginsburg's double-membrane model shown in Figure 5 (Ginsburg, 1971). While constructing it, Ginsburg assumed that, in the radial segment of the root symplastic route, water encountered two barriers (1 and 2: cf. Figure 3). He gave these barriers the status of membranes M_o and M_i , and ascribed filtration coefficients (L_{po} and L_{pi}), as well as reflection coefficients (σ_o and σ_i) to them respectively. In this model, the membrane M_o separates solutions of the concentrations C_{so} and C_s , while the membrane M_i – solutions of the concentrations C_s and C_{si} , where C_{so} , C_s and C_{si} are the concentrations of the solution in the soil, between the membranes and in



Membranes, Role in Water Transport in the Soil–Root–Xylem System, Figure 5 Two-membrane Ginsburg model (description in text).

the apoplast of the vascular cylinder. With the use of the Kedem–Katchalsky equation for the flow J_v (i.e., Equation 1), Ginsburg demonstrated that transport properties of his model are thus formulated:

$$\begin{aligned} J_{vr} &= -LRT(\sigma_i - \sigma_o)C_s + LRT(\sigma_{si}C_i - \sigma_iC_{so}) \\ &\quad - L(P_i - P_o), \end{aligned} \quad (12)$$

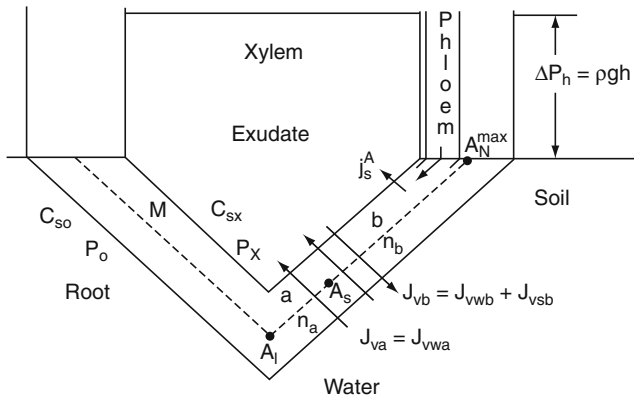
where J_{vr} is the volume flow; P_i and P_o are mechanical pressures in the soil and in the apoplast of the vascular cylinder; and $L = L_{po}L_{pi}(L_{po} + L_{pi})^{-1}$.

From an analysis of this equation, it follows that – depending on the value of the concentration C_s (which may be regulated with the active flow j_s^A of the solute (s)) – the flow J_{vr} may occur in accordance with the concentration gradient (at $C_{so} < C_{si}$), under iso-osmotic conditions (at $C_{so} = C_{si}$), as well as against the concentration gradient (at $C_{so} > C_{si}$). These conclusions, if referred to water transport across the root, are the main research achievement resulting from the Ginsburg model.

It must be added here that many membrane models have been developed to emulate the root radial water route, including multi-membrane models (Pitman, 1982; Taura et al., 1987; Kargol, 1995, 2007).

Single-membrane theory of two-way water transport along the root radial route

We shall presently consider the single-membrane model of the root radial water route, which we have developed (Kargol, 2007) on the basis of the MF formalism. Schematically, it has been presented in Figure 6. In this model, the assumption is that the membrane M is a heterogeneous porous structure, which emulates (in a manner analogous to the Fiscus model) the entire radial water route in the root. It contains the statistical number of N pores, which are permeable to water. Individual pores vary in areas (A) of their cross sections and are arranged randomly (arbitrarily). To facilitate our considerations, the pores have been arranged in one direction, from the smallest A_1 , to the largest A_N^{\max} . With reference to this membrane, it is possible to select such a solute (s), with the molecule



Membranes, Role in Water Transport in the Soil–Root–Xylem System, Figure 6 Single-membrane root model in which the membrane M is a heterogeneous porous structure (C_{so} , C_{sx} are concentrations; P_i , P_o are mechanical pressures; J_{va} , J_{vb} are volume flows; n_a and n_b are numbers of semipermeable and permeable pores; j_s^A is the active flow of the substance (s)).

cross-section area A_s , that the following relation will be satisfied: $A_1 < A_2 < \dots < A_s < \dots < A_N^{\max}$.

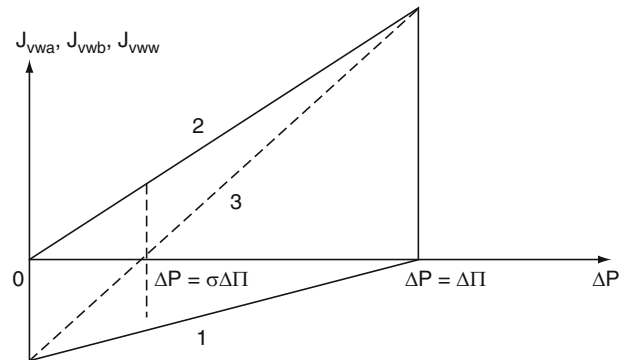
Under the circumstances, it is justified to divide the membrane M into Part (a) that contains n_a semipermeable pores and Part (b) that contains n_b permeable pores. These parts are to be ascribed the reflection coefficients $\sigma_a = 1$ and $\sigma_b = 0$ respectively. This membrane (according to Figure 6) separates the soil water with the solute (s) concentration C_{so} and the xylem solution (the exudate) with the solute concentration C_{sx} . Due to the occurrence of active transport j_s^A of the solute (s) in the root, it may be assumed that on the membrane M there occurs the pressure difference $\Delta C = C_{\text{sx}} - C_{\text{so}}$. Thus, there also occurs the osmotic pressure difference $\Delta\Pi = RT\Delta C = RT(C_{\text{sx}} - C_{\text{so}})$. As a consequence, within the pores n_a , the osmotic volume flow will be generated $J_{\text{va}} = J_{\text{vwa}}$ (which is in fact a water flow). This means, in turn, that the model root under consideration is able to generate root pressure $\Delta P_{\eta} = \rho gh$. In connection with the existence of this pressure, on the membrane at issue there also occurs, apart from the pressure difference $\Delta\Pi$, the mechanical pressure difference $\Delta P = P_x - P_o = \Delta P_h$. In the presented situation (according to the MF formalism), it may be written that [7]

$$\begin{aligned} J_{\text{vwa}} &= L_{\text{pa}}\Delta P - L_{\text{pa}}\Delta\Pi \\ &= L_{\text{pa}}(P_x - P_o) - L_{\text{pa}}RT(C_{\text{sx}} - C_{\text{so}}), \end{aligned} \quad (13)$$

where L_{pa} is the filtration coefficient of semipermeable pores n_a . Because $L_{\text{pa}} = L_{\text{pr}}\sigma_r$, the above equation, which describes the osmotic transport of water takes the following form:

$$J_{\text{vwa}} = L_{\text{pr}}\sigma_r(\Delta P - \Delta\Pi), \quad (14)$$

where L_{pr} is the filtration coefficient for the entire membrane (all N pores), and σ_r is the reflection coefficient of the membrane M.



Membranes, Role in Water Transport in the Soil–Root–Xylem System, Figure 7 Plots of relations of flows $J_{\text{vwa}} = f(\Delta P)$ and $J_{\text{vwb}}^{\Delta P} = f(\Delta P)$, obtained on the basis of Equation 13 – Plot 1, and Equation 16 – Plot 2. Plot 3 depicts the relation $J_{\text{vw}} = J_{\text{vwa}} + J_{\text{vwb}}^{\Delta P} = f(\Delta P)$.

In connection with the occurrence on the membrane M of the pressure difference ΔP , within its pores n_b the volume flow J_{vb} will be generated and given by the formula

$$J_{\text{vb}} = L_{\text{pb}}\Delta P = (1 - \sigma_r)L_{\text{pr}}\Delta P, \quad (15)$$

where $L_{\text{pb}} = (1 - \sigma)rL_{\text{pr}}$ is the filtration coefficient of the pores n_b . While analyzing Figure 5, it is easy to see that

$$J_{\text{vb}} = J_{\text{vwb}} + J_{\text{vsb}} = J_{\text{vwb}}^{\Delta P} + J_{\text{vwb}}^{\Delta\Pi} + J_{\text{vsb}}^{\Delta P} + J_{\text{vsb}}^{\Delta\Pi},$$

where J_{vwb} and J_{vsb} are the volume flows of water (w) and the solute (s); and $J_{\text{vwb}}^{\Delta P}$ and $J_{\text{vwb}}^{\Delta\Pi}$ are volume flows of water and the solute, driven by the pressure difference ΔP ; while $J_{\text{vsb}}^{\Delta P}$ and $J_{\text{vsb}}^{\Delta\Pi}$ are volume flows of water and the solute, driven by the pressure difference $\Delta\Pi$. The flow $J_{\text{vwb}}^{\Delta\Pi}$ may be expressed by the following formula (Kargol, 2007):

$$\begin{aligned} J_{\text{vwb}}^{\Delta P} &= (1 - \sigma_r)(1 - \bar{c}_s \bar{V}_s)L_{\text{pr}}\Delta P \\ &\approx (1 - \sigma_r)L_{\text{pr}}\Delta P, \end{aligned} \quad (16)$$

where \bar{c}_s is the mean concentration of the concentrations C_{sx} and C_{so} ; and \bar{V}_s is the molar volume of the substance (s). Equation 14 and the Formula 16 are the sought expressions that pertain to water transport along the root radial route. This transport is realized simultaneously in two opposite directions. Equation 14 formulates osmotic transport of water from the soil to the xylem of the vascular cylinder, and Equation 16 depicts water transport in the opposite direction. In order to clarify this, Plots 1 and 2 of these equations have been provided. They have been presented and explained in Figure 7. Plot 3, in turn, illustrates the relation of the net flow J_{vw} , given by the formula:

$$J_{\text{vw}} = J_{\text{vwa}} + J_{\text{vwb}}^{\Delta P} = L_{\text{pr}}\Delta P - L_{\text{pr}}\sigma_r\Delta\Pi. \quad (17)$$

From the discussion of the latter relation (Equation 17), two main conclusions follow. If $\Delta P = 0$,

then $J_{\text{vwa}} + J_{\text{vwb}}^{\Delta P} = -L_{\text{pr}} \sigma_r \Delta \Pi$. If $\Delta P = -\sigma \Delta \Pi$, then $J_{\text{vwa}} + J_{\text{vwb}}^{\Delta P} = 0$, which means that the amounts of water absorbed or removed by the root are the same.

Conclusions

- The above discussion of water transport across the plant root has demonstrated that the root is capable of generating root pressure. Under the influence of this pressure, water may be pumped through the stem xylem up to a certain height.
- The discussion has also demonstrated that the proposed single-membrane model of the root radial route (containing a heterogeneous porous membrane) displays the properties of simultaneous water transport in opposite directions (to the xylem of the vascular cylinder and out of the root – to the soil). This original investigation result is particularly important from the agrophysical viewpoint, particularly in terms of plants maintaining homeostasis.
- Due to this two-way water transport, the plant can also obtain necessary nutrients from the soil as well as simultaneously removing into the soil both water and superfluous (and frequently harmful) products of metabolism occurring in root cells. These unneeded products are food for many bacteria, which subsist in the direct vicinity of the root. Their superfluous metabolism products, in turn, may provide the plant with necessary nutrients.

Bibliography

- Fiscus, E. L., 1975. The interaction between osmotic- and pressure-induced water flow in plant roots. *Plant Physiology*, **55**, 917–922.
- Fiscus, E. L., 1986. Diurnal changes in volume and solute transport coefficient of Phaseolus roots. *Plant Physiology*, **80**, 752–759.
- Ginsburg, H., 1971. Model for iso-osmotic water flow in plant root. *Journal of Theoretical Biology*, **32**, 917–922.
- Kargol, M., 1994. Energetic aspect of radial water transport across the bean root. *Acta Physiologiae Plantarum*, **16**, 45–52.
- Kargol, M., 1995. *Introduction to Biophysics*. Ed. WSP, pp.189–215.
- Kargol, M., 2002. Mechanistic approach to membrane mass transport processes. *Cellular & Molecular Biology Letters*, **7**, 983–993.
- Kargol, M., 2006. *Physical Foundations of Membrane Transport of Non-electrolytes*. Poland: Copyright and printed by PPU “Ekspres Druk” Kielce, pp. 25–31.
- Kargol, M., 2007. *Mass Transport Processes in Membranes and Their Biophysical Implications*. Poland: WSTKT Kielce, pp. 19–144.
- Kargol, M., and Kargol, A., 2003a. Mechanistic formalism for membrane transport generated by Osmotic and mechanical pressure. *General Physiology and Biophysics*, **22**, 51–68.
- Kargol, M., and Kargol, A., 2003b. Mechanistic equations for membrane substance transport and their identity with Kedem-Katchalsky equations. *Biophysical Chemistry*, **103**, 117–127.
- Kargol, M., and Kargol, A., 2006. Investigation of reverse osmosis on the basis of the Kedem-Katchalsky equations and mechanistic transport equations. *Desalination*, **190**, 267–276.
- Katchalsky, A., and Curran, P. F., 1965. *Nonequilibrium Thermodynamics in Biophysics*. Cambridge, MA: Harvard University Press, pp. 113–132.

Pitman, G. M., 1982. Transport across plant roots. *Quarterly Review of Biophysics*, **15**, 481–553.

Steudle, E., Oren, R., and Schulze, E. D., 1987. Water transport in maize roots. *Plant Physiology*, **84**, 1220–1232.

Stryer, L., 2000. *Biochemistry*. Poland: PWN Warszawa, pp. 280–384.

Taura, T., Furumoto, M., and Katou, K., 1987. A model for water transport in stele of plants roots. *Protoplasma*, **140**, 123–132.

Cross-references

[Coupled Heat and Water Transfer in Soil](#)

[Plant Roots and Soil Structure](#)

[Root Water Uptake: Toward 3-D Functional Approaches](#)

[Soil Hydraulic Properties Affecting Root Water Uptake](#)

[Soil–Plant–Atmosphere Continuum](#)

[Stomatal Conductance, Photosynthesis, and Transpiration, Modeling](#)

[Water Budget in Soil](#)

[Water Effects on Physical Properties of Raw Materials and Foods](#)

[Water Reservoirs, Effects on Soil and Groundwater](#)

[Water Uptake and Transports in Plants Over Long Distances](#)

MICROBES AND SOIL STRUCTURE

Vadakattu Gupta

Entomology, CSIRO, Glen Osmond, SA, Australia

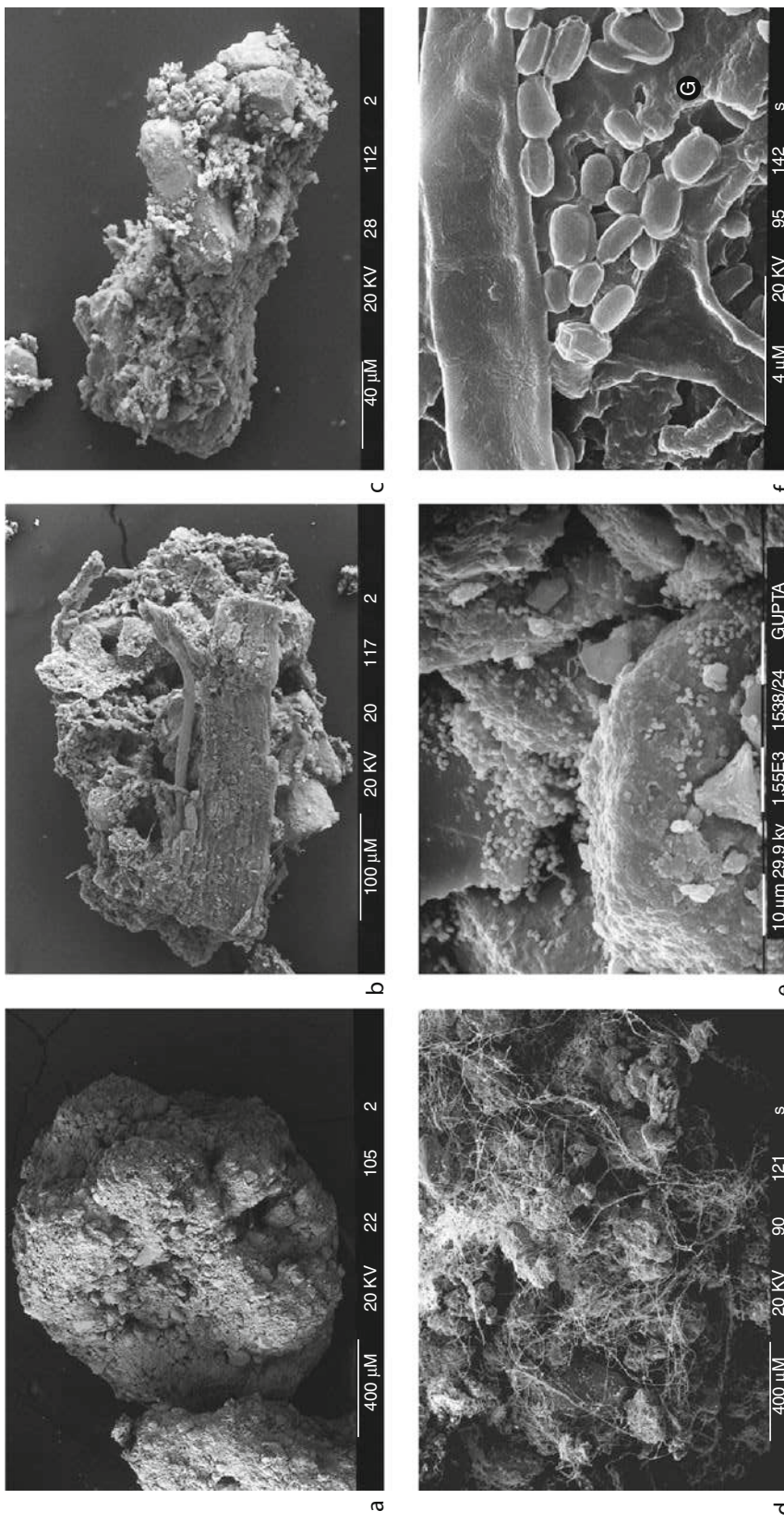
Definition

Microbes – Single and multicelled microorganisms that are microscopic in size (<100 µm in body width) including bacteria, fungi, algae, and protozoa.

Soil structure – The arrangement of primary soil particles and the pore spaces between them.

Soil particles are arranged together to form aggregates which are held together by organic matter and microbial agents (Tisdall and Oades, 1978). Aggregates that are stable to wetting are a key component of good soil structure as they help to maintain soil porosity and aeration at optimal levels for soil biota and plants.

Soil microorganisms play an important role in the formation and stabilization of aggregates. Bacteria and fungi produce a variety of mucilaginous polysaccharides, by utilizing the more easily available C substrates from fresh residues and roots, which act like glue and help them attach to clays, sands, and organic materials, resulting in the formation of new aggregates. Fungal hyphal networks facilitate the formation of macroaggregates (250–2,000 µm) through enmeshment of soil particles with organic debris (Gupta and Germida, 1988), whereas, decomposing plant residues and microbial debris encrusted with soil particles, by mucilages, form the core of microaggregates (20–250 µm) (Six et al., 2004). Both mycorrhizal and saprophytic fungi contribute to aggregate formation and stabilization. The influence of mucigels through their binding capacity is mostly seen at a scale <50 µm within the aggregates. As the decomposition of organic material progresses, microbial metabolites further permeate the surrounding mineral crust, increasing the interparticle cohesion and promoting the stability of aggregates. The production of hydrophobic



Microbes and Soil Structure, Figure 1 Scanning electron micrographs of soil aggregates: the backbone of soil structure: aggregates offer a diverse array of microsites for microbial colonization over short distances. Stable macroaggregates (a, b) are composed of decomposing crop residues (particulate organic matter), individual primary particles, microaggregates (c), pores of varying sizes, and biota remnants. Fungal hyphal networks (thread-like structures) hold soil particles and micro aggregates onto the surface of crop residues as part of the formation of macroaggregates (d). (e) Bacteria and fungi colonize the surfaces and small pores of macroaggregates (e). Organic compounds (glues, G) produced by bacteria (f) and fungi help bind the primary particles and plant debris to form stable aggregates.

substances by microorganisms increases the repellency of aggregates, which decreases the rate of soil wetting and influences aggregate stability. The relative importance of fungi vs. bacteria for aggregation is dependent on soil texture through its influence on porosity characteristics and nutrient availability (Figure 1).

Good soil structure provides an array of niches, i.e., in terms of redox potential and substrate availability, which can house diverse microbial communities. The distribution of bacterial and fungal communities and their function varies between different aggregate size classes (Gupta and Germida, 1988). Macroaggregates generally contain more labile organic matter with rapid turnover times and a greater proportion of fungal biomass. Mycelial networks of fungi help them exploit the heterogeneous soil matrix where carbon and nutrient resources are spatially separated (1) over extended distances at microbial scale and (2) in unconnected pore networks.

The coexistence of diverse bacterial communities within 1-cm³ area reflects the high degree of spatial heterogeneity in soil microniches. Bacteria often reside in pores and inner surfaces of aggregates as microcolonies of 2–16 bacteria each, and extensive colonization is restricted to microsites with higher C availability, e.g., rhizosphere and outer surfaces of freshly formed macroaggregates (Foster, 1988). Location of different phenotypic and functional groups of bacteria varies in different parts of aggregates, e.g., denitrifying bacteria and diazotrophs are generally located within inner parts of aggregates (Hattori, 1988; Mummy et al., 2006). However, location of aggregates in relation to roots, organic residues, and macropores is more important for determining the microbial community composition and their activity. Bacteria present within inner portions of larger aggregates, microaggregates, and micropores are protected from desiccation and grazing by protozoan predators. The turnover of these organisms is generally low compared to those located in macropores. Disturbance affects aggregation, aeration, and accessibility of substrates, thereby influencing diversity and activity of microbes in soil.

Bibliography

- Foster, R. C., 1988. Microenvironments of soil microorganisms. *Biology and Fertility of Soils*, **6**, 189–203.
- Gupta, V. V. S. R., and Germida, J. J., 1988. Distribution of microbial biomass and its activity in different soil aggregate size classes as affected by cultivation. *Soil Biology and Biochemistry*, **20**, 777–787.
- Hattori, T., 1988. Soil aggregates as microhabitats for microorganisms. *Report of the Institute of Agricultural Research*, Tohoku University, Vol. 37, pp. 23–36.
- Mummy, D., Holben, W., Six, J., and Stahl, P., 2006. Spatial stratification of soil bacterial populations in aggregates of diverse soils. *Microbial Ecology*, **51**, 404–411.
- Six, J., Bossuyt, H., Degryze, S., and Denef, K., 2004. A history of research on the link between microaggregates, soil biota, and soil organic matter dynamics. *Soil and Tillage Research*, **79**, 7–31.
- Tisdall, J. M., and Oades, J. M., 1978. Organic matter and water-stable aggregates in soils. *Journal of Soil Science*, **33**, 141–163.

Cross-references

- [Earthworms as Ecosystem Engineers](#)
[Microbes, Habitat Space, and Transport in Soil](#)
[Mineral–Organic–Microbial Interactions](#)
[Plant Roots and Soil Structure](#)
[Soil Aggregates, Structure, and Stability](#)
[Soil Biota, Impact on Physical Properties](#)
[Tillage, Impacts on Soil and Environment](#)

MICROBES, HABITAT SPACE, AND TRANSPORT IN SOIL

Karl Ritz

Natural Resources Department, National Soil Resources Institute, School of Applied Sciences, Cranfield University, Cranfield, UK

Definition

Microbes. Life forms that are nominally microscopic (not discernable with the unaided human eye) and typically comprised of one cell (unicellular).

Habitat space. Ecological or environmental volume, encompassing the physical, chemical, and biological environment that is inhabited by particular organisms, populations and communities.

Transport. Movement of entities (e.g., gases, liquids, solutes, particulates, organisms) from one region of a defined space to another.

Microbial life in soil

The living fraction of soils collectively known as the biomass, typically constitutes only a small percent of the total organic matter, but it is of great significance with regard to soil functioning (Paul, 2007). The biota play fundamental roles in delivering the majority of the ecosystem goods and services that soils provide, ranging from soil formation, carbon and nutrient cycling, modulating structural dynamics, regulating biotic populations, and providing biodiversity and genetic resources (Bardgett, 2005; Kibblewhite et al., 2008). Whilst the body size range of soil organisms spans several orders-of-magnitude from centimeters to micrometers (μm , 10^{-6} m), the majority of the soil biomass is always microbial, represented predominantly by bacteria, archaea, and fungi, plus to a lesser extent, protozoa. (Algal biomass in soils is generally present but relatively insignificant, except in some wetland rice systems in the tropics, and is then predominantly confined to the surface, since there is no light beyond a few millimeter depth in most soils, hence phototrophic organisms do not prevail beyond this zone. However, a small biomass does not necessarily mean algae are functionally unimportant in soil systems.) Multicellular organisms such as nematodes and the other soil fauna are not deemed microbial and hence are outside the scope of this entry. The soil microbial biomass typically ranges between different ecosystems from tens to thousands of

$\mu\text{g C g}^{-1}$ soil, depending upon the system and a wide variety of factors. However, there is generally a positive relationship between the concentration of organic matter in soil and microbial biomass, since carbonaceous material represents the primary energy source for the majority of the soil biota. Soil biodiversity is generally greater than in any other ecological compartment, particularly within microbial groups.

The soil habitat

The solid phases of soil are comprised of a diverse mixture of inorganic (“mineral” materials derived from the parent geology or glacial deposition) and organic (containing carbon) materials, made up of living matter (biota) or nonliving matter) components (Brady and Weil, 2002). Soils are produced by gradual processes of biogeochemical transformation, including “weathering,” a range of erosive chemical, physical, and biological mechanisms that produce a population of mineral particles of varying sizes. The small (nanometer), medium and large (millimeter) components are classified as the clay, silt, and sand fractions respectively. These mineral constituents eventually combine with organic components, predominantly originating from green plants, to form relatively thin “topsoils.” The inorganic and organic constituents of soil are arranged in space to form the so-called soil pore network. The origins of soil pore networks are that the fundamental sand-silt-clay components, mediated by organic materials, aggregate to form larger units (Tisdall and Oades, 1983). Generally, the forces binding such aggregates together are greater at smaller-size scales, and hence there tends to be a greater stability of soil structure at these smaller scales. These small units then aggregate further to create larger structures, with an associated hierarchy of scale and structural stability. Since the units are nonuniform, their packing creates a porous matrix, and since the constituents carry such a wide size range, the porous network is heterogeneous across a concomitantly wide range of scales. It is the pore network that comprises the physical, and primary, habitat for all soil organisms, representing a form of “inner space” in which the entirety of below-ground life inhabits (Figure 1). The nature of the pore network imparts a structural organization to soil communities and strongly influences the way they function and interact (Young and Ritz, 2005).

How soil structure affects microbial function

The exceptional heterogeneity of the soil pore network imparts some significant properties to the soil system from the perspective of the microbiota. First, it provides a huge surface area for potential colonization. Many soil bacteria are adapted to adhere to surfaces and occur as colonies on the surface of pore walls. Filamentous fungi are also well adapted to grow through soil pore networks by the process of hyphal elongation and branching, but also require some direct contact with substrates in order to absorb water and nutrients released by the action of the extracellular

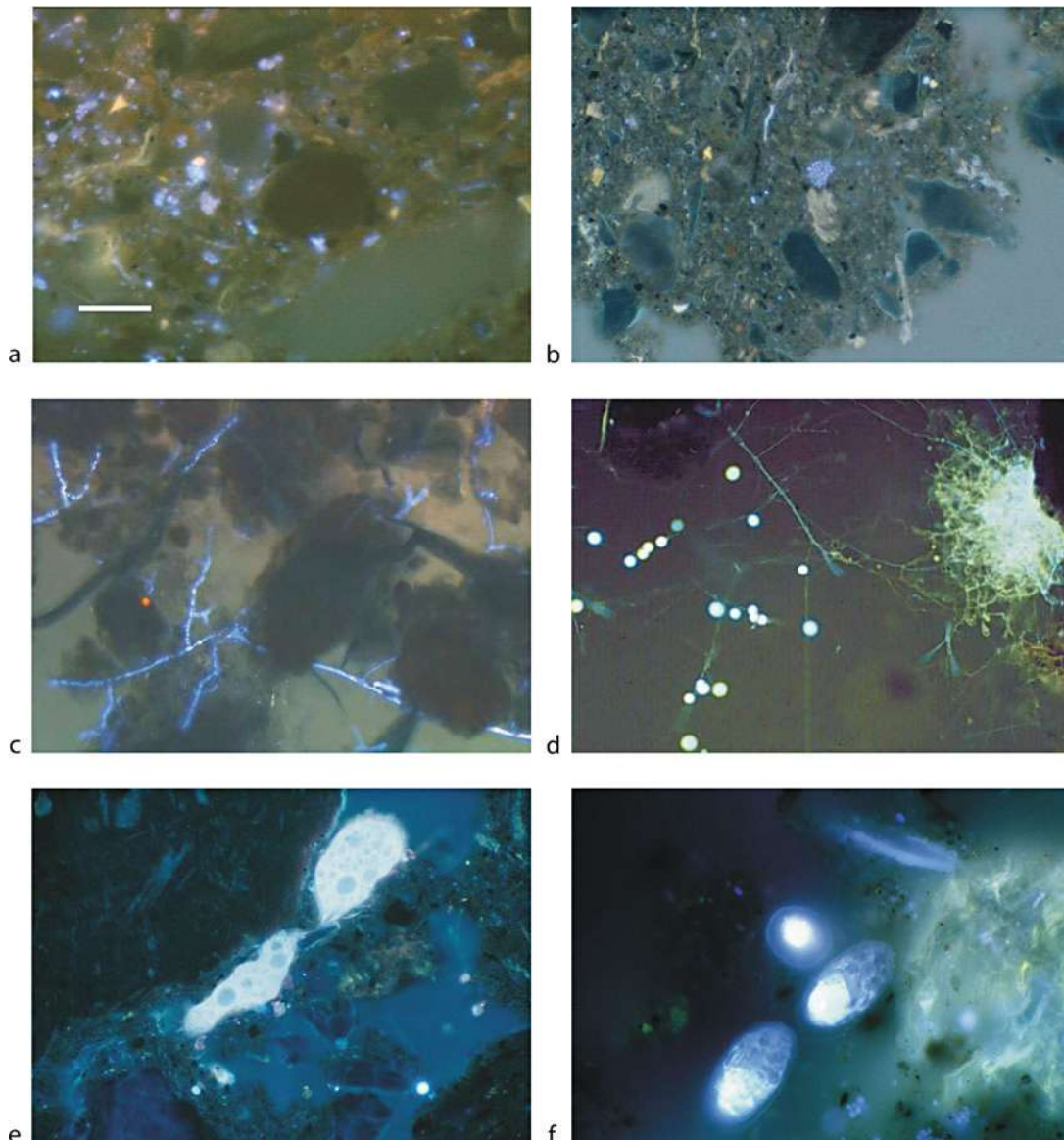
enzymes they produce. It is hypothesized that the extreme structural heterogeneity of soils is one basis for the exceptional diversity found in the soil microbiota, since it provides an extreme range of spatially isolated microhabitats which can lead to adaptive radiation (Zhou et al., 2002). Second, it governs the distribution and availability of nutrient resources to the biota. Unlike in aquatic systems, where most constituents are relatively well mixed by virtue of existing in a fluid matrix, the physical structure of soils essentially discretizes nutrient resources into spatially distinct patches, many of which will then be physically protected from being accessed by organisms. This can occur as a result of coating with soil minerals, or by being located in soil pores smaller than the physical size of potential consumer organisms. Such physical protection mechanisms can equally apply to dead organic matter, or potential prey in the case of active predators such as protozoa.

The connectivity and tortuosity of the pore network governs the movement of gases, liquids, and associated solutes, as well as particulates and organisms, through the matrix. Sessile organisms such as attached bacterial colonies rely upon the delivery of substrates to the colony, usually in water phases, as well as oxygen for aerobic respiration, via such pathways. The foraging distances taken by motile organisms when searching for substrate or prey – and hence the amount of energy consumed – will also be affected by path lengths for movement, which are related to these properties. There is a strong interaction between the pore network, water, and microbial activity, fundamentally linked to the relationships between the matric potential of a soil and the associated distribution of water between differently sized pores. Bacteria and protozoa require water films to move in, and their passage will be curtailed where there is no continuity in such features. Fungi are less constrained since hyphae can grow extended distances through air-filled pores.

As oxygen diffuses about 10,000 times more slowly in water than in air, water-filled pores – or narrow necks to larger pores – effectively act as valves, preventing the passage of oxygen and hence its availability to organisms for aerobic respiration. In these circumstances, many so-called facultative microbes can switch their metabolism to alternative biochemical pathways involving anaerobic processes.

How microbes affect soil structure

Whilst soil structure strongly affects the distribution and functioning of microbes and microbial communities, the microbiota also play important roles in soil structural dynamics (Brussaard and Kooistra, 1993). Microbes create soil structure by a number of direct and indirect processes, including (1) moving and aligning primary particles along cell or hyphal surfaces; (2) adhering particles together by the action of adhesives involved in colony cohesion, and other exudates, such as extracellular polysaccharides (EPS); (3) enmeshment and binding of



Microbes, Habitat Space, and Transport in Soil, Figure 1 Soil microbes in the soil habitat, visualized in thin sections of undisturbed soil, prepared appropriately to preserve biological tissue (cf. Nunan et al., 2001). (a) Bacterial cells in worm cast. (b) Bacterial colony embedded in soil matrix. (c) Mycelia of *Rhizoctonia solani* in sterilized soil. Note preferential growth in larger pores and apparent lack of penetration of denser masses of soil. (d) Unidentified mycelium in field soil, with abundant sporangia in main region of pore. (e) Naked amoeba passing through narrow pore in arable soil. (f) Testate amoebae accumulating near pore wall of arable soil. Scale bar ca. 25 μm .

aggregates by fungal hyphae and actinomycete filaments, and associated mycelia; and (4) coating pore walls with hydrophobic compounds, particularly by fungi which produce such polymers to insulate their mycelia, which have a relatively large surface area:volume ratio.

Soil structure is also destroyed by the action of microbes, since much of the organic material which serves to bind soil particles together is also potentially energy-containing substrate which microbes will

decompose if they can gain access to it. This is the reason why frequent soil disturbance, such as where repeated tillage is applied to soils, typically leads to a degradation of soil structure and a loss of soil C. Undisturbed soils have a high proportion of physically protected organic matter in them. When these are disturbed, such stabilizing material becomes available to microbial assimilation, is decomposed, and a proportion of the C is lost as respired CO₂.

Microbes and transport phenomena

Transport processes in soils are fundamentally affected by (1) the nature of the material being transported – gas, liquid, solute, colloid, particle, or organism; (2) the porosity, connectivity, and tortuosity of the pore network; (3) the exchange properties of the soil, and particularly their distribution in pore surfaces; (4) the distribution of water within the pore network; (5) interactions with the soil biota.

Microbial effects upon transport processes are generally indirect. Via their involvement with a plethora of elemental cycles, microbes transform the constitution and nature of compounds such that their propensity to be transported can be markedly altered, for example, by mineralizing elements from organic forms, or by altering the redox states of compounds, which can have profound effects upon transportability. Soil structure is affected by microbial actions as summarized above – and this in turn affects the moisture release curve, and hence distribution of water.

In relation to direct effects, bacterial movement through the soil matrix will result in a concomitant transport of elements bound in the bacterial cells, but given that the majority of bacteria in soils are sessile, this is not considered to be of great significance. Whilst motile, and hence prone to movement through the soil matrix, protozoan biomass is generally insufficient to likely influence nutrient transport phenomena directly. Protozoa can carry viable bacteria in their cells, including pathogenic forms, and hence may play a role in dispersal of such cells within soils. Fungi, however, have a much greater direct influence upon transport processes (Ritz, 2006). This arises as a result of the mycelium which is essentially a connected and integrated network, which is spatially isolated from the soil matrix. Materials can be translocated within mycelia by both active and passive processes, and are to some extent under the control of the fungal organism. Some primary nutrient elements which appear particularly prone to transport by filamentous fungi are C, N, P, K, S. Other elements, including some heavy metals and radionuclides, have been reported to be directly translocated by fungi. Of particular significance is the transport of P by mycorrhizal fungi to their host plants (Smith and Read, 2008).

Conclusions

Microbial activity creates soil structure which in turn affects the actual and potential function of such organisms. One way of conceptualizing the complex interplay between soil microbes – indeed, the entire soil biota – is that of “soil architecture,” which encompasses the notion of communities living in an appropriately physically structured environment, which allows, but modulates, a wide range of direct and indirect interactions which deliver the range of functions that lead to an integrated and sustainable system. An inappropriately structured soil (typically, one which has a low porosity) will be detrimental to the biota since there will be a compromised habitat,

manifest as inadequate space and a constrained potential for the dynamics of gases, liquids, solutes, and organisms. Without such dynamics, soil functioning will then inevitably also be impaired.

Bibliography

- Bardgett, R. D., 2005. *The Biology of Soil: A Community and Ecosystem Approach*. New York: Oxford University Press.
- Brady, N. C., and Weil, R. R., 2002. *The Nature and Properties of Soils*. Upper Saddle River: Prentice-Hall.
- Brussaard, L., and Kooistra, M. J., 1993. *Soil Structure/Soil Biota Interrelationships*. Amsterdam: Elsevier.
- Kibblewhite, M. G., Ritz, K., and Swift, M. J., 2008. Soil health in agricultural systems. *Philosophical Transactions of the Royal Society London B*, **363**, 685–701.
- Nunan, N., Ritz, K., Crabb, D., Harris, K., Wu, K., Crawford, J. W., and Young, I. M., 2001. Quantification of the *in situ* distribution of soil bacteria by large-scale imaging of thin-sections of undisturbed soil. *FEMS Microbiology Ecology*, **37**, 67–77.
- Paul, E. A., 2007. *Soil Microbiology, Ecology and Biochemistry*. Oxford: Academic.
- Ritz, K., 2006. Fungal roles in transport processes in soils. In Gadd, G. M. (ed.), *Fungi in Biogeochemical Cycles*. Cambridge: Cambridge University Press, pp. 51–73.
- Smith, S. E., and Read, D. J., 2008. *Mycorrhizal Symbiosis*. Third edition. London: Academic.
- Tisdall, J. M., and Oades, J. M., 1983. Organic matter and water-stable aggregates in soils. *Journal of Soil Science*, **33**, 141–163.
- Young, I. M., and Ritz, K., 2005. The habitat of soil microbes. In Bardgett, R. D., Usher, M. B., and Hopkins, D. W. (eds.), *Biological Diversity and Function in Soils*. Cambridge: Cambridge University Press, pp. 31–43.
- Zhou, J. Z., Xia, B. C., Treves, D. S., Wu, L. Y., Marsh, T. L., O'Neill, R. V., Palumbo, A. V., and Tiedje, J. M., 2002. Spatial and resource factors influencing high microbial diversity in soil. *Applied and Environmental Microbiology*, **68**, 326–334.

Cross-references

- [Biofilms in Soil](#)
[Earthworms as Ecosystem Engineers](#)
[Microbes and Soil Structure](#)
[Soil Biota, Impact on Physical Properties](#)

MICROCOSM

A little world; a world in miniature (opposed to macrocosm). Term often used in soil experiments.

Bibliography

- Kurt-Karakus, P., and Kevin C. Jones. 2006. Microcosm studies on the air–soil exchange of hexachlorobenzene and polychlorinated biphenyls. *Journal of Environmental Monitoring*, **8**:1227–1234.

MICRO-IRRIGATION

A water management irrigation technique using a micro-sprinkler or drip irrigation system to minimize water runoff.

Cross-references

[Water Use Efficiency in Agriculture: Opportunities for Improvement](#)

MICROSTRUCTURE OF PLANT TISSUE

Krystyna Konstankiewicz

Institute of Agrophysics, Polish Academy of Sciences,
Lublin, Poland

Synonyms

Microstructure; Structure

Definition

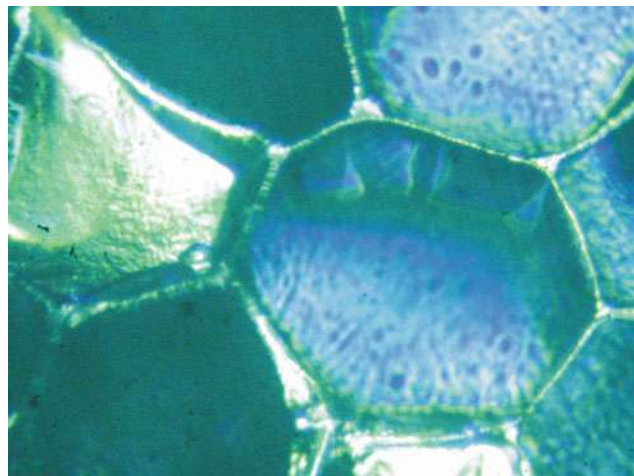
The *microstructure of plant tissue* is the geometric arrangement of cells as the fundamental elements of that structure. The packing of cells is not tight – between cells, surrounded by stiff cell walls, there are intercellular spaces. The system of plant microstructure is a three-phase one – the interior of the cells and of the intercellular spaces is filled with liquid and gas, while the cell walls are the solid phase. The shape and size of cells are determined by the cell walls which, due to their physical properties, play the role of “skeleton” of the whole object and affect its properties.

The *microstructure of plant tissue* is its fundamental material feature and determines its other properties – chemical, physical, and biological.

Introduction

The latest trends in research of plant tissues relate to the identification and description of the basic features of the material – on the microscale, and then to the search for their relations with the properties of whole objects, including their quality features (Mebatsion et al., 2008). One of the fundamental physical properties that characterize the material under study is its structure, which determines all of its other properties, for example, physical, chemical, and biological (Aguilera and Stanley, 1990). Material studies have a long tradition, supported by practical experience resulting from the production of a variety of materials (Kunzek et al., 1999). Based on the quantitative description of the structure of a material studied one can make comparisons between objects or record changes taking place within a single object as a result of, for example, a technological process, storage, or from non-homogeneity of the material (Wilkinson et al., 2000). Knowledge on the effect of structure on the properties of a material, in turn, can be utilized for controlling the technological processes so as to obtain materials with desired properties as well as for designing totally new materials (Bourne, 2002).

The fundamental structural element of plant tissue is the cell and that is the element to whose size relations of other properties of the material studied are sought (Konstankiewicz and Zdunek, 2005) (Figure 1).



Microstructure of Plant Tissue, Figure 1 Microstructure of potato parenchyma – preparation of sample: 1 mm sliced with a razor blade and washed with tap water. Image obtained with the Tandem Scanning Reflected Light Microscope (TSRLM), 0.47 mm × 0.65 mm.

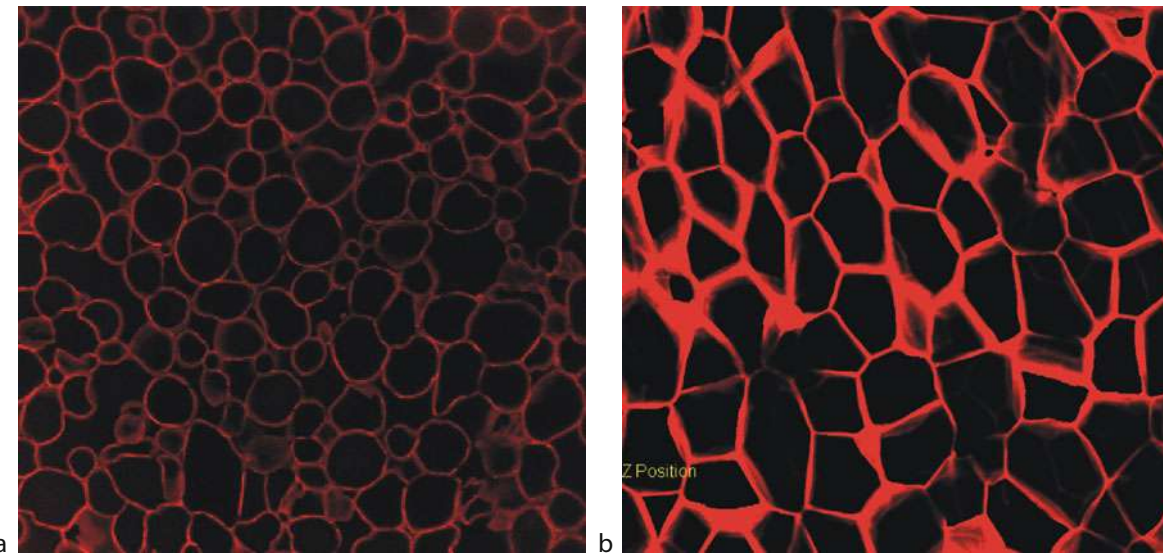
Many years of research in this field, including also my own, indicate that the cellular structure is a characteristic feature of plant tissues, and every conclusion may only be based on current results of quantitative analysis of structural parameters, especially those relating to cell size (Konstankiewicz et al., 2002; Zdunek and Umeda, 2005).

Microscope observations of cellular structures of plants

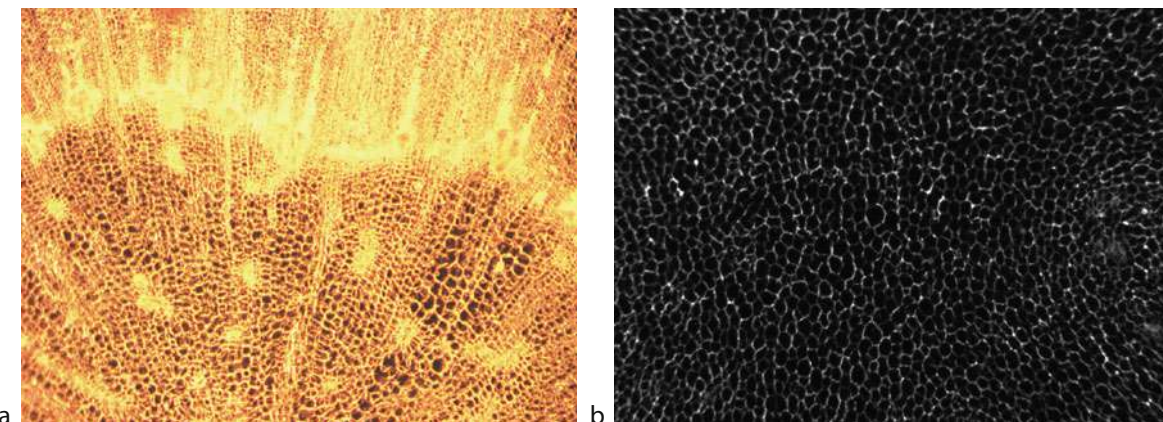
Microscope observations are the source of information on cellular structures. Commonly available and continually improved microscope methods permit the observation of cell structures at various rates of magnification, and digital techniques of recording the images obtained permit analysis of the information they contain. The broad array of microscopes of various types – optical, confocal, electron (scanning, transmission), acoustic, X-ray, atom force, Raman – with a variety of additional accessories and software, used for routine observations with very good results for various materials, provides a set of excellent research tools also with relation to plant tissues (Sargent, 1988; Pawley, 1989; Hemminga, 1992; Blonk and van Aalst, 1993; Kaláb et al., 1995; Davies and Harris, 2003; Konstankiewicz and Zdunek, 2005; Figure 2).

A separate group is constituted by methods of imaging of large sample areas – macrosopes, thanks to which it is possible to assess the spatial organization of structural elements, arrangement of cells, and to study identified directions and large zones of structural changes resulting from processes under study (Zdunek et al., 2007; Devaux et al., 2008; Figure 3).

The choice of suitable equipment is not easy, yet it frequently determines the successful solution of problems



Microstructure of Plant Tissue, Figure 2 Images of microstructure obtained with the Confocal Scanning Laser Microscope (CSLM), each one 1.4×1.4 mm (a) apple and (b) potato parenchyma, sample after preparation procedure.



Microstructure of Plant Tissue, Figure 3 Microstructure of carrot (a) and potato parenchyma (b) sample in natural state. Image obtained with the macroscope, $6 \text{ mm} \times 4.5 \text{ mm}$.

posed, and may also save time and cost. The objective of the research, that is, focusing on the significant elements of the structure and elimination of useless details while ensuring methodological correctness, is of fundamental importance. The location of specimen taking and the choice of the plane of observation are other significant elements. Whereas, the application of preliminary preparation of specimens, from simple slicing to the fixing of structure, may introduce disturbances in the structures under observation that have to be taken into account in subsequent examinations and in the formulation of conclusions (Sun and Li, 2003; Delgado and Rubiolo, 2005; Spector and Goldman, 2006; Otero et al., 2009).

In the studies on the physical properties of plant tissues, methods are sought for the obtainment of such images of

the structure that will provide distinct representation of cell walls that determine the overall dimensions of the cells, permit the measurement of those dimensions and then their correlation with other features of the tissue under study (De Smedt et al., 1998; Fornal et al., 1999; Konstankiewicz and Zdunek, 2001; Hepworth and Bruce, 2004).

For an image of a structure to be suitable for computer analysis, it must be of high quality, that is, primarily with a very good level of contrast. The structural elements of interest should be clearly defined, countable, and measurable. This is a difficult task in the case of plant tissues that have a low level of coloring, sometimes are even transparent, and additionally, due to their high content of water, tend to dry quickly and get deformed in the course of observation.

The quantitative description of a cellular structure requires the development of research methodology suitable for a given object. Even with well-developed procedures, the experience and knowledge of the observer are indispensable for correct interpretation of information contained in the images analyzed (Zdunek et al., 2004; Gancarz et al., 2007).

Image analysis of plant tissue microstructure

Good-quality microscope images of the structure of plant tissue can be subjected to detailed analysis leading to quantitative characterization of the object studied. Computer image analysis used for the purpose has been known since the beginning of the 1960s, and has undergone a violent development in the period of common availability of digital cameras and of various types (Serra, 1982; Serra, 1988; Kaláb et al., 1995; Abbott, 1999; Wojnar et al., 2002). Computers, cameras, and software are necessary equipment of every microscope set. The use of software for image analysis may appear to be a simple task, especially when there is easy access to professional offers and an abundance of promising results concerning other materials. It turns out, however, that the task is a complex one and requires good experience as well as knowledge not only about the object of study itself but also about the methods of image taking, acquisition, processing, and analysis. In spite of the continual advances of specialist knowledge in the field of image analysis, and the resultant occasional problems with its understanding, its possession at a basic level is a requirement for every user in order to avoid errors that may bring irreversible effects at the final stage of formulation of conclusions.

Computer image analysis is the most helpful when we need to make multiple computations or measurements, or when comparing images with one another. Such problems are encountered not only in research, but also in diagnostics or in quality control. These tasks require numerous replications and, most importantly, objectivity of the results obtained. For images with sufficiently good quality, it is possible to perform automatic analysis with the help of professional software (Bourne, 1981; Devaux et al., 2005; Cybulská et al., 2008). In practice, however, application of automated image analysis is not always possible even with good quality of the images, and very often image evaluation and manual corrections by an experienced observer are a necessity.

In a flat (2D) image, the size of a cell is defined by measured parameters: surface area, perimeter, diameters, and chords. However, the expected size of a cell as a spatial (3D) object should be its volume and shape and the dimensions of such a solid. Identification of a spatial structural element permits the modeling of the structure of the whole object.

The latest solutions propose highly specialized techniques of computer tomography for mathematic modeling of 3-D cell structures of plant tissues. Such models open

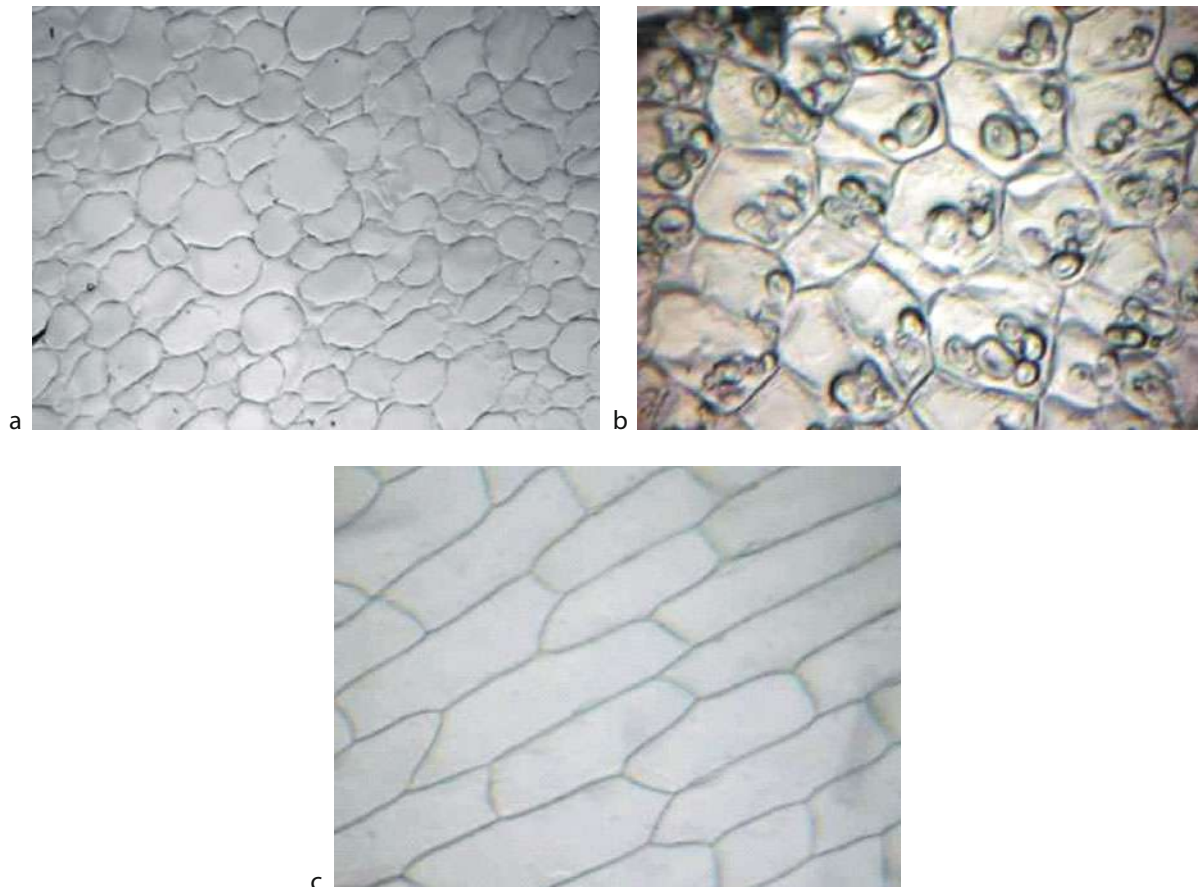
up new possibilities in the range of simulation studies on the transport of liquids and gases through the system of cell walls and intercellular spaces and on the processes of deformation under mechanical effects (Lee and Ghosh, 1999; Maire et al., 2003; Tijskens et al., 2003; Kuroki et al., 2004; Mebatson et al., 2006; Mebatson et al., 2009).

Stereological methods in studies on microstructure of plant tissue

The need for practical application of structural studies was at the root of the appearance of quantitative methods for structure description – the stereological methods (Underwood, 1970). The notable advance of theoretical stereology in recent years is related, among other things, with the development of microstructure observation techniques and precision sampling methods (Kurzydłowski and Ralph, 1995). It is the method of selection of objects to be studied that largely determines the systematic error of measurement. One of the fundamental errors is to conduct estimations of structure on the basis of a single cross section of a sample or a single selected area of the specimen. That is the erroneous assumption of homogeneity and isotropy of a medium (Ryś, 1995). Plant tissues have a nonhomogeneous and unstable cellular structure, with frequent discontinuities of notable dimensions (Haman and Konstankiewicz, 2000; Konstankiewicz et al., 2002). The morphology of their structure is a resultant of many factors – cultivar, object size and shape, type of tissue, method of cultivation, time of harvest, postharvest processing, and many others. Information on the heterogeneity of structure is obtained on the basis of microscope observation of natural or fixed specimens (Figure 4).

This permits the selection of characteristic areas in the section of the object – heterogeneity of position, as well as finding whether there occurs spatial orientation of elements of the structure – anisotropic heterogeneity (Gao and Pitt, 1991). Such a preliminary assessment determines the choice of the place and direction of taking specimens, as well as of their number, and in consequence determines the correctness of the final result. It is also important whether the results are to describe a specific area of the object studied or the object as a whole. Large areas of uniform structure permit the taking of specimens with sizes sufficient not only for microscope observation but also for other determinations, for example, of mechanical properties (Zdunek et al., 2004). This is important in the study of relations between the geometric parameters of the structure and other properties of plant tissue. In case of doubt as to the homogeneity of studied areas within the object, for example, the type of tissue or anisotropy features, specimens should be taken from various zones – close to the surface, from the center, and also from intermediate areas, varying the directions of specimen taking.

Based on the analysis of large sets of microscope images, it is possible to determine the minimum number of cells representative for the whole population



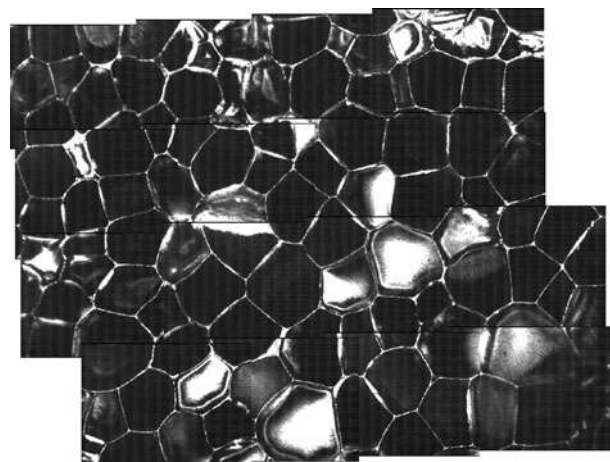
Microstructure of Plant Tissue, Figure 4 Cellular structure of apple (a) potato – cells with starch (b) and onion (c), respectively. Images obtained with optical microscope, samples after preparation, each one $1\text{ mm} \times 0.8\text{ mm}$.

(Maliński et al., 2000). As an example, for the parenchyma tissue of potato tuber the minimum number of cells cannot be less than 300, with high repeatability of results for several independent observers. Properly chosen number of cells under analysis permits the determination of not only the mean values of the geometric parameters of the cell but also their distributions within the object studied (Maliński et al., 1991; Figure 5).

Determination of parameters describing a cellular structure requires the development of suitable research methodology for a given object.

Due to the extensive range of variability of plant cell sizes, a microscope image may contain an insufficient number of whole objects. In such situations, it may be necessary to merge images so that the side of the resultant image be severalfold larger than the mean cell diameter.

The procedures relating to the choice of object, specimen, and area in the specimen for microstructure observation, have a significant effect on the final result and determine the weight of the relationships obtained.



Microstructure of Plant Tissue, Figure 5 Microstructure of potato parenchyma. Example for an image obtained by composing 16 images – TSRLM, $1.5 \times 1.2\text{ mm}$.

Summary

Structure is an important material feature of plant tissue. Investigation of the microstructure of plant tissue is difficult due to the large biological diversity of the material and to the necessity of simultaneous consideration of the effect of a large number of factors resulting from the complex conditions of cultivation and storage and from the increasingly demanding technological processes. Such complex materials, with the rapid development of measurement techniques – microscopes, image analysis – require particularly precise selection of proper measurement methods, preceded with fundamental studies. In most cases, there is no possibility of adaptation of measurement systems commonly used in studies on other materials, and the new research methods being developed require constant improvement due to the rapid development of measurement techniques and to the changing cultivar requirements related with the destined application of agricultural raw materials and products, and with the increasing expectations of the consumers. The utilization of knowledge on plant tissue structure in the process of plant production is the best method of obtaining, in a reproducible manner, materials with expected properties, and of rapid estimation of the quality of plant materials and products.

All the methods for the investigation of the structure, together with other properties, of plant tissues have potential for development, both due to the originality of methodological solutions and to the considerable potential of future practical applications.

Bibliography

- Abbott, J. A., 1999. Quality measurements of fruits and vegetables. *Postharvest Biology and Technology*, **15**, 201–225.
- Aguilera, J. M., and Stanley, D. W., 1990. *Microstructural Principles of Food Processing and Engineering*. London: Elsevier Applied Science.
- Blonk, J. C. G., and van Aalst, H., 1993. Confocal scanning light microscopy in food research. *Food Research International*, **26**, 297–311.
- Bourne, M., 1981. Physical properties and structure of horticultural crops. In Peleg, M., and Bagley, E. G. (eds.), *Physical Properties of Foods*. Westport: AVI, pp. 207–228.
- Bourne, M. C., 2002. *Food Texture and Viscosity: Concept and Measurement*. London: Academic.
- Cybulska, J., Zdunek, A., Konskyy, R., and Konstankiewicz, K., 2008. Image analysis of apple tissue cells after mechanical deformation. *Acta Agrophysica*, **11**(1), 57–69.
- Davies, L. M., and Harris, P. J., 2003. Atomic force microscopy of microfibrils in primary cell walls. *Planta*, **217**, 283–289.
- De Smedt, V., Pauwels, E., De Baerdemaeker, J., and Nicolaï, B. M., 1998. Microscopic observation of mealiness in apples: a quantitative approach. *Postharvest Biology and Technology*, **14**, 151–158.
- Delgado, A. E., and Rubiolo, A. C., 2005. Microstructural changes in strawberry after freezing and thawing processes. *Lebensmittel – Wissenschaft und Technologie*, **38**, 135–142.
- Devaux, M.-F., Barakat, A., Robert, P., Bouchet, B., Guillon, F., Navez, B., and Lahaye, M., 2005. Mechanical breakdown and cell wall structure of mealy tomato pericarp tissue. *Postharvest Biology and Technology*, **37**(3), 209–221.
- Devaux, M.-F., Bouchet, B., Legland, D., Guillon, F., and Lahaye, M., 2008. Macro-vision and grey level granulometry for quantification of tomato pericarp structure. *Postharvest Biology and Technology*, **47**, 199–206.
- Fornal, J., Jeliński, T., Sadowska, J., and Quattrucci, E., 1999. Comparison of endosperm microstructure of wheat and durum wheats using digital image analysis. *International Agrophysics*, **13**, 215–220.
- Gancarz, M., Konstankiewicz, K., Pawlak, K., and Zdunek, A., 2007. Analysis of plant tissue images obtained by confocal tandem scanning reflected light microscope. *International Agrophysics*, **21**(1), 49–53.
- Gao, Q., and Pitt, R. E., 1991. Mechanics of parenchyma tissue based on cell orientation and microstructure. *Transactions of the American Society of Agricultural Engineers*, **34**, 232–238.
- Haman, J., and Konstankiewicz, K., 2000. Destruction processes in the cellular medium of a plant – theoretical approach. *International Agrophysics*, **14**, 37–42.
- Hemminga, M. A., 1992. Introduction to NMR. *Trends in Food Science and Technology*, **3**, 179–186.
- Hepworth, D. G., and Bruce, D. M., 2004. Relationships between primary plant cell wall architecture and mechanical properties for onion bulb scale epidermal cells. *Journal of Texture Studies*, **35**(6), 586–602.
- Kaláb, M., Allan-Wojtas, P., and Miller, S. S., 1995. Microscopy and other imaging techniques in food structure analysis. *Trends in Food Science and Technology*, **6**, 177–186.
- Konstankiewicz, K., Czachor, H., Gancarz, M., Król, A., Pawlak, K., and Zdunek, A., 2002. Cell structural parameters of potato tuber tissue. *International Agrophysics*, **16**(2), 119–127.
- Konstankiewicz, K., and Zdunek, A., 2001. Influence of turgor and cell size on the cracking of potato tissue. *International Agrophysics*, **15**(1), 27–30.
- Konstankiewicz, K., and Zdunek, A., 2005. *Micro-structure Analysis of Plant Tissues*. Lublin: Centre of Excellence for Applied Physics in Sustainable Agriculture Agrophysics.
- Kunzek, H., Kabbert, R., and Gloyna, D., 1999. Aspects of material science in food processing: changes in plant cell walls of fruits and vegetables. *Zeitschrift Lebensmittel Untersuchung Forschung A*, **208**, 233–250.
- Kuroki, S., Oshita, S., Sotome, I., Kawagoe, Y., and Seo, Y., 2004. Visualisation of 3-D network of gas-filled intercellular spaces in cucumber fruit after harvest. *Postharvest Biology and Technology*, **33**, 255–262.
- Kurzydłowski, K. J., and Ralph, B., 1995. *The Quantitative Description of the Microstructure of Materials*. London: CRC Press.
- Lee, K., and Ghosh, S., 1999. A microstructure based numerical method for constitutive modelling of composite and porous materials. *Material Science and Engineering A*, **272**, 120–133.
- Maire, E., Fazekas, A., Salvo, L., Dendievel, R., Youssef, S., Cloetens, P., and Letang, J. M., 2003. X-ray tomography applied to the characterization of cellular materials. Related finite element modeling problems. *Composites Science and Technology*, **63**, 2431–2443.
- Maliński, M., Cwajna, J., and Chrąpolski, J., 1991. Grain size distribution. *Acta Stereologica*, **10**, 73–83.
- Maliński, M., Cwajna, J., and Mokry, W., 2000. Procedure for determination minimal number of measurements and for testing results repeatability in quantitative evaluation of materials microstructure. In *Proceedings of Sixth International Conference, Stereology and Image Analysis in Material Science, STERMAT 2000*, September 20–23, Cracow, pp. 259–264.

- Mebatsion, H. G., Verboven, P., Ho, Q. T., Mendoza, F., Verlinden, B. E., Nguyen, T. A., and Nicolaï, B. M., 2006. Modelling fruit microstructure using novel ellipse tessellation algorithm. *CMES – Computer Modelling in Engineering and Sciences*, **14**(1), 1–14.
- Mebatsion, H. G., Verboven, P., Ho, Q. T., Verlinden, B. E., and Nicolaï, B. M., 2008. Modeling fruit (micro)structure, why and how? *Trends in Food Science and Technology*, **19**, 59–66.
- Mebatsion, H. G., Verboven, P., Melese, E. A., Billen, J., Ho, Q. T., and Nicolaï, B. M., 2009. A novel method for 3-D microstructure modeling of pome fruit tissue using synchrotron radiation tomography images. *Journal of Food Engineering*, **93**, 141–148.
- Otero, L., Martino, M., Zaritzky, N., Solas, M., and Sanz, P. D., 2009. Preservation of microstructure in peach and mango during high-pressure-shift frizing. *Journal of Food Science*, **65**, 466–470.
- Pawley, J., 1989. *The Handbook of Biological Confocal Microscopy*. Madison: Electron Microscopy Society of America.
- Ryś, J., 1995. *Stereology of Materials*. Cracow: Fotobit-Design (in Polish).
- Sargent, J. A., 1988. The application of cold stage scanning electron microscopy to food research. *Food Microstructure*, **7**, 123–135.
- Serra, J., 1982. *Image Analysis and Mathematical Morphology*. London: Academic.
- Serra, J., 1988. Image analysis and mathematical morphology, Vol. 2: *Theoretical Advances*. London: Academic.
- Spector, D. L., and Goldman, R. D., 2006. *Basic Methods in Microscopy. Protocols and Concepts from Cells. A Laboratory Manual*. New York: Cold Spring Harbor Laboratory Press.
- Sun, D. W., and Li, B., 2003. Microstructural change of potato tissues frozen by ultrasound-assisted immersion freezing. *Journal of Food Engineering*, **57**, 337–342.
- Tijssens, E., Ramon, H., and De Baerdemaeker, J., 2003. Discrete element modelling for process simulation in agriculture. *Journal of Sound and Vibration*, **266**, 493–514.
- Underwood, E. E., 1970. *Quantitative Stereology*. Massachusetts: Addison Wesley.
- Wilkinson, C., Dijksterhuis, G. B., and Minekus, M., 2000. From food structure to texture. *Trends in Food Science and Technology*, **11**, 442–450.
- Wojnar, L., Kurzydłowski, K. J., and Szala, J., 2002. *Practice of Image Analysis*. Polish Society of Stereology: Cracov (in Polish).
- Zdunek, A., Konskyy, R., Cybulska, J., Konstankiewicz, K., and Umeda, M., 2007. Visual textureanalysis for cell size measurements from confocal images. *Acta Agrophysica*, **21**(4), 409–415.
- Zdunek, A., and Umeda, M., 2005. Influence of cell size and cell wall volume friction on failure properties of potato and carrot tissue. *Journal of Texture Studies*, **36**, 25–43.
- Zdunek, A., Umeda, M., and Konstankiewicz, K., 2004. Method of parenchyma cells parametrisation using fluorescence images obtained by confocal scanning laser microscope. *Electronic Journal of Polish Agricultural Universities, Agriculture Engineering*, <http://www.ejpau.media.pl>, 7, 1.

Cross-references

- [Agrophysics: Physics Applied to Agriculture](#)
[Physical Phenomena and Properties Important for Storage of Agricultural Products](#)
[Plant Biomechanics](#)
[Quality of Agricultural Products in Relation to Physical Conditions](#)
[Rheology in Agricultural Products and Foods](#)
[Shrinkage and Swelling Phenomena in Agricultural Products](#)

MINERAL FERTILIZERS

See [Fertilizers \(Mineral, Organic\), Effect on Soil Physical Properties](#)

MINERALISATION

Conversion to a mineral substance. In soil science the conversion by microbes of organic matter into simple inorganic compounds.

Cross-references

- [Mineral-Organic-Microbial Interactions](#)

MINERAL-ORGANIC-MICROBIAL INTERACTIONS

Małgorzata Dąbek-Szreniawska¹, Eugene Balashov²

¹Institute of Agrophysics PAN, Polish Academy of Sciences, Lublin, Poland

²Agrophysical Research Institute RAAS, Russian Academy of Agricultural Sciences, St. Petersburg, Russia

Introduction

Soil minerals, organic matter, and microorganisms are interacting with each other. These interactions play an important role in creating soil structure, controlling biogeochemical processes, and turnover of organic and inorganic substances in soil.

A great role of clay minerals in the formation of complexes with soil microorganisms and organic substances of microbial origin and new quantitative approaches and hypothesis to the studies of interactions between mineral soil solid phase and microorganisms are pointed out.

Minerals, organic matter, and microorganisms have significant higher-order interactions in terrestrial ecosystem. These reactions exert strong control over soil physical, chemical, and biological processes. Soil mineral surfaces play a vital role in catalysis of abiotic formation of humic substances. Soil minerals, especially noncrystalline minerals, have the ability to chemically stabilize soil organic matter. Organic substances also act as binding agents to promote and stabilize aggregation. There are distinct interactive mechanisms between soil minerals, organic matter, and microbes, which should have a direct influence on the stability and cycling of C, N, P, and S (Huang et al., 2005).

Emerson (1959) presented a physical aspect of the microstructure of a soil aggregate. Assuming that a soil aggregate is composed mainly of clay and quartz, these particles may be linked directly by organic matter or through two or more domains which are themselves linked by organic matter.

A mineral soil solid phase more or less easily adsorbs bacteria on the surface. Negatively charged adsorbents repel rather than attract bacteria of negative charge. An attention of scientists has been drawn to the fact that the type of microorganisms is more significant than the type of adsorbents. For instance, gram-positive, immobile microorganisms are characterized by the highest absorbing affinity to soil particles.

A particle-size fractionation of soils is commonly used to quantify the content of soil organic matter and microbial biomass in different particle-size fractions.

A great role of clay minerals is known in the formation of complexes with soil microorganisms and organic substances of microbial origin (Chenu, 1993; Golchin et al., 1995; Schnitzer et al., 1988). The formation of complexes between extracellular polysaccharides and montmorillonite decreases the rate of microbial decomposition of these polysaccharides and other labile organic matter. Therefore, clay soils have a greater capacity for the protection of biomass of microorganisms within the soil matrix than sand soils (Hassink et al., 1993).

The role of interactions of soil minerals with soil microorganisms and their metabolites in the formation of soil aggregates was being studied for a long-term period (Harris et al., 1966; Bossuyt et al., 2001; Six et al., 2004). An ability of fungi and bacteria to participate in aggregate formation is dependent on soil texture, its composition, and availability of C and N. Compared to bacteria, fungi play a dominant role especially in water-stable macroaggregation of light-textured soils with a poor fertility (Guggenberger et al., 1999).

Hattori and Hattori (1976) observed the physical environment in soil microbiology and undertook an attempt to extend the principles of microbiology to soil microorganisms. A formation of complexes was studied between *Escherichia coli* cells and loam soil particles of different mineralogical origin. Pyrophyllite and kaolinite complexes being combined with *E. coli* cells, showed an adhesion to loam particles and formed microaggregates. The “cell-loam particle” complexes treated with sodium ions were stable in acidic medium and unstable in alkaline medium. The loam particles treated with Cu⁺⁺, Co⁺⁺, or Fe⁺⁺ demonstrated stronger adhesion with bacterial cells than loam ones treated with Na⁺, and the complexes were stable in alkaline medium but labile in acidic medium (Hattori, 1970).

Three hypotheses have been proposed concerning mechanisms of the adsorption of the mineral's molecules on the surface of bacterial cells (Marshall, 1971):

- (a) Adsorption of the molecules could proceed through on the surfaces of bacteria and mineral particles (“face-to-face adsorption”).
- (b) Adsorption of the molecules could proceed through on their edges (“edge adsorption”).
- (c) Adsorption could result from both mentioned mechanisms (“mixed adsorption”).

Adsorption of sodium bentonite was studied on *Bacillus subtilis* cells (Lahav, 1962). The effect of sodium bentonite (molecules smaller than the bacterial cells) on the electrophoretic mobility of *Bacillus subtilis* was tested in solutions of sodium chloride and of sodium phosphate with different concentrations of hydrogen ions and ionic force. It was noted that the adsorption of sodium bentonite on bacteria was a reversible process. Bacterial population consisted of two types of microorganisms. The addition of bentonite affected the electrophoretic mobility of one bacterial type, while the other one was not affected. The first type represented bacteria-adsorbing bentonite, whereas the second one included bacteria not adsorbing bentonite on their surface. Moreover, the presence of both bacterial types was found only in the presence of bentonite. The effect of bentonite on bacterial mobility depended on pH, ionic force, and contents of electrolytes. The lower were the pH values and the higher was the ionic force, the more effective was the effect of bentonite.

Among different types of bacteria, for instance, the influence of the bacterial biomass of *Arthrobacter* sp. on the formation and stabilization of water-stable macroaggregates in the soil was studied after the addition of plant residues, mineral fertilizers (NPK, Ca), and bentonite (Dąbek-Szreniawska, 1974). The introduction of the bacterial biomass of *Arthrobacter* sp. resulted in an increased amount of water-stable macroaggregates (>250 µm). The highest increase in the water-stable aggregation was induced by a combined influence of bacterial biomass and plant residues during a 3-month incubation. Application of bentonite generally increased the water stability of aggregates. Application of mineral NPK fertilizers caused a decrease in the water stability of aggregates as a result of changes in the activity and the composition of soil microbial community.

New quantitative approaches to the studies of interactions between mineral soil solid phase and microorganisms give an opportunity to get more detailed information about structure and function of soil microbial community in micro- and macroaggregates (Väistönen et al., 2005).

Conclusions

The distinct interactive mechanisms between soil minerals, especially clay minerals, which form complexes with microorganisms and organic substances are confirmed. They affect the stability and cycling of soil chemical components and have a positive effect on soil microstructure and aggregation.

Bibliography

- Bossuyt, H., Denef, K., Six, J., Frey, S. D., Merckx, R., and Paustian, K., 2001. Influence of microbial population on aggregate stability. *Applied Soil Ecology*, **16**, 195–208.

- Chenu, C., 1993. Clay- and sand-polysaccharide associations as models for the interface between microorganisms and soil: water-related properties and microstructure. *Geoderma*, **56**, 143–146.
- Dąbek-Szreniawska, M., 1974. The influence of *Arthrobacter* sp. on the water stability of soil aggregates. *Polish Journal of Soil Science*, **7**, 169–179.
- Emerson, W. W., 1959. The structure of soil crumbs. *Journal of Soil Science*, **10**, 235–244.
- Golchin, A., Oades, J. M., Skjemstad, J. O., and Clarke, P., 1995. Structural and dynamical properties of soil organic matter as reflected by ^{13}C natural abundance, pyrolysis mass spectroscopy and solid-state ^{13}C NMR spectroscopy in density fractions of an oxisol under forest and pasture. *Australian Journal of Soil Research*, **33**, 59–76.
- Guggenberger, G., Elliott, E. T., Frey, S. D., Six, J., and Paustian, K., 1999. Microbial contributions to the aggregation of a cultivated soil amended with starch. *Soil Biology and Biochemistry*, **31**, 407–419.
- Harris, R. F., Chesters, G., and Allen, O. N., 1966. Dynamics of soil aggregation. *Advances in Agronomy*, **18**, 107–169.
- Hassink, J., Bouwman, L. A., Zwart, K. B., Bloem, J., and Brussaard, L., 1993. Relationships between soil texture, physical protection of organic matter, soil biota and C and N mineralization in grassland soils. *Geoderma*, **57**, 105–128.
- Hattori, T., 1970. Adhesion between cells of *E. coli* and clay particles. *Journal of General and Applied Microbiology*, **16**, 351–359.
- Hattori, T., and Hattori, R., 1976. The physical environment in soil microbiology: an attempt to extend principles of microbiology to soil microorganisms. *CRC Critical Reviews in Microbiology*, **4**, 423–461.
- Huang, P.-M., Wang, M.-K., and Chiu, Ch-Y, 2005. Soil mineral-organic matter-microbe interactions: Impact on biogeochemical processes and biodiversity in soils. *Pedobiologia*, **49**, 609–635.
- Lahav, N., 1962. Adsorption of sodium bentonite particles on *Bacillus subtilis*. *Plant and Soil*, **17**, 191–208.
- Marshall, K. C., 1971. Sorptive interactions between soil particles and microorganisms. *Soil Biochemistry*, **2**, 409–445.
- Schnitzer, M., Ripmeester, J. A., and Kodama, H., 1988. Characterization of the organic matter associated with a soil clay. *Soil Science*, **145**, 448–454.
- Six, J., Bossuyt, H., De Gryze, S., and Denef, K., 2004. A history of research on the link between (micro)aggregates, soil biota, and soil organic matter dynamics. *Soil and Tillage Research*, **79**, 7–31.
- Väistönen, R. K., Roberts, M. S., Garland, J. L., Frey, S. D., and Dawson, L. A., 2005. Physiological and molecular characterisation of microbial communities associated with different water-stable aggregate size classes. *Soil Biology and Biochemistry*, **37**, 2007–2016.

Cross-references

- [Clay Minerals and Organo-Mineral Associates](#)
[Microbes and Soil Structure](#)
[Organic Matter, Effects on Soil Physical Properties and Processes](#)
[Soil Aggregates, Structure, and Stability](#)

MIRE

See [Peats and Peatlands, Physical Properties](#)

MODELING THE THERMAL CONDUCTIVITY OF FROZEN FOODS

Vlodek R. Tarnawski¹, Wey H. Leong²,
Toshihiko Momose³

¹Division of Engineering, Saint Mary's University, Halifax, NS, Canada

²Department of Mechanical and Industrial Engineering, Ryerson University, Toronto, ON, Canada

³Bavarian Environment Agency, Hof/Saale, Germany

Definition

Thermal conductivity of foods. The bulk property of food products describing their ability to conduct heat resulting from a gradient of temperature. It is measured in Watts per Kelvin per meter ($\text{W K}^{-1} \text{ m}^{-1}$).

Frozen foods. Foods with their aqueous solutions converted into ice and then stored at a temperature below freezing point.

Thermal conductivity models. Equations describing the material ability to conduct heat.

Introduction

A large variety of foods (meat, fish, poultry, fruits, vegetables, bakery, dairy foods, etc.) require refrigeration (chilling and/or freezing) to maintain their high quality, edibility, and nutritive values. Solid foods are capillary, porous, colloidal materials consisting of water, solid constituents (e.g., carbohydrates, fats, proteins, vitamins, or minerals), and in some instances, air (bakery products, ice cream, cheese, etc.). The majority of fresh natural foods (meat, fish, fruits, vegetables) are fully saturated with aqueous solution (solid food components dissolved in water). During a freezing process, food water is converted into ice and the solution concentration increases; consequently, the food initial freezing point (T_f) decreases below 0°C . Good knowledge of frozen food thermophysical properties, particularly thermal conductivity (λ), is required in the design of freezing/thawing equipment and analysis of chilling, freezing, storage, and thawing processes. This property describes food's ability to distribute heat strictly by a conduction mode. It is very difficult to measure and also to estimate as it is influenced by numerous parameters such as initial water content, temperature (T), density, food composition, anisotropy, ice fraction, measuring techniques, etc. Available experimental data usually do not cover a full T range encountered during freezing, storing, and thawing processes; often λ data are contradictory and incomplete (missing measurement details, T , composition data, a sample preparation procedure, and uncertainty analysis). Therefore, there is a strong demand for the use of λ models in computer analysis of food freezing, storing, and thawing processes.

Thermal conductivity of food components

Water and ice are two main components of frozen foods. Thermal conductivity of water (λ_w) is approximately double that of other solid constituents, while with respect to ice it is approximately four times smaller. There is a weak λ_w dependence on T . On the contrary to water, the thermal conductivity of ice (λ_{ice}) increases considerably with decreasing T . As a result, ice has a dominant effect on the frozen food's ability to conduct heat. Several predictive equations, $\lambda_{ice}(T)$, λ_{ice} in W/m K and T in °C, have been published over the last 30 years (Sakazume and Seki, 1978; Yen, 1981; Choi and Okos, 1986; U.S. Army Corps of Engineers 1996).

$$\begin{aligned}\lambda_{Choi-Okos} &= 2.2196 - 0.0062489 \cdot T + 0.00010154 \cdot T^2 \\ \lambda_{Sakazume-Seki} &= 2.2156 - 0.0100456 \cdot T + 0.00003445 \cdot T^2 \\ \lambda_{Yen} &= 6.727 \cdot \exp[-0.0041 \cdot (T + 273.15)] \\ \lambda_{US-Army} &= 2.21 - 0.011 \cdot T\end{aligned}\quad (1)$$

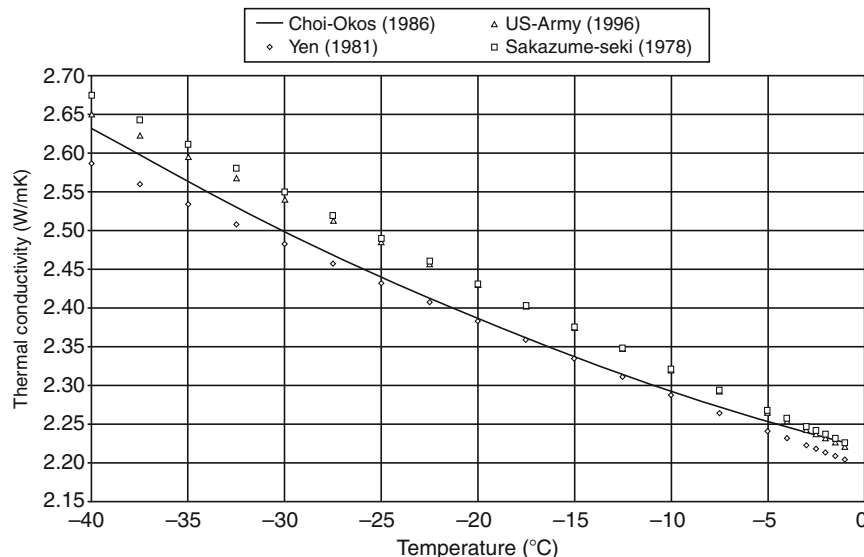
Fukusako (1990) reviewed available $\lambda_{ice}(T)$ data and fitting correlations and concluded that variations among the reported data were caused mainly by differences in sample purity, sample preparation, methods of measurement, and reproducibility of experimental data. The difference in predicted λ is on average below 0.05 W/m K (Figure 1). The predictive λ_{ice} equation by Choi and Okos (1986) is commonly used in food engineering for modeling λ of frozen foods within a range of T from −40°C to 0°C; λ_{ice} increases by about 18.6% as T decreases from −1°C to −40°C. Therefore, λ_{ice} dependence on T may strongly influence the λ of lean frozen foods that usually contain a large amount of ice. Thermal conductivities of remaining basic food components (including water) are

also estimated from equations given by Choi and Okos (1986) and in comparison to ice, λ shows a weak dependence on T .

$$\begin{aligned}\lambda_{water} &= 0.57109 - 0.0017625 \cdot T + 0.00000607036 \cdot T^2 \\ \lambda_{protein} &= 0.17881 - 0.0011958 \cdot T + 0.0000027178 \cdot T^2 \\ \lambda_{fat} &= 0.18071 - 0.00027604 \cdot T + 0.00000017749 \cdot T^2 \\ \lambda_{ash} &= 0.32962 - 0.0014011 \cdot T + 0.0000029069 \cdot T^2 \\ \lambda_{carbohydrates} &= 0.2014 - 0.0013874 \cdot T + 0.0000043312 \cdot T^2 \\ \lambda_{fiber} &= 0.18331 - 0.0012497 \cdot T + 0.0000031683 \cdot T^2\end{aligned}\quad (2)$$

Thermal conductivity of frozen foods

Two measuring techniques of λ are commonly used for frozen foods, namely: steady and transient state. The steady-state technique (a guarded hot plate) requires a long time to reach the equilibrium T of tested foods and therefore it is prone to moisture migration and spoilage. The transient state technique offers a smaller size of equipment, much shorter measuring times, smaller food samples and consequently, it is currently a preferable choice for λ measurement. Thermal conductivity probes, however, lack thorough verification at $T < T_f$ and latent heat of ice may considerably alter measured λ (Wang and Kolbe, 1990). Besides, thermal conductivity measurements are based on a highly simplified assumption that foods are homogeneous and isotropic materials. In fact, fibrous foods usually conduct different amount of heat in a perpendicular and parallel direction to fibers; this difference could be up to about 15% for frozen beef (Heldman, 2003). As a result, experimental data gathered may be burdened with errors of unknown magnitude. Fat has a very



Modeling the Thermal Conductivity of Frozen Foods, Figure 1 Thermal conductivity of ice as a function of temperature.

low λ (0.2–0.5 W/m K) and therefore, its increasing content has a decreasing effect on the frozen food's λ . The majority of frozen foods show a strong λ dependence on decreasing T . Figure 2 displays experimental λ data of selected foods, by Pham and Willix (1989) and Willix et al. (1998), undergoing freezing from -1°C to -40°C ; within this T range λ increases by a factor of 2–3.

Predicting ice fraction in frozen foods

Thorough knowledge of ice fraction in frozen foods is crucial for obtaining good λ estimates. One of the most frequently used m_{ice} models was proposed by Schwartzberg (1976).

$$m_{\text{ice}} = (m_w - m_b) \cdot \left(1 - \frac{T_f}{T}\right), \quad (3)$$

where m_w = mass fraction of water at T_f in $^{\circ}\text{C}$, m_b = mass fraction of bounded water, and T = temperature of frozen food in $^{\circ}\text{C}$. For example, for meat products, $T_f \approx -0.9^{\circ}\text{C}$ and $m_b = 0.4 \cdot m_{\text{protein}}$ (Pham and Willix, 1989).

The above equation gives good estimates for highly diluted solutions, i.e., T_f is close to 0°C .

Golovkin and Tchizov (1951) provided an empirical relation for ice fraction that follows closely experimental m_{ice} data of a variety of foods such as meat, fish, milk, eggs, fruits, and vegetables. Their experimental m_{ice} , from -1°C to -65°C , was refitted and coefficients of the original empirical relation were slightly adjusted.

$$m_{\text{ice}} = \frac{1.133}{1 + \frac{0.339}{\log[1+|T-T_f|]}} \quad (r^2 = 0.996). \quad (4)$$

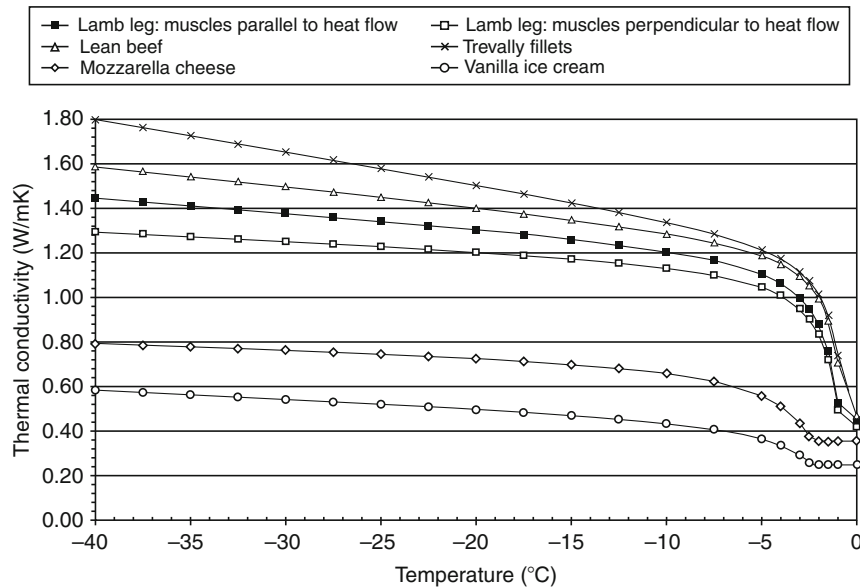
The initial freezing point is a key parameter in the above Equations 3 and 4; its value, however, is difficult to predict or measure. In general, T_f for fish, meats, fruits, and vegetables varies from -2°C to -0.5°C ; a summary of T_f predictive models for a variety of foods was published by Sun (2006). A comprehensive summary of m_{ice} modeling approaches was given by Fikiin (1998) and Rahman (2001).

Models predicting thermal conductivity of frozen foods

For modeling purposes, solid foods are often subdivided into two groups, namely: fully saturated with water (fish, meat, fruits, vegetables, etc.) and partly saturated with water (bread, butter, ice cream, etc.), i.e., food pores are filled with water and/or moist air, respectively. Measuring λ of porous saturated/unsaturated materials undergoing freezing is difficult, error prone, time consuming, laborious, and equipment expensive. Therefore, several predictive models of λ for frozen fully saturated porous systems (e.g., food and soils) were proposed in the past. In the majority of cases, these models are based on a system composition data and λ of their components. The models for saturated solid foods consider that heat is being distributed by conduction only, while for unsaturated foods more complex modeling attempts are required to take into account simultaneous phenomena of water evaporation, condensation, and ice formation. A concise review of selective predictive models is given below.

Maxwell–Eucken (Maxwell–E) model

Maxwell (1873) published a model for predicting electrical conductivity of randomly distributed and noninteracting



Modeling the Thermal Conductivity of Frozen Foods, Figure 2 Thermal conductivity of frozen foods vs. temperature.

homogeneously dispersed spheres (d) in a homogeneous continuous medium (con); and distances between spheres were assumed to be considerably larger than spheres' radii. Eucken (1932) extended this model to conduction heat flow in porous media and provided the following weighted average relation.

$$\lambda = \frac{k_{\text{con}} \cdot \theta_{\text{con}} \cdot \lambda_{\text{con}} + k_d \cdot \theta_d \cdot \lambda_d}{k_{\text{con}} \cdot \theta_{\text{con}} + k_d \cdot \theta_d}, \quad (5)$$

$$k_d = \frac{1}{3} \sum_{x=a,b,c} [1 + (\delta - 1) \cdot g_x]^{-1} \quad \delta = \frac{\lambda_d}{\lambda_{\text{con}}}, \quad (6)$$

where $k_{\text{con}} = 1$, θ are respective volume fractions, g_x is a shape factor for each particle's dimension in the dispersed phase. For solid spherical particles, $g_x = 1/3$ is applied to all three dimensions.

Levy model

Levy (1981) modified the Maxwell–E model by replacing the volume fraction of a dispersed phase, θ_d , by a new function F that eliminates a dilemma of phase designation.

$$F = \frac{1}{\sigma} - \frac{1}{2} + \theta_d - \frac{1}{2} \sqrt{\left(\frac{2}{\sigma} - 1 + 2 \cdot \theta_d\right)^2 - 8 \cdot \frac{\theta_d}{\sigma}} \quad (7)$$

$$\sigma = \frac{(\delta - 1)^2}{(\delta + 1)^2 + 0.5 \cdot \delta}.$$

In reality, porous media such as foods, however, are not necessarily composed of solid spheres and they may not be isolated from each other.

deVries model

Further modification of the Maxwell–E model was done by deVries (1963), who replaced a spherical shape of solid grains by rotated oblate ellipsoids dispersed in the continuous medium (water, air, ice), generating the following relation.

$$\lambda = \frac{k_{\text{con}} \cdot \theta_{\text{con}} \cdot \lambda_{\text{con}} + \sum_{j=1}^N k_j \cdot \theta_j \cdot \lambda_j}{k_{\text{con}} \cdot \theta_{\text{con}} + \sum_{j=1}^N k_j \cdot \theta_j}, \quad (8)$$

where N is the number of solid components; each solid grain component (j) has the same weighting factor k_j and the same thermal conductivity λ_j .

$$k_j = \frac{1}{3} \sum_{x=a,b,c} \left[1 + \left(\frac{\lambda_j}{\lambda_{\text{con}}} - 1 \right) \cdot g_x \right]^{-1}, \quad (9)$$

where g_x is a solid particle ellipsoidal shape factor for each of three ellipsoid axes (a , b , c); $g_a + g_b + g_c = 1$, $a = b = p \cdot c$, where p is a shape value; thus, $g_a = g_b$, while $g_c = 1 - 2 \cdot g_a$.

The models by Maxwell–E, Levy (Equations 5–7), and deVries (Equations 8–9) are at first sight, identical in form, but in fact a different shape of solid particles (sphere vs. rotated ellipsoid) is used in these models. The shape value for spheres is known ($p = 1$), while for rotated ellipsoid the p is usually obtained by fitting the model to experimental data. Consequently, the model by deVries is rarely used in food engineering.

Mascheroni model

Mascheroni et al. (1977) assumed that solid frozen meats are made of partially dehydrated fibers (f), surrounded by ice and/or water randomly dispersed in a continuous matrix of the remaining food tissue. The first version of the model considers that heat flow is perpendicular (\perp) to meat fibers:

$$\lambda_{\perp} = \frac{\lambda_{\text{ice}} \cdot \lambda_f \cdot (1 - \xi_{\text{ice}})}{\xi_{\text{ice}} \cdot \lambda_f + \lambda_{\text{ice}} \cdot (1 - \xi_{\text{ice}})} + \lambda_{\text{ice}} \cdot \xi_{\text{ice}}, \quad (10)$$

where $\xi_{\text{ice}} = 1 - \sqrt{1 - \theta_{\text{ice}}}$, $\theta_{\text{ice}} = m_{\text{ice}} \cdot \frac{\rho_b}{\rho_{\text{ice}}}$, ρ_b = food bulk density, ρ_{ice} = density of ice.

The second model option assumes that heat flow is parallel (\parallel) to the meat fibers:

$$\lambda_{\parallel} = \lambda_{\text{ice}} \cdot \xi_{\text{ice}} + (1 - \xi_{\text{ice}}) \cdot \left[\lambda_{\text{ice}} \cdot \xi_{\text{ice}}^2 + \lambda_f \cdot (1 - \xi_{\text{ice}})^2 + \frac{4 \cdot \xi_{\text{ice}} \cdot (1 - \xi_{\text{ice}})}{\frac{1}{\lambda_f} + \frac{1}{\lambda_{\text{ice}}}} \right]. \quad (11)$$

Gori model

Gori (1983) assumed that frozen meats (also used for frozen soils) are composed of cubic cells, each having a concentrically located cubicle, representing all solid food components (s), surrounded with the continuous medium (unfrozen water [w], ice [i], or a mixture of both [wi]). The first version of the model considers the horizontal parallel isotherms in the cubic cell.

$$\frac{1}{\lambda} = \frac{\beta - 1}{\lambda_{\text{wi}} \cdot \beta} + \frac{\beta}{\lambda_{\text{wi}} \cdot (\beta^2 - 1) + \lambda_s} \quad \beta = \sqrt[3]{\frac{1}{1 - \theta_{\text{wi}}}} \quad (12)$$

The second version of the model takes into account a vertical parallel heat flux in the cubic cell.

$$\lambda = \frac{1}{\frac{\beta \cdot (\beta - 1)}{\lambda_{\text{wi}}} + \frac{\beta}{\lambda_s}} + \lambda_{\text{wi}} \cdot \frac{\beta^2 - 1}{\beta^2}. \quad (13)$$

Effective medium theory (EMT) model

The EMT model was adapted to predicting λ of vegetable foods by Mattea et al. (1986).

$$\sum_1^n \theta_j \cdot \frac{\lambda_j - \lambda}{\lambda_j + 2\lambda} = 0. \quad (14)$$

For frozen foods, three phases were considered:

$$\begin{aligned}\lambda_1 &= \lambda_w \quad \theta_1 = \theta_w \quad \lambda_2 = \lambda_{ice} \quad \theta_2 = \theta_{ice} \\ \lambda_3 &= \lambda_s \quad \theta_3 = 1 - \theta_w - \theta_{ice}\end{aligned}$$

Modified resistor series model

Cleland and Valentas (1997) proposed a modified resistor series model for calculating λ of frozen foods, which may also contain bounded water (b).

$$\frac{\theta_w + \theta_b + \theta_s}{\lambda} = \frac{\theta_w + \theta_b}{\lambda_w} + \frac{\theta_s}{\sum_{j=1}^n \frac{\theta_j}{\lambda_j}}. \quad (15)$$

Geometric mean model (GMM)

The GMM was successfully used in predicting λ of frozen soils by Johansen (1975).

$$\lambda = \lambda_s^{\theta_s} \cdot \lambda_{ice}^{\theta_{ice}} \cdot \lambda_w^{\theta_w}. \quad (16)$$

Parallel model (/)

It assumes parallel configuration of the system components in the direction of heat flow.

$$\lambda_{//} = \frac{\sum_i^n \theta_i \cdot \lambda_i}{\sum_1^n \theta_i}. \quad (17)$$

Series model (Σ)

It assumes series configuration of the system components in the direction of heat flow.

$$\lambda_{\Sigma} = \frac{\sum_{j=1}^n \theta_j}{\sum_{j=1}^n \frac{\theta_j}{\lambda_j}}. \quad (18)$$

Pham (1990) carried out a comprehensive analysis of seven physical predictive models and one set of empirical equations for λ of frozen foods and concluded that the model by Levy (1981) was the most accurate followed by the effective medium theory (EMT) model and the Maxwell–Eucken model. Tarnawski et al. (2005) analyzed and compared eight models (deVries, Levy, Mascheroni, Maxwell–Eucken, Gori, geometric mean, effective medium theory, modified resistor) and their 54 versions, developed for frozen foods and soils, against λ data of 13 meat products (Pham and Willix, 1989) in T ranging from -1°C to -40°C . The thermal conductivity of ice and other food components were assumed to be T independent; the fraction of ice was modeled using a relation given by Schwartzberg (1976). The models by

deVries, Levy, and Mascheroni produced results very close to experimental data. In general, relatively small differences in predictions were observed, i.e., Relative Root Mean Squared-Error (RRMSE) was ranging from 5% to 7%; it was probably due to meat anisotropy, constant λ_{ice} , varying composition, measuring errors, and limitation of predictive models. A similar analysis carried out by Tarnawski et al. (2007) for T -dependent λ_{ice} showed that the models by Mascheroni et al. (1977) are marginally better than the other remaining models. Carson (2006) published a comprehensive review of models applied to unfrozen and frozen foods. Wang et al. (2006) verified 31 predictive models by comparing them with λ conductivity data for 22 meat and seafood products (Willix et al., 1998; Pham and Willix, 1989), with T ranging from -40°C to $+40^{\circ}\text{C}$. The results obtained showed that the best 15 models had RRMSE varying from 11.5% to 16.4%. van der Sman (2008) modeled thermophysical properties of frozen meat products using their composition data, $\lambda(T)$ for water and ice, with the ice fraction estimated by a relation given by Schwartzberg (1976). The λ model by Torquato and Sen (1990) was extended to ternary systems (frozen meats) by modeling two existing phases (unfrozen water and muscle fiber) as one continuous medium and handling ice crystals as the dispersed phase. The model introduces a factor dependent on the structure and orientation of protein fibers. This modeling attempt was compared with experimental λ data by Pham and Willix (1989) and Willix et al. (1998), and predictions with an error of 10% were reported. In the past, comprehensive reviews on modeling λ of foods were also given by Sweat (1985) and Sanz et al. (1989).

In terms of frozen unsaturated food products (internal pores filled in with moist air), λ modeling is much more intricate as porosity of foods and filling mediums (water, air) have to be considered. Cogné et al. (2003) measured λ of ice creams using a hot-wire probe technique. The measured λ was affected by T and the ice cream's apparent density. For λ modeling, ice cream was considered as a heterogeneous and multiphase system composed of a frozen concentrated continuous liquid phase matrix (carbohydrates, proteins, lipids, and unfrozen water) filled in with ice and air. The dispersed phase (liquid water and solid components) λ was estimated by a parallel model and then together with $\lambda_{ice}(T)$ was applied to de Vries model for obtaining λ of a standard mix at different T ; then, this λ with a value of λ_{air} was applied to Maxwell–Eucken model to obtain the overall λ . Jury et al. (2007) carried out λ measurements of bread with T ranging from -20°C to 80°C . Bread was assumed to be composed of dry fraction (proteins, carbohydrates, lipids, mineral salts, etc.) and pores containing moist air, both surrounded by water. When this system is exposed to $T < T_f$, very complex simultaneous heat and moisture transfer phenomena (evaporation–condensation effects, ice formation, etc.) take place (Hamdammi et al., 2004). Consequently, measuring and estimating effective λ for unfrozen and frozen breads still remains a very complex issue (Hamdammi et al., 2003).

Conclusions and recommendations

Accurate λ predictions for frozen foods are difficult due to a large number of modeling parameters involved, such as initial water content, temperature, density, food structure, anisotropy, initial freezing point, rate of ice formation, temperature-dependent thermal conductivity of ice, etc. Frozen foods are often considered as a mixture of homogeneous solid components being dispersed in continuous phase (ice, water, or water+ice). There are, however, still some dilemmas with a proper selection of a continuous medium and therefore, further studies are needed. A choice of water+ice as the continuous phase is promising as it improves λ predictions and eliminates discontinuity at the initial freezing point T_f , but nevertheless it requires further comprehensive testing. Temperature-dependent λ_{ice} has a strong influence on predicted λ of frozen lean meats; but, there are some unanswered concerns regarding the equations currently used for λ_{ice} estimation, as λ_{ice} also depends on ice structure and a freezing process for both water solution and pure water. Taking into account these issues and the enormous complexity of foods and the freezing process, developing an accurate mechanistic λ model for frozen foods is rather unrealistic. Review of frozen food literature reveals that Levy model and Mascheroni's equations produce very close results to experimental data (within approximately 10% error). The model by Mascheroni, however, is simpler in form, accounts for food fiber orientation, does not require any fitting, and it produces close predictions for low-fat meats. For high-fat meats, Levy's model gives better λ estimates, but the model structure is too complex and therefore it is not easy to use. Highly complex predictive models are difficult to handle when applied to food products of uncertain food structure, composition, and unknown thermal conductivity, because numerous rough assumptions have to be made. Besides, it is still unclear what the real impact of highly accurate λ predictions will have on the analysis of freezing processes and designing freezing/thawing equipment, due to a variety of foods having very diverse physical properties. It appears that, the demand for sophisticated and difficult to use λ models may not be fully justified and more attention should be paid to the use of simple models (e.g., geometric mean, series-parallel, etc.) applied to a wide variety of foods.

Bibliography

- Carson, J. K., 2006. Review of effective thermal conductivity models for foods. *International Journal of Refrigeration*, **29**(6), 958–967.
- Choi, Y., and Okos, M. R., 1986. Effects of temperature and composition on the thermal properties of foods. In Le Maguer, M., and Jelen, P. (eds.), *Food Engineering and Processes Applications*, I. Amsterdam: Elsevier Applied Science, pp. 93–101.
- Cleland, D. J., and Valentas, K. J., 1997. Prediction of freezing time and design of food freezers. In Singh, R. P., and Valentas, K. J. (eds.), 1997. CRC Press: Handbook of Food Engineering Practice, pp. 71–124.
- Cogné, C., Andrieu, J., Laurent, P., Besson, A., and Nocquet, J., 2003. Experimental data and modeling of thermal properties of ice creams. *Journal of Food Engineering*, **66**(4), 469–475.
- DeVries, D. A., 1963. Thermal properties of soils. In van Wijk, W. R. (ed.), *Physics of Plant Environment*. New York: Wiley, pp. 210–235.
- Eucken, A., 1932. Thermal conductivity of ceramics refractory materials. *Fortsch. Geb. Ing., B-3, Forschungsheft*, **53**, 6–21.
- Fikiin, K. A., 1998. Ice content prediction methods during food freezing: a survey of the eastern European literature. *Journal of Food Engineering*, **38**, 331–339.
- Fukusako, F., 1990. Thermophysical properties of ice, snow, and sea ice. *International Journal of Thermophysics*, **11**(2), 353–372.
- Golovkin, N. A., and Tchizov, G. B., 1951. Refrigeration technology of food products (in Russian). *Pischedromizdat*, **1951**, 232.
- Gori, F., 1983. A theoretical model for predicting the effective thermal conductivity of unsaturated frozen soils. In *Proceedings of the Fourth International Conference on Permafrost, Fairbanks (Alaska)*. Washington: National Academy Press, pp. 363–368.
- Hamdami, N., Monteau, J.-Y., and Le Bail, A., 2003. Effective thermal conductivity of a high porosity model at above and sub-freezing. *International Journal of Refrigeration*, **7**, 809–816.
- Hamdami, N., Monteau, J.-Y., and Le Bail, A., 2004. Thermophysical properties evolution of French partly baked bread during freezing. *Food Research International*, **37**, 703–713.
- Heldman, D. R., 2003. Encyclopedia of Agricultural, Food, and Biological Engineering. Marcel Dekker.
- Johansen, O., 1975. Thermal conductivity of soils. PhD Thesis, University of Trondheim, Norway, CRREL Translation 637.
- Jury, V., Monteau, J.-Y., Comiti, J., and Le-Bail, A., 2007. Determination and prediction of thermal conductivity of frozen part baked bread during thawing and baking. *Food Research International*, **40**, 874–882.
- Levy, F. L., 1981. A modified Maxwell–Eucken equation for calculating the thermal conductivity of two-component solutions or mixtures. *International Journal of Refrigeration*, **4**, 223–225.
- Mascheroni, R. H., Ottino, J., and Calvelo, A., 1977. A model for the thermal conductivity of frozen meat. *Meat Science*, **1**, 235–243.
- Mattea, M., Urbicain, M. J., and Rotstein, E., 1986. Prediction of thermal conductivity of vegetable foods by the effective medium theory. *Journal of Food Science*, **51**(1), 113–115.
- Maxwell, J. C., 1873. *A Treatise on Electricity and Magnetism*, 1st edn. Oxford: The Calerdon Press, Vol. 1, p. 440.
- Pham, Q. T., 1990. Prediction of thermal conductivity of meats and other animal products. In Spiess, W. E. L., and Schubert, H. (eds.), *Engineering and Food*, vol. 1st edn. London: Elsevier Applied Science, pp. 408–423.
- Pham, Q. T., and Willix, J., 1989. Thermal conductivity of fresh lamb meat, offal and fat in the range –40 to + 30°C: measurements & correlations. *Journal of Food Science*, **54**(3), 508–515.
- Rahman, M. S., 2001. Thermophysical properties of foods. In D-Wen Sun. (ed.), *Advances in Food Refrigeration*. Leatherhead Publishing: Surrey.
- Sakazume, S., and Seki, N., 1978. Thermal properties of ice and snow at low temperature region. *Trans. JSME*, **44**(382), 2059–2069.
- Sanz, P. D., Alonso, M. D., and Mascheroni, R. H., 1989. Equations for the prediction of thermophysical properties of meat products. *Latin American Applied Research*, **19**, 155–163.
- Schwartzberg, H. G., 1976. Effective heat capacity for the freezing and thawing of food. *Journal of Food Science*, **41**, 152–156.
- Sun, Da-Wen., 2006. *Handbook of Frozen Food Processing and Packaging*. Boca Raton: Taylor & Francis.

- Sweat, V. E., 1985. Thermal conductivity of food: present state of the data. *Trans. American society of heating refrigerating and airconditioning Engineers*, **19**(part B), 299–311.
- Tarnawski, V. R., Cleland, D. J., Corasaniti, S., Gori, F., and Mascheroni, R. H., 2005. Extension of soil thermal conductivity models to frozen meats with low and high fat content. *International Journal of Refrigeration*, **28**, 840–850.
- Tarnawski, V. R., Boveseccchi, G., Coppa P., and Leong, W. H., 2007. Modeling thermal conductivity of frozen foods with temperature dependent thermal conductivity of ice. *The 22nd International Congress of Refrigeration*, August 21–26, 2007, Beijing, China.
- Torquato, S., and Sen, A. K., 1990. Conductivity tensor of anisotropic composite media from microstructure. *Journal of Applied Physics*, **67**(3), 1145–1155.
- U.S. Army Corps of Engineers, 1996. Engineering & Design –Ice Engineering: Manual No. 1110-2-1162, Washington D.C. p. 2.
- van der Sman, R. G. M., 2008. Prediction of enthalpy and thermal conductivity of frozen meat and fish products from composition data. *Journal of Food Engineering*, **84**, 400–412.
- Wang, D., and Kolbe, E., 1990. Thermal conductivity of surimi-measurement and modeling. *Journal of Food Science*, **50**(5), 1458–1462.
- Wang, J. F., Carson, J. K., Cleland, D. J., and North, M. F., 2006. *A comparison of effective thermal conductivity models for frozen foods*, in *Innovative Equipment and Systems for Comfort and Food Preservation*, Proceedings, Auckland 2006, pp. 336–343.
- Willix, J., Lovatt, S. J., and Amos, N. D., 1998. Additional thermal conductivity values of foods measured by a guarded hot plate. *Journal of Food Engineering*, **37**, 159–174.
- Yen, Y. C., 1981. Review of thermal properties of snow, ice and sea ice. *CRREL Report*, **81**(10), 1–27.

Cross-references

[Databases on Physical Properties of Plants and Agricultural Products](#)

MODULUS OF ELASTICITY (YOUNG'S MODULUS)

The ratio of normal stress to corresponding strain below the proportional limit of a material (e.g., plant stalks and roots).

MODULUS OF RIGIDITY

The ratio of shear stress to the shear strain below the proportional limit of a material displacement per unit sample length.

MOHRE CIRCLE OF STRESS

A graphical representation of the components of stress acting across the various planes at a given point, drawn with reference to axes of normal stress and shear stress.

Bibliography

Glossary of Soil Science Terms. Soil Science Society of America. 2010. <https://www.soils.org/publications/soils-glossary>

Cross-references

[Friction Phenomena in Soils](#)

MONITORING PHYSICAL CONDITIONS IN AGRICULTURE AND ENVIRONMENT

Wojciech M. Skierucha

Department of Metrology and Modeling of Agrophysical Processes, Institute of Agrophysics, Polish Academy of Sciences, Lublin, Poland

Definition

Monitoring physical conditions in agriculture and environment is a collection and processing of data that allow to determine temporal and spatial variation of these conditions to make proper decisions in the future for the benefit of sustainable food production.

Introduction

Agriculture has both positive and negative influence on environment. Its primary function is meeting the growing demand for food. Agriculture creates habitats not only for humans but also for wildlife and plays an important role in sequestering carbon, managing watersheds, and preserving biodiversity. But agriculture degrades natural resources causing soil erosion, introducing unrecoverable hydrological changes, contributing in groundwater depletion, agrochemical pollution, loss of biodiversity, reducing carbon sequestration from deforestation, and carbon dioxide emissions from forest fires (Doran, 2002).

Physical conditions in agriculture and environment can be defined as physical properties and processes involved in mutual relation between the processes of food and fiber production and the impact of these processes on natural agro-environment. They include topography, surface water and groundwater distributions, heat-temperature distributions, wind direction changes, and intensity.

The measures of physical conditions in agriculture and environment should include a minimum number of measurable physical indicators, that can provide sufficient data not only for decision making in the production of food and fiber but also in ecosystem function and the maintenance of local, regional, and global environmental quality.

Agricultural sustainability and environmental quality are determined by the health of soil, which is a thin layer of the earth surface forming the interface between agriculture and environment. Soil quality, which can be described

by the combination of its physical, chemical, and biological properties and contamination by inorganic and organic chemicals is critical to environmental sustainability (Arshad and Martin, 2002). The physical properties of soils play a major role in controlling mass and energy transport in the subsurface environment.

The basic physical soil quality indicators recommended or used by soil researchers are as follows (Schoenholtz et al., 2000): texture (influence retention and transport of water and nutrients), soil depth and topsoil depth (major factor in total nutrient, water, and oxygen availability), bulk density (decides about root growth, rate of water movement, soil volume expression), soil water content, soil temperature, available water holding capacity (informs about plant available water, erosivity), soil roughness (erosivity, soil tilth), saturated hydraulic conductivity (water and air balance, hydrology regulation), resistance to penetration (root growth), porosity (water/air balance, water retention, root growth), and aggregate stability and size distribution (root growth, air/water balance).

The need for monitoring physical conditions in agriculture and environment is increasing, because of increasing pressure on natural resources, sustainability, and exhaustion of nonrenewable resources. Advances in sensors, computers, and communication devices result in great amounts of temporal and spatial information that should be processed in real-time (or near real-time) to produce unambiguous information for the decision-making stage.

Robust, low-cost, and preferably real-time sensing systems are needed for monitoring physical conditions in agriculture and environment. Commercial products have become available for some sensor types. Others are currently under development, especially in the field of precision agriculture.

Selection of the monitoring method

Monitoring is a series of measurements (or observations) done in a planned fashion in order to assemble a more complete view of existing conditions through time. Single observations or surveys are made at a point in time to record the current condition. Monitoring, in a formal sense, is a series of surveys.

The goals, applied sensors, data collection strategies, and methods of analysis used in monitoring must be defined in detail and in advance before taking further steps that sometimes require formal, technical, and financial arrangements. These elements and their relationship depend on the temporal and dimensional scale of planned observations. There are technical means to measure minute quantities of chemicals in the environment. At the other end of the dimensional scale, there are space-based satellite sensors routinely scanning and mapping the earth surface several times a day.

The choice of mass and volume of the sampled material, size of measurement probes, and temporal and spatial

locations should be chosen for assuring the measured sample to be representative of the target component. This is especially important for soil because it is not homogeneous both in space and in time.

The investigation of the agricultural and environmental physical conditions sometimes requires physical removal of samples from the environment, for example, collecting soil cores in the vadose zone disrupt soil profiles and can create preferential flow paths. Measurements involving unrecoverable destruction of the measured medium are called destructive. Nondestructive measurements or monitoring is becoming increasingly important with the technological miniaturization as well as the development of sensors, electronics and telecommunication. The example of nondestructive monitoring is by means of satellite-based sensors to measure topography, plant cover, or top-soil temperature.

Selectivity

The key feature of the applied measurement method is its selectivity, that is, the lack of sensitivity of the conversion function (calibration) on the influence from the factors other than the measured one. Proper selectivity liberates the user from frequent, specific for each soil, *in situ* calibrations.

The solution to the problem of electric measurement of the physical quantity in selective way is to find such an electric property of the medium conditioning it, which is specific to the considered medium. For example, the specific property of molecular oxygen in electrolyte ("soil water") is small activation energy of electrode reaction of its reduction. It can be concluded that electric measurement of oxygenation may be based on the ammetric measurement of the current of electrode reaction of oxygen molecules reduction (Malicki and Bieganowski, 1999).

Concerning the problem of electric soil moisture measurement, the medium conditioning moisture is water and its specific property is the polar structure of water molecules. Polarity of water molecules is the reason that dielectric permittivity (dielectric constant) of water is much higher than permittivity of soil solid phase (the relative dielectric constant of water in the electric field of frequency below 18 GHz and at room temperature is about 81, while the relative dielectric constant of solid phase is 4–5 at the same conditions). The dielectric constant of soil strongly depends on its water content, therefore it may be concluded that electric measurement of soil moisture should be based on the measurement of its dielectric constant.

Similarly, concerning the issue of electric measurement of soil salinity, the media conditioning salinity are salts present in soils and the specific property is their ionic form. The ability to transport electric charge by the ions in "soil water" allows the soil to conduct electric current. Therefore, the electric measurement of soil salinity should be based on the measurement of its electric conductivity.

Status of water as significant issue of agrophysics

Increasing demands of water management result in the continuous development of its tools. One of the most important, besides the simulation models of water balance, is monitoring of water status in porous materials defined as a space-temporal recording of the water properties that stimulate the phenomena and processes observed in the soil–plant–atmosphere system.

Concerning agrophysics, water status in porous materials is the issue of first priority, because each phenomenon or process examined in its scope depends on water status.

Monitoring of water status is accomplished using digital systems. The digital data acquisition systems react only on electric signals and the applied sensors must convert the measured value into the proportional electric signal.

Water status of soil, as a porous material should be expressed by minimum five variables: amount of water in the soil (i.e., soil moisture), soil potential, salinity, oxygenation, and temperature (Malicki, 1999).

The most difficult are the electric measurement of soil water potential and soil water content (soil moisture); therefore, they are the subject of permanent research. It is assumed here, that the method successfully verified for soils will be also applicable for other porous agricultural materials because their structure is not as complex as soil.

Monitoring physical conditions in agriculture and environment is done by sampling, automatic ground measurement systems or remote sensing with the use of planes or satellites.

Sampling

There are several soil basic physical properties that cannot be measured automatically and the necessary information about their variability in time and/or space is gathered by means of traditional sampling. Soil mechanical properties, that is, soil texture and soil density or porosity, which is functionally dependent on soil density, do not change in time in uncultivated areas because they present the effect of long-term geological processes.

Sampling strategy in agro-environmental monitoring depends on the objectives, which include increase agriculture productivity (yield indicators), optimize water use in irrigation systems, or increase carbon sequestration. Also, it depends on observation scale from the geographical or administrative point of view: an experimental plot, field, landscape, watershed, farm, district, or whole country. Spatial and temporal variability must also be taken into account in constructing time schedule and sampling locations to be representative.

Sampling usually affects the environment, that is, this type of measurement maybe destructive to the tested object or its immediate vicinity. Drilling a deep well to collect groundwater does not affect the groundwater environment but the geological profile is irreversibly damaged. Soil cores collected in the vadose zone disrupt soil profiles and can create preferential flow paths.

Ground monitoring systems with automated data acquisition and processing

The technological progress in material science, electronics, telecommunication, and informatics effects in the development of new sensing devices that can be adopted in examining objects of agricultural and environmental studies. They include Time Domain Reflectometry (TDR) and Frequency Domain Reflectometry (FDR) probes for the simultaneous measurement of soil moisture, electrical conductivity, and temperature (Skierucha et al., 2006). There sensing devices include sensors and transducers, where the former detects the signal or stimulus and the latter converts input energy of one form into output energy of another form. An example of the sensor is thermistor giving the change of resistance as the function of temperature. This sensor associated with electrical circuitry forms an instrument, also called a transducer, that converts thermal energy into electrical energy.

Another important element of a ground monitoring system is a data acquisition and processing unit, which monitors the output signal of the transducer and processes the resulting data into a form that can be understood by the end user. The basic features of this unit include user-friendly interface for the operator, large storage memory, physical communication interfaces preferably with serial transmission from the instrument to the operator's notebook. Telemetry with the application of wireless networks is becoming popular especially for distant ground monitoring systems (Wang et al., 2006).

Monitoring stations must meet strong requirements concerning power consumption. The hardware designers should use low-power electronic circuits and apply sleep mode operations whenever possible. Also, charging the internal battery is accomplished with a solar panel.

Remote sensing

Remote sensing in agriculture and environment is the acquisition of biological and geochemical information about the condition and state of the land surface by sensors that are not in direct physical contact with it. The transmission of this information is in the form of electromagnetic waves reflected from the land surface either in passive mode – when the source of energy is the sun and/or the Earth, or in active mode – when the source energy is artificially generated. The analyzed signal reflected from the land surface is composed with different wavelengths over the electromagnetic spectrum (Artiola et al., 2004a). Today a large number of satellite sensors observe the Earth at wavelengths ranging from visible to microwave, at spatial resolutions ranging from submeters to kilometers and temporal frequencies ranging from minutes to weeks or months (Rosenqvist et al., 2003).

The remote sensed data provide information about ecosystem stability, land degradation and desertification (Artiola et al., 2004b), carbon cycling (Rosenqvist et al., 2003), erosion and sediment yield, soil moisture

(Wigneron et al., 1998; Kerr, 2007), and plant and weeds cover (Thorp and Tian, 2004).

Conclusion

Monitoring physical conditions in agriculture and environment can be done in various temporal and dimensional scales and with the application of numerous instruments and methods reflecting the current development of technology. The received and processed data increase our knowledge for the benefit of social, political, and economic sustainable development as well as for better understanding the nature.

Bibliography

- Arshad, A. A., and Martin, S., 2002. Identifying limits for soil quality indicators in agro-ecosystems. *Agriculture, Ecosystems and Environment*, **88**, 152–160.
- Artiola, J., Pepper, I. L., and Brusseau, M. L., 2004a. Monitoring and characterization of the environment (Chapter 11). In *Environmental Monitoring and Characterization*. Burlington: Elsevier, pp. 1–9.
- Artiola, J., Pepper, I. L., and Brusseau, M. L., 2004b. Remote sensing for environmental monitoring (Chapter 11). In *Environmental Monitoring and Characterization*. Burlington: Elsevier, pp. 183–206.
- Doran, J. W., 2002. Soil health and global sustainability: translating science into practice. *Agriculture, Ecosystems and Environment*, **88**, 119–127.
- Kerr, Y. H., 2007. Soil moisture from space: where are we? *Hydrogeology Journal*, **15**, 117–120.
- Malicki, M. A., 1999. Methodical aspects of water status monitoring in selected bio-materials. *Acta Agrophysica (Series Monographs)*, **19** (in Polish).
- Malicki, M. A., and Bieganowski, A., 1999. Chronovoltammetric determination of oxygen flux density in the soil. *International Agrophysics*, **13**(3), 273–281.
- Rosenqvist, Å., Milne, A., Lucas, R., Imhoff, M., and Dobson, C., 2003. A review of remote sensing technology in support of the Kyoto Protocol. *Environmental Science & Policy*, **6**, 441–455.
- Schoenholtz, S. H., Van Miegroet, H., and Burger, J. A., 2000. A review of chemical and physical properties as indicators of forest soil quality: challenges and opportunities. *Forest Ecology and Management*, **138**, 335–356.
- Skierucha, W., Wilczek, A., and Walczak, R. T., 2006. Recent software improvements in moisture (TDR method), matric pressure, electrical conductivity and temperature meters of porous media. *International Agrophysics*, **20**, 229–235.
- Thorp, K. R., and Tian, L. F., 2004. A review on remote sensing of weeds in agriculture. *Precision Agriculture*, **5**, 477–508.
- Wang, N., Zhang, N., and Wang, M., 2006. Wireless sensors in agriculture and food industry – recent development and future perspective. *Computers and Electronics in Agriculture*, **50**, 1–14.
- Wigneron, J. P., Schmugge, T., Chanzy, A., Calvet, J. C., and Kerr, Y., 1998. Use of passive microwave remote sensing to monitor soil moisture. *Agronomie*, **18**, 27–43.

Cross-references

- [Climate Change: Environmental Effects](#)
[Nondestructive Measurements in Soil](#)
[Online Measurement of Selected Soil Physical Properties](#)
[Remote Sensing of Soils and Plants Imagery](#)
[Spatial Variability of Soil Physical Properties](#)

MUalem EQUATION

Model for predicting hydraulic conductivity of unsaturated porous media.

Bibliography

- Mualem, Y., 1976. A new model for predicting hydraulic conductivity of unsaturated porous media. *Water Resources Research*, **12**:513–522.

Cross-references

- [Water Budget in Soil](#)

MULCHING

See [Water Use Efficiency in Agriculture: Opportunities for Improvement](#)

MULCHING, EFFECTS ON SOIL PHYSICAL PROPERTIES

Antonio Jordán¹, Lorena M. Zavala¹,
 Miriam Muñoz-Rojas²

¹MED_Soil Research Group, Departamento de Cristalografía, Mineralogía y Química Agrícola, Universidad de Sevilla, Sevilla, Spain

²Instituto de Recursos Naturales y Agrobiología de Sevilla (CSIC), Sevilla, Spain

Definition

Mulch. Mulch is any material, other than soil, placed or left at the soil surface for soil and water management.

Mulching. In agriculture and gardening, mulching is the practice of leaving crop residues or other materials on the soil surface for soil and water conservation and keeping favorable and stable environments for plant growth.

Introduction

Mulching is a form of conservation tillage consisting of leaving a layer of crop residues (CR) or other materials on the soil surface. Mulch helps to preserve high and sustainable yields by increasing the soil organic matter (SOM) content and therefore improving soil physical quality. Mulch tilling is also a form of minimum tillage and a cost-efficient alternative for high-yield conservation agricultural practice.

Leaving CR or other substances on the soil surface is a traditional practice for protecting soil from erosion and enhancing fertility (Lal and Stewart, 1995). It has been reported that conventional agricultural practices, based

on intensive fertilization and chemical amendments, often lead to degradation processes, such as erosion (see entry *Tillage Erosion*), acidification, and the emission of greenhouse gases (see entry *Greenhouse Gases Sink in Soils*). Current global problems such as population growth, greenhouse effect, malnutrition, water quality, reduction of agricultural land, and soil degradation (see entry *Desertification: Indicators and Thresholds*) require the implementation of conservation tillage practices to address the problem of sustainability, food security, and environmental quality.

Materials used as mulch

A wide variety of materials can be used as mulch. Most of mulches are organic materials (e.g., CR, litter, straw, leaves, or weed biomass), but other inorganic or industry-derived materials can be also used (plastic film, gravels, or geotextiles). The election depends in both availability and objectives.

Organic mulches must be weed free, easy to apply, and readily available by farmers. The mulch decomposition time can vary greatly. Depending on the amount and type of mulch, varying quantities of nutrients and organic matter enter the soil during the decomposition process. In agriculture, the most commonly used organic mulches are crop/plant residues, produced on-site or off-site and left on the soil surface after cropping (e.g., wheat straw). A large quantity of residue is produced annually, so that it constitutes a renewable and easily available resource. Other mulches used in agriculture and gardening are wood chips, pine bark, and pine needles. Some wastes, such as shredded or composted clipped grass, litter, and small branches can also be used.

Inorganic materials such as geotextiles can be used as mulch. Some of the advantages of using geotextiles is the prevention of weed growth (at least in a great proportion), and the normal aeration and water exchange. Rock fragments and gravels can be used as inorganic mulch materials. They show low decomposition rates and do not require annual replacement, but cannot be suitable for all crops. Plastic films help control most weeds and contribute to water conservation. Plastic films are used predominantly in extensive crop areas, but show some problems: interruption of air, water, and nutrients flow between the topsoil and the atmosphere, as well as other environmental problems such as disposal of plastic materials.

Effects on soil physical properties

Soil structure and aggregate stability

Soil structure is extremely important for the maintenance of soil quality and productivity. Aggregate stability (AS) affects root density and elongation (see entry *Root Responses to Soil Physical Limitations*), air and water flow and erosion (Amézketa, 1999). Some of the main factors affecting soil aggregation are SOM content (see entry *Soil Aggregates, Structure, and Stability*), texture and moisture content, but external factors as crop type, tillage practices, or microfauna are also important. Long-term tillage affects AS (Angers et al., 1993; Unger et al., 1998; Álvaro-Fuentes et al., 2008), as tillage destroys aggregates leading to a decrease in aggregate size and pore clogging by fine particles. It has been reported that decomposition rates of SOM are lower with minimum tillage and residue retention, and consequently it increases over time (Loch and Coughlan, 1984; Dalal, 1989).

AS is determined by the cohesive forces between particles. Therefore, it can be used as an index of structure and physical soil stability. Soil texture, clay mineralogy, cations, and the quantity and quality of SOM are key factors controlling aggregation. Plant roots (see entry *Plant Roots and Soil Structure*), microorganisms (especially fungi), and organic substances are also involved in the formation of aggregates and AS. AS may vary seasonally (Hillel, 1998) or during tilling. After mulching, increased SOM content contributes to enhance aggregation, as it has been reported under a diversity of climate areas (Mulumba and Lal, 2008; Jordán et al., 2010) even in the short term (Hermawan and Bomke, 1997).

Inorganic mulches (e.g., plastic film) show limited or no effect on soil structure. Zhang et al. (2008), for example, reported that under no tillage, the increase in SOM content and AS in soils under straw cover was higher than under plastic film; in this case, soil quality under plastic mulch was similar or even lower than in non-covered soils. In contrast, geotextiles may increase SOM content, improving topsoil structure and AS (Bhattacharyya et al., 2010).

Bulk density and porosity

The effects of CR on soil bulk density (BD; see entry *Bulk Density of Soils and Impact on their Hydraulic Properties*) are highly variable. Although high BD has been observed under mulch relative to conventional tillage (Bottenberg et al., 1999), decreased bulk densities have also been reported by Oliveira and Merwin (2001) and Ghuman and Sur (2001). In other cases, there is no relationship between mulch rate and BD. This variability may be due to differences in management practices, soil type, and the type of mulch material used in the experiments. However, Mulumba and Lal (2008) found that BD increased for mulching rates between 0 and 5 Mg ha⁻¹ wheat straw mulch, but strongly decreased for higher rates.

Pores of different size (see entry *Pore Size Distribution*), shape, and continuity are created by abiotic and biotic factors (Kay and VandenBygaart, 2002). Mulumba and Lal (2008) found that total porosity increased significantly with increase in mulch rate after an 11-year treatment in the USA. Increased porosity due to mulch application has been also reported after shorter periods (Oliveira and Merwin, 2001; Jordán et al., 2010).

Penetration resistance

Many studies have reported greater penetration resistance in soils under no-tillage practices than in other conventionally tilled soils in the upper centimeters, and, generally, penetration resistance is higher under reduced tillage systems with residue cover. Mulch application has a significant effect on penetration resistance but only at certain stages of the crop production. After an experiment with Polish Luvisols under reduced and no-tillage practices, penetration resistance increased in the growing season, causing reduced plant growth and crop yield (Pabin et al., 2003). In this case, straw mulch did not counteract the negative changes in the parameters of the soil strength. According to Bielders et al. (2002), differences in penetration resistance after different treatments are mostly due to differences in intrinsic soil properties (e.g., cohesion, BD).

Crusting and sealing

Plant residues on the soil surface protect it against crusting (Sumner and Stewart, 1992), improving AS and infiltration rates (see entry *Soil Surface Sealing and Crusting*). Le Bissonnais and Arrouays (1997) observed that increasing SOM content decreased soil surface sealing. After a study in western Niger, Bielders et al. (2002) observed low permeability erosion crusts and discontinuous structural crusts with partially exposed clay skins in soils under conventional tillage, in contrast to mulched soils. As it has been reported in stone-covered soils (Martínez-Zavala and Jordán, 2008; Zavala et al., 2010), gravel mulch helps to avoid soil sealing and crusting (Poesen and Lavee, 1994).

The use of plastic film mulches has spread considerably as a way to reverse the low crop yields (e.g., Zhang and Ma, 1994), increasing the risk of crust formation (Li et al., 2005).

Soil temperature

Temperature affects the rate of soil biological and chemical processes (see entry *Temperature Effects in Soil*). The amount of energy entering the soil depends strongly on soil color, aspect, and the vegetative cover. CR on the soil surface can affect or completely modify the soil temperature regime by reducing the amount of energy entering the soil by the interception of radiation, shading the soil surface, and buffering temperature variations.

Soil temperature range is usually narrower in mulched than unmulched soils. Wheat straw has a higher albedo and lower thermal conductivity than bare soil, and therefore it reduces the input of solar energy (Horton et al., 1996). On the other hand, during colder periods, wheat straw mulch on the soil surface insulates it from the colder atmosphere (Zhang et al., 2009).

Results after application of inorganic mulches vary depending on the mulch material. After field experiments in the UK, Cook et al. (2006) demonstrated that soil temperature reduced with higher mulching rates. In contrast, the use of inorganic mulches can increase soil temperature. Nachtergael et al. (1998) reported that gravel mulch

increased soil temperature and decreased evaporation (see entry *Evapotranspiration*) in vineyard soils in Switzerland. Organic geotextiles can also attenuate extreme temperature fluctuations, reducing water loss through evaporation. Inorganic materials such as plastic mulches are often used to increase soil temperature in horticulture, leading to high yields. Apart from other environmental problems, intensive use of plastic mulches for increasing soil temperature shows some limitations. Enhanced mineralization rates can lead to exhaustion of SOM, affecting long-term soil physical and chemical fertility (Li et al., 2004).

Soil water

Mulching has a great impact on soil water and surface water. Mulching decreases runoff by improving infiltration rate and increases water storage capacity by improving retention (see entry *Field Water Capacity*). In addition, reduced evaporation rates help to extend the period of time during which soil remains moist.

Mulching improves considerably soil water characteristics, although different results have been reported. Organic mulches on the soil surface induce optimal soil conditions for plant growth, enhancing soil water retention and availability, and increasing macroporosity (Martens and Frankenberger, 1992). Much research has shown that use of mulch can increase infiltration and decrease evaporation, resulting in more water stored and reduced runoff rates (e.g., Smika and Unger, 1986).

Wheat straw mulch is considered the best way of improving water retention in the soil and reducing soil evaporation. High available water capacities have been reported under high mulching rates and reduced or no till practices. Mulumba and Lal (2008) and Jordán et al. (2010) found that even low mulch rates have a strong impact on the available water content. Contrasting data have been reported by Głab and Kulig (2008), who found no effect in available water content after applying mulch and different tillage systems. Results can also vary between the upper and lower layers of the soil profile.

Soil erosion risk

Many researchers have reported low or negligible soil losses in mulched soils in comparison with conventional soil tillage (see entry *Water Erosion: Environmental and Economical Hazard*). The hydrological/erosional response of mulched soils depends largely on the mulching rates applied during the crop period. It has been reported that the erosive consequences of moderate storms in the Mediterranean area could be strongly reduced by using just $5 \text{ Mg ha}^{-1} \text{ year}^{-1}$ mulching rates (Jordán et al., 2010). A mulch layer increases the roughness and the interception of raindrops, delaying runoff flow and favoring infiltration (García-Orenes et al., 2009). Low erosive responses of mulched soils have been reported from diverse climate areas of the world. In contrast, Jin et al. (2009) suggested that the relation between mulching rate

and interrill soil detachment is not unique and can vary depending on rainfall intensity. Increasing cover rates reduce infiltration and lead to an increasing net flux, which becomes deeper and faster in its concentrated flow part. In this case, ponding is faster and deeper, thus the water column pressure is greater and thereafter infiltration takes place more quickly and penetrates more deeply. However, this response can be overridden under moderate rainfall intensity by a dense soil cover or thick mulch layers.

Plastic mulches substantially accelerate runoff generation in slopes (Wan and El-Swaify, 1999). According to Bhattacharyya et al. (2010), the use of geotextiles is an effective soil conservation practice, but its efficiency decreases in large areas. Despite synthetic geotextiles dominating the commercial market, geotextiles constructed from organic materials are highly effective in erosion control and vegetation establishment (Ogbobe et al., 1998) and can be an ecological alternative for farmers (Giménez-Morera et al., 2010). Anyway, experimental studies under natural and simulated rainfall have demonstrated that cotton geotextiles reduce soil losses but increase water losses, probably due to water repellency of cotton. Although soil erosion can be severely reduced by geotextiles at the pedon or meter scale, surface runoff may result in high erosion rates at slope and watershed scales as more runoff will be available (Giménez-Morera et al., 2010).

Summary

During the last decades, conservation tillage techniques have displaced conventional tillage in many areas of the world. The use of CR left on the soil surface improves soil quality and productivity through favorable effects on soil physical properties. Mulch farming is a form of conservation tillage that preserves soil quality and the environment. Mulch affects soil physical properties by improving SOM content, increasing soil porosity and AS. Indirectly, mulching also regulates soil temperature, and increases water retention capacity.

An organic mulch layer serves as a protecting layer against rainfall-induced soil erosion by reducing drop impacts and modifying the hydrological response of the exposed surface. CR and other organic mulches intercept rainfall and contribute to decrease runoff rates and enhance infiltration, protecting soil from erosion. Inorganic mulches as geotextiles, gravels, or plastic films show a range of erosional responses to rainfall.

Bibliography

- Álvaro-Fuentes, J., Arrué, J. L., Gracia, R., and López, M. V., 2008. Tillage and cropping intensification effects on soil aggregation: temporal dynamics and controlling factors under semiarid conditions. *Geoderma*, **145**, 390–396.
- Amézketa, E., 1999. Soil aggregate stability: a review. *Journal of Sustainable Agriculture*, **14**, 83–151.
- Angers, D. A., Samson, N., and Légère, A., 1993. Early changes in water-stable aggregation induced by rotation and tillage in a soil under barley production. *Canadian Journal of Soil Science*, **73**, 51–59.
- Bhattacharyya, R., Smets, T., Fullen, M. A., Poesen, J., and Booth, C. A., 2010. Effectiveness of geotextiles in reducing runoff and soil loss: a synthesis. *Catena*, **81**, 184–195.
- Bielders, C. L., Michels, K., and Bationo, A., 2002. On-farm evaluation of ridging and residue management options in a Sahelian millet-cowpea intercrop. I. Soil quality changes. *Soil Use and Management*, **18**, 216–222.
- Bottenberg, H., Masiunas, J., and Eastman, C., 1999. Strip tillage reduces yield loss of snapbean planted in rye mulch. *HortTechnology*, **9**, 235–240.
- Cook, H. F., Valdes Gerardo, S. B., and Lee, H. C., 2006. Mulch effects on rainfall interception, soil physical characteristics and temperature under *Zea mays* L. *Soil and Tillage Research*, **91**, 227–235.
- Dalal, R. C., 1989. Long-term effects of no-tillage, crop residue, and nitrogen application on properties of a Vertisol. *Soil Science Society of America Journal*, **53**, 1511–1515.
- Garcia-Orenes, F., Cerdà, A., Mataix-Solera, J., Guerrero, C., Bodí, M. B., Arcenegui, V., Zornoza, R., and Sempere, J. G., 2009. Effects of agricultural management on surface soil properties and soil-water losses in eastern Spain. *Soil and Tillage Research*, **106**, 117–123.
- Ghuman, B. S., and Sur, H. S., 2001. Tillage and residue management effects on soil properties and yields of rainfed maize and wheat in a subhumid subtropical climate. *Soil and Tillage Research*, **58**, 1–10.
- Giménez-Morera, A., Ruiz Sinoga, J. D., and Cerdà, A., 2010. The impact of cotton geotextiles on soil and water losses from Mediterranean rainfed agricultural land. *Land Degradation and Development*, **21**, 210–217.
- Głab, T., and Kulig, B., 2008. Effect of mulch and tillage system on soil porosity under wheat (*Triticum aestivum*). *Soil and Tillage Research*, **99**, 169–178.
- Hermawan, B., and Bomke, A. A., 1997. Effects of winter cover crops and successive spring tillage on soil aggregation. *Soil and Tillage Research*, **44**, 109–120.
- Hillel, D., 1998. *Environmental Soil Physics*. San Diego: Academic.
- Horton, R., Bristow, K. L., Kluitenberg, G. J., and Sauer, T. J., 1996. Crop residue effects on surface radiation and energy balance – review. *Theoretical and Applied Climatology*, **54**, 27–37.
- Jin, K., Cornelis, W. M., Gabriels, D., Baert, M., Wu, H. J., Schietecatte, W., Cai, D. X., De Neve, S., Jin, J. Y., Hartmann, R., and Hofman, G., 2009. Residue cover and rainfall intensity effects on runoff soil organic carbon losses. *Catena*, **78**, 81–86.
- Jordán, A., Zavala, L. M., and Gil, J., 2010. Effects of mulching on soil physical properties and runoff under semi-arid conditions in southern Spain. *Catena*, **81**, 77–85.
- Kay, B. D., and VandenBygaart, A. J., 2002. Conservation tillage and depth stratification of porosity and soil organic matter. *Soil and Tillage Research*, **66**, 107–118.
- Lal, R., and Stewart, B. A., 1995. *Soil Management – Experimental Basis for Sustainability and Environmental Quality*. Boca Raton: Lewis. Advances in Soil Science.
- Le Bissonnais, Y., and Arrouays, D., 1997. Aggregate stability and assessment of soil crustability and erodibility. II. Application to humic loamy soils with various organic carbon contents. *European Journal of Soil Science*, **48**, 39–48.
- Li, F. M., Wang, J., Xu, J. Z., and Xu, H. L., 2004. Productivity and soil response to plastic film mulching durations for spring wheat on entisols in the semiarid Loess Plateau of China. *Soil and Tillage Research*, **78**, 9–20.
- Li, L. L., Huang, G. B., Zhang, R. Z., Jin, X. J., Li, G. D., and Chan, K. Y., 2005. Effects of conservation tillage on soil water regimes in rainfed areas. *Acta Ecologica Sinica*, **25**, 2326–2332.

- Loch, R. J., and Coughlan, K. J., 1984. Effects of zero tillage and stubble retention on some properties of a cracking clay. *Australian Journal of Soil Research*, **22**, 91–98.
- Martens, D. A., and Frankenberger, W. T., 1992. Modification of infiltration rates in an organic-amended irrigated soil. *Agronomy Journal*, **84**, 707–717.
- Martínez-Zavala, L., and Jordán, A., 2008. Effect of rock fragment cover on interrill soil erosion from bare soils in Western Andalucía, Spain. *Soil Use and Management*, **24**, 108–117.
- Mulumba, L. N., and Lal, R., 2008. Mulching effects on selected soil physical properties. *Soil and Tillage Research*, **98**, 106–111.
- Nachtergael, J., Poesen, J., and van Wesemael, B., 1998. Gravel mulching in vineyards of southern Switzerland. *Soil and Tillage Research*, **46**, 51–59.
- Ogbobe, O., Essien, K. S., and Adebayo, A., 1998. A study of biodegradable geotextiles used for erosion control. *Geosynthetics International*, **5**, 545–553.
- Oliveira, M. T., and Merwin, I. A., 2001. Soil physical conditions in a New York orchard after eight years under different groundcover management systems. *Plant and Soil*, **234**, 233–237.
- Pabin, J., Lipiec, J., Włodek, S., and Biskupski, A., 2003. Effect of different tillage systems and straw management on some physical properties of soil and on the yield of winter rye in monoculture. *International Agrophysics*, **17**, 175–181.
- Poesen, J. W. A., and Lavee, H., 1994. Rock fragments in top soils: significance and processes. *Catena*, **23**, 1–28.
- Singh, B., Chanasyk, D. S., McGill, W. B., and Nyborg, M. P. K., 1994. Residue and tillage management effects on soil properties of a typic cryboroll under continuous barley. *Soil and Tillage Research*, **32**, 117–133.
- Smika, D. E., and Unger, P. W., 1986. Effect of surface residues on soil water storage. *Advanced Soil Science*, **5**, 111–138.
- Sumner, M. E., and Stewart, B. A., 1992. *Soil Crusting – Chemical and Physical Processes*. Boca Raton: Lewis. Advances in Soil Science.
- Unger, P. W., Jones, O. R., McClenagan, J. D., and Stewart, B. A., 1998. Aggregation of soil cropped to dryland wheat and grain sorghum. *Soil Science Society of America Journal*, **62**, 1659–1666.
- Wan, Y., and El-Swaify, S. A., 1999. Runoff and soil erosion as affected by plastic mulch in a Hawaiian pineapple field. *Soil and Tillage Research*, **52**, 29–35.
- Zavala, L. M., Jordán, A., Bellinfante, N., and Gil, J., 2010. Relationships between rock fragment cover and soil hydrological response in a Mediterranean environment. *Soil Science and Plant Nutrition*, **56**, 95–104.
- Zhang, S. F., and Ma, T. L., 1994. Yield components and cultivation technology of corn with high grain yield through plastic film cover in West Yellow River area. *Gansu Agricultural Science and Technology*, **1**, 16–17.
- Zhang, Z., Zhang, S., Yang, J., and Zhang, J., 2008. Yield, grain quality and water use efficiency of rice under non-flooded mulching cultivation. *Field Crops Research*, **108**, 71–81.
- Zhang, S., Lövdahl, L., Grip, H., Tong, Y., Yang, X., and Wang, Q., 2009. Effects of mulching and catch cropping on soil temperature, soil moisture and wheat yield on the Loess Plateau of China. *Soil and Tillage Research*, **102**, 78–86.

[Plant Roots and Soil Structure](#)
[Pore Size Distribution](#)
[Root Responses to Soil Physical Limitations](#)
[Soil Aggregates, Structure, and Stability](#)
[Soil Surface Sealing and Crusting](#)
[Temperature Effects in Soil](#)
[Tillage Erosion](#)
[Water Erosion: Environmental and Economical Hazard](#)

MUNSELL COLOR SYSTEM

A color designation system that specifies the relative degrees of the three simple variables of color: hue, value, and chroma.

Cross-references

[Color in Food Evaluation](#)
[Color Indices, Relationship with Soil Characteristics](#)

MYCORRHIZAL SYMBIOSIS AND OSMOTIC STRESS

Juan M. Ruiz-Lozano
 Departamento de Microbiología del Suelo y Sistemas Simbióticos, Estación Experimental del Zaidín (CSIC), Granada, Andalucía, Spain

Definition

The term Mycorrhiza comes from the Greek words “mycos,” meaning fungus and “rhiza,” meaning root and applies to a mutualistic symbiosis between roots of most higher plants and a group of soil fungi belonging to the phyla Glomeromycota, Basidiomycota or Ascomycota. By this mutualistic association, the plant receives soil nutrients (especially phosphorus) and water, while the fungus receives a protected ecological niche and plant-derived carbon compounds for its nutrition (Varma, 2008).

The term Osmotic Stress refers to all the environmental conditions that induce a water deficit in the plant tissues, limiting plant growth and development. It generally includes drought, cold and salinity, which directly decreases the plant water content due to an also low soil water content (drought) or which difficult the right uptake of water from soil due to the diminution of soil water potential (cold and salinity).

Eco-physiological studies investigating the role of the mycorrhizal symbiosis against osmotic stresses have demonstrated that the symbiosis often results in altered rates of water movement into, through, and out of the host plants, with consequent effects on tissue hydration and plant physiology (Augé, 2001). Thus, it is accepted that the mycorrhizal symbiosis protects host plants against the detrimental effects of water deficit, and that this protection results from a combination of physical, nutritional and

Cross-references

[Bulk Density of Soils and Impact on their Hydraulic Properties](#)
[Desertification: Indicators and Thresholds](#)
[Evapotranspiration](#)
[Field Water Capacity](#)
[Greenhouse Gases Sink in Soils](#)

cellular effects. Several mechanisms have been proposed to explain these effects. The most important are: direct uptake and transfer of water through the fungal hyphae to the host plant, better osmotic adjustment of host plants, enhancement of plant gas exchange through hormonal changes, and protection against the oxidative damage generated by drought. Modulation by the mycorrhizal symbiosis of plant genes involved in the response of plants to water deficit have also been described, with special emphasis on the role of aquaporins (Ruiz-Lozano et al., 2006). Results obtained so far show that the mycorrhizal symbiosis up- or down-regulates aquaporin genes depending on the own intrinsic properties of the osmotic stress. In any case, the induction or inhibition of particular aquaporins by mycorrhizal symbiosis results in a better regulation of plant water status and contribute to the global plant resistance to the stressful conditions, as evidenced by the better

growth and water status of mycorrhizal plants under conditions of water deficit (Ruiz-Lozano and Aroca, 2009).

Bibliography

- Augé, R. M., 2001. Water relations, drought and vesicular-arbuscular mycorrhizal symbiosis. *Mycorrhiza*, **11**, 3–42.
- Ruiz-Lozano, J. M., and Aroca, R., 2009. Modulation of aquaporin genes by the arbuscular mycorrhizal symbiosis in relation to osmotic stress tolerance. In Sechback, J., and Grube, M. (eds.), *Symbiosis and Stress*. Germany: Springer. ISBN 978-90-481-9448-3 in press.
- Ruiz-Lozano, J. M., Porcel, R., and Aroca, R., 2006. Does the enhanced tolerance of arbuscular mycorrhizal plants to water deficit involve modulation of drought-induced plant genes? *The New Phytologist*, **171**, 693–698.
- Varma, A., 2008. *Mycorrhiza. State of the Art, Genetics and Molecular Biology, Eco-Function, Biotechnology, Eco-Physiology, Structure and Systematics*, 3rd edn. Berlin: Springer.

N

NANOMATERIALS IN SOIL AND FOOD ANALYSIS

Subramanian Viswanathan

Requimte, Grupo de Reacções e Análises Químicas,
Instituto Superior de Engenharia do Porto, Porto, Portugal

Synonyms

Nanomaterials application in soil and food testing

Definition

Nanomaterials: generally referring to materials with the size of 0.1–100 nm.

Carbon nanotube: allotropes of carbon with a cylindrical nanostructure.

Biosensor: a device for the detection of an analyte that combines a biological component with a physicochemical detector component.

Introduction

The Food and Agriculture Organization (FAO) is the main United Nations agency specializing in all aspects of food quality and safety, and in all the different stages of food production, harvest, postharvest handling, storage, transport, processing, and distribution. Food analysis is the discipline dealing with the development, application, and study of analytical procedures for characterizing the properties of foods (Nielsen, 2003). These analytical procedures are used to provide information about a wide variety of different characteristics of foods, including their composition, structure, physicochemical properties, and sensory attributes. This information is critical to our rational understanding of the factors that determine the properties of foods, as well as to our ability to economically produce foods that are consistently safe, nutritious, and desirable and for consumers to make informed choices about their diet. One of the most

important reasons for analyzing foods from both the consumers and the manufacturers' standpoint is to ensure that they are safe.

Precision farming has been a long-desired goal to maximize output (i.e., crop yields) while minimizing input (i.e., fertilizers, pesticides, and herbicides) through monitoring environmental variables and applying targeted action. A soil analysis is used to determine the level of nutrients found in a soil sample. Quality crops with high yields require a sufficient supply and maintenance of nutrient elements. As nutrients are utilized by one crop and not replaced for subsequent crop production, yields will decrease accordingly. Accurate monitoring of nutrient before and after crop production and soil analysis results will help the efficient management of fertilizer applications. Soil analysis can also help to reduce agricultural waste and thus keep environmental pollution to a minimum. Researchers are exploring to come up with sensors for detection of soil nutrients, pesticides, pollutants up to very minute fractions by exploiting novel properties of nanomaterials.

The definition of nanomaterial is based on the prefix “nano,” which is from the Greek word meaning “dwarf.” The word nanomaterials is generally used when referring to materials with the size of 0.1–100 nm; however, it is also inherent that these materials should display different properties from bulk (or micrometric and larger) materials as a result of their size (Rao et al., 2004). These differences include physical strength, chemical reactivity, electrical conductance, magnetism, and optical effects. The potential of nanomaterials to revolutionize the health care, textile, materials, information and communication technology, and energy sectors has been well publicized. In fact, several products enabled by nanomaterials are already in the market, such as antibacterial dressings, transparent sunscreen lotions, stain-resistant fabrics, scratch-free paints for cars, and self-cleaning windows.

Nanomaterials such as nanotubes (NTs), nanowires (NWs), and nanoparticles present new opportunities as sensing platforms for biological and environmental applications. Having micrometer-scale lengths and nanometer-scale diameters, NTs and NWs can be manipulated with current microfabrication, as well as self-assembly techniques to fabricate nanoscale devices and sensors (Rao et al., 2004). Examples of different nanomaterials-based analytical techniques for the detection of major families of environmental pollutants, i.e., organic contaminants, heavy metals, and air pollutants are reported. Application of the nanomaterials in the field of soil and food analysis is promising. This article covers the recent developments and issues in electrochemical biosensors for food analysis such as ease of preparation, robustness, sensitivity, and realizations of mass production of the detection strategies. This article also emphasizes the current development of electrochemical biosensors combined with nanotechnology.

The synthesis, characterization, and utilization of nanomaterials are part of an emerging and rapidly growing field. Nanomaterials may be grouped under nanoparticles (the building blocks), nano-intermediates, and nanocomposites. Nanostructured materials are synthesized by supramolecular chemistry yielding nanoassemblies (Rao et al., 2004). The nanoparticles serve as the building blocks of nanomaterials and devices. They include nanocrystalline materials such as ceramic, metal and metal oxide nanoparticles; fullerenes, nanotubes, nanorods, and related structures; nanofibers and wires, and precise organic as well as hybrid organic–inorganic nanoarchitectures such as dendrimers and polyhedral silsesquioxanes, liposomes, or nanosomes, respectively.

Nanocrystalline materials

Included here are ceramics, metals, and metal oxide nanoparticles. These materials are assembled from nanometer-sized building blocks, mostly crystallites. The building blocks may differ in their atomic structure, crystallographic orientation, or chemical composition. In other words, materials assembled of nanometer-sized building blocks are microstructurally heterogeneous, consisting of the building blocks (e.g., crystallites) and the regions between adjacent building blocks (e.g., grain boundaries). One of the primary applications of metals in chemistry is their use as heterogeneous catalysts in a variety of reactions (Rao et al., 2004). Due to their vastly increased surface area over macroscale materials, nanometals and oxides are ultrahigh activity catalysts. Nanometals and oxides are also widely used in the formation of nanocomposites. Aside from their synthetic utility, they have many useful and unique magnetic, electric, and optical properties.

Carbon nanotubes

Carbon nanotubes (CNTs) are hollow cylinders of carbon atoms. Their appearance is that of rolled tubes of graphite

such that their walls are hexagonal carbon rings and are often formed in large bundles. Generally speaking, there are two types of CNTs: single-walled carbon nanotubes (SWCNTs) and multi-walled carbon nanotubes (MWCNTs) (Rao et al., 2004). As their names imply, SWCNTs consist of a single, cylindrical graphene layer, whereas MWCNTs consist of multiple graphene layers telescoped about one another. CNT-based nanodevices are a hot research area at the moment. Applications could include novel semiconducting devices, chemical sensors, and ultrasensitive electromechanical sensors (Wang, 2005).

Nanocomposites

Nanocomposites are materials with a nanoscale structure that improve the macroscopic properties of products. Typically, nanocomposites are clay, polymer or carbon, or a combination of these materials with nanoparticle building blocks. Nanocomposites, materials with nanoscale separation of phases can generally be divided into two types: multilayer structures and inorganic/organic composites. Multilayer structures are typically formed by gas phase deposition or from the self-assembly of monolayers. Inorganic/organic composites can be formed by sol–gel techniques, bridging between clusters (as in silsequioxanes), or by coating nanoparticles, in polymer layers for example.

Biosensors

Biosensors are molecular sensors that combine a biological recognition mechanism with a physical transduction technique. They provide a new class of inexpensive, portable instrument that permit sophisticated analytical measurements to be undertaken rapidly at decentralized locations. The sampling component of a biosensor contains a bio-sensitive layer that can either contain bioreceptors or be made of bioreceptors covalently attached to the transducer. The interaction of the analyte with the bioreceptor is designed to produce an effect measured by the transducer, which converts the information into a measurable effect, for example, an electrical signal. There are four major types of transducers: electrochemical (electrodes), mass (piezoelectric crystals or surface acoustic wave devices), optical (optrodes) and thermal (thermistors or heat-sensitive sensors). Among the various types of biosensors, the electrochemical biosensors are the most common as a result of numerous advances leading to their well-understood biointeraction and detection process (Egging, 2002).

The state of the art of nanomaterials and nanotechnologies represents a new trend in the development of sensors and electronic chips that will have a big impact on the future of nanoscience. It is essential to distinguish between nanotechnology and nanomaterials, because in the first case nanotechnologies represent new possibilities for sensor construction and for the developing of novel methods. In the second case, nanomaterials have been widely used

to immobilize enzymes, antigens, and nucleic acids on transducer surfaces, to promote the direct electron transfer reactions, and to amplify and orient the analytic signal of the bio-recognition events.

Applications

In chromatography

Separation science, based on chromatographic and electrophoretic techniques, has achieved many advances employing nanomaterials. Separation media and channels in the above two approaches have sizes and shapes comparable to those of nanomaterials, which makes the latter useful for specific applications in separation science on a micro- and nanometer scale. Nanomaterials have played various roles (e.g., modifier, stabilizer, and stationary phase) in chromatography. The effective pi–pi interactions between fullerenes and phenyl group have utilized to develop fullerene-based stationary phases for the separation of solutes with phenyl moieties in their structures. The conjugated pi- electron system on the surface of SWCNT as well as surface functionalization provides an opportunity to synthesize a stationary phase with good selectivity (Zhang et al., 2006). Nanoparticles, including silica nanoparticles, gold nanoparticles, titanium oxide nanoparticles, polymer nanoparticles, molecularly imprinted polymers, molecular micelles, and dendrimers, used as pseudostationary phases in CEC, have been reviewed by Nilsson et al. (2006).

In optical sensors

Nanomaterials-based optical sensors have been much interested to the trace detection of analytes of interest in the agriculture and food industry. The changes in the optical properties of nanomaterials such spectral absorbance, photoluminescence (PL), and chemiluminescence (CL) phenomena induced by the interaction between nanomaterials and various analytes is utilized to the determination of chemical and biochemical analytes (Shi et al., 2004). Quantum dots (QDs) are nanocrystals of inorganic semiconductors that are somewhat restricted to a spherical shape of around 2–8 nm diameter (Smith and Nie, 2004). Their fluorescent properties are size-dependent and therefore they can be tuned to emit at desired wavelengths (between 400 and 2,000 nm) if synthesized in different composition and size. In this way, QDs of different sizes can be excited with a single wavelength and emission controlled at different wavelengths, thus providing for simultaneous detection. These, together with their highly robust emission properties, make them more advantageous for labeling and optical detection than conventional organic dyes (Patolsky et al., 2006). Their high quantum yields and their narrow emission bands produce sharper colors, lead to higher sensitivity and the possibility of multiplexing of analysis (Tully et al., 2006). The unique optical properties of plasmonic nanoparticles have led to the development of label-free chemical and environmental sensor since the surface plasmon resonance (SPR) is

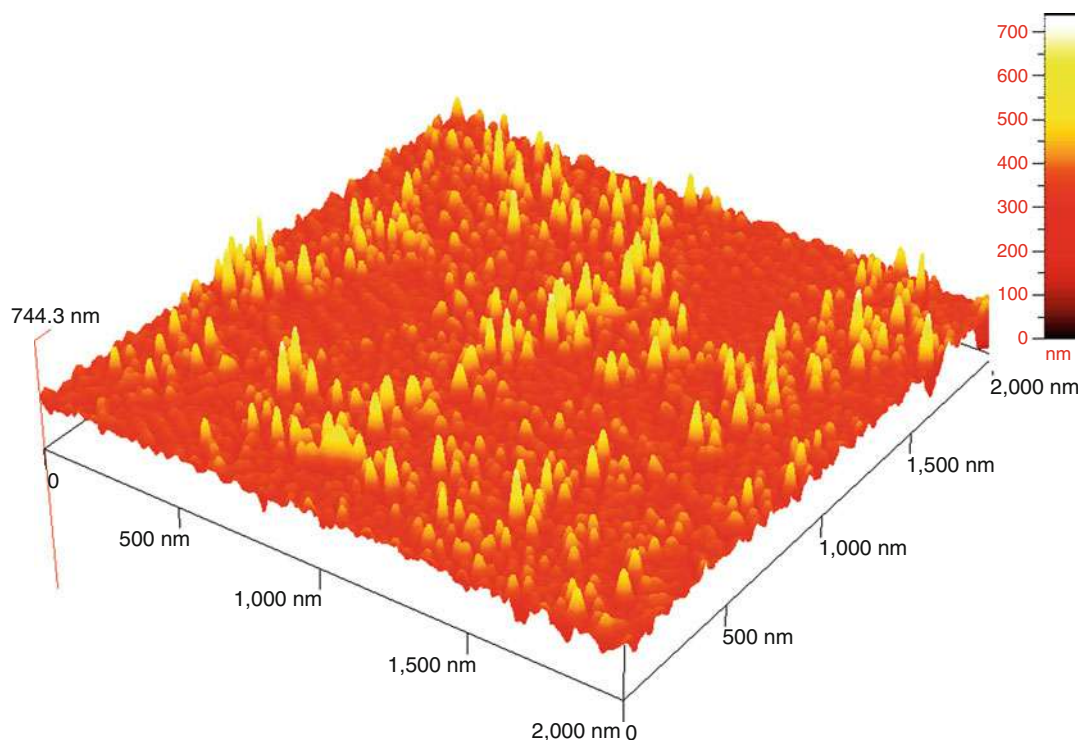
sensitive to the local environment. Some research groups are exploring biosensors based on the SPR exhibited by metal nanoparticles (Haes and Van Duyne, 2002).

In electrochemical biosensors

One-dimensional (1-D) nanostructures, such as CNT and semiconductor- or conducting polymer nanowires, are particularly attractive materials for working electrode in biosensors. Nature of biosensing surface is very important, namely, the prolonged use of the sensor and an anticipated extended storage and working stability. High surface-to-volume ratio and electron transport properties of CNT opens the possibility of developing superior electrochemical sensing devices, ranging from amperometric enzyme electrodes to label-free DNA hybridization biosensors (Zhang et al., 2009). The possibility of direct electron-transfer between enzymes and electrode surfaces could pave the way for superior reagentless biosensing devices, as it obviates the need for co-substrates or mediators and allows efficient transduction of the bio-recognition event. “Trees” of aligned CNT in the nanoforest, prepared by self-assembly, can act as molecular wires to allow electrical communication between the underlying electrode and redox proteins covalently attached to the ends of the SWCNT (Gooding et al., 2003). Viswanathan et al. (2009) demonstrated that vertically aligned SWCNT on gold electrode for pesticides determination (Figure 1). Arrays of nanoscopic gold tubes or wires have been prepared by electroless deposition of the metal within the pores of polycarbonate particle track-etched membranes (Marc and Sophie, 2003). A sensitive and selective genomagnetic assay for the electrochemical detection of food pathogens based on in situ DNA amplification with magnetic primers reported by Lermo et al. (2007). Liposomes are microscopic, fluid-filled, pouches with endless walls that are made of layers of phospholipids identical to the phospholipids that make up cell membranes. Electroactive marker encapsulated immuno liposomes are typically used as signal amplifier for electrochemical immunoassays (Viswanathan et al., 2006). Chitosan (CS) is the second abundant polysaccharide and a cationic polyelectrolyte present in nature. Chitosan nanoparticles are promising biometarials for various analytical applications. Ferrocene-conjugated chitosan nanoparticles were used as the electroactive indicator of hybridization (Kerman et al., 2008).

Electronic tongue

Electronic tongue systems are hybrid micro or nanoarrays of electronic sensors that measure and compare tastes. E tongue is mainly based on potentiometric, voltammetric, ion-selective field-effect transistor (ISFET), piezoelectric, and optical sensors with pattern recognition tools for data processing. The information given by each sensor is complementary and the combination of all sensors results generates a unique fingerprint. Most of the detection thresholds of sensors are similar or better than those of



Nanomaterials in Soil and Food Analysis, Figure 1 Atomic force microscopic image of ssDNA-wrapped single-walled carbon nanotube (SWCNT) self-assembled monolayer on Au(111) surface (Viswanathan et al., 2009).

human receptors. The electronic tongue appeared to be capable of distinguishing between different sorts of beverages: natural and artificial mineral waters, individual and commercial brands of coffee, flesh food, and commercial and experimental samples of soft drinks containing different sweeteners (Scampicchio et al., 2008). Ciosek and Wroblewski (2007) have reviewed about recent developments of multisensor array based electronic tongue for food and soil analysis.

Electronic nose

Electronic nose is a specific kind of semiconducting sensor arrays that can mimic the natural olfaction sense, according to the electronic response (e.g., voltage, resistance, conductivity) arising from the different gas sensors, usually metal-oxide chemosensors. After exposure of the volatile compounds to the sensor array, a signal pattern is collected and results are evaluated with multivariate analysis or processed by an artificial neural network. Arrays of these nanosensors are able to detect molecules on the order of one part per million, sniffing molecules out of the air or taste them in liquid, suggesting applications in foods and food industry. A novel hybrid chemical sensor array composed of individual In_2O_3 nanowires, SnO_2 nanowires, ZnO nanowires, and single-walled carbon nanotubes with integrated micromachined hotplates for sensitive gas discrimination was demonstrated by

Chen et al. (2009). Mycotoxins are secondary metabolites that mold produce naturally from some fungal species. Many researchers have reported efficient e-nose application such as mycotoxins analysis in grains (Falasconi et al., 2005), *Salmonella typhimurium* in stored beef (Zhang et al. 2008).

Mass-sensitive sensors

Researchers have taken advantage of the unique coupled semiconducting and piezoelectric properties of metal oxide nanowires to create a new class of electronic components and devices that could provide the foundation for a broad range of sensor applications. Plata et al. (2008) reported the microcantilever-based sensor for the determination of total carbonate in soil.

Conclusions

Soil and food analysis has become a very important and interesting area of research because of the rapid expansion of food trade and awareness of organic farming. Quality food is important both for consumer protection and also for the food industry. Nanomaterials such as nanoparticles, nanowires, and nanotubes open a new door as sensing platforms for sensor applications. They have allowed introducing novel strategies in sensors and bio-sensor technology. In particular, the development and application of nanomaterials in soil and food analysis are discussed, with focus on sensors, separation and

extraction techniques, including the use of nanomaterials as transducer elements for sensors. Although not fully implemented yet, tiny sensors and monitoring systems enabled by nanotechnology will have a large impact on future precision farming methodologies. The prediction is that nanotechnology will transform the entire food industry, changing the way food is produced, processed, packaged, transported, and consumed.

Bibliography

- Chen, P. C., Ishikawa, F. N., Chang, H. K., Ryu, K., and Zhou, C., 2009. A nanoelectronic nose: a hybrid nanowire/carbon nanotube sensor array with integrated micromachined hotplates for sensitive gas discrimination. *Nanotechnology*, **20**, 125503–125511.
- Ciosek, P., and Wroblewski, W., 2007. Sensor arrays for liquid sensing – electronic tongue systems. *The Analyst*, **132**, 963–978.
- Eggins, B., 2002. Chemical sensors and biosensors. In *Analytical Techniques in the Sciences*. West Sussex: Wiley.
- Falasconi, M., Gobbi, E., Pardo, M., Torre, M. D., Bresciani, A., and Sberveglieri, G., 2005. Detection of toxigenic strains of fusarium verticillioides in corn by electronic olfactory system. *Sensors and Actuators B*, **108**, 250–257.
- Gooding, J. J., Wibowo, R., Liu, J. Q., Yang, W., Losic, D., Orbons, S., Mearns, F. J., Shapter, J. G., and Hibbert, D. B., 2003. Protein electrochemistry using aligned carbon nanotube arrays. *Journal of the American Chemical Society*, **125**, 9006–9007.
- Haes, A. J., and Van Duyne, R. P., 2002. A nanoscale optical biosensor: sensitivity and selectivity of an approach based on the localized surface plasmon resonance spectroscopy of triangular silver nanoparticles. *Journal of the American Chemical Society*, **124**, 10596–10604.
- Kerman, K., Saito, M., and Tamiya, E., 2008. Electroactive chitosan nanoparticles for the detection of single-nucleotide polymorphisms using peptide nucleic acids. *Analytical and Bioanalytical Chemistry*, **391**, 2759–2767.
- Lermo, A., Campoy, S., Barbé, J., Hernández, S., Alegret, S., and Pividori, M. I., 2007. In situ DNA amplification with magnetic primers for the electrochemical detection of food pathogens. *Biosensors and Bioelectronics*, **22**, 2010–2017.
- Marc, D., and Sophie, D.-C., 2003. Immobilisation of glucose oxidase within metallic nanotubes arrays for application to enzyme biosensors. *Biosensor and Bioelectronics*, **18**, 943–951.
- Nielsen, S. S., 2003. Introduction to food analysis. In Nielsen, S. S. (ed.), *Food Analysis*, 3rd edn. New York: Kluwer academic/Plenum, pp. 3–15.
- Nilsson, C., and Nilsson, S., 2006. Nanoparticle-based pseudostationary phases in capillary electrochromatography. *Electrophoresis*, **27**, 76–83.
- Patolsky, F., Zheng, G., and Lieber, C., 2006. Nanowire-based biosensors. *Analytical Chemistry*, **78**, 4260–4269.
- Plata, M. R., Hernando, J., Zougagh, M., Contento, A. M., Villasenor, M. J., Sánchez-Rojas, J. L., and Ríos, A., 2008. Characterization and analytical validation of a microcantilever-based sensor for the determination of total carbonate in soil samples. *Sensors and Actuators – B*, **134**, 245–251.
- Rao, C. N. R., Muller, A., and Cheetham, A. K., 2004. *The Chemistry of Nanomaterials*. WILEY-VCH Verlag GmbH: Weinheim.
- Scampicchio, M., Ballabio, D., Arecchi, A., Cosio, S. M., and Mannino, S., 2008. Amperometric electronic tongue for food analysis. *Microchimica Acta*, **163**, 11–21.
- Shi, J., Zhu, Y., Zhang, X., Baeyens, W. R. G., and Campana, A. M. G., 2004. Recent developments in nanomaterial optical sensors. *Trends in Analytical Chemistry*, **23**, 351–360.
- Smith, A., and Nie, S., 2004. Chemical analysis and cellular imaging with quantum dots. *The Analyst*, **129**, 672–677.
- Tully, E., Hearty, S., Leonard, P., and Kennedy, R., 2006. The development of rapid fluorescence-based immunoassays, using quantum dot-labelled antibodies for the detection of *Listeria monocytogenes* cell surface proteins. *International Journal of Biological Macromolecules*, **39**, 127–134.
- Viswanathan, S., Radecka, H., and Radecki, J., 2009. Electrochemical biosensor for pesticides based on acetylcholinesterase immobilized on polyaniline deposited vertically assembled carbon nanotubes wrapped with ssDNA. *Biosensors and Bioelectronics*, **24**, 2772–2777.
- Viswanathan, S., Wu, L.-c., Huang, M.-R., and Ho, J.-a. A., 2006. Electrochemical immunosensor for cholera toxin using liposomes and poly(3, 4-ethylenedioxythiophene)-coated carbon nanotubes. *Analytical Chemistry*, **78**, 1115–1121.
- Wagner, G., and Guilbault, G. G. (eds), 1994. *Food Biosensor Analysis*. New York: Marcel Dekker, p. 31.
- Wang, J., 2005. Nanomaterial-based electrochemical biosensors. *The Analyst*, **130**, 421–426.
- Zhang, X., Guo, Q., and Cui, D., 2009. Recent advances in nanotechnology applied to biosensors. *Sensors*, **9**, 1033–1053.
- Zhang, Z., Tong, J., Chen, D.-h., and Lan, Y a-b., 2008. Electronic nose with an air sensor matrix for detecting beef freshness. *Journal of Bionic Engineering*, **5**, 67–73.
- Zhang, Z., Wang, Z., Liao, Y., and Liu, H., 2006. Applications of nanomaterials in liquid chromatography: opportunities for separation with high efficiency and selectivity. *Journal of Separation Science*, **29**, 1872–1878.

Cross-references

- [Agrophysical Objects \(Soils, Plants, Agricultural Products, and Foods\)](#)
[Chemical Imaging in Agriculture](#)
[DNA in Soils: Mobility by Capillarity](#)
[Electrochemical Measurements in Soils](#)
[Enzymes in Soils](#)
[Leaching of Chemicals in Relation to Soil Structure](#)
[Oxidation–Reduction Reactions in the Environment](#)
[Physical Degradation of Soils, Risks and Threats](#)
[Precision Agriculture: Proximal Soil Sensing](#)
[Quality of Agricultural Products in Relation to Physical Conditions](#)

NATURE CONSERVATION MANAGEMENT

Tadeusz J. Chmielewski

Department of Landscape Ecology and Nature Conservation, University of Life Sciences, Lublin, Poland

Synonyms

Biological resources management

Definition

Nature conservation management (NCM) is a system of actions aimed at permanent conservation and sustainable use of the resources and values of the natural environment.

The main elements of NCM system

The growing scale of anthropogenic transformation of the environment causes that NCM is becoming an increasingly important field of human activity and requires higher and higher qualifications. At present, the NCM system (NCMS) comprises the integrated functioning of five subsystems (Chmielewski, 2007): (1) subsystem of diagnosis (DS); (2) planning subsystem (PS); (3) decision-taking subsystem (DTS); (4) subsystem of tasks realization (TRS); (5) certificate and control subsystem (CCS).

- (1) For rational management of nature conservation we must first acquire knowledge about the functioning of natural ecosystems and about their responses to various human actions (Pullin, 2007; Wu and Hobbs, 2007). Organization for economic co-operation and development (OECD) presents the organization of the system of natural environment diagnosis as the following sequence: Drivers – Pressures – State – Impact – Response, referred to by the abbreviation DPSIR model (Watt and Young, 2007). **Driving forces** are anthropic activities and processes that cause pressures production (agriculture, industry, transport, etc.), consumption, recreation, etc. **Pressures** are described as direct stress from the anthropic system on the natural environment: release of polluting substances, radiation emissions, use of soil, intake of natural resources, and other changes of the natural environment. **State** – means conditions and tendencies in the natural environment, air, water and soil quality, global temperature, loss of biodiversity, etc. The description of the state of the environment is not easy: it should comprise at least four stages: (a) retrospection, that is, analysis of changes that have taken place in the environment over the last several decades; (b) inventory of nature resources; (c) valuation of nature resources; and (d) analysis of the potential of the natural environment (Chmielewski, 2001). **Impacts** are effects on the anthropic system due to changes in the natural environment: negative consequences on human health, economic loss in production activities, floods, etc. **Responses** are actions of the anthropic system aimed at solving environmental problems (prevention, pollutants elimination, biodiversity conservation, ecosystem restoration, ecological compensation, etc.) (Fiedler and Jain, 1992). The “**Responses**” element, however, is not a typical element of the diagnostic system as it comprises elements of three further subsystems of the NCMS (2–4).
- (2) The results of diagnosis of the state of the natural environment constitute the basis for initiating the planning subsystem, the main element of which are *nature management plans* (or nature conservation plans) for the most valuable areas: national parks, nature reserves, Natura 2000 sites, landscape parks, etc., as well as the *sustainable development strategies* and *local development plans* for the various levels of hierarchy of administrative organization of the country.

Nature management plans are mostly worked out by the governmental nature conservation services; however, in the process of their preparation local government representatives take part as well. Achievement of compatibility and agreement of the provisions of the nature conservation plans with the local development plans are of key importance for smooth management of resources of the natural environment.

- (3) On the basis of these two types of plans, the administrative decisions concerning nature conservation actions as well as land-use changes, housing and road construction, development of services, and other activities are undertaken. They may pertain, for example, to water damming, stand reconstruction, moor plant succession control, but also to the architecture style of buildings, tourist facilities, and creating tourist routes and educational paths. All administrative decision should contain relevant provisions concerning the conservation of natural values, sustainable utilization of nature resources, and harmonious scenic beauty design. Unfortunately, many decisions – particularly those concerning new economic investments, neglect the ecological conditions or marginalize them.
- (4) and (5) Observance of the provisions contained in administrative decisions is of fundamental importance for nature conservation and landscape quality. This purpose is served by a system of certification, control, standards, and indexes of quality of the environment (Keulartz and Leistra, 2008; Schmidt et al., 2008). However, losses observed in the resources and values of the natural environment indicate that in many regions that system is not effective. For a better nature conservation management it is necessary to develop urgently a network of biodiversity and landscape diversity monitoring as well as urban monitoring. It is also necessary to systemize the gathering of these data, by a common introduction of Spatial Information Systems based on advanced computing technologies. Such systems are one of the key instruments facilitating effective protection and sustainable management of resources and unique natural values areas on the world scale.

Key instruments for effective functioning of the five subsystems of NCMS

Each of the five subsystems of the NCMS has at its disposal specialist instruments that should ensure its effective functioning. Of key importance for the subsystem of diagnosing, the state of the natural environment is the financing and organization of research and of the network of monitoring of the natural environment. For better understanding of the functioning of nature and for the purpose of development of effective methods of nature resources management theories are constructed as well as models for conservation and wildlife management (Samson and

Knopf, 1996; Harris, 2007). For the quality of the planning subsystem, of fundamental importance is the legal system, the quality of education of landscape ecologists, landscape architects, space planners and engineers, as well as the operating conditions of design companies and offices. The quality of administrative decisions depends primarily on the quality of the relevant legislation and on the level of professionalism of administration officers and on the quality of internal audit. In the process of realization of the plans and decisions, that is, in the course of the practical utilization of nature resources, highly important is the ecological policy of the particular countries, their legal systems, ecological education of the people, education of the administrative cadre, organization of the system of certification and audit. At all levels of organization and at all stages of implementation an important instrument of the NCMS should be the cost-effectiveness analysis, permitting to identify which NCM methods and techniques should be applied for the invested funds and undertaken organization activities to bring the best ecological effects (Wätzold, 2005).

Conclusion

NCM is becoming a more and more extensive and highly specialist branch of knowledge and a broader and broader forum of practical activity. The NCM system has an extensive infrastructure and numerous instruments that should ensure its effective operation. In spite of all this, we are still witnessing many processes unfavorable for nature, such as the shrinking of the ecological space, landscape structure fragmentation, and loss of biodiversity. These challenges necessitate further intensive work on the ecological education of the society and on the development of the NCM system at the level of regions, countries, continents, and the whole biosphere.

Bibliography

- Chmielewski, T. J., 2001. *System of Spatial Planning Harmonizing Nature and Economy*. Lublin: Technical University in Lublin, Vols. 1–2, in Polish, English summary.
- Chmielewski, T. J. (ed.), 2007. *Nature Conservation Management: From Idea to Practical Results. European Commission 6th Framework Program: ALTER-Net*. Lublin/Łódź/Helsinki/Aarhus: PWZN Print 6.
- Fiedler, P. L., and Jain, S. K., 1992. *Conservation Biology: The Theory and Practice of Nature Conservation, Preservation and Management*. New York: Chapman and Hall.
- Harris, G., 2007. *Seeking Sustainability in an Age of Complexity*. New York/Melbourne/Madrid/Cape Town/Singapore/São Paulo: Cambridge University Press.
- Keulartz, J., and Leistra, G. (eds.), 2008. *Legitimacy in European Nature Conservation Policy. Case Studies in Multilevel Governance. The International Library of Environmental, Agricultural and Food Ethics*. Berlin/Heidelberg: Springer, Vol. 14.
- Pullin, A. S., 2007. *Conservation Biology*. New York/Melbourne/Madrid/Cape Town/Singapore/São Paulo: Cambridge University Press.
- Samson, F. B., and Knopf, F. K. (eds.), 1996. *Ecosystem Management. Selected Readings*. New York/Berlin/Heidelberg/Barcelona/Budapest/Hong-Kong/London: Springer.
- Schmidt, M., Glasson, J., Emmelin, L., and Helbron, H. (eds.), 2008. *Standards and Thresholds for Impact Assessment*. Berlin/Heidelberg: Springer, Vol. 3. Environmental Protection in the European Union.
- Watt, A. D., and Young, C., 2007. Nature Conservation in the EU and the DPSIR framework. In Chmielewski, T. J. (ed.), *Nature Conservation Management: From Idea to Practical Results. European Commission 6th Framework Program: ALTER-Net*. Lublin/Łódź/Helsinki/Aarhus: PWZN Print 6, pp. 15–35.
- Wätzold, F., 2005. Why be wasteful when preserving a valuable resource. A review article on the cost-effectiveness of European biodiversity conservation policy. *Biological Conservation*, **123**, 327–338.
- Wu, J., and Hobbs, R. J. (eds.), 2007. *Key Topics in Landscape Ecology*. New York/Melbourne/Madrid/Cape Town/Singapore/São Paulo: Cambridge University Press.

Cross-references

[Climate Change: Environmental Effects](#)

[Monitoring Physical Conditions in Agriculture and Environment Wetlands, Management, Degradation and Restoration](#)

NEURAL NETWORKS IN AGROPHYSICS

Krzysztof Lamorski

Institute of Agrophysics, Polish Academy of Sciences, Lublin, Poland

Synonyms

Artificial Intelligence; Artificial Neural Network; Neural Network

Definition

Artificial neural network (ANN) – a mathematical model, based on the calculations made by the network of interconnected artificial neurons or perceptrons. Neural networks are a subclass of wider range of calculation techniques called *soft learning techniques*.

Introduction

First ideas concerning artificial neural networks are dated back to 1940s, when for the first time model of an artificial neuron was formulated (McCulloch and Pitts, 1943) and basic methods of neural networks training was developed (Hebb, 1949). Further theoretical developments and first practical applications of neural networks took place in 1950s and 1960s. The first image classification system was built (Rosenblatt, 1958). A new effective method of network learning-supervised training was developed (Widrow and Hoff, 1960). The multipurpose neural networks ADALINE and MADALINE, used for weather forecasting, in adapting control systems, and for image recognition, was built (Widrow, 1962). After initial period of rapid developments, works on neural networks stagnated some, until 1980s, when performance of computational systems increased enough, to allow for new ANN applications. New types of neural networks were

discovered and a new type of training algorithm was developed (Hopfield, 1982; Kohonen, 1984). From 1980s period of rapid theoretical developments and increasing practical applications started.

Nowadays artificial neural networks emerged into one of the wider used soft learning techniques. The artificial neural networks are used in scientific developments and in wide range of practical applications. Many agrophysical objects and processes may be modeled by artificial neural networks.

Basic concepts of neural networks

Artificial neural networks are mathematical models which allows for data processing or information storage. These mathematical models consist of neural network themselves and algorithms or methods for neural network training and evaluation of its performance. Concept of artificial neural network was taken from organization of biological brain. Neural network is a set of interconnected artificial neurons and links between them.

Artificial neurons, called also in ANN nomenclature a perceptron, have properties similar to real brain's biological neuron. It has many inputs, called *dendrites*, and only one output – *axon*. In fact, behavior of the perceptron is modeled by simple nonlinear function of the form [Equation 1](#):

$$y = f_{\text{act}} \left(w_0 + \sum_{i=0}^n w_i x_i \right) \quad (1)$$

where y – is an output signal from neuron considered, x_i – are input signals from other neurons, w_i – are weights specific for i -th dendrite of artificial neuron, w_0 – is a constant bias signal used in many neural networks types (called also inhibitory input), finally f_{act} – is a so called activation function. Based on this equation, the output of each neuron is simply a weighted sum of input signals, processed by additional activation function.

There are many types of activation functions used in ANN developments. Some of them commonly used are grouped in [Table 1](#).

In neural networks, output from one neuron is connected to inputs of other neurons. This net of interconnected neurons has parallel data processing capabilities, and may be used to store the information.

There are many neural networks topologies, but in agrophysical research two of them are commonly used. For applications based on evaluation of the output, based on input variables, multilayer neural networks are used.

Neural Networks in Agrophysics, Table 1 Sample activation functions

Binary (0,1)	Log-sigmoid	Hyperbolic	Linear
$f_{\text{act}}(z) = \begin{cases} 0, & z < 0 \\ 1, & z \geq 0 \end{cases}$	$f_{\text{act}}(z) = \frac{1}{1 - e^{-z}}$	$f_{\text{act}}(z) = \frac{e^z - e^{-z}}{e^z + e^{-z}}$	$f_{\text{act}}(z) = z$

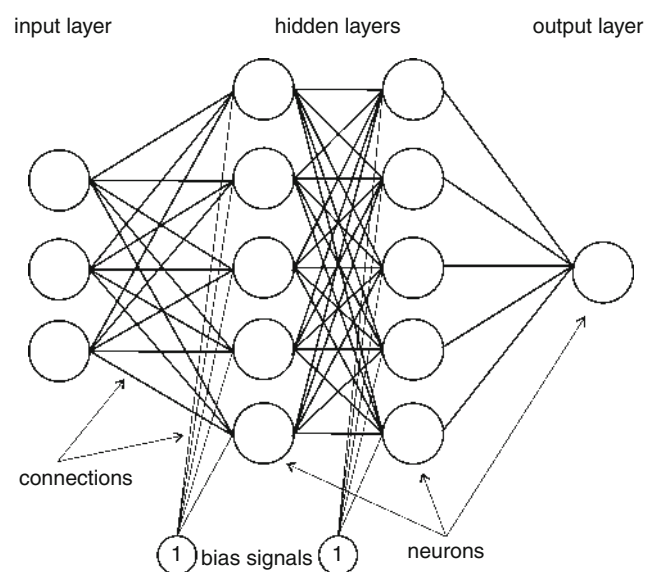
These neural networks are mainly feedforward neural networks, but some applications utilize feedback neural networks also. If modeled problem is based on some kind of classification, self-organizing map (SOM) neural networks are typically used.

The wider range of applications uses single layer or multilayer feedforward network. Such network has layered architecture, see [Figure 1](#). The first neuron layer consists of input neurons. These neurons are used to enter processed data into the network. Following input layer are one or more hidden layers. The last is the output layer, values of neurons from this layer represent results generated by neural network for specific input values. Outputs of neurons in feedforward networks from one layer are connected to inputs of neurons in the next layer. This allows for trained network to evaluate its output for input variables.

Common feature of feedback neural networks is its recurrence. Due to this, outputs of neurons from one layer are connected to input of the same layer. This kind of neural network may be used for modeling of processes, because of calculated output values changes for each subsequent evaluation.

Training of the neural networks

Neural network consists of neurons and weights describing connections between neurons. While number and type of neurons for specific neural network is fixed, weights for each connection may be changed. Processes of adjustment of weight values have a crucial role for applications of neural networks, and it is called neural network training. There are many algorithms/methods used for ANN training. Generally each neural network topology has specific



Neural Networks in Agrophysics, Figure 1 Feedforward neural network.

training method. Training methods may be generalized into two categories: supervised training and unsupervised training.

In most of agrophysical applications, where feedforward or feedback neural networks are used, proper method of network training is some kind of supervised training technique. Supervised training assumes knowledge of proper output responses for set of inputs. The origin of this dataset is application dependent, but the most frequent source of training data is some kind of experiment, survey, or measurement. The basic idea of supervised neural network training is to compare results/outputs generated by neural network for inputs, for which proper output values are known. Based on difference between evaluated by network output results and known outputs from training dataset, called training error, weights of neural network are subsequently adjusted.

Data which are used for learning neural network are commonly divided into two disjointed datasets: training dataset and testing dataset. Training dataset is used for training of the neural network, while on the testing dataset performance of trained neural network is evaluated. The aim of neural network training is to adjust neural network weights in such way that error for testing dataset, called test error, will be minimal. The smaller the test error is, the better generalization properties the neural network has, and will better perform for new, unknown input data.

Presentation of training data to the network and weight adjustments are repeated many times, until neural network performs well. Generally, training error decreases in subsequent neural network training procedure repetitions. However testing error, which is the criterion for neural network evaluation, in some circumstances, may remain at constant level, or even grow up slightly after initial decrease. This phenomenon is known as over learning that occurs especially when training dataset is too small in comparison to number of neurons in the neural network. When over learning happens, testing error increases for subsequent steps of learning, while training error decreases.

Agrophysical applications

Basic tool for scientific development utilizing artificial neural networks methodology is appropriate software. There are many commercially and freely software packages available. Beside many others, some freely available software is worth to mention: SNNS (Zell et al., 1995) and its successor JavaNNS. EMERGENT (Aisa et al., 2008), and program R (R Development Core Team, 2010) with appropriate modules are free multiplatform neural network solutions.

Neural networks may be used in many fields of agrophysical developments. Typical applications include: modeling of transport processes in the soil medium, modeling of hydrophysical properties of soils, soil classification based on different criteria, crop production modeling, or food quality evaluation. These applications

of neural networks can be generalized into two categories: problems based on prediction of some property and problems based on some kind of classification.

Soil science

One of the fields where neural networks are extensively used is pedotransfer functions (PTF) development. Pedotransfer functions are mathematical models, which allow for approximating difficult measurable soil parameters, based on some easily measurable input information. Typically, soil water retention curve and hydraulic conductivity of soils are evaluated by PTFs. For PTF development many techniques may be used (Wösten et al., 2001), from legacy regression models (Walczak et al., 2006) to neural networks and beyond (Lamorski et al., 2008).

For PTFs development feed forward neural networks are used, as these applications are based on approximation. Typically among others input parameters for PTFs evaluating retention curve are: particle size distribution, soil porosity, bulk density, and organic carbon content. Some PTF models use as input parameter measured water content for one specific value of water potential. The output of neural network is a retention curve approximation. There are numerous models used for evaluating soil water retention curve, which may be divided into two classes: models which evaluate water content for selected values of water potential (Lamorski et al., 2008; Pachepsky et al., 1995) and models which evaluate parameters of some kind of retention curve approximation function, mainly in the form of Mualem and van Genuchten approximation (Schaap and Leij, 1998; Minasny and McBratney, 2002).

The other usage of ANN to evaluation of hydrological properties of soils are PTFs for soil hydraulic conductivity approximation. Soil hydraulic conductivity is one of parameters which influences soil water transport phenomena. For many purposes approximations of value of hydraulic conductivity may be used instead of measured values. One of the method, which may be used for soil hydraulic conductivity approximation, is to use neural network modeling. This approach includes models for saturated hydraulic conductivity evaluation (Merdun et al., 2006; Schaap et al., 1998). Unsaturated soil hydraulic conductivity may be approximated by neural networks also (Schaap and Leij, 2000).

Soil classification is the other application of ANN to soil science. One of the commonly used soil classification systems are texture based classification systems. They allow for determination to which class soil belongs, based on its granulometric distribution. For other purposes, different classification criteria than soil texture may be used. The common problem in soil classification systems is that one wants to determine some kind of qualitative in nature soil parameter. In soil surveys such parameters evaluation are made by properly trained and experienced researcher. It is not easy task to map such soil features from a set of quantitative, easily measurable soil parameters, but there are attempts to build such

expert systems. One of important soil properties is its aggregation structure. Soil aggregation is a qualitative parameter which cannot be directly connected to soil quantitative parameters. Although there were attempts to classify soil to one of three aggregate classes (granular, blocky or massive) based on soil granulometric composition and organic carbon content using feed forward neural networks (Levine et al., 1996).

Crop production and food quality

The other field of investigations where artificial neural networks are used is crop production, especially with precision agriculture relying on advanced monitoring, measurement ([Precision Agriculture: Proximal Soil Sensing](#)) and modeling techniques. Fertilization is one of the key practices used in crop production, proper dosage of fertilizer, appropriate for current field conditions may be determined by neural networks (Yu et al., 2010). Prediction of crop growth is another example of usage of neural network. There are ANN models which allow for crop yield prediction based on some input parameters (Green et al., 2007). Irrigation is a common agricultural technique. Effective usage of water is an important objective; artificial neural networks may be also used in optimization of water usage (Morimoto et al., 2007). Food quality is very important and may be influenced by many external factors, during crop harvesting, storage, and processing. Some properties of crops important for food quality may be modeled by ANN. Example applications include method of estimation of sorption isotherm for rice (Amiri-Chayjan and Esna-Ashari, 2010), which is important factor influencing rice storage conditions and has impact on rice quality. Chemicals are commonly used in tillage practice, for crop fertilization, or protection against pests. Unfortunately, if inappropriately used, chemical compounds may accumulate in crops and influence quality of food produced. The key point is to prevent food contamination, by optimization of chemicals usage (Du et al., 2008). In some circumstances toxins may be introduced to food in naturally occurring phenomena. One of application of ANN allows for predicting contamination of peanuts by aflatoxin produced by naturally occurring mildew (Henderson et al., 2000) in dependence of plant growth conditions.

Modeling approaches

Processes occurring in agrophysical objects may be modeled using strict mathematical, physical, or chemical methodology. In such approach phenomena are modeled exactly. Although in some practical applications rigorous modeling methodology is not needed. Artificial neural networks are the tool which may be used in such circumstances. The main idea of learning based modeling is to build and train ANN which will predict approximated values, based on previously registered values. Forecasting neural networks may be used for modeling wide range of agrophysical processes. Possible applications include

forecasting of soil moisture, soil temperature, or contaminant concentration. There is a known model (Raju, 2001) utilizing ANN to evaluate soil temperature and evaporation, based on air relative humidity, wind speed, and air temperature. The other study (Han and Felker, 1997) describes method of estimation daily soil water evaporation, where neural network input factors are: air humidity, air temperature, wind speed, and soil water content. Soil moisture predictions are also possible (Liu et al., 2008), neural network was used for prediction of future soil moisture at specified depth, based on previous values of soil moisture readings from the same depth. Also they are successfully used for modeling of post-harvest drying process ([Neural Networks in the Modeling of Drying Processes](#)).

Summary

Proper description of processes occurring in the soil–plant–atmosphere continuum has a crucial role in agrophysical development. Artificial neural networks are useful for a range of agrophysical applications, including estimates of soil water retention, movement, evaporation, temperature, crop growth, post-harvest drying process, and food quality. ANN descriptions are particularly useful when strict measurement or modeling methods cannot be used.

Bibliography

- Asua, B., Mingus, B., and O'Reilly, R. C., 2008. The emergent neural modeling system. *Neural Networks*, **21**, 1146–1152. <http://grey.colorado.edu/emergent>
- Amiri-Chayjan, R., and Esna-Ashari, M., 2010. Comparison between mathematical models and artificial neural networks for prediction of sorption isotherm in rough rice. *International Agrophysics*, **24**, 1–7.
- Du, C., Tang, D., Zhou, J., Wang, H., and Shaviv, A., 2008. Prediction of nitrate release from polymer-coated fertilizers using an artificial neural network model. *Biosystems Engineering*, **99**, 478–486.
- Green, T. R., Salas, J. D., Martinez, A., and Erskine, R. H., 2007. Relating crop yield to topographic attributes using Spatial Analysis Neural Networks and regression. *Geoderma*, **139**, 23–37.
- Han, H., and Felker, P., 1997. Estimation of daily soil water evaporation using an artificial neural network. *Journal of Arid Environments*, **37**, 251–260.
- Hebb, D., 1949. *The Organization of Behaviour: A Neuropsychological Theory*. New York: Wiley.
- Henderson, C. E., Potter, W. D., McClendon, R. W., and Hoogenboom, G., 2000. Predicting aflatoxin contamination in peanuts: a genetic algorithm/neural network approach. *Applied Intelligence*, **12**, 183–192.
- Hopfield, J., 1982. Neural networks and physical systems with emergent collective computational abilities. *Proceedings of the National Academy of Sciences of the United States of America*, **79**, 2554–2558.
- Kohonen, T., 1984. *Self-Organization and Associative Memory*. Berlin: Springer-Verlag.
- Lamorski, K., Pachepsky, Y., Śląwiński, C., and Walczak, R., 2008. Using support vector machines to develop pedotransfer functions for water retention of soils in Poland. *Soil Science Society of America Journal*, **72**, 1243–1247.
- Levine, E., Kimes, D., and Sigillito, V., 1996. Classifying soil structure using neural networks. *Ecological Modelling*, **92**, 101–108.

- Liu, H., Xie, D., and Wu, W., 2008. Soil water content forecasting by ANN and SVM hybrid architecture. *Environmental Monitoring and Assessment*, **143**, 187–193.
- McCulloch, W., and Pitts, W., 1943. A logical calculus of the ideas imminent in nervous activity. *The Bulletin of Mathematical Biophysics*, **5**, 115–133.
- Merdun, H., Cinar, Ö., Meral, R., and Apan, M., 2006. Comparison of artificial neural network and regression pedotransfer functions for prediction of soil water retention and saturated hydraulic conductivity. *Soil & Tillage Research*, **90**, 108–116.
- Minasny, B., and McBratney, A. B., 2002. The Neuro-m method for fitting neural network parametric pedotransfer functions. *Soil Science Society of America Journal*, **66**, 352–361.
- Morimoto, T., Ouchi, Y., Shimizu, M., and Baloch, M. S., 2007. Dynamic optimization of watering Satsuma mandarin using neural networks and genetic algorithms. *Agricultural Water Management*, **93**, 1–10.
- Pachepsky, Y. A., Timlin, D., and Varallyay, G., 1995. Artificial neural networks to estimate soil water retention from easily measurable data. *Soil Science Society of America Journal*, **60**, 727–733.
- Raju, G. K., 2001. Prediction of soil temperature by using artificial neural networks algorithms. *Nonlinear Analysis*, **46**, 1737–1748.
- R Development Core Team, 2010. R: A language and environment for statistical computing. R foundation for statistical computing, Vienna, Austria (<http://www.R-project.org>).
- Rosenblatt, F., 1958. The perceptron: a probabilistic model for information storage and organization in the brain. *Psychological Review*, **65**, 386–408.
- Schaap, M. G., and Leij, F. J., 1998. Using neural networks to predict soil water retention and soil hydraulic conductivity. *Soil & Tillage Research*, **47**, 37–42.
- Schaap, M. G., and Leij, F. J., 2000. Improved prediction of unsaturated hydraulic conductivity with the Mualem-van Genuchten model. *Soil Science Society of America Journal*, **64**, 843–851.
- Schaap, M. G., Leij, F. J., and van Genuchten, M. T., 1998. Neural network analysis for hierarchical prediction of soil hydraulic properties. *Soil Science Society of America Journal*, **62**, 847–855.
- Walczak, R., Moreno, F., Ślawiński, C., Fernandez, E., and Arregi, J., 2006. Modeling of soil water retention curve using soil solid phase parameters. *Journal of Hydrology*, **329**, 527–533.
- Widrow, B., 1962. Generalisation and information storage in networks of Adaline ‘neurons’. In Jovitz, M., Jacobi, G., and Goldstein, G. (eds.), *Self-Organizing Systems*. New York: Spartan Books, pp. 435–461.
- Widrow, B., and Hoff, M., 1960. Adaptive switching circuits. *Western Electric Show and Convention Record*, **4**, 96–104.
- Wösten, J. H., Pachepsky, Y. A., and Rawls, W., 2001. Pedotransfer functions: bridging the gap between available basic soil data and missing soil hydraulic characteristics. *Journal of Hydrology*, **251**, 123–150.
- Yu, H., Liu, D., Chen, G., Wan, B., Wang, S., and Yang, B., 2010. A neural network ensemble method for precision fertilization modeling. *Mathematical and Computer Modelling*, **51**, 1375–1382.
- Zell, A., Mamier, G., Vogt, M., Mache, N., Hübner, R., Döring, S., Hermann Kai-Uwe, Soyez, T., Schmalzl, M., Sommer, T., Hatzigeorgiou, A., Posselt, D., Schreiner, T., Kett, B., Clemente, G., and Wieland, J., 1995. SNNS, Stuttgart Neural Network Simulator – User Manual, Version 4.1. Stuttgart: University of Stuttgart. (<http://www.ra.cs.uni-tuebingen.de/SNNS/>).

Cross-references

- [Agophysical Objects \(Soils, Plants, Agricultural Products, and Foods\)](#)
- [Databases on Physical Properties of Plants and Agricultural Products](#)

[Databases of Soil Physical and Hydraulic Properties](#)
[Hydraulic Properties of Unsaturated Soils](#)
[Hydrometeorological Processes in Soils](#)
[Neural Networks in the Modeling of Drying Processes](#)
[Pedotransfer Functions](#)
[Physical Phenomena and Properties Important for Storage of Agricultural Products](#)
[Physical Properties as Indicators of Food Quality](#)
[Precision Agriculture: Proximal Soil Sensing](#)

NEURAL NETWORKS IN THE MODELING OF DRYING PROCESSES

Istvan Farkas

Department of Physics and Process Control, Szent Istvan University, Gödöllő, Hungary

Synonyms

Artificial intelligence modeling

Definition

Neural network (NN) is an artificial intelligence method in order to determine the relationship between the moisture distribution in the material bed to be dried and the physical parameters of the drying air temperature, humidity, and airflow rate. During its application, an emphasis should be given on the selection aspects of neural network structure and specifically to the influencing parameters as sampling time, randomized training, different training algorithms, number of hidden neurons, number of linked data series, and type of validation data. A properly selected structure of neural network model can be used to determine the moisture distribution in the drying bed. It can also be stated that besides other factors the selection of training and validation input data for NN model has a strong influence on the applicability.

Introduction

Concerning the postharvest processes, besides the energy consumption impacts, the quality issues remain the most determining factor. The main problem in the grain drying process is to determine the moisture content in the material bed. Overdrying requires excessive energy and even can damage the quality of the dried material, especially in case of seed. On the other hand, the grain will be vulnerable to mildew if the moisture content remains high. There is an option to determine the moisture content in the drying bed by measurement but the accuracy of this approach is probably not satisfactory. Weather conditions and dust have a great effect on the accuracy, as well. Another way to determine the moisture distribution is to calculate the moisture content based on drying air parameters using physically based or black-box models. Physically based models give a moderately good result in most cases but it normally takes a great effort to identify their parameters and also to solve the model itself. Derivation of the

classical black-box models seems to be an uncomplicated approach. However, the application of such models is mainly limited to process control.

The artificial neural network is a well-known tool for solving complex problems and it can give reasonable solutions even in extreme cases or in the event of technological faults (Lin and Lee, 1995). Huang and Mujumdar (1993) created a neural network in order to predict the performance of an industrial paper dryer. The neural network model by Jay and Oliver (1996) was used for predictive control. Trelea et al. (1997) successfully used explicit time and recurrent neural networks for modeling the moisture content of thin-layer (5 cm) corn during the drying process and for wet-milling quality at constant airflow rate and absolute humidity and variable temperature. Thyagarajan et al. (1997) modeled an air heater plant for a dryer using a neural network. Sreekanth et al. (1998) predicted psychometric parameters using various neural network models. Kaminski et al. (1998) used a neural network for data smoothing and for modeling material moisture content and temperature. The literature cited clearly encourages further study of the application of artificial neural networks to modeling of postharvest and within that the drying process. However, application of neural networks for drying processes takes a significant consideration to the influence of sampling time, randomized training, different training algorithms, number of hidden neurons, number of linked data series, and type of validation data. The structure of the NN is to be selected to include all the inputs and outputs of the drying system.

Modeling approaches

As a classical way of modeling, the physically based models (PBM) are normally used to determine the performance evaluation of drying process. However, the PHBs make some difficulties in setting up the most appropriate equations, to determine the accurate values of their parameters, and to find the most efficient methods for the solution. At the same time, there is a good option of the use of NN for modeling purposes along with their uncertainties and difficulties in determination their optimal topology and parameters for the given problem, for example, postharvest technology this time. Sometimes, in order to provide input data for training the neural network a well-identified physically based model are considered to use instead of full-scale or laboratory measurements.

Several NN topologies could be considered for the use of modeling the drying process as it was suggested by Farkas et al. (2000a). The choice of a topology depends on careful selection of the input system variables and the controlled output variables, for example, moisture contents in the different layers of the material bed. It should be stated that the selection of NN topology is an essential step.

Training the neural networks

Input data used for training the neural network of different structure should be the same. The drying air

temperature, airflow, and absolute humidity have to be changed randomly to train higher order dynamics, as well. The outlet air temperature and absolute humidity in the layers could be calculated on the basis of an appropriate physically based model because of its difficulty in measurements. In each training loop, each data record can be trained, for example, with back-propagation algorithm (Lin and Lee, 1995). One training step means to calculate the error between the network output and the desired output and to modify the weight of the neural network. During the training process, all the introduced neural network structures have different training speed, for example, the number of calculation loops in order to reach the required accuracy. The cost function expresses the stop condition of the training. The selection of training input data for NN model has a strong influence on the applicability.

Validation the neural networks

For validation purposes, constant and multi-flow data are normally chosen because of the real industrial drying processes. The validation data for multi-flow dryer are taken from outside weather parameters. The airflow is switched between two states to simulate intermittent drying, the air temperature, and humidity considered based on weather condition. The selection of validation input data for NN model has a strong influence on the applicability. During the validation calculation beside the correlation coefficients the average and maximal deviation could be used to estimate the behavior of the neural network model.

Sensitivity of the neural networks

Extensive studies on validation of the NN model have been carried out along with the influences different parameters as the sampling time, the randomized training, the different training algorithms, the number of hidden neurons, the number of linked data series, and the type of the data as it was suggested by Farkas et al. (2000b). In this experiment, a three layer feed-forward neural network with six hidden neurons was used. The NN contained also delayed feedback from the output to the input.

It was found that increasing the time step decreases the average deviation between the original training points and the outputs of the NN. It can be observed that the fluctuations are larger at the beginning of the drying if small sampling time is selected, because of the large number of points. The explanation of this effect can be that the back-propagation algorithm minimizes the difference between one input-output training pair in one step, and then it modifies the network weights based on the calculation point by point. In such a way, the neural network partly "forgets" the behavior of the process at the beginning. The more points are used the higher fluctuation will be at the beginning of the process. Randomized training can be used for reducing this effect

when the points are randomly selected to train the neural network.

In order to avoid high fluctuation at the beginning of the process, the training pairs are randomly selected from the entire drying period. Using randomized training pairs for back-propagation algorithm caused considerable improvement in the results even in case of a large number of training pairs. The result shows furthermore that there is no fluctuation effect at the beginning of drying process, so using randomized training pairs is to be recommended for real applications.

Preliminary studies showed that the original back-propagation algorithm could be slightly improved after some modifications. The first changing was to introduce an adaptive learning constant during the training. Another modification was changing the weights. After such experiments it can be concluded that there is almost no influence caused by the modifications, so it can be concluded that the original algorithm could be efficiently used without any modification.

A sensitivity study was performed in order to determine the influence of the number of hidden neurons in the NN. The sampling time was selected as 120 s along with randomized training pairs and the original back-propagation algorithm. From the results, it can be concluded that the best approximation was achieved when the number of hidden neurons was between 3 and 5. So the number of neurons in the hidden layer could be optimized in any special application cases.

As it was said before, it has been realized that a single data series is not reasonably enough for training the NN. Training with one data series, validation results can be unsatisfactory in case of changing in input data. To achieve better performance in neural network modeling it seems a good idea to link together different number of data series as one virtual drying process. The result shows that increasing the number of linked data series for training increases the accuracy of the NN model. Fast random signals caused the largest fluctuation at low number of linked data series.

There were several trials to validate the NN with different (constant, slow, and fast random) type of data. It can be observed that the case of slow random training gives reasonable good result for both constant and fast random validations. Constant training gives the worse result for the case of fast validation signal.

Summary

Neural network modeling is a reliable tool for determining the moisture and temperature distribution in the course of drying process. In order to set up an appropriate model, sufficient number of measurements should be available for training the neural network. The sensitivity aspect of the neural network model should be taken into account during the training and validation. Generally saying, the NN can be successfully applied especially for process control purposes.

Bibliography

- Farkas, I., Reményi, P., and Biró, A., 2000a. A neural network topology for modelling grain drying. *Computers and Electronics in Agriculture*, **26**, 147–158.
- Farkas, I., Reményi, P., and Biró, A., 2000b. Modelling aspects of grain drying with a neural network. *Computers and Electronics in Agriculture*, **29**, 99–113.
- Huang, B., and Mujumdar, A. S., 1993. Use of neural network to predict industrial dryer performance. *Drying Technology*, **11**(3), 525–541.
- Jay, S., and Oliver, T. N., 1996. Modelling and control of drying processes using neural networks. In *Proceedings of the 10th International Drying Symposium (IDS'96)*. Kraków, Poland, 30 July–2 August, 1996, Vol. B, pp. 1393–1400.
- Kaminski, W., Strumillo, P., and Tomczak, E., 1998. Neurocomputing approaches to modelling of drying process dynamics. *Drying Technology*, **16**(6), 967–992.
- Lin, C.-T., and Lee, C. S. G., 1995. *Neural fuzzy systems*. Englewood Cliffs: Prentice Hall.
- Sreekanth, S., Ramaswamy, H. S., and Sablani, S., 1998. Prediction of psychrometric parameters using neural networks. *Drying Technology*, **16**(3–5), 825–837.
- Thyagarajan, T., Panda, R. C., Shanmugam, J., Rao, P. G., and Ponnavaikko, M., 1997. Development of ANN model for nonlinear drying process. *Drying Technology*, **15**(10), 2527–2540.
- Trelea, I. C., Courtois, F., and Trystram, G., 1997. Dynamic models for drying and wet-milling quality degradation of corn using neural networks. *Drying Technology*, **15**(3 and 4), 1095–1102.

Cross-references

[Drying of Agricultural Products](#)

[Grain Physics](#)

[Neural Networks in Agrophysics](#)

[Physical Phenomena and Properties Important for Storage of Agricultural Products](#)

[Physical Properties of Raw Materials and Agricultural Products](#)

[Quality of Agricultural Products in Relation to Physical Conditions](#)

[Rheology in Agricultural Products and Foods](#)

[Shrinkage and Swelling Phenomena in Agricultural Products](#)

[Solar Drying of Biological Materials](#)

NITRIFICATION

The oxidation in biological process of ammonia to nitrate, via nitrite.

NONDESTRUCTIVE MEASUREMENTS IN FRUITS

Francisco J. García-Ramos

Escuela Politécnica Superior, University of Zaragoza,
Huesca, Spain

Synonyms

Nondestructive measurement of fruit quality

Definition

Technologies used to measure quality parameters in fruit of not destructive form.

Introduction

Nondestructive testing was, and still is, a priority research area for specialty crops; its aim is to assess or quantify product properties and characteristics for the purpose of quality and safety monitoring and control. Sensors have been widely recognized for their potential to identify product properties, and they have been translated into industrial technologies, as evidenced by thousands of engineering research publications during the past 50 years.

Fruit quality is related to both internal variables (firmness, sugar content, acid content, and internal defects) and external variables (shape, size, external defects, and damage). Increasing consumer demand for high-quality fruit has led to the development of optical, acoustic, and mechanical sensors that determine this quality (Nicolai et al., 2006). Fruit packing companies need to measure these quality variables, but they need to do so in a nondestructive manner. Manufacturers and research groups have understood this complexity and are currently developing sensors with this aim.

The development of sensors to measure fruit internal and external quality variables on a nondestructive way is one of the challenges of postharvest technology. These include static and online sensors that use different technologies for determining fruit quality parameters. Although many techniques are under development, some companies already market instruments that determine the internal quality of fruit.

Internal fruit quality parameters

Fruit firmness

Fruit firmness is one of the most important quality variables; it is an indirect measurement of ripeness and its accurate assessment allows appropriate storage periods and optimum transport conditions to be established.

Traditionally, fruit firmness has been estimated in a destructive manner by means of the Magness Taylor test. This can be performed in the laboratory or with portable equipment, and is based on the introduction of a cylindrical head into the flesh of a peeled fruit to measure the maximum penetration force. Depending on the equipment used, other variables can be measured such as maximum force, deformation, and the values for different relationships between force and deformation. However, the Magness Taylor test has three main drawbacks: it is destructive, measurements are highly variable (by up to 30%), and it cannot be used in online situations. Nevertheless, this technique is well accepted and used for classifying fruit by many packing companies and quality laboratories.

Technical advances over the last few decades have led to the development of nondestructive devices capable of measuring fruit internal variables (Delwiche et al., 1996). Originally, these devices were developed for use in the laboratory, but have been adapted for online use (as have weight or diameter-measuring devices).

Fruit firmness can be estimated by different techniques including the measurement of variables extracted from force-deformation curves, the analysis of impact forces, the rebound technique, the measurement of acoustic responses to vibrations and impacts, the measurement of optical properties, and nuclear magnetic resonance (Garcia-Ramos et al., 2005).

Sugar content, acid content, and internal defects

The interaction between light and fruit tissues can be used to measure fruit internal quality (Nicolaï et al., 2007). An optical sensor consists of a light source and a receiver that records the optical signal. The optical signal has different wavelengths. According to the light pathway inside the sample, there are two main optical techniques: reflectance (incident light penetrates the external tissues and exits toward the sensor near the entering point) and transmittance (incident light goes through the tissues and hits the sensor on the opposite side of the fruit – or at least 90° away from entrance point).

The technology more used is the near infrared reflectance spectroscopy (NIR). This technique, which measures the reflected spectrum of a sample lit with halogen light is closely related to that employed by optical equipment (e.g., cameras). Much research effort is currently being made in this area.

Commercial, online, optical devices based on NIR spectroscopy are available. Some devices were developed for use with melons but have been successfully used with pears, apples, peaches, and Sharon fruit. These sensors can handle 2–5 fruits/s depending on the species. The internal variables measured are sugar content plus an indirect measurement of firmness (“ripeness”).

External fruit quality parameters

Shape and size

The estimation of the size and form of the fruit is realized by means vision systems in the range of the visible and near infrared spectrum (Moreira et al., 2009). Nevertheless, commercial vision systems do not yield in general the high precision volume estimates required for density sorting, because they compute volume from two-dimensional (2D) images. Nowadays, three-dimensional (3D) machine vision systems are beginning to be introduced in some food industries. This trend could eventually spread to fresh produce packinghouses, where 3D cameras could be used, apart from calculating accurate volume, shape sorting, and surface area.

Weight

Fruit weight estimation is commonly performed with an electronic weight sizer. These sensors are implemented in commercial fruit packing lines and can be recalibrated for different weight groups. The accuracy achieves ± 1 g working at speeds of 1 m/s (until 10 fruits/s).

Color

Light in the visible region (approximately 400–780 nm) can provide color and/or pigment information about horticultural products. Skin color may be indicative of maturity for some horticultural products such as banana, mango, and tomato (Edan et al., 1997). However, for many other horticultural products, skin color is not a good and reliable indicator of their maturity/quality. Color more directly relates to product appearance, which is important to the consumer perception of product quality (Abbott, 1999). Hence, color vision technology is widely used in the horticultural industry to ensure consistent product items in size, shape, and color.

Summary

The increasing demand of fruit quality by consumers makes necessary the development of technology to achieve this goal. Most of the fruit packing lines already have equipments capable of quantifying the parameters of external quality of a fruit (size, weight, and color) in line and of not destructive form. During the recent years, the enterprises and research groups have developed technologies for the nondestructive measure of internal quality parameters (sugar content, acids content, firmness, etc.). These include static and online sensors that use different technologies for determining fruit quality parameters. Although many techniques are under development, some companies already market instruments that determine the internal quality of fruit.

Bibliography

- Abbott, J. A., 1999. Quality measurement of fruits and vegetables. *Postharvest Biology and Technology*, **15**(3), 207–225.
- Delwiche, M. J., Arévalo, H., and Mehlschau, J., 1996. Second generation impact force response fruit firmness sorter. *Transactions of the ASAE*, **39**(3), 1025–1033.
- Edan, Y., Pasternak, H., Shmulevich, I., Rachmani, D., Guedalia, D., Grinberg, S., and Fallik, E., 1997. Color and firmness classification of fresh market tomatoes. *Journal of Food Science*, **62**(4), 793–796.
- García-Ramos, F. J., Valero, C., Homer, I., Ortiz-Cañavate, J., and Ruiz-Altisent, M., 2005. Non-destructive fruits firmness sensors: a review. *Spanish Journal of Agricultural Research*, **3**(1), 61–73.
- Moreda, G. P., Ortiz-Cañavate, J., García-Ramos, F. J., and Ruiz-Altisent, M., 2009. Non-destructive technologies for fruit and vegetable size determination – a review. *Journal of Food Engineering*, **92**(2), 119–136.
- Nicolaï, B. M., Beullens, K., Bobelyn, E., Hertog, M., Schenk, A., Vermeir, S., and Lammertyn, J., 2006. Systems to characterise internal quality of fruit and vegetables. *Acta Horticulturae*, **712**, 59–66.
- Nicolaï, B. M., Beullens, K., Bobelyn, E., Peirs, A., Saeys, W., and Theron, K. I., 2007. Nondestructive measurement of fruit and vegetable quality by means of NIR spectroscopy: a review. *Postharvest Biology and Technology*, **46**, 99–118.

Cross-references

- [Agriculture and Food Machinery, Application of Physics for Improving](#)

Color in Food Evaluation

[Fruits, Mechanical Properties and Bruise Susceptibility](#)

[Machine Vision in Agriculture](#)

[Physical Properties as Indicators of Food Quality](#)

[Quality of Agricultural Products in Relation to Physical Conditions](#)

NONDESTRUCTIVE MEASUREMENTS IN SOIL

Wojciech M. Skierucha

Department of Metrology and Modeling of Agrophysical Processes, Institute of Agrophysics, Polish Academy of Sciences, Lublin, Poland

Definition

Nondestructive measurements in soil are a wide group of techniques used in science and agriculture and applying ground-installed sensors to evaluate the properties of soil without causing damage.

Nondestructive and destructive measurements

Contrary to destructive measurements in soil, where the original physical, chemical, or biological properties of the measured object cannot be recovered, in nondestructive testing the measured object can function correctly after the measurement process. For example, the standard thermogravimetric method for the measurement of soil volumetric water content is destructive, while TDR (time-domain reflectometry) method is nondestructive. In thermogravimetric method, the soil sample is permanently removed from its original location and during the process of drying its structure and biological components are destroyed. In TDR method, after one-time installation disturbance in a fixed location, repeated and automated measurements are allowed without causing any damage to any soil constituent.

Nondestructive measurements or tests should be distinguished from noninvasive ones, which include diagnostics, that is, procedures that do not involve tools breaking the soil structure (see [Noninvasive Quantification of 3D Pore Space Structures in Soils](#)) and the skin or physically enter the body (ultrasound, X-rays, endoscopes, computer tomography). The noninvasive measurements that do not use sensors installed in the soil include: NIRS (near infrared reflectance spectroscopy) for determination of soil texture and carbon content, airborne and satellite remote sensing for characterizing soils for plant available water capacity and topsoil properties (Schmidhalter et al., 2008), GPR (Ground Penetrating Radar), electromagnetic induction for collecting information about field heterogeneity of soil texture and soil water content, NIRS (near infrared spectroscopy) for determination of soil texture and carbon content. Their primary application is precision agriculture and site-specific soil treatment to achieve optimal plant production under sustainable agricultural and environmental conditions.

These methods usually require additional and traditional ground measurements for calibration purposes.

Nondestructive measurement techniques are commonly used in industry because they do not permanently alter the article being inspected saving both money and time in product evaluation, troubleshooting, and research.

Elements of nondestructive measurements in soil

Agrophysics as an applied and interdisciplinary science adopts nondestructive measurement techniques from other fields of science and industry. The fundamental elements

for successful nondestructive measurements in soil apart from a sensor, usually working in the indirect measurement mode, are: data-logging features of the applied measurement equipment, battery supply (frequently supported by charging solar panel) powerful enough to work without replacement for at least one measurement season, and communication option (preferably wireless) to transmit measured data as well as the experiment configuration in both direction between the field location and the operator's computer. **Table 1** presents the selection of the most popular nondestructive measurements in soil, which are used for the measurement of soil water status.

Nondestructive Measurements in Soil, Table 1 Selection of the most popular nondestructive and noninvasive soil water status measurements methods

Measurement method	Directly measured quantity, physical principle, soil property measured, and references	Remarks
TDR (time domain reflectometry)	Velocity of propagation of electromagnetic wave (step or needle pulse) along the metallic parallel or coaxial waveguide (TDR probe) fully inserted into the soil. It is very well correlated with the real part of the soil complex dielectric permittivity as well as the amount of water in soil. (Topp et al., 1980; Noborio, 2001) Attenuation of the electromagnetic wave during its travel in the TDR probe, which results mainly from the soil electrical conductivity-dependent ion conduction. Signal attenuation is correlated with the soil bulk electrical conductivity and soil salinity defined as electrical conductivity of soil extract. (Malicki and Walczak, 1999; Robinson et al., 2003)	<ul style="list-style-type: none"> – Commonly recognized alternative for the thermogravimetric method – Instruments are still very expensive – Usually no site calibration required
FDR (frequency domain reflectometry)	Phase shift (dependent on soil bulk dielectric permittivity) and amplitude attenuation (dependent on soil salinity) of a probe inserted into the soil treated as a lossy capacitor. Measurement is done in single frequency generated by the probe internal probe oscillator (50–150 MHz). (Veldkamp and O'Brien, 2000)	<ul style="list-style-type: none"> – Not applicable for very saline soils and long probe rods – Limited accuracy caused by the possible change of the TDR probe geometry
Neutron scattering	Number of slow neutrons that are produced from the collision of fast neutrons with hydrogen molecules in soil, which is linearly related to the soil volumetric water content. Fast neutron generator and the counter are installed in the vertical access tube for the measurements in different layers of soil. (Evett and Steiner, 1995)	<ul style="list-style-type: none"> – Requires soil site calibration – Probes and meters are commercially available and cheaper than TDR instrumentation – Low power consumption as compared to TDR technique – Requires soil-site calibration – Precise but expensive – Additional cost with special licensing, operator training, handling, radiation materials waste disposal – Health hazard – Limited range of work (down to about –85 kPa) – Require frequent servicing (air bubbles) – In drought conditions water moves from the tensiometer to the soil – Sensitive to soil salinity and temperature – Requires soil-specific calibration – Very economic and field installations can work for several years – Supplementary to tensiometers in the range up to –1,500 kPa
Tensiometry	Suction force or pressure exerted on a pressure transducer in a water-filled tube connected with soil matrix by a porous cap. The measured physical quantity is a matrix potential of soil water, which is a basic element of the total potential of water in the soil. (Mullins, 2001; Sisson et al., 2002)	
Electrical resistance blocks	Electrical resistance, measured with an alternating current bridge (usually \approx 1,000 Hz) of electrodes encased in some type of porous material (gypsum, nylon fabric, fiberglass) that within about 2 days will reach a quasi-equilibrium state with the soil. This method determines soil water content and water potential as a function of electrical resistance. (Hillel, 1998; Spaans and Baker, 1992)	
Nuclear magnetic resonance (NMR) spectroscopy	Structure and composition of soil, soil organic matter and nutrients (Randall et al., 1997), plant nitrogen metabolism. (Mesnard and Ratcliffe, 2005)	<ul style="list-style-type: none"> – High spectral resolution – Problems with equipment availability
X-ray computed tomography	Description and quantitative measurements of soil structure elements, especially of soil pores and pore network features, investigation the hydro-physical characteristics of the soil, in a functional and temporal manner, analysis of the biotic factor influence on soil. (Taina et al., 2008; Peth et al., 2008)	<ul style="list-style-type: none"> – High spatial resolution (\sim 1 μm) – Lack of unity, not only in the utilized methods, but also in terminology

There is a tendency to construct noninvasive integrated sensors that measure more than one physical soil property at the same time and in the same soil volume, for example, TDR or FDR soil water content and soil salinity integrated with an easy to implement temperature sensor (Skierucha et al., 2006), bulk density, and water content using low- and high-energy sources for CT scanning (Rogasik et al., 1999; Lipiec and Hatano, 2003), penetrometers with TDR probe sensors (Young et al., 2000; Vaz and Hopmans, 2001) and with thermal sensors (Marczewski et al., 2004), combined measurements system of TDR and tensiometry (Malicki et al., 1992; Walczak et al., 1993; Whalley, 1993), thermo-time domain reflectometry probe for measuring soil thermal properties and water content (Ren et al., 2003; Usowicz et al., 2006).

Summary

Nondestructive measurement methods in soil and other environmental objects develop rapidly following the technological advances in electronics, informatics, and materials engineering. They are on the application front of modern technology developments. Agrophysics should take advantage of the progress of nondestructive methods of measurements in medicine, satellite, and others branches of science financially supported by governmental and private funds and look for the new applications in the field of food quality and environmental protection.

Bibliography

- Evett, S. R., and Steiner, J. L., 1995. Precision of neutron scattering and capacitance type moisture gages based on field calibration. *Soil Science Society of America Journal*, **59**, 961–968.
- Hillel, D., 1998. *Environmental Soil Physics (Chapter 6: Content and Potential of Soil Water)*. San Diego: Academic, pp. 132–134.
- Lipiec, J., and Hatano, R., 2003. Quantification of compaction effects on soil physical properties and crop growth. *Geoderma*, **116**, 107–136.
- Malicki, M. A., and Walczak, R. T., 1999. Evaluating soil salinity status from bulk electrical conductivity and permittivity. *European Journal of Soil Science*, **50**(3), 505–514.
- Malicki, M. A., Plagge, R., Renger, M., and Walczak, R. T., 1992. Application of time-domain reflectometry (TDR) soil moisture miniprobe for the determination of unsaturated soil water characteristics from undisturbed soil cores. *Irrigation Science*, **13**, 65–72.
- Marczewski, W., Schröer, K., Seiferlin, K., Usowicz, B., Banaszkiewicz, M., Hlond, M., Grygorczuk, J., Gadomski, S., Krasowski, J., Gregorczyk, W., Kargl, G., Hagermann, A., Ball, A. J., Kührt, E., Knollenberg, J., and Spohn, T., 2004. Prelaunch performance evaluation of the cometary experiment MUPUS-TP. *Journal of Geophysical Research*, **109**(E7), E07S09.
- Mesnard, F., and Ratcliffe, R. G., 2005. NMR analysis of plant nitrogen metabolism. *Photosynthesis Research*, **83**, 163–180.
- Mullins, C. E., 2001. Matric potential. In Smith, K. A., and Mullins, C. E. (eds.), *Soil and Environmental Analysis: Physical Methods*. New York: Marcel Dekker, pp. 65–93.
- Noborio, K., 2001. Measurement of soil water content and electrical conductivity by time domain reflectometry: a review. *Computers and Electronics in Agriculture*, **31**, 213–237.
- Peth, S., Horn, R., Beckmann, F., Donath, T., Fischer, J., and Smucker, A. J. M., 2008. Three-dimensional quantification of intra-aggregate pore-space features using synchrotron-radiation-based microtomography. *Soil Science Society of America Journal*, **72**, 897–907.
- Randall, E. W., Mahieu, N., and Ivanova, G. I., 1997. NMR studies of soil, soil organic matter and nutrients: spectroscopy and imaging. *Geoderma*, **80**, 307–325.
- Ren, T., Ochsner, T. E., and Horton, R., 2003. Development of thermo-time domain reflectometry for vadose zone measurements. *Vadose Zone Journal*, **2**, 544–551.
- Robinson, D. A., Jones, S. B., Wraith, J. M., and Friedman, S. P., 2003. A review of advances in dielectric and electrical conductivity measurement in soils using time domain reflectometry. *Vadose Zone Journal*, **2**, 444–475.
- Rogasik, H., Crawford, J. W., Wendorth, O., Young, I. M., Joschko, M., and Ritz, K., 1999. Discrimination of soil phases by dual energy X-ray tomography. *Soil Science Society of America Journal*, **63**(4), 741–751.
- Schmidhalter, U., Maidl, F. X., Heuwinkel, H., Demmel, M., Auernhammer, H., Noack, P. O., and Rothmund, M., 2008. Precision farming – adaptation of land use management to small scale heterogeneity (chapter 2.3). In Schröder, P., Pfadenhauer, J., and Munch, J. C. (eds.), *Perspective for Agroecosystem Management*. Amsterdam: Elsevier, pp. 121–186.
- Sisson, J. B., Gee, G. W., Hubbel, J. M., Bratton, W. L., Ritter, J. C., Ward, A. L., and Caldwell, T. G., 2002. Advances in tensiometry for long-term monitoring of soil water pressures. *Vadose Zone Journal*, **1**, 310–315.
- Skierucha, W., Wilczek, A., and Walczak, R. T., 2006. Recent software improvements in moisture (TDR method), matric pressure, electrical conductivity and temperature meters of porous media. *International Agrophysics*, **20**, 229–235.
- Spaans, E. J. A., and Baker, J. M., 1992. Calibration of Watermark soil moisture sensors for soil matric potential and temperature. *Plant and Soil*, **143**, 213–217.
- Taina, I. A., Heck, R. J., and Elliot, T. R., 2008. Application of X-ray computed tomography to soil science: a literature review. *Canadian Journal of Soil Science*, **88**(1), 1–19.
- Topp, G. C., Davis, J. L., and Annan, A. P., 1980. Electromagnetic determination of soil water content: measurement in coaxial transmission lines. *Water Resources Research*, **16**, 574–582.
- Usowicz, B., Lipiec, J., and Ferrero, A., 2006. Prediction of soil thermal conductivity based on penetration resistance and water content or air-filled porosity. *International Journal of Heat and Mass Transfer*, **49**, 5010–5017.
- Vaz, C. M. P., and Hopmans, J. W., 2001. Simultaneous measurements of soil penetration resistance and water content with a combined penetrometer–TDR moisture probe. *Soil Science Society of America Journal*, **65**, 4–12.
- Veldkamp, E., and O'Brien, J. J., 2000. Calibration of a Frequency Domain Reflectometry Sensor for Humid Tropical Soils of Volcanic Origin. *Soil Science Society of America Journal*, **64**, 1549–1553.
- Walczak, R. T., Śląwiński, C., Malicki, M. A., and Sobczuk, H., 1993. Measurement of water characteristics in soil using TDR technique. Water characteristics of loess soil under different treatment. *International Agrophysics*, **7**, 175–182.
- Whalley, W. R., 1993. Considerations on the use of time domain reflectometry (TDR) for measuring soil water. *European Journal of Soil Science*, **44**, 1–9.
- Young, G. D., Adams, B. A., and Topp, G. C., 2000. A portable data collection system for simultaneous cone penetrometer force and volumetric soil water content measurements. *Canadian Journal of Soil Science*, **80**, 23–31.

Cross-references

- [Electrical Properties of Agricultural Products](#)
[Electrical Properties of Soils](#)

Magnetic Resonance Imaging in Soil Science
 Nondestructive Measurements in Fruits
 Noninvasive Quantification of 3D Pore Space Structures in Soils
 Precision Agriculture: Proximal Soil Sensing
 Remote Sensing of Soils and Plants Imagery
 X-Ray Method to Evaluate Grain Quality

NONINVASIVE QUANTIFICATION OF 3D PORE SPACE STRUCTURES IN SOILS

Stephan Peth

Institute for Plant Nutrition and Soil Science, Christian-Albrechts-University zu Kiel, Kiel, Germany

Definitions

Noninvasive research facilitates the understanding of physical, chemical, and biological processes in soils and their dependency on soil structure. The most commonly employed method or device used for noninvasive examinations of porous materials and their 3D architectures is X-ray Computed (Micro)Tomography (XCT, μ CT), which can be either based on synchrotron radiation (SR- μ CT) or microfocus tube sources (MF- μ CT).

XCT = X-ray computed tomography

μ CT = X-ray computed microtomography

SR = Synchrotron radiation

SR- μ CT = Synchrotron radiation-based microtomography

Voxel = Three-dimensional equivalent to pixel

CCD = Charge-coupled device

Introduction

Soil pore spaces are of interest to soil researchers for various reasons where the traditional soil science disciplines usually take different perspectives. The soil physicist, for example, treats soil pore spaces mostly with respect to water, gas, and solid particle movements, while the soil biologist and soil chemist understands pore spaces predominantly as an environment for root growth and microbial activity and a pathway to access and retain nutrients or contaminants, respectively. Recent research on the soil-microbe system emphasizes that the interaction of physical, biological, and biogeochemical processes occurring within soil pore space structures deserves more appreciation (Young and Crawford, 2004). Soil scientists now begin to recognize that the physical heterogeneity of soil structures controls both abiotic and biotic functions within soil habitats with feedback loops between the two. In other words, soil structure and its dynamic functional properties regulate soil biodiversity (Crawford et al., 2005; Ettema and Wardle, 2002) while soil microbes in turn can alter soil structure and hence pore spaces (Six et al., 2004). Detailed insights into pore space realms are important not only from a soil microbial habitat perspective. Given that the interacting mechanisms operate across scales virtually all soil environmental processes (from transport

to sorption and turnover) maintaining biogeochemical cycling in the pedosphere depend on pore space structures.

How to study soil pore space structures

Past research on soil structure and its associated pore space was strongly based on traditional techniques, which can be distinguished into direct (e.g., thin section analysis) and indirect (e.g., water retention function) methods. Despite profound conceptual understanding on soil structure formation and stability has been achieved the major drawback of this traditional approach is that the techniques are either destructive (e.g., preparation of thin sections) or that results refer to statistical values averaged over a bulk volume (e.g., pore size distribution) lacking detail on the spatial configuration of pores. Another problem is that soil structure is inherently three dimensional and that 2D analysis from thin sections bears some risk for inaccurate interpretations of structural morphologies. When we consider the soil pore space as a dynamic, three-dimensional, interconnected network of voids with a complex hierarchical organization we have to acknowledge that traditional methods are insufficient for deriving an adequate quantitative characterization of pore space morphologies. Noninvasive imaging techniques have made significant progress in the last decade ([Nondestructive Measurements in Soils](#)) promising to overcome some of the limitations involved in studying dynamic 3D soil pore spaces.

Applications of X-ray computed tomography in soil structure analysis

X-ray computed tomography (XCT) is the most widely used noninvasive imaging technique to study soil structure. The technique was introduced in the discipline of soil science by the pioneering work of Petrovic et al. (1982) investigating soil bulk density and later followed up by Crestana et al. (1986), who studied the spatial distribution and temporal dynamics of water in soil. Both used medical scanners achieving a voxel resolution in the submillimeter range. Later efforts were made to extend the noninvasive visualization of pore spaces beyond larger macropores ($>50 \mu\text{m}$) toward smaller pore sizes down to the mesopore range ($<10 \mu\text{m}$). However, because of the strong X-ray attenuation of the mineral soil components, resolution is generally limited by the distance the X-ray beam has to travel from the entry to the exit of the specimen and hence decreases with increasing sample size. As a rule of thumb, the resolution achieved is in the range of 1/1,000 of the sample thickness. A main limitation of conventional medical scanners for analyzing small samples at high resolution, however, is that because they are built for larger objects (human bodies) they do not reach the required precision in terms of angular rotation of the detector and sample positioning during image acquisition.

With synchrotron radiation sources becoming more accessible to the scientific community, the potential of this high energy radiation for X-ray microtomography of

environmental samples was recognized. Pioneering work on synchrotron radiation-based X-ray microtomography (SR- μ CT) was conducted by Flannery and colleagues about 20 years ago (Flannery et al., 1987). They introduced SR- μ CT as a “new form of microscope” that produces three-dimensional images with a spatial resolution comparable to that of a light microscope ($\sim 1 \mu\text{m}$). The use of SR- μ CT for analyzing soil pore spaces at micrometer resolution was introduced by Spanne et al. (1994) but surprisingly only recently the technique was applied to study small-scale soil structure of natural undisturbed soils (Altman et al., 2005; Feeney et al., 2006; Nunan et al., 2006; Peth et al., 2008a; Peth et al., 2008b). Synchrotron radiation sources offer a variety of special techniques (fluorescence, absorption, diffraction, infrared) providing excellent perspectives for plant and soil research with a superior performance in terms of sensitivity, speed, and resolution (Lombi and Susini, 2009). Recent developments of high-resolution laboratory μ CT systems, however, will make X-ray computed microtomography (μ CT) a more readily available tool in soil structure analysis allowing for the visualization and quantification of soil pore architectures at a resolution down to a few microns with a quality that is very close to what is obtained from SR facilities (Brunke et al., 2008).

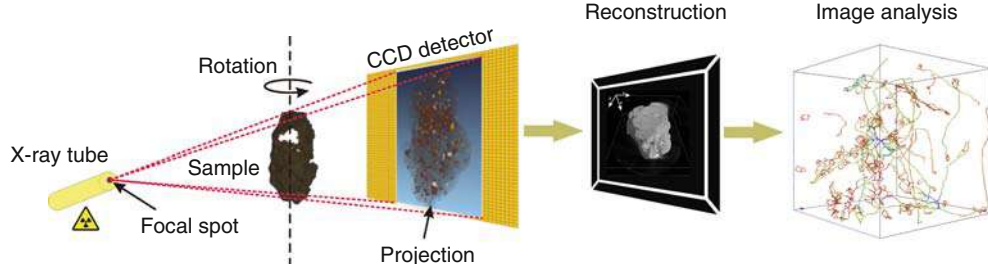
Principles of X-ray computed tomography

X-ray computed tomography is based on the differences in X-ray attenuation where an incident beam of intensity I_0 is absorbed by the internal components of the radiated object resulting in a transmitted beam with reduced intensity (I). This relationship is described by Lambert-Beer’s law:

$$I = I_0 \exp(-\mu D) \quad (1)$$

where μ is the overall linear attenuation coefficient (L^{-1}) and D is the sample thickness (L^{-1}). The linear X-ray attenuation coefficient (μ) is a function of density and atomic number of the components as well as the X-ray energy used. For porous media consisting of different phases (solid, water, and air) Equation 1 must be extended accounting for the different phase specific attenuation coefficients to

$$I = I_0 \exp\left(-[(1 - \theta_p)\mu_s\rho_s D + \theta_p S_w \mu_w \rho_w D]\right) \quad (2)$$



Noninvasive Quantification of 3D Pore Space Structures in Soils, Figure 1 Typical layout of a tomography experiment with a laboratory X-ray computed microtomography (μ CT) system.

where ρ_s and ρ_w are the densities and μ_s and μ_w the linear attenuation coefficients of solid matter and water, respectively. S_w denotes the water saturation and θ_p the total porosity. Due to the low linear attenuation of air, the contribution of the gaseous phase to the overall attenuation is considered negligible and therefore omitted in Equation 2.

The incident fan-shaped X-ray beam is generated in a high vacuum X-ray tube and transmitted through the sample, which is mounted on a precision rotation table (Figure 1). The sample is rotated at 0.25–0.50° steps between 0° and 360° and at each angular step the integral attenuation of the X-ray beam transmitting the sample is recorded by the CCD detector. The measured angular projections of the sample are finally reconstructed into a 3D linear attenuation coefficient map. Commonly, attenuation coefficients are converted to grayscale values ranging from [255] for the highest attenuation coefficient to [0] for the lowest attenuation coefficient. Reconstructed images finally contain the spatial configuration of soil voids and soil components with sufficient attenuation contrast. Hence, the architecture of soil pore networks is available in digital format and can be analyzed quantitatively with 3D image analysis algorithms.

A readable introduction to principles of computerized tomography is given by Kak and Slaney (1988).

Visualization and quantification of soil pore space structures in 3D

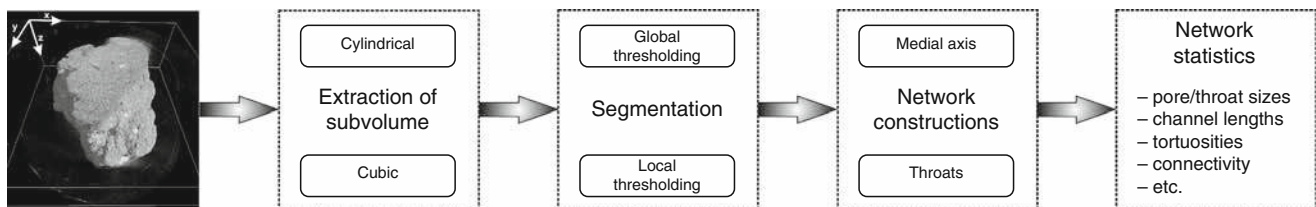
During a microtomography scan usually a couple of hundred (often $>1,000$) grayscale image slices are recorded and subsequently rendered into a 3D volume of the sample. Tools exist to visualize the 3D structure of the sample providing some qualitative information about the pore space architecture, e.g., the spatial arrangement and continuity of pores. However, in order to make objective comparisons between different samples, some kind of morphological and topological quantification is desired.

Morphological and topological features of pore networks may be quantified by means of 3D image analysis using algorithms that are based on the principles of mathematical morphology (e.g., Serra, 1982; Soille, 2003). Different sets of such morphometric algorithms that are suitable for analyzing soil pore spaces are available, e.g., *DXSoil* (Delerue and Perrier, 2002) and *3dma* (Lindquist

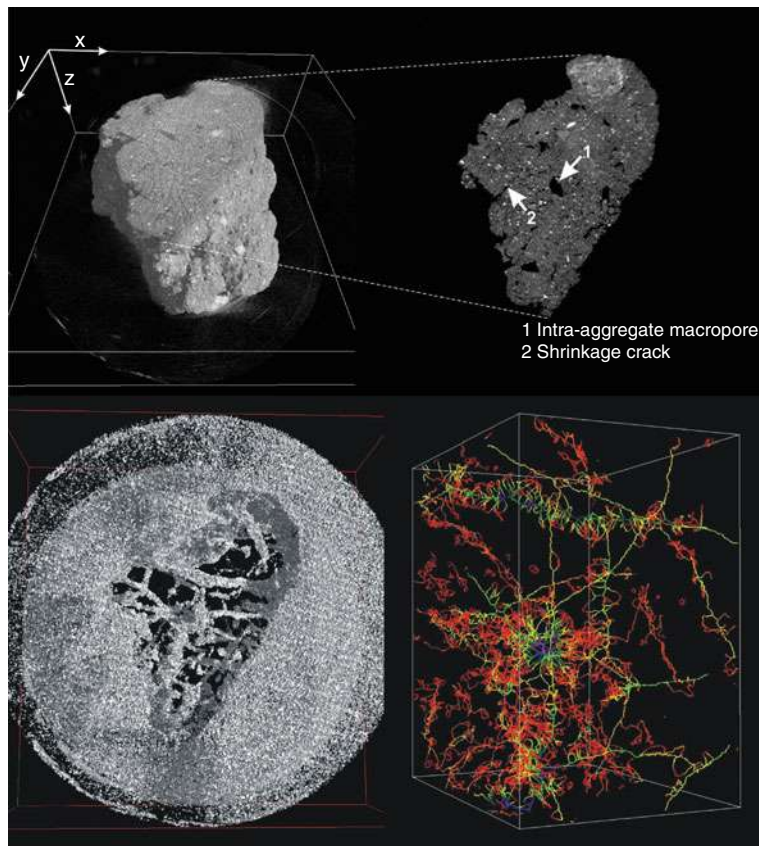
et al., 2005). Image analysis involves the stepwise transformation of the image data into sets (Horgan, 1998) from which a variety of geometrical features of the pore space structure can be calculated (e.g., size, shape, connectivity and tortuosity of pore channels; pore interface area; pore bottlenecks). Basic operations during image analysis with the software *3dma* are shown in Figure 2.

The application of *3dma* for analyzing the intra-aggregate pore space architecture of different soil aggregates was demonstrated by Peth et al. (2008a). Figure 3 shows

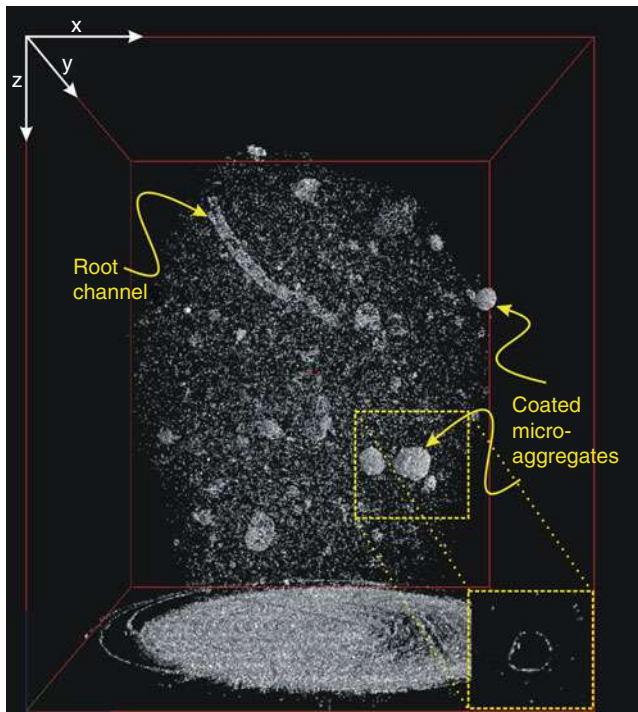
an example of the reconstructed 3D X-ray attenuation map of a small-scale soil aggregate (5-mm diameter) and the extracted shape of the internal macropore architecture. The calculation of the skeleton (medial axis) reveals the existence of numerous convoluted narrow pores and a few continuous pore channels. Pore channels become visible when the 3D representation is restricted to a short range of grayscale values corresponding to specific attenuation coefficients. Obviously, larger pore channels are plagued with highly absorbing material in this case.



Noninvasive Quantification of 3D Pore Space Structures in Soils, Figure 2 Basic image analysis steps in *3dma*. (Reprinted from Peth et al., 2008b with permission from SPIE.)



Noninvasive Quantification of 3D Pore Space Structures in Soils, Figure 3 Three-dimensional reconstruction (top, left) of a soil aggregate (Alfisol, Rotthalmünster/Germany) and an xy-image slice showing shrinkage cracks and intra-aggregate macropores (top, right). Reconstructed pore channels (bottom, left) and medial axis representation of the main pore network (bottom, right). (Reprinted from Peth et al., 2008b with permission from SPIE.)



Noninvasive Quantification of 3D Pore Space Structures in Soils, Figure 4 X-ray attenuation map of a specific grayscale range of a paddy rice field soil aggregate (*Stagnic Cambisol*, Yingtan/China) showing coatings around root channels and microaggregates.

This phenomenon is also often visible around root channels and microaggregates (Figure 4).

Summary

Functional traits of soil structure, irrespective of scale, rely on the connectivity, tortuosity, and the heterogeneity of pore spaces in 3D (Young et al., 2001). This is often neglected using conventional approaches of investigating soil structure morphologies. Data concerning 3D architectures of pore spaces are invaluable when studying structural genesis, gas and water transport, habitat functions, water uptake, etc. Visualizing and quantifying the complex geometry of the pore network and soil structure on various scales is promising to enhance our understanding of the multiple interacting physical, biological, and biogeochemical processes taking place in soil pore spaces.

Bibliography

- Altman, S. J., Peplinski, W. J., and Rivers, M. L., 2005. Evaluation of synchrotron X-ray computerized microtomography for the visualization of transport processes in low-porosity materials. *Journal of Contaminant Hydrology*, **78**, 167–183.
- Brunke, O., Brockdorff, K., Drews, S., Müller, B., Donath, T., Herzen, J., and Beckmann, F., 2008. Comparison between X-ray tube based and synchrotron radiation based μ CT. In Stock, S. R. (ed.), *Developments in X-ray Tomography VI*. San Diego: SPIE, Vol. 7078, pp. 70781U–1.
- Crawford, J. W., Harris, J. A., Ritz, K., and Young, I. M., 2005. Towards an evolutionary ecology of life in soil. *Trends in Ecology and Evolution*, **20**, 81–87.
- Crestana, S., Cesareo, R., and Mascarenhas, S., 1986. Using a computed tomography miniscanner in soil science. *Soil Science*, **142**, 56–61.
- Delerue, J. F., and Perrier, E., 2002. DXSoil, a library for 3D image analysis in soil science. *Computers and Geosciences*, **28**, 1041–1050.
- Ettema, C. H., and Wardle, D. A., 2002. Spatial Soil Ecology. *Trends in Ecology and Evolution*, **17**, 177–183.
- Feeney, D. S., Crawford, J. W., Daniell, T., Hallett, P. D., Nunan, N., Ritz, K., Rivers, M., and Young, I. M., 2006. Three-dimensional microorganization of the soil-root-microbe system. *Microbial Ecology*, **52**, 151–158.
- Flannery, B. P., Deckman, H. W., Robarge, W. G., and D'Amico, K. L., 1987. Three-dimensional X-ray microtomography. *Science*, **237**, 1439–1444.
- Horgan, G. W., 1998. Mathematical morphology for analysing soil structure from images. *European Journal of Soil Science*, **49**, 161–173.
- Kak, A. C., and Slaney, M., 1988. *Principles of Computerized Tomographic Imaging*. New York: IEEE.
- Lindquist, W. B., Lee, S.-M., Oh, W., Venkatarangan, A. B., Shin, H., and Prodanovic, M., 2005. 3DMA-Rock: a software package for automated analysis of rock pore structure in 3-D computed microtomography images. http://www.ams.sunysb.edu/~lindquis/3dma/3dma_rock/3dma_rock.html#Sec_intro (last accessed 26 August 2010).
- Lombi, E., and Susini, J., 2009. Synchrotron-based techniques for plant and soil science: opportunities, challenges and future perspectives. *Plant and Soil*, **320**, 1–35.
- Nunan, N., Ritz, K., Rivers, M., Feeney, D. S., and Young, I. M., 2006. Investigating microbial micro-habitat structure using X-ray computed tomography. *Geoderma*, **133**, 398–407.
- Peth, S., Horn, R., Beckmann, F., Donath, T., Fischer, J., and Smucker, A. J. M., 2008a. Three-dimensional quantification of intra-aggregate pore-space features using synchrotron-radiation-based microtomography. *Soil Science Society of America Journal*, **72**, 897–907.
- Peth, S., Horn, R., Beckmann, F., Donath, T., and Smucker, A. J. M., 2008b. The interior of soil aggregates investigated by synchrotron-radiation-based microtomography. In Stock, S. R. (ed.), *Developments in X-ray Tomography VI*. San Diego: SPIE, Vol. 7078, pp. 70781H.1–70781H.12.
- Petrovic, A. M., Siebert, J. E., and Rieke, P. E., 1982. Soil bulk density analysis in three dimensions by computed tomographic scanning. *Soil Science Society of America Journal*, **46**, 445–450.
- Serra, J., 1982. *Image analysis and mathematical morphology*. London: Academic.
- Six, J., Bossuyt, H., Degryze, S., and Denef, K., 2004. A history of research on the link between (micro)aggregates, soil biota, and soil organic matter dynamics. *Soil and Tillage Research*, **79**, 7–31.
- Soille, P., 2003. *Morphological Image Analysis – Principles and Applications*. Berlin: Springer.
- Spanne, P., Jones, K. W., Prunty, L., and Anderson, S. H., 1994. Tomography of soil-water-root processes. In Anderson, S. H., and Hopman, J. H. (eds.), *Potential applications of synchrotron computed microtomography to soil science*. *Soil Science Society of America Journal*. Special Publ. **36**, 43–57.
- Young, I. M., and Crawford, J. W., 2004. Interactions and self-organization in the soil-microbe complex. *Science*, **304**, 1634–1637.
- Young, I. M., Crawford, J. W., and Rappoldt, C., 2001. New methods and models for characterising structural heterogeneity of soil. *Soil and Tillage Research*, **61**, 33–45.

Cross-references

Microbes and Soil Structure
Microbes, Habitat Space, and Transport in Soil
Nondestructive Measurements in Soil
Pore Morphology and Soil Functions
Soil Aggregates, Structure, and Stability
Soil Structure, Visual Assessment

NORMAL STRESS

See *Soil Compactibility and Compressibility*

NON-LIMITING WATER RANGE (NLWR)

See *Soil Physical Quality*

NUMERICAL METHODS (MODEL)

Algorithms that use arithmetic and logical operations to obtain approximate solutions to complex formulas, such as differential equations, describing a soil process.

NON-THERMAL TECHNOLOGIES

See *Thermal Technologies in Food Processing*

Cross-references

Agrophysics: Physics Applied to Agriculture

O

OHM'S LAW

The law describing the movement of electricity as caused by a gradient in electrical potential.

Cross-references

[Agrophysics: Physics Applied to Agriculture](#)

ONLINE MEASUREMENT OF SELECTED SOIL PHYSICAL PROPERTIES

Abdul Mounem Mouazen
Natural Resources Department, Natural Soil Resources Institute, Cranfield University, Cranfield, Bedfordshire, UK

Synonyms

Soil physical properties measurement

Definition

Online measurement of soil properties. Installing a measurement system of soil properties on a tractor and driving across the field, while collecting data on soil.

Introduction

Online soil sensing requires advanced sensing technologies based on single or sensor fusion systems. Researchers have used a large variety of sensing technologies, while the majority of them did not consider the sensor fusion concept. Adamchuk et al. (2004) have listed six different categories of online sensing methods, namely, electrical and electromagnetic sensors, optical and radiometric sensors, mechanical sensors, electrochemical sensors,

acoustic sensors, and pneumatic sensors. Calibration of many of these technologies is a challenging task due to the interference of different soil physical properties that prevents extracting useful information about a given soil property.

Liu et al. (1996) reported the first sensor fusion system of soil physical properties. They combined draught sensor with a dielectric-based moisture content sensor, a radar gun to measure speed, a linear potentiometer to measure depth, and a Trimble global positioning system (GPS) unit. Based on this system they could perform online measurement of texture/compaction using an empirical model. Mouazen et al. (2003) stated that this model may have a narrow range of applicability due to relatively high soil heterogeneity and rather complex relationships among variables involved.

A more robotic type of soil sensor fusion system has been developed in Tokyo University of Agricultural Technology by Shibusawa et al. (2003). The most upgraded system consisted of several sensing units, including a penetration tine, whose tip was equipped with a resistance measurement cell, a fiber type visible (Vis), and near infrared (NIR) spectrophotometer from Zeiss (Carl Zeiss Ltd, Germany) with a measurement range of 400–1,700 nm, a micro CCD camera (Toshiba IK-UM42) to monitor the soil surface roughness, a micro NIR thermometer to monitor soil temperature, a line laser marker to monitor the flatness of soil surface, and an GPS (Trimble MS740) antenna and receiver to monitor the position of the system. An electrical conductivity device was attached to the system to acquire additional information about soil physical properties. The system proved applicable to acquire data on soil physical and chemical properties, namely, resistance, moisture content, organic matter, nitrate, and pH (Shibusawa et al., 2003).

A simplified sensor fusion system (Mouazen, 2006), as compared to that of Shibusawa et al. (2003) was later

reported by Mouazen and Ramon (2006). The system enabled indirect measurement of soil bulk density indicating soil compaction level. It was also used to measure soil gravimetric moisture content. A detailed description of the system is provided below.

Sun et al. (2006) developed a dual sensor consisting of a penetrometer equipped with strain-gage load cell to measure horizontal mechanical penetration resistance and a dielectric sensor to measure moisture content. Later, Zeng et al. (2008) have attached electrical conductivity (EC) sensor to measure soil texture to be accounted for during online measurement of soil resistance, since soil resistance is a function of moisture content, bulk density, and texture.

Among several versions of their sensing systems, Adamchuk and Christenson (2007) reported a sensor fusion system that consisted of an instrumented blade with strain gauges to measure the resistance of soil profile, a capacitance-based sensor to measure soil moisture constant, and an optical sensor to measure variability of soil organic matter. This paper describes on the online sensing system of soil physical properties of Mouazen and Ramon (2006).

Online sensor of soil properties

The online measurement system of soil properties developed by Mouazen and Ramon (2006) consists of three different sensing techniques, namely, a load cell to measure subsoiler draught, a wheel gauge to measure subsoiler depth, and an optical probe attached to a portable fiber type spectrophotometer (Zeiss Corona, Zeiss Ltd, Germany) to measure soil physical and chemical properties (Mouazen, 2006). With the last-mentioned sensor, the smooth soil surface prepared by the subsoiler and optical probe coming behind is illuminated and the diffuse light from the surface is captured and transferred back to the spectrophotometer by means of the illumination and detection fibers, respectively. The measurement system is equipped with a differential global positioning system (DGPS) to determine the position while moving over the field. This online measurement system was initially developed to measure soil physical properties, namely, bulk density and moisture content, but the implementation of the sensor was extended to the chemical properties of soil (Mouazen et al., 2007, 2009).

Online measurement of soil moisture content

Certainly, soil moisture content is the easiest property to be measured with Vis–NIR spectroscopy because of the important water absorption bands at 950, 1,450, and 1,950 nm (Mouazen et al., 2006; Plamer and Williams, 1974). However, the accuracy of measurement depends upon several factors including soil texture, color, and the scale of calibration model used (field, landscape, regional, continental, or global). Due to these variables a general calibration model developed for the measurement of moisture content for a large geographic area including Belgium

and northern France was less accurate ($R^2 = 0.91$ and root mean square error of prediction (RMSEP) = 0.015 kg kg⁻¹) than a model developed for one single field in Belgium with $R^2 = 0.97$ and RMSEP = 0.021 kg kg⁻¹ (Mouazen et al., 2006). This can be interpreted by the fact that the variation of these variables is much larger at large geographical area as compared to a single field scale. Although these results were under nonmobile laboratory measurement conditions, a similar tendency was reported for online field measurement conditions (Mouazen et al., 2005a, 2007).

Online measurement of bulk density indicating soil compaction

Reports on online measurement of soil compaction often consider penetration resistance and/or draught of soil cutting tools, measured by load cells or strain gauges as indicators of soil compaction. However, it is well known that draught and penetration resistance are functions of not only bulk density indicating soil compaction, but also moisture content and organic matter, in addition to soil texture type (Mouazen and Ramon, 2006). Therefore, a mathematical model is needed to account for these different influencing variables during the online measurement of soil compaction. Mouazen and Ramon (2002) have developed a hybrid numerical-statistical model to calculate bulk density indicating soil compaction as a function of draught, moisture content, and depth. In order to acquire data for all influencing factors considered in the model, a sensor fusion system has been developed as described above. The model and the measurement systems were successfully tested in a sandy loam field (Mouazen and Ramon, 2006), and later expanded to loamy sand, loam, silt loam, and silt soils (Mouazen and Ramon, 2009). They proved that the spatial pattern of bulk density maps produced using this mathematical model and the online measurement system were very realistic and similar to the measured bulk density maps by conventional core sampling method in sandy loam field ($R^2 = 0.56$) and in loamy sand, loam, silt loam, and silt field ($R^2 = 0.52$). A depth control system (Mouazen et al., 2005b) was developed, which resulted in improved accuracy of measurement of soil compaction. The authors suggested that online measurement of soil compaction has to consider bulk density instead of draught or penetration resistance, while a sensor fusion system and a mathematical model are essential for successful and accurate measurement.

Summary

Since agricultural soils are complex materials, online measurement of soil physical properties can be a difficult and sometimes misleading procedure if the approaches and techniques considered are not adequate. To arrive at realistic measurement methodologies, advanced measurement and modeling techniques might be worth considering. However, some soil physical properties might be possible

to be measured online with a single sensing technology; for example, soil moisture content can be measured successfully with Vis–NIR spectroscopy. Other properties such as soil compaction (bulk density) cannot be measured with simple techniques (e.g., penetration resistance), and a sensor fusion system is recommended.

Bibliography

- Adamchuk, V. I., and Christenson, P. T., 2007. An instrumented blade system for mapping soil mechanical resistance represented as a second-order polynomial. *Soil & Tillage Research*, **95**, 76–83.
- Adamchuk, V. I., Hummel, J. W., Morgan, M. T., and Upadhyaya, S. K., 2004. On-the-go soil sensors for precision agriculture. *Computers and Electronics in Agriculture*, **44**, 71–91.
- Liu, W., Upadhyaya, S. K., Kataoka, T., and Shibusawa, S., 1996. Development of a texture/soil compaction sensor. In Robert, P. C., Rust, R. H., and Larson, W. E. (eds.), *Proceedings of the Third International Conference on Precision Agriculture*. Wisconsin: American Society of Agronomy/Crop Science Society of America/Soil Science Society of America, pp. 617–630.
- Mouazen, A. M., 2006. Soil Survey Device. International publication published under the patent cooperation treaty (PCT). World Intellectual Property Organization, International Bureau. International Publication Number: WO2006/015463; PCT/BE2005/000129; IPC: G01N21/00; G01N21/00.
- Mouazen, A. M., and Ramon, H., 2002. A numerical–statistical hybrid modelling scheme for evaluation of draught requirements of a subsoiler cutting a sandy loam soil, as affected by moisture content, bulk density and depth. *Soil & Tillage Research*, **63**, 155–165.
- Mouazen, A. M., and Ramon, H., 2006. Development of on-line measurement system of bulk density based on on-line measured draught, depth and soil moisture content. *Soil & Tillage Research*, **86**, 218–229.
- Mouazen, A. M., and Ramon, H., 2009. Expanding implementation of an on-line measurement system of topsoil compaction in loamy sand, loam, silt loam and silt soils. *Soil & Tillage Research*, **103**, 98–104.
- Mouazen, A. M., Dumont, K., Maertens, K., and Ramon, H., 2003. Two-dimensional prediction of spatial variation in topsoil compaction of a sandy loam field-based on measured horizontal force of compaction sensor, cutting depth and moisture content. *Soil & Tillage Research*, **74**, 91–102.
- Mouazen, A. M., De Baerdemaeker, J., and Ramon, H., 2005a. Towards development of on-line soil moisture content sensor using a fibre-type NIR spectrophotometer. *Soil & Tillage Research*, **80**(1–2), 171–183.
- Mouazen, A. M., Anthonis, J., and Ramon, H., 2005b. An automatic depth control system for online measurement of spatial variation in soil compaction. Part 4: improvement of compaction maps by using a proportional integrative derivative depth controller. *Biosystems Engineering*, **90**, 409–418.
- Mouazen, A. M., Karoui, R., De Baerdemaeker, J., and Ramon, H., 2006. Characterization of soil water content using measured visible and near infrared spectra. *Soil Science Society of America Journal*, **70**, 1295–1302.
- Mouazen, A. M., Maleki, M. R., De Baerdemaeker, J., and Ramon, H., 2007. On-line measurement of some selected soil properties using a VIS–NIR sensor. *Soil & Tillage Research*, **93**, 13–27.
- Mouazen, A. M., Maleki, M. R., Cockx, L., Van Meirvenne, M., Van Holm, L. H. J., Merckx, R., De Baerdemaeker, J., and Ramon, H., 2009. Optimum three-point link set up for optimal quality of soil spectra collected during on-line measurement. *Soil & Tillage Research*, **103**, 144–152.
- Plamer, K. F., and Williams, D., 1974. Optical properties of water in the near infrared. *Journal of the Optical Society of America*, **64**, 1107–1110.
- Shibusawa, S. I., Made Anom, S. W., Hache, C., Sasao, A., and Hirako, S., 2003. Site-specific crop response to temporal trend of soil variability determined by the real-time soil spectrophotometer. In Stafford, J. V. (ed.), *Precision Agriculture. Proceedings of the Joint European Conference of ECPA-ECPLF*. Berlin: Wageningen, pp. 639–643.
- Sun, Y., Ma, D., Schulze Lammers, P., Schmittmann, O., and Rose, M., 2006. On-the-go measurement of soil water content and mechanical resistance by a combined horizontal penetrometer. *Soil & Tillage Research*, **86**, 209–217.
- Zeng, Q., Sun, Y., Schulze Lammers, P., Ma, D., Lin, I., and Hueging, H., 2008. Improvement of a dual-sensor horizontal penetrometer by incorporating an EC sensor. *Computers and Electronics in Agriculture*, **64**, 333–337.

Cross-references

- [Mapping of Soil Physical Properties](#)
[Monitoring Physical Conditions in Agriculture and Environment](#)
[Nondestructive Measurements in Soil](#)
[Precision Agriculture: Proximal Soil Sensing](#)
[Soil Compatability and Compressibility](#)
[Soil Penetrometers and Penetrability](#)

ORGANIC CARBON IN SOIL

See *Physical Protection of Organic Carbon in Soil Aggregates*

ORGANIC DUSTS, ELECTROSTATIC PROPERTIES

Wiktor Pietrzyk, Marek Horyński

Department of Computer and Electrical Engineering,
Lublin University of Technology, Lublin, Poland

Synonyms

Dielectrics; Dust pollutants; Dusts

Definition

Organic dust. Fraction of solid body particles contained in air.

Dielectric. Material that does not conduct electric current.

Electric permeability. Physical quantity characterizing electric properties of the environment – dust.

Electric susceptibility. Dimensionless physical quantity determining the dielectric polarizability.

Dielectric loss tangent. Parameter describing the losses in a dielectric in a variable electric field.

Introduction

The loose and grainy materials commonly occurring in nature are used in many industrial processes and characterized with respect to their phenomenology or structure. As a result of the first approach, they are classified in the group

consisting of expandable elastoplastic materials, and in accordance with structural approach, they are defined as a two or three phases substance consisting of solid particles and pores between them filled with fluid and gas.

The dusts are defined as solid body particles contained in air. They are subdivided into the following classes in accordance with the size of dust grains:

- Dusts characterized by macroscopic size of grains, that is, between 1 and 1,000 μm .
- Dusts characterized by colloidal size of grains, that is, between 0.001 and 1 μm .

Depending on the original source of the dust or the form of its occurrence, the following subdivision has been established:

- Dispersing dusts, that is, those created as a result of mechanical disintegration of solids (e.g., coal dust in course of coal crushing and milling in power generation plants).
- Condensing dusts, that is, those created as a result of condensation and solidification of vapors of various chemical substances (e.g., soot). They are usually occurring in the category characterized by colloidal size of grains.

With respect to their behavior under gravity, the dusts are subdivided into the following categories:

- Falling dust, that is, dust being subject to sedimentation.
- Dust suspended in air, that is, dust not being subject to sedimentation.

With respect to origin of dispersed phase, the dusts are subdivided into the following categories:

- Inorganic dusts
- Mineral dusts (silica, asbestos, chalk, coal)
- Metal dusts (iron, lead, copper, chromium)
- Organic dusts
- Plant origin dusts (wood, cotton, flour, pollen, hay)
- Animal origin dusts (hair, feathers, skin cells, hoofs)
- Chemical origin dusts (plastic)
- Mixed dusts (organic and inorganic)
- Organized dusts (microorganisms, spores)
- Radioactive dusts

Organic dusts

The plant and animal origin dusts constitute a huge family of dusts containing various types of plant and animal particles as their basic components. They usually occur in the form of mixtures consisting of inorganic particles as well as many fractions of microflora and microfauna with substances produced by their representatives except of the basic fractions consisting of plant and animal particles. It is the specific feature characterizing this family of dusts. This relationship is best visible in the agricultural dusts with the composition determined by the diversity of working materials and materials constituting the source of dust emissions, also including the chemicals introduced into

production process, for example, pesticides and mineral fertilizers as well as superimposing pollutants originating mainly from industrial waste and exhaust gases produced by the transport sector.

These dusts are diversified in respect to dimensions of particles contained therein. The percentage of fractions expressed as the number of particles under $<5 \mu\text{m}$ is included between 40% and 98%, and their weight percentage up to 60%.

Furthermore the microorganisms and endotoxins can be found in almost all plant and animal origin dusts. Free silica is contained in a significant part of these dusts. The highest content of SiO_2 in inhalable dust, even up to 60%, depending on the type of soil, takes place in the plant raw material production and harvesting phase; this content is reduced in the next processing phases to the level lower than 10% and most frequently to 0 in the final production phase. The role of this fraction in the dusts occurring in animal breeding and in animal raw material processing is not significant.

Electrostatic properties

The description of the electrostatic properties of organic dusts encompasses the properties of solid phase in the two-phase system: solid body–air. The dimensions of the dust grains are irregular and included between 10 and 500 μm .

The electrostatic properties of organic dusts are not well known. They belong to an inflammable and explosive group of materials. Therefore mechanical methods, that is, textile filters and cyclones are used for their elimination. Only the knowledge of particle size distribution is required in order to apply these methods.

The knowledge of electrostatic properties of the dust was not required before LV electrostatic bifilar filter was developed. An organic dust with humidity of 0 up to 20% is used as a dielectric.

The basic dielectric properties of the dust are described by the electric permeability ϵ , which is a complex number, that is:

$$\epsilon = \epsilon' + j\epsilon'' \quad (1)$$

In Equation 1, ϵ' is the real component of electric permeability, and ϵ'' – the imaginary component of electric permeability.

Knowing both components, we can calculate the dielectric loss tangent δ :

$$\operatorname{tg} \delta = \frac{\epsilon''}{\epsilon'} \quad (2)$$

and the electric conductivity of the dielectric:

$$\sigma = \omega \epsilon'' \quad (3)$$

where

$$\omega = 2\pi f \quad (4)$$

and f is the frequency of voltage variations.

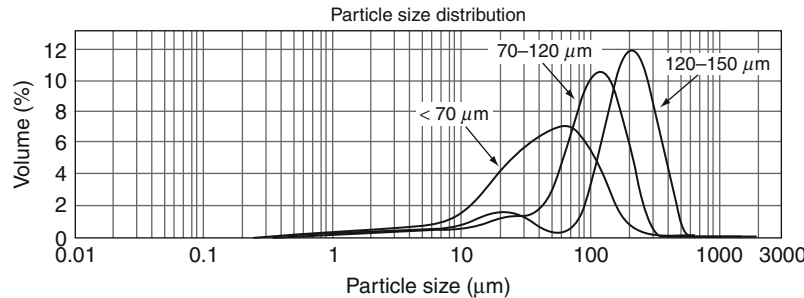
The facilities operating in food industry, particularly the corn mills, animal feed mixing, and manufacturing plants processing grains in course of various processes are the sources of organic dust emissions as a result of human activity. Wheat grains are most frequently used as the raw material. Therefore the dust obtained from the milling of "Zawisza" winter wheat by means of the laboratory disc mill has been examined as an example of organic dust.

The particle size distribution for three samples of dust obtained from wheat grains after passing through the sieves 150, 120, and 70 μm is illustrated in Figure 1.

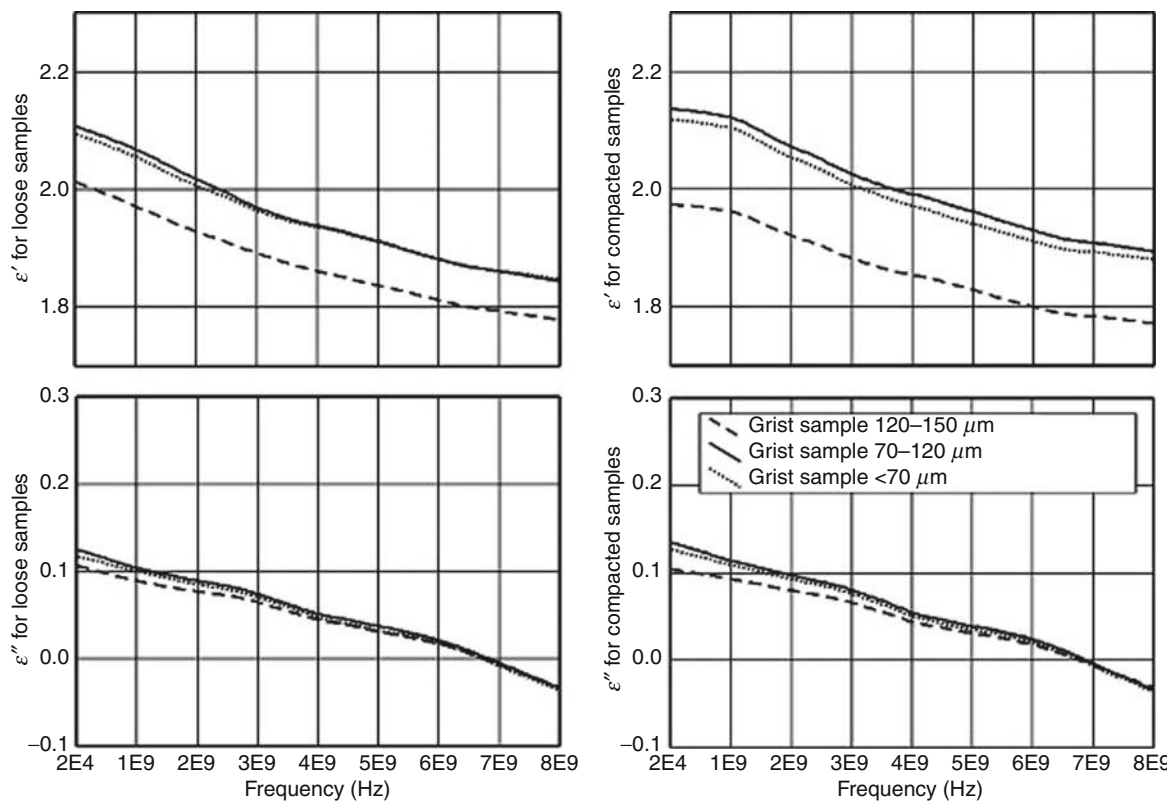
The values of electric permeability ϵ' and ϵ'' versus frequency have been illustrated in Figure 2 for loose samples. In course of examinations we have found that the impact of dust compression on frequency characteristics is insignificant in case of the real as well as imaginary component of electric permeability.

The value of component of electric permeability ϵ'' is small in comparison with the real component.

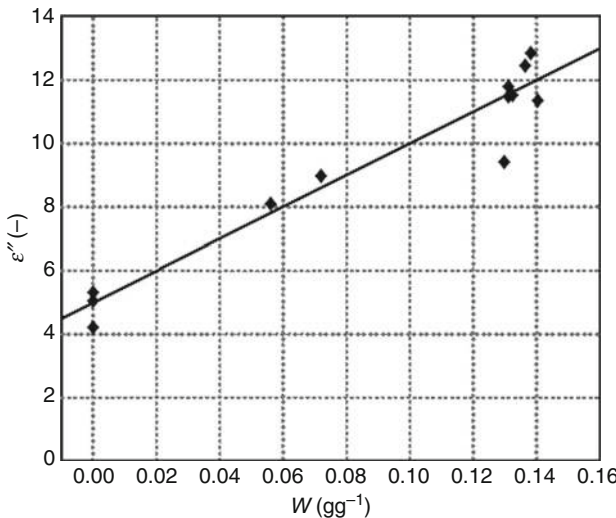
In case of wet samples (Figure 2), the values of the real ϵ' and imaginary component ϵ'' are insignificantly increased for compressed dust samples in comparison with the loose dust samples.



Organic Dusts, Electrostatic Properties, Figure 1 Particle size distribution for three samples of dust obtained from "Zawisza" wheat grains.



Organic Dusts, Electrostatic Properties, Figure 2 Frequency characteristics of the real ϵ' and imaginary component ϵ'' of complex electric permeability ϵ for the samples after moisture elimination, with diversified particle size distribution.



Organic Dusts, Electrostatic Properties, Figure 3 The value of imaginary electric permeability ϵ'' in dust solid phase versus moisture.

From the diagrams presented in the Figures 1 and 2 it appears that no relaxation phenomena are present because any significant increase of ϵ'' accompanied by reduction of ϵ' for the same frequency has been not found. Therefore it is possible to determine electric conductivity σ basing upon the measurements of the component ϵ'' (Equation 3).

The variability range σ for the dust under examination is included between 0.0 and $0.04 \text{ S} \cdot \text{m}^{-1}$, the higher value refers to wet samples.

The value of electric permeability for organic dusts is strongly influenced by their humidity and increases versus humidity in accordance with linear relationship.

An example of the curve of imaginary electric permeability measured by means of TDR method (Time Domain Reflectometry) has been illustrated in Figure 3.

The value of electric permeability in dust is reduced when its temperature is increased. The impact of the temperature is lower than that of moisture.

In case of increased density of the dust the value of its electric permeability is proportionally increased.

Summary

The organic dusts are produced in natural environments as well as in manufacturing processes carried out in the corn mills and in animal feed manufacturing plants. The plant dust particles are classified as dielectric materials characterized by low polarizability, diversified shapes, frequently nonuniform structures, and diversified particle sizes. The size of particles of dust occurring in agricultural and food industry and in nature is diversified, that is, large, medium, and small particles are contained. Therefore the classification of dust, that is, in coarse or fine category depends on the percentage of particles of a size, that is, particle size distribution of the dust.

Bibliography

- Hlaváčová, Z., 2005. Utilization of electric properties of granular and powdery materials. *International Agrophysics*, **19**, 209–213.
- Nelson, S. O., 2005. Density-permittivity relationships for powdered and granular materials. *IEEE Transactions on Instrumentation and Measurement*, **54**, 2003–2040.
- Pietrzyk, W., 2001. Models of cereal grains applied in electrodynamic analysis. *Acta Agrophysica*, **42**, 1–126 (in Polish).
- Pietrzyk, W., and Ścibisz, M., 2000. Electrostatic filter. Patent no. 315984. Polish Patent Office in Warsaw (in Polish).
- PN-91/Z-04018/04: Protection of air quality. Research of the content of free crystalline silica. Determination of free crystalline silica in total and respirable dust in the presence of silicates for work stations by means of colorimetric method. Polish standard (in Polish).
- PN-91/Z-04030/05: Protection of air quality. Dust content research. Determination of total dust content for work stations by means of filtration – weighing method. Polish standard (in Polish).
- PN-91/Z-04030/06: Protection of air quality. Dust content research. Determination of respirable dust content for work stations by means of filtration – weighing method. Polish standard (in Polish).
- Skierucha, W., and Wilczek, A., 2008a. Physical properties of technological dusts. In Pietrzyk, W. (ed.), *Bifilar Electrofilter Designed for the Elimination of Plant Origin Dusts*. Lublin: Scientific Publishing FRNA, Committee of Agrophysics – Polish Academy of Sciences, pp. 9–22 (in Polish).
- Skierucha, W., and Wilczek, A., 2008b. Influence of humidity on dielectric permeability of dust. In Pietrzyk, W. (ed.), *Bifilar Electrofilter Designed for the Elimination of Plant Origin Dusts*. Lublin: Scientific Publishing FRNA, Committee Agrophysics – Polish Academy of Sciences, pp. 23–32 (in Polish).
- Skierucha, W., Wilczek, A., Horyński, M., and Sumorek, A., 2008. Determination of electromechanical properties of dusts obtained from cereal grain. *Transactions of the American Society of Agricultural and Biological Engineers*, **51**, 177–184.

Cross-references

- [Dielectric Properties of Agricultural Products](#)
[Electrical Properties of Agricultural Products](#)
[Physical Properties as Indicators of Food Quality](#)

ORGANIC FARMING, EFFECT ON THE SOIL PHYSICAL ENVIRONMENT

Apostolos Papadopoulos

Research and Development, Branston Ltd, Branston, UK

Definition

Organic farming is based on the concept of sustainability, in which the inherent fertility and biological activity of the soil is returned such that, with careful management, the soil can remain consistently productive over long periods of time (Lampkin, 1990). As such, it relies on the use of crop rotations, animal and green manures, and biological pest control, combined with abstention from using synthetic fertilizers and pesticides (USDA, 1980).

Introduction

Conventional agriculture relies heavily on the use of synthetic fertilizers, pesticides, and intensive tillage methods

to meet its objectives of high yields and low labor requirements (Gerhardt, 1997). Conventional farming systems have evolved with a primary emphasis on high yield and quality of crop production, and secondary considerations for the condition of the soil (Reganold, 1995).

It has been suggested that organic farming systems are “a valid alternative approach,” which deliver agronomic and environmental benefits (Stockdale et al., 2001) and offer potential for better soil physical conditions (Shepherd et al., 2002). The basic philosophy within which all organic certification bodies work, is one of building and maintaining inherent soil fertility, through the employment of natural biological processes, as opposed to importing short-term fertility in the form of soluble mineral fertilizers and pesticides, as occurs in conventional farming (Defra, 2002).

Organic farming vs. conventional farming

Pulleman et al. (2003) found that when compared with conventional arable, organic soil showed increased total soil organic matter (SOM), earthworm activity, water-stable macro-aggregation, and N mineralization, which are important indicators of soil quality. Although less sensitive to slaking than soil under conventional arable, organic arable soil has been shown to be susceptible to compaction due to tillage, traffic, and grazing under Dutch climatic conditions. Structural degradation due to slaking or compaction results in unfavorable conditions for crop production, mineralization, and workability of the soil (Jensen et al., 1996; Droogers et al., 1997).

Droogers and Bouma (1996) found that greater SOM content under organic arable resulted in increased soil strength compared with conventional arable. SOM content is an important indicator of soil physical quality. Soils under long-term intensive arable agriculture, in which SOM levels decline compared to the value under native vegetation, permanent pasture, or ley-arable rotations, could become increasingly sensitive to physical damage. However, Watts et al. (2001) stated in less well-structured soils, a small loss of SOM may result in a dynamic lowering in soil physical quality. One factor that may help to prevent a continuous decline in soil quality is the ability of damaged soils to reaggregate around organic matter. Reganold (1988) in another study found organic soils had a more granular structure, a less hard and more friable consistency, and a significantly greater A horizon and SOM than conventional soils. Defra (2002) stated on average, comparisons with nonorganic systems did not show organically farmed soils to be consistently better or worse in terms of structure. Shepherd et al. (2002) concluded that a few differences in organic matter content have been found between organic and conventionally managed pasture soils, and only small differences found between conventional and organically managed arable soils in the UK.

Siegrist et al. (1998) emphasized the importance of the ley phase, and its duration, in maintaining large earthworm populations in organic rotations and it has been

argued that clover is particularly beneficial to earthworms because of its high protein content (Edwards and Bohlen, 1996). These findings are consistent with other studies. Berry and Karlen (1993) found higher populations of earthworms in organic as compared with conventional stockless systems. In contrast, Yeates et al. (1997) found greater earthworm biomass in conventional rather than organic grassland soils. Anon (1998) also found that in most cases, the benefits of leys did not persist much beyond the first year of arable cropping.

Defra (2002) concluded that organic farming practices have a positive effect on soil microbial numbers, processes, and activities. Van Diepeningen et al. (2006) reported that changing from conventional to organic farming leads to a gradual increase in biodiversity. They also indicated that higher biodiversity in organic soil can be due to the lower plow depth and especially the use of organic amendments and absence of mineral fertilizers. Pest and root diseases are generally less severe in organically managed soils than in conventionally managed soils (Van Bruggen and Termoshuizen, 2003). Much of the cited literature has made direct comparisons between organic/biodynamic and non-organically managed soils (i.e., Pulleman et al., 2003; Droogers and Bouma, 1996) with the evidence generally supporting greater microbial population size, diversity and activity, and benefits to other soil organisms. Little is currently known about the influence of changes in biomass size/activity/diversity on soil processes and rates of processes. Neither is it possible to conclude that all organic farming practices have beneficial effects while nonorganic practices have negative effects.

Tillage operations modify soil structure and distribute energy-rich organic substrates into the soil. Pulleman et al. (2003) mentioned the effects of mechanical disturbance during tillage and harvest might also explain why long-term organic matter protection in stable aggregates is not increased under organic arable.

Conclusion

The conventional soil management practices, such as frequent soil mixing by tillage, and by leaving the soil bare during crucial times, are associated with an increased oxidation of organic matter and subsequent reduction of organic matter levels, increasing the risk of erosion. Management practices such as the organic matter input, no tillage cultivations, the use of less synthetic pesticides, and more of soil improvement products based on biological activity, which are associated with organic farming, promote a more active soil physical environment with positive effects to the environment and agriculture.

Bibliography

- Anon, 1998. *Final Report: Modelling Earthworm Populations – Comparing Organic and Conventional Arable Rotations*. University of Aberystwyth and Elm Farm.
- Berry, E. C., and Karlen, D. L., 1993. Comparison of alternative farming systems II. Earthworm population density and species

- diversity. *American Journal of Alternative Agriculture*, **8**, 21–26.
- Defra, 2002. Understanding soil fertility in organically farmed soils. Defra (project OF0164).
- Droogers, P., and Bouma, J., 1996. Biodynamics vs. conventional farming effects on soil structure expressed by simulated potential productivity. *Soil Science Society of America Journal*, **60**, 1552–1558.
- Droogers, P., van der Meer, F. B. W., and Bouma, J., 1997. Water accessibility to plant roots in different soil structures occurring in the same soil type. *Plant and Soil*, **188**, 83–91.
- Edwards, C. A., and Bohlen, P. J., 1996. *Biology and Ecology of Earthworms*. London: Chapman and Hall.
- Gerhardt, R. A., 1997. A comparative analysis of the effects of organic and conventional farming systems on soil structure. *Biological Agriculture and Horticulture*, **14**, 139–157.
- Jensen, L. S., McQueen, D. J., and Shepherd, T. G., 1996. Effects of soil compaction on N-mineralisation and microbial –C and –N. I. Field measurements. *Soil and Tillage Research*, **38**, 175–188.
- Lampkin, N., 1990. *Organic Farming*. Ipswich: Farming.
- Pulleman, M., Jongmans, A., Marinissen, J., and Bouma, J., 2003. Effects of organic versus conventional arable farming on soil structure and organic matter dynamics in a marine loam in the Netherlands. *Soil Use and Management*, **19**, 157–165.
- Reganold, J. P., 1988. Comparison of soil properties as influenced by organic and conventional farming systems. *American Journal of Alternative Agriculture*, **3**, 144–154.
- Reganold, J. P., 1995. Soil quality and profitability of biodynamic and conventional systems: a review. *American Journal of Alternative Agriculture*, **10**, 36–45.
- Shepherd, M. A., Harrison, R., and Webb, J., 2002. Managing soil organic matter – implications for soil structure on organic farms. *Soil Use and Management*, **18**, 284–292.
- Siegrist, S., Schaub, D., Pfiffner, L., and Mäde, P., 1998. Does organic agriculture reduce soil erodibility? The results of a long-term field study on loess in Switzerland. *Agriculture, Ecosystems and Environment*, **69**, 253–264.
- Stockdale, E. A., Lampkin, N. H., Hovi, M., Keatinge, R., Lennartsson, E. K. M., MacDonald, D. W., Padel, S., Tattersall, F. H., Wolfe, M. S., and Watson, C. A., 2001. Agronomic and environmental implications of organic farming systems. *Advances in Agronomy*, **70**, 261–327.
- U.S. Department of Agriculture, 1980. Soil and water resources conservation act. Summary of Appraisal, Parts 1 and 2 and Program Report. Washington, D.C.: U.S. Government Printing Office.
- Van Bruggen, A. H. C., and Termoshouzen, A. J., 2003. Integrated approaches to root disease management in organic farming systems. *Australian Plant Pathology*, **32**, 141–156.
- Van Diepeningen, A. D., de Vos, O. J., Korthals, G. W., and van Bruggen, A. H. C., 2006. Effects of organic versus conventional management on chemical and biological parameters in agricultural soils. *Applied Soil Ecology*, **31**, 120–135.
- Watts, C. W., Whalley, W. R., Longstaff, D. J., White, R. P., Brooke, P. C., and Whitmore, A. P., 2001. Aggregation of a soil with different cropping histories following the addition of organic materials. *Soil Use and Management*, **17**, 263–268.
- Yeates, G. W., Bardgett, R. D., Cook, R., Hobbs, P. J., Bowling, P. J., and Potter, J. F., 1997. Faunal and microbial diversity in three Welsh grassland soils under conventional and organic management regimes. *Journal of Applied Ecology*, **34**, 453–470.

Cross-references

[Agrophysical Properties and Processes](#)

[Microbes and Soil Structure](#)

[Organic Matter, Effects on Soil Physical Properties and Processes](#)

[Soil Physical Quality](#)

ORGANIC FERTILIZERS

See [Fertilizers \(Mineral, Organic\), Effect on Soil Physical Properties](#)

ORGANIC MATTER

Substances containing carbon compounds of plant and animal origin.

ORGANIC MATTER, EFFECTS ON SOIL PHYSICAL PROPERTIES AND PROCESSES

Rattan Lal

Carbon Management and Sequestration Center, SENR,
The Ohio State University, Columbus, OH, USA

Synonyms

Aeration and gaseous exchange between soil and the atmosphere; Anaerobiosis and poor aeration or lack of O₂ in soil; Densification and compaction; Greenhouse gases and radiatively-active gases; Soil organic matter and soil organic carbon; Soil structure and aggregation

Definition

Aggregation: Formation of secondary particles through flocculation and cementation of primary particles.

Densification: Increase in soil bulk density that restricts root growth and inhibits aeration.

Erodibility: Susceptibility of soil to erosion.

Erosivity: Energy of rainfall and wind to cause soil erosion.

Humification: Conversion of biomass (plant and animal residues) into humus.

Illuviation: Transfer of material from surface into subsoil layers.

Nutrient Use Efficiency: Nutrient use per unit agronomic production (mg kg⁻¹).

Pedological Processes: Soil-related processes.

Saline Soils: Soils containing high concentration of salts and high electrical conductivity.

Soil C Sequestration: Transfer of atmospheric CO₂ into soil C pool.

Water Use Efficiency: Water use per unit agronomic production (mm kg⁻¹).

Introduction

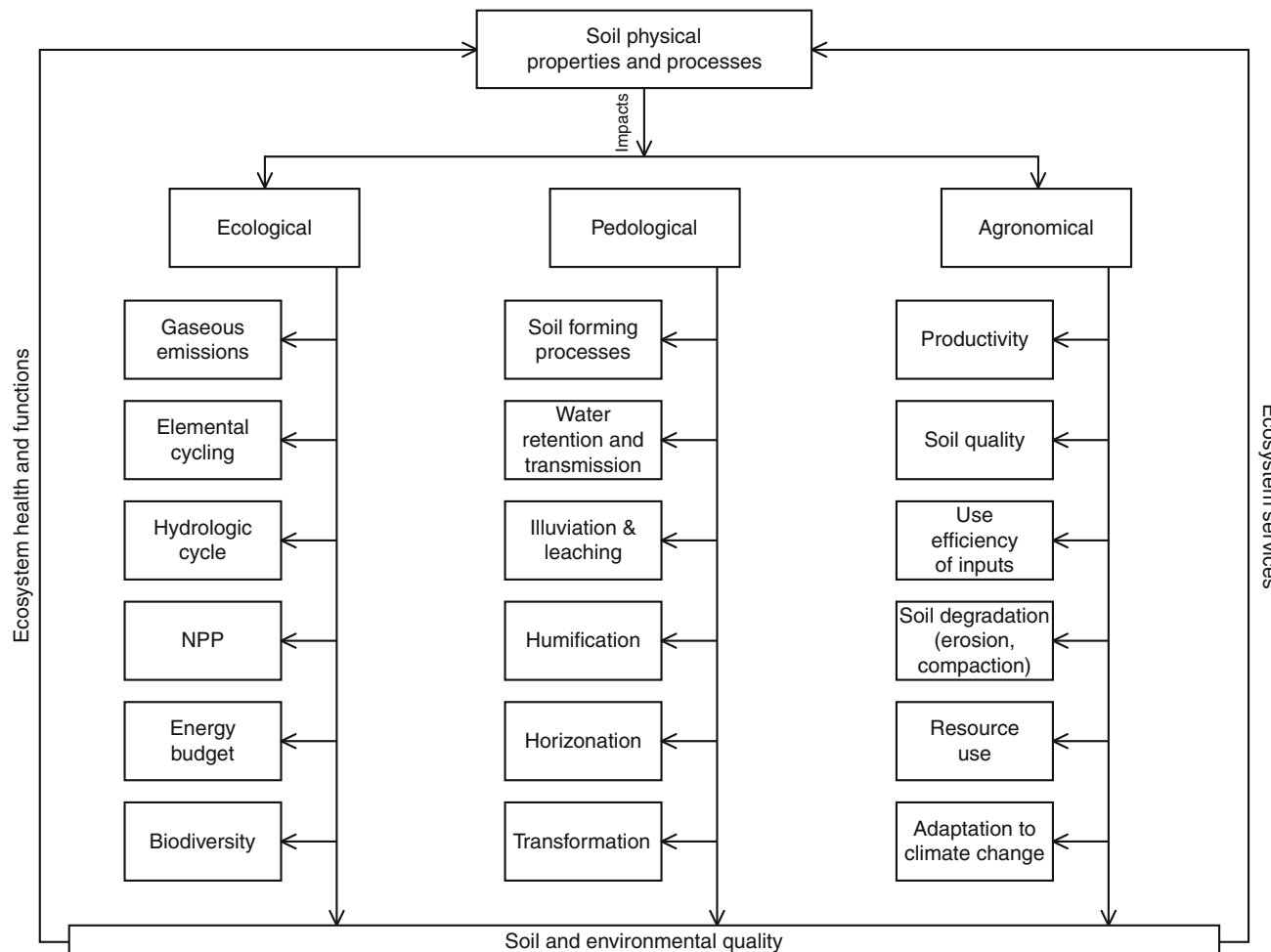
Soil physical properties include physical attributes related to: size distribution of particles (texture), arrangement of particles (structure), volume and continuity/stability of voids (porosity), amount of solids within a specified volume (density), movement of water into (infiltration) and through the soil (hydraulic conductivity), the amount of

water held in soil pores that plants (available water capacity) and microbes (residual water) can use, the amount of heat required to raise temperature of a unit mass of soil by 1°C (heat capacity), gaseous concentrations in soil atmosphere (soil air), and susceptibility of soil to erosion (erodibility). Principal processes mediated by key soil physical properties include: densification/compaction influenced by bulk density, crusting and infiltration by texture and structure, erosion by erodibility and texture, aeration by total/macropores and gaseous composition of soil air, soil warming by heat capacity, and runoff by infiltration rate and texture. These key properties strongly impact ecological, pedological, and agronomical processes with consequences to ecosystem services and ecological processes (Figure 1) at soilscape, landscape, and watershed scales and are affected by soil organic matter (SOM) and its dynamics (Janzen et al., 1997; Reynolds et al., 2002).

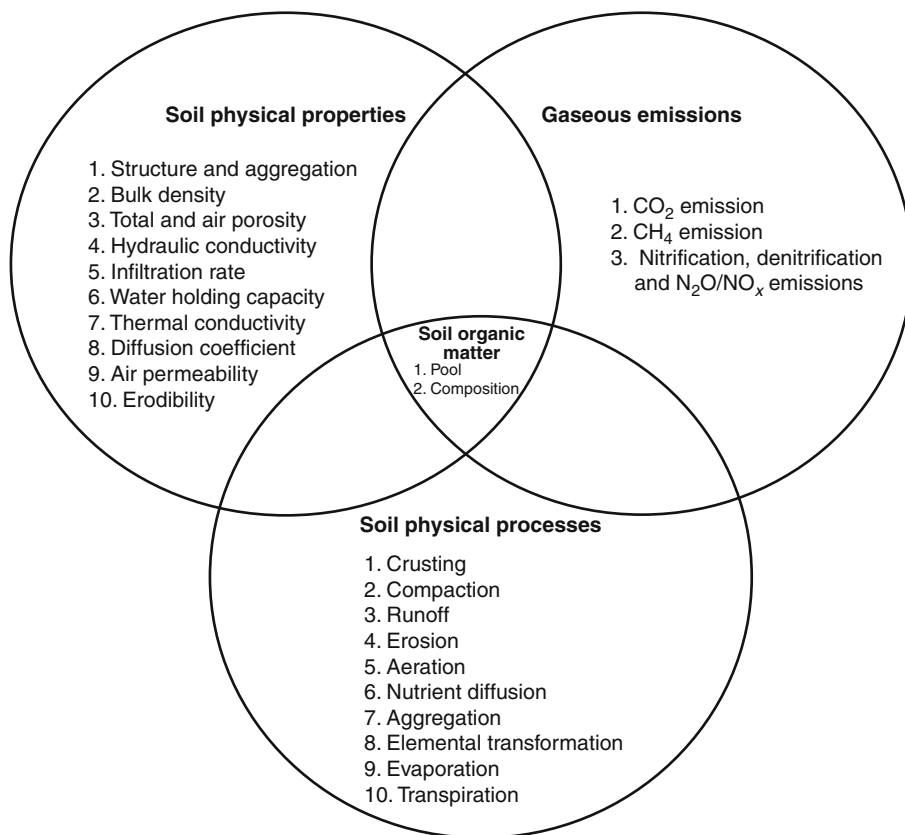
Soil physical properties mediate gaseous flux, elemental cycling, hydrological cycles, energy budgets,

biodiversity, and net primary productivity (NPP) among principal ecological processes. Similarly, rate of soil formation, humification, illuviation, horizonation and transformation, and leaching are examples of pedological processes affected by soil physical properties. Consequently, agronomic yield and productivity (use efficiency of input) is influenced by soil physical properties. Adaptation to climate, changes in seasonality and parameters affecting it, is mediated by soil physical properties and the related processes.

Changes in soil properties in turn affect soil organic matter (SOM) content and its turnover. For example, SOM affects soil properties (such as structure, porosity, density, hydraulic conductivity, water holding capacity, and thermal conductivity), which affect SOM pool and its dynamics. The latter also impacts principal processes such as crusting, compaction, water runoff, erosion, aeration, nutrient/elemental diffusion, and transformation. Furthermore, SOM is a key determinant of gaseous emissions including CO₂, CH₄, and N₂O. Strong connectivity



Organic Matter, Effects on Soil Physical Properties and Processes, Figure 1 Ecological, pedological, and agronomical impacts of soil physical properties and processes.



Organic Matter, Effects on Soil Physical Properties and Processes, Figure 2 Soil organic matter impacts on soil physical properties and processes.

and feedbacks among these properties and processes are mediated by SOM content, dynamic, and turnover. The SOM content and its quality impact soil physical properties and processes (Figure 2).

This article describes the importance of SOM on some soil physical processes mediated by physical properties and SOM content. Key processes discussed are gaseous flux between soil and the atmosphere, soil aggregation, water availability to plants, soil erosion, and soil compaction and densification.

Gaseous flux between soil and the atmosphere

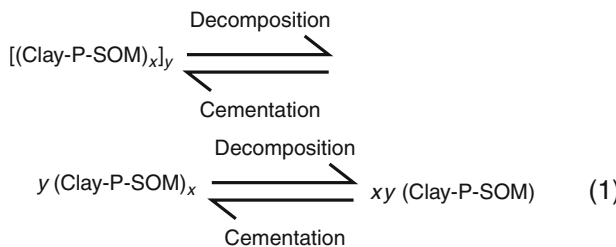
Soil can be a source or sink of greenhouse gases (GHGs) depending on land use, soil/vegetation management, and soil physical properties. Important soil physical properties affecting gaseous flux are bulk density, total and macro-porosity, and the degree of anaerobiosis or lack of oxygen in soil air. With good soil structure and adequate aeration, soil is a sink for CH₄ and vice versa. Similarly, soil aeration and structural properties moderate nitrification/denitrification process and the attendant emission of N₂O into the atmosphere. Annual flux of CO₂-C between soil and atmosphere, because of soil respiration, is about 60 Gt C year⁻¹ (Lal, 2004). With total soil organic carbon (SOC) pool of 2,500 Gt to 2 m depth (Batjes, 1999), the

mean residence time of C in world soils (pool/flux) is $2,500 \text{ Gt} \div (60 \text{ Gt C year}^{-1}) \cong 40 \text{ years}$. The site-specific residence time, however, varies among soil types and ecoregions depending on the SOC pool and CO₂-C flux. At soilscape scale, flux of CO₂-C from soil depends on both ambient and soil temperatures and moisture regimes, bulk density, and total and macro-porosity. Microbial activity increases with increase in soil temperature, leading to a strong variation in CO₂ flux among seasons, terrain aspect, landscape position, and management. The latter includes application of easily decomposable biomass (e.g., crop residues, compost, manure). The rate of soil respiration also depends on the presence of extracellular enzymes which degrade complex organic compounds and accentuate the rate of C turnover in soil (Allison and Jastrow, 2006). In contrast to C turnover that influences aggregation, turnover of aggregates can also influence the SOC pool and CO₂-C flux. Aggregate turnover directly controls the stabilization and physical protection of SOM (De Gryze et al., 2006). Soil microbial community dynamics is another important factor affecting CO₂ flux and C sequestration (Six et al., 2006). In view of the risks of projected global warming and the role of SOC in the global C cycle, understanding the magnitude and determinants of gaseous flux is important to mitigating

and adapting to climate change. Increasing aggregation, improving aeration, and creating positive C budgets are essential to making soil a net sink of CO₂ and CH₄ (Lal, 2004, 2010).

Soil aggregation

Soil structure and its formation are as important to biosphere as is photosynthesis but it is much less understood and is difficult to manage in intensive agroecosystems. Soil structure mediates many soil biological and physical processes and is influenced by SOM content, which acts as a cementing agent for binding clay particles into domains, domains into microaggregates (<250 µm), and microaggregates into macroaggregates (>250 µm). The SOM content is a key attribute of soil quality that strongly impacts formation and stabilization of soil aggregates (Franzluebbers, 2002). In general, bonds within microaggregates are stronger than those between microaggregates. Edwards and Bremner (1967) proposed the general model of aggregation as shown in **Equation 1**:



where P is a polyvalent cation, SOM is soil organic matter or humic substance, and x and y are number of units combined together to form microaggregates and macroaggregates. Tisdall and Oades (1982) indicated that microaggregates are formed in stages with different types of bonds at each stage. Soil aggregation is related to many biological processes in the root zone (Batten et al., 2005). Roots and external hyphae are also important to formation of macroaggregates (Jastrow et al., 1998). Macroaggregation is positively influenced by fungal activity (Bossuyt et al., 2001). Aggregation may also be affected by increase in atmospheric abundance of CO₂, especially to faster turnover of macroaggregates compared to microaggregates (Six et al., 2001).

There are numerous soil management practices which affect aggregation and SOM dynamics. Type and intensity of tillage, along with incorporation or maintenance of crop residues on the soil surface, strongly impacts aggregation and flux of soil C and N. Therefore, no-tillage (NT) and plow-based tillage affect soil structure differently (Six et al., 1998). Conversion of plow-based tillage to conservation tillage can enhance aggregation. Permanent raised bed systems, a form of conservation tillage, can also improve aggregation (Lichter et al., 2008). Use of NT farming enhances aggregation and improves soil structure (Six et al., 2002; Mahboubi and Lal, 1998). Aggregation is also strongly influenced by crop residue and its management. Removal of crop residues for other purposes

(e.g., biofuels) has adverse impact on soil physical properties, especially aggregation, crusting, infiltration rate, and hydraulic conductivity (Blanco-Canqui and Lal, 2007a, b, c, 2008). In general, aggregation increases linearly with increasing amounts of residue application (De Gryze et al., 2005; Duiker and Lal, 1999; Mulumba and Lal, 2008).

Plant available water capacity

The capacity of a soil to supply water to plant roots is an important attribute of soil physical quality especially in regions where rainfall is variable and soil-water storage is crucial to satisfying crop yields. Agronomic yield in arid and semiarid regions is sensitive to combination of small/variable rainfall and small available water capacity (AWC) of soils (Asseng et al., 2008). Soils with high AWC provide buffers to store water for use by plants between rainfall events (Wang et al., 2009). The AWC of soil (centimeter of water in the root zone), defined as the difference in field capacity and wilting point, differs among soils of different structural properties (Droogers et al., 1997). The AWC is defined by **Equation 2** as follows:

$$\text{AWC(cm)} = \sum_{i=1}^n (\theta_{fc} - \theta_{wp}) d_i \quad (2)$$

where θ_{fc} is the volumetric moisture content (cm³/cm³) retained in the soil after the free water (excess water) has been drained through the macropores by the force of gravity. In the laboratory, θ_{fc} is measured by subjecting a saturated undisturbed soil core (clod) to a pressure of 0.3 bar (30 kPa) for a fine-textured soil and 0.1 bar (10 kPa) for a coarse-textured soil. Soil moisture constant θ_{wp} is the volumetric soil moisture content when plants undergo permanent wilting and do not recover even when transferred to an atmosphere of 100% relative humidity. In the laboratory, θ_{wp} is measured when soil is subjected to a pressure of 15 bar (1,500 kPa). In coarse-textured soils, θ_{wp} may be attained at a low pressure of 1 bar (100 kPa). The term $(\theta_{fc} - \theta_{wp})$ is multiplied by the depth (d, in cm) and summed for the number of layers (n) comprising the effective/desired rooting depth (Dane and Hopmans, 2002; Topp et al., 1993). Management of θ_{fc} , determined by aggregation through interaction between texture and SOM content, is essential to enhancing AWC.

Increase in SOM concentration in soil increases θ_{fc} (Rakic et al., 2009) but has no or less impact on θ_{wp} . Thus, a soil with higher SOM content has more AWC than the same soil with lower SOM (Lowery et al., 1996; Lal, 1994). The beneficial impact of SOM on AWC is more on coarse-textured than fine-textured soils (Wesseling et al., 2009). Thus, AWC can be improved through adoption of those agricultural practices which enhance SOM content. Important among these are organic amendments (e.g., compost, farm yard manure) and use of crop residues (Becher, 1996; Bhogal et al., 2009). Incorporation of compost can increase AWC even in drastically disturbed soils (Curtis and Claassen, 2005) and in saline soils (Groenveld et al., 2004).

Soil compaction and densification

Increase in soil bulk density, more solids per unit volume, is a problem in intensively mechanized farm operations involving frequent traffic of heavy machinery. All other factors remaining the same (e.g., texture, vehicular traffic), soils with higher SOM content and stable aggregates are less susceptible to densification than those with lower SOM content and weak aggregates (Soane, 1988). In general, soil bulk density decreases linearly with increase in SOM content (Angers and Simard, 1986; Rawls, 1983; Zaytsev, 1967; Saini, 1966). Soil compaction adversely impacts agronomic production by decreasing crop growth (Nadian et al., 2005; Arvidsson, 1998; Gemtos and Lellis, 1997), reducing root penetration, and reducing AWC (Ohu et al., 1986). Therefore, addition of organic matter reduces risks of soil compaction (Mamman et al., 2007) by decreasing bulk density and increasing activity of earthworms and other soil biota (Jordan et al., 2000; Ruehlmann and Korschens, 2009). Reduction in compaction increases crop yields and the overall agronomic productivity (Ohu et al., 1986, 1987; Janssen and Vanderweert, 1977). Application of sphagnum peat can also decrease bulk density, improve AWC, and enhance potato (*Solanum tuberosum* L.) yield even in sandy soils (Li et al., 2004).

Soil erosion and organic matter content

Accelerated soil erosion (by water and wind) is among the serious global issues of the twenty-first century. Soil degradation by erosion affects agronomic productivity (Lal, 1998) and accentuates emissions of GHGs into the atmosphere (Lal, 2003). The potential hazard of soil erosion is determined by two factors: climatic erosivity and soil erodibility. The latter, susceptibility of a soil to erosional processes, depends on key soil physical properties including texture, structure, infiltration rate, permeability, and SOM content. In general, soil erodibility decreases with increase in structural stability, and the latter increases with increase in SOM content (Lal and Elliot, 1994). The SOM content can have a strong impact on detachment of particles, especially in soils of low activity clays (Kuhn, 2007). Therefore, management of SOM content is essential to an effective erosion control.

One of the co-benefits of soil C sequestration is erosion control and reduction of the nonpoint source pollution (Lal, 2004). Increase in SOM concentration reduces soil erosion risks by increasing aggregation, decreasing erodibility, reducing susceptibility to crusting and compaction, improving activity of earthworms and other soil fauna, increasing infiltration rate, and reducing runoff rate and amount, and decreasing dissolved and suspended loads in surface flow. Soils with high SOM content generate lower amounts of particles/sediments available for transport by soil and inter-soil processes.

Conclusions

The SOM content is important to enhancing and sustaining physical properties and processes. Soil physical

properties affected by SOM include bulk density, aggregation, water retention and movement, air composition, and heat capacity and transmission. Soil physical processes impacted by SOM content include crusting, compaction, water runoff, erosion, gaseous diffusion, and nutrient transformation and movement. These properties and processes are moderated by amount, quality, and dynamics (turnover) of SOM.

Thus, SOM content is an important property for improving and enhancing soil physical quality. Maintenance of SOM content above the critical threshold level is essential to formation and stabilization of soil aggregates, creation, and stabilization of transmission and retention pores and their continuity, buffering soils against compactive and erosive forces, and increasing plant available water capacity. Use efficiency of agronomic input is more for soils with high than low SOM content.

Therefore, strategy of sustainable soil management is to create positive C and elemental budgets (N, P, S, K). Soil and crop management practices which enhance SOM content include conservation tillage with use of crop residue mulch, cover cropping, use of organic amendments (e.g., manure, compost, biochar), and adoption of complex farming systems including agroforestry.

Through their strong impact on soil physical properties and processes, SOM content and dynamics affect ecosystem services such as moderation of atmospheric chemistry through rendering soil a source or sink of GHGs, catalysis of photosynthesis and increase in net primary production and food to ensure food/nutritional security, filtration and purification of natural waters with attendant impact on nonpoint source pollution and hypoxia of coastal ecosystems, and creation of habitat and energy source for soil microorganisms and other biota. Maintenance of SOM content above the threshold level is essential to the desirable/required level of soil's life support systems. Indeed, SOM pool is nation's precious resource. It must be improved, restored, and judiciously managed for the maintenance of the ecosystem services.

Bibliography

- Allison, S. D., and Jastrow, J. D., 2006. Activities of extracellular enzymes in physically isolated fractions of restored grassland soils. *Soil Biology and Biochemistry*, **38**, 3245–3256.
- Angers, D. A., and Simard, R. R., 1986. Relationships between organic-matter content and soil bulk density. *Canadian Journal of Soil Science*, **66**, 743–746.
- Arvidsson, J., 1998. Influence of soil texture and organic matter content on bulk density, air content, compression index and crop yield in field and laboratory compression experiments. *Soil and Tillage Research*, **49**, 159–170.
- Asseng, S., Milroy, S. P., and Poole, M. L., 2008. Systems analysis of wheat production on low water-holding soils in a Mediterranean-type environment, yield potential and quality. *Field Crops Research*, **105**, 97–106.
- Batjes, N. H., 1999. *Management Options for Reducing CO₂-Concentrations in the Atmosphere by Increasing Carbon Sequestration in the Soil*. ISRIC Technical Paper 30. Wageningen, Holland.

- Batten, K. M., Six, J., Scow, K. M., and Rillig, M. C., 2005. Plant invasion of native grassland on serpentine soils has no major effects upon selected physical and biological properties. *Soil Biology and Biochemistry*, **37**, 2277–2282.
- Becher, H. H., 1996. Influence of organic amendments on soil physical properties. *Zeitschrift für Pflanzenährung und Bodenkunde*, **159**, 121–127.
- Bhogal, A., Nicholson, F. A., and Chambers, B. J., 2009. Organic carbon additions: effects on soil biophysical and physicochemical properties. *European Journal of Soil Science*, **60**, 276–286.
- Blanco-Canqui, H., and Lal, R., 2007a. Impact of long-term wheat straw management on soil hydraulic properties under no-tillage. *Soil Science Society of America Journal*, **71**, 1166–1173.
- Blanco-Canqui, H., and Lal, R., 2007b. Soil and crop response to harvesting corn residues for biofuel production. *Geoderma*, **141**, 355–362.
- Blanco-Canqui, H., and Lal, R., 2007c. Soil structure and organic carbon relationships following 10 years of wheat straw management in no-till. *Soil and Tillage Research*, **95**, 240–254.
- Blanco-Canqui, H., and Lal, R., 2008. Stover removal impacts on microscale soil physical properties. *Geoderma*, **145**, 335–346.
- Bossuyt, H., Denef, K., Six, J., Frey, S. D., Merckx, R., and Paustian, K., 2001. Influence of microbial populations and residue quality on aggregate stability. *Applied Soil Ecology*, **16**, 195–208.
- Curtis, M. J., and Claassen, V. P., 2005. Compost incorporation increases plant available water in a drastically disturbed serpentine soil. *Soil Science*, **170**, 939–953.
- Dane, J. H., and Hopmans, J. W., 2002. Pressure plate extractor. In Dane, J. H., and Tupp, G. C. (eds.), *Methods of Soil Analysis, Part 4*. Madison: Soil Science Society of America, pp. 688–690.
- De Gryze, S., Six, J., Brits, C., and Merckx, R., 2005. A quantification of short-term macroaggregate dynamics; influences of wheat residue input and texture. *Soil Biology and Biochemistry*, **37**, 55–66.
- De Gryze, S., Six, J., and Merckx, R., 2006. Quantifying water-stable soil aggregate turnover and its implication for soil organic matter dynamics in a model study. *European Journal of Soil Science*, **57**, 693–707.
- Droogers, P., van der Meer, F. B. W., and Bourma, J., 1997. Water accessibility to plant roots in different soil structures occurring in the same soil type. *Plant and Soil*, **188**, 82–91.
- Duiker, S. W., and Lal, R., 1999. Crop residue and tillage effects on C sequestration in a Luvisol in central Ohio. *Soil and Tillage Research*, **52**, 73–81.
- Edwards, A. P., and Bremner, J. M., 1967. Micro-aggregates in soils. *Journal of Soil Science*, **18**, 64–73.
- Franzuebers, A. J., 2002. Water infiltration and soil structure related to organic matter and its stratification with depth. *Soil and Tillage Research*, **66**, 197–205.
- Gemtos, T. A., and Lellis, T., 1997. Effects of soil compaction, water and organic matter contents on emergence and initial plant growth of cotton and sugar beet. *Journal of Agricultural Engineering Research*, **66**, 121–134.
- Groenveld, P. H., Grant, C. D., and Murray, R. S., 2004. On water availability in saline soils. *Australian Journal of Soil Research*, **42**, 833–840.
- Janssen, B. H., and Vanderweert, R., 1977. Influence of fertilizers, soil organic matter and soil compaction on maize yields on Surinam Zanderij soils. *Plant and Soil*, **46**, 445–458.
- Janzen, H. H., Campbell, C. A., Ellert, B. H., and Bremer, E., 1997. Soil organic matter dynamics and their relationship to soil quality. In Gregorich, E. G., and Carter, M. R. (eds.), *Soil Quality for Crop Production and Ecosystem Health*. Amsterdam: Elsevier, pp. 277–291.
- Jastrow, J. D., Miller, R. M., and Lussenhop, J., 1998. Contributions of interacting biological mechanisms to soil aggregate stabilization in restored prairie. *Soil Biology and Biochemistry*, **30**, 905–916.
- Jordan, D., Hubbard, V. C., Ponder, F., and Berry, E. C., 2000. The influence of soil compaction and the removal of organic matter on two native earthworms and soil properties in an oak-hickory forest. *Biology and Fertility of Soils*, **31**, 323–328.
- Kuhn, N. J., 2007. Erodibility of soil and organic matter: independence of organic matter resistance to interrill erosion. *Earth Surface Processes and Landforms*, **32**, 794–802.
- Lal, R., 1994. *Methods and Guidelines for Assessing Sustainable Use of Soil and Water Resources in the Tropics*. SMSS Soils Bulletin 21. Washington, DC: USDA-NRCS.
- Lal, R., 1998. Soil erosion impact on agronomic productivity and environment quality. *Critical Reviews in Plant Sciences*, **17**, 319–464.
- Lal, R., 2003. Soil erosion and the global carbon budget. *Environment International*, **29**, 437–450.
- Lal, R., 2004. Soil carbon sequestration impacts on global climate change and food security. *Science*, **304**, 1623–1627.
- Lal, R., and Elliot, W., 1994. Erodibility and erosivity. In Lal, R. (ed.), *Soil Erosion Research Methods*, 2nd edn. Ankeny: SWCS, pp. 181–210.
- Lal, R., 2010. Managing soils and ecosystems for mitigating anthropogenic carbon emissions and advancing global food security. *BioScience*, **60**, 708–721.
- Li, H., Parent, L. E., Karam, A., and Tremblay, C., 2004. Potential of sphagnum peat for improving soil organic matter, water holding capacity, bulk density and potato yield in a sandy soil. *Plant and Soil*, **265**, 355–365.
- Lichter, K., Govaerts, B., Six, J., Sayre, K. D., Deckers, J., and Dendooven, L., 2008. Aggregation and C and N contents of soil organic matter fractions in a permanent raised-bed planting system in the highlands of Central Mexico. *Plant and Soil*, **305**, 237–252.
- Lowery, B., Arshad, M. A., Lal, R., and Hickey, W. J., 1996. Soil water parameters and soil quality. In Doram, J. W., and Jones, A. J. (eds.), *Methods for Assessing Soil Quality*. Madison: Soil Science Society of America, pp. 143–157. Special Publication 49.
- Mahboubi, A. A., and Lal, R., 1998. Long-term tillage effects on changes in structural properties of two soils in central Ohio. *Soil and Tillage Research*, **45**, 107–118.
- Mamman, E., Ohu, J. O., and Crowther, T., 2007. Effect of soil compaction and organic matter on the early growth of maize (*Zea mays L.*) in a vertisol. *International Agrophysics*, **21**, 367–375.
- Mulumba, L. N., and Lal, R., 2008. Mulching effects on selected soil physical properties. *Soil and Tillage Research*, **98**, 106–111.
- Nadian, H., Barzegar, A. R., Rouzitalab, P., Herbert, S. J., and Hashemi, A. M., 2005. Soil compaction, organic matter, and phosphorus addition effects on growth and phosphorus accumulation of clover. *Communications in Soil Science and Plant Analysis*, **36**, 1327–1335.
- Ohu, J., Raghavan, G. S. V., and McKyes, E., 1986. Effect of reduction of soil compaction through organic matter incorporation on crop yield. *Soil and Tillage Research*, **8**, 325–325.
- Ohu, J., Raghavan, G. S. V., Prasher, S., and Mehuy, G., 1987. Prediction of water-retention characteristics from soil compaction data and organic matter content. *Journal of Agricultural Engineering Research*, **38**, 27–35.
- Rakic, T., Quartacci, M. F., Cardelli, R., Navari-Izzo, F., and Stevanovic, B., 2009. Soil properties and their effect on water and mineral status of resurrection *Ramonda serbica*. *Plant Ecology*, **203**, 13–21.
- Rawls, W. J., 1983. Estimating soil bulk density from particle size analysis and organic matter content. *Soil Science*, **135**, 123–125.
- Reeve, M. J., and Carter, A. D., 1991. Water release characteristics. In Smith, K. A., and Mullins, C. E. (eds.), *Soil Analysis: Physical Methods*. New York: Marcel Dekker, pp. 111–160.

- Reynolds, W. D., Bowman, B. T., Drury, C. F., Tan, C. S., and Lu, X., 2002. Indicators of good soil physical quality: density and storage parameters. *Geoderma*, **110**, 131–146.
- Ruehlmann, J., and Korschens, M., 2009. Calculating the effect of soil organic matter concentration on soil bulk density. *Soil Science Society of America Journal*, **73**, 876–885.
- Saini, G. R., 1966. Organic matter as a measure of bulk density of soil. *Nature*, **210**, 1295.
- Six, J., Elliott, E. T., Paustian, K., and Doran, J. W., 1998. Aggregation and soil organic matter accumulation in cultivated and native grassland soils. *Soil Science Society of America Journal*, **62**, 1367–1377.
- Six, J., Carpentier, A., van Kessel, C., Merckx, R., Harris, D., Horwath, W. R., and Luscher, A., 2001. Impact of elevated CO₂ on soil organic matter dynamics as related to changes in aggregate turnover and residue quality. *Plant and Soil*, **234**, 27–36.
- Six, J., Feller, C., Denef, K., Ogle, S. M., Sa, J. C. D., and Albrecht, A., 2002. Soil organic matter, biota and aggregation in temperate and tropical soils – effects of no-tillage. In *11th International Nitrogen Workshop*, 9–12 September 2001, Reims, France; *Agronomie*, **22**, 755–775.
- Six, J., Frey, S. D., Thiet, R. K., and Batten, K. M., 2006. Bacterial and fungal contributions to carbon sequestration in agroecosystems. *Soil Science Society of America Journal*, **70**, 555–569.
- Soane, B. D., 1988. The role of organic matter in soil compaction. *Journal of the Science of Food and Agriculture*, **45**, 134–135.
- Tisdall, J. M., and Oades, J. M., 1982. Organic matter and water stable aggregates in soils. *Journal of Soil Science*, **33**, 141–163.
- Topp, G. C., Galganev, Y. T., Ball, B. C., and Carter, M. R., 1993. Soil water desorption curves. In Carter, M. R. (ed.), *Soil Analysis: Physical Methods*. New York: Marcel Dekker, pp. 111–160.
- Wang, E., Cresswell, H., Xu, J., and Jiang, Q., 2009. Capacity of soils to buffer impact of climate variability and value of seasonal forecasts. *Agricultural and Forest Meteorology*, **149**, 38–50.
- Wesseling, J. G., Stoof, C. R., Ritsema, C. J., Oostindie, K., and Dekker, L. W., 2009. The effect of soil texture and organic amendment on the hydrological behavior of coarse-textured soils. *Soil Use and Management*, **25**, 274–283.
- Zaytsev, B. D., 1967. Quantitative relationship between organic matter content and bulk density of top horizons of podzolic forest soil. *Soviet Soil Science – USSR*, **12**, 1695.

Cross-references

- [Agrophysical Properties and Processes](#)
- [Anisotropy of Soil Physical Properties](#)
- [Bulk Density of Soils and Impact on Their Hydraulic Properties](#)
- [Carbon Losses Under Dryland Conditions, Tillage Effects](#)
- [Climate Change: Environmental Effects](#)
- [Conditioners, Effect on Soil Physical Properties](#)
- [Coupled Heat and Water Transfer in Soil](#)
- [Crop Responses to Soil Physical Conditions](#)
- [Cropping Systems, Effects on Soil Physical Properties](#)
- [Databases of Soil Physical and Hydraulic Properties](#)
- [Desertification: Indicators and Thresholds](#)
- [Earthworms as Ecosystem Engineers](#)
- [Field Water Capacity](#)
- [Flooding, Effects on Soil Structure](#)
- [Greenhouse Gas Fluxes: Effects of Physical Conditions](#)
- [Greenhouse Gases Sink in Soils](#)
- [Hardsetting Soils: Physical Properties](#)
- [Hydraulic Properties of Unsaturated Soils](#)
- [Hysteresis in Soil](#)
- [Infiltration in Soils](#)
- [Management Effects on Soil Properties and Functions](#)

Mechanical Resilience of Degraded Soils

- [Organic Farming, Effect on the Soil Physical Environment](#)
- [Physical Protection of Organic Carbon in Soil Aggregates](#)
- [Puddling: Effect on Soil Physical Properties and Crops](#)
- [Root Responses to Soil Physical Limitations](#)
- [Salinity, Physical Effects on Soils](#)
- [Soil Biota, Impact on Physical Properties](#)
- [Soil Physical Quality](#)
- [Tropical Soils, Physical Properties](#)
- [Wetting and Drying, Effect on Soil Physical Properties](#)

ORNAMENTAL PLANTS, PHYSICAL PROPERTIES

Paweł Szot

Institute of Ornamental Plants and Architecture of Landscape, University of Life Sciences, Lublin, Poland

Ornamental plants, similar to other crop plants, are characterized by considerable differentiation of physical traits, both within the species and cultivars grown and in the course of harvest, storage, and transport.

Ornamental plants, especially after their cutting (i.e., separation from the organs that supply water and mineral salts) rapidly lose their resistance to the effect of mechanical forces. In a highly simplified sense, the anatomy of plants comprises specialized tissues – collenchyma and sclerenchyma that form the mechanical structure. However, in the broader sense it relates to all cells, and thus the mechanical system of the plants should be considered on the level of a plant organ and not that of tissue. In the case of cut ornamental plants used for making floral compositions, the stem plays a highly important role. Among the fundamental mechanical properties that may represent stem strength are the bending force, stress, and strain (**Table 1**). Stem stress may occur under the effect of tensile or compressive forces, as a result of which reversible or irreversible strain takes place. In actual structures, deformation of a stem is always accompanied by shearing stress and strain, caused by forces that are parallel to the surface under consideration. In plant organs, shearing stress does not usually exceed the respective strength. When that is exceeded, there takes place a shift or split in the shear plane. In the case of stems of ornamental plants, what is significant is the bending strength and rigidity of the stem, and its resistance to buckling (i.e., deformation caused by compressive forces and resulting in bending of the compressed body). Every deformation is accompanied by an input of work.

Basically, a non-lignified cell wall has only tensile strength, like a sheet of paper. A cell in the state of turgor becomes resistant to compression, torsion, and bending, as in that state of the cell all the deforming forces become converted to forces applying tensile stress to the cell wall; hence, the special importance of the tensile strength of cell walls. The cell wall may be stiff and resistant to direct compression if it contains lignin. Also the presence of endogenous plant hormones has an effect on the

Ornamental Plants, Physical Properties, Table 1 Examples of mean values of selected mechanical properties of flower or inflorescence stems of some ornamental plants

Plant	Force causing permanent damage to the stem (N)	Stem deformation corresponding to the force value (mm)	Energy causing permanent damage to the stem (mJ)
<i>Allium aflatunense</i>	12.7	6.9	66.7
<i>Allium sphaerocephalon</i>	5.8	6.4	29.1
<i>Dalia</i> sp.	5.8	5.7	3.0
<i>Gerbera</i> sp.	1.7	21.0	18.0
<i>Tulipa</i> sp.	2.5	12.8	23.6

mechanical properties of plant stems. Auxins cause greater plasticity and elasticity of cell walls, and their effect depends on the content of pectins that may retain or release ions (Ca, Mg, or K).

The mechanical properties of stems and another part of ornamental plants can be enhanced through optimisation of cultivation of particular species, and application of suitable growth regulators and conditioners that also extend the ornamental values of the plants in time (Hetman et al., 1994; Szot and Rybczyński, 2008; Szot et al., 2009).

Bibliography

- Hetman, J., Szot, P., and Stepniewski, A., 1994. Preliminary study on mechanical properties of inflorescences stems of some cultivars of gerbera (in Polish). *Hodowla i nasiennictwo roślin ogrodniczych*, pp. 374–379.
 Szot, P., and Rybczyński, R., 2008. Influence of conditioning on morphological features and mechanical properties of tulip stem (in Polish). *Acta Agrophysica*, **12**, 777–790.
 Szot, P., Pogroszewska, E., and Rybczyński, R., 2009. Effect of growth regulators on mechanical properties of strelitzia leaves. *International Agrophysics*, **23**, 87–96.

ORTSTEIN, PHYSICAL PROPERTIES

Jacek Chodorowski

Department of Soil Science, Maria Curie-Skłodowska University, Lublin, Poland

Definition

Ortstein (German: *ort*-place, *stein*-stone) is defined by Soil Survey Staff (1992) as all or part of the spodic horizon, when moist, it is at least weakly cemented into a massive horizon that is present in more than half of each pedon.

Origin: Ortstein is usually a hard, partly or entirely cemented illuvial horizon B of podzol or gley-podzol soils, formed as a result of illuviation of aluminum, iron, manganese, and humus compounds from the overlying horizons. In gley-podzol soils, some iron and manganese compounds may come from precipitation from groundwater (Chodorowski, 2009). A huge accumulation of the complexes leads to the formation of coherent aggregates,

and even of continuous, highly cemented layers referred to as ortstein.

Properties: Ortstein is 25 mm or more thick and 50% or more (by volume) cemented (Soil Survey Staff, 1999). As a rule, the horizon has sandy grain-size distribution. Compared to the adjacent non-cemented horizons, ortstein usually has a higher bulk density (Lambert and Hole, 1971; Wang et al., 1978). It is also stronger; the penetration resistance of cone of the ortstein horizon may amount to the value of approximately 8 MPa (Chodorowski, 2009). Water retention and capillary conductivity of ortstein are more influenced by moisture content or matric potential than those of the adjacent horizons (Lambert and Hole, 1971). Due to strong cementation and high concentration of toxic aluminum and manganese ions, ortstein is a mechanical and chemical barrier to the root growth of both forest and crop plants.

Bibliography

- Chodorowski, J., 2009. *Origin, Age and Diagnostic Properties of Ortstein in the Light of Study of Sandy Soils in the Sandomierz Basin*. Lublin: Maria Curie-Skłodowska University Press. 132 p.
 Lambert, J. L., and Hole, F. D., 1971. Hydraulic Properties of an Ortstein Horizon. *Soil Science Society of America Proceedings*, **35**(5), 785–787.
 Soil Survey Staff, 1992. Keys to Soil Taxonomy. SMSS Technical Monograph No. 19. 5th edn. Blacksburg: Pocahontas, 541p.
 Soil Survey Staff, 1999. Soil Taxonomy. A Basic System of Soil Classification for Making and Interpreting Soil Surveys. 2nd edn. USDA, NRCS. Agriculture Handbook, No. 436. 870 p.
 Wang, C., Beke, G. J., and McKeague, J. A., 1978. Site characteristics, morphology and physical properties of selected ortstein soils from the Maritime Provinces. *Canadian Journal of Soil Science*, **58**, 405–420.

OSMOSIS

Diffusion of water from a dilute solution to a more concentrated solution through a permeable membrane separating the two solutions.

Cross-references

- Membranes, Role in Water Transport in the Soil–Root–Xylem System
 Water Uptake and Transports in Plants Over Long Distances

OSMOTIC POTENTIAL

See *Water Use Efficiency in Agriculture: Opportunities for Improvement*

OVERBURDEN PRESSURE

A term used in soil science and storage of granular solids in silo denoting the pressure imposed by the weight of overlying layers of material.

OVERLAND FLOW

Elias Dimitriou
Institute of Inland Waters, Hellenic Centre for Marine Research, Anavissos, Attika, Greece

Synonyms

Hortonian overland flow; Infiltration excess overland flow; Saturation excess overland flow; Surface runoff

Definition

Overland flow is the movement of water over the land, downslope toward a surface water body.

Overland flow is a very important aspect of the water cycle and can be generated under two different physical mechanisms. The infiltration excess overland flow is formed (named also Hortonian overland flow after Horton E. R.), when the rainfall intensity exceeds the soil infiltration capacity in an area (Liu et al., 2004). Then water accumulates on the soil and starts moving downslope, due to gravity, towards the hydrographic network. The second mechanism occurs when the soil saturation exceeds its maximum level due to groundwater uplifting, baseflow, and lateral subsurface water discharges, resulting in the appearance of saturation excess overland flow (Beven, 2001).

Factors such as soil permeability, topographic slope, and type and density of vegetation affect the development and distribution of overland flow in both time and space. Bare soil areas will facilitate infiltration excess overland flow because the energy of raindrops can lead to the rearrangement of the surface soil particles which will then create a crust and reduce the infiltration capacity. On the other hand, vegetation protects the soil and creates pathways for water infiltration through its roots and thus can reduce overland flow in an area (Beven, 2001). Additionally, for the formulation of saturation excess overland flow, the initial conditions of the local aquifer (water level and hydraulic conductivity), and the soil storage deficit play an important role in achieving the necessary soil saturation. An aquifer with well developed fracture system and good connectivity with the unsaturated zone can

maintain subsurface and baseflows for long time periods facilitating soil saturation and overland flow.

Bibliography

- Beven, J. K., 2001. *Rainfall – Runoff Modeling*. England: Wiley, p. 360.
Liu, Q. Q., Chen, L., Li, J. C., and Singh, V. P., 2004. Two-dimensional kinematic wave model of overland-flow. *Journal of Hydrology*, **291**, 28–41.

OXIDATION-REDUCTION REACTIONS IN THE ENVIRONMENT

Zofia Stepniewska

Department of Biochemistry & Environmental Chemistry,
The John Paul II Catholic University of Lublin, Lublin,
Poland

Synonyms

Oxidation-reduction conditions; Redox processes; Redox reactions

Definition

Oxidation-reduction (redox) reactions – reactions that are connected with electrons transfer from the atom oxidized to the atom reduced.

Oxidation-reduction conditions are connected with changes, where an element's positive valence is increased (electron loss), accompanied by a simultaneous reduction of element's valence that is decreased (electron gain).

Redox processes – processes where electron transfer between donors and acceptors take place and in any redox transformations causing oxidation states of the two components.

Introduction

Numerous processes from the microenvironment to the macro environment scale dependent to their redox conditions where dynamics are connected with serious oxidation-reduction reactions and can be expressed by redox potential (E_h) or by free electron pressure (p_e) showing the tendency of an environment to receive or to supply electrons in water solution. In a water sample or in a soil solution, the redox potential is determined by the concentration of effective electron acceptors. In the case of heterogeneous nature of soil, presence of oxygen plays role as a first acceptor of electrons in the series of redox reactions and its consumption by organisms. In oxic environments where oxygen accepts electrons, high redox potential is observed. In environments rich in oxygen, heterotrophic organisms provide their living processes by the use of O_2 as a powerful electron acceptor. The metabolism of reduced organic compounds in the soil generates electrons, which transports to O_2 transform different forms of carbon to CO_2 (product of soil respiration).

Redox potential

Electron free energy scale for mole of electrons can be expressed in ΔG (joule) or in E_h (volts) as well as in pE (dimensionless). The energy gained in the transfer of 1 mole of electrons from oxidants to H_2 , expressed in volts, is the redox potential (E_h) (Stumm and Morgan, 1996). Redox potential measurement is made with the use of inert (e.g., platinum) and reference (saturated calomel or silver chloride) electrodes. Redox potential E_h for the redox reaction



is expressed by Nernst equation, as follows:

$$E_h = E^o - (0.0592/n) \bullet \log Q \quad (2)$$

where $Q = [(C)^c(D)^d]/[(A)^a(B)^b]$, n = number of electrons transferred in reaction, E^o is the standard electrode potential at $25^\circ C$ in which all substances are at 1.0 M concentrations at $pH = 7$ in equilibrium.

Standard redox potential (E^o) expresses a tendency of a reducing agent to donate electrons when $Q = 1$.

In soil heterogeneous conditions where not one but many parallel reactions take place connected with different electron acceptors formed redox potential, which is called mixed redox potential (Bohn, 1971).

Redox status of electrochemical systems is often expressed in terms of electron activity (pe), which is derived from the equilibrium constant of the oxidation-reduction reaction (James and Bartlett, 2000). For any reaction



the equilibrium constant, K, is determined by

$$\log K = \log [Red] - \log [Ox] - \log [e^-] - \log [H^+] \quad (4)$$

where Ox is the oxidized form of the substrate and Red is the reduced product of the reaction.

In the case when the concentrations of oxidized and reduced species are equal then

$$pe + pH = \log K. \quad (5)$$

As a consequence of this formula, every tenfold change in the activity ratio causes a unit change in pe.

Because the sum of pe and pH is constant, if one of them increases, the other must decline. When a given reaction occurs at lower pH, it means that it will occur at higher redox potential or pe.

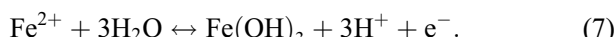
The value of redox potential can be converted to pe according to the formula

$$pe = \frac{E_h}{2.303(RT/F)} \quad (6)$$

where R = universal gas constant ($8.31447 \text{ J mol}^{-1} \text{ K}^{-1}$), F is Faraday's constant ($96,500 \text{ C mol}^{-1}$), T is the temperature in Kelvin, and 2.303 is a constant.

Effects of pH

Between redox conditions and pH there exists a strong relationship. In natural waters or soil solutions, which are in a highly dynamic state with regard to oxidation-reduction reactions the values of E_h (or pE) and pH are rather far from the thermodynamic equilibrium (Ponnamperuma, 1972). In the absence of biochemical catalysts (enzymes), most oxidation-reduction reactions under these conditions have a tendency to be much slower than acid-base reactions (Sposito, 1989). For example at pH 5, when equilibrium between Fe^{2+} and Fe^{3+} is established, the redox potential is about +400 mV.



At higher pH, the reaction equilibrium will shift to the right so Fe^{3+} will prevail in neutral and alkaline conditions. At lower pH, such as the acid anoxic waters of peat bogs, Fe^{2+} will prevail.

The redox potential (E_h) for the reaction $O_{2(Aq)} + 4H^+ + 4e^- \rightarrow 2H_2O$, taking place in any water solution containing soluble oxygen (e.g., $8 \text{ mg dm}^{-3} O_2 = 10^{-3.6} \text{ M} = 32 \text{ g mol}^{-1}$) at pH values of 5, 6, 7, 8, and 9 would be as follows: $E_{h_s} = 0.921 \text{ V}$, $E_{h_6} = 0.862 \text{ V}$, $E_{h_7} = 0.802 \text{ V}$, and $E_{h_9} = 0.684 \text{ V}$.

Changes in temperature also influence E_h . A rise in temperature by $1^\circ C$ will decrease E_h by 0.0016 V (Gliński and Stepniewski, 1985).

Under natural conditions at pH from 3 to 9 values of pE range from -6 to +12, and those of E_h from -600 to +400 mV (Figure 1).

Redox transformations of elements

Some macroelements such as C, N, O, S, Mn, and Fe, and trace elements or contaminants such as As, Se, Cr, Hg, U, Mo, V, Cu, Ag, and Pb can exist (Cicerone and Oremland, 1988; Faulkner and Patrick, 1992; Khalil et al., 1998) in a number of oxidation states in near-surface geologic environments (Figure 2).

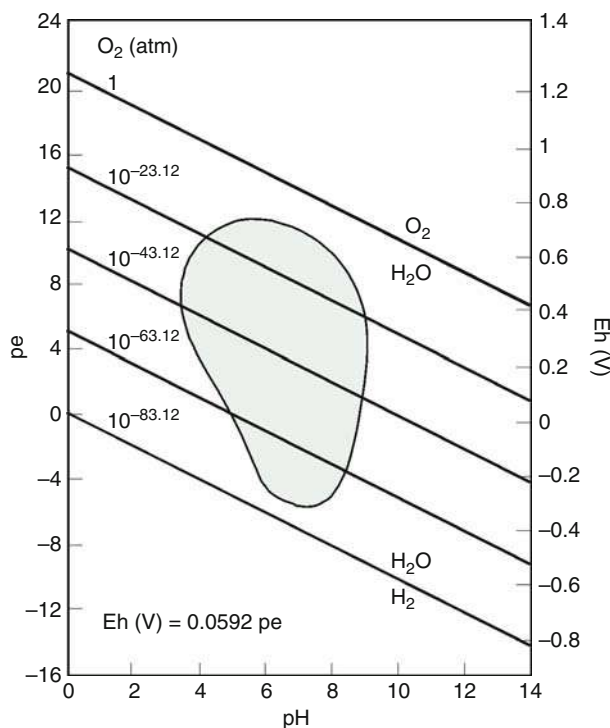
Redox processes in the environment

The values of redox potential in the environment according to oxygen availability are found as follows:

- (a) well-oxygenated water – $E_h \sim 0.802 \text{ V}$
- (b) oxygenated soils and surface waters – $E_h \sim 0.560 \text{ V}$
- (c) anaerobic waters or soils – $E_h \lesssim 0.300 \text{ V}$

As long as the system is exposed to the atmosphere, O_2 will maintain a high redox potential. In the absence of O_2 , a decline in redox potential and the reduction of oxidized forms (nitrate, Mn^{4+} , Fe^{3+} , and SO_4^{2-}) take place (Mosier, 1998).

The driving force causing a decrease in the redox potential is the consumption of oxygen by microbial respiration and the use of organic matter as a carbon source (Yu et al., 2006). All aerobic organisms must have O_2 to survive. Facultative anaerobes can tolerate periods of aerobic conditions (Brune et al., 2000).



Oxidation-Reduction Reactions in the Environment, Figure 1 The range of E_h found in natural environments (modified after Schlesinger (1997)).

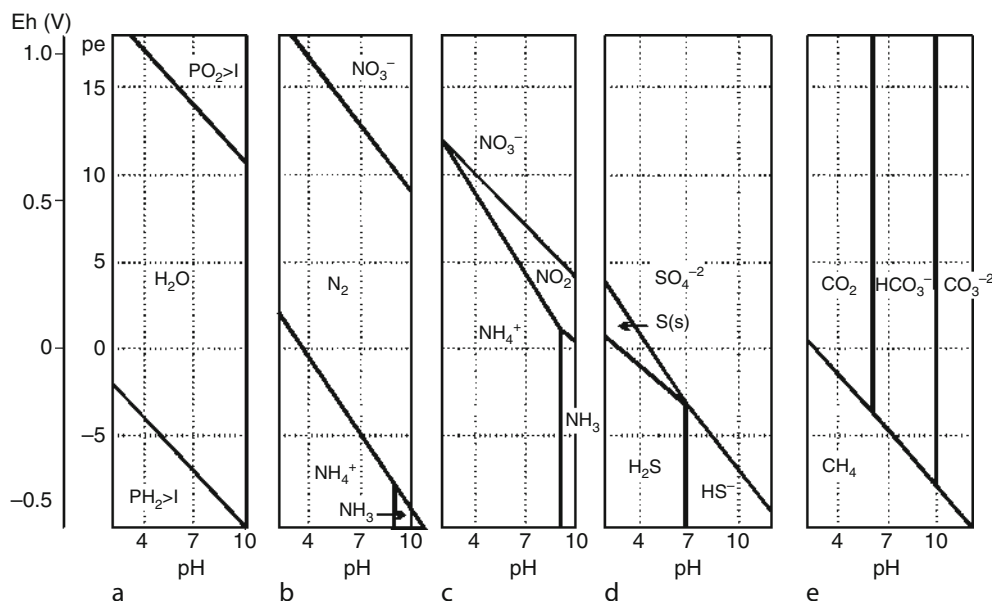
After O_2 is depleted by aerobic respiration, denitrification occurs within the redox potential interval from +750 to 300 mV, dependently on pH. Denitrifying bacteria use nitrate as an alternative electron acceptor during the oxidation of organic matter (Włodarczyk et al., 2004; Yu and Patrick, 2003). Below a redox potential of +500 mV, when nitrate is depleted, the reduction of Mn^{4+} begins. Reduction of manganese is performed also by facultative anaerobes (Stepniewska et al., 1997).

Obligate anaerobes at $E_h < -50$ mV perform the reduction of Fe^{3+} . Due to this, the appearance of reduced Fe^{+2} ions is used as the indicator of the transition from mildly reducing to strongly reducing conditions.

The oxidation processes proceed with some asymmetry versus redox potential (Figure 3). This is reflected by higher E_h (pe) values for the same reaction under oxidation conditions.

Seasonal fluctuations of water table or water level in surface waters may expose a previously flooded soil to the air, the boundary between oxidized and reduced conditions will shift downward in the profile, and the products of previous reduction reactions become substrates for oxidizing bacteria (Tiedje et al., 1984).

Denitrification is enhanced when seasonal periods of aerobic conditions stimulate the mineralization and nitrification of organic nitrogen (Smith et al., 1983), which makes nitrate more available for denitrifiers when the water level later rises (Stepniewska et al., 1996). Generally, pH and E_h (pe) are considered the master geochemical variables



Oxidation-Reduction Reactions in the Environment, Figure 2 The pe-pH diagrams for most biologically important elements (at 298K): (a) oxygen and hydrogen equilibrium with water; (b) and (c) nitrogen oxidation states with regard to N_2 ; (d) sulfur species stable for assumed conditions; (e) thermodynamically possible existence of C compounds (modified after Schlesinger (1997)).

controlling the geochemical reactions of elements in geo-logic and aquatic systems (Schlesinger, 1997).

Redox capacity – redox resistance

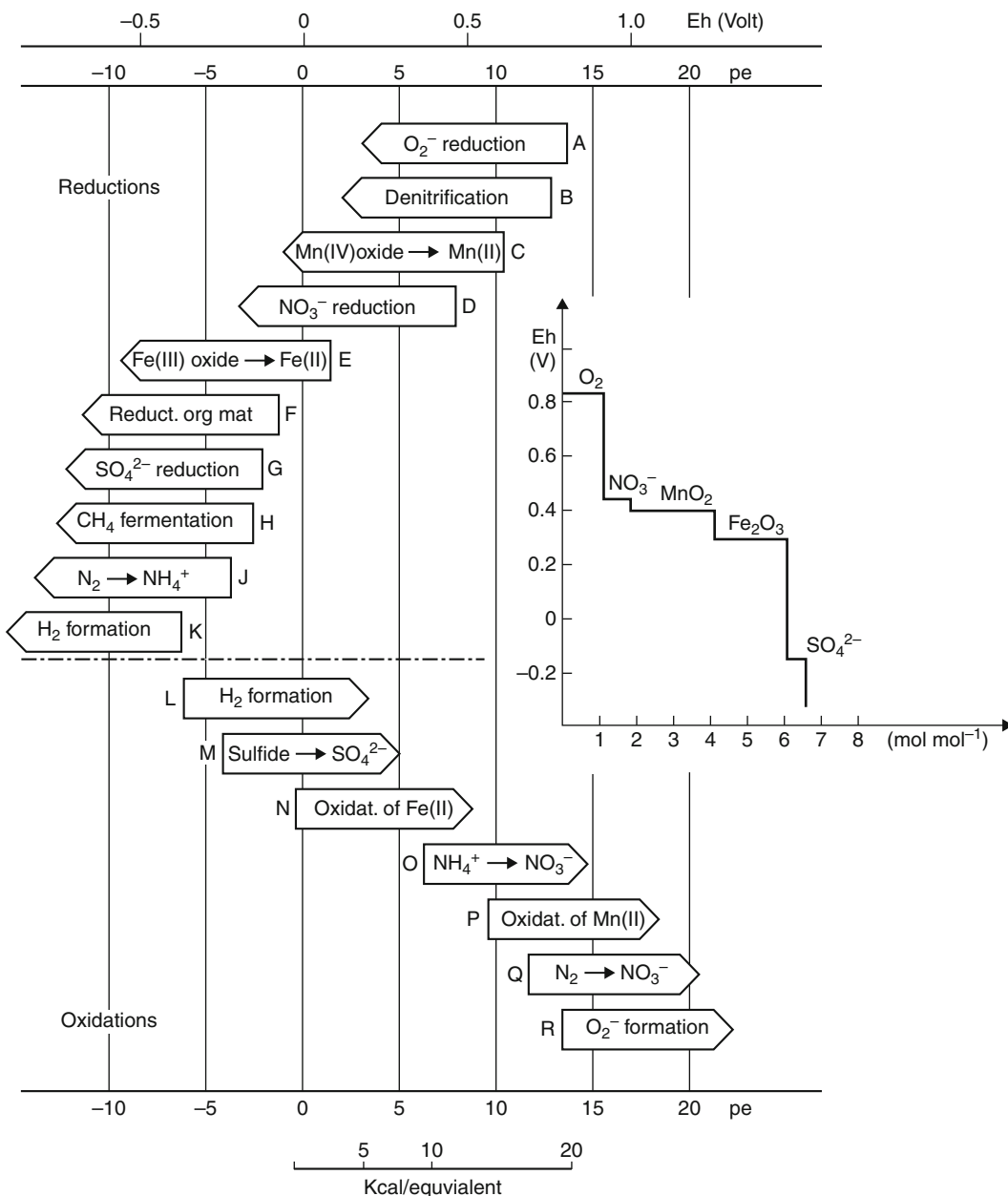
The stabilization of redox status of soils and sediments are express by resistance of changes in their redox potentials and is known as a redox resistance (Ponnamperuma, 1972). The term of buffering redox capacity r (eq/L) of the system express the ability of E_h stabilization and at

any E_h is defined as the quantity of strong reductant that must be added to reduce the E_h by 1 V,

$$r = dC/d(E_h) \quad (8)$$

or, as the time needed to decrease redox potential (E_h) to a given value to +400 mV corresponding to beginning of nitrate decomposition, or to +300 mV corresponding to the beginning of manganese and iron reduction.

Redox buffering capacity can help to interpret important reactions that control pH of natural waters and inform



Oxidation-Reduction Reactions in the Environment, Figure 3 Redox reactions that occur during wetting and rewetting of soils (modified after Schlesinger (1997)). The inset presents the E_h levels of particular compounds and their oxygen equivalents (width), that is, number of moles of a given compound substituting as electron acceptor 1 mole of oxygen (Stępniewski et al., 2005).

about stability of E_h in natural systems in connection with the mobilization and the accumulation of toxic substances (Yu et al., 2001; Stępniewska et al., 2003) as well the emission of greenhouse gases (Gorham, 1991; Chareonsilp et al., 2000; Le Mer and Roger, 2001; Mosier et al., 2002).

Summary

The application of redox transformation in recent years is connected with many different human activities. The first of all in agriculture for foreseen quality and quantity of food under controlling of water management as a irrigation of fields with water or waste water as well in respect to soil fertilization, nutrient availability, and cycling (Gliński and Stępniewski, 1985; Gorham, 1991; Faulkner and Patrick, 1992; Stępniewska et al., 1996; Włodarczyk et al., 2004). Transformations of Cr(III,VI) or As(III,V) in contaminated soils are controlled by oxidation states and response for pollution of ground and surface waters (Singh et al., 1999; James et al., 1997; Stępniewska and Bucior, 2001). Degradation of added to soil synthetic organic chemicals or pesticides by humans are resulted by oxidation-reduction (Vink et al., 1997). Quite fresh was found possibility for galvanic system, which generate electricity on the base of differentiation of redox potentials in the arid and saturated zone (Reimers et al., 2006; Rezaei et al., 2007; Kaku et al., 2008).

Bibliography

- Bohn, H. L., 1971. Redox potentials. *Soil Science*, **112**, 39–45.
- Brune, K., Kalden, J., Zacher, J., and Zeihofer, H. U., 2000. Selektive Inhibitoren der Zykloooxygenase-2. *Deutscher Ärzteblatt*, **97**, 1540.
- Chareonsilp, N., Buddhaboon, C., Promnart, P., Wassmann, R., and Lantin, R. S., 2000. Methane emission from deepwater rice fields in Thailand. *Nutrient Cycling in Agroecosystems*, **58**, 121–130.
- Cicerone, R. J., and Oremland, R. S., 1988. Biogeochemical aspects of atmospheric methane. *Global Biogeochemical Cycles*, **2**, 299–327.
- Faulkner, S. P., and Patrick, W. H. Jr., 1992. Redox processes and diagnostic wetland soil indicators in bottomland hardwood forests. *Soil Science Society of America Journal*, **56**, 856–865.
- Gliński, J., and Stępniewski, W., 1985. *Soil Aeration and Its Role for Plants*. Boca Raton: CRC Press.
- Gorham, E., 1991. Northern peatlands: role in the carbon cycle and probable responses to climate warming. *Ecological Applications*, **1**, 182–195.
- James, B. R., and Bartlett, R. J., 2000. Redox phenomena. In Summer, M. E. (ed.), *Handbook of Soil Science*. Boca Raton: CRC Press, pp. 169–194.
- James, B. R., Petura, J. C., Vitale, R. J., and Mussoline, G. R., 1997. Oxidation-reduction chemistry of chromium: relevance to the regulation and remediation of chromate-contaminated soils. *Journal of Soil Contamination*, **6**, 569–580.
- Kaku, N., Yonzewa, N., Kodama, Y., and Watanabe, K., 2008. Plant/microbe cooperation for electricity generation in a rice paddy field. *Applied Microbiology and Biotechnology*, **79**, 43–49.
- Khalil, M. A. K., Rasmussen, R. A., and Shearer, M. J., 1998. Effects of production and oxidation processes on methane emissions from rice fields. *Journal of Geographical Research – Atmosphere*, **103**, 25233–25239.
- Le Mer, J., and Roger, P., 2001. Production, oxidation, emission and consumption of methane by soils: a review. *European Journal of Soil Biology*, **37**, 25–50.
- Mosier, A. R., 1998. Soil processes and global change. *Biology and Fertility of Soils*, **27**, 221–229.
- Mosier, A. R., Morgan, J. A., King, J. Y., Le Cain, D., and Milchunas, D. G., 2002. Soil-atmosphere exchange of CH₄, CO₂, NO_x, and N₂O in the Colorado short grass steppe under elevated CO₂. *Plant and Soil*, **240**, 201–211.
- Ponnampерuma, F. N., 1972. The chemistry of submerged soils. *Advances in Agronomy*, **24**, 29–96.
- Reimers, C. E., Girgius, P., Stecher, H. A., Tender, M., Ryckelynck, N., and Whaling, P., 2006. Microbial fuel cell energy from an ocean cold seep. *Geobiology*, **4**, 123–136.
- Rezaei, F., Richard, T. L., Brennan, R. A., and Logan, B. E., 2007. Substrate-enhanced microbial fuel cells for improved remote power generation from sediment-based systems. *Environmental Science and Technology*, **41**, 4053–4058.
- Schlesinger, W. H., 1997. *Biogeochemistry: An Analysis of Global Change*. San Diego: Academic.
- Singh, J., Comfort, S. D., and Shea, P. J., 1999. Iron-mediated remediation of RDX-contaminated water and soils under controlled E_h/pH . *Environmental Science and Technology*, **33**, 1488–1494.
- Smith, C. J., Wright, M. F., and Patrick, W. H. Jr., 1983. The effect of soil redox potential and pH on the reduction and production of nitrous oxide. *Journal of Environmental Quality*, **12**, 186–188.
- Sposito, G., 1989. *The Chemistry of Soils*. New York: Oxford University Press.
- Stępniewska, Z., and Bucior, K., 2001. Chromium contamination of soils, waters, and plants in vicinity of a tannery waste lagoon. *Environmental Geochemistry and Health*, **23**, 241–245.
- Stępniewska, Z., Stępniewski, W., Gliński, J., and Ostrowski, J., 1996. Redox resistance as a feature determining fate and transport of pollutants in soils using the example of mineral soils of Poland. In *Chemistry for Protection of the Environment 2*. New York: Plenum, pp. 345–350.
- Stępniewska, Z., Stępniewski, W., Gliński, J., and Ostrowski, J., 1997. *Atlas of Redox Properties of Arable Soils of Poland*. Lublin/Falenty: IA PAN/IMUZ.
- Stępniewska, Z., Nosalewicz, M., and Ostrowska, A., 2003. Methane and carbon dioxide emissions from a loess soil treated with municipal waste water after second step of purification. *International Agrophysics*, **17**, 31–34.
- Stumm, W., and Morgan, J. J., 1996. Kinetics of redox processes. In *Aquatic Chemistry: Chemical Equilibria and Rates in Natural Waters*, 3rd edn. New York: Wiley-Interface, pp. 672–725.
- Tiedje, J. M., Sextone, A. J., Parkin, T. B., Revsbech, N. P., and Shelton, D. R., 1984. Anaerobic processes in soil. *Plant and Soil*, **76**, 197–212.
- Vink, J. P., Sjoerd, E. A., and Van der Zee, T. M., 1997. Effect of oxygen status on pesticide transformation and sorption in undisturbed soil and lake sediment. *Environmental Toxicology and Chemistry*, **164**, 608–616.
- Włodarczyk, T., Stępniewski, W., Brzezinska, M., and Stępniewska, Z., 2004. Nitrate stability in loess soils under anaerobic conditions – laboratory studies. *Journal of Plant Nutrition and Soil Science*, **167**, 693–700.
- Yu, K. W., and Patrick, W. H. Jr., 2003. Redox range with minimum nitrous oxide and methane production in a rice soil under different pH. *Soil Science Society of America Journal*, **67**, 1952–1958.
- Yu, K. W., Wang, Z. P., Vermoesen, A., Patrick, W. H. Jr., and Van Cleemput, O., 2001. Nitrous oxide and methane emissions from different soil suspensions: effect of soil redox status. *Biology and Fertility of Soils*, **34**, 25–30.

Yu, K. W., Faulkner, S. P., and Patrick, Jr. P., 2006. Redox potential characterization and soil greenhouse gas concentration across a hydrological gradient in Gulf coast forest. *Chemosphere*, **62**, 905–914.

Cross-references

- [Alkalinity, Physical Effects on Soils](#)
- [Buffer Capacity of Soils](#)
- [Greenhouse Gas Fluxes: Effects of Physical Conditions](#)
- [Hysteresis in Soil](#)
- [Liming, Effects on Soil Properties](#)
- [Oxygenology](#)
- [Peats and Peatlands, Physical Properties](#)
- [Soil Physical Quality](#)
- [Temperature Effects in Soil](#)
- [Wetting and Drying, Effect on Soil Physical Properties](#)

OXYGENOLOGY

Witold Stępniewski
Department of Land Surface Protection Engineering,
Lublin University of Technology, Lublin, Poland

Synonyms

Aeration (with respect to soils and plants only)

Definition

Oxygenology is defined as a scientific discipline comprising problems related to the presence and functions of oxygen in nature (Stępniewski and Stępniewska, 1998).

The term oxygenology, recently proposed by Stępniewski and Stępniewska (1998) is related to a scientific discipline, dealing with the presence and role of oxygen in the nature on Earth, which is an exceptional phenomenon on the cosmic scale. This discipline, constituting a branch of environmental sciences, covers issues of generation, storage, transport, absorption, turnover, functions, and measurement

of oxygen content in the environment. The name of oxygenology is analogous to that of hydrology.

Oxygen, as a dominant final acceptor of electrons, plays a unique role in the life of all macroorganisms and of most microorganisms, as well as in the chemical and biochemical processes occurring in the biosphere (Stępniewski et al., 2005). We can distinguish paleooxygenology related to the past geological époques and contemporary oxygenology focusing on the present-day processes and phenomena. In both cases, subbranches such as aquatic, lithospheric, atmospheric oxygenology can be distinguished. Moreover, we can talk about biooxygenology, that is, the oxygenology of biota.

Oxygenology of atmosphere is related to the presence of oxygen in its particular spheres. Thus, tropospheric, stratospheric, and mesospheric oxygenology as well as ozonology can be distinguished here. Aquatic oxygenology is divided into oceanic oxygenology, marine oxygenology, limnooxygenology (oxygenology of lakes), and potamic oxygenology (i.e., oxygenology of rivers). Oxygenology of lithosphere comprises such research areas as oxygenology of wetlands (natural, agricultural, and constructed), oxygenology of drylands (natural and agricultural), and oxygenology of anthropogenic systems (e.g., mines, buildings, and landfills). Biooxygenology is divided into microbial oxygenology, phytotoxic oxygenology, zoological oxygenology, and human oxygenology.

Bibliography

- Stępniewski, W., and Stępniewska, Z., 1998. Oxygenology as a new discipline in the environmental sciences – a proposal for discussion. *International Agrophysics*, **12**, 53–55.
- Stępniewski, W., Stępniewska, Z., Bennicelli, R. P., and Gliński, J., 2005. *Oxygenology in Outline. EU 5th Framework Program QLAM – 2001-00428*. Lublin: Institute of Agrophysics PAS.

Cross-references

- [Aeration of Soils and Plants](#)

P

PACKING DENSITY

The mass of particulate solids per unit bulk volume. A measure of the amount of particulate solids (e.g., soil, grains) in a given volume.

PAN

See [Claypan and its Environmental Effects](#)

PARENT MATERIAL AND SOIL PHYSICAL PROPERTIES

Andrzej Mocek, Wojciech Owczarzak
Department of Soil Sciences and Land Protection,
University of Life Sciences, Poznań, Poland

Synonyms

Mantle rock; Soil parent rock

Definition

Parent material. The unconsolidated and more or less chemically weathered mineral or organic matter from which the solum of soils is developed by pedogenic processes (Glossary of Soil Science Terms, 1987; Resource Conservation Glossary, 1982; Soil Taxonomy, 1976).

Physical properties (of soils). Those characteristics, processes, or reactions of a soil that are caused by physical forces and that can be described by, or expressed in, physical terms or equations (Glossary of Soil Science Terms, 1987; Resource Conservation Glossary, 1982; Soil Taxonomy, 1976).

Introduction

Soil was formed as a result of long-term and complex transformations of its mineral matter called parent material. Primordial, abiotic factors such as properties of the parent material, relief, climate, and time played a key role during the first stage of these transformations. In the course of the second phase, the results of the primary factors became intertwined with the effects of biotic factors, namely with the impact of microorganisms as well as the plant and higher animal kingdoms either coming into existence or just developing. During the last, relatively short time of the Earth history, still one more, important factor appeared, namely man's activities in the broad sense of the word. However, the basis of contemporary soils is the diverse, primary mineral substrate, which developed under the influence of complex actions of a number of physical, chemical, and biological factors.

Genesis

It is known that solid rock underwent breakup as a result of fairly complex processes commonly referred to as weathering. The primary factor of this process was physical weathering (see [Physical \(Mechanical\) Weathering of Soil Parent Material](#)). Frequent, periodical temperature changes in surface rock layers caused uneven strains and stresses leading to the development of pulsations. The higher was the amplitude of temperature fluctuations, the faster were the flaking processes in rocks, development of crevices, splinters, etc. The process was supported by the heterogeneity of the rock structure and by the different coefficient of expansion of its components (minerals). Another important factor taking part in the process was water, especially in the case of the phase change from liquid to solid (frost processes).

Physical weathering processes overlapped with processes of chemical weathering. Also in this case, the main factor here was water in which soluble gases

occurred: carbon dioxide and oxygen. Such water solution caused a change of some minerals into other minerals, while poorly soluble ones turned into more soluble.

In the result of physical and chemical processes of weathering, solid rock was transferred into rock mantle of various degree of disintegration and, hence, of diverse physical properties. It is commonly assumed that this kind of weathered rock constitutes not more than 5% of the terrestrial globe lithosphere and, at the same time, it occupies 75% of the land area.

Geological classification of soil parent material

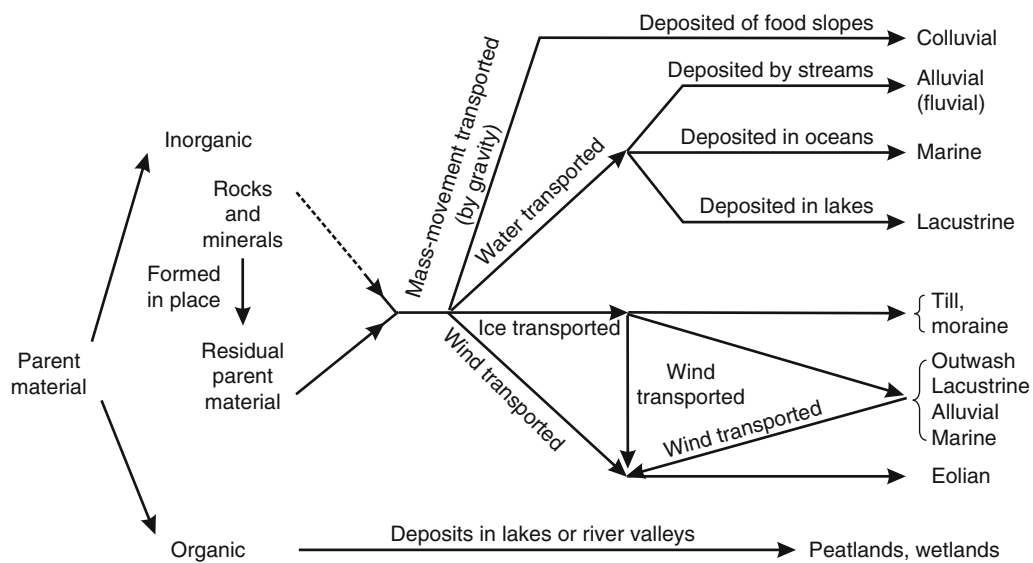
Bearing in mind the place of their development, mineral parent materials are divided into sedentary – formed in situ, and transported (Figure 1; Brady, 1990). Their characteristics are as follows:

Residual materials are usually formed from solid (compact) magmatic, sedimentary, and metamorphic rocks as a result of weathering processes. The developed mantle rock remains in place and is deposited on parent rocks (Buckman and Brady, 1969). It is partially impoverished by soluble components and, to a smaller extent, by particles floated by water currents and wind forces (slight translocation). The character of residual deposits depends on the intensity of weathering processes. Therefore, in warm and humid climates, regoliths undergo strong oxidation and fairly strong rinsing that explains their red, orange, or yellow color. In addition, they are characterized by low calcium content (Buckman and Brady, 1969). In colder conditions, which are also frequently drier, the weathering processes are less intensive. Oxidation processes and iron hydration in the regolith are less noticeable (colors are less intensive), while the content of calcium carbonate, as a rule, is higher. The discussed materials

can be found on all continents and their current characteristics depend on the diversification of intensity of individual soil-forming factors as well as on the degree of advancement of pedogenetic processes. Residual mantles most frequently exhibit the nature of clays or sand deposits.

Colluvial materials constitute heterogeneous rock raw material, which slides down from slopes as a result of gravitation forces (mass movements) from higher portions of slopes and which accumulates at their foot. Most frequently, they are unassorted deposits and are rarely found in poorly diversified geomorphological areas (Thompson and Troeh, 1973). Extensive colluvia can be found, primarily, in the mountains where steep slopes favor the formation of large slides and slips. One of the examples of colluvial formations includes the so-called scree, that is, loose rock debris consisting of pieces of rock broken away from the mountain face in the result of mechanical weathering as well as of slabbing rock blocks and stones covering slope sides (Pietkiewicz and Żmuda, 1973). They sometimes accumulate on slopes of these faces (mostly in gullies) but can be found mostly at the foot of mountains in the form of covers, heaps, or irregular steep cones.

Alluvial materials these are sediments deposited by waters of rivers and streams on the bottom of their beds, in flood lands (flood terraces), and in deltas at river mouths. The character of alluvial formations depends on the erosive-sedimentation activity of surface waters. Majority of stones and gravel are deposited in the river main current or in its upper course. Sandy formations accumulate along riverbanks, its arms, or on the flood plain neighboring the river. Fine particles float further on along the course of the river and are deposited further from



Parent Material and Soil Physical Properties, Figure 1 Classification of parent materials in relation to their kinds, development, transport, and deposition (Brady, 1990, modified).

the riverbed on the flood plain. Clays sediment along the lower course of the river where water velocity is minimal. Hence, three main groups of alluvial sediments are distinguished: flood terraces, alluvial cones, and delta sediments (Buckman and Brady, 1969; Brady, 1990). Flood terraces develop during river floodings (inundations). Sediments of a single flood exhibit similar particle-size distribution, which means that, in general, alluvial materials are characterized by stratified distribution; coarse sediments are deposited closer to the riverbed, while finer materials – further away from the river current. Alluvial cones constitute fan-like accumulation of alluvial sediments deposited by still or periodic waters in a place where a concave profile collapses and reduced inclination (distinct decrease in velocity) occurs on the way of these waters, for example, at the inlet of lateral valley (lateral river) to the main valley (main river). Alluvial cones are built, primarily, from sands and gravels. Coarser (gravel) material settles in the upper part of the developing cone, whereas finer particles are transferred toward its foot and toward the main river current. Sediments that form alluvial cones are sometimes referred to as proluvial sediments (Kowda, 1973). Materials forming them are badly graded, differently “turned” and, most frequently, improperly layered in an oblique manner. Silt sediments enriched in CaCO_3 can also occur along the periphery of proluvial cones. River delta deposits are formed at the mouth of rivers flowing into lakes or seas. The deposited finest material settles on an area whose shape is similar to a triangle. Deltas somewhat remind alluvial cones and their name derives from the Greek letter Δ (delta) (Thompson and Troeh, 1973). Sediments deposited in deltas are very fertile provided air-water conditions are controlled.

Marine materials are made up of sediments deposited in these reservoirs by surface waters and courses flowing in from inland areas. The above deposits were affected by various weathering-erosion factors and sorted first by flowing waters and then by sea waves. They form soil parent material when they emerge over the sea level. They can assume different shapes and forms of surface features such as delta bars, long river outwashes, sandbanks separated from the shore, which can give rise to lagoons, polders, bays, or swampy-saline areas (Kowda, 1973). In the majority of cases, delta bars and river outwashes are made of coarse-grained sandy material, while contemporary and old polders – from finer-grained clay material. In hot and dry climates, layers of chemical sediments in the form of soluble salts are formed at the bottom of lagoons and bays, whereas in the case of the occurrence of sandbanks – salines are developed ([Alkalinity, physical effects on soils](#)).

Limestones constitute an important group of sedimentary rocks, mainly of sea (less frequently of lake) chemical-organic origin. Their primary constituent is calcite or aragonite. Depending on various admixtures, limestone colors may vary from white, gray, yellow to brown, red, and bluish. As a rule, they are soft but sometimes they

can also be very hard and crystalline. This depends on the geological formation from which they derived. Mostly, they originate from residues of sea organisms (shell, coral and crinoid limestones, i.e., echinoids and crinoids). Some limestones contain glauconite (green), bituminous (black), or clay admixtures (Pietkiewicz and Źmuda, 1973). They constitute parent material of soils known as Rendzinas. Anhydrites (gypsum) belong to sediments of sea or lake origin. They develop as a result of drying of large water reservoirs (seas, less frequently lakes) forming extensive beds in tertiary deposits. They are also parent materials of soils known as anhydrite Rendzinas.

Lacustrine materials are formed from sediments deposited by rivers flowing into lakes from surrounding uplands. Coarser formations (gravel and sand) deposit along shores or in river deltas, whereas most of the silt and clay sediments are transferred further and settle in the central parts of lakes. Once lakes dry out, such sediments can constitute parent material for soil development. One of the examples of lake sediments can be varved clays consisting of numerous, alternative less than 5-mm thick light (aleurite) and dark (pearlite) layers occurring in stagnant lakes from ice period (Ryka and Maliszewska, 1991). Light layers derive from summer periods and dark ones from winter periods. Together with flowing waters, various chemical compounds in dissolved form are delivered into lake reservoirs and can undergo precipitation as chemical sediments (sediments of calcium carbonate). This is how limestones (oolitic limestones) – important soil parent materials – were formed.

Till (glacial) materials were formed as a result of glacier melting from deposits that were transported by them. They constitute a mixture of strongly diversified deposits, especially with regard to particle-size distribution. These deposits were deposited in the elements of postglacial landscape such as frontal and ground moraines, outwash zones, and marginal stream valleys (Prusinkiewicz, 1994). Frontal moraines, also known as terminal moraines, form a series of hills made up of variously grained rock material drifted and deposited by a glacier in a place in which the considerable speed of melting of the land-ice head made its further movement forward impossible. Frontal moraine ramparts are usually made of coarser rock material, that is, boulders, gravel, and sand and, therefore, constitute poor soil parent material. Ground moraines are made of deposits frozen to the base of the glacier or situated at its bottom. They consist of rock fragments broken away from the base by the carving action of the glacier. As a result of strong friction against the base and mutual wear of individual fragments, this material is scratched and rounded producing considerable quantities of boulder clay (glacial till) made up of fractions of clay, silt, sand, gravel, stones, and boulders mixed in different proportions. Ground moraines usually make flat or only fairly plicate forms and, hence, flat and corrugated ground moraines are distinguished. Top parts of ground moraines, sometimes called ablation moraines, contain more sand, whereas bottom parts exhibit more clayey

character (Prusinkiewicz, 1994). Boulder clays provide good soil parent material. The outwash zone consists of an extensive, flat cone slightly tilted in the distal direction situated directly in front of the frontal moraine. It is made up, mainly, from sands and gravels left by waters of the melting glacier. These deposits are frequently referred to as fluvioglacial sands containing significant quantities of skeletal deposits. Quartz (see *Estimation of Quartz Content in Mineral Soils*) is a dominant (60–90%) mineral in these sediments. Pradolinas (ice-marginal) valleys form wide valleys running latitudinally and are associated with extended periods of halts of the glacier during which they were furrowed by waters flowing along the melting front. They can be found in areas of all large quaternary glaciations. They are lined with variously grained deposits beginning with boulder clays through sands to more uniform alluvia of silt nature. Many old ice-marginal valleys were later covered by fluvioglacial deposits of later glaciations.

Eolian materials are developed as a result of relocation by wind of fine particles from all areas either deprived of all vegetation or poorly covered by plants, primarily from desert regions, seashore beaches, river flood terraces, and areas where fluvial deposits accumulate. Sand grains are transported not very far, while silt and clay fractions can be carried for considerable distances. Sand deposits are frequently referred to as sand dunes, whereas mainly silt and partly clay particles form loessic deposits. Dune sands most frequently form elevations called dunes built by wind. Seashore and inland as well as migrating and permanent dunes can be distinguished. They are of little value as soil parent material. Loesses constitute a classic sedimentary, porous, fine-grained, usually non-layered rock. They are straw yellow or dark yellow in color and their particle-size varies from 0.1 mm to 0.02 mm. They contain about 60–75% quartz silt, about 10–25% CaCO_3 , 4–6% clay minerals (see *Clay Minerals and Organo-Mineral Associates*) and dispersed iron hydroxides (Prusinkiewicz, 1994). Loesses belong to the best – albeit erosion-sensitive – soil parent materials and occupy approximately 4% of the earth's area. Loesses can be found, primarily, in China where their thickness reaches 200 m at places, although they also occur in Russia and America. In Western Europe, loesses are found in northern France, central Belgium, western and central Germany, southeastern Austria, in Moravia, southern Poland as well as in southern Slovakia, Hungary, and Romania (Pietkiewicz and Źmuda, 1973).

Parent materials of organic nature (most frequently of lake origin) occupy low, wet areas (see *Wetlands, Management, Degradation and Restoration*) where, at oxygen shortage, accumulation of organic matter known as peat takes place. This is an organic product of slow, structural, and chemical transformations of boggy plants undergo in conditions of high moisture and permanent anaerobiosis (Prusinkiewicz, 1994). Peat materials (see *Peats and Peatlands, Physical Properties*), apart from a certain amount of humus substances, also contain considerable

quantities of poorly decomposed plant residues and ash components. From the point of view of botanical composition, the following peats are usually distinguished: low-moor moss, sedge and rush peats as well as highmoor moss, heather peats, and boggy coniferous forest. Peats exhibit varying degrees of decomposition, hence, the following three groups are distinguished: poorly decomposed (*fabric*), medium-decomposed (*hemic*), and well-decomposed (*sapric*) peats (Soil Taxonomy, 1976). They constitute parent material of peat soils and, after advanced process of mineralization (drying), of muck soils. Also gyttia rocks, which make up the organic or mineral-organic sediment accumulating at the bottom of some eutrophic and well-aerated water reservoirs, constitute deposits of organic origin. The organic part of gyttia consists of decomposing plankton organisms including varying additions of clay particles. As a rule, gyttias constitute a thin, dark (jelly-like) layer of biomass in the bottom part of peats. Depending on the type and volume of co-components, the following gyttias are distinguished: calcareous (containing CaCO_3), clayey (presence of clay), and detritus (with plant detritus).

Soil physical properties

Soil physical properties are particularly important since they determine all its other properties, including chemical and biological ones. Soil is a porous, three-phase medium with its constituent elements found in solid, liquid, and gaseous phases (see *Soil Phases*). Soil solid phase is made up of mineral, organic, and organic-mineral particles of different degree of breakup. The liquid phase of the soil consists of water in which mineral and organic compounds are dissolved together making up soil solution. The gaseous phase is composed of a mixture of gases and water vapor and is also known as soil air. There is a continuous antagonism between liquid and gaseous phases since they can only occupy the same spatial volume (see *Spatial Variability of Soil Physical Properties*), which is not taken up by the solid phase, that is, soil pores (see *Pore Size Distribution*).

Primary and secondary soil physical properties are usually distinguished. Primary soil properties include those that constitute the quality of the soil material and its relation to the occupied space. They comprise texture (see *Soil Texture: Measurement Methods*), density (see *Bulk Density of Soils and Impact on Their Hydraulic Properties*), porosity, consistency, structure, viscosity, and compaction (see *Compaction of Soil*). Soil secondary properties are the function of primary properties and precondition soil properties as the environment and substrate for living organisms (plants and animals). They include water (see *Water Budget in Soil; Wetting and Drying, Effect on Soil Physical Properties*), air, and temperature (see *Temperature Effects in Soil*).

The basic and most important soil physical property is its texture, which describes the degree of size distribution of the mineral part of soil solid phase. This distribution

was developed during a long and complex geological process (weathering processes), in other words, in the course of the development of parent material and, at the present time, it is a constant property unchangeable even during a long period of time. The mineral part of the solid phase is both polydisperse, as it comprises particles of different sizes and heterodisperse because it exhibits diverse chemical-mineralogical composition.

Depending on the method of formation, transport, and sedimentation of the rock mantle deposition, it is possible to distinguish polyfraction materials – of different diameter span of mineral particles (till, moraine) and monofraction (alluvial, marine, outwash, eolian). Selective sedimentation and accumulation of more homogeneous material took place as a result of segregation processes. Soil colloids, that is, particle with the diameter smaller than 0.002 mm (clay minerals), constitute the most important fraction of the mineral part of the solid phase. Their extensive specific surface area (see *Specific Surface Area of Soils and Plants*) increases significantly water capacity (see *Field Water Capacity*) which, in the case of soil wetting, leads to soil swelling and during drying – to its shrinking, that is, to processes resulting in unfavorable soil volume changes – maximal soil loosening and compaction.

Apart from the size distribution of the soil material, its other important quality is the shape (sharp-edged, circular, elliptical, plate-like) and form (smoothness, roughness) of elemental particles. Both size distribution and the shape and form of elementary particles influence quantitative interrelationships of the three-phase soil medium affecting variations in the compactibility (see *Soil Compactibility and Compressibility*) of various soils.

Summary

Soil parent materials can be of mineral (magmatic, sedimentary, and metamorphic mantel rocks) or organic origin. According to geological classification of these deposits, the following mineral materials are distinguished: residual, colluvial, alluvial, marine, lacustrine, glacial, and eolian, whereas organic materials include peats and gyttias. The above-mentioned parent materials form three-phase systems (phases: solid, liquid, and gaseous). Mutual relationships between these phases are decisive with regard to both basic (texture, density, porosity, structure, compaction, etc.) and functional (air-water) soil properties.

Bibliography

- Brady, N. C., 1990. *The Nature and Properties of Soil*, 10th edn. New York: Macmillan; London: Collier Macmillan, 621pp.
- Buckman, H. C., and Brady, N. C., 1969. *The Nature and Properties of Soil*, 7th edn. London: Macmillan/Collier Macmillan.
- Glossary of Soil Science Terms, 1987. *Soil Science Society of America*. WI: Madison.
- Kowda, W. A., 1973. *Basic of Soil Science*. Moskwa: Izdatielstwo Nauka (in Russian).

- Pietkiewicz, S., and Żmuda, S., 1973. *Dictionary of Geographic Concepts*. Warszawa: Wiedza Powszechna (in Polish).
- Prusinkiewicz, Z., 1994. *Ecological – Soil Science Glossary*. Warszawa: PWN (in Polish).
- Resource Conservation Glossary, 1982. Ankeny, IA: Soil Conservation Society of America.
- Ryka, W., and Maliszewska, A., 1991. *Petrographic Dictionary*. Warszawa: Wydawnictwa Geologiczne (in Polish).
- Soil Taxonomy, 1976. Washington, D.C.: U.S. Department of Agriculture.
- Thompson, M. L., and Troeh, F. R., 1973. *Soil and Soil Fertility*, 3rd edn. New York: McGraw-Hill.

Cross-references

- [Alkalinity, Physical Effects on Soils](#)
[Bulk Density of Soils and Impact on their Hydraulic Properties](#)
[Compaction of Soil](#)
[Clay Minerals and Organo-Mineral Associates](#)
[Estimation of Quartz Content in Mineral Soils](#)
[Field Water Capacity](#)
[Peats and Peatlands, Physical Properties](#)
[Physical \(Mechanical\) Weathering of Soil Parent Material](#)
[Pore Size Distribution](#)
[Salinity, Physical Effects on Soils](#)
[Soil Phases](#)
[Soil Structure and Mechanical Strength](#)
[Soil Texture: Measurement Methods](#)
[Spatial Variability of Soil Physical Properties](#)
[Specific Surface Area of Soils and Plants](#)
[Subsoil Compaction](#)
[Temperature Effects in Soil](#)
[Water Budget in Soil](#)
[Wetlands, Management, Degradation and Restoration](#)
[Wetting and Drying, Effect on Soil Physical Properties](#)

PARTIAL PRESSURE

The pressure exerted by each gas in a mixture proportional to the amount of that gas in the mixture (e.g., proportion of oxygen in the soil atmosphere).

PARTICLE DENSITY

The density of the particles (e.g., soils and grains), the dry mass of the particles being divided by the solid (not bulk) volume of the particles, in contrast with bulk density.

PARTICLE FILM TECHNOLOGY

Michael Glenn
USDA-ARS Appalachian Fruit Research Station,
Kearneysville, WV, USA

Synonyms

Kaolin; Reflectant

Definition

Particle Film Technology involves establishing a mineral particle film on the surface of a plant or plant product that (1) is chemically inert, (2) has a mean particle diameter $<2\text{ }\mu\text{m}$, (3) is formulated to spread and create a uniform film, (4) does not physically disrupt gas exchange from the leaf, (5) transmits photosynthetically active radiation (PAR) to and partially reflects harmful ultraviolet (UV) and infrared (IR) radiation from the surface, (6) alters insect and/or pathogen behavior on the plant, and (7) can be removed from the plant or plant product. Particle Film Technology was developed using chemically inert kaolin mineral particles in aqueous formulations for application to crop plants to protect them from insect pests and environmental stresses. Field research demonstrated that this technology effectively provides a safe alternative to conventional insecticides for certain insect problems on a wide range of crops, including apple, pear, grape, blackberry, melons, tomato, onions, papaya, peach, nectarine, olive, pineapple, and citrus. Surround® Crop Protectant is the first particle film product to provide effective suppression of high heat damage and sunburn without the use of evaporative cooling. In organic agriculture, Particle Film Technology represents the first broad utility material that provides effective insect control and high produce quality in organic fruits and vegetables. Particle Film Technology represents a broadly based insect control system whose impact could be similar to the development of the first synthetic insecticides but without the adverse effects on ecosystems. Additionally, Particle Film Technology provides agriculture with the first sunburn and heat management tool that can manipulate ultraviolet, photosynthetically active infrared radiation. Surround is a registered trademark of Tessenderlo Kerley, Inc.

Bibliography

- Glenn, D. M., and Puterka, G. J., 2004. Particle film technology: a new technology for agriculture. In Janick, J. (ed.), *HortReviews*, Vol. 31, pp. 1–45.

PARTICLE-SIZE DISTRIBUTION

The fractions of the various particle sizes (soils, powders) often expressed as mass percentages.

PARTICULATE ORGANIC MATTER

Material of plant or animal source suspended in water and usually capable of being removed by filtration.

Cross-references

- [Organic Matter, Effects on Soil Physical Properties and Processes](#)

pe

The negative logarithm of the apparent electron activity which can be calculated by including the apparent activity of electrons in equilibrium calculations of redox half-cell reactions. It is used as an alternative to Eh (redox potential) and at 25°C can be calculated from Eh values expressed in volts by dividing by 0.059.

Cross-references

- [Oxidation–Reduction Reactions in the Environment](#)

PEATLANDS: ENVIRONMENTAL FUNCTIONS

Tadeusz J. Chmielewski¹, Danuta Urban²

¹Department of Landscape Ecology and Nature Conservation, University of Life Sciences, Lublin, Poland

²Institute of Soil Science and Environment Formation, University of Life Sciences, Lublin, Poland

Synonyms

Bogmoor; Moor; Peatland; Peat moor; Peat swamp

Definition

There are a number of various definitions of the word “peatland.” When defining peatlands, botanists will place emphasis on plant assemblages, geologists and soil scientists – on quality parameters and resources of peat deposits, whereas the ecologists prefer the habitat and ecosystem approach.

Peatland is:

1. One of the types of wetlands – strongly hydrogenic areas with the occurrence of specific vegetation and processes of accumulation of organic deposits. It is a habitat that is permanently waterlogged, developed on a hard-permeable substrate, covered with communities of mosses and moor-grassland vegetation (Keddy, 2004).
2. The biotope for moss–fruticose biocenosis, developing under conditions of strong hydration, with a peat layer with depth greater than 30 cm (Crum, 1992).
3. An ecosystem capable of permanent or periodical saturation or flooding with water, composed of hydric soils and hydrophytic vegetation (Committee on Characterization of Wetlands, 1995).
4. A plant community overgrowing a peat deposit created by itself (Weiner, 2000)
5. A deposit of peat – sedimentary rock formed as a result transformation, undergoing under specific conditions, of decayed plant residues, the youngest fossil coal. It contains less than 60% of carbon and is composed on non-decomposed plant residues and amorphous humus mass (Ilnicki, 2002).

6. Recently a new term is being introduced: suo (from the Finnish language), denoting areas of organic or mineral soils on which peat-forming vegetation is currently growing.

Occurrence and development

Peatlands occur primarily in the moderate humid and cool climate zone (in the northern part of Eurasia and North America, as well as in mountain regions).

Contemporary peatlands have been developing since the beginning of the oldest Dryas and Bölling, that is, from the time when the glaciations receded, i.e., for ca. 13,000 years. One of the oldest peatlands in Poland, probably also in the European Lowland, is the peatland Białe Ługi (Ilnicki, 2002).

In the moderate humid climate zone, the annual increment of a peatland is ca. 0.7–1.0 mm, on average.

Peatlands covering large areas (of the order of thousands of hectares) are referred to as peat complexes. The largest peat complex in Europe is Polesie.

Classification of peatlands

Classifications of peatlands take into account the trophy of habitats and the content of calcium compounds in the substrate that affect the composition of peatland vegetation assemblages. Another criterion is the water relations, resulting from the land relief. In Central Europe, the following are distinguished:

- Low moors – formed due to the flow or stagnation of eutrophic waters, most frequent in Europe; they develop within river valleys, fertile, and floristically rich: rush communities (reed, bulrush, horsetail) or turf communities (mosses, sedges)
- High moors – supplied with oligotrophic precipitation waters, morasses formed in depressions with no outlet, strongly acidic, poor in nutrients, and therefore also poor floristically (peat mosses, fruticose species from the genus *Ericaceae* such as *Ledum palustre*, *Vaccinium uliginosum*, *Oxycoccus palustris* and *Andromeda polifolia*, *Erica tetraix*, tawny cottongrass *Eriophorum vaginatum*, sedges, insectivorous plants); conditions suitable for bog forests develop here
- Transitional moors – encountered in intermediate habitat conditions. These moors are covered with morass-sedge communities composed of *Carex lasiocarpa*, *Carex limosa*, *Scheuchzeria palustris*, *Rhynchospora alba*, *Eriophorum angustifolium*, peat mosses (*Sphagnales*), and hypnaceous mosses (*Bryales*). Through natural succession, in those moors, there appear pine and birch, and in the northern part of Eurasia and in North America – also spruce.

Ecological significance

Peatlands fulfil significant functions in the natural environment: (1) they take part in water circulation and retention; (2) they are natural filters of environmental

pollutants; (3) they store organic matter and carbon, and thus affect global climate changes and carbon circulation; (4) they have a mollifying and stabilizing effect on the microclimate of the immediate environment; (5) they play an important role in the preservation of biodiversity; (6) they are an important characteristic element of landscape; (7) they constitute archaeological archives.

Ad. (1) Peatlands are considered to be important water reservoirs; they constitute some of the best retention reservoirs created by nature (Ilnicki, 2002; Mitsch and Gosselink, 1993). The retention capacity applies primarily to living peatlands, in which the peat-forming process continues. They can accept notably greater amounts of water and release it much more slowly than degraded peatlands do. Water is also stored in partially drained peat deposits. It is estimated that, e.g., the peatlands of Poland may hold ca. 34,000 million cubic meters of water, and the water retained in them would cover the whole territory of Poland with a layer of 1.10 cm (Tobolski, 2000). Valley peatlands play an important role in the shaping of the water level in the rivers and the adjacent valleys. River valleys with a high degree of conversion into peatlands have significantly increase water retention capacity and ensure more uniformly directed outflow of waters (Lipko, 2000).

Ad. (2) Through biogenic accumulation, peatlands play the role of efficient natural filters. The filtration properties of those ecosystems consist in the reduction of water solutions migrating vertically and horizontally, though their incorporation into solutions accumulated in peat. They can reduce the load of nutrients flowing to the rivers from the surrounding fields – limiting the flux of nitrogen, fixing phosphorus and sulphur compounds, and absorbing calcium and magnesium. Peatlands supplied with water from surface flooding participate in the process of purification of waters, and the efficiency of the process depends on the time of water retention and on the surface area of the peatland (Mitsch and Gosselink, 1993).

Ad. (3) Peatlands play also a significant role in the global balance of organic carbon and nitrogen. Depending on the way of their use, peatlands should be treated either as storage reservoirs for greenhouse gases or as a source of their emission. It is necessary to consider separately peatlands that are not drained and drained peatlands being used by agriculture, forestry, or the peat industry. Live peatlands, in which the peat-forming process continues, play an accumulative role and are natural reservoirs of carbon and nitrogen. Drained peatlands become emitters of greenhouse gases, releasing to the atmosphere compounds of carbon (carbon dioxide) and nitrogen (nitrous oxide). In the balance of greenhouse gases, another important element is the emission of methane which is high in non-drained peatlands, especially low moors, with a high level of ground water. It attains maximum values on flooded areas and also

increases on pastures fertilized with animal feces. No methane emission is observed in the case of extensively and intensively used grasslands and arable lands situated on peatlands (Klöve et al., 2009; Ilnicki, 2002).

Ad. (4) Peatlands, and especially their large complexes, significantly affect the climatic conditions in their surroundings. They are characterized by a specific microclimate – higher air humidity compared to mineral soils, greater frequency of occurrence of mists and dew, notably greater frequency of occurrence of ground frost, shorter periods without ground frost, lower air temperatures and lower topsoil temperatures in the summer period (Ilnicki, 2002).

Ad. (5) Peatlands are often treated as refuges of nature, enriching the biological diversity of neighboring areas, and especially of lowland regions. They are the habitats of numerous species of plants, animals, and fungi (Crum, 1992; Ilnicki, 2002), including species that are rare, covered with legal protection, and threatened. Valuable plant species occurring on transitional moors include, e.g., downy willow *Salix lapponum*, swamp willow *Salix myrtilloides*, bog orchid *Hammarbya paludosa*; on low moors, e.g., creeping marshwort *Apium repens*, marsh violet *Viola uliginosa*, dwarf marsh violet *Viola epipsila*. Peatlands are also considered to be major bird refuges in Central Europe, with the occurrence of such species as, e.g., Eurasian Bittern *Botaurus stellaris*, Jack Snipe *Lymnocryptes minimus*, Ruff *Philomachus pugnax*, Black Grouse *Tetrao tetrix*, Eurasian Curlew *Numenius arquata*, Aquatic Warbler *Acrocephalus paludicola*. Peatlands are also the sites of occurrence of numerous groups of relic species of plants and animals. Glacial (boreal) relicts include bush and fruticose species – dwarf birch *Betula humilis*, swamp willow *Salix myrtilloides*, downy willow *Salix lapponum*, marsh Labrador tea *Ledum palustre*, black crowberry *Empetrum nigrum*, herbaceous plants – yellow marsh saxifrage *Saxifraga hirculus*, royal loose-wort *Pedicularis sceptrum-carolinum*, creeping sedge *Carex chordorrhiza*, bryophytes – *Calliergon trifarium*, *Meesia triquetra*, *Scorpidium scorpioides*. The specific habitat conditions of peatlands cause that the flora of those ecosystems is characterized by a high share of species with a narrow ecological amplitude. Most plants occurring there are stenotopic species. In terms of water requirements, the largest group is hygrophytes, followed by hydrophytes. Dominant are photophilic species (heliophytes). As relates to the thermal requirements, oligothermic species dominate. The flora occurring on peatlands is varied in terms of tolerance to the level of nutrients in the soils (eutrophic, meso- and oligotrophic species) and to the soil reaction (acidophytes, species of weakly acid and alkaline habitats) (Ilnicki, 2002). One of the methods of adaptation of peatland plants to the habitat conditions (deficit of available nitrogen) is insectivorousness (carnivorousness), e.g., common butterwort *Pinguicula vulgaris*,

sundews *Drosera rotundifolia*, *Drosera intermedia*, *Drosera anglica*, and *Drosera × obovata*, as well as the waterwheel plant *Aldrovanda vesiculosa*, occurring in micro-reservoirs within transitional moors. Also important for the shaping of biodiversity are the large-area peatlands of river valleys and small midfield and mid-forest peat moors.

Ad. (6) Peatlands should be treated as a significant landscape-forming element. The role of peatlands in landscape, and especially their comprehensive effects in above-ecosystem systems, is more and more the object of analyses (Chmielewski, 2009; Succow and Joosten, 2001).

Ad. (7) Peatlands constitute archaeological archives created by the forces of nature. In the sequence of peat formations, there is a record of changes of climate and water relations, succession of plant assemblages, as well as of the conditions of human life (Crum, 1992; Ilnicki, 2002).

Threats to peatlands and problems of peatland conservation

Peatlands are highly susceptible to degradation and are among the fastest-disappearing ecosystems on Earth. The main reasons for the shrinkage of the area of peatland ecosystems are the following:

- Regulation of rivers, drainage of wetlands, and transformation of peatlands into grasslands and arable land
- Artificial afforestation of peatlands and processes of natural succession of trees and bushes onto drained peatland habitats
- Exploitation of peat deposits for use in agriculture, horticulture, balneology, and formerly also for fuel
- Climate warming and disappearance of species with cool climate preferences
- Eutrophisation of habitats and dwindling of species requiring habitats poor in biogens
- Fragmentation of landscape and of the spatial structure of peat complexes.

In view of the above, all peatlands that have still retained their natural character, or seminatural, require particular protection.

The fundamental international legal act concerning the protection of peatlands is the *Ramsar Convention on Wetlands* from 1971: <http://www.ramsar.org/cda/en/ramsar-home/main/ramsar/>. An important role in peatland protection in Europe is played also by the Council Directive 92/43/EEC on the Conservation of Natural Habitats and of Wild Fauna and Flora, from 1992 (*Habitats Directive*): http://ec.europa.eu/environment/nature/legislation/habitatsdirective/index_en.htm.

Since the 1980s, peatland restoration projects have been increasingly important in active conservation and restoration of the lost values of peatlands (Comin, 2010).

Conclusions

1. Peatlands belong to the most valuable and the most dangerous natural ecosystems in Eurasia and North America.
2. Peatlands fulfil significant functions in the natural environment: (1) they take part in water circulation and retention; (2) they are natural filters of environmental pollutants; (3) they store organic matter and carbon and thus affect global climate changes and carbon circulation; (4) they have a mollifying and stabilizing effect on the microclimate of the immediate environment; (5) they play an important role in the preservation of biodiversity; (6) they are an important characteristic element of landscape; (7) they constitute archaeological archives.
3. The fundamental international legal acts concerning the protection of peatlands are: *The Ramsar Convention on Wetlands* from 1971 and EU *Habitats Directive* from 1992.
4. Over the last 3 decades, increasing role in peatland conservation actions play wetland restoration projects.

Bibliography

- Chmielewski, T. J. (ed.), 2009. *Ecology of Hydrogenic Landscapes of the "West Polesie" Biosphere Reserve*. Lublin: Uniwersytet Przyrodniczy w Lublinie, Zakład Ekologii Krajobrazu i Ochrony Przyrody (in Polish, English Summary).
- Committee on Characterization of Wetlands, 1995. *Wetlands, Characteristic and Boundaries*. Washington, DC: National Academy of Sciences Press.
- Crum, H., 1992. *A Focus on Peatlands and Peat Mosses*. Michigan: The University of Michigan Press.
- Ilnicki, P., 2002. *Peatlands and Peat*. Poznań: Wydawnictwo Akademii Rolniczej im. Augusta Cieszkowskiego w Poznaniu (in Polish).
- Keddy, P. A., 2004. *Wetland Ecology. Principles and Conservation*. Cambridge, UK/New York/Melbourne/Madrid/Cape Town: Cambridge University Press.
- Klöve, B., Mrtilla, H., Öskarrsson, H., Grønlund, A., Berglund, K., Berglund, Ö., Maljanen, M., and Lægdsmann, M., 2009. Past and future of cultivated peatlands – Nordic environmental challenges. *Peatlands International*, **2**, 28–32.
- Lipko, K., 2000. Peatlands in the catchment basin of the Vistula river as an element of the natural environment. *Zeszyty Naukowe Akademii Rolniczej im. H. Kollataja w Krakowie*, **255**, 10–146 (in Polish).
- Mitsch, W. J., and Gosselink, J. G., 1993. *Wetlands*, 2nd edn. New York: Van Nostrand Reinhold.
- Succow, M., and Jeschke, L., 1986. *Moore in der Landschaft: Entstehung, Haushalt, Lebewelt, Verbreitung, Nutzung und Erhaltung der Moore*. Leipzig-Jena-Berlin: Urania-Verlag.
- Succow, M., and Joosten, H., 2001. *Landschaftsökologische Moorkunde*. Stuttgart: E. Schweizerbart Science Publishers.
- Tobolski, K., 2000. *Guide to the Determination of Peats and Lake Sediments*. Warszawa: Wydawnictwo Naukowe PWN (in Polish).
- Weiner, J., 2000. Peatlands. In Otalega, Z. (ed.) *Biological Encyclopedia*. Kraków: OPRES, Vol. IX, 38 pp (in Polish).

Cross-references

- [Climate Change: Environmental Effects](#)
[Nature Conservation Management](#)
[Wetlands, Management, Degradation and Restoration](#)

PEATS AND PEATLANDS, PHYSICAL PROPERTIES

Lech Wojciech Szajdak¹, Jan Szatyłowicz²,
Raimo Kõlli³

¹Department of Environmental Chemistry, Institute for Agricultural and Forest Environment, Polish Academy of Sciences, Poznań, Poland

²Department of Environmental Improvement, University of Life Sciences (SGGW), Warsaw, Poland

³Department of Soil Science and Agrochemistry, Institute of Agricultural and Environmental Sciences, Estonian University of Life Sciences, Tartu, Estonia

Definition

Peat. Sedentarily accumulated material consisting of at least 30% (per dry mass) of dead organic material.

Peatland. An area with or without vegetation with a naturally accumulated peat layer at the surface.

Mire. A peatland where peat is currently being formed.

Introduction

Peat accumulation generally takes place as a result of limited decay (decomposition) of plant material. An important factor for peat accumulation is the chemical and structural composition of the organic material, which determines its “ability to decay.” However, water seems to be the most important external factor limiting decay. The ability to decay varies with species, plant part, and chemical and biochemical compounds. This means that some plant species, organs, and compounds are more inclined to accumulate peat than others. A large number of plant species occurring in mires can contribute to peat formation, such as sedges, grasses, *Sphagnum* and other mosses, and woody plants. Consequently, a wide variety of “botanical” peat types exists. Thus, botanical composition, relative amounts of the main plant species or species groups is the fundamental property for determining the nature of peat and the physical and chemical properties of the peat. Moreover, a classification of peat reflects the peat that is laid down beneath the dominant kinds of vegetation. Thus, three basic peat types are recognized – *Sphagnum*, sedge, reed, and woody peats – and various subtypes are recognized based on abundant species or species groups (Rydin and Jeglum, 2006). The great majority of present-day peatlands originated in the last 15,000 years. It is estimated that 4 million km² on Earth (some 3% of the land area) is covered with peatlands (Joosten and Clarke, 2002). Over 90% of peatlands are in the temperate and cold belt in the Northern Hemisphere (Western Siberia, Canada and Alaska, and Northern Europe). The remaining area is located in tropical and subtropical latitudes, much of it under forest (Southeast Asia, and parts of the Amazon basin) (Lappalainen, 1996).

Peatland and mire type

There are many different ways of classifying wetlands, peatlands, and mires depending on the purposes of the classification. Two major types are *bogs* (which are mainly rain-fed and nutrient-poor) and *fens* (which are mainly fed by surface or ground water and are more nutrients rich) (Joosten and Clarke, 2002). *Bogs* represent ombrotrophic peatlands with the surface above the surrounding terrain or otherwise isolated from laterally moving, mineral-rich soil waters. Although some bogs are convex in shape (raised bogs), bogs can also be quite flat or sloping, with slight rises at the margin that isolate them from incoming mineralogenous water. The peat is usually more than 40-cm deep. The main physiognomic groups are open bog and wooded bog (bog forest). There is large variation of wetness in bogs with a pattern of hummocks and hollows. *Fens* characterize minerotrophic peatlands with water table slightly below, at, or just above the surface. Usually there is slow internal drainage by seepage, but sometimes with over-surface flow. Peat depth is usually greater than 40 cm, but sometimes less (for instance adjacent to the mineral edges). Two broad types are *topogenous* (basin) fen and *soligenous* (sloping) fen. The main physiognomic groups of fen are open fen and wooded fen (with *tree cover*, or a sparse tall shrub cover, sometimes called *shrub carr*) (Rydin and Jeglum, 2006). Peat layer growth and the degree of decomposition (or humification) depend principally on its composition and on the degree of waterlogging. Peat formed in very wet conditions accumulates considerably faster, and is less decomposed, than that in drier places. The average annual growing of peat in the majority of mires amounts to scarcely more than 0.5 mm; only under extremely favorable conditions do thicknesses of over 1 mm per year occur (Joosten and Clarke, 2002).

Functions of peatlands

In peatlands, water, peat, and specific vegetation are strongly interconnected. If any one of these components is removed, the nature of the peatland is fundamentally changed. Peatlands may be naturally forested or naturally open and vegetated with mosses or sedges. Peatlands seem to be the most important carbon stores of the world, and contain about 90% water, thus acting as vast reservoirs. Peatlands are used for grazing and for growing crops, and are exploited for timber harvesting. In addition, some kinds of peat are commonly used for the preparation of organic fertilizers for agriculture, as well as for substrate and growing media for horticulture, and pomology. Peat reveals energetic features because it is extracted for fuel both for domestic and industrial use. Thus, peatlands contribute importantly to the economy of local communities. In addition, peatland ecosystems play an important function as archives, and provide suitable habitats for unique flora and fauna (Charman, 2002; Joosten and Clarke, 2002).

Decomposition degree

The solid phase of peat soils is made up of plant fibers and amorphous humus and inorganic matter such as particles of different sizes (from sand to clay), as well as amorphous substances primarily in the form of carbonates, phosphates, and hydroxides. The rate at which plant material in peatlands is decomposed (humified) depends on many factors such as acidity, temperature, moisture, oxygen supply, plant composition, and composition of peat organisms. The degree of decomposition or degree of humification of the peat is assessed by measuring its fiber or humus content. In practice, peat decomposition is determined by a field method, the von Post pressing method (von Post, 1922). The method identifies ten classes of decomposition, with H1 being undecomposed peat and H10 completely decomposed peat (Table 1). Low humification is associated with high fiber content, and vice versa. The classification system for peat commonly uses humification and fibrosity at a high level. For example, the USA uses three classes – fibric, hemic, and sapric peats. The American Society for Testing and Materials has adopted a laboratory classification of peat based on fiber content, ash content, acidity, absorbance, and botanical composition. Canada uses three similar classes designation although with differences in terminology – fibric, mesic, and humic peats. Both divisions correspond to the level of decomposition (Richardson and Brinson, 2001). The ten classes from the von Post pressing method correspond to the three Canadian classes (Table 1).

Ash content

Ash content seems to be a useful factor for characterizing peat soils. It is determined by igniting the dried peat samples in a muffle furnace at about 550°C until their weight is constant. The ash content is expressed in terms of percentage of the ignition residue with respect to the original dry matter. The amount of ash content for sedge and woody peats is considerably higher than that of *Sphagnum* peat (Table 2). However, raised bog peats are characterized by low ash content (1–5% on dry mass basis). In addition, the quantity of ash in fen peats is greater than in raised bog peat and ranges from 5% to 20%. The ash content of transitional peats may range from 3% to 15% (Szajdak, 2002).

Peat bulk and particle density

Bulk density (BD) seems to be the most frequently used index of the density of the soil formation. It is expressed in dry mass per unit volume (kg m^{-3}). It depends both on the soil mass in a unit of volume and on its specific density which, in turn, depends on the content of mineral particles in the soil. The bulk density of peat deposits varies according to the botanical composition of the plant remains and degree of decomposition of the peat. Bulk density ranges from 20 kg m^{-3} in the surface layers to $100\text{--}260 \text{ kg m}^{-3}$ in lower layers (Boelter, 1969).

Peats and Peatlands, Physical Properties, Table 1 The von Post system of humification H1–H10 (given in Agriculture Canada Expert Committee on Soil Survey, 1987). It reveals the three-part fiber content system used in Canada (Lemasters et al., 1983). It is similar, but with different terminology, used in the USA

Class of fiber content, Canada (USA)	von Post humification
Fibric = Fibric (USA) weakly decomposed, botanical readily identified, 40% or more of rubbed fiber (by volume)	H1 Undecomposed: plant structures unaltered; yields only clear, colorless water when squeezed H2 Mostly undecomposed: plant structures distinct, yields yellow-brown water, still almost clear H3 Very weakly decomposed: plant structures distinct; yields somewhat turbid, brown water; no peat substance passes between the fingers. Residue is not mushy (pasty) H4 Weakly decomposed: plant structures distinct; yields very muddy, dark, and turbid water; no peat substance passes between the fingers, and no distinct ridges after squeezing. Residue slightly mushy(pasty) H5 Moderately decomposed: plant structures clear but becoming indistinct; yields much turbid brown water, some peat (about one tenth) escapes between the fingers, and distinct ridges remain after squeezing. Residue very mushy (pasty) H6 Strongly decomposed: plant structures somewhat indistinct, but clear in the squeezed residue than in the undisturbed peat; about one third of the peat escapes between the fingers. Residue strongly mushy H7 Strongly decomposed: plant structures indistinct but recognizable; about one half of the peat escapes between the fingers H8 Almost completely decomposed: plant structures very indistinct almost unrecognizable; nearly all the peat escapes between the fingers H9 Completely decomposed: plant structures unrecognizable; all the peat escapes between the fingers
Mesic = (USA) medium decomposed, botanical origin indistinct but still recognizable, material partly altered both physically and chemically into amorphous humus, 10–40% rubbed fiber	
Humic = Sapric (USA) strongly decomposed, botanical original very indistinct, in advanced stage of decomposition, dominated by amorphous humus. Less than 10% of rubbed fiber	

Peats and Peatlands, Physical Properties, Table 2 Basic physical properties of peat soils. (Based on data from Päivänen (1973) and Szymanowski (1993))

Peat type	Degree of decomposition (von Post scale)	Ash content (% per dry mass)	Bulk density (kg m^{-3})	Porosity ($\text{m}^3 \text{m}^{-3}$)
Raised bog				
<i>Sphagnum</i>	H1–H3	2.6	61.0	0.958
<i>Sphagnum</i>	H4–H6	3.0	97.0	0.929
<i>Sphagnum</i>	H7–H10	4.2	134.0	0.898
Fen peat				
Moss	H1–H3	8.4	114.0	0.927
Moss	H4–H6	11.8	168.0	0.895
Sedge	H1–H3	10.2	115.0	0.928
Sedge	H4–H6	11.4	141.0	0.912
Sedge	H7–H10	13.7	165.0	0.898
Reed	H4–H6	11.0	126.0	0.920
Reed	H7–H10	14.3	164.0	0.900
Alder	H4–H6	14.3	145.0	0.911
Alder	H7–H10	15.1	175.0	0.893

Päivänen (1973) and Szymanowski (1993) presented some results of bulk density for peat (Table 2). In addition, Päivänen (1973) revealed a positive and approximately linear relationship with von Post humification. Moss peats are generally characterized by a smaller bulk density than fen peats, mainly due to a lower degree of decomposition and lower ash content. With increasing degree of decomposition, an increase in bulk density is often observed.

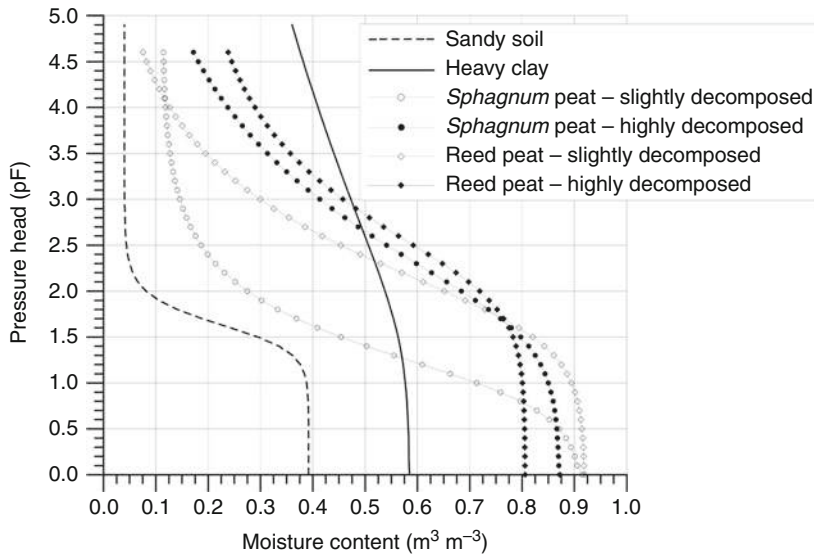
The particle density (density of solids), (SD) refers to the mass of dry solids divided by the volume of the solids. It is expressed in dry mass of solid packed matter (with no pore spaces) per unit volume. The average particle density of the organic soil mass is $1,450 \text{ kg m}^{-3}$ varying only slightly from $1,300 \text{ kg m}^{-3}$ to $1,600 \text{ kg m}^{-3}$ depending on the degree of decomposition (Okruszko, 1993). The particle density value for most mineral soils generally varies between $2,400 \text{ kg m}^{-3}$ and $2,650 \text{ kg m}^{-3}$.

Porosity

Peat is a porous material whose pores (macro- and micro-pore networks) differ in size and shape and are largely dependent on the plant residues and the degree of decomposition. Total pore space is often calculated as $\text{TP} = [1 - (\text{BD}/\text{SD})] \times 100\%$. The total porosity of peat is high, up to 96% for undecomposed, and about 90% for highly decomposed peats (Table 2). Porosity is high in fibric peats and decreases in mesic and humic peats. It seems that porosity decreases with increasing humification, bulk density, and the degree of compaction. With increasing humification and bulk density, the number of large pores decreases, but the number of small pores increases. In mineral soils, the total porosity is much lower, varying between 30% and 65%.

Moisture retention

The water retention curve of soil refers to the relationship between the soil water content and the soil water matric potential. The relationship between pressure (or matric



Peats and Peatlands, Physical Properties, Figure 1 Water retention curves for different peat and mineral soils. (Data for *Sphagnum* peat from Päivinen (1973).)

potential) and soil moisture in peat soils depends upon the degree of decomposition and the composition of the accumulated plant residues (Figure 1). The water retention capacity of peat soils is generally greater than that of mineral soils at low matric suction values. In the case of large matric suction values, too, coarse mineral soils usually retain less water than slightly decomposed *Sphagnum* peat, the water retention capacity of clay being of similar magnitude to that of moderately decomposed peat. Slightly decomposed peats contain a large quantity of water at saturation, but the water is released relatively easily with increasing matric suction.

Hydraulic conductivity

Darcy's law, an empirical relationship connecting the macroscopic velocity of water in a porous medium with the gradient of water potential down which the water flows, defines hydraulic conductivity. The hydraulic conductivity has various direct effects on the hydrology of peat and on the ecology of mire vegetation, and it varies with the degree of decomposition of the plant remains (Rycroft et al., 1975a, b). Undecomposed peats have a high hydraulic conductivity, which is of the order of 10^{-3} m s^{-1} to 10^{-5} m s^{-1} whereas highly decomposed peats have hydraulic conductivity around 10^{-8} m s^{-1} . Baden and Eggelmann (1963) found a negative hyperbolic relationship between the saturated hydraulic conductivity and the degree of decomposition of peats composed of *Sphagnum*, *Carex*, or *Phragmites* plant residues. The hydraulic conductivity of *Sphagnum* peat is usually considerably lower than that of fen peat.

Unsaturated hydraulic conductivity describes the ability of a porous medium to transmit water when the

whole cross section of the pores is not filled with water. The measured data for fen peat soils indicate the variation in unsaturated hydraulic conductivity, some of them are close to the data representing coarse soil while the others are close to the data representing very fine soil (Brandyk et al., 2003).

Peat shrinkage

The long-term intensive cultivation and agricultural use of peatlands is connected with drying. Drying of peat soils leads to soil volume decreases (Tuncer et al., 1986). Soil volume losses, usually between 53% and 70% compared with the initial peat volume (from saturation to oven-dry), vary with peat botanical composition and degree of decomposition. When peat shrinkage is larger, the greater is the degree of decomposition and the smaller is the ash content. An increased moss fraction decreases peat shrinkage. According to research performed by Ilnicki (1967), peats with a degree of decomposition over 45% show a clear tendency to cracking as a result of shrinkage induced by drying. The formation of cracks starts at volumetric moisture content of about 70% and becomes well visible at 50% volumetric water content. The intensity of cracking is proportional to an increase in the degree of the decomposition and is also dependent on peat type. Woody peats are most susceptible to cracking, followed by sedge, whereas moss peats are the least vulnerable to this process. In field soils, this shrinkage process results in the subsidence of the soil surface and in the occurrence of cracks. It is generally understood that the rate of subsidence varies strongly and depends on a number of factors, such as the type of peat, rate of decomposition, density and thickness of the peat layer, drainage depth and its duration,

climate, and land use (Ilnicki, 2003). Total subsidence due to drainage of peat soils can be subdivided into three following components:

1. "Wastage" of the peat resulting from loss of organic matter as a result of decomposition by biochemical processes
2. Shrinkage of the upper horizons as a result of water loss
3. Loss of buoyancy of the upper horizons by removal of water, which causes mechanical compression of permanently saturated peat layers below the groundwater level

Shrinkage of the upper horizons and loss of buoyancy are both a direct result of water removal from the upper horizons of the peat soil profile and depends on the amount of water stored in the profile. Subsidence rate of drained organic soils is typically found in the range of 0.3 cm year⁻¹ for grassland and 1.0–5.0 cm year⁻¹ for arable land (Ilnicki, 2003).

Summary

In peat soils, basic physical properties as well as water retention and hydraulic conductivity characteristics depend upon the degree of decomposition and the composition of the accumulated plant residues. Upon drying, most organic soils show a considerable shrinkage and hydrophobicity. The variability of peat physical properties is relatively large.

Bibliography

- Agriculture Canada Expert Committee on Soil Survey. 1987. The Canadian system of soil classification. 2nd edition. *Research Branch*, Agriculture Canada.
- Baden, W., and Eggelmann, R., 1963. Zur durchlässigkeit der moorböden. *Zeitschrift für Kulturtechnik und Flurbereinigung*, **4**, 226–254.
- Boelter, D. H., 1969. Physical properties of peats as related to degree of decomposition. *Soil Science Society of America Proceedings*, **33**, 606–609.
- Brandyk, T., Szatyłowicz, J., Oleszczuk, R., and Gnatowski, T., 2003. Water-related physical attributes of organic soils. In Parent, L.-E., and Ilnicki, P. (eds.), *Organic Soils and Peat Materials for Sustainable Agriculture*. Boca Raton: CRC Press and International Peat Society, pp. 33–66.
- Charman, D., 2002. *Peatlands and Environmental Change*. Chichester: Wiley.
- Ilnicki, P., 1967. The shrinkage of peat soils during drying as dependent on soil structure and physical properties. *Zeszyty Problemowe Postępów Nauk Rolniczych*, **76**, 197–311 (in Polish).
- Ilnicki, P., 2003. Agricultural production systems for organic soil conservation. In Parent, L.-E., and Ilnicki, P. (eds.), *Organic Soils and Peat Materials for Sustainable Agriculture*. Boca Raton: CRC Press and International Peat Society, pp. 187–199.
- Joosten, H., and Clarke, D., 2002. *Wise Use of Mires and Peatlands*. Jyväskylä: International Mire Conservation Group, International Peat Society.
- Lappalainen, E. (ed.), 1996. *Global Peat Resources*. Jyväskylä: International Peat Society and Geological Survey of Finland.
- Lemasters, G. S., Bartelli, L. J., and Smith, M. R., 1983. Characterization of organic soils as energy sources. In Jarrett, P. M. (ed.), *Testing of Peats and Organic Soils*. Special Technical Publication 820, West Conshohocken: American Society for Testing and Materials, pp. 122–137.
- Okruszko, H., 1993. Transformation of fen-peat soils under the impact of draining. *Zeszyty Problemowe Postępów Nauk Rolniczych*, **406**, 3–73.
- Päivinen, J., 1973. Hydraulic conductivity and water retention in peat soils. *Acta Forestalia Fennica*, **129**, 1–70.
- Richardson, J. L., and Brinson, M. M., 2001. Wetland soils and hydrogeomorphic classification of wetlands. In Richardson, J. L., and Vepraskas, M. J. (eds.), *Wetland Soils. Genesis, Hydrology, Landscapes and Classification*. Boca Raton: CRC Press, pp. 209–228.
- Rycroft, D. W., Williams, D. J. A., and Ingram, H. A. P., 1975a. The transmission of water through peat. I. Review. *Journal of Ecology*, **63**, 535–556.
- Rycroft, D. W., Williams, D. J. A., and Ingram, H. A. P., 1975b. The transmission of water through peat. II. Field Experiments. *Journal of Ecology*, **63**, 557–568.
- Rydin, H., and Jeglum, J., 2006. *The Biology of Peatlands*. Oxford: Oxford University Press.
- Szajdak, L., 2002. Chemical properties of peat. In Ilnicki, P. (ed.), *Peatlands and Peat*. Poznań: Wydawnictwo Akademii Rolniczej im. Augusta Cieszkowskiego w Poznaniu, pp. 432–450 (in Polish).
- Szymański, M., 1993. Basic physico-hydrological and retention properties and their relationship with bulk density of various weakly-sludged (low-ash) peat formations (in Polish, English summary). *Wiadomości IMUZ*, **XVII**(3), 153–174.
- Tuncer, B. E., Bosscher, P., and DeWitt, C. B., 1986. Composition and gravity drainage as means of dewatering peat. In Fuchsman, C. H. (ed.), *Peat and Water: Aspect of Water Retention and Dewatering in Peat*. Crown House: Elsevier Applied Science, pp. 21–36.
- von Post, L., 1922. Sveriges Geologiska Undersöknings torvinventering och några av dess hitills vunna resultat. *Svenska Mosskulturföreningens tidskrift*, **36**, 1–27 (in Swedish).

Cross-references

- [Bulk Density of Soils and Impact on their Hydraulic Properties](#)
[Hydraulic Properties of Unsaturated Soils](#)
[Organic Matter, Effects on Soil Physical Properties and Processes](#)
[Parent Material and Soil Physical Properties](#)
[Peatlands: Environmental Functions](#)
[Shrinkage and Swelling Phenomena in Soils](#)
[Soil Phases](#)
[Soil Water Flow](#)
[Wetlands, Management, Degradation and Restoration](#)

PEDON

A term used by pedology to describe structural elements block, column, granule, plate, or prism, formed by natural processes (in contrast with a clod, which is formed artificially in cultivated soils).

PEDON

A three-dimensional volume of soil with lateral dimensions large enough to permit the study of horizon shapes and relations. Its area ranges from 1 to 10 m².

PEDOTRANSFER FUNCTIONS

Yakov A. Pachepsky¹, Martinus Th. van Genuchten²
¹Environmental Microbial and Food Safety Laboratory, Animal and Natural Resource Institute, Beltsville Agricultural Research Center, USDA-ARS, Beltsville, MD, USA
²Department of Mechanical Engineering, COPPE/LTTC, Federal University of Rio de Janeiro, UFRJ, Rio de Janeiro, Brazil

Definition

Pedotransfer functions. Equations or algorithms expressing relationships between soil properties different in difficulty of their measurement or their availability.

Introduction

Parameters governing the retention and movement of water and chemicals in soils are notorious for the difficulties and high labor costs involved in measuring them. Often, there is a need to resort to estimating these parameters from other, more readily available data. Following Briggs and Shantz (1912), who were the pioneers in the field, generations of researchers quantified and interpreted relationships between soil properties. Such terms as “prediction of” or “predicting” soil properties, “estimation of” or “estimating” soil properties, “correlation of” or “correlating” soil properties, were used interchangeably to name the contents, procedures, and results of these type of studies (Carter and Bentley, 1991; Rawls et al., 1991; van Genuchten and Leij, 1992; Timlin et al., 1996; McBratney et al., 2002). Relatively recently, equations expressing relationships between soil properties were proposed to be called “transfer functions” (Bouma and van Lanen, 1987) and later “pedotransfer functions” or PTFs (Bouma, 1989). Large international databases, such as UNSODA (Leij et al., 1996), HYPRES (Lilly, 1997; Wösten et al., 1999), WISE (Batjes, 1996), the NRCS pedon database (NRCS, 2007), as well as national databases such as the Soil Profiles Bank of Polish Mineral Soils (Gliński et al., 1991) were established and used for the purpose of PTF development. Recently the number of PTF applications increased significantly due to development of geographic information system based regional modeling.

Pedotransfer functions to predict soil hydraulic properties are most numerous. Such PTFs have many potential user groups in agrophysics. For example, soil water retention and hydraulic conductivity data are needed to partition precipitation into runoff and infiltration, to assess evapotranspiration, to schedule management practices, especially irrigation and chemical applications, to establish components of the heat balance, and to predict contaminant transport.

For soil water retention, one approach (using point PTFs) consists of estimating soil water contents at several soil water pressure heads using a separate predictive

equation for each pressure head. Another approach (using parametric PTFs) involves estimating coefficients in equations that express the dependence of the water content on the soil water potential. The equations that are most often used for this purpose are the Brooks–Corey equation (Brooks and Corey, 1964)

$$\frac{\theta - \theta_r}{\theta_s - \theta_r} = \left(\frac{h_b}{h} \right)^\lambda \quad (1)$$

and the van Genuchten equation (van Genuchten, 1980)

$$\frac{\theta - \theta_r}{\theta_s - \theta_r} = \frac{1}{(1 + |\alpha h|^n)^m} \quad (2)$$

where θ is the volumetric water content, θ_s is the saturated water content, θ_r is the residual water content, h is the soil water pressure head, h_b is the soil water pressure head corresponding to the soil bubbling pressure or air entry value. The parameters θ_r , h_b , and λ in Equation 1, and θ_r , α , m , and n in Equation 2 are empirical coefficients. Pedotransfer functions have been constructed to estimate these coefficients using many local and regional data sets.

For the saturated hydraulic conductivity, K_{sat} , one approach is to estimate this coefficient from basic soil parameters without employing soil water retention data (e.g., Bloemen, 1980). Another approach benefits from the use of soil pore space models to derive K_{sat} equations in which the coefficients must be estimated from basic soil properties (e.g., Han et al., 2006). Estimates of the unsaturated hydraulic conductivity are based predominantly on pore size distribution models that relate the unsaturated hydraulic conductivity to K_{sat} as well as several geometric parameters of the pore space inferred from water retention data. A general form of such a model was proposed by Alexander and Skaggs (1987):

$$k(h) = K_{sat}[S(\theta)]^\beta \left\{ \frac{\int_0^S [h(\theta)]^{-\gamma} d\theta}{\int_0^1 [h(\theta)]^{-\gamma} d\theta} \right\}^\delta \quad (3)$$

where S is effective saturation give by $S = (\theta - \theta_r)/(\theta_s - \theta_r)$, and β , γ , and δ are parameters. Pedotransfer functions must be used to estimate both K_{sat} and $h(\theta)$ in Equation 3 to evaluate the integral and calculate the unsaturated hydraulic conductivity (Pachepsky et al., 2000).

Soil erosion prediction models frequently rely upon a variety of soil pedotransfer functions that most often estimate soil erodibility and soil infiltration parameters (Flanagan, 2004). Existing long-term historical erosion plot data (e.g., the USLE database) provide sufficient information to create pedotransfer equations for soil erosion models.

Solute and gas retention and transport parameters can be predicted reasonably well also from basic soil properties, although caution should be exercised because of

possible scale effects (i.e., the effect of the scale of solute transport on solute dispersion and retardation). Unified diffusivity models can use existing PTFs to estimate solute and gas diffusivities as a function of soil water content (Minasny and Perfect, 2004). Based on current knowledge, the pore size distribution appears to be an acceptable dispersivity predictor, with water retention PTFs being helpful in developing PTFs for the dispersivity.

Soil water retention has been related to soil rheology by defining several characteristic points on the water retention curve that separate segments of the retention curve where the forces causing water retention have a distinctly different physical nature (Voronin, 1990; Shein et al., 2004). Water contents at the characteristic points in this approach are termed key water contents and are related to the soil pressure head. The key water contents can be estimated from the liquid limit, the plastic limit, and data on evaporation from soil. As soon as they are estimated, their relationships with the soil matric potential provide several points on the water retention curve.

PTF inputs

Soil water retention and the soil hydraulic conductivity are essential hydraulic properties that can be estimated using PTFs. The particle size distribution and its parameters are used in almost all pedotransfer functions. Differences in the particle size classes of various national and international classifications have to be factored in when PTFs are used. It is very important to use the correct boundaries of the sand and silt textural classes from the classification used during PTF development, rather than from a specific national classification.

Water retention PTFs generally become more accurate when some experimental information about water retention is used as the PTF input (Ahuja et al., 1985). Soil organic carbon content and composition both affect soil structure and the adsorption properties, which imply that soil bulk density, water retention, and hydraulic conductivity may be affected by soil organic carbon. The effect of soil organic carbon on the soil hydraulic properties exhibits a complex dependence on proportions of textural components and amount of organic carbon (Rawls et al., 2003).

Using soil morphological attributes and soil structure in pedotransfer functions is extremely important because of the dominant role of soil structure in soil hydrology. Unfortunately, effectively using soil morphological attributes is also very difficult because of the semiqualitative nature of soil morphology and related soil structure descriptors. It is possible to develop pedotransfer relationships to predict soil hydraulic properties and soil hydrological functioning from soil morphology data, including soil structure (Lin et al., 1999). These relationships can be expressed as either pedotransfer functions or semiqualitative pedotransfer rules. A considerable volume of soil morphological data residing in national and regional databases can be of great use in providing

information on soil hydrology. However, future progress may require the acceptance of standardized methodologies to describe and quantify soil morphological attributes, as well as to measure soil hydraulic properties in the field.

Soil aggregate composition is often assumed to be related to soil structure and as such has been expected to affect soil water retention. That has indeed been the case when the quantiles of soil aggregate size distributions have been used, instead of contents of individual aggregate fractions (Guber et al., 2003).

Soil mineralogical and chemical properties are conceptually important factors of the ability of a soil to retain and transmit water. This may be one of the reasons why a preliminary genetic grouping of soils appears to be a useful way to improve PTF performance (Pachepsky and Rawls, 1999). Much can be gained in understanding and estimating soil hydraulic properties when mineralogical and chemical data are coupled with soil physical information (Bruand, 2004). Such coupling is especially beneficial for regions where soil salinity and alkalinity constitute environmental and management problems.

PTFs in a spatial context

PTFs generally are constructed using data from small point samples, but then are most often applied to large spatial units. Results of applications will depend on basic soil data availability within those units, on soil variability within those units, on the capability of PTFs to reproduce this variability, and on our ability to modify PTFs according to the scale of the application. The spatial dependencies in PTF input may not necessarily translate correctly to spatial dependencies in the PTF output, in which case corrections of the existing PTFs are needed to reflect the spatial dependencies (Romano, 2004).

A relatively new promising direction in PTF development is the use of spatially dense physical information related to the soil cover. Soil properties are known to be related to landscape position. Since geomorphic information has long been routinely used in soil mapping, geomorphometry may be a valuable data source to predict basic soil properties. In particular, soil texture, organic matter content, and bulk density are known to reflect both landscape position and land surface shape. Because these soil properties are most often included in pedotransfer functions, one can hypothesize that soil hydraulic properties should have some relationship to landscape position and land surface shape. Overall, the reported studies and related discussions confirm the usefulness of topographic attributes as ancillary data to indirectly estimate soil hydraulic properties. Geophysical techniques, such as ground-penetrating radar, penetrometers, electric conductivity surveys, and remote sensing provide spatial coverage that shows great potential to be included in PTFs.

Methods to develop PTF

Statistical regression has been a popular tool for PTF development for many decades (e.g., Rawls et al., 1982).

An advantage of regression techniques is the possibility to obtain rigorous estimates of the statistics of the predicted values and the coefficients in the PTF equations. However, as shown by Vereecken and Herbst (2004), the blind use of statistical computer packages without a preliminary and *a posteriori* data analysis can have a deleterious effect on the regression results. Model misspecification, the presence of outliers, multicollinearity, and other drawbacks, have to be anticipated and overcome. As such, constructing PTFs using regression is an iterative procedure that may require many iteration steps.

Applying statistical regression to predict soil properties that are difficult to measure requires (a) deciding which properties are to be used as predictors and (b) which regression equation to use. Those decisions are not straightforward, especially when the databases involved contain many potential predictors and the relationships between soil properties may be different in different parts of the databases. For this reason, PTF development recently has employed data mining and exploration methods, as well as machine learning algorithms, which automate predictor and equation selections. Artificial neural networks have become a common tool for modeling complex “input–output” dependencies in pedotransfer functions because of their ability to mimic the behavior of complex systems (Pachepsky et al., 1996; Schaap and Bouten, 1996).

While being powerful approximators, artificial neural networks often lack a built-in methodology to remove the less or least important input variables. PTF development for this reason benefits from methods that do not assume a certain type of dependency, while still being able to eliminate some predictors. The most important predictors may also be different in different parts of the database. The database then has to be quite large to permit the use of artificial neural networks. A data exploratory technique aimed at uncovering some structure in the data can be useful in such cases. Regression tree modeling (e.g., Rawls and Pachepsky, 2002) is such a technique that gives transparent results and can be applied not only to numerical but also to categorical soil data. Another drawback of using neural networks may be the inability of finding the best approximation for the entire database. Using support vector machines in PTF development may provide a good solution (Lamorski et al., 2008).

PTF development presumes that similarity in input will result in similarity in output. For large enough databases, one can find soils with properties that are very close to the soil for which the pedotransfer prediction is needed. In such case, finding the closest neighbors and using their hydraulic properties as the required PTF predictions has been shown beneficial (Nemes et al., 2006).

PTFs have also been developed based on the additivity hypothesis that the property of interest (e.g., water retention) is known for certain soil components (e.g., certain particles size ranges), and that this property then can be estimated for the entire soil by adding component values with appropriate weights (Zeliguier et al., 2000).

PTF evaluation and selection

Evaluation of PTFs is an essential element of their development and use. Pachepsky et al. (1999) broadly defined the accuracy of a PTF as the degree of correspondence between measured and estimated data for the data set *from which the PTF was developed*. The reliability of a PTF was assessed in terms of the correspondence between measured and estimated data for the data set(s) *other than the one used to develop the PTF*. Finally, the utility of a PTF in modeling was viewed as the degree of correspondence between *measured and simulated environmental variables*.

The concept of PTF uncertainty (Schaap and Leij, 1998) encompasses the ambiguity in PTF predictions and parameters caused by input data variability and uneven representation of soils with different properties in the database. The uncertainty in PTF estimates may be evaluated using replicated PTF development with data resampling by either the bootstrap (Schaap et al., 1998) or jackknife (Pachepsky and Rawls, 1999) methods.

The reliability of a PTF is not directly related to its utility (Pachepsky et al., 1999). The latter is affected by the sensitivity of the model to PTF predictions, and also by the uncertainty in other model inputs (Leenhardt, 1995). The functional evaluation of PTFs considers the evaluation of PTFs on the base of their utility and uses criteria directly related to specific applications rather than statistics to characterize the accuracy. PTF accuracy may be not an issue since at least four factors affect the performance of a PTF in simulations. These are the accuracy of basic soil data used as inputs in the PTFs, the accuracy of the PTF itself, specific features of the simulation model, and the output used in the functional criteria (Wösten and van Genuchten, 1988).

Database size and measurement method are among the more important factors affecting PTF accuracy and reliability. The number of samples has to be large enough to develop PTFs that are both accurate and reliable. When the reliability of USA-wide PTFs was compared with the accuracy of those based on several smaller databases, and the PTFs were ranked by their reliability, the all-USA PTFs usually had one of the highest rankings (Tietje and Tapkenhinrichs, 1993; Kern, 1995). However, PTFs based on local information appear to be more accurate in the area where the data were collected.

There are indications that PTFs developed from regional databases give good results in regions with similar soil and landscape histories. For example, water retention PTFs developed in Belgium (Vereecken et al., 1989) were the most accurate as compared with 13 PTFs based on a database of Northern Germany (Tietje and Tapkenhinrichs, 1993). Water retention PTFs developed for the Hungarian Plain (Pachepsky et al., 1992) were applicable to the Caucasian Piedmont Plain (Nikolaeva et al., 1988). The development of PTF equations adapted for the conditions of Brazilian weathered soils allowed much better estimates of the parameters in [Equation 2](#), as

compared to the performance of PTFs derived for soils from temperate climates (Tomasella et al., 2000). It remains to be seen whether this observation holds for other cases, and which soil and landscape features have to be similar in two regions to assure the mutual reliability of the PTFs developed.

The use of models depends on the easiness to operate them, and PTFs are no exception. A PTF user has to be able to make an informed choice of the PTF, and to have a convenient tool to apply the PTF technology. One example of creating a multipurpose PTF tool is the soil inference system (McBratney et al., 2002). Also, software packages like Rosetta (Schaap et al., 2001) and k-Nearest (Nemes et al., 2008) provide graphic user interfaces that substantially simplify PTF use and the interpretation of results.

Since pedotransfer functions are empirical regression-type relationships, their accuracy outside of their development region is essentially unknown. Instead of attempting to find a single best PTF, Guber et al. (2009) proposed the use of multimodeling. The approach involves assigning weights to the simulation results obtained with different PTFs and then using the weighted average of these results. Improvements in the predictions have been attributed to the fact that multimodeling provides better coverage of possible variations in PTF inputs.

Limits of PTF accuracy

The accuracy and reliability of a PTF is sometimes limited by temporal variations in soil properties caused by changes in vegetation and soil management. Incorporation of organic matter, soil erosion, and tillage practices can cause variations in hydraulic properties that are comparable with variations within regional databases (Wösten et al., 2001). The PTFs may require a temporal component and vegetation parameters to improve their reliability (Sharma et al., 2006). Differences in measurement techniques for the samples in the same database will definitely affect PTF performance. Future PTF improvements will strongly depend on advances in characterization of fine-scale soil physical and chemical heterogeneities that controls flow and transport in soils at PTF application scales.

Conclusions

The history and the current status of PTF development demonstrate the need in and value of integrative studies. Systematic coupling measurements of various soil properties add value to all of those measurements as pedotransfer relationships can be derived for a variety of agrophysical applications. PTF development contributes to understanding of soil functioning and enhances the role of soil information in multiple applications. PTFs hence are essential tools to translate data that we have to date we need in agrophysical research and management applications.

Bibliography

- Ahuja, L. R., Naney, J. W., and Williams, R. D., 1985. Estimating soil water characteristics from simpler properties or limited data. *Soil Science Society of America Journal*, **49**, 1100.
- Alexander, L., and Skaggs, R. W., 1987. Predicting unsaturated hydraulic conductivity from soil texture. *Journal of Irrigation and Drainage Engineering*, **113**, 184.
- Batjes, N. H., 1996. Development of a world data set of soil water retention properties using pedotransfer rules. *Geoderma*, **71**, 31.
- Bloemen, G. W., 1980. Calculation of hydraulic conductivities of soils from texture and organic matter content. *Zeitschrift für Pflanzenernährung und Bodenkunde*, **143**, 581.
- Bouma, J., 1989. Using soil survey data for quantitative land evaluation. *Advances in Soil Science*, **9**, 177.
- Bouma, J., and van Lanen, H. A. J., 1987. Transfer functions and threshold values: from soil characteristics to land qualities. In *Proceedings of the International Workshop on Quantified Land Evaluation Procedures*. 27/04–2/05/1986, Washington DC, p. 106.
- Briggs, L. J., and Shantz, H. L., 1912. The wilting coefficient and its indirect measurement. *Botanical Gazette*, **53**, 20.
- Brooks, R. J., and Corey, A. T., 1964. *Hydraulic Properties of Porous Media. Hydrology Paper 3*. Fort Collins: Colorado State University.
- Bruand, A., 2004. Utilizing mineralogical and chemical information in PTFs. In Pachepsky, Y., and Rawls, W. J. (eds.), *Development of Pedotransfer Functions in Soil Hydrology*. Amsterdam: Elsevier, pp. 153–158.
- Carter, M., and Bentley, S. P., 1991. *Correlations of Soil Properties*. London: Pentech Press.
- Flanagan, D. C., 2004. Pedotransfer functions for soil erosion models. In Pachepsky, Y., and Rawls, W. J. (eds.), *Development of Pedotransfer Functions in Soil Hydrology*. Amsterdam: Elsevier, p. 177.
- Gliński, J., Ostrowski, J., Stepniewska, Z., and Stepniewski, W., 1991. Bank próbek glebowych reprezentujących gleby mineralne Polski. (Bank of Soil Samples Representing Minerals Soils of Poland). *Problemy Agrofizyki*, 66.
- Guber, A. K., Rawls, W. J., Shein, E. V., and Pachepsky, Y., 2003. Effect of soil aggregate size distribution on water retention. *Soil Science*, **168**, 223.
- Guber, A. K., Pachepsky, Y., van Genuchten, M. Th., Simunek, J., Jacques, D., Nemes, A., Nicholson, T. J., and Cady, R. E., 2009. Multimodel simulation of water flow in a field soil using pedotransfer functions. *Vadose Zone Journal*, **8**, 1.
- Han, H., Gimenez, D., and Lilly, A., 2006. Textural averages of saturated soil hydraulic conductivity predicted from water retention data. *Geoderma*, **146**, 121.
- Kern, J. S., 1995. Evaluation of soil water retention models based on basic soil physical properties. *Soil Science Society of America Journal*, **59**, 1134.
- Lamorski, K., Pachepsky, Y., Slawinski, C., and Walczak, R., 2008. Using support vector machines to develop pedotransfer functions for water retention of soils in Poland. *Soil Science Society of America Journal*, **72**, 1243.
- Leenhardt, D., 1995. Errors in estimation of soil water properties and their propagation through a hydrological model. *Soil Use and Management*, **11**, 15.
- Leij, F. J., Alves, W. J., van Genuchten, M. Th., and Williams, J. R., 1996. *Unsaturated Soil Hydraulic Database, UNSODA 1.0. User's Manual. Report EPA/600/R96/095*. Ada: US Environmental Protection Agency.
- Lilly, A., 1997. A description of the HYPRES database (HYdraulic Properties of European Soils), In The use of pedotransfer functions in soil hydrology research. *Proceedings of the Second Workshop of the Project "Using Existing Soil Data to Derive*

- Hydraulic Parameters for Simulation Modeling in Environmental Studies and in Land Use Planning.*" Orleans, France, 10–12/10/1996, p. 161–184, INRA, Orleans and EC/JRC Ispra.
- Lin, H. S., McInnes, K. J., Wilding, L. P., and Hallmark, C. T., 1999. Effects of soil morphology on hydraulic properties: II Hydraulic pedotransfer functions. *Soil Science Society of America Journal*, **63**, 955.
- McBratney, A. B., Minasny, B., Cattle, S. R., and Vervoort, R. W., 2002. From pedotransfer functions to soil inference systems. *Geoderma*, **109**(12), 41–73.
- Minasny, B., and Perfect, E., 2004. Solute adsorption and transport parameters. In Pachepsky, Y., and Rawls, W. J. (eds.), *Development of Pedotransfer Functions in Soil Hydrology*. Amsterdam: Elsevier, p. 195.
- Nemes, A., Rawls, W. J., and Pachepsky, Y., 2006. Use of k-nearest neighbor algorithms to estimate soil hydraulic properties. *Soil Science Society of America Journal*, **70**, 327.
- Nemes, A., Roberts, R., Rawls, W. J., Pachepsky, Y., and van Genuchten, M. Th., 2008. Software to estimate –33 and –1500 kPa soil water retention using the non-parametric k-nearest neighbor technique. *Environmental Modeling and Software*, **23**, 254.
- Nikolaeva, S. A., Pachepskii, Ya. A., Shcherbakov, R. A., and Shcheglov, N. I., 1988. Simulation of the water regime of micellar calcareous ordinary chernozem. *Pochvovedenie*, 44.
- NRCS, 2007. *National Soil Survey Characterization Data*. Lincoln, Neb.: USDA-NRCS National Soil Survey Laboratory.
- Pachepsky, Y., and Rawls, W. J., 1999. Accuracy and reliability of pedotransfer functions as affected by grouping soils. *Soil Science Society of America Journal*, **63**, 1748.
- Pachepsky, Y., Mironenko, E. V., and Scherbakov, R. A., 1992. Prediction and use of soil hydraulic properties. In van Genuchten, M. Th., Leij, F. J., and Lund, L. J. (eds.), *Indirect Methods for Estimating the Hydraulic Properties of Unsaturated Soils*. Riverside: University of California, p. 203.
- Pachepsky, Y., Timlin, D. J., and Varallyay, G., 1996. Artificial neural networks to estimate soil water retention from easily measurable data. *Soil Science Society of America Journal*, **60**, 727.
- Pachepsky, Y., Rawls, W. J., and Timlin, D. J., 1999. The current status of pedotransfer functions: their accuracy, reliability, and utility in field- and regional-scale modeling. In Corwin, D. L., Loague, K., and Ellsworth, T. R. (eds.), *Assessment of Non-Point Source Pollution in the Vadose Zone*. Washington, D. C: American Geophysical Union. Geophysical Monograph 108, p. 223.
- Pachepsky, Y., Rawls, W. J., and Timlin, D. J., 2000. A one-parameter relationship between unsaturated hydraulic conductivity and water retention. *Soil Science*, **165**, 911.
- Rawls, W. J., and Pachepsky, Y., 2002. Soil consistency and structure as predictors of water retention. *Soil Science Society of America Journal*, **66**, 1115.
- Rawls, W. J., Brakensiek, D. L., and Saxton, K. E., 1982. Estimation of soil water properties. *Transactions of the American Society of Agricultural Engineers*, **25**, 1316.
- Rawls, W. J., Gish, T. J., and Brakensiek, D. L., 1991. Estimating soil water retention from soil physical properties and characteristics. *Advances in Soil Science*, **16**, 213.
- Rawls, W. J., Pachepsky, Y., Ritchie, J. C., Sobecki, T. M., and Bloodworth, H., 2003. Effect of soil organic carbon on soil water retention. *Geoderma*, **116**, 61.
- Romano, N., 2004. Spatial Structure of PTF estimates. In Pachepsky, Y., and Rawls, W. J. (eds.), *Development of Pedotransfer Functions in Soil Hydrology*. Amsterdam: Elsevier, p. 295.
- Schaap, M., and Bouten, W., 1996. Modeling water retention curves of sandy soils using neural networks. *Water Resources Research*, **32**, 3033.
- Schaap, M. G., and Leij, F. J., 1998. Database-related accuracy and uncertainty of pedotransfer functions. *Soil Science*, **163**, 765.
- Schaap, M. G., Leij, F. J., and van Genuchten, M. Th., 1998. Neural network analysis for hierarchical prediction of soil water retention and saturated hydraulic conductivity. *Soil Science Society of America Journal*, **62**, 847.
- Schaap, M. G., Leij, F. J., and van Genuchten, M. Th., 2001. Rosetta: a computer program for estimating soil hydraulic parameters with hierarchical pedotransfer functions. *Journal of Hydrology*, **251**, 163.
- Sharma, S. K., Mohanty, B. P., and Zhu, J., 2006. Including topography and vegetation attributes for developing pedotransfer functions. *Soil Science Society of America Journal*, **70**, 1430.
- Shein, E. V., Guber, A. K., and Dembovetsky, A. V., 2004. Key soil water contents. In Pachepsky, Y., and Rawls, W. J. (eds.), *Development of Pedotransfer Functions in Soil Hydrology*. Amsterdam: Elsevier, p. 241.
- Tietje, O., and Tapkenhinrichs, M., 1993. Evaluation of pedotransfer functions. *Soil Science Society of America Journal*, **57**, 1088.
- Timlin, D. J., Ahuja, L. R., and Williams, R. D., 1996. Methods to estimate soil hydraulic parameters for regional scale applications of mechanistic models. In *Application of GIS to the Modeling of Non-Point Source Pollutants in the Vadose Zone*. SSSA Special publication 48. Madison: American Society of Agronomy.
- Tomasella, J., Hodnett, M. G., and Rossato, L., 2000. Pedotransfer functions for the estimation of soil water retention in Brazilian soils. *Soil Science Society of America Journal*, **64**, 327.
- van Genuchten, M. T., 1980. A closed-form equation for predicting the hydraulic conductivity of unsaturated soils. *Soil Science Society of America Journal*, **44**, 892.
- van Genuchten, M. Th., and Leij, F., 1992. On estimating the hydraulic properties of unsaturated soils. In van Genuchten, M. Th., Leij, F. J., and Lund, L. J. (eds.), *Indirect Methods for Estimating the Hydraulic Properties of Unsaturated Soils*. Riverside: University of California, p. 1.
- Vereecken, H., and Herbst, M., 2004. Statistical regression. In Pachepsky, Y., and Rawls, W. J. (eds.), *Development of Pedotransfer Functions in Soil Hydrology*. Amsterdam: Elsevier, p. 3.
- Vereecken, H., Maes, J., Feyen, J., and Darius, P., 1989. Estimating the soil moisture retention characteristics from texture, bulk density and carbon content. *Soil Science*, **148**, 389.
- voronin, A. D., 1990. An energy-based concept for the physical state of soils. *Soviet Soil Science*, **22**, 53.
- Wösten, J. H. M., and van Genuchten, M. Th., 1988. Using texture and other soil properties to predict the unsaturated soil hydraulic functions. *Soil Science Society of America Journal*, **52**, 1762.
- Wösten, J. H. M., Lilly, A., Nemes, A., and Le Bas, C., 1999. Development and use of a database of hydraulic properties of European soils. *Geoderma*, **90**, 169–185.
- Wösten, J. H. M., Pachepsky, Y., and Rawls, W. J., 2001. Pedotransfer functions: bridging the gap between available basic soil data and missing soil hydraulic characteristics. *Journal of Hydrology*, **251**, 123.
- Zeiliger, A. M., Pachepsky, Y., and Rawls, W. J., 2000. Estimating water retention of sandy soils using the additivity hypothesis. *Soil Science*, **165**, 373.

Cross-references

- Agrophysical Properties and Processes
 Bulk Density of Soils and Impact on their Hydraulic Properties
 Databases of Soil Physical and Hydraulic Properties
 Field Water Capacity
 Hydraulic Properties of Unsaturated Soils
 Mapping of Soil Physical Properties

Neural Networks in Agrophysics
Organic Matter, Effects on Soil Physical Properties and Processes
Pore Size Distribution
Soil Hydraulic Properties Affecting Root Water Uptake
Soil Water Flow
Spatial Variability of Soil Physical Properties

PENETRABILITY

See *Soil Penetrability, Effect on Animal Burrowing; Soil Penetrometers and Penetrability*

PENETRATION RESISTANCE

See *Cropping Systems, Effects on Soil Physical Properties*

PENMAN EQUATION

An equation based on the simultaneous solution of the heat and mass balance equations, designed to estimate the potential evapotranspiration from a smooth, well-watered field with a dense, low crop.

Bibliography

Introduction to Environmental Soil Physics (First Edition) 2003
Elsevier Inc. Daniel Hillel (ed.) <http://www.sciencedirect.com/science/book/9780123486554>

Cross-references

Evapotranspiration

PENMAN-MONTEITH EQUATION

An extension of the Penman equation, estimating the rates of heat and vapor transfers from less-than-saturated surfaces. Specifically, this form of the equation accounts for the existence of “canopy resistance,” due to the physiological restriction of transpiration by the crop (the so-called “stomatal control mechanisms”).

Bibliography

Introduction to Environmental Soil Physics (First Edition) 2003
Elsevier Inc. Daniel Hillel (ed.) <http://www.sciencedirect.com/science/book/9780123486554>

Cross-references

Evapotranspiration

PERCHED GROUNDWATER

An accumulation of water that is under positive pressure, at some depth in or under the soil profile, resting on a relatively impermeable layer that lies above the general (regional) water table.

Bibliography

Introduction to Environmental Soil Physics (First Edition) 2003
Elsevier Inc. Daniel Hillel (ed.) <http://www.sciencedirect.com/science/book/9780123486554>

PERCOLATION

The downward flow of water through saturated or nearly saturated layers of the soil profile, generally due to gravity.

PERMAFROST

Permanently frozen material underlying the solum or perennially frozen soil horizon.

Cross-references

Snowmelt Infiltration

PERMANENT CHARGE

The net negative or positive charge of clay particles not affected by changes in pH of soil solution or ion-exchange reactions.

Cross-references

Surface Properties and Related Phenomena in Soils and Plants

PERMEABILITY

The property of a soil to permit water to pass through it.

PHOTOSYNTHESIS

See *Stomatal Conductance, Photosynthesis, and Transpiration, Modeling*

PHYSICAL DEGRADATION OF SOILS, RISKS AND THREATS

Winfried E. H. Blum

Institute of Soil Research, University of Natural Resources and Applied Life Sciences (BOKU) Vienna, Vienna, Austria

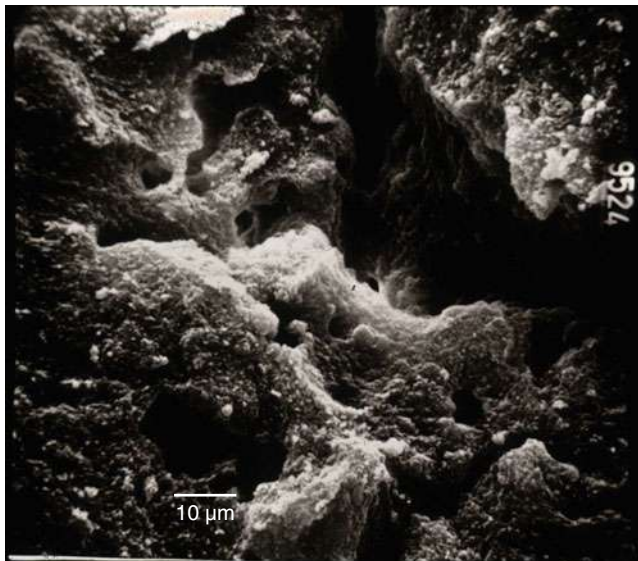
Definition

Physical soil degradation is one of the eight main risks and threats defined by the European Thematic Strategy for Soil Protection (COM(2002)179 final).

Physical degradation comprises very different processes and morphometric forms, mainly through the deformation of the inner soil structure by compaction, caused by tracking with heavy agricultural machinery, through vertical sheer stress caused by rotating parts of machines, e.g., wheels, as well as by chemical impacts such as salinization, especially alkalinization. Physical degradation also includes soil erosion by water and wind as well as the formation of crusts at the soil surface (soil crusting).

Physical degradation

The deformation of the inner soil structure, which comprises large ($>50 \mu\text{m}$ diameter) and small macropores ($50\text{--}10 \mu\text{m}$ diameter), medium pores ($10\text{--}0.2 \mu\text{m}$ diameter), and fine pores ($<0.2 \mu\text{m}$ diameter) (see Figure 1), occurs by heavy soil loading and results especially in the loss of soil macropores $>50 \mu\text{m}$ diameter or even smaller macropores $>10 \mu\text{m}$ diameter, under extreme conditions.



Physical Degradation of Soils, Risks and Threats,
Figure 1 Look into a soil by electronic microscopy (observe scale of $10 \mu\text{m}$), showing different types of pores, which are all interconnected (Blum, 2002).

Macropores are responsible for soil aeration and water conductivity and are also the living space of soil organisms, especially those which are not able to create own spaces in soil, like many earthworms. Therefore, the destruction of macropores, seldom medium pores ($10\text{--}0.2 \mu\text{m}$ diameter), means low water (rainwater) conductivity, causing stagnant water phases in soils, with anaerobic conditions changing soil chemistry as well as soil biology. Under specific topographical conditions, compaction also causes soil erosion by water surface flow. Sheer stress causes similar results, although less compacting, but smearing and closing or blinding pores, especially in the top soil, between 0 and 20 cm soil depth. A special form of sheer stress combined with loading and compaction is the formation of the so-called plough horizons, a compacted zone below the ploughed top soil with problems for root penetration and often changes in redox potential through decreased water infiltration, causing stagnant water conditions after intensive rainfall.

Compaction at soil depths $>50 \text{ cm}$ are nearly irreversible, because no technical measures are available to restore soil macroporosity, except biological processes, e.g., through earthworm activities, which is normally a very slow process and depends on further edafic conditions.

Moreover, physical soil degradation occurs also at the soil surface through the destruction of crumbly or blocky soil structures, mainly through the physical impact of rainwater, especially raindrops with high kinetic energy, called splash, destructing surface soil structures, causing smaller soil particles, which can be transported by water or wind (erosion) or may form crusts at the soil surface, especially under semiarid and arid climatic conditions. The physical degradation through splash by raindrops with high kinetic energy depends on the size of the raindrops, the wind velocity, and the type and stability of surface soil structures. Structure stability is highly influenced by soil organic matter. Through loss of soil organic matter in top soils, soil structures become unstable and therefore prone to erosion, especially crumbs or small blocks at the soil surface. Soils with a high silt content are most endangered by wind and water erosion. Soil erosion causes losses of the most fertile part of the soil, additionally decreasing soil fertility through a decrease of the rooting depth and consequently of the availability of water and nutrients for plant growth.

In climatic regions with long-lasting dry periods, fine soil particles produced by rain splash at the soil surface can form crusts, which are in most cases very resistant against deformation by water and wind, also because of fungal growth compacting these surfaces, additionally. Crusting occurs very often in soils under a mediterranean type of climate or in semiarid or semi-humid areas of the tropics and subtropics.

Conclusions

Physical soil degradation has negative impacts on nearly all soil characteristics and processes, e.g., space for plant

roots and soil biota, soil temperature, transport of water, air, and nutrients as well as natural attenuation of organic and inorganic contaminants.

Bibliography

- Blum, W. E. H., 2002. Soil pore space as communication channel between the geosphere, the atmosphere and the biosphere. In *17th World Congress of Soil Science, Transactions No. 2014, Abstracts, Vol. V, 1942, IUSS, August 14–21, Bangkok/Thailand (CD-ROM)*.
 Horn, R., Fleige, H., Peth, S., and Peng, X. (eds.), 2006. *Soil Management for Sustainability. Advances in GeoEcology 38*. Reiskirchen: Catena.

Cross-references

- [Aeration of Soils and Plants](#)
- [Bulk Density of Soils and Impact on their Hydraulic Properties](#)
- [Compaction of Soil](#)
- [Claypan and its Environmental Effects](#)
- [Field Water Capacity](#)
- [Hydraulic Properties of Unsaturated Soils](#)
- [Infiltration in Soils](#)
- [Microbes and Soil Structure](#)
- [Organic Matter, Effects on Soil Physical Properties and Processes](#)
- [Oxidation–Reduction Reactions in the Environment](#)
- [Physical Protection of Organic Carbon in Soil Aggregates](#)
- [Plant Roots and Soil Structure](#)
- [Soil Aggregates, Structure, and Stability](#)
- [Soil Surface Sealing and Crusting](#)
- [Soil Water Flow](#)
- [Solute Transport in Soils](#)
- [Subsoil Compaction](#)
- [Surface Roughness, Effect on Water Transfer](#)
- [Tillage, Impacts on Soil and Environment](#)
- [Water Erosion: Environmental and Economical Hazard](#)
- [Wind Erosion](#)

PHYSICAL DIMENSIONS AND UNITS USE IN AGRICULTURE

Wojciech Skierucha¹, Marcin Widomski²,
 Witold Stępniewski², Bogusław Usowicz¹

¹Institute of Agrophysics, Polish Academy of Sciences,
 Lublin, Poland

²Department of Land Surface Protection Engineering,
 Lublin University of Technology, Lublin, Poland

Definition

A unit and a number are factors expressing the value of a physical quantity.

Dimensions of a physical quantity are the powers to which the base units of a measurement system are raised to get one unit of the physical quantity.

Introduction

Real world should be described in terms of its biophysical and qualitative attributes, which are physical quantities. Agricultural objects and processes are interdisciplinary

and they deal with nearly all physical, chemical, and biological aspects of real world. Therefore dimensions' and units' use in agriculture includes the respective physical quantities.

The majority of physical quantities that we actually deal with in science and also in our daily life can be expressed in terms of one or more base units.

International system of units (SI)

The most popular and scientifically recognized system of units is the International System of Units, known as the SI (from the French *Système International d'Unités*). Use of SI is recommended by most scientific journals and in many it is now mandatory. Multiples and submultiples of units should be chosen to minimize the repetition of zeros before or after the decimal point. Several units related to SI (e.g., tonne and hectare) are convenient in speech as well as in writing but should be avoided in analysis to minimize the risk of numerical errors.

The fundamental part of the units in the system is called a set of base units describing base quantities and the other units describing remaining quantities are called derived units.

There are seven base quantities used in the SI system: length, mass, time, electric current, temperature, amount of substance, and luminous intensity. The base quantities are independent by definition. The corresponding base units are: the meter, the kilogram, the second, the ampere, the kelvin, the mole, and the candela. The definition of each base unit (The International System of Units (SI), 2006) of the SI is carefully drawn up so that it is unique and provides a sound theoretical basis upon which the most accurate and reproducible measurements can be made. The realization of the definition of a unit is the procedure by which the definition may be used to establish the value and associated uncertainty of a quantity of the same kind as the unit.

All derived quantities may be written in terms of base quantities by the equations of physics.

Table 1 presents base quantities and their corresponding symbols, symbols for dimension, units, and symbols for the

Physical Dimensions and Units Use in Agriculture, Table 1
 Base quantities and dimensions used in the SI

Base quantity	Symbol for quantity	Symbol for dimension	Base unit	Symbol for base unit
Length	l, x, r	L	Meter	m
Mass	m	M	Kilogram	kg
Time, duration	t	T	Second	s
Electric current	I, i	I,	Ampere	A
Temperature	T	Θ	Kelvin	K
Amount of substance	n	N	Mole	M
Luminous intensity	I_v	J	Candela	cd

Physical Dimensions and Units Use in Agriculture, Table 2 Selected quantities as well as the corresponding applications, units, and dimensions in the agriculture use

Quantity	Application	Unit		Generally accepted unit	SI unit	SI dimension
Length	Soil depth Plant height	Meter		m	m	L ¹
	X-ray Pot area	Ångström Square centimeter		$1 \text{ \AA} = 10^{-10} \text{ m}$ $1 \text{ cm}^2 = 10^{-4} \text{ m}^2$	m^2	L^2
Area	Leaf area Land area	Square meter Hectare		$1 \text{ ha} = 10^4 \text{ m}^2$		
	Specific surface area Lab	Square meter per kilogram		$\text{m}^2 \cdot \text{kg}^{-1}$	m^3	$\text{L}^2 \text{M}^{-1}$
Volume	Field	Cubic meter		m^3	m^3	L^3
Speed	Air	Meter per second		$\text{m} \cdot \text{s}^{-1}$	$\text{m} \cdot \text{s}^{-1}$	$\text{L}^1 \text{T}^{-1}$
Total porosity Air-filled porosity, differential porosity	Soil, plant Soil, plant	Cubic meter voids per cubic meter soil Cubic meter voids per cubic meter soil		$\text{m}^3 \cdot \text{m}^{-3}$ $\text{m}^3 \cdot \text{m}^{-3}$	$\text{m}^3 \cdot \text{m}^{-3}$ $\text{m}^3 \cdot \text{m}^{-3}$	$\text{L}^3 \text{L}^{-3}$ $\text{L}^3 \text{L}^{-3}$
Void ratio	Soil	Cubic meter voids per cubic meter solids		$\text{m}^3 \cdot \text{m}^{-3}$	$\text{m}^3 \cdot \text{m}^{-3}$	$\text{L}^3 \text{L}^{-3}$
Concentration	Pollutant transport Fertilizers application	Kilogram solute per cubic meter solution Mole solute per cubic meter solution Cubic meter solute per cubic meter solution		$\text{kg} \cdot \text{m}^{-3}$ $\text{M} \cdot \text{m}^{-3}$ $\text{m}^3 \cdot \text{m}^{-3}$	$\text{kg} \cdot \text{m}^{-3}$ $\text{M} \cdot \text{m}^{-3}$ $\text{m}^3 \cdot \text{m}^{-3}$	$\text{L}^{-3} \text{M}^1$ $\text{L}^{-3} \text{N}^1$ $\text{L}^3 \text{L}^{-3}$
Concentration of air components	Soil air Atmosphere	Cubic meter component per cubic meter air		$\text{m}^3 \cdot \text{m}^{-3}$	$\text{m}^3 \cdot \text{m}^{-3}$	$\text{L}^3 \text{L}^{-3}$
Molar fraction	Soil solution Atmosphere	Mole component per mole mixture		$\text{M} \cdot \text{M}^{-1}$	$\text{M} \cdot \text{M}^{-1}$	$\text{N}^1 \text{N}^{-1}$
Temperature	Air	Kelvin		K	K	Θ^1
	Water Plant					
Force	Soil and plant mechanics	Newton		N	$\text{kg} \cdot \text{m} \cdot \text{s}^{-2}$	$\text{L}^1 \text{M}^1 \text{T}^{-2}$
Pressure	Soil	Pascal		$1 \text{ Pa} = 1 \text{ N} \cdot \text{m}^{-2}$	$\text{kg} \cdot \text{s}^{-2} \cdot \text{m}^{-1}$	$\text{L}^{-1} \text{M}^1 \text{T}^{-2}$
Stress	Air	Newton per square meter		$\text{N} \cdot \text{m}^{-2}$		
Pressure equivalent of water potential	Water	Kilogram per square second meter		$\text{kg} \cdot \text{s}^{-2} \cdot \text{m}^{-1}$		
		Bar		$1 \text{ bar} = 10^5 \text{ Pa}$		
Energy	Soil	Millimeter of mercury		$1 \text{ mmHg} \approx 133.322 \text{ Pa}$		
Work	Water	Joule		$1 \text{ J} = 1 \text{ N} \cdot \text{m}$	$\text{m}^2 \cdot \text{kg} \cdot \text{s}^{-2}$	$\text{L}^2 \text{M}^1 \text{T}^{-2}$
Heat	Movement Air flow	Newton meter Square meter kilogram per square second		$\text{N} \cdot \text{m}$ $\text{m}^2 \cdot \text{kg} \cdot \text{s}^{-2}$		
	Heat transport Water movement Air flow	Erg Watt Joule per second		$1 \text{ erg} = 10^{-7} \text{ J}$ $1 \text{ W} = 1 \text{ J} \cdot \text{s}^{-1}$ $1 \text{ J} \cdot \text{s}^{-1} = 10^7 \text{ erg}$	$\text{m}^2 \cdot \text{kg} \cdot \text{s}^{-3}$	$\text{L}^2 \text{M}^1 \text{T}^{-3}$
Power		Square meter kilogram per cubic second				
Water content	Soil	Kilogram water per kilogram dry soil		$\text{kg} \cdot \text{kg}^{-1}$	$\text{kg}^1 \text{M}^{-1}$	$\text{L}^3 \text{L}^{-3}$
Water potential (matrix, gravitational, osmotic, total)	Soil Plant	Cubic meter water per cubic meter soil Joule per cubic meter water Joule per kilogram water		$\text{m}^3 \cdot \text{m}^{-3}$ $\text{J} \cdot \text{m}^{-3}$ $\text{J} \cdot \text{kg}^{-1} = 10^{-3} \text{ MPa} = 10^{-2}$	$\text{kg} \cdot \text{m}^{-3}$ $\text{kg} \cdot \text{m}^{-1} \cdot \text{s}^{-2}$ $\text{m}^2 \cdot \text{s}^{-2}$	$\text{L}^{-1} \text{M}^1 \text{T}^{-2}$ $\text{L}^2 \text{T}^{-2}$
	Laboratory	Joule per mole water		bar	$\text{kg} \cdot \text{m}^2 \cdot \text{M}^{-1} \cdot \text{s}^{-2}$	$\text{L}^2 \text{M}^1 \text{N}^{-1} \text{T}^{-2}$

Effective saturation	$1 \text{ J.N}^{-1} = 1 \text{ m}$	$\text{m}^3 \cdot \text{m}^{-3}$	$\text{m}^3 \cdot \text{m}^{-3}$	$\text{L}^3 \text{L}^{-3}$
Bulk density	Cubic meter water per cubic meter voids	$\text{kg} \cdot \text{m}^{-3}$	$\text{kg} \cdot \text{m}^{-3}$	$\text{L}^{-3} \text{M}^1$
Solid phase density	Kilogram per cubic meter soil	1 g.cm^{-3}	$1 \text{ Mg.m}^{-3} = 10^3 \text{ kg.m}^{-3}$	$\text{L}^{-3} \text{M}^1$
Electrical conductivity	Kilogram per cubic meter solids	$\text{kg} \cdot \text{m}^{-3}$	$\text{kg} \cdot \text{m}^{-3}$	$\text{L}^{-3} \text{M}^1$
Evapotranspiration	Siemens per meter	$1 \text{ S.m}^{-1} = 10 \text{ dS.m}^{-1} = 10$	$\text{s}^3 \cdot \text{A}^2 \cdot \text{m}^{-3} \cdot \text{kg}^{-1}$	$\text{I}^2 \text{L}^{-3} \text{M}^{-1} \text{T}^3$
Evaporation	Cubic meter water per square meter per second	$\text{m}^3 \cdot \text{m}^{-2} \cdot \text{s}^{-1}$	$\text{m} \cdot \text{s}^{-1}$	$\text{L}^1 \text{T}^{-1}$
Transpiration	Meter per second	mm.s^{-1}	m.s^{-1}	
Elongation rate	Millimeter per second	mm.d^{-1}	m.s^{-1}	$\text{L}^1 \text{T}^{-1}$
Photosynthetically active radiation (PAR)	Meter per day	$\mu\text{mol.s}^{-1} \cdot \text{m}^{-2}$	$\text{M} \cdot \text{s}^{-1} \cdot \text{m}^{-2}$	$\text{L}^{-2} \text{N}^1 \text{T}^{-1}$
Ion transport	Micromoles photons per second meter square			
	Mole per kilogram (of dry plant tissue) per second	$\text{M} \cdot \text{kg}^{-1} \cdot \text{s}^{-1}$	$\text{M} \cdot \text{kg}^{-1} \cdot \text{s}^{-1}$	$\text{M}^{-1} \text{N}^1 \text{T}^{-1}$
Stomatal diffusive resistance	Mole of charge per kilogram (of dry plant tissue) per second	$\text{s} \cdot \text{m}^{-1}$	$\text{s} \cdot \text{m}^{-1}$	$\text{L}^{-1} \text{T}^1$
Yield	Second per meter	$1 \text{ kg.ha}^{-1} = 10^{-1} \text{ g.m}^{-2}$	$\text{kg} \cdot \text{m}^{-2}$	$\text{L}^{-2} \text{M}^1$
	Kilograms per hectare			M^1
	Gram	g	kg	
Heat capacity, entropy	Joule per kelvin	J.K^{-1}	$\text{m}^2 \cdot \text{kg} \cdot \text{s}^{-2} \cdot \text{K}^{-1}$	$\text{L}^2 \text{M}^1 \text{T}^{-2} \Theta^{-1}$
Volumetric heat capacity	Joule per cubic meter kelvin	$\text{J.m}^{-3} \text{K}^{-1}$	$\text{m}_1^1 \cdot \text{kg}_s^2 \cdot \text{K}^{-1}$	$\text{L}^1 \text{M}^1 \text{T}^{-2} \Theta^{-1}$
Specific heat	Joule per kilogram kelvin	$\text{J.kg}^{-1} \cdot \text{K}^{-1}$	$\text{m}^2 \cdot \text{s}^{-2} \cdot \text{K}^{-1}$	$\text{L}^2 \text{T}^{-2} \Theta^{-1}$
Flux density	Watt per square meter	W.m^{-2}	$\text{kg} \cdot \text{s}^{-3}$	$\text{M}^1 \text{T}^{-3}$
Heat flow	Kilogram per cubic second	kg.s^{-3}		
Gas diffusion	Gram per square meter second	$\text{g.m}^{-2} \cdot \text{s}^{-1}$		
	Mole per square meter second	$\text{M} \cdot \text{m}^{-2} \cdot \text{s}^{-1}$		
Water flow	Kilogram per square meter second	$\text{kg.m}^{-2} \cdot \text{s}^{-1}$		
	Cubic meter per square meter second	$\text{m}^3 \cdot \text{m}^{-2} \cdot \text{s}^{-1}$		
	Watt per square meter	W.m^{-2}		
Net radiation	Watt per meter kelvin	$\text{W.m}^{-1} \cdot \text{K}^{-1}$	$\text{kg} \cdot \text{m} \cdot \text{s}^{-3} \cdot \text{K}^{-1}$	$\text{L}^1 \text{M}^1 \Theta^{-1} \text{T}^{-3}$
Thermal conductivity	Kilogram meter per cubic second kelvin	$\text{kg}_s^2 \cdot \text{m} \cdot \text{s}^{-1}$		
Gas diffusivity	Square meter per second	$\text{m}^2 \cdot \text{s}^{-1}$	$\text{m}^2 \cdot \text{s}^{-1}$	$\text{L}^2 \text{T}^{-1}$
Water diffusivity	Square meter per second	$\text{m}^2 \cdot \text{s}^{-1}$	$\text{m}^2 \cdot \text{s}^{-1}$	$\text{L}^2 \text{T}^{-1}$
Solute diffusivity	Mass transport			
Thermal diffusivity	Heat transport			
Water permeability	Square meter	m^2	m^2	L^2
Air permeability	Darcy	$1 \text{ D} = 10^{-12} \text{ m}^2$		
Hydraulic conductivity	Meter per second	m.s^{-1}	m.s^{-1}	$\text{L}^1 \text{T}^{-1}$
	Water flow	kg.s.m^{-3}	kg.s.m^{-3}	$\text{L}^{-3} \text{M}^1 \text{T}^1$
Solute amount retained by soil	Kilogram second per cubic meter	$\text{m}^3 \cdot \text{s} \cdot \text{kg}_s^1$	$\text{m}^3 \cdot \text{s} \cdot \text{kg}_s^1$	$\text{M}^1 \text{M}^{-1}$
	Cubic meter second per kilogram	$\text{kg} \cdot \text{kg}^{-1}$	$\text{kg} \cdot \text{kg}^{-1}$	$\text{M}^1 \text{L}^{-2}$
	Kilogram per kilogram	$\text{kg} \cdot \text{m}^{-2}$	$\text{kg} \cdot \text{m}^{-2}$	$\text{M} \cdot \text{m}^{-2}$
	Kilogram per square meter			
	Mole per square meter			

Physical Dimensions and Units Use in Agriculture, Table 2 (Continued)

Quantity	Application	Unit	Generally accepted unit	SI unit	SI dimension
Dynamic viscosity	Water and gas flow	Poise	$1 \text{ P} = 1 \text{ g} \cdot \text{cm}^{-1} \cdot \text{s}^{-1} = 10^{-1}$ $\text{Pa} \cdot \text{s}$	$\text{kg} \cdot \text{m}^{-1} \cdot \text{s}^{-1}$	$\text{L}^{-1} \text{M}^1 \text{T}^{-1}$
Kinematic viscosity	Wetting front	Kilogram per meter second	$1 \text{ Pa} \cdot \text{s} = 1 \text{ kg} \cdot \text{m}^{-1} \cdot \text{s}^{-1}$	$\text{m}^2 \cdot \text{s}^{-1}$	$\text{L}^2 \text{T}^{-1}$
	Water and gas flow	Stokes	$1 \text{ St} = 10^{-4} \text{ m}^2 \cdot \text{s}^{-1}$	s^{-1}	T^{-1}
Frequency	Wetting front	Square meter per second			
	Waves	Hertz			
		Unit per second			
Leaf area index (LAI)	Plants	Square meter leaves per square meter soil	$\text{m}^2 \cdot \text{m}^{-2}$	s^{-1}	$\text{L}^2 \text{L}^{-1}$
Soil respiration, root respiration,	Soil	Kilogram per kilogram second	$\text{kg} \cdot \text{kg}^{-1} \cdot \text{s}^{-1}$	$\text{s}^3 \cdot \text{kg}^{-1} \cdot \text{s}^{-1}$	$\text{L}^3 \text{M}^{-1} \text{T}^{-1}$
Field respiration	Plants	Cubic meter per kilogram second	$\text{m}^3 \cdot \text{kg}^{-1} \cdot \text{s}^{-1}$	$\text{m}^3 \cdot \text{s}^{-1}$	$\text{L}^3 \text{T}^{-1}$
		Cubic meter per square meter second	$\text{m}^3 \cdot \text{m}^{-2} \cdot \text{s}^{-1}$	$\text{kg} \cdot \text{m}^{-2} \cdot \text{s}^{-1}$	$\text{L}^2 \text{M}^1 \text{T}^{-1}$
Redox resistance	Soil	Kilogram per square meter second	s	s	T^1
Gas solubility	Soil solution	Second	$\text{m}^3 \cdot \text{m}^{-3}$	$\text{m}^3 \cdot \text{m}^{-3}$	$\text{L}^3 \text{L}^{-3}$
		Cubic meter gas per cubic meter solution	$\text{kg} \cdot \text{m}^{-3}$	$\text{kg} \cdot \text{m}^{-3}$	$\text{M}^1 \text{L}^{-3}$
		Kilogram gas per cubic meter solution	$\text{M} \cdot \text{m}^{-3}$	$\text{M} \cdot \text{m}^{-3}$	$\text{L}^{-3} \text{N}^1$
		Mole gas per cubic meter solution	$\text{kg} \cdot \text{kg}^{-1}$	$\text{kg} \cdot \text{kg}^{-1}$	$\text{M}^1 \text{M}^{-1}$
		Kilogram gas per kilogram solution	Ω	$\text{m}^3 \cdot \text{kg}^{-3} \cdot \text{A}^{-2}$	$\text{I}^{-2} \text{L}^2 \text{M}^1 \text{T}^{-3}$
Electrical resistance	Plant	Ohm	Ω	$\text{s}^4 \cdot \text{A}^2 \cdot \text{m}^{-2} \cdot \text{kg}^{-1}$	$\text{I}^2 \text{L}^{-2} \text{M}^{-1} \text{T}^4$
Electrical capacitance	Plant	Farad	F		
Magnetic flux density	Testing equipment	Tesla	T	$\text{kg} \cdot \text{s}^{-2} \cdot \text{A}^{-1}$	$\text{I}^{-1} \text{M}^1 \text{T}^{-2}$
Radioactivity	Soil	Bequerel	$1 \text{ Bq} = 1 \text{ s}^{-1}$	s^{-1}	T^{-1}
Humidity	Plants	Unit per second			
	Air	Kilogram	kg	kg	M^1
		Kilogram water vapor per kilogram dry air	$\text{kg} \cdot \text{kg}^{-1}$	$\text{kg} \cdot \text{kg}^{-1}$	$\text{M}^1 \text{M}^{-1}$
		Water vapor pressure per saturation vapor	$\text{Pa} \cdot \text{Pa}^{-1}$	$\text{Pa} \cdot \text{Pa}^{-1}$	
Surface tension	Water	Newton per length	$\text{N} \cdot \text{m}^{-1}$	$\text{kg} \cdot \text{s}^{-2}$	$\text{M}^1 \text{T}^{-2}$
	Soil	Joule per square meter			
	Plant	Farad per meter	F m^{-1}	$\text{m}^{-3} \text{kg}^{-1} \text{s}^4 \text{A}^2$	$\text{I}^2 \text{L}^{-3} \text{M}^{-1} \text{T}^4$
Aquametry	Soil				

units' dimension of any quantity, which is written using the SI system of units.

Traditional and popular units used in various parts of the world make some confusion and misunderstanding for others who are accustomed to other units. Conversion factors between most common units used in agrophysics is available in NIST Special Publication 1038 (Butcher et al., 2006).

Any derived physical quantity Q can then be dimensionally expressed as

$$[Q] = L^\alpha M^\beta T^\gamma I^\delta \Theta^\varepsilon N^\zeta J^\eta$$

where the exponents $\alpha, \beta, \gamma, \delta, \varepsilon, \zeta$, and η , which are generally small integers can be positive, negative, or zero, are called the dimensional exponents. The notation $[Q]$ means "the dimension of Q ."

The SI system adopted a series of prefix names and prefix symbols of the decimal multiples and submultiples of SI units ranging from 10^{12} to 10^{-12} . With the exception of da (deca), h (hecto), and k (kilo), all multiple prefix symbols are uppercase letters (e.g., 1 dag = 10 g, 1 hPa = 100 Pa, 1 km = 10^3 m, 1 Mg = 10^6 g, 1 GHz = 10^9 Hz), and all submultiple prefix symbols are lowercase letters (e.g., 1 mm = 10^{-3} m, 1 ps = 10^{-12} s). All prefix names are printed in lowercase letters, except at the beginning of a sentence. Compound prefix symbols as well as compound prefix names are not permitted, for example, nm (nanometer) is correct but not μm (millimicrometer).

Selected SI base and derived quantities, units, and dimensions used in agriculture

Agriculture, like other applied sciences, prefers specific quantities as well as corresponding units and dimensions, the selection of which is presented in Table 2 (American Society of Agronomy et al., 1988; Scott, 2000).

The examples for conversion of generally accepted units to SI base units are:

- Water potential: $J \cdot m^{-3} = (N \cdot m) \cdot m^{-3} = (kg \cdot m \cdot s^{-2} \cdot m) \cdot m^{-3} = kg \cdot m^{-1} \cdot s^{-2}$
- Thermal conductivity: $W \cdot m^{-1} \cdot K^{-1} = (J \cdot s^{-1}) \cdot m^{-1} \cdot K^{-1} = (N \cdot m \cdot s^{-1}) \cdot m^{-1} \cdot K^{-1} = (kg \cdot m \cdot s^{-2} \cdot m \cdot s^{-1}) \cdot m^{-1} \cdot K^{-1} = kg \cdot m \cdot s^{-3} \cdot K^{-1}$

Summary

The parallel use of traditional as well as formally acknowledged units is commonly applied by scientists representing agrophysics. As the interdisciplinary science agrophysics is particularly prone to the influences coming from other branches of science. To avoid ambiguity in presenting qualitative data it is advised to use International System of Units (SI).

Bibliography

American Society of Agronomy, Crop Science Society of America, and Soil Science Society of America, 1988. Conventions and style. In *Publications Handbook and Style Manual*. Madison, WI: American Society of Agronomy, Chap. 6.

Bureau International des Poids et Mesures, 2006. *The International System of Units (SI)*, 8th edn. Paris: Bureau International des Poids et Mesures. http://www.bipm.org/utils/common/pdf/si_brochure_8_en.pdf

Butcher, K., Crown, L., and Gentry, E. J., 2006. *The International System of Units (SI): Conversion Factors for General Use*. NIST Special Publication 1038. <http://ts.nist.gov/WeightsAndMeasures/Metric/upload/SP1038.pdf>.

Scott, H. D., 2000. Calculations and dimensions of physical quantities. In *Soil Physics: Agricultural and Environment Applications*. Ames, IA: Iowa State University Press, Chap. 2, pp. 12–34.

Cross-references

[Agrophysical Objects \(Soils, Plants, Agricultural Products, and Foods\)](#)

[Agrophysical Properties and Processes](#)

[Soil Physical Quality](#)

PHYSICAL PHENOMENA AND PROPERTIES IMPORTANT FOR STORAGE OF AGRICULTURAL PRODUCTS

Marek Molenda, Józef Horabik

Institute of Agrophysics, Polish Academy of Sciences,
Lublin, Poland

Definition

Main tasks during the storage are to protect products against undesirable changes, to improve their *quality*, and to preserve their nutritional value. Physical phenomena that may be observed by instrumental methods serve as indices of state of material and parameters used in the design of equipment and in process control.

Introduction

Progress in science initiated in the beginning of the twentieth century resulted in a substantial development in communication and information technologies in the second part of that period. These were followed by harsh global competition in economy also in storage and processing of agricultural products.

A large group of materials may be regarded as agricultural products, which may include plant materials, animal materials, and materials used in the agricultural production such as chemicals or mineral fertilizers. In this article, only products of plant origin will be covered.

Physical phenomena occurring during the storage of agricultural products may be a direct cause of damage, but on the other hand create environment for chemical and biological processes and as such may intensify or moderate their pace. Optimization of storage of agricultural products involve large spectrum of actions. This includes elaboration of new methods of preservation and treatment in order to maintain structure, firmness, color, taste, and aroma, and elimination of diseases and pesticide

residues: all to meet the demands of increasingly sophisticated markets. Storage loss may be considered in terms of either quantity or *quality*. Quantitative loss is a physical loss of substance as shown by a reduction in weight or volume. It is the form of loss that can most readily be measured and valued. Qualitative loss is more difficult to assess and is perhaps best estimated through comparison with standards. Nutritional loss and loss of seed are both aspects of *quality* losses.

Physical phenomena having the strongest influence on conditions of storage of agricultural plant products or those that may be used in process control are mechanical, acoustic, electrical, optical, and thermal. Mechanical are those associated with equilibrium or motion of objects, deformation or damage of products. Acoustic phenomena are those involving propagation of mechanical waves such as sounds, infra sounds, or ultra sounds. Electrical phenomena that may be observed in macroscale are manifestations of interactions between electrical fields on the atomic scale. Optical phenomena are those involving light, manifest themselves as visual appearance of objects, important factor in consumer preference. Thermal phenomena are those associated with addition or removal of energy from materials or maintaining temperature at a given level. Physical phenomena are usually described using relationships between independent and dependent variables presented in the form of equations involving factors called physical properties or, in the case of engineering applications, material parameters. Design and process control require values of those properties that may be taken from catalogs or have to be determined for specific application in laboratory tests. In the last case, standard method of determination of the property should be applied to ensure obtaining close value of the results in various laboratories.

Thus, *physical properties* are factors necessary to describe physical phenomena as relationships between variables. In this article, physical properties will be covered that are currently most frequently used in technological operations that are performed during the storage and handling of plant agricultural materials. Majority of definitions will be given after Mohsenin (1970), whose work even after 40 years remain very frequently cited reference for physical properties of agro-food materials and methods of their determination.

Physical characteristics used for the description of visual appearance of agro-food products

Such characteristics as shape, size, volume, density, or surface area are widely used for the characterization of agricultural products for trade as well as material parameters for design and process control. Some of those characteristics determine visual appearance of the product, which is an important factor for consumer's purchasing decision. Shape and color are considered main *quality* indicators of fruits.

Shape and size

Seeds, grains, fruits, and vegetables are irregular in shape and the measurement of several mutually perpendicular axes is necessary to approximately describe their shape. It may be determined precisely using specific measurements and/or mathematical relationships. For verbal description of shape, it may be described subjectively and compared with charted standards. Extreme variations in shape that may influence purchasing decisions are usually discarded during harvest or packing.

Size of individual units of product may influence consumer appeal, handling practices, storage potential, market selection, and final use. Size may be determined by one of the three methods: dimension (length, width, diameter, or circumference), weight, or volume. The most desired shape and size depend on the product, on its application, and on the preferences of specific market. Probably, very large potatoes will be used for starch production rather than for fresh market sales.

Volume and density

Volume and density of agro-food products play an important role in applications such as design of silos, *drying*, mechanical compaction, stability of pellets and wafers, separation and grading, evaluation of maturity, or *quality* evaluation. The irregular shape of most of the agricultural products, the small size of numerous materials (such as grains or seeds), and the porous nature of others (such as straw or grain in bulk) pose some difficulties in volume and density measurement. Because of the irregular shape of the product, volume is usually determined by liquid displacement and most frequently water is used.

Porosity

For applications involving flow of gases through porous material such as *aeration*, *drying*, cooling, or fumigation, the percent of voids in the material is crucial factor. For porous materials of high moisture content gas pycnometer method may be used as proposed by Sereno et al. (2007). The volume is obtained by measuring the change in pressure experienced by an amount of compressed gas filling a constant volume reference chamber when it expands into a second chamber containing a sample of the material to be tested. From such pressure change and the knowledge of the volumes of the two chambers, the volume of the sample solid matrix is determined. The gas pycnometer proposed by those authors offers reliable results of particle volume for any type of solids, specifically foods and other materials with high moisture content.

Surface area

Surface area is an important technological parameter considering both plant material parts (as leaf or fruit) and porous substances. Leaf area is an indicator of photosynthetic capacity and growth rate of a plant. Surface area of fruits is important in the determination of spray coverage,

respiration rate, light reflectance, color evaluation, or heat transfer in cooling or heating.

The surface area determines numerous processes in porous media such as dissolution of powders, moisture transport, or intensity of fumigation. The true surface area of porous material, including surface irregularities and pore interiors, may be determined at the atomic level by the adsorption of an unreactive or inert gas. The amount adsorbed is a function not only of the total amount of exposed surface, but also of (1) temperature, (2) gas pressure, and (3) the strength of interaction between gas and solid.

Mechanical properties

Strength, hardness, toughness, elasticity, plasticity, brittleness, and ductility are the mechanical properties used to measure the behavior of material under a load. These properties are described in terms of the types of load (force or stress) that the material must withstand without damage or loss of *quality*. Common types of stress are compression, tension, shear, torsion, impact, or a combination of these.

Compression stresses develop within a material when forces compress or crush the material. Grain column in a silo that acts on layers close to floor generate compression, and the internal stresses that develop within the lower layers are compression.

Tension (or tensile) stresses develop when a material is subject to a pulling load; for example, when using a rope to lift a load or a chain to transfer movement. Tensile strength is defined as resistance to longitudinal stress or pull and can be measured in Newtons per square meter of cross-section. Shearing stresses occur within a material when external forces are applied along parallel lines in opposite directions. Shearing forces can separate material by sliding part of it in one direction and the rest in the opposite direction.

Some materials are equally strong in compression, tension, and shear. Strength of biomaterials differs not only dependently on the type of load, but also on the load direction – this feature is called *anisotropy*. Describing of maximum strength, the type of loading and load direction should be always stated.

Strength

Strength is the property that enables a material to resist deformation under a load. The ultimate strength is the maximum strain a material can withstand. Tensile strength is a measurement of the resistance to being pulled apart when placed in a tension load.

Impact strength is the ability of a material to resist suddenly applied loads and is measured in kJ m^{-2} .

Hardness

Hardness is the property of a material to resist permanent indentation. Because there are several methods of

measuring hardness, the hardness of a material is always specified in terms of the particular test that was used to measure this property. Rockwell, Vickers, and Brinell are some of the methods of testing. Of these tests, Rockwell is the one most frequently used. The basic principle used in the Rockwell test is that a hard material can penetrate a softer one. We then measure the amount of penetration and compare it to a scale. For ferrous metals, which are usually harder than nonferrous metals, a diamond tip is used and the hardness is indicated by a Rockwell "C" number. On nonferrous metals, that are softer, a metal ball is used and the hardness is indicated by a Rockwell "B" number. To get an idea of the property of hardness, compare lead and steel. Lead can be scratched with a pointed wooden stick but steel cannot because it is harder than lead. For elastomers and rubbers, Shore method is used that better suits relatively soft biomaterials. Shore in 1920s developed a measurement device called durometer and currently 12 scales are used depending on the characterized material.

Toughness

Toughness is the property that enables a material to withstand shock and to be deformed without rupturing. Toughness may be considered as a combination of strength and plasticity and may be measured as the work done in making a unit surface of crack within it. In the case of biological materials, devices are used with scissors or with a wedge.

Elasticity

When a material has a load applied to it, the load causes the material to deform. Elasticity is the ability of a material to return to its original shape after the load is removed. Theoretically, the elastic limit of a material is the limit to which a material can be loaded and still recover its original shape after the load is removed. Since the modulus of elasticity is determined from the ratio of stress to corresponding strain in an elastic range of deformation knowing the upper limit of elastic range is essential. The interpretation of force–deformation curve must follow recommendation of one of established standards.

Plasticity

Plasticity is the ability of a material to deform permanently without breaking or rupturing. This property is the opposite of elasticity. In processing of agricultural materials, irreversible deformation is used to give shape feasible for transport and storage of products such as butter, cheese, or bakery doughs. To characterize plasticity yield, stress is used that may be measured by penetrometer or extrusion tests.

Brittleness

Brittleness is the opposite of the property of plasticity. A brittle material is one that breaks or shatters at relatively

low deformation. In the case of metals, temperature acts as a factor changing its properties from elastic solid, through plastic solid to viscous liquid in melted material. Some biological materials, particularly those containing high amount of starch similarly react to water content. Dry grain is brittle, while wet grain reveals plastic behavior.

The state of the art in predicting the mechanical and rheological properties is not developed to the same degree as it is in the case of thermal properties due to the much greater influence of the structure of the product on its mechanical properties.

Information of mechanical properties of agricultural materials is necessary for the design of optimum processes and equipment. Search of such information for the design of hemp conditioner and harvester was reported by Chen et al. (2004). Field operation for hemp harvesting includes swathing with a traditional windrower or a haybine harvester, and baling the windrows. The bales are stored for later processing for fibers. The authors conducted experiments to estimate mechanical properties of hemp by cutting stems using a sickle knife section and a countershear. The shear strength and resistance to penetration were found significantly affected by the interactions of stem moisture content and blade type. When cutting low moisture hemp, a serrated blade should be used, while a smooth blade edge may be chosen to cut higher moisture hemp.

Acoustic, ultrasound, and vibration

Acoustics is an interdisciplinary science that deals with the study of sound, ultrasound, and infrasound – all mechanical waves in solids, liquids, and gases. One of longtime used acoustic methods is ultrasonic inspection. This nondestructive test method employs high-frequency mechanical vibration energy to detect and locate structural discontinuities or differences and to measure the thickness of materials. Radiation frequency is of the order 0.1–25 MHz. The beam travels unimpeded through large objects, may be angled for testing layered stocks, and can impact materials immersed in liquids. Access is required to only one side of the material being tested. This nondestructive testing (NDT) method can detect microstructural alterations, such as microcracks, foreign particles, precipitates, grain boundaries, or interphase boundaries.

In recent decades, acoustic methods became extensively used to determine mechanical properties of agro-food materials. Ultrasonic velocity was used to evaluate textural properties of meat products, as well as to examine liquids and starch-based materials. Measurement of ultrasonic wave velocity and attenuation was used to monitor internal changes during ripening of avocado fruit, to determine firmness of muskmelons, or to investigate density and porosity of plant granular materials. Acoustics was employed to monitor development of fissures in rice, to

detect pistachio nuts with closed shells, or to determine hardness of wheat kernels.

Ultrasound pulse echo method has been used for the inspection of integrity of food packages. The technique was able to spot defects less than 10 µm and might distinguish what is in the channel of a defect – air, water, or strands of a protein. For certain applications, ultrasound process outperforms other nondestructive imaging techniques, such as machine vision, X-ray, infrared, or magnetic resonance.

Electric properties

Electric properties in practical use are essentially the dielectric permittivity and loss of the material (Nesvadba et al., 2004). Permittivity is related to material ability to transmit electrical field. In SI units, it is measured in farads per meter. It is not constant, but depends on location in the material, frequency of applied electrical field, moisture content of the material, and other parameters. Permittivity of considered material is usually related to the permittivity of vacuum and termed relative permittivity. Response of the vacuum does not depend on the frequency of the field, while response of regular materials does. Material polarization involved in response does not take place instantaneously to an applied field, but with certain delay that may be characterized through phase difference. Thus, permittivity is frequently treated as complex function since complex numbers allow for specification of magnitude and phase. Complex permittivity is naturally separated into real and imaginary parts:

$$\epsilon(\omega) = \epsilon'(\omega) + i\epsilon''(\omega) \quad (1)$$

where ω is angular frequency. Often the loss tangent, $\tan \delta = \epsilon''/\epsilon'$, or dissipation factor, as a descriptive dielectric parameter. Usually (as, e.g., Nelson, 1999) ϵ'' is interpreted to include energy losses in the dielectric due to all operating dielectric relaxation mechanisms and ionic conduction. The principal needs for information on the *dielectric properties of agricultural products* have been their use in explaining the behavior of the materials when exposed to dielectric or microwave heating and their use for rapid sensing.

Some other electrical properties, such as electrical resistance, resistivity, impedance, and conductivity of fruits and vegetables also have been investigated. Usually, the objective of these investigations was to establish relationships between electrical property and some *quality* factor of the product.

Measurement of dielectric properties may be used for the determination of moisture content of seeds, grain kernels, nuts, etc. Kraszewski and Nelson (1992) used microwave resonant cavities for making size independent moisture determination individual seeds, grain kernels of arbitrary shape and for simultaneous determination of both mass and moisture content in kernels of uniform shape. Resonant cavity is a dielectric region completely

surrounded by a conducting surface. In a proper configuration of hollow resonant cavity, standing wave pattern may be formed and may persist if energy is supplied to offset losses in the cavity. When a small dielectric sample object is placed in the cavity, the change in the resonant angular frequency takes place. Because the permittivity of practical materials is complex, the resonant angular frequency should be considered complex as well. The authors measured simultaneously the change in complex characteristic of the cavity reflected in two factors: frequency shift ΔF and the cavity transmission factor ΔT . In the case of spherically shaped seeds, the ratio $\Delta F/\Delta T$ was found to provide accurate moisture determination independent of seed size. Moisture content of objects of varying shape and size could also be determined accurately, but measurements of ΔF and ΔT at two perpendicular orientations were required. Both moisture content and mass of objects of uniform shape, such as peanut kernel, could be determined by a single measurement of ΔF and ΔT when the kernels were presented in uniform orientation with respect to the electric field vector in the cavity.

Optical properties

Some optical properties discernible by human sight are used since long time to distinguish between varieties or commercial types of products. For *quality* evaluation by consumer color, gloss and translucency are the most important engineering properties (Barbosa-Canovas et al., 2004).

Color is a general term applied to the reaction of human sight to visible range of electromagnetic radiation of frequency from 3.45×10^{14} to 7.5×10^{14} Hz, and is related to visual appearance of agro-food products (such as shape, size, surface, and flesh structure, and defects). It is essentially a beam of light composed of irregularly distributed energy emitted at different wavelengths. Depending on the type of illumination, the same materials can show different appearance.

Gloss is the name given to light reflected from a plain smooth surface. It can be characterized by a goniophotometric curve, which represents intensity of light reflected at the surface at different angles of incidence and viewing.

Translucency of agro-food products is defined using an opaque-to-translucent scale. This sensation reflects a degree of scatter of light inside the material. Many products (such as cloudy fruit juices) are neither fully opaque nor fully transparent, but are translucent. Measurements of color are very important for food manufacturer in order to achieve uniformity and consistency of color of the product. Several device independent systems of color analysis have been created but nearly universally accepted is CIE standard published in 1931, the first system for scientifically defining light colors. This standard uses a tristimulus model CIE XYZ in which each perceivable color is specified as a triplet of numbers. The CIE X, Y, and Z values

correspond to reactions of three types of color-sensing human retina cells, and are normally defined between 0% and 100%. The human eye photoreceptors have three sensitivity peaks in short (420–440 nm), medium (530–540 nm), and long (560–580 nm) wavelengths. Thus, three parameters describe color sensation. The tristimulus values of a color are amounts of three primary colors in the three-component additive color model needed to match the test color. The CIE has defined a set of three color matching functions, called $x(\lambda)$, $y(\lambda)$, and $z(\lambda)$. The tabulated numerical values of these functions are known collectively as the CIE standard observer.

Physicists search for objective and instrumental methods of description of human eye sensations or engineering properties through physical properties of materials. Optical properties can be represented by absorption or reflection spectra. For instrumental evaluation, not only visible but also infrared and ultraviolet ranges of electromagnetic radiation are used for measuring *quality* of products (Nesvadba et al., 2004). Instruments called spectrophotometers are used to measure light intensity as a function of wavelength (corresponding to color). Probably the most popular application of spectrophotometers is measurement of light absorption, but they may be used to measure light reflectance as well.

One of popular applications of optical techniques is estimation of state of maturation of fruits. Bodria et al. (2004) used optical techniques to assess the chlorophyll content in red-pigmented apples and peaches to estimate ripeness and to optimize harvesting and postharvest management. Application of dual-band reflectance probe was found promising, particularly because this system was simple, handheld, and relatively low cost. The R/IR index, defined as the ratio of the signals measured at 675–800 nm, was found to be accurate in estimating the chlorophyll content of apple and peach fruit. Moreover, the R/IR index monitored the postharvest ripening of fresh peaches, showing different evolution patterns for fruits harvested at different dates.

Thermal properties

Temperature and availability of light, water, and oxygen decide about the rate of respiration (enzymatic processes) in plant material. Moisture content of the product itself, as well as the humidity of surrounding air are very important for safe storage. Fruits during storage mature and age and these processes are dependent on the ambient temperature. Increase or decrease in the temperature may be used for the control of the rate of respiration, that is, enzymatic processes. The rate of chemical reactions in fruits generally doubles for every 10°C increase in the temperature. Changes in fruits during ripening include intensification of color and aroma, softening and manifestations of activity of harmful microorganisms.

Very common technique to prolong the shelf life of the product is storage under refrigeration or freezing, in which

case a decrease in the temperature of the product is brought about. There are three modes of heat transfer (Rha, 1975): conduction, convection, and radiation, each of which requires its own set of parameters to be described. Conduction is the prevalent mechanism of heat transfer, when product is placed in direct contact with a solid heating or cooling medium. Convection is macroscopic movement of fluid. Radiation is heat transmission between phases, and it depends on the temperature of radiating body.

In conduction, heat transfer is summarized in *thermal conductivity K* that is defined by Fourier equation:

$$q = -KA \frac{\partial T}{\partial x} \quad (2)$$

where q is conductive rate of heat transfer, A is the area for heat transfer, T is temperature, and x is the length.

In convection, heat transfer is accomplished by actual physical movement of heating medium, which is usually fluid. The equation that expresses the convective heat transfer is as follows:

$$q = h_c A (T_s - T_\infty) \quad (3)$$

where q is convective rate of heat transfer, h_c is coefficient of convective heat transfer, A is area for heat transfer, T_s is surface temperature, and T_∞ is temperature of heating medium.

In radiation, heat transfer electromagnetic waves travel along straight-line path at the speed of light. When radiation energy strikes a body it is partially absorbed, partially reflected. The heat transferred by radiation from body 1 to body 2 is the difference between the energy emitted by body 1 and body 2:

$$q_{1-2} = A\sigma f(e_1 T_1^4 - e_2 T_2^4) \quad (4)$$

where q_1 and q_2 are heat fluxes, T is absolute temperature, e_1 and e_2 are emissivities, A is area for heat transfer, and σ is Stefan–Boltzmann constant $= 5.670400 \times 10^{-8} \text{ W m}^{-2} \text{ K}^{-4}$.

Heat transfer by the three described modes depend on physical properties of the heating medium such as thermal conductivity, heat capacity, density, viscosity, coefficient of thermal expansion, emissivity, and absorptivity. Once the heat is transferred to the material, the change of its temperature depends on the properties of the material, specific heat and density, viscosity and thermal expansion, as well as on its thermal conductivity and enthalpy of phase change. Thermal properties are important for modeling processes (drying, heating, freezing, etc.), design of storage and processing equipment, calculating energy demand, etc. Important thermal properties are specific heat C_p , thermal conductivity K , and thermal diffusivity D .

Specific heat ($\text{J kg}^{-1} \text{ K}^{-1}$) determines the quantity of heat to be supplied or removed in order to bring the food material to the desired temperature.

Thermal conductivity ($\text{Wm}^{-1} \text{ K}^{-1}$) is the property of a material that indicates ability to conduct heat. Most of

fresh plant products contain a large percent of water and thermal conductivity of water may be used as a very rough approximation of the thermal conductivity of the material.

Thermal diffusivity ($\text{mm}^2 \text{ s}^{-1}$) defines a rate at which heat diffuses by conduction through a material. It is represented by the rate at which temperature changes in a certain volume of material, while transient heat is conducted through it in a certain direction in or out of the material.

In determining the thermal properties, usually the known quantity of heat is supplied to the system and change in the temperatures of the system is measured. In experimental determination of the thermal properties of plant agricultural material, it is necessary to select representative and homogeneous samples, as in other experiment with biological materials.

Temperature-dependant moisture migration is a very common process in the storage of grain in silos (Loewer et al., 1994). *Thermal conductivity* of grain is relatively low and when grain is placed in a silo in the fall, the center tends to remain near the initial temperature. The grain near the wall tends to cool to reach average ambient temperature. With a further decrease in ambient temperature, air currents develop where colder and denser air near the wall moves down forcing the warmer air up through the center of grain mass. As it reaches the top center surface of the grain, it cools to a point at which it cannot hold the moisture it had absorbed. The excess moisture condenses on the surface of the grain creating the environment that enhances molds and insects growth. The reverse situation occurs during the summer months. To minimize the problem of moisture migration temperatures near the silo wall and in the center should be kept relatively close, within 10°C range. This may be accomplished by using aeration fans that pull air down through the grain until the temperature of grain reach prescribed value.

Summary

To control physical phenomena occurring during the storage of agricultural products, knowledge of physical properties of the materials is necessary that are material parameters included in equations modeling processes. Methods of instrumental characterization of agricultural materials during storage still remain on the stage of development and standardization of methods is far from completing. Inherent feature of structure of biological material is its complexity and unhomogeneity. Material properties may vary depending on the location of the area of measurement (unhomogeneity). Even at the same area, properties may vary with direction (*anisotropy*). In general, biological materials do not follow single classical model, but usually their behavior combines a number of these classic effects. Design of efficient technologies of storage of agricultural materials require further work in advancing research, development, and implementation.

Bibliography

- Barbosa-Canovas, G. V., Julianio, P., and Peleg, M., 2004. *Engineering Properties of Food. Encyclopedia of life support systems*. Developed under the Auspices of the UNESCO. Oxford, UK: Eolss. (<http://www.eolss.net>).
- Bodria, L., Fiala, M., Giudetti, R., and Oberti, R., 2004. Optical techniques to estimate the ripeness of red-pigmented fruits. *Transactions of the ASAE*, **47**, 815–820.
- Chen, Y., Gratton, J. L., and Liu, J., 2004. Power requirements of hemp cutting and conditioning. *Biosystems Engineering*, **87**, 417–424.
- Kraszewski, A. W., and Nelson, S. O., 1992. Resonant microwave cavities for sensing properties of agricultural products. *Transactions of the ASAE*, **35**, 1315–1321.
- Loewer, O. J., Bridges, T. C., and Bucklin, R. A., 1994. *On-Farm Drying and Storage Systems*. St. Joseph, MI: American Society of Agricultural Engineers.
- Mohsenin, N. N., 1970. *Physical Properties of Plant and Animal Materials*. New York: Gordon and Beach Science.
- Nelson, S. O., 1999. Dielectric properties measurement techniques and applications. *Transactions of the ASAE*, **42**, 523–529.
- Nesvadba, P., Houska, M., Wolf, W., and Gekas, V., 2004. Database of physical properties of agro-food materials. *Journal of Food Engineering*, **61**, 497–503.
- Rha, Ch. (ed.), 1975. *Theory, determination and control of physical properties of food materials*. Dordrecht-Holland/Boston: D. Reidel.
- Sereno, A. M., Silva, M. A., and Mayor, L., 2007. Determination of particle density and porosity in foods and porous materials with high moisture content. *International Journal of Food Properties*, **10**, 455–469.

Cross-references

- [Aeration of Agricultural Products](#)
[Aeration of Soils and Plants](#)
[Anisotropy of Soil Physical Properties](#)
[Dielectric Properties of Agricultural Products](#)
[Drying of Agricultural Products](#)
[Electrical Properties of Agricultural Products](#)
[Physical Properties as Indicators of Food Quality](#)
[Physical Properties of Raw Materials and Agricultural Products](#)
[Quality of Agricultural Products in Relation to Physical Conditions](#)
[Thermal Technologies in Food Processing](#)

PHYSICAL PROCESSES

See *Agophysical Properties and Processes; Agrophysics: Physics Applied to Agriculture*

PHYSICAL PROPERTIES

See *Physical Properties as Indicators of Food Quality; Agophysical Properties and Processes; Agrophysics: Physics Applied to Agriculture; Physical Properties of Raw Materials and Agricultural Products*

PHYSICAL PROPERTIES AS INDICATORS OF FOOD QUALITY

Martin G. Scanlon

Department of Food Science, University of Manitoba, Winnipeg, Canada

Synonyms

Physical properties: constitutive properties; Quality: merit, grade or value; Quality: property or characteristic

Definition

Physical Properties: Essential attributes shared by all members of a class of material.

Introduction

Quality is defined by the *Encyclopedia Britannica* in two ways: as a synonym for “property” or “characteristic,” and in situations where merit, grade, or value is appraised. Inevitably, physical properties are assessed when either definition is applied to foods. For example, when evaluating its acceptability to a consumer, a quality of a fruit is that it is “pleasant to the eyes,” or the uniformity in characteristics of individual food items is such that, when adjudged by the appropriate standards, this particular batch of food commands a higher price. The latter definition, where a physical property is the basis for a trading specification, may be because it is directly relevant to consumer acceptability, such as the USDA quality standards for mechanical toughness in frozen carrots (USDA, 2010), or because the physical property is a predictor of quality in a derived food product, e.g., the battery of physical property tests on wheat flour doughs that are conducted by the Canadian Grain Commission to assure offshore millers and bakers of the quality of Canadian wheat (CGC, 2010). Measurement of physical properties as the basis for quality assurance in the trading of commodities or partly manufactured foods between different food manufacturers is a pervasive activity in food science. Notwithstanding this actuality, subsequent discussion of physical properties as indicators of food quality is restricted to physical properties as determinants of food acceptability to consumers, because the ultimate objective of trading specifications between food manufacturers is to ensure the delivery of high-quality products to their customers.

Creating quality in foods

Quality in foods can be defined in a multitude of ways, but at its most basic it is comprised of:

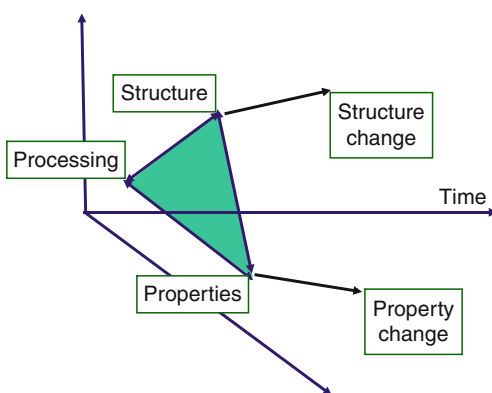
1. The maintenance of the as-harvested or as-processed condition of the food, i.e., prolongation of shelf-life
2. The sensory acceptability of the food – its appearance, flavor/aroma, and texture

3. Two quality criteria of ever-increasing allure – the food's nutritional quality and its quality of convenience

The physical properties that govern these quality definitions are in turn dependent on the structure of the food. Food is structurally complex (Donald, 2004; Ubbink et al., 2008), and so the effects of structure on physical properties can originate from a number of length scales. For example, differences in fatty acid substitution in the triacylglycerols that are expressed from olives exert a molecular-scale effect on the pouring properties of the olive oil, while the hierarchy of various structural levels, from subcellular to cellular to tissue, profoundly affects the flavor and texture of an apple. For processed foods, and foods that are manufactured in the kitchen, the manipulation of structure by process operations is the key to delivering convenience to consumers, to creating new taste sensations, and even to eliciting desirable satiety and digestive physiology responses. The relation between structure creation through manipulation of process and the structural governance of the physical properties that are the determinants of food quality is illustrated schematically (Figure 1). In addition to this triad of interrelated factors, there are also temporal changes in structure and properties that are ongoing from the time of manufacture of the food to the time of its consumption. An example of a time-dependent change in food structure that affects consumer perception of quality is the syneresis of yoghurt, a quality-degradation phenomenon that arises from structural rearrangements in the yoghurt's casein particle network (Tamime et al., 2007).

Determining physical properties

A cursory glance at DIN, ISO, or ASTM standards (DIN, 2010; ISO, 2010; ASTM, 2010) informs that many standardized tests exist for measuring the physical properties of food so that food quality can be determined. The numerous tests in these catalogs of conformity are



Physical Properties as Indicators of Food Quality,

Figure 1 Schematic illustrating the interdependence of physical properties on food structure and how that structure is manipulated by processing and the dynamic changes in properties and structure that can occur with time.

augmented by rigorously defined tests of physical properties for in-house use by food companies seeking to optimize the quality of their food products by controlling each of their unit process operations. Testing methods for physical properties can be grouped into four categories:

1. Methods to measure fundamental physical properties
2. Methods to measure fundamental physical properties when results are analyzed with an appropriate model
3. Methods to measure physical properties under conditions dictated by an appropriate model in order that measurements relate to sensory properties
4. Methods to measure physical properties of practical use in food quality assessments

An example associated with food quality will be used to illustrate each of these measurement categories. Crispness is an essential quality parameter for foods such as crackers (Luyten et al., 2004), and in evaluations of crispness, a three-point bending test may be employed. If the dimensions of the cracker are such that they conform to recommendations in ASTM D790, a valid measurement of the elastic modulus of the cracker can also be obtained from the quality assessment test. In indentation (penetrometer) testing of solid triacylglycerol samples, a consistency parameter derived from the measured force-displacement curve is commonly used for routine quality assurance (Wright et al., 2001). However, it is also possible to derive a fundamental mechanical characterization of the triacylglycerol sample's constitutive properties from its force-displacement curve if an appropriate constitutive model is utilized. In measuring the color quality of a frozen dessert, it is imperative that the dessert's optical properties are measured under standardized conditions. But, if the composition of the diffusively reflected light is spectrally weighted to match the spectral sensitivity of the human eye, then the measured optical properties of the dessert directly relate to human perception of the dessert's color (Hunter and Harold, 1991). Finally, in a multitude of empirical or imitative tests of food quality, physical properties strongly influence the measured quality parameter. However, the relation between physical properties and the measured quality parameter may not be readily apparent. Shearing of meat samples in the Warner–Bratzler test affords a force reading that correlates to meat textural quality (Bourne, 2002), while, on the basis of the intensity of light passing through red, yellow, and blue glasses, a Lovibond tintometer defines the color quality of beer (Hunter and Harold, 1991). In some tests, the causal relation between physical property and quality parameter is rather difficult to discern, e.g., measurement of flour color grade to predict whether the flour will produce an attractive loaf of bread.

Physical properties of foods

Specific physical properties can play a crucial role in many definitions of quality for a wide array of food products. Included here, necessarily brief, is a cursory

overview of significant physical properties in the context of food quality; comprehensive treatments of physical properties and food quality are given in the classic texts of Mohsenin (1970, 1986), and in the more current texts of Sahin and Sumnu (2006) and Figura and Teixeira (2007), emphasizing the enduring interest in evaluating the physical properties of foods and understanding the mechanisms that govern them.

Most texts on the physical properties of foods devote a chapter to definitions and assessments of physical characteristics. Although these extensively defined physical properties, such as product size and shape, are not true physical properties, they are frequently used as food quality indices. For example, in New Zealand, five size categories are used in partial definition of the quality of eggs (EPF, 2010). Similarly, shape standards are applied to quality definitions of some commodities, with misshapen eggs eliminated from the USDA's two top quality standards (USDA, 2010), and shape uniformity being a prerequisite for the higher official US quality grades of many food products (USDA, 2010). In addition, because of the multiphase nature of many foods, the size and shape of individual particles within the food product substantially influence perceived quality. For example, during frozen storage of ice cream, the rate of disproportionation of ice crystals may be such that ice crystals will grow to a size that the resulting perception of grittiness imparts a negative impression of product quality to the consumer (Marshall et al., 2003).

Density

Density is perhaps the single most important physical property for understanding the quality attributes of food products. Density governs instability in many multiphase food systems, e.g., the tendency of components to undesirably cream or sediment (Friberg et al., 2004); it is a critical factor in understanding the stability and textural quality of aerated food systems (Scanlon, 2004); and, it is an excellent predictor of overall end-product quality for a number of agricultural commodities, e.g., potatoes and tomatoes (Dauthy, 1995). In addition, very precise measurements of the density of solutions using vibrating tube technologies permit quantification of solution components that define product quality. An example is the routine quality assurance role for density meters in accurate assessment of ethanol concentration by brewers and vintners (Jacobson, 2006).

Optical and dielectric properties

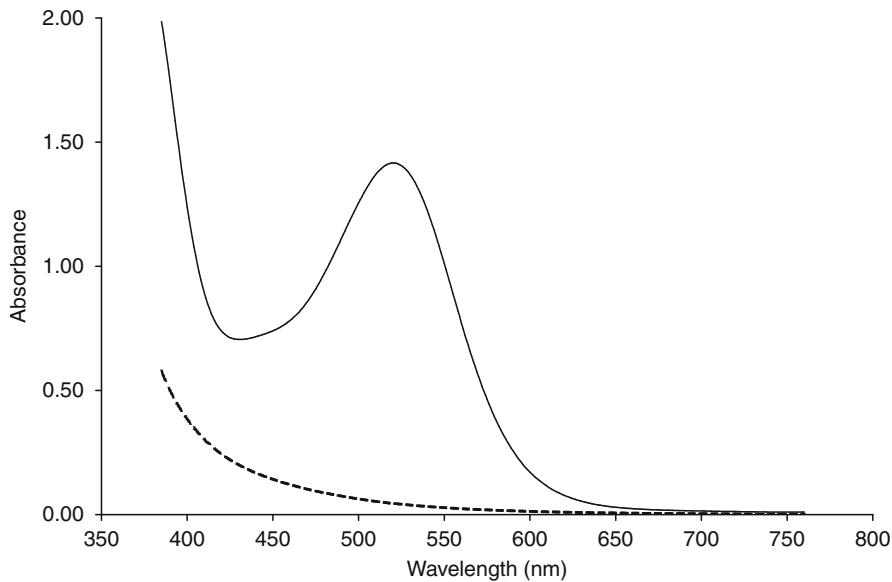
In an initial appraisal of food quality, appearance is undoubtedly the primary quality attribute (Clydesdale, 1993). Thus, optical properties are a highly relevant set of physical properties because the manner in which petahertz electromagnetic radiation interacts with food materials and structures ordains the appearance of the food. In addition, because the quality of convenience is an indispensable element of modern food product quality,

foods should heat up rapidly and evenly when exposed to an electromagnetic field of microwave wavelengths without undergoing physical and/or chemical changes that will undermine the gustatory attributes of the food. Therefore, the manner in which food components and food structures respond to low-frequency electromagnetic radiation is relevant to food manufacturers and to consumer evaluations of food quality.

When electromagnetic radiation of a given frequency strikes a food surface, it is either reflected or it is transmitted into the body of the food. Within the food, the radiation's propagation characteristics differ from those in air due to a difference in the velocity of propagation or in the absorptivity of the radiation, or both. In the absence of absorption, the refractive index (n), the ratio of the velocity of propagation of the radiation of a given frequency in vacuo to that in the food, is a useful physical property for characterizing food quality. The refractive index depends on how charged particles in the food materials respond to the electromagnetic radiation, electrons predominant in the visible region and dipolar molecules in the microwave region. Variation in the polarization of different molecules can serve as a signature for quality variation that can be determined by refractive index measurements. For example, the greater polarization of sucrose molecules compared to that of water molecules allows the refractive index to be a useful determinant of the amount of sucrose in syrups and the amount of water in honey (Figura and Teixeira, 2007).

The refractive index also determines how much energy of the electromagnetic field is reflected or transmitted at the surface of the food (although absorptivity is also a factor). The higher the refractive index, the higher the proportion of light reflected back, e.g., if absorptivity is ignored, ice with $n = 1.31$ reflects about 12% less light at 589 nm as water does with $n = 1.333$. If the food surface is smooth, such as the surface of a glazed donut, the specularly reflected light imparts a gloss or luster to the food, a distinctive food quality parameter for some foods, e.g., in a fruit packing house, the glossiness of apples is enhanced through wax applications in a series of polishing operations. More commonly, food surfaces are not smooth, and the structural organization of polarizable molecules is such that diffuse reflection occurs: the reflected light is reradiated over a wide range of angles, thereby lightening the overall appearance of the food.

Radiation transmitted into the food is very rarely unaffected by absorption. Accordingly, the intensity of the electromagnetic field is progressively reduced the further the radiation propagates into the food. For example, even in a transparent material such as pure water, optical absorption attenuates light transmission, with light intensity (at 550 nm) reaching the end of a meter-long column of water being only 85% of the intensity entering the column. Absorption mechanisms vary depending on the components in the food, but absorption is invariably frequency dependent (Figure 2). Thus, in the multiple-structured multi-materials that constitute food products, the process



Physical Properties as Indicators of Food Quality, Figure 2 Absorption spectra (relative to water) for a path length of 1 cm of apple juice (dashed line) and cranberry juice (solid line) in the visible region of the electromagnetic spectrum. (Data courtesy of Alison Ser.)

of multiple reflections and transmissions that takes place as the light encounters structural features within the food leads to its selective absorption, so that the diffusely re-reflected radiation gives rise to differences in food color; an example is β -carotene and lycopene, both conjugated alkene molecules of nutritional import (Miller et al., 1935). Although the features of their absorption spectra are fairly similar, the absorption maxima for lycopene occur at wavelengths that are approximately 20 nm longer than those of β -carotene. Thus, in the lycopene-rich structures of a tomato, there is greater loss of energy from the green region of the electromagnetic spectrum at each scattering event, and this establishes a red hue in tomatoes in contrast to the orange hue manifest in β -carotene-rich carrots. The greater the red hue of juiced tomatoes, the higher their quality grade. At microwave frequencies, higher absorptivity has both good and bad quality connotations. If the food materials effectively absorb microwave radiation, the food heats up quickly. However, too strong an absorptivity and microwave transmissivity into the interior of the food is hampered; an ensuing disparity between hot exterior and cold interior in a TV dinner or ready meal is not perceived as a desirable quality trait.

Mechanical properties

The evaluation of the mechanical properties of foods is central to definitions of food quality because food texture depends on mechanical behavior (Bourne, 2002). Mechanical properties also affect food quality by virtue of their maintenance of the integrity of solid foods, e.g., is the packet of cookies that one opens a friable mass of

crumbs or does it contain the same number of items that was packaged by the food manufacturer? Similarly, the mechanical and flow properties of liquid foods are important for mouthfeel and for factors associated with quality of convenience, e.g., does the tomato ketchup flow evenly or is it dispensed in a series of messy stick-slip events?

Kamyab et al. (1998) assumed that the textural characteristics of solid foods could be described by four mechanical properties – the Young's modulus, the yield stress, the coefficient of friction, and the fracture toughness. The importance of each of these mechanical properties to food quality can be illustrated with a specific textural attribute. In assessing the freshness of bread, a consumer squeeze test of crumb softness interrogates the elastic character of the crumb as defined by its Young's modulus (Scanlon and Zghal, 2001), albeit mediated by the customer's application of stress through the stiffer crust material. After an elastic response at small strains, a number of foods exhibit a yield stress, which may be defined as the minimum stress required to initiate flow in the food. A physical property defined in this manner is evidently a quality parameter for a number of spreadable foods, e.g., cream cheese (Steffe, 1996). There is increasing recognition of the relevance of the coefficient of friction between the surfaces of food materials and those of teeth, tongue, and palate in the oral appreciation of a number of foods. This appears to be more evident in foods with a creamy quality character (Dresselhuis et al., 2008), so that attaining the right coefficient of friction through food structure manipulation allows textural quality matching of fat-reduced foods with their full-fat counterparts. Although it is not easy to discount geometric effects and the mechanics of mastication

from the effect of mechanical properties, for those food products where crispiness and crunchiness are important quality criteria, fracture toughness is the relevant mechanical property in attaining desirable sensory characteristics (Luyten et al., 2004).

In beverages and in some solid-like foods, flow (rheological) properties govern mouthfeel quality (Bourne, 2002). Some relatively simple beverages display Newtonian behavior, so that regardless of the rate of testing, a single parameter, the viscosity, suffices to define the beverage's flow behavior; examples are fruit juices (Steffe, 1996). However, the vast majority of liquid foods are not this well behaved (Figure 3), and a statement on flow characteristics must also stipulate shear rate, with shear rates pertinent to those operative during mastication of special interest in relating the measured mechanical parameter to consumer oral quality assessments. A further hindrance to an exact characterization of mechanical performance by rheological methods is the fact that the properties of the vast majority of food materials are sensitive to their deformation history. To obviate ambiguity and to comprehensively evaluate the mechanical properties of food systems that are sensitive to temperature as well as time of testing, empirical evaluation of flow characteristics is conducted with rigorously controlled time-temperature treatments in instruments of well-defined geometry. An example is the evaluation of the pasting characteristics of starches or flours in the amylograph or rapid viscoanalyser.

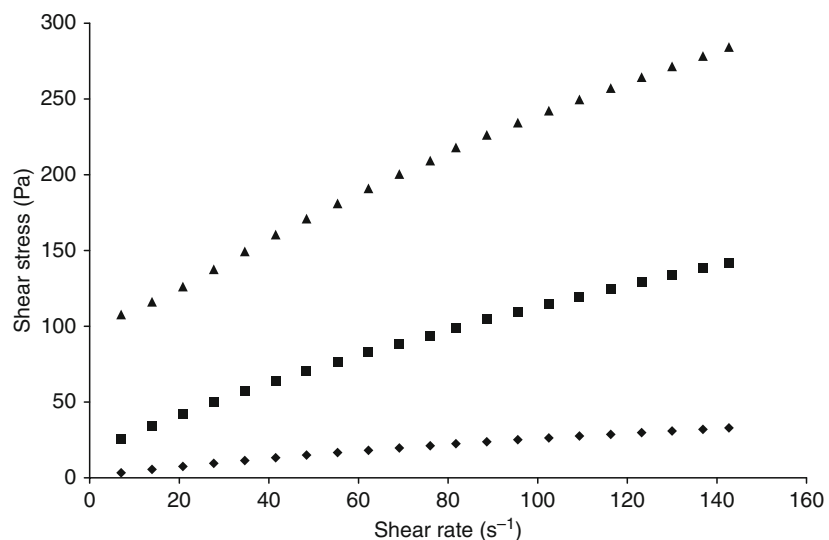
Thermal properties

The thermal properties of foods are unquestionably relevant to the attainment of good quality in most processed foods, e.g., see Lewis (1990) or Nesvadba et al. (2004).

An example from thermal process operations is thermal conductivity, a physical property that governs the degree of overprocessing, and thus the extent of quality degradation, that occurs in retorted foods as a consequence of ensuring that the coldest point in the food has an extremely low safety risk. However, as indicators of food quality per se, thermal properties are of lesser utility than other physical properties. Perhaps the most frequently used quality assurance assessment of thermal properties is obtained from differential scanning calorimetry, a technique that monitors specific enthalpy and melting points associated with phase transitions of food materials such as starch. Melting point determination is an informative quality criterion of shortening functionality for both domestic and industrial bakery applications, and so a simple test of this thermal property is measurement by drop point. A sample of shortening is heated in a glass tube and the temperature at which the sample slips defines its melting point (AOCS, 2009).

Other physical properties

The importance of water to so many facets of food quality means that many texts examining the physical properties of foods will devote a chapter or more to an examination of the adsorption of water to food materials (Rahman, 1995). Measurement of the shift in the vapor pressure of water molecules arising from the colligative properties of food molecules via water activity measurements is probably the most widely used technique for evaluating the effect of water content on product shelf life. In a similar vein, the change in electrical properties of a food resulting from moisture content changes can provide insights into the longevity of foods in storage facilities; for this purpose, the capacitance of grain samples is a relatively



Physical Properties as Indicators of Food Quality, Figure 3 Change in shear stress with increasing shear rate for a meringue mix (egg-whites and sucrose) with different volume fractions (ϕ) of bubbles entrained by mixing (\blacklozenge , $\phi = 0.46$; \blacksquare , $\phi = 0.65$; \blacktriangle , $\phi = 0.80$). (Data from Spencer and Scanlon [unpublished].)

simple means of evaluating moisture content and thus determining whether the grain should be dried in order that the quality of products derived from the grain is assured.

Temperature dependence of physical properties

All physical properties are affected by temperature, some more than others, e.g., cf. the temperature dependence of viscosity and density of food oils. The extent to which the quality of the food is changed depends on the food itself, but temperature-dependent effects are pronounced when a component in the food undergoes a phase transition as a result of the temperature change. Examples, with a resulting disastrous effect on food quality, are the melting of ice crystals in ice cream, and the melting of fat crystals in chocolate.

Conclusions

The structural and dynamic complexity of foods confounds a simplistic examination of the relationship between physical properties and food quality. Nevertheless, three driving forces impel food scientists to gain a better understanding of the causal relation between a given physical property and food quality: rapid advances in online detection technologies will permit physical property measurements by acoustic and electromagnetic fields to be related to online quality assurance provided the relation between the physical property and food quality is understood; the need for continuous innovation in the food industry, as well as in the culinary arts (Barham, 2001), demands a better understanding of how quality and physical properties are related if novel food products are to be created; the ongoing understanding from the nutritional sciences about relations between diet and health is driving product innovation to a focus on developing products that deliver greater health benefits without impairing food quality. These driving forces will undoubtedly shape the research that must be undertaken to better understand the relations between food materials, food structures, and quality changes as a function of time.

Bibliography

- AOCS, 2009. Recommended Practice Cc 18–80 (Reapproved) – Dropping Point. *American Oil Chemists' Society*. Champaign, IL: The Society.
- ASTM, 2010. *American Society for Testing and Materials*. <http://www.astm.org/>.
- Barham, P., 2001. *The Science of Cooking*. Berlin: Springer.
- Bourne, M. C., 2002. *Food Texture and Viscosity: Concept and Measurement*, 2nd edn. San Diego: Academic.
- CGC, 2010. Quality of western Canadian wheat exports. *Canadian Grain Commission*. <http://www.grainscanada.gc.ca/wheat-ble/method-methode/wmethod-methodeb-eng.pdf>.
- Clydesdale, F. M., 1993. Color as a factor in food choice. *Critical Reviews in Food Science and Nutrition*, **33**, 83–101.
- Dauthy, M. E., 1995. *Fruit and Vegetable Processing*. Rome: Food and Agriculture Organization of the United Nations.
- DIN, 2010. *Deutsches Institut für Normung*. <http://www.din.de/>.
- Donald, A., 2004. Food for thought. *Nature Materials*, **3**, 579–581.
- Dresselhuis, D. M., van Aken, G. A., de Hoogac, E. H. A., and Cohen Stuart, M. A., 2008. Direct observation of adhesion and spreading of emulsion droplets at solid surfaces. *Soft Matter*, **4**, 1079–1085.
- EPF, 2010. *Egg Producers Federation of New Zealand*. <http://www.eggfarmers.org.nz/egg-quality.asp>.
- Figura, L. O., and Teixeira, A. A., 2007. *Food Physics: Physical Properties – Measurement and Application*. Berlin: Springer.
- Friberg, S., Larsson, K., and Sjöblom, J. (eds.), 2004. *Food Emulsions*, 4th edn. New York: Marcel Dekker.
- Hunter, R. S., and Harold, R. W., 1991. *The Measurement of Appearance*, 2nd edn. New York: Wiley.
- ISO, 2010. *International Organization for Standardization*. <http://www.iso.org/iso/home.htm>.
- Jacobson, J. L., 2006. *Wine Laboratory Practices and Procedures*. New York: Springer.
- Kamyab, I., Chakrabarti, S., and Williams, J. G., 1998. Cutting cheese with wire. *Journal of Materials Science*, **33**, 2763–2770.
- Lewis, M. J., 1990. *Physical Properties of Foods and Food Processing Systems*. Chichester: Ellis Horwood.
- Luyten, A., Pluter, J. J., and van Vliet, T., 2004. Crispy/crunchy crusts of cellular solid foods: a literature review with discussion. *Journal of Texture Studies*, **35**, 445–492.
- Marshall, R. T., Goff, H. D., and Hartel, R. W., 2003. *Ice Cream*, 6th edn. New York: Kluwer Academic.
- Miller, E. S., Mackinney, G., and Zscheile, F. P., Jr., 1935. Absorption spectra of alpha and beta carotenes and lycopene. *Plant Physiology*, **10**, 375–381.
- Mohsenin, N. N., 1970. *Physical Properties of Plant and Animal Materials*. New York: Gordon and Breach.
- Mohsenin, N. N., 1986. *Physical Properties of Plant and Animal Materials: Structure, Physical Characteristics, and Mechanical Properties*, (2nd rev. ed.). New York: Gordon and Breach.
- Nesvadba, P., Houska, M., Wolf, W., Gekas, V., Jarvis, D., Sadd, P. A., and Johns, A. I., 2004. Database of physical properties of agro-food materials. *Journal of Food Engineering*, **61**, 497–503.
- Rahman, S., 1995. *Food Properties Handbook*. Boca Raton: CRC Press.
- Sahin, S., and Sumnu, S. G., 2006. *Physical Properties of Foods*. New York: Springer.
- Scanlon, M. G., 2004. Biogenic cellular solids. In Dutcher, J. R., and Marangoni, A. G. (eds.), *Soft Materials: Structure and Dynamics*. New York: Marcel Dekker, p. 321.
- Scanlon, M. G., and Zghal, M. C., 2001. Bread properties and crumb structure. *Food Research International*, **34**, 841–864.
- Steffe, J. F., 1996. *Rheological Methods in Food Process Engineering*, 2nd edn. East Lansing: Freeman.
- Tamime, A. Y., Hassan, A., Farnworth, E., and Toba, T., 2007. Structure of fermented milks. In Tamime, A. Y. (ed.), *Structure of Dairy Products*. Oxford: Blackwell, p. 134.
- Ubbink, J., Burbidge, A., and Mezzenga, R., 2008. Food structure and functionality: a soft matter perspective. *Soft Matter*, **4**, 1569–1581.
- USDA, 2010. *United States Department of Agriculture*. <http://www.usda.gov/wps/portal/usda/home>.
- Wright, A. J., Scanlon, M. G., Hartel, R. W., and Marangoni, A. G., 2001. Rheological properties of milkfat and butter. *Journal of Food Science*, **66**, 1056–1071.

Cross-references

[Adsorption Energy of Water on Biological Materials](#)

[Breads: Physical Properties](#)

[Color in Food Evaluation](#)

[Databases on Physical Properties of Plants and Agricultural Products](#)

[Dielectric Properties of Agricultural Products](#)

[Electrical Properties of Agricultural Products](#)

[Extrusion, Effect on Physical and Chemical Properties](#)

Fats: Rheological Characteristics
 Fruits, Mechanical Properties and Bruise Susceptibility
 Grain Physics
 Grains, Aerodynamic and Geometric Features
 Grass Fibers, Physical Properties
 Hysteresis in Foods
 Isotropy and Anisotropy in Agricultural Products and Foods
 Machine Vision in Agriculture
 Microstructure of Plant Tissue
 Modeling the Thermal Conductivity of Frozen Foods
 Nondestructive Measurements in Fruits
 Physical Dimensions and Units Use in Agriculture
 Physical Phenomena and Properties Important for Storage of Agricultural Products
 Physical Properties of Raw Materials and Agricultural Products
 Plant Physical Characteristics in Breeding and Varietal Evaluation
 Quality of Agricultural Products in Relation to Physical Conditions
 Rheology in Agricultural Products and Foods
 Soil Penetrometers and Penetrability
 Tropical Fruits and Vegetables: Physical Properties
 Water Effects on Physical Properties of Raw Materials and Foods
 X-Ray Method to Evaluate Grain Quality

PHYSICAL PROPERTIES OF RAW MATERIALS AND AGRICULTURAL PRODUCTS

Bohdan Dobrzański, Jr.^{1,2}, Rafał Rybczyński²

¹Pomology Department, University of Life Sciences, Lublin, Poland

²Institute of Agrophysics, Polish Academy of Sciences, Lublin, Poland

Synonyms

Physical properties of fresh and proceed agricultural crops

Definition

Physical property of agricultural material. A measurable property which describes a physical state of agricultural material at any given condition and time.

Agricultural raw materials. Biomaterials originating from farming or any agricultural production that are used as components for products processed by industries or human labor as a building material to create a new product or a new structure. Agrophysics focuses mostly on plant materials that are essential in creating agricultural products in food industry.

Agricultural products. Any goods created through farming or food processing based on usage of agricultural crops.

Introduction

The wide knowledge of physical properties of agricultural products is being used in the farming, planting, harvesting, drying, freezing, processing and storage of raw materials. Accurate design of machines and processes to harvest and handle raw materials and agricultural products and to change these crops into food requires an understanding of their physical properties. These properties include size,

shape, and density; deformation in response to applied forces; moisture content, adsorption and desorption of water, and hydrodynamic properties; and other characteristics describing physical state of agricultural material.

The physical properties of agricultural products are important in the design and processing of food (see also *Agriculture and Food Machinery, Application of Physics for Improving*). They can be classified as thermal, optical, electrical, mechanical, or structural properties. Most of these primary and secondary properties indicate changes in the chemical composition and structural organization of plant material consisting final product. The measurement techniques allow computation of these properties, which can provide information about the effects of processing conditions in fresh and proceeded foods. Some of characteristics, such as color, mechanical and rheological properties, thermal and electrical resistance, water content, and other physical quantities give excellent description of product quality.

This topic has been comprehensively covered by many researchers (Abbott and Harker, 2003; Barbosa-Cánovas et al., 2004; Dobrzański et al., 2006). When physical properties of agricultural products, such as grains, seeds, fruits and vegetables, dairy, meat and fish, oil crops, sugar crops, and fibers, are studied by considering either bulk or individual units of the material, it is important to have an accurate estimate of shape, size, volume, density, specific gravity, surface area, and other mechanical characteristics, which may be considered as designing parameters for food production.

Role of raw material in quality of agricultural products

The primary role of agriculture is, and should remain the production of agricultural raw materials for food and feed (CIAA, 2008). Agricultural raw materials are essential components for products processed by industries. The cost of agricultural raw materials represents between 30% and 80% of a food and drink manufacturer's operating costs.

Industry needs raw material supply that corresponds to specific quality criteria. According to the CIAA (2008) report, 70% of the European agricultural production is processed by the EU food and drink companies. Access to local supplies of raw materials remains a priority in certain food industries. The sustainable supply of agricultural materials represents an essential element in the long-term health and prosperity of the food and drink industry. Modern agriculture already provides the industry with products that respect a high and increasing level of requirement, notably in the area of environment and food safety. The coherence between farmers and the industrial sector in relation to consumers and market demand needs the researcher's access in study of physical properties of raw materials and is essential for ensuring competitive agricultural product. Measures and instruments developed under policies such as agricultural production, environment protection, biofuels promotion, food safety requirements, the

use of GMOs, and trade should be taken into consideration in study of physical properties of raw material and agricultural products. According to global production of top crops and raw materials ([Table 1](#)), the problem consists on the estimation of quality and sorting over 7,800 million tons of agricultural products.

Quality evaluation of raw materials and agricultural products has been a subject of interest to many researchers for many years (see [Quality of Agricultural Products in Relation to Physical Conditions](#)). Quality of agricultural products is an important factor to both the producers and the consumers. In this context the consumer is the person or organization receiving the product at every point in the production chain. This is important because quality will be perceived differently depending on the needs of the particular consumer: a packing shed operator will have a very different idea of quality to the ultimate eater of the fruit (Studman, [1994](#)). Quality factors for fresh fruits and vegetables listed by Kader ([1983](#)) are: hygiene and quarantine factors (parasites larvae, pupae, natural toxicants, contaminants, spray residues, heavy metals, etc.), cosmetic appearance (size, weight, volume, dimensions, shape, regularity, surface texture, smoothness, waxiness, gloss, color, uniformity, intensity, spectrum, physical defects, splits, cuts, dents, bruises), texture and flavor factors (firmness, hardness/softness, crispness, mealiness/grittiness, fibrousness, toughness), flavor (sweetness, sourness, astringency, bitterness, aroma, off-flavors, off-odors), and nutritional factors (dietary fiber, cancer inhibitors, carbohydrates proteins, lipids, vitamins, minerals).

Physical Properties of Raw Materials and Agricultural Products, Table 1 Production of crops and agricultural raw materials (million tons)

Agricultural products and raw materials, by crop types (including top individuals)

Cereals	2,263
Maize	721
Wheat	627
Rice	605
Barley	154
All types of fruit and vegetables	2,577
Tomato	120
Apple	45
Roots and tubers	715
Potatoes	328
Sugar crops	1,573
Sugar cane	1,324
Sugar beet	249
Dairy, meat and fish	1,075
Milk	619
Meat	259
Eggs	63
Fish	134
Oil crops	499
Soybean	204
Other oil crops	133
Oil palm fruit	162

Firstly, quality standards are affected by international and cultural preferences (Amos et al., [1994](#)). Secondly, standards can be affected by cultural changes or by strong marketing in the media. Quality standards may involve appearance, feel, taste, consistency, handling characteristics, ability to retain properties for long periods of time, or the absence of undesirable impurities (Kader, [1983](#)). There is no clear definition of quality, equal for all agricultural products. However, for each product and property interest, some objective means of measurement technique is required. Several methods are available for quality detection in horticultural commodities according to external and internal properties. The challenges are to make these techniques affordable in the market place and especially to relate the measurement parameters to the very subjective, sensory evaluation of quality by consumers.

Physical property of agricultural materials

In a Newtonian sense, the physical properties of an object may include many varietal properties; some of them are listed below alphabetically: absorption, area, boiling point, brittleness, capacitance, color, concentration, conductivity, density, dielectric (see [Dielectric Properties of Agricultural Products](#)), distribution, ductility, efficacy, electric charge, electric field, electric potential, emission, flow rate, fluidity, frequency, impedance, inductance, length, location, luminance, magnetic field, magnetic flux, malleability, mass, melting point, moment, permeability, permittivity, pressure, radiance, reflectivity, resistance, solubility, specific heat, spin, strength, temperature, tension, thermal transfer, velocity, viscosity, volume. These are frequently determined during the study of raw materials and agricultural products (see also [Databases on Physical Properties of Plants and Agricultural Products](#)).

Barbosa-Cánovas et al. ([2004](#)) divided physical properties into the following groups:

- Thermal properties such as specific heat, conductivity, diffusivity, and boiling point rise, freezing point depression (see also [Drying of Agricultural Products; Thermal Technologies in Food Processing](#))
- Optical properties, primarily color, but also gloss and translucency
- Electrical properties, primarily conductivity and permittivity (see also [Electrical Properties of Agricultural Products](#))
- Structural and geometrical properties such as density, particle size, shape, porosity, surface roughness, and cellularity
- Mechanical properties such as textural (including strength, compressibility, and deformability) and rheological properties (such as viscosity) (see also [Rheology in Agricultural Products and Foods](#))
- Others, including mass transfer related properties (diffusivity, permeability), surface tension, cloud stability, gelling ability, and radiation absorbance

Agricultural products and raw materials in general can display large compositional variations, inhomogeneities, and anisotropic structures. Composition can change due to seasonal variations and environmental conditions, or in the case of processed foods, properties can be affected by process conditions and material history.

Early physical property analyses of food and agricultural products required constant uniform values and were often oversimplified and inaccurate. Nowadays, computational engineering techniques, such as the finite element method, are much more sophisticated and can be used to evaluate nonuniform properties (e.g., thermal properties) that change with time, temperature, and location in food products that are heated or cooled. Improvements measuring the compositions of crop and food are now allowing predictions of physical properties that are more accurate than previously.

Physical methods for quality evaluation of agricultural products

Chen (1996) presents an overview of various quality evaluation techniques that are based on one of the following physical properties: density, firmness, vibration characteristics, x-ray and gamma-ray transmission, optical reflectance and transmission, electrical properties, aromatic volatile emission, and nuclear magnetic resonance (NMR) (see also *Physical Properties as Indicators of Food Quality*).

Zachriah (1976) reported that a number of researchers have investigated the electrical properties of fruits and vegetables, however, the results were not conclusive enough to permit development of a practical method for quality sorting of fruits and vegetables.

It was found that radiation in the near-infrared region of the spectrum can provide information related to many quality factors of agricultural products. Bellon and Sevilla (1993) developed an NIR system, which combined a CCD spectrophotometric camera and bifurcated fiber optics, for determining soluble solids in apples.

Short-wave radiations such as x-rays and gamma rays can penetrate through most agricultural products. The level of transmission of these rays depends mainly on the mass density and mass absorption coefficient of the material.

Nuclear magnetic resonance (NMR) is a technique that detects the concentration of hydrogen nuclei (protons) and is sensitive to variations in the concentration of liquid in the material. Although NMR imaging (MRI) has been used frequently in the medical field, however quality factors in raw materials and agricultural products has not been fully explored. Wang et al. (1988) used MRI methods to obtain images of water core and its distribution in Red Delicious apples. Chen et al. (1989) used MRI to evaluate various quality factors of crops.

One of the most practical and successful techniques for nondestructive quality evaluation and sorting of agricultural products is the electro-optical technique, based on

the optical properties of the product. Thus, determining such optical characteristics of an agricultural product can provide information related to quality factors of the product.

Texture and mechanical properties of tissue

Texture is a quality attribute that is critical in determining the acceptability of agricultural products. A few of the many terms used to describe sensory texture of crops are hard, firm, soft, crisp, limp, mealy, tough, leathery, melting, gritty, woolly, stringy, dry, and juicy. There are no accepted instrumental methods for measuring each of these attributes.

Abbott and Harker (2003) indicate that most important to understand the texture of a product is to identify the main elements of tissue strength and to determine which elements are responsible for the textural attributes of interest (see *Microstructure of Plant Tissue*). For example, it may be necessary to avoid tough strands of vascular material when measuring texture of soft tissues because the small amount of fiber produces an artificially high reading that does not agree with the sensory assessment of softness. On the other hand, it is important to measure the strength of fibers when determining toughness, such as in asparagus spears or broccoli stalks.

The arrangement and packing of parenchyma cells within the tissue is another factor that influences mechanical strength of raw material and products (Abbott and Harker, 2003). In carrots, the cells are small (approximately 50 µm in diameter), irregular in shape, and closely packed with a high degree of contact between neighboring cells and a small volume of intercellular gas-filled spaces. The cells can be arranged either as columns or as a staggered array where each cell overlays the junction of the two lower cells. These differences in cell packing may, in part, explain genotypic differences in susceptibility to harvest splitting in carrots. In the apple cortical tissue, the cells are large (up to 300 µm in diameter), elongated along the direction of the fruit radius, and organized into distinct columns (Vincent, 1989). As a result of this orientation of apple cells, the elastic modulus of tissue is higher and the strain at failure is lower when tissue plugs are compressed in a radial rather than a vertical or tangential orientation (Abbott and Lu, 1996; Vincent, 1989). Additionally, up to 25% of the volume of apple tissue may be gas-filled intercellular spaces, which indicates relatively inefficient cell packing and a low elasticity of tissue (Vincent, 1989).

Plant cells tend to maintain a small positive pressure, known as turgor pressure. This pressure develops when the concentration of solutes inside the cell is higher than outside the cell (Abbott and Harker, 2003). The extracellular solution fills the pores of the cell wall, sometimes infiltrates into gas-filled spaces, and usually is continuous with vascular (water conducting) pathways of the plant. Differences in solute concentration at the inner and outer surface of the plasma membrane cause water to flow into the cell

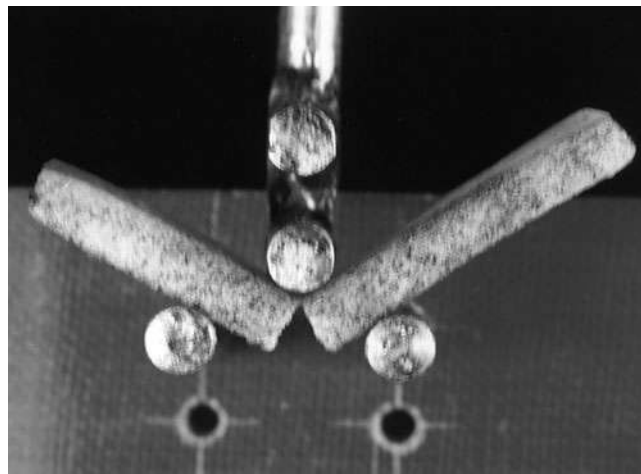
by the process of osmosis. This net movement of water is halted by the physical constraint of the rigid cell wall and, as a result of this, turgor develops inside the cell. At equilibrium, $\Psi = \Psi_p + \Psi_\pi$, where Ψ is the turgor (generally a positive value), Ψ_p is the water potential (water activity, generally a negative value) of the tissue, and Ψ_π is the osmotic pressure (generally a positive value) of the cell. Turgor has the effect of stressing the cell wall (see [Water in Forming Agricultural Products](#)). The consequences of this stressing depend on whether compressive or tensile loads are applied. When tissues are subjected to compressive loads, higher turgor tends to make the cell more brittle, that is, makes it fail at a lower force. When tissues are subjected to tensile measurements, turgor tends to harden the cell wall and a greater force is needed before cells fail (De Belie et al., 2000a). Also, turgor is thought to play a central role in softening and development of mealiness during storage of apples.

The strength of the cell wall relative to the adhesion between neighboring cells will determine whether cell rupture or cell-to-cell de-bonding is the mechanism of tissue failure. Cell rupture is generally associated with crisp and often juicy produce, as well as with unripe fruit and raw vegetables (Abbott and Harker, 2003). Cell-to-cell de-bonding is frequently associated with dry, unpleasant texture such as in mealy apples, chilling injured stone fruit and tomato, and juice loss in citrus (Harker et al., 1997). However, a dry texture is not always unacceptable to consumers, for example, banana.

Many crops contain a number of tissue zones – periderm, pericycle, and phloem parenchyma in carrot; skin, outer pericarp, inner pericarp, and core in kiwifruit; and outer pericarp, locular gel, seeds, and columella in tomato. These tissues differ in strength and biological properties and often need to be considered individually when measuring texture. For example, a very precise test for study the elasticity of apple was proposed and successfully used by Dobrzański et al. (2006). In this test, only a superficial layer of apple tissue with the skin over was loaded ([Figure 1](#)). It shows that fruit firmness was most influenced by elasticity of apple tissue and strength of apple skin and proves that strength of superficial layer of apple tissue more accurately indicates the mechanical properties of apple flesh in bending test (Rybczyński and Dobrzański, 2000) (see [Bending Properties of Plants](#)).

Instrumental measurement of texture

Szczesniak (1963) proposed a texture profile, a systematic approach to sensory texture analysis based on mechanical, geometrical, and other characteristics. Mechanical characteristics included basic parameters (hardness, cohesiveness, viscosity, elasticity, and adhesiveness) and secondary parameters (brittleness or fracturability, chewiness, and gumminess). Geometrical properties related to size, shape, and orientation of particles. The other characteristics comprised moisture and fat content. Moisture content is one of the most influential factor affected the mechanical



Physical Properties of Raw Materials and Agricultural Products, Figure 1 The failure of two layer tissue of apple beam (flesh with the skin) loaded in three-point support bending test.

resistance of raw material and agricultural products (see [Water Effects on Physical Properties of Raw Materials and Foods](#)). On the other hand, the change of moisture involves significant decrease or increase in volume of product observed as shrinkage or swelling (see also [Shrinkage and Swelling Phenomena in Agricultural Products](#)).

There are many types of mechanical loading: puncture, compression, shearing, twisting, extrusion, crushing, tension, bending, vibration, and impact. And there are four basic values that can be obtained from mechanical property tests: force (load), deformation (distance, displacement, penetration), slope (ratio of force to deformation), and area under the force/deformation curve (energy). The engineering terms based on these measurements are stress, strain, modulus, and energy, respectively. Stress is force per unit area, either of contact or cross-section, depending on the test. Strain is deformation as a percentage of initial height or length of the portion of sample subject to loading. Modulus of elasticity (tangent, secant, chord, or initial tangent) is a measure of stiffness based on the stress/strain ratio (see [Stress–Strain Relations](#)). Force and deformation values are more commonly used in food applications than stress and strain values and are sufficient, provided that the contact area and the distance the probe travels are constant and sample dimensions are similar from sample to sample. (Sample here means the portion of tissue tested, not necessarily the size of the fruit or vegetable.) In many horticultural texture tests, deformation is kept constant and the force value is reported. A typical force/deformation characteristic for a cylindrical piece of apple tissue compressed at constant speed gives F/D curve for puncture tests that look similar to compression curves. The portion of the initial slope up to point represents nondestructive elastic deformation; point is the inflection point where the curve begins to have a concave-downward shape and is called the elastic limit. The region before this point is where slope or elastic

modulus should be measured. Beyond the elastic limit, permanent tissue damage begins. There may be a biyield point where cells start to rupture or to move with respect to their neighbors, causing a noticeable decrease in slope (Abbott and Harker, 2003).

Mechanical properties of agricultural products and fruit firmness

Firmness is a property that is often used for evaluating the quality of fruits and vegetables. Firmness is not a physical quantity, however, is strongly related to numerous mechanical properties. In many agricultural products firmness is related to maturity. In general firmness of fruits decreases gradually as they become more mature and decreases rapidly as they ripen (Dobrzański and Rybczyński, 2000). Overripe and damaged fruits and vegetables become relatively soft. Several methods for measuring fruit firmness have been developed. Fekete and Felföldi (2000) reckoned firmness as a principal characteristic of fruits, importance for the quality, the optimum harvest date, and the evaluation of the maturity for storage and for shelf life (see *Physical Phenomena and Properties Important for Storage of Agricultural Products*). They divided the methods of fruit firmness measure on direct (contact: compression, shear, impact, rebound) and indirect (noncontact: vibration, sonic) techniques.

Firmness is related to maturity and it is well known; overripe and damaged fruits become relatively soft. Thus firmness can be used as a criterion for sorting of agricultural products into different maturity groups or for separating overripe and damaged fruits from good ones. Firmness is related to the quality factors, however, through use of simple penetrometers, only the maximum squeezing force has been frequently correlated with numerous quality factors. It is also well known, that the firmness should depends to the shape and size of fruit; size and contact area of plunger; rate of deformation; the way of fruit fixing, and other procedures influenced a final accuracy. Generally, determination of mechanical properties based on the high-precision measurement with expensive equipment requires a complete force/deformation curve. From the force/deformation curve, stiffness; modulus of elasticity; modulus of deformability; toughness; force and deformation to point of inflection, to biyield, and rupture; and maximum normal contact stress or stress index at low levels of deformation can be obtained. The force/deformation curve was frequently used in the study of physical properties of agricultural products; however, this measurement is not widely utilized in practice because of expensive and complicated procedures.

The most common texture tests of fruits and vegetables, the Magness-Taylor puncture and the Kramer Shear report only the maximum force attained, regardless of the deformation at which it occurs. Puncture testers (Magness and Taylor, 1925), are used to measure firmness of numerous fruits and vegetables to estimate harvest maturity or for postharvest evaluation of firmness (Abbott and Harker,

2003). Based on this procedure, Mizrach et al. (1992) used a 3-mm diameter pin as a mechanical thumb to sense firmness of oranges and tomatoes. Fekete and Felföldi (2000) have been reported four rapid penetration methods, where the values of force or deformation were measured. Bellon and Sevila (1993), reported the method, where the deformation was measured at constant force. Fekete and Felföldi (2000) designed device equipped with force sensor, an amplifier and A/D converter, connected to a hand-held microcomputer for data recording. Dobrzański and Rybczyński (2000) made the bases to develop a new device; nondestructive strain meter, where strain was measured at low constant force that allows estimating the modulus as firmness characteristic.

The Kramer Shear device is used extensively in the food processing industry and is used by some fresh-cut processors for quality control. Shearing in engineering terms does not mean cutting with a knife or scissors, but instead sliding adjacent parallel planes of cells past one another (Abbott and Harker, 2003). It does not measure true shear, however, the force measured by the test involves compression, shear, extrusion, and friction between the tissue and blades. As with the MT probe, comparisons should not be made between results from cells of different geometries.

Compression tests are also widely used in research on agricultural products (Abbott and Harker, 2003). Although raw materials and agricultural products are viscoelastic, they are often treated as elastic, so the force required to attain a specified deformation or to rupture (bruise or burst) the product is generally measured. Modulus of elasticity, stiffness, forces and deformation to biyield and to rupture, and contact stress can be calculated from elastic measurements, dimensions of the specimen, and Poisson's ratio. The elastic modulus or Young's modulus is often used by engineers. As the ratio of stress to strain or calculated from the slope of the force/deformation curve before the elastic limit, the modulus is the most accurate parameter of firmness.

Tensile measurement has not been as popular as puncture or compression testing because it is not intuitively as related to crushing or chewing as are puncture or compression and because it requires gripping or otherwise holding the ends of the sample so they can be pulled apart without crushing the tissues where they are held. Schoorl and Holt (1983) used clamps to hold apple tissue; however, only satisfactory results were obtained by Rybczyński and Dobrzański (1994).

Firmness of agricultural products can be measured at different force or deformation. Generally, these methods were based on the high precision measurement. F/D characteristics beyond the elastic limit may be more important than those before it because they simulate the destruction that occurs in bruising or eating (Bourne, 1980; Szczesniak, 1963).

Most force/deformation measurements are destructive. In these tests rupture forces usually provide the best correlation with sensory texture evaluations of foods.

Unfortunately destructive tests cannot be used in sorting of fruits and vegetables for subsequent sale, so a great deal of research has gone into developing nondestructive methods to estimate the mechanical properties and the textural quality of raw materials and agricultural products (Abbott and Harker, 2003; Chen and Sun, 1991).

Nondestructive techniques: frequency and product response

None of these nondestructive methods has attained wide commercial acceptance to date (see also *Nondestructive Measurements in Fruits*). After the relationship between an instrumental measurement and a quality attribute or acceptability is well established, the instrumental measurement is usually used to replace human evaluations (Peleg, 1994; Ruiz-Altisent et al., 1994; Wang et al., 1988). A nondestructive, noncontact firmness detector was elaborated and a laser to measure deflection caused by a short puff of high-pressure air was used. Under fixed air pressure, firmer products deflect less than softer ones. Laser-puff readings correlate well with destructive Magness-Taylor firmness values for apple, cantaloupe, kiwifruit, nectarine, orange, pear, peach, plum, and strawberry (McGlone and Jordan, 2000).

Impact, bounce, and vibration

Numerous studies have been conducted on the bounce responses of horticultural products and a number of impact parameters have been proposed to measure firmness, including peak force, coefficient of restitution, contact time, and the impact frequency spectrum (see *Mechanical Impacts at Harvest and After Harvest Technologies*). When one object collides with another object, its response is related to its mechanical properties, its mass, and the contact geometry (Abbott and Harker, 2003). The coefficient of restitution is the ratio of the velocities of the product just before and after impact and reflects the energy absorbed in the product during impact. Most impact tests involve dropping the agricultural product onto a sensor (McGlone and Schaare, 1993; Patel et al., 1993; Zapp et al., 1990) or striking the product with the sensor (Chen, 1996). Delwiche et al. (1991) developed a single-lane firmness sorting system for pear and peach. Impact measurements frequently do not correlate with the Magness-Taylor puncture measurement.

The force response of an elastic sphere impacting a rigid surface is governed by the impacting velocity, mass, radius of curvature, elastic modulus, and Poisson's ratio of the sphere. A problem inherent to the technique of dropping the fruit on a force sensor is that the impact force is also a function of the mass and radius of curvature of the fruit (Chen, 1996). Therefore, a large variation in these two parameters will affect the accuracy in firmness measurement.

A different approach is to impact the fruit with a small spherical impactor of known mass and shape and measuring the acceleration of the impactor. The advantage of this

method is that the impact-force response is independent of the fruit mass and is less sensitive to the variation of the fruit dimension. This technique was first described by Chen et al. (1985). A low-mass high-speed impact sensor was designed and tested with good results, however, only on kiwifruits and peaches.

The vibration characteristics of fruits are governed by their elasticity, mass, and size. Therefore, it is possible to evaluate firmness of fruits on the basis of their vibration characteristics. An extensive study of vibration characteristics of apples was conducted by Abbott et al. (1968). In general, the researchers detected a series of resonant frequencies. However, in the cases where the fruit was excited by a vibrator and the vibration was detected by an accelerometer. The lower resonant frequencies may not be those of the free vibration of the fruit, but may be resonant frequencies that were caused by the interaction between the fruit mass or accelerometer mass and the force developed by local deformation of the fruit.

Acoustic (sonic) and ultrasonic waves

Acoustic vibrations (sonic) are those within the human audibility range of frequency to 20,000 Hz. Sonic measurements provide a means of measuring fruit and vegetable firmness (Abbott and Harker, 2003). The traditional watermelon ripeness test is based on the acoustic principle, where one thumps the melon and listens to the pitch of the response. A number of sonic instruments and laboratory prototype sorting machines have been developed and tested (Abbott et al., 1968, 1992; Armstrong et al., 1990; Muramatsu et al., 2000; Peleg et al., 1990; Schotte et al., 1999; Stone et al., 1998; Zhang et al., 1994). When an object is caused to vibrate, amplitude varies with frequency of the vibration and will be at a maximum at some particular frequency determined by a combination of the shape, size, and density of the object; such a condition is referred to as resonance. Resonance measurement can be achieved by applying an impulse or thump that contains a range of frequencies. Kawano et al. (1994) reported a commercial sorting machine for detecting internal voids in Japanese watermelon. Shmulevich et al. (1995) developed a sonic instrument using a lightweight flexible piezoelectric film sensor to follow changes in fruit during storage. Muramatsu et al. (2000) examined the relationship of both phase shifts and resonant frequencies to firmness. Peleg et al. (1990) examined the sonic energy transmitted by the specimen rather than the resonant frequencies. Despite considerable research, sonic vibration has not yet become a viable option for the horticultural industry. However, there are several advanced commercial prototypes currently being evaluated.

Ultrasonic techniques have been used quite successfully for evaluating subcutaneous fat, total fat, lean, and other internal properties of live animals. However, researchers have not been so successful in using ultrasonic measurements to evaluate internal quality of fruits and vegetables.

On the other hand, ultrasonic wave range frequencies over >20,000 Hz are widely used in the medical field and for analyzing meat. Ultrasonic has been used with limited success for measuring physical properties of crops because of the high energy absorption of plant tissues. The commonly measured ultrasonic parameters are velocity, attenuation, and frequency spectrum composition. Bruises in apples (Upchurch et al., 1987) and hollow heart of potatoes (Cheng and Haugh, 1994) could be detected in the laboratory using ultrasonic wave. Mizrach et al. (1999) have followed the softening process in avocados, melons, and mangoes, respectively.

Visible light and color measurements

In physics, visible light is said to be composed of electromagnetic rays. The electromagnetic rays of visible light are different only in their frequency from the other rays such as: gamma rays, x-rays, ultraviolet, infrared, microwaves and rays carrying radio and television (Dobrzański et al., 2006). The frequency range reflected is influenced by the physical and chemical properties of the object and by the frequency ranges which are absorbed. However, the color of an object is unknown, because electromagnetic rays are colorless. An illuminated object reflects light, which is perceived and interpreted by persons. The human eye converts the electromagnetic rays and then brain interprets this information as sensation of color. The eye is able to convert varying frequencies of electromagnetic rays into information which the brain perceives as different colors. The eye is also able to convert the intensity of rays into information which the brain interprets as a sensation of lightness. Based on the fact that the retina of the human eye contains three different types of cone cells which are sensitive to the primary colors of red, green, and blue respectively.

Because humans are able to distinguish between several hundred thousand shades of color (approx. 350,000), it is necessary to introduce mathematical color models which enable each shade to be described exactly in terms of a numbered value. To enable colors to be described as geometrical interpretation, there are various 3-D models for color description. Some of these, e.g., the RGB color model are derived directly from the additive or CMY from the subtractive color mixing system. Therefore, each color in this cube is identified by its coordinates. Compared with the RGB and CMY color models, the HSV (hue, saturation, and value) color model, hexagon pyramid, has the advantage that the colors correspond closely to our perception of color. Consequently, this color space is often preferred for practical implementation of color measurement.

Most new colorimeters allow measurements of absolute color to be displayed in any of five color systems: Yxy, L*a*b*, L*C*H_o, Hunter Lab, or tristimulus values XYZ. Measurements of color difference can be displayed in any of four systems: $\Delta(L^*a^*b^*)/\Delta E^*ab$, $\Delta(L^*C^*H_o)/\Delta E^*ab$, $\Delta(Yxy)$, and Hunter $\Delta(\text{Lab})/\Delta E$ (Good, 2002).

Two of these systems is frequently applied in any quality estimation of raw materials and agricultural products.

The L*a*b* color system is one of the uniform color spaces recommended by CIE in 1976 as a way of more closely representing perceived color and color difference. In this system, L* is the lightness factor; a* and b* are the chromaticity coordinates.

The colorimeter measuring system is designed to provide accurate readings and uniform response. The light received by the meter is divided three ways and passed through special filters whose light absorbing characteristics combine with the spectral response of the photo cells. Upon reaching the silicon photocells, light energy is converted into electrical signals and sent to the microprocessor, where it is adjusted for the illuminating condition desired and then converted into co-ordinates according to the chosen color space. Readings are displayed on the LCD panel and can be transferred to a separate computer or processor through the data output terminal. For color readings, these values are translated into Yxy coordinates or in color L*a*b* standard. The device allows for different settings for illumination and CIE 2° – Standard Observer or CIE 10° – Supplementary Observer. All results were determined at daylight D65 of color temperature 6,500 K.

Crops and agricultural products behavior in visible light

With the increasing diversity of plant varieties, crop quality recognition is becoming more and more important. Along with quality estimation, color is one of the major factors in creating a consumer acceptance of crop and agricultural products (Alchanatis and Searcy, 1995; Dobrzański and Rybczyński, 2002; Kader, 1983; Kameoka et al., 1994; Lancaster, 1992; Molto et al., 1996; Motonaga et al., 1997; Studman, 1994). Therefore the appearance of products has a major influence on perceived quality. However, color as one of the most important quality parameter is influenced by cultural and consumer preferences (see *Color in Food Evaluation*).

The preferences of color depend on: uniformity of external color, repeatability of fruit color in crop, differences between high and ground color, intensity of blush and base color (saturation of red), size of blush, lightness-darkness, whiteness, physical defects, dents, browning, bruising, and stage of maturity (ripeness). After harvest, cosmetic appearance of apples seems to be the most important quality factor. However, the storage has substantial influence on final quality of fruits, as it affects the appearance and induces color changes (Dobrzański and Rybczyński, 2002; Dobrzański et al., 2006; Kader, 1999; Kameoka et al., 1994; Saks et al., 1999). Firstly, some of fruits are more influenced by storage conditions than others. Secondly, shelf-life is a period of storage, with unsuitable conditions, i.e., high temperature and low humidity, for keeping apple in good quality. At this

time, darkening of the skin observed by consumers, decreases perceptions of color, which influences the estimation of fruit quality. Impacts on fruits cause damages, and bruising leads to enzymatic browning of the tissue. Frequently, internal browning is visible externally.

One of the basic conditions for improvement of quality is proper sorting and handling of the fruit for market (Dobrzański et al., 2006). Hence, sorting for separating the fruit with the same blush or having the same base color should be the most important factor for improving quality and influence price. Separating ripe from over ripe or damaged would allow the “good” food (having adequate shelf life) to be shipped to fresh market while the less desirable, the green and the over ripe and bruised fraction, could be sent to a processing plant where quality could be enhanced by appropriate bioprocessing techniques (McClure, 1995).

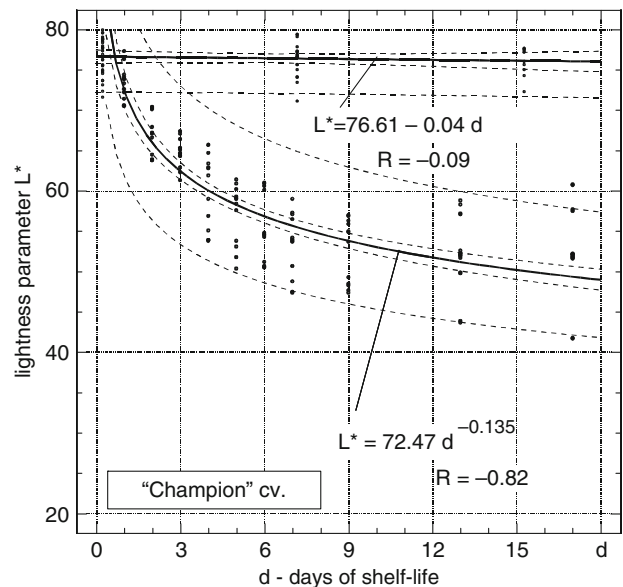
The change of fruit color as a result of storage, shelf-life, and bruising

The ground color of blush dependent on sun rays during growing. In this case, the low value of L^* parameter indicates dark skin of fruit. After five months of storage the color of apples was stable, however, some changes of color components at shelf-life were observed. The increases of the L^* coordinate in this case indicates, that the apples seem to become brighter during the shelf-life.

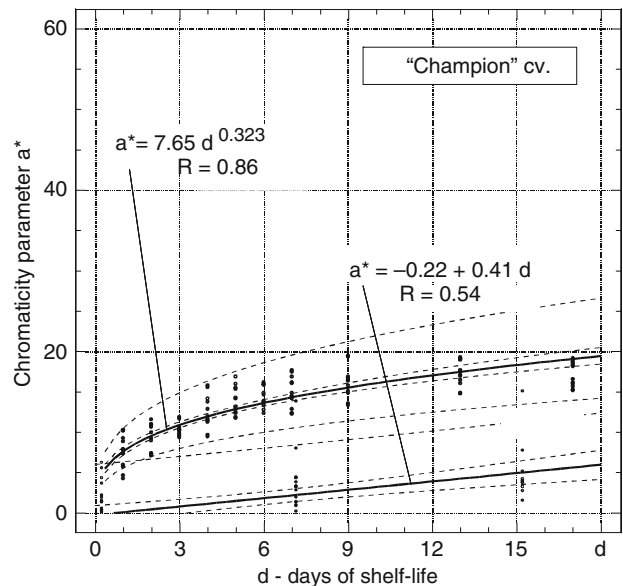
Some differences in color in 3-D Figures on the cube of color coordinates, where the lightness L^* and chromaticity coordinates of a^* and b^* of storage apple were presented by Dobrzański and Rybczyński (2002). For most apples, chromaticity a^* ranges negative values representing light green of the base color. The most sensitive parameter a^* , indicates blush reaching the values over 40. Further, the storage of apples for two additional months does not change the color of fruits, however, slight differences for all quality classes are observed.

Dobrzański et al. (2006), analyzed the $L^*a^*b^*$ color coordinates of bruised apples during the shelf-life (see also *Fruits, Mechanical Properties and Bruise Susceptibility*). More distinct differences are visible on the base color of fruit. The lightness coordinate L^* is stable during the shelf-life; however, darkening of apple increases each day and L^* parameter rapidly decrease indicating bruising after 5 days (Figure 2).

The blush color consists of more intensive components, which is frequently the reason why bruising is invisible on this surface. Only the component of red color presented by a^* decrease after bruising, while slightly increases at shelf-life (Figure 3). The red less skin of Champion apples indicates a^* value near zero. However, the bruising caused browning of tissue, which appearing intensity of red color component on the skin and increase of the index a^* . The red color of bruising is close to the blush color, being invisible on this area, while, the bruising appears on the base color of the opposite side of fruit.



Physical Properties of Raw Materials and Agricultural Products, Figure 2 The lightness coordinate L^* of ground color at shelf-life of Champion apples and the change of color after bruising.



Physical Properties of Raw Materials and Agricultural Products, Figure 3 The chromaticity coordinate a^* of ground color at shelf-life of Champion apples and the change of color after bruising.

The value of the chromaticity parameter a^* indicates the blush affecting the cosmetic's appearance. However, after 2 days of shelf-life the bruising on this area of base color looks not acceptable for the consumer.

Light scatter imaging

As light passes through tissue, cellular contents such as starch granules, cell walls, and intercellular spaces cause scatter. The extent of scatter of collimated light such as a laser beam may change during ripening due to changes in cell-to-cell contact and compositional changes. Measurement of the scatter using computer vision may thus provide an indirect indication of textural changes. Significant correlations between mechanical properties and image size have been shown in apples (De Belie et al., 2000b) and tomatoes (Tu et al., 2000). Interest is increasing in the development of machine vision systems to replace human visual inspection. One of the major requirements in developing machine vision systems for sorting fruits and vegetables is the ability to analyze an image accurately and quickly (Abbott and Harker, 2003).

Summary

Agricultural raw materials are essential components for products processed by industries. The top characteristics of raw materials and agricultural products, definitions, and methods for determination of the physical properties of agricultural materials are presented.

A measurable property which describes physical state of raw agricultural material at any given condition and time can be defined as a physical property of product. The physical properties of raw materials and agricultural products are wide knowledge being used in the farming, planting, harvesting, drying, freezing, processing and storage. Some characteristics, such as color, mechanical and rheological properties, thermal and electrical resistance, water content, and other physical quantities give excellent description of product quality. According to physical properties estimation, numbers of methods are available for quality detection in raw materials and are essential for ensuring competitive agricultural product.

Bibliography

- Abbott, J. A., and Harker, R., 2003. *Texture*, pp. 1–19. Available from <http://usna.usda.gov/hb66/021texture.pdf>.
- Abbott, J. A., and Lu, R., 1996. Anisotropic mechanical properties of apples. *Transactions of the American Society of Agricultural Engineers*, **39**, 1451–1459.
- Abbott, J. A., Bachman, G. S., Childers, N. F., Fitzgerald, J. V., and Matusik, F. J., 1968. Sonic techniques for measuring texture of fruits and vegetables. *Food Technology*, **22**, 101–112.
- Abbott, J. A., Affeldt, H. A., and Liljedahl, L. A., 1992. Firmness measurement of stored 'Delicious' apples by sensory methods, Magness-Taylor, and sonic transmission. *Journal of the American Society for Horticultural Science*, **117**, 590–595.
- Alchanatis, V., and Searcy, S. W., 1995. *A Selectable Wavelength Imaging Sensor for Multispectral Inspection of Agricultural Products*. ASAE Paper: 95-3210, St. Joseph.
- Amos, N. D., Opara, L. U., Studman, C. J., Wall, G. L., and Walsh, C., 1994. Techniques to assist with meeting international standards for the export of fresh produce. Section 6a, XII CIGR – AgEng 94, Milan.
- Armstrong, P., Zapp, H. R., and Brown, G. K., 1990. Impulsive excitation of acoustic vibrations in apples for firmness determination. *Transactions of the American Society of Agricultural Engineers*, **33**, 1353–1359.
- Barbosa-Cánovas, G. V., Juliano, P., and Peleg, M., 2004. Engineering properties of foods, in food engineering. In: Barbosa-Cánovas, G. V. (ed.), *Encyclopedia of Life Support Systems (EOLSS)*. Oxford, UK: EOLSS Publishers. <http://www.eolss.net>.
- Bellon, V., and Sevilla, F., 1993. Optimization of a non-destructive system for on-line infra-red measurement of fruit internal quality. In: *Proceedings of the Fourth International Symposium on Fruit, Nut, and Vegetable Production Engineering*, Zaragoza, Spain, pp. 317–325.
- Bourne, M. C., 1980. Texture evaluation of horticultural crops. *HortScience*, **15**, 51–57.
- Chen, P., 1996. Quality evaluation technology of agricultural products. In: *Proceedings of the ICAME'96*, Seoul, Korea, Vol. I, pp. 171–190.
- Chen, P., and Sun, Z., 1991. A review of non-destructive methods for quality evaluation and sorting of agricultural products. *Journal of Agricultural Engineering Research*, **49**, 85–98.
- Chen, P., Tang, S., and Chen, S., 1985. *Instrument for Testing the Response of Fruits to Impact*. American Society of Agricultural Engineers Paper No. 75-3537.
- Chen, P., McCarthy, M. J., and Kauten, R., 1989. NMR for internal quality evaluation of fruits and vegetables. *Transactions of the American Society of Agricultural Engineers*, **32**, 1747–1753.
- Cheng, Y., and Haugh, C. G., 1994. Detecting hollow heart in potatoes using ultrasound. *Transactions of the American Society of Agricultural Engineers*, **37**, 217–222.
- CIAA, 2008. TCO/091/08E-Final. (<http://ec.europa.eu>, accessed 21 April, 2010).
- De Belie, N., Hallett, I. C., Harker, F. R., and De Baerdemaeker, J., 2000a. Influence of ripening and turgor on the tensile properties of pears: a microscopic study of cellular and tissue changes. *Journal of the American Society for Horticultural Science*, **125**, 350–356.
- De Belie, N., Schotte, S., Coucke, P., and De Baerdemaeker, J., 2000b. Development of an automated monitoring device to quantify changes in firmness of apples during storage. *Postharvest Biology and Technology*, **18**, 1–8.
- Delwiche, M. J., Singh, N., Arevalo, H., Mehlschau, J., 1991. A second generation fruit firmness sorter. In: *Proceedings of the American Society of Agricultural Engineers*. Paper 916042.
- Dobrzański, Jr., B., and Rybczyński, R., 2000. *Requirements for the Measurement of Fruit Firmness*. CD-ROM of AgEng 2000 Papers, Warwick. Paper: 00-PH-047, pp. 1–7.
- Dobrzański, Jr., B., Rabcewicz, J., and Rybczyński, R., 2006. Handling of apple, Transport techniques and efficiency vibration, damage and bruising, texture, firmness and quality. *Centre of Excellence Agrophysics*. IA PAN, Lublin, pp. 1–234.
- Dobrzański, B., Jr., and Rybczyński, R., 2002. Colour as a quality parameter of fruits and vegetables. In Blahovec, J., and Kutilek, M. (eds.), *Physical Methods in Agriculture*. New York: Kluwer, pp. 375–398.
- Fekete, A., and Felföldi, J., 2000. *System for Fruit Firmness Evaluation*. CD-ROM of AgEng 2000 Papers, Warwick. Paper: 00-PH-034.
- Good, H., 2002. Measurement of colour in cereal products. *Cereal Foods World. New Technologies*, **47**, 5–6.
- Harker, F. R., Redgwell, R. J., Hallett, I. C., and Murray, S. H., 1997. Texture of fresh fruit. *Horticultural Reviews*, **20**, 121–224.
- Kader, A. A., 1983. Postharvest quality maintenance of fruits and vegetables in developing countries. In *Postharvest Physiology and Crop Production*. New York: Plenum, pp. 455–470.
- Kader, A. A., 1999. Fruit maturity, ripening, and quality relationships. *Acta Horticulturae*, **485**, 203–208.

- Kameoka, T., Hashimoto, A., and Motonaga, Y., 1994. Surface colour measurement of agricultural products during post-ripening. In: *Proceedings of Colour Forum Japan'94*, pp. 11–14.
- Kawano, S., Abe, H., and Iwamoto, M., 1994. Novel applications of nondestructive techniques for quality evaluation of fruits and vegetables. In Brown, G., and Sarig, Y. (eds.), *Nondestructive Technologies for Quality Evaluation of Fruits and Vegetables. Proceedings of the International Workshop, US-Israel BARD Fund*, June 1993, Spokane. American Society of Agricultural Engineers, St. Joseph, pp. 1–8.
- Lancaster, J. E., 1992. Regulation of skin colour in apples. *Critical Reviews in Plant Sciences*, **10**, 487–502.
- Magness, J. R., and Taylor, G. F., 1925. *An Improved Type of Pressure Tester for the Determination of Fruit Maturity*. US Department of Agriculture Circulation, pp. 350–358.
- McClure, W. F., 1995. Biological measurements for the 21st century. In: Keynote Paper at *Agricultural and Biological Engineering Conference*, “New Horizons, New Challenges”, Newcastle, 3, pp. 1–9.
- McGlone, V. A., and Jordan, R. B., 2000. Kiwifruit and apricot firmness measurement by the non-contact laser air-puff method. *Postharvest Biology and Technology*, **19**, 47–54.
- McGlone, V. A., and Schaare, P. N., 1993. *The Application of Impact Response Analysis in the New Zealand Fruit Industry*. ASAE Paper: 93-6537.
- Mizrach, A., Nahir, D., and Ronen, B., 1992. Mechanical thumb sensor for fruit and vegetable sorting. *Transactions of the American Society of Agricultural Engineers*, **35**, 247–250.
- Mizrach, A., Flitsanov, U., Schmilovitch, Z., and Fuchs, Y., 1999. Determination of mango physiological indices by mechanical wave analysis. *Postharvest Biology and Technology*, **16**, 179–186.
- Molto, E., Aleixos, N., Ruiz, L. A., Vazquez, J., and Juste, F., 1996. *An Artificial Vision System for Fruit Quality Assessment*. AgEng'96, Madrid, Paper: 96F-078, 2, pp. 956–957.
- Motonaga, Y., Kameoka, T., and Hashimoto, A., 1997. Constructing colour image processing system for managing the surface colour of agricultural products. *Journal of Japanese Society of Agricultural Machinery*, **59**, 13–21.
- Muramatsu, N., Sakurai, N., Wada, N., Yamamoto, R., Tanaka, K., Asakura, T., Ishikawa-Takano, Y., and Nevins, D. J., 2000. Remote sensing of fruit textural changes with a laser Doppler vibrometer. *Journal of the American Society for Horticultural Science*, **125**, 120–127.
- Patel, N., McGlone, V. A., Schaare, P. N., and Hall, H., 1993. “BerryBounce”: a technique for the rapid and nondestructive measurement of firmness in small fruit. *Acta Horticulturae*, **352**, 189–198.
- Peleg, K., 1994. A new sensor for non-destructive measurement and modelling in fruits. *International Agrophysics*, **8**, 431–438.
- Peleg, K., Ben-Hanan, U., and Hinga, S., 1990. Classification of avocado by firmness and maturity. *Journal of Texture Studies*, **21**, 123–129.
- Ruiz-Altsent, M., Barreiro, P., and Garcia, J. L., 1994. Non-destructive quality measurement and modelling in fruits. *International Agrophysics*, **8**, 445–454.
- Rybczyński, R., and Dobrzański, B., Jr., 1994. Mechanical resistance of apple in different place of fruit. *International Agrophysics*, **8**, 455–459.
- Rybczyński, R., and Dobrzański, B., Jr., 2000. Physical properties of apples after harvest. *Agricultural Engineering*, **32**, 89–94.
- Saks, Y., Hofman, P. J., and Meiburg, G. F., 1999. Potential for improvement of mango skin colour during storage. *Acta Horticulturae*, **485**, 325–329.
- Schoorl, D., and Holt, J. E., 1983. A practical method for tensile testing of apple tissue. *Journal of Texture Studies*, **14**, 155–164.
- Schotte, S., De Belie, N., and De Baerdemaeker, J., 1999. Acoustic impulse-response technique for evaluation and modelling of firmness of tomato fruit. *Postharvest Biology and Technology*, **17**, 105–115.
- Shmulevich, I., Galili, N., and Benichou, N., 1995. Development of a nondestructive method for measuring the shelf-life of mango fruit. In: *Proceedings of the Food Processing Automation IV Conference*, Chicago, pp. 275–287.
- Stone, M. L., Armstrong, P. R., Chen, D. D., and Brusewitz, G. H., 1998. Peach firmness prediction by multiple location impulse testing. *Transactions of the American Society of Agricultural Engineers*, **41**, 115–119.
- Studman, C. J., 1994. Fruit firmness measurement techniques – a new approach. *International Agrophysics*, **8**, 461–466.
- Szczesniak, A. S., 1963. Classification of textural characteristics. *Journal of Food Science*, **28**, 385–389.
- Tu, K., Jancsok, P., Nicolai, B., and De Baerdemaeker, J., 2000. Use of laser-scattering imaging to study tomato-fruit quality in relation to acoustic and compression measurements. *International Journal of Food Science & Technology*, **35**, 503–510.
- Upchurch, B. L., Miles, G. E., Stroshine, R. L., Furgason, E. S., and Emerson, F. H., 1987. Ultrasonic measurement for detecting apple bruises. *Transactions of the American Society of Agricultural Engineers*, **30**, 803–809.
- Vincent, J. F. V., 1989. Relationship between density and stiffness of apple flesh. *Journal of the Science of Food and Agriculture*, **47**, 443–462.
- Wang, S. Y., Wang, P. C., and Faust, M., 1988. Non-destructive detection of watercore in apples with nuclear magnetic resonance imaging. *Scientia Horticulturae*, **35**, 227–234.
- Zachariah, G., 1976. Electrical properties of fruits and vegetables for quality evaluation. In: *Quality Detection in Foods*. ASAE Publication 1-76, American Society of Agriculture Engineering, St. Joseph, pp. 98–101.
- Zapp, H. R., Ehlert, S. H., Brown, G. K., Armstrong, P. R., and Sober, S. S., 1990. Advanced instrumented sphere (IS) for impact measurements. *Transactions of the American Society of Agricultural Engineers*, **33**, 955–960.
- Zhang, X., Stone, M. L., Chen, D., Maness, N. O., and Brusewitz, G. H., 1994. Peach firmness determination by puncture resistance, drop impact, and sonic impulse. *Transactions of the American Society of Agricultural Engineers*, **37**, 495–500.

Cross-references

- [Agriculture and Food Machinery, Application of Physics for Improving Bending Properties of Plants](#)
[Color in Food Evaluation](#)
[Databases on Physical Properties of Plants and Agricultural Products](#)
[Dielectric Properties of Agricultural Products](#)
[Drying of Agricultural Products](#)
[Electrical Properties of Agricultural Products](#)
[Fruits, Mechanical Properties and Bruise Susceptibility](#)
[Mechanical Impacts at Harvest and After Harvest Technologies](#)
[Microstructure of Plant Tissue](#)
[Nondestructive Measurements in Fruits](#)
[Physical Phenomena and Properties Important for Storage of Agricultural Products](#)
[Physical Properties as Indicators of Food Quality](#)
[Quality of Agricultural Products in Relation to Physical Conditions](#)
[Rheology in Agricultural Products and Foods](#)
[Shrinkage and Swelling Phenomena in Agricultural Products](#)
[Stress–Strain Relations](#)
[Thermal Technologies in Food Processing](#)
[Water in Forming Agricultural Products](#)
[Water Effects on Physical Properties of Raw Materials and Foods](#)

PHYSICAL PROPERTIES FOR SOIL CLASSIFICATION

Johan Bouma
Soil Science Department, Wageningen University,
Rhenen, CA, The Netherlands

Definition

Soil Classification is the arrangement of soils into a hierarchy of groups on the basis of their similarities. There are many National Classification systems for different countries and two widely used international ones, Soil Taxonomy in the USA (Soil Survey Staff, 1998) and the World Reference Base (FAO, ISRIC and IUSS, 1998). Attention will be focused here on these two systems.

Introduction

General descriptions of soil classification systems and the underlying philosophy are well summarized in Eswaran et al. (2003) and in the *Handbook of Soil Science* (Summer, 2010). Attention will be confined here to the role being played by physical properties in defining the various categories. Any soil classification is the result of judgments being made as to the effects of soil formation processes that occurred in the past. Generally, five soil-forming factors are distinguished, as initially proposed by Jenny in 1941: parent material, topography, climate, biological factors, and time. Regarding the time aspect, some red tropical soils are millions of years old, while soils being formed in recent deposits are very young. Anything in between may be found in terms of age, whereby soil-forming processes in the past may have resulted in soils that can again act as parent material when the climate changes or when the original soil erodes and soil formation starts again after deposition at another location. Soils form in a given parent material by interacting physical, chemical, and biological processes, whereby physical processes related to water and temperature regimes are key driving factors. Topography has a major effect on the magnitude and direction of these processes as well as on the soil stability in a landscape. Water and temperature regimes during soil formation and the resulting physical soil properties are therefore logical choices when discussing physical properties for soil classification. Sometimes "man" is added as a sixth soil-forming factor because of his major impact on the earth and its soils. However, in the context of a geological time frame, man has only rather recently arrived on earth while his major (or better, often devastating) impact has only been felt after the industrial revolution. When discussing soil classification, three particular features may be surprising to outsiders and need therefore special consideration.

1. Soil classification focuses on the natural, undisturbed soil. This requires, for instance, mixing the top 30 cm of soil before a classification is made, to avoid possible changes in classification of a given soil as a result of

frequent human activity such as plowing. Be that as it may, different soil management may result in quite different properties of a given soil even if the classification remains the same and the land user will be particularly interested in such effects of management. The only aim of classification is, however, to correctly classify the soil being considered according to the system being followed. To avoid common misunderstandings about the aims of soil classification, Droogers and Bouma (1997) proposed the term *genoform* to represent soil conditions as defined in soil classification and the term *phenoform* for different functional properties as a result of different types of management in any given particular type of soil, such as, e.g., permanent pasture, arable land, and organic farming.

2. Modern soil classification systems try to use morphometric field characteristics as much as possible to allow on-site determination of the proper classification. If a classification would only be based on mineralogical, chemical, and physical analyses, the system would lose much of its attractiveness as the procedure would become very slow and discontinuous. The classifier is confronted with a given soil profile and is forced to hypothesize about the kind of interactions between soil-forming factors that are likely to have resulted in the soil being observed with all its morphological features. He has his experience to go by including analyses and observations of comparable soils and landscapes elsewhere, including measurements. There is, however, no possibility for experimental verification of hypotheses if only because conditions of the past cannot be reproduced. Examples to be discussed later will show that easily observable patterns of iron mottles (*Redoximorphic Features*) and occurrence of particular types of soil horizons can give indications about water and temperature regimes.
3. The relation between soil classification and soil mapping is not always clear to users of soil information. Soil maps show how natural soil bodies occur within a landscape. The delineated boundaries reflect the constraints of map scales and the conceptual landscape model of the surveyor who can only make a limited amount of soil observations by augering. The classification system is used to classify the soil bodies that have been observed in strategically localized soil pits or augerings. Broadening the interpretation from a point observation to the area of the mapping unit involves substantial generalization as map units may be quite heterogeneous, while sharp lines on the map separating different units are often arbitrary. The surveyor defines so-called "representative soil profiles" for a given map unit that is next being classified. This, however, involves largely unknown generalizations. Still, this step from point observation to mapping unit is very important for land users as the soil map report presents suitability assessments for any given mapping unit for a range of land uses. Land users will not be

particularly interested in soil classification, as such, but it is an important tool for soil survey as it helps to organize soil knowledge transferring it from point to point in a landscape.

The US soil taxonomy system

The US Soil Taxonomy system (Soil Survey Staff, 1998) consists of six categories: Orders, Suborders, Great Groups, Subgroups, Families and Series. For example, the soil studied by Droogers and Bouma (1997) was a loamy, mixed, mesic Typic Fluvaquent.

Order: Entisol: ..ent.

Suborder: Aquent: ..aqu.

Great Group: Fluvaquent: ..Fluv

Subgroup: Typic Fluvaquent: Typic...

Family: Texture (loamy), mineralogy (mixed), temperature regime (mesic)

Series: Not distinguished in the Netherlands. In the USA, the name of localities is often used where the soil occurs, e.g., Tama silt loam.

A number of differentiating characteristics are distinguished to allow placement of any soil into the classification system: (1) diagnostic epipedons (surface horizons), (2) diagnostic subsurface horizons, (3) other diagnostic soil characteristics, (4) soil moisture regimes, and (5) soil temperature regimes. These differentiating characteristics will now be discussed, emphasizing physical properties related to the water and temperature regime.

Ad (1): The *Folistic* epipedon (L.folia = leaf) contains high amounts of organic C but is not saturated with water for more than a few days after heavy rains. In contrast, the *Histic* epipedon (Gr.histos = tissue) is commonly saturated with water for long periods.

Ad (2): The *Albic* subsurface horizon (L.albus = white) is an eluvial horizon with a color that is largely determined by the color of the primary soil particles rather than of their coatings of iron and clay that have been removed by pedogenesis. The *Cambic* horizon (L.cambiare = to exchange) is formed by limited physical and chemical transformations, including effects of temporary saturation with water, leading to some limited mobilization of iron and manganese. The *Duripan* (L.durus = hard) is cemented by illuvial silica. The *Fragipan* (L.fragilis = brittle) is not cemented but very slowly permeable, resulting in stagnating water and limited root growth. The *Petrocalcic* (Gr.petra = rock) and *Petrogypsic* horizons are cemented by calcium carbonate and gypsum, respectively.

Ad (3): *Aquic conditions* arise in soils that currently experience continuous or periodic saturation and reducing conditions, mobilizing manganese and iron that may again oxidize in characteristic patterns when aeration occurs during drying. The soil matrix that has lost iron and manganese becomes grayish. The combination of gray and red colors (which is specifically defined in terms of color chromas and values) is called: *Redoximorphic Features*. Several types of saturation are distinguished:

Episaturation describes a perched water table on top of a slowly permeable subsoil horizon; *Endosaturation* describes saturation by a true water table as part of a continuous aquifer; and *Anthraquic* saturation describes controlled flooding such as that used to grow rice and cranberries. Each subtype is characterized by different types of *Redoximorphic Features*.

Ad (4): Six soil moisture regimes are distinguished:

- (a) Aquic: Signifies saturation with a reducing regime free of dissolved oxygen (to be observed by *Redoximorphic Features*).
- (b) Aridic: Occurs in arid climates; dry in more than half of the growing season and moist in less than 90 consecutive days.
- (c) Udic: Occurs in climates with sufficient rain in growing season. Rain plus stored moisture equals or exceeds evaporation.
- (d) Perudic: In climates where rainfall always exceeds evaporation in all months when the soil is not frozen.
- (e) Ustic: Is moister than Aridic and drier than Udic.
- (f) Xeric: In climates with cool moist winters and warm, dry summers.

Moisture conditions are defined in terms of soil water potentials, but regimes are usually estimated from limited experimental data, particularly with regard to the climate. Saturated conditions are estimated by observing *Redoximorphic Features*. For most Soil Orders, the moisture regime is used to determine placement of a soil at Suborder level.

Ad (5): Five soil temperature regimes are distinguished:

- (a) Cryic: Mean annual soil temp <8°C
- (b) Frigid: Same as previous but with higher summer temperatures
- (c) Mesic: Mean annual soil temperature between 8°C and 15°C
- (d) Thermic: Mean annual soil temperature between 15°C and 22°C
- (e) Hyperthermic: Same but >22°C

When the difference between mean summer and winter temperature is less than 6°C, “iso” is added to the name, e.g., isomesic. Soil temperature is used at the Family level of Taxonomy.

The world reference base for soil resources (WRB)

Since its endorsement by the IUSS (International Union of Soil Sciences) in 1998, the World Reference Base for Soil Resources (WRB) has established itself as a comprehensive soil correlation system. It has been translated in nine languages and is used all over the world. WRB is increasingly used as a soil classification system.

Much similarity exists with the US Taxonomy classification system, discussed above. Both systems try to use as many morphometric soil characteristics as possible to allow classifications in the field. But there are some differences as follows.

1. Soil Taxonomy uses climatic factors for its taxa but this is avoided in WRB, where using detailed climatic data as an overlay over soils data is preferred when preparing land evaluations.
2. WRB distinguishes 30 reference soil groups at the highest level of their system, whereas Soil Taxonomy has only 12 orders at the highest level.
3. WRB uses two categorical levels: Reference Soil Groups and Soil Units, the latter based on a set of diagnostic criteria “qualifiers,” while Soil Taxonomy uses six, as discussed above. WRB is “broad and shallow,” Soil Taxonomy is “small and deep.”
4. WRB uses more diagnostic horizons and properties than Soil Taxonomy.
5. Though there is considerable similarity between names of diagnostic horizons in WRB and Soil Taxonomy, the differences in definitions may be large as WRB has made an effort to simplify analytical requirements for classification. WRB also considers at the highest-level physical processes such as prolonged saturation with water (hydromorphy), while Soil Taxonomy does so at the second Suborder level. On the other hand, Soil Taxonomy defines and uses soil moisture and temperature regimes that are not being considered in WRB.

Physical properties and soil classification

Overall, physical properties play a relatively minor role in defining Taxa in soil classification systems. There are two notable exceptions: (1) soil saturation, as evidenced by *Redoximorphic Features* augmented by the measurements of water table levels, is clearly distinguished. Only Soil Taxonomy distinguishes soil moisture regimes at all levels, while soil temperature regimes are considered at family level. (2) Hardness of cemented soil horizons formed by soil processes displacing and accumulating silica, gypsum, or calcite, is also a notable physical property. But in general, chemical and biological processes rather than physical processes play a dominant role in defining differentiating criteria and, therefore, soil Taxa. Of course, chemical and biological processes can only occur when soils contain water and when water acts as a transporting medium. It is, therefore, difficult and somewhat artificial to separate the physical, chemical, and biological processes when defining different types of soil.

For practical applications, the reverse question as to how application of an existing soil classification system to a newly exposed soil profile can help define its soil physical properties is quite interesting as we will explore next.

Does soil classification allow relevant predictions of physical properties?

Both Soil Taxonomy and the WRB present a system that allows classifying soils all over the world. Several diagnostic criteria used in both systems to classify soils contain information about physical properties or processes, as

discussed above. Whether or not this allows relevant predictions depends on the spatial scale being considered. Land use studies at world level or for large regions depend on information obtained from soil classification as applied in small-scale soil maps because usually the alternative is to have no information at all. Here, soil classification and associated soil mapping is most valuable. For smaller areas, such as countries or regions within countries and certainly farms, the conclusion is often different because information from classification may be too qualitative, descriptive, or speculative to be of value for the specific management questions being raised. For example, when studying precision farming at farm level, we found that new quantitative approaches were necessary and that soil classification was of no value (e.g., Bouma et al, 2008). However, in regional studies, interpretations based on soil classification can be quite useful as a starting point for discussions with land users and politicians. Again, the alternative is to have nothing at all to start with, and interpretations based on soil maps are cheap and can be rapidly obtained, the more so since Geographic Information Systems are increasingly being used, even in developing countries. Interpretations can next be improved by initiating specific measurements or computer modeling studies that are, however, costly. But a cost/benefit analysis should always be made to balance the cost of additional procedures versus the added usefulness of new information obtained. Sometimes, qualitative information is adequate to answer certain questions and application of sophisticated simulation models represents overkill. Applying additional techniques can be done in steps and can in the end of the knowledge chain involve application of sophisticated state-of-the-art models and monitoring procedures (e.g., Bouma et al, 2008). Bouma (2001) has called this the “step-by-step” approach that also works well to gradually involve users of soil information into the decision process. Input of soil maps and soil classification in regional modeling studies can be quite helpful to improve the overall quality of the work because the implicit underlying assumption of flow equations being used in hydrological models is that porous media are isotropic and homogeneous, which they are not. Soil maps can help to better define boundary conditions for models in terms of occurrence of soil horizons and different soil units. Basic soil survey data can also be used to derive *Pedotransfer functions* that relate simple soil characteristics from the soil survey report to parameters used in simulation that are difficult and costly to measure (Pachepsky and Rawls, 2004).

Recently, Hydropedology has been proposed as an activity to combine pedological expertise in classification and mapping with expertise in measuring, monitoring, and modeling in soil physics and hydrology. This combines the best of two worlds: hydrologists can thus obtain more realistic representations of land areas for their models, while pedologists can improve their interpretations of soil maps by moving beyond qualitative and descriptive procedures (Lin et al., 2006). A representative example for

hydropedology was presented by Vepraskas et al. (2006), combining an analysis of *Redoximorphic Features* with use of a simulation model for regional water dynamics.

Summary

Soil physical properties play a minor role in defining differentiating criteria for soil classification. But soil moisture regimes, including saturation as deduced from *Redoximorphic Features*, and soil temperature regimes are being used as well as the hardness of various soil horizons with accumulations of silica, gypsum, and carbonate. Application of an existing soil classification system to a new soil allows estimates of physical soil properties of various soil horizons that are useful as a first step for regional characterizations of water and solute movement that can next be improved by computer simulation. The new discipline of hydropedology thus combines descriptive, often qualitative, expertise from soil mapping/classification with quantitative expertise from hydrologists.

Bibliography

- Bouma, J., 2001. The new role of soil science in a network society. *Soil Science*, **166**(12), 874–879.
- Bouma, J., de Vos, J. A., Sonneveld, M. P. W., Heuvelink, G. B. M., and Stoorvogel, J. J., 2008. The role of scientists in multiscale land use analysis: lessons learned from Dutch communities of practice. *Advances in Agronomy*, **97**, 175–238.
- Droogers, P., and Bouma, J., 1997. Soil survey input in exploratory modelling of sustainable soil management practices. *Soil Science Society of America Journal*, **61**, 1704–1710.
- Eswaran, H., Rice, T., Ahrens, R., and Stewart, B. A., 2003. *Soil Classification: A Global Desk Reference*. Boca Raton: CRC Press.
- FAO/ISRIC/UNESCO, 1998. *World reference base for soil resources*. World Resources Report 84. Rome: FAO.
- Lin, H., Bouma, J., Pachepsky, Y., Western, A., Thompson, J., van Genuchten, R., Vogel, H., and Lilly, A., 2006. Hydropedology: synergistic integration in pedology and hydrology. *Water Resources Research*, **42**, W05301, doi:10.1029/2005WR004085.
- Pachepsky, Y. A., and Rawls, W. J., 2004. *Development of Pedotransfer Functions in Soil Hydrology*. Boston: Elsevier. *Developments in Soil Science*. The Netherlands: Amsterdam, Vol. 30.
- Soil Survey Staff, 1998. *Keys to Soil Taxonomy*. Washington: USDA Natural Resources Conservation Service.
- Summer, M. E. (ed.), 2010. *Handbook of Soil Science*, 2nd edn. Boca Raton: CRC Press.
- Vepraskas, M. J., Huffman, R. L., and Kreizer, G. S., 2006. Hydrologic models for altered landscapes. *Geoderma*, **131**, 287–298.

Cross-references

[Agophysical Properties and Processes](#)

[Ecohydrology](#)

[Hydraulic Properties of Unsaturated Soils](#)

[Hydropedological Processes in Soils](#)

[Oxidation–Reduction Reactions in the Environment](#)

[Parent Material and Soil Physical Properties](#)

[Pedotransfer Functions](#)

PHYSICAL PROTECTION OF ORGANIC CARBON IN SOIL AGGREGATES

Tiphaine Chevallier

UMR Eco&Sols, Functional Ecology and Biogeochemistry of Soils and Agro-Ecosystems, Institut de Recherche pour le Développement (IRD), Montpellier, France

Definitions

Soil organic carbon (SOC): Soil organic carbon refers to the carbon occurring in the soil organic matter (SOM). In soils, carbon is either organic (SOC) or inorganic (mainly carbonates, CaCO_3). SOM comes from all living and dead organisms (roots, litter, fauna, microfauna, and microorganisms).

Soil aggregates: Soil aggregates are organic and mineral particles bound to each other more strongly than to adjacent particles (<http://soils.usda.gov/sqi/management/fils/RESQIS3.pdf>; http://ed.fnal.gouv/trc_new/pdandp/soil_research/soilaggregates.html). Aggregates are often separated with their ability to resist stresses such as wetting followed by shaking in water (Yoder, 1936; Kemper and Rosenau, 1986; Kay and Angers, 1999). They are named water-stable aggregates. There are also named after their size: macroaggregates ($>250 \mu\text{m}$) and microaggregates $50–250 \mu\text{m}$ (Tisdall and Oades, 1982; Elliott, 1986) ([Soil Aggregates, Structure, and Stability](#)).

Physical protection of soil organic carbon in soil aggregates: This term pools all the physical processes that limit microbial activities and then explain the stabilization or the accumulation of SOC in soil aggregates (Balesdent et al., 2000; Six et al., 2002).

Introduction

Sufficient soil organic matter (SOM) must be retained for biological, chemical, and physical soil functioning. Appropriate levels of SOM ensure soil fertility, maintain soil structure, minimize soil erosion, and preserve soil biodiversity (Feller and Beare, 1997). The sequestration of carbon in soil is also becoming increasingly important because of concern over rising levels of CO_2 in the atmosphere (Feller and Bernoux, 2008). Because soil is considered to be a larger pool of carbon than biomass and atmosphere, many studies try to identify and quantify the processes that limit soil carbon mineralization. Three main processes are usually distinguished: SOC can be (1) physically stabilized, that is, protected from mineralization by aggregation, (2) stabilized physically and chemically by intimate association with mineral particles, especially clays ([Clay Minerals and Organo-Mineral Associates](#)), and (3) biochemically stabilized by the formation of recalcitrant organic compounds (Six et al., 2002). The first process, physical protection of SOC in soil aggregates, is indicated by the positive influence of aggregation on the accumulation of SOC (Angers, 1992). Indeed, SOC

can be protected from microbial decomposition within macroaggregates ($>250\text{ }\mu\text{m}$) and within microaggregates ($<250\text{ }\mu\text{m}$) (Bossuyt et al., 2002; see Figure 1).

SOC protection

Tisdall and Oades (1982) and Elliott (1986) initiated many studies on the interaction between soil aggregates and soil organic matter dynamics (see *Organic Matter, Effects on Soil Physical Properties and Processes*). In the 1990s and even recently, lots of papers established SOC turnover with their location, inside or outside water-stable soil aggregates (Puget et al., 1995; Besnard et al., 1996; Puget et al., 2000; Six et al., 2000; Denef et al., 2004; Six et al., 2004). The lower turnover of SOM signed a protection from microbial attack when located in soil aggregates. Those studies displayed lower turnover for plant residues (particulate organic matter, POM) located in soil aggregates (40–49 years) compared to plant residues not located in soil aggregates (19–27 years) (Golchin et al., 1995). The main site of SOC protection seems to be especially situated in microaggregates with a SOC turnover of 209 ± 95 years compared to a SOC turnover within macroaggregates of 42 ± 18 years (Six et al., 2002; Denef et al., 2004; Pulleman and Marinissen, 2004).

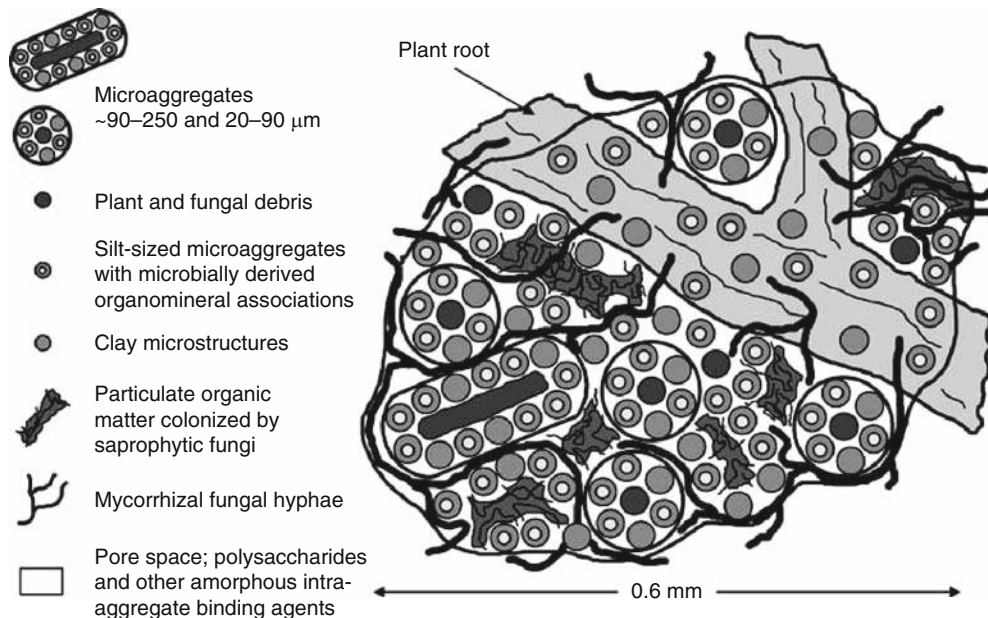
In addition, other studies evaluated the pool of aggregate-protected SOC by comparing crushed and uncrushed soil mineralization (Gupta and Germida, 1988; Beare et al., 1994; Balesdent et al., 2000; Chevallier et al., 2004; Pulleman and Marinissen, 2004; Razafimbelo et al., 2008). The additional carbon mineralized with soil crushing is considered to be the amount of aggregate

protected SOC. Protected SOC within aggregates is about 1–2% of the total SOC (Balesdent et al., 2000), but it can represent up to 40% of easily mineralizable SOC (Chevallier et al., 2004).

The main explanations for this protection against microbial decomposition are

- Substrates are inaccessible to microbes or enzymes because adsorbed on clay surfaces, or located in pores small enough to protect SOC against enzyme attack by physical exclusion (Sollins et al., 1996; Strong et al., 2004; Zimmerman et al., 2004).
- Poor water and air conditions to microbial activity (Sexstone et al., 1985; Young and Ritz, 2000).
- Hydrophobicity of SOM in soil aggregates (Chenu et al., 2000; Goebel et al., 2005).
- A Lack of appropriate microbial population to decompose SOM, indeed (microbial biomass, activities, and genetic structure are modified in soil aggregates) (Elliott, 1986; Gupta and Germida, 1988; Ranjard et al., 2000; Mumey et al., 2006).

Physical protection of SOC in soil aggregates depends on aggregate dynamics and aggregate formation, which depend on soil type, especially the amount of clay and oxyhydroxyde particles, soil management, i.e. soil tillage, soil occupation (see *Management Effects on Soil Properties and Functions*), root and soil fauna activities (see *Earthworms as Ecosystem Engineers*), and drying–rewetting or freezing–thawing events (Six et al., 2004). However, SOC stabilization is a combination of different mechanisms: physical, biochemical, and chemical mechanisms that do not play separately. The degree and amount



Physical Protection of Organic Carbon in Soil Aggregates, Figure 1 Conceptual diagram of aggregate hierarchy illustrating microaggregates inside a macroaggregate (Jastrow et al., 2007).

of protection of SOC depends on the chemical and physical properties of the mineral matrix and the morphology and chemical structure of the organic matter (Baldock and Skjemstad, 2000). Although organizing and quantifying the different processes are still difficult (Kogel-Knabner et al., 2008; Von Lützow et al., 2008), soil aggregation can be a master integrating variable that both controls and indicates the SOC stabilization status of a soil (Plante and McGill, 2002; Six et al., 2004; Jastrow et al., 2007). Soil aggregation is initiated by microbial decomposition of plant residues (Martens, 2000; Abiven et al., 2007) (see *Microbes and Soil Structure*). Indeed the microbial activity enhances the internal cohesion and hydrophobicity of aggregates, that is, the aggregates' stability (Cosentino et al., 2006). Within soil aggregates, particulate organic matter and SOC turnover are slowed down, so other SOC stabilization mechanisms can occur, such as getting a chemical recalcitrance and/or being adsorbed to clay particles (Baldock and Skjemstad, 2000; Kaiser and Guggenberger, 2000; Puget et al., 2000; Balabane and Plante, 2004; see Figure 1).

Conclusion

With respect to enhancing SOC protection against microbial mineralization, the main goals should involve maximizing the stability of soil microaggregates, the main site of soil physical protection of SOC, with an optimum rate of soil macroaggregate turnover to allow incorporation and stabilization of fresh SOC (Plante and McGill, 2002). Further studies on SOC stabilization should try to specify the combination of the different processes, i.e. physical, chemical, and biochemical processes. What are the main different combination with the soil type, occupation, and management?

Bibliography

- Abiven, S., Menasseri, S., Angers, D. A., and Leterme, P., 2007. Dynamics of aggregate stability and biological binding agents during decomposition of organic materials. *European Journal of Soil Science*, **58**, 239–247.
- Angers, D. A., 1992. Changes in soil aggregation and organic carbon under corn and alfalfa. *Soil Science Society of America Journal*, **56**, 1244–1249.
- Balabane, M., and Plante, A. F., 2004. Aggregation and carbon storage in silty soil using physical fractionation techniques. *European Journal of Soil Science*, **55**, 415–427.
- Baldock, J. A., and Skjemstad, J. O., 2000. Role of the soil matrix and minerals in protecting natural organic materials against biological attack. *Organic Geochemistry*, **31**(7–8), 697–710.
- Balesdent, J., Chenu, C., and Balabane, M., 2000. Relationship of soil organic matter dynamics to physical protection and tillage. *Soil and Tillage Research*, **53**, 215–230.
- Beare, M. H., Cabrera, M. L., Hendrix, P. F., and Coleman, D. C., 1994. Aggregate-protected and unprotected organic matter pools in conventional-tillage and no-tillage soils. *Soil Science Society of America Journal*, **58**, 787–795.
- Besnard, E., Chenu, C., Balesdent, J., Puget, P., and Arrouays, D., 1996. Fate of particulate organic matter in aggregates of silty soils with cultivation. *European Journal of Soil Science*, **47**, 495–503.
- Bossuyt, H., Six, J., and Hendrix, P. F., 2002. Aggregate-protected carbon in no-tillage and conventional tillage agroecosystems using carbon-14 labeled plant residue. *Soil Science Society of America Journal*, **66**, 1965–1973.
- Chenu, C., Le Bissonnais, Y., and Arrouays, D., 2000. Organic matter influence on clay wettability and soil aggregate stability. *Soil Science Society of America Journal*, **64**, 1479–1486.
- Chevallier, T., Blanchart, E., Albrecht, A., and Feller, C., 2004. The physical protection of soil organic carbon in aggregates: a mechanism of carbon storage in a Vertisol under pasture and market gardening (Martinique, West Indies). *Agriculture, Ecosystems and Environment*, **103**, 375–387.
- Cosentino, D., Chenu, C., and Le Bissonnais, Y., 2006. Aggregate stability and microbial community dynamics under drying-wetting cycles in a silt loam soil. *Soil Biology and Biochemistry*, **38**, 2053–2062.
- Denef, K., Six, J., Paustian, K., and Merckx, R., 2001. Importance of macroaggregate dynamics in controlling soil carbon stabilization: short-term effects of physical disturbance induced by dry-wet cycles. *Soil Biology and Biochemistry*, **33**, 2145–2153.
- Denef, K., Six, J., Merckx, R., and Paustian, K., 2004. Carbon sequestration in microaggregates of no-tillage soils with different clay mineralogy. *Soil Science Society of America Journal*, **68**, 1935–1944.
- Elliott, E. T., 1986. Aggregate structure and carbon, nitrogen and phosphorus in native and cultivated soils. *Soil Science Society of America Journal*, **50**, 627–633.
- Feller, C., and Beare, M. H., 1997. Physical control of soil organic matter dynamics in the tropics. *Geoderma*, **79**, 69–116.
- Feller, C., and Bernoux, M., 2008. Historical advances in the study of global terrestrial soil organic carbon sequestration. *Waste Management*, **28**, 734–740.
- Goebel, M.-O., Bachmann, J., Woche, S. K., and Fischer, W. R., 2005. Soil wettability, aggregate stability, and the decomposition of soil organic matter. *Geoderma*, **128**, 80–93.
- Golchin, A., Clarke, P., Oades, J. M., and Skjemstad, J. O., 1995. The effects of cultivation on the composition of organic matter and structural stability of soils. *Australian Journal of Soil Research*, **33**, 975–993.
- Gupta, V. V. S. R., and Germida, J. J., 1988. Distribution of microbial biomass and its activity in different soil aggregate size classes as affected by cultivation. *Soil Biology and Biochemistry*, **20**, 777–786.
- Jastrow, J. D., Amonette, J. E., and Bailey, V. L., 2007. Mechanisms controlling soil carbon turnover and their potential application for enhancing carbon sequestration. *Climatic Change*, **80**, 5–23.
- Kaiser, K., and Guggenberger, G., 2000. The role of DOM sorption to mineral surfaces in the preservation of organic matter in soils. *Organic Geochemistry*, **31**, 711–725.
- Kay, B. D., and Angers, D. A., 1999. Soil Structure. In Sumner, M. E. (ed.), *Handbook of Soil Science*. Boca Raton: CRC Press, pp. 229–276.
- Kemper, W. D., and Rosenau, R. C., 1986. Aggregate stability and size distribution. In Klute, A. (ed.), *Methods of Soil Analysis. Part 1. Physical and Mineralogical Methods – Agronomy Monographs*, 2nd edn. Madison: American Society of Agronomy, pp. 425–442.
- Kogel-Knabner, I., Ekschmitt, K., Flessa, H., Guggenberger, G., Matzner, E., Marschner, B., and von Lützow, M., 2008. An integrative approach of organic matter stabilization in temperate soils: Linking chemistry, physics and biology. *Journal of Plant Nutrition and Soil Science*, **171**, 5–13.
- Martens, D. A., 2000. Plant residue biochemistry regulates soil carbon cycling and carbon sequestration. *Soil Biology and Biochemistry*, **32**, 361–369.

- Mummey, D. L., Holben, W., Six, J., and Stahl, P. D., 2006. Spatial stratification of soil bacterial populations in aggregates of diverse soils. *Microbial Ecology*, **51**, 404–411.
- Plante, A. F., and McGill, W. B., 2002. Soil aggregate dynamics and the retention of organic matter in laboratory-incubated soil with differing simulated tillage frequencies. *Soil and Tillage Research*, **66**, 79–92.
- Puget, P., Chenu, C., and Balesdent, J., 1995. Total and young organic matter distributions in aggregates of silty cultivated soils. *European Journal of Soil Science*, **46**, 449–459.
- Puget, P., Chenu, C., and Balesdent, J., 2000. Dynamics of soil organic matter associated with particle-size fractions of water-stable aggregates. *European Journal of Soil Science*, **51**, 595–605.
- Pulleman, M. M., and Marinissen, J. C. Y., 2004. Physical protection of mineralizable C in aggregates from long-term pasture and arable soil. *Geoderma*, **120**, 273–282.
- Ranjard, L., Poly, F., Combrisson, J., Richaume, A., Gourbière, F., Thioulouse, J., and Nazaret, S., 2000. Heterogeneous cell density and genetic structure of bacterial pools associated with various soil microenvironments as determined by enumeration and DNA fingerprinting approach (RISA). *Microbial Ecology*, **39**, 263–272.
- Razafimbelo, T., Albrecht, A., Oliver, R., Chevallier, T., Chapuis-Lardy, L., and Feller, C., 2008. Aggregate associated-C and physical protection in a tropical clayey soil under Malagasy conventional and no-tillage systems. *Soil and Tillage Research*, **98**, 140–149.
- Sexstone, A. J., Revsbech, N. P., Parkin, T. B., and Tiedje, J. M., 1985. Direct measurement of oxygen profiles and denitrification rates in soil aggregates. *Soil Science Society of America Journal*, **49**, 645–651.
- Six, J., Elliott, E. T., and Paustian, K., 2000. Soil macroaggregate turnover and microaggregate formation: a mechanism for C sequestration under no-tillage agriculture. *Soil Biology and Biochemistry*, **32**, 2099–2103.
- Six, J., Conant, R. T., Paul, E. A., and Paustian, K., 2002. Stabilization mechanisms of soil organic matter: implications for C-saturation of soils. *Plant and Soil*, **241**, 155–176.
- Six, J., Bossuyt, H., Degryze, S., and Denef, K., 2004. A history of research on the link between (micro)aggregates, soil biota, and soil organic matter dynamics. *Soil and Tillage Research*, **79**, 7–31.
- Sollins, P., Homann, P., and Caldwell, B. A., 1996. Stabilization and destabilization of soil organic matter: mechanisms and controls. *Geoderma*, **74**, 65–105.
- Strong, D. T., De Wever, H., Merckx, R., and Recous, S., 2004. Spatial location of carbon decomposition in the soil pore system. *European Journal of Soil Science*, **55**, 739–750.
- Tisdall, J. M., and Oades, J. M., 1982. Organic matter and water-stable aggregates in soils. *Journal of Soil Science*, **33**, 141–163.
- Von Lützow, M., Kogel-Knabner, I., Ludwig, B., Matzner, E., Flessa, H., Ekschmitt, K., Guggenberger, G., Marschner, B., and Kalbitz, K., 2008. Stabilization mechanisms of organic matter in four temperate soils: development and application of a conceptual model. *Journal of Plant Nutrition and Soil Science*, **171**, 11–124.
- Yoder, R. E., 1936. A direct method of aggregate analysis of soils and a study of the physical nature of erosion losses. *Journal of American Society of Agronomy*, **28**, 337–351.
- Young, I. M., and Ritz, K., 2000. Tillage, habitat space and function of soil microbes. *Soil and Tillage Research*, **53**, 201–213.
- Zimmerman, A. R., Goyne, K. W., Chorover, J., Komarneni, S., and Brantley, S. L., 2004. Mineral mesopore effects on nitrogenous organic matter adsorption. *Organic Geochemistry*, **35**, 355–375.

Cross-references

- [Clay Minerals and Organo-Mineral Associates](#)
- [Earthworms as Ecosystem Engineers](#)
- [Management Effects on Soil Properties and Functions](#)
- [Microbes and Soil Structure](#)
- [Organic Matter, Effects on Soil Physical Properties and Processes](#)
- [Soil Aggregates, Structure, and Stability](#)

PHYSICAL QUALITY, SOIL

See [Soil Physical Quality](#)

PHYSICAL (MECHANICAL) WEATHERING OF SOIL PARENT MATERIAL

Stefan Skiba

Department of Pedology and Soil Geography, Institute of Geography and Spatial Management, Jagiellonian University, Cracow, Poland

Definition

Physical (mechanical) weathering is the granular disintegration of rocks and soils.

The processes of rock and mineral breakdown and disintegration taking place in the upper part (surface) of the lithosphere; minerals and rocks, which are the result of magmatic processes, diagenesis and metamorphism are not stable in the conditions on the surface and near the surface of the earth: they undergo changes that lead to the formation of new stable phases. Physical (mechanical) weathering is disintegration of rocks into blocks and grains of different size (block weathering, granular disintegration). Mechanical weathering leads to alterations in



Physical (Mechanical) Weathering of Soil Parent Material,
Figure 1 Insolation weathering on Hamada (Sahara Desert).



Physical (Mechanical) Weathering of Soil Parent Material,
Figure 2 Block weathering in Bieszczady Mts (Carpathians).

the rock cohesion, and the main causes are temperature (insolation, frost weathering) and humidity changes (salt weathering, clay rocks weathering). As a result of physical (mechanical) weathering, covers of various fraction are formed (rock, rubble, sand, silt, clay), and they provide parent material for pedogenesis. Genesis of the weathering covers, together with their evolution within the morphodynamic and soil-forming processes, determines the variety of taxonomical units that form the actual soil cover and its agrotechnical properties.

PHYSICO-CHEMICAL METHODS FOR REMEDIATION OF CONTAMINATED SOILS

Toshko Raytchev, Svetla Rousseva
Nikola Poushkarov Institute of Soil Science,
Sofia, Bulgaria

Definition

Contaminated soils are soils with increased content of compounds with harmful impact on vegetation, animals, and humans. Major contaminants are associated with heavy metals, organic compounds (mostly polyaromatic hydrocarbons, polychloride biphenyls, or chlororganic pesticides), and fertilizers.

Remediation technologies of contaminated areas are based on several basic approaches:

Activation of physico-chemical interactions, leading to the development of appropriate structural formations between the contaminants, the soil adsorbent, and the applied ameliorants. The aim is to influence the mobility of the contaminants.

Decreasing the mobility of the contaminants by their precipitation or co-precipitation in a form of chemical

compounds, which are less available for the vegetation. Organo-mineral liming is a traditionally applied method used mostly for detoxification of soil acidity as well as for soils contaminated with heavy metals and arsenic.

Increasing the mobility of the contaminants by intensification of their extraction through phytoextraction or applying of modified electrokinetics methods. Two strategies have been suggested: (a) *chelating* – addition of complex synthetic agents such as diethylene-triamine-penta-acetic acid/DTPA, nitrile-triacetic acid/NTA, or other natural products and (b) *soil acidification* – application of organic or inorganic acids (acetic or nitric) or fertilizers (as ammonium). Weakness – possibility for leaching of the contaminants toward subsoil or deeper layers.

Phytoremediation uses plants for transfer, stabilization, or annihilation of soil contaminants. It includes:

Phytostabilization – growing plants, which are tolerant to contaminants in the existing limits and stabilize the surface of contaminated soils.

Phytostimulation – is applied when the plants are stimulated by the existing excessive levels of the element or the group of compounds and/or their higher concentrations.

Phytoextraction – is using the opportunities of certain plant species to extract from soil or substrate excessive quantities of certain ions or compounds.

Phytoremediation is mainly applicable to contamination with heavy metals, pesticides, and petrochemicals. Weakness – the time requirements for economically viable recovery.

Electrokinetic remediation involves the application of direct current of low voltage through the soils between ceramic electrodes. Metal ions, ammonium ions, and positively charged organic compounds move toward the cathode. Anions (chlorine, cyanides, fluorine, nitrate and negatively charged organic compounds) are moving toward the anode. Extraction of contaminants is achieved by electroplating of the electrodes, precipitation or co-precipitation on them, pumping water from the space around electrode, or formation of complexes with ion-exchange resins.

Soil leaching – separation of contaminants from the selected soil volume in water system based on the size of soil particles. The leaching water may contain detergents, weak acids, or chelated agents to enable displacement of organics and heavy metals. Disadvantages – the method alone is not sufficient for remediation of contaminated soil.

In situ thermic methods are ways to transfer or mobilize of contaminants in soil and groundwater by heating. Movement through the soil is directed to underground drills for collecting and transferring toward the surface and subsequent implementation of some of the many available methods for remediation. The major advantage is the possibility for soil treatment without its digging and shifting.

Bibliography

<http://www.clu-in.org/remediation>

PHYSICS OF NEAR GROUND ATMOSPHERE

Evgeny V. Shein, Tatiana A. Arkhangelskaya
 Department of Soil Physics, Moscow State University,
 Moscow, Russia

Synonyms

Micrometeorology

Definition

Physics of near ground atmosphere is a branch of science studying physical processes within the near ground atmosphere mostly affected by the Earth surface.

Introduction

Physics of near ground atmosphere studies the processes of solar energy absorption and transformation in *soil–plant–atmosphere continuum*, and the regularities in forming the wind regime of plant environment. *Near ground atmosphere* is characterized by drastic changes of meteorological elements with height: the vertical gradients of wind speed, air temperature, and air humidity within the *near ground atmosphere* are tens and hundreds times greater as compared to corresponding gradients in the upper air layers. These gradients originate from *surface phenomena* – the interactions between soil, vegetation, air, and both short-wave and long-wave radiation. Physical processes, which take place within the *near ground atmosphere*, influence directly the agroecosystems' functioning and determine their productivity. So, we may point out that it is quite necessary for agrophysics both to develop the qualitative studies of the physical mechanisms of micrometeorological processes and to carry out the quantitative estimations of the intensity of energy and substance fluxes within the *near ground atmosphere*.

Physical processes

The Sun is a primary source of energy which is supplied to and redistributed in the *soil–plant–atmosphere continuum*. Solar radiation is a thermal radiation by its physical nature. Its spectrum and intensity are determined by the solar surface temperature (about 6,000 K) and are described by the laws of Stefan-Boltzmann, Planck, and Wien. About 99% of solar radiation is a shortwave radiation with wavelengths of 1×10^{-7} to 4×10^{-6} m. Solar spectrum includes the visible light with wavelengths $4-7.6 \times 10^{-7}$ m (47%), the infrared radiation with wavelengths of more than 7.6×10^{-7} m (44%), and ultraviolet radiation with wavelengths shorter than 4×10^{-7} m (9%). The maximum of the solar spectral intensity corresponds to the wavelength of 4.75×10^{-7} m in the green-blue area of visible spectrum (Khromov and Petrosyants, 1994).

Practically, all ultraviolet solar rays with wavelengths shorter than 2.9×10^{-7} m are entirely absorbed by ozone

when propagating through the Earth atmosphere and therefore do not achieve the Earth surface. Besides, the water vapor present in the atmosphere absorbs radiation within several intervals of visible and near-infrared spectral areas. So, the resulting spectrum of solar radiation coming to the Earth surface differs to some extent from that at the upper boundary of atmosphere.

The solar radiation income onto any surface is quantitatively characterized by the amount of energy supplied to unit surface area per unit time interval (W m^{-2}). In the case of parallel rays coming from a remote source, such as the Sun is for the Earth, one may speak about the intensity of radiation flux, which is equal to the amount of radiant energy, passing across the unit area section perpendicular to the direction of rays per unit time interval (W m^{-2}).

The intensity of solar radiation flux at the upper boundary of atmosphere varies throughout the year due to annual variability of the Earth–Sun distance. The average Earth–Sun distance is 1.496×10^{11} m; the corresponding value of solar radiation flux intensity is the solar constant $S_0^* = 1.367 \times 10^3 \text{ W m}^{-2}$ (Khromov and Petrosyants, 1994). About 30% of radiation coming to the upper boundary of atmosphere is reflected by the upper edge of clouds and is dissipated back to the cosmic space. Another 23% of incoming radiation is absorbed by water vapor, clouds, aerosol particles of atmospheric impurities, and ozone. Some of the remaining solar radiation is scattered within the atmosphere by atmospheric gases and aerosols. Due to these processes, the Earth surface gets both the direct solar radiation coming right from the Sun disk without changing the direction of rays while propagating through atmosphere and the diffuse sky radiation coming from the whole sky – from all directions possible. According to the Rayleigh law, the intensity of scattering of solar radiation within the atmosphere is inversely proportional to the wavelength of scattered rays: ultraviolet and blue rays are scattered much more effectively than red and infrared rays. Maximum of spectral intensity of scattered radiation is in the blue area of spectrum. This results in blue color of sky. The spectrum of direct solar radiation which avoided scattering is shifted to yellow area. The closer is the sun disk to the horizon and the longer is the way passed by solar beams propagating through atmosphere, the greater is the portion of scattered blue rays and the more yellow or even red is the Sun disk as seen by the on-ground observer.

The amount of direct solar radiation coming to the unit surface area per unit time interval is referred to as direct insolation of this surface. The direct insolation of a horizontal surface S' and the direct solar radiation flux S are related by formula $S' = S \sin h_{\text{sun}}$, where h_{sun} is the height of the Sun. The sum of direct insolation S' and the diffuse sky radiation D is (global) insolation, or global radiation Q : $Q = S' + D = S \sin h_{\text{sun}} + D$. The direct insolation of horizontal surface typical for July midday in Moscow is about 700 W m^{-2} for a clear sky and about 400 W m^{-2} for average cloudiness. The corresponding

values for global insolation are about 820 W m^{-2} and about 550 W m^{-2} .

Part of solar radiation is reflected from the Earth surface. The percent of reflected radiation Q_r depends on surface properties. The ratio $Q_r/Q = \alpha$ is the surface albedo (%). The albedo of a fresh snow is 80–85%, the albedo of dry soil varies between 15% and 35%, and the albedo of moist soil varies between 5% and 14%. The less the albedo is, the greater portion of solar energy is absorbed. Therefore, the lessening of surface albedo results in some extra amount of heat supplied into soil. In agrophysical practice, albedo is decreased by covering surface with dark films or black materials such as peat, soot, and the like.

It is important for agrophysical purposes and for the studies of production process that part of both incoming and reflected solar radiation may be accumulated during plant photosynthesis (Larcher, 2003). This part is a photosynthetically active radiation (PAR) with wavelengths $3.8\text{--}7.1 \times 10^{-7} \text{ m}$. About 50% of total solar radiation income to Earth surface is photosynthetically active radiation. But, only 1–3% of PAR is accumulated in the products of photosynthesis, and only rarely, in the cases of tropical forests, the sugarcane plantations and similar this value approaches 5%, and in the artificial conditions, 8% (Shein and Goncharov, 2006).

Most of the total shortwave solar radiation income is absorbed by the Earth surface and is transformed into heat. The heated surface emits its own thermal radiation with spectrum and intensity obeying the laws of Stefan-Boltzmann, Planck, and Wien – i.e., the same laws which describe the thermal emission of the Sun. But the temperature of the Earth surface is about 300 K, which is much less than that of the Sun surface. So the spectrum of Earth surface radiation is shifted to the long-wave interval of 4×10^{-6} to $1.2 \times 10^{-4} \text{ m}$ with maximum of spectral intensity at $1 \times 10^{-5} \text{ m}$. The intensity of surface long-wave radiation B_s depends on the surface temperature T_s and may be calculated using formula $B_s = \delta\sigma T_s^4$, where $\sigma = 5.7 \times 10^{-8} \text{ W m}^{-2} \text{ K}^{-4}$ is a Stefan-Boltzmann constant, $\delta = 0.95$ is emissivity factor for the gray body. For $T_s = 15^\circ\text{C} = 288 \text{ K}$, the intensity of surface thermal radiation $B_s = 373 \text{ W m}^{-2}$.

The long-wave surface radiation has a far lower air penetrating capability as compared with the shortwave solar radiation. The atmosphere is almost transparent for short-wave radiation and is almost opaque for long-wave radiation. So, about 80% of Earth surface thermal radiation is absorbed by *near ground atmosphere*, which results in heating of the latter. *Near ground atmosphere* is also heated due to the absorption of solar energy, though the portion of solar energy absorbed in the atmosphere is relatively small – about 15% of the whole income. The convective heat exchange within the *soil-plant-atmosphere continuum* and the condensation of water vapor evaporated from the Earth surface or transpired by plants also add to heating of the *near ground atmosphere*. But the main mechanism of this heating is the absorption of

long-wave radiation. The heated atmosphere also emits long waves obeying the same physical laws of thermal emission which describe the thermal emission of the Sun surface and the Earth surface. As the temperature of *near ground atmosphere* is close to the temperature of the Earth surface, the spectrum of atmospheric thermal radiation is close to that of the Earth surface. Atmosphere emits invisible long-wave radiation in the middle and the far-infrared spectrum areas. Due to the low penetrability of atmosphere for the long waves, they are absorbed and reemitted within the Earth-atmosphere continuum for many times before leaving the atmosphere and dissipating in the cosmic space. The part of atmospheric thermal radiation returns back to the Earth surface. This long-wave back radiation of atmosphere B_a is practically completely (95–99%) absorbed by the Earth surface being an important source of heat in addition to the solar radiation.

The radiation balance R of the Earth surface is a sum of all shortwave and long-wave radiation coming to and from the Earth surface:

$$R = S' + D - \alpha(S' + D) - B_s + B_a.$$

The difference between the Earth radiation and the back radiation of atmosphere is an effective radiation of Earth surface: $B_{\text{eff}} = B_s - B_a$. Taking into account $Q = S' + D$, the expression for the radiation balance may be rewritten as:

$$R = Q(1 - \alpha) - B_{\text{eff}}.$$

The radiation balance of Earth surface varies throughout day and night: in the daytime R is positive, during nighttime R is negative. The annual changes of the diurnal pattern of radiation balance are caused by changes in the height of the Sun and the day length. In Moscow, the clear sky midday radiation balance is about 500 W m^{-2} in July and only about 40 W m^{-2} in January. Radiation balance R is positive from 5 a.m. to 19 p.m. in July and from 10 a.m. to 14 p.m. in January (Khromov and Petrosyants, 1994). When speaking about the long-term average planetary data, the radiation balance is an incoming part of the Earth surface heat balance. All-planetary yearly Earth surface radiation balance is positive (Slatyer and McIlroy, 1961).

The essential constituents of Earth surface heat balance are the convective heat exchange between the Earth surface and the *near ground atmosphere* and the heat spent during evapotranspiration or released during condensation of water vapor.

Natural and forced convection are different: the natural convection is related to the upward movement of heated air, and the forced convection is related to wind and the wind-caused additional mixing of air masses. So, the intensity of convective heat exchange between the Earth surface and the *near ground atmosphere* depends on the surface temperature, the air temperature, and the wind speed.

It is important to accentuate the role of wind as a factor playing an important role in the formation of both heat and

humidity balance between *near ground atmosphere* and soil (Van Wijk, 1963). Lateral incomes of heat and water vapor and the heat exchange in the air layers are based on wind – the horizontal movement of air. The wind is a result of nonuniform heating of Earth surface. Therefore, the movement of air masses transfers heat from the places which are more heated by the Sun to the cooler places. In agrophysics, the local circulation is usually studied. It is necessary to distinguish between the horizontal and the vertical mass and heat transfers. The vertical transfer is primarily based on the mechanism of turbulent diffusion and the horizontal one, on advection. Turbulent diffusion is the result of movement of some air volumes, air currents at the boundaries between air layers. In laminar layers, the heat and vapor transfers are realized through the molecular diffusion due to the chaotic Brownian movement of molecules. At turbulent diffusion, these transfers are much faster and, say, more effective due to the mechanism of air currents. In most cases when studying phenomena at the landscape scale, the average free path of separate currents is of much higher order than that of separate molecules. So, the intensity of mass and heat transfer by turbulent diffusion is much higher than that by molecular one.

It should be said separately about the phenomenon of advection – the movement of air masses from other parts of the Earth to the place of interest. If the incoming air has a higher temperature, one can speak about the advection of heat; if the incoming air has a lower temperature, one can speak about the advection of cold. Due to the advection, the convective heat exchange is an incoming part of the planetary surface heat balance (Slatyer and McIlroy, 1961). This fact may seem to contradict the physics of absorption and redistribution of heat in *near ground atmosphere*: indeed, the sunlight passes through the atmosphere almost without being absorbed and therefore almost without heating the atmosphere. The absorption of solar energy and its transfer to heat occurs at the Earth surface, which is heated and therefore emits the long waves. It is this long-wave radiation emitted by the Earth surface which is the main source of heating the *near ground atmosphere*. Therefore, the *near ground atmosphere* is heated by the Earth surface, and the opposite is not true. The fact that the average planetary convective heat flux is directed from the *near ground atmosphere* to the Earth surface is related to advection: air which was heated after absorbing the surface radiation in the hot areas of planet moves to the cooler areas and transmits the heat it brought to the local surface by means of convective heat exchange.

So, both the radiation and the convection are the incoming components of the annual heat balance of planet surface. An essentially negative, spending component of the surface heat balance are the heat losses related to evapotranspiration. These heat losses depend on the surface temperature, air temperature, surface moisture conditions, air humidity, and wind speed. They distinguish between the evaporation from soil or water surface and vegetation

transpiration; the combination of these two processes is evapotranspiration.

The last part of the Earth surface heat balance is the heat flux into the soil G . The heated surface transmits the heat not only to the *near ground atmosphere* but also into the deep soil layers too. The amount of energy transferred to the deep soil layers depends both on the micrometeorological conditions at the surface and on *soil physical properties*, which are related to such relatively permanent soil properties as *soil bulk density*, *soil texture*, *parent material*, *organic matter*, *soil aggregation*, and *surface roughness*. Besides, *soil physical properties* are continually changing during *wetting and drying of soil*.

The surface heat balance equation may be written as follows:

$$Q(1 - \alpha) - B_{\text{eff}} - H - LE - G = 0,$$

where H is the convective heat flux, E is the intensity of evapotranspiration per unit surface area, $L = 2.514 \times 10^6$ J/kg is the specific heat of evaporation for water.

In the daytime Q is always positive and at night $Q = 0$. The effective radiation of the Earth surface B_{eff} may be both positive and negative, depending on the state of *near ground atmosphere*. The convective, evaporative, and soil heat fluxes also may be both positive and negative.

The physics of interactions between the *near ground atmosphere* and the Earth surface is basically the same for any types of this surface. The physical mechanisms discussed above work for bare soil, for the soil covered by vegetation or by snow, and even for open water surface. The same mechanisms determine the heat fluxes within the vegetation cover and the *energy balance in agrosystems*.

Conclusions

The physical processes in *near ground atmosphere* are interrelated processes. Besides, they are quick processes: the physical picture of what is happening in the *soil–plant–atmosphere continuum* may change dramatically within a few seconds. Examples are the abrupt change of the Sun disk state or a sudden blast. The physical processes in the *near ground atmosphere* are also characterized by the spatial variability, which is related to the *spatial variability of soil physical properties*, the vegetation cover properties, and the microrelief conditions. Open question is the quantitative estimation of energy and substance fluxes in *soil–plant–atmosphere continuum* for small time and space scales, which is required to forecast the ecosystem functioning during possible *climate changes* and also to create artificial agroecosystems.

Bibliography

- Khromov, S. P., and Petrosyants, M. A., 1994. *Meteorology and Climatology*. Moscow: MSU, in Russian.
Larcher, W., 2003. *Physiological Plant Ecology*, 4th edn. Berlin: Springer.

- Shein, E. V., and Goncharov, V. M., 2006. *Agrophysics*. Rostov-na-Donu: Phoenix, in Russian.
- Slatyer, R. O., and McIlroy, I. C., 1961. *Practical Microclimatology*. Paris: UNESCO.
- Van Wijk, W. R. (ed.), 1963. *Physics of Plant Environment*. Amsterdam: North Holland.

Cross-references

- [Bulk Density of Soils and Impact on their Hydraulic Properties](#)
[Climate Change: Environmental Effects](#)
[Energy Balance of Ecosystems](#)
[Organic Matter, Effects on Soil Physical Properties and Processes](#)
[Parent Material and Soil Physical Properties](#)
[Soil Aggregation and Evaporation](#)
[Soil–Plant–Atmosphere Continuum](#)
[Spatial Variability of Soil Physical Properties](#)
[Surface Properties and Related Phenomena in Soils and Plants](#)
[Surface Roughness, Effect on Water Transfer](#)
[Wetting and Drying, Effect on Soil Physical Properties](#)

PHYSICS OF PLANT NUTRITION

Evgeny V. Shein
 Department of Soil Physics, Moscow State University,
 Moscow, Russia

Definition

Physics of plant nutrition is the part of agrophysics that deals with the physical processes of mineral nutrient exchange, migration, and root consumption from soil.

Introduction

Being a part of agrophysics, physics of plant nutrition deals with the physical fundamentals of exchange of ions in diffusive double layer (DDL), their transfer to roots and within plants. As a rule, studies and the description of mentioned processes are conducted on a microscale; they consider equilibrium exchange and transport of separate ions in soil and root, special features of this transport, connected with characteristics of ions, soil solid phase and porous media, and root systems as well (Shein and Goncharov, 2006).

In some amount or other, 16 elements, forming groups of macro-, secondary, and microelements, are needed by a majority of plants. Each element plays its specific role. However, the fact that 95% of a plant consists of C, H, and O, which are received by plants from CO₂ of air and soil water, should be considered. The rest of the 13 elements are taken out by plants from soil solute in ionic form, though sometimes plants can take out and assimilate S and Cl from air in the form of SO₂ and Cl₂. A unique ability of leguminous plants to fix atmospheric nitrogen due to symbiosis with *Rhizobia* in root zone should be remembered as well. Sodium, silicon, cobalt, and vanadium can promote yield growth, but they do not determine its forming. Sometimes Na performs the function of K,

i.e., in beet plants, and Co can play a significant role in generating B₁₂, which takes part in nitrogen fixation by *Rhizobia*.

The importance of this part of agrophysics is determined by the fact that the physics of plant nutrition is central to the scientific regulation of the production process, the use of mineral fertilizers, evaluation and prognosis of plant growth in relation to features of nutrient transport in soil, and their availability to plants.

Physical processes

Two processes – convection and diffusion – are the main physical processes providing nutrient delivery and transfer to roots in ionic form. Convection is a movement of substances with solute mass flux. This flux to a vegetating plant is always supported by transpiration. That is why this mechanism of ion transport to root and throughout the whole plant is quite possible. Additionally, plants are able to take up selectively some ions, which are most important for their growth and development. This transfer is affected by concentration drops, as ion concentration in and around roots is less than that in soil solute, and the lower it is, the higher is the demand. Correspondingly, the more is concentration gradient between root surface and soil solute, the faster is a diffusive flux, and at that a plant is able to consume the most part of positively charged biophile elements from absorbed state by means of exchange reactions on DDL–soil solute and soil solute–root surface interfaces. Appropriate nutrient ions are delivered due to diffusion and convective solute flux to roots. A presence of these ions in soil solute is regulated by exchange reactions with corresponding DDL ions, which in their turn are also adjusted by activities (concentrations) of consumed ions in a solute.

The important role of *convection* in substances movement and their uptake by roots was revealed in the experiment, undertaken by Barber (1988). It might be suggested, that as a large amount of soil solute is delivered to plants to support transpiration flux, this very transfer would provide a receipt of a major part of nutrients. Barber used the balance method: knowing element content in a plant and its transpiration ratio (amount of water needed to form a unit of dry biomass), a concentration of this element in soil solute, necessary to draw up a balance, was calculated. Furthermore, a concentration of an element obtained in this balance calculation was compared with its real one in soil solute. If element concentration in soil solute is higher than the rated one, a supply of this element for plants can be provided by a convective flux alone. If lower, and element is taken by means other mechanisms, primarily by diffusion. The results of Barber experiment are given in Table 1.

Thus, it is obvious that K and P ions are taken from solute more rapidly than by convection. These ions are transferred by means of diffusion. It should be noted therewith, that ion diffusion in soil is a rather long-term process. Indeed, the diffusion coefficient for a majority of solute

Physics of Plant Nutrition, Table 1 A possibility of element takeover by plants in the form of convection with total transpiration flux

Element	Content in plants (mg g ⁻¹)	Necessary rated concentration in soil solute (mg L ⁻¹)	Real concentration in soil solute (mg L ⁻¹)	Possibility of element supply by means of convection
Ca	2.2	4.4	33.0	Possible
Mg	1.8	3.6	28.0	Possible
K	20.0	40.0	4.0	Impossible
P	2.0	4.0	0.5	Impossible

ions is no more than $1.73 \text{ cm}^2 \text{ day}^{-1}$. This coefficient is 1.71 for K^+ , 1.64 for NO_3^- , and 0.67 and $0.6 \text{ cm}^2 \text{ day}^{-1}$ for Ca^{2+} and Mg^{2+} respectively. At the same time, with porous media tortuosity and real water content in soil taken into account, it becomes necessary to use the effective coefficient of salt diffusion, which is usually two to three orders lower, instead of the diffusion one. According to Barber (1988), an ion of potassium can move no more than on 0.13 cm a day by means of diffusion, and H_3PO_4^- can move on yet less – only 0.004 cm a day. Thus, not only do ions move toward a root due to diffusion, but also a root itself is to “move,” to grow in order to get the needed amount of nutrients. Evidently, this factor of active root growth and development of new spaces in soil may determine nutrient supply for plants, and not just physical processes of convective and diffusive transfer of nutrients to roots. It is rather difficult to estimate the significance of this factor in direct experiments, as it is hard to separate processes of nutrient transfer to root due to a diffusion and root growth toward higher ion concentration. This kind of research can be held only with the help of mathematical modeling, making possible to assign individual parameters characterizing particular processes, and then to evaluate a relative influence of each parameter on resulting substance uptake one after another, assuming others to be constant. Let us look at this kind of model analysis with the help of mathematical model of nutrient consumption by root, developed by Barber and Cushman (1981).

Two major processes of ion transfer to root, a diffusion $(\frac{\partial c}{\partial t})_{\text{diff}}$ and a convection $(\frac{\partial c}{\partial t})_{\text{conv}}$, are described by the following equations:

$$\left(\frac{\partial c}{\partial t}\right)_{\text{diff}} = -D_h \frac{\partial^2 c}{\partial r^2}, \quad (1)$$

$$\left(\frac{\partial c}{\partial t}\right)_{\text{conv}} = v \frac{\partial c}{\partial r}, \quad (2)$$

where c is an ion concentration in pore solute, t is time, D_h is a hydrodynamic diffusion coefficient, r is a radius of a zone where nutrient consumption takes place, v is a macroscopic velocity of solute flux (i.e., an averaged movement velocity in soil capillaries).

In addition, an exchange of dissolved and absorbed ions takes place by a mechanism of instant linear absorption, i.e., according to the following equation:

$$c_3 = k_d \cdot c, \quad (3)$$

where c_3 is a concentration of an ion in absorbed state, k_d is a distribution constant.

This process produces an additional source-and-flow factor – J_s . As a whole, nutrient transfer to root can be expressed by an already known convective-diffusion equation, but written in cylindrical coordinates, as a flux to root is directed along a radius to a centrally set root

$$\frac{\partial c}{\partial t} = -\frac{1}{r} \cdot \partial \partial r \left(r D_h \frac{\partial c}{\partial r} + v c r_0 \right) \pm J_s, \quad (4)$$

where r_0 is a root radius.

A growth factor in the form of root growth coefficient K_r is also input, as well as a condition on root boundary in a form of nutrient consumption (J_r) according to Michaelis–Menten equation

$$J_r = \frac{J_{\max} \cdot K_m c}{1 + K_m c} - c_{\min}, \quad (5)$$

where J_{\max} is a nutrient flux in a root, maximum possible for a particular plant, K_m is the Michaelis constant, equal to an ion concentration in solute, at which the absorption reaches a half of its maximum value ($0.5 J_r$). Physically, this constant shows, how actively a plant can uptake nutrients from solute; the higher it is, the more active is a nutrient uptake by plant, c_{\min} is a minimum concentration of nutrients in solute, at which its uptake is possible.

Model development is based on the assumptions that soil is homogeneous, hydrodynamic diffusion and linear sorption rates do not depend on concentration, a root is cylindrical, and there is no microbial activity. These combined assumptions help to develop a numerical model and conduct its test for the sensitivity to particular parameters. A sensitivity test is a study of change in ion uptake by root at alternating change of each of model parameters. In a resultant notation, these parameters, both of plant and soil, are presented in Table 2.

Regarding these parameters, the analysis of K^+ uptake model results into the following. K^+ uptake mostly depends on root growth rate and radius (K_r and r_0 correspondingly), and it is these parameters change that causes maximum increase of the consumption. Soil parameters have much less influence on of K^+ uptake. At the same time, the Michaelis constant rise causes uptake decrease, which is the required result, as this parameter denotes a

Physics of Plant Nutrition, Table 2 The parameters of a model of ion uptake by plant roots

Plant parameters	Soil parameters
r_0 – root radius	c – nutrient concentration in pore solute
c_{\min} – minimum solute concentration, at which an uptake is possible	D_h – hydrodynamic diffusion
J_{\max} – the maximum possible uptake	K_d – distribution coefficient
K_m – the Michaelis constant	v – water flux to root
K_r – the parameter of root growth rate	

concentration, at which the absorption reaches a half of its maximum value. The more is this concentration, the less is the ability of a plant to uptake nutrients. The suggested physically validated model underlines parameters importance in regulation of ion flux in plant nutrition.

Conclusions

Nutrients delivery to roots, determining plant nutrition, goes in the form of convective and diffusive fluxes. Biophile elements like Ca^{2+} and Mg^{2+} can be transferred to roots by a convective flux simultaneously with total transpiration flux of solutes within a plant. Other biophile elements (potassium, phosphorus) are delivered to roots by means of diffusion.

Nutrients uptake rate is mostly determined by parameters like roots growth rate and their average diameter. This rate increase is much less at that of nutrient concentration in pore solute (c), hydrodynamic diffusion (D_h), distribution coefficient (K_d), and microscopical velocity of water flow to roots (v), which are physical transport parameters, related to soil conditions.

Bibliography

- Barber, S. A., 1988. *Biological Availability of Nutrients in Soil: Mechanistic Approach*. Moscow: Agropromzdat (Russian translation).
 Barber, S. A., and Cushman, J. H., 1981. Nitrogen uptake model for agronomic crops. In Iskandar, I. K. (ed.), *Modeling Waste Water Renovation-Land Treatment*. Wiley-Interscience: New York, pp. 382–409.
 Shein, E. V., and Goncharov, V. M., 2006. *Agrophysics*. Rostov-on-Don: Phoenix (in Russian).

Cross-references

- [Diffuse Double Layer \(DDL\)](#)
[Evapotranspiration](#)
[Infiltration in Soils](#)
[Plant Roots and Soil Structure](#)
[Root Responses to Soil Physical Limitations](#)
[Root System Architecture: Analysis from Root Systems to Individual Roots](#)
[Soil Aggregation and Evaporation](#)
[Soil Water Flow](#)
[Solute Transport in Soils](#)
[Water Uptake and Transports in Plants Over Long Distances](#)

PIEZOMETER HEAD

The elevation at which water stands in a piezometer in reference to a point in question in the soil.

PLANCK'S LAW

The intensity distribution of radiation (energy flux in a given wavelength range) emitted from a body as a function of absolute temperature.

PLANT BENDING

See [Bending Properties of Plants](#)

PLANT BIOMECHANICS

Tomasz Rusin¹, Paweł Koj²

¹MTS Systems Corporation, Warsaw, Poland

²Polish Academy of Sciences, Botanical Garden – Center for Biological Diversity Conservation, Warsaw, Poland

Synonyms

Mechanics of plants

Definition

Biomechanics – mechanics of living body; science of mechanical aspects of living bodies; *plant biomechanics* – interdisciplinary science describing behavior of plants subjected to forces and displacements at the level of molecules, cells, tissues, organs, whole organisms, and ecosystems. Because plant cells are surrounded by cell wall which gives the cells their shape and protection, it is the mechanical properties of the cell wall and its building materials which are of special interest to plant biomechanics studies. Mechanical changes in cell wall subjected to internal and external forces influence plant cell growth and morphogenesis.

Historical perspective

Some special mechanical features of the plant tissues and organs have been long known to man. Egyptians knew that dry wood when watered expands generating high forces. The same principles was used in many cultures for building different sorts of barrels. For more than 2,000 years it was known to man that the best material for making bows (the English longbow) was yew (*Taxus* species). It could take up to 4 years to make a good bow. The inner side of the bow consisted of heartwood (more resistive to compression) and the outer side of sapwood (more resistive in tension). This was one of the first

laminates used by men for the construction of a composite bow. The only other bow with comparable range and draw force was that Mongol bow of Genghis Khan – that was another composite made of horn (compression) and tendon (tension) (<http://www.huntingociety.org/MongolArchery.html>).

One of the first descriptions of the importance of mechanical factors (water flow) in plant growth and function was given by Leonardo da Vinci (<http://www.britannica.com/EBchecked/topic/336408/Leonardo-da-Vinci/59786/Mechanics-and-cosmology>).

In the second half of the nineteenth century many botanists performed experiments with the mechanical influence on the growth of algae, herbaceous plants, and trees. Julius von Sachs invented clinostat and used it in research on gravitropism and gravimorphism (Sachs, 1879). First experiment on the effect of mechanical traction on growth of sunflower seedlings was performed by Hegler (1893). In this experiment plants grew under longitudinal pull for 2 days. After this time their breaking strength increased nearly two times in comparison to their original breaking strength. Hegler noticed anatomical changes in plants grown under tension. They developed thicker cell walls and more mechanical tissue as he called epidermal and subepidermal cells. Plant biomechanics was greatly advanced by Wilhelm Pfeffer (Bunning, 1989; Pfeffer, 1904). Later the work on mechanical factors in plant development and adaptation to mechanical stimuli was continued by Bordner (1909), Newcombe (1895), Ball (1904), and many others. With increase of interest in biochemistry, plant biomechanics was not present in main stream botanical research for many years. With onset of the space race between east and west, more and more scientists investigated gravitropism and gravimorphism. Modern interest in plant biomechanics was catalyzed by the fact that biochemistry alone was not able to explain basic growth, development, and adaptation phenomena observed in plants. The most important contributors which brought plant biomechanics to mainstream botany were Niklas (1992), Vincent (1992), Steudle et al. (1977), Speck et al. (1996), Spatz et al. (1999), Mattheck (1998), Hejnowicz and Sievers (1995a, b), Cosgrove (1986, 1993), and many others.

Plant biomechanics

Plants in their environment are subjected to mechanical factors like gravity, wind, water flow, friction, and changes in temperature, pressure, and humidity. Plant biomechanics measures the mechanical response of plants and their building blocks to these mechanical factors and in reverse plant biomechanics explains how mechanical factors influence growth and development of plants.

Research in plant biomechanics focuses on the cell wall (Whitney et al., 1999) because it determines the shape of cells, tissues, organs, and whole plants. In a single celled plants the mechanical properties of cells depend on positive hydrostatic pressure (turgor) exerted by protoplast

on cell wall (Cosgrove, 1986). The simplest model representing this behavior would be balloon filled with water. Protoplast is compressed and cell wall is stretched. In herbaceous plants mechanical properties of organs depend on turgor and on tissue stresses. Tissue stresses arise in effect of interplay between tissues that differ mechanically – simplest case thick walled epidermal cells with small protoplast and thin walled parenchymal cells with large protoplast. As a result one tissue (for example epidermis) is under tension and other (parenchyma) under compression (Hejnowicz and Sievers, 1995a). In woody plants, in addition to turgor and tissue stresses, there are growth stresses that govern mechanical behavior of organs.

Studies on single intact cells can be performed using pressure probe technique developed by Steudle et al. (1977) and Tomos and Leigh (1999). This technique enables to measure mechanical properties of cell wall and turgor/cell wall deformation relations.

It is possible to measure local properties of cell wall at the scale of nanometers using nanoindenters. Some researchers measure mechanical behavior of single cells on universal testing machines (UTM). Instead of using small machines it is possible to use extra large cells of algae, for example, *Chara* species. Mechanical test using UTM can be performed also on isolated tissue in vitro and on whole organs (isolated or in vivo). Universal testing machines can be used both for the induction of mechanical stimulus and for measurement of plant response to that stimulus. Because modern UTM are computer controlled by very sophisticated software they can accurately reproduce any mechanical stimulus by precise application of force and displacement, stress, strain, energy, etc. UTM have very high displacement and force resolution. Standard force sensors (load cells) of 0.1 N capacity have 0.001 N accuracy. Standard displacement accuracy is about 1 μm. Recent developments in optical measurement techniques enable scientists to measure displacement and strain with unprecedented accuracy. Techniques of Digital Image Correlation (DIC) and Electronic Speckle Pattern Correlation (ESPI) enable full field (3D) displacement and strain measurement. For example, ESPI systems can measure area of 10×20 mm with 30 nm resolution.

UTM can be equipped with special chambers controlling accurately temperature, humidity, water flow, pH of the media. Measurements with UTM can be further enhanced by the use of special grips, gages, and adapters.

In situ plant tissues are rarely subjected to uniaxial stress; therefore, some researchers use specialized material testing machines capable of applying bidirectional stress to plant material – for example, isolated plant epidermis. This technique enables creation of planar biaxial stress field which more closely mimics the real stress field to which some tissues are subjected *in situ*.

Some biomechanical laws apply to the whole population of plants. The trees growing at the peripheral part of the forest are usually smaller because they are subjected

to stronger winds than trees deeper in the forest. But at the same time these trees are tougher than the tall trees inside forest. One could say that the trees at the periphery protect trees inside forest from strong wind.

From the perspective of material sciences plant cell wall is a highly complex anisotropic polymer. Most of the plant tissues can be considered as cellular solids which exhibit viscoelastic behavior. Many plants take advantage of the prestresses to optimize the use of the material (tissue) without compromising their mechanical strength. This building principle is widespread in all living organism at many different levels and is termed tensegrity (Ingber, 1998). Living plant cells, tissues, and organs have few important features which differentiate them from even most advanced man made materials. Their ability for self repair, self optimization, self cleaning, adaptation to mechanical environment, and biodegradability make them most sophisticated material known to men. Using biomechanical approach to plant structure and function we can learn a lot not only about plants but we can copy some of their patents and create materials with some of these features (biomimetics, bionics).

Summary

Plant Biomechanics is a large field of research with wide range of interest but which is unified by the tools and mathematical definitions used by physical sciences and mechanical engineering. Today it is a main stream research helping to understand plant growth, development, as well as structure–function relationships. Plant biomechanics help to understand evolutionary trends and adaptation to wide variety of physical conditions that exist in water, air, and soil. Niklas et al. (2006) divide plant biomechanics into subfields interested in cell wall and plant growth, tissue mechanical properties, mechanoperception and posture control, tree biomechanics, hydraulics and wood anatomy, and ecology. Plant Biomechanics gained a lot from engineering approach to plant structure and function but today we also see a reversed trend – the more we know about mechanics of plants the more nature inventions find practical use in modern technology (biomimetics, nanotechnology) (Milwiche et al., 2006; Forbes, 2008).

Bibliography

- Ball, O. M., 1904. Der Einfluss von Zug auf die Ausbildung von Festigungsgewebe. *Jahrbuch für Wissenschaft und Botanik*, **39**, 305–341.
- Bordner, J., 1909. The influence of traction on the formation of mechanical tissue in stems. *Botanical Gazette*, **48**, 251–274.
- Bunning, E., 1989. *Ahead of His Time: Wilhelm Pfeffer – Early Advances in Plant Biology*. Ottawa, Ontario, Canada: Carlton University Press.
- Cosgrove, D. J., 1986. Biophysical control of plant cell growth. *Annual Review of Plant Physiology*, **37**, 377–405.
- Cosgrove, D. J., 1993. Wall extensibility: its nature, measurement, and relationship to plant cell growth. *New Phytologist*, **124**, 1–23.

- Forbes, P., 2008. Self-cleaning materials: lotus leaf-inspired nanotechnology. *Scientific American Magazine*, July 30, 2008.
- Hegler, R., 1893. Ueber den Einfluss des mechanischen Zugs auf das Wachstum der Pflanze. *Beiträge zur Biologie der Pflanzen*, **6**, 383–432.
- Hejnowicz, Z., and Sievers, A., 1995a. Tissue stresses in organs of herbaceous plants. I. Poisson ratios of tissues and their role in determination of the stresses. *Journal of Experimental Botany*, **47**, 519–528.
- Hejnowicz, Z., and Sievers, A., 1995b. Tissue stresses in organs of herbaceous plants. II. Determination in three dimensions in the hypocotyl of sunflower. *Journal of Experimental Botany*, **46**, 1045–1053.
- Ingber, D. E., 1998. The architecture of life. *Scientific American*, **278**, 48–57.
- Mattheck, C., 1998. *Design in Nature*. Heidelberg: Springer Verlag.
- Milwiche, M., Speck, T., Speck, O., Stegmaier, T., and Planck, H., 2006. Biomimetics and technical textiles. Solving engineering problems with the help of nature's wisdom. *American Journal of Botany*, **93**, 1455–1465.
- Newcombe, F., 1895. The regulatory formation of mechanical tissue. *Botanical Gazette*, **20**, 441–448.
- Niklas, K. J., 1992. *Plant Biomechanics: An Engineering Approach to Plant Form and Function*. Chicago, IL: University of Chicago Press.
- Niklas, K. J., Spatz, H.-Ch., and Vincent, J., 2006. Plant biomechanics: an overview and prospectus. *American Journal of Botany*, **93**, 1369–1378.
- Pfeffer, W., 1904. Kraftwechsel. *Lehrbuch der Pflanzenphysiologie. Band 2*. Leipzig.
- Sachs, J., 1879. Ueber Ausschliessung der geotropischen und heliotropischen Krümmungen während des Wachsthums. *Würzburger Arbeiten*, **2**, 209–225.
- Spatz, H.-Ch., Köhler, L., and Niklas, K. J., 1999. Mechanical behavior of plant-tissues: composite-materials or structures. *Journal of Experimental Biology*, **202**, 3269–3272.
- Speck, T., Rowe, N. P., Brückert, F., Haberer, W., Gallenmüller, F., and Spatz, H.-Ch., 1996. How plants adjust the “material properties” of their stems according to differing mechanical constraints during growth: an example of smart design in nature. *Bioengineering – PD-Volume 77, Proceedings of the 1996 Engineering Systems Design and Analysis Conference, Volume 5*, ASME, pp. 233–241.
- Steudle, E., Zimmermann, U., and Luettge, U., 1977. Effect of turgor pressure and cell size on the wall elasticity of plant cells. *Plant Physiology*, **59**, 285–289.
- Tomos, A. D., and Leigh, R. A., 1999. The pressure probe: a versatile tool in plant cell physiology. *Annual Review of Plant Physiology and Plant Molecular Biology*, **50**, 447–472.
- Vincent, J. F. V., 1992. Plants. *Biomechanics-Material: A Practical Approach*. Oxford: IRL Press at Oxford University Press.
- Whitney, S. E. C., Gothard, M. G. E., Mitchell, J. T., and Gidley, M. J., 1999. Roles of cellulose and xyloglucan in determining the mechanical properties of primary plant cell walls. *Plant Physiology*, **121**, 657–663.

Cross-references

- [Bending Properties of Plants](#)
[Biospeckle](#)
[Crop Responses to Soil Physical Conditions](#)
[Databases on Physical Properties of Plants and Agricultural Products](#)
[Diurnal Strains in Plants](#)
[Rheology in Agricultural Products and Foods](#)
[Stress–Strain Relations](#)
[Tensiometry](#)
[Windbreak and Shelterbelt Functions](#)

PLANT DISEASE SYMPTOMS, IDENTIFICATION FROM COLORED IMAGES

Anyela Valentina Camargo Rodriguez, Jan T. Kim
School of Computing, University of East Anglia,
Norwich, UK

Definition

Apoptosis: Programmed cell death.

Attribute: A categorical or numerical characteristic of a target object (region).

Classification: Designation of a class label to an object, or to multiple objects.

Classifier: A function that designates class labels to input objects, thus performing classification.

Generalization: The ability of a classifier to designate correct labels to samples that are not part of the training set, i.e., to “predict” the correct label.

Learning (or training): Computational construction of a classifier.

Mathematical morphology: Thinning (erosion) or expansion (dilation) of a region. It assesses pixel similarity by estimating a measurement of distance between two neighboring pixels.

Overfitting: Object misclassification due to poor generalization.

Pathogen: An agent that causes disease, e.g., a microorganism such as a bacterium or fungus.

Postprocessing: Enhancement of regions for attribute determination.

Preprocessing: Enhancement of a raw image for segmentation (or other subsequent process).

Segmentation: Subdivision of an image into different regions.

Supervised learning: Learning based on labeled training data. Supervised learning aims to learn how attributes determine the class label.

Training data: Data used for training. Each data sample consists of a given set of attributes. Labeled data also provide the correct class label for each sample.

Unsupervised learning: Learning based on unlabeled training data. Unsupervised learning includes generating class labels, e.g., by partitioning the training data into clusters.

Introduction

Plants are constantly attacked by pathogen-related diseases and pests. Plants have developed complex, coordinated, and targeted mechanisms of defense that produce responses specific to the attack or stress. For example, plants induce apoptosis when attacked by a biotrophic pathogen, thus depriving it of food. On the contrary, plants do not induce apoptosis when attacked by necrotrophic pathogens which feed on dead tissue. They instead fight off the pathogen by using most of their energy sources to the protection of the affected area (Glazebrook, 2005).

Plants show different responses to stress. Depending on the attack they are under, different defense mechanisms are triggered. Under some circumstances plants might turn pale, slow down their development, or shed their fruits before time. Conspicuous visual signs of stress include cankers, streaks, and spots on leaves, stems, and fruits (Camargo and Smith, 2009). These visual symptoms of a disease can sometimes be perceived by the naked eye at an early stage. They can be used as the first step in a disease identification program where digital images of diseased regions of a plant are used to assess, by automatic or manual means, the current state of the crop. The ultimate purpose of this analysis is to reduce the economic loss that is caused when a disease is not countered in time (Chakraborty et al., 2000). The use of methods for the early detection of plant diseases have become increasingly important as social and biological factors such globalization, climate change, human mobility, and pathogen and vector evolution have forced plant pathogens to adapt to new environments more rapidly. The consequences of this rapid adaptation can be gauged by the way disease outbreaks are nowadays more frequent, more rapid and more severe.

Plant disease identification by the computerized assessment of colored images can be used as a tool to help farmers identify the presence of a disease when it is still possible to control it (Qin et al., 2009; Boissard et al., 2008; Gómez-Sanchis et al., 2008; Pydipati et al., 2006).

Machine vision for image classification

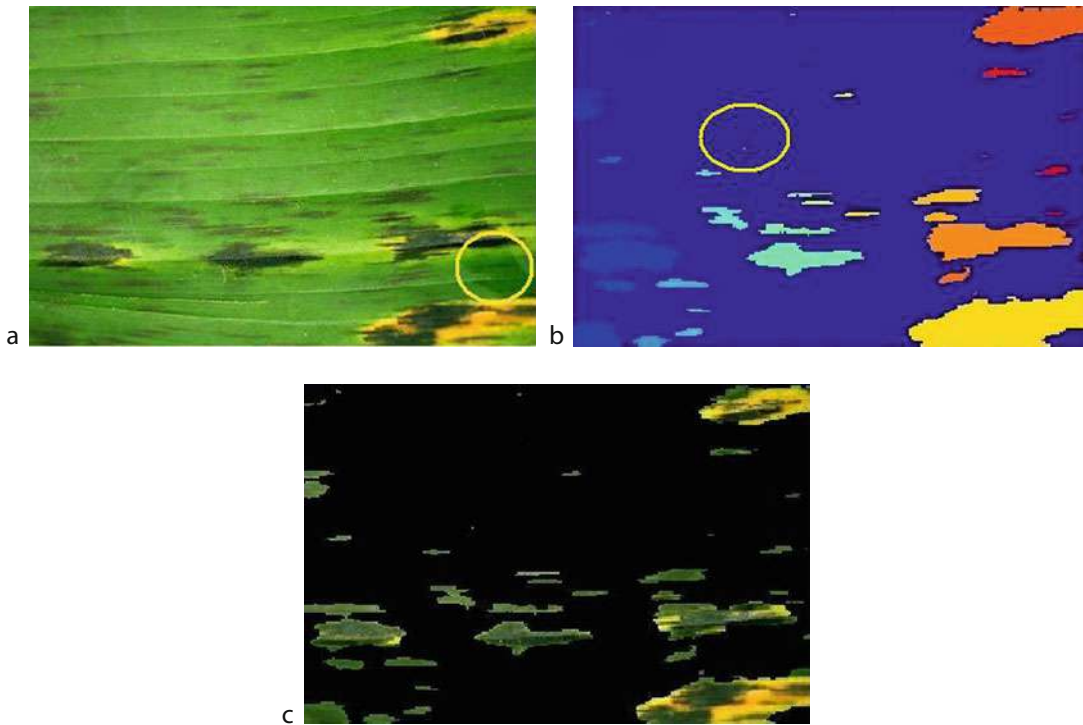
A machine vision system takes images as input and classifies them. A typical image analysis procedure includes the steps of (1) preprocessing the image, (2) segmenting the image to extract regions of defined relevance for classification and postprocessing the regions, (3) using a fixed set of attributes to characterize each region, and (4) using a classifier to designate a label to each region, based on its attributes. The choice of the segmentation method and of region attributes is critical for the performance of a machine vision system. For plant disease classification, segmentation is typically designed to identify regions that are affected by the disease (e.g., necrotic zones), and attributes are chosen to reflect characteristics such as color or aspects of shape. Figure 1 shows a raw image, segmentation, and the raw regions.

Distances

Many methods for image segmentation and for classification are based on distance measures. Such measures provide non-negative values that characterize how far two objects are apart. The Euclidean distance

$$d(\mathbf{x}, \mathbf{y}) = \sqrt{(\mathbf{x} - \mathbf{y})^T (\mathbf{x} - \mathbf{y})} = \sqrt{\sum_i (x_i - y_i)^2} \quad (1)$$

of two vectors $\mathbf{x} = (x_1, x_2, \dots, x_n)^T$ and $\mathbf{y} = (y_1, y_2, \dots, y_n)^T$ is one of the most well-known distance measures and widely used for various purposes in image processing. Alternatives to the Euclidean distance



Plant Disease Symptoms, Identification from Colored Images, Figure 1 Visual disease symptoms of Black Sigatoka (*M. fijiensis*) on leaves of Banana Plantain (*M. parviflora*). (a) Original Image. Yellow circle indicates human fingerprint. (b) Disease symptoms are segmented out. Yellow circle indicate a region wrongly segmented. (c) Segmented image is postprocessed to avoid including false positives (regions with similar characteristics to the target regions that in reality are part of the background).

include correlation-based divergences. Distances and divergences may be weighted by a weight vector $\mathbf{w} = (w_1, w_2, \dots, w_n)^T$. As an example, the weighted variant of the Euclidean distance is

$$d_{\mathbf{w}}(\mathbf{x}, \mathbf{y}) = \sqrt{\sum_i w_i (x_i - y_i)^2} \quad (2)$$

Preprocessing

The objective of preprocessing is to improve the visual traits of an image so that segmentation can be more efficient. The success of segmentation is determined by the accuracy with which target regions (in this document targets are visual symptoms of disease) are correctly identified. Two of the most popular methods used for image enhancement are intensity transformation and spatial filtering which operates on the Fourier Transform of an image (Gonzalez et al., 2009). A straightforward approach to intensity transformation is based on histograms and aims to produce a more even distribution of intensities. In the case of spatial filtering, there are several methods that can be used to suppress either low or high frequencies (intensities in histogram that are more or less frequent as opposed to those whose frequencies are around the average). For example, the Gaussian filter is a low-pass filter

that suppresses high frequencies to produce a smoother image. The degree of smoothing is determined by the convolution kernel size which is the standard deviation of the associated probability distribution. In general, the selection of what method to use very much depends on the image's characteristics and its quality. When dealing with images that are taken in the open, as is the case presented here, effects upon the digital image such as light intensity and shade can introduce noise to the original image. Therefore, raw digital images must be preprocessed before segmentation is carried out.

Image segmentation and postprocessing

Segmentation clusters image pixels into contiguous regions. For disease identification, segmentation typically aims to divide the image into foreground regions that contain plant parts that exhibit disease symptoms, and background regions, comprised of plant parts not affected by the disease and unrelated objects). Simple yet useful segmentation methods use reference points in color space and designate pixels to regions based on the distance of a pixel's color to these references. Even more simply, the space of colors or intensities may be partitioned, and contiguous pixels that fall in the same partition are combined into a region.

More sophisticated techniques can be used if the image is rather complex, for example, pixel clustering can be combined with a tree-search-like technique to connect spatially distant regions. [Figure 1](#) is an example of a complex image: the picture depicts a leaf of banana plantain (*Musa spp.*) showing the symptoms of the Black Sigatoka disease. Note that because every streak is different in shape, size, and intensity, a segmentation procedure that relies on intensities selection only might render inaccurate results. As an example, there is a fingerprint mark in [Figure 1a](#). That mark might have the same R, G, or B intensity as one of the target segments and therefore can be erroneously extracted as a disease symptom.

Further to segmentation, morphological binary open functions are used to join regions, fill holes, and remove small and isolated regions. [Figure 1b](#) shows that small regions wrongly segmented (yellow circle) were deleted after postprocessing. The picture also shows that as a result of applying a dilation procedure, some regions were expanded (bottom right) and therefore joined.

Attribute extraction

An attribute represents a categorical or numerical characteristic of a region in an image. Examples of attributes include the overall brightness of the object, its shape, texture (given by measures of energy, inertia, entropy, homogeneity and correlation which are calculated according to an angle and distance between two neighbor pixels) or size. As in segmentation, the selection of which attribute to extract will depend on the characteristics of the object. As illustrated by [Figure 1](#), characteristics of shape, intensity, and texture might be a good set of attributes representing any of the targets regions highlighted in [Figure 1c](#). Further useful attributes include solidity, extent, major axis length, minor axis length, eccentricity, centroid, diameter, lacunarity, and fractal dimensions. Each feature aims to capture an aspect of a visual symptom of the disease (Black Sigatoka in the example shown). It is important to mention that as well as representing image characteristics, attributes should be invariant to translation and rotation because images are normally captured from different angles and distances. Furthermore, lighting conditions are subject to variation that is irrelevant for disease classification. Therefore, attributes should be invariant to lighting conditions to the extent possible. The same set of attributes is determined for each region. As a result, each region r is characterized by an attribute vector $\mathbf{a}_r = (a_{r1}, a_{r2}, \dots, a_{rm})^T$.

Disease classification

Regions are classified based on distances or divergences between attribute vectors. Classifiers obtained by supervised learning may straightforwardly label regions with the disease that most likely causes the symptom shown by the region. Simple classifiers of this type contain reference attribute vectors. Each reference vector represents a symptom that is typical for a disease. Given an attribute

vector of a region from an image, the classifier determines the closest reference vector and designates the corresponding disease as the label of the region. The classification of an image is subsequently based on the classification of the regions in that image.

Construction of classifiers

Constructing classifiers for plant disease identification by supervised learning requires a set of training data, i.e., of images for which a human expert has determined and labelled regions. As an example, reference vectors may be computed by finding groups of regions in the training data which have the same label and are close in attribute space, and choosing their mean as the reference sample to represent that group. Weighted distances are a suitable and efficient approach where some attributes are more important for classification than others.

Simple classifiers operate on the attribute vectors directly and attempt to separate groups of samples using a linear hyperplane of separation. However, linear separation is not always possible. Where linear classifiers are not satisfactory, nonlinear classifiers, such as Artificial Neural Networks (ANNs) or Support Vector Machines (SVMs), may be used. SVMs notionally operate by nonlinearly mapping n -dimensional attribute vectors to a feature space of much higher dimensionality. The added dimensions enable construction of classifiers that are not feasible using linear techniques. However, this added power increases the risk of overfitting, i.e., of constructing a classifier that performs well on the training data but generalizes poorly to input that is not contained in the training data. Generally, a larger quantity and higher quality of training data is required to train a more powerful classifier, otherwise the classifier may produce unreliable results despite performing well on the training data.

Unsupervised learning may be useful where data is not fully labeled by human experts as its greatest strength is knowledge discovery from unknown data. As an example, consider a data set where the disease shown on each image is stated, but images are not segmented and consequently there are no labels for regions. In this situation, segmenting the images and clustering the regions may identify clusters of attribute vectors that represent visual symptoms of a plant disease but will not indicate to which diseases those cluster correspond.

Summary and outlook

In summary, while image based computational identification of plant diseases involves many challenges, a carefully designed image analysis pipeline can well complement and support disease assessment by human experts. The identification of the symptoms of plant diseases by means of a machine vision system may help to identify early symptoms of plant diseases. Here we described how digital images showing diseased regions of plants can be used as a tool for disease identification. These and other similar tools could become more useful

and widespread if they are available over the Internet as it has been shown that today's worldwide farmers (including those in poor countries) have more changes of accessing the Internet.

We also emphasized the importance of analyzing carefully the problem domain so as to select the best technique for each step in the pipeline that lead to the identification of plant diseases from colored images.

Plant disease detection ideally should not rely entirely on the assessment of images as visual symptoms might be similar among more than one disease (Miller et al., 2009) or might show up when it is too late to control the disease. However, machine vision systems may complement and speed up plant disease diagnosis, and it may be most beneficial to farmers in remote regions of developing countries, who have no support by agronomy or plant pathology experts, and therefore have limited knowledge of the pests and diseases that may attack their crops, but who rapidly gain access to the Internet in recent years.

Bibliography

- Boissard, P., Martin, V., and Moisan, S., 2008. A cognitive vision approach to early pest detection in greenhouse crops. *Computers and Electronics in Agriculture*, **62**, 81–93.
- Camargo, A., and Smith, J. S., 2009. Image pattern classification for the identification of disease causing agents in plants. *Computers and Electronics in Agriculture*, **66**, 121–125.
- Chakraborty, S., Tiedemann, A. V., and Teng, P. S., 2000. Climate change: potential impact on plant diseases. *Environmental Pollution*, **108**, 317–326.
- Glazebrook, J., 2005. Contrasting mechanisms of defense against biotrophic and necrotrophic pathogens. *Annual Review of Phytopathology*, **43**, 205–227.
- Gómez-Sanchis, J., Gómez-Chova, L., Aleixos, N., Camps-Valls, G., Montesinos-Herrero, G., Moltó, E., and Blasco, J., 2008. Hyperspectral system for early detection of rotteness caused by *Penicillium digitatum* in mandarins. *Journal of Food Engineering*, **89**, 80–86.
- Gonzalez, R. F., Woods, R. E., and Eddings, S. L., 2009. *Digital Image Processing Using MATLAB*. Knoxville, TN, US: Gatersmark Publishing.
- Miller, S. A., Beed, F. D., and Harmon, C. L., 2009. Plant disease diagnostic capabilities and networks. *Annual Review of Phytopathology*, **47**, 15–38.
- Pydipati, R., Burks, T. F., and Lee, W. S., 2006. Identification of citrus disease using color texture features and discriminant analysis. *Computers and Electronics in Agriculture*, **52**, 49–59.
- Qin, J. W., Burks, T. F., Ritenour, M. A., and Bonn, W. G., 2009. Detection of citrus canker using hyperspectral reflectance imaging with spectral information divergence. *Journal of Food Engineering*, **93**, 183–191.

Cross-references

[Climate Change: Environmental Effects](#)

[Crop Yield Losses Reduction at Harvest, from Research to Adoption](#)

[Image Analysis in Agrophysics](#)

[Quality of Agricultural Products in Relation to Physical Conditions](#)

[Stress–Strain Relations](#)

[Visible and Thermal Images for Fruit Detection](#)

PLANT DROUGHT STRESS: DETECTION BY IMAGE ANALYSIS

Istvan Farkas

Department of Physics and Process Control, Szent Istvan University, Gödöllő, Hungary

Synonyms

Plant condition; Speaking plant; Water shortage

Definition

Plant drought stress basically originated from the water shortage. That could be caused by the extreme weather conditions and/or by the insufficient amount of soil water within the rooting zone. The plants have an ability to regulate their water stress by transpiration process through stomata within a certain range.

Introduction

Drought is one of the most severe and extreme weather events affecting more people than any other form of natural disaster. According to the World Meteorological Organization nearly half of the worlds people will live in water-stressed areas by 2025. Beside desertification, climate change impacts, socioeconomic developments, and an increased agricultural production in addition to fresh water supply will further stress water resources. The International Solar Energy Society in his Solar World Congress organized in August 2005 put also the water into the focus of the discussions.

Drought stress of plants

The early and exact recognition of drought stress of crops (e.g., through extreme temperatures and water shortage) is of particular importance for sustainable crop production. However, the precise quantification of drought is difficult as no universal drought estimation method (e.g., drought indices, hydrological or soil water balance models) can be defined through the complexity of the problem. For precision farming two main features may be used for drought stress detection. On the one hand drought stress changes the leaf temperature of the plants. The leaf temperature as a result of its heat balance is linked with leaf surface characteristics, the leaf transpiration, and climatological factors such as wind speed and net radiation (Farkas et al., 2007).

Depending on the soil water content within the rooting zone and the related root water uptake, plants regulate their stomata and stop or continue their transpiration if water stress occurs. Transpiration is a means to keep leaf temperature low and protect them from heat stress. Plants differ significantly from their ability to regulate transpiration through stomata. Some drought resistant plants close their stomata at a very early stage of water stress, and some other less drought stress resistant plants will carry on with transpiration. Increased complexity results from the fact

that transpiration and stomatal resistance depend, beside soil water availability, on climatological factors such as radiation, saturation deficit, wind speed, and air temperature.

Drought stress detection by image analysis

In the last 2 decades several research experiments investigated the relationship between plant water status and visual appearance. It is a part of the speaking plant concept approach (Hashimoto et al., 1989).

Soybean leaves were studied by Oosterhuis et al. (1985) and found that soybean leaf-stem angle became smaller as the leaf-water potential and soil water potential declined.

Side projected canopy images can be used for such purposes in case of different plants as tomato, cucumber, and paprika. A camera is to be focused on the plant canopy from horizontal direction in order to obtain images covering the leaves. At defined time scales, images can be taken to analyze leaf and stem movements as the visual signs of plant state (Font and Farkas, 2008).

The image analyzing algorithm requires input files of preset operating parameters, camera position, and plants morphological features. These values should be adjusted for different plants, camera, or measurements. The leaves and stems on the image could be separated by the image processing algorithm according to the differences in their shape. A general leaf inclination value can be calculated from the local orientations at each point on the visible leaf's and stem's edge lines.

Algorithms have been developed for using side projected canopy images to determine *in vivo* and *in situ* the growth, shape, size, and leaf inclination angle of tomato and other plants in a climate-controlled indoor greenhouse along with an automatic irrigation technique.

Seginer et al. (1992) followed the vertical movement of the tip of fully expanded tomato leaves using machine vision imaging and reported that the movement can be used as an indicator of incipient drought stress before the appearance of visual wilt symptoms.

Another possibility to automated assessment of plant water status estimation is the image of the whole canopy rather than that of the individual plants or leaves. Kurata and Yan (1996) extracted lines reflecting inclinations of the rachides of tomato leaves from the whole canopy image obtained from a fixed position slightly above the canopy.

Another existing method for determination of leaf inclination is the LAI 2000 canopy analyzer. This method is based on the algorithms of LI-COR, Inc.

To draw a conclusion, the methods have been tested easily for different vegetable plants for instance tomato, paprika, and cucumber. Most of them have been tested in greenhouses and under completely controlled indoor conditions. They have not been adapted for many cultivars (e.g., maize) and also mostly not for outdoor environments.

Summary

Plant drought stress basically originated from the water shortage, which could be caused by the extreme weather conditions and/or by the insufficient amount of soil water within the rooting zone. The early and exact recognition of drought stress of crops is difficult as no universal drought estimation method can be defined through the complexity of the problem. Side projected canopy images can be used for such purposes in case of different plants as tomato, cucumber, and paprika. The images can be taken to analyze leaf and stem movements as the visual signs of plant drought state. Algorithms developed for using side projected canopy images can also be used for automatic irrigation of greenhouse crops.

Bibliography

- Farkas, I., Körösi, F., Seres, I., Font, L., Szabó, Z., Weihs, P., Eitzinger, J., and Werschonig, E., 2007. Drought experiments with maize plants, Research Report, Department of Physics and Process Control, Szent István University Gödöllő, No 41, July 2007, p. 43.
- Font, L., and Farkas, I., 2008. Wilting detection in greenhouse plants by image processing. *Acta Horticulturae*, **801**, 669–675.
- Hashimoto, Y., et al., 1989. *Dynamical Approach to Physiological Plant Ecology*. Matsuyama: Ehime University.
- Kurata, K., and Yan, J., 1996. Water stress estimation of tomato canopy based on machine vision. *Acta Horticulturae*, **440**, 389–394.
- Oosterhuis, D. M., Walker, S., and Eastham, J., 1985. Soybean leaflet movements as an indicator of crop water stress. *Crop Science*, **25**, 1101–1106.
- Seginer, L., Elster, R. T., Goodrum, J. W., and Rieger, M. W., 1992. Plant wilt detection by computer-vision tracking of leaf tips. *Transactions of the ASAE*, **35**, 1563–1567.

Cross-references

- [Drought Stress, Effect on Soil Mechanical Impedance and Root \(Crop\) Growth](#)
[Image Analysis in Agrophysics](#)
[Irrigation and Drainage, Advantages and Disadvantages](#)
[Light Interception by Plant Canopies](#)
[Plant Disease Symptoms, Identification from Colored Images](#)
[Plant Root Strength and Slope Stability](#)
[Plant Wellness](#)
[Physics of Plant Nutrition](#)
[Remote Sensing of Soils and Plants Imagery](#)
[Visible and Thermal Images for Fruit Detection](#)
[Water Uptake and Transports in Plants Over Long Distances](#)

PLANT LODGING, EFFECTS, AND CONTROL

Grażyna Podolska

Department of Cereal Crop Production, Institute of Soil Science and Plant Cultivation, National Research Institute, Puławy, Poland

The process by which the shoots of cereals are displaced from their vertical stance is called lodging. Lodging is a complicated phenomenon. There are many external

factors that have influence on lodging including: wind, rain, topography, soil type, forecrop, tillage, nitrogen fertilizers, diseases, sowing date, seed rate, and variety. Lodging has a negative influence on both the yield and the yield quality.

Smaller yield losses are observed when the angle of lodging is less than 90° from the vertical and when lodging occurs at the later stage of development. Artificial lodging at the ear emergence, milk, soft dough, and hard dough stage reduced yields by 31%, 25%, 20%, and 12%, respectively (Fischer and Stapper, 1987; Berry et al., 2004). Lodging during early grain filling affected grain quality, deducting falling number, thousand grain yield, and specific weight and increased the protein content (Cacak-Pietrzak et al., 2006; Stanca et al., 1979).

The resistance against lodging is associated with the plant resistance to mechanical stress and it is based on the mechanical and structural properties of the plant. Plant morphology, anatomy, chemical composition of the stem as well as the condition of the root system has an impact on the resistance against lodging. Morphological properties involved in lodging are: the length of the stem, the thickness of the bottom three internodes, as well as the diameter of the stem. Morphological properties decide upon the resistance to the pressure and forces put by wind or rain. Anatomical properties are mainly the thickness of the cell walls and the sclerenchyma width. Chemical composition involved in lodging, mainly refers to the cellulose and lignin content. Cellulose gives stiffness whereas lignins give resistance to the external pressure influencing the cell walls. Moreover the vertical distribution of the root system supports lodging resistance of the plant (Berry et al., 2004; Źebrowski, 1992).

The prevention of lodging is mainly focused on the cultivation of the resistant varieties, mainly through the introduction of so-called dwarf genes, but also by application of growth regulators (PGRs). Three major types of PGRs are currently in use, namely: chlormequat chloride, etephon, and trinexapac-ethyl (Cox and Otis, 1989).

Bibliography

- Berry, P. M., Sterling, M., Spink, J. H., Baker, C. J., Sylvester-Bradley, R., Mooney, S. J., Tams, A. R., and Ennos, A. R., 2004. Understanding and reducing lodging in cereals. *Advances in Agronomy*, **84**, 217–269.
- Cacak-Pietrzak, G., Ceglińska, A., and Leszczyńska, U., 2006. Influence of growth regulators on utility value of winter wheat. *Progress in Plant Protection*, **46**, 89–92 (in Polish).
- Cox, W. J., and Otis, D. J., 1989. Growth and yield of winter wheat as influenced by chlormequat chloride and etephon. *Agronomy Journal*, **81**, 264–270.
- Fischer, R. A., and Stapper, M., 1987. Lodging effects on high yielding crops of irrigated semi-dwarf wheat. *Field Crops Research*, **17**, 245–248.
- Stanca, A. M., Jenkins, G., and Hanson, P. R., 1979. Varietal response in spring barley to natural and artificial lodging and to a growth regulator. *Journal of Agricultural Science Cambridge*, **93**, 449–456.
- Źebrowski, J., 1992. Structural and mechanical determinants and methods of lodging resistance estimation in cereals. *Buletyn Instytutu Hodowli i Aklimatyzacji Roślin*, **183**, 74–93 (in Polish).

PLANT NUTRIENTS

See *Physics of Plant Nutrition*

PLANT PHYSICAL CHARACTERISTICS IN BREEDING AND VARIETAL EVALUATION

Bogusław Szot¹, Wojciech Rybiński²

¹Institute of Agrophysics, Polish Academy of Sciences, Lublin, Poland

²Institute of Plant Genetics, Polish Academy of Sciences, Poznań, Poland

Definition

The relations between agrophysics, and genetics and plant breeding are a measure of the *breeding and crop variety evaluation* progress in respect of the utilization of agrophysical studies in the creation of new plant cultivars. It has been proven that *plant physical characteristics* such as mechanical strength parameters (force, elasticity, deformation, energy) are inheritable to a very high extent and there is a possibility of selecting the parent forms in such a way as to obtain genotypes with favorable features with respect to cultivation, harvest, storage, and material quality for the food processing industry. The effects of such joint research efforts presented herein support the thesis that only interdisciplinary research may result in measurable achievements.

Introduction

The area of interest of agrophysics covers the physical processes and material properties that are important for sustainable agricultural production and for modern food processing technologies, and especially the physical and physicochemical interactions taking place in the soil-plant-atmosphere and soil-plant-machine-agricultural product systems, with special emphasis on the condition of the environment and on the quality of food products. At present, in the first decade of the twenty first century, a notable biological progress is observed, especially in the aspect of dynamic development of genetic engineering and biotechnologies, and agrophysics, which provides efficient support in solving the complex problems of the agricultural and natural sciences. As an example, knowledge of the physical properties of crop plants was utilized by mankind already in ancient times, and now knowledge of the range of physical properties of a given plant material is a necessary prerequisite for the estimation of the quality of a given plant material. From its very beginning agrophysics made extensive use of the research tools and the achievements of physics and mathematics. There is no doubt that also the natural sciences, genetics, and plant breeding included, often face the necessity of searching for interdisciplinary interpretations of mutual interactions.

Studies of the same object (e.g., a specific plant material) but at different levels of magnitude are frequently in the focus of interest of various disciplines of science. The resultant interactions are usually not simple sums of interactions taking place at different scales. As an example, the structure of cereal kernels can be accurately described in terms of their mechanical or physicochemical properties, but it is obvious that at the root of the observed variability of the physical or chemical parameters studied, there lie the fundamental transformations of genetic nature that remain in specific interactions with the environmental conditions. Hence, one of the fundamental challenges facing agrophysics is the interdisciplinary interpretation of studied interactions taking place in the natural environment, and especially in plant material.

In the interdisciplinary aspect, the plant geneticists and breeders on the one hand, and agrophysicists on the other, have now at their disposal modern research tools that permit in-depth determination of the genetic variability of traits and of the physical and physicochemical interactions taking place in the environment of plant growth and development in the broad sense. Irrespective of the two disciplines of science mentioned, the genetic-breeding aspects as well as the physical ones are analyzed in close relationship with the soil-plant-atmosphere system. This is a significant interdisciplinary bond that permits undertaking attempts at combining the results of genetic-breeding experiments with the effects studied in the field of agrophysics of plant materials. Doubtlessly, it is of interest to find out to what extent genetic-breeding experiments may contribute to elucidation of physical phenomena taking place in plant material, and vice versa, and how much the physical processes may help in the interpretation of a number of phenomena of genetic and breeding nature. To give an example, the process of pod cracking and seed shedding is closely related with processes of physical character that take place in the pod under specific environmental conditions, but on the other hand that phenomenon is genetically determined and specific for particular species, cultivars, or lines. Hence, the knowledge of the physical aspect of pod cracking with an accumulation of specific climatic factors (temperature, precipitations, air humidity etc.) is undoubtedly a significant element in studies on genetic improvement of crop plants.

In studies aimed at the introduction of new, high-yield cultivars resistant to biotic and abiotic stresses, both geneticists and plant breeders concentrate on the fundamental quality and quantity features of plants that guarantee high market competitiveness of new cultivars. Whereas, they do not have at their disposal precision research tools that would allow them to obtain basic information, e.g., on the physical (mechanical) properties of plant stems or stalks in the aspect of improving their resistance to lodging or the resistance of seeds to mechanical loading, which later has its consequences in the processes of harvest, storage, and processing of agricultural products. To meet the requirements of contemporary economy, crop plant cultivars used in agricultural production should permit the

obtainment of material and biological product that has to meet specific standard and requirements with simultaneous limitation of losses. This is closely related with the biological progress whose intensification, especially in recent years, is observed already on the global scale. The biological progress encompasses improvement of plant and animal organisms, and increase in the number of plant and animal species that are useful to man. In contemporary agriculture there are a number of concepts used alternately for the description of the progress brought in by the new cultivars – the most commonly used ones include genetic and varietal progress. The advances contributed by new crop plant cultivars form a part of the biological progress understood as improvement of living organisms. Among other things, the breeding progress is important that can be considered as all improvements related with breeding research and that may relate both to the development of specific breeding techniques and to the actual effects of breeding experiments, i.e., new plant cultivars. Breeding progress in relation to crop plants can be considered in the aspect of improvements to the yield quality indices – expressed, among other things, in increased content of protein, improvement of its amino acid composition, elimination of significant reduction of the content of anti-nutritional substances, as well as in improvement of the yield structure, reduction of the vegetation period, increased resistance of plants to lodging, drought, or pest or disease infestation. The ultimate effect aimed at by plant breeding is increase in crop yield and improvement of its quality features. An element that hitherto has been under-appreciated and little known is the degree of seed resistance to physical factors, expressed in the mechanical properties of kernels, which is – in turn – related with the limitation of losses involved in the harvest, transport, and storage of seeds. To meet this requirement, an attempt has been undertaken to estimate the physical properties of seeds in the context of the breeding progress as evidenced in the final product of the breeders, i.e., crop plant cultivars as well as strains, lines, mutants, or hybrids in the first generations after crossbreeding, obtained at early stages of breeding work. That study is an attempt at combining the breeding progress as exemplified by the abovementioned breeding materials with evaluation of their seeds in terms of their physical properties, mainly in the aspect of their resistance to mechanical loads. The study has been based on literature results relating to cereals and leguminous plants.

When the classical breeding methods are applied, the time elapsing from the first crossbreeding to the registration of a new cultivar is at least 10 years. The initial stages of the breeding cycle include the selection of the most promising genotypes which, in subsequent generations, are multiplied and tested in field experiments. The condition for effective selection is to obtain the broadest possible range of variability of traits, which permits selection of genotypes possessing properties sought by the breeder. Hence, it is important for the breeder to have at his disposal, already at early stages of the breeding program,

information on the breeding value of selected objects in terms of the most desirable traits, with the inclusion of the resistance of seeds to mechanical loads in the selection evaluations, a property often underestimated and neglected by the breeders but truly indispensable in the development of the optimum model of a new plant cultivar or variety. The valuation information obtained permits to limit, in the initial generations of a breeding cycle, the abundant crossbred material to the most valuable and promising genotypes. Among other things, this is of a measurable financial significance as it permits the limitation of the scope and therefore also the costs of breeding programs in progress.

Cereals

Evaluation of materials at early stages of breeding

An example of estimation of the resistance of kernels to mechanical loads at an early stage of wheat breeding can be a study by Milczak et al. (1977) with relation to generation F₂. The hybrids were obtained by crossbreeding the wheat line Z-70 (P₁) with the cultivated variety Kaukaz (P₂). Apart from the evaluation of the parent material and the F₂ hybrids in terms of their weight of kernels per year, weight of kernels per plant, weight of 1,000 kernels, grain vitreosity, and protein content, a novel element was the inclusion of kernel resistance to mechanical loads in the scope of the estimations. That last trait was analyzed on an apparatus designed at the Institute of Agrophysics, PAS, permitting systematic recording of increasing force values as a function of strain. This allows readings of the instantaneous force compressing the kernel, and of strains

within the range of linear elasticity. The levels of values of the studied traits P₁, P₂, and F₂ and the range of their variability are illustrated in Table 1. Comparison of mean values indicates high phenotypic similarity of both parental forms. In the context of the studied traits, considerable differences were observed with relation to the grain resistance to mechanical loading, which is closely related to the susceptibility of the grain to mechanical damage. The range of variability of that trait was notably different for P₁ (43.6 – 61.9 N) than for P₂ (65.0 – 96.0), which indicates genotype-inherent resistance of the parental forms with respect to that feature. The result of the separateness of the parental forms was the obtainment, through recombination, of considerable variability of grain resistance to mechanical loading in plants of generation F₂, the highest within the group of traits under study. This is confirmed by the coefficient of variation of ca. 9%, compared to 18.6% for the hybrids of F₂. Closely related with the range of variability of traits is an index that is very important in the prediction of genetic progress – heritability (H). The highest proportion of genotype variation with relation to phenotypic variation was found for the resistance of grains to static loads (H = ca. 78%). The obtained variability of grain resistance to mechanical loads at a high level of heritability of that trait in hybrids permits the selection of the most resistant forms from generation F₂ and their use for further crossbreeding and proper orientation of the breeding program. An important element in breeding is to identify the relations between the evaluated traits as expressed by the index of phenotypic correlation (Table 2).

Among the 21 correlations under study a particularly practical breeding aspect is represented by the relationship

Plant Physical Characteristics in Breeding and Varietal Evaluation, Table 1 Mean values and range of variability of studied traits of winter wheat (Milczak et al., 1977)

Trait	Generation	Mean value	Range of variability (from – to)	Coefficient of variation V (%)	Coefficient of heritability (H)
Weight of kernels per spike (g)	P ₁	2.50	1.2–3.9	28.2	0.418
	P ₂	2.70	1.9–3.9	17.5	
	F ₂	2.60	1.0–4.7	30.6	
Weight of kernels per plant (g)	P ₁	39.20	14.2–82.2	33.0	–
	P ₂	20.30	15.0–32.2	22.0	
	F ₂	27.60	15.0–55.4	32.5	
Weight of 1,000 kernels (g)	P ₁	35.80	28.9–43.4	11.2	0.567
	P ₂	35.40	30.3–39.4	7.6	
	F ₂	37.70	24.2–52.7	13.9	
Vitreosity of kernels (%)	P ₁	16.90	7.0–23.0	22.8	0.389
	P ₂	15.40	8.0–26.0	32.5	
	F ₂	16.70	7.0–30.0	35.2	
Protein content (%)	P ₁	15.30	13.0–18.0	8.2	0.402
	P ₂	15.90	14.0–18.5	8.5	
	F ₂	13.70	11.0–18.2	11.5	
Resistance to static loads (N)	P ₁	53.00	43.6–61.9	9.1	0.784
	P ₂	80.00	65.9–96.0	8.8	
	F ₂	63.20	34.8–92.1	18.6	
Elastic deformation (mm)	P ₁	0.29	0.20–0.40	21.5	–
	P ₂	0.41	0.35–0.52	19.0	
	F ₂	0.34	0.22–0.55	18.3	

Plant Physical Characteristics in Breeding and Varietal Evaluation, Table 2 Coefficient of phenotypic correlation (r_{xy}) for population F_2 (Milczak et al., 1977)

Trait	Weight of kernels per spike (g)	Weight of kernels per plant (g)	Weight of 1,000 kernels (g)	Kernel vitreosity (%)	Protein content (%)	Resistance to static loads (N)	Elastic deformation (mm)
Weight of kernels per spike (g)	—						
Weight of kernels per plant (g)	0.524*	—					
Weight of 1,000 kernels (g)	0.258*	0.375*	—				
Kernel vitreosity (%)	0.163	0.138	0.358*	—			
Protein content (%)	-0.092	-0.004	-0.121	0.016	—		
Resistance to static loads (N)	0.283*	0.244*	0.316*	0.537*	-0.011	—	
Elastic deformation (mm)	0.075	0.170	0.018	0.193	0.283*	0.398*	—

* Significant at the 0.05 level.

in population F_2 between the resistance of kernels to static loads and their vitreosity ($r_{xv} = 0.537$). For the breeder, this relation is of particular value as grain vitreosity is a trait easy to assess and can be used in selection as a morphological marker of grain resistance to mechanical damage. The dependence of the mechanical strength of grain on its vitreosity, long known in grain milling practice, has found support in literature data. The identification of the above marker is a good prognostic for breeding programs that take into account grain resistance to mechanical loads in the modeling of new cultivars. The presented results, based on the evaluation of breeding materials at early stages of creation of cultivars, are valuable in the sense that there is a general lack of studies of this kind and a review of literature has not yielded any pertaining publications.

The expression of traits observed and evaluated in breeding is based on changes of genetic nature, including modification caused by the effect of the environment. At present, for numerous plant species genetic maps are available, giving the precise location of a large number of genes on the chromosomes. Apart from the effect of specific genes on the expression of traits, studies are also conducted on the effect of additional chromosomes. This can be exemplified by the wheat-rye addition lines obtained by numerous researchers (e.g., Evans and Jenkins, 1960; Miller, 1973; Bernard, 1976). Series of addition lines have no practical application, and many authors analyzed the effect of additional chromosomes of rye on the process of meiosis and on plant development, and on the physiological and biochemical properties of wheat lines with additional rye chromosomes (Sears, 1967; Tnag and Hart, 1975; Schlegel, 1978; Liu and Gale, 1989). In spite of the existence of abundant literature on the subject, there is a lack of studies on the physical properties of kernels of wheat lines with additional rye chromosomes. Making use of the created series of lines of wheat cv. Grana with a set of additional chromosomes of

rye cv. Dańskowskie Złote and branches of chromosomes 1R, 2R, 3RS, 4R, 5R, 6R 6RL and 7R, a study was made of the properties of kernels of those lines as well as of the initial forms: wheat cv. Grana, rye cv. Dańskowskie Złote, and an octoploid triticale (Grana x Dańskowskie Złote). The authors (Miazga and Szot, 1996) studied, among other things, the internal damage to kernels using for the purpose an X-ray apparatus and analyzing the obtained X-ray images. Estimations of the resistance of the kernels to mechanical loads were performed with the use of the INSTRON model 6022 strength tester. The physical properties of kernels are determined by their morphology and anatomical structure, as well as by their chemical composition, which at the same time affects their physiology. Among the primary causes for the appearance of cracking in kernels one can mention the gradient of moisture related to the weather conditions (dew, rainfall-drought) in the phase of full ripeness of kernels and in the course of uneven filling of kernels which causes local weakening and cracking of endosperm. Internal damage to the kernels was evaluated on the basis of the index, with no effect of external forces. It was found that all the addition lines, including the triticale, were characterized by notably higher index of damage compared to kernels of wheat cv. Grana, while no damage to rye kernels was noted. Differentiation in internal damage in the addition lines was shown by defining the location and extent of damage to the kernels. In view of the fact that the environmental conditions in the field experiment were identical for all tested objects, the observed differences resulted from the genetic effect of the additional rye chromosomes in the addition lines. Kernel surface roughness (coarseness), in the physical aspect, is subject to the effect of forces causing various levels of friction and abrasion during threshing, transport, cleaning, and storage. Moreover, rough-surfaced kernels retain water (moisture) longer after rainfall or dew. The surface roughness (coarseness) of kernels was estimated by means of a microscope (BK 70 × 50) and the

results were given in micrometers. All addition lines were characterized by lower surface coarseness than the initial forms. The results related to surface coarseness alone, and not to kernel surface wrinkling, were observed for kernels of triticale. The results of compressive strength of kernels are given in Table 3. The values of the maximum force, i.e., force causing kernel destruction, varied from 65.9 N for line 4R, through 83.5 for line 3R, to 104.9 N for line 6R. Forms that were the most resistant to compression included lines 6R, 6RL, and 2R. The results suggest that probably those chromosomes include genes responsible for the mechanical strength of rye kernels. This trait may be related with the endosperm structure. Simmonds et al. (1973) describes the differences in endosperm structure between rye, wheat, and triticale, with special attention to the distribution of proteins and starch in the endosperm. The values of maximum force correspond with maximum strain at the point of damage to kernels and vary among the lines in the range from 0.18 to 0.28 mm, depending on the line. Rye kernels, being the strongest, require the greatest energy during crushing (25.0 mJ). All addition lines, with the exception of line 3R, required greater energy for kernel crushing compared to wheat. Concluding, the authors emphasize that, with high probability, the genes that determine the mechanical strength of rye (initial form Dańskowskie Złote) are found on chromosomes 6R, 6RL, and 2R, which constitutes significant information for geneticists and breeders in the process of selection and obtaining, at further stages of breeding work, of cultivars with increased resistance to mechanical damage.

The variability of the animated world is a result of the processes of recombination and mutation. While the subject of utilization of hybrids created through crossbreeding

followed by recombination has been discussed earlier in the text on the example of wheat, the application of induced mutation for the assessment of mechanical loading of kernels of hull-less barley is presented by other authors (Rybniński and Szot, 2006). Mutations and mutation breeding are a valuable complement to conventional breeding methods (Campbell et al., 1994). Mutations can be used for the creation of additional variability of traits, used by breeders for the development of cultivars with specific properties and with specific adaptive capabilities under given environmental conditions. Kernels of the hull-less bred line 1 N/86 were treated with a chemomutagen (MNU), and kernels not subjected to the effect of the mutagen constituted the control treatment. Mutant selection was conducted in generation M₂, and after a several-year cycle of multiplication kernels from a field experiment with selected mutants were assessed in terms of their geometric properties of resistance to mechanical loads. For comparison of the physical properties of kernels, estimations were also performed for hulled forms of spring barley. It was demonstrated that the mutagenic agent induced an extension of the range of variability of physical properties of the mutants compared to their initial form 1 N/86. Among other things, this concerned the geometric parameters of the kernels (thickness, width, and length), and especially their resistance to mechanical loads expressed by values of force, deformation, and energy. To give some examples, the mean value of force required to destroy a kernel of the initial form 1 N/86 was 168.5 N, and for the mutants it varied from 125.3 N to 227.3 N. The obtained variability permitted the selection of hull-less mutants that differed from the initial form in the geometric parameters and in greater resistance to

Plant Physical Characteristics in Breeding and Varietal Evaluation, Table 3 Mechanical strength parameters of kernels of initial forms: wheat cv. Grana, rye cv. Dańskowskie Złote, octoploid triticale (Grana x Dańskowskie Złote) and eight addition lines (Miazga and Szot, 1996)

Genotype	Maximum force (N)			Maximum elasticity (N)			Maximum deformation (mm)			Elastic deformation (mm)			Energy (mJ)		
	Mean	s.d.	c.v. (%)	Mean	s.d.	c.v. (%)	Mean	s.d.	c.v. (%)	Mean	s.d.	c.v. (%)	Mean	s.d.	c.v. (%)
Wheat cv. Grana	82.43	16.35	19.8	69.85	18.58	26.6	0.185	0.052	28.1	0.102	0.03	29.4	7.91	5.87	61.4
Rye cv. Dańskowskie Złote	131.33	35.45	27.0	100.29	35.06	35.0	0.338	0.104	30.	0.166	0.079	47.6	25.00	13.55	54.2
Triticale (Grana x Dańskowskie Złote)	86.72	24.17	27.9	62.73	28.13	44.8	0.338	0.103	30.5	0.160	0.079	49.4	16.56	7.91	47.8
1 R"	88.64	16.62	18.8	62.97	19.42	30.8	0.268	0.065	24.3	0.135	0.057	42.2	13.46	5.87	43.6
2 R"	102.72	18.51	18.0	79.74	17.59	22.1	0.221	0.070	31.7	0.113	0.041	36.3	13.04	6.36	48.8
3 R"	85.27	19.57	23.0	71.82	19.00	26.5	0.177	0.063	35.6	0.106	0.032	30.2	7.68	5.82	75.8
3 RS"	98.20	21.64	22.0	80.04	19.17	23.7	0.230	0.059	25.7	0.118	0.049	41.5	11.76	5.79	49.2
4 R"	65.96	18.73	28.4	46.61	20.73	44.5	0.284	0.088	31.0	0.135	0.059	43.7	10.76	5.63	52.3
5 R"	86.04	15.21	17.7	67.21	20.72	30.8	0.262	0.067	25.6	0.152	0.070	46.1	11.53	4.98	43.2
6 R"	107.93	25.02	23.2	94.77	28.51	30.1	0.236	0.067	28.4	0.157	0.065	41.4	132.41	7.07	57.0
6 RL"	107.04	26.73	25.0	90.03	32.70	36.3	0.282	0.081	28.7	0.203	0.115	56.7	14.87	7.44	50.0

mechanical loads. The selected mutants may constitute valuable initial material for the development of improved cultivars of hull-less barley. An interesting insight is provided by comparison of physical properties of kernels of hull-less mutants with those of the hulled forms. On average, the mutants were characterized by longer kernels and by higher compressive strength (141.2 N for the hulled forms and 175.0 N for the hull-less mutants), and by higher values of energy required – 25.6 and 38.2 mJ, respectively. The elimination of the hulls from the kernels, constituting 13% of the weight of a single kernel, is highly advantageous in the feeding of monogastric animals as it permits saving of energy that has to be expended on digestion of the hard to digest hulls composed mainly of fiber and cellulose. Hence, hull-less cultivars of barley provide a valuable complement to the array of hulled cultivars commonly used in animal feeding. However, the elimination of hulls results in reduced protection of the germ, which causes that incorrect settings of the threshing machine amplify the risk of damage to the germ, and that, in many cases, leads to disqualification of the grain as qualified sowing material.

Another batch of hull-less mutants were analyzed with regard to the status of damage to the parenchyma as measured by the number of cracks (recorded on X-ray film), and also, using mechanical tests on kernel sections under uniaxial compression, determinations were made of the strength of the kernels, their modulus of elasticity, deformation, and specific work during deformation (Woźniak et al., 2006). Kernels of the initial form 1 N/86 were characterized by low susceptibility to internal damage, at an average of three cracks per kernel. The mutants were characterized by decreased resistance, but a few forms with increased strength were also selected. This indicates that the mutagen caused a broadening of the range of variability of that trait. The observed cracks, however, did not cause any greater decrease in the compressive strength of kernels. Most of the mutants were characterized by kernels with modulus of elasticity values significantly higher than in the initial form. In the conclusion of the study, it was shown that mutation of barley permits the obtainment of forms with improved kernel strength parameters.

An important element of the quality of cultivars is their resistance to lodging. Strong tendency of plants to lodge causes notable losses in grain yield and leads to a significant deterioration of their quality (Jeżowski, 1981). The physical parameters of the stem affect the degree of lodging. For mutants of barley measurements were made of plant height, outer diameter of stem, stem wall thickness, and the ultrasonic method was employed to determine the index of stem elasticity – the Young modulus. The range of variability of the trait of plant height in the mutants was from 61.8 to 113.4 cm, with plant height of the initial form at 92.5 cm. High values of coefficient of variability were obtained for the traits that determine the resistance to lodging – stem wall thickness (14.8%) and Young modulus (13.3%). The relation between the degree

of lodging (measured in a scale from 1 to 9; 1 – no lodging, 9 – full susceptibility to lodging) and the values of traits determining resistance to lodging was reflected in high, significant values of correlation coefficient. For stem wall thickness and for the Young modulus, those values were $r = -0.695$ and $r = -0.902$, respectively. High value of the coefficient of correlation between the degree of lodging and stem elasticity, measured by the value of a physical parameter, the Young modulus, constitutes significant information for the breeder, permitting him to use the index of stem elasticity in the selection of forms with improved resistance to lodging. Such mutants have been created that, thanks to greater stem elasticity, displayed lower susceptibility to lodging than their initial forms. What needs to be emphasized here is that the factor that determines the degree of lodging is not only plant height (stem length), but primarily the physical parameters of the plant stem.

While the hybrids of generation F₂, addition lines and mutants discussed above are evaluated by the breeder at the early stages of the breeding cycle and selection, the last stage of the work prior to the submission of a form for cultivar registration tests is the evaluation of the selected breeding strains. The study on strains comprised, i.e., two lines of triticale – 46 and 51 – and in comparative estimations wheat cv. Grana and rye cv. Dańskowskie Selekcjyne were used (Szot and Tarkowski, 1977). Apart from evaluation of the geometric features of kernels, also the instantaneous resistance of single kernels to static loads was determined with accuracy of 1 N. Among the most valuable issues was the estimation of strength parameters of line 45 taking into account the kernel thickness fractions. A unique methodological approach in the aspect of breeding practice and technology was the attempt at relating the thickness of kernels to their resistance to static loads. It was demonstrated that the critical values of force increased with increase in the kernel thickness fractions. Significant differences were proved even between neighboring fractions. Mean values varied from 22.66 to 77.5 N, with kernels with thickness above 3.0 mm indicating a certain drop in strength. In the summary of results, the authors emphasize that the thickness and width of kernels of octoploid triticale and of the hexaploid lines 45 and 51 fall in between those of winter wheat cv. Grana and of rye cv. Dańskowskie Selekcjyne. Moreover, the instantaneous resistance of kernels to static loading increases with their thickness, and the absolute values obtained suggest that they are closer to those of wheat than of rye. This indicates that the strength traits in question are inherited to a greater degree on the part of wheat than of rye. A negative feature of triticale kernels is their frequent surface wrinkling that is genetically determined. It was observed that well-filled kernels were less susceptible to mechanical damage than wrinkled ones. Hence, breeding studies should aim at elimination of endosperm wrinkling and at increase content of lysine in the triticale as well as in barley kernels (Rybicki and Patyna, 1984).

Estimation of physical parameters of kernels on the example of commercial cultivars

The best breeding lines, with high yielding and the most advantageous utility features (and especially with improved resistance to biotic and abiotic stresses), are registered as cultivars and introduced on the market. As cultivars are the end product of breeding, their evaluation with regard to the geometric parameters and resistance to mechanical loads can be used as additional information for the users, for grain processing process engineers, or for breeders who can use the best cultivars in their own crossbreeding programs, treating them as parental components. The quality of agricultural products, or more generally agricultural materials (e.g., cultivars), is usually associated with their utility value as the essence of quality is their suitability for nutritional or extra-nutritional purposes. Estimation of the quality of a given material requires knowledge of the range of variability of its physical properties. New research programs already include even the level of a single kernel (Single Kernel Technology), which supports the sense of undertaking research programs aimed at determination of physical properties of individual kernels of particular cultivars, not only within a given material for the processing industry, but also with respect of materials used in breeding programs. It is important to determine changes in the values of physical properties of individual kernels in spikes of wheat (*Triticum aestivum* L.) of commercial winter and spring cultivars. The scope of the study included field experiments, and the selection of wheat cultivars for the study was based on the criterion of "quality" that defines the limit values of physical or technological traits of grain and determines its being qualified in a suitable quality type. The winter forms were represented in the evaluation by the quality wheat Zyta (type A), and the bread-fodder forms by cv. Kris (type B/C). Among the spring forms the selected cultivars were Nawra and Broma, meeting the same criteria as above. Among the numerous physical parameters of individual kernels on the length of a spike the determinations included the parenchyma damage index that provides information on the state of its destruction under the effect of moisture gradient. X-ray images of the kernels did not reveal any damage in the material under examination. This indicates that under the conditions of the field experiment the cultivars analyzed displayed notable genetic resistance to internal damage in kernels. A significant element of the evaluation was the distribution of hardness of successive kernels in spikelets on the length of the spike (Grundas, 2004). Kernel hardness was estimated on the Single Kernel Characterization System analyzer as hardness index, which is an abstract value and has no physical interpretation. Based on the mean hardness values of the first, second, third, and fourth kernels in the spikelets it was concluded that it is a trait that is highly correlated with hardness understood as the resistance of a kernel to the effect of static mechanical loads. As results from the study, kernel

hardness is largely determined by internal features. This follows from the fact that the successive kernels do not display the typical decreasing trend in the direction of the tip of the spikelet that is characteristic of the other traits. Moreover, apart from the bread-fodder wheat cv. Kris, all other cultivars are characterized by a fairly even level of that trait. In accordance with the rule confirmed in other studies, kernels of spring wheat are harder and more resistant to mechanical damage than kernels of winter wheat, which is especially visible in cv. Kris. Improvement of kernel hardness in certain winter wheat cultivars may be one of the selection criteria in breeding programs.

Estimations were also made of the physical properties of successive kernels on the length of spikes of triticale forms and of wheat cv. Grana and rye cv. Pancerne. Analysis was made of the kernel to spike bond force, and the measurements covered five spike zones to determine the distribution of force variability on the whole spike length. It was demonstrated that the bond forces, depending on the cultivar, varied within the broad range from 0.93 N to 1.94 N. The strongest set were the kernels in the lower zones of the spike, and the weakest – in the tip section of the spike. The notable differences between the forms under analysis indicate that they are susceptible to shedding to various degrees – from easily shedding to hard to thresh.

An important element of physical assessment of kernels used for examination of commercial cultivars is the compressive strength of kernels, specific work, and modulus of elasticity as related to the level of moisture, as illustrated in a study on wheat cv. Henika (Woźniak, 2003). The study showed a ca. 50% decrease in the values of those parameters as a result of wetting of the kernels. A negative correlation was found between the traits studied and the time of grain wetting. That correlation did not relate to deformation. Moreover, kernels with vitreous type of parenchyma were characterized by higher values of mechanical parameters than mealy kernels. Estimation of the effect of kernel wetting time in parenchyma cracking and mechanical damage was also continued for hull-less barley cv. Rastik. A notable susceptibility of the hull-less kernels to parenchyma cracking was observed, with mean number of cracks in the control sample (dry kernels) being 13.6 and increasing with increase in the time of prior kernel wetting up to 15.8 (after 3 h of wetting). Wetting lasting more than 3 h caused a decrease of modulus of elasticity by 15% and of compressive strength by ca. 10%. Moreover, changes in kernel strain and in specific energy caused by prior moistening were similar. A very important conclusion of practical significance in breeding and processing is the demonstrated lack of correlation of the mechanical parameters with the number of internal cracks.

In studies continued also for commercial cultivars of spring barley – Berac, Gryf, Kosmos, and Polon, kernels after harvest were wetted to 12, 18, and 22% moisture (Styk and Szot, 1984). It transpired that kernels of all cultivars responded negatively to the effect of mechanical

loads, both at the conditional moisture and when moistened to the level of 18 and 22%. Increase in the mechanical load level from 4 MPa to 8 MPa resulted in a considerable decrease in the germination capacity that fell within the range from 23% to 35%, depending on the cultivars and moisture content levels. Kernels with increased moisture content proved to be more susceptible to damage. The period of storage had a significant effect, lowering the biological value of kernels, and that phenomenon was especially pronounced in material that was earlier subjected to mechanical loads of the level of 8 MPa at higher initial moisture. Those conditions caused that the seeds of all cultivars germinated at the rate of 52–61%. Such a considerable decrease in germination capacity indicates high sensitivity of sowing material to the effect of external forces, and the inter-variety (genetic) differences, varied fertilization, as well as seed moisture are those elements that may largely shape the resistance of kernels to mechanical loads, causing a variety of damage to the seed coat, the germ, or the parenchyma.

Leguminous plants

The problem of worldwide deficit of protein fodders relates both to their quantity and quality. The basic fodders in this respect are the seeds of high-protein leguminous plants. In the context of the onset of the BSE disease, the effect of elimination of high-value fodders of animal origin and the controversies around genetically modified soybean (GMO) may further aggravate the deficit of proteins in animal feeding. Ensuring high quality proteins in human and animal feeding is a priority topic in the EU countries. At present in those countries, 70% of plant proteins is imported, mainly in the form of extraction meal and soybean seeds, primarily transgenic. Unfortunately, the area of cultivation, both in Poland and Europe (respectively 1% and 3% in the crop structure), does not correspond to the unquestionable advantages of high-protein leguminous plants, important, i.e., due to their binding of atmospheric nitrogen (reduced requirements for nitrogen fertilization), positive effect on the soil structure, and plant succession in crop rotation systems. Among the numerous and already mentioned in part advantages that make growing of legumes an attractive proposal, a less known, undervalued, and attributed only a marginal significance element is the physical properties of their seeds. Knowledge of the physical properties of seeds is of special significance for the optimization of harvest, drying, and storage, and is related with minimization of quantitative losses and mechanical damage.

Evaluation of materials at early stages of breeding

Sowing grasspea (*Lathyrus sativus* L.), as a high-protein leguminous plant, is characterized by exceptional resistance to biotic and abiotic stresses. In particular, this relates to resistance to drought, the highest among all leguminous plants and also other crop plant species. In the

aspect of the global climate change and the mentioned resistance to drought, grasspea has been accepted as the model plant for the needs of sustainable agriculture (Vaz Patto et al., 2006). Hence, an attempt was undertaken at performing an estimation of the genetic variability of the utility features of that little known species, and especially a study of the resistance of its seeds to mechanical damage, to fill a gap in the world literature (Rybniński et al., 2004). The object of the study was young breeding material – mutants obtained through subjecting seeds of the Polish cultivars Derek and Krab to the effect of chemomutagens. Selected utility features were analyzed on the basis of a field experiment and, after harvesting the seeds, their resistance to static loads was determined as expressed by the force (N), deformation (mm), and energy (mJ). It was found that induced mutation is an effective tool for expanding the genetic variability of utility features in mutants. Apart from the selection of grasspea mutants with utility features improved with relation to the initial cultivars, selection of forms with increased resistance of seeds to mechanical loads was also performed. With the mean force value (N) for seeds of cv. Krab being 279.2 N, the range of variability of that trait in the mutants was from 238.0 for mutant K 14 to 328.4 N for mutant K 50. The broad range of genetic variability of mutant seeds resistance to mechanical loads, in conjunction with the favorable values of utility features estimated in the field experiment, permits the breeder to effectively select the most desirable forms as initial material for further breeding work, combining in a single genotype the improved utility features with increased seed resistance to mechanical loads.

In many cases, in order to extend the genetic variability of features and to introduce new ones, currently not available to the breeder, breeding programs make use of unique material collected at world Gene Banks. In view of the fact that such collection materials represent practically all the regions of the world, the breeders have at their disposal unique materials that are characterized by features not found in local materials. Frequently, due to their specific adaptive capabilities and exotic origin, not all collection materials can be applied under the conditions in which the breeder introduces new cultivars that are to be used by farmers under similar conditions. The above can be exemplified by a study that used collection lines of sowing grasspea originating from the regions of South and Central Europe for the estimation of phenotypic features, seed yield structure, geometric properties of seeds, and their resistance to static loads. The estimations comprised the variability of 32 objects, 21 of which originated from Italy, five from Spain, two each from France, Germany, and Poland (Rybniński et al., 2008). The material under estimation was characterized by a broad range of phenotypic variability, field structure parameters, geometric parameters of seed, and its resistance to mechanical loads (Table 4). In terms of their morphology, the plants and seeds of forms from Central Europe (Germany, Poland) differed the most from forms from Italy and Spain. The greatest variability

Plant Physical Characteristics in Breeding and Varietal Evaluation, Table 4 Statistical characteristics of morphological traits and yield structure parameters of grasspea plants (Rybicki et al., 2008)

Traits	Mean values	Range of variability			Coefficient of variation V(%)
		Min.	Max.	Variance	
Time of flowering (days)	62.19	58.0	67.0	0.546	3.76
Plant height (cm)	50.79	31.4	67.4	0.574	14.93
Height of lowest pod (cm)	17.88	11.0	27.0	0.113	18.83
Number of branches per plant	5.13	3.0	7.4	0.731	16.66
Number of pods per plant	29.56	17.8	69.4	0.690	28.09
Pod length (cm)	3.99	3.2	4.7	0.949	7.70
Pod width (cm)	1.56	1.33	1.92	0.174	8.48
Number of seeds per pod	2.31	1.08	3.74	0.332	24.93
Weight of seeds per pod (g)	0.60	0.31	0.91	0.125	18.59
Number of seeds per plant	58.24	15.50	148.4	0.645	43.62
Weight of seeds per plant (g)	13.85	7.20	21.19	0.953	22.29
Weight of 100 seeds (g)	27.10	8.70	51.0	0.917	35.33
Maximum force (N)	264.81	131.21	407.62	3346.41	21.85
Force of elasticity (N)	216.3	92.28	382.69	3783.50	28.42
Maximum deformation (mm)	0.42	0.23	0.81	0.01	27.02
Elastic deformation (mm)	0.13	0.09	0.29	0.01	20.65
Energy (mJ)	29.42	13.50	47.20	56.33	25.51
Modulus of elasticity (MPa)	888.24	557.63	1273.70	22131.41	16.75
Seed thickness (mm)	5.35	4.42	8.34	0.29	10.00
Seed width (mm)	9.50	5.70	13.00	2.41	16.34
Seed length (mm)	10.46	6.30	14.55	3.05	16.70

was recorded for the number of seeds per plant and the weight of 100 seeds, at coefficient of variability values of 45.6 and 35.3%, respectively. A broad range of variability of seed resistance to static loads was accompanied by similar levels of variability of other mechanical parameters, with the exception of the modulus of elasticity. Similar, though lower, values of coefficient of variability were obtained for seed thickness and width. It was noted that next to the small-seeded forms originating from France, Germany, and Poland, large-seeded forms came only from Italy and Spain. In breeding work, the relations between the evaluated features, as expressed by the value of coefficient of correlation, provide important information for the breeder (Table 5). A number of significant correlations were demonstrated between the utility features concerning plant morphology and the yield structure of the plants (traits Nos. 1–12 in Table 5). For the breeder estimating those features in his own field experiments it is important to know to what extent they are related with the resistance of seeds to mechanical loads. A lack of significant correlations between was demonstrated, which means in practice that estimations of morphological traits and yielding cannot be a basis for conclusions concerning the degree of seed resistance to mechanical damage. Whereas, a strong and significant correlation was observed between the particular parameters of mechanical loads (traits Nos. 13–18 in Table 5), with the exception of an insignificant correlation between maximum strain and energy and modulus of elasticity, and between the modulus and elastic strain. All geometric parameters of seeds

were correlated with one another (traits Nos. 18–21 in Table 5), as well as with certain morphological features, yield structure parameters, and mechanical load parameters. Noteworthy is the obtainment of a positive correlation between seed thickness and elastic strain, and a negative correlation between seed thickness and modulus of elasticity. The notable differentiation of forms with relation to their geographic origin is supported by the positioning of the objects on the plane in the system of two first canonical variables with respect to the analyzed traits of yields and mechanical loads combined. The most different from all other forms is the Polish cultivar Derek, followed by cv. Krab and the objects from North France and Germany. A notable separateness within the group of forms from Italy and Spain is characteristic of the Italian forms. With respect to resistance for mechanical loads cv. Derek is similar with forms from France and Germany whereas cv. Krab - with Italian forms.

Estimation of physical parameters of seeds on the example of commercial cultivars

Lentil is a member of the family of papilionaceous plants (*Papilionaceus*) – (*Fabaceae* = *Papilionaceae*) comprising 18,000 species. Compared to other species popular in agriculture, such as pea, vetch, soybean or lupine, and lentil – as the mentioned sowing grasspea (*Lathyrus sativus L.*) is a species with rather a marginal importance in European agriculture. Lentil seeds are characterized by a high content of proteins (even up to 30%) and high nutritional

Plant Physical Characteristics in Breeding and Varietal Evaluation, Table 5 Coefficients of correlation for morphological traits of plants, yield structure, and mechanical loads of seeds

	1	2	3	4	5	6	7	8	9	10	11	12	13	14	15	16	17	18	19	20	
1	1																				
2	0.50**	1																			
3	0.42*	0.86***	1																		
4	0.25	0.47**	0.42*	1																	
5	0.26	0.43*	0.07	0.4*	1																
6	0.13	0.22	0.32	0.33	-0.29	1															
7	-0.31	-0.23	-0.01	-0.03	-0.44*	0.57***	1														
8	0.51**	0.63***	0.40*	0.43*	0.51**	0.04	-0.68***	1													
9	-0.38*	-0.08	0.12	0.04	-0.50**	0.56***	-0.29	1													
10	0.55***	0.66***	0.39*	0.49**	0.761***	-0.07	-0.65***	0.90***	1												
11	0.00	0.42*	0.34	0.38*	0.19	0.25	0.17	0.21	0.55***	0.24	1										
12	-0.35*	-0.41*	-0.16	-0.28	-0.53***	0.24	0.86***	-0.86***	0.62***	-0.81***	0.15	1									
13	-0.12	-0.11	-0.10	0.02	-0.01	0.18	-0.03	0.10	0.00	0.06	0.06	0.08	1								
14	-0.13	-0.15	-0.11	-0.02	-0.03	0.27	-0.12	0.15	-0.06	0.05	0.19	0.96***	1								
15	0.08	-0.03	-0.01	-0.14	-0.02	0.15	0.01	0.15	-0.03	0.15	-0.15	-0.10	0.26	0.31	1						
16	-0.32	-0.23	-0.20	-0.11	-0.04	0.12	0.16	-0.14	0.20	-0.11	0.02	0.15	0.58***	0.71***	0.46***	1					
17	-0.27	-0.11	-0.07	-0.02	-0.01	0.18	0.24	-0.06	0.15	-0.04	0.05	0.09	0.95***	0.91***	0.32	0.62***	1				
18	0.24	0.03	0.00	0.09	0.00	0.06	-0.14	0.19	-0.27	0.18	-0.25	0.58***	0.46***	-0.04	-0.09	0.36*	1				
19	-0.63***	-0.44*	-0.22	-0.19	-0.43*	0.01	0.45**	-0.62***	-0.54***	-0.61***	0.08	0.59***	0.05	0.16	-0.25	0.52**	0.16	-0.48**	1		
20	-0.43*	-0.44*	-0.18	-0.20	-0.61***	0.40*	0.90***	-0.84***	0.61***	-0.82***	0.04	0.9***	0.20	0.27	-0.08	0.19	0.22	-0.10	0.60***	1	
21	-0.39*	-0.47***	-0.23	-0.25	-0.58***	0.28	0.81***	-0.87***	0.51**	-0.81***	-0.01	0.88***	0.21	0.31	-0.12	0.21	0.19	-0.01	0.59***	0.96***	1
1	2	3	4	5	6	7	8	9	10	11	12	13	14	15	16	17	18	19	20		

* significant at $\alpha = 0.05$; ** significant at $\alpha = 0.01$; *** significant at $\alpha = 0.001$

1 – Time of flowering (days); 2 – Plant height (cm); 3 – Height of the lowest pod; 4 – Number of branches per plant; 5 – Number of pods per plant; 6 – Pod width (cm); 8 – Number of seeds per plant; 9 – Weight of seeds per plant (g); 10 – Number of seeds per pod (g); 11 – Weight of 100 seeds (g); 13 – Maximum force (N); 14 – Force of elasticity (N), 15 – Maximum deformation (mm); 16 – Elastic deformation (mm); 17 – Energy (mJ); 18 – Modulus (MPa); 19 – Seed thickness (mm); 20 – Seed width (mm); 21 – Seed length (mm)

value, which causes that in many countries lentil is now rediscovered by dieticians and nutritionists, who now classify it among so-called "safe foods" (Bhatti, 1988; Dębski and Dębska, 1989; Lampart-Szczapa, 1997). In spite of the unique nutritional qualities of its seeds, lentil is characterized by utility features that require genetic improvement in the process of breeding. One of such features is pod cracking. It takes place during ripening, when lentil pods tend to crack causing seed shedding. Seed losses resulting from this may reach up to ca. 20% of seed yield per hectare, and two-phase harvest reduced those losses to 14.2% compared to single-stage harvest (Sosnowski et al., 1993). In regions of East Asia and Africa, those losses may reach even 55% of the total yield of lentil seeds (Sidhamed and Jaber, 2004). Some literature data point out certain attempts at limiting lentil seed shedding or even total elimination of that unfavorable trait. Until the problem of premature cracking of pods and seed shedding has been solved through the creation of genetic resistance, one of the ways of reducing the levels of losses is the application of preparations inhibiting pod cracking under field conditions (Szot et al., 2005). Suitable measuring apparatus permitted the estimation of susceptibility of lentil pods to opening (in the phase of full ripeness), expressed by values of maximum force and energy causing the pods to break open. The measurement of both parameters, under the effect of opposing forces applied to both lateral sides of the pod, ended at the moment of its full opening. Measurement results were obtained for the commercial lentil cultivars Tina and Anita, for pods not subjected to the effect of desiccating agents (control treatment) and for pods after the application of such preparations. The results indicate varied responses of the cultivars as expressed by values of force required for pod opening – from 0.71 N for cv. Anita to 0.89 N for cv. Tina. When the desiccating preparations were applied, the best results were obtained using the spraying preparation Spodam and potato starch. With the application of Spodam, the force values increased by 0.32 N (36%) for cv. Tina and by 0.12 N (17%) for cv. Anita compared to the control treatment. Other preparations proved to be less effective, especially in the case of wheat starch and Reglone. The coefficient of variability for the preparations applied varied within the range from 41% to 60%. In spite of the positive results obtained for the Spodam preparation, it will not replace attempts by breeders at obtaining genetic resistance of pods to cracking and seed shedding. Nevertheless, the information from agrophysicists on the values of force required for pod opening relating to world collection materials, lines, and cultivars will permit better selection of parent components in crossbreeding aimed at the creation of cultivars with enhanced resistance to seed shedding. It is also important to demonstrate that the resistance of seeds to the effect of external forces is closely related with the level of damage to the seeds in the processes of harvest, transport, and at various stages of post-harvest processing, such as seed behavior in the course of various technological processes

to which seeds are subjected as raw material. Damage to seeds may be an important element of reduced germination capacity and lead to the disqualification of a seed batch as qualified sowing material. Differences between cultivars were observed in response to mechanical loading of seeds with moisture content of 9%. With respect to the force destroying seed structure, seeds of cv. Tina required the application of average force values at the level of 90 N, with range of variability from 53.7 N to 135.7 N. Seeds of cv. Anita proved to be more resistant, with mean force value of 125.5 N, minimum of 67.2 N and maximum of 194.0 N. Moreover, a rapid decrease in the force values was demonstrated for seed moisture increase from 9% to 15%, reaching even the level of 10 N. Noteworthy are the inter-variety differences in response to static loads, indicating their role in the estimation of seed quality for consumption purposes and as raw material for the food industry. The study was conducted for seeds of only two cultivars, demonstrating that their proneness toward shedding and mechanical damage had a genetic background. One can expect that examination of a large group of collection forms from various Gene Banks and cultivars will permit the selection of forms with the highest resistance. Data from agrophysical laboratories should provide valuable information that, given to the breeders, will help in finding proper directions in lentil breeding aimed at its genetic improvement.

Estimation of the physical properties of seeds of the most popular species of leguminous plants permits not only the assessment of varietal differentiation within a species, but also identification of differences between different species. Within the scope of particular species, farmers or the processing industry have at their disposal a large array of commercial cultivars representing a broad range of intra-species variability of traits, primarily in the aspects of their yielding capacity, chemical composition of seeds (e.g., protein, its amino acid composition, content of anti-nutritional substances), as well as resistance to biotic and abiotic stresses. The properties of cultivars regarding the abovementioned traits are generally available, mainly in the form of advertising material and cultivation recommendations published by plant breeding and seed producing institutions. The user of cultivars, however, will not find there significant information on the resistance of seeds to mechanical loads, for the simple reason that the author of a given cultivar has no data on that subject and, as a rule, does not conduct selection programs aimed at genetic improvement of that resistance. On the other hand, there are not many agrophysical publications that would present studies on a larger number of breeding materials (lines) or commercial cultivars. An example here may be a review of inter-cultivar and inter-species differences in the geometric parameters of seeds and their resistance to static loads. The object of the study were commercial cultivars of white, yellow, narrow-leaf and Andean lupine, and of sowing pea, sowing grasspea, lentil, and vetch. In total, 24 cultivars of those species were subjected to estimations. The results concerning the resistance to static loads indicate a broad range of variability

of the respective parameters. The calculated coefficient of variability shows that the most variable parameter was energy, and the least – elastic deformation. Similar values of the coefficient of variation were characteristic of the geometric parameters of seeds, as measured by their thickness, width, and length. An exception was the low coefficient of variability for seed length. With relation to the estimation of intra-species differences (among cultivars within a single species) in regard of the resistance of seeds to mechanical loads, it was demonstrated that the highest values of maximum force are characteristic of white lupine, followed by pea, and then by yellow lupine and narrow-leaf lupine. Notably different from all three lupine species are the low values of the Andean lupine, typical of South America. Analysis of other parameters of static loading confirmed the occurrence of the highest values for seeds of white lupine, indicating its genetic separateness from the other species and cultivars of lupine, as well as from the other species and cultivars of leguminous plants studied. A significant element is the estimation of relationships between the traits under study. With the exception of the modulus of elasticity, all remaining five parameters of mechanical loading (maximum force, force of elasticity, maximum deformation, elastic deformation, and energy) were positively and statistically significantly correlated with one another at the level of $\alpha = 0.001$. The modulus of elasticity was positively correlated only with the force of elasticity. Except for the modulus, all other load parameters were positively and significantly correlated with seed width. Seed thickness, in turn, was positively correlated with the force of elasticity and with elastic deformation. Seed length was not correlated with any of the parameters under assessment.

Estimation of similarity of all cultivars and lines in terms of mechanical loading of seeds, treated jointly in spatial form and in the system of two first canonical variables, showed that the most isolated spatial positioning was characteristic of two white lupine cultivars – Boros and Butan. The positions of the remaining cultivars indicate their greater mutual similarity and considerable separateness with relation to the white lupine cultivars.

Conclusion

Summing up, it should be clearly stated that the results of agrophysical studies are highly valuable for the geneticists and for breeders of crop plants. The presented correlations and their positive effects indicate the need for intensified scientific cooperation in this field that is a necessity for modern and interdisciplinary achievement of joint targets. As it has been shown above, the physical properties of plants are inherited to a large extent, and knowledge of those parameters may play a highly important role in the creation of new cultivars. Every species or variety is characterized by its own specific genetic potential. That potential is revealed in the specific expression of the utility features, hence the importance of proper selection of suitable initial material for breeding studies (at various stages

of the breeding cycle) and its analysis in the context of its genetic potential as well as with the inclusion of the effect on plants of specific, controlled as far as possible, environmental conditions. Therefore, it should be considered a necessity that agrophysical research methods are made available to the geneticists and plant breeders so as to allow them to test the parent forms for the selection of the most favorable traits and their heritability at the earliest possible stages of breeding programs.

Bibliography

- Bernard, M., 1976. Etude des caractéristiques cytologiques, morphologiques et agronomiques de six lignées d'addition blésigle. *Annales de l'Amélioration des Plantes*, **26**, 67–91.
- Bhatti, R. S., 1988. Composition and quality of lentil (*Lens culinaris Medic.*). *Canadian Institute of Food Science and Technology Journal*, **21**, 144–160.
- Campbell, C. G., Mehra, R. B., Agrawal, S. K., Chen, Y. Z., El Moneim, B., Khawaja, H. I. T., Yadow, C. R., Tay, J. U., and Araya, W. A., 1994. Current status and future strategy in breeding grasspea. (*Lathyrus sativus L.*). *Euphytica*, **37**, 167–175.
- Dębski, H., and Dębska, D., 1989. *Vegetables in the Kitchen (in Polish)*. Warszawa: Instytut Żywności i Żywienia.
- Evans, L. E., and Jenkins, B. C., 1960. Individual Secale cereale chromosome additions of *Triticum aestivum*. I. The addition of individual Dakold fall rye chromosomes to Kharkov winter wheat and their subsequent identification. *Canadian Journal of Genetics and Cytology*, **2**, 205–215.
- Grundas, S., 2004. Characteristics and physical properties of kernels in spikes of wheat (*Triticum aestivum L.*) (in Polish). *Acta Agrophysica*, **102**, 5–64.
- Jeżowski, S., 1981. Analysis of relationships between lodging grade and some morphological characters of spring barley varieties. *Genetica Polonica*, **22**, 45–61.
- Lampart-Szczapa, E., 1997. Seeds of leguminous plants in human nutrition. Biological and technological values (in Polish). *Zeszyty Problemowe Postępów Nauk Rolniczych*, **446**, 61–81.
- Liu, C. J., and Gale, M. D., 1989. Ibf-1 (lodging binding factor) a highly variable marker system in the Triticeae. *Theoretical and Applied Genetics*, **77**, 233–240.
- Miazga, D., and Szot, B., 1996. The influence of added rye chromosomes on physical properties of kernels of addition lines *T. aestivum Grana-S. Cereale Dankowskie Złote*. *Journal of Applied Genetics*, **37**, 37–47.
- Milczak, M., Segit, Z., and Szot, B., 1977. Variability, heritability and dependence of yield structure parameters and physicochemical properties of winter wheat kernels in population of F_2 (lines Z-70 x Kaukaz) (in Polish). *Hodowla Roślin Aklimatyzacja i Nasiennictwo*, **21**, 441–447.
- Miller, T. E., 1973. *Alien chromosome additions and substitutions*. Plant Breeding Institute Annual Report, p. 143.
- Rybicki, W., and Patyna, H., 1984. Field structure of spring barley (*Hordeum vulgare L.*) characterized by increase lysine content in grain. *Genetica Polonica*, **25**, 237–246.
- Rybicki, W., and Szot, B., 2006. Estimation of genetic variability of yielding traits and physical properties of seeds of spring barley (*Hordeum vulgare L.*) mutants. *International Agrophysics*, **20**, 219–227.
- Rybicki, W., Szot, B., and Pokora, L., 2004. Estimation of genetic variation and physical properties of seeds for grass pea mutants (*Lathyrus sativus L.*). *International Agrophysics*, **18**, 339–346.
- Rybicki, W., Szot, B., and Rusinek, R., 2008. Estimation of morphological and mechanical properties of grasspea seeds (*Lathyrus sativus L.*) originating from EU countries. *International Agrophysics*, **22**, 261–275.

- Schlegel, R., 1978. Configuration of chromosomes in wheat-rye addition lines (in Russian). *Genetyka*, **XIV**, 1365–1375.
- Sears, E., 1967. Induced transfer of hairy neck from rye to wheat. *Zeitschrift für Pflanzenzüchtung*, **57**, 4–25.
- Sidhamed, K. M., and Jaber, N. S., 2004. The design and testing of a cutter and feeder mechanism for the mechanical harvesting of lentil. *Biosystem Engineering*, **88**, 295–304.
- Simmonds, D. H., Barlow, K. K., and Wrigley, C. W., 1973. The biochemical basis of grain hardness in wheat. *Cereal Chemistry*, **50**, 553–562.
- Sosnowski, S., Jech, J., Rataj, V., and Ponican, J., 1993. Mechanized lentil collection in Slovakia. *Zeszyty Problemowe Postępu Nauk Rolniczych*, **339**, 243–246.
- Styk, B., and Szot, B., 1984. Evaluation of seed biological quality of several varieties of summer barley. *Buletyn IHAR*, **153**, 57–66.
- Szot, B., and Tarkowski, Cz., 1977. Preliminary investigation on some physical properties of *Triticale* grain. *Roczniki Nauk Rolniczych*, **72-C-3**, 15–24.
- Szot, B., Stępniewski, A., and Rudko, T., 2005. *Agrophysical Properties of Lentil*. Lublin: Institute of Agrophysics PAN.
- Tnag, K. S., and Hart, G. E., 1975. Use of isoenzymes as chromosome markers in wheat-rye addition lines and *Triticale*. *Genetics Research*, **26**, 187–201.
- Vaz Patto, M. C., Skiba, B., Pang, E. C. K., Ochatt, S. J., Lambein, F., and Rubiales, D., 2006. Lathyrus improvement for resistance against biotic and abiotic stresses: from classical breeding to marker assisted selection. *Euphytica*, **147**, 133–147.
- Woźniak, W., 2003. Application of uniaxial compression for evaluation of basic mechanical properties of wheat grain. *Acta Agrophysica*, **93**, 145–155.
- Woźniak, W., Gründas, S., and Rybiński, W., 2006. Mechanical characteristics of kernels of genetic variation of hull-less barley. *Acta Agrophysica*, **8**, 1041–1047.

Cross-references

- [Agrophysical Objects \(Soils, Plants, Agricultural Products, and Foods\)](#)
[Agrophysical Properties and Processes](#)
[Agrophysics: Physics Applied to Agriculture](#)

PLANT ROOT STRENGTH AND SLOPE STABILITY

Sekhar Lukose Kuriakose¹, L. P. H. van Beek²

¹United Nations University-ITC School for Disaster Geo-information Management, University of Twente, Enschede, The Netherlands

²Department of Physical Geography, Utrecht University, Utrecht, The Netherlands

Synonyms

Root pullout strength; Root tensile strength; Shallow landslides; Slope stability

Definition

- Plant root strength: Maximum force per unit area, causing a plant root in strained soil to break or to become detached along the soil–root interface.
- Slope stability: Force equilibrium of resistant and driving forces acting on a soil mass that can deform freely

under the influence of gravity (e.g., on sloping surfaces), leading to limited deformation that is inconsequential for the safety or serviceability of the slope or adjacent areas.

Introduction

Root reinforcement is the interaction between mobilized root strength, root morphology, and shear strength along the soil–root interface. At the plant level, this interaction ensures the stability of the aboveground biomass while, at the stand level, the reinforced soil may contribute positively to the overall stability of natural and man-made slopes. Root reinforcement is widely recognized as the most important beneficial effect of vegetation on slope stability. However, it is just one of the many ways by which vegetation influences slope stability, either directly by affecting the loads or resistance or indirectly through the hydrology. The influence of vegetation on slope stability has been widely attested with the frequency of mass movements such as shallow landslides increasing after the removal of the vegetation and the decay of roots, reaching as far back as Pliny, the Elder (Pliny the Elder or Gaius Plinius Secundus [23–79]: Roman officer and encyclopedist) who wrote “Often, disastrous torrents are formed after the felling of mountain woods, which used to hold back clouds and feed on them.”

Root reinforcement requires that plant roots anchor the soil mantle to bedrock or that roots act as fibrous binders of soil particles (Ziemer, 1981). The major biotic determinants of root reinforcement are root strength and root architecture which are primarily dependent on plant species, while the major abiotic determinants are soil texture, depth, moisture content, the local slope angle, water table depth, and the depth of the potential slip plane (Danjon et al., 2008; Genet et al., 2005).

Mechanisms of root reinforcement

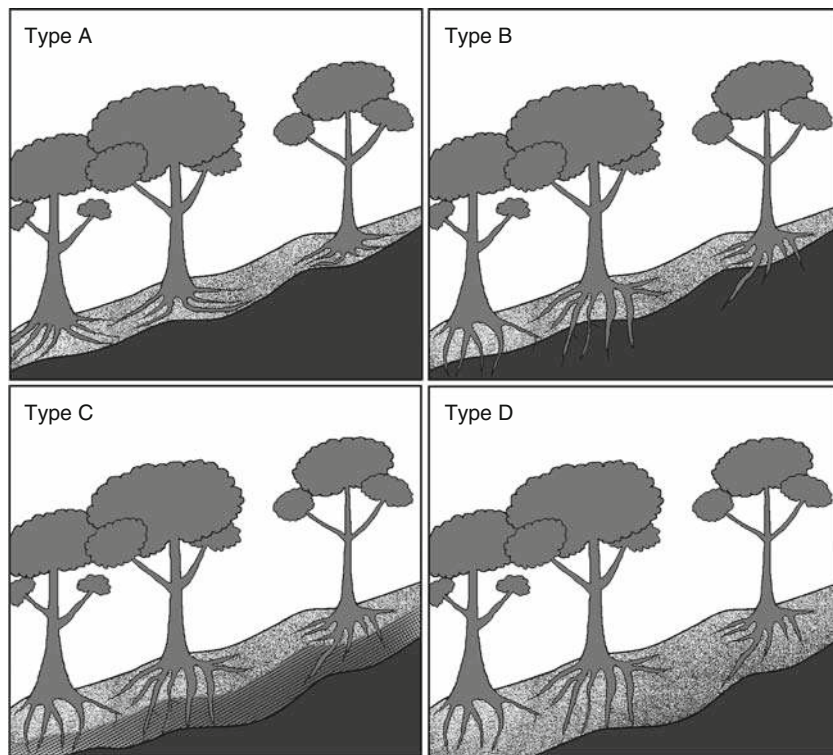
In soil possessing little if any tensile strength of its own, roots constitute elastic elements with high tensile strength. Upon deformation of the soil, elastic elongation of the roots mobilizes the available root strength. Given root orientation with respect to local displacement, total root reinforcement depends on the total number of roots loaded and the mobilized strength. Normal to the potential slip plane, root reinforcement contributes through the confining normal stress to the frictional resistance, while the tangential component reduces the applicable shear stress. With continued deformation, root reinforcement continues to increase until individual roots eventually fail by breakage or pullout (slippage). Thus, root reinforcement is only appreciable after some strain has occurred and a substantial number of roots has deformed, when those roots remain intact and bounded by the soil and when the strain is small enough to prevent the complete loss of integrity of the soil; when these conditions are not met, the slope may fail regardless without mobilizing the maximum available root reinforcement (Mulder, 1991).

Failure of individual roots occur when they rupture in tension or are pulled out from the surrounding soil. The latter usually requires less force than the former and most often in highly saturated fine-textured soils, pullout is the dominant root failure mechanism (van Beek et al., 2005; Waldron and Dakessian, 1981). Root strength of a single root segment ultimately depends on the effective normal stress acting on it, the cohesion and friction along the soil–root interface, and the area thereof in case of pullout or the root tensile strength, which is partly species dependent, partly dependent on wood age, and function. Branched roots can mobilize more strength than roots without branches that slip out of the ground with minimal resistance. Branched roots fail in two different modes, them being (1) the ones that reach a maximum strength and maintain this strength until it progressively decreases with the breakage of individual branches after crossing a threshold strain and (2) those that break with the progressive increase of force (Greenwood et al., 2004).

While root-reinforced soil contributes locally to the available shearing resistance, stable columns of soil may act as buttresses and prevent overall slope failure (Wang and Yen, 1974). Consequently, the relative location of plants with varying root architecture is an important determinant of total root reinforcement (Coutts, 1983). The presence of plants with heart roots and lateral roots is preferred along the toe and scarp of a potentially unstable

slope, while plants with tap roots that provide anchoring into bedrock or stable soil layers are favored along the mid-slopes (Danjon et al., 2008). In general, a large number of small roots will contribute more to slope stability as compared to a small number of large roots (De Baets et al., 2008). Based on the root–soil–bedrock interactions and the resultant slope stabilizing effects of roots, hill slopes can be classified into four types (Figure 1) (Tsukamoto and Kasakobe, 1984), them being:

- Type A: Characterized by shallow soil (<1 m) overlying an impenetrable bedrock. Roots grow laterally at the failure plane, binding the overlying soil and thus provide high soil cohesion, but lacks anchoring.
- Type B: Characterized by shallow soil (<1 m) overlying a bedrock with substantial density of fractures. Roots penetrate the bedrock, intersecting the potential failure plane and thus provide high soil cohesion and anchoring.
- Type C: Characterized by deeper soils (1–3 m) overlying a nondistinct weather bedrock material that acts as a hydrological transition zone, exhibiting increasing strength with depth, which in turn overlies the impenetrable bedrock. Roots penetrate the soil and the weathered parent material often through which passes the failure plane, and thus provide high soil cohesion and anchoring.



Plant Root Strength and Slope Stability, Figure 1 Four types of root reinforced hill slopes. (Modified after Tsukamoto and Kasakobe, 1984.)

- Type D: Characterized by very deep soil (>3 m) overlying an impenetrable bedrock. The failure plane in such slopes being very deep, often the roots do not intersect them and thus lacks any anchoring; however, given a certain root density there may be moderate soil cohesion.

Root strength measurements

Quantification of root reinforcement requires information on root densities, orientation, diameter, and species as well as on the available strength. For individual root segments, soil–root bond has to be measured by mimicking pullout, while root tensile strength has to be measured by loading a root segment in tension until failure occurs.

Root tensile strength

Root tensile strength is measured by subjecting a single root segment to elongation until the root breaks. The load at failure can be measured using a universal tensile and compression testing machines generally used for fiber tensile strength testing (De Baets et al., 2008) or specialized equipment (Ziemer, 1978) which can apply a constant strain rate to the clamped root. To avoid stress concentrations around the clamped ends, the overall length of a root segment should be several times its diameter and sufficiently large to provide for clamping (approximately 5 cm on either side). For roots under 10 mm, a total length of 15 cm often suffices. Clamping a root is a delicate work, and roots often either slip from the clamps or break where the root gets crushed by it. Epoxy resin or Plaster of Paris reinforcement at the tips can prevent this. A tensile strength test is counted successful if the breakage is at the middle nonreinforced part of the sample. Care has to be taken to avoid root desiccation or root decay during the period between sampling and testing. Roots should be kept as close to their original moisture content as possible or at least soaked for 24 h to approximate their green strength (Cofie and Koolen, 2001).

For most plants, the tensile strength is known to increase with a decrease in the diameter of roots based on a power law having the form

$$T_{ri} = aD^{-b},$$

where T_{ri} is the tensile strength of an individual root (measured in units of pressure, usually MPa or kPa), D the diameter of roots (measured in units of distance, usually mm), a the relationship constant, and b the scaling exponent.

Table 1 provides the parameters of the tensile strength-diameter power relationships for various plant species from published literature. **Figure 2** shows this relationship of five tropical plant species.

Root pullout strength

Pullout strength has to be measured in situ either by measuring the total strength necessary to pull out a whole plant

(Nilaweera and Nutalaya, 1999) or by testing individual root threads (van Beek et al., 2005). Studies have shown that there exists a theoretical threshold diameter between root pullout and root breaking. Above this threshold, the friction between the soil and roots exceeds the root tensile strength and below it, if the force required to break the root–soil friction bond is less than the force required to break the root, the roots will slip off the soil (Pollen, 2007). Pullout strength test needs minimum 10 cm of root protruding outside the soil. Ideally, the sample should be at least 0.5 m away from the base of the tree. A pullout strength test is counted successful if successive straining decreases the stress, indicating the loss of soil–root bond. If the roots break during a pullout test, they are registered separately, so as to identify the threshold diameter between root pullout and root breaking. Pullout strength is more site specific compared to the tensile strength because of the spatial variations in root-soil bond which in turn is influenced by factors such as soil cohesion, soil saturation, slope and root type (Schmidt et al., 2001).

Root reinforcement models

There are three models that abstract root reinforcement. The first and the most commonly used approach called simple perpendicular root model considers root–soil interaction within a shear band through force equilibrium (Waldron, 1977; Wu et al., 1979). The root reinforcement is translated as an additional amount of cohesion in the Coulomb equation, which depends on the amount and strength of roots present in the soil and assumes the form:

$$C_r = T_r(\sin\theta + \cos\theta\tan\phi)\left(\frac{A_R}{A}\right),$$

where C_r is the total root-induced cohesion, T_r is the average tensile strength of roots per unit area, A_R/A (unit less) is the root area ratio, ϕ is the angle of internal friction of the soil, and θ is the angle of deformed roots with respect to the shear surface. Based on the extensive sensitivity analysis, the value of $(\sin\theta + \cos\theta\tan\phi)$ is approximated to be 1.2 for most practical situations (Wu et al., 1979). As calculating, C_r necessitates site-specific information such as soil depth and root density, it is not attempted herein. The amount of additional cohesion induced by roots of a given species of plant presented in **Table 1** can be found in the respective articles.

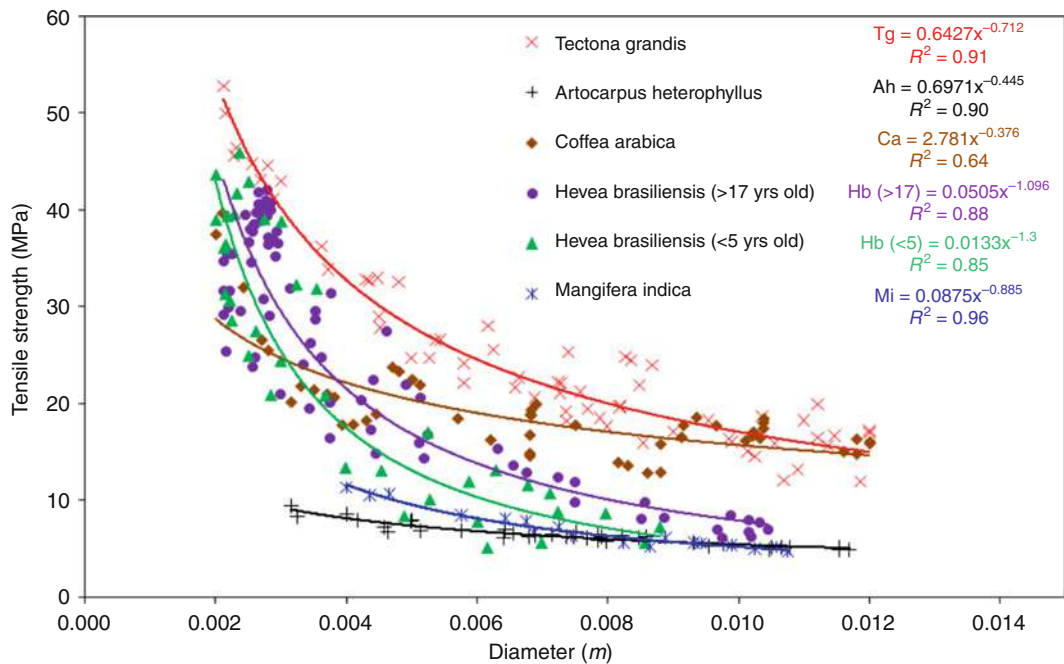
The second model considers root-included soil matrix as a composite material with a homogenous macroscopic behavior (Michałowski and Zhao, 1995). The third model (named RipRoot model) is based on the concept of fiber-bundle models in material sciences and attempts to capture the progressive breakage of roots having varying tensile strengths, with an associated redistribution of stress as each root segment breaks (Pollen and Simon, 2005).

Natural variability is the major source of uncertainty in computing root reinforcement. Root strength of different

Plant Root Strength and Slope Stability, Table 1 Parameters and R^2 values of the root tensile strength-root diameter power relationships

Species	Type	D range (mm)	a	b	R^2	N	Reference
<i>Atriplex halimus</i>	S	0.23–4.68	45.59	0.56	0.52	38	De Baets et al. (2008) (MPa)
<i>Salsola genistoides</i>	S	0.30–3.84	44.23	0.51	0.58	26	
<i>Thymelaea hirsuta</i>	S	0.18–2.70	33.31	0.64	0.55	52	
<i>Artemisia barrelieri</i>	S	0.16–2.15	30.12	0.61	0.37	32	
<i>Fumana thymifolia</i>	S	0.19–2.43	15.71	0.66	0.53	52	
<i>Dorycnium pentaphyllum</i>	S	0.27–4.35	16.32	0.62	0.31	48	
<i>Teucrium capitatum</i>	S	0.22–2.60	18.72	0.45	0.4	51	
<i>Dittrichia viscosa</i>	S	0.30–5.50	18.94	0.45	0.3	54	
<i>Thymus zygis</i>	S	0.12–2.88	19.31	0.73	0.63	34	
<i>Rosmarinus officinalis</i>	S	0.16–3.60	12.89	0.77	0.63	54	
<i>Nerium oleander</i>	S	0.09–4.11	4.41	1.75	0.91	30	
<i>Ononis tridentata</i>	S	0.88–5.53	9.59	n.s.	n.a.	46	
<i>Anthyllis cytisoides</i>	S	0.51–7.03	8.43	n.s.	n.a.	54	
<i>Retama sphaeroarpa</i>	S	0.41–3.77	16.36	n.s.	n.a.	28	
<i>Brachypodium retusum</i>	G	0.10–1.45	45.05	0.61	0.71	33	
<i>Stipa tenacissima</i>	G	0.43–1.34	24.34	0.61	0.22	57	
<i>Lygeum spartum</i>	G	0.26–2.72	19.28	0.68	0.44	50	
<i>Helictotrichon filifolium</i>	G	0.34–1.22	14.51	1.08	0.42	53	
<i>Piptatherum miliaceum</i>	G	0.10–0.64	11.49	1.77	0.63	48	
<i>Avenula bromoides</i>	G	0.15–0.32	4.77	1.52	0.6	52	
<i>Juncus acutus</i>	Ru	0.18–1.10	23.23	0.89	0.66	45	
<i>Phragmites australis</i>	R	0.10–7.91	34.29	0.78	0.92	20	
<i>Limonium supinum</i>	H	0.34–3.90	33.82	0.85	0.55	30	
<i>Plantago albicans</i>	H	0.21–2.55	16.75	0.52	0.47	50	
<i>Tamarix canariensis</i>	T	0.10–4.80	31.74	0.89	0.42	55	
<i>Cryptomeria japonica</i> (mature)	T	0.30–4.30	31.90	0.41	0.36	100	Genet et al. (2008) (MPa)
<i>Cryptomeria japonica</i> (intermediate)		0.45–4.20	25.79	0.37	0.36	100	
<i>Cryptomeria japonica</i> (juvenile)		0.25–3.50	21.59	0.34	0.15	100	
<i>Sesbania cannabina</i>	H	0.5–4.5	60.478	0.858	0.52	20	Fan and Su (2008) (kPa)
<i>Paraserianthes falcataria</i>	T	0.97–12.45	95.587	0.3175	0.85	19	Yonghong et al. (2006)
<i>Eucalyptus globulus</i>		1.25–15.12	92.141	0.2747	0.88	19	Equation used $T_{ri} = ae^{-bD}$ (MPa)
<i>Pinus nigra</i>	T	0.2–12	18.40	0.52	0.23	30	Genet et al. (2005) (MPa)
<i>Pinus pinaster</i>			23.40	0.87	0.51	34	
<i>Castanea sativa</i>			31.92	0.73	0.51	53	
<i>Salix purpurea</i>	S	0.18–4.10	26.33	0.95	0.55	150	Bischetti et al. (2005) (MPa)
<i>Salix caprea</i>	S	0.13–5.70	34.50	1.02	0.82	144	
<i>Fraxinus excelsa</i>	T	0.27–5.70	35.73	1.11	0.51	17	
<i>Alnus viridis</i>	S	0.65–5.91	34.76	0.69	0.34	49	
<i>Corylus avellana</i>	S	0.31–3.82	60.15	0.75	0.57	13	
<i>Larix decidua</i>	T	0.14–5.47	33.45	0.75	0.47	43	
<i>Fagus sylvatica</i>	T	0.14–4.59	41.65	0.97	0.62	168	
<i>Picea abies</i>	T	0.12–5.84	28.10	0.72	0.53	92	
<i>Ostrya carpinifolia</i>	T	1–10	21.89	0.43	0.55	42	Bischetti et al. (2009) (MPa)
<i>Lygeum spartum</i>	H	1.1–1.8	60.73	1.30	0.38	28	Mattia et al. (2005) (MPa)
<i>Pistacia lentiscus</i>	S	2.7–4.6	91.25	0.45	0.14	18	
<i>Rosa canina</i>	S	0.43–9.9	0.5642	2.5611	0.76	57	Tosi (2007)
<i>Inula viscosa</i>	H	0.40–13	0.7559	2.4814	0.88	63	Equation used $T_{ri} = -aD + b$ (MPa)
<i>Spartium junceum</i>	S	0.65–9.35	0.3413	2.6004	0.51	48	
<i>Vetiveria zizanioides</i>	G	0.3–1.4	3.3016	1.3134	0.71	20	Mickovski and van Beek (2009) (MPa)
<i>Pseudotsuga menziesii</i>	T	1–15	24.753	0.201	n.a.	n.a.	Nilaweera and Nutalaya (1999) (MPa)
<i>Dipterocarpus alatus</i>	T		68.953	0.447			
<i>Hopea odorata</i>	T		87.041	0.693			
<i>Alstonia macrophylla</i>	T		28.273	0.465			
<i>Ficus benjamina</i>	T		40.485	0.722			
<i>Alangium kurzii</i>	H		52.948	0.527			
<i>Hibiscus macrophyllus</i>	S		51.487	0.563			

T tree, S shrub, H herb, Ru rush, G grass, n.s. not significant, n.a. not available, N number of successfully tested samples. Wherever other equations are mentioned, the authors used these forms of power law. Unit of tensile strength is provided in parentheses in the reference column as (MPa) Mega Pascal or (kPa) Kilo Pascal



Plant Root Strength and Slope Stability, Figure 2 Root tensile strength-root diameter power relationships of five tropical tree species namely *Tectona grandis*, *Hevea brasiliensis* (plant age <5 and >17 years), *Artocarpus heterophyllus*, *Mangifera indica*, and *Coffea arabica*.

species of the same family can be considerably different (Greenway, 1987). Such high variability can also be observed with the strength of roots of the same species growing in different terrain conditions (Gray and Sotir, 1996).

Reliability of root reinforcement

Increased infiltration and permeability, desiccation of soil due to plant intake which results in large macropores, surcharge due to the presence of overgrown trees, and wind loading are some of the detrimental effects of vegetation on slopes susceptible to failure (Coppin and Richards, 1990). Such effects are clearly outweighed by the mitigating effects of root reinforcement (Fan and Su, 2008). However, the presence of roots does not increase the stability of slopes indefinitely. Root count rapidly decreases with increase in soil depth (Cammeraat et al., 2005), and hence root reinforcement is limited in such slopes (Type D slopes). Studies indicate that the root reinforcement on natural slopes is limited to a small range of critical hydrological conditions (van Beek et al., 2005).

In anthropogenically intervened landscapes, root development is significantly hampered by cyclical slope modifications and when trees are cut, the root system begins to decay, leading to the progressive weakening of soil–root fabric (Schmidt et al., 2001). Such decayed roots also act as preferential flow conduits, which transport water

directly to the potential failure planes. So also, after the reestablishment of vegetation in clear felled forests, it takes almost 3 decades for soil to regain the strength of that in the uncut forest (Ziemer, 1981).

Conclusion

It is evident from Table 1 that research on root reinforcement offered by plants is limited. Very little efforts have been directed toward understanding the relationships between the cellulose content and the tensile strength of roots. Most researchers consider root reinforcement as additional cohesion based on the first model, while the second and third models are not widely applied or researched upon. The root reinforcement model is by itself limited in certain aspects. For example, fine roots are not very flexible to be loaded in compression which in reality will affect root–soil bond and thereby limit the mobilization of root pullout strength. Laboratory studies are still lacking in this direction (van Beek et al., 2005). A significant root strength parameter, the Young's modulus (measure of the stiffness of root thread as an isotropic elastic material), is less frequently measured than the tensile strength (Wu, 2007).

Studies are limited on the three-dimensional (3D) distribution of woody roots, which is often not accountable by means of conventional methods for deriving the root area ratio. This will result in an over or under estimate of

net root reinforcement by trees growing on mountain slopes (Danjon et al., 2008). Root reinforcement does not assure long-term stability in anthropogenically modified landscapes. In natural forests, forest fires and plant diseases may lead to the eventual loss of root reinforcement. Despite such limitations, plant roots can provide considerable reinforcement and is the most cost effective means to increase the stability of natural and modified slopes.

Bibliography

- Bischetti, G. B., Chiaradia, E. A., Simonato, T., Speziali, B., Vitali, B., Vullo, P., and Zocco, A., 2005. Root strength and root area ratio of forest species in Lombardy (Northern Italy). *Plant and Soil*, **278**, 11–22.
- Bischetti, G. B., Chiaradia, E. A., Epis, T., and Morlotti, E., 2009. Root cohesion of forest species in the Italian Alps. *Plant and Soil*, doi:10.1007/s11104-009-9941-0.
- Cammeraat, E., van Beek, R., and Kooijman, A., 2005. Vegetation succession and its consequences for slope stability in SE Spain. *Plant and Soil*, **278**(1), 135–147.
- Cofie, P., and Koolen, A. J., 2001. Test speed and other factors affecting the measurements of tree root properties used in soil reinforcement models. *Soil and Tillage Research*, **63**(1–2), 51–56.
- Coppin, N. J., and Richards, I. G., 1990. *Use of Vegetation in Civil Engineering*. Burredworths: C.I.R.I.A.
- Coutts, M. P., 1983. Root architecture and tree stability. *Plant and Soil*, **71**(1–3), 171–188.
- Danjon, F., Barker, D. H., Drexhage, M., and Stokes, A., 2008. Using three dimensional plant root architecture in models of shallow-slope stability. *Annals of Botany*, **101**(8), 1281–1293.
- De Baets, S., Poesen, J., Reubens, B., Wemans, K., De Baerdemaeker, J., and Muys, B., 2008. Root tensile strength and root distribution of typical Mediterranean plant species and their contribution to soil shear strength. *Plant and Soil*, **305**, 207–226.
- Fan, C. C., and Su, C. F., 2008. Role of roots in the shear strength of root-reinforced soils with high moisture content. *Ecological Engineering*, **33**, 157–166.
- Genet, M., Stokes, A., Salin, F., Mickovski, S. B., Fourcaud, T., Dumai, J.-F., and van Beek, L. P. H., 2005. The influence of cellulose content on tensile strength in tree roots. *Plant and Soil*, **278**(1–2), 1–9.
- Genet, M., Kokutse, N., Stokes, A., Fourcaud, T., Cai, X., Ji, J., and Mickovski, S., 2008. Root reinforcement in plantations of *Cyptomeria japonica* D. Don: a tree age and stand structure on slope stability. *Forest Ecology and Management*, **256**, 1517–1526.
- Gray, D. H., and Sotir, R., 1996. *Biotechnical and Soil Bioengineering Slope Stabilization*. New York: Wiley.
- Greenway, D. R., 1987. Chapter 6: Vegetation and slope stability. In Anderson, M. G., and Richards, K. S. (eds.), *Slope Stability*. West Sussex: Wiley.
- Greenwood, J. R., Norris, J. E., and Wint, J., 2004. Assessing the contribution of vegetation to slope stability. *Proceedings of the ICE – Civil Engineering*, **157**(4), 199–207.
- Mattia, C., Bischetti, G. B., and Gentile, F., 2005. Biotechnical characteristics of root systems of typical Mediterranean species. *Plant and Soil*, **278**, 23–32.
- Michałowski, R. L., and Zhao, A., 1995. Continuum versus structural approach to stability of reinforced soil. *Journal of Geotechnical Engineering*, **121**(2), 152–162.
- Mickovski, S. B., and van Beek, L. P. H., 2009. Root morphology and effects on soil reinforcement and slope stability of young vetiver (*Vetiveria zizanioides*) plants grown in semi-arid climate. *Plant and Soil*, doi:10.1007/s11104-009-0130-y.
- Mulder, H. F. M., 1991. *Assessment of Landslide Hazard*. Ph.D. thesis, Utrecht University, The Netherlands, 150 p.
- Nilaweera, N. S., and Nutalaya, P., 1999. Role of tree roots in slope stabilization. *Bulletin of Engineering Geology and the Environment*, **57**(4), 337–342.
- Pollen, N., 2007. Temporal and spatial variability in root reinforcement of streambanks: Accounting for soil shear strength and moisture. *CATENA*, **69**(3), 197–205.
- Pollen, N., and Simon, A., 2005. Estimating the mechanical effects of riparian vegetation on streambank stability using a fiber bundle model. *Water Resources Research* **41**(W07025): doi: 10.1029/2004WR003801.
- Schmidt, R. L., Roering, J. J., Stock, J. D., Dietrich, W. E., Montgomery, D. R., and Schaub, T., 2001. The variability of root cohesion as an influence on shallow landslide susceptibility in the Oregon Coast Range. *Canadian Geotechnical Journal*, **35**(5), 995–1024.
- Tosi, M., 2007. Root tensile strength relationships and their slope stability implications of three shrub species in the Northern Apennines (Italy). *Geomorphology*, **87**, 268–283.
- Tsukamoto, Y., and Kasakobe, O., 1984. Vegetation influences on debris slide occurrences on steep slopes in Japan. In *Symposium on the Effect of Forest Land Use on Erosion and Slope Stability*, Honolulu, Hawaii, pp. 63–72.
- van Beek, L. P. H., Wint, J., Cammeraat, L. H., and Edwards, J. P., 2005. Observation and simulation of root reinforcement on abandoned Mediterranean slopes. *Plant and Soil*, **278**, 55–74.
- Waldron, L. J., 1977. The shear resistance of root-permeated homogenous and stratified soil. *Soil Science Society of America Journal*, **41**, 843–849.
- Waldron, L. J., and Dakessian, S., 1981. Soil reinforcement by roots: calculation of increased soil shear resistance from root properties. *Soil Science*, **132**, 427–435.
- Wang, W. L., and Yen, B. C., 1974. Soil arching in slopes. *Journal of Geotechnical Engineering Division, ASCE* **100**(GT1), 61–78.
- Wu, T. H., 2007. Reliability analysis of slopes. In Phoon, K. K. (ed.), *Reliability Based Design in Geotechnical Engineering*. London: Taylor & Francis.
- Wu, T. H., McKinnell, W. P. I., and Swanston, D. N., 1979. Strength of tree roots and landslides on Prince of Wales Island, Alaska. *Canadian Geotechnical Journal*, **16**, 19–33.
- Yonghong, Y., Shuzhen, L., Chenghua, W., and Chuan, T., 2006. A study of tensile strength tests of arborous species root system in forest engineering technique of shallow landslide. *Wuhan University Journal of Natural Sciences*, **11**(4), 892–896.
- Ziemer, R. R., 1978. An apparatus to measure the crosscut shearing strength of roots. *Canadian Journal of Forest Research*, **8**, 142–144.
- Ziemer, R. R., 1981. The role of vegetation in the stability of forested slopes. In *Proceedings of the International Union of Forestry Research Organizations, XVII World Congress*, 6–17 September, Kyoto, Japan, Vol. 1, pp. 297–308.

Cross-references

Physical (Mechanical) Weathering of Soil Parent Material

Plant Roots and Soil Structure

Plant–Soil Interactions, Modeling

Root Responses to Soil Physical Limitations

Root System Architecture: Analysis from Root Systems to Individual Roots

PLANT ROOTS AND SOIL STRUCTURE

A. Pierret¹, C. J. Moran²

¹Institut de Recherche pour le Developpement/
International Water Management Institute, Vientiane,
Lao PDR

²Sustainable Minerals Institute, The University of
Queensland, Brisbane, Qld, Australia

Definition

Roots anchor plants, provide access to water and nutrients, and store energy and carbon. Soil structure is the arrangement of pore space and solids. Soil without plants is extremely rare. Emerging from the coevolution of plants and soil is a complex and intermingled system that is often specific to the situation and its history. Agricultural and ecosystem management strategies tend to treat these as separate systems and consider the bulk soil and average plant root properties as representative of the function of the whole. Consequently, many problems arise because in fact local conditions and plant strategies to exploit these are a far better representation of the real conditions experienced and therefore reflect plant performance more accurately. Separation of soil structure and plant roots restricts man's capability to most effectively and sustainably manage soil production systems.

Introduction

Soils are highly complex environments that encompass physical and chemical heterogeneity across a wide range of spatial and temporal scales (Pierret et al., 2007). They bridge the mineral world with all the other trophic levels in the biosphere. Soil structure is central to such a fundamental linking role, as it provides the habitat for an extraordinary array of organisms (Young and Crawford, 2004; Watt et al., 2006) and the pathway for essential resources on which they depend for their survival. In turn, soil biological activity is one of the main drivers of soil structure and fertility formation and maintenance. Among the myriad of soil life forms, plants, through root growth and functioning, play a pivotal role with regards to all other soil processes. Plants deposit considerable amounts of carbon in the soil: up to about a third of photosynthates allocated to roots could be lost to the soil as cap cells, mucilages, soluble exudates and lysates, and decaying tissues (Hawes et al., 2003; Hutsch et al., 2002). Due to roots' inherent nutritional value as a carbon substrate and the wide range of metabolites that they secrete into the soil (Rovira, 1965), rhizosphere soil and root surfaces are also the main habitats for many soil organisms (Stewart et al., 1999).

The plant species that make up the vegetation in a given ecosystem have evolved to occupy different niches and thus often deploy different (both complementary and competitive) soil exploration strategies. A root system can be

regarded as a population of individual roots behaving (1) differently and independently from each other (Waisel and Eshel, 1992) (although coordinated to some degree at the root system level), (2) as a function of tissue differentiation, and (3) in response to changing environmental conditions (plasticity). The rooting pattern of a given plant species in a given environment represents an evolutionary response to the spatiotemporal variability in resource availability and the resulting constraints to growth. Roots of higher plants and their associated microbes play a major role in soil formation processes; as such they have coevolved plastic responses to their environment and thus differentiated as organs optimized to explore and utilize heterogeneously distributed soil resources (Leyser and Fitter, 1998) throughout geological times (Raven and Edwards, 2001). The interactions between plant roots and soil structure are of two types (1) root response to the heterogeneity of local soil conditions and (2) variations in root soil contact. The former includes reduced growth due to soil strength (Whalley et al., 1995) or low water and/or nutrient availability, and root proliferation in nutrient hotspots or in macropores (e.g., Tardieu, 1988)

Plant root types and functions

Roots are the organs of vascular plants that bear neither leaves nor nodes, and which are generally located below the soil surface. Roots have two major functions (1) the absorption of water and inorganic nutrients essential to plant growth and (2) the anchoring of the plant to its substrate. Roots also often function as storage organs. Roots are classified into several categories according to their ontogenesis and functions. Details about nomenclature used to describe root types and root system architectures can be found in Klepper (1992), Pagès et al. (2000), and Zobel (2005). Different root types play different functional roles (e.g., Navara, 1987; Mistrik and Mistrikova, 1995). Significant changes in physiological properties and activities also occur along individual roots, often as a function of root ontogenesis (Clarkson, 1996; Lazof et al., 1992). Root ability for water uptake varies according to (1) tissue differentiation, namely suberization, which affects the radial pathway (i.e., water transport from soil to xylem vessels) and xylem maturation (axial pathway, i.e., water transport along roots) (Steudle, 2000) and (2) transient changes in root water carrying capacity (short-term changes in xylem resistance Zwieniecki et al., 2003 or embolism Shane and McCully, 1999). There is good evidence that the few centimeters of unsuberized root tissue just behind root tips often act as active sinks through which soil water is absorbed while older parts of roots may predominantly be involved in carrying water extracted by younger and finer roots to the plant (Varney and Canny, 1993; Doussan et al., 1998). Together with litter fall, root production is believed to be the dominant input of organic carbon to soil and to correspond to a carbon stock more than twice that existing

above ground (Jackson et al., 1996). Among root types, fine roots may be the prominent sink for carbon in soils (Jackson et al., 1997; Norby et al., 2004).

Soil structure

Soil structure refers to the arrangement of the solid constituents of the soil and of the voids between them (Marshall and Holmes, 1979). It results from a range of factors such as the nature of the parent material from which soil constituents formed; the environmental conditions under which the soil formed; the mineralogy and organic matter content of the soil; the foraging activity of soil fauna; microbiological interactions; and the recent management history. Depending on soil mineralogy, the formation of zones of highly heterogeneous soil strength can result from purely physical processes such as cracking and swelling or freezing – thawing cycles. Human activities, such as agricultural practices, induce soil structural modifications that, although generally limited to the first 10–30 cm of the soil profile, are more rapid than natural processes, such as compaction due to tillage, wheel traffic or trampling by cattle, formation of plow pans, slotting, and deep ripping (Whalley et al., 1995). Soil particles combine into aggregates held together by binding forces exerted by clay particles and organic matter, shrink/swell dynamics, and cementing processes. The size, form, and strength (or persistence under degrading forces) of aggregation is used to characterize or describe soil structure. A well-structured soil will generally provide habitat for a wide range of life forms, conduit for fluids (air, water), preferential pathways for root growth, and reactive surfaces suitable for biochemical exchange and/or storage. Plant growth is both strongly influenced by soil structure and is one of the factors from which soil structure arises.

Root foraging strategies as a function of variable soil conditions

Hutchings and John (2004) outlined that most studies on root growth follow the premise that soil conditions are homogeneous, leaving serious gaps in our understanding of how plants function under natural and managed conditions and how they take advantage of patchy soil conditions. It has long been established that root system architecture of plants grown *in situ* is generally more complex and subject to greater inter- and intra-specific variability than that of roots grown in laboratory conditions (e.g., in agar). Soil is a physical environment where it is often difficult for roots, microorganisms, and soil fauna to move, and where resources (water, air, nutrients) are frequently scarce and patchy, with considerable spatial and temporal variability. Even when abundant, soil resources are often poorly available to organisms due to the capacity of the soil matrix to bind water and nutrients (Strong et al., 1999).

Variable soil conditions experienced locally by plant roots trigger, within species-specific limits, a range of physiological responses that help the plant minimize the

potential stress arising from soil heterogeneity and enable it to take advantage of “better-than-average” conditions (Drew, 1975; Robinson et al., 1999). Such plastic root responses to heterogeneous supplies of nutrients have been extensively reviewed by Hodge (2006). Plants have developed a range of complex strategies to exploit the soil’s inherent patchiness, such as proliferation, segregation, aggregative root placement (Bartelheimer et al., 2006), or preemption of nutrient supply (Craine et al., 2005).

Depending on local environmental conditions, a single species may deploy subtle combinations of foraging strategies. For example, one plant species was shown to switch between dichotomous and herringbone root architectures, the former topology being advantageous to compete for scarce nutrients while the latter restricts root length thus helping to minimize exposure to toxic compounds. The existence of opportunistic strategies has been confirmed experimentally: soil patchiness triggers costly “root races” between competing plants, in which large amounts of assimilates are spent into producing a great profusion of roots in an effort to secure exclusive benefit from resource enriched spots (Hodge et al., 1999). It has also been reported that rapid physiological plasticity consisting of opportunistic changes in nutrient uptake rates could be an important process for the capture of patchy resources by plants (Jackson et al., 1990).

Plant root growth in structured soil

The presence of zones of high mechanical resistance is one of the most common physical limitations to soil exploration by roots (Hoad et al., 1992). In soil volumes of higher mechanical strength, the development of soil structure is of paramount importance to root penetration (Tardieu and Manichon, 1986; Tardieu, 1988; Tardieu and Katerji, 1991); increases in soil strength reduce root elongation and alter root diameters and the average number of lateral roots that stem from primary axes (Dexter, 1987; Bengough, 1997) with direct consequences for resource acquisition by plants (Lynch and Nielsen, 1996; Pagès, 2002; Pagès et al., 2000). In very hard soil, the uptake of water and nutrients may become limiting because roots have difficulty penetrating the soil. In very soft soil, root length is not affected, but some have argued that the contact between the root and the soil may be so low that transport of water and nutrients is restricted (Herkelrath et al., 1977; Kooistra et al., 1992). In soils that impede root growth (e.g., because of high resistance to penetration), successive generations of roots tend to reuse paths of least mechanical resistance, such as preexisting structural features like cracks, biopores, or casts excreted by soil macrofauna. This co-location of roots and macropores (Stewart et al., 1999) leads to the formation of a specific environment that differs significantly chemically and biologically from the bulk soil (Pierret et al., 1999; Pankhurst et al., 2002).

Quantification of the root–soil interplay

Passioura (1985, 1991) hypothesized that roots are not evenly distributed throughout the soil matrix and are possibly trapped in large pores. This has been termed the root clumping model. Comparing plant growth in uniformly hard soil and in hard soil containing biopores, Stirzaker et al. (1996) found that while large biopores can provide the plant with access to extra water and nutrients from depth, this is offset by problems related to poor root–soil contact in biopores and impeded laterals in the compacted biopore walls. Based on microscopical observations of roots in thin sections of undisturbed soil, Kooistra et al. (1992) proposed the first detailed quantification of the relationship between soil structure and root–soil contact. Root–soil contact was found to increase nearly proportionally to soil bulk density. Plants can maximize root–soil contact in loose soil through branching (with some degree of species-specific variability); for example, in porous topsoils, very small roots (<0.1 mm radius) tend to explore the denser parts of the system (aggregates) (Moran et al., 2000). Yet, soil compaction significantly affects root–soil contact, which in turn influences plant uptake efficiency (Veen et al., 1992).

Combining microscopy and image analysis, Krebs et al. (1994) quantified the spatial distributions of roots relative to the locations of soil structural features such as channels, cracks, and pores and provided a first quantification of the spatial association between plant roots and soil structure. Stewart et al. (1999) assessed the root clumping model by comparing the frequency of roots in macropores with the frequency expected if the roots were randomly located in the soil volume. Some clumping was observed, however, a more significant effect was the location of a large proportion (80%) of roots in the soil within 1 mm of macropores. They termed the portion of the soil surrounding macropores with which roots are associated the macropore sheath. It was later found that the macropore sheath represents a local environment, only a few millimeters thick, that supports a biological activity and diversity orders of magnitude higher than that which prevails in the bulk soil (Pierret et al., 1999; Pankhurst et al., 2002). From this result, it was concluded that measurements of bulk soil properties may not be a good reflection of the environment experienced by the root system, and thus the plant, because the macropore sheath is a small proportion of the total soil. Using high resolution X-ray imaging, Moran et al. (2000) confirmed that roots are not spread evenly throughout the subsoil and showed that, as they grow preferentially in soil less dense than the soil bulk density, roots probably exploit a limited portion of the soil resources.

A conceptual model for root growth based on soil structure as the primary control for soil exploration was proposed by Pierret et al. (2005) to explain data published in that paper and by Moran et al. (2000). The most important data from X-ray analysis of thin soil slabs, showed that almost no roots occupied soil with density as great

as the average soil bulk density; roots (of all radii) strongly preferentially occupy low-density regions of the soil. Their model proposes that not only is root presence and length distribution likely controlled by the soil heterogeneity, as described earlier, but root radius as well. In brief, their model contends that the plant matches root radius to available pore size and thus exploits the soil resources through the structure rather than waste assimilate unnecessarily creating pores. As an example of supporting data, root radius was found to be smaller in denser soil and vice versa. This is the opposite of what is found using conventional experiments in which massive (structureless) soil or sand materials are equilibrated to a range of soil water tensions, seeds germinated, and root radius and elongation measured. This work demonstrates the importance of not relying on simplified physical models of soil to understand interactions with plants. A similar misunderstanding arises when soil biological and nutrient status measured from bulked soil samples are linked to root system characterization, because, as indicated earlier, the environment in the vicinity of roots can be radically different to the bulk soil.

Summary

There exists significant evidence in the literature that soil structure and plant roots can barely be considered separate entities. Plant root form, length distributions, radius distributions, branching, and overall plant vigor have all been demonstrated to be heavily influenced by soil structure. This has been illustrated using a number of different techniques in the laboratory and in the field. Similarly, characterization of soil structure has shown that plant roots and their associated local chemical and biological environments are strong determinants of the character of soil structure. The mineral nature of the soil, wetting and drying frequency, and intensity and disruption management history are the other major factors. Plants show tremendous plasticity in root system responses to heterogeneous soil conditions. Individual species and plant communities have evolved mechanisms to very effectively exploit available soil resources. In introduced monocultures, the evolved efficiency delivered by communities is absent and inefficient soil resource exploitation can be observed. There are many examples where measurements of bulk soil chemical, physical, and biological properties indicate that there should be sufficient resources for plant vigor but plants seem to suffer poor performance. Without a good understanding of the soil structure plant root interplay, it is unlikely that maximum plant performance will be achieved and over-allocation of resource such as fertilizers and water via irrigation will continue to be a heavy-handed risk mitigation strategy to avoid crop failure. For maximum carbon sequestration into soil that is stable into the long term, it is also likely that lessons regarding the strong interrelationships between soil structure and plants roots will need to be exploited.

Bibliography

- Bartelheimer, M., Steinlein, T., and Beyschlag, W., 2006. Aggregative root placement: a feature during interspecific competition in inland sand-dune habitats. *Plant and Soil*, **280**, 101–114.
- Bengough, A. G., 1997. Modelling rooting depth and soil strength in a drying soil profile. *Journal of Biology*, **186**, 327–338.
- Clarkson, D. T., 1996. Root structure and sites of ion uptake. In Waisel, Y. A., Eshel, A., and Kafkafi, U. (eds.), *Plant Roots: The Hidden Half*. New York: Marcel Dekker, pp. 483–510.
- Craine, J. M., Fargione, J., and Sugita, S., 2005. Supply pre-emption, not concentration reduction, is the mechanism of competition for nutrients. *The New Phytologist*, **166**, 933–940.
- Dexter, A. R., 1987. Mechanics of root growth. *Plant and Soil*, **97**, 401–406.
- Doussan, C., Vercambre, G., and Pagès, L., 1998. Modeling of the hydraulic architecture of root systems: an integrated approach to water absorption – 2. Distribution of axial and radial conductances in maize. *Annals of Botany (London)*, **81**, 225–232.
- Drew, M. C., 1975. Comparison of the effects of a localized supply of phosphate, nitrate, ammonium, and potassium on the growth of the seminal root system, and the shoot, in barley. *The New Phytologist*, **75**, 479–490.
- Hawes, M. C., Bengough, G., Cassab, G., and Ponce, G., 2003. Root caps and rhizosphere. *Journal of Plant Growth Regulation*, **2**, 352–367.
- Herkelrath, W. M., Miller, E. E., and Gardner, W. R., 1977. Water uptake by plants: II. The root contact model. *Soil Science Society of America Journal*, **41**, 1039–1043.
- Hoad, S. P., Russel, G., Lucas, M. E., and Bingham, I. J., 1992. The management of wheat, barley, and oat root systems. *Advances in Agronomy*, **74**, 193–246.
- Hodge, A., 2006. Plastic plants and patchy soils. *Journal of Experimental Botany*, **57**, 401–411.
- Hodge, A., Robinson, D., Griffiths, B. S., and Fitter, A. H., 1999. Why plants bother: root proliferation results in increased nitrogen capture from an organic patch when two grasses compete. *Plant, Cell and Environment*, **22**, 811–820.
- Hutchings, M. J., and John, E. A., 2004. The effects of environmental heterogeneity on root growth and root/shoot partitioning. *Annals of Botany (London)*, **94**, 1–8.
- Hutsch, B. W., Augustin, J., and Merbach, W., 2002. Plant rhizodeposition: an important source of carbon turnover in soils. *Journal of Plant Nutrition and Soil Science*, **165**, 397–407.
- Jackson, R. B., Manwaring, J. H., and Caldwell, M. M., 1990. *Nature*, **344**, 58–60.
- Jackson, R. B., Canadell, J., Ehleringer, J. R., Mooney, H. A., Sala, O. E., and Schulze, E. D., 1996. A global analysis of root distributions for terrestrial biomes. *Oecologia*, **108**, 389–411.
- Jackson, R. B., Mooney, H. A., and Schulze, E. D., 1997. A global budget for fine root biomass, surface area, and nutrient contents. *Proceedings of the National Academy of Sciences of the United States of America*, **94**, 7362–7366.
- Klepper, B., 1992. Development and growth of crop root systems. In Hatfield, J. L., and Stewart, B. A. (eds.), *Limitations to Plant Root Growth. Advances in Soil Science*, Vol. 19, pp. 1–25.
- Kooistra, M. J., Schoonderbeek, D., Boone, F. R., Veen, B. W., and Van Noordwijk, M., 1992. Root–soil contact of maize, as measured by a thin-section technique. II. Effects of soil compaction. *Plant and Soil*, **139**, 119–129.
- Krebs, M., Kretzschmar, A., Babel, U., Chadoeuf, J., and Goulard, M., 1994. Investigations on distribution patterns in soil: basic and relative distributions of roots, channels and cracks. In Ringrose-Voase, A. J., and Humphreys, G. S. (eds.), *Soil Micromorphology: Studies in Management and Genesis. Developments in Soil Science*, Amsterdam: Elsevier, Vol. 22, pp. 437–449.
- Lazof, D., Rufty, T. W., and Redingbaugh, M. G., 1992. Localization of nitrate absorption and translocation within morphological regions of corn roots. *Plant Physiology*, **100**, 1251–1258.
- Leyser, O., and Fitter, A., 1998. Roots are branching out in patches. *Trends in Plant Science*, **3**, 203–204.
- Lynch, J., and Nielsen, K. L., 1996. Simulation of root system architecture. In Waisel, Y., Eshel, A., and Kafkafi, U. (eds.), *Plant Roots: The Hidden Half*. New York: Marcel Dekker, pp. 247–257.
- Marshall, T. J., and Holmes, J. W., 1979. *Soil Physics*. Cambridge: Cambridge University Press.
- Mistrik, I., and Mistrikova, I., 1995. Uptake, transport, and metabolism of phosphate by individual roots of Zea mays L. *Biologia (Bratislava)*, **50**, 419–426.
- Moran, C. J., Pierret, A., and Stevenson, A. W., 2000. X-ray absorption and phase contrast imaging to study the interplay between plant roots and soil structure. *Plant and Soil*, **223**, 99–115.
- Navara, J., 1987. Participation of individual root types in water uptake by maize seedlings. *Biologia (Bratislava)*, **42**, 17–26.
- Norby, R. J., Ledford, J., Reilly, C. D., Miller, N. E., and O'Neill, E. G., 2004. Fine-root production dominates response of a deciduous forest to atmospheric CO₂ enrichment. *Proceedings of the National Academy of Sciences of the United States of America*, **101**, 9689–9693.
- Pagès, L., 2002. Modeling root system architecture. In Waisel, Y., Eshel, A., and Kafkafi, U. (eds.), *Plant Roots: The Hidden Half*. New York: Marcel Dekker, pp. 359–382.
- Pagès, L., Asseng, S., Pellerin, S., and Diggle, A., 2000. Modelling root system growth and architecture. In Smit, A. L., Bengough, A. G., Engels, C., van Noordwijk, M., Pellerin, S., and van de Geijn, S. C. (eds.), *Root Methods: A Handbook*. Paris: Springer, pp. 113–146.
- Pankhurst, C. E., Pierret, A., Hawke, B. G., and Kirby, J. M., 2002. Microbiological and chemical properties of soil associated with macropores at different depths in a red-duplex soil in NSW Australia. *Plant and Soil*, **238**, 11–20.
- Passioura, J. B., 1985. Roots and water economy of wheat. In Day, W., and Atkin, R. K. (eds.), *Wheat Growth and Modelling*. New York: Plenum, pp. 185–198.
- Passioura, J. B., 1991. Soil structure and plant growth. *Australian Journal of Soil Research*, **29**, 717–728.
- Pierret, A., Moran, C. J., and Pankurst, C. E., 1999. Differentiation of soil properties related to the spatial association of wheat roots and soil macropores. *Plant and Soil*, **211**, 51–58.
- Pierret, A., Moran, C. J., and Doussan, C., 2005. Conventional detection methodology is limiting our ability to better understand the roles and functions of fine roots. *The New Phytologist*, doi:10.1111/j.1469-8137.2005.01389.x.
- Pierret, A., Doussan, C., Capowicz, Y., Bastardie, F., and Pagès, L., 2007. Root functional architecture: a framework for modeling the interplay between roots and soil. *Vadose Zone Journal*, **6**, 269–281.
- Raven, J. A., and Edwards, D., 2001. Roots: evolutionary origin and biogeochemical significance. *Journal of Experimental Botany*, **52**, 381–408.
- Robinson, D., Hodge, A., Griffiths, B. S., and Fitter, A. H., 1999. Plant root proliferation in nitrogen-rich patches confers competitive advantage. *Proceedings of the Royal Society of London. Series B*, **266**, 431–435.
- Rovira, A. D., 1965. Interactions between plant roots and soil microorganisms. *Annual Reviews of Microbiology*, **19**, 241–266.
- Shane, M. W., and McCully, M. E., 1999. Root xylem embolisms: implications for water flow to the shoot in single-rooted maize plants. *Australian Journal of Plant Physiology*, **26**, 107–114.
- Steudle, E., 2000. Water uptake by roots: effects of water deficit. *Journal of Experimental Botany*, **51**, 1531–1542.

- Stewart, J. B., Moran, C. J., and Wood, J. T., 1999. Macropore sheath: quantification of plant root and soil macropore association. *Plant and Soil*, **211**, 59–67.
- Stirzaker, R. J., Passioura, J. B., and Wilms, Y., 1996. Soil structure and plant growth: impact of bulk density and biopores. *Plant and Soil*, **185**, 151–162.
- Strong, D. T., Sale, P. W. G., and Helyar, K. R., 1999. The influence of the soil matrix on nitrogen mineralization and nitrification: III. Predictive utility of traditional variables and process location within the pore system. *Australian Journal of Soil Research*, **37**, 137–149.
- Tardieu, F., 1988. Analysis of the spatial variability of maize root density: II. Distances between roots. *Plant and Soil*, **107**, 267–272.
- Tardieu, F., and Katerji, N., 1991. Plant-response to the soil–water reserve: consequences of the root–system environment. *Irrigation Science*, **12**, 145–152.
- Tardieu, F., and Manichon, H., 1986. Caractérisation en tant que capteur d'eau de l'enracinement du maïs en parcelle cultivée: II. Une méthode d'étude de la répartition verticale et horizontale des racines. *Agronomie*, **6**, 415–425.
- Varney, G. T., and Canny, M. J., 1993. Rates of water uptake into the mature root system of maize plants. *The New Phytologist*, **123**, 775–786.
- Veen, B. W., Van Noordwijk, M., De Willigen, P., Boone, F. R., and Kooistra, M. J., 1992. Root–soil contact of maize, as measured by a thin-section technique III. Effects on shoot growth, nitrate and water uptake efficiency. *Plant and Soil*, **139**, 131–138.
- Waisel, Y., and Eshel, A., 1992. Differences in ion uptake among roots of various types. *Journal of Plant Nutrition*, **15**, 945–958.
- Watt, M., Silk, W. K., and Passioura, J. B., 2006. Rates of root and organism growth, soil conditions, and temporal and spatial development of the rhizosphere. *Annals of Botany (London)*, **97**, 839–855.
- Whalley, W. R., Dumitru, E., and Dexter, A. R., 1995. Biological effects of soil compaction. *Soil and Tillage Research*, **35**, 53–68.
- Young, I. M., and Crawford, J. W., 2004. Interactions and self-organisation in the soil–microbe complex. *Science*, **304**, 1634–1637.
- Zobel, R. W., 2005. Primary and secondary root systems. In Zobel, R. W., and Wright, S. F. (eds.), *Roots and Soil Management: Interactions Between Roots and the Soil*. Agronomy Monograph 48. Madison: ASA.
- Zwieniecki, M. A., Thompson, M. V., and Holbrook, N. M., 2003. Understanding the hydraulics of porous pipes: tradeoffs between water uptake and root length utilization. *Journal of Plant Growth Regulation*, **21**, 315–323.

Cross-references

- Anisotropy of Soil Physical Properties
 Biochemical Responses to Soil Management Practices
 Bypass Flow in Soil
 Cracking in Soils
 Crop Responses to Soil Physical Conditions
 Cropping Systems, Effects on Soil Physical Properties
 Greenhouse Gases Sink in Soils
 Hardpan Soils: Management
 Hardsetting Soils: Physical Properties
 Image Analysis in Agrophysics
 Leaching of Chemicals in Relation to Soil Structure
 Microbes and Soil Structure
 Nondestructive Measurements in Soil
 Noninvasive Quantification of 3D Pore Space Structures in Soils
 Physical Protection of Organic Carbon in Soil Aggregates
 Plant–Soil Interactions, Modeling
 Pore Morphology and Soil Functions
 Pore Size Distribution

Rhizosphere

Root Responses to Soil Physical Limitations

Root System Architecture: Analysis from Root Systems to Individual Roots

Root Water Uptake: Toward 3-D Functional Approaches

Soil Aggregates, Structure, and Stability

Soil Biota, Impact on Physical Properties

Soil Hydraulic Properties Affecting Root Water Uptake

Spatial Variability of Soil Physical Properties

Tillage, Impacts on Soil and Environment

Water Balance in Terrestrial Ecosystems

PLANT TEMPERATURE

Piotr Baranowski

Institute of Agrophysics, Polish Academy of Sciences, Lublin, Poland

Definition

Plant temperature is the measure of its ability to exchange heat energy with surrounding (air, soil, water). It is an important quantity influencing plant growth and yielding. It is also an indicator of water availability for rooting system and the occurrence of abiotic or biotic stresses.

Biochemical reactions, cell growth and division, cell differentiation (generative/vegetative), and cell elongation depend on the temperature distribution within the plant and its daily variation. The actual value of plant temperature is continuously modified by changing environment and physiological activity. Meteorological parameters and soil temperature are the main factors modifying the temperature of particular plant organs and are responsible for considerable differentiation of temperature distribution within the whole plant. Roots of land and water plants possess temperature close to the surrounding (soil or water reservoir) temperature. The temperature of above-ground parts of plant often deviates considerably from air temperature. Plant temperature response to environmental factors, especially of leaves and stem, is regulated by stomata opening and closing mechanism, which is responsible for tuning transpiration intensity and gas exchange (Chalerle et al., 2005). Heat loss associated with transpiration is the result of energy demand for this process and equals the product of the rate of transpiration and the latent heat of vaporization of water. Transpiration is able to lower plant temperature by several degrees. Leaf cooling through transpiration may be regarded as beneficial for plants which are at high temperatures until water loss is made up by sufficient water uptake from soil. The energy balance equation for a leaf is fundamental for understanding the temperature regime in plant (Baranowski et al., 2005). Increase of plant temperature as result of stomata closing (especially, when compared with a reference plant surface temperature or actual air temperature) is an indicator of occurring stress. Depending on the origin or type of plant stress, it manifests itself through a local or overall increase of plant temperature. Thermal imaging is the most efficient way of

measuring plant temperature, being a powerful tool for the study of spatial variation in plant and canopy temperatures (Jones, 2004).

Bibliography

- Baranowski, P., Usowicz, B., Walczak, R. T., and Mazurek, W., 2005. *Evaporation into the Boundary Layer of the Atmosphere*. Lublin: Institute of Agrophysics, pp. 1–160.
- Cherelle, L., Saibo, N., and Van Der Straeten, D., 2005. Tuning the pores: towards engineering plants for improved water use efficiency. *Trends in Biotechnology*, **23**, 308–315.
- Jones, H. G., 2004. Application of thermal imaging and infrared sensing in plant physiology and ecophysiology. *Advances in Botanical Research*, **41**, 107–163.

Cross-references

- Databases on Physical Properties of Plants and Agricultural Products
 Diurnal Strains in Plants
 Plant Drought Stress: Detection by Image Analysis
 Soil–Plant–Atmosphere Continuum
 Stomatal Conductance, Photosynthesis, and Transpiration, Modeling

PLANT TROPISMS, PHYSICS

Fernando Migliaccio, Alessio Fortunati, Paola Tassone
 Institute of Agro-Environmental and Forest Biology (IBAF), National Research Council, Monterotondo, Rome, Italy

Definition

Plant tropisms are directional movements of plant organs, generally due to growth, induced by an external factor. The movement can be toward or away from the inducer, but the path is not predetermined as in the nastic movements. The most common kinds of tropisms are gravitropism and phototropism.

Introduction

Despite the fact that plants are usually seen as stationary organisms, they do, in fact move continuously in different ways, and for different reasons, among others: in search of light, water, nutrients, defense against predators, and reproduction. Several kinds of movements are recognized but the principal ones are nastic, circumnutational, and tropic. In the latter, the plants move in a direction, under an external stimulus, which induces a different elongation on opposite sides of an organ. The best known, most common, and most easily observable tropisms are gravitropism and phototropism. Although these are the main subjects of this contribution, other kinds of tropisms, known as thigmotropism, hydrotropism, and autotropism have also been described.

The fact that plants move has been known since antiquity (Larsen, 1962). However, apparently the first consistent experimental work on tropisms was carried out by

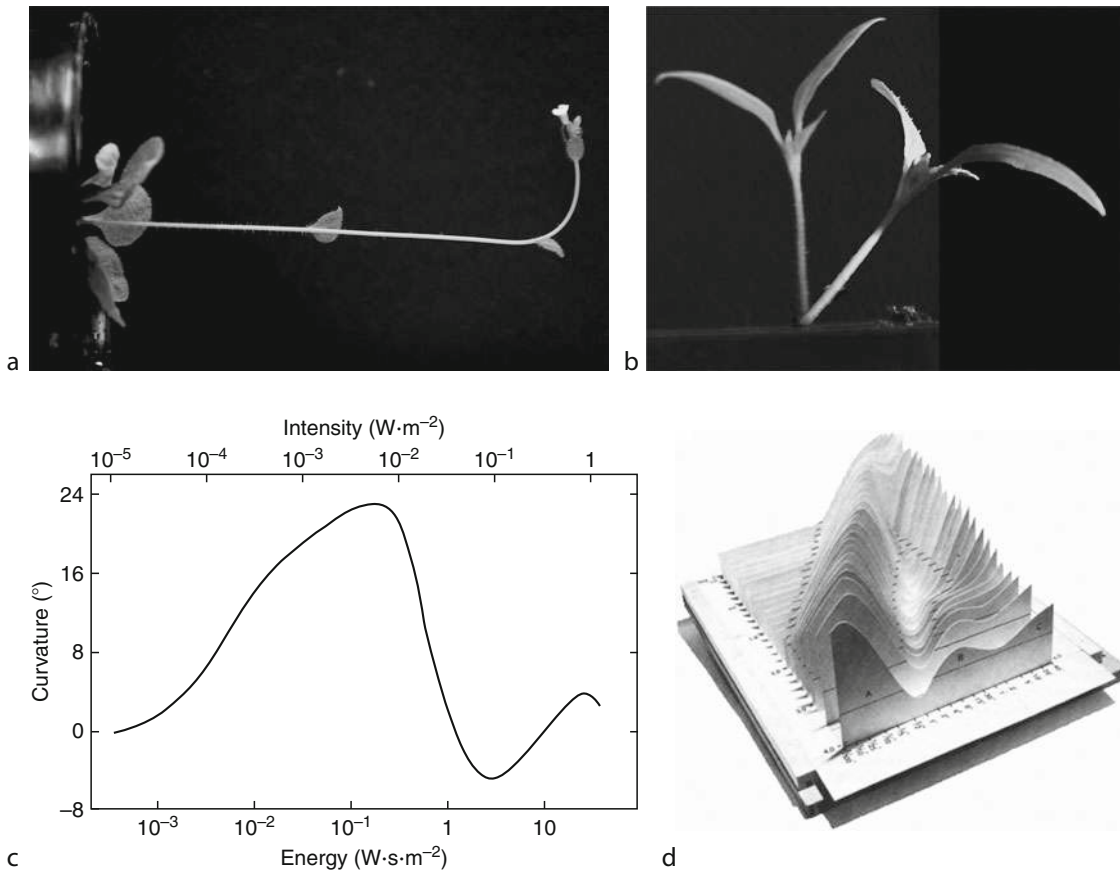
T.A. Knight in 1806. He thought, correctly as it turned out, that the movement induced by the gravitational force could be mimicked by the application of a centrifugal force (really a centripetal force). He built a device consisting of a wheel that could be rotated at different speeds and discovered that plant seedlings, rotated at a speed that produced about 3.5 times the earth gravity, ignored the gravitational force and redirected their shoots toward the center of the wheel, and the root away from it.

In the nineteenth century, experimentation on tropisms (and plant movements) progressed rapidly, but the seminal contributions were made by von Sachs and by Darwin. von Sachs invented and built the clinostat, a disc on which plants are fixed, that rotates at moderate speeds and thus does not produce centrifugal force. It does, however, simulate the absence of gravity, because the stimulation of the plant from all directions practically suppresses the gravitropic effect. Subsequently, the process of plants movements (and among them tropisms) was submitted to the powerful scientific mind of Darwin. The results of these researches were reported in a book about the movements of plants (Darwin, 1880). At about that time a large amount of research and experimentation on tropisms began.

Gravitropism

The term gravitropism (previously geotropism) applies to the process by which a plant grows with the shoot directed up and the root, downward (Figure 1a). This form of gravitropism is known as orthogravitropism, but other forms exist, such as plagiotropism, in which case the branches grow at an angle to the gravity vector. More precisely, the different organs of a plant keep a gravitationally set angle, to which they return if moved away (Digby and Firn, 1995). Plants, however, do not respond only to gravity but also to centrifugal force, as already mentioned, so that a more exact term for the process would be barytropism (Larsen, 1962).

Gravitropism has been traditionally classified into three steps: detection of the stimulus, transduction of the signal, and response. In this process some physical descriptors can be established: one is the *sine law*, which establishes that the response or curvature of the organ is the product of 1 g (acceleration of gravity on earth) and the sine of the angle made by the organ with respect to the gravity vector (response = $1 \text{ g} \times \sin a^\circ$). This law is not always respected. A second parameter is the *dose of stimulus*, i.e., the product of time of stimulation and intensity. In addition, the so-called presentation time, i.e., the time that a plant requires to respond after a gravistimulation at 90°. This parameter was at first calculated from the time of appearance of a curvature in 50% of the studied coleoptiles. In later work, however, plotting the extent of curvature against increasing periods of stimulation and extrapolating the curve back to zero time produced presentation times between 12 and 30 s (Volkman and Sievers, 1979). More sensitive methods, such as the submission



Plant Tropisms, Physics, Figure 1 (a) Response to gravity of an *Arabidopsis* plant. (b) Response to a lateral light source by a pea seedling. (c) Curvature of oat coleoptiles as a function of increasing light fluences. Exposure time: 30 s. (After Blaauw and Blaauw-Jensen, 1970.) (d) Curvature of oat coleoptiles as a function of both fluence rates (increasing from *back to front*) and exposure time (increasing from *left to right*). (From Blaauw and Blaauw-Jensen, 1970.)

of roots to periods of 1 s of gravistimulation, with intervals of 0.5 s revealed a further reduction of the presentation time. This can be taken as an indication that plants start responding almost immediately (Pickard, 1985). The *threshold angle*, i.e., the inclination of an organ with respect to the gravity vector also gives a value of the gravitropic response. Usually a deviation of 0.5–10° is sufficient to evoke a response, but the maximum of effectiveness normally is at 90°. These experiments are generally performed on shoots and roots that respond to a deviation from a plumb line. Different, however, is the case of cereals, where the responding part is the basal pulvinus of the shoot, which resumes elongation when the plant lies horizontal, and returns the shoot to vertical. As regards the minimum of g acceleration that can evoke a response, experiments on clinostats and biosatellites with lettuce hypocotyls and roots, indicate values of 2.9×10^{-3} – 1.5×10^{-4} (Halstead and Dutcher, 1987).

In the case of the root, the zone responding to gravity is different with respect to shoots and consists of only a few millimeters above the root cap, which cells

(statocytes), detecting the stimulus, carry the statolyts (amloplasts). The gravitropic message then moves basipetally down the root inducing the response in the elongation zone. Two zones have been described in roots, i.e., the distal elongation zone and the central elongation zone (Wolverton et al., 2000). On the contrary, in shoots the zone responding to gravity is relatively large, and the statocytes seem to be located around the vascular tissue.

Regarding the mechanism of gravity sensing, in the past it was thought (Volkmann and Sievers, 1979) that the statolyts (starch accumulating plastids), by way of their sedimentation to the bottom of the cell, were the detector of the stimulus, because no other organelle shows such sedimentation in cells. Recently however, considering that even the starchless mutants of some plants respond to gravity (though with less intensity) a new hypothesis was developed, which involves the full body of the cell in the detection of gravity (Harrison and Masson, 2008) through stretching sensors (possibly ion pumps).

To respond to gravity however, the plant's organs need to become asymmetric, through the redistribution of an inducer of growth. Already, Darwin advanced the hypothesis that an effector was redistributed, although he did not have the time to find it. It was, in fact, Frits Went who first found this unknown substance, which was able to redistribute asymmetrically in concentration in the plant organs (Thimann and Schneider, 1938). These studies were through biotests, but very soon a substance, named auxin (indole-3-acetic acid), able to dramatically accelerate growth, was found. This was the first hormone found in plants that acts at very low concentration (between 10^{-7} and 10^{-9} M). Consequently, it was not long before the hypothesis was advanced that this substance, at the right concentration, can accelerate growth on the lower part of gravistimulated shoots and slow growth on the lower part of the roots (roots are sensitive to lower concentrations). This idea is known as the Chodlony–Went hypothesis, having been advanced independently by two authors (the first a Russian, the second a Dutch). In spite of some criticism based on the grounds that the redistribution was not found in all cases, this hypothesis may be correct, and recent research using the powerful techniques of molecular biology seem to support it. Some of the work was performed by transforming *Arabidopsis* plants with a gene extremely sensitive to low concentrations of auxin, whose activation can easily be seen through fluorescence. In many cases, using this technique, increased auxin concentrations could be observed in the lower parts of shoots and roots (Li et al., 1991).

Today, a number of gravitropic mutants are known in which auxin redistribution is not apparent and which do not respond to gravity at all or only slowly. The ensemble of the data thus seems to support the Chodlony–Went hypothesis, but doubts persist in general on the function and action of this plant hormone (Trewavas, 1992). In addition, it is thought also that action potentials might be involved in the process, because of the swift, practically immediate response, shown by gravistimulated organs (Bjorkman and Leopold, 1987).

Frequently, more than one tropism acts on the same organ, so that the final growth behavior is the result of an interaction between different growth processes. For instance, the root of *Arabidopsis* shows a particular wavy pattern that seems to arise from gravitropism, circumnutation, and thigmotropism, when grown on a tilted vertical agar plate (Migliaccio and Piconese, 2001).

Phototropism

Phototropism is one of the many effects that light can have on plant organisms. It is because light can modify the growth direction of a plant (Figure 1b) by inducing an asymmetry inside the plant organs (for instance coleoptiles). More frequently, plants move toward the light source, but negative phototropism also exists. Research

goes back to the nineteenth century, but the initial and most important work was brought about, as in the case of gravitropism, by Darwin, and reported in the book describing the movements of plants already mentioned (Darwin, 1880). Through large arrays of experiments, Darwin established that the most important part of the plant for the phototropic response is the shoot tip, because seedlings immersed in light sand responded only when the tip was illuminated, whereas if a tip was covered with black paper, they did not respond at all. Thereafter, matters became far more complicated, because different zones of the shoot responded even in plants whose tips had been removed. For coleoptiles it has been reported, that the most sensitive zone is 100 μ m behind the tip (Curry, 1969). Obviously, not only the seed plants respond to light, but also algae, fungi, and ferns.

The phototropic response in coleoptiles and in dicots seedlings (Dennison, 1979) to increasing light spectrum shows the following feature. In the relative graph, there is a peak of activity in the near UV around λ 370 nm, and then two peaks in the blue region, corresponding to λ 450 and λ 475, plus a shoulder at λ 420. The most important wavelength range is thus the blue. On the other hand, when the plant shoots are subjected to increasing light fluences, a first positive response is seen (Figure 1c), then a negative one, and subsequently a second positive response. Considering natural light, the most important is the second positive response.

In particular, an extremely precise investigation was carried out by Blaauw and Blaauw-Jensen (1970) (Figure 1d). Using collected data they constructed a three-dimensional graph in which increasing light fluence rates were plotted from rear to front (z-axis), increasing irradiation times from left to right (x-axis), and the coleoptile curvature in degrees vertically (y-axis). The results showed that at high light intensity, around 10 W m^{-2} ($36.8 \mu\text{mol m}^{-2} \text{ s}^{-1}$), the plot shows three peaks named by them A, B, and C, corresponding to first, second, and third positive responses, plus a negative response between B and C. In the graph sections taken from the most intense to the lower fluence, area A and B, shift to longer exposures times, as does the negative response, and this shift is in accordance with the reciprocity law (exposure time \times fluence = k). Area C instead does not shift with decreasing intensities and thus in this case the reciprocity is not respected. In addition, area B at low intensities, i.e., at 10^{-3} W about ($0.003 \mu\text{mol m}^{-2} \text{ s}^{-1}$) merges with area A, and the negative region disappears. This means that at low fluence only two positive peaks are present (area A and C), the latter notably increased.

Regarding the nature of the light receptor(s), in the past two kinds of yellow compounds (as a consequence of their absorption in the blue region) were suggested. One is a carotenoid, in which case the receptor would be close to that utilized by animals, the other is a flavonoid. Both have absorption spectra notably similar to that regarding the phototropic response as a function of

wavelength, but not identical. Subsequently, the carotenoid hypothesis was abandoned, on the grounds that the inhibition of the carotenoids synthesis by the herbicide Norfluorazon does not stop the phototropic response (Viestra and Poff, 1981). The failure of the phototropic spectra to overlap exactly that of absorption by pigments was then variously interpreted, for instance with the presence of more than one pigment. The discussion on the receptor proceeded for years, and only in 1990 was the blue light absorption receptor identified (Whippo and Hangarter, 2006), through the mutant of *Arabidopsis nph* (non phototropic hypocotyl). This and similar receptors were renamed *phototropins*. In *Arabidopsis*, there are two of these genes and the relative proteins are named PHOT1 and PHOT2. The proteins are autophosphorylating serine/threonine kinases, with two LOV domains. These domains bind flavin as a photoreceptor (Lascèvre et al., 1999). The phototropins do not only function as photoreceptors, but also have other functions, for instance in photosynthesis.

Although the phototropins are the most important receptors of light in phototropism, there is another family of photoreceptors named chriptochromes, that are sensitive to blue light and are involved principally in photomorphogenesis (Lin et al., 1998), which also interact with the phototropins. Another family of photoreceptors are the phytochromes, mainly involved in photoperiodism (PHYA to E), which absorb red light, that can modify notably the phototropic reaction (Correll et al., 2003).

As regards the mechanism of response after the detection of light, what is known is that it is probably produced through a redistribution of auxin, as in the case of gravitropism. The existence of an auxin gradient has been known for a long time (Cholodny–Went hypothesis applied to phototropism) through the study of auxin redistribution. And, even though not everybody accepts the hypothesis, today we have confirmation of the involvement of auxin in phototropism through the study of the *pin* gene family, since the corresponding proteins are auxin transporters, which concentrate on the shaded side of a plant organ in the case of positive phototropism (Blakeslee et al., 2005).

Summary

Among the different kinds of movements performed by plants, tropisms are the most common. They consist of movements of the plant toward or away from an external environmental factor. Among the various tropisms, the most evident are gravitropism and phototropism. The first is a movement made through the sensing of the gravity vector, which leads the plant organs to grow at a precise angle with respect to it. Phototropism consists of a movement of a plant, induced by a light source, normally toward it, but also in some cases, away from it. The particular physical aspects of the two tropisms are described and discussed.

Bibliography

- Bjorkman, T., and Leopold, A. C., 1987. An electrical current associated with gravity sensing in maize roots. *Plant Physiology*, **84**, 841–846.
- Blaauw, O. H., and Blaauw-Jensen, G., 1970. The phototropic response of *avena* coleoptiles. *Acta Botanica Neerlandica*, **19**, 755–763.
- Blakeslee, J. J., Peer, W. A., and Murphy, A. S., 2005. Auxin transport. *Current Opinion in Plant Biology*, **8**, 494–500.
- Correll, M. J., Coveney, K. M., Raines, S. V., Mullen, J. L., Hangarter, R. P., and Kiss, J. Z., 2003. Phytochromes play a role in phototropism and gravitropism in *Arabidopsis* roots. *Advances in Space Research*, **31**, 2203–2210.
- Curry, G. M., 1969. Phototropism. In Wilkins, M. B. (ed.), *The Physiology of Plant Growth and Development*. New York: McGraw-Hill, pp. 241–273.
- Darwin, C., 1880. *The Power of Movement in Plants*. London: J. Murray.
- Dennison, D. S., 1979. Phototropism. In Haupt, W., and Feinleben, M. E. (eds.), *Encyclopedia of Plant Physiology*. Berlin: Springer, Vol. NS 7, pp. 507–566.
- Digby, J., and Firm, R. D., 1995. The gravitropic set-point angle (GSA): the identification of an important developmentally controlled variable governing plant architecture. *Plant, Cell and Environment*, **18**, 1434–1440.
- Halstead, T. W., and Dutcher, F. R., 1987. Plant in space. *Annual Review of Plant Physiology*, **38**, 317–345.
- Harrison, B. R., Masson, P. H., 2008. ARL2, ARG1, and Pin3 define a gravity signal transduction pathway in root statocytes. *Plant Journal*, **53**, 380–392.
- Larsen, P., 1962. Geotropism. An introduction. In Ruhland, W. (ed.), *Physiology of Movements, Encyclopedia of Plant Physiology*. Berlin: Springer, Vol. 17, Part 2, pp. 334–373.
- Lascèvre, G., Leymarie, J., Olney, M. A., Liscum, E., Christie, J. M., Vavasseur, A., and Briggs, W. R., 1999. *Arabidopsis* contains at least four independent blue-light-activated signal transduction pathways. *Plant Physiology*, **120**, 605–614.
- Li, Y., Hagen, G., and Guilfoyle, T. J., 1991. An auxin-Responsive promoter is differentially induced by Auxin gradients during tropisms. *The Plant Cell*, **3**, 1167–1175.
- Lin, C., Yang, H., Guo, H., Mockler, T., Chen, J., and Cashmore, A. R., 1998. Enhancement of blue-light sensitivity of *Arabidopsis* seedlings by a blue light receptor cryptochrome 2. *Proceedings of the National Academy of Sciences – USA*, **95**, 2686–2690.
- Migliaccio, F., and Piconese, S., 2001. Spiralisations and tropisms in *Arabidopsis* roots. *Trends in Plant Science*, **6**, 561–565.
- Pickard, B. G., 1985. Early events in geotropism of seedlings shoots. *Annual Review of Plant Physiology*, **63**, 55–75.
- Thimann, K. V., and Schneider, C. L., 1938. Differential growth in plant tissue. *American Journal of Botany*, **25**, 627–641.
- Trewavas, A. J., 1992. What remains of the Cholodny – Went theory? A summing up. *Plant, Cell and Environment*, **15**, 793–794.
- Viestra, R. D., and Poff, K. L., 1981. Role of carotenoids in the phototropic response of corn seedlings. *Plant Physiology*, **68**, 798–801.
- Volkmann, D., and Sievers, A., 1979. Graviperception in multicellular organs. In Haupt, W., and Feinleb, E. (eds.), *Physiology of Movements, Encyclopedia of Plant Physiology*. Berlin: Springer, Vol. NS 7, pp. 573–600.
- Whippo, C. W., and Hangarter, R. P., 2006. Phototropism: bending towards enlightenment. *The Plant Cell*, **18**, 1110–1119.
- Wolverton, C., Mullen, J. L., Ishikawa, H., and Evans, M. L., 2000. Two distinct regions of response drive differential growth in *Vigna* roots electrotropism. *Plant, Cell and Environment*, **23**, 1275–1280.

Cross-references

- Bending Properties of Plants
- Image Analysis in Agrophysics
- Microstructure of Plant Tissue
- Plant Biomechanics
- Plant Root Strength and Slope Stability
- Root System Architecture: Analysis from Root Systems to Individual Roots

PLANT WELLNESS

Istvan Farkas

Department of Physics and Process Control, Szent Istvan University, Gödöllő, Hungary

Synonyms

Plant health; Well-being of plants

Definition

Wellness refers generally to the state of being healthy. When the plants have the feeling of well-being they are more productive, and provide safe and secure food. Since plants do not change their location, temperature, humidity, CO₂, and other physical parameters of their environment are used to keep them in a healthy state. If all of these are similar to that which the plant would experience in its natural environment, it will generally fight off any insect or disease problems (Hashimoto, 1989).

Visual appearance is a useful sign for the grower, and monitoring the plant itself gives a straight diagnosis about the health of plant. Some of the wellness parameters that can be quantified by machine vision technique are plant color, growth rate, leaf and stem movement, and insect recognition (Kacira and Ling, 2001).

A computer vision method is to be used for detection and localization of leaves' wilting as a sign of visual appearance (Farkas and Font, 2008).

Bibliography

- Farkas, I., and Font, L., 2008. Plant wellness in greenhouse growing management. In Tüzel, Y., and Tunali, U. (eds.), *Second Coordinating Meeting of the Regional FAO Working Group on Greenhouse Crop Production in the SEE Countries*, Antalya, Turkey, April 7–11, 2008, pp. 45–56.
- Hashimoto, Y., 1989. Recent strategies of optimal growth regulation by the speaking plant concept, *Acta Horticulturae*, **260**, 115–121.
- Kacira, M., and Ling, P. P., 2001. Design and development of an automated and non-contact sensing system for continuous monitoring of plant health and growth. *Transactions of the American Society of Agricultural Engineers*, **44**, 989–996.

PLANT-SOIL INTERACTIONS, MODELING

Tiina Roose

School of Mathematics, University of Southampton, Southampton, UK

Definition

Plant–soil interaction modeling is a field of study which uses quantitative mathematical methods to assess the importance of different soil or plant properties on the interaction of plants and soil.

Modeling plant–soil interactions

The main emphasis in plant–soil interaction modeling is on describing the movement of nutrients in the soil surrounding the roots. The equations describing this typically include equilibrium nutrient binding to the soil particle surfaces, diffusion of nutrients in the soil pore water, and movement of nutrients due to water convection. The most general equation for the conservation of nutrients in the soil is given by (Tinker and Nye, 2000)

$$\partial_t(\theta c_L + c_S) + \nabla \cdot (\underline{v} c_L) = \nabla \cdot (D f \nabla c_L), \quad (1)$$

where c_L is the nutrient concentration in the soil pore water, c_S is the amount of nutrients bound to the soil particle surfaces, \underline{v} is the fluid movement velocity, D is the nutrient diffusion coefficient in water, and f is the diffusion impedance due to the tortuosity of fluid paths between the soil particles. Typically, the relationship between c_S and c_L is described either by linear, Langmuir or Michaelis-Menten adsorption isotherm, or something similar, i.e., for linear ($\alpha = 1$) and Langmuir ($\alpha > 1$) we would have $c_S = b c_L^\alpha$, and for the Michaelis-Menten we would have $c_S = f_m c_L / (k_m + c_L)$. Thus, Equation 1 is in fact a single equation for one variable c_L . In order to solve this equation one needs to describe the boundary conditions far from the plant and at the plant surface. Thus, typically Equation 1 is supplemented by a plant nutrient boundary condition describing the flow (flux) of nutrients into the root, and the most popular one of these is given by

$$\underline{n} \cdot (\underline{v} c_L - D f \nabla c_L) = \frac{F_m c_L}{K_m + c_L} - E \text{ on the root surface}, \quad (2)$$

where \underline{n} is the normal to the root surface, F_m and K_m are experimentally measured constants describing the root nutrient uptake, and E is the constant characterizing the concentration when the nutrient uptake by plant stops. The right hand side effectively means that at low nutrient concentration values the flux of nutrients increases linearly proportional to concentration, but at the high nutrient concentration values the flux is limited to a constant value.

Root systems are in general complex three dimensional objects and thus in general one would need to solve Equations 1 and 2 in three dimensions. However, it is usually unfeasible to solve Equations 1 and 2 explicitly for all specific situations. Thus, usually a certain level of simplification of root structure is needed in order to answer questions on the realistic timescale. Thus, if one wants to calculate the nutrient uptake by single cylindrical root, then one can use either numerical methods in cylindrical geometry (Tinker and Nye, 2000) or use one of the analytic solutions that has been derived for this situation (Roose et al., 2001; Roose and Kirk, 2008). For example, the simplest analytic function describing the flux of nutrient into single cylindrical root is given by (from Roose et al., 2001; Roose and Kirk, 2008)

$$F(t) = 2F_m \frac{c_0}{K_m} \sqrt{1 + \frac{c_0}{K_m} + (\lambda - Pe) \frac{L(t)}{2}} + \left\{ \left[1 - \frac{c_0}{K_m} + (\lambda - Pe) \frac{L(t)}{2} \right]^2 + 4 \frac{c_0}{K_m} \left(1 - Pe \frac{L(t)}{2} \right) \right\}^{1/2} \quad (3)$$

$$\text{Where } \lambda = \frac{F_m a}{Df K_m}, Pe = \frac{aV}{Df}, L = \ln \left(1 + 4e^{-v} t \frac{Df}{a^2(\theta+b)} \right),$$

where a is the root radius, V is the flux of water into the root, b is the soil buffer power, and v is Euler's constant.

The fact that we have an analytic expression for nutrient uptake by single cylindrical root proves to be a very powerful tool if one wants to now address questions on the root system scale. Single root solution serves as a basis on using homogenization and upscaling methods.

The challenge in plant-soil modeling is to upscale the modeling knowledge from a single root to a root branching structure scale. There are essentially two alternatives, full 3D computation or homogenization methods. Despite the increases in computing power, full 3D simulations are still not entirely realistic. In addition, one is not usually interested in the exact 3D solution since one is never measuring nutrient concentrations in 3D. Instead one is often interested in the overall uptake of nutrients or water from the soil, or in the horizontal profiles of nutrient concentration and water saturation in the soil. Thus, the method of homogenization proves to be one of the most popular alternatives (Roose and Schnepf, 2008; Fowler, 1997; Pavliotis and Stuart, 2008). This method essentially relies on the fact that one can consider many (infinitely many) simple elements in the system. The result is that one derives models describing the average concentration of nutrients or water or both in the soil and that these models contain all the necessary information about the microstructure in the system.

Summary

In conclusion, we can now firmly say that mathematics has much to offer to study of plant–soil interaction. The main challenges in this field deal with developing rigorous mechanistic multiscale models that have just the right

amount of detail in them so that they are still tractable analytically and numerically. Multiscale homogenization methods will undoubtedly be used further to answer these questions. However, this work needs to be done in a framework of experimental investigations.

Bibliography

- Fowler, A. C., 1997. *Mathematical Models in Applied Sciences*. Cambridge: Cambridge University Press.
- Pavliotis, G. A., and Stuart, A. M., 2008. *Multiscale Methods. Averaging and Homogenisation*. New York: Springer.
- Roose, T., and Kirk, G. J. D., 2008. The solution of convection-diffusion equations for solute transport to plant roots. *Plant and Soil*, **361**(1), 257–264.
- Roose, T., and Schnepf, A., 2008. Mathematical models of plant-soil interactions. *Philosophical Transactions of the Royal Society A: Physical Sciences*, **366**, 4597–4611.
- Roose, T., Fowler, A. C., and Darrah, P. R., 2001. Mathematical model of plant nutrient uptake. *Journal of Mathematical Biology*, **42**, 347–360.
- Tinker, P. B., and Nye, P. H., 2000. *Solute Movement in the Rhizosphere*. Oxford: Oxford University Press.

Cross-references

- Agriculture and Food Machinery, Application of Physics for Improving
- Agophysical Objects (Soils, Plants, Agricultural Products, and Foods)
- Agophysical Properties and Processes
- Buffer Capacity of Soils
- Drought Stress, Effect on Soil Mechanical Impedance and Root (Crop) Growth
- Enzymes in Soils
- Fertilizers (Mineral, Organic), Effect on Soil Physical Properties
- Irrigation and Drainage, Advantages and Disadvantages
- Microbes and Soil Structure
- Mycorrhizal Symbiosis and Osmotic Stress
- Nondestructive Measurements in Soil
- Physics of Plant Nutrition
- Plant Roots and Soil Structure
- Rheology in Soils
- Rheology in Agricultural Products and Foods
- Rhizosphere
- Root responses to Soil Physical Limitations
- Root System Architecture: Analysis from Root Systems to Individual Roots
- Root Water Uptake: Toward 3-D Functional Approaches
- Scaling of Soil Physical Properties
- Soil Aggregates, Structure, and Stability
- Soil Erosion Modeling
- Soil Functions
- Soil Hydraulic Properties Affecting Root Water Uptake
- Soil Physical Degradation: Assessment with the Use of Remote Sensing and GIS
- Soil Physical Quality
- Soil–Plant–Atmosphere Continuum
- Soil Water Flow
- Solute Transport in Soils
- Sorptivity of Soils
- Stomatal Conductance, Photosynthesis, and Transpiration, Modeling
- Water Balance in Terrestrial Ecosystems
- Water Uptake and Transports in Plants Over Long Distances
- Water Use Efficiency in Agriculture: Opportunities for Improvement

PLASTIC LIMIT

Boundary between non-plastic and plastic states of matter. With soils the limit corresponds to the minimum water mass content at which a soil sample can be deformed without rupture. See also *Atterberg Limits*.

PLASTICITY

The property of a solid body (e.g., clay soil, fruits) whereby it undergoes a permanent change in shape or size when subjected to a stress exceeding a particular value, called the yield value.

PLASTICITY NUMBER

The numerical difference between the liquid and the plastic limit or, synonymously, between the lower plastic limit and the upper plastic limit. Sometimes called "plasticity index." See also *Liquid Limit (Upper Plastic Limit, Atterberg Limit)*.

Bibliography

Glossary of Soil Science Terms. Soil Science Society of America. 2010. <https://www.soils.org/publications/soils-glossary>

PLATE SINKAGE TEST

See *Soil Compaction and Compressibility*

POISEUILLE'S LAW

The law governing laminar flow in an individual narrow tube in which the flow rate is proportional to the product of the pressure drop per unit distance and the pore radius to the fourth power.

POLISH SOCIETY OF AGROPHYSICS

Bogusław Szot
Institute of Agrophysics, Polish Academy of Sciences,
Lublin, Poland

The Polish Society of Agrophysics (PSA) is a professional and technical organization dedicated to the advancement of social, scientific, and educational activity in agrophysics as well as to the extension of results of research in the interest of national economy. The activity of the society is focused on: physics and physicochemistry of soil

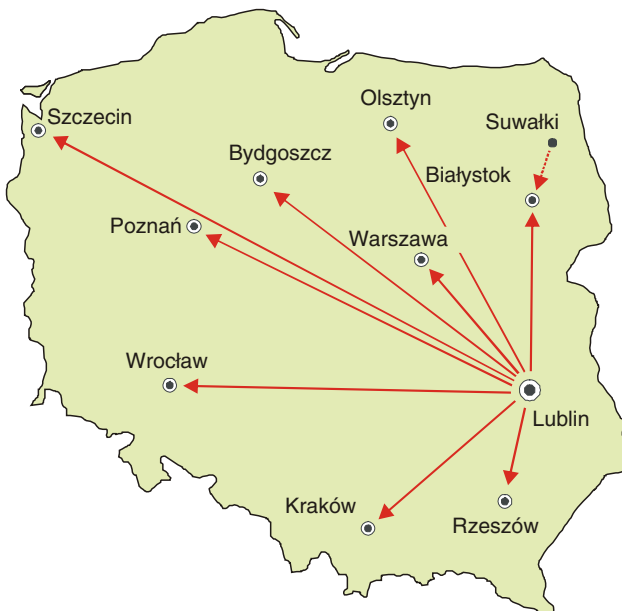
environment, physical processes in soil, physical properties of plants and crops, physical properties of foods, physical processes connected with harvesting, cleaning, drying, handling, and storing of plant products.

The goals of the Society are fulfilled by

- Organization of scientific meetings, conferences, congresses, seminars, symposia on national as well as international level
- Organization of public lectures and other forms of extension of results of investigations
- Education and popularization activity through media
- Organization and conducting of agrophysical research and development by appointed sections, committees, and working groups
- Publishing activity
- Advocating lifelong learning of the members and promoting the profession
- Issuing of opinions and expertises on the field of agrophysics
- Cooperation in advancement of unification of agrophysical terminology and standards
- Carrying out economical activity, performing investigations, analyses, expertises, and arrangement for prototype production
- Other type of activity conforming with the statute

Founded in 1996 and headquartered in Lublin, PSA comprises over 360 members, among whom over 150 hold the title of professor.

In the last 9 years, the Society grown to ten branches in major scientific centers in Poland, where agrophysical investigations are performed (Figure 1). Every year



Polish Society of Agrophysics, Figure 1 Location of PSA branches in Poland.



Polish Society of Agrophysics, Figure 2 Scientific Convention of PSA in Lublin, 2008.

branches organize meetings, seminars, and methodic symposia also for young scientists.

Until now, the society has organized nine national and international conferences with over 1,400 participants (115 of them from 29 countries outside Poland) (Figure 2). Summaries of the reports were published in proceedings, while the majority of full texts were published in International Agrophysics and Acta Agrophysica. Current information on the activity is spread through Information Bulletin of the PSA.

Statute of the PSA allows residents out of Poland to join the society. Annual dues levied on a calendar year basis is \$10. One of the member benefits is discounted meeting and conference registration fees.

PORE MORPHOLOGY AND SOIL FUNCTIONS

Marcello Pagliai

Agricultural Research Council (CRA), Research Centre for Agrobiology and Pedology (CRA-ABP), Florence, Italy

Synonyms

Pore shape; Soil porous system

Definition

The pore morphology is the shape, size, and spatial arrangement of the soil spaces representing the liquid and gaseous phases.

Introduction

Soil health is strictly related to structural conditions and many of the environmental damages in cultivated areas

(erosion, desertification, etc.) are determined by soil structure degradation.

Soil structure may be defined either as “the shape, size and spatial arrangement of individual soil particles and clusters of particles (aggregates)” or as “the combination of different types of pores with solid particles (aggregates).” Soil structure has generally been defined in the former way and measured in terms of aggregate characteristics. These can be related to plant growth only empirically. In fact, it is the shape, size distribution, and arrangement of pores that affect many of the most important processes in soil that influence plant root growth and development, the physical habitat for soil biota, such as storage and movement of water and gasses, and solute movements. Therefore, soil porosity is widely recognized as one of the best indicator of soil structure quality (Greenland, 1981; Pires et al., 2005). For this reason, measurements of pore space are increasingly being used to characterize soil structure. In fact, between the particles arranged singly or in aggregates, there is an intricate system of pore spaces on which plant roots, microorganisms, and soil fauna depend for the storage and movement of water and air.

The image analysis, among innovative techniques studying soil pore system entirely, allows to characterize soil structure by the quantification of soil porosity in all its aspects (pore shape, pore size distribution, irregularity, orientation, continuity, etc.) on thin sections, prepared from undisturbed soil samples (Bouma et al., 1977, 1982; Murphy et al., 1977a, b; Pagliai et al., 1983b, 1984; Pagliai, 1988; Mermut et al., 1992; Pagliai and Vignozzi, 2002). This morphometric technique has the advantage that the measurement and the characterization of pore space can be combined with a visual appreciation of the type and distribution of pores in soil at a particular

moment in its dynamic evolution. For this analysis, it is necessary to prepare thin sections of soil following a procedure that consists in taking undisturbed soil samples using appropriate tools, containers, and techniques taking care that the internal structure of the soil samples remains undisturbed. Then the soil samples, carefully packed, are transported to the laboratory, dried to avoid pronounced shrinkage phenomena, using appropriate methods, for example, acetone replacement of the water (Murphy, 1986), and impregnated, under vacuum, with a polyester resin, which has the characteristic of polymerizing slowly at room temperature without altering in any way the structure of the soil. Practically, this resin fills the pores of the soil. When the soil samples are hardened (generally after 4–6 weeks) they are made into vertically or horizontally oriented thin sections by using appropriate machines (Murphy, 1986). Their thickness is about 30 µm so that they can be analyzed by the microscope in transmitted light. The size depends on the kind of machines available; for porosity measurement, a size larger than 6 × 6 cm is recommended. Image analysis can be used not only on soil thin sections but also on polished faces of large soil blocks impregnated directly in the field with (fairly cheap) materials such as paraffin wax (Dexter, 1988), plaster of Paris (FitzPatrick et al., 1985), or resin (Moran et al., 1989).

The soil thin sections are analyzed with image analyzers (Murphy et al., 1977a, b; Pagliai et al., 1983b, 1984). Two-dimensional images can also be transformed into data representing three-dimensional area percentages that are representative for three-dimensional volumes. Stereology techniques have been applied to achieve this objective (Ringrose-Voase and Bullock, 1984; Ringrose-Voase and Nortcliff, 1987).

To characterize the microporosity (pores less than 50 µm), the thin sections must be covered by a layer of carbon, in order to allow conductivity to the electron beam, and analyzed by a scanning electron microscope (SEM) with a module for back-scattered electron scanning images (BESI) (Pagliai et al., 1983a). The thin sections can be examined by the SEM at several magnification. For example, if the analysis in the image analyzer starts with BESI taken at ×400 magnification, the size of the pixel will be 0.2 µm, therefore pores in the range of the storage pores 0.5–50 µm can be measured from the back-scattered electron scanning images (Pagliai and Vittori Antisari, 1993).

Basic measurements by image analysis include pores number, area, perimeter, diameters, projections, etc., and these are supplemented by derived quantities such as shape factors, size distribution, continuity, irregularity, and orientation. Detailed insight into the complexity of the pore system in soils can be obtained by using mercury intrusion porosimetry to quantify pores with equivalent pore diameter <50 µm (micropores) within the soil aggregates (Fiès, 1992).

Several methods are available to characterize soil structural attributes: image analysis and tomographic unit

profiles could successfully be used (Pires et al., 2005). X-ray computed tomography (CT-scanning) is a rapid, nondestructive method that has been applied in a variety of ways; for example, Mooney (2002) applied CT-scanning to undisturbed soil, preparing three-dimensional visualizations to quantitatively describe soil pore structure. Despite the advantages of this technique, access to scanners, resolution limitations, and the associated costs restrict its use.

Classification of soil pores

Pore shape, continuity, irregularity, and orientation A morphological distinction can be obtained by image analysis using, for example, the shape factor “roundness” [$P^2/(4\pi^*A)$] that relates area (A) and perimeter (P) of each pore.

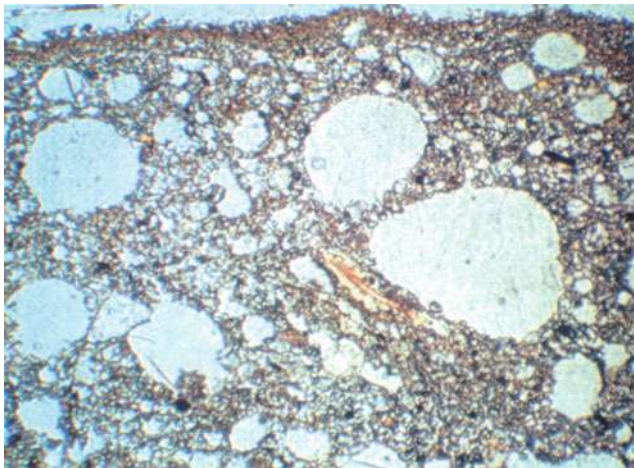
This parameter allows the division of pores into three main different shape groups such as, more or less rounded (regular) (roundness 1–2), irregular (roundness 2–5), and elongated pores (roundness >5) (Bouma et al., 1977; Pagliai et al., 1983b).

The regular pores are obviously those of a rounded shape and can be distinguished in two types according to their origin: the spherical pores formed by entrapped air during soil drying and the channels and chambers formed by biological activity (root growth and movement of soil fauna). Their distinction on soil thin sections is very evident because spherical pores (vesicles, according to Brewer [1964]) have very smooth walls, while channels, even though cut in a transversal way on thin section, present rough walls with deposits of insects’ excrements or root exudates. The presence of many spherical pores of the first type creates a vesicular structure.

Figure 1 shows an example of a vesicular soil structure. There are no single aggregates and the mass is broken up by rounded pores, “vesicles” (Bullock et al., 1985), which do not contribute to water movement. This kind of structure is an indicator of degraded soils. This is an excellent example of how it is important to characterize soil porosity, because sometime the same value of total porosity could originate extremely different types of soil structure, that behave in really different ways with respect to water storage and movement.

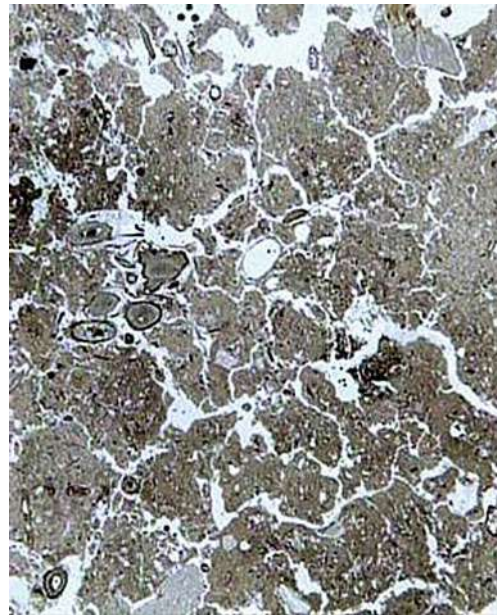
The irregular pores are the common soil voids with irregular walls (vughs, according to the micromorphological terminology of Brewer, 1964) and can be isolated (packing voids) or interconnected. The dominant presence of these pores produce the typical vughy structure (Bullock et al., 1985). In cultivated soils, these pores can be produced by the action of soil tillage implements.

Two types of elongated pores can be distinguished, cracks and thin fissures (planes). The former are typical of clay soils with a depleted soil organic matter content and they are visible at the surface when the soil is dry and has shrunk. The thin fissures are the most important, especially from an agronomic point of view, being the typical transmission pores. An adequate proportion of this



Pore Morphology and Soil Functions,

Figure 1 Microphotograph of a vertically oriented soil thin section showing an example of vesicular structure. The white areas represent the pores. Frame length 5×3 mm.



Pore Morphology and Soil Functions,

Figure 2 Macrophotograph of a vertically oriented thin section showing an example of subangular blocky structure. The white areas represent the pores. Frame length 3×5 cm.

type of pore (over 10% of the total porosity) generally creates an angular to subangular blocky structure of good quality. Obviously for this to be true, it is necessary for these pores to be homogeneously distributed in the soil matrix. In fact, for the characterization of these pores by image analysis, it is necessary to determine not only their shape and width, but also their length. With the same procedure of width determination, it is also possible to determine the length of these elongated pores, which may reflect their continuity, and it is well known that the flow of water through soil depends on the continuity of large pores. An example of a good pore continuity is reported in [Figure 2](#), which represents a subangular blocky structure. The soil aggregates are separated by elongated continuous pores (planes), are of different sizes, and can be rather porous inside. From an agronomic point of view, this is the best type of soil structure because the continuity of elongated pores allows good water movement and makes easy root growth. Moreover, it is a rather stable soil structure.

Therefore, the analysis of pore patterns allows the characterization and prediction of flow processes in soils.

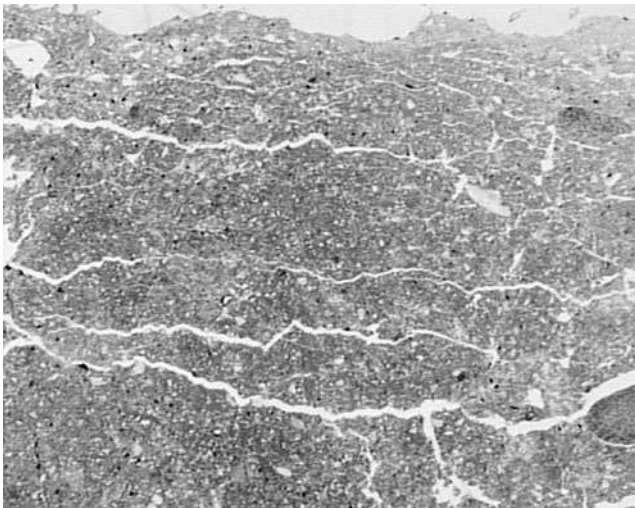
For root growth and water movement, not only the size and continuity of elongated pores are important but also their irregularity and orientation. The ratio convex perimeter/perimeter or convex area/area of elongated pores gives information about their irregularity, tortuosity, and reentrance. As regards water movement, for example, the very regular and the moderately regular elongated pores play a different role. The very regular elongated pores are flat and smooth pores with accommodating faces, which tend to seal when the soil is wet, thus preventing water movement. In contrast, the moderately regular elongated pores have walls that do not accommodate each other. Therefore, these pores permit water movement even when

the soil is wet and fully swollen ([Pagliai et al., 1984](#)). The ratio vertical/horizontal dimension gives the orientation of elongated pores ([Pagliai et al., 1984](#)). It is easily understandable that many soil processes, such as, water movement, leaching, clay migration, etc., are strongly related to the orientation of pores and these processes change dramatically depending on whether a vertical or horizontal pore orientation is dominant.

[Figure 3](#) shows an example of platy structure, that is, the thin and flat soil aggregates are separated by elongated pores oriented parallel to the soil surface and, therefore, not continuous in a vertical sense. This leads, as a consequence, to a drastic reduction of water infiltration capacity. Soils with this type of structure are subject to water stagnation or runoff and erosion depending on their slope. The platy structure is typical of compacted soils.

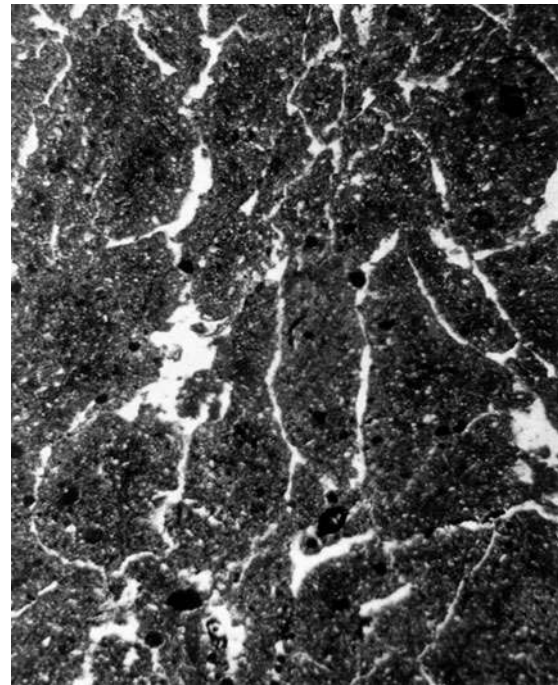
On the contrary, [Figure 4](#) shows an example of a prismatic structure, that is, the soil macroaggregates are divided into prisms separated by vertically oriented elongated pores with accommodating walls. Also, this type of structure is typical of clay soils, especially in the B horizon, and is not very stable because the swelling of the soil when wet causes the closing of pores.

Characterization of the soil pore system by image analysis of thin sections can give detailed information about soil structural conditions; moreover, if climate, agronomic, and management data are known, an evaluation of soil physical vulnerability is possible. Hence, the soil pore system can be considered a good indicator of soil



Pore Morphology and Soil Functions,

Figure 3 Macrophotograph of a vertically oriented soil thin section showing an example of platy structure. The white areas represent the pores. Frame length 5 × 3 cm.



quality, nevertheless, as for other indicators, threshold values have to be known.

According to the micromorphometric method, a soil can be classified as follows where the total porosity represents the percentage of area occupied by pores larger than 50 µm per thin section (Pagliai, 1988):

Soil very compact	When total porosity is	<5%
Soil compact	When total porosity is	5–10%
Soil moderately porous	When total porosity is	10–25%
Soil highly porous	When total porosity is	25–40%
Soil extremely porous	When total porosity is	>40%

Soil functions

The role of soil management in a sustainable environment is to provide multiple functions for the well-being of humans. In this context, the functions of soils for human societies and the environment are of special importance. According to Blum (2002), soils have at least six different functions for the social and economic development of humankind, which can be distinguished into three more ecological functions and three others directly linked to human activities defined as technical, industrial, and socioeconomic functions:

Soil ecological functions:

- Production of biomass, ensuring food, fodder, renewable energy, and raw biological materials
- Storing, filtering, buffering, and transforming substances and water, carbon sink, protecting the environment
- Biological habitat and gene reserve

Pore Morphology and Soil Functions,

Figure 4 Macrophotograph of a vertically oriented soil thin section showing an example of prismatic structure. The white areas represent the pores. Frame length 3 × 5 cm.

Soil socioeconomic functions:

- Physical basis for technical, industrial, socioeconomic, and cultural structures and their development
- Source of geogenic energy, raw mineral materials, and water
- Geogenic and cultural heritage, forming an essential part of the landscape, concealing and protecting paleontological and archeological treasures

It is obvious to underline the importance of pore morphology for the explication of soil ecological functions: the production of biomass, for example, depends on the soil structure quality and it has already been explained as the pore morphology determines the type of soil structure.

Summary

The soil pore system gives essential indications about soil health and vulnerability in relation to degradation events mainly connected with human activity. Such a characterization is especially useful in the study of the relationships between soil physical, chemical, and biochemical properties and provides a realistic basis for understanding water retention and water movement in soil.

The characterization of soil pore system, by means of image analysis on thin sections, can provide basic information for the study of soil. The major disadvantage of this technique is that the preparation of soil thin sections is both difficult and time consuming. However, many public and private laboratories are now equipped for the preparation of soil thin sections and the development of improved computer software has made the analysis of the images easy.

When the obstacle of the acquisition of soil thin sections is overcome, it is possible to benefit from the full potential of this technique, particularly valuable to quantify the changes in soil structure following human activities. Therefore, on the basis of the acquired experience, it is possible to go deep into the analysis of soil thin sections in relation to aspects of water movement. The quantification of the size, continuity, orientation, and irregularity of elongated pores allows the modeling of water movement and solute transport, or, at least, allows the prediction of the changes that can be expected following soil structural modifications, or following soil degradation due to compaction, formation of surface crusts, etc.

Bibliography

- Blum, W. E. H., 2002. Environmental protection through sustainable soil management – a holistic approach. *Advances in GeoEcology*, **35**, 1–8.
- Bouma, J., Jongerius, A., Boersma, O. H., Jager, A., and Schoonderbeek, D., 1977. The function of different types of macropores during saturated flow through four swelling soil horizons. *Soil Science Society of America Journal*, **41**, 945–950.
- Bouma, J., Belmans, C. F. M., and Dekker, L. W., 1982. Water infiltration and redistribution in a silt loam subsoil with vertical worm channels. *Soil Science Society of America Journal*, **46**, 917–921.
- Brewer, R., 1964. *Fabric and Mineral Analysis of Soils*. New York: Wiley.
- Bullock, P., Fedoroff, N., Jongerius, A., Stoops, G., and Tursina, T., 1985. *Handbook for Soil Thin Section Description*. Wolverhampton: Waine Research.
- Dexter, A. R., 1988. Advances in characterization of soil structure. *Soil and Tillage Research*, **11**, 199–238.
- Fiès, J. C., 1992. Analysis of soil textural porosity relative to skeleton particle size, using mercury porosimetry. *Soil Science Society of America Journal*, **56**, 1062–1067.
- Fitz Patrick, E. A., Makie, L. A., and Mullins, C. E., 1985. The use of plaster of Paris in the study of soil structure. *Soil Use and Management*, **1**, 70–72.
- Greenland, D. J., 1981. Soil management and soil degradation. *Journal of Soil Science*, **32**, 301–322.
- Mermut, A. R., Grevers, M. C. J., and de Jong, E., 1992. Evaluation of pores under different management systems by image analysis of clay soils in Saskatchewan, Canada. *Geoderma*, **53**, 357–372.
- Mooney, S. J., 2002. Three dimensional visualization and quantification of soil macroporosity and water flow patterns using computed tomography. *Soil Use and Management*, **18**, 142–151.
- Moran, C. J., McBratney, A. B., and Koppi, A. J., 1989. A rapid method for analysis of soil macropore structure. I. Specimen preparation and digital binary image production. *Soil Science Society of America Journal*, **53**, 921–928.
- Murphy, C. P., 1986. *Thin Section Preparation of Soils and Sediments*. Herts: AB Academic.
- Murphy, C. P., Bullock, P., and Turner, R. H., 1977a. The measurement and characterization of voids in soil thin sections by image analysis: part I. principles and techniques. *Journal of Soil Science*, **28**, 498–508.
- Murphy, C. P., Bullock, P., and Biswell, K. J., 1977b. The measurement and characterization of voids in soil thin sections by image analysis: part II. applications. *Journal of Soil Science*, **28**, 509–518.
- Pagliai, M., 1988. Soil porosity aspects. *International Agrophysics*, **4**, 215–232.
- Pagliai, M., and Vignozzi, N., 2002. Image analysis and microscopic techniques to characterize soil pore system. In Blahovec, J., and Kutilek, M. (eds.), *Physical Methods in Agriculture – Approach to precision and quality*. New York: Kluwer Academic/Plenum, pp. 13–38.
- Pagliai, M., and Vittori Antisari, L., 1993. Influence of waste organic matter on soil micro and macrostructure. *Bioresource Technology*, **43**, 205–213.
- Pagliai, M., Bisdom, E. B. A., and Ledin, S., 1983a. Changes in surface structure (crusting) after application of sewage sludges and pig slurry to cultivated agricultural soils in northern Italy. *Geoderma*, **30**, 35–53.
- Pagliai, M., La Marca, M., and Lucamante, G., 1983b. Micromorphometric and micromorphological investigations of a clay loam soil in viticulture under zero and conventional tillage. *Journal of Soil Science*, **34**, 391–403.
- Pagliai, M., La Marca, M., Lucamante, G., and Genovese, L., 1984. Effects of zero and conventional tillage on the length and irregularity of elongated pores in a clay loam soil under viticulture. *Soil and Tillage Research*, **4**, 433–444.
- Pires, L. F., Bacchi, O. O., Reichardt, K., and Timm, L. C., 2005. Application of Gamma-ray computer tomography to analysis of soil structure before density evaluations. *Applied Radiation and Isotopes*, **63**(4), 505–511.
- Ringrose-Voase, A. J., and Bullock, P., 1984. The automatic recognition and measurement of soil pore types by image analysis and computer programs. *Journal of Soil Science*, **35**, 673–684.
- Ringrose-Voase, A. J., and Nortcliff, S., 1987. The application of stereology to the estimation of soil structural properties: a review. In: Fedoroff, N., Bresson, L. M., and Courty M. A. (eds.), *Soil Micromorphology, Proc. VIIth Int. Working Meeting on Soil Micromorphology*. Plasir, France: Association Francaise pour l'Etude du Sol, pp. 81–88.

Cross-references

- [Aeration of Soils and Plants](#)
- [Cracking in Soils](#)
- [Field Water Capacity](#)
- [Flooding, Effects on Soil Structure](#)
- [Fractal Analysis in Agrophysics](#)
- [Hydropedological Processes in Soils](#)
- [Image Analysis in Agrophysics](#)
- [Infiltration in Soils](#)
- [Organic Matter, Effects on Soil Physical Properties and Processes](#)
- [Physical Degradation of Soils, Risks and Threats](#)
- [Pore Size Distribution](#)
- [Porosimetry](#)
- [Shrinkage and Swelling Phenomena in Soils](#)
- [Soil Biota, Impact on Physical Properties](#)
- [Soil Compaction and Compressibility](#)
- [Soil Functions](#)
- [Soil Phases](#)
- [Soil Physical Quality](#)
- [Soil Structure, Visual Assessment](#)
- [Soil Surface Sealing and Crusting](#)
- [Soil Water Flow](#)

[Soil–Wheel Interactions](#)

[Subsoil Compaction](#)

[Tillage, Impacts on Soil and Environment](#)

[Water Reservoirs, Effects on Soil and Groundwater](#)

[Wetting and Drying, Effect on Soil Physical Properties](#)

PORE SIZE DISTRIBUTION

Miroslav Kutílek

Emeritus Professor of Soil Science and Soil Physics,
Prague 6, Czech Republic

Definition

Soil pores vary in size and shape, and manifest an interconnected lattice. In a similar way, other porous materials can be defined but the soils belong to the most complicated porous systems. The frequency of pore sizes expressed as equivalent pore diameters when forming a continuous function is considered as a pore size distribution.

Soil porosity

The relative volume of pores is denoted as soil porosity

$$P = V_p/V_T$$

where V_p is the volume of pores and V_T the total bulk volume of soil. When this equation is multiplied by 100, we obtain P in percent. The volume of pores V_p is related to the volume of soil solid phase V_s by the void ratio

$$e = V_p/V_s$$

with mutual relations between P and e being

$$P = \frac{e}{1+e} \quad \text{and} \quad e = \frac{P}{1-P}$$

Void ratio is more appropriate than porosity if the reference term V_T is not constant as for example in clays when they swell or shrink. Estimating the proper size of V_T is obtained theoretically as the representative elementary volume (REV). Let us assume that when V_T is small enough ($V_T < V_p$) and centered in a pore, $P=1$. When V_T is centered in the solid phase and small enough ($V_T < V_s$), $P=0$. When V_T increases, we reach the situation when either $V_T=(V_p+\delta V_s)$ or $V_T=(V_s+\delta V_p)$ and porosity is neither 1 nor 0. Centering V_T in the solid phase, P is slightly above zero. With a gradual increase in V_T we obtain first a gradual decrease of P (center in the pore) or a gradual increase of P (center in the solid phase), until both values coincide. Before coincidence occurs, a damping oscillation of P may exist. At this stage of increasing V_T when porosity is independent upon the initial centering of V_T , we have reached the representative elementary volume (REV) (Kutilek and Nielsen, 1994).

Soils without structural development have an REV of about 100 cm³ or less. Because the REV of aggregated soils depends upon the size and shape of their peds, its value may be one or more orders of magnitude greater. The porosity of mineral soils lies between 0.4 and 0.6. Some organic soils have values of P close to 0.9. Porosity depends upon the composition, texture, and structure of soil. Soil structure is influenced by the content of organic matter, the quantity of inorganic cementing agents, the genesis of the soil and its horizons, and more recently by human activity. Theoretically, in the most dense arrangement of spherical particles of identical size, $P=0.26$. Although this value is sometimes taken as the theoretical minimum porosity of sands, even sandy soils are mixtures of particles of various sizes and shapes and for a model consisting of such a mixture of spherical particles the lowest value of porosity is well above 0.3. With an increase of clay content the porosity of soils rises, owing mainly to a greater opportunity for soil aggregation. The porosity of the A-horizon reaches its maximum value in loamy soils owing to the optimum conditions for aggregation. In clays, the tendency to slushiness leads to a slight decrease of P . The use of heavy machinery, the application of fertilizers in high quantities, and the decrease of organic matter in soils – all specific features of modern intensive agriculture – decrease aggregation and enhance soil compaction. In some clays and loams, P depends upon the soil water content θ as soil swells when wetted and shrinks when dried. In such soils P increases with θ . This relationship is linear for large values of θ . At smaller values of θ , P changes non-linearly with θ . In the soil profile, the maximum porosity usually occurs in the top of the A_o horizon. The porosity distribution with soil depth depends upon the development of each soil profile. For example, in the illuvial Bt horizon accumulated material causes a decrease in porosity. Or, the reduction of iron oxides and the destruction of the structure in hydromorphic gley G horizons lead to an abrupt decrease in porosity.

Classification of soil pores

The classification of soil pores should follow the laws of hydrostatics and hydrodynamics and leads to three major categories (Corey, 1977, completed by Pagliai and Kutilek, 2008).

1. Submicroscopic pores, which are so small that they preclude clusters of water molecules to form fluid particles or continuous water flow paths. Inasmuch as convection does not exist in these pores, the laws of fluid mechanics are not applicable. Pores belonging to this category are oftentimes neglected.
2. Capillary pores where the shape of the interface between air and water is determined by the configuration of pores and by the forces on the interface. The resulting air–water interface is called the capillary meniscus. The flow of water in these pores is

considered to be laminar and dominant in soils. This category is subdivided into two:

- (a) Matrix (intra-aggregate, intra-pedal, textural) pores within soil aggregates or soil blocks. The arrangement of the soil skeleton, coating of aggregates, cutans, and nodules typical for each soil taxon have main influence upon the soil water hydrostatics and hydrodynamics in the matrix domain. Hydraulic conductivity is strongly reduced when compared to conductivity of the whole soil.
 - (b) Structural (inter-aggregate, inter-pedal) pores between the aggregates, or eventually between the soil blocks. Their morphology and interconnection depends upon the shape, size, and stability of aggregates and blocks, or, generally upon the soil genesis and the type of soil use.
3. Macropores (non-capillary pores) are of sufficient size that capillary menisci are not formed. The shape of the interface between air and water is considered planar, and hence, capillary forces are nil. The flow of water inside of such pores can be either in the form of a film moving over all the irregularities of the walls induced by their roughness and shape, or in some cases, turbulent flow when the pores contain considerably more water. The shape of macropores is generally thought to be either tubular or planar. A tubular shape is caused by the action of soil fauna (e.g., earthworms) or originates after the decay of plant roots. Planar pores have the form of cracks and fissures owing mainly to cleavage planes and volume changes of the bulk soil when it dries. A more detailed classification of macropores is related to their stability and persistence in time:

- (a) Macropores formed by the activity of pedoedaphon such as decayed roots and earthworm channels. Their main characteristic is their high stability and persistence in time.
- (b) Fissures and cracks occurring as a consequence of volumetric changes of swelling–shrinking soils. They have planar form and they close when the soil matrix is saturated with water.
- (c) Macropores originating due to soil tillage. The depth of their occurrence is limited and they disappear usually in less than one vegetation season. Their persistence depends upon the genetic evolution of the soil, meteorological conditions, and the type of plants being grown.

Pore size distribution

The real size of pores, their continuity and forms are visualized microscopically on thin sections of soil. Computerized tomography (CT), nuclear magnetic resonance (NMR), and X-ray stereo radiographs offer insight into three-dimensional networks of pores. X-ray computerized tomography (CT) and nuclear magnetic resonance (NMR) produce an image of a slice of finite thickness of a soil. If there is sufficient number of successive slices in the

direction of the axis perpendicular to the slices, a three-dimensional image can be obtained. Both techniques are noninvasive and do not disturb the soil system, they are suitable for repetitive measurements on the same soil body. The form and distribution of soil pores can be quantified by the application of fractal theory and by methods of quantitative stereometry. The mercury porosimetry offers information on pore size distribution assuming that the pores are formed by cylindrical pores. Mercury is injected into the sample at increasing incremental pressures using nitrogen gas as the displacing medium. At each pressure increment, mercury intrusion is monitored while the pressure is held constant. The applied pressure is transformed to equivalent radius; the smaller are the pores, the higher pressure has to be applied to inject mercury into the pore. Thus a curve on pore size distribution is obtained. In soil hydraulics, the porous system is modeled and interpreted using soil water retention curves. Several different types of models have been used to describe experimentally measured soil water retention curves. The most frequent is derived from a bundle of parallel capillary tubes. The derivative curve to soil water retention curve with the pressure height h transformed to pore radius $r = a/h$ is then the pore size distribution. The model of lognormal pore size distribution $f(r)$ fits well for soils (Brutsaert, 1966; Pachepsky et al., 1992; Kosugi, 1994):

$$f(r) = \frac{\theta_S - \theta_R}{\sigma r \sqrt{2\pi}} \exp\left\{-\frac{[\ln(r/r_m)]^2}{2\sigma^2}\right\}$$

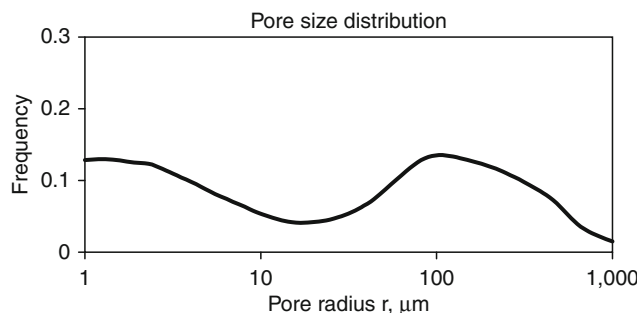
where r_m is the geometric mean radius, σ is the standard deviation, θ_S is the soil water content at full saturation of soil with water, and θ_R is the residual soil water content when the liquid flow is essentially zero. It is usually not measured but it is found as a fitting parameter of the retention curve. The detailed study of $h(\theta)$ of the porous system of majority of soils led to the discovery of bi- and multimodal porosity (Othmer et al., 1991; Durner, 1992; Pachepsky et al., 1992) due to the structural characteristics of soils, see the Figure 1. Then the pore size distribution equation is formulated for each domain separately

$$f(r)_i = \frac{\theta_{Si} - \theta_{Ri}}{\sigma_i r_i \sqrt{2\pi}} \exp\left\{-\frac{[\ln(r_i/r_{mi})]^2}{2\sigma_i^2}\right\}$$

where $i=1$ is for the matrix domain, and $i=2$ is for the structural domain. In spite of the generally lower value of the volume of structural pores, this domain influences mainly the transport processes and flow of water provided that the structural pores are at least partly saturated by water.

Summary

Pore size distribution is studied on the representative elementary volume and it depends upon the evolution and character of horizons and upon the soil structure and



Pore Size Distribution, Figure 1 Pore size distribution in a well-aggregated loamy soil. The peak on the right-hand side belongs to the structural domain and the peak on the left-hand side belongs to the matrix domain. The minimum at $r=27\text{ }\mu\text{m}$ denotes the boundary between the two domains.

texture. Soil pores belong to one of three basic categories: (1) submicroscopic pores, (2) capillary pores, and (3) macropores. The smooth function of pore size distribution in the capillary category is obtained from the derivative curve to the soil water retention curve.

Bibliography

- Brutsaert, W., 1966. Probability laws for pore size distribution. *Soil Science*, **101**, 85–92.
 Corey, A. T., 1977. *Mechanics of Heterogeneous Fluids in Porous Media*. Fort Collins: Water Resources.
 Durner, W., 1992. Predicting the unsaturated hydraulic conductivity using multi-porosity water retention curves. In van Genuchten, M. Th., Leij, F. J., and Lund, L. J. (eds.), *Indirect Methods for Estimating the Hydraulic Properties of Unsaturated Soils*. Riverside: University of California, pp. 185–202.
 Kosugi, K., 1994. Three-parameter lognormal distribution model for soil water retention. *Water Resources Research*, **30**, 891–901.
 Kutilek, M., and Nielsen, D. R., 1994. *Soil Hydrology*. Cremlingen-Destedt: Catena Verlag.
 Othmer, H., Diekkrüger, B., and Kutilek, M., 1991. Bimodal porosity and unsaturated hydraulic conductivity. *Soil Science*, **152**, 139–150.
 Pachepsky, Ya A, Mironenko, E. V., and Shcherbakov, R. A., 1992. Prediction and use of soil hydraulic properties. In van Genuchten, M. Th., Leij, F. J., and Lund, L. J. (eds.), *Indirect Methods for Estimating the Hydraulic Properties of Unsaturated Soils*. Riverside: University of California, pp. 203–213.
 Pagliai, M., and Kutilek, M., 2008. Soil micromorphology and soil hydraulics. In Kapur, S., Mermut, A., and Stoops, G. (eds.), *New Trends in Soil Micromorphology*. Berlin: Springer, pp. 5–18.

Cross-references

- [Bypass Flow in Soil](#)
[Hydraulic Properties of Unsaturated Soils](#)
[Infiltration in Soils](#)
[Nondestructive Measurements in Soil](#)
[Noninvasive Quantification of 3D Pore Space Structures in Soils](#)
[Organic Matter, Effects on Soil Physical Properties and Processes](#)
[Oxidation–Reduction Reactions in the Environment](#)
[Physical Degradation of Soils, Risks and Threats](#)
[Pore morphology and Soil Functions](#)
[Porosimetry](#)
[Soil Water Flow](#)

POROSIMETRY

Mieczysław Hajnos

Institute of Agrophysics, Polish Academy of Sciences,
 Lublin, Poland

Definition

Porosimetry is an analytical technique used to determine various quantifiable aspects of a material's porous nature such as pore diameter, total pore volume, surface area, and bulk and absolute densities.

Introduction

Total porosity and specific surface area are two characteristics of soils that contribute in a significant way to the relationship between the observed properties and behavior of soils (Antilén et al., 2004). The soil porosity, critical for its aeration, is a parameter related to the storage and plant availability of water. Porosity and pore size are considered as structural factors related to the thermal properties of the soil.

Pore size, specified as the pore width (d_{pore}), is classified by IUPAC into three types: macropores ($d_{\text{pore}} > 50\text{ nm}$), mesopores ($2\text{ nm} < d_{\text{pore}} < 50\text{ nm}$) and micropores ($d_{\text{pore}} < 2\text{ nm}$). In the soil, micropores are important in the physisorption processes and the physical sequestration of chemical pollutants from the environment. Micropores are also important in the soil physicochemical processes, such as the K-Ca cation exchange selectivity of soils, where the size and shape of micropores are involved.

Mesopores act as a transport system, and the soil mesoporosity is of special interest because it regulates accessibility to the micropores.

The proportion of micro- and macropores affects the soil's water holding capacity, and the higher the microporosity, the higher the soil resistance to desiccation.

Soil macropores provide living space for the soil biota. Pores with a diameter smaller than 200 nm are inaccessible to soil microorganisms; those with diameter 800 to 6,000 nm are accessible to bacteria and protozoa; and pores larger than 30,000 nm of diameter are needed by nematodes.

The porous structure can be characterized by integral or differential curves of pore volume distribution vs. pore radius (porosimetric curves or porograms) (Volkovich et al., 2005).

The following methods for measuring porograms are well known:

- Mercury porosimetry – mercury intrusion into a non-wettable porous material
- Small-angle X-ray scattering
- Electron, atomic force and tunnel microscopy; centrifugal porosimetry
- Displacement of wetting liquids from the pore volume by gas pressure capillary condensation and others

Each of these methods has advantages and limitations.

For example, small-angle X-ray scattering can be used only for pore radii ranging from 2 to 50 nm and often leads to ambiguous results. Centrifugal porosimetry, optical microscopy, and displacement methods are practically useless for $r < 10^3$ nm. Measurements by electron microscopy are associated with difficulties in sample preparation and results interpretation. The method of capillary condensation can be used only in the pore size range from 0.3 to 50 nm. The method of mercury porosimetry (MMP) provides the widest range of measurable pore radii (from 2 to 10^5 nm). A great disadvantage of this method is the necessity to apply high pressure of mercury (up to thousands of atmospheres), which can lead to sample deformation or even destruction as well as the distortion of programs. The problem is also toxicity of mercury. All methods of microscopy practically give only half-quantitative information.

Methods of porosity determination

Following are the main methods used for determination of soil porosity and they are shown in [Figure 1](#).

Adsorption/desorption isotherm of nitrogen

Pores can be determined from adsorption/desorption isotherms of nitrogen in temperature -185.8°C . Pore size distribution can be calculated by various software methods accompanied by the measuring device. Usually these are the following methods: Dollimore/Heal, Horvath/Kawazoe, and B.J.H. (Barret–Joyner–Halenda).

Adsorption/desorption isotherm of water vapors

The pore size distribution can be calculated assuming that adsorbate molecules, by a given vapor pressure p , undergo capillary condensation in cylindrical pores of radii $r(p)$. Dependence of pore radii against pressure fulfil the Thomson (Kelvin) equation:

$$r(p) = \frac{-2\gamma V_m \cos \theta}{RT \ln \frac{p}{p_0}}, \quad (1)$$

where γ – surface tension of water, V_m – molar volume of water, θ – contact angle of water on the solid surface.

With relative pressures lower than inflection point of isotherm, adsorption occurs in monolayer and it cannot be interpret as the condensation process. Because of that the volume of monolayer calculated from the BET equation should be subtracted from the condensate volume.

The method from adsorption/desorption isotherms of nitrogen and water vapors enables pore size distribution in the range of lower pores than determined by mercury porosimetry ($r < 0.0039 \mu\text{m}$).

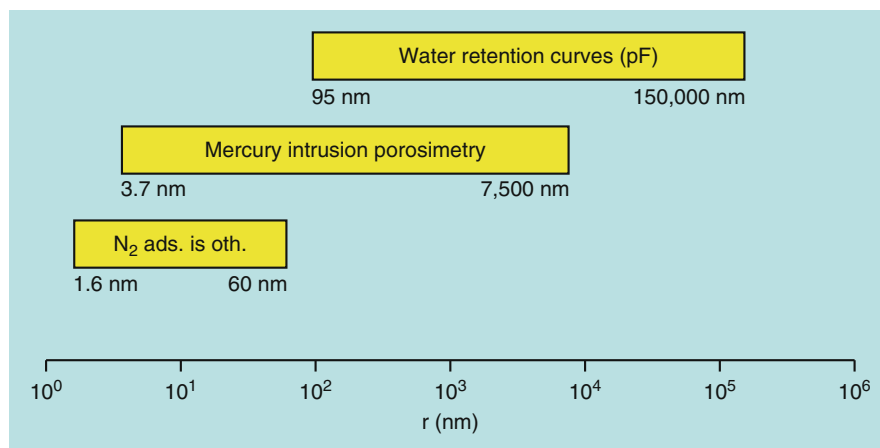
Mercury porosimetry

Mercury porosimetry and analysis of porosimetric curves is most often the method for determination of pore size distribution (Hajnos, 1998; Kozak, 1995). The basis of this method rests on the principle that a non-wetting fluid will not spontaneously intrude the pores of a solid, but will do so if sufficient pressure is applied. It is assumed that the sizes of pores intruded by mercury are inversely proportional to its pressure. The pressure indispensable for insertion of mercury to a capillary is the function of capillary radius according to the Washburn equation:

$$P = \frac{2\gamma_{\text{Hg}} \cos \theta}{r}, \quad (2)$$

where P – external pressure, γ_{Hg} – surface tension of mercury at 20°C (480 mN/m), θ – contact angle of mercury on soil material (average value 141.30°), r – determined pore radius.

Process of forcing of mercury into pores of investigated material under the influence of applied pressure underlies the basis of working of mercury porosimeter. It should be mentioned that determined pore radius r is not a real radius



Porosimetry, Figure 1 Ranges of porosity determined by various indirect methods. N_2 ads. isoth. – adsorption isotherm of nitrogen.

but so-called equivalent pore radius, depending on the mathematic model used for calculations.

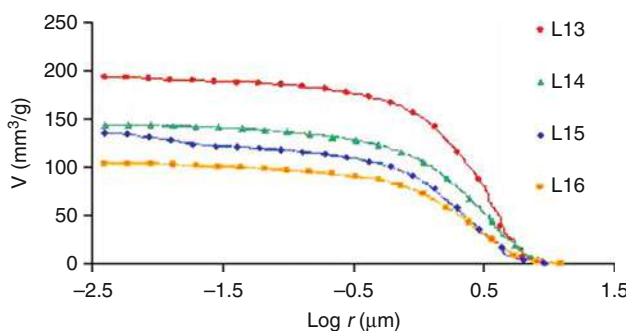
Usually pore size distribution is determined assuming cylindrical shape of pores. Because range of pores contains several orders of magnitude, cumulative distribution functions are often presented against logarithm of their radii:

$$f(\log r) = \frac{dV(\log r)}{d \log r}. \quad (3)$$

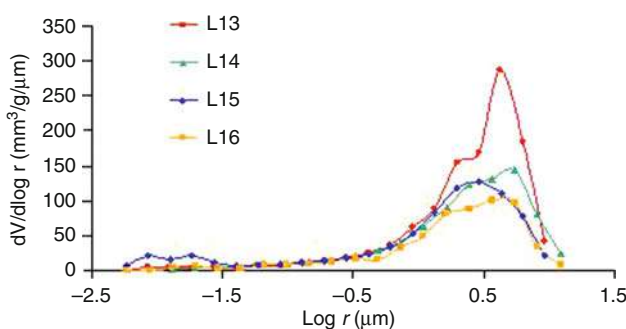
The modern mercury intrusion porosimeters allow usually for applying pressures up to 200 MPa, which corresponds to the equivalent pore size of 3.7 nm.

Range of pores measured by this method is from 0.0039 to about 12 μm .

Cumulative diagram of pore volume as a function of pore radius in logarithmic scale taking from the mercury porosimetry most often is presented as decreasing function, because total pore volume increases in the direction of low radii (Figure 2). The pore size distribution can be also presented by differential curves – $dV/d\log r = f(\log r)$ (Figure 3).



Porosimetry, Figure 2 Exemplary cumulative curves for orchard soils taken from the following horizons: L13 – 0–10 cm, L14 – 10–20 cm, L15 – 20–30 cm, L16 – 30–49 cm.



Porosimetry, Figure 3 Differential curves for orchard soils taken from the following horizons: L13 – 0–10 cm, L14 – 10–20 cm, L15 – 20–30 cm, L16 – 30–49 cm.

Soil water retention curves

In the unsaturated zone, the water is retained in the soil by capillary and molecular forces. As a result of these forces, the pressure in soil water is smaller than the atmospheric pressure. The atmospheric pressure is typically considered as the reference pressure in subsurface hydrology, and hence the pressure above the atmospheric pressure is positive, and similarly the pressure below the atmospheric level is negative. The negative pressure is also often called tension or suction.

The relationship between the volumetric water content and the soil water pressure can be described with a soil water retention curve (soil moisture characteristic curve) that plots the soil water pressure as a function of the soil water content. Often the soil water pressure is given as a pF value, which is the 10 base logarithm of the pressure in centimeters of water column h , i.e.,

$$\text{pF} = \log(-h). \quad (4)$$

Soil pore size can be determined on the basis of the water retention curve, because the given potential relates to definite pore radius, in which water is bonded. Relationship for the liquid perfectly wetting solid surface is given by the Laplace equation:

$$\Delta P = \frac{2\gamma}{r}. \quad (5)$$

Because the assumption of perfectly wetting soil samples, especially those with high content of organic matter (which means that water contact angle is equal zero), diverges from reality, the calculations performed on the basis of equation, taking into account measured contact angle (θ) (from the surface-free energy components):

$$r = \frac{2\gamma \cos \theta}{\Delta P} \quad (6)$$

Porosimetry is also applied to the structure determination of dried plant material (Rudko et al., 2004; Stawiński, 1976) and industrial plant products (Jamroz et al., 1999; Skiba et al., 2008).

Summary

Porosimetry is a technique used for the determination of pore diameter, total pore volume, surface area, and bulk and absolute densities. The following methods are applied for the determination of solid material porosity: mercury porosimetry – mercury intrusion into a non-wettable porous material, small-angle X-ray scattering, electron, atomic force, and tunnel microscopy, centrifugal porosimetry, and displacement of wetting liquids from the pore volume by gas pressure capillary condensation. The main methods used for the determination of soil and plant material porosity are the following: adsorption/desorption isotherm of nitrogen, adsorption/desorption isotherm of water vapors, mercury intrusion porosimetry, and water retention curves (pF).

Bibliography

- Antilén, M., Förster, J. E., del Confetto, S., Rodier, E., Fudym, O., Venezia, A. M., Deganello, G., and Escudey, M., 2004. Characterization of the porous structure of chilean volcanic soils by nitrogen adsorption and mercury porosimetry. *Journal of the Chilean Chemical Society*, **49**, 313–318.
- Hajnos, M., 1998. Mercury intrusion porosimetry as compared to other methods characterizing microstructure of soil materials (in Polish). *Zeszyty Problemowe Postępów Nauk Rolniczych*, **461**, 523–537.
- Jamroz, J., Hajnos, M., and Sokolowska, Z., 1999. Application of the mercury porosimetry to the porosity study of wheat flour extrudates. *International Agrophysics*, **13**, 445–449.
- Kozak, E., and Peida, M., 1995. Application of image analysis for evaluation of mercury intrusion porosimetry results. *International Agrophysics*, **9**, 337–341.
- Rudko, T., Sokołowska, Z., and Hajnos, M., 2004. Application of mercury porosimetry to determination of rape silique (in Polish). *Rośliny Oleiste*, IHAR Poznań, **25**, 81–87.
- Skiba, K., Hajnos, M., Tys, J., and Mościcki, L., 2008. Study of the microstructure of extruded rapeseed oil cake. *Polish Journal of Environmental Studies*, **17**, 284–289.
- Stawiński, J., and Szot, B., 1976. Application of mercury porosimetry to determination of wheat grain internal porosity (in Polish). *Hodowla Roślin Aklimatyzacja i Nasieniarnictwo*, **20**, 321–327.
- Volkovich, Y. M., Sakars, A. V., and Volinsky, A. A., 2005. Application of the standard porosimetry method for nanomaterials. *International Journal of Nanotechnology*, **2**, 292–302.

Cross-references

- [Compaction of Soil](#)
[Pore Morphology and Soil Functions](#)
[Pore Size Distribution](#)
[Soil Aggregates, Structure, and Stability](#)
[Soil Texture: Measurement Methods](#)
[Specific Surface Area of Soils and Plants](#)
[Stratification of Soil Porosity and Organic Matter](#)
[Surface Roughness, Effect on Water Transfer](#)

POROSITY

A measure of the void spaces in a material. A fraction of the volume of voids over the total volume, between 0–1. See [Soil Compaction and Compressibility](#)

Cross-references

- [Pore Morphology and Soil Functions](#)
[Pore Size Distribution](#)
[Porosimetry](#)

POTENTIAL EVAPOTRANSPIRATION

See [Evapotranspiration](#)

POWER SPECTRUM

See [Spatial Variability of Soil Physical Properties](#)

PRECISION AGRICULTURE: PROXIMAL SOIL SENSING

Viacheslav I. Adamchuk¹, Raphael A. Viscarra Rossel²

¹Bioresource Engineering Department, McGill University, Ste-Anne-de-Bellevue, QC, Canada

²Division of Land & Water Bruce E. Butler Laboratory, Commonwealth Scientific and Industrial Research Organisation (CSIRO), Canberra, ACT, Australia

Synonyms

On-the-Go Soil Sensing

Definitions

Precision agriculture: A management strategy that is based on information technologies implemented to optimize production agriculture.

Proximal soil sensing: Metering and data processing technology that allows *in situ* determination of physical, chemical, and other soil characteristics while placing sensor systems in close proximity to the soil being evaluated.

On-the-go soil sensing: Use of proximal soil sensing technologies while moving across a landscape.

Introduction

The concept of precision agriculture emerged from the belief that the variability of plant growing conditions is one of the major contributors to field-scale differences in yield, and that varying agricultural inputs according to local changes in soil properties could be beneficial. To engage in an effective decision-making process, it is important to obtain high-quality information about the spatial variability of different soil attributes that may limit yield in specific field areas ([Crop Responses to Soil Physical Conditions](#)). The inability to generate such information rapidly and at an acceptable cost using conventional means remains one of the biggest obstacles to the adoption of precision agriculture. Both proximal and remote sensing technologies have been implemented to provide high-density data layers relevant to the soil attributes of interest. Unlike remote sensing, which involves deployment of sensor systems using aerial platforms or space-crafts, proximal sensing requires placement of the sensor at a close range, contact, or it is even moved through the soil being measured. This allows real-time *in situ* determination of soil characteristics at or below the soil surface at specific locations.

Some proximal sensor systems can be operated in a stationary field position and can be used to: (1) make a single site measurement, (2) produce a set of measurements related to different depths at a given site, or (3) monitor changes in soil properties when installed at a site for a period of time. Although there are a variety of applications for which single site measurements can be beneficial, high-resolution thematic soil maps are typically obtained when measurements are conducted while the

sensor systems are moved across landscapes ([Online Measurement of Selected Soil Physical Properties](#)). Efforts to create these on-the-go proximal soil sensing technologies have become an interdisciplinary field of research and development with a goal of providing essential tools for precision agriculture and other areas of natural resources management (Hummel et al., 1996; Sudduth et al., 1997; Adamchuk et al., 2004; Shibusawa, 2006).

Proximal soil sensing concepts

Although the design concepts take a variety of forms, most on-the-go soil sensors being developed involve one of the following measurement methods: (1) electrical and electromagnetic sensors that measure electrical resistivity/conductivity or capacitance affected by the composition of the soil tested; (2) optical and radiometric sensors that use electromagnetic waves to detect the level of energy absorbed, reflected, or emitted by soil particles; (3) mechanical, acoustic, and pneumatic sensors that measure spatially variable interaction between a measuring tool and soil; and (4) electrochemical sensors that use ion-selective material, producing a voltage output in response to the activity of selected ions ([Figure 1](#)).

Usually, a sensor system based on one of these measurement principles is integrated with a global navigation satellite system (GNSS) receiver to locate and navigate a sensor carrier within a field. However, it is important to keep in mind that in addition to the geographic coordinates, high-accuracy GNSS receivers provide sufficiently accurate measurements of elevation (height above datum). In many instances, landscape relief as well as its derivatives (slope and aspect) can play key roles in forming the spatially variable crop growing environment. This means that frequently recorded field elevation data can also be useful when assessing soil variability. With optical

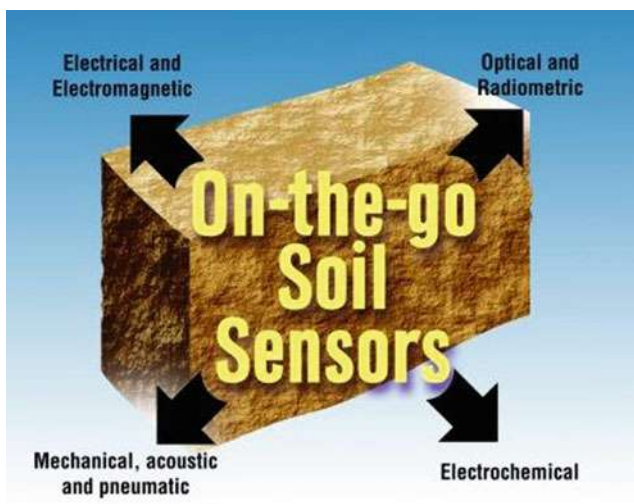
proximity distance sensors, researchers have also been able to study the micro-relief of the soil surface, which can be related to soil tilth and other attributes affecting soil resistance to erosion and other surface processes.

Electrical and electromagnetic sensors

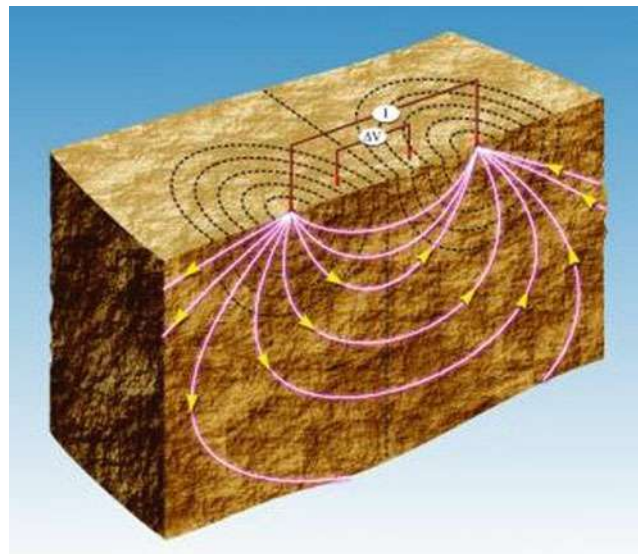
On-the-go proximal soil sensors that are based on electrical and electromagnetic principles use electric circuits to measure the capability of soil particles to conduct and/or accumulate electrical charge. When using these sensors, the soil becomes a part of an electromagnetic circuit, and the changing local conditions immediately affect the signal obtained ([Electrical Properties of Soils](#)).

To measure soil resistivity/conductivity ([Electrical Resistivity to Assess Soil Properties](#)), electrical current can be introduced using (1) galvanic contact, (2) capacitive coupling, or (3) electromagnetic induction methods. With the galvanic contact approach ([Figure 2](#)), at least two pairs of electrodes (typically in Wenner array configuration) must maintain stable contact with the soil surface (Allred et al., 2008). One pair of electrodes is used to create a low-frequency (<50 Hz) alternating current as other pairs measure the change of electrical potential, which is directly related to soil resistivity (the inverse of apparent electrical conductivity). By placing pairs of sensing electrodes at different distances from the current-injecting pair, it is possible to obtain multiple depths of investigation. Longer distance involves a deeper profile of soil affecting the signal.

Using the capacitively coupled resistivity method, current is injected into the soil using a coaxial cable serving as a large capacitor. The metal shield of the coaxial cable is one of the capacitor plates, the outer insulation of the cable is dielectric material, and the soil under the cable is the



Precision Agriculture: Proximal Soil Sensing,
Figure 1 On-the-go proximal soil sensing systems.



Precision Agriculture: Proximal Soil Sensing, Figure 2 A sensor based on the galvanic contact resistivity method.

other plate. The transmitter applies an alternating current to the coaxial cable, which causes an electrical current in the soil. At the receiver side, it is the current in the soil which causes current inside the coaxial cable. The difference in electric potential between the transmitter and the receiver is related to soil resistivity. As with the galvanic contact method, varying the distance between the transmitter and an array of receivers enables researchers to obtain measurements representing variable depths.

Popular in geophysical applications, the electromagnetic induction method is also used to determine soil apparent electrical conductivity (Daniels et al., 2008a). Unlike the sensor systems based on the galvanic contact and capacitively coupled resistivity methods, sensor systems based on electromagnetic induction do not require contact with soil. Instead, a transmitting inductor (a coil of wire with high-frequency (>1 kHz) alternating current) creates a magnetic field that causes a secondary (eddy) current in the soil (Figure 3). As with the capacitively coupled approach, electrical current in the receiving inductor is formed by the reverse process (current induced by the magnetic field from this secondary eddy current). From a number of parameters relating alternating current in the transmitting and receiving inductors (amplitude, time delay, and relative orientation), the measurements obtained can be used to quantify the apparent electrical conductivity as well as the magnetic susceptibility of the soil. Spacing between the transmitting and receiving inductors as well as their relative orientation affects the weight each layer of soil has when forming the output signal.

While using any of the on-the-go electrical resistivity/conductivity methods, measured electrical conductivity is

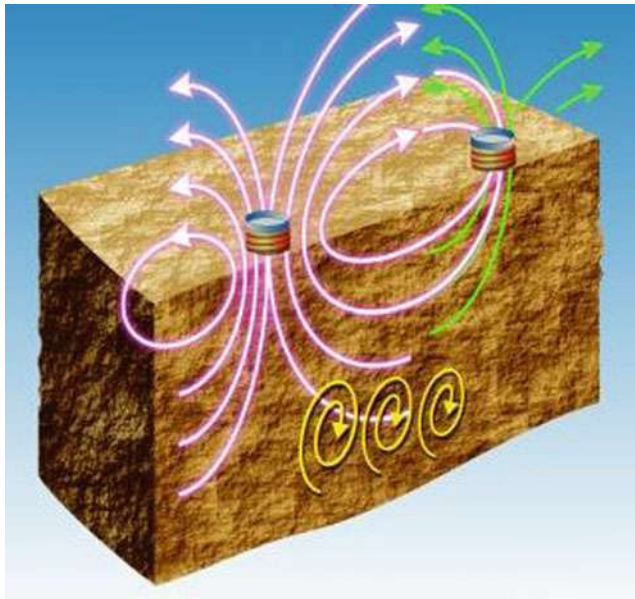
called “apparent” since it is different from a standardized solution-based test and is determined for a bulk media of soil containing different layers and inclusions. Various types of inverse modeling have been implemented attempting to predict the change of soil electrical conductivity with depth using measurements obtained with different geometrical parameters of an instrument.

In addition to electrical resistivity/conductivity sensing systems, capacitor-type sensors have been used to evaluate the soil dielectric properties. This differs from the capacitively coupled resistivity method in that the sensors use soil as a media between two capacitor plates. The direct relationship between the dielectric constant of soil and water content makes this type of sensor attractive for rapid measurement of volumetric soil moisture.

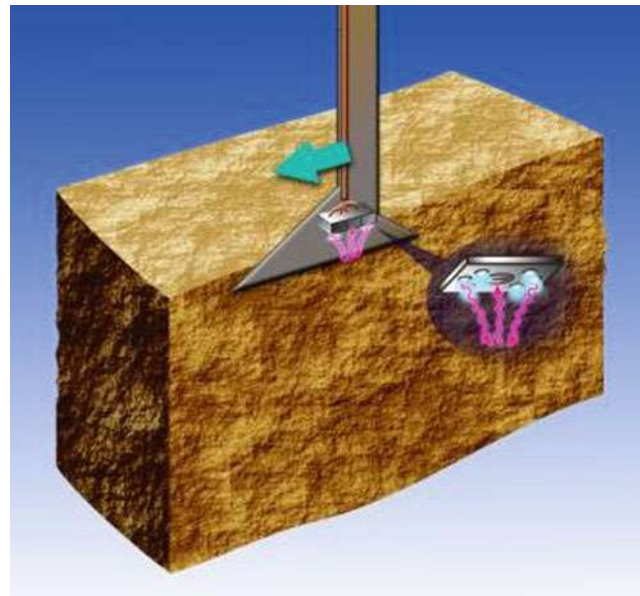
Optical and radiometric sensors

Proximal soil sensors that are used to measure the energy of electromagnetic waves can be active or passive. While optical sensor systems and ground-penetrating radars (GPR) detect energy provided by an artificial source (the active sensing approach), γ -radiometers used in agriculture detect radiation emitted by the soil (the passive sensing approach).

Optical sensors are used to determine soil’s ability to reflect light in different parts of the electromagnetic spectrum. Fundamentally, these can be similar to multispectral or hyperspectral remote sensing platforms but are deployed at the surface, or even below ground (Figure 4). Optical sensing systems can cover the visible (400–750 nm), near-infrared (750–2,500 nm), and/or mid-infrared (2,500–25,000 nm) wavelengths (Viscarra Rossel et al., 2006).



Precision Agriculture: Proximal Soil Sensing,
Figure 3 A sensor based on the electromagnetic induction method.



Precision Agriculture: Proximal Soil Sensing,
Figure 4 A subsurface optical reflectance sensor.

Typically, measurements are made using a combination of light-emitting diodes and photodiodes, or with spectrometers receiving the signal using fiber optics. Measurements obtained using optical sensors can be related (directly or indirectly) to a number of soil attributes such as soil mineral composition, clay content, soil color, moisture, organic carbon, pH, cation exchange capacity (CEC), etc. (Christy, 2008; Viscarra Rossel et al., 2009; Mouazen et al., 2010). Sensor calibration strategy ranges from simple linear regression to multivariate chemometrics and data mining methods. In any case, it appears that the relationship between soil characteristics of agronomic importance and soil reflectance may be limited to a particular set of conditions, and wider application of calibration models may not always be appropriate.

Ground-penetrating radars (GPR) have been used to investigate the behavior of 50–500 MHz electromagnetic waves directed toward the soil (Figure 5). A typical GPR output represents a sequence of amplitude traces with the depth of investigation related to the time of signal travel. Detectable changes in wave reflectance may indicate inconsistency in soil density or the existence of restricting soil layers (Daniels et al., 2008b). GPR has great potential for geophysics in general and agriculture in particular, especially to support water management.

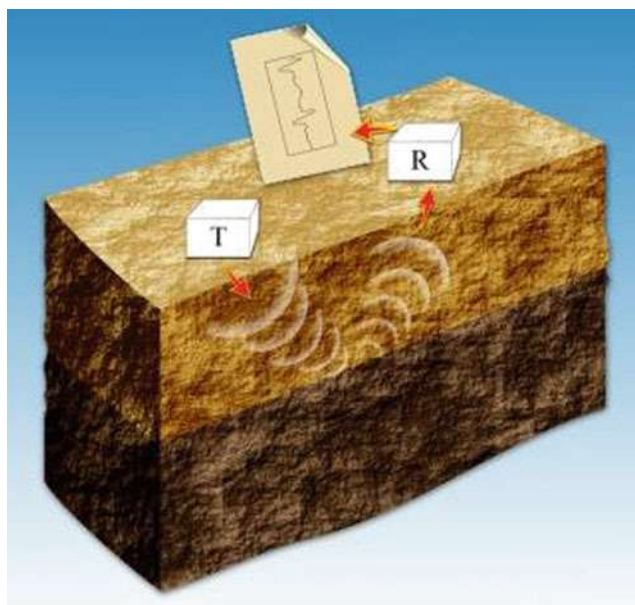
At the very short wavelength (i.e., high frequency) end of the electromagnetic spectrum, there is potential for the use of gamma (γ)-radiometric methods. All soils contain naturally occurring radioisotopes that can disintegrate to produce γ -rays. Gamma-rays are suited to spectroscopic detection because the energy of each photon is characteristic of the isotope from which it originates

(Hendriks et al., 2001). The attenuation of γ -rays through the soil varies with bulk density and water content. Also, γ -radiometrics has been used for field-scale mapping of some influential soil properties (Viscarra Rossel et al., 2007).

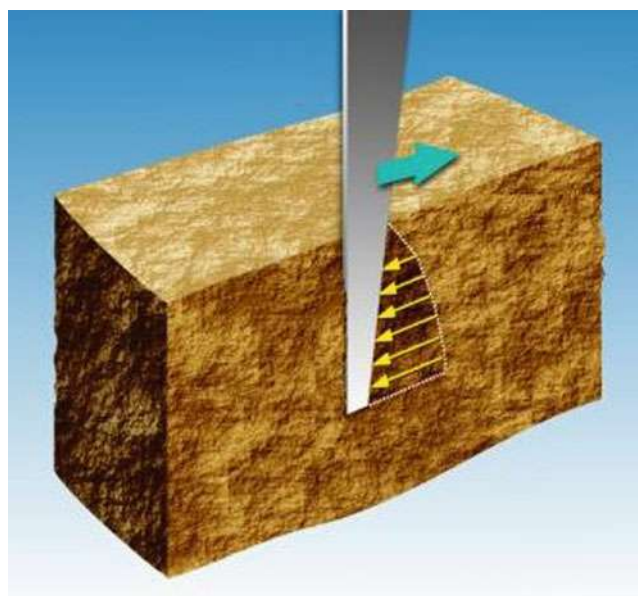
Mechanical, acoustic, and pneumatic sensors

Probably the most conceptually simple mechanical sensors are used to estimate soil mechanical impedance (resistance). By nature, these soil strength sensors measure resistance to soil failure (Hemmat and Adamchuk, 2008). As this type of sensor moves through the soil, it registers resistance forces arising from cutting, breakage, and displacement of soil, as well as from the parasitic (frictional and adhesive) forces that develop at an interface between the sensor surface and surrounding soil (Figure 6). Normally, soil mechanical resistance is expressed in units of pressure and represents the ratio of the force required to penetrate the soil media and the frontal (normal to the direction of penetration) area of the tool engaged with the soil.

A first step toward soil mechanical resistance sensing is to map the total horizontal (draft) and, sometimes, vertical force applied to a traditional fixed-depth implement engaged with the soil. Recorded measurements represent surrogate values affected by a variety of factors, including the type and shape of the tool working the soil, the speed and depth of the operation, and the surface conditions. Constructing a bulk soil strength sensor based on soil mechanics allows for better control of the type of soil failure and therefore produces more consistent measurements



Precision Agriculture: Proximal Soil Sensing, Figure 5 Ground penetrating radar.



Precision Agriculture: Proximal Soil Sensing, Figure 6 A mechanical resistance sensor.

in diverse soil conditions. In any case, bulk measurements can only reveal the spatial patterns of the overall soil strength. If a bulk soil strength sensor is actuated vertically (i.e., moved up and down) while mapping the field, the effective depth of engagement with the soil changes from location to location. Assuming a relatively strong spatial structure, this approach allows assessment of soil variability associated with the depth of operation in addition to the field location. On the other hand, adopted as a standard tool, a vertically actuated cone penetrometer is the most popular method for detecting changes in soil penetration resistance with depth at a given location. Traditionally, this tip-based sensor has been used manually; automated versions increase the number of simultaneous point measurements and/or labor efficiency. However, automated cone penetrometer sensors fail to provide economically justifiable mapping densities to determine spatial variability across large agricultural fields.

Single-tip horizontal sensors have been designed to generate high-resolution maps of horizontal soil penetration resistance obtained at a specific depth. Similar to the vertically actuated cone penetrometers, this method involves continuous logging of direct load measurements, which are frequently made using a load cell. Simultaneous deployment of multiple tips operated at different depths allows researchers to determine the spatial variability of soil mechanical resistance at any available depth as well as vertical variability in each location of the field. To avoid the expense of adding direct load sensing tips, a single-tip horizontal sensor can be actuated vertically in a way similar to a bulk soil strength sensor.

In addition to using a tip-based method, producers can measure the vertical distribution of soil mechanical resistance using an instrumented tine. This is done by measuring the direct load applied to the tine at discrete depths or by measuring the degree of bending using strain gauge technology (i.e., a cantilever beam approach). As with the inversion of apparent electrical conductivity, measurement arrays, the cantilever beam-like sensors, have been used to map the parameters of a modeled relationship between soil mechanical resistance and depth rather than using the discrete values at a given depth.

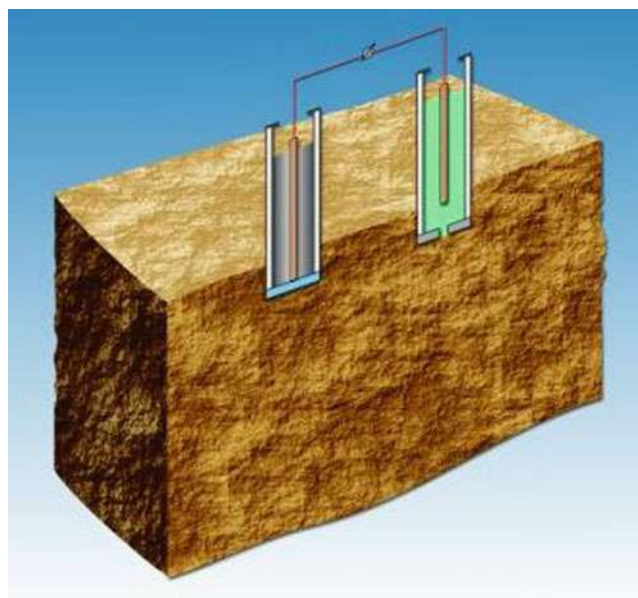
Acoustic and pneumatic sensors serve as alternatives to mechanical sensors when studying the interaction between the soil and an agricultural implement. Acoustic sensors have been investigated for determining soil texture and/or bulk density by measuring the change in the level of noise caused by the interaction of a tool with soil particles. Pneumatic sensors have been used for on-the-go sensing of air permeability in soil. The pressure required to force a given volume of air into the soil at a fixed depth was compared to several soil properties such as soil structure and compaction.

Electrochemical sensors

Finally, sensor systems that resemble a traditional wet-chemistry method to assess the content of certain chemical

compounds can provide the most important type of information needed for precision agriculture – soil nutrient availability and pH ([Electrochemical Measurements in Soils](#)). The measurements are conducted using either an ion-selective electrode (ISE) or an ion-selective field effect transistor (ISFET). These sensors detect the activity of specific ions at the interface between sensitive membranes and the aquatic part of either a soil solution or a naturally moist sample ([Figure 7](#)). A common ISE system consists of a membrane that is sensitive to specific ions and a reference electrode (Talibudeen, 1991). The difference in the potential between the sensitive membrane and the reference is measured and converted to the activity of specific ions in the tested solutions. The design of a combination ion-selective electrode allows both sensitive and reference parts to be assembled in one probe. Different electrode brands represent different designs of ion-selective membranes and reference junctions.

An ISFET integrates the ion selectivity of an ISE with the small size and robust nature of a field effect transistor (Artigas et al., 2001). In this case, the current between two semiconductor electrodes (source and drain) is controlled by a gate electrode represented by an ion-selective membrane. As ions of interest affect the gate, their charge impacts the source-drain current, providing an indication of ion activity. The main difference between an ISFET and an ISE is that an ISFET does not contain an internal solution, and the ion-selective membrane is affixed directly on the gate surface of the ISFET. Its compact size and theoretically high signal-to-noise ratio make ISFET technology attractive, especially when used to implement the flow injection analysis (FIA) method. However, the range of commercially available ISFETs



Precision Agriculture: Proximal Soil Sensing, Figure 7 An electrochemical sensor.

remains relatively narrow. In both the ISE and ISFET approaches, the sensitive membrane is made of glass (H^+ , Na^+), polyvinyl chloride (K^+ , NO_3^- , Ca^{2+} , Mg^{2+}), or metal (H^+).

The interface between an ISE or ISFET and a soil solution under investigation can involve a range of approaches, from methods involving soil processing to relatively simple methods. On one end of the spectrum, complete sample preparation with a prescribed controlled ratio between soil particles and extracting solution adds complexity to the measurement apparatus and may require a longer sampling and analysis cycle time. On the other end of the spectrum, a simple direct soil measurement (DSM) approach is relatively easy to implement (Adamchuk et al., 2005). However, real-time chemical extraction of the ions to be measured mimics conventional soil analysis procedures, while DSM-based measurements reveal specific ion content in a given soil state, which may not represent nutrient availability throughout the growing season.

Precision agriculture applications of proximal soil sensing

The decision-making process in precision agriculture requires knowledge and understanding of the soil's spatial variability in properties that are important for crop growth (e.g., nutrient availability, soil texture, organic matter, or water content). On the other hand, on-the-go proximal soil sensing systems provide high-density information on the spatial variability of specific measured quantities (e.g., field elevation, apparent electrical conductivity, optical reflectance, gamma radiation count). The relationships between sensor measurements and agronomic soil attributes are frequently specific to a certain agricultural environment.

For example, since clay particles are capable of transmitting more electrical charge than sand, popular maps of apparent electrical conductivity may be associated with the spatial distribution of different soil series in a given landscape. However, spatial and temporal variability in water content, salinity, and/or organic matter will affect electrical conductivity as well (sometimes even to a higher degree). Therefore, the same instrument can be used to identify localized patches of sand in one environment and sites with excessive salinity or manure deposition elsewhere. Although capacitive sensors have a more direct relationship with the amount of soil water stored, this relationship may also be affected by particle size distribution when predicting water content using either a volumetric or gravimetric basis.

Hyperspectral analysis of visual, near-infrared, and mid-infrared reflectance is an attractive approach for the prediction of various soil characteristics (both physical and chemical). Most reliable relationships have been found between light reflectance and soil carbon/organic matter content, soil moisture, clay content, mineral composition, and soil color. Significant secondary relationships have also been documented with CEC, calcium,

and magnesium as well as with soil pH, nitrate, and phosphate. In most of these cases, predictions require the development of multivariate calibrations, which may only generalize locally. Perhaps, some models currently under development could be applied to several geographic areas with similar soil mineralogy.

With ground-penetrating radars, it is possible to investigate soil layering without excavating the soil. Knowing the type of soil profile can help predict various physical processes that may have site-specific dynamics (e.g., water storage). Similarly, γ -radiometers have been used for surveying rather than for measuring. Like electrical conductivity sensing systems, these instruments are excellent tools for delineating soil spatial variability, with the goal of establishing management zones along with sampling or temporal monitoring sites.

Intuitively, measurements of soil strength are related to soil compaction (bulk density), which may be inappropriate if soil water content changes substantially at the time of mapping. However, when mapped at the beginning of a growing season, soil strength can reveal field areas with relatively high root penetration resistance (whether due to the dry soil or because of compaction). Measurement of soil strength at multiple depths allows researchers to detect variable depth hard pan, which suggests the use of variable depth tillage when appropriate ([Hardpan Soils: Management](#)).

It might seem that at least electrochemical measurements should have stable relationships with the content of important chemical elements. However, on-the-go measurements do not necessarily represent the same type of analysis as conventional laboratory tests. The differences may include sampling depth, preparation, and chemical extraction. Therefore, researchers have attempted to use prior information about soil buffering characteristics to define relationships between multiple proximal soil sensor measurements and chemical soil properties as well as the number of soil amendments needed.

Consequently, the integration of different proximal soil sensing technologies combined with the balanced use of different methods of sensor deployment has been the most promising strategy for successfully adopting soil sensing to support precision agriculture. Various innovative ideas and methods are on the horizon to unify different instruments and new geostatistical algorithms and make better use of the high-density data provided by the range of proximal soil sensing systems.

Summary

Information on the variability of different soil attributes within a field is essential to the decision-making process for precision agriculture. On-the-go proximal soil sensing is the most promising strategy to obtain much-needed high-density measurements of key soil properties. Proximal soil sensing systems are based on electrical and electromagnetic, optical and radiometric, mechanical, acoustic, pneumatic, and electrochemical measurement

concepts. The major benefit of on-the-go sensing is its ability to quantify the heterogeneity (nonuniformity) of soil within a field and to adjust other data collection and field management strategies accordingly. The integration of different sensing systems in multisensor platforms may allow better prediction of agronomic soil attributes.

Bibliography

- Adamchuk, V. I., Hummel, J. W., Morgan, M. T., and Upadhyaya, S. K., 2004. On-the-go soil sensors for precision agriculture. *Computers and Electronics in Agriculture*, **44**, 71–91.
- Adamchuk, V. I., Lund, E., Sethuramasamyraja, B., Morgan, M. T., Dobermann, A., and Marx, D. B., 2005. Direct measurement of soil chemical properties on-the-go using ion-selective electrodes. *Computers and Electronics in Agriculture*, **48**, 272–294.
- Allred, B. J., Groom, D., Ehsani, M. R., and Daniels, J. J., 2008. Resistivity methods. In Allred, B. J., et al. (eds.), *Handbook of Agricultural Geophysics*. Boca Raton, FL: CRC Press, pp. 85–108.
- Artigas, J., Beltran, A., Jimenez, C., Baldi, A., Mas, R., Dominguez, C., and Alonso, J., 2001. Application of ion sensitive field effect transistor based sensors to soil analysis. *Computers and Electronics in Agriculture*, **31**, 281–293.
- Christy, C. D., 2008. Real-time measurements of soil attributes using on-the-go near infrared reflectance spectroscopy. *Computers and Electronics in Agriculture*, **61**, 10–19.
- Daniels, J. J., Vendl, M., Ehsani, M. R., and Allred, B. J., 2008a. Electromagnetic induction methods. In Allred, B. J., et al. (eds.), *Handbook of Agricultural Geophysics*. Boca Raton, FL: CRC Press, pp. 109–128.
- Daniels, J. J., Ehsani, M. R., and Allred, B. J., 2008b. Ground-penetrating radar methods (GPR). In Allred, B. J., et al. (eds.), *Handbook of Agricultural Geophysics*. Boca Raton, FL: CRC Press, pp. 129–145.
- Hemmat, A., and Adamchuk, V. I., 2008. Sensor systems for measuring spatial variation in soil compaction. *Computers and Electronics in Agriculture*, **63**, 89–103.
- Hendriks, P. H. G. M., Limburg, J., and de Meijer, R. J., 2001. Full-spectrum analysis of natural γ -ray spectra. *Journal of Environmental Radioactivity*, **53**, 365–380.
- Hummel, J. W., Gaultney, L. D., and Sudduth, K. A., 1996. Soil property sensing for site-specific crop management. *Computers and Electronics in Agriculture*, **14**, 121–136.
- Mouazen, A. M., Kuang, B., De Baerdemaeker, J., and Ramon, H., 2010. Comparison among principal component, partial least squares and back propagation neural network analyses for accuracy of measurement of selected soil properties with visible and near infrared spectroscopy. *Geoderma* (in press).
- Shibusawa, S., 2006. Soil sensors for precision agriculture. In Srinivasan, A. (ed.), *Handbook of Precision Agriculture. Principles and Applications*. New York: Food Products Press, pp. 57–90.
- Sudduth, K. A., Hummel, J. W., and Birrell, S. J., 1997. Sensors for site-specific management. In Pierce, F. T., and Sadler, E. J. (eds.), *The State of Site-Specific Management for Agriculture*. Madison, WI: ASA-CSSA-SSSA, pp. 183–210.
- Talibudeen, O., 1991. Ion-selective electrodes. In Smith, K. A. (ed.), *Soil Analysis. Modern Instrumental Techniques*. New York: Marcel Dekker, pp. 111–182.
- Viscarra Rossel, R. A., Walvoort, D. J. J., McBratney, A. B., Janik, L. J., and Skjemstad, J. O., 2006. Visible, near infrared, mid infrared or combined diffuse reflectance spectroscopy for simultaneous assessment of various soil properties. *Geoderma*, **131**, 59–75.
- Viscarra Rossel, R. A., Taylor, H. J., and McBratney, A. B., 2007. Multivariate calibration of hyperspectral gamma-ray energy spectra for proximal soil sensing. *European Journal of Soil Science*, **58**, 343–353.
- Viscarra Rossel, R., Cattle, S., Ortega, A., and Fouad, Y., 2009. In situ measurements of soil colour, mineral composition and clay content by vis-NIR spectroscopy. *Geoderma*, **150**, 253–266.

Cross-references

- [Crop Responses to Soil Physical Conditions](#)
[Electrical Properties of Soils](#)
[Electrical Resistivity to Assess Soil Properties](#)
[Electrochemical Measurements in Soils](#)
[Hardpan Soils: Management](#)
[Online Measurement of Selected Soil Physical Properties](#)

PRE-COMPRESSION STRESS

See [Stress–Strain Relations](#) – a possibility to quantify soil strength defined as the precompression stress.

Cross-references

- [Management Effects on Soil Properties and Functions](#)
[Soil Structure and Mechanical Strength](#)
[Subsoil Compaction](#)
[Traficability and Workability of Soils](#)

PRE-COMPRESSION TEST

See [Soil Compaction and Compressibility](#)

PREFERENTIAL FLOW

Synonyms

Funnel flow; Macropore flow

See [Bypass Flow in Soil](#)

Cross-references

- [Soil Water Flow](#)
[Solute Transport in Soils](#)

PRESSURE HEAD

See [Physical Dimensions and Units Use in Agriculture](#)

PRESSURE POTENTIAL

The component of water potential due to the hydrostatic pressure that is exerted on water in a cell. In turgid plant

cells it usually has a positive value as the entry of water causes the protoplast to push against the cell wall (see *Turgor Pressure*). In xylem cells there is a negative pressure potential, or tension, as a result of transpiration.

Bibliography

A Dictionary of Biology., 2004. http://www.encyclopedia.com/topic/pressure_potential.aspx

PRIMING EFFECTS IN RELATION TO SOIL CONDITIONS – MECHANISMS

Evgenia Blagodatskaya^{1,2}, Yakov Kuzyakov¹

¹Department of Agroecosystem Research, University of Bayreuth, Bayreuth, Germany

²Institute of Physicochemical and Biological Problems in Soil Science, Russian Academy of Sciences, Pushchino, Russia

Definitions and terms

Priming effect is defined as a short-term change in the turnover of soil organic matter caused by treatments, usually addition of organic C to the soil (Kuzyakov et al., 2000) (Figure 1). Usually since the soil organic matter (SOM) turnover is not directly measured, but it is determined by changes in CO₂ efflux rates or N mineralization rates, the origin of extra CO₂-C (*primed carbon*) or N cannot be directly evaluated. Therefore, the *real priming effect* (RPE) cannot be assessed based only on extra CO₂. Other processes, such as accelerated microbial turnover may contribute to the changes in the CO₂ efflux rates or N mineralization rates (Dalenberg and Jager, 1981; Wu et al., 1993; De Nobili et al., 2001). Accelerated CO₂ evolution in response to the activation of microbial metabolism and higher microbial biomass turnover is not related to the SOM turnover and is termed as *apparent priming effect* (APE). Usually, the microbial succession initiated by the input of fresh organic matter is accompanied by activation of various, previously dormant microorganisms that respond specifically to the added substrate. Accelerated activity of such microorganisms may enhance the degradation of soil organic matter as a result of co-metabolism and higher enzyme production, i.e., RPE. Thus, both apparent and real priming actions are governed by microbial activity. Few studies, however, have evaluated PE as a function of abiotic factors such as temperature, moisture, pH, etc.

Jenkinson et al. (1985) suggested that RPE is an increase in the decomposition of recalcitrant SOM, whereas APE is an increase of microbial C turnover, which is not linked with changes of SOM decomposition. Usually the term “apparent” has been used in relation to primed CO₂-C originated from soil microorganisms (De Nobili et al., 2001; Gioacchini et al., 2002;

Bell et al., 2003; Fontaine et al., 2003; De Neve et al., 2004; Hamer and Marschner, 2005; Hopkins et al., 2006; Mondini et al., 2006). However, in a few cases, the term “apparent” priming has been also used to interpret extra CO₂ evolution derived from experimental errors due to the use of nonuniformly labeled substrate, incomplete trapping of evolved CO₂, addition of high amount of substrate to soil (Brookes et al., 1990; Conde et al., 2005), or enhanced decomposition of organic matter in response to improved soil moisture (Niklaus and Falloon, 2006). We suggest such PEs be termed as *artificial* to distinguish them from microbially originated apparent PE.

According to Jenkinson et al. (1985), most changes in N mineralization after addition of N to soil are to be considered as apparent effects caused by N displacement reactions (with fixed ammonium or with microbial N) or by pool substitution. They assumed that real acceleration of SOM mineralization requires an excess of fresh organic matter with a wide C/N ratio. We believe that this could be one cause, but not the sole one for real PE.

In recent years, new terms such as “signaling” and “triggering” (De Nobili et al., 2001; Mondini et al., 2006) have been proposed for some PEs but they were not clearly defined. Here we define the *triggering effect* as an acceleration of internal microbial metabolism with quick increase in the respiratory activity promoted by trace amounts of substrate. In many studies and under field conditions, the amount of C added to soil does not represent a significant source of energy but can promote changes whose energy demand can be much higher than the energy of the added substrate. This triggering effect can activate dormant soil microorganisms if promoted by the addition of available low molecular substrates such as glucose and amino acids to soil (De Nobili et al., 2001; Kuzyakov and Bol, 2006). The triggering effect induced by the input of external substrate should be distinguished from *quorum sensing*, which includes a wide range of signal exchanges *within* soil microbial community producing multiple cell–cell signaling molecules (Lazazzera, 2000; Burmolle et al., 2003; Wang and Leadbetter, 2005) and inducing gene expression, encoding a variety of both phenotypical and physiological responses upon reaching a critical threshold (Gray and Smith, 2005). Since the underlying molecular mechanisms of the triggering effect need to be investigated, we can hypothesize that permanent or occasional input of available low molecular weight substrates associated to plant residues, root exudates, excretes of soil animals etc., can act as *external inducer* and can *trigger* the mechanism of microbial communication similar to quorum sensing that can regulate the behavior of a group of organisms (Raffa et al., 2005). Thus, the triggering effect promoted by external compounds can represent the first step in a *signaling pathways cascade*, which alter the behavior on a population-wide scale by intra- and interspecies microbial interactions (Gray and Smith, 2005; Waters and Bassler, 2005; Little et al., 2008).

Introduction

The term priming effect (PE) was introduced to describe changes in the SOM turnover affected by the addition of organic or mineral substances (Jenkinson et al., 1985; Kuzyakov et al., 2000) (Figure 1). Depending on soil conditions, such changes can result in acceleration or retardation of SOM decomposition (positive or negative PE, respectively). The intensity of both processes is governed by physicochemical factors such as temperature, soil moisture, and pH, which act indirectly – mainly by affecting microbial activity that drives the mineralization of SOM and plant residues. Beyond these abiotic factors, however, many biotic factors directly affect C mineralization in soil. These changes are due to changes in the microbial activity as a response to altered amounts and availability of C. The increase in the number of investigations on priming effects during the last decade (see Blagodatskaya and Kuzyakov, 2008 for details) reflects the interest in biotic mechanisms of carbon (C) turnover in soil (Chander et al., 1997; Carreiro et al., 2000; Bell et al., 2003; Falchini et al., 2003; Fontaine et al., 2003; Cheng and Kuzyakov, 2005; Conde et al., 2005; Perelo and Munch, 2005; Zyakun and Dilly, 2005; Brant et al., 2006; Fontaine et al., 2007) (Figure 2). The indirect effect of abiotic factors, which are the main drivers of C turnover in soil, is not considered in most of these studies.

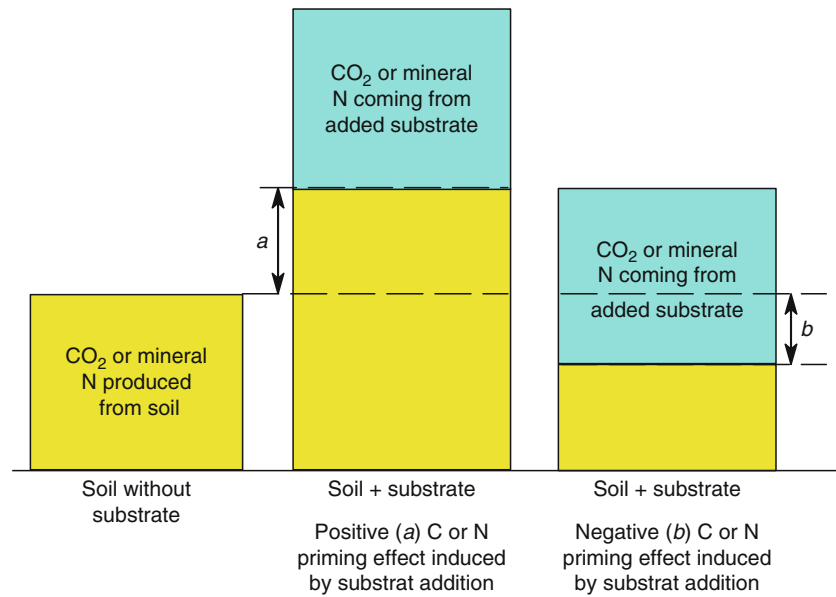
There might be various mechanisms for the changes in microbial activity in soil after adding organic or mineral substances (Jenkinson et al., 1985; Kuzyakov et al., 2000; De Nobili et al., 2001; Fontaine et al., 2003; Schimel and Weintraub, 2003). However, most studies failed to prove the suggested mechanisms because the

experiments were aimed at identifying priming effects (mainly by changes in CO₂ evolution) and not at identifying the mechanisms of these effects. This review will evaluate PE mechanisms based on CO₂ efflux data combined with other published data related to microbial biomass and activity. Therefore, we discuss the relationships linking the physicochemical soil conditions and the magnitude of priming effects observed in studies over the last decades. We distinguish real (SOM decomposition) and apparent (changes in microbial biomass turnover without effects on SOM decomposition) PE by considering the extra released C as affected by the amount of added C and microbial biomass C content (De Nobili et al., 2001; Luna-Guido et al., 2001; Hamer and Marschner, 2005; Mondini et al., 2006; Blagodatskaya et al., 2007). We also discuss the relationship between the phenomena of apparent or real priming effects and the role of soil properties, such as soil pH and aggregation, which were not considered earlier as affecting PE through their direct effect on biological activity.

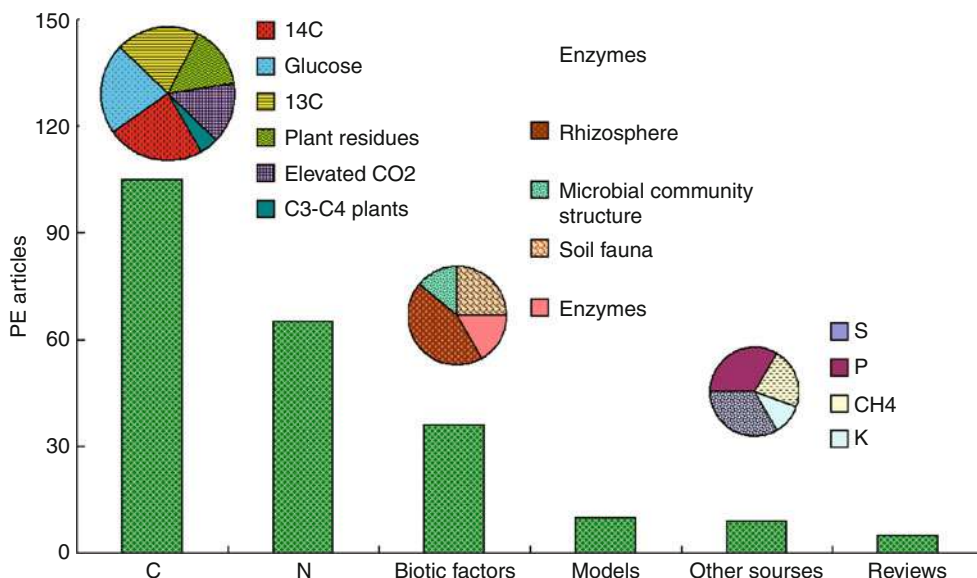
The amount of added substrate, the microbial biomass content, and priming effects

Adding easily available substances to soil provides C and energy sources to microorganisms. Depending on the amount of added C and energy, three types of changes can occur:

1. The amount of added substrate C is higher than the microbial biomass C content of soil and both microbial growth and changes in the community structure can occur.



Priming Effects in Relation to Soil Conditions – Mechanisms, Figure 1 Schema of the priming effect – nonadditive interactions between decomposition of the added substrate and of soil organic matter (SOM): (a) acceleration of SOM decomposition – positive priming effect, (b) retardation of SOM decomposition – negative priming effect.



Priming Effects in Relation to Soil Conditions – Mechanisms, Figure 2 Published papers to priming effects (PE) related to various questions: C and N mineralization, effect of biotic factors on PE, models simulating PE, release of S, P, CH₄, and K, and review articles from 1980 to late 2007. Web-of-Science citations with search options ("priming" AND "soil*") NOT "seed*" were evaluated.

2. The amount of added substrate C is similar or less than the microbial biomass C content of soil and changes in microbial activity and in turnover rate of the active microflora can occur, but the added substrate is not sufficient to induce microbial growth.
3. The amount of added C is much less than the microbial biomass C content of soil and the energy added is insufficient to directly accelerate microbial turnover. Either triggering or signaling effects can occur.

Here we discuss the threshold values for the three levels of substrate addition.

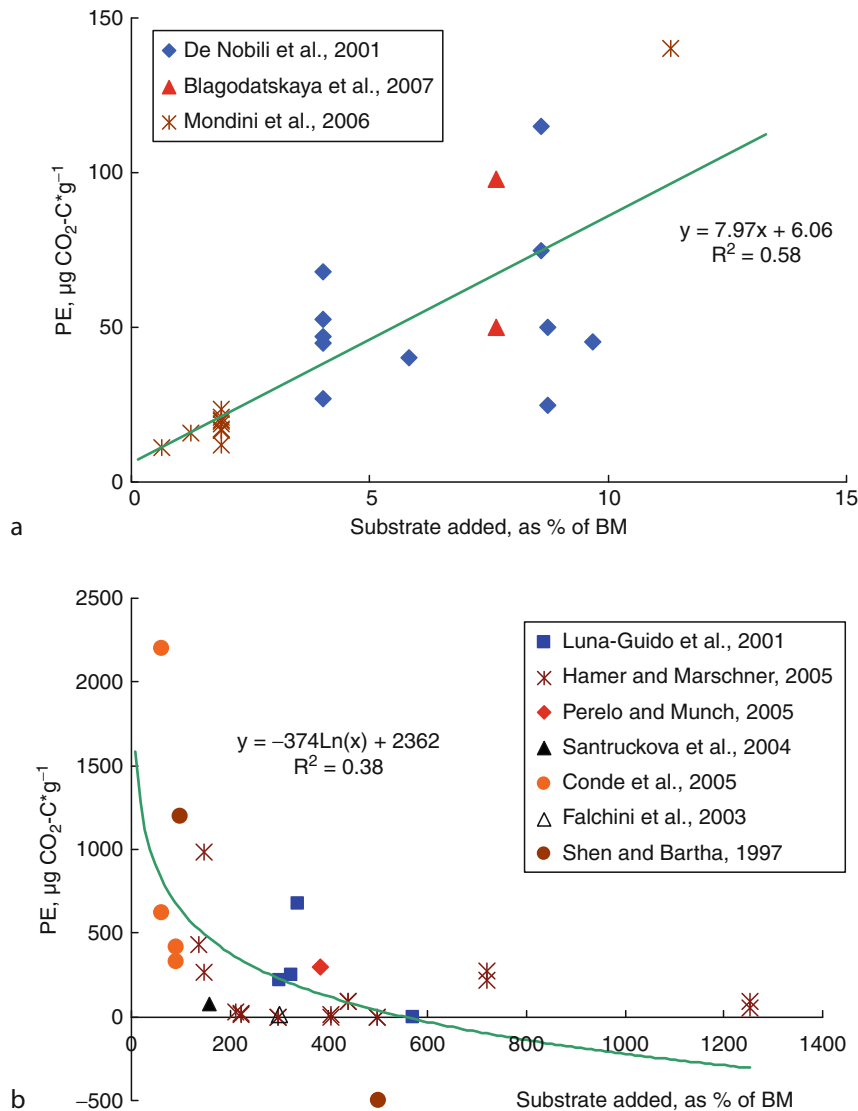
As the content of microbial biomass can differ in various soils, the amount of added substrate C should be expressed as the percentage of microbial biomass C (Figure 3). To find the threshold values for the three response possibilities mentioned above, we considered PE studies in which microbial biomass C was measured and a few studies (Shen and Bartha, 1997; Falchini et al., 2003; Fontaine et al., 2004; Conde et al., 2005), in which we calculated microbial biomass C considering that it represents 2% of the organic C content (Paul and Clark, 1989).

Surprisingly, two opposite relationships between the amount of added substrate and induced PE were found with different levels of added substrate C as related to microbial biomass C (Figure 3). When the amounts of added substrate C were lower than 15% of microbial biomass C, the magnitude of PE (here measured as extra CO₂) linearly increased with the amount of added C (Figure 3a). Therefore, for low levels of the added substrate, the PE is substrate limited and it confirms our hypothesis that priming effects are related to the energy

input to the soil microorganisms by easily available substrates such as glucose and amino acids (Figure 3). This means that microorganisms were able to utilize these substrates within a few hours or less, and thus, these inputs probably represent a pulse of available energy promoting the shift from dormant to active state.

When the amount of added substrates C exceeded 50% of the microbial biomass C value, the amount of primed CO₂-C decreased exponentially by increasing the added C (Figure 3b). At the rates of substrate C exceeding 200–500% of microbial biomass C, the priming effect tended to be zero or even negative. Thus, the amount of added substrates switches the direction of PE. If easily available substrates were added in sufficient amounts, soil microorganisms start growing within 4–10 h (Blagodatskaya et al., 2007) and end within 1–3 days, depending on the used substrate and available nutrients. The 1–3 day period coincides with the maximal intensity of the observed priming effects. We suggest that such short-term priming effects induced at high levels of added substrates (comparable or higher than microbial biomass C) are mainly related with changes in microbial community structure and also involves their demand for other nutrients, such as N.

With a level of added substrate C being 2–5 times higher than microbial biomass C, priming effects tended to be close to zero or even negative. We assume that preferential microbial substrate utilization (Kuzyakov, 2002; Cheng and Kuzyakov, 2005) is the main process occurring at these levels of added substrates with the switch of substrate conditions for soil microflora from low available SOM to easily available and highly accessible added substrate. This can cause a lower SOM decomposition



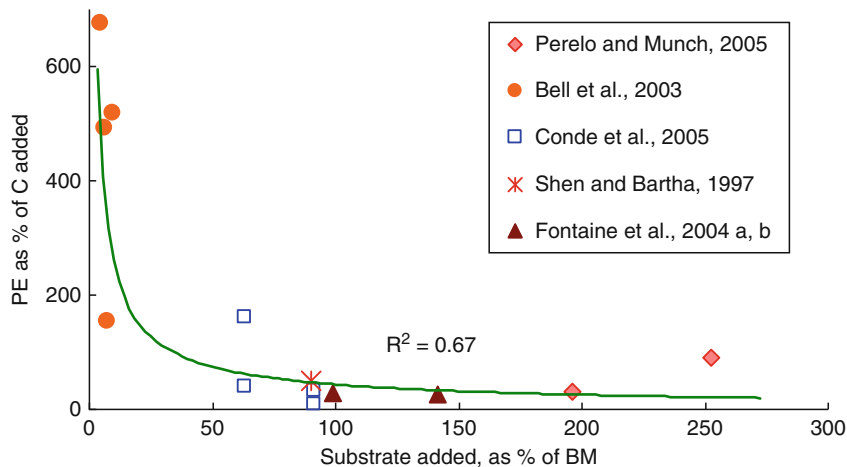
Priming Effects in Relation to Soil Conditions – Mechanisms, Figure 3 Primed $\text{CO}_2\text{-C}$ efflux as affected by the amount of easily available substrate C added and expressed as percent of microbial biomass C; added C is < 15% of microbial C (a); added C is > 50% of microbial C (b).

with a negative PE. It is important to underline that the magnitude of PE by high levels of the added substrate is about one order higher than the PE induced at levels of added organic C lower than 15% of microbial biomass C.

When plant residues were added to soil, the relationship between PE and the amount of added substrate was similar to that occurring when easily available substrates were added to soil (Figure 4). The highest PE (expressed as percent of added substrate from study of Bell et al., 2003) was observed when the amount of plant residue-C accounted for 4–9% of microbial biomass C. By increasing the amount of plant residues an exponential decrease in PE was observed.

Therefore, studies comparing priming effects in different soils or in different horizons, should consider the microbial biomass content that can differ among different soils, and among different soil horizons. By considering that microbial biomass C varied in the range of 0.2–1% of total organic C in the study of Hamer and Marschner (2005), the amount of organic C added to soil as 1.3% of the SOM C was 1.4–12.5 times higher than microbial biomass C. This caused the absence of PE in some soil horizons when microorganisms were oversaturated by the added substrate. Regrettably, many reports on PE did consider neither organic C nor microbial biomass C content in soil.

In conclusion, when the added substrate C accounted for less than 15% of microbial C, a linear increase of extra



Priming Effects in Relation to Soil Conditions – Mechanisms, Figure 4 Relationship between the input of less available substrate (plant residues) to soil expressed as percent of microbial biomass C and CO₂-C primed expressed as percent of added C.

CO₂ occurred by increasing amounts of added substrate C. When the amount of added substrate C was between 50% and 200% of microbial biomass C, an exponential decrease in primed CO₂-C was observed. When the amount of added substrate C accounted for more than 200% of microbial C, no PE or negative PE occurred. When the added substrate C was lower than 15% of microbial biomass C, the magnitude of PE was one order lower than PE induced by substrate C amounting to 50–200% of microbial biomass C.

Apparent and real priming effects

Until now, no clear-cut approach has been suggested to distinguish apparent from real priming effects and it is not clear if the source of primed CO₂-C is SOM or the endogenous microbial metabolism (Bell et al., 2003). At least two different kinds of *apparent PE* can be caused by microbial activity when fresh available substrates are added to soil:

1. A triggering effect that is an acceleration of internal microbial metabolism by trace amounts of substrate with an immediate (several minutes to several hours) increase in the respiratory activity.
2. A pool substitution with acceleration of microbial turnover revealed by a long-term (several days or weeks) increase in respiratory activity (Jenkinson et al., 1985).

The *real PE* depends on the composition of added substrate used by microorganisms. If some nutrients, mainly N, are lacking, this shortage can be supplemented by an accelerated SOM decomposition resulting in a real PE. When complex organic substrates are added, soil microorganisms can use the energy of most available compounds to synthesize enzymes hydrolyzing the low available compounds. Therefore, SOM can be co-metabolized by microorganisms. Thus, *real PE* can be due to:

1. Mineralization of soil organic N to supply available N
2. Co-metabolism of SOM

The difficulties in distinguishing real and apparent PE also reflect the fact that both effects may occur simultaneously (Mondini et al., 2006).

We suggest relating the response time with PE magnitude for a better interpretation of PE. The following situations can occur:

1. *Short-term response: the amount of the primed carbon (C_{primed}) exceeds the rate of substrate additions (C_{added}) but it is lower than microbial biomass C (C_{BM}): C_{added} < C_{primed} < C_{BM}.* This type of PE is usually observed from hours to days after applying trace amounts (5–50 µg C g⁻¹ soil) of substrate (De Nobili et al., 2001; Bell et al., 2003; Mondini et al., 2006; Blagodatskaya et al., 2007). It has been suggested that the quick short-term response with lower amount of primed CO₂-C versus microbial biomass C is a triggering effect that can be due to accelerated metabolism of soil microorganisms rather than to the decomposition of SOM. This hypothesis has been verified by adding unlabeled substrates to the ¹⁴C-labeled microbial pool (Dalenberg and Jager, 1981; Bell et al., 2003). The flush of microbial primed ¹⁴CO₂-C detected immediately after adding ¹²C derived from the increased turnover of microbial C. Therefore, if the amount of primed CO₂-C is much less than microbial biomass C, and if the additional CO₂ (or N_{min}) is released very shortly after substrate addition, then an apparent PE is probably observed.
2. *Long-term response: the amount of the primed carbon (C_{primed}) is higher than microbial biomass C: C_{primed} > C_{BM}.* This PE usually occurs during long-term incubation ranging from weeks to months (Shen and Bartha, 1997; Conde et al., 2005; Hamer and Marschner, 2005; Perelo and Munch, 2005) and can coincide

with a significant increase in microbial biomass. The presence of the apparent PE cannot be excluded even when the amount of extra CO_2 exceeds the initial microbial biomass C value since growing soil microorganisms can also contribute to the accelerated microbial turnover. Without applying isotopic labeled compounds, the real PE can only be evaluated if the amount of the primed carbon is higher than both microbial biomass C (C_{BM}) and the added C ($C_{\text{added}} < C_{\text{primed}} > C_{\text{BM}}$).

3. *Short and long-term responses.* Added substrate can accelerate both microbial turnover and decomposition of recalcitrant SOM. Thus, the observed PE may be the combination of both real and apparent PE. The triggering effect immediately after substrate addition is replaced by an apparent PE caused by pool substitution and occurring during the intensive substrate decomposition (Hamer and Marschner, 2005). Intensive mineralization results in a short-term increase in the active microbial biomass, which can also cause the real PE both during the intensive substrate mineralization and later at the beginning of microbial starvation. Thus, real PE can occur with apparent PE, as shown after the exhaustion of available ^{13}C -substrates added to soil (Perelo and Munch, 2005). It was shown that real PE occur as a significant increase in the incorporation of SOM-derived C in microbial biomass and this preceded the extra CO_2 evolution. Perelo and Munch (2005) suggested that substrate input increased the immobilization of soil organic C by soil microorganisms and then this microbial immobilized C was oxidized to CO_2 due to the accelerated microbial turnover.

To distinguish apparent from real PE in long-term incubation experiments, the amount of primed CO_2 -C should be related to changes in microbial biomass during the studied period. We suggest that the contribution of real and apparent PEs to the total PE can be estimated by distinguishing substrate-originated and SOM-originated pools in the newly formed microbial biomass (Schneckenberger et al., 2008). Further studies with different labeling of the three most important pools (added substrate, microbial biomass, and recalcitrant soil organic matter) are required to distinguish apparent from real PE (Kuzyakov and Bol, 2006) and to precisely estimate the real PE.

Priming effects as related to substrate and soil properties

Substrate properties

As already mentioned, the availability, composition, and amount of substrate determine the magnitude and the type (real or apparent) of PE. The decomposition of easily available C sources (glucose, fructose, alanine) led to a greater PE than the addition of less available substrates, such as catechol, oxalic acid, plant residues, manure, or slurry to soil (Conde et al., 2005; Hamer and Marschner, 2005). Among the easily available substrates, glucose

generally caused lower PE than L-glutamic acid (Mondini et al., 2006), a complex substrate mixture (root extract, rhizosphere soil extract; De Nobili et al., 2001), or an amino acid mixture (Mondini et al., 2006).

The amount of primed carbon is also dependent on the amount of available N in soil. Decrease in PE was observed when available N was applied to soil with organic C (Liljeroth et al., 1994; Cardon, 1996; van Ginkel et al., 1997; Martin-Olmedo et al., 2002; Blagodatskaya et al., 2007). This confirms the preferential substrate utilization (the added versus the SOM) if the main nutrients, such as N, are present. In the case of an input of C-rich substrates without N, soil microorganisms are activated to decompose SOM to acquire N with production of a real PE. However, it has been observed that N addition with glucose and plant residues can also produce a PE (Conde et al., 2005; Hamer and Marschner, 2005). Probably this depended on still high C-to-N ratio despite the N addition. The synthesis and the activity of various enzymes involved in C and N cycling are, respectively, controlled by N and C availability (Chander et al., 1997; Carreiro et al., 2000). Thus, N addition stimulated the activity of cellulases, while the activity of phenoloxidase, an important ligninolytic enzyme, was greatly reduced by the increased N availability (Carreiro et al., 2000). Similarly, the activity of amidohydrolases (Deng and Tabatabai, 1996) and other enzymes involved in N cycling (Skujins, 1976), was influenced by the organic C content of soils.

In conclusion, the addition of trace amounts of easily available substrates induces a short-term triggering effect, whereas the input of available substrate without nutrients in amounts sufficient for microbial growth leads to activation of SOM decomposition. If nutrients are present, no PE occurs or even preferential substrate utilization decreases SOM decomposition.

Soil physical properties

Since the effect of chemical (such as nutrient status and the C-to-N ratio of the active SOM pool) and physical soil properties on the PE were reviewed earlier (Kuzyakov et al., 2000; Kuzyakov, 2002), here we will focus on the effect of soil moisture, temperature, aggregation, and pH on PE as it is mediated by biological activity.

Soil moisture

Since soil moisture is the main driver of microbial activity, lower PE can be expected under limiting moisture conditions. The intensity of PE, however, can be also driven by the frequency and duration of drying–rewetting events. Rare rainfalls during long dry periods cause quick short-term activation of soil microorganisms metabolizing available substrates (microbial necromass, root exudates, plant residues). Quickly decreasing soil moisture is the main limiting factor of microbial activity under such conditions, so two types of PE can be expected before soil drying: (1) apparent PE caused by triggering microbial activity and by pool substitution mechanism or

(2) negative PE caused by preferential substrate utilization. Since SOM is not involved in such PE, carbon sequestration prevails under an arid climate. At high humidity the duration of decomposition processes can be relatively long, since microbial activity is not limited by soil moisture. So, other factors such as lack of nutrients become limiting at long-term wet periods. Microorganisms benefiting under such conditions can supply the lacking nutrients, degrading SOM and causing the real PE. Mineralization of SOM can occur under long-term high humidity resulting in accelerated SOM turnover. This mechanism can explain the relatively young age of humus in paleosoils formed during humid versus arid climatic periods (Alexandrovskiy and Chichagova, 1998). Thus, the alternation and duration of dry and wet periods are responsible for the type of PE prevailing in soil.

Soil temperature

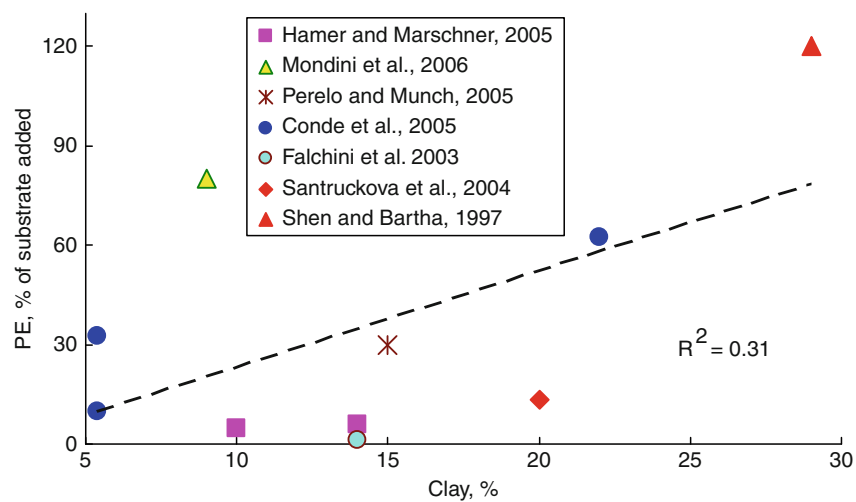
It is still unclear, what type of PE can prevail at global climate warming. On the one hand, greater amount and availability of substrate (e.g., from enhanced rhizodeposition), accelerated microbial and enzymatic activity caused by increasing temperature, can result in greater PE intensity. On the other hand, psychrophilic microorganisms benefiting at low temperatures have the enzyme system with higher affinity to low available substrates such as soil humus. Both increase and decrease in PE were observed in different studies at low versus high temperature. Such discrepancy can be explained by the interactive effect of temperature and substrate availability, which should be considered in PE studies at low amounts of substrate (S) (Davidson and Janssens, 2006). At high substrate amounts the decomposition rate does not depend on S and is only temperature dependent. Under substrate limitation, however, the rates of enzyme catalyzed reactions are mainly dependent on substrate affinity. Since psychrophilic

microorganisms have greater affinity to low available substrates, no changes or even increase in decomposition rate can occur at low versus high temperature in the interval of very low substrate amounts (Kuzyakov et al., 2007).

Aggregate and particle-size fractions

The accumulation and physical protection of SOM as well as its mineralization depends on soil-aggregate size (Denef et al., 2001; Six and Jastrow, 2002) and the mean residence time of C in macroaggregates is shorter than that of C in microaggregates (Six and Jastrow, 2002). This indicates that the PE due to the response of microorganisms to substrate addition may vary in aggregates with different size. Indeed, Degens and Sparling (1996) observed that only the middle-sized fraction (1–2 mm) showed a significant and positive PE as a quick response to glucose addition and this PE was apparently related to microbial biomass. Both larger (>2 mm) and smaller (<0.25 mm) particles showed PE, long (21 days) after glucose application and probably both PEs were real because they were not due to microbial turnover (Degens and Sparling, 1996). The intermediate-aggregate size fractions (0.25–1 mm) showed a negative PE. Probably the differences in response in various aggregates size classes was due to the different localization of soil microorganisms; generally fungi predominate in macroaggregates, whereas bacteria predominate in microaggregates (Guggenberger et al., 1999).

Silt mainly contributes to the formation of microaggregates, while sand particles are mostly associated with macroaggregates. According to Kandeler et al. (1999), invertase activity mainly due to intracellular activity, was abundant in the silt fraction, whereas extracellular enzyme activities were distributed among particle-size fractions; thus xylanase activity was associated with sand, alkaline phosphatase activity with silt and clay, and protease activity with sand and clay. It is important to underline



Priming Effects in Relation to Soil Conditions – Mechanisms, Figure 5 Relationship between primed CO_2 -C efflux expressed as percent of added C and clay content in soil.

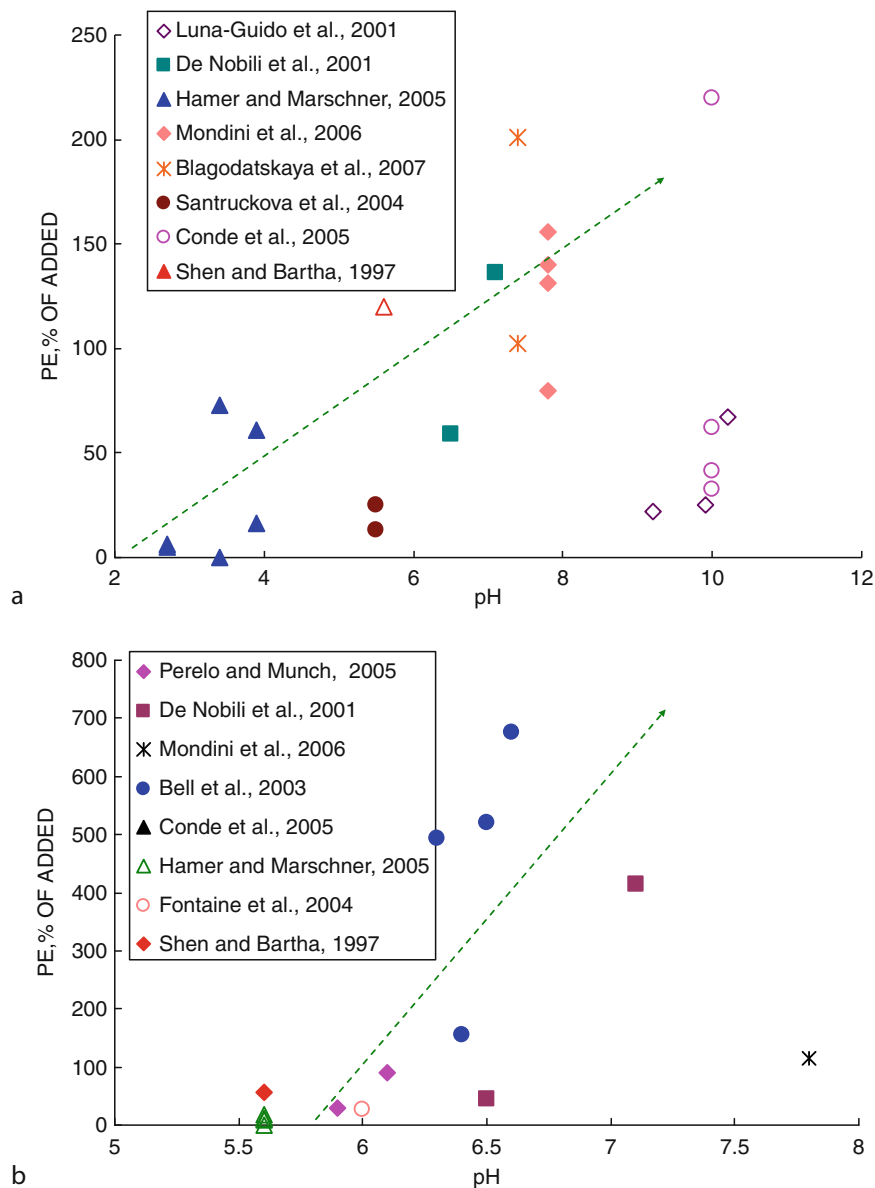
that since the present enzyme assays do not allow distinguishing the intracellular and extracellular enzyme activities, these are just hypotheses.

No differences in PE promoted by fructose and alanine were observed between soil fractions (sand, silt, and clay) obtained by mild sonication followed by wet sieving and sedimentation (Ohm et al., 2007). It is important to underline that available fractionation procedures can give artifacts. Sonication can promote not only disaggregation, but also desorption of microbial cells from soil particles and these desorbed microbial cells can redistribute during wet sieving to smaller size fractions. This

can smooth the differences in microbial activity between fractions. The dry sieving method used by Degens and Sparling (1996) seems to yield a more realistic distribution of microbial activity among the soil particles (Figure 5).

Soil acidity (pH)

The higher intensity of PE occurs in neutral soils – in the pH range between 6 and 8 – when both easily decomposable substances and plant residues are added to soil (Figure 6). The changes of microbial activity and community structure as well as the enzyme synthesis are higher in



Priming Effects in Relation to Soil Conditions – Mechanisms, Figure 6 Relationship between primed $\text{CO}_2\text{-C}$ efflux expressed as percent of added C and soil pH: easily available substrate (top) and plant residues (bottom).

soils with pH ranging from 5 to 8 than in acidic soils (Blagodatskaya and Anderson, 1998).

Most studies on priming effects are based on CO₂ measurements and artifacts can occur if the effect of soil pH on the solubility of CO₂ is neglected. Indeed, the equilibrium among H₂CO₃, CO₃²⁻, and HCO₃⁻, all derived from CO₂, in soil solution is pH dependent, and thus, the soil pH should be considered when interpreting results from CO₂ evolution. Possible misestimates of CO₂ evolution do not occur at pH values <5 because H₂CO₃ is the prevailing (about 98%) form that dissociates immediately into CO₂ and H₂O, and thus all CO₂ produced by soil microorganisms can be freely evolved as CO₂. At pH between 5 and 5.5, the contribution of H₂CO₃ decreases to 70% and some CO₂ can occur in soil solution as HCO₃⁻, and this can give a small underestimation of the produced CO₂. As the total amount of soluble CO₂ species is less than 0.03 mM l⁻¹ at pH 5–5.5, such underestimation does not exceed 0.1 µg CO₂-C g⁻¹ however, this value can be neglected considering that the CO₂ production rate in most unamended mineral soils is 1–2 µg CO₂-C g⁻¹ h⁻¹.

The prevailing forms of carbonate at pH values higher than 6.8 are HCO₃⁻ and CO₃²⁻. Therefore, CO₂ produced by microbial respiration will initially dissolve in soil water until the saturation capacity of the solution is reached. In such a case, CO₂ evolution depends on the volume of soil solution. Assuming the soil water content to be 30% of dry weight with a CO₂ evolution rate of about 30–40 µg CO₂-C g⁻¹ day⁻¹, the CO₂ evolution from soil can be underestimated by 10–100% at soil pH values of 8 and 9, respectively. This may explain the 1-day delay in the PE of alkaline soils (pH of 9.8–11.7) promoted by the addition of glucose or maize (Conde et al., 2005). Probably, CO₂ produced during the first day after treatment was accumulated as HCO₃⁻ and CO₃²⁻ in soil solution until the CO₂ saturation was reached; then the excess was evolved as CO₂. Therefore, the short-term PEs in soils at pH > 8, should be interpreted with caution. In soils with very high pH (9–11), the PE estimation is even more difficult because of carbonate recrystallization (Kuzyakov et al., 2006).

Summary

Priming effects are short-term changes in the turnover of soil organic matter caused by the addition of organic substances to the soil. Additions of easily available organic C up to 15% of microbial biomass C induce a linear increase of extra CO₂. When the added amount of easily available organic C is higher than 50% of the microbial biomass C, an exponential decrease of the PE or even a switch to negative values is often observed. PE increases with pH and clay content.

Bibliography

Alexandrovskiy, A. L., and Chichagova, O. A., 1998. Radiocarbon age of Holocene Paleosols of the East European forest-steppe zone. *Catena*, **34**, 197–207.

- Bell, J. M., Smith, J. L., Bailey, V. L., and Bolton, H., 2003. Priming effect and C storage in semi-arid no-till spring crop rotations. *Biology and Fertility of Soils*, **37**, 237–244.
- Blagodatskaya, E.V., and Anderson, T-H., 1998. Interactive effects of pH and substrate quality on the fungal-to-bacteria ratio and QCO₂ of microbial communities in forest soils. *Soil Biology and Biochemistry*, **30**, 1269–1274.
- Blagodatskaya, E. V., Blagodatsky, S. A., Anderson, T-H., and Kuzyakov, Y., 2007. Priming effects in Chernozem induced by glucose and N in relation to microbial growth strategies. *Applied Soil Ecology*, **37**, 95–105.
- Blagodatskaya, E., and Kuzyakov, Y., 2008. Mechanisms of real and apparent priming effects and their dependence on soil microbial biomass and community structure: critical review. *Biology & Fertility of Soils* **45**, 115–131.
- Brant, J. B., Sulzman, E. W., and Myrold, D. D., 2006. Microbial community utilization of added carbon substrates in response to long-term carbon input manipulation. *Soil Biology and Biochemistry*, **38**, 2219–2232.
- Brookes, P. C., Ocio, J. A., and Wu, J., 1990. The soil microbial biomass: its measurements, properties and role in soil nitrogen and carbon dynamics following substrate incorporation. *Soil Microorganisms*, **35**, 39–51.
- Burmolle, M., Hansen, L. H., Oregaard, G., and Sorensen, S. J., 2003. Presence of N-acyl homoserine lactones in soil detected by a whole-cell biosensor and flow cytometry. *Microbial Ecology*, **45**, 226–236.
- Cardon, Z. G., 1996. Influence of rhizodeposition under elevated CO₂ on plant nutrition and soil organic matter. *Plant and Soil*, **187**, 277–288.
- Carreiro, M. M., Sinsabaugh, R. L., Repert, D. A., and Parkhurst, D. F., 2000. Microbial enzyme shifts explain litter decay responses to simulated nitrogen deposition. *Ecology*, **81**, 2359–2365.
- Chander, K., Goyal, S., Mundra, M. C., and Kapoor, K. K., 1997. Organic matter, microbial biomass and enzyme activity of soils under different crop rotations in the tropics. *Biology and Fertility of Soils*, **24**, 306–310.
- Cheng, W., and Kuzyakov, Y., 2005. Root effects on soil organic matter decomposition. In: Wright S., and Zobel, R. (eds.), *Roots and Soil Management: Interactions Between Roots and the Soil*. Agronomy Monograph No. 48. ASA, Madison WI US, pp. 119–143.
- Conde, E., Cardenas, M., Ponce-Mendoza, A., Luna-Guido, M. L., Cruz-Mondragon, C., and Dendooven, L., 2005. The impacts of inorganic nitrogen application on mineralization of C-14-labelled maize and glucose, and on priming effect in saline alkaline soil. *Soil Biology and Biochemistry*, **37**, 681–691.
- Dalenberg, J. W., and Jager, G., 1981. Priming effect of small glucose additions to ¹⁴C-labeled soil. *Soil Biology and Biochemistry*, **13**, 219–223.
- De Neve, S., Saez, S. G., Daguilas, B. C., Sleutel, S., and Hofman, G., 2004. Manipulating N mineralization from high N crop residues using on- and off-farm organic materials. *Soil Biology and Biochemistry*, **36**, 127–134.
- De Nobili, M., Contin, M., Mondini, C., and Brookes, P. C., 2001. Soil microbial biomass is triggered into activity by trace amounts of substrate. *Soil Biology and Biochemistry*, **33**, 1163–1170.
- Degens, B., and Sparling, G., 1996. Changes in aggregation do not correspond with changes in labile organic C fractions in soil amended with C-14-glucose. *Soil Biology and Biochemistry*, **28**, 453–462.
- Denef, K., Six, J., Bossuyt, H., Frey, S., Elliott, E., Merckx, R., and Paustian, K., 2001. Influence of dry–wet cycles on the interrelationship between aggregate, particulate organic matter, and microbial community dynamics. *Soil Biology and Biochemistry*, **33**, 1599–1611.

- Deng, S. P., and Tabatabai, M. A., 1996. Effect of tillage and residue management on enzyme activities in soils 1. Amidohydrolases. *Biology and Fertility of Soils*, **22**, 202–207.
- Falchini, L., Naumova, N., Kuikman, P. J., Bloem, J., and Nannipieri, P., 2003. CO₂ evolution and denaturing gradient gel electrophoresis profiles of bacterial communities in soil following addition of low molecular weight substrates to simulate root exudation. *Soil Biology and Biochemistry*, **35**, 775–782.
- Fontaine, S., Bardoux, G., Abbadie, L., and Mariotti, A., 2004. Carbon input to soil may decrease soil carbon content. *Ecology Letters*, **7**, 314–320.
- Fontaine, S., Barot, S., Barre, P., Bdoui, N., Mary, B., and Rumpel, C., 2007. Stability of organic carbon in deep soil layers controlled by fresh carbon supply. *Nature*, **450**, 277–280.
- Fontaine, S., Mariotti, A., and Abbadie, L., 2003. The priming effect of organic matter: a question of microbial competition? *Soil Biology and Biochemistry*, **35**, 837–843.
- Gioacchini, P., Nastri, A., Marzadori, C., Giovannini, C., Antisari, L. V., and Gessa, C., 2002. Influence of urease and nitrification inhibitors on N losses from soils fertilized with urea. *Biology and Fertility of Soils*, **36**, 129–135.
- Gray, E. J., and Smith, D. L., 2005. Intracellular and extracellular PGPR: commonalities and distinctions in the plant–bacterium signalling processes. *Soil Biology and Biochemistry*, **37**, 395–412.
- Guggenberger, G., Elliott, E. T., Frey, S. D., Six, J., and Paustian, K., 1999. Microbial contributions to the aggregation of a cultivated grassland soil amended with starch. *Soil Biology and Biochemistry*, **31**, 407–419.
- Hamer, U., and Marschner, B., 2005. Priming effects in different soil types induced by fructose, alanine, oxalic acid and catechol additions. *Soil Biology and Biochemistry*, **37**, 445–454.
- Hopkins, D. W., Sparrow, A. D., Elberling, B., Gregorich, E. G., Novis, P. M., Greenfield, L. G., and Tilston, E. L., 2006. Carbon, nitrogen and temperature controls on microbial activity in soils from an Antarctic dry valley. *Soil Biology and Biochemistry*, **38**, 3130–3140.
- Jenkinson, D. S., Fox, R. H., and Rayner, J. H., 1985. Interactions between fertilizer nitrogen and soil nitrogen - the so-called ‘priming’ effect. *Journal of Soil Science*, **36**, 425–444.
- Kandeler, E., Palli, S., Stemmer, M., and Gerzabek, M. H., 1999. Tillage changes microbial biomass and enzyme activities in particle-size fractions of a Haplic Chernozem. *Soil Biology and Biochemistry*, **31**, 1253–1264.
- Kuzyakov, Y., 2002. Review: Factors affecting rhizosphere priming effects. *Journal of Soil Science and Plant Nutrition*, **165**, 382–396.
- Kuzyakov, Y., and Bol, R., 2006. Sources and mechanisms of priming effect induced in two grassland soils amended with slurry and sugar. *Soil Biology and Biochemistry*, **38**, 747–758.
- Kuzyakov, Y., Friedel, J. K., and Stahr, K., 2000. Review of mechanisms and quantification of priming effects. *Soil Biology and Biochemistry*, **32**, 1485–1498.
- Kuzyakov, Y., Shevtsova, E., and Pustovoytov, K., 2006. Carbonate re-crystallization in soil revealed by ¹⁴C labeling: Experiment, model and significance for paleo-environmental reconstructions. *Geoderma*, **131**, 45–58.
- Kuzyakov, Y., Hill, P. W., and Jones, D. L., 2007. Root exudate components change litter decomposition in a simulated rhizosphere depending on temperature. *Plant and Soil*, **290**, 293–305.
- Lazazzera, B. A., 2000. Quorum sensing and starvation: signals for entry into stationary phase. *Current Opinion in Microbiology*, **3**, 177–182.
- Liljeroth, E., Kuikman, P., and Vanveen, J. A., 1994. Carbon translocation to the rhizosphere of maize and wheat and influence on the turnover of native soil organic-matter at different soil-nitrogen levels. *Plant and Soil*, **161**, 233–240.
- Little, A. E. F., Robinson, C. J., Peterson, S. B., Raffa, K. F., and Handelsman, J., 2008. Rules of engagement: Interspecies interactions that regulate microbial communities. *Annual Review in Microbiology*, **62**, 375–401.
- Luna-Guido, M. L., Beltran-Hernandez, R. I., and Dendooven, L., 2001. Dynamics of ¹⁴C-labelled glucose in alkaline saline soil. *Soil Biology and Biochemistry*, **33**, 707–719.
- Martin-Olmedo, P., Rees, R. M., and Grace, J., 2002. The influence of plants grown under elevated CO₂ and N fertilization on soil nitrogen dynamics. *Global Change Biology*, **8**, 643–657.
- Mondini, C., Cayuela, M. L., Sanchez-Monedero, M. A., Roig, A., and Brookes, P. C., 2006. Soil microbial biomass activation by trace amounts of readily available substrate. *Biology and Fertility of Soils*, **42**, 542–549.
- Niklaus, P. A., and Falloon, P., 2006. Estimating soil carbon sequestration under elevated CO₂ by combining carbon isotope labelling with soil carbon cycle modelling. *Global Change Biology*, **12**, 1909–1921.
- Ohm, H., Hamer, U., and Marschner, B., 2007. Priming effects in soil size fractions of a podzol Bs horizon after addition of fructose and alanine. *Journal of Plant Nutrition and Soil Science-Zeitschrift fur Pflanzenernahrung und Bodenkunde*, **170**, 551–559.
- Paul, E. A., and Clark, F. E., 1989. *Soil Microbiology and Biochemistry*. Academic Press ed., San Diego.
- Perelo, L. W., and Munch, J. C., 2005. Microbial immobilisation and turnover of C-13 labelled substrates in two arable soils under field and laboratory conditions. *Soil Biology and Biochemistry*, **37**, 2263–2272.
- Raffa, R. B., Iannuzzo, J. R., Levine, D. R., Sacid, K. K., Schwartz, R. C., Sucic, N. T., Terleckyj O. D., and Young, J. M., 2005. Bacterial communication (“Quorum Sensing”) via ligands and receptors: A novel pharmacologic Target for the design of antibiotic drugs. *Journal of Pharmacology and Experimental Therapeutics*, **312**, 417–423.
- Schimel, J. P., and Weintraub, M. N., 2003. The implications of exoenzyme activity on microbial carbon and nitrogen limitation in soil: a theoretical model. *Soil Biology and Biochemistry*, **35**, 549–563.
- Schneckenberger, K., Demin, D., Stahr, K., and Kuzyakov, Y., 2008. Microbial utilization and mineralization of [¹⁴C] glucose added in six orders of concentration to soil. *Soil Biology and Biochemistry*, **40**, 1981–1988.
- Shen, J., and Bartha, R., 1997. Priming effect of glucose polymers in soil-based biodegradation tests. *Soil Biology and Biochemistry*, **29**, 1195–1198.
- Six, J., and Jastrow, J., 2002. *Organic Matter Turnover*, Marcel Dekker, New York.
- Skujins, J. J., 1976. Extracellular enzymes in soil. *CRC Critical Reviews in Microbiology*, **4**, 383–421.
- Van Ginkel, J. H., Gorissen, A., and vanVeen, J. A., 1997. Carbon and nitrogen allocation in *Lolium perenne* in response to elevated atmospheric CO₂ with emphasis on soil carbon dynamics. *Plant and Soil*, **188**, 299–308.
- Wang, Y. J., and Leadbetter, J. R., 2005. Rapid acyl-homoserine lactone quorum signal biodegradation in diverse soils. *Applied and Environmental Microbiology*, **71**, 1291–1299.
- Waters, C. M., and Bassler, B. L., 2005. Quorum sensing: cell-to-cell communication in bacteria. *Annual Review of Cell and Developmental Biology*, **21**, 319–346.
- Wu, J., Brookes, P. C., and Jenkinson, D. S., 1993. Formation and destruction of microbial biomass during the decomposition of glucose and ryegrass in soil. *Soil Biology and Biochemistry*, **25**, 1435–1441.
- Zyakun, A. M., and Dilly, O., 2005. Use of carbon isotope composition for characterization of microbial activity in arable soils. *Applied Biochemistry and Microbiology*, **41**, 512–520.

Cross-references

- Aeration of Soils and Plants
 Agrophysical Properties and Processes
 Carbon Losses Under Dryland Conditions, Tillage Effects
 Organic Matter, Effects on Soil Physical Properties and Processes

PROTON NUCLEAR MAGNETIC RESONANCE (NMR) RELAXOMETRY IN SOIL SCIENCE

Gabriele E. Schaumann

Department of Environmental and Soil Chemistry,
 Institute for Environmental Sciences, University
 Koblenz-Landau, Landau, Germany

Proton NMR relaxometry is a very powerful tool for investigating porous media and their interaction with water with organic molecules in solution. It is commonly used in material science or earth science and is increasingly applied in soil science as detailed in the review (Bayer et al., 2010). NMR relaxometry is sensitive and promising to study pore size distribution in soils (Jaeger et al., 2009), wetting (Schaumann et al., 2005; Todoruk et al., 2003), swelling (Jaeger et al., 2010; Schaumann et al., 2004), bio-film formation (Jaeger et al., 2006), or metal-NOM binding (Jaeger et al., 2008; Melton et al., 2007). It further helps to study interactions between molecules in soil organic matter (Schaumann and Bertmer, 2008). Relaxation times determined by NMR relaxometry are sensitive to various factors that play a role in soil–water interaction which is both an advantage and shortcoming of the method: NMR relaxometry is a versatile method, which can be applied to numerous investigations in soil science, but at the same time interpretation of the results in such complex and heterogeneous systems like soils requires expertise from both soil science and NMR.

Bibliography

- Bayer, J. V., Jaeger, F., and Schaumann, G. E., 2010. Proton Nuclear magnetic resonance (NMR) relaxometry in soil science applications. *The Open Magnetic Resonance Journal*, **3**, DOI: 10.2174/1874769801003020015.
- Jaeger, F., Grohmann, E., and Schaumann, G. E., 2006. ^1H NMR Relaxometry in natural humous soil samples: Insights in microbial effects on relaxation time distributions. *Plant and Soil*, **280**, 209–222.
- Jaeger, F., Rudolph, N., Lang, F., and Schaumann, G. E., 2008. Effects of soil solution's constituents on proton NMR relaxometry of soil samples. *Soil Science Society of America Journal*, **72**, 1694–1707.
- Jaeger, F., Bowe, S., and Schaumann, G. E., 2009. Evaluation of ^1H NMR relaxometry for the assessment of pore size distribution in soil samples. *European Journal of Soil Science*, **60**, 1052–1064.
- Jaeger, F., Shchegolikhina, A., van As, H., and Schaumann, G. E., 2010. Proton NMR Relaxometry as a Useful Tool to Evaluate Swelling Processes in Peat Soils. *The Open Magnetic Resonance Journal*, **3**, DOI: 10.2174/1874769801003020027.
- Melton, J. R., Kantzias, A., and Langford, C. H., 2007. Nuclear magnetic resonance relaxometry as a spectroscopic probe of the

coordination sphere of a paramagnetic metal bound to a humic acid mixture. *Analytica Chimica Acta*, **605**, 46–52.

Schaumann, G. E., and Bertmer, M., 2008. Do water molecules bridge soil organic matter molecule segments? *European Journal of Soil Science*, **59**, 423–429.

Schaumann, G. E., Hurraß, J., Müller, M., and Rotard, W., 2004. Swelling of organic matter in soil and peat samples: insights from proton relaxation, water absorption and PAH extraction. In Ghabbour, E. A., and Davies, G. (eds.), *Humic Substances: Nature's Most Versatile Materials*. New York: Taylor and Francis, pp. 101–117.

Schaumann, G. E., Hobley, E., Hurraß, J., and Rotard, W., 2005. H-NMR relaxometry to monitor wetting and swelling kinetics in high organic matter soils. *Plant and Soil*, **275**, 1–20.

Todoruk, T. R., Langford, C. H., and Kantzias, A., 2003. Pore-scale redistribution of water during wetting of air-dried soils as studied by low-field NMR relaxometry. *Environmental Science and Technology*, **37**, 2707–2713.

PROXIMAL SOIL SENSING

See *Precision Agriculture: Proximal Soil Sensing*

PUDDLING: EFFECT ON SOIL PHYSICAL PROPERTIES AND CROPS

Gunnar Kirchhof¹, T. P. Tuong², H. B. So¹

¹School of Land, Crop and Food Sciences, The University of Queensland, Brisbane, QLD, Australia

²International Rice Research Institute, Metro Manila, Philippines

Definition

Soil puddling for paddy rice production is the process of working saturated or near-saturated soil into soft structureless mud.

Tillage in lowland rice production systems (paddy rice) is synonymous with puddling. Puddling is achieved by cultivating the soil under saturated condition using animal drawn or tractor driven implements. Mechanical breaking and dispersing of soil aggregates destroys the soil structure and forms the puddled zone. Puddling softens the soil and assists manual transplantation of rice seedling, minimizes water use through reduced percolation losses and effective weed control. Over time, soil puddling also creates a compacted layer below the puddled zone which further reduces percolation losses. The least permeable zone is usually found just below the puddled layer where tillage implements created a thin smeared layer. The reduction in permeability is mainly caused by blocking of macropores with fine dispersed particles translocated during puddling process, and the smearing effect of the tillage implements.

Although lowland rice does not require saturated conditions to produce high yields, it is traditionally kept under submerged conditions to maximize water supply, mobilize

nutrients, and to control weeds, which is generally not possible without puddling.

However, preferential flow or bypass flow through macropores, cracks, or large biopores contributes to water losses in paddy systems. This includes water losses through bunds which are not puddled. Water moves laterally into the bunds and then percolates down through the under-bund areas that are not puddled.

Despite the benefits of puddling for rice production, there are adverse effects, especially on post-rice crop production. Due to its structureless nature, puddled soils tend to harden and crack upon drying, with the rate and size of crack development depending on the rate of drying, type of clay, and clay content. These characteristics are the main constraint to the establishment and growth of post-rice crops. Irrigation of dried paddy soils can result in excessive losses from bypass flow, while severe cracking can result in root breakage and excessive strength impedes root growth.

Although soil puddling reduces the percolation rates, the puddling process itself requires large amounts of water. With increasing water scarcity, alternative tillage methods to reduce water use are needed. Dry tillage prior to flooding can reduce water requirements substantially by filling cracks and disrupting bypass flow pathways. It has become apparent that soils have often been puddled excessively. On clay soils, sufficient reduction in hydraulic conductivities can be achieved with only one pass of the

puddling implement, but coarser textured soils may require several passes. Landscapes with very shallow water tables may not need puddling at all, while broad cast planting of pre-germinated seed can save labor without sacrificing yield. In the context of rice and upland crop rotations, minimizing puddling to reduce soil structural degradation will benefit post-rice crops such as legumes or wheat.

Bibliography

- IRRI, 1985. *Soil Physics and Rice*. Los Banos, Laguna, Philippines: International Rice Research Institute, ISBN 971-104-146-4, 430 pp.
- ACIAR, 1996. *Management of Clay Soils for Rainfed Lowland Rice-Based Cropping Systems*. Kirchhof, G., and So, H. B. Australian Centre for International Agricultural Research, ISBN 1 86320 176 9, 259 pp.

PUGGING

The compaction and waterlogging of soil caused by trampling of grazing animals.

Cross-references

- [Grazing-Induced Changes of Soil Mechanical and Hydraulic Properties](#)
[Soil Compatability and Compressibility](#)

Q

QUALITY OF AGRICULTURAL PRODUCTS IN RELATION TO PHYSICAL CONDITIONS

Guillermo P. Moreda, Margarita Ruiz-Alsent
Laboratorio de Propiedades Físicas y Tecnologías Avanzadas en Agro-Alimentación (LPF-TAGRALIA), Universidad Politécnica de Madrid, Madrid, Spain

Definition

Quality. Degree to which a set of inherent characteristics fulfills requirements (ISO 9000:2005).

Agricultural Products. In broad terms, food and fiber products. For more detail, see the Introduction section below.

Physical condition of agricultural products. In broad terms, everything related to the properties that can be observed or measured without changing the composition of the product matter. More specifically, the physical condition of, e.g., a fruit is related to textural aspects. Physical conditions determining agricultural products quality depend on the product considered.

Introduction

The quality of a commodity depends greatly on the intended use. As this entry deals with quality of agricultural products (see *Agophysical Objects (Soils, Plants, Agricultural Products, and Foods)*), it seems reasonable to start by identifying what commodities are included in the term *agricultural product*, and what their possible uses are. The United States Department of Agriculture (USDA) points out that agricultural products, sometimes also referred to as “food and fiber” products, cover a broad range of goods; specifically, all of the products found in Chapters 1–24 of the U.S. Harmonized Tariff Schedule – except for fishery products, manufactured tobacco

products like cigarettes and cigars, and spirits – are considered agricultural products. Agricultural products within these chapters generally fall into the following categories: grains, animal feeds, and grain products (like bread and pasta); oilseeds and oilseed products; livestock, poultry, and dairy products including live animals, meats, eggs, and feathers; horticultural products including all fresh and processed fruits, vegetables, tree nuts, as well as nursery products and wine; unmanufactured tobacco; and tropical products like sugar, cocoa, and coffee. Certain other products outside of Chapters 1–24, like raw rubber, raw animal hides and skins, and wool and cotton, are also considered agricultural products. To illustrate the wide variety of uses of agricultural products, let us take the corn grain as an example. While its main use is for livestock feed, corn grain is also used for human nourishment under the forms of corn cob, sweet tender canned corn, corn flakes, margarine elaborated from corn oil, etc., and through the industrial process of corn wet milling, to obtain starch and starch-derived chemicals. This corn-starch is then processed and used as food (e.g., as thickener in the food industry) and industrial products. It is routinely used as an adhesive, for manufacture of papers, and as an excipient or filler for pharmaceuticals. It can be converted into an enormous assortment of industrial chemicals now produced from petroleum sources. For example, new biodegradable plastic products are being made from corn, such as garbage bags, car parts, and packing “peanuts” (Olson and Warren, 2010).

Given the heterogeneity of agricultural products and their possible uses, to dissert on their quality it is convenient to focus on some agricultural products and specific uses. This article focuses on products obtained from cultivated plants for purposes of human nourishment, both in raw and processed form. More specifically, here we deal with grain and horticultural produce destined for human consumption. Other agricultural products as foods

obtained from animals (fish, meat, milk, eggs, etc.), or fibers of vegetal and animal origin (cotton, flax, wool, silk, etc.), are beyond the scope of this entry. Grains, and especially fruits and vegetables, are living, respiring, biologically active organisms that require optimal storage conditions (see *Physical Phenomena and Properties Important for Storage of Agricultural Products*) to maintain the quality that is present at harvest. A major difference between horticultural produce and grains is that horticultural products, mainly due to much higher water content, have to be stored under refrigeration, whereas grains do not.

According to Sloof et al., (1996), quality is a very elusive concept, which depends on several factors, the major of which are the product itself and its intended use. For instance, the required degree of ripeness of an olive depends on whether it will be seasoned for consumption as *table olive* or it will be processed for extracting olive oil. While most types of table olives are harvested before véraison, i.e., when they are green or immature, olives intended for oil extraction must be mature enough (véraison or purple turning to black). In both cases, the destination of olives is the food industry since these fruits, due to a glucoside in the flesh called *oleuropein*, are too bitter to be eaten raw. Olive is not the only horticultural produce that cannot be eaten raw; e.g., potatoes are never eaten raw, and quince flesh is so hard that all its production is processed. Another example of quality dependence on the intended use is in the fresh oranges we purchase for home consumption. Typically, there are two ways of using these oranges: one is eating the whole fruit – except the peel – and the other is making them juice. When a consumer buys *juice oranges*, he will normally expect a maximum content of juice, and the lesser fiber possible. But if he wants *table oranges*, i.e., oranges for being eaten whole, his preferences might differ. A third example can be mentioned for tomato. For fresh consumption, as in salads, a thick skin is a negative attribute, but if the tomato is to be processed, it should have a thick skin, in order to remain intact until it reaches the factory. The latter requirement arises because processing tomatoes are harvested mechanically, and this operation entails potential damage (see *Mechanical Impacts at Harvest and After Harvest Technologies*). If machine-harvested tomatoes had a thin skin, they would break easily, and the losses of juice would be considerable. In practice, processing tomato varieties are different from fresh-market varieties. Within fresh-market tomatoes, the quality desired by the consumer will vary depending on the intended use: ripe tomatoes for soup, hard tomatoes for salads. A last example can be addressed for peaches. Peach varieties can be classified as *freestone* or *clingstone*. Freestone peaches are destined for fresh consumption, whereas the peach canning industry demands exclusively clingstone peaches, since they have a harder flesh than their freestone counterparts. Apart from the product itself and the intended use, there are sociopsychological factors that play a role in defining the quality, since they affect the user's attitude toward

the product. For example, one person may be status conscious and prefer bananas from Spain's Canary Islands or plum tomatoes from Italy, another may be environmentally aware and prefer organically grown tomatoes. On the other hand, physical conditions determining the quality of grain and horticultural produce depend on the product under consideration.

Grain

Physiological maturity and maximum dry matter yield of winter cereals (wheat, barley, rye, oats) is reached when the grain moisture content is between 30% and 40%, but at this moisture content the grain is too soft to combine (see *Physical Properties of Raw Materials and Agricultural Products*). Grain is usually combine ready (sometimes referred to as "harvest ripe" or "grain ripe") when it has dried to about 15% moisture (Farrer et al., 2006). Besides, this is the moisture content limit required for safe storage. Harvest delay is not recommended, as it usually results in yield reduction due to hail damage, insects or birds attack, lodging, or shattering. Shattering occurs when the spikelets or grains fall from the plant. Moreover, when harvest is delayed the combine operation may be hindered by weeds infestation; weeds may even fructify, producing seeds that will be harvested together with the grain, contaminating it. In the case of rice, the drawbacks associated to harvest delay are the same as for winter cereals, plus the fact that rice will fissure while on the panicle if allowed to dry below certain levels and subsequently incur rapid moisture adsorption. Rain or exposure to high relative humidity could cause such adsorption. Therefore, in most countries, rice is not allowed to dry too much in the field after physiological maturity, but it is harvested with high moisture content (25–30%). Afterward, rice is dried down to safe storage conditions, about 15% moisture content, at dedicated facilities (see *Drying of Agricultural Products*).

The main cereals used for human nourishment internationally are wheat and rice. However, for the poorest rural people in the semiarid tropics of Asia and Africa, sorghum and millets are the most important staple foods, growing in harsh environments where other crops do not grow well (FAO, 1995). Barley is also important internationally insofar it constitutes the raw material for beer making (brewing). Rye is traditionally used for bread making in some European countries, competing with common bread made from wheat. Rye bread has the advantage over wheat bread of remaining tender during several days, while wheat bread soon dries and hardens (see *Water Effects on Physical Properties of Raw Materials and Foods*). Finally, white corn is of utmost importance in Spanish-American countries, such as Mexico or Peru, where it is used to produce *tortillas* and other traditional staple foods.

Wheat

Worldwide, the main use of wheat grain is for bread making. Species used in bread making is the *common wheat* or

bread wheat (*Triticum aestivum* L.), whereas *durum wheat* (*Triticum turgidum* ssp. *Durum*) is used to make pastas. Bread wheat mills to produce flour, whereas durum wheat mills to produce semolina, which has a coarser granulometry than flour. Depending on the variety, bread wheat can be soft or hard. Moreover, grain can be *white* or *red*. Attending to the duration of the vegetative cycle, there are winter wheat (long cycle) and spring wheat (short cycle) cultivars. Within bread wheat, soft wheat varieties are generally used to make biscuits and other bakery products, whereas hard cultivars are used to make loaf bread.

Wheat milling factories transform the grain into flour, which is then sold to bread-making facilities. According to the United Kingdom Home-Grown Cereals Authority (HGCA), the quality parameters analyzed by wheat millers for each grain delivery are: moisture content, specific weight (*test weight*), screenings and admixture, wheat variety, protein content, protein quality, Hagberg Falling Number, molds, damaged grain and odors, and

grain hardness. Grain moisture content does not directly affect grain quality, but can indirectly affect quality since grain will spoil at moisture contents above that recommended for storage (15%); this is because insects and molds, the causing agents of spoiling, require moisture to grow.

Thin, shriveled grain will not mill to produce adequate amounts of clean, white flour. Grain *test weight* is used as an indicator of general grain quality and is a measure of grain bulk density. The *test weight* measures the weight of wheat (in kg) that can be packed into a cylinder of fixed volume, normally 1 L. Wheat standards fix a minimum specific weight (Table 1). *Test weight* is composed of two components: the packing efficiency of the grain and the density of the individual kernels. Packing efficiency is dependent on genotype, while kernel density is primarily affected by environment (Farrer et al., 2006). Schuler et al. (1995) found that *test weight* did not predict flour yield in soft red winter wheat when shriveling was absent,

Quality of Agricultural Products in Relation to Physical Conditions, Table 1 Grades and grade requirements for all classes of wheat except Mixed wheat. Source: United States Standards for Wheat. Grain Inspection, Packers and Stockyards Administration. United States Department of Agriculture (2006)

Grading factors	Grades U.S. Nos.				
	1	2	3	4	5
Minimum pound limits of:					
Test weight per bushel					
Hard Red Spring wheat or White Club wheat	58.0	57.0	55.0	53.0	50.0
All other classes and subclasses	60.0	58.0	56.0	54.0	51.0
Maximum percent limits of:					
Defects:					
Damaged kernels					
Heat (part of total)	0.2	0.2	0.5	1.0	3.0
Total	2.0	4.0	7.0	10.0	15.0
Foreign material	0.4	0.7	1.3	3.0	5.0
Shrunken and broken kernels	3.0	5.0	8.0	12.0	20.0
Total ^a	3.0	5.0	8.0	12.0	20.0
Wheat of other classes: ^b					
Contrasting classes	1.0	2.0	3.0	10.0	10.0
Total ^c	3.0	5.0	10.0	10.0	10.0
Stones	0.1	0.1	0.1	0.1	0.1
Maximum count limits of:					
Other material in 1 kg:					
Animal filth	1	1	1	1	1
Castor beans	1	1	1	1	1
Crotalaria seeds	2	2	2	2	2
Glass	0	0	0	0	0
Stones	3	3	3	3	3
Unknown foreign substances	3	3	3	3	3
Total ^d	4	4	4	4	4
Insect-damaged kernels in 100 g	31	31	31	31	31
U.S. Sample grade is Wheat that:					
(a) Does not meet the requirements for U.S. Nos. 1, 2, 3, 4, or 5; or					
(b) Has a musty, sour, or commercially objectionable foreign odor (except smut or garlic odor) or					
(c) Is heating or of distinctly low quality.					

^aIncludes damaged kernels (total), foreign material, shrunken and broken kernels

^bUnclassed wheat of any grade may contain not more than 10.0% of wheat of other classes

^cIncludes contrasting classes

^dIncludes any combination of animal filth, castor beans, crotalaria seeds, glass, stones, or unknown foreign substance

but it was related to flour protein content, which is associated with bread-baking quality. Grain *test weight* normally increases as grain is dried ([Table 2](#)).

Screenings are undersized grains, and admixture comprises impurities, e.g., chaff, weed seeds and earth, which must be removed before milling marketable flour. Screenings and admixture represent a loss to the miller, so a maximum of 2% is normally allowed (HGCA). A synonym of admixture is *foreign matter*, and these terms should not be confused with the term *dockage*. The latter refers to any non-wheat material that can be easily removed from grain, and that must be removed in order that the grain can be assigned the highest grade for which it qualifies.

Protein content is specified for all bakery flours. For most bread-making flour, wheat with protein content above 13% dry matter is preferred (HGCA). When wetted, during dough making, some of the proteins in wheat flour form a viscoelastic (see [Rheology in Agricultural Products and Foods](#)) substance called gluten. This can hold gas produced during fermentation and supports the starch and bran producing well-risen loafs. For most biscuits and cakes, gluten formation is not required; hence, much lower protein flours may be used.

Visual examination assesses grain for molds, like *Fusarium* (pink grains) and particularly ergot. Ergot is a disease of cereal crops and grasses caused by the fungus *Claviceps purpurea*. It causes reduced yield and quality of grain. Although the crop loss caused by this disease is important, the effect of the ergot's alkaloid toxins on man and animals is of much greater significance. Most of the sclerotia (ergot bodies) can be removed from ergoty grain with modern cleaning machinery, unless broken pieces are present or the sclerotia are similar in size to the grain (Mc Mullen and Stoltenow, [2002](#)). Ergot is a particular problem in durum wheat because semolina is not sifted, as flour is for bread, and ergot shows up as dark spots in the pasta. Apart from visual examination for molds, checks are made for live insects and grain damaged by insects. Grain is also assessed for unusual odors; "mustiness" or "chemical" odors indicate storage problems.

Quality of Agricultural Products in Relation to Physical Conditions, Table 2 Test weight variation due to moisture content (Hellevang, [\[1995\]](#))

Grain	Moisture content (%)	Test weight (kg/hL) ^a
Wheat	11.5	79.2
	13.5	77.4
	15.5	75.6
Corn	13.5	73.9
	15.5	72.2
	17.5	70.5

^aOriginal values in lb/bu. Conversion factors applied: 1 lb = 0.454 kg; 1 U.S. bu = 35.24 L

The Hagberg Falling Number (HFN) is an internationally recognized measure that allows the indirect determination of α -amylase activity (α -amylases are enzymes that decompose starch). This activity may become excessive if germinated grains are present. The laboratory measurement of HFN aims to measure the viscosity of a mixture of ground wheat and water, placed in a bain-marie at 100°C. Low values for HFN (below 120 s) mean excessive levels of α -amylase, hence excessive activity, causing loaves to be discolored, sticky, and of poor resilience and texture (see [Rheology in Agricultural Products and Foods](#)). The ideal level of activity is between 180 s and 250 s (GeotraceAgri project, [2003](#)). Wheat grains whose α -amylase activity is too high do not suit bakery use and rather should be used for animal feeding.

In regards to durum wheat, Jiménez González ([1995](#)) pointed out the following quality criteria:

- Grain moisture content must be the lowest possible.
- Small grains are not valid for milling, due to the low endosperm/seed coat ratio.
- Grain size must be uniform.
- Germinated grains can yield pasta of bad cooking quality.

Rice

Rice, unlike most other cereals, is consumed as a whole grain. Therefore physical properties such as size, shape, uniformity, and general appearance are of utmost importance. A whole grain of rice, i.e., a grain of rice as it comes from the field after harvest (*paddy rice* or *rough rice*) has several constituent layers. More precisely defined, paddy rice is rice which has retained its husk after threshing (Codex Standard for Rice, [1995](#)). Only the outermost layer, the hull or husk, is removed to produce *husked rice*, more commonly known as *brown rice* or *cargo rice*. This process is the least damaging to the nutritional value of the rice and avoids the loss of nutrients that accompanies further processing. If brown rice is further milled to remove the bran and most of the germ, the result is a white rice, but also a rice that has lost many more nutrients. At this point, however, the rice is still unpolished, and it takes polishing to produce the white rice we are used to seeing. Polishing removes the aleurone layer of the grain, a layer filled with essential fats, to extend the shelf life of the product; polishing is important because fats in the aleurone layer, once exposed to air as a consequence of the previous stage in the refining process, are highly susceptible to oxidation. The drawback of the refining-polishing process is that the resulting white rice is largely bereft of its original nutrients (The George Mateljan Foundation, [2010](#)). To compensate the loss of nutrients, vitamins, minerals and specific amino acids may be added in conformity with the legislation of the country in which the rice is sold (Codex Standard for Rice, [1995](#)).

Because most rice is milled, the important physical properties are determined primarily by the milled endosperm. Several components of rice quality largely

determine market price and consumer acceptance. Milling yield is one of the most important criteria of rice quality. Two values of rice milling yield are *whole-grain yield* and *total* (whole plus broken) *milling yield*. Broken rice is generally valued at only 30–50% of whole grain (Mutters, 2003). Physical characteristics of rice considered important by the quality standards for rice in force in Japan include:

- The number of whole grains (damaged, opaque, immature, foreign matter)
- The number of damaged grains (germinated, diseased, insect-damaged, cracked grains, malformed)
- Morphology parameters (periderm thickness, filling status, softness, uniformity of grain size, shape, luster, abrasion, white core, white belly)

The second major criterion of quality in Japanese standards for rice is taste. Good eating quality relates to high stickiness, sweet flavor, gloss of cooked rice, and palatability.

Barley

There are two main types of barley: six-row and two-row. Generally, two-row barley has lower enzyme content, less protein, more starch, and a thinner husk than six-row barley (Goldammer, 2008). These characteristics make two-row barley the preferred one for brewing in most countries. However, six-row barley outperforms its two-row counterpart as to enzymes content. In those breweries or elaborations where *adjuncts* – corn and rice – are used in the elaboration process, six-row barley is preferred, since in this case a highest amount of enzymes is required. Brewing exclusively from barley produces strong-flavored beers, whereas blending with some percentage of rice or corn makes beer “lighter,” but more refreshing.

The brewing process begins at the malthouse. In these facilities, after cleaning the grain, the kernels are steeped to make them germinate. At a certain moment, germination is stopped by drying the grains (*kilning*), then the tiny sprouts developed at germination are removed. The produce obtained, *malted barley*, is the raw material for the breweries and differs from raw barley in that the original starch in the barley grain has suffered some amount of degradation by enzymes; in technical language it is said that the starch has been *modified*.

Correct harvesting of barley is critical to maximize both yield and quality. Grain that is overthreshed causing cracking and *skinning* will have poor viability and result in low malt extract as well as increased risk of microbial infection when malted. Maltsters and brewers require grain that is free from skinning. The presence of a complete husk on barley protects the embryo during handling (the embryo must be protected because it is the agent in charge of converting the barley into malt), retains the modified starch within a parcel, and is used as a filtration aid during brewing (Department of Agriculture and Food, Government of Western Australia, 2006).

The maltster wants little nitrogen in the barley because excessive proteins in the grain prolong the process of malting, making it more difficult and more expensive. Not only that, but excessive of protein in beer reduces both the quality and shelf life of the beer (Holder, 2002). For example, chill haze in beer is partly caused by excessive protein content. The brewer has to adopt a trade-off between reducing protein content to improve colloidal stability, i.e., preventing haze development, and affecting fermentation and beer quality (if the protein content is too low, the yeasts in charge of the alcoholic fermentation will not work well, and on the other hand, the “mouthfeel” of the beer will negatively be affected). Barley growers know that fertilizing the crop too much nitrogen can increase protein beyond levels acceptable to the malting industry’s standards.

The maltster wants barley varieties characterized by rapid and synchronous germination of the grains. An important quality test undertaken by maltsters upon reception of a lot of barley is the germinative capacity test. A highest germination capacity is crucial since only germinated grain will produce malted grain. The ideal germination capacity is of 100%. In practice, a minimum germination capacity of 95% is required for a grain delivery to be accepted.

Grain size is a term used to describe a morphological character (see *Grains, Aerodynamic and Geometric Features*) of barley grain. Large grain will usually provide a higher level of starch with a decreased level of protein (Fox et al., 2006). On the other hand, although barley varieties with small grains can provide satisfactory malting quality, these varieties risk producing commercially unacceptable levels of small grain and thereby reduce the chance for barley growers to meet malt barley specifications (Fox et al., 2006). Finally, varieties exhibiting varying grain size within a delivery can cause uneven malt modification.

Fruits and vegetables

Fruits and vegetables are irreplaceable in a wholesome diet. They constitute a fabulous source of vitamins, minerals, and dietary fiber (non-starch polysaccharides). The assortment of horticultural produce is enormous. There are green leafy vegetables as lettuce, spinach, and kale; bulb vegetables as onion, garlic and leek, root vegetables as carrot and turnip, flower vegetables as cauliflower and broccoli; stem vegetables as celery and asparagus; fruit vegetables as pepper, melon, watermelon, zucchini (courgette, marrow), cucumber, pumpkin, and aubergine (eggplant); tropical fruits as mango and papaya; sweet fruits of temperate areas like plums and apricots; berries, etc. There are also tree nuts and mushrooms – strictly speaking the latter are not plants – they belong to the Kingdom Fungi. In the last decade, some sweet fruits of temperate areas like kiwifruit or persimmon have experimented notable production increase. From a worldwide economic point of view, some of the more relevant fruits and

vegetables are apples, peaches, citrus fruits (orange, tangerine, lemon, grapefruit), potato, and tomato, and in following sections we focus on them.

Fruits and vegetables marketing standards establish the main quality criteria that fresh-market products have to meet. The European Communities (EC) Commission Regulation 1221/2008 provides a *general marketing standard* for 26 products, namely, apricots, artichokes, asparagus, aubergines, avocadoes, beans, Brussels sprouts, carrots, cauliflowers, cherries, zucchini, cucumbers, cultivated mushrooms, garlic, hazelnuts in shell, headed cabbage, leeks, melons, onions, peas, plums, ribbed celery, spinach, walnuts in shell, watermelons, and chicory. The foregoing Regulation also provides specific marketing standards for the ten most traded products in the European Union, namely, citruses, apples, pears, kiwifruits, lettuces, peaches and nectarines, tomatoes, strawberries, sweet peppers, and table grapes.

Now let us take one of the specific quality standards, e.g., that for kiwifruit, for examining some aspect of it. The marketing standard for kiwifruits (EC Commission Regulation 1221/2008) includes *minimum maturity requirements* consisting of that the fruit must have attained a degree of ripeness:

- At packing stage within the region of production and the subsequent delivery by the packer, as well as at import and export stage, of at least 6.2°Brix or an average dry matter content of 15%
- At all other marketing stages (e.g., at the sale point), of at least 9.5°Brix

The unit °Brix is a measure of sugar or soluble-solids content very much used for internal quality assessment of fruits. In the last few years, some packers have installed near-infrared spectrophotometers for online determination of fruit sugar content in their packinghouses (see [Nondestructive Measurements in Fruits](#)). This new capability is advertised by packers as *brix sensing*.

Apart from the minimum maturity requirements above-mentioned, the marketing standard for kiwifruits provides shape requirements for the fruits to be classified as *Extra class* or *Class I*. For qualifying *Extra class*, the ratio of the minimum/maximum diameter of the fruit, measured at the equatorial section, must be 0.8 or greater, while for qualifying *Class I*, the ratio must be 0.7 or greater. This means that a kiwifruit of *Extra class* has to present a rather round cross section. Three dimensionally considered kiwifruits feature a maximum length axis, called polar axis, plus an intermediate and a minimum length axis, the two latter contained in the fruit cross section. In the ideal case of a fruit featuring a perfect circular section, the major and minor axis of the equatorial section would coincide. If a kiwifruit has a ratio smaller than 0.7, it means that its cross section is rather elliptical or flattened, i.e., the fruit has an “ugly” shape. Finally, the marketing standard for kiwifruits includes provisions concerning the sizing of the fruits. Sizing means sorting by size, and the size of kiwifruits is determined by the

fruit weight. Likewise, for some other produce, e.g., lettuce, the size is determined by the weight of one unit; nevertheless, for other products such as citrus fruits, size is determined by the maximum diameter of the equatorial section.

The *minimum quality requirements* of the EC *general marketing standard* establish that the products shall be:

- Intact
- Sound; products affected by rotting or deterioration such as to make them unfit for consumption are excluded
- Clean, practically free of any visible foreign matter
- Practically free from pests
- Practically free from damage caused by pests affecting the flesh
- Free of abnormal external moisture
- Free of any foreign smell and/or taste

In each batch the standard allows a tolerance of 10% by number or weight of product not satisfying the foregoing *minimum quality requirements*. This tolerance does not, however, cover product affected by rotting or any other deterioration rendering it unfit for consumption. Unlike the specific marketing standards for the above-mentioned group of ten products, the EC *general marketing standard* does not include provisions concerning sizing or shape. It seems that this decision pursues that *off-size* and *off-shape* fruits can be dispatched to fresh market instead of being classified as culls and destined for processing or animal feeding. The advantage of diverting these “ugly” fruits to the fresh market is that their price should accordingly be lower, and this is good in the present world economic conjuncture of crisis.

Apparently trivial physical properties may have a definite effect on the quality of the end product. For example, from the wine-making point of view, grape berry has three major types of tissue: flesh, skin, and seed, with the sheer bulk of wine being derived from the flesh. These tissues vary considerably in composition, and therefore by extension, they contribute differently to overall wine composition. Because of this, the composition of wine can be manipulated by simply changing berry size. As a general rule, wines made from smaller berries will have a higher proportion of skin and seed derived compounds (Kennedy, 2002).

Most consumers prefer seedless fruits. Throughout the years, plant breeders have selected seedless tangerines, grapes, and watermelons. To meet consumer expectations, it is important that fruit labeled as *seedless* is effectively free of seeds. Nowadays, there is X-ray and magnetic resonance imaging (MRI)-based methods (see [Nondestructive Measurements in Fruits](#)) that allow detecting if a tangerine contains seeds. Sometimes, the production of a seedless variety carries problematic “side effects.” This has occurred with seedless watermelons, where some fruits develop an internal void, while this defect is less frequent in the traditional seeded watermelon.

Apples and peaches

Physiological disorders are abnormalities of the fruit that are not associated with diseases or insect pests. They can appear during the growing season or after harvest during storage, and affect the appearance and usability of the fruit. Some physiological disorders affecting apples are watercore, sunburn (sunscald), scald (common scald or superficial scald), bitter pit, internal browning (brown heart), and mealiness. Among them, bitter pit and mealiness are probably the best known by most consumers. Bitter pit reduces the fresh-market quality of fruit. It is recognized as an abiotic disorder found in all areas of the world where apples are grown. Bitter pit is influenced by climate and orchard cultural practices. Symptoms consist of small brown lesions of 2–10 mm in diameter in the flesh of the fruit. The tissue below the skin becomes dark and corky. Cultural practices that reduce the incidence of bitter pit are annual bearing, moderate tree vigor, smaller fruit size, calcium sprays, summer pruning, and harvesting mature fruit (Andris et al., 2002).

Horticultural produce must be stored under refrigeration to maintain freshness and reduce decay development. However, low-temperature disorders, chilling injury classified as internal breakdown, limit the storage life of produce under refrigeration. According to Lurie and Crisosto, (2005), chilling injury in peaches and nectarines manifests itself as fruit that are dry and have a mealy or woolly texture (mealiness or woolliness), or hard-textured fruit with no juice (leatheriness), fruit with flesh or pit cavity browning (internal browning), or with flesh bleeding (internal reddening). These authors mentioned a “killing temperature zone” comprehended between 2.2°C and 7.6°C, which must be avoided. Peach maximum storage life can be achieved near or below 0°C, depending on the soluble solids content of the fruit.

Two well-known textural disorders, mealiness in apples and wooliness in peaches and nectarines, diminish the quality of affected fruit in the fresh market. Both disorders share a lack of juiciness that is perceived when the fruit is chewed, and both of them are negative textural attributes because consumers systematically dislike them. According to Arana et al. (2004), there is a correlation between firmness and juiciness in apple, and this explains why firm apples are usually not mealy. The foregoing correlation makes mealiness detection based on firmness measurement feasible. Firmness (see *Fruits, Mechanical Properties and Bruise Susceptibility*) is one of the aspects of vegetable tissue texture. When a consumer bites a firm apple, the pressure of his teeth breaks cell walls, releasing juice. Nevertheless, when a soft apple is chewed, the pressure exerted by the teeth deforms instead of breaking the cell walls of the apple flesh tissue, and no juice is released, implying that it is a mealy apple.

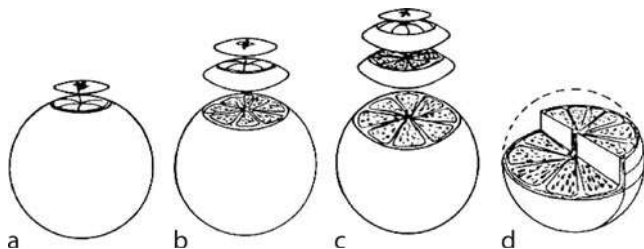
Citrus fruits

We can highlight three physiological disorders affecting citrus fruits: freeze damage as a potential accident in all

citrus species, puffiness in tangerines, and sheepnosing in grapefruit.

The symptoms of freeze injury are principally due to membrane damage. This applies to both the tough carpillary membranes around the individual segments, to the very frail vesicular membranes of the juice sacs, and of the individual cells within the juice sacs (Miller et al., 2006). Initially, frozen areas within the fruit tend to be wet and mushy with the normal radial arrangement of the segment membranes distorted by the action of the formation of ice crystals. At this stage, frozen fruit cannot be mechanically separated from sound fruit. The injured portions dry out within 4–5 weeks. A completely frozen fruit never shrivels because there is no membrane to be pulled inward (see *Shrinkage and Swelling Phenomena in Agricultural Products*). The water diffuses to the outside leaving hollow dried up areas within apparently sound fruit (see *Water Effects on Physical Properties of Raw Materials and Foods*). The severity of the freeze damage is determined by the total volume of desiccated or mushy tissue, following the procedure shown in Figure 1. Lorena Falcone Ferreyra et al. (2006) studied the effect of freeze injury on carbohydrate metabolism and fruit quality in Valencia oranges. They suggested that freezing temperatures provoke a notable metabolic switch in citrus fruit toward a fermentative stage, resulting in low-quality fruits.

Puffiness, also known as “floating skin” or “floating peel,” is a weakening and disintegration of the albedo tissues which is characteristic of mature tangerines. The rind becomes thick and separates from the pulp (segments), creating an air gap between the peel and the segments. Floating skin makes the fruit very susceptible to damage during picking and packing, due to punctures and fissures around the calyx. This can cause severe harvest and



Quality of Agricultural Products in Relation to Physical Conditions, Figure 1 To evaluate freeze damage in oranges, first cut a thin slice off the stem to expose the flesh (a). Then remove a 0.64 cm slice and examine the orange (b). If damage does not extend below this 0.64 cm slice, the fruit automatically grades No. 1 as far as internal quality is concerned. If some damage is noted, make another 0.64 cm cut (c), and depending on the extent of the damage noted, the fruit is graded No. 1 or No. 2. Additional cuts may be made as needed to determine the full extent of damage-down to the middle of the orange (d) and, in some cases, even lower. Inspectors must balance the area of damage with its depth. A 10% tolerance is allowed on fruit graded for the fresh market. Oranges for concentrate must be “wholesome.” (Miller et al., [2006]).

postharvest losses. Moreover, there are some markets, paradigmatically in Japan, where puffy tangerines are not acceptable. In these markets, the detection of a single puffy tangerine usually carries the rejection of the whole carton, and even of the whole pallet. Nowadays, it is technically feasible to detect puffy tangerines using techniques such as X-ray computer vision, MRI, or mechanical firmness assessment (see *Nondestructive Measurements in Fruits*). Occurrence of puffiness in some tangerine varieties is a usual phenomenon; in fact, this peel alteration can affect up to 50% of harvested fruit under the worst conditions (Gutiérrez et al., 1999).

Misshapen, sheepnosed fruit is consistently among the top five causes of fruit elimination at the packinghouse (Ritenour et al., 2003). Sheepnosing, or stem-end taper, is often associated with thick, puffy, or coarse rinds of relatively large fruit. Figure 2 shows some typical sheepnosed or pear-shaped grapefruits. Online detection of misshapen grapefruit at the packinghouse is possible using machine vision technology, i.e., with one or more video cameras that inspect the fruits (see *Image Analysis in Agrophysics*).

Finally, it is important to remark that consumers consider “easy-to-peel” as a quality attribute of utmost importance for tangerines.

Tomato

Tomatoes are consumed both fresh and in various processed foods, with more than 65% of the world tomato production being processed (Moraru et al., 2004). The most relevant quality attributes of tomatoes vary depending on their intended use: taste, appearance, color, and handling characteristics are crucial for fresh-market



Quality of Agricultural Products in Relation to Physical Conditions, Figure 2 Picture taken in a citrus packinghouse in Florida (USA), in 2003. The fruit handled on the date was red grapefruit. Note the defect known as “sheepnosing” or pear-shaped grapefruit in the fruits picked off the roller conveyor. Only the far-right grapefruit is of correct shape.

tomatoes; viscosity and soluble solids content are the most important attributes for triturated or sauce-processing tomatoes (Schuch and Bird, 1994); firmness and skin resistance are the most relevant properties in quality characterization of whole-peeled canned tomatoes (Arazuri et al., 2007). Depending on their industrial use, tomato varieties are classified into two groups: peeled and concentrated varieties. Peeled tomato requires oblong-shape varieties and high quality tomatoes with total absence of mechanical damages. Tomato processing companies are interested in developing varieties which carry oblong, almost square-shaped fruit, in order to pack them more efficiently. For example, some companies might be interested in developing extremely elongated tomatoes shaped like cucumbers. These fruits would be very advantageous when preparing sliced tomatoes for hamburgers, as less ends would have to be thrown away. For the larger fresh-market slicing tomatoes, the ideal is a high locule number (van der Knaap and Tanksley, 2003).

Potato

Physiologically mature potato tubers have high starch and protein levels and low respiration, water content, and sugar levels. Carbohydrates content of tubers can reach 85% of dry matter. Starch content represents usually over 95% of carbohydrates. At harvest, the content of reducing sugars (glucose, fructose) is usually very low (about 0.5%), but it increases during storage, depending on temperature conditions and mechanical damage (impacts, injuries, etc.) suffered by the tuber.

French fries manufacturers prefer long-oval or long tuber with a length of at least 50 mm. For the production of crisps (chips), round tubers are required with a diameter range of 40–60 mm. Potato varieties for frying must absorb little oil, show golden color, and have a crisp and firm texture. If the dry matter content (Table 3) is too low, the French fries or crisps will be too soft or too wet, whereas if it is too high, the French fries will be too hard and dry and the crisps too brittle. Chip color is a very important factor in determining consumer acceptability of potato chips or crisps. The browning of chips is primarily the result of the Maillard reaction which occurs between reducing sugars and amino compounds during

Quality of Agricultural Products in Relation to Physical Conditions, Table 3 Quality requirements for processing potatoes (Netherlands Potato Consultative Foundation [NIVAP Holland])

End product	Dry matter content (%)	Maximum reducing sugars content (% of fresh weight)
French fries	20–24	0.5
Potato chips or crisps	22–24	0.3
Dehydrated potato products (flakes, granules, flour)	>21	0.3

the frying operation at high oil temperature, with the amount of reducing sugars being the limiting factor.

The sugar content in potato tubers depend on many factors, both hereditary and environmental. Tubers of most chipping cultivars stored at temperatures below 9°C for sprouting control accumulate appreciable amounts of reducing sugars. These sugars are the result of starch hydrolysis. Due to the low respiration rate associated to the low storage temperature, sugars are not oxidized ("burned"), resulting in potatoes with a sweet taste. High sugar concentrations in the tubers result in an objectionable sweet flavor in baked or boiled potatoes and result in dark colored chips and French fries. The dark product in fried products is also bitter-tasting. Potatoes that are destined for use as chips or fries are usually taken from cold storage and reconditioned at 12–16°C for a period of 1–2 weeks to reduce the sugar level and make the potatoes satisfactory for processing. The effect of a warmer storage temperature is that sugars are oxidized at a higher rate compared to cold storage conditions.

Potatoes can present several internal defects, like hollow heart, internal discoloration, and "greening." Hollow heart (an irregular hole at the center of the tuber) is caused by excessively rapid growth. Internal discoloration may be caused by improper field or storage conditions, freezing or disease; each causes a different type of discoloration. Potatoes with severe internal discoloration should not be eaten. After harvest, potatoes should be kept away from natural or artificial light because exposure to light causes a green coloring – "greening" – to the tubers. Sometimes only the skin is affected, but greening may penetrate the flesh. The green portions contain the alkaloid *solanin*, which causes a bitter flavor and may have a poisonous effect when consumed in great quantities.

Summary

Grain and horticultural produce are irreplaceable in human nourishment. According to the opinion of some scientists, for a reasonable utilization of the planet resources we should be as vegetarian as possible. Eating beef is little efficient, as a bovid transforms into protein only the 5% of the protein it consumes. Chickens are more efficient, since their protein conversion rate is of 25%. From this point of view, it seems more reasonable to consume the vegetables directly. This does not imply that livestock industry should disappear since livestock provides us with products such as wool, milk, eggs, etc., which are of great nutritional interest and cannot be obtained from plants.

Although crucial vegetal foods in human nourishment as legumes and oilseeds have not been addressed here, some ideas have been presented on quality of emblematic grain and horticultural produce. An interesting reflection is that the quality of a product depends on the intended use. With the purpose of protecting public health and guaranteeing trade transparency, official organisms dictate quality or marketing standards for agricultural products.

Bibliography

- Andris, H., Mitcham, B., and Crisosto, C. H., 2002. *Fruit Physiological Disorders: Apples*. Davis, CA: University of California, Postharvest Technology Research and Information Center (available at <http://postharvest.ucdavis.edu/Produce/Disorders/apple/pdapbit.shtml>), accessed January 9th 2010.
- Arana, I., Jarén, C., and Arazuri, S., 2004. Apple mealiness detection by non-destructive mechanical impact. *Journal of Food Engineering*, **62**, 399–408.
- Arazuri, S., Jarén, C., Arana, J. I., and Pérez de Ciriza, J. J., 2007. Influence of mechanical harvest on the physical properties of processing tomato (*Lycopersicum esculentum* Mill.). *Journal of Food Engineering*, **80**, 190–198.
- Codex Alimentarius, Codex Standard for Rice, CODEX STAN 198-1995. FAO and WHO.
- Commission Regulation (EC) No 1221/2008, of 5 December 2008. Official Journal of the European Union L 336 of 13 December 2008.
- Department of Agriculture and Food, Government of Western Australia, 2006. Barley harvest damage: colour, protein, size. Available at: http://www.agric.wa.gov.au/PC_92002.html?s=1001. Accessed January 9th 2010.
- FAO, 1995. Sorghum and millets in human nutrition. Available at: <http://www.fao.org/docrep/t0818e/T0818E01.htm>. Accessed January 9th 2010.
- Farrer, D., Weisz, R., Heiniger, R., Murphy, J. P., and Pate, M. H., 2006. Delayed harvest effect on soft red winter wheat in the southeastern USA. *Agronomy Journal*, **98**, 588–595.
- Fox, G. P., Kelly, A., Poulsen, D., Inkerman, A., and Henry, R., 2006. Selecting for increased barley grain size. *Journal of Cereal Science*, **43**, 198–208.
- GeotraceAgri/IST Project 2001-34281, 2003. Indicator on Hagberg Falling Number determination. Available at: http://www.geotraceagri.net/proto/gta_lux1_en.php. Accessed January 9th 2010.
- Goldammer, T., 2008. *The Brewer's Handbook*, 2nd edn. Clifton, VA: Apex.
- Gutiérrez, A., Ramos, P., and Moltó, E., 1999. Desarrollo de una máquina para la detección de mandarinas bufadas basada en sensores de firmeza (Development of a machine for the detection of puffy tangerines based on firmness sensors). *Actas de Horticultura*, **27**, 67–72. Sociedad Española de Ciencias Hortícolas.
- Hellevang, K. J., 1995. *Grain Moisture Content Effects and Management*. Fargo, ND: North Dakota State University, Agriculture and University Extension (available at <http://www.ag.ndsu.edu/pubs/plantsci/crops/ae905w.htm>), accessed January 9th 2010.
- HGCA. Milling wheat quality criteria and tests. Available at: http://www.hgca.com/publications/documents/varieties/milling_wheat.pdf. Accessed January 9th 2010.
- Holder, J. D., 2002. *The Science Behind the Brew: The Biology of the Malting and Mashing Processes Used in Brewing Beer*. J. Holder, (available at <http://technocosm.org/brew/brewout.html>), accessed January 9th 2010.
- ISO 9000:2005. Quality management systems – Fundamentals and vocabulary.
- Jiménez González, A. T., 1995. Milling process of durum wheat. In di Fonzo, N., Kaan, F., and Nachit, M. (eds.), *Durum Wheat Quality in the Mediterranean Region*. Zaragoza: CIHEAM-IAMZ, pp. 43–51.
- Kennedy, J., 2002. Understanding grape berry development. Practical Winery and Vineyard, July/Aug: 14–18.
- Lorena Falcone Ferreyra, M., Perotti, V., Figueiroa, C. M., Garrán, S., Anderson, P. C., Vázquez, D., Iglesias, A. A., and Podestá, F. E., 2006. Carbohydrate metabolism and fruit quality are affected in

- frost-exposed Valencia orange fruit. *Physiologia Plantarum*, **128**, 224–236.
- Lurie, S., and Crisosto, C. H., 2005. Chilling injury in peach and nectarine (review). *Postharvest Biology and Technology*, **37**, 195–208.
- Mc Mullen, M., and Stoltenow, C., 2002. Ergot. Fargo, ND: North Dakota State University, Agriculture and University Extension (available at <http://www.ag.ndsu.edu/pubs/plantsci/crops/pp551w.htm>), accessed January 9th 2010.
- Miller, W. M., Wardowski, W. F., and Grierson, W., 2006. Separation and grading of freeze-damaged fruit. In Wardowski, W. F., Miller, W. M., Hall, D. J., and Grierson, W. (eds.), *Fresh Citrus Fruits*. Longboat Key, FL: Florida Science Source, pp. 299–306.
- Moraru, C., Logendra, L., Lee, T.-C., and Janes, H., 2004. Characteristics of 10 processing tomato cultivars grown hydroponically for the NASA Advanced Life Support (ALS) Program. *Journal of Food Composition and Analysis*, **17**, 141–154.
- Mutters, C., 2003. Rice quality. In *Rice quality workshop 2003* (available at <http://www.plantsciences.ucdavis.edu/ucceRice/QUALITY/rqw2003/C-1QualityConcepts2003.pdf>), accessed January 9th 2010.
- NIVAP Holland (Netherlands Potato Consultative Foundation). Tuber characteristics determining quality. Available at: http://www.nivaa.nl/uk/about_potatoes/agronomy/on_the_road_to_potato_processing/tuber_characteristics. Accessed August 26th 2010.
- Olson, E., and Warren, N. *Corn Wet Milling Lab*. Ottumwa, IA: Indian Hills Community College (available at <http://www.biolink.org/docs/corn.doc>), accessed January 9th 2010.
- Ritenour, M. A., Stover, E. W., and DuBois, M., 2003. Factors reducing fresh grapefruit packouts in Florida: can packouts be improved? *Proceedings of the Florida State Horticultural Society*, **116**, 219–223.
- Schuch, W., and Bird, C., 1994. Improving tomato fruit quality using bioscience. *Acta Horticulturae*, **376**, 75–80.
- Schuler, S. F., Bacon, R. K., Finney, P. L., and Gbur, E. E., 1995. Relationship of test weight and kernel properties to milling and baking quality in soft red winter wheat. *Crop Science*, **35**, 949–953.
- Sloof, M., Tijskens, L. M. M., and Wilkinson, E. C., 1996. Concepts for modelling the quality of perishable products (Review). *Trends in Food Science and Technology*, **7**, 165–171.
- The George Mateljan Foundation, 2010. Brown rice. Available at: <http://www.whfoods.com/genpage.php?tname=foodspice&id=128>. Accessed January 9th 2010.
- USDA. Grain Inspection, Packers and Stockyards Administration, 2006. United States Standards for Wheat.
- van der Knaap, E., and Tanksley, S. D., 2003. The making of a bell pepper-shaped tomato fruit: identification of loci controlling fruit morphology in yellow stuffer tomato. *Theoretical and Applied Genetics*, **107**, 139–147.

Cross-references

- Agrophysical Objects (Soils, Plants, Agricultural Products, and Foods)
- Drying of Agricultural Products
- Fruits, Mechanical Properties and Bruise Susceptibility
- Grains, Aerodynamic and Geometric Features
- Image Analysis in Agrophysics
- Mechanical Impacts at Harvest and After Harvest Technologies
- Nondestructive Measurements in Fruits
- Physical Phenomena and Properties Important for Storage of Agricultural Products
- Physical Properties of Raw Materials and Agricultural Products
- Rheology in Agricultural Products and Foods
- Shrinkage and Swelling Phenomena in Agricultural Products
- Water Effects on Physical Properties of Raw Materials and Foods

R

RADIATIVE PROPERTIES

See [Absorptivity](#); [Reflectivity](#); [Transmissivity](#)

RAINFALL INTERCEPTION BY CULTIVATED PLANTS

Józef Kołodziej

Department of Agrometeorology, University of Life Sciences, Lublin, Poland

Definition

Rainfall interception is a process of retention of rainwater by the plant cover. It is expressed in millimeters of water layer, similar to atmospheric precipitation, or as a percentage value in comparison to precipitation measured over open space. Water retention by abiotic objects (buildings, roots, etc.) is named *wetting*.

Introduction

The interception process is one of the phenomena of the hydrological-meteorological sequence in which permanent and periodically cultivated vegetation takes part. The vegetation affects the process of retention of rainwater that is mostly directly returned to the atmosphere through evaporation, and partly absorbed by plants, or flows along plant stems down to the ground. Rainfall interception investigations were concentrated mainly on tree and grass stands, ignoring seasonal crops, because of the significantly longer duration of tree and grass canopies during the annual hydrologic cycle (Savabi and Stott, 1994).

Rainfall interception

Methods of measurements

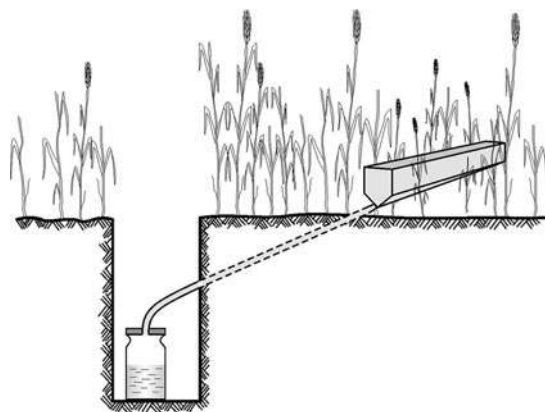
At the beginning of studies on rainfall interception by cultivated plants, measurements were carried out with the use of commonly used rain gauges placed among plants. Later, Stoltenberg and Wilson (1950) cut plants, weighed them, and then moistened and weighed them again. The difference in weight was a measure of water retention by plants. From the knowledge of the amount of plants on a given area, the retained rainfall was calculated. Kontorshchikov and Eremina (1963) cut plants in different growth stages and placed them in a vessel with a known amount of water. A decrease of water in the vessel, after removing the plants, was a measure of the amount of interception. In turn, Burg and Pomeroy (1958) measured the loss of water in a portable frame with grass, which was weighed before and after rain simulation.

Kołodziej and Orzeł (1978) used for interception investigations a drainpipe rain gauge of their own design, with dimensions 5 cm × 40 cm, matching the collecting surface of Hellmann's rain gauge (Figure 1). It enables the comparison of interception results with rainfall data made in open space. Its additional advantage is the possibility of making measurements during the whole vegetation period. Another type of device placed on soil with cultivated plants (Figure 2) was elaborated by Kołodziej and Orzeł (1978) for measuring the total amount of rain water coming to the surface of the ground.

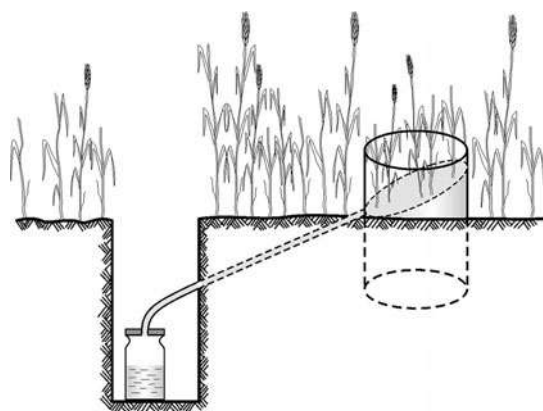
Results

An example of results of rainfall interception and the amount of water retained by various cereal plants during 8-year measurements is shown in Table 1.

The numbers of observations were different in the successive years of the study. They depended, among other



Rainfall Interception by Cultivated Plants, Figure 1 Drainpipe rain gauge for direct measurement of rainfall reaching ground surface inside plant canopy (Kołodziej and Orzeł, 1978).



Rainfall Interception by Cultivated Plants, Figure 2 Rain gauge for direct measurement of rainfall and water flowing down the stems to the surface of the ground (Kołodziej and Orzeł, 1978).

things, on the frequency of atmospheric precipitation and were characterized by the following values: under spring barley – from 51 to 77 days, under winter wheat – from 92 to 97 days, and under winter rye – from 91 to 97 days.

The rate of rainfall interception in the canopy of cultivated plants depends on the level of precipitation, its intensity and duration, on the kind of vegetation, its height, development stage, and its ground coverage. The rate of interception is negatively correlated with precipitation measured on the open space. During the most intensive growth and foliation of plants precipitation from 0.1 to 5.0 mm undergoes nearly total interception, but at higher levels the precipitation is intercepted only partly. A positive correlation is observed between the rate of interception and the height of vegetation. The dependence curve between chosen meteorological elements (amount, duration and intensity of precipitation, and also wind speed and evaporation) and the amount of interception has a logarithmic form and tends asymptotically to the final value of interception.

Among the cereals, the highest dependence of interception on the precipitation duration was found for spring barley. Leaf area and area of whole plant and also condensation on the unit surface affect the highest interception. At leaf area index (LAI) equal to 20, the mean value of rainfall interception during the whole vegetation seasons of 1977–2005 is directed to 33% for winter rye, 38% for winter wheat, and 36% for spring barley. How plant development stage affects rainfall interception by two different cereals is shown on the example of winter rye, where it is the highest from shooting to heading, and of spring barley – from heading to dough maturity. Such differences are due to differences in their morphological structure, canopy density, position of leaf angle, length of internodes, and time of drying up of the lowest leaf blades. A part (about 7%) of retained water is absorbed through plant stomata or flows down along the stems to soil surface, and the rest evaporates back to the atmosphere (Kołodziej et al., 1979, 1992, 2005; Kołodziej and Liniewicz, 1992, 1994; Bednarek et al., 2000).

Rainfall Interception by Cultivated Plants, Table 1 Mean values of rainfall interception and amount of water retained by various cereal plants during 8-year (1987–1995) measurements. Felin Agrometeorological Observatory, Lublin, Poland (Kołodziej et al., 2005)

Years	Spring barley		Winter wheat		Winter rye	
	Interception (%)	Amount of water (mm)	Interception (%)	Amount of water (mm)	Interception (%)	Amount of water (mm)
1987	45.6	39.3	37.4	65.2	30.1	48.7
1988	30.6	59.0	31.8	73.3	35.4	81.6
1989	34.4	54.1	35.3	74.4	38.6	81.2
1990	29.4	43.1	33.9	53.4	22.4	35.3
1991	41.0	51.2	37.7	74.5	23.8	48.6
1992	39.3	32.1	26.6	30.0	17.7	20.0
1993	30.2	48.0	26.4	42.2	29.9	53.1
1994	36.5	46.1	19.7	5.2	12.2	10.8
1995	17.8	19.6	42.1	58.0	34.6	47.7
Mean	33.1	43.6	33.8	52.9	28.9	47.5

On the basis of results from field experiments, prognostic mathematical models of rainfall interception for various cultivated plants in their stages of growth and development were elaborated (Wigneron et al., 1996; Kozak et al., 2007; Lorens and Domingo, 2007; Muzylo et al., 2009).

Conclusion

Rainfall interception is one of the most important elements in water budget of cultivated field. During the vegetative season, it can be in the range of 30–40%.

Bibliography

- Bednarek, H., Kołodziej, J., and Liniewicz, K., 2000. Selected features of interceptions of atmospheric precipitation in canopy of some arable crops (in Polish). *Acta Agrophysica*, **4**, 19–28.
- Burgy, R. H., and Pomeroy, C. R., 1958. Interception losses in grassy vegetation. *Transactions American Geographical Union*, **39**, 1095–1100.
- Kołodziej, J., and Liniewicz, K., 1992. Methods of measuring the interception in stands of cultivated plants. *Zeszyty Problemowe Postępów Nauk Rolniczych*, **398**, 101–106.
- Kołodziej, J., and Liniewicz, K., 1994. Interception of atmospheric rainfalls in the canopies of cultivated plants versus field water utilization of plants (1992–1994) (in Polish). *Annales University Mariae Curie-Skłodowska, Poland*. Vol. XLIX suppl.14, sec.E.: 107–114.
- Kołodziej, J., and Orzeł, W., 1978. Investigations on the methods of measuring rainfall interception in canopy of cultivated plants (in Polish, 20). *Folia Societatis Scientiarum Lublinensis*, **20** (Geogr. 2), 75–82.
- Kołodziej, J., Liniewicz, K., and Orzeł, W., 1979. Investigations into the relationship between the amount of precipitation, the precipitation interception, and the moisture of the soil under cultivated plants. *Zeszyty Problemowe Postępów Nauk Rolniczych*, **220**, 191–202.
- Kołodziej, J., Liniewicz, K., and Sadza-Monge, A., 1992. Interception of atmospheric precipitation in stands of cultivated plants. *Zeszyty Problemowe Postępów Nauk Rolniczych*, **398**, 107–111.
- Kołodziej, J., Liniewicz, K., and Bednarek, H., 2005. Rainfall interception in cereal fields (in Polish). *Acta Agrophysica*, **6**, 381–391.
- Kontorshikov, A. S., and Eremina, K. A., 1963. Interception of precipitation by spring wheat during the growing season. *Soviet Hydrology*, **2**, 400–409.
- Kozak, J. A., Ahuja, L. R., Green, T. R., and Ma, L., 2007. Modeling crop canopy and residue rainfall interception effects on soil hydrological components for semiarid agriculture. *Hydrological Processes*, **21**, 220–241.
- Lorens, P., and Domingo, F., 2007. Rainfall partitioning by vegetation under Mediterranean conditions. A review of studies in Europe. *Journal of Hydrology*, **335**, 37–54.
- Muzylo, A., Lorens, P., Valente, F., Keizer, J. J., Domingo, F., and Gash, J. H. C., 2009. A review of rainfall interception modelling. *Journal of Hydrology*, **370**, 191–206.
- Savabi, M. R., and Stott, D. E., 1994. Plant residue impact on rainfall interception. *Transactions of the ASAE*, **37**, 1093–1098.
- Stoltenberg, N. L., and Wilson, T. V., 1950. Interception storage of rainfall by corn plants. *Transactions American Geographical Union*, **31**, 443–448.
- Wigneron, J.-P., Calvet, J.-Ch., and Kerr, Y., 1996. Monitoring water interception by crop field from passive microwave observations. *Agricultural and Forest Meteorology*, **80**, 177–194.

Cross-references

- Infiltration in Soils
Irrigation and Drainage, Advantages and Disadvantages
Physics of Near Ground Atmosphere
Plant–Soil Interactions, Modeling
Soil–Plant–Atmosphere Continuum
Water Balance in Terrestrial Ecosystems

RAINFALL WATER USE EFFICIENCY

See *Water Use Efficiency in Agriculture: Opportunities for Improvement*

RAW MATERIALS

See *Physical Properties of Raw Materials and Agricultural Products*

REDOX POTENTIAL (E_h)

See *Oxidation-Reduction Reactions in the Environment*

REFLECTIVITY

Reflected part of incoming radiation/total incoming radiation.

REMOTE SENSING OF SOILS AND PLANTS IMAGERY

Ramsis B. Salama
Managed Water Resources, Ocean Reef, Australia

Definitions

Remote sensing can be defined as the study of make observations, take measurements, and produce images of phenomena that are beyond the limits of our own senses and capabilities without making actual contact with the object of study. It can also be defined as: Any of the technical disciplines for observing and measuring the Earth from a distance, “The acquisition and measurement of data/information on some property(ies) of a phenomenon, object, or material by a recording device including satellite imaging, Global Positioning Systems, Radar, Sonar and aerial photography which is not in physical or close contact with the feature(s) under surveillance” and generate digital or hard copy image data (Jensen, 2007, 2008; http://en.wikipedia.org/wiki/Remote_sensing).

Introduction

Remote sensing data are indispensable for measurement and evaluation of regional-to-global processes. Remote sensing is now widely used for collecting data, monitoring and studying the natural resources and environment conditions of the universe. Tens of new Earth-observing satellites and a larger number of airborne instruments are available for research. Instruments are better calibrated, more stable, and produce more channels of spectral data. An increasing number of instruments have capabilities that include imaging spectroscopy, multiple-view-angle, and/or multipolarization bands that can simultaneously capture information about the plants, soils, biochemistry of surface materials, and their structures. Use of remote sensing data is advancing from correlative studies to fundamental understanding of the physical variables and their interactions with electromagnetic radiation. This information is used in increasingly complex models to plan most of the activities of politicians, scientists, and human resources in all areas of agriculture and related environmental processes to assess ecosystem goods and services, and to evaluate sustainability of land use activities (Figure 1).

Remote sensing

Optical remote sensing makes use of visible, near-infrared, and shortwave infrared sensors to form images of the Earth's surface by detecting the solar radiation reflected from targets on the ground. Different materials reflect and absorb differently at variable wavelengths. Therefore, the targets can be differentiated by their spectral reflectance signatures in the remotely sensed

images. Remote sensing systems offer four basic components to measure and record data about an area from a distance.

- Energy source; electromagnetic energy is required to transmit information from the target to the sensor.
- As the energy travels from its source to the target, it will come in contact with and interact with the atmosphere it passes through.
- Once the energy makes its way to the target through the atmosphere, it interacts with the target depending on the properties of both the target and the radiation.
- After the energy has been scattered by, or emitted from the target, the energy is recorded by the sensor and transmitted electronically to a receiving and processing station where the data are processed into a hardcopy or digital image.

Quality of remote sensing data

The quality of remote sensing data consists of its spatial, spectral, radiometric, and temporal resolutions.

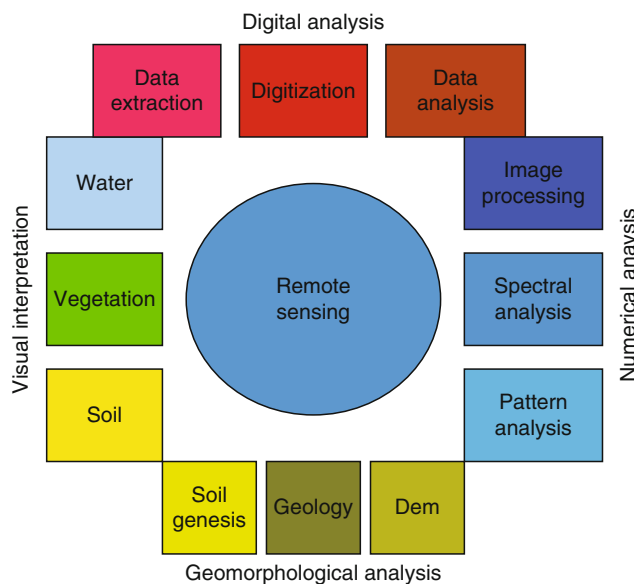
Spatial resolution

The size of a pixel that is recorded in a raster image – typically pixels may correspond to square areas ranging in side length from 1 to 1,000 m.

Spectral resolution

The number of different frequency bands recorded, this is equivalent to the number of sensors carried by the platform. Optical remote sensing systems are classified into the following types, depending on the number of spectral bands used in the imaging process: <http://www.crisp.nus.edu.sg/~research/tutorial/optical.htm>.

- Panchromatic imaging system:** Sensor is a single channel detector sensitive to radiation within a broad wavelength range. Examples of panchromatic imaging systems are: IKONOS PAN, SPOT HRV-PAN
- Multispectral imaging system:** Sensor is a multichannel detector with a few spectral bands. Each channel is sensitive to radiation within a narrow wavelength band. The resulting image is a multilayer image which contains both the brightness and spectral (color) information of the targets being observed. Examples of multispectral systems are: LANDSAT MSS, LANDSAT TM, SPOT HRV-XS, IKONOS MS
- Superspectral Imaging Systems:** A superspectral imaging sensor has many more spectral channels (typically >10) than a multispectral sensor. The bands have narrower bandwidths, enabling the finer spectral characteristics of the targets to be captured by the sensor. Examples of superspectral systems are: MODIS, MERIS
- Hyperspectral Imaging Systems:** Hyperspectral imaging system is also known as an “imaging spectrometer.” It acquires images in about a hundred or more contiguous spectral bands. The precise spectral information contained in a hyperspectral image enables better



Remote Sensing of Soils and Plants Imagery,
Figure 1 Remote sensing key components and inter-related areas (DEM = Digital Elevation Model).

characterization and identification of targets. Hyperspectral images have potential applications in such fields as precision agriculture (e.g., monitoring the types, health, moisture status, and maturity of crops), coastal management (e.g., monitoring of phytoplanktons, pollution, bathymetry changes). An example of a hyperspectral system is: Hyperion on EO1 satellite.

<http://www.crisp.nus.edu.sg/~research/tutorial/optical.htm>

Radiometric resolution

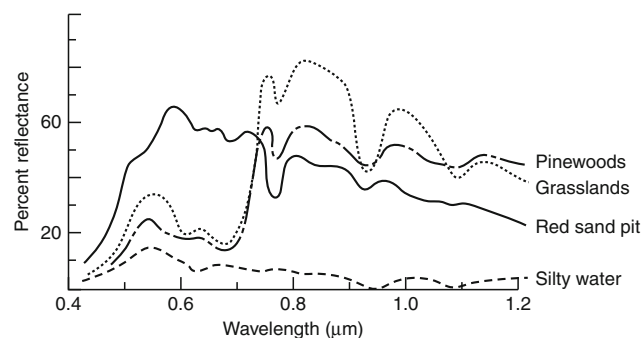
The number of different intensities of radiation the sensor is able to distinguish. Typically, this ranges from 8 to 14 bits, corresponding to 256 levels of the gray scale and up to 16,384 intensities or “shades” of color, in each band.

Temporal resolution

The frequency of flyovers by the satellite or plane, and is only relevant in time-series studies or those requiring an averaged or mosaic image as in deforesting monitoring. This was first used by the intelligence community where repeated coverage revealed changes in infrastructure, the deployment of units, or the modification/introduction of equipment. Cloud cover over a given area or object makes it necessary to repeat the collection of said location. http://en.wikipedia.org/wiki/Remote_sensing.

Electromagnetic spectrum: spectral signatures

For any given material, the amount of solar radiation that it reflects, absorbs, transmits, or emits varies with wavelength. When that amount (usually intensity, as a percent of maximum) coming from the material is plotted over a range of wavelengths, the connected points produce a curve called the material’s *spectral signature* (spectral response curve) http://en.wikipedia.org/wiki/Spectral_signature. This important property of matter makes it possible to identify different substances or classes and to separate them by their individual spectral signatures, as shown in Figure 2.



Remote Sensing of Soils and Plants Imagery, Figure 2 Spectral curves for Pine Wood, Grassland, Red Sand Pit, and Silty Water. (NASA remote sensing tutorial available at <http://rst.gsfc.nasa.gov> [accessed September 2009]).

Processing and classification of remotely sensed data; pattern recognition; approaches to data/image interpretation

Processing and classification of remote sensing system are to detect radiation signals, determine their spectral character, derive appropriate signatures, and inter-relate the spatial positions of the classes they represent. This ultimately leads to some type of interpretable display product, be it an image, a map, or a numerical data set, that mirrors the reality of the surface (affected by some atmospheric property [ies]) in terms of the nature and distribution of the features present in the field of view. The determination of these classes requires that either hard copy, i.e., images, or numerical data sets be available and capable of visual or automated analysis. http://rst.gsfc.nasa.gov/Intro/Part2_5a.html; http://rst.gsfc.nasa.gov/Intro/Part2_6.html.

There are several image processing techniques. Data from the several bands that are set up from spectral data in the visible and near-IR tend to be varyingly correlated for some classes. This correlation can be minimized by a reprocessing technique known as *Principal Components Analysis (PCA)*. New color images can be made from sets of three band ratios or three Principal Components. The color patterns will be different from natural or false color versions. Interpretation can be conducted either by visual means, using the viewer’s experience, and/or aided by automated interpretation programs, such as the many available in a computer-based Pattern Recognition procedure. A chief use of remote sensing data is the *classification* of the numerous features in a scene (usually presented as an image) into meaningful categories or classes. The image then becomes a *thematic map* (the theme is selectable, e.g., land use; geology; vegetation types; rainfall). This is done by creating an *unsupervised* classification when features are separated solely on their spectral properties and a *supervised* classification when we use some prior or acquired knowledge of the classes in a scene in setting up *training sites* to estimate and identify the spectral characteristics of each class http://rst.gsfc.nasa.gov/Intro/Part2_6.html.

Remote sensing for soils

Soil is a fundamental natural resource; it is the basis of human agriculture. Civilizations rise in regions blessed with fertile soil; they fall when humans fail to treat soil with respect. Further, soil plays an essential role in the biophysical and biogeochemical functioning of the planet. On continents, soil forms a porous boundary where the biosphere, hydrosphere, lithosphere, and atmosphere interact (Scull et al., 2003). Understanding the spatial distribution and management of soil is critical to maintain a productive society and to understand the complex balance of chemical and physical processes that make life possible on Earth.

Soil characteristics

Soil has properties that cause the ratio of near-infrared and visible red reflectance to plot in a linear fashion. This



Remote Sensing of Soils and Plants Imagery, Figure 3 Soil line, line of a bare field plot in a straight line when looking at the reflectance values of NIR vs. Red.

means that as light energy comes into contact with the individual soil particles, each particle will reflect a proportionately similar amount of near-infrared and red wavelengths. For very homogenous soils, this line may be very short and for soils that vary in type and moisture content, this line may be stretched significantly more. The soil line of the soil reflectance spectra characterizes the soil type, defines vegetation indices, and corrects the plant canopy reflectance from the optical soil property effects (Figure 3).

The line can be established by locating two or more patches of bare soil in the image having different reflectivities and finding the best fit line in spectral space. The soil line can also be calculated by the least-square regression method:

$$\text{NIR}(\text{soil}) = \alpha \text{RED}(\text{soil}) + \beta \quad (1)$$

where RED (Soil) = soil reflectance in the red band, NIR (soil) = soil reflectance in the near-infrared band, α , β = parameters of the soil line estimated by the least-square regression method. Other visible bands, such as green or blue ones, can be used instead of red ones.

Factors that influence soil reflectance in remote sensing

The properties of soils that govern their spectral reflectance are biogeochemical (mineral and organic) constituents, optical geometric scattering (particle size, aspect, roughness), and moisture conditions of the surface (Baumgardner et al., 1985; Irons et al., 1989; Ben-Dor et al., 1999).

(a) The mineral composition of soils affects the reflectance spectrum. Most soils exhibit increasing reflectance with wave length over the visible to NIR portion of the spectrum, since iron is fairly omnipresent (Mulders, 1987). Minerals with OH, CO_3 (Calcite), and SO_4 (gypsum) exhibit vibrational features

in the 1.8–2.5 μm region, while silicates with OH absorb near 1.4 and 2.2 μm (Baumgardner et al., 1985; Mulders, 1987).

- (b) Soil moisture has a strong influence on the amount and composition of reflected and emitted energies from a soil surface, and thus information about soil moisture condition can be derived from measurements in all parts of the electromagnetic spectrum. In the shortwave region, the major effect of adsorbed water on soil reflectance is a decrease in reflected energy, making soils darker when moistened, particularly in the water absorption bands centered at 1.45 and 1.9 μm (Reginato et al., 1977). The decrease in reflectance is proportional to the thickness of the water film around the soil particles and can be related to gravimetric water content as well as the energy status of the adsorbed water (Idso et al., 1975). Moisture of soil has an equal effect over the entire spectrum and the ratios between spectral bands such as red and near-infrared bands are independent of the soil moisture.
- (c) The presence of organic matter in the soil has been found to decrease the overall reflectance and result in decrease in the spectral contrast. Organic matter has a lower effect in the bands beyond 1.8 μm . Organic matter absorbs strongly in shorter wavelength as well as in the infrared region due to the presence of various functional groups and conjugate bonds (Hoffer, 1978; Hunt, 1980). High organic matter in soil may produce spectral interferences for band characteristics of minerals like Mn and Fe. This factor has an indirect spectral influence through its effect on soil structure and on water retention capacity.
- (d) Soil texture, which is the relative proportion of sand, silt, and clay, affects the spectral reflectance of the soils due to its influence on water-holding capacity and the size of soil particles. Large grain size exhibits numerous well-developed absorption features at wavelengths less than 1,600 nm, and smaller grains exhibit fewer less developed features in this region and well-developed features at wave lengths more than >1,600 nm. In smaller grains, the soil surface becomes smoother and more incoming solar energy is reflected. An increase in particle size causes a decrease in reflectance as light is trapped in the rough surfaces of the coarse soil particles. However, silt content of soil is considered as major controlling factor for spectral reflectance. The reflectance becomes lower as the silt content decreases (Hoffer, 1978). On the other hand, it is commonly observed that sandy soil exhibits higher reflectance than that of clayey soil, which is due to abundance of macro pores and air–soil interface that cause multiple reflection/scattering. For example, if iron and lime are present, a stronger reflectance is received than if the soil material was fine textured and dry. Variations in soil reflectance occur where there is a change in distribution of light and shadow areas with surface roughness areas. This factor is important in the thermal infrared and microwave spectral domains.

Plant characteristics

Vegetation has distinct properties when exposed to light energy. The reflective and absorptive properties of vegetation with respect to red and near-infrared radiation are much different than that of soil. Active vegetation uses light energy available in the atmosphere as an ingredient in the photosynthesis process. The plant uses water from the soil, CO₂ from the air, and light energy to produce sugar molecules used by the plant. The by-product is oxygen molecules, which are released into the air. For this process to take place, certain wavelengths of light are absorbed by the plant and used as fuel for the process. As light strikes the leafy surfaces of the plant, three things can occur. The light may either be reflected back into the atmosphere, it may be absorbed by the plant, or it may be transmitted through the plant onto other lower lying surfaces. In most cases, a combination of all three things happens. The light that is transmitted through the leaf will then come into contact with whatever lies beneath it. If it is another leaf, a combination of the above three circumstances will again occur. This explains how light energy that is not reflected but transmitted by the first leaf layer may eventually be reflected back into the atmosphere by lower leaf levels. In the same manner, some wavelengths that are transmitted through the first layer may eventually be absorbed by lower leaf layers. As the biomass of the vegetation increases over the soil, the amount of light reaching the soil decreases. Intense radiation can be harmful to vegetation, and therefore plants have adapted to absorb only what is necessary, and reflect the longer more harmful rays (Jensen, 2007). As the vegetation biomass increases, more and more visible red light is absorbed by the plants for photosynthetic purposes, while more and more near-infrared energy that can be damaging to the plant is reflected.

Vegetation indexes

The visible portion of the leaf reflectance spectrum is characterized by high absorption of pigments. The chlorophyll pigments absorb violet, blue, and red but green, so most vegetation has green appearance. The reflectance spectrum of green vegetation has maximum absorption at 420, 490, and 660 nm bands; all by chlorophyll. The electromagnetic absorption mechanism in the pigments of green vegetation is by atomic excitation. Pigments, such as chlorophyll and carotenes, absorb light in particular wavelength, causing an electron jump in the pigment molecular structures. The energy produced by de-excitation will be consumed for electrochemical reaction.

Numerous indices have been developed to quantify how vegetation responds to light energy as it grows. In fact, over 50 vegetation indices exist (Huete et al., 1994; Ray, 1994; Jensen, 2007).

Ratio vegetation index (RVI)

The first developed of these indices is the ratio vegetation index (RVI), which is simply the near-infrared reflectance values divided by the visible red reflectance values.

$$\text{The RVI is defined as : } RVI = \frac{NIR}{Red} \quad (2)$$

NIR=near infra-red reflectance, *Red*=visible red reflectance.

Red simple ratio

The near-infrared (NIR) to red simple ratio (SR) is the first true vegetation index:

$$SR = \frac{\rho Red}{\rho NIR} \quad (3)$$

(*ρRed* = reflectance in the red spectral range. *ρNIR* = reflectance in near-infrared range).

It takes advantage of the inverse relationship between chlorophyll absorption of red radiant energy and increased reflectance of near-infrared energy for healthy plant canopies (Cohen, 1991).

The generic normalized difference vegetation index (NDVI)

$$NDVI = \frac{(NIR - RED)}{(NIR + RED)} \quad (4)$$

(RED and NIR stand for the spectral reflectance measurements acquired in the red and near-infrared regions, respectively).

NDVI measures of the overall amount and quality of photosynthetic material in vegetation and provided a method of estimating net primary production over varying biome types (Tucker, 1979; Lenney et al., 1996) (Biomes are defined by factors such as plant structures (such as trees, shrubs, and grasses), leaf types (such as broadleaf and needleleaf), plant spacing (forest, woodland, savanna), and climate), identifying ecoregions (Ramsey et al., 1995) (Ecoregion is geographic area characterized by distinctive environmental characteristics including climate, geomorphology, vegetation, soil, water, fauna, and land use), monitoring phenological patterns (Phenology is the study of periodic plant and animal life cycle events) of the earth's vegetative surface, and of assessing the length of the growing season and dry-down periods (Huete and Liu, 1994).

Normalized difference moisture or water index (NDMI or MDWI)

Vegetation water content has widespread use in agriculture, forestry, and hydrology. Gao (1996) found that the normalized difference moisture or water index (NDMI or MDWI) based on Landsat TM near- and middle-infrared bands was highly correlated with canopy water content and more closely tracked changes in plant biomass than did the NDVI.

$$NDMI = \frac{NIR_{TM_4} - MidIR_{TM_5}}{NIR_{TM_4} + MidIR_{TM_5}} \quad (5)$$

Soil-adjusted vegetation index (SAVI)

Improved vegetation indices that may take advantage of calibrated hyperspectral sensor systems such as the moderate resolution imaging spectrometer – MODIS has been developed (Running et al., 1994; Zarco-Tejada et al., 2003). The improved indices incorporate a *soil adjustment factor* and/or a *blue band for atmospheric normalization*. The *soil-adjusted vegetation index* (SAVI) introduces a soil calibration factor, L , to the NDVI equation to minimize soil background influences resulting from first order soil–plant spectral interactions (Huete et al., 1994):

$$SAVI = \frac{(1+L)(\rho_{nir} - \rho_{red})}{\rho_{nir} + \rho_{red} + L} \quad (6)$$

An L value of 0.5 minimizes soil brightness variations and eliminates the need for additional calibration for different soils (Huete and Liu, 1994).

Atmospherically resistant vegetation index (ARVI)

SAVI was made less sensitive to atmospheric effects by normalizing the radiance in the blue, red, and near-infrared bands by the *atmospherically resistant vegetation index*:

$$ARVI = \frac{\rho^{*nir} - \rho^{*rb}}{\rho^{*nir} + \rho^{*rb}} \quad (7)$$

where

$$\rho^{*rb} = \rho^{*red} - \gamma(\rho^{*blue} - \rho^{*red}) \quad (8)$$

The technique requires prior correction for molecular scattering and ozone absorption of the blue, red, and near-infrared remote sensor data, hence the term ρ^* .

Aerosol free vegetation index (AFRI)

Karnieli et al. (2001) found that under clear sky conditions, the spectral bands centered on 1.6 and 2.1 μm are highly correlated with visible spectral bands centered on blue (0.469 μm), green (0.555 μm), and red (0.645 μm). Empirical linear relationships such as $\rho_{0.469\mu\text{m}} = 0.25\rho_{2.1\mu\text{m}}$; $\rho_{0.555\mu\text{m}} = 0.33\rho_{2.1\mu\text{m}}$, and $\rho_{0.645\mu\text{m}} = 0.66\rho_{1.6\mu\text{m}}$ were found to be statistically significant. Therefore, based on these and other relationships, two *Aerosol Free Vegetation Indices* were developed:

$$AFRI_{1.6\mu\text{m}} = \frac{(\rho_{nir} - 0.66\rho_{1.6\mu\text{m}})}{(\rho_{nir} + 0.66\rho_{1.6\mu\text{m}})} \quad (9)$$

$$AFRI_{2.1\mu\text{m}} = \frac{(\rho_{nir} - 0.5\rho_{2.1\mu\text{m}})}{(\rho_{nir} + 0.5\rho_{2.1\mu\text{m}})} \quad (10)$$

Enhanced vegetation index (EVI)

The MODIS Land Discipline Group proposed the *enhanced vegetation index* (EVI) for use with MODIS Data:

$$EVI = G \frac{\rho_{nir}^* - \rho_{red}^*}{\rho_{nir}^* + \rho_{red}^* - C_2 \rho_{blue}^* + L} \quad (11)$$

The EVI is a modified NDVI with a soil adjustment factor, L , and two coefficients, C_1 and C_2 , which describe the use of the blue band in correction of the red band for atmospheric aerosol scattering. The coefficients, C_1 , C_2 , and L , are empirically determined as 6.0, 7.5, and 1.0, respectively. This algorithm has improved sensitivity to high biomass regions and improved vegetation monitoring through a de-coupling of the canopy background signal and a reduction in atmospheric influences. G is a gain factor set to 2.5.

Triangular vegetation index

Broge and Leblanc (2000) developed a *triangular vegetation index* (TVI), which describes the radiative energy absorbed by pigments as a function of the relative difference between red and near-infrared reflectance in conjunction with the magnitude of reflectance in the green region, where the light absorption by chlorophyll *a* and *b* is relatively insignificant. The index is calculated as the area of the triangle defined by the green peak, the chlorophyll absorption minimum, and the near-infrared shoulder in spectral space. It is based on the fact that both chlorophyll absorption causing a decrease of red reflectance and leaf tissue abundance causing increased near-infrared reflectance will increase the total area of the triangle. The TVI index encompasses the area spanned by the triangle ABC with the coordinates given in spectral space:

$$TVI = \frac{1}{2} [120(\rho_{nir} - \rho_{green})] - 200(\rho_{red} - \rho_{green}) \quad (12)$$

where ρ_{green} , ρ_{red} , and ρ_{nir} are the reflectances centered at 0.55, 0.67, and 0.75 μm , respectively.

Visible atmospherically resistant index (VARI)

The index is minimally sensitive to atmospheric effects, allowing estimation of vegetation fraction with an error of <10% in a wide range of atmospheric optical thickness (Gitelson et al., 2002):

$$VARI_{green} = \frac{\rho_{green} - \rho_{red}}{\rho_{green} + \rho_{red} - \rho_{blue}} \quad (13)$$

The generic normalized difference vegetation index (NDVI) may be not be adequate for assessing crop vegetation due to confounding soil background effects in imagery and indices such as the *soil-adjusted vegetation index* was suggested (SAVI; Huete, 1988), *optimized soil-digital adjusted vegetation index* (OSAVI; Rondeaux et al., 1996), and *transformed soil-adjusted vegetation index* (TSAVI; Baret et al., 1989). On the other hand, Gitelson et al. (1996) proposed use of the *green normalized difference vegetation index* (GNDVI) (where the

green band substituted for the red band in the NDVI equation), which may prove to be more useful for assessing canopy variation in green crop biomass.

$$GNDVI = \frac{(NIR - Green)}{(NIR + Green)} \quad (14)$$

$$TSAVI = a \left[\frac{NIR - (ax Red) - b}{Red + (ax NIR) - (ax b)} \right] \quad (15)$$

where the a and b values represent the slope and intercept, respectively, of an equation fitted through a plot of red vs. NIR reflectance data for a variety of bare soil conditions (dry, wet, smooth, and rough).

Red edge

The abrupt change in the 680–800 nm region of reflectance spectra of leaves caused by the combined effects of strong chlorophyll absorption and leaf internal scattering is called the *red edge*. The *red edge position* (REP) is the point of maximum slope on a vegetation reflectance spectrum between the red and near-IR wavelengths. The red edge was first described by Collins (1978). The REP is highly correlated with foliar chlorophyll content and can be a sensitive indicator of vegetation stress.

A linear method proposed by Clevers (1994) can be used to compute the REP that makes use of four narrow bands and is computed as:

$$REP = 700 + 40 \left[\frac{\rho_{(red_edge)} - \rho_{(700\text{nm})}}{\rho_{(740\text{nm})} + \rho_{(700\text{nm})}} \right] \quad (16)$$

where

$$\rho(red_edge) = \frac{\rho_{670\text{nm}} + \rho_{780\text{nm}}}{2} \quad (17)$$

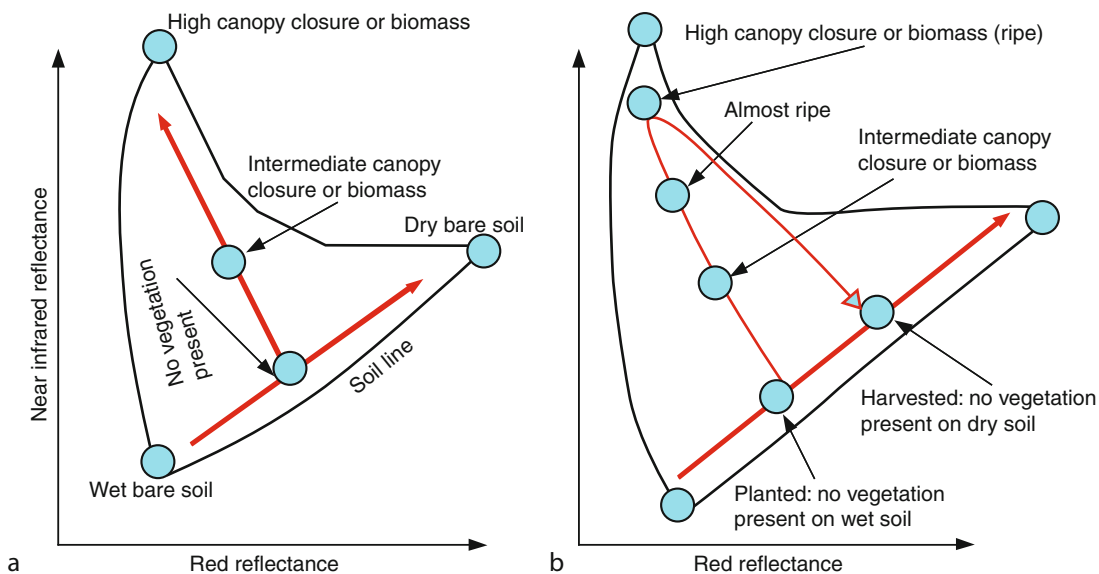
The red-infrared triangle (vegetation boater)

If we plot the red against the near-infrared reflectance for an entire image, we generally see a triangular shaped distribution as shown in Figure 4. The soil line represents areas on the ground that do not have significant vegetation cover but vary in reflectance based upon whether the soil is wet or dry. Areas where vegetation is present will be found somewhere above the soil line.

Pixels falling at the peak of the curve indicate the densest canopy, while pixels near the soil line indicate little to no vegetation. All areas between indicate a combination of soil and vegetation. Using a ratio such as this puts the data in a format that is easier to view and also removes factors that affect both bandwidths equally. Ideally the soil and vegetation in the index should be easily distinguishable.

Development of absorption and reflectance from active vegetation to senescence

Actively growing plants show a strong contrast between strong absorption in the red and high reflectance in the



Remote Sensing of Soils and Plants Imagery, Figure 4 (a) Distribution of reflectance values in a remote sensing image in the red and near-infrared regions of the electromagnetic spectrum is found inside the triangle. The greater the amount of photosynthetically active vegetation present, the greater the near-infrared reflectance and the lower the red reflectance. This condition moves a pixel's spectral location in a perpendicular direction away from the soil line. (b) The migration of a single vegetated agricultural pixel in red and near-infrared multispectral space during a growing season is shown. After the crop emerges, it departs from the soil line, eventually reaching complete canopy closure. After harvesting, the pixel will be found on the soil line, but perhaps in a drier soil condition. (Modified from Jensen, J. R., (2007) *Remote Sensing of the Environment: An Earth Resource Perspective*. New Jersey: Prentice-Hall, Figure 11.8 on p. 364.)

near-infrared regions of the spectrum. The amount of absorption in the red and reflectance in the near-infrared varies with both the type of vegetation and the vigor of the plants. Pigments such as chlorophyll and carotenes absorb light in particular wave length, causing an electron jump in the pigment molecular structures. The energy produced by de-excitation will be consumed for electrochemical reaction. The chlorophyll pigments absorb violet, blue, and red but green, so most vegetation has green appearance. The reflectance spectrum of green vegetation has maximum absorption at 420, 490, and 660 nm bands, all by chlorophyll. The natural change of a green leaf as it senesces is shown in Figure 5. We see that the healthy green leaf has very low reflectance values in the red (600–700 nm) due to chlorophyll absorption and very high reflectance values in the near-infrared (700–1,000 nm). However, as the plant begins to senesce, reflectance begins to decrease in the near-infrared and increase in the red regions. The electromagnetic absorption mechanism in the pigments of green vegetation is by atomic excitation (Ray, 1994; Jensen, 2007; Jensen, 2008).

In the period of senescence, faster degradation of chlorophylls compared to carotenes causes significant increase in the red wavelength due to the great decrease in the chlorophyll pigment density. In this case, carotenes absorb blue and reflect green and red, hence leaves will have yellow appearance. By death of brown pigments (tannins), leaf reflectance and transmittance in 400–700 nm decrease (Fourty et al., 1996); the decline in reflectance in the near-infrared is due to the spongy-mesophyll layer collapsing as the leaf comes under stress and the increase in reflectance in the red is caused by the die-off of chlorophyll and therefore a decrease in absorption. This

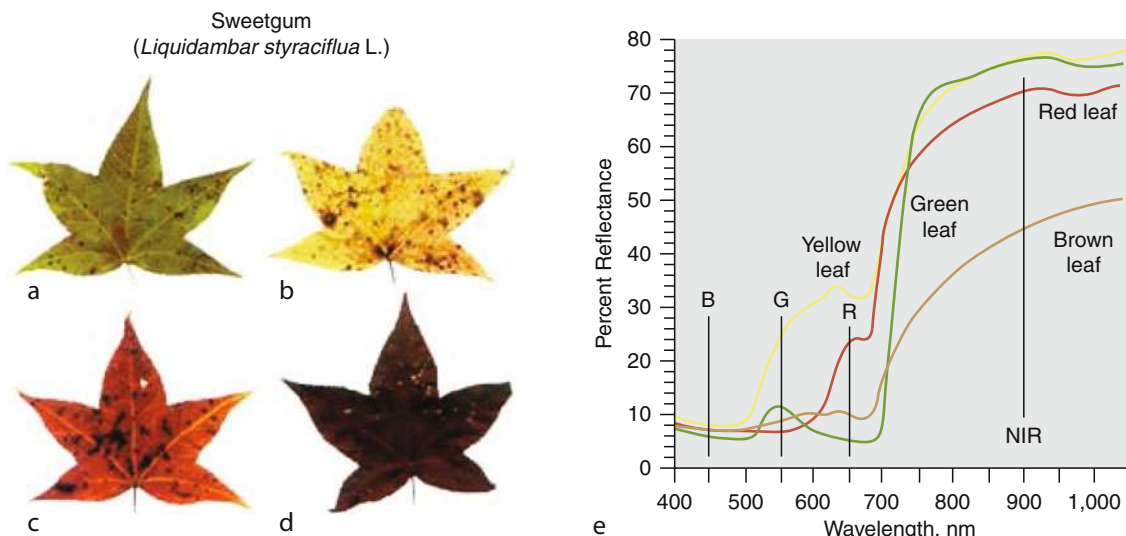
information can be used to evaluate vegetation type, condition, or density. One way of characterizing this relationship with a single variable is by dividing the near-infrared reflectance by the red reflectance (NIR/Red). The larger this ratio, the more photosynthetically active vegetation is present; the lower the ratio, the less photosynthetically active vegetation is present (Figure 5).

Remote sensing and grain yield

The goal of estimating green leaf or crop biomass has been to arrive eventually at some estimate of harvestable crop yield. Yield models that are related to remotely sensed data: reflectance-based and thermal-based models. Tucker et al. (1980) proposed a relationship between spectral reflectance and crop yield. This was similar to the approach suggested by Idso et al. (1978), Aase and Siddoway (1981), and Pinter et al. (1981). The general class of these models can be characterized as some form of a relationship between rate of change in the vegetation index (VI) and crop growth rate. The faster the rate of growth, the higher the harvestable crop yield.

Using a physiological approach, Hatfield (1983) developed a method using the maximum NIR/red ratio during the growing season as an indication of the maximum leaf area attained by the crop. He found that at 0.5 of the maximum ratio, 90% of the reproductive dry matter was attained. Spectral reflectance was coupled with thermal measurements as a combined approach to estimate stress and growth for both wheat and grain sorghum.

Idso et al. (1980) had found that grain yields in wheat were related to the rate of crop senescence. Recent observations by Shanahan et al. (2001) using TSAVI, NDVI, and a GNDVI, where the red reflectance is replaced by



Remote Sensing of Soils and Plants Imagery, Figure 5 (a) Healthy green sweet gum leaf obtained from a tree on November 11, 1998. (b–c) Senescing yellow and red sweet gum leaves obtained from the tree. (d) Senesced sweet gum leaf that was on the ground. (e) Reflectance measurements of the four leaves. (Jensen, J. R. (2007) *Remote Sensing of the Environment: An Earth Resource Perspective*. Prentice-Hall, New Jersey, Color Plate 11.1.)

green reflectance, showed a slight improvement in yield estimates for four corn hybrids grown with varying nitrogen and water levels. Usually, NDVI is useful as a tool for estimating net primary production over various biomes (Huete and Liu, 1994), but has a number of deficiencies. GNDVI acquired during midgrain filling could be used to produce relative yield maps depicting spatial variability in fields, offering a potentially attractive alternative to use of a combine yield monitor (Shanahan et al., 2001). Eldaw Elwadie et al. (2005) find that corn grain yield was strongly related to canopy reflectance for either individual wavelengths or for SVIs (spectral vegetation index), reaching an optimum ($R^2 > 0.9$) at R5 dent stage. Green reflectance based on simple ratio (green simple ratio index, GSRI) had the highest R^2 , lowest RMSE, and most consistent slope and intercept. In contrast, LAI was best predicted by NDVI (RMSE = 0.426) while GNDVI performed poorly (RMSE = 0.604).

Radar remote sensing for estimation of surface soil moisture at the watershed scale

A great deal of progress has been made in the use of spectral images from satellite sensors for surface soil moisture mapping, where surface soil moisture (SM) is the average moisture ($\text{cm}^3 \text{ cm}^{-3}$) in the top few centimeters of soil over a heterogeneous volume (Moran et al., 2004). The greatest progress has been made with passive microwave sensors. These sensors measure the intensity of microwave emission (at wavelengths $1=1 - 30 \text{ cm}$) from the soil, which is related to its moisture content because of the large differences in dielectric constant of dry soil (~ 3.5) and water (~ 80). This emission is proportional to the product of surface temperature and surface emissivity, which is commonly referred to as the microwave brightness temperature (BT). The relation between BT and SM varies with differences in surface roughness and vegetation biomass and is further affected by the changes in dielectric constant related to soil texture. The efficacy of the measurement is a function of wavelength, where longer wavelengths ($1 > 10 \text{ cm}$) probe deeper into the soil and have the ability to penetrate a vegetated canopy.

Moran et al. (1994) also developed the water deficit index (WDI), utilizing surface minus air temperatures and a spectral vegetation index to estimate the relative soil moistures. The WDI takes into account surface temperature variations resulting from plant water stress in partial canopies.

Remote sensing and precision farming

Precision farming is an integrated agricultural management system incorporating several technologies. The technological tools often include the *global positioning system*, *geographical information system*, *yield monitor*, *variable rate technology*, and *remote sensing*. Remote sensing provides practical insights into crop growth and vigor, stress presence, and moisture status. Crop growth and vigor determining plant "greenness" or nitrogen

content, plant cell density and biomass, and seedling emergence. Hyperspectral analysis has the ability of improving best practices in the field of precision farming. This technique allows the characterization of agri-environmental indicators and notably the estimation of certain terms of the nitrogen balance through the study of the soil organic matter content and the chlorophyll content in plants. These two parameters, linked to the soil nitrogen concentration, intervene in the plant answer to fertilizer applications and are essential in the establishment of the nitrogen balance within the framework of precision farming. Stress presence is useful to identify disease or weed effects. Moisture status is useful for irrigation scheduling. Remote sensing fits neatly within a management system that utilizes precision farming technologies (Moran et al., 1997).

Remote sensing's functional role in studies of land-use/land-cover change

The problem of identifying the causes and consequences of land-use/land-cover change requires that the functional aspects of ecosystems be examined (Golubiewski et al., 2007). This involves the incorporation of land-use change into models that can couple land use with biogeochemical, biophysical, and atmospheric dynamics. New techniques in quantitative data retrieval allow the application of remote sensing to expand from a role of mostly spatial description to one where functional relationships can be examined. The basic concept is to use the structural attributes that can be pulled from satellite imagery to relate directly to functional variables. These ecological variables can then be incorporated into models instead of literature values in order to make more realistic assessments of linkages between changes in canopy structure and biogeochemical processes (Golubiewski et al., 2007).

Use of remote sensing for detecting weeds and stress

Remote sensing techniques offer the advantage of rapid acquisition of data with generally short turnaround time and considerably less cost. Everitt et al., 1995 used remote sensing techniques to detect leafy spurge in an active phenological stage, which had higher visible (0.63- to 0.69- μm) reflectance than several associated plant species. Quantitative data obtained from digitized video images showed that leafy spurge had statistically different digital values from those of associated vegetation and soil.

Alterations in the chlorophyll absorption feature are also indicative of phenological and stress-induced changes in chlorophyll activity. Research suggests that other canopy biochemical constituents, such as cellulose and lignin, influence reflectance in the shortwave infrared and can potentially be quantified using imaging spectrometry. Capability to estimate biochemical properties in terrestrial ecosystems would aid in the assessment of carbon fixation/allocation patterns, metabolic processes,

and nutrient availability altered by a changing environment (Wessman, 2003).

Predictive soil mapping

All approaches to soil mapping rest on our ability to use knowledge of the process of soil genesis to predict the properties of soils at any point in the landscape. Predictive soil mapping (PSM) can be defined as the development of a numerical or statistical model of the relationship among environmental variables and soil properties, which is then applied to a geographic database to create a predictive map. PSM is made possible by geocomputational technologies developed over the past few decades. For example, advances in geographic information science, digital terrain modeling, remote sensing, and fuzzy logic have created a tremendous potential for improvement in the way that soil maps are produced. PSM research is being driven by a need to understand the role soil plays in the biophysical and biogeochemical functioning of the planet. (Scull et al., 2003).

Identification of soil heterogeneity

- (a) Combining ground measurements of morphological crop parameters collected from representative soil sites with multispectral information at visible, infrared, and thermal wavebands recorded from the airborne scanner Daedalus AADS 1268 using bioindicative transfer functions, based on cause and effect relationships of the soil–plant system, enabled the spatial detection and the quantification of soil properties. The available water capacity of the rooting zone accounted predominantly for the heterogeneity of crop stands and yield formation of winter wheat. The thermal emission and its relationship to the transpiration of crops was recognized as most suitable to detect quantitatively soil properties via crop stand conditions of winter wheat. Soil maps derived from remote sensing and bioindicative transfer functions explained the pattern of nitrogen uptake and yield information (Seliger and Schmidhalter, 2006).
- (b) Soil erosion, an important soil degradation process, can influence soil spectra. Soil erosion influences indirectly by influencing soil surface roughness and iron content in top soils. So the more is the erosion, the more will be soil reflectance in the longer wavelength of visible and NIR regions (Latz et al., 1984). Direct spectral measures indicative of soil erosion include changes in organic matter content, mineral composition, albedo, roughness, and soil structure (Mulders, 1987; Irons et al., 1989).
- (c) Ground radar can be used in combination with remote sensing, to detect changes of diagnostic soil horizons such as albic, spodic, and argillic horizons or soil/rock boundaries. Limitations with ground radar include soils with high salt content/clay/silt/moisture amounts. <http://www.ucalgary.ca/geog/Virtual/Remote%20Sensing/rssoils.html>.

Predicting types of soil processes from remote sensing data

Predicting the types of soil processes and their rates from remote sensing data will depend on strong correlations between canopy variables and the process of interest (Wessman, 2003). Soil plays an integral role in almost all remote observations of the land surface either because the vegetation cover is discontinuous or because multiple scattering of the radiation occurs between vegetation and the underlying soil surface. However, since vegetation covers most of the land surface, plant canopy can be considered as a primary interface to soil processes. In many ways, the canopy is an integrated expression of (and is mutually linked to) below-ground processes and can, as such, be used to infer ecosystem properties. Classifications of satellite imagery into vegetation communities in which soil processes have been characterized can be used to extrapolate those processes across the landscape based on the areal extent of the associated cover type. Ratios of reflectance values measured in the region of chlorophyll absorption to those in the highly reflected near-infrared region are sensitive to biomass quantity and, when integrated over time, strongly correlate with primary productivity. High spectral resolution measurements of the absorption characteristics of major foliar chemical constituents may permit assessment of canopy-level concentrations and related processes such as decomposition and nitrogen mineralization (Wessman, 2003).

Remote sensing for salinity studies

Remote sensing was extensively used for salinity studies in many parts of the world. Several remote sensing studies used MMS and TM and SPOT data for salinity studies (Szilágyi and Baumgardner, 1991; Dwivedi, 1992; Dwivedi and Rao, 1992). It has been found that saline soils give lower reflectance than non-saline throughout the range between 0.5 and 2.38 μm (Baumgardner et al., 1985). In the case of salt-affected soils, the white crust that forms on the surface tends to have higher reflectance in the visible and near-infrared part of the spectrum (Barnes et al., 2003).

Dutkiewicz et al. (2009) used hyperspectral images from three sensors (Airborne HyMap, satellite Hyperion imagery and airborne Compact Airborne Spectrographic Imager (CASI) imagery) to discriminate and map selected symptoms of salinity in a dry-land agricultural area in southern Australia. The evaluation of imagery included comparisons of spectral resolution, spectral range, spatial resolution, and landscape seasonality. Salinity symptoms were also characterized using field spectra collected with an ASD FieldSpecPro spectrometer. Saltpans were discriminated using the gypsum 1,750 nm absorption feature, whereas full-wavelength image spectra were necessary to map the halophytic plants. HyMap imagery produced the most accurate maps of samphire and saltpans, identifying substantial saline areas covered with samphire that had not been delineated in previous aerial photo-interpretation.

Salama et al., 1997 used combination of vegetation, soils, and geology from remote sensing imagery with digital elevation models to classify catchments to hydrogeomorphic units, which recognize and classify salinity hazard zones.

Outlook

With increasing population pressure throughout the world and the need for increased agricultural production there is a critical need for improved management of the world's agricultural resources which is the most important renewable, dynamic natural resources. Comprehensive, reliable and timely information on the quality, quantity and location of these resources must be acquired at the required frequency. Remote Sensing technology has been and will continue to be the best system for acquiring and generating agricultural and resources data. This is mainly due to easy data acquisition over inaccessible areas at different scales and resolutions and acquired data are analyzed in the laboratory, thus reducing the amount of fieldwork. One of the most successful applications of multispectral space imagery is monitoring the state of the world's agricultural production including detection, identification, measurement and monitoring of agricultural phenomena including crop identification, acreage, vigor, density, maturity, growth rates and yield forecasting as well as plant health, insect and disease infestation. Remote sensing is also used for land surveys including mapping of soil physical properties, soil types, fertility, toxicity, moisture content, and erosion and for irrigation requirements, water quality, water availability, and plant drought stress.

The science of remote sensing is rapidly developing and new areas are continuously emerging which makes it the most important and indispensable tool in monitoring all routine agricultural activities.

Bibliography

- Aase, J. K., and Siddoway, F. H., 1981. Spring wheat yield estimates from spectral reflectance measurements. *IEEE Transactions on Geoscience and Remote Sensing*, **GE-19**, 78–84.
- Baret, F., Guyot, G., and Major, D. J., 1989. TSAVI: a vegetation index which minimizes soil brightness effects on LAI and APAR estimation. In Proceedings of the 12th Canadian Symposium on Remote Sensing and IGARSS'89, Vancouver, Vol. 3, pp. 1355–1358.
- Barnes, E. M., Sudduth, K. A., Hummel, J. W., Lesch, S. M., Corwin, D. L., Yang, C. H., Daughtry, C. S. T., and Bausch, W. C., 2003. Remote and ground-based sensor techniques to map soil properties. *Photogrammetric Engineering and Remote Sensing*, **69**(6), 619–630.
- Baumgardner, M., Silva, L., Biehl, L., and Stoner, E., 1985. Reflectance properties of soil. *Advances in Agronomy*, **38**, 1–44.
- Ben-Dor, E., Irons, J. R., and Epema, G., 1999. Soil reflectance. In Rencz, A. N. (ed.), *Remote Sensing for the Earth Sciences*. New York: Wiley, pp. 111–188.
- Broge, N. H., and Leblanc, E., 2000. Comparing prediction power and stability of broadband and hyperspectral vegetation indices for estimation of green leaf area index and canopy chlorophyll density. *Remote Sensing of Environment*, **76**, 156–172.
- Clevers, J. G. P. W., 1994. Imaging spectrometry in agriculture – plant vitality and yield indicators. In Hill, J., and Mégier, J. (eds.), *Imaging Spectrometry – A Tool for Environmental Observations*. Dordrecht: Kluwer Academic, pp. 193–219.
- Cohen, W. B., 1991. Temporal versus spatial variation in leaf reflectance under changing water stress conditions. *International Journal of Remote Sensing*, **12**(9), 1865–1876.
- Collins, W., 1978. Remote sensing of crop type and maturity. *Photogrammetric Engineering and Remote Sensing*, **44**, 43–55.
- Dutkiewicz, A., Lewis, M., and Ostendorf, B., 2009. Evaluation and comparison of hyperspectral imagery for mapping surface symptoms of dryland salinity. *International Journal of Remote Sensing*, **30**, 693–719.
- Dwivedi, R. S., 1992. Monitoring and the study of the effects of image scale on delineation of salt-affected soils in the Indo-Gangetic alluvial plains. *International Journal of Remote Sensing*, **13**, 1527–1536.
- Dwivedi, R. S., and Rao, B. R. M., 1992. The selection of the best possible Landsat-TM band combinations for delineating salt-affected soils. *International Journal of Remote Sensing*, **13**, 2051–2058.
- Eldaw Elwadie, M., Pierce, F. J., and Qi, J., 2005. Remote sensing of canopy dynamics and biophysical variables estimation of corn in Michigan. *Agronomy Journal*, **97**, 99–105.
- Everitt, J. H., Anderson, G. L., Escobar, D. E., Davis, M. R., Spencer, N. R., and Andrascik, R. J., 1995. Use of remote sensing for detecting and mapping leafy spurge (*Euphorbia esula*). *Weed Technology*, **9**, 599–609.
- Fourty, T., Baret, F., Jacquemond, S., Schmuck, G., and Verdebout, J., 1996. Leaf optical properties with explicit description of its biochemical composition: direct and inverse problems. *Remote Sensing of Environment*, **56**, 104–117.
- Gao, B. C., 1996. NDWI – A normalized difference water index for remote sensing of vegetation liquid water from space. *Remote Sensing of Environment*, **58**, 257–266.
- Gitelson, A., Kaufman, Y., and Merzlyak, M., 1996. Use of a green channel in remote sensing of global vegetation from EOS-MODIS. *Remote Sensing of Environment*, **58**, 289–298.
- Gitelson, A., Kaufman, Y. J., Stark, R., and Rundquist, T. D., 2002. Novel algorithms for remote estimation of vegetation fraction. *Remote Sensing of Environment*, **80**, 76–87.
- Golubiewski, N. (Lead Author); Hussein, G. H. G. (Topic Editor). 2007. Remote sensing's functional role in studies of land-use/land-cover change. In Cleveland, C. J. *Encyclopedia of Earth*. Washington, DC: Environmental Information Coalition, National Council for Science and the Environment. (Published in the Encyclopedia of Earth March 15, 2007; Retrieved September 20, 2009). http://www.eoearth.org/article/Remote_sensing%27s_functional_role_in_studies_of_land-use/land-cover_change
- Hatfield, J. L., 1983. Remote sensing estimators of potential and actual crop yield. *Remote Sensing of Environment*, **13**, 301–311.
- Hoffer, R. M., 1978. Biological and physical considerations in application computer aided analysis techniques to remote sensing. In Swain, P. H., and Davis, S. M. (eds.), *Remote Sensing: Quantitative Approach*. New York: McGraw-Hill, pp. 237–286.
- Huete, A. R., 1988. A soil vegetation adjusted index (SAVI). *Remote Sensing of Environment*, **25**, 295–309.
- Huete, A. R., and Liu, H. Q., 1994. An error and sensitivity analysis of the atmospheric- and soil-correcting variants of the NDVI for the MODIS-EOS. *IEEE Transactions on Geoscience and Remote Sensing*, **32**(4), 897–905.
- Huete, A., Justice, C., and Liu, H., 1994. Development of vegetation and soil indices for MODIS-EOS. *Remote Sensing of Environment*, **49**(3), 224–234.
- Huete, A., Didan, K., Miura, T., Rodriguez, E. P., Gao, X., and Ferreira, L. G., 2002. Overview of the radiometric aiophysic

- performance of the MODIS vegetation indices. *Remote Sensing of Environment*, **83**, 195–213.
- Hunt, G. R., 1980. Electromagnetic radiation: the communication link in remote sensing. In Siegal, B. S., and Gillespie, A. R. (eds.), *Remote Sensing in Geology*. New York: Wiley, pp. 5–46.
- Idso, S. B., Jackson, R. D., Reginato, R. J., Kimball, B. A., and Nakayama, F. S., 1975. The dependence of bare soil albedo on soil water content. *Journal of Applied Meteorology*, **14**, 109–113.
- Idso, S. B., Hatfield, J. L., Reginato, R. J., and Jackson, R. D., 1978. Wheat yield estimation by albedo measurement. *Remote Sensing of Environment*, **7**, 273–276.
- Idso, S. B., Pinter, P. J., Jr., Jackson, R. D., and Reginato, R. J., 1980. Estimation of grain yields by remote-sensing of crop senescence rates. *Remote Sensing of Environment*, **9**, 87–91.
- Irons, J. R., Weismiller, R. A., and Petersen, G. W., 1989. Soil reflectance. In Asrar, G. (ed.), *Theory and Application of Optical Remote Sensing*. New York: Wiley, pp. 66–106.
- Jensen, J. R., 2007. Remote sensing of vegetation. In *Remote Sensing of the Environment, An Earth Resource Perspective*, 2nd edn. Chapter 11. Prentice-Hall, Upper Saddle River.
- Jensen, J. R., 2008. Remote sensing for vegetation. Power Point Presentation <http://www.cas.sc.edu/geog/rslab/551/>
- Karnieli, A., Kaufman, Y. J., Remer, L., and Wald, A., 2001. *Remote Sensing of Environment*, **77**(1), 10–21.
- Latz, K., Weismiller, R. A., Van Scyoc, G. E., and Baumgardner, M. F., 1984. Characteristic variations in spectral reflectance of eroded Alfisols. *Soil Science Society of American Journal*, **48**, 1130–1134.
- Lenney, M. P., Woodcock, C. E., Collins, J. B., and Hamdi, H., 1996. The status of agricultural lands in Egypt: the use of multitemporal NDVI features derived from landsat TM. *Remote Sensing of Environment*, **56**, 8–20.
- Moran, M. S., Clarke, T. R., Inoue, Y., and Vidal, A., 1994. Estimating crop water deficits using the relation between surface-air temperature and spectral vegetation index. *Remote Sensing of Environment*, **46**, 246–263.
- Moran, M. S., Inoue, Y., and Barnes, E. M., 1997. Opportunities and limitations for image-based remote sensing in precision crop management. *Remote Sensing of Environment*, **61**, 319–346.
- Moran, M. S., Peters-Lidard, C. D., Watts, J. M., and McElroy, S., 2004. Estimating soil moisture at the watershed scale with satellite-based radar and land surface models. *Journal of Remote Sensing*, **30**(5), 805–826.
- Mulders, M. A., 1987. *Remote Sensing in Soil Science*. Amsterdam: Elsevier, p. 379.
- Pinter, P. J., Jr., Jackson, R. D., Idso, S. B., and Reginato, R. J., 1981. Multidate spectral reflectance as predictors of yield in water-stressed wheat and barley. *International Journal of Remote Sensing*, **2**, 43–48.
- Ramsey, R. D., Falconer, A., and Jensen, J. R., 1995. The relationship between NOAA-AVHRR NDVI and Ecoregions in UTAH. *Remote Sensing of Environment*, **53**(3), 188–198.
- Ray, T., 1994. A FAQ on Vegetation in Remote Sensing. <http://www.yale.edu/ceo/Documentation/rsvegfaq.html>
- Reginato, R. J., Vedder, J. F., Idso, S. B., Jackson, R. D., Blanchard, M. B., and Goettelman, R., 1977. An evaluation of total solar reflectance and spectral band ratioing techniques for estimating soil water content. *Journal of Geophysical Research*, **82**, 2101–2104.
- Rondeaux, G., Steven, M., and Baret, F., 1996. Optimization of soil-adjusted vegetation indices. *Remote Sensing of Environment*, **55**, 95–107.
- Running, S. W., Loveland, T. R., and Pierce, L. L., 1994. A vegetation classification logic based on remote sensing for use in global biogeochemical models. *Ambio*, **23**, 77–81.
- Salama, R. B., Hatton, T. J., Elder, G. M., Ye, L., and Dowling, T., 1997. Hydrogeological characterisation of catchments using Hydrogeomorphic Analysis of Regional Spatial Data (HARSD): characterisation of Axe Creek Catchment. In: Taniguchi, M. (ed.), *Subsurface Hydrological Responses to Land Cover and Land Use Change*. Kluwer Academic, Victoria, Australia, pp. 153–166.
- Scull, P., Franklin, J., Chadwick, O. A., and McArthur, D., 2003. Predictive soil mapping: a review. *Progress in Physical Geography*, **27**(2), 171–197.
- Selige, T., and Schmidhalter, U., 2006. Remote sensing of soil properties to support site specific farming. *Developments in Plant and Soil Sciences*, **92**.
- Shanahan, J. F., Schepers, J. S., Francis, D. D., Varvel, G. E., Wilhelm, W. W., Tringe, J. M., Schlemmer, M. R., and Major, D. J., 2001. Use of remote-sensing imagery to estimate corn grain yield. *Agronomy Journal*, **93**, 583–589.
- Szilágyi, A., and Baumgardner, M. F., 1991. Salinity and spectral reflectance of soils, In: Proceedings American Society of Photogrammetry Remote Sensing Symposium, March 25–29, 1991, Baltimore, MD, pp. 430–437.
- Tucker, C. J., 1979. Red and photographic infrared linear combinations for monitoring vegetation. *Remote Sensing of Environment*, **8**, 127–150.
- Tucker, C. J., Holben, B. N., Elgin, J. H. Jr., and McMurtrey, J. E., III, 1980. Relationship of spectral data to grain yield variations. *Photogrammetric Engineering and Remote Sensing*, **46**, 657–666.
- Wessman, C. A., 2003. The use of remote sensing in following soil process, Remote sensing of soil processes. Agriculture, Ecosystems and Environment. In: Proceedings of the International Workshop on Modern Techniques in Soil Ecology Relevant to Organic Matter Breakdown, Nutrient Cycling and Soil Biological Processes, Volume 34, Issues 1–4, 15 February 1991, pp. 479–493.
- Zarco-Tejada, P. J., Rueda, C., and Ustin, S., 2003. Water content estimation in vegetation with MODIS reflectance data and model inversion methods. *Remote Sensing of Environment*, **85**, 109–124.

Cross-references

- [Agrogeology](#)
- [Agrophysical Objects \(Soils, Plants, Agricultural Products, and Foods\)](#)
- [Brightness Temperature in Monitoring of Soil Wetness](#)
- [Buffer Capacity of Soils](#)
- [Bypass Flow in Soil](#)
- [Chemical Imaging in Agriculture](#)
- [Climate Change: Environmental Effects](#)
- [Color Indices, Relationships with Soil Characteristics](#)
- [Cracking in Soils](#)
- [Crop Responses to Soil Physical Conditions](#)
- [Crop Yield Losses Reduction at Harvest, from Research to Adoption](#)
- [Cropping Systems, Effects on Soil Physical Properties](#)
- [Cultivation Under Screens, Aerodynamics of Boundary Layers](#)
- [Ecohydrology](#)
- [Field Water Capacity](#)
- [Ground-Penetrating Radar, Soil Exploration](#)
- [Image Analysis in Agrophysics](#)
- [Management Effects on Soil Properties and Functions](#)
- [Mapping of Soil Physical Properties](#)
- [Monitoring Physical Conditions in Agriculture and Environment](#)
- [Overland Flow](#)
- [Peats and Peatlands, Physical Properties](#)
- [Physical Properties for Soil Classification](#)
- [Plant Disease Symptoms, Identification from Colored Images](#)
- [Plant Drought Stress: Detection by Image Analysis](#)
- [Plant Physical Characteristics in Breeding and Varietal Evaluation](#)

Plant Temperature
 Plant Wellness
 Precision Agriculture: Proximal Soil Sensing
 Salinity, Physical Effects on Soils
 Scaling of Soil Physical Properties
 Soil Erosion Modeling
 Soil Physical Degradation: Assessment with the Use of Remote Sensing and GIS
 Soil Structure, Visual Assessment
 Soil Surface Sealing and Crusting
 Soil Water Management
 Soil–Plant–Atmosphere Continuum
 Spatial Variability of Soil Physical Properties
 Stable Isotopes, Their Use in Soil Hydrology
 Stomatal Conductance, Photosynthesis, and Transpiration, Modeling
 Stratification of Soil Porosity and Organic Matter
 Surface and Subsurface Waters
 Surface Properties and Related Phenomena in Soils and Plants
 Tillage, Impacts on Soil and Environment
 Tropical Soils, Physical Properties
 Tropical Watersheds, Hydrological Processes
 Urban Soils, Functions
 Water Budget in Soil
 Water Erosion: Environmental and Economical Hazard
 Water Reservoirs, Effects on Soil and Groundwater
 Weather, Effects on Plants
 Wind Erosion

REPRESENTATIVE ELEMENTARY VOLUME

See [Soil Water Flow](#)

RHEOLOGY IN AGRICULTURAL PRODUCTS AND FOODS

Jiří Blahovec
 Department of Physics, Czech University of Life Sciences, Prague 6-Suchdol, Czech Republic

Synonyms

Deformation in agricultural products and foods; Flowing in agricultural products and foods

Definition

Rheology is the part of science dealing with the flow of matter; mainly liquids but also soft solids or solids in states where they flow rather than deform elastically. It applies to substance aggregates of different properties (see [Agrophysical Objects \(Soils, Plants, Agricultural Products, and Foods\)](#)), including biological materials (see [Physical Properties of Raw Materials and Agricultural Products](#)). Complex materials of this type cannot be characterized by a single parameter like viscosity – in fact viscosity changes due to other factors. The experimental characterization of the rheological properties of a material is termed “rheometry.”

Shortly speaking, rheology is an extension of the “classical” disciplines of elasticity and (Newtonian) fluid mechanics (see [Stress–Strain Relations](#)) to materials whose mechanical behavior cannot be described by the classical theories.

Continuum Mechanics	Solid Mechanics	Elasticity	Rheology
	Viscoelasticity	Non-Newtonian Fluids	
Fluid mechanics		Newtonian Fluids	

One of the tasks of rheology is to empirically establish the relationships between deformations and stresses (*Stress–Strain Relations*), and their derivatives by adequate measurements. These experimental techniques are concerned with the determination of well-defined rheological material functions. Such relationships are then amenable to mathematical treatment by the established methods of continuum mechanics.

Introduction

Agricultural products and foods (see [Agrophysical Properties and Processes](#)) belong to a wide group of non-crystalline substances that can be included in the so-called “soft matter” (Jones, 2002) characterized by weak interaction between structural units, large thermal fluctuations, large numbers of internal degrees of freedom, macroscopic softness indicative of a weak modulus of elasticity, and sensitivity of their phase diagrams to external constraints. The physical properties are strongly dependent on temperature and pressure. Matter stability plays an important role in the multi-phase state.

Processed foods represent a typical example of soft matter of biological origin (see [Thermal Technologies in Food Processing](#)). Agricultural products before processing (see [Quality of Agricultural Products in Relation to Physical Conditions](#)) contain information on their biological content, mainly on structural character (organs, tissues, and cells). The cellular structure is a source of the special mechanical properties of the agricultural products. The soft matter can be divided into two groups: quasi-liquids described by means of liquid rheology, including the rheology of non-Newtonian liquids (not given here, for details see Steffe (1996), Steffe and Daubert (2006)), and quasi-solids described by theories and models presented here.

The real quasi-solid represents mixing of elastic (solid) and inelastic (fluid) properties. Crude assessment of participation of both properties in the resulting properties of a real product leads to determination of the degree of elasticity (DE) and/or hysteresis losses (HL) in a loading/unloading test or analysis of the corresponding tests: by stress relaxation, or in creep test. Results of the tests depend on many test parameters like temperature, strain rate, and type and level of deformation.

The first attempts to describe real rheological, i.e., inelastic, behavior of quasi-solid matter in macroscopic deformation tests were based on simple models combining serial (Maxwellian) and parallel (Kelvinian)

connection of ideal elastic and viscous elements. The rheological models of this type were not able to describe all details of deformation in real materials for which special functions (relaxation and creep) were developed. Their application to low level deformations of bodies is termed (linear) viscoelasticity. The deformation behavior is strongly influenced by strain rate-temperature scenario that can be unified in a complex theory. Temperature influences also the state of the deformed matter being the basis for the so-called thermomechanical analysis. Information on the polymer rheology is given by Ward (1983) and Ferry (1980).

Irreversibility in deformation of quasi-solid materials

The viscous-like processes represent irreversible part of the whole deformation process. They can be assessed using results of special tests (loading/unloading t., stress relaxation t., and creep t.).

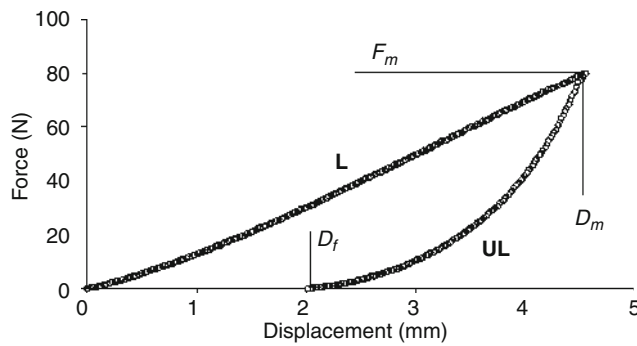
Loading/Unloading test

The loading/unloading test is presented by a Force–Displacement plot in Figure 1. From the figure it is clear that after reaching a displacement 4.55 mm, the compression loading was reversed and two branches of the test were obtained: the loading branch (L) and the unloading branch (UL). The participation of the irreversible inelastic deformation can be assessed by two ways (Blahovec, 2008) in this case.

Using characteristic deformations the “degree of elasticity” (DE) can be calculated as follows:

$$DE = 1 - \frac{D_f}{D_m} \quad (1)$$

where D_m is the maximum displacement (i.e., the displacement corresponding to the reversion of loading) and D_f



Rheology in Agricultural Products and Foods, Figure 1 Force-displacement curve in Loading/Unloading test. L denotes loading part, UL is unloading part, D_m is maximum displacement, D_f final displacement. Result of deformation of potato specimen in compression. Maximum displacement 4.55 mm, maximum force 80.08 N.

final (resulting) permanent displacement. Degree of elasticity varies between 0 ($D_f = D_m$) and 1 ($D_f = 0$). In our case (Figure 1) $DE \approx 0.553$.

The “hysteresis loss” (HL) is based on deformation work during loading (W_L) and unloading (W_{UL}). The deformation work is proportional to the area between the corresponding curve and the displacement axis. The area of the loop between L and UL curves represents the energy dissipated during the whole process. The hysteresis loss is expressed by its relative value as follows:

$$HL = \frac{W_L - W_{UL}}{W_L} = 1 - \frac{W_{UL}}{W_L} = 1 - \frac{\frac{D_m}{D_f} \int_0^{D_m} F_{UL} dD}{\int_0^{D_m} F_L dD} \quad (2)$$

where F_L denotes the loading force and F_{UL} the unloading force. The hysteresis loss varies between 1 for $W_{UL} = 0$ (inelastic, i.e., plastic deformation) and 0 for $W_{UL} = W_L$ (elastic deformation). In our case (Figure 1), $HL \approx 0.640$.

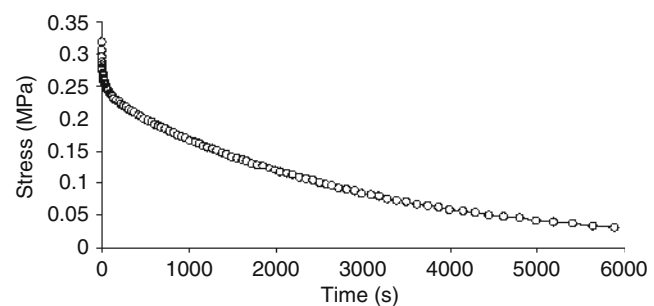
Stress relaxation

The stress relaxation test consists of a quick pre-strain that is followed by the proper relaxation step during which the strain is kept at constant value. The internal stresses in the tested specimen relax in this step and the stage is characterized by the falling down of the external stress value (see Figure 2). More detailed analysis of the individual stages is obtained by a slope analysis of the relaxation curve, calculating the so-called source f -function:

$$f = -\frac{d\sigma}{dt} \quad (3)$$

where σ is the stress. The source f -function serves to calculate of the activation volume v :

$$v = k_B T \frac{d \ln f}{d \sigma} \quad (4)$$



Rheology in Agricultural Products and Foods, Figure 2 Stress relaxation curve obtained at potato cylindrical specimen (diameter 15 mm, height 20 mm) deformed in compression (pre-strain 10%), time of relaxation 100 min.

where k_B is Boltzmann constant and T absolute temperature. For more information on this problem see Blahovec (2002).

In an elastic body, the stress is constant during the stress relaxation test so that the source f -function is constant and the activation volume v is constant, too. It means that the increasing values of the source f -function and the activation volume as well, indicate increasing participation of the inelastic deformations in the tested specimen.

Creep test

The creep test aims in the detection of inelastic deformation in the tested specimen at its constant loading in longer time interval (see, e.g., Ward 1983).

Rheological models

The simplest way in rheological models is based on models with springs and dampers. The springs are characterized by spring constants (elasticity modulus E) whereas the dampers are characterized by their viscosities (η). The serial connection of a spring and of a dumper represents the Maxwell's model, suitable for the description of stress relaxation in a body, i.e., time development of the stress (σ) in the body at constant strain ε_0 . This process is described by a simple differential equation:

$$\frac{d\varepsilon}{dt} = \frac{1}{E} \frac{d\sigma}{dt} + \frac{\sigma}{\eta} \quad (5a)$$

with solution:

$$\sigma = \sigma_0 e^{-\frac{Et}{\eta}} = \sigma_0 e^{-\frac{t}{T_{rel}}} \quad (5b)$$

where $\sigma_0 = E/\varepsilon_0$ is the initial stress and $T_{rel} = \eta/E$ is the relaxation time.

The parallel connection of a spring and a dumper represents the Kelvin's body that is suitable for description of creep. The creep determines the increase of strain (ε) during specimen constant loading by stress σ_0 as follows:

$$\varepsilon = \varepsilon_0 e^{-\frac{Et}{\eta}} = \varepsilon_0 e^{-\frac{t}{T_{ret}}} \quad (6)$$

where $\varepsilon_0 = \sigma_0/E$ is the initial strain and $T_{ret} = \eta/E$ retardation time. Equations 5b and 6 show that the exponential functions describe the development of the simple stress relaxation and creep processes.

The parallel connection of different Maxwell's models (of different parameters E_i and η_i) is termed Generalized Maxwell's model with the following expression for stress:

$$\sigma = \sum_{i=1}^n \left(\sigma_{0i} e^{-\frac{t}{T_i}} \right) \quad (7a)$$

where $\sigma_{0i} = E_i/\varepsilon_0$ and $T_i = \eta_i/E_i$. For $i=2$ and $\eta_2 \rightarrow \infty$ the model is termed standard linear body. The serial connection of different Kelvin's models (of different parameters E_i and η_i) is termed Generalized Kelvin's model with the following expression for strain:

$$\varepsilon = \sum_{i=1}^n \left(\varepsilon_{0i} e^{-\frac{t}{T_i}} \right) \quad (7b)$$

where $\varepsilon_{0i} = \sigma_0/E_i$ and $T_i = \eta_i/E_i$. The serial connection of a Maxwell's and a Kelvin's model is termed Burgers' model. More information on rheological models can be found in Gross (1953).

The rheological models were used for description rheology of agricultural materials mainly in 1950s and 1960s and they are widely described by Mohsenin (1986).

Rheological functions

Rheological functions are easily applicable to stress relaxation and creep of the viscoelastic bodies (Ferry, 1980; Ward, 1983). They are based on time dependent modulus of elasticity in tension $E(t)$ or in shear $G(t)$, so-called relaxation functions, or the corresponding time dependent creep compliances $D(t)$ and $J(t)$. The sense of the rheological functions is given by their application in the calculation of the strain and the stress (Ferry, 1980):

$$\varepsilon(t) = \int_{-\infty}^t D(t-\tau) \frac{d\sigma(\tau)}{d\tau} d\tau \quad (8a)$$

$$\sigma(t) = \int_{-\infty}^t E(t-\tau) \frac{d\varepsilon(\tau)}{d\tau} d\tau \quad (8b)$$

The shapes of rheological functions are sensitively dependent on deformation temperature and deformation rate. In some special cases, like at some polymers, it is possible to find some unifying principle for rheological functions determined at different conditions. The concept of rheological functions can be extended to the study of dynamic loading either by the initial harmonic periodic strain (ε) or by the initial harmonic periodic stress (σ). Both strain and stress are understood as complex functions as well as the rheological functions $E(\omega)$, $D(\omega)$, $G(\omega)$, $J(\omega)$, where the bold symbol denotes complex character of the function and ω angular frequency of the loading. In the frame of linear viscoelasticity, the rheological functions are interdependent as follows:

$$\begin{aligned} D(\omega)E(\omega) &= 1 \\ J(\omega)G(\omega) &= 1 \end{aligned} \quad (8c)$$

The rheological functions can be analyzed using spectral analysis of the relaxation and retardation times (Ferry, 1980).

The usual way of unifying the rheological functions is by using a "master curve" at reference temperature T_0 that is built using Williams-Landel-Ferry (WLF) transformation of data obtained at different temperatures. Two steps are used in this process:

- The time is multiplied by time-factor a_T :

$$a_T = \exp\left(\frac{-C_1(T - T_0)}{C_2 + T - T_0}\right) \quad (9a)$$

- The following parameter is defined:

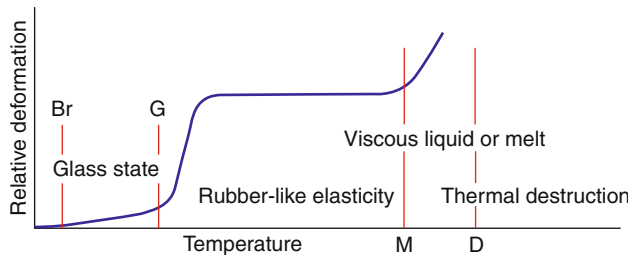
$$x(T, T_0) = \frac{T_0 \rho_0}{T \rho} \quad (9b)$$

where T and ρ are the experimental absolute temperature and density, respectively, and T_0 and ρ_0 are the same quantities at the reference state. The transformed rheological function is either multiplied by the factor $x(T, T_0)$ in the case of the functions E , G , their complex parts and the corresponding spectral functions or divided by the factor in all other cases.

Thermomechanics of biopolymers

(See also Tolstoguzov, 2000)

Quasi-solids of agricultural products and their ingredients are in different physical states: amorphous (liquid, rubber-like, solid) and crystalline. Whereas in crystalline solids the solid state is changed at the melting point into the liquid state, in amorphous solids the change from solid to liquid state is more complicated (Jones, 2002) and a new change, termed glass transition (T_g), is observed (Wunderlich, 2005). A typical temperature plot of the deformation of an amorphous polymeric material is given in Figure 3. The arbitrary temperature scale in Figure 3 is strain rate dependent: when strain rate increases, the



Rheology in Agricultural Products and Foods,

Figure 3 Thermomechanical curve of the amorphous polymeric material at the same stress plotted versus temperature. The temperature scale depends on deformation rate: at higher deformation rates the temperature scale is shifted to higher temperatures (Jones, 2002). At lowest temperatures the material is brittle; at brittle transition (Br) is changed into the brittle state changing at glass transition (G) into rubbery state characterized by relatively high but temperature sensitive deformation. M denotes melting of the polymer with transition to the viscous and/or viscoelastic state with temperature sensitive flow. In some cases the temperature corresponding to thermal destruction (D) can be observed.

temperature scale with the characteristic points is shifted to higher temperatures and vice versa (see *Rheology in Agricultural Products and Foods* and *Rheology in Soils*). The flow is temperature sensitive mainly in glassy and viscous states.

Therefore, the states of matter are distinguished by the energy ratio between the thermal movement and the intermolecular interaction, and by the mutual arrangement of individual macromolecules relative to one another (Strick et al. 2003). In the solid state, the energy of intermolecular interaction exceeds the energy of thermal motion, while in the liquid state, these values are comparable and macromolecules are in thermal motion. Accordingly, in the absence of external forces a solid body has a preferred shape, while a liquid has a definite volume but not shape. The liquid state is characterized by a relative molecular disorder. An external force, e.g., the weight of a liquid, directs the molecular movement. This corresponds to flow, i.e., an irreversible deformation of the liquid. Due to its extremely high viscosity, a glassy system behaves like a solid, and has both a definite shape and a definite volume. An amorphous glassy system exhibits the mechanical properties of a solid material and a structural arrangement typical for liquids. This reflects an increase in inter- and intramolecular interactions and a loss of molecular mobility (Rubinstein and Colby, 2003).

The glassy state of a macromolecular system only requires a mutual fixation of a certain proportion of the chain segments. The higher the rigidity of the chains, the lower the number of the chain segments which has to be fixed during change to glassy state. Mechanical stress can help to re-activate the motion of the fixed segments and makes possible longer deformation of glassy material. The stress necessary for this effect can reach the strength of the material as the temperature decreases from the glass transition to the temperatures of brittleness (crispness – see also *Physical Properties as Indicators of Food Quality*). The glassy state of a loaded viscoelastic system results in an accumulation of mechanical energy, which can be released above the glass transition temperature due to heating and/or addition of a plasticizer.

Unlike the amorphous state, the crystalline state is very rigid. The rate of crystallization (nucleation and crystal growth) increases as the temperature approaches the melting temperature (T_m). Since the probability of crystallization increases with time, crystallization can be avoided by cooling of a macromolecular liquid rapidly to below the melting point, where this liquid becomes super-cooled. On further cooling this liquid changes to glassy state, i.e., is converted into a solid-like system at around T_g . In the vicinity of T_g , the system's viscosity greatly rises with a decrease in temperature. Formation of a glass is accompanied by a gradual change in temperature dependencies of the mechanical properties, specific volume, and heat capacity. Normally, the specific heat capacity of a glass is close to that of the crystal, i.e., well below that of the liquid. The absolute values of the changes in thermodynamic

variables are quite comparable to those of crystallization/melting. Accordingly, T_g in both polymers and food systems can be measured by various techniques termed thermal analysis (Haines, 2002). The glass transition is a kinetically controlled structure formation process. Unlike T_m , which is well defined by an abrupt change in the temperature dependence of thermodynamic variables, the glass transition usually covers quite a wide region (up to 10–30°C around T_g) on the temperature scale. The size of this region depends on the rate of cooling/heating and loading.

Molecular parameters influencing T_g and T_m are chain stiffness, intermolecular interactions, and molecular weight. Other factors are the presence of other macromolecules, water, and other plasticizers. These parameters simultaneously and differently affect both T_g and T_m values. Figure 3 schematically shows a thermomechanical curve typical of both low moisture food systems and polymer materials. The thermomechanical curve characterizes a change in deformability of a material during heating at a constant rate (Jones, 2002). It presents the relative deformation-temperature (D-T) dependence at a constant value of periodically applied stress and constant loading-unloading times. The thermomechanical curve shows that during heating the deformability of a glassy material is greatly increased in the vicinity of T_g and T_m . These two jumps in deformability correspond to the transitions from the solid glassy state to the rubber-like elastic state at T_g and then to the viscous liquid state at T_m . Above T_g deformability increases (i.e., the elastic modulus sharply drops), becomes nearly constant and reversible, i.e., forms a so-called “rubbery plateau.” Deformability change with temperature is relatively small between the two transition temperatures, T_g and T_m , and below T_g . Both changes are reversible. Upon cooling, the viscoelastic melt and the rubber-like system are again glassy. Above T_m the deformation is partly irreversible. Figure 3 presents three sub-states of the amorphous solid state distinguishable on a temperature scale. These sub-states represent brittle, non-brittle glassy, and rubber-like materials. Many food systems can exist in each of these sub-states of matter. It should be noted the term “rubbery-like,” which is widely used in food science, is quite arbitrary.

The dynamics of polymer chains is different above, below and in the vicinity of T_g . The glass transition can be determined as the temperature range at which segment motion of macromolecules becomes thermally activated. The physical cross-links are labile above T_g and “frozen” below T_g . The cross-linking density decreases the distance between the cross-links. Movement of more flexible chains leads to a denser packaging of macromolecules in the glassy state.

We can distinguish materials with rigid (a) and flexible (b) macromolecular chains. Normally, biopolymer chains are rigid due to large side groups, high degree of conformation and presence of groups forming hydrogen bonds, i.e., strong inter- and intramolecular attractive forces. An increase in intermolecular attractive forces, i.e., in the

cohesive energy density, reduces chain flexibility and increases the T_g . Usually biopolymers exhibit high T_g values and form rigid dry materials, which are more similar to plastics than rubbers. Some biopolymers are more flexible and this property leads to higher deformability in rubbery and melted states.

Plasticizers and water

Water is the main solvent and plasticizer in biological and food systems (Jones, 2002). The effect of a plasticizer consists in decreasing the critical transitions temperatures T_g and T_m and increasing the deformability of the basic polymer above the glass transition temperatures. Addition of a plasticizer to a rigid chain material can transform the system to a highly viscous liquid or a rubber-like solid. The absence of rubber-like elasticity is typical for highly rigid macromolecules. A plasticizer decreases and brings closer both T_g and T_m , and reduces the viscosity and the elastic modulus of the system.

Plasticization is due to several factors. The first is an affinity of the plasticizer, water, to the macromolecular compound, and its interactions with charged and polar groups. The second factor is an increase in the distance between macromolecules (see *Shrinkage and Swelling Phenomena in Agricultural Products*) and a decrease in intermolecular interaction due to dilution with water. These plasticizing mechanisms, together with factors such as the lowest molecular weight of water, its low density, high dielectric constant, highly pronounced ability of forming H-bonds, and low T_g (see *Water in Forming Agricultural Products*), make water the most effective plasticizer for macromolecular structures of biological origin (see *Water Effects on Physical Properties of Raw Materials and Foods*) and the best solvent for polar and charged biopolymers. Relatively small amount of adsorbed water, which is not available as a solvent, is the most efficient plasticizer. Molecular mobility of a plasticizer usually results in its loss, by either evaporation or extraction by the medium (see *Drying of Agricultural Products*).

Aggregated bio-materials

(See also Blahovec, 2007)

The most biological structures are aggregated structures in which the substances of different state participate one with another. This is typical also for the other structures based on structure units of complicated properties. Generally, we can wait that all the basic matter states could participate at the aggregate architecture that could be crudely described in the three state diagrams (see *Water in Forming Agricultural Products*) based on participation of dry matter, water, and air in the product.

The three state diagram describes all the possible participations of the basic state components in the material. We can speculate about the state property of the aggregate and we have to take into account the main properties laying in basis of the state classification of the aggregate: its compressibility and shape change ability.

Analysis of the properties of many cellular (Gibson and Ashby, 1988) and particular materials (see [Soil Aggregates, Structure, and Stability](#)) shows that participation of the basic state components in the volume of the aggregated material is not important for the resultant state character of the aggregate. The concentration of the gaseous components is usually meaningless for the gaseous character of the aggregate. The aggregates with high gas concentration are usually unstable in the gravitational field and they form the real gas-like aggregates only in the special cases in which the gaseous state is stabilized by motion of the gaseous component to overcome gravitational sedimentation due to different densities of different state components. This is very frequent in dusts, fogs, boils, droplets, etc. The aggregates of this type then can be classified really as fluids during the permanent stabilization process.

The solid-like aggregates and liquid-like aggregates are more stable than the aggregates previously described. Most of them are built on the solid and/or liquid basis like solutions, colloids, gels, suspensions, emulsions, etc. The most frequent are the multi-state aggregates with relatively big structural units being in contact at their external surfaces. When the contact forces between the structural units are low, e.g., of the frictional character, then the structural units are relatively free and movable one from the other, and we speak about particles forming the particular materials. The particular materials easily change their shape in flowing processes, classifying them as fluids even in cases in which the important part of the material volume is formed by solids (see [Aeration of Soils and Plants](#)). The sands are a good example of this kind of material (see [Soil Aggregates, Structure, and Stability](#)); in sands about half of their volume is occupied by stony particles and the other volume, the inter-particle spaces, is occupied either by water or by air. It is well known that sands are fluid-like despite the high content of solids.

In other aggregates, the contact forces among the structural units are high, i.e., they are formed by chemical bonds of the soft character at least, and the connections among the structural units cover a big part of their surface. We speak then about cellular structures that behave rather as solid materials even in cases where big amounts of the cellular volume is represented by fluids (Fung, 1993). We use this method to classify some agricultural aggregates. Soil (see [Soil Aggregates, Structure, and Stability](#)) is a material that can be classified in many cases as a particular one: really, sands and light not-compressed soils are easy movable. Other aggregates, in which the bonding forces among particles is high (e.g., clay), are classified as the cellular structure. It is clear that the final decision about the state character of soils depends mainly on the level of the cohesion forces rather than on the dry matter content. Water and air contents in wood are very variable but the state character of the wood is not changed by their ratio and the wood is classified as solid.

The relative independence of the aggregates of biological origin on the relative participation of substances of different state is clearly demonstrated by fruit or vegetable tissues. The moisture content (see [Water in Forming Agricultural Products; Fruits, Mechanical Properties and Bruise Susceptibility, Microstructure of Plant Tissue](#)) in many of those aggregates is higher than 90% but these aggregates behave as solids (see [Physical Properties of Raw Materials and Agricultural Products](#))! These rather surprising results are based on tough cellular walls connected one to another by many bonds of medium strength and filled by quasi-liquid sap of high turgor pressure (see [Microstructure of Plant Tissue](#)). The solid properties of the cellular aggregates are determined by the complex properties of the cellular walls.

Role of water in cellular structure

(See also [Water Effects on Physical Properties of Raw Materials and Foods](#))

Moisture content in every material is not an independent value; storing the material in a box with some definite air humidity results in moisture content changes depending on the difference between water activity in the material and humidity of the surrounding air (see [Adsorption Energy of Water on Biological Materials](#)). These changes are drying or adsorption depending on the water activity and humidity difference (see [Drying of Agricultural Products](#)). The final spontaneous end of the process is the equilibrium – the state in which the air relative humidity has the same value as the water activity of the material (Oertli, 1976). It means that there exists some equilibrium moisture content for a given temperature and water activity. The plot of the equilibrium moisture content (usually based on dry basis – see [Water in Forming Agricultural Products](#)) versus water activity (e.g., different air humidity) at the same temperature is termed sorption isotherm (see [Adsorption Energy of Water on Biological Materials](#)). In many cases the details of sorption isotherms depend on the procedure leading to its values (drying or adsorption – see [Drying of Agricultural Products](#)) forming the so-called sorption hysteresis ([Hysteresis in Foods](#)). Water activity is a very important parameter because its value predetermines the rate of many biochemical and biological processes in the materials including the rate of microbial growth (see [Adsorption Energy of Water on Biological Materials; Physical Phenomena and Properties Important for Storage of Agricultural Products](#)).

At the same moisture content water activity increases with increasing temperature.

In the cellular structures, water is adsorbed on solid surfaces, in pores and forms solute solutions (see [Shrinkage and Swelling Phenomena in Agricultural Products](#)). The part of water bound in cell solute solutions is a source of cell wall “turgor pressure” as a result of selective cell permeability for water and solutes.

Cellular rheology

(See also *Microstructure of Plant Tissue* and *Plant Biomechanics*)

A crucial role in cell rheology is played by cell walls (Boal, 2002). Cell walls are formed by many biopolymers (Heimburg, 2007). Water serves as a plasticizer also in this case and the strength of the cell walls materials increases with increasing moisture content significantly. This trend is typical also for cellular materials with moisture content below 10% w.b. at the beginning of the corresponding sorption isotherm. The cell wall materials that form substantial part of the cellular material at these conditions can be classified as brittle and water as a plasticizer only reduces the probability of the brittle fracture. At higher moisture contents, the water plays more complicated role that affects mainly cell wall properties. Removing of water from the tissue structure can lead to substantial increase of the yield strain (for apples in order of hundreds% - Lin and Pitt, 1986) and also stress. In wet conditions, the moisture content in cells increases causing an increase of the turgor pressure and then also of the modulus of elasticity.

Rheology of cellular materials can be then divided into three different regions:

1. *Rheology of turbid cellular materials (turgor pressure is higher than zero).* Water penetrates cell walls and causes an increase of the internal (turgor) pressure on the cellular walls and thus it acts as a source of the product toughness. This process is influenced by the cellular solutions and the solutes concentration in the solutions depending on the cell wall properties. There are important differences among different products. Sources of the differences should be found not only in the cellular walls but also in the concentrations and properties of the cellular solutions. The role of water as plasticizer is limited. The toughness of the structure decreases with decreasing turgor pressure but the yield stress increases at the same conditions. The region in plants is well limited by the point of wilting at water potential approximately -1.5 MPa (Richter, 1976). The turbid state is typical for soft fruits and vegetables, with bigger cells and thin cell walls (Fung, 1993). Flowing of the materials included into this region increases with increasing level of loading (Blahovec, 2007).
2. *Rheology of flaccid cellular materials.* Turgor pressure does not play the previous most important role (there is zero in the basic state) but the yield stress increases with decreasing water activity as a result of the formation of the nonzero intercellular stress due to deformation. Water plays its role of the polymer plasticizer. The lower water potential, the lower the moisture content and then the yield point and the strength points are higher (Lin and Pitt, 1986). This group is formed by very wide spectrum of materials starting with soft flaccid products like wilted vegetable and fruits or soft animal organs and finishing with products like moist wood or moist cereals. Flowing in this group is very

variable and depends on the type of material, temperature, strain rate, and plasticizing in a similar way as it was described in thermomechanics of biopolymers.

3. *Rheology of cellular structure in brittle state.* At moisture content lower than 10%, water in the cellular structure is close to monomolecular state of water (Van den Berg and Bruin, 1981; Blahovec, 2007). Water plays its role of the polymer plasticizer. In this state, crack formation is so frequent that this process is an important source of strength decrease with decreasing moisture content. The brittle state in cellular structures does not differ from the same state of the other polymeric materials. All dry or dried products are included into this group, moreover all brittle components, like bones or shells, are included. Flowing of the materials of this group is observed sporadically.

Conclusion

Agricultural products and foods form very wide spectrum of materials with properties that vary with temperature and strain rate. At low temperatures and high deformation rates, the products are deformed as brittle solids. With increasing temperature, the deformability of the products increases but the changes are rather of step-wise character with characteristic temperatures. The first step is the glassing state with permanent increase of deformability with increasing temperature. At glass transition temperature, the state of the crucial components of the product is changed substantially and deformability strongly increases. In the rubbery state the deformability is approximately constant. This state is finished by “melting” of the crucial components and entrance of the system in the viscoelastic state, the state with typical flowing of the crucial components. The temperature scenario finishes by thermal destruction of the product.

In agricultural products, a big role in their rheology is usually played by the cell walls. Water plays two roles in the materials of this type (cellular), the first one is the traditional role of plasticizer in the cell wall system, and the second is its participation in forming the turgor pressure inside the cells due to cell walls with selective permeability.

There are two ways for the description of the rheological properties of the agricultural products. The first one is a macroscopic phenomenology, which is based on rheological functions that copy changes in the structural character of the products (different states) respecting temperature, strain rate, and water content and further additives. The second one is based on a deeper understanding of the microscopic processes, which control flowing at different conditions.

Bibliography

- Blahovec, J., 2002. Stress relaxation in potato. Before and after cooking. In Blahovec, J., and Kutilek, M. (eds.), *Physical Methods in Agriculture. Approach to Precision and Quality*. New York: Kluwer Academic/Plenum Publishers, pp. 137–155.

- Blahovec, J., 2007. Role of water in food and product texture. *International Agrophysics*, **21**, 209–215.
- Blahovec, J., 2008. *Agromaterials. Study Guide*. Prague: Czech University of Life Sciences.
- Boal, D., 2002. *Mechanics of the Cell*. Cambridge: Cambridge University Press.
- Ferry, J. D., 1980. *Viscoelastic Properties of Polymers*. New York: Wiley.
- Fung, I. C., 1993. *Biomechanics. Mechanical Properties of Living Tissues*. New York: Springer-Verlag.
- Gibson, L. J., and Ashby, M. F., 1988. *Cellular solids. Structure & Properties*. Oxford: Pergamon Press.
- Gross, B., 1953. *Mathematical Structure of the Theories of Viscoelasticity*. Paris: Herman.
- Haines, P. J., 2002. *Principles of Thermal Analysis and Calorimetry*. Cambridge: Royal Society of Chemistry.
- Heimburg, T., 2007. *Thermal Biophysics of Membranes*. Weinheim: Wiley-VCH Verlag GmbH&Co.KGaA.
- Jones, R. A. L., 2002. *Soft Condensed Matter*. Oxford: Oxford University Press.
- Lin, T.-T., and Pitt, R. E., 1986. Rheology of apple and potato tissue as affected by cell turgor pressure. *Journal of Texture Studies*, **17**, 291–313.
- Mohsenin, N. N., 1986. *Physical Properties of Plant and Animal Materials*. Emmapplein: Gordon & Breach Science Publishers Ltd.
- Oertli, J. J., 1976. The states of water in the plant. Theoretical considerations. In Lange, O. L., Kappen, L., and Schulze, E.-D. (eds.), *Water and Plant Life. Problems and Modern Approaches*. Berlin: Springer-Verlag, pp. 19–31.
- Richter, H., 1976. The water status in the plant experimental evidence. In Lange, O. L., Kappen, L., and Schulze, E.-D. (eds.), *Water and Plant Life. Problems and Modern Approaches*. Berlin: Springer-Verlag.
- Rubinstein, M., and Colby, R. H., 2003. *Polymer Physics*. Oxford: Oxford University Press.
- Steffe, J. F., 1996. *Rheological Methods in Food Process Engineering*. East Lansing, USA: Freeman Press.
- Steffe, J. F., and Daubert, C. R., 2006. *Bioprocessing Pipelines: Rheology and Analysis*. East Lansing, USA: Freeman Press.
- Strick, T. R., Dessinges, M-N., Charvin, G., Dekker, N. H., Allemand, J-F., Bensimon, D., and Croquette, V., 2003. Stretching of macromolecules and proteins. *Reports on Progress in Physics*, **66**, 1–45.
- Tolstoguzov, V. B., 2000. The importance of glassy biopolymer components in food. *Nahrung*, **44**, 76–84.
- Van den Berg, C., and Bruin, S., 1981. Water activity and its estimation in food systems: Theoretical aspects. In Rockland, L. B., and Stuards, G. F. (eds.), *Water Activity. Influence on Food Quality*. New York: Academic Press, pp. 1–61.
- Ward, I. M., 1983. *Mechanical Properties of Solid Polymers*. New York: John Wiley & Sons Inc.
- Wunderlich, B., 2005. *Thermal Analysis of Polymeric Materials*. Berlin: Springer-Verlag.
- Physical Properties as Indicators of Food Quality**
Physical Properties of Raw Materials and Agricultural Products
Plant Biomechanics
Quality of Agricultural Products in Relation to Physical Conditions
Shrinkage and Swelling Phenomena in Agricultural Products
Soil Aggregates, Structure, and Stability
Stress–Strain Relations
Thermal Technologies in Food Processing
Water Effects on Physical Properties of Raw Materials and Foods
Water in Forming Agricultural Products

RHEOLOGY IN SOILS

Wibke Markgraf

Institute for Plant Nutrition and Soil Science, Christian-Albrechts-University zu Kiel, Kiel, Germany

Definition

Rheology Greek: *rhei* ($\rho\epsilon\iota$): flow; *logos* ($\lambda\circ\gamma\circ\sigma$): science; science of flow behavior.

ta panta rhei ($\tau\alpha\pi\alpha\tau\alpha\rho\epsilon\iota$) Everything flows (Heraklit, ~2500 year BP).

Introduction

Rheology is a science dealing with the mechanical behavior of fluids and plastic bodies when subjected to external stresses. Hooke's law for a perfect elastic body, Newton's law for ideal fluids, and finally, Bingham's yield represent terms on which rheology is based (Bingham, 1922). Theoretical aspects of rheology are the relation of the flow/deformation behavior of material and its internal structure (e.g., the orientation of particles) and the flow/deformation behavior of materials that cannot be described by classical fluid mechanics or elasticity.

Fundamentals of rheology: thixotropy and rheopexy

Thixotropic (thixis ($\tau\iota\xi\iota\sigma$): touch; tropous ($\tau\rho\pi\circ\sigma$): turn, change) behavior is a time-dependent phenomenon. The viscosity η (Pa s) of a pseudoplastic non-Newtonian fluid decreases, the longer the influence of any applied shear stress σ (Pa) (= shear thinning). Hence, soil liquefaction (cp. quicksand) may occur due to mechanical disturbance (i.e., vibrations), or due to the influence of salt under saturated conditions. In opposite to this, the solidification of a non-Newtonian fluid due to an increasing shear rate $\dot{\gamma}$ (s^{-1}) is defined as rheoplectic, shear-thickening behavior (i.e., gypsum pastes), whereas dilatant flow is given under time-independent conditions (Bingham, 1922; McMillen, 1932; Barnes et al., 1989; Jasmund and Lagaly, 1993; Macosko, 1994; Mezger, 2002) (Figure 1).

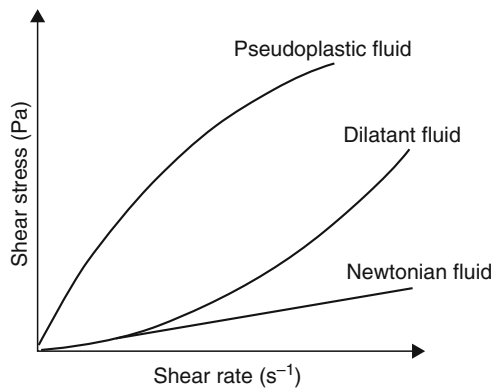
Rheometry

The measurement of rheological parameters (= rheometry) is commonly applied in chemical industry, e.g., food science (see *Rheology in Agricultural Products and Foods*),

Cross-references

- Adsorption Energy of Water on Biological Materials
- Aeration of Soils and Plants
- Agrophysical Objects (Soils, Plants, Agricultural Products, and Foods)
- Agrophysical Properties and Processes
- Drying of Agricultural Products
- Fruits, Mechanical Properties and Bruise Susceptibility
- Hysteresis in Foods
- Microstructure of Plant Tissue
- Physical Phenomena and Properties Important for Storage of Agricultural Products

polymer research, ceramics, coatings, or building material production, in which quality assurance is indispensable (Mezger, 2002). In soil science, rheological terms such as the liquid limit (yield stress), according to Atterberg

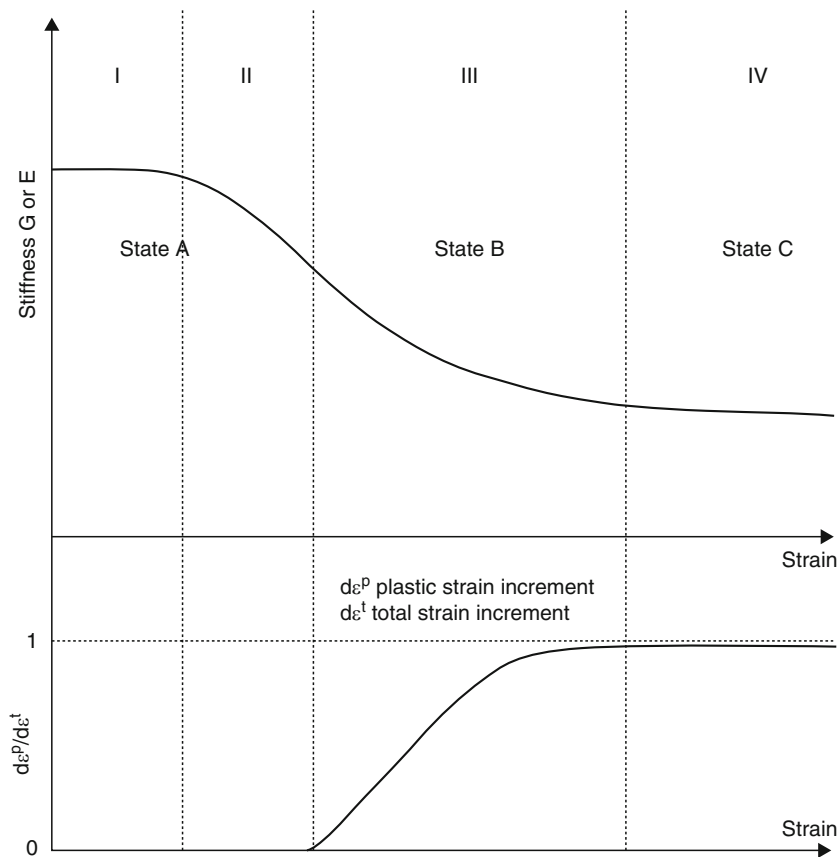


Rheology in Soils, Figure 1 Different types of responses (shear stress σ) to a change in strain rate ($d\varepsilon/dt$).

(1914), elasticity in terms of “full recovery,” plastic flow, or cohesion are well known but are generally regarded to mesoscale (core) stress–strain considerations. With regard to colloidal science, shear tests of clay suspensions have been applied to achieve rheological data (Jasmund and Lagaly, 1993); this knowledge has been transferred and adapted to soil scientific considerations. However, due to technical progress and development of new and powerful, sensitive measuring devices, rheometry could be established in the research field of soil micromechanics within the last 20 years. In research works of Ghezzehei and Or (2001), Markgraf (2006), Markgraf and Horn (2006a), Markgraf and Horn (2006b), Markgraf et al. (2006), Markgraf and Horn (2007), rheometry is introduced as soil mechanical method and is being optimized continuously (Markgraf and Horn, 2009).

Rheometry in soil micromechanics

Kézdi (1974) and Mitchell and Soga (2005) give a general introduction to deformation characteristics. They state that strains consist of elastic and plastic parts. Transferred to



Rheology in Soils, Figure 2 Four zones of deformation characterization: stiffness degradation and plastic strain development; an increasing stiffness degradation is associated by an increase of plastic strain. The part of plastic strain ($d\varepsilon^p$) is 0 in state A, the region of true and nonlinear elasticity, is approximating in state B, the region of pre-yielding, and equals total strain ($d\varepsilon^t$) in state C, the full plastic region. (After Jardine, 1992.)

rheological understanding, combinations of elastic and plastic or plastic and viscous compounds are possible. Soil can be defined as viscoelastic material (Markgraf et al., 2006). In soil mechanics, it is assumed that plastic strains develop only when the stress state satisfies some failure criterion (see [Stress–Strain Relations](#)).

According to this fundamental definition, the yield point differentiates the state of soil between elastic and plastic (viscous). From a soil mechanical point of view, there is no distinct transition from elastic to plastic behavior, which is related to cyclic loading. In solid mechanics, the small strain shear modulus G (Pa) (or Young's modulus E) is defined as:

$$G = \tau_c / \gamma_c \quad (1)$$

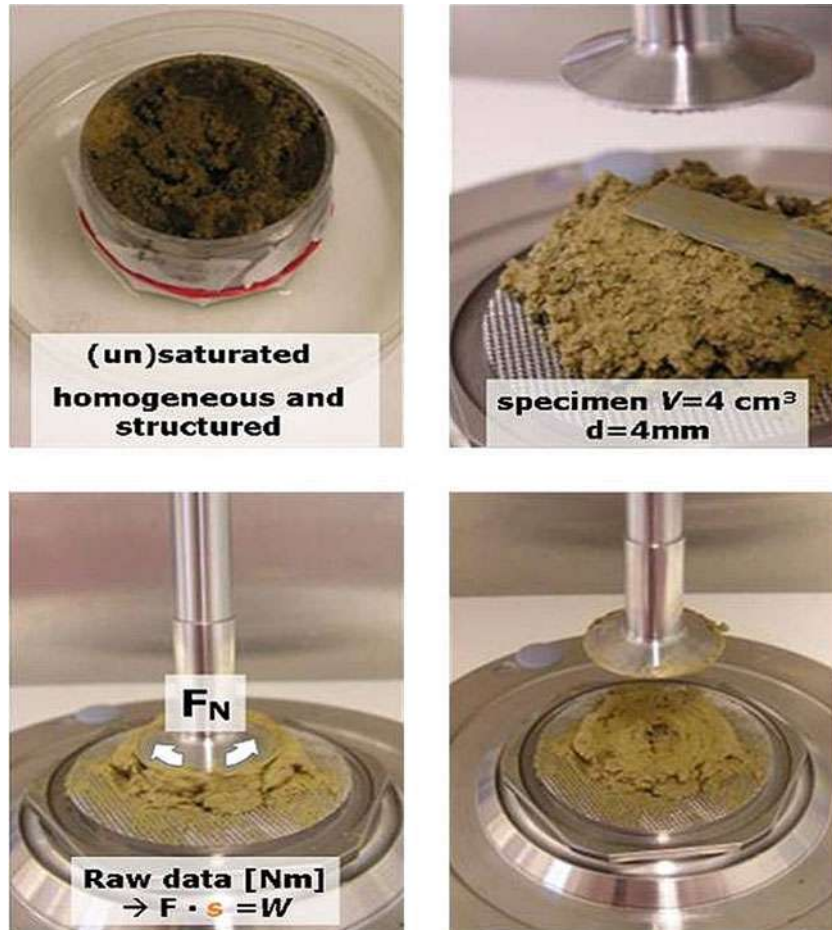
τ_c is the applied shear stress (Pa) and γ_c is the corresponding shear strain (%).

Under small stresses, strains of solid materials are more or less proportional to the applied stress. The constant of

proportionality (elasticity) is given by the inverse of Young's modulus of elasticity, which is a parameter of stiffness. Thus, elasticity is typically modeled by using the linear relationship between stress and strain. The classic theoretical example of linear elasticity is the perfect spring, whose behavior is described by Hooke's law. However, linear elasticity is an approximation, whereas natural, real materials exhibit some degree of nonlinear behavior.

Viscoelastic material models are frequently used to describe the behavior of plastics, polymers, or soil particles (soil network as three phase system). Commonly applied viscoelastic models are the Kelvin–Vogt and the Maxwell model for viscoelastic fluids or solids, respectively. Each model can be represented by spring and dashpot sets in combinations of series and parallel elements (Kézdi, 1974; Mezger, 2002).

Fundamental knowledge of soil stiffness in the linear elastic region is important for evaluating soil response



Rheology in Soils, Figure 3 Preparation and application of soil material for an Amplitude sweep test with controlled shear deformation. A rotational rheometer (MCR 300, Paar Physica, Ostfildern, Germany), profiled parallel-plate-measuring system (25 mm) is used; raw data is achieved by path-controlled force and recorded as torsional moment. This data defines storage and loss modulus G' (Pa); G'' (Pa), and deriving parameters, such as the dimensionless loss factor $\tan \delta$ ($= G''/G'$).

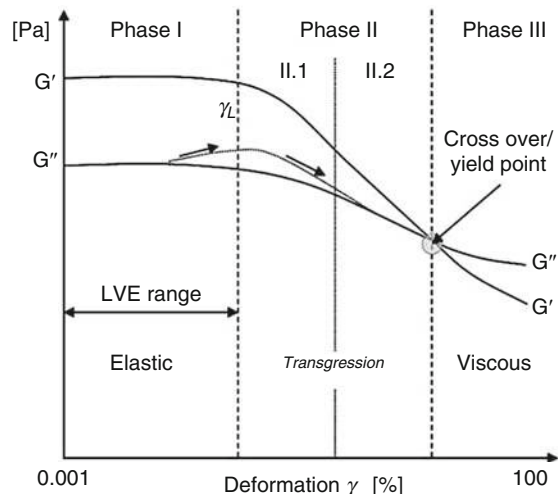
under dynamic loadings such as mechanical or vehicle vibrations (Garciano et al., 2001). It also provides indirect information regarding the state and structure of natural soil. Therefore, stiffness values can be used to assess the quality of soil samples. The linear elastic stiffness of soils is evaluated from measurements of elastic wave velocities or use of displacement transducers. Theoretical analyses of elastic waves are described in detail in Santamarina (2001). For a characterization of deformation, it is useful to differentiate between four zones and three states (Figure 2) (Jardine, 1992):

- Zone 1: True elastic region
- Zone 2: Nonlinear elastic region
- Zone 3: Pre-yield plastic region
- Zone 4: Full plastic region

Above a certain stress known as the elastic limit or the yield strength of an elastic material, the relationship between stress and strain is breaking down. Beyond this limit, the solid may deform irreversibly, exhibiting plasticity. This phenomenon is often observed using stress-strain curves.

Amplitude sweep test: quantifying stiffness degradation

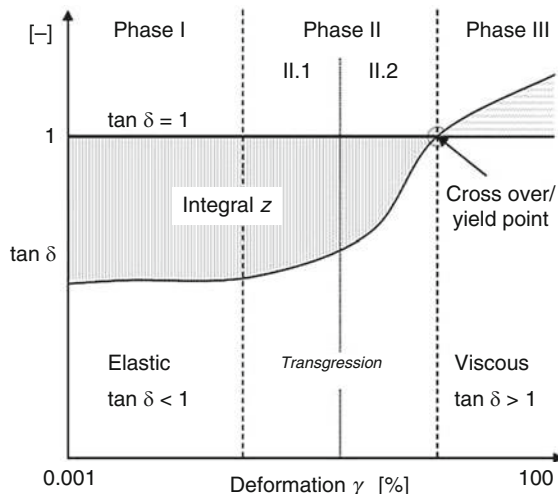
A rotational rheometer with a parallel-plate measuring device can be used to achieve parameters, which define soil as viscoelastic material (Figure 3) according to Maxwell's model, in which both Hooke's law of ideal elastic bodies and Newton's law of ideal viscous fluids are considered (Mezger, 2002). Amplitude sweep tests (AST) under oscillatory condition are conducted, with controlled shear deformation (CSD) $\gamma = 0.0001\dots$



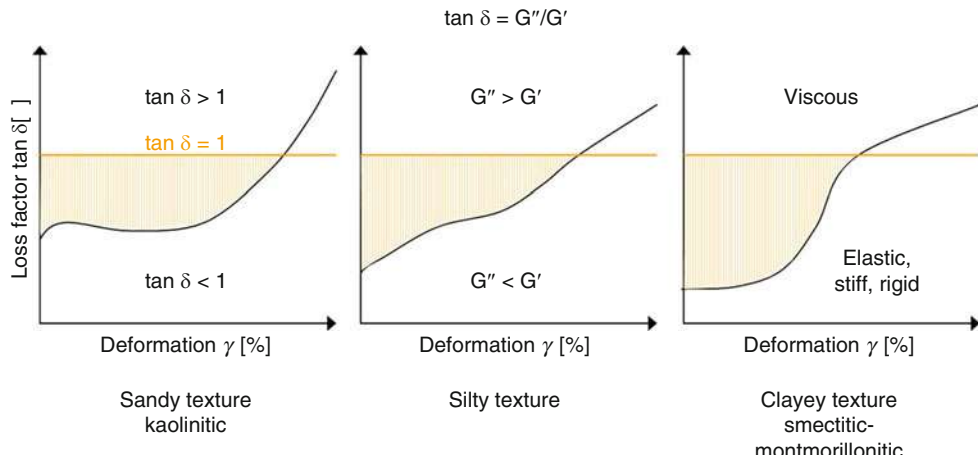
100%, an angular frequency $\omega = \pi s^{-1}$ ($f = 0.5$ Hz), and 30 measuring points, which lead to an average test duration of 15 min. A plate distance of 4 mm is preset according to a plate radius of the rotating bob of 25 mm and the given texture ($>2\text{ }\mu\text{m}$). Tests are operated by using the software US 200 (Paar Physica, Ostfildern, Germany). During all tests, a constant temperature of 20°C is maintained, regulated by a Peltier unit (see Video 1) (Markgraf, 2006; Markgraf et al., 2006).

From the stress-strain relationship in oscillation, with preset deformation γ (%), specific parameters such as the storage modulus G' (Pa), representing elasticity, stiffness, or rigidity of a material, the loss modulus G'' (Pa), representing viscosity, and the loss factor $\tan \delta$ ($= G''/G'$) are achieved, including the linear viscoelastic (LVE) deformation range, and deformation limiting value γ_L . Plots of storage and loss modulus (G' and G'') are generated automatically during a test. Three phases of elasticity loss can be identified (Figure 4).

In phase I, the initial or plateau phase, $G' > G''$, a quasi-elastic behavior can be observed. This can be described by an analog of a spring for ideal elastic substances according to Hooke's law. The quasi-elastic stage of soil as viscoelastic solid is defined by the linear viscoelastic (LVE) range and the deriving deformation limit γ_L . At this stage of low strain, a full recovery of the microstructure can be assumed. In phase II.1, a stage of pre-yielding occurs due to higher strain; soil particles are reorientating and microstructural stability is given, but decreasing. At the end of phase II.2, an intersection of G' and G'' indicates the yield point. In comparison, the intersection of $\tan \delta$ with the $\tan \delta = 1$ -line also indicates a complete loss of stiffness and rigidity of the soil microstructure (Markgraf



Rheology in Soils, Figure 4 Representative results from a conducted Amplitude sweep test with controlled shear deformation (CSD). Left: plots of storage and loss modulus G' (Pa); G'' (Pa) vs. deformation γ ; three phases of stiffness degradation are given: Phase I: quasi-elastic stage, Phase II: pre-yielding (II.1), yield point (end of II.2), Phase III: viscous stage, microstructural breakdown, yielding. Right: (same database) loss factor $\tan \delta$ (G''/G') vs. deformation γ ; if $\tan \delta = 1$ is crossed, a viscous character is given. By calculating integral z , stiffness (rigidity; elasticity) can be quantified.



Rheology in Soils, Figure 5 Plots of $\tan \delta$ vs. deformation γ : Classification of different textured soil material. Similar schemes are adaptable for, e.g., influence of cations, organic compounds, water content (menisci forces – pore water pressure).

and Horn, 2009). Due to a calculation of integral z (Figure 4 right), stiffness (structural strength), which includes quasi-elasticity, and pre-yielding behavior, can be quantified. Hence, phase III defines the final stage of structural collapse, $G' < G''$; a viscous character predominates, and substances are creeping or running. This behavior can be represented by a dashpot, an analog for ideal fluids according to Newton's law.

Classification of stiffness degradation

By using loss factor $\tan \delta$, a semiquantitative classification of rigid–nonrigid or elastic–viscous substrates can be done (Figure 5), considering, i.e., water content, sandy, silty, and/or clayey texture, clay mineralogy, (hydr)oxides, organic matter compounds (see *Organic Matter, Effects on Soil Physical Properties and Processes*), and ionic forces due to the application of fertilizer (see *Liming, Effects on Soil Properties*), irrigation water, or naturally given factor (e.g., soils in arid regions, coastal areas) (Markgraf and Horn, 2006b; Markgraf and Horn, 2007; Markgraf and Horn, 2009) (see *Alkalinity, Physical Effects on Soils* and *Salinity, Physical Effects on Soils*).

Conclusion

Rheological techniques are an appropriate tool to investigate and quantify microstructural stability and stiffness degradation of soil on a particle–particle scale. Furthermore, it can be combined with and extended by other methods that are intertwined in micromechanics and physico-chemical investigations on the microscale (microaggregate scale) (see *Soil Aggregates, Structure, and Stability*), i.e., ζ potential measurements (see *Diffuse Double Layer (DDL); Electrokinetic (Zeta) Potential of Soils; Flocculation and Dispersion Phenomena in Soils*), scanning electron microscopy (Markgraf and Horn, 2007), and X-ray diffractometry, or compared to well-known soil physical parameters that are used to achieve

soil mechanical data, i.e., shear strengths, angle of internal friction, cohesion, and soil hydraulics, i.e., shrinkage and swelling processes on the mesoscale (core scale) (see *Shrinkage and Swelling Phenomena in Soils*). With regard to upscaling concepts, rheometry is adaptable to several research areas that are related to soil mechanics and stress–strain considerations, i.e., geophysics, geohydrology, and geochemistry.

Bibliography

- Atterberg, A., 1914. Die Eigenschaften der Bodenkörper und die Plastizität der Böden. *Kolloidchemische Beihete*, **6**, 55–89.
 Barnes, H. A., Hutton, J. F., and Walters, K., 1989. *An Introduction to Rheology. Rheology Series*. Amsterdam, Oxford, New York, Tokyo: Elsevier, Vol. 3.
 Bingham, E. C., 1922. *Fluidity and Plasticity*. New York: McGraw-Hill.
 Garciano, L., Torisu, R., Takeda, J., and Yoshida, J., 2001. Resonance identification and mode shape analysis of tractor vibrations. *Journal of the Japanese Society of Agricultural Machinery*, **63**, 45–50.
 Ghezzehei, T. A., and Or, D., 2001. Rheological properties of wet soils and clays under steady and oscillatory stresses. *Journal of the Soil Science Society of America*, **65**, 624–637.
 Jardine, R. J., 1992. Some observations on the kinematic nature of soil stiffness. *Soils and Foundations*, **32**, 11–124.
 Jasmund, K., and Lagaly, G. (eds.), 1993. *Tonminerale und Tone: Struktur, Eigenschaften, Anwendungen und Einsatz in Industrie und Umwelt*. Darmstadt: Steinkopff-Verlag.
 Kézdi, Á., 1974. *Handbook of Soil Mechanics – Volume 1: Soil Physics*. Budapest: Akadémiai Kiadó.
 Macosko, C. W., 1994. *Rheology – Principles – Measurements, and Applications*. New York: VCH.
 Markgraf, W., 2006. *Microstructural Changes in Soils: Rheological Investigations in Soil Mechanics*. Cumulative Ph.D. Thesis. Christian-Albrechts-University zu Kiel. (available online).
 Markgraf, W., and Horn, R., 2006a. Rheometry in soil mechanics: microstructural changes in a Calcaric Gleysol and a Dystric Planosol. In Horn, R., Fleige, H., Peth, S., and Peng, Xh (eds.), *Soil Management for Sustainability. Advances in Geocology*, Vol. 38, pp. 47–58.

- Markgraf, W., and Horn, R., 2006b. Rheological strength analysis of K⁺-treated and of CaCO₃-rich soils. *Journal of Plant Nutrition and Soil Science*, **169**, 411–419.
- Markgraf, W., Horn, R., and Peth, S., 2006. An approach to rheometry in soil mechanics - structural changes in bentonite, clayey and silty soils. *Soil and Tillage Research*, **91**, 1–14.
- Markgraf, W., and Horn, R., 2007. Scanning electron microscopy – energy dispersive scan analyses and rheological investigations of South-Brazilian soils. *Journal of the Soil Science Society of America*, **71**, 851–859.
- Markgraf, W., and Horn, R., 2009. Rheological investigations in soil micro mechanics: measuring stiffness degradation and structural stability on a particle scale. In Gragg, L. P., and Cassell, J. M. (eds.), *Progress in Management Engineering*. Hauppauge, NY: Nova Science Publishers, 237–279.
- McMillen, E. L., 1932. Thixotropy and plasticity: I. The measurement of thixotropy; II. An empirical equation expressing thixotropic fluidity changes; III. The effect of thixotropy upon plasticity measurements. *Journal of Rheology*, **3**:74–94, 163–195.
- Mezger, T., 2002. *The Rheology-Handbook – For Users of Rotational and Oscillatory Rheometers*. Hannover: Vincentz Verlag.
- Mitchell, J. K., and Soga, K., 2005. *Fundamentals of Soil Behavior*, 3rd edn. Hoboken, NJ: Wiley.
- Santamarina, J. C., 2001. Soil behavior at the microscale: particle forces. In *Proceedings of the Symposium of Soil Behavior and Soft Ground Construction*, in honor of Charles C. Ladd., MIT. pp. 1–32.

Cross-references

- [Alkalinity, Physical Effects on Soils](#)
[Clay Minerals and Organo-Mineral Associates](#)
[Diffuse Double Layer \(DDL\)](#)
[Electrokinetic \(Zeta\) Potential of Soils](#)
[Flocculation and Dispersion Phenomena in Soils](#)
[Liming, Effects on Soil Properties](#)
[Organic Matter, Effects on Soil Physical Properties and processes](#)
[Rheology in Agricultural Products and Foods](#)
[Salinity, Physical Effects on Soils](#)
[Shrinkage and Swelling Phenomena in Soils](#)
[Soil Aggregates, Structure, and Stability](#)
[Stress–Strain Relations](#)

RHEOPEXY

See [Rheology in Soils](#)

RHIZOSPHERE

Jerzy Lipiec, Jan Gliński
Institute of Agrophysics, Polish Academy of Sciences,
Lublin, Poland

Synonyms

The hidden half (of plant) of the hidden half (of roots)

Definition

Considering the phenomena occurring at the root–soil boundary, it is essential to define such terms as: root–soil

interface, rhizoplane, rhizosphere, and bulk soil. The term root–soil interface is defined as a boundary between the outermost root tissues and the particles of soil which are closest to them. The rhizoplane refers to the zone of the external root surface itself (it is the external root surface) (Bowen and Rovira, 1991). The rhizosphere is a zone of soil or other growing medium in which the environment for microbial activity in general is influenced by any root growing in it, distinguishing it from the “bulk” or “non-rhizosphere” soil, which is influenced by growing roots only by the withdrawal of water and nutrients. A reasonable assumption is that the diameter of the rhizosphere at least equals that of the cylinder of soil around a root which root hairs explore and into which they may release root exudates (Russell, 1977). The rhizosphere can be divided into two regions (Lynch, 1982): endorhizosphere, including the inner root region (stele with conducting elements: xylem and phloem, epidermis, cortex, endodermis, and root cap), and ectorhizosphere, including the outer root region (plant and bacterial mucigel, root hairs, root mucilage, and sloughed root cap cells).

Introduction

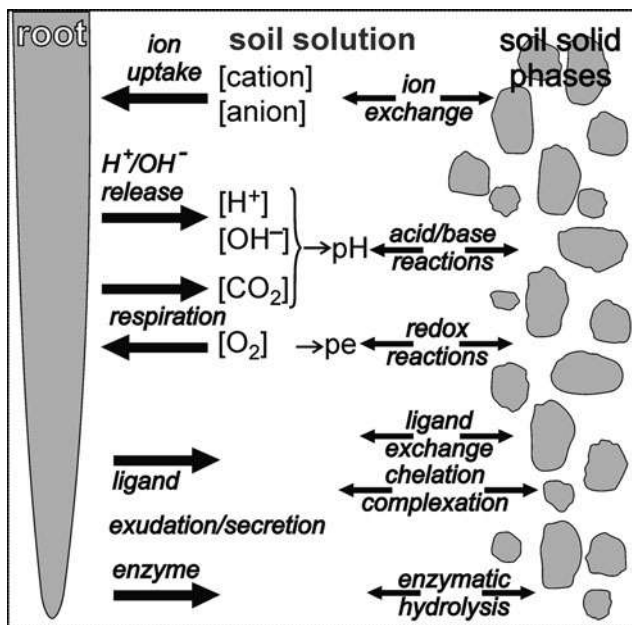
Roots of many higher plants release about 20% of C assimilated by photosynthesis into the soil as rhizodeposits that are substrate for the growth of microbial communities. As a result, the roots are embedded in mucilaginous layers released into the soil by outer root cap cells or produced by root-colonizing microorganisms. These enhance population and activities of microorganisms in the rhizosphere. Typical populations are 10⁹ bacteria, 10⁷ actinomycetes, 10⁶ fungi, 10³ protozoa, and 10³ algae per gram of rhizosphere soil being 50–100 times as many microorganisms as the bulk soil (the rhizosphere effect). Each gram of root can support 36 mg of bacteria which is equal to 2 × 10¹⁰ cells. Some are free-living; others are symbiotic (e.g., root nodule bacteria and mycorrhizal fungi) (Foster et al., 1983). The above microbial changes affect physical and chemical processes and characteristics of the soil. The processes occurring in the rhizosphere influence spatial and temporal heterogeneities in the soil and result in gradients of different sizes (Gliński and Lipiec, 1990; Hinsinger et al., 2005; 2009). The rhizosphere is considered as one of the most fascinating hot spots of activity and diversity in soils (Jones and Hinsinger 2008).

Physical aspects

Figure 1 illustrates the effects of root growth and functions on physical processes occurring in the rhizosphere. The processes affect soil structure and stability, bulk density, porosity, textural composition, root–soil contact, and water relations in the soil.

Soil structure

The role of plant roots in soil structure formation consists generally in soil aggregation (see [Plant Roots and Soil](#)



Rhizosphere, Figure 1 Schematic representation of root functions involved in changes in physical properties in the rhizosphere (After Hinsinger et al., 2005).

Structure. Roots and root hairs penetrating the soil produce lines of weakness along which the clod or soil mass break into smaller aggregates that are stabilized by root exudation with its associated rhizosphere microbial activity (Amellal et al., 1998; Six et al., 2004) and wetting-drying cycles during crop growth (see *Soil Aggregates, Structure, and Stability*). Also the pressure exerted by developing roots may enhance the aggregation. Root hairs and mucilage can form specific structures “rhizosheaths” (McCully, 1999; Hinsinger et al., 2005) around the roots that are particularly strong and affect root–soil water transfer and soil porosity. Functioning of “rhizosheaths” depends on their spatial and temporal geometry (Crawford et al., 2005; Hinsinger et al., 2009). Noninvasive methods (e.g., X-ray, neutron radio) may provide insight for visualizing spatial and temporal dimensions of rhizosphere processes (Hinsinger et al., 2009).

The effects of living roots on soil structure and stability depend on the plant species. Research showed that interactions of root- and microbial-derived mucilages with soil minerals appreciably improve soil structure and stability (see *Mineral–Organic–Microbial Interactions*) (Czarnes et al., 2000). The increase in aggregate stability by maize, soybeans, and wheat roots was attributed to the physical entanglement of aggregates by roots and to the increased production of root exudates resulting from increased root growth (Monroe and Kladivko, 1987). Maize roots, in some cases, can decrease structure stability of soils by chelating iron and aluminum, thus destroying chemical bonds with organic matter.

The mucilaginous layers around the roots affect water transport (Alami et al., 2000; Czarnes et al., 2000) and protect plants against heavy metal toxicity (Gliński and Lipiec, 1990). Soil structure and water status around the root affect spatial distribution of root pathogens (e.g., *Rhizoctonia solani*) (Harris et al., 2003) and minimize the effects of soil drying on bacterial populations within the biofilms (Alami et al., 2000; Hinsinger et al., 2009).

Association composed of fungal hyphae and roots, named mycorrhiza, alters soil acidity and enhances adhesion of soil particles to the root, microbial population, and root exudation; improves soil aggregation; and facilitates uptake of nutrient elements (Jones et al., 2004; Skwaryło-Bednarz and Krzepiłko, 2009). Recent results indicate that the use of arbuscular mycorrhiza may reduce the stressful effects of soil compaction on growth of wheat (Miransari et al., 2008) and maize (Miransari et al., 2007).

Bulk density and strength of soil

Roots growing in the soil occupy space that was previously occupied by soil pore space and soil particles. Since root diameters of most agricultural plants (0.1–3 mm) are usually larger than soil pores (0.002–0.2 mm), soil particles are pushed aside and the bulk density and porosity close to the root–soil interface change (Gliński and Lipiec, 1990; Young, 1998.). In a study by Bruand et al. (1996), maize root reduced porosity by 22–24% and increased bulk density up to 1.80 Mg m^{-3} close by the root–soil interface, although it was 1.54 Mg m^{-3} in the bulk soil. The modeling work of Dexter (1987) indicated that the soil density around roots decreases exponentially with distance from the root surface with an exponent, which is a constant multiple of the root diameter. This can be enhanced in compacted soil where roots are typically shorter and thicker (Lipiec and Simota, 1994). The area is characterized by a higher incidence of oriented clay and greater percent of elongated grains oriented within 30° tangent to the root surface (Gliński and Lipiec, 1990) and micropore porosity (Feeney et al., 2006). Also aggregates adherent to plant roots (“root aggregates”) were denser than those taken from bulk soil due to a decrease in the contribution of larger pores (Guidi et al., 1985). Increase in soil bulk density together with root network results in greater soil strength, shearing resistance, and bearing capacity (Gliński and Lipiec, 1990), and thus increases soil resistance to erosion. (see *Plant Root Strength and Slope Stability*).

Textural and mineralogical composition

Plant roots can modify the textural and mineralogical composition of the soil adjacent to the root. As shown by Sakkar et al. (1979), the rhizosphere in the silty loam compared to bulk soil was relatively higher in the finer fractions ($<6.3 \mu\text{m}$) of 25–35% and of the fine silt ($6.3\text{--}2.0 \mu\text{m}$) in particular, at the expense of the medium and coarse silt fractions. It was explained by an accelerated disaggregation of compound shale fragments into

their component silt/clay particles and by differential packing of soil particles in the volume near the root. The mineralogical changes in the same study were manifested most clearly in the finest clay fractions ($<0.0063\text{ }\mu\text{m}$) and involved a decrease in both regularly and irregularly interstratified $0.0010\text{--}0.0014\text{ }\mu\text{m}$ material: amorphous (extractable) Al, Fe, and C accumulated in the rhizosphere, while Si was depleted. It was due to intensified weathering of soil materials in the vicinity of the plant root.

Root–soil contact

An important physical aspect of the root–soil interface is the contact area between the root and the soil (Gliński and Lipiec, 1990). The degree of this contact affects the movement of water and nutrients from the bulk soil to the root. The contact area in the case of dicotyledons can be increased with time due to cambial increase in root diameter. The monocotyledons have no such progressive thickening. It is known that this contact is not continuous, and it can be weakened either by the enlargement of the cavities or by the decrease in diameter of the roots themselves due to shrinkage at low soil water potentials, and root aging and associated the degeneration of the cortex due to invasion by microorganisms or dessication.

Lack of contact between root and soil may be reduced by the following effects:

- Root hairs proliferation in the humid air of large soil pores and channels
- Formation of a film of water on the root and root hair surfaces, linking them to the soil moisture continuum
- Excretion a layer of root mucilage up to $5\text{ }\mu\text{m}$ thick (on average $1\text{ }\mu\text{m}$), which will bridge small gaps

Root–soil water relations

Root growth and uptake of water affect are primary functions of plant roots that directly alter physical properties of the rhizosphere (Hinsinger et al., 2005). In general, the root water uptake rate decreases with lowering soil water content. The decrease is explained by the increase of hydraulic resistance in the soil–plant system. This resistance, named “the rhizosphere resistance” or “interfacial resistance” appearing in the soil immediately adjacent to each single root, is distinguished from the so-called “pararhizal resistance,” which concerns the movement of water through the bulk soil to the roots (Russell, 1977; Gliński and Lipiec, 1990). If the interfacial resistance is sufficiently high, the roots of a rapidly transpiring plant may reduce the water potential of the neighboring soil to the value near the wilting point, even though the water potential at a short distance away is close to field capacity. Roots affect water in their immediate vicinity, and the quantity of water they can extract is closely related to the soil hydraulic conductivity, soil water potential gradients between roots and soil, and soil water–root contact area (Hasegawa, 1986). Enough water to plant roots was moved until the hydraulic conductivity of the soil fell to around the order of $10^{-5}\text{ cm day}^{-1}$. The root–soil water

relations affect proportion of water-filled and air-filled pores and thereby relative contribution of anaerobic and aerobic organisms (Young and Ritz, 2000).

Physicochemical and chemical aspects

Acidity and redox potential

Through many studies, it is clear that most plant species in their apical root zones increase: the acidification (expressed in pH values), the reducing capacity, and the rate of iron and manganese reduction and their uptake. Also soil microbes can contribute to rhizosphere acidification by producing organic acids (Casarin et al., 2004). Between the rhizosphere and bulk soil, distinct pH gradients up to two units are observed along the root axes (e.g., Nye, 1981). The pH changes are influenced by redox processes in the rhizosphere (Hinsinger et al., 2009).

A particular case of differences in rhizospheric pH within a root system can be observed in the so-called cluster-rooted plants (Gliński and Lipiec, 1990). The root system of these plants is characterized by clusters of finely divided, highly branched sections of roots, called the proteoid roots. Their capacity for acidification of the cluster-rhizosphere soil may drop pH to about 4.5 compared to about 7.0 in the other root zones. Increasing soil acidity leads to the deficiency in soil and uptake by plants of some elements, e.g., phosphate (e.g., Richardson et al., 2009), and decreasing the diversity and richness of soil microbial communities (Fierer and Jackson, 2006; Hinsinger et al., 2009). Root activity in calcareous soils is connected with the formation of water flux toward the root and acidification of root environment. These phenomena form various types of soil structure due to dissolution, movement, and reprecipitation of soil carbonates (Jaillard, 1987).

Two-dimensional developments for studying the changes of pH, redox potential (Eh), and partial pressure of O_2 provide new opportunities for improved understanding rhizosphere processes (Hinsinger et al., 2009).

Water and ions

The uptake behavior of roots changes water and ion movement and the accumulation profile in the rhizosphere differing salt concentration between the rhizosphere soil and the bulk soil (Jungk, 2002). The root system influences ion uptake directly through their flux in aqueous solution to the root surface by diffusion and mass flow induced by the transpiration stream and also by modification of the rhizosphere pH (Gliński and Lipiec, 1990). If water together with ions and other solutes arrive at the root faster than they are absorbed, their accumulation in the rhizosphere increases, increasing the osmotic potential. It causes the diffusion of ions away from the root until a steady state is reached when diffusion away just balances arrival by mass flow. Preferential uptake of either ions or water leads to depletion or accumulation profiles of ions. Examples of this are the depletion zones of phosphorus and potassium (Jungk and Claassen, 1986), the

accumulation in the rhizosphere of calcium (Malzer and Barber, 1971), and the accumulation of sodium and chloride in saline soils (Schleiff, 1980). The examples indicate that the rhizosphere effects on plant nutrition can be beneficial or detrimental.

Examining water content and ion concentration gradients (using the root plane technique) in soil near a plane of onion seedling roots, Dunham and Nye (1973) found that soil water potential gradients near roots were steeper in drier than in wetter soil. The process of root growth, if rapid enough, can reduce the effect of the localized draw down of both matric and osmotic potential around each root. In the rhizospheric saline soil, the water uptake rates by barley roots were reduced to a greater extent by decreasing soil matric water potentials than by decreasing soil osmotic water potential (Schleiff, 1986).

Summary

There is substantial evidence that the root-mediated processes within the rhizosphere enhance soil aggregation and stability, increase the soil bulk density and strength next to the roots, alter soil acidity, and affect accessibility of nutrients to the plants and root water uptake. The water extracted by roots is related to the soil hydraulic conductivity, soil water potential gradients between roots and soil and soil water–root contact area. The rhizosphere processes induce much spatial and temporal heterogeneity in the soil. Root–microbial–mineral interactions associations may reduce the stressful effects of soil drying and compaction on root growth and biological activity. Further research on holistic perception of the rhizosphere, including the connections between the biology, physics, and chemistry, and on how to bridge the rhizosphere of individual roots to soils at field scales and larger is needed (Hinsinger et al., 2009).

Bibliography

- Alami, Y., Achouak, W., Marol, C., and Heulin, T., 2000. Rhizosphere soil aggregation and plant growth promotion of sunflowers by an exopolysaccharide-producing *Rhizobium* sp. Isolated from sunflower roots. *Applied and Environmental Microbiology*, **66**, 3393–3398.
- Amellal, N., Burtin, G., Bartoli, F., and Heulin, T., 1998. Colonization of wheatroots by an exopolysaccharide-producing *Pantoea agglomerans* strain and its effects on rhizosphere soil aggregation. *Applied and Environmental Microbiology*, **64**, 3740–3747.
- Bowen, G. C., and Rovira, A. D., 1991. The rhizosphere – the hidden half of the hidden half. In Waisel, Y., Eshel, A., and Kaffkafi, U. (eds.), *The Roots-the Hidden Half*. New York: Marcel Dekker, pp. 641–649.
- Bruand, A., Cousin, I., Nicoullaud, B., Duval, O., and Begon, J. C., 1996. Backscattered electron scanning images of soil porosity for analyzing soil compaction around roots. *Soil Science Society of America Journal*, **60**, 895–901.
- Casarini, V., Plassard, C., Hinsinger, P., and Arvieu, J. C., 2004. Quantification of ectomycorrhizal fungal effects on the bioavailability and mobilisation of soil P in the rhizosphere of *Pinus pinaster*. *The New Phytologist*, **163**, 177–185.
- Crawford, J. W., Harris, J. A., Ritz, K., and Young, I. M., 2005. Towards an evolutionary ecology of life in soil. *Trends in Ecology & Evolution*, **20**, 81–86.
- Czarnes, S., Hallett, P. D., Bengough, A. G., and Young, I. M., 2000. Root- and microbial-derived mucilages affect soil structure and water transport. *European Journal of Soil Science*, **51**, 435–443.
- Dexter, A. R., 1987. Compression of soil around roots. *Plant and Soil*, **97**, 401–406.
- Dunham, R. J., and Nye, P. H., 1973. The influence of soil water content on the uptake of ions by roots. I. Soil water content gradients near a plane of onion roots. *Journal of Applied Ecology*, **10**, 585–598.
- Feeley, D. S., Crawford, J. W., Daniell, T., Hallett, P. D., Nunan, N., Ritz, K., Rivers, M., and Young, I. M., 2006. Three-dimensional microorganisation of the soil-root-microbe system. *Microbial Ecology*, **52**, 151–158.
- Fierer, N., and Jackson, R. B., 2006. The diversity and biogeography of soil bacterial communities. *Proceedings of the National Academy of Sciences of the United States of America*, **103**, 626–631.
- Foster, R. C., Rovira, A. D., and Cockk, T. W., 1983. *Ultrastructure of the Root-Soil Interface*. St. Paul, MN: American Phytopathological Society.
- Gliński, J., and Lipiec, J., 1990. *Soil Physical Conditions and Plant Roots*. Boca Raton, FL: CRC Press, p. 250.
- Guidi, G., Poggio, G., and Petruzzelli, G., 1985. The porosity of soil aggregates from bulk soil and from soil adhering to roots. *Plant and Soil*, **87**, 311–314.
- Harris, K., Young, I. M., Gilligan, C. A., Otten, W., and Ritz, K., 2003. Effect of bulk density on the spatial organisation of the fungus *Rhizoctonia solani* in soil. *FEMS Microbiology Ecology*, **44**, 45–56.
- Hasegawa, S., 1986. Changes in soil water contents in the vicinity of soybean roots. *Transactions 13th Congress International Society of Soil Science*, Vol. 2, Hamburg, West Germany, p. 73.
- Hinsinger, P., Gobran, G. R., Peter, J., Gregory, P. J., and Wenzel, W. R., 2005. Research review Rhizosphere geometry and heterogeneity arising from rootmediated physical and chemical processes. *The New Phytologist*, **168**, 293–303.
- Hinsinger, P., Bengough, A. G., Vetterlein, D., and Young, I. M., 2009. Rhizosphere: biophysics, biogeochemistry and ecological relevance. *Plant and Soil*, **321**, 117–152.
- Jaillard, B., 1987. *Rhizomorphic Carbonate Structures: Model of Rearrangement of Soil Minerals by Roots*. Ph.D. thesis, Montpellier, p. 221.
- Jones, D. L., and Hinsinger, P., 2008. The rhizosphere: complex by design. *Plant and Soil*, **312**, 1–6.
- Jones, D. L., Hodge, A., and Kuzyakov, Y., 2004. Plant and mycorrhizal regulation of rhizodeposition. *The New Phytologist*, **163**, 459–480.
- Jungk, A., 2002. Dynamics of nutrient movement at the soil–root interface. In Waisel, Y., Eshel, A., and Kaffkafi, U. (eds.), *Plant Roots: The Hidden Half*, 3rd edn. New York: Marcel Dekker, pp. 587–616.
- Jungk, A., and Claassen, N., 1986. Availability of phosphate and potassium as the result of interactions between root and soil in the rhizosphere. *Zeitschrift fur Pflanzenernahrung und Bodenkunde*, **149**, 411–427.
- Lipiec, J., and Simota, C., 1994. Role of soil and climate factors influencing crop responses to compaction in Central and Eastern Europe. In Soane, B. D., and van Ouwerkerk, C. (eds.), *Soil Compaction in Crop Production*. Amsterdam, The Netherlands: Elsevier, pp. 365–390.
- Lynch, J. M., 1982. The rhizosphere. In Burns, R. G., and Slater, J. H. (eds.), *Experimental Microbial Ecology*. Oxford: Blackwell Scientific, p. 395.
- Malzer, G. L., and Barber, S. A., 1971. Precipitation of calcium and trontium sulfates around plant roots and its evaluation. *Soil Science Society of America Proceedings*, **39**, 492–495.

- McCully, M. E., 1999. Roots in soil: unearthing the complexities of roots and their rhizospheres. *Annual Review of Plant Physiology and Plant Molecular Biology*, **50**, 695–718.
- Miransari, H., Bahrami, H. A., Rejali, F., Malakouti, M. J., and Torabi, H., 2007. Using arbuscular mycorrhiza to reduce the stressful effects of soil compaction on corn (*Zea mays* L.) growth. *Soil Biology and Biochemistry*, **39**, 2014–2026.
- Miransari, M., Bahrami, H. A., Rejali, F., and Malakouti, M. J., 2008. Using arbuscular mycorrhiza to alleviate the stress of soil compaction on wheat (*Triticum aestivum* L.) growth. *Soil Biology and Biochemistry*, **40**, 1197–1206.
- Monroe, C. D., and Kladivko, E. J., 1987. Aggregate stability of a silt loam soil as affected by roots of corn, soybeans and wheat. *Communications in Soil Science and Plant Analysis*, **18**, 1077–1087.
- Nye, P. H., 1981. Changes of pH across the rhizosphere induced by roots. *Plant and Soil*, **61**, 7–16.
- Richardson, A. E., Barea, J. M., McNeill, A. M., and Prigent-Combaret, C., 2009. Acquisition of phosphorus and nitrogen in the rhizosphere and plant growth promotion by microorganisms. *Plant and Soil*, **321**, 305–339.
- Russell, R. S., 1977. *Plant Root Systems*. London: McGraw-Hill, p. 298.
- Sakkar, A. N., Jenkins, D. A., and Wyn Jones, R. G., 1979. Modifications to mechanical and mineralogical composition of soil within the rhizosphere. In Harley, J. L., and Russell, R. S. (eds.), *The Soil-Plant Interface*. London: Academic, p. 125.
- Schleiff, U., 1980. Chloride content of onion roots and their adhering soil under irrigation with saline drainage water. *Zeitschrift für Pflanzenernährung und Bodenkunde*, **143**, 638–644.
- Schleiff, U., 1986. Water uptake by barley roots as affected by the osmotic and matric potential in the rhizosphere. *Plant and Soil*, **94**, 143–147.
- Six, J., Bossuyt, H., Degryze, S., and Denef, K., 2004. A history of research on the link between (micro)aggregates, soil biota, and soil organic matter dynamics. *Soil and Tillage Research*, **79**, 7–31.
- Skwaryło-Bednarz, B., and Krzepiło, A., 2009. Effect of different fertilization on enzyme activity in rhizosphere and non-rhizosphere of amaranth. *International Agrophysics*, **23**, 409–412.
- Young, I. M., 1998. Biophysical interactions at the root–soil interface: a review. *Journal of Agricultural Science*, **130**, 1–7.
- Young, I. M., and Ritz, K., 2000. Tillage, habitat space and function of soil microbes. *Soil and Tillage Research*, **53**, 201–213.

Cross-references

- Biofilms in Soil
 Bulk Density of Soils and Impact on their Hydraulic Properties
 Drought Stress, Effect on Soil Mechanical Impedance and Root (Crop) Growth
 Microbes and Soil Structure
 Microbes, Habitat Space, and Transport in Soil
 Mineral–Organic–Microbial Interactions
 Oxidation–Reduction Reactions in the Environment
 Plant Roots and Soil Structure
 Plant–Soil Interactions, Modeling
 Root Responses to Soil Physical Limitations
 Soil Aggregates, Structure, and Stability

RIGIDITY

The property of a body (e.g., soils, plant stalks) that makes it inflexible, or stiff.

RILL EROSION

An erosion process on sloping fields in which numerous and randomly occurring small channels of only several centimetres in depth are formed; occurs mainly on recently cultivated soils.

Bibliography

Glossary of Soil Science Terms. Soil Science Society of America. 2010. <https://www.soils.org/publications/soils-glossary>

Cross-references

Water Erosion: Environmental and Economical Hazard

ROOT LENGTH DENSITY

See *Soil Hydraulic Properties Affecting Root Water Uptake*

ROOT RESPONSES TO SOIL PHYSICAL LIMITATIONS

A. Glyn Bengough
 Scottish Crop Research Institute (SCRI), Dundee, UK

Synonyms

Effects of soil physical properties on root growth; Hypoxia; Root responses to mechanical impedance; Water stress

Definition

Root responses: Changes in the growth of individual roots and of the root system as a whole. This includes changes in elongation rate, diameter, number of roots, and branching pattern.

Soil physical limitations: The physical properties (soil strength, soil aeration, soil matric potential) of a soil that may restrict root growth.

Context – why soil physical limitations to roots are increasingly important

For good growth, plants require a root system of sufficient size to obtain water and mineral nutrients from the soil they are growing in. In nutrient-poor or dry soils, limitations to root system growth will often restrict water and nutrient uptake, resulting in slower plant growth and restricting crop yield of agricultural plants. Physical limitations – particularly mechanical impedance, hypoxia, water stress, and non-optimal temperature – represent a major restriction to root system growth in many soils (Bengough et al., 2006). The first three limitations occur when the soil water content is non-optimal for root growth and depend on the soil strength, structure, and water

regime. Mechanical impedance occurs where the strength of the soil physical matrix mechanically restricts root growth. Hypoxia occurs where oxygen diffusion to the root, and particularly growing root tips, limits growth. Water stress occurs when the soil water potential surrounding the root tip is sufficiently negative that it restricts water uptake for cell expansion and root tip growth. More than one stress can occur in different parts of a single root system, and even an individual root tip may experience multiple stresses.

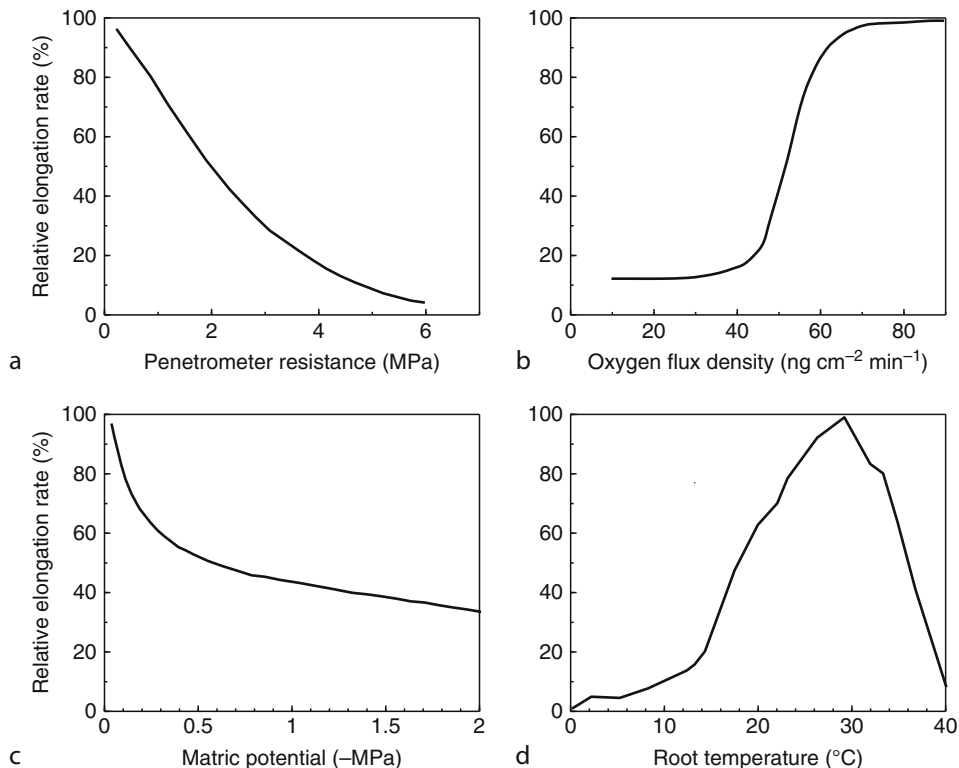
The pressure to increase food production, to satisfy the demand of a rising global population, increases the pressure to put more land under intensive agricultural production. Intensive cultivation, if not carefully managed, can lead to decrease in soil organic matter and hard-setting soils that restrict root growth (Mullins et al., 1987). Predictions of global climate change scenarios include greater local variability of rainfall patterns in many areas that may cause greater oscillations in soil water regime – more intense rainfall events, with longer periods of drought between in many parts of the world. Such large fluctuations in the soil water regime are likely to create adverse physical conditions for root growth. Global environmental change is therefore a strong motivation to understand and, where possible overcome, physical limitations to root

growth, through crop breeding and improved soil management.

In this article, root responses to soil physical stresses are considered, and it should be noted that root responses differ significantly from shoot responses. Readers interested in further information on root responses to the soil physical environment are referred to books by de Kroon and Visser (2003) and Gregory (2006).

Root response to mechanical impedance

Mechanical impedance will be a major restriction to root growth in soils where the penetrometer resistance is greater than 2 MPa, and there are no continuous channels available to provide an alternative pathway for root growth (Bengough and Mullins, 1990; Bengough et al., 2006). In hard soils roots elongate more slowly and root tips thicken (Figure 1a). Root cortical cells are shorter and fatter in mechanically impeded roots, and the cell flux (the rate of adding new cells onto a cell file) is also decreased. Border cells and mucilage are produced by the root tip to create a low-friction sheath around the root that eases its passage into hard soil. These border cells are root cap cells that become detached from the root cap like a disposable drilling tissue. Mucilage is a gel, produced by root cap cells,



Root Responses to Soil Physical Limitations, Figure 1 Examples of relations between root elongation rate and soil physical stresses. (a) Peanut root elongation slows as penetrometer resistance increases (Taylor and Ratliff, 1969). (b) Hypoxia – oat root elongation slows as oxygen diffusion decreases below threshold (Blackwell and Wells, 1983). (c) Maize root elongation slows as matric potential decreases (Sharp et al. 1988). (d) Pecan root growth is greatest at about 30°C (Woodroof, 1934).

that is very slippery and acts as a lubricant between the border cells and the root proper. Mucilage and border cell production are maintained or increased in mechanically impeded roots and have the advantage of decreasing root-soil friction – which is often a major component of penetration resistance for probes pushed into soil.

Root response to hypoxia

Hypoxia is likely to limit root growth if the soil air-filled porosity is less than 10% (i.e., less than 10% of the soil volume is filled with air). In hypoxic soil, root elongation slows, and root tips may thicken (Figure 1b; Blackwell and Wells, 1983). Plants may adapt to hypoxia, depending on species, by producing gas-filled passages in the root cortex called aerenchyma (Armstrong, 1979). Aerenchyma increases the rate of oxygen diffusion along the root axis to the root tip, helping to maintain the oxygen supply to the growing root tip where new cells are being produced in the meristem. In many flooding-resistant plants, new adventitious roots may appear on stem tissue in response to water logging (Blom et al., 1994). These roots contain aerenchyma and may have fewer branches than in non-waterlogged plants.

Root response to water stress

Studies of root responses to water stress are often confounded by changes in soil strength that occur as the soil dries: In most soils, soil drying causes major increase in mechanical impedance to root growth as well as in water stress (Bengough et al., 2006; Whalley et al., 2006). Studies that have carefully separated the effects of water stress from those of mechanical impedance have shown that root tips of non-transpiring seedlings can continue to extend even beyond the permanent wilting point of mesophytic plants (-1.5 MPa matric potential; Figure 1c) in soft growing media such as vermiculite (Sharp et al., 1988). This shows that roots are much less sensitive than shoots to water stress in loose growing media. Root elongation is decreased by water stress and roots become thinner, in contrast to the hypoxia and mechanical impedance responses. Root cortical cells in water-stressed roots are shorter and the rate of cell flux is slower.

Root response to temperature

Temperature affects both the processes of root development and root extension, with root growth slowing or halting if the temperature becomes too hot or too cold (Cooper, 1973; Kaspar and Bland, 1992). The optimum temperature for root growth is between 10°C and 35°C for most species that have been studied experimentally (e.g., Figure 1d; Cooper, 1973). The number of stem-borne (nodal) root axes for cereals increases with the number of leaf nodes – which can be predicted from accumulated thermal time above a base temperature. Indeed, the number of root axes increased linearly with accumulated thermal time at the shoot meristem for pearl millet (Vincent and Gregory, 1989). Primary roots of maize grown at cooler temperature

grew more slowly and were thinner than those at more optimal temperature (Pahlavanian and Silk, 1988). This slower elongation was associated with decreased growth strain rate in the elongation zone, but there was negligible change in the length of this zone.

Interactions between stresses and feedback effects

The underlying growth responses to physical stresses are mediated by biophysical changes in cell wall properties that control cell expansion and in changes in cell flux. More than one stress may affect a single root tip at a particular time. In dry compacted soil, both mechanical impedance and water stress may limit root tip growth whilst, in wet compacted soil, a combination of mechanical impedance and hypoxia may limit growth. Feedback effects will be of considerable importance for crop plants: For example, a compacted plow pan may limit root penetration to depth by creating a large mechanical impedance to growth, resulting in water stress that limits crop yield if sufficient water is not available in the topsoil.

Gaps in knowledge

The most important limitations to root growth in the many different climatic zones and soil types that exist worldwide have not been quantified adequately. The least limiting water range concept provides a useful framework for considering the major soil physical limitations to root growth as a function of time in different soils, and so may allow this problem to be addressed. This could be used to highlight the priorities for future plant breeding and root system selection for problem soils.

The extent to which it will be possible to overcome physical limitations to root growth by breeding plants better adapted to these physical stresses requires more study. Most plant breeding has been centered on improving the yield of crops grown in relatively optimum conditions, and so we need to address the problem of breeding varieties for stressed environments.

Summary

Soil physical stresses represent important limitations to root growth in many soils, and are likely to become of increasing importance in many regions of the world. Root elongation is slowed in response to mechanical impedance, hypoxia, water stress, and temperature stress. This results in decreased root system size with potential reductions in crop yield.

Bibliography

- Armstrong, W., 1979. Aeration in higher plants. *Advances in Botanical Research*, **7**, 226–332.
- Bengough, A. G., and Mullins, C. E., 1990. Mechanical impedance to root growth – a review of experimental techniques and root growth responses. *Journal of Soil Science*, **41**, 341–358.
- Bengough, A. G., Bransby, M. F., Hans, J., McKenna, S. J., Roberts, T. J., and Valentine, T. A., 2006. Root responses to soil physical

- conditions; growth dynamics from field to cell. *Journal of Experimental Botany*, **57**, 437–447.
- Blackwell, P. S., and Wells, E. A., 1983. Limiting oxygen flux densities for oat root extension. *Plant and Soil*, **73**, 129–139.
- Blom, C. W. P. M., Voesenek, L. A. C. J., Banga, M., Engelaar, W. M. H. G., Rijnders, J. H. G. M., Vandesteeg, H. M., and Visser, E. J. W., 1994. Physiological ecology of riverside species – adaptive responses of plants to submergence. *Annals of Botany*, **74**, 253–263.
- Cooper, A. J., 1973. *Root Temperature and Plant Growth*. Slough: Commonwealth Agricultural Bureaux, p. 73.
- de Kroon, D., and Visser, E. J. W., 2003. *Root Ecology*. Berlin: Springer, p. 394.
- Gregory, P. J., 2006. *Plant Roots*. Oxford: Blackwell, p. 318.
- Kaspar, T. C., and Bland, W. L., 1992. Soil-temperature and root-growth. *Soil Science*, **154**, 290–299.
- Mullins, C. E., Young, I. M., Bengough, A. G., and Ley, G. J., 1987. Hard-setting soils. *Soil Use and Management*, **3**, 79–83.
- Pahlavanian, A. M., and Silk, W. K., 1988. Effect of temperature on spatial and temporal aspects of growth in the primary maize root. *Plant Physiology*, **87**, 529–532.
- Sharp, R. E., Silk, W. K., and Hsiao, T. C., 1988. Growth of the primary maize root at low water potentials. I. Spatial distribution of expansive growth. *Plant Physiology*, **87**, 50–57.
- Taylor, H. M., and Ratliff, L. H., 1969. Root elongation rates of cotton and peanuts as a function of soil strength and water content. *Soil Science*, **108**, 113–119.
- Vincent, C. D., and Gregory, P. J., 1989. Effects of temperature on the development and growth of winter wheat roots. I. Controlled glasshouse studies of temperature, nitrogen and irradiance. *Plant and Soil*, **119**, 87–97.
- Whalley, W. R., Clark, L. J., Gowing, D. J. G., Cope, R. E., Lodge, R. J., and Leeds-Harrison, P. B., 2006. Does soil strength play a role in wheat yield losses caused by soil drying? *Plant and Soil*, **280**, 279–290.
- Woodroof, J. G., 1934. Pecan root growth and development. *Journal of Agricultural Science*, **49**, 511–530.

Cross-references

- [Aeration of Soils and Plants](#)
- [Climate Change: Environmental Effects](#)
- [Compaction of Soil](#)
- [Conditioners, Effect on Soil Physical Properties](#)
- [Crop Emergence, the Impact of Mechanical Impedance](#)
- [Crop Responses to Soil Physical Conditions](#)
- [Drought Stress, Effect on Soil Mechanical Impedance and Root \(Crop\) Growth](#)
- [Hardpan Soils: Management](#)
- [Hardsetting Soils: Physical Properties](#)
- [Mechanical Resilience of Degraded Soils](#)
- [Organic Matter, Effects on Soil Physical Properties and Processes](#)
- [Physical Degradation of Soils, Risks and Threats](#)
- [Plant Roots and Soil Structure](#)
- [Root System Architecture: Analysis from Root Systems to Individual Roots](#)
- [Soil Penetrometers and Penetrability](#)
- [Soil Structure and Mechanical Strength](#)
- [Spatial Variability of Soil Physical Properties](#)
- [Subsoil Compaction](#)

ROOT STRENGTH

See [Plant Root Strength and Slope Stability](#)

ROOT SYSTEM ARCHITECTURE: ANALYSIS FROM ROOT SYSTEMS TO INDIVIDUAL ROOTS

Loïc Pagès

INRA Centre d'Avignon, Avignon cedex 9, France

What is the root system architecture? Importance for functioning

The term “architecture” includes two important aspects of the root system: its shape and its structure.

The shape is the three-dimensional arrangement of roots that can be described through several geometrical criteria, as lateral root extension, root depth, or more thoroughly by the distribution of root length density throughout the soil.

The structure refers to the diversity of the components (roots) and their relationships. According to their age and position within the root system, roots have specific physiological characteristics and functions (Waisel and Eshel, 2002). The way they are distributed and connected to each other (i.e., the topology of the system) is usually specific and important for the functioning of the whole system (Fitter, 1987).

Water and mineral uptake, the main function of root systems, requires several steps which illustrate the role of the root system architecture: (1) during the soil-to-root transport of any resource, the shape of the system will determine the length of the transport pathways for this resource; (2) when entering into the plant, permeability of the root surface (a structural attribute) is a main parameter; (3) then, the within-plant transport, from the absorbing root to the final place of use, depends on the conducting capacities of the branching system.

Other functions, such as carbon efflux from the plants to the soil, or anchorage, are also linked to the architecture. Regarding anchorage especially, the geometry and mechanical properties of the main roots will determine the efficiency of the system for this function (Fourcaud et al., 2008).

The dynamics of the architecture are important to consider, since the plant is a changing organism in a changing environment. Moreover, the success of competition with other organisms at the same place depends usually on dynamic aspects and rates of development.

Overview of the root system architecture: classification and diversity

A first overview, although static, can be given through some words that often qualify the diversity of root systems. A common distinction is made between: (1) fibrous (or diffuse, or fasciculate) root systems on the one hand, that are formed by a large number of equivalent roots, directly connected to the stem, and (2) taproot (or central, or conical) root systems on the other hand, that are made by a central and vertical main root (often called the taproot) along which a number of lateral roots originate at various

depths. It is worth noticing that many plants may begin their life exhibiting a taproot system, because the taproot is the dominant root, developed from the embryonic root (radicle). Then, the root system will become fibrous if the lateral roots are numerous and have a dominant development. The distinction is still more difficult when the taproot stays short and the lateral roots are superficial.

Therefore, it is helpful to consider not only the morphology at a given stage, but also the developmental sequence (or “growth strategy”), as suggested by Cannon (1949). Cannon has classified the root system architecture, starting from two fundamental categories (see Figure 1): (1) the primary root system originates from the radicle, which grows downward, and branches acropetally (i.e., from its base to its tip); (2) the secondary root system (also called adventitious root system) originates from the shoot system: roots emerge continuously during shoot development, whereas the radicle gives only a small and temporary root system. In the first category, the architectural types are defined by the relative importance of the taproot and lateral roots, and the distribution of lateral roots’ vigor along the taproot. Most dicotyledonous plants and gymnosperms exhibit a primary root system, associated with a significant radial growth and storage function of the taproot. In the second category, the architectural types depend on the distribution of the adventitious root system on the shoots. It can be centralized when all adventitious roots appear at the shoot base, or diffuse when adventitious roots appear along a running shoot or rhizome or even throughout the erected shoot system. Monocotyledonous plants, which do not have radial growth, develop their root system according to this secondary strategy.

This classification has been applied and completed by Krasilnikov (1968) on trees (see Figure 2). Krasilnikov has also defined a number of morphological types in these two basic categories, and has shown that many root systems are built by combining the two categories. The primary root system is preeminent during the young stages of the plant, while secondary root system will superimpose during the older stages. This superposition makes what he called mixed root systems.

Even though these general developmental patterns of the root system are kept, root system architecture can be deeply modified by special adaptations of some roots. Among these adaptations, let us mention roots playing a particular role for anchorage or support: buttress and stilt roots. Buttress roots develop along the base of the trunk, stabilizing the tree, especially in shallow saturated soils. Stilt roots grow down from lateral branches, and branch into the soil. They are common among mangroves. Regarding nutrition, roots exhibit also several specializations. Aerating roots (or pneumatophores) rise above the ground, have breathing pores to catch air, and provide oxygen to the root system. Tuberous roots are modified lateral roots which work as storage organs, able to store and distribute later various resources. Haustorial roots can absorb water and nutrients from another plant, in the case of parasitic plants.

Because of particular morphogenetic capacities, roots can play an important role in extension and vegetative multiplication of plants. For example, in some species, roots produce shoot buds giving rise to suckers (e.g., Poplars, Black Locust, Cherry tree, Raspberry).

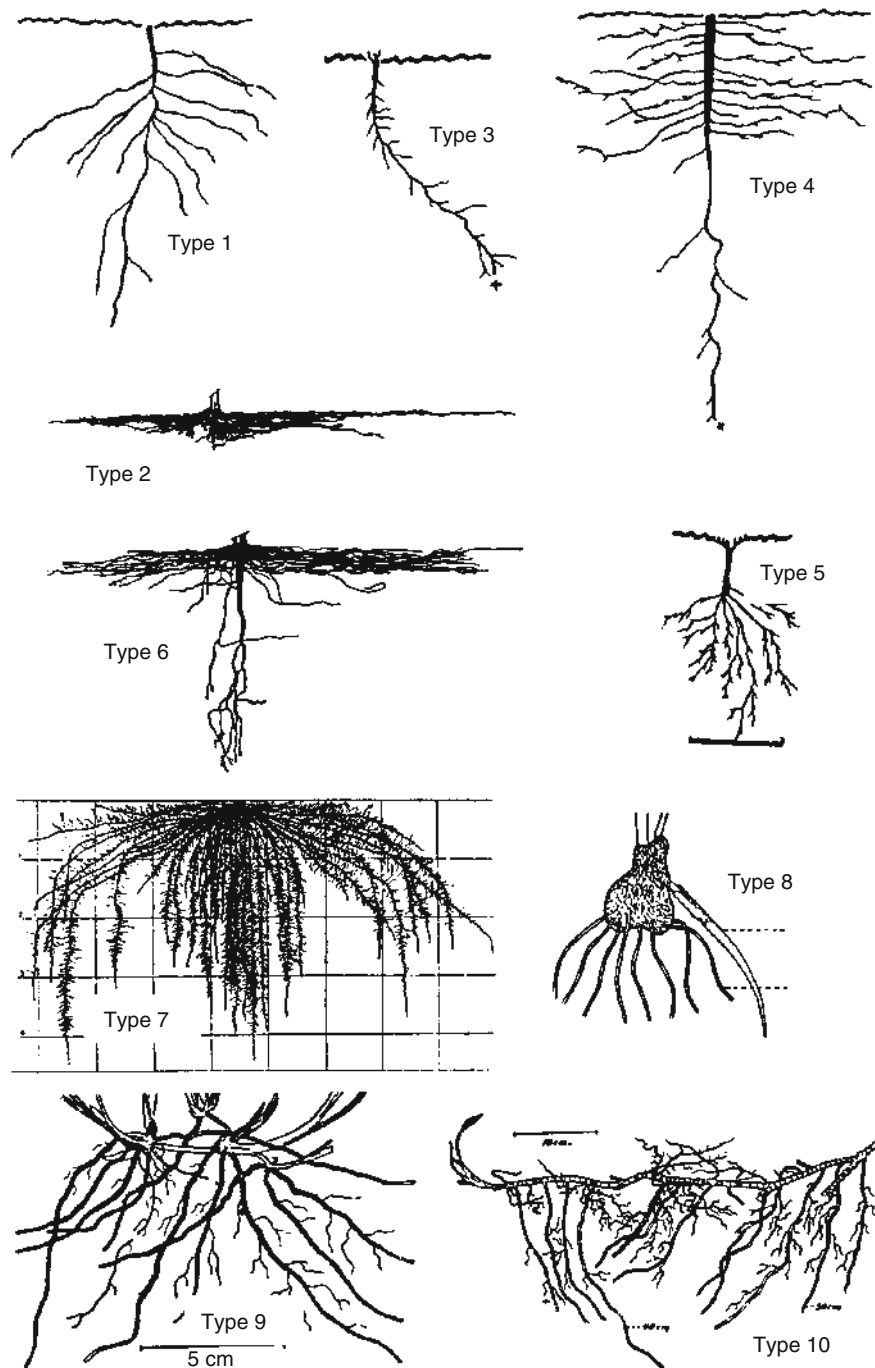
Analysis of the root system architecture through components and developmental processes

To understand better the root system architecture and its dynamics, it is worth considering the system through its main components and developmental processes.

A large part of the architectural diversity comes from the distribution and diversity of root apical meristems that are the key substructures for root elongation and generation of the young (subapical) root tissues. These meristems provide the new cells in the apical part of the root, allowing apical elongation and maintenance of the root cap. In many plants, apical meristems exhibit large variations in diameter, up to one or two orders of magnitude, and these variations are correlated to their morphogenetic capacities (Coutts, 1987). Big meristems generally make fast growing roots, with a long life span, able to orient themselves through various tropisms. These roots extend the volume colonized by the root system. On the opposite, small meristems make short roots, which follow the soil porosity and stop growing after some days. Then, they senesce and die quickly, and thus exploit only temporarily the very local soil. After having completed their role for the plant, their decomposition contributes also to the carbon efflux to the soil.

Branching is the major process for increasing root number and so root length and surface. It is spatially and temporally organized, since lateral roots appear acropetally on their mother root, i.e., following the progression of its tip. Lateral meristems are initiated as primordia very close to the meristem in the mother root, and emerge some days later as new lateral roots. Because of this process, the most distal lateral roots are also the youngest.

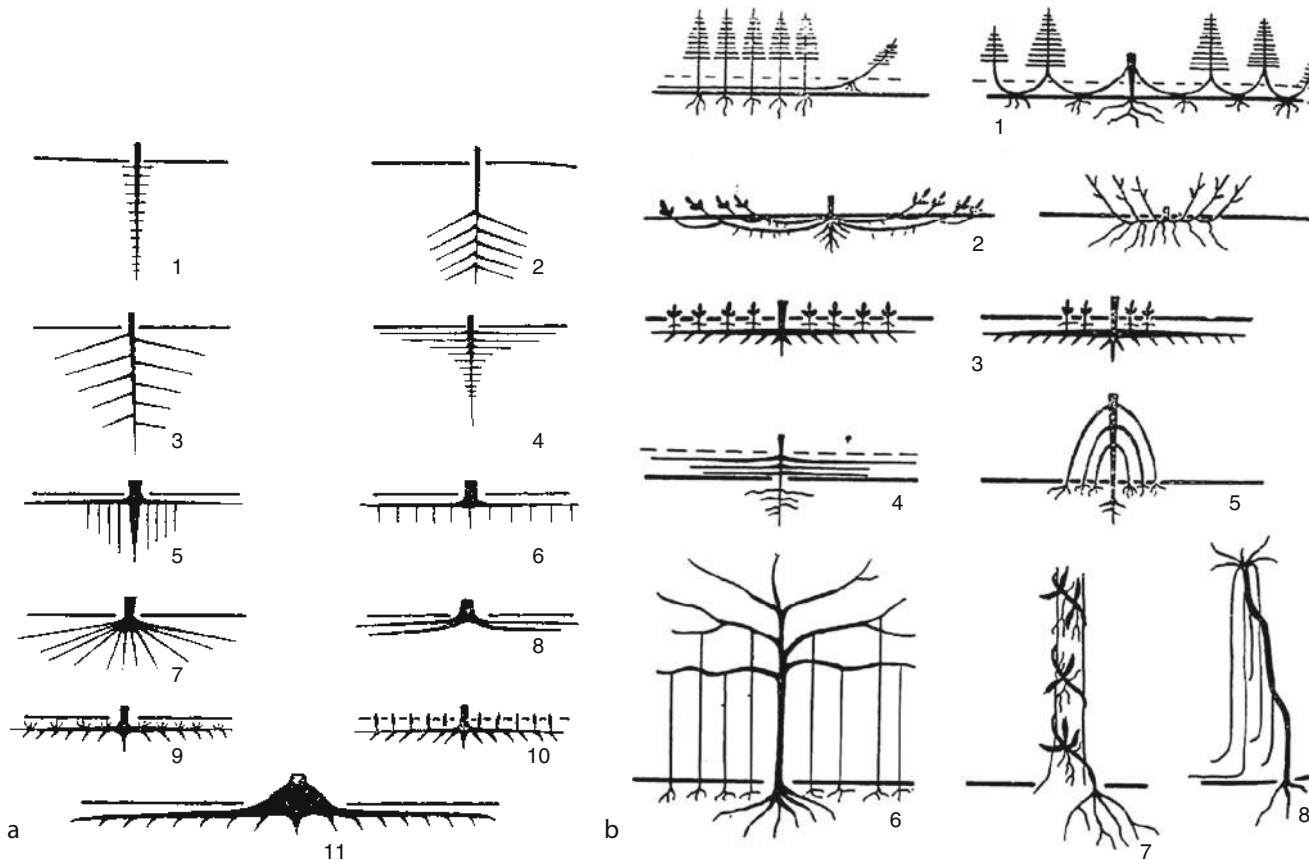
In order to reinforce conducting and support capacities of the roots, dicotyledonous plants have secondary meristems, which add layers of vessels and stiff tissues to the existing roots. Thanks to this secondary meristem functioning, the roots become thicker, highly conductive for sap, and are better protected against adverse organisms and mechanical constraints. In monocotyledonous plants, original tissues are gradually complemented by stiff and protective substances, like lignin and suberin, but without any significant radial growth, because there are not secondary meristems producing additional tissues. These different strategies induce large differences in the dynamics of these two categories of plants. The development of lateral roots is much higher on plants that exhibit radial growth. The increase of conducting capacity of the root allows it to bear daughter roots. On those plants with radial growth, tight relationships are observed at each branching point between the sectional area of a mother root and the sum of the sectional areas of its daughter roots.



Root System Architecture: Analysis from Root Systems to Individual Roots, Figure 1 Classification of root systems, according to Cannon (1949). Types 1–6 are primary root systems, where a taproot is developed from the radicle. Types 7–10 are secondary root systems, where most main roots emerge from the shoot system (adventitious roots).

It is also important to notice that a large number of roots are very short-lived. On trees, these fine and short-lived roots can be compared to the leaves on the shoot system. They represent a large area and have a transient role of exchange with the medium.

All these developmental processes are deeply affected by the soil, through a number of its physical and chemical characteristics. For example, the distribution of temperature in the soil modifies the developmental kinetics. Mechanical impedance of the soil is also a main factor



Root System Architecture: Analysis from Root Systems to Individual Roots, Figure 2 Classification of root systems for trees and shrubs, according to Krasilnikov (1968). (a) Primary root systems, with 11 different types. (b) Secondary and mixed root systems, with eight different types.

affecting root elongation and branching, and consequently the root system architecture.

Modeling the root system architecture

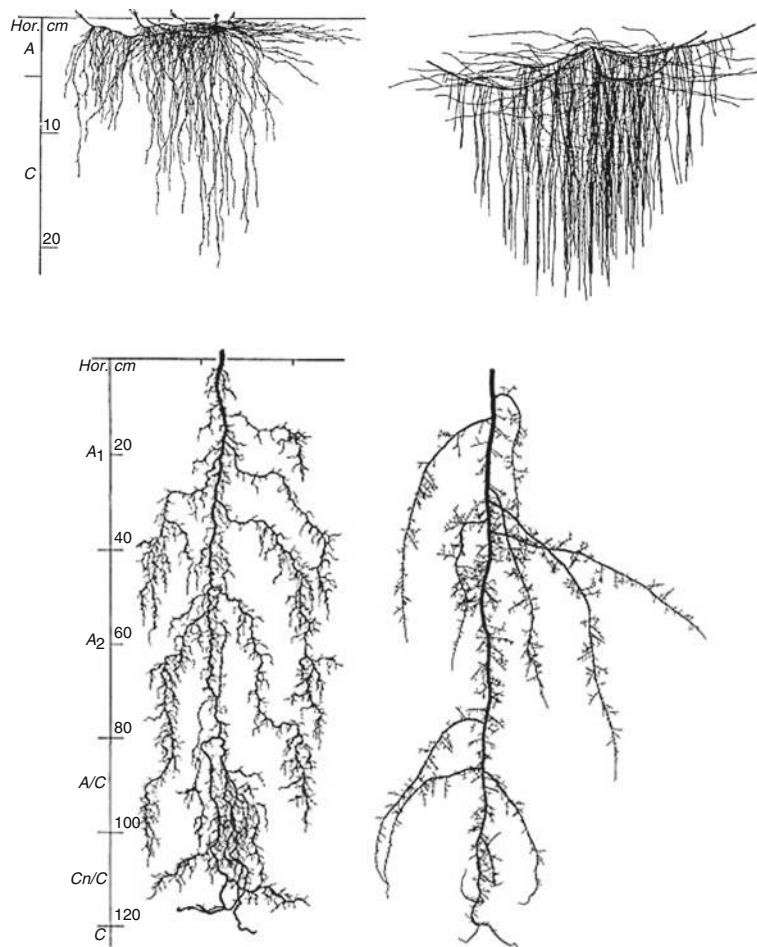
Mathematical modeling and simulation have been shown to be very important tools for representing both the combination of all these processes, together with interactions with soil and various organisms.

Early models of the three-dimensional architecture (Diggle, 1988; Pagès and Aries, 1988) have shown the interest of making such a combination of several developmental processes in order to get a dynamic and quantitative representation of this complex object, the root system architecture. These models made the link between the root level and the root system level. This link is important because comprehensive experimental data are usually easier to acquire on individual roots and on simple developmental processes at the root level (like elongation, branching), but the root system is an integrated system whose functioning comprehension requires standing back and looking at this higher organization level. The approach has been extended and validated on various plant species, including tree species.

Later architectural models have integrated several root–soil interactions (Pagès et al., 2004; see Figure 3) and have been merged with models of water and mineral transport in the soil (Clausnitzer and Hopmans, 1994). This approach allows a much more realistic simulation of plant development in a transient environment, and the quantitative study of the soil–plant system. Increasing the quality of our predictions regarding the soil–plant–atmosphere fluxes is an important challenge, in which architectural models have a prime position.

Another important comprehensive step has been made by modeling water (Doussan et al., 1998) and sugar (Bidel et al., 2000) transport within the root system architecture. These approaches make another bridge between functional and morphological aspects of the root system architecture, by integrating both developmental processes and transport processes of various resources described on root parts (meristems and root segments). These approaches make possible the emergence, at the root system organization level, of the overall consequences of local mechanisms described at the root part level.

Models allow the simulation of a virtual infinity of combinations, crossing plant and environmental



Root System Architecture: Analysis from Root Systems to Individual Roots, Figure 3 Examples of drawn and simulated root systems, after Pagès et al. (2004). Drawn root systems (on the left) have been observed in the field. Simulated root systems (on the right) come from a model which combines several developmental processes, and takes into account interactions with the soil.

situations. In this way, architectural diversity and functional consequences can be explored further.

Conclusions

The root system architecture (shape and structure) is a key concept that should be considered for understanding better many functions of the soil plant systems. For this purpose, it is helpful to consider architecture with a dynamic point of view, and to relate it to the developmental processes, which combine during the plant cycle. In this task, simulation models are necessary tools for representing a number of soil–plant interactions in a quantitative perspective.

Bibliography

- Bidel, L. P. R., Pagès, L., Rivière, L.-M., Pelloux, G., and Lorendeau, J.-Y., 2000. MassFlowDyn I: A carbon transport and partitioning model for root system architecture. *Annals of Botany*, **85**, 869–886.
- Cannon, W. A., 1949. A tentative classification of root systems. *Ecology*, **30**, 452–458.
- Clausnitzer, V., and Hopmans, J. W., 1994. Simultaneous modeling of transient three-dimensional root growth and soil water flow. *Plant and Soil*, **164**, 299–314.
- Coutts, M. P., 1987. Developmental processes in tree root systems. *Canadian Journal of Forest Research*, **17**, 761–767.
- Diggle, A. J., 1988. ROOTMAP - a model in three-dimensional coordinates of the growth and structure of fibrous root systems. *Plant and Soil*, **105**, 169–178.
- Doussan, C., Pagès, L., and Vercambre, G., 1998. Modelling the hydraulic architecture of root systems: An integrated approach of water absorption. I. Model description. *Annals of Botany*, **81**, 213–223.
- Fitter, A. H., 1987. An architectural approach to the comparative ecology of plant root systems. *The New Phytologist*, **106**(suppl), 61–77.
- Fourcaud, T., Ji, J. N., Zhang, Z. Q., and Stokes, A., 2008. Understanding the impact of root morphology on overturning mechanisms: A modelling approach. *Annals of Botany*, **101**, 1267–1280.
- Krasilnikov, P. K., 1968. On the classification of the root system of trees and shrubs. In Ghilanov, M. S., et al. (eds.), *Methods of Productivity Studies in Root Systems and Rhizosphere Organisms*. Leningrad: Nauka (URSS Academy of Sciences), pp. 106–114.

- Pagès, L., and Aries, F., 1988. SARAH: modèle de simulation de la croissance, du développement, et de l'architecture des systèmes racinaires. *Agronomie*, **8**, 889–896.
- Pagès, L., Vercambre, G., Drouet, J.-L., Lecompte, F., Collet, C., and Le Bot, J., 2004. RootTyp: a generic model to depict and analyse the root system architecture. *Plant and Soil*, **258**, 103–119.
- Waisel, Y., and Eshel, A., 2002. Functional diversity of various constituents of a single root system. In Waisel, Y., Eshel, A., and Kafkafi, U. (eds.), *Plant Roots, the Hidden Half*. New York: Marcel Dekker, pp. 157–174.

Cross-references

- [Crop Responses to Soil Physical Conditions](#)
[Plant Root Strength and Slope Stability](#)
[Plant Roots and Soil Structure](#)
[Rhizosphere](#)
[Root Responses to Soil Physical Limitations](#)
[Root Water Uptake: Toward 3-D Functional Approaches](#)
[Soil–Plant–Atmosphere Continuum](#)

ROOT WATER UPTAKE: TOWARD 3-D FUNCTIONAL APPROACHES

Mathieu Javaux^{1,4}, Xavier Draye², Claude Doussan³,
Jan Vanderborght¹, Harry Vereecken¹
¹ Agrosphere, ICG-4, Institute of Chemistry and Dynamics
of the Geosphere, Forschungszentrum Juelich GmbH,
Juelich, Germany

²Crop Physiology and Plant Breeding, Earth and Life
Institute - Agronomy, Université catholique de Louvain,
Louvain-la-Neuve, Belgium

³UMR 1114 EMMAH, INRA/UAPV, Avignon, France

⁴Earth and Life Institute - Environmental Sciences,
Université catholique de Louvain, Louvain-la-Neuve,
Belgium

Definition

Root water uptake (water extraction or water absorption): water flow from the soil to the root.

3D functional approaches (or functional–structural plant modeling): modeling approach aiming at representing virtual plants with their three-dimensional (3D) architecture and selected physiological functions.

Introduction

Water is an essential resource for plant life. Typically, cropped plants transpire 200–1,000 kg of water for each kilogram of dry matter produced (Martin et al., 1976), and this water is principally extracted from the soil by the roots. Therefore, modeling of soil water uptake by plant roots is of importance for a series of environmental and agronomic purposes. Numerous practical applications like yield prediction, irrigation management, or pollutant fate prediction under cropped fields need a detailed

understanding of the interactions between soil water and roots to be investigated as well as advanced modeling approaches.

The uptake of water by roots is mainly a passive process driven by water potential gradient between the soil around the root and the xylem (Steudle and Peterson, 1998). At the root scale, uptake depends on the local soil and root hydraulic properties (including the interface between soil and root). At the plant scale, the root water uptake (RWU) is, amongst others, linked to the plant root xylem network topology, the location of the roots in the soil, the distribution of the soil water, the regulation of transpiration by the leaves, and the vapor pressure deficit in the atmosphere (Feddes and Raats, 2004). Root locations and distribution in the soil but also root hydraulic properties and xylem network are therefore key parameters for modeling of root water uptake at the plant scale. Yet, they are relatively difficult to assess and are extremely variable in space and time.

Plant root systems develop spatially to optimize the extraction of nutrients and water from the heterogeneous and varying soil environment (Fitter, 1987; Schymanski et al., 2008). In turn, the spatial distribution of the roots impacts the soil water content distribution and the drainage to deeper layers. Across time, the root system growth and spatial deployment (its architecture) will result from genetic traits modulated by root plasticity, i.e., the capability of roots to adapt their development to soil spatio-temporal variations and growth constraints (see [Root Responses to Soil Physical Limitations](#)). In addition, within a root system, the size, diameter, location, and hydraulic properties (cortex and xylem conductivities) of root segments also vary with the root type (e.g., branching order) and age (Pierret et al., 2007) (see [Root System Architecture: Analysis from Root Systems to Individual Roots](#)). On the other hand, the distribution of water in soils is usually quite variable, especially close to the surface because of interception/redistribution processes (canopy interception, surface runoff, etc.) and soil natural heterogeneity. As a consequence, it is expected that root water uptake patterns will be spatially heterogeneous and vary with time as a function of soil and root properties and the climatic demand. The use of three-dimensional modeling based on an accurate description of the root architecture should thus help to gain better insights into soil exploration and foraging processes by roots (Draye et al., 2010).

Several models describing 3D root growth are now available (Wu et al., 2005). However, to date, only a few models with explicit account of the full 3D root architecture to predict water uptake have been developed (Green et al., 2006). Clausnitzer and Hopmans (1994) developed such a model. It consists of a three-dimensional root growth model combined with a three-dimensional, transient soil water flow and solute transport model based on the finite-element method. In their model, root growth depends on the spatial distribution of temperature, water content, and soil strength. Root water uptake is taken as

proportional to the local root length density. However, water flow within the root system is not modeled, and thus the distributed root sink term does not depend on the water potential gradient between the soil and roots but only on the soil water potential, by means of a stress function. On the other hand, Doussan et al. (1998) proposed a modeling of water uptake and flow within the root system, where the soil was not limiting water transfer. Recently, Doussan et al. (2006), Javaux et al. (2008), and Schneider et al. (2010) developed a fully coupled root architecture soil water transfer model, where the water flow equation is solved in both the soil matrix and the root xylem network. Such 3D functional models offer the possibility of explicitly considering the spatial and temporal changes of the root and soil conductivity and thus, are the basis of a fully integrated approach for modeling fluxes at the plant scale.

Other 2D or 2,5D approaches which attempt to simplify the 3D root systems to predict root water uptake (Roose and Fowler, 2004; Siqueira et al., 2008; Amenu and Kumar, 2008; De Willigen and Noordwijk, 1987) are also being developed, but these will not be reviewed here.

Modeling principles

3D Root water flow model

Doussan et al. (1998) proposed an algorithm to solve the water flow within the whole root system as a function of the soil water status. They simplified the root architecture as a series of interconnected nodes, in which radial (soil to root) and longitudinal (along xylem vessels) flow take place. Assuming that the osmotic potential gradient generates negligible water fluxes, the volumetric radial water flow [$L^3 T^{-1}$] between the soil–root interface and the root xylem can be written as

$$J_r = K_r s_r [H_s(z) - H_x(z)], \quad (1)$$

where H_s and H_x are the total water potentials (written on height basis, or water head) at the root surface and in the xylem [L], K_r is the radial conductivity [T^{-1}], and $s_r = 2\pi r_{int} l$ is the root–soil interface area [L^2] with l , length of the root segment and r , the root radius. Note that the total (negative) water potential is $H = h + z$ [L], where h is the matric (in soil) or the hydrostatic (in root) heads and z , the altitude (oriented upward). Longitudinal water flow in the xylem [$L^3 T^{-1}$] is defined as

$$J_x = -K_x^* A_x \frac{dH_x(z)}{dl} = -K_x \left[\frac{dh_x(z)}{dl} + \frac{dz}{dl} \right] \quad (2)$$

with H_x – the total xylem water head, A_x – the xylem cross-sectional area [L^2], dl – an infinitesimal segment length [L], K_x^* – the axial conductivity [$L T^{-1}$], and $K_x = K_x^* A_x$ [$L^3 T^{-1}$] – the xylem conductance. Note that, in Equations 1 and 2, radial and xylem conductivities may be considered as variables dependent on water potential value or root type and age.

Equations 1 and 2 can be used to define the water mass balance for a given root node i as:

$$\begin{aligned} & K_{x,i:i-1} \frac{(H_{x,i} - H_{x,i-1})}{l_{i:i-1}} \\ &= K_{x,i+1:i} \frac{(H_{x,i} - H_{x,i+1})}{l_{i+1:i}} + K_{r,i}^* s_r (H_s - H_x), \end{aligned} \quad (3)$$

where the right-hand side term refers to the water flow from node i to node $i - 1$ (mother node) through the segment $i : i - 1$ with a length $l_{i:i-1}$ and a root xylem conductance $K_{x,i:i-1}$ while the subscripts $i + 1 : i$ refer to the segment between the nodes $i + 1$ and i . Equations 1 and 2 (discretized by Equation 3) can be solved analytically for one-root segment (Landsberg and Fowkes, 1978). When generalized to the whole root system, the water potential distribution in the xylem is obtained by solving a system of linear equations derived from Equation 3, which writes in matrix notation (Doussan et al., 1998),

$$\mathbf{C} \cdot \mathbf{H}_x = \mathbf{Q}, \quad (4)$$

where \mathbf{C} (dimensions $n_p \times n_p$ with n_p the number of root nodes) is called the “conductance matrix,” \mathbf{Q} (dimensions $n_p \times 1$) contains the soil factors, and \mathbf{H}_x (dimensions $n_p \times 1$) is the unknown xylem water potential vector.

Soil water flow

Water flow in soils with root uptake can be described by the Richards equation with a 3D root sink term (Vrugt et al., 2001):

$$\frac{\partial \theta}{\partial t} = \nabla \cdot [\mathbf{K} \nabla (h + z)] - S, \quad (5)$$

where θ is the volumetric water content [$L^3 L^{-3}$], t is the time [T], \mathbf{K} the hydraulic conductivity tensor [LT^{-1}], h the matric head [L], S the sink term representing the distributed root water uptake [T^{-1}], and z the vertical coordinate [L]. Both θ and \mathbf{K} are nonlinear functions of the matric head, which are called the unsaturated hydraulic soil properties.

Different numerical solutions exist to this nonlinear equation based on finite element or finite volume methods, which require a soil discretization with a 3D grid (see [Soil Water Flow](#)).

Coupled model

Coupling soil and root water flow requires the merging of two very different geometrical domains: the three-dimensional numerical soil grid made of voxels and a tree-like root network. This coupling is necessary since the Richards equation (Equation 1) needs the sink term distribution S to be known, while the root system depends on soil water potential distribution h around the roots

(Equation 5). In the coupled model, the root sink term for soil a voxel j is defined as

$$S_j = \frac{\sum_{i=1}^{n_j} J_{r,i}}{V_j}, \quad (6)$$

where the numerator represents the sum of all the radial fluxes toward the n_j root nodes located inside a soil voxel j [$\text{L}^3 \text{T}^{-1}$], and V_j is the volume of the j th soil voxel [L^3].

To solve the root flow equation for the whole root system, the soil water potential around each root node $\langle H_s \rangle_i$ is needed. Assuming that the water potential at the soil–root interface would be the same as the bulk soil, water potential at the soil–root interface can be defined as a weighed average of the soil pressure head $H_{s,k}$ of the soil voxel nodes (n_{vox}) which surround the root node i as follows:

$$\langle H_s \rangle_i = \frac{\left(\sum_{k=1}^{n_{\text{vox}}} \frac{1}{dist_k} H_{s,k} \right)}{\sum_{k=1}^{n_{\text{vox}}} \frac{1}{dist_k}}, \quad (7)$$

where $dist_k$ [L] represents the spatial distance between the root node i and the soil node k . The radial flow rate from soil to root node i is then written as:

$$J_{r,i} = K_{r,i}^* s_{r,i} [\langle H_s \rangle_i - H_{x,i}]. \quad (8)$$

The radial fluxes of all root nodes located inside a soil voxel j are then summed up to estimate the soil sink term in Equation 6. The sink term is now defined as a function of the local root water uptake, which explicitly depends on the water potential gradient between soil and root.

Equation 7 holds for fine soil mesh (small soil voxel size). Indeed, in that case, the water potential at the soil nodes is relatively close to the water potential at the root–soil interface. However, alternatives to Equation 7 exist for estimating the water potential at the soil–root interface with greater voxel sizes, like adding an analytical solution of the soil water flow equation at the sub-voxel scale (Schroder et al., 2009a). Also, local grid refinement may be used to describe the water potential field around the roots more accurately (Schroder et al., 2009b).

For coupling the water flow in both the soil and root systems, an implicit iterative scheme must be used (Garrigues et al., 2006; Javaux et al., 2008). First, the root flow is solved, given an initial estimate of the pressure head distribution in the soil. This generates a first estimate of the xylem pressure head H_x and water flow distribution (Equation 7). A 3D sink term distribution can thus be calculated from Equation 6 and used in the numerical solution of the Richards equation (Equation 1). These two steps are repeated until the maximum change in root and

soil pressure head over all the nodes does not exceed a given threshold value and there is no change in the total water uptake between consecutive iterations.

Potentials of 3D RWU models

Figure 1 illustrates typical outcome of 3D RWU model simulations. It shows the distribution of the water potential distribution in the soil and within the xylem network for a maize root subject to a 1-week dry period and the corresponding sink-term profile from Equation 6 aggregated in 1D. Doussan et al. (2006) used such a model to investigate the effect of root architecture on water uptake. He showed that tap-rooted architecture induced more concentrated uptake zone than fibrous systems. Javaux et al. (2008) showed that classical stress function could not be used to account for the effect of soil water availability on root water uptake and suggested that such models could be used to deduce effective stress equation for simpler models.

Other uses for soil–plant models include the investigation of water uptake with root architectural traits (De Dorlodot et al., 2007; Lynch, 2007), the study of the influence of the soil heterogeneity or irrigation conditions (Hodge et al., 2009), the simulation of the responses of virtual plants carrying diverse combinations of alleles under different scenarios of abiotic stress (Tardieu, 2003), or the understanding of optimal root development under various climate conditions. Such models can also be used as tools to integrate our knowledge on plant uptake processes and when confronted to real measurements, emphasize gaps in our knowledge and models.

Challenges

Numerous challenges associated with the development of these detailed 3D root water uptake models still remain. Two types of challenges can be identified.

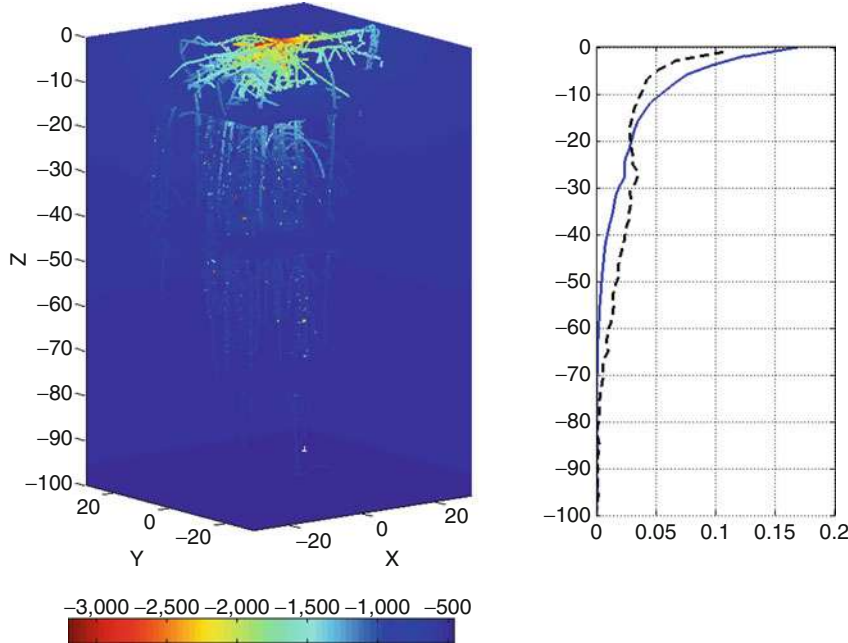
Improving numerical solutions

Such models are complex and computationally demanding. Further development in the numerical solutions of the underlying model equations includes:

- Improvement of model numerical accuracy: in particular, very heterogeneous and rapid changes in water fluxes induced by plant uptake may render the solution of the flow equations difficult and prone to errors. On the other hand, analytical solutions hardly exist and this makes the comparison difficult.
- Reduction of model computation time: 3D models are computationally expensive and time demanding. Parallelization is one way to speed up the computation time (Hardelauf et al., 2007).

Improving process modeling

Soil–Plant/Root water uptake models are relatively demanding regarding parameters. Each root segment has its own hydraulic properties. Root architecture in three



Root Water Uptake: Toward 3-D Functional Approaches, Figure 1 *Left:* Distribution of the soil and xylem water potential (cm) after a 7-day dry period for a maize root. *Right:* depth-normalized root length density profile (—) (dashed line) and depth-normalized sink term profile (—) (blue line) computed from 3D computations.

dimensions as well as the parameterization of the soil must be known. Many of these parameters are not readily available, which makes the use of such complex models difficult today. In addition, some processes are still unknown. Improvement of such models will require strong interaction between modelers, soil hydrologists, agronomists, and biologists. Amongst others, remaining open issues are:

- Root architecture characterization: Root architecture can either be modeled or measured. New imaging methods have recently been developed and allow the detailed assessment of the root architecture needed for these 3D models (Oswald et al., 2008; Pohlmeier et al., 2008; Moradi et al., 2009). Root growth models could also be used to generate replicates of probable root systems in case no real data is available.
- Root soil interface: a model is always a simplified representation of the reality. The level of details involved in the root description cannot explicitly resolve root hairs or very fine roots or mycorrhiza, which may actually be an important pathway or uptake. Air gaps may appear and change the interface area between soil and roots (Carminati et al., 2009). This could be taken into account by varying s_r in Equation 1 in function of the root water potential.
- Rhizosphere: the rhizosphere is the volume of soil shared by bacteria, where roots have a direct influence

(Gregory, 2006). Many biological, biochemical, chemical, and physical processes occur in rhizosphere, and these will have a direct influence on the root and soil properties, potentially affecting the root water uptake. Incorporating rhizospheric processes in a plant scale model still remains challenging (Luster et al., 2009) (**Rhizosphere**).

- Biological processes and parameterization: knowledge gaps still exist regarding how certain parameters vary with time. Lateral flow through plant cortex, for instance, depends on active mechanisms which may change the root radial conductivity (Vandeleur et al., 2005). Xylem vessels are also prone to embolism (Sperry et al., 2003), which would make xylem conductance (K_x in Equation 2) dependent to water potential as well. On the other hand, very complex mechanisms mediate the response of plants to biotic and abiotic stresses (Hodge et al., 2009). Many of these mechanisms are likely to affect the water flow resistance through the soil–plant atmosphere system but are still unknown.

Conclusions

The development of numerical facilities and the current interests for sustainable food productions open new avenues for investigating root–soil interactions with water uptake models based on root architecture. New models have recently been developed and are today capable of

dealing with complex soil and plant descriptions. These 3D soil–plant functional models represent the basis of a coupled model, where energy and matter fluxes and related biochemical, chemical, and physical processes are fully integrated at the plant level. Advances made in noninvasive measurement techniques and in understanding the mechanisms underlying the plant water regulation will probably improve the prediction performance of such models in the near future and make them an instrumental to understanding the complex mechanisms controlling water and nutrient fluxes in the soil/plant continuum.

Bibliography

- Amenu, G. G., and Kumar, P., 2008. A model for hydraulic redistribution incorporating coupled soil-root moisture transport. *Hydrology and Earth System Sciences*, **12**, 55–74.
- Carminati, A., Vetterlein, D., Weller, U., Vogel, H. J., and Oswald, S. E., 2009. When roots lose contact. *Vadose Zone Journal*, **8**, 805–809.
- Clausnitzer, V., and Hopmans, J. W., 1994. Simultaneous modeling of transient 3-dimensional root-growth and soil-water flow. *Plant and Soil*, **164**, 299–314.
- De Dorlodot, S., Forster, B., Pages, L., Price, A., Tuberrosa, R., and Draye, X., 2007. Root system architecture: opportunities and constraints for genetic improvement of crops. *Trends in Plant Science*, **12**, 474–481.
- De Willigen, P., and Van Noordwijk, M., 1987. *Roots, Plant Production and Nutrient Use Efficiency*. PhD thesis, University of Agriculture, Wageningen.
- Doussan, C., Pages, L., and Vercambre, G., 1998. Modelling of the hydraulic architecture of root systems: an integrated approach to water absorption - model description. *Annals of Botany*, **81**, 213–223.
- Doussan, C., Pierret, A., Garrigues, E., and Pages, L., 2006. Water uptake by plant roots: II - modelling of water transfer in the soil root-system with explicit account of flow within the root system - comparison with experiments. *Plant and soil*, **283**, 99–117.
- Draye, X., Kim, Y., Lobet, G., and Javaux, M., 2010. Model-assisted integration of physiological and environmental constraints affecting the dynamic and spatial patterns of root water uptake from soils. *Journal of Experimental Botany*, **61**, 2145–2155, doi:10.1093/jxb/erq077.
- Feddes, R.A., and Raats, PAC., 2004. Parameterizing the soil–water–plant root system. In Feddes, R. A. et al. (eds.), *Unsaturated-Zone Modeling: Progress, Challenges, Applications*. Wageningen UR Frontis Series, pp. 95–141.
- Fitter, A. H., 1987. An architectural approach to the comparative ecology of plant-root systems. *New Phytologist*, **106**, 61–77.
- Garrigues, E., Doussan, C., and Pierret, A., 2006. Water uptake by plant roots: I -Formation and propagation of a water extraction front in mature root systems as evidenced by 2D light transmission imaging. *Plant and soil*, **283**, 83–98.
- Green, S., Kirkham, M., and Clothier, B., 2006. Root uptake and transpiration: from measurements and models to sustainable irrigation. *Agricultural Water Management*, **86**, 165–176.
- Gregory, P. J., 2006. Roots, rhizosphere and soil: the route to a better understanding of soil science? *European Journal of Soil Science*, **57**, 2–12.
- Hardelauf, H., Javaux, M., Herbst, M., Gottschalk, S., Kasteel, R., Vanderborght, J., and Vereecken, H., 2007. PARSWMS: a parallelized model for simulating 3-D water flow and solute transport in variably saturated soils. *Vadose Zone Journal*, **5**, 255–259.
- Hodge, A., Berta, G., Doussan, C., Merchan, F., and Crespi, M., 2009. Plant root growth, architecture and function. *Plant and Soil*, **321**, 153–187.
- Javaux, M., Schröder, T., Vanderborght, J., and Vereecken, H., 2008. Use of a three-dimensional detailed modeling approach for predicting root water uptake. *Vadose Zone Journal*, **7**, 1079–1088.
- Landsberg, J. J., and Fowkes, N. D., 1978. Water-movement through plant roots. *Annals of Botany*, **42**, 493–508.
- Luster, J., Gottlein, A., Nowack, B., and Sarret, G., 2009. Sampling, defining, characterising and modeling the rhizosphere-the soil science tool box. *Plant and Soil*, **321**, 457–482.
- Lynch, J. P., 2007. Roots of the second green revolution. *Australian Journal of Botany*, **55**, 493–512.
- Martin, J., Leonard, W., and Stamp, D., 1976. *Principles of Field Crop Production*, 3rd edn. New York: Macmillan.
- Moradi, A. B., Conesa, H. M., Robinson, B., Lehmann, E., Kuehne, G., Kaestner, A., Oswald, S., and Schulin, R., 2009. Neutron radiography as a tool for revealing root development in soil: capabilities and limitations. *Plant and Soil*, **318**, 243–255.
- Oswald, S. E., Menon, M., Carminati, A., Vontobel, P., Lehmann, E., and Schulin, R., 2008. Quantitative imaging of infiltration, root growth, and root water uptake via neutron radiography. *Vadose Zone Journal*, **7**, 1035–1047.
- Pierret, A., Doussan, C., Capowicz, Y., Bastardie, F., and Pages, L., 2007. Root functional architecture: a framework for modeling the interplay between roots and soil. *Vadose Zone Journal*, **6**, 269–281.
- Pohlmeier, A., Oros-Peusquens, A., Javaux, M., Menzel, M. I., Vanderborght, J., Kaffanke, J., Romanzetti, S., Lindenmair, J., Vereecken, H., and Shah, N. J., 2008. Changes in soil water content resulting from ricinus root uptake monitored by magnetic resonance imaging. *Vadose Zone Journal*, **7**, 1010–1017.
- Roose, T., and Fowler, A. C., 2004. A model for water uptake by plant roots. *Journal of Theoretical Biology*, **228**, 155–171.
- Schneider, C. L., Attinger, S., Delfs, J. O., and Hildebrandt, A., 2010. Implementing small scale processes at the soil-plant interface - the role of root architectures for calculating root water uptake profiles. *Hydrology and Earth System Sciences*, **14**, 279–289.
- Schroder, T., Javaux, M., Vanderborght, J., Korfgen, B., and Vereecken, H., 2009a. Implementation of a microscopic soil-root hydraulic conductivity drop function in a three-dimensional soil-root architecture water transfer model. *Vadose Zone Journal*, **8**, 783–792.
- Schroder, T., Tang, L., Javaux, M., Vanderborght, J., Korfgen, B., and Vereecken, H., 2009b. A grid refinement approach for a three-dimensional soil-root water transfer model. *Water Resources Research*, **45**, W10412, doi:10.1029/2009WR007873.
- Schymanski, S. J., Sivapalan, M. et al., 2008. An optimality-based model of the coupled soil moisture and root dynamics. *Hydrology and Earth System Science*, **12**, 913–932.
- Siqueira, M., Katul, G., and Porporato, A., 2008. Onset of water stress, hysteresis in plant conductance, and hydraulic lift: scaling soil water dynamics from millimeters to meters. *Water Resources Research*, **44**, W01432.
- Sperry, J. S., Stiller, V., and Hacke, U. G., 2003. Xylem hydraulics and the soil-plant-atmosphere continuum: opportunities and unresolved issues. *Agronomy Journal*, **95**, 1362–1370.
- Steudle, E., and Peterson, C. A., 1998. How does water get through roots? *Journal of Experimental Botany*, **49**, 775–788.
- Tardieu, F., 2003. Virtual plants: modelling as a tool for the genetics of tolerance to water deficit. *Trends in Plant Science*, **8**, 9–14.
- Vandeleur, R., Niemietz, C., Tilbrook, J., and Tyerman, S. D., 2005. Roles of aquaporins in root responses to irrigation. *Plant and Soil*, **274**, 141–161.

- Vrugt, J. A., Van Wijk, M. T., Hopmans, J. W., and Simunek, J., 2001. One-, two-, and three-dimensional root water uptake functions for transient modeling. *Water Resources Research*, **37**, 2457–2470.
- Wu, L., Mcgechan, M. B., Watson, C. A., and Baddeley, J. A., 2005. Developing existing plant root system architecture models to meet future agricultural challenges. *Advances in Agronomy*, **85**, 181–219.

Cross-references

Rhizosphere

Root Responses to Soil Physical Limitations

Root System Architecture: Analysis from Root Systems to Individual Roots

Soil Water Flow

ROUGHNESS

Irregularities, protuberances, or ridges of a surface.

RUNOFF

The volume of water that runs off the soil surface that exceeds the soil's infiltrability.

S

SALINITY, PHYSICAL EFFECTS ON SOILS

Lajos Blaskó
Karcag Research Institute of Centre for Agricultural and Technical Sciences, Debrecen University, Karcag, Hungary

Synonyms

Saline and saline-sodic soils; Solonchak soils

Definition

Salinity is the presence of soluble salts in soils or waters. It is a general term used to describe the presence of elevated level of different salts such as sodium chloride, magnesium and calcium sulfates, and bicarbonates in liquid phase of soil and in water.

Introduction

The natural and man-induced salt accumulation is a major threat for agricultural activity in arid and semi-arid regions. Several processes of climate change might strengthen the salt accumulation. Because of the decreasing amount of precipitation, leaching is getting more and more limited. The rising temperature increases the evaporation, which accompanied with upward water movement, transferring salts from underground to the soil surface. The consequence of the increasing frequency of drought situation is the rising demand for irrigation water.

The global warming would substantially impact the availability and quality of irrigation water. Scarcity of good quality water emphasizes the use of marginal waters with higher salt content. Because of the possible increasing salt stress, it is very important to investigate the effect of salts on soil properties for establishing a sustainable land use on the areas threatened by secondary salinization.

Indicators of salinity

Soil salinity is estimated from the electrical conductivity (EC) of a saturated soil paste. It is expressed in dSm^{-1} . The sodium adsorption ratio (SAR) is a measure of comparative concentration of Na^+ to Ca^{2+} and Mg^{2+} ions in a soil solution or in irrigation water.

Effect of salinity on soil structure

It is generally accepted that an increasing electrolyte concentration has a flocculating effect on the soil colloids and strengthens the stability of micro-aggregates (Abu-Shara et al., 1987; Goldberg et al., 1988; Tajik et al., 2003). Regarding the macro-aggregate stability, the positive effect of higher salt concentration is not unanimously proved. In several experiments, despite the better microaggregate stability, the macro-aggregates were not affected by the electrolyte concentration (Goldberg et al., 1988; Shainberg et al., 1992).

Effect of EC and SAR on soil permeability

The simply saline soils usually occur on parent materials with low colloid content. On soils with colloidal particles, both the water soluble and the exchangeable forms of cations can be found.

For characterizing the simultaneous effect of EC and SAR or ESP, the threshold concentration concept was elaborated by Quirk and Schofield (1955). They measured the permeability of soils saturated to varying degrees with exchangeable sodium, and obtained a threshold concentration that was defined as that concentration of electrolyte at which clay swelling and deflocculation had an appreciable effect in decreasing the permeability.

Several investigators concluded that a higher EC value (especially if it is caused by neutral salts) could counterbalance the adverse effect of SAR or ESP on the hydraulic conductivity (Quirk, 1971; Agassi et al., 1981; Várallyay, 1981; Shainberg and Letey, 1984; Abu-Shara et al., 1987).

Effect of Ca^{2+} and Mg^{2+} on physical properties of soils

The effect of salinity on the structural properties and transport processes depends not only on the salt and sodium concentration of the soil or of the irrigation water, but on the other cation and anion composition of water as well. Among the cations, the positive effect of Ca^{2+} on the soil structural and transport properties has been proved. The main goal of the chemical amelioration of waters and soils is increasing the Ca^{2+} concentration in the water and the Ca^{2+} saturation of the colloidal surface. The usual amelioration practice of saline soils is to apply gypsum or other soluble calcium compounds to the soil to keep a high electrolyte concentration with low SAR level, which is suitable to maintain a high infiltration rate and to leach the sodium salts with irrigation water.

The judgment of the soil physical role of Mg^{2+} is not so consistent. From the viewpoint of potentially different physical effect, the Ca^{2+} and Mg^{2+} are not distinguished when calculating the SAR value of waters by Richards (1954). Negative effects of Mg^{2+} were observed in the countries where well-water with high Mg^{2+} content was used due to the scarcity of good quality water. Girdhar and Yadav (1981) pointed out that increasing Mg^{2+} in water caused increased water retention of the soil at 15 bar suction. They found that the irrigation water with high Mg content increased the exchangeable Mg content of a CaCO_3 containing soil lesser than that of non-calcareous soil. Alperovich et al. (1981) found that exchangeable Mg did not have a specific effect on the clay dispersion and on the hydraulic conductivity in calcareous soils. In contrast with these findings, Keren (1991) concluded from the result of a rainfall simulation experiment that the Mg soil surface was more susceptible to sealing than the Ca soil, regardless of the presence of CaCO_3 .

There are results showing a higher dispersion of montmorillonite and illite in the presence of Na and Mg, than in a Ca and Na system (Bakker and Emerson, 1973; Emerson and Chi, 1977).

Blaskó and Karuczka (2001) investigated the effect of water with increasing MgSO_4 concentration (from 0 to 30 meq l^{-1}) on some physical properties of the soil. The infiltration rate, in accordance with the general rule by which a higher electrolyte concentration causes faster infiltration, was higher under the influence of higher Mg^{2+} concentration in irrigation water. The stability of micro-aggregates of the irrigated soils did not change. The swelling and shrinking properties were not influenced by the MgSO_4 in spite of the fact that the exchangeable magnesium percentage, as a consequence of irrigation with water of high magnesium content, got higher than 30, which was considered according to Ellis and Caldwell (1935) to be limit value of "magnesium solonet." Beside the high magnesium saturation, the exchangeable sodium content was negligible. It seems from the results, that the damaging effect of Mg to soil physical properties is expressed more in the presence of Na than in Ca–Mg system.

The partly contradictory results on the physical effects of Mg^{2+} give the reason for further investigations, especially in countries where irrigation water rich in magnesium is widely used.

Effect of anions on physical properties of soil

Taking into account the anion components of soils, two main groups of salt-affected soils can be distinguished (Szabolcs, 1969):

- Soils affected by neutral sodium salts (NaCl , Na_2SO_4).
- Soils affected by sodium salts capable of alkaline hydrolysis (NaHCO_3 , Na_2CO_3 , Na_2SiO_3).

The specific effects of different anions are well known. The carbonate and hydrocarbonate type of salinization is much more dangerous from the viewpoint of soil physical properties than the chloride and sulfate type of salinization, especially in soils with smectite type clay mineral. Even a very little amount (0.1%) of sodium carbonate can cause dispersion and swelling reducing the soil hydraulic conductivity and leading to a stop of the leaching process (Szabolcs, 1969; Várallyay, 1981).

Salinity, availability of water and osmotic stress

In spite of the positive effect of neutral salt content on the water transport in the soil, the whole water regime of the soil–plant system is adversely affected by increasing salt content, because the total available water is much less in soils with high salinity than in non-salt-affected soils (Ayers and Westcot, 1976). Because of the high wilting percentage and higher osmotic potential of the soil water, a salty soil needs more frequent irrigation and higher leaching fraction of irrigation water to leach out the salts from the root zone.

From the point of view of osmotic stress, salinity caused by soluble calcium salts is the same or sometimes more dangerous than the salinity caused by sodium salts (Aceves et al., 1975).

Conclusions

Increasing salinity, in general, caused by neutral salts, creates better conditions for flocculation and mitigates the swelling of clay minerals. The consequences of these processes are the better structural and water transport characteristics. The cation and anion composition of the soil water can modify the general rule. The higher the SAR value of the soil or of the irrigation water, the higher EC volume is necessary to maintain the good structural and transport properties.

The diverse effect of neutral and alkali sodium salts is well defined, but there are partly contradictory results concerning the physical effects of Mg^{2+} .

In spite of the favorable physical effects of neutral salts, the extreme increase of their concentration must not be the solution for the soil physical problems, because the high salt concentration causes an osmotic stress even in the case of neutral calcium and magnesium salts.

Bibliography

- Abu-Shara, T. M., Bingham, F. T., and Rhoades, J. D., 1987. Stability of soil aggregates as affected by electrolyte concentration and composition. *Soil Science Society of America Journal*, **51**, 309–314.
- Aceves-N, E., Stolzy, L. H., and Mehuys, G. R., 1975. Effects of soil osmotic potential produced with two salt species on plant water potential, growth, and grain yield of wheat. *Plant and Soil*, **42**, 619–627.
- Agassi, M., Shainberg, I., and Morin, J., 1981. Effect of electrolyte concentration and soil sodicity on infiltration rate and crust formation. *Soil Science Society of America Journal*, **48**, 848–851.
- Alperovich, N., Shainberg, I., and Keren, R., 1981. Specific effect of magnesium on the hydraulic conductivity of soils. *Journal of Soil Science*, **32**, 543–554.
- Ayers, R. S., and Westcot, D. W., 1976. Water quality for agriculture. *FAO Irrigation and Drainage Paper No. 29 (Rev 1)*, Food and Agriculture Organization of the United Nations.
- Bakker, A. C., and Emerson, W. W., 1973. The comparative effect of exchangeable calcium, magnesium and sodium on some physical properties of red-brown earth subsoil III. The permeability of Shepperton soil and comparison methods. *Australian Journal of Soil Research*, **11**, 159–165.
- Blaskó, L., and Karuczka, A., 2001. Role of magnesium in some physical properties of soils (In Hungarian). *Agrokémia és Talajtan*, **50**, 383–396.
- Ellis, J. H., and Caldwell, O. G., 1935. Magnesium clay solonet. In *Proceedings 3rd International Congress of Soil Science*, Vol. 1, pp. 348–350.
- Emerson, W. W., and Chi, C. L., 1977. Exchangeable calcium, magnesium, and sodium and the dispersion of illite in water II. Dispersion of illite in water. *Australian Journal of Soil Research*, **15**, 255–262.
- Girdhar, I. K., and Yadav, J. S. P., 1981. Role of magnesium in varying quality irrigation waters in influencing soil properties and wheat crop. *Agrokémia és Talajtan*, **30**, 148–157.
- Goldberg, S., Suarez, D. L., and Glaubig, R. A., 1988. Factors affecting clay dispersion and aggregate stability of arid-zone soils. *Soil Science*, **146**, 317–325.
- Keren, R., 1991. Specific effect of magnesium on soil erosion and water infiltration. *Soil Science Society of America Journal*, **55**, 783–787.
- Quirk, J. P., 1971. Chemistry of saline soils and their physical properties. In Talsma, T., and Philip, J. R. (eds.), *Salinity and Water Use*. London: Australian Academy of Science, MacMillan, pp. 79–91.
- Quirk, J. P., and Schofield, R. K., 1955. The effect of electrolyte concentration on soil permeability. *Journal of Soil Science*, **6**, 163–178.
- Richards, L. A. (ed.), 1954. *Diagnose and Improvement of Saline and Alkali Soils*. Handbook No. 60. USDA.
- Shainberg, I., and Letey, J., 1984. Response of soils to sodic and saline conditions. *Hilgardia*, **61**, 21–57.
- Shainberg, I., Levy, G. J., Rengasamy, P., and Frenkel, H., 1992. Aggregate stability and seal formation as affected by drop's impact energy and soil amendments. *Soil Science*, **154**, 113–119.
- Szabolcs, I., 1969. The influence of sodium carbonate on soil forming processes and soil properties. *Agrokémia és Talajtan*, **18**, 37–68.
- Tajik, F., Rahimi, H., and Pazira, E., 2003. Effects of electrical conductivity and sodium adsorption ratio of water on aggregate stability in soils with different organic matter content. *Journal of Agricultural Science and Technology*, **5**, 67–75.
- Várallyay, G., 1981. Extreme moisture regime as the main limiting factors of the fertility of salt affected soils. *Agrokémia és Talajtan*, **30**, 73–96.

Cross-references

- Irrigation and Drainage, Advantages and Disadvantages
Leaching of Chemicals in Relation to Soil Structure
Physical Degradation of Soils, Risks and Threats
Shrinkage and Swelling Phenomena in Soils
Soil Aggregation and Evaporation
Soil Water Flow
Solute Transport in Soils

SCALE (DEPENDENCY, INVARIANCE)

See *Scaling of Soil Physical Properties*

SCALING OF SOIL PHYSICAL PROPERTIES

Asim Biswas, Bing Cheng Si
Department of Soil Science, University of Saskatchewan,
Saskatoon, SK, Canada

Definition

Soil spatial variability. Soil properties measured at different locations exhibit different values.

Self similarity. Soil properties measured at points close to each other are more similar than those located far apart.

Scale. It is a characteristic length or time.

Scale dependency. The statistical measure of soil properties change with change in scale.

Scale invariance. A measure of a soil property at a scale is a power function of the scale with the exponent independent of scale.

Introduction

Soil physical properties are highly variable and exhibit scale-dependent spatial variability (Nielsen et al., 1973; Burrough, 1983). For environmental, hydrological, and agricultural applications, some questions are always being asked about soil physical properties: What is the most representative scale of variability and at which scale should we measure the soil physical properties? How does the variability change with scales? How can we interpret and correlate soil processes over scales, given the information collected at a given scale? Can we interpolate (disaggregation) or extrapolate (aggregation) the information from one measurement scale to others? Can we transfer the information from local observation to large scales?

These issues arise as the scale of measurements differs from the scale of application. In another word, the scale at which the information is collected is different from the scale at which the prediction is necessary or the information will be used. Similarly, the actual scale of soil processes is quite different from our scale of observation. There is always a gap between the scales at which real soil processes are going on; we measure the soil physical

properties, and we predict them or we want to use the information. To make a bridge for the gap, we need to understand the scaling of soil physical properties.

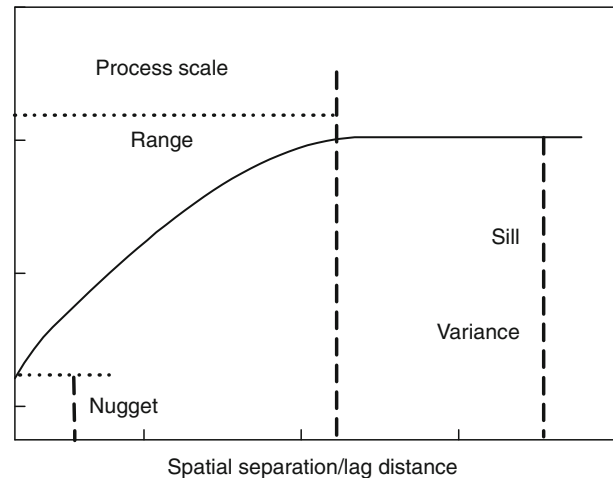
Concept of scale

Soil physical properties can vary frequently in space and are called small-scale variability. Similarly, they can vary slowly in space and are called large-scale variability. The scale at which the actual soil processes are going on is generally considered as process scales, whereas the scale at which measurements of soil physical properties are taken in field is known as measurement scale or observation scale. The scale, at which a model is established or used for validation and prediction, is known as model scale.

Process scale

Though the process scales are related to the spatial dimension of the natural variability of soil processes, it is defined as the range of their correlation. This correlation range is the representative spatial distance within which a soil physical property behaves similar or the relationship between multiple soil physical properties does not change. Within this range, soil physical properties are autocorrelated as a result of spatial continuity or inter-sample dependence and are explained as self-similar (Goovaerts, 1997). The correlation range can be estimated from the experimental semivariogram, which is the backbone of geostatistics. A detailed review of geostatistics can be found in Trangmar et al. (1985) and Si et al. (2007). Semivariogram measures the average dissimilarity between the pairs of data points. It is a plot of semivariance (half of the average squared difference between points that are separated by lag distances) as a function of spatial separation or lag distance. A well-behaved semivariogram (Figure 1) increases from a minimum value at smallest lag (lag = 1) distance or unit separation until a plateau is reached, where the semivariance remains constant with increasing lag. The extrapolated minimum semivariance at lag = 0 is known as the “nugget,” the lag at which the semivariance reaches its maximum is called “range,” and the maximum semivariance value is known as the “sill” (Figure 1).

Different soil physical property may have different correlation range. For example, Zeleke and Si (2005) reported the correlation range of different soil physical properties including sand (116 m), silt (173 m), clay (43 m), and organic carbon (43 m) from a gently undulating field in cold and subhumid climate in Canada. Further, for the same soil physical properties, the correlation range changes from field to field. For example, Ceddia et al. (2009) reported the correlation length of 56.9 and 86.8 m for bulk density and sand, respectively in a Brazilian soil. Sometimes, there may be several processes operating together contributing to the variability of soil physical properties, which can be represented as the nested spatial structure with multiple ranges. Each range is the characteristic scale of a particular process. Biswas and Si (2009)



Scaling of Soil Physical Properties, Figure 1 A typical semivariogram showing its components and indicating process scale.

reported two ranges of 20 and 120 m, suggesting two different processes that controlled the variability of soil physical properties including bulk density, sand, silt, and clay. The joint correlation length for two soil physical properties can be identified from the cross semivariogram analysis. Once the characteristic scales are identified, the scale information can be used to interpolate the information for unsampled locations through a process called “kriging.” Kriging can produce a detailed map of soil properties once the dominant scale is identified from the semivariogram spatial structure.

Multiple processes can operate together at different scales, thus creating multiple ranges in soil physical properties. Similarly, the intensity of the processes can vary over scales and make their contribution to the total variance scale dependent. For example, one process contributes majority of variance to the total variance at one scale, while at other scales, it has a different level of contribution or even may not have any contribution to the total variance. Some of the processes can also be transient in time and/or location. Like mean and variance, semivariogram is a global measure and cannot deal with transient and location-specific, nonstationary features. Wavelet analysis can be used in this situation to identify and separate out dominant scales of variability of soil physical properties. It is an advanced statistical method that can partition total variation into different scales and locations. For example, using wavelet analysis, Si and Zeleke (2005) reported the scale for organic carbon as 6–24, 60, and 100 m. The dominant scale of variation between two physical properties can also be identified from wavelet coherency analysis. The details of wavelet and wavelet coherency analysis technique in explaining the variability of soil properties is available in Lark and Webster (1999), Si (2003), Si and Zeleke (2005), and Biswas and Si (2008).

Measurement scale

The scale at which measurements for any soil properties has been taken is called measurement scale. According to Blöschl and Sivapalan (1995), measurement scale consists of three important characteristics: spacing, extent, and support, which are also known as the “scale triplet” (Figure 2).

Spacing is the distance between samples, extent refers to the total coverage of the measurements, and support is the area over which a measurement is taken. All the three components are needed to uniquely specify the space dimension of a measurement. The measurement scale can be small and restricted to ground-based measurement of a small field (where spacing and extent is small, but support can be little bigger as each point averages the soil property over a certain area) or an aerial measurement by remote sensing for a large area (spacing can be variable based on image resolution, extent is large, and support is small and represented by a point).

Model scale

Model scale also consists of the “scale triplet” (Blöschl and Sivapalan, 1995) similar to the measurement scale (Figure 2). However, it is related to the spatial properties of model rather than those of measurements. Scale triplets depend on the resolution of the map to be produced, the area to be mapped and the area, of which each point in the map is representative.

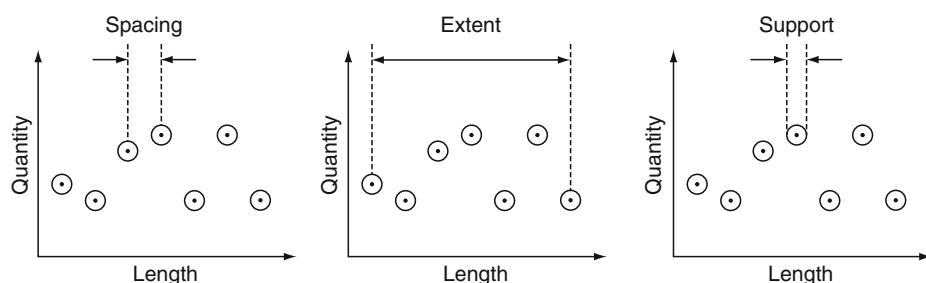
Scaling

We often need to use the information from one scale to another. This change in scale is known as scaling (Beven, 1995). Generally, there are two changes in scale, from the true processes to the observation (i.e., scaling by measurement) and from the observation to the prediction (i.e., scaling by model). How the measurement scale triplets change the true pattern to be reflected in the observation and how the model scale triplets change the observation to be reflected in predictions are the main interest in understanding scaling. There are some similarities in this scaling (Blöschl and Sivapalan, 1995; Blöschl, 1999). For example, small-scale variability will not be captured if the observation spacing is too large and the large-scale

variability will not be captured if the extent is too small. Similarly, if the support of the observation is too large, most of the variability will be averaged and smoothed out. Therefore, the pattern reflected in the measurement is a filtered true pattern in a real field. The effect of filter is closely related to the ratio of the measurement scale to process scales. The small-scale variability will not be captured if the spacing of the measurement is too large compared to the process scales. Model scale also has the similar effect. If the model scale is larger than the process scales, most of the variability will not be captured in prediction. The interpolation, extrapolation, disaggregation, and aggregation of information always imply the change in scales, which can also be viewed as filtering. This scaling issue can merely be solved by simply considering the differences in space. It is further compounded by the spatial variability of soil properties and the nonlinear nature of soil processes. The spatial variability of soil properties can be taken into account using geostatistics as a linear stochastic filter, and the nonlinearity of soil processes can be taken into account through physically based modeling as nonlinear deterministic filter.

In linear approximation, the small-scale variability within elements and large-scale variability between elements add up to the total variability (Isaaks and Srivastava, 1989). The large-scale processes (larger than element size) are explicitly presented in the model, and the small-scale processes (smaller than element size) are parameterized through some lumped relationships (Blöschl, 1999). In most cases, the small-scale variability within an element is unknown (Beven, 1995), and hence a lumped representation as sub-grid variability (variability within a sub-grid cells) is appropriate and necessary. The spatial interpolation through geostatistics is used to represent the spatial variability of soil processes between elements.

In geostatistics, the processes can be aggregated through simple arithmetic averaging and therefore, it assumes that (1) upscaling from measurements through simple arithmetic averaging will not have an effect on the expectation (of mean) and (2) the variable to be examined is a second-order stationary random variable. In nature, sometimes it is difficult to satisfy both



Scaling of Soil Physical Properties, Figure 2 The scale triplet (spacing, extent, and support). (After Blöschl and Sivapalan, 1995.)

assumptions as many processes aggregate nonlinearly. Nonlinearity does not allow aggregating the processes through simple arithmetic averaging. For example, suppose that soil hydraulic conductivity is measured at every $5 \times 5 \text{ cm}^2$ from an area of $10 \times 10 \text{ m}^2$. The simple arithmetic average of the 4,000 small-scale soil hydraulic conductivity measurements will be much smaller than the measurement made at $10 \times 10 \text{ m}^2$. If soil pores are vertically straight, then the simple arithmetic averaging will lead to a similar result to the large-scale measurement. In reality, soil pores are extremely tortuous, and pore connectivity (especially preferential pores) is much smaller in small soil cores than in a large area, resulting in much smaller hydraulic conductivity from small-scale than from large-scale measurements. This nonlinearity requires a distributed physically based model that incorporates the complexity of the physical processes as much as possible. In distributed modeling, the extent of a scale is subdivided into different square grid cells. This is done through splitting the total spatial variability into a small-scale part of variability within elements and large-scale parts of variability between elements (Blöschl, 1999).

The above-mentioned scaling methodology is very pragmatic but is limited to mean and variances. And there are no theoretical bases for determining if the proposed scaling method is accurate. An elegant theory was proposed by Mandelbrot (1982) and is very applicable in upscaling or downscaling of these statistical moments. The spatial patterns of soil properties observed at different scales may be related to each other by a power function (power law relations) (Mandelbrot, 1982), whose exponent is known as fractal dimension:

$$\langle X^q \rangle(s) \rightarrow s^\alpha, \quad (1)$$

where X is the spatial series representing soil physical property, q is the order of moment, s represents scale, and α is the fractal dimension. Therefore, any statistical moment of the soil physical property at any scale can be obtained, once the fractal dimension is known. Fractal theory has been utilized to investigate and quantitatively characterize spatial variability over a range of measurement scales (Mandelbrot, 1982; Burrough, 1983). Fractals were first introduced into soil science in representation of the particle size distribution, where cumulative mass or volume is a power function of particle size (Tyler and Wheatcraft, 1992; Taguas et al., 1999; Millán et al., 2003). A detail presentation of fractal theory and its application to soil science is available in Mandelbrot (1982), Tyler and Wheatcraft (1992), Perfect and Kay (1995), and Millán et al. (2003). When the variability of a soil property can be explained by a single fractal dimension, it is known as monofractal. Zeleke and Si (2006) found the monofractal behavior of bulk density and sand and silt contents in an agricultural field. More often than not, any spatial statistical moments of soil physical properties

exhibit fractal properties (obey the power law), but the exponents are different for different order of statistical moments:

$$\langle X^q \rangle(s) \rightarrow s^{\alpha(q)}, \quad (2)$$

where $\alpha(q)$ is a function of moment order q . We call this soil physical property multifractal. For each order of moment, the soil physical property is monofractal, but different q requires a different α . Multifractal soil properties are governed by a random multiplicative process, and systematic analysis of this behavior enables characterization of complex phenomenon in a fully quantitative fashion (Stanley and Meakin, 1988). Multifractal is also a technique that transfers irregular observation into a more compact form and amplifies slight differences among the variables distribution (Lee, 2002). The knowledge of soil physical properties being monofractal or multifractal is very important for scaling. For monofractal soil properties, any statistical moments can be scaled through a single exponent (fractal dimension). For multifractal soil properties, scaling can be done for any statistical moment, but the scaling exponent is different for different order of statistical moments. While fractal analysis is a very powerful tool for obtaining scaling exponents, different soil physical properties can be fractal or nonfractal, and there are a priori methods to determine if a soil physical property is fractal or nonfractal. Therefore, measurements at different scales have to be taken before we can determine whether the soil properties are fractal or not. The organic matter (Kravchenko et al., 1999; Zeleke and Si, 2005; Zeleke and Si, 2006) and clay content (Zeleke and Si, 2005; Zeleke and Si, 2006) showed multifractal behavior, while bulk density, sand, and silt (Zeleke and Si, 2005; Zeleke and Si, 2006) showed monofractal behavior, indicating that organic matter and clay content are more heterogeneous than bulk density, sand, or silt.

Summary

Soil physical properties vary from location to location and at scales. This article addresses the basic concepts of scale and the scaling or the transfer of information from one scale to another. The spatial distance of the natural variability of soil processes, which can be identified as the distance within which a soil property behaves similar or the correlation between multiple properties does not change is known as the processes scale. Geostatistics can identify the distance of spatial correlation as the “range.” The process scale varies with field and environmental situation. Sometimes, there can be several processes operating together in a field representing through multiple ranges. These processes sometimes may operate at different intensities and at different locations. Wavelet, an advanced mathematical analysis, can deal with scale- and location-specific variability. The scale- and location-specific variability between two properties can be identified through wavelet coherency analysis. The characteristic scales can

be used to predict the soil properties at unsampled locations through “kriging.” The process scale is the actual scale of occurrence of soil processes. However, the measurements are not always recorded at process scales. The measurement scale depends on the spacing or distance between measurement, extent, or total coverage of measurement, and the support or the area of the measurement. These “scale triplets” are also important for model scale, which depends more on the spatial properties of models than measurements.

Now the change in information from true processes to observation and from observation to prediction is known as scaling. The aggregation, disaggregation, interpolation, and extrapolation always imply change in scale or scaling. However, the spatial variability and the nonlinear nature of soil process do not allow simple consideration of space. The former can be taken into consideration as a linear stochastic filter and the later through physically based modeling as deterministic filter. However, these methods are limited to means and variances. The higher-order statistical moments can be upscaled or downscaled if the spatial pattern of soil properties observed at different scale can be represented through a power function. This is known as power law relationship. Once the relationship is observed, any statistical moments of soil physical properties can be obtained at any scales. This is known as fractal relationship. The relationship over scales can be represented through a single dimension, which is known as monofractal or can be different for different statistical moments, which is known as multifractal. This type of behavior of soil properties is important for scaling.

Bibliography

- Beven, K., 1995. Linking parameters across scales: subgrid parameterizations and scale dependent hydrological. *Hydrological Processes*, **9**, 507–25.
- Biswas, A., and Si, B. C., 2009. Spatial relationship between soil hydraulic and soil physical properties in a farm field. *Canadian Journal of Soil Science*, **89**, 473–488.
- Biswas, A., Si, B. C., and Walley, F. L., 2008. Spatial relationship between $\delta^{15}\text{N}$ and elevation in agricultural landscapes. *Nonlinear Processes in Geophysics*, **15**, 397–407.
- Blöschl, G., 1999. Scaling issues in snow hydrology. *Hydrological Processes*, **13**, 2149–2175.
- Blöschl, G., and Sivapalan, M., 1995. Scale issues in hydrological modelling: a review. *Hydrological Processes*, **9**, 251–290.
- Burrough, P. A., 1983. Multiscale sources of spatial variation in soil: I. The application of fractal concepts to nested levels of soil variation. *Journal of Soil Science*, **34**, 577–597.
- Ceddia, M. B., Vieira, S. R., Villela, A. L. O., Mota, L. D. S., dos Anjos, L. H. C., and de Carvalho, D. F., 2009. Topography and spatial variability of soil physical properties. *Scientia Agricola*, **66**, 338–352.
- Goovaerts, P., 1997. *Geostatistics for Natural Resources Evaluation*. New York: Oxford University Press.
- Isaaks, E., and Srivastava, R., 1989. *An Introduction to Applied Geostatistics*. Oxford: Oxford University Press.
- Kravchenko, A. N., Boast, C. W., and Bullock, D. G., 1999. Multifractal analyses of soil properties. *Agronomy Journal*, **91**, 1033–1041.
- Lark, R. M., and Webster, R., 1999. Analysis and elucidation of soil variation using wavelets. *European Journal of Soil Science*, **50**, 185–206.
- Lee, C. K., 2002. Multifractal characteristics in air pollutant concentration time series. *Water Air and Soil Pollution*, **135**, 389–409.
- Mandelbrot, B. B., 1982. *The Fractal Geometry of Nature*. San Francisco: Freeman.
- Millán, H., González-Posada, M., Aguilar, M., Domínguez, J., and Céspedes, L., 2003. On the fractal scaling of soil data. Particle size distributions. *Geoderma*, **117**, 117–128.
- Nielsen, D. R., Biggar, J. W., and Erh, K. T., 1973. Spatial variability of field measured soil water properties. *Hilgardia*, **42**, 214–259.
- Perfect, E., and Kay, B. D., 1995. Applications of fractals in soil and tillage research: a review. *Soil and Tillage Research*, **36**, 1–20.
- Si, B. C., 2003. Spatial and scale dependent soil hydraulic properties: a wavelet approach. In Pachepsky, Y., Radcliffe, D., and Selim, H. M. (eds.), *Scaling Method in Soil Physics*. New York: CRC Press, pp. 163–178.
- Si, B. C., and Zeleke, T. B., 2005. Wavelet coherency analysis to relate saturated hydraulic properties to soil physical properties. *Water Resources Research*, **41**, W11424, doi:10.1029/2005WR004118.
- Si, B. C., Kachanoski, R. G., and Reynolds, W. D., 2007. Analysis of soil variability. In Gregorich, E. G. (ed.), *Soil Sampling and Methods of Analysis*. Boca Raton: CRC Press, pp. 1163–1191.
- Stanley, H. E., and Meakin, P., 1988. Multifractal phenomena in physics and chemistry. *Nature*, **335**, 405–409.
- Taguas, F. J., Martín, M. A., and Perfect, E., 1999. Simulating and testing of self similar structures for soil particle size distributions using iterated function systems. *Geoderma*, **88**, 191–203.
- Trangmar, B. B., Yost, R. S., and Uehara, G., 1985. Application of geostatistics to spatial studies of soil properties. *Advances in Agronomy*, **38**, 45–94.
- Tyler, S. W., and Wheatcraft, S. W., 1992. Fractal scaling of soil particle size distribution: analysis and limitations. *Soil Science Society of America Journal*, **56**, 362–369.
- Zeleke, T. B., and Si, B. C., 2005. Scaling relationships between saturated hydraulic conductivity and soil physical properties. *Soil Science Society of America Journal*, **69**, 1691–1702.
- Zeleke, T. B., and Si, B. C., 2006. Characterizing scale dependent spatial relationship between soil properties using multifractal techniques. *Geoderma*, **134**, 440–452.

Cross-references

- [Agrophysical Properties and Processes](#)
[Fractal Analysis in Agrophysics](#)
[Mapping of Soil Physical Properties](#)

SEED

See [Grain Physics](#)

SEEPAGE

Percolation of water through the soil from e.g., a pond, ditches, watercourses, or water storage facilities.

SELF SIMILARITY

See [*Scaling of Soil Physical Properties*](#)

SENSORY EVALUATION

The application of design and statistical analysis to the use of the senses to evaluate food products.

SHEAR STRENGTH

The ability of a material to withstand shear stress.

SHEAR STRESS

A stress state resulting in a change of material (e.g., soil, plants) shape.

Bibliography

http://www.wordiq.com/definition/Shear_stress

SHEET EROSION

The removal of relatively uniform thin layer of soil from the land surface by rainfall.

Cross-references

[Water Erosion: Environmental and Economical Hazard](#)

SHEET FLOW

Overland water flow in a thin sheet of uniform thickness.

Cross-references

[Overland Flow](#)

SHRINKAGE

See [*Shrinkage and Swelling Phenomena in Agricultural Products; Shrinkage and Swelling Phenomena in Soils*](#)

SHRINKAGE AND SWELLING PHENOMENA IN AGRICULTURAL PRODUCTS

Bohdan Dobrzański, Jr.

Pomology Department, University of Life Sciences,
Lublin, Poland

Institute of Agrophysics, Polish Academy of Sciences,
Lublin, Poland

Synonyms

Shrinkage and swelling of food

Definition

Shrinkage—The physical phenomenon of a body becoming smaller frequently observed during drying.

Swelling—The physical phenomenon where a porous body becomes larger by absorbing water or during imbibition and hydration processes.

Introduction

The present demand for high-quality products in the food market requires dehydrated foods that maintain most of the quality characteristic of the fresh product. Dehydration of agricultural products is one of the most common processes used to improve food stability, because it decreases considerably the water activity of the material, reduces microbiological activity, and minimizes physical and chemical changes during its storage (Mayor and Sereno, 2004).

One of the most important physical changes that agricultural products undergo during drying is reduction of external volume due to shrinkage. Shrinkage of food materials has a negative impact on the quality of the dehydrated product. Loss of water and heating cause collapse in the cellular structure of products. Changes in shape and volume increase hardness, which in most cases has a negative impression on the consumer. However, some dried food, such as raisins, dried plums, peaches, and dates, have consumer acceptance as traditionally shrunken products.

Shrinkage of agricultural products and food

When water is removed from material, a pressure unbalance is produced between the interior of the material and the exterior, generating contracting stresses that lead to material shrinkage or collapse, changes in shape, and occasionally cracking of the product. For this reason, drying under vacuum, as in freeze-drying, leads generally to much less shrinkage (Mayor and Sereno, 2004). Shrinkage of food materials increases with the volume of water removed. In some cases, the mechanical equilibrium is reached when shrinkage of the material equals volume of removed water. This behavior is observed during the whole drying process. In other cases, however, the volume of removed water during the final stages of drying is larger than the reduction in sample volume. This behavior can be explained by the decrease in the mobility of the solid matrix of the material at low moisture contents, as described below.

In food systems shrinkage is rarely negligible, and it is advisable to take it into account when predicting moisture content profiles in the material undergoing dehydration. For such purposes, different types of models that predict volume change in the material are available and should be used. Several authors have reviewed the process of food dehydration both from an experimental and modeling viewpoint, pinpointing new approaches and methodologies (Mayor and Sereno, 2004).

White and Bell (1999) tried to relate the effect of collapse and porosity with the kinetics and extension of some chemical reactions in foods undergoing drying and further storage. In this case, a model food system was composed by glucose and glycine included in an inner matrix. They tried to eliminate porosity due to structural collapse by decreasing the glucose loss rate constant, but this had a minimal effect on the rate of brown pigment development associated with the Maillard reaction.

Mechanism of shrinkage

Given a physical description of the shrinkage mechanism, a classification of the different models was presented by Mayor and Sereno (2004) to describe this behavior in food and agricultural materials undergoing dehydration. The models were classified in two main groups: empirical and fundamental models. Empirical models are obtained by means of regression analysis of shrinkage data. Fundamental models are based on a physical interpretation of the structure of food materials and try to predict dimensional changes due to volume variation of the different phases in the food system during the drying process. Several models were compared with experimental data on air drying of several fruits and vegetables. Average relative deviations between experimental and predicted values of shrinkage found were, in most cases, less than 10% (Mayor and Sereno, 2004). This approach is more fundamental and based on a physical interpretation of the food system and tries to predict geometrical changes based on conservation laws of mass and volume. In both cases, linear and nonlinear models result to describe shrinkage behavior versus moisture content.

Most of agricultural products are solid or semi-solid food and are highly heterogeneous materials that may be considered as consisting of a three-dimensional solid network or matrix holding usually large quantities of a liquid phase, in most cases an aqueous solution. Biopolymers are the common structural elements of the solid matrix. The particular structure of the material and the mechanical characteristics of its elements at equilibrium define sample volume and determine its size and shape.

The mobility of the solid matrix is closely related to its physical state; high mobility corresponds to a viscoelastic behavior typical of a rubbery state while low mobility corresponds to an elastic behavior typical of a glassy state. Levi and Karel (1995) found that mobility of the solid matrix is a dynamic process with rates that depend on the difference of temperature of the sample undergoing

dehydration and glass transition temperature. At high moistures, when the material is in the rubbery state, shrinkage almost entirely compensates for moisture loss, and volume of the material decreases linearly with moisture content. At low moisture content, glass transition temperature increases, allowing the material to pass from the rubbery to glassy state, and the rate and extension of shrinkage decreases significantly. When the drying process is in the range of low moisture content where phase transition from rubbery to glassy state is going on, rigidity of the material stops shrinkage and parallel pore formation may occur.

The mechanism of shrinkage in seeds and grain

In the early 1970s, Overhults et al. (1973) observed the physical damage in soybeans, as indentations or cracks and splits, during drying. In view of these problems, especially in the legume seed industry, several authors elaborated on the optimum drying conditions for minimizing seed coat cracking. The major problem in the drying of beans and seeds with heated air is the splitting of the seed coat (Liu et al., 1989; 1990). However, in the study of stress cracking due to drying, the decreasing moisture content of grains is essential to this mechanism. On the other hand, the modulus of elasticity of the seed coat varies with moisture level (Dobrzański, 1998; 2000). Looking for the mechanism responsible for the splitting of seed coat, a determination of the elasticity limit of the seed coat and its resistance to tension for various legume seeds, was the essential in understanding the mechanism of cracking due to seed coat shrinkage.

All results reported by Dobrzański (2002a) made the bases for the shrinkage model of the seed coat being drying with a hot air. The model presents a spherical seed in a stream of hot air. The wet seed of large volume is surrounded by the seed coat. During drying, the seed coat reduces its size, which leads to rapid shrinkage. The shrinkage leads to a tension stress in the seed coat, involving an increase of inner pressure of low compressibility cotyledons. In this case, each point of spherical shell represents a plane stress, where the principal stress in each direction is equal. To determine a criterion of tension strength for the seed coat, it is sufficient to estimate circumferential stress in a cross-section of the seed (Dobrzański, 1998).

Unbalanced seed coat shrinkage of the seed in layer

Most seeds in real conditions are located on the layer or inside the layer where each seed has three or more contacts with others. In these areas, the contact zone limits the inflow of air so that free parts only are subject to shrinkage. The shrinkage leads to tension and elongation in the wet part of the contact area. Determination of the strain of the seed coat and elasticity modulus allows estimating criteria of tension. For this purpose, the shrinkage, strain, ultimate elongation at rupture, and modulus of elasticity

must be determined experimentally at wide ranges of moisture. The results obtained at tension of the seed coat showed that the increase of moisture content involves the decrease of force at breakage. In seed coat strength-differentiated cultivars, however, shrinkage stress was frequently higher than tension strength of the seed coat. The force induced by the shrinkage also depended on drying conditions. The highest shrinkage of the seed coat for all cultivars was noticed in heated air. Low temperature and slow stream of air involved less shrinkage. The relevance was the phenomenon that rapid decrease of temperature during drying involved additional 25% shrinkage. Dobrzański (1998) clarified the reason for the coat split in cold air after drying in hot air. He observed this phenomenon for all beans, peas, and other legume seeds. Shrinkage of the seed coat at drying lead to its stress and splitting. The results obtained in all experiments proved that frequently the stress was higher than the strength of the seed coat. It is the main reason for seed coat cracking during drying (Dobrzański, 2002b).

Surface cracking

Surface cracking is another phenomenon that may occur during drying. This happens when shrinkage is not uniform during the drying process, leading to the formation of unbalanced stresses and failure of the material. Cracking of food materials has been reported by several authors: in soybeans (Mensah et al., 1984; Dobrzański, 2000) and corn (Fortes and Okos, 1980). This cracking phenomenon has been successfully modeled by coupling equations of heat and mass transfer by Akiyama et al. (1997) and Litchfield and Okos (1988). Another important consequence of shrinkage is the decrease of rehydration capability of the dried product. McMinn and Magee (1997), in the air drying of potatoes at different process temperatures, reported that when comparing samples with the same moisture content but a different degree of shrinkage due to the different drying conditions used, a lower dehydration capacity corresponded to most shrunk samples.

Swelling of seeds and grain

Shrinkage of seeds is a physical phenomenon observed during maturing or dehydrating processes. On the other hand, swelling of seeds is the opposite process and physical phenomena observed during soaking of grain or during hydration of formerly dried material for long storage as sieving material. For legume seeds, the first stage only, connected with imbibitions of water is a physical phenomenon; however, further hydration is related to biological or chemical processes.

Dobrzański (1998) has tested the influence of water capacity on seed volume increase of different pea seed, soya, french bean (yellow-pod and green-pod), bean, faba bean, and bread bean. The effect of moisture content on expansion volume and dimensions of beans was observed in the initial phase of swelling. Further, a rapid decrease of moisture content of the seed coat caused the shrinkage

during drying, leading to stress. With an increase of moisture content, the seed coat of legume seeds decreased its strength (Dobrzański, 2002b). The increase of moisture content of legume seeds caused considerable deformations in its shape that lead to increase of volume. In the initial phase of swelling, only the shell is soaked and its shrunken area increased. Further, seed cotyledons become larger, causing seed coat filling, leading the shell tensioning till its disruption. The relative elongation of the seed coat allows calculating stress during seed swelling. The problem consists of determining the surface area of the seed coat surrounding two cotyledons. It is characteristic that the shape and volume of wet seed is not equal after drying and second soaking.

Rate and temperature of drying

If rapid drying rate conditions are used and intense moisture gradients through the material are observed, low moisture content of the external surface may induce a rubber–glass transition and the formation of a porous outer rigid crust or shell that fixes the volume and complicates subsequent shrinkage of the still rubbery inner part of the food. If low drying rate conditions are used, diffusion of water from the inner to the outer zone of the material happens at the same rate as evaporation from the surface and no sharp moisture gradients are formed in the material, which shrinks uniformly until the last stages of drying. This behavior was noticed by Mayor and Sereno (2004). The shell formation effect cannot be observed if drying conditions do not allow a phase transition in the outer zone material, even at high drying rates. Willis et al. (1999), during drying of pasta, observed a higher shrinkage when samples were dehydrated at higher temperature (100°C) than in samples dehydrated at 40°C at the same relative humidity of air. In the first case, drying temperature was greater than the glass transition temperature of the pasta, and the product remained in the rubbery state and shrank uniformly during the whole drying process. In the second case, the case hardening effect was observed due to a glass transition in the surface of the material that decreased shrinkage and increased residual stresses in the dried material, which underwent cracking and breakage during storage. Mayor and Sereno (2004) presented the influence of different process conditions in volume change of the materials during dehydration. In most cases, such analysis has been done, studying the effect of each single process condition like temperature, velocity of air, or relative humidity of air. Unfortunately, the results of these works are often unclear as to the influence of these process conditions on shrinkage.

Drying of foods is a complex process involving simultaneous mass and energy transport in a system that suffers different changes in its chemical composition, structure, and physical properties. As suggested before, it is the combined effect of process conditions when facilitating the formation of a crust or shell in the external surface of

the product during the initial stage of the drying process that determines the type and extent of shrinkage.

The force induced by the shrinkage depended also on drying conditions. Dobrzański (1998) presented that, in some cases, an increase of drying temperature produced less shrinkage. However, the highest shrinkage of the seed coat for all cultivars was noticed in heated air. Low temperature and slow stream of air involve less shrinkage. This approach is more fundamental and is based on a physical interpretation of the food system that tries to predict geometrical changes based on conservation laws of mass and volume. In this case, both linear and nonlinear models result to describe shrinkage behavior versus moisture content.

Summary

Shrinkage of agricultural products is a common physical phenomenon observed during different dehydration processes. On the other hand, swelling of various agricultural products is a physical phenomenon observed during soaking of plant materials or during hydration of formerly prepared-for-preservation dried food. For some plant materials, e.g., legume seeds, the first stage only, connected with imbibition of water, is a physical phenomena, however, further hydration is related to biological or chemical processes. Shrinkage of food materials increases with the volume of water removed, since the more water removed, the more contraction stresses are originated in the material. In some cases, the mechanical equilibrium is reached when shrinkage of the material equals volume of removed water. These changes affect the quality of the hydrated or dehydrated product and should be taken into consideration when predicting moisture and temperature profiles in the dried or soaked material. Temperature and moisture gradients can cause stresses in agricultural products. However, shrinkage in the seed coat is a phenomenon observed during drying, leading to its stress and splitting.

Bibliography

- Akiyama, T., Liu, H., and Hayakawa, K., 1997. Hygrostress-micracking formation and propagation in cylindrical viscoelastic food undergoing heat and moisture transfer processes. *International Journal of Heat and Mass Transfer*, **40**, 1601–1609.
- Dobrzański, B., Jr., 1998. The cracking mechanisms of the legume seeds (in Polish). *Acta Agrophysica*, **13**, 1–98.
- Dobrzański, B., Jr., 2002a. The shrinkage stress of the seed coat at grain legume drying. In Zude, M., Herold, B., and Geyer, M. (eds.), *Fruit Nut and Vegetable Production Engineering*. Potsdam: Institut für Agrartechnik Bornim e.V. (ATB), pp. 403–408.
- Dobrzański, B., Jr., 2002b. The cracking mechanisms of grain legume. In Blahovec, J., and Kutilek, M. (eds.), *Physical Methods in Agriculture*. Kluwer Academic: USA, pp. 167–194.
- Dobrzański, B., Jr., 2000. The analysis of seed cracking at grain legume processing. CD-ROM of *AgEng'2000 Warwick UK, Papers from the conference*, Paper: 00-PHI-050, 1–10.
- Fortes, M., and Okos, M. R., 1980. Changes in physical properties of corn during drying. *Transactions of the American Society of Agricultural Engineers*, **23**, 1004–1008.
- Levi, G., and Karel, M., 1995. Volumetric shrinkage (collapse) in freeze-dried carbohydrates above their glass transition temperature. *Food Research International*, **28**, 145–151.
- Litchfield, J. B., and Okos, M. R., 1988. Prediction of corn kernel stress and breakage induced by drying, tempering, and cooling. *Transactions of the American Society of Agricultural Engineers*, **31**, 585–594.
- Liu, M., Haghghi, K., and Stroshine, R. L., 1989. Viscoelastic characterization of the soybean seedcoat. *Transaction of the American Society of Agricultural Engineers*, **32**, 946–952.
- Liu, M., Haghghi, K., Stroshine, R. L., and Ting, E. C., 1990. Mechanical properties of the soybean cotyledon and failure strength of soybean kernels. *Transaction of the American Society of Agricultural Engineers*, **33**, 559–566.
- Mayor, L., and Sereno, A. M., 2004. Modelling shrinkage during convective drying of food materials: a review. *Journal of Food Engineering*, **61**, 373–386.
- McMinn, W. A. M., and Magee, T. R. A., 1997. Physical characteristics of dehydrated potatoes – Part II. *Journal of Food Engineering*, **33**, 49–55.
- Mensah, J. K., Nelson, G. L., Herum, F. L., and Richard, T. G., 1984. Mechanical properties related to soybean seedcoat cracking during drying. *Transactions of the American Society of Agricultural Engineers*, **27**, 550–560.
- Overhults, D. G., White, H. E., Hamilton, H. E., and Ross, I. J., 1973. Drying soybeans with heated air. *Transaction of the American Society of Agricultural Engineers*, **16**, 112–113.
- White, K. L., and Bell, L. N., 1999. Glucose loss and Maillard browning in solids as affected by porosity and collapse. *Journal of Food Science*, **64**, 1010–1014.
- Willis, B., Okos, M., and Campanella, O., 1999. Effects of glass transition on stress development during drying of a shrinking food system. In *Proceedings of the Sixth Conference of Food Engineering (CoFE099)* Dallas, TX, 496.

Cross-references

Grain Physics

Grains, Aerodynamic and Geometric Features

Physical Phenomena and Properties Important for Storage of Agricultural Products

Physical Properties as Indicators of Food Quality

Quality of Agricultural Products in Relation to Physical Conditions

Shrinkage and Swelling Phenomena in Soils

Stress–Strain Relations

Thermal Technologies in Food Processing

Water in Forming Agricultural Products

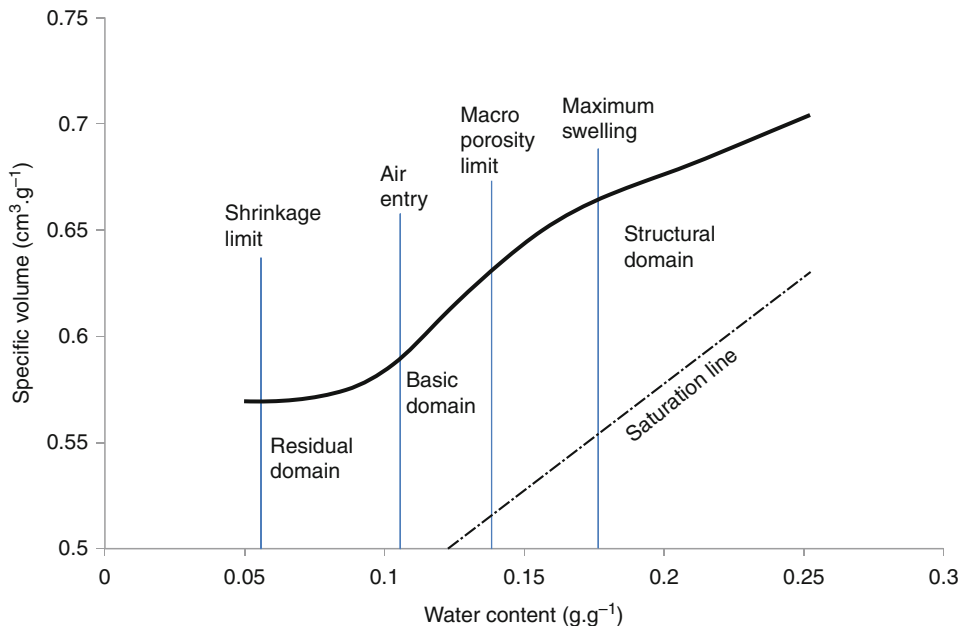
SHRINKAGE AND SWELLING PHENOMENA IN SOILS

Pascal Boivin

University of Applied Sciences of Western Switzerland (HES-SO), Geneva, Switzerland

Definition

The soil shrinkage is defined as the specific volume change of soil relative to its water content and is mainly due to clay swelling properties (Haines, 1923; Stirk, 1954). It can be measured in most soils with more than 10% clay content (Boivin et al., 2006) and shows a typical S-shape (Figure 1). This process is reversible with changes in water content and the reverse to shrinkage is swelling.



Shrinkage and Swelling Phenomena in Soils, Figure 1 Typical shrinkage curve of an undisturbed soil sample, with the transition points between the shrinkage domains. Note the position of the saturation line, delimiting air in the porosity (above) and water in the porosity (below).

Shrinkage is due to the volume change of the soil plasma and to some extent of the structural porosity with water content. The plasma is made of the colloidal constituents of the soil and is often referred to as clay matrix. Its porosity is often assimilated to the textural porosity as introduced by Childs (1969). The swelling factors in the plasma are the phyllosilicates and the organic matter, while binding elements (e.g., oxides and salts) tend to limit the plasma swelling. Therefore, soil shrinkage is closely related to the type of and content in colloids (Braudeau and Bruand, 1993; Boivin et al., 2004, 2009). Shrinkage is at the origin of crack forming in soils, and is, therefore, a major factor of soil structure resilience.

Soil shrinkage was first studied with the aim to quantify the soil structural behavior (Haines, 1923; Lauritzen and Stewart, 1941; Stirk, 1954; McGarry and Daniells, 1987), based on the observation that the swelling capacity of the soil quantifies the ability of the structure to withstand the drying forces, thus quantifying the hydrostructural stability with the slope of the shrinkage curve (Schäffer et al., 2008).

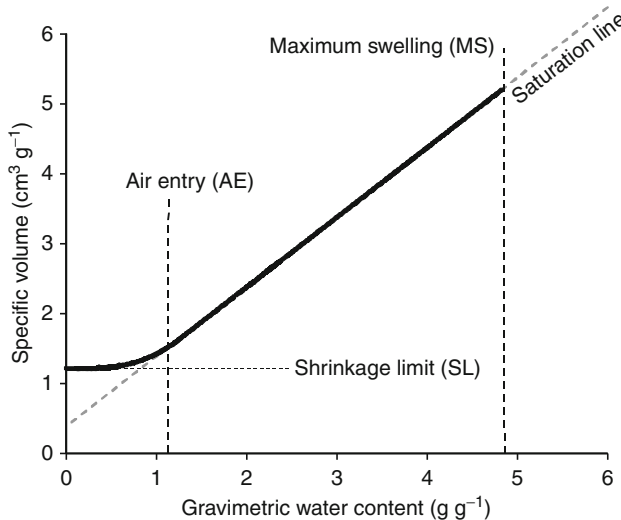
Based on the modeling of the shrinkage curve with the conceptual model XP (Braudeau et al., 1999), shrinkage analysis is now used to provide a full quantification of the soil pore systems (plasma and structural porosity), their deformation and air and water content at any soil water content, the pore size distribution of the structural pores, and the hydrostructural stability (Schäffer et al., 2008; Milleret et al., 2009), with applications to the

diagnosis of soil biota or soil management impact on soil properties.

The shrinkage curve of undisturbed soil clods was first estimated by measuring the volume of multiple soil clods at different water content (Haines, 1923). It is now determined continuously together with the water retention curve using a shrinkage apparatus, thus providing inexpensive, accurate, and reliable data (Braudeau et al., 1999; Boivin et al., 2004). In some cases it has been determined in situ (Coquet et al., 1998; Cabidoche and Ruy, 2001).

Shrinkage models were developed at two scales: namely plasma (clay matrix) and soil clods. All plasma models (Sposito, 1973; Chertkov, 2003) acknowledge the shrinkage behavior of clay pastes (Tessier et al., 1992), which remain saturated along most of their water content range, thus following the saturation line (load line) until the limit of plasma deformation allows air to enter the plasma porosity upon loss of water (air entry point) (Figure 2).

Shrinkage models can be split in shape fitting, deterministic and conceptual models. In the first category, Peng and Horn (2005) proposed to fit the Van Genuchten Equation to both shrinkage and water retention curves, and Boivin et al. (2006) follow this line using the XP model to show the similarity between the curves. In the second category, Chertkov (2008) proposed to model the S-shape behavior based on the clay-paste behavior and simple assumptions on aggregate structure. The conceptual XP model is widely used because it allows a unique



Shrinkage and Swelling Phenomena in Soils, Figure 2 Typical shrinkage curve of a clay paste. Note the clay paste following the saturation line from saturation to air entry: on this water content range there is no air in the clay porosity.

characterization of the soil physical properties with shrinkage analysis (cited refs).

Summary

Shrinkage is a general property of soils mostly due to its colloidal constituents, and play a major role in structure forming and resilience. The shrinkage curve of an undisturbed soil clod can be measured easily and quasi continuously together with the water retention curve. Shrinkage analysis based on the fitting of a conceptual model on the shrinkage curve allows a full characterization of the soil pore systems and their swelling dynamic with water. The corresponding properties show large correlations with the content in soil colloids and allow unique assessment of the impact of soil management on soil properties. Shrinkage analysis is, therefore, of growing interest in soil science as acknowledged by the increasing number of references.

Bibliography

- Boivin, P., Garnier, P., and Tessier, D., 2004. Relationship between clay content, clay type and shrinkage properties of soil samples. *Soil Science Society of America Journal*, **68**, 1145–1153.
- Boivin, P., Garnier, P., and Vauclin, M., 2006. Modeling the soil shrinkage and water retention curves with the same equations. *Soil Science Society of America Journal*, **70**, 1082–1093.
- Boivin, P., Schaeffer, B., and Sturmy, W., 2009. Quantifying the relationship between soil organic carbon and soil physical properties using shrinkage modelling. *European Journal of Soil Science*, **60**, 265–275.
- Braudeau, E., and Bruand, A., 1993. Determination of the clay shrinkage curve using the shrinkage curve of the undisturbed soil sample – application to a soil sequence in Ivory-Coast. *Comptes Rendus de l'Académie des Sciences Serie II*, **316**, 685–692.

- Braudeau, E., Costantini, J. M., Bellier, G., and Colleuille, H., 1999. New device and method for soil shrinkage curve measurement and characterization. *Soil Science Society of America Journal*, **63**, 525–535.
- Cabidoche, Y.-M., and Ruy, S., 2001. Field shrinkage curves of a swelling clay soil: analysis of multiple structural swelling and shrinkage phases in the prisms of a Vertisol. *Australian Journal of Soil Research*, **39**, 143–160.
- Chertkov, V. Y., 2003. Modelling the shrinkage curve of soil clay pastes. *Geoderma*, **112**, 71–95.
- Chertkov, V. Y., 2008. The physical effects of an intra-aggregate structure on soil shrinkage. *Geoderma*, **146**, 147–156.
- Childs, E. C. (ed.), 1969. *An Introduction to the Physical Basis of Soil Water Phenomena*. New York: Wiley.
- Coquet, Y., Touma, J., and Boivin, P., 1998. Comparison of soil linear shrinkage curve from extracted cores and in situ. *Australian Journal of Soil Research*, **36**, 765–781.
- Haines, W. B., 1923. The volume changes associated with variations of water content in soil. *Journal of Agricultural Science*, **13**, 296–311.
- Lauritzen, C. W., and Stewart, A. J., 1941. Soil volume changes and accompanying moisture and pore space relationships. *Soil Science Society of America Proceedings*, **6**, 113–116.
- McGarry, D., and Daniells, I. G., 1987. Shrinkage curve indices to quantify cultivation effects on soil structure of a vertisol. *Soil Science Society of America Journal*, **51**, 1575–1580.
- Milleret, M., Le Bayon, C., Lamy, F., Gobat, J. M., and Boivin, P., 2009. Impact of root, mycorrhiza and earthworm on soil physical as assessed by shrinkage analysis. *Journal of Hydrology*, **373**, 499–507.
- Peng, X., and Horn, R., 2005. Modeling soil shrinkage curve across a wide range of soil types. *Soil Science Society of America Journal*, **69**, 584–592.
- Schäffer, B., Schulin, R., and Boivin, P., 2008. Changes in shrinkage of restored soil caused by compaction beneath heavy agricultural machinery. *European Journal of Soil Science*, **59**, 771–783.
- Sposito, G., 1973. Volume changes in swelling clays. *Soil Science*, **115**, 315–320.
- Stirk, G. B., 1954. Some aspects of soil shrinkage and the effect of cracking upon air entry into the soil. *Australian Journal of Soil Research*, **5**, 279–290.
- Tessier, D., Lajudie, A., and Petit, J. C., 1992. Relation between the macroscopic behavior of clays and their microstructural properties. *Applied Geochemistry*, **7**, 151–161.

Cross-references

- [Bulk Density of Soils and Impact on their Hydraulic Properties](#)
[Clay Minerals and Organo-Mineral Associates](#)
[Cracking in Soils](#)
[Organic Matter, Effects on Soil Physical Properties and Processes](#)
[Pore Size Distribution](#)
[Soil Physical Quality](#)
[Wetting and Drying, Effect on Soil Physical Properties](#)

SLAKING

The partial breakdown of soil aggregates in water due to the swelling of clay and the expulsion of air from pore spaces. <http://dictionary.babylon.com/slaking/>
See [Shrinkage and Swelling Phenomena in Agricultural Products](#)

SLOPE STABILITY

See [Plant Root Strength and Slope Stability](#)

SNOWMELT INFILTRATION

Yukiyo Iwata

Climate and Land-use Change Research Team, National Agricultural Research Center for Hokkaido Region, NARO, Sinsei Memuro, Hokkaido, Japan

Definition

Snowmelt infiltration is the process by which snowmelt water enters the soil.

In this process, the winter precipitation stored on the soil surface as snow melts and infiltrates the soil when the snow temperature rises to above 0°C. This may occur in response to periods of warm weather during winter, but primarily occurs in early spring.

The infiltration rate is heavily influenced by the existence of frozen soil and a layer of ice on the soil surface. However, soil does not freeze in the field when there is enough snowcover to insulate the soil from the cold air during winter (Iwata et al., 2010). In such cases, the infiltration process of the snowmelt water is the same as that of rainwater in summer and the infiltration rate is determined by pore geometry and its continuity. However, the process of the snowmelt infiltration into the frozen ground is significantly different from that of rainwater infiltration. During the early snowmelt period, the water infiltrating into large pores, such as macropores, freezes quickly and does not percolate to deeper soil layers. However, the snowmelt water can infiltrate into small pores because the water in such pores does not freeze (Miller, 1980), even when the soil temperature is below zero, although the movement of water through these pores is slow. During the late snowmelt period, the soil temperature of the frozen layer increases to almost 0°C. The liquid water can move through large pores during this stage, but the ice in large pores, which is formed by the soil freezing during winter or the refreezing of infiltrated meltwater in early spring, reduces the rate at which water infiltrates frozen soil. Snowmelt water or surface ponding after the snowmelt period infiltrates the ground rapidly after the ice in the large pores melts in response to heat supply from the upper and bottom portion of the frozen layer. The ice layer at the soil surface, which is formed by surface ponding by rain or snowmelt in the beginning of winter or refreezing of snowmelt water in late winter, also impedes the infiltration of snowmelt (Bayard et al., 2005). Therefore, snowmelt infiltration into the frozen ground is determined by the movement of heat and water in the soil and snow layers, and it is strongly influenced by ice and liquid water content, air porosity, soil temperature, frost depth, and the presence of an ice layer at the soil surface, and not simply pore geometry.

Snowmelt infiltration has some harmful effects on agriculture. For example, a poor snowmelt infiltration rate induces a substantial amount of runoff, which is accompanied by soil erosion in some regions, even when the rate of snowmelt is not high. Prolonged surface ponding in level frozen lands causes excess water injury for grass and winter wheat. Decreased snowmelt infiltration into the ground results in shortages in the water available to plants in subsequent seasons.

Bibliography

- Bayard, D., Stähli, M., Parriaux, A., and Flühler, H., 2005. The influence of seasonally frozen soil on the snowmelt runoff at two Alpine sites in southern Switzerland. *Journal of Hydrology*, **309**, 66–84.
- Iwata, Y., Hirota, T., Hayashi, M., Suzuki, S., and Hasegawa, S., 2010. Effects of frozen soil and snow cover on cold-season soil water dynamics in Tokachi, Japan. *Hydrological Processes*, **24**, 1755–1765.
- Miller, R. D., 1980. Freezing phenomena in soils. In Hillel, D. (ed.), *Applications of Soil Physics*. New York: Academic, pp. 254–299.

SOIL AERATION

See [Aeration of Soils and Plants](#)

SOIL AGGREGATES

See [Physical Protection of Organic Carbon in Soil Aggregates](#)

SOIL AGGREGATES, STRUCTURE, AND STABILITY

Apostolos Papadopoulos

Research and Development, Branston Ltd, Branston, UK

Synonyms

Soil clod; Soil stability; Soil structure

Definition

Primary soil particles held together by cohesive forces, secondary particles and organic matter, form soil aggregates. Stability of an aggregate is its ability to resist stresses such as tillage, swelling, and shrinking processes and fast wetting by raindrops which cause aggregate disintegration.

Introduction

Soil aggregates vary in size and shape and the arrangement of soil aggregates is called soil structure which is

an important soil physical property. A well-structured soil aggregate, typically associated with agricultural importance, consists of primary particles in such arrangement to offer good aeration, water movement and storage, biological activity, and stability, which are vital for optimum plant growth. Soil aggregate stability is an important measure for assessing soil structural quality. Stable soil aggregates form a stable soil structure, which allows optimum movement and storage of gases, water, nutrients, biological activity, and energy. These activities occur in the pore structure which is created between the aggregated primary particles and are constantly at a dynamic state. The stability of soil structure is responsible for soil degradation, i.e., soil erosion and crusting, which affects negatively soil sustainability, crop establishment, and eventually, yield.

Measuring aggregate stability

Measuring soil aggregate stability is a mean of assessing soil structural condition. Various methods exist to measure soil aggregate stability and each of them simulates a mechanism of aggregate breakdown. Le Bissonnais (1996) reported four main mechanisms of aggregate breakdown: (a) slaking due to compression of entrapped air during wetting, (b) microcracking due to differential swelling, (c) mechanical breakdown, and (d) physico-chemical dispersion due to osmotic stress. A short overview of methods used for aggregate stability measurement can be found, e.g., in Le Bissonnais (1996) or in Diaz-Zorita et al. (2002). Selection of the methods and interpretation of its results depends on the purpose of the measurement. The most common method used for aggregate stability measurement is wet sieving. Other methods are based, e.g., on the simulation of raindrop energy impact, ultrasonic dispersion, or breakdown of aggregates after sudden immersion in water (Rohoskova and Valla, 2004). Among soils containing much organic carbon, fast wetting will probably give a better separation of values than slow wetting. By contrast, the low-energy slow-wetting treatments will be better for distinguishing among weak aggregate soils (Le Bissonnais, 1996).

Soil aggregation and stability

Oades (1984) suggested that macro-aggregates ($>250\text{ }\mu\text{m}$ diameter) do not just bind existing micro-aggregates ($<250\text{ }\mu\text{m}$ diameter) together, but that new micro-aggregates are formed preferentially within stable macro-aggregates. Mucilage produced during decomposition of organic fragments inside the macro-aggregate interacts with clay, which begins to encrust the organic fragment, eventually to an extent where the degradation of the organic material is retarded. Over time, binding agents in macro-aggregates degrade, resulting in a loss of macro-aggregate stability and the release of stable micro-aggregates, which become the building blocks of the next cycle of macro-aggregate formation (Six et al., 2000). Micro-aggregates exhibit greater stability than macro-aggregates and better protect soil organic matter

(SOM) against microbial decay (Tisdall and Oades, 1982; Skjemstad et al., 1990). Six et al. (2000) and Denef et al. (2001) reported that the formation of these micro-aggregates within macro-aggregates is negatively related to the rate of macro-aggregate turnover and therefore is strongly affected by management factors such as tillage and residue management. Therefore, the degree of stable micro-aggregation, rather than stable macro-aggregation, might play a more important and direct role in the relation between SOM sequestration and management of agricultural soils (Pulleman et al., 2005). Watts et al. (2001) also found that an understanding of the formation and stabilization of micro-aggregates is crucial not only because they are a key component of the soil structural hierarchy but also because they help control the dynamics of soil organic matter turnover. In addition to being the primary cause of crusting, aggregate breakdown is responsible for the production of micro-aggregates and particles, which are easily transported by runoff and splash (Le Bissonnais, 1996).

The measurement of aggregate stability is a particularly destructive method where thoroughly desiccated aggregates are submerged in water. The water drawn in to each aggregate over its entire periphery may trap and compress the air originally present in the dry aggregate. As the cohesive strength of the outer part of the aggregate is reduced by swelling, and as the pressure of the entrapped air builds up in proportion to its compression, the latter may eventually exceed the former and the clod may actually explode. More typically, however, a series of small explosions, each marked by the escape of a bubble of air, shatters the clod into fragments (Hillel, 1998).

Angers and Caron (1998) observed that wetting and drying cycles caused by crop roots influence the extent of soil fragmentation and aggregate formation, i.e., drying produces cracks and induces fracture of aggregates. Plant growth will influence the magnitude, frequency, and effects of these cycles on aggregation (Semmel et al., 1990). For instance, Materechera et al. (1992) observed that repeated wetting/drying cycles associated with root growth resulted in the production of smaller aggregates. Penetrating roots can mechanically break up existing aggregates, but they also stabilize surrounding aggregates through drying the soil and root exudation with its associated microbial activity (Six et al., 2004). Materechera et al. (1994) found that, even at constant water potentials, roots decreased the proportions of already formed large water stable aggregates by 20–50%.

Haynes et al. (1991) suggested that increase in aggregate stability during a short-term pasture is due principally to production of binding carbohydrates by the large microbial biomass present in the pasture rhizosphere. When pasture is ploughed under, the microbial biomass declines as does aggregate stability, and the increase in aggregate stability following pasture establishment is considerably more rapid than the increase in clod porosity. Six et al. (1998) suggested that the very small effect of organic farming on micro-aggregate characteristics and associated

carbon (C) stabilization may be caused by the effect of tillage on aggregate turnover. The paucity of organic resources that stimulate the formation of micro-aggregates during passage through earthworms and other biotic processes that result in the formation or stabilization of micro-aggregates may also play an important role. Hillel (1998) stated that in addition to increasing the strength and stability of intra-aggregate bonding, organic products may further promote aggregate stability by reducing wettability and swelling. Some of the organic materials are inherently hydrophobic, or become so as they dehydrate, so that the organo-clay complex may have a reduced affinity for water. It has been established that the inclusion of organic materials within soil aggregates reduces their decomposition rate (Oades, 1984). Six et al. (1998) suggested that increased macroaggregate turnover under conventional tillage is a primary mechanism causing decreases of soil C.

Organic matter and aggregate stability

Organic matter (OM) and soil structure are strongly related: OM binds mineral particles into aggregates and reduces the susceptibility of soil to slaking (Tisdall and Oades, 1982). In turn, stable aggregates may enhance the physical protection of OM against decomposition under grassland or reduced tillage compared with conventional tillage systems (Six et al., 1998). OM concentration and soil aggregate stability have therefore been proposed as important soil quality indicators (Six et al., 2000; Saggar et al., 2001). Organic matter is routinely added to soils in organic farming, while intensive arable agriculture can lead to a decline in both organic matter levels and stability of soil structure (Watts et al., 2001). The effects of organic amendments on aggregate stability will depend also on their composition and subsequent effects on biological activity. The important role of fresh OM in aggregate stability explains why most research has found better correlation between components of OM (e.g., water-soluble carbohydrates) and stability than between total OM and stability (Shepherd et al., 2002).

Concerns have been expressed that soils might suffer long-term degradation under intensive agriculture, particularly to soil structure, due to reductions in soil organic matter levels (MacRae and Mehuijs, 1985; Sommerfeldt and Chang, 1985). This has wide-reaching negative secondary effects, e.g., the ameliorative actions of soil organisms are decreased, resulting in a soil with a reduced A horizon, reduced range and size of pores, and less-developed, finer and weaker aggregates (Kay, 1990). These traits are associated with soils susceptible to physical degradation, i.e., erosion and surface crusting (Poincelot, 1986) resulting in poor crop establishment, and eventually, yield.

Six et al. (1998) developed a conceptual model to explain the influence of disturbance (e.g., tillage) on soil carbon (C) stabilization rates. Their model links a proportion of the C lost upon disturbance to the increased turnover of macro-aggregates. A disturbance-induced increase in

macro-aggregate turnover inhibits formation of micro-aggregates within macro-aggregates and the long-term sequestration of C within micro-aggregates.

Golchin et al. (1994) proposed that when fresh plant material (as surface residues or roots) enters the soil, it induces the formation of aggregates because it stimulates the production of microbial-derived binding agents by being a C source for microbial activity. During decomposition, plant material fragments or particulate organic matter (POM) gradually becomes encrusted with clay particles and microbial products to form the core of stable micro-aggregates. Microbial mucilages and metabolites further impregnate the mineral crust surrounding the still decomposing organic cores to form very stable micro-aggregates (Six et al., 2004).

Soil aggregation, slaking and pore morphology

Six et al. (2000) and Denef et al. (2001) reported that the formation of micro-aggregates within macro-aggregates is negatively related to the rate of macro-aggregate turnover and is therefore strongly affected by management factors such as tillage and residue incorporation. Aggregates released by the slaking of macro-aggregates contain less OM on average and appear unable to form stable macro-aggregates (Six et al., 1998, 2000). Papadopoulos et al. (2009) found contrasted results as the analysis of OM fractionation demonstrated that neither the light fraction nor the intra-aggregate fraction of OM affected aggregate stability. This suggests soil aggregates may be at different stages of aggregate turnover at the time of sampling. Therefore, within a soil sample, some macro-aggregates may have been formed recently by stable micro-aggregates, while others may be breaking down to release micro-aggregates. This would provide false results by applying the slaking method, although it has been proved stability measurements by slaking are constant and not affected by the aggregate turnover stage. Therefore, observations of stability can advise on the rate of aggregate turnover and how long stable-formed aggregates may last. It is likely that conventional management promotes a faster aggregate turnover (macro-aggregate breakdown) resulting in the production of unstable macro-aggregates comprised of micro-aggregates with less OM than organic management, as they are formed in less time inside macro-aggregates and typically there is less OM supplied in conventional management (Papadopoulos et al., 2009).

Slaking is dependent on increased pressure inside soil pores; therefore, pore morphology is an important factor influencing this process. These pores are formed by the binding of micro-aggregates into stable macro-aggregates. During this process, intra-aggregate pore morphology depends on the assemblage of the micro-aggregates which can be measured by pore roughness. Papadopoulos et al. (2009) performed fractal analysis between organic and conventionally managed soils which showed that organic

soils promoted the formation of soil aggregates which consisted of pores with slightly greater perimeter fractal D compared to conventional soils. Therefore, proposed that one of the factors affecting soil aggregate stability is the morphology of pores within both micro- and macro-aggregate pore spaces, the “rougher” the pores, the greater the aggregate stability. This is partially supported by the findings of Bresson and Moran (2004), who reported that aggregate stability does not necessarily decrease with decreasing macroporosity but is rather related to the balance between changes in macro- and microporosity.

Hallett et al. (2000) found that the soil aggregate strength increased exponentially with decreasing aggregate size. Fracture mechanics theory predicts that at each level of aggregate breakdown, the largest cracks are consumed. Results show a decrease in the proportion of cracks on soil fracture surfaces with decreasing aggregate size which is direct evidence that at each level of aggregate breakdown, the “weakest link” is stronger. Cracks are thought to affect soil strength by one of two mechanisms. The most basic is that cracks weaken soil by reducing the number of particle bonds. More recently, it has been disputed that this theory is incorrect and that cracks reduce strength by intensifying stresses at their tips as described by fracture mechanics theory (Hallett et al., 2000).

X-ray Computed Tomography (CT) together with other 3D imaging techniques including NMR and synchrotron are becoming increasingly popular in geoscience, offering the ability to further investigate the intact properties of soil aggregates. At the microscale, the topology and connectivity of the intra-aggregate pore network is of crucial importance for microbial processes, the sequestration of organic carbon, water storage, and transport properties which are greatly associated with processes evolving at the larger scale (for more reading see *Noninvasive Quantification of 3D Pore Space Structures in Soils*).

Summary

Soil aggregate stability is an important measure for the evaluation of soil structural quality. Several methodologies have been developed to assess aggregate stability in a destructive manner which has proved very useful and accurate. The study of aggregate formation and stability has received great attention in the last few decades, typically associated with soil organic matter. Nowadays, with the availability of sophisticated equipment (X-ray Computed Tomography, rheology, mechanical precision stress inducer, etc.) allowing the investigation of the intact aggregate pore structure and networks, the strength and degree of degradation, we are able to improve our understanding of soil aggregate formation and stability as it is a dynamic and complex process. Soil aggregation is a multi-scale, multi-temporal, and multi-spatial property which is essential for making improvements in agriculture as it is related to soil–root interactions, hydrological properties, and environmental issues.

Bibliography

- Angers, D. A., and Caron, J., 1998. Plant-induced changes in soil structure: processes and feedbacks. *Biogeochemistry*, **42**, 55–72.
- Bresson, L. M., and Moran, C. J., 2004. Micromorphological study of slumping in a hardsetting seedbed under various wetting conditions. *Geoderma*, **118**, 277–288.
- Denef, K., Six, J., Pausian, K., and Merckx, R., 2001. Importance of macroaggregate dynamics in controlling soil carbon stabilization: short-term effects of physical disturbance induced by dry-wet cycles. *Soil Biology and Biochemistry*, **33**, 2145–2153.
- Diaz-Zorita, M., Perfect, E., and Grove, J. H., 2002. Disruptive methods for assessing soil structure. *Soil and Tillage Research*, **64**, 3–22.
- Golchin, A., Oades, J. M., Skjemstad, J. O., and Clarke, P., 1994. Study of free and occluded particulate organic matter in soils by solid state ¹³C P/MAS NMR spectroscopy and scanning electron microscopy. *Australian Journal of Soil Research*, **32**, 285–309.
- Hallett, P. D., Dexter, A. R., Bird, N. R. A., and Seville, J. P. K., 2000. Scaling of the structure and strength of soil aggregates. *Advances in GeoEcology*, **32**, 22–31.
- Haynes, R. J., Swift, R. S., and Stephen, R. C., 1991. Influence of mixed cropping rotations pasture-arable on organic matter content water stable aggregation and clod porosity in a group of soils. *Soil Tillage Research*, **19**, 77–87.
- Hillel, D., 1998. *Environmental Soil Physics*. London: Academic.
- Kay, B. D., 1990. Rates of change of soil structure under different cropping systems. In Stewart, B. A. (ed.), *Advances in Soil Science*, Vol. 12, New York: Springer, pp. 1–44.
- Le Bissonnais, Y., 1996. Aggregate stability and assessment of soil crustability and erodibility: I. Theory and methodology. *European Journal of Soil Science*, **47**, 425–437.
- MacRae, R. J., and Mehys, G. R., 1985. The effects of green manuring on the physical soil properties of temperate-area soils. In Stewart, B. A. (ed.), *Advances in Soil Science*, Vol. 3, New York: Springer, pp. 71–94.
- Materechera, S. A., Dexter, A. R., and Alston, A. M., 1992. Formation of aggregates by plant-roots in homogenized soils. *Plant and Soil*, **142**(1), 69–79.
- Materechera, S. A., Kirby, J. M., Alston, A. M., and Dexter, A. R., 1994. Modification of soil aggregation by water regime and roots growing through beds of large aggregates. *Plant and Soil*, **160**, 57–66.
- Oades, J. M., 1984. Soil organic matter and structural stability: mechanisms and implications for management. *Plant and Soil*, **76**, 319–337.
- Papadopoulos, A., Bird, N. R. A., Whitmore, A. P., and Mooney, S. J., 2009. Investigating the effects of organic and conventional management on soil aggregate stability using X-ray computed tomography. *European Journal of Soil Science*, **60**(3), 360–368.
- Poincelot, R. P., 1986. *Toward a More Sustainable Agriculture*. Westport Connecticut: AVI.
- Pulleman, M. M., Six, J., Van Breemen, N., and Jongmans, A. G., 2005. Soil organic matter distribution and microaggregate characteristics as affected by agricultural management and earthworm activity. *European Journal of Soil Science*, **56**, 453–467.
- Rohoskova, M., and Valla, M., 2004. Comparison of two methods for aggregate stability measurements – a review. *Plant, Soil and Environment*, **50**(8), 379–382.
- Saggar, S., Yeates, G. W., and Shepherd, T. G., 2001. Cultivation effects on soil biological properties, microfauna and organic matter dynamics in Eutric Gleysil and Gleyic Luvisol soils in New Zealand. *Soil and Tillage Research*, **58**, 55–68.

- Semmel, H., Horn, R., Hell, U., Dexter, A. R., and Schulze, E. D., 1990. The dynamics of soil aggregate formation and the effects on soil physical properties. *Soil Technology*, **3**, 113–129.
- Shepherd, M. A., Harrison, R., and Webb, J., 2002. Managing soil organic matter – implications for soil structure on organic farms. *Soil Use and Management*, **18**, 284–292.
- Six, J., Elliot, E. T., Paustian, K., and Doran, J. W., 1998. Aggregation and soil organic matter accumulation in cultivated and negative grassland soils. *Soil Science Society of America Journal*, **62**, 1367–1377.
- Six, J., Elliott, E. T., and Paustian, K., 2000. Soil macroaggregate turnover and microaggregate formation: a mechanism for C sequestration under no-tillage agriculture. *Soil Biology and Biochemistry*, **32**, 2099–2103.
- Six, J., Bossuyt, H., Degryze, S., and Denef, K., 2004. A history of research on the link between (micro)aggregates, soil biota, and soil organic matter dynamics. *Soil and Tillage Research*, **79**, 7–31.
- Skjemstad, J. O., Le Feuvre, R. P., and Prebble, R. E., 1990. Turnover of soil organic matter under pasture as determined by ^{13}C natural abundance. *Australian Journal of Soil Research*, **28**, 267–276.
- Sommerfeldt, T. G., and Chang, C., 1985. Changes in soil properties under annual application of feedlot manure and different tillage practices. *Soil Science Society of America Journal*, **49**, 983–987.
- Tisdall, J. M., and Oades, J. M., 1982. Organic matter and water-stable aggregates in soils. *Journal of Soil Science*, **33**, 141–163.
- Watts, C. W., Whalley, W. R., Longstaff, D. J., White, R. P., Brooke, P. C., and Whitmore, A. P., 2001. Aggregation of a soil with different cropping histories following the addition of organic materials. *Soil Use and Management*, **17**, 263–268.

Cross-references

- [Agrophysical Properties and Processes](#)
[Microbes and Soil Structure](#)
[Noninvasive Quantification of 3D Pore Space Structures in Soils](#)
[Organic Matter, Effects on Soil Physical Properties and Processes](#)
[Parent Material and Soil Physical Properties](#)
[Physical Degradation of Soils, Risks and Threats](#)
[Physical Protection of Organic Carbon in Soil Aggregates](#)
[Plant Roots and Soil Structure](#)
[Pore Morphology and Soil Functions](#)
[Soil Aggregation and Evaporation](#)
[Soil Physical Quality](#)

SOIL AGGREGATION AND EVAPORATION

Barbara Witkowska-Walczak
 Institute of Agrophysics, Polish Academy of Sciences,
 Lublin, Poland

The primary particles of soil tend, in favorable circumstances, to group themselves into composite structural units known as *aggregates*. The presence of aggregates in soil is called *soil aggregation*. The soil aggregates are characterized neither by any universally fixed size nor by the stability. The aggregates of the order of several millimeters are called *macroaggregates*, the smaller ones are called *microaggregates*. The arrangement of aggregates and primary particles in the soil is called *soil structure*.

Evaporation is the process of change of the state of water from a liquid to gaseous phase. It is a principal process of water cycling in the environment. Evaporation of water from bare soil is one of the simple processes of water loss from land to atmosphere. Evaporation in soil involves the next events: transport of water to surface within soil profile, a phase change from liquid water to vapor water, and the transfer of water vapor from the soil surface to atmosphere. The evaporation management can be done by reducing the total energy responsible for it, modifying the albedo parameters, or reducing the water movement to soil surface.

Soil aggregation is one of the best important factors of the evaporation decrease, because it changes the transport of water to soil surface by reducing the upward flux of water by either lowering the water table or decreasing the diffusivity and conductivity of the soil profile. The upper layer of soil built of macroaggregates can be worked as mulching and it caused several times decrease in water loss from soil profiles in comparison to soil without aggregation.

Bibliography

- Brutsaert, W., 1991. *Evaporation into the Atmosphere*. Dordrecht/Boston/London: Kluwer.
- Hillel, D., 1998. *Environmental Soil Physics*. San Diego/London/Boston/New York/Sydney/Tokyo/Toronto: Academic.
- Kutilek, M., and Nielsen, D., 1994. *Soil Hydrology*. Cremlingen-Destedt: Catena.
- Lal, R., and Shukla, M. K., 2004. *Principles of Soil Physics*. New York/Basel: Marcel Dekker.

SOIL BIOTA, IMPACT ON PHYSICAL PROPERTIES

Pascal Boivin¹, Roxane Kohler-Milleret²

¹University of Applied Sciences of Western Switzerland (HES-SO), Geneva, Switzerland

²Institute of Biology, Soil & Vegetation Group, University of Neuchâtel, Neuchâtel, Switzerland

Definition

The *soil biota* is made of all soil living organisms from microorganisms to macrofauna, including roots. Most of these organisms are considered as soil ecosystem engineers (Jones et al., 1994) involved in the formation of aggregates in soils and in the generation of the structural porosity. Their impact greatly differs according to the type of organism, soil conditions, and the soil biodiversity.

Soil biota: impact on physical properties

The soil living organisms range from eye-invisible microbes (bacteria and fungi) to macrofauna (termites, earthworms, etc.) with organisms of intermediary size as microfauna (protozoa, nematodes, etc.) and mesofauna (microarthropods, enchytraeids, etc.). Furthermore, although plants are primary producers and determine the

amounts of carbon that enter the system via the above-ground system (Wardle, 2002), the root system, as a heterotrophic part of the plant, may also be considered as a soil organism as it is in close relationship with other soil biota. All these soil organisms are interacting together in very complex trophic and nontrophic webs (Wardle, 2002; Bardgett, 2005; Coleman, 2008) that affect in turn the aboveground system (Van der Putten et al., 2001; Wardle, 2002; Coleman, 2008). Moreover, they utilize the soil as a habitat and a source of energy (Bardgett, 2005) and have therefore a strong effect on soil properties.

It is first worthwhile to recall that a major factor of soil structure formation and stabilization is the soil organic matter (SOM). An increase in organic matter content results in a proportional increase in most soil physical properties such as porosity and aggregate stability (Kay, 1998). Hence, plants as a source of SOM have a strong impact on soil physical properties. Root-related processes affecting soil structure are reviewed by Angers and Caron (1998): root penetration, enhancement of wetting–drying cycles, root entanglement of soil particles, production of binding agents, and stimulation of the microbial activity.

The impact of bacteria and fungi on soil aggregation has received growing interest (Six et al., 2002; Young and Crawford, 2004). Arbuscular mycorrhizal fungi (AMF) influence soil aggregation via three processes. First, AMF affect soil aggregation formation or stabilization physically by the enmeshment of primary particles, organic matter, and small aggregates to macro aggregates, and the alignment of primary particles (Thomas et al., 1993; Andrade et al., 1998). Second, AMF affect soil aggregation chemically by the secretion of extracellular compounds as mucilages, polysaccharides, or glomalin-related soil proteins (Wright and Upadhyaya, 1996). These compounds have been shown to act as a glue substance (Six et al., 2004; Bronick and Lal, 2005). Finally, AMF affect soil aggregation biologically by interacting with the soil food web, thus influencing bacterial communities that would in turn influence soil aggregation through the secretion of polysaccharides (Andrade et al., 1997, 1998; Artursson et al., 2005).

Earthworms play a very important role on soil structure. By creating soil biogenic structures (casts, burrows), which are called drilosphere soil (Lavelle et al., 1997), earthworms influence physical, chemical, and biological soil properties. Through casting and burrowing activities, they affect the soil physically, by modifying soil porosity, aggregation, stability, aeration, and hydraulic conductivity (Shipitalo and Protz, 1989; Edwards and Bohlen, 1996). The burrow walls can form a stable structure that may persist in soil for several months, or even years (Lee, 1985). Earthworms may be cause to preferential flow (Zehe and Flühler, 2001). They are assumed to be a sign of “healthy” soil and to provide an improvement of soil permeability and structure.

Cases of heavy soil compaction by earthworms have been, however, reported (Chauvel et al., 1999; Milleret et al., 2009). In both cases, the compaction was attributed

to an exceptional development of endogeic species. The study of Milleret et al. (2009) shows that combined with root and AMF activity, the earthworm activity leaved the soil structure as it is. Further experiments showed that the compaction occurs with all worm species when alone on a soil which is not compacted, but mixing species and/or working with compacted soils leads to a soil decompaction (unpublished results).

Showing that roots generate a large volume of pores that cannot be attributed to the direct mechanical effect of the roots, Milleret et al. (2009) assumed that root exudates stimulated bacteria activity which in turn developed the structural porosity, thus supporting the “self-organization of the soil–plant–microbe system” theory.

Summary

The soil biota can be considered as the permanent engineer of the soil. Obviously, either by contribution to the SOM dynamic, direct entanglement of particles, and active interactions in between species, it contributes to renew and improve the soil structure. A “living soil” is, therefore, to be promoted. The impact of soil biota can be observed on short time ranges (e.g., from day to months), while the contribution of SOM occurs on larger time range dynamics (over years). The role of soil biota remains, however, largely unknown, and recent studies suggest that the positive role of soil biota on soil structure is only observed when the soil biodiversity is satisfactory, which means that the interaction between species is the key factor.

Bibliography

- Andrade, G., Mihara, K. L., Linderman, R. G., and Bethlenfalvay, G. J., 1997. Bacteria from rhizosphere and hyphosphere soils of different arbuscular mycorrhizal fungi. *Plant and Soil*, **192**, 71–79.
- Andrade, G., Linderman, R. G., and Bethlenfalvay, G. J., 1998. Bacterial associations with the mycorrhizosphere and hyphosphere of the arbuscular mycorrhizal fungus *Glomus mosseae*. *Plant and Soil*, **202**, 79–87.
- Angers, D. A., and Caron, J., 1998. Plant-induced changes in soil structure: processes and feedbacks. *Biogeochemistry*, **42**, 55–72.
- Artursson, V., Finlay, R. D., and Jansson, J. K., 2005. Combined bromodeoxyuridine immunocapture and terminal restriction fragment length polymorphism analysis highlights differences in the active soil bacterial metagenome due to *Glomus mosseae* inoculation or plant species. *Environmental Microbiology*, **7**, 1952–1966.
- Bardgett, R. D., 2005. *The Biology of Soil. A Community and Ecosystem Approach*. Oxford: Oxford University Press.
- Bronick, C. J., and Lal, R., 2005. Soil structure and management: a review. *Geoderma*, **124**, 3–22.
- Chauvel, A., Grimaldi, M., Barros, E., Blanchart, E., Desjardins, T., Sarrazin, M., and Lavelle, P., 1999. Pasture damage by an Amazonian earthworm. *Nature*, **398**, 32.
- Coleman, D. C., 2008. From peds to paradoxes: linkage between soil biota and their influences on ecological processes. *Soil Biology and Biochemistry*, **40**, 271–289.
- Edwards, C. A., and Bohlen, P. J., 1996. *Biology and Ecology of Earthworms*. London: Chapman and Hall.

- Jones, C. G., Lawton, J. H., and Shachak, M., 1994. Organisms as ecosystem engineers. *Oikos*, **69**, 373–386.
- Kay, B. D., 1998. Soil structure and organic carbon: a review. In Lal, R., Kimble, J. M., Follett, R. F., and Stewart, B. A. (eds.), *Soil Processes and the Carbon Cycle*. Boca Raton: CRC Press, pp. 169–197.
- Lavelle, P., Bignell, D., Lepage, M., Wolters, V., Roger, P., Ineson, P., Heal, O. W., and Dhillon, S., 1997. Soil function in a changing world: the role of invertebrate ecosystem engineers. *European Journal of Soil Biology*, **33**, 159–193.
- Lee, K. E., 1985. *Earthworms, their Ecology and Relationships with Soils and Land Use*. Australia: Academic.
- Milleret, R., Le Bayon, C., Lamy, F., Gobat, J.-M., and Boivin, P., 2009. Impact of roots, mycorrhizas and earthworms on soil physical properties as assessed by shrinkage analysis. *Journal of Hydrology*, **373**, 499–507.
- Shipitalo, M. J., and Protz, R., 1989. Chemistry and micromorphology of aggregation in earthworm casts. *Geoderma*, **45**, 357–374.
- Six, J., Feller, C., Denef, K., Ogle, S. M., Sa, J. C. D., and Albrecht, A., 2002. Soil organic matter, biota and aggregation in temperate and tropical soils – effects of no-tillage. *Agronomie*, **22**, 755–775.
- Six, J., Bossuyt, H., Degryze, S., and Denef, K., 2004. A history of research on the link between (micro) aggregates, soil biota and soil organic matter dynamics. *Soil and Tillage Research*, **79**, 7–31.
- Thomas, R. S., Frauson, R. L., and Bethlenfalvay, G. J., 1993. Separation of vesicular-arbuscular mycorrhizal fungus and root effects on soil aggregation. *Soil Science Society of America Journal*, **57**, 77–81.
- Van der Putten, W. H., Vet, L. E. M., Harvey, J. A., and Wackers, F. L., 2001. Linking above- and belowground multitrophic interactions of plants, herbivores, pathogens, and their antagonists. *Trends in Ecology and Evolution*, **16**, 547–554.
- Wardle, D. A., 2002. *Communities and Ecosystems: Linking the Aboveground and Belowground Components*. Princeton: Princeton University Press.
- Wright, S. F., and Upadhyaya, A., 1996. Extraction of an abundant and unusual protein from soil and comparison with hyphal protein of arbuscular mycorrhizal fungi. *Soil Science*, **161**, 575–586.
- Young, I., and Crawford, J. W., 2004. Interactions and self-organization in the soil–microbe complex. *Science*, **304**, 1634–1637.
- Zehe, E., and Flühler, H., 2001. Preferential transport of isoproturon at a plot scale and a field scale tile-drained site. *Journal of Hydrology*, **247**, 100–115.

Cross-references

- [Biofilms in Soil](#)
[Earthworms as Ecosystem Engineers](#)
[Microbes and Soil Structure](#)
[Microbes, Habitat Space, and Transport in Soil](#)
[Organic Matter, Effects on Soil Physical Properties and Processes](#)
[Rhizosphere](#)

SOIL COLOUR INDEX

See [Color Indices, Relationship with Soil Characteristics](#)

Cross-references

- [Color in Food Evaluation](#)

SOIL COMPACTIBILITY AND COMPRESSIBILITY

Stephan Peth

Institute for Plant Nutrition and Soil Science, Christian-Albrechts-University zu Kiel, Kiel, Germany

Definitions

k_0 -loading = vertical compression under confined lateral deformation

σ_i = normal stress [kPa], with $i = x, y, z$ indicating horizontal (x, y) and vertical (z) direction

n = porosity = ratio of pore volume to total volume [$\text{cm}^3 \text{ cm}^{-3}$]

ε = void ratio = ratio of pore volume to solid volume [$\text{cm}^3 \text{ cm}^{-3}$]

CCT = confined compression test (oedometer test)

PST = plate sinkage test

C_p = compaction point

P_c = pre-compaction stress

C_c = compressibility index

C_s = swelling index

C_n = cyclic compressibility

Introduction

Physical quality and functionality of soils is a prerequisite for sustainable land use. This target is increasingly compromised by the expansion of highly mechanized crop production systems with intensive field traffic. A fourfold mass increase of agricultural vehicles over the past 3–4 decades have put soils more and more under pressure (Horn et al., 2006). Moreover, heavier loads have to be borne by soils often under unfavorable moisture conditions (e.g., during sugar beet harvesting). Deep penetrating soil compaction under heavy machinery has therefore become a great concern in arable land (Peth et al., 2006), where repeated wheeling over years exacerbate compaction effects (Kirby, 2007). The consequence is a long term irreversible deterioration especially of subsoil functions. About 33 million ha of arable land in Europe and 68 million ha worldwide are seriously degraded by soil compaction (Oldeman, 1994). Detimental effects for crop yield and soil erosion are reported in many cases (Alakukku et al., 2003; Håkansson, 1994; Hamza and Anderson, 2005) and problems will probably be aggravated in the future by climate change.

Given the inevitable threat for subsoil compaction due to highly mechanized land use indicators for soil stability and compressibility are very important to assess the susceptibility of soils to mechanical loads. A commonly used value defining the potential risk for soil compaction is the so-called pre-compaction stress P_c , which determines the maximum mechanical stress a soil can sustain without experiencing significant plastic (=irreversible) deformation. The underlying principle dates back to Casagrande (1936) who proposed a method to estimate the geological stress history of clay deposits by determining the

pre-consolidation load by means of a confined compression test (*CCT*). CASAGRANDE outlined the practical significance of the method for settlement analysis and the test is still widely used due to its easy conductibility and reproducibility. The basic concept assumes that as long as stresses remain below P_c soil deformation is fully elastic while upon exceeding P_c plastic soil deformation will take place. While P_c is a suitable indicator for the overall soil stability it lacks information on the actual soil compressibility under specific stresses when the threshold stress P_c is exceeded. Such information, however, is very important because soils with the same P_c value may react quite differently with respect to deformation (i.e., volume changes) and hence also with respect to changes in soil functions. Soil compressibility indices are therefore additionally required to allow estimating the degree to which soils become compressed by mechanical loads during field traffic or animal trampling.

Soil compactibility/compressibility and its measurement

Soil compactibility and soil compressibility are often used in the literature as synonyms with a somewhat indistinct terminology. According to the definition suggested by Håkansson (2005) compaction denotes a process where a soil decreases its air filled pore volume after the application of an external mechanical stress. Håkansson (2005) hence distinguishes between the change in pore volume or void ratio associated with the expulsion of air and pore volume changes caused by drainage of excess pore water. Latter is usually referred to as consolidation. In contrast soil compressibility describes the overall sensitivity of a soil to react to a unit change in mechanical stress with a unit change in pore volume irrespective if water or air is expelled from the pore space. In any case solid particles are assumed to be incompressible so that each volume change is equal to a change in porosity n . However, while under field traffic conditions mostly short loading times prevail and predominantly air will be expelled from the soil, mechanical soil testing is usually conducted in a way that some equilibrium in settlement is reached for a given stress magnitude. Under such conditions water has sufficient time to drain from or redistribute within the pore space (internal drainage) which contributes to the total pore volume change. In this sense soil compactibility may be the more appropriate term to describe pore volume changes associated with short single stress applications encountered during field operation, whereas compressibility describes pore volume changes measured during field and laboratory soil testing where longer loading times or frequent successive load applications are imposed to the soil following a particular stress path. Depending on the stress path different compressibility indices may be defined as a sensitivity measure for volumetric soil deformation.

Although a full treatment of volume change behavior of soils would require also the consideration

of shrinking-swelling processes caused by hydraulic stresses (see *Stress–Strain Relations*) here we concentrate our view on soil compression evoked by external mechanical loads. This is justified because we are interested in the immediate change in pore volume after field traffic or animal trampling. Soil compression is influenced by many factors: three-dimensional stress state, time (duration of loading), stress path, pore water pressure, drainage and hydraulic conductivity, inter-particle and aggregate strength. These factors are not acting independently from each other and some of them (e.g., hydraulic conductivity, pore water pressure and hence effective stress) are continuously modified during the deformation process by particle rearrangements and associated changes in pore network geometries. Consequently, determining the relative influence of each individual factor on compaction is difficult and the description of soil deformation processes mostly relies on empirical soil tests. During soil testing external (e.g., drainage) and internal (e.g., pore water pressure) boundary conditions should therefore be well defined, measured, or if possible even controlled.

Depending on the expected in situ stress state/path and loading boundary conditions different soil tests are employed to derive volume change indices. The most commonly used laboratory test for determining compressibility of arable soils is the confined compression test (*CCT*), also standard oedometer test. It is a one-dimensional compression test where deformation is allowed only in the vertical direction (k_0 -loading: $d\sigma_x = d\sigma_y = \text{undefined}$). The advantage of the *CCT* is that vertical displacements during loading can readily be translated into porosity changes (Δn) which are usually expressed as changes in void ratio ($\Delta \varepsilon$) in order to keep the reference volume constant (volume of the solid phase). Soil tests with *uniaxial* ($d\sigma_x = d\sigma_y = 0$), *isotropic* ($d\sigma_x = d\sigma_y = d\sigma_z$), and *plane stress* ($d\sigma_x \neq d\sigma_z \neq 0, d\sigma_y = 0$) loading conditions shall not be treated here as they describe special situations useful for particular geotechnical problems. A comprehensive literature review on volume change theories and corresponding laboratory experiments for measuring volume change coefficients of unsaturated soils under specific loading conditions is presented in Fredlund and Rahardjo (1993). Although *triaxial* loading ($d\sigma_x = d\sigma_y \neq d\sigma_z$) would in terms of stress state be the closest representation of in situ stresses under wheels (at least assuming static loading) triaxial tests are seldom used in practice because they require special equipment and compared to oedometer tests are more difficult to conduct. Oedometer tests allow a higher number of replicate measurements which is beneficial for characterizing soil heterogeneities of field soils. A limitation, however, is that lateral soil displacement is prevented which is not necessarily the case in situ where additional lateral deformation may occur depending on the confining pressure.

Attempts have been made to use in situ methods such as the plate sinkage test (*PST*) to determine both pre-compaction stress and soil compressibility. Comparing the result to laboratory tests (*CCT*) it was found that up to a so-called compaction point (C_p), where lateral stresses

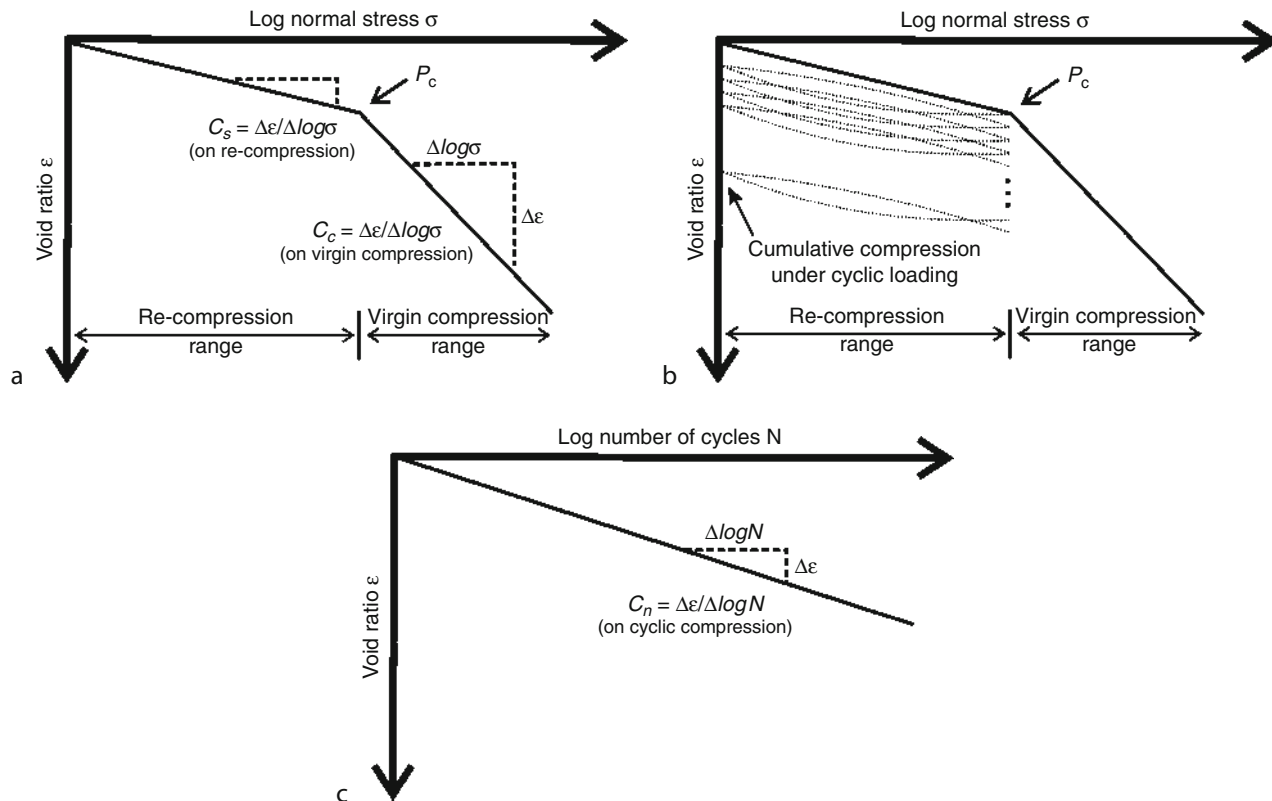
reach the confining stress, settlement under confined compression is very similar to the settlement measured in situ with a semi-confined *PST*. But as soon as stresses exceed C_p stress-strain curves of the two tests significantly deviate from each other, which is attributed to the change in mode of deformation with additional lateral soil displacement in the *PST* (Earl and Alexandrou, 2001). Deformation in this stage is a combination of both compaction and lateral displacement of the soil by shear. The determination of soil compressibility from *PST* measurements is limited since neither the two displacement components – compression and volume constant shear deformation – can be accurately separated nor is the volume affected by compaction constant and defined.

Compressibility indices

Compression and swelling index (re-compression index)

Soil compressibility under static loading is most commonly obtained from measurements of the pre-compaction stress by *CCT*. Compressibility is the change in pore volume or void ratio ($\Delta\varepsilon$) with stress increment ($\Delta\sigma$). The *CCT* is conducted under stepwise increasing loads until the sample settlement is considered to be

completed under the prevailing stress. Void ratios ε are calculated from corresponding final settlements for each load and plotted against the applied vertical stress σ on logarithmic scale. The obtained curve is referred to as *compression curve* which can be approximated by two linear lines separated by P_c . The re-compression line describes the deformation below P_c while the virgin compression line describes the deformation above P_c (Figure 1a). In the re-compression stress range deformation is considered fully elastic whereas in the virgin compression stress range elasto-plastic deformation is taking place. The respective slopes reflect the compressibility of the soil while under load and are referred to as the *compression index* C_c for the virgin compression line ($C_c = \Delta\varepsilon/\Delta\log\sigma$, for $\sigma > P_c$) and *swelling index* C_s for the re-compression line ($C_s = \Delta\varepsilon/\Delta\log\sigma$, for $\sigma < P_c$). Note that the linear lines in Figure 1 – virgin compression and re-compression line – represent approximations to the non-linear compression curve. The slope $\Delta\varepsilon/\Delta\log\sigma$ is strictly speaking a function of stress where the compressibility index $C_c(\sigma)$ increases with $\log\sigma$. Nevertheless, above mentioned linear approximation is reasonably accurate and provides a single parameter characterization of the soil sensitivity against compression under static loading.



Soil Compactibility and Compressibility, Figure 1 (a) Soil compression under static loading in the re-compression and virgin compression range, (b) cumulative soil compression in the re-compression range by repeated loading, (c) compressibility under cyclic loading.

Cyclic compressibility

The assumption of fully elastic soil behavior in the re-compression stress range does not hold true for a higher number of load repetitions (Figure 1b). Repeated (cyclic) loading tests have shown that loads even well below the pre-compression stress may cause significant cumulative soil deformation associated with changes in soil functions (Peth and Horn, 2006). High numbers of load repetitions may be assumed in the field due to repeated wheeling over long time spans (several years) resulting in irreversible cumulative deformation effects in the subsoil. Volume change behavior under repeated loading conditions can be investigated by *cyclic compression tests*. Samples are measured in a standard oedometer device with a constant load applied for a number of load cycles (e.g., 100 cycles). Loads are applied for a short time (e.g., 30 s) followed by unloading and subsequent reloading with one loading–unloading path corresponding to one loading cycle. Cumulative soil deformation expressed as change in void ratio ϵ in general follows a logarithmic trend with \log number of load cycles (Figure 1c). The slope of the log-linear trend is referred to as *cyclic compressibility* ($C_n = \Delta\epsilon/\Delta\log N$) which indicates the sensitivity of a soil against cyclic compression upon repeated loading. C_n is a useful parameter for estimating cumulative effects of specific loads on subsoil compaction with respect to long term field traffic. Modification of the loading–unloading time as a test boundary condition can change the cumulative deformation and consequently C_n values. Therefore, standardization of the measurement protocol is needed to allow for comparison between samples. Ideally loading time is short (few seconds) followed by a rest time after unloading allowing pore water pressure to dissipate.

Summary and conclusion

Determination of soil compressibility is crucial for estimating the impact of field traffic or animal trampling on soil porosity and related soil physical functions. The Compressibility index C_c is derived from compression curves obtained from standard oedometer tests (CCT) allowing to calculate volumetric soil deformation that may be expected when P_c is exceeded by a certain stress value. The index is determined under static loading conditions meaning that the slope reflects a loaded stress situation. While this stress condition is a realistic assumption for many geotechnical problems, where permanent loads are applied (e.g., building foundations), for arable land permanent loads do seldom occur. Instead soils are usually loaded for a short time (seconds) in the incidence of field traffic and then subsequently unloaded again. During unloading elastic rebound recovers a part of the plastic deformation which unfortunately is not quantified by applying standard CCT procedures. On the other hand soils are repeatedly loaded during long term land use and also on a short term basis by multiple axle machines. Concerning long term field traffic, especially in intensive cropping systems, the subsoil may be exposed to hundreds of load applications.

Considering the cumulative soil compression associated with this repeated loading the assumption of full elasticity in the re-compression stress range is not valid. Cyclic compressibility (C_n) of subsoils for estimated expected mean stresses of employed farm machinery should additionally be determined by repeated (cyclic) loading tests.

Soil compression depends on multiple interrelated factors where especially loading time, pore water pressure, stress path and stress state affect the parameters obtained from soil mechanical tests. Derivation of soil compressibility indices requires an adaption of the boundary conditions in soil mechanical laboratory testing to a more realistic representation of in situ stress paths, i.e., short loading time; short and long term repeated loading. Finally, due to the coupling of hydraulic and mechanical stresses in the course of loading, it is indispensable to standardize initial soil pore water pressure and measure its change during the loading process.

Bibliography

- Alakukku, L., Weisskopf, P., Chamen, W. C. T., Tijink, F. G. J., van der Linden, J. P., Pires, S., Sommer, C., and Spoor, G., 2003. Prevention strategies for field traffic-induced subsoil compaction: a review: Part 1. Machine/soil interactions. *Soil and Tillage Research*, **73**, 145–160.
- Casagrande, A., 1936. The determination of pre-consolidation load and its practical significance. *International Conference on Soil Mechanics and Foundation Engineering*, Harvard University, Cambridge, MA, pp. 60–64.
- Earl, R., and Alexandrou, A., 2001. Deformation processes below a plate sinkage test on sandy loam soil: theoretical approach. *Journal of Terramechanics*, **38**, 163–183.
- Fredlund, D. G., and Rahardjo, H., 1993. *Soil Mechanics for Unsaturated Soils*. New York: John Wiley & Sons.
- Håkansson, I., 2005. Machinery-induced compaction of arable soils: incidence – consequences – counter measures. Swedish University of Agricultural Sciences Uppsala, Reports from the division of soil management, Report no. 109, 153 pp.
- Håkansson, I., 1994. Subsoil compaction caused by heavy vehicles: a long-term threat to soil productivity. *Soil and Tillage Research*, **29**, 105–110.
- Hamza, M. A., and Anderson, W. K., 2005. Soil compaction in cropping systems: A review of the nature, causes and possible solutions. *Soil and Tillage Research*, **82**, 121–145.
- Horn, R., Fleige, H., Peth, S., and Peng, X. (eds.), 2006. *Soil Management for Sustainability*. Reiskirchen, Germany: Catena.
- Kirby, M., 2007. Whither soil compaction research? *Soil and Tillage Research*, **93**, 472–475.
- Oldeman, L. R., 1994. The global extent of soil degradation. In Greenland, D. J., and Szabolcs, I. (eds.), *Soil Resilience and Sustainable Land Use*. Wallingford: CAB International, pp. 99–118.
- Peth, S., and Horn, R., 2006. The mechanical behavior of structured and homogenized soil under repeated loading. *Journal of Plant Nutrition and Soil Science*, **169**, 401–410.
- Peth, S., Horn, R., Fazekas, O., and Richards, B. G., 2006. Heavy soil loading and its consequences for soil structure, strength and deformation of arable soils. *Journal of Plant Nutrition and Soil Science*, **169**, 775–783.

Cross-references

- Pre-Compression Stress
Stress–Strain Relations

SOIL ERODIBILITY

A measure of the soil's susceptibility to raindrop impact and runoff.

SOIL EROSION MODELING

John N. Quinton

Lancaster Environment Centre, Lancaster University,
Lancaster, UK

Soil erosion is a globally significant environmental process. It degrades the soil upon which we rely on for food, fuel, clean water, carbon storage, and as substrate for buildings and infrastructure. Soil erosion also acts as a mechanism for transferring pollutants to surface waters and can reduce water availability for crops and increase flooding. Given soil erosion's importance it is not surprising that there have been a number of attempts to produce mathematical models of varying complexity to predict its magnitude and in some cases its spatial and temporal distribution.

Soil erosion models broadly fit into two groups: empirical and process-based models, and the reader is referred to edited volumes by Morgan and Nearing (in press) and Harmon and Doe III (2001) for more detailed information. The Universal Soil Loss Equation (USLE) (Wischmeir and Smith, 1978) is the most dominant empirical model. The USLE was developed from over 10,000 plot years of data collected across the eastern half of the USA. The result was a simple equation to predict annual field scale erosion rates, which had six parameters: slope, erodibility, slope length, erosivity, cover, and management and support practice (conservation measures) factor. This allowed the USLE to be adopted by the US soil conservation service as a simple tool for extension officers. The USLE has been incorporated into watershed models, revised, and re-calibrated and used throughout the world.

As a response to the lack of physical representation of erosion processes in the USLE the 1980s saw a number of groups begin to develop process-based approaches to soil erosion modeling. These included the Water Erosion Prediction Project (WEPP) (Nearing et al., 1989), European Soil Erosion Model (EUROSEM) (Morgan et al., 1998), and Griffith University Erosion System Template (GUEST) (Hairsine and Rose, 1992), originating from teams in the USA, Europe, and Australia, respectively. These models offered the potential to be transferable than the USLE, since they used mathematics to represent erosion processes without, for the most part, recourse to empiricisms. Because of their distributed nature they could also identify sites of erosion and deposition in the landscape and compute the delivery of sediment to surface waters. While this group of models were more

satisfying scientifically than the USLE, their predictions suffered from uncertainties associated with high numbers of parameters which were hard to measure in the field, e.g., Quinton (1997).

As we have become more aware of diffuse pollution problems and soil erosion's role in global biogeochemical cycling erosion modeling has responded. Erosion models have been linked to contaminant and carbon transport at scales ranging from tens of square meters up to the global scale. For example, Sander has further developed the Hairsine Rose model to simulate the selective erosion of contaminant containing soil particles. To address the impact of soil erosion on the global carbon cycle, Van Oost et al. (2007) have applied simple models of erosion across the globe to estimate the impact of these processes on the global carbon cycle.

There are now more erosion models available to use than ever before and they are being used to answer an ever wider number of questions – yet there is still room for development. Although scientific progress pushes us toward adding more complexity to our models by including new processes, it is likely that modelers will be forced to be more open and honest about model uncertainties and the ability of models to predict the soil erosion at a variety of temporal and spatial scales. This may focus model development on the production of parsimonious models which can be applied to data sets using uncertainty estimation procedures, such as Generalized Likelihood Uncertainty Estimation (GLUE) (Freer et al., 1996), allowing their predictive uncertainty to be quantified.

Bibliography

- Freer, J. E., Beven, K. J., and Ambroise, B., 1996. Bayesian estimation of uncertainty in runoff prediction and the value of data: an application of the GLUE approach. *Water Resources Research*, **32**, 2161–2173.
- Hairsine, P., and Rose, C., 1992. Modelling water erosion due to overland flow using physical principles: I. Uniform flow. *Water Resources Research*, **28**, 237–243.
- Harmon, R. S., and Doe III, W. W. (eds.), 2001. *Landscape Erosion and Evolution Modelling*. New York: Kluwer Academic.
- Morgan, R. P. C., and Nearing, M. A., (in press). *Handbook of Erosion Modelling*. Oxford, UK: Wiley-Blackwell.
- Morgan, R. P. C., Quinton, J. N., Smith, R. E., Govers, G., Poesen, J. W. A., Auerswald, K., Chisci, G., Torri, D., and Styczen, M. E., 1998. The European Soil Erosion Model (EUROSEM): A dynamic approach for predicting sediment transport from fields and small catchments. *Earth Surface Processes and Landforms*, **23**, 527–544.
- Nearing, M. A., Foster, G. R., Lane, L. J., and Finckner, S. C., 1989. A process based soil erosion model for USDA water erosion prediction technology. *Transactions of the American Society of Agricultural Engineers*, **32**, 1587–1593.
- Quinton, J. N., 1997. Reducing predictive uncertainty in model simulations: a comparison of two methods using the European Soil Erosion Model (EUROSEM). *Catena*, **30**, 101–117.
- Van Oost, K., Quine, T. A., Govers, G., De Gryze, S., Six, J., Harden, J. W., Ritchie, J. C., McCarty, G. W., Heckrath, G., Kosmas, C., Giraldez, J. V., Marques da Silva, J. R., and Merckx, R., 2007. The impact of agricultural soil erosion on the global carbon cycle. *Science*, **318**, 626–629.

Wischmeir, W. H., and Smith, D. D., 1978. Predicting rainfall erosion losses: a guide to conservation planning. *USDA Agricultural Handbook No. 537*. Washington, DC: U.S. Department of Agriculture.

Cross-references

[Flooding, Effects on Soil Structure](#)
[Hydrophobicity of Soil](#)
[Overland Flow](#)
[Physical Degradation of Soils, Risks and Threats](#)
[Surface Roughness, Effect on Water Transfer](#)
[Tillage Erosion](#)
[Water Erosion: Environmental and Economical Hazard](#)

SOIL FUNCTIONS

Winfried E. H. Blum
Institute of Soil Research, University of Natural Resources and Applied Life Sciences (BOKU) Vienna, Vienna, Austria

Definition

Soil as a natural resource performs six environmental, social, and economic functions.

Introduction

Soil functions reflect the capacity of soil to function within natural or managed ecosystem boundaries, to sustain plant and animal productivity, maintain or enhance water and air

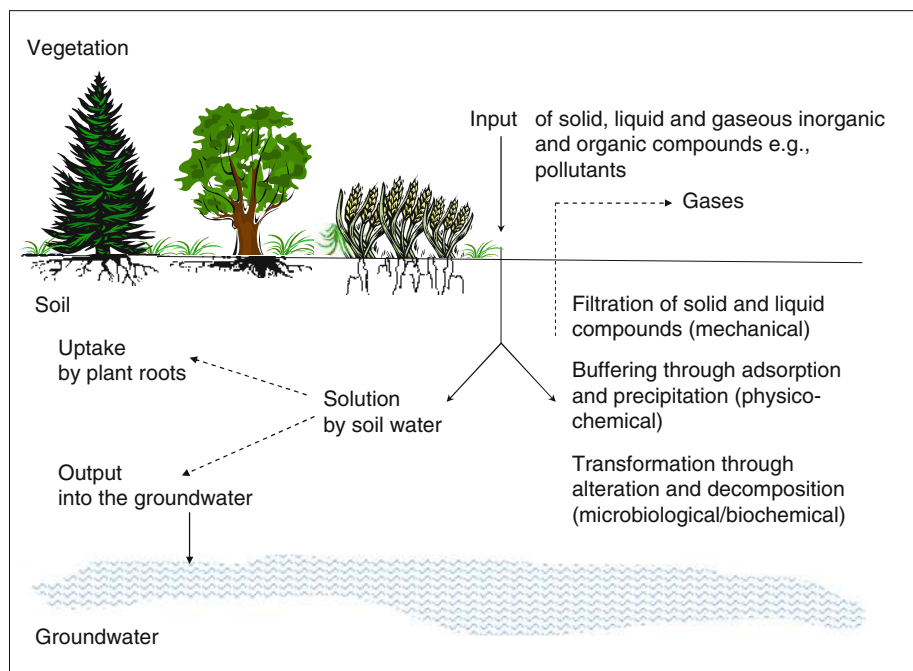
quality, and support human health and habitation (Mausbach and Tugel, 1995, modified).

Soil functions

The three ecological functions are:

1. Production of biomass, ensuring food, fodder, renewable energy, and raw materials. This function is the basis of human and animal life (Blum and Eswaran, 2004).
2. Filtering, buffering, and transformation between the atmosphere, the ground water, and the plant cover, strongly influencing the water cycle at the earth surface as well as the gas exchange between terrestrial and atmospheric systems, and protecting the environment, including human beings, against the contamination of ground water and the food chain (Blum, 1998). This function is most important, because of the many solid, liquid or gaseous, inorganic or organic depositions on which soils react through mechanical filtration, physico-chemical absorption, and precipitation or micro-biological and biochemical mineralization and metabolization, see [Figure 1](#).

These biological reactions may also contribute to global change through the emission of gases from the soil into the atmosphere, because globally the total pool of organic carbon of soils is about three times higher than the total organic carbon in the above ground biomass and about twice as high as the total organic carbon in the atmosphere. Therefore, soils are a central link in the biotransformation of organic carbon and continually play a role in releasing CO₂ and



Soil Functions, Figure 1 Soil as a filter, buffer and transformation substrate.

- other trace gases (e.g., N₂O and CH₄) into the atmosphere. These gases are most important for processes of global change, which in this case involves large-scale feed-back of many local small-scale processes. As long as these filtering, buffering, and transformation capacities can be maintained, there is no danger to the ground water or to the food chain. However, these capacities of soils are limited and vary according to the specific soil conditions.
3. Gene reservoir: Soils are a biological habitat, with a large variety of organisms. They contain two to three times more species in number and quantity than all other above ground biota together. Therefore, soils are the main basis of biodiversity. Human life depends on this biodiversity, because we do not know if we will need new genes for maintaining human life from soils in the near or the remote future. Moreover, genes from the soil are increasingly important for many biotechnological and bioengineering processes.

The three non-ecological functions are:

1. The physical basis for technical, industrial, and socio-economic structures and their development, e.g., industrial premises, housing, transport, sports, recreation, dumping of refuse etc. One of the main problems in this context is the sealing of soils through the continuous increase of urban and peri-urban as well as industrial areas, including transport facilities between them.
2. A source of raw materials, e.g., clay, sand, gravel, and minerals in general, as well as a source of energy and water. Raw materials are the basis for technical, industrial, and socio-economic development. The use of soils for infrastructural development and for the extraction of raw materials can be considered as irreversible.
3. Soils are also important as a geogenic and cultural heritage, forming an essential part of the landscape in which we live, concealing and protecting palaeontological and archaeological remains of importance for the understanding of the history of the earth.

Under holistic aspects, soil and land use can be defined as the temporarily and spatially simultaneous use of all these functions, minimizing irreversible ones.

Outlook

In view of the soil as an absolutely limited resource, which cannot be extended or enlarged, the harmonization between the uses of these six functions, which are often concomitant in the same area, is a key issue of sustainability. However, this is not a scientific but a political task (see COM(2006)231 final, 2006).

Bibliography

- Blum, W. E. H., 2005. Functions of soil for society and the environment. *Reviews in Environmental Science and Biotechnology*, **4**, 75–79.

- Blum, W. E. H., and Eswaran, H., 2004. Soils for sustaining global food production. *Journal of Food Science*, **69**(2), CRH37–CRH42 (published online 02/20/2004).
- COM(2006)231 Final, 2006. EU – *Thematic Strategy for Soil Protection*, Brussels.
- Mausbach, M., and Tugel, A., 1995. *A decision Document for Establishing a Soil Quality Institute. White Paper*. USA: Natural Resources Conservation Service.

Cross-references

- [Agroforestry Systems, Effects on Water Balance in Cropping Zone](#)
[Agrophysical Properties and Processes](#)
[Buffer Capacity of Soils](#)
[Clay Minerals and Organo-Mineral Associates](#)
[Climate Change: Environmental Effects](#)
[Coupled Heat and Water Transfer in Soil](#)
[Diffusion in Soils](#)
[Earthworms as Ecosystem Engineers](#)
[Electrical Properties of Soils](#)
[Enzymes in Soils](#)
[Fertilizers \(Mineral, Organic\), Effect on Soil Physical Properties](#)
[Greenhouse Gases Sink in Soils](#)
[Horticulture Substrates, Structure and Physical Properties](#)
[Hydrophobicity of Soil](#)
[Lysimeters: A Tool for Measurements of Soil Fluxes](#)
[Magnetic Properties of Soils](#)
[Management Effects on Soil Properties and Functions](#)
[Microbes and Soil Structure](#)
[Nature Conservation Management](#)
[Organic Farming, Effect on the Soil Physical Environment](#)
[Peatlands: Environmental Functions](#)
[Physical Degradation of Soils, Risks and Threats](#)
[Plant–Soil Interactions, Modeling](#)
[Pore Morphology and Soil Functions](#)
[Root Responses to Soil Physical Limitations](#)
[Soil Hydraulic Properties Affecting Root Water Uptake](#)
[Soil Penetrability, Effect on Animal Burrowing](#)
[Soil Physical Quality](#)
[Soil Water Flow](#)
[Soil Water Management](#)
[Soil–Plant–Atmosphere Continuum](#)
[Solute Transport in Soils](#)
[Sorptivity of Soils](#)
[Subsoil Compaction](#)
[Temperature Effects in Soil](#)
[Urban Soils, Functions](#)
[Water Balance in Terrestrial Ecosystems](#)

SOIL HYDRAULIC PROPERTIES AFFECTING ROOT WATER UPTAKE

Leilah Krounbi, Naftali Lazarovitch

Wyler Department of Dryland Agriculture, French
 Associates Institute for Agriculture and Biotechnology of
 Drylands, Jacob Blaustein Institutes for Desert Research,
 Ben-Gurion University of the Negev, Israel

Definitions

Soil water potential. The energy required to move a unit quantity of pure water from one point in the soil to another.

Compensatory uptake. The ability of a plant to transpire at its potential rate under drying conditions through root water uptake from the sparsely rooted, but wetter and less saline regions in the soil profile.

Root length density. The root length per unit volume of soil.

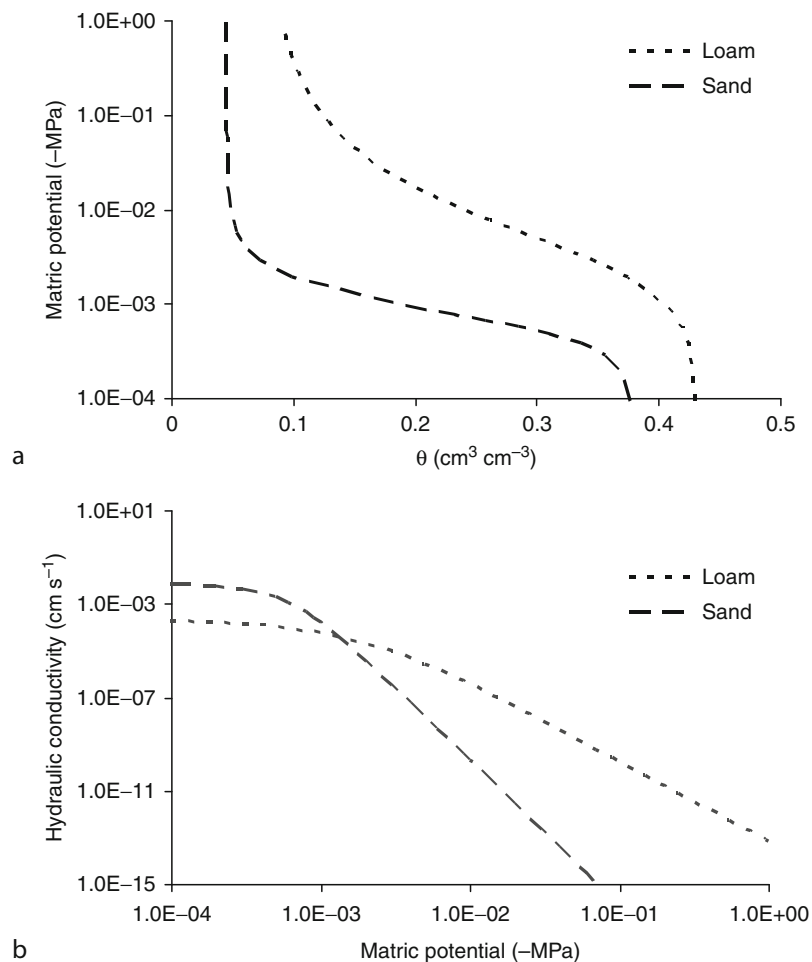
Introduction

Contemporary agriculture, with its dependence on irrigation, fertilizers, and pesticides, contributes significantly to water and solute fluxes through the soil, specifically in arid and semi-arid areas. The quality and quantity of this water as it passes through the vadose zone is governed primarily by plant water uptake (Vrugt et al., 2001; Simunek and Hopmans, 2008; Skaggs and Shouse, 2008). In non-limiting conditions, the atmospheric demand controls uptake, while in water deficit soils characteristic of field conditions, the soil hydraulic properties seem to determine root water uptake (Feddes and Raats, 2004). Compensatory uptake is one example of the latter scenario.

Therefore, accurately predicting the temporal and spatial root water uptake pattern in a drying soil, as a function of the soil hydraulic properties, is important for sustainable agricultural resource management that minimizes soil and groundwater pollution.

Soil hydraulic properties

The high nonlinearity of the soil hydraulic functions describing the relation between the soil water potential, water content, and the hydraulic conductivity (Lazarovitch et al., 2007) can be seen in the retention and conductivity curves depicted in Figure 1. Soil particle size distribution, or texture, is a primary factor in determining the slope of both the water content and hydraulic conductivity curves as a function of the soil water potential. Sand is characterized by larger sized soil particles, which aggregate into larger water-conducting pores. The wall surfaces of these soil capillaries adsorb a relatively small percentage of water molecules in the flow stream. The limited water holding capacity of sand therefore



Soil Hydraulic Properties Affecting Root Water Uptake, Figure 1 (a) The soil water content at varying water potentials for two soils, loam and sand. (b) The soil hydraulic conductivity at varying water potentials for two soils, loam and sand.

confers greater hydraulic conductivity, or easier drainage, near the saturation range. This is made evident by the drastic drop in the soil water content of sand at the onset of low potentials, depicted in [Figure 1a](#). The small-diameter pores typical of loamy soils are comprised primarily of finer particles characterized by a high water holding capacity. Slight changes in the soil water content necessitate the application of lower water potentials, and the residual water content of loam is markedly higher than that of sand ([Hillel, 1998](#)). The gradual change in the hydraulic conductivity of loamy soil with decreasing soil water potentials, as shown in [Figure 1b](#), can be attributed to the higher percentage of water molecules adsorbed to pore walls, coupled with the increasing difficulty of releasing them at low potentials. The change in the hydraulic conductivity of sandy soil with decreasing potentials is much more drastic, eventually dropping below that of loam once most of the soil water has been drained.

Water flow through the soil–plant–atmosphere continuum (SPAC)

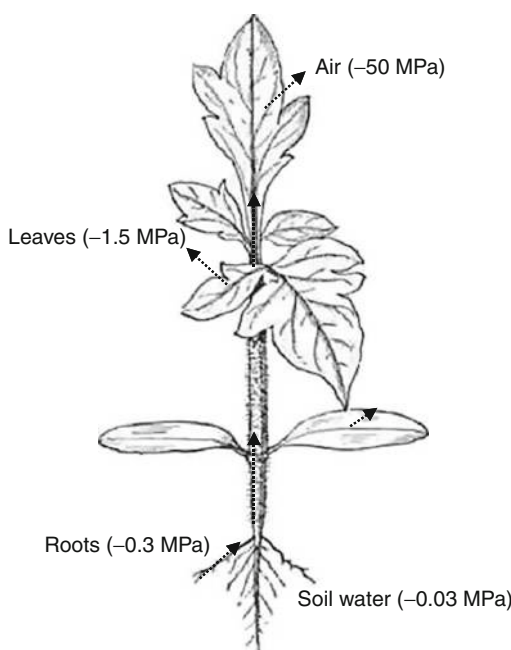
Water potential gradients serve as the force inducing flow within and between adjacent compartments in the SPAC ([Boyer, 1995](#); [van der Ploeg et al., 2008](#)). [Figure 2](#) highlights the typical potential differences between soil water and atmospheric water vapor, oftentimes amounting to tens of megapascals (MPa). The effectiveness of plants in meeting a continuous evaporative demand through

increased water extraction is primarily determined by the soil's ability to deliver water to the root surface. As the soil dries, the soil water potential decreases, leading to a subsequent reduction in the hydraulic conductivity. To maintain the water potential gradient powering the transpiration stream, the root water potential must decrease beyond that of the soil. But while the soil water potential can decrease to very low values, the root water potential is limited by a critical value, around -1.6 MPa for most agricultural crops ([Koorevaar et al., 1983](#)), below which plant death ensues. While root water uptake is often equated to transpiration, water flow through the SPAC may be affected by fluxes between the xylem and adjacent parenchyma cells. The lag time between the onset of maximum water potential gradients in the leaves and xylem demonstrates a lack of coordination in water potential changes between SPAC compartments, pointing to the effect of plant capacitance on the transpiration stream ([Nobel and Jordan, 1983](#)).

An Ohm's law type of relationship ([van den Honert, 1948](#); [Feddes and Raats, 2004](#)) describes the water flow through the SPAC. The flux is expressed as a function of the operating water potential per unit distance, and a proportionality factor that defines either the conductance or the resistance of the transmitting media to water flow; the flux is assumed constant from soil to atmosphere so that segments characterized by large gradients will also have large flow resistances. The definition of the proportionality factor changes between soil and plant systems according to the spatial scale of the water-transferring media ([Hopmans and Bristow, 2002](#)). The overall resistance is defined as the series combination of all resistances in the SPAC ([Campbell, 1985](#)). Water evaporation from the stomatal cavity to the atmosphere is met with the largest resistance in the SPAC.

While multiple methods exist for measuring both soil and leaf water fluxes and potentials from which respective compartmental flow resistances can be deduced, little success has resulted from attempts at measuring soil–root interface potentials and fluxes, and much controversy remains surrounding this subject ([Personne et al., 2003](#)). Steep water potentials and hydraulic conductivity gradients at the soil–root interface have been demonstrated experimentally ([Duham and Nye, 1973](#); [Hainsworth and Aylmore, 1989](#); [Schmidhalter, 1997](#)). Experimental data presented by [Taylor and Klepper \(1975\)](#) for water uptake by cotton roots show that in a wet soil, the soil–root interface hydraulic conductivity was up to six orders of magnitude smaller than the bulk soil hydraulic conductivity. These results indicate that in field conditions, most of the flow resistance from soil to plant lies in the soil–root interface. In very dry soils, the conductivities of both the bulk soil and the soil–root interface are of similar magnitude ([Raats, 2007](#)).

Recent research highlights the dominance of soil hydraulic conductivity in affecting root water uptake. [Schroeder et al. \(2008\)](#) used a three-dimensional numerical model to assess root water uptake with and without



Soil Hydraulic Properties Affecting Root Water Uptake,
Figure 2 The transpiration stream through the soil–plant–atmosphere continuum, with representative potential values indicated for various compartments.

a hydraulic conductivity drop in the rhizosphere. Results show that a sharp decrease in the hydraulic conductivity near the root greatly affects root water uptake, specifically in cases where the radial root hydraulic conductivity is greater than that of the bulk soil. Experiments designed to isolate the effects of the soil water potential and the soil hydraulic conductivity on root water uptake show that the latter has a much more pronounced effect on uptake patterns (Zeelim, 2009). The presence of dry soil layers within the rhizosphere has been put forth as one explanation for the steep hydraulic conductivity gradient in the vicinity of the root surface (Rendig and Taylor, 1989). Herkelrath et al. (1977) postulated that the soil hydraulic conductivity drop at the soil–root interface results from a decrease in the effective area of contact between root and soil with decreasing water content. During drying periods, soil and root shrinkage can result in roots diminishing to 60% of their original size, and in much of the root epidermis detaching from soil particles (Rendig and Taylor, 1989).

Root water uptake under stressed conditions

Root water uptake is a function of both a physical root parameter, commonly referred to as the root length density (Gardner, 1964; Taylor and Klepper, 1975; Feddes and Raats, 2004), and the soil water status (de Jong van Lier et al., 2008). The location of maximum water uptake in a homogenous soil profile of uniform water content and hydraulic conductivity is correlated with the soil layer containing the largest root length density. Under field conditions, plants are both subject to, and the source of, great spatial variability in the soil water content. The upper soil layers containing the bulk of the root zone are usually the most water depleted, while the deeper regions of the soil profile containing fewer roots are wetter.

Although plants can minimize transpiration and the resulting growth rates under limiting conditions to conserve water, many plants maintain a constant, potential transpiration rate long after the commencement of the drying process. One explanation for this is the elongation of deeper, finer roots into soil regions, saturated with untapped water stores. Experimentation with *Arabidopsis* seedlings subjected to drought and osmotic stress showed an increase in primary root growth in the deeper soil regions in response to stress, while lateral root elongation was temporarily arrested (Xiong et al., 2006). Another mechanism by which plants sustain potential transpiration rates in drying soils is compensatory uptake, whereby plants respond to nonuniform, limiting conditions by increasing water uptake from areas in the root zone characterized by more favorable conditions (Skaggs et al., 2006).

Reicosky et al. (1972) report on a pronounced example of compensatory uptake, where, in the vicinity of a water table, 20–25% of plant roots extracted 80–90% of the transpired water. In their study of alfalfa root uptake in a drying soil, Nimah and Hanks (1973a) found that plants

were able to continue transpiring at their potential rate by compensating for the loss in water uptake from the root dense, but drier surface soil layers through uptake from the deeper, wetter regions in the soil. They report that, in agreement with Reicosky et al. (1972), the maximum root extraction zone of alfalfa deepened over time as a result of upward flow from a water table (Nimah and Hanks (1973b)). The observed increase in uptake from the wetter soil regions under drying conditions, as reported by Reicosky et al. (1972) and Nimah and Hanks (1973b), sheds light on the more dominant role of the soil hydraulic properties over the root distribution in affecting root water uptake.

Devices to explore root water uptake

Root water uptake can be monitored using both invasive and noninvasive techniques. In situ devices such as tensiometers, time domain reflectrometry (TDR), and dual probe heat/temperature sensors can measure local changes in the soil water status over time. Studying soil–root water fluxes using invasive devices requires microsensors at the scale of millimeters, a range much smaller than presently available devices. Other difficulties in using invasive technology include the site-specific calibrations necessary for indirect methods such as heat dissipation and TDR, and the limited measurement range of tensiometers. Noninvasive techniques such as computer tomography (CT) and magnetic resonance imaging (MRI) produce two- and three-dimensional, high-resolution images of the rhizosphere from which root growth and changes in the soil water content can be measured. Noninvasive methods have significantly improved our understanding of plant responses to drought stress (Garrigues et al., 2006), but are complicated to operate and not suitable for field use.

Vetterlein and Reinhold (2004) used a ceramic capillary microtensiometer 1 mm in diameter and 5 mm in length to measure the differences between the soil water potential in the rhizosphere and the bulk soil. Segal et al. (2008) developed a pliable-tipped microtensiometer from a plastic pipette tip lined with geotextile, filled with milled quartz in contact with a water reservoir, and attached to a pressure transducer. A wick extending from the pipette tip into the rhizosphere enabled a close monitoring of rhizosphere water potentials from distances as close as 1 mm from the root surface. Segal et al. (2008) studied the soil water potential as a function of distance from the root surface using a growth container sectioned off into two portions by a diagonal screen, which confined root growth. Opposite the screen, six identical microtensiometers were inserted at 2.5 mm depth intervals, such that the distance of each microtensiometer tip from the screen upon which a root mat eventually formed, increased with depth. Results showed that the development of a significant potential gradient, or drawdown zone, as near as 3 mm from the root surface became noticeable following 1 day of root water extraction. van der Ploeg et al. (2008) recently developed a polymer tensiometer able to measure the full

range of soil water potentials encountered in a cropped soil, down to the wilting point value of -1.6 MPa . Root water uptake was monitored in cropped lysimeters subjected to three irrigation regimes – minimum, intermediate, and maximum stress – with both polymer tensiometers and TDR sensors. Results from the maximum stress treatment showed that after severe drying down to -0.7 MPa , larger potential gradients indicating water removal were detected between 0.4 and 0.6 m depths than at 0.2 and 0.4 m depths. TDR measurements showed a vertically uniform water content profile. The ability of the polymer tensiometers to detect extremely low potential gradients across various depth increments helped to identify root water uptake zones that would not have been noticeable from TDR measurements in that particular soil.

X-ray imaging techniques such as CT have been used to measure a variety of soil properties such as bulk density (Anderson et al., 1988), porosity (Phogat and Aylmore, 1999), and water content (Hopmans et al., 1992). CT outputs a series of linear attenuation coefficients for each image pixel that can be calibrated to known water content values (Hamza et al., 2001). Root imaging using CT on the scale of a few centimeters was reported by Gregory et al. (2003) and Perret et al. (2007). Hanisworth and Aylmore (1983, 1986) used CT to measure changes in the soil water content with time, and were able to calculate root water uptake from radishes transpiring at high and low rates. Hamza et al. (2001) studied the effect of low soil water content on prolonged radish root water uptake using CT scans. Results showed that as the water content decreased from 0.3 to $0.1\text{ cm}^3\text{ cm}^{-3}$, the transpiration rate decreased tenfold. The ability of plants to maintain transpiration in such dry conditions was attributed to osmotic adjustment by leaves. In addition, it was shown that the water content at the soil–root interface was 2.5 times smaller at the end of the experiment in drier soils than in wetter soils, and that the extent of the sharp potential gradient immediate to the root surface was also less.

Another noninvasive method for quantifying the water content in the root zone is MRI. MRI scans have been used to monitor water infiltration into soils (Vortrubova et al., 2003), image roots two-dimensionally (Cofer et al., 1989), and visualize root water uptake in porous media (Brown et al., 1990). Segal et al. (2008) used MRI images of the soil water content distribution in the rhizosphere to study the effect of water uptake by a single barley root on soil water depletion patterns. The soil water content of the imaged rhizosphere was quantified using a calibration curve of the MRI signal/noise ratio and the volumetric water content of two sandy soils. Results showed the development of a steep water content gradient near the soil–root interface 2 h after water uptake commenced, which gradually increased with distance from the root until approaching the bulk soil water content. Pohlmeier et al. (2008) used MRI to image the root architecture of 4-week old castor bean plants, and to study changes in the soil water content following root uptake. Results from

both types of imaging showed that soil regions containing the highest root densities, near the bottom and toward the surface of the plant container, experienced the greatest change in the soil water content due to root water uptake.

Summary

Various environmental and plant physiological factors play a role in determining root water uptake patterns. The soil physical properties such as the particle distribution affect the amount of soil water available for plant consumption, and the rate of water transfer from soil to root. Climate conditions determine the evaporative demand that is met by transpiring plants primarily through root water uptake. Steep water potential and hydraulic conductivity gradients have been observed in the vicinity of the root surface due to an increase in the flow resistance from the bulk soil to the soil–root interface. In drying soils, the soil hydraulic properties have a more dominant role in regulating water uptake than the physical properties of roots, and the effect of the soil hydraulic conductivity on root water uptake has recently been shown as much more significant than the soil water potential. Compensatory uptake is one example of how root water uptake patterns are controlled by the soil hydraulic properties in suboptimal conditions. The development of both invasive and noninvasive soil sensors has alleviated much of the difficulty in researching below-ground processes, and has enabled imaging of root development and changes in the soil water content due to root water uptake.

While much research has been carried out to examine the effect of drought conditions on root water uptake, the effects of other stresses, such as salinity, oxygen stress, and temperature extremes, as well as the combined effect of multiple stresses, are also important topics of research. Root water uptake studies usually focus on fully developed root zones, thereby taking the root density distribution throughout the soil profile as constant. New experiments should be performed to look at dynamic root water uptake patterns as a function of both variable soil conditions as well as a changing root density distribution. Nutrient uptake as affected by the water flow and nutrient transport in the soil remains another important topic of research, and can help in planning fertigation regimes that maximize root water uptake and the resulting crop yields while minimizing groundwater pollution by leachate.

Bibliography

- Anderson, S. H., Gantzer, C. J., Boone, J. M., and Tully, R. J., 1988. Rapid nondestructive bulk density and soil–water content determination by computer tomography. *Soil Science Society of America Journal*, **52**, 35.
- Boyer, J. S., 1995. *Measuring the Water Status of Plants and Soils*. San Diego: Academic.
- Brown, J. M., Kramer, P. J., Cofer, G. P., and Johnson, G. A., 1990. Use of nuclear magnetic resonance microscopy for noninvasive observations of root–soil water relations. *Theoretical and Applied Climatology*, **42**, 229.
- Campbell, G. S., 1985. *Soil Physics with BASIC: Transport Models for Soil–Plant Systems*. Amsterdam: Elsevier.

- Cofer, G. P., Brown, J. M., and Johnson, G. A., 1989. In vivo magnetic resonance microscopy at 5 μm . *Journal of Magnetic Resonance*, **83**, 608.
- Duham, R. J., and Nye, P. H., 1973. The influence of the soil water content on the uptake of ions by roots: I/Soil water content gradients near a plant onion roots. *Journal of Applied Ecology*, **10**, 585.
- Feddes, R. A., and Raats, P. A. C., 2004. Parameterizing the soil–water–plant root system, In Feddes, R. A., de Rooij, G. H., and van Dam, J. C. (eds.), *Unsaturated-Zone Modeling: Progress, Challenges, Applications*. Wageningen UR Frontis Series. Vol. 6, pp. 95–141 (Chapter 4 in <http://library.wur.nl/frontis/unsaturated/tocunsaturated.html>)
- Gardner, W. R., 1964. Relation of root distribution to water uptake and availability. *Agronomy Journal*, **56**, 41.
- Garrigues, E., Doussan, C., and Pierret, A., 2006. Water uptake by plants: 1. Formation and propagation of a water extraction front in mature root systems as evidenced by 2D light transmission imaging. *Plant and Soil*, **173**, 317.
- Gregory, O. J., Hutchison, D. J., Read, D. B., Jenneson, P. M., Gilboy, W. B., and Morton, E. J., 2003. Non-invasive imaging of roots with high resolution X-ray micro-tomography. *Plant and Soil*, **255**, 351.
- Hainsworth, J. M., and Aylmore, L. A. G., 1983. Use of computer-assisted tomography to determine spatial distribution of soil water content. *Australian Journal of Soil Research*, **21**, 435.
- Hainsworth, J. M., and Aylmore, L. A. G., 1989. Non-uniform soil water extraction by plant roots. *Plant and Soil*, **113**, 112.
- Hamza, M. A., Anderson, S. H., and Aylmore, L. A. G., 2001. Studies of soil water drawdowns by single radish roots at decreasing soil water contents using computer-assisted tomography. *Australian Journal of Soil Research*, **39**, 1387.
- Hanisworth, J. M., and Aylmore, L. A. G., 1986. Water extraction by a single plant root. *Soil Science Society of America Journal*, **50**, 841.
- Herkelrath, W. M., Miller, E. E., and Gardner, W. R., 1977. Water uptake by plants: II. The root contact model. *Soil Science Society of America Journal*, **41**, 1039.
- Hillel, D., 1998. *Environmental Soil Physics*. San Diego: Academic. 565.
- Hopmans, J. W., and Bristow, K. L., 2002. Current capabilities and future needs of root water and nutrient uptake modeling. *Advances in Agronomy*, **7**, 104.
- Hopmans, J. W., Vogel, T., and Koblik, P. D., 1992. X-ray tomography of soil water distribution in one-step outflow experiments. *Soil Science Society of America Journal*, **56**, 355.
- Jong, D., van Lier, Q., van Dam, J. C., Metselaar, K., de Jong, R., and Duijnisveld, W. H. M., 2008. Macroscopic root water uptake distribution using a matric flux potential approach. *Vadose Zone Journal*, **7**, 1065.
- Koorevaar, P., Menelik, G., and Dirksen, C., 1983. Elements of soil physics. *Developments in Soil Science*, Vol. 13. Amsterdam: Elsevier.
- Kramer, P. J., 1983. *Water relations of plants*. London: Academic.
- Lazarovitch, N., Ben-Gal, A., Simunek, J., and Shani, U., 2007. Uniqueness of soil hydraulic parameters determined by a combined Wooding inverse approach. *Soil Science Society of America Journal*, **571**, 860.
- Nimah, M. N., and Hanks, J. R., 1973a. Model for estimating soil water, plant, and atmospheric interrelations: I. Description and sensitivity. *Soil Science Society of America Journal Proceedings*, **37**, 522.
- Nimah, M. N., and Hanks, J. R., 1973b. Model for estimating soil water, plant, and atmospheric interrelations: II. Field test of model. *Soil Science Society of America Journal Proceedings*, **37**, 528.
- Nobel, P. S., and Jordan, P. W., 1983. Transpiration stream of desert species: Resistances and capacitances for a C₃, a C₄, and a CAM plant. *Journal of Experimental Botany*, **34**, 1379.
- Perret, J. S., Al-Belushi, M. E., and Deadman, M., 2007. Non-destructive visualization and quantification of roots using computed tomography. *Soil Biology and Biochemistry*, **39**, 391.
- Personne, E., Perrier, A., and Tuzet, A., 2003. Simulating water uptake in the root zone with a microscopic-scale model of root extraction. *Agronomie*, **23**, 153.
- Phogat, V. K., and Aylmore, L. A. G., 1999. Evaluation of soil structures by using computer assisted tomography. *Australian Journal of Soil Research*, **27**, 313.
- Pohlmeier, A., Peusquens, A., Javaux, M., Menzel, M. I., Vanderborght, J., Kaffanke, J., Romanzetti, S., Lindenmair, J., Vereecken, H., and Shah, N. J., 2008. Changes in soil water content resulting from *Ricinus* root uptake monitored by magnetic resonance imaging. *Vadose Zone Journal*, **7**, 1010.
- Raats, P. A. C., 2007. Uptake of water from soils by plant roots. *Transport in Porous Media*, **68**, 5, doi:10.1007/s11242-006-9055-6.
- Reicosky, D. C., Millington, R. J., Klute, A., and Peters, D. B., 1972. Patterns of water uptake and root distribution of soybeans in the presence of a water table. *Agronomy Journal*, **64**, 292.
- Rendig, V. V., and Taylor, H. M., 1989. *Principles of Soil–Plant Interrelationships*. New York: McGraw-Hill, 123pp.
- Schmidhalter, U., 1997. The gradient between pre-dawn rhizoplane and bulk soil matric potentials, and its relations to the pre-dawn root and leaf water potentials of four species. *Plant, Cell and Environment*, **20**, 953.
- Schroeder, T., Javaux, M., Vanderborght, J., Koerfgen, B., and Vereecken, H., 2008. Effect of local soil hydraulic conductivity drop using a three-dimensional root water uptake model. *Vadose Zone Journal*, **7**, 1089.
- Segal, E., Kushnir, T., Mualem, Y., and Shani, U., 2008. Microsensing of water dynamics and root distributions in sandy soils. *Vadose Zone Journal*, **7**, 1018.
- Simunek, J., and Hopmans, J. W., 2008. Modeling compensated root water and nutrient uptake. *Ecological Modeling*, doi:10.1016/j.ecolmodel.2008.11.004.
- Skaggs, T. H., and Shouse, P. J., 2008. Roots and root function: introduction. *Vadose Zone Journal*, **7**, 1008.
- Skaggs, T. H., van Genuchten, M. T., Shouse, P. J., and Poss, J. A., 2006. Macroscopic approaches to root water uptake as a function of water and salinity stress. *Agricultural Water Management*, **86**, 140.
- Smith, J. A. C., and Griffiths, H., 1993. *Water deficits, plant responses from cell to community*. Oxford: BIOS Scientific.
- Taylor, H. M., and Klepper, B., 1975. Water uptake by cotton root systems: An examination of assumptions in the single root model. *Soil Science*, **120**, 57.
- van den Honert, T. H., 1948. Water transport in plants as a catenary process. *Discussions of the Faraday Society*, **3**, 146.
- van der Ploeg, M., Gooren, H. P. A., Bakker, G., and Rooji, G. H., 2008. Matric potential measurements by polymer tensiometers in cropped lysimeters under water-stressed conditions. *Vadose Zone Journal*, **7**, 1048.
- Vetterlein, D., and Reinhold, J., 2004. Gradients in soil solution composition between bulk soil and rhizosphere: In situ measurement with changing soil water content. *Plant and Soil*, **258**, 307.
- Votruba, J., Cislerova, M., Amin, M. H. G., and Hall, L. D., 2003. Recurrent ponded infiltration into structures soil: a magnetic resonance imaging study. *Water Resources Research*, **39**(12), 1371, doi:10.1029/2003WR002222.
- Vrugt, J. A., van Wijk, M. T., Hopmans, J. W., and Simunek, J., 2001. One-, two-, and three-dimensional root water uptake functions from transient modeling. *Water Resources Research*, **37**, 2457.

Xiong, L., Wang, R., Mao, G., and Kozcan, J. M., 2006. Identification of drought tolerance determinants by genetic analysis of root response to drought stress and abscisic acid. *Plant Physiology*, **142**, 1065.

Zeelim, E., 2009. The influence of water potential gradient between the rhizosphere and the atmosphere on plant water uptake. Thesis submitted to the Faculty of Agriculture of the Hebrew University of Jerusalem.

Cross-references

[Hydraulic Properties of Unsaturated Soils](#)

[Plant–Soil Interactions, Modeling](#)

[Root Water Uptake: Toward 3-D Functional Approaches](#)

[Soil Water Flow](#)

[Soil–Plant–Atmosphere Continuum](#)

[Spatial Variability of Soil Physical Properties](#)

[Water Use Efficiency in Agriculture: Opportunities for Improvement](#)

Bibliography

Bachmann, J., Deurer, M., and Arye, G., 2007. Modeling water movement in heterogeneous water-repellent soil: 1. Development of a contact angle-dependent water-retention model. *Vadose Zone Journal*, **6**, 436–445.

Bauters, T. W. J., Steenhuis, T. S., DiCarlo, D. A., Nieber, J. L., Dekker, L. W., Ritsema, C. J., Parlange, J. Y., and Haverkamp, R., 2000. Physics of water repellent soils. *Journal of Hydrology*, **231–232**, 233–243.

Hillel, D., 1980. *Fundamentals of Soil Physics*. New York: Academic.

Ritsema, C. J., and Dekker, L. W., 2000. Preferential flow in water repellent sandy soils: principles and modeling implications. *Journal of Hydrology*, **231–232**, 308–319.

Wang, Z., Wu, Q. J., Wu, L., Ritsema, C. J., Dekker, L. W., and Feyen, J., 2000. Effects of soil water repellency on infiltration rate and flow instability. *Journal of Hydrology*, **231–232**, 265–276.

Cross-references

[Bypass Flow in Soil](#)

[Hydrophobicity of Soil](#)

[Infiltration in Soils](#)

[Soil Water Flow](#)

[Sorptivity of Soils](#)

[Wetting and Drying, Effect on Soil Physical Properties](#)

SOIL HYDROPHOBICITY AND HYDRAULIC FLUXES

Peter Hartmann

Department of Soils and Environment, Forest Research Institute Baden-Wuerttemberg, Freiburg, i. Br., Germany

Synonyms

Soil hydrophobicity = soil water repellency

Definitions

Hydrophobicity derives from the Greek “hydro” and “phobos” that means water and fearing. The reverse is hydrophilic, from “philos” – loving.

Hydraulic derives from Greek “hydraulikos” – “aulos” means hollow tube.

Flux derives from Latin “fluere,” which means flow.

Soil hydrophobicity affects the soil water contact angle (CA) and thus the capillary forces of soil (Bauters et al., 2000). Hydraulic fluxes in soil are mainly capillary flows, which are driven by gravity and interfacial pressure differences. These depend on the geometry of the pores and on local wetting properties that are a time-dependent function of moisture content (Bachmann et al., 2007). Hydrophobicity is strongest in dry soils and decreases with remoistening and higher water contents. In a hydrophobic soil ($CA > 90^\circ$) water infiltrates not until the persistence of hydrophobicity is exceeded respectively a positive water entry pressure value is applied. In the latter case, first large pores will fill with water before fine pores are moistened and infiltration increases with time (Wang et al., 2000). Contrary is the infiltration in a hydrophilic soil ($CA < 90^\circ$), where water infiltrates first in fine pores with a constant infiltration rate (Hillel, 1980). Hydrophobicity causes unstable wetting fronts and is assumed to induce preferential flow, which is of major importance in the spatial distribution of water in soil (Ritsema and Dekker, 2000).

SOIL PARENT MATERIAL

See [Parent Material and Soil Physical Properties](#)

SOIL PENETRABILITY, EFFECT ON ANIMAL BURROWING

Petr Heneberg

Charles University in Prague, Prague 10, Czech Republic

Synonyms

Soil hardness, effect on animal burrowing; Soil penetrability, effect on animal digging behavior; Soil penetration resistance, effect on animal burrowing

Definition

Soil penetrability. Measure of the ease with which an object can be pushed or driven into the soil.

Burrow. A hole or tunnel dug into the ground by an animal, for habitation, temporary refuge, or as a byproduct of locomotion.

Introduction

Burrowing behavior evolved independently in species separated by >500 million years of evolution from two phyla (*Arthropoda* and *Chordata*), seven classes (*Arachnida*, *Insecta*, *Malacostraca*, *Osteichthyes*, *Amphibia*, *Reptilia*, and *Mammalia*). These species vary

by six orders of magnitude in their body mass, and occupy both marine and terrestrial habitats (White, 2005).

Numerous species of burrowing animals bear morphological and physiological adaptations for subterranean life, with strongly convergent traits, showing structural reduction of limbs, tails, eyes, and external ears, together with structural developments of incisors, forelimbs, pectoral girdle, claws, sense organs, and pineal gland that complement each other to optimize burrowing capacities and efficiency (Nevo, 1979).

For semifossorial or fossorial species, any reduction in burrowing costs increases the net energy yield from a given section of burrow. Given that burrowing cost is proportional to the volume of soil excavated (Vleck, 1979), it is apparent that any reduction in construction costs achieved through a reduction in burrow length, or cross section, will similarly reduce the energy yield from the burrow (White, 2005). However, the available habitat patches are not equal to each other. Among the main differences is the soil penetrability, which is not uniformly distributed either vertically or horizontally.

Soil penetrability and vertebrates

Soil penetrability was shown to affect burrowing behavior of mammals, such as tuco-tucos (*Ctenomys talarum*; Luna and Antinuchi, 2006), and wombats (*Lasiorhinus latifrons*, Walker et al., 2007). In birds, ~18% of bird species was shown to be primary or secondary cavity nesters (Newton, 1994), and the burrowing behavior of sand martins (*Riparia riparia*), bee-eaters (*Merops apiaster* and *Merops philippinus*), and Eurasian kingfishers (*Alcedo atthis*) were shown to be dependent on the soil penetrability (Yuan et al., 2006; Heneberg, 2009). Even the non-burrowing bird species that specialize in feeding on soil invertebrates were found to be soil-penetrability-dependent, among them lapwing (*Vanellus vanellus*; Lister, 1964), snipe (*Gallinago gallinago*; Green et al., 1990), song thrush (*Turdus philomelos*; Peach et al., 2004), and yellow wagtails (*Motacilla flava*; Gilroy et al., 2008). These birds were found to check the soil or intertidal substrates by probing with the bill. For the common snipe, the penetrability of wet grassland soils was even found to be a more important determinant of the duration of the breeding season and foraging site selection than prey abundance (Green et al., 1990).

Soil penetrability and semifossorial insect

Among semifossorial insect, soil penetrability has been studied in relation to the presence and nesting of numerous solitary hymenopteran species (wasps and bees). A large number of these species is ground-nesting, and soil is considered as a limiting factor for local bee communities (Kim et al., 2006). Nesting of at least 10 bee and wasp species was already shown to be dependent on the soil penetrability (Ghazoul, 2001; Kim et al., 2006; etc), thus one might speculate that the dependency on soil penetrability

is a shared phenomenon among all ground-nesting aculeate hymenopterans. However, individual species differ in their soil penetrability requirements, suggesting that these preferences may contribute to the decrease of potential interspecies competition. Some species tend to utilize the whole spectrum of substrates with low and medium penetrability resistance values (*Lasioglossum sp.*), some others were found to prefer soils with medium (*Halictus tripartitus*, *Sphex ichneumoneus*), or low penetrability resistance only (*Halictus ligatus*) (Brockman, 1979; Kim et al., 2006). The habitat selection may be even more complicated, as *Halictus rubicundus* was found to prefer localities with low penetrability resistance. However, within site, this species selects spots with medium soil penetrability (Potts and Willmer, 1997).

The semifossorial hymenopterans spend long time with predigging search, a complex behavioral pattern involving search for soil with appropriate penetrability, granulometrical characteristics, temperature, and plant cover (Brockman, 1979; Field, 1989). Simply, if the soil is too soft, it tends to collapse. If the soil is too hard-packed, the fossorial hymenopteran resumes the predigging search. Depending on the burrow length, species-specific techniques, and penetrability resistance, the digging of one burrow may last only 20 min, but it can take also more than 24 h.

Some species, such as *Mellinus arvensis*, were reported to prolong the time of digging accordingly to the increasing soil penetrability resistance (Ghazoul, 2001). Some other species, such as *Episyron quinquenotatus*, were reported to decrease the length of their burrows when the soil penetrability resistance increases (Kurzewski, 2001). Thus, the higher penetrability resistance leads to the increase of costs of nesting, or, alternatively, to the decrease of the burrow length. This in turn may lead to higher predation, higher nest usurpation rate, or to higher susceptibility to damage of the nest cells due to erosion or other external disturbances. At habitat patches lacking soils with low penetrability resistance, various species of wasps and bees were even shown to increase the frequency of nest usurpation and nest sharing. Such behavior has been shown for *Mellinus arvensis*, *Cerceris antipodes*, *Cerceris australis*, *Cerceris cibrosa*, *Cerceris simplex*, and *Andrena erythronii*. Nesting in substrates with higher penetrability resistance may also lead to the decreased fitness of digging individuals, as in fossorial ant communities the increased energy expenditure and desiccation due to cuticular abrasion is thought to be related to higher mortality rate of adult excavation specialists compared to the nonspecialists.

Soil penetrability and other invertebrates

Representatives of several other groups of invertebrates were also shown to be dependent on soil penetrability. Among them are springtails (*Collembola*), the density of which is reduced with decreasing penetrability and increasing bulk densities. This behavior is shared among

at least nine springtail species (Dittmer and Schrader, 2000; Larsen et al., 2004) and thus seems to be characteristic for springtails as a typical soil-specialist invertebrate group. Some of the arachnids (*Arachnida*) were also shown to be dependent on proper soil penetrability, as Bradley (1986) reported it for scorpion *Paruroctonus utahensis*. Soil penetrability and compaction is also a strong determinant of presence and activity of earthworms (*Lumbricina*), such as *Aporrectodea caliginosa* and *Lumbricus terrestris* (Joschko et al., 1989; Stovold et al., 2004). Despite very few studies being focused on fossorial invertebrates, it is highly probable that the soil penetrability dependence is associated with most of the other groups of invertebrate soil specialists.

Burrowing in aquatic species

Penetrability is also known to have strong influence on density and distribution of marine macrofauna in coastal intertidal zones. Among the groups influenced are *Mollusca* (*Bivalvia*), *Annelida* (*Polychaeta*), *Oligochaeta*, *Nemertea*, *Sipuncula*, *Arthropoda* (*Amphipoda*, *Brachyura*), and *Insecta* (Hsu et al., 2009). Among others, penetrability of coastal intertidal zones affects density and distribution of economically important species, such as shrimps (*Caridea*) (Eckrich and Holmquist, 2000). Marine sediments are dominated by mud – elastic solids that fracture under small tensile forces exerted by burrowers. Thus, numerous aquatic species had been shown to burrow by crack propagation, not by various forms of digging common among terrestrial burrowers. Among the groups shown to use crack propagation are polychaetes (*Nereis virens*) and bivalves (*Yoldia*) (Dorgan et al., 2005, 2006). However, it is still unclear how often and under what conditions a crack becomes a burrow.

The historical view of the function of animal burrow is that it represents a microrefuge, or shelter from environmental stresses such as temperature extremes, fire, or predation. Despite the burrowing costs, the burrowers have been extremely successful in the reinforcement of social life, in the alteration of habitats, in the exploitation of the resources of others, and in the invasion in new habitats.

Summary

Soil penetrability was shown to affect burrowing of both, terrestrial and aquatic animals. As soil penetrability is not uniformly distributed either vertically or horizontally, species-specific soil penetrability preferences result in spatiotemporal separation of habitats utilized by different burrowing species, and thus contribute to decrease in overlap between available resource patches.

Bibliography

Bradley, R. A., 1986. The relationship between population density of *Paruroctonus utahensis* (Scorpionida: Vaejovidae) and characteristics of its habitat. *Journal of Arid Environments*, **11**, 165–171.

- Brockman, H. J., 1979. Nest site selection in the golden digger wasp (*Sphecius ichneumoneus* L.). *Animal Behavior*, **28**, 426–445.
- Dittmer, S., and Schrader, S., 2000. Longterm effects of soil compaction and tillage on Collembola and straw decomposition in arable soil. *Pedobiologia*, **44**, 527–538.
- Dorgan, K. M., Jumars, P. A., Johnson, B. D., Boudreau, B. P., and Landis, E., 2005. Burrow elongation by crack propagation. *Nature*, **433**, 475.
- Dorgan, K. M., Jumars, P. A., Johnson, B. D., and Boudreau, B. P., 2006. Macrofaunal burrowing: the medium is the message. *Oceanography and Marine Biology: An Annual Review*, **44**, 85–121.
- Eckrich, C. E., and Holmquist, J. G., 2000. Trampling in a seagrass assemblage: direct effects, response of associated fauna, and the role of substrate characteristics. *Marine Ecology Progress Series*, **201**, 199–209.
- Field, J., 1989. Nesting tactics in a solitary wasp. *Behaviour*, **110**, 219–243.
- Ghazoul, J., 2001. Effect of soil hardness on aggression in the solitary wasp *Mellinus arvensis*. *Ecological Entomology*, **26**, 457–466.
- Gilroy, J. J., Anderson, G. Q. A., Grice, P. V., Vickery, J. A., Bray, I., Watts, P. N., and Sutherland, W. J., 2008. Could soil degradation contribute to farmland bird declines? Links between soil penetrability and the abundance of yellow wagtails *Motacilla flava* in arable fields. *Biological Conservation*, **141**, 3116–3126.
- Green, R. E., Hirons, G. J. M., and Cresswell, B. H., 1990. Foraging habitats of female Common Snipe *Gallinago gallinago* during the incubation period. *Journal of Applied Ecology*, **27**, 325–335.
- Heneberg, P., 2009. Soil penetrability as a key factor affecting the nesting of burrowing birds. *Ecological Research*, **24**, 453–459.
- Hsu, C.-B., Chen, C.-P., and Hsieh, H.-L., 2009. Effects of sediment compaction on macrofauna in a protected coastal wetland in Taiwan. *Marine Ecology Progress Series*, **375**, 73–83.
- Joschko, M., Diestel, H., and Larink, O., 1989. Assessment of earthworm burrowing efficiency in compacted soil with a combination of morphological and soil physical measurements. *Biology and Fertility of Soils*, **8**, 191–196.
- Kim, J., Williams, N., and Kremen, C., 2006. Effects of cultivation and proximity to natural habitat on ground-nesting native bees in California sunflower fields. *Journal of the Kansas Entomological Society*, **79**, 309–320.
- Kurzewski, F. E., 2001. Comparative nesting behavior of *Episyron quinquenotatus* (Hymenoptera: Pompilidae) in the Northeastern United States. *Northeastern Naturalist*, **8**, 403–426.
- Larsen, T., Schjønning, P., and Axelsen, J., 2004. The impact of soil compaction on euedaphic Collembola. *Applied Soil Ecology*, **26**, 273–281.
- Lister, M. D., 1964. The Lapwing habitat enquiry, 1960–1961. *Bird Study*, **11**, 128–147.
- Luna, F., and Antinuchi, D. C., 2006. Cost of foraging in the subterranean rodent *Ctenomys talarum*: effect of soil hardness. *Canadian Journal of Zoology*, **84**, 661–667.
- Nevo, E., 1979. Adaptive convergence and divergence of subterranean mammals. *Annual Review of Ecology, Evolution, and Systematics*, **10**, 269–308.
- Newton, I., 1994. The role of nest sites in limiting the numbers of hole-nesting birds: a review. *Biological Conservation*, **70**, 265–276.
- Peach, W. J., Robinson, R. A., and Murray, K. A., 2004. Demographic and environmental causes of the decline of rural song thrushes *Turdus philomelos* in lowland Britain. *Ibis*, **146**(suppl. 2), 50–59.
- Potts, S. G., and Willmer, P., 1997. Abiotic and biotic factors influencing nest-site selection by *Halictus rubicundus*, a ground-nesting halictine bee. *Ecological Entomology*, **22**, 319–328.

- Stovold, R. J., Whalley, W. R., Harris, P. J., and White, R. P., 2004. Spatial variation in soil compaction, and the burrowing activity of the earthworm *Aporrectodea caliginosa*. *Biology and Fertility of Soils*, **39**, 360–365.
- Vleck, D., 1979. The energy cost of burrowing by the pocket gopher *Thomomys bottae*. *Physiological Zoology*, **52**, 122–136.
- Walker, F. M., Taylor, A. C., and Sunnucks, P., 2007. Does soil type drive social organization in southern hairy-nosed wombats? *Molecular Ecology*, **16**, 199–208.
- White, C. R., 2005. The allometry of burrow geometry. *Journal of Zoology*, **14**, 395–403.
- Yuan, H.-W., Wang, M.-K., Chang, W.-L., Wang, L.-P., Chen, Y.-M., and Chiou, C.-R., 2006. Soil composition affects the nesting behavior of blue-tailed bee-eaters (*Merops philippinus*) on Kinmen Island. *Ecological Research*, **21**, 510–512.

Cross-references

- [Earthworms as Ecosystem Engineers](#)
[Microbes and Soil Structure](#)
[Microbes, Habitat Space, and Transport in Soil](#)
[Nature Conservation Management](#)
[Soil Biota, Impact on Physical Properties](#)

SOIL PENETROMETERS AND PENETRABILITY*

- Francisco J. Arriaga¹, Birl Lowery², Randy Raper³
¹U.S. Department of Agriculture-Agricultural Research Service, National Soil Dynamics Laboratory, Auburn, AL, USA
²Department of Soil Science, University of Wisconsin-Madison, Madison, WI, USA
³U.S. Department of Agriculture-Agricultural Research Service, Dale Bumpers Small Farm Research Center, Booneville, AR, USA

Synonyms

Cone penetrometer; Profile penetrometer

Definition

Penetrability. The ability or ease at which an instrument can penetrate the soil.

Soil penetrometer. Device consisting of a rod (shaft) with a pointed or blunt tip on one end that is pushed or hammered into the soil to measure soil penetration resistance, soil penetrability or strength.

Introduction

Soil penetrometers are instruments that can be used to measure the strength, compactness, or cohesiveness of a soil. Originally, penetration tests were conducted to determine soil load bearing capacity for engineering purposes. They have also been used extensively in geotechnical engineering to describe the stratigraphy of geological layers. In agriculture, penetrometers are traditionally used

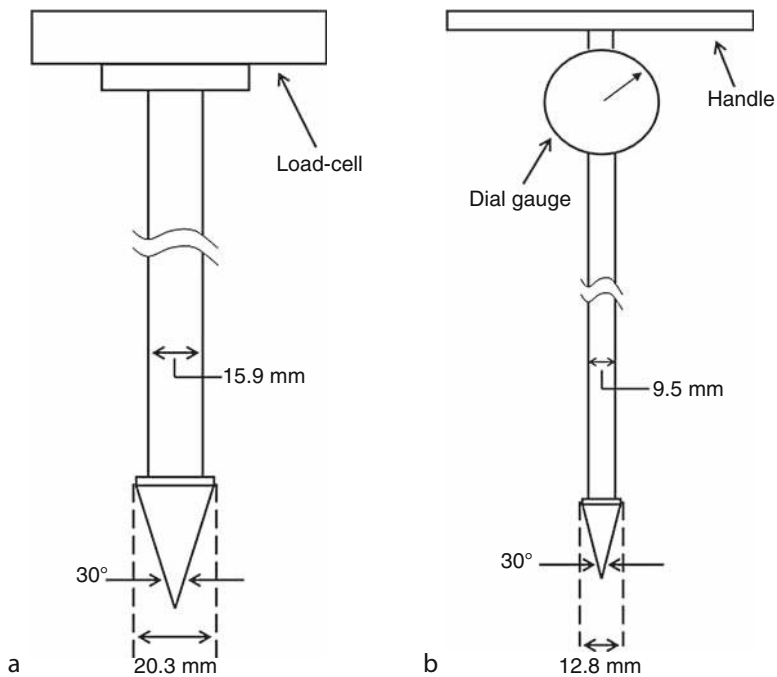
to measure soil compaction, although other uses, including soil mapping, have been implemented.

Design

Several designs have been proposed and are in use today, with many commercially available devices. Soil penetrometers in their most simple form consist of a metal rod that can be pushed or hammered into the ground manually. If it is pushed, the individual pushing the penetrometer would “sense” the force required to penetrate the soil. This requires a certain level of training and experience. However, most penetrometer designs incorporate a dial, spring loaded scale, or load cell to measure the force required to push the rod into the ground. The rod or shaft can have evenly spaced markings to measure the depth of readings. More complex designs incorporate electronic load cells and will be discussed in more detail later. Pocket penetrometers are convenient since, as the name implies, they can be easily carried in a pocket or bag. However, they have a blunt tip and only measure penetrability of very shallow depths, the soil surface, or exposed soil layers (Lowery and Morrison, 2002). Drop penetrometers are not pushed into the soil surface but rather dropped from a given height. The depth to which the drop penetrometer inserts itself into the ground gives the user an idea of soil compaction and penetrability at the soil surface. A laboratory version of the drop-cone penetrometer can be used to determine the liquid limit of cohesive soils (McBride, 2002). The dynamic cone penetrometer (Herrick and Jones, 2002) is yet another very simple device for measuring cone penetration resistance. According to Herrick and Jones (2002), the dynamic penetrometer method does not require one to push the penetrometer through the soil, nor does it need one to apply continuous force to the penetrometer. Dynamic penetrometers supply a known amount of kinetic energy (KE) to the penetrometer, which causes the penetrometer to move some distance through the soil. Penetration distance depends on the KE applied, the geometry of the penetrometer tip, and the soil penetration resistance.

The dimensions and geometry of the tip and the rod itself can affect penetration measurements. For agricultural purposes, most penetrometers consist of a stainless steel rod with a threaded, replaceable, tip attached to one end and a handle on the other. The tip is constructed of stainless steel with a 30° angle and can have two different base diameters, 12.8 or 20.3 mm (Figure 1) (ASAE, 1999a). The American Society of Testing and Materials (ASTM) suggests using a 60° cone; however, the application of this design is mainly intended for civil engineering purposes (ASTM, 2007). It is important to note that penetrometers with a cone that have an angle greater than 30° will exhibit lower penetrability (i.e., greater cone index values), while decreasing the diameter of its base will have the opposite effect. If one desires to make comparisons between treatments or soil conditions, it is important that the same type of penetrometer is used.

*All rights reserved



Soil Penetrometers and Penetrability, Figure 1 Soil penetrometer dimensions and examples of two common designs: (a) using a load-cell for force data measurement and, (b) a manual design with a dial gauge. Adapted from ASAE, 1999a.

Cone index and insertion speed

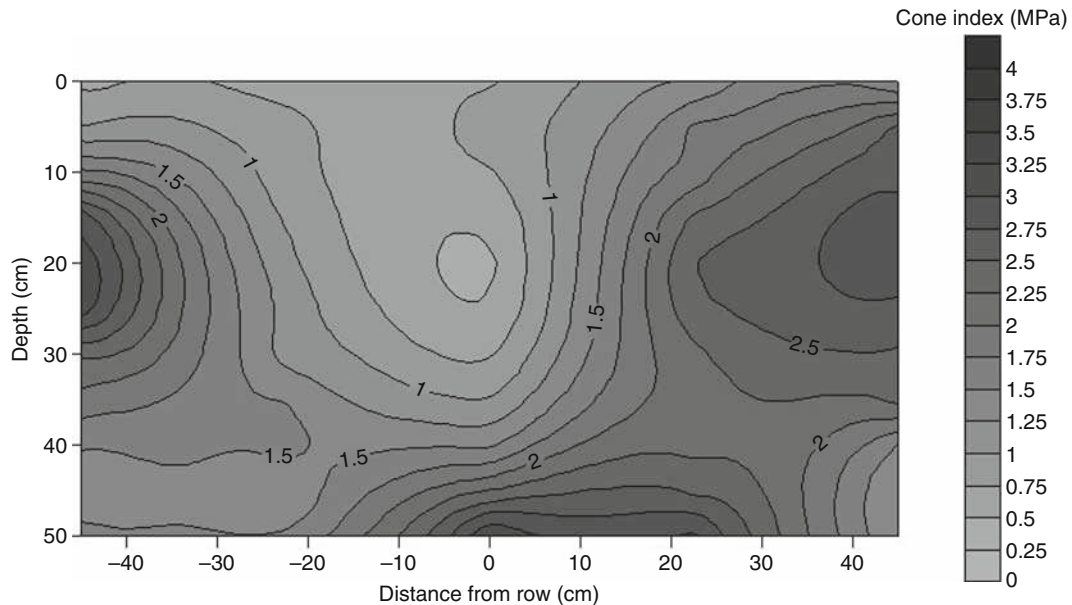
Penetrability measurements taken with a soil penetrometer can be expressed as the force required to push the cone into the ground. This force is typically referred to as the cone index and is defined as the force per unit base area (ASAE, 1999b). Further, it is recommended that a constant insertion rate of 30 mm/s be used when acquiring data with a soil penetrometer (ASAE, 1999b). However, it is noted that lower insertion rates would not introduce significant error to the measurement. In any case, it is important for the penetrometer rod to be pushed at a constant rate to avoid artificial spikes in the data.

Uses of soil penetrometers

Soil penetrometer designs also vary in the manner they record cone index and in the manner they are pushed. The most common and simple soil penetrometers are pushed into the soil manually by the user and measure cone index with either a dial or spring gauge. The main information that can be obtained with this type of device is the maximum cone index value and depth of the maximum value. This would be useful to determine the presence of hardpans and depth of subsoiling required to alleviate this condition. Cone index values >2 MPa are often considered to be root restricting (Taylor and Gardner, 1963; Raper et al., 1994).

Soil penetrometers used for most research purposes are designed to allow for the recording of the cone index data digitally as the rod/tip is pushed into the soil/material, as

well as the soil depth associated with the reading. This provides the user with a picture of the penetrability of a given soil profile. The force is typically measured with a load cell and the depth with a sonic depth indicator, an encoder, or a potentiometer. Various commercially available models rely on human power to push the device into the soil. However, Lowery (1986) developed a portable soil penetrometer that fits between crop rows and can be electrically driven into the soil at a constant speed, improving the quality of data collected compared to a manually pushed penetrometer. Other soil penetrometers have been designed to be driven hydraulically, thus allowing for constant insertion rates. Raper et al. (1999) developed a multi-probe soil penetrometer consisting of an array of five rods, each one with its own independent load-cell. This setup provides cone index data at five locations simultaneously and can be used to create contour plots of penetrability for soil profiles (Figure 2). Others have used soil penetrometers to map soil variability in agricultural landscapes since penetrometers can measure differences in penetrability between soil layers and depth to these layers (Grunwald et al., 2000, 2001). Arriaga and Lowery (2005) developed a three-dimensional (3-D) map of an eroded landscape with data collected with a soil penetrometer and used this and other information to estimate the total amount of soil organic carbon stored in various soil horizons. Other penetrometer designs have incorporated simultaneous determination of soil water content with some success (Morrison et al., 2000; Young et al., 2000).



Soil Penetrometers and Penetrability, Figure 2 Contour plot of cone index data collected with a multiple cone soil penetrometer for a soil profile in the autumn. Notice the area with lower cone index values is associated with the location of a bent-leg subsoiling operation conducted in the spring, and the area to the right with greater cone index values relates to the traffic middle. (Unpublished data)

Soil properties that affect penetrability

Penetrability is a function of several soil properties including soil water content and bulk density. Typically, penetrability and cone index values are directly correlated with soil bulk density (Lowery and Schuler, 1994; Grunwald et al., 2001). However, soil particle size distribution also affects penetrability, particularly clay content. The manner in which clay content affects cone index values is affected by soil moisture. Also, past tillage and traffic practices often cause increased bulk density in wheel tracks. Differences in cone index due to inherent soil conditions are sometimes difficult to determine due to differences caused by tillage and traffic events. Therefore, it is difficult to develop so-called pedo-transfer functions that would predict clay content, bulk density, or soil moisture from cone index values alone. Additionally, it is recommended to take data with soil penetrometers as close as possible to field capacity conditions (i.e., after a significant rainfall event) to minimize differences between treatments that might be caused by soil water content during soil investigations.

Summary

Soil penetrometers are useful tools that measure the penetrability, or strength, of a soil. They can be as simple as a rod or shaft with a blunt or sharp end, or complicated mechanically driven instruments with digital data collection systems. Regardless of their design, soil penetrometers measure soil penetrability and can detect differences in soil strength within a soil profile. Traditionally,

penetrometers in agriculture have been used to detect soil compaction issues and depth to compacted soil layers. However, with advances in electronics and computing power, several researchers have created innovative uses for soil penetrometers such as the development of pedotransfer functions and 3-D mapping of soil landscapes from cone index data. With the advent of new technologies and coupling of other sensors, soil penetrometers will continue to be important useful tools in agrophysics.

Bibliography

- American Society for Testing and Materials (ASTM). 2007. ASTM Standard D5778-07, *Standard test method for electronic friction cone and piezocone penetration testing of soils*. Book of Standards 04.08. West Conshohocken, PA.
- American Society of Agricultural Engineering (ASAE), 1999a. *Soil Cone Penetrometer*. ASABE Standard S313.3, February 1999 (rev. 2009).
- American Society of Agricultural Engineering (ASAE), 1999b. *Procedures for Using and Reporting Data Obtained with the Soil Cone Penetrometer*. ASABE Standard EP542, February 1999 (rev. 2009).
- Arriaga, F. J., and Lowery, B., 2005. Spatial distribution of carbon over an eroded landscape in southwest Wisconsin. *Soil and Tillage Research*, **81**(2), 155–162.
- Grunwald, S., Barak, P., McSweeney, K., and Lowery, B., 2000. Soil landscape models at different scales portrayed in virtual reality modeling language (VRML). *Soil Science*, **162**, 598–615.
- Grunwald, S., Rooney, D. J., McSweeney, K., and Lowery, B., 2001. Development of pedotransfer functions for a profile cone penetrometer. *Geoderma*, **100**, 25–47.

- Herrick, J. E., and Jones, T. L., 2002. A dynamic cone penetrometer for measuring soil penetration resistance. *Soil Science Society of America Journal*, **66**, 1320–1324.
- Lowery, B., 1986. A portable constant-rate cone penetrometer. *Soil Science Society of America Journal*, **50**, 412–414.
- Lowery, B., and Morrison, J. E., Jr., 2002. Soil penetrometers and penetrability. In Dane, J. H., and Topp, G. C. (eds.), *Methods of Soil Analysis, Part 4: Physical Methods*. Madison: Soil Science Society of America, pp. 363–388.
- Lowery, B., and Schuler, R. T., 1994. Duration and effects of compaction on soil and plant growth in Wisconsin. *Soil and Tillage Research*, **29**, 205–210.
- McBride, R. A., 2002. Atterberg limits. In Dane, J. H., and Topp, G. C. (eds.), *Methods of Soil Analysis, Part 4: Physical Methods*. Madison: Soil Science Society of America, pp. 389–398.
- Morrison, Jr., J. E., Lowery, B., and Hart, G. L., 2000. Soil penetrometer for sensing soil water content as in soil characterization for site-specific farming. In *Proceedings of Agrophysical and Ecological Problems of Agriculture in the 21st Century*. 6–9 September 1999, St. Petersburg: International Soil and Tillage Research Organization, Vol. 2, pp. 121–129.
- Raper, R. L., Reeves, D. W., Burt, E. C., and Torbert, H. A., 1994. Conservation tillage and traffic effects on soil condition. *Transactions of the ASAE*, **37**(3), 763–768.
- Raper, R. L., Washington, B. H., and Jarrell, J. D., 1999. A tractor-mounted multiple-probe soil cone penetrometer. *Applied Engineering in Agriculture*, **15**(4), 287–290.
- Taylor, H. M., and Gardner, H. R., 1963. Penetration of cotton seedling taproots as influenced by bulk density, moisture content, and strength of soil. *Soil Science*, **96**(3), 153–156.
- Young, G. D., Adams, B. A., and Topp, G. C., 2000. A portable data collection system for simultaneous cone penetrometer force and volumetric water content measurements. *Canadian Journal of Soil Science*, **80**, 23–31.

Cross-references

- [Bulk Density of Soils and Impact on their Hydraulic Properties](#)
[Compression Index](#)
[Crop Responses to Soil Physical Conditions](#)
[Cropping Systems, Effects on Soil Physical Properties](#)
[Databases of Soil Physical and Hydraulic Properties](#)
[Drought Stress, Effect on Soil Mechanical Impedance and Root \(Crop\) Growth](#)
[Field Water Capacity](#)
[Hardpan Soils: Management](#)
[Hardsetting Soils: Physical Properties](#)
[Management Effects on Soil Properties and Functions](#)
[Mapping of Soil Physical Properties](#)
[Pedotransfer Functions](#)
[Soil Compatability and Compressibility](#)
[Soil Penetrability, Effect on Animal Burrowing](#)
[Spatial Variability of Soil Physical Properties](#)

SOIL PHASES

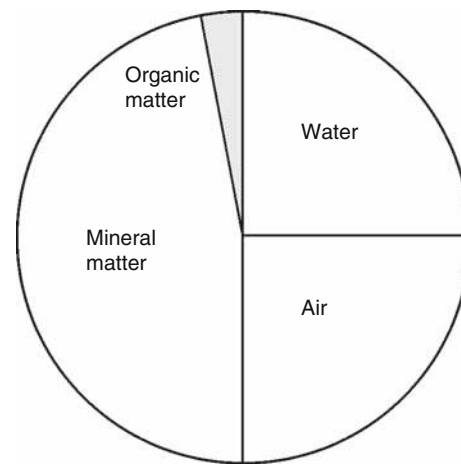
Jan Gliński
Institute of Agrophysics, Polish Academy of Sciences,
Lublin, Poland

Soil phase is a portion of a mixture that has: (1) differing properties from the contiguous material and (2) definite bounding surfaces (Fredlund and Rahardjo 1993).

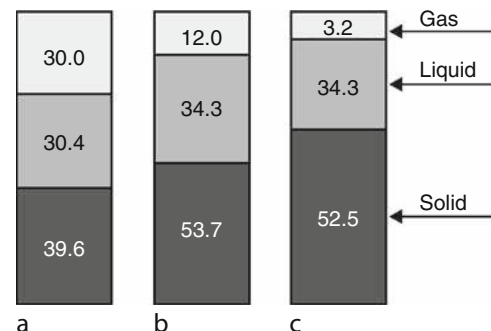
Soil is a heterogeneous, multiphase, disperse, and porous system. It is built of four phases: solid, liquid, gaseous, and living phase composed of organisms that participate in soil metabolism. In unsaturated soils, additionally, the air-water interface as an independent phase (or contractile skin) is distinguished (Fredlund and Rahardjo 1993). Phases play a significant role in formation soil, physical properties, and processes. A typical example of the proportion of phases in mineral soils is shown in Figure 1. In organic soils, which are in minority (about 1.2% of the world land area), these proportions are other, to the advantage of organic matter (at least 30%).

The distribution of solid, gaseous, and liquid phases within soil profile creates soil structure (soil architecture). When soil is dry, only solid particles and air within the pores are present, creating two-phase composition.

Phases have own volume and weight (except air phase), and they are not evenly distributed within the soil.



Soil Phases, Figure 1 Approximate proportions of phases in mineral soils (From Lal and Shukla, 2004; changed).



Soil Phases, Figure 2 Changes of a three-phasic system (in volumetric percent) of an upper layer of loess soil (acc. to Turski et al., 1997, changed), (a) after ploughing (soil density $1.06 \times 10^3 \text{ kg m}^{-3}$), (b) after wheat harvest (soil density $1.40 \times 10^3 \text{ kg m}^{-3}$), and (c) shortly after compaction by tractor (soil density $1.69 \times 10^3 \text{ kg m}^{-3}$).

The relative proportion of the phase change strongly depends on soil management practices. An example of such change due to soil compaction is shown in [Figure 2](#).

To determine numerous soil ecological functions, such as transport processes, buffering and transformation capacities, biological habitat, production of biomass (Blum, 2008), drainage and irrigation practices, phase diagram, and phase relationships based on ratios of the volume and mass are useful (Lal and Shukla, 2004).

The term *soil phase* is also used as a “subdivision of a soil type of other unit of classification having characteristics that affect the use and management of the soil, but which do not vary sufficiently to differentiate it as a separate soil type. A variation in a property of characteristic (e.g., degree of slope, degree of erosion, stone content)” (Gregorich et al., 2002).

Bibliography

- Blum, W. E. H., 2008. Threats to soil quality in Europe. In Tóth, G., Montanarella, L., and Rusco, E. (eds.), *JRC Scientific and Technical Reports*. Luxembourg: Office for Official Publications of the European Communities, pp. 5–10.
- Fredlund, D. G., and Rahardjo, H., 1993. *Soil Mechanics for Unsaturated Soils*. New York: Wiley, p. 14.
- Gregorich, E. G., Turchenek, L. W., Carter, M. R., and Angers, D. A. (eds.), 2002. *Soil and Environmental Science Dictionary*. Boca Raton: CRC Press LLC.
- Lal, R., and Shukla, M. J., 2004. *Principles of Soil Physics*. Boca Raton: CRC Press.
- Turski, R., Domżał, H., Borowiec, J., Flis-Bujak, M., and Misztal, M., 1997. *Soil Science. Exercises for Students of Agricultural Faculties AR (in Polish)*. Lublin: University of Agriculture.

Cross-references

- [Aeration of Soils and Plants](#)
[Field Water Capacity](#)
[Irrigation and Drainage, Advantages and Disadvantages](#)
[Oxidation-Reduction Reactions in the Environment](#)
[Pore Size Distribution](#)
[Root Responses to Soil Physical Limitations](#)

SOIL PHYSICAL DEGRADATION: ASSESSMENT WITH THE USE OF REMOTE SENSING AND GIS

Stanisław Białousz

Department of Photogrammetry, Remote Sensing and GIS, Warsaw University of Technology, Warsaw, Poland

Synonyms

Information systems; Satellite images; Soil degradation; Soil harms; Soil threats

Definitions and introduction

Soil physical degradation is involved in more general notion “soil degradation.” In common understanding, soil degradation is defined as “the general process by which

soil gradually declines in quality and is thus made less fit for a specific purpose, such as crop production” (Soil Science Glossary Terms Committee, 2008).

“Remote sensing (fr. télédétection) means combination of techniques and methods to recognize, identify and investigate objects (e.g., soils) and phenomena (e.g., temperature) from a distance, i.e., without contact with those.” Remote sensing offers also the possibility to study the relationship between objects and phenomena as well as the study of development in their properties” (Białousz, 1999, 511).

In many books and dictionaries different definitions of remote sensing could be found. For example, Sabins (1997) defines it as: “The term remote sensing refers to methods that employ electromagnetic energy, such as light, heat, and radio waves, as the means of detecting and measuring target characteristics.... The science of remote sensing excludes geophysical methods such as electrical, magnetic and gravity surveys that measure force fields rather than electromagnetic radiation.”

“A geographic information system (GIS) is the combination of skilled persons, spatial and descriptive data, analytic methods, and computer software and hardware-all organized to automate, manage, and deliver information through geographic presentation” (Zeiler, 1999, 46). GIS provides the tools to collect, manage, and display geographic data very efficiently and effectively (Longley et al., 2005, 438). Recently acronym GIS is developed also as Geographic Information Science. “GIScience is the set of fundamental issues (scale, accuracy, relationship between humans and computers) arising from the use of geographic information systems” (Longley et al., 2005, 438).

Many interdependent processes occur in soil at the same time, but only some of them, fortunately, lead to soil degradation. According to scientific research methods and based on them indicators of degradation, one can talk about the degradation of biological, chemical, or physical properties of soil and caused by them the degradation of soil functions. In this text we examine the types of physical soil degradation and their influence on the degradation of soil functions and the methods of their study.

In the ultimate approach, soil physical degradation could be also understood as the total destruction of the soil as a biologically active body, creating a medium for plant growth and food production. Total physical degradation means total disappearance of the soil (e.g., by erosion of river or sea, or open mining of minerals) or change in the function of the biological substrate of the living soil environment for plant development platform (the base) on which the road or buildings are constructed.

Many countries and international organizations direct their attention to soil degradation, analysis of the causes of this processes, methods of preventing degradation, and methods of degraded soils’ rehabilitation. In the USA there is a Soil Conservation Service, while in the European Union ongoing work leads to establishment of Soil Protection Strategy (EC Proposal for a Directive, 2006).

Studies on soil degradation take into account all elements of the cause and effect relationship. There is a reason (cause), which causes processes (acting factors). The receptor of these processes is the soil, in which harms occur.

Analyzing the causes and processes of degradation and knowing the properties of soil and surrounding environment, areas vulnerable to degradation could be delineated and the intensity of degradation could be predicted. Such studies require a lot of time and resource; therefore, they often examine the effects of degradation processes (harms). Harms are expressed by, among other things, a deterioration of soil physical properties (increasing of density – compaction, reduced permeability, reduced water holding capacity, deterioration of structure, crusting, cracking, loss of organic matter), reducing the depth of active soil layer by water and wind erosion, creeping, solifluction, landslides, and in extreme cases by soil erosion leading to the point where soil is biologically inactive until the rocks or soil are covered with a layer of asphalt or concrete.

Currently, new approach that it is cheaper and better to anticipate risks and prevent them, than to remedy their consequences later is creating. Thus, development of methods that allow the delineation of priority areas for soil risk is begun. European Soil Bureau Network formed a special working group for this purpose. Notion of priority areas for soil risk correspond with notion of soil threats. The concept of strategy for soil protection contained in the European Soil Framework Directive (EC Proposal for a Directive, 2006) distinguishes eight major threats of soils:

- Erosion, loss of organic matter, contamination, salinization, compaction, decrease in biodiversity in the soil, sealing, landslides, and floods.

All these risks and their effects, regardless of their position in the cause and effect chain, could be studied using three different approaches (Eckelman et al., 2006):

1. Qualitative approach, based on expert knowledge
2. Quantitative approach, based on measured data
3. Model approach, based on prediction of the extent of soil degradation from modeling, considering site factors and soil management

Remote sensing and GIS for soil degradation survey: general information

In examining both the risk of degradation, degradation processes, as well as its effects, methods that utilize GIS and remote sensing are useful. Soil as a continuous layer on the Earth surface and the processes occurring in it are interesting subjects to investigate using remote sensing methods, but also difficult because it is a three-dimensional layer, mostly covered by plants which hinder observation from the air. Therefore, three main elements of remote sensing technology must be carefully utilized:

acquiring, processing, and interpreting image and related data obtained from aircraft and satellites that record the interaction between soil and electromagnetic radiation.

Technology of data acquisition uses different ranges of electromagnetic spectrum (UV, visible, infrared, microwave) and recording equipment adapted to these needs: analog (photographic) and digital cameras, multispectral scanners, radars, radiometers and image radiometers. Now available are images recorded almost entirely digitally. Therefore, their processing and interpretation are quite easy. It should be kept in mind, however, that for comparative researches, for example, for studies of progression or regression of soil degradation, which also use photos that are 20–50 years old, require ability to work with pictures taken with photographic cameras.

Remote sensing data for study and modeling of soil degradation should satisfy several conditions. First of all, they should be recorded in the spectral ranges, and in those seasons in which environmental elements affecting the degradation and their effects are most visible (Bonn, 1996; Białousz, 1999; Girard and Girard, 1999). These conditions, though theoretically known, are very difficult to satisfy because of cloud cover, and availability and cost of equipment (satellite images programmed on a specific date are much more expensive). Only in a few research projects such registrations were feasible. Thus, in most cases the study of soil degradation makes use of images recorded for other purposes (map updating, cadastre, LPIS for Common Agricultural Policy) and images taken during current satellite missions. For that reason the digital processing of such data must be handled in a manner that eliminates image features, which obscure the effects of soil degradation, and when interpreting the results, using many elements of deductive reasoning and the available knowledge bases (Mulders, 1987; Białousz, 1999).

Remote sensing methods used in soil study utilize differentiation behavior of electromagnetic radiation in contact with the soil as it reaches the soil surface. This differentiation lies in the fact that the soil, depending on its state and its properties, absorbs and reflects in different spectral ranges of various amounts of radiation falling on it from the Sun, or from a radar antenna, and radiates different amounts of energy depending on properties, especially humidity. Differences between the soils can be detected and then interpreted, when the differences of their characteristics or properties cause measurable differences of energy reflected or radiated by the soil.

The identification of soil in images registered in the optical band utilize the knowledge that soils with higher organic matter content, wetter, and cloudy reflect less solar energy and appear darker in photographs, while soils with low organic matter content, drier, and with smooth surfaces, or that contain carbonates in the surface layer reflect more energy, and hence appear brighter in the pictures. There are many examples, where the boundaries of soils with different organic matter content or with differences in humidity are very clearly visible on aerial

photographs and satellite images (Soil Atlas of Europe, 2005). A large amount of research has been performed to determine the relationship between organic matter content, soil moisture, carbonate content, soil pigments and spectral characteristics of soils, and associated soil images in photographs (Baumgardner et al., 1970; Escadafal and Girard, 1988; Białousz, 1999). Based on these correlations, attempts at automatic mapping of organic matter and soil moisture have been made. Due to the complexity of these relationships, only few attempts have been successful.

A number of models describing the relationships between the geometry of the structural aggregates on the soil surface, the position of the Sun as a source of radiation, the position of the observing sensor, and the spectral characteristics of soils have been developed (Cieriewski and Verbrugghe, 1997; Cieriewski et al., 2004).

Methods of remote sensing studies of soil degradation

General research on the recognition and interpretation of soils in aerial and satellite images have provided a basis to analyze whether, and if so how remote sensing methods can be used to study soil degradation. The logic of these methods is, as it follows:

1. To determine the risk of degradation:
 - (a) For each type of threats to determine the set of internal factors, arising from the soil characteristics and external factors (climate, relief, land cover, anthropopressure) causing danger of degradation and its intensity
 - (b) Specify remote sensing data; what methods of their processing and interpretation will provide data to the model simulating the threat, or will immediately (without model) predict these risks and determine their spatial extent
2. To study the effects of degradation (degraded soil inventory)
 - (a) To determine how degradation processes influenced physical and chemical properties of surface soil layers: loss of organic matter, deterioration or loss of crumb structure, increasing compaction, worsening air, and water properties. These cases are generally known from studies on physical properties of soil
 - (b) To determine how changes in these properties affect the spectral characteristics of the soils, on soil temperature, the density and intensity of vegetation cover
 - (c) To determine how it will effect on the radiometric value of remote sensing images and on the images of soils obtained from various digital processing of initial data
 - (d) To determine whether the resulting differences in images of soil (or vegetation cover) are sufficient to detect the occurrence of soil degradation and

their delineation, according to the types of degradation

In both cases (1 and 2) the final goal of application of remote sensing methods is assessment of the risk of degradation or a statement regarding degradation already present. It is a broader approach than a simple one informing that the change of physical properties.

Remote sensing data can often be understood as a radiometric value of pixels being still subject to digital processing as well as data recorded during satellite missions brought for radiometric and geometric correction of images. For environmental research, including soil, not only are used radiometric values of pixels, but also derived products such as DTM and land cover maps.

For the study of different types of degradation, it is recommended that various types of remote sensing data and different methods of processing and interpretation are used. Source data and methods must also take into account the territorial scope of research: on a scale of one field, micro regional, and regional. We will perform such an analysis for the most important types of soil threats.

Soil erosion

“Soil erosion is the wearing away of the land surface by physical forces such as rainfall, flooding water, wind, ice, temperature change, gravity or other natural or anthropogenic agents that abrade, detach or remove soil or geological material from one point on the earth’s surface to be deposited elsewhere” (Soil Science Glossary Terms Committee, 2008). The result of erosion caused by rain and melting water is the loss of soil mass in the upper parts of the terrain and its deposition at the foot of the slopes, at the water reservoirs and transfer by rivers to seas and oceans. Measurable effect of erosion is a lowering of the surface of the eroded area. With the reference to the morphology of the soil profile the result of erosion is reduced thickness of humus horizon, its total removal and the exposure of the deeper horizons, or even the mother rock (parent material). The most common indicator of the intensity of the erosion is the amount of eroded soil expressed in tones per hectare per year. It is obtained from measurements in the field or from modeling.

Remote sensing and photogrammetric methods can be used both to measure the effects of erosion (small area) and to assess the risks of erosion through modeling. For small areas, parameters calculated with use of remote sensing data, useful to estimate the effects of erosion are: value slope angle, slope length, elevation, the area of land occupied by ravines (gullies) and rills and their volume, surface covered by permanent and annual vegetation, the area without vegetation during the greatest threat of erosion.

Many of these data can be obtained from large-scale aerial photographs (altitude, slope angle, slope length,

area and volume of gullies and rills) and from periodic registration of LIDAR.

The utility of remote sensing data to model the risks of erosion depends on the type of model, namely, the parameters used in the model. The most commonly used parameters are: slope angle, slope length, class of land cover, type of agriculture, terrain dissection by hydrography network, and density of road networks. All these parameters can be determined from the DTM and satellite imagery of high (Landsat ETM, SPOT, IRS), and very high (IKONOS, Quick Bird, WorldView) spatial resolution (Białousz and Baritz, 2006).

Beside the measurement, the real effects of erosion performed on small plots of experimental fields the erosion hazard modeling an inventory of the larger areas already affected by erosion of varying intensity are carried out.

Traditional methods of photointerpretation (the interpretation of stereoscopic aerial photographs), computer-assisted interpretation of digital aerial photographs or satellite images classification, and an object-oriented approach can be used. In each of the methods a relationship between the effects of erosion and soil eroded images is used. It is assumed in general that woodland soils and permanent meadows are not affected by erosion. Pastures, because of the possibility of overgrazing, too early or too late season of grazing can be affected by erosion.

In the early stages of erosion, when there is still a preserved (though shallower) humus horizon, eroded soils (in the upper parts of the slopes) are lighter, while in the foothills in the deluvial accumulation zone they are darker. They also have a distinctive texture image composed of bright streaks of fine material, stretching along the slope line.

In subsequent phases, when on the surface deeper horizons of soil or rock appear, the color of eroded sites may also be light, if lighter soils horizons (E) or bright rocks (limestone, sandstone) where exposed or dark, when on the surface is illuvial horizon, clay parent material, or other dark rock.

Advanced erosion of the loess areas is visible through the dendrites of ravines (gullies) with a depth of several meters. The intenseness of erosion at such sites can be expressed by the density of the network of ravines. This is readily calculated almost automatically using the appropriate functions of GIS software. The ravines are very clearly visible on all types of aerial and satellite images.

GIS technologies allow connecting satellite and aerial images with different thematic layers, such as: soil types, texture, geology, geomorphology, land cover, slopes, aspect and others. This allows by modeling or by a simple visual analysis to delineate eroded areas and the intenseness of erosion. Results of both, modeling and visual analysis require verification in the field.

Delimitation of eroded areas is easier if specially processed image (enhancement of clear tones, maps of brightness indices) is overlayed on a three-dimensional

image derived from a DTM that has been magnified vertically.

Landslides

Landslide is defined as “the movement of a mass of rock, debris, artificial fill or earth down a slope, under the force of gravity, causing a deterioration or loss of one or more soil functions” (Huber et al., 2009). There are two types of landslides: slow moving landslides and fast moving landslides.

As in the case of erosion there is the possibility:

1. Of inventory of landslide activity occurrence with estimation of volume of displaced material
2. To assess landslide hazard
3. To create a system for landslide control measures

In all of these cases the role of remote sensing and GIS technology could be meaningful.

During the mapping, where landslides have occurred, facts observed on the ground are taken into consideration (they can be marked on a map or their coordinates measured using GPS) as well as specific terrain microforms identifiable in stereoscopic aerial photographs, or satellite imagery complemented by a DTM. In recent years, to identify these forms satellite radar interferometry and three-dimensional images generated from LIDAR have also been used.

For landslide hazard assessment models, the following key parameters are used: slope angle, slope length, land cover, drainage network and road network (as GIS layers), parent material (texture, aggregate stability, sequence of permeable and impermeable layers, depth of impermeable layers) climatic date, and current site of identified landslides.

The parameters for the slopes and forms of the terrain (convex, concave, flat) can be obtained from the DTM. The DTM should have a spatial resolution from 15 to 20 m. and a vertical precision of 30–50 cm. It should therefore be created from aerial photographs, or from aerial LIDAR registration. DTMs created from aerial photographs for the LPIS require careful checking before using it for such purposes. Classes of land use can be obtained from high resolution satellite images, or from orthophotomaps performed for LPIS.

Layers of parent material can be obtained from maps (databases) of soil, geological, or geomorphological maps at scales of 1:25,000 and larger.

System for landslide control measures should include fixed points for field measurements (analogous to the geodetic measurements of displacement), a base for terrain registration by LIDAR and reference points for processing LIDAR aerial images. Analysis of all mentioned data should take into account also data on rainfall (seasonal distribution and extreme values), snow cover, and freezing depth of soil to obtain information making possible to predict what amount of rainfall in a given area can cause landslides to occur.

Floods

Three kinds of applications of remote sensing and GIS technology can be identified:

1. To delineate the areas flooded by the flood waters. Theoretically, aerial infrared photographs are the best, but clouding associated with flooding causes the limitation to their implementation as well as for registration of satellite images in the optical band. Cloudless skies usually appear a few days following the peak flood wave, so the images do not register all the flooded areas. Radar images can be taken regardless of the weather and often they are the only documents that show all the flooded areas. There is an international agreement in effect by which the owners of remote sensing systems may at the request of interested countries pass along, as soon as possible transfer (usually for the next day), images recorded for flooded areas. This facilitates the tracking of the flood wave propagation as well as organizational measures for rescue operations. Such images of the Vistula River Valley were registered on 11 May 2010 by the TerraSAR-X system during the floods of May 2010. Images registering flooded areas make it easy to assess the damage and work on removing the effects of floods.
2. To control the state of flood banks. Levees along rivers in some countries are tens of thousands of kilometers in length. Current monitoring of their condition directly in the field requires much time and ample manpower. Aerial photographs taken for other purposes can be used to analyze levees and their environs. On enlarged and processed images, results of damage to the ramparts are visible, often due to damage by people and cattle in areas outside the paved passages, losses caused by animals by the river zone, and leakages of water. The best for these purposes are infrared images taken in early spring at high water levels in the river, but this kind of pictures is not always available.
3. To model flood risk. This pertains to two kinds of models. Models predicting the status (height) of water in the river and models of risk of land flooding. For the first type of models, data for the whole catchment are necessary, and for the second type of models, only data for the valley in the range of potential flooding.

In both cases, essential data are: land cover classes, DMT, and hydrography network. Land cover classes and their area could be determined with precision satisfying modeling by classification of multispectral satellite images or by visual interpretation of color composite

images obtained from multispectral images. They should register one or two infrared spectral bands and have pixel of 5 m or less.

Land cover classes are used to determine terrain roughness indices necessary to calculate speed of flood wave and to estimate soil retention ability. Images should be registered when it is the easiest to identify land cover classes, which affect terrain roughness: arable land, meadows and pastures, bushes, forests, and built-up areas. Consequently, in temperate zone the best time for it is May, second half of August, and September. Lately, new attempts to determine terrain roughness indices have been made with LIDAR, but there is no need for such high accuracy in modeling.

DTM should have vertical accuracy around 20–30 cm. Only direct measurement in the terrain (too costly), large-scale aerial images or LIDAR images can provide such precision. The same large-scale aerial images used to create DTM might be useful to perform land cover maps, but such procedure takes significantly more time and funds, than based on satellite images.

Land cover maps or color composite images from satellite images supply data not only to determine terrain roughness indices, but are proved to be useful to assign polders and storage reservoirs location as well as to planning valley monitoring or to carrying out rescue action. Nevertheless, those are commonly overlooked, as liable services prefer using maps.

Loss of organic matter

Loss of organic matter in common language means the loss of organic matter in the topsoil. It is a process that naturally occurs in all arable soils and in drained organic soils. In a good agrotechnical situation, these losses on mineral soils are offset by organic fertilization and crop rotation. When can a loss of organic matter be considered as soil degradation? This is difficult to determine, because the thresholds may be different depending on climate zone and soil use. It is understood that in Europe under conditions where the soil has less than 1% of soil organic carbon, and without organic fertilization deficit of mineral nitrogen may occur, which leads to a reduction in biomass production and to a decrease in soil organic matter (SOM) content (Soil biodiversity, 2010).

Remote sensing and GIS technologies can help in analysis of soil organic matter diminution in arable land. As with other phenomena, the SOM inventory and delineation, the areas with a greater risk of loss of SOM should be differentiated. In the case of inventory the mentioned earlier relationship, that soils with higher organic matter content are darker and reflect less solar energy (below 10%) in each of the ranges of visible and near infrared band is used. This leads to darker tones of these soils (dark gray, black) on aerial photographs and to lower radiometric values of pixels in the digital images.

Several attempts have been made to determine the quantitative correlation between the amount of reflected

solar energy, the optical density of aerial photographs, radiometric values of pixels, and the content of SOM. A set of indices has been used, among others: brightness indices, image enhancement, contrast stretching, and other digital image processing to increase the strength of correlation. The aim of these studies was to elaborate and test automated methods of delineation of soil boundaries according to content of SOM. However, results have been modest, because the appearance of soil on remote sensing images also depends on other soil properties as well as external factors. Practically it is possible to delineate the areas with a similar SOM content. The amount of SOM for each area should be measured by laboratory methods. Remote sensing data thus should be recommended as supporting material (Baumgardner et al., 1970; Białousz, 1999; Girard and Girard, 1999).

For analyzing loss of SOM multi-temporal remote sensing data could be useful. They may show diminution of the surface of soils rich in SOM as a result of artificial drainage or erosion. The second case is observed in the chernozems of Central and Eastern Europe formed on loess, particularly in countries where large-area state farms are operated.

Remote sensing methods can also be useful to investigate the loss of SOM in organic soils as a result of their drainage and tillage, because interpretation of images helps delineation of areas that are in intensive cultivation. Also, in particular cases make possible to detect differentiation of soil cover by differences of soil temperature and humidity, which are calculated on the basis of data registered in the thermal and microwave band. In connection with ground-based surveys, areas with different diminution of SOM could be detected and delineated.

In advanced studies, performed in the framework of the global balance of CO₂, remote-sensing data from the optical, thermal, and microwave bands are used to calculate LAI, biomass, evapotranspiration, moisture, soil temperature, and other indices. These parameters together with land cover data are implemented to the models that allow to calculate the ecosystem's CO₂ balance (Hese et al., 2005; Calvet et al., 2005). Positive balance of CO₂ (CO₂ released more than assimilated by plants) means a degradation of SOM. Studies of this type were designed and partially executed in the USA and Europe (CarboEurope, Geoland 2 programs).

Soil surface sealing

Soil surface sealing in the broader sense includes "all land development for human settlement-related activities by which previously undeveloped land is urbanized, i.e., agricultural, forest or natural land are turned into built-up areas" (Jones et al., 2008). It is also called as a land consumption. In more specific form, "soil sealing means the destruction or covering of soil for buildings, constructions, and layers or other bodies of artificial material that may very slowly permeable to water causing a deterioration or loss of one or more soil functions" (EC Proposal for a Directive, 2006).

Indicator of soil surface sealing may be the absolute area of sealed soils, the rate of sealed soils such as per 1 km², or per capita (Huber et al., 2009). Experience has shown that remote sensing data and GIS technology are indeed useful for the determination of these indicators. It would seem that the surface of sealed soils can be quickly calculated from cadastral data. However, the cadastral data do not include all surfaces that are sealed. Because the problem concerns mainly urban areas and their surroundings, the full data for those areas can be obtained from the base maps in scales of 1:500 or 1:1,000, but this requires a lot of work, even when the maps are already in digital form.

Each country protecting soils draws up an annual soil balance, which shows how much new agricultural and forested land has been converted to urban areas. Such data is available in each country's cadastral and statistics offices, urban planning and environmental organizations. But national or regional registers of sealed soils do not exist. Some cities in Europe calculated the surface of sealed soils, to estimate how much water flowing to the sewage treatment plant comes from households, and how much from the roofs of buildings and concrete-covered spaces. Some cities have introduced a so-called roof tax.

However, this is not the most important reason to know how large the surface of sealed soils is. Equally important is the impact of those areas on the city's microclimate. At the time of the writing of this text, it was 32°C out of the building. Some windows of the room are overlooking the garden (non-sealed soil), and the others the street with asphalt and concrete (sealed soil). Even without any measurements, impact of sealed soils on microclimate of the room and on the mood of the writer was perceptible. Sealed soils cause also a rapid runoff of rainwater into rivers and increase the risk of high water flooding.

The quickest way to calculate the area of sealed soils is to use large-scale digital maps showing buildings, concrete-covered surfaces, bitumen, and green areas as well as orthophotomaps generated from aerial photographs or from satellite images with a size of pixel around 1 m. In the first step homogeneous areas in terms of development intensity are delimited on orthophotomaps. In each homogenous area test zones are determined (randomly or systematically). For which test zone the surface of sealed soils is calculated using the detailed digital maps. Then, using the orthophotomaps, sealed surfaces and the various indicators are calculated for homogeneous areas and for the whole city. Calculations made by this method for Warsaw (Białousz, 2008) showed that in the district with the nineteenth century buildings, sealed soils occupy 96% of the total area and, respectively, 52% in the zone of big blocks, 26% in residential zone, and 20% in urban green areas. On average, sealed soils cover 47% of the built-up areas and 22% of the area within the administrative borders of Warsaw. The rate per inhabitant amounted to 66 m².

Surfaces of sealed soils and new urban areas (land consumption) will be calculated quickly after the creation of

CORINE Land Cover (CLC) database based on satellite images of very high spatial resolution (pixel 1 m and less). Reference zones will be needed, however, because part of the terrain is covered by trees and bushes; therefore the real surfaces of these terrains are not visible on orthophotomaps.

Salinization

Soil salinization is defined as “accumulation of water soluble salts in the soil, causing a deterioration or loss of one or more soil functions. The accumulated salts include sodium, potassium, magnesium and calcium chlorides, sulphates, carbonates and bicarbonates” (Huber et al., 2009).

Soil salinization causes salt efflorescence on the surface of soil, the disappearance of crumb structures, susceptibility to dispersion of the surface layer at a higher moisture content, the creation of superficial crust when dry, and less dense vegetation causing smaller biomass. For the delimitation of extent and intensity of the salty soil direct features could be used: increasing the brightness of the soil surface, and indirect features: lower density of vegetation and diminished plant vigor. Under natural conditions, meadows and pastures salted soils give rise to specific distinctive vegetation of a darker color than of vegetation on salt-free soils, which is visible on the images.

Many studies proved the usefulness of aerial photographs and satellite images later in the inventory of saline soils (USA, India, Pakistan, Iraq, Egypt, the European Mediterranean area, regions around the Caspian Sea, and other areas of semidry zone). Apart from satellite images, GIS thematic layers that provide data on irrigation systems, groundwater depth, and the parameters characterizing the soil and water for irrigation are commonly used. With such a multifactorial analysis the relationship between groundwater depth and salinity of the surface layer in the Nile Delta has been found as well as salinity and the efficiency of drainage system in the delta of the Rhone. GIS technology together with satellite images and historical data makes modeling of salinization risks a lot easier.

Compaction

“Soil compaction occurs when soil is subject to mechanical stress often through the use of heavy machinery or overgrazing, especially in wet soils conditions. Compaction reduces the coarse pore space between soil particles, thereby increasing the bulk density with the result that the soil partially or fully loses its capacity to absorb water. Compaction also affects subsoil layers” (Eckelman et al., 2006).

Application of remote sensing data and GIS technology to inventory the areas affected by the soil compaction and to threat's modeling is more difficult than to other types of soil degradation. Soil compaction causes changes in certain soil properties, which can be recognized by remote sensing methods, that is, deterioration of soil structure, restriction of root growth, decrease in water storage

capacity, fertility, and biological activity, thus reducing the density of vegetation and biomass. Rainwater periodically stagnant on the soil surface may be supplementary feature characterizing compacted soils. Detection of these features directly on the surface of bare soil or indirectly by the vegetation lead to identification of this type of degradation.

Because of the repetition of passages of heavy machinery by the same places (zones near the edges of plots, area of relapses, strips between the trees in the orchards), the intensity of soil compaction in these places is higher than in other parts of the field. For that reason a minimum and maximum values within the field, rather than one average value, should be shown.

At the scale of one field it is recommended to determine soil compaction on the basis of direct field measurements (analysis of the soil profile and soil density measurements with penetrometer). For larger areas, aerial photographs or satellite images can be used to determine the sample plots and to extrapolate the results obtained on the sample plots, and GIS technologies to take into account other factors contributing to soil compaction. Modeling based on soil texture, slope value, CEC, water regime, and economical data (type of farming, saturation by heavy machinery, frequency and periods of use of fertilizers and pesticides, etc.) can separate the zones with different susceptibility to soil compaction. According to the simplified model, for example, such zones have been separated for the southwestern Poland with an accuracy corresponding to a map at the scale of 1:250,000 (Białousz and Rozycki, 2006).

This type of soil degradation, which so far mainly has been studied in laboratory-scale and in a single field scale, has an impact not only on the yield of plants, but like soil sealing accelerate also runoff of rainwater into the rivers, therefore increase the risk of flooding. More accurate models to determine the areas already affected by the soil compaction, and delimitation areas that can be potentially affected are not yet completely tested.

Contamination

This type of degradation is the hardest to investigate using remote sensing and GIS methods. Such analysis, as well as on the other types of degradation use the physical properties of soil changes and vegetation cover changes caused by the contamination of soils. These changes (properties of soil and vegetation) depend on the type of contamination. If it is, for example, fallout dust from the cement plant, they will lighten the soil surface and reduce the acidity, which will affect the structure of the surface layer. Both of these changes, as well as the impact of emission from the chimneys of other types of industrial plants influence weekly on the differentiation of soils in the images. However, there are spectacular examples. Few days after precipitation of snow the darker area around the chimney of industrial plants was visible on the satellite images. Contamination, like soil compaction generally impairs

soil biodiversity, soil fertility and consequently reduces the density and biomass crops (European Atlas of Soil Biodiversity, 2010).

There have been successful attempts carried already (Zawadzka, 2005) at exploring the correlation between soil contamination and the results of processing multispectral satellite images. Processing was supported by data input from GIS thematic layers. A significant correlation was found between the content of lead, zinc, and copper, and the weighted sum of the spectral channels of the ASTER system. Color composites generated from multispectral satellite images and GIS thematic layers can be fully used to design monitoring networks in the areas affected by contamination, primarily from industrial sources.

Desertification

Desertification is not only an ecological problem, but also a social and economical, and in some regions a political one. The term “desertification” is not about enlarging the area of deserts, but refers to a loss of productivity of the land due to farming practices in dryland areas.

Drylands are characterized by a precipitation/potential evaporation ratio of less than 0.65 (wiki/Desertification, 2010). Drylands called also as the hyperarid, arid, semi-arid, and dry subhumid zones cover 35% of Earth land surface, and hosts a billion people in more than a hundred countries (Middleton and Thomas, 1997). The largest areas of degraded drylands are in sub-Saharan Africa, in Asia, and Latin America. The consequences of desertification are visible also in Mediterranean zone, in Central and Eastern Europe (Toth et al., 2008; Soil Atlas of Europe, 2005).

Problem of desertification is so serious that many international organizations, governments of majority of countries, and also scientific institutions have intensively taken care of it. The United Nations has formulated in 1994 Convention to Combat Desertification (UNCCD). It has been ratified by 184 institutions and governments, 38 European governments among this number. According to this Convention, “Desertification means land degradation in arid, semi-arid and dry sub-humid areas resulting from various factors, including climatic variations and human activities”.

The main factors causing this kind of degradation are: overgrazing, cutting trees and bushes for fuel, overexploitation of water and lowering of groundwater table caused by this, and cultivation of the terrain that should be protected by permanent vegetation. Visible results of desertification are: soil erosion, vegetation disappearance, and dunes transgression. That is why the effects of desertification are very well visible in aerial and satellite images. Rare appearance of clouds in dry and semidry zones facilitates registration of images.

Analogically to the investigation of the results of desertification, one can observe extent and efficiency of remediation actions, such as plantation of trees and bushes

bands, protecting soils against wind and erosion, fixation of the structure of topsoil layer, irrigation infrastructure and its extent. Actually there are many kinds of remote sensing data and it is easy to choose images of adequate spatial resolution, acquisition date, and spectral bands; so we do not enumerate the preferred images. Even simple color compositions generated from multispectral Landsat images are very useful for these purposes. One can use also images from systems dedicated to vegetation analysis, ex. SPOT Vegetation or from meteorological satellites. Images registered by ground penetrating radar can give information on presence and depth of groundwater table.

Very important advantage of remote sensing and GIS methods is that satellite images give synoptic view of terrain, facilitating connection of analyzed phenomena with landscape. GIS thematic layers and DTM provide data for analysis of causes and also for designing of remediation.

In Internet, conference proceedings, and journals one can find thousands of articles about desertification, remediation methods, and examples of successes and failures. World Atlas of Desertification has been also published (Middleton and Thomas, 1997). Research results show that it is easier to solve technical and ecological problems of desertification, than problems resulting from poverty, local traditions, lack of initiative of local governments.

Soil drought is an intermediary state between desertification and normal conditions for vegetation growth. Soil drought means that during the vegetation period there are weeks or even months of deficit of water available for plants. This deficit decreases yield, even 30% and more, but they do not cause a visible degradation of soil besides the loss of organic matter.

Areas touched by soil drought, like desertification, are investigated with use of satellite images and field measurements. The most frequently calculated indices in consecutive decades of vegetation periods are: NDVI, plant moisture and temperature, soil moisture in roots layer. In many countries maps of spatial distribution of these indices and maps of soil drought are published regularly. Besides cognitive goals, these maps are also useful for models of yield prediction with use of remote sensing methods.

Conclusion

Soil degradation causes changes in the appearance of the surface layer of soil: usually brightens it, reduces water capacity, alters thermal emissivity, and changes dielectric properties. Some of these changes can be measured by remote sensing methods, which facilitates the detection and delimitation of areas with degraded soil. From satellite and aerial images and from GIS thematic layers one can generate data like: morphometric parameters of the terrain, land cover classes, biomass, temperature and humidity of the surface layer, which implemented to models, make possible to predict risk of various types of degradation, its range, and intensity.

Abbreviations

- CEC—Cation exchange capacity
 CORINE—Coordination of information on the environment
 DTM—Digital Terrain Model
 E—Elluvial horizon
 EC—European Communities
 ESBN—European Soil Bureau Network
 ENVASSO—Environmental assessment of soil for monitoring
 ETM—Enhanced Thematic Mapper
 GIS—Geographical Information System
 GPS—Global Positioning System
 IRS—Indian Remote Sensing Satellites
 LIDAR—Light detection and ranging
 LPIS—Land Parcel Identification System
 NDVI—Normalized Difference Vegetation Index
 SOM—Soil organic matter
 SPOT—Satellite pour l'Observation de la Terre
 UNCCD—United Nations Convention to Combat Desertification
 UV—Ultra violet

Bibliography

- Baumgardner, M., Kristof, S., Johannsen, C., and Zachary, L., 1970. Effects of organic matter on multispectral properties of soils. *Proceedings of the Indian National Science Academy*, **79**, 413–422.
- Bialousz, S., 1999. Soil cover investigation with use of remote sensing. In Zawadzki, S. (ed.), *Gleboznawstwo*. Warsaw: PWRiL, pp. 511–538 (in Polish).
- Bialousz, S., 2008. Current problems in soil protection as seen from Poland. In *Europaischer Bodenschutz*. Berlin: Universitätsverlag der TU Berlin, pp. 117–140.
- Bialousz, S., and Baritz, R., 2006. Auxiliary data for risk assessment in soil protection. In Eckelman, W., Baritz, R., Bialousz, S., Bielek, P., Carre, F., Houskova, B., Jones, R. J. A., Kibblewhite, M., Kozak, J., La Bas, Ch., Toth, G., Varallyay, G., Halla, M. Y., and Zupan, M. (eds.), *Common Criteria for Risk Area Identification According to Soil Threats*. Italy: JRC Ispra. ESBN Research Report No. 20. EUR 22 185 EN.
- Bialousz, S., and Rozycki, S., 2006. *Simplified model for soil compaction risk delimitation with use of soil database, DTM and satellite data*. Discussion paper for Soil Information Working Group ESBN, JRC Ispra.
- Bonn, F., 1996. *Precis de Teledetection*. Sainte-Foy: Press de l'Université de Québec.
- Calvet, J. C., Viterbo, R., and Friend, A., 2005. Assimilation of remote sensing data to monitor the terrestrial carbon cycle. *Geographical Research Abstracts*, **7**, 4647–4650.
- Cierniewski, J., and Verbrugge, M., 1997. Influence of soil surface roughness on soil bidirectional reflectance. *International Journal of Remote Sensing*, **18**, 1277–1288.
- Cierniewski, J., Gdala, T., and Karnieli, A., 2004. A hemispherical-directional reflectance model as a tool for understanding image distinctions between cultivated and uncultivated bare surfaces. *Remote Sensing of Environment*, **90**, 505–523.
- EC Proposal for a Directive of the European Parliament and of the Council establishing a framework for the protection of soil and amending Directive, 2006. Bruxelles COM (2006), 232 final.
- Eckelman, W., Baritz, R., Bialousz, S., Bielek, P., Carre, F., Houskova, B., Jones, R. J. A., Kibblewhite, M., Kozak, J., La Bas, Ch., Toth, G., Varallyay, G., Halla, M. Y., and Zupan, M., 2006. *Common Criteria for Risk area Identification According to Soil Threats*. Italy: JRC Ispra. ESBN Research Report No. 20, EUR 22185 EN.
- Escadafal, R., and Girard, M. C., 1988. La couleur des sols: appréciation, mesure et relations avec les propriétés spectrales. *Agronomie*, **8**(2), 147–154.
- European Atlas of Soil Biodiversity, 2010. *European Soil Bureau Network EC*. Luxembourg: Office for Official Publications of the European Communities.
- European Commission, 2010. *Soil biodiversity: functions, threats and tools for policy makers*. Report for European Commission. Bruxelles: EC DG Environment, 250 pp.
- European Soil Bureau Network, E. C., 2005. *Soil Atlas of Europe*. Luxembourg: Office for Official Publications of the European Commission. 128 pp.
- Girard, M. C., and Girard, C. M., 1999. *Traitemet des Donnees de Teledetection*. Paris: Dunod.
- Hese, S., Lucht, W., and Schmullius, C., 2005. Global biomass mapping for an improved understanding of the CO₂ balance. *Remote Sensing of Environment*, **94**, 94–104.
- <http://en.wikipedia.org/wiki/Desertification>
<http://pubs.usgs.gov/gip/deserts/desertification>
<http://soils.usda.gov/use/worldsoils/landdeg/degradation.html>
<http://www.fao.org/docrep/010/a1598e06.htm>
<http://www.unccd.int/cop8/docs/parl-disc.pdf>
- Huber, S., Prokop, G., Arrouays, D., Banko, G., Bispo, G., Jones, R. J. A., and Kibblewhite, M., 2009. *Environmental Assessment of Soil for Monitoring*. Luxembourg, Office for the Official Publications of the European Communities, EUR 23490 EN/1. Indicators and Criteria, Vol. I.
- Jones, R. J. A., Verheijen, F. G. A., Reuter, H. I., and Jones, A. R., 2008. *Environmental Assessment of Soil for Monitoring*. Luxembourg: Office for the Official Publications of the European Communities, EUR 23490 EN/5. Procedures and Protocols, Vol. V.
- Longley, P., Goodchild, M., Maguire, D., and Rhind, W., 2005. *Geographic Information Systems and Science*. New York: Wiley.
- Middleton, N., and Thomas, D., 1997. *World Atlas of Desertification*. London: Arnold. 182 pp.
- Mulders, M. A., 1987. *Remote Sensing in Soil Science*. Amsterdam, The Netherlands: Elsevier.
- Sabins, F. F., 1997. *Remote Sensing: Principles and Interpretation*. New York: W.H. Freeman.
- Soil Science Glossary Terms Committee, 2008. *Glossary of Soil Science Terms 2008*. Madison: Soils Science Society of America, p. 92.
- Toth, G., Montanarella, L., and Rusco, E., 2008. *Threats to Soil Quality in Europe*. Luxembourg: Office for Official Publications of the European Communities, EUR 23438 EN.
- Zawadzka, B., 2005. *Use of Satellite Images for Estimation of Quantity of Trace Metals in the Soil*. Ph.D. thesis, Pulawy, Institute of Soil Science and Plant Cultivation (in Polish).
- Zeiler, M., 1999. *Modeling Our World*. Redlands: ESRI Press.

Cross-references

- Color Indices, Relationship with Soil Characteristics
 Cracking in Soils
 Desertification: Indicators and Thresholds
 Ground-Penetrating Radar, Soil Exploration
 Image Analysis in Agrophysics
 Physical Degradation of Soils, Risks and Threats
 Remote Sensing of Soils and Plants Imagery
 Salinity, Physical Effects on Soils

[Shrinkage and Swelling Phenomena in Soils](#)
[Soil Compaction and Compressibility](#)
[Surface Roughness, Effect on Water Transfer](#)
[Water Erosion: Environmental and Economical Hazard](#)

SOIL PHYSICAL QUALITY

Blair M. McKenzie¹, Judith M. Tisdall², Wendy H. Vance³

¹Environment–Plant Interactions, Scottish Crop Research Institute, Dundee, UK

²Department of Agricultural Sciences, La Trobe University, Bundoora, VIC, Australia

³School of Environmental Science, Murdoch University, Murdoch, WA, Australia

Synonyms

Soil physical health

Definition

Soil Physical Quality is the ability of a given soil to meet plant and ecosystem requirements for water, aeration, and strength over time and to resist and recover from processes that might diminish that ability. Concepts of soil physical quality can be applied to individual soil horizons, profiles, or areas classified to a common soil type.

Introduction

Soil physical quality is determined by a combination of soil texture, structure, and morphology and relates to the capacity of a soil to function (Karlen et al., 1997). Soil texture, the relative proportions of sand, silt, and clay in the soil and soil structure, the arrangement of these mineral components with soil organic matter, are described elsewhere (see [Soil Phases](#)). Soil morphology describes how soil looks, is handled, and behaves in the field. Morphology is usually determined through soil survey taking into account soil depth, stoniness, and the presence and depth of various horizons and other soil layers.

Soil properties that limit or lead to improved crop yields have been identified and are often taken as standards (Tisdall and Adem, 1988; Reynolds et al., 2008). An example is that a soil with a penetrometer resistance of greater than 2 MPa will decrease root elongation by more than 50% (Gregory, 2006). More detailed explanations of this example can be found elsewhere (see [Root Responses to Soil Physical Limitations](#)). The standards may apply to an individual plant species, a crop or plant community in a managed ecosystem, or may relate to a process of root growth. Standards for root, plant, or crop growth quantify soil characteristics that may decrease crop yield. By comparison of specific soil properties with the standards for root growth, soil management may be identified to improve deficient soil characteristics (Tisdall and Adem, 1988). Measurements associated with different standards can be combined and indicators that provide relative

measures or indexes of soil physical quality developed. Pedotransfer functions (see [Pedotransfer Functions](#)) have been used (da Silva and Kay, 1997) to predict one soil characteristic from one or more other characteristics. This estimation may enable faster or cheaper estimation of soil physical quality.

The physical characteristics of the soil, such as soil water, infiltration, soil aeration, soil temperature, and mechanical resistance, are considered individually elsewhere (see [Soil Water Flow](#); [Aeration of Soils and Plants](#); [Temperature Effects in Soil](#)). Here, the combination of the physical characteristics is related to soil physical quality and the ability of the soil to be used for particular purposes, particularly plant growth. When limiting nutrients, water, aeration, temperature or mechanical resistance can impair seedling emergence and root growth. A productive soil environment requires coordination of these soil physical characteristics. The structure of the soil does not directly affect plant growth but does affect the supply of water and gases, temperature and mechanical resistance that directly influence plant growth (Letey, 1985; Boone, 1988). The magnitude of the soil physical characteristics differs with time and position in the soil profile, especially in relationship to rainfall and irrigation. Values for soil physical characteristics that allow a balance for optimum plant growth need to be understood, because different crops may have different responses. Rice (*Oryza sativa* L.) grown as paddy (i.e., under waterlogged condition) is the basis of feeding a large proportion of the world's population. Other cereals would not be productive if grown under the same conditions. Similarly, if only one soil characteristic were considered, the overall growth of the plant may be limited by another (Letey, 1985). The relationship between water and aeration is opposite to that between water and soil strength. If the water content increases toward a waterlogged condition, aeration decreases and may impair root growth. An increase in water content also decreases mechanical resistance and allows penetration of roots and emergence of seedlings. Thus, soil physical quality needs to be properly defined, understood, and managed.

Because soil physical quality can, to varying degrees, be manipulated by soil management, several indexes or scales have been, and are being, developed to specifically quantify soil physical quality. In some cases, these scales are being linked to soil survey techniques and to the visual assessment of soil structure (see [Soil Structure, Visual Assessment](#)).

Soil survey and the assessment of soil physical quality

The definition of soil physical quality above includes "of a given soil." It is thus necessary to define what is meant, in this context, by a given soil. Soil survey is "the systematic examination, description, classification and mapping of soils in an area" (Soil Science Society of America, 2001). A given soil, sometimes termed the soil type,

whether taken as a sample or in situ, has properties that can be measured, estimated, or inferred. There may be variation around a mean for any given property of a soil type, but that variation cannot be sufficiently extreme as to prevent the classification as a type.

Soil survey traditionally uses a range of morphological measures to characterize the soil, allowing comparison between classes. These morphological measures are used to infer the characteristics of the soil that directly affect plant growth. These measures typically include color, texture, structure, and consistence of the material for each horizon (e.g., Kerry et al., 2009) and are at least in part related to the physical performance of the soil. A simple example is that the soil color may indicate the likelihood of waterlogging and poor aeration of the profile. Soil survey that adds soil chemical and biological criteria to soil physical analysis is often used to define potential land use. As some of the values that contribute to soil physical quality may be subjective, some authors (e.g., Bouma and Droogers, 1998) have considered quality in terms of the ability to meet requirements relative to a potential in the absence of other constraints.

The key feature of soil physical quality that soil survey reveals is the depth of soil available to fulfil a function. The depth of the soil available is determined by the depth of horizons above weathering bedrock (usually taken as the A and B horizons). The amount of plant available water that can be stored in the profile is directly determined by the soil depth. Plant productivity can be directly linked to the depth of soil available for root development (Wheaton et al., 2008). In some cases, the proportion of the soil horizons that are occupied by stones or gravel must be subtracted from the soil depth as these components prevent soil function. For example, Chow et al. (2007) report some detrimental impacts of coarse fragment content on soil properties and potato production.

Traditional concepts of soil physical quality

Water intake and delivery

A key concept that underlies most indexes of soil physical quality is that of plant available water. Plants cannot grow without access to water. The ability of a soil to store water in a manner that is available to the plant roots is thus the most important single function of the soil (see *Root Water Uptake: Toward 3-D Functional Approaches*). Traditionally, water that is held in soil between the energy states of field capacity and permanent wilting point is described as the plant available water (White, 2006). Field capacity is defined simply as the amount of water that is held within a soil after the soil has been saturated and allowed to drain freely for 2 days (Kirkham, 2005). While there may be some local variations in the value ascribed to field capacity, it is, for this purpose, usually taken as equivalent to a matric suction of -10 kPa . Similarly, $-1,500\text{ kPa}$ is usually taken as the energy state of soil water at which it can no longer be extracted by plant roots.

The volume of plant available water held by a soil can be related to precipitation by the depth of soil as in a water budget (see *Water Budget in Soil*). The root depth determines the plant available water (Boone, 1988). The full relationship between the amount of water in a soil and its energy state is described by a water retention curve. Explanations of terms such as field capacity, permanent wilting point, matric suction, and water retention curve can be found in standard soil physics texts such as Hillel, (1998) or Marshall et al. (1996). Traditionally, the pores holding water between the limits of field capacity and permanent wilting point have been described as mid-range or mesopores. A soil with greater plant available water is generally regarded as having better soil physical quality.

In addition to storing water, a functioning soil must be able to accept rainfall or irrigation and transmit and distribute that water. The movement of water through the soil depends on the number, size distribution, and orientation of pores that conduct water. Various authors have suggested values for the functions of infiltration and hydraulic conductivity. These are sometimes related to particular plant types, e.g., Cass et al. (1993) suggested for adequate root growth of a tree or vine, the infiltration rate of the soil needs to be greater than 0.5 m day^{-1} . Others have suggested more general values such as Dexter (1988), who concluded that the minimum hydraulic conductivity of the bulk soil must be in the range $0.1\text{--}0.01\text{ m day}^{-1}$ if water supply is not to restrict plant development.

Aeration

Aeration is the process of gas exchange between life in the soil, particularly plant roots and the atmosphere. As noted in the introduction, with the exceptions of certain hydrophytes, oxygen is required from the soil for root growth and is supplied by diffusion to the respiration site. The delivery of oxygen to roots and the removal of carbon dioxide to the atmosphere are thus essential functions of the soil physical structure. Because gas diffuses through water at only $1/10^4$ that of diffusion through air, the air-filled porosity of the soil has been used as an indicator of the soils' ability to function. Diffusion of air through the soil profile is related to air-filled pore space and hence is connected to soil water retention. Moldrup et al. (2000) have developed gas diffusion models based on as few as two points from a soil water retention curve, provided that one of the points corresponded to a matric suction of -10 kPa (the value often used for field capacity). Values of air-filled porosity below which the soil cannot adequately support root growth have been variously suggested as at between 10% and 15% (Cockroft and Olsson, 1997). Dexter (1988) suggested that 10% of the soil volume is needed to comprise gas-filled pores and for at least 10% of the gas to be oxygen for supply to roots to be adequate. Macropores, defined as those pores that are air-filled when the soil is at field capacity, are often taken as an indicator of the ability of the soil to deliver

its aeration function. A macroporosity of 10% may be viewed as a critical limit for soil physical quality. Czyż (2004), in a study of barley (*Hordeum vulgare*) growth found that increased soil density and the associated loss of macroporosity resulted in decreased oxygen diffusion rates through the soil and suggested that this contributed to decreased crop yield.

Mechanical impedance

For a plant to achieve its genetic potential, it must access water and nutrients from the soil. Expressing this alternatively, the root system must explore a sufficient volume of soil to meet the requirements of the plant for water and nutrients. To explore the soil, roots must either grow along existing pore spaces or create pores by pushing soil from their path. The mechanical impedance of the soil is the force that plant roots and shoots must generate to deform the soil and allow growth. If a plant root cannot generate a force greater than the soil strength, the root is not able to elongate (Gregory, 2006). The mechanical impedance of the soil affects the volume of rooted soil, the distribution of roots in this volume, the extent to which crop emergence is mechanically impeded, and the mechanical stability of the plant.

The volume of soil occupied by large pores is less in a dense soil, and hence dense or compacted soils have smaller volumes through which roots can grow. Roots in loose soil move through continuous cracks, large pores, and planes of weakness. The roots move through the easiest path, i.e., those with minimal resistance. Roots are unable to decrease in diameter to enter rigid soil pores. Roots may be able to penetrate the soil by expanding the pores, but this depends on the strength of the soil which in turn is determined by factors including the nature and extent of the solid material and the soil water content. When dense layers appear in soil, either naturally at textural changes or as a result of compaction by traffic roots, they may be deflected and may not grow through the compacted layer. Roots accumulate above soil layers with greater mechanical impedance and plants growing with confined roots are at greater risk of drought and other stresses. Definitions and understanding of soil physical quality need to reflect the risks to crops associated with dense soil layers or horizons.

Each plant species has a mechanical resistance that it is able to overcome. The turgor pressure that roots can exert is limited, with all reliably reported values less than 1 MPa (Clark et al., 2003). These can be related to critical values for easily measured penetrometer resistance at which root growth is inhibited. Penetrometer resistances of 1 MPa slow root growth with all elongation ceasing by 3–4 MPa (Kirkegaard et al., 1992). Because penetrometers can quickly assess soil strength conditions and the results are related to root growth, many measures of soil physical quality incorporate penetrometer data (see also *Soil Penetrometers and Penetrability* and *Root Responses to Soil Physical Limitations*).

Temperature

Metabolic processes are temperature dependent; therefore soil temperature is important in crop production (Letey, 1985) (see *Temperature Effects in Soil*). The temperature regime in a soil is a function of many factors including surface radiation, reflection, absorption, and emission characteristics; aerodynamic roughness and subsurface soil thermal properties influence the heat flux. These factors can be changed by management, e.g., irrigation of dry soil increases the heat stored in the soil and thus may decrease the risk of frosts detrimental to crop production. Similarly, metabolic processes that lead to greenhouse gas emissions from soil depend on temperature, and as such, the soil thermal regime is linked to the function of ecosystems both above and below ground.

The degree to which the soil temperature varies depends on the soil surface properties. Mulch diminishes the variation in soil surface temperature. A well-drained, loose, finely crumbed seedbed dries out earlier and increases the variation in temperature of the soil surface (Boone, 1988). Soil temperature influences plant growth rates, and interacts with other soil physical properties including water relations (Licht and Al-Kaisi, 2005).

Soil structure and stability

The definition of soil physical quality given above acknowledges that soil is subject to external and internal forces over a wide range of time scales. The ability of the soil to resist, and recover from, processes that might diminish the ability to function is inherent in its quality and so the stability of the soil in response to stress, particularly stresses related to water and mechanical loading have been included in traditional thinking about soil quality (see *Soil Aggregates, Structure, and Stability*).

Soils consist of primary particles that may be combined to form secondary particles, called aggregates. Oades and Waters (1991) describe a porosity exclusion principle in which larger aggregates have a greater porosity (contain more pores of all size ranges) than do smaller aggregates. Thus, smaller aggregates are more dense and likely to be stronger than larger aggregates, as described by Utomo and Dexter (1981). The size distribution of pores within a soil is thus governed by the extent of aggregation.

Aggregates and pores are formed by a range of processes including:

- (a) Coagulation and flocculation
- (b) Soil fauna which ingest and excrete soil and organic matter
- (c) The movement of soil fauna and roots through the soil profile
- (d) The physical process of wetting and drying, and freezing and thawing (Oades, 1993)

Changes in the water status of the soil, freezing, thawing, and tillage cause shrinkage and swelling. All these processes thus change the soil structure. The ability of a soil to maintain coherence under external forces, particularly

forces associated with water has been used to understand mechanisms underlying the soil quality (Tisdall and Oades, 1982) and to assess the suitability of soil for crop production (Vance et al., 2002).

Assembling the components of soil physical quality into indexes

The soil is the environment for root growth. Soil properties can be manipulated to maximize root growth and hence the soil physical quality can be changed. A simple example is that the addition of farm yard manure changes aggregation of soil particles, leading to improved soil water relations and crop productivity (Singh et al., 2007). Manipulation of soil to change soil structure is costly but can be justified by increased production or by changes to the soils' ability to resist or recover from threats such as erosion or salinization. It is therefore important to quantify changes in soil physical quality, and to have quantitative relationships between soil structure and plant or crop production. To this end, there have been several attempts to unify the various aspects of the traditional descriptors of soil physical quality, provided above, into individual indexes.

Many of the traditional concepts discussed above rely on the soil structure and explicitly the degree of aggregation, generating a wide range of pore sizes (see *Pore Morphology and Soil Functions*). Pores of different sizes deliver different functions, e.g., macropores controlling aeration, mesopores controlling water storage, and micropores influencing the material strength. The nature and extent of these pores can be influenced by soil management. Macroporosity can be increased by cultivation or the activity of soil fauna, mesoporosity can be changed by organic amendments or root growth and exudation, and microporosity can be changed by changing cation concentrations by adding calcium or other salts. For this reason, many of the indexes of soil quality that have been developed have sought to reflect the degree of aggregation and the stability thereof, or the diversity of pore sizes. The indexes or specific measures of soil quality that follow are not a complete list. Rather they are some of the more common examples which can be and are being widely used.

Friability

Aggregates are assemblages of primary particles that cohere into structural units. Friability (see *Soil Tilt: What Every Farmer Understands but No Researcher Can Define*) was defined by Bodman (1949) as the propensity of a soil to crumble and break down into smaller fragments or aggregates under a given load. This concept was used as a basis for an index of soil physical quality by Utomo and Dexter (1981) and has been modified by Watts and Dexter (1998) to indicate the coefficient of variation in soil tensile strength. The measurement of friability involves assessing the strength, by brittle fracture, of multiple aggregates from a soil. Thus, friability cannot be determined on soils with no aggregation. The aggregatory need to be crushed

at the same water content, usually air-dry or oven-dry. For this reason, the assessment of friability is a laboratory-based method.

Tensile strength depends on the microstructure of the soil within the aggregate. The strength is limited by the largest flaw, usually the largest pore within the aggregate. From multiple crushed aggregates, a distribution of the extent of flaws within aggregates from that soil is assembled and from this the statistical coefficient of variation can be obtained. For aggregates of a given size, this coefficient of variation is a measure of the friability. Alternatively, aggregates of different sizes can be crushed. By the porosity exclusion principle, larger aggregates contain larger flaws, and thus are weaker than are smaller aggregates. The slope of a plot of the natural log of the aggregate strength against the natural log of the aggregate volume is similarly a measure of the soil friability. The relative methods of calculating soil friability have been assessed by Watts and Dexter (1998).

Because friability depends on the distribution of cracks within soil aggregates, factors that influence soil microstructure change friability. Natural processes, such as swelling and shrinking in response to water content, changes throughout a season, generate cracking within aggregates and hence change the friability. Processes that homogenize soil and remove large pore spaces, e.g., soil compaction by machinery, result in decreased friability. Agricultural management and changes in land use from continuous cropping to grassland can result in improved friability (Munkholm and Kay, 2002).

Aggregate stability in water

As aggregates are assemblages, their ability to resist change that will be detrimental to their integrity is a measure of their quality (see *Soil Aggregates, Structure, and Stability*). The ability of aggregates to resist abrasion when dry has been used to assess the risk of wind erosion (Chepil, 1962), but this is a specific use, and for the purposes of this review, beyond the scope of general measures of soil physical quality. In a similar manner to the friability measure, just described, the ability of aggregates to remain coherent after exposure to water has been used as a measure of soil quality. Aggregates collected from the field are brought to the laboratory. Depending on the severity of the test required, the aggregates may be dried, or other pretreatments imposed. The distribution of aggregate sizes may be determined prior to testing for later comparison (Six et al., 2000a). Known weights of aggregates are placed on sieves with different apertures and the soil and sieve oscillated in water for a fixed time interval. The amount of soil remaining on each sieve is determined after drying. From the amount of soil that remains on the different sieves, a mean weight diameter of stable soil can be calculated and used as a measure of soil quality.

The processes that lead to the breakdown of aggregates in water can be described as slaking and dispersion. Slaking is the rapid wetting of dry aggregates, and the ability to

withstand this rapid wetting is a measure of the manner in which aggregates typically larger than 100 mm are held together. The coherence of aggregates of this size is determined by the nature of organic matter in the soil and by other biologically-induced mechanisms. Dispersion is the separation of aggregates into their primary particles and can be seen as the reverse of coagulation. Dispersion is influenced by the mineralogy of the primary mineral particles and the salts offsetting the associated changes.

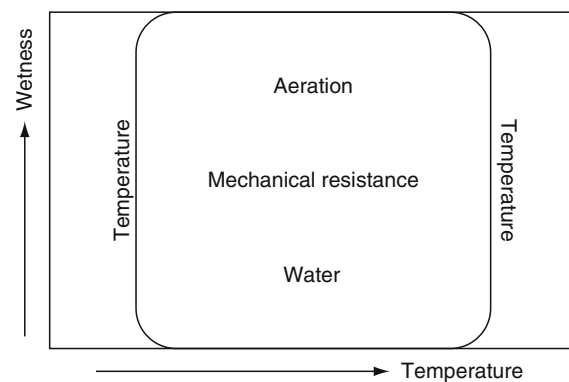
Because of the different mechanisms involved in the stability of aggregates in water changes, in that stability can reflect management and thus seen as a measure of soil physical quality. By comparison with initial aggregate size distribution, an index can be determined (Six et al., 2000b).

Least limiting water range

Letey (1985) introduced the non-limiting water range (NLWR) to link the separate effects that water, aeration, and mechanical resistance have on root growth. The NLWR is a single parameter that defines a range of water contents at which available water, aeration, and mechanical resistance do not restrict root growth (Letey, 1985). Values of soil aeration and mechanical resistance that limit root growth have been reported by various researchers (see *Root Responses to Soil Physical Limitations*). As the water content of the soil changes, mechanical resistance and aeration change and may exceed limiting values for root growth. The limits of available water are between the matric suction at wilting point (1,500 kPa), where plant roots are unable to access water required for growth and the matric suction at field capacity (10 kPa). The NLWR is the range where root growth is not limited by available water, aeration, or mechanical resistance. The maximum water content is the drier of field capacity, or the water content at which root growth is limited by aeration. The minimum water content is the wetter of wilting point or the water content at which mechanical resistance limits root growth.

The NLWR has since been termed the least limiting water range (LLWR) by da Silva et al. (1994), and has continued to be used by researchers (da Silva and Kay, 1996, 1997; Tormena et al., 1999; Leao et al., 2006). The change was made because plant growth occurs continuously in response to changes in available water, aeration, and mechanical resistance and may be limited, although the growth not totally prevented. Inside the range, growth is least limited, while outside the range, growth is most limited (da Silva et al., 1994). da Silva and Kay (1997) defined the LLWR as “the range in soil water content after rapid drainage has ceased within which limitations to plant growth associated with water potential, aeration and mechanical resistance to root penetration are minimal.”

Soil physical characteristics are linked. In Figure 1, adapted from Boone (1988), soil water content and soil temperature are independent variables. At very low or very high temperatures, root growth is limited. When the



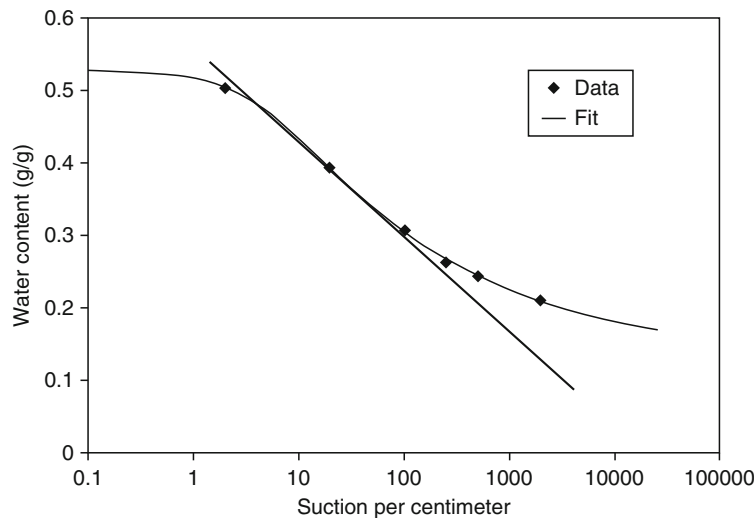
Soil Physical Quality, Figure 1 Representation of the least limiting water range (LLWR) after Boone (1988).

soil temperature is non-limiting and the soil is very wet, aeration is limiting. As the soil dries, water becomes limiting and high mechanical resistance restricts root growth, which also limits crop water availability. Boone et al. (1986) investigated the relationship between soil water and soil structure (Figure 1) to determine the limits of soil aeration and soil mechanical resistance. With combined limits of soil mechanical resistance with soil water and soil structure and limits of soil aeration with soil water and soil structure, it can be determined at what soil water contents root growth and function are not limited (Boone, 1988).

The period of least-limited root growth is when neither mechanical resistance nor aeration is limiting. To these two parameters, the water contents associated with plant available water are added as limits, the matric suctions of field capacity, and wilting point. The LLWR is then calculated from the water content values associated with the values of mechanical resistance and aeration that limit root growth and matric suctions of wilting point and field capacity. It is possible to have a negative LLWR, which da Silva et al. (1994) considered as zero.

S-theory or S-index

Dexter (2004a, b) describes an index, S, as representing soil physical quality. The S-value represents the slope of the water retention curve at its point of inflection when the curve has been plotted as gravimetric water content against the natural logarithm of the pore water suction. Figure 2 shows a soil water retention curve. Typical raw data are presented and the curve, fitted to the van Genuchten (1980) parameters, follows these points. The slope at the point of inflection is shown as a straight line. The slope at the point of inflection is not arbitrary but has been related to physical management of soil, e.g., it has been suggested that the water content at the point of inflection is the optimum condition for soil manipulation through tillage (Dexter and Bird, 2001). Because the water retention curve is a measure of the pore-size distribution, an increase in slope at the point of inflection indicates



Soil Physical Quality, Figure 2 Water retention curve showing data and fitted curve with the slope at the point of inflection as a line.

greater pore diversity. The larger pore classes, the often-termed structural pores, are responsive to soil management, while pores that result from texture are less sensitive to management. So when the different pore types are connected, the S-index can be changed by management. Typical values of the S-index are >0.05 for a soil with very good structural quality, while a value <0.02 classes it as a degraded soil or one with very poor quality. While the vast majority of soils exhibit a single inflection point, the approach is more difficult in soils with more than one inflection point.

There is currently an increasing use of the S-index approach to assess soil physical quality. Keller et al. (2007) connected the optimum water content for conducting tillage operations with the S-index of the soil. They found that the optimum water content for tillage was close to the point of inflection on the water retention curve, and that tillage operations when the soil was in this state produced a better seedbed with fewer large clods. Similarly, Cavalieri et al. (2009) have found the S-index sensitive to small increases in the bulk density of particular layers within a given soil and by inference suggested that it is a good measure of soil physical quality.

Resistance and resilience

The indexes described in the text above are based on the state of the soil as it exists at a given time. They are responsive to management; values increase under conditions that improve crop performance and decrease when the soil is compacted or has decreased concentrations of organic matter. However, the indexes may not reflect the ability of a soil to resist change by poor management or other stress and do not explicitly reveal how rapidly, if at all, the soil will recover from being degraded. Lal (1993) introduced the idea that, implicit in the concept of soil quality a soil needs to be able to resist degradation and

that, rapid recovery to the preexisting state (not to an inferior state) was part of the concept of soil quality. Gregory et al. (2007) defined resilience as the ability of a soil to recover its original property, capacity, or function when an applied stress is removed. While the stresses can be physical (e.g., compaction), chemical (e.g., toxic elements), or biological (e.g., pathogens), the risks of compaction in modern agriculture make physical resilience a key parameter. A soil deemed to have good soil physical quality will show rapid and total recovery. Gregory et al. (2007) suggest that self-mulching surface soils as described by Grant et al. (1995) provide an example of this good quality (see *Shrinkage and Swelling Phenomena in Soils*). Griffiths et al. (2005) studied several measures of soil condition in response to amendments with heavy-metal contaminated sewage sludge. They suggested that the recovery or resilience of the soil to imposed physical stresses resulting from compaction and long-term waterlogging and stresses, on the biological function resulting from heat or contamination, were linked. Strong interconnection between the physics, chemistry, and biology of soil are well known. The concepts of resistance and resilience may provide opportunities to unify them for measures of soil quality.

Soil physical quality: the future

There is clearly a need for more practical, rigorous testing of the current indexes of soil physical quality. This should include comparisons between the different approaches to test how they perform relative to each other and how they might be connected. Because the soil physical quality is not isolated from chemical fertility or biological function, the opportunity to unite approaches from different disciplines needs to be explored. It will not be simple to combine different ways of thinking, but to place an environmental as well as an economic value on soil, dialog

between the disciplines is needed. One novel approach is to supplement physical measurement with expert or stakeholder knowledge (e.g., Kaufmann et al., 2009) through expert systems. Mixing human experience with multi-criteria scientific analysis of soil quality is being tested to develop approaches for soil monitoring (Aalders et al., 2009). Whether this can be used to quantify the ability of a given soil to meet plant and ecosystem requirements for water, aeration, and strength over time remains to be seen.

Bibliography

- Aalders, I., Hough, R. L., Towers, W., Black, H. I. J., Ball, B., Griffiths, B., Hopkins, D. W., Lilly, A., McKenzie, B. M., Rees, R. M., Sinclair, A., Watson, C., and Campbell, C. D., 2009. Considerations for Scottish soil monitoring in the European context. *European Journal of Soil Science*, **60**, 833–843.
- Bodman, G. B., 1949. Methods of measuring soil consistency. *Soil Science*, **68**, 37–56.
- Boone, F. R., 1988. Weather and other environmental factors influencing crop responses to tillage and traffic. *Soil and Tillage Research*, **11**, 283–324.
- Boone, F. R., van der Werf, H. M. G., Kroesbergen, B., ten Hag, B. A., and Boers, A., 1986. The effect of compaction of the arable layer in sandy soils on the growth of maize for silage. 1. Critical matric water potentials in relation to soil aeration and mechanical impedance. *Netherlands Journal of Agricultural Science*, **34**, 155–171.
- Bouma, J., and Droogers, G., 1998. A procedure to derive land quality indicators for sustainable agricultural production. *Geoderma*, **85**, 103–110.
- Cass, A., Cockcroft, B., and Tisdall, J. M., 1993. New approaches to vineyard and orchard soil preparation and management. In Hayes, P. F. (ed.), *ASVO seminar vineyard development and redevelopment, Mildura, Victoria*. Adelaide: ASVO, pp. 18–24.
- Cavalieri, K. M. V., da Silva, A. P., Tormena, C. A., Leao, T. P., Dexter, A. R., and Hakansson, I., 2009. Long-term effects of no-tillage on dynamic soil physical properties in a Rhodic Ferrisol in Paraná, Brazil. *Soil and Tillage Research*, **103**, 158–164.
- Chepil, W. S., 1962. A compact rotary sieve and the importance of dry sieving in physical soil analysis. *Soil Science Society of America Proceedings*, **26**, 4–6.
- Chow, T. L., Rees, H. W., Monteith, J. O., Toner, P., and Lavoie, J., 2007. Effects of coarse fragment content on soil physical properties, soil erosion and potato production. *Canadian Journal of Soil Science*, **87**, 565–577.
- Clark, L. J., Whalley, W. R., and Barraclough, P. B., 2003. How do roots penetrate strong soil. *Plant and Soil*, **255**, 93–104.
- Cockcroft, B., and Olsson, K. A., 1997. Case study of soil quality in south-eastern Australia: management of structure for roots in duplex soils. In Gregorich, E. G., and Carter, M. R. (eds.), *Soil Quality for Crop Production and Ecosystem Health*. Amsterdam: Elsevier, pp. 339–350.
- Czyż, E., 2004. Effects of traffic on soil aeration, bulk density and growth of spring barley. *Soil and Tillage Research*, **79**, 153–166.
- da Silva, A. P., and Kay, B. D., 1996. The sensitivity of shoot growth of corn to the least limiting water range of soils. *Plant and Soil*, **184**, 323–329.
- da Silva, A. P., and Kay, B. D., 1997. Effect of soil water content variation on the least limiting water range. *Soil Science Society of America Journal*, **61**, 884–888.
- da Silva, A. P., Kay, B. D., and Perfect, E., 1994. Characterization of the least limiting water range of soils. *Soil Science Society of America Journal*, **58**, 1775–1781.
- Dexter, A. R., 1988. Advances in the characterization of soil structure. *Soil and Tillage Research*, **57**, 203–212.
- Dexter, A. R., 2004a. Soil physical quality. Part 1 theory, effects of soil texture, density, and organic matter, and effects on root growth. *Geoderma*, **120**, 210–214.
- Dexter, A. R., 2004b. Soil physical quality. Part 11. Friability, tillage, tilth and hard-setting. *Geoderma*, **120**, 215–225.
- Dexter, A. R., and Bird, N. R. A., 2001. Methods for predicting the optimum and the range of water contents for tillage based on the water retention curve. *Soil and Tillage Research*, **11**, 199–238.
- Grant, C. D., Watts, C. W., Dexter, A. R., and Frahn, B. S., 1995. An analysis of the fragmentation of remoulded soils, with regard to self-mulching behavior. *Australian Journal of Soil Research*, **33**, 569–583.
- Gregory, P. J., 2006. *Plant Roots Growth, Activity and Interaction with Soils*. Oxford: Blackwell Publishing.
- Gregory, A. S., Watts, C. W., Whalley, W. R., Kuan, H. L., Griffiths, B. S., Hallett, P. D., and Whitmore, A. P., 2007. Physical resilience of soil to field compaction and the interactions with plant growth and microbial community structure. *European Journal of Soil Science*, **58**, 1221–1232.
- Griffiths, B. S., Hallett, P. D., Kuan, H. L., Pitkin, Y., and Aitken, M. N., 2005. Biological and physical resilience of soil amended with heavy metal-contaminated sewage sludge. *European Journal of Soil Science*, **56**, 197–205.
- Hillel, D., 1998. *Environmental Soil Physics*. San Diego: Academic.
- Karlen, D. L., Mausbach, M. J., Doran, J. W., Cline, R. G., Harris, R. F., and Schuman, G. E., 1997. Soil quality: a concept, definition, and framework for evaluation (a guest editorial). *Soil Science Society of America Journal*, **61**, 4–10.
- Kaufmann, M., Tobias, S., and Schulin, R., 2009. Quality evaluation of restored soils with a fuzzy logic expert system. *Geoderma*, **151**, 290–302.
- Keller, T., Arvidsson, J., and Dexter, A. R., 2007. Soil structures produced by tillage as affected by soil water content and the physical quality of soil. *Soil and Tillage Research*, **92**, 45–52.
- Kerry, R., Rawlins, B. G., Olivari, M. A., and Lacinska, A. M., 2009. Problems with determining the particle size distribution of chalk soil and some of their implications. *Geoderma*, **152**, 324–337.
- Kirkegaard, J. A., So, H. B., and Troedson, R. J., 1992. The effect of soil strength on the growth of pigeon pea radicles and seedlings. *Plant and Soil*, **140**, 65–74.
- Kirkham, M. B., 2005. *Principles of Soil and Plant Water Relations*. Boston: Elsevier Academic Press.
- Lal, R., 1993. Tillage effects on soil degradation, soil resilience, soil quality, and sustainability — introduction. *Soil and Tillage Research*, **27**, 1–8.
- Leao, T. P., da Silva, A. P., Macedo, M. C. M., Imhoff, S., and Euclides, V. P. B., 2006. Least limiting water range: a potential indicator of changes in near-surface soil physical quality after the conversion of Brazilian Savanna into pasture. *Soil and Tillage Research*, **88**, 279–285.
- Letey, J., 1985. Relationship between soil physical properties and crop production. In Stewart, B. A. (ed.), *Advances in Soil Science*. New York: Springer, Vol. 1.
- Licht, M. A., and Al-Kaisi, M., 2005. Strip-tillage effect on seedbed soil temperature and other soil physical properties. *Soil and Tillage Research*, **80**, 233–249.
- Marshall, T. J., Holmes, J. W., and Rose, C. W., 1996. *Soil Physics*, 3rd edn. Cambridge: Cambridge University Press.
- Moldrup, P., Olesen, T., Schjonning, P., Yamaguchi, T., and Rolston, D. E., 2000. Predicting the gas diffusion coefficient in undisturbed soil from soil water characteristics. *Soil Science Society of America Journal*, **64**, 94–100.
- Munkholm, L. J., and Kay, B. D., 2002. Effect of water regime on aggregate-tensile strength, rupture energy and friability. *Soil Science Society of America Journal*, **66**, 702–709.

- Oades, J. M., 1993. The role of biology in the formation, stabilization and degradation of soil structure. *Geoderma*, **56**, 377–400.
- Oades, J. M., and Waters, A. G., 1991. Aggregate hierarchy in soils. *Australian Journal of Soil Research*, **29**, 815–828.
- Reynolds, W. D., Drury, C. F., Yang, X. M., and Tan, C. S., 2008. Optimal soil physical quality inferred through structural regression and parameter interactions. *Geoderma*, **146**, 466–474.
- Singh, G., Jalota, S. K., and Singh, Y., 2007. Manuring and residue management effects on physical properties of a soil under rice-wheat system in Punjab, India. *Soil and Tillage Research*, **94**, 229–238.
- Six, J., Paustian, K., Elliott, E. T., and Combrink, C., 2000a. Soil structure and organic matter: I. Distribution of aggregate-size classes and aggregate-associated carbon. *Soil Science Society of America Journal*, **64**, 681–689.
- Six, J., Elliott, E. T., and Paustian, K., 2000b. Soil structure and soil organic matter: II. A normalized stability index and the effect of mineralogy. *Soil Science Society of America Journal*, **64**, 1042–1049.
- Soil Science Society of America Inc, 2001. *Glossary of Soil Science Terms*. Madison: Soil Science Society of America Inc.
- Tisdall, J. M., and Adem, H. H., 1988. An example of custom prescribed tillage in south-eastern Australia. *Journal of Agricultural Engineering Research*, **40**, 23–32.
- Tisdall, J. M., and Oades, J. M. H., 1982. Organic matter and water-stable aggregates in soils. *Journal of Soil Science*, **33**, 141–163.
- Tormena, C. A., da Silva, A. P., and Libardi, P. L., 1999. Soil physical quality of a Brazilian Oxisol under two tillage systems using the least limiting water range approach. *Soil and Tillage Research*, **52**, 223–232.
- Utomo, W. H., and Dexter, A. R., 1981. Soil friability. *Journal of Soil Science*, **32**, 203–213.
- van Genuchten, M. T., 1980. A closed-form equation for predicting the hydraulic conductivity of unsaturated soils. *Soil Science Society of America Journal*, **44**, 892–898.
- Vance, W. H., McKenzie, B. M., and Tisdall, J. M., 2002. The stability of soils used for cropping in northern Victoria and southern New South Wales. *Australian Journal of Soil Research*, **40**, 615–624.
- Watts, C. W., and Dexter, A. R., 1998. Soil friability: theory, measurement and the effects of management and organic carbon content. *European Journal of Soil Science*, **49**, 73–84.
- Wheaton, A. D., McKenzie, B. M., and Tisdall, J. M., 2008. Management to increase the depth of soft soil improves soil conditions and grapevine performance in an irrigated vineyard. *Soil and Tillage Research*, **98**, 68–80.
- White, R. E., 2006. *Principles and Practice of Soil Science The Soil as a Natural Resource*, 4th edn. Oxford: Blackwell Publishing.

Cross-references

- [Aeration of Soils and Plants](#)
- [Pedotransfer Functions](#)
- [Pore Morphology and Soil Functions](#)
- [Root Responses to Soil Physical Limitations](#)
- [Root Water Uptake: Toward 3-D Functional Approaches](#)
- [Shrinkage and Swelling Phenomena in Soils](#)
- [Soil Aggregates, Structure, and Stability](#)
- [Soil Penetrometers and Penetrability](#)
- [Soil Phases](#)
- [Soil Structure, Visual Assessment](#)
- [Soil Tilth: What Every Farmer Understands but No Researcher Can Define](#)
- [Soil Water Flow](#)
- [Temperature Effects in Soil](#)
- [Water Budget in Soil](#)

SOIL PORE

The least volume of a body limited by solid phase and narrowings.

Bibliography

- Czachor, H., Gozdz, A., 2001. Modelling of granular and cellular materials. *Transaction of ASAE*, **44**, 439–445.

SOIL SEPARATES

Mineral particles, <2.0 mm in equivalent diameter, ranging between specified size limits. The names and size limits of separates recognized in the USA are: *very coarse sand* (Prior to 1947 this separate was called “fine gravel;” now fine gravel includes particles between 2.0 mm and about 12.5 mm in diameter), 2.0 to 1.0 mm; *coarse sand*, 1.0 to 0.5 mm; *medium sand*, 0.5 to 0.25 mm; *fine sand*, 0.25 to 0.10 mm; *very fine sand*, 0.10 to 0.05 mm; *silt*, 0.05 to 0.002 mm; and *clay* (Prior to 1937, “clay” included particles <0.005 mm in diameter, and “silt,” those particles from 0.05 to 0.005 mm) <0.002 mm. The separates recognized by the International Society of Soil Science are: (i) *coarse sand*, 2.0 to 0.2 mm; (ii) *fine sand*, 0.2 to 0.02 mm; (iii) *silt*, 0.02 to 0.002 mm; and (iv) *clay*, <0.002 mm.

Bibliography

- Glossary of Soil Science Terms. Soil Science Society of America. 2010. <https://www.soils.org/publications/soils-glossary>

Cross-references

- [Soil Texture: Measurement Methods](#)

SOIL STRUCTURE AND MECHANICAL STRENGTH

Rainer Horn, Heiner Fleige

Institute for Plant Nutrition and Soil Science, Christian-Albrechts-University zu Kiel, Kiel, Germany

Definition

Soil strength is typically referred to the maximum amount of stress a solid material can stand before it fails, thus exceeding soil strength results in soil failure or yield.

Stress is defined as force per area within a solid body. Stress can be induced by external or internal forces which lead, if the body is nonrigid, to a change in the body's volume and/or shape expressed as deformations or strains. The mechanical behavior of a soil can therefore be characterized by its stress-strain relationships. The transition from the recompression to the virgin compression state is defined as precompression stress.

Introduction

The determination of soil strength always coincides with a link to physical soil properties like hydraulic conductivity, pore size distribution, and pore continuity, and is also linked with plant growth and yield, climate change aspects as well as groundwater recharge, and water quality.

The determination of soil and/or aggregate strength has always to be subdivided into (1) mechanically, hydraulically, or chemically prestressed and (2) virgin conditions, which also ultimately affect the predictability of physical properties. These general ideas have been described in greater detail by Hartge (1965), Toll (1995), Baumgartl and Horn (1999), Groenevelt and Grant (2002), Grant et al. (2002), Horn et al. (2000, 2006), and Horn and Fleige (2003).

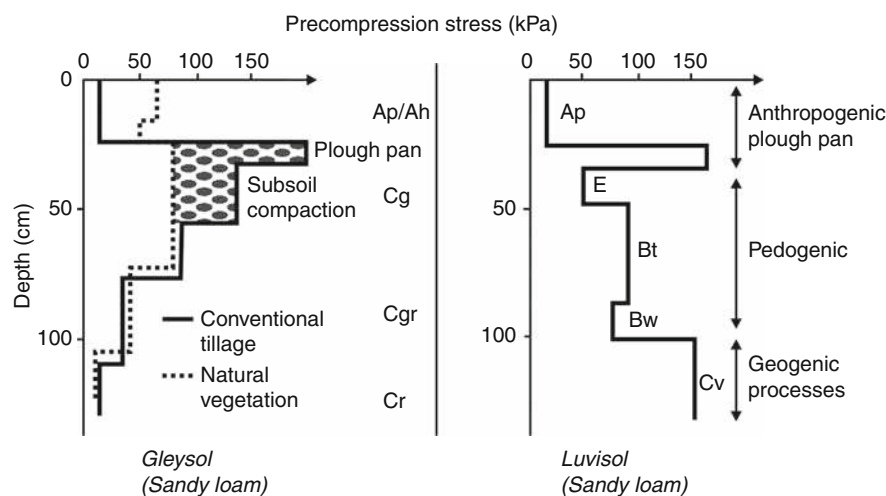
Mechanical strength of structured soils

The mechanical strength of structured soils depends on aggregation and history of hydraulic stresses (degree of maximum pre-drying), as well as the shape and internal arrangement of particles, micro-aggregates, and voids. At comparable grain size distribution, bulk density, and pore water pressure, soil strength increases with aggregation (i.e., coherent < prismatic < blocky < subangular blocky < crumbly). In the case of a platy structure, the strength depends on the direction of shear forces relative to the preferred orientation of the particles. In the direction of the elongated axes of aligned particles, shear strength is lower than perpendicular to it. This means that not only mechanical stresses are anisotropic but also strength properties which in turn are a function of aggregation. However, both the magnitude of previous hydraulic stresses (pre-drying intensity) and their dynamic changes determine soil strength. Therefore, mechanical properties also depend on the frequency of swell/shrink and wet/dry events and on the actual pore water pressure at the time

of loading. Soils become stronger when re-dried and rewetted and when pore water pressure gradients over longer distances promote particle movement and rearrangement until entropy is minimized (Semmel et al., 1990). The effect of pore water pressure on strength itself is governed by the theory of effective stresses in unsaturated soils (e.g., BISHOP's effective stress equation). The χ factor in this equation quantifies the water-filled pores in soils relative to water saturation (=1) and complete dryness (=0). Thus, if the relative reduction in water-filled pores is smaller than the actual decrease in pore water pressure (more negative matric potential), soil strength increases. Conversely, drier soils become weaker when the effective surface of water menisci decreases above average ($\chi \rightarrow 0$).

In principle, soil strength is promoted by two different mechanisms: (1) the increase in strength results from an increase in the total number of contact points between single particles (i.e., an increase in effective stress) and (2) the increase in shear resistance per contact point (Hartge and Horn, 1984). Therefore, even if soil bulk densities are similar, strength properties may be quite different. Also freezing and thawing affects soil strength, because aggregates become denser or are destroyed by ice lens formation during freezing. Aggregates may act as rigid bodies which allow exfoliation processes to start from the outer skin due to ice lens formation. Both effects are called soil curing but result in completely different strength values and physical properties of the bulk soil (Horn, 1985; Kay, 1990).

Pedogenic effects on natural soil mechanical strength are illustrated in Figure 1. A Gleysol derived from marine sediments can be defined as very loose, linked with a high air capacity and plant available water capacity as well as high values for hydraulic conductivity, which can be also linked to the high biological activity. This soil also shows a pronounced effect of natural drying intensity and



Soil Structure and Mechanical Strength, Figure 1 Precompression stress values for two soil profiles under various land use and geological origin (marin sediments, weichselian glacial till) at an initial soil matric potential $\Psi_m = -6$ kPa.

aggregate formation with increasing distance to the groundwater table as well as of land use. Under natural vegetation, soil strength (defined as precompression stress P_c) increases from coherent (=weak) structure (C_r horizon) to prismatic structure ($C_{gr\ hor.}$) and blocky structure ($C_g\ hor.$) due to a more often and more intense swelling and shrinkage and drying intensity. If these natural soils are wheeled and ploughed, a more compressed, dense, and more rigid plow pan layer is created, which can also be detected by the increased P_c value at this depth. Additionally, the soil deformation alters the soil properties over depth as can be derived from the higher P_c values which only fade off at depths >50 cm.

Soils derived from glacial till are characterized both by their geological origin and soil genetic processes. The latter can be derived for the Luvisol from the effect of clay illuviation, which results in strength decrease in the E-horizon and an increase in the Bt-horizon due to aggregation based on the improved swell shrink behavior of the clay. In general, the parent material (C-horiz.) is weakest as long as it was deposited as an aeolian or fluvial sediment. If, however, the geological origin (glacial pressure) dominates, then the former higher strength caused by, e.g., 150 m of (weichselian) glacier height in northwest Germany and the long-term backward and forward shearing movement of the glacier can be still detected and quantified even after more than 10,000 years of postglacial soil development.

Anthropogenic processes such as annual plowing and wheeling create very strong plow pan layers with P_c values similar to the contact pressure of a tractor tire or even higher (up to 300%) due to lug effects, while the loosened Ap horizon has been mostly homogenized and consequently weakened by the reduction of the contact points between particles, a height increase of the soil horizon. Thus, the strength decreases in the Ap-horizon due to plowing and, seedbed preparation can be observed until texture-dependent values are reached. Pronounced strength decreases are also found in soil profiles which have been deep loosened or deep plowed (up to 60 cm) or loosened and/or mixed with other soil material. In the case of a partial deep loosening by a trenching slit plow (Blackwell et al., 1989; Horn, 1994), traffic must be restricted by use of smaller and lighter machinery or controlled tracks perpendicular to the homogenized soil volume.

Soils with a well-developed vertical pore system are stronger than those with randomized or horizontal pore arrangements since elongated pores are more stable with their symmetry axis oriented in the direction of the major principle stress (σ_1) than perpendicular to it. Therefore, vertical (bio-) pores are less prone to compression than horizontally oriented pores and, thus, untilled or minimum tilled soils are stronger than conventionally tilled ones (Horn, 1986, 2004).

However, each soil deformation affects air-filled pore space and continuous coarse pores because each settlement requires a reduction in coarse pores and a hydraulic

conductivity which allows during compression to drain off excess pore water. The smaller the hydraulic conductivity, the hydraulic potential gradient, and the pore continuity, the more stable is the soil especially during short-term loading. It is often described with termini-like aquaplaning or the waterskiing effects. In sandy soils, this effect is small and the initial settlement equals the total strain. With increasing clay content, however, the proportion of initial to primary and secondary consolidation is reduced and the time-dependent soil settlement becomes more important (Horn, 1988). This results in an increase of P_c for short-term loading due to an increase in the pore water pressure-related soil strength that dissipates only slowly depending on the local hydraulic conductivity. Consequently, it is to be expected in mainly fine-textured soils (sand < silt < clay) with increasing bulk density, with mostly minor aggregation, higher degree of soil disturbance, e.g., by plowing, and less continuous pores. More detailed information is given in Horn: Management Effects on Soil Properties and Functions.

Conclusions

Soil strength depends on the kind and arrangement of aggregates as well as on the pore geometry and rigidity. The coupled mechanical and hydraulic processes affect the time-dependent soil strain and the alteration of the pore functioning, e.g., aeration and water fluxes.

Geogenic, pedogenic, and anthropogenic processes can be differentiated by the parameter precompression stress and can therefore also be used to define the actual internal soil strength as a function of matric potential.

Bibliography

- Baumgartl, T., and Horn, R., 1999. Influence of mechanical and hydraulic stresses on hydraulic properties of swelling soils. In van Genuchten, M. Th., Leij, F. J., and Wu, L. (eds.), *Characterisation and Measurement of the Hydraulic Properties of Unsaturated Porous Media*. Riverside: University of California, pp. 449–457.
- Blackwell, J., Horn, R., Jayawardane, N. S., White, R., and Blackwell, P. S., 1989. Vertical stress distribution under tractor wheeling in a partially deep loosened typic paleustalf. *Soil and Tillage Research*, **13**(1), 1–12.
- Grant, C. D., Groenevelt, P. H., and Bolt, G. H., 2002. On hydrostatics and matrastatics of swelling soils. In: Raats, P. A. C., et al. (eds.), *Environmental Mechanics: Water, Mass, and Energy Transfer in the Biosphere*. Geophysical Monograph 129, AGU, pp. 95–105.
- Groenevelt, P. H., and Grant, C. D., 2002. Curvature of shrinkage lines in relation to the consistency and structure of a Norwegian clay soil. *Geoderma*, **106**, 235–247.
- Hartge, K. H., 1965. Vergleich der Schrumpfung ungestörter Böden und gekneteter Pasten. Wiss Zeitschrift Friedr Schiller Uni Jena. *Math. Naturw. Reihe*, **14**, 53–57.
- Hartge, K. H., and Horn, R., 1984. Untersuchungen zur Gültigkeit des Hook'schen Gesetzes bei der Setzung von Böden bei wiederholter Belastung. *Zeitschrift f. Acker- und Pflanzenbau*, **153**, 200–207.
- Horn, R., 1985. Die Bedeutung der Trittverdichtung durch Tiere auf physikalische Eigenschaften Alpiner Böden. *Z. f. Kulturtechnik und Flurbereinigung*, **26**, 42–51.

- Horn, R., 1986. Auswirkung unterschiedlicher Bodenbearbeitung auf die mechanische Belastbarkeit von Ackerböden. *Journal of Plant Nutrition and Soil Science*, **149**(1), 9–18.
- Horn, R., 1988. Compressibility of arable land. In Drescher, J., Horn, R., de Boodt, M. (eds.), *Interaction of Structured Soils with Water and External Forces*. *Catena Supplement* 11, 53–71. ISBN: 3-923381-11-5.
- Horn, R., 1994. Stress transmission and recompaction in tilled and segmentally disturbed soils under trafficking. In Jayawardane, N. S., and Stewart, B. A. (eds.), *Subsoil Management Techniques*. Advances in Soil Science: CRC Press, pp. 53–87. ISBN: 1-56670-020-5.
- Horn, R., 2004. Time dependence of soil mechanical properties and pore functions for arable soils. *Soil Science Society of America Journal*, **68**, 1131–1137.
- Horn, R., and Fleige, H., 2003. A method for assessing the impact of load on mechanical stability and on physical properties of soils. *Soil and Tillage Research*, **73**, 89–99.
- Horn, R., van den Akker, J. J. H., Arvidsson, J., 2000. Subsoil compaction – distribution, processes and consequences. *Advances in Geocology* **32**, ISBN: 3-923381-44-1, 462S.
- Horn, R., Fleige, H., Peth, S., and Peng, X. H. (eds.), 2006. Soil management for sustainability. *Advances in Geocology* **38**, 497 pp. 3-923381-52-2.
- Kay, B. D., 1990. Rates of change of soil structure under different cropping systems. *Advances in Soil Science*, **12**, 1–41.
- Semmel, H., Horn, R., Hell, U., Dexter, A. R., and Schulze, E. D., 1990. The dynamics of soil aggregate formation and the effect on soil physical properties. *Soil Technology*, **3**, 113–129.
- Toll, D. G., 1995. A conceptual model for the drying and wetting of soil. In Alonso, E. E., and Delage, P. (eds.), *Proceeding of the International Conference on Unsaturated Soils*. Rotterdam: Balkema, pp. 805–810. ISBN: 9054105852.

Cross-references

- [Agophysical Objects \(Soils, Plants, Agricultural Products, and Foods\)](#)
[Cracking in Soils](#)
[Hydrophobicity of Soil](#)
[Infiltration in Soils](#)
[Mechanical Impacts at Harvest and After Harvest Technologies](#)
[Noninvasive Quantification of 3D Pore Space Structures in Soils](#)
[Shrinkage and Swelling Phenomena in Soils](#)
[Soil Structure, Intersecting Surface Approach, and its Applications](#)
[Soil Water Flow](#)

SOIL STRUCTURE, INTERSECTING SURFACE APPROACH, AND ITS APPLICATIONS

Victor Yakov Chertkov

Division of Environmental, Water, and Agricultural Engineering, Technion – Israel Institute of Technology, Haifa, Israel

Definitions

Soil structure. The arrangement and organization of the different soil particles in a soil.

Intersecting surfaces approach (ISA). The physical approach to soil (and rock) structure and properties description and prediction that originates from the obvious presence and superposition in any (sufficiently large) soil

volume of the enormous number of natural intersecting surfaces having a different scale and physical nature and meeting several simple geometrical conditions.

Applications of ISA. The physical derivation of such geometrical characteristics of soil structure underlying any soil properties and processes, as (1) interconnected size and shape distributions of soil solids and voids between them; and (2) porosity, connectedness, and tortuosity relating to the voids.

Development history

Initially, the prototype of the ISA only related to multiple cracking of rocks and their corresponding fragmentation, natural- and explosion-induced (Chertkov, 1985; Chertkov, 1986; Chertkov, 1991). The prototype model is based on a concentration criterion of crack accumulation and connection (Zhurkov et al., 1981) and effective independence of cracks in the case of multiple cracking (Hudson and Priest, 1979). In the case of the natural blockiness of a rock mass (this is interesting for the extension to soils), the model is in good agreement with the following principal observations: (1) the ratio of the maximum size of a structural block of rock mass to the average size is approximately equal to 4 (Hudson and Priest, 1979); (2) severe, but incomplete disintegration is observed in rock masses due to natural cracks; (3) the average number of faces on a fragment, at randomly oriented cracking, is approximately equal to 8 (Curran et al., 1977); (4) the observed size distributions of structural blocks for deposits of granite, diorite, and diabase (Azovtsev, 1984); (5) the shape characteristics of rock blocks – average ratios of the second and third fragment sizes to the first one (Repin, 1978).

The prototype of the ISA was applied to multiple cracking ([Cracking in Soils](#)) and fragmentation of swelling soils as they dry and shrink ([Shrinkage and Swelling Phenomena in Soils](#)) (Chertkov, 1995; Chertkov and Ravina, 1998; Chertkov and Ravina, 1999). Comparison between the model prediction (Chertkov, 1995) and data (Guidi et al., 1978) for two-dimensional fragmentation showed good agreement. The model of multiple cracking considers cracks to be surfaces (without openings). For this reason, in the three-dimensional case the model gives parameters of the crack network itself – crack spacing and depth – as functions of soil depth. Crack opening and volume are found by accounting for the soil shrinkage. Comparison between predicted parameters of crack networks (Chertkov and Ravina, 1998; Chertkov and Ravina, 1999) and available observations for different clay soils from Yaalon and Kalmar (1984), Zein el Abedine and Robinson (1971), and Dasog et al. (1988) showed good agreement.

After application of the multiple cracking and fragmentation model to rocks and soils, in which the crack network develops (for different reasons), it was realized that the geometrical entity of the model, that is, the division of a volume by a surface system meeting some conditions,

can likely be relevant to many geometrically similar issues of soil structure with another physical nature of the dividing surfaces. Before formulation of ISA, such an approach (“by analogy”), inspired by the multiple cracking model, was used to describe the pore structure of a clay matrix as applied to the physical modeling of clay shrinkage (Chertkov, 2000; Chertkov, 2003). With that, clay particles meeting some conditions played the part of surfaces (instead of cracks) dividing the space into the clay matrix pores (in place of soil or rock fragments). The comparison between prediction and data from Bruand and Prost (1987) and Tessier and Pedro (1984) was promising. There is a review of the prehistory of ISA (Chertkov and Ravina, 2004).

Major concepts of ISA

S- and V-objects

Geometrically, soils consist of volume-like objects (V-objects – blocks, fragments, aggregates, silt and sand grains, and 3D pores) ([Soil Aggregates, Structure, and Stability](#)) and surface-like objects (S-objects – boundaries of V-objects as well as cracks, and clay particles). S-objects have limited sizes and random orientations in space. The ratio of connected S-objects to the total number of S-objects defines the so-called connectedness of their system, $0 < C \leq 1$. S-objects do not stick together at their surfaces. Connections of S-objects of close sizes, $\sim x$, lead to the development of an S-object of a larger scale $\sim (K+1)x$ according to the concentration criterion at $K \cong 5$ (Zhurkov et al., 1981). The condition of the effective independence of S-objects: the spacing x between neighboring intersections of the S-objects with a straight line is distributed as $\exp(-x/d)$ where d is an average value (Hudson and Priest, 1979 – data for rocks; Scott et al., 1986 – data for soils). The condition of V-object formation at S-object connection: at least part of the S-objects outline V-objects totally or nearly so. The V-objects have sizes in the range, $x_{\min} \leq x \leq x_m$ (x_{\min} and x_m being the minimum and maximum sizes) and constitute a volume fraction $P \leq 1$ of the soil (rock) volume where P is a function of connectedness C (see below).

ISA distributions

If the S-objects fulfill the above geometrical conditions, the physical size distribution of V-objects originates from the division of a volume by a large number of intersecting S-objects. The elementary ISA distribution of V-objects of a given type, $F(x)$ (a volume fraction of V-objects of size $< x$ of their total volume) is given as (Chertkov, 2005):

$$F(x) = \left[1 - (1 - P)^{I(\xi(x))/8.4} \right] / P, \quad x_{\min} \leq x \leq x_m \quad (1)$$

where $I(\xi) = \ln(K+1)(4\xi)^4 \exp(-4\xi)$, ($K=5$); $\xi \equiv (x-x_{\min})/(x_m-x_{\min})$; and P is a volume fraction of V-objects (of the total volume). P is coupled with connectedness C as $P \cong 1 - \exp(-8.4C)$. Thus, the V-object size

distribution is characterized by the P , x_{\min} , and x_m parameters.

If the soil contains two different types of V-objects, for example, inter-aggregate pores with volume fraction $P = P_p$ ([Pore Size Distribution](#)) and aggregates with volume fraction $P = P_a = 1 - P_p$, the above distribution $F(x)$ can be separately written for the pores ($F(x) = F_p(x)$, $P = P_p$, $x_{\min} = x_{\min p}$, $x_m = x_{\max p}$) and aggregates ($F(x) = F_a(x)$, $P = P_a$, $x_{\min} = x_{\min a}$, $x_m = x_{\max a}$). In the general case of more than two different V-object types, the sum of all volume fractions P_j ($j = 1, \dots, J$) should be equal to unity.

The size distribution of the mixture of V-objects of a given type (e.g., I modes of pores) can be presented as the sum of I terms of corresponding elementary ISA distributions multiplied by the weights $P_i / \sum_{i=1}^I P_i$ (P_i is the porosity of the i th pore mode; $i = 1, \dots, I$) as (Chertkov, 2005):

$$F(x) = \sum_{i=1}^I \left[1 - (1 - P_i)^{I(\xi_i(x))/8.4} \right] / \sum_{i=1}^I P_i, \quad x_{\min 1} \leq x \leq x_{\max I} (x_{\min 1} < x_{\min 2} < \dots < x_{\max I}) \quad (2)$$

where $\xi_i \equiv (x-x_{\min i})/(x_{\max i}-x_{\min i})$, ($i = 1, \dots, I$). The case of $I=1$ corresponds to the elementary ISA distribution. If the $F(x)$ function gives a [Pore Size Distribution](#), $P = \sum_{i=1}^I P_i$ is the total porosity, and P_i is the volume fraction of pores of the i -th mode (of the soil volume). If the $F(x)$ function gives a solids-size distribution (e.g., for several sand-grain modes) $\sum_{i=1}^I P_i = 1 - P$ where P again is the total porosity, and P_i is the volume fraction of solids of the i -th mode (of the soil volume). The above generalized ISA distribution was checked (Chertkov, 2005) in the case of two modes ($I=2$) of sand pores (data from Day and Luthin, 1956), aggregates (data from Wittmuss and Mazurak, 1958), and silty fine sand (data from Mualem, 1976).

The presentation of [Equations 1](#) and [2](#) is relevant to both rigid and nonrigid soil matrices. However, in the case of the clay of a shrink-swell matrix the soil parameters P_i , $x_{\min i}$, and $x_{\max i}$ (for pore modes or aggregate modes) become functions of the water content (for a clay porosity example, see Chertkov, 2004).

Features of ISA

1. The ISA distribution of V-objects that fulfills the abovementioned geometrical conditions is a universal function of V-object size, x . The view of the function ([Equations 1](#) and [2](#)) does not depend on V-object type, for example, soil (rock) fragments, clay matrix pores or soil aggregates, and their methods of preparation. Materials and methods can only influence values of the P , x_{\min} , and x_m parameters (universality).

2. Except for the size distributions, ISA allows one to estimate the tortuosity of the connected S-objects (Chertkov and Ravina, 1999; Chertkov, 2005) (tortuosity estimation).
3. In connection with the soil heterogeneity and variability of a different type, the P , x_{\min} , and x_m parameters become functions of spatial coordinates and time (locality).
4. The approach enables consideration of an actual soil as a superposition of S-objects of different physical nature, for example, clay particles and cracks, and different scales, such as cracks of essentially different sizes (superposition of different S-object systems).
5. One can also estimate any shape characteristic of V-objects (Chertkov, 2005).
6. Part of the actual S-objects (cracks, slits, and clay particles) has small, but finite (nonzero) thickness (or aperture) and volume. The small thickness of such S-objects is found by independent means from physical conditions of a task.

Recent applications and perspectives

The recent physical explanation and prediction of soil shrinkage (Chertkov, 2007a, b; Chertkov, 2008a, b) essentially relies on ISA concepts in the estimation of the relevant size distributions of pores and aggregates. Without a doubt, the similar use of ISA will be needed in future physical approaches to soil swelling, residual cracking (after soil wetting), [Hydraulic Properties of Unsaturated Soils](#), and water flow.

Summary

ISA leads to the scale invariant fragment and [Pore Size Distribution](#) and permits one to take into account the superposition of S-objects of a different physical nature and scale, the connectedness and tortuosity of the S-objects, the shape characteristics, and the swelling-shrinkage of the corresponding V-objects.

Bibliography

- Azovtsev, S. N., 1984. Characteristic features of the structure and explosive disintegration of igneous rocks. In *Improving the Mining and Reprocessing Procedure for Mineral Ore* (in Russian). Moscow: Izd. Minstroimaterialov SSSR.
- Bruand, A., and Prost, R., 1987. Effect of water content on the fabric of a soil material: an experimental approach. *Journal of Soil Science*, **38**, 461–472.
- Chertkov, V. Y., 1985. Chip development during multiple crack formation in a brittle rock. *Soviet Mining Science*, **21**, 489–495.
- Chertkov, V. Y., 1986. Model of fragment formation for short-delay detonation of a series of elongated charges in fissured rock. *Soviet Mining Science*, **22**, 447–455.
- Chertkov, V. Y., 1991. Characteristics of the shape of blasted rock fragments. *Soviet Mining Science*, **27**, 528–532.
- Chertkov, V. Y., 1995. Mathematical simulation of soil cloddiness. *International Agrophysics*, **9**, 197–200.
- Chertkov, V. Y., 2000. Modeling the pore structure and shrinkage curve of soil clay matrix. *Geoderma*, **95**, 215–246.
- Chertkov, V. Y., 2003. Modelling the shrinkage curve of soil clay pastes. *Geoderma*, **112**, 71–95.
- Chertkov, V. Y., 2004. A physically based model for the water retention curve of clay pastes. *Journal of Hydrology*, **286**, 203–226.
- Chertkov, V. Y., 2005. Intersecting-surfaces approach to soil structure. *International Agrophysics*, **19**, 109–118.
- Chertkov, V. Y., 2007a. The reference shrinkage curve at higher than critical soil clay content. *Soil Science Society of America Journal*, **71**, 641–655.
- Chertkov, V. Y., 2007b. The soil reference shrinkage curve. *Open Hydrology Journal*, **1**, 1–18.
- Chertkov, V. Y., 2008a. The physical effects of an intra-aggregate structure on soil shrinkage. *Geoderma*, **146**, 147–156.
- Chertkov, V. Y., 2008b. Estimating the aggregate/intraaggregate mass ratio of a shrinking soil. *Open Hydrology Journal*, **2**, 7–14.
- Chertkov, V. Y., and Ravina, I., 1998. Modeling the crack network of swelling clay soils. *Soil Science Society of America Journal*, **62**, 1162–1171.
- Chertkov, V. Y., and Ravina, I., 1999. Tortuosity of crack networks in swelling clay soils. *Soil Science Society of America Journal*, **63**, 1523–1530.
- Chertkov, V. Y., and Ravina, I., 2004. Networks originating from the multiple cracking of different scales in rocks and swelling soils. *International Journal of Fracture*, **128**, 263–270.
- Curran, D. R., Shockley, D. A., Seaman, L., and Austin, M., 1977. (Stanford Research Institute, Menlo Park, California). Mechanisms and models of cratering in earth media. In Roddy, D. J., Repin, R. O., and Merrill, R. B. (eds.), *Impact and Explosion Cratering*. New York: Pergamon, pp. 1057–1087.
- Dasog, G. S., Acton, D. F., Mermut, A. R., and De Jong, E., 1988. Shrink-swell potential and cracking in clay soils of Saskatchewan. *Canadian Journal of Soil Science*, **68**, 251–260.
- Day, P. R., and Luthin, J. N., 1956. A numerical solution of the differential equation of flow for a vertical drainage problem. *Soil Science Society of America Proceedings*, **20**, 443–447.
- Guidi, G., Pagliai, M., and Petruzzelli, G., 1978. Quantitative size evaluation of cracks and clods in artificially dried soil samples. *Geoderma*, **19**, 105–113.
- Hudson, J. A., and Priest, S. D., 1979. Discontinuities and rock mass geometry. *International Journal of Rock Mechanics, Mining Science, and Geomechanical Abstracts*, **16**, 339–362.
- Mualem, Y., 1976. *A Catalogue of the Hydraulic Properties of Unsaturated Soils*. Research Project No. 442. Haifa, Israel: Technion, Israel Institute of Technology.
- Repin, N. Y., 1978. *Preparation and Excavation of Overburden of Coal Strip Mines* (in Russian). Nedra, Moscow.
- Scott, G. J. T., Webster, R., and Nortcliff, S., 1986. An analysis of crack pattern in clay soil: its density and orientation. *Journal of Soil Science*, **37**, 653–668.
- Tessier, D., and Pedro, G., 1984. Recherches sur le rôle des minéraux argileux dans l'organisation et le comportement des soles. In *Livre Jubilaire du Cinquantenaire*, AFES. pp. 223–234.
- Wittmuss, H. D., and Mazurak, A. P., 1958. Physical and chemical properties of soil aggregates in a Brunizem soil. *Soil Science Society of America Proceedings*, **22**, 1–5.
- Yalon, D. H., and Kalmar, D., 1984. Extent and dynamics of cracking in a heavy clay soil with xeric moisture regime. In Bouma, J., and Raats, P. A. C. (eds.), *Proceedings of ISSS Symposium on Water and Solute Movement in Heavy Clay Soils*. Wageningen. The Netherlands, pp. 45–48.
- Zein el Abedine, A., and Robinson, G. H., 1971. A study on cracking in some vertisols of the Sudan. *Geoderma*, **5**, 229–241.
- Zhurkov, S. N., Kuksenko, V. S., and Petrov, V. A., 1981. Physical principles of prediction of mechanical disintegration. *Soviet Physics, Doklady*, **26**, 755–757.

Cross-references

- [Cracking in Soils](#)
- [Hydraulic Properties of Unsaturated Soils](#)
- [Pore Size Distribution](#)
- [Shrinkage and Swelling Phenomena in Soils](#)
- [Soil Aggregates, Structure, and Stability](#)

SOIL STRUCTURE, VISUAL ASSESSMENT

Lothar Müller

Leibniz – Centre for Agricultural Landscape Research (ZALF), Institute of Landscape Hydrology, Müncheberg, Germany

Definition

Visual assessment of soil structure is a procedure for obtaining and evaluating information on the feature and function of soils from macro-morphological characteristics of the soil structure.

Role and purpose

Soil structure is a soil property and a criterion of agricultural soil quality. Soil structure is vulnerable to change by management and degradation processes like

compaction and erosion, and its preservation is key to sustaining soil function. Visual soil structure refers to macro-morphological features of soil structure that can be detected and evaluated in the field. Soil structural features meet the farmers' perception of soil quality (Shepherd, 2000; Batey and McKenzie, 2006) and are correlated with measured data of physical soil quality (Shepherd, 2003; Lin et al., 2005) and crop yield (Mueller et al., 2009a). Visual assessment of soil structure may serve as a diagnostic tool for the recognition and evaluation of the morphological and functional status of soil. Structure features and function result from soil substratum and genetic and management factors. This offers the potential to provide semiquantitative information for use in extension and monitoring or even modeling (Roger-Estrade et al., 2009). Visual soil structure assessment may also serve as a research tool in conjunction with measurements and analyses of soils. Some methods identify layers and can provide useful guidance for locating further measurements. Visual soil structure evaluation plays a particularly important role in organic farming where good structure is vital to mineralize nutrients and where poor soil structure cannot be compensated by an extra input of agrochemicals in those systems (Munkholm et al., 2003). Visual soil structure assessment may explain only part of crop yield variability, as the influence of inherent soil properties and climate on crop yield is dominant, particularly over larger regions.



Soil Structure, Visual Assessment, Figure 1 Assessment of soil structure by the visual soil assessment (VSA) method of Shepherd (2009) (Photo: T. Graham Shepherd). (a) Good conditions, VS = 2: soil dominated by friable, fine aggregates with no significant clodding. Aggregates are generally sub-rounded and often quite porous. (b) Moderate conditions, VS = 1: soil contains significant proportions (50%) of both coarse clods and friable fine aggregates. The coarse clods are firm, sub-angular or angular in shape and have few or no pores. (c) Poor conditions, VS = 0: soil dominated by coarse clods with very few finer aggregates. The coarse clods are very firm, angular or sub-angular in shape and have very few or no pores.

Methods

Visual assessment of soil structure includes (1) recognition and description of soil structure and rooting features, visible to the naked eye; (2) classification, evaluation, and parameterization of visual soil structure, and sometimes (3) conclusions on the functional status of soil. Visual-tactile recognizable soil features like type, size, and hierarchy of aggregates, inter- and intra-aggregate porosity, and number and size of biogenic pores including earthworm casts may serve to evaluate and classify the quality of soil structure. Over the past decades, several methods have been evolved. Most of them differ in several important ways including depth of the soil under consideration, handling the soil prior to assessment, emphasis placed on particular features of soil structure, and application of size increments and direction of scoring scales. One of the most accepted methods is that of Peerlkamp (1967).

It has a conjoint scale referring to type and size of aggregates and pores. The main advantages of this method are speed and minor soil disturbance, providing comparative statistical analyses both in large fields and also in small plots of long-term trials. However, the scoring framework has potential for subjective errors. Methods like the “Le profil cultural” (Roger-Estrade et al., 2004), SOILpak (McKenzie, 2001), or the method of Werner and Thaemert (1989) or Munkholm et al. (2005) provide single scorings of different structure features. This is more time-consuming, a total assessment is sometimes difficult, and a total numerical score, though desirable, may not be part of the test. The New Zealand Visual Soil Assessment (VSA) method (Shepherd, 2000) is a multi-parameter technique based on scoring a spadeful of soil by different criteria. Disaggregation of soil after a drop-shatter test is a key criterion for assessing soil structure (Figure 1) and helps minimize

Structure quality	Ease of break up (moist soil)	Size and appearance of aggregates	Visible porosity	Roots	Appearance after break-up: various soils	Appearance after break-up: same soil different tillage	Distinguishing feature
Sq1 friable (tends to fall off the spade)	Aggregates readily crumble with fingers	Mostly <6 mm after crumbling	Highly porous	Roots throughout the soil			 Fine aggregates
Sq2 intact (most is retained on the spade)	Aggregates easy to break with one hand	A mixture of porous, rounded aggregates from 2 mm to 7 cm. No clods present	Most aggregates are porous	Roots throughout the soil			 High aggregate porosity
Sq3 firm	Most aggregates break with one hand	A mixture of porous aggregates from 2 mm to 10 cm; less than 30% are <1 cm. Some angular, non-porous aggregates (clods) may be present	Macropores and cracks present. Some porosity within aggregates shown as pores or roots.	Most roots are around aggregates			 Low aggregate porosity
Sq4 compact	Requires considerable effort to break aggregates with one hand	Mostly large >10 cm and sub-angular non-porous: horizontal/platy also possible; less than 30% are <7 cm	Few macropores and cracks	All roots are clustered in macropores and around aggregates			 Distinct macropores
Sq5 very compact	Difficult	Mostly large >10 cm, very few <7 cm, angular and non-porous	Very low; macropores may be present; may contain anaerobic zones	Few, if any, restricted to cracks			 Grey-blue colour

Soil Structure, Visual Assessment, Figure 2 Visual soil structure quality assessment by the revised Peerlkamp method (Ball et al., 2007). (Photo: Bruce C. Ball.)

the subjective handling of the soil prior to assessment. A quantitative comparison of some methods and their correlations with measured physical parameters after standardizing data revealed that many methods provided similar results (Mueller et al., 2009a). Types and sizes of aggregates and abundance of biological macropores were the most reliable criteria relating to measurement data and crop yields. Differences in soil management or effects of compaction may be detected by visual assessment of the soil (Batey and McKenzie, 2006; Mueller et al., 2009b). Unfavorable visual structure scores were associated with increased dry bulk density, higher soil strength, and lower infiltration rate but correlations were site specific. Visual soil structure assessments may form part of overall soil characterizations (FAO, 2006; WRB, 2006). Field data of this method may be parameterized by a simple coding scheme given by Mueller et al. (2009a). Overall soil and land quality rating schemes like the Muencheberg Soil Quality Rating (Mueller et al., 2007) include soil structure indicators.

Recommendation

Visual methods based on, or supplemented by illustrations, have clear advantages for the reliable assignment of a rating score based on visual diagnostic criteria. The latest development of the Peerlkamp method provided by Ball et al. (2007) (Figure 2) is well illustrated. Also, the New Zealand Visual Soil Assessment (VSA) (Shepherd, 2009) as an illustrated multi-criteria method, enabling reliable assessments of the soil structure status.

Summary

Methods of visual soil structure examination enable semi-quantitative information on the morphological and functional status of soil for use in extension, monitoring, modeling, and research. Type and size of aggregates and number and size of biogenic pores are reliable criteria.

Illustrated methods like the updated Peerlkamp method (Ball et al., 2007) and the Visual Soil Assessment (Shepherd, 2009) lead to ordinally scaled scores are easy to learn and use and are reliable in handling.

Bibliography

- Ball, B. C., Batey, T., and Munkholm, L. J., 2007. Field assessment of soil structural quality – a development of the Peerlkamp test. *Soil Use and Management*, **23**, 329–337.
- Batey, T., and McKenzie, D. C., 2006. Soil compaction: identification directly in the field. *Soil Use and Management*, **22**, 123–131.
- FAO, 2006. *Guidelines for Soil Description*, 4th edn. Rome: FAO.
- Lin, H., Bouma, J., Wilding, L. P., Richardson, J. L., Kutilek, M., and Nielsen, D. R., 2005. Advances in hydromechanics. In Sparks, D. L. (ed.), *Advances in Agronomy*. Amsterdam: Elsevier Academic, Vol. 85, pp. 2–76.
- McKenzie, D. C., 2001. Rapid assessment of soil compaction damage. I. The SOILpak score, a semi-quantitative measure of soil structural form. *Australian Journal of Soil Research*, **39**, 117–125.
- Mueller, L., Kay, B. D., Hu, C., Li, Y., Schindler, U., Behrendt, A., Shepherd, T. G., and Ball, B. C., 2009a. Visual assessment of soil structure: Evaluation of methodologies on sites in Canada, China and Germany: Part I: comparing visual methods and linking them with soil physical data and grain yield of cereals. *Soil and Tillage Research*, **103**, 178–187.
- Mueller, L., Kay, B. D., Deen, B., Hu, C., Wolff, M., Eulenstein, F., and Schindler, U., 2009b. Visual assessment of soil structure: Part II. Implications of tillage, rotation and traffic on sites in Canada, China and Germany. *Soil and Tillage Research*, **103**, 188–196.
- Mueller, L., Schindler, U., Behrendt, A., Eulenstein, F., and Dannowski, R., 2007. Das Muencheberger Soil Quality Rating (SQR): Ein einfaches Verfahren zur Bewertung der Eignung von Boeden als Farmland. *Mitteilungen der Deutschen Bodenkundlichen Gesellschaft*, **110**, 515–516.
- Munkholm, L. J., Schjonning, P., Jorgensen, M. H., and Thorup-Kristensen, K., 2005. Mitigation of subsoil recompaction by light traffic and on-land ploughing. II. Root and yield response. *Soil and Tillage Research*, **80**, 159–170.
- Munkholm, L. J., Schjonning, P., Rasmussen, K. J., and Tanderup, K., 2003. Spatial and temporal effects of direct drilling on soil structure in the seedling environment. *Soil and Tillage Research*, **71**, 163–173.
- Peerlkamp, P. K., 1967. Visual estimation of soil structure. In de Boodt, M., de Leenherr, D. E., Frese, H., Low, A. J., and Peerlkamp, P. K. (eds.), *West European Methods for Soil Structure Determination*. Belgium: State Faculty of Agricultural Sciences Ghentvol, Vol 2, No. 11, pp. 216–223.
- Roger-Estrade, J., Richard, G., Caneill, J., Boizard, H., Coquet, Y., Dé Fossez, P., and Manichon, H., 2004. Morphological characterisation of soil structure in tilled fields. From a diagnosis method to the modelling of structural changes over time. *Soil and Tillage Research*, **79**, 33–49.
- Roger-Estrade, J., Richard, G., Dexter, A. R., Boizard, H., De Tourdonnet, S., Bertrand, M., and Caneill, J., 2009. Integration of soil structure variations with time and space into models for crop management. A review. *Agronomy of Sustainable Development*, **29**, 135–142.
- Shepherd, T. G., 2000. *Visual Soil Assessment. Volume 1. Field Guide for Cropping and Pastoral Grazing on Flat to Rolling Country*. Palmerston North: Horizons.mw/Landcare Research, pp. 84.
- Shepherd, T. G., 2003. Assessing soil quality using visual soil assessment. In Currie, L. D., and Hanly, J. A. (eds.), *Tools for Nutrient and Pollutant Management: Applications to Agriculture and Environmental Quality*. Occasional Report No. 17. Palmerston North: Fertilizer and Lime Research Centre, Massey University, pp. 153–166.
- Shepherd, T. G., 2009. *Visual Soil Assessment. Volume 1. Field Guide for Pastoral Grazing and Cropping on Flat to Rolling Country*, 2nd edn. Palmerston North: Horizons Regional Council, 119 pp.
- Werner, D., and Thaemert, W., 1989. Zur Diagnose des physikalischen Bodenzustandes auf Produktionsflächen. *Archive für Acker-Pflanzenbau und Bodenkunde*. Berlin, **33**, 729–739.
- WRB, 2006. World Reference Base for Soil Resources 2006, A Framework for International Classification, Correlation and Communication, FAO Rome, 2006, World Soil Resources Reports 103.

Cross-references

- [Soil Aggregates, Structure, and Stability](#)
[Soil Structure, Intersecting Surface Approach, and its Applications](#)

SOIL SURFACE SEALING AND CRUSTING

Shmuel Assouline

Environmental Physics and Irrigation, Institute of Soil, Water and Environmental Sciences, Agricultural Research Organization – Volcani Center, Bet Dagan, Israel

Definition

Often, the surface of bare soils is topped with a relatively thin and hard layer that tends to peal when it dries. This layer was named “crust,” and the process of its formation was addressed as “soil surface crusting.” Many different causes to its formation were identified: high-intensity rain-storm, fire, microbiological activity, mechanical compaction, or chemical treatments. In some cases, like during rainstorms for example, the formation of that particular layer on top of the soil profile occurs under wet conditions. In those cases, the term “crust” is replaced by the term “seal” to differentiate the layer during its formation from that obtained after drying. When rainfall is the cause to seal formation, structural seals generated by the impact of raindrops, and depositional seals resulting from the settling of suspended solids in runoff can be formed.

Presence of seals or crusts at the soil surface can induce severe agricultural, hydrological, and environmental hazards: decrease of the infiltration rate; reduction of the available water to plants; diminution of aquifers’ recharge; increase of runoff; and limitation of seedlings and crop yields. In semiarid regions, crust presence can enhance a vicious cycle that intensifies desertification by reducing vegetation cover, initiating overgrazing, and finally leaving the soil surface bare and prone to seal formation. On the other hand, it can be beneficial as it augments runoff and improves the efficiency of water harvesting installations.

Introduction

Soil surface sealing may result from different causes such as raindrop impacts, fire, biological activity, and mechanical or chemical treatments. This complex phenomenon has been studied through extensive laboratory and field experimental investigations and different conceptual and empirical models of seal formation were suggested.

Rainfall-induced seals, also called structural seals, form at the surface of bare soils exposed to the direct impact of raindrops. Their formation is dominated by a wide variety of factors involving soil properties, rainfall characteristics, and flow conditions. Different reviews on the subject are available (Mualem et al., 1990a; Bradford and Huang, 1992; Assouline, 2004).

Depositional seals are formed when water rich in suspended solids infiltrates into the soil. The nature, the composition, the thickness, and the hydraulic properties of such seal layers depend on soil clay mineralogy and the chemical conditions in the soil-water system

prevailing during their formation. Depositional seals reduce the hydraulic conductivity of the soil profile and therefore affect infiltration and evaporation processes. Detailed information can be found in Shainberg (1992), Lado et al. (2007), and Bhardwaj et al. (2009).

Biological, or microbiotic, crusts are composed of lichens, cyanobacteria, algae, mosses, and fungi. These components improve the binding of soil particles together, thereby increasing soil surface stability and resistance to water and wind erosion. They affect soil physicochemical properties and, consequently, soil wetting and drying processes. Detailed information on this topic could be found in Evans and Johansen (1999), Belnap (2003), Eldridge and Greene (1994), and Eldridge et al. (2000).

In the following lines, the methodology applied to characterize seal morphology and properties, formation, and effects on flow processes is presented through the study of structural crusts formed under high-kinetic energy rainfalls.

Morphology and properties of rainfall-induced crusts

Reviews on seal morphology and properties were presented by Mualem et al. (1990a), West et al. (1992), and Assouline (2004). Various methods were applied to determine crust morphology: examination of thin sections of the crusted soil surface by means of light microscope, electron microscope, or X-rays radiography and tomography; mechanical analysis of the upper soil layer; measurements of hydraulic head distribution in the upper soil layer; and analysis of data from infiltration tests. The characteristics of structural crusts appear to strongly relate to the conditions prevailing during their formation.

The two-layer structure of McIntyre (1958a, b), which consists of a 0.1-mm skin overlying a 2.0-mm washed-in layer, is the most widely adopted description of the crust (Tackett and Pearson, 1965; Onofio and Singer, 1984; Tarchitzky et al., 1984; Wakindiki and Ben-Hur, 2002). It is interesting to note that this two-layer structure resulted from visual examination of the crust. When different methods were applied, like porosity or bulk density measurements, the results showed that gradual changes of structure within the crust were more likely to exist (Epstein and Grant, 1973; Eigel and Moore, 1983; Roth, 1997; Fohrer et al., 1999; Bresson et al., 2004; Augeard et al., 2007).

The reported crust thickness based on laboratory experiments varied by two orders of magnitude, from 0.1 mm (Chen et al., 1980; Wakindiki and Ben-Hur, 2002) to 10.0 mm and more (Sharma et al., 1981; Bresson and Boiffin, 1990; Roth, 1997; Fohrer et al., 1999; Bresson et al., 2004). Under field conditions, larger thicknesses than those observed in the laboratory, up to 20.0 mm, were reported (Hadas and Frenkel, 1982). Similarly, the ratio between the saturated hydraulic conductivities of the seal and that of the undisturbed soil underneath presents a huge variability, from 20% (Tackett and Pearson,

1965) to 1% (Hadas and Frenkel, 1982; Simunek et al., 1998) and even to 0.1% or 0.01% (Morin et al., 1981; Perez et al., 1999). Crust saturated hydraulic conductivity also is related to the conditions prevailing during seal formation: Baumhardt et al. (1990) reported that the conductance of the upper 10 mm of a sealed soil profile ranges between 0.013 h⁻¹ and 0.071 h⁻¹, depending on the applied rainfall intensity.

The crust layer is more compacted than the undisturbed soil underneath. A gradual increase of the bulk density from a depth of 10 mm below soil surface to the crust surface was measured (Eigel and Moore, 1983; Roth, 1997; Fohrer et al., 1999; Bresson et al., 2004). Augeard et al. (2008) showed that this distribution depends on the flow conditions during seal formation.

Different conceptual models of the crust layer were proposed. Hillel and Gardner (1969, 1970) suggested the simplified model of a single uniform saturated layer of constant low permeability, generally assumed to be 5-mm thick. This model was widely adopted to study infiltration into sealed soils (Ahuja, 1983; Brakensiek and Rawls, 1983; Parlange et al., 1984; Vandevaere et al., 1998). Mualem and Assouline (1989) have proposed the model of a nonuniform layer where the bulk density, ρ_c , decreases exponentially with depth, h , to that of the undisturbed soil, ρ :

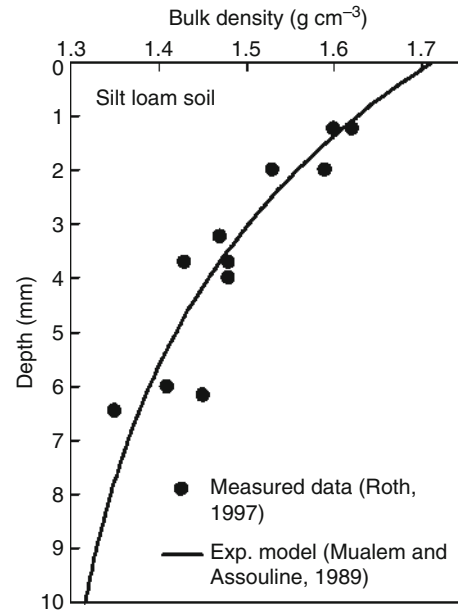
$$\rho_c(h) = \rho + \Delta\rho_o e^{-\gamma h}; \quad h = -Z \quad (1)$$

where Z is the elevation taken positive upward, $\Delta\rho_o$ is the maximum change in bulk density at the soil surface ($h = 0$), and γ is a characteristic parameter of the soil–rainfall interaction. This model was validated by the experimental results of Roth (1997), Bresson et al. (2004), and Augeard et al. (2008). Figure 1 depicts the distribution with depth of ρ_c measured by Roth (1997) in a crusted silt loam soil, and the fitted exponential model in Equation 1.

Formation of structural seals

During rainfall on a bare soil surface, transfer of kinetic energy from the raindrop to the surface and soil wetting occur simultaneously. Consequently, the processes involved in seal formation are (1) destruction of the soil aggregates exposed to the direct impact of the rain drops (Farres, 1978), (2) compaction (McIntyre, 1958a, b; Epstein and Grant, 1973; Bresson and Boiffin, 1990), (3) slaking (Moore, 1981b; Valentin and Ruiz Figueroa, 1987), (4) particle segregation (Eigel and Moore, 1983; Radcliffe et al., 1991), and (5) pore filling and clogging by wash-in of fine material (McIntyre, 1958a, b; Farres, 1978; Valentin and Bresson, 1992). Chemical dispersion resulting from the specific chemistry of the soil–rainfall system could play an additional significant role (Agassi et al., 1981). The relative importance of each of these processes depends upon the initial and boundary conditions that prevail during seal formation.

The study of seal formation addressed morphological aspects (Tackett and Pearson, 1965; Edwards and



Soil Surface Sealing and Crusting, Figure 1 Distribution with depth of ρ_c as measured by Roth (1997) in a crusted silt loam soil, and the fitted exponential model of Equation 1.

Larson, 1969; Farres, 1978; Bresson and Boiffin, 1990; Fohrer et al., 1999; Augeard et al., 2008) and impact on infiltration (Morin and Benyamin, 1977; Romkens et al., 1986; Baumhardt et al., 1990; Assouline and Mualem, 2000; 2001; Augeard et al., 2008). Modeling approaches for the different aspects of seal formation were suggested (Farres, 1978; Edwards and Larson, 1969; Baumhardt et al., 1990; Mualem et al., 1990b). In these models, the rainfall was represented by its duration, t (Moore, 1981b; Ahuja, 1983) or cumulative kinetic energy, E (Brakensiek and Rawls, 1983; Mualem et al., 1990b).

Assouline and Mualem (1997) proposed to model seal formation in terms of the temporal increase of the bulk density of the soil surface during the rainfall. This model relates the dynamics of the process to the initial soil mechanical and hydraulic properties as well as the physical characteristics of the regional rainfall. The bulk density increase at the soil surface, $\Delta\rho_o$, resulting from raindrop impact and wetting is related to rainfall intensity, I , and duration, t :

$$\Delta\rho_o(I, t) = \Delta\rho_o^*(1 - e^{-\xi t}) \quad (2)$$

where $\Delta\rho_o^*$ is the maximal change characterizing the final seal and the soil–rainfall characteristic, ξ , is defined by

$$\xi = \frac{6\omega kI}{d_{\max} \Delta\rho^* \tau(\rho_i, \psi_i)} \int_0^{d_{\max}} d^2 f(d, I) \delta d \quad (3)$$

where $f(d, I)$ is the raindrop size distribution, d_{\max} , the maximal drop diameter, k , a rainfall parameter

interrelating raindrop velocity and drop diameter d , ω , a fitting parameter, and $\tau(\rho_i, \psi_i)$, the initial soil shear strength. Figure 2 depicts the $\Delta\rho_o(t)$ relationship measured by Augeard et al. (2008) and the fitted dynamic model in Equations 2 and 3.

The theoretical analysis leading to Equation 3 indicated that rainfall cumulative kinetic energy, E , and intensity, I , determine the seal formation rate, in agreement with the result from the statistical analysis of Romkens et al. (1986).

Several physical, chemical, and mineralogical soil and rainfall properties were found to affect seal formation (Bradford and Huang, 1992; Shainberg, 1992). Rainfall intensity and kinetic energy were found to be decisive in determining the seal properties and the rate of seal formation (Morin and Benyamin, 1977; Romkens et al., 1986; Baumhardt et al., 1990). Soil properties affecting the cohesive power between the soil particles were found also to play a role in seal formation. These properties included soil mineralogy, texture, and structure (Mannering, 1967; Moldenhauer and Kemper, 1969; Farres, 1978; Tarchitzky et al., 1984; Freebairn et al., 1991; Bradford and Huang, 1993; Wakindiki and Ben-Hur, 2002); aggregate stability (Bryan, 1969; Le Bissonnais, 1996); initial bulk density and water content (Francis and Cruse, 1983; Luk, 1985; Le Bissonnais and Singer, 1992; Augeard et al., 2008); application of phosphogypsum or polymers to the upper soil layer (Helalia et al., 1988; Shainberg, 1992); slope (Poesen, 1987; Bradford and Huang, 1993; Fox et al., 1997); organic matter content (Le Bissonnais and Arrouays, 1997); soil exchangeable sodium percentage (ESP); and electrical conductivity (EC) of the applied water (Agassi et al., 1981; Hadas and Frenkel, 1982; Shainberg, 1992).

Effect of soil sealing on flow processes

The complexity of the soil-sealing phenomenon requires the use of physically based quantitative models to study the

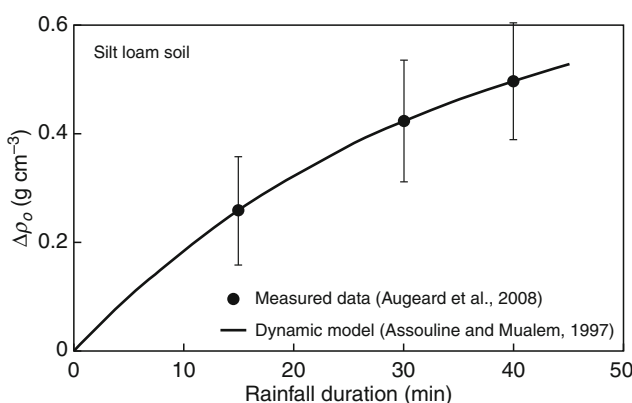
impact of seal formation on flow processes. Such models have to address two main aspects: the definition of the seal hydraulic properties and the simulation of the dynamics of seal formation.

The simplest model of the seal properties assumed a saturated soil layer with constant hydraulic conductivity and thickness (Hillel and Gardner, 1970; Ahuja and Swartzendruber, 1973). Although technically appropriate for simulating infiltration, it cannot simulate redistribution and drying processes, for which the entire hydraulic functions, i.e., water retention curve and hydraulic conductivity function, are needed. Approximated hydraulic properties were suggested by Moore (1981a), Philip (1998), Baumhardt et al. (1990), and Smith et al. (1999). Mualem and Assouline (1989) proposed a conceptual link between the hydraulic properties of the seal layer and those of the undisturbed seal underneath.

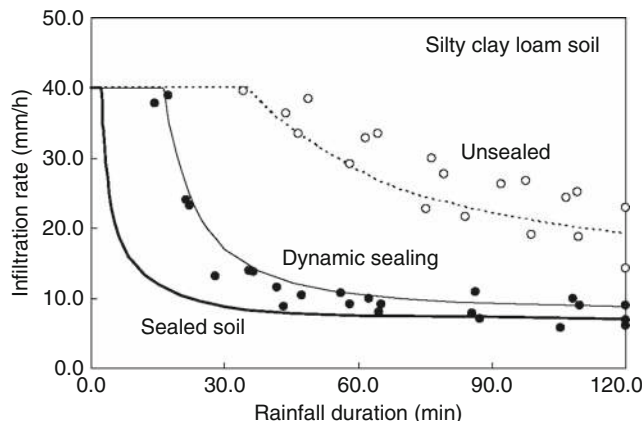
The first solution of infiltration into a sealed soil profile was proposed by Hillel and Gardner (1969, 1970), where the Green and Ampt (1911) approach was applied to a uniform soil profile capped with a saturated thin layer of low permeability and prescribed constant properties. This basic approach was adopted in a series of studies on infiltration through sealed soils with constant seal properties (Ahuja, 1983; Moore, 1981a; Parlange et al., 1984), or time-dependent ones (Farrell and Larson, 1972; Moore, 1981b; Ahuja, 1983; Brakensiek and Rawls, 1983; Vandevaere et al., 1998). The Green–Ampt approach was considered inappropriate to the simulation of infiltration into crusted soils sealed by Philip (1998), who preferred the flux-concentration method (Philip, 1973).

A different approach solving numerically the one-dimensional water flow equation was proposed by Baumhardt et al. (1990), Mualem et al. (1993), and Assouline and Mualem (1997). In these studies, the hydraulic properties of the seal layer are derived from the soil–rainfall system characteristics. This approach was extended to evaluate the combined effect of soil seal formation and areal heterogeneity of soil hydraulic properties on infiltration (Assouline and Mualem, 2002) and on runoff at the watershed scale (Assouline and Mualem, 2006). Figure 3 illustrates the effect of a completely formed seal and the effect of a seal under formation on infiltration compared to an undisturbed (mulched) soil for a constant rainfall intensity of 40 mm/h. The measured data were reported by Baumhardt (1985). The measured data were reported by Baumhardt (1985). The dashed curve results from the solution of the flow equations for the unsealed soil, the thin solid line corresponds to the calibrated dynamic model of Assouline and Mualem (1997), and the bold line is the predicted infiltration curve for a sealed soil profile following the model of Mualem and Assouline (1989).

Soil crusting affects also evaporation. Besides the fact that crust formation reduces water penetration and consequently, soil water content, it was shown to reduce evaporation directly (Bresler and Kemper, 1970; Jones et al., 1994). Assouline and Mualem (2003) have simulated the impact of constant evaporation on the water regime of



Soil Surface Sealing and Crusting, Figure 2 The change of ρ_c at the soil surface, $\Delta\rho_o$, during rainfall as measured by Augeard et al. (2008) and the fitted dynamic model of Assouline and Mualem (1997).



Soil Surface Sealing and Crusting, Figure 3 Infiltration through (1) a completely formed seal (bold line), (2) a seal under formation (thin solid line), and (3) an undisturbed silty clay loam soil (dashed line). The measured data (dots) are from Baumhardt (1985).

sealed soil profiles, showing that the sealed surface dries quicker than the undisturbed one, indicating that the seal surface acts as a barrier preventing further evaporation.

Summary

Bare soil surface can be prone to seal or crust formation. Different types of seals or crusts resulting from various processes are identified: structural seals resulting from high-intensity rainstorm; depositional seals or crusts resulting from the percolation of runoff water rich in suspended solids; post-fire crusts; biological or microbiotic crusts formed by nonvascular plants. Soil surface sealing can have severe agricultural, hydrological, and environmental effects. It decreases infiltration rate, reduces available water to plants, diminishes natural recharge of aquifers, increases runoff, and decreases crop yields. Seal formation is a complex phenomenon that involves several factors characterizing soil and rainfall physicochemical properties and flow initial and boundary conditions prevailing during the process. This entry presents the methodology applied to the investigation of rainfall-induced soil surface sealing, in terms of morphology, phenomenology, and modeling approaches to simulate the effect of on flow processes, as an illustrative case study of all the different seal types.

Bibliography

- Agassi, M., Shainberg, I., and Morin, J., 1981. Effect of electrolyte concentration and soil sodicity on infiltration rate and crust formation. *Soil Science Society of America Journal*, **45**, 848–851.
- Ahuja, L. R., 1983. Modeling infiltration into crusted soils by the Green-Ampt approach. *Soil Science Society of America Journal*, **47**, 412–418.
- Ahuja, L. R., and Swartzendruber, D., 1973. Horizontal soil-water intake through a thin zone of reduced permeability. *Journal of Hydrology*, **19**, 71–89.
- Assouline, S., 2004. Rainfall-induced soil surface sealing: a critical review of observations, conceptual models and solutions. *Vadose Zone Journal*, **3**, 570–591.
- Assouline, S., and Mualem, Y., 1997. Modeling the dynamics of seal formation and its effect on infiltration as related to soil and rainfall characteristics. *Water Resources Research*, **33**(7), 1527–1536.
- Assouline, S., and Mualem, Y., 2000. Modeling the dynamics of soil seal formation: analysis of the effect of soil and rainfall properties. *Water Resources Research*, **36**, 2341–2349.
- Assouline, S., and Mualem, Y., 2001. Soil seal formation and its effect on infiltration: Uniform versus nonuniform seal approximation. *Water Resources Research*, **37**, 297–305.
- Assouline, S., and Mualem, Y., 2002. Infiltration during soil sealing: The effect of areal heterogeneity of soil hydraulic properties. *Water Resources Research*, **38**(12), doi:10.1029/2001WR001168.
- Assouline, S., and Mualem, Y., 2003. Effects of rainfall-induced soil seals on the soil water regime: drying intervals and subsequent wetting. *Transport in Porous Media*, **53**, 75–94.
- Assouline, S., and Mualem, Y., 2006. Runoff from heterogeneous small bare catchments during soil surface sealing. *Water Resources Research*, **42**, W12405, doi:10.1029/2005WR004592.
- Augeard, B., Assouline, S., Fonty, A., Kao, C., and Vauclin, M., 2007. Estimating hydraulic properties of rainfall-induced soil surface seals from infiltration experiments and X-ray bulk density measurements. *Journal of Hydrology*, **341**, 12–26, doi:10.1016/j.jhydrol.2007.04.018.
- Augeard, B., Bresson, L. M., Assouline, S., Gaskuel, C., Kao, C., and Vauclin, M., 2008. Dynamics of soil surface bulk density: Role of water table elevation and rainfall duration. *Soil Science Society of America Journal*, **72**, 412–423, doi:10.2136/sssaj2006.0429.
- Baumhardt, R. L., 1985. *The effect of rainstorm characteristics on soil sealing and infiltration*. PhD thesis, Mississippi: Mississippi State University.
- Baumhardt, R. L., Romkens, M. J. M., Whisler, F. D., and Parlange, J. Y., 1990. Modeling infiltration into a sealing soil. *Water Resources Research*, **26**, 2497–2505.
- Belnap, J., 2003. Biological soil crusts in desert: a short review of their role in soil fertility, stabilization and water relation. *Archiv fuer Hydrobiologie supplement*, **148**, 113–126.
- Bhardwaj, A. K., McLaughlin, R. A., Shainberg, I., and Levy, G. J., 2009. Hydraulic characteristics of depositional seals as affected by exchangeable cations, clay mineralogy, and polyacrylamide. *Soil Science Society of America Journal*, **73**, 910–918.
- Bradford, J. M., and Huang, C., 1992. Physical components of crusting. In Sumner, M. E., and Stewart, B. A. (eds.), *Soil Crusting: Chemical and Physical Processes*. Boca Raton: Lewis, pp. 55–72.
- Bradford, J. M., and Huang, C., 1993. Comparison of interill soil loss for laboratory and field procedures. *Soil Technology*, **6**, 145–156.
- Brakensiek, D. L., and Rawls, W. J., 1983. Agricultural management effects on water processes, II, Green and Ampt parameters for crusting soils. *Transactions of the ASAE*, **26**, 1753–1757.
- Bresler, E., and Kemper, W. D., 1970. Soil water evaporation as affected by wetting methods and crust formation. *Soil Science Society of America Journal*, **34**, 3–8.
- Bresson, L. M., and Boiffin, J., 1990. Morphological characterisation of soil crust development stages on an experimental field. *Geoderma*, **47**, 301–325.
- Bresson, L. M., Moran, C. J., and Assouline, S., 2004. Use of bulk density profiles from X-radiography to examine structural crusts models. *Soil Science Society of America Journal*, **68**(4), 1169–1176.

- Bryan, R. B., 1969. The relative erodibility of soils developed in the Peak District of Derbyshire. *Geografiska Annaler*, **51A**, 145–149.
- Chen, Y., Tarchitzky, J., Brouwer, J., Morin, J., and Banin, A., 1980. Scanning electron microscope observations on soil crusts and their formation. *Soil Science*, **130**, 49–55.
- Edwards, W. M., and Larson, W. E., 1969. Infiltration of water into soils as influenced by surface seal development. *Transactions of the ASAE*, **12**(463–465), 470.
- Eigel, J. D., and Moore, I. D., 1983. Effect of rainfall energy on infiltration into bare soil. In *Proceedings of the National Conference on Advances in Infiltration*. December 12–13, 1983, Chicago, ASAE.
- Eldridge, D. J., and Greene, R. S. B., 1994. Microbiotic soil crusts – a review of their roles in soil and ecological processes in the rangelands of Australia. *Australian Journal of Soil Research*, **32**, 389–415.
- Eldridge, D. J., Zaady, E., and Shachak, M., 2000. Infiltration through three contrasting biological soil crusts in patterned landscapes in the Negev, Israel. *Catena*, **40**, 323–336.
- Epstein, E., and Grant, W. J., 1973. Soil crust formation as affected by raindrop impact. In Hadas, A., Swartzendruber, D., Rijtema, P. E., Fuchs, M., and Yaron, B. (eds.), *Physical Aspects of Soil Water and Salts Eco-Systems*. New York: Springer, pp. 195–201.
- Evans, R. D., and Johansen, J. R., 1999. Microbiotic crust and ecosystem processes. *Critical Reviews in Plant Sciences*, **18**, 183–225.
- Farrell, D. A., and Larson, W. E., 1972. Dynamics of the soil–water system during a rainstorm. *Soil Science*, **113**, 88–96.
- Farres, P., 1978. The role of time and aggregate size in the crusting process. *Earth Surface Processes*, **3**, 243–254.
- Fohrer, N., Berkenhagen, J., Hecker, J.-M., and Rudolph, A., 1999. Changing soil and surface conditions during rainfall – single rainstorm/subsequent rainstorms. *Catena*, **37**, 355–375.
- Fox, D. M., Bryan, R. B., and Price, A. G., 1997. The influence of slope angle on final infiltration rate for interrill conditions. *Geoderma*, **80**, 181–194.
- Francis, P. B., and Cruse, R. M., 1983. Soil water matric potential effects on aggregate stability. *Soil Science Society of America Journal*, **47**, 578–581.
- Freebairn, D. M., Gupta, S. C., and Rawls, W. J., 1991. Influence of aggregate size and microrelief on development of surface soil crusts. *Soil Science Society of America Journal*, **55**, 188–195.
- Green, W. H., and Ampt, G. A., 1911. Studies on soil physics, 1, the flow of air and water through soils. *Journal of Agricultural Science*, **4**, 1–24.
- Hadas, A., and Frenkel, H., 1982. Infiltration as affected by long-term use of sodic-saline water for irrigation. *Soil Science Society of America Journal*, **46**, 524–530.
- Helalia, A. M., Letey, J., and Graham, R. C., 1988. Crust formation and clay migration effects on infiltration rate. *Soil Science Society of America Journal*, **52**, 251–255.
- Hillel, D., and Gardner, W. R., 1969. Steady infiltration into crust topped profiles. *Soil Science*, **108**, 137–142.
- Hillel, D., and Gardner, W. R., 1970. Transient infiltration into crust topped profiles. *Soil Science*, **109**, 69–76.
- Jones, O. R., Hauser, V. L., and Popham, T. W., 1994. No-tillage effects on infiltration, runoff, and water conservation on dryland. *Transactions of the ASAE*, **37**, 473–479.
- Lado, M., Ben-Hur, M., and Shainberg, I., 2007. Clay mineralogy, ionoc composition, and pH effects on hydraulic properties of depositional seals. *Soil Science Society of America Journal*, **71**, 314–321.
- Le Bissonnais, Y., 1996. Aggregate stability and assessment of soil crusting and erodibility: I. Theory and methodology. *European Journal of Soil Science*, **47**, 425–437.
- Le Bissonnais, Y., and Arrouays, D., 1997. Aggregate stability and assessment of soil crustability and erodibility II. Application to humic loamy soils with various organic carbon contents. *European Journal of Soil Science*, **48**, 39–48.
- Le Bissonnais, Y., and Singer, M. J., 1992. Crusting, runoff and erosion response to soil water content and successive rainfalls. *Soil Science Society of America Journal*, **56**, 1898–1903.
- Luk, S. H., 1985. Effect of antecedent soil moisture content on rain-wash erosion. *Catena*, **12**, 129–139.
- Manning, J. V., 1967. *The relationship of some physical and chemical properties of soils to surface sealing*. PhD thesis. West Lafayette: Purdue University, 206 pp.
- McIntyre, D. S., 1958a. Permeability measurements of soil crusts formed by raindrop impact. *Soil Science*, **85**, 261–266.
- McIntyre, D. S., 1958b. Soil splash and the formation of surface crusts by raindrop impact. *Soil Science*, **85**, 185–189.
- Moldenhauer, W. C., and Kemper, W. D., 1969. Interdependence of water drop energy and clod size on infiltration and clod stability. *Soil Science Society of America Journal*, **33**, 297–301.
- Moore, I. D., 1981a. Infiltration equations modified for surface effect. *Journal of Irrigation and Drainage Division ASAE*, **107**, 71–86.
- Moore, I. D., 1981b. Effect of surface sealing on infiltration. *Transactions of the ASAE*, **24**, 1546–1553.
- Morin, J., and Benyamin, Y., 1977. Rainfall infiltration into bare soils. *Water Resources Research*, **13**, 813–817.
- Morin, J., Benyamin, Y., and Michaeli, A., 1981. The effect of drop impact on the dynamics of soil surface crusting and water movement in the profile. *Journal of Hydrology*, **52**, 321–335.
- Mualem, Y., and Assouline, S., 1989. Modeling soil seal as a non-uniform layer. *Water Resources Research*, **25**, 2101–2108.
- Mualem, Y., and Assouline, S., 1992. Flow processes in sealing soils: Conceptions and solutions. In Sumner, M. E., and Stewart, B. A. (eds.), *Soil Crusting: Chemical and Physical Processes*. Boca Raton: Lewis.
- Mualem, Y., Assouline, S., and Rohdenburg, H., 1990a. Rainfall-induced soil seal A, a critical review of observations and models. *Catena*, **17**, 185–203.
- Mualem, Y., Assouline, S., and Rohdenburg, H., 1990b. Rainfall-induced soil seal C, a dynamic model with kinetic energy instead of cumulative rainfall as independent variable. *Catena*, **17**, 289–303.
- Mualem, Y., Assouline, S., and Eltahan, D., 1993. Effect of rainfall induced soil seals on soil water regime: wetting processes. *Water Resources Research*, **29**(6), 1651–1659.
- Onofio, O., and Singer, M. J., 1984. Scanning electron microscope studies of surface crusts formed by simulated rainfall. *Soil Science Society of America Journal*, **48**, 1137–1143.
- Parlange, J.-Y., Hogarth, W. L., and Parlange, M. B., 1984. Optimal analysis of surface crusts. *Soil Science Society of America Journal*, **48**, 494–497.
- Perez, P., Todoroff, P., Touma, J., and Fortier, M., 1999. Determining the hydraulic properties of a Sahelian crusted soil. I. in field experiments and measurements. *Agronomie*, **19**, 331–340.
- Philip, J. R., 1973. On solving the unsaturated flow equation, I, the flux-concentration relation. *Soil Science*, **116**, 328–335.
- Philip, J. R., 1998. Infiltration into crusted soils. *Water Resources Research*, **34**(8), 1919–1927.
- Poesen, J., 1987. The role of slope angle in surface seal formation. In Gardiner, V. (ed.), *International Geomorphology Part II*. Chichester: Wiley, pp. 437–447.
- Radcliffe, D. E., West, L. T., Hubbard, R. K., and Asmussen, L. E., 1991. Surface sealing in coastal plains loamy sands. *Soil Science Society of America Journal*, **55**, 223–227.
- Romkens, M. J. M., Baumhardt, R. L., Parlange, M. B., Whisler, F. D., Parlange, J. Y., and Prasad, S. N., 1986. Rain-induced surface seals: their effect on ponding and infiltration. *Annales Geophysicae*, **4**, 417–424.
- Roth, C. H., 1997. Bulk density of surface crusts: depth functions and relationships to texture. *Catena*, **29**, 223–237.

- Shainberg, I., 1992. Chemical and mineralogical components of crusting. In Sumner, M. E., and Stewart, B. A. (eds.), *Soil Crusting: Chemical and Physical Processes*. Boca Raton: Lewis.
- Sharma, P. P., Gantzer, C. J., and Blake, G. R., 1981. Hydraulic gradients across simulated rain-formed soil surface seals. *Soil Science Society of America Journal*, **45**, 1031–1034.
- Simunek, J., Angulo-Jaramillo, R., Schaap, M. G., Vandervaere, J.-P., and van Genuchten, M. Th., 1998. Using an inverse method to estimate the hydraulic properties of crusted soils from tension-disc infiltrometers data. *Geoderma*, **86**, 61–81.
- Smith, R. E., Corradini, C., and Melone, F., 1999. A conceptual model for infiltration and redistribution in crusted soils. *Water Resources Research*, **35**(5), 1385–1393.
- Tackett, J. L., and Pearson, R. W., 1965. Some characteristics of soil crusts formed by simulated rainfall. *Soil Science*, **99**, 407–413.
- Tarchitzky, J., Banin, A., Morin, J., and Chen, Y., 1984. Nature, formation and effects of soil crusts formed by water drop impact. *Geoderma*, **33**, 135–155.
- Valentin, C., and Bresson, L. M., 1992. Soil crust morphology and interactions forming processes in loamy and sandy soils. *Geoderma*, **55**, 225–245.
- Valentin, C., and Ruiz Figueroa, J. F., 1987. Effects of kinetic energy and water application rate on the development of crusts in a fine sandy loam soil using sprinkling irrigation and rainfall simulation. In Fedoroff, N., Bresson, L. M., and Courty, M. A. (eds.), *Micromorphologie des Solis/Soil Micromorphology*. Plaisir: Association française pour l'étude des sols, pp. 401–408.
- Vandervaere, J.-P., Vauclin, M., Haverkamp, R., Peugeot, C., Thony, J.-L., and Gilfedder, M., 1998. A simple model of infiltration into crusted soils. *Soil Science*, **163**, 9–21.
- Wakindiki, I. I. C., and Ben-Hur, M., 2002. Soil mineralogy and texture effects on crust micromorphology, infiltration and erosion. *Soil Science Society of America Journal*, **66**, 897–905.
- West, L. T., Bradford, J. M., and Norton, L. D., 1992. The morphology of surface crusts. In Sumner, M. E., and Stewart, B. A. (eds.), *Soil Crusting: Chemical and Physical Processes*. Boca Raton: Lewis.

Cross-references

- [Agrophysics: Physics Applied to Agriculture](#)
- [Anisotropy of Soil Physical Properties](#)
- [Bulk Density of Soils and Impact on their Hydraulic Properties](#)
- [Compaction of Soil](#)
- [Conditioners, Effect on Soil Physical Properties](#)
- [Cracking in Soils](#)
- [Crop Emergence, the Impact of Mechanical Impedance](#)
- [Crop Responses to Soil Physical Conditions](#)
- [Desertification: Indicators and Thresholds](#)
- [Ecohydrology](#)
- [Flocculation and Dispersion Phenomena in Soils](#)
- [Flooding, Effects on Soil Structure](#)
- [Hardsetting Soils: Physical Properties](#)
- [Hydraulic Properties of Unsaturated Soils](#)
- [Infiltration in Soils](#)
- [Layered Soils, Water and Solute Transport](#)
- [Management Effects on Soil Properties and Functions](#)
- [Overland Flow](#)
- [Pore Size Distribution](#)
- [Soil Aggregates, Structure, and Stability](#)
- [Soil Aggregation and Evaporation](#)
- [Soil Compatability and Compressibility](#)
- [Soil Erosion Modeling](#)
- [Soil Penetrometers and Penetrability](#)
- [Soil Physical Quality](#)
- [Soil Tilth: What Every Farmer Understands but no Researcher Can Define](#)

- [Soil Water Flow](#)
- [Soil Water Management](#)
- [Spatial Variability of Soil Physical Properties](#)
- [Subsoil Compaction](#)
- [Tillage Erosion](#)
- [Tillage, Impacts on Soil and Environment](#)
- [Trafficability and Workability of Soils](#)
- [Water Budget in Soil](#)
- [Wetting and Drying, Effect on Soil Physical Properties](#)

SOIL TEMPERATURE EFFECT

See [Temperature Effects in Soil](#)

SOIL TEXTURE: MEASUREMENT METHODS

Andrzej Bieganowski, Magdalena Ryżak
Institute of Agrophysics, Polish Academy of Sciences,
Lublin, Poland

Synonyms

Particle size distribution

Definition

The percentage content of groups of particles with specific sizes in the soil is known as the *texture or the particle size distribution of the soil*. Soil texture determines the probability of finding a particle with a specific size in the set of all particles.

Introduction

The soil, also referred to as the pedosphere, is a natural formation of the upper layer of the earth crust, formed from weathered rock as a result of the effect of various factors changing over time (climate, biosphere, hydrosphere, relief, and human activity). The component elements of the soil are in the solid, liquid, and gaseous phases (see [Soil Phases](#)). The solid phase of the soil is made up mainly of mineral, organic, and organic-mineral particles with various degrees of fragmentation. The degree of their fragmentation has a significant effect on many of the properties of the soil. The percentage content of groups of particles with specific sizes in the soil is known as the texture or the particle size distribution of the soil. The size of soil particles and their packing affect the pore distribution (see [Pore Morphology and Soil Functions](#) and [Pore Size Distribution](#)) in the soil, and thus determine, among other things, the possibility of gas exchange (see [Aeration of Soils and Plants](#)), water retention, as well as the thermal and sorptive properties of the soil (see [Coupled Heat and Water Transfer in Soil](#)) and its content of mineral components. An important feature of the particle size distribution is its stability in time and relatively easy measurability, thanks to which it serves as a parameter for many models,

for example, for the estimation of water retention curves or hydraulic conductivity.

Sample dispersion

While analyzing the particle size distribution of soils, it should be kept in mind that it reflects the original properties of the soils only when the measurement is concerned with the “elementary” soil particles, that is, those properties that do not break up under the effect of various dispersing factors. Under natural conditions, every soil is characterized by specific aggregation; hence, for many years there has been a search for effective methods of soil sample dispersion in soil particle size distribution measurements. At present, the most frequently used methods of soil sample preparation for measurement include methods consisting in stirring, addition of suitable chemical agents, for example, calgon (solution of sodium hexametaphosphate and anhydrous sodium carbonate), or ultrasonic treatment (Day, 1965; Chappell, 1998; ISO 11277, 1998).

Mechanical methods

One of the oldest methods for the separation of substances with different particle sizes are the decantation and sieve methods, used already in the ancient Greece. However, documented sources give the year 1692 as the date of the first application of the decantation method for the separation of soil particles. It is accepted that the first described application of a sieve for the separation of sand fractions took place in 1704, while the term “mechanical analysis” itself was introduced in 1800 (Krumbein, 1932).

Sedimentation methods

Based on the fundamental laws of physics (and the Stokes law in particular), a succession of new methods for the determination of particle size distribution was created. Those methods can be classified into two categories – field and laboratory methods.

The sensory identification of soil type is highly useful in fieldwork when it is necessary to make an estimation of the content of particular soil particle fractions. The simplest of those is the so-called finger method, which permits the identification of soil composition on the basis of analysis of its behavior when rubbed between fingers in dry state, and after wetting. When analyzing a soil in the dry state, we estimate its coarseness or hardness and slipperiness. With wet soil, we can make an estimation of its viscosity, compaction, and capacity for rolling. Correct identification of soil type using the finger method requires a lot of experience. The method can only be used for preliminary classification of soils in field conditions.

The sieve method is used for the separation of the skeleton fractions (stones and gravel) from the earth fractions (sand, silt, and clay) of the soil, and for the determination of the coarser earth fractions. To be able to make comparison of results obtained with the sieve method one should

keep in mind that the result depends on the shape of apertures in the sieve; results obtained with sieves with square apertures will not be equivalent to results obtained with sieves with round holes. The probability of a particle passing through a given sieve during a given time of screening will depend both on the properties of the particle and on those of the sieve, as well as on the distribution of sizes and the number of particles on the sieve, on the physical properties of the particles (shape and type of surface), and on the method of sieve shaking. Analysis performed with the help of sieves consists in the selection of a suitable set of sieves. A specific weight of a soil sample is placed on the upper sieve, and then, after covering the upper sieve, the whole set of sieves is placed on the shaker. When the screening is over, the particles remaining on each of the sieves are weighed, and on this basis, the percentage share of a given fraction is determined as the ratio of the weight of the particles that remained on a given sieve to the weight of the whole soil sample.

The sedimentation methods are based on measurement of the settlement rate of soil particles in a water suspension. The basis for the sedimentation methods is the fact of balancing of forces acting on a particle suspended in a liquid, which causes it to settle to the bottom in a uniform motion. The forces that act on the particle are the following – the downward force of gravity F_g , the upward force of buoyant force F_w (resulting from the Archimedes law), and the force of friction F_t (resulting from the viscosity of the medium, expressed by the Stokes law). In measurements based on the sedimentation methods, the following assumptions are made:

- (a) The soil particles are hard and smooth spheres
- (b) The suspension has a Reynolds number below ca. 0.2, that is, it is a liquid in which particles settle with a laminar motion.
- (c) Soil particles in the suspension are at such a rate of dilution that none of them disturbs the settlement of any other.
- (d) There are no interactions between the particles and the liquid.
- (e) The diameter of the suspension column compared to particle diameter is large, that is, the fluid volume is “infinitely great.”
- (f) The soil particles have attained the terminal velocity.
- (g) The soil particles have the same specific density.

The most frequently applied sedimentation methods include the pipette method and the hydrometric method (in Poland, the latter method is mainly used in the Prószyński modification).

The pipette method consists in using a pipette to take a specific volume of water suspension of a soil. Samples are taken after a specific time from suspension stirring, at a specific depth, and using a pipette with known volume. Next, the samples taken are evaporated and dried to constant weight. Based on the sample weight after drying, the content of particles with a given diameter in the whole soil sample is determined (ISO 11277, 1998).

Another sedimentation method is the Casagrande hydrometer method (Day, 1965). In its classical form, the method consists in using a hydrometer to measure the density of water suspension of a soil at time intervals at which soil particle fractions with specific decreasing diameters settle at the bottom of the measurement cylinder. Obtaining results of measurements taken with the hydrometric method required the plotting of many graphs and making prior calculations. The modification of the method developed by Prószyński (Mocek et al., 2000) consisted in the application of a hydrometer of his own design and in the development of sedimentation tables, which permits direct determination of the percentage share of particles remaining in the suspension at the moment of measurement. Determination of particle size distribution with the Casagrande method in Prószyński modification (Mocek et al., 2000) requires a preliminary measurement to be made after ca. 10 min from the stirring of the suspension. That measurement permits the determination of approximate content of the fraction of <0.02 mm, and thus permits the selection of a suitable sedimentation table from which, depending on the ambient temperature, times are taken after which a reading should be taken on the hydrometer so as to calculate the content of a given fraction of particles in the soil tested (Mocek et al., 2000).

As in any other measurement, so also in the case of the sedimentation methods, one should remember the sources of uncertainty. One of the more important sources is the observed fact that thin blade-shaped particles settle much more slowly than the equivalent spheres adopted for them, which causes the obtainment of overestimated measurement results for such particles. In turn, for particles whose equivalent sphere diameter is less than 1 μm , the cause of measurement errors may be attributed to Brownian motions interfering with particles settling under the effect of gravity (Allen et al., 1996).

The standard ISO 11277 recommends that determinations of particle size distribution for air-dry soil samples can be done using the sieve–pipette method. Such an analysis should be performed as follows: particles that do not pass through sieve with 2-mm mesh are to be determined with the dry sieving method; particles passing through a 2-mm mesh sieve and retained on a sieve with mesh diameter of 0.063 mm are to be determined with the wet sieving method, while particles that have passed through the last sieve are to be determined with the sedimentation (pipette) method.

Laser diffraction method

A method that recently found an application in soil science is the laser diffraction method (Buurman et al., 1997). Diffraction is a phenomenon consisting in light being deflected when passing close to an obstacle, such as the edge of a slot. Diffraction takes place when the head of a light wave is partially stopped by an opaque object. Such a nontransparent object may be a particle that happens to be in the way of a light beam. Falling on that

particle the light beam is deflected. Measuring the angle of the deflection and the intensity of the deflected light we can obtain information about the size of the particle that caused the diffraction. The angle at which the laser light beam becomes deflected/scattered on the particle is inversely proportional to the particle size. Small particles deflect/scatter light at large angles, while large particles do so at small angles. Based on the angles of deflection/scattering of laser light beam calculation of particle sizes is made on the basis of the Fraunhofer or Mie theories. Contemporary apparatus for the determination of particle size distribution with the method commonly referred to as the laser diffraction method take into account four types of interactions between the electromagnetic wave (laser light) and the particle (ISO 13320, 1999), and namely:

- (a) Diffraction on the outer surface (contour) of the particle – Fraunhofer diffraction,
- (b) Reflection from particle surface (internal as well as external),
- (c) Refraction of laser light at the medium-particle and particle medium phase interface,
- (d) Absorption within the particle.

It takes two steps to obtain information about particle size distribution on the basis of analysis of deflected/scattered light falling onto detectors. The first step is the choice of mathematical model describing light deflection/scattering by the particles (the choice is between two possibilities – the Fraunhofer approximation and the Mie theory). The second step is to convert the information from the angular distribution of intensity of deflected/scattered light onto the size distribution of particles under analysis in accordance with the selected mathematical model. This step is realized automatically by the software supplied by the manufacturer of the apparatus. The growth of the computing power of computers that took place over the recent years permitted the application of the Mie theory for the determination of particle size distribution, as the Mie theory requires the solution of significantly more complex equations. The Mie theory treats the electromagnetic field in the space surrounding the particle as a superposition of the falling field and the scattered field.

The application of the Mie theory for the determination of particle size distribution requires the definition of the optical parameters of the particles, that is, the coefficient of light refraction and the coefficient of light absorption.

The Mie theory is recommended for the determination of size distribution of particles with dimensions below 25 μm in accordance with standard ISO 13320. However, application of the Mie theory with relation to a nonhomogeneous material such as soil, whose optical properties (refraction and absorption coefficients) for various particles are different, causes that it is hard to assume in prior which theory will be better. Especially as the determination of the optical parameters of the material studied may not only be costly and time consuming, but may also constitute a significant source of uncertainty in the determination of particle size distribution. All these inferences may lead to a situation

when the theoretically less precise Fraunhofer theory may have a better practical application for soil material, even taking into account the presence of smaller particles in the sample (Loizeau et al., 1994).

Summary

Particle size distribution is one the most important properties of soils. The size of soil particles and their packing affect the pore distribution in the soil, and thus determine, among other things, the possibility of gas exchange, water retention, as well as the thermal and sorptive properties of the soil. An important feature of particle size distribution is its stability in time and relatively easy measurability, thanks to which it serves as a parameter for many models, for example, for the estimation of water retention curves or hydraulic conductivity. The most important methods for measurements of soil particle size distribution are the following: (a) sieve methods; (b) methods based on Stokes law (aerometric and pipette ones); and (c) the new laser diffraction method.

Bibliography

- Allen, T., Davies, R., and Scarlett, B. (eds.), 1996. *Particle Size Measurement*. London: Chapman and Hall, 2 vols.
- Buurman, P., Pape, Th., and Muggler, C. C., 1997. Laser grain-size determination in soil genetic studies. 1. Practical problems. *Soil Science*, **162**, 211–218.
- Chappell, A., 1998. Dispersing sandy soil for the measurement of particle size distribution using optical laser diffraction. *Catena*, **31**, 271–281.
- Day, P. R., 1965. Particle fractionation and particle-size analysis. In Black, C. A., et al. (eds.), *Methods of Soil Analysis, Part I. Agronomy*, 9, pp. 545–567, Madison: American Society of Agronomy, Wis.
- ISO 11277, 1998. Soil quality – determination of particle size distribution in mineral soil material – method by sieving and sedimentation.
- ISO 13320, 1999. Particle size analysis – laser diffraction methods – part 1.
- Krumbein, W. C., 1932. A history of the principles and methods of mechanical analysis. *Journal of Sedimentary Petrology*, **2**, 89–124.
- Loizeau, J.-L., Arboville, D., Santiago, S., and Vernet, J.-P., 1994. Evaluation of wide range laser diffraction grain size analyser for use with sediments. *Sedimentology*, **41**, 353–361.
- Mocek, A., Drzymala, S., and Maszner, P., 2000. Genesis, analysis and classification of soils. *AR Poznań* (in Polish), pp. 416.

Cross-references

- [Aeration of Soils and Plants](#)
[Coupled Heat and Water Transfer in Soil](#)
[Pore Morphology and Soil Functions](#)
[Pore Size Distribution](#)
[Soil Phases](#)

SOIL TILLAGE

See [Tillage, Impacts on Soil and Environment](#)

SOIL TILTH: WHAT EVERY FARMER UNDERSTANDS BUT NO RESEARCHER CAN DEFINE

Douglas L. Karlen

National Laboratory for Agriculture and the Environment (NLAE), Ames, IA, USA

Synonyms

Soil condition; Soil quality

Definition

Tilth – The physical condition of soil as related to its ease of tillage, fitness as a seedbed, and its impedance to seedling emergence and root penetration.

Introduction

The farmer's understanding of soil tilth is nearly as old as agriculture itself. For example, Fitzherbert wrote in his 1523 *Boke of Husbandry* that a farmer could determine if soil was ready to be sown by going onto the plowed land and “if it syng or crye, or make any noise under thy fete, then it is to wete to sowe: and if it make no noyse, and wyll beare thy horses, thane sowe in the name of God.” Similarly, in the seventeenth century, Thomas Tusser is reported to have stated that “good tilth brings seeds, ill tilture weeds.” Evidenced by these quotes and many other examples, tilth has a long history of intriguing people because of its connection with the soil (Karlen et al., 1990), yet the concept confuses scientists because of their inability to provide an exact definition or protocol for measuring it. Soil tilth thus describes a soil property that is better visualized than quantified; however, the principles that underlie tilth are fundamental to the quality of all soil resources.

In the 1930s, several authors began to describe how climatic conditions and various soil, crop, and animal management practices affected soil tilth. Keen (1931) provided a summary of previous observations regarding the importance of tilth for the planting of crops into a proper seedbed, the impact of frost on soil, how hard rains after plowing would create a crust, and how grazing animals could compact soils. Keen's treatise on soil physical conditions was followed by Yoder's, 1937 paper that described soil tilth as a “blanket” term describing the soil conditions that determine the degree of fitness for growth and development of crop plants. By sieving soil samples and separating the material into different sizes, researchers showed how freezing, drying wind, rainfall, tillage, animal compaction, and other management factors affected the soil. Tilth was ultimately recognized as providing a fundamental understanding of soil structure and how it changes in response to tillage, organic matter additions, crop rotations, and environmental factors such as rainfall or temperature. Changes in soil structure and the impact on soil tilth are probably most quickly recognized by

gardeners and small farmers because they work their soil either by hand or with small tools. Effects of improving soil tilth are readily apparent because hard soil requires more energy to prepare a seedbed and generally produces less vigorous plants. It has also been recognized that not all soils respond to inputs and management practices in the same way because of fundamental differences in their sand, silt, clay, and organic matter composition.

Yoder (1937) defined the ideal tilth as offering minimum resistance to root penetration, allowing for good infiltration and storage of soil water, having good exchange of gases between the soil and atmosphere, sustaining an adequate air supply in the soil, having a proper balance of water and air in soil pores, resisting erosion, promoting biological activity, facilitating decomposition of green manure and other organic residues, and providing a stable foundation for farm implements. This is a very inclusive list that covers many soil functions and demonstrates the interactions among the physical, biological, and chemical processes that are occurring within a profile. Yoder also recognized that green manure and crop residue additions were crucial for developing good soil tilth.

Soil tilth has gradually become recognized as a dynamic soil condition. As virgin grassland or forest soils were cultivated, organic matter concentrations, base (cation) saturation, and porosity decreased while bulk density increased. These changes reduced the tendency of soil to form stable aggregates and gradually resulted in a deteriorated soil structure. Declining soil tilth became associated with increased runoff, erosion potential, need for tillage to prepare an adequate seedbed, and fertilizer to sustain reasonable and profitable crop yields. Conversely, as soil tilth is improved, water exchange, gas exchange, and the ability of a plant to explore the profile and capture nutrients and water were enhanced. Soils with good tilth generally have greater biodiversity and provide structural support for land management operations. Soil tilth continues to be important as humankind depends on soil resources for food, feed, fiber, and most recently fuel (i.e., bioenergy). Understanding how to manage soils for long-term improvement and enhanced sustainability of tilth are lessons that all must be aware of now and in the future (National Academy of Sciences NAS, 2009).

Critical soil tilth concepts

Organic matter is one of the primary factors affecting soil tilth because of its role in soil aggregation. Studies with disturbed and undisturbed soils show that as organic matter increases, compaction decreases and there is more space for air and water exchange. The constant addition of organic matter throughout the soil profile is one reason that virgin grassland soils generally have excellent aggregation and structure. Those soils, especially in humid regions, generally have higher organic matter content, an increased percentage of water-stable aggregates, and

a structure that accommodates rapid plant growth with unlimited root proliferation. Those soil characteristics occur because in humid regions, grasses replace most of their roots and top growth each year. Also, when the above ground plant material dies, it falls on the soil surface where it is decomposed or mixed into the upper part of the soil by earthworms and other soil organisms. The dead roots and plant residue provide a food source for fungal and bacterial decomposition processes leading to the formation of soil aggregates, which modify effects of soil texture with regard to water and air relationships and root penetration. Increased water-stable aggregation, annual proliferation of plant roots, and the associated wetting and drying cycles gradually develop a soil structure that is stable and with good management resists degradation.

Whiteside and Smith (1941) were among the first to examine how crop production affected soil productivity. They cited several reports showing that total N and organic matter in the surface of tilled soils decreased relative to adjacent untilled forest and grassland areas. They found that cropping systems had a great influence on the amount and direction of change in soil N and organic C. The greatest changes were associated with continuous row crops, followed by cereal crops, then legume and sod crops. These and similar studies gradually led to development of conservation practices with an increased emphasis on incorporating perennial crops into extended rotations, reducing tillage intensity and frequency, using cover crops and optimizing nutrient and water management.

Surface mulch from crop residues, cover crops, animal manure, municipal sludge, leaves, or other carbonaceous sources can enhance soil tilth by providing physical protection from raindrop impact and a food source for earthworms and other soil fauna. Surface mulch also moderates soil temperature and moisture extremes at the soil-air interface. If soils are left bare and exposed, surface temperatures can be very high causing the soil to become very dry. When this occurs, earthworms and other soil insects will move deeper into the soil leaving a surface zone that contains very few active organisms. Bacteria and fungi that live in thin films of water will die or become inactive, slowing the natural process of organic matter cycling and aggregation.

Tillage effects on soil tilth

Tillage can improve tilth over the short term by loosening surface soil, disrupting crusts and creating a more favorable soil-water-air environment for plants, but it is also a primary cause for the long-term deterioration of tilth. The loosening process that often has positive short-term plant production benefits has negative long-term effects because it increases the rate of organic matter decomposition through chemical and microbial mineralization. This occurs because previously protected organic matter is exposed by the tillage and subsequently used as a food source by many

microorganisms. The loss of organic matter decreases aggregate stability, thus increasing the potential for surface crusting, poor seedling emergence, runoff, erosion, and other indicators of poor soil tilth (e.g., decreased infiltration of rainfall or irrigation water, decreased soil water retention, and decreased nutrient cycling). Tillage itself or the wheel-traffic associated with tillage operations can further reduce tilth by increasing compaction. This reduces total pore space and frequently increases water-filled pore space leading to reduced aeration, slower nutrient cycling, and a decreased volume of soil for plant root proliferation. Traffic-induced compaction obviously occurs in fields used for crop production, but similar negative effects can be found at construction sites, in forests due to logging operations, on campgrounds, athletic fields, or even desert areas where off-road recreational vehicles are allowed.

Extended crop rotation effects on soil tilth

Soil tilth is affected in two ways by incorporating forage or hay crops into an extended rotation. First, soil organic matter decomposition decreases because the soil is not disturbed or tilled each year. Second, grass and legume sods develop extensive root systems, part of which dies each year, adding new organic matter to the soil. The dead roots provide a food source for fungal and bacterial decomposition processes leading to the formation of soil aggregates and improved tilth.

To demonstrate the effect of perennial root systems on soil aggregation, researchers compared aggregate size distributions for soils under continuous corn (*Zea mays* L.) with those where corn was grown in rotation with oat (*Avena sativa* L.) and meadow. The data showed that with continuous corn aggregate size was less than half that for corn grown in rotation. The studies also showed that aggregation decreased slowly but consistently over a 7-year period of continuous corn. In related studies, comparisons among crop sequences showed that aggregation increased by switching to a corn-oat-meadow rotation after 11 years of continuous corn (Karlen et al., 1990). Also, it took only 4 years of continuous corn to decrease the aggregation established under either bluegrass or alfalfa to less than that found after 18 years of the corn-oat-meadow rotation. The highly significant correlation between crop yield and aggregate size confirmed that soil tilth and productivity were both affected by crop rotation.

Cover crop effects on soil tilth

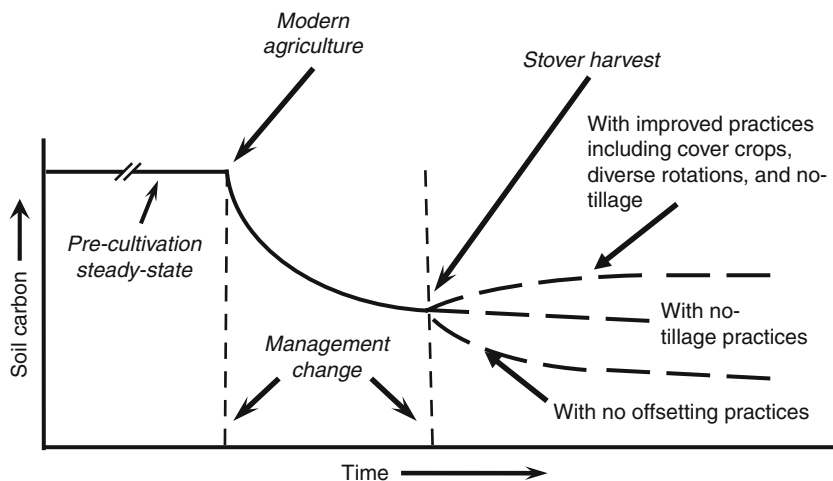
Growing cover crops can improve soil tilth by decreasing erosion, increasing infiltration, and adding organic residues to the soil. Although in orchards and vineyards the cover crops are frequently grown year-round, they are most often grown only during seasons when the soil is especially susceptible to erosion. The leaves and stems of the cover crop intercept rainfall and dissipate the energy while roots bind the soil and hold it in place. The amount

of benefit from cover crops depends on the above and below ground biomass and rooting structure of the plant being grown and the length of time before the soil is prepared for the next crop. For example, in the southeastern US crimson clover (*Trifolium incarnatum* L.) can be grown successfully as a cover crop prior to cotton (*Gossypium barbadense* L.). Initially planted in late autumn, the clover grows slowly throughout the winter and early spring, often reseeding itself for the next year before the cotton crop is planted. In more northern areas such as the US Corn and Soybean Belt where cold temperatures significantly shorten the growing season, crops such as crimson clover simply cannot survive. Oat, rye (*Secale cereale* L.), and hairy vetch (*Vicia villosa* L.) are some of the possible cover crops for the northern states, but the amount of protection against soil erosion and especially the amount of nitrogen supplied by the vetch are generally much less than in the southern USA. Also, in semiarid regions where water is often the most limiting factor, growing cover crops may not be a viable management practice.

Additional benefits of cover crops include sequestering nutrients (especially nitrate N) so they cannot be leached below the crop root zone, suppressing weeds, breaking pest cycles, providing habitat for beneficial insects and other fauna, and supplying nutrients (usually N) to the following crop. However, before a farmer or anyone else decides to grow a cover crop to maintain or improve soil tilth, it is important to determine what needs to be accomplished. Is the main purpose to add available nitrogen to the soil or to provide large amounts of carbon? Is erosion control during the late autumn and early spring the primary objective? Does the soil have a compaction problem that needs to be alleviated? Will the combination of cover crop, climate and water-holding capacity of the soil result in excess water depletion that adversely affects the primary crop? Once the primary purpose for growing a cover crop has been determined, decisions on plant species (i.e., legume or grass), the optimum date of planting, and when to kill the cover crop will be easier to make.

Potential biofuel feedstock production effects on soil tilth

Increasing worldwide energy demand, high commodity prices, rapid economic growth in developing countries, and growing evidence that atmospheric carbon dioxide (CO₂) is an important contributor to global climate change have significantly increased interest in using agricultural biomass to simultaneously increase energy supplies and reduce worldwide greenhouse-gas emissions (NAS, 2009b). Figure 1 illustrates the potential impact of meeting these needs on soil tilth because of their effect on the soil carbon balance. Worldwide, the pre-agriculture soil carbon content was generally at least twice that found in soils approaching equilibrium with current tillage and cropping practices. Harvesting additional stover or crop residues as



Soil Tilth: What Every Farmer Understands but no Researcher Can Define, Figure 1 Changes in soil carbon content (a primary factor influencing soil tilth) as native soils are subjected to cultivation and management changes including stover removal.

feedstock for biofuels or other bioproducts will have a negative impact on the C balance unless offsetting practices such as reduced tillage, cover crops, or diversified crop rotations are also implemented. Initial efforts to produce biofuel from corn, soybean (*Glycine max* [L.] Merr.) or other food crops have been questioned from social, economic, and environmental perspectives and induced fear of having global competition between food and fuel (Doornbosch and Steenblik, 2007).

As a feedstock, cellulosic biomass has numerous advantages over corn, soybean, and other grains, including its availability from sources that do not compete with food and feed production. Biofuels made from renewable feedstock are an attractive alternative to gasoline because they can decrease the net release of greenhouse gases (GHG) from the transportation sector. An unknown and current research question is what impact harvest of this material will have on soil tilth.

Corn stover, the aboveground material left in fields after corn grain harvest, was identified as a primary biomass source (Perlack et al., 2005), because it and other crop residues are frequently referred to as “trash” or agricultural waste (Wilhelm et al., 2007). This would suggest that stover has minimal value (Lal, 2004) but, when returned to the land, crop residues replenish soil organic carbon (SOC), a soil quality indicator that has been reduced by 30–50% (Schlesinger, 1985) compared to pre-cultivation levels. These decreases have occurred because of crop production activities that include artificial drainage, intensive annual tillage, and less diverse plant communities; factors also affecting soil tilth.

Removing crop residues for biofuel feedstock or any purpose will decrease the annual carbon input, and gradually diminish soil organic carbon and threaten the soil’s production capacity (Johnson et al., 2006). Therefore,

even though harvesting corn stover or any other crop residue as a feedstock for transportation biofuels could have many benefits, these must be evaluated in the context of other ecosystem services that crop residues provide. This includes conserving soil water, reducing surface runoff and evaporation, increasing infiltration rates, controlling soil erosion, recycling plant nutrients, providing habitat and energy for earthworms and other soil macro- and microorganisms, improving water quality by denaturing and filtering of pollutants and improving soil structure, preserving native habitats, maintaining biodiversity, and sustaining soil tilth. Crop residues also help reduce non-point source pollution, decrease sedimentation, minimize risks of anoxia and dead zones in coastal ecosystems, increase agronomic productivity, advance food security, and mitigate flooding by holding water on the land rather than allowing it to run off into streams and rivers (Kimble et al., 2007).

So why is soil tilth important?

Good soil tilth provides a stable base for agricultural production. The ability of a plant to explore the soil profile to extract water, nutrients, and air reduces a potential limitation to plant growth. A limited soil profile reduces the amount and vigor of plant growth. Good soil tilth is also associated with good soil structure. This is important because a vast majority of the world’s agriculture depends upon rainfall to produce a reliable supply of food, feed, or fiber and when the soil has an unstable structure, infiltration of rainwater into the soil is often very limited. This is critical when rainfall occurs in intense storms. The other limitation comes when soil water holding capacity is diminished by reductions in organic matter and the rainfall leaches through the profile and is not available to the plant. The simple change in the soil creates a limitation to plant

growth and yield because of reduced water availability. Fields with poor soils often show poor plant growth because of water limitations even in years that have normal rainfall for that location. Efficient use of stored soil water is critical to providing food, feed, and fiber for the world's population and the process begins with a soil that has good tilth. Soil with good tilth has improved nutrient cycling because of the role of the microbiological activity within the soil and supply of nutrients to plants is as critical as water in terms of sustaining plant productivity.

Conclusions

Soil tilth has both direct and indirect effects on plant production often overlooked or even ignored. Healthy soils with good tilth have better resistance to insects and diseases. This aspect has not been fully studied and offers an additional piece of evidence for the proper management of the soil resource. It is also critical to consider soil tilth as part of the ecosystem that contributes to improved ecosystem health and ecosystem services, e.g., water quality, air quality, biodiversity, and efficient use of resources. Soil provides the foundation for existence of humankind, but it is the soil tilth that increases the value of that foundation with regard to its ability to produce a reliable and sustained supply of food, feed, fiber, and now fuel from the soil. Soil is precious and good tilth increases the value of the soil for all future generations.

Bibliography

- Doornbosch, R., and Steenblik, R., 2007. Biofuels: Is the cure worse than the disease? In Roundtable on Sustainable Development. Organisation for Economic Cooperation and Development. Paris, France.
- Johnson, J. M. F., Allmaras, R. R., and Reicosky, D. C., 2006. Estimating source carbon from crop residues, roots, and rhizodeposits using the national grain-yield database. *Agronomy Journal*, **98**, 622–636.
- Karlen, D. L., Erbach, D. C., Kaspar, T. C., Colvin, T. S., Berry, E. C., and Timmons, D. R., 1990. Soil Tilth: A review of past perceptions and future needs. *Soil Science Society of America Journal*, **54**, 153–161.
- Keen, B. A., 1931. The physical properties of the soil. Rothamsted monograph on agricultural science. Ser. Longmans, Green and Coi., London.
- Kimble, J. M., Rice, C. W., Reed, D., Mooney, S., Follett, R. F., and Lal, R. (eds.), 2007. *Soil Carbon Management, Economic, Environmental, and Societal Benefits*. Boca Raton: Taylor and Francis.
- Lal, R., 2004. Soil carbon sequestration impacts on global climate change and food security. *Science*, **304**, 1623–1627.
- NAS, 2009. *Liquid Transportation Fuels from Coal and Biomass: Technical Status, Costs, and Environmental Impacts*. Washington: National Academy of Engineering and National Research Council, National Academy.
- National Academy of Sciences (NAS), 2009. *Frontiers in Soil Science Research: Report of a Workshop*. Washington: National Research Council, National Academy.
- Perlack, R. D., Wright, L. L., Turhollow, A. F., Graham, R. L., Stokes, B. J., and Erbach, D. C., 2005. Biomass as feedstock for a bioenergy and bioproducts industry: The technical feasibility of a billion-ton annual supply DOE/GO-102005-2135 and ORNL/TM-2005/66. Available at http://feedstockreview.ornl.gov/pdf/billion_ton_vision.pdf (accessed 25 May, 2010). NTIS, Springfield.
- Schlesinger, W. H., 1985. Changes in soil carbon storage and associated properties with disturbance and recovery. In Trabala, J. R., and Reichle, D. E. (eds.), *The Changing Carbon Cycle: A Global Analysis*. New York: Springer-Verlag, pp. 194–220.
- Whiteside, E. P., and Smith, R. S., 1941. Soil changes associated with tillage and cropping in humid areas of the United States. *Agronomy Journal*, **33**, 765–777.
- Wilhelm, W. W., Johnson, J. M. F., Karlen, D. L., and Lightle, D. T., 2007. Corn Stover to sustain soil organic carbon further constrains biomass supply. *Agronomy Journal*, **99**, 1665–1667.
- Yoder, R. E., 1937. The significance of soil structure in relation to the tilth problem. *Soil Science Society of America Proceedings*, **2**, 21–33.

Cross-references

- [Bulk Density of Soils and Impact on their Hydraulic Properties](#)
[Compaction of Soil](#)
[Crop Responses to Soil Physical Conditions](#)
[Cropping Systems, Effects on Soil Physical Properties](#)
[Hardpan Soils: Management](#)
[Management Effects on Soil Properties and Functions](#)
[Microbes and Soil Structure](#)
[Organic Matter, Effects on Soil Physical Properties and Processes](#)
[Physical Degradation of Soils, Risks and Threats](#)
[Plant Roots and Soil Structure](#)
[Rhizosphere](#)
[Root Responses to Soil Physical Limitations](#)
[Soil Aggregates, Structure, and Stability](#)
[Soil Aggregation and Evaporation](#)
[Soil Physical Quality](#)
[Subsoil Compaction](#)
[Traficability and Workability of Soils](#)
[Wetting and Drying, Effect on Soil Physical Properties](#)

SOIL WATER FLOW

Miroslav Kutílek
Prague 6, Czech Republic

Definition

Soil water flow is conditioned by the existence of a gradient of the total potential of soil water in both, the soil fully saturated by water (saturated flow) as well as in soil not fully saturated by water (unsaturated flow).

Basic concepts

The flow of water in soil can be described microscopically and macroscopically. On the microscopic scale, the flow in each individual pore is considered and for each defined continuous pore, the Navier–Stokes equations apply. For their solution, we lack detailed knowledge of the geometrical characteristics of individual pores to obtain a solution for the bulk volume of soil of the size about $0.1\text{--}1\text{ m}^3$, derived theoretically as the representative elementary

volume (REV). This type of procedure is applied in some theoretical investigations where the basic laws of fluid mechanics are invoked. In such studies, the real porous system is usually defined by a very simplified model.

The macroscopic or phenomenological approach of water transport relates to the entire cross section of the soil in REV. In order to emphasize the fact that water does not flow through the entire macroscopic areal cross section (REA), the term flux density (or flux ratio, or macroscopic flow rate) is used to describe the flow realized through only that portion of the area not occupied by the solid phase and, by the air phase eventually when we deal with unsaturated soil. The size of REA in soils is usually in the range of 100 cm^2 to m^2 . The dimension of the flux density is the volume of water (L^3) flowing through the area (L^2) in time (T), i.e., $(\text{L}^3/\text{L}^2 \text{T}) = (\text{LT}^{-1})$. The principal equation derived for this macroscopic approach is Darcy's equation developed in 1856. Water flow in soils is comparable to other transport processes such as heat flow and molecular diffusion when the appropriate driving force is defined. For water flow, it is the difference of total potentials between two points in the soil.

Saturated flow

We assume that water is flowing in all pores of the soil under a positive pressure head h . In field situations, the soil rarely reaches complete water saturation. Usually it is quasi-saturated with the soil water content $\theta = mP$ where m has values of 0.85–0.95 and P is the porosity. Entrapped air occupies the volume $P(1 - m)$. Further on we assume for the sake of simplicity that $m = 1$ and the impact of entrapped air is not considered. Darcy equation governing the saturated flow in the vertical direction is

$$q = K_S \frac{\Delta h}{L} = K_S I_h$$

where $\Delta h/L$ is the hydraulic gradient I_h , Δh the difference between water levels in piezometers at the vertical distance L . Since the dimension of h is (L) and of the distance L is also (L), the hydraulic gradient is dimensionless and the saturated hydraulic conductivity K_S has the dimension of q (LT^{-1}). When we read piezometer levels (or pressure heads) h_1 and h_2 at elevations z_1 and z_2 , respectively, we have in terms of the total potential $H = (h + z)$ a general form of the Darcy equation

$$q = -K_S \text{grad}H$$

When K_S is constant in the studied domain, then with $\Phi = K_S H$ is

$$q = -\text{grad}\Phi$$

The value of K_S depends upon the nature of the soil and is numerically equal to the flow rate when the hydraulic gradient is unity. Values of K_S commonly range from

less than 0.1 cm day^{-1} (10^{-8} m s^{-1}) to more than 10^2 cm day^{-1} (10^{-5} m s^{-1}). If the total potential H is not expressed as the height of the water column, but when we use $J \text{ kg}^{-1}$ ($\text{L}^2 \text{T}^{-2}$) then the potential gradient is $J \text{ kg}^{-1} \text{ m}^{-1}$ (LT^{-2}) and K_S has the dimension (T), usually s . K_S should be considered a scalar quantity for isotropic soils, and a tensor of rank 2 for anisotropic soils with the value of K_S dependent upon the direction of flow. When the tensor K_S is assumed to be symmetric, its principal axes, defined by six values, are identical to those of an ellipsoid of conductivity. If the gradient of the potential is not in the direction of a principal axis, the direction of flow is different from that of the gradient. The simplest expression of K_S was derived by Kozeny (1927) for the soil porosity modeled as a bundle of parallel capillary tubes. The flow is assumed to be laminar and its mean value is expressed by the Hagen-Poiseuille's equation. For P porosity [dimensionless], specific surface A ($\text{L}^2 \text{ L}^{-3}$) = (L^{-1}), g the acceleration of gravity (LT^{-2}), ρ_w the density of water (ML^{-3}), and μ the dynamic viscosity ($\text{ML}^{-1} \text{ T}^{-1}$) is

$$K_S = \frac{\rho_w g P^3}{2 \mu A^2}$$

Since the real flow paths in soil are curved and not straight as in the model, the term tortuosity τ was introduced as the ratio between the real flow path length L_e and the straight distance L between the two points of the soil. Because $L_e > L$, then $\tau > 1$. For example, in a monodispersed sand, $\tau = 2$. The permeability K_P valid for all fluids is

$$K_P = \frac{c P^3}{\tau A^2}$$

with c taken as an empirical constant. Permeability K_P has then the dimension (L^2). The unusual dimension represents the cross-sectional area of an equivalent pore. Although now almost obsolete, the historical unit of 1 Darcy = $1 \mu\text{m}^2$ was used for describing permeability. Kozeny's equation shows that K_S is sensitive to porosity. However, in his model the pore radii are considered uniform while those in real soils have great variability of pore size distribution, which is changed due to the aggregation or disaggregation of soil, by the compaction, etc. Due to the aggregation of soil, K_S may increase by orders of magnitude, yet the porosity may change slightly or even remain nearly the same. And, vice versa, soil dispersion or disaggregation substantially decreases K_S . For example, in a loess soil, the saturated hydraulic conductivity of its surface after a heavy rain decreases three to four orders of magnitude compared with its original value owing mainly to two processes – disaggregation and the blockage of pores by the released clay particles. Compaction of soil in the A-horizon and in the bottom of the plowed sub horizon causes a much greater decrease of K_S than that predicted from a decrease of porosity in the

simple Kozeny equation because compaction reduces primarily the content of large soil pores associated with values of pressure head $h=0$ to -100 cm. Although the textural class of a soil may have a large influence on the value of K_S , any attempt to establish a correlation between them usually fails. Only for those soils and soil horizons of the same genetic development occurring in the same region and being similarly managed will a correlation between texture and K_S be manifested. In sandy soils, the lowest value of K_S is about 100 cm day $^{-1}$, in silty loams about 10 cm day $^{-1}$, and in clays about 0.1 cm day $^{-1}$. In peats, K_S decreases with an increasing degree of decomposition of the original organic substances. When the degree of decomposition of a peat is more than 50%, the value of K_S diminishes to values of K_S of nonconsolidated clays. In loams and clays, the nature of the prevalent exchangeable cation plays an important role upon the value of K_S . In vertisols, an increase of the percentage of exchangeable sodium (ESP) is accompanied by a significant decrease in K_S when the ESP reaches 15–20%, provided that the soluble salt content of the soil water is small. For example, with the electrical conductivity of the soil paste EC = 1 mS cm $^{-1}$ or less, the value of K_S can decrease two or three orders of magnitude (Hillel, 1998). In not frequent events the linear relationship of Darcy equation is not applicable. This non-Darcian flow in clays is caused by the shift of clay particles due to the imposed hydraulic gradient and due to the changed of the water viscosity in clays having extremely large specific surface. In coarse sands, the nonlaminar flow could exist causing the deviation of linearity of Darcy equation (Kutilek and Nielsen, 1994).

Unsaturated flow

When the soil is not fully saturated by water, the Darcy equation was modified by Buckingham in 1907 to the form

$$q = -K(h)\text{grad}H$$

or with the relationship $\theta(h)$ known as the soil water retention curve is

$$q = -K(\theta_E)\text{grad}H$$

where q is flux density (LT $^{-1}$), h is the pressure head (L), and since the soil is not fully saturated with water, it is negative, sometimes denoted also as soil water potential. H is the total potential (L), the same as for saturated flow, but with h negative. K is unsaturated conductivity (LT $^{-1}$), no more a constant value, but functionally dependent either upon h or physically better expressed as dependent upon the relative saturation of soil by water $\theta_E = \theta/\theta_S$. The volumetric soil water content is the volume of water in the volume of soil (L 3 L $^{-3}$) and θ_S is soil water content at the full saturation of soil by water. In rigid soils is then $\theta_S=P$, porosity. Both equations are usually named Darcy-Buckingham equations.

When the soil is modeled as the bundle of capillary pores of variation of pore radii with radius size distribution $f(r)$ and when the laminar fluxes in individual capillaries are summed then the model of relative unsaturated conductivity is

$$K_R = \theta_E^\alpha \left[\frac{\int_0^r r^\beta f(r) dr}{\int_0^\infty r^\beta f(r) dr} \right]^\gamma$$

where $K_R = K/K_S$, α , β represent tortuosity, and γ is assumed to express the pores connectivity (Mualem, 1976). When $f(r)dr$ is approximated by $d\theta_E(h)$, i.e., by the derivative of the soil water retention curve and for the relation between the pore radius and the pressure head ($r=c/h$), we obtain

$$K_R = \theta_E^\alpha \left\{ \frac{\int_0^{\theta_E} \frac{d\theta_E}{[h(\theta_E)]^\beta} dr}{\int_0^1 \frac{d\theta_E}{[h(\theta_E)]^\beta} dr} \right\}^\gamma$$

among the various models of the soil water retention curve $h(\theta_E)$ the most frequently used is the equation of van Genuchten (1980)

$$\theta_E = \frac{1}{[1 + (a|h|)^n]^m}$$

where a , n , m are empirical fitting parameters to the soil water retention curve determined on the undisturbed soil sample. The value of K_R sinks in orders of magnitude when the soil water content decreases, e.g., when its value is lowered to the for plants still well available water content at $h = -500$ cm, then K_R falls by about three orders of magnitude in loams and to seven orders of magnitude in sands.

Richards' equation

The above Darcy–Buckingham equation of flux density is fully applicable to steady unsaturated flow when $\nabla q = 0$, $dq/dt = 0$ and $d\theta/dt = 0$. In practical situations, unsteady flow frequently exists with one of the conditions not fulfilled. In these situations, two equations are needed to describe the flux density and the rate of change of θ in time. The flux density is described by the Darcy–Buckingham equation and the rate of filling or emptying of the soil pores is described by the equation of continuity. The final equation derived by Richards (1931) is

$$\begin{aligned} \frac{\partial \theta}{\partial t} &= \frac{\partial}{\partial x} \left[K(h) \frac{\partial H}{\partial x} \right] + \frac{\partial}{\partial y} \left[K(h) \frac{\partial H}{\partial y} \right] \\ &\quad + \frac{\partial}{\partial z} \left[K(h) \frac{\partial H}{\partial z} \right] \end{aligned}$$

provided that the soil is homogeneous on REV scale and isotropic. In one-dimensional form for $H=h+z$ the above equation becomes

$$\frac{\partial \theta}{\partial t} = \frac{\partial}{\partial z} \left[K(h) \frac{\partial h}{\partial z} \right] + \frac{\partial K}{\partial z}$$

The equation is sometimes used as the Fokker–Planck equation (Kutilek and Nielsen, 1994) either in the capacitance form with water capacity $C_w = d\theta/dh$ (L^{-1})

$$C_w \frac{\partial h}{\partial t} = \frac{\partial}{\partial z} \left[K(h) \frac{\partial h}{\partial z} \right] + \frac{\partial K}{\partial z}$$

or in the diffusivity form

$$\frac{\partial \theta}{\partial t} = \frac{\partial}{\partial z} \left[D(\theta) \frac{\partial \theta}{\partial z} \right] + \frac{dK \partial \theta}{d\theta \partial z}$$

with the soil water diffusivity D ($L^2 T^{-1}$)

$$D(\theta) = K(\theta) \frac{dh}{d\theta}.$$

Preferential flow

The soil porous system is rarely homogeneous even on the REV scale and rigid, with pore size distribution constant and not dependent upon soil water content. Various types of irregularities cause the existence of small domains with a more rapid flow rates responsible for accelerated transport of pollutants or pathogens and dispersed clay particles than obtained by a simple application of the Richards' equation. This rapid flow is named preferential flow. It is realized in four physically defined types (Kutilek et al., 2009):

1. Preferential flow in the structural domain containing inter-pedal (inter-aggregate) pores, a subcategory of capillary pores. Richards' equation has been applied for this domain in simulation models since the pores belong to capillary pores. However, there is an indication that the flow in those pores could exist as transition to flow defined in item 2. The fluxes are accelerated when compared to fluxes in the matrix (intra-pedal) pores, if infiltration and redistribution are considered.
2. Preferential flow in real macropores (or non-capillary pores). Richards' equation is not applicable. Kinematic wave equation is mainly used. The fluxes are usually accelerated even when compared to fluxes due to item 1 (inter-pedal fluxes).
3. Preferential flow due to the unstable wetting front.
 - (a) Fingering, which occurs most frequently at the interface of less permeable layer above more permeable layer. Solution by Richards' equation exists provided that the geometry of fingering is defined. Rate of fluxes is comparable to item 1.
 - (b) Preferential flow due to irregularities in hydrophilicity. It occurs when initial soil water content is below critical value. Rate of fluxes is comparable to item 1.

In the majority of instances, the flow in matrix system of pores coexists with the flow in the structural system of pores. In each of the domains the unsaturated conductivity is expressed by the equation where the pore size distribution function $f(r)_i$ belongs either to matrix pores with $i=1$ or to the structural pores with $I=2$ and the unsaturated conductivity is then composed of matrix conductivity K_1 and of structural conductivity K_2

$$K = K_1 + K_2.$$

Summary

Soil water flow is described by the application of the Darcy's equation. In soils fully saturated with water, a constant hydraulic conductivity is defined. In unsaturated soils, Darcy's equation is modified by defining the unsaturated conductivity as a characteristic dependent upon the partial saturation of soil pores by water. Unsaturated conductivity is then no more a constant for the given soil. Its value decreases up to by order of magnitude with the decrease of soil water content. The governing equations of the solution of the water transport and soil water content change are partial differential equations. The existence of different domains of soil pores leads to the existence of bimodal or multimodal porous systems causing preferential flow.

Bibliography

- Buckingham, E., 1907. *Studies on the Movement of Soil Moisture*. Bureau of Soils, Bulletin No. 38. Washington DC: US Department of Agriculture.
- Hillel, D., 1998. *Environmental Soil Physics*. San Diego: Academic.
- Kozeny, I., 1927. Über Kapillarleitfähigkeit des Wassers im Boden. *Sitzungsberichte der Kaiserliche Akademie der Wissenschaften in Wien Sitzungsb.*, **136**, 303.
- Kutilek, M., and Nielsen, D. R., 1994. *Soil Hydrology*. Cremlingen-Destedt: Catena Verlag.
- Kutilek, M., Jendele, L., and Krejca, M., 2009. Comparison of empirical, semi-empirical and physically based models of soil hydraulic functions derived for bi-modal soils. *Journal of Contaminant Hydrology*, **104**, 84–89.
- Mualem, Y., 1976. A new model for predicting the hydraulic conductivity of unsaturated porous media. *Water Resources Research*, **12**, 2187–2193.
- Richards, L. A., 1931. Capillary conduction of liquids through porous media. *Physics*, **1**, 318–333.
- Van Genuchten, M Th., 1980. A closed-form equation for predicting the hydraulic conductivity of unsaturated soils. *Soil Science Society of America Journal*, **44**, 892–898.

Cross-references

- [Bulk Density of Soils and Impact on their Hydraulic Properties](#)
[Bypass Flow in Soil](#)
[Hydraulic Properties of Unsaturated Soils](#)
[Hydrophobicity of Soil](#)
[Infiltration in Soils](#)
[Peats and Peatlands, Physical Properties](#)
[Pore Size Distribution](#)
[Soil Aggregates, Structure, and Stability](#)
[Soil Surface Sealing and Crusting](#)

SOIL WATER MANAGEMENT

Willibald Loiskandl, Gerhard Kammerer
 Department of Water, Atmosphere and Environment,
 Institute of Hydraulics and Rural Water-Management,
 University of Natural Resources and Life Sciences,
 Vienna, Austria

Definition

Soil water management can be defined as active involvement in controlling soil water content at an optimal state for all given purposes, including environmental needs. An optimal state is often a compromise between competing uses and needs to account for long-term sustainability of the soil water system.

Progression of soil water management

Endeavors to maintain soil water balance have a long tradition and have been performed in many parts of the world. The irrigation schemes of the Mesopotamian plain are a well-documented example, but there is also evidence that drainage measures – the counterpart to irrigation – were undertaken in the same region. Lugalbanda, king of Uruk, an early settlement at the river Euphrates in ancient Mesopotamia ordered melioration of the swamps as a land reclamation measure over a 50-year period (C. Wilcke, Wiesbaden 1969, cited by Strommenger, 1980). In the past, irrigation with saline or brackish water and neglected drainage led to soil salinization; productive farmland had to be abandoned and some early civilizations declined or even disappeared (Evans and Fausey, 1999). Strictly speaking, this was not sustainable soil water management and until recently, water and soil were incorrectly considered as inexhaustible resources in many parts of the world.

It cannot be overemphasized that good drainage is an indispensable requirement for irrigation practice as well. As an example, an irrigated field in Ethiopia is highly at risk of crop failure due to nonexisting drainage and therefore, farmers decided to dig an “emergency drain” (Loiskandl 2006; Figure 1).

The beginning of modern land management practices in Central Europe (German “Kulturtechnik” = land preparation for agricultural and in a broader sense for human use including infrastructure) can be dated with the works of Dünkelberg (Kastanek, 1998). In the humid environment of his sphere of activity, the excess water was dominant and hence soils were drained intensively. However, he proposed the use of the drain systems for irrigation during dry periods (Dünkelberg, 1865).

A recent way to control soil water in certain cases is the application of soil additives. By mixing water retaining particles with soil, the hydraulic properties of the substrate should be improved and two hydrological effects should be achieved: (1) minimization of seepage losses and (2) reduction of evaporation, that is, water is kept in the root zone for the productive use by plants.

In a changing world, due to climate change and human interventions on land use, soil water management is still of growing importance. Subsurface water (water in the vadose zone and groundwater) forms the major volume of terrestrial water resources. For soil water Gusev and Novak (2007) distinguished three major functions in terrestrial ecosystems:

- Soil water is the most active link in the interchange of continental waters.
- Soil water is an element of the global climatic system (owing to its location at the atmosphere–lithosphere interface, soil water notably contributes to the formation of climate).
- Soil water is the most important factor governing the existence and development of the vegetation cover, which is the basic link in the trophic chain of land ecosystem.

To quantify the stress to which soil water is objected in an indicator-based assessment (EEA, 2008), the following key messages were delivered:

- Water retention capacity and soil moisture content will be affected by rising temperatures and by a decline in soil organic matter due to both climate change and land-management changes.
- Projections (for 2070–2100) show a general reduction in summer soil moisture over most of Europe, significant reductions in the Mediterranean region, and increases in the north-eastern part of Europe.
- Maintaining water retention capacity is important to reduce the impacts of more frequent intense rainfall and droughts.

Water in general, and soil water in particular, is fundamental to all life. It is vital to maintain its various functions in an optimum and sustainable manner and to safeguard its



Soil Water Management, Figure 1 Farmers at Godino are working on an emergency drain of an over-irrigated field to conduct excess water (Loiskandl, 2006).

use and protection. Modern soil water management has to acknowledge this fact.

Management and soil water

Soil water management has to be seen in the frame of the hydrological water cycle, especially when an integrated approach is proposed. It takes place in that part of the water cycle where water interacts with soil. In the hydrological glossary of UNESCO (2009), watershed management is defined as controlled use of drainage basins in accordance with predetermined objectives. In a process understanding, soil water is a subsystem of the hydrology of a basin (Figure 2), and soil water management activities are determined by the prevailing conditions and dynamics in the system in which it is embedded.

Classical melioration is defined as a long-term measure to maintain or to increase a higher productivity of the soil to enable an easier agriculture and to protect the soil from devastation and deterioration (Hunkeler et al., 1970). Drainage can be defined as artificial or natural, surface or subsurface dewatering with the aim to achieve a sustainable soil water condition at a certain location, whereas the Austrian standard ÖNORM B 2580 (ON, 1972) describes it as diversion of excessive soil water to ensure a better soil structure und aeration. Technical devices are required to control of soil water and are a major topic of rural water systems management. This classical approach is dominated by the planning and construction of hydraulic structures. Soil water management consists not only in technical measures, but aims to optimize the utilization of water for all purposes. Such an integrated water management approach is proposed by many authors (e.g., Bouwer, 2000). Management has to take into account that soil water governs the transport of solutes like

nutrients and contaminants and influences chemical and biological processes, hence water quality aspects are also object of soil water management activities.

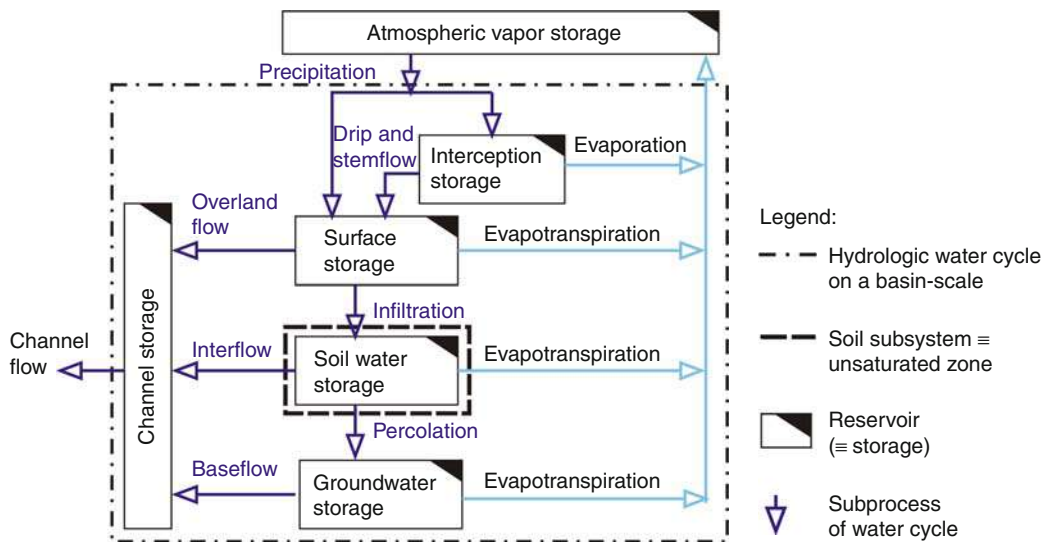
Agriculture and soil water

Agriculture may not be the most important user of soil water in economic terms, but due to its impact on the environment it is treated separately. Agricultural soil water management comprises traditionally irrigation and drainage.

In Europe, the purpose of water controlling has changed in the last decades from an application for agricultural production and purely technical measures to soil water management as an integrated and multipurpose task. Modern soil water management includes other elements like land use, variation of tillage operations, and adapted vegetation covers.

Good agricultural practice refers to establish optimum soil water content, fertilizer application, plant protection, soil conservation, and livestock production. Adequate technology is required for a homogeneous distribution of mineral or organic fertilizers. A combination of cover cropping with reduced tillage, thereby leaving part or all of the residues on the soil surface, is particularly recommended to achieve an optimum control of surface runoff losses and erosion.

A main concern of farmers in semiarid regions is the additional water consumption of cover crops, which is supposed to deplete soil water to the detriment of the succeeding cash crops. However, it could be shown by perennial monitoring of soil water dynamics under different cover crops in a low-rainfall region of eastern Austria that yield losses due to competition for soil water in the crop rotation are an exception (Bodner et al., 2008). On



Soil Water Management, Figure 2 Soil water management subsystem within the hydrologic cycle for a basin. (Adapted from Thompson, 1999.)

the contrary, also bare soil can undergo high evaporation losses during late summer and early autumn without providing the benefits of a plant covered field. Site characteristics such as soil water storage capacity and rainfall distribution have to be considered to accurately assess the impact of cover crops on soil water dynamics. "Storage driven" environments – i.e., climatic conditions with a distinct minimum of precipitation in summer and soil water storage in winter, making up a high percentage of total cash crop water use – are more prone to result in yield losses due to cover crop induced soil water depletion than "input driven" ecosystems, where crop growth usually relies on timely rainfall input during the vegetation period.

Reuse of water is a common practice in water-scarce regions for a long time. The problems that have to be solved in this context include available effluent flow, crop water requirements, storage, chemical composition of the treated wastewater (heavy metal and salt concentrations), hygienic conditions, potential health risks, as well as plant, soil, and groundwater protection.

In the dry areas, water, not land, is the limiting factor in improving agricultural production. Appropriate measures are irrigation or – where not enough water is available – increasing of water productivity. It was shown by Oweis and Hachum (2003) that substantial and sustainable improvement in water productivity can only be achieved through integrated farm resource management. In order to increase plant available soil water, current policies look at the whole set of technical, institutional, managerial, legal and operational activities required to plan, develop, operate and manage the water resources system at all scale, i.e., farm, project, basin, and national scale, while considering all sectors of the national economy that depend on water.

Economy and soil water

Long-term water storage – also referred to as water "banking" – is an option to remediate climate change impacts on temporal rainfall distribution. Compared to storage basins, underground storage of water has some advantages: it is not related to a land loss and evaporation losses are prevented. Using the word "banking" indicates that water gets a value in an economic term. Pratt already (1994) introduced the concept of water banking (Pratt, 1994), and a working definition for it is provided by Singletary (2009): water banking is a tool for leasing water for a limited period of time on a voluntary basis between willing water rights holders and users. It provides temporary transfers of water entitlements based on how much water a user needs and when it is needed without a permanent change in water rights. The result is that an individual can decide to lease water, based upon a personal perception of

- Operational needs
- Current market value of the water
- Risk involved in the transaction
- Market value of the crop or product requiring water input
- Cost of the transaction

Saving or exchanging currency through monetary banks is strictly a choice. Similarly, water banking is strictly a choice. Water banking transactions take place without the threat of outside coercion.

Legislation and soil water

Growing environmental concerns led to regional and European regulations and consequently to the European Water Framework Directive (WFD), which provides a comprehensive legislative instrument. In this respect, soil water protection is equal to groundwater protection and is part of land use. Measures for groundwater protection are connected to the functioning of soil as buffer and filter zone. As an immediate result, a code of good agricultural practice which refers to fertilizers, plant protection, soil conservation, and livestock production is defined (BMLFUW, 2007). Adequate spreading technology and homogeneous fertilizer distribution are required. Special threshold values of heavy metal contents in mineral fertilizers are introduced and the application of liquid fertilizer and liquid manure are allowed only on fallow land and if runoff is not possible. If sewage sludge is applied a certified quality has to be ensured.

The view of legislation on agricultural practices is mostly negative as potential contaminator. The positive aspects of nutrient supply into the agro-ecosystem for securing soil fertility, increasing the organic matter not only for agricultural productivity, but also for maintaining the vital functions of soil as filter, buffer, gene reserve and the role in carbon sequestration are often not seen alike.

Conclusions

Increasing pressure on the environment needs measures to protect soil water in terms of quantity and quality. Soil water management needs to be embedded in the bigger frame of catchment resource management. Besides traditional hydro-melioration practices like irrigation and drainage, other measures like tillage, cover cropping soil amendments, crop rotation and plant adaptations are equally important to keep the soil water content in an optimal state.

Bibliography

- BMLFUW – Bundesministerium für Land- und Forstwirtschaft, Umwelt und Wasserwirtschaft (ed.), 2007. Sonderrichtlinie des BMLFUW für das Österreichische Programm zur Förderung einer umweltgerechten, extensiven und den natürlichen Lebensraum schützenden Landwirtschaft (ÖPUL 2007). Wien: BMLFUW-LE.1.1.8/0073-II/8/2007.
- Bodner, G., Loiskandl, W., Buchan, G., and Kaul, H.-P., 2008. Natural and management-induced dynamics of hydraulic conductivity along a cover-cropped field slope. *Geoderma*, **146**, 317–325.
- Bouwer, H., 2000. Integrated water management: emerging issues and challenges. *Agricultural Water Management*, **45**, 217–228.
- Dünkelberg, F., 1865. *Der Landwirth als Techniker*. Braunschweig: Friedrich Vieweg und Sohn.
- EEA – European Environment Agency (ed.), 2008. *Impacts of Europe's changing climate—2008 indicator-based assessment*. EEA Report No. 4.

- Evans, R. O., and Fausey, N. R., 1999. Effects of inadequate drainage on crop growth and yield. In Skaggs, R. W., and van Schilfgaarde, J. (eds.), *Agricultural Drainage (Agronomy No. 38)*. Madison: Soil Science Society of America, pp. 13–54.
- Gusev, Y., and Novak, V., 2007. Soil water–main water resources for terrestrial ecosystems of the biosphere. *Journal of Hydrology and Hydromechanics*, **55**(1), 3–15.
- Hunkeler, K., Grubinger, H., and Tanner, E., 1970. *Landwirtschaftliches Meliorationswesen*, 5th edn. Bern: Verbandsdruckerei.
- Impacts of Europe's changing climate – 2008 indicator-based assessment
- Kastanek, F., 1998. Die tradition der Kulturtechnik. Wiener Mitteilungen: Wasser – Abwasser – Gewässer. *Das Band*, **149**, 1–59.
- Loiskandl, W., 2006. Hydrogeology and water utilization in Ethiopia. In Fiebig, M. (ed.), *Beiträge zur Angewandten Geologie – Festband Jean F Schneider*. Wien: Schriftenreihe des Departments für Bautechnik und Naturgefahren, Vol. 11, pp. 99–110.
- ON – Austrian Standards Institute (ed.), 1972. ÖNORM B 2580: Landwirtschaftlicher Wasserbau (Begriffsbestimmungen). Wien: Österreichisches Normungsinstitut.
- Oweis, T. Y., and Hachum, A. Y., 2003. Improving water productivity in the dry areas of West Asia and North Africa. In Kijne, J. W., Barker, R., and Molden, D. (eds.), *Water Productivity in Agriculture: Limits and Opportunities for Improvement*. Oxon: CABI.
- Pratt, K. B., 1994. Water banking: a new tool for water management. *The Colorado Lawyer*, **23**(3), 595–597.
- Singletary, L., 2009. Water Banking: What Is It And How Does It Work? Fact Sheet 98-09, Western Resource Issues Education Series No. 6 (Online). Available from World Wide Web: <http://www.unce.unr.edu/publications/files/ho/other/fs9809.pdf>.
- Stommenger, E. (ed.), 1980. *Sumer Assur Babylon: Sieben Jahrtausende Kunst und Kultur an Euphrat und Tigris*. Mainz: Verlag Philipp von Zabern.
- Thompson, S. A., 1999. *Hydrology for Water Management*. Rotterdam: A A Balkema.
- UNESCO (ed.), 2009. International Glossary of Hydrology (Online). Available from World Wide Web: <http://webworld.unesco.org/water/ihp/db/glossary/glu/EN/GF1380EN.HTM>, assessed 21.9. 2009.

Cross-references

- [Irrigation and Drainage, Advantages and Disadvantages](#)
[Management Effects on Soil Properties and Functions](#)
[Soil Water Flow](#)
[Water Budget in Soil](#)
[Water Use Efficiency in Agriculture: Opportunities for Improvement](#)

SOIL WATER POTENTIAL (PRESSURE, HEAD)

The amount of work that must be done per unit of a specified quantity of pure water in order to transport reversibly and isothermally an infinitesimal quantity of water from a specified source to a specified destination. If the specified quantity is volume, the potential is referred to as pressure (Pa). If the specified quantity is weight, the potential is referred to as head (m). If the specified quantity is mass, the potential is the term used ($J \text{ kg}^{-1}$).

See [Soil Hydraulic Properties Affecting Root Water Uptake](#)

Bibliography

Glossary of Soil Science Terms. Soil Science Society of America. 2010. <https://www.soils.org/publications/soils-glossary>

Cross-references

- [Hydraulic Properties of Unsaturated Soils](#)
[Hysteresis in Soil](#)
[Infiltration in Soils](#)
[Pedotransfer Functions](#)
[Physical Dimensions and Units Use in Agriculture](#)
[Soil–Plant–Atmosphere Continuum](#)
[Soil Water Flow](#)

SOIL WELDING

Soil welding is the formation of the solum of a ground soil through a thin cover sediment and mergence with the solum of a buried soil formed in a substratum material.

Bibliography

- Ruhe, R.V.; Olson, C. G. 1980. *Soil welding*. *Soil Science*, **130**(3):132–139.

SOIL-PLANT-ATMOSPHERE CONTINUUM

Cezary Ślawiński¹, Henryk Sobczuk²

¹Institute of Agrophysics Polish Academy of Sciences, Lublin, Poland

²Department of Thermal Techniques, Lublin University of Technology, Lublin, Poland

Synonyms

Soil–plant–atmosphere system

Definition

Soil–plant–atmosphere continuum is the near-surface environment in which water and energy transfer occurs from soil through plants to the atmosphere.

Introduction

John Philip (Philip, 1966) was the first to use the phrase “soil–plant–atmosphere continuum” (SPAC). According to his concept, SPAC integrates all components (soil, plant, animals, and the surrounding atmosphere) into a dynamic system in which the various transport processes involving energy and matter occur simultaneously.

The purpose of human activity in the areas being under agricultural use is plant production. The main aim of utilization of all agro-technical treatments is to create in the

soil an optimal condition for plant growth and development. This activity influences all constituents of SPAC.

The specific feature of soil–plant–atmosphere system parameters is their time and space variability and biological activity.

The soil system is composed of three major components: solid particles (minerals and organic matter), water with various dissolved chemicals, and air. The percentage of these components varies greatly with soil texture and structure. An active root system requires a delicate balance between the three soil components; but the balance between the liquid and gas phases is most critical, since it regulates root activity and plant growth process. It is necessary to mention about soil biota, which defines all organisms living within the soil. Soil organisms play a key role in cycling nutrients, which in turn impacts soil fertility and soil physical properties. They are also the indicators of soil health.

The role of soil in the soil–plant–atmosphere continuum is crucial. It is known that soil is not an essential factor for plant growth, and indeed plants can be grown hydroponically just with the application of water with proper fertilizers. However, usually plants are grown in the soil and soil properties directly affect the availability of water and nutrients to plants. Soil water affects plant growth directly through its controlling effect on plant water status and indirectly by its effect on oxygen availability through aeration, temperature variation, nutrient transport, uptake, and transformation. The understanding of these properties and processes is indispensable for irrigation system design and management.

Plants in SPAC play the role of water transmission from soil to the atmosphere. Actually few stages of long-distance translocation in plants are recognized, e.g., uptake of water by root system and its transport across root to the xylem, continued transport through xylem often several meters distance to the leaves and then transpiration. Some amount of water takes part in biochemical reactions in plant and in transport of assimilation products through phloem from leaves to organs where assimilation products are utilized.

The problem of scale

Environmental processes, their intensity and direction, originate from the basic processes of mass and energy transfer like evaporation, diffusion, and heat transport. These processes can be, in principle, described in a leaf scale with accurate physical equations. Most of the practical models are defined in a large scale of landscape or region. When scaling up the spatial coordinates, one is forced to include the description of more and more heterogeneous objects, which makes the model intractable. The way to solve this problem is hierarchical modeling of processes in different scales.

There are several scales of practical interest defined (Anderson et al., 2003):

- Leaf scale
- Plant scale

- Canopy scale
- Landscape scale
- Mesoscale

In each scale, processes and objects can be treated uniformly. Measurement data can be collected to provide parameters for the models specific for certain scale. The model results are then applied as part of input, or boundary description, to a higher scale model. Thus, the chain of hierarchical models allows spatial upscaling without loss of details of lower scale objects.

This kind of coupled model structure allows to gain reliable results for models like weather prediction model or yield prediction model from detailed data gained on a local scale.

Downscaling is also of practical interest. Remotely collected data by satellite means carry a lot of information, which in a sense is mixed due to the heterogeneity of area envisioned in pixels. Multi-scale model framework can be applied to support remote sensing data interpretation.

Soil–water–plant relationship

The soil is the main object that decides about water circulation in biosphere. It is a distributor of water, i.e., it receives and retains rainwater, transmits the water into deeper layers supplying underground water, as well as releases water into the atmosphere by evaporation and transpiration. Soil hydrophysical characteristics play a key role in the creation of plant growth conditions. They determine water availability for plant root system and water movement in soil profile.

Climatic factors such as air temperature, solar radiation, and wind speed control soil temperature. Solar radiation increases soil temperature, while other factors can cause increase or decrease of soil temperature. Temperature of soil under given conditions of thermal factors depends on soil thermal parameters: heat capacity and heat conductivity. Soil thermal properties in natural conditions are usually heterogeneous, and conditions of heat transfer are different in different positions in soil profile. This causes soil temperature spatial variability.

Water plays a crucial role in the process of plant growth, which involves cell division and cell expansion. The latter process occurs as each pair of divided cell imbibes water. The resulting internal pressure, called turgor pressure, stretches the elastic walls of the new cells, which thicken on account of the deposition of newly synthesized material.

Various terms used to characterize the status of water in different parts of the soil–plant–atmosphere system are merely alternative expressions of the energy level or potential of water. In order to describe the interlinked processes of water transport throughout the soil–plant–atmosphere continuum, one should evaluate the pertinent components of water energy potential and their effective gradients as they vary in space and time.

Soil water content and water potential, which is defined as the potential energy of water per unit volume relative to pure water in reference conditions gives the information

about amount of water present in the root zone and its availability for plants root system. Therefore, soil water content along with soil water potential should both be considered when dealing with plant growth and irrigation. For a specific soil, the soil water content and soil water potential are related to each other, and the soil water characteristic curve provides a graphical representation of this relationship.

The mechanisms of mass and energy transport in soil include molecular liquid diffusion, molecular vapor diffusion, capillary flow, convective transport, evaporation-condensation processes together with latent heat flow, pure hydrodynamic flow, and movement due to gravity. It is necessary to refer to freezing-thawing processes, which modify water transport through soil profile.

The mass flux is affected by the temperature and temperature gradient due to temperature dependence of bound water properties, as well as by the complicated pore network, which is difficult to describe in a given soil. The dominant mechanism under a specific set of conditions in a particular material often does not exist, and it is more likely that the mass and energy transport results from a combination of mechanisms. Due to this inherent complexity, theoretical models generally require assumptions that limit their applicability and a lot of measurement to verify them.

Water uptake by plants

A plant takes water mainly by the root system (Baranowski et al., 2005). At the first stage of water transport it finds its way along the root radius to the xylem, i.e., the bunch of conducting vessels. Then, water moves in xylem towards leaves. It is evaporated through the cells of mesophyll and cuticula and mainly through stomata into the atmosphere. A part of water taken by the plant is transported through phloem into cells, where the photosynthesis takes place.

Both passive and active water movement from the soil into the plant are the result of transpiration into the atmosphere. The passive process of water movement in the soil–plant–atmosphere system occurs under intensive transpiration. The intensity of transpiration is influenced by the difference of water potential in the plant and the water potential in the atmosphere. The water vapor potential in the atmosphere at the relative air humidity of 50% in temperature of 20°C is -94.1 MPa . In plant leaves in the same conditions, the water potential can reach values of minus several MPa. Such large difference of potentials confirms that the atmosphere is a huge “pump,” causing the water movement from plants into the surrounding air. Water losses in plants are compensated with water taken from soil, depending on the difference of water potentials between the soil and plant.

Water evaporates from plants by pores in the cell walls of mesophyll and cuticula. In these pores, concave menisci are created as a result of surface tension. In this case, the pressure lower than atmospheric arises, causing upward water movement in the xylem of whole plant. The pressure

of capillary rise reaches the value of -3 MPa . It is a cohesive mechanism of water uptake and conduction in plants.

The active water uptake and conduction in plants is based on root pressure. The root pressure is the result of water potential difference between the root xylem (higher solution concentration) and the soil (lower concentration). The osmotic movement is responsible for the water transfer from soil into roots. In case of strong salinization, the concentration of solution in the root can be much lower than in the soil solution. Then, the plant cannot take the soil water.

The soil water uptake can be hampered by the small coefficient of soil water diffusion. Despite high difference of water potentials in plant and soil, and therefore high potential evapotranspiration, the rate of water flow in soil towards roots can be too small, and the actual evapotranspiration can be strongly limited. Such situation leads to plant water stress.

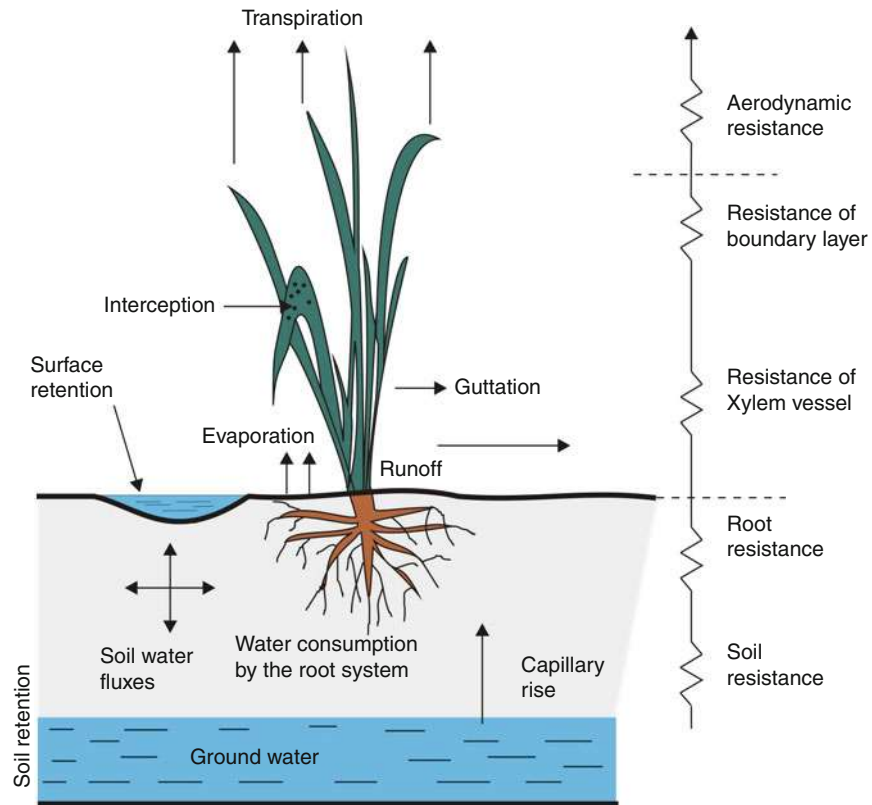
To explain the phenomenon of root pressure, many models were created, in which the transition into particular anatomical parts of the root, such as epidermis, endodermis, or xylem are treated as semipermeable membranes.

Another attempt to explain water uptake and conduction in plants is the theory of graviosmosis. The plant xylem is represented by a system of vertically placed compartments filled with solutions of various concentrations, connected by horizontally oriented semipermeable membranes. In this system, the graviosmosis force appears, causing the vertical water movement.

The resistance theory of water transport is used in many models of water flow in the soil–plant–atmosphere system. According to this theory, the flux density of moving water is proportional to the differences of water potential between the succeeding elements of the system, and inversely proportional to the resistance within these elements and at their interfaces. The resistance models are constructed as analogs of electrical circuits, and the role of resistors is played by water transport barriers, whereas the role of capacitors by the elements of water storage. In Figure 1, the water movement from the groundwater level through the plant into the atmosphere as well as accompanying resistances are presented. The groundwater enters into the unsaturated zone due the capillary rise. In this zone, water movement takes place in various directions, depending on the soil water potential gradients. The properties of the soil matrix, such as bulk density of the solid phase, grain size distribution, mineralogical and aggregate composition, water content, and water potential determine soil resistance for water transport in the root direction.

The root resistance for water transport is determined by intrinsic root structure which between others influences water potential in root. The resistance of the soil–root interface influences water potential difference in it as well as the quality of the soil–root contact, which is especially important in case of swelling and shrinking soils.

In plants, water is conducted by bunches of conducting vessels. In fact, they are the passive elements of the water



Soil-Plant-Atmosphere Continuum, Figure 1 Water movement in soil-plant-atmosphere system.

transport, and the resistance of the conducting vessels has an impact on the root pressure and the water potential in leaves. In a special case of some plants, where the root pressure occurs and simultaneously the water potential in leaves is equal to zero, which place under the relative air humidity close to 100%, water flows out on the plant's surface. This phenomenon is called guttation.

The resistance of the boundary layer includes the resistance for the water vapor transfer from the inside of the stoma chamber to the outside, which determines the pressure difference within the stoma chamber and on the leaf's surface, and the aerodynamic resistance of the air which has an effect on the water vapor pressure difference on the leaf's surface and in the atmosphere. The aerodynamic resistance depends on wind speed, atmospheric stability over the plant cover, and the architecture of the crop (its height and roughness).

Gas exchange in SPAC

It is generally agreed that soils play an important role in gaseous exchange and water and matter dynamics in terrestrial ecosystems. Much experimental work has been undertaken in the last few years in attempts to quantify the emission of greenhouse gases in terrestrial ecosystems and to identify the key factors that govern them. However,

fluxes vary greatly between ecosystems, and are often subject to great spatial and temporal variations within ecosystems. Consequently, there is an essential role for modeling, to scale-up observations made on relatively small areas to larger regions and ultimately to global level, and also to be able to predict the effects of environmental changes and changes in land management on future emissions.

The main components of soil oxygen demand are the microbial respiration of soil and the respiration of plant roots (Stepniewski et al., 2005). The contribution of the respiration of mezofauna as well as the contribution of chemical reactions is considered to be negligible and is usually neglected in models. Thus, the soil oxygen demand is used as synonymous for the soil respiration rate. Soil respiration rate is often expressed also as carbon dioxide production, as under aerobic respiration consumption of oxygen by volume is equivalent to that of carbon dioxide produced. The intensity of root respiration is usually higher by two orders of magnitude compared to the soil microbial respiration. Thus, the roots present themselves as linear objects of high oxygen demand on the background of the much less active soil matrix. Soil oxygen demand decreases with soil depth because both its components, i.e., microbial respiration and root density (and thus root respiration), decrease with depth.

Details of mass flux in SPAC

There is still a limited knowledge about mass flux details in SPAC and especially in plants. New investigations clarify some topics. Schroll and Kuehn (2004) developed a method and test system for determination of mass balance for organic compounds marked with isotope C14 in SPAC. Their experiment applies a lysimeter for the determination of C14 flux thus concluding the soil or the plant as the source of carbon in the flux. The stable oxygen isotopes were tracked to provide information on water use in walnut trees in paper (Lauteri et al., 2006). Analysis of concurrence conditions in a complex canopy is provided. Another attempt to investigate iodine isotope fate in plant is shown in Muramatsu et al., (1995) where the transfer factors of iodine were widely varied dependent on the plant type. Accumulation effects were discovered for the different plants in leaves. An important aspect of chemical compounds movement in the SPAC is phyto-remediation. Ouyang (2002) analyzed the fate of 1,4-dioxane with the application of SPAC idea with the application of model for coupled transport and accumulation of this pollutant. It comes out again that lives are very important in the accumulation of various pollutants.

Water and heat balance

The heat balance that includes radiation usually refers to a layer of the medium at the boundary with the atmosphere (water, soil, plant cover). Theoretically, it can be infinitely thin or it can have a specific thickness, e.g., corresponding to the thickness of plant cover. To express the basic processes of energy exchange in the system, the following form of the heat balance equation is used.

$$R_n - L \cdot E - H + L_p \cdot F_p - G + A_h = \frac{\partial W}{\partial t}$$

where R_n is the net radiative flux density at the upper surface of the layer (W m^{-2}), H is the sensible heat flux density (W m^{-2}), G is the density of the heat flux in the soil (W m^{-2}), L is the latent heat of vaporization ($2,448,000 \text{ J kg}^{-1}$), E is the water vapor flux density ($\text{kg m}^{-2} \text{ s}^{-1}$), L_p is the thermal conversion factor for fixation of CO_2 (J kg^{-1}), F_p is the specific flux of CO_2 ($\text{kg m}^{-2} \text{ s}^{-1}$), A_h is the energy advection into the layer expressed as specific flux (W m^{-2}), $\frac{\partial W}{\partial t}$ is the rate of change in energy storage per unit area in the layer (W m^{-2}).

Depending on the application, some components of this equation may be relatively less important and can be omitted. The most frequently used form of the heat balance equation takes into account four quantities: $L \cdot E$, H , R_n , and G .

The methods, which are based on the heat balance equation, assume one component of this equation as the unknown (usually it is $L \cdot E$ or H) and determine other components by direct or indirect methods.

A qualitatively new approach towards the problem of evapotranspiration determination with the use of the heat balance method was developed to measure remotely the

evaporating surface temperature. The radiation temperature, measured by remote sensing instruments with high accuracy and for large areas, creates an opportunity to modify the heat balance method to apply it for regional scale. The sensible heat flux, expressing the transport of heat energy from the evaporating surface into the atmosphere, is proportional to the difference of the air temperature at some level and the temperature of the studied surface.

Modeling of mass and energy transfer in SPAC

For the description of physical processes taking place in the SPAC, the constitutive physical equations are used, expressing the laws of momentum, mass, and energy conservation. The equations resulting from the conservation laws, describing a chosen phenomenon in this system, e.g., transport of water, salt and heat in the soil, soil deformation and stress as a result of reaction of wheels and working parts of machines and cultivation tools, need for their solution, the knowledge of transport coefficients characterizing the investigated object. Furthermore, for the proper verification of the solution of the applied equation, the knowledge of the dynamics of a studied physical quantity is indispensable, e.g., the dynamics of soil water content, salinity, gases and temperature, agro-climatic parameters such as amount of rainfall, radiation, air humidity, and temperature. Therefore, it is necessary to monitor the parameters of the investigated systems.

For modeling of mass and energy transport in SPAC, different transport processes should be taken into consideration occurring in soil as porous medium, in plants on short and long distances and from plants to ambient atmosphere.

Modeling processes taking place in the soil profile is an important and difficult task due to many transport processes occurring simultaneously and interacting with each other. These processes, among others, are transport of liquid water and water vapor, heat, soil air, dissolved salts and others chemicals. Which processes we are to consider depends on physical problem one wants to solve.

The common mathematical and physical framework for describing multicomponent and multiphase transport in porous medium is the linear thermodynamics of nonequilibrium processes. The partial differential equations, which describe such processes after several simplifications, are in general of the advection-diffusion nonlinear type with source terms.

The transport of water and heat are the basic processes, which must be taken into consideration almost independently apart from physical problem one is solving. Soil physical parameters depend on water content and/or temperature, whereas nonisothermal conditions in the soil influence nearly all the transport phenomena in the soil.

Water transport is described by Richard's equation of the form:

$$Cw(h) \frac{\partial h}{\partial t} = \nabla(K(h)\nabla(h - z))$$

where h is a pressure head [mH_2O], z is a distance from reference level, positive downward [m], $Cw(h) \equiv \frac{\partial \theta}{\partial h}$ is a soil water differential capacity function [m^{-1}], θ is volumetric soil water content [$m^3 m^{-3}$], $K(h)$ is an unsaturated hydraulic conductivity function [$m s^{-1}$].

The heat transport in soil occurs due to heat conduction and radiation. The heat flux caused by these phenomena is proportional to the gradient of soil temperature. The mean heat conductivity function describes soil heat transport properties. But apart from conduction and radiation, there may be also the convective heat transport, caused by liquid soil water migrating through the soil [4,5,8].

The equation which takes into account that transport phenomena has the form:

$$Cv(h) \frac{\partial T}{\partial t} = \nabla(\lambda(h, T) \nabla T) - c_{lw} \rho_{lw} \vec{q} \cdot \nabla T$$

where $C_v(h)$ is a volumetric heat capacity ($J m^{-3} \circ C^{-1}$) T is a temperature $\lambda(h)$ is the soil conductivity ($W m^{-1} \circ C^{-1}$) c_{lw} is a specific heat of liquid water ($J kg^{-1} \circ C^{-1}$) ρ_{lw} is a liquid water density ($kg m^{-3}$) The \vec{q} is Darcy velocity described by equation

$$\vec{q} \equiv K(h) \nabla(h - z)$$

which expresses the soil water movement velocity.

Summary

The concept of SPAC recognizing soil–plant–atmosphere system as integrated, dynamic system of all constituents, including living entities is widely accepted as way of understanding the system. In this sense, all the constituents and processes in the system should be considered together as embedded in it, interconnected mutually, and dependent of each other. Dynamic properties of each part of the system influence all other parts. Constituents and processes may be considered on various time or space scales. Mathematical description on different scales can vary according to the importance of constituents and processes at a given scale.

Bibliography

- Anderson, M. C., Kustas, W. P., and Norman, J. M., 2003. Upscaling and downscaling – a regional view of the soil–plant–atmosphere continuum. *Agronomy Journal*, **95**, 1408–1423.
- Baranowski, P., Usowicz, B., Walczak, R. T., and Mazurek, W., 2005. *Evapotranspiration into the Boundary Layer of the Atmosphere*. Lublin: Institute of Agrophysics Polish Academy of Sciences.
- Kirkham, M. B., 2002. The concept of soil–plant–atmosphere continuum and application. In Raats, P. A. C., Smiles, D., and Warrick, A. W. (eds.), *Environmental Mechanics: Water, Mass and Energy Transfer in Biosphere: The Philip Volume*. American Geophysical Union, Washington, DC: Geophysical Monograph, Vol. 129, pp. 327–335.
- Lauteri, M., Alessio, G. A., and Paris, P., 2006. Using oxygen isotopes to investigate the soil–plant–atmosphere hydraulic continuum in complex stands of walnut. *Acta Horticulturae*, pp. 223–230.

Mueller, T., Jensen, L. S., Magid, J., and Nielsen, N. E., 1997. Temporal variation of C and N turnover in soil after oilseed rape straw incorporation in the field: simulations with the soil–plant–atmosphere model DAISY. *Ecological Modelling*, **99** (2,3), 247–262.

Muramatsu, Y., Yoshida, S., and Ban-Nai, T., 1995. Tracer experiments on the behavior of radioiodine in the soil–plant–atmosphere system. *Journal of Radioanalytical and Nuclear Chemistry*, **194**(2), 303–310.

Ouyang, Y., 2002. Phytoremediation: modeling plant uptake and contaminant transport in the soil–plant–atmosphere continuum. *Journal of Hydrology (Amsterdam, Netherlands)*, **266**(1–2), 66–83.

Philip, J. R., 1966. Plant water relations: some physical aspects. *Annual Review of Plant Physiology*, **17**, 245–268.

Schroll, R., and Kuehn, S., 2004. Test system to establish mass balances for ^{14}C -labeled substances in soil–plant–atmosphere systems under field conditions. *Environmental Science and Technology*, **38**(5), 1537–1544.

Stepniewski, W., Stepniewska, Z., Bonnicelli, R. P., and Gliński, J., 2005. *Oxygenology in Outline*. Lublin: Institute of Agrophysics.

Cross-references

[Coupled Heat and Water Transfer in Soil](#)

[Plant Roots and Soil Structure](#)

[Plant–Soil Interactions, Modeling](#)

[Soil Functions](#)

[Soil Hydraulic Properties Affecting Root Water Uptake](#)

SOIL-WHEEL INTERACTIONS

Hiroshi Nakashima

Agricultural Systems Engineering Laboratory, Division of Environmental Science and Technology, Graduate School of Agriculture, Kyoto University, Oiwake-cho, Kitashirakawa, Sakyo-ku, Kyoto, Japan

Synonyms

Off-road wheel locomotion; Soil–tire interactions

Definition

Soil–wheel interactions are action and reaction relations between two contacting bodies – soil and a wheel – that occur during off-road locomotion and are foundations for the evaluation of the performance of wheeled vehicles.

Introduction

In agricultural operations in natural open fields, soil is a working material that is often encountered, the types of which are classifiable from clay to sand depending on the particle size distribution. In fact, softening of soil is the main purpose of tillage work. For agricultural vehicles, however, the capability of locomotion should be maintained in all soil conditions at the time of machinery operations. This kind of off-road wheel locomotion is often observed not only in agricultural vehicles but also in construction and military vehicles on earth and in extraterrestrial exploration vehicles. In principle, the

performance of wheeled vehicles depends on the contact mechanics at soil–wheel interfaces, where normal and tangential reactions play an important role. The analysis of contact interactions in relation with off-road vehicle performance is called terramechanics, which originated from rational studies by Bekker (1956, 1960). However, terramechanics belongs to typical nonlinear problems, in which the shape of the contact surface as well as the contact reaction can be determined only after the contact of two bodies – the soil and a wheel. Consequently, a simplification procedure should be applied to solve such problems approximately to reach an engineering solution. Two mathematical expressions of contact reactions – namely pressure–sinkage relations and shear stress–shear displacement relations – were introduced into the soil–wheel interface with the a priori assumption of the contact surface, which is now known as the semiempirical method (Wong, 1989). Moreover, further intensive studies of this framework have realized the development of a computer-aided performance prediction model for off-road vehicles based on the semiempirical method (Wong, 1989; Wong, 2008). Regarding numerical methods for soil–wheel interactions, the discrete element method (DEM) has recently become popular in performance analysis of wheels for off-road locomotion with various tread patterns (e.g., Oida and Ohkubo, 2000). For simplicity, the following explanation is limited to two dimensions unless otherwise stated.

Semiempirical model of soil–wheel interactions

The semiempirical method proposed by Bekker has contributed considerably to the understanding of soil–wheel interactions by introducing mathematical expressions for pressure–sinkage and shear stress–shear displacement relations on a simple contact interface with experimental identification of parameters used in those expressions.

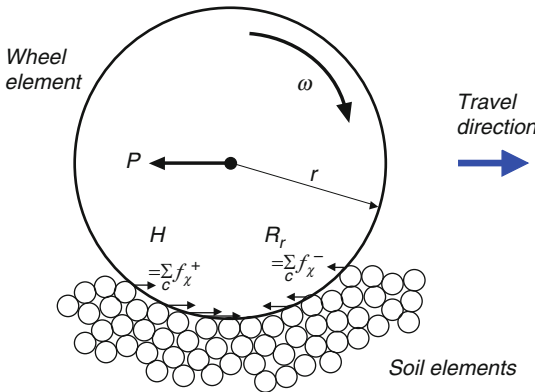
The pressure p in the pressure–sinkage relations might be understood as the contact pressure at the lowest wheel sinkage, which can be expressed as the given wheel contact load over a horizontally projected contact area, and which is a function of sinkage z to the n -th power, namely $p = k_{\text{eq}} z^n$, where $k_{\text{eq}} = k_c/b + k_\phi$ (Wong, 1989). Parameters k_c , k_ϕ , and n are obtained from measurement data using a *Bevameter*; b is the smallest width of a plate used in the measurements (Bekker, 1960). Moreover, the pressure distribution at the soil–wheel contact interface is assumed to be the same as the normal stress distribution over the contact length of the wheel as a function of sinkage. Therefore, for any value of parameter n , the maximum contact pressure is always generated at the largest wheel sinkage, or at the bottom dead center of a rigid wheel, as far as the pressure–sinkage relation is concerned. It is noteworthy that previously reported experimental results exhibited no such behavior and that the peak of contact pressure was generally observed before the bottom dead center of the wheel (e.g., Onafeko and Reece, 1967).

Shear stress–shear displacement relations were first incorporated from the response of a damping vibration model with explicit overshoot, or hump, behavior to express the brittle soil response. However, because of the difficulty in its use and because of the fact that plastic soils show rather monotonous response of shear stress without overshooting, a simpler and more useful exponential expression presented by Janosi and Hanamoto (1961), $\tau/\tau_{\max} = 1 - \exp(-j/K)$, has become popular to characterize the shear stress–shear displacement relation. In that equation, K is the shear deformation modulus, and τ_{\max} is the maximum shear strength, which might be expressed as $\tau_{\max} = c + p \tan \phi$ using the Mohr–Coulomb equation, where c signifies cohesion and ϕ denotes the angle of internal friction. The shear strength of soil depends on the loading condition. Therefore, the deviation of shear stress–shear displacement curves was introduced as a function of the applied normal contact stress p at the soil–wheel interface to connect two separate relations (Wong, 1989).

Although the semiempirical method depends on the assumption of two simple relations and although there exist different behaviors of the pressure–sinkage relation as evidenced from the experimental observations stated above, the analysis of traction performance for an off-road wheel using this method has been updated for use as a practical tool in terramechanics (e.g., Wong and Asnani, 2008).

Recent developments in traction analysis

Wheel performance depends on the wheel's surface condition as well as soil properties such as the soil shear strength. A lug-patterned wheel, called a lugged wheel, is generally assumed as a basic model for off-road wheels. Various tread patterns on a wheel might also be introduced depending on the mission of off-road vehicles for a given terrain condition. With improved performance of computers, numerical methods have been applied increasingly to various interaction problems in terramechanics. Among others, the discrete element method (DEM) developed by Cundall and Strack (1979) has become popular for analyses of lugged wheel performance on off-road terrain because the action of the tread pattern can be modeled easily using DEM. In DEM, virtual elements of a circle (Oida and Ohkubo, 2000; Nakashima et al., 2007), sphere (Horner et al., 2001), ellipsoid (Hopkins et al., 2008), clumped circles (Asaf et al., 2006), or other shape might be used as the soil element. Contact reactions between soil elements and between soil and wheel elements can be expressed simply as a parallel-connected linear spring and damper system in normal and tangential directions. Alternatively, nonlinear expressions such as the normal contact model of Hertz (Johnson, 1987) or the Mindlin–Deresiewicz tangential contact model (Mindlin and Deresiewicz, 1953) might be introduced. Coulomb friction is also installed in a tangential direction. Moreover, a tensile spring might be added to express the cohesive



Soil-Wheel Interactions, Figure 1 Soil-wheel interface.

effect between soil elements for analyses of cohesive soil-wheel interactions. Once all contact reactions are obtained, the equations of motion are constructed for all DEs; they are then integrated explicitly with a stable time step to obtain updated accelerations, velocities, and displacements. Parameters used in DEM must be prepared, but they cannot be determined through experiments because the radii of soil elements are usually larger than those of the soil particles.

Traction analysis of wheels using DEM is usually conducted as follows: (1) generation of discrete elements and consolidation of soil elements by their own weight, (2) free sinkage of wheel on soil elements until the vertical contact load condition is satisfied, and (3) wheel travel analysis with a given drawbar load condition. **Figure 1** portrays a typical soil-wheel interface in the wheel locomotion by DEM. To maintain simplicity, the tread pattern on the wheel surface is not presented in the figure.

For analysis of wheel performance using DEM, the gross tractive effort H of the wheel is calculated as the summation of all positive components of contact reactions at contacting wheel and soil elements. The running resistance R_r of the wheel is obtainable as the summation of all negative components of contact reactions. Then, the net traction P_n of wheel is calculable as $P_n = H - R_r$ (Oida and Ohkubo, 2000; Nakashima et al., 2007). The net traction P_n equals the drawbar load P shown in the figure. The expression of tread patterns can be realized by additional virtual small discrete elements embedded into the wheel rim surface (Nakashima et al., 2007). The result of DEM in general shows vibratory behavior of data. It should be averaged to obtain the required traction-related interactions at soil-wheel interfaces. The accuracy of analysis by DEM must be verified through precise experiments to assess the common conditions between experiments and simulations. For necessary verifications, the recent development of small force sensors is expected to contribute to such measurement of local normal and tangential contact reactions on the contact surface of a wheel or tire running on soil (Kasetani et al., 2010).

Summary

Soil-wheel interactions were analyzed traditionally using semiempirical methods from an engineering perspective. The development of computer capabilities will surely contribute to a deeper understanding of soil-wheel interactions. Moreover, it seems clear that not only conventional conditions but also some extended conditions related to soil-wheel interactions are solvable using such numerical methods as the discrete element method. Through these parametric analyses, we will be able to construct a new perspective for innovative running devices that might yield higher traction performances than conventional wheel systems.

Bibliography

- Asaf, Z., Shmulevich, I., and Rubinstein, D., 2006. Predicting soil-rigid wheel performance using distinct element methods. *Transactions of the ASABE*, **49**(3), 607–616.
- Bekker, M. G., 1956. *Theory of Land Locomotion*. Ann Arbor: University of Michigan Press.
- Bekker, M. G., 1960. *Off-the-Road Locomotion*. Ann Arbor: University of Michigan Press.
- Cundall, P. A., and Strack, O. D. L., 1979. Discrete numerical model for granular assemblies. *Geotechnique*, **29**(1), 47–65.
- Hopkins, M. A., Johnson, J. B., and Sullivan, R., 2008. *Discrete element modeling of a rover wheel in granular material under the influence of Earth, Mars, and Lunar Gravity*. In Proceedings of the Earth and Space 2008, 11th ASCE Aerospace Division International Conference on Engineering, Science, Construction, and Operations in Challenging Environments, Long Beach, March 3–5, pp. 1–7 (CD-ROM).
- Horner, D. A., Peters, J. F., and Carrillo, A., 2001. Large scale discrete element modelling of vehicle-soil interaction. *Journal of Engineering Mechanics*, **127**(10), 1027–1032.
- Janosi, Z., and Hanamoto, B., 1961. *The analytical determination of drawbar pull as a function of slip for tracked vehicle*. In Proceedings of the First International Conference on Mechanics of Terrain-Vehicle Systems, Turin.
- Johnson, K. L., 1987. *Contact Mechanics*. Cambridge: Cambridge University Press.
- Kasetani, T., Nakashima, H., Shinone, H., Shimizu, H., Miyasaka, J., and Ohdoi, K., 2010. Tri-axial contact reaction at the tire-soil interface. *Engineering in Agriculture, Environment and Food*, **3**(1), 14–19.
- Mindlin, R. D., and Deresiewicz, H., 1953. Elastic spheres in contact under varying oblique forces. *Journal of Applied Mechanics*, **20**, 221–227.
- Nakashima, H., Fujii, Y., Oida, A., Momozu, M., Kawase, Y., Kanamori, H., Aoki, S., and Yokoyama, T., 2007. Parametric analysis of lugged wheel performance for a lunar microrover by using DEM. *Journal of Terramechanics*, **44**, 153–162.
- Oida, A., and Ohkubo, S., 2000. Application of DEM to simulate interaction between soil and tire lug. *Agricultural and Biosystems Engineering*, **1**, 1–6.
- Onafeko, O., and Reece, A. R., 1967. Soil stresses and deformations beneath rigid wheels. *Journal of Terramechanics*, **4**(1), 59–80.
- Wong, J. Y., 1989. *Terramechanics and Off-Road Vehicles*. Amsterdam: Elsevier.
- Wong, J. Y., 2008. *Theory of Ground Vehicles*, 4th edn. Hoboken: Wiley.
- Wong, J. Y., and Asnani, V. M., 2008. Study of the correlation between the performances of lunar vehicle wheels predicted by the Nepean wheeled vehicle performance model and test data. *Proceedings of the Institution of Mechanical Engineers, Part D: Journal of Automobile Engineering*, **222**(11), 1755–1770.

Cross-references

Compaction of Soil
Friction Phenomena in Soils
Stress–Strain Relations
Subsoil Compaction
Traficability and Workability of Soils

SOILBORNE DISEASES, CONTROL BY PHYSICAL METHODS

Jaacov Katan¹, Abraham Gamliel²

¹Department of Plant Pathology and Microbiology, The Hebrew University of Jerusalem, Food and Environment, Rehovot, Israel

²The Laboratory for Pest Management Research, Institute of Agricultural Engineering, The Volcani Center, Agricultural Research Organization, Bet Dagan, Israel

Synonyms

Soil disinfestation; Soil pasteurization

Definitions

Soilborne pathogens. Soil-dwelling organisms (e.g., fungi, bacteria, or nematodes), which attack the roots of host plants and cause damage.

Root diseases. Malfunction in plant development and production caused by soilborne pathogens.

Disease control. Management of plant malfunction that aims at killing the pathogen or suppressing its activity, hence resulting in reduced disease incidence or severity.

Introduction: soilborne diseases and their control (management)

Soilborne pathogens (fungi, bacteria, nematodes) cause plant diseases, and consequently severe losses, in all major economic crops. These pathogens live in the soil and are therefore affected by the soil's physical, chemical, and biological characteristics, as well as by the agricultural practices applied to it, for example, irrigation, fertilization, and tillage. The close connection between soilborne pathogens and soil, their natural habitat, complicates their control, since it is difficult to reach all of the propagules at all soil sites. The basic principle of root-disease control is to manipulate or interfere with the interactions between pathogen, host, and their biotic and abiotic environments, in order to achieve an economic reduction in disease. The basic means used to achieve this goal are chemical, physical, biological, and cultural. There is increasing public concern over environmental pollution by pesticides. Consequently, there is increasing interest in physical methods of disease control which do not pollute the environment with chemicals. However, their use may involve problems of safety, energy transfer, technology, and cost.

Soil disinfestation in its present form was established at the end of the nineteenth century. Two approaches were developed at that time: chemical, for example, the use of fumigants, and physical, for example, soil steaming. It was only about 100 years later that a third approach for soil disinfestation – soil solarization, which involves heating the soil by solar energy – was developed. The amount of time taken for this third approach to emerge emphasizes the difficulties involved in introducing new approaches for soil disinfestation. Chemical soil disinfection, which is still the major soil-disinfestation practice, is not the focus of this entry and will therefore not be discussed.

Soil disinfestation involves the use of drastic means to treat the soil (Katan, 1984; Tjamos et al., 1999). It is carried out before planting, and is aimed at maximal reduction of the pathogen population in the soil to the desired soil depth (30–50 cm in soil or 10–20 cm in soilless culture). Soil disinfestation should create minimal disturbance of the biological equilibrium as a whole (especially beneficial microorganisms), and minimal changes in the soil's chemical or physical properties. Moreover, the control agent, or its decomposition product, has to dissipate before planting to avoid harmful residual effects. The execution of soil disinfestation is sophisticated and expensive, but it is also an effective method of eradicating soilborne pathogens, as well as other pests, for example, soil arthropods and weeds. Soil disinfestation was initially developed only for the control of harmful biotic agents. However, later on, its effects on abiotic soil components, for example, improvement of the plant's mineral nutrition status, were reported (Chen et al., 1991 and see further on). Although soil disinfestation should control a wide spectrum of soilborne pests, it does not protect the soil against contamination from outside sources once the disinfestation effect has ceased. Hence, a supplementary step needs to be taken, following soil disinfestation and during crop production to avoid reinfestation by soilborne pests from outside sources.

Physical methods of soil disinfestation: soil heating

The main approaches to disinfecting soil, which involve the utilization of heat energy in the form of hot water are the application of steam or flooding the soil with hot water. Heating the soil by applying hot air or microwave radiation has also been tested, but commercial implementation is questionable. Steam sterilization consists of applying pressurized steam under a mulched cover, and its penetration to the depth of the cultivation layer (Baker, 1962; McGovern and McSorley, 1997). Steam disinfection is very expensive as it consumes a high rate of energy (fuel), and involves expensive and sophisticated machinery. In sandy soils, penetration of the steam to deep soil layers requires a sucking infrastructure which is buried in the soil as a permanent

component of the greenhouse. Furthermore, the capacity of this process is low, enabling its application only on a small-farm scale.

Hot water treatment consists of a similar energy of water heating, but to a much lower water temperature. This soil-disinfestation approach consists of pouring water at a temperature of 70–95°C on the soil. Hot water treatment was developed in Japan, where it showed high control efficacy of fungal and bacterial pathogens and nematodes down to a soil depth of 30 cm (Nishi et al., 2003). However, the use of this approach did not expand beyond that country. The practical aspects of steam disinfection (energy consumption, equipment, etc.) also apply to hot water treatment.

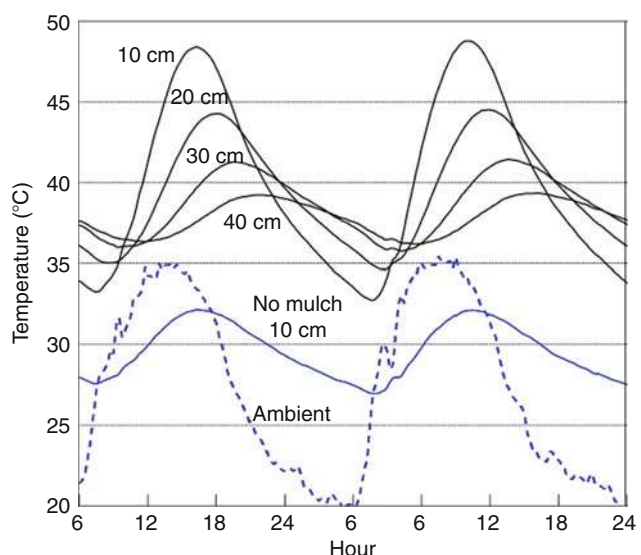
Attempts have been made to utilize electromagnetic energy as a means for dry heating. However, the energy and time needed to achieve pathogen control makes this approach impractical for soil disinfestation.

Soil solarization

Soil solarization in its present form for soil disinfestation was first described and reported in 1976 (Katan et al., 1976). Solarization consists of using solar energy to elevate soil temperatures by mulching a wet soil with transparent polyethylene under the appropriate climatic conditions (hot season with high solar irradiation). The heated soil kills soilborne pests, improves plant health and consequently, increases crop yield. This process has also been variously referred to as: solar heating of the soil, solar pasteurization, and solar disinfestation. However, the term “soil solarization” is the accepted and most widely used term.

Soil solarization can be carried out directly in the open field or in the greenhouse. Solar heating results in relatively mild temperatures, as compared to artificial and intense heating methods which are usually carried out at 70–100°C. The principles of soil solarization have been described in detail in many reviews and books (e.g., Katan, 1981; Katan and DeVay, 1991; McGovern and McSorley, 1997; Stapleton, 2000; Gamliel and Katan, 2009) and are summarized as follows:

1. Solar heating elevates soil temperatures through repeated daily cycles. At increasing soil depths, the maximal temperatures are lower than in the upper layers. In the deep layers, the maximal temperature is achieved later in the day, but it is maintained for longer periods (Figure 1).
2. The best time for mulching the soil and applying soil solarization relies on the appropriate climatic conditions, that is, periods of high temperature and extended daylight. These can be determined experimentally by tarping the soil and measuring the temperatures at various depths. Meteorological data from previous years and predictive models (see further on) are very useful in this decision-making process.
3. Adequate soil moisture during solarization is crucial. The water in the soil enables heat transfer, increases



Soilborne Diseases, Control by Physical Methods,

Figure 1 The daily course of soil heating by polyethylene (solarization) at three soil depths, as compared to nonsolarized (no mulch) soil at a depth of 10 cm. Typical results obtained during July–August in Rehovot, Israel.

the thermal sensitivity of the target organisms, and enables biological activity during solarization.

4. Proper preparation of a soil for planting is essential since after plastic removal, the soil should not be disturbed, in order to avoid recontamination.
5. The soil is mulched with thin, transparent sheets of polyethylene or other plastic material for 3–6 weeks. Mulching the soil in a closed greenhouse (glass or plastic) further improves soil heating. Novel technologies, such as the use of sprayable plastics (Gamliel et al., 2001), can enable plastic mulching of the soil in large-scale areas such as for field crops.
6. Solarization alters the chemical, physical, and biological properties of the soil, which further affects pest control and may benefit plant growth and yield (Chen et al., 1991).

Under appropriate conditions, many soilborne pathogens, such as fungi (e.g., *Verticillium*, *Fusarium*, *Phytophthora*, *Pythium*, *Pyrenophaeta*), nematodes (e.g., *Pratylenchus* and *Ditylenchus*), and bacteria (e.g., *Clavibacter michiganensis*), as well as a variety of weeds, especially annuals, are controlled by solarization and consequently, yields increase.

As with any soil-disinfestation method, soil solarization has its advantages and limitations. It is a nonchemical method that has less drastic effects on the biotic and abiotic components of the soil. Nevertheless, the possibility of negative side effects should not be ignored. Soil solarization is very simple to apply and it is frequently less expensive than chemical disinfestation. The limitations of this method stem from its dependence

on appropriate climatic conditions: it can only be used in certain climatic regions and during limited periods of the year. In addition, during the solarization process (3–6 weeks), the soil remains without a crop. Nevertheless, this method has attracted many researchers from over 60 countries (Gamliel and Katan, 2009) and it is also used by farmers, especially in combination with other methods. It has been commercially adopted and is currently being used in Israel, Jordan, Greece, Turkey, Spain and Latin American countries, among others.

Physical principles

The principles of soil heating and the energy balance of bare and mulched soils have been described in various publications (e.g., Mahrer, 1991). The main factors involved in soil heating are climatic (e.g., solar radiation, air temperature, air humidity, and wind speed), soil properties, and photometric and physical characteristics of the mulch. The fluxes of energy that have to be considered are:

R_g Global radiation (waveband of approximately 0.3–4 μm)

R_L Atmospheric (long-wave) radiation (waveband of approximately 4–80 μm)

S Conduction of heat in the soil (soil heat flux)

H Vertical heat exchanges with the air enclosed between the mulch and soil by conduction and with the surrounding air by convection (sensible heat flux)

E Condensation and evaporation of water (latent heat flux)

The two basic equations describing the energy balance of bare and mulched soils, respectively, are:

$$R_{sn} + R_{Ln} - H - E - S = 0 \quad (1)$$

$$R_{snm} + R_{Lnm} - H_m - E_m - S_m = 0 \quad (2)$$

where subscript m stands for mulched soil and R_{sn} and R_{Ln} are the net fluxes of short- and long-wave radiation at the bare soil surface, respectively; S , H , E are soil heat flux, vertical heat exchanges, and condensation and evaporation of water, respectively.

Using these equations, a one-dimensional numerical model to predict the diurnal cycle of soil temperature in mulched and bare soils was developed, with good agreement between observed and predicted soil temperatures. Calculations showed that increased soil temperature in wet mulched soil is mainly due to a reduction in heat loss through sensible and latent heat fluxes during the day, and partially due to the greenhouse effect of the wet cover (owing to the formation of small water droplets on its inner surface). A model suitable for humid areas was described (Wu et al., 1996).

Application

Continuous mulch is desirable for effective soil solarization as it enables effective disinfestation of a wide area

and also improves control efficacy and reduces soil reinfestation. However, strip solarization applied to raised beds also increases soil temperatures and results in effective pathogen control under appropriate conditions. Moreover, relatively small plots can be covered manually. The edges of the sheet should be firmly embedded in the soil, while ensuring film tightness. For relatively small plots, a continuous plastic covering can be achieved by manually anchoring the edge of two adjacent sheets together in one furrow (Grinstein and Hetzroni, 1991). Mechanized plastic mulch is preferred and used in large plots. It is applied essentially as soil fumigation is performed. The tarp-laying machine unrolls plastic strips (2–4 m width), each of which is anchored to the soil on one side and connected to the other sheet by means of glue or welding. Sheet glue is moist and is sprayed in a 5- to 8-cm strip along the edge of the previously laid sheet near the border of the anchored area. Since solarization requires a minimum period of 30 days, the glue has to be long-lasting. In recent years, suitable glues have been developed and are used for continuous mulching. An alternative system to weld polyethylene sheets together was developed in Israel (Grinstein and Hetzroni, 1991): sheet fusing is accomplished with hot air streams, emitted from a combustion chamber and directed onto the plastic sheets.

Sprayable polymers offer a feasible and cost-effective alternative to plastic tarps for soil solarization. The plastic-based polymers are sprayed on the soil surface in the desired quantity and form a membrane film, which maintains its integrity in soil and elevates soil temperature. Nevertheless, the formed membrane is porous, allowing overhead irrigation. The soil-heating process with sprayable mulch is faster than that with plastic film, but the soil also cools down to lower temperatures at night. The thickness of the sprayed coat is critical to obtaining effective heating mulch. Soil solarization using sprayable mulches was shown to be effective at controlling Verticillium wilt and potato scab in potato (Gamliel et al., 2001). The level of control was as effective as that achieved by solarization using plastic films. Nevertheless, the use of sprayable polymers needs to be further improved.

Another application of soil solarization is structural solarization for controlling pathogens and other pests remaining in the greenhouse structure (Shlevin et al., 2003). This is accomplished by closing the greenhouse between crops and during the hot season. The temperatures are raised to 60°C and higher, resulting in pest control, namely, sanitation. A model simulating the heating process under structural solarization has been developed (Shlevin et al., 2003).

Concluding remarks

Soil disinfestation for controlling soilborne pathogens is much needed for an ever-growing world population. However, there is an urgent need to replace the widely used polluting fumigants with environmentally acceptable

methods. Physical methods can meet this demand, but so far their use has been limited. To further expand their use, we have to further improve their effectiveness in pest control and methods of application in an attempt to reduce their cost and make them economically acceptable.

Bibliography

- Baker, K. F., 1962. Principles of heat treatment of soil and planting material. *Journal of the Australian Institute of Agricultural Science*, **28**, 118–126.
- Chen, Y., Gamliel, A., Stapleton, J. J., and Aviad, T., 1991. Chemical, physical and microbial changes related to plant growth in disinfested soil. In Katan, J., and DeVay, J. E. (eds.), *Soil Solarization*. Boca Raton: CRC Press, pp. 103–129.
- Gamliel, A., and Katan, J., 2009. Control of plant disease through soil solarization. In Walter, D. (ed.), *Disease Control in Crops: Biological and Environmentally Friendly Approches*. Oxford: Blackwell, pp. 196–220.
- Gamliel, A., Skutelski, Y., Peretz-Alon, Y., and Becker, E., 2001. Soil Solarization Using Sprayable Plastic Polymers to Control Soilborne Pathogens in Field Crops. In *Proceedings of the 8th Annual International Research Conference on Methyl Bromide Alternatives and Emission Reduction*. San Diego, 10-1–10-3.
- Grinstein, A., and Hetzroni, A., 1991. The technology of soil solarization. In Katan, J., and DeVay, J. E. (eds.), *Soil Solarization*. Boca Raton: CRC Press, pp. 193–204.
- Katan, J., 1981. Solar heating (solarization) of soil for control of soilborne pests. *Annual Review of Phytopathology*, **19**, 211–236.
- Katan, J., 1984. *The Role of Soil Disinfestation in Achieving High Production in Horticultural Crops*. Brighton: British Crop Protection Conference, pp. 1189–1196.
- Katan, J., and DeVay, J. E., 1991. *Soil Solarization*. Boca Raton: CRC Press.
- Katan, J., Greenberger, A., Alon, H., and Grinstein, A., 1976. Solar heating by polyethylene mulching for the control of diseases caused by soilborne pathogens. *Phytopathology*, **66**, 683–689.
- Mahrer, Y., 1991. Physical principles of solar heating. In Katan, J., and DeVay, J. E. (eds.), *Soil Solarization*. Boca Raton: CRC Press, pp. 75–86.
- McGovern, R. J., and McSorley, R., 1997. Physical methods of soil sterilization for disease management including soil solarization. In Rechcigl, N. A., and Rechcigl, J. E. (eds.), *Environmentally Safe Approaches to Disease Control*. Boca Raton: CRC Lewis, pp. 283–313.
- Nishi, K., Kita, N., and Uematsu, S., 2003. Hot water soil sterilization begins in Japan. *Farming Japan*, **37**(2), 35–41.
- Shlevin, E., Saguy, S., Mahrer, Y., and Katan, J., 2003. Modeling the survival of two soilborne pathogens under dry structural solarization. *Phytopathology*, **93**, 1247–1257.
- Stapleton, J. J., 2000. Soil solarization in various agricultural production systems. *Crop Protection*, **19**, 837–841.
- Tjamos, E. C., Grinstein, A., and Gamliel, A., 1999. Disinfestation of soil and growth media. In Alfajes, R., Gullino, L. M., Van Lentern, J. C., and Elad, Y. (eds.), *Integrated Pest and Disease Management in Greenhouse Crops*. Dordrecht: Kluwer Academic, pp. 130–149.
- Wu, Y., Perry, K. B., and Ristaino, J., 1996. Estimating temperature of mulched and bare soil from meteorological data. *Agricultural Meteorology and Forestry*, **81**, 299–323.

Cross-references

- [Climate Change: Environmental Effects](#)
[Cultivation Under Screens, Aerodynamics of Boundary Layers](#)
[Energy Balance of Ecosystems](#)
[Microbes, Habitat Space, and Transport in Soil](#)

SOILS AND PLANTS AERATION

See [Aeration of Soils and Plants](#)

SOILS AND PLANTS OXYGENATION

See [Aeration of Soils and Plants](#)

SOLAR DRYING OF BIOLOGICAL MATERIALS

Istvan Farkas

Department of Physics and Process Control, Szent Istvan University, Gödöllő, Hungary

Synonyms

Solar dehydration; Sun drying

Definition

The solar drying of different grains, fruits, vegetables, and other materials of biological origin plays an important role in influencing energy savings, quality of end-products, and environmental impacts. There is a number of drying methods currently available, but it is worth taking into account the technical and economical benefits of solar drying, with the substantial number of commercially available solar dryers in operation today. However, for some special cases, individually designed solar dryers have also been developed. The applicable temperature range and energy requirement for moisture removal are the most important parameters in designing a safe and cost-effective drying system. During the drying of biological materials, the solar-assisted preheating of drying air fits to such requirements.

Introduction

There is no doubt that using solar energy is a promising solution in attaining the technical, economical, and environmental demands raised in the course of a drying process. For this reason, several new approaches in the application of dryers and biological materials are under development in order to produce a high quality of product at competitive cost. The new approaches include designing of new type of solar dryers, revising of existed traditional dryers with solar preheating unit and use the multipurpose operation of solar units. For example, dried material cases can be as barley, rice, peach, apple, grape, plum, cherry, blackthorn, pineapple, carrot, onion, chili, tomato, pegaga leaf, hay, tobacco, timber, fish sardines, and shark fillets. The feasibility of solar drying must include several additional factors, such as local climate, variety of biological materials, the amount of material to be dried, etc. In addition to the practical issues, the

research and development priorities in solar drying fall into similar directions.

Solar grain drying

The traditional use of solar energy for grain drying is in a forced convection heated air system. A small-scale solar dryer can be used effectively for drying of various agricultural crops (Farkas, 2004, 2008). A design method for sizing solar-assisted crop-drying systems and assessing the combination of solar collector area and auxiliary energy needs that meets the load. Two empirical correlations were compared for their use with high thermal inertia solar collectors, which are cheap and adequate in rural areas. The grain drying with partial air heating by solar energy can provide an annual economy of about 30% in the fuel consumption (Santos et al., 2004).

Solar fruit drying

There are several types and sizes of fruit that often need to be handled together during the drying process, using the same equipment. For that purpose, a modular solar tray dryer was designed (Farkas, 2004, 2008). Two basic variations were considered of which one is a surface dryer, the other one is a batch or “overflowing” solution. The modular construction of a dryer means that the equipment does not need to contain all of its parts for operation. It can be used with or without the solar collector, with natural (without fan) or forced airflow. The dryer has four main sections: a drying chamber with different trays, a photovoltaic (PV) module, a grid connected fan, and a solar collector unit. With a modular construction, the dryer can be operated with natural ventilation by ambient air, artificial ventilation of ambient air with PV module, artificial ventilation of collector preheated air, and combined uses as well. During the drying experiments, several types of fruit were tested, e.g., grape, peach, plum, cherry, and blackthorn. Carrot and apple in the same solar dryer have been studied in order to evaluate the weight losses during the drying period and to present the temperature and moisture content distributions in the modular solar dryer (Romano et al., 2009).

A hybrid solar dryer has been constructed relying on solar energy to heat forced airflow for drying fruits (Amer et al., 2006). A heat exchanger placed inside the collector is used during sunny days to heat water from the heated air and the direct solar radiation. While at night, hot water flows through the exchanger to heat air in the reverse direction. Additionally, electric energy can be applied during the night to complete the heating of water in case the stored energy in the water tank is insufficient for heating the drying air during the night.

Solar vegetable drying

There are several type of vegetables dried in both direct sun drying and in solar dryers all over the world. Due to the long drying time during sun drying, however, the quality parameters as color, flavor, and nutrients are often

affected and solar drying may be preferably recommended (Prakash et al., 2004; Praveenkumar et al., 2006).

A batch type solar dryer was designed for different agricultural products and used recently for drying onion (Bennamoun and Belhamri, 2002). The dryer is constructed from brick walls, supporting ten trays to hold the material to be dried. The solar air collector is constructed from glass Pyrex plate and a black painted aluminum plate serves as the absorber. An auxiliary heater could be mounted to the dryer.

Recently specialists are opting for forced convection solar tunnel drying for drying of various crops (Pangavhane and Sawhney, 2002). A mixed mode type forced convection solar tunnel drier was used to dry hot red and green chillies (Hossain and Bala, 2007). The drier consisted of transparent plastic covered flat-plate collector and a drying tunnel connected in series to supply hot air directly by two fans operated by a photovoltaic module. The drier has a loading capacity of 80 kg of fresh chilies.

Tomato is a widely used vegetable. A vacuum-assisted solar dryer have been developed to study the drying kinetics of tomato slices (Rajkumar et al., 2007). The drying time for drying of tomato slices of 4, 6, and 8 mm thicknesses starting from initial moisture content of 94.0% to a final one of $11.5 \pm 0.5\%$ (w.b.) was 360, 480, and 600 min in vacuum-assisted solar dryer and 450, 600, and 750 min in open sun drying, respectively. Beside the drying time taken for drying the additional benefit of vacuum-assisted drying was that the quality of tomato slices dried in such solar dryer was higher in terms of color retention.

Solar drying of medical plants

Simple solar dryers are the most useful equipment in maintaining the medicinal properties of medicinal herbs. Their construction costs are cheap and maintenance costs tend to be low, whilst being used for drying different sorts of herbs. It has been studied the drying kinetics and quality (color degradation) of the pegaga leaf by varying the inlet air temperature and relative humidity using a solar assisted dehumidification drying system (Yahya et al., 2004). They concluded that there the solar drying system is suitable for drying of pegaga leaf without significant loss of quality.

Solar wood drying

The main parameters affecting the process in a drying kiln are the temperature, humidity, and velocity of the air stream. There are presented several theoretical models for solar drying of timber based on conventional mass transfer equations (Khater et al., 2004; Helwa et al., 2004). The effect of several parameters on the drying rate was studied in order to accomplish minimal drying defects. These parameters include ventilation conditions, wood volume, wood timber thickness, season of drying, and the drying air velocity. It has been concluded that the most influencing parameter using solar energy for timber drying is the drying air relative humidity. It is advised to leave open the fans through the night, especially within

the first period of drying. It is better to load the kiln with its full capacity to save the duration of drying of smaller timber volumes. Proper design is needed for the absorber area and the timber volume to be dried. The experiments showed that timber boards were dried inside solar kiln to moisture content of 12% within 17 days, meanwhile the drying air humidity was limited to 20%.

Solar fish drying

Solar drying of fresh fish sardines was investigated in terms of drying rate and quality (Sablani et al., 2002). Four different solar dryers, namely, rack dryer, multi-rack dryer, wooden, and plexiglas cabinet dryer were used. The wooden cabinet provided the fastest drying rate as it generated higher air temperatures followed by the multi-rack, rack, and plexiglas cabinet dryer.

The sun versus solar drying of salted shark fillets was investigated (Sankat and Mujaffar, 2004). Salted slabs were dried in direct sunlight and compared to drying using two natural convection solar dryers of similar design but employing direct and indirect drying. Of the three drying treatments, slabs dried in the open air dried the fastest, while drying was slowest in the indirect dryer. Sun-dried slabs were of acceptable quality, but somewhat inconsistent in color. Slabs dried in the direct solar dryer had a pleasing and even color and texture. The solar drying of salted shark is therefore an attractive option for small-scale fish processors.

Multipurpose use of solar dryers

An attractive advantage of solar dryer is their versatile use, i.e., the same design of solar dryer can be used for different sorts of crops. A solar assisted indirect dryer may consist of a solar air collector, a heat storage unit, a drying chamber, and a solar chimney, and it can be used for different crops such as rice, tobacco, etc. (Vlachos et al., 2002).

A new solution of a solar, mobile, universal, and ecological chamber dryer that satisfies the basic three requirements in the drying process: maximal process intensity, good quality of the dried material, and minimal energy consumption was designed (Topic and Topic, 2006). The solar dryer characteristics are based on a construction solution which met the following requirements: operation at any location (mobile solution), low costs, possible drying of different products, better quality of the dried material, and a better economic effect. The dryer was successfully used for drying biological materials such as fruits and vegetables, medicinal and aromatic herbs, and spices.

Integrated solar drying systems

In a typical agricultural farm, there is an impetus to maximize collection of all available energy resources, including solar, and distribute them optimally among the different consumers, including dryers, which require a fairly great portion of the total energy. This task requires an integrated solar energy/technology approach (Farkas, 2004, 2008). Setting up a solar preheating system can be economically justified if the solar energy is used throughout the year.

The integration of solar energy into the farm energy system seems to be economically possible.

An indirect type natural convection solar dryer with integrated collector-storage solar and biomass backup heaters have been designed and constructed (Madhlopa and Ngwalo, 2007). The dryer was fabricated using simple materials, tools, and skills, and it was tested in three modes of operation as solar alone, biomass combustion alone, and a combined solar-biomass combustion by drying 12 batches of fresh pineapple. It appears that the solar dryer is suitable for dehydrating pineapples and other fresh foods.

A direct solar-biomass dryer was developed when the biomass burner has a rock slab on the top part which assists in moderating the temperature of drying air (Prasad and Vijay, 2005). Such dryer designs have a backup heater without thermal storage of captured solar energy. Consequently, the air temperature in the drying chamber drops down to ambient after the sunset, requiring backup heating even when the preceding day was sunny. This leads to wasting of both solar and fuel resources.

A solar dryer can be installed with a thermal storage system (El-Sebaii et al., 2002). The air heater part is designed to be able to insert various storage materials (e.g., sand) under the absorber plate. The dryer was tested with and without thermal storage. The thermal storage system reduces the drying period, as for example, in the case of seedless, grapes the reduction was 12 h.

A natural convection solar dyer and a simple biomass burner can be combined for small-scale processing of different fruits and vegetables (Bena and Fuller, 2002).

Summary

The solar drying of materials of biological origin plays an important role in energy savings, quality of end-products, and environmental impacts. The applicable temperature range and energy requirement for moisture removal are the most important parameters in designing a safe and cost-effective drying system. The traditional use of solar energy for drying is a forced convection heated air system, which can be used effectively for drying of various agricultural as grains, fruits, vegetables, medical plants, wood, fish, etc. An attractive advantage of solar dryer is that the same design of solar dryer can be used for different sorts of crops. The integrated use of solar energy means to maximize collection of all available energy resources, including solar, and distribute them optimally among the different consumers, including dryers.

Bibliography

- Amer, B. A. A., Gottschalk, K., and Hahn, J., 2006. New design for constructing a proto-type of solar dryer. In Farkas, I. (ed.), *15th International Drying Symposium*. Budapest, Hungary, August 20–23, Vol. B, pp. 790–796.
- Bennamoun, L., and Belhamri, A., 2002. Study of a solar dryer for agriculture products. In Cao, C. W., Pan, Y. K., Liu, X. D., and Qu, Y. X. (eds.), *Proceedings of the 13th International Drying Symposium IDS 2002*. Beijing, China, August 27–30, Vol. A, pp. 1413–1422.

- Bena, B., and Fuller, R. J., 2002. Natural convection solar dryer with biomass back-up heater. *Solar Energy*, **72**, 75–83.
- El-Sebaii, A. A., Aboul-Enein, S., Ramadan, M. R. I., and El-Gohary, H. G., 2002. Experimental investigation of an indirect type natural convection solar dryer. *Energy Conversion and Management*, **43**, 2251–2266.
- Farkas, I., 2004. Solar-drying of materials of biological origin. In Mujumdar, A. S. (ed.), *Dehydration of Products of Biological Origin*. Enfield-Plymouth: Science Publishers, pp. 317–368. Chap. 13.
- Farkas, I., 2008. Solar drying. *Stewart Postharvest Review*, **2**, 2–8.
- Helwa, N. H., Khater, H. A., Enayet, M. M., and Hashish, M. I., 2004. Experimental evaluation of solar kiln for wood drying. *Drying Technology*, **22**, 703–717.
- Hossain, M. A., and Bala, B. K., 2007. Drying of hot chilli using solar tunnel drier. *Solar Energy*, **81**, 85–92.
- Khater, H. A., Helwa, N. H., Enayet, M. M., and Hashish, M. I., 2004. Optimization of solar kiln for drying wood. *Drying Technology*, **22**, 677–701.
- Madhlopa, A., and Ngwalo, G., 2007. Solar dryer with thermal storage and biomass-backup heater. *Solar Energy*, **81**, 449–462.
- Pangavhane, D. R., and Sawhney, R. L., 2002. Review of research and development work on solar driers for grape drying. *Energy Conversion and Management*, **43**, 45–61.
- Prakash, S., Jha, S. H., and Datta, N., 2004. Performance evaluation of blanched carrots dried by three different dryers. *Journal of Food Engineering*, **62**, 305–313.
- Prasad, J., and Vijay, V. K., 2005. Experimental studies on drying of *Zingiber officinale*, *Curcuma l.* and *Tinospora cordifolia* in solar-biomass hybrid drier. *Renewable Energy*, **30**, 2097–2109.
- Praveenkumar, D. G., Umesh Hebber, H., and Ramesh, M. N., 2006. Suitability of thin layer models for infrared-hot air drying of onion slices. *Lebensmittel-Wissenschaft und Technologie*, **39**, 700–705.
- Rajkumar, P., Kulanthaisami, S., Raghavan, G. S. V., Gariépy, Y., and Orsat, V., 2007. Drying kinetics of tomato slices in vacuum assisted solar and open sun drying methods. *Drying Technology*, **25**, 1349–1357.
- Romano, G., Kocsis, L., and Farkas, I., 2009. Analysis of energy and environmental during solar cabinet drying of apple and carrot. *Drying Technology*, **27**, 574–579.
- Sablani, S. S., Rahman, M. S., Mahgoub, O., and Al-Marzouki, A. S., 2002. Sun and solar drying of fish sardines. In Cao, C. W., Pan, Y. K., Liu, X. D., and Qu, Y. X. (eds.), *Proceedings of the 13th International Drying Symposium IDS 2002*. Beijing, China, August 27–30, Vol. A, pp. 1662–1666.
- Sankat, C. K., and Mujaffar, S., 2004. Sun and solar cabinet drying of salted shark fillets. In *CD-ROM Proceedings, 14th International Drying Symposium*. Sao Paulo City, Brazil, August 22–25, 2004, pp. 1584–1591.
- Santos, B. M., Queiroz, M. R., and Borges, T. P. F., 2004. A solar collector design procedure for crop drying. In *CD-ROM Proceedings, 14th International Drying Symposium*. Sao Paulo City, Brazil, August 22–25, pp. 1042–1048.
- Topic, R. M., and Topic, G. R., 2006. Solar dryer for biological materials and drying kinetics. In Farkas, I. (ed.), *15th International Drying Symposium*. Budapest, Hungary, August 20–23, Vol. C, pp. 1655–1659.
- Vlachos, N. A., Karapantsios, T. D., Balouktsis, A. I., and Chassapis, D., 2002. Design and testing of a new solar tray dryer. *Drying Technology*, **20**, 1243–1271.
- Yahya, M., Othman, M. Y., Sopian, K., Daud, W. R. W., and Yatim, B., 2004. Quality of pegaga leaf in a solar assisted dehumidification drying system. In *CD-ROM Proceedings, 14th International Drying Symposium*. Sao Paulo City, Brazil, August 22–25, pp. 1049–1054.

Cross-references

- Drying of Agricultural Products
Grain Physics
Neural Networks in the Modeling of Drying Processes
Physical Phenomena and Properties Important for Storage of Agricultural Products
Physical Properties of Raw Materials and Agricultural Products
Quality of Agricultural Products in Relation to Physical Conditions
Rheology in Agricultural Products and Foods
Shrinkage and Swelling Phenomena in Agricultural Products
Solar Drying of Biological Materials

SOLUTE TRANSPORT IN SOILS

Yves Coquet, Valérie Pot
UMR 1091 INRA/AgroParisTech Environment and Arable Crops, AgroParisTech, Thiverval-Grignon, France

Synonyms

Solute transfer in soils

Definition

Solute. A substance dissolved in a solvent, both forming a solution.

Soil solution. The soil water that contains various solutes.

Solute transport. Group of processes by which solutes are transported through a medium.

Introduction

Soil is a natural medium at the interface between rocks, air, water bodies, and biota. As a result of this particular position in the biosphere, soil is crossed through by multiple flows: flow of air, water, heat, energy, solutes, solid particles, cells, organisms. Most of the transport processes in soil occur through its pores, either filled with air in the case of gases, or filled with water in the case of solutes and suspended particles. From the quantitative point of view, the transport of matter in soil is occurring in large majority via the soil solution, which refers to the soil water including all substances that can be found in it (solutes, suspended particles, dissolved gases). Even important gases for soil organisms, such as oxygen, carbon dioxide, and nitrogen, are transported at some stage in dissolved state through the soil solution. Most of the chemical elements and substances are transported in soil as solute in the soil solution. Nitrate, phosphate, carbonates, calcium, potassium, pesticides, etc., are all transported as solutes in the soil solution, but at rate which are largely dependent on their solubility in water. It is in the soil solution that soil organisms, including plants, take up the chemical elements and substances necessary for their growth. It is also through the soil solution that pollutants are put in contact with living organisms and can then enter and contaminate their bodies. Knowledge about solute transport in soils is

therefore essential to the understanding of plant nutrition and environmental contamination.

Solute transport processes

As water moves through the soil, it carries any substance dissolved in it. The transport of solutes together with soil water is referred to as *advection* (from Latin: “transport next to”) or *convection* (“transport with”). From the macroscopic point of view, this process can be expressed by the following mathematical [Equation 1](#) (Hillel, 1998; Jury and Horton, 2004):

$$\mathbf{J}_c = C_l \cdot \theta \cdot \mathbf{J}_w, \quad (1)$$

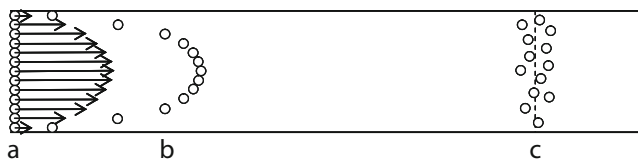
where \mathbf{J}_c is the tensor of solute flux density in soil due to macroscopic convection [$M L^{-2} T^{-1}$], C_l is the solute mass concentration in the soil solution [$M L^{-3}$], θ is the volumetric soil water content [$L^3 L^{-3}$], and \mathbf{J}_w is the tensor of water flux density [$L T^{-1}$]. \mathbf{J}_w may be described by Darcy’s law generalized to unsaturated-saturated soils.

The second process governing solute transport in soil is *molecular diffusion*. This process occurs in soil, disregarding whether water is moving through soil or not. Molecular diffusion is the macroscopic result of the microscopic agitation of molecules due to temperature. It can be expressed by the following [Equation 2](#), also known as Fick’s second law:

$$\mathbf{J}_d = -\theta \cdot \mathbf{D}_s \bullet \overrightarrow{\text{grad}} C_l, \quad (2)$$

where \mathbf{J}_d is the tensor of solute flux density in soil due to molecular diffusion [$M L^{-2} T^{-1}$], and \mathbf{D}_s is the molecular diffusion coefficient tensor of the solute in the soil [$L^2 T^{-1}$].

Convection and molecular diffusion being the two fundamental solute transport processes in soil, one could be tempted of simply adding [Equations 1](#) and [2](#) to get the general solute transport equation in soil. This would be wrong because [Equation 1](#) does not actually describe properly the convection process at the macroscopic scale. As [Equation 1](#) is put, it says that all solute molecules have the same velocity as that of the bulk water, which is obviously wrong because water is a viscous fluid. As a result, not all water molecules in soil move at the same velocity. Those located close to the soil solid surfaces hardly move, while those located far from the soil solid surfaces near the axis of soil pores move faster than the average water velocity. This process, called *mechanical dispersion*, is pictured in [Figure 1a](#), where solute molecules entering a soil cylindrical pore have different instantaneous velocities with the maximum value along the axis. Poiseuille’s law states that for Newtonian liquids, such as water, the solute velocity vector profile in the pore is parabolic, its value on the axis being twice the average value along the profile. A short time after they entered the pore ([Figure 1b](#)), solute molecules will have conserved their initial velocity. After some time ([Figure 1c](#)), solute molecules will have changed their velocity by moving



Solute Transport in Soils, Figure 1 (a) Solute molecules entering a soil cylindrical pore have a parabolic speed vector profile; (b) a short time after entering the pore, each solute molecule keeps its speed vector; (c) after some time, solute molecules move transversally due to molecular diffusion and, thereby, experience different speed values (dashed line shows the average position).

transversally to the pore axis because of molecular diffusion. As a result, some solute molecules will have moved a little bit faster than average and some others slower than average. For the mathematical point of view, this can be described macroscopically with an equation formally similar to that of Fick’s diffusion law ([Equation 3](#)):

$$\mathbf{J}_m = -\mathbf{D}_m \bullet \overrightarrow{\text{grad}} C_l, \quad (3)$$

where \mathbf{J}_m is the tensor of solute flux density in soil due to mechanical dispersion [$M L^{-2} T^{-1}$], and \mathbf{D}_m is the mechanical dispersion coefficient tensor of the solute in the soil [$L^2 T^{-1}$]. To the difference of molecular diffusion, mechanical dispersion vanishes as soon as water is immobile.

Finally, solute transport in soil is the result of three processes: (macroscopic) convection, molecular diffusion, and mechanical dispersion. The general solute transport equation in soil may thus be expressed by [Equation 4](#):

$$\mathbf{J}_s = \mathbf{J}_c + \mathbf{J}_d + \mathbf{J}_m, \quad (4)$$

where \mathbf{J}_s is the tensor of total solute flux density in soil [$M L^{-2} T^{-1}$]. Molecular diffusion and mechanical dispersion being described by the same type of mathematical equations, both processes may be summed up into a single equation. The resulting *hydrodynamic dispersion* process is then written by [Equation 5](#):

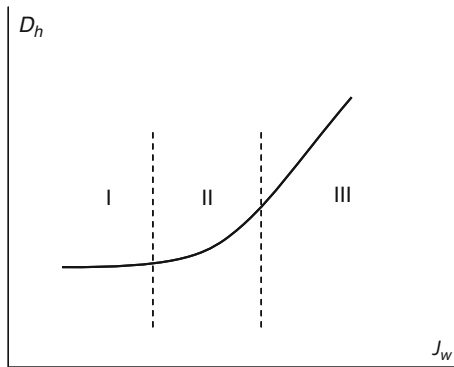
$$\mathbf{J}_h = -\mathbf{D}_h \bullet \overrightarrow{\text{grad}} C_l, \quad (5)$$

where \mathbf{J}_h is the tensor of solute flux density in soil due to hydrodynamic dispersion [$M L^{-2} T^{-1}$], and \mathbf{D}_h is the hydrodynamic dispersion coefficient tensor of the solute in the soil [$L^2 T^{-1}$].

Pfannkuch (1963) demonstrated that \mathbf{D}_h was linearly dependent on \mathbf{J}_w for high values of \mathbf{J}_w ([Figure 2](#)). In this case, \mathbf{D}_m can be written by [Equation 6](#):

$$\mathbf{D}_m = \lambda \bullet \mathbf{J}_w, \quad (6)$$

where λ is the dispersivity tensor of the soil [L]. Soil dispersivity has been shown to be dependent on the spatial scale at which transport processes are studied (Vanderborght and Vereecken, 2007).



Solute Transport in Soils, Figure 2 Evolution of the hydrodynamic dispersion coefficient, D_h , with water flux density in soil, J_w . Three regimes may be distinguished: regime I, where molecular diffusion dominates over mechanical dispersion; regime II, where both molecular diffusion and mechanical dispersion are equivalently important; regime III, where mechanical dispersion dominates over molecular diffusion.

Finally, the total solute flux density in soil may be written as [Equation 7](#):

$$\mathbf{J}_s = \mathbf{J}_c + \mathbf{J}_h = C_l \cdot \mathbf{J}_w - \theta \cdot \mathbf{D}_h \bullet \overrightarrow{\text{grad}}C_l. \quad (7)$$

When coupled to the conservation of mass equation, [Equation 7](#) gives [Equation 8](#):

$$\begin{aligned} \frac{\partial(\theta \cdot C_l)}{\partial t} &= -\mathbf{div}\mathbf{J}_s \\ &= -\mathbf{div}(C_l \cdot \mathbf{J}_w - \theta \cdot \mathbf{D}_h \bullet \overrightarrow{\text{grad}}C_l), \end{aligned} \quad (8)$$

where t is time [T]. [Equation 8](#) is known as the *convection-dispersion equation* (CDE). This equation is more frequently encountered in its vertical mono-dimensional form and for steady-state water regime ([Equation 9](#)):

$$\frac{\partial C_l}{\partial t} = D_h \frac{\partial^2 C_l}{\partial z^2} - V_w \frac{\partial C_l}{\partial z}, \quad (9)$$

where z is depth [L] and $V_w = J_w/\theta$ is the average pore water velocity [$L T^{-1}$].

The formulation of the CDE as [Equation 9](#) is adapted to inert (non-sorbing) conservative (nondegraded) solutes. For solutes that interact with soil solid surfaces, either organic or mineral, such as cations or uncharged organic micropollutants, or for solutes that are degraded or transformed by the soil microflora, such as nitrate or most organic molecules, the CDE must be coupled to other equations describing sorption and/or degradation processes in soil.

Coupling with physicochemical and microbiological processes

The vast majority of solutes in soils interacts with soil solid surfaces and/or undergoes transformation. The main

interaction of solutes with soil solid surfaces is through *adsorption*, the process by which solutes may be retained at the surface of soil particles due to weak physicochemical interactions (hydrogen bonds, van der Waals' forces). Adsorption is considered to be instantaneous and fully reversible. In soils, adsorbed solutes may be subjected to further processes like molecular diffusion inside the soil "solid" particle, such as diffusion into the interfoliar space of clay particles or diffusion into organic macromolecules. Interaction with the adsorbing surfaces may evolve toward strong physicochemical interactions such as covalent bonds. Finally, interaction of solutes with soil solid surfaces covers a large array of processes themselves in interaction, which are referred to globally through the term of *sorption*. The simplest way to describe sorption is by limiting it to adsorption, i.e., by considering it as an instantaneous reversible process. Adsorption is described by an *adsorption isotherm*, which relates the concentration of the solute adsorbed onto soil solid surfaces, C_s [$M M^{-1}$], to C_l . The term "isotherm" refers to the fact that adsorption is sensitive to temperature, so that the relationship between C_s and C_l is measured experimentally at constant temperature. The solute adsorption isotherm may be linear or non linear. In the first instance, it can be described by [Equation 10](#):

$$C_s = K_d \cdot C_l, \quad (10)$$

where K_d is the linear adsorption coefficient or partitioning coefficient [$L^3 M^{-1}$]. Non linear isotherms are often described by the Langmuir isotherm, if C_s values reach a plateau for large C_l values, or by the Freundlich isotherm, if C_s does not reach any plateau for large C_l values. The Freundlich isotherm is written as [Equation 11](#):

$$C_s = K_f \cdot C_l^{n_f}, \quad (11)$$

where K_f is the Freundlich adsorption coefficient [$L^{3n_f} M^{-nf}$] and n_f the Freundlich exponent [-]. The exponent n_f is generally lower than unity for pesticides.

For sorbing solutes, the mass balance [Equation 8](#) must account for the quantity of solute adsorbed onto the soil solid phase, resulting in [Equation 12](#):

$$\frac{\partial(\theta \cdot C_l + \rho_b \cdot C_s)}{\partial t} = -\mathbf{div}\mathbf{J}_s \quad (12)$$

where ρ_b is the soil bulk density [$M \cdot L^{-3}$], i.e., the mass of dry soil per unit of bulk soil volume. For steady-state water flow and linear-sorbing solutes, the CDE ([Equation 9](#)) is written by [Equation 13](#):

$$\frac{\partial C_l}{\partial t} = \frac{D_h \partial^2 C_l}{R \partial z^2} - \frac{V_w \partial C_l}{R \partial z}, \quad (13)$$

with $R = 1 + \rho_b \cdot K_d/\theta$ [-]. The CDE for linear-sorbing solutes ([Equation 13](#)) has a similar form to that for inert solutes ([Equation 9](#)), which means that the transport of linear-sorbing solutes in soils happens R times more slowly

than inert solutes. This is why R is also called the *retardation factor*.

If sorption is not instantaneous, one has to account of the rate of the sorption process. *Kinetic sorption* for linear-sorbing solutes may be written by [Equation 14](#):

$$\frac{\partial C_s}{\partial t} = \omega \cdot (K_d C_l - C_s), \quad (14)$$

where ω is the first-order rate constant of the kinetic sorption process [T^{-1}]. [Equation 13](#) is then modified with an additional term accounting for kinetic sorption ([Equation 15](#)):

$$\frac{\partial C_l}{\partial t} = \frac{D_h \partial^2 C_l}{R \partial z^2} - \frac{V_w \partial C_l}{R \partial z} + \omega \frac{\rho_b}{R \cdot \theta} (C_s - K_d C_l). \quad (15)$$

Solute degradation, transformation, or absorption all result in the disappearance of the solute from the soil. These processes are generally accounted for by introducing a sink term, r_s [$M L^{-3} T^{-1}$], in the mass conservation [Equation 8](#) to give [Equation 16](#):

$$\frac{\partial (\theta \cdot C_l)}{\partial t} = -\mathbf{div} \mathbf{J}_s - r_s. \quad (16)$$

When the sink term is due to microbiological degradation, it is generally described as a linear first-order process ([Equation 17](#)):

$$r_s = -\mu \cdot C_l, \quad (17)$$

where μ is the degradation rate constant [T^{-1}]. Rather than using a rate value, degradation is often quantified by the half-life of the solute $t_{1/2} = \ln 2 / \mu$ [T].

When the sink term is due to absorption by plant roots, it may be described by [Equation 18](#):

$$r_s = -\alpha \cdot C_l \cdot r_w, \quad (18)$$

where r_w is the water sink term [T^{-1}], that is the quantity of water removed from the soil by plant roots per unit of time, and α is a parameter [-] varying between 0 (no absorption) to 1 (fully passive absorption).

All the processes that have been described so far can be found in models such as HYDRUS-1D (Simunek et al., 2005; available at www.pc-progress.com). The simulation of transport processes coupled to more complex geochemical processes may be realized by using the HP1 model, which is a coupled version of HYDRUS-1D with PHREEQC (also available at www.pc-progress.com). The HYDRUS-1D model is also capable of simulating preferential flow of solutes in soil.

Preferential flow

In many situations, it has been observed that solutes can be transported more rapidly in the soil than what is expected from the solute transport equation describing the three above-mentioned transport processes: convection, molecular diffusion, and mechanical dispersion. It is as if

solutes were bypassing part of the soil porosity, thereby covering longer distances than they would have done if they would have explored the whole available porosity. This process is named *preferential flow*. The bypass pathways or *preferential pathways* can be many in soils: biopores (earthworm galleries, dead roots), fractures, and fissures. Parts of the soil porosity can also be regions of lower hydraulic conductivities, like dead-end pores, intra-aggregate pores, that are accessible to the solutes only through diffusion process. The result is that a large fraction of the solutes undergoes a higher velocity than the bulk velocity since they are transported through a restricted portion of the available water-filled porosity, resulting in an earlier breakthrough or preferential flow. Preferential flow can thus be a major factor of environmental pollution. Indeed, by this process a fraction of the pollutants can bypass the soil surface horizon where transformation processes (degradation of pollutants by biological activity) and retention processes are the most active.

Different models have been proposed to describe preferential flow (Šimůnek et al., 2003). The mobile-immobile model (MIM) or dual-porosity model assumes that the liquid phase of the soil is partitioned into mobile (flowing) and immobile (stagnant) flow regions (Coats and Smith, 1964), which gives [Equation 19](#):

$$\theta = \theta_m + \theta_{im}, \quad (19)$$

where θ_m and θ_{im} are the volumetric fractions of soil mobile and immobile water, respectively [$L^3 L^{-3}$]. Mobile region corresponds to inter-aggregate pores and macropores while immobile region corresponds to intra-aggregate pores or soil matrix. Water flow is assumed to occur in the mobile region only and solute is transported in the mobile region by both convection and hydrodynamic dispersion. Solute transfer between the dynamic flowing region and the stagnant region is described by a first-order mass transfer process. The general governing transport equations are thus written in vertical monodimensional form as [Equations 20](#) and [21](#):

$$\frac{\partial(\theta_m C_m)}{\partial t} + \frac{\partial(\theta_{im} C_{im})}{\partial t} = \frac{\partial}{\partial z} \left(\theta_m D_h \frac{\partial C_m}{\partial z} \right) - \frac{\partial J_w C_m}{\partial z} \quad (20)$$

$$\frac{\partial \theta_{im} C_{im}}{\partial t} = \alpha_{ph} (C_m - C_{im}), \quad (21)$$

where C_m and C_{im} are the solute concentrations in the soil solution of the mobile and immobile regions, respectively [$M \cdot L^{-3}$], and α_{ph} is the mass transfer coefficient [T^{-1}].

The dual-permeability model (DP) differs from the MIM model in that water flow is also assumed to move in the intra-aggregate pores (matrix) as well, but with a lower permeability than in the inter-aggregate pores (macropores). Water content and flow velocity are defined for each system as [Equations 22](#) and [23](#):

$$\theta = w \theta_f + (1 - w) \theta_{ma} \quad (22)$$

$$J_w = wJ_f + (1 - w)J_{ma}, \quad (23)$$

where $w = V_f/V$ [–] is the ratio of the volume of the macropores, V_f [L^3], to the volume of the total porosity, V [L^3], θ_f and θ_{ma} are the volumetric water contents of the macropores and matrix systems, respectively, and J_f and J_{ma} are the water density flux in both systems. Note that θ_f and θ_{ma} are different from θ_m and θ_{im} of the MIM model since they represent the water contents of each pore system and not absolute values of water content referred to the total soil volume.

Thus, mass conservation is calculated for each system such that the transport of solutes is described using two coupled convection–dispersion Equations 24 and 25:

$$\frac{\partial(\theta_f C_f)}{\partial t} = \frac{\partial}{\partial z} \left(\theta_f D_f \frac{\partial C_f}{\partial z} \right) - \frac{\partial J_f C_f}{\partial z} - \frac{\Gamma_s}{w} \quad (24)$$

$$\frac{\partial(\theta_{ma} C_{ma})}{\partial t} = \frac{\partial}{\partial z} \left(\theta_{ma} D_{ma} \frac{\partial C_{ma}}{\partial z} \right) - \frac{\partial J_{ma} C_{ma}}{\partial z} + \frac{\Gamma_s}{w}, \quad (25)$$

where Γ_s is the solute mass transfer term [$\text{ML}^{-3} \text{T}^{-1}$] defined as the sum of the diffusive mass transfer due to the solute concentration difference between the two pore systems and a convective mass transfer due to water mass exchange, Γ_w [T^{-1}], between the two pore systems (Equation 26):

$$\Gamma_s = \alpha_{ph}(1 - w)\theta_{ma}(C_f - C_{ma}) + \Gamma_w C_i, \quad (26)$$

where C_i is equal to C_f if $\Gamma_w \geq 0$ and to C_{ma} if $\Gamma_w < 0$.

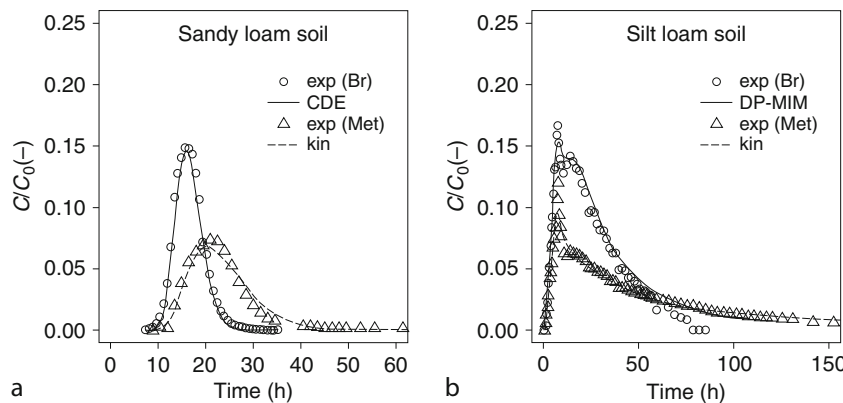
Other approaches consider only gravitational flow in the macropore systems (Jarvis, 1994). Based on the same

approaches, the division of the soil water phase can be further complicated by creating additional pore regions (Gwo et al., 1995).

Many studies of solute transport in the field and in the laboratory have shown evidence of preferential flow. When a pulse of solute is transported under equilibrium conditions, the distribution of the solute concentration in the soil outflow exhibits a Gaussian shape. When preferential flow occurs, the peak position is markedly advanced together with a long elution tail corresponding to diffusion process of solutes from and to regions of low permeability. In some cases, the solute concentration distribution can show a double peak which is indicative of dual-permeability flow. Figure 3 shows examples of an inert conservative solute (bromide) undergoing classical convection–dispersion transport at equilibrium conditions in a sandy loam soil column (Figure 3a) and the same solute undergoing preferential flow in a silt loam soil column (Figure 3b). In these examples, a pesticide was simultaneously injected in the soil columns together with bromide: for equilibrium conditions (Figure 3a), the pesticide exhibited delay due to sorption processes, while in the second case (Figure 3b) the pesticide arrived simultaneously as the tracer because of preferential flow.

Summary

Solute transport processes in soils are at the basis of plant nutrition and environmental contamination. Three main processes are governing solute transport in soil: convection, molecular diffusion, and mechanical dispersion. As most solutes are subjected to physicochemical interactions with the soil solid surfaces and/or physicochemical or biological transformation, models of solute transport in soil



Solute Transport in Soils, Figure 3 Breakthrough curves of bromide and the herbicide metribuzin in a sandy loam soil column (a) and in a silt loam soil column (b), measured under constant near-saturated flow conditions. The convection–dispersion equation (CDE) describes correctly bromide transport through the sandy loam soil column (a), while the model DP-MIM (three porosity domains, dual-permeability model) describing preferential transport must be used to correctly describe the double peaks and long elution tail of the bromide breakthrough curve in the silt loam soil. Metribuzin exhibits delay compared to bromide, due to sorption process in the sandy loam soil. In the silt loam soil, metribuzin is not delayed compared to bromide as it is rapidly transported through preferential pathways (macropores) at the same speed as that of bromide. In these examples, kinetic sorption processes were needed to correctly describe metribuzin transport in both soils.

need to account for these processes. However, such representations of solute transport in soil may still be found unsuitable when solutes are transported by preferential flow processes. Preferential flow results in solutes being transported more rapidly than expected through a limited fraction of soil porosity. As such, it is regarded as a major factor of groundwater contamination.

Bibliography

- Coats, K. H., and Smith, B. D., 1964. Dead-end pore volume and dispersion in porous media. *Society of Petroleum Engineers Journal*, **1964**, 73–84.
- Gwo, J. P., Jardine, P. M., Wilson, G. V., and Yeh, G. T., 1995. A multiple-pore-region concept to modeling mass transfer in subsurface media. *Journal of Hydrology*, **164**, 217–237.
- Hillel, D., 1998. *Environmental Soil Physics*. San Diego: Academic.
- Jarvis, N. J., 1994. *The MACRO Model (Version 3.1). Technical Description and Sample Simulations. Reports and Dissertations 19. Department of Soil Science*. Uppsala: Swedish University of Agricultural Science, p. 51.
- Jury, W. A., and Horton, R., 2004. *Soil Physics*, 6th edn. Noboken: Wiley.
- Pfannkuch, O., 1963. Contribution à l'étude des déplacements de fluides miscibles dans un milieu poreux. *Revue de l'Institut Français du Pétrole*, **18**, 215–268.
- Šimůnek, J., van Genuchten, M. Th., and Sejna, M., 2005. *The HYDRUS-1D Software Package for Simulating the Movement of Water, Heat, and Multiple Solutes in Variably Saturated Media*. Version 3.0. Department of Environmental Sciences; University of California; Riverside.
- Šimůnek, J., Jarvis, N. J., van Genuchten, M. Th., and Gardenas, A., 2003. Review and comparison of models for describing non-equilibrium and preferential flow and transport in the vadose zone. *Journal of Hydrology*, **272**, 14–35.
- Vanderborght, J., and Vereecken, H., 2007. Review of dispersivities for transport modeling in soils. *Vadose Zone Journal*, **6**, 29–52.

Cross-references

- [Agrophysics: Physics Applied to Agriculture](#)
[Buffer Capacity of Soils](#)
[Bypass Flow in Soil](#)
[Crop Responses to Soil Physical Conditions](#)
[Hydrogeological Processes in Soils](#)
[Layered Soils, Water and Solute Transport](#)
[Leaching of Chemicals in Relation to Soil Structure](#)
[Soil Water Flow](#)

SORPTION

The process in which one substance takes up or holds another.

Bibliography

- <http://www.thefreedictionary.com/sorption>

Cross-references

- [Absorption](#)
[Adsorption](#)
[Conditioners, Effect on Soil Physical Properties](#)

SORPTIVITY OF SOILS

Budiman Minasny¹, Freeman Cook²

¹Food & Natural Resources, The University of Sydney, Sydney, NSW, Australia

²CSIRO Land and Water, CSIRO Long Pocket Laboratories - Indooroopilly, Indooroopilly, QLD, Australia

Definition

Sorptivity is a measure of the capacity of the medium to absorb or desorb liquid by capillarity.

Theory

When water is applied into a dry soil, initially, most of the water is absorbed by the capillary potential of the soil matrix. The capillary force dominates the initial water infiltration process, however, as infiltration proceeds, the gravitational force dominates. Sorptivity is related to the infiltration that is driven by the capillary forces alone. Cumulative absorption or desorption of water into or out of a horizontal (minimal gravity effects) column of soil with uniform properties and moisture content is proportional to the square root of time and has been termed sorptivity (S [$L T^{-1/2}$]) by Philip (1957). He also defined the intrinsic sorptivity (ζ [$L^{1/2}$]) (that associated with the porous material) from the S and the fluid properties, by Philip (1969):

$$\zeta = (\mu/\sigma)S, \quad (1)$$

where μ is the dynamic viscosity ($ML^{-1} T^{-1}$) and σ (MT^{-2}) is the surface tension of the fluid. Sorptivity depends on initial uniform water content (θ_n) or potential (ψ_n) of the soil and the water content (θ_0) or potential (ψ_0) on the intake surface, so that strictly we should write sorptivity as $S(\theta_n, \theta_0)$ or $S(\psi_n, \psi_0)$. The latter form is needed when the potential at the intake surface is positive.

Sorptivity can be defined analytically as a function of soil water content and diffusivity (Philip and Knight, 1974). The calculation of the sorptivity involves iterative numerical procedures, and because of technical difficulties, several approximations have been proposed (Elrick and Robin, 1981; Kutílek and Valentová, 1986). The approximation by Parlange (1975) has been found to give good results (Elrick and Robin, 1981):

$$S_0^2 = 2\sqrt{\theta_0 - \theta_n} \int_{\theta_n}^{\theta_0} \sqrt{\theta - \theta_n} D(\theta) d\theta, \quad (2)$$

where θ_0 is the water content at applied potential ψ_0 , θ_n is the initial water content of the soil, and D is the soil diffusivity.

Measurement

In practice, Philip (1969) showed that sorptivity can be measured relatively easily from horizontal infiltration,

where water flow is only controlled by capillary absorption:

$$I = S_0 \sqrt{t}, \quad (3)$$

where I is the cumulative infiltration at time t . Talsma (1969) proposed measurement of sorptivity in the field from short-time ring infiltrometer data. Cook (2008) presented methods for measuring it in the laboratory for the early time vertical infiltration into soil cores.

Algebraic models for infiltration, which satisfy the condition that cumulative infiltration is proportional to the square root of time at short times and reaches a steady state rate at long times (Collis-George, 1977; Philip, 1987), have been developed. From these, the sorptivity component of the infiltration can be estimated.

For vertical three-dimensional (3D) infiltration from the infiltrometers or disk permeameters, sorptivity can be determined from early stages of flow where capillary force dominates (White et al., 1992; Cook and Broeren, 1994; Cook, 2002):

$$\lim_{t \rightarrow 0} \frac{dI}{d\sqrt{t}} \approx S_0. \quad (4)$$

In 3D infiltration, sorptivity does not only affects the early stage of infiltration but also the whole infiltration process.

Smith (1999) proposed a simple field method, which consists of inserting a 100-mm-diameter steel tube into the soil, pouring a volume of water equivalent to 1 cm depth (I_v) into the tube, and recording the time needed for water to imbibe until half of the soil surface is not ponded (t_v). Sorptivity is calculated from $S_0 = I_v/t_v^{1/2}$. This is a rough estimate and only measures sorptivity at saturation.

Values of sorptivity are quite variable, with standard deviations of the same order as those found for hydraulic conductivity (Talsma, 1969).

Applications

White and Perroux (1989) showed how sorptivity measured at different intake potentials could be used to estimate hydraulic conductivity, and this was tested by Cook and Broeren (1994) and was found to give good results. Minasny and McBratney (2000) showed the overestimation of sorptivity when contact sand materials were used with a disk permeameter for estimating sorptivity. Other disk permeameter methods such as those of Vandervaere et al. (2000a, b) also rely on the estimation of sorptivity to obtain the hydraulic conductivity.

Philip (1984) used the sorptivity in deriving travel times from buried and surface point sources which was later used by Cook et al. (2003a, b) for predicting wetting patterns for trickle irrigation. Broadbridge and White (1987) used sorptivity in the estimation of the time-to-ponding which has applications in the design of spray irrigation systems and erosion control. Leeds-Harrison and

Youngs (1997) described a measurement procedure for obtaining hydraulic conductivity of soil aggregates from measurements of water uptake at negative potential (sorptivity). This procedure was employed by Hallett and Young (1999) for quantifying water repellency, which was determined from the sorptivity measurements of soil aggregates using two wetting liquids with different soil–liquid contact angles.

Summary

Sorptivity is a component of the flow processes and needs to be incorporated in any application where adsorption or desorption of a fluid from a porous media is occurring due to a potential change at a surface boundary.

Bibliography

- Broadbridge, P., and White, I., 1987. Time to ponding: comparison of analytic, quasi-analytic and approximate predictions. *Water Resources Research*, **23**, 2302–2310.
- Collis-George, N., 1977. Infiltration equations for simple soil systems. *Water Resources Research*, **13**, 395–403.
- Cook, F. J., 2002. The twin-ring method for measuring saturated hydraulic conductivity and sorptivity in the field, Chapter 7. In McKenzie, N. J., Couglen, K. J., and Cresswell, H. P. (eds.), *Soil Physical Measurements and Interpretation for Land Evaluation. Australian Soil and Land Survey Handbook Series 5*. Australia: CSIRO, pp. 108–118.
- Cook, F. J., 2008. Near-saturated hydraulic conductivity and sorptivity: laboratory measurement, Chapter 80. In Carter, M. R., and Gregorich, E. G. (eds.), *Soil Sampling and Methods of Analysis (Canadian Society of Soil Science)*. Boca Raton: Taylor & Francis, pp. 1075–1087.
- Cook, F. J., and Broeren, A., 1994. Six methods for determining sorptivity and hydraulic conductivity with disc permeameters. *Soil Science*, **157**, 2–11.
- Cook, F. J., Fitch, P., Thorburn, P. J., Charlesworth, P. B., and Bristow, K. L., 2003a. Modelling trickle irrigation: comparison of analytical and numerical models for estimation of wetting front position with time. *Environmental Modelling and Software*, **21**, 1353–1359.
- Cook, F. J., Thorburn, P. J., Fitch, P., and Bristow, K. L., 2003b. WetUp: a software tool to display approximate wetting patterns from drippers. *Irrigation Science*, **22**, 129–134.
- Elrick, D. E., and Robin, M. J., 1981. Estimating the sorptivity of soils. *Soil Science*, **132**, 127–132.
- Hallett, P. D., and Young, I. M., 1999. Changes to water repellence of soil aggregates caused by substrate-induced microbial activity. *European Journal of Soil Science*, **50**, 35–40.
- Kutílek, M., and Valentová, J., 1986. Sorptivity approximations. *Transport in Porous Media*, **1**, 57–62.
- Leeds-Harrison, P. B., and Youngs, E. G., 1997. Estimating the hydraulic conductivity of aggregates conditioned by different tillage treatments from sorption measurements. *Soil and Tillage Research*, **41**, 141–147.
- Minasny, B., and McBratney, A. B., 2000. Estimation of sorptivity from disc-permeameter measurements. *Geoderma*, **95**, 305–324.
- Parlange, J. Y., 1975. On solving the flow equation in unsaturated soils by optimization: horizontal infiltration. *Soil Science Society of America Proceedings*, **39**, 415–418.
- Philip, J. R., 1957. The theory of infiltration: 4. Sorptivity and algebraic infiltration equations. *Soil Science*, **84**, 257–264.
- Philip, J. R., 1969. The theory of infiltration. *Advances in Hydroscience*, **5**, 215–296.

- Philip, J. R., 1984. Steady infiltration from spherical cavities. *Soil Science Society of America Journal*, **48**, 724–729.
- Philip, J. R., 1987. The infiltration joining problem. *Water Resources Research*, **23**, 2239–2245.
- Philip, J. R., and Knight, J. H., 1974. Solving unsaturated flow equation. 3. New quasi-analytical technique. *Soil Science*, **177**, 1–13.
- Smith, R. E., 1999. Rapid measurement of soil sorptivity. *Soil Science Society of America Journal*, **63**, 55–57.
- Talsma, T., 1969. In situ measurement of sorptivity. *Australian Journal of Soil Research*, **7**, 269–276.
- Vandervaere, J. P., Vauclin, M., and Elrick, D. E., 2000a. Transient flow from tension infiltrometers. I. The two-parameter equation. *Soil Science Society of America Journal*, **64**, 1263–1272.
- Vandervaere, J. P., Vauclin, M., and Elrick, D. E., 2000b. Transient flow from tension infiltrometers. II. Four methods to determine sorptivity and conductivity. *Soil Science Society of America Journal*, **64**, 1272–1284.
- White, I., and Perroux, K. M., 1989. Estimation of unsaturated hydraulic conductivity from field sorptivity measurements. *Soil Science Society of America Journal*, **53**, 324–329.
- White, I., Sully, M. J., and Perroux, K. M., 1992. Measurement of surface-soil hydraulic properties – disk permeameters, tension infiltrometers, and other techniques. In Topp, G. C., Reynolds, W. D., and Green, R. E. (eds.), *Advances in Measurement of Soil Physical Properties: Bringing Theory into Practice*. Madison: Soil Science Society of America. Soil Science Society of America Special Publication, Vol. 5, pp. 69–103.

Cross-references

- [Databases of Soil Physical and Hydraulic Properties](#)
[Hydraulic Properties of Unsaturated Soils](#)
[Infiltration in Soils](#)
[Pedotransfer Functions](#)
[Pore Size Distribution](#)
[Soil Hydraulic Properties Affecting Root Water Uptake](#)
[Soil Hydrophobicity and Hydraulic Fluxes](#)

SPACE SOIL PHYSICS

Robert Heinse
 Department of Plant, Soil and Entomological Sciences,
 University of Idaho, Moscow, ID, USA

Synonyms

Microgravity soil physics

Definition

Space Soil Physics is the study of physical properties of soils, and more generally porous media, and its relations to water- and air-distribution and transport under reduced gravity conditions experienced during spaceflight and on extraterrestrial habitats.

Space soil physics is a subsection of soil physics that aims to identify, characterize, and predict critical physical phenomena that are affected by, or play a more pronounced role in, reduced gravity necessitated by practical questions of fluid management in partially saturated media, and dust behavior on extraterrestrial bodies. As the gravitational

level is reduced below that of Earth, phenomena relating to competing forces are altered as body forces become less significant compared to surface forces. The influence of such a shift in competing phenomena can be difficult to predict, and poses challenges for engineered systems addressed by Space Soil Physics (National Research Council (U.S.). Committee on Microgravity Research, 2000).

The main focus of Space Soil Physics is on multiphase flow and liquid behavior in porous media in the absence of gravity, where capillarity is the dominant mechanism for fluid management applications ranging from plant-based bioregenerative life support to power generating systems, the design and management of gas and liquid separation and recovery technology, and numerous other functions such as wastewater storage and treatment, and fuel management that operate in the near absence of gravity in terrestrial orbit or on spaceflight missions. Recent evidence suggests that fluid displacement patterns become unstable and enhance phase entrapment in the absence of gravity, thereby modifying macroscopic transport properties essential for fluid management decisions (Or et al., 2009).

Space soil physics plays a critical role in space agriculture for research and design of root-zone hydraulic processes for plant growth in reduced gravity (Bingham et al., 2000). The shift to capillary-dominated fluid distributions provides physical constraints that require novel considerations for growth-media selection, plant hydration (i.e., watering), and aeration (i.e., gas exchange) designs to maintain adequate supplies of water and gas exchange to plant roots (Scovazzo et al., 2001; Steinberg and Poritz, 2005).

Bibliography

- Bingham, G. E., Jones, S. B., Or, D., Podolski, I. G., Levinikh, M. A., Sytchov, V. N., Ivanova, T., Kostov, P., Sapunova, S., Dandolov, I., Bubenheim, D. B., and Jahns, G., 2000. Microgravity effects on water supply and substrate properties in porous matrix root support systems. *Acta Astronautica*, **47**, 839–848.
- National Research Council (US). Committee on Microgravity Research, 2000. *Microgravity Research in Support of Technologies for the Human Exploration and Development of Space and Planetary Bodies*. Washington, DC: National Academy Press.
- Or, D., Tuller, M., and Jones, S. B., 2009. Liquid behavior in partially saturated porous media under variable gravity. *Soil Science Society of America Journal*, **73**, 341–350.
- Scovazzo, P., Illangasekare, T. H., Hoehn, A., and Todd, P., 2001. Modeling of two-phase flow in membranes and porous media in microgravity as applied to plant irrigation in space. *Water Resources Research*, **37**, 1231–1243.
- Steinberg, S. L., and Poritz, D., 2005. Measurement of hydraulic characteristics of porous media used to grow plants in microgravity. *Soil Science Society of America Journal*, **69**, 301–310.

Cross-references

- [Aeration of Soils and Plants](#)
[Hydraulic Properties of Unsaturated Soils](#)
[Soil Water Flow](#)
[Solute Transport in Soils](#)

SPATIAL VARIABILITY OF PROPERTIES AND PROCESSES

The non-uniform distribution of specifiable attributes of an area, whether random or systematic (structured), and the range of their variation expressed by means of statistical (probabilistic) criteria.

See *Scaling of Soil Physical Properties*

Bibliography

Introduction to Environmental Soil Physics (First Edition) 2003
Elsevier Inc. Daniel Hillel (ed.) <http://www.sciencedirect.com/science/book/9780123486554>

SPATIAL VARIABILITY OF SOIL PHYSICAL PROPERTIES

Ole Wendoroth, Edwin L. Ritchey, Susmitha Nambuthiri,
John H. Grove, Robert C. Pearce
Department of Plant and Soil Sciences, College of
Agriculture, University of Kentucky, Lexington, KY,
USA

Definition

Autocovariance. A measure of association between neighboring observations taken in space or time (Equation 2), manifested in the autocovariance function, which describes the autocovariance behavior versus separation or lag distance between observations. The normalized version of autocovariance is autocorrelation (Equation 1) (Shumway and Stoffer, 2000).

Power spectrum. A graph depicting the decomposition of cyclic variance components of different frequency, wavelength, or period based on the integration of the autocorrelation function (Shumway and Stoffer, 2000).

Spatial process. The change of a variable, or a state vector consisting of several variables, across a spatial domain caused by underlying effects. The spatial process of soil water content across a landscape can be influenced by spatial changes in soil type, topography, vegetation, rainfall, evapotranspiration, management, etc. (Wendoroth et al., 2011).

Introduction

The spatial variability of soil properties generally determines the change of a soil property's magnitude in space. This change is observed at different spatial locations on the land surface, or at some soil depths. The change can be considered across a spatial domain of any size, at any separation distance and for any sample volume. According to Blöschl and Sivapalan (1995), synonyms for domain, separation distance, and sample volume are extent, spacing, and support, respectively. We distinguish between structured and random spatial variability.

A change in a soil property observed across a domain, when observations taken close to each other are more similar than those sampled farther apart, manifests structured variability. If, on the other hand, the magnitude of change or fluctuation remains constant regardless of the separation distance between observations, the spatial variability is random. The structure of variability is usually quantified with a semivariogram (Journel and Huijbregts, 1991) or with the autocorrelation function (Shumway, 1988). Only if spatial variability exhibits structure can values at locations between the observation locations be interpolated by using, e.g., kriging or cokriging (Isaaks and Srivastava, 1989; Goovaerts, 1997; Deutsch and Journel, 1997) and autoregressive state-space models (Morkoc et al., 1985; Shumway and Stoffer, 2000; Nielsen and Wendoroth, 2003). Analysis of variance (ANOVA) applied to observations in randomized treatment experiments assumes random variability, i.e., spatial independence of observations. With structured variability, a spatial range of representativeness can be derived, i.e., the statistical area, or sphere, of influence. Note that, the statistical range of influence differs from the physical range of influence, the latter being determined by the size of the equipment or sample volume.

The spatial range of dependence not only leads to the opportunity to interpolate between measured locations, it also manifests a spatial process, which is the continuous or nonrandom change of an observed magnitude across a spatial domain (Wendoroth et al., 2011). In order to quantify the relationship between two variables measured in a spatial domain, their individual range of representativeness needs to be known, as well as their common range of dependence, manifested by the cross-semivariogram (Deutsch and Journel, 1997; Nielsen and Wendoroth, 2003) or the crosscorrelation function (Shumway, 1988). This consideration is especially relevant for cases in which observations cannot be taken at exactly the same location or are based on a different support size, and the investigator asks, "Although measurements of two variables were not taken exactly at the same location or their individual support volume differs, can I still statistically relate them?" Examples would be (a) the relation of a soil textural observation taken as a bulk composite of four auger samples within an area of 1 m² with a grain yield measurement taken over an area of 100 m² by a combine harvester; (b) the field measurement of a soil water retention curve where the soil water content sensor cannot be installed at exactly the same location but only in close proximity to a tensiometer (Greminger et al., 1985; Nielsen and Wendoroth, 2003).

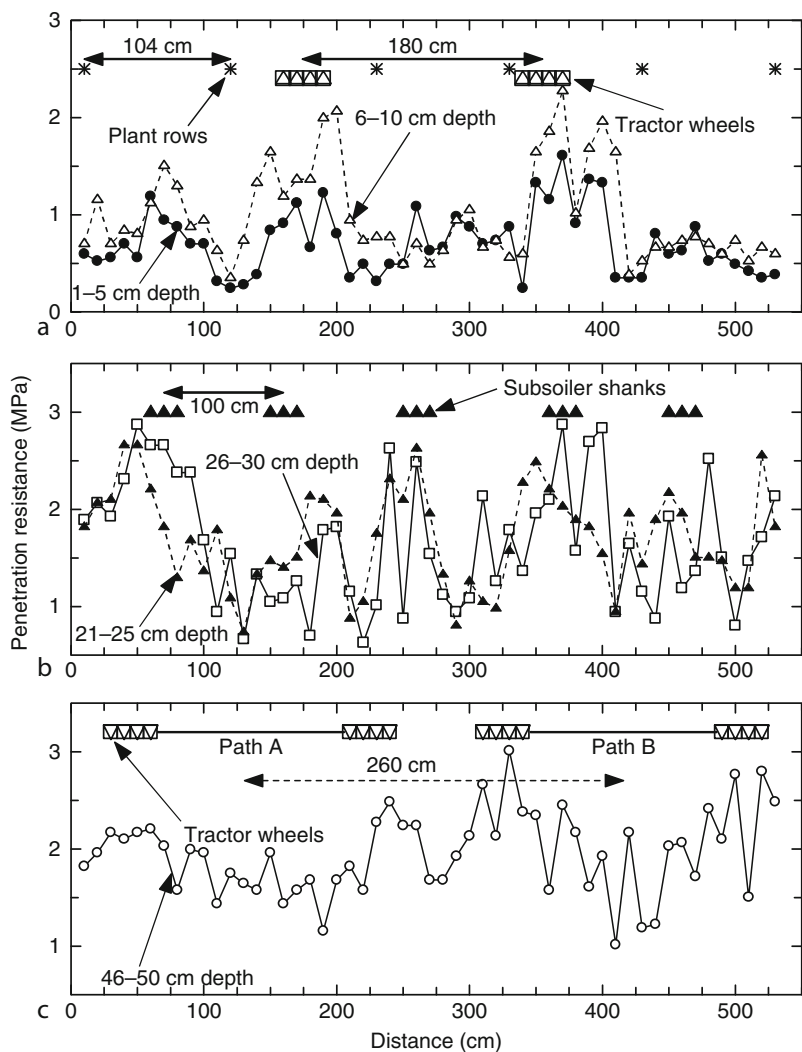
Autocovariance and frequency-domain variability analysis of soil penetration resistance and its relation to vehicle traffic patterns

In many agrophysical investigations of soil properties, management influences on soil state variables, e.g., quantitative measures of soil structure, are studied. Typically,

intensively managed soils exhibit a variability of soil physical properties that reflects the repetitive patterns of field management. These patterns are often times related to the pattern of surface topography, e.g., in furrow irrigation systems or row crops (Nielsen et al., 1983), or to field traffic and soil tillage operations (Domsch and Wendroth, 1997; House et al., 2001; Perfect and Caron, 2002; Wendroth and Nielsen, 2002). Investigations of soil structure carried out perpendicular to the main direction of tillage exhibit a repetitive or sinusoidal variability pattern. To detect these patterns would be impossible with random sampling, but instead requires systematic and equally spaced sampling along a transect.

In a study at the Kentucky Agricultural Station (Spindletop) near Lexington, tobacco was grown at a row spacing of 104 cm. Along a transect laid out

perpendicular to the tobacco rows, vertical cone penetrometer resistance (*PR*) was measured every 10 cm, giving 53 locations. Measurements of *PR* were recorded in units of MPa at every centimeter of depth and averaged over depth intervals of 5 cm. In Figure 1a, *PR* results are shown for the two upper depths, i.e., 1–5 and 6–10 cm, together with the location of the six plant rows perpendicular to the transect. Moreover, the locations of the left and right wheels (180 cm apart) of a heavy tractor that pulled a subsoiler through the plot in one direction prior to tobacco planting are shown. It is obvious that in close vicinity to plant rows *PR* yields relatively small values, whereas between plant rows *PR* values are relatively higher, and they reach the largest levels in zones of tractor wheel traffic during the subsoiling operation. The *PR* values proceed relatively synchronous, spatially, in the



Spatial Variability of Soil Physical Properties, Figure 1 Soil cone penetration resistance along a transect at five depths (a, 1–5, 6–10 cm; b, 21–25, 26–30 cm; c, 46–50 cm) in an intensively tilled tobacco plot. Location of one tractor wheel path with a wheel distance of 180 cm (a) pulling a subsoiler with five shanks separated by 100 cm (b), and of bidirectional tractor paths (A and B, separated by 260 cm) (c) for disk tillage are indicated.

upper two measured layers. The impact of tractor wheel tracks at distances of around 180 and 360 cm, causing larger *PR* values, is more pronounced in the 6–10 cm depth than 1–5 cm depth (Figure 1a).

A different spatial *PR* behavior is observed for the 21–25 and 26–30 cm depth compartments (Figure 1b). Measurements in the 21–25 cm layer proceed more continuously than those at 26–30 cm, which exhibit larger fluctuations from one location to the next. These larger local fluctuations may be ascribed to the paths of subsoiler shanks pulled through soil zones whose locations are also indicated in Figure 1b.

In general, *PR* values proceed higher in the 46–50 cm layer than in the layers above (Figure 1c). Moreover, the spatial *PR* series measured at this depth fluctuates more gradually than in the layers above. However, locally higher *PR* levels are found in those zones that correspond to the back-(path A) and-forth (path B) wheel paths of a tractor pulling a disk after subsoiling and prior to planting. The locations of the four wheels are shown in Figure 1c. The disking operation was repeated three times in both paths and at the locations of the wheels, an effect on *PR* was apparent at the 46–50 cm depth.

For the following analysis, the spatial autocorrelation function $r(h)$ of each series is calculated by Shumway (1988)

$$r(h) = \frac{\text{cov}[A_i(x), A_i(x + h)]}{\sqrt{\text{var}[A_i(x)]} \sqrt{\text{var}[A_i(x + h)]}} \quad (1)$$

where the sample autocovariance is

$$\begin{aligned} \text{cov}[A_i(x), A_i(x + h)] \\ = \frac{1}{N} \sum_{i=1}^{N-h} [A_i(x_i) - \bar{A}] [A_i(x_i + h) - \bar{A}], \end{aligned} \quad (2)$$

and the sample variance is

$$\text{var}[A_i(x)] = \frac{1}{N} \sum_{i=1}^N (A_i(x_i) - \bar{A})^2. \quad (3)$$

In Equations 1–3, A_i denotes observations being taken at locations x_i , \bar{A} denotes the arithmetic mean of A_i , and N the total number of observations.

Typically, a series of soil observations that is autocorrelated or structured exhibits large values of $r(h)$ at short lag distances and $r(h)$ decays with increasing lag distance h and equals zero at some distance, manifesting the fact that at and beyond this distance observations vary randomly. However, the resulting autocorrelation functions for the *PR* measurements at the five soil depth compartments are depicted in Figure 2, and they behave different from a regularly declining $r(h)$ behavior. In the layer 1–5 cm, $r(h)$ obviously oscillates and peaks of $r(h)$ occur regularly at every 100 cm of lag distance, or at every tenth observation. Regardless of where an observation is taken within the 530 cm transect, at 100, 200, 300, and

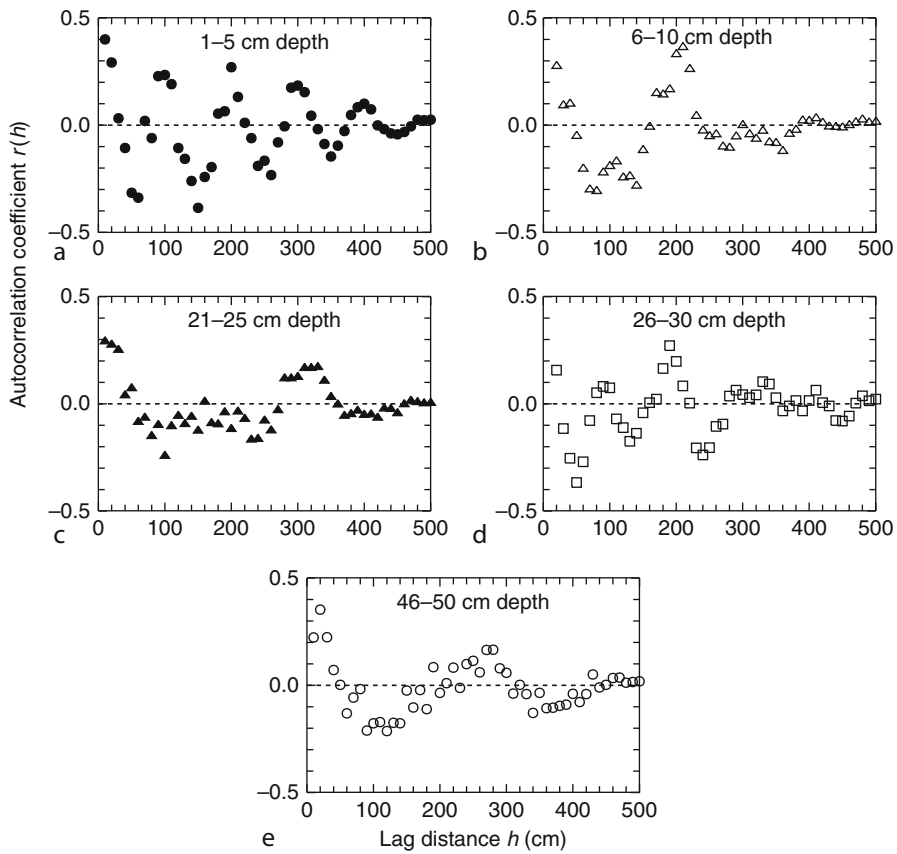
400 cm away from it, the magnitude of the observation is very similar. Notice the minimum magnitude of $r(h)$ at distances separated from the current location at $h = 50, 150, 250, 350$, and 450 cm, manifesting the opposite or inverse behavior of *PR*. Why does the amplitude of oscillations in the autocorrelation function decrease with increasing lag distance? Because in the sample autocovariance and sample variance, the sums of deviations are divided by N , regardless of the number of pairs of observations considered for a particular lag class. Since the sum term in the covariance equation (Equation 2) declines with increasing lag distance due to a decreasing number of differences in the particular lag class, the autocovariance and the variance decrease as well.

For the autocorrelation function of the 6–10 cm depth, a drop of $r(h)$ can be observed over the first lag intervals to $h = 60$ cm, from where $r(h)$ only slightly increases for the following lag distances but remains negative (Figure 2b). Only up to distances of around $h = 210$ cm, $r(h)$ increases again, implying a repetitive behavior at every 210 cm. The shape of the autocorrelogram for 21–25 cm depth (Figure 2c) is similar to the one at 6–10 cm, but the range of lag intervals at which $r(h)$ represents a repetitive pattern is approximately 320 cm. An autocorrelation behavior similar to that for 1–5 cm (Figure 2a) can be observed for *PR* measurements at 26–30 cm (Figure 2d). However, the cyclic autocorrelation is pronounced only at lag distances between 180 and 200 cm, and to some extent at $h = 100$ cm. This result may be caused by the compaction of tractor wheels that are spaced 180 cm apart from each other (Figure 1c). The signal at approximately 100 cm being less pronounced than the one at 180–200 cm may relate to the distance of subsoiler shanks being approximately 100 cm apart from each other. Their soil loosening effect every 100 cm is diminished by wheel compaction caused by the disking operations that followed.

Upon learning that the autocorrelation function reflects repetitive or periodic patterns of observations, spectral analysis, a specific tool for identifying periodicity- or frequency-based variance components is next applied (Davis, 1986; Shumway, 1988). Spectral analysis builds on Fourier transformation and on the theory that each data series can be considered as a combination of an infinite number of sine and cosine waves with their specific lengths and amplitudes. Hence, as ANOVA is focused on ascribing variance among treatments and their interactions, spectral analysis decomposes variance into cyclic components. Periodic variance components are depicted in the power spectrum $S(f)$ defined as (Shumway, 1988)

$$S(f) = 2 \int_0^\infty r(h) \cos(2\pi f h) dh \quad (4)$$

where f refers to the frequency, the inverse of the period (wavelength), given in length units. The unit for frequency depicted in the abscissa of the power spectrum is the inverse of the basic sampling interval, i.e., in this case $[0.1 \text{ m}]^{-1}$.



Spatial Variability of Soil Physical Properties, Figure 2 Sample autocorrelation functions for penetration resistance data at five depths shown in [Figure 1](#).

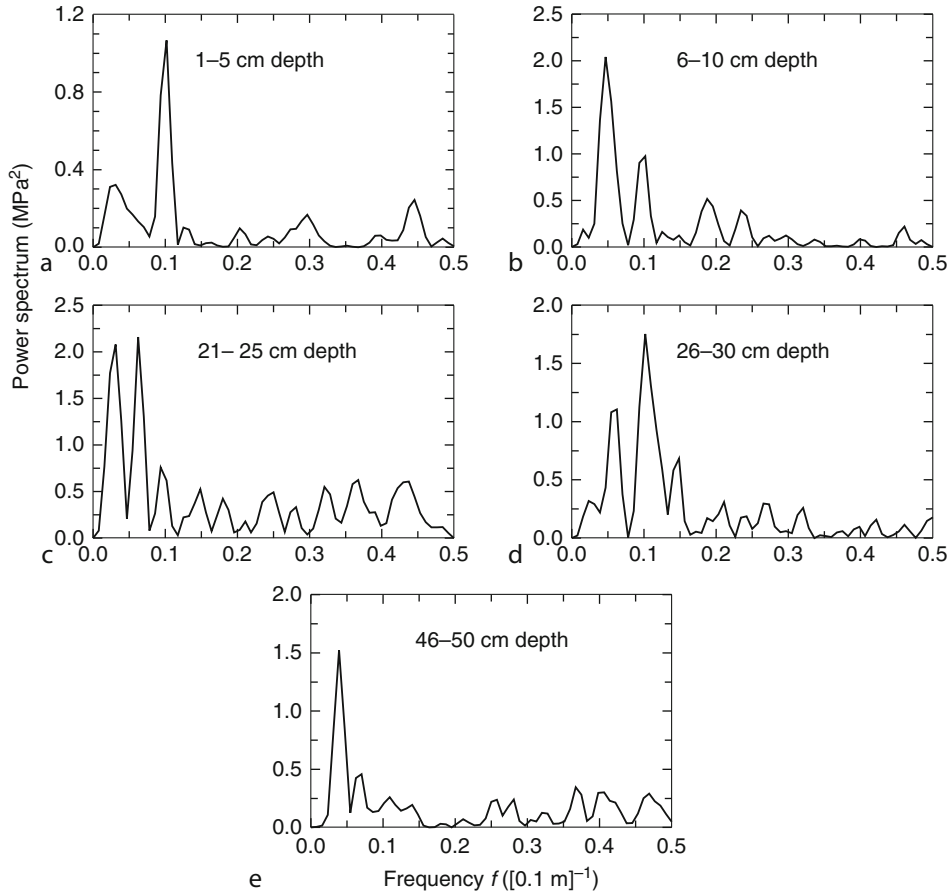
The power spectrum or periodogram derived from *PR* measurements at 1–5 cm depth is shown in [Figure 3a](#). In the graph, the abscissa depicts the frequency of the signal. For example, $f = 0.5$ refers to a period length of 0.5^{-1} , hence a period length of 2 observation intervals, equal to 20 cm for the *PR* data set. This is the minimum length of a period because the shortest fashion of a periodic fluctuation is a series of alternating high and low observed values. Such alternating data behavior would result in a spectral peak at a frequency of 0.5, or a period of 2. The smaller the frequency, the larger is the scale or characteristic wavelength at which cyclic variation occurs. The peak in the power spectrum of the 1–5 cm depth observed at a frequency of 0.1, a wavelength of 0.1^{-1} or 10 basic observation intervals (10 cm each), refers to the peaks in the autocorrelation function ([Figure 2a](#)) occurring periodically at lag distances of approximately 100, 200, 300, and 400 cm. A cyclic variance component at a frequency of 0.1 can also be observed at the 6–10 cm depth ([Figure 3b](#)). However, it is less pronounced than that at the 1–5 cm depth ([Figure 3a](#)). Instead, the strongest variance signal exists at a smaller frequency band around 0.05, corresponding to a wavelength of 200 cm. Notice the

consistency of this result with the peak in the autocorrelation function at $h = 200$ cm ([Figure 2b](#)).

At the 21–25 cm depth, the two strongest variance signals exist at frequencies of around 0.03 and 0.06, corresponding to wavelengths of approximately 320 and 160 cm, respectively ([Figure 3c](#)). In our calculations, the lengths of periods in the neighborhood of 320 cm are 426 and 256 cm, respectively, and in the neighborhood of 160 cm are 183 and 142 cm, respectively, which is determined by the number of spectral estimates being a power of 2. No clearer distinction can be made at the spectral resolution chosen in our calculations. At periods of approximately 160 cm ($f = 0.06$) and at 100 cm ($f = 0.1$) major variance components are detected ([Figure 3d](#)).

As is apparent in the original *PR* data for the 46–50 cm depth ([Figure 1c](#)), its variation is dominated by relatively long periods, manifested in the power spectrum with a distinctive peak at $f = 0.039$, corresponding to a period length of 260 cm ([Figure 3e](#)). This period length corresponds to the distance between the center of wheel paths A and B, the traffic pattern due to disking displayed in [Figure 1c](#).

In the following, analytical procedures for calculating spatial statistical relationships between different variables



Spatial Variability of Soil Physical Properties, Figure 3 Power spectra for penetration resistance data at five depths shown in Figure 1. Respective autocorrelograms are displayed in Figure 2. The frequency units reflect the inverse of the basic sampling interval.

are applied and discussed. First, the crosscorrelation function $r_c(h)$ is calculated with (Shumway, 1988)

$$r_c(h) = \frac{\text{cov}[A_i(x_i), B_i(x_i + h)]}{\sqrt{\text{var}[A_i(x_i)]} \sqrt{\text{var}[B_i(x_i + h)]}} \quad (5)$$

where the numerator term refers to the covariance between variable A_i observed at location x_i and variable B_i observed at separation distance h away from x_i . In the denominator, the individual variance terms of both variables are given.

In the crosscorrelation function, the relationship between two variables is measured when they are not sampled at the same location but at a separation distance h apart from each other. In Figure 4a, the crosscorrelation function for the PR data measured at 1–5 cm versus those at 6–10 cm, is plotted. The crosscorrelation coefficient $r_c(h)$ at $h = 0$ is equal to the classical correlation coefficient. Crosscorrelation coefficients displayed for positive lags h on the right-hand side of the crosscorrelogram manifest the relationship of the current PR values at 1–5 cm depth with PR values at 6–10 cm depth for previous lag distances, h . The left side of the crosscorrelation function

displays the spatial relationships for PR at 6–10 cm versus PR at 1–5 cm for prior distances h . On both sides of the crosscorrelation function, the cyclically proceeding relationship between the two variables is obvious. Although both series vary periodically (Figure 1a) their characteristic wavelengths differ, i.e., the most important periods are 100 and 200 cm for the 1–5 and 6–10 cm depth, respectively (Figure 3a and b). Hence, in the crosscorrelogram, the common wavelength is reflected through relatively large correlation coefficients at $h = \pm 200$ cm.

The crosscorrelation of PR at 1–5 and 26–30 cm depth is shown in Figure 4b, indicating common fluctuations every 100 cm. Interestingly, the maximum crosscorrelation coefficient is not observed at a lag $h = 0$, but at $h = 20$ cm. This phenomenon is often observed for two time series when a fluctuation occurs over the same characteristic wavelength in both series but with a certain spatial or temporal delay, e.g., daily soil temperature series at different soil depths (Rose, 1966). One way of understanding this phenomenon is to identify the causes of PR variation in the two layers considered. In both layers, a significant periodic variation component was observed

for wavelengths of 100 cm. At the 1–5 cm depth, the main cause for periodic fluctuations may have been the position of plant rows at every 104 cm, whereas at the 26–30 cm depth the subsoiler shanks were pulled through the ground at a similar interval, but slightly shifted relative to the plant rows. Note that the subsoiling happened before planting, and both field operations were spatially not coordinated.

The PR series measured at 6–10 and 46–50 cm are inversely crosscorrelated and are not perfectly synchronous, being shifted by 40 cm (Figure 4c). Wherever high PR values are observed at 6–10 cm depth, the 46–50 cm depth exhibits low PR , with a phase shift of 40 cm. Higher PR values occur at the 6–10 cm depth in the wheel path of the tractor pulling the subsoiler (Figure 1a). At 46–50 cm, repeated paths of tractor wheels originating from the above-mentioned post-subsoiling but preplanting disk tillage operations cause relatively higher PR (Figure 1c). Recompaction of the previously loosened subsoil might have occurred during the disking operations and the associated wheeling paths (A and B), which are laterally shifted relative to the subsoil shanks by about 40 cm (Figure 1b and c). Note that lower PR values occur in

the zones of subsoiling (Figure 1b), whereas the tractor wheels cause subsoil compaction with higher PR . This pattern of tillage operations causes the inverse relationship between PR values found at the two different depths.

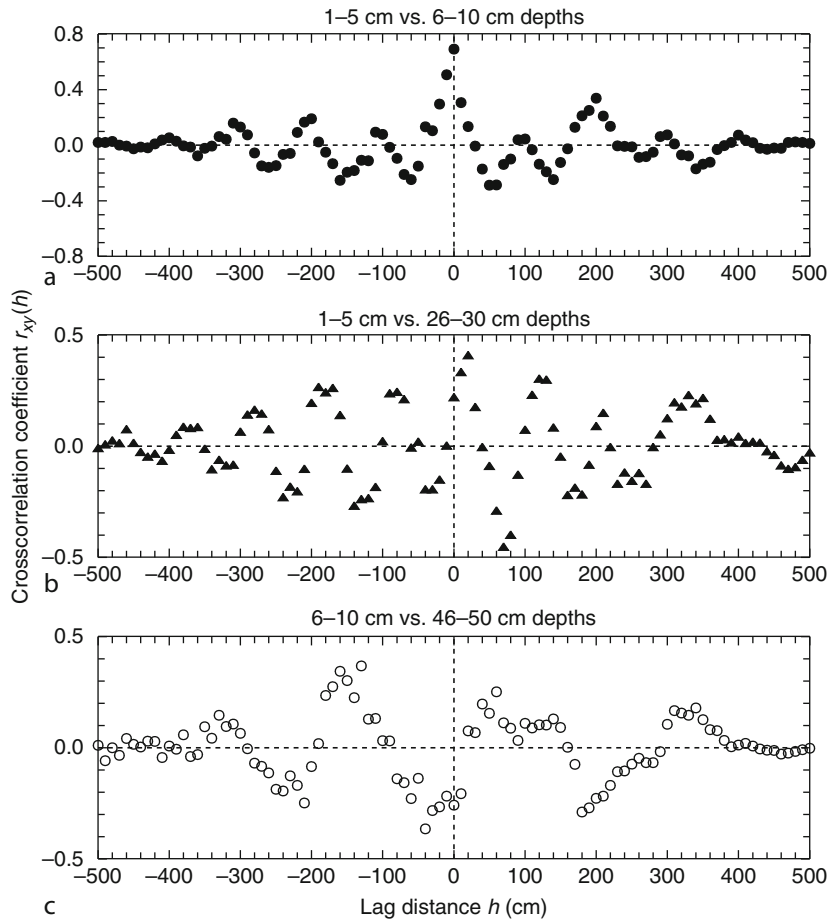
The detection of common frequency-based variance sources is accomplished through cross-spectral analysis consisting of two basic components, i.e., the co-spectrum and the quad-spectrum. Similar to the integration of the autocorrelation function for the power spectrum, the crosscorrelation function needs to be integrated for the co-spectrum $Co(f)$ through (Shumway, 1988)

$$Co(f) = 2 \int_0^\infty r_c(h) \cos(2\pi fh) dh \quad (6)$$

Before the crosscorrelation function can be integrated, both the right-hand side and left-hand side of the correlogram are averaged with

$$r_c(h) = 0.5[r_c(h < 0) + r_c(h > 0)]. \quad (7)$$

Through this averaging, fluctuations described by a cosine function are emphasized, and those described by a sine



Spatial Variability of Soil Physical Properties, Figure 4 Crosscorrelograms for three pairs of layer-specific penetrometer resistance data shown in Figure 1.

function are diminished. The second element, i.e., the quad-spectrum $Q(f)$ is calculated with (Shumway, 1988)

$$Q(f) = 2 \int_0^{\infty} r'_c(h) \sin(2\pi f h) dh. \quad (8)$$

This element of cross-spectral analysis is necessary in order to properly emphasize the fluctuations described by a sine function rather than cosine function by averaging both branches of the crosscorrelogram with

$$r'_c(h) = 0.5[r_c(h > 0) - r_c(h < 0)] \quad (9)$$

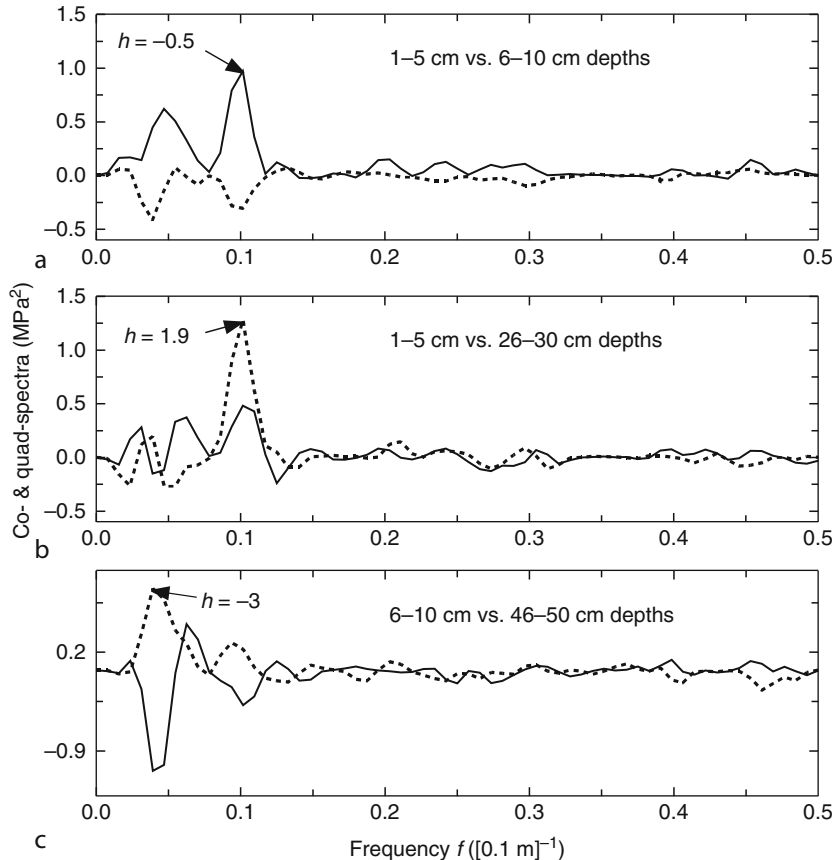
A perfect sine wave is equal to a perfect cosine wave when it is delayed by an angle of 90° . Both the co- and the quad-spectra need to be considered in cross-spectral analysis because two series may exhibit periodic fluctuations at the same wavelengths, but they may be shifted against each other. This shift is quantified for each particular frequency through the so-called phase spectrum defined as (Shumway, 1988)

$$h_{\phi}(f) = \frac{1}{2\pi f} \tan^{-1} \left[\frac{Q(f)}{Co(f)} \right]. \quad (10)$$

In Figure 5, co- and quad-spectra are shown for PR compared for the same pairs of depths for which crosscorrelation functions are depicted in Figure 4. The phase lag $h_{\phi}(f)$ for the peaks for PR at the 1–5 and 6–10 cm depths observed for $f = 0.1$ (Figure 5a) yields a low value of -0.5 sampling intervals, manifesting the almost synchronous behavior of the two series obvious from the corresponding crosscorrelation function (Figure 4a). At the same frequency, the periodic variation between PR in 1–5 and 26–30 cm (Figure 5b) is shifted by $+1.9$, corresponding to the maximum crosscorrelation coefficient observed at $h = 2$ (Figure 4b). For the band of even larger wavelengths ($f = 0.039$), the co- and quad-spectra (Figure 5c) result in a phase of -3 lags, which only approximately corresponds to the lag of -4 in the crosscorrelation (Figure 4c). This slight discrepancy is due to the coarse resolution of frequencies at this scale.

Variance scales of soil water storage, clay content, and corn yield

The spatial variation in soil profile water storage differs with time. Depending on the season, on the magnitude of soil water content or matric potential, and on the

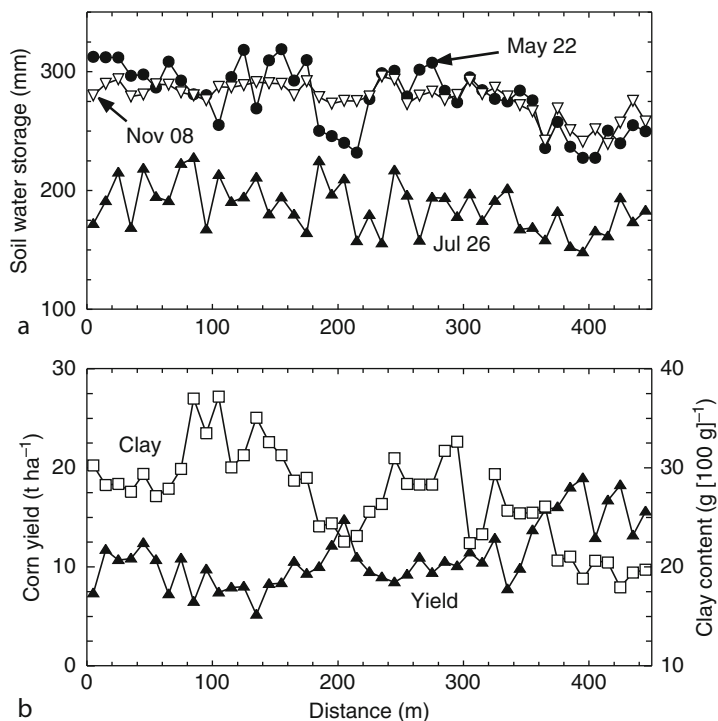


Spatial Variability of Soil Physical Properties, Figure 5 Co-(solid line) and quad-spectra (dashed line) for layer-specific pairs of penetration resistance measurements displayed in Figure 1. Respective crosscorrelograms are shown in Figure 4. The phase lag is denoted with h .

vegetation and its status, different patterns of spatial soil water distribution enunciate processes within the vadose zone whose relevance for soil water storage (SWS) changes throughout the year and, perhaps, over longer time intervals (Nielsen, 1997). In other words, the dominance of a spatial process on soil water storage distribution is not maintained throughout the year, but varies. Hence, for some seasons of the year, the spatial pattern in soil moisture distribution exhibits temporal persistence (Vachaud et al., 1985; Hu et al., 2010), but there are times when the distribution of soil moisture follows a pattern that is not consistent with that observed at other times. There are many ways to characterize the change in variation behavior over time. Roth (1995) derived the variation behavior for soil water status and flux from two-dimensional computer simulations of a Miller-similar medium. Under dry conditions, variance in soil water status is large in general and related to soil textural effects. With increasing soil water content, variance in water status and fluxes may decrease and reaches a minimum at a soil water potential level that is often called field capacity. With further increasing soil water content, variance increase is caused by soil structural effects (Roth, 1995). Field measurements by Wendoroth et al. (1999) confirmed this postulation. For a variety of different soils, Vereecken et al. (2007) reported standard deviation in soil water content versus average soil water content. Besides temporal

changes in the magnitude of the variance, the spatial autocovariance can change with time as a manifestation of cause controlling variance. Kachanoski and De Jong (1988) applied the above-mentioned frequency domain-based analyses to discriminate different spatial scales in field soil water content variation prevailing at particular times during their experimental period.

For deriving the scale of variance for profile soil water storage at different times and its relation to profile-average clay content and yield of corn, soil water content was measured in a farmer's field in Western Kentucky along a transect with 45 regularly spaced locations separated by 10 m. At each location, water content was measured and integrated over the 0–80 cm soil depth with a capacitance probe. In Figure 6a, soil water storage is depicted for three measurement dates in 2007, i.e., May 22, July 26, and November 08. The two series measured in May and November differ substantially from the one measured in July, the latter reflecting a situation of stored water depletion due to dry weather conditions and crop water uptake. The series observed in May and November exhibit a spatial process on a similar average level, and they behave similarly over the domain measured, but they differ in their local fluctuations. The May series exhibits more local noise whereas the November water storage proceeds smoother at the local scale. Neglecting the general water storage level, the July series manifests the



Spatial Variability of Soil Physical Properties, Figure 6 Profile soil water storage (SWS) integrated over a 0–80-cm soil depth at 45 locations separated by a 10-m distance, for 3 days in 2007 (a) and corn yield in 2007 and profile-average soil clay content (b), all in a farmer's field in Western Kentucky.

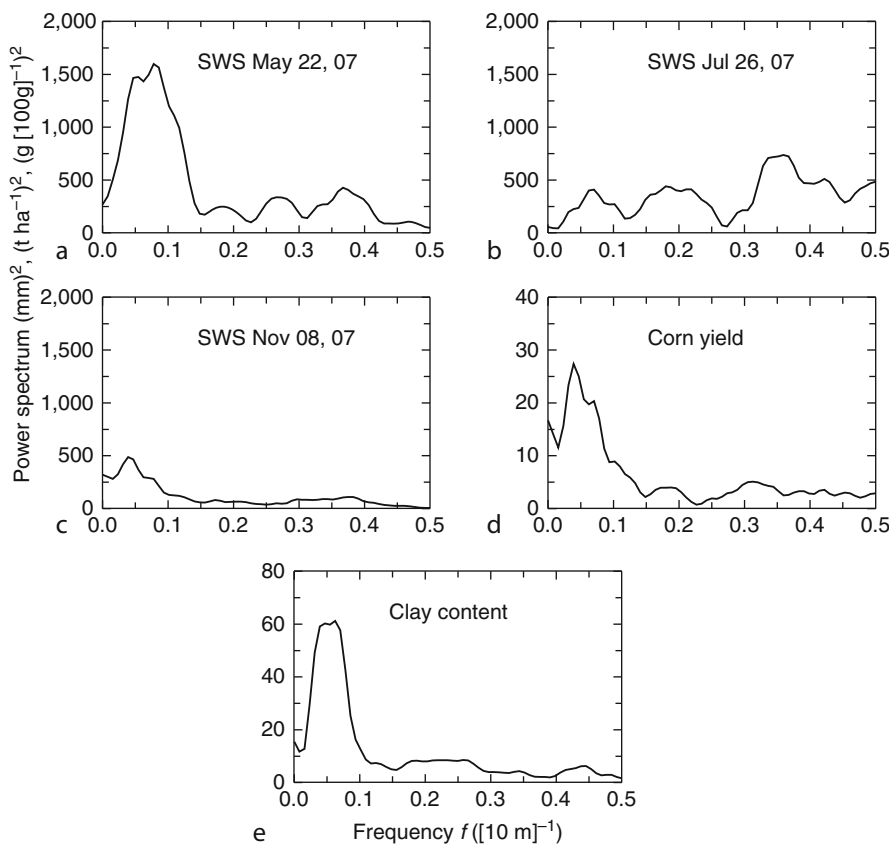
largest local variance, i.e., the storage differences between neighboring profiles are largest on this summer day. For the same transect, corn yield and profile-average soil clay content are illustrated in Figure 6b. In a very general way, clay content and corn yield are negatively related, and clay content and soil water storage in May and November behave spatially similar.

In what follows, the application of spectral analysis illustrates an example unlike the penetration resistance data set discussed above, because these data are not affected by cyclically repeated patterns related to soil management but are influenced by the curvature and characteristics caused by landscape morphology, soil genesis, vegetation, and crop establishment, irrigation, etc. This has been shown in the work of Warrick and Gardner (1983) and Kachanoski and De Jong (1988).

Power spectra for the three spatial series of soil water storage are shown in Figure 7a–c, which are purposely plotted with the same y -axis scale. The spectrum for the May 22 series reflects a strong weight on the large-scale variance for $f < 0.1$, corresponding to substantial variance observed over a distance of 100–200 m in the field. Small-scale peaks indicate variability at frequencies of 0.27 and 0.37, corresponding to every 40–30 m, respectively, but

these are less pronounced than the large-scale variance. Overall, due to similar large-scale behavior, the power spectrum for water storage measured in November (Figure 7c) is consistent with the one obtained for May (Figure 7a), but the overall variance is smaller in November, reflected by a smaller area under the peak profile. Notice that at small scales, the November series is smooth, manifested by the absence of peaks at $f > 0.1$. The spectrum for the July series (Figure 7b) manifests more pronounced small-scale fluctuations every 30–50 m. This small-scale variability contributes to a larger magnitude in total variance of the July series than the barely pronounced large-scale peak at a similar frequency that dominated variance in the May and November series (Figure 7a and c). The two remaining spectra for corn yield and clay content (Figure 7d and e) manifest the same dominating large-scale variance that is observed for the May and November water storage series.

Above, the degree of periodic coincidence in two PR series measured at different depths was illustrated with cross-spectral analysis. An additional statistical measure is the coherency spectrum defined by (Shumway, 1988)



Spatial Variability of Soil Physical Properties, Figure 7 Power spectra for the data depicted in Figure 6, i.e., soil water storage (SWS) on May 22, 2007 (a), July 26 (b), November 08 (c), corn yield (d), and clay content (e), all measured in a farmer's field in Western Kentucky in 2007.

$$Coh(f) = \frac{Co^2(f) + Q^2(f)}{S_A(f) S_B(f)} \quad (11)$$

which – similar to the coefficient of determination in regression analysis – quantifies the relationship between two variables for the spectrum of different frequencies. Coherency spectra for various combinations of the variables presented in Figure 6 are depicted in Figure 8. Common variance scales of 30–50 m dominate the coherency between the May and July water storage series (Figure 8a). However, a broader range of common frequencies is obtained for the May and November series (Figure 8a). While the soil water storage measured in May and yield have many, not extremely pronounced common frequencies, water storage in July is related to corn yield only at scales above 100 m (Figure 8b). Water storage measured in November varies consistently with corn yield over large but also small common scales, and there are a variety of different common scales between clay content and yield (Figure 8c).

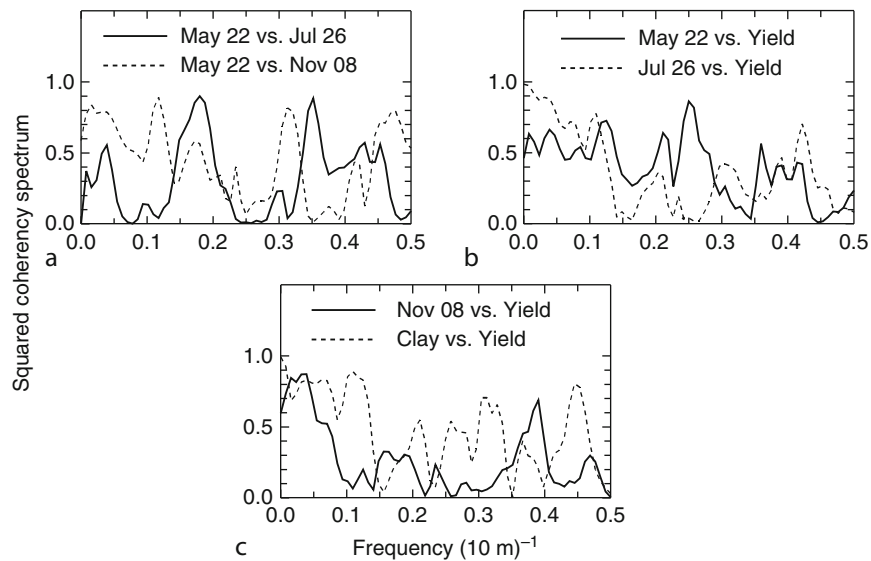
For two series, their common scales of variation are quantified in the coherency spectrum. It is important to note that spatial series separated by a longer time interval can exhibit more common scale variability than those observed over a shorter interval. For example, the water storage series observed in May and November display more common variability scales with corn yield than storage measured in late July, which was close to harvest. The physiological or functional relevance of a state variable and its spatial pattern can prevail over much longer time intervals and periods than is often assumed. Erroneous assumptions about functional relationships can lead to

measurements taken at closer, but functionally rather irrelevant times.

Outlook

Frequency domain-based analysis provides many opportunities to study agrophysical processes in systems even without any imposed treatments. Folorunso and Rolston (1985) discovered soil water content to vary in wavelengths of 4–5 m. Moreover, these periodic fluctuations coincided with the spatial pattern of greenhouse gas emissions. An additional frequency component, caused by water-soluble organic carbon was found in their study. In their investigations of surface topography, horizon thickness and density, Kachanoski et al. (1985a, b) detected common wavelengths between 2 and 10 m length at which variations in surface curvature, slope gradient, and A-horizon mass occurred. When the same relationships were investigated for the B-horizon, characteristic periodicities were found again at 10-m wavelengths, but were barely observable for shorter wavelengths that dominated variability in the A-horizon.

The first two-dimensional application of spectral analysis was performed by Bazza et al. (1988) who investigated variation in soil surface temperature in a 6-ha field that had previously been irrigated with water at different salinity levels. Those prior treatments could not be laid out in a random fashion but had to be arranged in a regular repetitive pattern. Perpendicular to the direction of different treatments, soil temperature and salinity level exhibited a close inverse relationship whose periodic coincidence was obvious. On the other hand, along the differently treated strips, soil temperature showed only minor and



Spatial Variability of Soil Physical Properties, Figure 8 Coherency spectra for pairs of data depicted in Figure 6, i.e., soil water storage series measured on May 22, July 26, and November 08, respectively (a), May and July storage series versus corn yield (b), and November storage and clay content versus yield (c), all measured in a farmer's field in Western Kentucky in 2007.

rather random variation. This was one of the first studies in soil science in which treatments were laid out non-randomly but in a cyclic spatial pattern.

Spectral analysis has also been applied to study crop competition (Samra et al., 1993) and two-dimensional vegetation patterns (Renshaw, 1997). Samra et al. (1993) investigated the competing interactions between Bhabbar grass planted in between rows of Eucalyptus trees. Growth performance of Bhabbar significantly differed depending on plant position relative to the tree row. Moreover, little difference was observed in the ecological impact of the trees on the grass in a dry year. It is extremely hard, if not impossible, to imagine a study in which these findings could have been derived from samples taken randomly in a randomized treatment experiment. Similar to ANOVA, Samra et al. (1993) applied F statistics for the identification of significant frequency-based variation components in their analysis of power (ANOPO).

In a pine stand forest ecosystem, Böttcher et al. (1997) investigated the spatial variation in solute input into the ground water, i.e., sulfate concentration of canopy throughfall. Their analysis revealed that the spatial pattern of solute input proceeded in a spatially synchronous fashion with the distributional pattern of pine canopy coverage of the ground. Maximum sulfate concentrations were found at the locations corresponding to the edges of the canopies, minima in zones of maximum canopy coverage. Note that the sulfate concentrations in the uppermost ground water sampled in 1989 were stronger related to the canopy coverage pattern than in 1993 due to more pronounced canopy variation in younger trees.

Management-induced variation in crop growth is often times an unintended effect that can be discovered by frequency-domain analysis of integrative crop state variables. In their investigation, Wendoroth et al. (1997) found that the position of sprinklers in an almond orchard caused systematic differences in almond tree growth, reflected in trunk circumference. One-year yield observations would not have obviously shown this cyclic and systematic effect.

Tillage-induced horizontal variability has been analyzed with spectral techniques (Petersen et al., 1997; Wendoroth and Nielsen, 2002). In their study, Petersen et al. (1997) detected periodic variation in dye patterns as an indicator of flow at a frequency that corresponded to the furrow width of the plow. The furrow width was also one of the main factors causing horizontal variability in soil chloride concentration and soil water content in the study of Wendoroth and Nielsen (2002). In addition, they discovered that an additional cyclic impact corresponded to the width of the plow.

Interestingly, the topographic curvature index and corn grain yield varied coincidentally in a landscape morphology study of Timlin et al. (1998). While yield maps in subsequent years were temporally unstable, pronounced surface curvature caused yield patterns to vary depending on whether curvatures were convex or concave in shape,

and on whether the year was relatively dry or wet. Moreover, depth to fragipan caused yield fluctuations in dry years.

Decomposition of soil water content variability, along several transects and with depth, using spectral coherency manifested strong relationships between the scale of variation at the surface layer and those at deeper soil layers in a study by Cassel et al. (2000). The same analysis was applied to detect common frequency-based variability components during subsequent sampling dates. Relatively large-scale fluctuations, at a scale of 50 m, dominated common variability behavior in surface soil water content measured at different times.

Recently, R.L. Fox's idea of applying nitrogen not in randomized plots but at continuously varying rates across the landscape was applied in experiments of Shillito et al. (2009) and Wendoroth et al. (2011). The study of Shillito et al. (2009) resulted in systematic differences in nitrogen response of potato yield to the amount of nitrogen applied. The regular and repetitive pattern of applied nitrogen evidently showed nonunique response caused by systematic soil variability. In the study of Wendoroth et al. (2011), less pronounced but still obvious differences in nitrogen response of winter wheat were observed across a field with sinusoidal nitrogen application. Spectral and another frequency-based analysis, i.e., the wavelet spectrum, revealed a strong periodic component at the treatment scale, and in addition a large-scale component based on soil textural differences manifesting a trend in soil quality underlying the field investigated.

Experimentalists who intend to answer a question related to scale and frequency of variation in a soil or crop property, impact of surface topography, soil management, and other sources of variation by using spectral analysis need to remember that observations undergoing frequency-domain analysis must be taken equally spaced. Moreover, a prior assumption or investigation of fundamental wavelengths affecting the variability of observations needs to be seriously considered in the design of the experiment. A process is under sampled if the shortest periodic fluctuation is covered with just three observations over a distance $2\Delta x$ where Δx is the basic sampling interval, which would result in a spectral peak at a frequency $f = 0.5$, the so-called Nyquist frequency (Davis, 1986). The shortest periodic fluctuation needs to be covered by more than three observations. As shown in the examples of penetration resistance analyzed, measurements of different variables do not necessarily need to be taken at exactly the same point. Observations undergoing crosscorrelation and cross-spectral analysis can be taken at the same location, or at locations along a parallel line transect, at the same location but at a different depth, at the same or a parallel location at a different time, etc. Any combination of observations along a space or time axis is possible. Prior to the analysis of the frequency domain, autocovariance analysis needs to be employed to identify the spatial or temporal representativity of observations. The next step is to identify the spatial or

temporal distance over which two variables are still meaningfully related with each other, information that is depicted in the crosscorrelogram. Still, in too many agronomic and soil-related studies these two essential characteristics of observations are disregarded, misleading the investigators to conclusions about the lack of relationships among the two or more variables investigated.

In the original applications of Fourier-transform-based analysis, time series analyses were applied to electric signals, collected using data-logging devices, resulting in significant power spectra that were not affected by data shortage. In many soil science applications, especially in the spatial domain, observed series may cover only a limited number of waves. Nevertheless, new soil sampling and sensor technologies provide increasing opportunities for which frequency domain analysis is the tool of choice (Pringle and Lark, 2007). Experiments with a frequency-based layout of treatments – different treatments should cover different wavelengths – allow studying treatment response while discerning whether underlying soil processes gradually alter the response.

Summary

According to the French mathematician J.B. Fourier (1768–1830), any continuous single-valued function can be represented by an infinite number of sinusoidal waves of different length, amplitude, and phase. If the variance of soil state variables taken across a spatial or temporal domain is not random, it follows some pattern at various scales, manifested as local trends. Managed soils often exhibit a spatially cyclic variation in properties caused by the repetitious pattern of management, e.g., row spacing, wheel traffic, tillage, irrigation, and fertilization. Landscape topography, pedogenesis, hydropedologic conditions, and vegetation cause trends and curvature in the spatial series of data observed over larger scales. The variance in regularly repeating observation patterns and their causal factors can be decomposed in spectral analysis. Typical contributions to the variance are illustrated in the power spectrum, which depicts the main frequencies, periods, wavelengths, or scales over which variance occurs. In a study of intensive soil tillage for tobacco, spatial soil penetration resistance data series, measured perpendicular to the main tillage direction and at different soil depths, exhibited typical variation patterns at different scales. Spectral and cross-spectral analysis quantified cyclic variation components. Their typical wavelengths varied with depth and could be linked to different wheel traffic and soil management patterns. In a landscape-scale study on soil water storage, soil texture and crop yield, spectral analysis was helpful in detecting different spatial patterns in soil water storage throughout the year. Coherency spectra identified the main common scales of variation. Typical variation scales for corn yield, after a relatively dry growing season, were related mainly to those for soil water storage measured when that

storage was relatively high. In order to predict significant spatial patterns for important variates and their spatial processes such as crop yield, optimum times for measuring the distribution pattern of underlying soil state variables can be identified using cross-spectral and coherency analysis.

Bibliography

- Bazza, M., Shumway, R. H., and Nielsen, D. R., 1988. Two-dimensional spectral analyses of soil surface temperature. *Hilgardia*, **56**, 1–28.
- Blöschl, G., and Sivapalan, M., 1995. Scale issues in hydrological modeling – a review. *Hydrological Processes*, **9**, 251–290.
- Böttcher, J., Lauer, S., Strelbel, O., and Puhlmann, M., 1997. Spatial variability of canopy throughfall and groundwater sulfate concentrations under a pine stand. *Journal of Environmental Quality*, **26**, 503–510.
- Cassel, D. K., Wendoroth, O., and Nielsen, D. R., 2000. Assessing spatial variability in an agricultural experiment station field: opportunities arising from spatial dependence. *Agronomy Journal*, **92**, 706–714.
- Davis, J. C., 1986. *Statistics and Data Analysis in Geology*, 2nd edn. New York: Wiley.
- Deutsch, C. V., and Journel, A. G., 1997. *GSLIB. Geostatistical Software Library and User's Guide*. New York: Oxford University Press, 340 pp.
- Domsch, H., and Wendoroth, O., 1997. On-site diagnosis of soil structure for site specific management. In Stafford, J. V. (ed.), *Precision Agriculture. Proceedings of First European Conference on Precision Agriculture*. Oxford, UK: BIOS Scientific, pp. 95–102.
- Folorunso, O. A., and Rolston, D. E., 1985. Spatial and spectral relationships between field-measured denitrification gas fluxes and soil properties. *Soil Science Society of America Journal*, **49**, 1087–1093.
- Goovaerts, P., 1997. *Geostatistics for Natural Resources Evaluation*. New York: Oxford University Press, 483 pp.
- Greminger, P. J., Sud, K., and Nielsen, D. R., 1985. Spatial variability of field-measured soil-water characteristics. *Soil Science Society of America Journal*, **49**, 1075–1082.
- House, M. L., Powers, W. L., Eisenhauer, D. E., Marx, D. B., and Fekersillasse, D., 2001. Spatial analysis of machine-wheel traffic effects on soil physical properties. *Soil Science Society of America Journal*, **65**, 1376–1384.
- Hu, W., Shao, M., and Reichardt, K., 2010. Using a new criterion to identify sites for mean soil water storage evaluation. *Soil Science Society of America Journal*, **74**, 762–773.
- Isaaks, E. H., and Srivastava, R. M., 1989. *Applied Geostatistics*. New York: Oxford University Press.
- Journel, A. G., and Huijbregts, Ch J., 1991. *Mining Geostatistics*. London: Academic, 600 pp.
- Kachanoski, R. G., and De Jong, E., 1988. Scale dependence and the temporal persistence of spatial patterns of soil water storage. *Water Resources Research*, **24**, 85–91.
- Kachanoski, R. G., Rolston, D. E., and De Jong, E., 1985a. Spatial and spectral relationships of soil properties and microtopography. I. Density and thickness of A-horizon. *Soil Science Society of America Journal*, **49**, 804–812.
- Kachanoski, R. G., De Jong, E., and Rolston, D. E., 1985b. Spatial and spectral relationships of soil properties and microtopography. II. Density and thickness of B-horizon. *Soil Science Society of America Journal*, **49**, 812–816.
- Morkoc, F., Biggar, J. W., Nielsen, D. R., and Rolston, D. E., 1985. Analysis of soil water content and temperature using state-space approach. *Soil Science Society of America Journal*, **49**, 798–803.

- Nielsen, D. R., 1997. A challenging frontier in hydrology – the vadose zone. In Buras, N. (ed.), *Reflections on Hydrology: Science and Practice*. Washington, DC: AGU, pp. 205–226.
- Nielsen, D. R., and Wendoroth, O., 2003. *Spatial and Temporal Statistics – Sampling Field Soils and their Vegetation*. Reiskirchen: Catena, 416 pp.
- Nielsen, D. R., Tillotson, P. M., and Vieira, S. R., 1983. Analyzing field-measured soil water properties. *Agricultural Water Management*, **6**, 93–109.
- Perfect, E., and Caron, J., 2002. Spectral analysis of tillage-induced differences in soil spatial variability. *Soil Science Society of America Journal*, **66**, 1587–1595.
- Petersen, C. T., Hansen, S., and Jensen, H. E., 1997. Tillage-induced horizontal periodicity of preferential flow in the root zone. *Soil Science Society of America Journal*, **61**, 586–594.
- Pringle, M. J., and Lark, R. M., 2007. Scale- and location-dependent correlations of soil strength and the yield of wheat. *Soil and Tillage Research*, **95**, 47–60.
- Renshaw, E., 1997. Spectral techniques in spatial analysis. *Forest Ecology and Management*, **94**, 165–174.
- Rose, C. W., 1966. *Agricultural Physics*. Oxford: Pergamon.
- Roth, K., 1995. Steady state flow in an unsaturated, two-dimensional, macroscopically homogeneous, Miller-similar medium. *Water Resources Research*, **31**, 2127–2140.
- Samra, J. S., Grewal, S. S., and Singh, G., 1993. Modelling competition of paired columns of Eucalyptus on interplanted grass. *Agroforestry Systems*, **21**, 177–190.
- Shillito, R. M., Timlin, D. J., Fleisher, D., Reddy, V. R., and Quebedeaux, B., 2009. Yield response of potato to spatially patterned nitrogen application. *Agriculture, Ecosystems and Environment*, **129**, 107–116.
- Shumway, R. H., 1988. *Applied Statistical Time Series Analysis*. Englewood Cliffs: Prentice Hall, 379 pp.
- Shumway, R. H., and Stoffer, D., 2000. *Time Series Analysis and Its Applications*. New York: Springer, 549 pp.
- Timlin, D. J., Pachepsky, Y., Snyder, V. A., and Bryant, R. B., 1998. Spatial and temporal variability of corn grain yield on a hillslope. *Soil Science Society of America Journal*, **62**, 764–773.
- Vachaud, G., Passerat de Silans, A., Balabanis, P., and Vauclin, M., 1985. Temporal stability of spatially measured soil water probability density function. *Soil Science Society of America Journal*, **49**, 822–828.
- Vereecken, H., Kamai, T., Harter, T., Kasteel, R., Hopmans, J., and Vanderborght, J., 2007. Explaining soil moisture variability as a function of mean soil moisture: a stochastic unsaturated flow perspective. *Geophysical Research Letters*, **30**, L22402, doi:10.1029/2007GL031813.
- Warrick, A. W., and Gardner, W. R., 1983. Crop yield as affected by spatial variations of soil and irrigation. *Water Resources Research*, **19**, 181–186.
- Wendoroth, O., and Nielsen, D. R., 2002. Time and space series. In Dane, J. H., and Topp, G. C. (eds.), *Methods of Soil Analysis*, Part 4, 3rd edn. Soil Science Society of America Book Series, no. 5. Madison, WI: Soil Science Society of America, Inc., pp. 119–137.
- Wendoroth, O., Reynolds, W. D., Vieira, S. R., Reichardt, K., and Wirth, S., 1997. Statistical approaches to the analysis of soil quality data. In Gregorich, E. D., and Carter, M. R. (eds.), *Soil Quality for Crop Production and Ecosystem Health. Developments in Soil Science* 25. Amsterdam: Elsevier, pp. 247–276.
- Wendoroth, O., Pohl, W., Koszinski, S., Rogasik, H., Ritsema, C. J., and Nielsen, D. R., 1999. Spatio-temporal patterns and covariance structures of soil water status in two Northeast-German field sites. *Journal of Hydrology*, **215**, 38–58.
- Wendoroth, O., Koszinski, S., and Vasquez, V., 2011. Soil spatial variability. In Huang, P. M., Li, Y. C., and Sumner, M. E. (eds.), *Handbook of Soil Science*, 2nd edn. Boca Raton, FL: Taylor & Francis (in press).

Cross-references

- [Agrophysical Objects \(Soils, Plants, Agricultural Products, and Foods\)](#)
- [Agrophysical Properties and Processes](#)
- [Compaction of Soil](#)
- [Cropping Systems, Effects on Soil Physical Properties](#)
- [Field Water Capacity](#)
- [Management Effects on Soil Properties and Functions](#)
- [Soil Penetrometers and Penetrability](#)
- [Soil Water Management](#)
- [Subsoil Compaction](#)

SPECIFIC SURFACE AREA OF SOILS AND PLANTS

Zofia Sokołowska

Institute of Agrophysics, Polish Academy of Sciences,
Lublin, Poland

Definitions

Different kinds of the surface area may be found in soil. The *geometric surface area* is calculated on the data of shapes and dimension of representative soil particles. The *internal surface area* is the surface of inter walls of the microcapillaries (the term “internal surface” is usually restricted in its application to those cavities, which have an opening to exterior of the grains). The *external surface area* is defined as the sum of geometric and internal surface area. The *interlayer surface area* is the surface of interlayer walls of minerals of the montmorillonite type. The *total surface area* is the sum of the external and internal surface areas, as well as the surface area of organic matter.

The total, external and internal surface areas are the main types of specific surface that can be used to characterize each adsorbent. Sometimes other kinds of surface area are invoked, but all of them are special cases of the definitions given above.

Specific surface area of a soil sample is combined surface area of all the particles in the sample, as determined by some experimental technique and expressed per unit mass of the sample, mostly in $\text{m}^2 \text{ g}^{-1}$. As its definition implies, term “specific surface area” is an operational concept.

Introduction

Surface area is recognized to play a complementary part to porosity in adsorption phenomena for a vast range of solids. Solid phase of a soil is a mixture of different inorganic constituents as nonporous materials of different size and shape, porous materials with microcapillaries or pores, and phyllosilicates with the interlayer structure, as well as organic species, mainly organic matter.

Methods of measurements of specific surface area

Physical methods

Direct physical methods for measuring specific surface area (the crystallographic or geometric surface area) are

based on light or electron microscopy and on X-ray diffraction methods. All these techniques can be used to determine the shape and dimensions of individual soil particles and, additionally to assess crystallographic structure and interlayer spacing of clay minerals. Providing that a characteristic particle size and shape can be determined, the specific surface area can be obtained from mass–volume relationships. To estimate the specific surface area of clay minerals, the structural formula and unit cell dimensions must be known.

Chemical methods

The majority of chemical methods are based on measurement of adsorption of polar and nonpolar gases, vapors or dissolved molecules (Schofield, 1947; Everett and Ottewill, 1970; Tiller and Smith, 1990; Chiou and Rutherford, 1993; Sivapullaiah et al., 2008). The adsorbable compounds used to determine specific surface area are chosen on the basis of their molecular properties. Polar adsorbates include water vapor, ethylene glycol, or ethylene glycol monoethyl and they are employed to measure the total surface area. Typical nonpolar adsorbates are nitrogen, argon, krypton and they are applied to measure the external surface area. Nitrogen is commonly used as the adsorbate because it interacts weakly with a broad array of surface functional groups and therefore permits for the determination of exposed area of soil.

The application of the physical adsorption of gases to the estimation of the specific surface area of soils.

The physical adsorption is also called “the van der Waals adsorption.” The adsorbate molecules are accumulated at a surface in result of their physical interactions with that surface. These interactions include: dispersion forces (which are attractive in nature) and short-range repulsive forces. In addition, there may exist forces due to permanent dipoles within the adsorbed molecules. The process of physical adsorption is reversible, the heat of adsorption is low, and the thickness of adsorbed layers may be a few molecular diameters of a gas molecule.

The amount of gas adsorbed per gram of solid, N , depends on the equilibrium pressure, p , the temperature, T , and also on the nature of the gas and solid. The adsorbed amount at a constant T is called the adsorption isotherm when the measurements were carried out at consecutively increasing pressures, and the desorption isotherm, when the adsorption data were obtained along decreasing pressures branch. The amount of adsorbed, N , may be measured in any suitable units, i.e., grams or milligrams, moles or millimoles, and cubic centimeter under normal temperature and pressure (NTP) conditions. The adsorption isotherm is the most popular way to express the adsorption data.

The isotherms start at the origin of the coordinates and they end is at a nearly of the saturated vapor pressure. No simple interpretation can be given to describe the main part of the curve. The initial part of the isotherm is used

to obtain the surface area, whereas its end-part to evaluate the pore structure of a solid body. A number of different theories have been proposed for the interpretation of adsorption data, but only a few equations have been found to reproduce with a reasonable precision a large number of experimental isotherms. The best known and probably the most frequently used theory is that proposed by Brunauer, Emmett, and Teller (BET). The BET theory not only leads to a simple analytical equation (called the BET equation) for the adsorption isotherm, but also provides the way to classify the isotherm into five distinct categories. The BET theory has proved remarkably successful in the calculation of specific surface area of several isotherms, providing that they belong to an appropriate type (specifically, to the type II), according to the BET classification scheme. Other theory that also can be employed to determine the specific surface area is that proposed by Langmuir. The latter theory is usually applied to calculate the specific surface area for the isotherms of type I according to the BET classification.

The Langmuir equation describes localized monolayer adsorption on a homogeneous surface. It has the form:

$$N = \frac{N_m kp}{1 + kp} \quad (1)$$

In the above, N_m is the monolayer capacity, that is, the amount of adsorbed molecules necessary to cover the surface with a monomolecular film, and k is a constant.

In contrast to the Langmuir isotherm that characterizes monolayer adsorption, the BET equation describes localized multilayer adsorption on a homogeneous surface. It reads:

$$N = \frac{N_m x C_{BET}}{(1 - x)[1 + (C_{BET} - 1)x]}, \quad (2)$$

where $x = p/p_0$ is the relative pressure of a vapor (p_0 is the saturated vapor pressure), and C_{BET} is a constant, usually called “the BET constant.” The range of validity of the BET equation does not always extend to relative pressure higher than 0.5.

Calculation of the specific surface area from adsorption data

The surface area of soil samples is evaluated from adsorption–desorption isotherms as follows. The first step in the application of the Langmuir or BET method is to obtain the monolayer capacity, N_m . The second step is to calculate the specific surface area from the value of N_m .

The monolayer capacity from Langmuir plot

A linear form of the Langmuir equation (the so-called Langmuir plot) has the form:

$$\frac{p}{N} = \frac{1}{N_{mk}} + \frac{1}{N_m} p. \quad (3)$$

The parameters k and N_m can be directly evaluated fitting experimental data by a straight line. If p/N data are plotted against p , the resulting straight line slope, s , gives $s = 1/N_m$ and the intercept $i = 1/k N_m$. From the above quantities, we obtain $N_m = 1/s$ and $k = (1/(N_m)(1/i))$.

The monolayer capacity from BET plot

The linearized form of the BET isotherm has the form:

$$\frac{x}{N(1-x)} = \frac{1}{C_{BET}N_m} + \frac{(C_{BET}-1)}{C_{BET}N_m}x. \quad (4)$$

If $x/N(1-x)$ is plotted against p/p_0 , a straight line should result with the slope $s = (C_{BET}-1)/N_m C_{BET}$ and the intercept $i = 1/N_m C_{BET}$. From the above quantities we obtain N_m and C_{BET} , namely, $N_m = 1/(s+i)$ and $C_{BET} = (s/i) + 1$. Note that the most reliable results are usually obtained if the approximation is carried out within the range of relative pressures of $0 < p/p_0 < 0.35$.

Calculation of the surface area

The second step is to calculate the surface area from the dependence:

$$S = N_m M^{-1} L \omega, \quad (5)$$

where L is the Avogadro number (6.02×10^{23} molecules per mole), M is the molecular weight of gas or vapor (in gram per mole) and ω is the molecule cross-sectional area of an adsorbate molecule, expressed in m^2 per molecule. If N_m is obtained from water vapor isotherm and is expressed in grams of water per gram of solid, ω is $10.8 \times 10^{-20} \text{ m}^2$ for water molecule then the specific surface area $S(\text{m}^2 \text{ g}^{-1})$ is $S = 3,612 \times N_m$. One should note, however, that in the case of porous (or "wiggly") solids, the value of N_m may depend on ω , i.e., on the kind of the adsorbate. This is quite obvious, because large molecules cannot enter pores of a diameter smaller than their dimension, whereas smaller molecules can probe such parts of the adsorbent. Therefore, N_m increases with a decrease of ω in general. If the dependence between N_m and ω has the form of a power law, then the exponent can be interpreted in terms of fractal concepts and the adsorbent may be a surface fractal.

The molecule cross-sectional area

Emmett and Brunauer proposed that ω should be calculated from the density of the adsorbate in the ordinary liquid (or solid) phase. This leads to the formula:

$$\omega = f(M/\rho L)^{2/3} \times 10^{16}, \quad (6)$$

where f is the packing factor and ρ is the mass density of the bulk liquid. With the hexagonal close packing of bulk liquid phase the value of f is 1.091 and if ρ is expressed in kilograms per cubic meter, ω is expressed

in square nanometers. For nitrogen as adsorbate at -195°C $\omega = 0.162 \text{ nm}^2$.

The adsorption of water vapor is a complex process in such sense that it is highly specific and thus it may appear that the application of the BET equation to water vapor isotherms in many cases will have no real validity. Early works indicated that the value of the molecule cross-sectional area is 0.106 nm^2 . McClellan and Harnsberg (1967) given cross section surface areas of different molecules adsorbed on solid surfaces.

Adsorption from solution

The adsorption of dissolved molecules from solution can also be used to estimate the specific surface area of solid. Usually, the adsorption isotherms obtained are classified as the type I in the BET classification scheme and therefore the Langmuir model can be used. Several organic molecules have been used to determine specific surface area from Langmuir equation. Those are: organic dyes (methylene blue, crystal violet), cationic surfactants (cetylpyridinium bromide, CPB) or other compounds, e.g., carbon tetrachloride, ortho-phenanthroline, and so on.

Retention of polar liquids

Retention data of EG (ethylene glycol) and EGME (ethylene glycol monoethyl ether) can be used to estimate the total (i.e., internal and external) surface area of expandable clay minerals and soil organic matter because EG and EGME molecules are able to penetrate the interlayer space of clay minerals. This method also has been applied to natural soil. However, the use of the retention method is complicated because the polar EG/EGME molecules exhibit a tendency to form multilayers around exchangeable cations and, additionally, they undergo partition into soil organic matter.

Other methods

More recently, new methods for soil-specific surface area determination have been proposed. These methods are based, among others, on the measurements of adsorption of polyvinyl alcohol from aqueous suspension (Pagel-Wieder and Fischer, 2001), investigations of the soil-moisture potential (Filgueira et al., 2006), evaluation of hygroscopic water content (Moiseev, 2008), and determination of fractal dimension of particle-size distribution (Ersahin et al., 2006).

Specific surface area of mineral and organic solid (soils and plants)

Specific surface area can be related to various chemical and physical properties of soils (Zawadzki et al., 1971; Gliński et al., 1988; Wilczyński et al., 1993; Petersen et al., 1996; Theng et al., 1999; Stawiński et al., 2000; Ferreiro et al., 2002; Sokołowska, 2004; Pennell, 2005; Dolinar et al., 2007; Sivapullaiah et al., 2008).

The relationships between the specific surface area and some physical and chemical properties of mineral soils are presented in [Table 1](#) (modified from Sokołowska, 2004).

Dobrzański et al. (1977) found for 724 Polish mineral soil samples a wide range of the specific surface areas from a few to several hundreds $\text{m}^2 \text{ g}^{-1}$. The relationships between the specific surface area and the content of soil fractions <0.02 (a), <0.002 mm (b), and the organic matter content (c) for these soils were expressed by:

$$R = x_1a + x_2b + x_3c + w, \quad (7)$$

where x_1 , x_2 and x_3 are the multiple regression coefficients for the values a , b and c and w is a constant.

In particular, for mineral soils there exist a linear relationship between specific surface area and the content of the granulometric fractions. For the clay fraction the correlation coefficient is very high (cf. [Table 1](#) and [Figure 1](#)). Similarly, for several soils, the specific surface area is strongly correlated with the cation exchange capacity and the correlation coefficient is again very high for several soils (see [Table 1](#) and [Figure 2](#)). There also exist exceptions – poor correlations between those quantities were reported (Martel et al., 1979) for very organic-rich soils.

Soil organic matter is one of the import factors determining surface properties of soils and can also change the value of the specific surface area. However, the effect of the soil organic matter on the specific surface area is not unequivocal in general (Sokołowska et al., 2009). No correlation between the content of organic matter and surface area were found (Feller et al., 1992; Sokołowska et al., 2001; Sokołowska et al., 2002). The removal of organic matter from soils may either lead to a decrease of the

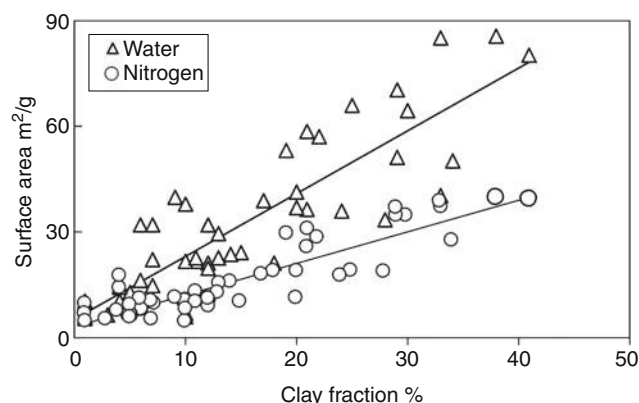
Specific Surface Area of Soils and Plants, Table 1 Correlation coefficients of linear regression between the specific surface area (S) obtained from water vapor and nitrogen adsorption data and selected properties of soils (data for 482 Polish mineral soil samples)

Sorbant	Soil fraction (%)		
	<0.02 mm	<0.002 mm	CEC ($\text{cmol} \cdot \text{kg}^{-1}$)
Soils formed from loess			
$S(\text{N}_2)$	0.519	0.705	0.589
$S(\text{H}_2\text{O})$	0.701	0.976	0.936
Soils formed from clay			
$S(\text{N}_2)$	0.720	0.656	0.542
$S(\text{H}_2\text{O})$	0.627	0.832	0.579
Soils formed from silt			
$S(\text{N}_2)$	0.547	0.679	0.673
$S(\text{H}_2\text{O})$	0.696	0.875	0.535
Soils formed from loam			
$S(\text{N}_2)$	0.805	0.792	0.666
$S(\text{H}_2\text{O})$	0.936	0.902	0.667
Soils formed from sand			
$S(\text{N}_2)$	0.561	0.641	0.425
$S(\text{H}_2\text{O})$	0.589	0.770	0.700

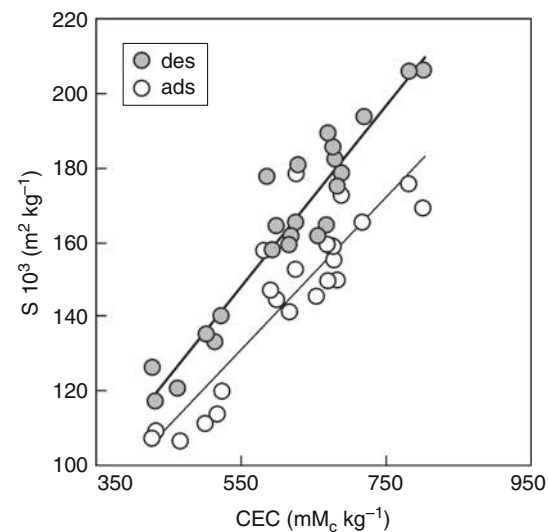
CEC cation exchange capacity

surface area (Sequi and Aringheri, 1977; Pachepsky et al., 1995) or to its increase (Sokołowska et al., 1993) (see [Figure 3](#)).

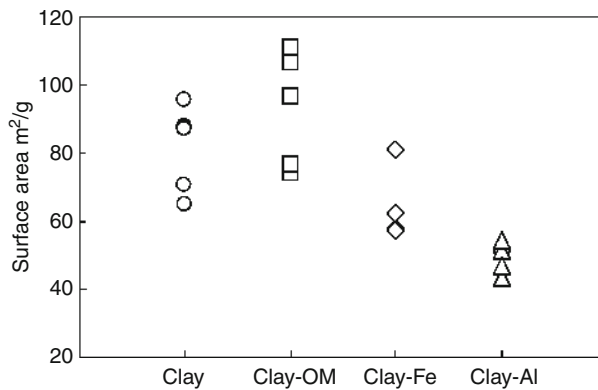
The numerical value of the surface area found for a given soil depends on which experimental method has been used. There are two principal reasons for this very important characteristic. First, the properties of the solid surfaces in soils can often be altered during preparation of the sample for a surface measurement. Second, if a surface reaction is involved in the measurement of the specific surface area, the data obtained reflect only characteristics of the surface functional groups that participate in the reaction, and provide information only about the solid



Specific Surface Area of Soils and Plants, Figure 1 Specific surface area obtained from water vapor and nitrogen sorption data vs. content of the clay fraction.



Specific Surface Area of Soils and Plants, Figure 2 The correlation between the specific surface area (S) obtained from adsorption and desorption data, and the cation exchange capacity (CEC) for vertisol (data taken from Sokołowska et al., 2004a).



Specific Surface Area of Soils and Plants, Figure 3 Specific surface area of clay fractions before and after removal of organic matter, iron, and aluminum.

surfaces that were reactive under the condition of the measurement (Figure 3) (Purin and Murari, 1963; Everett and Ottewill, 1970; Newman, 1983; Churchman et al., 1991; Ferreiro et al., 2002). Frequently the nitrogen surface area has been interpreted as the “external” surface, and the water surface area as the “total” one. In most cases, the total surface area exceeding the external one is measured. For soil minerals the water surface area is higher than the nitrogen surface area: for bentonite and zeolite about 10 times, for vermiculite more than 25 times, whereas for the other minerals around 2–3 times.

For an ideal adsorption, the adsorption and desorption isotherms should coincide (provided no phase transformations, e.g., a two-dimensional condensation within a monolayer, occur in the system). However, in the case of many experimentally measured isotherms one observes that the desorption branch deviates within some range of pressures from the adsorption one. When adsorption and desorption data are plotted together, then the upper curve corresponds to desorption, while the lower branch indicates adsorption. This behavior is called adsorption hysteresis. Adsorption hysteresis is very common. Generally, hysteresis loop is connected with porosity and their shape is determined by the character of adsorbent and adsorbate and by the interactions between them (Gregg and Sing, 1978; Oćik, 1982; Sing, 1982). Generally, the values of the specific surface area obtained from adsorption and desorption data are different (Figure 2) (Sokołowska, 2004).

The term adsorption presently used in the physical chemistry for mineral adsorbents and soils, is not adequate for organic soils, because the accumulation of gaseous molecules occurs not only at surfaces, but they can also enter the interior of organic phase, i.e., they can undergo absorption. In such cases the term *sorption* is more appropriate. The term *sorption* embraces both types of phenomena, adsorption and absorption.

The BET surface areas of the organic soils and other organic materials, evaluated by using polar substances,

usually locate in high ranges of surface areas of mineral soils (Mayer and Xing, 2001; Józefaciuk and Szatanik-Kloc, 2003; Sokołowska et al., 2004b, 2008; Szatanik-Kloc et al., 2009). Polar compounds (like EG) can partition into soil organic matter and this should hamper their use for measuring reliable value of specific surface area (Pennell et al., 1995). For the surface area determined by the EG method, the term “apparent surface area” was proposed, while the surface area determined by N₂-BET method was called “the free surface area” (Chiou et al., 1990). The last term corresponds to the interfacial area of a solid, which exist before the adsorption and can be unequivocally measured by an adsorbate that does not change the structure of the solid.

Conclusion

Two factors, surface area and porosity are recognized to play complementary part in adsorption phenomena for a vast range of solids. Specific surface area is an important feature of soil. It characterizes both quantity and quality of mineral and organic components and also their physical and physicochemical properties. These properties treated separately do not give such exact information about the state of the soil as specific surface area. The idea of estimate of the surface area is to find the number of adsorbate molecules that cover the adsorbing surface as a monolayer, and multiply this number by the area occupied by a single molecule. The specific surface area is usually determined by adsorption methods. Therefore, methods are needed for the rapid determination of the specific surface area, especially in routine analysis. Regression relationships (pedotransfer function) were developed for the approximate estimation of the specific soil surface area.

Bibliography

- Chiou, C. T., and Rutherford, D. W., 1993. Sorption of N₂ and EGME vapors on some soils, clays, and mineral oxides and determination of sample surface areas by use of sorption data. *Environmental Science & Technology*, **27**, 1587–1594.
- Chiou, C. T., Lee, J.-F., and Boyd, S. A., 1990. The surface area of soil organic matter. *Environmental Science & Technology*, **24**, 1164–1166.
- Churchman, G. J., Burke, C. M., and Parfitt, R. L., 1991. Comparison on various methods for the determination of specific surfaces of subsoils. *Journal of Soil Science*, **42**, 449–461.
- Dobrzański, B., Dechnik, I., Gliński, J., Podel, H., and Stawiński, J., 1977. Surface area of Polish soils (in Polish). *Roczniki Nauk Rolniczych*, D-165.
- Dolinar, B., Mišić, M., and Trauner, L., 2007. Correlation between surface area and Atterberg limits of fine-grained soils. *Clays and Clay Minerals*, **55**, 519–523.
- Ersahin, S., Gunal, H., Kutlu, T., Yetgin, B., and Coban, S., 2006. Estimating specific surface area and cation exchange capacity in soils using fractal dimension of particle size distribution. *Geoderma*, **136**, 588–597.
- Everett, D. H., and Ottewill, R. H., 1970. Surface area determination. In *Proceedings of the International Symposium on Surface Area Determination*, July 16–18, 1969, University of Bristol; London, Butterworths.

- Feller, C., Schouller, E., Thomas, F., Rouiller, J., and Herbillon, A. J., 1992. N₂-BET specific surface areas of some low activity clay soils and their relationships with secondary constituents and organic matter contents. *Soil Science*, **153**, 293–299.
- Ferreiro, E. A., de Bussetti, S. G., and Helmy, A. K., 2002. Determination of surface area of soil by adsorption methods. *European Journal of Soil Science*, **53**, 475–480.
- Filgueira, R. R., Ruiz, H. A., Schaefer, C. E. G. R., and Sarli, G. O., 2006. Specific surface of Oxisols determined by soil-moisture potential. In *18th World Congress of Soil Science*, July 9–15, 2006, Philadelphia, Pennsylvania.
- Gliński, J., Borowiec, J., and Stawiński, J., 1988. The specific surface area of eroded soils formed from loess. *Polish Journal of Soil Science*, **21**, 15–22.
- Gregg, S. J., and Sing, K. S. W., 1978. *Adsorption, Surface Area and Porosity*. London: Academic.
- Józefaciuk, G., and Szatanik-Kloc, A., 2003. Changes in specific area and energy of root surface of cereal plants in Al-solution cultures. Water vapor adsorption studies. *Plant and Soil*, **250**, 129–140.
- Martel, Y. A., de Kimpe, C. R., and Lverdier, M. R., 1979. Cation-exchange capacity of clay-rich soils in relation to organic matter, mineral composition and surface area. *Soil Science Society of America Journal*, **42**, 764–767.
- Mayer, L. M., and Xing, B., 2001. Organic matter-surface area relationships in acid soils. *Soil Science Society of America Journal*, **65**, 250–258.
- McClellan, A. L., and Harnsberg, H., 1967. Cross sectional areas of molecules adsorbed on solid surfaces. *Journal of Colloid and Interface Science*, **23**, 577–599.
- Moiseev, K. G., 2008. Determination of the specific soil surface area from the hygroscopic water content. *Eurasian Soil Science*, **41**, 744–749.
- Newman, A. C. D., 1983. The specific surface of soils determined by water sorption. *Soil Science*, **34**, 23–32.
- Oćisk, J., 1982. *Adsorption*. Chichester: PWS Ellis Horwood.
- Pachepsky, Ya A., Polubesowa, T. A., Hajnos, M., Jozefaciuk, G., and Sokołowska, Z., 1995. Parameters of surface heterogeneity from laboratory experiments on soil degradation. *Soil Science Society of America Journal*, **59**, 410–417.
- Pagel-Wieder, S., and Fischer, W. R., 2001. Estimation of the surface area of soil particles by adsorption of polyvinylalcohol in aqueous suspension. *Journal of Plant Nutrition and Soil Science*, **164**, 441–443.
- Pennell, K. D., 2005. Specific surface area. In Hillel, D. (ed-in-chief). *Encyclopedia of Soils in the Environment*. Elsevier, Oxford, pp 13–19.
- Pennell, K. D., Boyd, S. A., and Abriola, L. M., 1995. Surface area of soil organic matter reexamined. *Soil Science Society of America Journal*, **59**, 1012–1018.
- Petersen, L. W., Moldrup, P., Jacobsen, O. H., and Rolston, D. E., 1996. Relation between specific surface area and soil physical and chemical properties. *Soil Science*, **161**, 9–21.
- Purin, B. R., and Murari, K., 1963. Studies in surface area measurements of soils I. Comparison of different methods. *Soil Science*, **96**, 331–336.
- Schofield, R. K., 1947. Calculation of surface area from measurements of negative adsorption. *Nature*, **160**, 408–410.
- Sequi, P., and Aringhieri, R., 1977. Destruction of organic matter by hydrogen peroxide in presence of pyrophosphate and its effect on soil specific surface area. *Soil Science Society of America Journal*, **41**, 340–342.
- Sing, K. S. W., 1982. Reporting physisorption data for gas/solid systems, with special reference to determination of surface area and porosity. *Pure and Applied Chemistry*, **54**, 2201–2218.
- Sivapullaiah, P. V., Gurit, P. B., and Allam, M. M., 2008. Methylene blue surface area method to correlate with specific surface soil properties. *Geotechnical Testing Journal*, **31**, 503–512.
- Sokołowska, Z., 2004. Adsorption and surface area of agricultural materials. In Matyka-Sarzyńska, D., and Walczak, R. T. (eds.), *Basic Problems of Agrophysics*. Lublin: Institute of Agrophysics PAS, pp. 117–124.
- Sokołowska, Z., Józefaciuk, G., Sokołowski, S., and Ourumova-Pesheva, A., 1993. Adsorption of water vapour by soils: investigations of the influence of organic matter, iron, and aluminum on energetic heterogeneity of soil clays. *Clays and Clay Minerals*, **41**, 346–352.
- Sokołowska, Z., Hajnos, M., Hoffman, C., Renger, M., and Sokołowski, S., 2001. Comparison of fractal dimensions of soils estimated from adsorption isotherms, Mercury intrusion, and particle size distribution. *Journal of Plant Nutrition and Soil Science*, **164**, 591–599.
- Sokołowska, Z., Borówko, M., Reszko-Zygmont, J., and Sokołowski, S., 2002. Adsorption of nitro gen and water vapor by alluvial soils. *Geoderma*, **107**, 33–54.
- Sokołowska, Z., Hajnos, M., Elias, E. A., and Alaily, F., 2004a. Characteristics of the surface area of vertisols from the Gezira region in Sudan. *International Agrophysics*, **18**, 83–90.
- Sokołowska, Z., Matyka-Sarzyńska, D., and Bowanko, G., 2004b. Specific surface area of Lublin Polesie mucks determined from water vapour and nitrogen adsorption data. *International Agrophysics*, **18**, 363–368.
- Sokołowska, Z., Jamroz, J., and Bańska, P., 2008. Apparent surface area of selected meal extrudates. *International Agrophysics*, **22**, 75–80.
- Sokołowska, Z., Warchulska, P., and Sokołowski, S., 2009. Trends in soil fractal parameters caused by accumulation of soil organic matter as resulting from the water vapor adsorption isotherms. *Ecological Complexity*, **6**, 254–262.
- Stawiński, J., Gliński, J., Ostrowski, J., Stepniewska, Z., Sokołowska, Z., Bowanko, G., Józefaciuk, G., Książkowska, A., and Matyka-Sarzyńska, D., 2000. Spatial characterization of specific surface area of arable soils in Poland. *Acta Agrophysica*, **33**, 1–52.
- Szatanik-Kloc, A., Boguta, P., and Bowanko, G., 2009. Effect of aluminum ions on free surface area and energetic characteristics of barley and clover roots. *International Agrophysics*, **23**, 383–389.
- Theng, B. K. G., Rostori, G. G., Santi, C. A., and Percival, H. J., 1999. An improved method for determining the specific surface areas of topsols with varied organic matter, texture and clay mineral composition. *European Journal of Soil Science*, **50**, 309–316.
- Tiller, K. G., and Smith, L. H., 1990. Limitations of EGME retention to estimate the surface area of soils. *Australian Journal of Soil Research*, **28**, 1–26.
- Wilczyński, A. W., Renger, M., Józefaciuk, G., Hajnos, M., and Sokołowska, Z., 1993. Surface area and CEC as related to qualitative and quantitative changes of forest organic matter after liming. *Zeitschrift für Pflanzenernährung und Bodenkunde*, **156**, 235–238.
- Zawadzki, S., Michałowska, K., and Stawiński, J., 1971. The application of surface area measurements of soils for determination of the content of water unavailable for plants. *Polish Journal of Soil Science*, **IV**, 89–92.

Cross-references

- [Adsorption Energy and Surface Heterogeneity in Soils](#)
- [Adsorption Energy of Water on Biological Materials](#)
- [Agophysical Objects \(Soils, Plants, Agricultural Products, and Foods\)](#)
- [Clay Minerals and Organo-Mineral Associates](#)
- [Fractal Analysis in Agrophysics](#)
- [Organic Matter, Effects on Soil Physical Properties and Processes](#)
- [Soil Texture: Measurement Methods](#)

STABLE ISOTOPES IN EVALUATION OF GREENHOUSE GAS EMISSIONS*

Kurt A. Spokas
United States Department of Agriculture, Agricultural Research Service, St. Paul, MN, USA

Definitions

Isotopes. Atoms of the same element with differing number of neutrons, but with the same number of protons.

Stable isotopes. A particular grouping of isotopes that do not undergo radioactive decay (thereby are stable).

Introduction

Isotopes offer a unique opportunity to have natural tracers present in the ecosystem to track produced greenhouse gasses (GHG; [Climate Change: Environmental Effects](#)) through multiple scales. Isotopes are atoms of the same element with differing number of neutrons, but with the same number of protons. For example, carbon-12 (^{12}C) and carbon-13 (^{13}C) are two naturally occurring isotopes of carbon, both have six protons, except ^{12}C has six neutrons and ^{13}C has seven neutrons. This differing number of neutrons leads to differences in the atomic masses of the elements. There are two basic types of isotopes, which are grouped by their stability. The first group of isotopes that do not decay are referred to as stable isotopes and those that do decay are called radioactive isotopes. Radioactive isotopes undergo radioactive decay by which the unstable atom loses energy (emitting radiation/ionizing particles). Radioactive isotopes are mainly used for energy production (Ferguson, [2007](#)) as well as geological dating of materials (Arnold and Libby, [1949](#)). These radioactive isotopes can also be used in the evaluation of greenhouse gas emissions, particularly in mechanistic studies (e.g., Turnbull et al., [2006](#)). However, the main focus here is on the stable isotopes.

Isotopic compositions at or near natural abundance levels are reported in delta notation (δ), a value which is in parts per 1,000 or per million ("‰"). Delta values are not absolute isotope measurements but rather differences between sample readings and a reference material ([Table 1](#)).

These reference materials are considered to have a delta value of zero ($\delta = 0\text{‰}$). Absolute isotope ratios (R) are measured for both the sample and reference standard, and then delta is calculated by the following equation:

$$\delta X \text{ per mil versus standard} = \left(\frac{R_{\text{sample}} - R_{\text{std}}}{R_{\text{std}}} \right) \times [1,000 \text{ ‰}],$$

where X is the particular element and R is the ratio of the atomic percentages of the heavier isotope to the lighter isotope, e.g., for nitrogen this would be

$$R = \left(\frac{\text{Atomic \% } ^{15}\text{N}}{\text{Atomic \% } ^{14}\text{N}} \right)$$

The major benefit to stable isotopes as opposed to radioactive isotopes is that stable isotopes do not decay. Since stable isotopes do not decay, their abundance is not a function of time, which improves the use of the stable isotopes as tracers of GHG emissions. For many biological (microbial reactions, enzyme reactions, plant respiration, etc.) and abiotic processes (diffusion, photolysis, solution equilibrium, phase transitions, etc.), there are differences in the reaction rates for different isotopes (Galimov, [1985](#)). These differences in reaction rates lead to differences in the distribution of the isotopes in the end products compared to the starting material, which is referred to as fractionation (Hayes, [1982](#)). However, this fractionation can be a function of several variables (e.g., microbial species, temperature, substrate availability) and presents a potential source of error in isotopic interpretations (e.g., Morris et al., [2005](#)). Recent observations have also revealed the potential for water vapor flux fractionation in addition to thermal and gravitational fractionation in soil gas transport (Severinghaus et al., [1996](#)).

Different sources of trace gasses often show characteristic variations in their isotopic signatures, which allow one to distinguish the sources of the GHG. However, atmospheric sink reactions cause kinetic isotope fractionations which contribute to the naturally occurring variations of isotopic composition and need to be accounted for in global estimates (Kohen and Limbach, [2005](#)). There are approximately 250 known stable isotopes (Lajtha and Michener, [1994](#)). However, for GHG emission research, the focus is predominately on isotopes of carbon, nitrogen, hydrogen, oxygen, and sulfur ([Table 1](#)). In general, lighter isotopes react faster than heavier isotopes (Kohen and Limbach, [2005](#)), although exceptions exist such as gravitational fractionation where the heavier isotope is preferentially settled by gravity (Gibbs, [1970](#)). This small difference in reaction rates (fractionation) between isotopes leads to differences in the isotopic signature of the products as compared to the reactants. Provided the amount of fractionation is known along with the reactant and product isotopic distribution, the relative contribution of different processes can be calculated from the changes in the isotopic distribution.

The use of stable isotopes for mechanistic studies falls into two different categories. The first are those that utilize the natural abundance distribution ([Table 1](#)) to track processes, which is referred to as natural abundance isotope techniques. On the other hand, there are methods that add amounts of the rarer isotope (typically the heavier isotope) to the system under investigation to track the flow of the element through the system, which is referred to as isotope tracer techniques.

Stable Isotopes in Evaluation of Greenhouse Gas Emissions, Table 1 Abundances of stable isotopes of the major elements for greenhouse gas studies. (Data taken from Rundel et al. (1989).) Incidentally, all original supplies of both SMOW and PDB have been used up and replaced by secondary standards (U.S. National Bureau of Standards and International Atomic Energy Agency)

Element	Isotope	Abundance (%)	Reference material
Hydrogen	¹ H	99.985	Standard mean ocean water (SMOW)
	² H	0.015	
Carbon	¹² C	98.890	Peedee Belemnite (PDB)
	¹³ C	1.110	(Belemnitella Americana—Peedee formation of South Carolina, USA)
Nitrogen	¹⁴ N	99.63	Atmospheric air
	¹⁵ N	0.37	
Oxygen	¹⁶ O	99.759	SMOW or PDB
	¹⁷ O	0.037	
Sulfur	¹⁸ O	0.204	
	³² S	95.00	Canyon Diablo meteorite
	³³ S	0.76	
	³⁴ S	4.22	
	³⁶ S	0.014	

Background

Presented is a very brief history of isotopic studies; for further background on isotopes the reader is encouraged to consult Clark and Fritz (1997), Kendall and Caldwell (1998), and Kohen and Limbach (2005). As summarized recently by Kaiser (2002), isotopes have a fairly recent history. The initial research on stable isotopes was first conducted about 50 years ago (nitrogen metabolism using ¹⁵N [Dugdale et al., 1959]). The first measurements of the ¹⁵N content of atmospheric nitrous oxide (N_2O) were carried out in the early 1970s (Moore, 1974) and it was observed that stratospheric N_2O was enriched in ¹⁵N relative to troposphere N_2O , an observation that is still confirmed today (Yoshida and Matsuo, 1983; Crutzen, 2001). These large-scale measurements were soon followed by mechanistic studies utilizing isotopes for N mineral cycling (e.g., Dugdale et al., 1959; Garber and Hollocher, 1982). For C, the initial stable isotope work utilizing ¹³C was not conducted until the late 1970s (e.g., Slawyk et al., 1977), partly due to the previous focus on the radioactive ¹⁴C isotope (Kamen, 1963). The major contribution of this early research was confirmation that GHG (particularly N_2O , methane [CH_4] and carbon dioxide [CO_2]) produced from different processes have differing isotopic compositions. These differences are the foundation for the use of isotopes as tracers and results in isotopic analyses being pivotal to numerous research areas. Since we can quantify the differences in these stable isotopes, they have an immense utility to act as tracers for various biogeochemical applications to study both small as well as large global source–sink relationships (Rundel et al., 1989).

The use of stable isotopes in research has paralleled instrumentation improvements. Within the last 10 years,

new analytical techniques for determining intra-molecular ¹⁵N-site preference in the asymmetric N_2O molecule have been created (Toyoda and Yoshida, 1999), which has contributed to substantial new insights into fundamental nitrogen cycling quantification (Mariotti et al., 1981; Baggs, 2008). Intra-molecular preferences have been made possible by instrumentation improvements such as the first dual-isotope measurements (¹⁵N and ¹⁸O) (Wahlen and Yoshinari, 1985; Kim and Craig, 1990; Kim and Craig, 1993; Röckmann et al., 2001). Isotopic measurements typically have required expensive and dedicated stable isotope mass spectrometer systems in order to quantify the isotopic compositions. Recent instrumentation advances have eliminated this requirement with the use of tunable diode and quantum cascade lasers in the early 2000s (Petrov et al., 1998; Kosterev et al., 1999). These lasers can be located in the laboratory or field setting. These advancements have allowed coupling of isotopic data along with eddy covariance data to allow real-time calculation of various isotope fluxes across diverse ecosystems (e.g., Bowling et al., 2003; Schaeffer et al., 2008). Furthermore, these new analytical techniques allow isotopic ratios to be monitored in real-time and without the periodic sampling (in gas flasks or other containers) that was the high-labor burden of initial work with isotope research.

When we refer to isotopes in the evaluation of greenhouse gas emissions, there are two different scales of processes. The first is large-scale emissions (global) and the other is mechanistic determination of soil microbial processes (small scale). These two approaches will be discussed separately. However, these processes are not separate since the mechanistic studies feed into the global-scale studies.

Global-scale studies

As first noted back in the 1970s, isotope measurements provide a means to constrain the global budgets of GHG since different sources typically have different isotopic signatures. Isotopes initially were utilized in global circulation models in the 1980s focusing on the isotopes of water with very coarse spatial resolution (Joussaume et al., 1984; Grew et al., 1987; [Stable Isotopes, Their Use in Soil Hydrology](#)). However, more recently isotopes have been utilized in global top-down modeling approaches to constrain the global GHG budgets, since isotope measurements provide additional data to constrain these budgets. A couple of examples of this are given below.

Isotopic signatures of atmospheric CH_4 ($\delta^{13}\text{C}$) were recently used to more accurately constrain the contribution of atmospheric CH_4 from vegetation. Back in 2006, Keppler et al. (2006) presented results of a combination laboratory and bottom-up modeling that feasibly showed terrestrial vegetation as a yet unknown major contributor to global CH_4 budgets. From this research, they estimated that this discovered source from terrestrial plants would result in 62–236 Tg CH_4 year⁻¹ contribution to the global CH_4 budget (10–40% of total global CH_4 sources).

However, Ferretti et al. (2007) utilized $\delta^{13}\text{C}$ data to illustrate through a top-down modeling approach that this source of CH_4 was significantly lower than Keppler et al.'s (2006) estimates. From the isotopic data, both from atmospheric sampling and ice core data, they restricted this source down in the range of 0–42 Tg $\text{CH}_4 \text{ year}^{-1}$. Still the CH_4 from terrestrial plants is a source, but not to the degree that was suggested by the upscale modeling (bottom-up) of Keppler et al. (2006).

The isotopic signatures of N_2O have advanced the understanding of the contribution of various sources to the global N_2O budget (Baggs, 2008). However, major complications exist in the ability to differentiate a true isotopic signal due to the variety of production/consumption reactions that are possible in soils with the fractionation factor being dependent on the rate of N_2O reduction (Vieten et al., 2007). There is also uncertainty in the size of the global source for N_2O from oceans (Bange, 2006) as well as soils (Pérez et al., 2001; Conen and Neftel, 2007). Despite all the uncertainties, current estimates have established closure of the N_2O budget within an error of 10% (Houghton et al., 1994). Recent developments in the isotopologues of N_2O (or site preference for isotopic substitution) have provided new insights in potential differences between reaction pathways (Well et al., 2008). Röckmann et al. (2001) have utilized this new research data in the development of a refined model for the reconstruction of the global isotopic average N_2O source for present and preindustrial atmospheres.

Mechanism level research

Soil is a complex system. Recent advancements in DNA and RNA extractions from soils have improved our estimates on the diversity and abundance of microbes in the soil system. It has been estimated that up to 1,000,000 genomes exist per gram of soil (Chatzinotas et al., 1998; Gans et al., 2005). Putting this into a more tangible analogy, there are more than 10^{16} microbes in a ton of soil compared to a mere 10^{11} stars in our total galaxy (Curtis and Sloan, 2005). This makes it clear, that the soil is a very diverse and complicated system. Given these vast populations, a daunting task is to assess soil microbial processes. Further complicating matters, fewer than 1% of soil microorganisms can be cultured in the laboratory (Torsvik et al., 1990), leading to significant gaps in the fundamental understanding of microbial mechanisms and assessments of microbial functionality in the soil. However, soil microbial communities are instrumental in the emissions of GHG from the soils (Conrad, 1996; [Greenhouse Gases Sink in Soils](#)). A useful tool for the tracking and detection of microbial functionality is the use of stable isotopes in the assessment of microbial processes.

One particular application of stable C isotopes is in the determination of the percent of CH_4 being oxidized as the gas migrates through the cover soils at a landfill site. Stable carbon isotopic methods, which rely on the difference between the $\delta^{13}\text{C}$ of emitted CH_4 compared to the $\delta^{13}\text{C}$ of

un-oxidized CH_4 in the anaerobic zone (landfill), provide an estimate of the fractional CH_4 oxidation. In other words, the percentage of CH_4 that is oxidized during transport through the landfill cover soil materials. Isotopic methods have been developed over the last decade and rely on the preference of methanotrophs for the isotope of smaller mass (^{12}C rather than ^{13}C) (Liptay et al., 1998; Chanton and Liptay, 2000). In general, $\delta^{13}\text{C}$ values for un-oxidized CH_4 in the anaerobic zone are from about –57 to –60. However, when the CH_4 undergoes oxidation, these values undergo a positive shift to –35 or more, due to the microbial preference for the lighter isotope. This methodology has been pivotal in the improved estimation of the percent oxidation within landfill covers (Chanton et al., 2009). Additional improvements in the methodology are underway with the combined use of $\delta^{13}\text{C}$ and $\delta^2\text{H}$ methods since the hydrogen isotope has a larger relative fractionation factor in microbial processes (e.g., Hackley et al., 1996). This is analogous to the use of ^{18}O in the N_2O studies mentioned above and should provide additional insights into the active microbial mechanisms.

The most vital development in recent years in N_2O has been the research on isotopologues and ^{15}N site preference for the elucidation of major microbial pathways of N_2O production/consumption in soils (Baggs, 2008). N_2O is produced by a series of biogeochemical reactions. The most important are nitrification and denitrification (Firestone and Davidson, 1989). Since these processes are linked and use the same substrates, it is difficult to separate the contribution of each. Initially, it was assumed that a high $\delta^{15}\text{N}$ indicated a denitrification dominated system and a lower delta value indicated that nitrification dominated (Boontanon et al., 2000). However, this approach is problematic due to the wide isotopic variations (^{15}N) in the precursors of N_2O (nitrate or ammonia), which directly affects the distribution in N_2O (Pérez et al., 2000). Recent advantages in the dual-isotope methodology and site preference measurements have aided our understanding (e.g., Johnston et al., 1995). Pérez et al. (2006) have observed different site preferences in resulting N_2O for nitrifying versus denitrifying bacteria in incubations of Amazon forest soils. Sutka et al. (2006) utilized site preference differences to demonstrate the existence of two different nitrifying enzymatic pathways for N_2O production as well as the ability to detect denitrification. Baggs (2008) presents a good review on the current state of stable isotope research with N_2O . Site preference will be a useful tool in separating the microbial influences on N_2O production/consumption and potentially aid to the determination of the overall N_2O source strength of soils. The advantage to site preference is the lack of isotopic fractionation effects (Sutka et al., 2006) that has complicated the straight stable isotope approaches (Pérez et al., 2000). However, additional research is needed to fully evaluate these initial observations and results to be fed into the global-scale modeling effort to ascertain the contributions of the various sources.

Conclusions

The use of stable isotopes in tracking environmental processes is a very powerful tool across multiple disciplines, particularly in the quantification and tracking of GHG emissions. Some of the most important advancements in environmental research have utilized stable isotopic data. This overview provided a brief introduction, but by no means an exhaustive description, particularly in light of the growth of the research in this field. Stable isotopes offer a unique means of assessing GHG emissions from a variety of sources. However, as recent research has demonstrated, the complexity of the soil system and the number of simultaneous processes occurring limit the straightforward application of stable isotopes (e.g., Hayatsu et al., 2008), and the newer methods of dual-isotope and position specific isotope preference appear to be the future key into unlocking some the complexity of the natural system. With these new-found keys, we are gaining an increased knowledge of the global GHG cycles. This knowledge is vital not only for determining global GHG sources and sinks, but also for the potential mitigation of GHG emissions, particularly from soils. In other words, once we know the dominant processes we can alter management decisions to minimize sources.

Bibliography

- Arnold, J. R., and Libby, W. F., 1949. Age determinations by radio-carbon content: checks with samples of known age. *Science*, **110**, 678–680.
- Baggs, E. M., 2008. A review of stable isotope techniques for N₂O source partitioning in soils: recent progress, remaining challenges and future considerations. *Rapid Communication in Mass Spectrometry*, **11**, 1664–1672.
- Bange, H. W., 2006. New directions: the importance of oceanic nitrous oxide emissions. *Atmospheric Environment*, **40**, 198–199.
- Boontanon, N., Ueda, S., Kanatharana, P., and Wada, E., 2000. Intramolecular stable isotope ratios of N₂O in the tropical swamp forest in Thailand. *Die Naturwissenschaften*, **87**, 188–192.
- Bowling, D. R., Sargent, S. D., Tanner, B. D., and Ehleringer, J. R., 2003. Tunable diode laser absorption spectroscopy for stable isotope studies of ecosystem-atmosphere CO₂ exchange. *Agricultural and Forest Meteorology*, **118**, 1–19.
- Chanton, J., and Liptay, K., 2000. Seasonal variation in methane oxidation in a landfill cover soil as determined by an in situ stable isotope technique. *Global Biogeochemical Cycles*, **14**, 51–60.
- Chanton, J. P., Powelson, D. K., and Green, R. B., 2009. Methane oxidation in landfill cover soils, is a 10% default value reasonable? *Journal of Environmental Quality*, **38**, 654–663.
- Chatzinotas, A., Sanda, R. A., Schonhuber, W., Amann, R., Daae, F. L., Torsvik, V., Zeyer, J., and Hahn, D., 1998. Analysis of broad-scale differences in microbial community composition of two pristine forest soils. *Systematic and Applied Microbiology*, **21**, 579–587.
- Clark, I. D., and Fritz, P., 1997. *Environmental Isotopes in Hydrogeology*. Boca Raton: Taylor and Francis, LLC.
- Conen, F., and Neftel, A., 2007. Do increasingly depleted δ¹⁵N values of atmospheric N₂O indicate a decline in soil N₂O reduction? *Biogeochemistry*, **82**, 321–326.
- Conrad, R., 1996. Soil microorganisms as controllers of atmospheric trace gases (H₂, CO, CH₄, OCS, N₂O, and NO). *Microbiological Reviews*, **60**(4), 609–640.
- Crutzen, P. J., 2001. Isotopic enrichment of nitrous oxide (¹⁵N¹⁴NO, ¹⁴N¹⁵NO, ¹⁴N¹⁴N¹⁸O) in the stratosphere and in the laboratory. *Journal of Geophysical Research*, **106**, 403–410.
- Curtis, T. P., and Sloan, W. T., 2005. Exploring microbial diversity – a vast below. *Science*, **309**, 1331–1332.
- Dugdale, R. C., Dugdale, V. A., Ness, J. C., and Goering, J. J., 1959. Nitrogen fixation in lakes. *Science*, **130**, 859–860.
- Ferguson, C. D., 2007. *Nuclear Energy: Balancing Benefits and Risks*. New York: Council on Foreign Relations.
- Ferretti, D. F., Miller, J. B., White, J. W. C., Lassey, K. R., Lowe, D. C., and Etheridge, D. M., 2007. Stable isotopes provide revised global limits of aerobic methane emissions from plants. *Atmospheric Chemistry and Physics*, **7**, 237–241.
- Firestone, M. K., and Davidson, E. A., 1989. Microbiological basis of NO and N₂O production and consumption in soil. In Andreae, M. O., and Schimel, D. S. (eds.), *Exchange of Trace Gases Between Terrestrial Ecosystems and the Atmosphere*. New York: Wiley, pp. 7–21.
- Galimov, E. M., 1985. *The Biological Fractionation of Isotopes*. New York: Academic.
- Gans, J., Wolinsky, M., and Dunbar, J., 2005. Computational improvements reveal great bacterial diversity and high metal toxicity in soil. *Science*, **309**, 1387–1390.
- Garber, E. A. E., and Hollocher, T. C., 1982. ¹⁵N, ¹⁸O tracer studies on the activation of nitrite by denitrifying bacteria. *The Journal of Biological Chemistry*, **257**, 8091–8097.
- Gibbs, J. W., 1970. *Collected Works, Vol. 1, Thermodynamics*. Cambridge: MIT Press.
- Grew, K. E., Jouzel, J., Russell, G. L., Suozzo, R. J., Koster, R. D., White, J. W. C., and Broecker, W. S., 1987. Simulations of the HDO and H₂¹⁸O atmospheric cycles using the NASA GISS General Circulation Model: The seasonal cycle for present-day conditions. *Journal of Geophysical Research*, **92**, 14739–14760.
- Hackley, K. C., Liu, C. L., and Coleman, D. D., 1996. Environmental isotope characteristics of landfill leachates and gases. *Ground Water*, **34**, 827–836.
- Hayatsu, M., Tago, K., and Saito, M., 2008. Various players in the nitrogen cycle: diversity and functions of the microorganisms involved in nitrification and denitrification. *Soil Science and Plant Nutrition*, **54**, 33–45.
- Hayes, J. M., 1982. Fractionation: an introduction to isotopic measurements and terminology. *Spectra (Finigan Corp)*, **8**, 3–8.
- Houghton, J. T., Meira Filho, L. G., Bruce, J., Lee, H., Callander, B. A., Hailes, E., Harris, N., and Maskell, K., 1994. *Climate Change 1994: Radiative Forcing of Climate Change and an Evaluation of the IPCC IS 92 Emission Scenarios*. Cambridge: Cambridge University Press.
- Johnston, J. C., Cliff, S., and Thiemens, M., 1995. Measurement of multioxygen isotopic (δ¹⁸O and δ¹⁷O) fractionation factors in the stratospheric sink reactions of nitrous oxide. *Journal of Geophysical Research*, **100**, 16801–16804.
- Joussaume, S., Sadourny, R., and Jouzel, J., 1984. A general circulation model of water isotope cycles in the atmosphere. *Nature*, **311**, 24–29.
- Kaiser, J., 2002. Stable isotope investigations of atmospheric nitrous oxide. PhD Dissertation. Mainz: Gutenberg University. <http://archimed.uni-mainz.de/pub/2003/0004/diss.pdf>.
- Kamen, M. D., 1963. Early history of Carbon-14: discovery of this supremely important tracer was expected in the physical sense but not in the chemical sense. *Science*, **140**, 584–590.
- Kendall, C., and Caldwell, E. A., 1998. Fundamentals of isotope geochemistry. In Kendall, C., and McDonnell, J. J. (eds.), *Isotope Tracers in Catchment Hydrology*. Amsterdam: Elsevier Science, pp. 51–86.

- Keppler, F., Hamilton, J. T. G., Brass, M., and Röckmann, T., 2006. Methane emissions from terrestrial plants under aerobic conditions. *Nature*, **439**, 187–191.
- Kim, K. R., and Craig, H., 1990. Two isotope characterization of N₂O in the Pacific Ocean and constraints on its origin in deep water. *Nature*, **347**, 58–61.
- Kim, K. R., and Craig, H., 1993. Nitrogen-15 and oxygen-18 characteristics of nitrous oxide: a global perspective. *Science*, **262**, 1855–1857.
- Kohen, A., and Limbach, H.-H., 2005. *Chemistry and Biology*. Boca Raton: Taylor and Francis Group, LLC.
- Kosterev, A. A., Curl, R. F., Tittel, F. K., Gmachl, C., Capasso, F., Sivco, D. L., Baillargeon, J. N., Hutchinson, A. L., and Cho, A. Y., 1999. Methane concentration and isotopic composition measurements with a mid-infrared quantum-cascade laser. *Optical Letters*, **24**, 1762–1764.
- Lajtha, K., and Michener, R. H., 1994. *Stable Isotopes in Ecology*. Oxford: Blackwell.
- Liptay, K., Chanton, J., Czepiel, P., and Mosher, B., 1998. Use of stable isotopes to determine methane oxidation in landfill cover soils. *Journal of Geophysical Research*, **103**, 8243–8250.
- Mariotti, A., Germon, J. C., Hubert, P., Kaiser, P., Letolle, R., Tardieu, A., and Tardieu, P., 1981. Experimental determination of nitrogen kinetic isotope fractionation: some principles; illustration for the denitrification and nitrification processes. *Plant and Soil*, **62**, 413–430.
- Moore, H., 1974. Isotopic measurement of atmospheric nitrogen compounds. *Tellus*, **XXVI**, 169–174.
- Morris, A. E. L., Stark, J. M., and Gilbert, B. K., 2005. Evaluation of isotopic fractionation error on calculations of marine-derived nitrogen in terrestrial ecosystems. *Canada Journal of Forestry Research*, **35**, 1604–1616.
- Pérez, T., Trumbore, S. E., Tyler, S. C., Davidson, E. A., Keller, M., and de Camargo, P. B., 2000. Isotopic variability of N₂O emissions from tropical forest soils. *Global Biogeochemical Cycles*, **14**, 525–535.
- Pérez, T., Trumbore, S. E., Tyler, S. C., Matson, P. A., Ortiz-Monasterio, I., Rahn, T., and Griffith, D. W. T., 2001. Identifying the agricultural imprint on the global N₂O budget using stable isotopes. *Journal of Geophysical Research*, **106**(D9), 9869–9878.
- Pérez, T., Garcia-Montiel, D., Trumbore, S., Tyler, S., De Camargo, P., Moreira, M., Piccolo, M., and Cerri, C., 2006. Nitrous oxide nitrification and denitrification ¹⁵N enrichment factors from Amazon forest soils. *Ecological Applications*, **16**, 2153–2167.
- Petrov, K. P., Curl, R. F., and Tittel, F., 1998. Compact laser difference-frequency spectrometer for multicomponent trace gas detection. *Applied Physics B*, **66**, 531–538.
- Röckmann, T., Kaiser, J., Brenninkmeijer, C. A. M., Crowley, J. N., Borchers, R., Brand, W. A., and Crutzen, P. J., 2001. Isotopic enrichment of nitrous oxide (¹⁵N¹⁴NO, ¹⁴N¹⁵NO, ¹⁴N¹⁴N¹⁸O) in the stratosphere and in the laboratory. *Journal of Geophysical Research*, **106**, 10403–10410.
- Rundel, P. W., Ehleringer, J. R., and Nagy, K. A., 1989. *Stable Isotopes in Ecological Research*. New York: Springer Verlag.
- Schaeffer, S. M., Miller, J. B., Vaughn, B. H., White, J. W. C., and Bowling, D. R., 2008. Long-term field performance of a tunable diode laser absorption spectrometer for analysis of carbon isotopes of CO₂ in forest air. *Atmospheric Chemistry and Physics Discussions*, **8**, 9531–9568.
- Severinghaus, J. P., Bender, M. L., Keeling, R. F., and Broecker, W. S., 1996. Fractionation of soil gases by diffusion of water vapor, gravitational settling and thermal diffusion. *Geochemistry et Cosmochimica Acta*, **60**, 1005–1018.
- Slawyk, G., Collos, Y., and Auclair, J. C., 1977. The use of the ¹³C and ¹⁵N isotopes for the simultaneous measurement of carbon and nitrogen turnover rates in marine phytoplankton. *Limnology and Oceanography*, **22**, 925–932.
- Sutka, R. L., Ostrom, N. E., Ostrom, P. H., Breznak, J. A., Gandhi, H., Pitt, A. J., and Li, F., 2006. Distinguishing nitrous oxide production from nitrification and denitrification on the basis of isotopomer abundances. *Applied and Environmental Microbiology*, **72**, 638–644.
- Torsvik, V., Goksoyr, J., and Daee, F. L., 1990. High diversity in DNA of soil bacteria. *Applied and Environmental Microbiology*, **56**, 782–787.
- Toyoda, S., and Yoshida, N., 1999. Determination of nitrogen isotopomers of nitrous oxide on a modified isotope ratio mass spectrometer. *Analytical Chemistry*, **71**, 4711–4718.
- Turnbull, J. C., Miller, J. B., Lehman, S. J., Tans, P. P., Sparks, R. J., and Sounthor, J., 2006. Comparison of ¹⁴CO₂, CO, and SF₆ as tracers for recently added fossil fuel CO₂ in the atmosphere and implications for biological CO₂ exchange. *Geophysical Research Letters*, **33**, L01817.
- Vieten, B., Blunier, T., Neftel, A., Alewell, C., and Conen, F., 2007. Fractionation factors for stable isotopes of N and O during N₂O reduction in soil depend on reaction rate constant. *Rapid Communications in Mass Spectrometry*, **21**, 846–850.
- Wahlen, M., and Yoshinari, T., 1985. Oxygen isotope ratios in N₂O from different environments. *Nature*, **313**, 780–782.
- Well, R., Flessa, H., Xing, L., Xiaotang, J., and Romheld, R., 2008. Isotopologue ratios of N₂O emitted from microcosms with NH₄⁺ fertilized arable soils under conditions favoring nitrification. *Soil Biology and Biochemistry*, **40**, 2416–2426.
- Yoshida, N., and Matsuo, S., 1983. Nitrogen isotope ratio of atmospheric N₂O as a key to the global cycle of N₂O. *Geochemical Journal*, **17**, 231–239.

Cross-references

- Aeration of Soils and Plants
 Climate Change: Environmental Effects
 Enzymes in Soils
 Greenhouse Gas Fluxes: Effects of Physical Conditions
 Greenhouse Gases Sink in Soils
 Soil Biota, Impact on Physical Properties
 Stable Isotopes, their Use in Soil Hydrology

STABLE ISOTOPES, THEIR USE IN SOIL HYDROLOGY

Peggy Macaigne
 Soil and Water Management and Crop Nutrition Section,
 Joint FAO/IAEA Division, International Atomic Energy Agency (IAEA), Vienna, Austria

Synonyms

Stable nuclides in the soil–plant–water system

Definitions

Isotopes. One of two or more atoms having the same atomic number (same chemical element) but different mass numbers due to different numbers of neutrons in their nucleus.

Stable isotopes. An isotope of an element that does not undergo radioactive breakdown. Stable isotopes are nonradioactive.

Stable isotopes in soil hydrology. Stable isotopes used to investigate soil–water interactions with the biological, hydrological, and atmospheric spheres.

Introduction

The Greek term “isotope” was coined in 1913 by Margaret Todd, a Scottish doctor and the British chemist Frederick Soddy to describe elements occupying the same place in the periodic table but with different atomic weights. In 1912, Joseph John Thomson proved the existence of stable isotopes: measuring the deflection of a stream of ionized neon gas, induced by magnetic and electrical fields, on a photographic plate. His assistant Francis William Aston pursued these discoveries developing mass spectrometry techniques to separate isotopes. Research has since continued on isotope properties and their characteristics; however, it is the application of isotope techniques and the information they can yield that has led to the most revolutionary advances in many fields of science. Using isotopes it is possible to trace the origin and pathway of different entities or to characterize complex natural phenomena, these techniques have been developed in a range of disciplines from medicine, to cure disease to earth sciences, using hydrology-based studies to solve environmental problems. Recent advances have been made using stable isotopes as high precision tools to explore the complex soil–plant–water continuum responding to the problems facing modern society such as water scarcity and resource management by improving water use efficiency (see *Water Use Efficiency in Agriculture: Opportunities for Improvement*), assuring food security, and reducing environmental impacts such as diffuse pollution and soil salinization (see *Salinity, Physical Effects on Soils*).

Natural abundance of stable isotopes

A number of elements in the periodic table have one or more stable isotopes with distinct concentrations in nature or natural abundance. In soil water studies the isotopes of interest are the isotopes of water itself (isotopes of oxygen and hydrogen) or those of associated elements that are dissolved in water (e.g., isotopes of nitrogen and carbon). Oxygen has three stable isotopes: oxygen-16 (^{16}O), oxygen-17 (^{17}O), and oxygen-18 (^{18}O), and their respective natural abundance on earth is 99.76%, 0.035%, and 0.2%. Oxygen-18 is usually preferred to oxygen-17 in environmental studies, because it is more abundant and therefore easier to measure.

Hydrogen has two stable isotopes: hydrogen (^1H) and deuterium (^2H or D) with natural abundances of 99.985% and 0.015%, respectively. ^{18}O and ^2H are extremely useful in hydrological studies, as they allow the direct tracing of water pathways.

Nitrogen has two stable isotopes: ^{14}N and ^{15}N with natural abundances of 99.634% and 0.366%, respectively. Carbon also has two stable isotopes: ^{12}C and ^{13}C with natural abundances of 98.9% and 1.1%, respectively.

Expression mode of stable isotope

Stable isotopes of an element are expressed as a ratio of the rarer isotope to the abundant isotope (e.g., $^{18}\text{O}/^{16}\text{O}$, $^{15}\text{N}/^{14}\text{N}$, $^2\text{H}/^1\text{H}$) as it is easier to measure isotopic ratios, rather than absolute values. Isotope ratio analysis is traditionally undertaken using isotope ratio mass spectrometry (IRMS), recently other successful spectroscopic techniques have been developed. In natural abundance studies, where there are minute differences, isotope ratios are reported, referenced against international standards, in delta (δ) units, parts per thousand ‰. This is also called the “isotopic signature” (Equation 1). The accepted reference for water is VSMOW (Vienna Standard Mean Ocean Water) (Clark and Fritz, 1997; Hoefs, 1997).

$$\delta^{18}\text{O}_{\text{sample}} = \left(\frac{(^{18}\text{O}/^{16}\text{O})_{\text{sample}}}{(^{18}\text{O}/^{16}\text{O})_{\text{VSMOW}}} - 1 \right) 1000 \text{ ‰ VSMOW} \quad (1)$$

In environmental studies it is sometimes useful to trace an artificially isotopically enriched source (e.g., fertilizer, irrigation water), especially if there is no natural isotopic variation in the different natural sources. Enrichments of the isotopes are then expressed as atom% enrichments (Equation 2 example for ^{15}N) (Knowles and Blackburn, 1993).

$$\%^{15}\text{N}/\text{N}_{\text{tot}} = 100 \frac{^{15}\text{N}}{^{15}\text{N} + ^{14}\text{N}} \quad (2)$$

If there is sufficient isotopic distinction of one element (natural abundances or enrichment) between sources it is possible to follow the pathways of the individual sources in the environment, as the isotopic signature of the mixed pool will be the result of the isotopic signature and contribution of each component to the final pool, based on mass balance equations. If there are only two sources and the isotope values of all pools are known then it is possible to quantify the contribution of each individual source to the final pool, from the isotope values alone, using an isotope mixing model. If there are three possible sources, an additional isotope signature is required to resolve the mixing model using this approach.

Specific properties of stable isotopes useful for environmental studies

Small differences in physical and chemical reaction rates caused by kinetic and equilibrium effects induce minute variations in the isotopic ratios of both substrates and products. The alteration in isotopic ratio between substrate and product is called fractionation. The specific sensitivity of isotopes during phase changes or reactions can be exploited to track changes in the environment. For example, during the process of water evaporation, the liquid phase becomes preferentially enriched in ^{18}O isotopes compared to the vapor phase.

There are two main phenomena that lead to isotopic fractionation: (i) isotope exchange reactions occurring at equilibrium and (ii) kinetic processes.

For reactions at equilibrium, modifications of the isotopic signature are quantified by the fractionation factor α , which is expressed as the ratio between the substrate and the product (Equation 3).

$$\alpha = \frac{R_{\text{substrate}}}{R_{\text{product}}} \quad (3)$$

For example, for oxygen isotopes in the liquid water (substrate) and vapor phase (product), the fractionation factor α at equilibrium during the process of evaporation (Majoube, 1970) is expressed as follow (Equation 4):

$$\alpha^{18}\text{O}_{\text{water-vapor}} = \frac{(^{18}\text{O}/^{16}\text{O})_{\text{water}}}{(^{18}\text{O}/^{16}\text{O})_{\text{vapor}}} \quad (4)$$

The fractionation factor between the liquid and vapor phases during evaporation of water is temperature dependent (Majoube, 1971). During evaporation of liquid water, the isotopic ratio $^{18}\text{O}/^{16}\text{O}$ increases in the liquid phase simultaneously inducing a depleted ratio in the vapor phase of the atmosphere. This is of practical importance when measuring isotopes in the Earth's atmosphere as the size of a cloud during rainfall is continuously diminishing. This type of reaction is well described by the Rayleigh equations (Clark and Fritz, 1997; Kendall and Caldwell, 2000). Kinetic processes also occur in nature due to incomplete and unidirectional reactions such as evaporation, dissociation reactions, biological mediation, and diffusion (Hoefs, 1997), contributing to slight global differences in isotopic signatures as predicted by the fractionation factors at equilibrium.

Numerous natural phenomena induce the modification of the isotopic signature of a considered element, allowing further interpretations and quantifications of natural processes and environmental tracing.

Factors influencing the isotopic signature of rainfalls, a source for soil water

Precipitation is a major input to the soil–plant–water system. It is therefore important to understand the natural processes influencing the isotopic signature of precipitation. Several factors have an impact on the isotopic signature of precipitation at the moment of its formation, such as temperature latitude/annual temperature, season, distance to coast, altitude, amount of rainfall leading to interannual variation, and small-scale variations (Clark and Fritz, 1997; Mook, 2006). Precipitation events can be individually traced in the Soil–Plant–Atmosphere Continuum (qv) of a specific field provided it has a distinct isotopic signature, which is the result of the environmental effects described above. Therefore, prior to starting any isotopic measurements, it is recommended to be aware of impact of such site-specific factors on isotope ratios, especially temperature.

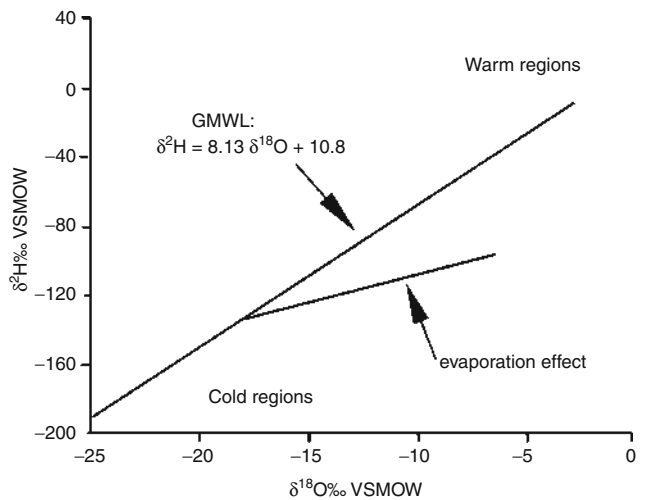
A clear relationship has been established between $\delta^{18}\text{O}$ and $\delta^2\text{H}$ in rainfall collected at different locations on Earth, known as the Global Meteoric Water Line (GMWL, Craig (1961)). It is also possible to establish a local

relationship (LMWL) at the site of measurement by collecting precipitations. Comparing the isotopic signature of collected soil water samples to the GMWL or the established LMWL allows determining the occurrence of evaporation (see Figure 1).

The use of stable isotopes in soil hydrology

Soil hydrology is a vast and complex domain, where water acts as the vector to transport dissolved nutrients, chemical compounds, and pollutants (see *Solute Transport in Soils*) in a medium interacting with the biological, hydrological, and atmospheric spheres (see *Soil Water Flow*). Water is also essential for assuring plant growth and facilitates the absorption of nutrients.

In the soil–plant–water system hydrological mass balance, the water inputs (qv *Water Budget in Soil*) are precipitation and/or irrigation, while the outputs are runoff, downward percolation and *Evapotranspiration* (qv), the combination of both soil evaporation and plant transpiration. Improving *Soil Water Management* (qv) by optimizing the hydrologic mass balance (qv *Water Budget in Soil*) in the soil–plant–water system is the key to solving many pressing environmental problems related to soils such as: (i) reducing diffuse pollution due to diluted nutrients or pollutants (qv *Leaching of Chemicals in Relation to Soil Structure*), (ii) improving *Water Use Efficiency in Agriculture: Opportunities for Improvement* (qv) and nutrient uptake by plants in cropped area to assure food security, (iii) reducing the water erosion, and (iv) reducing soil salinization (qv *Salinity, Physical Effects on Soils*). Therefore, there is a need to improve the knowledge of the driving processes associated to water such as *Evapotranspiration*, leaching, and plant water and nutrient uptake.



Stable Isotopes, Their Use in Soil Hydrology,

Figure 1 The GMWL established by Rozanski et al. (1993) and a schematic representation of the evaporation effect on the $\delta^2\text{H}$ versus $\delta^{18}\text{O}$ ratio of collected water. Evaporation induces a relative enrichment in $\delta^{18}\text{O}$ versus $\delta^2\text{H}$ compared to the original rainfall sample. The slope value of the trend decreases with increasing aridity.

Stable isotopes of water (^{18}O and ^2H) are tools that can be used in association with conventional methods to explore (i) water movement in the [Soil–Plant–Atmosphere Continuum](#) (qv), which includes impacts of management on downward percolation, runoff, soil evaporation, and plant transpiration; and (ii) the origins of soil water coming from precipitation, irrigation, groundwater capillary rise, river, and marine intrusion.

Previous research studies have specifically used isotopes of water (^{18}O and ^2H) to investigate water mechanisms, origins, and pathways within the soil–plant–water system.

Some studies have used the isotopic signature of soil water of bare soils to model soil water flux: percolation (see [Layered Soils, Water and Solute Transport](#)) and evaporation (see [Laminar and Turbulent Flow in Soils](#)) as shown on [Figure 2](#) (Allison et al., 1983; Barnes and Allison, 1984, 1988; Barnes et al., 1989; Barnes and Turner, 2000). Based on these models, it is possible to understand complex problems driven by water flux such as soil salinization (qv [Salinity, Physical Effects on Soils](#)), for example, Grunberger et al. (2008).

The percolation of precipitation through soil can be traced by comparing the isotopic signature of soil water with the signature of collected precipitation, for example, Gazis et al. (2004). This approach is useful to determine risky periods for diluted nutrient leaching in cropped area, for example, Macaigne (2007).

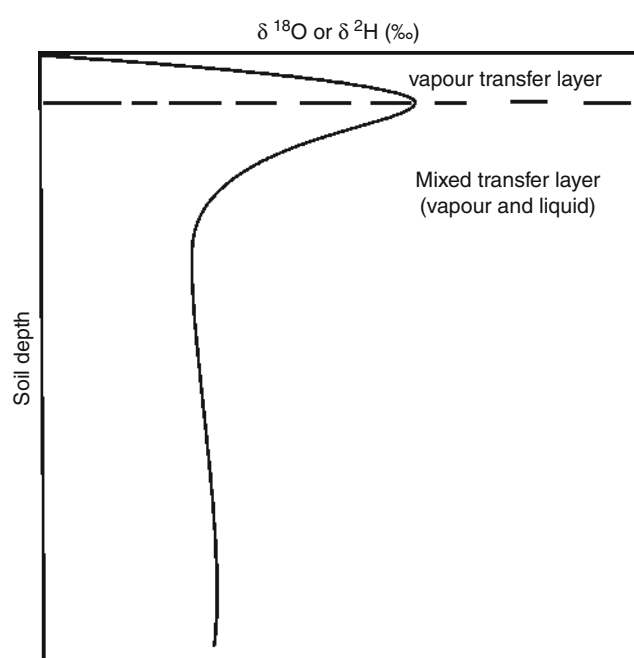
The isotopic signature of ^{18}O and ^2H in water extracted from soils and plants helps in characterizing plant water use and determining the influence of plants at a catchment scale perspective, especially the impact of deeply rooted trees on the hydrological cycle (Dawson and Ehleringer, 2000).

Specific studies have investigated plant transpiration from plant tissue as reviewed by Barbour (2007). Gas exchanges in ecosystems such as transpiration and CO_2 flux can also be studied with ^{18}O and ^{13}C (Yakir and Sternberg, 2000). Furthermore, soil evaporation (E) can be separated from plant transpiration (T) in the evapotranspiration flux (ET) based on isotopic measurement of ^{18}O and ^2H in soil water associated with soil water mass balance (Hsieh et al., 1998); or with more complex transport models integrated heat (see [Coupled Heat and Water Transfer in Soil](#)) and kinetic effects on the isotopic fractionation factor (Braud, 1995; Braud et al., 2005a, b); or with measurements of the ET flux (Wang, 2000; Yakir and Sternberg, 2000; Williams, 2004; Yepez et al., 2007) (see also [Stomatal Conductance, Photosynthesis, and Transpiration, Modeling](#)). Since transpiration reflects the true plant water use, separating E from T can help developing knowledge-based management strategies for improving water use efficiency in cropping systems.

In conjunction with ^{18}O and ^2H , other stable isotopes are used to characterize specific problems such as nitrate leaching and plant resistance to drought (qv [Drought Stress, Effect on Soil Mechanical Impedance and Root \(Crop\) Growth](#)). Movements of nutrients such as nitrate in the soil–plant–water system can be explored with nitrogen 15 (^{15}N) (Knowles and Blackburn, 1993). A slight enrichment in ^{15}N in the fertilizer allows investigating the fraction of fertilizer recovered by the plant (IAEA-TCS-29/CD, 2008). These and similar techniques have been widely used to test the efficiency of agricultural practices and biological nitrogen fixation (BNF) (Hardarson and Broughton, 2003). It is also possible to investigate NO_x gas emissions and nitrate removal from agricultural catchments to improve land management, for example, Zaman et al. (2008). Since ^{18}O is also present in phosphates (PO_4), it can be used to identify phosphate sources in aquatic systems coming from waste water, fertilizer, or plant effluent (Young et al., 2009). [Drought Stress, Effect on Soil Mechanical Impedance and Root \(Crop\) Growth](#) (qv) has also been well explored by using a methodology based on the isotopic ^{13}C signature also called carbon isotopic discrimination (CID) (Farquhar et al., 1988; Condon et al., 1993; Dercon et al., 2006).

Summary

Specific properties of stable isotopes can be exploited in soil hydrology to investigate and understand complex mechanisms and to identify the origins of water. The isotopic signature of individual precipitation events determined by temperature and other natural effects allows tracing its pathways in the soil–plant–atmosphere system. The use of stable isotopes (^{18}O and ^2H , ^{15}N , ^{13}C) associated to models



Stable Isotopes, Their Use in Soil Hydrology,

Figure 2 Schematic representation of the isotopic signature of soil water ($\delta^{18}\text{O}$ or $\delta^2\text{H}$) along the soil profile. An isotopic peak delineated the vapor transfer layer from the mixed transfer layer as described in Barnes et al. (2000).

and/or conventional measurements gives greater certainty to measurements and leads to better understanding of the complex mechanisms related to soil water phenomena such as water percolation, leaching, and soil salinity and plant-related factors such as resistance to drought, evapotranspiration, and water use efficiency.

Acknowledgments

Acknowledgments comments and suggestions to improve this manuscript from Rebecca Hood, Lee Heng and Long Nguyen of the Soil and Water Management & Crop Nutrition Subprogramme of the Joint FAO/IAEA Division in Nuclear Techniques in Food and Agriculture.

Bibliography

- Allison, G. B., Barnes, C. J., and Hughes, M. W., 1983. The distribution of deuterium and O-18 in dry soils.2. Experimental. *Journal of Hydrology*, **64**(1–4), 377–397.
- Barbour, M. M., 2007. Stable oxygen isotope composition of plant tissue: a review. *Functional Plant Biology*, **34**(2), 83–94.
- Barnes, C. J., and Allison, G. B., 1984. The distribution of deuterium and O-18 In Dry Soils.3. Theory for non-isothermal water-movement. *Journal of Hydrology*, **74**(1–2), 119–135.
- Barnes, C. J., and Allison, G. B., 1988. Tracing of water-movement in the unsaturated zone using stable isotopes of hydrogen and oxygen. *Journal of Hydrology*, **100**(1–3), 143–176.
- Barnes, C. J., Allison, G. B., and Hughes, M. W., 1989. Temperature-gradient effects on stable isotope and chloride profiles in dry soils. *Journal of Hydrology*, **112**(1–2), 69–87.
- Barnes, C. J., and Turner, J. V., 2000. Isotopic exchange in soil water. In Kendall, C., and McDonnell, J. J., (eds.), *Isotope Tracers in Catchment Hydrology*. Amsterdam: Elsevier, pp. 137–163.
- Braud, I., Bariac, T., Gaudet, J. P., and Vauclin, M., 2005a. SiSPAT-Isotope, a coupled heat, water and stable isotope (HDO and (H₂O)-O-18) transport model for bare soil. Part I. Model description and first verifications. *Journal of Hydrology*, **309**(1–4), 277–300.
- Braud, I., Bariac, T., Vauclin, M., Boujamloui, Z., Gaudet, J. P., Biron, P., and Richard, P., 2005b. SiSPAT-Isotope, a coupled heat, water and stable isotope (HDO and (H₂O)-O-18) transport model for bare soil. Part II. Evaluation and sensitivity tests using two laboratory data sets. *Journal of Hydrology*, **309**(1–4), 301–320.
- Braud, I., Dantas-Antonino, A. C., Vauclin, M., Thony, J. L., and Ruelle, P., 1995. A simple soil-plant-atmosphere transfer model (SiSPAT) development and field verification. *Journal of Hydrology*, **166**, 213–250.
- Clark, I. D., and Fritz, P., 1997. *Environmental Isotopes in Hydrogeology*. Boca Raton, FL: Lewis.
- Condon, A. G., Richards, R. A., and Farquhar, G. D., 1993. Relationships between carbon-isotope discrimination, water-use efficiency and transpiration efficiency for dryland wheat. *Australian Journal of Agricultural Research*, **44**(8), 1693–1711.
- Craig, H., 1961. Isotope variations in meteoric waters. *Science*, **133**, 1702–1703.
- Dawson, T. E., and Ehleringer, J. R., 2000. Plants, isotopes and water use: a catchment-scale perspective. In Kendall, C., and McDonnell J. J., (eds.), *Isotope Tracers in Catchment Hydrology*. Amsterdam, The Netherlands: Elsevier, pp. 165–202.
- Dercon, G., Clymans, E., Diels, J., Merckx, R., and Deckers, J., 2006. Differential C-13 isotopic discrimination in maize at varying water stress and at low to high nitrogen availability. *Plant and Soil*, **282**(1–2), 313–326.
- Farquhar, G. D., Hubick, K. T., and Condon, A. G., 1988. Carbon isotope discrimination and water use efficiency. In Rundel (ed.), *Stable Isotopes in Ecological Research*. New York: Springer-Verlag, pp. 21–46.
- Gazis, C., and Feng, X. H., 2004. A stable isotope study of soil water: evidence for mixing and preferential flow paths. *Geoderma*, **119**(1–2), 97–111.
- Grunberger, O., Macaigne, P., Michelot, J. L., Hartmann, C., and Sukchan, S., 2008. Salt crust development in paddy fields owing to soil evaporation and drainage: Contribution of chloride and deuterium profile analysis. *Journal of Hydrology*, **348**, 110–123.
- Hardarson, G., and Broughton, W. J., (eds.) 2003. *Maximising the use of biological nitrogen fixation in agriculture, Report of the FAO/IAEA Technical Expert Meeting held in Rome, 13–15 March 2001*. Developments in plant and soil sciences, FAO and Kluwer Academic Publishers.
- Hoefs, J., 1997. *Stable Isotope Geochemistry*. Berlin: Springer-Verlag.
- Hsieh, J. C. C., Chadwick, O. A., Kelly, E. F., and Savin, S. M., 1998. Oxygen isotopic composition of soil water: Quantifying evaporation and transpiration. *Geoderma*, **82**(1–3), 269–293.
- IAEA-TCS-29/CD. 2008. Guidelines on Nitrogen Management in Agricultural Systems. *IAEA Training Course CD Series No. 29*. S. s. unit. Vienna, Austria.
- Kendall, C., and Caldwell, E. A., 2000. Fundamentals of isotope geochemistry. In Kendall, C., and McDonnell, J. J., (eds.), *Isotope Tracers in Catchment Hydrology*. Amsterdam, The Netherlands: Elsevier, pp. 51–86.
- Knowles, R., and Blackburn, T. H., 1993. *Nitrogen Isotope Techniques*. San Diego: Academic Press.
- Macaigne, P., 2007. *Suivi du devenir de l'eau et des nitrates sous culture de pommes de terre (*Solanum tuberosum* L.) à l'aide du traçage isotopique ¹⁸O, ²H et ¹⁵N et d'un échantillonnage représentatif de la microtopographie*. Ph.D thesis (<http://www.theses.ulaval.ca/2007/24946/24946.html>). Québec, Canada: Université Laval.
- Majoube, M., 1970. Fractionation factor of sup ¹⁸O between water vapour and ice. *Nature*, **226**, 1242.
- Majoube, M., 1971. Fractionnement en oxygène-18 et en deutérium entre l'eau et sa vapeur. *Journal of Chemical Physics*, **197**, 1423–1436.
- Mook, W. G., 2006. *Introduction to Isotope Hydrology: Stable and Radioactive Isotopes of Hydrogen, Oxygen and Carbon*. London/Leiden/New York/Philadelphia/Singapore: Taylor & Francis.
- Rozanski, K., Araguás-Araguás, L., and Gonfiantini, R., 1993. Isotopic patterns in modern global precipitation. In e. a. Swart, P. K., (ed.), *Climate Change in Continental Isotopic Records. Geophys. Monogr. Ser. 78*. Washington, DC: AGU, pp. 1–36.
- Wang, X. F., and Yakir, D., 2000. Using stable isotopes of water in evapotranspiration studies. *Hydrological Processes*, **14**: 1407–1421.
- Williams, D. G., Cable, W., Hultine, K., Hoedjes, J. C. B., Yepez, E. A., Simonneaux, V., Er-Raki, S., Boulet, G., de Bruin, H. A. R., Chehbouni, A., Hartogensis, O. K., and Timouk, F., 2004. Evapotranspiration components determined by stable isotope, sap flow and eddy covariance techniques. *Agricultural and Forest Meteorology*, **125**, 241–258.
- Yakir, D., and Sternberg, L. D. L., 2000. The use of stable isotopes to study ecosystem gas exchange. *Oecologia*, **123**(3), 297–311.
- Yepez, E. A., Scott, R. L., Cable, W. L., and Williams, D. G., 2007. Intraseasonal variation in water and carbon dioxide flux components in a semiarid riparian woodland. *Ecosystems*, **10**(7), 1100–1115.
- Young, M. B., McLaughlin, K., Kendall, C., Stringfellow, W., Rollog, M., Elsbury, K., Donald, E., and Paytan, M., 2009. Characterization of oxygen isotope composition of phosphate sources to aquatic ecosystems. *Environmental Science and Technology*, **43**, 5190–5197.

Zaman, M., Nguyen, M. L., Gold, A. J., Groffman, P. M., Kellogg, D. Q., and Wilcock, R. J., 2008. Nitrous oxide generation, denitrification, and nitrate removal in a seepage wetland intercepting surface and subsurface flows from a grazed dairy catchment. *Australian Journal of Soil Research*, **46**, 565–577.

Cross-references

Coupled Heat and Water Transfer in Soil
 Drought Stress, Effect on Soil Mechanical Impedance and Root (Crop) Growth
 Evapotranspiration
 Laminar and Turbulent Flow in Soils
 Layered Soils, Water and Solute Transport
 Leaching of Chemicals in Relation to Soil Structure
 Salinity, Physical Effects on Soils
 Soil–Plant–Atmosphere Continuum
 Soil Water Flow
 Soil Water Management
 Solute Transport in Soils
 Stomatal Conductance, Photosynthesis, and Transpiration, Modeling
 Water Budget in Soil
 Water Use Efficiency in Agriculture: Opportunities for Improvement

Technical Committees (TC). Considering ISO the following TC should be mainly taken into consideration (in the order of significance):

- TC 190 Soil quality – the most important
- TC 23 Tractors and machinery for agriculture and forestry
- TC 134 Fertilizers and soil conditioners
- TC 182 Geotechnics

After reviewing the agrophysical literature, it should be stated that agro-physicists relatively seldom use the standards in their methodology and that great effort should be made to develop new and much needed agrophysical standards.

Bibliography

EN 45020:2006. Standardization and related activities – general vocabulary.
www.cen.eu
www.iso.org

STANDARDIZATION IN AGROPHYSICS

Andrzej Bieganowski, Magdalena Ryżak
 Institute of Agrophysics, Polish Academy of Sciences,
 Lublin, Poland

Definition

According to EN 45020:2006 (EN – European Standard), *standardization* is an activity of establishing, with regard to actual or potential problems, provisions for common and repeated use, aimed at the achievement of the optimum degree of order in given context.

There are two notes that complete the definition and explain the aim of standardization in the same standard:

- (a) *Note 1.* In particular, the activity consists of the processes of formulating, issuing, and implementing standards.
- (b) *Note 2.* Important benefits of standardization are improvement of suitability of products, processes, and services for their intended purposes, prevention of barriers to trade and facilitation of technological cooperation.

Standardization in agrophysics is realized on three levels:

- International level – ISO standards (ISO – International Organization for Standardization)
- Continental level – for instance EN – standards in Europe
- National level – for instance DIN (German Standards), BS (British Standards), or PN (Polish Standards)

Because agrophysics is an interdisciplinary science, the agrophysical standards are published by different

STEADY FLOW

The condition in which flow velocity do not vary with time.

STICKY

Having the property of adhering or sticking to a surface.

STOCHASTIC MODEL

Models based upon the concept that the variable of interest is represented by variability or uncertainty in the input values and the output represents probability distributions functions.

Bibliography

Glossary of Soil Science Terms. Soil Science Society of America. 2010. <https://www.soils.org/publications/soils-glossary>

Cross-references

[Agrophysics: Physics Applied to Agriculture](#)

STOKES' LAW

Law that defines the settling velocity of a particle based on its density and size.

STOMATAL CONDUCTANCE, PHOTOSYNTHESIS, AND TRANSPERSION, MODELING

Andrée J. Tuzet

Unité Mixte de Recherche, Environnement et Grandes Cultures, Institut National de la Recherche Agronomique (INRA), Thiverval Grignon, France

Definition

Stoma. Stomata are small pores on the epidermis of plant leaves. The aperture of the pore is controlled by the conformation of the two guard cells surrounding the pore. When the guard cells are relatively flaccid, the stomatal pore is nearly closed, and when they are turgid, it is open. **Stomatal conductance.** Stomatal conductance expresses the aptitude of stomatal aperture to control gas exchanges from or into the leaf.

Photosynthesis. Photosynthesis is a plant process that converts atmospheric carbon dioxide into more complex organic compounds, especially sugars, using energy from sunlight.

Transpiration. Transpiration is water taken up from the soil and lost through the stomata in the leaves. This loss of water as vapor through stomata is directly related to the degree of stomatal opening, the supply of water to the leaves, and the evaporative demand of the atmosphere surrounding the leaf.

Introduction

Modeling, like scientific observation and experimentation, is a method for increasing our understanding of cause-and-effect relationships. It requires classifying the processes involved according to importance, which results in the creation of a simplified reality. The modeling approach selected for a given problem depends on implied objectives, which can be expressed as a combination of precision, generality, and reality (Levins, 1966).

In order to utilize water resources effectively, and to quantitatively evaluate plant production and interaction between the vegetation and the environment, we need to model mass and energy-exchange processes within the soil–plant–atmosphere system through stomatal conductance, photosynthesis, and transpiration. The processes of transpiration and photosynthesis are closely related since they are regulated by the same stomatal feedback control mechanism. This feedback mechanism constantly modifies the conductance to water vapor and carbon dioxide exchanges in response to changing environmental conditions. The use of mechanistic models is ideally suited for gaining a better insight into the integrative behavior of the soil–plant–atmosphere system.

Stomatal conductance

Stomata have evolved physiological control mechanisms to satisfy the conflicting demands of allowing a net carbon gain by leaves while restricting water loss to acceptable

levels, under a range of environmental conditions. Therefore, it is very important to understand responses of stomata to environmental factors and to simulate stomatal conductance. In these aspects, numerous researchers have contributed to the study, and important advances have been achieved in understanding and mathematically modeling the physiology of stomatal movement (Jarvis, 1976; Cowan, 1977, 1982; Ball et al., 1987).

Jarvis (1976) presents an early empirical model in which stomatal resistance is estimated as multiplicative response functions of environmental variables (solar radiation, leaf temperature, water vapor pressure deficit) and soil or leaf moisture status. The environmental dependences are assumed to be separable, so that the dependence on each environmental variable is described by an individual response function which varies between 0 and 1. Predicted values of stomatal conductance are derived as the product of the maximum stomatal conductance and each of these functions. This approach is often employed in various forms for different vegetation surfaces; it is mainly guided by the concern to keep the number of physical variables low, while preserving the main mechanisms controlling the opening and closing movement of the stomata. The general problem arising with this approach is its specificity to particular vegetation–climate systems and parameters, such as the maximal stomatal conductance, or the sensitivity of stomatal conductance to environmental variables, and it must be therefore constantly readjusted to fit a particular vegetation type or prevailing condition.

Cowan (1977) is one of the first to analyze the role of stomatal conductance in regulating the balance between transpiration and net uptake of CO₂ for photosynthesis, in order to assess the transpiration-use efficiency (amount of C gained per water used). He considers functional and theoretical constraints that are presumably major factors in the evolution of the regulatory mechanisms of stomata, and he proposes to link stomatal control to an optimization between changes in assimilation and transpiration (Cowan, 1982). The mechanistic basis of this theory remains unresolved. The reason for this is that while diffusion is a well-defined physical process, and photosynthesis is essentially a reaction involving identifiable molecular components including CO₂, stomatal function is a control process depending on numerous feedbacks between poorly defined physiological and biochemical processes. Numerous empirical models of stomata behavior are developed on the basis of these experimental and observational studies. The model proposed by Ball et al. (1987) and later extended by Leuning et al. (1995) which links conductance to photosynthesis received wide attention and applications. This model expresses the dependence of stomatal conductance on net carbon assimilation, relative humidity or vapor pressure deficit, and leaf CO₂ concentration. The great interest in this approach relies on the opportunity to integrate it in general circulation models by coupling stomatal conductance transpiration and CO₂ concentration for predicting

greenhouse gas-induced climate change. It is also advantageous because the dependence of stomatal conductance on various factors can be achieved indirectly through their effects on photosynthesis since the model operates as a function of carbon assimilation. Correct parameterization of the model provides close agreement between simulated and observed stomatal conductance values and carbon assimilation rates. However, the empirical nature of this model makes it difficult to extrapolate it into different environmental conditions. For example, the effect of soil water stress on stomatal conductance is not explicitly included in this model.

To account for the dynamic response of stomata to the competing atmospheric demand and supply of water to leaves Tuzet et al. (2003) developed a model which fully couples stomatal conductance, water transport through the plant and soil, CO₂ assimilation, and the leaf energy balance. In this model, the parametrization of stomatal conductance is a variant of the Ball–Berry model which includes the responses of stomata to leaf water status. This stomatal feedback control mechanism is activated by the level of leaf water potential. It is expressed in terms of stomatal sensing of the soil water uptake, via changes in the gradient of water potential between the leaves and roots. An empirical logistic function is used to describe the sensitivity of stomata to leaf water potential. In this approach, water uptake by the roots is calculated dynamically to get the detailed distribution of water near the roots. This precise description is particularly important as the soil dries out because of the strongly nonlinear relationship between the moisture content and the hydraulic conductivity, which affects the water transport from the bulk soil to the root surfaces. This new scheme calculates directly the effects of supply and loss of water by leaves on stomatal conductance, an approach also adopted by Williams et al. (1996) and Grant et al. (1999).

Photosynthesis

Photosynthesis is the process of converting light energy to chemical energy and storing it as carbohydrates. This process occurs in plants and some algae. Plants need light energy, CO₂, and H₂O to make sugars. Photosynthesis takes place in the chloroplasts and involves the interception of light energy and its conversion to chemical energy in the intermediates of high chemical potential, which are then used to drive the catalytic fixation of CO₂ into sugars and others compounds. Photosynthesis is not a single reaction; rather, it is composed of many individual steps that work together with remarkably high overall efficiency. Despite this complexity, there are several key biochemical processes that allow simplification in photosynthesis modeling.

Over the past 25 years, models of photosynthesis integrated to the leaf level have progressed from a collection of partial process models to an integrated mathematical form, with an undeniable dominance of Farquhar, von Caemmerer, and collaborators in the process. Today almost

all mechanistic models of leaf photosynthesis are based on the kinetic properties of the enzyme Ribulose-1,5-bisphosphate (RuBP) carboxylase/oxygenase (RuBisCO). This enzyme is used in a dark reaction to catalyze the first major step of carbon fixation and the competing reaction of RuBP oxygenation. This reaction does not directly need light to occur, but it does need the products of the light reaction: ATP (Adenosine Triphosphate) and NADPH (Nicotinamide adénine dinucléotide phosphate). The dark reaction involves a cycle called the Calvin cycle in which CO₂ and energy from ATP are used to form sugars.

According to the model (Farquhar et al., 1980; Farquhar and von Caemmerer, 1982), the net rate of carbon assimilation is the carbon fixed by the rate of RuBisCO carboxylation minus the carbon released by the photorespiratory cycle (half the rate of RuBisCO oxygenation) and minus day respiration (CO₂ release occurring in the light other than that of photorespiration). Farquhar's model assumes that for C3 plants, the rate of RuBisCO carboxylation is limited by the slower of the two processes: (1) the maximum rate of Rubisco-catalyzed carboxylation (Rubisco-limited) or (2) the regeneration of RuBP controlled by the electron transport rate (RuBP-limited). The rate of regeneration of RuBP is dependent upon the concentration of the high-energy nucleotides ATP and reduced NADPH, both of which dependent on photochemical energy supply, which is controlled by Photosynthetic Photon Flux.

At the level of the individual C3 leaf, Farquhar's model enjoys general acceptance, and it is widely used to interpret leaf-scale photosynthesis data. However, considerable skill is needed in using it for a plant canopy. Although the big-leaf approximation is successful for modeling evapotranspiration for plant canopies, the same approximation may be erroneous for photosynthesis because of the additional leaf internal control on carbon assimilation. From this perspective, the big-leaf methodology needs to be further examined using experimental data. Many studies demonstrate successful use of Farquhar's model at the canopy level using other approaches such as vertical integration against radiation gradient (Baldocchi, 1993) and separation of a canopy into sunlit and shaded portions (Norman, 1993; De Pury and Farquhar, 1997).

Transpiration

Transpiration is the process by which water is taken up from the soil and lost through the stomata in the leaves. It is only a part of the total evaporation that may occur from vegetation. In transpiration, water flows through the plant in response to physical forces. There is a decreasing water potential from the soil to the roots, up through the xylem and leaves, and out into the atmosphere. Therefore, water moves by bulk flow in response to water potential gradients, pulling water from regions of high water potential toward areas of lower water potential. The atmosphere, even with only small humidity

deficits, is a large sink for water vapor and draws water away from the leaves through the stomata, thus allowing cooling of the leaf surface in the evaporating process.

The driving force of water through the plant is determined by factors such as solar and atmospheric radiations, wind speed, temperature, and air humidity. In the air spaces within the leaf, the liquid water becomes vapor. If the stomata are open, water vapor will usually diffuse into the atmosphere because of the relative dryness of the atmosphere compared to the near saturation inside the leaf.

The flow of water through the transpiration stream can be thought of in terms of supply and demand. Most of the time, water lost through transpiration is replaced by water absorbed from the soil by the roots. Short-term water deficits can occur in plants even when there is adequate soil water available. This can occur if the atmospheric demand exceeds the capacity of the roots to meet it. These deficits can be partly made up for by the closure of stomata. We can say that transpiration processes depend on biologically mediated responses to aerial and soil environments that can, in turn, exercise feedback effects via the plant on the energy balance, turbulent exchanges, and air characteristics (temperature and humidity), thereby determining the state of the environment itself. Therefore, the prediction of transpiration fluxes under changing climates involves suitable models describing the complex interaction of plant and environmental variables.

For many decades, transpiration models based on the energy balance were mostly derived from the Penman equation (Penman, 1948). Priestley and Taylor (1972) show that transpiration is a rather conservative variable, which can be determined primarily by the available energy. Combined with temperature and vapor pressure deficit, they obtain good results for well-watered vegetation. Monteith (1965) enlarges the Penman model with a stomatal conductance model. However, the use of simplistic approaches often fails to account for a number of interacting effects such as energy balance and soil water availability. More sophisticated approaches are proposed to account for interactive effects and to view the water transfer system in the three domains of soil, plant, and atmosphere as a whole. This need for a soil–plant–atmosphere continuum (SPAC) approach was first recognized by Philip (1966) and Cowan (1977) and by many other authors later. In these models, root water uptake is determined by a potential transpiration calculated from atmospheric conditions and a reducing function, which depends on the mean soil water content. Use of mean soil moisture content, rather than the value near to the roots, may lead to incorrect values for the resistance to water flow in the soil. Furthermore, the spatial distribution in moisture content also changes through the day, and hence the dynamics of water flow to the roots will not be captured when mean soil moisture content is used to calculate soil hydraulic resistance. To overcome this deficiency, the model of Tuzet et al. (2003, 2008) uses Richards' equation for water flow from the soil to the roots, rather than using soil hydraulic resistances. Plant water relations are

modeled as an analog to a simple electrical circuit including plant hydraulic resistances and plant capacitance. This approach ensures a complete coupling between stomatal conductance, plant energy balance, transpiration, and water transport in the soil–plant–atmosphere continuum and describes the dynamics of the different water fluxes.

Summary and conclusions

To survive and grow, plants must take up carbon dioxide through the stomata while avoiding desiccation and death. Stomata play a pivotal role in regulating water loss and CO₂ uptake by plant leaves. The degree of regulation varies continually in response to changing environmental factors such as light intensity, leaf temperature, water vapor pressure deficit, CO₂ concentration, and soil or leaf water status. Therefore, understanding stomatal behavior must involve a description of the *coupled* processes of leaf energy balance, transpiration, photosynthesis, and the dynamics of water transport within the soil and plant.

The development of such models is important not only in improving water use efficiency of cropland but also in studying the interactions between the vegetation and the atmosphere under variable climatic environmental conditions.

Bibliography

- Baldocchi, D. D., 1993. Scaling water vapor and carbon dioxide exchange from leaves to a canopy: rules and tools. In Ehleringer, J. R., and Field, C. B. (eds.), *Scaling Physiological Processes: Leaf to Globe*. San Diego: Academic, pp. 77–114.
- Ball, J. T., Woodrow, I. E., and Berry, J. A., 1987. A model predicting stomatal conductance and its contribution to the control of photosynthesis under different environmental conditions. In Biggs, J. (ed.), *Progress in Photosynthesis Research*. Dordrecht: Martinus Nijhoff, Vol. IV, pp. 221–224.
- Cowan, I. R., 1977. Stomatal behaviour and environment. *Advances in Botanical Research*, **5**, 117–228.
- Cowan, I. R., 1982. *Regulation of Water Use in Relation to Carbon Gain in Higher Plants. Physiological Plant Ecology 11, Water Relations and Carbon Assimilation*. Berlin: Springer, pp. 589–614.
- De Pury, D. G. G., and Farquhar, G. D., 1997. Simple scaling of photosynthesis from leaves to canopies without the errors of big-leaf models. *Plant, Cell and Environment*, **20**, 537–557.
- Farquhar, G. D., and von Caemmerer, S., 1982. Modelling of photosynthetic response to environmental conditions. In Lange, O. L., Nobel, P. S., Osmond, C. B., and Ziegler, H., Jr. (eds.), *Encyclopedia of Plant Physiology, New Series: Physiological Plant Ecology II*. Berlin: Spring, Vol. 12B, pp. 549–587.
- Farquhar, G. D., von Caemmerer, S., and Berry, J. A., 1980. A biochemical model of photosynthetic CO₂ assimilation in leaves of C3 species. *Planta*, **149**, 78–90.
- Grant, R. F., Wall, G. W., Kimball, B. A., Frumau, K. F. A., Pinter, P. J., Jr., and Hunsaker, D. J., 1999. Crop water relations under different CO₂ and irrigation: testing of *ecosys* with the free air CO₂ enrichment (FACE) experiment. *Agricultural and Forest Meteorology*, **95**, 27–51.
- Jarvis, P. G., 1976. The interpretation of the variations in leaf water potential and stomatal conductance found in canopies in the field. *Philosophical Transactions of the Royal Society of London B*, **273**, 593–610.

- Leuning, R., Kelliher, F. M., DePury, D. G. G., and Schulze, E. D., 1995. Leaf nitrogen, photosynthesis, conductance and transpiration: scaling from leaves to canopies. *Plant, Cell and Environment*, **18**, 1183–1200.
- Levins, R., 1966. The strategy of model building in population biology. *American Scientist*, **54**, 421–431.
- Monteith, J. L., 1965. Evaporation and environment. In Fogg, G. E. (ed.), *The State and Movement of water in Living Organisms, Sympos. Soc. Exper. Biol.*, Vol. 19, New York: Academic, pp. 205–234.
- Norman, J. M., 1993. Scaling processes between leaf and canopy levels. In Ehleringer, J. R., and Field, C. B. (eds.), *Scaling Physiological Processes: Leaf to Globe*. San Diego: Academic, pp. 41–76.
- Penman, H. L., 1948. Natural evaporation from open water, bare soil and grass. *Proceedings of the Royal Society of London Series A*, **194**, 120–145.
- Philip, J. R., 1966. Plant water relations: Some physical aspects. *Annual Review of Plant Physiology and Plant Molecular Biology*, 245–268.
- Priestley, C. H. B., and Taylor, R. J., 1972. On the assessment of surface heat flux and evaporation using large-scale parameters. *Monthly Weather Review*, **100**(2), 81–92.
- Tuzet, A., and Perrier, A., 2008. *Modeling the dynamics of water flow through plants: role of capacitance in stomatal conductance and plant water relations*. In Response of Crops to Limited Water: Understanding and Modeling Water Stress Effects on Plant Growth Processes, Advances in Agricultural Systems Modeling Series 1, Chap. 5, Madison: ASA/CSSA/SSSA, pp. 145–164.
- Tuzet, A., Perrier, A., and Leuning, R., 2003. A coupled model of stomatal conductance, photosynthesis and transpiration. *Plant, Cell and Environment*, **26**(7), 1097–1116.
- Williams, M., Rastetter, E. B., Fernandes, D. N., Goulden, M. L., Wofsy, S. C., Shaver, G. R., Melillo, J. M., Munger, J. W., Fan, S. M., and Nadelhoffer, K. J., 1996. Modelling the soil–plant–atmosphere continuum in a *Quercus-Acer* stand at Harvard Forest: the regulation of stomatal conductance by light, nitrogen and soil/plant hydraulic conductance. *Plant, Cell and Environment*, **19**, 911–927.

environment, and an environmental buffer in the formation, attenuation, and degradation of natural and xenobiotic compounds. A favorable balance between solids and voids in soil is needed to optimize air exchange, to allow plants to extract water, and for soil to store water in pores. In addition, the organic contents of soil are vitally important in providing energy, substrates, and the biological diversity necessary to sustain many important ecosystem functions.

The soil surface is the vital interface that (1) receives much of the fertilizers and pesticides applied to cropland, (2) receives the intense impact of rainfall, and (3) partitions the flux of gases into and out of soil. Optimizing porosity and organic matter content of surface soil is necessary to optimize soil functioning, since characteristics at the soil surface oftentimes control functions deeper in the soil. As well, the soil surface is the most dynamic portion of soil that can be manipulated by management, and therefore, is the most sensitive to damaging or enhancing activities.

As soil organic matter increases, soil porosity also increases (Figure 1), in response to the positive effect of organic matter on soil aggregation, tilth, and biopore development (Kay and VandenBygaart, 2002). The degree of soil organic matter stratification can be viewed as an indicator of soil quality or soil ecosystem functioning, because surface soil organic matter is essential for erosion control, water infiltration, and conservation of nutrients (Franzluebbers, 2002).

Surface enrichment in soil organic matter and an improvement in soil porosity are dependent on (1) continuous surface residue cover and (2) minimal traffic, especially under wet conditions. Lack of residue cover and exposure of soil to high-intensity rainfall leads to poor aggregation, reduced plant-water availability, erosion,

STRATIFICATION OF SOIL POROSITY AND ORGANIC MATTER

Alan J. Franzluebbers

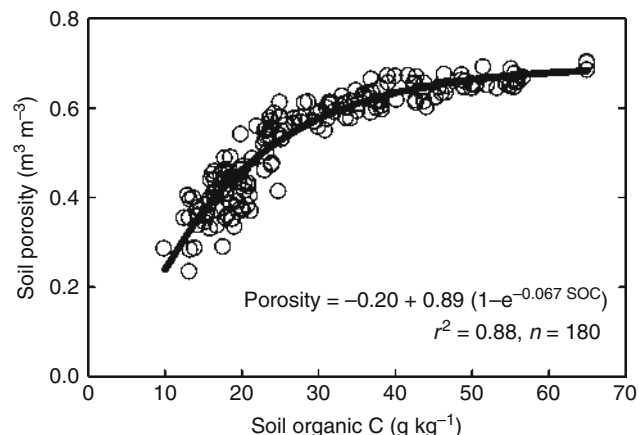
United States Department of Agriculture, Agricultural Research Service, Watkinsville, GA, USA

Definition

Soil porosity is the volume of soil not occupied by solids and can be filled with air or water. Volume of soil pores and concentration of organic matter are greatest nearest the soil surface and decline with depth. This characteristic is typical of undisturbed soils under grassland, forest, and conservation-tilled cropland. Soil porosity is strongly linked to soil organic matter concentration.

Soil organic matter and soil porosity stratification

Soil is an essential natural resource that provides several important ecosystem functions, e.g., medium for plant growth, regulation, and partitioning of water flow in the

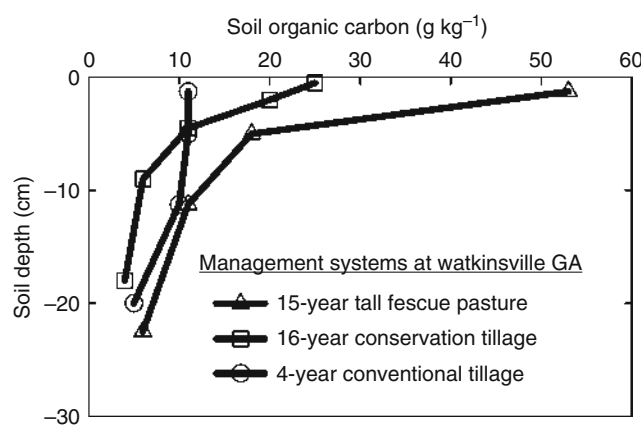


Stratification of Soil Porosity and Organic Matter

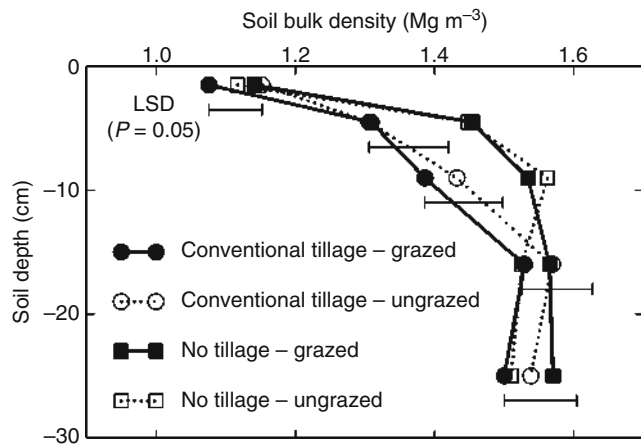
Figure 1 Relationship between soil porosity and soil organic carbon in 180 soil samples taken from the surface 2 cm of a Typic Kanhapludult in Georgia, USA under different grassland management systems. (Data from Franzluebbers et al., 2001.)

off-site sedimentation, and poor water quality, of which, all are characteristics of poor soil quality.

On cropland, soil organic C is uniform with depth when using traditional, inversion tillage systems (Figure 2). However, with conservation-tillage management (systems that leave >30% residue cover on the surface with minimum tillage, reduced tillage, mulch tillage, ridge tillage, or no tillage), soil organic C becomes concentrated at the soil surface and declines with depth (Figure 2). Pastures in a warm, humid climate are capable of increasing surface-soil organic C even more than under cropland (Figure 2). Perennial pastures encourage surface-soil



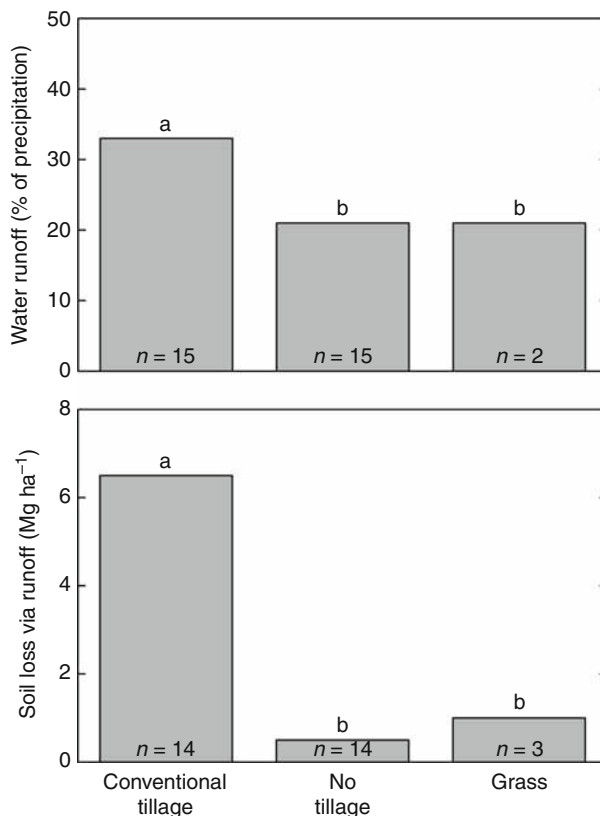
Stratification of Soil Porosity and Organic Matter,
Figure 2 Soil organic carbon as a function of depth and management on a Typic Kanhapludult in Georgia. (Data from Schnabel et al., 2001.)



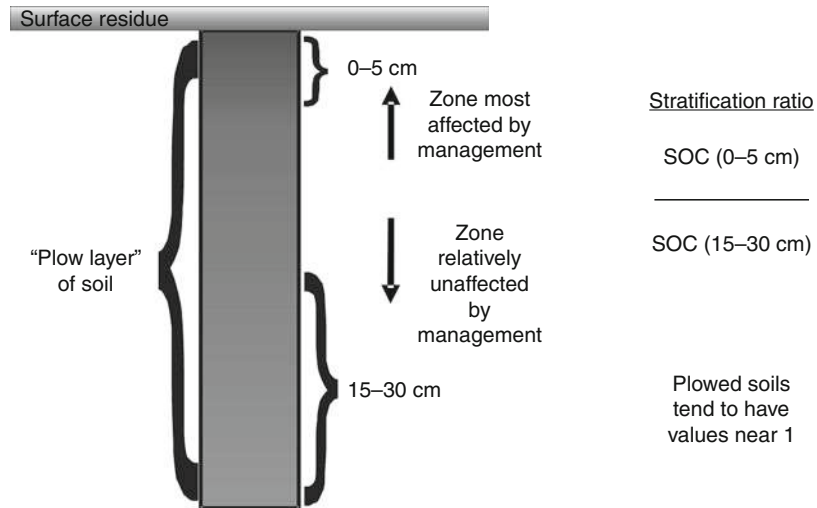
Stratification of Soil Porosity and Organic Matter,
Figure 3 Soil bulk density (inversely related to soil porosity) as a function of depth and management on a Typic Kanhapludult in Georgia. (Data from Franzluebbers and Stuedemann, 2008). Note: Bulk density of 1.1, 1.3, and 1.5 Mg m⁻³ would correspond to porosity of 0.58, 0.51, and 0.43 m³ m⁻³, respectively.

organic matter accumulation due to increases in C input (a longer growing period than most annual crops that fix C in plant biomass and greater transfer of C to an extensive root system) and decreases in C output (reduced decomposition due to lack of soil disturbance, more thorough soil drying, and large proportion of substrates at the soil surface).

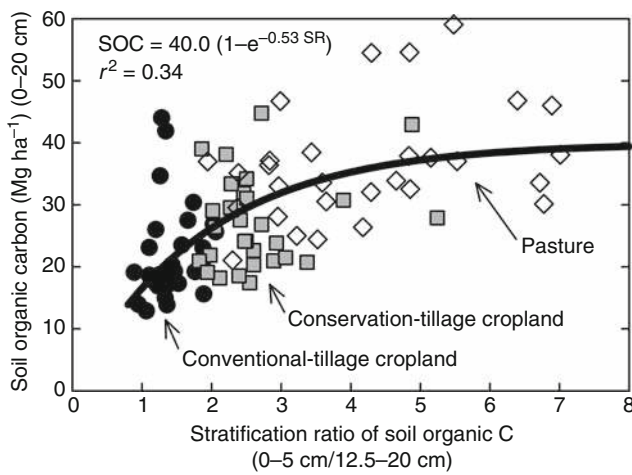
Soils under conservation-tillage cropland generally have lower soil porosity (conversely higher bulk density) in much of the previous “plow layer” than under conventionally tilled cropland (Figure 3), except at the soil surface with very high organic C concentration and consequently high soil porosity. Loss of porosity at depths below the soil surface with conservation tillage is often associated with changes in pore size distribution (Kay and VandenBygaart, 2002). Volume of macropores (>30 µm) usually decreases with conservation tillage (such pores are temporarily built through the loosening action of inversion tillage implements). However, biopores (rounded pores >500 µm) often increase with increasing number of years under conservation tillage.



Stratification of Soil Porosity and Organic Matter,
Figure 4 Water runoff and soil loss from water catchments throughout the USA under conventional and no-tillage cropland and grassland. Data from multiple sources summarized in Franzluebbers (2008). Different letters above bars within a panel indicate significant differences ($p < 0.05$). n number of observations.



Stratification of Soil Porosity and Organic Matter, Figure 5 Illustration of sampling zones and calculation of stratification ratio of soil organic matter.



Stratification of Soil Porosity and Organic Matter, Figure 6 Stock of soil organic C as a function of stratification ratio of soil organic C across 87 sites in the Piedmont and coastal plain regions of Alabama, Georgia, South Carolina, North Carolina, and Virginia. (Data from Causarano et al., 2008.)

Kay and VandenBygaart (2002) suggested that stabilized pore size distribution can only be expected with at least 15 years of conservation tillage.

Stratification ratio of soil organic matter has been calculated in several soils as an indicator of soil ecosystem functioning. Soils with high stratification ratio under long-term conservation-tillage cropland or under grassland often have greater water infiltration, lower soil loss from erosion, and lower nutrient loss in runoff than soil with low stratification ratio under conventional, inversion tillage (Franzluebbers, 2008). From a compilation of

water catchments with relevant data in the USA, water runoff and soil loss were lower in conservation-tillage cropland and grasslands than in conventionally tilled cropland (Figure 4). The effect of stratified organic matter is often greater on soil erosion control than on water runoff, since water can fill pores and runoff, but soil is stabilized with high organic matter even with excess rainfall.

Stratification ratio is calculated from the concentration of soil organic C at a sampling depth near the soil surface divided by the concentration of soil organic C at a sampling depth near the bottom of the “plow layer” (Figure 5). The depth increments for sampling are somewhat arbitrary at this point, until greater definition can be established as to what the impact of different sampling depths might be on predicting soil ecosystem functioning. Various numerator-depth increments sampled have been 0–3, 0–5, and 0–6 cm, while denominator-depth increments have been 12.5–20, 15–30, and 20–30 cm.

Stratification ratio of soil organic C (0–5/12.5–20 cm) has been related to the potential of conservation agricultural systems to sequester soil organic C in the southeastern USA (Franzluebbers, 2010). In a land-use survey, stratification ratio of soil organic C explained 34% of the variation in the stock of soil organic C under a diversity of management and soil conditions (Piedmont and coastal plain regions of Alabama, Georgia, South Carolina, North Carolina, and Virginia) (Figure 6). This relationship indicates that the majority of C stored with conservation management in Ultisols and Alfisols of the region occurred within the surface 5 cm. However, when stratification ratio of soil organic C was calculated as concentration at 0–2.5 cm divided by concentration at 7.5–15 cm, there was little relationship with soil organic C stock of conservation-tilled coastal plain soils in Virginia (Spargo et al., 2008). The surface 2.5 cm was

not adequately deep enough to represent the accumulation of soil organic C in these soils.

Conclusions

Quantity of soil organic matter is important to ecosystem functioning. However, stratification of soil organic matter appears to be even more important to ecosystem functioning. Soil quality and ecosystem functioning could be assessed with calculation of stratification ratio.

Stratification ratio increases the most on soils with low native organic matter. Such soils can be found in extreme environments with coarse texture and low precipitation or high temperature. Conservation management of these soils low in native organic matter are therefore, most improved in soil quality with the accumulation of organic matter at the soil surface.

Bibliography

- Causarano, H. J., Franzluebbers, A. J., Shaw, J. N., Reeves, D. W., Raper, R. L., and Wood, C. W., 2008. Soil organic carbon fractions and aggregation in the Southern Piedmont and Coastal Plain. *Soil Science Society of America Journal*, **72**, 221–230.
- Franzluebbers, A. J., 2002. Soil organic matter stratification ratio as an indicator of soil quality. *Soil and Tillage Research*, **66**, 95–106.
- Franzluebbers, A. J., 2008. Linking soil and water quality in conservation agricultural systems. *Electronic Journal of Integrative Biosciences*, **6**, 15–29.
- Franzluebbers, A. J., 2010. Achieving soil organic carbon sequestration with conservation agricultural systems in the southeastern United States. *Soil Science Society of America Journal*, **74**, 347–357.
- Franzluebbers, A. J., and Stuedemann, J. A., 2008. Early response of soil organic fractions to tillage and integrated crop-livestock production. *Soil Science Society of America Journal*, **72**, 613–625.
- Franzluebbers, A. J., Stuedemann, J. A., and Wilkinson, S. R., 2001. Bermudagrass management in the Southern Piedmont USA: I. Soil and surface residue carbon and sulfur. *Soil Science Society of America Journal*, **65**, 834–841.
- Kay, B. D., and VandenBygaart, A. J., 2002. Conservation tillage and depth stratification of porosity and soil organic matter. *Soil and Tillage Research*, **66**, 107–118.
- Schnabel, R. R., Franzluebbers, A. J., Stout, W. L., Sanderson, M. A., and Stuedemann, J. A., 2001. The effects of pasture management practices. In Follett, R. F., Kimble, J. M., and Lal, R. (eds.), *The Potential of U.S. Grazing Lands to Sequester Carbon and Mitigate the Greenhouse Effect*. Boca Raton: Lewis, pp. 291–322.
- Spargo, J. T., Alley, M. M., Follett, R. F., and Wallace, J. V., 2008. Soil carbon sequestration with continuous no-till management of grain cropping systems in the Virginia coastal plain. *Soil and Tillage Research*, **100**, 133–140.

Cross-references

- Aeration of Soils and Plants
 Biochemical Responses to Soil Management Practices
 Bulk Density of Soils and Impact on their Hydraulic Properties
 Compaction of Soil
 Crop Responses to Soil Physical Conditions
 Cropping Systems, Effects on Soil Physical Properties
 Earthworms as Ecosystem Engineers

- Enzymes in Soils
 Fertilizers (Mineral, Organic), Effect on Soil Physical Properties
 Grazing-Induced Changes of Soil Mechanical and Hydraulic Properties
 Greenhouse Gas Fluxes: Effects of Physical Conditions
 Hardsetting Soils: Physical Properties
 Hydrophobicity of Soil
 Infiltration in Soils
 Management Effects on Soil Properties and Functions
 Microbes and Soil Structure
 Organic Farming, Effect on the Soil Physical Environment
 Organic Matter, Effects on Soil Physical Properties and Processes
 Pedotransfer Functions
 Physical Degradation of Soils, Risks and Threats
 Physical Protection of Organic Carbon in Soil Aggregates
 Plant Roots and Soil Structure
 Pore Size Distribution
 Root Responses to Soil Physical Limitations
 Soil Aggregation and Evaporation
 Soil Biota, Impact on Physical Properties
 Soil Compatability and Compressibility
 Soil Functions
 Soil Physical Quality
 Soil Surface Sealing and Crusting
 Soil Tilth: What Every Farmer Understands but no Researcher can Define
 Subsoil Compaction
 Surface and Subsurface Waters
 Surface Properties and Related Phenomena in Soils and Plants
 Trafficability and Workability of Soils
 Water Erosion: Environmental and Economical Hazard
 Water Use Efficiency in Agriculture: Opportunities for Improvement
 Wind Erosion

STRENGTH

The capacity of a body to withstand stresses without experiencing failure, whether by rupture, fragmentation, collapse, or flow. In quantitative terms, it is the maximal stress a given body can bear without undergoing failure, or the minimal stress that will cause the body to fail.

Bibliography

- Introduction to Environmental Soil Physics (First Edition) 2003 Elsevier Inc. Daniel Hillel (ed.): <http://www.sciencedirect.com/science/book/9780123486554>

Cross-references

- Soil Penetrometers and Penetrability
 Soil Structure and Mechanical Strength
 Subsoil Compaction
 Trafficability and Workability of Soils

STRESS RELAXATION

The time-dependent decrease in stress under constant strain.

STRESS-STRAIN RELATIONS

Stephan Peth, Rainer Horn

Institute for Plant Nutrition and Soil Science, Christian-Albrechts-University zu Kiel, Kiel, Germany

Definition

σ_i =Normal stress (kPa)

τ_i =Shear stress (kPa)

ε_i =Strain (-)

i =Directional indices, with $i=x, y, z$ for horizontal (x, y) and vertical (z) direction or with $i=1, 2, 3$ for maximum, intermediate, and minimum principle stress/strain.

MNS=Mean normal stress (kPa)

OCTSS=Octahedral shear stress (kPa)

P_c =Pre-compression stress

v_k =Concentration factor

SST=Stress state transducer

FEM=Finite element method

Synopsis

The quantification of stress propagation and associated deformation processes in soils requires a detailed analysis of stress-strain relationships due to the nonlinear elastoplastic soil behavior. Deformation responses to loads are stress-strain path dependent, where deformation by compression and shear in turn controls stress distribution in the soil profile. Stress-strain relationships and resulting alterations of physical soil properties like hydraulic, gas, and thermal conductivity, as well as rooting need to be considered as an interactive process.

Introduction

It is well known that soils as three-phase systems can always mobilize internal tensile strength and shear forces over depth, which may attenuate applied external stresses. If, however, the external forces exceed the internal soil strength, a further deformation will occur until a new equilibrium will be reached and the rearrangement of particles as well as of soil aggregates has led to an equilibrated new, more rigid, denser volume orientation with the applied forces (Kezdi, 1969; McCarthy, 2007; Hartge Horn, 1999; Fredlund and Rahardjo, 1993; Horn et al., 2006). Within the last 4 decades, the mechanical stresses applied by agricultural (also forestry) machinery as well as the frequency of wheeling throughout the year have quadrupled and “final (=highest) maximum” values are still not to be seen (Hakansson, 2005).

Stress theory

The extent of soil deformation can be predicted by stress-strain processes and by their relative proportions. In the absence of gravitational and other applied forces, stresses in three-phase soil systems are subdivided into three normal stresses (σ) and six shear stresses (τ) acting on a cube; at equilibrium, the shearing forces reduce to three

components. Therefore, three normal-stress ($\sigma_x, \sigma_y, \sigma_z$) and three shear-stress ($\tau_{xy}, \tau_{xz}, \tau_{yz}$) components must be determined to fully define the stress state at a point (Nichols et al., 1987; Horn et al., 1992). This stress state can be then described completely by a symmetric matrix:

$$\begin{bmatrix} \sigma_x & \tau_{xy} & \tau_{xz} \\ \tau_{xy} & \sigma_y & \tau_{yz} \\ \tau_{xz} & \tau_{yz} & \sigma_z \end{bmatrix}. \quad (1)$$

For a single-valued characterization of the stress state, two invariants of the stress matrix are often used, the mean normal stress (MNS) and the octahedral shear stress (OCTSS) (Koolen and Kuipers, 1983):

$$MNS = \frac{1}{3}(\sigma_1 + \sigma_2 + \sigma_3) \quad (2)$$

$$OCTSS = \frac{2}{3}\sqrt{(\sigma_1 - \sigma_2)^2 + (\sigma_2 - \sigma_3)^2 + (\sigma_3 - \sigma_1)^2}. \quad (3)$$

Strain theory

All stresses exceeding the internal soil strength initiate a plastic (irreversible) deformation. The latter is a process more complex than a volume reduction which is same as the volumetric strain, expressing only one degree of freedom, whereas deformation at constant volume (shearing) summarizes five degrees of freedom. Although it is useful to distinguish between shear and compaction/decompaction processes as they typically exhibit very different effects, all deformations in soils are combinations of both, utilizing the full range of six degrees of freedom. Analogous to the stress theory, strain can be described by normal ($\varepsilon_x, \varepsilon_y, \varepsilon_z$) and shear strain ($\varepsilon_{xy}, \varepsilon_{xz}, \varepsilon_{yz}$) components, being described completely by the symmetric strain matrix:

$$\begin{bmatrix} \varepsilon_x & \varepsilon_{xy} & \varepsilon_{xz} \\ \varepsilon_{xy} & \varepsilon_y & \varepsilon_{yz} \\ \varepsilon_{xz} & \varepsilon_{yz} & \varepsilon_z \end{bmatrix}. \quad (4)$$

In the corresponding principal axis system, the strain matrix reduces to:

$$\begin{bmatrix} \varepsilon_1 & 0 & 0 \\ 0 & \varepsilon_2 & 0 \\ 0 & 0 & \varepsilon_3 \end{bmatrix}. \quad (5)$$

The strain matrix completely describes the local soil deformation. For example, the volumetric strain (ε_{vol}) can be calculated as:

$$\varepsilon_{vol} = \varepsilon_1 + \varepsilon_2 + \varepsilon_3 = \varepsilon_x + \varepsilon_y + \varepsilon_z. \quad (6)$$

Note that the trace of a matrix is invariant under coordinate transformations. Furthermore, the strain components

and their proportions depend on internal and external parameters and require the determination of all components in a three-dimensional volume.

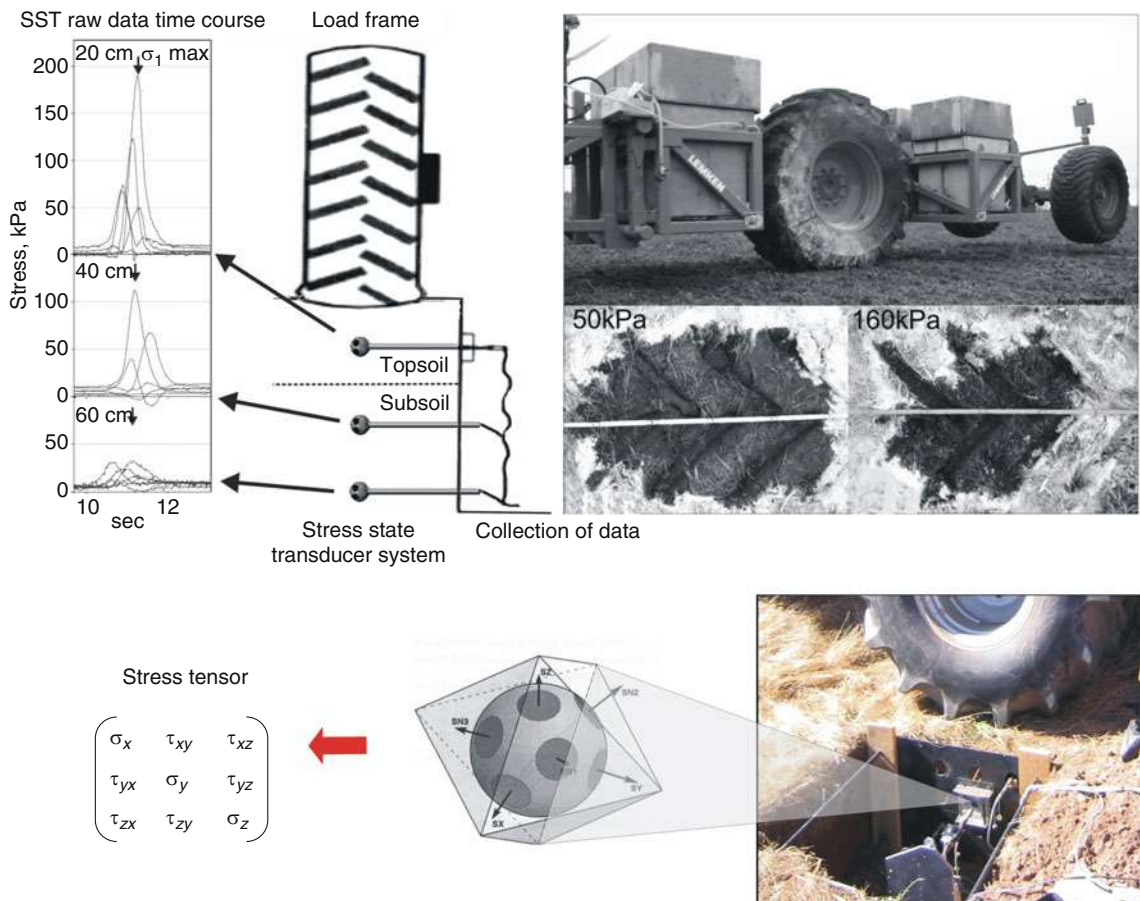
Stress propagation

Each applied stress is transmitted into the soil in three dimensions and can alter the physical, chemical, and biological properties if the internal mechanical strength ([Pre-Compression Stress](#)) is exceeded. The type of external force applied, time dependency, and number of compaction events can either change properties to depths by divergent processes or destroy a given structure by shear forces known as kneading. The latter case may result in complete homogenization and reversal to normal shrinkage behavior (Horn, 1988). [Figure 1](#) shows some general measurement techniques for in situ stress registration and analysis.

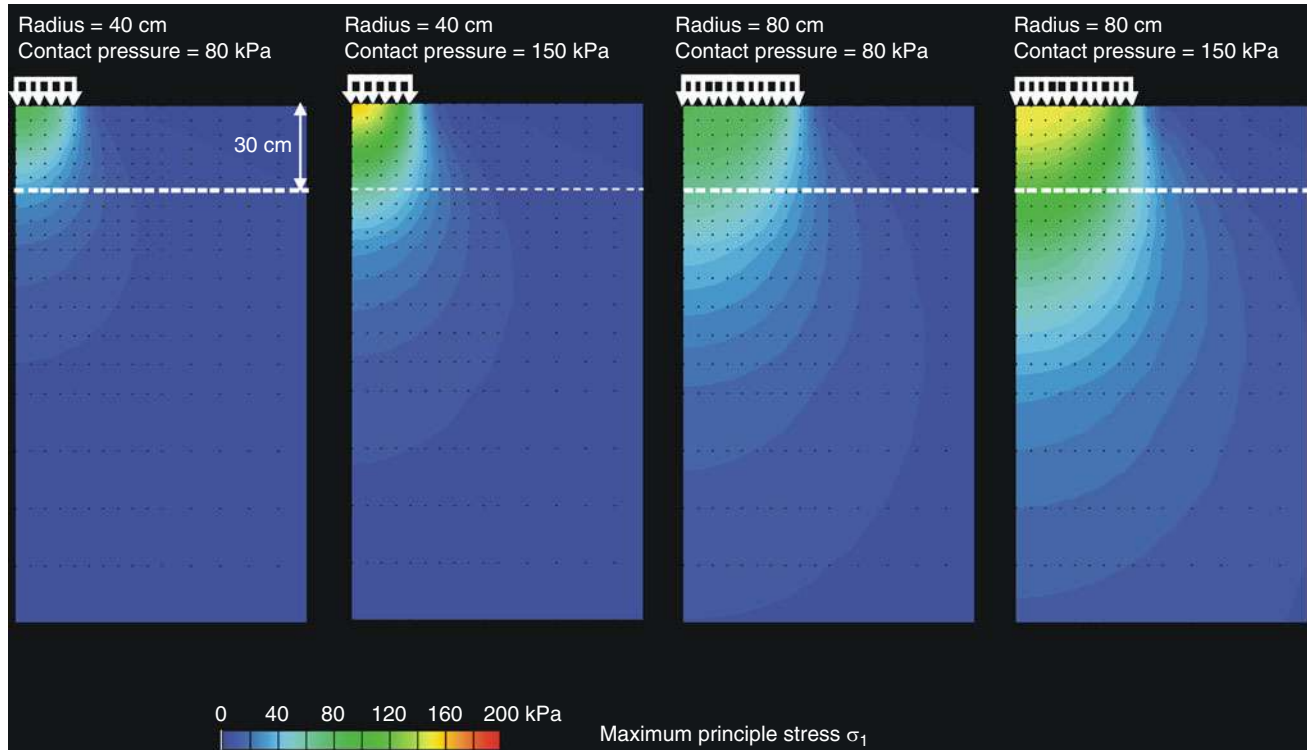
Stress propagation theories are rather old and have been often modified and adapted to in situ situations.

The fundamental theories introduced by Boussinesq (1885) are only valid for completely elastic material. Fröhlich (1934) and Soehne (1958) included elastoplastic properties through the introduction of concentration factor values (v_k) which allowed a more realistic description of the deeper stress penetration in soft soils. More comprehensive descriptions of these models are obtained by finally introducing pre-compression stress (P_v)—dependent values of the concentration factor, which are smaller in the recompression stress range, while they increase within the virgin compression stress range ([Pre-Compression Stress](#)). The latter can be explained by the plastic deformation behavior which causes a deeper stress transmission with a stress concentration more close to the perpendicular line of the load center.

The stress distribution in soils obeys the following physical laws: At a given contact area (defined as radius in [Figure 2](#)), the stress penetration is the stronger the greater the contact pressure. However, at a given contact



Stress–Strain Relations, Figure 1 (a) Experimental setup of a stress state transducer system (SST) and ballasted field load frame to simulate different wheel loads (in this case 3.3 Mg) and tyre inflation pressures. Tyre inflation pressures influence the distribution of the load on the soil surface resulting in different ground contact pressures which is demonstrated by the two footprint areas. (b) Detailed sketch of the stress measurement device showing the geometrical arrangements of stress transducers on the sensor head. From the various orientations of the stress transducers the full stress tensor can be calculated.



Stress–Strain Relations, Figure 2 Simulated distribution of the maximum principle stress (σ_1) for different tyre sizes and ground contact pressures. The dashed horizontal line indicates the depth of the plowed topsoil. Simulation was done with a finite element model (FEM) with a rotational symmetry of the elastoplastic half-space. The left border of the half-space corresponds to the centre of the load surface.

pressure, stresses are transmitted the deeper the greater the contact area (Figure 2).

Additionally, wheeling always induces shear stresses resulting in shear deformation. Shear stress and shear displacement are shown in Figure 3 for the case of a static wheel load with different ground contact pressures. Shear stresses significantly increase when traction forces are considered (not shown), which are generated when the vehicle is moving. In the case where shear stresses exceed the shear strength of a soil, both soil compression and shear deformation will increase and consequently further deteriorate pore functions down to deeper soil levels.

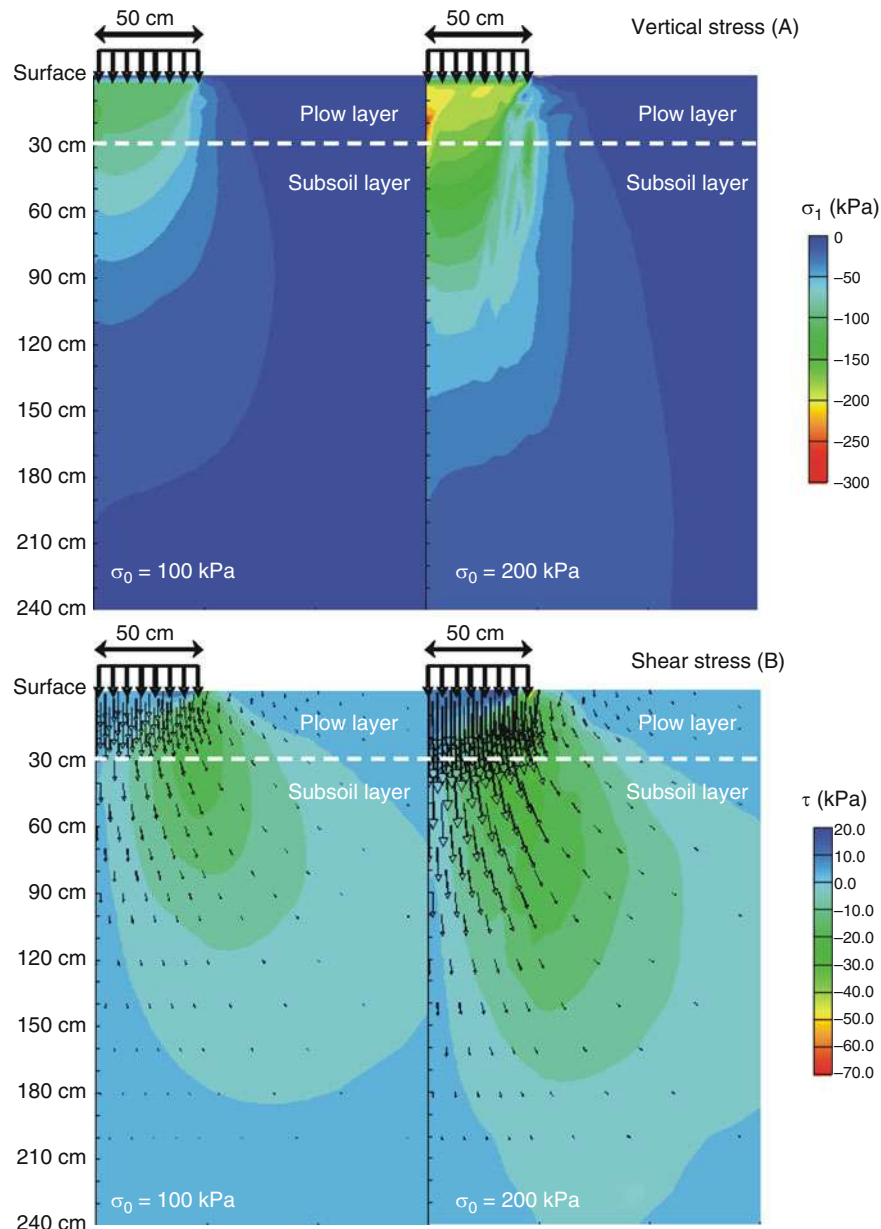
Precompression stress versus load

In order to quantify soil horizon-dependent specific stress attenuation and the consequences for stress-induced changes in physical properties, the combination of P_c of different soil horizons with the stress distribution in the soil profile is required. The concentration factor v_k as a measure of the stress transmission calculated from the Newmark equation (Newmark, 1942) is a function of the equivalent radius of the tire contact area, the effective contact pressure at the top of the respective horizon, and the calculated/measured P_c of each soil horizon. The mechanical strength of a soil can be derived from the

horizon-specific P_c , the actual soil pressure, and the strength-dependent concentration factor v_k of the respective horizon. It can further be deduced up to which depth additional deformation can be expected because the ratio of the applied stress and the strength of each consecutive soil horizon is >1 . The stress propagation theory and the calculation method are described in detail in Horn and Fleige (2003).

An example will elucidate the effect of stress propagation-dependent and internal strength-dependent attenuation for a natural (forest) Luvisol derived from loess and an arable site (Figure 4). If we assume natural properties of a Luvisol derived from loess (under forest) and compare the theoretical stress distribution for various agricultural machinery with depth, it becomes obvious that all stresses applied down to a depth of 60 cm exceed by far the internal soil strength of the Ah horizon with a crumbly structure and that of the clay derived Al horizon with a coherent (=weak) structure. Only the Bt horizon with a more rigid polyhedral and prismatic structure attenuates the remaining stresses more completely apart from the stresses exerted by the heavier sugar beet harvester.

The chosen arable site with an identical Luvisol derived from loess had been wheeled not only over decades with various agricultural machines and had a pronounced platy structure but also by the sugar beet harvester that had



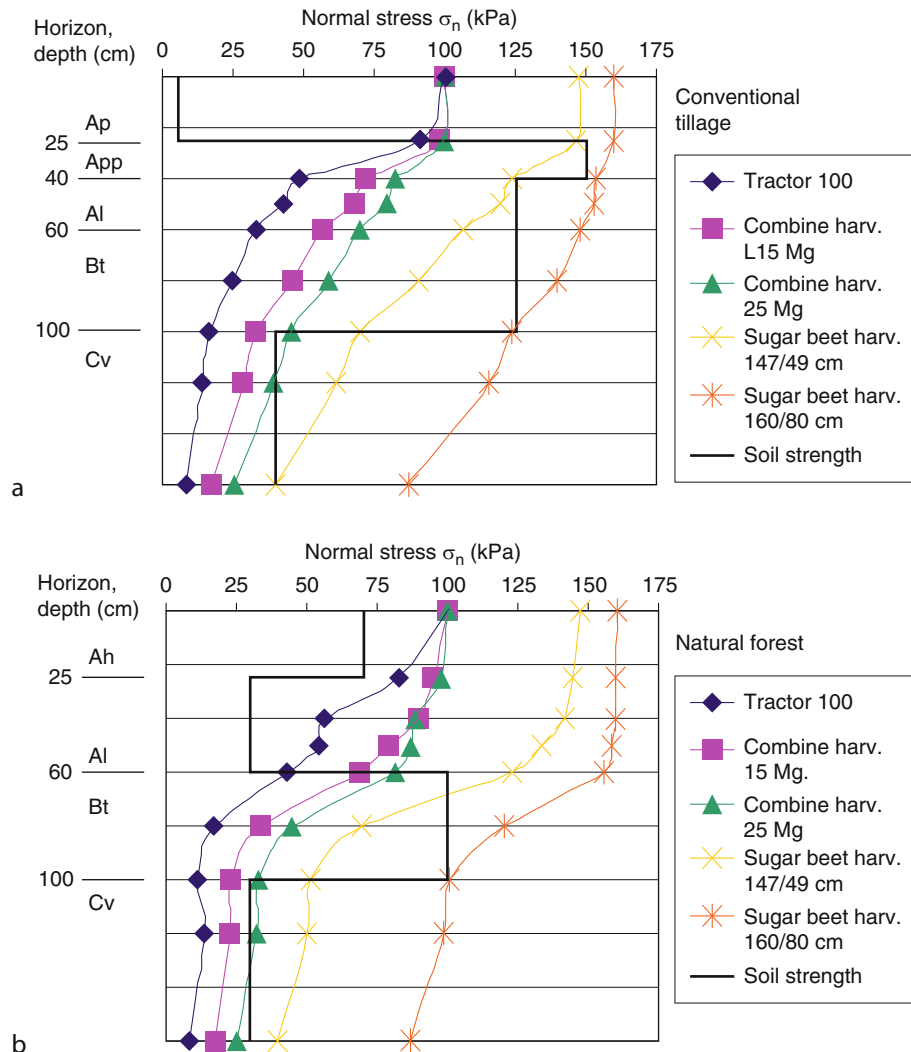
Stress–Strain Relations, Figure 3 Simulated (FEM) distribution of vertical normal σ_z (a) and shear stress τ (b) associated with different ground contact pressures. Arrows indicate corresponding shear displacements. Wheel loads in this case were considered static (no traction force).

passed the site for the first time. Thus, the soil was more rigid, which is expressed by increased actual precompression stresses over depth. Comparable machinery on this site caused the following stress distribution (under consideration of altered concentration factor values): higher values for the precompression stresses in the soil profile as a consequence of the long-term arable land management, including a reduced pore volume and reduced hydraulic functions. The transmitted stresses are attenuated within the soil horizons below the Ap horizon

completely, but stresses associated with heavier machinery (e.g., sugar beet harvesters) still cause additional plastic deformation at greater depth (Figure 4).

Some thoughts on consequences for sustainable land use

Soils are increasingly exposed to mechanical stresses during land use. Knowledge on stress–strain relations in soils and stress distribution within soil profiles is the basis for evaluating soil deformation and to protect soil



Stress–Strain Relations, Figure 4 Comparison between the depth dependent soil strength (pre-compression stress) and vertical stresses under arable land (a) and natural (forest) (b) soil conditions after the first wheeling event with a corresponding sugar beet harvester (35 Mg, 147 kPa contact pressure). The stress distribution was calculated based on strength dependent variation of the concentration factor for the various horizons.

functions. Long-term effects of soil deformation on soil functions include: increased uncertainty of crop yield, reduction in root growth, reduced plant available water and higher sensitivity to drought or stagnic conditions, cooler soils in springtime, enhanced greenhouse gas emission potential, altered nutrient adsorption behavior and retarded accessibility, consequences for microbial activity, retarded drinking water production, and higher sensitivity for overland flow or soil water erosion.

Bibliography

- Boussinesq, I., 1885. *Applications des potentiels à l'étude de l'équilibre et du mouvement des solides élastiques*. Paris: Gauthier-Villars.
- Fredlund, D. G., and Rahardjo, H., 1993. *Soil Mechanics for Unsaturated Soils*. New York: Wiley.
- Fröhlich, O. K., 1934. *Druckverteilung im Baugrund*. Wien: Springer.
- Hakansson, I., 2005. *Machinery-Induced Compaction of Arable Soils: Incidence – Consequences – Counter Measures*. Uppsala: Swedish University of Agricultural Sciences, p. 153.
- Hartge, K. H., and Horn, R., 1999. Introduction to Soil Physics (in German). *Einführung in die Bodenphysik*. 3. Auflage. Stuttgart: Enke Verlag.
- Horn, R., 1988. Compressibility of arable land. In Drescher, J., Horn, R., de Boodt, M. (eds.), *Interaction of Structured Soils with Water and External Forces*. Catena Supplement 11, 53–71, ISBN 3-923381-11-5.
- Horn, R., and Fleige, H., 2003. A method of assessing the impact of load on mechanical stability and on physical properties of soils. *Soil and Tillage Research*, 73, 89–100.

- Horn, R., Semmel, H., Schafer, R., Johnson, C., and Lebert, M., 1992. A stress state transducer for pressure transmission measurements in structured unsaturated soils. *Zeitschrift für Pflanzenernährung und Bodenkdunde*, **155**, 269–274.
- Horn, R., Fleige, H., Peth, S., and Peng, X. H. (eds.), 2006. Soil management for sustainability. *Advances in Geocology*, **38**, 497 pp. 3-923381-52-2.
- Kezdi, A., 1969. *Handbuch der Bodenmechanik Teil 1 Bodenphysik*. Berlin: VEB Verlag.
- Koole, A. J., and Kuipers, H., 1983. *Agricultural Soil Mechanics. Advanced Series in Agricultural Sciences*. Vol. 13, Berlin: Springer.
- McCarthy, D. F., 2007. *Essentials of Soil mechanics and Foundations*, 7 Auflage. Pearson.
- Newmark, N. M., 1942. *Influence charts for computation of stresses in elastic foundations*. University of Illinois, Engineering Experiment Station Bulletin 40.
- Nichols, T. A., Bailey, A., Johnson, C., and Grisso, R., 1987. A stress state transducer for soil. *Transactions of the American Society of Agricultural Engineers*, **30**(5), 1237–1241.
- Söhne, W., 1958. The mechanical behaviour of arable land under loading due to rolling wheels and tillage. (in German) *Grundlagen der Landtechnik*(Heft 1), 87–94.

Cross-references

- [Pre-Compression Stress](#)
[Soil Compaction and Compressibility](#)

STRESS-STRAIN RELATIONSHIPS: A POSSIBILITY TO QUANTIFY SOIL STRENGTH DEFINED AS THE PRECOMPRESSION STRESS

Rainer Horn, Stephan Peth
Institute for Plant Nutrition and Soil Science, Christian-Albrechts-University zu Kiel, Kiel, Germany

Definition

Concerning their mechanical properties, soils are defined neither by a complete elasticity nor by a complete plastic deformation behavior but as elastoplastic if the relationship between stress and strain is defined.

Precompression stress

Each stress applied to a completely homogenized substrate (e.g., seedbed) will result in a proportional strain or settlement (if plotted as semilog relation) and will define the virgin compression, that is, the normal compression curve. Thus, after stress release the deformation remains preserved. During a following restressing with a new but smaller stress, nearly any additional substantial strain occurs until the former, that is, the maximal mechanical stress applied is reached again. Now, this stress range, smaller than the original one, causes mostly elastic strain behavior and only minor additional volume changes. Exceeding, however, the former maximum stress results in an intense strain (= soil deformation, settlement, and volume decline) in the mostly texture and hydraulic

conductivity (= drainage off the excess pore water) dependent virgin (= normal) compression range.

Synopsis

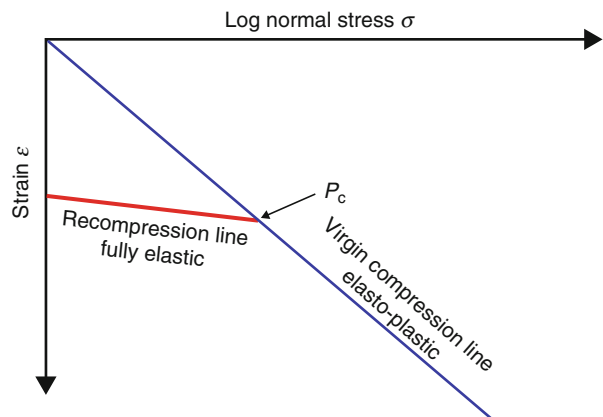
The quantification of the precompression stress of soils and soil horizons allows the overall determination of the internal soil strength and the transition from the elastic, that is, mostly reversible from the plastic deformation in the virgin compression load range.

Introduction

The compression of a soil means a change not only in total pore volume but is generally accompanied by a change in pore size distribution including related soil functions (e.g., permeability, storage of water, and aeration). Hence, the determination of the soils' resistance to compaction (i.e., its stability) and the magnitude of volume changes in soils exposed to external mechanical stresses are of primary importance for preserving soil physical quality.

The precompression stress (P_c) (often also defined as preconsolidation load, precompaction stress) is determined as the transition of elastic to plastic deformation if plotted as a semi-logarithmic stress-settlement (strain, void ratio) behavior. It can be quantified by the semiquantitative method of Casagrande (1936). In soil science, the P_c value and the corresponding graphical method (Figure 1) was introduced and validated for soil profile properties as a threshold value for internal soil strength by Horn (1981).

It is proofed to be a sufficiently good approximation of the stress and strain state of the various soil horizons for a given predrying intensity in numerous research papers (e.g., see Drescher et al. 1988; Horn et al., 2000; Pagliai and Jones, 2002). For more than 500 soil profiles under various land use systems and climates, this method was



Stress-Strain Relationships: A Possibility to Quantify Soil Strength Defined as the Precompression Stress,
Figure 1 Schematic diagram of a stress-strain relation and the definition of the precompression stress P_c (= internal soil strength).

applied to quantify not only the genetic soil processes, but also anthropogenic and climatic site effects (Horn and Fleige, 2003). Thus, the pre-compression stress values give three observations: (1) they are an indicator for the mechanical stability of a soil with respect to compressive deformation (compaction), (2) they record the maximum value of former stresses applied to the soil as long as there has no homogenization taken place since then, and (3) within the virgin compression stress range, each stress applied results in a plastic = irreversible deformation and consequently also reduces the pore volume, pore continuity, the hydraulic, gas, heat conductivity, and the corresponding diffusivity values.

The origins of this strengthening can range from pure mechanical stress application, biological activity (like the strength of earthworm casts or burrow (created by lateral stress application of up to 290 kPa by the worms), to chemical bindings' and also precipitation, hydraulic stresses, that is, shrinkage and swelling-induced aggregate formation.

Besides this Casagrande approach, additional methods were defined mostly by civil engineers like Hvorslev, van Zelst, and Ohde (all cited in Bölling, 1971). Their approaches include the rebound curve after the highest stress was applied in order to derive the precompression stress value. Thus, the latter ones all include the uncertainty of the rebound curve pattern caused by the wall friction effects, which is excluded by the Casagrande method and therefore more defined.

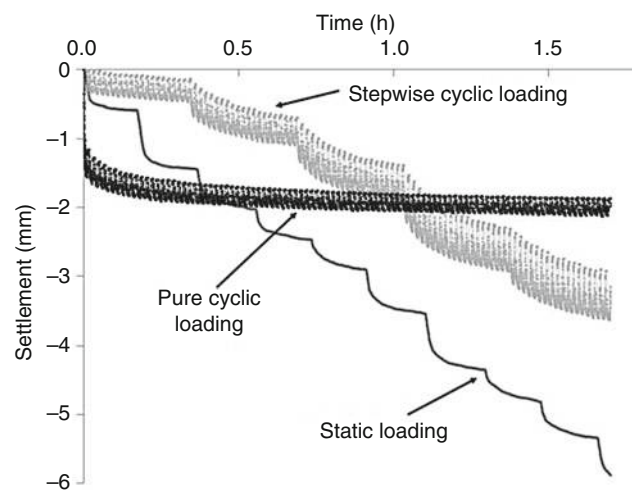
Comparison of various test approaches

Usually this compressive deformation is measured under laboratory conditions using undisturbed soil samples in a confined compression test (cf. Peth and Horn, 2006) whereby stresses in the σ_2 and σ_3 direction are undefined (rigid wall of the soil cylinder).

Three different tests can be carried out to define the internal soil strength (= precompression stress).

1. The stress-strain curve will be defined as a function of loading time and results especially in finer-textured soil samples in a flatter pattern and higher precompression stress values (time-controlled test).
2. The incremental changes in soil strain for a given stress applied can be defined as a criterion before the next stress is applied (height-controlled test).
3. The simultaneous control of the stress-and strain-induced changes of the pore water pressure during the test is used as a measure to define the application of the next stress (= pore water pressure-controlled test). The smaller the hydraulic conductivity due to loading and/or with increasing bulk density, the longer lasts each step – especially after exceeding the precompression stress the re-equilibration to the initial pore water pressure will not occur even after weeks.

Each of these tests can be furthermore prepared as (see Figure 2)



Stress–Strain Relationships: A Possibility to Quantify Soil Strength Defined as the Precompression Stress,

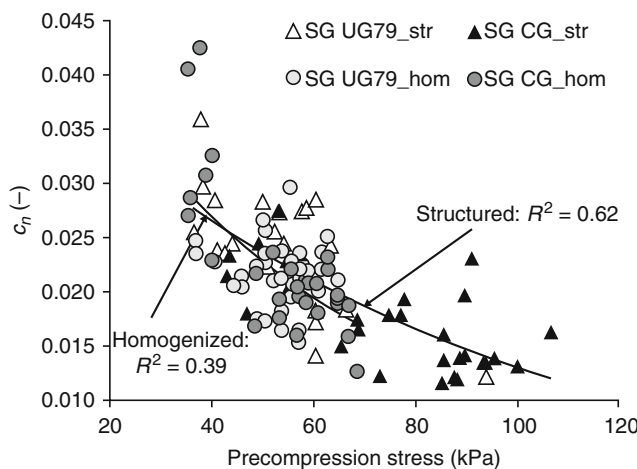
Figure 2 Examples of time–displacement curves during static, pure cyclic, and stepwise cyclic loading tests (taken from Reszkowska et al., 2010).

1. Static loading test (The sample will be loaded for a given time, for example, 10 min for each step and numerous defined stresses are applied successively while the height changes are recorded.)
2. Dynamic soil testing
 - (a) Cyclic loading. During this test, the load will be applied cyclically by repeated loading and unloading. This kind imitates the conditions, for example, due to animal movement or trampling with a given stress. The time intervals between loading and unloading can be defined.
 - (b) Stepwise cyclic loading. During this test, both the applied stresses and the number of cycles vary. Each load can be, for example, applied in 20 cycles (and each cycle may consist of 30 s loading and 30 s of unloading), which will result in a total loading and unloading time of 10 min each.

The results of such loading tests quantify the mechanical soil strength, which depends on soil parameters such as particle size distribution, type of clay minerals, nature, and amount of adsorbed cations, content and type of organic matter, aggregation induced by swelling and shrinking, stabilization by roots and humic substances, bulk density, pore size distribution and pore continuity of the bulk soil and single aggregates, water content, and/or water suction (Horn, 1981).

It can be stated that at a given soil type, the precompression stress value, that is, the internal soil strength is

1. the higher the more pronounced is the aggregation (coh<pris<pol<subangular blocky<crumbs<plat).



Stress–Strain Relationships: A Possibility to Quantify Soil Strength Defined as the Precompression Stress,
Figure 3 Correlation between precompression stress determined using 20th loading cycle (P_c') and coefficient of cyclic compressibility (C_n) for structured and homogenized samples of SG UG79 and SG CG for both investigated soil layers (4–8 and 18–22 cm); $n = 30$ (taken from Reszkowska et al., 2010).

2. the drier, that is, the more negative the matric potential is within the soil.
3. the higher is the organic carbon content. At a given amount of C org. strength increases with an higher proportion of humic acids.
4. the smaller the soil disturbance (conservation tillage results in stronger soils than conventional tilled sites).
5. the higher is the biological activity.
6. the more intense was the previous maximum and the duration of previous drying (for more detailed info see Hartge and Horn, 1999; Drescher et al., 1988; Fredlund and Rahardjo, 1993; Parry, 2004; McCarthy, 2007; Horn et al., 2000, 2005, 2006).
7. the higher because there is a significant correlation between the precompression stress and the rigidity of soil structure during cyclic loading expressed as coefficient of cyclic compressibility (C_n) (for more details see Reszkowska et al., 2010 submitted) (Figure 3).

Conclusions

The determination of the precompression stress is the most effective measure to quantify the internal soil strength as a consequence of soil mechanical, hydraulic, chemical, and biological impacts. This value depends also on the actual matric potential, is the basis for small up to large-scale soil mechanical strength maps, and can serve as a decision tool to predict the alteration in physical but also physicochemical and microbial site properties.

Bibliography

Bölling, W. H., 1971. Zusammendrückung und Scherfestigkeit von Böden. New York: Springer, Wien, ISBN: 3-211-81039-0.

- Drescher, J., Horn, R., and de Boodt, M. (eds.), 1988. Impact of water and external forces on soil structure. Catena Supplement 11, ISBN 3-923381-11-5, 171 S.
- Enache, K. R., de la Rosa, D., and Simota, C., 2005. SIDASS project part 5: prediction of mechanical strength of arable soils and its effects on physical properties at various map scales. *Soil and Tillage Research*, **82**, S.47–S.56.
- Fredlund, D. G., and Rahardjo, H., 1993. *Soil mechanics for unsaturated soils*. New York: Wiley.
- Hartge, K. H., and Horn, R., 1999. Introduction to soil physics. (in German) Einführung in die Bodenphysik. 3.Aufl. Enke Verlag Stuttgart.
- Horn, R., 1981. Effect of soil aggregation on the mechanical soil strength and its consequences on physical properties. (in German) Schriftenreihe des FB 14 TU Berlin, H.10, 2005. ISBN 379830792 X.
- Horn, R., and Fleige, H., 2003. A method of assessing the impact of load on mechanical stability and on physical properties of soils. *Soil and Tillage Research*, **73**, 89–100.
- Horn, R., Fleige, H., Richter, F.-H., Czyz, E. A., Dexter, A., Diaz-Pereira, E., Dumitru, E., Enache, R., Rajkai, K., de la Rosa, D., and Simota, C., 2005. Prediction of mechanical strength of arable soils and its effects on physical properties at various map scales. *Soil and Tillage Research*, **82**, 47–56.
- Horn, R., van den Akker, J. J. H., and Arvidsson, J., 2000. Subsoil compaction – distribution, processes and consequences. *Advances in Geoenvironmental Engineering*, **32**, ISBN 3-923381-44-1, 462S.
- Horn, R., Fleige, H., Peth, S., and Peng, X. H. (eds.), 2006. Soil management for sustainability. *Advances in Geoenvironmental Engineering*, **38**, 497pp. ISBN 3-923381-52-2.
- McCarthy, D. F., 2007. Essentials of soil mechanics and foundations. 7. Aufl. New York: Pearson.
- Pagliai, M., and Jones, R., 2002. *Advances in Geoenvironmental Engineering*, **35**, 480pp. Reiskirchen: Catena, ISBN: 3-923381-48-4.
- Parry, R. H. G., 2004. Mohr circles, stress paths and geotechnics, 2nd edn. 264pp. London: Spon, ISBN 0-415-27297-1.
- Peth, S., and Horn, R., 2006. The mechanical behaviour of structured and homogenized soils under repeated loading. *Journal of Plant Nutrition and Soil Science*, **169**, pp. 401–411.
- Reszkowska, A., Peth, S., and Horn, R., 2010. Effect of grazing on soil compressibility of steppe ecosystem in Inner Mongolia, China. *Soil and Tillage Research* submitted.

Cross-references

- [Agrophysical Properties and Processes](#)
[Infiltration in Soils](#)
[Management Effects on Soil Properties and Functions](#)
[Mechanical Resilience of Degraded Soils](#)
[Shrinkage and Swelling Phenomena in Soils](#)
[Trafficability and Workability of Soils](#)

SUBDRAINAGE

The control and removal of excess groundwater, usually by means of pipe drains that intercept seepage and/or lower the water table.

Bibliography

Library of Congress Cataloging-in-Publication Data Environmental engineering dictionary and directory/Thomas M. Pankratz <http://www.docstoc.com/docs/2845196/CRC-Press>

SUBIRRIGATION

The water is applied in open ditches or tile lines until the water table is raised sufficiently to supply water to the rooting depth of the crop.

Bibliography

Glossary of Soil Science Terms. Soil Science Society of America. 2010. <https://www.soils.org/publications/soils-glossary>

Cross-references

[Irrigation and Drainage, Advantages and Disadvantages](#)
[Irrigation with Treated Wastewater, Effects on Soil Structure](#)

SUBSOIL

The solum below the plough layer.

SUBSOIL COMPACTION

Rainer Horn, Heiner Fleige

Institute for Plant Nutrition and Soil Science, Christian-Albrechts-University zu Kiel, Kiel, Germany

Definition

Soil compaction and especially subsoil compaction are defined as one out of the ten major threats concerning soil degradation worldwide. The reduction of pore space and especially of coarse pores, the additional formation of finer pores, as well as the consequences for hydraulic, pneumatic, and heat transport processes are all linked to compaction. It can also be defined as increase in soil mass per volume and in combination with the shear induced rearrangement of particles at a given bulk density.

Introduction

According to the German Soil Protection Law (1998) and the European Soil Framework Directive (2006), soil compaction is besides water and wind erosion is one of the main physical reasons and threats of soil degradation. It is estimated, that 32% of the subsoils in Europe are highly degraded and 18% moderately vulnerable to compaction (Fraters, 1996, cited in Van den Akker, 2002). Thus, also the effects of soil deformation on crop yield, ground water recharge, soil loss by water and wind erosion, gas production, and emission (global warming) are to be considered if the mechanical strength in the top- and subsoil are exceeded (e.g., Horn et al., 2000, 2006; Pagliai and Jones, 2002).

Subsoil compaction is regarded as the major problem because it is defined as permanent and the pore functions

are not renewable after their deterioration or at least alteration. In Germany, the problem of compaction was defined in the German Federal Soil Protection Law (1998) by (1) the *obligation of precaution toward soil compaction*, which includes the request that soil compaction should be avoided “as far as possible,” and (2) the *obligation to prevent harmful changes of the soil*. Test and action values have to be defined for soil strength or maximal stress application, which is still on debate but some preliminary values are given in Horn and Fleige (2009). According to the concept “precompression stress P_c ” (Horn and Fleige, 2003, 2009; Horn et al., 2005; Stress-strain Relations by Peth and Horn) the value P_c can be used as precaution value to avoid subsoil compaction in general. The prediction of the change of soil functions/parameters after exceeding the P_c allows an assessment if critical values caused by subsoil compaction are already exceeded. These maps can be created for all scales and at different accuracy. As a general approach, the developed PDF (pedotransfer functions) can be used to derive for the dominant soil types corresponding PC-maps and stress dependent changes in physical functions up to the farm scale with actual controlled values based on a farm soil map (1:5,000).

Examples for PC maps at various scales

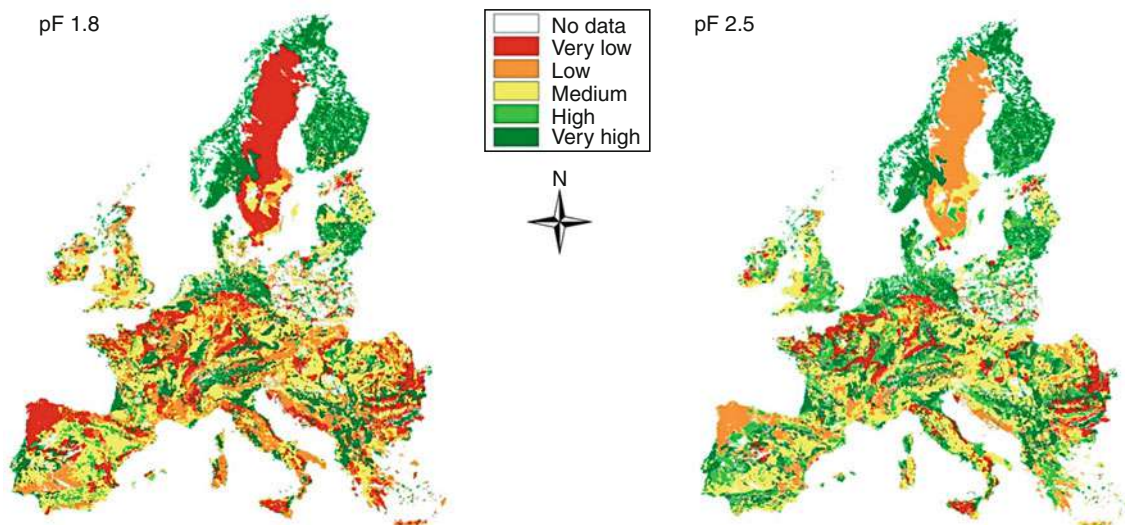
Based on the PDF (for more details see DVWK 1995, 1997, and Horn and Fleige 2003) developed within various projects (e.g., SIDASS, Horn et al., 2005) during the last decades, the map of the internal soil strength for the representative soil types 1/50 km² approximately can be derived (see Figure 1).

It gives a rough overview about the most sensitive soil areas with the most sensitive subsoils but requires further details at large scales if applied for an exact land use planning. A further precision increase is given if a detailed soil map is available, which can be used to derive the corresponding subsoil strength values (Figure 2).

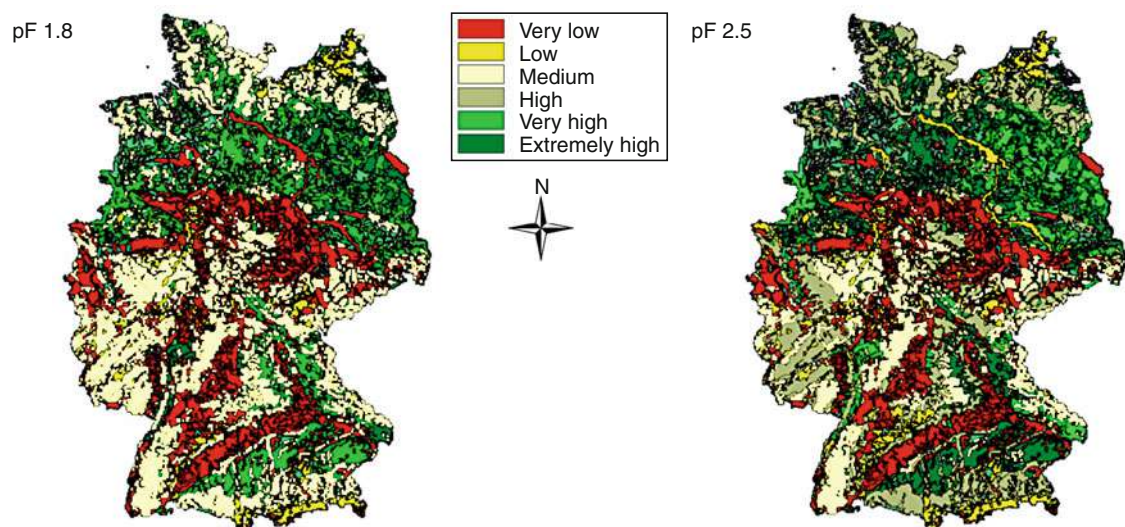
Areas with very weak subsoils can be detected, for example, at a pF value of 1.8 in the loess region while the sandy outwash area (Lower Saxony in Germany) is very rigid. An increase in drying (pF1.8–pF2.5) always results in higher precompression values.

The highest degree of certainty is given in the actual soil regions (e.g., a farm is completely mapped and the precompression stress values for the representative soil types measured (Figure 3).

The farm (155 ha) is located in the hilly weichselian moraine area, which results in a high pedodiversity. The parent material of the soils is derived from glacial till and results in a dominance of sandy loam, loamy sand, and sand. The main soils are partly eroded (Stagnic) Luvisols, associated with Stagnosols, Gleysols, Cambisols, Anthrosols, and in addition Histosols (according to WRB 2006). Areas with low soil strength even within a single field can be detected and consequently also the actual farming processes adjusted to these site properties.



Subsoil Compaction, Figure 1 Mechanical strength (precompression stress) for subsoils (30–60 cm). European scale (1:1,000,000). Classification of the precompression stress (kPa): very low <30, low 30–60, medium 60–90, high 90–120, very high 120–150, extremely high >150.

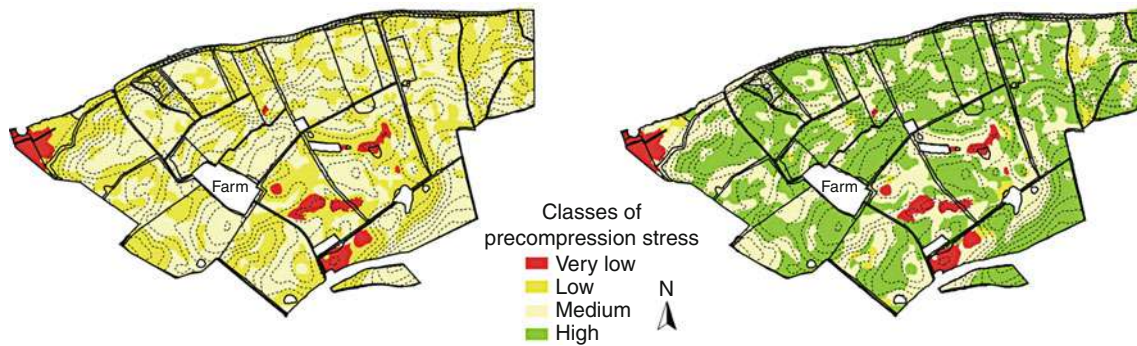


Subsoil Compaction, Figure 2 Precompression stress ranges for subsoils in Germany as a function of predrying: pF 1.8 (−60 hPa) = analog to the springtime, pF 2.5 (−300 hPa) = early summertime = drier (scale: 1:1,000,000). Classification of the precompression stress (kPa): very low <30, low 30–60, medium 60–90, high 90–120, very high 120–150, extremely high >150.

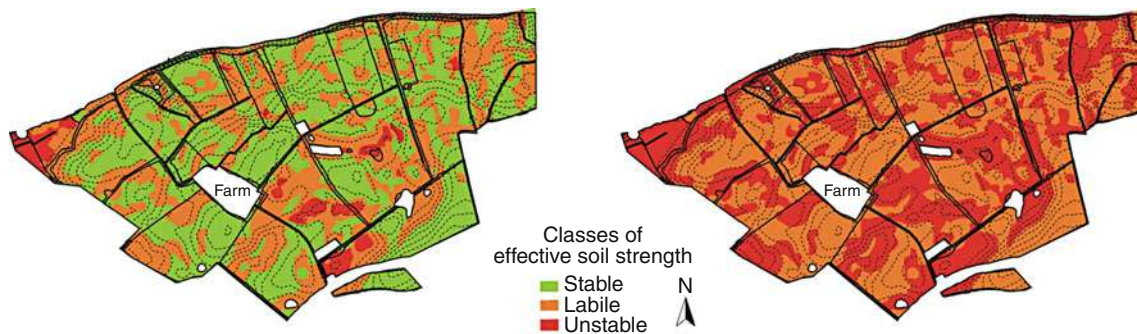
Quantification of the sensitive soils (areas) for defined applied stresses

According to Horn and Fleige (2003, 2009), the relationship of P_c to soil pressure can be determined by considering the stress propagation theory and the ratio $P_c/\text{overburden pressure}$ for classification. If the strength of the soil horizon is lower than the applied stress, the ratio is smaller than 0.8 and the horizon is defined as

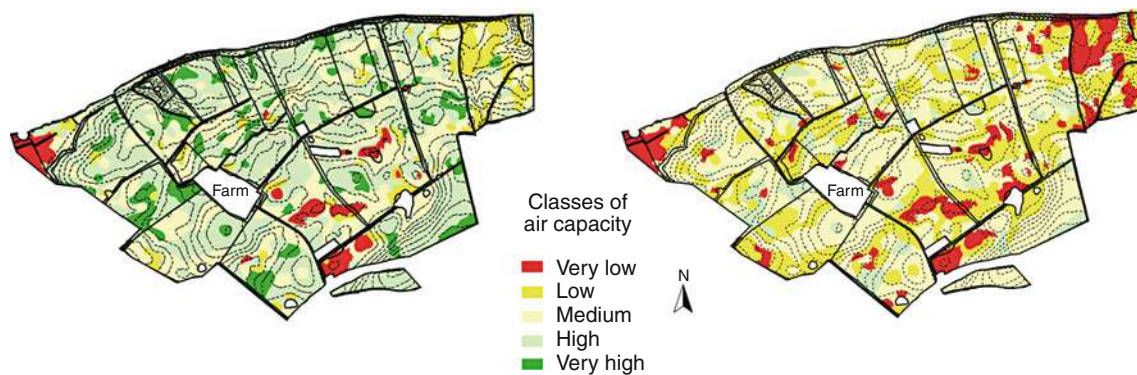
plastic/fluent. If the ratio exceeds 1.2, the soil is defined as rigid (stable and very stable). If the ratio is between 0.8 and 1.2, we classify the applied stress mostly too high (unstable). If the stress distribution under agricultural machinery is now modeled by the method of Newmark 1942 and compared with the actual internal soil strength per horizon, we can quantify the unavoidable consequences for soil functions within the virgin compression



Subsoil Compaction, Figure 3 Modeling of precompression stress P_c at pF 1.8 (-60 hPa) resp. $<\text{pF} 1.8$ (hydromorphic soils) (left) and pF 2.5 (-300 hPa) resp. pF 1.8 (hydromorphic soils) (right) for subsoils (40 cm) at farm scale. Classification of P_c (kPa): very low <30 , low 30–60, medium 60–90, high 90–120.



Subsoil Compaction, Figure 4 Relationship between the precompression stress and actual soil pressure for subsoils (40 cm) at farm scale. Subsoil stress: 60 kPa (left), subsoil stress: 90 kPa (right). Classification of the effective soil strength is defined by the relationship of precompression stress to soil pressure: 1.5–1.2 stable, 1.2–0.8 labile, <0.8 unstable, additional plastic deformation.



Subsoil Compaction, Figure 5 Modeling changes of air capacity at pF 1.8 (-60 hPa), respectively, at $<\text{pF} 1.8$ (stagnic and gleyic horizons) for subsoils (40 cm) at a stress of 90 kPa (right) in comparison to the initial state (left) at farm scale. Classification (Vol. %): very low: <2 , low: 2 to <5 , medium: 5 to <13 , high: >13 .

load range. [Figure 4](#) compares the application of a soil stress of 60 and 90 kPa in the subsoil (40 cm depth) at field capacity. It is obvious that a stress of 90 kPa exceeds the P_c of all subsoils, because the effective soil strength is too small and classified as labile to unstable. At a stress of 60 kPa, about 30% of the subsoils react labile to unstable, whereby there are differences resulting from pedodiversity between the fields.

Consequence of subsoil compaction on the air capacity as a function of stress applied

The analysis stress dependent changes of soil physical properties can again be determined on the basis of corresponding PDF for various texture classes (Horn and Fleige [2003](#)) and results in the differentiation of soil types, regions, landscapes concerning the long-term alterations, and possibly negative effects on soil properties that are responsible not only for crop yield, rooting but also for soil erodibility, filtering, and buffering processes or even gas emission.

A more detailed analysis on the large (farm) scale allows a better and more complete insight also in the irreversible processes and can become the basis for a more site-adjusted land use management ([Figure 5](#)).

It shows the potential effects at a defined stress of 90 kPa at field capacity in comparison to the initial state in the subsoil at the example of the air capacity (macro porosity, pores $>50 \mu\text{m}$). Because the oxygen supply of hydromorphic soils is restricted, a reduction of one air capacity class (e.g., medium to low) is assumed. The P_c of all soils at a stress of 90 kPa is exceeded, but "harmful changes of the soil" by modeling the parameter air capacity exist only for approximately 25% of the soils. On the side, this is attributed to all soils with loamy texture (e.g., eroded Luvisols with Bt-horizon near to the surface) and on the other side furthermore to all loamy sandy hydromorphic soils. Such soils, for example, Gleysols show in many cases medium- to high-air capacity values, but despite a sandy texture a low oxygen supply, because of incomplete air-filled macro pores.

Conclusions

The P_c value and the concept of critical values can be applied for the description of the soil mechanical strength. The P_c value is used as the precaution value to conserve the existing soil structure. P_c -maps of (sub) soils at all scales are a helpful tool for decision makers, agricultural advisers, or farmers for a site-adjusted land use. The decision about the site-adjusted machinery of a farm or a company can be related to the internal soil strength data at the weakest, that is, wettest site conditions in the subsoil and used for the specification of an appropriate agricultural machine. Thus, it will be possible to avoid additional subsoil compaction and define sustainable land use systems.

Bibliography

- DVWK, 1995. Soil strength in structured unsaturated soils. Part I: precompression stress. (in German, with English summary and captures) Gefügestabilität ackerbaulich genutzter Mineralböden. Teil I: Mechanische Belastbarkeit. Merkblätter 234, Wirtschafts- und Verlagsges. Gas und Wasser, Bonn.
- DVWK, 1997. Gefügestabilität ackerbaulich genutzter Mineralböden, Teil 2: Auflastabhängige Veränderung von bodenphysikalischen Kennwerten. DVWK-Merkblatt 235, ATV-DVWK, Germany, p. 7.
- European Soil Framework Directive, 2006. Proposal for a directive of the European parliament and of the council establishing a framework for the protection of soil and amending directive 2004/35/EC. p. 30.
- Fraters, B., 1996. Generalized soil map of Europe. Aggregation of the FAO-Unesco soil units based on the characteristics determining the vulnerability to degradation processes. RIVM report no. 481505006, Bilthoven/The Netherlands, p. 60.
- German Soil Protection Law, 1998. Gesetz zum Schutz des Bodens vom 17.03.1998. BGBI.I, p. 502.
- Horn, R., and Fleige, H., 2003. A method for assessing the impact of load on mechanical stability and on physical properties of soils. *Soil and Tillage Research*, **73**, 89–99.
- Horn, R., and Fleige, H., 2009. Risk assessment of subsoil compaction for arable soils in Northwest Germany at farm scale. *Soil and Tillage Research*, **102**, 201–208.
- Horn, R., van den Akker, and J. J. H., Arvidsson, J. (eds.), 2000. Subsoil compaction – distribution, processes and consequences. *Advances in Geocology*, **32**, 462.
- Horn, R., Fleige, H., Richter, F.-H., Czyz, E. A., Dexter, A., Diaz-Pereira, E., Dumitru, E., Enarche, R., Mayol, F., Rajkai, K., De la Rosa, D., and Simota, C., 2005. SIDASS project part 5: prediction of mechanical strength of arable soils and its effects on physical properties at various map scales. *Soil and Tillage Research*, **82**, 47–56.
- Horn, R., Fleige, H., Peth, S., and Peng, X., (eds.), 2006. Soil management for sustainability. *Advances in Geocology*, **38**, 497.
- Newmark, N. M., 1942. Influence charts for computation of stresses in elastic foundations, University of Illinois Bulletin No. 338.
- Pagliai, M., and Jones, R. (eds.), 2002. Sustainable land management environment protection – a soil physical approach. *Advances in Geocology*, **35**, 588.
- Van den Akker, J. J. H., 2002. Soil compaction. Determination of the susceptibility of subsoils to compaction and ways to prevent subsoil compaction. In Pagliai, M., and Jones, R. (eds.), Sustainable Land Management – Environmental Protection – A Soil Physical Approach. *Advances in Geocology*, **35**, 291–305.
- WRB, 2006. World Reference Base for Soil Resources. A framework for international classification, correlation and communication. WRB Resources Reports, p. 103.

Cross-references

- [Agrophysics: Physics Applied to Agriculture](#)
[Compression Index](#)
[Databases of Soil Physical and Hydraulic Properties](#)
[Mechanical Resilience of Degraded Soils](#)
[Soil Compatability and Compressibility](#)
[Stress–Strain Relations](#)

SURFACE AND SUBSURFACE WATERS

Todd C. Rasmussen

Warnell School of Forestry & Natural Resources, The University of Georgia, Athens, GA, USA

Synonyms

Ground water; Soil water; Streamflow

Definitions

Surface water – liquid water (H_2O , including all isotopic forms) found above the ground surface, including lotic (flowing) water in channels and as overland flow, and lentic (non-flowing) water in lakes, ponds, and wetlands, but does not include water found in plants, animals, or the atmosphere.

Subsurface water – liquid water found below the ground surface, including soil water above the water table and ground water below the water table, but does not include water chemically bound to minerals or organic matter.

Introduction

Water is a chemical compound with three dominant phases on Earth – gas, liquid, and solid. Gaseous water has a high vapor pressure, especially at warm temperatures, making it readily transportable through the atmosphere. Liquid water has a low viscosity, making it highly mobile, and is polar, making it an excellent solvent. Solid water is less dense than its liquid form, making it float.

Accounting for the movement and distribution of water resources is important because water is a vital component of world economic activity, including transportation and commercial, industrial, and energy production (Cech, 2009; Glennon, 2009). It is also important to agriculture, especially in climates where precipitation is insufficient to satisfy crop water requirements (Hillel, 1994).

The vast majority of water on Earth lies within its oceans (Gleick, 1996), while most of the remainder is present in polar icecaps (Table 1). That small residual not found in oceans or icecaps is predominately found in the subsurface, which is more abundant (but generally less accessible) than surface water. The volume of water found

in plant life is only a small fraction of the next larger reservoir, the atmosphere. The residence times (defined as the volume of water, V , in the reservoir divided by the average flux, Q , through the reservoir, $\tau = V/Q$) of water in our oceans and icecaps are much longer than in the soil, atmosphere, and plant life.

Understanding the source of water in streams and groundwater is critical to their management. Water in streams is generated by a range of mechanism, including

- Precipitation on saturated surfaces (e.g., channel surfaces, wetlands, lakes, riparian areas);
- Exfiltration from shallow, perched aquifers and subsurface piping (e.g., root and animal holes);
- Ground-water discharge from aquifers (both unconfined (An unconfined aquifer is a geologic unit capable of transmitting adequate water to wells when pumped, overlain by a water table, that allows gravity drainage from pores when pumped) and confined (A confined aquifer is a geologic unit capable of transmitting adequate water to wells when pumped, overlain by a confining layer that prevents gravity drainage from pores; water released from storage is due to expansion of pore fluids and matrix as the pore fluid pressure declines)).

Subsurface water is found as soil water either above the *water table* (A water table is the water-level elevation in a well completed in an unconfined aquifer), or as ground water below the water table (Figure 1). Recharge to the unconfined aquifers originates as infiltration into soil water, and then percolation through the unsaturated zone to the water table. Recharge is less than infiltration due to plant water uptake in the root zone. Recharge to confined aquifers can occur either in the zone where the aquifer outcrops, or by flow from an adjacent aquifer through a confining layer.

At the local scale, water flow obeys the conservation equation (Hillel, 1998)

$$\nabla \cdot \vec{q} + \frac{d\theta}{dt} \pm r = 0 \quad (1)$$

where \vec{q} (L/T) is the flux vector, θ (L^3 -water/ L^3) is the volumetric water content, and r (L^3 -water/ L^3/T) is the local source/sink term.

At larger, watershed scales, the conservation (or water-budget) equation is

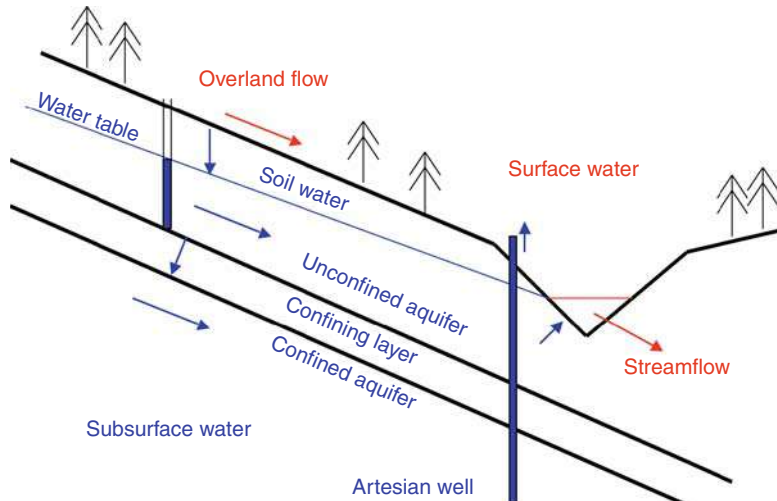
$$P = Q + ET + W \pm \Delta S \quad (2)$$

where P is the precipitation, Q is discharge from the outlet of the watershed, ET is the evapotranspiration, W includes other consumptive water withdrawals, and ΔS is the change in storage per unit time within the watershed. Note that the units of these variables can be or volume per time, (L^3/T), or volume per area per time, which is a depth per time, (L/T).

While water is generally considered to be a renewable resource (i.e., it is replenished by precipitation), the extraction of surface and ground water can exceed the rate

Surface and Subsurface Waters, Table 1 Water volumes and approximate residence times

Reservoir	% of Water		Residence Time
	Global	Fresh	
Oceans and seas	97.5	–	2,643 years
Glaciers	1.75	68.7	12,000 years
Ground water	0.79	30.9	5,400 years
Surface water	0.008	0.3	2.26 years
Soil water			7 weeks
Atmosphere	0.0009	0.04	9 days
Plants	0.00008	0.003	5 days



Surface and Subsurface Waters, Figure 1 Surface and subsurface water schematic.

of natural replenishment (i.e., $W > P$), causing unsustainable declines in local and regional water resources (i.e., $\Delta S < 0$) (Hillel, 1992; Glennon, 2004; Cech, 2009). Even in areas with abundant precipitation, water is often limiting due to asynchronicity between water supply and demand. Increasing water storage using surface and subsurface reservoirs is an important mechanism for synchronizing water supplies with demands.

Modern investments in dams to store surface water have multiple benefits including mitigating floods, augmenting flows for irrigation, and assuring sufficient flows for navigation. Yet the adverse impacts on sediment loads, as well as failure to provide sufficient environmental flows to support endemic fish species, have had grave effects on natural ecologic functions (Ward, 2002). Relying on subsurface water for storage can reduce the ecologic impacts, but these impacts are often difficult to eliminate entirely (Glennon, 2004).

Surface water

Surface water has long been used for agricultural purposes, primarily irrigation and aquaculture (fish production) (Hillel, 1994; Yoo and Boyd, 1994). Most of the earliest agricultural centers were located in subtropical to warm-temperate climates along major waterways, including the Indus, Nile, Tigris/Euphrates, Yellow, and Ganges rivers (Cech, 2009).

Measuring the quantity of flows in streams is important for their allocation and management. Streamflow discharge, Q (L^3/T), is measured using

$$Q = \int_A v(A) dA = \sum_{i=1}^n v_i A_i \quad (3)$$

where v_i (L/T) is the flow velocity determined using a flowmeter at point i within the stream, $A_i = w_i h_i$ is the incremental cross-sectional area surrounding the

measurement point, and where $w_i(L)$ is the distance between velocity measurements, and $h_i(L)$ is the total depth of the stream at the point of measurement. Note that $\bar{v} = Q/A$ is the mean water velocity, where $A = \sum_i A_i (L^2)$ is the total stream cross-sectional area.

Repeated measurements of discharge over a range of stages (water level elevations) are used to construct a rating curve, with the general form

$$Q = a (h - h_o)^b \quad (4)$$

where a and b are fitted coefficients, and h_o is the stage at which $Q = 0$. More accurate measurements of streamflow can be obtained using control structures, such as *flumes* and *weirs*, which provide a uniform cross-section and stable stage-discharge relationships.

For ungaged streams (those without control structures or rating curves), the mean velocity can be estimated using the *Manning formula*

$$\bar{v} = \frac{1}{n} R^{2/3} S^{1/2} \quad (5)$$

where n ($T/L^{1/3}$) is the Manning friction factor, a function of channel characteristics, $R = A/P(L)$ is the hydraulic radius, a function of the stream cross-sectional area, A (L^2), and the wetted perimeter, $P(L)$, which is the length of the streambed interface, and $S(L/L)$ is the channel energy slope, approximately equal to the water surface slope.

Flooding is a major concern along rivers and streams, and occurs when streamflow exceeds the channel flow capacity. The *kinematic velocity*, or *celerity*, (L/T), is used to account for the velocity of the flood wave (McCuen, 2005)

$$c = \frac{dQ}{dA} = \bar{v} + A \frac{d\bar{v}}{dA} \quad (6)$$

The kinematic ratio, k , is a dimensionless number that is the ratio of the celerity to the mean water velocity

$$k = \frac{c}{\bar{v}} = 1 + \frac{A}{\bar{v}} \frac{d\bar{v}}{dA} \quad (7)$$

The kinematic ratio is commonly greater than one because water usually flows faster as the flow area (or depth) increases (i.e., $d\bar{v}/dA > 0$). Yet the marginal velocity may decrease once floods overtop the floodplain (i.e., $d\bar{v}/dA < 0$), introducing additional friction losses, so that $k < 1$. The flood wave velocity can be predicted for a range of stages as a function of the mean water velocity and the kinematic ratio.

A more complete description of the dynamic behavior of flood waves that incorporates the continuity and momentum equations is given by (McCuen, 2005)

$$\frac{\partial h}{\partial x} + \frac{1}{g} \left[v \frac{\partial v}{\partial x} + \frac{\partial v}{\partial t} \right] = S_o - S_f \quad (8)$$

where h is the water surface elevation, v is water velocity, g is the gravitational constant, x and t are distance and time, respectively and S_o and S_f are the bed and friction slopes, respectively.

Subsurface water

Subsurface water is less accessible for exploitation due to the need for mechanical devices (such as pumps) to lift the water to the surface. Early agricultural societies in Central Asia and the Middle East developed the ability to harvest ground water in unconfined aquifers using *qanats*, which are near-horizontal tunnels that intersect the water table and allow the water to flow by gravity to the surface (Hillel, 1994; Cech, 2009). In some areas, vertical boreholes tapped into *confined aquifers* support *artesian* wells, which flow to the surface without pumping.

Modern wells provide access to the ground-water reservoir, but can be limited by the total storage and permeability of the units. Flow through an aquifer is described using *Darcy's law*

$$\vec{q} = -K \nabla h \quad (9)$$

where \vec{q} (L/T) is the three-dimensional flux vector, K (L/T) is the hydraulic conductivity (a measure of permeability), and ∇h is the hydraulic gradient. This formulation is appropriate for flow through an unconfined aquifer.

For a confined aquifer, Darcy's law is written in two dimensions:

$$\vec{q} = -T \nabla h \quad (10)$$

where \vec{q} (L²/T) is the two-dimensional flux vector, and

$$T = \int_b K(b) db = \sum_{i=1}^n K_i b_i \quad (11)$$

is the aquifer transmissivity (L²/T), which represents the integrated hydraulic conductivity across the aquifer thickness, b (L).

Water flow through the soil above the water table is primarily vertical. Because the soil is not fully saturated, an unsaturated flow equation is used

$$\vec{q} = -K(\psi) \nabla h \quad (12)$$

where $K(\psi)$ is the soil-tension-dependent hydraulic conductivity, ψ is the *soil tension* (The soil tension is a negative pressure head that accounts for the cohesive and adhesive forces between water and soil, respectively), and $h = z - \psi$ is the total head, with z being the elevation. Note that

$$\begin{aligned} \nabla h &= [0, 0, 1] - \nabla \psi \\ &= \left[-\frac{\partial \psi}{\partial x}, -\frac{\partial \psi}{\partial y}, 1 - \frac{\partial \psi}{\partial z} \right] \end{aligned} \quad (13)$$

The function $K(\psi)$ can also be written as $K(\theta)$, where θ is the soil water content, and the function $\psi(\theta)$ is the soil characteristic curve that relates the soil tension to the water content.

Modern agriculture relies heavily on ground-water extraction for all or part of their irrigation needs. Declines in water levels due to pumping have resulted in reductions in ground-water flows to streams, causing a reduction in streamflow in these areas (Glennon, 2004). *Subsidence* of the ground surface results when the pore pressure (which partially supports the mineral matrix) is reduced.

Water quality

Water pollution from point and nonpoint sources may compromise the value of water for subsequent use by downstream users. Surface water quality can be compromised by stormwater runoff from agricultural lands, as well as contamination of ground water (Boyd, 2000). Stormwater has been shown to transport a wide diversity of potential contaminants (e.g., nutrients, sediments, pesticides, herbicides, pathogens).

Soil salinization results when flows are insufficient to remove accumulated salts from soils, causing the loss of agricultural productivity. Also, natural sediment transport can be reduced by trapping in reservoirs or by reduced sediment transport capacity, or increased by erosion from land-disturbing activities.

Contaminant migration is commonly represented using the advection-dispersion equation (ADE)

$$\frac{\partial C}{\partial t} = D \frac{\partial^2 C}{\partial x^2} - v \frac{\partial C}{\partial x} \quad (14)$$

where C is the solute concentration, D is the effective dispersion coefficient, v is the velocity, x is distance, and t is time. This equation describes both the advective

component of transport, along with Taylor dispersion. The solution to the ADE for a Heaviside (step) input (release) of a conservative tracer is (Ogata 1970)

$$C(x, t) = \frac{1}{2} \left[\operatorname{erfc} \left(\frac{x - vt}{2\sqrt{Dt}} \right) + \exp \left(\frac{vx}{D} \right) \operatorname{erfc} \left(\frac{x + vt}{2\sqrt{Dt}} \right) \right] \quad (15)$$

Besides advection and dispersion, a wide range of other processes affects the fate and transport of contaminants (e.g., biological uptake and degradation, sorption, volatilization, and settling).

The effects of water quality degradation depend upon the use of the water. Elevated nutrients may be desired for agricultural uses, but not for environmental or drinking water uses. Elevated salinity may be desired for specific forms of aquaculture, but not for others.

Water-quality degradation can be mitigated using a broad array of agricultural practices (e.g., no-till agriculture, riparian buffers, animal exclusion from streams, grass filter strips, terracing, and farm ponds). Efforts to control contamination commonly focus on reducing pollutant loading to levels that do not exceed the *assimilative capacity* of aquatic systems.

Summary

Surface and subsurface waters are a small component of the global water budget, yet are vital for a wide range of economic activities, including agricultural irrigation and aquaculture. Surface and subsurface waters are widely used to augment precipitation, and to carry away salts and other waste materials. Measuring the quantity and flow of surface and subsurface waters is an important component of water management. Adverse environmental and social impacts may occur when water utilization exceeds available supplies, or when contaminant loading exceeds the assimilative capacity of aquatic systems.

Bibliography

- Boyd, C. E., 2000. *Water Quality: An Introduction*. New York: Springer.
 Cech, T. V., 2009. *Principles of Water Resources: History, Development, Management, and Policy*, 3rd edn. New York: Wiley.
 Gleick, P. H., 1996. Water resources. In Schneider, S. H. (ed.), *Encyclopedia of Climate and Weather*. New York: Oxford University Press, Vol. 2, pp. 817–823.
 Glennon, R., 2004. *Water Follies: Groundwater Pumping and the Fate of America's Fresh Waters*. Washington: Island Press.
 Glennon, R., 2009. *Unquenchable: America's Water Crisis and What to Do About It*. Washington: Island Press.
 Hillel, D., 1992. *Out of the Earth: Civilization and the Life of the Soil*. Berkeley: University of California Press.
 Hillel, D., 1994. *Rivers of Eden: The Struggle for Water and the Quest for Peace in the Middle East*. Oxford: Oxford University Press.

- Hillel, D., 1998. *Environmental Soil Physics: Fundamentals, Applications, and Environmental Considerations*. New York: Academic.
 McCuen, R. H., 2005. *Hydrologic Analysis and Design*, 3rd edn. Upper Saddle River: Pearson Prentice Hall.
 Ogata, A., 1970. Theory of Dispersion in a Granular Medium. U.S. Geological Survey Professional Paper 411-I.
 Ward, D. R., 2002. *Water Wars: Drought, Flood, Folly, and the Politics of Thirst*. New York: Penguin Putnam.
 Yoo, K. H., and Boyd, C. W., 1994. *Hydrology and Water Supply For Pond Aquaculture*. New York: Springer.

Cross-references

- [Field Water Capacity](#)
[Flooding, Effects on Soil Structure](#)
[Hydraulic Properties of Unsaturated Soils](#)
[Infiltration in Soils](#)
[Irrigation and Drainage, Advantages and Disadvantages](#)
[Leaching of Chemicals in Relation to Soil Structure](#)
[Salinity, Physical Effects on Soils](#)
[Soil Erosion Modeling](#)
[Soil Water Flow](#)
[Soil Water Management](#)
[Solute Transport in Soils](#)
[Tropical Watersheds, Hydrological Processes](#)
[Water Balance in Terrestrial Ecosystems](#)
[Water Budget in Soil](#)
[Water Reservoirs, Effects on Soil and Groundwater](#)

SURFACE AREA

See [Specific Surface Area of Soils and Plants](#)

SURFACE CHARGE

See [Surface Properties and Related Phenomena in Soils and Plants](#)

SURFACE PROPERTIES AND RELATED PHENOMENA IN SOILS AND PLANTS

Grzegorz Józefaciuk
 Institute of Agrophysics, Polish Academy of Sciences,
 Lublin, Poland

Definition

A *surface phenomenon* is a phenomenon that takes place on or near a surface, that is, in a common boundary among contacting phases (including solid–liquid, solid–gas, and liquid–gas interfaces). The specific properties of surfaces of plant tissues and of mineral and organic surfaces occurring in soils result from their complex chemical buildup, large area and charge, and primarily, from a range of interactions (forces) between the molecules present in the interfaces.

Intermolecular interactions

Chemical forces. The contacting molecules may form a chemical compound at the join. The strongest bonds are where atoms of the two materials swap (ionic bonding) or share (covalent bonding) outer electrons. These attractive forces are effective only over very small distances, less than a nanometer. A weaker bond is formed if an (electron poor) hydrogen atom in one molecule is attracted to a free electron pair of, for example, nitrogen, oxygen, or fluorine atom in another molecule, which is called hydrogen bonding.

Electrostatic (Coulomb) forces. Forces between electric charges of the magnitude (for point charges) directly proportional to the product of the magnitudes of each of the charges and inversely proportional to the square of the total distance between them. Charges of the same sign (like charges) repel and of the opposite signs (unlike charges) attract each other. Linear superposition is applied to calculate the force exerting on one charge by a system of several discrete charges. For a charge distribution in a space (surface) an integral over the region containing the charge is applicable, treating each infinitesimal element of space as a point charge.

Dispersive (van der Waals) forces. These very weak forces compared to chemical bonds forces, also of electrostatic origin, have four major contributions: repulsive forces preventing the collapse of molecules as they move closer to one another due to electronic shells repulsion (Pauli exclusion principle) and three attractive components: the electrostatic (Keesom) force between permanent charges on a molecular ion and permanent multipoles on the other molecule; induction (Debye) forces between a permanent multipole (charge) on one molecule with an induced multipole on the other; and attraction (London) forces between momentary multipole occurring on one molecule due to permanent variation of electrons density around atoms and induced by it momentary multipole on the other molecule. Dispersive forces are generally anisotropic, which means they depend on the relative orientation of the molecules and are effective over very small distances (less than 1 nm).

Diffusive forces. This type of interaction occurs when a mobile part(s) of a molecule penetrate into an adjacent phase while still being bound to the phase of origin.

Steric forces. The sterical join occurs when one molecule locates inside a space within the other molecule to which it fits merely well.

Intermolecular attraction forces between like-molecules in a single phase are called cohesion forces, while these forces between molecules present in two adjacent phases are forces of adhesion.

Adsorption

In a bulk material, all intermolecular forces between the constituent molecules (atoms) are generally neutralized by surrounding neighbors, however, molecules on the surface are not wholly surrounded and therefore they attract

molecules from the adjacent phase that is known as adsorption process. If weak van der Waals forces are responsible for the process, it is classified as physisorption while if chemical bonds are formed in consequence of adsorption, it is called chemisorption. Thus during chemisorption only a single layer (monolayer) of the adsorbed molecules (adsorbate) can form chemical bonds with the surface of the solid (adsorbent) and the process is characterized by high energies ($80\text{--}300\text{ kJ mol}^{-1}$). In chemisorption, the minimum in potential energy occurs at a distance less than 3 Å corresponding to the length of a chemical bond. Physisorption is a general phenomenon and occurs at any surface. Usually the adsorbed molecules (especially from a gas phase) can form several layers on the adsorbent surface (multilayer adsorption). For physisorption, a minimum in potential energy, between 2 kJ mol^{-1} and 15 kJ mol^{-1} , exists at a distance corresponding to the Van der Waals radius (ca. 6 Å) and the quantity of the fluid phase adsorbed decreases with increasing temperature.

Physical adsorption of water vapor on surfaces of soil constituents plays important role in formation of water films under unsaturated soil conditions. Usually adsorption of water vapor on plant root surfaces is more energetically favored than on soil materials (more strongly polar groups on root surfaces) and water films at the same conditions are thicker on the roots. The adsorption of natural organic matter on inorganic particle surfaces such as clay and quartz is an important geochemical process that occurs in soil and aquatic media. Adsorption to mineral phases can stabilize organic matter against microbial decay in soil. Formation of strong bonds that reduce desorbability can explain that effect. With time, the adsorbed organic matter may undergo changes in configuration, migrate into pores, or intraparticle spaces in minerals or rearrange structural configurations of organo-mineral associates so its stability may increase with residence time. Stabilization of low-molecular-weight organic compounds may result from their diffusion and adsorption into pores small enough to prevent hydrolytic exoenzymes from entering.

Catalysis

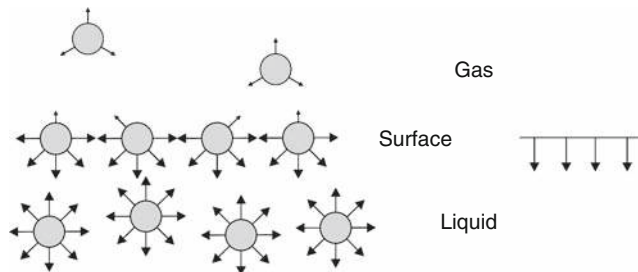
Molecules adsorbed on a surface may react with each other. Usually the rate of the reaction is different than in their own phase due to increase in concentration of the adsorbed reagents, their specific orientation or deformation, weakening intramolecular bonds, dissociation or lysis to reactive forms (new bonds to the surface are favored), or changing the frequency of contact of the reactants. The adsorbent (catalyst) can fasten (positive catalysis) or break the process (inhibition). The adsorbed species are bound to active sites on the catalyst; therefore, the rate of the process is highly related to the total surface area of the adsorbent. In a reaction catalyzed by a solid (heterogeneous catalysis), the diffusion of reagents to the surface and of products out from the surface are frequently

rate-determining steps. Surfaces having acidic character can catalyze many reactions in soils involving water, as hydrolysis and its reverse. Catalytically active are zeolites, alumina, and humic substances. Transition metals catalyze redox reactions (oxidation, hydrogenation).

Surface free energy (surface tension)

A molecule within a bulk phase attracts the surrounding molecules and in turn it is attracted by them (cohesion forces). To create a surface one has to input enough energy to break cohesion bonds. Because at a break two surfaces are formed, the energy given to the surface (surface tension Y , joule per square meter or newton per meter) equals half of the energy of cohesion (ideal case). All surfaces exhibit surface tension that is of most importance for liquid surfaces. The surface of the liquid differs from its bulk. Inside a liquid, all cohesion forces between molecules neutralize each other while on the surface, the molecules are much more attracted by the neighboring liquid molecules, than by the gas molecules outside. As a result, a force directed inside the liquid is formed on the surface and the latter behaves like an elastic membrane, which covers and compresses the liquid tending to diminish the area of its surface ([Figure 1](#)).

The surface tension expresses the force with which the surface molecules attract each other. Surface tension can be modified by other compounds added into the liquid. For example, low-molecular hydrocarbons (e.g., sugar) dissolved in water have little or no effect on the surface tension, as their hydroxyls interact with water molecules via hydrogen bonds, as water molecules bond themselves. Ions of dissociated soluble salts strongly interact with water molecules (hydration); thus, they can further increase the surface tension. Dissolved alcohols decrease water surface tensions, as their nonpolar (hydrocarbon) chains interact with water molecules only by weak dispersion forces. Special molecules having strongly polar hydrophilic head and a long nonpolar hydrophobic tail can markedly diminish water surface tension. Such compounds, called surfactants reduce the surface tension of water by accumulating at the liquid–gas interface, with the head remaining in water and a tail directing outside. Many surfactants can also assemble in the bulk solution



Surface Properties and Related Phenomena in Soils and Plants, Figure 1 Intermolecular forces at liquid–gas interface.

into aggregates (micelles). Examples of such aggregates are phospholipid membranes in plants (e.g., cell vacuoles used for osmotic control and nutrient storage). Soil humic acids have an amphiphilic nature because of the presence of both hydrophilic and hydrophobic fragments in their structure; thus, they are able to reduce water surface tension as well, and can form micelle-like aggregates. In soil environments, such surface activities of humic acids can play an important role in the transport, bioavailability, and biodegradability of hydrophobic organic pollutants (a pollutant is bound to a hydrophobic part of humic acid and so follows its pathway). Usually the surface activity of humic acids is facilitated at lower pH of soil solution. Similarly, hydrophobic fragments of bacterial cell walls can adsorb hydrophobic molecules affecting contaminant mobility.

Evaporation and condensation

The number of bulk neighbors interacting with a molecule located on the liquid surface depends on the surface curvature. If it is convex, fewer neighbors and if concave, more neighbors are in close contact with surface molecule than for flat surface. The cross section of the space containing direct members of the surface molecule (interaction sphere) on various menisci is imagined in [Figure 2](#).

Therefore less energy is needed to move a molecule to the gas phase (evaporate the liquid) from a convex surface than from flat surface and than from concave surface. So the vapor pressure p over convex surface is higher and over concave surface is lower than the pressure over flat surface, p_0 (saturated vapor pressure). Obvious is that the greater surface curvature, that is, the smaller the curvature radius r , the effects are more pronounced (small liquid droplets evaporate much faster than bigger ones), which is described by a Kelvin equation

$$\log(p/p_0) \sim Y/r \quad (1)$$

As an environmental process, evaporation and transpiration of water are collectively termed evapotranspiration. Transpiration is the evaporation of water from the aerial parts of plants, mostly leaves. Transpiration cools plants and enables mass flow of water (and mineral nutrients) through the xylem from roots to shoots that is caused by the increase in water potential in the upper parts of the plants due to the evaporation of water out of stomata into the atmosphere. Plants can regulate transpiration by changing water–atmosphere contact area, that is, by closing or opening stomata depending on external air and soil



Surface Properties and Related Phenomena in Soils and Plants, Figure 2 Surface molecule interaction sphere on convex, flat, and concave surface.

conditions or they adapt their tissue structures to permanent unfavorable conditions (e.g., thick cuticles, reduced leaf areas, sunken stomata, and hairs to reduce transpiration and conserve water).

When vapor of a liquid is adsorbed on a wall of a thin tube (capillary) or on pore walls of a porous body, the film of adsorbed liquid forms a concave meniscus over which the equilibrium liquid vapor pressure is lower than over a liquid flat surface. Therefore, water vapor may condense in capillaries under lower pressure than under the saturated water pressure. The thinner the capillary, the lower water vapor pressure is needed to condense water and after this process is started, the whole volume of the capillary becomes instantaneously filled by the liquid because the radius of liquid meniscus in the tube decreases with the amount of condensed vapor, which is called capillary condensation. As the vapor pressure decreases, the liquid evaporates from the capillary to the atmosphere as vapor molecules. Various pore geometries (different types of menisci curvature) often lead to differences in condensation and evaporation pathways (liquid menisci are different at the same vapor pressure if the pore is empty or filled) that is called a hysteresis. In naturally occurring porous structures (soils), the geometry of pores is very complicated. Soils and their constituents form networks of pores, much like spaces between spherical granules with large voids connected by smaller necks and "snake-like" capillaries. In such structures, the concept of capillary condensation is used to determine pore-size distribution using adsorption-desorption isotherms.

For water vapor, the relation of equilibrium vapor pressure to the saturation vapor pressure can be considered as a relative humidity of the atmosphere, so capillary condensation is an important factor in soil water retention and transport (via gaseous phase). Due to adsorption and capillary condensation, soil stores water even in dry atmospheric conditions.

Capillary condensation is responsible for bridging between mineral and organic grains in soils at low moistures. The condensed layer of water in the pore formed at a contact point between grains adheres the grains. This consolidation mechanism is particularly important in soils poor in structure-stabilizing organic matter and amorphous mineral materials.

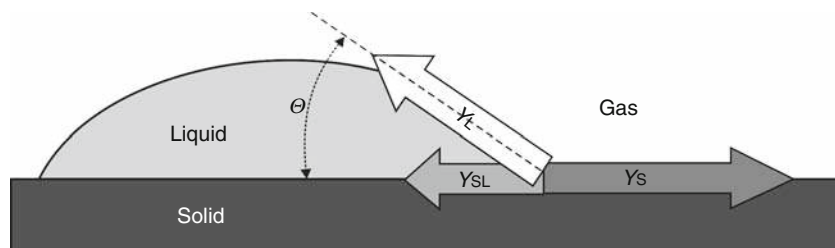
Wettability

The ability of a liquid to maintain contact with a solid surface results from a balance between adhesion and cohesion forces. The cohesive forces tend to keep liquid molecules together, and the adhesive forces tend to bind them to the surface and to spread the liquid upon it (wetting). When the forces of adhesion are greater than the forces of cohesion, the liquid tends to spread on (to wet) the surface, while in the opposite situation, the liquid tends to refuse the surface. Solids in which cohesion forces are very strong (covalent, ionic, or metallic bonds) have thus surfaces of high free energy (high-energy solids) and they are well wettable by most liquids. If cohesion forces are weak (e.g., van der Waals or hydrogen bonds) the solid has low surface free energy (low-energy solids) so it is consequently wetted only by liquids of low surface tension. Depending on wettability, a drop of a liquid placed on a solid surface forms a truncated sphere of which the angle at the solid surface contact point (contact angle) ranges from 0 for completely wettable to 180° for totally nonwettable solids. The contact angle θ results from a tendency of surface tensions to reduce the area of their own surfaces. The surface tension of the solid Y_S (solid-air interface) tends to reduce solid area by covering it with the liquid and consequently to enlarge the area of the liquid; in opposition, the surface tension of the liquid Y_L (liquid-air interface) tends to reduce liquid area by shrinking a drop and the surface tension of the solid-liquid interface Y_{SL} tends to reduce its area by repelling liquid from the contact surface. An equilibrium of interfacial surface tensions at the contact point for homogeneous flat surface is presented in Figure 3.

The force balance at the contact point can be described by the Young equation

$$Y_S = Y_L \cos\theta + Y_{SL} \quad (2)$$

Natural surfaces are usually chemically and geometrically heterogeneous and the wettability of such surfaces is a complex function of heterogeneity. The contact angle observed on rough surface is higher than the (intrinsic) contact angle on the respective flat surface and depends on the ratio of the true area of the solid surface to the apparent contact area (roughness ratio). For example, the lotus petal has uniformly spread hydrophobic



Surface Properties and Related Phenomena in Soils and Plants, Figure 3 Surface tensions balance at solid–liquid–gas contact point.

micropapillae on the surface and a water contact angle on such rough surface increases almost to 180° so water on the petal forms droplets of a spherical shape (superhydrophobicity), which roll out easily (self-cleaning effect). The contact angle observed on a surface build from different patches of various wettabilities (contact angles) relates to the input of the areas of these patches into the whole surface, which is of great importance for water movement in soils. By reducing liquid surface tension, surfactants in general should enhance wettability. However if strong interactions with the surfactant polar head and the polar surface of wettable material occur, the effect can be opposite due to decrease in solid surface free energy by adsorbed surfactant layer. Such effect is important in soils. Polar heads of humic compounds may be bound to mineral surfaces (or to each other) by ion-dipole or dipole-dipole interactions. Under water-saturated conditions, the stability of such associates is not high because weak electrostatic bonds are destabilized by water molecules; however, in undersaturated conditions they become increasingly important. Drying leaves organo-mineral and organic-organic associates with hydrophobic parts directed outward and (if enough organic matter is present) the soil becomes strongly hydrophobic, requiring a long time of watering to restore its original hydrophilic properties.

Capillary rise

When one end of a capillary is immersed in a liquid, it adheres to the surface of the tube with definite contact angle, forming a concave meniscus inside the tube if adhesion interactions overcome the cohesion ones (wettable solids), and a convex meniscus in opposite situation. The tendency to minimize area of the highest energy surface causes that the liquid tends to cover the solid surface and in consequence the liquid column in the tube is pulled up in the case of wettable solids and down in the case of nonwettable solids (here the highest energetic is liquid-air surface). The above phenomenon is called capillary action. Surface tension forces proportional to the curvature of the liquid meniscus surface r (equal practically to the capillary radius) act until they are balanced by weight of the liquid column (proportional to liquid density ρ , the area of the column cross section, and the height of the column H):

$$rY_L \cos\theta \sim \rho r^2 H \quad (3)$$

Thus, the height of the capillary rise is higher in thinner tubes. This phenomenon is important in movement of water in soil and transpirational pull in plants as it allows water to move up without the need for special transport mechanism. Capillary rise pulls water in soil up to the surface of the ground, where from it evaporates. This loss of soil water is minimized by plowing – mechanical disruption of upper soil layer enlarges diameter of capillaries and breaks capillary rise.

Osmosis

When a bulk liquid is separated by a membrane having pores permeable to liquid molecules, statistically the same amount of molecules will pass through the membrane from one side to another and vice versa. If into one part of the separated liquid a soluble substance is added, which molecules are too large to pass through the membrane pores (semipermeable membrane), statistically more liquid molecules passes the membrane from the side of pure liquid than from the side of solution (instead of some liquid molecules that should pass through, molecules of the dissolved substance collide with the membrane being reversed), and as a result the solution is diluted. This dilution may be stopped by exerting an external pressure on the solution thus forcing the liquid molecules to move in opposite direction (to counteract the osmotic pressure). The osmotic pressure Π is directly proportional to the concentration of the dissolved substance c :

$$\Pi \sim c \quad (4)$$

If the other side of the membrane is in contact not with pure solvent but with other solution, the total pressure on the membrane is the difference between osmotic pressures on its two sides. In isotonic situation when the osmotic pressures on both sides of the membrane are the same, no solvent movement occurs. Similar to capillary rise, osmosis is a physical process in which water moves, without input of energy. Seeds use osmotic pressure to crush rocks. Net movement of solvent from the less-concentrated (hypotonic) to the more-concentrated (hypertonic) solution is a frequent phenomenon responsible for water transport into and out of plant cells as many biological membranes are semipermeable (permeability may depend on solute charge and size). Osmosis is responsible for the ability of plant roots to uptake soil water, for the turgor pressure of a cell and for regulating an aperture of stomata. When a plant cell is placed in a hypertonic solution, the water in the cells moves out and the cell shrinks, which finally can lead to plasmolysis, while in the opposite situation the cell expands and can finally explode. To reach a balance in osmotic pressure, plants developed a homeostasis mechanism known as osmoregulation.

Solubility

Solubility is the property of a solid, liquid, or gas (solute) to dissolve in a liquid forming a homogeneous solution. The opposing process to dissolution is precipitation (or crystallization) of a solid. The solubility prolongs until these two processes reach the same rate (saturated solution). Temperature, presence of other species that can react with solute molecules, or pressure (especially for gases) can alter these rates and can thus influence the solubility. Solubility results from prevalence of intermolecular interactions between molecules of the solvent with that of the solute

over those among the molecules of the solute itself and is supported by the entropy factor (dissolved molecules are more dissipated). The solute dissolves better in a solvent having similar polarity to itself (like dissolves like). The solute molecules may form several species in the solution by dissociation, hydrolysis, and polymerization.

Solubility depends on the size (surface area) of the (solid or liquid) solute (similarly as evaporation). So smaller crystals are better soluble than larger ones that results in precipitate aging (the crystal size spontaneously increases in time). Therefore in soils, the solubility of amorphous phases of silicon, aluminum, and iron oxides rather than their more crystalline forms govern the concentration of respective ions in soil solution. Solubility depends also on the polymorphic form of the crystal solid; thus, weathering rates of different rocks of the same chemical composition may significantly differ. Contrary to most solids, the solubility of gases in water decreases with temperature, which may cause root oxygen stress in soils at warm seasons.

Many solids dissolve congruently, which means that the composition of the solid and the dissolved solute are identical. However, some substances dissolve incongruently, that is, the composition of the solute in solution differs from that of the solid. This process is accompanied by alteration of the solid being dissolved and formation of a secondary solid phase. Formation of metamorphic rocks results from incongruent dissolution. Most soil clay minerals dissolve incongruently.

Different soils have diverse solutions depending on soil composition and environmental conditions. Its composition is determined by weathering of parent rock, mineralization of plant residues, dissolution of primary minerals by carbonic acid that liberates calcium, magnesium, and potassium ions, and exchange of gases with the soil atmosphere. Soil solutions can contain dissolved sugars, fulvic and other organic acids, plant micronutrients such as zinc, iron, and copper, plus other metals, ammonium plus a host of others. Calcium is common in forest soils, some soils have high amount of sodium ions that greatly impact plant growth. The upper layers of soil water usually have higher organic content than the lower soil layers. Surface waters with high content of dissolved organic compounds (DOC) are typically found in peat and bogs

areas. Soil pH effects the type and amount of anions and cations that soil solutions contain.

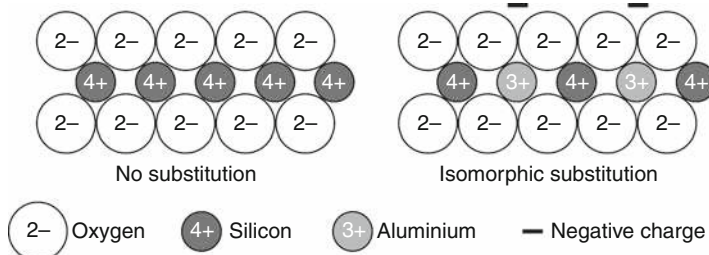
Colloids

Solutes dissolved in a solvent behave as a part of the liquid phase and they do not exhibit their surfaces (no phase boundary). If larger and larger particles (molecules) are dispersed in a liquid, they start to exhibit defined boundaries against the liquid and behave as individual phases (particles of approximate sizes above 0.002 µm). Such particles form a suspension named colloid. If particles size increase further to more than 0.2 µm, the mixture is formed, from which the particles tend to separate out quickly from the liquid phase. Colloids constitute the most chemically active fraction in soils, because the higher the contact surface in respect to the phase volume the more pronounced are surface phenomena. They are mineral or organic (humus) and could be crystalline (e.g., minerals and clay minerals of definite structure) or amorphous (e.g., hydrous oxides of iron, aluminum, and silicon). Behavior of soil colloidal systems depends on composition of soil solution in which finely dispersed mineral and organic particles are suspended.

Surface charge of soil constituents

The sources of charges on soil colloids are permanent (constant) charges due to isomorphic substitutions in clay minerals, and variable (pH dependent) charges due to broken edge, OH, and COOH groups.

Clay minerals are finely divided crystalline aluminosilicates. The basic building elements of the clay minerals are two-dimensional silicon–oxygen tetrahedral sheets and aluminum- or magnesium–oxygen–hydroxyl octahedral sheets. Kaolinite type minerals are built from one silica and one alumina sheet by sharing oxygen atoms between them (1:1 two-layer minerals). Montmorillonite type minerals are built from one octahedral sheet sharing oxygen atoms with two silica sheets (2:1 three-layer minerals). Isomorphic substitution of Si- and/or Al-ions in the crystal lattice by lower positive valence ions and accompanied “unsaturation” of oxygen bonds results in that clay lamellae achieve permanent negative charge exhibited on basal planes of the minerals (Figure 4).



Surface Properties and Related Phenomena in Soils and Plants, Figure 4 Isomorphic substitution of silicon by aluminum in the clay lattice.

Depending on the degree of substitution (influenced by conditions of mineral genesis) the layer charge density differs among different clay minerals. For most frequently occurring clay minerals, this charge amounts from a few thousands (kaolin group) by few tens thousands (mica group – illites) to hundreds thousands (smectites, zeolites) of coulombs per kilogram of the mineral (1 coulomb = $6,24 \times 10^{18}$ elementary charges). Frequently a part of the permanent lattice charge is neutralized by specifically bound cations inside the spaces between several subsequent structural layers of the mineral, as this occurs in illites due to binding of potassium cations. Permanent charge minerals dominate in mineral soils of the temperate climatic zone; therefore, soils of these regions are called permanent charge soils.

Contrary to the permanent charge, some mineral soil constituents can have either positive, zero, or negative charge of the magnitude depending on the composition of the soil solution (pH, concentration, ionic composition). In relatively low pH range, surface hydroxyl groups of these constituents may associate protons from soil solution via hydrogen bonds, thus, the surface becomes positively charged. In relatively high pH range, these surface hydroxyls may undergo acidic dissociation, resulting in formation of negative charge. At a defined pH value, the surface hydroxyls neither associate the protons from the solution nor dissociate their own ones and the surface has no charge. The latter value of pH is called point of zero charge (PZC). One can imagine the above reactions are similar to those illustrated in Figure 5 for aluminum (or iron) oxide.

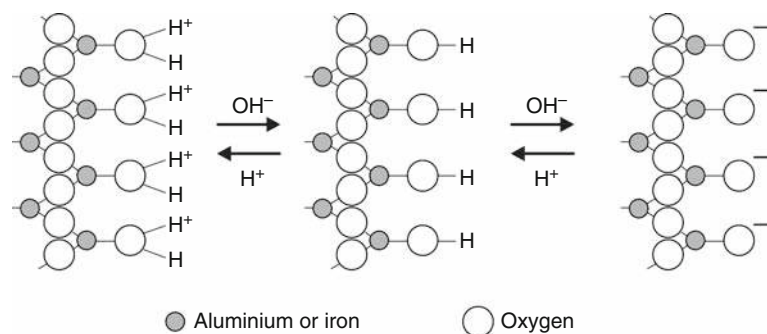
The point of zero charge for some most frequently occurring soil constituents is at pH values between 3 and 4 for silicon oxides, 5 and 8 for iron oxides, 6 and 10 for aluminum oxides. Tetrahedral Si–OH (silanol) and octahedral Al–OH (aluminol) groups situated at the mineral edges and hydroxyl-terminated planes of clay lamellae may be also involved in proton donor–acceptor reactions of hydroxylic groups; however, only 5–10% of the negative charge on 2:1 layer silicates is pH dependent, whereas 50% or more of the charge developed on 1:1 minerals can

be pH dependent. The PZC of edge surfaces of clay minerals is most frequently around 8.

Reactions of proton association/dissociation reactions on variable charge surfaces constitute important mechanisms of soil acid–base buffering systems.

Electrostatic charges dependent on pH are present to some extent in nearly all terrestrial ecosystems, however, they are predominately found in highly weathered soils of humid tropics and subtropics, as Oxisols, Ultisols, Alfisols, Spodosols, and Andisols (variable-charge soils), which collectively cover nearly one third of the global ice-free land surface area.

Humus is a major part of soil organic matter. It originates from a decomposition of animal and plant residues by soil flora and fauna to a point where it is highly resistant to further breakdown or alteration. Humic and fulvic acids are most important constituents of humus and their relative ratio increases with organic matter oxidation (mineralization). Humic substances are very complex, molecularly flexible polyelectrolyte materials with almost acidic (mostly carboxylic and phenolic) surface functional groups. Humic acids are larger and more aromatic than fulvic acids. Fulvic acids are more water soluble and more oxygenated than humic acids and have more total acidity and more carboxylic acid functional groups than humic acids. Surface functional groups of soil organic matter have very different acidic strength, depending not only on the kind of the group, but also on its locality. Surface groups of stronger acidic character are neutralized at lower pH values leaving a negative charge on the surface. The weaker acidic is the group, its neutralization requires higher pH value. Therefore the higher is the soil pH, the larger negative surface charge occurs on organic matter surfaces. Acidic surface groups located closely to each other, create common electric field surrounding these groups and within this field their protons become delocalized (proximity effect). The delocalized protons behave as strong acids and so the neighboring groups are very strongly acidic so the soil organic matter has some negative charge even at very low pH values. Charging of organic matter surfaces also markedly contribute to soil buffering.



Surface Properties and Related Phenomena in Soils and Plants, Figure 5 Formation of variable charge on surface of aluminum or iron oxides.

Bacterial cell walls expose numerous carboxyl, phosphate, and phenolic types of functional groups to the aqueous phase, and are negatively charged at pH values above approximately 2–3.

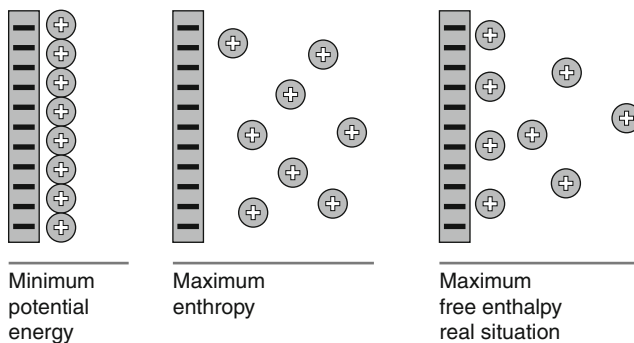
Electric double layer

The charged surface attracts ions of opposite sign of charge (counterions) from soil solution and repels ions of the same sign (coions). The tendency of the whole system to reach minimum potential energy would request the counterions to locate just near the surface and the coions to be repelled. The simultaneous tendency to reach maximum dissipation (entropy) would request a uniform distribution of both counter and coions in the solution. Thus, in the system, the potential energy factor is responsible for accumulation of most counterions close to the surface and repulsion of the coions while the entropy factor causes diffusion of some counterions out from the surface and of coions to the surface. As a result of these two opposite tendencies, the specific distribution of the ions near the surface occurs, which meets the conditions of minimum free enthalpy. The ions balancing surface charge together with the charged surface are called electric double layer (DDL) or diffuse double layer (DDL). The schematic buildup of this layer is shown in [Figure 6](#) wherein only counterions distribution is depicted.

The double layer can be roughly approximated as an electric condenser of one plate being the surface and the second being the layer containing counterions. The electric capacity of the condenser C equal to the plate (surface) net charge q divided by the electric potential U is proportional to the area between plates (i.e., area of the charged surface) S divided by the distance between the condenser plates d (i.e., the DDL thickness):

$$C = q/U \sim S/d \quad (5)$$

The rise in concentration and/or in counterion valence leads to the drop of the DDL thickness that, because the area of the charged surface is constant, leads to increase



Surface Properties and Related Phenomena in Soils and Plants, Figure 6 Distribution of counterions near negatively charged surface.

in DDL-condenser capacity. In the case of permanent charge soil constituents, (q is constant) this is connected with surface potential decrease. For variable charge components, the surface potential is governed by the point of zero charge PZC and this is constant at a given pH:

$$U \sim \text{PZC} - \text{pH} \quad (6)$$

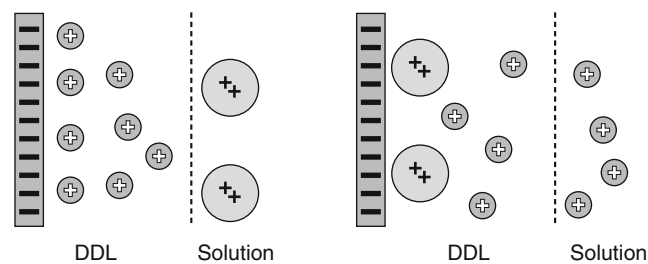
Thus, for such components, the increase of salt concentration and/or counterion valence leads to the increase of surface charge by the dissociation of surface protons to the solution (above PZC) or association of the solution protons to the surface (below PZC).

Prevalence of negatively charged surfaces in temperate climatic zone soils causes that they bound mainly cations. And so the troubles with anionic fertilization may arise. For example, the negatively charged nitrate anions are repelled to the solution and they are easily washed out from the soil with the rainwater. Therefore, this is better to apply the nitrate fertilizers in a few doses rather than in a single one, or to use foliar application. In mineral soils of humid tropics, having usually lower pH than the PZC, the deficit of cationic nutrients is a frequent phenomenon.

Ion exchange

The counterions present in the DDL may be easily exchanged with other ions being actually in an excess in soil solution as soluble salts. This process is called ion exchange and is schematically presented in [Figure 7](#). The formal boundary between the DDL and the bulk solution is drawn as a dashed vertical line.

Higher electrostatic force exerted by the charged surface on the higher valence counterions causes that they are better electrostatically adsorbed so their ratio to lower valence counterions is higher near the surface than in the bulk solution. When the surface potential drops to zero, this ratio approaches the ionic ratio in the bulk solution. The higher is the charge of the counterion and the higher is its mass, the higher is the force of its binding and so this ion is more difficult to be exchanged by other ions. Therefore, acidic soils may lose their ability to bind nutrient cations: trivalent aluminum cations or polymeric aluminum cations of large charge and mass may be so strongly bound that the soil charge becomes almost totally blocked.



Surface Properties and Related Phenomena in Soils and Plants, Figure 7 Schematic view on cation exchange.

Deblocking of soil surface charge and renovation of exchange properties of the soil requests neutralization of aluminum and its precipitation as oxides, which can be performed by liming.

Cations adsorbed in the DDL (cations of soil exchange complex) are easily taken by plants. To fulfill the condition of an electric neutrality of the system, the plant should release the equivalent amount of cations to the soil. These are hydrogen ions, because the plant cannot produce the other ones. This is one of the important mechanisms of soil acidification, and is more pronounced in agricultural areas from which the soil nutrients are removed from soils together with the taken biomass. Therefore, the crops need the mineral nutrients supply. In natural environments the cations taken from soils, or at least their large part, may return to the soil after decomposition of the dead plants. From this reason, this is advantageous to leave the crop residues in the field after harvesting.

The quantity of exchangeable cations in the zone adjacent to the charged surface that can be exchangeable for other cations is called the cation exchange capacity (CEC). Agricultural sciences regard CEC as the ability of the soils to supply cations. The range of soil colloid CEC ranges from about 4 cmol kg^{-1} for Si oxides to about 600 cmol kg^{-1} for humic acids. Thus, humus has the highest CEC in comparison with minerals like kaolinite, monmorillonite, smectite, and even zeolite. Contrary to constant charge clay minerals, organic matter does not have a fixed CEC and it increases markedly with increasing pH. So to measure the actual CEC of a soil, pH must be constant during the procedure.

The CEC of plant roots is mainly determined by the number and density of carboxylic groups of pectines and proteins present in cell walls, thus, this is dependent on pH. It is responsible for cations uptake from soil. The lower the CEC of the roots (lower surface charge density and lower surface potential), the lower is the ratio of polyvalent to monovalent cations at the root surface at the same composition of the soil solution and the uptake of polyvalent cations by the plant is respectively smaller. Therefore low root CEC ensures with plant tolerance on soil acidity (aluminum). As a rule, dicotyledonous plants have markedly higher CEC than monocotyledonous plants; therefore, they uptake relatively more polyvalent cations

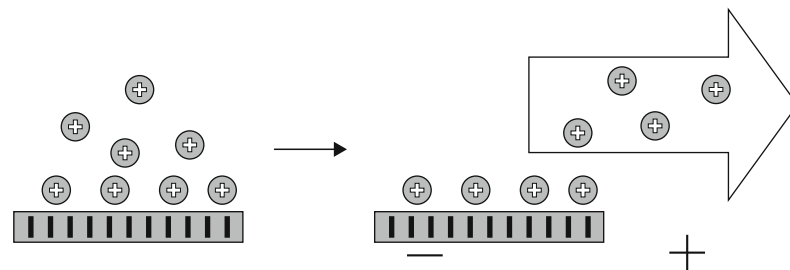
(e.g., Ca and Mg) and in natural environments poor in calcium and magnesium they eliminate monocots from mixed populations. And the opposite occurs in potassium poor habitats. The plant can modify the root CEC depending on nitrogen and phosphorus supply, availability of microelements, soil density (compaction), as well as oxygen, heavy metals, or aluminum stresses. During, the Al stress the density of variable surface charge of the roots decreases markedly that may lead to significant depression of the relative amount of multivalent aluminum ions present at the root cation exchange sites that may serve as a kind of plant self-protection mechanism.

Electrokinetic phenomena

Because counterions in DDL diffuse into the surrounding solution, they can move together with the liquid phase. So if an external force causes a movement of the liquid in respect to the charged solid, some of the counterions are taken apart from the surface by the migrating liquid as this is shown in Figure 8.

As a result, the electric field arises that brakes the further movement of the counterions. This electric field exists until the liquid movement stops. Thus the movement of the solution through a capillary tube with charged walls or a porous body composed from charged particles (soil) creates an electric potential between inlet and outlet of the liquid that is called streaming potential. Similarly, if the charged particle settles down in a liquid due to gravity (sedimentation process) or during centrifuging, the electric potential along the liquid phase arises that is called sedimentation potential.

On the other hand, if the external electric field is applied on two ends of a charged capillary tube or on opposite sides of a porous body composed from charged particles, the charges in DDL separate and the gradient of counterions concentration arises on both ends of the body inducing an osmotic pressure along it and a related movement of the liquid phase to "dilute" the counterions that is called electroosmosis. If the capillary tube is placed vertically, the electroosmosis goes until the hydrostatic pressure of the water column (plus capillary rise term) equals the electroosmotic pressure. However if the capillary is placed horizontally the electroosmosis lasts until the liquid is



Surface Properties and Related Phenomena in Soils and Plants, Figure 8 Separation of charges in diffuse double layer (DDL) due to relative movement of solid and liquid phases.

present at the inlet, so this whole liquid may be transferred through the capillary or porous body.

Electroosmosis has been frequently used in geotechnical and environmental soil engineering as a method of soil improvement including electroosmotic dewatering, contaminant removal, electrobioremediation, and electrochemical remediation. Electroosmosis is applied for consolidation of foundation soils and drying building structures. However numerous disadvantages accompany electroosmotic treatment in soils as electrolysis, hydrolysis, oxidation, reduction, local changes in pH, mineral decomposition, precipitation of salts, or secondary minerals.

Electroosmosis is applied in plant physiology to explain movement of water via the phloem. Preferential uptake of similar charge ions (e.g., K^+) to the interior results of the cells in ions unbalance alongside the phloem and accompanied electric field forces water molecules and other solutes present to move upward.

Movement of soil animals (having charged surface of the body) causes the electroosmotic flow in a micro thin layer of water at the body surface that serves as a lubricant against the rough particles of the surrounding soil.

If the electric field is applied to a liquid containing suspended charged particle, separation of diffuse layer charges on sides of the opposite particle results in differences in osmotic pressure that causes the movement of liquid around the particle to more ion concentration region. Thus, a liquid pressure is exerted on the respective side of the particle and it is pushed forward that is called electrophoresis. Electrophoresis is a very important tool to study biomolecules (genes, proteins, and enzymes).

Aggregation

The interaction between the colloidal mineral phases, with special reference to clay minerals, and colloidal humic substances, is a crucial step for the formation and stabilization of organo-mineral aggregates in soil. Since organic anions are normally repelled from the negatively charged surface of soil minerals, the interaction with humic substances occurs only when cations, present on the exchange complex, act as a bridge between the mineral and the organic phases. The effectiveness of cations in binding clay minerals and humic substances increases with their charge, so that polyvalent cations are more able to stabilize the aggregates than monovalent cations.

Although the overall particle charge of clay minerals is negative in general, both negatively and positively charged parts on the surface of clay mineral particles exist simultaneously below PZC that favors positively charged edge-to negatively charged face aggregation.

Repulsion forces between permanent charges of clay minerals may be diminished by increased concentration of soil solution due to decrease in DDL electric potential and in this case face-to-face aggregation takes place.

Below their PZC, positively charged iron and aluminum oxides act as cementing agents for clay minerals and humic particles.

Summary

A vast number of environmentally important processes occur on surface of soil solid phase. This surface is extremely complex due to diversified mineral, organic and ionic composition of soil constituents, and it constantly changes under various environmental factors. Soil surface become increasingly used for description and modeling of soil physical, chemical, and biological processes as fertility, mass and energy exchange, accumulation of various species, water retention, microbial life, catalysis, pollution, acidification and alkalization, soil organic matter leaching, and oxidation as well as for quantitative analysis of soil typological and genetic properties. Surfaces of plant tissues play very important role in plant transport processes, their reaction on stresses, and adaptation to environmental conditions.

Bibliography

- Bolt, G. H., and Bruggenwert, M. G. M., 1976. *Soil Chemistry. A. Basic Elements*. Amsterdam: Elsevier.
 Sparks, D. L., 1999. *Soil Physical Chemistry*. Boca Raton: CRC Press.
 Sposito, G., 1984. *The Surface Chemistry of Soils*. New York: Oxford Press.
 Sumner, M. E., 2000. *Handbook of Soil Science*. Boca Raton: CRC Press.

Cross-references

- [Adsorption Energy of Water on Biological Materials](#)
[Biocolloids: Transport and Retention in Soils](#)
[Buffer Capacity of Soils](#)
[Clay Minerals and Organo-Mineral Associates](#)
[Diffuse Double Layer \(DDL\)](#)
[Electrokinetic \(Zeta\) Potential of Soils](#)
[Evapotranspiration](#)
[Flocculation and Dispersion Phenomena in Soils](#)
[Hydraulic Properties of Unsaturated Soils](#)
[Hydrophobicity of Soil](#)
[Infiltration in Soils](#)
[Membranes, Role in Water Transport in the Soil–Root–Xylem System](#)
[Mycorrhizal Symbiosis and Osmotic Stress](#)
[Organic Matter, Effects on Soil Physical Properties and Processes](#)
[Root Water Uptake: Toward 3-D Functional Approaches](#)
[Salinity, Physical Effects on Soils](#)
[Shrinkage and Swelling Phenomena in Soils](#)
[Soil Aggregates, Structure, and Stability](#)
[Soil Aggregation and Evaporation](#)
[Soil Hydrophobicity and Hydraulic Fluxes](#)
[Soil Phases](#)
[Soil Water Flow](#)
[Sorptivity of Soils](#)
[Specific Surface Area of Soils and Plants](#)
[Stomatal Conductance, Photosynthesis, and Transpiration, Modeling](#)
[Water Uptake and Transports in Plants Over Long Distances](#)
[Wetting and Drying, Effect on Soil Physical Properties](#)

SURFACE ROUGHNESS, EFFECT ON WATER TRANSFER

Frédéric Darboux
UR 0272 Science du sol, INRA, Centre de recherche d'Orléans, Orléans Cedex 2, France

Synonyms

Micro-relief; Micro-topography

Definition

Surface roughness is the height changes in reference to the general shape of a surface. For soils, surface roughness is the shape of a surface when the topographic slope has been removed.

Introduction

Roughness is the second most obvious feature of the soil surface after its color. Being at the interface between soil and atmosphere, surface roughness affects water transfer. Surface roughness can store water in puddles, enhance infiltration, and limit overland flow. It can also affect the path, depth, and velocity of overland flow.

Because surface roughness can present various characteristics due to field work and rainfall, its effect on water transfer vary in space and time. The complexity in determining roughness effects comes from this variability but also from its time-consuming measurement. However, relationship between characteristics of surface roughness and water transfer can be drawn. Defining several kinds of roughness helps in understanding them.

Surface roughness characteristics

Soil surface roughness is usually divided into two components: the random roughness and the oriented roughness (Allmaras et al., 1966). Oriented roughness is related to fieldwork and to soil erosion. When related to fieldwork, oriented roughness is described as ridges and furrows. It can be characterized by a wavelength (about 1 dm), an amplitude (ranging between 1 cm and 1 dm), and a direction. All these features depend on the type of fieldwork. As a soil erosion feature, oriented roughness consists in the rill network. It is characterized through the rill density (length of rills per unit area) and rill depth.

By contrast, random roughness is isotropic, meaning that its features do not change significantly with direction. It is related to clods and aggregates created by fieldwork at the soil surface. The amplitude of random roughness ranges between a few millimeters and 1 dm. When analyzing the correlation of height with the distance (e.g., through a semi-variogram), a correlation length is usually found. This correlation length ranges between a few millimeters and 1 dm. At distances smaller than the correlation length, a correlation is present. For distances larger than the correlation length, little correlation exists. So, even if

it has some randomness in its features, random roughness has nevertheless a spatial structure.

Usually soil cracks are not considered as part of the surface roughness. They are seen as vertical objects included in the soil and, as such, a constituent of soil porosity.

Surface roughness measurement

Because the geometry of the interface between the soil and the atmosphere affects transfer through this interface and on this interface, measurement of surface roughness is an important issue (Jester and Klik, 2005). The simplest device to measure surface roughness consists in a chain placed across the soil surface. The distance between the two ends of the chain is measured. Comparing the actual length of the chain with this distance gives an estimate of the roughness. The shorter the distance between the ends is, the rougher the surface is.

The most used device is called a “pin meter.” A pin meter consists of a frame holding a set of equally spaced pins. Set vertically above the soil surface, the pins slide down up to come into contact with the soil surface. Reference lines drawn on the frame allow for manual or automatic reading of pin heights. Hence, a profile of the surface roughness can be measured. The most sophisticated versions of pin meter replace the pins by a single laser pointer traveling along the frame. They allow for a smaller step of about 1 mm.

The most sophisticated devices are able to build digital maps of surface heights with a millimeter resolution. First devices were using a single laser pointer traveling over a surface of about 1 square meter. Most recent devices can measure the heights along a profile simultaneously. By acquiring a set of profiles parallel to each other, a height map can be built. Another way to build height maps is to use stereophotogrammetry, i.e., a set of two pictures of the soil surface taken from slightly different locations. First manual, automatic computing of height maps is now possible. The main interest of height maps is in the direct quantification of features such as flow network and volume of puddles.

It should be noted that, whatever the device used to measure the roughness, some features are ignored – such as overhangs under clods for example.

Another way of estimating the surface roughness is through the use of satellite or aerial radars. Radars are able to estimate surface roughness with a resolution of about 100 m² over large surface areas and can be of great help in estimating the roughness pattern at watershed scale.

A lot of work has been devoted to define indices to characterize random roughness. These indices aim at summarizing the random roughness features into a single number. Most of these indices are statistical values, such as the standard deviation of heights. Currently, there is no universal index accepted by all soil specialists. The random roughness index (usually noted RR) should not be confused with the random roughness: RR is a number aiming

at summarizing some features of the roughness while the random roughness per se is an object.

Surface roughness effects on infiltration

Infiltration is a vertical transfer of water. A surface will have a higher infiltration capacity if it consists of numerous clods or if it can hold water in puddles. The spaces between the clods are large pores able to conduct rainfall or irrigation water downward. With the addition of water, pores will be more and more occluded through sealing and crusting. This phenomenon will decrease soil roughness. Therefore, roughness amplitude and infiltration capacity will decrease with time, but the relationship between them is not linear: infiltration capacity can become very low with the roughness amplitude still being high (Helming et al., 1998a; Darboux and Huang, 2005). More than the roughness amplitude, it is the kind of roughness that is relevant to infiltration, specifically its cloddiness and the presence of surface depressions.

Both ridge-and-furrow oriented roughness and random roughness can create depressions on the surface. Depressions are able to store water into puddles (Planchon et al., 2001). Though temporary, this storage can represent a significant volume of the inflow water. It can also be important because the water stored in puddles will not take part in overland flow but will infiltrate or evaporate instead. The volume of water that can be stored on a surface unit is called surface storage capacity. Because of sealing and crusting, depressions can have a low infiltration capacity compared to other parts of the surface. Hence, because surface roughness cause variability in sealing and crusting, it leads to spatial variability in infiltration capacity.

Surface roughness effects on overland flow

The surface roughness can delay the triggering of overland flow. This effect is due to surface porosity and to puddle filling and has been discussed previously.

Surface roughness also affects flow path. In the case of rills, the direction of oriented roughness is also the flow paths. Except for this special case, above the scale of a few square meters, flow direction is controlled by the interaction between the slope gradient, and the amplitude and direction of oriented roughness (Souchère et al., 1998; Takken et al., 2001). If the slope gradient is large, flow paths will be controlled by the slope. Otherwise, flow path can be in the direction either of the slope or of the furrows. Hence, in agricultural fields with low slope gradient, the actual flow network can be quite different from the flow network computed from the digital elevation model of a watershed only. This strongly advocates for including the effect of ridge-and-furrow into the computation of flow networks of watershed management models.

Random roughness has several effects on overland flow: it can change the overland flow velocity, depth,

and direction. The effect of random roughness on flow direction can be characterized at the scale of 1 m² (Römkens et al., 2002). The geometry of flow networks in interrill areas is similar to the one of river networks. Because the depth of overland flow is similar to the height of random roughness, numerous mounds protrude through the flow. Therefore, in interrill areas, though this flow is usually called sheet flow, it looks more like a net than a sheet.

A larger random roughness is usually expected to slow down the flow. Hydraulic studies, mainly carried out in open channels, account for the random roughness of the walls through a friction coefficient (such as Manning and Darcy Weisbach coefficients). In these studies, the height of the roughness is always much lower than the water depth. The roughness of the channel affects the water velocity without changing the flow direction. Such roughness is termed hydraulic roughness.

Because overland flow in interrill area is very different from channel flow, the applicability of hydraulic roughness concept and coefficients to overland flow, though widespread, remains debated by the scientific community (Smith et al., 2007). Because the flow occurs between mounds, random roughness can cause the flow to be deeper than expected (Helming et al., 1998b). Consequently, flow velocity could be increased – and not decreased – by a larger roughness. In order to better account for this specificity of overland flow on agricultural fields without abandoning the hydraulic roughness concept, “equivalent” friction coefficient values are used.

Summary

The usual splitting of surface roughness into oriented and random roughness has been of great help to understand the effects of surface roughness on water transfers. Other sub-components, such as mounds and depressions are also meaningful in better inferring the interaction between roughness and water flow. The roughness measurement remains an issue for improving our knowledge.

Bibliography

- Allmaras, R. R., Burwell, R. E., Larson, W. E., Holt, R. F., and Nelson, W. W., 1966. Total porosity and random roughness of the interrow zone as influenced by tillage. *Conservation Research Report 7, U.S.D.A. Conservation Resource*, U.S. Gov. Print. Office, Washington, DC. Available at <http://www.ars.usda.gov/sp2UserFiles/Place/36221500/cswq-t1914-allmaras.pdf>
- Darboux, F., and Huang, C., 2005. Does soil surface roughness increase or decrease water and particle transfers? *Soil Science Society of America Journal*, **69**, 748–756.
- Helming, K., Römkens, M. J. M., and Prasad, S. N., 1998a. Roughness and sealing effect on soil loss and infiltration on a low slope. *Advances in GeoEcology*, **31**, 589–595.
- Helming, K., Römkens, M. J. M., and Prasad, S. N., 1998b. Surface roughness related processes of runoff and soil loss: a flume study. *Soil Science Society of America Journal*, **62**, 243–250.

- Jester, W., and Klik, A., 2005. Soil surface roughness measurement – methods, applicability, and surface representation. *Catena*, **64**, 174–192.
- Planchon, O., Esteves, M., Silvera, N., and Lapetite, J.-M., 2001. Micrelief induced by tillage: measurement and modelling of Surface Storage Capacity. *Catena*, **46**, 141–157.
- Römkens, M. J. M., Helming, K., and Prasad, S. N., 2002. Soil erosion under different rainfall intensities, surface roughness, and soil water regimes. *Catena*, **46**, 103–123.
- Smith, M. W., Cox, N. J., and Bracken, L. J., 2007. Applying flow resistance equations to overland flows. *Progress in Physical Geography*, **31**, 363–387.
- Souchère, V., King, D., Daroussin, J., Papy, F., and Capillon, A., 1998. Effects of tillage on runoff directions: consequences on runoff contributing areas within agricultural catchments. *Journal of Hydrology*, **206**, 256–267.
- Takken, I., Govers, G., Steegen, A., Nachtergael, J., and Guérif, J., 2001. The prediction of runoff flow directions on tilled fields. *Journal of Hydrology*, **248**, 1–13.

Cross-references

- Anisotropy of Soil Physical Properties
 Mapping of Soil Physical Properties
 Nondestructive Measurements in Soil
 Overland Flow
 Soil Surface Sealing and Crusting

SURFACE RUNOFF

Precipitation, snow melt, or irrigation in excess of what can infiltrate the soil surface and be stored in small surface depressions.

Bibliography

- Library of Congress Cataloging-in-Publication Data Environmental engineering dictionary and directory/Thomas M. Pankratz <http://www.docstoc.com/docs/2845196/CRC-Press>

SURFACE STORAGE CAPACITY

The maximal volume of water per unit area that can accumulate over the surface during periods of intense rainfall (i.e., rainfall exceeding the soil's infiltrability). When surface storage capacity is exceeded, overland flow begins.

Bibliography

- Introduction to Environmental Soil Physics (First Edition) 2003 Elsevier Inc. Daniel Hillel (ed.) <http://www.sciencedirect.com/science/book/9780123486554>

SURFACE TENSION

The resistance of a liquid body to an increase in its surface area. It is due to the cohesion between the liquid molecules and is expressed quantitatively as the force per unit length or the energy per unit area needed to overcome that resistance and to increase the surface of the liquid.

Bibliography

- Introduction to Environmental Soil Physics (First Edition) 2003 Elsevier Inc. Daniel Hillel (ed.) <http://www.sciencedirect.com/science/book/9780123486554>

SURFACE-WATER EXCESS

The excess of rainfall intensity over the infiltration rate.

SUSPENSION

A system in which very small particles are uniformly dispersed in a liquid or gaseous medium.

Bibliography

- Library of Congress Cataloging-in-Publication Data Environmental engineering dictionary and directory/Thomas M. Pankratz <http://www.docstoc.com/docs/2845196/CRC-Press>

SWELLING

See *Shrinkage and Swelling Phenomena in Agricultural Products*; *Shrinkage and Swelling Phenomena in Soils*

T

TEMPERATURE EFFECTS IN SOIL

Graeme D. Buchan

Soil and Physical Sciences Department and Centre for Soil and Environmental Research, Lincoln University, Christchurch, Canterbury, New Zealand

Definition

Temperature effects in soil. The effects of temperature and its variations on the properties of soil, and on processes occurring in soil, including soil formation, physical properties and processes, and biological processes.

Introduction

Soil temperature plays a central role in all soil processes. Soil and near-ground air temperatures are powerful “biocontrollers.” In temperate climates, the transition from the nongrowing to the growing season occurs when temperature rises above a threshold or “base temperature,” T_b (e.g., about 5°C for temperate pastures). Temperature drives chemical and biological processes, leading to the Q_{10} concept described below. Biological “clocks” (e.g., the clock which determines the developmental stages of a plant) run not by time alone but by time (e.g., in days) multiplied by temperature (in degrees). This leads to the concept of “thermal time” (expressed as a “day-degree sum”).

Soil properties and processes are controlled by a complex set of factors, most strongly by soil water and soil temperature. Thus, it may be impossible to isolate and quantify the temperature dependence of a process in simple mathematical form, due to confounding effects, especially of soil water. Where possible, equations for temperature dependences are given below.

Climate change increases our need to understand temperature effects in soil. Globally, the “temperature increase

from 1850–1899 to 2001–2005 is 0.76°C” (IPCC, 2007). Of key importance for future climate are the changes in soil’s ability to act as a “carbon store,” and to emit or absorb other greenhouse gases (GHGs), and hence provide feedbacks on climate change (Smith et al., 2003; see *Greenhouse Gas Fluxes: Effects of Physical Conditions*; *Greenhouse Gases Sink in Soils*). Such feedbacks will operate until some new steady state between soil and atmosphere is achieved.

Soil temperatures cover a wide range, from subzero in frozen or tundra soils to hundreds of degrees Celsius under scrub or forest fires (see *Wildfires, Impact on Soil Physical Properties*).

This article summarizes the effects of temperature on the following:

- *Pedogenic processes*, including the weathering of minerals and soil formation and the accumulation of soil organic carbon
- *Physical properties and processes*, including the storage, flow and measurement of soil water, and the dissolution and diffusion of gases
- *Biological processes*, including the transformations of organic matter, CO₂ release from soil, microbial activity, and seed germination

Note that purely chemical processes (e.g., hydrolysis of soil minerals) are omitted above, since (a) they may be part of pedogenic weathering (e.g., clay formation) or (b) they may be part of a mixed system of chemical and biotic transformations (e.g., in the nitrogen cycle).

Pedogenic processes

The Jenny model of soil development (Jenny, 1994) identifies climate (i.e., temperature plus precipitation) as one of the five main controllers of soil formation. The effect of temperature is approximated by the van’t Hoff rule: *For every 10°C rise in temperature the rate of*

a chemical reaction increases by a factor of typically two to three. This approximate rule holds for numerous chemical reactions and biological processes. It applies to soil weathering and the process of “mineralization” (i.e., the release of soil mineral components from unavailable chemical combinations into available forms in the soil solution). Thus rates of soil formation are strongly temperature controlled, varying from roughly 0.02 mm/year or less (e.g., resistant parent material combined with cold or dry climate) to 1 mm/year (e.g., softer parent material, warmer and wetter climate) (Schertz and Nearing, 2006).

Physical properties and processes

Temperature differences in soil drive flows of both heat and of water (Buchan, 2001).

Here, we consider other less obvious effects of temperature, particularly on soil water.

Measurement of soil water content

The two main methods used to measure volumetric water content, θ_v ($\text{m}^3 \text{ water/m}^3$ soil) are the neutron probe (NP) and electromagnetic (EM) methods. The NP method can be regarded as unaffected by variations in soil temperature. EM methods (which include time-domain reflectometry [TDR], capacitance, and other methods) measure water content via the large dielectric permittivity of water, ϵ_w , which varies approximately as follows (Woodhead et al., 2003):

$$\epsilon_w = 89 - 0.37T \quad (1)$$

Thus, EM probe readings require correction for temperature variations (Stangl et al., 2009; Gong et al., 2003). For EM probes operating at higher (~ 1 GHz) frequencies (e.g., TDR probes), Equation 1 indicates a temperature sensitivity of ca. 4% per 10°C . However, for EM probes which operate at lower (e.g., 10–100 MHz) frequencies, variation of the soil’s electrical conductivity may further increase probe sensitivity to temperature (Western and Seyfried, 2005; Carrick, 2009).

Soil water potential

The total potential of water in soil is the sum of three main components: the pressure potential, ψ_p ; the solute (or osmotic) potential, ψ_s ; and the gravitational potential, ψ_g .

The pressure potential (or “suction”)

In unsaturated soil, ψ_p is negative. To simplify, we drop the negative sign and refer more intuitively to the soil water “suction,” s (i.e., $s = -\psi_p$). As temperature increases, suction decreases. The Philip–de Vries theory (Hopmans and Dane, 1986) postulates that this is accounted for by the decrease in the surface tension of water. However, experimental results indicate a temperature coefficient that is about two to three (or more) times larger than the value predicted by this theory (Hopmans and Dane, 1986).

Solute potential, ψ_s

For dilute solutions, ψ_s (in kPa) is given by (Or and Wraith, 2002):

$$\psi_s = -RTC_s \quad (2)$$

Here, $R = 8.314 \text{ J K}^{-1} \text{ mol}^{-1}$, T (in K) is absolute temperature, and C_s (mol m^{-3}) is the solute concentration.

Water flow

The literature reports conflicting results for the effect of temperature on hydraulic conductivity, $K(\Psi_p)$ (a function of the pressure potential Ψ_p). Some authors (e.g., Constantz, 1982; Hopmans and Dane, 1986) report that, as temperature rises, the rate of increase in K is well explained by the decrease in the viscosity of water, $\eta(T)$. By contrast, Stoffregen et al. (1999) report that it can be described using the exponential function:

$$K_{10^\circ\text{C}}(\psi_p) = K(\psi_p) \exp[0.04(10 - T)] \quad (3)$$

Here, $K(\Psi_p)$ is corrected to a reference temperature of 10°C , from the soil temperature (T) at which K was obtained. Equation 3 gives a temperature dependence about twice that based on the viscosity of water alone. The viscosity of water decreases by a factor of about 2, over the range 0 – 30°C . Therefore, infiltration and drainage rates will at least double over this range – a common winter-to-summer range near the soil surface in temperate regions (see *Soil Water Flow; Infiltration in Soils*).

Water vapor in the soil air space

Temperature controls the saturated vapor pressure (SVP) of water, $e_s(T)$. Of several approximate equations for the $e_s(T)$ function (Vomel, 2009), the simplest is the Bolton equation, accurate within 0.3% over the range -35°C to $+35^\circ\text{C}$:

$$e_s(T) = 6.112 \exp[17.67T/(T + 243.5)] \quad (4)$$

Here, T is in $^\circ\text{C}$ and $e_s(T)$ in hPa (=mbar). (Note: Equation 4 applies over liquid water, not ice). As the water potential $\psi_w = \psi_p + \psi_s$ decreases (i.e., becomes more negative), water is held more tightly, and hence the relative humidity (RH) in the soil air space also decreases, according to Equation 5:

$$RH = e/e_s = \exp\left[\frac{M_w\psi_w}{\rho_w RT}\right] \quad (5)$$

Here, e (mbar) is the actual vapor pressure in the soil air space, ρ_w (kg m^{-3}) and M_w (kg mole^{-1}) are the density and molar mass of water, respectively, ψ_w is in Pascal, and T (K) is temperature. Equation 5 is exploited in the technique called “psychrometry”: by measuring RH in the soil air space, one can determine the water potential, ψ_w (Mullins, 2001; Or and Wraith, 2002). If ψ_s is negligible, psychrometry gives the pressure potential, ψ_p .

Gases: dissolution and diffusion

The dissolution and transport of O₂ and CO₂ in soil water control root and microbial respiration, the redox conditions in soil, the pH of the soil solution and hence, the weathering and development of soils (see *Aeration of Soils and Plants*). As temperature increases, water will progressively “de-gas,” until the concentrations of O₂ and CO₂ become effectively zero at the boiling point (The Engineering Toolbox, 2005). The diffusivity D of a gas in the soil air space increases with temperature T as follows (Rolston, 1986):

$$D_{T2} = D_{T1}(T_2/T_1)^{1.72} \quad (6)$$

Coupled flows of heat and water (*Coupled Heat and Water Transfer in Soil*)

Temperature gradients drive flows of water, in both liquid and vapor phases. Vapor flows from warmer to cooler soil via a “distillation” process, carrying water itself and also latent heat. This can occur strongly in near-surface soil, and also in some “engineering” situations. The heat generated in underground electric cables can cause moisture to migrate away from the cable, drying the surrounding soil and increasing its thermal resistance, which can lead to overheating of the cables (Campbell and Bristow, 2009). Under paved surfaces, moisture can migrate upward and accumulate beneath the paving material (Morgenroth and Buchan, 2009).

Thermal properties and processes

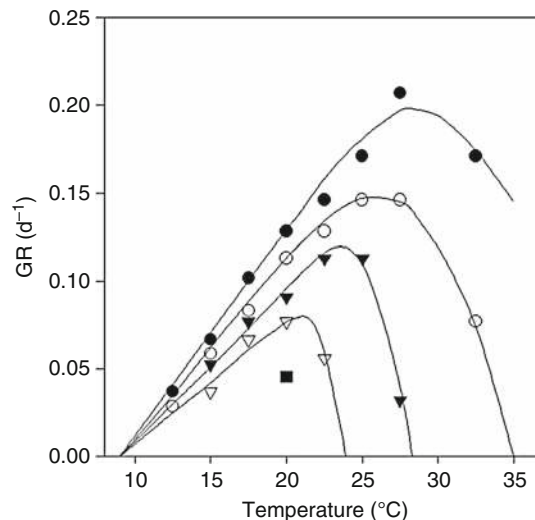
Soil thermal properties (heat capacity, thermal conductivity, and diffusivity) are weakly temperature dependent, so that the heat flow equation can be treated as linear. Freezing leads to expansion of water (Buchan, 1996). Freeze-thaw cycles contribute to soil weathering and microbial die-off, and can rearrange soil components, e.g., migration of stones to the soil surface (Kessler and Werner, 2003).

Biotic processes

Biotic processes are catalyzed by enzymes and typically respond to temperature as shown in **Figure 1**. The process rate increases in a rising (or thermo-stimulation) stage from c. zero at a base temperature, T_b , up to some optimum temperature, T_o (typically in the range 20–35°C). Above T_o the rate decreases, mainly due to denaturing (i.e., thermally induced deformation) of enzyme molecules.

The rising or suboptimal stage ($T_b < T < T_o$) illustrated in **Figure 1** may cover most of the actual temperature range in a soil, especially as temperature rises in spring, and is quantified in two distinct ways. The first and simpler approach assumes that the rising stage is approximately linear. Then, assuming T is within this range, the cumulative effect of soil temperature (e.g., on seed germination) can be described via the concept of “thermal time” or a “day-degree sum,” DD:

$$DD = \Sigma(T_{ave} - T_b) \quad (7)$$



Temperature Effects in Soil, Figure 1 Effect of temperature T on Germination Rate (GR) of radiata pine tree seeds. The diagram illustrates: (a) the typical T -dependence of biotic processes, starting at a base temperature T_b (here $\sim 9^\circ\text{C}$), then increasing approximately linearly to an optimum temperature, followed by decline due to thermo-inhibition; (b) the added complexity that real biological populations (here, a set of seeds) show variability in their response – the different curves represent the different responses of subpopulations, from fast responders (*uppermost curve*) to slow responders (*lowest curve*). (From Bloomberg et al., 2009.)

Here, Σ denotes a day-by-day sum and T_{ave} is the average temperature for the day. (Note: Days with $T_{ave} < T_b$ count zero in the sum).

However, soil moisture is also a strong determinant of some processes, so the thermal time concept has been extended to the concept of “hydrothermal time” (e.g., Bloomberg et al., 2009). **Equation 7** is then extended by multiplying it by a term $(\psi_p - \psi_b)$, where ψ_b is a base water pressure potential.

The second approach to quantifying the thermo-stimulation or rising stage recognizes that it is more generally curvilinear and should follow van't Hoff's rule, written as:

$$R_T = R_0 \exp(BT) \quad (8)$$

Here, R_T and R_0 are the process rates at temperatures $T^\circ\text{C}$ and 0°C , and B is a constant. This leads to the definition of the “ Q_{10} ” factor, i.e., the factor by which the rate of a process increases for a 10°C temperature increase:

$$Q_{10} = R_{T+10}/R_T = \exp(10B) \quad (9)$$

Q_{10} values vary with the process involved, and also with temperature, but are predominantly of order 2–3. The Q_{10} concept applies to a wide range of processes. It expresses the effect that increased molecular kinetic energy causes molecules to increase the frequency with which they either (a) escape from a phase (e.g., via

evaporation or volatilization) or (b) exceed the activation energy of a chemical or biochemical reaction.

Soil respiration, organic C content and climate change

Soil respiration (i.e., the rate of production of CO₂, caused by decomposition of organic substrates) is the sum of respiration by (1) roots and (2) microbial decomposers in soil. The latter represents the rate of organic matter (OM) decomposition in soil, a key quantity controlling the soil's carbon budget under climate change. Considering whole-soil respiration (i.e., both 1 and 2 above), Zheng et al. (2009) found that average Q_{10} values in soils in China followed the order forest (2.51 ± 0.78) > grassland (2.15 ± 0.44) > cropland (1.99 ± 0.24).

They also showed that Q_{10} is itself temperature dependent:

$$Q_{10} = a \exp(-kT_{\text{ave}})$$

Kirschbaum (1995) separated out the rate of microbial OM decomposition (under non-limiting soil water conditions) and found that Q_{10} decreased with soil temperature from about 8 at 0°C through 4.5 at 10°C to 2.5 at 20°C. This decrease of Q_{10} with temperature assists the simplifying assumption that the rising stage in Figure 1 is approximately linear, and hence the usefulness of the thermal time (day-degree) concept.

Note that the actual effect of climate change on the soil's carbon budget will be the net effect of two opposing processes: (a) increased OM decomposition due to rising temperatures versus (b) increased plant productivity due to the "fertilization effect" of increased atmospheric CO₂. Studies indicate that (b) is likely to be greater, so that (depending also on land use change) C sequestration by soils should increase under climate change.

Microbiological effects

Microbes such as bacteria can exist in two phases: the vegetative or normal growth phase; and the survival phase, when bacteria form resistant spores. Temperature controls die-off in the vegetative phase. However, to kill off spores typically requires either very high or very low temperatures. Microorganisms can survive longer in cold soils than in warm soils. Bacterial die-off rate approximately doubles with each 10°C rise in temperature between 5°C and 30°C (Reddy et al., 1981; Gerba and Goyal, 1985). In cold soils (<5°C) bacteria can survive for up to 100 days.

Manipulation of soil temperature

Techniques to manipulate soil temperature include mulching the soil surface, altering plant cover, ridging the surface, and soil solarization (see *Soilborne Diseases, Control by Physical Methods*). These techniques also alter near-ground air temperature, e.g., frost intensity is commonly reduced by controlling or removing plant cover in the inter-row spaces of frost-sensitive horticultural crops.

Conclusions

Temperature controls a wide range of soil processes, often in ways difficult to quantify, due to the confounding effects of other controlling variables, especially soil moisture. Key areas requiring further research include: (1) The net effect of future climate change on greenhouse gas exchanges between the atmosphere and soil-plant systems, due to the combined actions of (a) increasing temperature (which tends to decrease soil organic matter content, but increase plant productivity) (Portner et al., 2009), and (b) rising atmospheric CO₂ (which increases plant productivity via an atmospheric "fertilization effect"). (2) Description of the synergistic (coacting) effects on soil processes of temperature and other variables (especially soil moisture) e.g., via concepts such as hydrothermal time (Bloomberg et al., 2009).

Bibliography

- Bloomberg, M., Sedcole, R., Mason, E., and Buchan, G., 2009. Hydrothermal time germination models for radiata pine (*Pinus radiata* D.Don). *Seed Science Research*, **19**, 171–182.
- Buchan, G. D., 1996. Ode to H₂O. *The Journal of Soil and Water Conservation*, **51**, 467–470. See also <http://hdl.handle.net/10182/333>
- Buchan, G. D., 2001. Soil temperature regime. In Smith, K. A., and Mullins, C. (eds.), *Soil and Environmental Analysis: Physical Methods*. New York: Marcel Dekker, pp. 539–594.
- Campbell, G., and Bristow, K. Underground power cable installations: soil thermal resistivity. <http://www.ictinternational.com/brochures/kd2/Paper%20-%20AppNote%202%20Underground%20power%20cable.pdf> Verified Oct 2009.
- Carrick, S., 2009. *The dynamic interplay of mechanisms governing infiltration into structured and layered soil columns*. PhD thesis, Lincoln University, NZ.
- Constantz, J., 1982. Temperature dependence of unsaturated hydraulic conductivity of two soils. *Soil Science Society of America Journal*, **46**, 466–470.
- Gerba, C., and Goyal, S., 1985. Pathogen removal from wastewater during groundwater recharge. In Asano, T. (ed.), *Artificial Recharge of Groundwater*. Boston: Butterworth, pp. 283–318.
- Gong, Y., Cao, Q., and Sun, Z., 2003. The effects of soil bulk density, clay content and temperature on soil water content measurement using time-domain reflectometry. *Hydrological Processes*, **17**, 3601–3614.
- Hopmans, J. W., and Dane, J. H., 1986. Temperature dependence of soil hydraulic properties. *Soil Science Society of America Journal*, **50**, 4–9.
- IPCC, 2007. Summary for Policymakers. In *Climate change 2007: the physical science basis. Contribution of working group I to 4th assessment report of the Intergovernmental Panel on Climate Change*. UK: Cambridge University Press.
- Jenny, H., 1994. *Factors of soil formation: a system of quantitative pedology*. New York: Dover.
- Kessler, M. A., and Werner, B. T., 2003. Self-organization of sorted patterned ground. *Science*, **299**, 380–383.
- Kirschbaum, M. U. F., 1995. The temperature dependence of soil organic matter decomposition, and the effect of global warming on soil organic C storage. *Soil Biology and Biochemistry*, **27**, 753–760.
- Lin, C., Greenwald, D., and Banin, A., 2003. Temperature dependence of infiltration rate during large-scale water recharge into soils. *Soil Science Society of America Journal*, **67**, 487–493.

- Morgenroth, J., and Buchan, G. D., 2009. Soil moisture and aeration beneath pervious and impervious pavements. *Arboriculture and Urban Forestry*, **35**, 135–141.
- Mullins, C., 2001. Matric Potential. In Smith, K. A., and Mullins, C. (eds.), *Soil and environmental analysis: physical methods*. NY: Marcel Dekker, pp. 65–93.
- Nassar, I. N., and Horton, R., 1992. Simultaneous transfer of heat, water and solutes in porous media. I. Theoretical development. *Soil Science Society of America Journal*, **56**, 1350–1356.
- Or, D., and Wraith, J., 2002. Soil water content and water potential relationships. In Sumner, M. E. (ed.), *Soil Physics Companion*. Boca Raton: CRC Press LLC.
- Portner, H., Bugmann, H., and Wolf, A., 2009. Temperature response functions introduce high uncertainty in modelled carbon stocks in cold temperature regimes. *Biogeosciences*, **6**, 8129–8165.
- Reddy, K. R., Khaleel, R., and Overcash, M., 1981. Behavior and transport of microbial pathogens and indicator organisms in soils treated with organic wastes. *Journal of Environmental Quality*, **10**, 255–266.
- Rolston, D., 1986. Gas diffusivity. In Klute, A. (ed.), *Methods of Soil Analysis*. Madison: American Society of Agronomy.
- Schertz, D. L., and Nearing, M. A., 2006. Erosion tolerance/soil loss tolerance. In Lal, R. (ed.), *Encyclopedia of Soil Science*. Boca Raton: CRC Press, pp. 640–642.
- Smith, K. A., Ball, T., Conen, F., Dobbie, K. E., Massheder, J., and Rey, A., 2003. Exchange of greenhouse gases between soil and atmosphere: interactions of soil physical factors and biological processes. *European Journal of Soil Science*, **54**, 779–791.
- Stangl, R., Buchan, G., and Loiskandl, W., 2009. Field use and calibration of a TDR-based probe for monitoring water content in a high-clay landslide soil. *Geoderma*, **150**, 23–31.
- Stoffregen, H., Wessolek, G., and Renger, M., 1999. Effect of temperature on hydraulic conductivity. In Van Genuchten, M. T., et al. (eds.), *Characterization and Measurement of the Hydraulic Properties of Unsaturated Porous Media. Proceedings, International Workshop on Characterization and Measurement of Hydraulic Properties of Unsaturated Porous Media*, Riverside, California, pp. 497–506.
- The Engineering Toolbox, 2005. Solubility of gases in water. http://www.engineeringtoolbox.com/gases-solubility-water-d_1148.html Verified Oct 2009.
- Vomel, H., 2009. *Saturation vapor pressure formulations*. CIRES, University of Colorado, Boulder. <http://cires.colorado.edu/~voemel/vp.html>. Verified Oct 2009.
- Western, A. W., and Seyfried, M. S., 2005. A calibration and temperature correction procedure for the water-content reflectometer. *Hydrological Processes*, **19**, 3785–3793.
- Woodhead, I., Buchan, G., Christie, J., and Irie, K., 2003. A general dielectric model for time domain reflectometry. *Biosystems Engineering*, **86**, 207–216.
- Zheng, Z.-M., Yu, G.-R., Fu, Y.-L., Wang, Y.-S., Sun, X.-M., and Wang, Y.-H., 2009. Temperature sensitivity of soil respiration is affected by prevailing climatic conditions and soil organic carbon content: A trans-China based case study. *Soil Biology and Biochemistry*, **41**, 1531–1540.

Cross-references

[Aeration of Soils and Plants](#)

[Coupled Heat and Water Transfer in Soil](#)

[Greenhouse Gas Fluxes: Effects of Physical Conditions](#)

[Greenhouse Gases Sink in Soils](#)

[Infiltration in Soils](#)

[Soilborne Diseases, Control by Physical Methods](#)

[Soil Water Flow](#)

[Wildfires, Impact on Soil Physical Properties](#)

TENSILE STRENGTH

The maximum tensile stress that a material is able to withstand.

Bibliography

Library of Congress Cataloging-in-Publication Data Environmental engineering dictionary and directory/Thomas M. Pankratz <http://www.docstoc.com/docs/2845196/CRC-Press>

TENSIOOMETRY

Krzysztof Lamorski

Institute of Agrophysics, Polish Academy of Sciences, Lublin, Poland

Definition

Tensiometry – methods and techniques of measuring soil water potential, by means of using tensiometers.

Introduction

Soil water potential is one of the key concepts in soil physics. Water potential determines many soil processes, including soil water movement, soil solutes and pollutants transport, and others e.g., soil heating phenomena. Availability of soil water for plants and its evaporation or transpiration is also influenced by soil water potential.

Soil water potential

Energetic state of soil water is formally defined as a total soil water potential. There are four main components of the total soil water potential (Campbell, 1988), which takes its source in different physical phenomena: matric, osmotic, pneumatic and gravitational forces. Matric potential results from interactions of soil water with soil solid phase. It is known also as a capillary potential. Osmotic or solute potential is associated with chemical solutes existing in water. Pressure or pneumatic potential is attributed to pressure differences between the place in the soil medium where it is determined, and pressure in reference to free water. Gravitational potential takes into account differences in water energy associated with the work done by gravitational force. Gravitational potential is calculated in relation to some reference level, where it is assumed to be equal to zero.

Matric potential plays special role in many soil processes and is very important for agriculture. Especially soil water content is related to matric potential via so called retention curve. Soil matric potential may be measured by devices called – tensiometers.

The first use of tensiometers is commonly attributed to Willard Gardner or Lorenzo Richards, which took place about 1920s. However, recent developments (Or, 2001) shows possibility that the tensiometer like devices were

used earlier. Burton E. Livingston in 1908 developed auto-irrigator device in which the same concepts as in tensiometer were used. In old tensiometers pressure was measured, by mercury pressure gauges, so these devices were neither portable nor easy to use.

Tensiometer

Tensiometers are devices used to measure value of the soil water matric potential. The name tensiometer, is taken from old soil science nomenclature, where soil water potential was called water tension.

The tensiometer consists of three main components (see Figure 1): a *porous cup* fixed on an impermeable *tensiometer body* and a *pressure gauge*. Dimensions and shape of the porous cup determines the place in the soil medium where soil water matric potential is measured. The device body is fully filled up with deaerated water.

The key concept in tensiometer functioning is equilibrium state achieved between soil medium and tensiometer cavity. When soil is dried water flows out from the tensiometer via ceramic cup, until pressure drop in the tensiometer, equilibrate suction from the soil medium. When soil moisture increases, water from the soil medium flows into the tensiometer, until a new state of equilibrium is reached. Water exchange between the tensiometer and soil medium

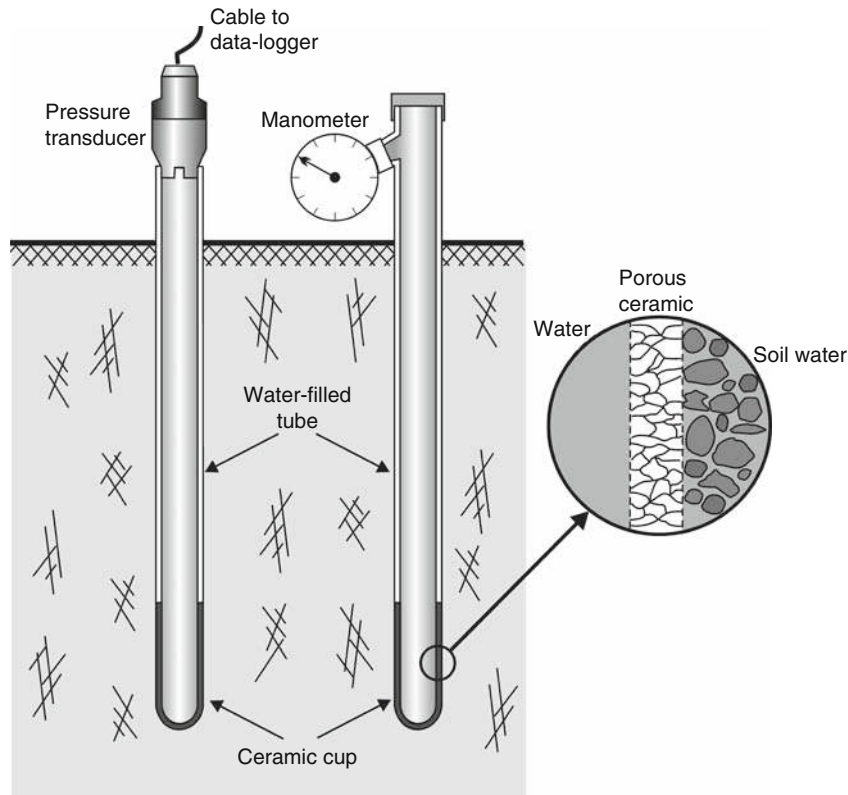
causes water pressure changes in the tensiometer itself. This pressure is related to the soil water potential.

Different kinds of pressure gauges may be used in the tensiometer measurements. Nowadays the most standard way of pressure measurements used in the tensiometers, is to use manometer, especially in the field devices. Electronic pressure transducers are also often used. They allow for automatic and remote soil water matric potential measurements.

Difficulties in tensiometer measurements

There are some technical issues with using tensiometer. Properties of the porous cup and its contact with the soil medium are the most important.

First of all, the tensiometer is not working properly for dry conditions. As the soil becomes dry, pressure in tensiometer decreases reaching the point when air enter into tensiometer. The measured pressure is no longer related to the value of soil matric potential. The pressure value in which this phenomenon occurs depends on pore sizes, of the applied ceramic cup. The thinner the pores are, there higher pressure is needed to remove water from them, and at higher pressure air entry occurs. Typical value of pressure at which air entry take place is about -100 kPa although ceramic cups with higher and lower air entry pressures are produced.



Tensiometry, Figure 1 Tensiometer.

The required condition of accurate tensiometer measurements is a good contact between pressure cup and the soil medium. Unfortunately, it may be difficult to ensure proper contact, due to improper device installation or soil shrinking and swelling. When there are gaps between soil medium and the tensiometer's ceramic cup, the measured pressure is not equal to the soil matric potential value and/or the tensiometer response time is longer.

The basic requirement for correct tensiometer measurements is to achieve equilibrium state between device and the soil medium. This may be an issue when the soil water content changes rapidly. The response time of tensiometer depends not only on the device itself, but also on water permeability of soil in which measurement occurs (Towner, 2006). When device response time is high, in comparison to rate of soil moisture changes, the device readings will lag behind true soil matric potential values.

Alternative methods of soil water potential measurements

The other devices for measuring soil matric potential are osmometers and psychrometers. The *osmometers* or *polymer tensiometers* used in soil potential measurements, are generally tensiometers, but filled up with other substances than water, e.g., polymer, which ceramics are semipermeable (de Rooij et al., 2009). Semipermeable ceramic cup is made of substances, which are permeable to water but non-permeable to polymer. Due to osmosis, water is exchanged between soil medium and the device, which cause registered pressure changes.

The *psychrometers* are generally devices for measuring the relative humidity of air, but in soil measurements *micro-psychrometers* are used for indirect measurement of soil water potential (Hillel, 1998). The concept of measurement is based on assumption that in equilibrium conditions soil vapor potential is equal to the sum of the matric and osmotic potential components. In soil measurements thermocouple micro-psychrometer are used, in which chromel-constantian thermocouple is placed in small ceramic cup. This thermocouple is cooled below the dew point of soil vapor phase, and the temperature is recorded. In the next step the condensed water evaporate and the temperature of the junction equilibrates with the temperature of soil medium. The difference of these two temperature values is related to the soil water potential.

Summary

Measurements of soil water potential belong to the first soil physical measurements performed in the past. Due to importance of water potential in the soil-plant-water system, the tensiometry is still technique widely used in agriculture and soil science research. Tensiometers used in such measurements, evolved and now are often controlled by electronic transducers and data-loggers. New type devices, such as psychrometers or osmometers are emerging in this field of usage.

Bibliography

- Campbell, G. S., 1988. Soil water potential measurement: an overview. *Irrigation Science*, **9**, 265–273.
de Rooij, G. H., van der Ploeg, M. J., Gooren, H. P. A., Bakker, G., Hoogendam, C. W., Huiskes, C., Kruidhof, H., and Koopal, L. K., 2009. Measuring very negative water potentials with polymer tensiometers: principles, performance and applications. *Biologia*, **64**, 438–442.
Hillel, D., 1998. *Environmental Soil Physics*. Amsterdam: Academic Press.
Or, D., 2001. Who invented the tensiometer? *Soil Science of America Journal*, **65**, 1–3.
Towner, G. D., 2006. Theory of time response of tensiometers. *European Journal of Soil Science*, **31**, 607–621.

Cross-references

- [Coupled Heat and Water Transfer in Soil](#)
[Field Water Capacity](#)
[Laminar and Turbulent Flow in Soils](#)
[Soil Water Flow](#)
[Surface and Subsurface Waters](#)
[Water Budget in Soil](#)

TERRESTRIAL ECOSYSTEM

See [Water Balance in Terrestrial Ecosystems](#)

TEXTURE

See [Soil Texture: Measurement Methods](#)

Cross-references

- [Fruits, Mechanical Properties and Bruise Susceptibility](#)
[Physical Properties of Raw Materials and Agricultural Products](#)

THERMAL CAPACITY

Synonyms

Heat capacity

Represents the amount of heat needed to cause a 1°C change in temperature of a unit volume of a body.

Cross-references

- [Agrophysics: Physics Applied to Agriculture](#)

THERMAL CONDUCTIVITY

See [Modeling the Thermal Conductivity of Frozen Foods](#)

Cross-references

- [Coupled Heat and Water Transfer in Soil](#)

THERMAL DIFFUSIVITY

Thermal diffusivity is the thermal conductivity divided by the volumetric heat capacity. It has the SI unit of $\text{m}^2 \text{ s}^{-1}$.

Cross-references

[Coupled Heat and Water Transfer in Soil](#)
[Modeling the Thermal Conductivity of Frozen Foods](#)

THERMAL IMAGING

See [Visible and Thermal Images for Fruit Detection](#)

THERMAL TECHNOLOGIES IN FOOD PROCESSING

António A. Vicente, Luís F. Machado
IBB – Institute for Biotechnology and Bioengineering,
Center of Biological Engineering, Universidade do
Minho, Braga, Portugal

Definition

The term *thermal technologies* encompasses the processes and equipment especially designed to heat a food with the purpose of processing it. This term is often used in opposition to *non-thermal technologies*, where food is processed but virtually no heat is involved.

Introduction

Thermal processing is probably the most important process in food industry that has been used since prehistoric times, when it was discovered that heat enhanced the palatability and the life of the heat-treated food. Thermal processing comprehends the heating of foods at a defined temperature for a certain length of time. However, in some foods, the high thermotolerance of certain enzymes and microorganisms, their physical properties (e.g., high viscosity), or their components (e.g., solid fractions) require the application of extreme heat treatments that not only are energy intensive, but also will adversely affect the nutritional and organoleptic properties of the food. Technologies such as ohmic heating, dielectric heating (which includes microwave heating and radio-frequency heating), inductive heating, and infrared heating are available to replace, or complement, the traditional heat-dependent technologies (heating through superheated steam, hot air, hot water, or other hot liquid, being the heating achieved either through direct contact with those agents – mostly superheated steam – or through contact with a hot surface which is in turn heated by such agents). Given that the “traditional” heat-dependent technologies are thoroughly described in the literature, this text will be mainly devoted to the so-called “novel” thermal technologies.

These novel thermal technologies have a common characteristic: heat is generated directly from inside the food, which allows the food thermal treatment while offering potential for improvement on preservation of vitamins and nutrients. The principal differences between ohmic, dielectric, and infrared heating are (Fellows, 2000):

- In ohmic heating, heat is generated due to the electrical resistance of a food, while in dielectric heating, heat is produced by friction of water molecules and infrared energy is simply absorbed and converted into heat.
- Ohmic heating depends on the electrical resistance of the food, dielectric heating is determined by the moisture content of the food, and infrared heating depends on the surface characteristics and of the color of the food.
- Ohmic heating generally is applied at normal electrical supply frequencies (50–60 Hz). The used frequencies of microwaves and radio frequency are defined in closed intervals to prevent interference with radio transmissions, whereas the infrared frequencies have a wider range.
- The used frequency defines the capacity of the energy penetration into a food. While ohmic heating penetrates throughout the food instantly, the lower frequencies used in dielectric heating allow a higher penetration rate than the ones of infrared heating.
- Electrical conductivity has a decisive role in the effectiveness of ohmic and dielectric heating, whereas in infrared heating, it is the thermal conductivity that limits the efficacy of the treatment.

Inductive heating

Inductive heating is based on the generation of an electric current through the food by electromagnetic induction. Heating occurs due to the induction of eddy current in the food that is placed in the generated magnetic field. An induction heater is constituted by an inductor (coil) which generates an electromagnetic field when an alternating electric current flows through it. The heating can be confined to an area immediately opposite to the coil where a secondary coil is placed and through it pass the food that is instantaneously heated (Piyasena et al., 2003). The existing information in the literature using this technology is nonexistent and was not possible to find studies of the application of inductive heating to food processing.

Ohmic heating

Ohmic heating (OH) presents itself as an alternative thermal method, being defined as a process where electric current is passed through foods to heat them. As the electric current passes throughout the food, heat is internally generated within the food which works like an electrical resistance.

OH has distinctive features that allow its distinction from other electric heating processes. In OH processing the direct contact of the foods with the electrodes is

required, whereas in microwave it is not necessary to have electrodes; OH does not have waveform restrictions, even though the sinusoidal type is preferred; and OH can use unrestricted frequency, excluding the defined radio or microwave frequency range.

Ohmically heated products present unique characteristics, with highly added value when compared to other products sterilized by alternative methods; this is especially the case of viscous products and of products with solid phases. The main advantages of OH are:

- Fast and uniform heating of liquids and solid phases by internal heat generation (without the limitations of the conventional heat transfer or microwave heating due to the dielectric penetration limit into solid phases).
- Continuous processing without heat-transfer surfaces, providing uniform heating that results in less thermal damage.
- High energy efficiency (approximately 90% of the electrical energy is converted into heat).
- Multiphase mixtures are not subjected to shear forces, as in scraped surface heat exchangers, due to low flow velocity and no moving parts.
- Reduced fouling and overprocessing of the food when compared with conventional heating, resulting in mechanical damage and better nutrients and vitamins retention.
- Simpler process control, with instant switch-on/switch-off and with reduced maintenance costs.

OH technology presents some disadvantages, such as the higher initial operational costs and the little information available on validation procedures for this heating process. In addition, the main advantage of OH (the heating is volumetric and dependent on electrical resistance) can, in some specific cases, be a significant disadvantage when heating products that are not ionically loaded, like products that include in their composition high amounts of fats, oils, and distilled water (Leadley, 2008).

Commercial applications

The longest running ohmic commercial system in England is a 75 kW unit which has been in operation since the 1990s. This system processed low-acid meat and vegetable products that were packed in bags. In Japan, a system with similar capacity was used to process whole fruits, including whole strawberries (Mans and Swientek, 1993).

Also in Japan, tofu is being processed using OH. Conventionally, the commercial tofu manufacturers use steam injection to heat the soymilk to denature the soybean proteins. Since steam temperature is higher than 100°C and steam condenses after injection, uneven heating and soymilk dilution are unavoidable. With OH, not only liquid food can be heated evenly, but also heating temperature and time could be accurately adjusted or controlled (Wang et al., 2007).

In the USA, a system for the pasteurization of liquid egg is being used, achieving flow rates over 10,000 kg h⁻¹. The

use of this system allowed not only the extension of the shelf life of the product to 12 weeks, but also the cleaning costs and downtime were reduced when comparing with the conventional heating exchange units (Raztek Corporation, 2009).

This technology is useful for the treatment of proteinaceous foods, which tend to denature and coagulate when thermally processed. Juices can be treated to inactivate proteins without affecting the final flavor. Other potential applications of ohmic heating include blanching, thawing, and peeling of fruits (eliminating the need of lye that is an environmental hazard) (Ramaswamy et al., 2005).

OH also has shown potential for a wide array of processes with great promise in future applications. The applications include the acceleration of fermentations; detection of starch gelatinization in solutions and pastes; pretreatments for drying, extraction, and expression; and reduction of water use during blanching (Sastry et al., 2002).

It is estimated that there are at least 18 commercial plants in operation across Europe, the USA, and Japan. As an example, Table 1 shows a summary of industrial plants, with the respective location, year of installation, product that is processed (Leadley, 2008).

Microwave heating

Microwave (MW) heating technology is based on the transfer of electromagnetic energy to the food product. Heat is generated mostly due to the presence of water in the food products. Because of the dipolar nature of this molecule, water is forced to move with the applied electromagnetic field – dielectric effect. This is an extremely fast oscillatory movement (due to the very high frequency of the field) that provokes molecular friction, which in turn causes the volumetric heating of the food. Furthermore, MW also provokes the generation of heat due to the oscillatory movement of ionic charges toward oppositely charged areas that causes multiple collisions and disruption of hydrogen bonds with water, both generating heat within the food (Kinn, 1947).

MW is characterized by wavelength and frequency. Frequencies used for MW heating are internationally established by Electromagnetic Compatibility regulations, and the respective frequency bands (known as Industrial and Scientific and Medical bands) are described in Table 2.

Generally, the frequencies of 2,540, 896, and 915 MHz are used for food processing. The 2,540 MHz frequency is used for home ovens and the three are used for industrial heating.

MW heating has a major advantage over conventional technologies, i.e., the ability to cause a rapid and volumetric temperature rise within the food. This characteristic leads to a number of significant advantages over the traditional heating techniques, namely:

- Increased product throughput: the time required to achieve the desired process temperature is reduced to one-quarter resulting in improved product quality, especially for particulate foods.

Thermal Technologies in Food Processing, Table 1 List of OH plants, year, processed product, process temperature, heating power and location installed until 2006 (Adapted from Leadley (2008))

Products	Installation year	Country	Heating power (kW)
Tomato sauces and pastes	1994	Italy	50
Tomato paste and mango purée	1996	Ivory Coast	64
Fruit slice and dices	1996	Italy	100
Peach and apricot slices and dices	1998	Greece	150
Peach and apricot dices, slices, and halves	1999/2000	Greece	150, 200, and 240, respectively
Diced pears and apples	2000	Italy	150
Low-acid vegetable purées	2001	Italy	100
Strawberries	2002	Mexico	250
Fruit preparations	2002	France	100
Meat preparations	2003	France	50
Tomato dices and peeled	2004	Italy	480
Vegetable sauces	2005	Italy	60
Diced mushrooms and tomato	2006	Italy	240
Tomato dices, pulp and sauces	2006	Italy	480
Tomato sauces and derivatives	2006	Italy	100
Peach and apricot dices and slices	2006	Greece	120

Thermal Technologies in Food Processing, Table 2 Specific frequencies for industrial, scientific, and medical uses (Adapted from Leadley (2008))

	Frequency (MHz)
Microwaves	896 (UK) and 915 (USA)
	2,450
	5,800
	24,125

- Improved energy efficiency: the heat is generated in the product, so it is possible to attain a more uniform temperature distribution in the product, simplifying the control of thermal treatment and avoiding overprocessing.
- The process can be instantly switched on or off.
- The food product can be pasteurized after being packaged.

The main disadvantages of this technology are the high equipment and operating costs and the difficulties in validating the heat treatment due to changes of dielectric properties during the heating process that are not yet fully understood, resulting in wide distributions of temperature across the food product. Being so, the validation of the process has to be done almost individually for each food product, which becomes a barrier for a wide propagation of MW heating in the food industry.

Commercial applications

Although MW heating is very popular in the domestic use, there has been a slow uptake of this technology in industrial food processing.

A combination of MW and hot air has been successful in speeding the drying process, of pasta drying (Decareau, 1985) and for producing dried onions (Metaxas and Meredith, 1983). Also, MW heating is used for drying

snack foods (e.g., puffed rice cake, seaweeds), vegetables, fruits, chocolate powder, and milk cake (Chen et al., 1982).

The use of MW heating allows the reduction of baking time, making possible the use of flour with high α -amylase content and low protein content (Leadley, 2008).

MW can be used to speed up the process of meat tempering, which is currently used in France for beef, lamb, and ham.

Pasteurization and sterilization processes where MW heating is used include yogurt and pouch-packet meals and the continuous pasteurization of milk (Decareau, 1985; Rosenberg and Bögl, 1987).

Radio-frequency heating

Radio frequency (RF) operates under the same principle as that of MW heating, allowing fast and volumetric heating of the food product. Heat is generated within the product and throughout its mass simultaneously due to the frictional interactions of polar dielectric molecules disturbed by the applied AC electric field (Kinn, 1947).

RF (as well as MW) are both non-ionizing radiations because they have insufficient energy (< 10 eV) to ionize atoms. The allowed frequencies for RF heating processes are 13.56, 27.12, and 40.68 MHz (Piayesena et al., 2003).

RF heating present similar advantages to ohmic and MW when compared with conventional processing technologies that are essentially due to the generation of heat throughout the volume of the food being processed. However, RF has some specific advantages over those volumetric technologies (Rowley, 2001):

- In contrast with OH, there is no need for electrodes in direct contact with the food (as well as for MW).
- The RF longer wavelength allows a deeper penetration of the radiation (tens of centimeters) in the foods than MW energy (several centimeters), depending on the dielectric properties of foods.

- RF systems are simpler in their construction than MW systems. RF is better suited for large industrial applications, having a straightforward application to continuous processes.

RF's main disadvantages are the higher equipment and operating costs, when compared to conventional systems, and are even more expensive than OH-based processes; RF systems are significantly bigger than MW systems for equivalent power output and have slower heating rates than MW.

As in MW heating, it is difficult to achieve the validation of RF due to lack of data regarding the RF dielectric properties of foods. Being so, it is necessary to gain full understanding of parameters that affect the dielectric properties of foods, such as mass, shape, water content, chemical composition, temperature, and frequency of treatment to solve common problems such as dielectric arcing and thermal runaway heating, allowing further development of this technology (Rowley, 2001).

Commercial applications

RF dielectric heating has been used in the food industry to replace conventional heating methods in a wide range of applications (Table 3).

Infrared heating

Infrared (IR) energy is a form of electromagnetic energy. It is transmitted as a wave, which penetrates into the food and is then converted to heat by interaction with molecules of the food. Heat passes throughout the food from the surface layer by conduction. The IR spectra can be divided in three classes, depending on the wavelength: short waves (0.7–2.0 μm); medium waves (2.0–4.0 μm); and long waves (4.0 μm–1 mm). The wavelengths from medium to long waves are the most advantageous to use in industrial applications since maximum radiation absorption occurs in the range of 3–10 μm for the majority of food products.

IR heating present similar advantages to the other types of electromagnetic heating when compared with conventional processing technologies, namely:

- The heat transfers occurs instantaneously, reducing processing time and energy costs (the savings can reach 50%).

- IR energy is only absorbed at the material being heated, allowing differentiating heating in nearby zones. Furthermore, the surrounding air does not absorb IR energy, so it does not heat up.
- The equipment can be compact and very easily controlled and with low-risk operation as no by-products are produced.

IR technology use in food industry is expected to grow as the main advantage of this technology over the traditional ones is the drastic reduction of processing times (up to 70% reduction), which, in turn, increases productivity while maintaining product quality. Nevertheless, it is still necessary to increase understanding of the interactions between energy transfer and its effects on the foods organoleptic and nutritional properties; in the area of process control; and innovations on IR heating equipment.

Commercial applications

Although IR heating is widely used in nonfood industries, such as medical, dye, automobile, electronics, and paper industries, for heating and drying purposes, in the food industry, IR heating is still relatively new. Recently, interest in short-wave IR (wavelengths approximately of 1 μm) and in intermediate IR (wavelengths approximately of 10 μm) has increased, since these wavelengths allow a rapid transfer of high amounts of energy reaching working temperatures in seconds. Nevertheless, in the food industry, long-wave IR is still used more than the other IR methods because the high-load energy is more difficult to control and it can damage the food. Being so, the industrial food applications described next are using long-wave IR heating.

IR heating has been successfully used in practical applications as a substitute of conventional processes, such as baking of bread and cookies (Nakamura, 1999; Kiyohira and Yoneda, 1999), roasting of coffee and green tea (Kino, 1999; Takeo, 1999), cooking of beef patties (Sheridan and Shilton, 2002), heating of legume seeds (Oladiran et al., 2001), drying of edible seaweed, vegetables, fish products, and pasta (Kimura, 1999; Itoh, 1986; Tokunaga, 1987; Ratti and Mujumdar, 1995).

IR pasteurization is particularly effective at the surface of foods and has been successfully used for the pasteurization

Thermal Technologies in Food Processing, Table 3 Examples of RF heating applications for food processing

Process	Food products	Reference
Heating	Bread	Cathcart et al. (1947)
Blanching	Vegetables, fruit	Moyer and Stotz (1947)
Thawing	Meat, sausages, bacon, pies, frozen eggs, fruits, vegetables and fish	Sanders (1966); Cathcart et al. (1947)
Cooking	Turkey breast rolls	Tang et al. (2005)
Drying (Roasting)	Cocoa beans	Cresko and Anantheswaran (1998)
Pasteurization	Ham	Orsat et al. (1999)
Heating (continuous)	Carrots, potatoes	Zhong et al. (2004)

of oysters (Kutsunai, 1988) as well as in packaged products such as sausages and boiled fish paste (Ishi, 1985).

Summary

In recent years, consumers started to demand food products with enhanced safety and quality, along with extended shelf life. The traditional thermal processing is always associated with some undesirable degradation of heat-sensitive quality attributes. This all added to research and development of novel thermal-processing technologies that could take action towards these new challenges. The novel thermal-processing technologies addressed here are: ohmic, microwave, radio frequency, inductive heating, and infrared heating.

Bibliography

- Cathcart, W. H., Parker, J. J., and Beattie, H. G., 1947. The treatment of packaged bread with high frequency heat. *Food Technology*, **1**, 174–177.
- Chen, S. C., Shen, Z. Y., Fu, C. S., and Wu, D., 1982. The development of microwave power applications in China. *Journal of Microwave Power*, **17**, 11–15.
- Cresko, J. W., and Anantheswaran, R. C., 1998. Dielectric drying and roasting for food manufacturing. In *Proceedings of 33rd Microwave Power Symposium*. Chicago, pp. 95–98.
- Decareau, R. V., 1985. *Pasteurization and Sterilization. Microwaves in the Food Processing Industry*. Orlando: Academic.
- Fellows, P. J., 2000. *Food Processing Technology: Principles and Practice*, 2nd edn. Cambridge: Woodhead Publishing.
- Itoh, K., 1986. Drying of vegetable by far infrared radiation. *Shokuhin Kikai Souchi*, **23**, 45–53.
- Ishi, T., 1985. Possibility of far infrared radiation to food processing. *Food Processing (Shokuhin To Kaihatu)*, **20**, 28–31.
- Kimura, Y., 1999. Far infrared roasting of lumps of unprocessed “Nori”, edible seaweed. *The Food Industry (Shokuhin Kogyo)*, **42**, 32–37.
- Kinn, T. P., 1947. Basic theory and limitations of high frequency heating equipment. *Food Technology*, **1**, 161–173.
- Kino, T., 1999. Application of far-infrared heating on roasting of coffee beans. *The Food Industry (Shokuhin Kogyo)*, **42**, 29–38.
- Kiyohira, K., and Yoneda, T., 1999. Rice cookie baking machines and chikuwa baking machines. *The Food Industry (Shokuhin Kogyo)*, **42**, 52–61.
- Kutsunai, T., 1988. Heating equipment for oyster by far infrared radiation. *Japan Food Science*, **27**, 53–56.
- Leadley, C., 2008. Novel commercial preservation methods. In Tucker, G. S. (ed.), *Food Biodegradation and Preservation*. Oxford: Blackwell Publishing, pp. 211–244.
- Mans, J., and Swientek, B., 1993. Electrifying progress in aseptic technology - food processing - food plant ideas. Prepared Foods Magazine, http://findarticles.com/p/articles/mi_m3289/is_n9_v162/ai_14462699/.
- Metaxas, A. C., and Meredith, R. J., 1983. *Industrial Microwave Heating*. London: Polu Pelegrinus Ltd.
- Moyer, J. C., and Stotz, E., 1947. The blanching of vegetables by electronics. *Food Technology*, **1**, 252–257.
- Nakamura, A., 1999. Far-infrared heating and heating process in bread baking. *The Food Industry (Shokuhin Kogyo)*, **42**, 46–51.
- Oladiran, F., Tyer, B., Pickad, M., Zhen, G. H., and Wang, N., 2001. Effect of infrared heating on the properties of legume seeds. *International Journal of Food Science and Technology*, **36**, 79–80.
- Orsat, V., Bai, L., and Raghavan, G. S. V., 1999. Radio-frequency pasteurization of ham to enhance shelf life in vacuum packaging. In *ASAE Annual International Meeting*. Toronto: Paper No. 996091.
- Piyasena, P., Dussault, C., Koutchma, T., Ramaswamy, H., and Awuah, G., 2003. Radio frequency heating of foods: principles and applications and related properties – a review. *Critical Reviews in Food Sciences and Nutrition*, **43**(6), 587–606.
- Ramaswamy, R., Jin, T., Balasubramaniam, V. M., and Zhang, H., 2005. Pulsed electric field processing. In *FactSheet Extension*, FSE-2-05, pp. 1–3.
- Ratti, C., and Mujumdar, A. S., 1995. Infrared drying. In Mujumdar, A. S. (ed.), *Handbook of Industrial Drying*. New York: Marcel Dekker, pp. 567–588.
- Raztek Corporation, 2009. url: <http://www.raztek.com/>.
- Rosenberg, U., and Bögl, W., 1987. Microwave pasteurization, sterilization, blanching and pest control in the food industry. *Food Technology*, **41**, 92–99.
- Rowley, A. T., 2001. Radio frequency heating. In Richardson, P. (ed.), *Thermal Technologies in Food Processing*. Cambridge: Woodhead Publishing, pp. 163–177.
- Ruan, R., Ye, X., Chen, P., Doona, C., and Taub, I., 2002. Ohmic heating. In Henry, C. J. K., and Chapman, C. (eds.), *The Nutrition Handbook for Food Processors*. Boca Raton, FL: CRC Press, pp. 407–422.
- Sanders, H. R., 1966. Dielectric thawing of meat and meat products. *Journal of Food Technology*, **1**, 183–192.
- Sastray, S. K., Yousef, A., Cho, H. Y., Unal, R., Salengke, S., Wang, W. C., Lima, M., Kulshrestha, S., Wongsa-Ngasri, P., and Sensoy, I., 2002. Ohmic heating and moderate electric field (MEF) processing. In Welti-Chanes, J., Barbosa-Canovas, G. V., and Aguilera, J. M. (eds.), *Engineering and Food for the 21st Century*, Boca Raton, FL: CRC Press, pp. 785–794.
- Sheridan, P. S., and Shilton, N. C., 2002. Analysis of yield while cooking beefburger patties using far infrared radiation. *Journal of Food Engineering*, **51**, 3–11.
- Takeo, T., 1999. Firing and roasting of green tea. *The Food Industry (Shokuhin Kogyo)*, **42**, 18–24.
- Tang, X., Cronin, D. A., and Brunton, N. P., 2005. The effect of radio frequency heating on chemical, physical and sensory aspects of quality in Turkey breast rolls. *Food Chemistry*, **93**, 1–7.
- Tokunaga, T., 1987. Drying of marine products by far-infrared rays. *New Food Industry*, **29**, 10–15.
- Wang, L. -J., Li, D., Tatsumi, E., Liu, Z. -S., Chen, X. D., and Li, L.-T., 2007. Application of two-stage ohmic heating to tofu processing. *Chemical Engineering and Processing*, **46**, 486–490.
- Zhong, Q., Sandeep, K. P., and Swartzel, K. R., 2004. Continuous flow radio frequency heating of particulate foods. *Innovative Food Science and Emerging Technologies*, **5**, 475–483.

Cross-references

- [Dielectric Properties of Agricultural Products](#)
[Electrical Properties of Agricultural Products](#)
[Physical Properties as Indicators of Food Quality](#)

THERMOSEQUENCE

A group of related soils that differ, one from the other, as a result of differences in temperature as a soil formation factor.

THIXOTROPY

See [Rheology in Soils](#)

TILLAGE, IMPACTS ON SOIL AND ENVIRONMENT

Márta Birkás

Department of Soil Management, Institute of Crop Production, Szent István University Gödöllő, Gödöllő, Hungary

Definition

Soil tillage. Preserving or improving the soil physical and biological condition in a way and to a depth suitable for the required tasks of soil protection and cropping.

Arable land use. Production of plants regarding their various biological requirements and after-effects and the relevant cropping technologies; Categories: early extensive, conventional, early intensive, integrated, modern intensive, modern extensive, and organic.

Conventional tillage. Working the entire soil surface, using conventional plow for primary tillage, creating soil conditions assumed to be favorable for plant growth by an unreasonably large number of tillage passes and with excessive time, energy, and cost input; inconsistent, if any, adaptation to soil condition and, typically, repeating ineffective tillage interventions.

Environment conserving tillage. Creating and maintaining a harmonious balance between the requirements of the environment and those of cropping, by preserving or improving the quality of the soil.

Adaptable tillage. Improving or preserving the quality of the soil in harmony with ecological, climatic, and farming requirements.

Climate risk. Defects in the soil quality condition along with likely consequences of soil disturbance.

Climate stress mitigation tillage. Alleviation of soil sensitivity by reasonably controlling the soil water transport and the carbon balance.

Introduction

European authors of past centuries used to describe the importance of tillage in terms of satisfying plant requirements, thus, the era dominated by their concepts may also be referred to as the age of *crop-focused* tillage. The over-estimating of “crop requirements” contributed to the damaging of the soil both directly and indirectly. Soil degradation and its consequences inevitably drew attention in the early seventies to the need for protecting the soil as a multi-functional environmental element. According to the principle of *soil-focused* tillage, conserved soil meets the requirements of growing crops. Since the first years when the alarming signs of climate change began to appear, there has been a growing need for adopting

a *climate-focused* approach to tillage as well, since losses caused by climate change can be alleviated by preserving and improving the quality of the soil (Birkás, 2009).

Soil and land use

Soil is the loose fertile layer of the solid crust of the Earth; it is an environmental element whose condition and quality can be changed, renewed, or degraded (Várallyay, 2008). The use of soil for agricultural purposes is considered to be reasonable if the requirements for its renewal are met. The soil special capability of renewal can be maintained by continuous treatment adapted to the local circumstances (Birkás, 2008). The primary tasks of arable land use include, within the framework of landscape and environment protection, maintaining and improving favorable soil characteristics as well as preventing undesirable changes.

Direct impacts on soil by tillage

Tillage is a groundwork type element of cropping, preceding other technological components of crop production. Tillage does not influence the soil natural characteristics (e.g., clay content, particle size distribution, acidity/alkalinity), but it does change the soil physical state both directly and indirectly. Factors of importance for cropping, which can be altered by tillage, include the looseness of the root zone, the depth of the loosened layer, the soil structure, the shape of the surface, and the surface coverage. The *root zone looseness* can be described by well-known parameters such as bulk density, pore volume, and penetration resistance (Håkansson, 1990). These parameters give a numerical indication of the soil state – as well as the favorable or unfavorable impacts of a given tillage technique – at the given point in time (Sajko et al., 2009). Plants are less sensitive to the soil looseness if the soil contains enough water and nutrients. A compact soil is not a suitable habitat for plants, and this is particularly true if compactness is coupled with insufficient water and nutrient supply or with excessive water content. In dry years, the lack of water and excessive compactness are mutually aggravating risk factors. The *depth of the loosened layer* either helps or retards the plant root development. The depth of the loosened layer brought about by primary tillage is usually the same as the depth of the soil layer suitable for taking in water and for crops to take up water. A loosened state can be preserved if subsequent tillage passes are carried out when the soil moisture content is suitable for tillage, using tools that do not create watertight compact layers in the soil. What is referred to as *agronomical structure*, that is, the relative proportions of clods (>10 mm), crumbs (0.25–10 mm), and dust (<0.25 mm) is indicative of the processes occurring in regularly tilled soil. A ratio of crumb over 75–80% crumb fraction is characteristic of a climate stress-tolerant state. The *shape and coverage* (by chopped field residues) of the *soil surface* are important indicators of the soil water retaining capacity. More water is usually lost through

a larger surface and less water is lost through a smaller surface (Birkás, 2008). Bare soil is equally exposed to heat- or rain-induced stress and to the structure deterioration. The minimum cover ratios recommended are between 40% and 50% after harvest in the summer and 20–35% after primary tillage.

Indirect impacts on soil by tillage

Changes in the soil water transport patterns (the balance between intake, storage, and loss), in its biological activity and in its organic material balance are indirect changes but they are extremely important from the aspect of the future of soils and cropping. *Water intake* is the proportion of precipitation that actually ends up in the soil, it is up to 80% in favorable cases but most often it is around 65–70%. Tillage improves the soil water intake capacity but it may just as well increase its water loss. Outside the growing season, the degree of water loss is affected by the shape of the tilled surface, by the cover of the soil surface, and the depth of disturbance. *The ratio of water released from the soil* are affected by land use, tillage (loss increasing or decreasing), and crop water consumption. Drought-induced losses cannot be prevented in soils where water-loss increasing tillage has been applied for years. A soil with a large bare surface loses the largest amount of water in the summer, in the early autumn, or in the spring. Up to 40–48 mm of water may be lost from a clay loam soil after deep plowing (0.28–0.32 m), left in clods, in two dry summer months, in contrast to the 18–24 mm of water lost from a soil tilled to a similar depth but rolled after plowing (Birkás, 2009). The loss of water from soil with a large surface is further increased by persistent warm or windy weather. Owing to the current climate change, more attention needs to be paid to the loss of water from soils plowed and left without surface leveling. Up to 40–56 mm of water may be lost from a clay loam soil left in clods, during the mild winter months, while not more than 20–26 mm of water is lost from the same soil conditions if the soil surface is flattened. The soil *biological activity* has become a focal issue, as a consequence of the current climate change. By boosting aerobic activity, too frequent inverting and excessive airing of the soil will increase the loss of humus, an indispensable soil component for structure building (Szabó, 2008). Loosening and crumb-forming tillage coupled with adequate pressing are more advantageous from a biological perspective as well, since they result in reduced aeration of the soil, which in turn, limits aerobic microbial activity. Soil *humus or carbon balance* is a function of composition and decomposition. Soils that have never been tilled are in a state of balance, but once they are broken up, decomposition will be occurred. Continuous application of humus-conserving tillage may result in a balance near the original level. Under favorable conditions, the quantity of humus produced during a year equals or may even exceed the amount decomposed over the same period. Problems begin when the amount of

humus decomposed exceeds the amount produced. In a year of average precipitation, if there are 5 t ha⁻¹ wheat straw and 2.5 t ha⁻¹ root residues in the soil (since approximately 40% of it is carbon (La Scala et al., 2006)), the expected carbon yield is approximately 3 t ha⁻¹. The whole of this quantity may be released into the atmosphere if the soil is plowed deeply without surface flattening, while only about a third of the same quantity will be lost if a carbon-conserving tillage is adopted. If the straw is fully removed, leaving only the carbon content of the roots in the soil, carbon-conserving tillage will result in a smaller loss of carbon (0.6–1.2 t ha⁻¹) while a carbon-wasting tillage will lead to a greater loss (3.0–3.5 t ha⁻¹). Concern is raised by the cyclical carbon loss where plowing in the summer is the usual practice. Moreover, the soil state resulting in carbon loss is exactly the same soil state that induces water loss. While the water absorbing capacity of humus colloids is as great as that of clay minerals, so humus improves the water retaining capacity. From the aspect of their impacts on CO₂, flux tillage interventions qualify as preserving, balance keeping, or waste increasing techniques. *Earthworm activity* is a good soil condition indicator. Compacted, bare, or over disturbed soils make poor habitats for earthworms. Earthworm-friendly tillage has a loosening and crumb-forming impact, creating a small soil surface, with adequate (35–45%) mulch cover. Soil moisture content ensuring favorable workability is also good for earthworms.

Tillage impact to the environment

The quality of the soil affects the landscape and the quality of the environment. Therefore, one crucial requirement to be met by tillage is that neither the process, nor the soil state created over a shorter or a longer period should be detrimental. This expectation is a result of a multitude of tillage-induced soil defects caused by conventional tillage systems.

Tillage defects qualifying as environmental damage and their consequences

Multiple tillage traffics and excessive disturbance boost CO₂ emission and increase the loss of organic material (Chatterjee and Lal, 2009). The fuel consumption of multiple tillage passes is an indirect environment pollution factor. Diminishing organic materials in frequently and intensively disturbed soils undermines the soil bearing capacity and workability and it leads to growing exposure to the risk of compaction and pulverization (Lal, 2007). A deteriorated soil structure is more exposed to water and wind erosion, water causes silting in such soils while when they dry out crusting and capping appears. Tillage to the same depth year after year leads to detrimental compaction in the root zone (Birkás et al., 2009). Compacted state reduces water intake and transport in the soil and the water, accumulating above the compact layers inducing airless condition. Field residues are often inverted or burnt instead of being used for soil surface protection.

Conventional tillage

More than 3 decades of increasingly intensive criticism of conventional tillage inevitably raises the question of how, despite the detrimental impacts, this could remain one of the predominant prerequisites for crop production. The power required for conventional tillage and the clearly visible effects on the soil (inverting, clean surface), as well as the sentiments relating to the *plow* must have played a dominant role in this. Despite its large time, energy, and labor requirement, conventional tillage remained more attractive (Table 1) than the risks possibly entailed by a new method that should have had to be learned. These views were changed both by increasing fuel prices and by the recognition of the deterioration of soil condition.

Water, carbon, and structure conserving tillage

Distinguishing between tillage trends (conventional, reduced, soil conserving, etc.) and endeavors (energy saving, sustaining, etc.) has been enabled – in even a clearly defined way during the past 4 decades – by two crucial factors: (1) though much soil disturbance conventional crop-focused tillage leads to soil and environment threat and to reduced output, (2) crop needs concerning soil condition have proven to be possible to meet even without the conventional methods, with reduced inputs. The deterioration of the environmental conditions is forced to adopt techniques preventing and alleviating damage, that is, to use adaptable tillage.

Recommendations for soil and environmentally sound tillage

Tillage may cause soil defects, but proper techniques are also available for remedying damage so caused. Preserving soil quality requires avoiding techniques causing defects, along with applying remedial procedures (Birkás, 2008). Special recommendations have been worked out for the Central European region, in view of its particular climate. Because of the danger of moisture and carbon loss and because of the climate risk, the

depth and methods of tillage interventions in the summer will have to be changed. Conserving moisture and soil quality calls for shallow stubble treatment, and mulching the soil surface. Since the lack of knowledge of the soil state leads to wrong decisions, there is a need for regular soil state assessments. Recognition of soil defects helps choosing the most suitable techniques and avoiding losses. Adequate (35–45%) cover of disturbed soils protects soils against heat and rain stress in the summer, against desiccation, and the diminishing of biological life. The covering material is utilized as organic material, mixed into the soil after the passage of the critical months. Smaller soil surface – through which water is lost – must be created in all seasons, but most importantly in the summer months. Milder autumn and winter weather conditions call for extending the use of water conservation to primary tillage minimizing the surface for evaporation. Soil in clods in the surface is not favorable for weathering in the winter months without snow cover. Exceptions to this include too wet soils in the seasons, where the damage would be aggravated by secondary tillage. If the soil is suitable for traffic, however, the evaporative surface must be reduced. In the summer and in the spring soil surface evening and pressing, while before wintering, surface levelling is the preferred method following primary tillage (or soil disturbance). Compact layers blocking water intake and the seeping of water down into the root zone must be broken up, restoring thereby the soil harmonious water transports. The use of tools forming tillage pan should be avoided in wet soil, regardless of the tillage type. This requires knowledge of the water content range ensuring optimum workability of the soil. Crumb forming requires a favorable carbon balance, adequate moisture, and earthworm activity in the soil. The soil organic material content must be protected, since it is indispensable for retaining water, for keeping the soil workable, for resisting compaction, and for mitigating climate risk. Field residues should not be removed (e.g., for generating energy)

Tillage, Impacts on Soil and Environment, Table 1 Main characteristics of conventional and environmentally sound tillage

Factor	Conventional	Environmentally sound
Purpose of tillage	Meeting plant requirements	Soil quality conserving or improving
Depth	Excesses (deep or shallow)	Depending on soil condition
Mode	Inverting	Plowless
Surface	Free of residues	Covered to various degrees
Field residues	Something impeding tillage	Valuable material
Organic material	Diminishing	Preserving
Carbon balance	Input in soil < loss	Input in soil > loss
Tillage tool	Subordinated to tillage concept	Adapted to soil condition
Energy input	Excessive	Realistic
Adaptability to soil	Limited	Wide
Risks	Soil quality deterioration	Weeds, pests, pathogens
Impact on soil	Varying	Protection, renewal
Impact on plants	Sometimes positive	Positive
Long-term impacts	Increasing climate-induced sensitiveness	Alleviating climate-induced threats

where there is no other way for recycling organic materials. Soils that still have optimum levels of organic material should be taken care of just as much as those of low organic material contents.

Summary

Creating soil conditions best suiting crop requirements used to be considered as the most important goal of tillage for centuries. This type of crop-focused tillage is largely to be blamed for the degradation of soils. The old approach has necessarily been replaced by a soil-focused tillage approach to improve damaged soils and to preserve soil quality. Tillage can have peculiar effects, as it can just as easily damage the soil as it can remedy most of the damage already caused. The importance of the protection of soil quality and of alleviating tillage-induced environmental damage has been confirmed yet again, this time by the threats imposed by global climate change. Science assumes an important role and, based on soil quality research, offers a good chance for reducing climate-induced harvest losses. Soil- and environmentally sound tillage helps carrying out the tasks of climate stress alleviation by means of soil moisture, organic material, and soil structure protection.

Bibliography

- Birkás, M., 2008. *Environmentally-sound Adaptable Tillage*. Budapest: Akadémiai Kiadó.
- Birkás, M., 2009. Conventional tillage requirements and the pressure of the need for alleviating climate-induced damage. *Növénytermelés*, **2**, 123–134 (in Hungarian).
- Birkás, M., Stingli, A., Farkas, C., and Bottlik, L., 2009. Relationship between Tillage-induced Compaction and Climate-induced Damage. *Növénytermelés*, **3**, 5–26 (in Hungarian).
- Chatterjee, A., and Lal, R., 2009. On farm assessment of tillage impact on soil carbon and associated soil quality parameters. *Soil and Tillage Research*, **104**, 270–277.
- Håkansson, I., 1990. A method for characterizing the condition of compactness of the plough layer. *Soil and Tillage Research*, **16**, 105–120.
- La Scala, N., Jr., Bolonhezi, D., and Pereira, G. T., 2006. Short-term Soil CO₂ emission after conventional and reduced tillage of a no-till sugar cane area in southern Brazil. *Soil Tillage Research*, **91**, 241–248.
- Lal, R., 2007. Farming carbon. *Soil and Tillage Research*, **96**, 1–5.
- Sajko, K., Kisic, I., Basic, F., and Sabolic, M., 2009. Bulk density and soil resistance variability in different soil moisture conditions under different tillage systems. *Cereal Research Communications*, **37**, 371–374.
- Szabó, I. M., 2008. *Biological Fundamentals of General Soil Science*. Budapest: Mundus Kiadó (in Hungarian).
- Várallyay, G., 2008. Dedication to the English edition. In Birkás, M. (ed.), *Environmentally-sound Adaptable Tillage*. Budapest: Akadémiai Kiadó, pp. 9–10.

Cross-references

- [Compaction of Soil](#)
[Soil Physical Quality](#)
[Soil Water Management](#)
[Subsoil Compaction](#)

TILLAGE EROSION

Jianhui Zhang

Institute of Mountain Hazards and Environment, Chinese Academy of Sciences and Ministry of Water Conservancy, Chengdu, Sichuan, PR China

Synonyms

Soil erosion by tillage

Definition

Tillage erosion. Tillage erosion refers to the net soil translocation on the hillslope due to tillage operations, expressed in units of volume, mass, or depth per unit width of tillage. The transport and resultant displacement of soil during tillage is referred to as tillage translocation.

Introduction

In agricultural practices, tillage has been used to prepare the soil for seeding, to improve soil physical properties, to enhance a rapid release of nutrients from the soil organic material, to control weeds, and the like. However, a major drawback of tillage arises when it becomes intensive and continuous, which causes soil erosion. Soil erosion is usually thought of as a natural process induced by natural driving forces such as water, wind, and gravity. Nevertheless, soil erosion is also caused by human driving forces, mainly derived from tillage in agricultural practices, independent of these natural processes. Tillage operation moves the soil mechanically in the tractive force direction, and on the hillslope this movement is enhanced by gravity during a downslope tillage operation. Soil is moved upslope during an upslope tillage operation, and likewise, a downslope soil displacement occurs during a downslope tillage operation under tractor-plow tillage. However, the distance over which the soil is displaced during the downslope tillage operation is normally greater than the displacement distance of the upslope tillage operation. In the case of animal-drawn plow and manual hoeing tillage, the soil is typically turned downslope to minimize energy requirements, and thus only downslope soil displacement occurs without upslope soil displacement. Tillage erosion redistributes soil in a landscape, and is typically characterized by soil loss from convexities (or upper slope positions) and soil accumulation in concavities (or lower slope positions) in the case of complex slopes (or linear slopes).

Although research on tillage erosion first emerged in 1929 (Aufrère, 1929), the first attempts were made to carry out a more systematic study on tillage translocation and erosion until the late 1980s and the early 1990s. During the several decades, only a few studies on tillage erosion had been conducted to specifically examine downslope soil translocation on the hillslope. Tillage erosion were quantitatively examined by Lindstrom et al. (1990, 1992) to comprehensively assess soil translocation and

erosion, showing that soil displacement from convex to concave slope positions was far from insignificant.

Measurement of tillage translocation and tillage erosion

Tillage translocation, defined as the transport and resultant displacement of soil by tillage, is normally measured with a tracer method, i.e., a volume of soil is labeled and tilled, and then changes in tracer concentrations (or weights) before and after tillage are used to calculate soil translocation (Lobb et al., 1995). The change in tracer concentrations as a result of tillage portrays soil shift during tillage, assuming that tracers moved along with soil. Several techniques including physical and chemical ones are used to trace the soil displacement by tillage. Physical tracer used in measuring tillage translocation has so far involved metal cubes (e.g., Govers et al., 1994), rock fragments (e.g., Nyssen et al., 2000) and stone chips (e.g., Zhang et al., 2004a, b), and chemical tracer radiocaesium (e.g., Lobb et al., 1995) and chloride (e.g., Lobb et al., 1999). Recently, the low-induction electromagnetic (EM) (De Alba et al., 2006) and magnetic tracer techniques (Zhang et al., 2009) are also used to measure soil displacement, which are characterized by a simple and quick manipulation.

For up- and downslope tillage, which is common in mechanized agriculture areas, tillage is conducted by successive passes in opposing directions. The soil flux due to tillage is expressed as:

$$Q_s = kS \quad (1)$$

In non-mechanized agriculture areas, tillage is typically conducted downslope. The soil flux due to tillage is expressed as:

$$Q_s = k_3 + k_4 S \quad (2)$$

where k , k_3 , and k_4 are soil transport coefficients (kg m^{-1} tillage pass $^{-1}$), and S the slope gradient (m m^{-1}).

The above empirical equations indicate that tillage erosion is mostly affected by slope gradient under controlled tillage implements. However, other studies also indicate that additional factors including soil conditions (e.g., soil bulk density, soil moisture) and tillage operations (e.g., tillage depth, speed) would be associated with tillage erosion rates (Lobb et al., 1999; Van Muysen et al., 1999).

Tillage transport coefficient in selected regions

Tillage erosion rates vary from 15 to 150 Mg ha^{-1} year $^{-1}$ depending on tillage implements and landforms in different parts of the world. In Europe, tillage erosion has been considered as the dominant process of soil redistribution in the landscape (Quine and Zhang, 2002). In shoulder slope landscape positions, tillage erosion was estimated to account for at least 70% of total soil erosion in southwestern Ontario, Canada (Lobb et al., 1995). High ratios of tillage erosion to water erosion have also been found on sloping terraces of hilly areas, southwestern China,

with tillage erosion accounting for about 70–80% of total soil losses from water and tillage erosion (Zhang et al., 2006, 2010). The tillage transport coefficient is an important indicator reflecting tillage erosion intensity, as it clearly indicates the process causing the soil transport. In mechanized agriculture areas, the tillage transport coefficient k ranges from 111 to 330 kg m^{-1} tillage pass $^{-1}$, and varies between 68 and 108 kg m^{-1} tillage pass $^{-1}$ in some parts of non-mechanized agriculture areas. In the other part of non-mechanized agriculture areas, tillage transport coefficients k_3 , k_4 are 31–89, 108–243 kg m^{-1} tillage pass $^{-1}$, respectively (Table 1). Under animal-drawn plow and manual hoeing tillage, farmers are accustomed to till downslope on the slope with downslope turning and/or pulling on every occasion, which is different from the mechanized tillage in which the soil is turned in opposing directions on successive occasions. As a result, there are still great tillage transport coefficients to be found in non-mechanized agriculture areas.

Tillage erosion versus water and wind erosion

Tillage erosion largely causes soil loss in shoulder slope or downslope sides of the field boundary, while water erosion usually occurs in middle to lower back-slope positions. Typically, tillage erosion is most severe in areas (in convex slope positions and downslope sides of the field boundary) where water erosion is weakest, whereas soil accumulation by tillage is present in areas (in depression positions) where water erosion is most intense, thereby showing that there are different patterns of water erosion and tillage erosion along the transect of the slope. Unlike water erosion that transports the soil off the field and over a long distance, tillage erosion moves the soil within the field and over a short distance in the course of each event. As a result, soil deposition by tillage occurs towards the downslope boundary of the field, resulting in an approximate balance between soil loss and gain within the field. Among landform factors, slope gradients and slope lengths are the two important factors controlling rates of both tillage erosion and water erosion. However, the tillage erosion rate is negatively proportional to slope length in contrast to the water erosion rate, while both are of similar effects with respect to slope gradients, i.e., the erosion rate increases with increasing slope gradient.

Soil loss by tillage occurs in surface soils, thereby impacting soil erodibility to water and wind erosion, as the removed topsoil has more organic matter, and thus more stable soil structure than subsoils. The process of tillage erosion may create an accelerating mechanism of soil erosion, i.e., tillage erosion continuously delivers soil into convergent areas of overland water flow where there is the most severe water erosion, resulting in more severe soil losses, as sediments are delivered beyond the field (Lobb et al., 1995; Zhang et al., 2010). In the terrace system where water erosion is insignificant, however, soil deposition by tillage is evident at lower parts of the terraces, as individual terraces represent a closed system in which

Tillage Erosion, Table 1 Tillage transport coefficients in mechanized and non-mechanized agriculture areas

Tillage implement	Tillage transport coefficient k (or k_3, k_4) (kg m^{-1} tillage pass $^{-1}$)	Location	Data source
Mechanized agriculture			
Mouldboard	330	USA	Lindstrom et al. (1992)
Chisel	111	Belgium	Govers et al. (1994)
Mouldboard	234	Belgium	Govers et al. (1994)
Mouldboard	254	Portugal	Van Muyzen et al. (1999)
Non-mechanized agriculture			
Manual hoe	107	Thailand	Poesen et al. (2000)
Manual hoe	31 (k_3); 141 (k_4)	Sichuan, China	Zhang et al. (2004a)
Manual hoe	84–108	Tanzania	Kimaro et al. (2005)
Manual hoe	37 (k_3); 118 (k_4)	Chongqing, China	Zhang et al. 2009
Animal-drawn plow (chisel)	89 (k_3); 108 (k_4)	Sichuan, China	Quine et al. (1999)
Animal-drawn plow (duckfoot)	79 (k_3); 113 (k_4)	Chinamora, Lesotho	Quine et al. (1999)
Animal-drawn plow (mouldboard by two animals)	79 (k_3); 243 (k_4)	Ha Sofonia, Zimbabwe	Quine et al. (1999)
Animal-drawn plow (chisel)	68	Ethiopia	Nyssen et al. (2000)

major changes in soil redistribution occurs close to upslope and downslope boundaries of the field (Zhang et al., 2008).

Soil profile modification by tillage erosion

As has been stated, tillage causes soil loss in upper slope positions. In middle slope positions, the soil in the till layer is only transported downslope and the removed soil was replaced by the soil from upslope, and therefore the depth of soil profiles was not changed by tillage. Tillage operation mostly plays a transport role, creating zero soil loss and gain in middle slope positions, where the downslope transport of the till layer is similar to a conveyor belt from top to bottom of the slope (De Alba et al., 2004). In the toe-slope positions, tillage mixes the soil of the till layer in the short-term and the original soil profile becomes buried under the accumulated materials from upslope soils in the long term. Progressive effects of the long-term tillage create truncated soil profiles in convex (or upper) slope positions, and deep topsoil accumulations in concave (or lower) slope positions with inverted soil profiles, where subsurface soil material is deposited over original surface horizons (De Alba et al., 2004). The long-term tillage deletes surface soils in convex (or upper) slope positions due to no soil replacement from upslope, leaving subsoils, parent materials, or bedrocks exposed. In North America and Europe, farmers have to till into the subsoil, and therefore materials from subsoils are incorporated into the till layer. In order to offset such soil losses at the proximity of the upslope boundary in Asia, the farmers need to till into parent materials or bedrocks that are soft enough to be crushed by hoes or plows to obtain a replacement (e.g., in the case of Regosols derived from mudstone of Jurassic Age), which remains a certain thickness of the soil layer (generally <20 cm deep). In practice, although the exposure of bedrocks is not widespread, the thin soil layer with a high content of gravel and coarse texture is always found at the summit positions,

as a result of the incorporation of parent materials or mudstone fragments into the cultivated soil layer. In most cases, at the summit of the slope, the depth of soil profiles is generally so small that only the cultivated layer could appear due to soil erosion by tillage (Zhang et al., 2004b). This situation is different from that of the soil profile with multi-genetic horizons (e.g., Ap, AB, B), in which an original subsurface horizon becomes directly exposed at the surface and constitutes a new till layer (De Alba et al., 2004).

Control of tillage erosion

Conversions of conventional tillage to conservation tillage can diminish tillage erosion rates to a great extent. Contour tillage is a common technique and one of the most effective ones to control soil loss by tillage. In southeast Spain, by using a duckfoot chisel, contour tillage reduces soil translocation by 51% (tillage transport coefficient decreased to 139 from 282 kg m^{-1} tillage pass $^{-1}$), compared to conventional up- and downslope tillage (Poesen et al., 1997). Tillage-induced soil loss was also found to be reduced by approximately 70% using contour ridge tillage compared to moldboard plowing up- and downslope on steep lands in Claveria, Philippines (Thapa et al., 1999). A similar reduction (77%) was found in the Sichuan Basin, China, when contour tillage was performed by hoeing in comparison to downslope tillage (Zhang et al., 2004a). In some specific situations, a significant effect of reducing tillage erosion rates has been gained by “the non-overturning tillage,” in which tillage erosion rates can be decreased by 63% compared to those by conventional tillage (i.e., turning soil and pulling it downslope) (Zhang et al., 2009).

Conclusion

Tillage erosion is a gradual soil translocation downslope induced by tillage operations in agricultural landscapes. Several techniques including physical and chemical ones

can be used to trace the soil displacement, and therefore measuring tillage erosion rates. Among those techniques, the low-induction electromagnetic (EM) and magnetic tracer techniques are considered to be characterized by a simple and quick manipulation. Tillage erosion is far from negligible in agricultural ecosystems and is the dominant process of soil redistribution in most agricultural landscapes. The process of tillage erosion may create an accelerating mechanism of soil erosion by water, resulting in more severe soil losses. Tillage erosion rates in non-mechanized agriculture areas may be comparable to those in mechanized agriculture areas, as a result of much steeper slope of the former, despite smaller tillage transport coefficients with the former. As a whole, tillage erosion rates are equivalent to or even surpass water erosion rates, irrespective of agriculture area types. Consequently, tillage erosion is an important process of soil degradation on sloping cultivated land. However, such a degraded process can be reduced significantly by adopting conservation tillage methods, some of which are common to farmers in different parts of the world, e.g., contour tillage.

Bibliography

- Aufrère, L., 1929. Les rideaux, étude topographique. *Annales de Géographie*, **38**, 529–560.
- De Alba, S., Borselli, L., Torri, D., Pellegrini, S., and Bazzoffi, P., 2006. Assessment of tillage erosion by mouldboard plough in Tuscany (Italy). *Soil and Tillage Research*, **85**, 123–142.
- De Alba, S., Lindstrom, M., Schumacher, T. E., and Malo, D. D., 2004. Soil landscape evolution due to soil redistribution by tillage: a new conceptual model of soil catena evolution in agricultural landscapes. *Catena*, **58**, 77–100.
- Govers, G., Vandaele, K., Desmet, P., Poesen, J., and Bunte, K., 1994. The role of tillage in soil redistribution on hillslopes. *European Journal of Soil Science*, **45**, 469–478.
- Kimaro, D. N., Deckers, J. A., Poesen, J., Kilasara, M., and Msanya, B. M., 2005. Short and medium term assessment of tillage erosion in the Uluguru Mountains, Tanzania. *Soil and Tillage Research*, **81**, 97–108.
- Lindstrom, M. J., Nelson, W. W., and Schumacher, T. E., 1992. Quantifying tillage erosion rates due to moldboard plowing. *Soil and Tillage Research*, **24**, 243–255.
- Lindstrom, M. J., Nelson, W. W., Schumacher, T. E., and Lemme, G. D., 1990. Soil movement by tillage as affected by slope. *Soil and Tillage Research*, **17**, 255–264.
- Lobb, D. A., Kachanoski, R. G., and Miller, M. H., 1995. Tillage translocation and tillage erosion on shoulder slope landscape positions measured using ^{137}Cs as a tracer. *Canadian Journal of Soil Science*, **75**, 211–218.
- Lobb, D. A., Kachanoski, R. G., and Miller, M. H., 1999. Tillage translocation and tillage erosion in the complex upland landscapes of southwestern Ontario, Canada. *Soil and Tillage Research*, **51**, 189–209.
- Nyssen, J., Poesen, J., Haile, M., Moeyersons, J., and Deckers, J., 2000. Tillage erosion on slopes with soil conservation structures in the Ethiopian highlands. *Soil and Tillage Research*, **57**, 115–127.
- Poesen, J., Turkelboom, F., Ohler, I., Ongprasert, A. S., and Vlassak, K., 2000. Tillage erosion in Northern Thailand: intensities and implications. *Mededelingen Koninklijke Academie Voor Overzeese Wetenschappen*, **46**, 489–512.
- Poesen, J., Van Wesemael, B., Govers, G., Martinez-Fernandez, J., Desmet, P. J. J., Vandaele, K., Quine, T. A., and Degrer, G., 1997. Patterns of rock fragment cover generated by tillage erosion. *Geomorphology*, **18**, 183–197.
- Quine, T. A., and Zhang, Y., 2002. An investigation of spatial variation in soil erosion, soil properties, and crop production within an agricultural field in Devon, United Kingdom. *Journal of Soil and Water Conservation*, **57**, 55–65.
- Quine, T. A., Walling, D. E., Chakela, Q. K., Mandiringana, O. T., and Zhang, X., 1999. Rates and patterns of tillage and water erosion on terraces and contour strips: evidence from caesium-137 measurements. *Catena*, **36**, 115–142.
- Thapa, B. B., Cassel, D. K., and Garrity, D. P., 1999. Ridge tillage and contour natural grass barrier strips reduce tillage erosion. *Soil and Tillage Research*, **51**, 341–356.
- Van Muysen, W., Govers, G., Bergkamp, G., Roxo, M., and Poesen, J., 1999. Measurement and modelling of the effects of initial soil conditions and slope gradient on soil translocation by tillage. *Soil and Tillage Research*, **51**, 303–316.
- Zhang, J. H., Frielinghaus, M., Tian, G., and Lobb, D. A., 2004a. Ridge and contour tillage effects on soil erosion from steep hill-slope in the Sichuan Basin, China. *Journal of Soil and Water Conservation*, **59**, 277–284.
- Zhang, J. H., Lobb, D. A., Li, Y., and Liu, G. C., 2004b. Assessment for tillage translocation and tillage erosion by hoeing on the steep land in hilly areas of Sichuan, China. *Soil and Tillage Research*, **75**, 99–107.
- Zhang, J. H., Nie, X. J., and Su, Z. A., 2008. Soil profile properties in relation to soil redistribution by intense tillage on a steep hillslope. *Soil Science Society of America Journal*, **72**, 1767–1773.
- Zhang, J. H., Ni, S. J., and Su, Z. A., 2010. Dual roles of tillage erosion in lateral SOC movement in the landscape. *Soil Science Society of America Journal* (in press).
- Zhang, J. H., Quine, T. A., Ni, S. J., and Ge, F. L., 2006. Stocks and dynamics of SOC in relation to soil redistribution by water and tillage erosion. *Global Change Biology*, **12**, 1834–1841.
- Zhang, J. H., Su, Z. A., and Nie, X. J., 2009. An investigation of soil translocation and erosion by conservation hoeing tillage on steep lands using a magnetic tracer. *Soil and Tillage Research*, **105**, 177–183.

Cross-references

- [Carbon Losses Under Dryland Conditions, Tillage Effects](#)
[Hardpan Soils: Management](#)
[Overland Flow](#)
[Physical Degradation of Soils, Risks and Threats](#)
[Soil Erosion Modeling](#)
[Tillage, Impacts on Soil and Environment](#)
[Water Erosion: Environmental and Economical Hazard](#)
[Wind Erosion](#)

TILLAGE PAN

An induced soil pan which has a higher bulk density and a lower total porosity than the soil directly above or below it and is produced as a result of pressure applied by normal tillage operations or by other artificial means.

Bibliography

- <http://www.answers.com/topic/pressure-pan>

TILTH

See *Soil Tilth: What Every Farmer Understands but no Researcher Can Define*

TOP SOIL

The upper part of the solum, essentially the part affected directly by plowing (the plow-layer), synonymous with the A horizon.

TOPOSEQUENCE

A sequence of related soils that differ, one from the other because of topography as a soil-formation factor.

TRACE ELEMENTS IN CROPS: EFFECTS OF SOIL PHYSICAL AND CHEMICAL PROPERTIES

Holger Kirchmann, Jan Eriksson

Department of Soil and Environment, Swedish University of Agricultural Sciences, Uppsala, Sweden

Definitions

Elements present in crops at concentrations of milligrams per kilogram dry matter are defined as *trace elements* (Kabata-Pendias, 2001). A large number of trace elements are found in crops including rare earth metals (Gundersen et al., 2000). The trace elements boron, iron, copper, manganese, molybdenum, nickel, and zinc are essential for crops and are therefore often named *micronutrients*. Selenium has recently been also pointed out to be an essential micronutrient (Hartikainen, 2005). Some trace elements not required by crops are, however, essential for humans and animals, that is, fluoride, iodine, chromium, cobalt, and selenium. The term “heavy metal” refers to elements with a density higher than 4.5 kg dm^{-3} , but provides no information on the toxicity and effect of metals on organisms (Niebor and Richardson, 1980). Knowledge about the functions of *rare earth* metals in crops is scarce, some may be essential, others toxic or without any effect (Markert, 1993).

Soil properties

A number of different factors determine trace element concentrations in crops such as (1) soil properties; (2) addition of trace elements with fertilizers or manures; (3) atmospheric deposition; (4) crop variety; (5) weather conditions; and (6) developmental stage of the crop. Among soil-related factors, physical, chemical, and biological soil ones like soil structure, bulk density (pore

volume), water content, texture, redox conditions, soil pH, soil organic matter content, nutrient content, and microorganism activity are of importance. These factors interact often in a rather complicated manner and some have a direct effect on plant uptake of trace elements, while others have a more indirect effect. For example, texture and organic matter content determine soil structure. A well-structured soil with a low bulk density allows crops to develop large root systems resulting in accessibility to nutrients and trace elements in large soil volume. Soil pH, on the other hand, has a direct effect on uptake since it strongly influences trace metal solubility. Below, some important soil factors are discussed more in detail.

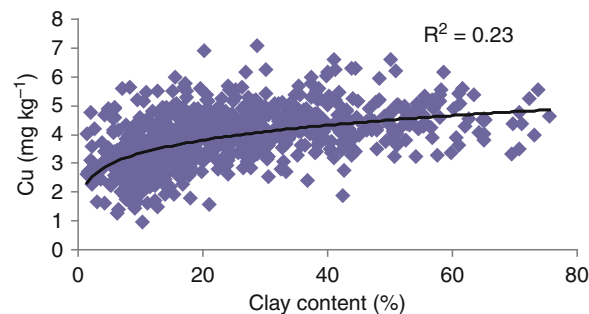
Soil texture

In general, soils with naturally high concentrations of trace elements also produce crops rich in trace metals. Many trace metals are bound to clay particles and consequently clay soils contain more trace metals than lighter soils. Eriksson et al. (2000) showed that there is a strong positive correlation between clay contents in soil and total concentrations of trace elements in soil (R^2 -values: Cr = 0.87; V = 0.83; Ni = 0.80; Co = 0.79; Cu = 0.73; Zn = 0.71). Also, concentrations of boron, manganese, molybdenum, and selenium in soil are correlated with soil clay contents, but weaker. This induces a positive correlation between clay content and trace metals in crops. For V, Ni, Co, and Cu, R^2 values range from 0.15 to 0.5. How the copper concentration in cereal crop increases with clay content in soil is illustrated in Figure 1. The data are from a large number of Swedish arable soils with varying clay content.

Redox conditions

The micronutrient manganese, taken up by crops in reduced form as a divalent ion, is rather easily reduced in soil. Thus, reducing microenvironments in soil are very important for Mn availability. Such conditions are most common in heavy soils, where small pores inside peds are temporally water-filled also when the soil on the whole is well aerated.

However, under strong reducing conditions (complete waterlogging for a period of time) root uptake of nutrients



Trace Elements in Crops: Effects of Soil Physical and Chemical Properties, Figure 1 Relation between copper concentration in cereal crops and clay content in soil.

may be inhibited for most crops, while, for example, a crop like paddy rice is adapted to high tissue concentrations of manganese. In addition, several trace metals may form sulfides (CuS , MoS , ZnS) under such conditions, which means very low or no crop availability.

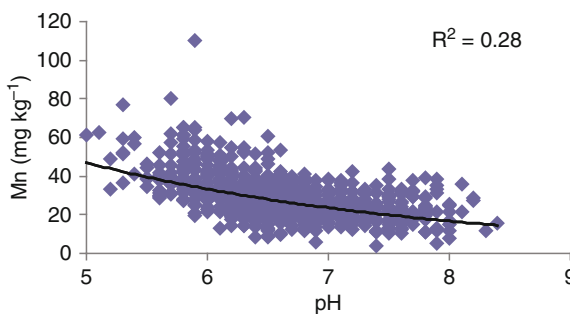
Soil pH

It is well-known that soil pH has a major influence on the solubility of trace metals. Changes in soil pH are followed by changes of the electrical charge on soil particles. At lower soil pH values, hydrogen ions are adsorbed that increase the positive charge on both inorganic and organic soil components resulting in weaker adsorption of positively charged ions. Thereby, cations such as manganese, zinc, iron, boron, and copper become more plant available. On the other hand, higher pH values in soil result in higher negative charge and anions including molybdate are repelled and become more soluble (Lindsay, 1974; Fageria et al., 2002).

Consequently, trace metal concentrations in crops are highly affected by changes in soil pH values (e.g., Öborn et al., 1995; Kirchmann and Eskilsson, 2010). Data in Figure 2 illustrate how manganese concentrations in cereals significantly decline at higher pH values in soil. The large variation in Mn concentration at all pH-levels illustrates that many other factors than pH influence trace metal uptake. The influence of redox conditions on manganese is mentioned above. In fact, manganese deficiency is most common on sandy soils high in pH. In addition, in acid arable soils, mycorrhiza can function as a supplier of copper, zinc, and nickel to crops (Clark and Zeto, 2000).

Soil organic matter and dissolved organic matter

According to a data set from Swedish arable soils (Eriksson et al., 2000), the organic matter content in soil is only weakly correlated with trace element concentrations in crops. For some metals, manganese, copper, cobalt, and zinc, correlations exist but for other metals there is no positive relationship. Selenium, for example, is selectively bound to soil organic matter and concentrations in crops actually decrease with higher soil organic matter content (Johnsson, 1992). Copper deficiency in



Trace Elements in Crops: Effects of Soil Physical and Chemical Properties, Figure 2 Relation between manganese concentration in cereal crops and pH values in soil.

crops grown on peat soils is another example of the insufficient supply of trace metals by soil organic matter.

However, dissolved organic matter can increase trace elements availability due to its capability to form complexes with metals. Functional groups (e.g., $-\text{COOH}$; $-\text{OH}$) of dissolved organic matter bind metal ions electrostatically or covalently. If the ion is bound by five or six functional groups, a chelate complex of high stability is formed. Chelated trace metals are efficiently taken up by crops (Chen et al., 2001). At higher soil pH, the role of dissolved organic matter as carrier molecules for trace metals becomes very important as their negative charge increase and thus the binding of cationic trace metals.

Outlook

Between 1974 and 1982, a total of 3,538 arable soils from 30 countries were analyzed for micronutrient levels by the Food and Agriculture Organization (FAO), (Sillanpää, 1982). In 10% of the soils of each country, micronutrient deficiency was found. In global assessments, it has been estimated that ca 1 billion people are affected by deficiency of iron, iodine, and zinc caused by too low intake. The basis for this, as pointed out many times, is a too low content of essential trace elements in soil leading to low levels in crops and thereby an insufficient supply of humans (e.g., Sanchez and Swaminathan, 2005). Nutrient deficiency in soils of the world is a major task to be overcome and requires our whole-hearted efforts.

Bibliography

- Chen, Y., Magen, H., and Clapp, C. E., 2001. Plant growth stimulation by humic substances and their complexes with iron. In *Proceedings No 470*, International Fertilizer Society, York, 14 p.
- Clark, R. B., and Zeto, S. K., 2000. Mineral acquisition by arbuscular mycorrhizal plants. *Journal of Plant Nutrition*, **23**, 867–902.
- Eriksson, J., Stenberg, B., Andersson, A., and Andersson, R., 2000. Tillståndet i svensk åkermark och spannmålsgröda – jordartens betydelse för markegenskaperna, samband markfaktorer och elementhalter i kärna. *Swedish Environmental Protection Agency, Report 5062* (Summary and captions of figures and tables in English).
- Fageria, N. K., Baligar, C., and Clark, R. B., 2002. Micronutrients in crop production. *Advances in Agronomy*, **77**, 186–268.
- Gundersen, V., Ellegaard Bechmann, I., Behrens, A., and Stürup, S., 2000. Comparative investigation of concentrations of major and trace elements in organic and conventional Danish agricultural crops 1. Onions (*Allium cepa* Hysam) and peas (*Pisum sativum* Ping Pong). *Journal of Agricultural and Food Chemistry*, **48**, 6094–6102.
- Hartikainen, H., 2005. Biogeochemistry of selenium and its impact on food chain quality and human health. *Journal of Trace Elements in Medicine and Biology*, **18**, 309–318.
- Johnsson, L., 1992. Selenium in Swedish soil. Factors influencing soil content and plant uptake. *Reports and Dissertation 10*. Department of Soil Sciences, Swedish University of Agricultural Sciences. Uppsala, Sweden.
- Kabata-Pendias, A., 2001. *Trace Elements in Soils and Plants*. Boca Raton: CRC Press, p. 413.
- Kirchmann, H., and Eskilsson, J., 2010. Low manganese (Mn) and copper (Cu) concentrations in cereals explained yield losses after

- lime application to soil. *Acta Agriculturae Scandinavica, Section B, Soil and Plant Science* **60**, 569–572.
- Lindsay, W. L., 1974. *Chemical Equilibria in Soils*. New York: Wiley. 449.
- Markert, B., 1993. Occurrence and distribution of chemical elements in plants – outlook and further research plans. *Toxicological and Environmental Chemistry*, **40**, 31–41.
- Niebor, E., and Richardson, D. H., 1980. The replacement of the nondescript term “heavy metals” by a biologically and chemically significant classification of metal ions. *Environmental Pollution*, **1**, 3–26.
- Öborn, I., Jansson, G., and Johansson, L., 1995. A field study on the influence of soil pH on trace element levels in spring wheat (*Triticum aestivum*), potatoes (*Solanum tuberosum*) and carrots (*Daucus carota*). *Water, Air, and Soil Pollution*, **85**, 835–840.
- Sanchez, P. A., and Swaninathan, M. S., 2005. Hunger in Africa: the link between unhealthy people and unhealthy soils. *Lancet*, **365**, 442–444.
- Sillanpää, M., 1982. Micronutrients and the nutrient status of soils: a global study. *FAO Soils Bulletin 48*. Food and Agriculture Organization of the United Nations, Rome.

Cross-references

- [Alkalinity, Physical Effects on Soils](#)
[Crop Responses to Soil Physical Conditions](#)
[Liming, Effects on Soil Properties](#)
[Physics of Plant Nutrition](#)
[Plant–Soil Interactions, Modeling](#)
[Plant Wellness](#)
[Soil Physical Quality](#)

TRAFFIC FARMING

See [Controlled Traffic Farming](#)

TRAFFICABILITY AND WORKABILITY OF SOILS

Lothar Müller¹, Jerzy Lipiec², Ted S. Kornecki³, Stephan Gebhardt⁴

¹Leibniz – Centre for Agricultural Landscape Research (ZALF), Institute of Landscape Hydrology, Müncheberg, Germany

²Institute of Agrophysics, Polish Academy of Sciences, Lublin, Poland

³USDA-ARS, National Soil Dynamics Lab. Research Unit, Auburn, AL, USA

⁴Institute for Plant Nutrition and Soil Science, Christian Albrechts University of Kiel, Kiel, Germany

Definition

Trafficability and *workability* are soil capabilities supporting operations of agricultural machinery. Trafficability is a soil capability supporting agricultural traffic without degrading soils and ecosystems. Workability is a soil capability supporting tillage.

Introduction

Agriculture is associated with mechanical impacts on soils to provide optimum conditions for all processes relevant to plant production. Processes like tillage, seeding, fertilization or harvesting are highly mechanized and require agricultural traffic. Soils have to support those operations, but the soil status may include periods that are unsuitable for agricultural traffic and tillage. Agriculture is climate and weather dependent. Due to basic soil properties, climatic and weather conditions and land use and management, the status of soils varies both temporally and spatially. Main limitations both of the mobility function of tractors and the risk of soil compaction are due to excessive soil water content. The term trafficability refers largely to soil moisture conditions providing or restricting field traffic by machinery. Trafficability is a significant factor in carrying out farm field operations, especially after rainfall events when poor trafficability can cause delays in planting, cultivating, harvesting, and transporting of field crops (Kornecki and Fouss, 2001). But also in forests and on grassland, trafficability of soils is a necessary operation. Besides this, some common traffic and transport is off-road in rural areas worldwide.

Workability refers to soil tillage and is most relevant to agroecosystems. In cropping agriculture, a soil structure of the main rooting zone has to be provided by primary tillage like plowing or cultivating. Operational parameters depend on soil status, specific requirements of crops and the kind of general tillage purpose to be produced by special tillage implements. The desired result will only be achieved if the soil has an appropriate workability. Tillage has many advantages in producing a desirable soil structure, but may be harmful also. Intensive tillage, plowing in particular, decreases soil stability, eliminates organic mulch from the soil surface and diminishes humus content at the soil surface and can cause greater surface crusting and erosion (Kay and Munkholm, 2004). If the diagnosis of the soil reveals a need for tillage, the soil's workability becomes relevant. Main possible limitations are due to too wet or too dry soil conditions. Important questions associated with workability are: (a) Which ranges of soil moisture in terms of water content and water potential are suitable for workability? (b) What is the probability that soil moisture states for optimum workability will be reached?

Ignoring the rules of trafficability and workability may lead to soil compaction, a threat to many ecosystems worldwide. Compaction is a kind of physical degradation of soils which has negative impact on almost all soil functions.

Interactions of soils with vehicles and tillage implements

The definition of trafficability and workability as soil capabilities is a simplification of more complex operational processes. In the case of field traffic, wheels or tracks interact with soils. The Association of German Engineers (VDI, 2007) defines trafficability as a property of the soil/chassis system, which is determined by physical parameters of the

soil, by biological and ecological parameters, as well as by technical parameters (wheel load, slip, and contact area of the chassis, etc.). This definition of trafficability as an interacting process between a particular vehicle and terrain is in accordance with others both in civil and military engineering. Depending on the discipline, this definition refers to the question of whether the status of soil will provide the mobility function of a particular vehicle. This holds for civil and military engineering. Additional to the mobility function, in agriculture including forestry, grassland and range-land management, damage to the ecosystem must be avoided.

Workability is concerned with soil-implement interactions. At tillage, plastic deformation of the soil has to be avoided as it leads to smearing and clodding of soil. Depending on the purpose of tillage, for example, basic tillage, seedbed preparation or crop management by hoeing, tillage implements have been optimized and work at different depths (Koolen and Kuipers, 1983). Thus, both the requirements of different tillage procedures to the soil moisture status may be different, and the requirements of tillage and associated field traffic to the field moisture status as well.

Soil criteria and measurement methods of trafficability and workability

Soil properties and states affect both the mobility function of vehicles, for example, the drawbar pull of a tractor, and the resistance against soil structural damage. Important factors are soil strength (Terzaghi et al., 1996), affecting the bearing capacity of soils, traction parameters of vehicles, and the energy required for tillage. Soil strength is largely influenced by soil water content and density and thus varies with climate, weather, soil hydrologic conditions, and status of pre-compaction. Common physically based soil measurement methods of the soil strength are shear resistance measured by vane shear testers (Kezdi, 1969), penetrometer resistance (Campbell and O'Sullivan, 1991) measured by soil penetrating cones, cone pressure resistance (Müller et al., 1990) measured by the sinking depth of a cone or drop-cone penetration (Campbell, 1976), precompression stress (P_c) determined as the transition of elastic to plastic deformation if plotted as a semi-logarithmic stress-settlement (Horn and Fleige, 2009). Also, plate sinking depth is a common measure of strength and bearing capacity (Kezdi, 1969). Penetrometer measurements are very often used in field studies because of their fast and simple handling and reliability to detect heterogeneities in soil strength (Usowicz and Lipiec, 2009). Results of those measurements can be expressed as units of pressure, for example, in MPa at a given soil depth.

The soil status directly at the surface is particularly sensitive to weather and external forces. Factors like a too wet soil surface leads to stickiness and slipperiness, which may seriously diminish both the mobility of vehicles on wet cohesive soil and the quality of the soil structure by remolding.

Soil engineering properties related to trafficability and workability

Indices based on soil engineering properties describe the behavior of soil in dependence on water content. They are a basis of planning in civil and underground engineering worldwide and may also be used to calculate trafficability and workability states.

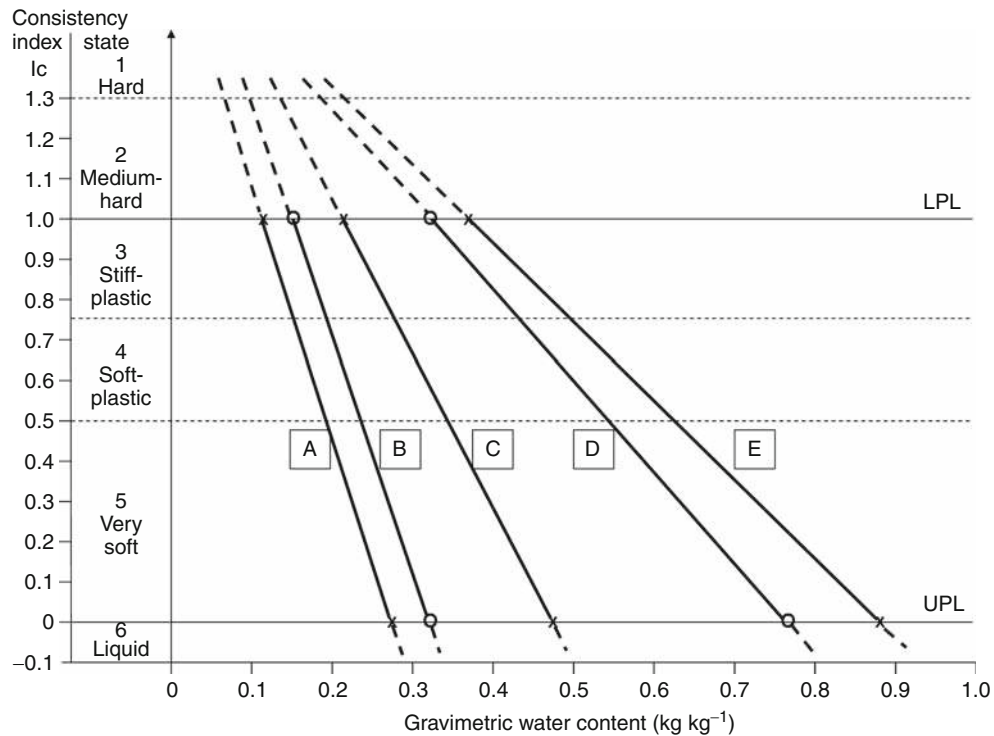
The Atterberg consistency diagram is suited to describe the moisture-dependent soil strength behavior in a simple manner. It is based on the upper plastic limit (UPL) and the lower plastic limit (LPL) (Kretschmer, 1996). The consistency index I_c is a crucial measure of relative soil strength.

$$I_c = (UPL - w)(UPL - LPL)^{-1}$$

(Kretschmer, 1996) where w is the actual soil water content, I_c is dimensionless, UPL, LPL and w are given in kilogram water per kilogram dry soil. A consistency index of $I_c = 0.75$ is an acknowledged arbitrary limit of workability. Figure 1 shows a consistency diagram for some soils of different texture. It demonstrates that soils of lower clay content change their mechanical behavior more rapidly with alterations in water content. The arbitrary workability limit ($I_c = 0.75$) ranges from about 0.16 kg kg^{-1} to 0.50 kg kg^{-1} over the range of soils indicated in Figure 1. A field assessment of consistency states and indices can be provided by Table 1.

In other studies, the soil water content corresponding to the Atterberg lower plastic limit (LPL) has often been used as an arbitrary threshold of workability (Thomasson, 1982). This limit is considered as a water content at which soil can be worked without causing structural damage (Tisdall and Adem, 1986). Arvidsson et al. (2004) found tillage at a water content close to the plastic limit produced the largest proportion of small aggregates. An advantage of the consistency concept is that it is suitable for field assessment (Mueller et al., 2003). However, it cannot be applied for non-cohesive soils which are either not plastic or highly compacted (Dexter and Bird, 2001).

Another important soil engineering procedure is the Proctor compaction test (Kezdi, 1969), which characterizes alterations in soil density with water content using a standardized energy input and compaction procedure. The maximum bulk density of the soil and the water content at this maximum are the most important parameters of this test. The water content indicates the moisture status for maximum compaction at a defined energy impact and has, like the plasticity limits, a crucial meaning in civil engineering (Terzaghi et al., 1996). Atterberg limits maximum dry bulk densities estimated by Proctor's test and the corresponding water contents belong to soil engineering properties. Those indices based on soil engineering properties can be used to define trafficability and workability criteria. Parallel measurements of field soil strength confirmed the suitability of consistency indices, to conclude on trafficability and workability of soil (Müller et al., 1997). Databases and pedotransfer functions for



Trafficability and Workability of Soils, Figure 1 Consistency diagram based on lower plastic limit (LPL) and upper plastic limit (UPL) including ranges of five typical topsoil substrates in north-eastern Germany (A, B: Glacial till, clay contents 15% and 20%; C: Holocene, clay content 30%, drained; D, E Holocene, clay contents 40% and 50%, wetland.) Field characteristics of consistency states are given in Table 1.

Trafficability and Workability of Soils, Table 1 Field assessment of consistency states for cohesive substrates

Consistency state	I_c	Field diagnosis
1. Hard	>1.3	Very dry, light, hard, brittle, no clods formable
2. Medium hard	1–1.3	Dry, not rollable to 3-mm-diameter thread, fissuring, and crumbling, weakly stable clod can be formed
3. Stiff plastic	0.75–1	Moist, rollable into 3-mm-diameter thread without crumbling, nonsticky
4. Soft plastic	0.5–0.75	Wet, easily deformable, rollable into 3-mm-diameter thread without crumbling, sticky
5. Very soft	0–0.5	Very wet and sticky, not rollable
6. Liquid	<0	Extremely wet, muddy, sliding out of the hand

the calculation of soil engineering properties from texture and organic carbon content exist (Mueller et al., 2003).

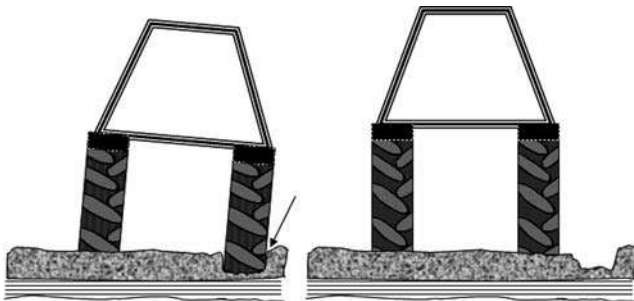
Matric potential and water retention curve defining trafficability and workability

For modeling purposes, suitable soil states for tillage and associated field traffic can be assessed by knowing the matric potential (suction) and the water retention curve of soil. This curve describes the relationship between suction and soil moisture content. Suction shall have positive defined values in this paper, and pF values are decadic logarithms of suction in hPa. Important fixed points on these curves relevant to trafficability and workability, are water contents at field capacity (FC) or at a defined equivalent of FC, mainly at suctions between 5 kPa (pF 1.7) and 30 kPa (pF 2.5), and the water content at the inflection point (Dexter and Bird, 2001).

Recommended suction thresholds of soils for trafficability and workability range from about 6 kPa in the upper 15 cm (Paul and de Vries, 1979) to 10 kPa in the upper 20 cm (Wösten and Bouma, 1985). This can be checked in the field by measurements using tensiometers (Earl, 1996). Those suction thresholds are arbitrary criteria of trafficability and workability and only rough estimates of acceptable conditions for field working operations. They do not consider real distribution of strains in the soil and possible compaction profiles during trafficking.

Discrepancies between trafficability and workability

In mechanized agriculture, soil tillage requires the use of tractors and thus field traffic. What trafficability and workability have in common is that both processes are combined in the case of tillage and that the desirable soil



Trafficability and Workability of Soils, Figure 2 Offland-plowing, i.e., running tractor wheels in the plow furrow (left) is responsible for serious subsoil compaction. It has to be banned from agricultural practice. If any plowing will be necessary, it should be done as onland plowing (right).

status is largely soil moisture dependent. During very wet conditions, both are limited, but if the soil gets drier, optimum soil states for both trafficability and workability do not coincide. Another main reason for conflicting decisions is the different soil depth of impact. During early spring periods the soil surface may be workable for seedbed preparation, but at the same time the subsoil may be too wet to bear traffic (Lipiec and Simota, 1994). Such situations may enhance vulnerability of soil to compaction.

In contrast, during or after harvest, too dry soil states or high soil densities may limit workability but provide best trafficability of most soils. At a given level soil surface, the higher the soil strength, the better the bearing capacity and the mobility function of vehicles. Also, a high tractor weight increases the drawbar pull. This may be conflicting with ecological soil functions like aeration and rooting ability, if thresholds of soil dry bulk density (Håkansson and Lipiec, 2000) or air capacities will be exceeded.

The discrepancy between trafficability and workability is most clearly demonstrated by the fact that optimum water content for workability is at maximum of the Proctor compaction curve (Wagner et al., 1992). This is the water content, at which soil is prone to be extremely highly compressed. In conclusion, soil tillage is responsible for soil compaction problems if the compaction impact exceeds the pre-compaction status at a depth deeper than the effective working depth of the following tillage implement. This extremely bad condition may often occur at “offland plowing,” i.e., the tractor tire runs in the furrow of the plow (Figure 2). Keller et al. (2002) revealed this by measuring the deep compaction effect, and Chamen et al. (2003) found this procedure most responsible for subsoil compaction in Europe. In conclusion, defining criteria for and assessing trafficability and workability, the first mentioned one is the decisive and more critical process (Botta et al., 2009).

Wheel ruts as a criterion of trafficability

Unsuitable soil structure features (see *Soil Structure, Visual Assessment*) indicate damage of the soil structure

by compaction or other over-consolidation. In the field, wheel rut depths are site-specific proper measures of the damage to soil structure (Lebert et al., 2003). Wheel rut depths of 5 cm or deeper on cropland (Müller et al., 1990), or deeper than 10 cm on peat grassland (Schmidt and Rohde, 1986), indicate exceedance of trafficability limits. Values on cropland refer to consolidated soil, not to freshly plowed soil, which is over-loosened. In soils under forest, Wronski et al. (1990) reported on acceptable rut depths of 15 cm. Lüscher et al. (2009) found rut depths more than 10 cm indicate clear compaction damage in forests.

Increased soil compactness may result in improved trafficability due to greater mechanical stability (higher densities and strengths) of soil as assessed by pre-compression stress (Horn et al., 1994). Sommer and Petelkau (1990) proposed conservation tillage, which is characterized by a higher top-soil pre-consolidation status, to improve trafficability. Botta et al. (2009) found that field traffic both in conventional tillage and direct sowing caused both topsoil and subsoil compaction. Higher pre-compacted soils have a potential for better trafficability only if the soil drainage is not hampered. However, as compaction may diminish infiltration and hydraulic conductivity (Gebhardt et al., 2009), stagnant water at the soil surface or perched water tables may appear. This is an indicator of a degree of soil compaction that does both exceed ecological thresholds (air capacities for plant growth) and the field’s capability to bear traffic or to suggest tillage operations. Stagnant water in wheel ruts over some days indicates that soil has been trafficked though trafficability was not given. Those wheel tracks are preferential flow paths for water and sediment transport and may initiate fast runoff and erosion (Basher and Ross, 2001). Roth et al. (1999) showed that the variability of soil hydraulic properties can be increased by field traffic and tillage, since wheel tracks in particular can influence local soil water balances.

Wheel ruts are indicators of ex-post assessments, for example, may indicate a damage that has occurred. Modeling (Hambleton and Drescher, 2009) or direct measurement of wheel rut depth can be used as preventive strategies to avoid damaging soil structure.

Off-road traffic and ecosystems

Outside of agriculture, the problem of trafficability is often less complex as the mobility of vehicles has priority. Studies in nonagricultural disciplines as military and civil engineering focus on having a terrain providing safe and rapid movement of vehicles. A most relevant topic of trafficability in engineering disciplines is developing and optimizing terrain mobility of cars and other vehicles including construction of planetary vehicles (Li et al., 2010). However, concerns about negative impacts of off-road traffic on the status of soil and vegetation in global ecosystems are growing. In forests and on grasslands, including range-land, awareness of possible impacts of machinery on the ecosystem status is increasing (Eisenbies et al., 2007). Keeping equipment out of wet lands is the single most important practice for avoiding soil compaction.

On agricultural land, installation of effective surface and subsurface drainage can minimize soil compaction due to increased water infiltration thus allowing for a soil moisture content suitable for sustaining agricultural equipment traffic. Controlled traffic farming can mitigate soil compaction of entire fields, by permanently using the same wheel tracks. This requires that tractors and agricultural machinery have identical tire spacing to fit the required path width. Implementation of controlled traffic patterns may be possible due to utilization of GPS and auto steering systems. But this would also require fixed field shapes and working width of machinery over several years. Another important factor in reducing compaction is to keep tire inflation pressure at the recommended minimum required to support heavy loads. Also using wider tires, dual wheels, or tracks can reduce soil compaction (Cramer, 2006). Reduced tillage or no-till can also minimize compaction by reducing or eliminating trips across the field.

Clearly defined rules in terms of soil trafficability thresholds or intensity of trafficking are still missing. Common approaches of calculating compaction depth and intensity are based on the assumption of free soil drainage profiles. However, for many soils worldwide, in particular in lowlands, for layered soils or heavy soils, this assumption is not valid, and natural soil drainage profiles show higher water contents in topsoils and subsoils by impeded drainage. Alakukku (1997) found a significant relationship between axle load and depth of soil compaction. Axle loads of 30–40 Mg compacted soils down to depths of 0.8–1 m. From compaction test, it is known that the water content of maximum compaction decreases with higher energy impact (Schultze and Muhs, 1967, p. 410). This means, dry soils may experience extreme compactions with increasing energy impacts. As long as loads of machinery will increase, the process of compaction of ecosystems, agroecosystems in particular, will continue. Besides agricultural fields, deep soil compaction occurs during ground construction work like pipeline construction (Berli, 2001).

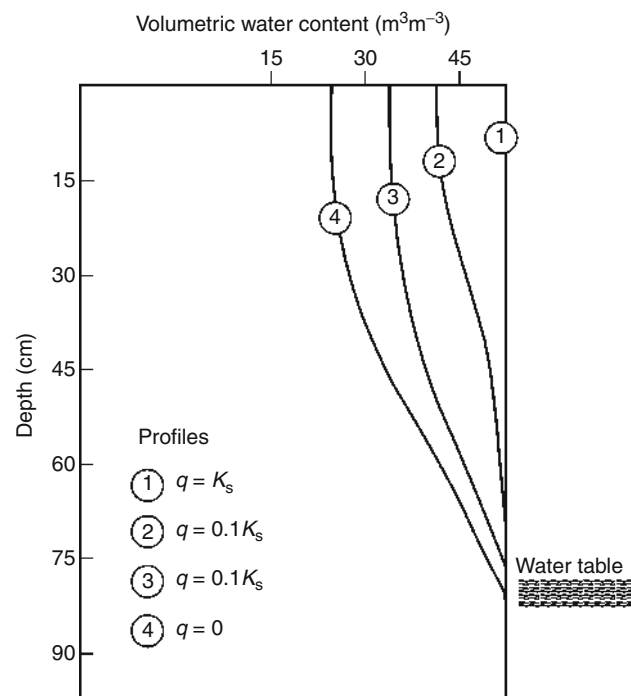
Risk assessment methods for soil compaction based on same principles like in common civil engineering, for example, containing probability and uncertainty criteria, do not exist. Environmental Impact Assessment procedures containing those criteria for very heavy vehicles would be a potential way to halt deep soil degradation through compaction.

Risk areas of trafficability

From a prevalent technical and economic point of view, soils of impeded drainage are risk areas of trafficability. Deep sinking or even tractor immobility may cause restrictions in soil management, and direct and indirect economic losses are a consequence. In very wet soils, structural damage is mainly due to soil remolding (plastic state of cohesive soils and oversaturated, quasi-plastic state of non-cohesive soils). If soils are cohesive and very

wet, they are not compactible in terms of increased density. Sometimes, remolding damage can be recovered by natural processes like alternating wetting and drying.

In boreal and temperate climates, frozen soil layers in spring may cause temporally impeded drainage and critical mechanical states on all soils. In lowland areas with shallow water tables, information on suitable water tables for providing soil trafficability in critical periods is necessary. Because the strength of the soil changes with water content, land drainage may alter the conditions for trafficability in lowlands or other soils of impeded drainage (Fausey, 2006). Figure 3 shows some possible soil moisture steady state profiles which may occur in a lowland soil in a humid climate. Profile 1 is fully saturated and drainage occurs with a maximum hydraulic gradient of 1, and the flow rate q is equal to the saturated hydraulic conductivity (K_s) of soil. Profiles 2–3 are transient hypothetical profiles, and profile 4 indicates the final drainage stage where the soil has reached a maximum drainage status. This profile is particularly important showing the minimum water content that can be achieved by gravitational drainage. The values of this curve are valid for a sandy loam. If, for example, the threshold moisture content required for workability of the particular soil is lower than the value of curve 4 at a given depth, additional evapotranspiration has to take place. Theoretically, also a very intensive and deep drawdown of the groundwater table could improve the situation slightly,



Trafficability and Workability of Soils, Figure 3 Field soil moisture profiles of a groundwater influenced soil (After Smedema, 1986).

but drainage curves of most soils (steep course of curve 4 in the upper part) show that there would be no real effect.

Several studies resulted in recommendations of water tables (see *Soil Water Management*). Kuntze and Wetjen (1984) found satisfactory trafficability with springtime water tables more than 75 cm below the surface in heavy marsh soils. Those recommendations are valid for the corresponding soil and climatic conditions but not transferrable to other regions. In a study of Müller et al. (1990), the trafficability of clay soils with shallow water table was analyzed. Alterations of trafficability and workability with time were derived from consistency and cone resistance data. The upper topsoil was trafficable if the cone resistance exceeded 0.3 MPa. At this resistance only shallow wheel sinkage (less than 4 cm) and no ponding in wheel tracks was observed.

Soft soils of high water table, peatlands, for example, are particularly sensitive to disturbances (see *Peats and Peatlands, Physical Properties*). High water tables may be tolerated by adapted vegetation but the bearing capacity of soils may be critical for any use of land if only common agricultural machinery will be available. Adapted machines lower in weight may provide for the agricultural use of those soils too, even at shallow water tables of about 40 cm (Prochnow et al., 2000).

From a prevalent ecological point of view, there are no areas of trafficability free of compaction risk. In other terms, soils that can be trafficked with any vehicle at any time do not exist. All soils have a potential to become severely and persistently compacted and degraded by heavy machinery. Rooting restrictions and crop yield losses are a consequence. This potential is even higher for lighter textured soils. Unsorted soil substrates (Sands, loamy Sands, and Loams of Moraine parent material) have a particularly high compaction risk (see *Soil Compaction and Compressibility*).

Operational forecasting of trafficability

Among strategies to halt soil degradation by compaction, operational forecasting could become an emerging tool in agriculture. In order to provide a sustainable use of resources in agriculture by planning or operational decision support systems of machinery use, models of trafficability of soils can be helpful. Predicting possible subsoil compaction by particular machinery is possible (Keller et al., 2007b). As a precondition, relevant parameters must be quantified. In a comparative field study over several years on heavy alluvial soils, Müller et al. (1997) measured some soil parameters along with field observations and ratings of trafficability. They found that the topsoil status in the upper two centimeters in terms of measured and field estimated parameters like consistency index or suction was most important. The main finding was that gradients or differences in the soil moisture and density status over the depth have to be taken into consideration. Averaged values over the total topsoil do not allow a reliable assessment of trafficability. Babeir et al. (1985)

used mainly soil moisture and climatic data for their prediction model. They calculated soil moisture dynamics for layers at depths of 0–15 cm and 15–30 cm, characterizing the soil as “workable” or “non-workable.”

Operational forecasting of field trafficability has not yet been resolved in agriculture. One reason may be the need to optimize too many ecological, economic, and technological factors. It is necessary to compromise between mobility function of vehicles and risk of soil compaction on the one hand and between different soil states across fields (spatial heterogeneity) on the other hand. Finally, ecological and economic risks of postponing or omitting field engaging operations have to be taken into consideration.

Available knowledge on soil engaging processes would provide a basis for the development of decision tools for operational forecasting of trafficability in agriculture based on weather forecasting. Anderson (1983) coupled a deterministic soil moisture submodel to a principal empirical soil moisture-trafficability model. Müller and Schindler (1998) proposed the combination of soil water models with expert-based matrices and presented a sample matrix for a wheeled tractor (Table 2). Based on available spatio-temporal data of field soil moisture and density states, and depths of wheel tracks, application of statistical approaches of auto-regressive one-step-ahead forecasting (Müller et al., 1997) seems also to be a feasible way to develop operational forecasting tools. A combination of both approaches, field validated and controlled by wheel rut depth and slip control sensors, seems to be most promising to resolve this problem.

Example for the use of the matrix

Referring to soil C of Figure 1, soil bears winter wheat which at field traffic time for spreading fertilizers (end of March) yields about 4 cm plant height. The effect of plant cover is negligible at this time. The density status is medium. The surface layer is dry with a consistency state of 1 which implies a water content less than 0.15 kg kg⁻¹. Layer 2 (2–10 cm) has a consistency state of 2 (water content about 0.15–0.22 kg kg⁻¹). Layer 3 has a consistency state of 3 (water content about 0.22–0.28 kg kg⁻¹). The resulting trafficability score is 1, practicable. After a rainfall of 3 mm the water content of layer 1 moves to a consistency state of 4 and the resulting consistency score is 2.5, limited practicable to bad practicable. Scores and threshold of 1.5 compromise both vehicle mobility and soil damage (rut depths, remolding). The matrix has been validated with more than 60 soils at different moisture conditions.

Defining appropriate moisture conditions for workability

The soil moisture status affecting mechanical behavior and aggregate friability, is the most influential factor of workability (Mosaddeghi et al., 2009). When drier, aggregates are stronger, so it is difficult to reduce their size, and when wetter, aggregates are weaker and can be compacted

Trafficability and Workability of Soils, Table 2 Trafficability in dependence of consistency and density of soils, wheeled tractor, medium tractive force requirements (Müller and Schindler, 1998, slightly modified)

Consistency at depth 0–2 cm	Consistency at depth 2–10 cm	Consistency at depth 10–30 cm																		
		Soil density low						Soil density medium						Soil density high						
		1	2	3	4	5	6	1	2	3	4	5	6	1	2	3	4	5	6	
1	1	1	1	1	1	2	3.5	1	1	1	1	2	3.5	1	1	1	1	2	3.5	
Hard	2	1	1	1	2	3	4	1	1	1	2	3	4	1	1	1	1	1.5	3	4
$I_c > 1.3$	3	1	1	1.5	2.5	3.5	4	1	1	1.5	2	3	4	1	1	1	1	2	3	4
	4	1.5	1.5	2	3	4	4	1.5	1.5	1.5	2.5	3.5	4	1.5	1.5	1.5	2.5	3.5	4	
	5	2.5	2.5	3	3.5	4	4	2.5	2.5	3	3	3.5	4	2.5	2.5	3	3	3.5	4	
	6	3	3	3.5	4	4	4	3	3	3.5	4	4	4	3	3	3.5	4	4	4	
2	1	1	1	1.5	2	4	1	1	1	1	2	4	1	1	1	1	1	2	4	
Medium-hard	2	1	1	1.5	2	3	4	1	1	1	2	2.5	4	1	1	1	1	2	2.5	4
$I_c = 1–1.3$	3	1	1	1.5	2.5	3.5	4	1	1	1.5	2	3.5	4	1	1	1	1	2	3	4
	4	2	2	2.5	3.5	4	4	2	2	2	2.5	3.5	4	2	2	2	2.5	3.5	4	
	5	2.5	2.5	3	3.5	4	4	2.5	2.5	3	3.5	4	4	2.5	2.5	3	3.5	4	4	
	6	3	3	3.5	4	4	4	3	3	3.5	4	4	4	3	3	3.5	4	4	4	
3	1	1	1	1	2	3	4	1	1	1	2	3	4	1	1	1	1	2	3	4
Stiff-plastic	2	1	1	1.5	2.5	3.5	4	1	1	1	2	3.5	4	1	1	1	1	2	3.5	4
$I_c = 0.75–1$	3	1	1.5	2.5	3	4	4	1	1	2	3	4	4	1	1	1	1	2	2.5	4
	4	2	2	3.5	4	4	4	2	2	3	3.5	4	4	2	2	2	2.5	2.5	4	
	5	2.5	3	3.5	4	4	4	2.5	3	3	3.5	4	4	2.5	3	3	3.5	4		
	6	3	3	4	4	4	4	3	3	3.5	4	4	4	3	3	3.5	4	4	4	
4	1	1.5	1.5	2	3	3	4	1.5	1.5	2	3	3	4	2	2	2	3	3	4	
Soft-plastic	2	1.5	2.5	2.5	3	3.5	4	1.5	2	2.5	3	3.5	4	2.5	2.5	2.5	3	3.5	4	
$I_c = 0.5–0.75$	3	2	2.5	3.5	4	4	4	2	2	3	4	4	4	2.5	2.5	3	4	4	4	
	4	2.5	3	4	4	4	4	2.5	2.5	3.5	4	4	4	3	3	3	4	4	4	
	5	3	3	4	4	4	4	3	3	3	4	4	4	3	3	3	4	4	4	
	6	4	4	4	4	4	4	4	4	4	4	4	4	4	4	4	4	4	4	
5	1	2.5	3	3	4	4	4	2.5	3	3	4	4	4	3	3	3	4	4	4	
Very soft-	2	3	3	3.5	4	4	4	3	3	3.5	4	4	4	3	3	3.5	4	4	4	
$I_c = 0–0.5$	3	3	3	4	4	4	4	3	3	4	4	4	4	3	3	4	4	4	4	
	4	3	3.5	4	4	4	4	3	3.5	4	4	4	4	3	3.5	4	4	4	4	
	5	3.5	3.5	4	4	4	4	3.5	3.5	4	4	4	4	3.5	3.5	4	4	4	4	
	6	4	4	4	4	4	4	4	4	4	4	4	4	4	4	4	4	4	4	
6	1	3	3	3.5	4	4	4	3	3	3.5	4	4	4	3.5	3.5	3.5	4	4	4	
Liquid	2	3	3	4	4	4	4	3	3	4	4	4	4	3.5	3.5	4	4	4	4	
$I_c < 0$	3	3.5	3.5	4	4	4	4	3.5	3.5	4	4	4	4	3.5	3.5	4	4	4	4	
	4	4	4	4	4	4	4	4	4	4	4	4	4	4	4	4	4	4	4	
	5	4	4	4	4	4	4	4	4	4	4	4	4	4	4	4	4	4	4	
	6	4	4	4	4	4	4	4	4	4	4	4	4	4	4	4	4	4	4	

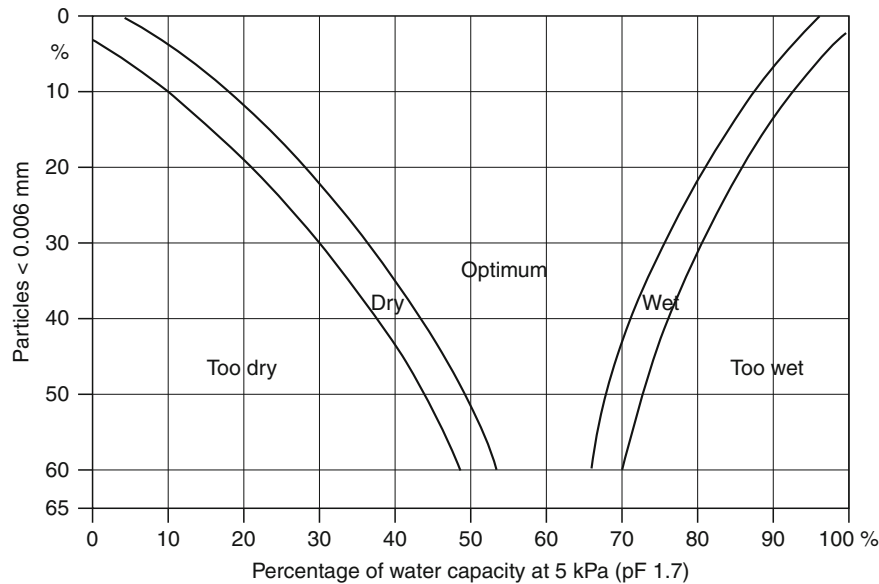
Consistency states coincide with Figure 1 and Table 1 but refer to three layers of the upper 30 cm. Low soil density refers to freshly ploughed soils, medium soil density is valid for common consolidated soils, and high density for no-till soils. Numbers from 1 to 4 in the matrix characterize trafficability: 1 practicable, 2 limited practicable, 3 bad practicable, 4 not practicable. A score of 1.5 is a threshold for trafficability

and remolded (Dexter and Bird, 2001). Rübensam and Rauhe (1968) emphasized differences in soil texture on workability. Whilst sandy soils are workable at almost any water content, it is very difficult for farmers to find an optimum water content for clay soils.

In humid environments, workability will be mainly hampered by excessive soil moisture. Soil water contents often exceed the common field water capacity (Van Wijk and Buitendijk, 1988). An important soil hydrological parameter affecting workability is poor drainage, formation of perched water and increasing wetness of surface soils (Chamen et al., 2003). Soil and land drainage in combination with evaporation have to provide suitable conditions for tillage operations (Kværnø et al., 2007).

Petelkau (1984) recommended ranges of moisture contents of Figure 4 for workability. He used the water content at a suction of 5 kPa (pF 1.7) as a reference basis. The Figure demonstrates that sandy soils (upper part of the graph) are workable at about any water content if a free drainage status that corresponds to field capacity of sandy soils, will be reached. With higher proportion of fine particles (lower part of the graph), soil moisture states either too wet or too dry, may occur. In the field, the wetter range is commonly larger, as also states of free water may occur.

In lowlands, associated with drainage problems, thresholds of soil water potential for predicting number of traffable and workable days depend on soil texture and type of operation. In the Netherlands, Van Wijk and



Trafficability and Workability of Soils, Figure 4 Ranges of water content for tillage (After Petelkau, 1984, mod).

Buitendijk (1988) proposed water suction thresholds for operations preceding spring and autumn sowing or planting of spring cereals, sugar beet, and potatoes varied from 50 to 110 hPa and for harvesting from 50 to 180 hPa in variously textured soils. A wider workable range was reported for plowing than for seedbed preparation (Larson et al., 1994). The water content at the inflection point interpreted as the “breakthrough” matric potential of the water retention curve at which air first penetrates through the soil (mid-point between the lower plastic limit and the shrinkage limit) was found to be the optimum for tillage of Rothamsted soils (Dexter and Bird, 2001). Authors developed equations for prediction of the optimum water content for tillage (OPT), the upper tillage limit (wet, UTL) and the lower tillage limit (dry, LTL) which can be combined with the use of pedotransfer functions for the prediction of the parameters of the van Genuchten equation (Van Genuchten, 1980) for soil hydraulic properties. Figure 5 shows the relations of the limits to soil clay content indicating that the range of water contents for tillage decreases with increasing soil clay content. Keller et al. (2007a) confirmed the water content at the inflection point of the water retention curve as a workability criterion in field experiments.

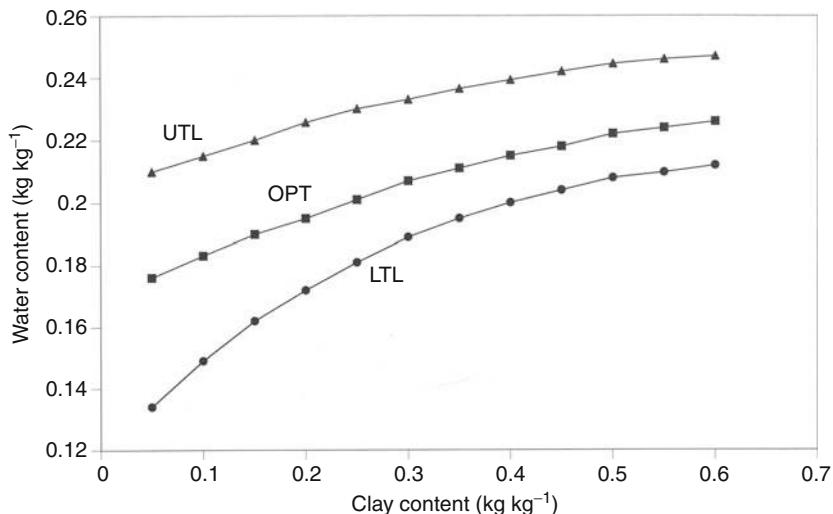
A comparison of some estimation methods of water contents for optimum workability revealed that most of them agreed well (Mueller et al., 2003). However, if the inflection point of the water retention curve will be calculated from existing databases, too high moisture contents are being expected, and the calculated value has to be tuned down by the factor 0.8 (Table 3). The coincidence between optimum water contents for tillage and for maximum compaction ($W_{optE} = W_{Proct}$) points up the risk of soil compaction by tractors during tillage operations.

Soil water status and specific energy for tillage

In drier as compared to wetter climates, workability concepts have to raise both problems of too wet and too dry moisture states (Canarache and Dumitru, 2000). Optimum workable range in terms of soil moisture is often quantified based on measurements of draft resistance to tillage implements and assessment of in-field implement effects on the structure (Dawidowski et al., 1988). Recent tillage studies showed tillage at a water content close to the plastic limit provided the lowest energy use for soil fragmentation (Arvidsson et al., 2004).

In terms of soil water potentials, the optimum working moisture obtained in a field study ranged between pF 1.9 and 3.1 for the loam soil and between pF 2.1 and 3.4 for the clay soil in Mexico (Cadena-Zapata et al., 2002, Figure 6). In this range of soil water matric potentials, specific energy applied in the loosening operation showed a minimum and an adequate seedbed was produced. Comparable workable ranges for same soils were also obtained by laboratory assessment based on a drop test (dry limit) and by air permeability and compression tests (wet limit) (Hoogmed et al., 2003).

Van Bergeijk et al. (2001) reported that plow draft varied between 30 and 50 kN m⁻² in a field where topsoil moisture content and clay content varied from 120 to 300 g kg⁻¹ and from 6% to 22%, respectively. The effect of soil moisture was lower in sandy than in clayey soils. The relation between optimum working range and soil texture and soil strength has been used to predict the draft requirement of primary tillage implements (Desbiolles et al., 1999). Greater resistance for tillage of compacted and stronger soil was accompanied by production of greater aggregate size (Guérif, 1994). Increased soil



Trafficability and Workability of Soils, Figure 5 Values of the upper tillage limit UTL, the optimum tillage moisture content OPT (inflection point), and the lower tillage limit LTL as functions of soil clay content (After Dexter and Bird, 2001).

Trafficability and Workability of Soils, Table 3 Orientation values of water contents for optimum tillage and tuning factors for alternative estimation methods (Mueller et al., 2003, shortened)

Texture classes	Orientation value of water content, [kg * kg⁻¹]	Tuning factors for alternative estimation methods			
		B	C	D	E
LS	Method A 0.13	1.1	0.8	0.8	1.2
SL	0.15	1.0	0.9	0.7	1.0
iL	0.19	1.0	0.8	0.6	0.9
L	0.20	1.0	1.0	0.7	1.0
SiC	0.21	0.9	0.7	0.5	0.9
CL	0.23	1.0	0.8	0.7	1.0
C	0.26	0.9	0.7	0.7	0.9

Methods: $W_{optA} = LPL - 0.15 * (UPL - LPL)$ (Kretschmer, 1996), Reference method, $W_{optB} = 0.9 * LPL$ (Dexter and Bird, 2001), $W_{optC} = W_{Infl}$ (Dexter and Bird, 2001), $W_{optD} =$ water content at 5 kPa, $W_{optE} = W_{Proct}$ (Wagner et al., 1992) UPL upper plastic limit (liquid limit acc. to Casagrande, Kezdi, 1969), LPL lower plastic limit (plastic limit acc. to Atterberg, : Kezdi, 1969), W_{Infl} water content at the inflection point of the water retention curve, W_{Proct} water content at maximum proctor density

compactness results in a smaller range of water content for tillage (Dexter and Bird, 2001).

In the procedure proposed by Canarache and Dumitru (2000) for droughty conditions in Romania, six classes of workability and six classes of trafficability were set based on the soil droughtiness and water logging risks as related to climate and soil hydrological parameters. The classes were defined by the number of days when tillage and traffic are impeded by too dry or too wet soil as determined by soil water models. Using GIS procedure, specific maps with classes of workability and trafficability were drawn.

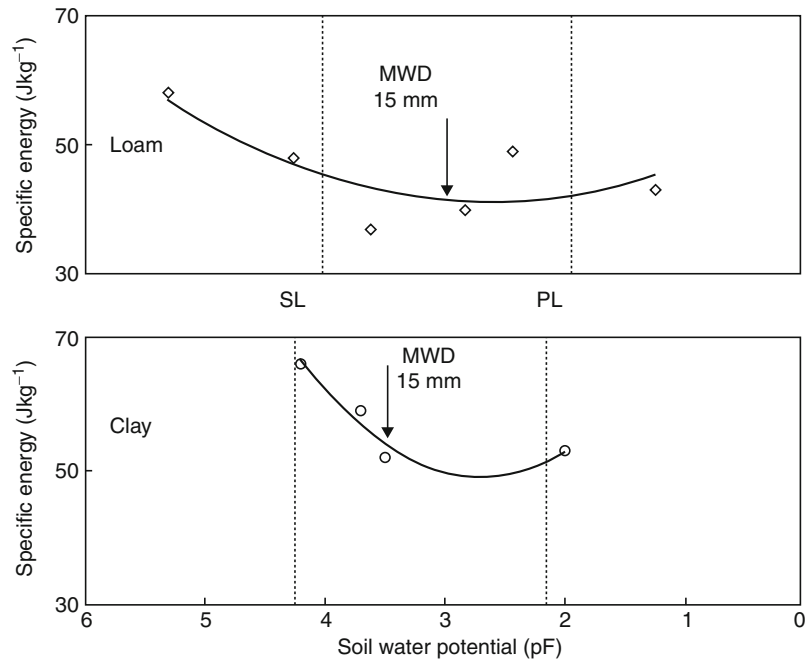
Consideration of natural effects forming a secondary soil structure

Tillage has to produce a favorable soil structure status for optimum establishment and development of crops. The desired and attainable soil structure in terms of aggregate size may be related to specific requirements of crops and has to consider possible changes of soil due to weather. For seedbed, preparation a very fine soil structure is being required. An old rule of thumb is that for seedbed preparation, the average diameter of aggregates should not exceed the threefold diameter of seed (Rübensam and Rauhe, 1968, p. 127).

While defining soil states for optimum effects of tillage, crop-specific requirements and natural forces on the tillage-induced primary soil structure have to be taken into consideration. In some cases, a soil drier than optimum for fine crumbling combined with a lower tillage intensity is more favorable. For example, fine seedbed consisting mostly of aggregates < 5 mm is suitable for emergence (Guérif et al., 2001; Håkansson et al., 2002) of most crops. However, in case of erosion risk, the seedbed has to be coarser and the surface rougher. Larger aggregates, for example, 15 mm are then more favorable because they provide depressions for water and thus allow more time for infiltration delaying runoff generation (Braunack and Dexter, 1989). Those processes may have implications for workability by the opportunity to accept suboptimum moisture conditions for tillage.

Achievable depth of tillage: soil moisture deficit and critical depth

The necessary soil moisture deficit (S_{MD}) is the amount of water that must be drained and/or evaporated from a typical wet springtime moisture status of soil to reach appropriate moisture for tillage (workability limit).



Trafficability and Workability of Soils, Figure 6 Specific energy applied for disc plowing. Curve fits: loam $r^2 = 0.77$, std. = 7.0, conf. ($P < 0.05$) = 7.4, clay $r^2 = 0.98$, std. = 6.2, conf. ($P < 0.05$) = 9.8. SL shrinkage limit, PL plastic limit, MWD mean weight diameter (After Cadena-Zapata et al., 2002)

S_{MD} is useful to calculate climate impacts on workability. The timespan in that S_{MD} can be reached, may be readily calculated from the climatic water balance obtained from agrometeorological databases (Earl, 1997). Depending on working depth and the difference between springtime soil moisture content and workability limit, S_{MD} ranges from about 10 to 200 mm in humid landscapes of central and northern Europe. In the case of heavy soils and deep tillage, it may be even higher.

Because of low water balance deficits in spring, appropriate soil moisture conditions for tillage of cohesive soils will be seldom reached. Only shallow tillage operations (<10 cm) are possible. Even small necessary soil moisture deficits of 10–20 mm can be rarely provided by evaporation. In Norway, Kværnø et al. (2007) calculated the time required for obtaining water contents for workability to about 5 days, which is longer than an average length of period without precipitation in the area, which is only 3.7 days.

Soil moisture deficits are of importance for quality drainage work or tillage of compacted subsoils. Subsoiling is a non-inversion deep tillage that utilizes shanks designed to disrupt subsurface compacted layers that restrict root growth and water movement. Though soils can be slightly wetter for some deep operating implements and procedures (Müller et al., 1990), soil moisture deficits for deep tillage are very high and cannot be provided in many years. Those situations can be used to adapt deep tillage implements to soil states. If soils require drainage, forming mole channels below the critical depth

may be a proper way to improve the soil moisture regime for arable farming (Mittelstedt and Müller, 1989).

Summary

In agriculture, soil management for plant production is provided by the use of efficient machinery. Many operations like tillage, fertilization, or harvesting require the application of tractors or other self-propelled and/or load-bearing machinery. Trafficability is a capability of land to provide field traffic operations without degradation of the ecosystem, particularly the compaction status of soil. Ecosystems include agroecosystems, forests, and grasslands including rangelands. Degradation includes all significant detrimental effects on soil structure, fertility, and vegetation. In agroecosystems, trafficability should be a precondition for mechanized soil tillage and is thus related to workability.

Trafficability can be measured and assessed by different parameters, characterizing shear strength, moisture, and density states of soil. Soil engineering properties as Atterberg's consistency limits are suited for the calculation and assessment of the soil's capability to provide for agricultural traffic. Weather conditions and ground or perched water tables influence trafficability significantly. Land drainage may reduce periods of limited trafficability. Based on available knowledge on field trafficking processes, evolving operational trafficability forecasting models seems to be feasible. This can be resolved by a combination of weather data with soil moisture models

and expert-based relational trafficability matrixes. Model combinations should include deterministic, probabilistic, and auto-regressive statistical approaches.

Workability is a capability of soil to be tilled. It is largely dependent on soil moisture and, thus, climate and weather. Defining appropriate moisture criteria and calculating suitable field moisture states may be important for planning tillage operations and land drainage. Parameters used for indicating potential soil wetness in relation to workability may be derived from the soil water retention curves (field water capacity, soil water potentials, inflection point of the water retention curve), from Atterberg limits or from Proctor compaction tests. Pedotransfer functions are available. In humid landscapes, soil moisture deficits for springtime tillage are critical and provide for only shallow operations. In subhumid and semiarid regions, restrictions of workability due to dry and hard soil conditions have to be considered.

While workability states can be reliably assessed, trafficability limits are largely unknown. Accelerated compaction of soils worldwide indicates failure to meet trafficability criteria by now. Besides existing recommendations for avoiding accelerated soil compaction, new measures should be taken into account. These are (1) restricting loads of machinery by environmental impact assessment procedures for heavy vehicles and (2) evolving operational forecasting of trafficability.

Acknowledgment

Authors thank Dr. Bruce C. Ball, Edinburgh and Dr. Uwe Schindler, Müncheberg, for helpful comments and suggestions.

Bibliography

- Alakukku, L., 1997. *Long-Term Soil Compaction Due to High Axle Load Traffic*. Agricultural Research Centre of Finland, Institute of Crop and Soil Science. Academic Dissertation. Jokioinen, Finland 1997.
- Anderson, M. G., 1983. Forecasting off-road trafficability. *Applied Geography*, **3**, 239–253.
- Arvidsson, J., Keller, T., and Gustafsson, K., 2004. Specific draught for mouldboard plough, chisel plough and disc harrow at different water contents. *Soil & Tillage Research*, **79**, 221–232.
- Babeir, A., Colvin, T. S., and Marvin, S. S., 1985. *Predicting Field Tractability with A Simulation Model*. ASAE Paper No. 85-1025, pp. 1–15.
- Basher, R., and Ross, C. W., 2001. Role of wheel tracks in runoff generation and erosion under vegetable production on a clay loam soil at Pukekohe, New Zealand. *Soil & Tillage Research*, **62**, 117–130.
- Berli, M., 2001. *Compaction of Agricultural Subsoils by Tracked Heavy Construction Machinery*. Swiss Federal Institute of Technology, Zurich PhD Dissertation No. 14132.
- Botta, G. F., Becerra, A. T., and Melcon, F. B., 2009. Seedbed compaction produced by traffic on four tillage regimes in the rolling Pampas of Argentina. *Soil & Tillage Research*, **105**, 128–134.
- Braunack, M. V., and Dexter, A. R., 1989. Soil aggregation in the seedbed: a review. I. Properties of aggregates and beds of aggregates. *Soil & Tillage Research*, **14**, 259–279.
- Cadena-Zapata, M., Hoogmoed, W. B., and Perdok, U. D., 2002. Field studies to assess the workable range of soils in the tropical zone of Veracruz, Mexico. *Soil & Tillage Research*, **68**, 83–92.
- Campbell, D. J., 1976. Plastic limit determination using a drop-cone penetrometer. *Journal of Soil Science*, **27**, 295–300.
- Campbell, D. J., and O'Sullivan, M. F., 1991. The cone penetrometer in relation to trafficability, compaction and tillage. In Smith, K. A., and Mullins, C. E. (eds.), *Soil Analysis: Physical Methods*. New York: Marcel Dekker, pp. 399–429.
- Canarache, A., and Dumitru, S., 2000. Estimating workability and trafficability in Romania. In Morrison, J. E. (ed.), *Proceedings of the 15th International Conference of the International Soil Tillage Reserach Organization, "ISTRO-2000"*, Fort Worth, text on CD.
- Chamen, W. C. T., Alakukku, L., Pires, S., Sommer, C., Spoor, G., Tijink, F., and Weisskopf, P., 2003. Prevention strategies for field traffic-induced subsoil compaction: a review. Part 2. Equipment and field practices. *Soil & Tillage Research*, **73**, 161–174.
- Cramer, B., 2006. Überprüfung von Bewertungsmodellen zur Identifikation und Prognose von Bodenschadverdichtungen auf Ackerböden in Nordrhein-Westfalen. PhD Thesis, Bonner Bodenkundl. Abh. 44, Bonn, p. 178.
- Dawidowski, J. B., Worona, M., and Hencel, A., 1988. The determination of plough draught from soil penetration resistance. In *Proceedings of the 11th International Soil and Tillage Research Organization Conference: Tillage and Crop Production*, Edinburgh, Scotland, pp. 457–462.
- Desbiolles, J. M. A., Godwin, R. J., Kilgour, J., and Blackmore, B. S., 1999. Prediction of tillage implement draught using cone penetrometer data. *Journal of Agricultural Engineering Research*, **73**, 65–76.
- Dexter, A. R., and Bird, N. R. A., 2001. Methods for predicting the optimum and the range of soil water contents for tillage based on the water retention curve. *Soil & Tillage Research*, **57**, 203–212.
- Earl, R., 1996. Prediction of trafficability and workability using tensiometers. *Journal of Agricultural Engineering Research*, **63**, 27–33.
- Earl, R., 1997. Prediction of trafficability and workability from soil moisture deficit. *Soil & Tillage Research*, **40**, 155–168.
- Eisenbies, M. H., Burger, J. A., Aust, W. M., and Patterson, S. C., 2007. Changes in site productivity and the recovery of soil properties following wet- and dry-weather harvesting disturbances in the Atlantic Coastal Plain for a stand of age 10 years. *Canadian Journal of Forest Research.*, **37**, 1336–1348, doi:10.1139/X07-038.
- Fausey, N. R., 2006. Drainage, aeration, and trafficability. In Lal, R. (ed.), *Encyclopedia of Soil Science*. New York: Marcel Dekker, pp. 361–363. 10.1081/E-ESS-120042665.
- Gebhardt, S., Fleige, H., and Horn, R., 2009. Effect of compaction on pore functions of soils in a North German Saalean moraine landscape. *Journal of Plant Nutrition and Soil Science*, **172**, 688–695, doi:10.1002/jpln.200800073.
- Guérif, J., 1994. Effects of compaction on soil strength parameters. In Soane, B. D., and van Ouwerkerk, C. (eds.), *Soil Compaction in Crop Production*. Amsterdam, Netherlands: Elsevier, pp. 191–214.
- Guérif, J., Richard, G., Dürr, C., Machet, J. M., Recous, S., and Roger-Estrade, J., 2001. A review of tillage effects on crop residue management, seedbed conditions and seedling establishment. *Soil Tillage Research*, **61**, 13–32.
- Håkansson, I., and Lipiec, J., 2000. A review of the usefulness of relative bulk density values in studies of soil structure and compaction. *Soil & Tillage Research*, **53**, 71–85.
- Håkansson, I., Myrbeck, A., and Etana, A., 2002. A review of research on seedbed preparation for small grain in Sweden. *Soil & Tillage Research*, **64**, 23–40.

- Hambleton, J. P., and Drescher, A., 2009. Modeling wheel-induced rutting in soils: rolling. *Journal of Terramechanics*, **46**, 35–44.
- Hoogmed, W. B., Cadena-Zapata, M., and Perdok, U. D., 2003. Laboratory assessment of the workable range of soils in the tropical zone of Veracruz, Mexico. *Soil & Tillage Research*, **74**, 169–178.
- Horn, R., and Fleige, H., 2009. Risk assessment of subsoil compaction for arable soils in Northwest Germany at farm scale. *Soil & Tillage Research*, **102**, 201–208.
- Horn, R., Werner, D., Baumgartl, T., and Winterot, C., 1994. Effect of wheeling on stress distribution and changes in macro- and microstructure of a cambic phaeozem derived from loess. *Journal of Plant Nutrition and Soil Science*, **157**, 433–440.
- Kay, B. D., and Munkholm, L. J., 2004. Chapter 11: Management-induced Soil Structure Degradation- Organic Matter Depletion and Tillage. In Schjoenning, P., Elmholt, S., and Christensen, B.T. Managing Soil Quality. Challenges in Modern Agriculture. CAB International 2004.
- Keller, T., Arvidsson, J., and Dexter, A. R., 2007a. Soil structures produced by tillage as affected by soil water content and the physical quality of soil. *Soil & Tillage Research*, **92**, 45–52.
- Keller, T., Défossez, P., Weisskopf, P., Arvidsson, J., and Richard, G., 2007b. SoilFlex: a model for prediction of soil stresses and soil compaction due to agricultural field traffic including a synthesis of analytical approaches. *Soil & Tillage Research*, **93**, 391–411.
- Keller, T., Trautner, A., and Arvidsson, J., 2002. Stress distribution and soil displacement under a rubber-tracked and a wheeled tractor during ploughing, both on-land and within furrows. *Soil & Tillage Research*, **68**, 39–47.
- Kezdi, A., 1969. *Handbuch der Bodenmechanik. Band 1, Bodenphysik, 259 pp., Band 3, Bodenmechanisches Versuchswesen*, 1st edn. Berlin/Kiado Budapest: VEB Verlag für Bauwesen, p. 274.
- Koolen, A. J., and Kuipers, H., 1983. *Agricultural soil mechanics, Advanced Series in Agricultural Sciences*. Heidelberg: Springer, Vol. 13, p. 241.
- Kornecki, T. S., and Fouss, J. L., 2001. Quantifying soil trafficability improvements provided by subsurface drainage for field crop operations in Louisiana. *Applied Engineering in Agriculture, ASAE*, **17**, 777–781.
- Kretschmer, H., 1996. Chapter 2.6.1.1. *Koernung und Konsistenz*. 46 pp. In Blume, H.-P., Felix-Henningsen, P., Fischer, W. R., Frede, H. G., Horn, R., and Stahr, K. 1996. *Handbuch der Bodenkunde*. Vol I, ecomed, 1th ed.
- Kuntze, H., and Wetjen, F., 1984. Bodenhydrologische Auswirkungen einer kombinierten Dränung eines Auengleyes. *Zeitschrift für Kultertechnik und Flurbereinigung*, **25**, 360–369.
- Kværnø, S. H., Haugen, L. E., and Børresen, T., 2007. Variability in topsoil texture and carbon content within soil map units and its implications in predicting soil water content for optimum workability. *Soil & Tillage Research*, **95**, 332–347.
- Larson, W. E., Eynard, A., Hadas, A., and Lipiec, J., 1994. Control and avoidance of soil compaction in practice. In Soane, B. D., and van Ouwerkerk, C. (eds.), *Soil Compaction in Crop Production*. Amsterdam: Elsevier, pp. 597–625.
- Lebert, M., Brunotte, J., Sommer, C., and Böken, H., 2003. Bodengefüge gegen Verdichtungen schützen - Lösungsansätze für den Schutz landwirtschaftlich genutzter Böden. *Journal of Plant Nutrition and Soil Science*, **169**, 633–641.
- Li, W., Huang, Y., Cui, Y., Dong, S., and Wang, S., 2010. Trafficability analysis of lunar mare terrain by means of the discrete element method for wheeled rover locomotion. *Journal of Terramechanics*, **47**, 161–172.
- Lipiec, J., and Simota, C., 1994. Role of soil and climate factors influencing crop responses to compaction in Central and Eastern Europe. In Soane, B. D., and van Ouwerkerk, C. (eds.), *Soil Compaction in Crop Production*. Amsterdam: Elsevier, pp. 365–390.
- Lüscher, P., Frey, B., Sciacca, S., and Frutig, F., 2009. *Physikalischer Bodenschutz im Wald – Datengrundlagen und Umsetzungsstrategie*. Tagungsbeitrag zu: Jahrestagung der DBG. Kommission VIII, Böden- eine endliche Ressource, September 2009, Bonn, Berichte der DBG, <http://www.dbges.de>
- Mittelstedt, R., and Müller, L., 1989. Kräfteanalyse an Penetrometerspitzen in alluvialen Tonböden als Grundlage für die Gestaltung und den Einsatz von Meliorationswerkzeugen. *Archiv für Acker und Pflanzenbau und Bodenkunde*, **33**, 111–120.
- Mosaddeghi, M. R., Morshedizad, M., Mahboubi, A. A., Dexter, A. R., and Schulin, R., 2009. Laboratory evaluation of a model for soil crumbling for prediction of the optimum soil water content for tillage. *Soil & Tillage Research*, **105**, 242–250.
- Müller, L., and Schindler, U., 1998. Wetness criteria for modelling trafficability and workability of cohesive arable soils. In Drainage in the 21th century: food production and the environment. *Proceedings of the 7th Annual Drainage Symposium*, March 8–10, Orlando, FL, pp. 472–479.
- Müller, L., Tille, P., and Kretschmer, H., 1990. Trafficability and workability of alluvial clay soils in response to drainage status. *Soil & Tillage Research*, **16**, 273–287.
- Müller, L., Schindler, U., and Rogasik, H., 1997. Topsoil status of cohesive soils as related to trafficability. *Archives of Agronomy and Soil Science*, **41**, 403–414.
- Mueller, L., Schindler, U., Fausey, N. R., and Lal, R., 2003. Comparison of methods for estimating maximum soil water content for optimum workability. *Soil & Tillage Research*, **72**, 9–20.
- Paul, C. L., and deVries, J., 1979. Effect of soil water status and strength on trafficability. *Canadian Journal of Soil Science*, **59**, 313–324.
- Petelkau, H., 1984. *Auswirkungen von Schadverdichtungen auf Bodeneigenschaften und Pflanzenertrag sowie Massnahmen zu ihrer Minderung*. Tagungsbericht-Akademie der Landwirtschaftswissenschaften D.D.R. Berlin, 215, 39–48.
- Prochnow, A., Kraschinski, S., Tölle, R., and Hahn, J., 2000. Appropriate machinery for trafficking grasslands on organic soils. In *Proceedings of the International Conference on Agricultural Engineering, Part 2*, Warwick, pp. 228–229.
- Roth, C. H., Bristow, K. L., Brunotte, J., Facklam-Moniak, M., and Wessolek, G., 1999. Impact of tillage and field traffic induced variability of hydraulic properties on unsaturated conductivity and water balance calculations. In Van Genuchten, M., Leij, F., Wu, L. (eds.), Characterization and measurement of the hydraulic properties of unsaturated porous media, *Proceedings of the International Workshop*, Part 1, October 1997, Riverside, CA, pp. 489–496.
- Rübensam, E., and Rauhe, K., 1968. *Ackerbau*. 2. Ausgabe, VEB Deutscher Landwirtschafts-verlag Berlin, p. 544.
- Schmidt, W., and Rohde, S., 1986. Untersuchungen zur Befahrbarkeit von Niedermoorgrasland. *Archiv für Acker und Pflanzenbau und Bodenkunde*, **30**, 25–35.
- Schultze, E., and Muhs, H., 1967. *Bodenuntersuchungen für Ingenieurbauten*, 2nd edn. Berlin, Heidelberg, New York: Springer, p. 722.
- Smedema, L. K., 1986. Some technical and economic aspects of groundwater drainage for mechanized farming in temperate humid climates. *ICID Bulletin*, **35**(1), 37–42.
- Sommer, C., and Petelkau, H., 1990. Bodenverdichtung, Definition, Meßmethoden, Analyse, Lösungsansätze und offene Fragen. *Landtechnik*, **45**, 404–406.
- Terzaghi, K., Peck, R. B., and Mesri, G., 1996. *Soil Mechanics in Engineering Practice*, 3rd edn. New York: Wiley.

- Thomasson, A. J., 1982. Soil and climatic aspects of workability and trafficability. *Proceedings of the 9th Conference of the International Soil Tillage Research Organisation (ISTRÖ)*, Osijek, Yugoslavia, pp. 551–557.
- Tisdall, J. M., and Adem, H. H., 1986. Effect of water content at tillage on size-distribution of aggregates and infiltration. *Australian Journal of Experimental Agriculture*, **26**, 193–195.
- Usowicz, B., and Lipiec, J., 2009. Spatial distribution of soil penetration resistance as affected by soil compaction: The fractal approach. *Ecological Complexity*, **6**, 263–271.
- Van Bergeijk, J., Goense, D., and Speelman, L., 2001. Soil tillage resistance as a tool to map soil type differences. *Journal of Agricultural Engineering Research*, **79**, 371–387.
- Van Genuchten, M. T., 1980. A closed-form equation for predicting the hydraulic conductivity of unsaturated soils. *Soil Science Society of America Journal*, **44**, 892–898.
- Van Wijk, A. L. M., and Buitendijk, J., 1988. A method to predict workability of arable soils and its influence on crop yield. In Drescher, J., Horn, R., and de Boodt, M. (eds.), *Impact of Water and External Forces on Soil Structure*. Catena, Cremlingen, Germany: Catena, Suppl. 11, pp. 1–14.
- VDI, 2007. *VDI 6101. Richtlinie "Machine Operation with Regard to the Trafficability of Soils Used for Agriculture"*, Verein Deutscher Ingenieure, Düsseldorf November 2007, p. 62
- Wagner, L. E., Ambe, N. M., and Barnes, P., 1992. Tillage-induced soil aggregate status as influenced by water content. *Transactions of the ASAE*, **35**, 499–504.
- Wösten, J. H. M., and Bouma, J., 1985. Using simulation to define moisture availability and trafficability for a heavy clay soil in The Netherlands. *Geoderma*, **35**, 187–196.
- Wronski, E. B., Stodart, D. M., and Humphreys, N., 1990. Trafficability assessment as an aid to planning logging operations. *Appita*, **43**, 18–22.

Cross-references

- [Bulk Density of Soils and Impact on their Hydraulic Properties](#)
- [Compaction of Soil](#)
- [Controlled Traffic Farming](#)
- [Field Water Capacity](#)
- [Grazing-Induced Changes of Soil Mechanical and Hydraulic Properties](#)
- [Hydraulic Properties of Unsaturated Soils](#)
- [Peats and Peatlands, Physical Properties](#)
- [Pedotransfer Functions](#)
- [Physical Degradation of Soils, Risks and Threats](#)
- [Soil Aggregates, Structure, and Stability](#)
- [Soil Compatability and Compressibility](#)
- [Soil Functions](#)
- [Soil Penetrometers and Penetrability](#)
- [Soil Physical Quality](#)
- [Soil Structure, Visual Assessment](#)
- [Soil Water Management](#)
- [Spatial Variability of Soil Physical Properties](#)
- [Subsoil Compaction](#)
- [Tillage Erosion](#)
- [Water Erosion: Environmental and Economical Hazard](#)

TRANSMISSIVITY

Transmitted part of incoming radiation/total incoming radiation.

TRANSPIRATION

See [Stomatal Conductance, Photosynthesis, and Transpiration, Modeling](#)

TRANSPIRATION RATIO

The ratio of the mass of water lost to atmosphere through transpiration and the weight of dry plant.

TREATED WASTE WATER

See [Irrigation with Treated Wastewater, Effects on Soil Structure](#)

TRIAXIAL COMPRESSION TEST

Marek Molenda

Institute of Agrophysics, Polish Academy of Sciences, Lublin, Poland

Definition

Triaxial compression test – a test for the compressive strength in all directions of a sample of particulate material, using a triaxial cell.

Tests in which drainage is prevented are called undrained, when pores are allowed to empty tests are called drained. The specimen for triaxial compression test forms a circular cylinder of height-to-diameter ratio between 2 and 2.5 and contains volume of material representative for investigated bedding. The largest particle size shall be smaller than one sixth of the specimen diameter. The specimen stands, with axis vertical, on a pedestal containing porous plate. A stiff impermeable disc forms a loading cap. A flexible impermeable closely fitting membrane of negligible thickness envelopes the specimen and is sealed to the loading cap and to the pedestal. The specimen with loading cap, membrane, and pedestal is immersed in water in a transparent cell. The cell is connected with the pipe to the source of hydraulic confining pressure that generates normal stress acting on the cylindrical specimen. A stiff ram slides freely through the gland in the top of the cell coaxially with the specimen axis. With the assumption of uniformity of stress throughout the specimen, an axisymmetric state of stress can be induced, with two equal principal stresses $\sigma_2 = \sigma_3$ either smaller or greater than the remaining third principal stress σ_1 . In conventional strain-controlled tests, the loading ram is driven down at a constant rate that results in axial pressure acting through the length of the specimen. Axial

strain is applied at a rate of approximately 1%/min for plastic materials and 0.3%/min for brittle materials (ASTM D2850-03a, 2007). Loading is continued to 15% of axial strain, except loading may be stopped when the deviator stress ($\sigma_1 - \sigma_2$) has peaked then dropped 20% or the axial strain has reached 5% beyond the strain at which the peak in deviator stress. In a more sophisticated test, the confining pressure may vary to follow prescribed sequence of axisymmetric stress states. Obtained stress-strain curves represent behavior of a given material, and may serve for the selection of mathematical constitutive model.

Bibliography

ASTM D2850-03a, 2007. Standard test method for unconsolidated-undrained triaxial compression test on cohesive soils.

TRICKLE IRRIGATION

Method in which water drips to the plant growth medium from perforated tubes or emitters.

TROPICAL FRUITS AND VEGETABLES: PHYSICAL PROPERTIES

K. P. Baiyeri¹, F. D. Ugese²

¹Department of Crop Science, University of Nigeria, Nsukka, Enugu State, Nigeria

²Department of Crop Production, University of Agriculture, Makurdi, Benue State, Nigeria

Introduction

The tropical environment of the world is broadly defined as the equatorial region of the earth that lies within latitudes 23.4° north and south of the equator; generally bordered by the Tropic of Cancer in the north and Tropic of Capricorn in the south [<http://en.wikipedia.org/wiki/Tropics>]. The region is generally hot and humid, and houses the world largest plant genetic diversity. The annual rainfall pattern demarcates two distinct seasons as rainy and dry seasons. The peculiar climatic factors and the soil types predicated the types of fruits and vegetables grown in this region. In this brief, few but economically important tropical fruits and vegetable will be discussed.

Fruit is any mature or ripen ovary, in botanical definition; however, culinary definition of fruits vary with peoples' group or context. In a general sense, fruits (when ripen) are usually any sweet tasting plant components associated with seed(s), and eaten with little or no cooking, as dessert. The Wikipedia (the free encyclopedia) loosely defines *vegetable* as an edible plant or part of

a plant; this definition is largely based on culinary and cultural tradition, thus, the application of the word is somewhat arbitrary and subjective.

Commonly cultivated tropical fruits

Musa species

Family: Musaceae

Common name(s): Bananas, Cooking banana, Plantains

Bananas and plantains are staple food in most part of the humid tropics. They are sources of rural income particularly for the smallholders who produce them in compound farms. Plantain (*Musa spp.* AAB) is a natural hybrid of *Musa acuminata* and *Musa balbisiana*. Desert bananas are either of the acuminata origin (having the AA genome) or the hybrids dessert banana having genomic complement of both the ancestral parents. Plantain is a giant herbaceous plant with a pseudostem (false stem) which is made up of overlapping leaf bases, tightly rolled around each other to form a ridged bundle. They can attain a height of 3–4 m with a short rhizome producing aerial shoot from lateral buds on the rhizome.

An underground stem (corm) functions primarily to perpetuate the plant by production of rhizome, and suckers, that are used for propagation. Plantain is shallow rooted and because it grows fairly tall, it is not well anchored. The leaf is very large. The fruits are formed parthenocarpically, each fruit is called a finger while a cluster of fingers is called hand (Figure 1).

Anacardium occidentale

Family: Anacardiaceae

Common name(s): Cashew

It is an evergreen, medium-sized tree with a mature height of 10–15 m. It has a spreading canopy which branches close to the ground. Leaves are long, simple, leathery, entire, lanceolate or ovoid, pale to dark-green, about 15 cm long, 7.5 cm wide, borne on short petioles. The leaves have reticulate venation.

The inflorescence is either axillary or terminal, has many floret bearing spikes. Panicles often consist of male and female flowers occurring together with the ratio of male to hermaphrodite flowers in the range of 6–7:1. The flowers are regular, with green calyx and red corolla, making them appear generally reddish.

The fruit has two parts – the cashew apple, which is pear shaped, swollen, and juicy, and the cashew nut which is the kidney shaped ovary at the end of the apple. The nut has a hard double shell. The kernel of the nut is rich in oil. The cashew has a deep taproot with deeply penetrating anchorage roots while the feeding roots occupy the top 50 cm of the soil layers. Generally, the lateral root system is vigorous (Figure 2).

Mangifera indica L.

Family: Anacardiaceae

Common name(s): Mango



Plantain hybrid [PITA 24]



Dessert banana [Nsukka Local]



Landrace plantain fruits



Banana fruits

Tropical Fruits and Vegetables: Physical Properties, Figure 1 *Musa* species.



Twig



Cluster of immature fruits



Ripe fruits

Tropical Fruits and Vegetables: Physical Properties, Figure 2 Cashew [*Anacardium occidentale*].

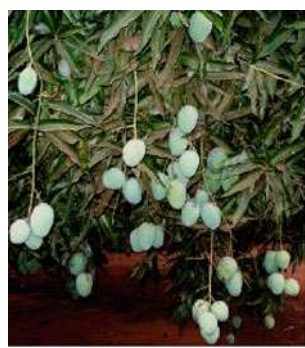
It is an erect tree, about 10–30 m tall. Canopy is oval shaped and upright; could attain a width of up to 3–8 m and with many branches. Leaves are alternate and entire, occurring mainly in clusters at the tips of branches or twigs, borne on petioles 2.5–10 cm long. Young leaves are pink or yellow, changing to green or dark-green with a shiny upper surface upon maturity. The mid ribs and the veins are quite pronounced. Mature leaves could be 10–32 cm long and 2–5.4 cm wide. The inflorescences consist of axillary or terminal panicles with hundreds or thousands of (sometimes up to 4,000) flowers. The flowers are small, regular, yellow, red, pink, or white, hermaphrodite, or male (25–98% male), both borne on the same panicle, normally without pedicels. Calyx is usually penta-sepalous, although number of sepals could sometimes be as high as seven or as low as three. Similar situation occurs with petals making up the corolla.

The fruit is a drupe showing remarkable variation in such attributes as shape, size and color. The fruit could be somewhat kidney shaped, round, oval or ovoid-oblong, 5–25 cm in length with a leathery, waxy, smooth skin whose color may be green, yellow, orange, yellow-orange, red-pink or purple-red when ripe. The mesocarp of the fruit is the main edible part in which is embedded a large flattened oval or kidney shaped seed called the stone.

The taproot is deeply penetrating (up to 6 m in some cases), the feeder root system is wide spreading with deeply penetrating anchor roots ([Figure 3](#)).

Persea americana Miller Syn:*Persea gratissima* Gaertn.
Family: Lauraceae
Common name(s): Avocado, avocado pear, alligator pear, butter pear

It is an evergreen, medium sized tree that can grow to a height of 10–20 m tall. Trees planted from seeds exhibit strong apical dominance giving rise to erect and vertical habit while grafted trees may be erect, round, or pyramidal. The root system is generally shallow, but deep in rare cases, reaching a depth of 1 m or more. The leaves are persistent, simple, coriaceous, lanceolate, 12–25 cm long, alternately arranged along the stem. They appear light



Plants carrying immature fruits



Ripe fruits

Tropical Fruits and Vegetables: Physical Properties,
[Figure 3](#) Mango [*Mangifera indica* L.]

green when young, appearing deep green at the mature stage.

Flowers are borne on axillary or terminal panicles. They are small, inconspicuous, greenish yellow, fragrant, about 5–8 mm long and 5–10 mm wide. A single inflorescence may contain from a few flowers to over a hundred. Flowers are androgynous. The fruit is a berry which could be pear shaped, spherical, oval, or elongated, measuring 7–20 cm in length with a weight of 50–1,000 g. The skin could be green, red, purple, or black and varies in thickness (from thin to thick). The creamy textured flesh is yellow-green to light-yellow in color with a pleasant smell. The seed is positioned in the central cavity of the fruit. The fruit is 3–5 cm in diameter, conical, spherical, or elongated with a double outer layer (seed coat) ([Figure 4](#)).

Citrus species

Family: Rutaceae

Some of the most important citrus species grown in West Africa are:

Citrus sinensis – sweet orange

Citrus aurantium – sour orange

Citrus aurantifolia – lime

Citrus limon – lemon

Citrus reticulata – tangerine, mandarine

Citrus species are small to medium sized evergreen trees, reaching a height of 5–15 m, the stems are often thorny. The leaves are unifoliate, margins entire with petioles that are most often winged. The leaves, oval and glossy, are alternately arranged on the shoot.

Flowers are strongly scented, large, perfect, and usually white in color. Each measures 2.4 cm in diameter with five- but sometimes four-membered perianth segments and numerous stamens. The stamens are usually arranged in five groups. The flowers occur singly (solitary) or in small clusters. The fruit of citrus is a hesperidium which is a specialized berry with the inner fleshy parts divided into various sections or segments (8–18) with an outer rind. The exocarp and mesocarp have a leathery texture. The fruit is more or less spherical or somewhat elongated, 4–30 cm long and 4–20 cm wide. Each of the easily separated segments or carpels or sections has many juice cells and several seeds covered by a leathery skin (exocarp) containing many oil glands. Some, like the tangelo, have no seeds while some have only few seeds. Rind color may be yellow to orange when ripe ([Figure 5](#)).

Psidium guajava

Family: Myrtaceae

Common name(s): Guava

The guava is a small tree that can attain a height of 6 m. The leaves are simple, elliptic to ovate, 5–15 cm long, very tough and dark, with entire margins. The white flowers are penta-petaloid but the stamens are numerous and conspicuous.

The fruit is a berry, round or pear shaped, 3–12 cm in diameter, with a soft or rough and thin or thick skin.



Mature fruits



Harvested mature fruits



Non-fruiting young tree

Tropical Fruits and Vegetables: Physical Properties, Figure 4 Avocado pear [*Persea americana* Miller Syn:*Persea gratissima* Gaertn.].



Sweet orange plant



Plant carrying immature fruits



Young non-fruiting plant

Tropical Fruits and Vegetables: Physical Properties, Figure 5 Citrus species.

Skin color of ripe fruit could be pale green, yellow, or pink as distinct from the green color of unripe fruit. The pulp is creamy white to deep pink and contains many usually hard seeds ([Figure 6](#)).

Carica papaya

Family: Caricaceae

Common name(s): Pawpaw

It is a soft wooded evergreen tree, 5–10 m tall, usually unbranched. The leaves occur at the top position of the trunk and are spirally arranged. Characteristically, they are compound or palmately lobed with each leaf having seven lobes. Usually, leaves are large, 50–70 cm in

Tropical Fruits and Vegetables: Physical Properties, Figure 6 Guava [*Psidium guajava*].

diameter, and borne on exceptionally long hollow petioles. Lower portion of the trunk is marked by scars of former leaves and fruits.

The plant is dioecious, with small unisexual flowers. They occur in leaf axils. Fruits could be spherical or elongated, measuring 15–45 cm long and 10–30 cm wide and could weigh up to 9 kg. Many shiny black or grayish-black seeds are contained in the large central cavity of

the fruit. Ripe fruit shows an amber or orange colored skin ([Figure 7](#)).

Ananas comosus (L.) Merr. Syn: *Ananas sativus* Schult. f.

Family: Bromeliaceae

Common name(s): Pineapple

It is a herbaceous plant growing to a height of 0.75–1.5 m with a spread of 0.9–1.2 m. The stem is short and thick. It is surrounded by a rosette of large sword-shaped leaves, 30–180 cm long, about 30 or more in number. The leaves are waxy, with pointed tips and sharp spines on the margins. Leaf color may be green or have red or yellow stripes close to the margin or at the middle. The apical portion of the stem lengthens and enlarges to accommodate a head of small blue, purple, or red flowers. Each flower has a single bract, red, yellow, or green in color.

Each flower transforms into a fleshy fruitlet. The fruitlets become united with adjacent ones to form a single compound, juicy fleshy fruit, 30 cm tall or more. The pine cone-shaped fruit could be dark-green, greenish-orange, yellow-green, yellow, or reddish when ripe. The rind is composed of tough, waxy, leaf-like floral bracts arranged in hexagonal units. Flesh color could vary from somewhat white to yellow. Continuation in growth of the stem culminates in the formation of the crown at the tip of the fruit. The crown or top is made up of a compact tuft of stiff, much smaller and shorter leaves. Suckers arise from the

base of the plant. While offshoots (slips) grow from stem portion near the base of the fruit, shoots occur in the axils of leaves ([Figure 8](#)).

Passiflora edulis Sims

Family: Passifloraceae

Common name(s): Yellow or Purple passion fruit

The passion fruit is a woody perennial climbing plant with tendrils. The leaves are green, alternate, finely toothed, glossy on the upper side, duller on the underside, oval in shape, and 7.5–20 cm long. Fully developed leaves have three deep lobes. The leaves, young stems, and tendrils have red or purple taints.

Flowers are fragrant, solitary, 5–10 cm in diameter, positioned at the nodes. They have three bracts, green in color; five sepals, greenish-white in color; and five white petals. Flowers generally are predominantly purple. Fruits are oblong, 4–7.5 cm in diameter, green-brown, dark-purple, or light-yellow in color, with a smooth but tough rind. The juicy flesh is yellow or orange and could hold up to 250 seeds. The seeds are small, hard brown, or black in color.

The plant has a shallow root system ([Figure 9](#)).

Commonly cultivated vegetables

Leafy vegetables

Amaranthus cruentus L. Syn: *Amaranthus paniculatus* L.

Family: Amaranthaceae

Common name(s): Amaranth, African spinach, Indian spinach

Amaranthus cruentus is the most popular in Africa. It is an erect annual herb reaching up to 2 m in height. The often stout stems may have some red color taints and varying degrees of hairiness. The leaves are two to three times longer than wide and very often have pointed tips. They are typically described as lanceolate. Generally, they could be 2–18 cm × 2–15 cm although leaf length could be up to 30 cm in some cases. The leaves are simple, have no stipules, and are spirally arranged on the stem. They have long stalks.

The pronounced inflorescence is plume-like with raceme diameter of 10 mm and above, while terminal inflorescence could be up to 2 mm in length. The



Fruiting plant

Tropical Fruits and Vegetables: Physical Properties,
[Figure 7](#) Pawpaw [*Carica papaya*].



Young plant



Horizontal view of fruit



Vertical view of the fruit

Tropical Fruits and Vegetables: Physical Properties, [Figure 8](#) Pineapple [*Ananas comosus* (L.) Merr. Syn: *Ananas sativus* Schult. f.].



Mature fruiting vines



Ripe fruits

Tropical Fruits and Vegetables: Physical Properties, Figure 9 Yellow passion fruit [*Passiflora edulis* Sims].

unisexual flowers could have five petals of up to 2 mm length. The fruit is a capsule, 2.0–2.5 mm long, and contains the shiny and tiny (c. 1 mm long) seeds which are produced in great quantities.

Telfairia occidentalis Hook. f

Family: Cucurbitaceae

Common name(s): Fluted pumpkin, fluted gourd

It is a perennial herb and a recognized climber. Its climbing habit is facilitated by its tendrils which easily coil round objects. The vine can reach and even exceed a height of 20 m. The compound leaves are spirally arranged, have no stipules while petiole length vary from 2 to 15 cm. The leaflets have petiolules with lengths up to 3.5 cm. To a great extent, female plants have characteristically stronger and bigger shoots and larger leaves than male plants, although this is only reliably detected about 3 months after sowing.

The male inflorescence has small white flowers which attaches to the terminal point of the stem. Female flowers are solitary, borne on short stalks, and are found in the leaf axils, often hidden from view by leaves. The nectar is exclusively produced by male flowers. The cream colored flowers have pedicels (up to 4 cm long) and sepals measuring up to 5 mm in length. Of the two to three fruits that form on a plant, only one to two develop to maturity. The fruit is a berry, typically weighing 5–7 kg or even more, 40–95 cm × 20–50 cm, has 10 pronounced ridges, and is coated with waxy material. The pale green fruit has a yellow pulp housing the seeds. Each fruit contains 30–110 seeds. The oval shaped seeds could be black, reddish-brown, or dark-red and measure about 5 cm long.

The root system is mainly distributed in the top soil layers. Under dry conditions, female plants, which have better adaptive capacity than male plants, could develop thick and enlarged roots ([Figure 10](#)).

Vernonia amygdalina Delile Syn: *Gymnanthemum amygdalinum* (Delile) Walp

Family: Asteraceae (Compositae)

Common name(s): Bitter leaf, common bitter leaf



Horizontal view of pod



Vertical view of the pod

Tropical Fruits and Vegetables: Physical Properties, Figure 10 *Telfairia occidentalis* Hook. F [Fluted pumpkin, fluted gourd].

It is a shrub that can grow to a height of 3–5 m, in some cases reaching up to 10 m. When young, that is less than or up to 1 year, the rough basal portion of the stem is grayish while the apical portion is green in color. Trunk could be 40 cm in diameter. Wood is hard but not brittle. Stem is supple when bent. Leaves are simple, without stipules, alternate, petioles 2–4 cm long, lamina measuring 4–28 cm × 1–15 cm. Edges are uneven and toothed (dented). Leaf lamina appears greenish while main rib is pale in color. Leaves at the base of the shoot have wider laminas and longer petioles compared to those at the apex, near the flowers. The petiole emerges gradually into the leaf blade.

The inflorescence is a head. The flowers are white and pleasantly scented and are less than 1 cm in diameter. The fruit is an achene, 10-ribbed, and could be up to 3.5 mm long. The seeds are surmounted by a pappus ([Figure 11](#)).

Fruit vegetables

Lycopersicon esculentum Mill. Syn: *Solanum lycopersicum* L., *Lycopersicon lycopersicum* (L.) H. Korst

Family: Solanaceae

Common name(s): Tomato



Tropical Fruits and Vegetables: Physical Properties, Figure 11 *Vernonia amygdalina* Delile Syn: *Gymnanthemum amygdalinum* (Delile) Walp [Bitter leaf].

It is a seasonal herb with stems up to 2–4 m long. Usually, the hairy stems are prostrate while the tips are erect. Branches trail from the stems, normally, profusely. The large, hairy leaves have many leaflets, seven to nine. The leaves measure about 7 cm long while the outline of larger leaves could be up to 50 cm long and 30 cm wide. Leaflets have toothed margins. Both the leaves and the stems have a strong odor.

Flowers are small and yellow and grow in clusters of 4–12 on stems between leaves and could measure up to 1–2 cm in diameter. At times, the inflorescence could be compound with up to 100 flowers. Tomato fruit is typically a berry, 2–15 cm in diameter. Immature fruit is green and could have hairs. Ripe fruit is hairless and shiny with red, pink, or yellow color. Fruits exist in various shapes: could be large and round or elongated or could be small in size with diameter up to 2 cm. The brown and hairy seeds are flat-oval in shape with mean dimensions of 4 mm × 3 mm.

The main root system is fibrous, though there is a strong taproot reaching a depth of 50 cm or more into the soil. The stems readily give rise to numerous adventitious roots.

Abelmoschus esculentus (L.) Moench Syn: *Hibiscus esculentus* L.

Family: Malvaceae

Common name(s): Common okra, okro, lady's finger

It has a strong, erect stem up to 4 m tall, branched to a greater or lesser extent. The erect stem has many stiff somewhat prickly hairs. Branches arising from the stem could be straight or they could bend downwards. Okra leaves are simple, borne on long petioles up to 50 cm long, three to seven lobed, more or less divided, cordate at base, veins present on both abaxial and adaxial sides, with stiff hairs, 20–40 cm long and up to 50 cm broad. Petiole is normally red tinged.

The axillary, solitary flowers have five petals, large and pink, white or yellow in color. The center of the calyx is dark-purple or crimson. Epicalyx segments are 7–18 in number, 5–25 mm in length, and 0.5–3 mm in width. Fruits, cylindrical to pyramidal in shape, often vary in

color, from purple to green to pale green to yellow or even black. It is a capsule varying in size from 5–25 cm in length and 1–5 cm in width. Fruits could be borne on stem tips or the axes of leaves or on spurs. The inside of each fruit is made up of several narrow spaces or cavities called loculi in which up to 100 seeds, round, 4.5 mm in diameter, gray or brown when ripe are embedded.

The taproot is strong and firmly establishes the plant in the soil with the aid of secondary roots arising therefrom.

Solanum melongena L. Syn: *Solanum insanum* L.,
Solanum incanum auct. non L.

Family: Solanaceae

Common name(s): Eggplant, Aubergine, brinjal

The plant can grow up to 1.5–2 m tall although normal height is about 1 m, with many branches. Leaves are simple, without stipules, entire but most often lobed, with 8 cm long petioles and with rounded or cordate leaf bases. The leaves could be 3–30 cm long and 2–15 cm wide, alternately arranged along the stem. Hairs occur both on the leaves and the stems.

Flowers are violet or purple, with an average diameter of 4 cm. The inflorescence is a cyme with one to five flowers, although flowers most often occur singly (solitary). Petals are united. The fruit is a berry, 2–35 cm long, and 2–20 cm broad, often single. When ripe, fruit is normally yellow, brown or intermediate between the two colors or even reddish. Unripe fruit however appears white, green, violet-purple, black, sometimes striped. The fruits contain flattened light brown seeds 3 mm × 4 mm.

It has a long taproot.

Citrullus lanatus (Thunb.) Matsum. & Nakai Syn: *Citrullus vulgaris* Schrad. Ex Eckl. & Zeyh., *Colocynthis citrulus* (L.) Kuntze

Family: Cucurbitaceae

Common name(s): Water melon, egusi melon, egusi water melon, West African water melon

It is a trailing annual plant, could reach 4–10 m in length. Presence of tendrils facilitates climbing ability. Stem is soft and ridged. Leaves are simple, but deep clefts

gives rise to irregular lobes. Leaves are $4-25 \times 3-19$ cm, with serrate margins, alternate. Petioles are 2–14 cm long.

Flowers are solitary and axillary, 2–3.5 cm in diameter, yellow in color. Male flowers are borne on long peduncles with petals united at the base. Female flowers are borne on shorter peduncles, have an inferior hairy ovary. Fruit is a berry, green, white, with white stripes (markings) or yellow. The shape is round or oval to round, 5–80 cm long, 15–20 cm in diameter, weighing 0.1–30 kg. The flesh is white, pale green, yellow, red or pink. The seeds are oval, flattened, smooth, although margins rough and thick, 0.5–1.5 cm long, 0.5–1 cm wide, yellow or brown in color.

It has a tap root with numerous lateral roots although root system is generally shallow.

Capsicum annuum L.

Family: Solanaceae

Common name(s): Sweet pepper, bell pepper, paprika

It is a fast growing herbaceous annual plant that can reach a height of 1 m. The lance-shaped leaves are simple, hairless or pubescent, alternate, petioles up to 10 cm long. Flowers are white, solitary, and pending. Fruits are large, 3–12 cm in diameter, red, yellow, orange, purple or green when ripe, fleshy with a mild flavor. Ripe fruit is hollow with the center anchoring many seeds. It has a strong taproot and numerous lateral roots.

Capsicum frutescens L.

Family: Solanaceae

Common name(s): Bird pepper, chilli

It is a fast growing annual herb reaching a height of up to 2 m. Leaves are simple, glabrous or pubescent, alternate with petiole length up to 10 cm. Flowers are white, solitary, or in clusters of two to three in leaf axils, pending, 1–2 cm in diameter. Fruits are ovoid or elongated, 1.5–16 cm long, bright red or sometimes yellow or orange when ripe, and highly pungent. The central cavity has several seeds. It has a taproot and numerous lateral roots.

Root vegetables

Zingiber officinale

Family: Zingiberaceae

Common name(s): Ginger, garden ginger

It is an erect herb that grows 0.3–1.2 m tall and 3–6 mm in diameter. The leaves are green, thin or narrow, 1–3 cm wide, 5–30 cm long, sharp, arranged at right angles to the stem. Flowers, yellow or yellowish-green, are produced in dense or compressed spikes on a basal stem. The root system is an enlarged rhizome, 3–25 cm long, 2–3 cm in diameter, is highly aromatic. Flesh color is white to yellow or pale greenish yellow (Figure 12). Adventitious roots arise from the rhizome in the upper soil layers.

Daucus carota

Family: Umbelliferae (Apiaceae)

Common name(s): Carrot

The plant is a biennial usually cultivated as an annual. During the first season of its growth, it develops a rosette of finely divided leaves and stores its food in the stout taproot which becomes enlarged and fleshy. The taproot could be globular, elongated, or tapering. It is most often orange or yellow in color. If it is not harvested in the first season, the plant will utilize its resources to grow a flowering stem the next season. Thus, a central terminal bud grows into a stem, 0.9–1.5 m tall, bearing an umbel of small, radially symmetrical flowers. The flowers, white or pinkish, have five each of petals, sepals, and stamens. The central flower is normally purple. The fruit of the plant has two nutlets each containing one seed.

Summary

The tropical environment has a highly diverse nature of fruits and vegetables that have remarkable nutritional and economic importance. Fruits and vegetables are generally low in protein, fat, and calories, but they are rich sources of important minerals and vitamins. Some,



Rhizomes of Ginger



Sliced rhizomes showing yellowish or whitish color

Tropical Fruits and Vegetables: Physical Properties, Figure 12 *Zingiber officinale* [Ginger].

especially fruits, contain anti-carcinogenic and antioxidant compounds that protect the body against cancer and slow down the ageing process respectively. Their high fibre content is known to impact a number of health benefits such as lowered risk of obesity and heart disease, as well safeguarding against constipation and enhancing bowel movement.

Tropical fruits and vegetables exhibit wide variation in their physical attributes. For instance the stems of fruits which are mostly woody vary in height from very short to very tall while their diameters could range from less than a meter to few or several meters. Branches could be loose or compact, dense or sparse. Some tropical fruit species are evergreen while others are deciduous.

Most tropical vegetables have soft stem, which is normally a few to several centimeters long, except for some (like those with vines) where the stem could be few to several meters long. The diameter is also very small, usually not exceeding a few centimeters, except in a few cases.

For both fruits and vegetables, the leaves could be few or numerous, simple or compound with various sizes. Arrangement on the stem could be opposite, alternate, or whorled. Venation also varies as well as types of margin. Certain portions of the leaf could have projections or be completely without projections. The texture of the lamina could vary between smooth and rough or dull and glossy. Leaf color is variable and could range from pure to a mixture or blend of various colors. Flowers are equally variable. In some plants they occur singly while in others they occur in clusters or groups called inflorescence. They could be terminal or axillary, prominent or inconspicuous, scented or not. Some plants are monoecious, diecious, or hermaphrodite.

Fruits show variation in shape, size, skin and flesh color, texture, and seed quality. Seeds within a fruit could be single, few or many with varying sizes and shapes. Rooting profile could vary between the extremes of shallow rootedness to deep rootedness. Thus, the tropical environment is endowed with numerous fruits and vegetables with diverse physical and rich nutritional attributes.

Bibliography

- Anonymous, 2009. *Capsicum Peppers: The Whole Story*. USA: California-Antilles Trading.
- Bosch, C. H., 2004. *Moringa oleifera*. In Grubben, G. J. H., and Denton, O. A. (eds.), *Plant Products of Tropical Africa 2: Vegetables*. Wageningen: PROTA Foundation, pp. 392–395.
- Bosch, C. H., Sie, K., and Asafa, B. A., 2004. *Adansonia digitata*. In Grubben, G. J. H., and Denton, O. A. (eds.), *Plant Products of Tropical Africa 2: Vegetables*. Wageningen: PROTA Foundation, pp. 36–41.
- Bukenya-Ziraba, R., 2004. *Hibiscus cannabinus*. In Grubben, G. J. H., and Denton, O. A. (eds.), *Plant Products of Tropical Africa 2: Vegetables*. Wageningen: PROTA Foundation, pp. 316–320.
- Bukenya-Ziraba, R., and Bonsu, K. O., 2004. *Solanum macrocarpon*. In Grubben, G. J. H., and Denton, O. A. (eds.), *Plant Products of Tropical Africa 2: Vegetables*. Wageningen: PROTA Foundation, pp. 484–488.
- Daunay, M. C., and Chadha, M. L., 2004. *Solanum melongena*. In Grubben, G. J. H., and Denton, O. A. (eds.), *Plant Products of Tropical Africa 2: Vegetables*. Wageningen: PROTA Foundation, pp. 488–493.
- Denton, O. A., 2004. *Celosia argentea*. In Grubben, G. J. H., and Denton, O. A. (eds.), *Plant Products of Tropical Africa 2: Vegetables*. Wageningen: PROTA Foundation, pp. 167–171.
- Dupriez, H., and DeLeener, P., 1989. *African Gardens and Orchards: Growing Vegetables and Fruits*. London: Macmillan, p. 333.
- Egunjobi, J. K., and Adebisi, A. A., 2004. *Cucumeropsis mannii*. In Grubben, G. J. H., and Denton, O. A. (eds.), *Plant Products of Tropical Africa 2: Vegetables*. Wageningen: PROTA Foundation, pp. 235–237.
- ENCARTA, 2005. *Microsoft Encarta Encyclopedia Standard, 2005*. USA: Microsoft.
- Fomum, F. U., 2004a. *Vernonia amygdalina*. In Grubben, G. J. H., and Denton, O. A. (eds.), *Plant Products of Tropical Africa 2: Vegetables*. Wageningen: PROTA Foundation, pp. 543–546.
- Fomum, F. U., 2004b. *Vernonia hymenolepis*. In Grubben, G. J. H., and Denton, O. A. (eds.), *Plant Products of Tropical Africa 2: Vegetables*. Wageningen: PROTA Foundation, pp. 546–549.
- Fondio, L., and Grubben, G. J. H., 2004. *Corchorus olitorius*. In Grubben, G. J. H., and Denton, O. A. (eds.), *Plant Products of Tropical Africa 2: Vegetables*. Wageningen: PROTA Foundation, pp. 271–221.
- Gaillard, J. P., and Godefroy, J., 1995. *Avocado*. Wageningen: Macmillan, p. 120.
- Greensil, T. M., 1968. *Growing Better Vegetables: A Guide for Tropical Gardeners*. London: Evans Brothers, p. 159.
- Grubben, G. J. H., 2004a. *Amaranthus cruentus*. In Grubben, G. J. H., and Denton, O. A. (eds.), *Plant Products of Tropical Africa 2: Vegetables*. Wageningen: PROTA Foundation, pp. 67–72.
- Grubben, G. J. H., 2004b. *Amaranthus dubius*. In Grubben, G. J. H., and Denton, O. A. (eds.), *Plant Products of Tropical Africa 2: Vegetables*. Wageningen: PROTA Foundation, pp. 72–76.
- Grubben, G. J. H., and El Tahir, I. M., 2004. *Capsicum annuum*. In Grubben, G. J. H., and Denton, O. A. (eds.), *Plant Products of Tropical Africa 2: Vegetables*. Wageningen: PROTA Foundation, pp. 154–163.
- Jacquemard, J. C., 1998. *Oil Palm*. Wageningen: Macmillan, p. 144.
- Joker, D., 2000a. *Tamarindus indica*. *Seed Leaflet No.45*. Denmark: Danida Forest Seed Centre.
- Joker, D., 2000b. *Vitellaria paradoxa*. *Seed Leaflet No.50*. Denmark: Danida Forest Seed Centre.
- Lester, R. N., and Seck, A., 2004. *Solanum aethiopicum*. In Grubben, G. J. H., and Denton, O. A. (eds.), *Plant Products of Tropical Africa 2: Vegetables*. Wageningen: PROTA Foundation, pp. 472–477.
- Maundu, P. M., and Grubben, G. J. H., 2004. *Amaranthus graecizans*. In Grubben, G. J. H., and Denton, O. A. (eds.), *Plant Products of Tropical Africa 2: Vegetables*. Wageningen: PROTA Foundation, pp. 76–78.
- McChintok, N. C., and El Tahir, I. M., 2004. *Hibiscus sabdariffa*. In Grubben, G. J. H., and Denton, O. A. (eds.), *Plant Products of Tropical Africa 2: Vegetables*. Wageningen: PROTA Foundation, pp. 321–326.
- Messiaen, C. M., and Fagbayide, J. A., 2004. *Cucurbita pepo*. In Grubben, G. J. H., and Denton, O. A. (eds.), *Plant Products of Tropical Africa 2: Vegetables*. Wageningen: PROTA Foundation, pp. 273–277.
- Mnzava, N. A., 2004. *Corchorus tridens*. In Grubben, G. J. H., and Denton, O. A. (eds.), *Plant Products of Tropical Africa 2: Vegetables*. Wageningen: PROTA Foundation, pp. 221–223.
- Morton, J. F., 1987. Fruits of warm climates. Miami, FL. www.hort.purdue.edu/newcrop/morton.html. Accessed August 28, 2009.

- New World Encyclopedia. www.wikipedia.org. Accessed August 28, 2009.
- Odiaka, N. I., and Schippers, R. R., 2004. *Telfairia occidentalis*. In Grubben, G. J. H., and Denton, O. A. (eds.), *Plant Products of Tropical Africa 2: Vegetables*. Wageningen: PROTA Foundation, pp. 522–527.
- Opeke, L. K., 1987. *Tropical Tree Crops*. Ibadan: Spectrum Books, p. 327.
- Opeke, L. K., 2005. *Tropical Commodity Tree Crops*. Ibadan: Spectrum Books, p. 503.
- Purseglove, J. W., 1972. *Tropical Crops: Monocotyledons*. London: Longman Group.
- Rice, R. P., Rice, L. W., and Tindall, H. D., 1987. *Fruit and Vegetable Production in Africa*. London: Macmillan, p. 170.
- Samson, J. A., 1986. *Tropical Fruits*. London: Longman Group, p. 607.
- Schippers, R. R., 2000. *African Indigenous Vegetables: An Overview of the Cultivated Species*. Chatham: Natural Resources Institute/CTA, p. 214.
- Siemonsma, J. S., and Kouame, C., 2004. *Abelmoschus esculentus*. In Grubben, G. J. H., and Denton, O. A. (eds.), *Plant Products of Tropical Africa 2: Vegetables*. Wageningen: PROTA Foundation, pp. 25–29.
- Sina, S., and Traore, S. A., 2002. *Parkia biglobosa*. Record from Protibase. In Oyen, L. P. A., and Lemmens, R. H. M. J. (eds.), *PROTA*. Wageningen Agricultural University.
- Tindall, H. D., 1968. *Commercial Vegetable Growing*. London: Oxford University Press, p. 300.
- Umali, B. E., and Nikiema, A., 2002. *Vitellaria paradoxa* C. F. Gaertn. Record from Protibase. In Oyen, L. P. A., and Lemmens, R. H. M. J. (eds.), *PROTA*. Wageningen: Wageningen Agricultural University.
- van der Vossen, H. A. M., Denton, O. A., and El Tahir, I. M., 2004a. *Citrullus lanatus*. In Grubben, G. J. H., and Denton, O. A. (eds.), *Plant Products of Tropical Africa 2: Vegetables*. Wageningen: PROTA Foundation, pp. 185–191.
- van der Vossen, H. A. M., Nono-Womdin, R. A., and Messiaen, C. M., 2004b. *Lycopersicon esculentum*. In Grubben, G. J. H., and Denton, O. A. (eds.), *Plant Products of Tropical Africa 2: Vegetables*. Wageningen: PROTA Foundation, pp. 373–379.
- Verheij, E. W. M., 2002. *Dactyloctenium edulis*. Record from Protibase. In Oyen, L. P. A., and Lemmens, R. H. M. J. (eds.), *PROTA*. Wageningen: Plant Resources of Tropical Africa.
- Wikipedia – The On-line Encyclopedia. www.wikipedia.org. Accessed August 28, 2009.

TROPICAL SOILS, PHYSICAL PROPERTIES

Charles A. Igwe

Department of Soil Science, University of Nigeria,
Nsukka, Enugu State, Nigeria

Synonyms

Equatorial; Subtropical; Tropical

Definition

Soil. This is the unconsolidated mineral material on the immediate surface of the earth that serves as a medium for plant growths. It is also a product of soil formation.

Tropical soils. These are soils found within the vicinity and overlap the two tropics, Cancer and Capricorn.

Equatorial soils. Terminology often used to describe soils that overlap the equator and extend northward to the Tropic of Cancer and southward to the Tropic of Capricorn.

Subtropical soils. Soils formed on the periphery of the two tropics – Cancer and Capricorn.

Introduction

Of all the major soils of the world, the ones least understood by soil scientists are the soils of the tropics. Most soil scientists describe them as useless soils that are often lateritic and drastically leached. The Soil Survey Staff (1975) attempted to classify world soils to a very low level of generalization, but found it necessary to classify in detail the order of ultisols and oxisols, which are the very prominent tropical soils. It was in the subsequent editions and upgrading that further classification of these soils was attempted. Some years later, Soil Survey Staff (1999) again described the major soil orders of the world. Those identified in the tropics are Oxisols, Ultisols, Alfisols, Aridisols, Inceptisols, and Entisols. These soils occur in most tropical areas of Africa, Asia, and North and South America. They have certain properties in common. Most of these soils are very fragile and possess the characteristics of not holding water for a long time when saturated. In spite of all the literature highlighting the negative side of these soils, they still support agriculture, forestry, wildlife conservation, recreation, and other types of land use such as industrial, mining, sewage disposal, highway development, and rural/urban development. Most soils are deep, highly weathered except for some few mountainous soils. The soils however, offer some challenges in the management and its restoration following degradation. Sometime they are very fragile due to their physical properties.

In order to manage these soils better and put them to sustainable productivity, their physical properties have to be understood. There should be an understanding between the soil properties, their management, and land use strategies. A number of soil physical properties influence the nature of the soil and their productivity potential. These soil physical properties are soil texture, structure, rheology, and soil water retention and transmissivity.

Texture of the soils

A variety of soil textures occur in tropical soils. The International Soil Science Society (ISSS) recognized 12 classes of soils in the soil textural triangle. Almost all of these 12 soil groups occur in the tropics. However, the finesse or the coarseness of soil often depends on the soil-forming parent materials. In most tropical areas with heavy rainfall and excessive leaching, the soils are mostly coarse because the fine materials are removed by erosion, leaving behind the coarse particles. Igwe et al. (1995) reported that most of the soils they studied were mainly sandy loam to sandy clay in the subsoil. The clay contents they observed are low to moderate while the silt contents are very low except for profiles in floodplain as Atami

Tropical Soils, Physical Properties, Table 1 Physical properties of some selected tropical soils

Depth (cm)	Clay%	Silt%	Sand%	Textural class	Bulk density (Mg m^{-3})	Ksat (cm h^{-1})	Permeability class
Ukehe ^a							
0–15	8	20	72	sl	1.66	39.3	Very rapid
15–35	12	8	80	sl	1.86	3.8	Moderate
35–68	20	2	78	sl	1.64	8.9	Moderately rapid
68–97	18	2	80	sl	1.73	23.4	Rapid
97–145	28	4	68	scl	1.62	21.7	Rapid
145–189	24	4	72	scl	1.68	3.7	Moderate
Nsukka ^b							
0–18	22	2	76	scl	1.54	24.6	Rapid
18–35	24	2	74	scl	1.56	16.5	Rapid
35–77	18	2	80	sl	1.34	18.6	Rapid
77–122	38	4	58	sc	1.50	1.32	Slow
122–185	38	2	60	sc	1.47	1.65	Slow
Atani ^c							
0–12	26	14	60	scl	1.70	1.43	Slow
12–27	34	10	56	scl	1.54	0.16	Slow
27–60	32	10	58	scl	1.38	0.11	Very slow
60–80	34	12	54	scl	1.50	0.09	Moderately slow
80–125	36	14	50	sc	1.81	0.05	Very slow

^aSource: Akamigbo and Igwe, 1990.

^bIgwe et al. 2005.

^cIgwe 2003a.

sl sandy loam, scl sandy clay loam, sc sandy clay.

(Table 1). The low silt content is attributed to the nature of the parent materials and the advanced stage of weathering. Sometime there are exceptions to these especially in floodplain soils that are entisols and inceptisols.

Structure of the soils and aggregate stability

One of the most remarkable characteristics of the tropical soils is their very high bulk density values. In most tropical ultisols and alfisols, bulk density values can sometime be more than 1.80 Mg m^{-3} . In the soils studied by Akamigbo and Igwe (1990), Igwe (2003b), and Igwe et al. (2005) bulk density values of between 1.34 Mg m^{-3} and 1.86 Mg m^{-3} were obtained for various soils (Table 1). These high bulk density values have been attributed to structure degradation and alterations within the profiles. The low level of soil organic matter (SOM) obtained in these soils also contribute significantly in the increased bulk density values. Studies by Mbagwu et al. (1983) and Igwe et al. (1995) indicated that bulk density of soils increased as organic matter decreased in the soil. The high temperature in the tropics and over use of the soil due to tillage contribute significantly to high mineralization of soil organic matter, thus low values of SOM in the soil. The negative influence of high bulk density is the development of compaction in the soil and sometimes development of hardpan or impervious layers, which hinders water movement in the soil.

One good characteristic of tropical soils is the stable aggregate potentials. The soils mostly are composed of kaolinite, oxides, and quartz. These minerals do not expand rapidly when wet and thus contribute to high aggregate

stability (AS) potential of the soils. Igwe et al. (1999) showed that for most soils the values of water-stable aggregates (WSA) greater than 0.5 mm can be as high as 85% for some soils while the unstable aggregates (WSA $< 0.25 \text{ mm}$) can be as low as 8%. Values of aggregate stability in most tropical soils are high. In some Nigerian soils, aggregate stability (AS) were between 10% in a degraded ultisol and 82% for highly weathered tropical soil.

The soil dispersion ratio (DR), which is the ratio of total clay and silt obtained with chemical dispersant and clay+silt obtained with deionized water dispersion only is moderate to high. Most often values of DR may range from values as low as 0.13–0.94. According to Igwe (2005) soils with high DR are very erodible while those with low DR are less erodible. The ease with which the soil disperses is also related to the level of sesquioxides, organic matter, and other cementing or binding agents in the soils.

Consistency

The pedological system of soil consistency determination indicates that the tropical soils can be regarded as being granular crumbs on the top soils while the subsoil is blocky to massive. The blocky structure can be angular blocky or subangular blocky depending on the over burden pressure and mode of soil formation. In the arid and semiarid areas, the structure of the B-horizon can be prismatic to columnar structure due to the effect of salt and other solutes. The aggregates are strong when dry, friable to firm when wet. Except the soils that contain a lot of clay particles, they are not very sticky and often not very

plastic. The *van der Waal's* forces binding the aggregates seem to be strong and make the soil particles adhere to one another very strongly.

Shrink–swell characteristics

Shrink–swell potential as a soil quality that determines its volume change with variation in the soil moisture regime is very important in citing agronomic and engineering infrastructure. As already stated, tropical soils with high 2:1 and oxides content hardly pose any problem associated with shrink–swell characteristics. Igwe (2003a) remarked that in some studied tropical soils with old parent materials, the coefficient of linear extensibility (COLE) were between 0.006 and 0.082 with corresponding volumetric shrinkage (VS) as 1.81 and 26.67. In another study on different soils, Igwe and Okebalama (2006) showed that COLE ranged from 0.03 to 0.09 with corresponding VS as 9.27 and 29.50. The shrink–swell hazard rating indicates that the soils fall within the class of slight shrink–swell class to very few severe shrink–swell hazard class. In most cases, the top soils fall within the slight shrink–swell hazard category while the soils with moderate shrink–swell hazard classes are those of the subsoil where there is increased clay size particle concentration due to translocation and accumulation of clay by illuviation or residual accumulation of clay.

Soil moisture retention

The moisture retention characteristics of the soils vary from soil to soil depending on texture, the inherent soil organic matter content, colloidal content, and other soil properties. The soils can retain about 10% to more than 60% moisture at 0.01 MPa suction and as low as <5% and 25% at 1.5 MPa. In most tropical soils, the available water content (AWC) have been shown from studies to range from <1% in coarse sandy soils to as high as >40% in clayey soils. In most cases, the topsoil retains more moisture than the subsoil except when there is accumulation of clay size particles.

Hydraulic conductivity, permeability, and infiltration rate

Land use, soil properties, and nature of soil biological activities determine to a large extent the hydraulic conductivity and infiltration rates of tropical soils. Hydraulic conductivity of soils can vary in tropical soils from very slow to rapid. In most soils, the conductivity is reduced due to structure degradation, high bulk density, and loss of structure due to soil erosion. These results are very rapid over land flow if there is reduced water intake into the soil. Numerical values obtained in the field and laboratories indicate that hydraulic conductivity of some tropical soils range from <0.12 cm h⁻¹ to >40 cm h⁻¹.

The high biological activities of the tropical soils and high porosity of the soils induces high infiltration rates. Values obtained from coarse-textured soils indicate that infiltration rates ranges from about 10 cm h⁻¹ to

>35 cm h⁻¹, while in fine-textured soils, Nnabude and Mbogwu (1999) obtained an infiltration rate of >20 cm h⁻¹. In floodplain soils, the infiltration rates are high, thus reflecting the excellent soil structure and increased biological activities on the top soil. Lithological discontinuity can also affect the easy flow of water into the soil and hence distorted infiltration rate.

Management of tropical soils

The greatest problem in management of tropical soils is soil erosion and problems associated with aridity. In areas of high tropical rainstorms, soil erosion by water remains the major problem. Soil erosion in these areas can be in the form of rill erosion, and interrill and gully erosion (Figure 1). Lal (1976) discussed in details the problems associated with soil erosion by water in a humid tropical environment. Associated with high rainfall is leaching of soil nutrient leading to decrease soil pH. As soil erosion by water poses problem in humid tropical environment, the tropical areas with less rainfall suffer from wind erosion. This form of erosion creates very serious



Tropical Soils, Physical Properties, Figure 1 Two different sites devastated by gully erosion in southern Nigeria.

environmental problem. Also associated with very low rainfall is the problem of aridity and salinity degradation of the soil. Salt-related problems can cause very severe damage to agricultural productivity.

Severe deforestation in this region has not helped in checking the erosion menace. Intensive afforestation and agroforestry programs are therefore recommended for soil erosion control in the region. Agricultural practices such as mulching, no-till farming, or zero tillage are also recommended. Other practices are contour plowing, strip cropping, and ridging across slope.

Summary

The soils of the tropical region are Oxisols, Ultisols, Alfisols, Aridisols, Inceptisols, and Entisols and occur in most tropical areas of Africa, Asia, and North and South America. They have some certain properties in common. Most of these soils are very fragile and possess the characteristics of not holding water for a long time when saturated. Their textures and particle distribution vary from location to location. They are well aggregated in that they lack swelling minerals and often do not undergo swell-shrink hazard except those with swelling clays. The greatest problem in management of tropical soils is soil erosion and problems associated with aridity and salinity. In areas of high tropical rainstorms, soil erosion by water remains the major problem.

Bibliography

- Akamigbo, F. O. R., and Igwe, C. A., 1990. Physical and chemical characteristics of four gullied soils locations in Anambra State, Nigeria. *Nigerian Agricultural Journal*, **25**, 29–48.
- Igwe, C. A., 2003a. Shrink-swell potential of a floodplain soil in Nigeria in relation to moisture content and mineralogy. *International Agrophysics*, **17**, 47–55.
- Igwe, C. A., 2003b. Erodibility of soils of the upper rainforest zone, southeastern Nigeria. *Land Degradation and Development*, **14**, 323–334.
- Igwe, C. A., 2005. Erodibility in relation to water-dispersible clay for some soils of Eastern Nigeria. *Land Degradation and Development*, **16**, 87–96.
- Igwe, C. A., and Okebalama, C. B., 2006. Soil strength of some central eastern Nigeria soils and effect of potassium and sodium on their dispersion. *International Agrophysics*, **20**, 107–112.
- Igwe, C. A., Akamigbo, F. O. R., and Mbagwu, J. S. C., 1995. Physical properties of soils of southeastern Nigeria and the role of some aggregating agents in their stability. *Soil Science*, **160**, 431–441.
- Igwe, C. A., Akamigbo, F. O. R., and Mbagwu, J. S. C., 1999. Chemical and mineralogical properties of soils in southeastern Nigeria in relation to aggregate stability. *Geoderma*, **92**, 111–123.
- Igwe, C. A., Zarei, M., and Stahr, K., 2005. Mineral and elemental distribution in soils formed on the river Niger floodplain, Eastern Nigeria. *Australian Journal of Soil Research*, **43**, 147–158.
- Lal, R., 1976. Soil erosion on alfisols in western Nigeria, IV. Nutrient element losses in runoff and eroded sediments. *Geoderma*, **16**, 403–417.
- Mbagwu, J. S. C., Lal, R., and Scott, T. W., 1983. Physical properties of three soils in southern Nigeria. *Soil Science*, **136**, 48–55.
- Nnabude, P. C., and Mbagwu, J. S. C., 1999. Soil water relations of a Nigerian Typic Haplustult amended with fresh and burnt rice-mill wastes. *Soil and Tillage Research*, **50**, 207–214.
- Soil Survey Staff, 1975. *Soil Taxonomy: A basic system of soil classification for making and interpreting soil surveys*. Washington, DC: USDA Agricultural Handbook No. 436.
- Soil Survey Staff, 1999. *Soil Taxonomy*. United States Department of Agriculture Handbook 436, 2nd edn. Washington, DC: United States Department of Agriculture.

Cross-references

- Friction Phenomena in Soils
 Hydraulic Properties of Unsaturated Soils
 Infiltration in Soils
 Organic Matter, Effects on Soil Physical Properties and Processes
 Shrinkage and Swelling Phenomena in Soils
 Soil Aggregates, Structure, and Stability
 Soil Texture: Measurement Methods
 Soil Water Flow
 Soil Water Management
 Water Erosion: Environmental and Economical Hazard

TROPICAL WATERSHEDS, HYDROLOGICAL PROCESSES

Juergen Baumann

Hydroagricultural Infrastructure (SGIH-GDTT), National Water Commission (CONAGUA), Mexico City, Federal District, D.F, Mexico

Definition

Tropical watersheds refer to watersheds in the wet and seasonally wet (humid) tropics, including type A climates according to the Köppen classification system and tropical regions that fit with the criteria defined by Chang and Lau (1993). Hydrological processes in tropical watersheds are strongly influenced by particular climatic, geomorphologic, and soil conditions.

Climate: Rain amount and rainfall intensities are commonly much higher than in other climates. Erosivity of single rainstorms (EI_{30}) can be higher than total annual rainerosivity (R-factor) in temperate wet or semiarid regions. High temperature and wetness accelerate rock weathering.

Vegetation: Runoff in undisturbed forested tropical watersheds is generally low and Hortonian Overland Flow (HOF) is strongly reduced by high infiltration rates of the topsoil layers (Bonell, 2005). Disturbance of natural forest cover decreases interception and reduces the infiltration capacity, leading to increased superficial runoff and streamflow (Chaves et al., 2008).

Soils and Geology: The formation of deep weathered soil profiles (Regolith, Saprolite) is widely shown in the tropics, and catchments may have a high water storage capacity. Soil texture, clay mineralogy, soil hydraulic properties, and especially drainage conditions of the subsoil and depth of regolith are key factors in determining hydrologic flowpaths and runoff (Brujinzeel, 2004; Chappell et al., 2007).

Topography: Hillslope hydrology in the humid tropics is driven by a combination of fast vertical flows, near surface lateral flows, lateral subsurface storm flows, as well as saturated overland flow. The dominance of a certain flowpath depends strongly on soil and subsoil conditions (Elsenbeer, 2001). The influence of slope gradient as a controlling factor on runoff will increase with rainfall amount and intensity of single storms or rainfall accumulations.

Bibliography

- Bonell, M., 2005. Runoff generation in tropical forests. In Bonell, M., and Bruijnzeel, L. A. (eds.), *Forests, Water and People in the Humid Tropics*. UNESCO, International Hydrology Series. Cambridge: Cambridge University Press, pp. 314–406.
- Bruijnzeel, L. A., 2004. Hydrological functions of tropical forests: not seeing the soil for the trees. *Agriculture, Ecosystems and Environment*, **104**, 185–228.
- Chang, J.-H., and Lau, L. S., 1993. A definition of the humid tropics. In Bonell, M., Hufschmidt, M. M., and Gladwell, J. S. (eds.), *Hydrology and Water Management in the Humid Tropics*. UNESCO. Cambridge: Cambridge University Press, pp. 571–574.
- Chappell, N. A., Sherlock, M., Bidin, K., McDonald, R., Najman, Y., and Davies, G., 2007. Runoff processes in Southeast Asia: role of soil, regolith and rock type. In Sawada, H., Araki, M., Chappell, N. A., La Frankie, J. V., and Shimizu, A. (eds.), *Forest Environments in the Mekong River Basin*. Japan: Springer, pp. 3–23.
- Chaves, J., Neill, Ch., Germer, S., Gouveia Neto, S., Krusche, A., and Elsenbeer, H., 2008. Land management impacts on runoff sources in small Amazon watersheds. *Hydrological Processes*, **22**, 1766–1775.
- Elsenbeer, H., 2001. Hydrologic flowpaths in tropical rainforest soils: a review. *Hydrological Processes*, **15**, 1751–1759.

Cross-references

- [Ecohydrology](#)
[Hydropedological Processes in Soils](#)
[Infiltration in Soils](#)
[Parent Material and Soil Physical Properties](#)
[Rainfall Interception by Cultivated Plants](#)
[Tropical Soils, Physical Properties](#)

TROPISMS

See [Plant Tropisms, Physics](#)

TURBIDITY

Ewa A. Czyz^{1,2}, Anthony R. Dexter¹

¹Department of Soil Science Erosion and Land Conservation, Institute of Soil Science and Plant Cultivation (IUNG-PIB), Puławy, Poland

²Rzeszów University, Rzeszów, Poland

Introduction

Turbidity basics

The term turbidity refers to the cloudiness of a suspension. This cloudiness is caused by the presence of colloidal

particles that have sizes smaller than about 1,000 nm. These particles scatter light because they have a refractive index that is different from that of the suspending liquid. When the particles have sizes smaller than the wavelength, λ , of visible light (red light has $\lambda \approx 750$ nm whereas violet light has $\lambda \approx 380$ nm), then the Rayleigh scattering theory may be used. In the more general case of any ratio between particle size and the wavelength of the radiation, then the more complex Mie solution to Maxwell's equations must be used.

Measurement of the proportion of light that is scattered is the preferred method of turbidity measurement. Measurement of absorption of light is not satisfactory because absorption is also sensitive to the color of a solution whereas the scattering of light is not. Scattering is a function of the solid particles in suspension only.

Here, as an example, we consider the dispersion of soil colloidal particles in aqueous suspension, although the same principles apply to other types of dispersed particles. In the case of soils, it is mostly the clay particles that cause turbidity although there may also be a contribution from organic colloids present.

Dispersion and flocculation of colloidal particles

Colloidal particles can spontaneously disperse (separate) or flocculate (group together) when in suspension depending on several factors. These processes are extremely important for the environment and for agriculture as well as for a wide range of industrial processes.

It is necessary to be careful with terminology here: the term *stable* is used by colloid scientists to refer to the stability of a suspension (i.e., a fully dispersed state). In contrast, soil scientists use the term *stable* to refer to the flocs (i.e., a fully flocculated state). Usually, in soil science, we want the colloidal particles to be flocculated so that they can contribute to the structure and stability of soil.

Dispersion is greater when soil has a low content of organic matter, a high input of mechanical energy (i.e., is intensively tilled), a high content of exchangeable sodium, and a high pH. Also, a low concentration of dissolved salts in the pore water (as can be measured by electrical conductivity, EC), increases colloid dispersion. Flocculation can be increased by replacement of sodium by calcium, by using lower energy tillage practices and by building up the soil organic matter content.

Environmental consequences of dispersed particles

Dispersible clay within soil makes the soil hard setting upon drying. In simple terms, we can imagine that the clay “clogs” the micro-cracks that otherwise make the soil friable and easy to till. Such a soil will also tend to have a lower hydraulic conductivity and water infiltration rate and will tend to be anaerobic. Dispersible clay contributes in this way to the problems of surface sealing and crusting. The presence of dispersible clay is therefore associated with poor soil quality whereas the absence of dispersible clay is associated with good soil quality.

The brown coloration of runoff water from land during storms indicates the presence of soil particles in suspension. The turbidity of runoff water therefore shows that soil erosion is occurring. This turbidity travels with the water down into streams and rivers where the turbidity is a sensitive measure of the water quality.

A range of materials can be adsorbed onto the surfaces of soil particles and will therefore be transported in the environment if the particles are transported. These materials include plant nutrients (such as phosphate) that can cause eutrophication (e.g., algal “blooms”) in water reserves such as lakes and the sea, heavy metals that can be toxic in the food chain, and also microorganisms that can have the potential to spread diseases.

Methodology

Equipment

Turbidity is measured with a turbidimeter. This equipment has a source of white light (most commonly a tungsten filament lamp). The intensity of light that is scattered at some angle (e.g., 90°) by the particles in suspension is detected and measured as a proportion of the forward-transmitted light. This is the principle of a ratio turbidimeter. The ratio mode of operation has the advantage that the measured values are independent of fluctuations in the intensity of the light source due to power supply variations or aging of the filament lamp.

A valuable feature of this method is the highly linear relationship between the turbidimeter measurements in NTU (or nephelometric turbidity units) and the concentration of the colloids in the suspension (mass colloids per volume of suspension). Colloid concentrations in suspension can be measured easily by turbidimetry over a range of 1:10⁵. A turbidimeter should be calibrated periodically using freshly prepared Formazin primary turbidity standards.

Factors to be considered

(a) Antecedent water content

It has been found that drying of soil samples causes big reductions in the content of readily dispersible clay (RDC) and that this effect can be essentially irreversible (Dexter et al., 2010). Therefore, soil for assessment of RDC should be collected at the end of a long, wet period (e.g., winter in Europe), and should not be allowed to dry during storage before measurement. It is recommended that soil to be measured should have a water content corresponding to field capacity (here defined as a pore water suction of 100 cm water).

Note that soil that has been dried cannot be rewetted and used to assess the condition of soil as it was in the field. Drying and rewetting changes the soil profoundly and in effect, it produces a new material. Therefore, soil should be used only when it is freshly collected in a moist condition from the field.

Some effects of climate on the RDC content of soil and the consequences for soil strength were reported by Kay and Dexter (1992).

(b) Dispersion techniques

As a standard, but arbitrary, procedure we take a known weight (about 5 g) of moist soil that has been collected in the field with minimum disturbance, and drop it into about 50 mL of distilled water in a 150 mL plastic bottle. We then add distilled water to make a total of 125 mL of suspension. Note that the remaining 25 mL of air space in the bottle must be accurate because it affects strongly the energy imparted when the bottles are inverted.

The soil is allowed to stand in the water for 1 h, then the bottles are inverted four times to apply a small, standard input of mechanical energy to disperse the readily dispersible particles. Then the bottles are allowed to stand overnight for 18 h for the larger particles to settle to the bottom of the bottles leaving the RDC in suspension. The next morning, 30 mL of suspension is collected from the center of each plastic bottle and put into a clean, glass turbidimeter cell. The turbidity is then measured with the turbidimeter in NTU.

The turbidity due to the RDC is then expressed in terms of dry mass of soil per liter of suspension to give a normalized result in NTU/(g L⁻¹). The dry mass is calculated from the known sample weight and the gravimetric water content of the soil, which must be measured on a separate sample. It is also useful to measure the electrical conductivity (EC) of the suspension after measurement of the turbidity to check that conditions for flocculation were not present.

Experimental procedures for measurement of RDC by turbidimetry have been described in greater detail by Czyż et al. (2002), Czyż and Dexter (2008) and updated procedures are given in Dexter et al. (2010).

Examples of results

Effects of mechanical energy inputs

Any process that disturbs soil, for example, by shearing or compaction, can break bonds between soil particles and therefore has the potential to make soil particles more dispersible. Mechanical energy inputs from agricultural machinery (e.g., tillage implements) can destabilize soil in this way. Reducing the energy input can reduce the degree of destabilization. For example, it has been found that the use of reduced tillage (tynes working at 10-cm depth) instead of conventional tillage (moldboard plowing to 25-cm depth) resulted in lower content of RDC in soil (Czyż and Dexter, 2008).

A simple laboratory apparatus for applying known amounts of mechanical energy to soil samples has been developed (Watts et al., 1996a). These applied energies were related to the energies applied by different tillage implements to soil in the field (Watts et al., 1996b). Specific energy inputs of 100 and 300 J kg⁻¹ were found to correspond to deep plowing and to tractor-powered rotary cultivation, respectively. RDC increased with increasing energy input only at water contents wetter than the lower plastic (Atterberg) limit.

Effects of organic matter

Land use, including different cropping, affects the content of RDC in soil. The greatest effect is on the amount of organic matter, but there is also an effect of the quality of the organic matter. The most effective seems to be the organic matter produced by the decomposition of grasses. This has a high content of hydroxyl and carboxyl chemical groups.

How much organic matter is required to stabilize soil? It has been found for a range of French, Polish, and UK soils that the content of organic matter (%) required to stabilize soils is approximately 0.172 times the clay content (%). This content of organic matter, if it is in humified form, is sufficient to form stable complexes with all of the clay present (Dexter et al., 2008). The non-complexed clay in soils comprises the RDC. Clay-organic complexing can reduce the RDC to very low levels.

Organic matter not only stabilizes soil through reducing the content of RDC, but it also reduces the sensitivity of soil to destabilization by mechanical energy inputs (Watts and Dexter, 1997).

Dispersible clay in relation to soil physical quality

The physical quality of soil relates to its ability to fulfill a range of functions. For agriculture and the environment, it is important that excess water can drain rapidly, that the soil is well aerated and that the soil is easily workable by tillage implements over a reasonable range of water contents. Soil can fulfill all of these functions if it has a suitable structure that is stable in water. We have already seen above that the presence of RDC indicates lack of stability in water.

The S-index of soil structure is based on the shape of the water retention curve, which is itself a function of the pore size distribution in soil (Dexter and Czyż, 2007). It has been found that the S-index is a good indicator of soil physical quality.

Correlation of values of RDC with values of the index S of soil physical quality show that soil has a “good” soil physical quality if less than 40% of the clay is RDC and has a “poor” soil physical quality if more than 40% of the clay is RDC.

This inference illustrates how the value of RDC, as can be easily measured with a turbidimeter, can be used as an indicator of the physical condition of soil.

Bibliography

- Czyż, E. A., and Dexter, A. R., 2008. Soil physical properties under winter wheat grown with different tillage systems at selected locations. *International Agrophysics*, **22**, 191–200.
- Czyż, E. A., Dexter, A. R., and Terelak, H., 2002. Content of readily-dispersible clay in the arable layer of some Polish soils. In Pagliai, M., and Jones, J. (eds.), *Sustainable Land Management – Environmental Protection – A Soil Physical Approach. Advances in GeoEcology* 35. Reiskirchen: Catena, pp. 115–124.

Dexter, A. R., and Czyż, E. A., 2007. Application of S-theory in the study of soil physical degradation and its consequences. *Land Degradation and Development*, **18**, 369–381.

Dexter, A. R., Richard, G., Arrouays, D., Czyż, E. A., Jolivet, C., and Duval, O., 2008. Complexed organic carbon controls soil physical properties. *Geoderma*, **144**, 620–627.

Dexter, A. R., Richard, G., Czyż, E. A., and Davy, J., 2010. Clay dispersion from soil as a function of antecedent water potential. *Soil Science Society of America Journal*, (in press).

Kay, B. D., and Dexter, A. R., 1992. The influence of dispersible clay and wetting/drying cycles on the tensile strength of a red-brown earth. *Australian Journal of Soil Research*, **30**, 297–310.

Watts, C. W., and Dexter, A. R., 1997. The influence of organic matter in reducing the destabilization of soil by simulated tillage. *Soil and Tillage Research*, **42**, 253–275.

Watts, C. W., Dexter, A. R., Dumitru, E., and Arvidsson, J., 1996a. An assessment of the vulnerability of soil structure to destabilisation during tillage. Part I – a laboratory test. *Soil and Tillage Research*, **37**, 161–174.

Watts, C. W., Dexter, A. R., and Longstaff, D. J., 1996b. An assessment of the vulnerability of soil structure to destabilisation during tillage. Part II – field trials. *Soil and Tillage Research*, **37**, 175–190.

Cross-references

[Flocculation and Dispersion Phenomena in Soils](#)

[Hardsetting Soils: Physical Properties](#)

[Organic Matter, Effects on Soil Physical Properties and Processes](#)

[Soil Aggregates, Structure, and Stability](#)

[Soil Physical Quality](#)

[Soil Surface Sealing and Crusting](#)

TURF

A block from the soil surface with the grass growing on it, and with roots and soil cohering.

TURGOR PRESSURE

The pressure exerted by water inside the plant cell against the cell wall.

TWO-PHASE FLOW

The simultaneous flow in the soil of two fluids, either immiscible (e.g., air and water, or petroleum and water) or miscible (e.g., saline and fresh water).

Bibliography

- Introduction to Environmental Soil Physics (First Edition) 2003
Elsevier Inc. Daniel Hillel (ed.) <http://www.sciencedirect.com/science/book/9780123486554>

U

UNDERGROUND RUNOFF

Water that leaks to stream channels after infiltration into the ground.

UNSATURATED ZONE

See [Vadose Zone](#)

Cross-references

[Hydraulic Properties of Unsaturated Soils](#)

UNSTEADY FLOW

Water flow in soil which properties of the flow change with respect to time.

URBAN SOILS, FUNCTIONS

Thomas Nehls, Gerd Wessolek
Department Soil Conservation, Technische Universität Berlin, Berlin, Germany

Definition

Urban soils are anthropogenically altered soils characterized by contamination, compaction, soil sealing, as well as deposition, removal, or mixing of technogenic and natural substrates. Urban soils are primarily situated in urban areas and exhibit a high spatial heterogeneity, but are also

typical of industrialized, transport, and mining sites (Morel et al., 2005).

They are formed over a dynamic sequence of soil-building processes, influenced by frequently changing of land use types and a spectrum of human impacts throughout history. Even when ecological characteristics are substantially changed, urban soils can still fulfill the same functions as natural soils (see [Soil Functions](#)), although to varying extents.

Urban soils predominantly provide the physical basis for technical, industrial, and socioeconomic structures in cities. Soils are used to support housing settlements, traffic infrastructure, all kinds of cultural life, waste disposal facilities, and to supply natural resources. Due to these functions, soils are often mixed, compacted, or sealed to meet construction requirements. Industrial production, automotive traffic, and waste disposal often result in soil contamination, leading to a significant restriction of other vital soil functions.

In developed countries, urban soils are usually not used for [Biomass](#) production except in urban forests, inner-city gardens, and parks. In contrast, urban agriculture is of increasing importance in developing countries, especially in mega cities, where populations often engage in subsistence or subsidiary farming within city limits (Mugeot, 2005).

Inner-city agricultural plots are often irrigated and fertilized with sewage, which improves productivity but involves risks of food contamination (Singh et al., 2004).

Urban soils act as a biodiversity pool and gene reservoir as they comprise a great variability of ecological niches. Extreme site characteristics of urban soils such as high temperature, salinity, drought, or contaminations, as well as special carbon sources such as sewage, oil, or polycyclic aromatic hydrocarbons, can promote changes

in the abundance of rare species. (Lysak et al., 2000; Reineke, 2001).

Urban soils can still fulfill storage, filter, buffer, and transformation functions, which are of high ecological relevance as urban areas are often polluted. These soil functions may be limited due to soil sealing, conductive and sorption-low construction materials, diminished biological activity, and old contamination deposits (Nehls et al., 2008). The thickness of urban soils often increased due to deposition of materials while the groundwater often depleted due to drinking water abstraction (e.g., Mexico City). Thus, the larger soil column may filter, store and transform more pollutants, carbon, and nutrients. The higher soil pH of urban soils compared to nonurban soils may positively influence the filter and transformation function for some contaminants.

Urban soils can also provide *Raw Materials*. Apart from drinking water and water for industrial production, soil raw materials like gravel, sand, clay, minerals, and organic material are of minor relevance in urban areas. Urban soils especially function as archives of geological and archaeological heritage. For hundreds and thousands of years, cities grew on the residues of the former civilizations. Urban soils contain and preserve artifacts from every phase of settlement periods. Wood, tiles, bricks, perfume or milk bottles, ammunition, plastics, or chocolate wrappers shed light on various aspects of everyday life of former urban populations.

Bibliography

Lysak, L. V., Sidorenko, N. N., Marfenina, O. E., and Zvyagintsev, D. G., 2000. Microbial complexes in urban soils. *Eurasian Soil Science*, **33**, 70–75.

- Morel, J.-L., Schwartz, C., Florentin, L., and de Kimpe, C., 2005. Urban soils. In Hillel, D. (ed.), *Encyclopedia of Soils in the Environment*. Oxford: Elsevier, pp. 202–208.
- Mugeot, L. J. A., 2005. *Agropolis: The Social, Political, and Environmental Dimensions of Urban Agriculture*. London/Sterling: Earthscan.
- Nehls, T., Jozefaciuk, G., Sokolowska, Z., Hajnos, M., and Wessolek, G., 2008. Filter properties of seam material of paved urban soils. *Hydrology and Earth System Sciences*, **12**, 691–702.
- Reineke, W., 2001. Aerobic and anaerobic biodegradation potentials of microorganisms. In Beek, B. (ed.), *The Handbook of Environmental Chemistry*. Berlin: Springer, Vol. 2, Part K, pp. 1–161.
- Singh, K. P., Mohan, D., Sinha, S., and Dalwani, R., 2004. Impact assessment of treated/untreated wastewater toxicants discharged by sewage treatment plants on health, agricultural, and environmental quality in the wastewater disposal area. *Chemosphere*, **55**, 227–255.

Cross-references

- Compaction of Soil
Horticulture Substrates, Structure and Physical Properties
Irrigation with Treated Wastewater, Effects on Soil Structure
Management Effects on Soil Properties and Functions
Nature Conservation Management
Subsoil Compaction
Soil Functions
Soil Surface Sealing and Crusting
Water Balance in Terrestrial Ecosystems

UTILITY VALUE OF CEREALS

See *Cereals, Evaluation of Utility Values*

V

VADOSE ZONE

The generally unsaturated soil and the underlying porous strata that overlie the permanent water table. It is also called the “unsaturated zone” or the “aerated zone,” in contrast with the saturated zone that lies underneath the water table.

Bibliography

Introduction to Environmental Soil Physics (First Edition) 2003
Elsevier Inc. Daniel Hillel (ed.) <http://www.sciencedirect.com/science/book/9780123486554>

VAN DER WAALS FORCES

Binding force which arises from an induced dipole in a normal molecule which induces a dipole in another molecule thus causing an attraction between them.

Bibliography

Glossary of Soil Science Terms. Soil Science Society of America. 2010. <https://www.soils.org/publications/soils-glossary>

Cross-references

[Conditioners, Effect on Soil Physical Properties](#)

VAN GENUCHTEN EQUATION

Model for predicting the hydraulic conductivity of unsaturated soils.

Bibliography

Van Genuchten, M. Th. 1980. A closed form equation for predicting hydraulic conductivity of unsaturated soils. *Soil Society of America Journal*, **44**: 892–898.

Cross-references

[Hydraulic Properties of Unsaturated Soils](#)
[Pedotransfer Functions](#)
[Soil Water Flow](#)

VAPOR PRESSURE

The partial pressure of water vapor in the atmosphere. It depends on the pressure and temperature of the atmosphere, as well as on the state of water in a water-containing body (such as soil) at equilibrium with the atmosphere.

Bibliography

Introduction to Environmental Soil Physics (First Edition) 2003
Elsevier Inc. Daniel Hillel (ed.) <http://www.sciencedirect.com/science/book/9780123486554>

VISCOSITY

The resistance of a fluid to shear (i.e., to a force causing the adjacent layers of the fluid to slide over each other). That resistance is proportional to the velocity of the shearing. As such, viscosity can be visualized as the fluid's internal friction.

Bibliography

Introduction to Environmental Soil Physics (First Edition) 2003
Elsevier Inc. Daniel Hillel (ed.) <http://www.sciencedirect.com/science/book/9780123486554>

VISIBLE AND THERMAL IMAGES FOR FRUIT DETECTION

Duke M. Bulanon¹, Thomas F. Burks¹, Victor Alchanatis²

¹Agricultural and Biological Engineering Department,
University of Florida, Gainesville, FL, USA

²Agricultural Research Organization, Volcani Center,
Institute of Agricultural Engineering, Bet Dagan, Israel

Definition

Machine Vision. A combination of imaging sensor and image processing to provide visual perception to machines.

Visible imaging. The application of machine vision using imaging sensors that operate within the visible region of the electromagnetic spectrum (400–700 nm).

Thermal imaging. The application of vision systems using imaging sensors that are sensitive to infrared radiation (7.5–15 μm).

Fruit robotic harvesting

Fruit and vegetable production in the USA is facing growing national and international market pressures that is affecting the economic viability of the agricultural products. Inexpensive imported produce, which freely flows in the US market, is a pressing concern resulting in the US Congress passing the Food, Conservation, and Energy Act, which provides funding for the Specialty Crop Research Initiative. This initiative is aimed toward specialty crop research, which includes fruits and vegetables, to develop science-based tools and technologies that can improve production efficiency, production quality, and postharvest operations (Burks et al., 2008).

Harvesting is a labor-intensive process and takes about 30–60% of the fruit production cost for apples and citrus. This has become a problem for farm producers with the uncertain availability of farm labor force and the increasing cost of harvesting. Mechanization of farming operation such as harvesting could solve this labor shortage dilemma and increase production efficiency (Srivastava et al., 2006). In the 1960, the mechanization of harvesting started with root and surface crops. By mid-1980, researchers developed mechanical mass harvesters for tree crops, and citrus had received much attention. Mechanical citrus harvesters remove fruit by some form of mechanical shaking applied to the tree (Brown, 2002). Some of the harvesters developed were canopy shaker, canopy pull and catch, trunk shake and catch, and continuous air shake. However, the commercial use of these harvesters has been limited mainly because of the damage to fruit and tree. Schertz and Brown (1966) recognized the

potential of individual fruit removal by mechanical means when they observed that 70–100% of oranges were visible from outside the canopy. The idea of Schertz and Brown gave way to the line of sight concept and eventually to robotic harvesting. This concept requires the detection of a fruit using an optical sensor, and then a fruit picking device can be guided along this line of sight toward the fruit.

Over the years, researchers have developed robotic harvesting prototypes for fruits like apples (Bulanon and Kataoka, 2010), cherries (Tanigaki et al., 2008), cucumbers (Van Henten et al., 2003), oranges (Plebe and Grasso, 2001; Bulanon et al., 2009), and tomatoes (Kondo et al., 1996). The robots developed by these researchers include four basic components: machine vision to detect the fruit, end-effector to detach the fruit, manipulator to extend the end-effector, and traveling system. In the following sections, we will cover machine vision systems for fruit detection, specifically visible imaging and thermal imaging.

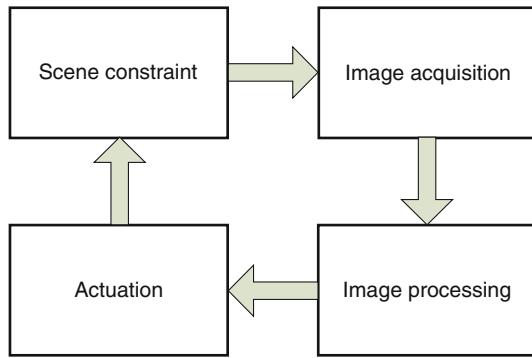
Machine vision

The first major task of a fruit harvesting robot is to recognize the fruit on the tree. Although locating the fruit on the tree is easy for human pickers, this task is challenging when applied to robotic harvesting. The robot has to locate the fruit, with variable color, shape, and size, and is randomly positioned in the tree. The robot is also subjected to various environmental conditions and usually operates under natural lighting condition. However, Parrish and Goksel (1977) demonstrated the feasibility of using machine vision to locate fruits on the tree. Since then, several researchers have used machine vision as a visual sensor to guide their harvesting robot prototypes.

Machine vision can be defined as a combination of an imaging sensor and image processing to provide visual perception to machines. The typical components of a machine vision system are lighting, image acquisition system, and a processing unit, usually a personal computer. In addition, a special software is developed to perform image processing functions. Awcock and Thomas (1996) defined a generic model for a machine vision system and this model can be adapted to robotic fruit harvesting application. The model, which is shown in Figure 1, is composed of four elements: scene constraint, image acquisition, image processing, and actuation.

Scene constraint

The scene constraint refers to the environment where the machine vision will operate. For fruit harvesting, the environment is the orchard or possibly a greenhouse. Included in the scene constraint is lighting. Lighting is a critical component in machine vision because it illuminates the object of interest. The color of an object is perceived differently depending on illumination. In the orchard, the primary source of lighting is the sun. This natural source of illumination is affected by the solar angle and cloud cover; therefore,



Visible and Thermal Images for Fruit Detection,
Figure 1 Generic model of machine vision system. The model has four elements: scene constraint (where target object is located), image acquisition, image processing, and actuation.

the machine vision implementation should take into account the lighting variability. Some researchers have supplemented their vision system with artificial lighting to eliminate lighting variation but this is still difficult to do in the field. Artificial lighting is useful for nighttime image acquisition. Results of fruit detection for nighttime-acquired images had a better performance compared to images acquired during the daytime (Sites and Delwiche, 1988).

Another component of scene constraint is the structure of the environment. In factory application, the object of interest is fixed, thus it is easy to locate. Moreover, the designer could simplify the background to facilitate image processing. However, in orchard application, the trees come in different shapes and sizes, and the fruits are randomly positioned in the tree. There are two ways to approach the unstructured condition of the orchard (Sarig, 1993). One is to adapt the robotic system to the present crop cultivation practice. The second approach to change the plant training system to adapt to the robotic system.

Image acquisition

Image acquisition is the subsystem responsible for capturing the scene into an image and saving to memory or disk, which can be processed to extract the required features. For example, in robotic harvesting, the robot needs the 3-D position of the fruit to pick it from the tree. Although the captured image provides 2-D information, there are techniques like stereo imaging that provides the depth information (Kondo and Ting, 1998).

The images can be acquired using a simple photodiode array, a monochrome or color video camera, or a thermal camera. At present, the solid-state image sensor is commonly used in robotic applications. Most monochrome and color video cameras use this type of sensor. The solid-state sensor consists of an array of photosensitive elements. One of the most popular solid-state sensor is the charge-coupled device (CCD), which has a high resolution and has a sensitivity from the visible region to the infrared region (400–1,200 nm).

On the other hand, a thermal camera or an infrared camera images the emitted infrared radiation from a scene. The sensor of a typical thermal camera consists of an array of infrared sensitive detectors known as microbolometer. When infrared radiation strikes a microbolometer, the radiation changes its electrical resistance, which can be measured, and creates the thermal image.

Image processing

After the image is acquired, the next task is to extract the features. Image processing is a technique to manipulate images with the goal of enhancing the image for human consumption or extracting useful information from the image (Castleman, 1996).

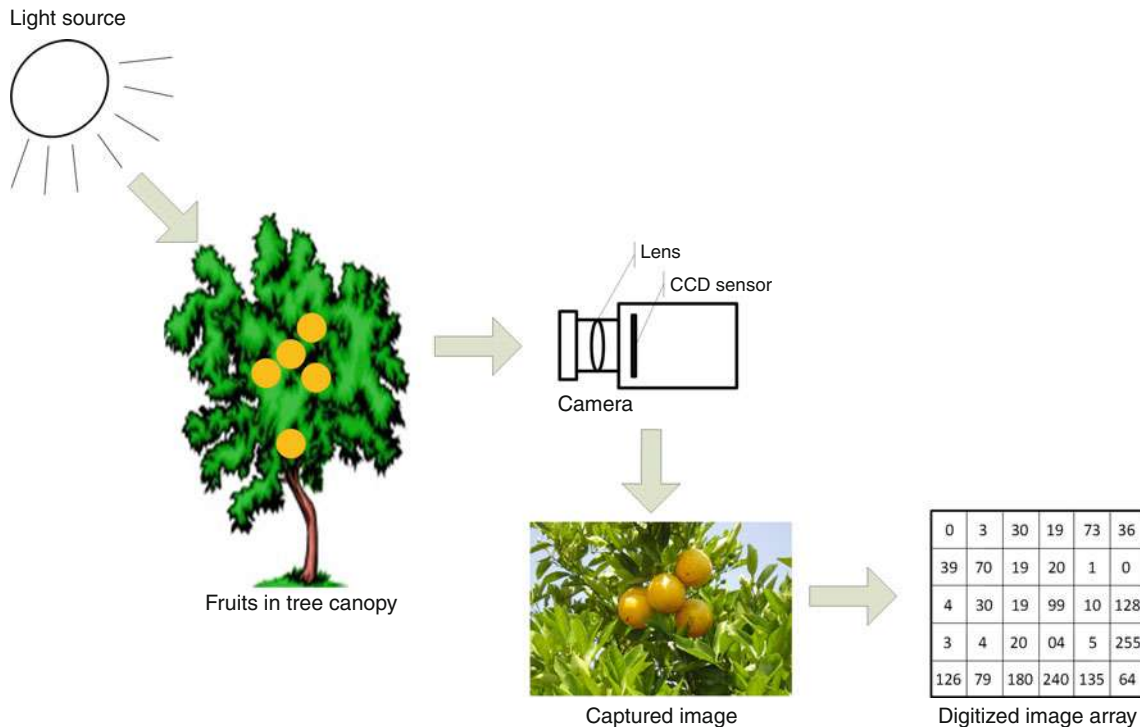
For robotic fruit harvesting application, the goals of image processing are to recognize the fruit and determine its position. The image processing for robotic application has four steps: preprocessing, segmentation, feature extraction, and classification. Preprocessing involves the manipulation of the image to make it suitable for the subsequent operation. Examples of preprocessing are cleaning up noise in the image and separating the red, blue, and green channels of a color image, or transformation from spatial domain to frequency domain. The next step, which is segmentation, is the most critical stage in fruit recognition. Segmentation separates the fruit from the background such as leaves, branches, sky, and ground. In the simplest case, the image is separated into a fruit region and a non-fruit region. Thresholding is one of the widely used segmentation techniques especially if the object has a different intensity than the background (Gonzalez and Woods, 1992). After the fruit is separated, the features of the fruit region are extracted. These are the area, perimeter, radius, and the number of the fruits. These features are used to guide the approach of the robot toward the fruit.

Actuation

Actuation completes the machine vision system model. It is the response of the system to the scene. When applied to robotic fruit harvesting, first the robot explores the scene and looks for mature high-quality fruits. Second, when the fruit is found and its position is determined, the robot approaches the fruit using the information from the image. This method of using an image to control robot motion is known as visual servoing (Spong et al., 2006).

Visible imaging

Figure 2 shows the basic process of visible image acquisition in the field. A light source, usually the sun, provides the source of illumination. Artificial light source may also be used when natural lighting is not available. When the canopy is illuminated, the light is reflected and the intensity of the reflected light, which is primarily dependent on the spectral characteristic of the object, is sensed. The captured image is then converted to an array of numbers, which can be manipulated to extract the important features, in this case the fruit.



Visible and Thermal Images for Fruit Detection, Figure 2 Visible imaging in the orchard under natural lighting condition. Spectral reflectance of the canopy is captured by a visible imaging sensor and processing the image to produce a matrix of the numerical representation of the scene.

In visible imaging, the machine vision system is operating in the visible region of the electromagnetic spectrum. The visible region ranges from 400 to 700 nm. Operating in the visible region works very well for fruits that have contrasting color compared to their canopy. Investigation of the spectral reflectance of orange fruits and leaves showed that the mature orange fruit has a different spectral reflectance than the leaf within the visible region specifically at 680 nm, which is the chlorophyll absorption band. It is well established that plants need light for photosynthesis, which is mostly the red and blue light; thus, the leaves reflect the green light (Kondo and Ting, 1998).

Taking advantage of the plant's reflectance properties, researchers used imaging sensors that are sensitive in the visible region. The first published attempt to apply visible imaging for fruit detection was reported by Parrish and Goksel (1977). They used a black and white camera combined with a red filter. The red filter allowed the camera to capture the red wavelength portion of the scene. Sites and Delwiche (1988) also used a monochrome camera supplemented with several different wavelength filters to detect peaches and apples. When color CCD cameras came out to the market, Slaughter and Harrel (1989) were the first of several researchers who used color cameras instead of specific wavelength filtering the scene. They used the color features of citrus fruits combined with a statistical pattern approach to segment the image. Using color has the

advantage of obtaining three bands, which are the red, green, and blue, of the scene instantaneously.

Image processing for visible images

In order to recognize and locate the fruits, the images need to be processed. Jiminez et al., (2000) categorized the basic approaches to image processing for fruit detection into two main groups: local-based and shape-based. These approaches are based on the extracted features used to detect the fruit.

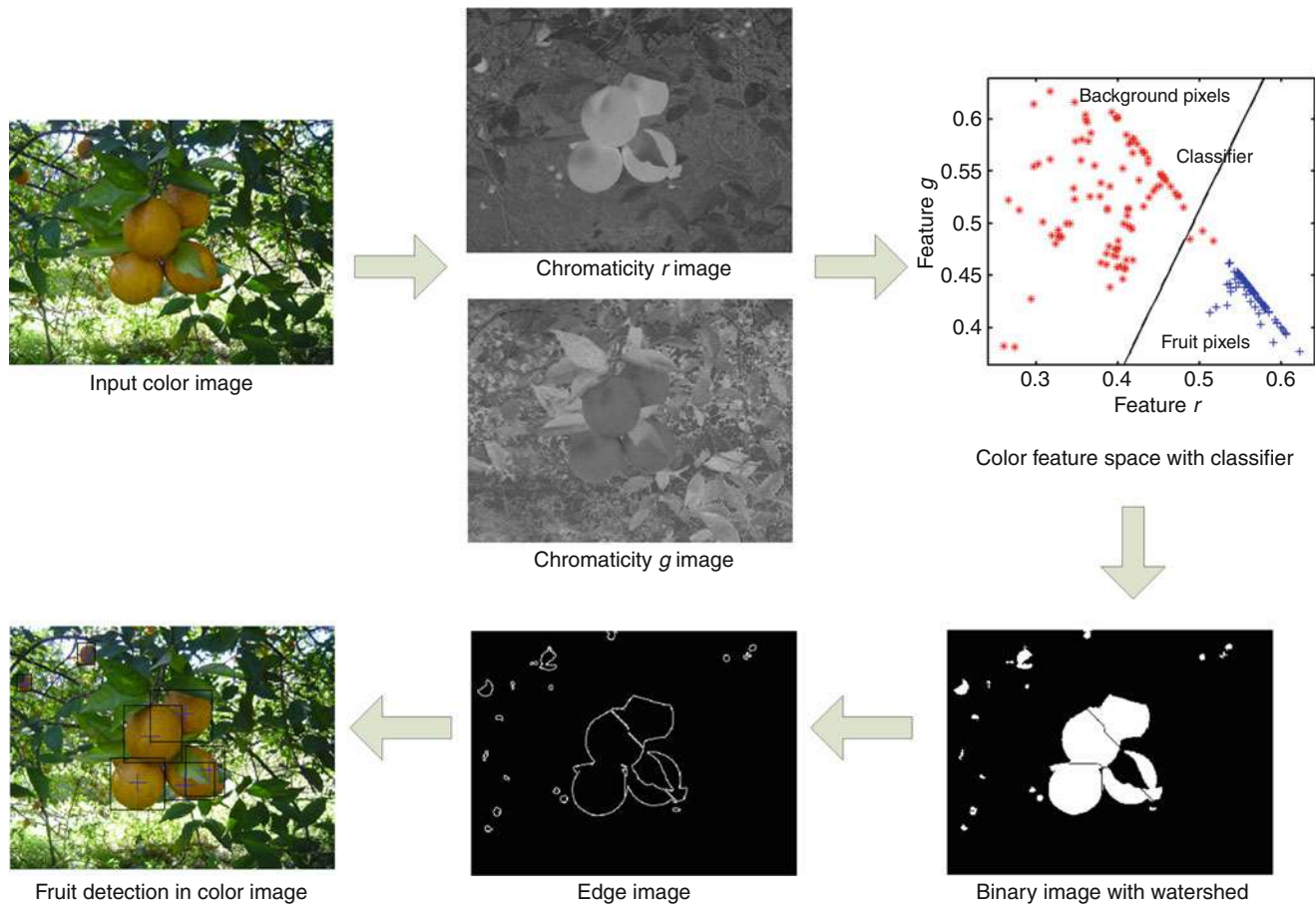
Local-based approach uses the value associated with each image pixel to determine whether it belongs to the fruit class or the non-fruit class (background). For a monochrome camera, the pixel value is based on intensity only, while pixels for color cameras are a function of the red, green, and blue values. These parameters (intensity and RGB) are used in an image segmentation technique to divide the image into regions of identical properties. Generally, for intensity images, the gray level thresholding is used to segment the fruit from the background. This thresholding operation uses the statistical properties of the image (e.g., gray level histogram) to segment the fruit from the image. Also, it requires that objects and background have different levels of intensity. Gray level thresholding is easily implemented in hardware and can be very fast. However, fruit and background are not easily segmented in the orchard.

The color segmentation method is a much better approach than gray level thresholding. However, the challenge of using color segmentation is to determine a group of color characteristics and a pattern recognition technique that would result in an efficient segmentation. Color can be represented using several color models (Gonzalez and Woods, 1992). The RGB color model represents any color using a combination of the three primary colors, red, green, and blue. Another color model that is used is the chromaticity model, which uses the chromaticity coefficients to describe hue and saturation. The chromaticity coefficients are defined as ratio between the intensity of one of the primary colors and the sum of all three. Once the color model is established, the next step is to develop a pattern recognition technique, which uses the color parameters as pattern, to segment the image into fruit class and non-fruit class. Statistical approaches such as linear discriminant classification and Bayesian classifier, and nonstatistical techniques like artificial neural networks are some of the pattern classification methods that have been successfully tested (Burks et al., 2000).

While the local-based approach depends on each pixel value, shape-based approaches analyze edge properties of region that form circular arcs to take advantage of the spherical shape of most fruits. The Circular Hough Transform is commonly used to find circular objects in the image. However, results of shape-based approaches for fruit detection are characterized by significant false detections. Illumination, transitions, shadows, and fruit and leaf occlusions are some of the factors that cause false detection (Plebe and Grasso, 2001).

A visible imaging system for orange fruit detection

In this section, a machine vision system for orange fruit detection is shown here as an example of developing a machine vision system. The machine vision system is composed of a 24-bit color CCD camera that has resolution of 640×480 pixels. The camera is connected to a personal computer through a frame grabber board. Solar lighting provided the source of illumination. The fruit detection process, which is shown in Figure 3, starts with



Visible and Thermal Images for Fruit Detection, Figure 3 Image processing for fruit detection using visible imaging. The chromaticity r and g images of the RGB image is calculated, which enhances the fruit. A linear discriminant classifier can be derived from the chromaticity plot and this can be used to segment the image (binary image). Digital image processing techniques such as watershed algorithm, edge extraction, and blob analysis are combined to detect the fruits in the image.

the color image acquisition. Using the RGB values, the chromaticity r gray level image and the chromaticity g gray level image were created. These two chromaticity coefficients enhance the fruit in the image and they are robust to varying lighting conditions. When the color properties of the fruit and the leaf background were plotted using these two color features, a linear discriminant classifier could be easily derived. The linear classifier was used to separate the fruit from the background, which is shown in the binary image. After segmenting the fruit, a filtering operation removed noise and small segmented regions. Then we applied a watershed algorithm (Gonzalez and Woods, 1992) to separate the fruits in clusters and identify individual fruits. Once the fruits were separated, we extracted the edge of the segmented region and analyzed the circular properties (e.g., radius) of the edge. This edge analysis allows us to detect circles in the region and ultimately detect the location of the fruit in the image. This image processing algorithm is a combination of both local-based and shape-based approaches. It has the advantage of dealing with the illumination problems by using the chromaticity color model, which decouples intensity and solves the problem of occlusion by using the spherical properties of the orange fruit. A similar image processing approach was also applied for the detection of apple fruits with minor modifications in the discriminant's classifier coefficients, and it had good fruit detection performance (Bulanon et al., 2001).

Thermal imaging

In contrast to visible imaging, thermal imaging does not rely on a light source to acquire an image. Instead, thermal imaging uses the electromagnetic radiation emitted from an object, processes the data, and produces a pseudo-image of the thermal distribution of the object. All objects, which have temperature greater than absolute zero, emit thermal radiation. The total amount of thermal radiation is expressed by the Stefan–Boltzmann Law:

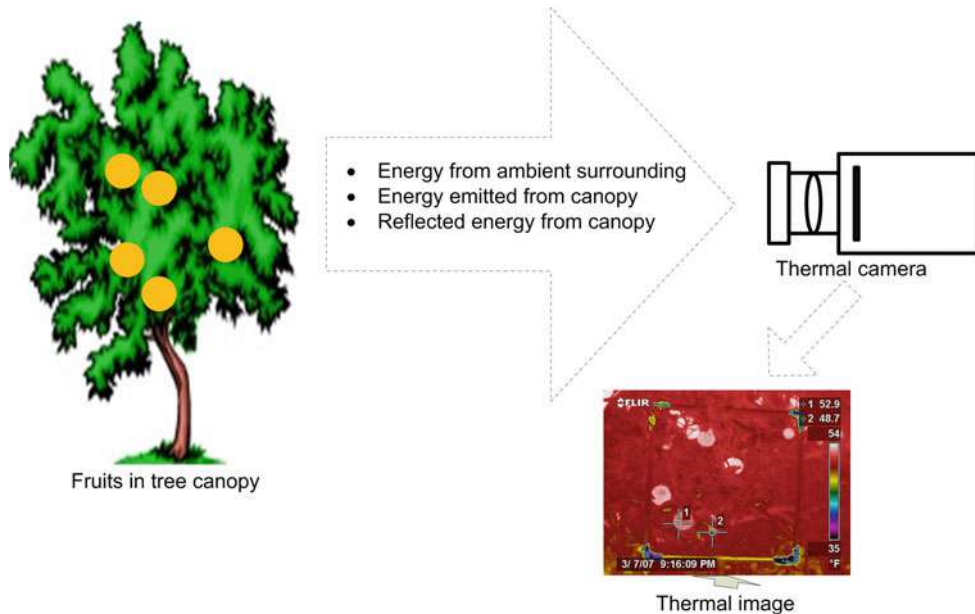
$$E = \varepsilon\sigma T^4 \quad (1)$$

where E is the emitted thermal radiation, ε is the emissivity of the object, σ is the Stefan–Boltzman constant, and T is the absolute temperature. The measurement of the emitted thermal radiation can be used as an indicator of the temperature of the emitting object. This is the underlying concept behind thermal imaging.

When applying thermal imaging to detect fruits in the orchard, other variables aside from the emitting object are taken into consideration. Figure 4 shows the thermal imaging process for fruit detection. The total radiation, E_{total} , received by the camera is:

$$E_{\text{total}} = \varepsilon E_{\text{canopy}} + (1 - \varepsilon)E_{\text{ref}} + (1 - \tau)E_{\text{atm}} \quad (2)$$

where E_{canopy} is the radiation emitted by the canopy (fruit, leaf, and branches), E_{ref} is the radiation from the surrounding environment, which is reflected by the canopy, ε is the emissivity of the canopy, E_{atm} is the radiation emitted by



Visible and Thermal Images for Fruit Detection, Figure 4 Thermal imaging in the orchard. The thermal camera senses the infrared radiation of the canopy including the radiation from the surrounding environment and its reflected radiation. A pseudo-RGB image of the temperature distribution of the canopy is created and this can be used to analyze the thermal variation of the scene.

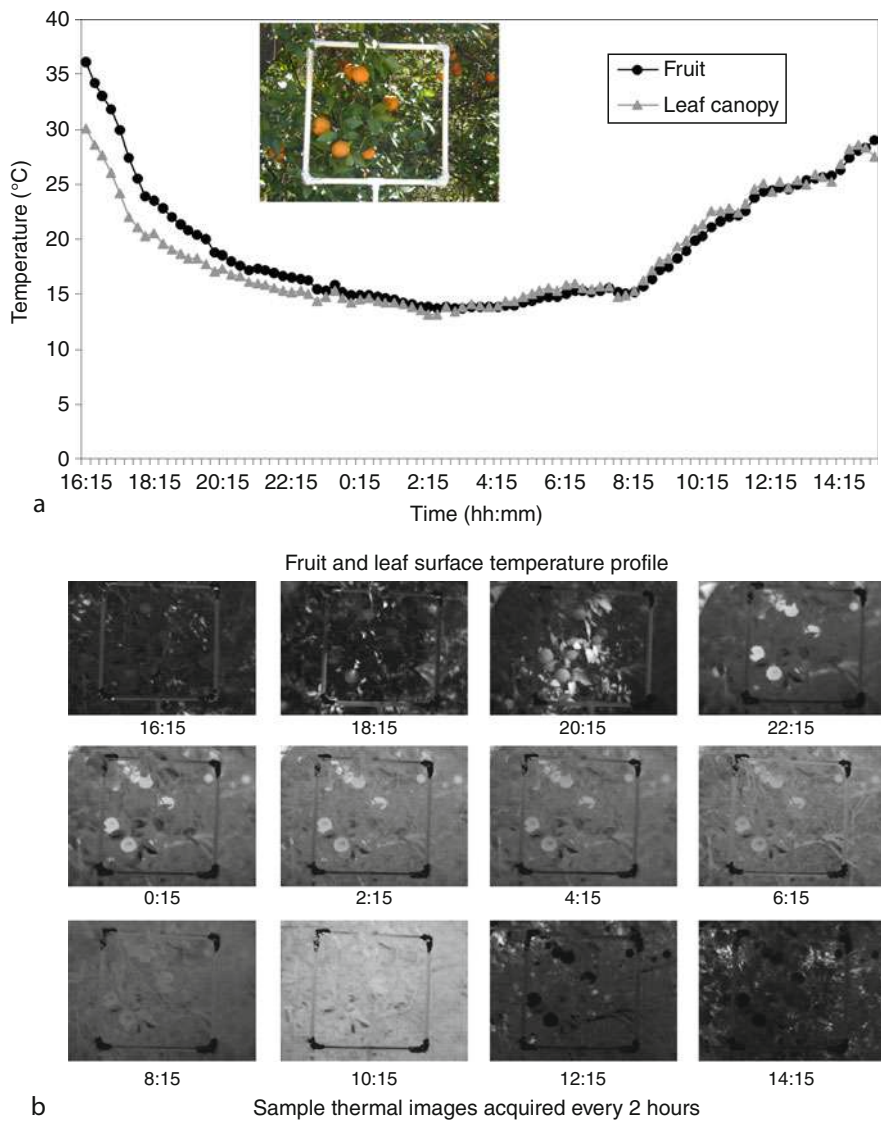
the surrounding environment, and τ is the transmittance of the ambient surrounding. And since we are interested on the fruit, which is part of the canopy, the emitted reflectance of the canopy can be expressed as:

$$E_{\text{canopy}} = \frac{E_{\text{total}}}{\varepsilon} - \frac{(1-\varepsilon)}{\varepsilon} E_{\text{ref}} - \frac{(1-\tau)}{\varepsilon} E_{\text{atm}} \quad (3)$$

which is the general measurement formula to create a thermal image.

Since we are interested in detecting the fruit using the thermal image, there should be a temperature variation between the fruits and the other parts of the canopy such as the leaves to differentiate the fruit using temperature. **Figure 5a** shows a typical 24-h temperature profile

between the fruit and the leaf of an orange canopy. The profile is comparable to a half sinusoid where the temperature rises in the morning until early afternoon and falls from mid-afternoon until early morning. There is not much difference between the fruit and leaf temperature in the early morning until early afternoon; however, temperature variation appears in the mid-afternoon and continues until late in the evening. **Figure 5b**, which are sample images taken over a 24-h-period, shows that the fruits are visible when the temperature of the fruits and the leaves are different. This temperature variation is due to the difference of heat capacity between the two objects and we can take advantage of this phenomenon to detect the fruit using thermal imaging. In the yield monitoring system for apples, Stajnko et al., (2004) acquired apple



Visible and Thermal Images for Fruit Detection, Figure 5 Sample thermal imaging in the field (a) Typical surface temperature profile of fruits and leaves (b) Sample thermal images acquired within a 24-h-period at 2-h-interval.

fruit images late in the afternoon to enhance the detection of fruit in the thermal images.

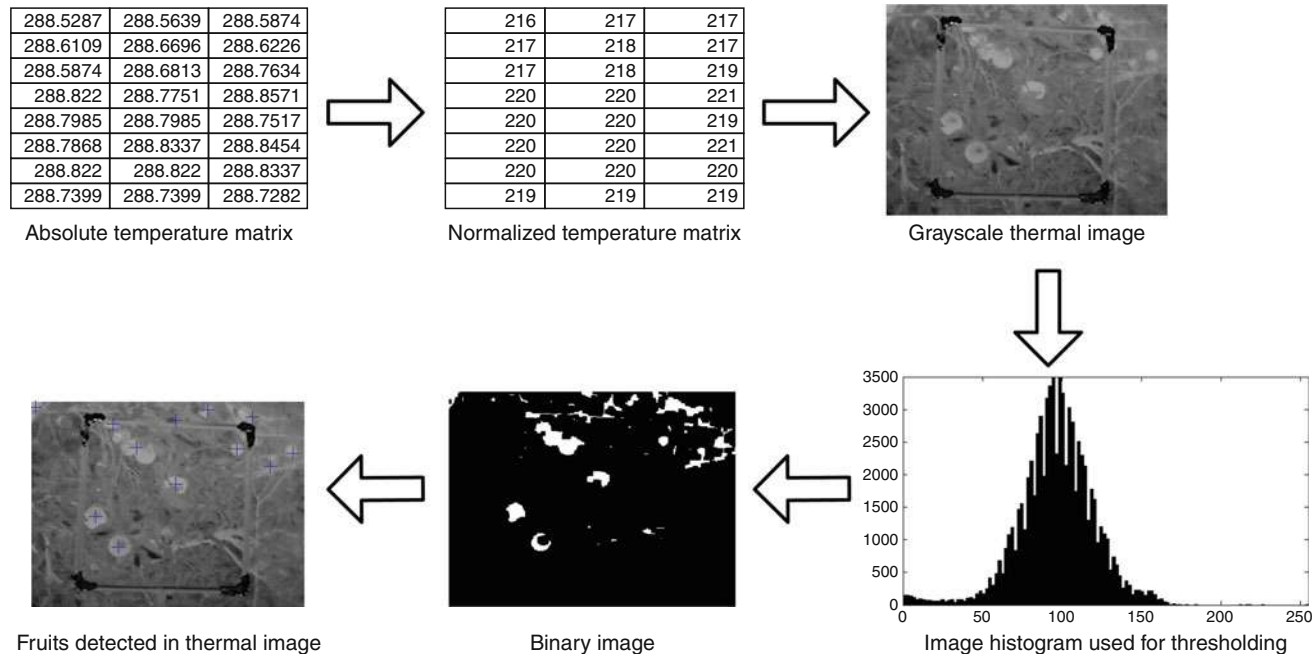
Thermal image processing for fruit detection

The raw data obtained from a thermal camera is a temperature array of the thermal distribution of the object's surface. Transforming this temperature array into an image format is required to create a thermal image and extract the relevant features of the object. [Figure 6](#) shows the flowchart of the digital image processing approach for thermal images. Although this flowchart was designed for orange fruit detection, this could be adapted for other applications as well. First, the raw data of 320×240 matrix of absolute temperature values is converted to an 8-bit gray level image. This transformation allows us to operate on the image using digital image processing techniques. By visual examination of the histogram and knowing that the fruit is warmer than the leaves, we used a thresholding technique called the "histogram-tail" method where the threshold is the sum of the mean intensity of the image and the standard deviation. Pixels with values greater than the threshold were designated as fruit pixels, and pixels below the threshold were marked as background pixels. After thresholding the image, standard digital image processing techniques such as blob analysis, labeling, perimeter and centroid detection are applied to detect the size and position of the individual fruits. Using this method, a fruit detection rate of 0.70 was achieved with a false detection rate of 0.06 ([Bulanon et al., 2008](#)).

Fusion of visible and thermal images

We have seen the potential of visible imaging to detect the fruit especially if it has a color contrast with the canopy. By using thermal imaging, fruits can also be detected provided there is a temperature difference within the canopy. Both imaging systems has its advantages and disadvantages. Thermal cameras do not require a light source for illumination; however, the fruit and the canopy must have a temperature variation. This variation is not constant and changes throughout the day. On the other hand, visible imaging requires illumination and in the orchard, illumination is mainly dependent on natural lighting. The changing solar angles and cloud cover causes lighting variations making fruit detection challenging. Nevertheless, we can combine the advantages of both imaging systems using image fusion.

Image fusion is a branch of multi-sensor fusion where the main goal is to combine information from two or more images of a scene into a single composite image ([Blum and Liu, 2006](#)). The images could come from the same or different sources, for example, combining a visible image and a thermal image. There are several image fusion techniques. These techniques can be classified as being pixel level, feature level, and symbolic level. At pixel level, the fused image is created by combining the individual pixels of the source images. Pixel correspondence between the source images is required for this method; thus the source images are registered prior to fusion. At feature level, feature from the source images are extracted and then combined to generate a new image.



Visible and Thermal Images for Fruit Detection, Figure 6 Image processing for fruit detection using thermal imaging. The temperature matrix is converted to a gray level image. The thermal gray level image can now be processed using techniques applied to RGB images. In this figure, a simple thresholding approach was implemented to compute the binary image and then blob analysis was used to detect the fruit.

Symbolic level fusion refers to processing the source images individually to acquire information and then use a higher level decision technique to combine the information.

Figure 7 shows a flowchart of image fusion to detect fruits using fuzzy logic (Bulanon et al., 2009). Fuzzy logic is widely used in control applications. Using fuzzy logic in image fusion is similar to a weighted averaging approach where the weights are determined using the fuzzy logic inference engine. The first step is fuzzification to convert the source images into information that can be applied to the fuzzy logic fusion rules. The two input membership functions, one for each source image, perform the fuzzification. Then we combine the fuzzified images using the fuzzy fusion rules as follows:

If (thermal is warm) then (fused is fruit)
 If (visible is red) then (fused is fruit)
 If (thermal is cold) and (visible is red) then (fused is fruit)
 If (thermal is average) then (fruit is non-fruit)
 If (visible is non-red) then (fruit is non-fruit)

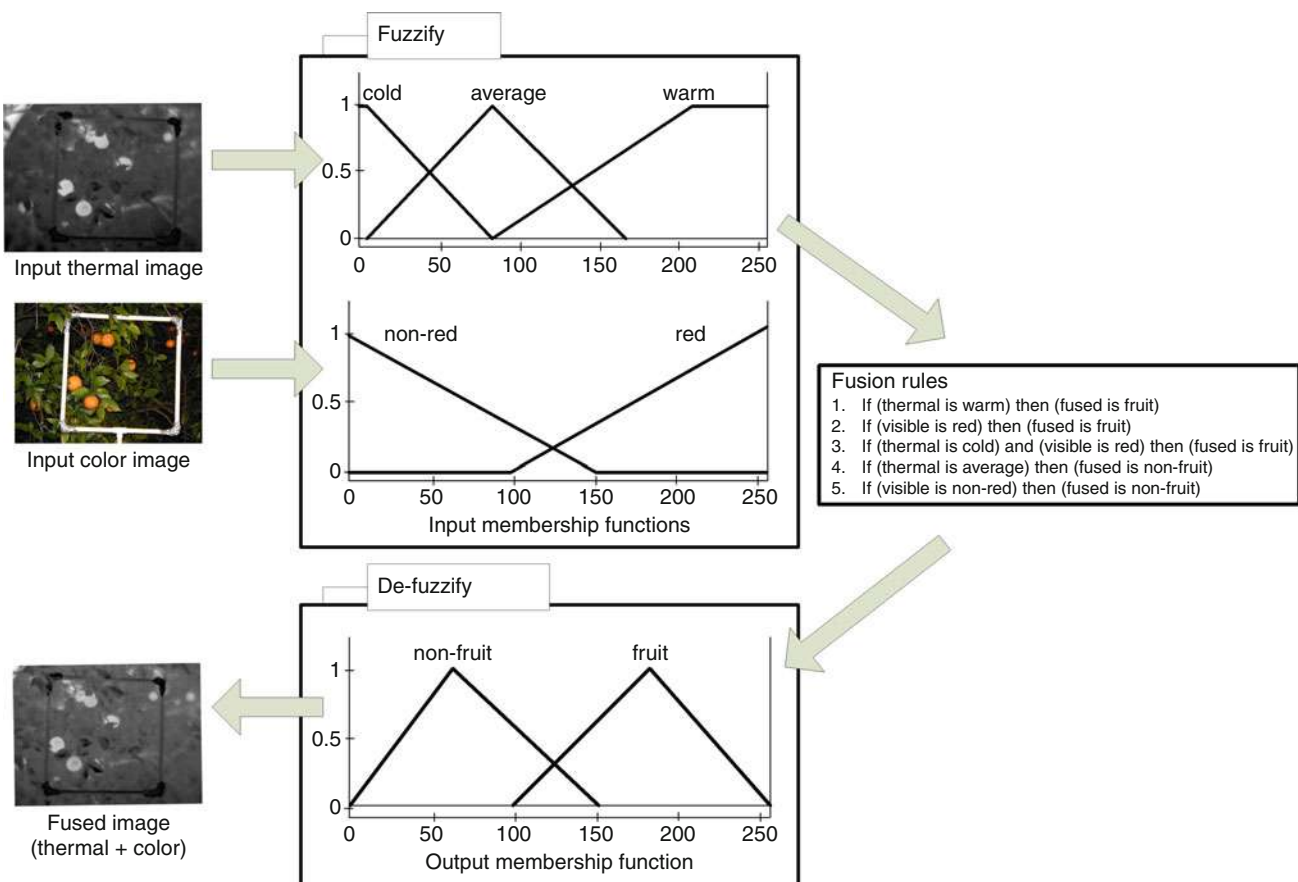
After applying the rules, defuzzification using the output membership function created the fused image.

We found that fruit detection was improved when image fusion was applied. Although there are other fusion techniques available, fuzzy logic is an intuitive approach to combine the thermal and visible images. The membership functions and the fusion rules, which are based on heuristics, closely resemble how humans approach a problem.

Image fusion will play an integral part in future orchard management and planning. Several studies have established the potential of thermal imaging like determining crop stress, irrigation requirement, and disease detection (Alchanatis et al., 2006). Combining these thermal images with other information using fusion techniques will be an effective tool for decision making.

Multispectral imaging

Multispectral imaging is another type of imaging system that has gained increasing popularity in the field of remote sensing, defense, medical field, manufacturing, and agriculture. This imaging system acquires images over contiguous narrow-wavelength intervals across the visible and near-infrared regions and can generate a pixel-level reflectance spectra. Each image is often referred to as a band



Visible and Thermal Images for Fruit Detection, Figure 7 Fusion of visible and thermal images for fruit detection using fuzzy logic. The source input images, color and thermal, are fuzzified so that they can be combined using the fusion rules. These fusion rules were based on the properties of the fruits and its background. The combined data is defuzzified to produce the fused image.

or a channel. Multispectral images contain information about a number of spectral bands where the human eye fails to capture.

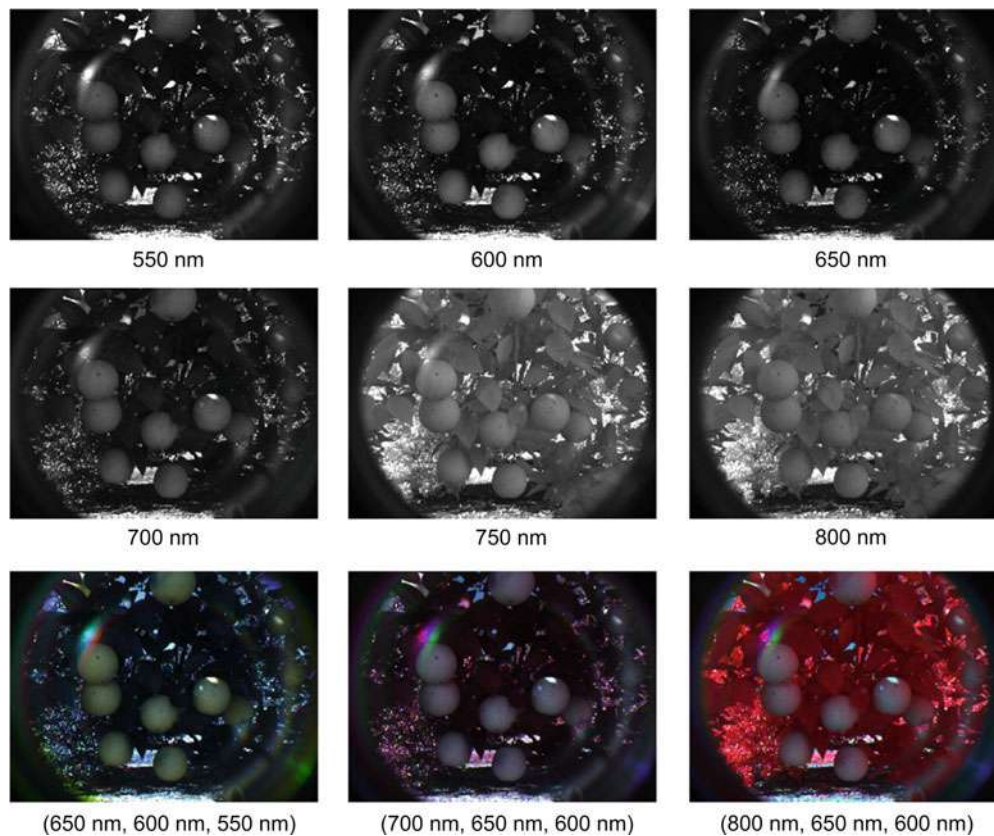
The simplest way to acquire multispectral images is a combination of a CCD monochrome camera and several narrow or broadband optical filters. The images can then be processed using conventional digital image processing. Other methods of obtaining multispectral images are by using a liquid crystal tunable filter, an acoustic-optic tunable filter, a common aperture multichannel imaging camera, and hyperspectral imaging.

Multispectral imaging for fruit detection

Bulanon et al., (2010) developed a multispectral imaging system to detect mature orange fruits. The imaging system was composed of a 12-bit monochrome CCD camera fitted with a filter wheel that holds six optical band-pass filters with central wavelengths of 550, 600, 650, 700, and 800 nm and each filter has a bandwidth of 50 nm. The selection of these filters was based on the high discriminability between fruit and leaf within this region. A sample scene of an orange canopy taken with this multispectral imaging system is shown in Figure 8. The first

six images are the individual bands and the last three are different combinations of three bands, which are pseudo-RGB images. In all the bands the fruits have high reflectance while the leaves have low reflectance in the visible bands. When the visible bands are combined with a near-infrared band, the different plant parts and the background can be easily distinguished.

As compared to visible imaging and thermal imaging, multispectral imaging has more images to deal with. One effective approach to reduce the number of features while increasing the variance is principal component analysis (PCA). PCA is a projection method used to analyze the variance of a multivariate dataset to simplify and reduce dimensionality. However, the loss of dimension does not cause any loss of information. The projection (principal component) is calculated by obtaining the eigenvectors of the covariance matrix of the multispectral images. In our study, the first three principal components were used as input to an artificial neural network that was developed for fruit detection. A fruit detection rate of about 0.90 was achieved. In an analysis of the weights of the principal components combined with feature selection, three wavelengths were found to effectively discriminate the fruit from the background: 600, 650, and 700 nm.



Visible and Thermal Images for Fruit Detection, Figure 8 Sample multispectral images acquired in the orchard under natural lighting condition. The first six images are the individual bands and the last three are different combinations of three bands, which are pseudo-RGB images.

Summary

Robots will play an integral role in the future of agriculture to maintain food sustainability and economic viability. An important component of the robot is its visual sensor, to be able to perceive its environment and interact with it. In the development of robotic fruit harvesting, recognizing and locating the fruits is the first task of the robot. Integrating visual sense to robots can be done using machine vision. Vision systems for apple, cherries, cucumbers, oranges, peaches, and tomatoes have been developed to guide robotic harvesting prototypes. Since most of the fruits have colors different from their background, sensors for detecting the fruit use the visible region of the electromagnetic spectrum. Once the image of the fruit is acquired, digital image processing combined with pattern recognition techniques detects and locates the fruit in the image and uses these 2-D information to determine the 3-D location of the fruit to guide the robot. Aside from spectral reflectance, the thermal radiation of the fruit can also be used to differentiate it from the leaves. Thermal cameras are able to image the infrared radiation of the canopy and transform the data into a thermal image that can be processed using digital image processing. Other than visible and thermal imaging, multispectral imaging is an emerging technology in agriculture. Multispectral imaging acquires images of a scene at different wavelengths, determined to have a high discriminability between fruits and the background. The detection of fruits using these imaging systems is critical to the success of the fruit harvesting robot development. Furthermore, these imaging systems have the potential to become as one of the tools used for agricultural management such as disease scouting, yield monitoring, and pesticide application.

Bibliography

- Alchanatis, V., Cohen, Y., Cohen, S., Moller, M., Meron, M., Tsipris, J., Orlov, V., Naor, A., and Charit, Z., 2006. Fusion of IR and multispectral images in the visible range for empirical and model based mapping of crop water status. *American Society of Agricultural and Biological Engineers, Paper No. 061171.*
- Acock, G., and Thomas, R., 1996. *Applied Image Processing*. New York: McGraw-Hill.
- Blum, R., and Liu, Z., 2006. *Multi-Sensor Image Fusion and Its Applications*. Boca Raton: CRC Press.
- Brown, G. K., 2002. Mechanical harvesting systems for the Florida citrus juice industry. *American Society of Agricultural and Biological Engineers, Paper No. 021108.*
- Bulanon, D. M., and Kataoka, T., 2010. A fruit detection system and an end effector for robotic harvesting of Fuji apples. *Agricultural Engineering International: CIGR Journal*, **12**, 203–210.
- Bulanon, D. M., Kataoka T., Zhang, S., Ota, Y., and Hiroma T., 2001. Optimal thresholding for the automatic recognition of apple fruits. *American Society of Agricultural and Biological Engineers, Paper No. 01-3133.*
- Bulanon, D. M., Burks, T. F., and Alchanatis, V., 2008. Study on temporal variation in citrus canopy using thermal imaging for citrus fruit detection. *Biosystems Engineering*, **101**, 161–171.
- Bulanon, D. M., Burks, T. F., and Alchanatis, V., 2009a. Fruit visibility analysis for robotic citrus harvesting. *Transactions of the American Society of Agricultural and Biological Engineers*, **52**, 277–283.
- Bulanon, D. M., Burks, T. F., and Alchanatis, V., 2009b. Image fusion of visible and thermal images for fruit detection. *Biosystems Engineering*, **103**, 12–22.
- Bulanon, D. M., Burks, T. F., and Alchanatis, V., 2010. A multispectral imaging system for citrus fruit detection. *Environmental Control in Biology*, **48**, 81–91.
- Burks, T. F., Shearer, S. A., and Payne, F. A., 2000. Classification of weed species using color texture features and discriminant analysis. *Transactions of the American Society of Agricultural and Biological Engineers*, **43**, 441–448.
- Burks, T. F., Schmoldt, D. L., and Steiner, J. J., 2008. U.S. specialty crops at a crossroad. *Resource*, **15**, 5–6.
- Castleman, K. R., 1996. *Digital Image Processing*. New Jersey: Prentice Hall.
- Gonzalez, R., and Woods, R., 1992. *Digital Image Processing*. Reading: Addison-Wiley.
- Jiminez, A. R., Ceres, R., and Pons, J., 2000. A survey of computer vision methods for locating fruit on trees. *Transactions of the American Society of Agricultural and Biological Engineers*, **43**, 1911–1920.
- Kondo, N., and Ting, K. C., 1998. *Robotics for Bioproduction Systems*. St. Joseph: American Society of Agricultural Engineers.
- Kondo, N., Nishitsuji, Y., Ling, P., and Ting, K. C., 1996. Visual feedback guided robotic cherry tomato harvesting. *Transactions of the American Society of Agricultural and Biological Engineers*, **39**, 2331–2338.
- Parrish, E., and Goksel, K., 1977. Pictorial pattern recognition applied to fruit harvesting. *Transactions of the American Society of Agricultural and Biological Engineers*, **20**, 822–827.
- Plebe, A., and Grasso, G., 2001. Localization of spherical fruits for robotic harvesting. *Machine Vision and Applications*, **13**, 70–79.
- Sarig, Y., 1993. Robotics of fruit harvesting: a state-of-the-art review. *Journal of Agricultural Engineering Research*, **54**, 265–280.
- Schertz, C. E., and Brown, G. K., 1966. Determining fruit bearing zones in citrus. *Transactions of the American Society of Agricultural and Biological Engineers*, **9**, 366–368.
- Sites, A., and Delwiche, M. J., 1988. Computer vision to locate fruit on a tree. *American Society of Agricultural and Biological Engineers, Paper No. 85-3039.*
- Slaughter, D., and Harrel, R. C., 1989. Discriminating fruit for robotic harvest using color in natural outdoor scenes. *Transactions of the American Society of Agricultural and Biological Engineers*, **32**, 757–763.
- Spong, M. W., Hutchinson, S., and Vidyasagar, M., 2006. *Robot Modeling and Control*. John Wiley and Sons, Inc.
- Srivastava, A. K., Goering, C. E., Rohrbach, R. P., and Buckmaster, D. R., 2006. *Engineering Principles of Agricultural Machines*, 2nd edn. St. Joseph: American Society of Agricultural and Biological Engineers.
- Stajnko, D., Lakota, M., and Hocevar, M., 2004. Estimation of number and diameter of apple fruits in an orchard during the growing season by thermal imaging. *Computers and Electronics in Agriculture*, **42**, 31–42.
- Tanigaki, K., Fujiura, T., Akase, A., and Imagawa, I., 2008. Cherry harvesting robot. *Computers and Electronics in Agriculture*, **63**, 65–72.
- Van Henten, E. J., Hemming, J., Van Tuijl, B. A. J., Kornet, J. G., and Bontsema, J., 2003. Collision-free motion planning for a cucumber picking robot. *Biosystems Engineering*, **86**, 135–144.

Cross-references

Chemical Imaging in Agriculture
Color in Food Evaluation
Color Indices, Relationship with Soil Characteristics
Image Analysis in Agrophysics
Neural Networks in Agrophysics
Plant Disease Symptoms, Identification from Colored Images

VISUAL ASSESSMENT

See *Soil Structure, Visual Assessment*

VITREOSITY

Having the nature of glassy (wheat grain).

VOID RATIO

See *Soil Compactibility and Compressibility*

VOLUMETRIC WATER CONTENT

The volume of liquid water per volume of soil.

VUGHS

Relatively large voids, usually irregular and not normally interconnected with other voids of comparable size; at the magnifications at which they are recognized they appear as discrete entities.

Bibliography

Glossary of Soil Science Terms. Soil Science Society of America.
2010. <https://www.soils.org/publications/soils-glossary>

W

WATER APPLICATION EFFICIENCY

The net amount of water added to the root zone as a fraction of the amount applied to the field. Surface irrigation methods such as flooding or furrowirrigation may result in runoff and/or in percolation beyond the root zone, thus reducing the application efficiency. Sprinkling irrigation may involve losses due to wind-drift. Microirrigation methods, if well managed, offer the potential for relatively high application efficiency.

Bibliography

Introduction to Environmental Soil Physics (First Edition) 2003
Elsevier Inc. Daniel Hillel (ed.) <http://www.sciencedirect.com/science/book/9780123486554>

WATER BALANCE IN TERRESTRIAL ECOSYSTEMS

Joanna Sposób
Department of Hydrography, Institute of Earth Sciences,
Maria Curie-Skłodowska University, Lublin, Poland

Synonyms

Hydrologic budget; Hydrologic cycle; Hydrologic equation

Definition

Water balance. The cyclical movement of water between the atmosphere and the ground surface, considering precipitation, evaporation, and runoff (Whittow, 1984).

Water balance equation. Equation presenting elementary parts of water balance: precipitation, evapotranspiration, and runoff, expressed as volume of water.

Terrestrial ecosystem. The continental as distinct from marine and atmospheric ecosystem.

Ecosystem. Ecological system formed by the interaction of all living organisms with each other and with the chemical and physical factors of the environment in which they live, linked by the transfer of energy and materials (Clark, 2003, p. 130).

Introduction

The hydrological cycle is the occurrence and movement of all waters above, on and below the Earth's surface. Nearly all water is continually in motion and it obeys basic universal laws – especially the principle of mass conservation. The water balance equation for a river catchment (terrestrial ecosystem) indicates the relative values of inflow, outflow, and change in water storage for the area. The water balance equation components may be expressed as a mean depth of water over the basin or water body (mm), as a volume of water (m^3), or in the form of discharge ($\text{m}^3 \cdot \text{s}^{-1}$) (Scientific framework of world water balance, 1971; Sokolov and Chapman, 1974). The hydrologic cycle is the term applied to the general circulation of water, but the term the runoff cycle describes portion of the hydrologic cycle between precipitation over land areas and subsequent discharge through river channels or direct return to atmosphere through evapotranspiration (Linsley et al., 1949).

Development of the water balance concept

The first quantitative approach, based on the water balance concept, was that of P. Perrault in 1674, who showed that the annual volume of precipitation on the River Seine basin in France was at least seven times the volume of discharge of the river. He also correctly established the concept of the allocation of precipitation as evaporation, transpiration, runoff, and groundwater recharge. In 1802, J. Dalton inquired into the quantitative relations between precipitation, evaporation, and runoff, he also was the first one

who determined the water balance of England (Scientific framework of world water balance, 1971). The problem of water balances also attracted much attention of Russian scientists S. G. Gmelin, M. V. Lomonosov, P. I. Rychkov, and others (Scientific framework of world water balance, 1971) who were concerned with the water balance of the Caspian Sea basin. After the invention of reliable velocity meters in the nineteenth century, discharge measurements were systematized. This permitted more effective study of the relations among hydrological parameters of the river basins. In 1894, F. H. Newell presented a direct relation between runoff and precipitation and prepared maps showing their mean values in the USA.

A. Penck in 1896 and E. V. Oppokov in 1906 made some theoretical generalizations and were the first to develop a water balance equation (known under the name Penck–Oppokov equation) for river basins:

$$R = P - E \pm \Delta G \quad (1)$$

or, after modification:

$$P = R + E \pm \Delta G \quad (2)$$

where: R – runoff; P – precipitation; E – evaporation; and G – ground water (Scientific framework of world water balance, 1971).

Oppokov also introduced the term of the catchment retention, which was equal to ground retention. Thus, it was denoted in the form

$$P + S_1 = R + E + S_2 \quad (3)$$

or

$$P = R + E \pm \Delta S \quad (4)$$

where: P – precipitation; R – runoff; E – evaporation; S_1 – the state of retention at the beginning of the balance period; S_2 – the state of retention at the end of the balance period; ΔS – variations of retention.

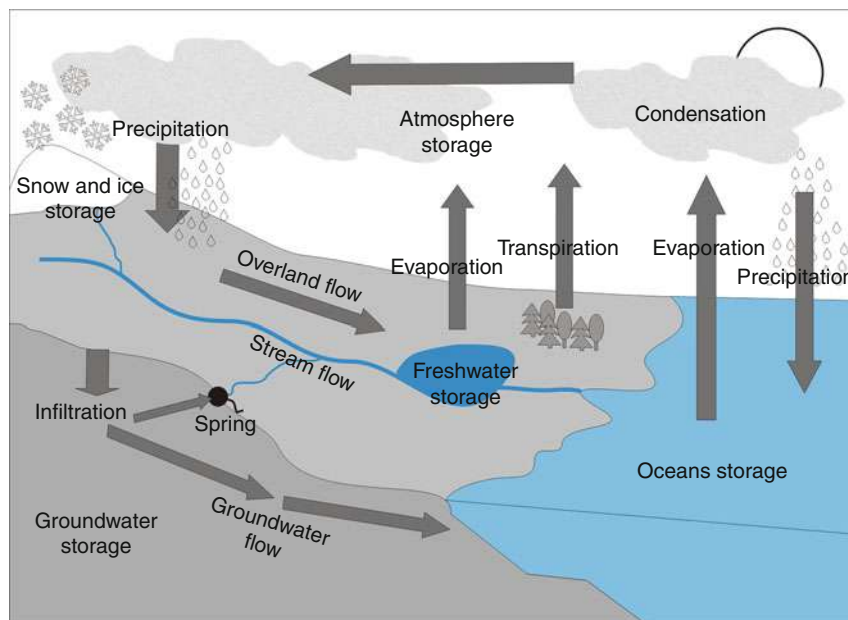
For a long time, water balance equation was treated in the form described above (Equations 3 and 4), which was developed by M. I. Lvovich (Scientific framework of world water balance, 1971) and C. Dębski (1963), who introduced two more parts: surface and ground runoff. Thus, the water balance equation can be expressed as the formula

$$P = R_g + R_s + E \quad (5)$$

where: P – precipitation; R_g – groundwater flow; R_s – overland flow; E – evaporation.

Global water balance

Global water balance comprises circulation of water between atmosphere, lithosphere, and hydrosphere. Water from the surface of oceans is evaporated into the atmosphere (Figure 1). This vapor is condensed by various processes, and falls as precipitation on the seas (80% of total), and the remaining 20% the lands. A portion of that precipitation falling on the land is retained temporarily in the soil, in surface depressions, and on vegetation and other objects until it is returned to the atmosphere by processes of evaporation and



Water Balance in Terrestrial Ecosystems, Figure 1 Global water circulation.

transpiration, or generally evapotranspiration. The remainder, moving by devious surface and underground channels to rivers, lakes, and eventually to the sea, is likewise subject to evaporation and transpiration throughout its travels.

Hydrological cycle is also determined as water balance equation. Water cycle for the Earth is characterized by balance between precipitation and evaporation:

$$P = E \quad (6)$$

where: P – total precipitation falling on seas and lands; E – total evaporation from the seas and lands surfaces.

Each phase of hydrological cycle can be described as separate water balance equation. For land phase of water cycle, it can be as follows:

$$P_L - E_L - R_L = \Delta S_L \quad (7)$$

where: P_L – total precipitation on the land surface; E_L – total evaporation from the land surface; R_L – total runoff from lands to seas; ΔS_L – changes of water retention on lands.

Following parts of the water balance can be denoted for oceanic phase of the cycle

$$P_O - E_O + H_L = \Delta R_O \quad (8)$$

where: P_O – total precipitation on the ocean surface; E_O – evaporation from ocean surface; R_L – total runoff from lands; ΔS_O – changes of water retention in the ocean.

In accordance to modern estimates, the Earth's hydrosphere contains amount of water of about 1,386 million cubic kilometers. However, 97.5% of this amount are saline water and only 2.5% fresh water. The greater portion of the fresh water (68.7%) is in the shape of ice and permanent snow cover (Table 1).

Water Balance in Terrestrial Ecosystems, Table 1 Global water distribution (Shiklomanov, 1993)

Parameter	Volume (km^3)	Percent of freshwater	Percent of total water
World oceans	1,340,000,000	–	96.5
Glaciers	24,064,000	68.7	1.74
Groundwater	23,500,000	–	1.7
Soil moisture	16,500	0.05	0.001
Permafrost	300,000	0.86	0.022
Lakes	176,400	–	0.013
Atmosphere water	12,900	0.04	0.001
Wetlands	11,500	0.03	0.0008
Rivers	2,120	0.006	0.0002
Biological water	1,120	0.003	0.0001
Total	1,386,000,000	–	100

Rhythm of the water cycle in the catchment – the runoff cycle

In the hydrological cycle of the ecosystem can be considered in four phases determined by the rhythm of precipitation. Presented cross section (Figure 2) shows part of the catchment – stream valley and adjacent areas in a humid climate, assuming the absence of snow, ice or frost (Linsley et al., 1949).

I phase of the cycle: end of dry period

All surface and channel storage resulting from the last previous rainfall has been depleted, except for that in reservoirs, lakes, and ponds. The only source of streamflow is groundwater feeding the channel from groundwater resources (Figure 2a). The streamflow, known also as base or sustained, has decreased with time in accordance to the storage depletion curve, slightly modified by transpiration from vegetation along the stream bank and evaporation from the stream surface. Evapotranspiration and discharge from subterranean storage result in gradual lowering of the groundwater table. If the dry period has been sufficiently long to allow the water table to drop below the level of the stream channel at all points above the cross section, streamflow ceases (Linsley et al., 1949).

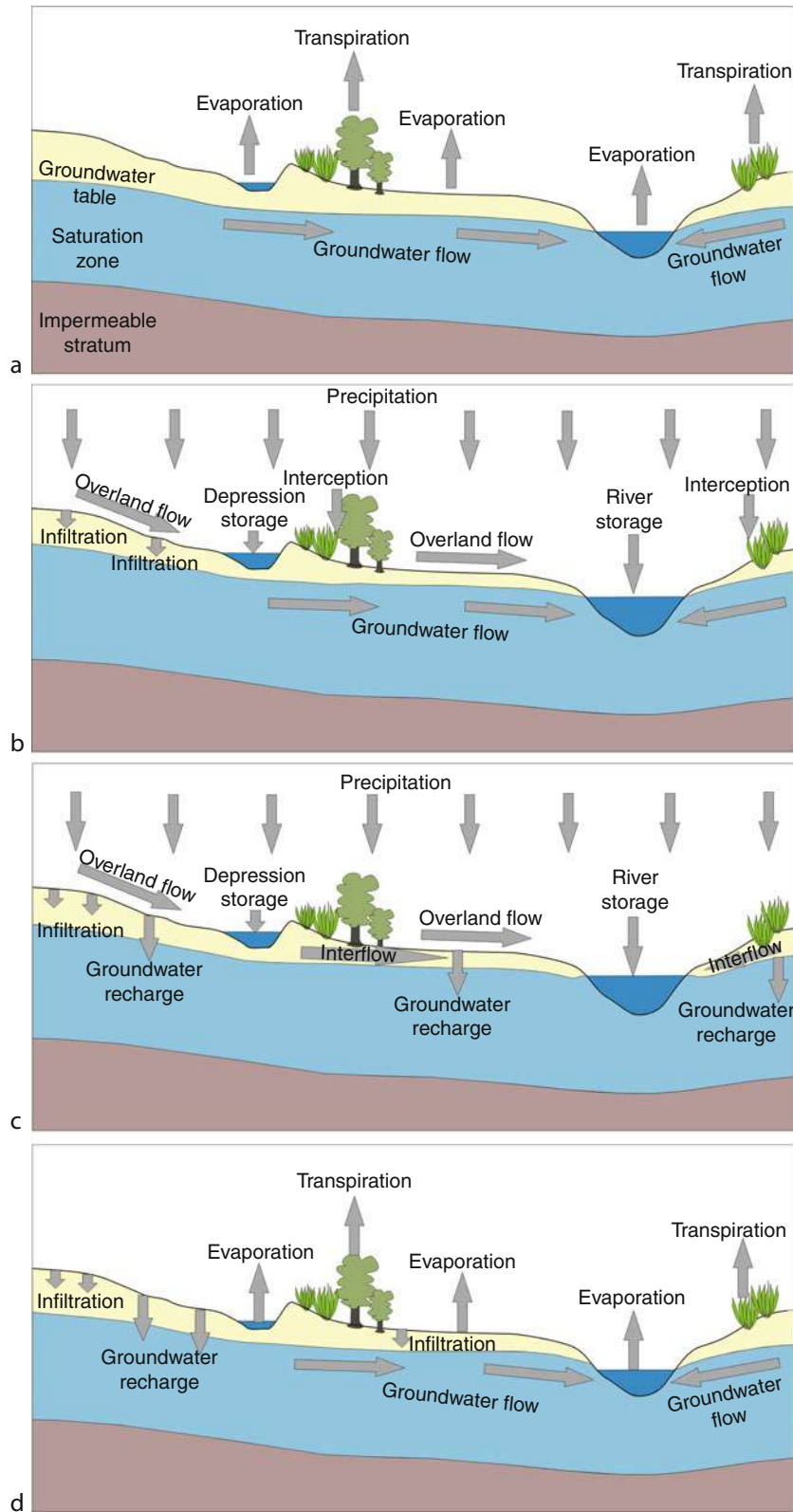
II phase of cycle: after beginning of rainfall

Part of the rain intercepted by vegetation (Figure 2b) does not contribute to runoff, but can be eventually returned to the atmosphere through transpiration. Most of the rain reaching the ground surface is retained on the surface as depression storage or passes through the soil surface as infiltration. Once below the surface, the water begins to satisfy the soil-moisture deficiency, which has gradually built up in the aeration zone during the dry period.

During the initial stage of rainfall, overland flow occurs only from impervious areas (urban roads, roofs, and other surfaces), and extremely steep slopes. On the most of the area, infiltration, interception, and depression storage preclude overland flow unless the intensity of rainfall is very great (torrential rains). The rate of groundwater flow during the initial stages of the storm is probably about the same as just prior to the beginning of rainfall. Flow may or may not be taking place, depending on the elevation of the groundwater table with respect to the water surface in the channel. High humidity is the reason for extremely slow rates of evaporation and transpiration as compared with those under fair-weather conditions.

III phase of cycle: near end of rainfall

After many hours of heavy rainfall, all depression and interception storage is filled, the soil-moisture deficiency is satisfied to considerable depths, and the infiltration rate is near a minimum (Figure 2c). The vegetation is saturated, and rain falling on it is balanced by an equal amount



Water Balance in Terrestrial Ecosystems, Figure 2 Water balance in the catchment.

falling from the vegetation to the ground, except for the small quantity being returned to the atmosphere through evaporation. The flow into filled surface depressions is essentially balanced by overland flow and infiltration.

Overland flow is taking place over nearly the entire basin, and streamflow is beginning to bear some relation to the rate of precipitation. Subsurface flow is contributing to stream discharge, and subterranean storage is being replenished in some portion of the basin.

IV phase of cycle: after end of rain

Rainfall and overland flow have ceased and that streamflow is composed of groundwater and channel storage. Evaporation is taking place at an active rate from soil moisture and depression and interception storage (Figure 2d). Transpiration has begun to take place from vegetal cover. Water in surface depressions is continuing to enter the soil mantle through infiltration, while gravity water within the aeration zone continues to replenish subterranean storage. The groundwater table is either raising or falling, depending on whether the downward-percolation rate exceeds the rate at which groundwater is contributing to streamflow.

Summary

Water balance in terrestrial ecosystems is the cyclical movement of water between the atmosphere and the ground surface in the water divide of the catchment. It can be presented in the form of water balance equation concerning elementary parts of water circulation: precipitation, evapotranspiration, and runoff.

Bibliography

- Clark, A. N., 2003. *Dictionary of Geography*. London: Penguin.
 Dębski, C., 1963. *A Developed Equation for the Water Balance and Means to Its Knowledge*. General Assembly of Berkeley Committee for Evaporation, No. 62. Gentbrugge.
 Linsley, R. K., Kohler, M. A., and Paulhus, J. L. H., 1949. *Applied Hydrology*. New York: McGraw-Hill/Kōgakusha.
 Scientific framework of world water balance, 1971. Technical Papers in Hydrology, No. 7. Paris: UNESCO.
 Shiklomanov, I. A., 1993. World fresh water resources. In Gleick, P. H. (ed.), *Water in Crisis*. New York: Oxford University Press, pp. 13–24.
 Sokolov, A. A., and Chapman, T. G. (eds.), 1974. *Methods for Water Balance Computations. An International Guide for Research and Practice. Studies and Reports in Hydrology 17*. Paris: UNESCO.
 Whittow, J. B., 1984. *Dictionary of Physical Geography*. London: Penguin.

Cross-references

- [Evapotranspiration](#)
[Infiltration in Soils](#)
[Overland Flow](#)
[Snowmelt Infiltration](#)
[Water Budget in Soil](#)

WATER BUDGET IN SOIL

Alberto Pistocchi
 GECOsistema srl, Cesena (FC), Italy

Synonyms

Water balance in soils; Hydrologic budget or balance

Definition

Water budget – the quantification of water volume and water fluxes in soils.

Introduction

This entry deals with the quantification of the water balance in soils using mathematical models. Topics such as the measurement and modeling of soil hydraulic properties, direct measurement of soil moisture, and water fluxes are deliberately not dealt with in this entry. Moreover, we focus explicitly on the hydrological processes relevant at the point and field scale, while deliberately letting apart catchment scale and stream hydrological processes. Also, precipitation is considered an input to the soil, and measurement and modeling of rainfall, snowfall, accumulation, and melting are not a topic of this entry. References to these topics are provided at the end of this entry. We rather focus here on the definition of soil hydrological properties determining the distribution of water within a soil profile, the identification and quantification of the different types of water flows within the soil, and their interplay in the definition of the soil water budget. The soil water budget can be calculated for daily and monthly time steps, the former being generally needed for management applications, while the latter being often satisfactory for planning applications and general assessments, e.g., in the field of land use or climate change effects modeling.

Soil hydrologic and hydraulic properties

Water in soils occupies the empty spaces (pores) to a degree depending on the properties of soils themselves. A first essential parameter of soils is porosity, i.e., the ratio of the volume of the pores over the total volume of a soil sample, which we will denote with the symbol φ . Porosity is related to the soil bulk density ρ_b by the relationship

$$\rho_b = \rho_g(1 - \varphi) \quad (1)$$

ρ_g being the density of soil solid grains, usually not appreciably different from 2700 kg m^{-3} . Porosity φ is a dimensionless measure of the total empty volume within a soil sample, and is usually in the order of 0.4–0.6 for agricultural soils, which corresponds to usual values of ρ_b of 1.1–1.6. Porosity, or bulk density, depends on the degree of compaction of soils. Often, the total volume of pores quantified by porosity is not completely available

to be filled with water. It is therefore preferred to refer to a measure of “effective porosity,” which is usually between 50% and 100% of the total porosity. It is also current practice to distinguish between “primary” or “matrix” porosity, i.e., the volume of pores present in an undisturbed soil sample, and “secondary” or “macro-” porosity, which includes the volume of cracks, animal burrows, litter and debris enclosures, and other empty spaces appearing in soils in the field but typically not measured in the collected samples. Due to the complexity and variety of processes originating soil porosity, this parameter is in itself rather difficult to predict *a priori* on the sole basis of other elementary soil properties such as texture and structure. It is worth noting that porosity usually decreases significantly within the first 100 cm or less of the soil column, being as high as 0.6 at the top and usually approaching 0.4 lower down.

Porosity or effective porosity does not account for the water content of soils, but only for its upper bound. The actual conditions of soil water are usually described in terms of soil moisture θ , i.e., the ratio of the volume of water to the bulk volume of a soil sample. The ratio of soil moisture to soil porosity is usually termed soil water saturation. When the soil moisture equals soil porosity, the soil is said to be saturated.

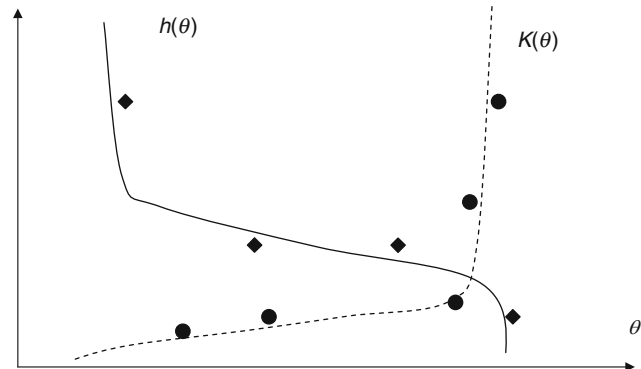
Water is retained in soils against the action of gravity, which tends to drive it downward. The forces by which soils retain water can be interpreted as pressures lower than the atmospheric pressure, so that the pressure difference on each drop of water contrasts the force of gravity. These forces are sometimes called “suction pressures.” It can be checked experimentally that suction pressures increase in absolute value with decreasing soil moisture. An experimental curve representing soil suction pressure as a function of soil moisture is sometimes termed “soil retention curve.” The suction pressure represents ideally the action plants have to provide to extract water from the soil.

In field conditions, soils tend to keep a minimum amount of water even after long dry periods and persistent high air temperatures. This amount is referred to as “residual soil moisture.”

Moreover, when soil moisture in a soil sample exceeds a given threshold, dripping starts to occur from the sample. This threshold is often called “field capacity.” Below a certain threshold of soil moisture, on the other hand, plants are not able to effectively extract water from the soil and start to wilt. This threshold is called therefore “wilting point.” The definition of wilting point and field capacity is essentially conventional. In order to make these quantities unambiguously measurable, it is common practice to refer to the soil moisture at the pressure of 150 cm and 15,000 cm of water head as “field capacity” and “wilting point” respectively.

Another essential property of soils is hydraulic conductivity. This is the measure of the discharge of water conveyed downward by a vertical soil column with cross section of 1 m², when the soil is at saturation. One may think of water flow through soils as the combination of

two processes: one of filling of pores by water, and another of transfer of water through the saturated soil. In reality, some transfer of water occurs simultaneously to filling, and reaches appreciable intensity after field capacity. Most numerical models of soil water budget represent this combination of the two processes by introducing the concept of “partially saturated hydraulic conductivity,” i.e., an experimentally derived curve relating the hydraulic conductivity (or vertical water discharge through a 1-m² cross section of soil) to the soil moisture conditions. Typically, when the soil is above field capacity, the hydraulic conductivity would be quite close to the hydraulic conductivity measured in saturated soil, while below field capacity it sharply drops to much lower values. For reasons of mathematical convenience, in numerical models soils are described using predefined functional forms of retention curves and partially saturated hydraulic conductivity curves, among which the most commonly used are the Brooks–Corey (Brooks and Corey, 1964) and Mualem–Van Genuchten (Mualem, 1976; Van Genuchten, 1980) models. These models predict the suction pressure (h) and the hydraulic conductivity (K) as a function of θ , using appropriate parameters calibrated on the basis of experimental curves (Figure 1). When no experimental curve is available, it is common practice to assign parameters on the basis of elementary soil properties such as texture, bulk density, and organic matter content. Rules to assign parameters based on such properties are derived from databases of soil hydraulic properties, often in the form of regression equations or through inference techniques such as the artificial neural networks (ANN). A database and software package commonly used worldwide for the parameters of the Mualem–Van Genuchten model is Rosetta (<http://www.ars.usda.gov/Services/docs.htm?docid=8953>). Wosten et al. (1999), have derived rules for the prediction of Van Genuchten parameters representative for western European soils.



Water Budget in Soil, Figure 1 Typical shape of retention $h(\theta)$ and hydraulic conductivity $K(\theta)$ curves in soils. Spots represent experimental measurements (♦ = suction, ● = conductivity), while continuous lines represent the interpolating mathematical models.

Fluxes of water affecting the soil water budget

Following a rainfall or snowmelt event, the soil absorbs water up to its capacity. Water fluxes in excess originate surface runoff, and water absorbed by the soil undergoes evaporation, transpiration through plants, infiltration to deeper soil, and eventually to the groundwater, possibly intercepted by soil draining mechanisms operating through artificial devices (e.g., subsurface tile drains, man-made ditches) or through the natural drainage network. Each of the types of fluxes described above has been extensively studied and represented in mathematical models, which are briefly recalled in the following.

The capacity of the soil surface to absorb water

When pouring water to a very dry soil, it can be observed that water initially tends to remain on the surface. After a few seconds, while the soil is wetted, infiltration through the surface starts. The initial difficulty of dry soils to absorb water can be associated to the experimental result that the hydraulic conductivity decreases in dry soils ([Figure 1](#)).

Occasionally, the presence of cracks due to soil drying facilitates infiltration. When the topsoil is completely saturated with water, it is common to observe that the rain tends to originate ponds, which may later disappear as the drainage progresses. These observations suggest that there is an optimal range of conditions for infiltration, corresponding to soils sufficiently wet to allow infiltration, but not so wet to be saturated, hence not able to accept additional water. Up to now, no widely accepted theoretical model is available to describe the flow at the interface between the surface and the soil, and the description of water absorption at the soil surface is completely conventional and phenomenological. Commonly used models of infiltration at the soil surface are the ones of Horton, Philip, and Green and Ampt. For an overview and description of these models, the reader may consult Ravi and Williams ([1998](#)). These models predict infiltration at a rate decreasing with increasing soil water content, or – equivalently – with increasing duration of the water input (rainfall). Usually, in water budget calculations, soil water absorption in dry conditions is simply not considered, and soils are assumed to be able to absorb up to their water holding capacity, in excess of which surface runoff starts to occur.

Surface runoff

The occurrence of surface runoff can be interpreted through two distinct mechanisms, namely “infiltration excess” and “saturation excess.” The first one is identified when rainfall or snowmelt intensity exceeds the capacity of soils to absorb water. This may happen in soils with low hydraulic conductivity, besides the trivial case of sealed soils. The other one occurs when the soil is completely saturated, so that it is not able to accept further water input. A commonly used method is to assume that a percentage of the water input ends in surface runoff without infiltrating.

Evapotranspiration

Usually, the sum of evaporation from bare soils and transpiration by vegetation is lumped together in a term called “evapotranspiration.” If the soil is supplied with water in quantities sufficient not to limit plant transpiration, the amount of water lost by evapotranspiration corresponds to the “potential” evapotranspiration. Potential evapotranspiration (PET) depends on the climate (the solar radiation and thermodynamic conditions of the atmosphere driving water vapor volatilization) and the type of vegetation present on the soil. It is common practice to refer to grass with conventional characteristics to determine a “reference” potential evapotranspiration. Formulas to calculate such reference potential evapotranspiration have been derived on more or less empirical grounds, among which one of the most widely used is the Penman formula. An overview of common formulas is provided by the food and agriculture organization (FAO) ([Allen et al., 1998](#)), along with practical guidance on their application. It is worth stressing that potential (non water-limited) evapotranspiration is a very complex process, for which no widely accepted theoretical model has been developed yet.

When the availability of water limits evapotranspiration, the latter will be less than its potential value. Calculations of soil water budget account in different ways for the reduced availability of water, and in more complex models the specific type of vegetation is also accounted for, by distributing evapotranspiration according to the plant rooting depth, stage of development, and water availability. The detailed assessment of evapotranspiration is usually included in plant models, among which WOFOST (e.g., [Supit et al., 1994](#)) is operationally applied for crop yield forecasting.

Flow in variably saturated soil

Once water has crossed the soil surface, it flows within the soil subject to fluid-dynamics laws, which are rather complex and not fully understood. Factors determining the complexity of water flow in soils, just to mention a few, include the presence of two fluid phases (air and water), macropores, variable soil properties, and complex boundary conditions. A widely accepted phenomenological description of the water flow is the well-known law of Darcy, stating that the water discharge q through a unit-area soil cross section is given by the product of the hydraulic gradient ($\text{grad}(h)$) by the soil hydraulic conductivity K , the latter depending on soil moisture

$$q = -K(\theta)\text{grad}(h) \quad (2)$$

Darcy’s law with soil moisture-dependent hydraulic conductivity, combined with the continuity equation of mass in soil, can be shown to yield the so-called Richards’ equation, which can be solved numerically in one and two dimensions (e.g., [Campbell, 1985](#)) or three dimensions (e.g., the InHM code: <http://inhm.org>; CRITERIA3D, [Bittelli et al., 2010](#)).

Richards' equation describes processes including redistribution of soil moisture within the soil, deep percolation, lateral drainage, once appropriate boundary conditions, and particularly an upper ("atmospheric") boundary condition (water input from rain, snowmelt, and output from evapotranspiration), and a "bottom" one (e.g., an impervious base layer in the soil profile, free drainage, a prescribed level of the water table) are specified.

Soil water budget calculations

In principle, soil water budget calculations may be conducted using numerical models solving Richards' equation. However, in practice simpler methods allow the quantification of the average soil moisture and water fluxes using only the continuity equation for water mass, or a simplified form of Richards' equation not requiring numerical solution. Here we present one well-known and widely applied method, originally developed by Thornthwaite (Thornthwaite, 1948; Thornthwaite and Mather, 1955), applicable at daily as well as monthly steps.

The method can be applied both at monthly and at daily time step. We refer here to the daily step, but replacing in the equations monthly quantities to daily ones would yield consistent monthly results for the soil water content. The method takes precipitation (P , mm day $^{-1}$) and potential evapotranspiration (PET , mm day $^{-1}$) as an input to compute a water mass balance in soil. The latter is characterized by an available water capacity (AWC , mm), which is the amount of water that the soil profile can hold. A possibility to compute AWC (in mm) is

$$AWC = (FC - WP) \times RD \quad (3)$$

where FC and WP (dimensionless) represent field capacity and wilting point soil water content, and RD (mm) is the crop rooting depth. The calculation is performed daily as follows (subscript i indicates the generic day). We first compute the net input to the soil (mm day $^{-1}$) as

$$\Delta P_i = P_i - PET_i \quad (4)$$

Subsequently, if $\Delta P_i > 0$ or $AW_i > AWC$, daily soil water content AW (mm) is computed as

$$AW_i = AW_{i-1} + \Delta P_i \quad (5)$$

Otherwise, we may assume that soil depletion is proportional to ΔP_i through the AW/AWC ratio

$$\frac{dAW}{dt} = \frac{AW}{AWC} (P - PET) \quad (6)$$

or, equivalently

$$AW_i = AW_{i-1} e^{(\Delta P / AWC)} \quad (7)$$

Water in excess of soil AWC (mm day $^{-1}$) contributes to surface runoff and infiltration; the method does not distinguish between the two fluxes, for which additional

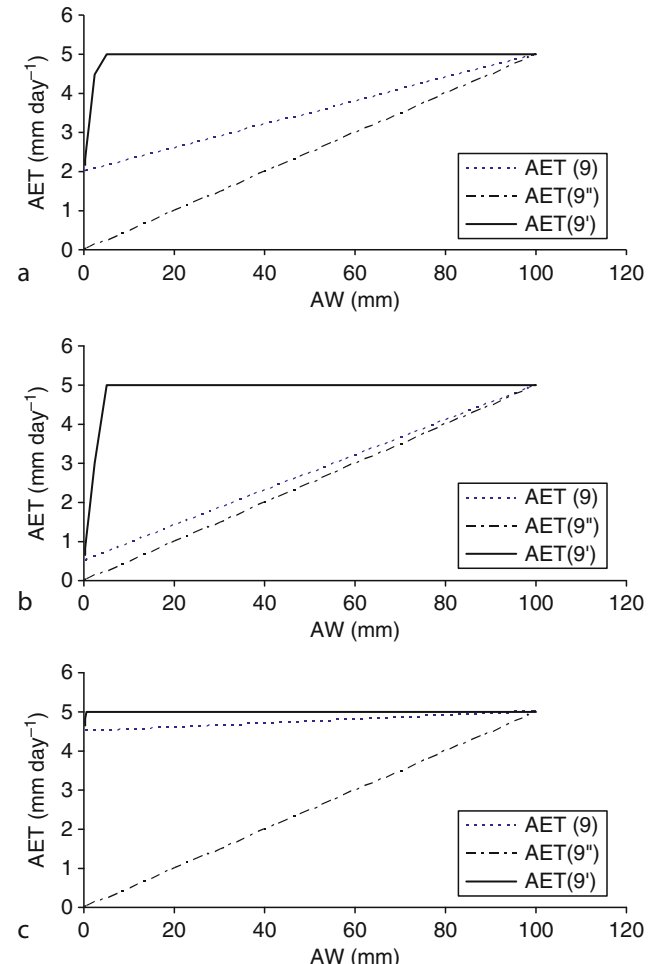
assumptions need to be done (e.g., Steenhuis and Van der Molen, 1986); it is computed daily as

$$E = \max(0, \Delta P_i + AW_i - AWC) \quad (8)$$

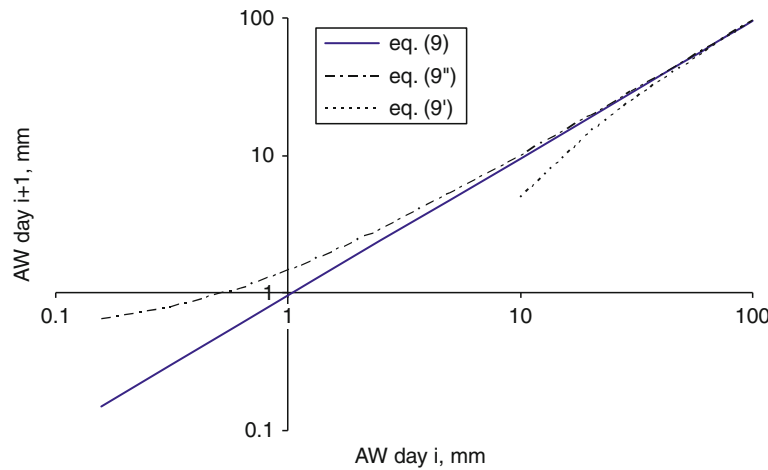
The depletion term $\frac{AW}{AWC} (P - PET)$ equates the difference between precipitation and actual evapotranspiration (AET), so that the latter may be computed as

$$AET = \frac{AW}{AWC} (1 - P) + \frac{AW}{AWC} PET \quad (9)$$

It is worth noting that the assumption of Equation 7 is rather arbitrary. As alternatives, one may select other functions. If we assume that actual evapotranspiration during the day is limited only by potential evapotranspiration and the availability of water, i.e., water is extracted at the same rate irrespective of the soil water content AW , we get



Water Budget in Soil, Figure 2 Behavior of actual evapotranspiration (AET) according to Equations 9, 9' and 9'', for Potential evapotranspiration (PET) = 5 mm day $^{-1}$ and available water capacity (AWC) = 100 mm. Case (a): $P = 2$ mm day $^{-1}$; Case (b): $P = 0.5$ mm day $^{-1}$; Case (c): $P = 4.5$ mm day $^{-1}$.



Water Budget in Soil, Figure 3 Computed AWC depending on the depletion equation (case of $P = 0.5 \text{ mm day}^{-1}$, $PET = 5 \text{ mm day}^{-1}$, $AWC = 100 \text{ mm}$).

$$AET = \min(P + AW_0, PET) \quad (9')$$

Neglecting precipitation during the days when $\Delta P_i < 0$ would yield instead

$$AET = \frac{AW}{AWC} PET \quad (9'')$$

This assumption corresponds to situations where precipitation is not immediately available for evapotranspiration during the same day (e.g., nighttime precipitation). Equations 9' and 9'' are two extreme cases of Equation 9. In (Figure 2) it is shown how, depending on P in relationship with PET , AET according to Equation 9 tends to approach the one according to Equations 9' and 9'', highlighting that Equation 9 modulates AET so to maintain it close to PET when precipitation is high, and close to a linear function of PET when precipitation is low. The different equations affect the soil water content at the end of the day: water balance calculations with Equations 9' and 9'' yield results close to the ones with Equation 9 at high water content, while they diverge at low contents (see Figure 3).

A relatively simple, but more detailed method has been proposed by Pistocchi et al. (2008) for the calculation of the soil water budget at daily step. In this case, aggregation at the monthly step is made not just by taking monthly quantities, but specific semiempirical functions. An alternative approach is the one presented by Eagleson (1978), referred to the yearly water balance. However, the above described Thornthwaite method remains a simple and widely adopted model of soil water budget that can be flexibly adapted to many practical situations.

Bibliography

- Allen, R. G., Pereira, L. S., Raes, D., and Smith, M., 1998. Crop evapotranspiration – Guidelines for computing crop water

requirements – Food and Agriculture Organization (FAO) Irrigation and drainage paper 56. Available at <http://www.fao.org/docrep/X0490E/X0490E00.htm>.

Bittelli, M., Tomei, F., Pistocchi, A., Flury, M., Boll, J., Brooks, E. S., and Antolini, G., 2010. Development and testing of a physically based, three-dimensional model of surface and subsurface hydrology. *Advances in Water Resources*, **33**, 106–122.

Brooks, R. H., and Corey, A. T., 1964. *Hydraulic Properties of Porous Media, Hydrology Papers*, 3. Fort Collins: Colorado State University.

Campbell, G. S., 1985. *Soil Physics with Basic – Transport Models for Soil-Plant Systems*. Amsterdam: Elsevier. Developments in Soil Science, 14.

Eagleson, P. S., 1978. Climate, soil and vegetation – 1. Introduction to water balance dynamics. *Water Resources Research*, **14**, 705–712.

Mualem, Y., 1976. A new model for predicting the hydraulic conductivity of unsaturated porous media. *Water Resources Research*, **12**, 593–622.

Pistocchi, A., Bouraoui, F., and Bittelli, M., 2008. A simplified parameterization of the monthly topsoil water budget. *Water Resources Research*, **44**, W12440, doi:10.1029/2007WR006603.

Ravi, V., and Williams, J. R., 1998. *Estimation of Infiltration Rate in the Vadose Zone: Compilation of Simple Mathematical Models - Volume I*. EPA/600/R-97/128a. Available at <http://epa.gov/ada/csmos/infiltration/infilvol1.pdf>.

Steenhuis, T. S., and Van Der Molen, W. H., 1986. The Thornthwaite-Mather procedure as a simple engineering method to predict recharge. *Journal of Hydrology*, **84**, 221–229.

Supit, I., Hooijer, A., and Van Diepen, C., 1994. *System Description of the WOFOST 6.0 Crop Simulation Model Implemented in CGMS, Volume 1: Theory and Algorithms*. An Agricultural Information System for the European Community, EUR15956 EN.

Thornthwaite, C. W., 1948. An approach toward a rational classification of climate. *Geographical Review*, **38**, 55–94.

Thornthwaite, C. W., and Mather, J. R., 1955. *The Water Balance*. No. 8, Centerton NJ: Laboratory of Climatology.

Van Genuchten, Th., 1980. A closed form equation for predicting the hydraulic conductivity of unsaturated soils. *Soil Science Society of America Journal*, **44**, 892–898.

Wosten, J. H. M., Lilly, A., Nemes, A., and Le Bas, C., 1999. Development and use of a database of hydraulic properties of European soils. *Geoderma*, **90**, 169–185.

Cross-references

Bulk Density of Soils and Impact on their Hydraulic Properties
 Bypass Flow in Soil
 Databases of Soil Physical and Hydraulic Properties
 Evapotranspiration
 Field Water Capacity
 Hydraulic Properties of Unsaturated Soils
 Laminar and Turbulent Flow in Soils
 Layered Soils, Water and Solute Transport
 Pedotransfer Functions
 Soil Water Flow
 Surface and Subsurface Waters
 Water Balance in Terrestrial Ecosystems

WATER DIFFUSION

See [Diffusion in Soils](#)

WATER EFFECTS ON PHYSICAL PROPERTIES OF RAW MATERIALS AND FOODS

Piotr P. Lewicki

Department of Food Engineering and Process Management, University of Life Sciences (SGGW), Warsaw, Poland

Synonyms

Dihydrogen monoxide; Hydrogen hydroxide; Hydroxilic acid; Oxidane

Definition

Water is a chemical compound made of two hydrogen atoms and one oxygen atom. Its structure is H_2O . It is the most abundant chemical and the only compound occurring in all three states – gas, liquid, and solid under the Earth conditions. It is a universal solvent conditioning life. Water is the main component of plant and animal tissues, in which it serves as solvent and reagent. Solid raw materials and liquids usually contain large amounts of water while some processed products are poor in water. In raw materials, the water is constitutive, but in many processes, water is added to obtain special properties of the final product. Water content in raw materials and foods varies from 99.5% in some gels to less than 1% in freeze-dried foods.

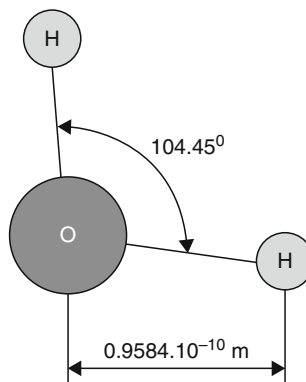
Properties of water

Water is an unusual chemical and its properties differ substantially from other hydrides of the oxygen family. Basic properties of water are collected in [Table 1](#).

Spatial configuration of atoms in the water molecule is well known ([Figure 1](#)). The van der Waals diameter of the water molecule is 0.282 nm. The bonds between

Water Effects on Physical Properties of Raw Materials and Foods, Table 1 Selected properties of pure water

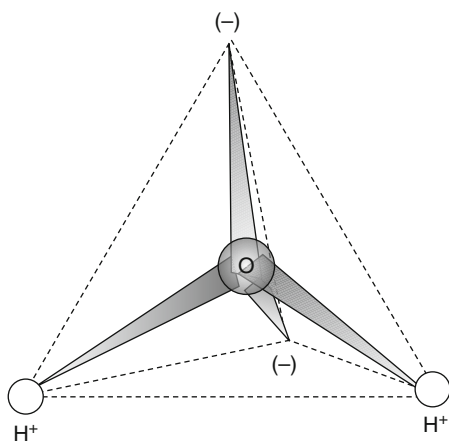
Property	Temperature (°C)	Value	Units
Molecular weight		18.01528 (33)	$g\ mol^{-1}$
Dipole moment		1.85	D
Density	3.98	1,000	$kg\ m^{-3}$
Viscosity	20	10^{-3}	$Pa\cdot s$
Surface tension	20	$72.75 \cdot 10^{-3}$	$N\ m^{-1}$
Specific heat	15	4.1868	$kJ\ (kg\cdot K)^{-1}$
Melting point		0 (273.15)	$^{\circ}C\ (K)$
Boiling point	Pressure 101,325 Pa	100 (373.15)	$^{\circ}C\ (K)$
Thermal conductivity	20	0.598	$W\ (m\cdot K)^{-1}$
Latent heat of vaporization	100	2.26	$MJ\ kg^{-1}$
Latent heat of fusion	0	333.55	$kJ\ kg^{-1}$
Dielectric constant	20	80.08	
Electrical resistivity	25	182	$k\Omega\cdot m^2\ m^{-1}$
Electrical conductivity	25	$55 \cdot 10^{-7}$	$S\ m^{-1}$
Refractive index	20	1.333	
Sound velocity	15	1,460	$m\ s^{-1}$



Water Effects on Physical Properties of Raw Materials and Foods, Figure 1 Water molecule.

hydrogen and oxygen are polarized because of high electronegativity of oxygen. Hence, electrons reside often at the oxygen atom than at hydrogen atoms. Because of that, at oxygen atom a partial negative charge occurs, while at hydrogen atoms partial positive charges appear. Bjerrum proposed in 1951 (Siniukow, 1994) to picture water molecule as a regular tetrahedron ([Figure 2](#)). Inside of the solid, there is an atom of oxygen, and in corners, there are either partial charges or hydrogen atoms.

Water molecule, due to partial positive and negative charges located in the tetrahedron corners, behaves as a dipole and interacts with neighboring molecules. A hydrogen bond is formed and its nature is not strictly



Water Effects on Physical Properties of Raw Materials and Foods, Figure 2 Spatial distribution of charges in water molecule.

electrostatic. Molar energy of hydrogen bond is estimated as 20–35 kJ, and the distance between oxygen and hydrogen atoms is from 0.26 nm to 0.30 nm (Franks, 1988). Hydrogen bond is linear, although can be stretched or bent. Hydrogen bond is formed between water molecules, water and solute molecules as well as between solute molecules containing electronegative atoms bonded with hydrogen. All those interactions affect substantially properties of raw materials and foods.

Small ions dissolved in water are surrounded by ordered water molecules, due to intermolecular interactions, and form hydration shell. The surface charge density of the ion affects ordering of water molecules in the hydration shell (Franks, 1988). Ions with large surface charge density are called structure formers because they form well-ordered hydration shells. Ions with small surface charge density are not able to overcome interactions between water molecules but disturb structure of solvent near the ion. These ions are considered as structure breakers.

In macromolecules such as proteins or polysaccharides, besides formation of hydration shell, some water molecules are built in the structure of biopolymers. Hence, structure water and hydration water are associated with biopolymer molecule. Structure water is immobilized in the macromolecule and moves together with biopolymer. On the other hand, hydration shell can be deformed and movement of water molecules is not completely restricted. The number of water molecules associated with macromolecule depends on its energy and ionization state.

In the presence of apolar compounds and groups, degrees of freedom of water are reduced. It stabilizes water molecules in space and the liquid acquires a structure similar to the structure of a solid. This type of interactions is called hydrophobic hydration.

Structure and hydration water arising from hydrophilic interactions as well as hydrophobic interactions all are

responsible, to some extent, for stability and spatial conformation of biopolymers.

Due to all kinds of interactions, with prevailing hydrogen bonding, water in a material occurs in states from completely bound, as structure water, to bulk water. The thermodynamic state of water in a material is expressed by the activity coefficient – a thermodynamic measure of chemical potential of water in the system. Scott (1953, 1957) proposed to express availability of water for microbial growth by the ratio of vapor pressure of water in material p (Pa) to the vapor pressure of pure water p_o (Pa) at the same temperature and total pressure.

$$a_w = \left[\frac{p}{p_o} \right]_{P,T} \quad (1)$$

Water activity calculated from the above equation differs less than 0.5% from the real thermodynamic value. Water activity is from 0 for completely dried materials to 1 for pure water. The lower is the water activity the stronger the water is bound to material constituents.

Water effects

Rheological properties

Water affects rheological properties of liquids and solids. In liquids, the effect is pronounced by changes in viscosity and consistency, while in solids, water affects their response to force. In liquids, increased concentration of solubles, due to structuring of water, increases viscosity of the solution. For Newtonian liquids the relationship is either exponential or a power type (Rao, 1986). The equation of the form

$$\mu = \mu_0 \cdot c^a \quad (2)$$

where μ_0 – viscosity of pure water, Pa·s; c – solubles concentration, %; a – adjustable parameter.

Macromolecules soluble in water cause non-Newtonian behavior of solution and affect strongly its rheological properties. Rheological properties become either time independent or time dependent. Interactions with water molecules are responsible for the size and shape of hydrated macromolecules and their behavior in sheared solution. The weight of solvent associated with a unit weight of solute, called as hydrodynamic hydration, is estimated to be between 0.2 g water g⁻¹ and 0.5 g water g⁻¹ of different proteins. The larger the macromolecule, the larger the friction between hydrated polymer and solvent. Moreover, macromolecules subjected to shearing forces become oriented according to the flow direction and their hydration shell deforms. Shear thinning is observed and consistency of the liquid decreases with increasing shear rate.

Polyelectrolytes are special type of macromolecules, whose size and shape depend on the ionic strength of the solution. In the presence of water, swelling of a polymer occurs and that affects viscosity of the solution. For

polyelectrolytes, the variation of viscosity with concentration is described by empirical equations.

In solids, interactions between water and constituents of the solid, at low water activities, are so strong that water is devoid of solvent properties (Duckworth, 1981). Under these conditions, mobility of small molecules as well as macromolecules is very much reduced and material is regarded as crisp or crunchy.

Increasing water content in solid material causes either plasticization or antiplasticization. Mobility of molecules and polymer chains increases and plasticization of the material occurs. For many brittle materials, there is a narrow range of water activities, within which there is an abrupt change in their mechanical properties (Lewicki and Wolf, 1995; Harris and Peleg, 1996). Further increase in water activity leads to minute changes in mechanical properties of the material. In some cases, increase in moisture causes toughening of the material (Harris and Peleg, 1996; Seow et al., 1999; Marzec and Lewicki, 2006).

Thermal properties

Specific heat of water is high in comparison to other materials. It can be interpreted as the ability of the material to accumulate heat. Hence, even small amount of water strongly affects specific heat of the material. Generally, it is accepted that specific heat obeys the rule of additivity. It means that specific heat of a product is equal to the sum of the fractional specific heats of the main constituents.

Using additivity principle, specific heat can be calculated from the following equation:

$$c_p = c_{pw} \cdot w + c_{pp} \cdot p + c_{pf} \cdot f + c_{pc} \cdot c \quad (3)$$

where c_p is specific heat at constant pressure, $\text{J}(\text{kg}\cdot\text{K})^{-1}$; w, p, f, c – water, protein, fat, and carbohydrate content, respectively, fraction; subscripts w, p, f, c correspond to specific heats of respective constituents. Such models were reviewed by Sweat (1986). In this formula when $w = 1$ the specific heat is equal to the specific heat of pure water.

Thermal conductivity of solid material depends on its structure and chemical composition (Sweat, 1986). At temperatures above freezing, thermal conductivity increases with increasing water content. Thermal conductivity λ , in $\text{W}(\text{m}\cdot\text{K})^{-1}$, of materials with high water content is calculated from the following formula:

$$\lambda = a_1 + a_2 \cdot w \quad (4)$$

where a_1 and a_2 are constants; w – water content, fraction.

Equations 3 and 4 approximate thermal properties of the material with good precision at high water contents; at low water contents differences become marked.

Mass transfer properties

Differences in concentration, strictly speaking in chemical potential, cause molecular mass transfer called diffusion.

The random movement of molecules is expressed by the Fick's first law giving the flux, in $\text{kg}(\text{s m}^2)^{-1}$, of component A diffusing in a stationary component B:

$$n_A = D \cdot \left(-\frac{dc_A}{dx} \right) \quad (5)$$

where c_A is the concentration of component A, kg m^{-3} ; x – the diffusion path, m; D – diffusivity or diffusion coefficient, $\text{m}^2 \text{s}^{-1}$. Diffusing substance undergoes hydration (change in size and shape), and moving collides with neighboring molecules and is subjected to friction (viscosity). In solids, movement of molecules is also affected by collisions with solid matrix and the winding of the path. Hence, diffusion coefficient is affected by interactions between diffusing substance and the surrounding, and becomes intrinsic property of the system.

Electrical properties

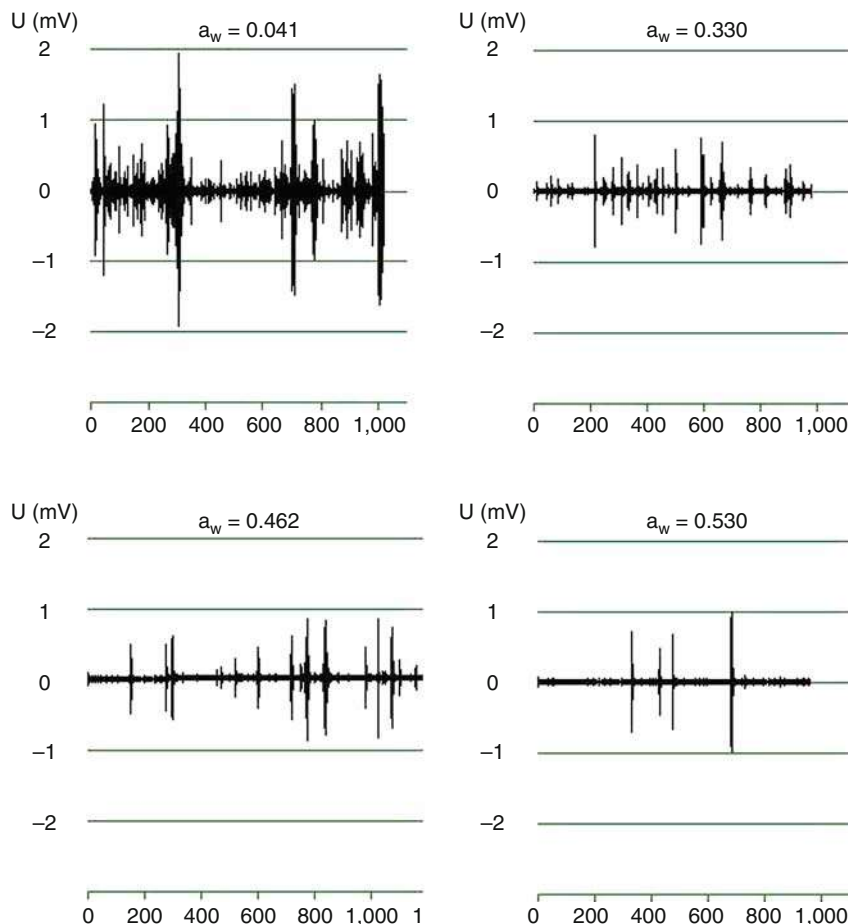
Electrical properties of the material depend primarily on current frequency and temperature, as well as its chemical composition and physical structure (Mudgett, 1987). Dielectric constant and loss factor varies with moisture content. High-moisture materials are generally linear dielectrics. Moreover, the wetter is the material the more its dielectric properties depend on temperature. Dried solids show a little or no variation of dielectric properties with temperature.

Electromagnetic field at radio- and microwave frequencies interacts with material constituents, especially with water. Dipole rotation of free water and conductive migration of charged molecules occur in the material exposed to electromagnetic field. Dipole rotation results in the disruption of tetrahedrally hydrogen bonding patterns.

Electrical conductivity occurs in media that contain electrically charged molecules. Low molecular weight electrolytes and charged macromolecules move in the electric field. This movement is dependent on those events, which are responsible for diffusion of molecules. Hence, increased concentration of ions increases electrical conductivity, but above certain concentration, resistance to movement becomes so large that conductivity decreases. For most solutions, the inflection point in electrical conductivity occurs at concentration between 20% and 30% of solubles.

Optical properties

Infrared radiation reaching surface of a body is partly absorbed and partly reflected. Materials containing water show significant ability to absorb infrared energy. In some products infrared radiation is capable to penetrate the material as deep as 30 mm, and penetration to a depth of 4–5 mm is very common (Ginzburg, 1969). Generally, the shorter the wavelengths the more energy penetrate the material. Hence, in processing of materials with high water content it is recommended to use infrared radiation at wavelength close to the first water maximum, i.e., 1.3–1.4 μm .



Water Effects on Physical Properties of Raw Materials and Foods, Figure 3 Influence of water activity on acoustic emission of flat wheat crisp bread.

Optical properties of materials are responsible for their color and appearance. These include such attributes as translucency and gloss. Free water on the surface of the material often increases its apparent shininess and visual impression of freshness. Treatment of porous materials with water decreases air content in pores, reduces light scattering, and results in more intense color.

Acoustic emission

It has already been mentioned that mechanical properties of solids are strongly influenced by water content (water activity). During breaking of brittle materials a sound is generated, which is perceived by the consumer as the sign of freshness (crisp vegetables) or use of appropriate technology (crackers, biscuits). Decreasing the turgor in fresh fruits or vegetables or increasing water content in crisp products changes their acoustic properties. Influence of water activity on acoustic emission is presented in Figure 3, and was published in numerous papers (Decremont, 1995; Duizer et al., 1998; Roudaut et al., 1998; Gondek et al., 2006; Marzec et al., 2007). It was

shown that each product has a specific frequency pattern for the generated sound and crunchiness disappears at water activities between 0.45 and 0.65.

Conclusions

Water is an important component of raw materials and foods, and affects practically all their physical properties. The influence of water on material properties arises from unusual properties of water per se, and interactions between water molecules and other constituents of the material. The interactions depend on chemical composition, concentration, ionization, surrounding environment, and applied force, and all of them determine the state of water in the material. Hence, many physical properties of food become related to water activity.

Bibliography

- Decremont, C., 1995. Spectral composition of eating sounds generated by crispy, crunchy and crackly foods. *Journal of Texture Studies*, **26**, 27–43.

- Duckworth, R. B., 1981. Solute mobility in relation to water content and water activity. In Rockland, L. B., and Stewart, G. F. (eds.), *Water Activity: Influences on Food Quality*. New York: Academic, pp. 295–317.
- Duizer, L. M., Campanella, O. H., and Barnes, G. R. G., 1998. Sensory, instrumental and acoustic characteristics of extruded snack food products. *Journal of Texture Studies*, **29**, 397–411.
- Eisenberg, D., and Kauzmann, W., 2005. *Structure and Properties of Water*. Oxford: Oxford University Press.
- Franks, F. (ed.), 1973. *Water: A Comprehensive Treatise*. New York: Plenum, Vols. 1–7.
- Franks, F., 1988. *Water*. WNT: Warszawa (in Polish).
- Franks, F. (ed.), 2009. *Water Science Reviews*. Cambridge: Cambridge University Press, Vols. 1–5.
- Ginzburg, A. S., 1969. *Infrared Heating in Food Industry*. WNT: Warszawa (in Polish).
- Gondek, E., Lewicki, P. P., and Ranachowski, Z., 2006. Influence of water activity on the acoustic properties of breakfast cereals. *Journal of Texture Studies*, **37**, 497–515.
- Harris, M., and Peleg, M., 1996. Patterns of textural changes in brittle cellular cereal foods caused by moisture sorption. *Cereal Chemistry*, **73**, 225–231.
- Lewicki, P. P., 2004. Water as the determinant of food engineering properties: a review. *Journal of Food Engineering*, **61**, 483–495.
- Lewicki, P. P., and Wolf, W., 1995. Rheological properties of raisins. Part II. Effect of water activity. *Journal of Food Engineering*, **26**, 29–43.
- Marzec, A., and Lewicki, P. P., 2006. Antiplasticization of cereal-based products by water. Part I. Extruded flat bread. *Journal of Food Engineering*, **73**, 1–8.
- Marzec, A., Lewicki, P. P., and Ranachowski, Z., 2007. Influence of water activity on the acoustic emission of flat extruded bread. *Journal of Food Engineering*, **79**, 410–422.
- Mudgett, R. E., 1987. Electrical properties of foods: a general review. In Jowitt, R., Escher, F., Kent, M., McKenna, B., and Roques, M. (eds.), *Physical Properties of Foods – 2*. London: Elsevier Applied Science, pp. 159–170.
- Rahman, S. M. (ed.), 2009. *Food Properties Handbook*. Boca Raton: CRC Press.
- Rao, M. A., 1986. Rheological properties of fluid foods. In Rao, M. A., and Rizvi, S. S. H. (eds.), *Engineering Properties of Foods*. New York: Marcel Dekker, pp. 1–47.
- Roudaut, G., Decremont, C., and Le Meste, M., 1998. Influence of water on the crispness of cereal-based foods: acoustic, mechanical, and sensory studies. *Journal of Texture Studies*, **29**, 199–213.
- Scott, W. J., 1953. Water relations of *Staphylococcus aureus* at 30°C. *Australian Journal of Biological Science*, **6**, 549–564.
- Scott, W. J., 1957. Water relations of food spoilage microorganisms. *Advances in Food Research*, **7**, 83–124.
- Seow, C. C., Chean, P. B., and Chang, Y. P., 1999. Antiplasticization by water in reduced-moisture food systems. *Journal of Food Science*, **64**, 576–581.
- Siniukow, W., 1994. *Water – Intrinsic Substance*. Warszawa: Wiedza Powszechna.
- Sweat, V. E., 1986. Thermal properties of foods. In Rao, A. A., and Rizvi, S. S. H. (eds.), *Engineering Properties of Foods*. New York: Marcel Dekker, pp. 49–87.

[Layered Soils, Water and Solute Transport Membranes, Role in Water Transport in the Soil–Root–Xylem System](#)
[Modeling the Thermal Conductivity of Frozen Foods](#)
[Rheology in Agricultural Products and Foods](#)
[Soil Water Flow](#)
[Stress–Strain Relations](#)
[Water in Forming Agricultural Products](#)

WATER EROSION: ENVIRONMENTAL AND ECONOMICAL HAZARD

Jerzy Rejman

Institute of Agrophysics, Polish Academy of Sciences, Lublin, Poland

Water erosion

Water erosion is a part of soil erosion process in which water is an erosive force in soil detachment and transport. It finally provides to setting of sediment at footslopes and valley floors or direct delivery of sediment to water courses or reservoirs. During the first phase of water erosion, the impact of raindrops causes soil crusting, that is, limits infiltration and leads to development of runoff, initially in the form of laminar flow and with increase of its depth and velocity – turbulent flow. The change of flow nature is reflected in separation of water erosion into sheet, rill, and gully (ephemeral and permanent). Dynamics of the process is ruled by energy input (rainfall amount and intensity, shear stress of overland flow) and resistance of soil and landscape features. The latter is changing with rainfall duration, providing higher connectivity of the flow system (surface, subsurface) to transport water and sediment during present and next events. Water erosion causes on- and off-site environmental effects, and part of them of significant economical extension.

On-site effects

Soil truncation, redeposition of sediment and nutrients inside fields and catchments, and total soil loss with the development of gullies are the main on-site effects. Soil profile truncation can be quantified as proportion of upper horizons (A/E) that have been removed. These criteria become a basis of separation of four erosion classes (Soil Survey Division Staff, 1993). Whilst upper horizons may range widely in thickness, the absolute amount of erosion cannot be specified by this method. Such division well describes initial phases of soil transformation due to erosion and poorly – larger soil profile changes (that are all put into fourth class). For the latter, separation of erosion classes based on the pedological attitude seems to be more suitable. Such classification was proposed for soils developed from loess (Haplic luvisols), in which lost

Cross-references

- [Adsorption Energy of Water on Biological Materials](#)
[Color in Food Evaluation](#)
[Dielectric Properties of Agricultural Products](#)
[Electrical Properties of Agricultural Products](#)
[Hydrophobicity of Soil](#)

of particular horizon/subhorizon becomes a criteria to separate five classes of erosion (Turski et al., 1992). Availability of this method to assess total amount of erosion is also restricted by the limited presence of non-eroded soil (reference sites). Nevertheless, both attitudes clearly show that in the eroded areas, rate of soil formation is lower than the rate of erosion. Soil truncation generally leads to lowering of soil productivity by lowering SOC content, lowering of infiltration capacity, and decreasing the retention of plant available water. In dependence on soil texture, water erosion affects crop yields also by creation of root barrier and increased compaction. Analyses of Bakker et al. (2004) based on extensive literature review showed 4% decrease of crop yield per 10 cm of lost topsoil. Usually, crop yields on severely eroded soils are reduced by 12–30% in comparison to non-eroded sites (Pimentel et al., 1995). Whilst in well-developed countries, the decrease could be diminished by excessive fertilization, in developing countries – due to limitation of its application (high costs), soil erosion leads to dramatic yield decrease (Boardman, 2006). Soil truncation and accumulation of sediment evoke spatial variation of soil properties over the landscape. The older concept of non-eroded soils on hilltops and eroded – on slopes is rather misleading, especially in the areas of complex landscape (as loess mantles). In these areas, present-day uplands and slopes are covered by mosaic of non-eroded soils, eroded soils, and colluvials (Turski et al., 1992). Spatial variation of soil properties over the landscape affects the intensity of water erosion process. Twofold differences in soil loss between slightly/moderately and very severely (developed directly from parent loess)/colluvial sites located in the same topographical conditions (9% slope) were reported in runoff-plot studies by Rejman et al. (1996). Largest erosion by water took place on bare, temporarily unprotected arable land, overgrazed areas, and badlands. Plot studies in Europe show that this sheet and rill erosion could have the extent of the annual average of 23, 20, and 14 Mg ha⁻¹ for bare soil, vineyards, and maize, respectively (Cerdan et al., 2006). Higher soil erosion rates are estimated for Asia, Africa, and South America with an average of 30–40 Mg ha⁻¹ year⁻¹, and lower for the USA (17 Mg ha⁻¹ year⁻¹), although in some USA regions soil losses reach 30 Mg ha⁻¹ year⁻¹ (Pimentel et al., 1995). Despite these forms, agricultural fields suffer from the formation of ephemeral gullies, and its contributions to total soil loss by water erosion is assessed between 10% and 80%, ranging in dependence on the environmental conditions (Poesen et al., 2006). However, the largest landscape transformation is caused by the development of permanent gullies, which totally exclude land from agricultural land use and lead to badlands evolution (Poesen and Valentin, 2003). The role of water erosion in soil transformation in northern hemisphere is decreasing in comparison to tillage erosion (Van Oost et al., 2005). However, new approach on water erosion shows that during less-intensive rainfalls, soil is transported over limited distance (Wainwright et al., 2008). Thus, sedimentation could take place even on uniform slope in the

case of break of energy input, and magnitude of sheet and rill erosion could be larger than soil losses measured at the plot outlet.

Off-site effects

With breaking of the resistance of landscape elements, overland flow and transported sediment evoke off-site effects (i.e., outside fields or farms). Muddy floods, siltation, and eutrophication of water reservoirs belong to most important effects. Term “muddy flood” was introduced to characterize water flowing from agricultural fields carrying large quantities of soil as suspended sediment or bedload (Boardman et al., 2006). These phenomena usually take place in loess areas, and there appears a close relation between its occurrence and development of ephemeral gullies. Muddy floods can cause serious financial damage to people and public infrastructure being located at the outlet of dry basin systems. It is estimated that each year, muddy floods lead to a total societal cost of 16×10^6 – 172×10^6 € in Central Belgium, depending on the extent and intensity of thunderstorms and monetary values damaged (Evrard et al., 2007). Deposition of sediment within water reservoirs and ponds is the other important off-site consequence of soil erosion by water. Number of these water bodies per unit area (density) is assessed on 0.33, and 0.1–0.2 km⁻², for the USA and Europe, respectively (Verstraeten et al., 2006). At the world scale, the estimation shows that annual loss in storage capacity is around 0.5–1%, and for individual reservoirs these values can be as high as 4–5% (WCD, 2000). For Europe, annual loss of storage capacity is 0.26% which corresponds to 63 hm³ year⁻¹, and the highest annual losses (above 5%) were found for small ponds of loess areas of Belgium. The latter value referred to the catchment areas give sediment yield ranging from 2 to 5 Mg ha⁻¹ year⁻¹ with maximum values of 20–50 Mg ha⁻¹ year⁻¹ (Verstraeten et al., 2006). Estimates for the USA show that about 880×10^6 Mg of agricultural soils are deposited into reservoirs and aquatic systems each year (Pimentel et al., 1995). Together with runoff and sediment, nutrients (C, N, P) and pesticides are transferred to water reservoirs. Subsurface flow is the other pathway of pollutant transfer, especially in the areas of low groundwater table. From the nutrients, phosphorus being considered as the limiting factor for algae growth is the most dangerous for the environment, and its additional load provides to potentially toxic algae blooms, oxygen deficiency, and destruction of wildlife habitats. Amounts of phosphorus discharged through rivers to oceans are estimated between 18.7 and 31.4 Tg year⁻¹, from which 3.1–4 to 10.1 Tg year⁻¹ is potentially biogeochemically reactive (Compton et al., 2000). Usually, it is assumed that the main source of P delivery is agricultural fields, where high inorganic fertilization resulted in its accumulation in topsoil layer, being removed during erosion events. Recent studies of Withers et al. (2009) show however that P sources associated with the functioning of rural communities (impervious surfaces, detergents, and

wastewater) may be more ecologically relevant than those associated with agriculture. Some economical extent of the off-site effects gives estimates for the UK made by Pretty et al. (2000). To the most significant external costs of agriculture belonged pollution of sources of drinking water by pesticides (120), phosphates (55), and nitrates (16), whilst the off-site damage to the soil was assessed on 14, and organic matter and carbon dioxide losses from soil on 82 (all values in millions of pounds).

Water erosion problems in perspective

Environmental and economical effects of water erosion effects are largely connected with changes in agriculture being the result of common acceptance by farmers, the rules of economic efficiency. Characteristic present-day tendencies in worldwide modern agriculture well describes Pimentel et al.'s (1995, p. 1117) description of changes in the US agriculture, "During the past 50 years, the average farm size has more doubled from 90 to 190 ha. To create larger farms and fields, farmers removed the grass strips, shelterbelts, and hedgerows that once protected soil from erosion. Crop specialization has also led to the use of heavier machines that damage the entire ecosystem." To better adopt to market demands, farmers resign from crop rotation, introduce of maize instead of winter wheat, or change meadows into fields, and ignore the off-site impacts of water erosion (Boardman, 2006). The other important factor increasing economical extension of water erosion is an urban sprawl into agricultural land, being one of the components responsible for more frequent occurrence of muddy floods (Evrard et al., 2007). Summarizing, the increase of on- and off-site effects of water erosion is expected to arise in the future, mainly due to improper land use changes from the environmental point of view.

Bibliography

- Bakker, M. M., Govers, G., and Rounsevell, M. D. A., 2004. The crop productivity – erosion relationship: an analysis based on experimental work. *Catena*, **57**, 55–76.
- Boardman, J., 2006. Soil erosion science: reflections on the limitations of current approaches. *Catena*, **68**, 73–86.
- Boardman, J., Verstraeten, G., and Bielders, C., 2006. Muddy floods. In Boardman, J., and Poesen, J. (eds.), *Soil Erosion in Europe*. Chichester: Wiley, pp. 743–755.
- Cerdan, O., Poesen, J., Govers, G., Saby, N., Le Bissonnais, Y., Gobin, A., Vacca, A., Quinton, J., Auerswald, K., Klik, A., Kwaad, F. P. M., and Roxo, M. J., 2006. Sheet and rill erosion. In Boardman, J., and Poesen, J. (eds.), *Soil Erosion in Europe*. Chichester: Wiley, pp. 501–514.
- Compton, J. D., Mallison, C. R., Glenn, G., Fillipelli, K., Follmi, K., Shields, G., and Zanin, Y., 2000. Variations in the global phosphorus cycle. In *Marine Authigenesis: from Global to Microbial*. SEPM Special Publication No 66. SEPM (Society for sedimentary Geology), Tulsa, Oklahoma, pp. 21–33.
- Evrard, O., Bielders, C. L., Vandaele, K., and van Wesemael, B., 2007. Spatial and temporal variation of muddy floods in central Belgium, off-site impacts and potential control measures. *Catena*, **70**, 443–454.
- Pimentel, D., Harvey, C., Resosudarmo, P., Sinclair, K., Kurz, D., McNair, M., Crist, S., Shpritz, L., Fitton, L., Saffouri, R., and Blair, R., 1995. Environmental and economic costs of soil erosion and conservation benefits. *Science*, **267**, 1117–1123.
- Poesen, J., and Valentin, C. (eds.), 2003. Gully erosion and global change. *Catena*, **50**(2–4):87–564.
- Poesen, J., Vanwalleghem, T., De Vente, J., Knapen, A., Verstraeten, G., and Martinez-Casasnovas, J. A., 2006. Gully erosion in Europe. In Boardman, J., and Poesen, J. (eds.), *Soil Erosion in Europe*. Chichester: Wiley, pp. 515–536.
- Pretty, J. N., Brett, C., Gee, D., Hine, R. E., Mason, C. F., Morison, J. I. L., Raven, H., Rayment, M. D., and van der Bijl, G., 2000. An assessment of the total external costs of UK agriculture. *Agricultural Systems*, **65**, 113–136.
- Rejman, J., Turski, R., and Paluszek, J., 1996. Spatial and temporal variations in erodibility of loess soil. *Soil and Tillage Research*, **46**, 61–68.
- Soil Survey Division Staff, 1993. *Soil survey manual*. Soil Conservation Service. U.S. Department of Agriculture Handbook 18. <http://soils.usda.gov/technical/manual>.
- Turski, R., Paluszek, J., and Ślowińska-Jurkiewicz, A., 1992. The effect of erosion on the spatial differentiation of the physical properties of Orthic Luvisols. *International Agrophysics*, **6**, 123–136.
- Van Oost, K., Van Muysen, W., Govers, G., Deckers, J., and Quine, T. A., 2005. From water to tillage erosion dominated landform evolution. *Geomorphology*, **72**, 193–203.
- Verstraeten, G., Bazzoffi, P., Łajczak, A., Radoane, M., Rey, F., Poesen, J., and de Vente, J., 2006. Reservoir and pond sedimentation in Europe. In Boardman, J., and Poesen, J. (eds.), *Soil Erosion in Europe*. Chichester: Wiley, pp. 769–774.
- Wainwright, J., Parsons, A. J., Muller, E. N., Brazier, R. E., Powel, D. M., and Fenti, B., 2008. A transport-distance approach to scaling erosion rates: I. Background and model development. *Earth Surface Processes and Landforms*, **33**, 813–826.
- WCD, 2000. *Dams and Development. A New Framework for Decision Making*. Report of the World Commission on Dams. London: Earthscan.
- Withers, P. J. A., Jarvie, H. P., Hodgkinson, R. A., Palmer-Felgate, E. J., Bates, A., Neal, M., Howells, R., Withers, C. M., and Wickham, H. D., 2009. Characterization of phosphorus sources in rural watersheds. *Journal of Environmental Quality*, **38**, 1998–2011.

Cross-references

- [Crop Responses to Soil Physical Conditions](#)
- [Field Water Capacity](#)
- [Infiltration in Soils](#)
- [Laminar and Turbulent Flow in Soils](#)
- [Leaching of Chemicals in Relation to Soil Structure](#)
- [Nature Conservation Management](#)
- [Overland Flow](#)
- [Physical Degradation of Soils, Risks and Threats](#)
- [Rainfall Interception by Cultivated Plants](#)
- [Soil Erosion Modeling](#)
- [Soil Surface Sealing and Crusting](#)
- [Soil Water Flow](#)
- [Soil Water Management](#)
- [Solute Transport in Soils](#)
- [Snowmelt Infiltration](#)
- [Spatial Variability of Soil Physical Properties](#)
- [Surface and Subsurface Waters](#)
- [Surface Roughness, Effect on Water Transfer](#)
- [Tillage Erosion](#)
- [Water Reservoirs, Effects on Soil and Groundwater](#)

WATER IN FORMING AGRICULTURAL PRODUCTS

Jiří Blahovec

Department of Physics, Czech University of Life Sciences, Prague 6-Suchdol, Czech Republic

Synonyms

Moisture content; Water content

Definition

Moisture content (MC) is defined as the derivative of water mass (m_w) versus the basic mass (m_b) in the matter:

$$MC = \frac{dm_w}{dm_b} \quad (1)$$

MC is a dimensionless quantity, which is sometimes expressed in percent. Two versions of moisture content are used: MC d.b. (dry basis), where m_b is mass of dry matter and MC w.b. (wet basis), where m_b is total mass of the analyzed part of matter.

Introduction

Water represents a fundamental component of agricultural products and organisms (Fennema, 1976). The most important property of a biological product is its nontrivial composition with different components (see *Water Uptake and Transports in Plants Over Long Distances*). Generally, MC of one part of a product differs from the MC of the other parts even if the parts are located in the tight neighborhood. This is typical property of animal or plant tissues (see *Stomatal Conductance, Photosynthesis, and Transpiration, Modeling*) (Oertli, 1976). This is why the MC is defined in Equation 1 as a local differential quantity that can vary in different points. Generally we can find differences in the MC in species, organs, tissues, cells, and cellular substructures, that is, in the whole spectrum of the product structural units. The differences in moisture content are connected with the variability of physical properties (see *Physical Phenomena and Properties Important for Storage of Agricultural Products; Physical Properties as Indicators of Food Quality; Physical Properties of Raw Materials and Agricultural Products*). Water plays the role of plasticizer in the agricultural products (Blahovec, 2007), so that it increases their flowing ability (see *Rheology in Agricultural Products and Foods*).

The lack of water leads to deficiency disease (living organisms – see also *Stomatal Conductance, Photosynthesis, and Transpiration, Modeling*) and/or deterioration (products). On the other hand, too high content of water usually increases the danger of microbial deterioration.

Water properties

Water is the only substance that occurs abundantly in all three basic physical states on this planet. There is mostly in liquid state as in the living organisms but the other two states are also frequent in contact with them. The basic

state constants of water are given in the following table (based on data of Fennema (1976)):

Constant	Value	Unit
Molecular weight	0.01801534	kg mol^{-1}
Phase transition properties		
Melting point (at 101.325 kPa)	0	$^{\circ}\text{C}$
Boiling point (at 101.325 kPa)	100	$^{\circ}\text{C}$
Critical temperature	373.946	$^{\circ}\text{C}$
Critical pressure	22.058	MPa
Triple point temperature	0.0099	$^{\circ}\text{C}$
Pressure	611.73	Pa
Heat of fusion at 0°C	6.010	kJ mol^{-1}
Heat of vaporization	40.62	kJ mol^{-1}
Heat of sublimation at 0°C	50.89	kJ mol^{-1}

Further properties of water and ice are as follows (based on data in Fennema, 1976):

Parameter at normal pressure	Unit	Liquid water		Ice	
		20°C	0°C	0°C	-20°C
Density	kg m^{-3}	998.203	999.841	916.8	919.3
Viscosity	Pa s	0.001002	0.001787	–	–
Surface tension against air	N m^{-1}	0.07275	0.0756	–	–
Vapor pressure	kPa	2.338	0.6105	0.6105	0.1035
Heat capacity	$\text{kJ kg}^{-1} \text{K}^{-1}$	4.114	4.216	2.050	1.943
Thermal conductivity	$\text{W m}^{-1} \text{K}^{-1}$	0.593	0.559	2.22	2.39
Thermal diffusivity	$\text{mm}^2 \text{s}^{-1}$	0.144	0.133	1.18	1.34
Dielectric constant	–				
Static		80.36	88	91 ^a	98 ^a
at 3 GHz		76.7	80.5		3.2 ^a

^aIn direction parallel to crystallographic axis c

Comparing water physical properties with physical properties of substances with molecules of similar molecular weight, like CH_4 , NH_3 , HF , and H_2S , we see that water has unusually high values for melting point, boiling point, surface tension, dielectric constant, heat capacity and heats of fusion, vaporization and sublimation; a moderately low value for density; an unusual density maximum at 3.98°C ; an unusual attribute of expanding upon solidification; and viscosity which, in light of the above, is strangely normal. In addition, the thermal conductivity of water is large compared to other liquids, and the same can be concluded also for ice. Thermal conductivity of ice at 0°C is approximately four times higher than liquid water at the same temperature; the bigger difference was observed at thermal diffusivity that is about nine times higher in ice than in liquid water at the same temperature. These data indicate deep anomalies in the water properties that have to be caused by special properties of the water molecule and its space asymmetry.

Water's large intermolecular attractive forces are caused by its ability to engage in multiple hydrogen

bonding on a three-dimensional basis (see *Adsorption Energy of Water on Biological Materials*). Compared to covalent bonds (bond energy few hundreds of kJ mol^{-1}), hydrogen bonds are weaker (less than 40 kJ mol^{-1}) but of greater and more variable length.

Water as a part of agricultural products

Water exists in different parts of agricultural products where it is more or less bound. Crudely, we can divide the locations into three basic types (see *Microstructure of Plant Tissue*, see also Kollmann et al., 1968 and Hultin, 1976):

Location	State of water	Bond degree
Pores	Soft solution or pure water	Surface and capillary forces
Protoplasm	Solutions of different types	Osmotic forces
Cell walls	Bound	Chemical forces of different kinds

When the content of water in cell walls and the content of solids in water solute solutions can be omitted then unit volume of agricultural product can be expressed as (Blahovec, 2008)

$$1 = v_{\text{DM}} + v_a + v_w = v_{\text{DM}} + v_p \quad (2)$$

where v are relative volumes of basic components of the agricultural products (DM : dry matter, a : air, w : water, and P : pores). Equation 2 well operates in many cases where swelling and shrinkage does not play important role. Porosity P in this case is expressed as

$$P = v_a + w_w = 1 - v_{\text{DM}} \quad (2a)$$

Physical properties of an agricultural (see *Water Effects on Physical Properties of Raw Materials and Foods*) product can be estimated in many cases by superposition of the physical properties of the main components

$$PP = v_{\text{DM}}PP_{\text{DM}} + v_aPP_a + v_wPP_w \quad (3)$$

where PP is physical property of the agricultural product and PP_{DM} , PP_a , PP_w are the same physical properties of dry matter, air, and water, respectively. This principle (the so-called superposition principle, see Blahovec, 2008) can be used, for example, for estimation of density of agricultural materials in cases where swelling and/or shrinkage can be omitted (see *Drying of Agricultural Products*).

In cases where the mass balance is used, the presence of air could be usually omitted due to its low density ($\sim 1.3 \text{ kg m}^{-3}$ exact value depends on temperature and pressure) and the mass of the agricultural product m_{ap} can be expressed as a sum of the mass of water m_w and the mass of dry matter m_{DM} . In this case, a simple relation between different based moisture contents – see Equation 1 – can be expressed (Blahovec, 2008):

$$MC \text{ d.b.} = \frac{MC \text{ w.b.}}{1 - MC \text{ w.b.}} \quad (4)$$

Equation 4 shows that when the theoretical range of 0–1 (0–100%) is accepted for $MC \text{ w.b.}$, the $MC \text{ d.b.}$ moves in the range $0\text{--}\infty$, irrespective of whether it is expressed as a simple ratio or as a percent part.

Moisture content in agricultural products

Moisture content in raw agricultural products is very variable (see *Drying of Agricultural Products; Water Uptake and Transports in Plants Over Long Distances*):

Product	MC w.b. (%)	MC d.b. (%)
Vegetables (Fennema, 1976)		
High MC (asparagus, green beans, cabbage, lettuce, etc.)	90–95	900–1,900
Medium MC (beets, broccoli, carrots, potatoes, etc.)	80–90	400–900
Low MC (avocado, bananas, green peas, etc.)	75–80	300–400
Fruits (Fennema, 1976)		
High MC (rhubarb, strawberries, tomatoes, etc.)	90–95	900–1,900
Medium MC (apples, peaches, oranges, grapefruit, etc.)	85–90	570–900
Low MC (berries cherries, pears, etc.)	80–85	400–570
Grain Crops (in harvest, Haard, 1976)	15–20	18–25
Wood (in time of felling – Kollmann et al., 1968)	44–55	80–120
Meat (Fennema, 1976; Hultin, 1976)		
Fish, muscle proteins	65–81	185–426
Chicken (without skin)	74	285
Beef	70–73	233–270
Pork	68–70	210–233
Milk (Brunner, 1976)	85–88	566–730

The increase in MC of agricultural products leads to an increase in their water activity and a decrease in adsorption energy (see *Adsorption Energy of Water on Biological Materials*).

Conclusion

Water represents one of the three basic components of agricultural products: dry matter, water, and air. With air, water participates in filling of the internal pores. When no important swelling or shrinkage of dry matter accompanies possible changes of water content, the so-called superposition principle can be used, that is, the total volume of the product is the sum of volumes of dry matter, water, and air. In this case, many physical properties of the product can be estimated as a weighted sum of the components. When the composition of the product is given in mass units, the role of air can usually be omitted.

Bibliography

- Blahovec, J., 2007. Role of water in food and product texture. *International Agrophysics*, **21**, 209–215.
- Blahovec, J., 2008. *Agromaterials. Study Guide*. Prague: Czech University of Life Sciences.
- Brunner, J. R., 1976. Characteristics of edible fluids of animal origin: milk. In Fennema, O. R. (ed.), *Principles of Food Science; Part I. Food Chemistry*. New York: Marcel Dekker, pp. 619–658.
- Fennema, O., 1976. Water and ice. In Fennema, O. R., (ed.), *Principles of Food Science; Part I. Food Chemistry*. New York: Marcel Dekker, pp. 13–38.
- Haard, N. F., 1976. Characteristics of edible plant tissue. In Fennema, O. R. (ed.), *Principles of Food Science; Part I. Food Chemistry*. New York: Marcel Dekker, pp. 677–764.
- Hultin, H. O., 1976. Characteristics of muscle tissue. In Fennema, O. R. (ed.), *Principles of Food Science; Part I. Food Chemistry*. New York: Marcel Dekker, pp. 577–617.
- Kollmann, F., Kuenzi, E., and Stamm, A., 1968. *Principles of Wood Technology. I. Solid Wood*. New York: Springer.
- Oertli, J. J., 1976. The states of water in the plant. Theoretical considerations. In Lange, O. L., Kappen, L., and Schulze, E.-D. (eds.), *Water and Plant Life. Problems and Modern Approaches*. Berlin: Springer, pp. 19–31.

Cross-references

- [Adsorption Energy of Water on Biological Materials](#)
[Drying of Agricultural Products](#)
[Microstructure of Plant Tissue](#)
[Physical Phenomena and Properties Important for Storage of Agricultural Products](#)
[Physical Properties as Indicators of Food Quality](#)
[Physical Properties of Raw Materials and Agricultural Products](#)
[Rheology in Agricultural Products and Foods](#)
[Stomatal Conductance, Photosynthesis, and Transpiration, Modeling](#)
[Water Uptake and Transports in Plants Over Long Distances](#)
[Water Effects on Physical Properties of Raw Materials and Foods](#)

WATER MANAGEMENT

See [Soil Water Management](#)

WATER PRODUCTIVITY

See [Magnetic Treatment of Irrigation Water, Effects on Crops](#)

WATER RELEASE CURVE

The relationship between the soil-water content (by mass or volume) and the soil-water matric potential. Also called the water retention curve.

Cross-references

- [Hydraulic Properties of Unsaturated Soils](#)

WATER RESERVOIRS, EFFECTS ON SOIL AND GROUNDWATER

Waldemar Mioduszewski

Department of Water Resources, Institute of Technology and Life Sciences, Falenty, Poland

Definition

A *water reservoir* is an artificial pond, formed in a river valley or other basin by a barrier or dam and having controlled or uncontrolled outlets. The rising of surface water level have some impact on the groundwater level in adjacent areas.

Water reservoirs were always an important element in the human environment and for many centuries were built for economic or ornamental purposes. There are many types of water reservoirs. Basic division distinguishes the *dug* and the *dam* reservoirs.

Dug reservoirs, usually named ponds, are formed as a result of digging the natural substratum and filling it with water. The sources of water may be different. Usually dug reservoirs are filled with groundwater. The impact of ponds on soils and groundwaters is small, and hence they are not considered in the further parts of the paper.

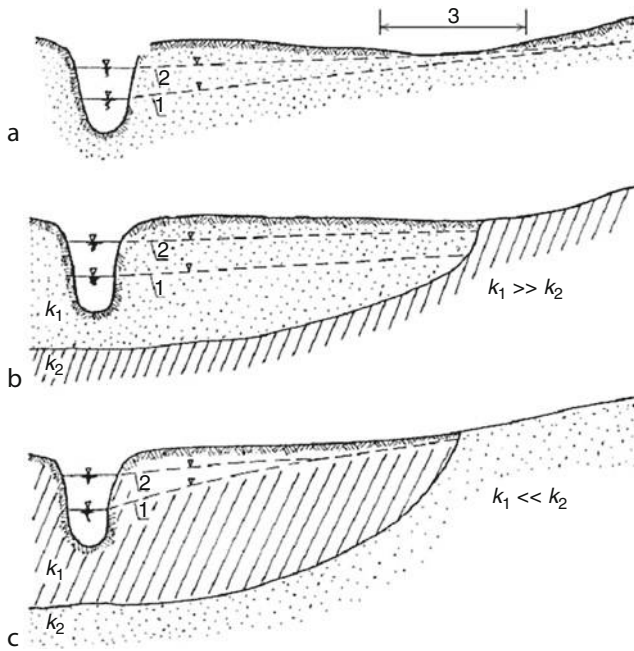
Dam reservoirs are formed as a result of damming the river channel or the whole valley with a water lifting hydraulic structure, usually an earthen dyke with a sluice. After damming, the water level is lifted and the river valley is flooded.

Reservoirs of quite variable sizes are being built worldwide, sometimes huge ones of a volume of several billion cubic meters, heavily affecting many components of the natural environment. This article mainly pertains to small dam reservoirs of a volume less than 0.5 million cubic meters and a water lifting height of 1.5 m.

In practice, every new or reconstructed water reservoir affects soil moisture and the hydrologic regime of a water course, creates favorable conditions for the development of aquatic macrophytes, etc. In most cases, these are positive changes from the biological and economic point of view. Small reservoirs form valuable wetlands with high biological diversity in a monotonous agricultural landscape.

Every dam reservoir that keeps the water level higher than before damming increases the groundwater table and soil moisture in the close vicinity of the reservoir. The range of a reservoir's impact depends not only on land relief and the height of damming but also on the geological structure and hydrogeologic conditions. When the reservoir is surrounded by poorly permeable soils, the range is small – from a few to several dozen meters. In catchments dominated by sandy formations, however, it may reach several hundred meters.

Figure 1 presents an example of the groundwater table depth before and after the construction of a reservoir in



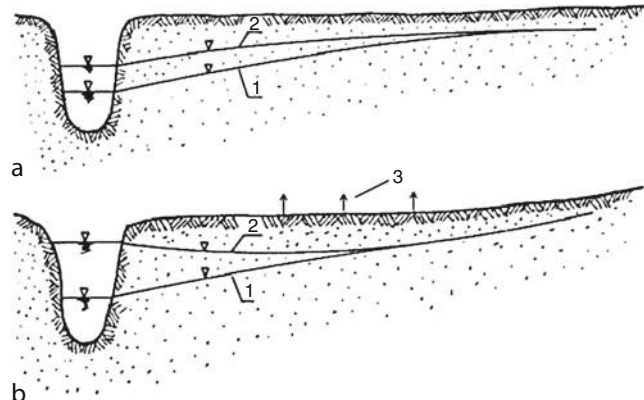
Water Reservoirs, Effects on Soil and Groundwater,
Figure 1 The influence of a reservoir on groundwater level:
 (a) uniform and permeable soil, (b) the erosion valley in
 permeable soil, (c) the valley covered with impermeable soil
 underlying permeable structures; 1: phreatic line before reservoir
 construction, 2: after water level rising, 3: waterlogged area.

relation to geological structure of the valley and uplands. Far range of reservoir's impact may be expected when the upland and valley are built of permeable, uniform formations (Figure 1a). The effect of damming may sometimes manifest itself far from the reservoir by flooding terrain depressions (Figure 1a).

When the erosion valley is made of older, poorly permeable formations (Figure 1b), the range of reservoir's impact is limited by the width of permeable valley. Reservoirs situated in poorly permeable soils exert their impact on groundwaters only in their close vicinity (Figure 1c). It has been estimated that in the soils of a hydraulic coefficient of 10^{-6} to $10^{-7} \text{ cm s}^{-1}$, water lifting by 1 m affects groundwaters not farther than several dozen meters.

The effect of dam reservoirs on soil moisture depends on the depth of groundwaters before and after reservoir construction. At deep groundwater table depths (deeper than the height of capillary rising), water lifting has no effect on soil moisture (Figure 2a). It may, however, cause water logging of terrain depressions as shown in Figure 1a.

When the reservoir is built in relatively flat area and is surrounded by grasslands, which is often the case in localization of small reservoirs, the elevation of groundwater table may be a form of capillary irrigation and may improve water relations in drained wetlands. Increased



Water Reservoirs, Effects on Soil and Groundwater,
Figure 2 The influence of a reservoir on the groundwater level:
 (a) in the winter season, (b) in the growing season; 1:
 groundwater level before the reservoir construction, 2:
 after water rising, 3: evapotranspiration.

soil moisture makes water more available for plants. This leads to increasing biomass production and to increased evapotranspiration. At a high evapotranspiration, the reservoir starts to supply water during the vegetation period (Figure 2b).

Summary

Elevation of groundwater table depth may exert a negative impact on areas used as arable lands. High groundwater table level causes excessive soil moisture and the deficit of air. Some changes of physical and chemical composition of soils can be expected. To maintain agricultural production, it is necessary to construct a draining system in order to discharge excess water and to increase air content in soil pores.

Maintaining high groundwater table makes agricultural utilization impossible and transforms the character of vegetation cover into such typical of hydrogenic habitats. Sometimes such approach is justified since it enlarges wetland areas and increases biological diversity of agricultural landscape.

Bibliography

- Design of Small Dams, 1987. *Water Resources Technical Publication*, 3rd edn. New York: SBS and Distributions.
- Mioduszewski, W., 1995. *Designing, Construction and Management of Small Water Reservoirs* (in Polish). Materiały Informacyjne 32. Falenty: Wydawnictwo IMUZ Multilingual Technical Dictionary on Irrigation and Drainage, 1971. English–French–German. Stuttgart: Franckh'sche Verlagshandlung.
- The World Commission on Dams, 2000. Final Report, Dams and Development: A Framework for Decision Making. New York.

Cross-references

- Agrogeology
- Ecohydrology
- Evapotranspiration

Flooding, Effects on Soil Structure
 Infiltration in Soils
 Irrigation and Drainage, Advantages and Disadvantages
 Soil Water Flow
 Soil Water Management
 Surface and Subsurface Waters

WATER RETENTION CURVE

See [Water Release Curve](#)

WATER STRESS

It occurs when the plant demand for water exceeds the available amount during a certain growth period.

Cross-references

[Crop Responses to Soil Physical Conditions](#)
[Plant Drought Stress: Detection by Image Analysis](#)

WATER TABLE

The upper surface of ground water.

WATER UPTAKE AND TRANSPORTS IN PLANTS OVER LONG DISTANCES

Marian Kargol
 Independent Department of Environment Protection and Modelling, The Jan Kochanowski University of Humanities and Sciences, Kielce, Poland

Introduction

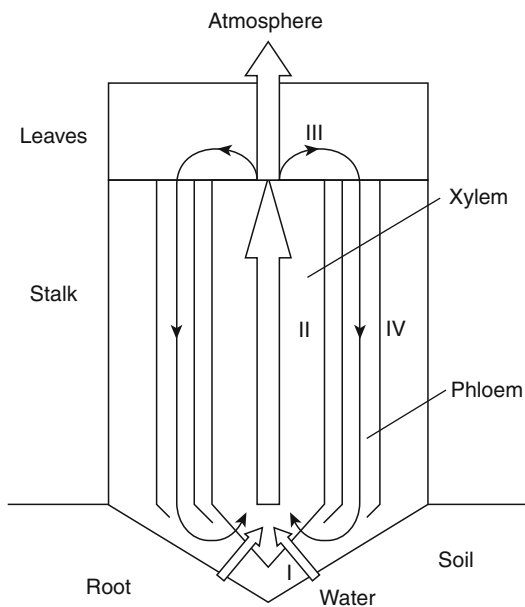
The subject of the present considerations shall be some basic issues pertaining to agrophysical aspects of long-distance water translocation in land plants. We shall be interested in plants with a root system, a stalk, and leaves. These plants take in soil water with the root, and then the water is transported through the root radial route to the xylem of the vascular cylinder. It is then transported through the xylem, along the stalk, to the leaves. Here, its major part transpires (evaporates) into the atmosphere. This is treated as long-distance water transport. Conventional literature also distinguishes another type of long-distance transport in these plants: this is the transport of water and assimilates that occurs through the phloem. Both of these transport types have generally been investigated separately. In several works (Kargol, 1995, 1996, 2007; Kargol and Kargol, 1996; Kargol et al., 2001), we have, however, attempted to formulate long-distance

water transport as part of the so-called integrated water translocation system. It comprises four stages. This idea has been illustrated in [Figure 1](#). At the first stage (I), soil water is taken in and transported from the soil to the xylem of the vascular cylinder. At the second stage (II), translocation occurs through the xylem (most frequently, rising) to the leaves. Next, the water is transported, at the third stage (III), through leaf tissues. From the leaves, the majority of the water evaporates into the atmosphere. The remaining part of the water (relatively small) is taken from the leaf apoplast by sieve tube members, which begin the water routes of the phloem. Next, it is moved (together with assimilates) through the phloem along the plant.

Within phloem water transport (which is the fourth stage [IV] of water translocation), water is – together with the assimilates – delivered to all locations in the plant in which the assimilates are to be used. Our further considerations will pertain to water translocation mechanisms in plants at respective distances. The above shall be done on the basis of the idea, which we have proposed for the integrated water translocation system in plants.

Soil water uptake – theories of xylem water transport in plants

It is believed that the plant root may be, for the sake of a model, treated as an osmometer. It can then be assumed that water intake from the soil and its movement along the radial route (to the xylem of the vascular cylinder) is osmosis-driven. It has also been assumed that osmosis can generate a certain pressure in the root, called root pressure. Due to that, water may also ascend through the xylem to a certain height. This is how the xylem water



Water Uptake and Transports in Plants Over Long Distances, Figure 1 Illustration of the idea for the integrated water translocation system in plants.

ascent theory has been formulated, called *the root pressure theory* (Wilkins, 1969; Zimmermann, 1971; Salisbury and Ross, 1976; Kargol, 1995, 2007). Yet, the most convincing theory of xylem water transport, referred to as *the transpiration-cohesion theory*, has been developed by Dixon and Renner (Wilkins, 1969; Zimmermann and Brown, 1971; Salisbury and Ross, 1976; Kargol, 1992, 2007). A certain amount of attention should also be paid to *the gravi-osmotic idea* of xylem water ascent, formulated by Kargol (1971, 1992, 1995, 2007) and Przestalski and Kargol (1987).

All the above are membrane theories. At this junction, let us explain that membrane transport properties are described by three parameters, that is, the filtration coefficient L_p , the reflection coefficient σ , and the solute permeability coefficients ω and ω_d (Kargol, 1995, 2007; Katchalsky and Kedem, 1965).

The Dixon–Renner transpiration-cohesion theory

As already indicated, xylem water transport can be driven by root pressure. Yet, from experimental investigations it follows that this pressure is able to pump water to relatively low heights. How then does water ascend through the xylem to leaves in tall plants? This question was answered by Dixon and Renner, who formulated the transpiration-cohesion theory (Wilkins, 1969; Zimmermann and Brown, 1971; Salisbury and Ross, 1976; Kargol, 1995, 2007). According to this theory, xylem water ascent occurs in unbroken routes of the xylem, which fork as needed along the plant length. In the last phase, water permeates across leaf tissues (mainly via the apoplastic route). From here, its majority evaporates (transpires) into the atmosphere, mostly from the mesophyll and cuticle cell wall surface. To be precise, it is the water contained in the pores of the cell walls that evaporates. In these pores, free water surfaces (from which water evaporates) are formed in concave menisci. Under the circumstances, under these curved surfaces a certain mean pressure is generated (negative with respect to atmospheric pressure). This pressure, called capillary (P_k), may be calculated from the formula:

$$P_k = \rho g h = \frac{2u}{r}, \quad (1)$$

where u is the surface tension, g is the acceleration of gravity, h is the height, and r is the mean pore cross-section radius. This pressure underlies the Dixon–Renner theory. This theory is, as can be seen, very simple. Notwithstanding the above, it very well explains the agrobiophysical bases of xylem water transport.

The Kargol and Przestalski gravi-osmotic hypothesis of xylem vessel water transport

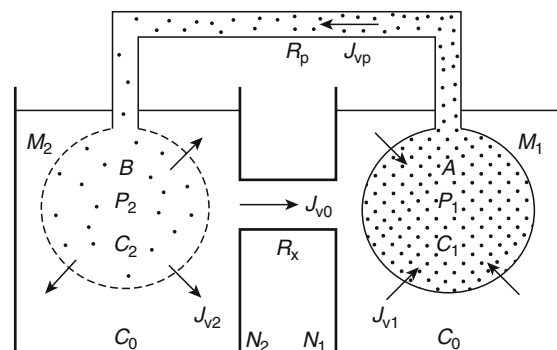
In the year 1971, the so-called gravi-osmotic hypothesis of xylem water transport was proposed (Kargol, 1971). It was subsequently developed by Kargol (1992, 1995, 2007) and Przestalski and Kargol (1987). It postulates that

water may ascend through xylem vessel elements at their respective development phases, with the use of gravi-osmotic mechanisms.

Biophysical theories of phloem transport of water and assimilates

Energy supply to living plant cells occurs by means of assimilates. These high-energy substances are produced in leaves (in photosynthesis processes occurring therein). Next, these assimilates are distributed all over the plant by means of phloem conducting elements, that is, sieve tube members. So far, several hypotheses have been developed pertaining to explanation of the long-distance translocation. They include *the electro-osmotic theory*, *the hypothesis of diffusion and natural cytoplasm movement*, as well as *the Münch pressure-flow theory* (Wilkins, 1969; Zimmermann, 1971; Salisbury and Ross, 1976). We shall focus on the latter as it is the most widely recognized and also because in recent years we have considerably modified and expanded this theory (Kargol, 1996; Kargol and Kargol, 1996; Kargol et al., 2001).

The classic version of *the Münch pressure-flow theory* claims that assimilates are moved through the phloem on the principle of convection in water. This transport, understood as a mass flow, can be best explained with the use of the membrane model as developed by Münch. The classic version of this model consists of two osmometers A and B, joined in opposition by means of the tube R_p . They are plunged in a solution of communicating vessels N_1 and N_2 , which has been more precisely illustrated in Figure 2. The osmometer A of this model, filled with the concentrated solution C_1 , represents a generalization of leaf photosynthesis cells. It is here, as a source effect, that assimilates are created. Hence, their concentration C_1 is high here. If it is also assumed that the membrane M_1 of the osmometer A (which emulates plasmalemmae of the cells at issue) is highly selective, then the osmosis-driven



Water Uptake and Transports in Plants Over Long Distances, Figure 2 The Münch model (classic version): A, B are osmometers; R_p , R_x are tubes emulating the conducting elements of the phloem and the xylem; C_1 , C_2 , and C_0 are concentrations; J_{vp} , J_{vo} are volume flows in the phloem and the xylem; N_1 , N_2 are vessels simulating the leaf apoplast; P_1 , P_2 are mechanical pressures; J_{v1} , J_{v2} are volume flows.

turgor pressure P_1 in these cells will also be high. The osmometer B, in turn, which contains the diluted solution C_2 corresponds to the locations in the plant where assimilates are used. These may be root and fruit cells, or flower buds. The membrane M_2 of this osmometer must be relatively well-permeable, both to water and assimilates. It formulates, for the sake of a model, the cell membranes of the phloem sieve tube members in the locations in the plant where assimilates are used.

It is believed that it is out of these conducting elements of the phloem that the outflow of water and assimilates occurs, driven by reverse osmosis (Wilkins, 1969; Zimmermann and Brown, 1971; Salisbury and Ross, 1976; Kargol, 1995, 1997).

In the presented model, it is also assumed that the tube R_p , which connects both hypothetical osmometers, symbolizes phloem sieve tube members. The containers N_1 and N_2 (together with the concentration C_0) emulate the plant apoplast together with the water and substances dissolved therein contained in it. The tube R_s , in turn, which connects the containers N_1 and N_2 , represents the xylem.

Generally, it may be stated that in the light of the above-presented conventional model of Münch, the phloem mass transport J_{vp} (of water and assimilates), also called pressure transport, occurs under the influence of the mechanical pressure difference $\Delta P = P_1 - P_2$.

On the whole, Münch's theory is essentially very adequate. Yet, since it was published in the year 1930 many significant experimental discoveries have been made, pertaining to long-distance water translocation in plants. As a result, clear possibilities have arisen to introduce to the Münch model significant modifications and additions.

Integrated water translocation system in plants and its modifications

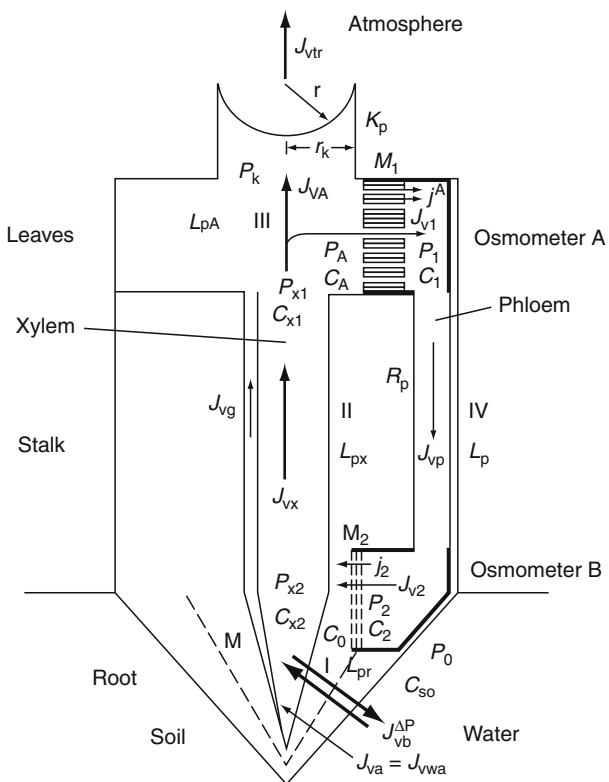
In the light of the conventional Münch model, phloem transport of water is driven by turgor pressure of leaf photosynthesis cells. The value of this pressure is too low, however, for it to be able to transport water and assimilates with sufficient efficiency.

It results mainly from the fact that hydraulic conductivity of the phloem conducting elements (sieve tube members) is relatively small. It also results from the very high viscosity of the phloem sap. Moreover, it has been experimentally demonstrated (with the use of aphids' proboscises) that the phloem sap, contained in leaf sieve tube members, is under very high positive mechanical pressure P_1 . This pressure, calculated with regard to the atmospheric pressure ($P_a = 1,013$ [hPa]), may reach values up to +3 (MPa). It has also been found, through microscope investigations, that pore radius dimensions in the walls of the leaf mesophyll and cuticle cells (from which pore water transpires into the atmosphere) represent the order of magnitude of $r \approx 48 \times 10^{-9}$ (m). On this basis, it has been accurately calculated, from the formula (1), that the negative mechanical pressure P_A in the leaf apoplast may take very high negative values, reaching even $P_A = P_k = -3$ (MPa). The above-quoted

discoveries (Wilkins, 1969; Zimmermann and Brown, 1971; Salisbury and Ross, 1976; Kargol, 1997) have contributed to our developing the long-distance integrated water translocation system in plants (Kargol, 1995, 1996; Kargol and Kargol, 1996; Kargol, 2007; Kargol et al., 2001). They have provided the basis for introducing significant modifications to the Münch model thanks to which that model could become closer to the biological reality.

In this system, as presented in Figure 3, four stages of water translocation have been distinguished (Kargol, 1996; Kargol and Kargol, 1996; Kargol, 2007; Kargol et al., 2001). At the first (I), the flow J_{vr} , which comprises water taken in from the soil, permeates across the root to the xylem of the vascular cylinder. At the second stage (II), the water flow J_{vx} is translocated through the xylem along the plant. Most frequently, water ascent against gravity occurs. The flow J_{vg} is generated by gravi-osmosis. The remaining part of the water that has reached the leaves is, together with the assimilates, transported through the phloem (as the flow J_{vp}), to those locations in the plant where assimilates are used. This translocation of water constitutes the fourth stage (IV) of its long-distance transport.

Agrobiophysical bases of water translocation along the former three distances are well known. Presently, we shall deal with the biophysical interpretation of phloem



Water Uptake and Transports in Plants Over Long Distances,
Figure 3 Long-distance integrated water translocation system in plants (as described).

transport of water and assimilates. This shall be done basing on the Münch model that we have modified, as part of the integrated water translocation system (cf. [Figure 3](#)).

While modifying the Münch model, it has been assumed that the membrane M_1 of the osmometer A emulates the route of water transport from the leaf apoplast to the inside of sieve tube members, which start the phloem water routes in leaves. This route is the tissue which comprises, for example, photosynthesis cells, sieve tube members, and cells adjacent to the tubes. It must be stressed (Kargol, [1995, 2007](#)) that in the leaf apoplast, there occurs negative pressure $P_A = -3$ (MPa). In contrast, in sieve tube members that start the leaf phloem water routes, we deal with positive pressure, which may reach the value of $P_1 = +3$ (MPa).

Under the circumstances, it should be assumed that the inside of the osmometer A emulates the insides of sieve tube members, which start the phloem leaf water routes. In order for the high pressure to originate in the sieve tube members, it should be assumed that transport of assimilates J^A , which occurs across the membrane M_1 , is realized actively. Thanks to that, they have a high concentration of assimilates. Water, when penetrating osmotically from the apoplast to the inside of leaf sieve tube members, is then capable of generating such a high pressure P_1 . The membrane M_1 ought to be ascribed particular properties as well. To be precise, this membrane must be semipermeable (i.e., have the reflection coefficient $\sigma_1 = 1$). To continue the considerations pertaining to the modification of the Münch model, it has to be said that water – together with assimilates contained in the osmometer A – is transported through the tube R_p (which emulates the phloem conducting elements) to the osmometer B. This transport, marked with the symbol J_{vp} , understood as mass transport, is driven by the mechanical pressure difference $\Delta P_f = P_1 - P_2$. In order to make further considerations more precise, let us assume that the osmometer B refers to the root system as the main location of assimilate use. It emulates in a generalized manner sieve tube members, which end the phloem water routes here. Across the membrane M_2 of this osmometer, the volume flow J_{v2} shall permeate, containing water as well as assimilates. This flow is driven by *reverse osmosis* (Kargol, [1995, 2007](#), Kargol and Kargol, [1996](#)). For this to happen, it is justified to assume that the reflection coefficient of the membrane M_2 amounts to $\sigma_2 \approx 0$. Under the considered conditions, water – together with assimilates – is transported (with the flow J_{v2}) to the apoplast of the root vascular cylinder. For particular long distances, the following laws of continuity can be written: $A_x J_{vx} = A_{tr} J_{vtr} + A_1 J_{v1}$ and $A_1 J_{v1} = A_p J_{vp} = A_2 J_{v2}$, where A_x , A_{tr} , A_1 , A_p , and A_2 are surfaces of permeation by the flows: J_{vx} , J_{vtr} , J_{v1} , J_{vp} , and J_{v2} , respectively (cf. [Figure 3](#)).

Conclusions

It must be stressed that solutes, delivered together with the water (through the xylem) to the leaf apoplast, are

absorbed in a completely active manner by the leaf cells where they are then used in metabolic processes, or simply accumulated. If this was not the case, the process of water transpiration would lead to progressive concentration of the leaf apoplastic solution. That would be utterly disadvantageous from the agrobiophysical viewpoint.

The main element of the integrated water translocation system in plants (as well as symptoms of its circulation) is the adequately modified Münch model. As a result of the introduced modifications, it necessarily becomes closer to the biological and agrophysical reality.

The water delivered to the root apoplast may also be removed from it to the soil due to root pressure. Together with this water, redundant (and frequently harmful) products of metabolism in the plant root may be removed to the soil. This aspect has considerable agrophysical significance as the products removed from the root are the food for bacteria. Their removed components may be needed by the plant. It must be noted that water (as the flow J_{v2}) is delivered to the root vascular cylinder. From here, it may be taken over by the xylem and again ascend along the plant.

Bibliography

- Kargol, M., 1971. *Nonelectrolytes and Electrolytes Transport Through Membrane System*. Poland: Department of Physics, WSP Opole, pp. 10–110.
- Kargol, M., 1992. The graviosmotic hypothesis of xylem transport of water in plants. *General Physiology and Biophysics*, **11**, 469–487.
- Kargol, M., 1995. Introduction to Biophysics. Kielce WSP (ed.), pp. 189–215.
- Kargol, M., and Kargol, A., 2003. Mechanistic equations for membrane substance transport and their identity with Kedem-Katchalsky equations. *Biophysical Chemistry*, **103**, 117–127.
- Kargol, A., 1996. An integrated approach to water transport in plant over long distances. *Journal of Biological Physics*, **23**, 157–173.
- Kargol, M., and Kargol, A., 1996. A synthetic approach to biophysical theories of water translocation in plants occurring over long distances. *Current Topics in Biophysics*, **20**, 149–153.
- Kargol, M., 2007. Mass Transport Processes in Membranes and Their Biophysical Implications. Wyd. WSTKT Kielce. pp. 106–131.
- Kargol, M., Suchanek, G., and Kargol, A., 2001. Modification and quantitative analysis of the Münch model in the integrated system of water translocation in plants. *General Physiology and Biophysics*, **20**, 191–202.
- Katchalsky, A., and Curran, P. F., 1965. *Nonequilibrium Thermodynamics in Biophysics*. Cambridge: Harvard University Press, pp. 113–132.
- Przestalski, S., and Kargol, M., 1987. Graviosmosis. *Comments on Molecular and Cellular Biophysics*, **4**, 249–263.
- Salisbury, F. B., and Ross, C., 1976. *Plant Physiology*. Warszawa: PWRiL, pp. 28–215.
- Wilkins, M. B., 1969. *The Physiology of Plant Growth and Development*. New York: MacGraw-Hill, pp. 15–308.
- Zimmermann, M. H., and Brown, C. L., 1971. *Trees, Structure and Function*. New York: Springer, pp. 213–383.

Cross-references

- [Coupled Heat and Water Transfer in Soil Membranes, Role in Water Transport in the Soil–Root–Xylem System](#)

Plant Roots and Soil Structure

[Root Water Uptake: Toward 3-D Functional Approaches](#)

[Soil Hydraulic Properties Affecting Root Water Uptake](#)

[Soil–Plant–Atmosphere Continuum](#)

[Stomatal Conductance, Photosynthesis, and Transpiration, Modeling](#)

[Water Budget in Soil](#)

[Water Effects on Physical Properties of Raw Materials and Foods](#)

[Water Reservoirs, Effects on Soil and Groundwater](#)

WATER USE EFFICIENCY IN AGRICULTURE: OPPORTUNITIES FOR IMPROVEMENT

Meni Ben-Hur

Soil Chemistry, Institute of Soil, Water, and Environmental Sciences, The Volcani Center, ARO, Bet Dagan, Israel

Definition

Any concept of efficiency addresses the output obtainable from a given input. According to this concept, the *general water use efficiency* (WUE_g) index in the context of agricultural and environmental activities determines the yield (Y) of the relevant plant attribute (e.g., biomass, grain, fruit, fiber, and merchandisable yield) per unit volume of water (W) (naturally available and added) per unit plant-growing area, according to [Equation 1](#).

$$\text{WUE}_g = \frac{Y}{W} \quad (1)$$

in which WUE_g can be defined as a specific index for a specific context, for example,

1. *Irrigation water use efficiency* (WUE_i), which is defined in [Equation 2](#)

$$\text{WUE}_i = \frac{Y_i}{W_i} \quad (2)$$

in which Y_i is the harvest or merchandisable yield of irrigated crop per unit growing area and W_i is the volume of irrigation water per unit growing area; or

2. *Rainfall water use efficiency* (WUE_r), which is defined in [Equation 3](#)

$$\text{WUE}_r = \frac{Y_r}{W_r} \quad (3)$$

in which Y_r is the harvest or merchandisable crop yield under “rainfed” conditions (farming watered only by rainfall) per unit growing area, and W_r is the seasonal volume of rainfall per unit growing area.

Introduction

With respect to water availability and use, regions can be divided into two main classes: (1) water-limited and (2) water-non-limited. This classification can be applied

by reference to the “aridity index” (AI), defined in [Equation 4](#) (Thornthwaite, 1948).

$$\text{AI} = \frac{P}{ET_p} \quad (4)$$

in which P = annual precipitation in millimeters; ET_p = annual potential evapotranspiration in millimeters. According to this index, regions with $\text{AI} \geq 1$ are considered to be water-non-limited regions and those with $\text{AI} < 1$ to be water-limited. In some regions, water-limited conditions could be temporary, because of high variability of the rainfall during the year. In regions under permanent or temporary water-limited conditions, in order to increase food production, on the one hand, and to relieve pressure on the earth’s natural ecosystems, on the other hand, it is important to increase water use efficiency (WUE) in agriculture.

Factors affecting water use efficiency

Plants absorb water mostly from the soil, via their root systems, therefore soil water content (water weight or volume per unit of weight or volume of soil) and soil water potential (the energy state of the water in the soil) are important factors in controlling the water availability for plants. The main sources of soil water are rainfall, irrigation water that is supplied by various irrigation systems, and upward movement of water into the root zone from shallow groundwater reservoirs. Four major factors can affect the WUE:

1. Environmental conditions in the vicinity (underground and aboveground) of the plant: plant growth, yield, and reproduction (plant production) depend on environmental factors such as soil fertility and structure, nutrients availability, soil and atmosphere aeration, and solar radiation, in the vicinity of the plant. Absence or deficiency of any of these factors could impair plant production, even under optimal water conditions, and could also decrease the water absorption capability of the plant.
2. Water status in the soil – the soil water can be characterized in terms of its energy state, called the “water potential.” Two main components of soil water potential can affect water uptake by the plant. (a) *The matric potential* (Ψ_m), which expresses the water-retaining strength of the soil matrix, and which is functionally related to the soil water content. In practice, when soil is saturated, that is, all soil pores are filled with water, the water $\Psi_m = 0$; as the soil water content decreases, also the value of water Ψ_m decreases, that is, becomes more negative. For soil solution with given electrolyte concentration, the lower the Ψ_m , the more the energy the plant needs to invest to extract the water from the soil matrix. (b) *The osmotic potential* (Ψ_p) of the water, which depends on the differences between the electrolyte concentrations in the solutions in the soil and in the root tissues: solutions that are separated by the root membrane which acts as a semipermeable membrane. For low and moderate ranges of electrical

conductivity (EC) values, the Ψ_p can be related to the EC of the saturated soil-extracted paste according to [Equation 5](#)

$$\Psi_p(\text{bar}) = -0.36 \cdot EC(\text{dS} \cdot m^{-1}) \quad (5)$$

The Ψ_p value is negative, and the more negative its value, the less the availability of soil water to the plant.

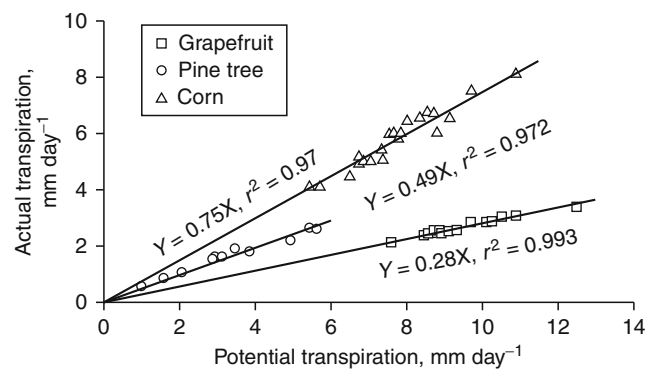
3. Plant properties – the effects of plant properties on WUE are discussed in detail below.
4. Water losses – from the standpoint of WUE, water loss can be classified into two main types. (a) *Internal losses*, that is, losses from soil water in the root zone, examples of which include deep water percolation below the root zone, and direct water evaporation from the soil surface. (b) *External losses*, that is, losses from water supplies before their infiltration into the soil, examples of which include water intercepted by foliage, following overhead sprinkler irrigation or rainfall, and which evaporates without entering either the soil or the plant; water that leaks from the irrigation system and is not used by the plant; and the fraction of the rainfall and irrigation water that is removed by surface runoff.

Plant water requirement

The plant water requirement is the amount of water needed by a plant for its production under any given climatic conditions. However, most of the water taken up by a plant (e.g., 99% in open fields in arid regions) is transpired in order to meet the climatic demand. Under arid and semi-arid climates, that is, climates with a high percentage of bright sunshine, the dry biomass yield of the plant (Y_b) tends to increase linearly with increasing transpiration, according to [Equation 6](#) (de Wit, 1958):

$$Y_b = m \frac{E_a}{E_p} \quad (6)$$

in which m is an empirical coefficient, E_a is the actual transpiration, and E_p is the potential transpiration. Under conditions of unlimited supplies of water, nutrients, and CO₂ to the plant (desirable conditions), and under any given climatic conditions, the plant E_a attains its maximal value, which is the maximum plant water requirement (E_r) for these specific climatic conditions. Values of E_r are presented as functions of E_p in [Figure 1](#), for grapefruit (*Citrus paradisi*), pine (*Pinus halepensis*), and corn (*Zea mays*). For these three plants, the E_r values increased linearly and significantly with increasing E_p , but with differing slopes, which indicates that water requirement depends on both climatic conditions and plant characteristics. In this case, the slope of each regression line ([Figure 1](#)), which expresses the plant water requirement per unit of potential transpiration, could be defined as the plant specific water requirement (SWR), which is an inherent plant characteristic that depends on the genetic properties of the plant: the values of SWR for grapefruit, pine, and corn are 0.28, 0.49, and 0.75, respectively



Water Use Efficiency in Agriculture: Opportunities for Improvement, Figure 1 The actual transpiration values as functions of potential transpiration values for three different crops (Data were taken from Cohen, 1992).

([Figure 1](#)). Under these conditions, [Equation 1](#) can be converted to

$$\text{WUE}_p = \frac{Y_u}{\text{SWR}} \quad (7)$$

in which WUE_p is the WUE of a specific plant, and Y_u is the plant yield of interest under desirable conditions. Thus, WUE_p could be considered as an inherent plant characteristic that indicates the crop productivity per unit volume of transpiration.

Approaches and methods to increase water use efficiency

In the following sections we discuss some major approaches and methods that can be used to increase WUE in agriculture.

Improving irrigation techniques and management

Under rainfed conditions, sporadic, low precipitation, with even short dry spells, often reduces crop production, and a prolonged drought can cause total crop failure. In contrast, irrigation involves supplying water artificially to permit farming during dry periods and droughts, therefore it can increase the WUE, because the potential productivity of irrigated land per unit volume of supplied water (i.e., from rainfall + irrigation) generally exceeds that of rainfed land. The old, traditional irrigation management practice involved repeated, infrequent but massive applications of water that were intended to replenish the soil water reservoir to its field capacity. Each irrigation event was followed by a prolonged period of depletion, nearly to the point of permanent wilting, before the next irrigation event. The concept behind this irrigation management was that the availability of water for plants is constant within the range between field capacity and wilting point. However, it was found that plants responded with a pronounced increase in production when irrigation was provided in sufficient quantity and frequency to prevent the occurrence of moisture stress during the growing

season. However, this favorable water condition in the root zone is difficult to achieve with the traditional surface and sprinkler irrigation methods.

Drip or trickle and microsprayer irrigation systems – collectively called microirrigation systems – currently are being introduced in many irrigated areas. The major advantages of microirrigation systems with respect to WUE are (Hillel, 1997; Coelho and Or, 1999; Assouline et al., 2006):

1. Ability to maintain favorable moisture conditions in the root zone, in accordance with the plant requirements, while still maintaining unsaturated conditions, so that the gas exchange capability between soil air and the atmosphere is high. Under irrigation with microirrigation systems, these favorable moisture conditions in the root zone can be maintained even in problematic soils.
2. Microirrigation systems wet the soil only in the immediate vicinity of the plants. As a result, a large proportion of the field, especially the inter-row areas, remains dry, which, in turn, makes the field less prone to weed infestation and to water evaporation directly from the soil surface.
3. Because microirrigation systems generally apply the water underneath the plant canopy, water loss through interception and the hazards of leaf scorch and fungal diseases are avoided.
4. They enable incorporation of equipment such as fertilizer injectors, filters, timers, and metering valves into the irrigation system. These complementary devices can enable optimization of the water, nutrients, and air regimes in the root zone, and thereby, in turn enable enhancement of the WUE (Nadler and Tyree, 2008).
5. Under saline conditions, the continuous supply of water by microirrigation systems ensures that the Ψ_p of the soil solution remains relatively high (less negative) in the root zone, which increases water availability and plant production.

Preventing surface runoff

Surface runoff is formed when the rainfall intensity or the application rate of the irrigation system exceeds the soil infiltration rate and the water-holding capacity of the field surface. According to the field characteristics, the runoff may flow out of the field and/or accumulate in small depressions within the field. Runoff can affect crop production in three main ways: (a) runoff from a cultivated field usually is lost for plant production; (b) local runoff within a cultivated field leads to poor water distribution within the field; and (c) runoff accelerates erosion of fertile soil out of the field, and depletion of fertilizer and pesticides from the field. Ben-Hur (2008) indicated that when soils with unstable structures are exposed to water-drop impact under rainfall or sprinkler irrigation, seal formation at the soil surface could lead to a drastic decrease in infiltration. Soils in many parts of the world – such as arid and semiarid regions – are characterized by relatively low organic matter

content, high levels of salinity and sodicity, high percentages of expandable clay minerals, and low vegetative cover, all of which decrease the stability of the soil structure (Ben-Hur et al., 2009). Consequently, high surface runoff is expected in these regions (Ben-Hur, 2008).

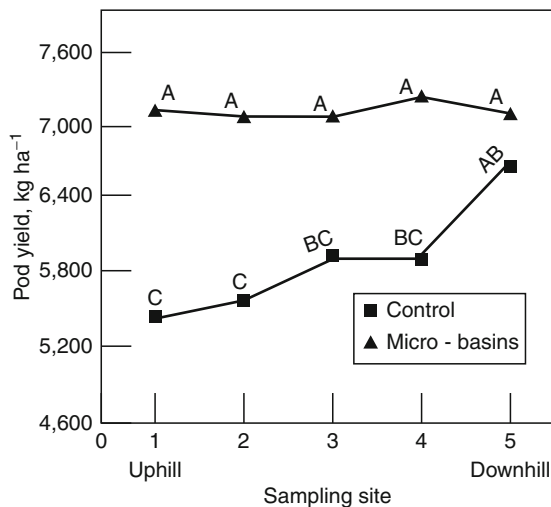
Advantages of self-propelled moving sprinkler irrigation systems (MSISs) include automation, wide-area coverage, ability to operate on relatively rough terrain, and reduced labor requirements; thus, the MSIS has become increasingly popular in recent years. However, since MSISs are designed to apply controlled amounts of water within relatively short periods, the instantaneous rate of water application rate of an MSIS with spray-nozzle emitters might be as high as 300 mm h^{-1} , compared with about 10 mm h^{-1} under traditional sprinkler irrigation. Consequently, this high water application rate increases the expectation of runoff during irrigation, particularly in soils with low infiltration rates (Stern et al., 1992; Ben-Hur, 2008).

Surface soil tillage practices

Field-surface tillage practices involve means such as microbasins (pits) and dikes across the furrows (Figure 2, lower), which can be formed by special



Water Use Efficiency in Agriculture: Opportunities for Improvement, Figure 2 Microbasin cultivator (upper) and microbasins (lower) in field irrigated by moving sprinkler irrigation system (Pictured by M. Ben-Hur).



Water Use Efficiency in Agriculture: Opportunities for Improvement, Figure 3 Peanut pod yields for two tillage treatments and five sampling sites along a slope. Within sites, symbols labeled with different letters indicate significant differences between the yields ($p < 0.05$).

machinery (Figure 2, upper). These tillage practices can increase the surface storage capacity of the field and, in turn, decrease the runoff flow within and out of the field under rainfall and irrigation with MSIS (Morin et al. 1984; Ben-Hur and Assouline, 2002). In a field experiment with peanut (*Arachis hypogaea* L.) and a slope of 3%, which was irrigated with a lateral MSIS with an average application rate of $\sim 100 \text{ mm h}^{-1}$, it was found that pod yield in plots with microbasin treatment were fairly uniform along the slope (Figure 3) whereas, in contrast, in control (without microbasin) plots pod yield increased in the downhill direction (Figure 3). Preventing runoff decreased water loss and improved the distribution uniformity of available water in the field, which, in turn, increased average pod yield by 880 kg ha^{-1} .

Soil amendments

Increased aggregate stability and prevention of seal formation, runoff, and soil erosion can be achieved by spraying soil amendments, such as gypsum or synthetic polymers, over the soil surface before a rainstorm or irrigation event (Levy and Sumner, 1998; Ben-Hur, 2006). The polymer molecules are adsorbed on the surfaces of soil particles, where they act as cement, holding particles together against the destructive forces of water drops, and preventing seal formation and runoff development (Ben-Hur, 2006). Ben-Hur (2001) studied the effects of spraying a low-molecular-weight, nonionic polymer (P-101) at 40 kg ha^{-1} on the soil surface in a field in the western Negev, Israel on runoff and potato (cv. Chloster) yield. The field was routinely irrigated with a linear MSIS fitted with three different emitters, Sprayer No. 1, Spinner, and Super Spray, with discharges of

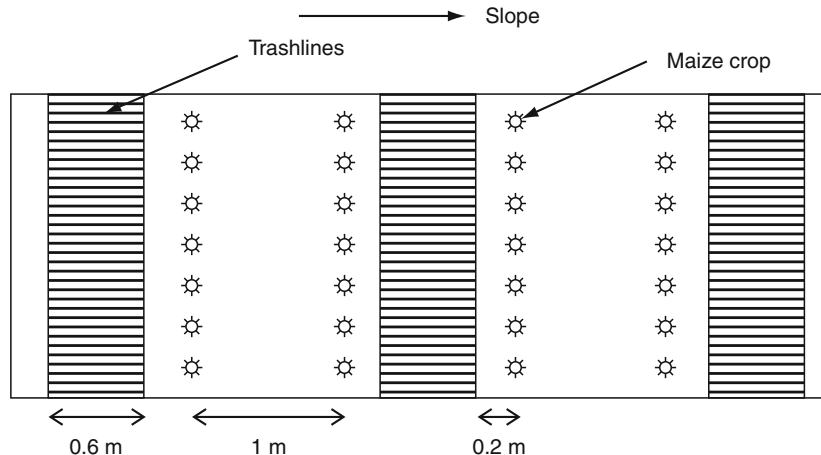
$1,254$, $2,713$, and $1,777 \text{ l h}^{-1}$, respectively. Ben-Hur (2001) found that the polymer reduced runoff by 75%, 60%, and 65% compared with the control treatment (untreated soil), for the Sprayer No. 1, Spinner, and Super Spray emitters, respectively, and the WUE_i values achieved with the MSIS fitted with these emitters were 56 , 31 , and 43 kg mm^{-1} , respectively, on untreated soil, and 66 , 49 , and 65 kg mm^{-1} , respectively, under the 40-kg ha^{-1} polymer treatment.

Soil mulching

To combat the massive problems of runoff and erosion, and the resulting low yields, poor smallholder farmers in arid and semiarid regions often use inexpensive, indigenous soil- and water-conservation techniques. The trash lines technique is among the most common and popular methods of conserving land in many areas of semiarid Africa, and is particularly valued for its positive effect on soil fertility. Wakindiki and Ben-Hur (2002) modified the traditional trash lines technique as the close-space trash lines (CSTL) technique (Figure 4). In this technique, the spacing between the trash lines was reduced to 2 m, and the plants, which are sown between the trash lines, could optimize the benefits from the water that infiltrates in the trash-covered area (Figure 4). Wakindiki and Ben-Hur (2002) studied the effects of a CSTL technique with 0.6-m-wide trash lines on runoff and soil loss, and on corn (*Zea mays* L.) and cowpea (*Vigna unguiculata*) production in semiarid Tunyai, Kenya, during five rainy seasons. The seasonal, average rainfall runoff percentage decreased significantly from 9% in untreated plots to 4% in CSTL-treated plots, and the seasonal, average soil loss decreased significantly from 3.35 Mg ha^{-1} in untreated plots to 1.17 Mg ha^{-1} in CSTL plots. These decreases in runoff and soil loss in the CSTL plots led to significant increases in the seasonal dry biomass (grain + stover) yield of corn, from 1.48 Mg ha^{-1} in the untreated plots to 3.63 Mg ha^{-1} in the CSTL plots.

Increasing crop productivity per unit transpiration, and plant selection

A different approach to increasing WUE is through increasing crop productivity per unit transpiration. To obtain progress via this approach, the closely linked processes of transpiration and yield formation need to be uncoupled, which involves two main, distinct objectives: (1) to achieve a substantial reduction of crop transpiration without a corresponding decrease in yield; and (2) to substantially increase crop yield without incurring a corresponding increase in transpiration. However, because little progress has been made toward the first objective, it is not discussed in this chapter. In contrast, much progress has already been achieved towards the second objective, by increasing the proportion of total dry matter in the harvested crop yield. For example, in some modern wheat varieties, which are grown today, the dry matter content of the grain is half of the plant total dry



Water Use Efficiency in Agriculture: Opportunities for Improvement, Figure 4 Schematic layout of the close-space trash lines technique.

matter, as compared with one-third or less in the wheat varieties that were grown at the beginning of the twentieth century (Stanhill, 1992). The modern varieties have a smaller leaf area and shorter height, and also a shorter crop cycle. All of these improvements decrease transpiration and increase WUE values by 1.5-fold compared with the values that were achieved 100 years ago (Stanhill, 1992). The potential for further progress in this direction is expected to be realized by transferring the carbon metabolism that is responsible for the high net dry matter production of C₄ plants to C₃ crop species (Ting, 1976). This would enable major increases in yields of many agricultural crops to be achieved without significant increases in transpiration. Increasing the crop productivity per unit transpiration by means of plant breeding and genetic engineering, and by growing selected crop varieties with high WUE_p, would enable substantial increases in WUE in agriculture.

Conclusions

In order to increase food production and to relieve pressure on the earth's natural ecosystems in water-limited regions, it is important to increase the WUE in agriculture. Four major factors can affect the WUE: (1) environmental conditions in the vicinity of the plant; (2) the availability of the soil water to the plant; (3) plant properties; and (4) water losses in the field. Some major approaches and methods that can be used to increase WUE in agriculture are: (1) using microirrigation systems for irrigation and improving the irrigation management; (2) preventing surface runoff in cultivated fields by using appropriate surface soil tillage practices, using soil amendments and mulching; and (3) increasing crop productivity per unit transpiration by means of plant breeding and genetic engineering. Using the above means and growing selected crop varieties with high WUE_p would enable substantial increases in WUE in agriculture.

Bibliography

- Assouline, S., Möller, M., Cohen, S., Ben-Hur, M., Grava, A., Narkis, K., and Silber, A., 2006. Soil-plant system response to pulsed drip irrigation and salinity: bell pepper case study. *Soil Science Society of America Journal*, **70**, 1556–1568.
- Ben-Hur, M., 2001. Soil conditioner effects on runoff, erosion and potato yield under sprinkler irrigation with different emitters. *Agronomy Journal*, **93**, 1156–1163.
- Ben-Hur, M., 2006. Using synthetic polymers as soil conditioners to control runoff and soil loss in arid and semiarid regions – a review. *Australian Journal of Soil Research*, **44**, 191–204.
- Ben-Hur, M., 2008. Seal formation effects on soil infiltration and runoff in arid and semiarid regions under rainfall and sprinkler irrigation conditions. In Zereini, F., and Jaeschke, W. (eds.), *Climatic Changes and Water Resources in the Middle East and in North Africa*. New York: Springer, pp. 429–452.
- Ben-Hur, M., and Assouline, S., 2002. Tillage effects on water and salt distribution in a Vertisol during effluent irrigation and rainfall. *Agronomy Journal*, **94**, 1295–1304.
- Ben-Hur, M., Yolcu, G., Uysal, H., Lado, M., and Paz, A., 2009. Soil structure changes: aggregate size and soil texture effects on hydraulic conductivity under different saline and sodic conditions. *Australian Journal of Soil Research*, **47**, 688–696.
- Coelho, E. F., and Or, D., 1999. Root distribution and water uptake patterns of corn under surface and subsurface drip irrigation. *Plant and Soil*, **206**, 123–136.
- Cohen, Y., 1992. A combined transpiration measurement and meteorological approach for determining water requirements in the field and orchard. In Shalhevet, J., Changming, L., and Yuexian, X. (eds.), *Water Use Efficiency in Agriculture. Proceedings of the Binational China-Israel Workshop*, Beijing, China, April 22–26, 1991. Rehovot: Priel Publishers, pp. 170–180.
- De Wit, C. T., 1958. Transpiration and plant yields. *Versl Landbouwk Onderz*, **646**, 59–84.
- Hillel, D., 1997. *Small-Scale Irrigation for Arid Zones: Principles and Options*. Rome: United Nations Food and Agriculture Organization. Development Monograph No. 2.
- Levy, G. J., and Sumner, M. E., 1998. Mined and by-product gypsum as soil amendments and conditioners. In Wallach, A. (ed.), *Handbook of Soil Conditioners*. New York: Marcel Dekker, pp. 399–428.
- Morin, J., Rawitz, E., Benyamin, Y., Hoogmoned, W. B., and Ethkin, H., 1984. Tillage practices for soil and water conservation in the

- semi-arid zone. 2. Development of the basin-tillage system in wheat fields. *Soil and Tillage Research*, **4**, 155–164.
- Nadler, A., and Tyree, M. T., 2008. Substituting stem's water content by electrical conductivity for monitoring water status changes. *Soil Science Society of America Journal*, **72**, 1006–1013.
- Stanhill, G., 1992. Irrigation in Israel: past achievements, present challenges and future possibilities. In Shalhevet, J., Changming, L., and Yuexian, X. (eds.), *Water Use Efficiency in Agriculture. Proceedings of the Binational China-Israel Workshop*, Beijing, China, April 22–26 1991. Rehovot: Priel Publishers, pp. 63–77.
- Stern, R., Ven Der Merwe, A. Z., Laker, M. C., and Shainberg, I., 1992. Effect of soil surface treatments on runoff and wheat yields under irrigation. *Agronomy Journal*, **84**, 114–119.
- Thornthwaite, C. W., 1948. An approach toward a rational classification of climate. *Geographical Review*, **38**, 55–94.
- Ting, I. P., 1976. Crassulacean acid metabolism in natural ecosystems in relation to annual CO₂ uptake patterns and water utilization. In Barris, R. M., and Black, C. C. (eds.), *CO₂ Metabolism and Plant Productivity*. Baltimore: University Park Press, pp. 251–268.
- Wakindiki, I. I. C., and Ben-Hur, M., 2002. Indigenous soil and water conservation techniques: effects on runoff, erosion, and crop yield under semi-arid conditions. *Australian Journal of Soil Research*, **40**, 367–379.

Cross-references

- Conditioners, Effect on Soil Physical Properties
 Crop Responses to Soil Physical Conditions
 Evapotranspiration
 Field Water Capacity
 Irrigation and Drainage, Advantages and Disadvantages
 Mulching, Effects on Soil Physical Properties
 Root Water Uptake: Toward 3-D Functional Approaches
 Soil Hydraulic Properties Affecting Root Water Uptake
 Soil Water Management
 Stomatal Conductance, Photosynthesis, and Transpiration, Modeling
 Tillage, Impacts on Soil and Environment
 Water Balance in Terrestrial Ecosystems
 Water Budget in Soil
 Water in Forming Agricultural Products

WATER-REPELLENT

Resistant to penetration by water but not entirely waterproof.

WATERLOGGED SOIL

A soil that is nearly saturated with water much of the time, such that its air phase is restricted and anaerobic conditions prevail. In extreme cases of prolonged waterlogging, anaerobiosis occurs, the roots of mesophytes suffer, and chemical reduction processes occur (including denitrification, methangensis, and the reduction of iron and manganese oxides).

Bibliography

Introduction to Environmental Soil Physics (First Edition) 2003
 Elsevier Inc. Daniel Hillel (ed.) <http://www.sciencedirect.com/science/book/9780123486554>

WATERSHED

See [Tropical Watersheds, Hydrological Processes](#)

WEATHER, EFFECTS ON PLANTS

Vlasta Štekauerová

Institute of Hydrology, Slovak Academy of Sciences,
 Bratislava 3, Slovakia

Definition

Weather is the state of the atmosphere on a particular place and at a defined time or a defined time interval. It is characterized by a set of data of the meteorological elements and phenomena, as precipitation, sunshine duration, air temperature, air pressure, wind velocity, air humidity, cloudiness, or other characteristics. The weather impact upon the vegetation can be evaluated either directly through its particular components (i.e., meteorological elements) or through transpiration impact upon the biomass production.

Introduction

Weather is influencing the environment permanently. Its course throughout the year is influencing both, the qualitative and quantitative properties of plants. For some production branches, weather presents in relation to vegetation, an objective production factor. For ecosystems, it is a factor on which the life can depend, at extreme, long-lasting conditions, even the plant's some species survival can depend.

Weather conditions are one of the factors influencing biomass production and its variability. Weather impact manifests differently on various species of the vegetation cover.

To determine weather impact upon the vegetation cover is fairly difficult; namely, weather in its effect should be understood as a multicomponent characteristic. It should also be noted that vegetation belongs to the atmosphere–plant–soil system, and that the biomass production depends upon all these three system components.

Long-term weather regime represents the climate representing an average weather state of a particular region. This state is derived from time courses of the meteorological elements, of a long-term period. Climate, differently from the weather, is influencing permanently on the vegetation cover structure and its biomass production. Based on this, it is possible to optimize the plant production structure, in various production regions.

Weather, and its dynamic in particular years, often differs expressively in relation to long-year mean values. Factors influencing the biomass production in a great extent are the weather extremes.

Solar radiation

For weather formation, the most important is the energy transfer from the Sun to the Earth through the cosmic

space, in the form of electromagnetic waves. Solar radiation is only slightly influenced by the cosmic space. It changes only when passing through the atmosphere. There it comes to its reflection, absorption, and dispersion, by clouds, water vapor, molecules of gases, and dust particles.

Electromagnetic spectrum of the solar radiation expands within a broad wavelength interval. Only a negligible part of it (400–760 nm) is noted for physiological effects (photosynthetically active radiation [FAR]), which condition the growth and the development of the green plants. This part of the energetic spectrum is also called the light. It is a part of the plant's photosynthesis.

Physiological radiation effect (photochemical) is materialized in process of the photosynthetic assimilation. Physical result of radiation is the plant's warming and consequent acceleration or deceleration of several physiological processes. Appearance of the plant depends upon the ratio of particular spectrum components. According to the plant's demands for light, we divide them into demanding light, demanding shade, and indifferent.

Photosynthesis is a decisive process for the plant production. Through it, the substances originate basic for the plant's body, and the energy needed for the physiological processes and reactions in the plant's mass exchange.

Portion of FAR in all radiation amount is not constant. It is influenced by the sun's elevation above the horizon, by the cloudiness, by the precipitation intensity, etc. The highest FAR portion in total global radiation was detected at cloudless sky, immediately prior to sunrise (70%), and the lowest at cloudless sky at noon hours (40%). Based upon the observation results, it was agreed internationally that this ratio be constant and equal to 45% of the global energy radiation. This means that the photosynthesis consumes only a small part of it. Photosynthetic efficiency of the real agricultural plants, forests, and marshes, as a rule does not exceed 2.5% of the global radiation energy, in the vegetational period.

Thus the plant production substance is the accumulation of the transformed energy of the sun into yield, and the amount of this energy upon the soil unit area is quasi constant. From it follows, that to achieve the maximum biomass production, it is necessary to utilize maximum ratio of the total solar radiation energy used for photosynthesis, during the production period on the area covered with vegetation.

Maximum biomass production (U_{\max}) is possible to express by [Equation 1](#), where G_{vo} (kWh m^{-2}) is the total global radiation falling during the vegetation period in the given conditions, and ε_{\max} is the maximum utilization degree of the radiation energy for photosynthesis, for a particular plant.

$$U_{\max} = \frac{G_{vo}\varepsilon_{\max}}{100Q} [\text{kg m}^{-2}] \quad (1)$$

Q is energy equivalent needed for the production of 1 kg of organic matter dry substance. Photosynthesis integral part is the transpiration, i.e., the water transfer from soil

through the plant into the atmosphere. Part of water flowing through the plant becomes a part of the transpiration and simultaneously is transporting to plant the nutrients. Transpiration is subordinated to the solar energy inflow. Its substantial part is consumed for the water phase change from liquid to water vapor, and simultaneously for cooling of the surrounding environment and adjusting it for vegetational living conditions.

There is another important process – evaporation. It also depends upon the solar energy input and upon its transformation into heat. The sum of evaporation and transpiration is evapotranspiration, the important water balance component and is also an important thermoregulatory element.

Sunshine

Sunshine duration and thus the solar energy input is governed by regular natural laws and shows a cyclic influence upon the vegetation cover – the yearly seasons. Depending on them directly is the vegetation transpiration.

Temperature

Air temperature is the state quantity determined by the mean kinetic energy of the chaotic air molecules motion.

When passing through the clean atmosphere, the solar radiation takes only a negligible role in the air warming up. The mean source of heat for the earth air enfold is the earth surface, called as active surface. There the sun's short-wave radiation is being transformed, increasing the earth surface temperature, which on the other hand, radiates the long-wave radiation, warming up the atmosphere.

It is surface of the earth, snow cover, rock, vegetation, or arbitrary body, which absorbs, transfers, and radiates energy. This all is of importance even for deeper soil layers.

Among the most important atmospheric processes belongs the heat exchange, forming the atmospheric thermal regime. Heat exchange takes part between the atmosphere, the active earth surface, vertical and horizontal transport of water, and energy.

Temperature presents one of the basic living conditions of plants. It is the base and is inevitable for life and its functions, as the nutrients receipt, transpiration, photosynthesis, breathing, and others. Plants can grow only at a particular temperature interval. Its lower and upper limits are called the critical temperatures. Dependence of the photosynthesis intensity upon the air temperature has form of the normal probability distribution, limited by the minimum air temperatures (biological temperature minimum), within the limits 2–5°C. It is also limited by the high air temperatures (lethal temperature), at which plants are dying in consequence of decay of their tissues (45–50°C). The maximum photosynthesis efficiency takes part at the optimum temperature, depending on the plant species. Optimum air temperature for potatoes is around 30°C, for warm-living plants (tomatoes, cucumbers) it is approximately 35°C. With the air temperature rise, the photosynthesis intensity is dropping down fast, until it stops at the critical air temperatures.

Air pressure

Air pressure is defined as the force, by which the air column (from the earth surface up to the upper atmosphere limit) is acting upon the surface unit.

Irregular air pressure distribution and its changes are due to irregular earth surface warming up. This irregular air pressure distribution results in horizontal and vertical airflow (wind). The air pressure changes cause, in most cases, the weather extremes.

Air pressure depends upon the altitude above sea level, acceleration gravity, and temperature. Neither its direct influence upon plants nor its changes have been detected so far. Its indirect influence is manifested through the weather change, depending directly upon the air pressure changes.

Air pressure changes are also manifested in the unsaturated soil zone, in its water retention and flow. This soil zone is one of the decisive factors influencing the plant's growth. Air pressure is affecting also the groundwater level. It is decreasing (lowering) at the air pressure rise, and vice versa, rising at pressure drop. These changes can make up to tens of centimeters, thus influencing the soil water regime.

Air humidity

Through air humidity the air water vapor content is expressed. A dry air does not exist at natural conditions. Water vapor has a decisive importance for the meteorological phenomena related to the water physical phase changes. The air water vapor content is changing continuously within particular limits, in consequence of the water phase changes. Depending on the temperature, the air can contain only a particular amount of water vapor. It is an equilibrium state, when the air is saturated with water vapor at a given temperature. At this state, that amount of water vapor molecules condensate into water, same molecules amount of water will evaporate at this temperature.

Air humidity is influencing the transpiration intensity and thus indirectly, the vegetation cover. The lower the air humidity, the higher is the transpiration. When the air is saturated with water vapor, the transpiration is zero. Air humidity is of the highest importance in periods when evaporation is of such intensity, that water inflow from soil is not sufficient for the plants water consumption. Vegetation then wilts and fades away inevitably.

Direct effect of air humidity upon the plant production can be observed also at incidence of plant diseases and insects. Many plant diseases and incidence of insects, except the air temperature, depend also upon the air humidity.

Cloudiness

Degree of the sky coverage by clouds is called cloudiness, expressed by the ratio of the sky covered by clouds, e.g., within the range from 0 to 10, or in percent (%).

Cloudiness plays an important role in view of the earth energy balance. Clouds absorb and reflect the direct solar

radiation and increase its dispersion. Thus, it decreases the positive balance of the long-wave radiation falling on the earth surface, and through this, it changes the conditions of its illumination.

Formation of clouds is due to irregular air water vapor distribution. Existence of the condensation nuclei is inevitable for that, together with saturation of the air by water vapor around the nuclei. Regardless of the cloud origin conditions, it is always formed either by tiny water droplets or by very small ice crystals. For vegetation are important those clouds bringing precipitation.

Precipitation

From meteorological elements or phenomena influencing most the plant's nutrients intake, belongs the precipitation amount. It influences primarily its water regime as well as that of the soil. Water as a base of the soil water solution and the plant nutrients carrier is influencing nutrients reception by a dominant way.

Precipitation deposited from the clouds is falling on the earth surface in a liquid or solid phase. The liquid precipitation is rain, which can be either of a long-term character (regional rain) or of a short-term one (short-term downpour). Important is also snow precipitation of a solid phase. It supplies water to soil in sufficient amount at the beginning of the vegetation season, and also protects vegetation against freezing out. Water is a basic building component of the plant complexes, where it plays important vital functions. Precipitation belongs to the natural water resource, in many cases only single supplying vegetation by water. In order to secure in plant cells normal vital functions, these cells must be sufficiently saturated by water – hydrated. Hydration level is not a stable quantity, because each cell, each plant organ, and the whole plant has its own water balance, i.e., its inflow and outflow.

The plant water content is not static, it is dynamic. The receipt and release water balance components in the same time interval are not the same. The balance can be positive at water saturation or negative when water deficit originates, and the plant suffers with lack of water. The water deficit can be of a permanent character, caused by a low soil moisture (by prevailing transpiration), or transient caused by a transient passive water balance, e.g., during daily time course.

In general, plants utilize water mostly from the soil resources. Soil water storage is formed by the precipitation and does not have the properties of free water. It is held in soil mainly by the capillary soil forces. So the soil water resources magnitude, except precipitation, depends upon the soil water type and its retention storage capacity. Whether this storage will be satisfactory for the production process during the vegetation season depends upon the soil hydrophysical properties and upon the plant characteristics. There exist such moisture soil states, according to which it is possible to determine whether the soil water is able to supply plant by it. Such soil moisture states can be expressed by the basic hydrophysical

soil characteristic – moisture retention curve. The field water capacity is characterizing by moisture lasting in soil profile a relatively longer time, when simultaneously the soil aeration zone is sufficient for the vegetation cover development. The point decreased soil water availability is characterizing the state of soil water when vegetation cover physiological processes are limited by water shortage. In case of the soil moisture increase (e.g., by precipitation), the plant is developing and growing further on. The soil moisture wilting point is characterizing the state when vegetation cover is not sufficiently supplied by water, and the plant is in stress and it is permanently wilting, perishing. This state is usually irreversible. The latest research shows that plants are able to use water from soil also in case when soil moisture is lower than soil moisture subsistent to wilting point, if they can adapt to the stressed conditions. (Ritchie and Burnett, 1971).

When extreme precipitation occurs, the soil can be flooded, soil aeration is low (anaerobiosis range of soil moisture), and not suitable for vegetation cover further development. Similarly, at longer precipitation absence, the dried soil is not able to supply vegetation by water. To what extent these extremes will show up upon the plant production decrease depends on their durations and on their occurrence frequency during the vegetation season, respectively.

Conclusions

It is rather complicated to express impacts of weather upon the vegetation. The weather is a multicomponent system, where individual components are mutually influencing each other. Impact of these components upon vegetation can be expressed also individually, but it should be kept in mind that they all act together influencing the weather in a complex way.

Weather and its changes show up in change of the vegetation cover production. It can be expressed in relation to the plant dry matter production Y_d , and to the total transpiration E_t during the whole vegetation season, according to Equation 2:

$$Y_d = nE_t \quad (2)$$

where n is water efficiency coefficient.

The total transpiration is a function of weather as a whole. The Penman–Monteith equation (Penman, 1948; Monteith, 1965) based on the transpiration model is using the above-described weather components as the model input variables. These weather components, either directly or indirectly, influence the transpiration or evapotranspiration velocity, respectively.

The weather manifests specifically by its extremes, like flooding, long periods of droughts (periods without precipitation), strong windstorms, etc. These extreme events usually influence the vegetation cover production only once in a way.

Bibliography

- Monteith, J. L., 1965. Evaporation and environment. In Fogg, G. E. (ed.), *The State and Movement of Water in Living Organisms*. Cambridge: Cambridge University Press, pp. 205–234.
 Penman, H. L., 1948. Natural evaporation from open water, bare soil and grass. *Proceedings of the Royal Society of London A*, **193**, 120–145.
 Ritchie, J. T., and Burnett, E., 1971. Dryland evaporative flux in a subhumid climate. II. Plant influences. *Agronomy Journal*, **63**, 56–62.

Cross-references

- [Ecohydrology](#)
[Evapotranspiration](#)
[Physics of Near Ground Atmosphere](#)
[Soil Water Flow](#)
[Stomatal Conductance, Photosynthesis, and Transpiration, Modeling](#)
[Water Balance in Terrestrial Ecosystems](#)
[Water Budget in Soil](#)

WELLNESS

See [Plant Wellness](#)

WETLANDS, MANAGEMENT, DEGRADATION AND RESTORATION

Kathrin Kiehl

University of Applied Sciences Osnabrück, Osnabrück, Germany

Definition of wetlands

For wetlands many definitions exist, which are generally based on three components: hydrology, physicochemical environment, and biota (Mitsch and Gosselink, 2000). The most comprehensive definition of wetlands was presented by the U.S. Fish and Wildlife Service (Cowardin et al., 1979):

Wetlands are lands transitional between terrestrial and aquatic systems, where the water table is usually at or near the surface or the land is covered by shallow water. [...] Wetlands must have one or more of the following three attributes: (1) at least periodically the land supports predominantly hydrophytes; (2) the substrate is predominantly undrained hydric soil; and (3) the substrate is [...] saturated with water or covered by shallow water at some time during the growing season of each year.

This definition covers both coastal and freshwater wetlands. The following text will focus on freshwater wetlands such as shallow lakes, ponds, freshwater marshes, swamps, and riparian ecosystems. Peatlands such as bogs and fens are another type of freshwater wetlands characterized by the accumulation of peat under wet conditions. Environmental

functions of peatlands are described by Vasander ([Peatlands: Environmental Functions](#)) and physical properties by Szajdak ([Peats and Peatlands, Physical Properties](#)).

Functions of wetland ecosystems

Both in natural and in cultural landscapes, wetland ecosystems play a major role in the ecological functioning of watersheds as they are often located in transition zones between terrestrial and open-water aquatic ecosystems. Their morphology and hydrologic conditions influence not only the retention and release of water but also biogeochemical transformations of carbon, nutrients, and pollutants and the availability of habitats for specialized plant and animal species (Bobbink et al., 2006; van der Valk, 2006).

Water budget and water retention

Wetlands can be characterized by their hydroperiod and their water budget ([Ecohydrology, Water Budget in Soil](#)). The hydroperiod is defined as the seasonal pattern of the water level (Mitsch and Gosselink, 2000). Examples for freshwater wetlands with different hydroperiods are permanently flooded wetlands (e.g., ponds, shallow lakes), seasonally flooded wetlands (e.g., riparian wetlands and freshwater marshes affected by floodings), and wetlands with water-saturated substrates but without surface water during most of the year (e.g., fens and bogs, see [Peatlands: Environmental Functions; Surface and Subsurface Waters](#)).

The water budget of a freshwater wetland is affected by precipitation and “evapotranspiration” as well as by inflow, outflow, and storage of water as a result of geomorphological and geological conditions. The balance between water storage, inflow, and outflow can be expressed as

$$\frac{\Delta V}{\Delta t} = P_n + S_i + G_i + ET + S_o + G_o$$

where

V = Volume of water stored in the wetland

$\Delta V/\Delta t$ = Change of volume of water stored in the wetland per time unit t

P_n = Net precipitation

S_i = Surface inflows (incl. flooding by streams)

G_i = Groundwater inflows

ET = Evapotranspiration

S_o = Surface outflows

G_o = Groundwater outflows

(modified for freshwater wetlands after Mitsch and Gosselink, 2000)

The capacity of wetlands to store water is one of their main ecosystem functions (Davidsson et al., 2000; Zedler, 2003; McAlpine and Wotton, 2009). There is strong evidence that water retention in wetlands located in floodplains or in headwaters of rivers can significantly reduce or delay floods and therefore reduce flood damage downstreams (Bullock and Acreman, 2003; Zedler and Kercher, 2005; Brody et al., 2007; Ming et al., 2007). Only in few cases, an increase of downstream flood flows has been

reported for saturated headwater wetlands (Bullock and Acreman, 2003).

Transformation and retention of nutrients and pollutants

The improvement of water quality during the flow through wetlands is another ecosystem function of both ecological and economical significance (Zedler, 2003; McAlpine and Wotton, 2009). All over the world, constructed wetlands are used for the treatment of wastewater (Vymazal et al., 2006; Lee et al., 2009; Zhang et al., 2009). Natural and seminatural wetlands, however, have also a high potential for removing nutrients from surface waters and groundwater, for example, in agricultural landscapes with high nutrient discharges (Jansson et al., 1994; Kronvang et al., 1999; Saunders and Kalff, 2001; Hoffmann and Baattrup-Pedersen, 2007; Bavor and Waters, 2008).

As human activities (e.g., agricultural fertilization and burning of fossil fuels) have altered the global nitrogen cycle, the nitrogen load to freshwaters has strongly increased, especially in industrialized and agriculturally used areas (Vitousek et al., 1997). It has been shown that diffuse nitrogen discharges from agricultural land can be lowered by a reduction of fertilizer application, by nitrogen uptake of crops, and by nitrogen removal in natural and constructed wetlands (Saunders and Kalff, 2001; Verhoeven et al., 2006; Lee et al., 2009).

In wetlands, three processes contribute to nitrogen retention: denitrification, sedimentation, and uptake by aquatic plants. During denitrification, facultative anaerobic bacteria in sediments or in biofilms on the surface of aquatic plants transform nitrate finally to gaseous atmospheric nitrogen (N_2):



The efficiency of nitrogen removal is affected by the nitrate concentration, the availability of organic carbon, the presence and type of wetland vegetation, and the retention time of the water within the wetland (Davidsson, 1997; Lee et al., 2009). Under certain conditions (e.g., at high temperatures or in partly aerated wetland soils), the intermediate product nitrous oxide (N_2O), instead of the end product N_2 , may be released to the atmosphere during denitrification (Vymazal et al., 2006), which is problematic because N_2O is one of the greenhouse gases contributing to global warming (see [Greenhouse Gas Fluxes: Effects of Physical Conditions](#)). For constructed wetlands, however, which generally receive the highest nitrogen loads, the contribution to global warming potential is usually neglectable due to their small scale (Stadmark and Leonardson, 2005; Vymazal et al., 2006). In natural wetlands, the production of greenhouse gases can be reduced by careful management of the water table (see below).

Phosphorus discharges from agricultural areas to surface waters are mostly due to soil erosion because phosphorus is bound to soil particles (Blume et al., 2002; see [Water Erosion: Environmental and Economical Hazard](#)).

The processes for the removal of phosphorus from surface waters are sedimentation of P bound to soil particles, soil adsorption, plant uptake, and microbial uptake (Uusi-Kämppä et al., 2000; Hogan et al., 2004; Hoffmann et al., 2009). In contrast to nitrogen, phosphorus cannot be totally eliminated from wetlands by bacteria. It can be accumulated in wetland sediments or released later depending on the interactions between groundwater and surface water. In riparian buffer zones and other temporarily or permanently flooded wetlands, P-retention by sedimentation can reach high rates, while immobilization rates by plant uptake are much lower (Kronvang et al., 1999; Hoffmann et al., 2009). Particle-bound phosphorus can be released from wetlands, however, when sediments are remobilized and washed out, for example, due to high flow velocity of flooding water. Furthermore, dissolved P can be released from wetland soils or sediments due to interactions with iron and aluminum oxides or other minerals under anaerobic conditions (Hoffmann et al., 2009). The sorption, precipitation, and release of different P-fractions under changing redox potentials (see *Oxidation-Reduction Reactions in the Environment*) is a complex field that still needs further research.

Apart from nutrient retention, constructed wetlands have also been used successfully for the removal of industrial pollutants such as heavy metals or organic compounds from wastewater (Yang et al., 2006; Haberl et al., 2008; Vymazal and Kröpfelová, 2009).

Wetlands as habitats for native plants and animals

Worldwide, wetlands are important habitats for specialized plant and animal species (Mitsch and Gosselink, 2000). Wetland plants such as hydrophytes (water plants) or helophytes (semiaquatic plants with aboveground organs above the water table) need special morphological and physiological adaptations to cope with temporal or permanent submergence and anoxic conditions in the root zone (Jackson, 2006; van der Valk, 2006; *Aeration of Soils and Plants*).

Many invertebrates such as aquatic insects, crustaceans, or mollusks depend on wetland habitats (van der Valk, 2006). Typical wetland vertebrates include amphibians (e.g., frogs and newts), reptiles (e.g., alligators and crocodiles), birds (e.g., ducks, waders, herons), mammals (e.g., beavers, otters, moose), and fish species typical for shallow water.

Apart from some widespread species, many native wetland plant and animal species have become rare due to wetland loss and degradation (see below). Today, a high proportion of species typical for wetlands and other freshwater ecosystems is even threatened with extinction (Bobbink et al., 2006).

Wetland degradation and loss

With increasing human activity, in particular since the nineteenth century, large areas of natural wetlands have been degraded or destroyed by drainage and

intensification of land use (e.g., Wolff, 1993; Finlayson and Rea, 1999; van der Valk, 2006). Especially in industrialized countries, natural wetlands declined due to reclamation of floodplains, poldering, river regulation, peat mining, and drainage for agriculture and forestry. Worldwide, the dramatic loss of wetlands has reached 50%; in densely populated regions of Europe, North America, or East Asia even more than 80% of wetlands are lost or severely degraded (Bobbink et al., 2006).

Many natural wetlands are degraded due to drainage by artificial ditches or restricted flooding regimes, which can change the soil structure (see *Physical Degradation of Soils, Risks and Threats*) and the whole biogeochemical cycling of nutrients and other chemicals in soils and sediments and hence affect the quality of resident and outflowing water (Updegraff et al., 1995; Olde Venterink et al., 2002; Hoffmann et al., 2009). Furthermore, the drainage and cultivation of wetland soils with high contents of accumulated organic matter (especially in peatlands; see *Peatlands: Environmental Functions*) leads to tremendous losses of CO₂, N₂O, and other greenhouse gases (Zedler and Kercher, 2005; see *Greenhouse Gas Fluxes: Effects of Physical Conditions*).

Although wetlands show a high capacity for retention and transformation of nutrients (see above), nutrient loads to natural wetlands have reached a critical level in many parts of the world with negative effects on wetland biodiversity and ecosystem functioning (Khan and Ansari, 2005; Lamers et al., 2006; Hogan and Walbridge, 2009). Therefore, wetland management and restoration have to consider the conflict between the optimization of nutrient retention and the optimal conservation of species-rich wetland communities adapted to oligo- and mesotrophic conditions (Verhoeven et al., 2006).

Wetland management

Natural wetlands are often unmanaged but in many parts of the world, both, natural and especially constructed wetlands are managed for nature conservation, environmental protection, and recreation or for the production of food and renewable resources (Mitsch and Gosselink, 2000; Zedler and Kercher, 2005; Welcomme et al., 2006; see *Nature Conservation Management*). Management practices differ strongly between different types of wetlands depending on desirable ecosystem services and other management goals.

In constructed wetlands, the management of floods and nutrient retention includes the optimization of wetland topography in order to control the water table, the in- and outflow as well as the retention time of the water (Trepel and Opitz 2000; Vymazal et al., 2006). Periodic removal (“harvest”) of vegetation and organic detritus or sediments (if necessary) enhances the water flow through the wetland and removes nutrients that cannot be eliminated by bacterial transformations (e.g., phosphorus, see above). Furthermore, the removal of vegetation and detritus can have a positive effect on wetland biodiversity

because the dominance of competitive species is reduced and conditions for early successional plants (like many threatened water plants) are improved.

Due to the fact that water and nutrient budgets of wetlands within one catchment area are often related and biocenoses are linked to each other, it is advisable to develop management concepts for whole watersheds (Kronvang et al., 1999; Zedler, 2003; Pittock et al., 2006). For a sustainable management of natural and seminatural wetlands, it is a challenge to take into account conflicting interests of biodiversity conservation and agricultural or industrial land use as well as ecosystem services (Maltby, 2006; Verhoeven et al., 2006).

Wetland restoration

Although damages to natural wetlands are often not reversible (e.g., loss of organic matter and soil compaction due to drainage), many projects have shown that it is possible to restore at least part of the ecosystem functions of degraded wetlands (Zedler and Kercher, 2005). For the restoration of drained wetlands, it is essential to improve the water balance (see above) by rewetting and to restore the hydroperiod, for example, by filling up ditches, inflow of surface water or restoration of natural flooding regimes (e.g., Pfadenhauer and Grootjans, 1999; Hoffmann and Baattrup-Pedersen, 2007). However, not only the quantity but also the quality of the water used for rewetting has to be considered in order to avoid negative effects of high loads of nutrients and pollutants on species-rich oligo- and mesotrophic ecosystems (Lamers et al., 2006; Verhoeven et al., 2006). In areas with high nutrient discharges from agricultural fields, it is recommendable to use series of consecutive wetlands. First, nutrient-rich water can be cleaned, for example, in constructed wetlands optimized for nutrient retention (e.g., Vymazal et al., 2006) or in (semi) natural wetlands with high productive but species-poor vegetation like reed (*Phragmites australis*) with high potential for nutrient retention. Afterwards, the cleaned discharge water can be used for rewetting of oligo- and mesotrophic wetlands with high value for biodiversity.

In rewetting projects, it has to be considered that soil physical properties and the biogeochemical cycling of nutrients in formerly drained wetland soils can be changed dramatically by drying and rewetting (Olde Venterink et al., 2002; Lamers et al., 2006; see *Wetting and Drying, Effect on Soil Physical Properties*). Under certain conditions, rewetting can, for example, induce phosphorus discharges from eutrophied wetland soils (Hoffmann et al., 2009) or enhance the production of greenhouse gases if water tables are not carefully adjusted (Verhoeven et al., 2006).

Wetland restoration can be limited not only by abiotic but also by biotic constraints (Zedler and Kercher, 2005). As many alien invasive species spread easily along watercourses, the restoration of natural or seminatural wetlands can be hampered by dominant invasive species (Zedler and Kercher, 2004). On the other hand, wetland target

species, which have disappeared from the wetland and its surroundings due to drainage or changed land use, often show a limited dispersal in fragmented landscapes (e.g., Klimkowska et al., 2007). Recent studies indicate, however, that dispersal limitation can be overcome by measures of target species introduction (Pfadenhauer and Grootjans, 1999; Zedler and Kercher, 2005).

Summary

Freshwater wetlands as transitional ecosystems between terrestrial and aquatic systems have important ecological functions in watersheds. Calculations of water budgets have shown that the capacity of wetlands to store water is generally high. The quality of water loaded with nutrients or pollutants can be strongly improved during the flow through wetlands due to sedimentation and nutrient transformation processes (e.g., denitrification). Therefore, constructed wetlands can be used for wastewater treatment. Natural wetlands as habitats of many specialized plant and animal species and globally important sinks for carbon have dramatically declined all over the world. Furthermore, drainage and restricted flooding regimes have led to tremendous carbon losses from wetlands and often changed the biogeochemical cycling of nutrients and other chemicals in soils and sediments. Management and restoration concepts for the improvement of the retention and habitat function of wetlands should be developed for whole watersheds. They have to consider the conflicting interests of biodiversity conservation and agricultural or industrial land use as well as the ecosystem services of wetlands.

Bibliography

- Bavor, H. J., and Waters, T. M., 2008. Buffering performance in a Papyrus-dominated wetland system of the Kenyan portion of the Lake Victoria Basin. In Vymazal, J. (ed.), *Wastewater Treatment, Plant Dynamics and Management in Constructed and Natural Wetlands*. Heidelberg: Springer, pp. 33–38.
- Blume, H.-P., Brümmer, G. W., Schwertmann, U., Horn, R., Kögel-Knabner, I., Stahr, K., Auerswald, K., Beyer, L., Hartmann, A., Litz, N., Scheinost, A., Stanjek, H., Welpe, G., and Wilke, B.-M., 2002. *Scheffer-Schachtschabel - Lehrbuch der Bodenkunde*, 15th edn. Heidelberg Berlin: Spektrum Akademischer Verlag.
- Bobbink, R., Whigham, D. F., Beltman, B., and Verhoeven, J. T. A., 2006. Wetland functioning in relation to biodiversity conservation and restoration. In Bobbink, R., Beltman, B., Verhoeven, J. T. A., and Whigham, D. F. (eds.), *Wetlands: Functioning, Biodiversity Conservation, and Restoration*. Berlin, Heidelberg: Springer. Ecological Studies, Vol. 191.
- Brody, S. D., Highfield, W. E., Ryu, H. C., and Spanel-Weber, L., 2007. Examining the relationship between wetland alteration and watershed flooding in Texas and Florida. *Natural Hazards*, **40**, 413–428.
- Bullock, A., and Acreman, M., 2003. The role of wetlands in the hydrological cycle. *Hydrology and Earth System Sciences*, **7**, 358–389.
- Cowardin, L. M., Carter, V., Golet, F. C., and LaRoe, E. T., 1979. *Classification of Wetlands and Deepwater Habitats of the United States*. Washington DC: U.S. Department of the Interior, Fish and Wildlife Service.

- Davidsson, T., 1997. *Nitrogen Transformations in Wetlands: Effects of Water Flow Patterns*. Ph. D. Thesis, Lund/Sweden: Lund University.
- Davidsson, T., Kiehl, K., and Hoffmann, C. C., 2000. Guidelines for monitoring of wetland functioning. In Trepel, M., and Opitz, S. (eds.), *Guidelines for Wetland Monitoring, Designing and Modelling*. EcosSys, Vol. 8, pp. 5–50.
- Finlayson, C. M., and Rea, N., 1999. Reasons for the loss and degradation of Australian wetlands. *Wetlands Ecology and Management*, **7**, 1–11.
- Haberl, R., Grego, S., Langergraber, G., Kadlec, R. H., Ciccalini, A.-R., Martins Dias, S., Novais, J. M., Aubert, S., Gerth, A., Thomas, H., and Hebner, A., 2008. Constructed wetlands for the treatment of organic pollutants. *Journal of Soils and Sediments*, **3**, 109–124.
- Hoffmann, C. C., and Baattrup-Pedersen, A., 2007. Re-establishing freshwater wetlands in Denmark. *Ecological Engineering*, **30**, 157–166.
- Hoffmann, C. C., Kjaergaard, C., Uusi-Kämppä, J., Bruun Hansen, H. C., and Kronvang, B., 2009. Phosphorus retention in riparian buffers: review of their efficiency. *Journal of Environmental Quality*, **38**, 1942–1955.
- Hogan, D. M., Jordan, T. E., and Walbridge, M. R., 2004. Phosphorus retention and soil organic carbon in restored and natural freshwater wetlands. *Wetlands*, **24**, 573–585.
- Hogan, D. M., and Walbridge, M. R., 2009. Recent land cover history and nutrient retention in riparian wetlands. *Environmental Management*, **44**, 62–72.
- Jackson, M. B., 2006. Plant survival in wet environments: resilience and escape mediated by shoot systems. In Bobbink, R., Beltman, B., Verhoeven, J. T. A., and Whigham, D. F. (eds.), *Wetlands: Functioning, Biodiversity Conservation, and Restoration*. Berlin Heidelberg: Springer. Ecological Studies, Vol. 191, pp. 15–36.
- Jansson, M., Andersson, R., Berggren, H., and Leonardson, L., 1994. Wetlands and lakes as nitrogen traps. *Ambio*, **23**, 320–325.
- Khan, F. A., and Ansari, A. A., 2005. Eutrophication: an ecological vision. *The Botanical Review*, **71**, 449–482.
- Klimkowska, A., van Diggelen, R., Bakker, J. P., and Grootjans, A. O., 2007. Wet meadow restoration in Western Europe: A quantitative assessment of the effectiveness of several techniques. *Biological Conservation*, **140**, 318–328.
- Kronvang, B., Hoffmann, C. C., Svendsen, L. M., Windolf, J., Jensen, J. P., and Dørge, J., 1999. Retention of nutrients in river basins. *Aquatic Ecology*, **33**, 29–40.
- Lamers, L., Loeb, R., Antheunisse, A., Miletto, M., Lucassen, E., Boxman, A., Smolders, A., and Roelofs, J., 2006. Biogeochemical constraints on the ecological rehabilitation of wetland vegetation in river floodplains. *Hydrobiologia*, **565**, 165–186.
- Lee, C. G., Fletcher, T. D., and Sun, G., 2009. Nitrogen removal in constructed wetland systems: a review. *Engineering in Life Sciences*, **9**, 11–22.
- Maltby, E., 2006. Wetland conservation and management: Questions for science and society in applying the ecosystem approach. In Bobbink, R., Beltman, B., Verhoeven, J. T. A., and Whigham, D. F. (eds.), *Wetlands: Functioning, Biodiversity Conservation, and Restoration*. Berlin Heidelberg: Springer. Ecological Studies, Vol. 191, pp. 93–116.
- McAlpine, K. G., and Wotton, D. M., 2009. *Conservation and the Delivery of Ecosystem Services: A Literature Review*. In New Zealand Department of Conservation (ed.), Science for Conservation, 295. Wellington (New Zealand), pp. 1–81.
- Ming, J., Xian-guo, L., Lin-shu, X., Li-juan, C., and Shouzheng, T., 2007. Flood mitigation benefit of wetland soil – a case study in Momoge National Nature Reserve in China. *Ecological Economics*, **61**, 217–223.
- Mitsch, W. J., and Gosselink, J. G., 2000. *Wetlands*, 3rd edn. New York: Wiley.
- Olde Venterink, H., Davidsson, T. E., Kiehl, K., and Leonardson, L., 2002. Impact of drying and re-wetting on N, P and K dynamics in a wetland soil. *Plant and Soil*, **243**, 119–130.
- Pfadenhauer, J., and Grootjans, A., 1999. Wetland restoration in Central Europe: aims and methods. *Applied Vegetation Science*, **2**, 95–106.
- Pittock, J., Lehner, B., and Lifen, L., 2006. River basin management to conserve wetlands and water resources. In Bobbink, R., Beltman, B., Verhoeven, J. T. A., and Whigham, D. F. (eds.), *Wetlands: Functioning, Biodiversity Conservation, and Restoration*. Berlin Heidelberg: Springer. Ecological Studies, Vol. 191, pp. 169–196.
- Saunders, D. L., and Kalff, J., 2001. Nitrogen retention in wetlands, lakes and rivers. *Hydrobiologia*, **443**, 205–212.
- Stadmark, J., and Leonardson, L., 2005. Emission of greenhouse gases from ponds constructed for nitrogen removal. *Ecological Engineering*, **25**, 542–51.
- Trepel, M., and Opitz, S., 2000. Guidelines for wetland monitoring, designing and modelling. *EcoSys*, **8**, 1–140.
- Updegraff, K., Pastor, J., Bridgeman, S. D., and Johnston, C. A., 1995. Environmental and substrate controls over carbon and nitrogen mineralization in northern wetlands. *Ecological Applications*, **5**, 151–163.
- Uusi-Kämppä, J., Braskerud, B., Jansson, H., Syversen, N., and Uusitalo, R., 2000. Buffer zones and constructed wetlands as filters for agricultural phosphorus. *Journal of Environmental Quality*, **29**, 151–158.
- van der Valk, A. G., 2006. *The Biology of Freshwater Wetlands*. Oxford: Oxford University Press.
- Verhoeven, J. T. A., Arheimer, B., Yin, C., and Hefting, M. M., 2006. Regional and global concerns over wetlands and water quality. *Trends in Ecology & Evolution*, **21**, 96–103.
- Vitousek, P. M., Aber, J. D., Howarth, R. W., Likens, G. E., Matson, P. A., Schindler, D. W., Schlesinger, W. H., and Tilman, D., 1997. Human alteration of the global nitrogen cycle: sources and consequences. *Ecological Applications*, **7**, 737–750.
- Vymazal, J., Greenway, M., Tonderski, K., Brix, H., and Mander, Ü., 2006. Constructed wetlands for wastewater treatment. In Verhoeven, J. T. A., Beltman, B., Bobbink, R., and Whigham, D. F. (eds.), *Wetlands and Natural Resource Management*. Berlin Heidelberg: Springer. Ecological Studies, Vol. 190, pp. 69–96.
- Vymazal, J., and Kröpfelová, L., 2009. Removal of organics in constructed wetlands with horizontal sub-surface flow: a review of the field experience. *The Science of the Total Environment*, **407**, 3911–3922.
- Welcomme, R. L., Brummet, R. E., Denny, P., Hasan, M. R., Kaggwa, R. C., Kipkemboi, J., Mattson, N. S., Sugunan, V. V., and Vass, K. K., 2006. Water management and wise use of wetlands: enhancing productivity. In Verhoeven, J. T. A., Beltman, B., Bobbink, R., and Whigham, D. F. (eds.), *Wetlands and Natural Resource Management*. Berlin Heidelberg: Springer. Ecological Studies, Vol. 190, pp. 155–180.
- Wolff, W. J., 1993. Netherlands wetlands. *Hydrobiologia*, **265**, 1–14.
- Yang, B., Lan, C. Y., Yang, C. S., Liao, W. B., Chang, H., and Shu, W. S., 2006. Long-term efficiency and stability of wetlands for treating wastewater of a lead/zinc mine and the concurrent ecosystem development. *Environmental Pollution*, **143**, 499–512.
- Zhang, D., Gersberg, R. M., and Keat, T. S., 2009. Constructed wetlands in China. *Ecological Engineering*, **35**, 1367–1568.
- Zedler, J. B., 2003. Wetlands at your service: reducing impacts of agriculture at the watershed scale. *Frontiers in Ecology and the Environment*, **1**, 65–72.
- Zedler, J. B., and Kercher, S., 2004. Causes and consequences of invasive plants in wetlands: opportunities, opportunists and outcomes. *Critical Review of Plant Sciences*, **23**, 431–452.

Zedler, J. B., and Kercher, S., 2005. Wetland resources: status, trends, ecosystem services, and restorability. *Annual Review of Environment and Resources*, **30**, 39–74.

Cross-references

Aeration of Soils and Plants
 Ecohydrology
 Evapotranspiration
 Greenhouse Gas Fluxes: Effects of Physical Conditions
 Nature Conservation Management
 Oxidation–Reduction Reactions in the Environment
 Peatlands: Environmental Functions
 Peats and Peatlands, Physical Properties
 Physical Degradation of Soils, Risks and Threats
 Surface and Subsurface Waters
 Water Budget in Soil
 Water Erosion: Environmental and Economical Hazard
 Wetting and Drying, Effect on Soil Physical Properties

WETNESS

Water content of soil solids per unit mass (mass-wetness); or per unit bulk volume of the soil (volume-wetness).

WETTABILITY

The tendency of a soil to accept water (in contrast with the opposite tendency of some soils to repel water, called “hydrophobicity”). Water applied to a wettable soil typically forms an acute contact angle, and is drawn into the soil’s pores.

Bibliography

Introduction to Environmental Soil Physics (First Edition) 2003
 Elsevier Inc. Daniel Hillel (ed.) <http://www.sciencedirect.com/science/book/9780123486554>

Cross-references

Conditioners, Effect on Soil Physical Properties
 Hydrophobicity of Soil
 Wildfires, Impact on Soil Physical Properties

WETTING AND DRYING, EFFECT ON SOIL PHYSICAL PROPERTIES

Sudhakar M. Rao
 Department of Civil Engineering, Indian Institute of Science, Bangalore, India

Definitions

Wetting is defined as the process leading to increase in water content of an unsaturated soil upon ingress of water.

Drying is defined as the process leading to reduction in water content and degree of saturation of a soil due to evaporation or evapotranspiration.

Introduction

Residual soils often exist where the climate is characterized by alternate wet and dry seasons. During dry period, the soil zone located above the water table and near the ground surface (up to depths of 6 m or more) begins to dry out with concomitant reduction in degree of saturation (S_r) in the soil mass. The loss in water by evaporation causes water to flow from the deeper regions of the soil mass toward the surface by capillary action. During drying process, capillary menisci form between adjacent soil particles at the air-water interface, with the pore water pressure (u_w) in the convex inner side being lower than the atmospheric pressure (u_a) on the concave outer side of the menisci (Yong and Warkentin, 1975). This pressure difference ($u_a - u_w$) constitutes the matric suction in unsaturated ($S_r < 1$) soils (Fredlund and Rahardjo, 1993). It has been suggested that the matric suction acts as a “modified” effective stress and increases the shear strength of unsaturated soils that mainly manifests as the apparent cohesion (Brand, 1982; Ho and Fredlund, 1982). The matric suction contribution to effective stress can be represented through a suction stress component, $\chi(u_a - u_w)$, where χ is a material property (Bishop and Blight, 1963; Lu and Likos, 2004) that depends on the degree of saturation, varying between zero (perfectly dry soil) to unity (saturated soil). According to Burland (1961), Jennings and Burland (1962), the high curvature capillary menisci formed at the grain contact points during drying tend to glue or bond the particles. These bonded particles offer considerable resistance to local shear stresses induced by addition of loads. Consequently, soils develop larger shear strength and resistance to volumetric deformations in the unsaturated state. However, infiltration of water causes loss of matric suction strength component and the soil mass responds by experiencing shear failure or swell/collapse strains when subjected to K_0 loading condition (i.e., the soil cannot experience lateral strains).

Effect on strength

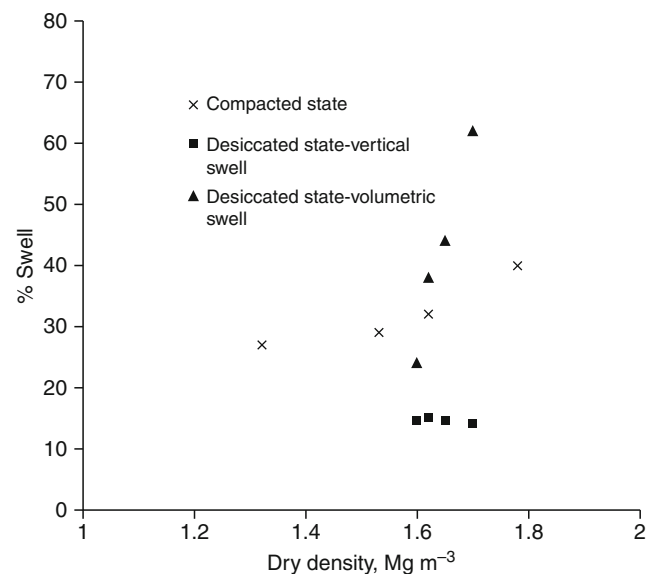
The influence of cyclic wetting and drying on certain engineering properties of residual soils has been investigated. Blight (1966) observed that repeated wetting and drying of residual soils produced an irreversible and significant increase in shear strength of the desiccated clay. The effect of intense wetting and drying appears to be equivalent to those produced by heavy overconsolidation. Grant (1974) investigating lateritic soils of Australia found that lightly tamped specimens subjected to cyclic wetting and drying mobilized unconfined compressive strength of the order of 50–100 kPa starting from a negligible strength at the beginning of the experiment. Grant (1974) attributed this gain in strength to creation of cementation bonds. Allam (1977), Allam and Sridharan (1981), Allam and Sridharan (1984) and Sridharan and Allam (1982) had

investigated the effect of repeated wetting and drying on the shear strength and consolidation characteristics of red soils from Bangalore District. Their results suggested that a microstructure was created on repeated wetting and drying of the red soil specimens due to cementation of the soil particles by chemical compounds. The generated microstructure in turn increased the shear strength, made the soil less compressible and more porous.

Swell behavior of expansive soils

Several researchers have performed laboratory investigations to understand the swelling behavior of expansive soils subjected to cycles of wetting and drying. The laboratory studies broadly categorize in two groups depending on the amount of drying experienced by the expansive soil specimens during the wetting–drying cycles. Repeated cycles of full wetting and partial drying are observed to reduce the vertical swell potentials of compacted soil specimens (Chu and Mou, 1973; Chen and Ma, 1987; Subba Rao and Satyadas, 1987; Al-Homoud et al., 1995). Comparatively, exposure of expansive soils to full wetting–drying cycles can almost double their vertical swell potentials (Popesco, 1980; Osipov et al., 1987; Dif and Bluemel, 1991; Day, 1994). In both the cases, the vertical swell potentials reached an equilibrium state after about three to five cycles. The reduction in swell potential in the first case is attributed to aggregation of clay particles during full wetting – partial drying cycles leading to reduction in clay content and hence swell potential of the specimens (Al-Homoud et al., 1995). The increase in swell potential in case two is attributed to destruction and disorientation of the soil elements during full wetting and drying cycles (Osipov et al., 1987); equilibrium in particle orientation and fabric is apparently reached after three to four cycles as illustrated by equilibrium swell potentials of the soil specimens.

Variations in initial dry density and compaction water content are known to significantly influence the swell potentials of compacted expansive soils (Chen, 1988). Subba Rao et al. (1998) and Subba Rao et al. (2000) have examined the role of the initial compaction conditions (dry density, water content) on the swell potential of expansive clay specimens subjected to four cycles of full wetting and drying. Figure 1 illustrates their results for an expansive soil (liquid limit = 75%, plasticity index = 44%, clay content = 55%) subjected to four cycles of wetting and drying at 40 °C at vertical stress of 6.25 kPa in odometer cells. The clay specimens develop greater vertical swell magnitudes with increase in dry density ρ_d (from 1.32 $Mg\ m^{-3}$ to 1.78 $Mg\ m^{-3}$) in the compacted state (Figure 1). However, near identical vertical swell potentials (defined as $\Delta h/H \times 100\%$, where Δh is increase in sample thickness on swelling and H is initial thickness of the specimen) of 15% are developed by the specimens after four wetting–drying cycles irrespective of the compaction dry density values (Figure 1). Further, following the cyclic wetting drying process, the dry densities of the



Wetting and Drying, Effect on Soil Physical Properties,
Figure 1 Dry density-swell magnitude relations for compacted and desiccated specimens

clay specimens were observed to vary in a narrow band of 1.6 $Mg\ m^{-3}$ to 1.7 $Mg\ m^{-3}$ (Figure 1). Unlike mobilization of near unique vertical swell potentials, the clay specimens subjected to cyclic wetting and drying process developed volumetric swell potentials (defined as $\Delta e/1 + e \times 100\%$, where Δe is increase in sample void ratio on swelling and e is initial void ratio of the compacted specimen) that vary from 24% to 62%. The volumetric swell potentials of the desiccated clay specimens (specimens subjected repeated wetting–drying cycles) were observed to linearly vary with volumetric shrinkage strains (Figure 2); the volumetric shrinkage strain is defined as

$$\Delta e_{\text{shrinkage}} = e_{\text{compacted}} - e_{\text{shrinkage}}, \quad (1)$$

In Equation 1, $e_{\text{compacted}}$ and $e_{\text{shrinkage}}$ represent the void ratios of clay specimens in the compacted state and at the end of four cycles of wetting and drying (termed desiccated state) respectively. The linear relation in Figure 2 suggests that specimens experiencing larger shrinkage strain or larger reduction in void ratio on wetting and drying are liable to develop larger volumetric swell potentials.

Figure 3 explores the role of initial void ratio in influencing the shrinkage strain magnitudes of expansive soil specimens subjected to wetting and drying cycles by plotting $\Delta e_{\text{shrinkage}}$ versus compaction density of the expansive soil specimens. The plot reveals that densely compacted specimens tend to shrink less upon cyclic wetting and drying. Further, the plot reveals that specimens compacted to dry density of 1.66 $Mg\ m^{-3}$ (point A in Figure 3, termed optimum dry density) would not experience any change in void ratio even after repeated wetting and drying under vertical stress of 6.25 kPa. Collating the

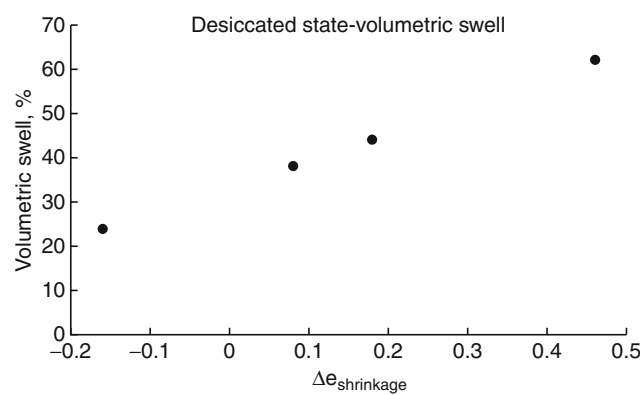
results in Figures 1 and 3 it follows that tendency of compacted clay specimens to experience increase in volumetric swell potential upon wetting and drying reduces as their initial dry density increases; volumetric swell potentials of clay specimens compacted at optimum dry density appear to be immune to the influence of cycles of wetting and drying. The optimum dry density is expected to be function of (a) the surcharge pressure at which the unsaturated soil is wetted and dried and (b) the amount of shrinkage (partial or complete) permitted during each drying cycle.

Swell behavior of lime-stabilized expansive soils

Table 1 presents the swell potential values of compacted expansive soil specimen (liquid limit = 65%, plasticity index = 46%, clay content = 40%) prior to and after lime

stabilization (lime content ranges from 2% to 7% on dry soil mass basis). The table also includes the swell potentials of the lime-stabilized specimens subjected to four cycles of wetting and drying (drying temperature = 40 °C) in odometer cells at vertical stress of 6.25 kPa (Rao et al., 2001). Lime addition modifies the swelling soil (swell potential = 10%) to mildly collapsing soil (collapse potential = -0.02 to -0.1%) brought about by the lime modification and pozzolanic reactions (Herrin and Mitchell, 1961; Bell, 1993).

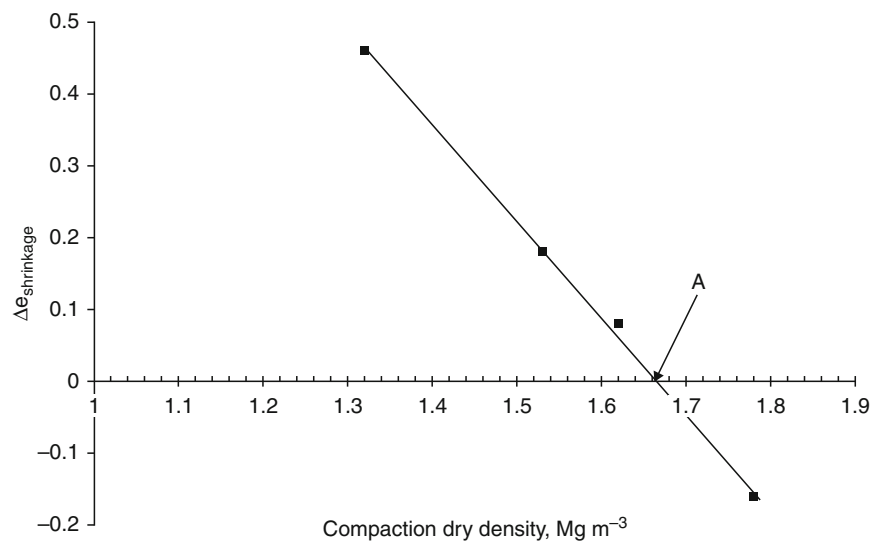
Cyclic wetting and drying degrades the cementation bonds in the lime-stabilized specimens causing them to exhibit vertical swell potentials of 1.2% to 4.2%. The initial consumption of lime (ICL) of the expansive soil corresponds to 3% (Rao et al., 2001). The vertical swell potentials in **Table 1** imply that inadequate lime addition (lime additions below ICL, e.g., 2% lime treated specimen) makes the treated soil more vulnerable to the effects of wetting and drying. Addition of lime in excess of ICL value (e.g., 4% and 7% lime-treated specimens) minimizes the destabilizing influence of wetting-drying cycles on the swelling behavior of lime-stabilized clays.



Wetting and Drying, Effect on Soil Physical Properties, Figure 2 Variation of volumetric swell of desiccated specimen with $\Delta\epsilon_{\text{shrinkage}}$

Collapse behavior

Table 2 examines the influence of cyclic wetting and drying on the swell/collapse behavior of the compacted red soil specimens (liquid limit = 37%, plasticity index = 18 %, clay content = 32%) at vertical stress of 6.25 kPa and 100 kPa (Rao and Revanasiddappa, 2006). The clay fraction of red soils is generally dominated by kaolinite and hydrous oxides of iron and aluminum with some amount of smectite. The compacted red soil specimens were subjected to four cycles of complete wetting and drying at 40 °C in odometer cells at vertical stresses of 6.25 kPa and 100 kPa. The table



Wetting and Drying, Effect on Soil Physical Properties, Figure 3 Influence of compaction density on $\Delta\epsilon_{\text{shrinkage}}$

Wetting and Drying, Effect on Soil Physical Properties, Table 1 Influence of wetting and drying on axial deformations of lime-stabilized soil

Soil state	Vertical swell potential/Collapse potential, %			
	Compacted	2% lime treated specimen	4% lime treated specimen	7% lime treated specimen
Compacted	10	-0.02	-0.04	-0.10
Subjected to four wetting-drying cycles	13	4.16	1.88	1.16

Wetting and Drying, Effect on Soil Physical Properties, Table 2 Index properties of compacted and desiccated specimens

Series	Specimen state	ρ_d ($Mg\ m^{-3}$)	w (%)	Void ratio	% swell at vertical stress of 6.25 kPa	% collapse at vertical stress of 100 kPa
1	Compacted	1.49	10.6	0.81	1	-5.2
1	Desiccated	1.51	2.0	0.78	2.2	-1.8
2	Compacted	1.49	17.6	0.81	0	-3
2	Desiccated	1.54	3.5	0.74	2	-1
3	Compacted	1.49	26.4	0.81	0	0
3	Desiccated	1.66	5.5	0.62	1	-0.5

illustrates that the wetting–drying process causes larger reduction in void ratio for an initially wetter specimen.

Since the swelling tendency of compacted soils increase, while, their tendency to collapse decrease with reduction in void ratio (Popescu, 1986), the wetting–drying process differently impacts the swell and collapse potential of the red soil specimens (Table 2). At a given compaction water content, the reduction in void ratio from wetting–drying process therefore increases the swell magnitude of the soil specimen at the vertical stress of 6.25 kPa but reduces the collapse magnitude at the vertical stress of 100 kPa.

Summary

Cyclic wetting and drying impacts the strength, swell, and collapse behavior of soil specimens. Cyclic wetting and drying increase the strength of natural soil specimens from growth of bonds. Though dry density impacts the vertical swell magnitude of expansive soils in the compacted state, it is unable to control the vertical swell magnitude of expansive soils subjected to repeated wetting and drying. The compaction dry density plays a significant role in the volumetric swell magnitudes of expansive specimens subjected to cycles of wetting and drying. Densely compacted specimens experience lesser shrinkage and therefore develop smaller volumetric swell potential upon subject to wetting–drying cycles. Wetting–drying processes degrade the cementation bonds in lime-stabilized specimens. Expansive soils treated with lime contents that are below the ICL value are more vulnerable to the wetting–drying effects. Soils that can experience both swelling and collapse strains on saturation (example red soils) react differently to wetting–drying effects. The reduction in void ratio from cyclic wetting and drying increases the swelling tendency but reduces the collapse tendency of the red soils.

Bibliography

- Allam, M. M., 1977. *Shear Strength and Volume Change Behaviour of Desiccated Soils*. Ph.D. dissertation. Bangalore, India: Indian Institute of Science.
- Allam, M. M., and Sridharan, A., 1981. Effect of repeated wetting and drying on shear strength. *Journal of the Geotechnical Engineering, ASCE*, **107**, 121–138.
- Allam, M. M., and Sridharan, A., 1984. Shear strength behaviour of desiccated soils. *Indian Geotechnical Journal*, **14**, 40–66.
- Al-Homoud, A. S., Basma, A. A., Husein Malkawi, A. J., and al Bashabsheh, M. A., 1995. Cyclic swelling behavior of clays. *Journal Geotechnical Engineering, ASCE*, **121**, 562–565.
- Bell, F. G., 1993. *Engineering Treatment of Soils*. London: E & FN Spon.
- Bishop, A. W., and Blight, G. E., 1963. Some aspects of effective stress in saturated and unsaturated soils. *Geotechnique*, **13**, 177–197.
- Blight, G. E., 1966. Strength characteristics of desiccated clays. *Journal of Soil Mechanics and Foundations Division, Proceedings of the ASCE*, **92**, 19–37.
- Brand, E. W., 1982. Analysis and design in residual soils. *Proceedings of the ASCE Geotechnical Conference, Engineering and Construction in Tropical and Residual Soils*, Honolulu: ASCE, pp. 89–143.
- Burland, J. B., 1961. Discussion on collapsible soils. *Proceedings of the 5th International Conference on Soil Mechanics and Foundation Engineering*, Paris, Vol. 3, pp. 219–220.
- Chen, F. H., 1988. *Foundation on Expansive Soils*. New York: Elsevier.
- Chen, F. H., and Ma, G. S., 1987. Swelling and shrinkage behavior of expansive clays, *Proceedings 6th International Conference on Expansive Soils*, New Delhi, Boca Raton, FL: CRC Press, Vol. 1, pp. 127–129.
- Chu, T. Y., and Mou, C. H., 1973. Volume change characteristics of expansive soils determined by controlled suction tests. *Proceedings 3rd International Conference on Expansive Soils*, Haifa, Isreal, Jerusalem: Academic press, Vol. 1, pp. 177–185.
- Day, R. W., 1994. Swell-shrink behavior of compacted clay. *Journal Geotechnical Engineering, ASCE*, **120**, 618–623.

- Dif, A. E., and Bluemel, W. F., 1991. Expansive soils under cyclic drying and wetting. *ASTM Geotechnical Testing Journal*, **14**, 96–102.
- Herrin, M., and Mitchell, H., 1961. Lime-soil mixtures. *Highway Research Board Bulletin*, **304**, 99–138.
- Ho, D. F. Y., and Fredlund, D. J., 1982. Increase in shear strength due to suction in two Hong Kong soils, tropical and residual soils. *Proceedings of the ASCE Geotechnical Conference*, Reston, VA: ASCE, pp. 263–295.
- Fredlund, D. G., and Rahardjo, H., 1993. *Soil Mechanics for Unsaturated Soils*. New York: John Wiley and Sons.
- Grant, K., 1974. The composition of some Australian laterites and lateritic gravel. *Proceedings 2nd International Congress of the International Association of Engineering Geology*, pp. IV-32.1–IV-32.15.
- Jennings, J. E., and Burland, J. B., 1962. Limitations to the use of effective stress in partly saturated soils. *Geotechnique*, **12**, 125–144.
- Lu, N., and Likos, W. J., 2004. *Unsaturated Soil Mechanics*. New York: Wiley.
- Osipov, V. I., Bik, N. N., and Rumjantseva, N. A., 1987. Cyclic swelling of clays. *Applied Clay Science*, **2**, 363–374.
- Popescu, M., 1980. Behavior of expansive soils with crumb structure. *Proceedings of the 4th International Conference on Expansive Soils*, Denver, New York: ASCE, Vol. 1, pp. 158–171.
- Popescu, M. E., 1986. A comparison between the behaviour of swelling and collapsing soils. *Engineering Geology*, **23**, 145–163.
- Rao, S. M., and Revanasiddappa, K., 2006. Influence of cyclic wetting drying on collapse behaviour of compacted residual soil. *Geotechnical and Geological Engineering*, **24**, 725–734.
- Rao, S. M., Reddy, B. V. V., and Muttharam, M., 2001. The impact of cyclic wetting and drying on the swelling behaviour of stabilized expansive soils. *Engineering Geology*, **60**, 223–233.
- Sridharan, A., and Allam, M. M., 1982. Volume change behaviour of desiccated soils. *Journal of Geotechnical Engineering Division, ASCE*, **108**, 1057–1071.
- Subba Rao, K. S., Rao, S. M., and Gangadhara, S., 1998. Band width of vertical movement of expansive soils. *Proceedings Indian Geotechnical Conference*, **1**, 71–74.
- Subba Rao, K. S., and Satyadas, C. G., 1987. Swelling potential with cycles of swelling and partial shrinkage. *Proceedings of the 6th International Conference on Expansive Soils*, New Delhi, Boca Raton, FL: CRC Press, Vol. 1, pp. 137–142.
- Subba Rao, K. S., Rao, S. M., and Gangadhara, S., 2000. Swelling behaviour of a desiccated clay. *ASTM Geotechnical Testing Journal*, **23**, 193–198.
- Yong, R. N., and Warkentin, B. P., 1975. *Soil Properties and Behaviour*. New York: Elsevier.

Cross-references

- [Shrinkage and Swelling Phenomena in Soils](#)
[Soil Surface Sealing and Crusting](#)
[Stress–Strain Relations](#)

WETTING FRONT

Interface between soil that is unaffected from the initial state and the wetted zone from an infiltration or irrigation event.

WIEN'S LAW

A statement that the wavelength of maximal radiation intensity emitted by a blackbody is inversely proportional to the absolute temperature of the body's surface.

Bibliography

Introduction to Environmental Soil Physics (First Edition) 2003
 Elsevier Inc. Daniel Hillel (ed.) <http://www.sciencedirect.com/science/book/9780123486554>

WILDFIRES, IMPACT ON SOIL PHYSICAL PROPERTIES

Henryk Czachor
 Institute of Agrophysics, Polish Academy of Sciences,
 Lublin, Poland

Definition

Wildfire is a raging, rapidly spreading fire.

The overall effects of wildfire on forest ecosystems cause the reduction or elimination of aboveground biomass and impact belowground soil physical, chemical, and microbial properties. Low-impact burning can promote a herbaceous flora, increase plant available nutrients, and thin overcrowded forests, all of which can foster healthy systems. Severe fires can often cause changes in successional rates, alter above- and below-ground species composition, generate volatilization of nutrients and ash entrainment in smoke columns, produce rapid or decreased mineralization rates, alter C:N ratios, and result in subsequent nutrient losses through accelerated runoff and erosion, leaching, and denitrification. In addition, changes in soil hydrologic functioning, degradation of soil physical properties, decreases in micro- and macrofauna, and alterations in microbial populations and associated processes can occur. The direct effect of fire on belowground systems is a result of the burning severity, which integrates aboveground fuel loading (live and dead), soil moisture and subsequent soil temperatures, and duration of the burn (Neary et al., 1999). Soil erosion limited only by post-fire rainfall intensity and quantity, or until bedrock is exposed, might be expected after wildfire on steep slopes in the forests, given the noncohesive sandy soils and their water repellent character (Shakesby et al., 2007).

The transfer of heat downward in the upper part of the soil combined with the vaporization and movement of water and organic compounds enhances the formation of a highly water-repellent soil condition during fire (DeBano, 2000; Wang et al., 1978).

Bibliography

- DeBano, L. F., 2000. The role of fire and soil heating on water repellency in wild land environments: a review. *Journal of Hydrology*, 231–232, 4–32.
- Neary, D. G., Klopatek, C. C., DeBano, L. F., and Ffolliott, P. F., 1999. Fire effects on belowground sustainability: a review and synthesis. *Forest Ecology and Management*, 122, 1–2.
- Shakesby, R. A., Wallbrink, P. J., Doerr, S. H., English, P. M., Chafer, C. J., Humphreys, G. S., Blake, W. H., and Tomkins, K. M., 2007. Distinctiveness of wildfire effects on soil erosion in south-east Australian eucalypt forests assessed in a global context. *Forest Ecology and Management*, 122, 1–2.
- Wang, C., Beke, G. J., and McKeague, J. A., 1978. Site characteristics, morphology and physical properties of selected ortstein soils from the Maritime Provinces. *Canadian Journal of Soil Science*, 58, 405–420.

WILTING POINT

The point when soil water content (usually at soil water potential of -1.5 MPa) is insufficient to meet a plants need due to use water from its own tissues for transpiration.

WIND EROSION

Christof Gromke, Katrin Burri
WSL Institute for Snow and Avalanche Research SLF,
Davos Dorf, Switzerland

Synonyms

Aeolian erosion; Aeolian particle transport

Definition

Erosion. Removal of surface material by any fluid motion.
Wind Erosion. Wind-induced removal of surface material like soil aggregates, grains, and snow.

Introduction

The implications of wind erosion on the Earth's surface are exemplified by several phenomena. Among them are such spectacular events as sand and dust storms or the relatively slow but persistent movement of shifting sand dunes in deserts, desert-like areas, or along coastlines (Schwämmle and Hermann, 2003). In many parts of the world, wind erosion causes substantial soil loss, leading to land degradation and desertification. Cornice formations due to intense snow deposition near ridge locations (Mott and Lehning, 2009), sastrugi and ripples are products of the erosive power of wind in alpine terrain and polar regions, respectively (Clifton et al., 2006).

The examples above show that wind erosion has the power to form the Earth's surface. Moreover, it affects the global dust particle concentration in the atmosphere,

which in turn influences the Earth's climate via the global radiation balance. Implications for human health, in particular respiratory diseases, are also evident as well as for agricultural land use and settling practices. Thus, wind erosion profoundly influences the natural environment and consequently human behavior and society.

Starting from a rather global perspective, the general conditions and prerequisites for wind erosion are introduced in the next section. The physical mechanisms on the particle scale are dealt with in the paragraph [Processes](#). Reference and relevance to agriculture is provided in the next two sections [Interaction with Agriculture](#) and [Mitigation Measures](#), before the conclusions are given.

Background

The occurrence of wind erosion is generally the result of a complex interplay between several factors including surface properties, topography, climate, and atmospheric conditions. The intensity of wind erosion depends on the erodibility of a surface on the one hand and on the erosivity of a wind event on the other. Erodibility is the potential of the surface to be eroded, while erosivity is the potential of the fluid to cause erosion (Shao, 2008). From this, it becomes clear that dry, less cohesive soils are especially susceptible to wind erosion. Large erosion events involving transport of soil material usually take place in arid and semi-arid regions with little or no vegetation cover since the surface erodibility is intrinsically high there. Besides desert areas in the lower latitudes, elevated plains (e.g., Tibetan Plateau) embedded in mountain ranges located in the temperate latitudes are often prone to wind erosion. This is because the local orography favors wind erosion friendly climatic conditions. Air masses approaching a mountain range are forced to elevate and to rain out when the condensation level is reached. The low humidity wind on the ridge's lee side warms up during the descent and dries out the soil surface, increasing its erodibility. Relatively strong winds can now easily cause wind erosion events.

Processes

Looking more closely at the processes occurring during a wind erosion event at the scale of a single particle (soil aggregate, grain, snow particle), three different states can be distinguished: particle entrainment, transport, and deposition. Particle entrainment is the state when the particle becomes mobile, leaves the surface, and becomes airborne. Entrainment can be caused either by aerodynamic forces (aerodynamic entrainment) or by impact with other airborne particles (splash or bombardment entrainment). Transport is the state in which spatial displacements are accomplished by the particle. Three modes of particle transport are generally distinguished: surface creep (also known as rolling, reptation, or surface traction), saltation, and suspension (also turbulent suspension). Surface creep is when the moving particles jostle and roll over the

surface in direct contact with the ground. Saltation is a hopping motion of the particles in which they follow almost parabolic trajectories. Typical saltation distances of sand grains are in the order of a few meters with maximum trajectory heights of 0.1–0.2 m. Suspension is a long-range transport mechanism and occurs when particles get caught by turbulent eddies, which lift them up into higher air streams. Some authors also distinguish a fourth mode of transport: modified saltation (Nishimura and Hunt, 2000). This mode is when a saltating particle gets slightly affected by turbulent eddies and shows a parabolic trajectory superimposed by a fluctuating motion. Deposition is when the moving particle hits the surface or stops rolling and remains at a fixed location.

The most likely transport mode, creep, saltation, or suspension, depends primarily on particle size. Larger-sized particles (>1 mm) preferentially move by creeping. Saltation is the typical transport mode for most sand-sized particles (0.1–0.5 mm). Dust particles (<0.02 mm) are susceptible to suspension because of their low terminal fall velocity. Once entrained, they are transported for long distances (some 1,000 km).

Each transport mode is the result of a certain balance of forces acting on the particle. Six types of forces are distinguished: gravitational force F_G , aerodynamic drag force F_D , aerodynamic lift force F_L , Magnus force F_M , electric force F_E , and cohesive force F_C . Forces originating from particle–particle interactions in the air such as collisions are generally not considered to be important as the particle number density in air is rather low and direct collisions are very rare.

When it comes to overall mass transport by wind erosion, saltation is the most important transport mode. A key parameter for understanding and quantifying saltation is the friction velocity u_* , which is a measure of the shear stress transported downward to the surface by the wind. The friction velocity u_* is the square root of the correlation of the fluctuating velocity parts $u'(t)$ and $w'(t)$ of the streamwise horizontal and vertical wind velocity components, respectively, i.e., $u_* = \sqrt{\langle u'(t) w'(t) \rangle^{1/2}}$. Here, the brackets denote the averaging operation and t denotes time. A rough estimate for the friction velocity is given by $u_* = 0.05 \dots 0.1 U_\delta$, where U_δ is the wind velocity at the top of the atmospheric boundary layer. Typical values for u_* range from 0.1 m s^{-1} to 2 m s^{-1} for normal, average atmospheric conditions. A particle is entrained and starts to saltate when a certain friction velocity, the so-called threshold friction velocity $u_{*,f}$, is exceeded. It is further distinguished between a fluid and an impact threshold. The fluid threshold $u_{*,f}$ is the value that needs to be exceeded for aerodynamic particle entrainment, whereas the impact threshold $u_{*,i}$ is required to maintain saltation when surface particles get ejected by splash and bombardment entrainment and is smaller than $u_{*,f}$ ($u_{*,i} \approx 0.8 u_{*,f}$). Owen (1964) hypothesized saltation to be a self-balancing process, meaning that the concentration of saltating particles in the air is governed by the momentum exchange, i.e., shear stress partitioning between the particle and the fluid phase. In the case of low concentration, only a small

fraction of the momentum of the fluid phase is absorbed by the airborne particles, but the shear stress acting directly on the surface is high and causes large entrainment rates. With increasing concentration, more momentum is absorbed by the airborne particles and consequently less shear stress acts on the ground. When the concentration increases further, the momentum transfer to each single airborne particle is too low to maintain the entrainment of surface particles by impact, leading to reduced entrainment rates. According to this argument, the airborne particle concentration adjusts itself to an equilibrium state.

In the following, simple equations for estimating the threshold friction velocity $u_{*,f}$, the total sediment mass flux Q , the vertical profile of sediment mass flux $q(z)$, and the saltation layer height h_s are provided. The equations were mostly derived by the pioneer of wind erosion studies – Ralph Alger Bagnold (1896–1990). His book “The Physics of Blown Sand and Desert Dunes” is the standard work in wind erosion science (Bagnold, 1941). Assuming the saltation process to be a balance of the aerodynamic drag force F_D and gravitational force F_G only, Bagnold (1941) derived for the threshold friction velocities $u_{*,f}$ and $u_{*,i}$:

$$(u_{*,f}, u_{*,i}) = (A_{t,f}, A_{t,i}) \sqrt{\frac{\rho_p}{\rho_a} g d} \quad (1)$$

with indices f and i indicating the fluid and impact threshold quantities, respectively, ρ_p the particle density, ρ_a the air density, g the gravitation constant and d the particle diameter. The values for $A_{t,f}$ and $A_{t,i}$ were empirically found to lie in the range between 0.1 and 0.2, with lower values corresponding to larger particles (for $d > 0.2$ mm $A_{t,f}=0.1$). The density ratio ρ_p/ρ_a is typically of order 2.5.

For the total sediment mass flux Q including creep and saltation Bagnold (1941) gives

$$Q = C \sqrt{\frac{d \rho_a}{d_s g}} \left(1 - \frac{u_{*,f}^2}{u_*^2} \right) u_*^3 \quad (2)$$

Here, C is a dimensionless coefficient depending on the particle size distribution ($C = 1.5$ for nearly uniform sand, $C = 1.8$ for naturally graded sand, and $C = 2.8$ for poorly sorted sand). d_s is Bagnold’s “standard” grain diameter of 0.25 mm. Equation 2 satisfactorily agrees with experimental results for sand particles of diameter $d > 0.1$ mm, but shows rather poor agreement for smaller particles, e.g., for dust.

The variation of the sediment mass flux with height, i.e., the vertical profile of mass flux $q(z)$ is generally assumed to a first approximation to be exponential. Nishimura and Hunt (2000) suggest

$$q(z) = \rho_a u_* \lambda C \sqrt{\frac{d}{d_s}} \exp(-\lambda/(u_*^2/g) z) \quad (3)$$

where λ is a dimensionless parameter, which typically but not necessarily decreases as the particle diameter

d increases. Wind tunnel saltation experiments with various kinds of particles of different shapes, diameters, and densities suggest $\lambda = 0.15\text{--}1.5$ (Nalpanis et al., 1993; Nishimura and Hunt, 2000).

Finally, an estimate for the saltation layer height h_s is provided. The idea is that the component of vertical kinetic energy, which is transferred to a surface particle in the entrainment state is converted into potential energy. Assuming the vertical lift-off velocity is proportional to the friction velocity u_* , implies $E_{\text{kin}} \sim \frac{1}{2} m u_*^2$ (m is particle mass). The potential energy of a particle in the highest point of its trajectory h_s is $E_{\text{pot}} = m g h_s$. This gives an estimate for the saltation layer height h_s :

$$h_s = \alpha \frac{u_*^2}{2g} \quad (4)$$

Values for the dimensionless parameter α range typically between 1 and 2.5.

The equations for saltation given above should be considered as estimates rather than exact mathematical formulations. However, they involve the basic physical principles of saltation and show fairly good agreement with experimental observations of saltating sand particles. More recent and sophisticated models and estimates can be found in the literature (Greeley and Iversen, 1985; Shao, 2008). These models can be seen as enhancements of the ideas presented above. They also contain empirical parts requiring input parameters, but are often applicable for broader particle size ranges including dust.

Interaction with agriculture

Wind erosion is influenced by agriculture and agriculture is simultaneously affected by wind erosion. For example, plowing activities break up larger soil aggregates into smaller ones and thus considerably increase the surface erodibility at least for some time. On the other hand, cultivation of crops, vegetables, and fruits shelters the ground from direct exposure to atmospheric wind. By absorbing fluid momentum (shear stress partitioning), vegetation reduces the wind erosivity. Additionally, since the soil structure is reinforced by the roots, the surface erodibility is reduced. Vegetation can also trap particles in motion, thus reducing the total sediment mass flux. Overgrazing, leading to lower grass covers or sometimes even to the destruction of low-rise vegetation by trampling also has a negative impact on the surface erodibility. The implications of wind erosion for agriculture and the multifaceted interactions involved are illustrated by the following example. The entrainment and suspension of dust particles often initiates a gradual degradation of the land. This is because fine particles contain most of the soil's organic matter and nutrients. Without artificial fertilizing, less, or in extreme cases, no vegetation will grow on the eroded ground, and the vegetation sheltering effect described above will become diminished and eventually vanish giving rise to increased wind erosion activity. Tegen and Fung (1995) estimate that 30–50% of the total atmospheric dust

loading originates from human disturbed soil surfaces to which activities like cultivation and deforestation contribute a major part.

Mitigation measures

According to the following five basic principles, wind erosion can be controlled by either reducing the wind force at the soil surface or by making the soil more resistant to the wind force (Tibke, 1988):

- (1) Reduce field widths along the prevailing wind direction by strip cropping or establishing wind barriers and thereby reduce wind velocity and erosivity. Wind barriers can either be planted, e.g., trees, shrubs, grasses, or constructed from inert materials, e.g., earth and rock walls, wooden fences, straw rows (Frank and Ruck, 2005).
- (2) Establish and maintain vegetation or vegetative residues to protect the soil, e.g., by stubble mulch tillage, no-till farming, or cover crops. In situations where it is not feasible to protect the soil with a vegetation cover, gravel, crushed rock, and various chemical surface films are used alternatively.
- (3) Produce, or bring to the soil surface, stable aggregates or clods large enough to resist the wind force.
- (4) Roughen the land surface, e.g., by tillage ridges, to reduce the wind velocity and trap drifting soils.
- (5) Level or bench land to reduce effective field widths and erosion rates on slopes and hilltops where converging streamlines of wind flow cause increased velocities and wind forces.

These measures are primarily targeted at cultivated land. However, wind erosion control is a major issue also on grazing land and in severely degraded areas with drifting sand. Trampling damages on grazing land can be avoided by proper management such as rotational grazing, limiting of livestock numbers, and fencing of highly erosive areas. On severely degraded bare land, the objective is to establish permanent vegetation. Vegetation can directly shelter the soil from the wind by reducing its erosive force on the surface, by trapping windborne particles, and by providing locations for sediment deposition (Wolfe and Nickling, 1993; Burri et al., 2009). Furthermore, plants affect wind erosion by altering soil and climatic characteristics, such as soil structural stability and near-surface soil moisture. However, revegetation practices often face major difficulties with low rates of plant establishment and survival. In areas with drifting sand dunes, stabilization by artificial barriers or covers and irrigation are usually required before seeding or planting vegetation. Reclamation success in limiting habitats can also be improved by applying symbiotic mycorrhizal fungi, as they are able to improve both plant growth and soil structure (Graf et al., 2006). Furthermore, it is important to consider native, adapted plant species and natural succession patterns.

Conclusions

Wind erosion processes and their effects are apparent all over the world, ranging from long time land forming

processes to spectacular short time events such as sand or dust storms. They have a direct impact on human society by affecting public health and imposing constraints on our habits and opportunities. Since world climate change is expected to favor wind erosion, it is considered to be among the most serious environmental problems the world is facing today and in the near future. Agricultural cultivation can have positive and negative effects on wind erosion. Appropriate agricultural measures help to stop and reverse land degradation and desertification.

The vivid imagery of a beginning sand storm given by Ondaatje (1992, p. 137) in his famous book “The English Patient” when citing the Egyptian explorer Ahmed Hassanein Pasha shall conclude this article on wind erosion:

It is as though the surface were underlaid with steam-pipes, with thousands of orifices through which tiny jets of steam are puffing out. The sand leaps in little spurts and whirls. Inch by inch the disturbance rises as if the desert were rising in obedience to some upthrusting force beneath. Larger pebbles strike against the skins, the knees, the thighs. The sand-grains climb the body till it strikes the face and goes over the head. The sky is shut out, all but the nearest objects fade from view, the universe is filled.

Bibliography

- Bagnold, R. A., 1941. *The Physics of Blown Sand and Desert Dunes*. Mineola: Dover.
- Burri, K., Gromke, C., and Graf, F., 2009. *A wind tunnel study of aeolian sediment transport and PM10 emission in grass canopies of different planting densities*. In Proceedings of the Second International Conference Wind Effects on Trees 2009, Freiburg, October 2009, pp. 39–44.
- Clifton, A., Ruedi, J. D., and Lehning, M., 2006. Snow saltation threshold measurements in a drifting-snow wind tunnel. *Journal of Glaciology*, **52**, 585–596.
- Frank, C., and Ruck, B., 2005. Double-arranged mound-mounted shelterbelts: influence of porosity on wind reduction between the shelters. *Environmental Fluid Mechanics*, **5**, 267–292.
- Graf, F., Frei, M., Schwarz, M., and Böll, A., 2006. *Use and importance of mycorrhiza in site-specific restoration*. In Proceedings Soil-Bioengineering: Ecological Restoration with Native Plant and Seed Material, pp. 155–160.
- Greeley, R., and Iversen, J. D., 1985. *Wind as a Geological Process on Earth, Mars, Venus and Titan*. Cambridge: Cambridge University Press.
- Mott, R., and Lehning, M., 2009. Meteorological modelling of very high resolution wind fields and snow deposition for mountains, (in press, *Journal of Hydrometeorology*, doi:10.1175/2010JHM1216.1).
- Nalpanis, P., Hunt, J. C. R., and Barrett, C. F., 1993. Saltating particles over flat beds. *Journal of Fluid Mechanics*, **251**, 661–685.
- Nishimura, K., and Hunt, J. C. R., 2000. Saltation and incipient suspension above a flat particle bed below a turbulent boundary layer. *Journal of Fluid Mechanics*, **417**, 77–102.
- Ondaatje, M., 1992. *The English Patient*. London: Bloomsbury.
- Owen, P. R., 1964. Saltation of uniform grains in air. *Journal of Fluid Mechanics*, **20**, 225–242.
- Schwämmle, V., and Hermann, H. J., 2003. Solitary wave behaviour of sand dunes. *Nature*, **426**, 619–620.
- Shao, Y., 2008. *Physics and Modelling of Wind Erosion*. Cologne: Springer, Netherlands.
- Tegen, I., and Fung, I., 1995. Contribution to the atmospheric mineral aerosol load from land surface modifications. *Journal of Geophysical Research*, **100**, 18707–18726.
- Tibke, G., 1988. Basic principles of wind erosion control. *Agriculture, Ecosystems and Environment*, **22**(23), 103–122.
- Wolfe, S. A., and Nickling, W. G., 1993. The protective role of sparse vegetation in wind erosion. *Progress in Physical Geography*, **17**, 50–68.

Cross-references

- [Air Flux \(Resistance\) in Plants and Agricultural Products](#)
[Cultivation under Screens, Aerodynamics of Boundary Layers](#)
[Desertification: Indicators and Thresholds](#)
[Grains, Aerodynamic and Geometric Features](#)
[Physical Degradation of Soils, Risks and Threats](#)
[Physics of Near Ground Atmosphere](#)
[Plant Roots and Soil Structure](#)
[Soil Erosion Modeling](#)
[Soil–Plant–Atmosphere Continuum](#)
[Soil Surface Sealing and Crusting](#)
[Tillage Erosion](#)
[Water Erosion: Environmental and Economical Hazard](#)
[Windbreak and Shelterbelt Functions](#)

WINDBREAK AND SHELTERBELT FUNCTIONS

Andrzej Kędziora

Institute for Agricultural and Forest Environment,
Polish Academy of Sciences, Poznań, Poland

Definition

A *windbreak* or *shelterbelt* is a plantation usually made up of one or more rows of trees or shrubs planted around the edges of fields on farms, down the roads and ditches, and across big fields, improving the structure of landscape toward maintaining and enhancing ecosystem services.

History

Living windbreaks (trees and hedgerows) have been used for thousands of years. Some of the oldest shelterbelts were planted in England at the end of the eighteenth century, in Poland in Wielkopolska region in the early years of the nineteenth century, and in Russia in steep region at the same time. Some of the first serious windbreak research started in the dustbowl years in the US Midwest. Years of removing trees and of finely tilling the soil had created a classic wind erosion problem.

In the early 1980s, the kiwifruit boom created a need for artificial windbreaks. The first kiwifruit needed to be sheltered because the hairs on the fruit were rubbed off if the vines were shaken by the wind. This devalued the fruit. Scientists then discovered that the growth and fruit production of the vines were very sensitive to wind speed too, so windbreaks were quickly accepted as an essential part of a viable kiwifruit orchard.

First, the windbreaks were used mainly to protect the fields against erosion and give shelter to animals against

very high temperature in summer and low ones in winter. But the recent investigation on windbreaks has showed new functions of the shelterbelt which are very important for sustainable development of agricultural landscape and rural areas.

Introduction

The knowledge on processes underpinning ecosystem services opened new frontiers for the management of landscapes' structures toward enhancing their capacities to deliver requested services. Forests and shelterbelts show similar functions in the landscape, but a network of shelterbelts perform many similar services like forests growing on smaller part of landscape area. According to the studies carried out by the Institute for Agricultural and Forest Environment in Poland, the following functions of shelterbelts are similar to those shown by forests when 4–5% of the landscape area is under the network of shelterbelts:

- Modify the microclimatic conditions and heat and water balances
- Control the water chemistry composition (control of diffuse pollution)
- Limit water and wind erosion
- Protect the biodiversity
- Increase the survival of the game animals
- Enhance recreational value of the region
- Provide wood and other products
- Promote aesthetic values of the countryside

The first four of these functions are most important for functioning of the landscape as a whole, so they will be

presented in more detail below. The paradigm for proper use of shelterbelts in agricultural landscape must be an aspiration for the creation of the net of shelterbelts instead of planted individual windbreaks ([Figure 1](#)). Shelterbelt networks can better improve water and wind conditions and reduce diffuse pollution in agricultural areas. They should approximately run perpendicular to the direction of dominating winds and cross fields transverse to the directions of water runoff. Tree species composition in shelterbelts should be adapted to local habitat conditions. Shelterbelts should preferably be located on marginal lands and areas of low agricultural utility. This condition is usually fulfilled by connecting their networks with infrastructure elements in fields (roadsides, canals, streams, swamps, etc.). The distance between wind protective belts should generally be 500–700 m, while optimal distances for water quality protection are 400–500 m.

Modification of microclimatic conditions and heat and water balances

The shelterbelts introduced into grain monoculture landscape change the microclimatic conditions of the field as well as aerodynamic characteristics of an active surface. Shelterbelts reducing wind speed ([Jansz, 1959](#)), stomatal resistance, and increasing the humidity ([Rosenberg, 1974](#)), turbulence, and net radiation cause a little increase of actual evapotranspiration of landscape taken as a whole but decrease it from the cultivated field lying between shelterbelts ([Kędziora and Olejnik, 2002](#)). The various ecosystems use net radiation energy in different ways. The shelterbelt uses about 40% more energy for evapotranspiration than does the wheat field. There are two main



Windbreak and Shelterbelt Functions, Figure 1 Net of shelterbelts in the agricultural landscape, Turew, Poland.

reasons for this difference. First, there is a difference in the structure of plant cover. Trees have much longer roots than wheat, which allows them to absorb water from deeper layers of the soil. In effect, more water is within reach of the tree roots. Since trees have greater amounts of water available for their use than cereals, tree leaves have smaller stomatal resistance than cereal leaves. Shelterbelts also have a greater canopy roughness than wheat, which together with a higher wind speed in the shelterbelt canopy, results in more intensive turbulent exchange over shelterbelt.

In the landscape composed of cultivated fields and shelterbelts, one can observe two opposite tendencies in water cycling (Kędziora, 1996). The trees increase evapotranspiration rates. At the same time, the protecting effects of trees stimulate a decrease in wind speed and a lower saturation of vapor pressure deficits which decrease evapotranspiration. It is for this reason that fields between shelterbelts conserve moisture which can increase yields (Ryszkowski and Karg, 1976; Grace, 1988; Brandle et al., 2004).

Controlling the water chemistry composition (control of diffuse pollution)

The increasing use of artificial fertilizers, as well as liquid manure from big farms, usually applied in one dose, and the increasing use of pesticides together with simplification of agricultural landscape structure led to very high pollution of environment. Shelterbelts and stretches of meadows located in upland parts of watersheds also influence the chemistry of water flowing within the reach of plant's root systems. It was observed that nitrate concentrations were decreasing substantially when the groundwater carrying them from under fields passed

under biogeochemical barriers. Both, shelterbelts or small mid-field forests could decrease concentrations of incoming N-NO₃ from fields in range of 63–98%. In meadows the detected decrease of nitrate concentrations was similar and ranged from 79% to 98% of the input (Ryszkowski et al., 2002). The decrease of phosphate concentration under the biological barriers is also clearly evident although not in cases when plant residues underwent rapid decomposition and release phosphorus compounds (Hillbricht-Ilkowska et al., 1995). When the waterborne migration of mineral compounds from the mosaic watershed was compared with their outputs from uniform drainage basin, more than tenfold lower outputs of inorganic ions were detected (Lowrance et al., 1983; Peterjohn and Correll, 1984; Kędziora et al., 1995; Haycock et al., 1997).

Controlling of water and wind erosion

One of the major threats for agricultural activity is water or wind erosions which destroy the soil structure and fertility. Water erosion is a danger in regions with high precipitation and silty soil, while wind erosion usually occurs in dry regions with strong wind. But sometimes, especially in a uniform landscape, after removing all shelterbelts and strips of bushes, erosion can be a substantial threat for ploughed soil layers (Figure 2). Wind erosion can occur in early spring under special weather conditions. At this time, there are many bare fields in the agricultural landscape. When under such conditions the cold weather is accompanied by very intensive solar radiation and very high wind speed, very high water vapor saturation deficit in the near surface air layer is observed. It is generated by intensive heating of soil aggregates surface and very low concentration of water vapor in the cold air. It, in turn,



Windbreak and Shelterbelt Functions, Figure 2 Wind erosion in open landscape in the dry and windy spring, Turew, Poland.

brings to extremely intensive evapotranspiration from the soil aggregated. In such conditions, the hydraulic conductivity within soil aggregates is too low to ensure enough water flux density from inside of aggregates to its surface to cover the needs of evapotranspiration. This process leads to the drying up of the surface of the aggregates and its crumbling. These small mineral particles as well as organic matter are intensively blown away bringing to real silt-storm. One of the best measures to counteract the wind and water erosion is introduction of net of shelterbelt into uniform landscape. Suitable dens of shelterbelt net can reduce the wind speed up to 60% of this in open landscape (Jansz, 1959) and reduce runoff up to 10% in comparison with open landscape (Kędziora and Olejnik, 2002). The reduction of wind up to 60% brings to reduction of wind erosion tenfold.

Biodiversity protection and enhance

Conversion of pristine ecosystems into cultivated fields and intensification of agricultural production brought an impoverishment of biological diversity which was recognized not only by scientists (e.g., Wilson, 1992; Collins and Qualset, 1999; Loreau et al., 2002) but also by politicians (Convention on Biological Diversity opened in 1992 at the Earth Summit in Rio de Janeiro for endorsing; COM 1999 and many other documents).

The results of long-term studies on above ground insect show that more insect families were found in mosaic landscapes with shelterbelts and their recurrent detections were more frequent in consecutive years. The distribution of insect families along a distance gradient from a refuge site (shelterbelts) was well described by a negative exponential equation. An increase in cereal share in crop patterns as well as changes in precipitation had a much smaller impact on insect diversity than mosaic of perennial vegetation patches. The main factors counteracting the decline of biodiversity in agroecosystems are the mosaic structure of the landscapes, reach in shelterbelts. The negative impacts of various agrotechnologies on biodiversity are well documented, but refuges in mosaic landscapes counterbalance the loss of insect biodiversity due to intensification of agriculture production. It was found that a number of families and diversification of the residual families depend on the distance from the shelterbelts,

Summary

Diversification of agricultural landscape structure formed by the introduction of shelterbelts changes evapotranspiration and water runoff rates and therefore influences water cycling in the region. The reported cleansing effects of shelterbelts on groundwater chemistry enable to use higher doses of fertilizers and by that token to achieve higher crop production without stimulation of water pollution by chemicals leached from fields than this will happen

in agricultural landscape consisting of large cultivated fields only. Thus, the introduction of shelterbelts into the agricultural landscape will help to develop new environment-friendly agrotechnologies which at the same time allow intensive production balanced with the ability of agricultural landscape to absorb the side effects of agriculture without being damaged. Landscape, agronomic, and technical methods should mutually support themselves in order to achieve effective and economical system of water management in rural areas.

Bibliography

- Brandle, J. R., Hodges, L., and Zhou, H. H., 2004. Windbreaks in North American agricultural systems. In Nair, P. K. R., Rao, M. R. L. E., and Buck, L. E. (eds.), *New Vistas in Agroforestry*. Dordrecht: Kluwer, pp. 65–78.
- Collins, W. W., and Qualset, C. D., 1999. *Biodiversity in Agroecosystems*. Boca Raton: CRC Press.
- Grace, J., 1988. Plant response to wind. *Agriculture ecosystems and environment*, **22**(23), 71–88.
- Haycock, N. E., Piney, G., Burt, T. P., and Goulding, K. W. T., 1997. Buffer zones: current concerns and future directions. In Haycock, N. E., Burt, T. P., Goulding, K. W. T., and Piney, G. (eds.), *Buffer Zones: Their Processes and Potential in Water Protection*. Harpenden: Quest Environmental, pp. 305–312.
- Hillbricht-Illkowska, A., Ryszkowski, L., and Sharplay, A. N., 1995. Phosphorus transfers and landscape structure: riparian sites and diversified land use pattern. In Tissen, H. (ed.), *Phosphorus in the Global Environment*. Chichester: Wiley, pp. 210–228.
- Jansz, A., 1959. Impact of shelterbelts in Rogaczewo on microclimate of adjoining fields. *Roczniki Nauk Rolniczych, Seria A*, **t.79**, 91–1125 (in Polish).
- Kędziora, A., 1996. Hydrological cycle in agricultural landscapes. In Ryszkowski, L., French, N., and Kędziora, A. (eds.), *Dynamics of an Agricultural Landscape*. Poznań: Państwowe Wydawnictwa Rolnicze i Leśne, pp. 65–78.
- Kędziora, A., and Olejnik, J., 2002. Water balance in agricultural landscape and options for its management by change in plant cover structure of landscape. In Ryszkowski, L. (ed.), *Landscape Ecology in Agroecosystems Management*. Boca Raton: CRC Press, pp. 57–110.
- Kędziora, A., Ryszkowski, L., and Kundzewicz, Z., 1995. *Phosphate Transport and Retention in a Riparian Meadow – A Case Study*. Chichester: Wiley, pp. 229–234.
- Loreau, M., Naeem, S., and Inchausti, P. (eds.), 2002. *Biodiversity and Ecosystem Functioning*. Oxford: Oxford University Press.
- Lowrance, R., Todd, R., and Asmussen, L., 1983. Waterborne nutrient budgets for the riparian zone of an agricultural watershed. *Agriculture, Ecosystems and Environment*, **10**, 371–384.
- Molga, M., 1983. *Agrometeorology*. Warszawa: Państwowe Wydawnictwa Rolnicze i Leśne (in Polish).
- Peterjohn, W. T., and Correll, D. L., 1984. Nutrient dynamics in agricultural watershed: observations on the role of a riparian forest. *Ecology*, **65**, 1466–1475.
- Rosenberg, N. J., 1974. *Microclimate: The Biological Environment*. New York: Wiley, p. 315.
- Ryszkowski, L., and Karg, J., 1976. Role of shelterbelts in agricultural landscape. In Missonnier, J. (ed.), *Les Bocages-Historie, Ecologie, Economie*. Rennes: CNRS INRA Univ. de Rennes, pp. 305–309.
- Ryszkowski, L., Bartoszewicz, A., and Kędziora, A., 1997. The potential role of mid-field forests as buffer zones. In Haycock,

- N. E., Burt, T. P., Goulding, K. W. T., and Piney, G. (eds.), *Buffer Zones: Their Processes and Potential in Water Protection*. Harpenden: Quest Environmental, pp. 171–191.
- Ryszkowski, L., Szajdak, L., Bartoszewicz, A., and Życzyńska-Baloniak, I., 2002. Control of diffuse pollution by mid-field shelterbelts and meadow strips. In Ryszkowski, L. (ed.), *Landscape Ecology in Agroecosystems Management*. Boca Raton: CRC Press, pp. 111–143.
- Wilson, E. O., 1992. *The Diversity of Life*. Cambridge: Belknap Press.

[Evapotranspiration](#)
[Management Effects on Soil Properties and Functions](#)
[Nature Conservation Management](#)
[Rainfall Interception by Cultivated Plants](#)
[Tropical Watersheds, Hydrological Processes](#)
[Water Balance in Terrestrial Ecosystems](#)
[Water Erosion: Environmental and Economical Hazard](#)

Cross-references

- [Climate Change: Environmental Effects](#)
[Ecohydrology](#)

WORKABILITY

See [Trafficability and Workability of Soils](#)

X

X-RAY METHOD TO EVALUATE GRAIN QUALITY

Alexander M. Demyanchuk¹, Leonid P. Velikanov², Michael V. Arhipov¹, Stanislaw Grundas³

¹Laboratory of Seed Biophysics, Agrophysical Research Institute of Russian Academy of Agricultural Sciences, St. Petersburg, Russia

²Laboratory of Seed Biophysics, Agrophysical Research Institute, St. Petersburg, Russia

³Institute of Agrophysics, Polish Academy of Sciences, Lublin, Poland

Synonyms

Roentgen's radiation; X-ray

Definition

X-ray is the electromagnetic waves in which energy of photons on a power scale is between ultraviolet and gamma radiation. X-ray is a key element of a method of nondestructive diagnostics of grain and seeds.

Introduction

Quality of grain is estimated by indicators of over 20 of its physical, biochemical, and technological properties. X-ray method (XRM) occupies more than a modest place among approximately three tens of methods to estimate the quality of grain. It is included into the standard as a method to estimate a contamination and insects' colonization of grain including the quarantine species. Not destroying an object, XRM enables to reveal its internal structure and make it observable and accessible for qualitative and quantitative estimation. This method distinguishes many defects of an internal structure of kernel that affect significantly the quality of kernel:

1. Endosperm cracks caused by natural and anthropogenic reasons
2. Damage caused by Sunn pest (*Eurygaster integriceps* Put.)
3. The enzyomo-mycotic exhaustion
4. The damage of a germ of the various origin and level
5. The hidden insect colonization including early stages of larvae development
6. The internal germination had still begun in the field or in a heap and then stopped by drying
7. Contamination and damage caused by fungi

All these defects reduce the quality of kernel both as seed and as technological raw material. In some cases it makes kernel suitable (the presence of an insect, the beaten out germ) neither for crops nor for processing.

The physical parameters of a separate kernel and grains in weight or in heaps such as the kernel size, grain nature, impurities, etc., are evaluated by XRM. The other possibilities in demand of X-ray method applications for the analysis of grain quality have recently come to light.

X-ray is defined as an electromagnetic radiation with wavelength from 0.001 to 50 nm located in a spectrum between areas of gamma- and ultraviolet radiations. These rays were discovered by Roentgen (1895); later in 1901, he was awarded the Nobel Prize for this discovery – the first award in history in the area of physics. The opportunities of the discovered phenomenon have demonstrated their inexhaustibility until now. The area of its application continues to broaden. The most desirable X-ray property for use is its ability to penetrate through objects being partially absorbed by them in proportion depended on density or thickness of matter. Due to this property radiation penetrating through the complex body consisting of many parts of different size, form, and density displays a shadow "portrait" of body internal structure on the fluorescing screen revealing its defects. X-ray films and now – CCD-matrices can be used instead of the

fluorescing screen. Roentgen tubes are used for emission of X-rays.

It is known from the history that the first features that attracted attention on the X-ray pictures of seeds were the signs of the content absence in the seed coat ("empty seeds") or the signs of the obvious morphological deviations of a germ meaning non-viability of a seed.

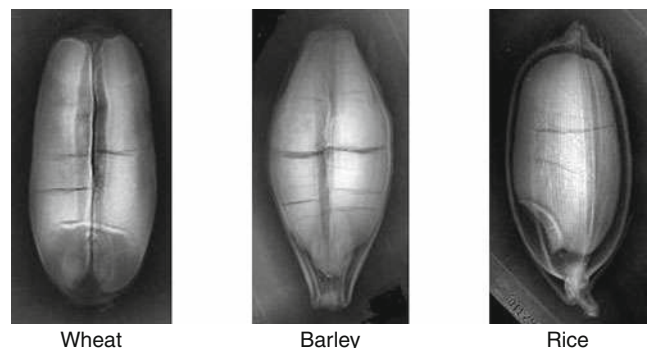
For the first time the radiographic analysis of seeds has found practical application in 50th years of the twentieth century. It was used for quarantine entomological examinations of seeds (Varshalovich, 1958). However, the method has not received development because of low productivity and labor content. It should be taken into account that there was no special equipment, and medical or technical ones were used instead of it. The later did not fit structurally and did not satisfy the needed radiation parameters. At a later stage X-ray radiation has been studied at the Institute for Agrophysics. Firstly, these studies were focused on mutagenic and suppressing growth of plants factor, then its classic application has been studied as well. These works gave an impetus to design special equipment for the analysis of grain and seeds. The microfocus soft-ray X-ray device "Elektronika-25" specially designed for X-ray shooting of seeds and grain was made. It consisted of a monoblock in which the X-ray radiator and a power unit were placed as well as of a film-making chamber and a control panel. It was used to receive the radiation generated under 15–25 kV and tube current up to 100 μ A and expositions from 1 to 16 min on a flat film of sensitivity equaled approximately to 100 on ISO scale. The focus spot sized from 40 to 100 μ m was observed. The chamber had side wall grooves into which the objective frame with grains could be inserted on different heights; the cartridge with X-ray sensitive film was placed under the frame.

The device enabled to shoot with direct X-ray enlargement that could be up to ten times as large. The experiments proved the fact that the shooting with twofold to threefold enlargement was needed to reveal the defects of grain structure (kernel) considering its small size. During 20 years in the past the device had been serving as the main tool for the radiographic analysis of grain and seeds in Russia and Poland (Grundas and Velikanov, 1998; Grundas et al., 1999; Nawrocka et al., 2010; Velikanov et al., 1994, 2008; Yakushev et al., 2002).

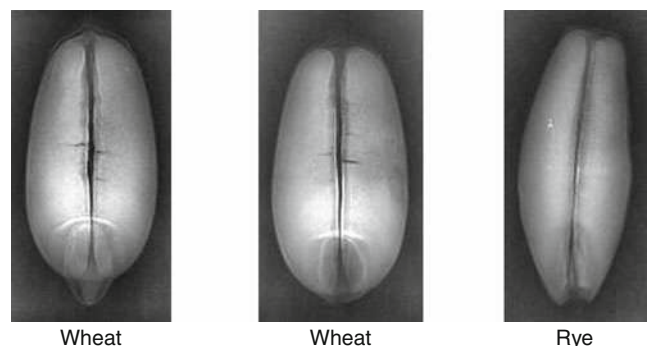
The used range of wavelengths (0.05–0.1 μ m) at specified tube current, expositions, sensitivity of a film, size of a focus spot made possible to distinguish steadily enough contours of a based germ and its details while internal germination has begun. The local irregular changes of optical density (dimness) of an image allowed to judge about presence or absence and also about damages of a germ and endosperm. Considering a character of dimness and its localization it was possible to conclude on the nature of damages.

Examples of X-ray images of cereal grain

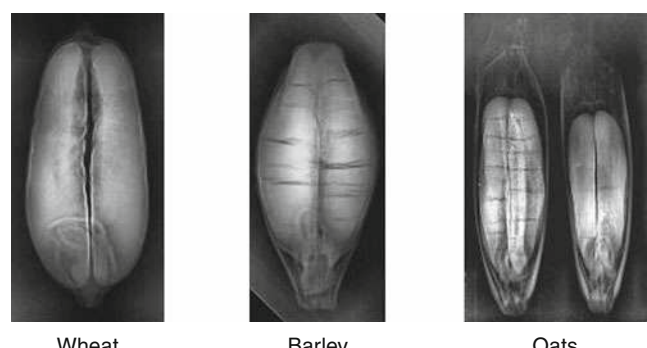
Some examples of X-ray images of kernels of basic cereals with internal defects of various origins are shown below and commented (Figures 1–6).



X-ray Method to Evaluate Grain Quality, Figure 1 Cracking of endosperm in wheat, barley, and rice. (Collection from authors.)



X-ray Method to Evaluate Grain Quality, Figure 2 Full or partial loss of a germ. (Collection from authors.)

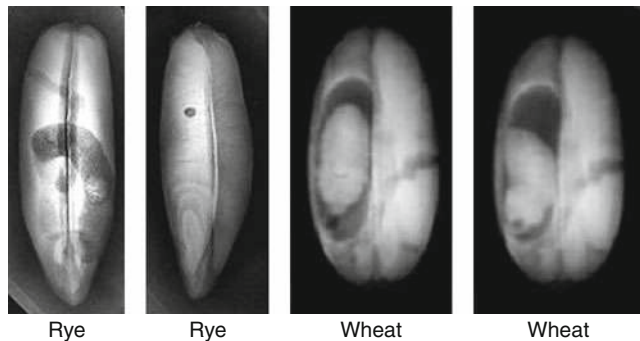


X-ray Method to Evaluate Grain Quality, Figure 3 The latent germination (wheat, barley, oats). (Collection from authors.)

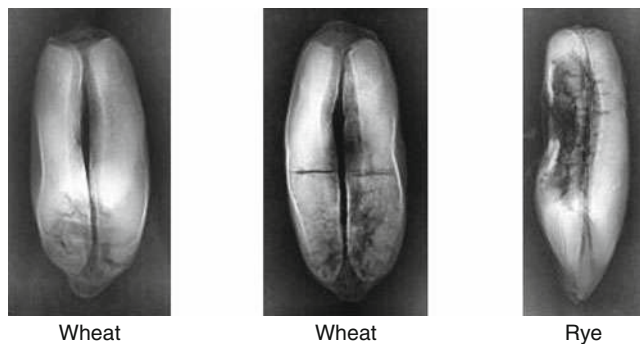
Endosperm of grain's kernel can get cracking while maturing in a field due to drops in air temperature and humidity as well as while drying, preprocessing, and transportation of grain. Strongly expressed cracking reduces both sowing properties of seeds and technological properties of grain (oxidation of spare substances,

reduction of admissible periods of storage, impossibility of getting the whole grits).

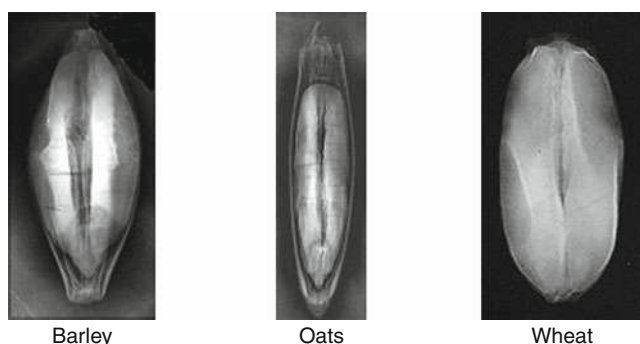
Full or partial loss of a germ at a kernel of any cereal (examples for wheat and a rye are shown in [Figure 2](#); the left picture demonstrates a kernel of wheat with a normal germ) leads toward a nonemergence of seeds and an



X-ray Method to Evaluate Grain Quality, Figure 4 Infestation and colonization of grain by insects.
(Collection from authors.)



X-ray Method to Evaluate Grain Quality, Figure 5 Damage of grain by a Sunn pest bug (*Eurygaster integriceps*).
(Collection from authors.)



X-ray Method to Evaluate Grain Quality, Figure 6 The enzymo-mycotic exhaustion of grain (barley, oats, wheat).
(Collection from authors.)

encapsulation of grains, i.e., the opening for air and malicious agents access if the later is not made specially due to the technological requirements just before grinding.

It is known that grain can sprout in the field in standing, in heaps, and while storage. The initial stages of germination revealed in X-ray pictures ([Figure 3](#)) cannot be found out visually, however biochemical and morphogenetic changes in grains reduce their sowing and technological properties. In the case of glumiferous even the advanced internal germination can be not noticed visually (in the right picture two oat kernels are shown in a smaller scale: the length of the sprout of the left kernel hidden by a film is almost equal to the length of endosperm).

The cavities inside the kernel that have been eaten away by larvae of insects can be easily seen in pictures ([Figure 4](#)) as a specific dimming irrespective of their size (two pictures of rye kernels at the left). The reshoot made in some seconds gives possibility to identify live insects in grain (pictures of two wheat kernels at the right). Presence of insects in grain is inadmissible. The selective visual analysis is unreliable. Only separation can guarantee the absence of infected kernels.

Specific moiré dimming in pictures of kernels in a unique manner indicates on decondensation of endosperm as the result of active hydrolytic enzymes introduction by bugs ([Figure 5](#)). If 2–3% of kernels with signs of such damages are presented in a sample it transfers grain of hard wheat into the category of soft weak. The visual analysis results in an underestimation or overestimation. The X-ray analysis gives a possibility of more accurate quantitative estimation of damages.

The pictures ([Figure 6](#)) demonstrate the loss of density of a kernel tissue in lateral parts and along a groove as a result of own enzyme activity under the increased air humidity in the field, and then of fungi enzymes, which have developed on a kernel surface with appeared hydrolyzates.

Visual estimation is difficult especially for glumiferous kernels. The X-ray analysis is accurate; the quantitative estimation of damage is possible. Sowing and technological parameters of kernels with signs of enzymo-mycotic exhaustion are decreased.

Discussion

The digital technologies have been recently widespread. The focus spot of produced X-ray tubes was reduced from 40–100 μm for tubes made in 1980–1990s to several microns that considerably increased the quality of image. Quality of X-ray images was improved by using the phenomenon of phase contrast (Zernike, 1935). Zernike the Nobel Prize in 1953 for, opening of a method of contrast of a phase and construction of the first contrast phase microscope has been awarded.

The method of phase contrast provides a high spatial resolution visualization of an internal structure of low absorbing objects with small gradients of substance density.

In spite of considerable progress in development of XRM, its use for diagnostics of seeds and grain quality remains significantly restricted. Concerning the problem of seeds and grains quality, what can be said about the situation in a whole?

Huge grain masses are estimated for their sowing and technological properties on the basis of the smallest samples. The previous studies proved that the size of these samples (2 kg) is sufficient for correct estimation of material state. It means the great risk especially for the minimum acceptability features such as a presence of insects or part damaged by a Sunn pest bug (*Eurygaster integriceps*). The quantitative estimation of kernels with these signs can be overestimated or underestimated while the decision about the whole party is made. Now the diagnosis itself if the state of grain party is concerned is not a reason to change this state in case if it is bad. On the basis of such diagnosis the price can be lowered, the decision on its processing by insecticides is made, as well as customer may decide to use this grain after applying additives to improve, but quality of initial party has no prospects for improvement. The situation can be significantly changed only by separation by critical feature, for example, by insect presence. However, such separation is impossible because the initial material is destroyed for diagnostics.

The big number of the parameters that are confidently found out by XRM allocates this method among others even at present time. In spite of indisputable advantages, X-rays are limited by two reasons. First, the control of protein and other grain biochemistry is required. Secondly, technologies should allow the total control. Today there are all premises to solve these problems.

Still in 1953, Watson and Crick were awarded the Nobel Prize for the discovering of the structure of double DNA helix by means of comparison of X-ray analysis data with the cardboard model proposed by them. The biochemical diagnostics required for an estimation of grain and seeds quality can be carried on by methods of the X-ray structural analysis. It is determined by possibility to study an atomic structure of substance by means of diffraction of X-rays. Considering the diffractive picture an electronic density of substance is estimated, then using the latter a sort of atoms and their arrangement are determined in its turn. The X-ray structural analysis is used to find out the structure of crystals, liquids, protein molecules, etc. To receive the images of the large molecules with the atomic resolution the rays with shorter wavelengths are used, i.e., not soft but hard X-ray is applied.

To solve the second problem the fast analysis of great volumes of a grain material is required. Usually to provide sharpness of the image at X-ray shooting object is illuminated during the exposing of a frame only. To gain it a switch linked to the mechanism of movie camera sends impulses of a current to the control grid of an X-ray tube of the X-ray device. In such a way using X-ray tube with cold emission 10^{-7} s exposition at frequency of shooting 100 shots per second is reached. Now it has reached the frequency of filming in a range from 1 to 100,000 frames

per second with a frame exposition up to 15 ns. The adaptation of these technologies to the needs of the diagnostics of cereals makes possible to exclude almost completely a poor-quality material by separation. The start of industrial application of X-ray separation that means the moving from diagnostics of several kilograms in hour to diagnostics of several tons in hour initiates the revision of a number of concepts. To solve the arbitrage problems it is not enough to declare that we observe signs of quality and its grade as well as deficiency. The limits of features should be defined quantitatively and proved to be true by specially developed standard documents. It means that modern problems of X-ray application demand the radical revision of the existing quality standards for cereals. It will allow the move to the full control of parameters for seeds rating and grain quality. It will require the obligatory introduction of elements of fast separation in the systems of X-ray diagnostics.

Conclusion

As shown, the XRM is unique for instant recognition of internal kernel defects. In parallel it allows to identify specific both high-quality features and fractional grain composition. The biochemical analysis of grain is also possible at use of more short-wave part of X-ray radiation spectrum. Thus, XRM may be potentially treated as a universal method of diagnostics and processing of initial parties of grain to the quality of high standards.

Bibliography

- Grundas, S., and Velikanov, L. P., 1998. Methodical and technological aspects of X-ray imaging of wheat grain. *Book of Abstracts of the 16th ICC Conference on Cereal Science – Its Contribution to Health and Well Being*, Vienna, Austria, 9–12 May 1998, p. 31.
- Grundas, S., Velikanov, L. P., and Archipov, M. V., 1999. Importance of wheat grain orientation for the detection of internal mechanical damage by the X-ray method. *International Agrophysics*, **13**, 355–361.
- Nawrocka, A., Grundas, S., and Grodek, J., 2010. Losses caused by granary weevil larva in wheat grain using digital analysis of X-ray image. *International Agrophysics*, **24**, 63–68.
- Roentgen, W. K., 1895. Über eine neue Art von Strahlen. *Sitzungsberichte der Physikalisch – medizinischen Gesellschaft zu Wurzburg*, pp. 132–141.
- Varshalovich, A. A., 1958. *Guide to Quarantine Entomological Expertise Seeds by X-ray* (in Russian). Moscow, USSR: USSR Ministry of Agriculture.
- Velikanov, L. P., Archipov, M., and Grundas, S., 1994. Signification of kernel orientation related to direction of X-ray beam for evaluation of inner cracks. *Abstract of Poster Session: Testing Methods, P.6.8. 14th ICC Congress*. The Hague, The Netherlands.
- Velikanov, L. P., Grundas, S., Archipov, M. V., Demyanchuk, A. M., and Gusakova, L. P., 2008. Agophysical direction of further development and application of X-ray method. *Proceedings of International Conference on New Trends in Agrophysics*. Lublin, Poland, pp. 147–148.
- Watson, J. D., and Crick, F. H. C., 1953. Molecular structure of nucleic acids. *Nature*, **171**, 738–740.

- Yakushev, V., Grundas, S., Velikanov, L. P., and Archipov, M. V.,
2002. X-ray pattern analysis of seeds and other vegetative materials. *Workshop on Applied Physics in Life Science*, Prague, Czech Republic, pp. 55–60.
- Zernike, F. 1935. Das Phasenkontrastverfahren bei der mikroskopischen Beobachtung. *Zeitschrift für technische Physik*, 16.

[Grain Physics](#)

[Grains, Aerodynamic and Geometric Features](#)

[Image Analysis in Agrophysics](#)

[Microstructure of Plant Tissue](#)

[Physical Properties as Indicators of Food Quality](#)

[Quality of Agricultural Products in Relation to Physical Conditions](#)

Cross-references

- [Agophysical Objects \(Soils, Plants, Agricultural Products, and Foods\)](#)
[Cereals, Evaluation of Utility Values](#)

Author Index

A

- Adamchuk, V.I., 650
Addiscott, T.M., 421
Alaoui, A., 148
Alchanatis, V., 944
Alekseev, A., 436
Alekseeva, T.V., 117
Anderson, S.H., 122, 180
Anken, T., 153
Arhipov, M.V., 1005
Arkhangelskaya, T.A., 597
Arriaga, F.J., 757
Assouline, S., 95

B

- Bachmann, J., 378
Baiyeri, K.P., 925
Balashov, E., 481
Bandyopadhyay, K., 296
Baranowski, P., 632
Baumann, J., 937
Ben-Hur, M., 979
Bengough, A.G., 709
Besson, A., 256
Białousz, S., 761
Bieganowski, A., 260, 791, 854
Billingsley, J., 433
Birkás, M., 903
Biswas, A., 725
Blagodatskaya, E., 657
Blahovec, J., 5, 60, 693, 971
Blaskó, L., 49, 400, 723
Blum, W.E.H., 562, 747
Boivin, P., 162, 733, 740
Bouma, J., 589
Brzezińska, M., 62, 274
Buchan, G.D., 891
Bulanon, D.M., 944
Burks, T.F., 944
Burmölle, M., 70
Burri, K., 997
Busscher, W.J., 357

C

- Cakmak, M.E., 66
Camargo Rodriguez, A.V., 605
Caurie, M., 384
Ceccherini, M.T., 224

C

- Chertkov, V.Y., 780
Chesworth, W., 29
Chevallier, T., 592
Chibowski, E., 301
Chmielewski, T.J., 503, 548
Chodorowski, J., 535
Cieśla, J., 260, 264
Clark, L.J., 228
Cook, F., 824
Coquet, Y., 819
Cousin, I., 256
Czachor, H., 378, 413, 996
Czaczyk, K., 75
Czyż, E.A., 938

D

- da Silva, A.P., 360
Dabek-Szreniawska, M., 481
Darboux, F., 887
de Lima, H.V., 360
Dębicki, R., 145
Demyanchuk, A.M., 1005
Dexter, A.R., 938
Dimitriou, E., 536
Diserens, E., 148
Dobrzański, B. Jr., 579, 730
Doolittle, J., 354
Doussan, C., 717
Draye, X., 717
Dutilleul, P., 424
Dziki, D., 110

E

- Eriksson, J., 910

F

- Fank, J., 428
Farkas, I., 338, 509, 608,
637, 816
Fernández, P.L., 304
Filipek, T., 425
Finch-Savage, W.E., 163
Fleige, H., 464, 777, 870
Fortunati, A., 633
Frąć, M., 49
Fraczek, J., 460
Franzluebbers, A.J., 858
Friedman, S.P., 242

G

- Gamliel, A., 813
García-Ramos, F.J., 511
Gebhardt, S., 912
Gerke, H.H., 100
Giarola, N.F.B., 360
Giráldez, J.V., 299
Glenn, M., 547
Gliński, J., 34, 35, 455, 705, 760
Górnicki, K., 48, 189
Grewal, H., 444
Gromke, C., 997
Grove, J.H., 827
Grundas, S., 323, 1005
Gupta, V., 470

H

- Hajnos, M., 94, 264, 647
Hallett, P.D., 378
Hartmann, P., 754
Hatano, R., 339
Hati, K., 296
Heinse, R., 826
Heitman, J.L., 155
Heneberg, P., 754
Hlaváčová, Z., 237
Holpp, M., 153
Horabik, J., 35, 393, 407, 567
Horn, R., 316, 447, 777, 862, 867, 870
Horton, R., 155
Horyński, M., 523
Hriberník, S., 333

I

- Igwe, C.A., 934
Iwata, Y., 736

J

- Jaroszuk-Sierocińska, M., 364
Javaux, M., 717
Jayas, D.S., 231
Jordán, A., 492
Józefaciuk, G., 393

K

- Kaleta, A., 48, 189
Kammerer, G., 802
Kang, S.P., 138

- Kargol, M., 465, 975
 Karlen, D.L., 794
 Katan, J., 813
 Kędziora, A., 26, 270, 323, 1000
 Kiehl, K., 987
 Kim, J.T., 605
 Kirchhof, G., 667
 Kirchmann, H., 910
 Kjøller, A., 70
 Kohler-Milleret, R., 740
 Kojs, P., 220, 602
 Kõlli, R., 551
 Kolodziej, J., 679
 Konstankiewicz, K., 476
 Koper, J., 62
 Kornecki, T.S., 912
 Kowalik, P., 52
 Kram, B.B., 327
 Krounbi, L., 748
 Krümmelbein, J., 334
 Kuczyński, A.P., 113
 Kuderna, M., 200
 Kuriakose, S.L., 622
 Kutílek, M., 125, 390, 645, 798
 Kuzyakov, Y., 657
- L**
 Lal, R., 528
 Lamorski, K., 505, 895
 Laredo, T., 289
 Laskowski, J., 91, 110
 Lavelle, P., 233
 Lazarovitch, N., 748
 Leong, W.H., 275, 483
 Levy, G.J., 403
 Lewicki, P.P., 964
 Lipiec, J., 35, 167, 705, 912
 Loiskand, W., 802
 Lowery, B., 757
- M**
 Macaigne, P., 849
 Machado, L.F., 898
 Madejón, E., 108
 Maheshwari, B., 444
 Marangoni, A.G., 289
 Markgraf, W., 700
 Martin, M.A., 309
 Matula, S., 376
 McKenzie, B.M., 770
 Mieszkalski, L., 14
 Migliaccio, F., 633
 Minasny, B., 824
 Mioduszewski, W., 973
 Mocek, A., 543
 Mojid, A. Md., 213
 Molenda, M., 7, 407, 567, 924
 Momose, T., 275, 483
 Morales, V.L., 66
 Moran, C. J., 628
 Moreda, G.P., 318, 669
 Moreno, F., 108
 Mościcki, Ł., 284
 Mouazen, A.M., 521
 Müller, L., 783, 912
 Muñoz-Rojas, M., 492
 Murillo, J.M., 108
 Myszka, K., 75
- N**
 Nakashima, H., 810
 Nambuthiri, S., 827
 Nawrocka, A., 323
- Nehls, T., 941
 Nelson, S.O., 207
 Nemes, A., 194
 Nosalewicz, A., 167
 Novák, V., 280
- O**
 Openshaw, K., 78
 Ostrowski, J., 455
 Owczarzak, W., 543
- P**
 Pachepsky, Y., 309, 368, 556
 Pagès, L., 712
 Pagliai, M., 640
 Papadopoulos, A., 526, 736
 Pearce, R.C., 827
 Pecen, J., 323
 Peng, X., 55
 Persson, M., 387
 Peth, S., 516, 742, 862, 867
 Peyronel, F., 289
 Pierret, A., 628
 Pietramellara, G., 224
 Pietrusiewicz, J., 167
 Pietruszewski, S., 267
 Pietrzky, W., 523
 Pinskiy, D.L., 135
 Piper, D.J.W., 275
 Pistocchi, A., 959
 Podolska, G., 609
 Pohlmeier, A., 439
 Pot, V., 819
- Q**
 Quinton, J.N., 746
- R**
 Rao, S.M., 992
 Raper, R., 757
 Rasmussen, T.C., 874
 Raytchev, T., 596
 Rejman, J., 968
 Richard, G., 256
 Ritchey, E.L., 827
 Ritz, K., 472
 Roose, T., 637
 Rousseva, S., 596
 Różyło, R., 91
 Ruiz-Altsent, M., 318, 669
 Ruiz-Lozano, J.M., 496
 Rusin, T., 220, 602
 Rybczyński, R., 579
 Rybiński, W., 610
 Ryzak, M., 791, 854
- S**
 Salama, R.B., 681
 Salvucci, A.E., 66
 San José Martínez, F., 309
 Sánchez-Marañón, M., 141
 Scanlon, M.G., 573
 Schaumann, G.E., 667
 Séger, M., 256
 Selim, H.M., 414
 Sfiligoj Smole, M., 333
 Shein, E.V., 597, 600
 Si, B.C., 725
 Singh, C.B., 231
 Skiba, S., 595
 Skierucha, W.M., 489,
 513, 563
 Śląwiński, C., 385, 805
- Ślipek, Z., 460
 Słowińska-Jurkiewicz, A., 364
 Smal, H., 116
 So, H.B., 667
 Sobczuk, H., 214, 805
 Sokołowska, Z., 2, 839
 Sokołowski, S., 2
 Sørensen, S.J., 70
 Spokas, K.A., 845
 Sposób, J., 955
 Steenhuis, T.S., 66
 Štekauerová, V., 984
 Stępniewska, Z., 536
 Stępniewski, W., 8, 214,
 541, 563
 Szajdak, L.W., 551
 Szatyłowicz, J., 551
 Szot, B., 176, 610, 639
 Szot, P., 534
 Szpryngiel, M., 176
- T**
 Taboada, M.A., 304
 Tamny, J., 185
 Targoński, Z., 89
 Tarnawski, V.R., 275, 483
 Tassone, P., 633
 Tisdall, J.M., 770
 Trabelsi, S., 207
 Tuong, T.P., 667
 Tuzet, A.J., 855
 Tys, J., 176
- U**
 Ugese, F.D., 925
 Urban, D., 548
 Urbanek, E., 378
 Uskov, I.B., 396
 Usowicz, B., 59, 563
 Usowicz, J., 93
- V**
 van Beek, L.P.H., 622
 van Genuchten, M.T., 368, 556
 Vance, W.H., 770
 Vanderborght, J., 717
 Vanderlinde, K., 299
 Varela, M.F., 304
 Velikanov, L.P., 1005
 Vereecken, H., 717
 Vicente, A.A., 898
 Viscarra Rossel, R.A., 650
 Viswanathan, S., 499
- W**
 Wendroth, O., 827
 Wessolek, G., 941
 Whalley, W.R., 163, 228
 Widomski, M., 214, 563
 Witkowska-Walczak, B., 740
 Włodarczyk, T., 351
- Y**
 Yakushev, V.P., 396
- Z**
 Zalewski, M., 235
 Zavala, L.M., 492
 Zdunek, A., 88
 Zhang, B., 378
 Zhang, J., 906
 Zhang, W., 66
 Zsolnay, A., 200

Subject Index

A

- Absorption, 1
 - energy, 7
 - isotherms, 7
- Adhesion, 1
- Adsorbate, 4
- Adsorption, 2, 5
 - energy, 3, 4
- Adsorption hysteresis, 843
- Advection-dispersion equation (ADE), 876–877
- Aeration, 12
 - air-filled porosity, 8
 - airflow rates, 8
 - air permeability, 9
 - grain, 8
 - plants, 8
 - silo, 8
 - soils, 8
- Aerodynamic characteristics
 - coefficient of aerodynamics, 328
 - coefficient of fineness, 328
 - critical velocity, 328
- Aerodynamic properties, 328
- After harvest technology, 461
- Aggregated bio-materials, 697–698
- Aggregate formation, soils, 448–449
- Agricultural landscape, 271
 - heat balance, 270
 - radiation balance, 270
 - water balance, 270
- Agricultural management
 - biochemical activity, 63
 - conservation tillage, 63
 - no-tillage, 63
 - reduced tillage, 63
- Agricultural material
 - brittleness, 569–570
 - elasticity, 569
 - hardness, 569
 - plasticity, 569
 - strength, 569
 - toughness, 569
- Agricultural plant products
 - porosity, 568
 - shape and size, 568
 - surface area, 568–569
 - volume and density, 568

Agricultural products, 207–212, 231–232, 237–241, 699

- aeration, 7
- airflow, 48
- anisotropy, 407–408
- color measurements, 585
- compression tests, 583
- degree of elasticity, 694
- density, 972
- dielectric properties, 208
- drying/dehydration, 232
- electrical properties, 237, 240, 241
- electric conductivity, 238
- firmness, 583
- force-displacement curve, 694
- heat transfer, 572
- hysteresis loss, 694
- isotropy, 407
- length, 189
- loading/unloading test, 694
- Magness-Taylor puncture, 583
- measurement of texture, 582–583
- moisture content, 972
- permittivity, 238
- physical condition, 669
- physical properties, 579–587
- production, 580
- quality, 669
- raw materials, 579, 580
- resistivity, 240
- rheological functions, 695
- rheology, 693
- shrinkage, 730–733, 972
- specific heat, 572
- storage, 6, 232, 567–572
- stress relaxation, 694
- swelling, 730–733, 972
- tensile measurement, 583
- thermal conductivity, 572
- thermal diffusivity, 572
- thickness, 189
- water, 971–972
- width, 189

Agriculture

- and environment, monitoring, 490
- irrigation water, 979
- machine vision, 433–436

rainfall water, 979

- wind erosion, 999

Agro-food products

- colour, 571
- gloss, 571
- thermal properties, 571–572
- translucency, 571

Agroforestry, 123, 124

- alley cropping, 27
- biodiversity, 27, 29
- environmental services, 29
- forest farming, 28
- riparian buffers, 28
- silvopasture, 27
- windbreaks or shelterbelts, 28

Agrogeology, 29

- agricultural science, 31

Agrophysical objects

- agricultural plants, 34
- agricultural products, 34
- foods, 34
- soils, 34

Agrophysics, 16, 37, 610

- agrophysical objects, 36
- agrophysical processes and properties, 36
- conferences, 38
- definition, 35
- fractal analysis, 309–315
- fractal geometry, 315
- history, 36
- image analysis, 387–389
- journals, 38
- neural networks, 505–508
- properties, 36
- research, 38
- scale dependence, 313
- standardization, 854

Air capacity

- classification, 872
- modeling, 872

Algae, source of fuel, 49

Alkalinity, soils, 50

Amplitude sweep test, 703

Animal burrowing, soil penetrability, 754

Anisotropy, 8, 335, 407–408

- description, 408
- granular solid, 408

Archie's empirical law, 243
Arrhenius formula, 240

B

Backscattering, physical forms, 59
Bacteria
 retention, 69
 transport, 69
Beer-Lambert law, 424

Biocolloids
 retention, 67
 soils, 67
 transport, 67

Biofilms
 bacteria, 76
 control, 76
 exopolymers (EPS), 75
 formation, 75
 microorganisms, 75
 pathogens, 76
 removal, 77
 soil, 69
Biological materials, 5, 7
 cooling, 8
 heating, 8
 isotropic, 8
 solar drying, 816

Biomass
 availability, 79
 charcoal, 80
 clearing land, 83, 84
 crops, 85
 energy, 80, 87
 energy source, 78
 energy value, 79
 environmentally benign, 87
 fuels, 79–81
 greenhouse gases (GHG), 81
 hydrogen, 80
 income, 84
 renewable energy, 52, 81

Biosphere, 31
 soil, 32

Biotechnology
 biomass, 89
 bioreactors, 89
 chemical processes, 90
 enzyme biocatalysis, 90
 physical processes, 89

Boltzmann's law, 440

Bread
 crumb, 91
 crust, 92, 93
 mechanical properties, 92
 physical properties, 93
 quality, 91
 raw material quality, 91
 raw materials, 91
 storage, 92

Breeding, 611
 physical characteristics, 610–621

Brightness temperature
 emissivity, 94
 microwave radiometers, 94
 soil, 94

Brooks and Corey hydraulic conductivity
 expression, 300

Brooks–Corey equation, 556

Bruise susceptibility
 citrus fruit, 320
 kiwifruit, 320
 pome fruit, 319
 stone fruit, 319–320
 tomato, 320

Brunauer, Emmett, and Teller (BET), 3, 840
Buffer capacity
 soil, 94
 sorption, 94
Bulk density, 190
 compaction, 96
 tillage, 96
Bypass flow
 cracks, 100
 funnel flow, 100
 macropore flow, 100
 macropores, 103
 preferential flow, 100
 water movement, 100

C

Campbell equation, 257
Capillary rise, 881
Carbon dioxide, 11, 13
 greenhouse gases, 12
 oxygen, 12
Cartesian coordinates, 2

Cation exchange capacity (CEC)
 plant roots, 885
 soil, 885

Cellular rheology, 699

Cereals, 324
 falling number, 112
 flour, 111
 flour milling, 111
 grain hardness, 111
 sedimentation test, 112
 utility values, 112
 wheat, 111, 112

Chemical imaging
 agriculture, 113
 image processing, 113–114
 techniques, 113

Chemical potential, 5, 6
Chemical time bomb (CTB), 116–117
 concept, 116

Clay minerals, 882

Claypan soils, 183
 agrichemical leaching, 124
 agrichemical runoff, 123–124
 best management practices (BMPs), 125
 erosion, 123–125
 permeability, 122
 plant productivity, 124
 preferential flow, 124
 saturated hydraulic conductivity (K_{sat}), 122, 123

structure, 122
texture, 122
tillage, 122–124

Cleavage plane, 125

Climate change
 aerosol concentration, 133
 aerosols, 129–130, 132, 133
 albedo, 129, 131, 132
 atmospheric CO₂, 131, 133, 134
 deforestation, 130

desertification, 134
environmental effects, 125–134
geologic history, 130–133

glaciers, 133

global aridization, 134
global cooling, 133

global warming, 134
greenhouse effect, 134
greenhouse gases, 128–130

mechanisms, 131

Milankovich cycles, 128, 133
seawater level, 126, 133

snow cover, 126
solar activity, 133
solar radiation, 128, 130
temperature, 126, 127, 129–131
thermohaline circulation, 129, 133
vegetation cover, 130
volcanic activity, 133
volcanoes, 129–130, 133
warming, 127
weather changes, 133

Clod, 135

Clusters, 310

absorption of heavy organic matter, 137
adsorption of heavy metals, 137
formation, 135–136
functions, 136
life time, 136
parent rock, 137
properties, 136
structures, 137
weathering, 137

Coherency spectra

clay content, 836
corn yield, 836
soil water storage, 836

Cohesion, 138

Colloidal particles

dispersed particles, 938–939
dispersion, 938
flocculation, 938

Colloids

aggregation, 67, 266
coagulation, 266
flocculation, 67, 266–267
peptization, 267
retention, 67
soils, 67
transport, 67

Color

CIELAB color space, 139–141
CIELAB system, 142, 143
CIE system, 142
color variation, 140
food, 140
fruit, 140
HSI color space, 139
HSV color space, 139
indices, 143
measurement, 140

Color composite (multiband photography), 138

Colored images

machine vision, 605
plant disease, 605–608

Compaction

bulk density, 334
of soil, 145
soil bulk density, 149, 218

Compressibility indices

compression and swelling index, 744
compression curve, 744
cyclic compressibility, 745
void ratios, 744

Conditioners

characteristics, 146
classification, 146
organic substances, 145
soil physical properties, 145
synthetic agents, 146

Conductivity, 148

Consistency, 148

Consolidation, 148

Contact area

inflation pressure, 148, 151
penetration resistance, 151

- soil resistance, 151
 trailer tyres, 150–151
 tyres, 149
 tyre size, 150
 wheel load, 151
- Contaminated soils, remediation, 596
- Continuity equation, 153
- Contour-furrow irrigation, 153
- Convection-dispersion equation (CDE), 415, 821
- Copper concentration in cereal crops
 clay content, 910
 soil organic matter, 911
- Coulomb's law, 155
- Cracks, soil, 163
- Creep test, 695
- Crop emergence
 germination, 166
 matric potential, 164–166
 mechanical impedance, 166
 oxygen diffusion rate, 168
 penetrometer resistance, 164
 seedbed, 164
 seedbed structure, 169
 shoot elongation, 166
- Crop growth
 air filled porosity, 170
 compaction, 174
 deep soil loosening, 174
 degree of compactness, 170
 least limiting water range (LLWR), 169
 soil physical conditions, 174
 soil strength, 170
 soil structural discontinuity, 170
 tillage managements, 174
- Cropping systems
 aggregate stability, 181, 182
 bulk density, 182
 physical properties, 180
 porosity, 182
 soil aggregate stability, 181
 soil saturated hydraulic conductivity, 183
 soil shear strength, 182
 water retention, 183
- Crop productivity
 plant selection, 982–983
 rainfall runoff, 982
 transpiration, 982–983
- Crops, 444–446, 667–668
 management, 183
 rotations, 181
- Crop yield losses
 cereals and grasses, 177
 reduction at harvest, 176–179
- Crop yields
 compaction, 173
 generalization, 173
 irrigation, 173
 practices, 173
 soil compactness, 173
 stomatal resistance, 172
 subsoil compactness, 173
 tillage, 173
- Crushing strength, 184
- Crusted soils, evaporation, 788
- Cultivated plants, rainfall interception, 679
- Cultivation under screens
 aerodynamic properties, 185–186
 aerodynamics of boundary layers, 185
 air flow, 186
 banana, 186
 citrus trees, 186
 pepper, 186
 plant canopies, 185
- resistance to the wind, 186
 screen constructions, 185
 turbulence, 186
- Cumulative infiltration, 187
 Cutan, 187
- D**
- Darcy-Buckingham equation, 368, 392
 Darcy-Buckingham flow, 157
 Darcy's equation, 10, 214, 799
 Darcy's law, 189, 216, 876, 961
 Databases, 189–198
 availability, 197
 challenges, 197–198
 compatibility and standardization, 197
 contents, 195
 Data and Information System of the International Geosphere Biosphere Programme (IGBP-DIS), 195
 Global Soil Data Task (GSDT), 195
 Grenoble Catalogue of Soils (GRIZZLY), 194
 history, 194–195
 Hydraulic Properties of European Soils (HYPRES), 194
 limitations, 195
 National Soil Survey Characterization database (NSSC), 195
 structure, 195
 Unsaturated Soil Hydraulic Database (UNSODA), 194
 World Inventory of Soil Emission Potentials (WISE), 195
- Deflation, 200
- Deflocculation, 200
- Deformation
 loading tests, 868
 loss factor, 704
 time-displacement curves, 868
- Degradation of soil, 200
- Denitrification, 200
- Derjaguin-Landau-Verwey-Overbeek (DLVO) theory, 302
- Desertification, 200–206
 indicators, 201, 202
 reforestation, 205
 remediation, 201, 202
 soil degradation, 202, 205
 soil erosion, 203
 soil parameters, 202
 soil quality, 201, 202
 soil remediation, 204
 thresholds, 202
 types of agriculture, 203
 vegetation types, 203
- Detachment, 207
- Deterministic model, 207
- Dew point, 207
- 3-D functional approaches, root water uptake, 717–721
- Dielectric properties, 207–212
 agricultural products, 208
 apple juice, 211
 apples, 210
 cereal grains, 209
 fruits, 210
 melons, 210
 oilseeds, 209
 orange, 211
 poultry products, 211–212
 rice, 210
 vegetables, 210
 wheat, 210
- Diffuse double layer (DDL), 213–214
 features, 214
- formation, 213
 models, 213–214
- Diffusion**
 bulk density, 10
 diffusion coefficient, 10
 equations, 216
 of gases, 218
 moisture diffusivity, 214
 moisture tension, 10
 in soils, 214–219
 of solutes, 219
 water, 216
- Dilatancy, 220
- Dimensions and units**
 agriculture, 563
 International system of units (SI), 563–567
 physical quantity, 563
- Discharge, 220
- Discrete element method (DEM), 811
- Disease classification, 607
- Dispersible clay, soil physical quality, 940
- Dispersion, 220, 301–306
 aggregates soil, 303
- Dispersivity, 220
- Diurnal strains, 220–223
 fluctuation, 221, 222
 measurements, 222
 shrinkage, 223
 stomata, 221
 swelling, 223
 water stress, 221
- Dixon-Renner transpiration-cohesion theory, 976
- DNA, 224–227
 bacteria, 225
 deoxyribonucleic acid, 224
 fungal cells, 225
 plant cells, 225
 water flow by capillarity, 227
- 3D pore space, noninvasive examinations, 513, 516–519
- Drainage, 228, 400–402
 advantages, 401
 disadvantages, 401
- Drip irrigation, 228
- 3D root water flow model, 718
- Drought, 228
 stress, 228–231
- Drying, 231–232
 cracking, 732
 infrared, 232
 microwave, 232
 neural networks, 508–511
 seeds and grain, 732
 solar, 232
 temperature, 732
- 3D soil-plant functional models, 721
- Dual-permeability model (DP), 822
- Dust, particle size distribution, 524–526
- E**
- Earthworms
 biogenic structures, 234
 C sequestration, 234
 ecosystem engineers, 233, 235
 management, 235
 powerful bioturbators, 233
 water supply, 234
- Ecohydrology, 235–237
 aquatic, 235
 terrestrial, 235
- Ecological principles, 236
- Ecosystem, 270–273
- Effective rainfall, 237
- Elasticity, 237

- Elastoplasticity, 237
 Electrical conductivity
 measurement, 243
 soil solution, 246
 Electrical double layer, 246
 charged surface, 884
 Electrical properties, 242–253
 complex conductivity, 242
 complex permittivity, 242
 complex resistivity, 242
 dielectric constant, 242
 dielectric permittivity, 242
 dielectric susceptibility, 242
 effective permittivity, 242
 electrical conductivity, 242
 measurements, 242
 relative permittivity, 242
 Electrical resistivity, 255–259
 cracks, 259
 measurements, 256
 profiles, 258
 soil, 259
 Electrochemical measurements, 260–263
 methods, 260
 potentiometric method, 260
 Electrochemical methods
 conductometric, 263
 potentiometric, 263
 voltammetric, 263
 Electrokinetic phenomena, 885–886
 diffuse double layer (DDL), 885
 Electromagnetic field
 germination, 269
 plants, 267
 seed, 268, 269
 Electrophoresis, 886
 Elektrokinetic phenomena
 diffuse layer, 264
 electrical double layer, 265
 electroosmosis, 265
 electrophoresis, 265
 sedimentation potential, 265
 streaming potential, 265
 Elektrokinetic zeta potential, 264–267
 clay minerals, 264
 diffuse layer, 264
 electric charge, 264
 elektrokinetic phenomena, 265
 soil colloids, 264
 Elutriation, 269
 Eluviation, 270
 Emergence
 critical stresses, 165
 mechanical impedance, 165
 shoot elongation, 164–165
 soil air, 168
 soil strength, 165, 168, 169
 temperature, 167–168
 water content, 167
 water potential, 165
 Emission, acoustic, 1
 Emissivity, 270
 Emmet and Teller (BET) equation, 3
 Empirical model, 270
 Energy
 balance, 270–273
 crops, 53
 renewable, 52
 Energy resources, biomass, 52
 Enthalpy, 274
 Entropy, 274
 Environment
 land use, 903
 tillage, 903
 Enzyme, 274
 Equivalent diameter, 190
 Erosion, 275
 Evaporation, 280
 and condensation, 879–880
 Evapotranspiration
 aerodynamic resistance, 283
 biomass production, 280
 canopy resistance, 283
 daily courses, 281
 determination, 282–283
 energy balance, 280
 evaporation, 282
 plants, 280
 seasonal courses, 281–282
 soil surface, 280, 282
 transpiration, 281, 283
 water balance, 280
 Evolution, soil, 30
 Exchangeable ions, 284
 Exchange complex, 284
 Extrudates
 thermoplastic processing, 286
 water absorption index, 285
 water solubility index, 285
 Extrusion, 284–287
 application, 284–285
 effects, 285–286
 extrudates, 285
 extrusion cooking, 285–286
 starch extrudates, 286
 vegetable raw materials, 284
 Exudate, plant roots, 287
- F**
- Fabric, 289
 Failure, 289
 Fat, 289–298
 cocoa butter, 294, 295
 fluids, 290–291
 plastic behavior, 292
 rheological behavior, 291
 rheological parameters, 293–294
 rheology, 292–293
 rheometer, 292–293, 295
 shear modulus, 294
 strain, 294
 stress, 289–290, 295
 Fatigue strength, 289
 Fertilizers, 296–299
 advantages, 297
 bulk density and porosity, 298
 detrimental effects, 299
 hydraulic conductivity, 298
 infiltration, 298
 limitations, 297
 mineral, 297
 organic, 297
 soil aggregates, 298, 303
 water retention, 298
 water transmission, 298
 Fibers, 333–334
 content, 333
 grasses, 333
 morphology, 333
 properties, 333
 Fick's equation, 216
 Fick's law, 10, 218, 299
 Field water capacity
 available soil water, 300
 field capacity, 300
 permanent wilting point, 300
 Fingering, 300
 Firmness, 300
 Fissures, 300
 Flexural strength, 301
 Flocculation, 301–303
 sodium adsorption ratio (SAR), 302
 Flooding, 304–307
 mechanical properties, 305, 307
 soils, 305
 structural stability, 305
 Flowability, 308
 Fluvial erosion, 308
 Food, 20–22, 25, 284, 286, 290, 324,
 407–408, 485
 absorption spectra, 576
 anisotropy, 407
 dielectric properties, 241
 electrical heating, 241
 electrical properties, 577
 electromagnetic heating, 241
 evaluation, 139–140
 freezing, 308
 isotropy, 407
 mechanical properties, 576–577
 microwave heating, 899–900
 nanomaterials, 499–503
 of plant origin, 34
 processes/processing, 18, 19, 24, 110
 production, 24
 products, 900
 RGB color space, 139
 rheology, 693
 shear deformation, 290
 shear rate, 577
 shear stress, 577
 strain, 289–290
 stress, 289–290
 thermal properties, 577
 Food processing
 commercial applications, 899
 heating applications, 901
 inductive heating, 898
 infrared heating, 901
 machines, 15
 microwave heating, 899–900
 ohmic heating, 898–899
 pasteurization, 902
 thermal technologies, 898–902
 Food products, 14, 17
 testing, 16
 thermal-processing technologies, 902
 Food quality
 optical and dielectric properties, 575–576
 physical properties, 574–576
 Fourier equation, 216, 572
 Fourier's law, 217, 308–309
 Fourier transformation, 440
 Fractals
 analysis, 309–315
 model, 309–311, 313–315
 objects, 309–311
 properties, 310
 Fracture, 315
 Fragipan, 315
 Freundlich and Langmuir reactions,
 layered soil, 416
 Friction, 316
 Mohr-Coulomb failure, 317
 Frozen foods, thermal conductivity, 483–488
 Fruit
 bruise susceptibility, 318–320
 bruising, 586
 color, 586

- mechanical damage, 318–320
 mechanical properties, 318–320
 nondestructive measurements, 511–513
 texture, 318
- Fruit detection
 fusion of visible and thermal images, 951
 multispectral images, 951–952
 thermal imaging, 950
- Fruit harvesting
 image acquisition, 945
 image processing, 945
 machine vision, 944
 machine vision system, 945
 robotics harvesting, 944
 scene constraint, 944–945
 thermal imaging, 944
 visible imaging, 944–947, 950
- Functions, urban soil, 941–942
- Furrow
 erosion, 321
 irrigation, 321
- G**
- Gas diffusion
 bulk density, 218
 soil moisture tension, 218
- Gas exchange
 air-filled pores, 10
 air-filled porosity, 9
 air flux, 10
 air permeability, 9, 10
 diffusion, 9
 laminar flow, 10
 mass flow, 9
 oxygen diffusion rate (ODR), 10
 transport, 9
- Generalized Kelvin's model, 695
- Generalized Maxwell's model, 695
- Geo-fertility cycle, 34
- Geological cycle, 30
- Geological soil, 30
- Geologic erosion, 323
- Geometric mean diameter, 190
- Geostatistics, 323
- Gibbs free energy, 323
- Gibbs potential, 6
- Global climate change, 21
- Global warming, deforestation, 87
- Global water circulation, water balance, 956
- Grain, 323–330, 332
 aerodynamics, 327, 331
 corn, 672
 physical properties, 324
 quality, 670, 672, 1005–1008
 rice, 672
 wheat, 672
- Grains/seeds
 color, 325
 density, 325
 hardness, 325
 impact, 325
 internal cracks, 325
 porosity, 325
 shear resistance, 325
 specific gravity internal cracks, 325
 strength, 325
 surface area, 325
- Gravimetric water content, 334
- Gravitational potential, 334
- Gravitropism, 636
 roots, 634
 threshold angle, 634
- Gravity head (gravity potential), 334
- Grazing
 animals, 334
 bulk density, 334
 compaction, 335
 infiltration, 335
 recovery of soil structure, 336
 saturated hydraulic conductivity, 335
 shearing, 334, 335
 soil deformation, 334
 soil recovery, 335
 soil structure, 334, 335
 trampling effect, 334
 water erosion, 335
 water repellency, 335
- Greenhouse, climate control, 338–339
- Greenhouse effect, 134, 339
- Greenhouse gas emission
 evaluation, 845
 stable isotopes, 845
- Greenhouse gases, 128–130
 carbon dioxide, 339
 fluxes, 49
 global warming, 134, 339
 methane, 339
 nitrous oxide, 339
 sink, 353
- Ground-penetrating radars (GPRs), 653, 655
 soil, 354–355
- Groundwater, 357
- Gully (linear) erosion, 357
- H**
- Hagberg falling number (HFN), 672
- Hardening, 357
- Hard layer
 management, 359
 penetration resistance, 358
 polyacrylamide (PAM), 359
 root growth, 358
 tillage, 358
- Hardpan soils
 penetration resistance, 357
 tillage, 357–360
- Hardsetting horizons
 resistance to penetration, 362
 structural arrangement, 362
- Hardsetting soils
 bulk densities, 361, 363
 characteristics, 360–361
 exchangeable sodium percentage (ESP), 361
 physical behavior, 361–363
 plant growth, 363
 processes, 361
 strength, 361
 tensile strength (TS) of aggregates, 363
- Harvest and after harvest processes
 agrophysical aspects, 463–464
 fruits and vegetables, 463–464
 grain crops, 463
 impacts, 462
- Harvest technology, 461
- Heat
 of adsorption, 7
 of condensation, 364
 of evaporation, 6
 isosteric, 6
 of sorption, 6
 of sublimation, 364
 of vaporization, 364
 of wetting, 364
- Heat and water transfer in soil
 background and applications, 156
 coupled, 155
 heat transfer, 159–160
- latent heat flux, 160–162
 moisture transfer, 159
 non-isothermal moisture transfer (NIMT), 156
 soil, 162
- theory, 157
- thermal moisture transfer (TMT), 156
- thermocapillary film flow, 157
- thermo-capillary meniscus flow, 157
- thermomictic effect, 157
- thermoosmotic flow, 157
- transfer mechanisms, 156–157
- water flow, 156
- Heat balance, 271–272, 364
 components, 273
 structure, 272–273
- Heat capacity, 364
- Heating
 commercial applications, 900
 infrared heating, 901
 radio-frequency, 900–901
- Henry's law, 364
- Hooke's law, 364
- Horticultural substrates, 364–367
 aggregate structure, 367
 air capacity, 366
 bulk density, 366
 classification, 365
 physical properties, 365–367
 porosity, 366
 type, 366
 water capacity, 366
 water retention, 366
 water retention curves, 367
- Humus, 367
- Humus parameters, 206
- Hydraulic diffusivity, 367
- Hydraulic fluxes, soil hydrophobicity, 754
- Hydraulic gradient, 368
- Hydraulic head, 368
- Hydraulic properties, 372, 374
 bimodal water retention, 376
 hydraulic conductivity, 369
 macropore conductivity, 373
 pedotransfer functions, 96
 pressure head, 369
 soil bulk density
 soil structure, 96
 soil texture, 96
 water retention curve, 369
 water retention function, 370
- Hydrodynamic dispersion, 376
- Hydrological processes, tropical watersheds, 937–938
- Hydrometeorological processes
 erosion, 376
 gleyization, 377
 illuviation, 377
 lateritization, 377
 overland flow, 377
 podsolisation, 377
 salinization, 377
 soil, 376
- Hydrophobicity
 advantages, 381
 aggregate stability, 381
 algae, 379
 bacterial exudates, 379
 capillary rise method (CSR), 380
 causes, 379
 contact angle, 379
 disadvantages, 381
 ethanol droplet test, 380
 geographical occurrence, 379
 organic compounds, 379

- H**
- Hydrophobicity (*Continued*)
 plant leaves, 379
 root mucilage, 379
 sessile drop method, 380
 severity, 381
 soil, 378, 382
 soil-water contact angle, 380
 surface tension of water, 382
 water drop penetration time test (WDPT), 380
 water repellency, 379–381
- Hypobaric storage, 384
- Hysteresis
 capillary water, 385
 foods, 384
 hygroscopic water, 385
 loop, 385
 soil, 385
 soil water retention curve (SWRC), 385
 types, 384
- I**
- Ice erosion (glacial erosion, thermal erosion), 387
- Illuviation, 387
- Image acquisition, 945
- Image analysis
 agrophysics, 387, 388
 applications, 388–389
 color, 388
 plant drought stress, 608–609
- Image processing, 946, 947, 950
- Imaging system
 flow processes, 442
 plant growth, 442
 root system architecture, 443
 root-water-soil relations, 442
- Imaging systems, 682
- Imbibition, 390
- Indicator plants, 390
- Infiltrability, 390
- Infiltration, 393
 cumulative, 391
 horizontal, 391
 rainfall, 392
 soil, 390–392
 sorptivity, 391
 unsaturated conductivity, 391
 unsteady, 390–391
 vertical, 391
- Insolation, 393
- Institute of Agrophysics
 in Lublin, 393–396
 in Saint-Petersburg, 396–399
- Integrated drainage, 399
- Interflow, 400
- Intermolecular interaction
 adsorption, 878
 catalysis, 878–879
 chemical forces, 878
 diffusive forces, 878
 dispersive (van der Waals) forces, 878
 electrostatic (Coulomb) forces, 878
 steric forces, 878
- Internal drainage, 400
- International Organization for Standardization (ISO)
 TC 23 Tractors and machinery for agriculture and forestry, 854
 TC 134 Fertilizers and soil conditioners, 854
 TC 182 Geotechnics, 854
 TC 190 Soil quality, 854
- International Soil Physical and Hydraulic Databases, 196
- Interrill erosion, 400
- Intrasectioning surface approach, soil structure, 780
- Intrinsic permeability, 400
- Ion exchange, 400, 884–885
 cation exchange, 884
 counterions, 884
- Ion hydration, 400
- Ion uptake
 plant parameters, 602
 soil parameters, 602
- Irrigation, 400–402, 406
 advantages, 401
 aggregate stability, 404
 disadvantages, 401
 erosion, 405
 exchangeable sodium percentage (ESP), 405
 permeability, 405
 runoff, 405
 sealing, 405
 soil loss, 405
 soils, 404
 treated wastewater, 403
- Irrigation water, 444–446
 water productivity, 444–445
- Isoelectric point, 407
- Isotropy, 407–408
- K**
- Kargol and Przestalski gravi-osmotic hypothesis, 976
- Kedem & Katchalsky (KK) formalism equations, 465
- Kernels, 323
 barley, 326
 compressive strength, 616
 cracks, 615
 cultivars, 615–617
 genotype, 614
 hardness, 616
 mechanical strength parameters, 614
 modulus of elasticity, 615
 near-infrared hyperspectral imaging (NIR HSI), 326
 parenchyma cracking, 616
 physical properties, 613
- Single Kernel Characterization system, 616
- TD-NMR technology (time-domain nuclear magnetic resonance), 326
- X-ray, 326
- Kinematic viscosity, 411
- Kirchhoff's Laws, 411
- Kriging, 411
- L**
- Lambert-Beer's law, X-ray computed tomography, 517
- Landfill, 414
- Land management, soil properties and functions, 454
- Land reclamation, 414
- Landslide, 414
- Land use, 9
 agroforestry, 26
- Langmuir equation, 3, 840
- Langmuir-Freundlich isotherm, 3
- Laplace equation, 414, 649
- Latent heat, 414
- Layered soils
 adsorption, 415
 aggregates, 423
 chemicals, 414
 convection-dispersion equation (CDE), 415
 equilibrium retention models, 416
 kinetic retention, 417
- kinetic retention reactions, 419
- Langmuir-type adsorption, 417
- layered soil linear adsorption, 416
- nonlinear Freundlich adsorption, 416
- pore volume, 416, 417, 420
- preferential flow, 420
- solute transport, 414, 418–420
- water and solute transport, 414
- water flow, 414
- water flux, 419
- water suction, 418
- water-unsaturated, 418
- Leaching
 of chemicals, 421
 cracks, 422
 diffusion, 422, 423
 macro-pores, 422
 soil structure, 421, 422
 solutes, 422, 423
- Legumes, 324
- Light interception, plant canopies, 424
- Limes
 characteristics, 426
 neutralizing power, 426
- Liming
 cation exchange capacity (CEC), 427
 infiltration, 427
 soil, 427
 soil permeability, 427
 soil structure, 427
- Liquid limit (upper plastic limit, Atterberg limit), 428
- Load, precompression stress, 864
- Losses
 harvest, 178
 leguminous plants, 178
 rapeseed, 178–179
- Lysimeters, 431
 application, 430
 evapotranspiration, 428–430
 history, 429
 percolating water, 430
 soil, 430
 solute transport, 428
 water balance, 428–430
- M**
- Machine-plant interaction theory, 461–463
- Machine-plant material system, 461
- Machines, 14–20, 24, 25
 agriculture, 14
 designing, 14
 food, 20
 GIS technology, 20
 GPS navigation, 20
 intelligent, 20
- Machine vision
 agriculture, 433
 animals, 435
 automatic picking, 435
 detection of weeds, 433
 fruits, 435
 quality assessment, 433
 sorting by color, 433
- Magnetic properties
 applications, 437–438
 measurements, 437
 soils, 436–439
 susceptibility, 438
- Magnetic resonance imaging (MRI), 439
 applications, 441–443
 basics, 440
- Larmor frequency, 440

- longitudinal relaxation, 440
 magnetic resonance sounding, 441
 pulse, 440
 pulses of electromagnetic irradiation, 441
 spin echo, 440, 441
 transverse, 440
Magnetic resonance tomography (MRT), 439
Magnetic treatment
 effects, 445
 plant growth, 445, 446
 plant roots, 445
 seed germination, 445–446
 water productivity, 446
Management practices, 448
 biological activity, 64
 enzyme activities, 64
 fertilization, 64
 liming, 64
 microbial activity, 64
 rotation, 64
 soil, 64, 449
Manganese concentration in cereal crops
 soil organic matter, 911
 soil pH, 911
Manning formula, 875
Mapping, 455–460
Maps
 color, 456
 construction, 456–457
 hydro-physical properties of soils, 457–458
 Polish soils, 459
 potential denitrification in soils, 458
 soil-cartographic database, 456
 soil redox properties, 458
 soil specific surface area, 458
 water retention, 459
Marketing standards
 fruits, 674
 vegetables, 674
Mass, 190
Material
 acoustic emission, 967
 electrical properties, 966
 mass transfer properties, 966
 optical properties, 966–967
 rheological properties, 965–966
 thermal properties, 966
Matrix of the soil, 460
Maximum principle stress
 contact pressure, 864
 tyre sizes, 864
Maxwell-De Loor mixing model, 249
Maxwell's model, 695
Mean particle size, 190
Measurement methods
 mechanical, 792
 sedimentation, 792
Mechanical damage, 320
Mechanical impedance, 163–166, 228
Mechanical properties
 cereal plants, 177
 leguminous plants, 178
 rapeseed pods, 178
 seed grasses, 177
Mechanical resilience, soils, 464
Mechanical strength
 land use, 778
 precompression stress (Pc), 779
 soils, 779
 structured soils, 778
Membranes
 Ginsburg model, 468
 mechanistic formalism, 466
 porous structures, 467
 soil-root-xylem system, 465
 water transport, 465–470
Mercury intrusion porosimeters
 cumulative curves, 649
 differential curves, 649
Methods
 adsorption/desorption isotherm, 648
 adsorption from solution, 841
 advantages and limitations, 648
 chemical imaging in agriculture, 113
 conductometric, 260
 coulometric, 260
 differential thermal analysis, 276
 direct, 7
 electrolytic, 260
 electron microscopy, 114
 fluorescence techniques, 114
 indirect, 7
 magnetic resonance, 114
 mass spectrometry, 114
 mercury porosimetry, 648–649
 molecule cross-sectional area, 841
 near-infrared hyperspectral imaging (NIR-HSI), 326
 nuclear magnetic resonance, 114
 potentiometric, 260
 real-time PCR, 225
 retention of polar liquids, 841
 single kernel characterization system (SKCS), 111
 TD-NMR technology (time-domain nuclear magnetic resonance), 326
 tunnel microscopy, 647
 ultrafast spectroscopy, 114
 vibrational imaging, 114
 voltammetric, 260
 X-ray, 325, 326, 647
 X ray diffraction (XRD), 276
 X ray spectroscopy, 114
Michaelis-Menten equation, 601
Microbes
 soil habitat, 474
 soil structure, 470, 473–474
 transport, 472
 transport processes, 475
Microbial parameters, 206
Microcosm, 475
Micro-irrigation, 475–476
Microstructure
 apple, 477, 479
 carrot, 477
 image analysis, 478
 images, 477, 479
 onion, 479
 plant tissue, 476–480
 potato, 479
 potato parenchyma, 477
 stereological methods, 478–479
Mindlin-Deresiewicz tangential contact model, 811
Mineralisation, 481
Mineral-organic-microbial interactions
 adsorption, 482
 interactions, 481
 microorganisms, 481
 organic matter, 481
 soil minerals, 481
Mineral soil, 275–279
Mobile-immobile model (MIM), 822
Models, 485
 analogue, 42
 conceptual, 387
 crop, 44
 empirical, 387
 equilibrium and kinetic type, 416
 erosion, 44
European Soil Erosion Model (EUROSEM), 746
 food, 42
Griffith University Erosion System Template (GUEST), 746
Langmuir-type adsorption, 417
mathematical-physical, 43
mathematical-statistical, 43
phenomenological, 42
real, 42
 soil swelling, 306
statistical-physical, 43
Universal Soil Equation (USLE), 746
Water Erosion Prediction Project (WEPP), 746
Modulus of elasticity (Young's modulus), 489
Modulus of rigidity, 489
Mohr-Coulomb equation, 811
Mohre circle of stress, 489
Moisture, 8
Monitoring
 agriculture and environment, 489
 electrical conductivity, 491
 frequency domain reflectometry (FDR), 491
 physical conditions, 489
 remote sensing, 491–492
 salinity, 490
 soil moisture, 491
 temperature, 491
 time domain reflectometry (TDR), 491
Mualem equation, 492
Mulching
 effects, 493–495
 materials, 493
 soils, 494
Multispectral images
 fruit detection, 951–952
 robotic fruit harvesting, 951
Münch model, 977
 gravi-osmosis, 977
 osmometers, 977, 978
 phloem transport, 977
 turgor pressure, 977
Münch pressure-flow theory, 976
Munsell color system, 496
Mycorrhizal symbiosis, osmotic stress, 496–497

N
Nanomaterials
 biosensors, 499–501
 carbon nanotubes, 500
 in chromatography, 501
 in electrochemical biosensors, 500, 501
 electronic nose, 502
 electronic tongue, 501–502
 food, 499–503
 mass sensitive sensors, 502
 nanocomposites, 500
 nanocrystalline materials, 500
 nanometals, 500
 nanoparticles, 500–502
 nanowires, 500–502
 in optical sensors, 501
 soil, 499
 ssDNA-wrapped single-walled carbon nanotube (SWCNT), 502
Natural environment, 25
Nature conservation
 certificate and control subsystem, 504
 decision taking subsystem, 504
 management, 504
 planning subsystem, 504

- Nature conservation (*Continued*)
 subsystem of diagnosis, 504
 subsystem of tasks realization, 504
- Near ground atmosphere
 albedo, 598
 heat balance, 598
 photosynthetically active radiation (PAR), 598
 physics, 597–599
 radiation balance, 598
 solar radiation, 598
 temperature, 598
- Neural networks
 agrophysical applications, 507, 508
 applications, 506
 concepts, 506
 crop production, 507, 508
 drying process, 509
 food quality, 502, 507–508
 modelling approaches, 508
 modelling of hydrophysical properties, 507
 sensitivity, 510–511
 soil surveys, 507
 training, 505–507
 validation, 509–511
- Newton's laws, 214
- Nondestructive measurements
 color, 513
 electrical resistance blocks, 514
 frequency domain reflectometry (FDR), 514
 fruit, 511
 neutron scattering, 514
 nuclear magnetic resonance spectroscopy, 512, 514
 soil, 513
 tensiometry, 514, 515
 time domain reflectometry (TDR), 513–515
 X ray computed tomography, 514
- Nondestructive methods, fruits, 584
- Nondestructive testing
 acid content, 512
 firmness, 512
 fruits, 512
 internal defects, 512
 shape and size, 512
 sugar content, 512
 weight, 512
- Noninvasive quantification
 3D architectures, 516
 X ray computed tomography, 516–517
- Nuclear magnetic resonance (NMR), 440
 quality evaluation, 581
- Numerical methods (model), 520
- O**
- Ohm's law, 521
- Online measurements
 bulk density, 522
 soil compaction, 522
 soil moisture content, 522, 523
 soil physical properties, 521–523
- Organic dusts
 electric permeability, 525
 electrostatic properties, 523–526
- Organic farming, soil structure, 527
- Organic matter, 528, 594
- Organic soil
 hydrophobicity, 555
 shrinkage, 555
 subsidence, 555
- Ornamental plants
 resistance to buckling, 534
 rigidity, 534
- tensile strength, 534
 tensile stress, 534
- Ornamental plants, physical properties, 534–535
- Orstein
 penetration resistance, 535
 water retention, 535
- Osmometers, 977
- Osmosis, 881
- Osmotic adjustment, diurnal strains, 222
- Overburden pressure, 536
- Overland flow
 infiltration capacity, 536
 rainfall, 536
 topographic slope, 536
 vegetation, 536
- Oxidation-reduction conditions
 effects of pH, 537
 redox potential, 537
 soil, 536
- Oxygen, 13
 availability, 11
- Oxygen diffusion rate (ODR), 262
- Oxygen flux density (OFD), 262
- Oxygenology
 oxygen in nature, 541
 subbranches, 541
- P**
- Packing density, 543
- Pan
 claypans, 122
 fragipans, 122
 hardpans, 122
 plowpans, 122
 plowsoles, 122
 pressure pans, 122
 traffic pans, 122
- Parent material
 alluvial, 544–545
 colluvial, 544
 eolian, 546
 geological classification, 544–546
 glacial, 545–546
 lacustrine, 545
 marine, 545
 organic nature, 546
 physical weathering, 543
 residual, 544
 rocks, 543
 soil, 543–547
 till, 545
- Partial pressure, 547
- Particle density, 547
- Particle film technology, 547
 application, 548
 crop plants, 548
 fruits and vegetables, 548
 insect control, 548
- Particle size distribution, 190, 549
 Fraunhofer/Mie theories, 793
 laser light beam, 793
- Particulate organic matter, 549
- Peat
 ash content, 552
 bulk density, 552–553
 decomposition degree, 552
 functions, 550
 particle density, 552–553
 physical properties, 551–555
 types, 552
- Peatlands
 classification, 549
 conservation, 550
 ecological significance, 549–550
- functions, 548–551
 occurrence and development, 549
- peats, 552
 threats, 550
 types, 552
- Peat soil
 ash content, 553
 bulk density, 553
 degree of decomposition, 553
 hydraulic conductivity, 554
 moisture retention, 553–554
 peat shrinkage, 554–555
 porosity, 553
 von Post system of humification, 553
 water retention curves, 554
- Ped, 555
- Pedon, 555
- Pedotransfer functions, 43, 507, 591
 accuracy and reliability, 559
 agrophysical research, 559
 evaluation and selection, 558–559
 hydraulic conductivity, 556
 inputs, 557
 methods to develop, 557–558
 pressure head, 557
 soil, 556, 557
 spatial context, 557
 water retention, 556
 water retention curve, 557
- Penck-Oppokov equation, 956
- Penetrability, 561
- Penetration resistance, 561, 828
 autocorrelation functions, 830
 power spectra, 831
 soil depth, 829
- Penetrometer resistance
 crosscorrelograms, 832
 pedotransfer function, 229
- Penman-Monteith (PM) equation, 283, 561
- Penman's equation, 283, 561
- Perched groundwater, 561
- Percolation, 561
- Permafrost, 561
- Permanent charge, 561
- Permeability, 561
- Philip's equation, 391, 392
- Photosynthesis, 561, 854
 C3 plants, 856
 stomatal conductance, 855
- Phototropism, 636
 light intensity, 635
- Phyllosilicates, classification, 117
- Physical characteristics
 agricultural products, 568
 breeding, 610–621
- Physical conditions, 490
 agricultural products, 669
- Physical degradation
 compaction, 562
 crusting, 562
 pores, 562
 redox potential, 562
 soil, 562
 water infiltration, 562
- Physical phenomena, agricultural products, 568
- Physical processes and properties
 agricultural products, 34
 impact on soil and plants, 6
- Physical properties
 acoustic, 324
 agricultural products, 579–587
 electrical, 324
 food quality, 574–576

- food structure, 574
 grain, 326–329
 hardness, 591
 magnetic, 324
 mechanical, 324
 optical, 324
 of plants and agricultural products, 189–193
 quality in foods, 573–578
 raw materials, 579
 redoximorphic features, 591
 seeds, 325
 soil classification, 589–592
 soil saturation, 591
 thermal, 324
 tropical soils, 934–937
Physical properties of food, density, 575
Physical properties of grains
 crushing strength, 110
 density, 110
 hardness, 110
 rapture energy, 110
 rapture force, 110
 shear strength, 110
Physical soil parameters, 206
Physics
 near ground atmosphere, 597–599
 plant nutrition, 600
Piezometer head, 602
Planck's law, 602
Plant biomechanics
 bidirectional stress, 603
 historical perspective, 602–603
 mechanical strength, 604
 tensegrity, 604
 tissue stresses, 603
 turgor, 603
Plant breeding
 cereals, 612–617
 grain resistance to mechanical damage, 613
Plant canopy, light interception, 424
Plant diseases
 classification, 605
 colored images, 605–608
 machine vision systems, 608
 visual disease symptom, 606
Plant drought stress
 image analysis, 608–609
 leaf temperature, 608
 leaf transpiration, 608
 leaf-water potential, 609
 machine vision imaging, 609
Plant lodging
 cereals, 609
 resistant varieties, 610
 yield losses, 610
Plant nutrition
 convection, 600
 diffusion, 600
 diffusive double layer (DDL), 600
 physics, 600–602
 solute flux, 600
Plant production
 air temperature, 985
 solar radiation, 984–985
 sunshine, 985
 weather, 984
Plant root
 slope stability, 622
 soil structure, 628–630
 strength, 622–627
Plants, 12, 220–223, 267, 333, 877–886
 airflow, 47
 atmospheric carbon, 80
 beam deflection, 61
 bending, 61, 602
 bending toughness, 61
 breeding, 41
 diurnal strains, 220, 222
 electromagnetic field, 268
 electroosmosis, 886
 elementary supply, 601
 growth, 40, 267–269
 lodging, 41, 61
 mechanical properties, 61–62
 morphological traits, 618, 619
 osmotic stress, 497
 photosynthesis, 12
 productivity, 40
 quality, 40
 renewable energy, 78
 rhizosphere, 63
 rod bending, 62
 shrinkage, 223
 specific surface area, 839
 stalks, 61
 stems, 61
 stomatal closure, 12
 surface phenomenon, 877
 swelling, 223
 transpiration, 879
 water-atmosphere contact area, 879
 yield structure, 618, 619
Plants and agricultural products
 aerodynamic properties, 191
 electromagnetic properties, 193
 hygroscopic properties, 192
 mechanical properties, 192–193
 thermal properties, 191–192
Plants growth
 air humidity, 986
 air pressure, 986
 cloudiness, 986
 precipitation, 986
Plant-soil interactions, modeling, 637, 638
Plant species, critical velocity, 332
Plant temperature, 633
 stomata, 632
 transpiration, 632
Plant tissue, microstructure, 476–480
Plant tropisms, gravitropism, 633–635
Plant water requirement
 climatic conditions, 980
 irrigation techniques and management, 980–981
 specific water requirement (SWR), 980
 transpiration, 980
Plant wellness, machine vision technique, 637
Plasticity, 639
Plasticity number, 639
Plasticizers and water, 697
Plastic limit, 639
Poiseuille's law, 370, 639
Polish Society of Agrophysics
 branches, 639
 location, 639
Polymerase chain reaction (PCR), 225
Pores
 elongated, 641
 macrophotograph, 642
 microphotograph, 642
 morphology, 642–644
 soil, 641, 643
 thin sections, 642
 voids, 641
 water movement, 642
Pore size distribution, 647
 bi- and multimodal, 646
 lognormal, 646
 measurements, 646
 soil, 645, 646
Porosimetry, 649
 soil, 647
Porosity, 190, 650
Power spectra
 clay content, 835
 corn yield, 835
 soil water storage (SWS), 835
Precision agriculture, 21
 hyperspectral analysis, 655
 proximal soil sensing, 650
Precompression stress (Pc), 656, 868
 actual soil pressure for subsoils, 872
 classification, 871
 cyclic compressibility, 869
 effective soil strength, 872
 load, 864
 loading cycle, 869
 maps, 870
 modeling, 872
 soil strength, 866
 subsoils, 871
Pressure potential, 656–657
Primed CO₂-C efflux, 664
Priming effects
 apparent, 661–662
 CO₂-C, 661
 CO₂-C efflux, 660
 mechanisms, 657–665
 microbial biomass, 658, 660
 real, 661–662
 soil acidity (pH), 664–665
 soil organic matter, 657
 substrate C, 658–660
 substrate properties, 662
Processes, wind erosion, 997–1000
Proton nuclear magnetic resonance, soil-water interaction, 667
Proximal soil sensing
 applications, 655
 concepts, 651–655
 global navigation satellite system (GNSS), 651
 precision agriculture, 650, 655
Proximal soil sensors, 652
Puddling
 cracking, 668
 lowland rice, 667
 preferential flow, 668
 soil aggregates, 667
 soil structural degradation, 668
Pugging, 668
- Q**
- Quality**
 apples, 675
 barley, 673
 citrus fruits, 675
 fruits, 673, 674
 peaches, 675
 potato, 676
 rice, 673
 tomato, 676
 vegetables, 673, 674
Quality in foods, physical properties, 573–578
Quartz, 275–279
 content, 277–278
 determination, 276
 estimation, 278
 thermal conductivity, 275
Quenching, 4

R

Radiation balance, 271
 Rainfall interception
 cereal plants, 680
 cultivated plants, 679
 measurement, 679, 680
 Raoult's law, 6
 Raw materials, 14–18, 20, 24,
 25, 587
 measurement of texture, 582–583
 testing, 16
 Raw materials and foods, 964
 acoustic emission, 967
 Redox processes
 natural environments, 538
 soils, 537
 transformation of elements, 537
 Redox resistance of soil, 458
 Reflectivity, 681
 Remediation, contaminated
 soils, 596
 Remote sensing
 components, 682
 data/image interpretation, 683
 electromagnetic spectrum, 683
 grain yield, 688
 land-use/land-cover change, 689
 organic matter, 765–766
 precision farming, 689
 radiometric resolution, 683
 reflectance values, 687
 salinity, 690
 soil compaction, 767
 soil heterogeneity, 690
 soil mapping, 690
 soil moisture, 689
 soil physical degradation, 761
 soil processes, 690
 soil reflectance, 684
 soil salinization, 767
 soil surface sealing, 766–767
 spatial resolution, 682
 spectral curves, 683
 spectral resolution, 682
 temporal resolution, 683
 weeds and stress, 689
 Remote sensing and GIS
 desertification, 768
 floods, 765
 soil contamination, 767–768
 soil degradation survey, 762
 Remote sensing and photogrammetric methods
 landslides, 764
 soil erosion, 763–764
 Renewable energy, hydrogen, 78
 Reservoirs
 groundwater level, 974
 soil moisture, 974
 Resistivity
 compaction, 257
 cracks, 259
 profiles, 257
 Reynolds number, 10, 413
 Rheological functions, 695–696
 Rheological models, 695
 Rheological parameters, 206
 Rheology, 289, 699
 agricultural products, 693
 foods, 693
 micromechanics, 701
 rheopexy, 700
 shear stress, 701
 soil, 701
 stiffness, 701

strain, 701
 thixotropy, 700
 Rhizosphere, 705–708
 acidity, 707
 mucilaginous layers, 706
 plant roots, 705, 706
 redox potential, 707
 root-colonising microorganisms, 705
 root-soil contact, 707
 root-soil water relations, 707
 soil, 706
 soil bulk density, 706
 soil strength, 706
 soil structure, 705–706
 water and ions, 707–708
 Richards equation, 368, 372–374,
 800, 809
 Rigidity, 709
 Rill erosion, 709
 Robotic fruit harvesting
 machine vision, 953
 multispectral imaging, 951, 953
 Robots, 24, 25
 Root
 anatomical structure, 467
 apoplastic route, 467
 bending stiffness, 230
 crops, soil strength, 173
 elongation, 229, 231
 matric potential, 229
 membrane model, 468
 nutrient transfer, 601
 nutrient uptake, 601
 penetration, 230
 radial water transport, 468
 respiration, 12
 single-membrane model, 467
 symplastic route, 467
 water transport, 467–470
 Root growth, 170
 bulk density, 229
 elongation rate, 228
 macropores, 171
 matric potential, 228
 mechanical resistance, 629
 pressure, 229
 soil structure, 629
 strength, 229
 Root growth and function
 optimum root size, 172
 pores, 171
 soil strength discontinuity, 170
 water uptake, 171
 Root reinforcement
 hill slopes, 623
 mechanisms, 622–624
 models, 624, 626
 pullout strength, 624
 soil, 623
 tensile strength, 624
 Root responses
 hypoxia, 710, 711
 matric potential, 710
 mechanical impedance, 710
 penetrometer resistance, 710
 soil physical limitations, 709
 temperature, 711
 water stress, 711
 Root-soil interplay, quantification,
 630
 Root system architecture
 classification, 712–713
 diversity, 712–713
 modelling, 715–716

Root systems

 architecture, 713–715
 classification, 714, 715
 Root tensile strength-root diameter, 626
 species, 625
 Root-to-shoot signaling
 abscisic acid (ABA), 172
 mechanisms, 172
 stomatal diffusive resistance, 172
 Root water uptake
 3-D functional approaches, 717–721
 polymer tensiometers, 752
 soil hydraulic properties, 749
 stressed conditions, 751
 TDR measurements, 752
 Roughness, 722
 Runoff, 722

S

Salinity
 anions, 724
 availability of water, 724
 electrical conductivity(EC), 723
 osmotic stress, 724
 sodium adsorption ratio (SAR), 723
 soil permeability, 723
 soils, 723
 soil structure, 723
 Saturated hydraulic conductivity, irrigation, 404
 Scaling
 fractal analysis, 728
 measurement scale, 727
 methodology, 728
 model scale, 727
 nonlinearity, 728
 particle size distribution, 728
 scale triplet, 727
 soil hydraulic conductivity, 728
 soil physical properties, 725
 Scene constraint, 944
 Sealed soils
 hydraulic properties, 788
 infiltration, 789
 Seedbed, hydraulic conductivity, 165
 Seeds, 324
 aerodynamic properties, 330
 commercial cultivars, 618–621
 cracking, 732
 cultivars, 621
 deformation, 621
 elastic deformation, 621
 geometry, 330
 germination, 267–269
 leguminous plants, 617
 mechanical damage, 617
 mechanical loads, 619, 621
 plant species, 330
 resistance to mechanical loads, 617
 swelling, 732
 Seeds and grains, aerodynamic characteristics,
 329
 Seepage, 729
 Sensors
 acoustic, 653–654
 electrical, 651–652
 electrochemical, 654–655
 electromagnetic, 651–652
 mechanical, 653–654
 mechanical resistance, 653
 optical, 652–653
 pneumatic, 653–654
 radiometric, 652–653
 Sensory evaluation, 730
 Shear resistance, 317

- Shear strength, 730
 Shear stress, 730
 Sheet erosion, 730
 Sheet flow, 730
 Shelterbelt, 1000–1003
 agricultural landscape, 1001
 agricultural production, 1003
 biodiversity protection, 1003
 biogeochemical barriers, 1002
 chemistry of water flowing, 1002
 functions, 1001
 heat and water balances, 1001–1002
 microclimatic conditions, 1001–1002
 wind erosion, 1002
 Shrinkage, 190
 agricultural products, 730
 curve, 734
 mechanism, 731
 models, 734
 seeds and grain, 731
 soil, 733
 Slaking, 736
 Slope stability
 plant root, 622
 root reinforcement, 622
 Snowmelt infiltration, 736
 Soil(s), 123, 224–231, 236, 242–253, 256–267,
 274, 301–303, 305–307, 310, 316–317,
 336, 339, 393, 402, 439–443, 652, 653,
 655, 683–684, 821, 823, 877–886
 acidification, 425
 adsorption isotherm, 821
 aggregate formation, 448–449
 aggregates, 403, 423, 518
 aggregate stability, 404
 aggregation, 147, 531, 886
 aggregation of clay particles, 993
 air-entry value, 371
 air-filled pores, 11
 air-filled porosity, 11, 218
 air permeability, 10
 alkalinity, 51
 amelioration, 382
 amplitude sweep test, 702
 anisotropy, 56, 98
 anisotropy of pore functions, 451
 anthropogenic ferrimagnetics, 438
 atmospheric carbon, 80
 atmospheric CO₂, 108
 available moisture range (AMR), 41
 available water capacity (AWC), 531
 bacteria, 72
 bare and mulched, 815
 base cations, 450
 bending force, 534
 bimodal water retention, 373
 biochemical activity, 63
 biocolloids, 66, 67
 biofilms, 70, 72
 biogenic structures, 234
 buffer capacity, 94
 bulk density, 10, 11, 98, 218, 229, 334,
 335, 522
 bypass flow, 100
 capillarity, 226–227
 capillary rise method, 380
 capillary water, 385
 carbon sink, 353–354
 cation exchange capacity (CEC), 245, 263, 427
 cementation, 528, 535
 cementation bonds, 994
 chemicals, 414
 CH₄ fluxes, 343–345, 349, 352
 clay minerals, 117, 136, 264
 CO₂ fluxes, 341–343
 cohesion, 317
 colloids, 66, 265
 color index, 141
 coloring process, 142
 compaction, 21, 97, 258, 277, 334, 335, 358,
 451–453, 532, 993
 compaction curves, 97
 computer tomography (CT), 751
 conditioners, 146
 conductivity, 251
 conservation tillage, 495
 convection-dispersion equation (CDE), 415
 cracks, 163, 259
 crop yield, 453
 crusting, 39, 40
 crusting and sealing, 494
 crusts, 786
 C sequestration, 234
 3D architectures, 516
 deformation, 449–450, 453, 454
 denitrification, 538
 densification, 532
 density-swell magnitude relations, 993
 dielectric permittivity, 247, 248, 253
 diffusion, 215, 422, 423
 diffusion coefficient, 10, 11
 diffusivity, 391
 disinfection, 814
 dispersion, 301–303
 DNA, 224, 225
 Dokuchaiev, 141
 drainage, 400
 3D structure, 517
 dualpermeability equation, 103
 dual-permeability models, 372
 dual-porosity models, 372
 3D X-ray attenuation map, 518, 519
 effective permittivity, 248
 electrical conductivity, 243, 247, 253
 electrical profile, 259
 electrical properties, 242
 electrical resistivity tomography, 259
 electrochemical methods, 263
 electron (pe) and proton (pH) variable, 31
 electroosmosis, 886
 emissivity, 94
 energetically heterogeneous surfaces, 4
 energetic heterogeneity, 4
 energy distribution functions, 4
 enzymes, 63
 erosion, 40, 377, 405, 453, 532
 erosion risk, 494–495
 ethanol droplet test, 380
 evaporation, 282, 377
 exchangeable cations, 450
 exchangeable sodium percentage (ESP), 405
 ferromagnetic minerals, 437
 flocculation, 301
 flooding, 305
 flow processes, 788
 food, 499
 fractals, 311
 fragmentation, 259
 freezing and thawing, 97
 friction, 316–317
 functions, 449–450
 funnel flow, 100
 gas and solute diffusion, 217
 gas composition, 451
 gas diffusion, 218
 gaseous flux, 529, 530
 gases, 9
 gas exchange, 808
 gleyization, 377
 global positioning system (GPS), 354
 greenhouse gases, 234
 ground-penetrating radar, 354–355
 hard layer, 358, 359
 hardpan, 357
 hardsetting, 360
 heat capacity, 219
 heat flow, 158–159
 heating, 814
 heat transfer, 217
 humus, 136
 hydraulic functions, 371, 373
 hydraulic conductivity, 51, 97, 147, 161, 215,
 370, 372, 373, 449, 451, 453, 556, 749
 hydraulic conductivity function, 369, 373
 hydraulic parameters, 371
 hydraulic properties, 234, 368, 370
 hydrologic and hydraulic properties, 959
 hydropedological processes, 376
 hydrophobicity, 378, 380
 hygroscopic water, 385
 hyperacid soils, 31
 hysteresis, 369, 385
 illuviation, 377
 image analysis, 389, 517, 518
 imaging, 442
 infiltration, 335, 377, 390, 391, 427
 infiltration rate, 405–406
 intra-aggregate macropores, 518
 irrigation, 400, 404, 405
 isothermal vapor diffusivity, 161
 laminar flow, 413
 land use, 778
 latent heat flux, 160, 161
 lateritization, 377
 layered, 414, 416, 418
 leaching, 423
 lime additions, 994
 liming, 425, 427
 loading tests, 868
 macroaggregates, 593
 MACRO model, 103
 macropore conductivity, 373
 macropore flow, 100
 magnetic iron oxides/sulfides, 437
 magnetic minerals, 437
 magnetic parameters, 438
 magnetic properties, 436, 437
 magnetic resonance imaging, 441, 751
 magnetic susceptibility, 437, 438
 magnetism, 438
 management practices, 448
 management systems, 454
 mass flux, 809
 matric potential, 228, 229, 316, 341, 451, 749
 mechanical and hydraulic properties, 335
 mechanical properties, 307
 mechanical resilience, 464
 mechanical stress, 452
 methane oxidation, 352
 methanotrophic bacteria, 352
 microaggregates, 593
 microbes, 63
 microbial activity, 340
 microbial biomass, 472
 microbial function, 473
 microhabitats, 473
 micromechanics, 701
 micromorphology, 147
 microorganisms, 11
 microsites, 63
 mineral permittivities, 252
 minerals, 250

- Soil(s) (Continued)**
- moisture diffusivity, 214, 216
 - moisture potential, 215
 - moisture profile, 916
 - moisture tension, 11, 218
 - mulching, 494
 - multilayered, 415
 - Munsell soil-color charts, 142
 - nanomaterials, 499–503
 - NO emissions, 345
 - N₂O emissions, 345, 348
 - N₂O fluxes, 346, 347, 349
 - nondestructive measurements, 513–515
 - nonecological functions, 748
 - noninvasive examinations, 516
 - N₂O sink, 353
 - organic matter, 342, 358–359
 - organo-mineral associations, 117
 - organo-mineral matrixes, 136
 - overland flow, 377
 - oxidation processes, 538
 - oxidation-reduction reaction, 12
 - oxygen, 11
 - oxygen diffusion rate (ODR), 10
 - parent rocks, 135
 - particle size distribution, 245, 252, 371
 - pathogen, 814
 - pathogenic bacteria, 73
 - pedology, 376–377
 - pedotransfer functions, 371, 374
 - penetration resistance, 96, 359, 494
 - penetrometer resistance, 229
 - pe-pH diagrams, 538
 - permeability, 56, 377, 405
 - permittivity, 250, 251
 - permittivity contrasts, 248
 - pF curve, 368
 - phylosilicates, 117
 - physical characteristics, 276
 - physical properties, 278
 - physical properties and processes, 528
 - podsolisation, 377
 - polyacrylamide (PAM), 359
 - pore channels, 518
 - pore-connectivity parameter, 371
 - pore network, 473, 514, 517–519
 - pore-size distribution, 371
 - pore-size distribution models, 371
 - pore spaces, 516, 517, 519
 - pore water pressure, 11
 - porosity, 147, 278
 - potentiometric method, 261
 - precompression stress (Pc), 779
 - preferential flow, 100, 372, 822
 - pressure head, 369, 557
 - priming effect, 657
 - processes, 24
 - quartz, 275, 277–279
 - redox buffering capacity, 539
 - redox potential (Eh), 353, 452, 539, 562
 - redox reactions, 539
 - redox resistance, 539
 - resistance to penetration, 362
 - respiration, 12, 340, 538
 - retention curve, 371
 - rheology, 700
 - root and microbial activity, 108
 - rotational rheometer, 702
 - runoff, 405
 - salinization, 377
 - saturated hydraulic conductivity, 335, 404
 - seal formation, 787
 - sealing, 51, 405
 - seals, 787
 - seed germination, 358
 - sessile drop method, 380
 - shearing, 334, 335
 - shear strength, 316
 - shrinkage, 56, 305, 306, 733–735
 - shrinkage cracks, 518
 - single point imaging, 442
 - sodic/sodicity, 50, 51
 - soil microorganisms, 11
 - solarization, 814
 - solute retention, 416
 - solute transport, 819
 - sorption, 95
 - sorptivity, 824
 - specific surface area (SSA), 120, 251, 839
 - stiffness, 701
 - stiffness degradation, 704
 - strain, 701
 - strength, 56, 147, 229, 230, 992
 - stress and soil effects, 451
 - stress-strain relationship, 703
 - structural arrangement, 362
 - structural stability, 305, 307
 - structure, 50, 56, 96, 258, 317, 403, 449, 450, 453, 473
 - subsoil compaction, 453
 - subsurface downslope flow, 377
 - superhydrphobicity, 378
 - surface heterogeneity, 4
 - surface tension of water, 382
 - swell behavior, 994
 - swell/collapse behavior, 994
 - swelling, 56, 305, 306, 733–735, 993
 - swell potential, 994
 - synthetic agents, 146–147
 - temperature, 161, 340–342, 494, 891–894
 - texture, 96, 317
 - thermal conductivity, 161, 219, 275, 279
 - thermal diffusivity, 218, 219
 - thermal liquid diffusivity, 161
 - thermal properties and process, 893
 - thermal vapor diffusivity, 161
 - thermo-dielectric effect, 252
 - tillage, 359, 905
 - time-displacement curves, 868
 - trafficability, 912
 - trafficability and workability, 912
 - transport processes, 51, 475
 - treated wastewater, 403
 - turbulent flow, 413
 - unimodal hydraulic properties, 373
 - unsaturated, 368
 - unsaturated flow, 372
 - unsaturated flow theories, 369
 - vapor flux, 158
 - void ratio, 994
 - voltammetric methods, 262
 - volumetric heat capacity, 161
 - water, 494
 - water and heat balance, 809
 - water content, 98
 - water diffusivity, 369
 - water drop penetration time test (WDPT), 380
 - water erosion, 335
 - water filled pore space (WFPS), 341, 342, 346
 - water flow, 370, 376
 - water flow by capillarity, 227
 - water flux, 158
 - water management, 281
 - water movement, 100
 - water repellency, 335, 380
 - water retention, 51, 556
 - water retention curve (WRC), 97, 369, 385
 - water retention function, 368
 - weathering, 135
 - wetting and drying, 96, 992–995
 - workability, 912
 - X ray attenuation map, 518, 519
 - X ray computed microtomography, 516, 517
 - X ray computed tomography, 514, 516–517
 - X-ray imaging, 752
 - Soil aggregates/Soil aggregation, 594
 - bacteria, 471
 - evaporation, 740
 - fungi, 471
 - hierarchy, 593
 - microsites, 471
 - organic carbon, 592
 - organic matter, 593, 738
 - pedotransfer functions, 556
 - physical protection, 592
 - pore morphology, 738, 739
 - slaking, 738, 739
 - stability, 738, 739
 - stability, measuring, 737
 - strength, 739
 - Soil and root water flow, coupled model, 718
 - Soil biota
 - engineer of the soil, 741
 - impact on physical properties, 740
 - Soilborne diseases, control (management), 813
 - Soilborne pathogens, disinfestation, 813
 - Soil classification
 - physical properties, 589–592
 - redoximorphic features, 591
 - Soil color
 - CIELAB, 143
 - Munsell, 143
 - quantifying, 142–143
 - Soil compactibility/compressibility
 - measurement, 743–744
 - precompaction stress, 742
 - Soil compression
 - cyclic loading, 744
 - repeated loading, 744
 - static loading, 744
 - Soil deformation
 - ground contact pressures, 865
 - shear displacements, 865
 - shear stress, 865
 - wheel loads, 865
 - Soil degradation, 768
 - remote sensing methods, 763
 - Soil disinfection
 - heating, 813
 - solarization, 814
 - Soil erodibility, 746
 - Soil erosion, models, 746
 - Soil fluxes, lysimeters, 428
 - Soil functions
 - ecological, 643, 747
 - macrophotograph, 643
 - pore morphology, 642
 - socioeconomic, 643
 - Soil hydraulic properties, 370
 - compaction, 96
 - hydraulic conductivity function (HCF), 97
 - root water uptake, 749
 - texture, 96
 - water retention curve (WRC), 97
 - Soil hydrology, stable isotopes, 849
 - Soil hydrophobicity, hydraulic fluxes, 754
 - Soil matrix potential
 - osmometers, 897
 - psychrometers, 897
 - Soil organic carbon (SOC), physical protection, 592–594

- Soil organic matter (SOM), 529, 658, 860
stratification, 858
- Soil parental materials, 547
weathering, 595–596
- Soil particles
laser diffraction method, 793
sedimentation methods, 792
sieve pipette method, 793
- Soil penetrability
animal burrowing, 754
aquatic species, 756
invertebrates, 755
semifossorial insect, 755
vertebrates, 755
- Soil penetrometers, 757, 758
cone index, 758
contour plot of cone index, 759
insertion speed, 758
penetrability, 758, 759
tools in agrophysics, 759
- Soil phases, 249, 760–761
concentric arrangements, 249
three-phasic system, 760
- Soil physical and hydraulic properties, 194–198
- Soil physical conditions
crop establishment, 167–169
emergence, 167–169
germination, 167–169
root growth, 167
- Soil physical degradation, 761–768
remote sensing, 761
- Soil physical limitations, root responses, 709
- Soil physical properties, 180–184, 546–547,
667–668, 827
aggregate and particle-size fractions,
663–664
aggregate stability, 493
bulk density, 493
concept of scale, 726
kriging, 726
mapping, 455–460
maps, 456
moisture, 662–663
mulching, 492
online measurements, 521–523
porosity, 493
primed CO₂–C efflux, 663
process scale, 726
scale dependency, 725
semivariogram, 726
structure, 493
structure and aggregation, 298
temperature, 663
water retention, 298
water transmission, 298
wavelet analysis, 726
wildfires, 996–1000
- Soil physical quality
aeration, 771–772
aggregate stability, 773–774
assessment, 770–771
concepts, 771–773
 friability, 773
least limiting water range (LLWR),
774
mechanical impedance, 772
resistance and resilience, 775
S-index, 774
structure and stability, 772–773
temperature, 772
water intake and delivery, 771
water retention curve, 775
- Soil physical stresses, feedback, 711
- Soil-plant-atmosphere continuum (SPAC), 9, 598,
599, 805, 857
scale, 806
transpiration, 750
water flow, 751
- Soil-plant-atmosphere system
modeling of mass and energy transfer, 809
resistance theory, 807
stomatal conductance, 855
water movement, 808
- Soil-plant models
3D root water uptake, 719
soil and xylem water potential, 720
- Soil-plant-water system, 851
- Soil pores, 777
capillary, 645–646
classification, 645–646
continuity, 641
image analysis, 640
irregularity, 641
macropores, 646
orientation, 641
shape, 641
submicroscopic, 645
system, 643
thin sections, 641
- Soil porosity, stratification, 858
- Soil recovery, 337
- Soil reflectance
mineral composition, 684
moisture, 684
organic matter, 684
texture, 684
- Soil-root-xylem system
membranes, 465–467
water transport, 465–467
- Soil separates, 777
- Soil solarization
controlling pathogens, 815
mulch, 815
sprayable polymers, 815
- Soil solution, electrical conductivity, 246
- Soil strength, 164–166
- Soil structure, 304–307, 780
cracks, 421
fungal hyphal networks, 470
intersecting surfaces approach (ISA), 780
leaching, 421, 422
lysimeters, 430
macro-pores, 422
mechanical strength, 778
microbes, 470
microorganisms, 470
percolating water, 430
plant root, 628–630
visual assessment, 783
- Soil surface
crusting, 786
sealing, 786
- Soil texture, 791
- Soil tilth, 798
biofuel feedstock production effects, 796
carbon content, 797
concepts, 795
cover crop effects, 796
crop rotation effects, 796
tillage effects, 795
- Soil water
agriculture, 803
economy, 804
European Water Framework Directive,
804
fingering, 801
function, 802
- hydrologic cycle, 803
legislation, 804
management, 803
management subsystem, 803
preferential flow, 801
retention capacity, 802
unsaturated, 800
- Soil water budget
actual evapotranspiration, 962
available water capacity, 962
calculations, 962
evapotranspiration, 961
field capacity, 960
fluxes of water, 961
hydraulic conductivity, 960
soil moisture, 960
surface runoff, 961
water absorption, 961
water flow, 961
wilting point, 960
- Soil water flow, 801
concepts, 798
model, 718
saturated, 799
- Soil water management
progression, 802
- Soil-water-plant relationship
mass and energy transport, 807
- Soil water potential (pressure, head), 805
- Soil welding, 805
- Soil-wheel interactions, 812
semiempirical model, 811
- Soil-wheel interface, traction analysis, 811
- Solar drying systems
biological materials, 816
dryers, 818
fish, 818
fruit, 817
grain, 817
medical plants, 817
vegetables, 817
wood, 817
- Solid (true) density, 190
- Solubility, 881–882
- Solute flux
hydrodynamic dispersion, 820
mechanical dispersion, 820
molecular diffusion, 820
- Solutes
adsorption isotherm, 821
preferential flow, 822
- Solute transport, 823
advection, 820
convection, 820
molecular diffusion, 820
soil, 819
- Sorption, 7, 824
isotherm, 6
- Sorptivity
application, 825
measurement, 824
soil, 824
theory, 824
- Space soil physics
reduced gravity, 826
space agriculture, 826
- Spatial relationship
crosscorrelation function, 831
soil temperature, 831
tractor wheels, 832
- Spatial scales
corn yield, 834
soil clay content, 834
soil water storage (SWS), 834

- Spatial variability, 827
of properties and processes, 827
soil penetration resistance, 827
traffic patterns, 827
- Spatial variation
clay content, 833
corn yield, 833
crosscorrelograms, 833
penetration resistance, 833
soil water storage, 833
- Specific surface area, 190, 843
calculation, 840
cation exchange capacity (CEC), 842
chemical methods, 840
clay fraction, 842
external, 843
methods, 841
physical methods, 839
plants, 841
soil organic matter, 842
soils, 839, 841, 842
total, 843
- Spectral analysis, 837
- Spectral and cross-spectral analysis, 838
- Spectral techniques, 837
- Sphericity, 190
- Stable isotopes, 845
abundance, 846, 850
background, 846
environment, 850
expression mode, 850
global-scale studies, 846
greenhouse gas, 846
isotopic signature, 852
microbial functionality, 847
nitrate leaching, 852
properties, 850
rainfalls, 851
soil, 847
soil hydrology, 849, 851
soil-plant-atmosphere system, 852
- Standardization, agrophysics, 854
- Steady flow, 854
- Stefan-Boltzman law, 948
- Sticky, 854
- Stochastic model, 854
- Stokes' law, 854
- Stomata, 857
- Stomatal conductance
empirical models, 855
modeling, 855
soil-plant-atmosphere system, 855
- Storage, agricultural products, 567–572
- Stratification, 860
management system, 859
soil bulk density, 859
soil organic carbon, 859
soil organic matter, 858
soil porosity, 858
- Straw, 21
briquettes, 22
energy resource, 22
- Strength, 861
- Stress, elastic deformation, 291
- Stress relaxation, 861
- Stress relaxation curve, 694
- Stress state transducer system (SST)
ground contact pressures, 863
stress transducers, 863
tyre inflation pressures, 863
wheel loads, 863
- Stress–strain relationship, 862
precompression stress P_c (internal soil strength), 867
soil strength, 867
strain theory, 862
stress propagation, 863
stress theory, 862
- Subdrainage, 869
- Subirrigation, 870
- Subsoil compaction
air capacity, 873
German Soil Protection Law, 870
- Subsoil, European Soil Framework Directive, 870
- Subsurface water, 874
artesian wells, 876
confined aquifers, 876
qanats, 876
- Surface and subsurface water
schematic, 875
streamflow discharge, 875
- Surface and subsurface waters, 877
- Surface area, 190
- Surface charge
electrostatic, 883
formation, 883
humus, 883
permanent, 883
point of zero charge (PZC), 883
- Surface free energy (surface tension)
intermolecular forces, 879
liquid-gas interface, 879
- Surface phenomena
colloidal systems, 882
surface charge, 882–884
- Surface properties, 877–886
soils, 877
- Surface roughness
characteristics, 887
infiltration, 888
measurement, 887–888
overland flow, 888
soil, 888
water transfer, 887
- Surface runoff, 889
- Surface storage capacity, 889
- Surface tension, 889
- Surface water, 874
- Surface-water excess, 889
- Suspension, 889
- Swelling
agricultural products, 730
seeds and grain, 732
soil, 733
- T**
- Temkin isotherm, 3
- Temperature, 8
bacteria, 894
biotic processes, 893–894
coupled heat and water transfer, 893
gases, dissolution and diffusion, 893
germination rate (GR), 893
mulching the soil surface, 894
soil, 891–894
soil respiration, 894
soil water content, 892
soil water potential, 892
- Tensile strength, 895
- Tensiometer
functioning, 896
soil water matric potential, 896
soil water potential, 897
- Tensiometry, 895–897
soil water potential, 895
- Terrestrial ecosystems, water balance, 955
- Thermal capacity, 897
- Thermal conductivity
deVries model, 486
effective medium theory (EMT) model, 486–487
frozen foods, 483–488
geometric mean model (GMM), 487
Gori model, 486
Levy model, 486
Mascheroni model, 486
Maxwell-Eucken (Maxwell-E) model, 485–486
modified resistor series model, 487
parallel model (//), 487
series model (Σ), 487
temperature, 484, 485
- Thermal diffusivity, 898
- Thermal imaging, 948–950
fruit detection, 950
fruit harvesting, 944
image processing, 946
orchard, 946
temperature profile of fruits and leaves, 949
visible imaging, 950
- Thermal properties and process
biotic processes, 893
germination rate (GR), 893
soil, 893
- Thermal radiation, brightness temperature, 94
- Thermal technologies
food, 898
food processing, 898–902
inductive heating, 898
ohmic heating, 898–899
- Thermomechanics of biopolymers, 696–697
- Thermosequence, 902
- Thixotropy, 903
- Thomson (Kelvin) equation, 648
- Tillage, 64, 181, 357–358
adaptable, 1
 CO_2 emissions, 108
conventional, 905
critical depth, 920–921
effects on carbon losses, 108
environmentally sound, 905
inflection point, 920
lower tillage limit (dry, LTL), 919
mean weight diameter, 921
optimum tillage moisture content
OPT, 920
recommendations, 905
soil, 905
soil aeration, 108
soil erosion, 108
soil moisture deficit, 920–921
soil structure, 920
soil water status, 919–920
specific energy, 921
tractive force requirements, 918
upper tillage limit (wet, UTL), 919
weight diameter, 921
wheel ruts, 915
- Tillage erosion
control, 908
downslope, 906
hillslope, 906
measurement, 907
soil displacement, 906
soil flux, 907
soil profile modification, 908
soil transport coefficients, 907
tillage translocation, 907
transport coefficients, 908

- Tillage pan, 909
 Tilth, 910
 Tissue
 elastic modulus, 581
 mechanical strength, 581
 texture, 581
 Tomography, acoustic, 1
 Toposequence, 910
 Top soil, 910
 Trace elements in crops
 redox conditions, 910–911
 soil texture, 910
 Traffability
 consistency and density of soils, 918
 ecosystems, 915–916
 forecasting, 917
 impeded drainage, 916
 moisture profiles, 916
 off-road traffics, 915–916
 soil, 912
 soil compaction, 915
 soil compactness, 915
 soil hydraulic properties, 915
 soil structure, 920
 soil water potential, 921
 Traffability and workability
 Atterberg consistency, 913
 biological activity, 904
 carbon balance, 904
 climate change, 894
 consistency diagram, 914
 consistency states, 914
 coupled heat and water transfer, 893
 environment, 904
 matrix potential (suction) and the water retention curve of soil, 914
 measurement methods, 913
 moisture profiles, 916
 offland plowing, 915
 onland plowing, 915
 organic C content, 894
 pedogenic processes, 891–892
 ratio of water, 904
 soil, 912
 soil criteria, 913
 soil hydraulic properties, 915
 soil-implement interaction, 913
 stickiness and slipperiness, 913
 temperature, 891–894
 thermal properties and processes, 893
 tillage, 903
 tillage implements, 912–913
 traffability, 912
 traffability and workability, 913
 water intake, 904
 wheel ruts, 915
 workability, 912
 Traffic farming
 advantages, 155
 controlled, 153
 history, 154–155
 traffic lanes, 153
 Transmissivity, 924
 Transpiration, 854, 856, 924
 models, 857
 stomatal conductance, 855
 Transpiration ratio, 924
 Transport, microbes, 472
 Treated wastewater, 924
 characteristics, 403
 sodium adsorption ratio (SAR), 403
 Triaxial compression test, 924–925
 Trickle irrigation, 925
- Tropical fruits and vegetables, 925–933
 colour, 933
 shape, 933
 Tropical soils
 aggregate stability, 935
 bulk density, 935
 consistency, 935–936
 dispersion ratio, 935
 gully erosion, 936
 hydraulic conductivity, 936
 infiltration rate, 936
 management, 936–937
 permeability, 935, 936
 physical properties, 934–937
 shrink-swell characteristics, 936
 soil moisture retention, 936
 structure, 935
 texture, 934
 Tropical watersheds
 climate, 937
 hillslope hydrology, 938
 hydrological processes, 937–938
 soils and geology, 937
 topography, 938
 vegetation, 937
- Turbidity
 basics, 938
 measurements, 939
 nephelometric turbidity units, 939
 readily dispersible clay (RDC), 939
- Turf, 940
 Turgor pressure, 940, 977
 Two-phase flow, 940
- Tyres
 braking force, 148
 bulldozing effect, 149
 contact area, 149–150
 contact pressure, 151
 inflation pressure, 149
 rolling resistance, 148
 size, 150
 traction force, 148
 trailer, 149
- U**
 Underground runoff, 941
 Units and dimensions
 agriculture, 564–567
 application, 564–566
 quantities, 564–566
 Unsteady, 392–393
 Unsteady flow, 941
 Urban soils, functions
 biodiversity pool and gene reservoir, 941
 buffer, 942
 filter, 942
 geological and archaeological heritage, 942
 raw materials, 942
 storage, 942
 transformation functions, 942
 US Soil Taxonomy System, 590
- V**
 Vadose zone, 943
 van der Waals attraction forces, 266
 van der Waals forces, 145, 302, 943
 van Genuchten equation, 371, 556, 943
 van't Hoff's rule, 893–894
 Vapor pressure, 943
 Vegetation
 absorption, 687
 aerosol free vegetation index (AFRI), 686
 atmospherically resistant vegetation index (ARVI), 686
 enhanced vegetation index (EVI), 686
 generic normalized difference vegetation index (NDVI), 685, 686
 green normalized difference vegetation index (GNDVI), 687
 normalized difference moisture/normalized difference water index (NDMI/NDWI), 685
 ratio vegetation index, 685
 red edge, 687
 red-infrared triangle (vegetation boater), 687
 red simple ratio, 685
 reflectance, 687
 soil-adjusted vegetation index (SAVI), 686
 triangular vegetation index, 686
 visible atmospherically resistant index (VARI), 686
 Vessel water transport, 976
 Dixon-Renner transpiration-cohesion theory, 976
 Kargol and Przestalski gravi-osmotic hypothesis, 976
 Münch pressure-flow theory, 976–977
 Viscosity, 943
 Visible imaging
 fruit detection, 947, 950
 fruit harvesting, 944, 946
 image processing, 945
 orchard, 946
 Visual assessment, soil structure, 783
 Visual soil assessment (VSA)
 aggregates, 784
 soil structure, 783
 Visual soil structure quality, pores, 784
 Vitreosity, 954
 Void ratio, 954
 Volume, 190
 Volumetric water content, 954
 Vughs, 954
- W**
 Washburn equation, 648
 Water
 activity, 6
 agricultural products, 971–972
 agriculture, 983
 application efficiency, 955
 in cellular structure, 698
 fresh, 874
 global, 874
 physical properties, 964–967, 971
 residence times, 874
 Water balance, 963
 concept, 955–956
 global water circulation, 956–957
 terrestrial ecosystem, 955–959
 Water budget
 soil, 959–963
 soil hydrologic and hydraulic properties, 959
 Water cycle in catchment, 958
 after beginning of rainfall, 957
 end of dry period, 957
 global water distribution, 957
 near end of rainfall, 957
 Water erosion
 off-site effects, 969–970
 on-site effects, 968–969
 perspective, 970
 water flow, 892
 Water for plants
 irrigation systems, 981
 preventing surface runoff, 981
 rainfall runoff, 982
 soil amendments, 981–982

- Water for plants (*Continued*)
 soil mulching, 982
 tillage practices, 981
- Waterlogged soil, 984
- Water movement, equations, 217
- Water phenomenon, 977
- Water potential, 6
 enthalpy, 5
- Water quality, 876–877
 pollution, 876
 soil salinization, 876
- Water release curve, 973
- Water-repellent, 984
- Water reservoirs
 dam, 973
 dug, 973
- Watershed, 984
- Water stress, 975
- Water table, 975
- Water transfer, 893
 surface roughness, 887–888
- Water translocation system in plants
 agrophysical aspects, 975
 long distances, 975–978
 Münch model, 977, 978
 osmometer, 978
 phloem, 978
 plant root, 975
 reverse osmosis, 978
 theories, 975–976
 xylem, 978
- Water uptake, agrophysical aspects, 975
- Water uptake by plants
 passive and active water movement, 807
 transpiration, 807
- Water use efficiency (WUE)
 agriculture, 979–983
 approaches and methods, 980–983
 irrigation techniques and management, 980–981
 irrigation water, 979
 opportunities for improvement, 979–983
 rainfall water, 979
- Water vapor in soil, 892
- Weather
 air humidity, 986
 air pressure, 986
 air temperature, 985
 atmosphere-plant-soil system, 984
 biomass production, 984, 985
 cloudiness, 986
 plants, 984–987
- precipitation, 986
 solar radiation, 984–985
 sunshine, 985
 vegetation, 987
- Wetlands
 degradation and loss, 989
 ecosystem functions, 990
 functions, 988
 habitats for native plants and animals, 989
 management, 989–990
 restoration, 990
 retention of nutrients and pollutants, 988
 transformation, 988
 water budgets, 988, 990
 water retention, 988
- Wetness, 992
- Wettability, 880–881, 992
 solid-liquid-gas contact, 880
 surface tensions, 880
- Wetting and drying
 aggregation of clay particles, 993
 axial deformations, 995
 cementation bond, 994
 compaction, 993
 density-swell magnitude relations, 993
 lime addition, 995
 lime stabilized soil, 995
 soil, 992–995
 swell behavior, 994
 swell/collapse behavior, 994
 void ratio, 994
- Wetting-drying cycles
 aggregation of clay particles, 993
 compaction, 993
- Wetting front, 996
- Wheat
 grading factors, 671
 grain, 671
 quality, 670, 671
- Wien's law, 996
- Wildfires, soil physical properties, 996–1000
- Williams-Landel-Ferry (WLF)
 transformation, 695
- Wilting point, 997
- Windbreak, 1000–1003
 functions, 1001
 heat and water balances, 1001–1002
 microclimatic conditions, 1001–1002
- Wind erosion, 997–1000
 aerodynamic drag force, 998
 aerodynamic lift force, 998
- agriculture, 999
 background, 997
 cohesive force, 998
 electric force, 998
 gravitational force, 998
 Magnus force, 998
 mitigation measures, 999
 processes, 997–998
 saltation, 998, 999
 sediment mass flux, 998
 transport coefficients, 907–908
- Workability
 lower tillage limit (dry, LTL), 919
 Petelkau, 918
 soil, 912
 soil compaction, 919
 soil moisture, 918
 soil moisture status, 917
 soil texture, 918
 soil water status, 919–920
 upper tillage limit (wet, UTL), 919
- World reference base (WRB) for soil resources, 590–591
- X**
- X-ray images
 cereal grain, 1006–1007
 cracking of endosperm, 1006
 loss of a germ, 1006
- X-ray method (XRM), 1005–1008
 quality of grain, 1005
- X-ray pictures
 damage of grain, 1007
 infected kernels, 1006
- X-ray radiation, 24
- X-ray structural analysis, grain, 1008
- Y**
- Young's equation, 379, 880
- Young's modulus, 702
- Young's modulus of elasticity, 291
- Z**
- Zeta potential, 269
 electrokinetic sonic amplitude, 266
 electroosmosis, 265
 electrophoresis, 265
 laser Doppler velocimetry, 266
 measurement, 265
 streaming potential, 266